Scientific Programming

Next-Generation Optimization Models and Algorithms in Cloud and Fog Computing

Lead Guest Editor: Punit Gupta
Guest Editors: Kashif Zia

Next-Generation Optimization Models and Algorithms in Cloud and Fog Computing

Scientific Programming

Next-Generation Optimization Models and Algorithms in Cloud and Fog Computing

Lead Guest Editor: Punit Gupta
Guest Editors: Kashif Zia

Contents

Contents

Contents

Contents

Contents

Contents

Hindawi
Scientific Programming
Volume 2023, Article ID 9867894, 1 page
https://doi.org/10.1155/2023/9867894

Retraction

Retracted: Ice and Snow Sports Education Based on 5G Cloud Computing to Improve the Social Adaptability of Southern University Students

Scientific Programming

Received 31 October 2023; Accepted 31 October 2023; Published 1 November 2023

This article has been retracted by Hindawi following an investigation undertaken by the publisher [1]. This investigation has uncovered evidence of one or more of the following indicators of systematic manipulation of the publication process:

(1) Discrepancies in scope
(2) Discrepancies in the description of the research reported
(3) Discrepancies between the availability of data and the research described
(4) Inappropriate citations
(5) Incoherent, meaningless and/or irrelevant content included in the article
(6) Peer-review manipulation

The presence of these indicators undermines our confidence in the integrity of the article's content and we cannot, therefore, vouch for its reliability. Please note that this notice is intended solely to alert readers that the content of this article is unreliable. We have not investigated whether authors were aware of or involved in the systematic manipulation of the publication process.

Wiley and Hindawi regrets that the usual quality checks did not identify these issues before publication and have since put additional measures in place to safeguard research integrity.

We wish to credit our own Research Integrity and Research Publishing teams and anonymous and named external researchers and research integrity experts for contributing to this investigation.

The corresponding author, as the representative of all authors, has been given the opportunity to register their agreement or disagreement to this retraction. We have kept a record of any response received.

References

[1] D. Zhang and C. Xia, "Ice and Snow Sports Education Based on 5G Cloud Computing to Improve the Social Adaptability of Southern University Students," *Scientific Programming*, vol. 2021, Article ID 3828624, 12 pages, 2021.

Hindawi
Scientific Programming
Volume 2023, Article ID 9821378, 1 page
https://doi.org/10.1155/2023/9821378

Retraction

Retracted: Enlightenment of Physical Education Teaching Experiment Based on Cloud Computing to the Current Physical Education Reform

Scientific Programming

Received 26 September 2023; Accepted 26 September 2023; Published 27 September 2023

This article has been retracted by Hindawi following an investigation undertaken by the publisher [1]. This investigation has uncovered evidence of one or more of the following indicators of systematic manipulation of the publication process:

(1) Discrepancies in scope
(2) Discrepancies in the description of the research reported
(3) Discrepancies between the availability of data and the research described
(4) Inappropriate citations
(5) Incoherent, meaningless and/or irrelevant content included in the article
(6) Peer-review manipulation

The presence of these indicators undermines our confidence in the integrity of the article's content and we cannot, therefore, vouch for its reliability. Please note that this notice is intended solely to alert readers that the content of this article is unreliable. We have not investigated whether authors were aware of or involved in the systematic manipulation of the publication process.

Wiley and Hindawi regrets that the usual quality checks did not identify these issues before publication and have since put additional measures in place to safeguard research integrity.

We wish to credit our own Research Integrity and Research Publishing teams and anonymous and named external researchers and research integrity experts for contributing to this investigation.

The corresponding author, as the representative of all authors, has been given the opportunity to register their agreement or disagreement to this retraction. We have kept a record of any response received.

References

[1] F. Wang, "Enlightenment of Physical Education Teaching Experiment Based on Cloud Computing to the Current Physical Education Reform," *Scientific Programming*, vol. 2021, Article ID 6607539, 11 pages, 2021.

Hindawi
Scientific Programming
Volume 2023, Article ID 9804141, 1 page
https://doi.org/10.1155/2023/9804141

Retraction

Retracted: Retrospection of the Optimization Model for Designing the Power Train of a Formula Student Race Car

Scientific Programming

Received 29 August 2023; Accepted 29 August 2023; Published 30 August 2023

This article has been retracted by Hindawi following an investigation undertaken by the publisher [1]. This investigation has uncovered evidence of one or more of the following indicators of systematic manipulation of the publication process:

(1) Discrepancies in scope
(2) Discrepancies in the description of the research reported
(3) Discrepancies between the availability of data and the research described
(4) Inappropriate citations
(5) Incoherent, meaningless and/or irrelevant content included in the article
(6) Peer-review manipulation

The presence of these indicators undermines our confidence in the integrity of the article's content and we cannot, therefore, vouch for its reliability. Please note that this notice is intended solely to alert readers that the content of this article is unreliable. We have not investigated whether authors were aware of or involved in the systematic manipulation of the publication process.

Wiley and Hindawi regrets that the usual quality checks did not identify these issues before publication and have since put additional measures in place to safeguard research integrity.

We wish to credit our own Research Integrity and Research Publishing teams and anonymous and named external researchers and research integrity experts for contributing to this investigation.

The corresponding author, as the representative of all authors, has been given the opportunity to register their agreement or disagreement to this retraction. We have kept a record of any response received.

References

[1] M. N. Kumar, V. Jagota, and M. Shabaz, "Retrospection of the Optimization Model for Designing the Power Train of a Formula Student Race Car," *Scientific Programming*, vol. 2021, Article ID 9465702, 9 pages, 2021.

Hindawi
Scientific Programming
Volume 2023, Article ID 9828120, 1 page
https://doi.org/10.1155/2023/9828120

Retraction

Retracted: The Process and Model Innovation of Ideological Education Network Communication in Colleges and Universities Based on Cloud Computing

Scientific Programming

Received 8 August 2023; Accepted 8 August 2023; Published 9 August 2023

This article has been retracted by Hindawi following an investigation undertaken by the publisher [1]. This investigation has uncovered evidence of one or more of the following indicators of systematic manipulation of the publication process:

(1) Discrepancies in scope
(2) Discrepancies in the description of the research reported
(3) Discrepancies between the availability of data and the research described
(4) Inappropriate citations
(5) Incoherent, meaningless and/or irrelevant content included in the article
(6) Peer-review manipulation

The presence of these indicators undermines our confidence in the integrity of the article's content and we cannot, therefore, vouch for its reliability. Please note that this notice is intended solely to alert readers that the content of this article is unreliable. We have not investigated whether authors were aware of or involved in the systematic manipulation of the publication process.

Wiley and Hindawi regrets that the usual quality checks did not identify these issues before publication and have since put additional measures in place to safeguard research integrity.

We wish to credit our own Research Integrity and Research Publishing teams and anonymous and named external researchers and research integrity experts for contributing to this investigation.

The corresponding author, as the representative of all authors, has been given the opportunity to register their agreement or disagreement to this retraction. We have kept a record of any response received.

References

[1] H. Zhan, "The Process and Model Innovation of Ideological Education Network Communication in Colleges and Universities Based on Cloud Computing," *Scientific Programming*, vol. 2021, Article ID 7302877, 7 pages, 2021.

Hindawi
Scientific Programming
Volume 2023, Article ID 9810957, 1 page
https://doi.org/10.1155/2023/9810957

Retraction

Retracted: Construction of the Luxury Marketing Model Based on Machine Learning Classification Algorithm

Scientific Programming

Received 8 August 2023; Accepted 8 August 2023; Published 9 August 2023

This article has been retracted by Hindawi following an investigation undertaken by the publisher [1]. This investigation has uncovered evidence of one or more of the following indicators of systematic manipulation of the publication process:

(1) Discrepancies in scope
(2) Discrepancies in the description of the research reported
(3) Discrepancies between the availability of data and the research described
(4) Inappropriate citations
(5) Incoherent, meaningless and/or irrelevant content included in the article
(6) Peer-review manipulation

The presence of these indicators undermines our confidence in the integrity of the article's content and we cannot, therefore, vouch for its reliability. Please note that this notice is intended solely to alert readers that the content of this article is unreliable. We have not investigated whether authors were aware of or involved in the systematic manipulation of the publication process.

Wiley and Hindawi regrets that the usual quality checks did not identify these issues before publication and have since put additional measures in place to safeguard research integrity.

We wish to credit our own Research Integrity and Research Publishing teams and anonymous and named external researchers and research integrity experts for contributing to this investigation.

The corresponding author, as the representative of all authors, has been given the opportunity to register their agreement or disagreement to this retraction. We have kept a record of any response received.

References

[1] Q. Chen, S. Cai, and X. Gu, "Construction of the Luxury Marketing Model Based on Machine Learning Classification Algorithm," *Scientific Programming*, vol. 2021, Article ID 6511552, 11 pages, 2021.

Hindawi
Scientific Programming
Volume 2023, Article ID 9804737, 1 page
https://doi.org/10.1155/2023/9804737

Retraction

Retracted: Research on the Optimization Strategy of Innovation Behavior and Entrepreneurship Intention in Entrepreneurship Teaching

Scientific Programming

Received 8 August 2023; Accepted 8 August 2023; Published 9 August 2023

This article has been retracted by Hindawi following an investigation undertaken by the publisher [1]. This investigation has uncovered evidence of one or more of the following indicators of systematic manipulation of the publication process:

(1) Discrepancies in scope
(2) Discrepancies in the description of the research reported
(3) Discrepancies between the availability of data and the research described
(4) Inappropriate citations
(5) Incoherent, meaningless and/or irrelevant content included in the article
(6) Peer-review manipulation

The presence of these indicators undermines our confidence in the integrity of the article's content and we cannot, therefore, vouch for its reliability. Please note that this notice is intended solely to alert readers that the content of this article is unreliable. We have not investigated whether authors were aware of or involved in the systematic manipulation of the publication process.

Wiley and Hindawi regrets that the usual quality checks did not identify these issues before publication and have since put additional measures in place to safeguard research integrity.

We wish to credit our own Research Integrity and Research Publishing teams and anonymous and named external researchers and research integrity experts for contributing to this investigation.

The corresponding author, as the representative of all authors, has been given the opportunity to register their agreement or disagreement to this retraction. We have kept a record of any response received.

References

[1] J. Huang, J. Wu, B. Deng, and S. Bao, "Research on the Optimization Strategy of Innovation Behavior and Entrepreneurship Intention in Entrepreneurship Teaching," *Scientific Programming*, vol. 2021, Article ID 4872108, 6 pages, 2021.

Hindawi
Scientific Programming
Volume 2023, Article ID 9780749, 1 page
https://doi.org/10.1155/2023/9780749

Retraction

Retracted: A Global Optimization Algorithm for Intelligent Electromechanical Control System with Improved Filling Function

Scientific Programming

Received 8 August 2023; Accepted 8 August 2023; Published 9 August 2023

This article has been retracted by Hindawi following an investigation undertaken by the publisher [1]. This investigation has uncovered evidence of one or more of the following indicators of systematic manipulation of the publication process:

(1) Discrepancies in scope
(2) Discrepancies in the description of the research reported
(3) Discrepancies between the availability of data and the research described
(4) Inappropriate citations
(5) Incoherent, meaningless and/or irrelevant content included in the article
(6) Peer-review manipulation

The presence of these indicators undermines our confidence in the integrity of the article's content and we cannot, therefore, vouch for its reliability. Please note that this notice is intended solely to alert readers that the content of this article is unreliable. We have not investigated whether authors were aware of or involved in the systematic manipulation of the publication process.

Wiley and Hindawi regrets that the usual quality checks did not identify these issues before publication and have since put additional measures in place to safeguard research integrity.

We wish to credit our own Research Integrity and Research Publishing teams and anonymous and named external researchers and research integrity experts for contributing to this investigation.

The corresponding author, as the representative of all authors, has been given the opportunity to register their agreement or disagreement to this retraction. We have kept a record of any response received.

References

[1] S. Zhang, K. Srividya, I. Kakaravada et al., "A Global Optimization Algorithm for Intelligent Electromechanical Control System with Improved Filling Function," *Scientific Programming*, vol. 2022, Article ID 3361027, 10 pages, 2022.

Hindawi
Scientific Programming
Volume 2023, Article ID 9753907, 1 page
https://doi.org/10.1155/2023/9753907

Retraction

Retracted: Study on Resource Sharing Strategy of e-Commerce Innovation and Entrepreneurship Education Based on Cloud Computing

Scientific Programming

Received 8 August 2023; Accepted 8 August 2023; Published 9 August 2023

This article has been retracted by Hindawi following an investigation undertaken by the publisher [1]. This investigation has uncovered evidence of one or more of the following indicators of systematic manipulation of the publication process:

(1) Discrepancies in scope
(2) Discrepancies in the description of the research reported
(3) Discrepancies between the availability of data and the research described
(4) Inappropriate citations
(5) Incoherent, meaningless and/or irrelevant content included in the article
(6) Peer-review manipulation

The presence of these indicators undermines our confidence in the integrity of the article's content and we cannot, therefore, vouch for its reliability. Please note that this notice is intended solely to alert readers that the content of this article is unreliable. We have not investigated whether authors were aware of or involved in the systematic manipulation of the publication process.

Wiley and Hindawi regrets that the usual quality checks did not identify these issues before publication and have since put additional measures in place to safeguard research integrity.

We wish to credit our own Research Integrity and Research Publishing teams and anonymous and named external researchers and research integrity experts for contributing to this investigation.

The corresponding author, as the representative of all authors, has been given the opportunity to register their agreement or disagreement to this retraction. We have kept a record of any response received.

References

[1] Q. Cao, "Study on Resource Sharing Strategy of e-Commerce Innovation and Entrepreneurship Education Based on Cloud Computing," *Scientific Programming*, vol. 2021, Article ID 8268000, 8 pages, 2021.

Hindawi
Scientific Programming
Volume 2022, Article ID 2419291, 10 pages
https://doi.org/10.1155/2022/2419291

Review Article

Next-Generation Optimization Models and Algorithms in Cloud and Fog Computing Virtualization Security: The Present State and Future

Rohit Verma,[1] Dheeraj Rane ,[2] Ravi Shankar Jha ,[3] and Wubshet Ibrahim [4]

[1]*Department of CSE, Manipal Institute of Technology, MAHE, Manipal 576104, India*
[2]*Department of CSE, Indore Institute of Science and Technology, Indore 453331, India*
[3]*Department of CSE, Sharda University, Greater Noida 201310, India*
[4]*Department of Mathematics, Ambo University, Ambo, Ethiopia*

Correspondence should be addressed to Wubshet Ibrahim; wubshet.ibrahim@ambou.edu.et

Received 28 January 2022; Revised 19 April 2022; Accepted 26 May 2022; Published 30 July 2022

Academic Editor: Debo Cheng

Virtualization is becoming popular and is gaining widespread attention in recent years. However, with its popularity comes the challenge of securing the virtualized environment. Security measures for virtualized systems cannot always be applied in the same manner as in physical systems. Virtualized environments may have multiple virtual systems on the same physical machine, so different levels of security one needed. The hypervisor is the controlling program that provides the virtual systems' effective isolation and security. In this article, we present a comprehensive review of the existing security ideas and architectures for virtualized environment and some of the open issues in virtualization security.

1. Introduction

Since the 1960s, with the advent of the first virtual machine-enabled operating system for mainframes by IBM, virtualization has become very popular [1]. Currently, virtualization can be deployed on high end servers, normal personal computers, or even mobile devices such as mobile phones or handy tablets [2]. It divides the physical system into multiple virtual systems and gives the end user an illusion that he is working on the actual physical system. Nowadays, several information services and new technology paradigms, such as infinite computing (grid computing, cloud computing), web services, and other on-demand services, use virtualization as their core technology because of its economy and efficiency [3]. Most of the datacenters today rely on this technology for their functioning. Several big players in the market are introducing novel features and aspects to this technology on a continuous basis, such as VMware, Citrix, and KVM [4]. A report on Server Virtualization MCS 2010, by Kaspersky (server virtualization shipment forecast 2005 to 2014), stated that in 2010 more than half of the industry's installed workload was virtualized and in 2013 it is expected to surpass two-thirds of the installed workload [5]. Figure 1 show the tremendous increase in the number VMs (virtual machines) used in the industry for their different workloads (development/test/critical).

It is a fallacy to believe that virtualized settings are more secure than physical ones. Unfortunately, even though this idea has no basis in fact or logic, it might mislead some organizations into a false feeling of security when it comes to security requirements for virtualization initiatives. A virtual computer "looks" and performs exactly like any physical machine from the perspective of everything that interfaces or interacts with it. The hypervisor is usually the only thing that knows the machine is virtual. As a result, it is a basic fact that virtualized environments must still deal with all of the possible security issues that physical environments must deal with.

The virtualization provider operates, manages, and controls all components from the bare metal host operating system and hypervisor virtualization layer down to the

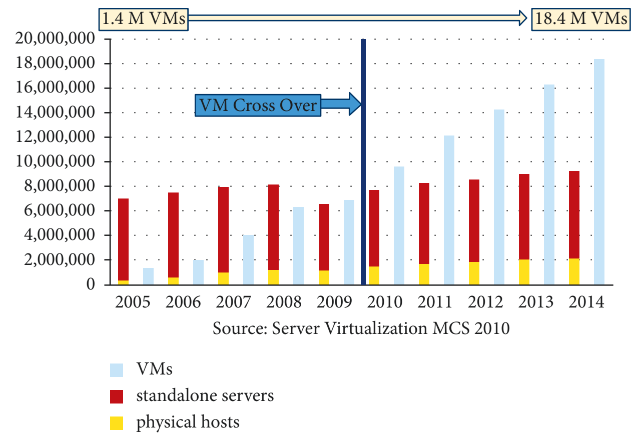

Figure 1: Increased number of VMs over the timeline.

physical security of the facilities where the services are provided under the shared responsibility paradigm [6]. It means that the virtualization provider oversees safeguarding the global infrastructure that underpins all of the services provided.

Physical security of datacenters with controlled, need-based access, location in nondescript facilities with 24/7 security guards, two-factor authentication, access logging and review, video surveillance, and disc degaussing and destruction are all things that your virtualization provider is responsible for. Provider's hardware infrastructure includes servers, storage devices, and other appliances. Operating systems, service applications, and virtualization software are all hosted on software infrastructure. Routers, switches, load balancers, firewalls, and cabling are examples of network infrastructure. Virtualization provider also keeps an eye on the network from the outside, safeguards access points, and offers redundant infrastructure with intrusion detection.

While the virtualization infrastructure is secured and maintained by provider, customers are responsible for security of everything they put in the cloud.

The customer is responsible for what is implemented by using provider services and for the applications that are connected to AWS. The security steps that customer must take depend on the services that they use and the complexity of the system.

Customer responsibilities include selecting and securing any instance operating systems, securing the applications that are launched on virtualization resources, security group configurations, firewall configurations, network configurations, and secure account management.

When customers use virtualization services, they maintain complete control over their content. Customers are responsible for managing critical content security requirements, including

(i) what content they choose to store on infrastructure
(ii) which provider services are used with the content
(iii) in what country that content is stored
(iv) the format and structure of that content and whether it is masked, anonymized, or encrypted
(v) who has access to that content and how those access rights are granted, managed, and revoked.

Customers retain control of what security they choose to implement to protect their own data, environment, applications, IAM configurations, and operating systems.

Along with its benefits and increased popularity, virtualization brings with it several security concerns. These are very critical and if not addressed properly the security of most datacenters and information services are at risk. Several security protection programs are emerging in research communities and markets, which emphasizes various aspects of virtualization.

In this paper, we organize these security architectures, threats, and solutions in a consolidated manner. Section 2 presents a brief overview of virtualization and virtual infrastructure. Section 3 discusses the vulnerabilities in a virtual infrastructure. Section 4 is a discussion on the various attack surfaces of virtualization. Sections 5 and 6 comprise brief discussion on the various attacks, mitigation, and other proposed architectures. Section 7 is an overview of future trends and various open issues in the virtualization security.

2. Background

In addition to the development and test workloads, organizations are now in the process of virtualizing even their most critical workloads. Also, virtualization is the core technology for many modern computing paradigms such as cloud computing [7, 8]. Commercial cloud providers use virtualization to provide and host different cloud services such as IaaS (Infrastructure as a Service). This allows users to benefit from virtualization in the form of reduced costs, easy availability, disaster recovery, and greater agility. They however need to realize that there are security risks that come along with these, such as easy creation/deletion/modification of VM and the fact that there is an entirely new infrastructure layer that needs to be secured. Attack on the virtual infrastructure can result in damage to the business drastically. The focus of this paper is to survey the current security vulnerabilities of virtualization.

2.1. Virtualization. Virtualization is the term commonly used to define abstraction of the underlying physical resources with logical objects [9]. This enables running multiple logical servers on a single physical server. Use of virtualization saves physical space, reduces power consumption, and saves network and storage cabling. Apart from this, virtualization also helps in providing hardware independence to operating systems and applications, dynamic provisioning to logical objects (operating systems or applications), better business continuity, better utilization of the physical resources, increased efficiency and responsiveness, better platform for legacy applications, and better isolation from other logical objects. All this is provided by a layer which lies in between the physical entity and the logical object known as the Virtual Machine Monitor (VMM). This layer decouples the physical resource from the multiple logical resources. Mainly three approaches are used to implement virtualization:

(i) *Full Virtualization.* In this approach, the logical object (may be VM) need not be modified to run over the VMM. Also, the VM or guest OS is not aware of the virtualization, as the whole physical system (BIOS, memory, storage, processor, etc.) is emulated to logical objects.

(ii) *Paravirtualization.* In this, the guest OS is aware of the presence of virtualization, as it is modified before being used in the virtual environment. This results in better performance of the guest OS than that in full virtualization.

(iii) *Hardware-Assisted Virtualization.* In this approach, virtualization is enabled at the hardware level. Intel's VT-x and AMD's SVM technology are examples of this. This runs the VMM at the higher privilege mode or ring than that of the guest OS and the VMM is responsible for all resource allocation and memory management using extended/nested page table.

In Figure 2, different types of virtualization techniques are shown. These are represented based on protection ring or hierarchical protection domains and privileges of different parts of virtualization.

2.2. Virtual Machine Monitor. Virtual Machine Monitor or VMM is the software layer used to provide a virtual environment [2]. This control program is responsible for monitoring and managing the virtual machines. VMM keeps track of the happenings in the VM such as resource allocation, device redirection, and policy enforcement. There are two types of VMM:

(i) Type 1: this VMM runs directly on the bare metal or hardware. This does not require any hosting OS. Type 1 VMM is popularly called hypervisor [10]. This type of VMM itself runs as an OS and then spawns the virtual machine after booting. Citrix XenServer, KVM, VMware ESX/ESXi, and Microsoft Hyper-V are examples of modern hypervisors. Bare metal architecture in Figure 2 uses type 1 VMM.

(ii) Type 2: this VMM runs on top of the hosting operating system and then spawns the virtual machines. It relies on the hosting OS for device support and physical resource management. This VMM runs as software inside the hosting OS. VMware Workstation and VirtualBox are example of this type of VMM. Hosted architecture shown in Figure 2 uses type 2 VMM.

2.3. Virtual Machine. The concept of virtual machine came into picture when IBM Corporation in the 1960s first created logical instances of the large mainframe computers for concurrent access. This logical instance or virtual machine gave an environment of the actual physical machine. Virtual machines are the OS installed in the virtual environment onto the VMM. VMs are the set of files which are used by the hypervisor/VMM for giving the end user an illusion of the physical machine. These VMs are easy to move or copy or manage. VMs provide isolation as the root of a guest virtual machine cannot access the host OS or host hardware or other VM.

3. Vulnerabilities

Virtualization improves resource utilization, eases the management of VM, and provides isolation and greater agility. At the same time, it adds vulnerabilities to the infrastructure. In virtualization, multiple VMs reside on the same physical host.

This may lead to compromising the VMs if any of the VMs or hypervisor or physical infrastructure is compromised, thus putting virtualization at higher risk of attack. Intra-VM communication is also one of the vulnerabilities, as the communication is through the hypervisor and does not need to go through the external network security solutions. Dynamicity of the infrastructure also adds to the vulnerability as the static security policy enforcement is uncertain over dynamic provisioning, decommission, and migration. "VM escape" is also one of the vulnerabilities; if the attacked VM can bypass the hypervisor and access the underlying host directly, it can attack at the hardware level in several ways such as DoS (Denial of Service) as it will get the root privileges. One of the vulnerabilities is "VM capturing," if an attacked VM can access the other VM and attack through it such as DDoS (Distributed DoS). Modifications to the hypervisor are also one of the vulnerabilities worth securing.

4. Attack Surface

Despite providing several benefits to the industry, the virtualization infrastructure also exposes a larger attack surface to the attacker, which is shown in Figure 3. The following are the major attack surfaces:

(i) Hypervisor

(ii) Virtual machine

(iii) Host machine

(iv) Management console.

As the hypervisor is the control point of the virtualization ecosystem, it has direct access to the underlying physical hardware and hosted virtual machines. It typically has full access to the environment which enables it to violate the security policies, privileges, and aggregation of duties. This makes it a crucial attack surface. According to IBM X-Force's Trend and Risk report [10], hypervisor is the largest attack surface. Also, the hypervisor has a very large number of lines of codes, which somewhat make it more vulnerable to attacks. Attack on the hypervisor, be it on the single point of failure gives the attacker root level (highest privilege) access to the hardware. This attack is analogous to the "man-in-the-middle" attack as it gives the attacker place

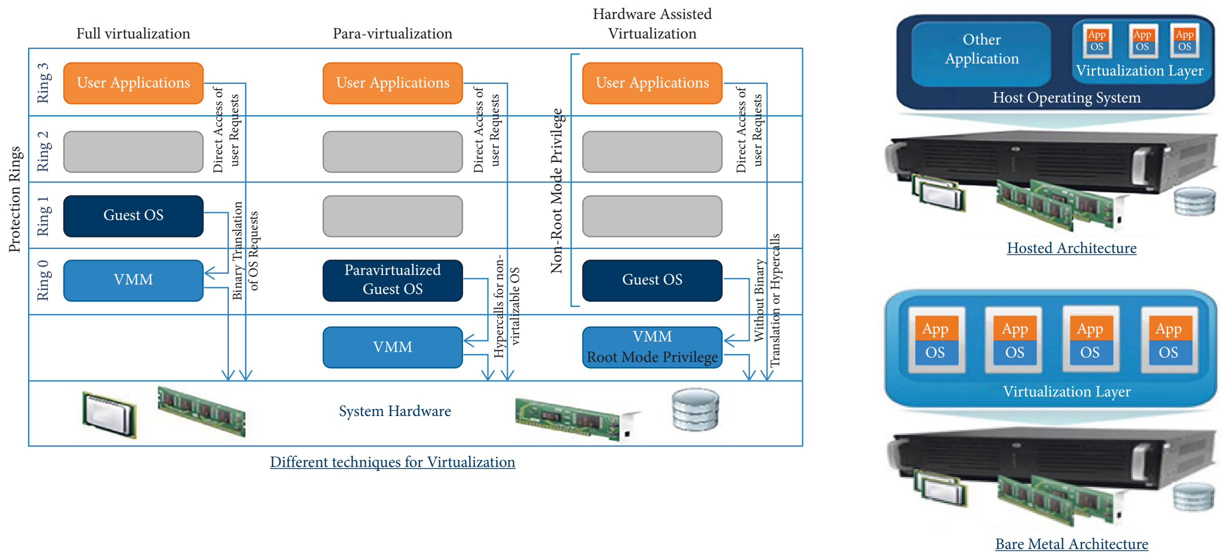

Figure 2: Different techniques and architectures in virtualization.

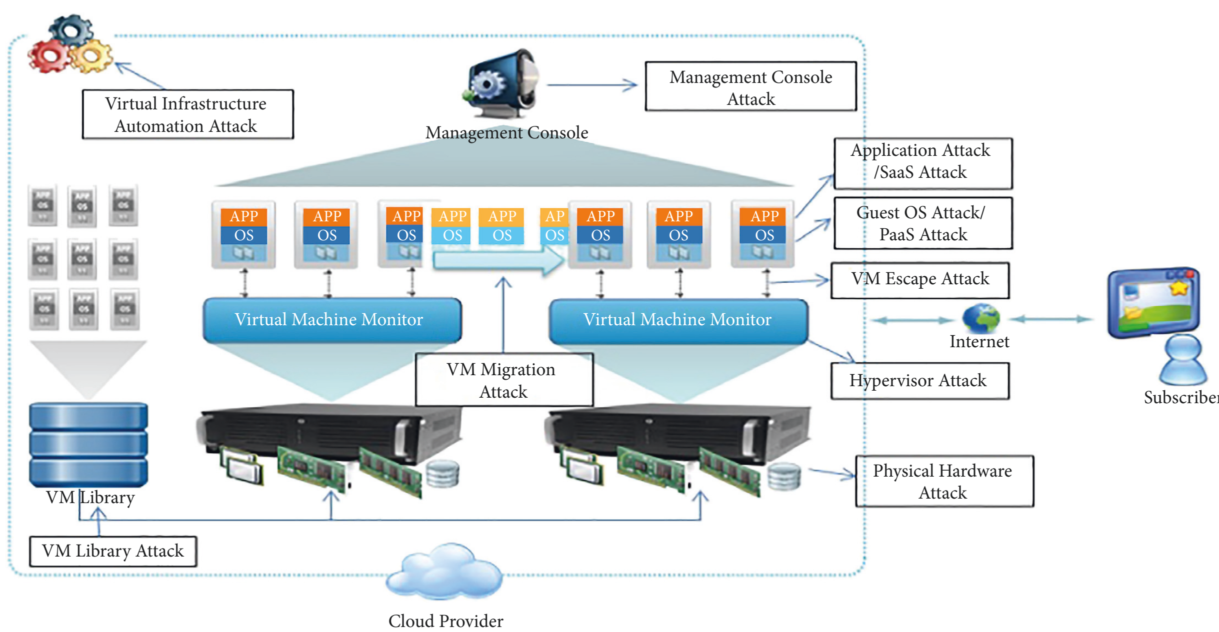

Figure 3: Different attack surfaces in virtual environment.

between the VMs and/or the hardware. This enables it to eavesdrop or modify the communication or system calls or register's/memory's value between VMs and/or hardware as the attacker. Attack on the hypervisor will also enable the attacker to attack actively by crashing the hypervisor or shutting down the VM. It may attack passively by modifying/controlling the VM or enabling the communication channel between the VMs such that they need not go through the hypervisor or also by changing resource allocation and usage.

Attack on the VM involves attack on the installed guest OS. The attacker may take advantage of the well-known vulnerabilities of the operating system and exploit them in a virtualized environment. Also, the unique configuration of each OS will have security concerns which if not addressed strictly may act as a channel for the attack. Even the state restoring capability of the VMs can be exploited for an attack; the VM can be restored to the state at which it was compromised, which will nullify the effect of the applied security patches. This would also enable the attacker to perform VM to VM attack, which may turn to DDOS attacks or use them as the attack launcher.

The host machine provides an attack surface mainly to the attacker that has direct access to the host, for example, through SSH, Rlogin, or by having access to the network of the host machine. This enables the attacker to launch DOS or to install the rouge hypervisor or change the network flow. The management console also provides a significant attack surface if it is not hardened properly. The management console can be accessed through SSH or web interface or custom console, which once compromised can control the hypervisor or the VM or the underlying hardware. Other than this, there is need to secure Guest operating system (Virtual Machines (VMs)).

All physical resources are controlled by the VMM, and it may create multiple logical objects to serve each VM. These logical objects dynamically bound to physical resources are several other attack surfaces which need to be hardened for a secure virtual infrastructure, such as attack on the VM Library which can put the security of the VM image or the whole repository at risk and attack on the VM in transit (during VM migration or VM deployment from the VM library) which also gives way to the man-in-the-middle attack. The VM in transit attack may be passive, that is, by only sniffing the contents of the VMs or creating an illegitimate copy of the VM. Attack may be active, that is, by modifying the VM state or contents or causing DOS attacks. An attack surface may have poorly written automation APIs (Application Program Interface). Virtualization vendor offers customizable APIs for better management, automation, and customization of the virtual infrastructure according to the customer's need. The APIs, if poorly written, can prove to be a significant avenue of attack. Besides the mentioned attack surfaces, there are also ones related to the vulnerabilities of the kernel used in the hypervisor.

5. Threat and Mitigation

With increasing reliance on virtualization and the hypervisor, cost is reduced, and management is getting easier; however, the threats are evolving. Most of the known threats are categorized as "hypothetical" rather than real. Hypothetical threats are those that are realized in the lab considering the worst-case scenario, while real threats are operational threats in practical scenarios [11]. A few of the operational threats or real threats are VM sprawl [12], lack of visibility [13], separation of duties (of users or devices or applications) at the virtualization layer, and too many rights (direct or indirect control of the whole infrastructure is given at different levels). Operational threats are more challenging and should be mitigated carefully. However, we cannot neglect hypothetical threats as they also have got very strong proof of concept. Here, we categorize different threats (including hypothetical as well as real) based on core principles of security.

5.1. Confidentiality. Confidentiality is said to be violated if information is disclosed to an unauthorized system or person. In a virtual infrastructure, if the communication between VMs or between VMs and the host is intercepted or modified by an unauthorized system, the confidentiality is said to have been compromised. Multiple VMs can be hosted on a single physical hardware, which may serve a different purpose, namely, a web server, a DNS server, or an FTP server. Such VMs may need to communicate with each other and/or the host. This communication may involve some common shared memory area or the system calls (hypercalls otherwise). This communication channel may also provide a gate to the attacker for "man-in-the-middle" attack. The attacker may modify the common memory area or may intercept and masquerade the system calls (hypercalls). In turn, this can result in malicious behavior of the VMs. The communication between the VM and the underlying host may involve hypercalls, which run in a higher privilege mode than the VM. Modification to these hypercalls can result in the control of the hardware and can lead to other threats.

This threat can be mitigated by maintaining isolation wherever possible. Further mitigation can be ensured by allowing all communication to happen only through the hypervisors and managing efficient MAC—Mandatory Access Control—policies [14] at the hypervisor such as Biba, Bell-LaPadula, Caernarvon, Type Enforcement, and Chinese Wall policies (as used in IBM's sHype [7]). This also controls resource sharing (e.g., virtual resource—shared memory, event channel, local resource—vLANs, vDisks). This in turn will monitor and minimize suspicious communication. Further, security of the communication is ensured by using HTTPS, TLS, SSH, or encrypted VPNs [15]. Other than the above mitigation strategies, one more way may be by conducting all communication through the physical networking devices which are already well hardened using various security policies rather than the virtual network and vSwitch. This is however done at the cost of compromising performance and increased network traffic.

Another well-known threat to confidentiality is the virtual machine-based rootkit (VMBR) [16] which is popularly known as the "Blue Pill" attack. Blue Pill attack is an advanced form of VMBR that installs a VM underneath an existing operating system and hoists the original operating system into the virtual machine. In Blue Pill attack, the running VM is intercepted or monitored by running it under the thin hypervisor which is malicious and remains undetected by the VM. This malicious hypervisor runs in the lower layer and can control and monitor the higher layers. The lower layers comprise the inner ring of the hierarchical protection rings, which run at the highest privileged level (kernel level) and can control the hardware. The malicious thin hypervisor can intercept any of the system calls of the VM. At the same time, the OS of the VM can reference all of its existing system calls, files, or devices and is unable to detect the presence of any of the rootkit. This malicious hypervisor can see all the states and events in the VM, such as keystrokes, network packets, disk states, and memory states [16]. Hyperjacking is also one of the attacks, which involves installing a malicious hypervisor underneath and taking full control of the server based on the Blue Pill or VMBR [17].

VMBR can be mitigated only after it has been detected. VMBR can be detected by using detector software that run below the VMBR that can view the system (physical memory or disk) and look for the signatures of the VMBR [16]. Other ways to control the VMBR are secure boot, use of secure hardware, use of secure VMM [5], and observing overhead caused due to VMBR at the native system resources, such as system clock, paging activity, and virtual I/O device behavior. Red Pill [18] is also able to detect the rootkit. Red Pill detects the presence of a malicious hypervisor by executing the nonprivileged instructions like sidt, at the lower privilege level. GuardHype [17] also provides mitigation from hyperjacking (hijacking of hypervisor).

VM fingerprinting is also a threat worth considering; an adversary may know about the VM by analyzing different registers values, memory dumps, etc. Also, details on older VMs may be recovered if the allocated memory to the deleted VM is not cleared properly, using memory recovery operations.

5.2. Integrity. Integrity is said to be violated in the context of virtualization if the modification has been done to the virtual infrastructure in a manner that is undetectable. In a virtualized environment, if the code of the hypervisor is modified or else a malicious kernel module is installed in the hypervisor, the integrity of the hypervisor is compromised. The idea behind this attack is to increase the complexity and size of the OS kernel, which also gives way to the higher security vulnerabilities. The main component of the hypervisor is its kernel, and it installs the other kernel modules to enable virtualization. This makes the system vulnerable as the kernel runs at a high privilege mode and it can control the whole system, thus compromising the kernel will bring the whole system's security at stack. Also, the compromised hypervisor's kernel can give up control of the hypervisor, which can provide a means to launch other attacks such as VM manipulation (start/stop, allocated resources) and zombie attack (controlling a VM for further attacks). This category of attacks is also known as external modification to the hypervisor [3].

This threat can be mitigated by only allowing user approved code in the kernel privilege. This can be done by checking all the code against the supplied user policy. This also ensures that once approved code cannot be further modified [15].

Other attacks related to exploiting zero day or other well-known vulnerability in the kernels are injecting malicious code and performing kernel buffer flow. Another kind of attack can be done by controlling the peripheral DMA and corrupting the kernel memory by frequent DMA writes or by manipulating IOMMU's translation. Such attacks are mitigated or minimized by making use of hardware memory protection schemes and AMD's Secure Virtual Machine (SVM) [15].

5.3. Availability. For any system availability is an important property. Availability is necessary to meet the requirements in SLAs and for ensuring continuity of business relationship. Any type of DoS (Denial of Service) or DDoS (Distributed Denial of Service) attack is a threat to availability. Such attacks are the result of vulnerabilities in the system. If the attacker gets access to the VM or hypervisor, it may make the service currently running on the VM unavailable either by stopping the VM or crashing the hypervisor or deleting the required files of the VM. Also, the external modification of the VM can be a threat to its availability. These types of attack are critical as the unavailability of the system can cause damage to the financial, business, and social reputation of the industry.

Other types of attack could be improper configuration of the hypervisor. An improper or careless configuration of the hypervisor provides one VM to capture all the physical resources. Suppose a compromised VM consumes all the processing power or networking resources and makes other VMs to starve. In such a situation, legitimate VMs will not have sufficient hardware resource to carry out their tasks. This will lead to DOS for users of those VMs. These types of attack can be mitigated by proper security policies at hypervisor level.

5.4. Authorization. Authorization is said to have been compromised if the system is able to perform a task that it is not allowed to. In the context of virtualization, threat to authorization is huge. If an attacker escalates its privileges and performs a task that it is not authorized, authorization is said to have been compromised. This is the most common form of attack in virtualized environment.

"VM escape" is one of the major attacks seen in a virtualized environment. In this attack, the VM can completely bypass the hypervisor and gain direct access to the hardware. When a program running on the VM gains the root privilege of the hardware, it may misuse the root access for active attacks like external modification of VM/hypervisor, or passive attacks such as VM monitoring from the host. Even the data cache is susceptible to being monitored and modified. This attack can lead to complete collapse of the security framework [3].

Other attacks along with this principle include obtaining access to the root in the management console and performing unauthorized tasks, such as VM modification, monitoring VM externally. These can be mitigated by properly managing different management consoles—local and web access.

In general, to mitigate various attacks and threats, focus should be towards hardening the infrastructure, proper configuration, timely patching, and change management. Various external tools and technologies may be adopted like virtualization-aware firewalls/IDS/IPS/antimalware, external vSwitch, and Virtual Encryption.

6. Other Secure Architectures

Several breakthroughs and models have been suggested for securing virtualization environments [19]. We did a comparison of various security models with security applied at the hypervisor level. Security implemented at the hypervisor level may reduce the resources required. These models comprise varied parameters of security and consider various threat models, as shown in Figure 4. Table 1 is a tabulation of these models.

$$x = \frac{-b \pm \sqrt{b^2 - 4ac}}{2a}. \tag{1}$$

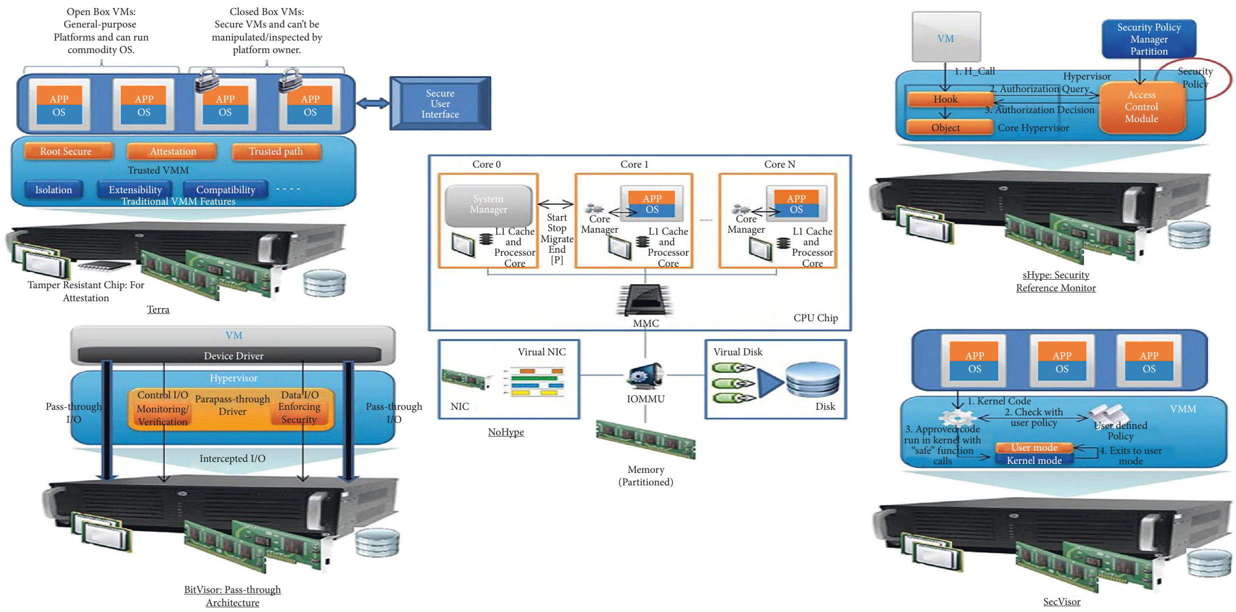

Figure 4: Comparison between different security models for virtualization [11, 21–23].

Table 1: Comparison between different security models for virtualization.

	SecVisor [15, 20]	sHype [7]	NoHype [21]	BitVisor [11, 22]	Terra [2]
Basis	Kernel occupies a privileged position in software stack and compromising it will give the attacker complete control of system.	Malicious OS can compromise the security of other OSes. Thus, secure cooperation of OS is needed at hypervisor layer.	Virtualization layer gives large attack surface to adversary.	Eliminating device drivers and device models from hypervisor may minimize hypervisor size.	Need for diverse security requirements in government, consumer, and enterprise application.
Concept	Ensure only user approved code should execute with kernel privilege.	Implementation of security reference monitor interface in hypervisor to enforce information flow constraints between VMs.	Elimination of hypervisor layer and giving virtualization at the hardware level directly.	Minimizing the hypervisor size by using the device drivers of guest OS to handle devices and I/O.	Flexible architecture for trusted computing with variable security requirements.
Threat model	(i) Misuse of modularization support from the kernels in the form of malicious code injection. (ii) Exploitation of software vulnerabilities in the kernel code. (iii) Malicious devices may corrupt kernel memory through DMA writes.	(i) Application set with conflicting security requirement may compromise other's security. (ii) Security above OS level can be bypassed by many threats, e.g., trap doors, malicious developers, and boot-sector viruses. (iii) Uncontrolled information flow between VMs.	(i) Large KLOC of hypervisor may have more vulnerability. (ii) Customer may run any software on the VM without any restriction. (iii) Compromised hypervisor may disturb the functionality of the whole infrastructure.	(i) Security of Virtual Machine Monitors is crucial if security is enforced at VMM. (ii) Vulnerabilities of hypervisor with large code may compromise security of the whole system.	(i) OS are complex programs with low assurance, to provide trusted computing base. (ii) Poor isolation of different applications may cause compromising the entire platform. (iii) Absence of trusted path between user and application.

Table 1: Continued.

	SecVisor [15, 20]	sHype [7]	NoHype [21]	BitVisor [11, 22]	Terra [2]
Security benefits	(i) Reduced code size. (ii) Reduced attack surface at kernel interface. (iii) Customized security policy of user.	(i) Strong isolation. (ii) Better access control. (iii) Boot-time and run-time guarantee.	(i) Confidentiality. (ii) Availability. (iii) Integrity. (iv) Reduced side channel attacks.	(i) Reduced code size of hypervisor. (ii) Improved reliability of hypervisor. (iii) Better I/O device security.	(i) Secure isolation. (ii) Better privacy, confidentiality, and integrity. (iii) Better application security assurance.
Assumptions in model	(i) Hardware has the virtualization support on which model is running. (ii) User and kernel share address spaces. (iii) Kernel does not make BIOS calls after initialization.	sHype was for single hypervisor infrastructure and all the communication was through virtual network not real network.	Hardware has virtualization capability; as vendor of network switches, multicore memory controller, IOMMU, and processors provide virtualization support.	Hardware has virtualization support and also platforms are equipped with IOMMU. Disk image of hypervisor cannot be modified externally. Firmware and BIOS are trusted entities.	(i) Attestation relies on security of standard SSL session key exchange protocol. (ii) Hardware platform with tamper-resistance, virtualization-enabled technology.
Brief design	SecVisor design based on mainly two principles: (i) CPU only executes the approved code in the kernel mode. (ii) Approved code should only be modified by SecVisor and its TCB (trusted computing base). For these, SecVisor used hardware memory protections and properly managing all kernel mode entries and exits.	sHype implemented different policies and modules; for example, for isolation, ring-based security is implemented. For access control enforcement, security hooks are inserted into code path inside the hypervisor, to guard the access to the virtual resources. Access control module (ACM) is implemented for policy management, making policy decision and other security decisions.	Implement virtualization at the hardware level with features: (i) one VM per core. (ii) Hardware enforced memory partitioning. (iii) Dedicated virtual IO devices to each VM. This design ensures that the working of one VM does not interrupt other VMs and isolate VMs from one another.	BitVisor implemented "parapass-through architecture," in which most of the access to the hardware from guest device driver is passed through the hypervisor. Part of I/O accesses are intercepted to (i) protect hypervisor from guest OS and (ii) enforce security policy.	Terra design is based on using a traditional VMM, to allow properties like isolation, extensibility, efficiency, and compatibility. Along with this, some more additional capabilities are included for making trusted VMM: (i) root secure, (ii) attestation (using tamper resistant hardware), and (iii) trusted path (using secure user interface).
Limitations	(i) Only provide integrity of code but not the integrity of control flow. (ii) Only single CPU support. (iii) No measures for self-modifying codes.	(i) Information leakage through covert channel. (ii) Lack of scalability: only for single hypervisor. (iii) Security of VM in transit.	(i) Lack of scalability. (ii) Underutilization. (iii) Performance may degrade. (iv) Security of VM in transit.	(i) Information leakage through covert channels. (ii) Hypervisor has limited functionalities. (iii) No support for USB and ethernet devices. (iv) Security of VM in transit.	(i) No measures for untrusted device drivers. (ii) Information leakage through covert channel. (iii) Security of VM in transit.

7. Future Trends and Concerns

From the time of IBM's first virtual machine-enabled mainframe until today, virtualization is evolving continuously, unfortunately though, so are attacks on virtual environments. Several sophisticated attacks are still at large and need to be properly understood and researched. An example of these attacks is "VM in transit," VMs when brought from VM library to the VMM or VM migration from one VMM to another VMM [24]. If the network for VM migration is compromised or, in future, when the customer has the flexibility to move his VMs between other machines via any network, attacks on VM in transit will become more sophisticated.

One other concern is related to the popularity of mobile phone virtualization. Though mobile virtualization enables the user to have two different OSs on the same device, on one OS personal data may reside, while on the other corporate data, with efficient separation by virtualization. However, this road to mobile virtualization is not smooth, because mobile platforms have several limitations as compared to servers and desktops, in terms of available resources, real-time computation, power limitations, and dependence on other technologies. Although mobile virtualization is a good way to provide security at the enterprise level (in form of BYOD—Bring Your Own Device—security), mobile virtualization in itself is prone to many challenges, such as limitation of computing resources, variable connectivity to the network, performance overhead by the virtualization layer, lost device issues, ruggedized devices, data ownership conflicts, rapid changes in mobile industries, and foremost jailbreaking, in which warranty from the vendor may become void owing to the installation of third-party software.

VMception or "virtualization inside virtualization" is another issue that needs to be addressed. We noted that most available measures cater to physical machines, meaning that models and measures require physical hardware for deployment. However, the attacks in nested virtualized environments need a different approach. The hardware would be virtual hardware and that too is hosted on a virtual machine, which will make traditional mechanisms inefficient.

More concrete security guidelines are needed for nested virtualization and mobile virtualization, which however would result in a trade-off between security and performance.

8. Conclusion

In this article, we have articulated various security related ideas and architectures in context of virtualization. In true sense, it is a virtualization-aware security implemented over the virtualized framework. Existing techniques that have been numbered in the article prove to secure the core of various information services. This is however not sufficient for ensuring security holistically. Computing paradigms such as cloud computing pose several other vulnerabilities and require addendum security measures. Also, security measures must be chosen to balance with the functional requirement and considerations of "Security vs Performance vs Economy."

Virtualization emerges as a powerful yet economic solution to reduce operational expenses in current computing paradigm. It easily becomes a threat to the environment if the configuration is not integrated with fine security. A full-proof virtualization security model to withstand probable attacks is the need of the hour. As quoted at several instances through the run of the paper, significantly monitoring new developments in this domain is important. A summarized state of the art and projecting newer strategies are the scope of the work presented in the paper.

Data Availability

No data were used to support the findings of the study.

Conflicts of Interest

The authors declare that there are no conflicts of interest regarding the publication of this paper.

References

[1] P. M. Chen and B. D. Noble, "When virtual is better than real [operating system relocation to virtual machines]," in *Proceedings of the 18th workshop on hot topics in operating systems*, pp. 133–138, IEEE, Bertinoro, Italy, May 2001.

[2] A. Kivity, Y. Kamay, D. Laor, U. Lublin, and L. Anthony, "kvm: the Linux virtual machine monitor," *Proceedings of the Linux symposium*, vol. 1, no. 8, pp. 225–230, 2007.

[3] L. Wang, G. von Laszewski, A. Younge et al., "Cloud computing: a perspective study," *New Generation Computing*, vol. 28, no. 2, pp. 137–146, 2010.

[4] J. P. Walters, A. J. Younge, I. K. Dong et al., "GPU pass-through performance: a comparison of KVM, Xen, VMWare ESXi, and LXC for CUDA and OpenCL applications," in *Proceedings of the 2014 IEEE 7th international conference on cloud computing*, pp. 636–643, IEEE, Anchorage, AK, USA, June 2014.

[5] T. Garfinkel, B. Pfaff, J. Chow, M. Rosenblum, and D. Boneh, "Terra," *ACM SIGOPS-Operating Systems Review*, vol. 37, no. 5, pp. 193–206, 2003.

[6] E. Keller, J. Szefer, J. Rexford, and R. B. Lee, "NoHype," *ACM SIGARCH-Computer Architecture News*, vol. 38, no. 3, pp. 350–361, 2010.

[7] C. Liu, C.-L. Sia, and K.-K. Wei, "Adopting organizational virtualization in B2B firms: an empirical study in Singapore," *Information & Management*, vol. 45, no. 7, pp. 429–437, 2008.

[8] K. Adams and O. Agesen, "A comparison of software and hardware techniques for x86 virtualization," *ACM SIGOPS-Operating Systems Review*, vol. 40, no. 5, pp. 2–13, 2006.

[9] S. Chiueh, T.-C. Nanda, and S. Brook, "A survey on virtualization technologies," *Rpe Report*, vol. 142, 2005.

[10] IBM, "IBM X-force 2010 trend and risk report," 2011, http://public.dhe.ibm.com/common/ssi/ecm/en/wgl03007usen/WGL03007USEN.PDF.

[11] A. Seshadri, M. Luk, N. Qu, and A. Perrig, "SecVisor," *ACM SIGOPS-Operating Systems Review*, vol. 41, no. 6, pp. 335–350, 2007.

[12] M. Lindner, F. McDonald, B. McLarnon, and P. Robinson, "Towards automated business-driven indication and mitigation of VM sprawl in Cloud supply chains," in *Proceedings of the 12th IFIP/IEEE International Symposium on Integrated Network Management (IM 2011) and Workshops*, pp. 1062–1065, IEEE, Dublin, Ireland, May 2011.

[13] S. J. Vaughan-Nichols, "Virtualization sparks security concerns," *Computer*, vol. 41, no. 8, pp. 13–15, 2008.

[14] R. Sailer, T. Jaeger, E. Valdez et al., "Building a MAC-based security architecture for the Xen open-source hypervisor," in *Proceedings of the IEEE Computer Security Applications Conference 21st Annual*, p. 10, Washington, DC, USA, December 2005.

[15] J. Kirch, "Virtual machine security guidelines" the center for Internet Security," 2007, http://www.cisecurity.org/tools2/vm/CIS_VM_Benchmark_v1.0.pdf.

[16] S. T. King and P. M. Chen, "SubVirt: implementing malware with virtual machines," in *Proceedings of the IEEE Security and Privacy Symposium*, p. 14, Berkeley/Oakland, CA, May 2006.

[17] M. Carbone, D. Zamboni, and W. Lee, "Taming virtualization," *IEEE Security and Privacy Magazine*, vol. 6, no. 1, pp. 65–67, 2008.

[18] Y. J. Rutkowska, "Red Pill... or how to detect VMM using (almost) one CPU instruction," 2005, http://invisiblethings.org/papers/redpill.html.

[19] S. Jin, J. Ahn, S. Cha, and J. Huh, "Architectural support for secure virtualization under a vulnerable hypervisor," in *Proceedings of the 44th Annual IEEE/ACM International Symposium on Microarchitecture*, pp. 272–283, Porto Alegre Brazil, December 2011.

[20] K. Lab, "Rethinking security for virtual environments," 2012, http://media.kaspersky.com/documents/business/brfwn/en/IDC-technology-spotlight_Kaspersky-Security-for-Virtualization-white-paper.pdf.

[21] R. Sailer, E. Valdez, T. Jaeger et al., "Secure hypervisor approach to trusted virtualized systems," *Techn. Rep.*, vol. RC23511, 2005.

[22] T. Shinagawa, H. Eiraku, K. Tanimoto et al., "BitVisor: a thin hypervisor for enforcing i/o device security," in *Proceedings of the 2009 ACM SIGPLAN/SIGOPS international conference on Virtual execution environments*, pp. 121–130, Washington, DC, USA, March 2009.

[23] R. Perez, L. Van Doorn, and R. Sailer, "Virtualization and hardware-based security," *IEEE Security and Privacy Magazine*, vol. 6, no. 5, pp. 24–31, 2008.

[24] M. Christodorescu, R. Sailer, L. S. Douglas, D. Sgandurra, and D. Zamboni, "Cloud security is not (just) virtualization security: a short paper," in *Proceedings of the 2009 ACM workshop on Cloud computing security*, pp. 97–102, Chicago, Illinois, USA, November 2009.

Hindawi
Scientific Programming
Volume 2022, Article ID 4841196, 31 pages
https://doi.org/10.1155/2022/4841196

Research Article

Cyber-Security and Social Media Risks Assessment by Using the Novel Concepts of Complex Cubic T-Spherical Fuzzy Information

Bushra Akram,[1] Naeem Jan,[1] Abdul Nasir,[1] Amerah Alabrah,[2] Mohsin S. Alhilal,[2] and Naziha Al-Aidroos[3]

[1] *Department of Mathematics, Institute of Numerical Science, Gomal University, Dera Ismail Khan 29050, KPK, Pakistan*
[2] *STC's Artificial Intelligence Chair, Department of Information Systems, College of Computer and Information Sciences, King Saud University, Riyadh 11543, Saudi Arabia*
[3] *Department of Computer Science, College of Computers and Information Technology, Hadhramout University, Al Mukalla, Hadhramout, Yemen*

Correspondence should be addressed to Amerah Alabrah; aalobrah@ksu.edu.sa and Naziha Al-Aidroos; naz.moh@hu.edu.ye

Received 24 November 2021; Revised 24 December 2021; Accepted 28 December 2021; Published 20 May 2022

Academic Editor: Punit Gupta

Over the past 20 years, the emergence of social media and its developments have rapidly changed communication and information technology. Social media plays a necessary part in accessing information and communication. In spite of its many advantages, users have also been facing many threats on social media platforms. This research aims to analyze and resolve these threats by using the new concepts of complex cubic T spherical fuzzy sets (CCuTSFS) that have a broad structure including degrees of membership, neutral-membership, and non-membership. It does a better job of modeling uncertainty than any other preexisting structure. Furthermore, we defined the concepts of the Cartesian product (CP) between CCuTSFSs, complex cubic T spherical fuzzy relation (CCuTSFR) and the types of CCuTSFRs with appropriate examples. This study looked at the relationship between different types of security and threats on social media for the first time in fuzzy set theory. The proposed methods demonstrate how to control the effects of threats by using valid security methods. Finally, the benefits of the presented strategies are explained in the comparative study.

1. Introduction

Uncertainty is an essential element of life, resulting from a range of factors ranging from a lack of judgment to a lack of knowledge. The nature of modeling and computing approaches is frequently precise, unavoidable, and crisp. In crisp set theory, a statement has only two options: true or false. Thus, decisions based on crisp knowledge are clear and unambiguous. Information is frequently complicated, uncertain, and confusing because people cannot deal with uncertainty. Mathematics is largely concerned with the precise and proper representation of data. After the introduction of crisp knowledge, some life-changing novelty in mathematics was made by the introduction of fuzzy sets and fuzzy logic.

In 1965, Zadeh [1] established the theory of fuzzy sets (FS) and fuzzy logic, which is one of the most prosperous theories for representing data uncertainty. Every element in the set is assigned a level of membership by an FS. The membership level is a function that takes values from the [0, 1] unit interval. Klir and Folger [2] introduced relations between classical sets. The classical set theory only deals with yes and no situations, hence a relation of classical sets enumerates the existence and nonexistence of a relationship. Mendel et al. [3] proposed the fuzzy relation (FR) for FSs. Unlike classical relations, FRs are not limited to yes-or-no problems. Based on their membership level, they can indicate the level, intensity, and degree of good connection between any two FSs. The higher the degree of membership, the better the relationship, whereas the lower the degree of membership, the worse the relationship. FR is a more comprehensive concept than a classical relationship because it deals with issues in both situations. Zadeh [4] introduced the idea of an interval-valued fuzzy set (IVFS) in 1975. The IVFSs are a more broader version of the FS. These sets describe the membership degree in the form of the subset from the unit interval. Because it can be difficult for an expert to accurately explain the level of certainty using a real number. As a result, an interval that represents the amount of confidence is a solid option. Bustince and Burillo [5] invented the interval-valued fuzzy relation (IVFRs), and they generalized the classical relation and FRs. Deschrijver and Kerre [6] derived the connection between different extensions of fuzzy set theory. Bustince et al. [7] employed matrices to create IVFSs and used them to detect edges. De Baets and Kerre [8] defined the application of FRs.

Atanassov [9] proposed the intuitionistic fuzzy set (IFS), which consists of membership and nonmembership degrees and satisfies the condition that the sum of the two degrees is less than or equal to 1. It is the generalization form of FS. Burillo and Bustince [10] invented the intuitionistic fuzzy relation (IFR), which studies the relationship between two IFSs. It is a broader form of the FR. Further, Atanassov [11] introduced a novelty concept called the interval-valued intuitionistic fuzzy set (IVIFSs) by showing the degree of membership and nonmembership of an IFS in the form of intervals. De et al. [12] used the IFSs in medical diagnosis. Yager [13] created the notion of the Pythagorean fuzzy set (PyFS) by changing the constraint of IFSs, which increases the space of membership and nonmembership by imposing some new restriction, i.e., the sum of the squares of membership and nonmembership must be interval, according to the innovative requirements. Zhou et al. [14] discussed and implemented a new PyFS divergence measure in medical diagnosis. Yager [15] recognized the constraints of assigning degrees to objects in PyFSs and proposed the concept of q-rung orthopair fuzzy set (qROFSs). By removing the limits imposed by the earlier set theories, these sets allow professionals and researchers to freely award membership and nonmembership degrees. The total of the nth power of membership and nonmembership degrees in qROFSs must be in the unit interval, with n being a natural number.

Cuong and Kreinovich [16] established the concept of picture fuzzy set (PFS) by the inclusion of a neutral degree in an IFS. The membership, neutral, and nonmembership degrees take on values from the unit interval, and the sum of all these degrees is accommodated within the unit interval [0,1]. Mahmood et al. [17] flourish the concept of spherical fuzzy set (SFS) by changing the constraint such that the sum of squares of membership, neutral, and nonmembership degrees consists of the unit interval. They also introduced the notion of T SFS (TSFS). The sum of membership, neutral, and nonmembership degrees must be contained in the unit interval in TSFSs when raised to the power n, where n is a natural number. Guleria and Bajaj [18] activated the Eigen SFSs in decision making problems. Ullah et al. [19] defined the similarity measures for TSFS and applied them in pattern recognition. Ullah et al. [20] conceive the correlation coefficients for TSFSs and used them in clustering and multiattribute decision making. Van Dinh et al. [21] presented a picture of fuzzy database applications and theories. Dutta [22] used the PFSs in the field of medical diagnosis.

After FS, a new theory of complex fuzzy sets (CFSs) was introduced by Ramot et al. [23], which is a broad form of FS. The CFS represents the membership degree in the form of a complex number. Instead of a real number in the unit interval, the degree of membership in a CFS is a complex number in a unit circle in the complex plane. The CFSs make it easier to represent multidimensional issues, particularly those that are time dependent. In addition, they defined the complex fuzzy relation (CFR). Lie et al. [24] investigated the application of CFSs. Greenfield et al. [25] introduced the concept of an interval-valued complex fuzzy set by changing the degree of membership of a CFS from a single number to an interval (IVCFS). Nasir et al. [26] recently defined interval-valued complex fuzzy relations as a tool for analyzing relationships between two or more IVCFSs. Alkouri and Salleh [27] proposed the notion of a complex intuitionistic fuzzy set (CIFS). In the complex plane, CIFS limit the sum of the degree of membership and nonmembership to the unit disc. Jan et al. [28] provide the CIFR which was applied to cybersecurities and cybercrimes in oil and gas industries. The concept of an interval-valued complex intuitionistic fuzzy set (IVCIFS) was established by Garg and Rani [29]. Using this relationship between two or more IVCFS, Nasir et al. [30] introduced the idea of interval-valued complex intuitionistic fuzzy relation (IVCIFR). Dick et al. [31] suggested the complex Pythagorean fuzzy set (CPyFS) by modifying the codomain of CIFS. Garg et al. [32] further expanded on CPyFS to create a complex q-rung orthopair fuzzy set (CqROFSs). The complex-valued membership and nonmembership degrees are assigned to the elements of a set in CqROFSs, when increased to the power n, the sum of modulus of membership and nonmembership degrees must be within the unit interval, where n is a natural number.

Nasir et al. [33] recommended the concept of a complex picture fuzzy set (CPFS). Ali et al. [34] defined the concepts of a complex spherical fuzzy set (CSFS) and, in addition, proposed the concepts of a complex T spherical fuzzy set (CTSFS) as a generalization of the CSFS. Jun et al. [35] developed some logic operations of the cubic set and introduced the idea of the cubic fuzzy set (CuFS) by combining both interval-valued fuzzy numbers and fuzzy numbers. Cubic fuzzy set is the improved form of both FS and IVFS because they cover the same set of information. Kaur and Garg [36] defined the generalization of cubic fuzzy with t-norm operators. Kim et al. [37] defined the new innovative results of cubic fuzzy relations (CuFR). Garg and Kaur [38] concocted the concept of a cubic intuitionistic fuzzy set (CuIFS), which is expressed by two sections, i.e., an interval-valued intuitionistic fuzzy set and another by an intuitionistic fuzzy set. The CuIFS includes more information than the general IVIFS and IFS because it is composed of both these sets. Talukdar and Dutta [39] developed the cubic Pythagorean fuzzy set (CuPyFS) with the application of multicriteria decision making. They are the generalization form of CuIFS. They improve the limitation. Zhang et al. [40] introduced the concept of cubic q-rung orthopair fuzzy set (CuqROFS). They are the generalization form of CuPyFS.

The constraint of the CuqROFS increased the space, so the sum of the power n will be less than or equal to 1. Gumaei and Hussain [41] proposed a new operator of cubic picture fuzzy set (CuPFS) with application. The cubic picture fuzzy set also includes the neutral degree. They are the three levels of degree, i.e., cubic membership, cubic neutral, and cubic nonmembership. Devaraj and Aldring [42] developed the cubic spherical fuzzy set (CuSFSs). The cubic spherical fuzzy set solves more complexities. Chinnadurai et al. [43] introduced the notion of a complex cubic fuzzy set (CCuFS). The CCuFS covered both sets of information, i.e., the complex fuzzy set and the cubic set. Zhou et al. [44] used the CCuFS in multiattribute decision making. Chinnadurai et al. [45] proposed the idea of the complex cubic intuitionistic fuzzy set (CCuIFS), which is a combined form of the cubic membership degree and cubic nonmembership degree. They are covered by both internal and external results. They are investigating the relationship between studying the two or more Cartesian products (CP) of CuFSs. He [46] gave the idea of social media security. Social media security is the more effective way they work to combat the social media threat.

In this article, we introduced the novel concepts of the complex cubic T spherical fuzzy set (CCuTSFS) and CCuTSFR. In addition, the CP between the two or more CCuTSFSs is considered. In addition, different types of CCuTSFRs are defined, such as reflexive, irreflexive, symmetric, antisymmetric, transitive, equivalence classes, and many more. Every definition with appropriate examples and results of CCuTSFRs has also been defined. The CCuTSFR is an improved form of the CFR, CCuFR, CIFR, CCuIFR, CPyFR, CCuPyFR, CqROFR, CCuqROFR, CPFR, CCuPFR, CSFR, CCuSFR, CTSFR, and CuTSFR. The CCuTSFR is more efficient of the T spherical fuzzy relation (TSFR) and complex T spherical fuzzy relation (CTSFR) because this structure covers both the results of the TSFR and IVTSFR. The CCuTSFR is discussing all of the three stages; membership, neutrals, and nonmembership with complex numbers. The CCuTSFR is the multidimensional structure that is described in both amplitude and phase terms. The phase term is used to define the time frame or periodicity. The CCuTSFR increases the space with the power of n if $n = 2$ and $n = 1$, then the CCuTSFR are converting to the CCuSFR and CCuPFS, respectively. In this manuscript, we examine the relationship between social media security against particular threats. The CCuTSFR, including all of the stages if the neutral will be equal to zero, then the CCuTSFR are changed to the CCuIFR, and if the nonmembership will also be equal to zero then the CCuTSFR are converting to the CCuFR, and the space $n = 1$. As a result, the CCuTSFRs are the better framework to use because it can encompass all aspects of the situation, including positive, no, and bad effects with time. The concepts of CCuTSFR are used to determine the best security methods. The novel idea of CCuTSFRs covers the present and the future. Further, this structure can be extended to other fuzzy set theory model that can be applied to many other fields such as economics, statistics, sports, computer science, medical, information technology, etc.

The arrangements of this paper are defined as follows.

In Section 2, a few predefined ideas of fuzzy algebra are described. In Section 3, the new concepts of CCuTSFS, CCuTSFR, and their types are defined. In Section 4, an application of the CCuTSFRs to study the relationship between social media security and threats is proposed. In Section 5, the proposed methods with the predefined structures are compared. Section 6 concludes the research.

2. Preliminaries

In this section, we defined some basic definitions of CuFS, CuFR, CCuFS, CIFS, CIVIFS, CPFS, and CqROFS.

Definition 1 (see [35]). For a non-empty set U, a cubic fuzzy set (CuFS) $\dot{C}$ on U is defined as

$$\dot{C} = \left\{ (\text{ţ}, D(\text{ţ}), \bar{E}(\text{ţ})) \colon \text{ţ} \in U \right\}, \tag{1}$$

where $(\text{ţ}) = \{ (\text{ţ}, [\acute{u}^{-}(\text{ţ}), \acute{u}^{+}(\text{ţ})]) \colon \text{ţ} \in U \}$ represents the IVFS defined on U and $\bar{E}(\text{ţ}) = \{ (\text{ţ}, \acute{u}(\text{ţ})) \colon \text{ţ} \in U \}$ represents the FS. Moreover, $\acute{u}^{-}(\text{ţ}), \acute{u}^{+}(\text{ţ})$ are called the lower and upper degrees of membership respectively, and $\acute{u}(\text{ţ})$ is called membership degree. Such that $\acute{u}(\text{ţ}) \colon U \longrightarrow [0, 1]$, and also $0 \leq \acute{u}^{-}(\text{ţ}) \leq \acute{u}^{+}(\text{ţ}) \leq 1$.

Therefore, a CuFS can be written as

$$\dot{C} = \{ (\text{ţ}, [\acute{u}^{-}(\text{ţ}), \acute{u}^{+}(\text{ţ})], \acute{u}(\text{ţ})) \colon \text{ţ} \in U \}. \tag{2}$$

Definition 2 (see [37]). Let us take two CuFSs in a nonempty set U,

$$\begin{aligned} j &= \left\{ (\text{ţ}), \left(\left[\acute{\alpha}^{-}_{j(\acute{u})}(\text{ţ}), \acute{\alpha}^{+}_{j(\acute{u})}(\text{ţ}) \right], \left(\acute{\alpha}_{j(\acute{u})}(\text{ţ}) \right) \right) \colon \text{ţ} \in U \right\}, \\ \mathscr{K} &= \left\{ (\acute{g}), \left(\left[\acute{\alpha}^{-}_{\mathscr{K}(\acute{u})}(\acute{g}), \acute{\alpha}^{+}_{\mathscr{K}(\acute{u})}(\acute{g}) \right], \left(\acute{\alpha}_{\mathscr{K}(\acute{u})}(\acute{g}) \right) \right) \colon \acute{g} \in U \right\}. \end{aligned} \tag{3}$$

Then, their CP is defined as

$$j \times \mathscr{K} = \left\{ (\text{ţ}, \acute{g}), \left(\left[\acute{\alpha}^{-}_{j\times\mathscr{K}(\acute{u})}(\text{ţ}, \acute{g}), \acute{\alpha}^{+}_{j\times\mathscr{K}(\acute{u})}(\text{ţ}, \acute{g}) \right] \right), \left(\acute{\alpha}_{j\times\mathscr{K}(\acute{u})}(\text{ţ}, \acute{g}) \right) \right\}, \tag{4}$$

where

$$\begin{aligned} \acute{\alpha}^{-}_{j\times\mathscr{K}(\acute{u})}(\text{ţ}, \acute{g}) &= \min\left\{ \acute{\alpha}^{-}_{j(\acute{u})}(\text{ţ}), \acute{\alpha}^{-}_{\mathscr{K}(\acute{u})}(\acute{g}) \right\}, \\ \acute{\alpha}^{+}_{j\times\mathscr{K}(\acute{u})}(\text{ţ}, \acute{g}) &= \min\left\{ \acute{\alpha}^{+}_{j(\acute{u})}(\text{ţ}), \acute{\alpha}^{+}_{\mathscr{K}(\acute{u})}(\acute{g}) \right\}, \\ \acute{\alpha}_{j\times\mathscr{K}(\acute{u})}(\text{ţ}, \acute{g}) &= \min\left\{ \acute{\alpha}_{j(\acute{u})}(\text{ţ}), \acute{\alpha}_{\mathscr{K}(\acute{u})}(\text{ţ}) \right\}. \end{aligned} \tag{5}$$

The subset of the CP of two CuFS is called a cubic fuzzy relation (CuFR).

Example 1. Let two CuFSs F and G on U is defined as

$$\begin{aligned} F &= \{ (a, [0.1, 0.5], (0.3)), (b, [0.2, 0.6], (0.4)) \}, \\ G &= \{ (c, [0.3, 0.7], (0.8)), (d, [0.2, 0.4], (0.1)) \}. \end{aligned} \tag{6}$$

Then, their CP is

$$F \times G = \left\{ \begin{array}{l} ((a, c), [0.1, 0.5], (0.3)), ((a, d), [0.1, 0.4], (0.1)), \\ ((b, c), [0.2, 0.6], (0.4)), ((b, d), [0.2, 0.4], (0.1)) \end{array} \right\}. \tag{7}$$

From the subset of $F \times G$ is called relation

$$Ŗ = \{((a, c), [0.1, 0.5], (0.3)), ((b, d), [0.2, 0.4], (0.1))\}. \tag{8}$$

Definition 3 (see [43]). For a nonempty set U, a complex cubic fuzzy set (CCuFS) $\dot{C}$ on U is defined as

$$\dot{C} = \{ (ţ, [\dot{u}_c^-(ţ), \dot{u}_c^+(ţ)], (\dot{u}_c(ţ))): ţ \in U\}, \tag{9}$$

where $\dot{u}_c^-(ţ), \dot{u}_c^+(ţ)$ represent the lower and upper degrees of membership, respectively. Thus, $\dot{u}_c^-(ţ) = \acute{\alpha}_{\dot{u}}^-(ţ)e^{2\pi i\eta_{\dot{u}}^-}(ţ)$, $\dot{u}_c^+(ţ) = \acute{\alpha}_{\dot{u}}^+(ţ)e^{2\pi i\eta_{\dot{u}}^+(ţ)}$ such that $0 \leq |\dot{u}_c^-(ţ)| \leq |\dot{u}_c^+(ţ)| \leq 1$, and $\dot{u}_c(ţ) = \acute{\alpha}_{\dot{u}}(ţ)e^{2\pi i\eta_{\dot{u}}(ţ)}$. Moreover, $\acute{\alpha}_{\dot{u}}^-, \acute{\alpha}_{\dot{u}}^+, \acute{\alpha}_{\dot{u}} \in [0, 1]$ are called the amplitude term of membership degree, and satisfy the inequalities $\acute{\alpha}_{\dot{u}}^- \leq \acute{\alpha}_{\dot{u}}^+$, and $\eta_{\dot{u}}^-$, $\eta_{\dot{u}}^+, \eta_{\dot{u}} \in [0, 1]$ are called the phase term of degree of membership, and satisfy the inequality. $\eta_{\dot{u}}^- \leq \eta_{\dot{u}}^+$.

Definition 4 (see [27]). For a nonempty set U, a complex intuitionistic fuzzy set (CIFS) $\dot{C}$ on U is defined as

$$\dot{C}(ţ) = \{ (ţ, \dot{u}_c(ţ), ŋ_c(ţ)): ţ \in U\}, \tag{10}$$

where $\dot{u}_c(ţ) = ŋ_c(ţ)$ is a complex-valued mapping i.e., $\dot{u}_c, ŋ_c: U \longrightarrow \{\mathscr{Z} : \mathscr{Z} \in C\, and\, |\mathscr{Z}| \leq 1\}$, which represents the membership and nonmembership degree of the CIFS, respectively. Where C is the set of complex numbers. Thus, $\dot{u}_c(ţ) = \acute{\alpha}_{\dot{u}}(ţ)e^{2\pi\eta_{\dot{u}}(ţ)i}$ and $ŋ_c(ţ) = \acute{\alpha}_{ŋ}(ţ)e^{2\pi\eta_{ŋ}(ţ)}$. Moreover, $\acute{\alpha}_{\dot{u}}, \acute{\alpha}_{ŋ} \in [0, 1]$ are called amplitude term of the membership and nonmembership degree, respectively, and $\eta_{\dot{u}}, \eta_{ŋ} \in [0, 1]$ are called phase term of the membership and nonmembership degree, respectively. On condition that $0 \leq \acute{\alpha}_{\dot{u}}(ţ) + \acute{\alpha}_{ŋ}(ţ) \leq 1$ and $0 \leq \eta_{\dot{u}}(ţ) + \eta_{ŋ}(ţ) \leq 1$.

Definition 5 (see [29]). For a nonempty set U, a complex interval-valued intuitionistic fuzzy set (CIVIFS) $\dot{C}$ on U is defined as

$$\dot{C}(ţ) = \{ (ţ, \dot{u}_c(ţ), ŋ_c(ţ)): ţ \in U\}, \tag{11}$$

where $\dot{u}_c(ţ) = [\dot{u}_c^-(ţ), \dot{u}_c^+(ţ)]$, $ŋ_c(ţ) = [ŋ_c^-(ţ), ŋ_c^+(ţ)]$, and $\dot{u}_c^-(ţ), \dot{u}_c^+(ţ)$ are called the lower and upper membership degrees, while $ŋ_c^-(ţ), ŋ_c^+(ţ)$ are called the lower and upper nonmembership degrees. $\dot{u}_c^-(ţ) = \acute{\alpha}_c^-(ţ)e^{2\pi\eta_c^-(ţ)i}$, $\dot{u}_c^+(ţ) = \acute{\alpha}_c^+(ţ)e^{2\pi\eta_c^+(ţ)i}$, $ŋ_c^-(ţ) = \acute{\alpha}_c^-(ţ)e^{2\pi\eta_c^-(ţ)i}$ and $ŋ_c^+(ţ) = \acute{\alpha}_c^+(ţ)$ $e^{2\pi\eta_c^+(ţ)i}$, given that,

$$0 \leq |\dot{u}_c^+(ţ)| + |ŋ_c^+(ţ)| \leq 1. \tag{12}$$

Equivalently, CIVIFS can be written as

$$\dot{C}(ţ) = \left\{ ţ,\ [\acute{\alpha}_{\dot{u}}^-(ţ), \acute{\alpha}_{\dot{u}}^+(ţ)]e^{2\pi[\eta_{\dot{u}}^-(ţ), \eta_{\dot{u}}^+(ţ)]i},\ [\acute{\alpha}_{ŋ}^-(ţ), \acute{\alpha}_{ŋ}^+(ţ)]e^{2\pi[\eta_{ŋ}^-(ţ), \eta_{ŋ}^+(ţ)]i} \right\}. \tag{13}$$

Definition 6 (see [32]). For a nonempty set U, a complex q-rung orthopair fuzzy set (CqROFS) $\dot{C}$ on U is defined as

$$\dot{C}(ţ) = \{ (ţ, \dot{u}_c(ţ), ŋ_c(ţ)): ţ \in U\}, \tag{14}$$

where $\dot{u}_c(ţ), ŋ_c(ţ)$ is a complex-valued mapping i.e., $\dot{u}_c, ŋ_c: U \longrightarrow \{\mathscr{Z} : \mathscr{Z} \in C\, an\, d\, |\mathscr{Z}| \leq 1\}$, which represents the membership and nonmembership degree of the qROFS, respectively. Where C is the set of complex numbers. Thus, $\dot{u}_c(ţ) = \acute{\alpha}_{\dot{u}}(ţ)e^{2\pi\eta_{\dot{u}}(ţ)i}$ and $ŋ_c(ţ) = \acute{\alpha}_{ŋ}(ţ)e^{2\pi\eta_{ŋ}(ţ)}$. Moreover, $\acute{\alpha}_{\dot{u}}, \acute{\alpha}_{ŋ} \in [0, 1]$ are called amplitude terms of the membership and nonmembership degree, respectively, and $\eta_{\dot{u}}, \eta_{ŋ} \in [0, 1]$ are called phase terms of the membership and nonmembership degree, respectively. On condition that, $0 \leq (\acute{\alpha}_{\dot{u}}(ţ))^n + (\acute{\alpha}_{ŋ}(ţ))^n \leq 1$ and $0 \leq (\eta_{\dot{u}}(ţ))^n + (\eta_{ŋ}(ţ))^n \leq 1$, $n\mathbb{N}$.

Definition 7 (see [33]). For a nonempty set U, a complex picture fuzzy set (CPFS) $\dot{C}$ on U is defined as

$$\dot{C}(ţ) = \{ (ţ, \dot{u}_c(ţ), P_c(ţ), ŋ_c(ţ)): ţ \in U\}, \tag{15}$$

where $\dot{u}_c(ţ), P_c(ţ), ŋ_c(ţ)$ is a complex-valued mapping i.e., $\dot{u}_c, p_c, ŋ_c: U \longrightarrow \{\mathscr{Z} : \mathscr{Z} \in C\, an\, d\, |\mathscr{Z}| \leq 1\}$, which represents the membership, neutral, and nonmembership degree of the CPFS, respectively. Thus, $\dot{u}_c(ţ) = \acute{\alpha}_{\dot{u}}(ţ)e^{2\pi\eta_{\dot{u}}}(ţ)i$, $p_c(ţ) = \acute{\alpha}_P(ţ)e^{2\pi\eta_P(ţ)}$, and $ŋ_c(ţ) = \acute{\alpha}_{ŋ}(ţ)e^{2\pi\eta_{ŋ}(ţ)}$. Moreover, $\acute{\alpha}_{\dot{u}}, \acute{\alpha}_P, \acute{\alpha}_{ŋ} \in [0, 1]$ are called amplitude term of the membership, neutral, and nonmembership degree, respectively, and $\eta_{\dot{u}}, \eta_P, \eta_{ŋ} \in [0, 1]$ are called phase term of the membership, neutral, and nonmembership degree, respectively. On condition that $0 \leq \acute{\alpha}_{\dot{u}}(ţ) + \acute{\alpha}_P(ţ) + \acute{\alpha}_{ŋ}(ţ) \leq 1$ and $0 \leq \eta_{\dot{u}}(ţ) + \eta_P(ţ) + \eta_{ŋ}(ţ) \leq 1$.

3. Complex Cubic T Spherical Fuzzy Relation

This section introduces the novel concepts of cubic T spherical fuzzy set (CuTSFS), complex cubic T spherical fuzzy set (CCuTSFS), the CP of two CCuTSFS, complex cubic T spherical fuzzy relation (CCuTSFR), and its types.

Definition 8. For a nonempty set U, a cubic T spherical fuzzy set (CuTSFS) $\dot{C}$ on U is defined as

$$\dot{C} = \{ (ţ, \mathbb{F}(ţ), \mathbb{G}(ţ)),\ ţ \in U\}, \tag{16}$$

where $\mathbb{F}(ţ) = \{(ţ, [\dot{\mathrm{U}}^-(ţ), \dot{\mathrm{U}}^+(ţ)], [\mathrm{P}^-(ţ), \mathrm{P}^+(ţ)], [ņ^-(ţ), ņ^+(ţ)]): ţ \in U\}$ represent the interval-valued TSFS and $\mathbb{G}(ţ) = \{(ţ, \dot{\mathrm{U}}(ţ), \mathrm{P}(ţ), ņ(ţ): ţ \in U)\}$ represent the TSFS of U. Where $\dot{\mathrm{U}}(ţ), \mathrm{P}(ţ), ņ(ţ)$ are called the membership, neutral, and nonmembership degrees, respectively. Such that $0 \le \dot{\mathrm{U}}^-(ţ) \le \dot{\mathrm{U}}^+(ţ) \le 1$, $0 \le \mathrm{P}^-(ţ) \le \mathrm{P}^+(ţ) \le 1$, and $0 \le ņ^-(ţ) \le ņ^+(ţ) \le 1$. Moreover, $\dot{\mathrm{U}}(ţ), \mathrm{P}(ţ), ņ(ţ) \in [0,1]$, on condition that $0 \le |\dot{\mathrm{U}}(ţ)|^n + |\mathrm{P}(ţ)|^n + |ņ(ţ)|^n \le 1$, $n \in \mathbb{N}$.

Definition 9. For a nonempty set U, a complex cubic T-spherical fuzzy set $\dot{\mathrm{C}}$ on U is defined as

$$\dot{\mathrm{C}} = \{(ţ, ([\dot{\mathrm{U}}_c^-(ţ), \dot{\mathrm{U}}_c^+(ţ)], [\mathrm{P}_c^-(ţ), \mathrm{P}_c^+(ţ)], [ņ_c^-(ţ), ņ_c^+(ţ)])), (\dot{\mathrm{U}}_c(ţ), \mathrm{P}_c(ţ), ņ_c(ţ)): ţ \in U\}, \tag{17}$$

where $\dot{\mathrm{U}}_c^-(ţ), \dot{\mathrm{U}}_c^+(ţ), \mathrm{P}_c^-(ţ), \mathrm{P}_c^+(ţ), , ņ_c^-(ţ), ņ_c^+$ are called the lower and upper membership, neutral, and nonmembership degrees, respectively, while $\dot{\mathrm{U}}_c(ţ), \mathrm{P}_c(ţ), ņ_c(ţ)$ are called membership, neutral, and nonmembership degrees defined as $\dot{\mathrm{U}}_c(ţ): U \longrightarrow \{\mathscr{Z}_{\dot{\mathrm{U}}}: \mathscr{Z}_{\dot{\mathrm{U}}} \in \dot{\mathrm{C}}\, and\, d\, |\mathscr{Z}_{\dot{\mathrm{U}}}| \le 1\}$, $\mathrm{P}_c(ţ): U \longrightarrow \{\mathscr{Z}_{\mathrm{P}}: \mathscr{Z}_{\mathrm{P}} \in \dot{\mathrm{C}}\, an\, d\ |\mathscr{Z}_{\mathrm{P}}| \le 1\}$, $ņ_c(ţ): U \longrightarrow \{\mathscr{Z}_{ņ}: \mathscr{Z}_{ņ} \in \dot{\mathrm{C}}\, an\, d\, |\mathscr{Z}_{ņ}| \le 1\}$. $\dot{\mathrm{C}}$ is the set of complex numbers and the complex numbers can be written as $\dot{\mathrm{U}}_c(ţ) = \dot{\alpha}_{\dot{\mathrm{U}}}(ţ)e^{\eta_{\dot{\mathrm{U}}}(ţ)2\pi i}$ $\mathrm{P}_c(ţ) = \dot{\alpha}_{\mathrm{P}}(ţ)e^{\eta_{\mathrm{P}}(ţ)2\pi i}$, and $ņ_c(ţ) = \dot{\alpha}_{ņ}(ţ)e^{\eta_{ņ}(ţ)2\pi i}$. Therefore, CCuTSFS can be expressed as

$$\dot{\mathrm{C}} = \left\{\left(ţ, \begin{pmatrix} [\dot{\alpha}_{\dot{\mathrm{U}}}^-(ţ), \dot{\alpha}_{\dot{\mathrm{U}}}^+(ţ)]e^{2\pi[\eta_{\dot{\mathrm{U}}}^-, \eta_{\dot{\mathrm{U}}}^+]i}, \\ [\dot{\alpha}_{\mathrm{P}}^-(ţ), \dot{\alpha}_{\mathrm{P}}^+(ţ)]e^{2\pi[\eta_{\mathrm{P}}^-, \eta_{\mathrm{P}}^+]i}, \\ \left[\dot{\alpha}_{ņ}^-(ţ), \dot{\alpha}_{ņ}^+(ţ)\right]e^{2\pi\left[\eta_{ņ}^-, \eta_{ņ}^+\right]i} \end{pmatrix}, \begin{pmatrix} \dot{\alpha}_{\dot{\mathrm{U}}}(ţ)e^{2\pi i\eta_{\dot{\mathrm{U}}}(ţ)}, \\ \dot{\alpha}_P(ţ)e^{2\pi i\eta_P(ţ)}, \\ \dot{\alpha}_{ņ}(ţ)e^{2\pi i\eta_{ņ}(ţ)} \end{pmatrix}\right)\right\}. \tag{18}$$

Moreover, $\dot{\alpha}_{\dot{\mathrm{U}}}^-(ţ), \dot{\alpha}_{\dot{\mathrm{U}}}^+(ţ), \dot{\alpha}_{\dot{\mathrm{U}}}(ţ), \eta_{\dot{\mathrm{U}}(ţ)}^-, \eta_{\dot{\mathrm{U}}(ţ)}^+, \eta_{\dot{\mathrm{U}}(ţ)}: U \longrightarrow [0,1]$ are the elements of membership degree, $\dot{\alpha}_{\mathrm{P}}^-(ţ), \dot{\alpha}_{\mathrm{P}}^+(ţ), \dot{\alpha}_{\mathrm{P}}(ţ), \eta_{\mathrm{P}}^-, \eta_{\mathrm{P}}^+, \eta_{\mathrm{P}}(ţ): U \longrightarrow [0,1]$ are the elements of neutral degree, $\dot{\alpha}_{ņ}^-(ţ), \dot{\alpha}_{ņ}^+(ţ), \dot{\alpha}_{ņ}(ţ), \eta_{ņ}^-, \eta_{ņ}^+, \eta_{ņ}: U \longrightarrow [0,1]$ are the elements of nonmembership degree, such that $0 \le (\dot{\alpha}_{\dot{\mathrm{U}}}(ţ))^n + (\dot{\alpha}_{\mathrm{P}}(ţ))^n + (\dot{\alpha}_{ņ}(ţ))^n \le 1$ and $0 \le (\eta_{\dot{\mathrm{U}}}(ţ))^n + (\eta_{\mathrm{P}}(ţ))^n + (\eta_{ņ}(ţ))^n \le 1$ $n \in \in \mathbb{N}$.

Definition 10. Let us take two CCuTSFSs in a nonempty set U,

$$j = \left\{(ţ), \left(\begin{pmatrix} \left[\dot{\alpha}_{j(\dot{\mathrm{U}})}^-(ţ)e^{2\pi i\eta_{j(\dot{\mathrm{U}})}^-(ţ)}, \dot{\alpha}_{j(\dot{\mathrm{U}})}^+(ţ)e^{2\pi\eta_{j(\dot{\mathrm{U}})}^+(ţ)i}\right], \\ \left[\dot{\alpha}_{j(P)}^-(ţ)e^{2\pi i\eta_{j(P)}^-(ţ)}, \dot{\alpha}_{j(P)}^+(ţ)e^{2\pi\eta_{j(P)}^+(ţ)i}\right], \\ \left[\dot{\alpha}_{j(ņ)}^-(ţ)e^{2\pi i\eta_{j(ņ)}^-(ţ)}, \dot{\alpha}_{j(ņ)}^+(ţ)e^{2\pi\eta_{j(ņ)}^+(ţ)i}\right], \end{pmatrix}, \begin{pmatrix} \dot{\alpha}_{j(\dot{\mathrm{U}})}(ţ)e^{2\pi i\eta_{j(\dot{\mathrm{U}})}(ţ)}, \\ \dot{\alpha}_{j(P)}(ţ)e^{2\pi i\eta_{j(P)}(ţ)}, \\ \dot{\alpha}_{j(ņ)}(ţ)e^{2\pi i\eta_{j(ņ)}(ţ)} \end{pmatrix}\right): ţ \in U\right\} and,$$

$$\mathscr{K} = \left\{(\dot{g}), \left(\begin{pmatrix} \left[\dot{\alpha}_{\mathscr{K}(\dot{\mathrm{U}})}^-(\dot{g})e^{2\pi i\eta_{\mathscr{K}(\dot{\mathrm{U}})}^-(\dot{g})}, \dot{\alpha}_{\mathscr{K}(\dot{\mathrm{U}})}^+(\dot{g})e^{2\pi\eta_{\mathscr{K}(\dot{\mathrm{U}})}^+(\dot{g})i}\right], \\ \left[\dot{\alpha}_{\mathscr{K}(P)}^-(\dot{g})e^{2\pi i\eta_{\mathscr{K}(P)}^-(\dot{g})}, \dot{\alpha}_{\mathscr{K}(P)}^+(\dot{g})e^{2\pi\eta_{\mathscr{K}(P)}^+(\dot{g})i}\right], \\ \left[\dot{\alpha}_{\mathscr{K}(ņ)}^-(\dot{g})e^{2\pi i\eta_{\mathscr{K}(ņ)}^-(\dot{g})}, \dot{\alpha}_{\mathscr{K}(ņ)}^+(\dot{g})e^{2\pi\eta_{\mathscr{K}(ņ)}^+(\dot{g})i}\right], \end{pmatrix}, \begin{pmatrix} \dot{\alpha}_{\mathscr{K}(\dot{\mathrm{U}})}(\dot{g})e^{2\pi i\eta_{\mathscr{K}(\dot{\mathrm{U}})}(\dot{g})}, \\ \dot{\alpha}_{\mathscr{K}(P)}(\dot{g})e^{2\pi i\eta_{\mathscr{K}(P)}(\dot{g})}, \\ \dot{\alpha}_{\mathscr{K}(ņ)}(\dot{g})e^{2\pi i\eta_{\mathscr{K}(ņ)}(\dot{g})} \end{pmatrix}\right): \dot{g} \in U\right\}. \tag{19}$$

Then, their CP is defined as

$$j\times\mathscr{K}=\left\{(\text{ţ},\dot{g}),\left(\left(\begin{array}{c}\left[\dot{\alpha}^{-}_{j\times\mathscr{K}(\dot{u})}(\text{ţ},\dot{g})e^{2\pi i\eta^{-}_{j\times\mathscr{K}(\dot{u})}(\text{ţ},\dot{g})},\dot{\alpha}^{+}_{j\times\mathscr{K}(\dot{u})}(\text{ţ},\dot{g})e^{2\pi\eta^{+}_{j\times\mathscr{K}(\dot{u})}(\text{ţ},\dot{g})i}\right],\\ \left[\dot{\alpha}^{-}_{j\times\mathscr{K}(P)}(\text{ţ},\dot{g})e^{2\pi i\eta^{-}_{j\times\mathscr{K}(P)}(\text{ţ},\dot{g})},\dot{\alpha}^{+}_{j\times\mathscr{K}(P)}(\text{ţ},\dot{g})e^{2\pi\eta^{+}_{j\times\mathscr{K}(P)}(\text{ţ},\dot{g})i}\right],\\ \left[\dot{\alpha}^{-}_{j\times\mathscr{K}(\text{ŋ̧})}(\text{ţ},\dot{g})e^{2\pi i\eta^{-}_{j\times\mathscr{K}(\text{ŋ̧})}(\text{ţ},\dot{g})},\dot{\alpha}^{+}_{j\times\mathscr{K}(\text{ŋ̧})}(\text{ţ},\dot{g})e^{2\pi\eta^{+}_{j\times\mathscr{K}(\text{ŋ̧})}(\text{ţ},\dot{g})i}\right],\end{array}\right),\left(\begin{array}{c}\dot{\alpha}_{j\times\mathscr{K}(\dot{u})}(\text{ţ},\dot{g})e^{2\pi i\eta_{j\times\mathscr{K}(\dot{u})}(\text{ţ},\dot{g})},\\ \dot{\alpha}_{j\times\mathscr{K}(P)}(\text{ţ},\dot{g})e^{2\pi i\eta_{j\times\mathscr{K}(P)}(\text{ţ},\dot{g})},\\ \dot{\alpha}_{j\times\mathscr{K}(\text{ŋ̧})}(\text{ţ},\dot{g})e^{2\pi i\eta_{j\times\mathscr{K}(\text{ŋ̧})}(\text{ţ},\dot{g})}\end{array}\right)\right)\right\}, \tag{20}$$

where

$$\begin{aligned}
\dot{\alpha}^{-}_{j\times\mathscr{K}(\dot{u})}(\text{ţ},\dot{g})e^{2\pi i\eta^{-}_{j\times\mathscr{K}(\dot{u})}(\text{ţ},\dot{g})} &= \min\left\{\dot{\alpha}^{-}_{j(\dot{u})}(\text{ţ}),\dot{\alpha}^{-}_{\mathscr{K}(\dot{u})}(\dot{g})\right\}e^{\min\left\{\eta^{-}_{j(\dot{u})}(\text{ţ}),\eta^{-}_{\mathscr{K}(\dot{u})}(\dot{g})\right\}2\pi i},\\
\dot{\alpha}^{+}_{j\times\mathscr{K}(\dot{u})}(\text{ţ},\dot{g})e^{2\pi\eta^{+}_{j\times\mathscr{K}(\dot{u})}(\text{ţ},\dot{g})i} &= \min\left\{\dot{\alpha}^{+}_{j(\dot{u})}(\text{ţ}),\dot{\alpha}^{+}_{\mathscr{K}(\dot{u})}(\dot{g})\right\}e^{\min\left\{\eta^{+}_{j(\dot{u})}(\text{ţ})i,\eta^{+}_{\mathscr{K}(\dot{u})}(\dot{g})\right\}2\pi i},\\
\dot{\alpha}^{-}_{j\times\mathscr{K}(P)}(\text{ţ},\dot{g})e^{2\pi i\eta^{-}_{j\times\mathscr{K}(P)}(\text{ţ},\dot{g})} &= \min\left\{\dot{\alpha}^{-}_{j(P)}(\text{ţ}),\dot{\alpha}^{-}_{\mathscr{K}(P)}(\dot{g})\right\}e^{\min\left\{\eta^{-}_{j(P)}(\text{ţ}),\eta^{-}_{\mathscr{K}(P)}(\dot{g})\right\}2\pi i},\\
\dot{\alpha}^{+}_{j\times\mathscr{K}(P)}(\text{ţ},\dot{g})e^{2\pi\eta^{+}_{j\times\mathscr{K}(P)}(\text{ţ},\dot{g})i} &= \min\left\{\dot{\alpha}^{+}_{j(P)}(\text{ţ}),\dot{\alpha}^{+}_{\mathscr{K}(P)}(\dot{g})\right\}e^{\min\left\{\eta^{+}_{j(P)}(\text{ţ}),\eta^{+}_{\mathscr{K}(P)}(\dot{g})\right\}2\pi i},\\
\dot{\alpha}^{-}_{j\times\mathscr{K}(\text{ŋ̧})}(\text{ţ},\dot{g})e^{2\pi i\eta^{-}_{j\times\mathscr{K}(\text{ŋ̧})}(\text{ţ},\dot{g})} &= \max\left\{\dot{\alpha}^{-}_{j(\text{ŋ̧})}(\text{ţ}),\dot{\alpha}^{-}_{\mathscr{K}(\text{ŋ̧})}(\dot{g})\right\}e^{\max\left\{\eta^{-}_{j(\text{ŋ̧})}(\text{ţ}),\eta^{-}_{\mathscr{K}(\text{ŋ̧})}(\dot{g})\right\}2\pi i},\\
\dot{\alpha}^{+}_{j\times\mathscr{K}(\text{ŋ̧})}(\text{ţ},\dot{g})e^{2\pi\eta^{+}_{j\times\mathscr{K}(\text{ŋ̧})}(\text{ţ},\dot{g})i} &= \max\left\{\dot{\alpha}^{+}_{j(\text{ŋ̧})}(\text{ţ}),\dot{\alpha}^{+}_{\mathscr{K}(\text{ŋ̧})}(\dot{g})\right\}e^{\max\left\{\eta^{+}_{j(\text{ŋ̧})}(\text{ţ}),\eta^{+}_{\mathscr{K}(\text{ŋ̧})}(\dot{g})\right\}2\pi i}.
\end{aligned} \tag{21}$$

Example 2. Let two CCuTSFSs $\mathscr{S}$ and $\mathscr{T}$ for $n=5$ on U is defined as

$$\begin{aligned}
\mathscr{S} &= \left\{\begin{array}{c}\left(\begin{array}{c}a,\left([0.2,0.6]e^{2\pi i[0.3,0.6]},[0.4,0.8]e^{2\pi i[0.2,0.4]},[0.5,0.6]e^{2\pi i[0.8.0.9]}\right),\\ \left(0.5e^{(0.4)2\pi i},0.3e^{(0.7)2\pi i},0.5e^{(0.3)2\pi i}\right)\end{array}\right),\\ \left(\begin{array}{c}b,\left([0.3,0.7]e^{2\pi i[0.1,0.2]},[0.3,0.6]e^{2\pi i[0.3,0.5]},[0.6,0.9]e^{2\pi i[0.3,0.8]}\right),\\ \left(0.3e^{(0.2)2\pi i},0.2e^{(0.1)2\pi i},0.7e^{(0.5)2\pi i}\right)\end{array}\right)\end{array}\right\},\\
\mathscr{T} &= \left\{\begin{array}{c}\left(\begin{array}{c}c,\left([0.4,0.7]e^{2\pi i[0.3,0.5]},[0.2,0.7]e^{2\pi i[0.3,0.5]},[0.5,0.8]e^{2\pi i[0.4,0.6]}\right),\\ \left(0.4e^{2\pi i(0.2)},0.6e^{2\pi i(0.8)},0.5e^{2\pi i(0.3)}\right)\end{array}\right),\\ \left(\begin{array}{c}d,\left([0.4,0.5]e^{2\pi i[0.5,0.7]},[0.3,0.6]e^{2\pi i[0.5,0.9]},[0.1,0.3]e^{2\pi i[0.4,0.7]}\right),\\ \left(0.5e^{2\pi i(0.2)},0.4e^{2\pi i(0.4)},0.8e^{2\pi i(0.3)}\right)\end{array}\right),\end{array}\right\}.
\end{aligned} \tag{22}$$

Then, their CP is

$$\mathcal{S}\times\mathcal{T}=\left\{\begin{array}{l}\left((\mathfrak{a},\mathfrak{c}),\begin{array}{c}\left([0.2,0.6]e^{2\pi i[0.3,0.5]},[0.2,0.7]e^{2\pi i[0.2,0.4]},[0.5,0.8]e^{[0.8.0.9]}\right),\\ \left(0.4e^{(0.2)2\pi i},0.3e^{(0.7)2\pi i},0.5e^{(0.3)2\pi i}\right)\end{array}\right),\\ \left((\mathfrak{a},d),\begin{array}{c}\left([0.2,0.5]e^{2\pi i[0.3,0.6]},[0.3,0.6]e^{2\pi i[0.2,0.4]},[0.5,0.6]e^{[0.8.0.9]}\right),\\ \left(0.5e^{(0.2)2\pi i},0.3e^{(0.4)2\pi i},0.8e^{(0.3)2\pi i}\right)\end{array}\right),\\ \left((\mathfrak{b},\mathfrak{c}),\begin{array}{c}\left([0.3,0.7]e^{2\pi i[0.1,0.2]},[0.2,0.6]e^{2\pi i[0.3,0.5]},[0.6,0.9]e^{3\pi i[0.4,0.8]}\right),\\ \left(0.3e^{(0.2)2\pi i},0.2e^{(0.1)2\pi i},0.7e^{(0.5)2\pi i}\right)\end{array}\right),\\ \left((\mathfrak{b},d),\begin{array}{c}\left([0.3,0.5]e^{2\pi i[0.1,0.2]},[0.3,0.6]e^{2\pi i[0.3,0.5]},[0.6,0.9]e^{2\pi i[0.4,0.7]}\right),\\ \left(0.3e^{2\pi i(0.2)},0.2e^{2\pi i(0.1)},0.8e^{2\pi i(0.5)}\right)\end{array}\right)\end{array}\right\}. \tag{23}$$

Definition 11. A complex cubic T spherical fuzzy relation (CCuTSFR) denoted by Ŗ is a subset of the CP of two complex cubic T spherical fuzzy sets (CCuTSFSs).

Example 3. From equation (23), the subset of $\mathcal{S}\times\mathcal{T}$ is

$$\text{Ŗ}=\left\{\begin{array}{l}\left((\mathfrak{a},d),\begin{array}{c}\left([0.2,0.5]e^{2\pi i[0.3,0.6]},[0.3,0.6]e^{2\pi i[0.2,0.4]},[0.5,0.6]e^{[0.8.0.9]}\right),\\ \left(0.5e^{(0.2)2\pi i},0.3e^{(0.4)2\pi i},0.8e^{(0.3)2\pi i}\right)\end{array}\right),\\ \left((\mathfrak{b},\mathfrak{c}),\begin{array}{c}\left([0.3,0.7]e^{2\pi i[0.1,0.2]},[0.2,0.6]e^{2\pi i[0.3,0.5]},[0.6,0.9]e^{3\pi i[0.4,0.8]}\right),\\ \left(0.3e^{(0.2)2\pi i},0.2e^{(0.1)2\pi i},0.7e^{(0.5)2\pi i}\right)\end{array}\right)\end{array}\right\}. \tag{24}$$

Definition 12. Let Ŗ be a CCuTSFR on a CCuTSFS Ċ

$$\begin{array}{l}\left((\text{ţ}),\left(\begin{array}{c}\left[\acute{\alpha}^{-}_{(\dot{u})}(\text{ţ})e^{2\pi i\eta^{-}_{(\dot{u})}(\text{ţ})},\acute{\alpha}^{+}_{(\dot{u})}(\text{ţ})e^{2\pi\eta^{+}_{(\dot{u})}(\text{ţ})i}\right],\\ \left[\acute{\alpha}^{-}_{(\text{ꝑ})}(\text{ţ})e^{2\pi i\eta^{-}_{(\text{ꝑ})}(\text{ţ})},\acute{\alpha}^{+}_{(\text{ꝑ})}(\text{ţ})e^{2\pi\eta^{+}_{(\text{ꝑ})}(\text{ţ})i}\right],\\ \left[\acute{\alpha}^{-}_{(\text{ŋ̧})}(\text{ţ})e^{2\pi i\eta^{-}_{(\text{ŋ̧})}(\text{ţ})},\acute{\alpha}^{+}_{(\text{ŋ̧})}(\text{ţ})e^{2\pi\eta^{+}_{(\text{ŋ̧})}(\text{ţ})i}\right]\end{array}\right),\left(\begin{array}{c}\acute{\alpha}_{(\dot{u})}(\text{ţ})e^{2\pi i\eta_{(\dot{u})}(\text{ţ})},\\ \acute{\alpha}_{(\text{ꝑ})}(\text{ţ})e^{2\pi i\eta_{(\text{ꝑ})}(\text{ţ})},\\ \acute{\alpha}_{(\text{ŋ̧})}(\text{ţ})e^{2\pi i\eta_{(\text{ŋ̧})}(\text{ţ})},\end{array}\right)\right),\\ \left((\dot{g}),\left(\begin{array}{c}\left[\acute{\alpha}^{-}_{(\dot{u})}(\dot{g})e^{2\pi i\eta^{-}_{(\dot{u})}(\dot{g})},\acute{\alpha}^{+}_{(\dot{u})}(\dot{g})e^{2\pi\eta^{+}_{(\dot{u})}(\dot{g})i}\right],\\ \left[\acute{\alpha}^{-}_{(\text{ꝑ})}(\dot{g})e^{2\pi i\eta^{-}_{(\text{ꝑ})}(\dot{g})},\acute{\alpha}^{+}_{(\text{ꝑ})}(\dot{g})e^{2\pi\eta^{+}_{(\text{ꝑ})}(\dot{g})i}\right],\\ \left[\acute{\alpha}^{-}_{(\text{ŋ̧})}(\dot{g})e^{2\pi i\eta^{-}_{(\text{ŋ̧})}(\dot{g})},\acute{\alpha}^{+}_{(\text{ŋ̧})}(\dot{g})e^{2\pi\eta^{+}_{(\text{ŋ̧})}(\dot{g})i}\right]\end{array}\right),\left(\begin{array}{c}\acute{\alpha}_{(\dot{u})}(\dot{g})e^{2\pi i\eta_{(\dot{u})}(\dot{g})},\\ \acute{\alpha}_{(\text{ꝑ})}(\dot{g})e^{2\pi i\eta_{(\text{ꝑ})}(\dot{g})},\\ \acute{\alpha}_{(\text{ŋ̧})}(\dot{g})e^{2\pi i\eta_{(\text{ŋ̧})}(\dot{g})}\end{array}\right)\right),\\ \left((z),\left(\begin{array}{c}\left[\acute{\alpha}^{-}_{(\dot{u})}(z)e^{2\pi i\eta^{-}_{(\dot{u})}(z)},\acute{\alpha}^{+}_{(\dot{u})}(z)e^{2\pi\eta^{+}_{(\dot{u})}(z)i}\right],\\ \left[\acute{\alpha}^{-}_{(\text{ꝑ})}(z)e^{2\pi i\eta^{-}_{(\text{ꝑ})}(z)},\acute{\alpha}^{+}_{(\text{ꝑ})}(z)e^{2\pi\eta^{+}_{(\text{ꝑ})}(z)i}\right],\\ \left[\acute{\alpha}^{-}_{(\text{ŋ̧})}(z)e^{2\pi i\eta^{-}_{(\text{ŋ̧})}(z)},\acute{\alpha}^{+}_{(\text{ŋ̧})}(z)e^{2\pi\eta^{+}_{(\text{ŋ̧})}(z)i}\right]\end{array}\right),\left(\begin{array}{c}\acute{\alpha}_{(\dot{u})}(z)e^{2\pi i\eta_{(\dot{u})}(z)},\\ \acute{\alpha}_{(\text{ꝑ})}(z)e^{2\pi i\eta_{(\text{ꝑ})}(z)},\\ \acute{\alpha}_{(\text{ŋ̧})}(z)e^{2\pi i\eta_{(\text{ŋ̧})}(z)}\end{array}\right)\right),\in \acute{C}.\end{array} \tag{25}$$

(i) A CCuTSFR Ŗ is said to be reflexive, if

$$\forall\left\{(\text{ţ}),\left(\begin{array}{l}\left[\dot{\alpha}^{-}_{(\dot{u})}(\text{ţ})e^{2\pi i\eta^{-}_{(\dot{u})}(\text{ţ})},\dot{\alpha}^{+}_{(\dot{u})}(\text{ţ})e^{2\pi\eta^{+}_{(\dot{u})}(\text{ţ})i}\right],\\ \left[\dot{\alpha}^{-}_{(P)}(\text{ţ})e^{2\pi i\eta^{-}_{(P)}(\text{ţ})},\dot{\alpha}^{+}_{(P)}(\text{ţ})e^{2\pi\eta^{+}_{(P)}(\text{ţ})i}\right],\\ \left[\dot{\alpha}^{-}_{(\text{ņ})}(\text{ţ})e^{2\pi i\eta^{-}_{(\text{ņ})}(\text{ţ})},\dot{\alpha}^{+}_{(\text{ņ})}(\text{ţ})e^{2\pi\eta^{+}_{(\text{ņ})}(\text{ţ})i}\right]\end{array}\right),\left(\begin{array}{l}\dot{\alpha}_{(\dot{u})}(\text{ţ})e^{2\pi i\eta_{(\dot{u})}(\text{ţ})},\\ \dot{\alpha}_{(P)}(\text{ţ})e^{2\pi i\eta_{(P)}(\text{ţ})},\\ \dot{\alpha}_{(\text{ņ})}(\text{ţ})e^{2\pi i\eta_{(\text{ņ})}(\text{ţ})}\end{array}\right)\right\}\in\dot{C},$$

$$\text{implies}\left\{(\text{ţ},\text{ţ}),\left(\begin{array}{l}\left[\dot{\alpha}^{-}_{(\dot{u})}(\text{ţ},\text{ţ})e^{2\pi i\eta^{-}_{(\dot{u})}(\text{ţ},\text{ţ})},\dot{\alpha}^{+}_{(\dot{u})}(\text{ţ},\text{ţ})e^{2\pi\eta^{+}_{(\dot{u})}(\text{ţ},\text{ţ})i}\right],\\ \left[\dot{\alpha}^{-}_{(P)}(\text{ţ},\text{ţ})e^{2\pi i\eta^{-}_{(P)}(\text{ţ},\text{ţ})},\dot{\alpha}^{+}_{(P)}(\text{ţ},\text{ţ})e^{2\pi\eta^{+}_{(P)}(\text{ţ},\text{ţ})i}\right],\\ \left[\dot{\alpha}^{-}_{(\text{ņ})}(\text{ţ},\text{ţ})e^{2\pi i\eta^{-}_{(\text{ņ})}(\text{ţ})},\dot{\alpha}^{+}_{(\text{ņ})}(\text{ţ},\text{ţ})e^{2\pi\eta^{+}_{(\text{ņ})}(\text{ţ},\text{ţ})i}\right]\end{array}\right),\left(\begin{array}{l}\dot{\alpha}_{(\dot{u})}(\text{ţ},\text{ţ})e^{2\pi i\eta_{(\dot{u})}(\text{ţ},\text{ţ})},\\ \dot{\alpha}_{(P)}(\text{ţ},\text{ţ})e^{2\pi i\eta_{(P)}(\text{ţ},\text{ţ})},\\ \dot{\alpha}_{(\text{ņ})}(\text{ţ},\text{ţ})e^{2\pi i\eta_{(\text{ņ})}(\text{ţ},\text{ţ})}\end{array}\right)\right\}\in\text{Ŗ}. \tag{26}$$

(ii) A CCuTSFR Ŗ is said to be irreflexive, if

$$\forall\left\{(\text{ţ}),\left(\begin{array}{l}\left[\dot{\alpha}^{-}_{(\dot{u})}(\text{ţ})e^{2\pi i\eta^{-}_{(\dot{u})}(\text{ţ})},\dot{\alpha}^{+}_{(\dot{u})}(\text{ţ})e^{2\pi\eta^{+}_{(\dot{u})}(\text{ţ})i}\right],\\ \left[\dot{\alpha}^{-}_{(P)}(\text{ţ})e^{2\pi i\eta^{-}_{(P)}(\text{ţ})},\dot{\alpha}^{+}_{(P)}(\text{ţ})e^{2\pi\eta^{+}_{(P)}(\text{ţ})i}\right],\\ \left[\dot{\alpha}^{-}_{(\text{ņ})}(\text{ţ})e^{2\pi i\eta^{-}_{(\text{ņ})}(\text{ţ})},\dot{\alpha}^{+}_{(\text{ņ})}(\text{ţ})e^{2\pi\eta^{+}_{(\text{ņ})}(\text{ţ})i}\right]\end{array}\right),\left(\begin{array}{l}\dot{\alpha}_{(\dot{u})}(\text{ţ})e^{2\pi i\eta_{(\dot{u})}(\text{ţ})},\\ \dot{\alpha}_{(P)}(\text{ţ})e^{2\pi i\eta_{(P)}(\text{ţ})},\\ \dot{\alpha}_{(\text{ņ})}(\text{ţ})e^{2\pi i\eta_{(\text{ņ})}(\text{ţ})}\end{array}\right)\right\}\in\dot{C}. \tag{27}$$

Implies

$$\left\{(\text{ţ},\text{ţ}),\left(\begin{array}{l}\left[\dot{\alpha}^{-}_{(\dot{u})}(\text{ţ},\text{ţ})e^{2\pi i\eta^{-}_{(\dot{u})}(\text{ţ},\text{ţ})},\dot{\alpha}^{+}_{(\dot{u})}(\text{ţ},\text{ţ})e^{2\pi\eta^{+}_{(\dot{u})}(\text{ţ},\text{ţ})i}\right],\\ \left[\dot{\alpha}^{-}_{(P)}(\text{ţ},\text{ţ})e^{2\pi i\eta^{-}_{(P)}(\text{ţ},\text{ţ})},\dot{\alpha}^{+}_{(P)}(\text{ţ},\text{ţ})e^{2\pi\eta^{+}_{(P)}(\text{ţ},\text{ţ})i}\right],\\ \left[\dot{\alpha}^{-}_{(\text{ņ})}(\text{ţ},\text{ţ})e^{2\pi i\eta^{-}_{(\text{ņ})}(\text{ţ})},\dot{\alpha}^{+}_{(\text{ņ})}(\text{ţ},\text{ţ})e^{2\pi\eta^{+}_{(\text{ņ})}(\text{ţ},\text{ţ})i}\right]\end{array}\right),\left(\begin{array}{l}\dot{\alpha}_{(\dot{u})}(\text{ţ},\text{ţ})e^{2\pi i\eta_{(\dot{u})}(\text{ţ},\text{ţ})},\\ \dot{\alpha}_{(P)}(\text{ţ},\text{ţ})e^{2\pi i\eta_{(P)}(\text{ţ},\text{ţ})},\\ \dot{\alpha}_{(\text{ņ})}(\text{ţ},\text{ţ})e^{2\pi i\eta_{(\text{ņ})}(\text{ţ},\text{ţ})}\end{array}\right)\right\}\notin\text{Ŗ}. \tag{28}$$

(iii) A CCuTSFR Ŗ is said to be symmetric, if

$$\forall\left\{\begin{array}{l}(ţ),\left(\begin{array}{c}\left[\dot{\alpha}^{-}_{(\dot{u})}(ţ)e^{2\pi i\eta^{-}_{(\dot{u})}(ţ)},\dot{\alpha}^{+}_{(\dot{u})}(ţ)e^{2\pi\eta^{+}_{(\dot{u})}(ţ)i}\right],\\ \left[\dot{\alpha}^{-}_{(P)}(ţ)e^{2\pi i\eta^{-}_{(P)}(ţ)},\dot{\alpha}^{+}_{(P)}(ţ)e^{2\pi\eta^{+}_{(P)}(ţ)i}\right],\\ \left[\dot{\alpha}^{-}_{(ņ)}(ţ)e^{2\pi i\eta^{-}_{(ņ)}(ţ)},\dot{\alpha}^{+}_{(ņ)}(ţ)e^{2\pi\eta^{+}_{(ņ)}(ţ)i}\right]\end{array}\right),\left(\begin{array}{c}\dot{\alpha}_{(\dot{u})}(ţ)e^{2\pi i\eta_{(\dot{u})}(ţ)},\\ \dot{\alpha}_{(P)}(ţ)e^{2\pi i\eta_{(P)}(ţ)},\\ \dot{\alpha}_{(ņ)}(ţ)e^{2\pi i\eta_{(ņ)}(ţ)}\end{array}\right)\end{array}\right\},$$

$$\left\{\begin{array}{l}(\dot{g}),\left(\begin{array}{c}\left[\dot{\alpha}^{-}_{(\dot{u})}(\dot{g})e^{2\pi i\eta^{-}_{(\dot{u})}(\dot{g})},\dot{\alpha}^{+}_{(\dot{u})}(\dot{g})e^{2\pi\eta^{+}_{(\dot{u})}(\dot{g})i}\right],\\ \left[\dot{\alpha}^{-}_{(P)}(\dot{g})e^{2\pi i\eta^{-}_{(P)}(\dot{g})},\dot{\alpha}^{+}_{(P)}(\dot{g})e^{2\pi\eta^{+}_{(P)}(\dot{g})i}\right],\\ \left[\dot{\alpha}^{-}_{(ņ)}(\dot{g})e^{2\pi i\eta^{-}_{(ņ)}(\dot{g})},\dot{\alpha}^{+}_{(ņ)}(\dot{g})e^{2\pi\eta^{+}_{(ņ)}(\dot{g})i}\right]\end{array}\right),\left(\begin{array}{c}\dot{\alpha}_{(\dot{u})}(\dot{g})e^{2\pi i\eta_{(\dot{u})}(\dot{g})},\\ \dot{\alpha}_{(P)}(\dot{g})e^{2\pi i\eta_{(P)}(\dot{g})},\\ \dot{\alpha}_{(ņ)}(\dot{g})e^{2\pi i\eta_{(ņ)}(\dot{g})}\end{array}\right)\end{array}\right\}\in \dot{C},$$

$$\left\{\begin{array}{l}(ţ,\dot{g}),\left(\begin{array}{c}\left[\dot{\alpha}^{-}_{(\dot{u})}(ţ,\dot{g})e^{2\pi i\eta^{-}_{(\dot{u})}(ţ,\dot{g})},\dot{\alpha}^{+}_{(\dot{u})}(ţ,\dot{g})e^{2\pi\eta^{+}_{(\dot{u})}(ţ,\dot{g})i}\right],\\ \left[\dot{\alpha}^{-}_{(P)}(ţ,\dot{g})e^{2\pi i\eta^{-}_{(P)}(ţ,\dot{g})},\dot{\alpha}^{+}_{(P)}(ţ,\dot{g})e^{2\pi\eta^{+}_{(P)}(ţ,\dot{g})i}\right],\\ \left[\dot{\alpha}^{-}_{(ņ)}(ţ,\dot{g})e^{2\pi i\eta^{-}_{(ņ)}(ţ,\dot{g})},\dot{\alpha}^{+}_{(ņ)}(ţ,\dot{g})e^{2\pi\eta^{+}_{(ņ)}(ţ,\dot{g})i}\right]\end{array}\right),\left(\begin{array}{c}\dot{\alpha}_{(\dot{u})}(ţ,\dot{g})e^{2\pi i\eta_{(\dot{u})}(ţ,\dot{g})},\\ \dot{\alpha}_{(P)}(ţ,\dot{g})e^{2\pi i\eta_{(P)}(ţ,\dot{g})},\\ \dot{\alpha}_{(ņ)}(ţ,\dot{g})e^{2\pi i\eta_{(ņ)}(ţ,\dot{g})}\end{array}\right)\end{array}\right\}\in Ŗ,\ \text{And} \tag{29}$$

$$\left\{\begin{array}{l}(\dot{g},ţ),\left(\begin{array}{c}\left[\dot{\alpha}^{-}_{(\dot{u})}(\dot{g},ţ)e^{2\pi i\eta^{-}_{(\dot{u})}(\dot{g},ţ)},\dot{\alpha}^{+}_{(\dot{u})}(\dot{g},ţ)e^{2\pi\eta^{+}_{(\dot{u})}(\dot{g},ţ)i}\right],\\ \left[\dot{\alpha}^{-}_{(P)}(\dot{g},ţ)e^{2\pi i\eta^{-}_{(P)}(\dot{g},ţ)},\dot{\alpha}^{+}_{(P)}(\dot{g},ţ)e^{2\pi\eta^{+}_{(P)}(\dot{g},ţ)i}\right],\\ \left[\dot{\alpha}^{-}_{(ņ)}(\dot{g},ţ)e^{2\pi i\eta^{-}_{(ņ)}(\dot{g},ţ)},\dot{\alpha}^{+}_{(ņ)}(\dot{g},ţ)e^{2\pi\eta^{+}_{(ņ)}(\dot{g},ţ)i}\right]\end{array}\right),\left(\begin{array}{c}\dot{\alpha}_{(\dot{u})}(\dot{g},ţ)e^{2\pi i\eta_{(\dot{u})}(\dot{g},ţ)},\\ \dot{\alpha}_{(P)}(\dot{g},ţ)e^{2\pi i\eta_{(P)}(\dot{g},ţ)},\\ \dot{\alpha}_{(ņ)}(\dot{g},ţ)e^{2\pi i\eta_{(ņ)}(\dot{g},ţ)}\end{array}\right)\end{array}\right\}\in Ŗ.$$

(iv) A CCuTSFR Ŗ is said to be antisymmetric, if

$$
\begin{aligned}
&\forall \left\{ (\text{ţ}), \begin{pmatrix} \left[\acute{\alpha}^{-}_{(\dot{\upsilon})}(\text{ţ})e^{2\pi i\eta^{-}_{(\dot{\upsilon})}(\text{ţ})}, \acute{\alpha}^{+}_{(\dot{\upsilon})}(\text{ţ})e^{2\pi\eta^{+}_{(\dot{\upsilon})}(\text{ţ})i}\right], \\ \left[\acute{\alpha}^{-}_{(\mathrm{P})}(\text{ţ})e^{2\pi i\eta^{-}_{(\mathrm{P})}(\text{ţ})}, \acute{\alpha}^{+}_{(\mathrm{P})}(\text{ţ})e^{2\pi\eta^{+}_{(\mathrm{P})}(\text{ţ})i}\right], \\ \left[\acute{\alpha}^{-}_{(\text{ņ})}(\text{ţ})e^{2\pi i\eta^{-}_{(\text{ņ})}(\text{ţ})}, \acute{\alpha}^{+}_{(\text{ņ})}(\text{ţ})e^{2\pi\eta^{+}_{(\text{ņ})}(\text{ţ})i}\right] \end{pmatrix}, \begin{pmatrix} \acute{\alpha}_{(\dot{\upsilon})}(\text{ţ})e^{2\pi i\eta_{(\dot{\upsilon})}(\text{ţ})}, \\ \acute{\alpha}_{(\mathrm{P})}(\text{ţ})e^{2\pi i\eta_{(\mathrm{P})}(\text{ţ})}, \\ \acute{\alpha}_{(\text{ņ})}(\text{ţ})e^{2\pi i\eta_{(\text{ņ})}(\text{ţ})} \end{pmatrix} \right\}, \\
&\left\{ (\dot{g}), \begin{pmatrix} \left[\acute{\alpha}^{-}_{(\dot{\upsilon})}(\dot{g})e^{2\pi i\eta^{-}_{(\dot{\upsilon})}(\dot{g})}, \acute{\alpha}^{+}_{(\dot{\upsilon})}(\dot{g})e^{2\pi\eta^{+}_{(\dot{\upsilon})}(\dot{g})i}\right], \\ \left[\acute{\alpha}^{-}_{(\mathrm{P})}(\dot{g})e^{2\pi i\eta^{-}_{(\mathrm{P})}(\dot{g})}, \acute{\alpha}^{+}_{(\mathrm{P})}(\dot{g})e^{2\pi\eta^{+}_{(\mathrm{P})}(\dot{g})i}\right], \\ \left[\acute{\alpha}^{-}_{(\text{ņ})}(\dot{g})e^{2\pi i\eta^{-}_{(\text{ņ})}(\dot{g})}, \acute{\alpha}^{+}_{(\text{ņ})}(\dot{g})e^{2\pi\eta^{+}_{(\text{ņ})}(\dot{g})i}\right] \end{pmatrix}, \begin{pmatrix} \acute{\alpha}_{(\dot{\upsilon})}(\dot{g})e^{2\pi i\eta_{(\dot{\upsilon})}(\dot{g})}, \\ \acute{\alpha}_{(\mathrm{P})}(\dot{g})e^{2\pi i\eta_{(\mathrm{P})}(\dot{g})}, \\ \acute{\alpha}_{(\text{ņ})}(\dot{g})e^{2\pi i\eta_{(\text{ņ})}(\dot{g})} \end{pmatrix} \right\} \in \dot{C}, \\
&\left\{ (\text{ţ}, \dot{g}), \begin{pmatrix} \left[\acute{\alpha}^{-}_{(\dot{\upsilon})}(\text{ţ},\dot{g})e^{2\pi i\eta^{-}_{(\dot{\upsilon})}(\text{ţ},\dot{g})}, \acute{\alpha}^{+}_{(\dot{\upsilon})}(\text{ţ},\dot{g})e^{2\pi\eta^{+}_{(\dot{\upsilon})}(\text{ţ},\dot{g})i}\right], \\ \left[\acute{\alpha}^{-}_{(\mathrm{P})}(\text{ţ},\dot{g})e^{2\pi i\eta^{-}_{(\mathrm{P})}(\text{ţ},\dot{g})}, \acute{\alpha}^{+}_{(\mathrm{P})}(\text{ţ},\dot{g})e^{2\pi\eta^{+}_{(\mathrm{P})}(\text{ţ},\dot{g})i}\right], \\ \left[\acute{\alpha}^{-}_{(\text{ņ})}(\text{ţ},\dot{g})e^{2\pi i\eta^{-}_{(\text{ņ})}(\text{ţ},\dot{g})}, \acute{\alpha}^{+}_{(\text{ņ})}(\text{ţ},\dot{g})e^{2\pi\eta^{+}_{(\text{ņ})}(\text{ţ},\dot{g})i}\right] \end{pmatrix}, \begin{pmatrix} \acute{\alpha}_{(\dot{\upsilon})}(\text{ţ},\dot{g})e^{2\pi i\eta_{(\dot{\upsilon})}(\text{ţ},\dot{g})}, \\ \acute{\alpha}_{(\mathrm{P})}(\text{ţ},\dot{g})e^{2\pi i\eta_{(\mathrm{P})}(\text{ţ},\dot{g})}, \\ \acute{\alpha}_{(\text{ņ})}(\text{ţ},\dot{g})e^{2\pi i\eta_{(\text{ņ})}(\text{ţ},\dot{g})} \end{pmatrix} \right\} \in \text{Ŗ}, \\
&\text{And} \left\{ (\dot{g}, \text{ţ}), \begin{pmatrix} \left[\acute{\alpha}^{-}_{(\dot{\upsilon})}(\dot{g},\text{ţ})e^{2\pi i\eta^{-}_{(\dot{\upsilon})}(\dot{g},\text{ţ})}, \acute{\alpha}^{+}_{(\dot{\upsilon})}(\dot{g},\text{ţ})e^{2\pi\eta^{+}_{(\dot{\upsilon})}(\dot{g},\text{ţ})i}\right], \\ \left[\acute{\alpha}^{-}_{(\mathrm{P})}(\dot{g},\text{ţ})e^{2\pi i\eta^{-}_{(\mathrm{P})}(\dot{g},\text{ţ})}, \acute{\alpha}^{+}_{(\mathrm{P})}(\dot{g},\text{ţ})e^{2\pi\eta^{+}_{(\mathrm{P})}(\dot{g},\text{ţ})i}\right], \\ \left[\acute{\alpha}^{-}_{(\text{ņ})}(\dot{g},\text{ţ})e^{2\pi i\eta^{-}_{(\text{ņ})}(\dot{g},\text{ţ})}, \acute{\alpha}^{+}_{(\text{ņ})}(\dot{g},\text{ţ})e^{2\pi\eta^{+}_{(\text{ņ})}(\dot{g},\text{ţ})i}\right] \end{pmatrix}, \begin{pmatrix} \acute{\alpha}_{(\dot{\upsilon})}(\dot{g},\text{ţ})e^{2\pi i\eta_{(\dot{\upsilon})}(\dot{g},\text{ţ})}, \\ \acute{\alpha}_{(\mathrm{P})}(\dot{g},\text{ţ})e^{2\pi i\eta_{(\mathrm{P})}(\dot{g},\text{ţ})}, \\ \acute{\alpha}_{(\text{ņ})}(\dot{g},\text{ţ})e^{2\pi i\eta_{(\text{ņ})}(\dot{g},\text{ţ})} \end{pmatrix} \right\} \in \text{Ŗ}. \text{ Then,} \\
&\left\{ (\text{ţ}, \dot{g}), \begin{pmatrix} \left[\acute{\alpha}^{-}_{(\dot{\upsilon})}(\text{ţ},\dot{g})e^{2\pi i\eta^{-}_{(\dot{\upsilon})}(\text{ţ},\dot{g})}, \acute{\alpha}^{+}_{(\dot{\upsilon})}(\text{ţ},\dot{g})e^{2\pi\eta^{+}_{(\dot{\upsilon})}(\text{ţ},\dot{g})i}\right], \\ \left[\acute{\alpha}^{-}_{\mathrm{P}}(\text{ţ},\dot{g})e^{2\pi i\eta^{-}_{(\mathrm{P})}(\text{ţ},\dot{g})}, \acute{\alpha}^{+}_{(\mathrm{P})}(\text{ţ},\dot{g})e^{2\pi\eta^{+}_{(\mathrm{P})}(\text{ţ},\dot{g})i}\right], \\ \left[\acute{\alpha}^{-}_{(\text{ņ})}(\text{ţ},\dot{g})e^{2\pi i\eta^{-}_{(\text{ņ})}(\text{ţ},\dot{g})}, \acute{\alpha}^{+}_{(\text{ņ})}(\text{ţ},\dot{g})e^{2\pi\eta^{+}_{(\text{ņ})}(\text{ţ},\dot{g})i}\right] \end{pmatrix}, \begin{pmatrix} \acute{\alpha}_{(\dot{\upsilon})}(\text{ţ},\dot{g})e^{2\pi i\eta_{(\dot{\upsilon})}(\text{ţ},\dot{g})}, \\ \acute{\alpha}_{(\mathrm{P})}(\text{ţ},\dot{g})e^{2\pi i\eta_{(\mathrm{P})}(\text{ţ},\dot{g})}, \\ \acute{\alpha}_{(\text{ņ})}(\text{ţ},\dot{g})e^{2\pi i\eta_{(\text{ņ})}(\text{ţ},\dot{g})} \end{pmatrix} \right\}, \\
&= \left\{ (\dot{g}, \text{ţ}), \begin{pmatrix} \left[\acute{\alpha}^{-}_{(\dot{\upsilon})}(\dot{g},\text{ţ})e^{2\pi i\eta^{-}_{(\dot{\upsilon})}(\dot{g}\,\text{ţ})}, \acute{\alpha}^{+}_{(\dot{\upsilon})}(\dot{g},\text{ţ})e^{2\pi\eta^{+}_{(\dot{\upsilon})}(\dot{g},\text{ţ})i}\right], \\ \left[\acute{\alpha}^{-}_{(\mathrm{P})}(\dot{g},\text{ţ})e^{2\pi i\eta^{-}_{(\mathrm{P})}(\dot{g},\text{ţ})}, \acute{\alpha}^{+}_{(\mathrm{P})}(\dot{g},\text{ţ})e^{2\pi\eta^{+}_{(\mathrm{P})}(\dot{g},\text{ţ})i}\right], \\ \left[\acute{\alpha}^{-}_{(\text{ņ})}(\dot{g},\text{ţ})e^{2\pi i\eta^{-}_{(\text{ņ})}(\dot{g},\text{ţ})}, \acute{\alpha}^{+}_{(\text{ņ})}(\dot{g},\text{ţ})e^{2\pi\eta^{+}_{(\text{ņ})}(\dot{g},\text{ţ})i}\right] \end{pmatrix}, \begin{pmatrix} \acute{\alpha}_{(\dot{\upsilon})}(\dot{g},\text{ţ})e^{2\pi i\eta_{(\dot{\upsilon})}(\dot{g},\text{ţ})}, \\ \acute{\alpha}_{(\mathrm{P})}(\dot{g},\text{ţ})e^{2\pi i\eta_{(\mathrm{P})}(\dot{g},\text{ţ})}, \\ \acute{\alpha}_{(\text{ņ})}(\dot{g},\text{ţ})e^{2\pi i\eta_{(\text{ņ})}(\dot{g},\text{ţ})} \end{pmatrix} \right\}.
\end{aligned}
\tag{30}
$$

(v) A CCuTSFR Ŗ is said to be transitive, if

$$
\begin{aligned}
&\forall\left\{(\text{ţ}),\begin{pmatrix}\left[\acute{\alpha}^{-}_{(\dot{u})}(\text{ţ})e^{2\pi i\eta^{-}_{(\dot{u})}(\text{ţ})},\acute{\alpha}^{+}_{(\dot{u})}(\text{ţ})e^{2\pi\eta^{+}_{(\dot{u})}(\text{ţ})i}\right],\\ \left[\acute{\alpha}^{-}_{(\mathrm{P})}(\text{ţ})e^{2\pi i\eta^{-}_{(\mathrm{P})}(\text{ţ})},\acute{\alpha}^{+}_{(\mathrm{P})}(\text{ţ})e^{2\pi\eta^{+}_{(\mathrm{P})}(\text{ţ})i}\right],\\ \left[\acute{\alpha}^{-}_{(\text{ņ})}(\text{ţ})e^{2\pi i\eta^{-}_{(\text{ņ})}(\text{ţ})},\acute{\alpha}^{+}_{(\text{ņ})}(\text{ţ})e^{2\pi\eta^{+}_{(\text{ņ})}(\text{ţ})i}\right]\end{pmatrix},\begin{pmatrix}\acute{\alpha}_{(\dot{u})}(\text{ţ})e^{2\pi i\eta_{(\dot{u})}(\text{ţ})},\\ \acute{\alpha}_{(\mathrm{P})}(\text{ţ})e^{2\pi i\eta_{(\mathrm{P})}(\text{ţ})},\\ \acute{\alpha}_{(\text{ņ})}(\text{ţ})e^{2\pi i\eta_{(\text{ņ})}(\text{ţ})}\end{pmatrix}\right\},\\
&\left\{(\dot{g}),\begin{pmatrix}\left[\acute{\alpha}^{-}_{(\dot{u})}(\dot{g})e^{2\pi i\eta^{-}_{(\dot{u})}(\dot{g})},\acute{\alpha}^{+}_{(\dot{u})}(\dot{g})e^{2\pi\eta^{+}_{(\dot{u})}(\dot{g})i}\right],\\ \left[\acute{\alpha}^{-}_{(\mathrm{P})}(\dot{g})e^{2\pi i\eta^{-}_{(\mathrm{P})}(\dot{g})},\acute{\alpha}^{+}_{(\mathrm{P})}(\dot{g})e^{2\pi\eta^{+}_{(\mathrm{P})}(\dot{g})i}\right],\\ \left[\acute{\alpha}^{-}_{(\text{ņ})}(\dot{g})e^{2\pi i\eta^{-}_{(\text{ņ})}(\dot{g})},\acute{\alpha}^{+}_{(\text{ņ})}(\dot{g})e^{2\pi\eta^{+}_{(\text{ņ})}(\dot{g})i}\right]\end{pmatrix},\begin{pmatrix}\acute{\alpha}_{(\dot{u})}(\dot{g})e^{2\pi i\eta_{(\dot{u})}(\dot{g})},\\ \acute{\alpha}_{(\mathrm{P})}(\dot{g})e^{2\pi i\eta_{(\mathrm{P})}(\dot{g})},\\ \acute{\alpha}_{(\text{ņ})}(\dot{g})e^{2\pi i\eta_{(\text{ņ})}(\dot{g})}\end{pmatrix}\right\},\\
&\left\{(\mathrm{z}),\begin{pmatrix}\left[\acute{\alpha}^{-}_{(\dot{u})}(\mathrm{z})e^{2\pi i\eta^{-}_{(\dot{u})}(\mathrm{z})},\acute{\alpha}^{+}_{(\dot{u})}(\mathrm{z})e^{2\pi\eta^{+}_{(\dot{u})}(\mathrm{z})i}\right],\\ \left[\acute{\alpha}^{-}_{(\mathrm{P})}(\mathrm{z})e^{2\pi i\eta^{-}_{(\mathrm{P})}(\mathrm{z})},\acute{\alpha}^{+}_{(\mathrm{P})}(\mathrm{z})e^{2\pi\eta^{+}_{(\mathrm{P})}(\mathrm{z})i}\right],\\ \left[\acute{\alpha}^{-}_{(\text{ņ})}(\mathrm{z})e^{2\pi i\eta^{-}_{(\text{ņ})}(\mathrm{z})},\acute{\alpha}^{+}_{(\text{ņ})}(\mathrm{z})e^{2\pi\eta^{+}_{(\text{ņ})}(\mathrm{z})i}\right]\end{pmatrix},\begin{pmatrix}\acute{\alpha}_{(\dot{u})}(\mathrm{z})e^{2\pi i\eta_{(\dot{u})}(\mathrm{z})},\\ \acute{\alpha}_{(\mathrm{P})}(\mathrm{z})e^{2\pi i\eta_{(\mathrm{P})}(\mathrm{z})},\\ \acute{\alpha}_{(\text{ņ})}(\mathrm{z})e^{2\pi i\eta_{(\text{ņ})}(\mathrm{z})}\end{pmatrix}\right\}\in\dot{\mathrm{C}},\\
&\left\{(\text{ţ},\dot{g}),\begin{pmatrix}\left[\acute{\alpha}^{-}_{(\dot{u})}(\text{ţ},\dot{g})e^{2\pi i\eta^{-}_{(\dot{u})}(\text{ţ},\dot{g})},\acute{\alpha}^{+}_{(\dot{u})}(\text{ţ},\dot{g})e^{2\pi\eta^{+}_{(\dot{u})}(\text{ţ},\dot{g})i}\right],\\ \left[\acute{\alpha}^{-}_{(\mathrm{P})}(\text{ţ},\dot{g})e^{2\pi i\eta^{-}_{(\mathrm{P})}(\text{ţ},\dot{g})},\acute{\alpha}^{+}_{(\mathrm{P})}(\text{ţ},\dot{g})e^{2\pi\eta^{+}_{(\mathrm{P})}(\text{ţ},\dot{g})i}\right],\\ \left[\acute{\alpha}^{-}_{(\text{ņ})}(\text{ţ},\dot{g})e^{2\pi i\eta^{-}_{(\text{ņ})}(\text{ţ},\dot{g})},\acute{\alpha}^{+}_{(\text{ņ})}(\text{ţ},\dot{g})e^{2\pi\eta^{+}_{(\text{ņ})}(\text{ţ},\dot{g})i}\right]\end{pmatrix},\begin{pmatrix}\acute{\alpha}_{(\dot{u})}(\text{ţ},\dot{g})e^{2\pi i\eta_{(\dot{u})}(\text{ţ},\dot{g})},\\ \acute{\alpha}_{(\mathrm{P})}(\text{ţ},\dot{g})e^{2\pi i\eta_{(\mathrm{P})}(\text{ţ},\dot{g})},\\ \acute{\alpha}_{(\text{ņ})}(\text{ţ},\dot{g})e^{2\pi i\eta_{(\text{ņ})}(\text{ţ},\dot{g})}\end{pmatrix}\right\}\in\text{Ŗ}\ \text{and},\\
&\left\{(\dot{g},\mathrm{z}),\begin{pmatrix}\left[\acute{\alpha}^{-}_{(\dot{u})}(\dot{g},\mathrm{z})e^{2\pi i\eta^{-}_{(\dot{u})}(\dot{g},\mathrm{z})},\acute{\alpha}^{+}_{(\dot{u})}(\dot{g},\mathrm{z})e^{2\pi\eta^{+}_{(\dot{u})}(\dot{g},\mathrm{z})i}\right],\\ \left[\acute{\alpha}^{-}_{(\mathrm{P})}(\dot{g},\mathrm{z})e^{2\pi i\eta^{-}_{(\mathrm{P})}(\dot{g},\mathrm{z})},\acute{\alpha}^{+}_{(\mathrm{P})}(\dot{g},\mathrm{z})e^{2\pi\eta^{+}_{(\mathrm{P})}(\dot{g},\mathrm{z})i}\right],\\ \left[\acute{\alpha}^{-}_{(\text{ņ})}(\dot{g},\mathrm{z})e^{2\pi i\eta^{-}_{(\text{ņ})}(\dot{g},\mathrm{z})},\acute{\alpha}^{+}_{(\text{ņ})}(\dot{g},\mathrm{z})e^{2\pi\eta^{+}_{(\text{ņ})}(\dot{g},\mathrm{z})i}\right]\end{pmatrix},\begin{pmatrix}\acute{\alpha}_{(\dot{u})}(\dot{g},\mathrm{z})e^{2\pi i\eta_{(\dot{u})}(\dot{g},z)},\\ \acute{\alpha}_{(\mathrm{P})}(\dot{g},\mathrm{z})e^{2\pi i\eta_{(\mathrm{P})}(\dot{g},z)},\\ \acute{\alpha}_{(\text{ņ})}(\dot{g},\mathrm{z})e^{2\pi i\eta_{(\text{ņ})}(\dot{g},z)}\end{pmatrix}\right\}\in\text{Ŗ}\ \text{implies},\\
&\left\{(\text{ţ},\mathrm{z}),\begin{pmatrix}\left[\acute{\alpha}^{-}_{(\dot{u})}(\text{ţ},\mathrm{z})e^{2\pi i\eta^{-}_{(\dot{u})}(\text{ţ},\mathrm{z})},\acute{\alpha}^{+}_{(\dot{u})}(\text{ţ},\mathrm{z})e^{2\pi\eta^{+}_{(\dot{u})}(\text{ţ},\mathrm{z})i}\right],\\ \left[\acute{\alpha}^{-}_{(\mathrm{P})}(\text{ţ},\mathrm{z})e^{2\pi i\eta^{-}_{(\mathrm{P})}(\text{ţ},\mathrm{z})},\acute{\alpha}^{+}_{(\mathrm{P})}(\text{ţ},\mathrm{z})e^{2\pi\eta^{+}_{(\mathrm{P})}(\text{ţ},\mathrm{z})i}\right],\\ \left[\acute{\alpha}^{-}_{(\text{ņ})}(\text{ţ},\mathrm{z})e^{2\pi i\eta^{-}_{(\text{ņ})}(\text{ţ},\mathrm{z})},\acute{\alpha}^{+}_{(\text{ņ})}(\text{ţ},\mathrm{z})e^{2\pi\eta^{+}_{(\text{ņ})}(\text{ţ},\mathrm{z})i}\right]\end{pmatrix},\begin{pmatrix}\acute{\alpha}_{(\dot{u})}(\text{ţ},\mathrm{z})e^{2\pi i\eta_{(\dot{u})}(\text{ţ},\mathrm{z})},\\ \acute{\alpha}_{(\mathrm{P})}(\text{ţ},\mathrm{z})e^{2\pi i\eta_{(\mathrm{P})}(\text{ţ},\mathrm{z})},\\ \acute{\alpha}_{(\text{ņ})}(\text{ţ},\mathrm{z})e^{2\pi i\eta_{(\text{ņ})}(\text{ţ},\mathrm{z})}\end{pmatrix}\right\}\in\text{Ŗ}.
\end{aligned}
\tag{31}
$$

(vi) A CCuTSFR Ŗ is said to be equivalence, if it is

(1) Reflexive
(2) Symmetric
(3) Transitive

(vii) A CCuTSFR Ŗ is said to be preorder, if it is

(1) Reflexive
(2) Transitive

(viii) A CCuTSFR Ŗ is said to be partial order, if it is

(1) Reflexive
(2) Antisymmetric
(3) Transitive

(ix) A CCuTSFR Ŗ is said to be CCuTS strict order, if it is

(1) Irreflexive

(2) Transitive

(x) Let $Ŗ_1$ and $Ŗ_2$ be two CCuTSFRs. Then, $Ŗ_1 \circ Ŗ_2$ is composite relation if

$$\left\{ (ţ, ġ), \begin{pmatrix} \left[ά^{-}_{(\dot{U})}(ţ, ġ) e^{2\pi i \eta^{-}_{(\dot{U})}(ţ,ġ)}, ά^{+}_{(\dot{U})}(ţ, ġ) e^{2\pi \eta^{+}_{(\dot{U})}(ţ,ġ) i} \right], \\ \left[ά^{-}_{(P)}(ţ, ġ) e^{2\pi i \eta^{-}_{(P)}(ţ,ġ)}, ά^{+}_{(P)}(ţ, ġ) e^{2\pi \eta^{+}_{(P)}(ţ,ġ) i} \right], \\ \left[ά^{-}_{(ņ)}(ţ, ġ) e^{2\pi i \eta^{-}_{(ņ)}(ţ,ġ)}, ά^{+}_{(ņ)}(ţ, ġ) e^{2\pi \eta^{+}_{(ņ)}(ţ,ġ) i} \right] \end{pmatrix}, \begin{pmatrix} ά_{(\dot{U})}(ţ, ġ) e^{2\pi i \eta_{(\dot{U})}(ţ,ġ)}, \\ ά_{(P)}(ţ, ġ) e^{2\pi i \eta_{(P)}(ţ,ġ)}, \\ ά_{(ņ)}(ţ, ġ) e^{2\pi i \eta_{(ņ)}(ţ,ġ)} \end{pmatrix} \right\} \in Ŗ_1 \text{ and,}$$

$$\left\{ (ġ, z), \begin{pmatrix} \left[ά^{-}_{(\dot{U})}(ġ, z) e^{2\pi i \eta^{-}_{(\dot{U})}(ġ,z)}, ά^{+}_{(\dot{U})}(ġ, z) e^{2\pi \eta^{+}_{(\dot{U})}(ġ,z) i} \right], \\ \left[ά^{-}_{(P)}(ġ, z) e^{2\pi i \eta^{-}_{(P)}(ġ,z)}, ά^{+}_{(P)}(ġ, z) e^{2\pi \eta^{+}_{(P)}(ġ,z) i} \right], \\ \left[ά^{-}_{(ņ)}(ġ, z) e^{2\pi i \eta^{-}_{(ņ)}(ġ,z)}, ά^{+}_{(ņ)}(ġ, z) e^{2\pi \eta^{+}_{(ņ)}(ġ,z) i} \right] \end{pmatrix}, \begin{pmatrix} ά_{(\dot{U})}(ġ, z) e^{2\pi i \eta_{(\dot{U})}(ġ,z)}, \\ ά_{(P)}(ġ, z) e^{2\pi i \eta_{(P)}(ġ,z)}, \\ ά_{(ņ)}(ġ, z) e^{2\pi i \eta_{(ņ)}(ġ,z)} \end{pmatrix} \right\} \in Ŗ_2 \text{ implies,} \tag{32}$$

$$Ŗ_1 \circ Ŗ_2 = \left\{ (ţ, z), \begin{pmatrix} \left[ά^{-}_{(\dot{U})}(ţ, z) e^{2\pi i \eta^{-}_{(\dot{U})}(ţ,z)}, ά^{+}_{(\dot{U})}(ţ, z) e^{2\pi \eta^{+}_{(\dot{U})}(ţ,z) i} \right], \\ \left[ά^{-}_{(P)}(ţ, z) e^{2\pi i \eta^{-}_{(P)}(ţ,z)}, ά^{+}_{(P)}(ţ, z) e^{2\pi \eta^{+}_{(P)}(ţ,z) i} \right], \\ \left[ά^{-}_{(ņ)}(ţ, z) e^{2\pi i \eta^{-}_{(ņ)}(ţ,z)}, ά^{+}_{(ņ)}(ţ, z) e^{2\pi \eta^{+}_{(ņ)}(ţ,z) i} \right] \end{pmatrix}, \begin{pmatrix} ά_{(\dot{U})}(ţ, z) e^{2\pi i \eta_{(\dot{U})}(ţ,z)}, \\ ά_{(P)}(ţ, z) e^{2\pi i \eta_{(P)}(ţ,z)}, \\ ά_{(ņ)}(ţ, z) e^{2\pi i \eta_{(ņ)}(ţ,z)} \end{pmatrix} \right\}.$$

(xi) A CCuTSFR Ŗ is said to be CCuTS linear order, if it is

(1) Reflexive
(2) Antisymmetric
(3) Transitive
(4) Complete

Example 4. Let a CCuTSFS Ă on U is defined as

$$\breve{A} = \left\{ \begin{pmatrix} ţ, \left([0.3, 0.4] e^{[0.2,0.7]2\pi i}, [0.1, 0.2] e^{[0.1,0.4]2\pi i}, [0.5, 0.6] e^{[0.3,0.5]2\pi i} \right), \\ \left(0.2 e^{2\pi i (0.3)}, 0.4 e^{2\pi i (0.5)}, 0.1 e^{2\pi i (0.2)} \right) \end{pmatrix}, \begin{pmatrix} ġ, \left([0.2, 0.6] e^{[0.1,0.5]2\pi i}, [0.3, 0.5] e^{[0.2,0.7]2\pi i}, [0.5, 0.9] e^{[0.1,0.9]2\pi i} \right), \\ \left(0.4 e^{2\pi i (0.5)}, 0.2 e^{2\pi i (0.1)}, 0.7 e^{2\pi i (0.7)} \right) \end{pmatrix}, \begin{pmatrix} z, \left([0.7, 0.9] e^{[0.2,0.5]2\pi i}, [0.2, 0.3] e^{[0.1,0.4]2\pi i}, [0.5, 0.7] e^{[0.4,0.9]2\pi i} \right), \\ \left(0.9 e^{2\pi i (0.6)}, 0.4 e^{2\pi i (0.2)}, 0.7 e^{2\pi i (0.3)} \right) \end{pmatrix} \right\}, \tag{33}$$

Then, its self-CP is

$$\breve{A} \times \breve{A} = \left\{ \begin{array}{l} \left((ţ,ţ), \begin{array}{c} \left([0.3, 0.4]e^{[0.2,0.7]2\pi i}, [0.1, 0.2]e^{[0.1,0.4]2\pi i}, [0.5, 0.6]e^{[0.3,0.5]2\pi i}\right), \\ \left(0.2e^{2\pi i(0.3)}, 0.4e^{2\pi i(0.5)}, 0.1e^{2\pi i(0.2)}\right) \end{array} \right), \\ \left((ţ,\dot{g}), \begin{array}{c} \left([0.2, 0.4]e^{[0.1,0.5]2\pi i}, [0.1, 0.2]e^{[0.1,0.4]2\pi i}, [0.5, 0.9]e^{[0.3,0.9]2\pi i}\right), \\ \left(0.2e^{2\pi i(0.3)}, 0.2e^{2\pi i(0.1)}, 0.7e^{2\pi i(0.7)}\right) \end{array} \right), \\ \left((ţ, z), \begin{array}{c} \left([0.3, 0.4]e^{[0.2,0.5]2\pi i}, [0.1, 0.2]e^{[0.1,0.4]2\pi i}, [0.5, 0.7]e^{[0.4,0.9]2\pi i}\right), \\ \left(0.2e^{2\pi i(0.3)}, 0.4e^{2\pi i(0.2)}, 0.7e^{2\pi i(0.3)}\right) \end{array} \right), \\ \left((\dot{g},ţ), \begin{array}{c} \left([0.2, 0.4]e^{[0.1,0.5]2\pi i}, [0.1, 0.2]e^{[0.1,0.4]2\pi i}, [0.5, 0.9]e^{[0.3,0.9]2\pi i}\right), \\ \left(0.2e^{2\pi i(0.3)}, 0.2e^{2\pi i(0.1)}, 0.7e^{2\pi i(0.7)}\right) \end{array} \right), \\ \left((\dot{g},\dot{g}), \begin{array}{c} \left([0.2, 0.6]e^{[0.1,0.5]2\pi i}, [0.3, 0.5]e^{[0.2,0.7]2\pi i}, [0.5, 0.9]e^{[0.1,0.9]2\pi i}\right), \\ \left(0.4e^{2\pi i(0.5)}, 0.2e^{2\pi i(0.1)}, 0.7e^{2\pi i(0.7)}\right) \end{array} \right), \\ \left((\dot{g}, z), \begin{array}{c} \left([0.2, 0.6]e^{[0.1,0.5]2\pi i}, [0.2, 0.3]e^{[0.1,0.3]2\pi i}, [0.5, 0.9]e^{[0.4,0.9]2\pi i}\right), \\ \left(0.4e^{2\pi i(0.5)}, 0.2e^{2\pi i(0.1)}, 0.7e^{2\pi i(0.7)}\right) \end{array} \right), \\ \left((z,ţ), \begin{array}{c} \left([0.3, 0.4]e^{[0.2,0.5]2\pi i}, [0.1, 0.2]e^{[0.1,0.4]2\pi i}, [0.5, 0.7]e^{[0.4,0.9]2\pi i}\right), \\ \left(0.2e^{2\pi i(0.3)}, 0.4e^{2\pi i(0.2)}, 0.7e^{2\pi i(0.3)}\right) \end{array} \right), \\ \left((z,\dot{g}), \begin{array}{c} \left([0.2, 0.6]e^{[0.1,0.5]2\pi i}, [0.2, 0.3]e^{[0.1,0.3]2\pi i}, [0.5, 0.9]e^{[0.4,0.9]2\pi i}\right), \\ \left(0.4e^{2\pi i(0.5)}, 0.2e^{2\pi i(0.1)}, 0.7e^{2\pi i(0.7)}\right) \end{array} \right), \\ \left((z, z) \begin{array}{c} \left([0.7, 0.9]e^{[0.2,0.5]2\pi i}, [0.2, 0.3]e^{[0.1,0.4]2\pi i}, [0.5, 0.7]e^{[0.4,0.9]2\pi i}\right), \\ \left(0.9e^{2\pi i(0.6)}, 0.4e^{2\pi i(0.2)}, 0.7e^{2\pi i(0.3)}\right) \end{array} \right) \end{array} \right\}. \tag{34}$$

(1) The reflexive relation $Ŗ_1$ is

$$Ŗ_1 = \left\{ \begin{array}{l} \left((ţ, ţ), \begin{array}{c} \left([0.3, 0.4]e^{[0.2,0.7]2\pi i}, [0.1, 0.2]e^{[0.1,0.4]2\pi i}, [0.5, 0.6]e^{[0.3,0.5]2\pi i}\right), \\ \left(0.2e^{2\pi i(0.3)}, 0.4e^{2\pi i(0.5)}, 0.1e^{2\pi i(0.2)}\right) \end{array} \right), \\ \left((\dot{g}, \dot{g}), \begin{array}{c} \left([0.2, 0.6]e^{[0.1,0.5]2\pi i}, [0.3, 0.5]e^{[0.2,0.7]2\pi i}, [0.5, 0.9]e^{[0.1,0.9]2\pi i}\right), \\ \left(0.4e^{2\pi i(0.5)}, 0.2e^{2\pi i(0.1)}, 0.7e^{2\pi i(0.7)}\right) \end{array} \right), \\ \left((z, z), \begin{array}{c} \left([0.7, 0.9]e^{[0.2,0.5]2\pi i}, [0.2, 0.3]e^{[0.1,0.4]2\pi i}, [0.5, 0.7]^{[0.4,0.9]2\pi i}\right), \\ \left(0.9e^{2\pi i(0.6)}, 0.4e^{2\pi i(0.2)}, 0.7e^{2\pi i(0.3)}\right) \end{array} \right) \end{array} \right\}. \tag{35}$$

(2) The symmetric relation $Ŗ_2$ is

$$\text{R}_2 = \left\{ \begin{array}{l} \left((\text{ţ},\text{ţ}), \begin{array}{c} \left([0.3, 0.4]e^{[0.2,0.7]2\pi i}, [0.1, 0.2]e^{[0.1,0.4]2\pi i}, [0.5, 0.6]e^{[0.3,0.5]2\pi i}\right), \\ \left(0.2e^{2\pi i(0.3)}, 0.4e^{2\pi i(0.5)}, 0.1e^{2\pi i(0.2)}\right) \end{array} \right), \\ \left((\text{ţ},\text{z}), \begin{array}{c} \left([0.3, 0.4]e^{[0.2,0.5]2\pi i}, [0.1, 0.2]e^{[0.1,0.4]2\pi i}, [0.5, 0.7]e^{[0.4,0.9]2\pi i}\right), \\ \left(0.2e^{2\pi i(0.3)}, 0.4e^{2\pi i(0.2)}, 0.7e^{2\pi i(0.3)}\right) \end{array} \right), \\ \left((z, \text{ţ}), \begin{array}{c} \left([0.3, 0.4]e^{[0.2,0.5]2\pi i}, [0.1, 0.2]e^{[0.1,0.4]2\pi i}, [0.5, 0.7]e^{[0.4,0.9]2\pi i}\right), \\ \left(0.2e^{2\pi i(0.3)}, 0.4e^{2\pi i(0.2)}, 0.7e^{2\pi i(0.3)}\right) \end{array} \right), \\ \left((\text{ġ}, \text{z}), \begin{array}{c} \left([0.2, 0.6]e^{[0.1,0.5]2\pi i}, [0.2, 0.3]e^{[0.1,0.3]2\pi i}, [0.5, 0.9]e^{[0.4,0.9]2\pi i}\right), \\ \left(0.4e^{2\pi i(0.5)}, 0.2e^{2\pi i(0.1)}, 0.7e^{2\pi i(0.7)}\right) \end{array} \right), \\ \left((\text{ġ}, \text{ġ}), \begin{array}{c} \left([0.2, 0.6]e^{[0.1,0.5]2\pi i}, [0.3, 0.5]e^{[0.2,0.7]2\pi i}, [0.5, 0.9]e^{[0.1,0.9]2\pi i}\right), \\ \left(0.4e^{2\pi i(0.5)}, 0.2e^{2\pi i(0.1)}, 0.7e^{2\pi i(0.7)}\right) \end{array} \right), \\ \left((\text{z}, \text{ġ}), \begin{array}{c} \left([0.2, 0.6]e^{[0.1,0.5]2\pi i}, [0.2, 0.3]e^{[0.1,0.3]2\pi i}, [0.5, 0.9]e^{[0.4,0.9]2\pi i}\right), \\ \left(0.4e^{2\pi i(0.5)}, 0.2e^{2\pi i(0.1)}, 0.7e^{2\pi i(0.7)}\right) \end{array} \right), \end{array} \right\}. \quad (36)$$

(3) The transitive relation Ŗ_3 is

$$\text{Ŗ}_3 = \left\{ \begin{array}{l} \left((\text{ţ}, \text{ġ}), \begin{array}{c} \left([0.2, 0.4]e^{[0.1,0.5]2\pi i}, [0.1, 0.2]e^{[0.1,0.4]2\pi i}, [0.5, 0.9]e^{[0.3,0.9]2\pi i}\right), \\ \left(0.2e^{2\pi i(0.3)}, 0.2e^{2\pi i(0.1)}, 0.7e^{2\pi i(0.7)}\right) \end{array} \right), \\ \left((\text{ġ}, \text{z}), \begin{array}{c} \left([0.2, 0.6]e^{[0.1,0.5]2\pi i}, [0.2, 0.3]e^{[0.1,0.3]2\pi i}, [0.5, 0.9]e^{[0.4,0.9]2\pi i}\right), \\ \left(0.4e^{2\pi i(0.5)}, 0.2e^{2\pi i(0.1)}, 0.7e^{2\pi i(0.7)}\right) \end{array} \right), \\ \left((\text{ţ}, \text{z}), \begin{array}{c} \left([0.3, 0.4]e^{[0.2,0.5]2\pi i}, [0.1, 0.2]e^{[0.1,0.4]2\pi i}, [0.5, 0.7]e^{[0.4,0.9]2\pi i}\right), \\ \left(0.2e^{2\pi i(0.3)}, 0.4e^{2\pi i(0.2)}, 0.7e^{2\pi i(0.3)}\right) \end{array} \right), \end{array} \right\}. \quad (37)$$

(4) The equivalence relation Ŗ_4 is

$$\text{Ŗ}_4 = \left\{ \begin{array}{l} \left((\text{ţ},\text{ţ}), \begin{array}{c} \left([0.3, 0.4]e^{[0.2,0.7]2\pi i}, [0.1, 0.2]e^{[0.1,0.4]2\pi i}, [0.5, 0.6]e^{[0.3,0.5]2\pi i}\right), \\ \left(0.2e^{2\pi i(0.3)}, 0.4e^{2\pi i(0.5)}, 0.1e^{2\pi i(0.2)}\right) \end{array} \right), \\ \left((\text{ţ},\text{ġ}), \begin{array}{c} \left([0.2, 0.4]e^{[0.1,0.5]2\pi i}, [0.1, 0.2]e^{[0.1,0.4]2\pi i}, [0.5, 0.9]e^{[0.3,0.9]2\pi i}\right), \\ \left(0.2e^{2\pi i(0.3)}, 0.2e^{2\pi i(0.1)}, 0.7e^{2\pi i(0.7)}\right) \end{array} \right), \\ \left((\text{ġ}, \text{ţ}), \begin{array}{c} \left([0.2, 0.4]e^{[0.1,0.5]2\pi i}, [0.1, 0.2]e^{[0.1,0.4]2\pi i}, [0.5, 0.9]e^{[0.3,0.9]2\pi i}\right), \\ \left(0.2e^{2\pi i(0.3)}, 0.2e^{2\pi i(0.1)}, 0.7e^{2\pi i(0.7)}\right) \end{array} \right), \\ \left((\text{ġ}, \text{ġ}) \begin{array}{c} \left([0.2, 0.6]e^{[0.1,0.5]2\pi i}, [0.3, 0.5]e^{[0.2,0.7]2\pi i}, [0.5, 0.9]e^{[0.1,0.9]2\pi i}\right), \\ \left(0.4e^{2\pi i(0.5)}, 0.2e^{2\pi i(0.1)}, 0.7e^{2\pi i(0.7)}\right) \end{array} \right), \\ \left((\text{z}, \text{z}), \begin{array}{c} \left([0.7, 0.9]e^{[0.2,0.5]2\pi i}, [0.2, 0.3]e^{[0.1,0.4]2\pi i}, [0.5, 0.7]e^{[0.4,0.9]2\pi i}\right), \\ \left(0.9e^{2\pi i(0.6)}, 0.4e^{2\pi i(0.2)}, 0.7e^{2\pi i(0.3)}\right) \end{array} \right) \end{array} \right\}. \quad (38)$$

(5) The partial order relation Ŗ_5 is

$$\text{Ŗ}_5 = \left\{ \begin{array}{l} \left((\text{ţ},\text{ţ}), \begin{array}{c} \left([0.3,0.4]e^{[0.2,0.7]2\pi i}, [0.1,0.2]e^{[0.1,0.4]2\pi i}, [0.5,0.6]e^{[0.3,0.5]2\pi i}\right), \\ \left(0.2e^{2\pi i(0.3)}, 0.4e^{2\pi i(0.5)}, 0.1e^{2\pi i(0.2)}\right) \end{array} \right), \\ \left((\text{ţ},\dot{g}), \begin{array}{c} \left([0.2,0.4]e^{[0.1,0.5]2\pi i}, [0.1,0.2]e^{[0.1,0.4]2\pi i}, [0.5,0.9]e^{[0.3,0.9]2\pi i}\right), \\ \left(0.2e^{2\pi i(0.3)}, 0.2e^{2\pi i(0.1)}, 0.7e^{2\pi i(0.7)}\right) \end{array} \right), \\ \left((\text{ţ},z), \begin{array}{c} \left([0.3,0.4]e^{[0.2,0.5]2\pi i}, [0.1,0.2]e^{[0.1,0.4]2\pi i}, [0.5,0.7]e^{[0.4,0.9]2\pi i}\right), \\ \left(0.2e^{2\pi i(0.3)}, 0.4e^{2\pi i(0.2)}, 0.7e^{2\pi i(0.3)}\right) \end{array} \right), \\ \left((\dot{g},\dot{g}), \begin{array}{c} \left([0.2,0.6]e^{[0.1,0.5]2\pi i}, [0.3,0.5]e^{[0.2,0.7]2\pi i}, [0.5,0.9]e^{[0.1,0.9]2\pi i}\right), \\ \left(0.4e^{2\pi i(0.5)}, 0.2e^{2\pi i(0.1)}, 0.7e^{2\pi i(0.7)}\right) \end{array} \right), \\ \left((z,\dot{g}) \begin{array}{c} \left([0.2,0.6]e^{[0.1,0.5]2\pi i}, [0.2,0.3]e^{[0.1,0.3]2\pi i}, [0.5,0.9]e^{[0.4,0.9]2\pi i}\right), \\ \left(0.4e^{2\pi i(0.5)}, 0.2e^{2\pi i(0.1)}, 0.7e^{2\pi i(0.7)}\right) \end{array} \right), \\ \left((z,z), \begin{array}{c} \left([0.7,0.9]e^{[0.2,0.5]2\pi i}, [0.2,0.3]e^{[0.1,0.4]2\pi i}, [0.5,0.7]e^{[0.4,0.9]2\pi i}\right), \\ \left(0.9e^{2\pi i(0.6)}, 0.4e^{2\pi i(0.2)}, 0.7e^{2\pi i(0.3)}\right) \end{array} \right) \end{array} \right\}. \tag{39}$$

(6) The relation Ŗ_6 is a CCuTS composite fuzzy relation between CCuTSFR Ŗ_a and Ŗ_b.

$$\begin{gathered} \text{Ŗ}_b = \left\{ \begin{array}{l} \left((\dot{g},\text{ţ}), \begin{array}{c} \left([0.2,0.4]e^{[0.1,0.5]2\pi i}, [0.1,0.2]e^{[0.1,0.4]2\pi i}, [0.5,0.9]e^{[0.3,0.9]2\pi i}\right), \\ \left(0.2e^{2\pi i(0.3)}, 0.2e^{2\pi i(0.1)}, 0.7e^{2\pi i(0.7)}\right) \end{array} \right), \\ \left((z,\dot{g}), \begin{array}{c} \left([0.2,0.6]e^{[0.1,0.5]2\pi i}, [0.2,0.3]e^{[0.1,0.3]2\pi i}, [0.5,0.9]e^{[0.4,0.9]2\pi i}\right), \\ \left(0.4e^{2\pi i(0.5)}, 0.2e^{2\pi i(0.1)}, 0.7e^{2\pi i(0.7)}\right) \end{array} \right), \\ \left((\dot{g},\dot{g}), \begin{array}{c} \left([0.2,0.6]e^{[0.1,0.5]2\pi i}, [0.3,0.5]e^{[0.2,0.7]2\pi i}, [0.5,0.9]e^{[0.1,0.9]2\pi i}\right), \\ \left(0.4e^{2\pi i(0.5)}, 0.2e^{2\pi i(0.1)}, 0.7e^{2\pi i(0.7)}\right) \end{array} \right) \end{array} \right\}, \\ \text{Ŗ}_a \circ \text{Ŗ}_b = \left\{ \begin{array}{l} \left((\text{ţ},\text{ţ}), \begin{array}{c} \left([0.3,0.4]e^{[0.2,0.7]2\pi i}, [0.1,0.2]e^{[0.1,0.4]2\pi i}, [0.5,0.6]e^{[0.3,0.5]2\pi i}\right), \\ \left(0.2e^{2\pi i(0.3)}, 0.4e^{2\pi i(0.5)}, 0.1e^{2\pi i(0.2)}\right) \end{array} \right), \\ \left((\text{ţ},\dot{g}), \begin{array}{c} \left([0.2,0.4]e^{[0.1,0.5]2\pi i}, [0.1,0.2]e^{[0.1,0.4]2\pi i}, [0.5,0.9]e^{[0.3,0.9]2\pi i}\right), \\ \left(0.2e^{2\pi i(0.3)}, 0.2e^{2\pi i(0.1)}, 0.7e^{2\pi i(0.7)}\right) \end{array} \right), \\ \left((z,\text{ţ}), \begin{array}{c} \left([0.3,0.4]e^{[0.2,0.5]2\pi i}, [0.1,0.2]e^{[0.1,0.4]2\pi i}, [0.5,0.7]e^{[0.4,0.9]2\pi i}\right), \\ \left(0.2e^{2\pi i(0.3)}, 0.4e^{2\pi i(0.2)}, 0.7e^{2\pi i(0.3)}\right) \end{array} \right), \\ \left((z,\dot{g}), \begin{array}{c} \left([0.2,0.6]e^{[0.1,0.5]2\pi i}, [0.2,0.3]e^{[0.1,0.3]2\pi i}, [0.5,0.9]e^{[0.4,0.9]2\pi i}\right), \\ \left(0.4e^{2\pi i(0.5)}, 0.2e^{2\pi i(0.1)}, 0.7e^{2\pi i(0.7)}\right) \end{array} \right) \end{array} \right\}. \end{gathered} \tag{40}$$

Definition 13. The equivalence class ţ of modulo Ŗ is written as

$$\mathrm{R}[\mathrm{t}]=\left\{\begin{array}{c}\left(\dot{g}),\left(\begin{array}{c}\left[\acute{\alpha}^{-}_{(\dot{u})}(\dot{g})e^{2\pi i\eta^{-}_{(\dot{u})}(\dot{g})},\acute{\alpha}^{+}_{(\dot{u})}(\dot{g})e^{2\pi\eta^{+}_{(\dot{u})}(\dot{g})i}\right],\\ \left[\acute{\alpha}^{-}_{(\text{ᵽ})}(\dot{g})e^{2\pi i\eta^{-}_{(\text{ᵽ})}(\dot{g})},\acute{\alpha}^{+}_{(\text{ᵽ})}(\dot{g})e^{2\pi\eta^{+}_{(\text{ᵽ})}(\dot{g})i}\right],\\ \left[\acute{\alpha}^{-}_{(\text{ŋ̧})}(\dot{g})e^{2\pi i\eta^{-}_{(\text{ŋ̧})}(\dot{g})},\acute{\alpha}^{+}_{(\text{ŋ̧})}(\dot{g})e^{2\pi\eta^{+}_{(\text{ŋ̧})}(\dot{g})i}\right],\end{array}\right),\left(\begin{array}{c}\acute{\alpha}_{(\dot{u})}(\dot{g})e^{2\pi i\eta_{(\dot{u})}(\dot{g})},\\ \acute{\alpha}_{(\text{ᵽ})}(\dot{g})e^{2\pi i\eta_{(\text{ᵽ})}(\dot{g})},\\ \acute{\alpha}_{(\text{ŋ̧})}(\dot{g})e^{2\pi\eta_{(\text{ŋ̧})}(\dot{g})}\end{array}\right)\right):\\ \left((\dot{g},\text{ţ}),\left(\begin{array}{c}\left[\acute{\alpha}^{-}_{(\dot{u})}(\dot{g},\text{ţ})e^{2\pi i\eta^{-}_{(\dot{u})}(\dot{g},\text{ţ})},\acute{\alpha}^{+}_{(\dot{u})}(\dot{g},\text{ţ})e^{2\pi\eta^{+}_{(\dot{u})}(\dot{g},\text{ţ})i}\right],\\ \left[\acute{\alpha}^{-}_{(\text{ᵽ})}(\dot{g},\text{ţ})e^{2\pi i\eta^{-}_{(\text{ᵽ})}(\dot{g},\text{ţ})},\acute{\alpha}^{+}_{(\text{ᵽ})}(\dot{g},\text{ţ})e^{2\pi\eta^{+}_{(\text{ᵽ})}(\dot{g},\text{ţ})i}\right],\\ \left[\acute{\alpha}^{-}_{(\text{ŋ̧})}(\dot{g},\text{ţ})e^{2\pi i\eta^{-}_{(\text{ŋ̧})}(\dot{g},\text{ţ})},\acute{\alpha}^{+}_{(\text{ŋ̧})}(\dot{g},\text{ţ})e^{2\pi\eta^{+}_{(\text{ŋ̧})}(\dot{g},\text{ţ})i}\right],\end{array}\right),\left(\begin{array}{c}\acute{\alpha}_{(\dot{u})}(\dot{g},\text{ţ})e^{2\pi i\eta_{(\dot{u})}(\dot{g}),\text{ţ}},\\ \acute{\alpha}_{(\text{ᵽ})}(\dot{g},\text{ţ})e^{2\pi i\eta_{(\text{ᵽ})}(\dot{g},\text{ţ})},\\ \acute{\alpha}_{(\text{ŋ̧})}(\dot{g},\text{ţ})e^{2\pi\eta_{(\text{ŋ̧})}(\dot{g},\text{ţ})}\end{array}\right)\right)\in\text{Ŗ}\end{array}\right\}. \tag{41}$$

Example 5. The CCuTSF equivalence relation Ŗ is given

$$\text{Ŗ}=\left\{\begin{array}{c}\left((\text{ţ},\text{ţ}),\begin{array}{c}\left([0.3,0.4]e^{[0.2,0.7]2\pi i},[0.1,0.2]e^{[0.1,0.4]2\pi i},[0.5,0.6]e^{[0.3,0.5]2\pi i}\right),\\ \left(0.2e^{2\pi i(0.3)},0.4e^{2\pi i(0.5)},0.1e^{2\pi i(0.2)}\right)\end{array}\right),\\ \left((\text{ţ},\dot{g}),\begin{array}{c}\left([0.2,0.4]e^{[0.1,0.5]2\pi i},[0.1,0.2]e^{[0.1,0.4]2\pi i},[0.5,0.9]e^{[0.3,0.9]2\pi i}\right),\\ \left(0.2e^{2\pi i(0.3)},0.2e^{2\pi i(0.1)},0.7e^{2\pi i(0.7)}\right)\end{array}\right),\\ \left((\dot{g},\mathrm{t}),\begin{array}{c}\left([0.2,0.4]e^{[0.1,0.5]2\pi i},[0.1,0.2]e^{[0.1,0.4]2\pi i},[0.5,0.9]e^{[0.3,0.9]2\pi i}\right),\\ \left(0.2e^{2\pi i(0.3)},0.2e^{2\pi i(0.1)},0.7e^{2\pi i(0.7)}\right)\end{array}\right),\\ \left((\dot{g},\dot{g}),\begin{array}{c}\left([0.2,0.6]e^{[0.1,0.5]2\pi i},[0.3,0.5]e^{[0.2,0.7]2\pi i},[0.5,0.9]e^{[0.1,0.9]2\pi i}\right),\\ \left(0.4e^{2\pi i(0.5)},0.2e^{2\pi i(0.1)},0.7e^{2\pi i(0.7)}\right)\end{array}\right),\\ \left((\mathrm{z},\mathrm{z}),\begin{array}{c}\left([0.7,0.6]e^{[0.2,0.5]2\pi i},[0.2,0.3]e^{[0.1,0.4]2\pi i},[0.5,0.7]e^{[0.4,0.9]2\pi i}\right),\\ \left(0.9e^{2\pi i(0.6)},0.4e^{2\pi i(0.1)},0.7e^{2\pi i(0.3)}\right)\end{array}\right)\end{array}\right\}. \tag{42}$$

Now, their equivalence classes are

$$\begin{gathered}\text{Ŗ}[\text{ţ}]=\left\{\begin{array}{c}\left(\text{ţ},\left(\begin{array}{c}[0.3,0.4]e^{[0.2,0.7]2\pi i},\\ [0.1,0.2]e^{[0.1,0.4]2\pi i},\\ [0.5,0.6]e^{[0.3,0.5]2\pi i}\end{array}\right),\left(\begin{array}{c}0.2e^{2\pi i(0.3)},\\ 0.4e^{2\pi i(0.5)},\\ 0.1e^{2\pi i(0.2)}\end{array}\right)\right),\\ \left(\dot{g},\left(\begin{array}{c}[0.2,0.6]e^{[0.1,0.5]2\pi i},\\ [0.3,0.5]e^{[0.2,0.7]2\pi i},\\ [0.5,0.9]e^{[0.1,0.9]2\pi i}\end{array}\right),\left(\begin{array}{c}0.4e^{2\pi i(0.5)},\\ 0.2e^{2\pi i(0.1)},\\ 0.7e^{2\pi i(0.7)}\end{array}\right)\right)\end{array}\right\},\\ \text{Ŗ}[\dot{g}]=\left\{\begin{array}{c}\left(\text{ţ},\left(\begin{array}{c}[0.3,0.4]e^{[0.2,0.7]2\pi i},\\ [0.1,0.2]e^{[0.1,0.4]2\pi i},\\ [0.5,0.6]e^{[0.3,0.5]2\pi i}\end{array}\right),\left(\begin{array}{c}0.2e^{2\pi i(0.3)},\\ 0.4e^{2\pi i(0.5)},\\ 0.1e^{2\pi i(0.2)}\end{array}\right)\right),\\ \left(\dot{g},\left(\begin{array}{c}[0.2,0.6]e^{[0.1,0.5]2\pi i},\\ [0.3,0.5]e^{[0.2,0.7]2\pi i},\\ [0.5,0.9]e^{[0.1,0.9]2\pi i}\end{array}\right),\left(\begin{array}{c}0.4e^{2\pi i(0.5)},\\ 0.2e^{2\pi i(0.1)},\\ 0.7e^{2\pi i(0.7)}\end{array}\right)\right)\end{array}\right\},\\ \text{Ŗ}[z]=\left\{\left(\mathrm{z},\left(\begin{array}{c}[0.7,0.9]e^{[0.2,0.5]2\pi i},\\ [0.2,0.3]e^{[0.1,0.4]2\pi i},\\ [0.5,0.7]e^{[0.4,0.9]2\pi i}\end{array}\right),\left(\begin{array}{c}0.9e^{2\pi i(0.6)},\\ 0.4e^{2\pi i(0.2)},\\ 0.7e^{2\pi i(0.3)}\end{array}\right)\right)\right\}.\end{gathered} \tag{43}$$

Theorem 1. *A CCuTSFR* Ŗ *is a CCuTS symmetric fuzzy relation on a CCuTSFS* Ċ *if and only if* $\text{Ŗ} = \text{Ŗ}^{-1}$.

Proof: Suppose that Ŗ is a CCuTS symmetric fuzzy relation on a CCuTSFS Ċ, then

$$\forall\left\{(\text{ţ},\text{ġ}),\left(\begin{array}{c}\left[\text{ά}^-_{(\text{u̇})}(\text{ţ},\text{ġ})e^{2\pi i\eta^-_{(\text{u̇})}(\text{ţ},\text{ġ})},\text{ά}^+_{(\text{u̇})}(\text{ţ},\text{ġ})e^{2\pi\eta^+_{(\text{u̇})}(\text{ţ},\text{ġ})i}\right],\\ \left[\text{ά}^-_{(\text{p})}(\text{ţ},\text{ġ})e^{2\pi i\eta^-_{(\text{p})}(\text{ţ},\text{ġ})},\text{ά}^+_{(\text{p})}(\text{ţ},\text{ġ})e^{2\pi\eta^+_{(\text{p})}(\text{ţ},\text{ġ})i}\right],\\ \left[\text{ά}^-_{(\text{ņ})}(\text{ţ},\text{ġ})e^{2\pi i\eta^-_{(\text{ņ})}(\text{ţ},\text{ġ})},\text{ά}^+_{(\text{ņ})}(\text{ţ},\text{ġ})e^{2\pi\eta^+_{(\text{ņ})}(\text{ţ},\text{ġ})i}\right]\end{array}\right),\left(\begin{array}{c}\text{ά}_{(\text{u̇})}(\text{ţ},\text{ġ})e^{2\pi i\eta_{(\text{u̇})}(\text{ţ},\text{ġ})},\\ \text{ά}_{(\text{p})}(\text{ţ},\text{ġ})e^{2\pi i\eta_{(\text{p})}(\text{ţ},\text{ġ})},\\ \text{ά}_{(\text{ņ})}(\text{ţ},\text{ġ})e^{2\pi i\eta_{(\text{ņ})}(\text{ţ},\text{ġ})}\end{array}\right)\right\}\in\text{Ŗ},$$
$$\text{And}\left\{(\text{ġ},\text{ţ}),\left(\begin{array}{c}\left[\text{ά}^-_{(\text{u̇})}(\text{ġ},\text{ţ})e^{2\pi i\eta^-_{(\text{u̇})}(\text{ġ},\text{ţ})},\text{ά}^+_{(\text{u̇})}(\text{ġ},\text{ţ})e^{2\pi\eta^+_{(\text{u̇})}(\text{ġ},\text{ţ})i}\right],\\ \left[\text{ά}^-_{(\text{P})}(\text{ġ},\text{ţ})e^{2\pi i\eta^-_{(\text{P})}(\text{ġ},\text{ţ})},\text{ά}^+_{(\text{P})}(\text{ġ},\text{ţ})e^{2\pi\eta^+_{(\text{P})}(\text{ġ},\text{ţ})i}\right],\\ \left[\text{ά}^-_{(\text{ņ})}(\text{ġ},\text{ţ})e^{2\pi i\eta^-_{(\text{ņ})}(\text{ġ},\text{ţ})},\text{ά}^+_{(\text{ņ})}(\text{ġ},\text{ţ})e^{2\pi\eta^+_{(\text{ņ})}(\text{ġ},\text{ţ})i}\right]\end{array}\right),\left(\begin{array}{c}\text{ά}_{(\text{u̇})}(\text{ġ},\text{ţ})e^{2\pi i\eta_{(\text{u̇})}(\text{ġ},\text{ţ})},\\ \text{ά}_{(\text{P})}(\text{ġ},\text{ţ})e^{2\pi i\eta_{(\text{P})}(\text{ġ},\text{ţ})},\\ \text{ά}_{(\text{ņ})}(\text{ġ},\text{ţ})e^{2\pi i\eta_{(\text{ņ})}(\text{ġ},\text{ţ})}\end{array}\right)\right\}\in\text{Ŗ}. \tag{44}$$

But

$$\left\{(\text{ġ},\text{ţ}),\left(\begin{array}{c}\left[\text{ά}^-_{(\text{u̇})}(\text{ġ},\text{ţ})e^{2\pi i\eta^-_{(\text{u̇})}(\text{ġ},\text{ţ})},\text{ά}^+_{(\text{u̇})}(\text{ġ},\text{ţ})e^{2\pi\eta^+_{(\text{u̇})}(\text{ġ},\text{ţ})i}\right],\\ \left[\text{ά}^-_{(\text{P})}(\text{ġ},\text{ţ})e^{2\pi i\eta^-_{(\text{P})}(\text{ġ},\text{ţ})},\text{ά}^+_{(\text{P})}(\text{ġ},\text{ţ})e^{2\pi\eta^+_{(\text{P})}(\text{ġ},\text{ţ})i}\right],\\ \left[\text{ά}^-_{(\text{ņ})}(\text{ġ},\text{ţ})e^{2\pi i\eta^-_{(\text{ņ})}(\text{ġ},\text{ţ})},\text{ά}^+_{(\text{ņ})}(\text{ġ},\text{ţ})e^{2\pi\eta^+_{(\text{ņ})}(\text{ġ},\text{ţ})i}\right]\end{array}\right),\left(\begin{array}{c}\text{ά}_{(\text{u̇})}(\text{ġ},\text{ţ})e^{2\pi i\eta_{(\text{u̇})}(\text{ġ},\text{ţ})},\\ \text{ά}_{(\text{P})}(\text{ġ},\text{ţ})e^{2\pi i\eta_{(\text{P})}(\text{ġ},\text{ţ})},\\ \text{ά}_{(\text{ņ})}(\text{ġ},\text{ţ})e^{2\pi i\eta_{(\text{ņ})}(\text{ġ},\text{ţ})}\end{array}\right)\right\}\in\text{Ŗ}^{-1}. \tag{45}$$

Hence, $\text{Ŗ}=\text{Ŗ}^{-1}$.

Conversely, suppose that $\text{Ŗ}=\text{Ŗ}^{-1}$, then

$$\forall\left\{(\text{ţ},\text{ġ})\left(\begin{array}{c}\left[\text{ά}^-_{(\text{u̇})}(\text{ţ},\text{ġ})e^{2\pi i\eta^-_{(\text{u̇})}(\text{ţ},\text{ġ})},\text{ά}^+_{(\text{u̇})}(\text{ţ},\text{ġ})e^{2\pi\eta^+_{(\text{u̇})}(\text{ţ},\text{ġ})i}\right],\\ \left[\text{ά}^-_{(\text{P})}(\text{ţ},\text{ġ})e^{2\pi i\eta^-_{(\text{P})}(\text{ţ},\text{ġ})},\text{ά}^+_{(\text{P})}(\text{ţ},\text{ġ})e^{2\pi\eta^+_{(\text{P})}(\text{ţ},\text{ġ})i}\right],\\ \left[\text{ά}^-_{(\text{ņ})}(\text{ţ},\text{ġ})e^{2\pi i\eta^-_{(\text{ņ})}(\text{ţ},\text{ġ})},\text{ά}^+_{(\text{ņ})}(\text{ţ},\text{ġ})e^{2\pi\eta^+_{(\text{ņ})}(\text{ţ},\text{ġ})i}\right]\end{array}\right),\left(\begin{array}{c}\text{ά}_{(\text{u̇})}(\text{ţ},\text{ġ})e^{2\pi i\eta_{(\text{u̇})}(\text{ţ},\text{ġ})},\\ \text{ά}_{(\text{P})}(\text{ţ},\text{ġ})e^{2\pi i\eta_{(\text{P})}(\text{ţ},\text{ġ})},\\ \text{ά}_{(\text{ņ})}(\text{ţ},\text{ġ})e^{2\pi i\eta_{(\text{ņ})}(\text{ţ},\text{ġ})}\end{array}\right)\right\}\in\text{Ŗ}, \text{ we have,}$$
$$\left\{(\text{ġ},\text{ţ}),\left(\begin{array}{c}\left[\text{ά}^-_{(\text{u̇})}(\text{ġ},\text{ţ})e^{2\pi i\eta^-_{(\text{u̇})}(\text{ġ},\text{ţ})},\text{ά}^+_{(\text{u̇})}(\text{ġ},\text{ţ})e^{2\pi\eta^+_{(\text{u̇})}(\text{ġ},\text{ţ})i}\right],\\ \left[\text{ά}^-_{(\text{P})}(\text{ġ},\text{ţ})e^{2\pi i\eta^-_{(\text{P})}(\text{ġ},\text{ţ})},\text{ά}^+_{(\text{P})}(\text{ġ},\text{ţ})e^{2\pi\eta^+_{(\text{P})}(\text{ġ},\text{ţ})i}\right],\\ \left[\text{ά}^-_{(\text{ņ})}(\text{ġ},\text{ţ})e^{2\pi i\eta^-_{(\text{ņ})}(\text{ġ},\text{ţ})},\text{ά}^+_{(\text{ņ})}(\text{ġ},\text{ţ})e^{2\pi\eta^+_{(\text{ņ})}(\text{ġ},\text{ţ})i}\right]\end{array}\right),\left(\begin{array}{c}\text{ά}_{(\text{u̇})}(\text{ġ},\text{ţ})e^{2\pi i\eta_{(\text{u̇})}(\text{ġ},\text{ţ})},\\ \text{ά}_{(\text{P})}(\text{ġ},\text{ţ})e^{2\pi i\eta_{(\text{P})}(\text{ġ},\text{ţ})},\\ \text{ά}_{(\text{ņ})}(\text{ġ},\text{ţ})e^{2\pi i\eta_{(\text{ņ})}(\text{ġ},\text{ţ})}\end{array}\right)\right\}\in\text{Ŗ}^{-1}, \tag{46}$$
$$\left\{(\text{ġ},\text{ţ}),\left(\begin{array}{c}\left[\text{ά}^-_{(\text{u̇})}(\text{ġ},\text{ţ})e^{2\pi i\eta^-_{(\text{u̇})}(\text{ġ},\text{ţ})},\text{ά}^+_{(\text{u̇})}(\text{ġ},\text{ţ})e^{2\pi\eta^+_{(\text{u̇})}(\text{ġ},\text{ţ})i}\right],\\ \left[\text{ά}^-_{(\text{P})}(\text{ġ},\text{ţ})e^{2\pi i\eta^-_{(\text{P})}(\text{ġ},\text{ţ})},\text{ά}^+_{(\text{P})}(\text{ġ},\text{ţ})e^{2\pi\eta^+_{(\text{P})}(\text{ġ},\text{ţ})i}\right],\\ \left[\text{ά}^-_{(\text{ņ})}(\text{ġ},\text{ţ})e^{2\pi i\eta^-_{(\text{ņ})}(\text{ġ},\text{ţ})},\text{ά}^+_{(\text{ņ})}(\text{ġ},\text{ţ})e^{2\pi\eta^+_{(\text{ņ})}(\text{ġ},\text{ţ})i}\right]\end{array}\right),\left(\begin{array}{c}\text{ά}_{(\text{u̇})}(\text{ġ},\text{ţ})e^{2\pi i\eta_{(\text{u̇})}(\text{ġ},\text{ţ})},\\ \text{ά}_{(\text{P})}(\text{ġ},\text{ţ})e^{2\pi i\eta_{(\text{P})}(\text{ġ},\text{ţ})},\\ \text{ά}_{(\text{ņ})}(\text{ġ},\text{ţ})e^{2\pi i\eta_{(\text{ņ})}(\text{ġ},\text{ţ})}\end{array}\right)\right\}\in\text{Ŗ}.$$

So, Ŗ is a CCuTS symmetric fuzzy relation on Ċ. □

Theorem 2. *A CCuTSFR Ŗ is a CCuTS transitive fuzzy relation on a CCuTSFS Ċ if and only if Ŗ ∘ Ŗ ⊆ Ŗ.*

Proof: Suppose that Ŗ is a CCuTS transitive fuzzy relation on a CCuTSFS Ċ, assume that

$$\left\{(ţ, z), \left(\begin{array}{c}\left[\dot{\alpha}^{-}_{(\dot{u})}(ţ, z)e^{2\pi i\eta^{-}_{(\dot{u})}(ţ,z)}, \dot{\alpha}^{+}_{(\dot{u})}(ţ, z)e^{2\pi\eta^{+}_{(\dot{u})}(ţ,z)i}\right],\\ \left[\dot{\alpha}^{-}_{(P)}(ţ, z)e^{2\pi i\eta^{-}_{(P)}(ţ,z)}, \dot{\alpha}^{+}_{(P)}(ţ, z)e^{2\pi\eta^{+}_{(P)}(ţ,z)i}\right],\\ \left[\dot{\alpha}^{-}_{(ņ)}(ţ, z)e^{2\pi i\eta^{-}_{(ņ)}(ţ,z)}, \dot{\alpha}^{+}_{(ņ)}(ţ, z)e^{2\pi\eta^{+}_{(ņ)}(ţ,z)i}\right]\end{array}\right), \left(\begin{array}{c}\dot{\alpha}_{(\dot{u})}(ţ, z)e^{2\pi i\eta_{(\dot{u})}(ţ,z)},\\ \dot{\alpha}_{(P)}(ţ, z)e^{2\pi i\eta_{(P)}(ţ,z)},\\ \dot{\alpha}_{(ņ)}(ţ, z)e^{2\pi i\eta_{(ņ)}(ţ,z)}\end{array}\right)\right\} \in Ŗ \circ Ŗ, \tag{47}$$

there exists an element $\dot{g} \in\in$ Ŗ, Then, by the transitivity of Ŗ

$$\begin{gathered}\left\{(ţ, \dot{g}), \left(\begin{array}{c}\left[\dot{\alpha}^{-}_{(\dot{u})}(ţ, \dot{g})e^{2\pi i\eta^{-}_{(\dot{u})}(ţ,\dot{g})}, \dot{\alpha}^{+}_{(\dot{u})}(ţ, \dot{g})e^{2\pi\eta^{+}_{(\dot{u})}(ţ,\dot{g})i}\right],\\ \left[\dot{\alpha}^{-}_{(P)}(ţ, \dot{g})e^{2\pi i\eta^{-}_{(P)}(ţ,\dot{g})}, \dot{\alpha}^{+}_{(P)}(ţ, \dot{g})e^{2\pi\eta^{+}_{(P)}(ţ,\dot{g})i}\right],\\ \left[\dot{\alpha}^{-}_{(ņ)}(ţ, \dot{g})e^{2\pi i\eta^{-}_{(ņ)}(ţ,\dot{g})}, \dot{\alpha}^{+}_{(ņ)}(ţ, \dot{g})e^{2\pi\eta^{+}_{(ņ)}(ţ,\dot{g})i}\right]\end{array}\right), \left(\begin{array}{c}\dot{\alpha}_{(\dot{u})}(ţ, \dot{g})e^{2\pi i\eta_{(\dot{u})}(ţ,\dot{g})},\\ \dot{\alpha}_{(P)}(ţ, \dot{g})e^{2\pi i\eta_{(P)}(ţ,\dot{g})},\\ \dot{\alpha}_{(ņ)}(ţ, \dot{g})e^{2\pi i\eta_{(ņ)}(ţ,\dot{g})}\end{array}\right)\right\} \in Ŗ, \text{ and}\\
\left\{(\dot{g}, z) \left(\begin{array}{c}\left[\dot{\alpha}^{-}_{(\dot{u})}(\dot{g}, z)e^{2\pi i\eta^{-}_{(\dot{u})}(\dot{g},z)}, \dot{\alpha}^{+}_{(\dot{u})}(\dot{g}, z)e^{2\pi\eta^{+}_{(\dot{u})}(\dot{g},z)i}\right],\\ \left[\dot{\alpha}^{-}_{(P)}(\dot{g}, z)e^{2\pi i\eta^{-}_{(P)}(\dot{g},z)}, \dot{\alpha}^{+}_{(P)}(\dot{g}, z)e^{2\pi\eta^{+}_{(P)}(\dot{g},z)i}\right],\\ \left[\dot{\alpha}^{-}_{(ņ)}(\dot{g}, z)e^{2\pi i\eta^{-}_{(ņ)}(\dot{g},z)}, \dot{\alpha}^{+}_{(ņ)}(\dot{g}, z)e^{2\pi\eta^{+}_{(ņ)}(\dot{g},z)i}\right]\end{array}\right), \left(\begin{array}{c}\dot{\alpha}_{(\dot{u})}(\dot{g}, z)e^{2\pi i\eta_{(\dot{u})}(\dot{g},z)},\\ \dot{\alpha}_{(P)}(\dot{g}, z)e^{2\pi i\eta_{(P)}(\dot{g},z)},\\ \dot{\alpha}_{(ņ)}(\dot{g}, z)e^{2\pi i\eta_{(ņ)}(\dot{g},z)}\end{array}\right)\right\} \in Ŗ. \text{ Implies,}\\
\left\{(ţ, z), \left(\begin{array}{c}\left[\dot{\alpha}^{-}_{(\dot{u})}(ţ, z)e^{2\pi i\eta^{-}_{(\dot{u})}(ţ,z)}, \dot{\alpha}^{+}_{(\dot{u})}(ţ, z)e^{2\pi\eta^{+}_{(\dot{u})}(ţ,z)i}\right],\\ \left[\dot{\alpha}^{-}_{(P)}(ţ, z)e^{2\pi i\eta^{-}_{(P)}(ţ,z)}, \dot{\alpha}^{+}_{(P)}(ţ, z)e^{2\pi\eta^{+}_{(P)}(ţ,z)i}\right],\\ \left[\dot{\alpha}^{-}_{(ņ)}(ţ, z)e^{2\pi i\eta^{-}_{(ņ)}(ţ,z)}, \dot{\alpha}^{+}_{(ņ)}(ţ, z)e^{2\pi\eta^{+}_{(ņ)}(ţ,z)i}\right]\end{array}\right), \left(\begin{array}{c}\dot{\alpha}_{(\dot{u})}(ţ, z)e^{2\pi i\eta_{(\dot{u})}(ţ,z)},\\ \dot{\alpha}_{(P)}(ţ, z)e^{2\pi i\eta_{(P)}(ţ,z)},\\ \dot{\alpha}_{(ņ)}(ţ, z)e^{2\pi i\eta_{(ņ)}(ţ,z)}\end{array}\right)\right\} \in Ŗ.\end{gathered} \tag{48}$$

Hence, Ŗ ∘ Ŗ ⊆ Ŗ.

Conversely, let us assume that Ŗ ∘ Ŗ ⊆ Ŗ, then the composition of CCuTSFR implies that,

$$\begin{gathered}\left\{ (\text{ţ},\dot{g}), \begin{pmatrix} \left[\acute{\alpha}^-_{(\dot{u})}(\text{ţ},\dot{g})e^{2\pi i\eta^-_{(\dot{u})}(\text{ţ},\dot{g})}, \acute{\alpha}^+_{(\dot{u})}(\text{ţ},\dot{g})e^{2\pi\eta^+_{(\dot{u})}(\text{ţ},\dot{g})i}\right], \\ \left[\acute{\alpha}^-_{(P)}(\text{ţ},\dot{g})e^{2\pi i\eta^-_{(P)}(\text{ţ},\dot{g})}, \acute{\alpha}^+_{(P)}(\text{ţ},\dot{g})e^{2\pi\eta^+_{(P)}(\text{ţ},\dot{g})i}\right], \\ \left[\acute{\alpha}^-_{(\text{ņ})}(\text{ţ},\dot{g})e^{2\pi i\eta^-_{(\text{ņ})}(\text{ţ},\dot{g})}, \acute{\alpha}^+_{(\text{ņ})}(\text{ţ},\dot{g})e^{2\pi\eta^+_{(\text{ņ})}(\text{ţ},\dot{g})i}\right] \end{pmatrix}, \begin{pmatrix} \acute{\alpha}_{(\dot{u})}(\text{ţ},\dot{g})e^{2\pi i\eta_{(\dot{u})}(\text{ţ},\dot{g})}, \\ \acute{\alpha}_{(P)}(\text{ţ},\dot{g})e^{2\pi i\eta_{(P)}(\text{ţ},\dot{g})}, \\ \acute{\alpha}_{(\text{ņ})}(\text{ţ},\dot{g})e^{2\pi i\eta_{(\text{ņ})}(\text{ţ},\dot{g})} \end{pmatrix} \right\} \in \text{Ŗ}, \text{and} \\
\left\{ (\dot{g},z), \begin{pmatrix} \left[\acute{\alpha}^-_{(\dot{u})}(\dot{g},z)e^{2\pi i\eta^-_{(\dot{u})}(\dot{g},z)}, \acute{\alpha}^+_{(\dot{u})}(\dot{g},z)e^{2\pi\eta^+_{(\dot{u})}(\dot{g},z)i}\right], \\ \left[\acute{\alpha}^-_{(P)}(\dot{g},z)e^{2\pi i\eta^-_{(P)}(\dot{g},z)}, \acute{\alpha}^+_{(P)}(\dot{g},z)e^{2\pi\eta^+_{(P)}(\dot{g},z)i}\right], \\ \left[\acute{\alpha}^-_{(\text{ņ})}(\dot{g},z)e^{2\pi i\eta^-_{(\text{ņ})}(\dot{g},z)}, \acute{\alpha}^+_{(\text{ņ})}(\dot{g},z)e^{2\pi\eta^+_{(\text{ņ})}(\dot{g},z)i}\right] \end{pmatrix}, \begin{pmatrix} \acute{\alpha}_{(\dot{u})}(\dot{g},z)e^{2\pi i\eta_{(\dot{u})}(\dot{g},z)}, \\ \acute{\alpha}_{(P)}(\dot{g},z)e^{2\pi i\eta_{(P)}(\dot{g},z)}, \\ \acute{\alpha}_{(\text{ņ})}(\dot{g},z)e^{2\pi i\eta_{(\text{ņ})}(\dot{g},z)} \end{pmatrix} \right\} \in \text{Ŗ}, \text{then} \\
\text{Ŗ} \circ \text{Ŗ} \subseteq \text{Ŗ}, \left\{ (\text{ţ},z), \begin{pmatrix} \left[\acute{\alpha}^-_{(\dot{u})}(\text{ţ},z)e^{2\pi i\eta^-_{(\dot{u})}(\text{ţ},z)}, \acute{\alpha}^+_{(\dot{u})}(\text{ţ},z)e^{2\pi\eta^+_{(\dot{u})}(\text{ţ},z)i}\right], \\ \left[\acute{\alpha}^-_{(P)}(\text{ţ},z)e^{2\pi i\eta^-_{(P)}(\text{ţ},z)}, \acute{\alpha}^+_{(P)}(\text{ţ},z)e^{2\pi\eta^+_{(P)}(\text{ţ},z)i}\right], \\ \left[\acute{\alpha}^-_{(\text{ņ})}(\text{ţ},z)e^{2\pi i\eta^-_{(\text{ņ})}(\text{ţ},z)}, \acute{\alpha}^+_{(\text{ņ})}(\text{ţ},z)e^{2\pi\eta^+_{(\text{ņ})}(\text{ţ},z)i}\right], \end{pmatrix}, \begin{pmatrix} \acute{\alpha}_{(\dot{u})}(\text{ţ},z)e^{2\pi i\eta_{(\dot{u})}(\text{ţ},z)}, \\ \acute{\alpha}_{(P)}(\text{ţ},z)e^{2\pi i\eta_{(P)}(\text{ţ},z)}, \\ \acute{\alpha}_{(\text{ņ})}(\text{ţ},z)e^{2\pi i\eta_{(\text{ņ})}(\text{ţ},z)} \end{pmatrix} \right\} \in \text{Ŗ} \circ \text{Ŗ}, \\
\left\{ (\text{ţ},z), \begin{pmatrix} \left[\acute{\alpha}^-_{(\dot{u})}(\text{ţ},z)e^{2\pi i\eta^-_{(\dot{u})}(\text{ţ},z)}, \acute{\alpha}^+_{(\dot{u})}(\text{ţ},z)e^{2\pi\eta^+_{(\dot{u})}(\text{ţ},z)i}\right], \\ \left[\acute{\alpha}^-_{(P)}(\text{ţ},z)e^{2\pi i\eta^-_{(P)}(\text{ţ},z)}, \acute{\alpha}^+_{(P)}(\text{ţ},z)e^{2\pi\eta^+_{(P)}(\text{ţ},z)i}\right], \\ \left[\acute{\alpha}^-_{(\text{ņ})}(\text{ţ},z)e^{2\pi i\eta^-_{(\text{ņ})}(\text{ţ},z)}, \acute{\alpha}^+_{(\text{ņ})}(\text{ţ},z)e^{2\pi\eta^+_{(\text{ņ})}(\text{ţ},z)i}\right] \end{pmatrix}, \begin{pmatrix} \acute{\alpha}_{(\dot{u})}(\text{ţ},z)e^{2\pi i\eta_{(\dot{u})}(\text{ţ},z)}, \\ \acute{\alpha}_{(P)}(\text{ţ},z)e^{2\pi i\eta_{(P)}(\text{ţ},z)}, \\ \acute{\alpha}_{(\text{ņ})}(\text{ţ},z)e^{2\pi i\eta_{(\text{ņ})}(\text{ţ},z)} \end{pmatrix} \right\} \in \text{Ŗ}.\end{gathered} \tag{49}$$

Hence, Ŗ is CCuTS transitive FR. □

Theorem 3. *If Ŗ is a CCuTS equivalence FR on a CCuTSFS $\dot{C}$, then Ŗ ∘ Ŗ = Ŗ.*

Proof: As Ŗ is a CCuTS equivalence FR on a CCuTSFS $\dot{C}$,

$$\text{For} \left\{ (\text{ţ},\dot{g}), \begin{pmatrix} \left[\acute{\alpha}^-_{(\dot{u})}(\text{ţ},\dot{g})e^{2\pi i\eta^-_{(\dot{u})}(\text{ţ},\dot{g})}, \acute{\alpha}^+_{(\dot{u})}(\text{ţ},\dot{g})e^{2\pi\eta^+_{(\dot{u})}(\text{ţ},\dot{g})i}\right], \\ \left[\acute{\alpha}^-_{(P)}(\text{ţ},\dot{g})e^{2\pi i\eta^-_{(P)}(\text{ţ},\dot{g})}, \acute{\alpha}^+_{(P)}(\text{ţ},\dot{g})e^{2\pi\eta^+_{(P)}(\text{ţ},\dot{g})i}\right], \\ \left[\acute{\alpha}^-_{(\text{ņ})}(\text{ţ},\dot{g})e^{2\pi i\eta^-_{(\text{ņ})}(\text{ţ},\dot{g})}, \acute{\alpha}^+_{(\text{ņ})}(\text{ţ},\dot{g})e^{2\pi\eta^+_{(\text{ņ})}(\text{ţ},\dot{g})i}\right] \end{pmatrix}, \begin{pmatrix} \acute{\alpha}_{(\dot{u})}(\text{ţ},\dot{g})e^{2\pi i\eta_{(\dot{u})}(\text{ţ},\dot{g})}, \\ \acute{\alpha}_{(P)}(\text{ţ},\dot{g})e^{2\pi i\eta_{(P)}(\text{ţ},\dot{g})}, \\ \acute{\alpha}_{(\text{ņ})}(\text{ţ},\dot{g})e^{2\pi i\eta_{(\text{ņ})}(\text{ţ},\dot{g})} \end{pmatrix} \right\} \in \text{Ŗ}. \tag{50}$$

The CCuTS symmetric FR implies that

$$\left\{ (\dot{g},\text{ţ}), \begin{pmatrix} \left[\acute{\alpha}^-_{(\dot{u})}(\dot{g},\text{ţ})e^{2\pi i\eta^-_{(\dot{u})}(\dot{g},\text{ţ})}, \acute{\alpha}^+_{(\dot{u})}(\dot{g},\text{ţ})e^{2\pi\eta^+_{(\dot{u})}(\dot{g},\text{ţ})i}\right], \\ \left[\acute{\alpha}^-_{(P)}(\dot{g},\text{ţ})e^{2\pi i\eta^-_{(P)}(\dot{g},\text{ţ})}, \acute{\alpha}^+_{(P)}(\dot{g},\text{ţ})e^{2\pi\eta^+_{(P)}(\dot{g},\text{ţ})i}\right], \\ \left[\acute{\alpha}^-_{(\text{ņ})}(\dot{g},\text{ţ})e^{2\pi i\eta^-_{(\text{ņ})}(\dot{g},\text{ţ})}, \acute{\alpha}^+_{(\text{ņ})}(\dot{g},\text{ţ})e^{2\pi\eta^+_{(\text{ņ})}(\dot{g},\text{ţ})i}\right] \end{pmatrix}, \begin{pmatrix} \acute{\alpha}_{(\dot{u})}(\dot{g},\text{ţ})e^{2\pi i\eta_{(\dot{u})}(\dot{g},\text{ţ})}, \\ \acute{\alpha}_{(P)}(\dot{g},\text{ţ})e^{2\pi i\eta_{(P)}(\dot{g},\text{ţ})}, \\ \acute{\alpha}_{(\text{ņ})}(\dot{g},\text{ţ})e^{2\pi i\eta_{(\text{ņ})}(\dot{g},\text{ţ})} \end{pmatrix} \right\} \in \text{Ŗ}. \tag{51}$$

The CCuTS transitive FR implies that

$$\left\{\left(ţ, ţ\right), \begin{pmatrix} \left[\dot{\alpha}^{-}_{(\dot{u})}(ţ, ţ)e^{2\pi i\eta^{-}_{(\dot{u})}(ţ, ţ)}, \dot{\alpha}^{+}_{(\dot{u})}(ţ, ţ)e^{2\pi\eta^{+}_{(\dot{u})}(ţ, ţ)i}\right], \\ \left[\dot{\alpha}^{-}_{(P)}(ţ, ţ)e^{2\pi i\eta^{-}_{(P)}(ţ, ţ)}, \dot{\alpha}^{+}_{(P)}(ţ, ţ)e^{2\pi\eta^{+}_{(P)}(ţ, ţ)i}\right], \\ \left[\dot{\alpha}^{-}_{(ņ)}(ţ, ţ)e^{2\pi i\eta^{-}_{(ņ)}(ţ)}, \dot{\alpha}^{+}_{(ņ)}(ţ, ţ)e^{2\pi\eta^{+}_{(ņ)}(ţ, ţ)i}\right], \end{pmatrix}, \begin{pmatrix} \dot{\alpha}_{(\dot{u})}(ţ, ţ)e^{2\pi i\eta_{(\dot{u})}(ţ, ţ)}, \\ \dot{\alpha}_{(P)}(ţ, ţ)e^{2\pi i\eta_{(P)}(ţ, ţ)}, \\ \dot{\alpha}_{(ņ)}(ţ, ţ)e^{2\pi i\eta_{(ņ)}(ţ, ţ)} \end{pmatrix}\right\} \in Ŗ. \tag{52}$$

Also, the CCuTS composite FR implies that

$$\left\{\left(ţ, ţ\right), \begin{pmatrix} \left[\dot{\alpha}^{-}_{(\dot{u})}(ţ, ţ)e^{2\pi i\eta^{-}_{(\dot{u})}(ţ, ţ)}, \dot{\alpha}^{+}_{(\dot{u})}(ţ, ţ)e^{2\pi\eta^{+}_{(\dot{u})}(ţ, ţ)i}\right], \\ \left[\dot{\alpha}^{-}_{(P)}(ţ, ţ)e^{2\pi i\eta^{-}_{(P)}(ţ, ţ)}, \dot{\alpha}^{+}_{(P)}(ţ, ţ)e^{2\pi\eta^{+}_{(P)}(ţ, ţ)i}\right], \\ \left[\dot{\alpha}^{-}_{(ņ)}(ţ, ţ)e^{2\pi i\eta^{-}_{(ņ)}(ţ, ţ)}, \dot{\alpha}^{+}_{(ņ)}(ţ, ţ)e^{2\pi\eta^{+}_{(ņ)}(ţ, ţ)i}\right] \end{pmatrix}, \begin{pmatrix} \dot{\alpha}_{(\dot{u})}(ţ, ţ)e^{2\pi i\eta_{(\dot{u})}(ţ, ţ)}, \\ \dot{\alpha}_{(P)}(ţ, ţ)e^{2\pi i\eta_{(P)}(ţ, ţ)}, \\ \dot{\alpha}_{(ņ)}(ţ, ţ)e^{2\pi i\eta_{(ņ)}(ţ, ţ)} \end{pmatrix}\right\} \in Ŗ \circ Ŗ. \tag{53}$$

Therefore, $Ŗ \subseteq Ŗ \circ Ŗ$ (1). Conversely, suppose that

$$\left\{\left(ţ, z\right), \begin{pmatrix} \left[\dot{\alpha}^{-}_{(\dot{u})}(ţ, z)e^{2\pi i\eta^{-}_{(\dot{u})}(ţ, z)}, \dot{\alpha}^{+}_{(\dot{u})}(ţ, z)e^{2\pi\eta^{+}_{(\dot{u})}(ţ, z)i}\right], \\ \left[\dot{\alpha}^{-}_{(P)}(ţ, z)e^{2\pi i\eta^{-}_{(P)}(ţ, z)}, \dot{\alpha}^{+}_{(P)}(ţ, z)e^{2\pi\eta^{+}_{(P)}(ţ, z)i}\right], \\ \left[\dot{\alpha}^{-}_{(ņ)}(ţ, z)e^{2\pi i\eta^{-}_{(ņ)}(ţ, z)}, \dot{\alpha}^{+}_{(ņ)}(ţ, z)e^{2\pi\eta^{+}_{(ņ)}(ţ, z)i}\right] \end{pmatrix}, \begin{pmatrix} \dot{\alpha}_{(\dot{u})}(ţ, z)e^{2\pi i\eta_{(\dot{u})}(ţ, z)}, \\ \dot{\alpha}_{(P)}(ţ, z)e^{2\pi i\eta_{(P)}(ţ, z)}, \\ \dot{\alpha}_{(ņ)}(ţ, z)e^{2\pi i\eta_{(ņ)}(ţ, z)} \end{pmatrix}\right\} \in Ŗ \circ Ŗ, \tag{54}$$

Then there exists an element $\dot{g}$ in

$$\begin{gathered} \left\{\left(ţ, \dot{g}\right), \begin{pmatrix} \left[\dot{\alpha}^{-}_{(\dot{u})}(ţ, \dot{g})e^{2\pi i\eta^{-}_{(\dot{u})}(ţ, \dot{g})}, \dot{\alpha}^{+}_{(\dot{u})}(ţ, \dot{g})e^{2\pi\eta^{+}_{(\dot{u})}(ţ, \dot{g})i}\right], \\ \left[\dot{\alpha}^{-}_{(P)}(ţ, \dot{g})e^{2\pi i\eta^{-}_{(P)}(ţ, \dot{g})}, \dot{\alpha}^{+}_{(P)}(ţ, \dot{g})e^{2\pi\eta^{+}_{(P)}(ţ, \dot{g})i}\right], \\ \left[\dot{\alpha}^{-}_{(ņ)}(ţ, \dot{g})e^{2\pi i\eta^{-}_{(ņ)}(ţ, \dot{g})}, \dot{\alpha}^{+}_{(ņ)}(ţ, \dot{g})e^{2\pi\eta^{+}_{(ņ)}(ţ, \dot{g})i}\right] \end{pmatrix}, \begin{pmatrix} \dot{\alpha}_{(\dot{u})}(ţ, \dot{g})e^{2\pi i\eta_{(\dot{u})}(ţ, \dot{g})}, \\ \dot{\alpha}_{(P)}(ţ, \dot{g})e^{2\pi i\eta_{(P)}(ţ, \dot{g})}, \\ \dot{\alpha}_{(ņ)}(ţ, \dot{g})e^{2\pi i\eta_{(ņ)}(ţ, \dot{g})} \end{pmatrix}\right\} \in Ŗ, \\ \left\{\left(\dot{g}, ţ\right), \begin{pmatrix} \left[\dot{\alpha}^{-}_{(\dot{u})}(\dot{g}, ţ)e^{2\pi i\eta^{-}_{(\dot{u})}(\dot{g}, ţ)}, \dot{\alpha}^{+}_{(\dot{u})}(\dot{g}, ţ)e^{2\pi\eta^{+}_{(\dot{u})}(\dot{g}, ţ)i}\right], \\ \left[\dot{\alpha}^{-}_{(P)}(\dot{g}, ţ)e^{2\pi i\eta^{-}_{(P)}(\dot{g}, ţ)}, \dot{\alpha}^{+}_{(P)}(\dot{g}, ţ)e^{2\pi\eta^{+}_{(P)}(\dot{g}, ţ)i}\right], \\ \left[\dot{\alpha}^{-}_{(ņ)}(\dot{g}, ţ)e^{2\pi i\eta^{-}_{(ņ)}(\dot{g}, ţ)}, \dot{\alpha}^{+}_{(ņ)}(\dot{g}, ţ)e^{2\pi\eta^{+}_{(ņ)}(\dot{g}, ţ)i}\right] \end{pmatrix}, \begin{pmatrix} \dot{\alpha}_{(\dot{u})}(\dot{g}, ţ)e^{2\pi i\eta_{(\dot{u})}(\dot{g}, ţ)}, \\ \dot{\alpha}_{(P)}(\dot{g}, ţ)e^{2\pi i\eta_{(P)}(\dot{g}, ţ)}, \\ \dot{\alpha}_{(ņ)}(\dot{g}, ţ)e^{2\pi i\eta_{(ņ)}(\dot{g}, ţ)} \end{pmatrix}\right\} \in Ŗ. \end{gathered} \tag{55}$$

since Ŗ is a CCuTS equivalence FR. Hence, the CCuTS transitive FR Ŗ implies that

$$\left\{ (\text{ţ}, z), \begin{pmatrix} \left[\dot{\alpha}^{-}_{(\dot{u})}(\text{ţ}, z)e^{2\pi i\eta^{-}_{(\dot{u})}(\text{ţ},z)}, \dot{\alpha}^{+}_{(\dot{u})}(\text{ţ}, z)e^{2\pi\eta^{+}_{(\dot{u})}(\text{ţ},z)i}\right], \\ \left[\dot{\alpha}^{-}_{(\text{P})}(\text{ţ}, z)e^{2\pi i\eta^{-}_{(\text{P})}(\text{ţ},z)}, \dot{\alpha}^{+}_{(\text{P})}(\text{ţ}, z)e^{2\pi\eta^{+}_{(\text{P})}(\text{ţ},z)i}\right], \\ \left[\dot{\alpha}^{-}_{(\text{ņ})}(\text{ţ}, z)e^{2\pi i\eta^{-}_{(\text{ņ})}(\text{ţ},z)}, \dot{\alpha}^{+}_{(\text{ņ})}(\text{ţ}, z)e^{2\pi\eta^{+}_{(\text{ņ})}(\text{ţ},z)i}\right] \end{pmatrix}, \begin{pmatrix} \dot{\alpha}_{(\dot{u})}(\text{ţ}, z)e^{2\pi i\eta_{(\dot{u})}(\text{ţ},z)}, \\ \dot{\alpha}_{(\text{P})}(\text{ţ}, z)e^{2\pi i\eta_{(\text{P})}(\text{ţ},z)}, \\ \dot{\alpha}_{(\text{ņ})}(\text{ţ}, z)e^{2\pi i\eta_{(\text{ņ})}(\text{ţ},z)} \end{pmatrix} \right\} \in \text{Ŗ}. \quad (56)$$

Therefore, Ŗ ∘ Ŗ ⊆ Ŗ. (2).

Equations (23) and (56) prove that Ŗ ∘ Ŗ = Ŗ. □

4. Application

In this section, the application of the proposed concepts is discussed. The CCuTSFS, CCuTSFR, and their types are used in this study of social media applications. We observe cybersecurity and cyber threats on social media.

4.1. Security of Social Media Platforms. Social media security is a critical aspect of modern business or personal success. It encompasses a wide range of technologies, strategies, and procedures. Social media has been constructed by the relations between users and bodies on the basis of modern Internet technology and platform carriers. Social media security has enabled organizations to safeguard the information that is shared over the network. All industries, organizations, and businesses require some kind of social media security clarification to save them from increasing cyber threats in today's wild world. In the following sections, we discussed some threats that are faced by social media and the social media security methods. The flow diagram for the application activity is shown in Figure 1.

The above flowchart can be explained as

(i) Collect the securities and threats methods.

(ii) Give the values of every set of securities and threats.

(iii) Find the CP between two CCuTSFS.

(iv) Read the information.

4.1.1. Threats. The different types of social media platforms attract a variety of threats towards them, which tend to steal users' identities or attack their privacy. Some threats are discussed that are prominent over social media. The objective of an attacker influences how they tackle a social media threat. Furthermore, each threat has been allocated to the membership, neutral, and nonmembership degrees. The membership degree is assigned to the professional according to their performance. The membership degree of threats shows the weakness, neutral degree demonstrates the neutral effect of threats and nonmembership degree indicates the strength of the threats. The different types of social media threats are shown in Table 1.

(1) *Identity Theft (IT).* Personal information becomes registered on one or more social media sites. This data become important as hackers and identity thieves use this information to reorganize passwords, claim for loans, or other various goals.

$$\left\{IT, \left([0.3, 0.5]e^{\pi i[0.3,0.4]}, [0.1, 0.3]e^{\pi i[0.2,0.5]}, [0.1, 0.2]e^{\pi i[0.2,0.3]}\right), \left(0.2e^{\pi i(0.4)}, 0.4e^{\pi i(0.5)}, 0.3e^{\pi i(0.2)}\right)\right\}. \quad (57)$$

(2) *Phishing Attacks (PA).* Phishing happens when someone conveys a fraudulent message sketch to trick a human victim into providing sensitive personal information like passwords or credit card numbers.

$$\left\{PA, \left([0.2, 0.4]e^{\pi i[0.1,0.3]}, [0.4, 0.7]e^{\pi i[0.3,0.8]}, [0.3, 0.5]e^{\pi i[0.2,0.5]}\right), \left(0.3e^{\pi i(0.2)}, 0.4e^{\pi i(0.6)}, 0.5e^{\pi i(0.7)}\right)\right\}. \quad (58)$$

(3) *Social Engineering (SE).* Employees may be contacted by attackers in an attempt to persuade them to give personal details, prove credentials, or send money to the attacker. In a more sophisticated approach, an attacker can mimic a high-ranking executive to persuade the intended victim to send money to the attacker's accounts.

$$\left\{SE, \left([0.3, 0.5]e^{\pi i[0.1,0.2]}, [0.2, 0.6]e^{\pi i[0.1,0.5]}, [0.4, 0.5]e^{\pi i[0.2,0.4]}\right), \left(0.2e^{\pi i(0.3)}, 0.4e^{\pi i(0.1)}, 0.3e^{\pi i(0.4)}\right)\right\}. \quad (59)$$

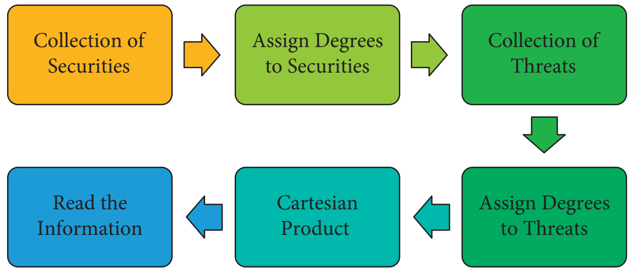

FIGURE 1: Flowchart for the process being followed.

TABLE 1: Details of threats.

Threats	Abbreviations	Membership	Neutral	Nonmembership
Identity theft	IT	$([0.3, 0.5]e^{\pi i[0.3,0.4]}), (0.2e^{\pi i(0.4)})$	$([0.1, 0.3]e^{\pi i[0.2,0.5]}), (0.4e^{\pi i(0.5)})$	$([0.1, 0.2]e^{\pi i[0.2,0.3]}), (0.3e^{\pi i(0.2)})$
Phishing attempts	PA	$([0.2, 0.4]e^{\pi i[0.1,0.3]}), (0.3e^{\pi i(0.2)})$	$([0.4, 0.7]e^{\pi i[0.3,0.8]}), (0.4e^{\pi i(0.6)})$	$([0.3, 0.5]e^{\pi i[0.2,0.5]}), (0.5e^{\pi i(0.7)})$
Social engineering	SE	$([0.3, 0.5]e^{\pi i[0.1,0.2]}), (0.2e^{\pi i(0.3)})$	$([0.2, 0.6]e^{\pi i[0.1,0.5]}), (0.4e^{\pi i(0.1)})$	$([0.4, 0.5]e^{\pi i[0.2,0.4]}), (0.3e^{\pi i(0.4)})$
Malware attacks	MR	$([0.1, 0.4]e^{\pi i[0.2,0.3]}), (0.3e^{\pi i(0.1)})$	$([0.3, 0.5]e^{\pi i[0.3,0.5]}), (0.2e^{\pi i(0.4)})$	$([0.2, 0.5]e^{\pi i[0.2,0.4]}), (0.5e^{\pi i(0.3)})$
Image retrieval and analysis	IRA	$([0.4, 0.7]e^{\pi i[0.2,0.5]}), (0.7e^{\pi i(0.5)})$	$([0.1, 0.3]e^{\pi i[0.3,0.5]}), (0.3e^{\pi i(0.4)})$	$([0.3, 0.4]e^{\pi i[0.1,0.2]}), (0.2e^{\pi i(0.3)})$
Celebrity name misuse	CNM	$([0.3, 0.6]e^{\pi i[0.2,0.6]}), (0.5e^{\pi i(0.6)})$	$([0.1, 0.2]e^{\pi i[0.3,0.4]}), (0.2e^{\pi i(0.3)})$	$([0.2, 0.3]e^{\pi i[0.1,0.4]}), (0.3e^{\pi i(0.2)})$

(4) *Malware Attacks (MA)*. They are becoming increasingly popular on social media platforms these days. When criminals create malicious software and install it on someone else's device without their consent, in order to steal personal details or cause device destruction for financial gain.

$$\left\{MA, \left([0.1, 0.4]e^{\pi i[0.2,0.3]}, [0.3, 0.5]e^{\pi i[0.3,0.5]}, \left[0.2, 0.5\right]e^{\pi i[0.2,0.4]}\right]\right), \left(0.3e^{\pi i(0.1)}, 0.2e^{\pi i(0.4)}, 0.5e^{\pi i(0.3)}\right)\right\}. \tag{60}$$

(5) *Image Retrieval and Analysis (IRA)*. The attackers here use several face and image identification technologies to learn more about the target and its correlated description. It not only affects the target but also his or her friends and family. The aim of this attack is to accumulate photographs and videos from the target.

$$\left\{IR\&A, \left([0.4, 0.7]e^{\pi i[0.2,0.5]}, [0.1, 0.3]e^{\pi i[0.3,0.5]}, \left[0.3, 0.4\right]e^{\pi i[0.1,0.2]}\right]\right), \left(0.7e^{\pi i(0.5)}, 0.3e^{\pi i(0.4)}, 0.2e^{\pi i(0.3)}\right)\right\}. \tag{61}$$

(6) *Celebrity Name Misuse (CNM)*. This is one of the most widely used social media platforms for threats nowadays. In several cases, hackers have been known to create a new account in the name of a celebrity. Fake accounts like this can be used to propagate false information.

$$\left\{CNM, \left([0.3, 0.6]e^{\pi i[0.2,0.6]}, [0.1, 0.2]e^{\pi i[0.3,0.4]}, \left[0.2, 0.3\right]e^{\pi i[0.1,0.4]}\right]\right), \left(0.5e^{\pi i(0.6)}, 0.2e^{\pi i(0.3)}, 0.3e^{\pi i(0.2)}\right)\right\}. \tag{62}$$

Therefore, the CCuTSFS $\mathbb{G}$ summarizing the threat is given as follows:

$$\mathbb{G} = \left\{ \begin{array}{l} \left(IT, \left([0.3, 0.5]e^{\pi i[0.3,0.4]}, [0.1, 0.3]e^{\pi i[0.2,0.5]}, \left[0.1, 0.2\right]e^{\pi i[0.2,0.3]}\right]\right), \left(0.2e^{\pi i(0.4)}, 0.4e^{\pi i(0.5)}, 0.3e^{\pi i(0.2)}\right)\right), \\ \left(PA, \left([0.2, 0.4]e^{\pi i[0.1,0.3]}, [0.4, 0.7]e^{\pi i[0.3,0.8]}, \left[0.3, 0.5\right]e^{\pi i[0.2,0.5]}\right]\right), \left(0.3e^{\pi i(0.2)}, 0.4e^{\pi i(0.6)}, 0.5e^{\pi i(0.7)}\right)\right), \\ \left(SE, \left([0.3, 0.5]e^{\pi i[0.1,0.2]}, [0.2, 0.6]e^{\pi i[0.1,0.5]}, \left[0.4, 0.5\right]e^{\pi i[0.2,0.4]}\right]\right), \left(0.2e^{\pi i(0.3)}, 0.4e^{\pi i(0.1)}, 0.3e^{\pi i(0.4)}\right)\right), \\ \left(MA, \left([0.1, 0.4]e^{\pi i[0.2,0.3]}, [0.3, 0.5]e^{\pi i[0.3,0.5]}, \left[0.2, 0.5\right]e^{\pi i[0.2,0.4]}\right]\right), \left(0.3e^{\pi i(0.1)}, 0.2e^{\pi i(0.4)}, 0.5e^{\pi i(0.3)}\right)\right), \\ \left(IRA, \left([0.4, 0.5]e^{\pi i[0.2,0.3]}, [0.1, 0.3]e^{\pi i[0.3,0.5]}, \left[0.3, 0.5\right]e^{\pi i[0.3,0.4]}\right]\right), \left(0.4e^{\pi i(0.5)}, 0.3e^{\pi i(0.4)}, 0.2e^{\pi i(0.3)}\right)\right), \\ \left(CNM, \left([0.3, 0.6]e^{\pi i[0.2,0.6]}, [0.1, 0.2]e^{\pi i[0.3,0.4]}, \left[0.2, 0.3\right]e^{\pi i[0.1,0.4]}\right]\right), \left(0.5e^{\pi i(0.6)}, 0.2e^{\pi i(0.3)}, 0.3e^{\pi i(0.2)}\right)\right) \end{array} \right\}. \quad (63)$$

4.1.2. Security. The social media techniques, procedures, and applications against threats are discussed. The social media security platform was built to protect the channels that are most important to your organization. Employees who openly share too much personal and corporate information on social media are the source of the bulk of social media threats. Because these accounts are personal, corporations cannot prevent users from using social media. Consumers, on the other hand, maybe educated on the best ways to protect their data and credentials. Avoiding social media risks requires education. The values of membership, neutrality, and nonmembership are assigned to each security mechanism. The strength is determined by the security's membership degree. Thus, a higher amplitude term and a higher phase term value of its membership degree indicate better security; no effect of amplitude term with a phase term value of its neutral degree indicates no effect of security; and lower amplitude term and phase term values of its nonmembership degree indicate lower security. Some of the major social media security methods are explained with their fuzzy grades. The different types of social media security are shown in Table 2.

(1) *Unique Password (UP)*. Make sure that each of your social media accounts have its own password. Make account passwords long and strong. Do not utilize the information shared on social media accounts to create a password. A strong password is one that is easy to remember but difficult for others to guess. Employees should not share passwords with another people. It is essential to not use the same passwords for Twitter as for Facebook, Instagram, and other social media tools.

$$\left\{UP, \left([0.3, 0.7]e^{\pi i[0.2,0.7]}, [0.2, 0.4]e^{\pi i[0.1,0.3]}, [0.1, 0.2]e^{\pi i[0.1,0.2]}\right), \left(0.6e^{\pi i(0.4)}, 0.4e^{\pi i(0.3)}, 0.2e^{\pi i(0.1)}\right)\right\}. \quad (64)$$

(2) *Enable Multifactor Authentication (MFA)*. This should be standard security procedure for everybody who uses the Internet today. Anyone attempting to log into an account is required to provide a code transmitted to an external device.

$$\left\{MFA, \left([0.2, 0.7]e^{\pi i[0.1,0.4]}, [0.3, 0.4]e^{\pi i[0.3,0.5]}, [0.1, 0.3]e^{\pi i[0.2,0.4]}\right), \left(0.3e^{\pi i(0.3)}, 0.3e^{\pi i(0.2)}, 0.4e^{\pi i(0.1)}\right)\right\}. \quad (65)$$

(3) *Update Security Settings (USS).* Update the security framework on all digital and social channels consistently. There are many fantastic step-by-step privacy instructions available online to assist with setting up secure. They are often renovated, so revise them from time to time to make sure that nothing has changed.

$$\left\{USS, \left([0.4, 0.5]e^{\pi i[0.3,0.6]}, [0.3, 0.6]e^{\pi i[0.2,0.4]}, [0.2, 0.4]e^{\pi i[0.3,0.5]}\right), \left(0.7e^{\pi i(0.5)}, 0.1e^{\pi i(0.4)}, 0.3e^{\pi i(0.3)}\right)\right\}. \quad (66)$$

(4) *Use the Block Button (UBB).* The links sent by spammers should be ignored. Always report the account as spam for the sake of others who are less knowledgeable. The social networking service will monitor it and, if enough people take the same actions, remove the account. Use ad blockers on corporate devices. The most immature method is to block that person on social media.

Table 2: Details of security.

Security	Abbreviations	Membership	Neutral	Nonmembership
Unique password	UP	$([0.3, 0.7]e^{\pi i[0.2,0.7]}),$ $(0.6e^{\pi i(0.4)})$	$([0.2, 0.4]e^{\pi i[0.1,0.3]}),$ $(0.4e^{\pi i(0.3)})$	$([0.1, 0.2]e^{\pi i[0.1,0.2]}),$ $(0.2e^{\pi i(0.1)})$
Multifactor authentication	MFA	$([0.2, 0.7]e^{\pi i[0.1,0.4]}),$ $(0.3e^{\pi i(0.3)})$	$([0.3, 0.4]e^{\pi i[0.3,0.5]}),$ $(0.3e^{\pi i(0.2)})$	$([0.1, 0.3]e^{\pi i[0.2,0.4]}),$ $(0.4e^{\pi i(0.1)})$
Update security settings	USS	$([0.4, 0.5]e^{\pi i[0.3,0.6]}),$ $(0.7e^{\pi i(0.5)})$	$([0.3, 0.6]e^{\pi i[0.2,0.4]}),$ $(0.1e^{\pi i(0.4)})$	$([0.2, 0.4]e^{\pi i[0.3,0.5]}),$ $(0.3e^{\pi i(0.3)})$
Use block button	UBB	$([0.5, 0.8]e^{\pi i[0.3,0.9]}),$ $(0.8e^{\pi i(0.5)})$	$([0.3, 0.5]e^{\pi i[0.2,0.3]}),$ $(0.2e^{\pi i(0.4)})$	$([0.2, 0.3]e^{\pi i[0.1,0.3]}),$ $(0.3e^{\pi i(0.2)})$
Do not accept friend request	FR	$([0.4, 0.5]e^{\pi i[0.5,0.7]}),$ $(0.5e^{\pi i(0.4)})$	$([0.1, 0.4]e^{\pi i[0.1,0.2]}),$ $(0.1e^{\pi i(0.4)})$	$[0.2, 0.6]e^{\pi i[0.2,0.4]},\ (0.3e^{\pi i(0.5)})$

$$\left\{UBB, \left([0.5, 0.8]e^{\pi i[0.3,0.9]}, [0.3, 0.5]e^{\pi i[0.2,0.3]}, [0.2, 0.3]e^{\pi i[0.1,0.3]}\right), \left(0.8e^{\pi i(0.5)}, 0.2e^{\pi i(0.4)}, 0.3e^{\pi i(0.2)}\right)\right\}. \tag{67}$$

(5) *Declining Friend Request (FR).* Friend's invitations from known people should be accepted. The request should be declined even if the users have several mutual friends. By looking for verified accounts, it is critical to identify the genuine social media profiles of celebrities, public figures, and businesses.

$$\left\{FR, \left([0.4, 0.5]e^{\pi i[0.5,0.7]}, [0.1, 0.4]e^{\pi i[0.1,0.2]}, [0.2, 0.6]e^{\pi i[0.2,0.4]}\right), \left(0.5e^{\pi i(0.4)}, 0.1e^{\pi i(0.4)}, 0.3e^{\pi i(0.5)}\right)\right\}. \tag{68}$$

Therefore, the CCuTSFS $\mathbb{H}$ summarizing the security is given as follows:

$$\mathbb{H} = \left\{\begin{array}{c} \left(UP, \left([0.3, 0.7]e^{\pi i[0.2,0.7]}, [0.2, 0.4]e^{\pi i[0.1,0.3]}, [0.1, 0.2]e^{\pi i[0.1,0.2]}\right), \left(0.6e^{\pi i(0.4)}, 0.4e^{\pi i(0.3)}, 0.2e^{\pi i(0.1)}\right)\right), \\ \left(MFA, \left([0.2, 0.7]e^{\pi i[0.1,0.4]}, [0.3, 0.4]e^{\pi i[0.3,0.5]}, [0.1, 0.3]e^{\pi i[0.2,0.4]}\right), \left(0.3e^{\pi i(0.3)}, 0.3e^{\pi i(0.2)}, 0.4e^{\pi i(0.1)}\right)\right), \\ \left(USS, \left([0.4, 0.5]e^{\pi i[0.3,0.6]}, [0.3, 0.6]e^{\pi i[0.2,0.4]}, [0.2, 0.4]e^{\pi i[0.3,0.5]}\right), \left(0.7e^{\pi i(0.5)}, 0.1e^{\pi i(0.4)}, 0.3e^{\pi i(0.3)}\right)\right), \\ \left(UBB, \left([0.5, 0.8]e^{\pi i[0.3,0.9]}, [0.3, 0.5]e^{\pi i[0.2,0.3]}, [0.2, 0.3]e^{\pi i[0.1,0.3]}\right), \left(0.8e^{\pi i(0.5)}, 0.2e^{\pi i(0.4)}, 0.3e^{\pi i(0.2)}\right)\right), \\ \left(FR, \left([0.4, 0.5]e^{\pi i[0.5,0.7]}, [0.1, 0.4]e^{\pi i[0.1,0.2]}, [0.2, 0.6]e^{\pi i[0.2,0.4]}\right), \left(0.5e^{\pi i(0.4)}, 0.1e^{\pi i(0.4)}, 0.3e^{\pi i(0.5)}\right)\right) \end{array}\right\}. \tag{69}$$

4.1.3. Calculations. We use the following mathematics to examine the effectiveness and ineffectiveness of every social media security measure and threat. We have the following two CCuTSFSs $\mathbb{G}$ and $\mathbb{H}$, corresponding to the set of security and threats, respectively.

$$\mathbb{G}=\left\{\begin{array}{c}\left(IT,\left([0.3,0.5]e^{\pi i[0.3,0.4]},[0.1,0.3]e^{\pi i[0.2,0.5]},[0.1,0.2]e^{\pi i[0.2,0.3]}\right),\left(0.2e^{\pi i(0.4)},0.4e^{\pi i(0.5)},0.3e^{\pi i(0.2)}\right)\right),\\ \left(PA,\left([0.2,0.4]e^{\pi i[0.1,0.3]},[0.4,0.7]e^{\pi i[0.3,0.8]},[0.3,0.5]e^{\pi i[0.2,0.5]}\right),\left(0.3e^{\pi i(0.2)},0.4e^{\pi i(0.6)},0.5e^{\pi i(0.7)}\right)\right),\\ \left(SE,\left([0.3,0.5]e^{\pi i[0.1,0.2]},[0.2,0.6]e^{\pi i[0.1,0.5]},[0.4,0.5]e^{\pi i[0.2,0.4]}\right),\left(0.2e^{\pi i(0.3)},0.4e^{\pi i(0.1)},0.3e^{\pi i(0.4)}\right)\right),\\ \left(MA,\left([0.1,0.4]e^{\pi i[0.2,0.3]},[0.3,0.5]e^{\pi i[0.3,0.5]},[0.2,0.5]e^{\pi i[0.2,0.4]}\right),\left(0.3e^{\pi i(0.1)},0.2e^{\pi i(0.4)},0.5e^{\pi i(0.3)}\right)\right),\\ \left(IRA,\left([0.4,0.5]e^{\pi i[0.2,0.3]},[0.1,0.3]e^{\pi i[0.3,0.5]},[0.3,0.5]e^{\pi i[0.3,0.4]}\right),\left(0.4e^{\pi i(0.5)},0.3e^{\pi i(0.4)},0.2e^{\pi i(0.3)}\right)\right),\\ \left(CNM,\left([0.3,0.6]e^{\pi i[0.2,0.6]},[0.1,0.2]e^{\pi i[0.3,0.4]},[0.2,0.3]e^{\pi i[0.1,0.4]}\right),\left(0.5e^{\pi i(0.6)},0.2e^{\pi i(0.3)},0.3e^{\pi i(0.2)}\right)\right)\end{array}\right\},$$

$$\mathbb{H}=\left\{\begin{array}{c}\left(UP,\left([0.3,0.7]e^{\pi i[0.2,0.7]},[0.2,0.4]e^{\pi i[0.1,0.3]},[0.1,0.2]e^{\pi i[0.1,0.2]}\right),\left(0.6e^{\pi i(0.4)},0.4e^{\pi i(0.3)},0.2e^{\pi i(0.1)}\right)\right),\\ \left(MFA,\left([0.2,0.7]e^{\pi i[0.1,0.4]},[0.3,0.4]e^{\pi i[0.3,0.5]},[0.1,0.3]e^{\pi i[0.2,0.4]}\right),\left(0.3e^{\pi i(0.3)},0.3e^{\pi i(0.2)},0.4e^{\pi i(0.1)}\right)\right),\\ \left(USS,\left([0.4,0.5]e^{\pi i[0.3,0.6]},[0.3,0.6]e^{\pi i[0.2,0.4]},[0.2,0.4]e^{\pi i[0.3,0.5]}\right),\left(0.7e^{\pi i(0.5)},0.1e^{\pi i(0.4)},0.3e^{\pi i(0.3)}\right)\right),\\ \left(UBB,\left([0.5,0.8]e^{\pi i[0.3,0.9]},[0.3,0.5]e^{\pi i[0.2,0.3]},[0.2,0.3]e^{\pi i[0.1,0.3]}\right),\left(0.8e^{\pi i(0.5)},0.2e^{\pi i(0.4)},0.3e^{\pi i(0.2)}\right)\right),\\ \left(FR,\left([0.4,0.5]e^{\pi i[0.5,0.7]},[0.1,0.4]e^{\pi i[0.1,0.2]},[0.2,0.6]e^{\pi i[0.2,0.4]}\right),\left(0.5e^{\pi i(0.4)},0.1e^{\pi i(0.4)},0.3e^{\pi i(0.5)}\right)\right)\end{array}\right\}. \tag{70}$$

For each social media threat and security, we assign degrees of membership, neutral, non-membership and interval-valued degrees of membership, neutral, and nonmembership. These functions in the set $\mathbb{G}$ and $\mathbb{H}$ represent both the present and future influences of each threat and security. The CP between the CCuTSFS $\mathbb{H}$ and $\mathbb{G}$ is used to define the effectiveness of each security method against a particular threat. Table 3, shows the CP between the CCuTSFS $\mathbb{H}$ and $\mathbb{G}$.

The CP $\mathbb{H}\times\mathbb{G}$ describes the relationship between each set of elements, i.e., the condition and impact of a security on a threat. The levels of a membership indicate how effective a social media security system is in detecting a specific threat over a period of time. The level of abstinence reflects whether a security system has no effect or has a neutral effect in the face of a threat over a time period. The degree of nonmembership levels denotes a security inefficiency in the face of a certain threat with a time period. For example, the ordered pair $\left((UP,IRA),\begin{pmatrix}[0.3,0.7]e^{\pi i[0.2,0.5]},\\ [0.1,0.3]e^{\pi i[0.1,0.3]},\\ [0.3,0.4]e^{\pi i[0.1,0.2]}\end{pmatrix},\begin{pmatrix}0.6e^{\pi i(0.4)},\\ 0.3e^{\pi i(0.3)},\\ 0.2e^{\pi i(0.3)}\end{pmatrix}\right)$ describes the unique password against image retrieval and analysis. The UP protects the IRA because of this reason that unauthorized person does not access to the user's device. Furthermore, it explains the present and future effects and impact of the ordered pair. The UP overcomes the threat of the IRA in the present because security effectiveness is better than the degree of ineffectiveness. A given ordered pair predicts the future security in the form of an interval.

5. Comparative Analysis

In this part, we compare the presented structure of CCuTSFR with some other preexisting structures such as FR, CuFR, CCuFR, IFR, CuIFR, CCuIFR, PyFR, CuPyFR, CCuPyFR, qROFR, CuqROFR, CCuqROFR, PFR, CuPFR, CCuPFR, SFR, CuSFR, CCuSFR, TSFR, and CuTSFR.

5.1. Comparison of FR, CuFR, and CCuFR with CCuTSFRs. The structure of FR and CuFR discuss only the membership degree with only one dimension. They are not capable of solving the multidimensional problem. The CuFR expressed the membership degree in both the present and future, but the FR described the membership degree only present aspect. These structures are unable to model periodicity. The structures of CCuFR discuss only the membership degree, which only shows the effectiveness of security measures on the threats. Consequently, they cannot offer a complete solution to the problem. The CCuTSFR examines all three levels, i.e., membership, neutral, and nonmembership with a complex number. They are capable to solve the periodicity. We consider the following two CCuFSs $\mathbb{G}$ and $\mathbb{H}$, which represent the threat and security sets, respectively.

$$\mathbb{G}=\left\{\begin{array}{c}\left(IT,\left([0.3,0.5]e^{\pi i[0.3,0.4]}\right),\left(0.2e^{\pi i(0.4)}\right)\right),\left(PA,\left([0.2,0.4]e^{\pi i[0.1,0.3]}\right),0.3e^{\pi i(0.2)}\right)\\ \left(SE,\left([0.3,0.5]e^{\pi i[0.1,0.2]}\right),\left(0.2e^{\pi i(0.3)}\right)\right),\left(MA,\left([0.1,0.4]e^{\pi i[0.2,0.3]}\right),0.3e^{\pi i(0.1)}\right)\\ \left(IRA,\left([0.4,0.7]e^{\pi i[0.2,0.5]}\right),\left(0.7e^{\pi i(0.5)}\right)\right),\left(CNM,\left([0.3,0.6]e^{\pi i[0.2,0.6]}\right),\left(0.5e^{\pi i(0.6)}\right)\right)\end{array}\right\},$$

$$\mathbb{H}=\left\{\begin{array}{c}\left(UP,\left([0.3,0.7]e^{\pi i[0.2,0.7]}\right),\left(0.6e^{\pi i(0.4)}\right)\right),\left(MFA,\left([0.2,0.7]e^{\pi i[0.1,0.4]}\right),\left(0.3e^{\pi i(0.3)}\right)\right)\\ \left(USS,\left([0.4,0.5]e^{\pi i[0.3,0.6]}\right),\left(0.7e^{\pi i(0.5)}\right)\right),\left(UBB,\left([0.5,0.8]e^{\pi i[0.3,0.9]}\right),\left(0.8e^{\pi i(0.5)}\right)\right)\\ \left(FR,\left([0.4,0.5]e^{\pi i[0.5,0.7]}\right),\left(0.5e^{\pi i(0.4)}\right)\right)\end{array}\right\}. \tag{71}$$

Table 3: CP of two CCuTSFSs.

Relation element	Complex T spherical fuzzy set	Complex interval-valued T spherical fuzzy set
(UP, IT)	$(0.2e^{\pi i(0.4)}, 0.2e^{\pi i(0.3)}, 0.3e^{\pi i(0.2)})$	$\left([0.3,0.5]e^{\pi i[0.2,0.4]}, [0.1,0.3]e^{\pi i[0.1,0.3]}, [0.1,0.2]e^{\pi i[0.2,0.3]}\right)$
(UP, PA)	$(0.3e^{\pi i(0.2)}, 0.4e^{\pi i(0.3)}, 0.5e^{\pi i(0.7)})$	$\left([0.2,0.4]e^{\pi i[0.1,0.3]}, [0.2,0.4]e^{\pi i[0.1,0.3]}, [0.3,0.5]e^{\pi i[0.2,0.5]}\right)$
(UP, SE)	$(0.2e^{\pi i(0.3)}, 0.4e^{\pi i(0.1)}, 0.3e^{\pi i(0.4)})$	$\left([0.3,0.5]e^{\pi i[0.1,0.2]}, [0.2,0.4]e^{\pi i[0.1,0.3]}, [0.4,0.5]e^{\pi i[0.2,0.4]}\right)$
(UP, MA)	$(0.3e^{\pi i(0.1)}, 0.2e^{\pi i(0.3)}, 0.5e^{\pi i(0.3)})$	$\left([0.1,0.4]e^{\pi i[0.2,0.3]}, [0.2,0.4]e^{\pi i[0.1,0.3]}, [0.2,0.5]e^{\pi i[0.2,0.4]}\right)$
(UP, IRA)	$(0.6e^{\pi i(0.4)}, 0.3e^{\pi i(0.3)}, 0.2e^{\pi i(0.3)})$	$\left([0.3,0.7]e^{\pi i[0.2,0.5]}, [0.1,0.3]e^{\pi i[0.1,0.3]}, [0.3,0.4]e^{\pi i[0.1,0.2]}\right)$
(UP, CNM)	$(0.5e^{\pi i(0.4)}, 0.2e^{\pi i(0.3)}, 0.3e^{\pi i(0.2)})$	$\left([0.3,0.6]e^{\pi i[0.2,0.6]}, [0.1,0.2]e^{\pi i[0.1,0.3]}, [0.2,0.5]e^{\pi i[0.1,0.4]}\right)$
(MFA, IT)	$(0.2e^{\pi i(0.3)}, 0.3e^{\pi i(0.2)}, 0.4e^{\pi i(0.2)})$	$\left([0.2,0.5]e^{\pi i[0.1,0.4]}, [0.1,0.3]e^{\pi i[0.2,0.5]}, [0.1,0.3]e^{\pi i[0.2,0.4]}\right)$
(MFA, PA)	$(0.3e^{\pi i(0.2)}, 0.3e^{\pi i(0.2)}, 0.5e^{\pi i(0.7)})$	$\left([0.2,0.4]e^{\pi i[0.1,0.3]}, [0.3,0.4]e^{\pi i[0.3,0.5]}, [0.3,0.5]e^{\pi i[0.2,0.5]}\right)$
(MFA, SE)	$(0.2e^{\pi i(0.3)}, 0.3e^{\pi i(0.1)}, 0.4e^{\pi i(0.4)})$	$\left([0.2,0.5]e^{\pi i[0.1,0.2]}, [0.2,0.4]e^{\pi i[0.1,0.5]}, [0.4,0.5]e^{\pi i[0.2,0.4]}\right)$
(MFA, MA)	$(0.3e^{\pi i(0.1)}, 0.2e^{\pi i(0.2)}, 0.5e^{\pi i(0.3)})$	$\left([0.1,0.4]e^{\pi i[0.1,0.3]}, [0.3,0.4]e^{\pi i[0.3,0.5]}, [0.2,0.5]e^{\pi i[0.2,0.4]}\right)$
(MFA, IRA)	$(0.3e^{\pi i(0.3)}, 0.3e^{\pi i(0.2)}, 0.4e^{\pi i(0.3)})$	$\left([0.2,0.5]e^{\pi i[0.2,0.3]}, [0.1,0.3]e^{\pi i[0.3,0.5]}, [0.3,0.5]e^{\pi i[0.3,0.4]}\right)$
(MFA, CNM)	$(0.3e^{\pi i(0.3)}, 0.2e^{\pi i(0.2)}, 0.4e^{\pi i(0.2)})$	$\left([0.2,0.6]e^{i[0.1,0.4]}, [0.1,0.2]e^{\pi i[0.3,0.4]}, [0.2,0.3]e^{\pi i[0.2,0.4]}\right)$
(USS, IT)	$(0.2e^{\pi i(0.4)}, 0.1e^{\pi i(0.4)}, 0.3e^{\pi i(0.3)})$	$\left([0.3,0.5]e^{\pi i[0.3,0.4]}, [0.1,0.3]e^{\pi i[0.2,0.4]}, [0.2,0.4]e^{\pi i[0.3,0.5]}\right)$
(USS, PA)	$(0.3e^{\pi i(0.2)}, 0.1e^{\pi i(0.4)}, 0.5e^{\pi i(0.7)})$	$\left([0.2,0.4]e^{\pi i[0.1,0.3]}, [0.3,0.6]e^{\pi i[0.2,0.4]}, [0.3,0.5]e^{\pi i[0.3,0.5]}\right)$
(USS, SE)	$(0.2e^{\pi i(0.3)}, 0.4e^{\pi i(0.1)}, 0.3e^{\pi i(0.4)})$	$\left([0.3,0.5]e^{\pi i[0.1,0.2]}, [0.2,0.6]e^{\pi i[0.1,0.5]}, [0.4,0.5]e^{\pi i[0.3,0.5]}\right)$
(USS, MA)	$(0.3e^{\pi i(0.1)}, 0.2e^{\pi i(0.4)}, 0.5e^{\pi i(0.3)})$	$([0.1,0.4]e^{\pi i[0.2,0.3]}, [0.3,0.5]e^{\pi i[0.3,0.5]}, [0.2,0.5]e^{\pi i[0.3,0.5]})$
(USS, IRA)	$(0.4e^{\pi i(0.5)}, 0.3e^{\pi i(0.4)}, 0.3e^{\pi i(0.3)})$	$([0.4,0.5]e^{\pi i[0.2,0.3]}, [0.1,0.3]e^{\pi i[0.3,0.5]}, [0.3,0.4]e^{\pi i[0.3,0.5]})$
(USS, CNM)	$(0.5e^{\pi i(0.6)}, 0.2e^{\pi i(0.3)},, 0.3e^{\pi i(0.3)})$	$([0.3,0.6]e^{\pi i[0.2,0.6]}, [0.1,0.2]e^{\pi i[0.3,0.4]}, [0.2,0.4]e^{\pi i[0.3,0.5]}))$
UBB, IT	$0.2e^{\pi i(0.4)}, 0.4e^{\pi i(0.5)}, 0.3e^{\pi i(0.2)}$	$(\pi[0.3,0.5]e^{\pi i[0.3,0.4]}, [0.1,0.3]e^{\pi i[0.2,0.5]}, [0.2,0.3]e^{\pi i[0.2,0.3]})$
(UBB, PA)	$(0.3e^{\pi i(0.2)}, 0.4e^{\pi i(0.6)}, 0.5e^{\pi i(0.7)})$	$([0.2,0.4]e^{\pi i[0.1,0.3]}, [0.4,0.7]e^{\pi i[0.3,0.8]}, [0.3,0.5]e^{\pi i[0.2,0.5]})$
(UBB, SE)	$(0.2e^{\pi i(0.3)}, 0.4e^{\pi i(0.1)}, 0.3e^{\pi i(0.4)})$	$([0.3,0.5]e^{\pi i[0.1,0.2]}, [0.2,0.6]e^{\pi i[0.1,0.5]}, [0.4,0.5]e^{\pi i[0.2,0.4]})$
(UBB, MA)	$(0.3e^{\pi i(0.1)}, 0.2e^{\pi i(0.4)}, 0.5e^{\pi i(0.3)})$	$([0.1,0.4]e^{\pi i[0.2,0.3]}, [0.3,0.5]e^{\pi i[0.3,0.5]}, [0.2,0.5]e^{\pi i[0.2,0.4]})$
UBB, IRA	$(0.4e^{\pi i(0.5)}, 0.3e^{\pi i(0.4)}, 0.3e^{\pi i(0.3)})$	$([0.4,0.5]e^{\pi i[0.2,0.3]}, [0.1,0.3]e^{\pi i[0.3,0.5]}, [0.3,0.4]e^{\pi i[0.1,0.3]})$
UBB, CNM	$(0.5e^{\pi i(0.6)}, 0.2e^{\pi i(0.3)}, 0.3e^{\pi i(0.2)})$	$([0.3,0.6]e^{\pi i[0.2,0.6]}, [0.1,0.2]e^{\pi i[0.3,0.4]}, [0.2,0.6]e^{\pi i[0.1,0.4]})$
(FR, IT)	$(0.2e^{\pi i(0.4)}, 0.4e^{\pi i(0.5)}, 0.3e^{\pi i(0.5)})$	$([0.3,0.5]e^{\pi i[0.3,0.4]}, [0.1,0.3]e^{\pi i[0.2,0.5]}, [0.2,0.6]e^{\pi i[0.2,0.4]})$
(FR, PA)	$(0.3e^{\pi i(0.2)}, 0.4e^{\pi i(0.6)}, 0.5e^{\pi i(0.7)})$	$([0.2,0.4]e^{\pi i[0.1,0.3]}, [0.4,0.7]e^{\pi i[0.3,0.8]}, [0.3,0.6]e^{\pi i[0.2,0.5]})$
(FR, SE)	$(0.2e^{\pi i(0.3)}, 0.4e^{\pi i(0.1)}, 0.3e^{\pi i(0.5)})$	$([0.3,0.5]e^{\pi i[0.1,0.2]}, [0.2,0.6]e^{\pi i[0.1,0.5]}, [0.4,0.6]e^{\pi i[0.2,0.4]})$
(FR, MA)	$(0.3e^{\pi i(0.1)}, 0.2e^{\pi i(0.4)}, 0.5e^{\pi i(0.5)})$	$([0.1,0.4]e^{\pi i[0.2,0.3]}, [0.3,0.5]e^{\pi i[0.3,0.5]}, [0.2,0.6]e^{\pi i[0.2,0.4]})$
(FR, IRA)	$(0.4e^{\pi i(0.5)}, 0.3e^{\pi i(0.4)}, 0.3e^{\pi i(0.5)})$	$([0.4,0.5]e^{\pi i[0.2,0.3]}, [0.1,0.3]e^{\pi i[0.3,0.5]}, [0.3,0.6]e^{\pi i[0.2,0.4]})$
(FR, CNM)	$(0.5e^{\pi i(0.6)}, 0.2e^{\pi i(0.3)}, 0.3e^{\pi i(0.5)})$	$([0.3,0.6]e^{\pi i[0.2,0.6]}, [0.1,0.2]e^{\pi i[0.3,0.4]}, [0.2,0.6]e^{\pi i[0.2,0.4]})$

The CP of $\mathbb{H}\times\mathbb{G}$

$$\mathbb{H}\times\mathbb{G}=\left\{\begin{array}{c}\left((UP,IT),\left([0.3,0.5]e^{\pi i[0.2,0.4]}\right)\left(0.2e^{\pi i(0.4)}\right),(UP,PA),\left([0.2,0.4]e^{\pi i[0.1,0.3]}\right),\left(0.3e^{\pi i(0.2)}\right)\right),\\ \left((UP,SE),\left([0.3,0.5]e^{\pi i[0.1,0.2]}\right)\left(0.2e^{\pi i(0.3)}\right),(UP,MA),\left([0.1,0.4]e^{\pi i[0.2,0.3]}\right),\left(0.3e^{\pi i(0.1)}\right)\right),\\ \left((UP,IRA),\left([0.3,0.7]e^{\pi i[0.2,0.5]}\right)\left(0.6e^{\pi i(0.4)}\right),(UP,CNM),\left([0.3,0.6]e^{\pi i[0.2,0.6]}\right),\left(0.5e^{\pi i(0.4)}\right)\right),\\ \left((MFA,IT),\left([0.2,0.5]e^{\pi i[0.1,0.4]}\right)\left(0.2e^{\pi i(0.3)}\right),(MFA,PA),\left([0.2,0.4]e^{\pi i[0.1,0.3]}\right),\left(0.3e^{\pi i(0.2)}\right)\right),\\ \left((MFA,SE),\left([0.2,0.5]e^{\pi i[0.1,0.2]}\right)\left(0.2e^{\pi i(0.3)}\right),(MFA,MA),\left([0.1,0.4]e^{\pi i[0.1,0.3]}\right),\left(0.3e^{\pi i(0.1)}\right)\right),\\ \left((MFA,IRA),\left([0.2,0.5]e^{\pi i[0.2,0.3]}\right)\left(0.3e^{\pi i(0.1)}\right),(MFA,CNM),\left([0.2,0.6]e^{\pi i[0.1,0.4]}\right),\left(0.3e^{\pi i(0.3)}\right)\right),\\ \left((USS,IT),\left([0.3,0.5]e^{\pi i[0.3,0.4]}\right)\left(0.2e^{\pi i(0.4)}\right),(USS,PA),\left([0.2,0.4]e^{\pi i[0.1,0.3]}\right),\left(0.3e^{\pi i(0.2)}\right)\right),\\ \left((USS,SE),\left([0.3,0.5]e^{\pi i[0.1,0.2]}\right)\left(0.2e^{\pi i(0.3)}\right),(USS,MA),\left([0.1,0.4]e^{\pi i[0.2,0.3]}\right),\left(0.3e^{\pi i(0.1)}\right)\right),\\ \left((USS,IRA),\left([0.4,0.5]e^{\pi i[0.2,0.3]}\right)\left(0.4e^{\pi i(0.5)}\right),(USS,CNM),\left([0.3,0.5]e^{\pi i[0.2,0.6]}\right),\left(0.5e^{\pi i(0.5)}\right)\right),\\ \left((UBB,IT),\left([0.3,0.5]e^{\pi i[0.3,0.4]}\right)\left(0.2e^{\pi i(0.4)}\right),(UBB,PA),\left([0.2,0.4]e^{\pi i[0.1,0.3]}\right),\left(0.3e^{\pi i(0.2)}\right)\right),\\ \left((UBB,SE),\left([0.3,0.5]e^{\pi i[0.1,0.2]}\right)\left(0.2e^{\pi i(0.3)}\right),(UBB,MA),\left([0.1,0.4]e^{\pi i[0.2,0.3]}\right),\left(0.3e^{\pi i(0.1)}\right)\right),\\ \left((UBB,IRA),\left([0.4,0.5]e^{\pi i[0.2,0.3]}\right)\left(0.4e^{\pi i(0.5)}\right),(UBB,CNM),\left([0.3,0.6]e^{\pi i[0.2,0.6]}\right),\left(0.5e^{\pi i(0.5)}\right)\right),\\ \left((FR,IT),\left([0.3,0.5]e^{\pi i[0.3,0.4]}\right)\left(0.2e^{\pi i(0.4)}\right),(FR,PA),\left([0.2,0.4]e^{\pi i[0.1,0.3]}\right),\left(0.3e^{\pi i(0.2)}\right)\right),\\ \left((FR,SE),\left([0.3,0.5]e^{\pi i[0.1,0.2]}\right)\left(0.2e^{\pi i(0.3)}\right),(FR,MA),\left([0.1,0.4]e^{\pi i[0.2,0.3]}\right),\left(0.3e^{\pi i(0.1)}\right)\right),\\ \left((FR,IRA),\left([0.4,0.5]e^{\pi i[0.2,0.3]}\right)\left(0.4e^{\pi i(0.4)}\right),(FR,CNM),\left([0.3,0.5]e^{\pi i[0.2,0.6]}\right),\left(0.5e^{\pi i(0.4)}\right)\right)\end{array}\right\}. \tag{72}$$

CCuFR shows only the effectiveness of security against a particular threat. The membership grade effect of the first element on the second element in an ordered pair. As a result, these structures have limitations and consequently provide restricted information. Meanwhile, the CCuTSFR gives the complete information.

5.2. Comparison of IFR, CuIFR, and CCuIFR with CCuTSFR. The structures of IFR, CuIFR, and CCuIFR discuss the membership degree and nonmembership degree. The membership degree shows the effectiveness of security measures on the threats, and nonmembership shows the ineffectiveness of security measures on the particular threat. Therefore, they cannot show the neutral values of security measures against the threat. The IFR and CuIFR can solve only one-dimensional problems. The IFR and CuIFR are unable to multivariable difficulties. But CCuIFR can solve the periodicity. The CCuTSFR is superior to this structure because they are also discussing the neutral effect of the first element to the other. So, the structure of CCuTSFR discusses all stages, i.e., membership, neutral, and nonmembership with both aspects of the present and future. We consider the two CCuIFSs, $\mathbb{G}$, and $\mathbb{H}$, which describe the threat and security sets, respectively.

$$\begin{aligned}\mathbb{G}&=\left\{\begin{array}{c}\left(IT,\left([0.3,0.5]e^{\pi i[0.3,0.4]},[0.1,0.3]e^{\pi i[0.2,0.5]}\right),\left(0.2e^{\pi i(0.4)},0.4e^{\pi i(0.5)}\right)\right),\\ \left(PA,\left([0.2,0.4]e^{\pi i[0.1,0.3]},[0.4,0.7]e^{\pi i[0.3,0.8]}\right),\left(0.3e^{\pi i(0.2)},0.4e^{\pi i(0.6)}\right)\right),\\ \left(SE,\left([0.3,0.5]e^{\pi i[0.1,0.2]},[0.2,0.6]e^{\pi i[0.1,0.5]}\right),\left(0.2e^{\pi i(0.3)},0.4e^{\pi i(0.1)}\right)\right),\\ \left(MA,\left([0.1,0.4]e^{\pi i[0.2,0.3]},[0.3,0.5]e^{\pi i[0.3,0.5]}\right),\left(0.3e^{\pi i(0.1)},0.2e^{\pi i(0.4)}\right)\right),\\ \left(IRA,\left([0.4,0.5]e^{\pi i[0.2,0.3]},[0.1,0.3]e^{\pi i[0.3,0.5]}\right),\left(0.4e^{\pi i(0.5)},0.3e^{\pi i(0.4)}\right)\right),\\ \left(CNM,\left([0.3,0.6]e^{\pi i[0.2,0.6]},[0.1,0.2]e^{\pi i[0.3,0.4]}\right),\left(0.5e^{\pi i(0.6)},0.2e^{\pi i(0.3)}\right)\right)\end{array}\right\},\\ \mathbb{H}&=\left\{\begin{array}{c}\left(UP,\left([0.3,0.5]e^{\pi i[0.2,0.7]},[0.2,0.4]e^{\pi i[0.1,0.3]}\right),\left(0.6e^{\pi i(0.4)},0.4e^{\pi i(0.3)}\right)\right),\\ \left(MFA,\left([0.2,0.7]e^{\pi i[0.1,0.4]},[0.3,0.4]e^{\pi i[0.3,0.5]}\right),\left(0.3e^{\pi i(0.3)},0.3e^{\pi i(0.2)}\right)\right),\\ \left(USS,\left([0.4,0.5]e^{\pi i[0.3,0.6]},[0.3,0.6]e^{\pi i[0.2,0.4]}\right),\left(0.7e^{\pi i(0.5)},0.1e^{\pi i(0.4)}\right)\right),\\ \left(UBB,\left([0.5,0.8]e^{\pi i[0.3,0.9]},[0.3,0.5]e^{\pi i[0.2,0.3]}\right),\left(0.8e^{\pi i(0.5)},0.2e^{\pi i(0.4)}\right)\right),\\ \left(FR,\left([0.4,0.5]e^{\pi i[0.5,0.7]},[0.1,0.4]e^{\pi i[0.1,0.2]}\right),\left(0.5e^{\pi i(0.4)},0.1e^{\pi i(0.4)}\right)\right)\end{array}\right\},\end{aligned} \tag{73}$$

The CP of $\mathbb{H}\times\mathbb{G}$

$$\mathbb{H}\times\mathbb{G}=\left\{\begin{array}{c}
((UP, IT), ([0.3, 0.5]e^{\pi i[0.2,0.4]}), [0.2, 0.4]e^{\pi i[0.2,0.5]}(0.2e^{\pi i(0.4)}, 0.4e^{\pi i(0.5)})),\\
((UP, PA), ([0.2, 0.4]e^{\pi i[0.1,0.3]}), [0.4, 0.7]e^{\pi i[0.3,0.8]}(0.3e^{\pi i(0.2)}, 0.4e^{\pi i(0.6)})),\\
((UP, SE), ([0.3, 0.5]e^{\pi i[0.1,0.2]}), [0.2, 0.6]e^{\pi i[0.1,0.5]}(0.2e^{\pi i(0.3)}, 0.4e^{\pi i(0.1)})),\\
((UP, MA), ([0.1, 0.4]e^{\pi i[0.2,0.3]}), [0.3, 0.5]e^{\pi i[0.3,0.5]}(0.3e^{\pi i(0.1)}, 0.2e^{\pi i(0.4)})),\\
((UP, IRA), ([0.3, 0.5]e^{\pi i[0.2,0.7]}), [0.2, 0.4]e^{\pi i[0.1,0.3]}(0.6e^{\pi i(0.4)}, 0.4e^{\pi i(0.3)})),\\
((\mathrm{UP, CNM}), ([0.3, 0.5]\,\mathrm{e}^{\pi\mathrm{i}[0.2,0.7]}, [0.2, 0.4]\mathrm{e}^{\pi\mathrm{i}[0.1,0.3]}), (0.6\mathrm{e}^{\pi\mathrm{i}(0.4)}, 0.4\mathrm{e}^{\pi i(0.3)})),\\
((\mathrm{MFA, IT}), ([0.2, 0.7]\mathrm{e}^{\pi i[0.1,0.4]}, [0.3, 0.4]\mathrm{e}^{\pi i[0.3,0.5]}), (0.3\mathrm{e}^{\pi i(0.3)}, 0.3\mathrm{e}^{\pi i(0.2)})),\\
((\mathrm{MFA, PA}), ([0.2, 0.4]\mathrm{e}^{\pi i[0.1,0.3]}, [0.4, 0.7]\mathrm{e}^{\pi\mathrm{i}[0.3,0.8]}), (0.3\mathrm{e}^{\pi i(0.2)}, 0.4\mathrm{e}^{\pi i(0.6)})),\\
((\mathrm{MFA, SE}), ([0.2, 0.7]\mathrm{e}^{\pi i[0.1,0.4]}, [0.3, 0.4]\mathrm{e}^{\pi i[0.3,0.5]}), (0.3\mathrm{e}^{\pi i(0.3)}, 0.3\mathrm{e}^{\pi i(0.2)})),\\
((\mathrm{MFA.MA}), ([0.1, 0.4]\mathrm{e}^{\pi\mathrm{i}[0.2,0.3]}, [0.3, 0.5]\mathrm{e}^{\pi\mathrm{i}[0.3,0.5]}), (0.3\mathrm{e}^{\pi\mathrm{i}(0.1)}, 0.2\mathrm{e}^{\pi\mathrm{i}(0.4)})),\\
((\mathrm{MFA, IRA}), ([0.2, 0.7]\mathrm{e}^{\pi\mathrm{i}[0.1,0.4]}, [0.3, 0.4]\mathrm{e}^{\pi i[0.3,0.5]}), (0.3\mathrm{e}^{\pi\mathrm{i}(0.3)}, 0.3\mathrm{e}^{\pi\mathrm{i}(0.2)})),\\
((\mathrm{MFA, CNM}), ([0.2, 0.7]\mathrm{e}^{\pi\mathrm{i}[0.1,0.4]}, [0.3, 0.4]\mathrm{e}^{\pi i[0.3,0.5]}), (0.3\mathrm{e}^{\pi i(0.3)}, 0.3\mathrm{e}^{\pi i(0.2)})),\\
((\mathrm{USS, IT}), ([0.3, 0.5]\mathrm{e}^{\pi i[0.3,0.4]}, [0.1, 0.3]\mathrm{e}^{\pi i[0.2,0.5]}), (0.2\mathrm{e}^{\pi i(0.4)}, 0.4\mathrm{e}^{\pi i(0.5)})),\\
((\mathrm{USS, PA}), ([0.2, 0.4]\mathrm{e}^{\pi i[0.1,0.3]}, [0.4, 0.7]\mathrm{e}^{\pi i[0.3,0.8]}), (0.3\mathrm{e}^{\pi i(0.2)}, 0.4\mathrm{e}^{\pi i(0.6)})),\\
((\mathrm{USS, SE}), ([0.3, 0.5]\mathrm{e}^{\pi i[0.1,0.2]}, [0.2, 0.6]\mathrm{e}^{\pi i[0.1,0.5]}), (0.2\mathrm{e}^{\pi i(0.3)}, 0.4\mathrm{e}^{\pi i(0.1)})),\\
((\mathrm{USS, MA}), ([0.1, 0.4]\mathrm{e}^{\pi i[0.2,0.3]}, [0.3, 0.5]\mathrm{e}^{\pi i[0.3,0.5]}), (0.3\mathrm{e}^{\pi i(0.1)}, 0.2\mathrm{e}^{\pi i(0.4)})),\\
((\mathrm{USS, IRA}), ([0.4, 0.5]\mathrm{e}^{\pi i[0.2,0.3]}, [0.1, 0.3]\mathrm{e}^{\pi i[0.3,0.5]}), (0.4\mathrm{e}^{\pi i(0.5)}, 0.3\mathrm{e}^{\pi i(0.4)})),\\
((\mathrm{USS, CNM}), ([0.3, 0.6]\mathrm{e}^{\pi i[0.2,0.6]}, [0.1, 0.2]\mathrm{e}^{\pi i[0.3,0.4]}), (0.5\mathrm{e}^{\pi i(0.6)}, 0.2\mathrm{e}^{\pi i(0.3)})),\\
((\mathrm{UBB, IT}), ([0.3, 0.5]\mathrm{e}^{\pi i[0.3,0.4]}, [0.1, 0.3]\mathrm{e}^{\pi i[0.2,0.5]}), (0.2\mathrm{e}^{\pi i(0.4)}, 0.4\mathrm{e}^{\pi i(0.5)})),\\
((\mathrm{UBB, PA}), ([0.2, 0.4]\mathrm{e}^{\pi i[0.1,0.3]}, [0.4, 0.7]\mathrm{e}^{\pi i[0.3,0.8]}), (0.3\mathrm{e}^{\pi i(0.2)}, 0.4\mathrm{e}^{\pi i(0.6)})),\\
((\mathrm{UBB, SE}), ([0.3, 0.5]\mathrm{e}^{\pi i[0.1,0.2]}, [0.2, 0.6]\mathrm{e}^{\pi i[0.1,0.5]}), (0.2\mathrm{e}^{\pi i(0.3)}, 0.4\mathrm{e}^{\pi i(0.1)})),\\
((\mathrm{UBB, MA}), ([0.1, 0.4]\mathrm{e}^{\pi i[0.2,0.3]}, [0.3, 0.5]\mathrm{e}^{\pi i[0.3,0.5]}), (0.3\mathrm{e}^{\pi i(0.1)}, 0.2\mathrm{e}^{\pi i(0.4)})),\\
((\mathrm{UBB, IRA}), ([0.4, 0.5]\mathrm{e}^{\pi i[0.2,0.3]}, [0.1, 0.3]^{\mathrm{e}\pi i[0.3,0.5]}), (0.4\mathrm{e}^{\pi i(0.5)}, 0.3\mathrm{e}^{\pi i(0.4)})),\\
((\mathrm{UBB, CNM}), ([0.3, 0.6]\mathrm{e}^{\pi i[0.2,0.6]}, [0.1, 0.2]\mathrm{e}^{\pi i[0.3,0.4]}), (0.5\mathrm{e}^{\pi i(0.6)}, 0.2\mathrm{e}^{\pi i(0.3)})),\\
((\mathrm{FR, IT}), ([0.3, 0.5]\mathrm{e}^{\pi i[0.3,0.4]}, [0.1, 0.3]\mathrm{e}^{\pi i[0.2,0.5]}), (0.2\mathrm{e}^{\pi i(0.4)}, 0.4\mathrm{e}^{\pi i(0.5)})),\\
((\mathrm{FR, PA}), ([0.2, 0.4]\mathrm{e}^{\pi i[0.1,0.3]}, [0.4, 0.7]\mathrm{e}^{\pi i[0.3,0.8]}), (0.3\mathrm{e}^{\pi i(0.2)}, 0.4\mathrm{e}^{\pi i(0.6)})),\\
((\mathrm{FR, SE}), ([0.3, 0.5]\mathrm{e}^{\pi i[0.1,0.2]}, [0.2, 0.6]\mathrm{e}^{\pi i[0.1,0.5]}), (0.2\mathrm{e}^{\pi i(0.3)}, 0.4\mathrm{e}^{\pi i(0.1)})),\\
((\mathrm{FR, MA}), ([0.1, 0.4]\mathrm{e}^{\pi i[0.2,0.3]}, [0.3, 0.5]\mathrm{e}^{\pi i[0.3,0.5]}), (0.3\mathrm{e}^{\pi i(0.1)}, 0.2\mathrm{e}^{\pi i(0.4)})),\\
((\mathrm{FR, IRA}), ([0.4, 0.5]\mathrm{e}^{\pi i[0.2,0.3]}, [0.1, 0.3]\mathrm{e}^{\pi i[0.3,0.5]}), (0.4\mathrm{e}^{\pi i(0.5)}, 0.3\mathrm{e}^{\pi i(0.4)})),\\
((\mathrm{FR, CNM}), ([0.3, 0.6]\mathrm{e}^{\pi i[0.2,0.6]}, [0.1, 0.2]\mathrm{e}^{\pi i[0.3,0.4]}), (0.5\mathrm{e}^{\pi i(0.6)}, 0.2\mathrm{e}^{\pi i(0.3)}))
\end{array}\right\}. \tag{74}$$

It is clear from the CCuIFR, that it describes the effectiveness and ineffectiveness of the security measures against a certain threat. They are not discussing neutral value.

Table 4: Summary of comparison.

Structure	Membership	Neutral	Non-membership	Multidimensional	Dual degree	Space
FR	Yes	No	No	No	No	$n = 1$
CuFR	Yes	No	No	No	Yes	$n = 1$
CCuFR	Yes	No	No	Yes	Yes	$n = 1$
IFR	Yes	No	Yes	No	No	$n = 1$
CuIFR	Yes	No	Yes	No	Yes	$n = 1$
CCuIFR	Yes	No	Yes	Yes	Yes	$n = 1$
PyFR	Yes	No	Yes	No	No	$n = 2$
CuPyFR	Yes	No	Yes	No	Yes	$n = 2$
CCuPyFR	Yes	No	Yes	Yes	Yes	$n = 2$
qROFR	Yes	No	Yes	No	No	$n \geq 1$
CuqROFR	Yes	No	Yes	No	Yes	$n \geq 1$
CCuqROFR	Yes	No	Yes	Yes	Yes	$n \geq 1$
PFR	Yes	Yes	Yes	No	No	$n = 1$
CuPFR	Yes	Yes	Yes	No	Yes	$n = 1$
CCuPFR	Yes	Yes	Yes	Yes	Yes	$n = 1$
SFR	Yes	Yes	Yes	No	No	$n = 2$
CuSFR	Yes	Yes	Yes	No	Yes	$n = 2$
CCuSFR	Yes	Yes	Yes	Yes	Yes	$n = 2$
TSFR	Yes	Yes	Yes	No	No	$n \geq 1$
CuTSFR	Yes	Yes	Yes	No	Yes	$n \geq 1$
CCuTSFR	Yes	Yes	Yes	Yes	Yes	$n \geq 1$

5.3. Comparison of PyFR, CuPyFR, and CCuPyFR with CCuTSFR. These structures discuss membership and nonmembership. These structures are used to show the effectiveness and ineffectiveness of the security measures against a certain threat. These are the generalization forms of CuIFR. As the framework of IFS has its limitations in assigning the membership and nonmembership because their sum exceeds from [0,1] in many cases. For example, the ordered pair $(0.8, 0.5)$ cannot be considered as an intuitionistic fuzzy number (IFN) because their sum exceeds 1, but sum $(0.8^2, 0.5^2) = 0.89 \in [0, 1]$. This shows that the range of the Pythagorean fuzzy set (PyFS) is greater than that of IFS. The PyFR and CuPyFR are only one-dimensional. The CCuPyFR is discussing both amplitude and time frame. The CuPyFR and CCuPyFR have certain limitations as compared to the CCuTSFR because these structures do not describe the neutral effect.

5.4. Comparison qOFR, CuqOFR, and CCuqOFR with CCuTSFR. The qOFR, CuqROFR, and CCuqROFR describe the only success and failure effects. They do not describe the values of success and failure. CuPyFS improved the limitations that occurred in CuIFS, but there are still some duplets that cannot be categorized as IFN or PyFN. For example, the duplet $(0.9, 0.6)$ is neither an IFN nor a PyFN because sum $(0.9, 0.6) = 1.5 \notin [0, 1]$ and sum $(0.9^2, 0.6^2) = 1.17 \notin [0, 1]$. If for $\mathbb{N} = 3$, then their duplet sum exists to the range of [0,1]. These structures are the generalization of CuPyFR and CCuPyFR, but these structures have certain limitations as compared to CCuTSFR.

5.5. Comparison of PFR, CuPFR, CCuPFR with CCuTSFR. These structures discuss all values such as membership, neutral, and nonmembership. These structures show the effectiveness of security measures against the threat; the neutral structure shows the ordered pair that has no effect; and nonmembership shows the ineffectiveness of the security against threat. The PFR and CuPFR are not showing the complex value with time frame i.e., PFR and CuPFR are only single dimensions. The CCuPFR describes the time frame or periodicity. The structure CuPFR and CCuPFR are using $\mathbb{N} = 1$. So, there are some limitations to selecting the degree of membership, neutral, and degree of nonmembership because their sum exists to the unit interval of [0, 1]. The CCuTSFR has improved the limitations to choosing the membership. neutral, and nonmembership degrees are using $\mathbb{N} = n$.

5.6. Comparison of SFR, CuSFR, and CCuSFR with CCuTSFR. The structure of SFR, CuSFR, and CCuSFR improve the limitations of CuPFR using $\mathbb{N} = 2$. A CuSFR based on membership, neutral, and nonmembership degrees, respectively, with the constraint that the sum of the square must exceed 1. The CuSFR increased the range of a CuPFR. These structures, SFR and CuSFR are discussing only one-dimensionally. The CCuSFR is the generalization form of a PFR, CuPFR, and CCuPFR. But the CCuSFR faces some limitations in choosing the degrees of membership, neutral, and nonmembership as compared to the CCuTSFR.

5.7. Comparison of TSFR and CuTSFR with CCuTSFR. The structure TSFR and CuTSFR improve the limitations of CuPFR and CuSFR using $\mathbb{N} = n$. The CuTSFR increased the range of the CuSFR and CuPFR. The CCuTSFR is the generalization form of the CuSFR and CCuSFR. Some ordered pairs exist that their sum of the squares exceeds the unit interval then occurs the CuTSFR for using the parameter $\mathbb{N} = n$. These structures TSFR and CuTSFR are discussing only one-dimensional. They have not defined the duration of time. The CCuTSFR has defined both amplitude and time frame. The CCuTSFR is the better form of all the preexisting frameworks. The summary of all fuzzy preexisting structures is defined in Table 4.

6. Conclusion

In this paper, we explored the novel concepts of the complex cubic T spherical fuzzy set (CCuTSFS), complex cubic T spherical fuzzy relation (CCuTSFR), and CP of two CCuTSFSs. Moreover, numerous types of CCuTSFR are also discussed, including CCuTS-reflexive-FR, CCuTS-irreflexive-FR, CCuTS-symmetric-FR, CCuTS-transitive FR, CCuTS-equivalence classes-FR, and many more. The CCuTSFS is the generalization form of the TSFR and IVTSFR. The novel concept of the CCuTSFRs is the more generalized form of all the predefined structures. Because this structure covers all levels i.e., membership, neutral, and nonmembership with complex number, this structure describes all levels of both present and future aspects. They are better at dealing with fuzziness. The goal of these new frameworks and novel modeling procedures is to solve social media security problems. The proposed study is used to analyze the relationship between various types of security methods and threats. They define the effectiveness, neutral, and ineffectiveness degrees of both the present and future. The advantage of these structures is that they are used to define all the three stages membership, neutral, and nonmembership with both the amplitude and phase term. The presented framework is compared to the other previous methods. As a result, the CCuTSFR is more advanced than all the other preexisting structures. In the future, the CCuTSFR will be used for better outcomes. This idea can be used for several interesting and diverse applications.

Data Availability

No data set was generated or analyzed during the current study.

Conflicts of Interest

The authors declare that there are no conflicts of interest with this study.

Acknowledgments

The authors are grateful to the Deanship of Scientific Research, King Saud University for funding through Vice Deanship of Scientific Research Chairs.

References

[1] L. A. Zadeh, "Fuzzy sets," *Information and Control*, vol. 8, pp. 338–353, 1965.
[2] G. J. Klir and T. A. Folger, *Fuzzy Sets, Uncertainty, and Information*, Prentice-Hall, Englewood Cliffs, NJ, 1988.
[3] J. M. Mendel, "Fuzzy logic systems for engineering: a tutorial," *Proceedings of the IEEE*, vol. 83, no. 3, pp. 345–377, 1995.
[4] L. A. Zadeh, "The concept of a linguistic variable and its application to approximate reasoning—I," *Information Sciences*, vol. 8, no. 3, pp. 199–249, 1975.
[5] H. Bustince and P. Burillo, "Mathematical analysis of interval-valued fuzzy relations: application to approximate reasoning," *Fuzzy Sets and Systems*, vol. 113, no. 2, pp. 205–219, 2000.
[6] G. Deschrijver and E. E. Kerre, "On the relationship between some extensions of fuzzy set theory," *Fuzzy Sets and Systems*, vol. 133, no. 2, pp. 227–235, 2003.
[7] H. Bustince, E. Barrenechea, M. Pagola, and J. Fernández, "Interval-valued fuzzy sets constructed from matrices: application to edge detection," *Fuzzy Sets and Systems*, vol. 160, no. 13, pp. 1819–1840, 2009.
[8] B. De Baets and E. Kerre, "Fuzzy relations and applications," *Advances in Electronics and Electron Physics*, vol. 89, pp. 255–324, 1994.
[9] K. T. Atanassov, "Intuitionistic fuzzy sets," *Fuzzy Sets and Systems*, vol. 20, pp. 87–96, 1986.
[10] P. Burillo and H. Bustince, "Intuitionistic fuzzy relations (Part I)," *Mathware and Soft Computing*, vol. 2, no. 1, pp. 5–38.
[11] K. T. Atanassov, "Interval valued intuitionistic fuzzy sets," in *Intuitionistic Fuzzy Sets*, pp. 139–177, Physica, Heidelberg, 1999.
[12] S. K. De, R. Biswas, and A. R. Roy, "An application of intuitionistic fuzzy sets in medical diagnosis," *Fuzzy Sets and Systems*, vol. 117, no. 2, pp. 209–213, 2001.
[13] R. R. Yager, "Properties and applications of Pythagorean fuzzy sets," in *Imprecision and Uncertainty in Information Representation and Processing*, pp. 119–136, Springer, Cham, 2016.
[14] Q. Zhou, H. Mo, and Y. Deng, "A new divergence measure of pythagorean fuzzy sets based on belief function and its application in medical diagnosis," *Mathematics*, vol. 8, no. 1, p. 142, 2020.
[15] R. R. Yager, "Generalized orthopair fuzzy sets," *IEEE Transactions on Fuzzy Systems*, vol. 25, no. 5, pp. 1222–1230, 2016.
[16] B. C. Cuong and V. Kreinovich, "Picture Fuzzy Sets-a new concept for computational intelligence problems," in *Proceedings of the 2013 third world congress on information and communication technologies (WICT 2013)*, pp. 1–6, IEEE, Hanoi, Vietnam, 2013, December.
[17] T. Mahmood, K. Ullah, Q. Khan, and N. Jan, "An approach toward decision-making and medical diagnosis problems using the concept of spherical fuzzy sets," *Neural Computing & Applications*, vol. 31, no. 11, pp. 7041–7053, 2019.
[18] A. Guleria and R. K. Bajaj, "Eigen spherical fuzzy set and its application to decision-making problem," *Scientia Iranica*, vol. 28, no. 1, pp. 516–531, 2021.
[19] K. Ullah, T. Mahmood, and N. Jan, "Similarity measures for T-spherical fuzzy sets with applications in pattern recognition," *Symmetry*, vol. 10, no. 6, p. 193, Jun. 2018.
[20] K. Ullah, H. Garg, T. Mahmood, N. Jan, and Z. Ali, "Correlation coefficients for T-spherical fuzzy sets and their applications in clustering and multi-attribute decision making," *Soft Computing*, vol. 24, no. 3, pp. 1647–1659, 2020.
[21] N. Van Dinh, N. X. Thao, and N. M. Chau, "On the picture fuzzy database: theories and application," *Journal of Science*, vol. 13, no. 6, pp. 1028–1035, 2015.
[22] P. Dutta, "Medical diagnosis based on distance measures between picture fuzzy sets," *International Journal of Fuzzy System Applications*, vol. 7, no. 4, pp. 15–36, 2018.
[23] D. Ramot, R. Milo, M. Friedman, and A. Kandel, "Complex fuzzy sets," *IEEE Transactions on Fuzzy Systems*, vol. 10, no. 2, pp. 171–186, 2002.

[24] C. Li, T. Wu, and F. T. Chan, "Self-learning complex neuro-fuzzy system with complex fuzzy sets and its application to adaptive image noise canceling," *Neurocomputing*, vol. 94, pp. 121–139, 2012.
[25] S. Greenfield, F. Chiclana, and S. Dick, "Interval-valued complex fuzzy logic," in *Proceedings of the 2016 IEEE International Conference on Fuzzy Systems (FUZZ-IEEE)*, pp. 2014–2019, IEEE, Vancouver, BC, Canada, 2016, July.
[26] A. Nasir, N. Jan, A. Gumaei, and S. U. Khan, "Medical diagnosis and life span of sufferer using interval valued complex fuzzy relations," *IEEE Access*, vol. 9, pp. 93764–93780, 2021.
[27] A. M. D. J. S. Alkouri and A. R. Salleh, "Complex intuitionistic fuzzy sets," *AIP Conference Proceedings*, vol. 1482, no. 1, pp. 464–470, 2012.
[28] N. Jan, A. Nasir, M. S. Alhilal, S. U. Khan, D. Pamucar, and A. Alothaim, "Investigation of cyber-security and cyber-crimes in oil and gas sectors using the innovative structures of complex intuitionistic fuzzy relations," *Entropy*, vol. 23, no. 9, p. 1112, 2021.
[29] H. Garg and D. Rani, "Complex interval-valued intuitionistic fuzzy sets and their aggregation operators," *Fundamenta Informaticae*, vol. 164, no. 1, pp. 61–101, 2019.
[30] A. Nasir, N. Jan, A. Gumaei, S. U. Khan, and F. R. Albogamy, "Cybersecurity against the loopholes in industrial control systems using interval-valued complex intuitionistic fuzzy relations," *Applied Sciences*, vol. 11, no. 16, p. 7668, 2021.
[31] S. Dick, R. R. Yager, and O. Yazdanbakhsh, "On Pythagorean and complex fuzzy set operations," *IEEE Transactions on Fuzzy Systems*, vol. 24, no. 5, pp. 1009–1021, 2015.
[32] H. Garg, J. Gwak, T. Mahmood, and Z. Ali, "Power aggregation operators and VIKOR methods for complex q-rung orthopair fuzzy sets and their applications," *Mathematics*, vol. 8, no. 4, p. 538, 2020.
[33] A. Nasir, N. Jan, S. U. Khan, A. Gumaei, and A. Alothaim, "Analysis of communication and network securities using the concepts of complex picture fuzzy relations," *Computational Intelligence and Neuroscience*, vol. 2021, pp. 1–20, 2021.
[34] Z. Ali, T. Mahmood, and M. S. Yang, "TOPSIS method based on complex spherical fuzzy sets with Bonferroni mean operators," *Mathematics*, vol. 8, no. 10, p. 1739, 2020.
[35] Y. B. Jun, C. S. Kim, and K. O. Yang, "Cubic sets," *Ann. Fuzzy Math. Inform*, vol. 4, no. 1, pp. 83–98, 2012.
[36] G. Kaur and H. Garg, "Generalized cubic intuitionistic fuzzy aggregation operators using t-norm operations and their applications to group decision-making process," *Arabian Journal for Science and Engineering*, vol. 44, no. 3, pp. 2775–2794, 2019.
[37] J. Kim, P. K. Lim, J. G. Lee, and K. Hur, "Cubic relations," *Ann. Fuzzy Math. Inform*, vol. 19, no. 1, pp. 21–43, 2020.
[38] H. Garg and G. Kaur, "Cubic intuitionistic fuzzy sets and its fundamental properties," *Journal of Multiple-Valued Logic and Soft Computing*, vol. 33, no. 6, 2019.
[39] P. Talukdar and P. Dutta, "Distance measures for cubic Pythagorean fuzzy sets and its applications to multicriteria decision making," *Granular Computing*, vol. 6, no. 2, pp. 267–284, 2021.
[40] B. Zhang, T. Mahmood, J. Ahmmad, Q. Khan, Z. Ali, and S. Zeng, "Cubic q-Rung orthopair fuzzy Heronian mean operators and their applications to multi-attribute group decision making," *Mathematics*, vol. 8, no. 7, p. 1125, 2020.
[41] A. Gumaei and A. Hussain, "New operators of cubic picture fuzzy information with applications," *Journal of Mathematics*, vol. 2021, pp. 1–16, 2021.
[42] A. Devaraj and J. Aldring, "Tangent similarity measure of cubic spherical fuzzy sets and its application to MCDM," in *Proceedings of the International Conference on Intelligent and Fuzzy Systems*, pp. 802–810, Springer, Istanbul, Turkey, 2021, August.
[43] V. Chinnadurai, S. Thayalana, and A. Bobin, "Complex cubic set and their properties," *Advances in Mathematics*, vol. 9, pp. 1561–1567, 2020.
[44] X. Zhou, Y. Deng, Z. Huang, F. Yan, and W. Li, "Complex cubic fuzzy aggregation operators with applications in group decision-making," *IEEE Access*, vol. 8, pp. 223869–223888, 2020.
[45] V. Chinnadurai, S. Thayalana, and A. Bobin, "Complex cubic Intuitionistic fuzzy set and its decision making," *Advances in Mathematics*, vol. 9, pp. 7933–7946, 2020.
[46] W. He, "A review of social media security risks and mitigation techniques," *Journal of Systems and Information Technology*, vol. 14, no. 2, pp. 171–180, 2012.

Hindawi
Scientific Programming
Volume 2022, Article ID 2090681, 11 pages
https://doi.org/10.1155/2022/2090681

Research Article

Smart Healthcare: Disease Prediction Using the Cuckoo-Enabled Deep Classifier in IoT Framework

Ashwani Kumar,[1] **S. Sai Satyanarayana Reddy**,[2] **Gouse Baig Mahommad**,[3] **Baseem Khan**,[4] **and Rahul Sharma**[5]

[1]*Department of Computer Science & Engineering, Sreyas Institute of Engineering and Technology, Hyderabad 500068, India*
[2]*Sreyas Institute of Engineering and Technology, Hyderabad 500068, India*
[3]*Department of CSE, Vardhaman College of Engineering, Hyderabad, India*
[4]*Department of Electrical and Computer Engineering, Hawassa University, Hawassa, Ethiopia*
[5]*Tallinn University of Technology, Tallinn, Estonia*

Correspondence should be addressed to Baseem Khan; basseemk@hu.edu.et

Received 26 January 2022; Revised 6 April 2022; Accepted 8 April 2022; Published 6 May 2022

Academic Editor: Jianping Gou

The Internet of Things (IoT) is commonly employed to detect different kinds of diseases in the health sector. Presently, disease detection is performed using MRI images, X-rays, CT scans, and so on for diagnosing the diseases. The manual detection process is found to be time-consuming and may result in detection errors that affect the diagnosis. Hence, there is a need for an automatic system for which the deep learning methods gain a major interest. Hence, the idea to combine deep learning and disease prediction to effectively predict the disease is initiated. In this research, the deep learning method is combined with deep learning for the effective prediction of diseases, where the IoT network is employed in the data collection from the patients. The proposed cuckoo-based deep convolutional long-short term memory (deep convLSTM) classifier is employed for disease prediction, where the cuckoo search optimization is utilized for tuning the deep convLSTM classifier. The proposed method is compared with the conventional methods, and it achieved a training percentage of 97.591%, 95.874%, and 97.094%, respectively, for accuracy, sensitivity, and specificity. The comparative analysis proved that the proposed method obtained higher accuracy than other methods.

1. Introduction

IoT [9] is an emerging new technology for the upcoming later generation technology that interconnects specific smart objects with the system. IoT is a combination of various objects that are fixed invisibly around the globe [5, 10]. Health monitoring (HM) is one of the major research sectors in terms of skin attachable electronic devices. Smart HM means controlling and computing of the remote HM devices along with IoT [5, 11]. Employing advanced modern hardware sensors in the medical sector helps to generate a new technology called the Internet of medical things (IoMT) [4]. The aim of smart healthcare is the efficient monitoring of the patients through efficient patient information sharing, emergency servicing, patient monitoring, and so on to reduce the risk of the patient's life. The smart healthcare field imposes information technology for developing advanced applications to improve medication and diagnostic procedures [25, 26]. Kumar et al. gave many solutions for detecting the object from images using machine learning algorithms [27–30]. Modern methods and research theories are the majority structures that produce large amounts of digital information [4]. Diabetes is a long-lasting disease all over the world, which begins when the human body losses the capability to synthesize a hormone called insulin. The world health organization (WHO) announced that diabetes was a chronic disease that resulted in 1.6 million deaths in the year 2016 [6, 7]. Patients affected with diabetes produce high levels of glucose in the blood that damages the organs of the body [6]. The features of the healthcare models comprise insufficient medical data, clogged information, warnings in data, and so on. Hence, to overcome this challenge, skin attachable sensors that are associated with the Internet of Things (IoT) with big data emerged in the present world [3, 8]. When compared to the olden days, nowadays IoT and AI methods help to predict the various health issues accurately [6].

In the smart healthcare scenario, the patient's information is stored in the server, and as per the requirement, it can be retrieved and the necessary diagnosis can be performed. For the diagnosis of the disease, various deep learning techniques are implemented on the basis of the structural data of the anatomical system known as artificial neural networks (ANNs). Widely known deep learning methods, such as recurrent neural networks (RNN), deep belief networks (DBN), convolutional neural networks (CNN), hybrid neural networks, and deep neural networks (DNN), are employed to process the health data. In the last few years, deep learning methods have gained attention in the field of IoT to enhance security by finding solutions to threats [2]. The accuracy of the deep learning techniques can be further enhanced by using the optimization algorithms such as cuckoo optimization [17, 20], particle swarm optimization [18], crow search algorithm [24], and so on.

1.1. Internet of Health Things. Recently, IoT (Internet of Things) has been said to be one of the promising technologies from which healthcare received significant benefits, as illustrated in Figure 1. In such a way, [31] presented a comprehensive review on IoT in healthcare, which could be determined as IoHT (Internet of Health Things). Furthermore, this study identifies technical advances and its corresponding limitations to be overcome. The study also suggested that further studies are more essential in this field for improvising the current challenges faced by IoHT. Finally, the study stated that this comprehensive review will be a great information source to the healthcare providers, technology specialists, researchers, as well as general population for improvising IoHT. An efficient cryptosystem for securing the transmission of MRI images in the IoHT (Internet of Health Things) environment has been reported by [32]. This study investigated the dynamic of 2-dimension trigonometric map, which has infinite solutions. Furthermore, the study utilized phase portrait, bifurcation diagram, and Lyapunov exponent for demonstrating the complex dynamics of the map. From the performance analysis of the suggested cryptosystem, it can be concluded that it is highly secure and can be utilized in the internet of health things for the transmission of medical images in a secured manner.

Normally, deep learning techniques are implemented to improve the performance to predict the security threats in IoT [2]. The PIMA dataset is used for disease prediction, which is subjected to pre-processing for eliminating the unwanted noises in the data. The preprocessed data are then fed to the feature extractor for extracting the required features, which are then passed to the classifier that classifies the data. The biases and weights of the classifier are tuned optimally using the cuckoo search optimization, which altogether efficiently predicts the disease.

1.2. Proposed Cuckoo Search-Based Conv LSTM Classifier. The proposed disease prediction model is designed based on the cuckoo search-based deep LSTM classifier such that the internal modal parameters of the classifier are tuned using the cuckoo search optimization, which is a nature-inspired algorithm that chooses the best parameter set for predicting the diseases.

The accomplishment of the research is as follows: section 1 enumerates the purpose for the disease prediction, section 2 explains the existing works and the vulnerabilities, section 3 explains the methodology for the proposed method, section 4 illustrates the results and the comparative analysis of the proposed over the exiting conventional methods, and section 5 deliberates the conclusion of the research work.

2. Motivation

In this segment, the reviews of the existing methods and the vulnerabilities of the existing methods are explained in detail.

2.1. Literature Review. The review of various pieces of research is as follows: Huma Naz and Sachin Ahuja [1] implemented a machine learning algorithm using the PIMA dataset. This method used different classifiers to predict the disease accurately but failed to diagnose the disease in the early stage. Usman Ahmad and others. [2] employed an artificial neural network (ANN) that effectively predicted the disease in the case of small datasets. Yet, this method is ineffective for larger datasets. Nithya Rekha Sivakumar and Faten Khalid Diaaldin Karim [3] explained the equidistant heuristic and duplex deep neural network (EH-DDNN) that enhanced the detection accuracy of diabetics. Though this method outperformed the existing methods, the prediction time must be lowered. Romany Fouad Mansour and others. [4] illustrated a new AI and IoT convergence-based disease diagnosis model for a smart healthcare system. This method had a higher prediction accuracy regarding the diagnoses of heart diseases and diabetes, however, there is no feature selection method, and hence, it had complex computations. Simanta Shekhar Sarmah [5] explained that the deep learning modified neural network (DLMNN) achieved higher data security, however, the disease detection rate had to be enhanced. The prediction based on machine learning using optimization was developed by [17]. The developed method obtained better accuracy in prediction with minimal computational cost, however, the slow convergence is considered to be the drawback of the method. The fuzzy-based classification using optimization was developed by [18] for the pattern classification. The minimal computation time with enhanced classification accuracy was obtained but failed to consider the preprocessing or postprocessing technique that enhances the quality of output. Disease prediction using the fuzzy technique was modeled by [19],

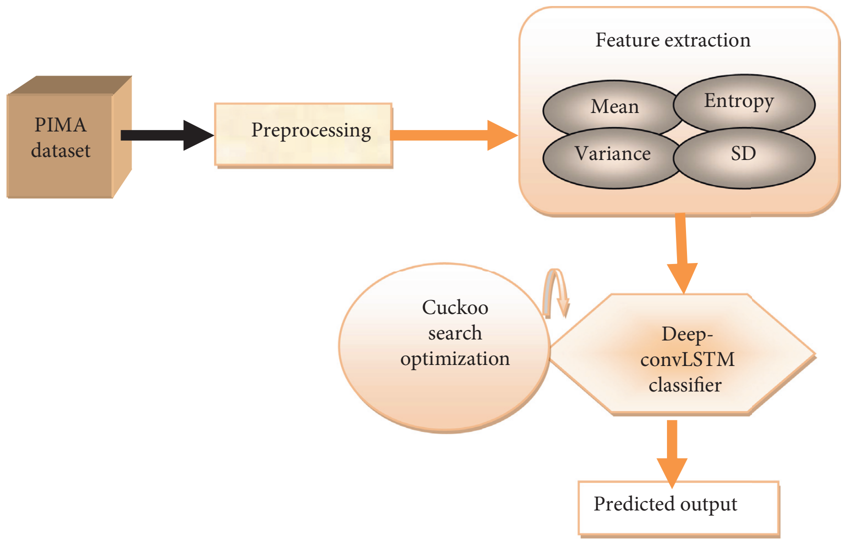

FIGURE 1: Disease prediction model using optimized convLSTM.

which obtained better classification accuracy. However, the updation of the fuzzy rules, and hence, the accuracy of the prediction is compromised under certain criteria. The estimation of the properties using the data was modeled by [20] using the optimization-based deep learning technique and obtained a more accurate estimation, however, the feature extraction is not considered, which may enhance the computational complexity of the system. The disease classification using the digital computer was developed by [21] using the segmentation and feature extraction with the support vector machine (SVM) but failed to enhance the accuracy by tuning the kernel function of the classifier. The ensemble-based classification of the disease was designed by [22, 23]. They obtained better classification accuracy using the most significant information selection but failed to consider the optimization that enhances the accuracy further. The healthcare monitoring using the IoMT was developed by [24] for the disease diagnosis. They obtained enhanced classification accuracy but failed to consider some of the significant features that may enhance the classification accuracy. IoT (Internet of things) is a combination of various communication devices and smart electronics that sense and communicate with each other. In recent years, IOT devices brought a revolution in the field of biomedical applications by looking at several challenges and complications faced in the past [33]. These IoT devices can generate a significant amount of biomedical data and also play a vital role in the development of existing automatic medical-data collection systems. When IoT devices are integrated with advanced ML (machine learning) algorithms, big data is essential for improvising these health systems in diagnosis, decision making, and treatment. IOT in biomedical applications has developed research areas in applications of IOE (Internet of everything), such as symptomatic treatments, observation of patients, and monitoring [25]. Additionally, the innovation of miniaturized healthcare sensors in monitoring the vital signs of the patient provided more security to the human healthcare system, and it offers more potential for early diagnosis and treatment. The security issues in IoT devices are bound to increase gradually because of the expeditious development and deployment of IoT systems. The importance of security further increases in H-IoT because security breach in it can lead to the loss of lives. Various pieces of research are employed for the accurate disease prediction using IoT devices, however, in a broader perspective, it is quite difficult to accurately predict the disease most of the times. Basically, the prediction is performed using the empirical and dynamic methods. The empirical approach utilizes the previous information or historical prediction, and this approach is most commonly used in the regression and artificial neural networks. The dynamic approach is utilized by the physical and statistical methods. The advancement of technology in recent years promotes disease prediction using the techniques of regression, support vector machine (SVM), and K-nearest neighbor (KNN). Deep learning models are useful in examining large datasets, and they provide factual information. It is useful in computational applications [34]. Numerous methods are used in disease prediction and are categorized into three groups, namely statistical, dynamic, and satellite-based methods [35, 36], and the statistical methods are frequently used because of their inexpensive and time-consuming nature [37]. In this context, the review of the existing prediction models with the challenges of the research is presented, which motivated the researchers in designing a prediction model based on ANN and optimization. Kaur et al. [38] presented disparate ML techniques that were aimed at real-time along with remote HM on IoT infrastructure and associated with cloud computing. In their proposed approach, it uses numerous input attributes associated with that disease. The prediction systems were employed in evaluating certain diseases, for instance, HD, breast cancer, liver disorders, diabetes, thyroid, dermatology, spect_heart, along with surgical data. Mohan et al. [39] proposed a method that found significant good features by applying ML techniques, resulting in enhancing the accuracy on the forecast of cardiovascular disease.

Shailendra Tiwari et al. proposed a hybrid-cascaded framework for image reconstruction [40–43].

2.2. Challenges. The vulnerabilities gone through by the researchers are as follows:

(i) Even though rapid miners are widely known for their data flow structure, the automatic optimization of larger medical data is vulnerable [1].

(ii) It is challenging to combine the larger medical information in the form of websites or applications with higher detection accuracy [1].

(iii) One of the main challenges is to get higher disease prediction performance for larger datasets on which most of the classifier depends [2].

The challenges faced by the existing disease prediction techniques are the failure to consider the preprocessing and postprocessing techniques that enhance the quality of prediction. Besides, the insignificant feature selection degrades the classification accuracy, and the failure to consider the same may enhance the computational complexity. Also, the failure to consider the optimization in the deep learning techniques reduces the classification accuracy. The above-mentioned challenges were solved using the proposed cuckoo search optimization based deep convolutional LSTM as it utilizes the pre-processing, most significant feature selection and optimization based deep learning mechanism to enhance the classification accuracy.

3. Proposed Disease Prediction Model Using Cuckoo Search-Based Deep Convolutional LSTM Classifier

Disease detection is essential to prevent serious health problems. Nowadays, IoT merged with deep learning methods is widely employed in various sectors. Hence, the healthcare sector is trying to implement IoT-based devices with the patients to effectively track the activities and disease-related capture for suggesting an effective diagnosis. Hence, in this research, a cuckoo search-based deep LSTM classifier is proposed for disease prediction for which the PIMA dataset [13] is used, which is preprocessed to remove the unwanted data, such as a negative value or infinity values. The processed data is then fed to the feature extractor, which draws only the appropriate features for evaluating the data. The extracted features are then sent to the classifier, where the cuckoo search algorithm is integrated to tune the biases and weights in the classifier. Figure 2 presented the disease prediction model using optimized convLSTM.

3.1. Read the Input Data. Initially, the data is obtained from the PIMA dataset [13], which is from the National Institute of Diabetes and Digestive and Kidney Diseases. The data is acquired from female patients above the age of 21 years and from an Indian background. The dataset is a combination of independent variables, such as insulin level, age, BMI index, and one dependent variable.

3.2. Preprocessing the Input Data. Preprocessing the data is one of the main processes to improve the performance of the method. It also transforms the raw data into processable data. Here, to execute the healthcare PIMA dataset, the missing value imputation method is employed, which removes the infinity values for efficient processing.

3.3. Feature Extraction. Feature extraction is the process of extracting the significant and essential data for prediction, which assures the effective presentation of the raw input data. In this research, feature extraction, including the statistical features, such as variance, mean, standard deviation, and entropy, are acquired.

3.3.1. Mean. Mean is a statistical feature, which is the ratio of the sum of the data to the total number of the data present in the database. It is mathematically represented as follows:

$$\text{mean} = \frac{1}{a}\sum_{t=1}^{a} R_t, \tag{1}$$

where a indicates the total instances and R_t indicates the t^{th} data.

3.3.2. Variance. The variance is the mean squared difference between each data and the mean, which is given by the following:

$$\text{variance} = \frac{1}{a-1} t \sum_{t=1}^{a} \left(R_t - \text{mean}\right)^2. \tag{2}$$

At different instances of time, the variance concentrates on minute changes, which enhances the prediction accuracy.

3.3.3. Standard Deviation (SD). Standard deviation shows the amount of variation or dispersion that exists at each instance of the data concerning mean. It is measured as the root of variance, which is given as follows:

$$\text{standard deviation} = \sqrt{\frac{1}{a-1} t \sum_{t=1}^{a} \left(R_t - \text{mean}\right)^2}. \tag{3}$$

3.3.4. Entropy. Entropy is the probability of the total number of ways the data can be arranged, which is formulated as follows:

$$\text{entropy} = -\sum_{x=1}^{A} b_x \log_2 b_x, \tag{4}$$

where b_x denotes the probability of the data, and x indicates the possible sample values.

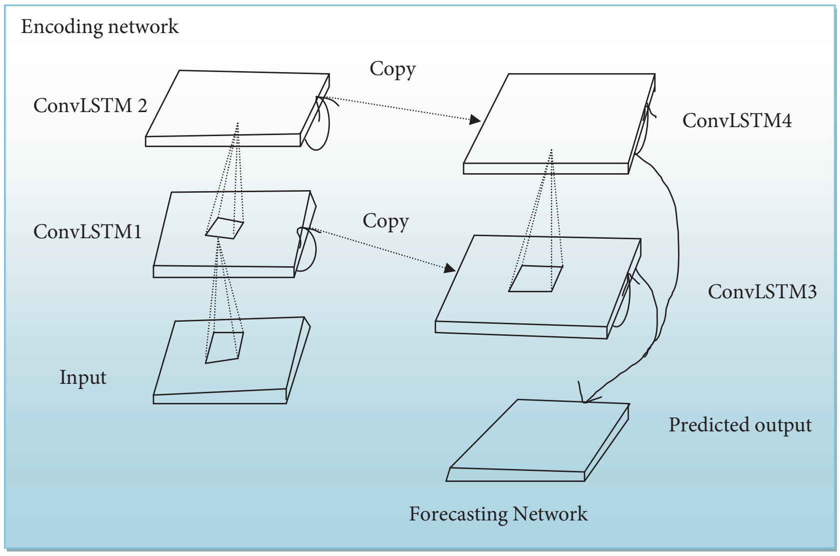

Figure 2: Architecture of deep-ConvLSTM.

3.4. Disease Prediction Using the Proposed Cuckoo-Based Deep-ConvLSTM Classifier. Disease prediction at the early stage is essential to improve the health of the patients. Hence, in this research, a deep learning model is implemented in the IoT systems for the efficient prediction of diseases. In the deep convolutional LSTM classifier, the convolution operation is merged with the long-short term memory. Here, the multiplication operation is replaced with a convolution operation, which records the essential spatial features for effective disease prediction. The cuckoo search algorithm is employed for tuning the weights and bias of the deep-convLSTM classifier. In this optimization, this bird has the best communication nature and chooses only the best eggs, and the selection characteristics of the cuckoo are integrated with the classifier in the internal modal parameter tuning that improves the prediction performance.

3.4.1. Architecture of Deep-ConvLSTM Classifier. Figure 1 shows the architectural explanation for the deep Conv LSTM classifier. The Conv LSTM is arranged as 3D tensors with $F_1, \ldots\ldots\ldots F_\beta$ as inputs, $G_1, \ldots\ldots\ldots G_\beta$ as cell outputs, $K_1, \ldots\ldots\ldots\ldots K_\beta$ as the hidden states, and $H_\beta, I_\beta, J_\beta$ as the gates of the Conv LSTM. Conv LSTM uses a large transitional kernel for efficient feature patterns. For efficient prediction, they are assembled as encoding layers and forecasting layers. The cell output and the initial states of the encoding layer are copied to the forecasting network. The dimensions of the predicted output are the same as the input. Hence, they are combined and sent to the [1 × 1] convolutional layer for the final prediction of output. The output of the input gate is expressed as follows:

$$H_\beta = \alpha\left(\eta_H^F * F_\beta + \eta_H^K * K_{\beta-1} + \eta_H^G \circ G_{\beta-1} + \gamma^H\right). \tag{5}$$

Here, F_β denotes the input vector, η_H^F denotes the weight between the input layer and input gate, α is the gate activation function, η_H^K denotes the weight between the input layer and the memory output, η_H^G denotes the input layer and the cell output, and $K_{\beta-1}, G_{\beta-1}$ are the preceding outputs of the cell and memory unit, respectively. γ^H denotes the bias of the input layer, $*$ is the convolutional operator, and $\circ$ is the element-wise multiplication. The forget gate output is expressed as follows:

$$I_\beta = \alpha\left(\eta_I^F * F_\beta + \eta_J^K * K_{\beta-1} + \eta_J^G \circ G_\beta + \gamma^J\right). \tag{6}$$

Here, η_I^F denotes the weight in between the input layer and the forget gate, η_I^K denotes the weights for the connections in between the output gate and the memory units of the previous layers, η_I^G denotes the weight in between the output gates and the cell, and γ^I is the bias regarding the forget gate. The result of the output gate is expressed as follows:

$$J_\beta = \alpha\left(\eta_J^F * F_\beta + \eta_J^K * K_{\beta-1} + \eta_J^G \circ G_\beta + \gamma^J\right). \tag{7}$$

Here, η_J^F indicates the weight in between the output gate and the input layer, η_J^K indicates the weight in between the output gate and the memory unit, η_J^G indicates the weight in the middle of the output gate and the cell, and γ^J is the output gate. The output of the temporary cell state is formulated as follows:

$$\widetilde{G}_\beta = \tanh\left(\eta_L^F * F_\beta + \eta_L^K * K_{\beta-1} + \gamma^L\right). \tag{8}$$

Here, η_L^F denotes the weight in the middle of the cell and the input layer, η_L^K denotes the weight in between the cell and the memory unit, and γ^L is the bias of the cell. The output of the cell is given as follows:

$$\begin{aligned} G_\beta &= I_\beta \circ G_{\beta-1} + H_\beta \circ \widetilde{G}_\beta G_\beta \\ &= I_\beta \circ G_{\beta-1} + H_\beta \circ \tanh\left(\eta_L^F * F_\beta + \eta_L^K * K_{\beta-1} + \delta^L\right). \end{aligned} \tag{9}$$

The output from the memory unit is expressed as follows:

$$K_\beta = J_\beta \circ \tan h\left(G_\beta\right). \quad (10)$$

Here, K_β is the output of the memory block, and J_β denotes the output gate. The output of the output layer is expressed as follows:

$$N_\beta = \lambda\left(\eta_N^K \cdot K_\beta + \gamma^N\right), \quad (11)$$

where η_N^K denotes the weight between the output vector and the memory unit, and γ^N is the bias of the output layer. Hence, the bias and the weights are represented as follows:

$$\begin{aligned} &\gamma \in \left\{\gamma^L, \gamma^I, \gamma^J, \gamma^H\right\}, \\ &\eta \in \left\{\eta_N^K, \eta_L^F, \eta_L^K, \eta_J^F, \eta_J^K, \eta_J^G, \eta_I^F, \eta_I^K, \eta_I^G, \eta_H^F, \eta_H^K, \eta_H^G\right\}. \end{aligned} \quad (12)$$

3.4.2. Mathematical Model for Cuckoo Search Optimization. The weights η and bias γ for the deep Conv LSTM classifier are generated using the cuckoo search algorithm, where the cuckoos are known for their wonderful voices and their breeding process. They lay their eggs in the nest of other birds, which resemble their eggs. Hence, the host bird considers the cuckoo eggs to be their eggs and feeds them. Thus, the cuckoos protect their eggs from dying, and when eggs are hatched, the cuckoo chick throws out the host eggs from the nest. Hence, they receive more food from the host nest, however, if the host bird discovers these eggs, they throw these eggs or leave their nest and build a new one [12]. There are three basic rules in cuckoo search optimization, which are as follows:

(1) Cuckoos choose a host nest for preserving their eggs.
(2) Nests with high quality have good eggs that are taken to the future generation.
(3) The total number of the host nests will be decided along with the probability that the host can find the cuckoo eggs.

Population initialization: cuckoos initialize the chosen nests for preserving their hatched eggs. The objective function is indicated as, $d(g), g = (g_1, \ldots, g_i)$.

The equation for initializing the host nest is expressed as, $g_j\,(j = 1, 2, \ldots, y)$., where y denotes the nest.

Fitness evaluation: fitness evaluation is carried out on the basis of accuracy. If the obtained fitness value is greater than the previous iteration, then the obtained value is chosen as the best solution, which is given as the condition $Q_j > Q_v$., where Q denotes the fitness, and v is the randomly chosen nest in y.

Position updating: the generation of new solutions, $g_j^{(k+1)}$, for cuckoo j, a levy flight can be carried out.

$$g_j^{(k+1)} = g_j^{(k)} + \mu \oplus \mathrm{Levy}(\theta), \quad (13)$$

where $\mu > 0$ denotes the step size of the problem, and $\oplus$ denotes the entry-wise multiplication.

Levy distribution for a large number of steps is expressed as follows:

$$\mathrm{Levy} \sim h = k^{-\theta}, \quad (1 < \theta \leq 3). \quad (14)$$

Termination: cuckoos find the eggs of other birds in the nest, with the probability given as $P_c \in [0, 1]$. The cuckoos discard them from the nest and build a new nest by updating their position through levy flights, thereby repeating the iteration until it reaches the best fitness solution to generate a global optimal solution. Algorithm 1 presented the pseudocode for the proposed cuckoo-based deep convLSTM.

Algorithm 1: the pseudocode for the proposed cuckoo-based deep convLSTM.

S.NO Pseudocode for the proposed cuckoo-based deep convLSTM

(1) Input: g_j
(2) Output: $g_{j,\mathrm{best}}$
(3) Initialize the population
(4) Fitness evaluation termination
(5) If $Q_j > Q_v$
(6) Replace the new solution
(7) end
(8) While $k <$ maximum generation
(9) New solution generated using the equation (13) and (12)
(10) Re-evaluate the fitness
(11) New optimal global solution, g_{best}
(12) End while
(13) end

4. Results and Discussion

This section illustrates the experimental analysis and the comparative results acquired while using the proposed cuckoo-based deep convLSTM model.

4.1. Experimental Setup. The MATLAB tool is used for the implementation of the proposed method for predicting diseases. The MATLAB tool is established in the Windows 10 OS and 64 bit operating systems with 16 GB RAM, which provides an efficient and simple implementation of the proposed method.

4.2. Data Description. PIMA dataset is employed for the prediction of the diabetic disease. Originally, this dataset is obtained from the National Institute of Diabetes and Digestive and Kidney Diseases. The dataset includes female patients above 21 years with an Indian background. The dataset is the combination of independent variables, such as insulin level, age, BMI index, and one dependent variable. The sample record is depicted in Figure 3.

4.3. Evaluation Metrics. The disease prediction ability of the proposed cuckoo-based deep convLSTM is analyzed based

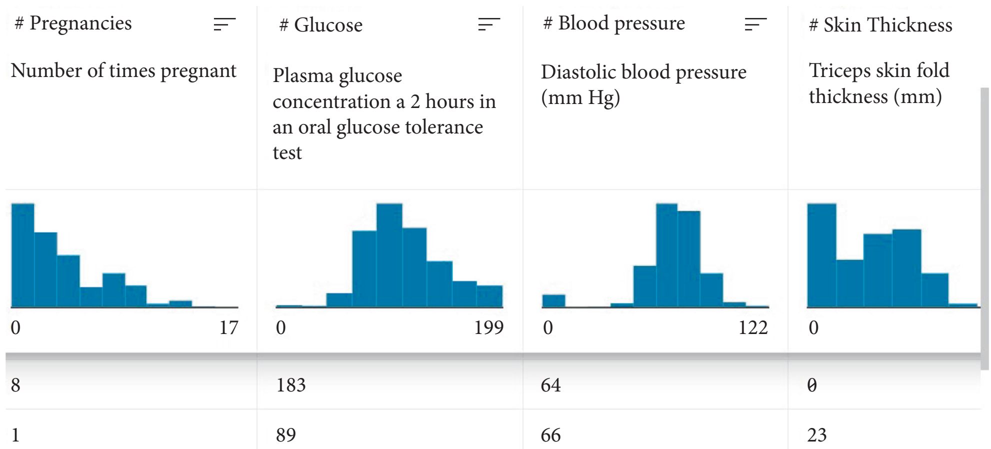

Figure 3: Sample record of database.

on accuracy, sensitivity, and specificity. They are enumerated as follows:

4.3.1. Accuracy. Accuracy is the nearness of the predicted output obtained by the proposed method to the standard value, which is mathematically expressed as follows:

$$\text{accuracy} = \frac{\text{measured positive} + \text{measured negative}}{\text{true positive} + \text{true negative}}. \tag{15}$$

4.3.2. Sensitivity. Sensitivity is the ability to identify patients with the diabetic disease correctly by the proposed method for efficient prediction, which is mathematically formulated as follows:

$$\text{sensitivity} = \left(\frac{\text{true positives}}{\text{total diseased}}\right). \tag{16}$$

4.3.3. Specificity. Specificity is the ability to identify patients with nondiabetic diseases correctly by the proposed method, which is mathematically formulated as follows:

$$\text{specificity} = \left(\frac{\text{true negative}}{\text{total real negative cases}}\right). \tag{17}$$

4.4. Comparative Analysis. In this section, the comparative analysis of the proposed cuckoo-based deep convLSTM is deployed for the efficient detection of diabetic disease. The methods considered for comparative analysis are ANN [14], CNN [15], deep convLSTM [16], MDCNN [23], and MSSO-ANFIS [24].

4.4.1. Comparative Analysis in terms of the Training Percentage. The proposed cuckoo-based deep Conv LSTM is compared with the existing conventional methods, such as ANN, CNN, and deep convLSTM. Figure 4(a) illustrates the analysis concerning the accuracy. The accuracy of the conventional methods and the proposed methods in terms of the training percentage of 80% are 91.99%, 95.56%, 82.96%, 87.02%, 94.17%, and 96.95%, respectively, for the methods, such as MSSO-ANFIS, MDCNN, ANN, CNN, Deep-Conv LSTM, and proposed Cuckoo-based Deep-Conv LSTM. Figure 4(b) illustrates the analysis with respect to sensitivity. The sensitivity of the conventional methods and the proposed methods in terms of the training percentage of 70% are 88.56%, 92.08%, 80.61%, 83.73%, 90.78%, and 93.39%, respectively, for the methods, such as MSSO-ANFIS, MDCNN, ANN, CNN, Deep-Conv LSTM, and proposed Cuckoo-based Deep-Conv LSTM. Figure 4(c) illustrates the analysis with respect to the specificity. The specificity of the conventional methods and the proposed methods in terms of the training percentage of 40% are 89.05%, 90.70%, 83.34%, 86.80%, 90.09%, and 91.30%, respectively, for the methods, such as MSSO-ANFIS, MDCNN, ANN, CNN, Deep-Conv LSTM, and proposed Cuckoo-based Deep-Conv LSTM.

4.4.2. Comparative Analysis in terms of K-fold. The proposed cuckoo-based deep convLSTM is compared with the existing conventional methods, such as ANN, CNN, and deep convLSTM. Figure 5(a) illustrates the analysis with respect to the accuracy. The accuracy of the conventional methods and the proposed methods in terms of the k-fold = 5 are 79.80%, 80.39%, 75.62%, 78.74%, 79.92%, and 80.87%, respectively, for the methods, such as MSSO-ANFIS, MDCNN, ANN, CNN, Deep-Conv LSTM, and proposed Cuckoo-based Deep-Conv LSTM. Figure 5(b) illustrates the analysis with respect to the sensitivity. The sensitivity of the conventional methods and the proposed methods in terms of the k-fold of 7 are 77.83%, 78.44%, 73.49%, 76.04%, 77.25%, and 79.63%, respectively, for the methods, such as MSSO-ANFIS, MDCNN, ANN, CNN, Deep-Conv LSTM, and proposed Cuckoo-based Deep-Conv LSTM. Figure 5(c) illustrates the analysis with respect to specificity. The specificity of the conventional methods and the proposed methods in terms of the k-fold of 9 are 88.26%, 88.38%, 85.80%, 87.63%, 87.86%, and 88.90%, respectively,

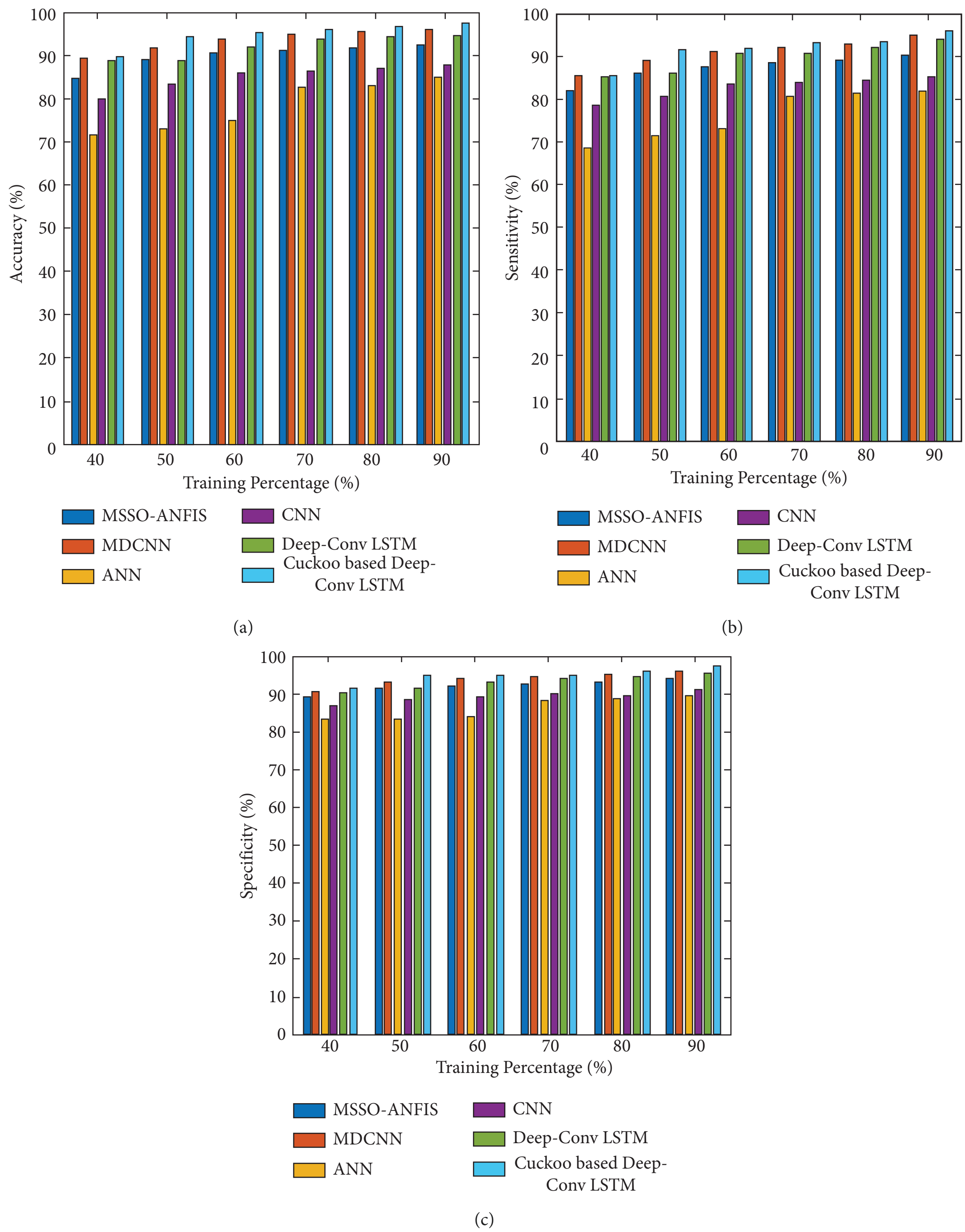

Figure 4: Analysis of the methods based on training percentage, (a) accuracy, (b) sensitivity, and (c) specificity.

for the methods, such as MSSO-ANFIS, MDCNN, ANN, CNN, Deep-Conv LSTM, and proposed Cuckoo-based Deep-Conv LSTM.

4.5. Comparative Discussion. Table 1 depicts the comparative Analysis of the proposed method, in which the best performance is obtained by the proposed method in terms of the performance metrics by varying the training and the K-Fold values. The maximal accuracy obtained by the proposed method is 97.59%, which shows 5.01%, 1.46%, 12.74%, 10.03%, and 2.92% superior performance as compared to the existing MSSO-ANFIS, MDCNN, ANN, CNN, and Deep-Conv LSTM methods, respectively. The maximal sensitivity obtained by the proposed method is 95.87%, which shows 5.63%, 0.99%, 14.55%, 11.26%, and 1.98% superior performance as compared to the existing MSSO-ANFIS, MDCNN, ANN, CNN, and Deep-Conv LSTM

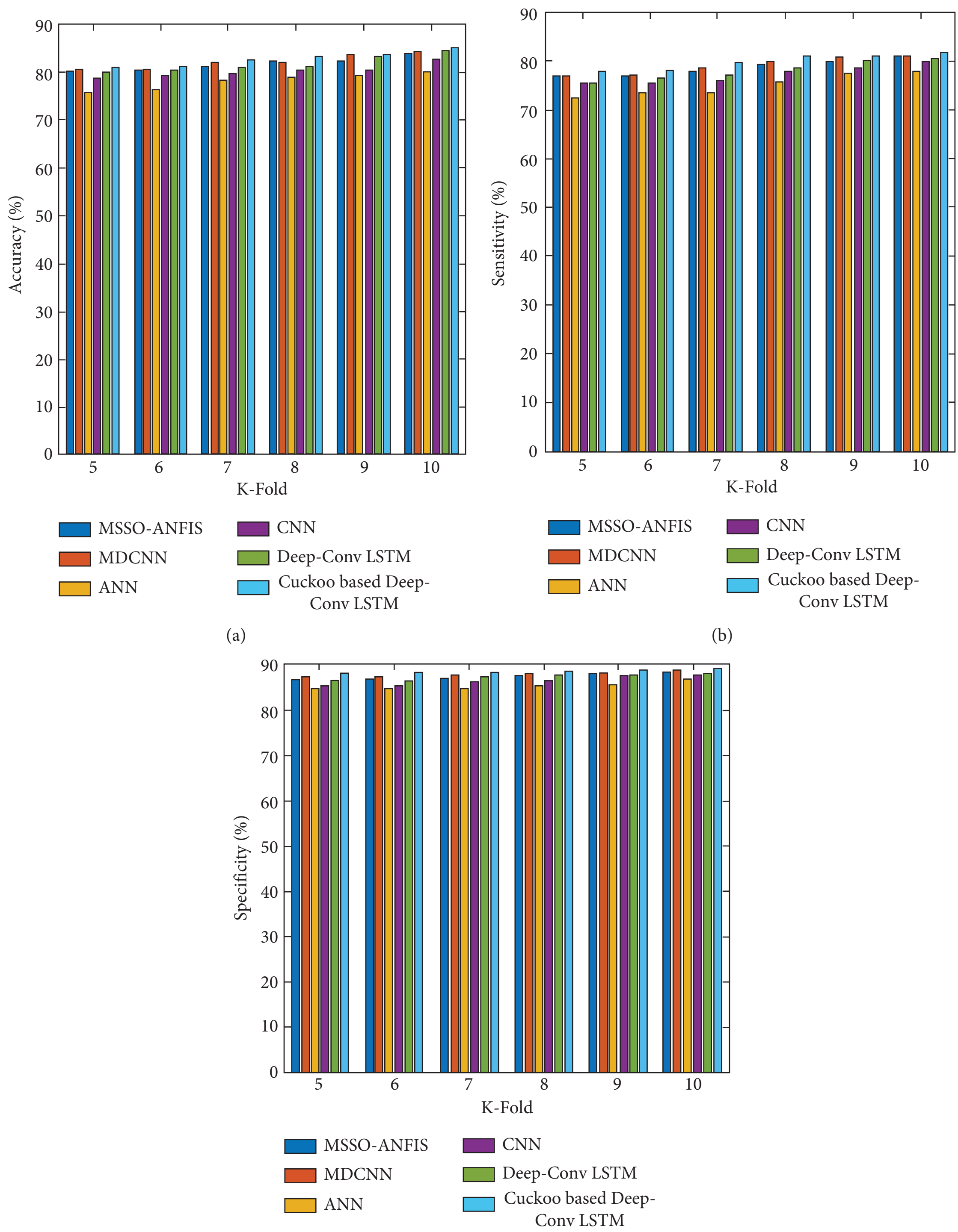

Figure 5: Analysis of the methods based on k-fold. (a) Accuracy, (b) sensitivity, and (c) specificity.

Table 1: Comparative analysis.

Method/Metrics		MSSO-ANFIS	MDCNN	ANN	CNN	Deep-conv LSTM	Proposed cuckoo-based deep-conv LSTM
Training percentage	Accuracy (%)	92.70	96.17	85.15	87.80	94.74	97.59
	Sensitivity (%)	90.47	94.92	81.92	85.08	93.97	95.87
	Specificity (%)	94.07	96.13	89.14	91.04	95.17	97.09
K-fold	Accuracy (%)	83.95	84.67	80.03	82.72	84.17	85.18
	Sensitivity (%)	80.86	81.12	77.78	79.97	80.50	81.74
	Specificity (%)	88.53	88.63	86.80	87.85	88.04	89.22

methods, respectively. The maximal specificity obtained by the proposed method is 97.09%, which presents 3.11%, 0.98%, 8.19%, 6.23%, and 1.97% superior performance as compared to the existing MSSO-ANFIS, MDCNN, ANN, CNN, and Deep-Conv LSTM methods, respectively.

The proposed method obtained elevated performance compared to the existing techniques in terms of performance metrics. It is because the proposed method utilizes the preprocessing of the input data, which removed the noises and artifacts. Then, the most significant feature extraction reduces the computational complexity by eliminating the less informative features. Finally, the diabetic disease prediction using the proposed cuckoo search optimization-based Deep-Conv LSTM enhances the prediction accuracy through the optimal tuning of weights and biases.

5. Conclusion

The proposed cuckoo-based deep convLSTM model is deployed for the prediction of diseases with higher efficiency. The data from the PIMA dataset is used and for effective prediction missing value imputation method is employed for processing the data. The cuckoo search optimization, which is a nature-inspired algorithm, is deployed with a deep convLSTM classifier as it effectively predicts the disease by transferring the information, thus reducing time consumption. A deep convLSTM classifier enhances the disease prediction ability through a convolution operation based on the weights and features, which generates highly refined information regarding the input data. The proposed method is compared with the conventional methods and revealed that the proposed method achieved 97.591%, 95.874%, and 97.094% of accuracy, sensitivity, and specificity, respectively. In the future, more datasets and highly advanced algorithms will be designed to further boost the classifier performance.

Data Availability

Data will be available on request. For the data related queries, kindly contact Ashwani Kumar at ashwani.kumarcse@gmail.com.

Conflicts of Interest

The authors declare that they have no conflicts of interest.

References

[1] H. Naz and S. Ahuja, "Deep learning approach for diabetes prediction using PIMA Indian dataset," *Journal of Diabetes and Metabolic Disorders*, vol. 19, no. 1, pp. 391–403, 2020.

[2] U. Ahmad, H. Song, A. Bilal et al., "A novel deep learning model to secure internet of things in healthcare," in *Machine Intelligence and Big Data Analytics for Cybersecurity Applications*, pp. 341–353, Springer, Cham, 2021.

[3] N. R. Sivakumar and D. K. Faten Khalid, "An IoT based big data framework using equidistant heuristic and duplex deep neural network for diabetic disease prediction," *Journal of Ambient Intelligence and Humanized Computing*, pp. 1–11, 2021.

[4] R. F. Mansour, A. E. Amraoui, I. Nouaouri, V. G. Diaz, D. Gupta, and S. Kumar, "Artificial intelligence and internet of things enabled disease diagnosis model for smart healthcare systems", *IEEE Access*, vol. 9, pp. 45137–45146, 2021.

[5] S. S. Sarmah, "An efficient IoT-based patient monitoring and heart disease prediction system using deep learning modified neural network," *IEEE Access*, vol. 8, pp. 135784–135797, 2020.

[6] A. K. Jaiswal, P. Tiwari, S. Kumar, M. S. Al-Rakhami, M. Alrashoud, and A. Ghoneim, "Deep learning-based smart IoT health system for blindness detection using retina images," *IEEE Access*, vol. 9, pp. 70606–70615, 2021.

[7] W. H. Organization, "Death among diabetic patients," 2016, http://www.who.int/diabetes/global-report/en.

[8] B. A. Muthu, C. B. Sivaparthipan, G. Manogaran et al., "IOT based wearable sensor for diseases prediction and symptom analysis in healthcare sector," *Peer-to-peer networking and applications*, vol. 13, no. 6, pp. 2123–2134, 2020.

[9] P. K. Gupta, B. T. Maharaj, and R. Malekian, "A novel and secure IoT based cloud centric architecture to perform predictive analysis of users activities in sustainable health centres," *Multimedia Tools and Applications*, vol. 76, no. 18, pp. 18489–18512, 2017.

[10] P. Verma, S. K. Sood, and S. Kalra, "Cloud-centric IoT based student healthcare monitoring framework," *Journal of Ambient Intelligence and Humanized Computing*, vol. 9, no. 5, pp. 1293–1309, 2018.

[11] M. Subramaniyam, D. Singh, S. J Park et al., "IoT based wake-up stroke prediction-Recent trends and directions," in *IOP Conference Series: Materials Science and Engineering*vol. 402, no. 1, IOP Publishing, Article ID 012045, 2018.

[12] A. H. Gandomi, X.-S. Yang, and A. Hossein Alavi, "Cuckoo search algorithm: a metaheuristic approach to solve structural optimization problems," *Engineering with Computers*, vol. 29, no. 1, pp. 17–35, 2013.

[13] Pima, 2021, https://www.kaggle.com/kumargh/pimaindiansdiabetescsv.

[14] H. Kukreja, N. Bharath, C. S. Siddesh, and S. Kuldeep, "An introduction to artificial neural network," *International Journal of Advance Research and Innovative Ideas in Education*, vol. 1, pp. 27–30, 2016.

[15] U. R. Acharya, L. O. Shu, Y. hagiwara et al., "A deep convolutional neural network model to classify heartbeats," *Computers in Biology and Medicine*, vol. 89, pp. 389–396, 2017.

[16] S. H. I. Xingjian, Z. Chen, H. Wang, D.-Y. Yeung, W.-K. Wong, and W.-C. Woo, "Convolutional LSTM network: a machine learning approach for precipitation nowcasting," in *Advances in Neural Information Processing Systems*, pp. 802–810, 2015.

[17] P. K. Jain, E. Admasu Yekun, R. Pamula, and G. Srivastava, "Consumer recommendation prediction in online reviews using Cuckoo optimized machine learning models," *Computers & Electrical Engineering*, vol. 95, 2021.

[18] S. Ganapathy, R. Sethukkarasi, P. Yogesh, P. Vijayakumar, and A. Kannan, "An intelligent temporal pattern classification system using fuzzy temporal rules and particle swarm optimization," *Sādhanā*, vol. 39, pp. 283–302, 2014, Part 2.

[19] U. Kanimozhi, S. Ganapathy, D. Manjula, and A. Kannan, "An intelligent risk prediction system for breast cancer using fuzzy temporal rules," *National Academy Science Letters*, vol. 42, no. 3, 2018.

[20] G. Zargara, A. Ayatizadeh Tanhaa, A. Parizada, M. Amouri, and H. Bagheri, "Reservoir Rock Properties Estimation Based

on Conventional and NMR Logdata using ANN-Cuckoo," *A case study in one of super fields in Iran southwest", Petroleum*, vol. 6, pp. 304–310, 2020.
[21] V. Halampathy Jeyapaul, L. Naidu, H. Khanna Nehemiah, G. Sannasi, and A. Kannan, "Identification and classification of pulmonary nodule lung modality using digital computer," *Appl. Math. Inf. Sci*, vol. 12, no. 2, pp. 451–459, 2018.
[22] B. Chithra and R. Nedunchezhian, "Dynamic neutrosophic cognitive map with improved cuckoo search algorithm (DNCM-ICSA) and ensemble classifier for rheumatoid arthritis Disease," *Journal of King Saud University – Computer and Information Sciences*, vol. 7, 2020.
[23] M. A. Khan, "An IoT framework for heart disease prediction based on MDCNN classifier," *IEEE Access*, vol. 8, no. No, 2020.
[24] M. A. Khan and F. Algarni, "A healthcare monitoring system for the diagnosis of heart disease in the IoMT cloud environment using MSSO-ANFIS," *IEEE Access*, vol. 8, 2020.
[25] M. A. Khan, M. T. Quasim, N. S. Alghamdi, and M. Y. Khan, "A secure framework for authentication and encryption using improved ECC for IoT-based medical sensor data," *IEEE Access*, vol. 8, 2020.
[26] S. K. Patel, "Attack detection and mitigation scheme through novel authentication model enabled optimized neural network in smart healthcare," *Computer Methods in Biomechanics and Biomedical Engineering, Priniting ahead*, vol. 4, 2022.
[27] A. Kumar, "A cloud-based buyer-seller watermarking protocol (CB-BSWP) using semi-trusted third party for copy deterrence and privacy preserving," *Multimedia Tools and Applications*, pp. 1–32, 2022.
[28] A. Kumar, "Design of secure image fusion technique using cloud for privacy-preserving and copyright protection," *International Journal of Cloud Applications and Computing*, vol. 9, no. 3, pp. 22–36, 2019.
[29] A. Kumar, "A review on implementation of digital image watermarking techniques using LSB and DWT," in *Proceedings of the Third International Conference on Information and Communication Technology for Sustainable Development (ICT4SD 2018)*, Goa, India, August 30-31,2018.
[30] A. Kumar, Z. J. Zhang, and H. Lyu, "Object detection in real time based on improved single shot multi-box detector algorithm," *EURASIP Journal on Wireless Communications and Networking*, vol. 2020, no. 1, pp. 1–18, 2020.
[31] J. J. Rodrigues, D. B. D. R. Segundo, H. A. Junqueira, M. H. Sabino, R. M. Prince, J. Al-Muhtadi et al., "Enabling technologies for the internet of health things," *IEEE Access*, vol. 6, pp. 13129–13141, 2018.
[32] N. Tsafack, S. Sankar, B. Abd-El-Atty, J. Kengne, K. Jithin, A. Belazi et al., "A new chaotic map with dynamic analysis and encryption application in internet of health things," *IEEE Access*, vol. 8, pp. 137731–137744, 2020.
[33] A. Chandy, "A review on IoT based medical imaging technology for healthcare applications," *Journal of Innovative Image Processing (JIIP)*, vol. 1, pp. 51–60, 2019.
[34] R. Venkatesh, C. Balasubramanian, and M. Kaliappan, "Rainfall prediction using generative adversarial networks with convolution neural network," *Soft Computing*, vol. 25, no. 6, pp. 4725–4738, 2021.
[35] S. Davolio, M. M. Miglietta, T. Diomede, C. Marsigli, A. Morgillo, and A. Moscatello, "A meteo-hydrologicalprediction system based on a multi-model approach for precipitation forecasting," *Natural Hazards and Earth System Sciences*, vol. 8, pp. 143–159, 2008.
[36] T. Diomede, S. Davolio, C. Marsigli et al., "Discharge prediction based on multi-model precipitation forecasts," *Meteorology and Atmospheric Physics*, vol. 101, pp. 245–265, 2008.
[37] A. Tran, T. D. D. Duong, and V. Song Pham, "Improved rainfall prediction using combined pre-processing methods and feed-forward neural networks," *D-J Series*, vol. 2, no. 1, pp. 65–83, 2019.
[38] R. K. PavleenKaur and M. Kumar, "'A healthcare monitoring system using random forest and Internet of Things (IoT)," *Multimedia Tools and Applications*, vol. 78, no. 14, pp. 19905–19916, 2019.
[39] S. Mohan, C. Thirumalai, and G. Srivastava, "'Effective heart disease prediction using hybrid machine learning techniques," *IEEE Access*, vol. 7, pp. 81542–81554, 2019.
[40] M. Devi, S. Singh, S. Tiwari, S. C. Patel, and M. T. Ayana, "A survey of soft computing approaches in biomedical imaging," *Journal of Healthcare Engineering*, vol. 2021, Article ID 1563844, 11 pages, 2021.
[41] S. Tiwari, "A variational framework for low-dose sinogram restoration," *International Journal of Biomedical Engineering and Technology*, vol. 24, no. 4, pp. 356–367, 2017.
[42] V. P. Singh, R. Srivastava, Y. Pathak, S. Tiwari, and K. Kaur, "Content-based image retrieval based on supervised learning and statistical-based moments," *Modern Physics Letters B*, vol. 33, no. 19, Article ID 1950213, 2019.
[43] S. Tiwari and R. Srivastava, "An OSEM-based hybrid-cascaded framework for PET/SPECT image reconstruction," *International Journal of Biomedical Engineering and Technology*, vol. 18, no. 4, pp. 310–332, 2015.

Hindawi
Scientific Programming
Volume 2022, Article ID 5812546, 9 pages
https://doi.org/10.1155/2022/5812546

Research Article

Deep Reinforcement Learning for Stock Prediction

Junhao Zhang [1] and Yifei Lei [2]

[1] *Zhejiang University, School of Economics, Zhejiang, China*
[2] *Zhejiang University, School of the Public Affairs, Zhejiang, China*

Correspondence should be addressed to Junhao Zhang; 12101010@zju.edu.cn

Received 11 December 2021; Revised 21 January 2022; Accepted 25 January 2022; Published 30 April 2022

Academic Editor: Punit Gupta

Investors are frequently concerned with the potential return from changes in a company's stock price. However, stock price fluctuations are frequently highly nonlinear and nonstationary, rendering them to be uncontrollable and the primary reason why the majority of investors earn low long-term returns. Historically, people have always simulated and predicted using classic econometric models and simple machine learning models. In recent years, an increasing amount of research has been conducted using more complex machine learning and deep learning methods to forecast stock prices, and their research reports also indicate that their prediction accuracy is gradually improving. While the prediction results and accuracy of these models improve over time, their adaptability in a volatile market environment is questioned. Highly optimized machine learning algorithms include the following: FNN and the RNN are incapable of predicting the stock price of random walks and their results are frequently not consistent with stock price movements. The purpose of this article is to increase the accuracy and speed of stock price volatility prediction by incorporating the PG method's deep reinforcement learning model. Finally, our tests demonstrate that the new algorithm's prediction accuracy and reward convergence speed are significantly higher than those of the traditional DRL algorithm. As a result, the new algorithm is more adaptable to fluctuating market conditions.

1. Introduction

One of the most common concerns of financial analysts and investors is making accurate predictions about stock prices [1], but it is also a difficult task for them [2]. This is because the majority of stock prices are highly volatile. Numerous different types of factors influence stock prices. Direct economic indicators such as fluctuations in consumer supply and demand and commodity price indexes are complex enough. Stock price changes have become increasingly elusive as a result of the global environment and investor's behavior [3]. Each factor generates forces in distinct directions, which eventually result in a change in the stock price. The correlation between various factors is frequently so obscure that it is difficult to identify the factors affecting stock prices, let alone build a model for stock price prediction on this basis.

According to today's popular value investment theory, the true value of a stock is usually determined by the market value of the company that issued it. Occasionally, however, stock prices deviate from rational market expectations. The volatility and dynamics of the stock price directly contradict the statistical model's and foundation's assumptions, frequently resulting in inaccurate or even negative prediction results [4, 5].

The well-known efficient market hypothesis argues that it is impossible to forecast the value of stocks and that their movement is random, effectively invalidating numerous attempts to forecast stock prices using historical data. However, a ten-year technical analysis reveals that the values of the majority of stocks are contained within their historical stock prices; thus, collecting and analyzing historical stock price movements is critical for forecasting future stock prices [6].

Machine learning (ML) is a highly effective technique that enables machines to learn autonomously via algorithms. Academia generally believes that machine learning has a strong ability to identify useful data and generalize patterns [7]. The advent of machine learning has resolved one of the most perplexing problems in stock price prediction: nonlinearity. Machine learning is particularly adept at detecting nonlinear patterns in data. Additionally, deep learning (DL), a method for extracting critical information from nonlinear time series that uses a multilevel network structure, performs even better.

Recent advances in machine learning and deep learning have enabled more accurate stock forecasting, and the majority of papers and studies have demonstrated that their models can outperform the market average or generate quite high returns. Certain fundamental machine learning (ML) models, such as feedforward neural networks (FFNN) and deep learning models, such as recurrent neural networks (RNN) with memory structure and dynamics, are, however, incapable of forecasting data with unstable time series and long-term autoregression [8].

Reinforcement learning (RL) is a subfield of deep learning that is distinct from other fields such as statistical data analysis and supervised learning. It is a strategy that seeks to maximize profits while adapting constantly to changes in the environment in which it operates. Supervised learning's objective is to condense the mapping from input to output, which frequently results in the omission of critical information. Due to the frequency and duration of stock price fluctuations, reinforcement learning (RL) is a more suitable predictive tool for statistical analysis of data than supervised learning.

RL can be classified into five categories based on its sample efficiency: (1) model-based, (2) off-policy, (3) actor-critic, (4) on-policy, and (5) evolutionary gradient-free. In this case, 1 is the most efficient sample size option, while 5 is the least efficient. Among them, model-based and non-policy methods, such as TD-learning [9] and Q-learning [10], are referred to as "the critic-only methods" [11] and are used to solve discrete area optimization problems. Luo et al. pioneered the use of the TD algorithm [12]. She believes that the stock price prediction problem can be optimized using reinforcement learning algorithms as a Markov process. She used a reinforcement learning algorithm called TD (0), which only learns through experience, to determine the state value of each state that corresponds to the current stock price trend.

On-policy and evolutionary gradient-free methods are often referred to as "the actor-only method" [13]. One of its applications is policy gradient [14], which can learn parameterized strategies via continuity. The middle section, dubbed "the actor-critic method," [15], is a synthesis of the two methods discussed previously. It is capable of optimizing the ultimate return while also calculating the parameterized strategy and adhering to the value creation of benefits principle.

In RL, the agent chooses which action to take in order to maximize his or her reward. This means that throughout the learning process, the agent maximizes the accumulated rewards and thus develops optimal strategies for a variety of problems. Now, researchers can apply reinforcement learning to a variety of interesting projects, including solving the Rubik's cube [16], improving unmanned driving [17], and Atari and first-person shooter game play [18, 19].

There have been many studies using reinforcement learning to predict stock prices and construct trading models. Lee et al. expanded the research field from simple stock forecasting to a trading system with risk management capabilities [8] and after that they changed the original single-agent research into a multiagent research, which increased the complexity of the system and more adapted to the research method of stocks in 2007 [1].

Other researchers approach the problem from the standpoint of raw data input. Moody et al. and others use financial data from the company as a quantitative basis [20]. Yue et al. proposed an optimal trading system inspired by sparse coding that is well suited for real-time high-frequency trading [21]. This method significantly improves the outcome of raw data selection.

However, the previous study did not completely extract useful financial data due to the noise and fluctuations inherent in a fluctuating market. This article will analyze and predict data using two machine learning frameworks: "critic-only DQN" and "actor-critic deep PG." DQN converts a single-layer network to a convolutional network with multiple layers. It not only enables experience replay but also enables our network to self-train using its memorized history, which more closely matches the time autocorrelation and intertemporal correlation that have emerged in the American market. The PG gradient descent algorithm is a superior strategy to the "Greedy Policy." It determines the rising direction of the objective function by computing its gradient and then adjusts the probability of the action based on its performance to maximize the return. Due to the stock market's relatively weak market power, it is frequently vulnerable to other factors. The optimal strategy based on greedy concepts frequently requires a significant amount of time to learn and is prone to overload problems. After implementing PG, the machine's load can be significantly reduced, and the time required for optimization strategies can be significantly reduced.

2. Fundamentals of Reinforcement Learning

In the context of reinforcement learning, an agent obtains information from the environment. The agent adapts the received data to the environment's current state. The AI then decides on an action to be taken based on the rewards associated with each choice. Moreover, each action alters the environment and the total number of reward points. Reinforcements for rewarding or punishing specific actions are immediately added on the basis of the new state. This interaction between action and environment will persist until the agent masters the art of choosing a decision strategy that maximizes the total return.

The terms above, rewards and environment, refer to two of the four critical factors affecting the RL problem as described by Sutton and Barto. Policies are similar to the rules we impose on ourselves when we operate in the environment. The reward function serves as the overarching goal of training and serves as the standard against which all other factors are measured. A value function specifies the value of a state or state-action pair, which indicates the long-run goodness of the state or state-action pair.

The flowchart is shown in Figure 1. The flowchart of RL illustrates the RL procedure for agent-environment interaction at a high level. In one process, the agent performs an action, in reply to the current state. Then, as a result of this action, the system receives a signal, a reward, r_{t+1}, to direct the behavior of the action in the subsequent time step and to adjust the state in the subsequent time step, using the probability function $f\,(a_t,\,s_t)$.

2.1. Agent-Environment Interaction in Reinforcement Learning. The goal of RL is to maximize the agent's reward in a limited number of actions by mapping environmental states to actions. The Markov decision process (MDP) is a mathematical model for the RL problem. Quad $(S,\,A,\,\rho,\,f)$ often expressed as a state of MDP.

In this case, S denotes the collection of all environmental states. $s_t \in S$ denotes the current state in the collection of all environmental states at time t; the set of possible actions taken by the agent is denoted by the letter A. $a_t \in A$ denotes the agent's action at time t; ρ: $S \times A \longrightarrow R$ is the reward function. $r_t \sim \rho(s_t, a_t)$ is a reward and punishment table. It summarizes all of the benefits that a single possible action, a_t, can obtain in a given state, s_t. $f\colon S \times A \times S \longrightarrow [0,1]$ is the probability distribution function for state transitions. The probability of state s_t successfully transitioning to state, s_{t+1}., is denoted by $s_{t+1} \sim f(s_t, a_t)$.

In reinforcement learning, the ultimate goal is to enable the agent to discover an optimal action mode, and thus, the strategy we use during this process is critical. The strategy, π: $\mathbf{S} \longrightarrow \mathbf{A}$, indicates that a_t is the optimal action step determined by the current environmental conditions s_t, that is, $\pi\,(s_t) = a_t$. Assuming that the immediate rewards obtained at each future period should be multiplied by a discount factor in order to avoid infinite returns and to discount future value into the present, time T denotes the plot's conclusion. The following here is an example of a typical function:

$$R_t = r_{t+1} + \gamma r_{t+2} + \gamma^2 r_{t+3} + \cdots = \sum_{k=0}^{T-1} \gamma^k r_{t+k+1}. \tag{1}$$

Here, γ $(0 < \gamma < 1)$ denotes a constant discount rate for future and current rewards. The strategy is followed until the training is complete while equation (2) refers to action a in the current state s. In another way, it shows a state action value function. The agent's cumulative return during this procedure is stated as follows:

$$Q^\pi(s,a) = E\left[R_t | s_{t=s}, a_{t=a}, \pi\right]. \tag{2}$$

If there is a strategy π^*, with an expected return greater than or equal to that of any other strategy for all state action pairs, we refer to it as the optimal strategy. For the strategy, which is called the optimal state action value function, the formula is as follows:

$$Q^\pi(s,a) = \max_\pi E\left[R_t | s_{t=s}, a_{t=a}, \pi\right]. \tag{3}$$

Then follows the Bellman optimality equation, we have the following:

$$Q^*(s,a) = E_{s' \sim S}\left[r + \gamma \max_{a'} Q(s', a') | s, a\right]. \tag{4}$$

The Q-value function is typically solved by iterating the Bellman equation in a traditional reinforcement learning framework as follows:

$$Q_{i+1}(s,a) = E_{s' \sim S}\left[r + \gamma \max_{a'} Q(s', a') | s, a\right]. \tag{5}$$

This formula automatically means when $i \longrightarrow \infty$, $Q_{i+1} \longrightarrow Q^*$,which suggests that if the state action value function is iterated continuously, it will ultimately converge on the optimal strategy:

$$\pi^* = \arg\max v^\pi(s),\ (\forall s). \tag{6}$$

In practice, however, iterating the Bellman equation to determine the Q-value is impractical in huge sample spaces due to the unimaginably large number of calculations.

2.2. Deep Reinforcement Learning Based on Value Function. Mnih was the first to propose a deep Q network (DQN) model by combining convolutional neural networks in deep learning and the Q learning algorithm in conventional reinforcement learning [18, 22]. This model incorporates a convolutional layer, which significantly improves the learning efficiency and performance [23].

Four preprocessed images preceding the current moment are fed into the DQN model. It becomes nonlinear after passing through three convolutional layers and two fully connected layers. Finally, the output layer produces the Q value associated with each action. TheDQN structure is depicted in Figure 2:

DQN made three significant improvements to the traditional Q learning algorithm to address the nonstationary as well as other issues associated with the nonlinear network used to represent the value function. DQN algorithm flow is shown in Figure 3.

DQN's training process makes use of the experience replay mechanism [24] (experience replay). The transferred samples $e_t = (s_t, a_t, r_t, s_{t+1})$. When an agent and environmental samples are transferred to a playback memory unit $D = \{e_1, \ldots, e_t\}$ at a given time t, they are stored there. Small batches of random transfer samples are selected from D each time, and the Stochastic Gradient Descent (the SGD) algorithm is used to update network parameter θ during training. When developing deep networks, it is common to require samples to be self-contained. Along with increasing the algorithm's stability, this random sampling method significantly reduces intersample relevance.

In this process, the agent and the transferred samples $e_t = (s_t, a_t, r_t, s_{t+1})$. obtained from environmental interaction are stored in the playback memory unit $D = \{e_1, \ldots, e_t\}$ at each time step t. When training deep networks, each sample must be completely independent of the rest of the data set. Random sampling improves the algorithm's stability by reducing intersample relevance.

In addition to the prior value function, DQN uses a deep convolutional network to estimate when another network is employed alone to obtain the desired Q value. The current

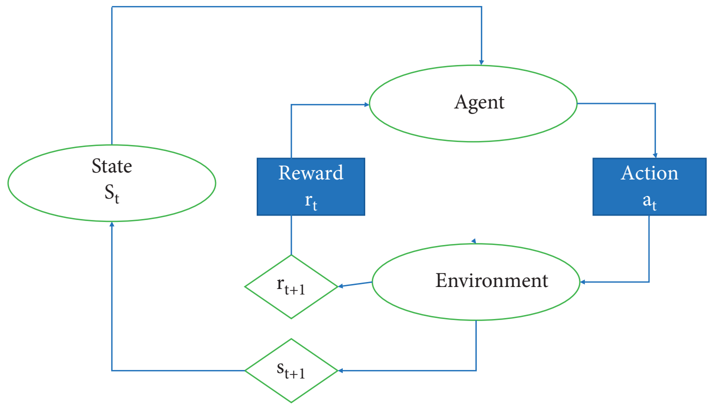

Figure 1: Flowchart of RL.

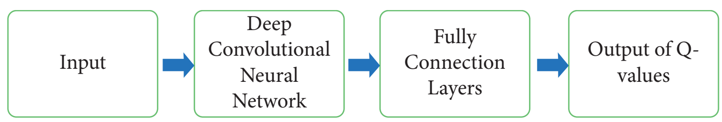

Figure 2: DQN structure.

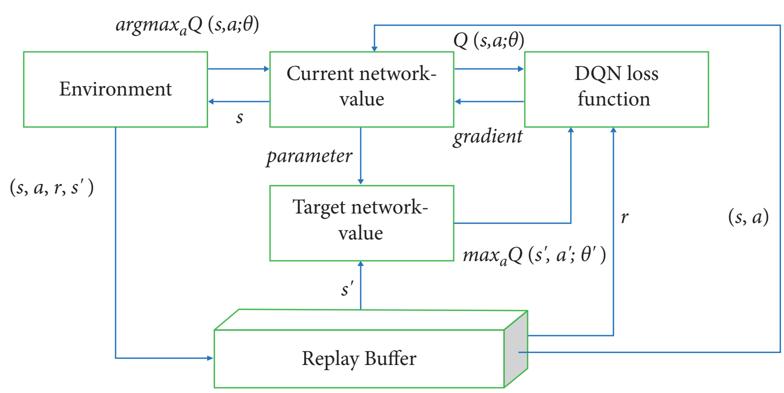

Figure 3: DQN algorithm flow.

value network's output, $Q(s,a|\theta_i)$, is used to calculate the value function of the current state action pair. The output of the target value network is represented as $Q(s,a|\theta_i^-)$ using the following formula:

$$Y_i = r + \gamma \max_{a'} Q(s', a'|\theta_i^-). \tag{7}$$

This is a rough representation of the value function optimization, with the purpose of obtaining the target Q value. The current value network's parameters θ are changed in real time. The parameters of the current value network will be used as the parameters of the target value network after N iterations. The principle of minimization reduces the joint variance of the desired Q value and the present Q value. The error function is as follows:

$$L(\theta_i) = E_{s,a,r,s'}\left[\left(Y_i - Q(s,a|\theta_i)\right)^2\right]. \tag{8}$$

Differentiate the parameter θ to get the following gradient:

$$\nabla_{\theta_i} L(\theta_i) = E_{s,a,r,s^s}\left[\left(Y_i - Q(s,a|\theta_i)\right)\nabla_{\theta_i} Q(s,a|\theta_i)\right]. \tag{9}$$

After introducing the target value network, the target Q value remains constant for a period of time, increasing the algorithm's stability by decreasing the correlation between the current and target Q values. By utilizing DQN, the reward and error terms are constrained to a small range, the Q and gradient values are guaranteed to be within a tolerable range, and the algorithm's stability is improved. DQN has been shown in experiments to be capable of resolving issues found in Atari 2600 games. When confronted with complex real-world situations [19], it demonstrates a competitive level comparable to that of human players. Even in less difficult nonstrategic games, DQN outperforms experienced human players. DQN uses the same network models, parameter settings, and training methods for visual perception as it does for auditory perception in the DRL task. This demonstrates how adaptable and flexible the DQN method can be.

3. Stock Prediction with RL

3.1. Deep Reinforcement Learning Based on the Policy Gradient for Stock Prediction. The policy gradient strategy (PG) is primarily achieved by modifying the settings in order to optimize the reward function. The key to this strategy is to alter the policy's parameters through extensive computation and iteration. Adjusted parameters will be included in the policy-making equation and will be modified on a continuous basis to accommodate more accurate policies. By fitting this approach, it will eventually converge on the optimal plan, which maximizes the reward value [15]. That is, in the optimal state, the strategy set contains specific parameters (or strategies) that ensure that the reward value of this strategy is equal to or greater than the reward value of any other strategy.

Parameterization is necessary to solve the DRL optimization problem. After constructing the fundamental equations in deep learning, the PG is typically used to pick parameters, alter the variable weights in the computer-constructed model, and finally choose the approach that maximizes the function's reward value. There are various advantages to this strategy, the primary one being that it reduces the computer's performance. This method streamlines the time-consuming dynamic iterative process, allows for a more precise optimization of the projected reward value, and also eliminates the need for heavy intermediate operations, which significantly reduces computing resource consumption. As a result, when compared to DQN and its advanced models, the DRL technique frequently achieves superior optimization results and has the lowest computing occupancy in model optimization when using the policy dimension reduction method. Additionally, the policy dimensionality reduction method may directly get the best policy from the policy set, significantly reducing computing costs. As a result, the bar for implementing this technology in practice is lower, and the area of its application is broader.

In practice, the strategy gradient method is a technique that uses an approximator directly to approximate and optimize the strategy, resulting in the optimal strategy. This method maximizes the strategy's projected total reward as follows:

$$\max_\theta E[R|\pi_\theta]. \tag{10}$$

$R = \sum_{t=0}^{T-1} r_t$ denotes the total number of rewards obtained in a plot. The most frequently used approach gradient is to enhance the likelihood of encountering a higher total reward plot. The strategy gradient approach operates in the following manner: We will assume here that the state, action sequence, and reward sequence of a complete plot are as follows, $\tau = (r_1, \ldots, s_{T-1}, a_{T-1}, r_{T-1}, s_0, a_0, r_0, s_1, a_1, s_T)$. The PG formula is then represented as follows:

$$g = R\nabla_\theta \sum_{t=0}^{T-1} \log \pi(a_t|s_t;\theta). \tag{11}$$

This gradient can be used to adjust policy parameters: $\theta \leftarrow \theta + \alpha g$. Among these, α determines how frequently policy parameters are updated, and it is called the learning rate. $\nabla_\theta \sum_{t=0}^{T-1} \log\pi(a_t|s_t;\theta)$, the gradient term, The gradient term denotes the potential direction in which the occurrence of a trajectory can be increased. The greater the total reward (in a single plot), the more "stretched" the probability density becomes after multiplying by R. The probability density will tend toward the trajectory with the highest total reward if a large number of paths with varying total rewards are collected, thereby increasing the likelihood of high-reward trajectories.

However, in some circumstances, the total reward R of each plot is positive, implying that all gradient g values are larger than or equal to 0. At this point, each trajectory τ met during the training process causes the probability density to "pull in" in a positive direction, significantly slowing the learning rate. This results in a relatively big variance for the gradient g. Thus, lower the variance of the gradient g by using any standardization operation in R. This strategy enables the algorithm to raise the likelihood of trajectories τ occurrence (for a greater total reward R) and decrease the probability of trajectories τ occurrence (for a lower total reward R).

Williams et al. [25, 26] proposed the REINFORCE method, which transformed the policy gradient into the following form:

$$\nabla_\theta \sum_{t=0}^{T-1} \log\pi(a_t|s_t;\theta)(R-b). \tag{12}$$

R's variance can be reduced by using an expected estimate of b as a baseline for the current trajectory. There is a strong correlation between R and b differences and the likelihood of a larger associated trajectory being chosen. For large-scale DRL challenges, the strategy parameters can be parameterized using deep neural networks and the optimal strategy can be solved using the standard strategy gradient method.

Additionally, another strategy to optimize strategies is to enhance the likelihood of performing "good" activities. In reinforcement learning, an advantage function is frequently used to quantify the quality of an action. As a result, the strategy gradient can be constructed using the following advantage function term:

$$g = \nabla_\theta \sum_{t=0}^{T-1} \widehat{A}_t \log \pi(a_t|s_t;\theta). \tag{13}$$

Among them, $\widehat{A}_t$ represents an estimate of (s_t, a_t) dominance function of the state action, which is usually constructed as follows:

$$\widehat{A}_t^\gamma = r_t + \gamma_{t+1} + \gamma^2 r_{t+2} + \cdots - V(s_t), \tag{14}$$

$\gamma \in (0,1)$ indicates discount factor. Sum of rewards with discount at this time $r_t + \gamma_{t+1} + \gamma^2 r_{t+2} + \cdots$ and the discounted state value function $V(s_t)$ is identical to R and the benchmark b in equation (12). When $\widehat{A}_t^\gamma > 0$, the likelihood of the appropriate action being chosen increases. When $\widehat{A}_t^\gamma < 0$, it will decrease the likelihood of the relevant action being chosen.

Figure 4: Training and testing results.

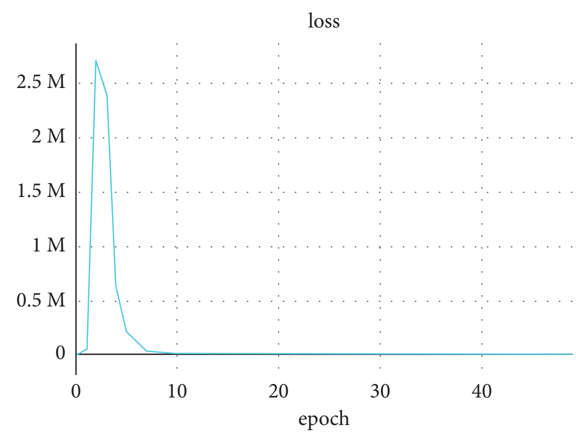

Figure 5: Loss function.

Figure 6: Reward convergence.

Hafner et al. [27] estimated the discounted reward summation using the value function, thereby lowering the gradient term's variance. At this point, the one-step truncated, $\widehat{A}_t^{\gamma}$'s expression is as follows:

$$\widehat{A}_t^{\gamma} = r_t + \gamma V(s_{t+1}) - V(s_t). \tag{15}$$

Additionally, the two-step truncated $\widehat{A}_t^{\gamma}$'s expression is as follows:

$$\widehat{A}_t^{\gamma} = r_t + \gamma_{t+1} + \gamma^2 V(s_{t+2}) - V(s_t). \tag{16}$$

However, this strategy introduces an element of estimating bias. To minimize variance while maintaining a little bias, Schulman et al. [28] proposed a generalized advantage function to solve this weakness as follows:

$$\widehat{A}_t^{\gamma} = \delta_t + (\gamma\lambda)\delta_{t+1} + (\gamma\lambda)^2\delta_{t+2} + \cdots + (\gamma\lambda)^{T-t-1}\delta_{T-1}. \tag{17}$$

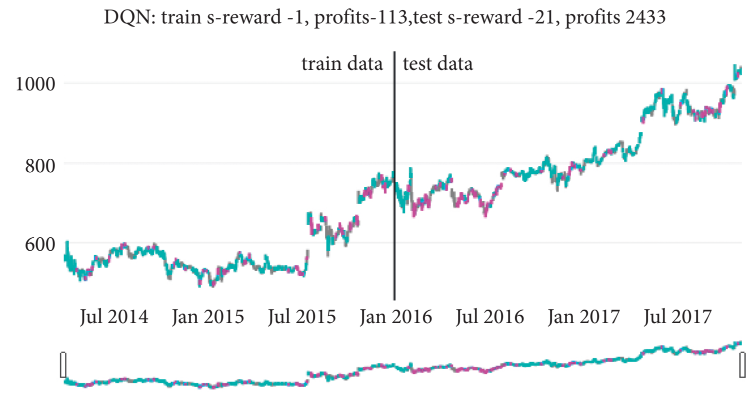

Figure 7: DQN training and testing results.

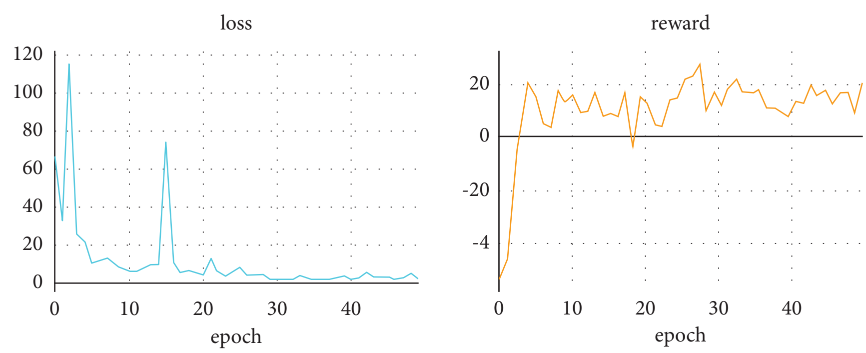

Figure 8: Loss function and convergence of DQN.

To take it a step further, Schulman et al. [29] then introduced a technique known as trust region policy optimization (TRPO). To broaden the application to large-scale state space DRL tasks, the TRPO method parameterizes the strategy using deep neural networks and achieves end-to-end control using only the original input image.

3.2. RL Application. In practice, during the day, when the trading system predicts that the stock price will continue to rise, there will be a judgement of whether to buy. When the stock price is predicted to fall continuously, a sell operation will be performed.

In the research, we use the single-agent training method. The rate of change of the price of a single stock in the market environment is what we focused, and we assumed that all the information in the market has been included in the environmental information and the state of the stock itself. Although the market is complex and changeable and the obtained market price is also the final expression of the game behavior of many Chinese investors. However, after a relatively long-term RL training, the result can theoretically reflect the information contained in the market more comprehensively, and therefore, this assumption is also harmless.

State is a unique parameter in the policy equation. Therefore, if it is assumed that the policies of all investors are inflexible, the choice of action is only based on a given state. Therefore, under 5-minute data, the policies of other investors can be regarded as the state of the market.

The indicators of stock information include the following: (1) Opening price, (2) Closing price, (3) Daily highest value, (4) Daily lowest value, (5) Daily average value, and (6) Trades Quantity. The above six data will serve as state indicators in the stock market environment.

s O: Opening price of the day.

s C: Closing price of the day.

s H: Highest price during the day.

s L: Lowest price during the day.

s A: Average price of the day.

Aq: the quantity and number of the successful trades of the day.

4. Results and Discussion

4.1. Simulated Results. The goal of this article is to establish a short-term stock price prediction framework with retrospective characteristics. In other words, the stock price fluctuations in the past are used as one of the references for predicting today's stock price. We used the historical daily prices and volumes of all U.S. stocks and ETFs to verify the methods we proposed. First, we trained the DRL model with the data from JUL 2014 to Jan 2016 and tested the model using the data from Jan 2016 to Jul 2017. The results are shown in Figure 4As can be seen from the figure, in the training phase and the test phase, the output results of the model are very consistent with the actual stock prices.

In the process of using the data set to train the model, as the epoch data increases, the loss function will gradually decrease. During this training process, the training result of the loss function is shown in Figure 5. It can be seen from the figure that starting from 10 epoch data, the loss function tends to be the smallest.

In addition, in the process of training and testing the data set, we will observe the changes of reward in the DRL model, as shown in Figure 6. As illustrated in Figure 4, the reward changes dramatically at the start of training and testing, but stabilizes as the number of epochs increases, indicating that the DRL model is trained.

Following that, we predict the stock price using the DRL-based policy gradient method proposed in this paper, as illustrated in Figure 7. As illustrated in Figure 7, this paper's method is more accurate at forecasting the trend of stock price data. The results of analyzing the model's loss function and reward function are shown in Figure 8. When compared to the DRL results, it is discovered that while the method in this paper has poor loss function stability, it quickly stabilizes on the reward curve.

5. Conclusion and Discussion

To improve the accuracy of daily stock price predictions, this paper proposes a new reinforcement learning method that incorporates policy gradients. A comparison was made between the daily stock price changes predicted by the basic DRL and the daily stock price changes predicted by the proposed DRL based policy gradient method in this study. Despite the fact that the convergence time of the loss function is longer as a result of the use of different dimensionality reduction methods, the experimental results show that the accuracy of the new method in prediction as well as the stability of rapid prediction have both been significantly enhanced. This shows that our new method will be able to more easily capture the information of market changes. Therefore, it is more suitable for use in periods of turbulent market compared to traditional methods. However, this research still has room for improvement. For stock price research, the intraday volatility of stock prices is often large. Using the results of this research to trade can sometimes reduce the rate of return, which will cause certain losses to investors who hold a large number of stocks when they reduce their holdings. In addition, in terms of data volume, because there are only a few pieces of data generated every day, the data used to predict daily stock prices often have a long-time span, and market information in different years cannot be generalized. Therefore, raising the forecast frequency of daily stock prices to the 5-minute or even 1-minute level may be of greater reference for investors. Compared with the daily data, the data every five minutes have less information density, but they will more clearly reflect the overall picture of stock price fluctuations, which is conducive to the prediction of future stock price fluctuations and can also provide a better reference for investors to increase returns.

Data Availability

The datasets used and/or analyzed during the current study are available from the corresponding author on reasonable request.

Conflicts of Interest

The authors declare that they have no conflicts of interest.

References

[1] F. Agostinelli, S. Mcaleer, A. Shmakov, and P. Baldi, "Solving the Rubik's cube with deep reinforcement learning and search," *Nature Machine Intelligence*, vol. 1, no. 8, pp. 356–363, 2019.

[2] S. Asadi, E. Hadavandi, F. Mehmanpazir, and M. M. Nakhostin, "Hybridization of evolutionary Levenberg-Marquardt neural networks and data pre-processing for stock market prediction," *Knowledge-Based Systems*, vol. 35, pp. 245–258, 2012.

[3] Y. Deng, Y. Kong, F. Bao, and Q. Dai, "Sparse coding-inspired optimal trading system for HFT industry," *IEEE Transactions on Industrial Informatics*, vol. 11, no. 2, pp. 467–475, 2015.

[4] R. Hafner and M. Riedmiller, "Reinforcement learning in feedback control," *Machine Learning*, vol. 84, no. 1-2, pp. 137–169, 2011.

[5] V. Konda and J. Tsitsiklis, "Actor-critic algorithms," *Advances in Neural Information Processing Systems*, vol. 12, 1999.

[6] G. Lample and D. S. Chaplot, "Playing FPS games with deep reinforcement learning," 2017, https://arxiv.org/abs/1404.3978.

[7] J. W. Lee, "Stock price Prediction Using Reinforcement Learning," in *Proceedings of the 2001 IEEE International Symposium on Industrial Electronics Proceedings*, pp. 690–695, Pusan, South Korea, June 2001.

[8] J. W. Lee, E. Hong, and J. Park, "A Q-Learning Based Approach to Design of Intelligent Stock Trading Agents," in *Proceedings of the 2004 IEEE International Engineering Management Conference*, pp. 1289–1292, Singapore, October 2004.

[9] J. Lehoczky and M. Schervish, "Overview and history of statistics for equity markets," *Annual Review of Statistics and Its Application*, vol. 5, no. 1, pp. 265–288, 2018.

[10] L.-J. Lin, *Reinforcement Learning for Robots Using Neural Networks (Tech. Rep.)*, DTIC Document, 1993.

[11] J. W. Lee, J. Park, J. O, J. Lee, and E. Hong, "A m approach to Q-Learning for daily stock trading," *IEEE Transactions on Systems, Man, and Cybernetics-Part A: Systems and Humans*, vol. 37, no. 6, pp. 864–877, 2007.

[12] B. Luo, D. Liu, H.-N. Wu, D. Wang, and F. L. Lewis, "Policy gradient adaptive dynamic programming for data-based optimal control," *IEEE Transactions on Cybernetics*, vol. 47, pp. 3341–3354, 2016.

[13] K. Miao, F. Chen, and Z. G. Zhao, "Stock price Forecast Based on Bacterial colony RBF Neural Network," *Journal of Qingdao University (Natural Science Edition)*, vol. 2, 2007.

[14] V. Mnih, K. Kavukcuoglu, D. Silver et al., "Playing Atari with deep reinforcement learning," 2013, https://arxiv.org/abs/1312.5602.

[15] V. Mnih, K. Kavukcuoglu, D. Silver et al., "Human-level control through deep reinforcement learning," *Nature*, vol. 518, no. 7540, pp. 529–533, 2015.
[16] J. E. Moody, M. Saffell, Y. Liao, and L. Wu, *Reinforcement Learning for Trading Systems and Portfolios*, pp. 279–283, 1998, https://www.aaai.org/Papers/KDD/1998/KDD98-049.pdf.
[17] M. Nabipour, P. Nayyeri, H. Jabani, A. Mosavi, E. Salwana, and S. Shahab, "Deep learning for stock market prediction," *Entropy*, vol. 22, no. 8, p. 840, 2020.
[18] M. P. Naeini, H. Taremian, and H. B. Hashemi, "Stock market value prediction using neural networks," in *Proceedings of the 2010 International Conference on Computer Information Systems and Industrial Management Applications*, pp. 132–136, IEEE, Krakow, Poland, October 2010.
[19] E. S. Olivas, J. D. M. Guerrero, M. Martinez-Sober, J. R. Magdalena-Benedito, and L. Serrano, *Handbook of Research on Machine Learning Applications and Trends: Algorithms, Methods, and Techniques: Algorithms, Methods, and Techniques*, IGI global, Hershey, PA, USA, 2009.
[20] D. S. S. Pinto and K. R. G. Da Silva, "Robot position control in pipes using *Q* learning," in *Proceedings of the 2016 IEEE International Conference on Systems, Man, and Cybernetics*, pp. 004609–004613, IEEE, Budapest, Hungary, October 2016.
[21] J. Schulman, S. Levine, P. Abbeel, M. Jordan, and P. Moritz, "Trust region policy optimization," in *Proceedings of the 32nd International Conference on Machine Learning*, pp. 1889–1897, PMLR, Lille, France, July 2015.
[22] J. Schulman, P. Moritz, S. Levine, M. Jordan, and P. Abbeel, "High-dimensional continuous control using generalized advantage estimation," 2015, https://arxiv.org/abs/1506.02438.
[23] R. S. Sutton, D. Mcallester, S. Singh, and Y. Mansour, "Policy gradient methods for reinforcement learning with function approximation," *Advances in Neural Information Processing Systems*, vol. 12, 1999.
[24] H. Wang, Y. Wu, G. Min, J. Xu, and P. Tang, "Data-driven dynamic resource scheduling for network slicing: a deep reinforcement learning approach," *Information Sciences*, vol. 498, pp. 106–116, 2019.
[25] C. J. C. H. Watkins, "Learning from delayed rewards," 1989.
[26] R. J. Williams, "Simple statistical gradient-following algorithms for connectionist reinforcement learning," *Machine Learning*, vol. 8, no. 3-4, pp. 229–256, 1992.
[27] P. Wolf, C. Hubschneider, M. Weber et al., "Learning How to Drive in a Real World Simulation with Deep Q-Networks," in *Proceedings of the 2017 IEEE Intelligent Vehicles Symposium*, pp. 244–250, IEEE, Los Angeles, CA, USA, July 2017.
[28] T. Xu, S. Zou, and Y. Liang, "Two time-scale off-policy TD learning: non-asymptotic analysis over Markovian samples," *Advances in Neural Information Processing Systems*, vol. 32, 2019.
[29] Y. Yuan, Z. L. Yu, Z. Gu et al., "A novel multi-step Q-learning method to improve data efficiency for deep reinforcement learning," *Knowledge-Based Systems*, vol. 175, pp. 107–117, 2019.

Hindawi
Scientific Programming
Volume 2022, Article ID 8194140, 12 pages
https://doi.org/10.1155/2022/8194140

Review Article

Descriptive Literature Review and Classification of Community Cloud Computing Research

Nouf S. Aldahwan [1,2] and Muhammed S. Ramzan [1]

[1] *Department of Information System, King Abdulaziz University, Jeddah, Saudi Arabia*
[2] *Department of Information System, King Khaled University, Abha, Saudi Arabia*

Correspondence should be addressed to Nouf S. Aldahwan; naldhwan@kku.edu.sa

Received 13 October 2021; Revised 11 January 2022; Accepted 16 March 2022; Published 21 April 2022

Academic Editor: Punit Gupta

Cloud computing has been devoted to the development of recent advanced technology, aiding in improving a government's functioning and the services it offers to its people and organizations. It has achieved widespread popularity due to the rising number of benefits, including scalability, versatility, reliability, safety, confidentiality, pay-per-use, and dynamicity for the distribution of IT services. This paper explores a descriptive literature review and aims to classify the scattered communities involved in cloud computing research in information technology. This involves 51 referred published articles between 2010 and 2020 relating to the inception of community cloud computing by various organizations. Based on a systematic structured of reviewed literature and grounded theory approach, articles are categorized with respect to the eleven key influencing variables: cost, security, performance, QoS, trust, accuracy, ease of use, usefulness, architecture, framework, and model. Following that, those variables are comprehended into final one in order to envisage the community cloud computing adoption factors and concepts. This will consent for a strong examination of the community cloud computing phenomenon. The study is a novel attempt to demonstrate the differences in key factors for cloud computing in varying community settings and their causal relationships among the considered variables. The findings from the long-term systematic review contribute by assisting a collection of determinants for the penetration of community clouds services and potential adopters. It could serve as a basis for future directions and the development of theories in the exploring the community cloud computing in the field of information systems. This study contributes to identify various existing research gaps by providing holistic insights and future exploratory approaches that are anticipated to result in a robust unified structure for the adoption of community cloud computing services in the higher education institution (HEIs).

1. Introduction

Cloud computing has become an emerging technology involved in the provision of information technology (IT) solution services in recent years, which is interconnected and is a dynamically Internet-based computing service agreement between users and cloud service providers. It is widely growing popular across the world in the IT industry, which prosecutes greater opportunity in the business sector [1]. This technology offers numerous benefits, including cost savings, increased scalability, integrity, security, ease of access, and risk reduction for business [3]. Cloud computing systems have proven to be effective in meeting the varying demands for computing distributed sharing resources and services. This has become a revolutionary integral computing paradigm in the field of information technology, contributing significantly as an unprecedented computing power and flexibility in the distributed community computing to science, education, and research sectors in recent years [3].

The private cloud application as a community cloud permits its use for research and education purposes in a variety of institutions. Different types of applications and usage scenarios have also been explored including web applications, blog, web hosting, networking, and dispersed data storage services. Additionally, a cloud system of this type can do provisioning activities in the form of computing infrastructure, software, and platform development to meet the demand of researchers or scientist's [4] It is also a technique in which users might access their own pool of computing resources in a network community [5].

Similarly, this research has shown its benefits in academic organizations, which has also been highlighted in this paper. The execution of parallel simulations was undertaken during the project's deployment, and the performance of the community cloud system was comparison functioning to that of the supercomputers [3]. Cloud computing is based on the fundamentals of distributed computing networks, service orientation, virtualization, grid computing system, and so on [6]. Further, the usage of grid technologies has also been introduced as a method for accessing cloud computing resources, enabling the monitoring and management of cloud resources.

Despite its benefits, cloud computing faces of several technical, management, and economic challenges, such as security and privacy [7, 8] and resource scheduling [8], that must be addressed,. Community is an integral aspect of cloud computing, and it is critical for its adoption and growth, particularly in the community cloud environment, which is highly accessible to users—considering that the community model is an advantage through perceived risks, shared resources, and saving costs. The community difficulties and challenges have been discussed in a variety of perspectives in cloud computing information systems [9, 10]. It has also been involved in security communication, resource distribution, security storage, and a variety of other facts of cloud computing [11].

Therefore, to deal with such problems, the need to implement better strategies arises, making use of community cloud computing one of them. The community cloud resides between the public and private clouds. The infrastructure and computing services, while like a private cloud, are not limited to one entity but are shared between two or more entities with common privacy, data integrity, security, identity, and regulatory considerations [12, 13]. However, despite the fact of the community cloud computing, the comprehensive and systematic review and background of the information about framework/model/architecture related to the community cloud adoption in HEIs is still the constraint that served as the primary impetus for performing this research. Therefore, the contribution of this study is to determine the community view in cloud computing with review the extant systematic literature review to identify the key frameworks/model/architecture. Furthermore, this study specifies which issues are being investigated and their relevant outcomes.

The structure of this paper is organized as follows: Section 1 is the introduction. Section 2 briefly discussed cloud computing and its characteristics. Section 3 explained related studies of the community cloud. Section 4 explains the methodology. Section 5 presented a detailed discussion. The final sections contain the conclusions and references.

2. Cloud Computing Overview

Cloud computing refers to "access to computing resources that are owned and managed by a third-party provider on a consolidated basis in one or more data center locations" [14]. Cloud computing is distinguished by on-demand provisioning and pay-as-you-use resource invoicing, with minimal upfront payment; cloud computing services minimize capital, transform running expenses into actual use, and lower staffing costs. It serves as a kind of application and a platform for providing computing services and infrastructures. The platform provisions configure, reconfigure, and de-provision servers as dynamically as required with the servers being virtual or physical machines. It establishes a paradigm shift from computing as a purchased product to computing supplied as a service to users over the Internet via huge databases or the cloud. The cloud infrastructure enables easily scalable, useful, virtually available, and customizable IT resources. Hardware support and maintenance for middleware and applications is not necessary with providing the cloud computing platform and service to users. Cloud computing is changing the development of the application and the way business decisions are taken [14].

Three common cloud services can be considered according to the different types of services offered.

(1) Software as a service (SaaS). In SaaS, the provider's applications on cloud infrastructure can be used by consumers, but they do not control the cloud networks, operating, and infrastructure. SaaS, considered a delivery model, will aid technologies supporting service-oriented architecture (SOA) and web services. Examples are Google's Gmail and Yahoo [12, 15].

(2) Platform as a service (PaaS). In PaaS, the provider's applications can be used by the consumer while deploying applications to the cloud infrastructure. This model offers the customer some control over the deployed applications but not the cloud infrastructure (networks, server, and storage).

Examples include Salesforce's Force.com and Microsoft's Azure [12, 15].

PaaS combines additional qualities such as built-in scalability, security, and dependability; facilitates developer collaboration; and ensures an uncompromised user experience. [16].

(3) Infrastructure as a service (IaaS). In IaaS, the consumer could use storage, network, and processes owned by the provider on-demand. The consumer can deploy and run the software. This model does not

give the consumer the ability to control the hardware cloud infrastructure, for example, Amazon's Elastic Compute Cloud (EC2) [12, 15].

2.1. Cloud Computing Deployment Models. Private clouds, public clouds, hybrid clouds, and community clouds are the four different types of cloud deployment methods available.

(1) Public Cloud. The public cloud is a type of cloud hosting whereby the cloud services are available in the open network for the public to use. This service may be offered for free or on a pay-per-use basis, for example, the Google App Engine [12].

(2) Private Cloud. A private cloud is a type of cloud computing concept that entails a secure cloud and a discrete cloud-based environment. This environment is entirely controlled by the given client. Private clouds that make use of actual computing resources offer computational power as a service within a virtual environment. In the model, the cloud or resources are available only to a single organization with greater privacy and control [14]. Examples of this are the VMware Private Cloud.

(3) Hybrid Cloud. This is an integrated type of cloud computing that involves the combination of private and public clouds [17]. Hybrid cloud refers to combining two separate clouds to form a combined cloud. It might be a mix of public and private cloud servers or it could be a mix of virtual cloud servers and real hardware. The many clouds are merged to provide a unified service [14]. The common type of combination is private data and the public cloud. Three key products are available are as follows: Azure, Microsoft System Center, and Windows Server.

(4) Community Cloud. When multiple organizations require identical infrastructure and wish to share it, a community cloud is formed. By pooling resources, enterprises may reap the benefits of cloud computing. The community cloud expenditures are distributed to fewer users than the public cloud, but not to a person or a tenant. Therefore, the community cloud is more expensive although it provides a high level of privacy, policy compliance, and security [14]. An example of the community cloud is the Gov Cloud by Google [12].

The remainder of this paper is structured as follows: The main literature related to community cloud computing is investigated and analyzed in Section 2 to address the frameworks, models, and architectures addressing various community cloud-related problems, an empirical analysis of the papers published during the period (2010–2020) is presented. The approach used is discussed in Section 3, and Section 4 summarizes the key findings. Finally, the conclusion presented in Section 5.

3. Community Cloud Adoption

A few architectures were suggested by researchers [18–32], as well as frameworks [33–44] and models [45–68] for the adoption of community cloud computing. The data set includes 51 articles that provided comprehensive frameworks, architectures, or models.

3.1. Frameworks. The article by Rodrigues studies a novel approach toward cloud architecture using the academic community cloud [13]. The two ways that can be used in the case of cloud burst or disaster recovery management are multicloud federation and cloud service standardization. The results reveal how the challenges and troubles faced due to old approaches can be solved by employing new ones.

These days, community clouds are used to save costs, and many organizations tend to use this service for their betterment [19]. Dubey et al. [19] offer a novel management approach for enterprises' use of community clouds. Additionally, IDA, a novel scheduling algorithm, was initiated. Research has shown that this system can improve the monetary cost of an organization.

Wahab et al. [20] illustrates how community-based cloud computing is a significant step in enhancing community services and networking, resulting in improved service management and resource utilization.

Yokoyama and Yoshioka's study [21] aims to perform new research on community clouds, with a particular emphasis on on-demand cloud extensions, which are typically built on remote sites for intercloud collaboration. The cloud on-demand approach enables the integration of private cloud computing systems horizontally.

In the current era of digitalization, Internet access is essential for all community members, and cloud computing systems need to be installed, especially in less developed areas and yearn for Internet accessibility [22]. The project shows that a community-owned local computing cloud can effectively be employed and sustained in a locality if appropriate tools and mechanisms are used.

Kawa and Ratajczak-Mrozek develop solutions for diverse businesses based on cloud communities and e-clusters [23]. The e-clusters are digital panoramas for collaboration that make use of communication and information technology. Using this information technology, the distances between widely dispersed networks can be reduced and the business process made effective.

Zhang et al. [24] study how community clouds provide a secure ambiance for organizations and business models. The risks of cyber incidents would also be mitigated and the decision-making within an organization improved.

The study conducted by Os and Bressan [25] demonstrates that for members of this environment, the concept of decentralized engineering is dependent on the community cloud's worldview, the creation of a heuristic function H, and research on mechanisms and policies for adapting physical and virtual networks to improve performance.

Valluripally et al. [26] propose a new community cloud infrastructure to make it possible for clinicians and scientists to increase accessibility from multiple sources to data sets, though it is also not compromised to ensure the data provider's security compliance.

Wu et al. [27] compare public and community clouds and propose a MeePo Cloud architecture. The results indicate that the MeePo Cloud architecture is well-suited for intensive big data sharing via digital disks and metadata servers.

The study presented by Baiardi and Sgan [28] provides the overlay of VMs, which helps manage a cloud more simply and easily. These specialized virtual machines (VMs) safeguard shared data and aid with the cloud community. Additionally, they oversee the cloud's infrastructure and are safe and dependable.

Filiposka and Juiz [29] provide a new model for the network architecture of the data center. The model has a large bandwidth and resilience. The result show that the cost and energy can be saved by modifying the structure of a community [30].

Selimi and Freitag focus on the attainability of application arrangements on cloud-based community frameworks. Tahoe-LAFS was used in conjunction with the cloud storage application to provide a graphical user interface and end-to-end encryption. Bit Torrent was also used, as it appeared to be better suitable for huge media storage files. The operation should be executed with real users where the community cloud will be the user's first choice [31].

The distributed file system on a cloud infrastructure attaching the Tahoe-LAFS and Extreme FS with their cloud storage gave a good end-user application with adequate security and privacy and web-based GUI. The importance of the distributed system lies in the interaction of users and providers, which gives dynamic results [32].

Mobile computing has been proposed for sharing and managing data across mobile communities. We can join the LAS service with the mobile communities by using the cloud infrastructure, and iPhone and Android phones can also benefit from it. Further research on it is essential for better outcomes as it is difficult to predict success in this field [32].

3.2. Architectures. The purpose of the study by Ojugo et al. is to investigate the benefits of a cloud framework for smartphones. Because of the study, it was determined that smartphones are vulnerable to attack. The Puch Cloud service thereby enables the users to hold the data by ensuring a backup. This system also allows users to solve security-related issues, with the data being recovered via a remote server [33].

Baig, Freitag, and Navarro studied and explained the upcoming computers system [34] that the emphasis is on CCs, or community clouds. The creation of the guifi.net community network has been cited as a successful example of digital infrastructure development. CCs can efficiently serve CN members by increasing the quality of existing services.

Alsaghier et al. [35] suggest based on the DRM community cloud (DCC) and the banking community cloud, a stable and lightweight protocol for mobile digital rights management (DRM). Using the wireless public key infrastructure, universal client-side integrated circuit board, DRM community cloud at the cloud provider, and banking community cloud, the non-repudiation property is attained.

In a cloud computing context, Ahmad et al. [36] suggest parallel virtualization. The authors sought to optimize the community cloud's hardware, cost, and workload while enhancing speed and performance.

In this rapidly developing era of digital objects, the Internet and IT technology have made it possible for communities to communicate more efficiently and effectively [37]. The costs of the networks have also been lowered, and local interests are served. [37].

Wen et al. [38] divided the cloud service part into many cooperative communities using the technique for community finding. The data indicate that using a community partitioning strategy improves the success rate of cloud services.

Zhao and Yang [39] proposed to include a bandwidth warranty for the sharing of social media content. The results showed that BRAC is efficient and effective in meeting social multimedia content bandwidth requirements and enhancing bandwidth usage.

Petri et al. [40] studied social community clouds and social clouds that are becoming a new environment where users can trade resources by social networks. The study finds the revenue as a metric affecting number of peer nodes [40].

According to Sus et al., climate research can be conducted using a community cloud structure based on several satellite image sensors. The findings demonstrate the system's versatility as a way for passive satellite sensor data generation from cloud objects. [41].

In many fields, such as education and research, the community cloud CC has emerged as a swiftly developing notion [42]. The business processes (BP) that facilitates the functioning of an organization plays an important role in community cloud. BP helps the community members achieve the activity flow in an organization for specific requirements. CC application tends to affect the efficiency of business processes.

Li [43] discussed the mechanism of fast collaboration and the method that used in process drive. Additionally, it is referred to as community cloud computing, and it provides a novel foundation for workflow systems. It enables structured and rapid communication, as well as a scheduled approach dubbed unified scheduling strategy.

3.3. Models. A self-coordinated cloud working framework can be fabricated and can convey a really circulated multicenter framework support. Its adaptability features the benefits of this client-driven cloud engineering. Traditional IaaS, PaaS, and SaaS can be altered to include angles as client claimed foundation, administrator less cloud stage, and character-driven data handling and capacity [44].

Mohan et al. [40] propose COMPAC (A Community Cloud Pricing Model) depending on the cost of services being offered. A web-based pricing tool was proposed and is available for use by other suppliers. Indian Banking leverages our pricing strategy to launch the country's first public cloud. The use of the group cloud has increased facilities [45].

Shirazi and Iqbal [46] focuses on analyzing m-commerce-related privacy problems. It encompasses the aspects of privacy and privacy expectations. This overviews current models, including innovations that design enhances privacy. The result shows that it can be achieved through socio-cultural solutions to fix privacy. Trust and security can be a mixture of technology and business policies [46].

To improve the user interest in cloud computing, Yoro and Ojugo propose a client-trusted security system. The suggested architecture includes a user-centric virtual process paradigm for cloud computing security. The results show that the ability of the proposed framework to increase the user's trust level by 67% [47].

The wireless networking service has proven to be a cost-effective IP networking infrastructure service in the less developed areas [48]. Providing services and applications by deploying their availability in these areas through a wireless network can be extremely helpful for the users.

Baig, Freitag, and Navarro focus on the research model of cooperative edge cloud deployment. The project demonstrated how the container method used in this community cloud system enabled community members to exchange services via the networking edge [49].

Another work by Hao et al. [50] proposes a social collaboration model for a two-layer multicommunity cloud cloudlet to allocate subtasks to community clouds in mobile edge computing. The findings show that the proposed algorithm will reduce the number of access costs, the sum of monetary costs, the consumption of electricity, and increase the level of protection.

For large-scale distributed infrastructures, the most significant procedure is cloud computing [51]. The use and application of an energy-aware brokering algorithm in a community cloud ecosystem can result in improved performance and increased sustainability. Several metrics were taken into account. This will also take into account the cost-saving element of using this method.

MC3 (Multi-Community-Cloud Social Collaboration Model) is a model that selects the most efficient, secure, and trustworthy tasks to complete complex tasks. The model is optimized in four ways: minimizing the cost of access and monetary costs and optimizing the agreement at the security level and confidence between group clouds. [52].

The world is rapidly progressing concerning IT systems and applications. When it comes to big companies, many must encounter challenges regarding the changing environment [53]. Cloud computing has proven to enhance the IT infrastructure for various companies. The companies can improve their ability to integrate within the supply chain by investing effectively in collaborative capability.

The model presented by Al-Mashat et al. [54] acts as a mediator between service providers and customers in a community in order to offer them with the best possible assistance. Through the usage of this system, end-users will be able to select the services that are most appropriate for their needs and preferences. Furthermore, it was verified that the quality of service offered was of a high enough standard to be relied upon by the users.

According to Khan, Freitage, and Rodrigues [55], the community clouds use user-contributed resources either through the user systems or augmentation with existing cloud infrastructures. The aim is to integrate the various options available in the cloud computing model with the help of resource availability to satisfy users' critical needs and interacting with them in long term [55].

Container-based virtualization is used to build a multipurpose execution environment on a single computer to address the issue of resource sharing in low-capacity systems. A single system can be built to give the user and the community with a multipurpose environment for isolation and security of community cloud resources while also providing the user with a single point of contact. The finding reveals that community networks are underutilized and that resources might be allocated to provide more services to more people [56].

Big data clusters on community clouds could benefit from this efficient and cheap resource distribution approach. In a quasi-real-time mode, tested with OpenStack-based community cloud tests, and SERAC3 is able to smartly pick a configuration within 2.2% of the exact optimal solution, saving around 80.1% of search costs compared to an exhaustive search. [57].

Liu [58] et al discussed the application of Swift as a system operating in a data center cloud environment. Usually, the community clouds that are established on a community network require a dispersed ambiance to serve. The result shows the functioning of Open Stack in a community setup. The most simulated environment was developed while working on the project, and the important community environment factors were used in the process.

The study by Saovapakhiran and Devetsikiotis inferred new confirmation control and directing algorithms in community clouds, advancing benefits while apportioning the extreme assets, subject to the SLA requirements. Additionally, they presented the idea of social evaluating and consolidated it into the algorithm to help the system focus on the appearances and control disappointments [59].

Cloud computing was proposed in the Garlick research proposal for data preservation. The loss of data by a sudden event can be disastrous for a company. Community cloud is also like public cloud, but both have their pros and cons. So, the main aim for business resilience is to get the data recovered after catastrophes damage [60].

Ren et al. [61] considered a community cloud that performs real-time stream mining across a wireless network for many users, addressed the problem of dynamic resource provisioning, and developed a selection and frequency algorithm that can achieve an arbitrary close-to-minimum average energy classification cost for each customer, thereby satisfying the average power restriction.

The study conducted by Keung [62] aims to enhance BIM with the help of the cloud community. It can solve many problems of BIM. First, in the construction market, they will remain competitive. Second, privacy problems and interpersonal interaction can be readily resolved through virtual interaction. Finally, a virtual communities focused on the cloud can increase productivity and collaboration. It can ease storage and increase the efficiency of BIM [62].

Khan et al. [63] applied different valuing instruments from the writing to transfer speed designation issue of cloud applications in the community network, examined their effect on the social government assistance and honesty.

The Web 2.0 is used to transfer patient information between the doctor, nurse, or caretaker. The study by Shirazi [64] proposes a home care system (HCC) that transfers information with the help of sensors, and it uses a cloud computing system. There are many drawbacks of this system as well.

Mullins et al. [65] explore the efficacy of a protocol for allocating lightweight resources in the allocation of services in a heterogeneous environment consisting mainly of low power nodes. The authors show that services can be provided on nodes with the correct resource brokering strategy without adversely affecting individual nodes in the network where the least effect on overall performance is achieved.

Jimenez et al. [66] conducted research on the expansion of community networking using community clouds. These clouds can boost the usage of many applications and provide many facilities at one point. In guifi.net, the extension and application of existing platforms and systems are available to deploy applications on clouds.

The study by Zhao et al. [67] discusses the problem of developing community-based cloud computing, specifically problems of resources' trading. Community-based community provides one-to-one communication to many users at once. The result showed that multiagent-based optimization improves the decision in the trading selection process.

Deebak and Al-Turjman proposed an integrated plan to develop collaboration between trusted neighbors. The test included three real-world data sets, and the results showed remarkable improvements in the traditional system [68].

4. Methodology

The aim of this paper is to conduct a systematic review of the literature to reflect the current state of IS research on community cloud adoption. This review process adhered to the manner of [70] basic guidelines for performing an efficient pertinent literature review, the query from papers was identified in those released between 2010 and 2020 with selected search keywords. A total of 51 publications were selected and added into the study based on their relevance to the research area from the first search, in accordance with our selected paper criteria.

A key strategy is to frame research questions and then select articles from within the domain using conceptualize research areas and survey and synthesize past research in line with the identified research gaps [71–73]. This comprehensive literature review provides a pictorial depiction of published results in linked study areas. The first stage is to define the research question and to take advantage of the chance for a review. All papers on community-based could computing are then searched for the primary stage. After that, all of the reviewed papers are categorized so that the relevant ones may be identified. Cloud computing research is then categorized and conceptualized through data extraction. Finally, these various approaches were used to produce a community-based cloud computing research theme.

4.1. Research Questions. For a systematic review of relevant literature, the study primary goal is to gain an in-depth understanding about the type and quality of existing research in a particular field and where it has been published. It is important to consider all these influencing factors while formulating the research questions. The following major research questions (RQs) are framed in accordance with the research gaps listed below to attain the study's objectives.

RQ 1. What is the proposed approach used in the researches?

RQ 2. What are the community cloud factors?

RQ 3. What are the limitations of the researches?

4.2. Conduct of Search and Selection Process. When conducting a review, the search phase is typically the first step in the process. The search for primary studies is typically carried out by exploring significant databases. Searching for publications on digital libraries was an important phenomenon for this systematic literature analysis. The significant databases were only incorporated because of scientific indexes and their high impact factor. Using this search query, researchers were able to find information on interventions, comparisons, and outcomes. The title of this study was analyzed to determine the keywords that would be utilized in a search. Cloud and computer science search results were involved into this study.

The selection criteria used in this study are critical since they ensure that only relevant papers are reviewed. Hence, the inclusion and exclusion criteria were used to select relevant publications in the domain of community cloud computing policy and research classification. According to this selection criteria, abstracts with little or no specific relation to the subject matter, as well as articles describing study summaries and the like were excluded in this selection process. It was decided to focus on cloud computing and the community domain in the primary investigations. For this study, a fundamental literature review on community cloud computing is the main wording for this work.

4.3. Data Extraction and Publication Statistics. Articles relevant to the community cloud computing strategy were grouped into different classifications schemes.

The results of a review of 51 publications are reported in four dimensions: article distribution across the year, publication sources, research methodologies used, and cloud

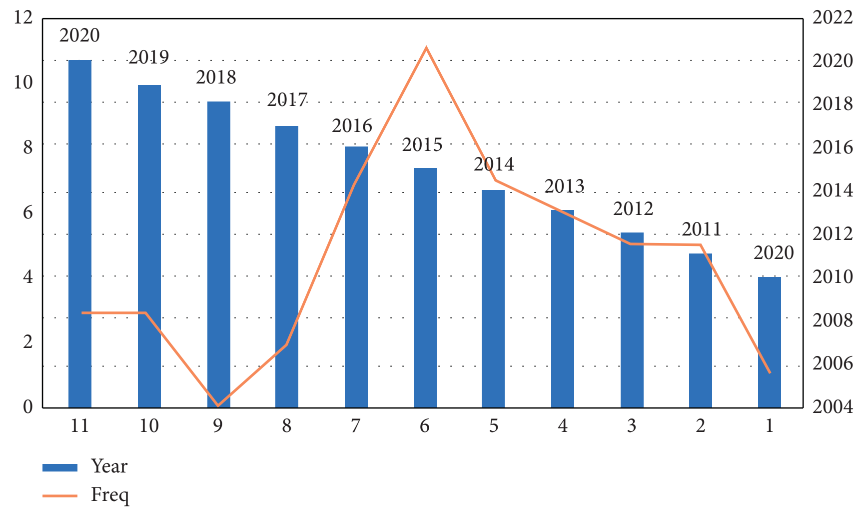

Figure 1: Distribution of articles per year.

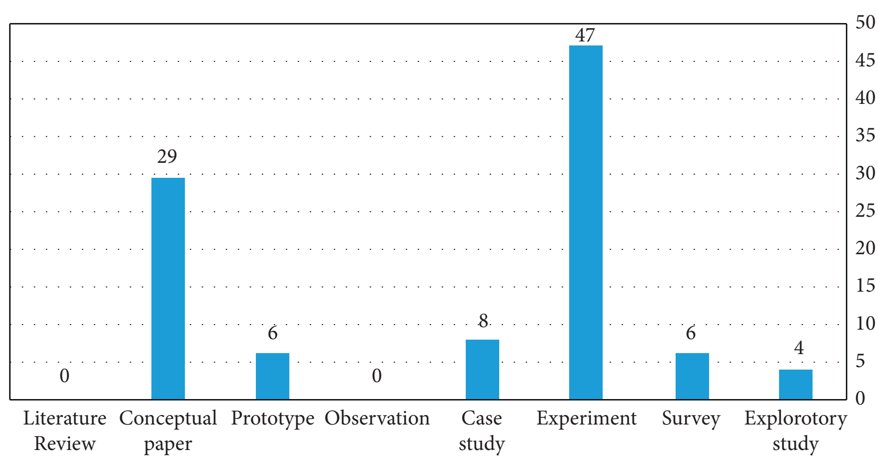

Figure 2: Summary of research methodology base on identified articles.

computing adoption factors and concepts. From 2010 through 2020, interest in exploring community cloud computing adoption has increased enormously, as depicted in Figure 1; however, the frequency did not the follow the similar trend of community cloud interest phenomenon.

5. Discussion

The study mainly focuses on community cloud computing and systematic research approach based on articles classification theme. The research may necessitate identifying the sources of publishing. Graphs and tables used to analyze the outcomes of the reviewed papers allowed us to determine which study topics and kinds lacked sufficient articles. It was found that certain topics had a high number of papers devoted to them. This study took into account variables such as security, cost, and performance linked with cloud computing as well as community cloud factors and research technique based on specified article categories.

5.1. Applied Approach. The results indicated that out of the 51 identified articles, 47% undertook experiments, 29% displayed conceptual papers, and 8% were case studies on the implementation and use of community cloud services, 6% was prototypes and surveys, 4% was exploratory studies, and the total data set is as shown in Figure 2. In comparison to quantitative studies, the findings show that qualitative studies have contributed less to understanding community cloud computing factors and concepts. In comparison of the identified articles, more articles were published on experimental, and conceptual research; however, minimum articles were published on prototype, case study, survey, and exploratory study. On the other hand, there were no articles on observation and literature review scheme. A quite consistent study conducted by the [74, 75] on the cloud computing literature review and they concluded the similar finding which aligned with current study.

There are several interesting facets of this cloud computing community research. For evaluation and validation

Table 1: Community cloud factors.

(Concept)	(Factors) Architecture	Framework	Model
Cost	[18, 19, 22, 23, 26, 27]	[33, 36]	[46, 47, 49–51, 53]
Security	[24, 25]	[33, 35, 37]	[45, 46, 50, 55, 56]
Performance	[14, 20, 21]	[33]	[53, 56]
QoS	[14, 20]	[37–39], [40]	[55]
Trust	—	—	[46, 50, 55]
Accuracy	[15]	—	[51]
Ease of use	—	[37]	[46, 53]
Usefulness	—	[37]	[46]

Table 2: Summary of limitations presented in adopting community cloud computing.

Concept	Limitations	Ref
Architecture	Expect to completely support Oracle-VM and suggest frameworks to demonstrate real-time resource savings and automate network border protection	[18]
	Additional security solutions for the cloud service provider are also considered to find out the cost variation, length, and other parameters in the real cloud environment	[19]
	It can be expanded to reduce the dependence on the master as a trustworthy central agent regarding the misbehavior detection system and includes a tri rather than binary classifier based on the gravity of their threats	[20]
	This architecture can be extended to broad-area networks using SINET L2VPN and VPLS services	[21]
	Components are being developed to calculate and account for contributions to and usage of the cloud CPR	[22]
	More on other model options to explore the model's local functions, which are currently missing from OpenStack	[24]
	Best practices can also focus non-experts with more intuitive user interfaces to query using parallel programming APIs in high-performance computing quickly	[26]
	It is needed to update community cloud systems to support several organizations The cloud protection structure of MeePo should be applied to multiple levels Using strong authentication to advance the protection of data creation, and transition	[27]
	(1) Physical attack protection so that it is not appropriate to trust the cloud provider and the cloud administrators (2) Explore how redundancy can be transparently introduced into an overlay without migrating a VM to cover hardware component faults	[28]
	To focus on a deeper investigation of the possibilities for performance boosting based on populations and other network metrics	[29]
	To extend the experiments and real use as the end-users become active	[30]
	Study for an in-depth understanding of mobile community specifications, the implications of cloud computing infrastructure and mobile communities	[32]
Framework	The contribution to and utilization of cloud CPR is measured and accounted for in order to be able to spread the costs equally and facilitate reinvestment, and the ability to identify and mitigate risks	[34]
	The BAN logic and scyther instrument are used to validate the proposed protocol	[35]
	To examine the cloud providers' non-functional functionality for the discovery and optimization algorithms of the cloud service community	[38]
	Another noteworthy concern is the replica selection process as in the next step	[42]
	The scheduling method will be further enhanced to use a fast collaboration process and other associated workflow system application improvements	[43]
Models	Pricing for PaaS and SaaS can also be further enhanced because of the service's differential value and can be dependent on transactions/use.	[45]
	Focus on this architecture's full-scale implementation and how the cloud can be protected from the deliberate malicious behavior of the cloud provider	[47]
	Includes multi-service implementations, reliance on the docker center, and ease of creating docker files	[49]
	Extend the proposed model to other cloud server services and applications in the community	[50]
	Explore a strategy to balance sustainability intelligently with many other success indicators	[51]
	Investigate the effect of the mutual implementation of internal and external integration activities on organizational efficiency	[53]
	Identify configuration or security problems that could affect the services' efficiency.	[56]
	The assessment as a real community of OpenStack swift cloud implementation is needed	[58]
	To get input from the involvement of end-users to further form the creation of the components of the group cloud	[66]
	To determine the normalization and user attributes, create a suitable testbed	[68]

research, it is important to note that there are indications of a lack of publication in particular domains. Using cloud computing to do research is a boon for researchers since it allows them to synthesize and display their findings in a way that piques their interest. Because it is so easy to discover the gaps in many areas of study, a community cloud computing scheme without conducting a follow-up systematic literature review offers a unique value of its own. It has been shown in this work that there is a dearth of community cloud computing studies that have been conducted in a systematic manner.

5.2. Community Cloud Factors. In this study, community cloud are influenced by many factors, including, cost, security, performance, QoS, trust, accuracy, and usefulness [76] as shown in the following Table 1. In addition, eight areas were also discussed in terms of tools, models, and methods as well as in terms of the evaluation and validation of solutions, as well as in terms of the evaluation of philosophical and subjective research. The observation is in alignment with the funding obtained by [77] in their studies on the systematic literature review on cloud computing factors evaluation.

5.3. Limitations of the Research. The following Table 2 shows the limitation of previous studies that adopted community cloud computing.

Based on earlier studies, there is a problem to determine the factors affecting the adoption of community clouds in higher education institutions from a decision-maker's perspective. The analysis concluded that cloud computing technology provides higher education institutions with great opportunities and a need for a centralized, well-structured framework. Different institutions of higher education are deploying this cloud computing system. In addition, there are some limitations in previous studies that are as follows:

(1) Consider security services for the cloud service provider [22].
(2) Make span to evaluate other factors [22] such as cost, availability, security, privacy, adequate resource, compatibility, ease of use, usefulness, integration, environment factors, complexity, QoS, and resource access.
(3) Investigate the influence of the adoption of community cloud on operational performance factors [50].
(4) Understand the factors that mitigate the risks [59], such as privacy, availability, and confidentiality.

Based on these gaps, this work will cover the development of the proposed standard comprehensive community cloud framework using technology, organization, environmental, human, security, and advantages factors. There is a need for a well-structured conceptual framework to be applied by different Saudi HEIs. This study involves the construction of a conceptual framework that considers the technology, organization, environment, people, advantages, and security that various Saudi HEIs could apply.

6. Conclusion

This paper performed a systematic literature review on community cloud adoption and the usage of community cloud technologies in various sectors. An extensive analysis was carried out from journals and conference papers that have been issued during the time (2010–2020).

A systematic review of the literature was utilized to find and collect the necessary research papers. The study concluded that community cloud computing technology offers great opportunities to higher education institutions and that a centralized, well-structured system is required. Various higher education institutions are implementing this cloud system. The contribution to the field is the direction for future research on the adoption of community cloud, to support the overall growth of IS theory and to expand their research and understanding of adoption decisions. Second, we offer guidance to practitioners on the design and implementation of community cloud services. This research offers valuable insights for both cloud service providers and companies exploring the application of technology.

7. Limitations

This study has concentrated on a systematic literature review to different designated areas lacking in studies in terms of community cloud regulation in a wider range of end users. The major limitation of this study is that the initial search consisting of small number of articles; however, the numbers of search articles should be increased a lot in varying identified subject areas with community cloud factors. A decision-point makers of view is needed to identify the elements influencing adoption of community clouds in higher education institutions.

8. Suggestions for Future

8.1. Work. This study found that community cloud technology provides great opportunities and requires a well-structured centralized, unified framework for various HEIs to incorporate the cloud. Based on this paper, further work will involve designing the proposed unified integrated framework that uses adoption technology with numerous factors and considering the previous limitations. This systematic literature search process is restricted to journals, conferences, and book chapters. As a result, only a few dissertations and other electronic media sources, such as periodicals and newspapers, can be considered for future work.

Unfortunately, due to the connection constraints, bandwidth and data transmit, data processing and synchronization, and distributed nature of community cloud computing environments, various problems regarding community cloud computing environments still needed to be resolved as future challenges.

Data Availability

The primary and secondary data used to support the findings of this study are available from the corresponding author upon request.

Conflicts of Interest

The authors declare that they have no conflicts of interest.

References

[1] S. Z. Mohammadi and J. N. Navimipour, "Invalid cloud providers' identification using the support vector machine," *International Journal Of Next-Generation Computing*, vol. 8, no. 1, 2017.

[2] Q. Zhang, L. Cheng, and R. Boutaba, "Cloud computing: state-of-the-art and research challenges," *Journal of internet services and applications*, vol. 1, no. 1, pp. 7–18, 2010.

[3] P. Heinzlreiter, M. Krieger, and W. Hennerbichler, "Usage Scenarios for a Community Cloud in Education and Research," in *Proceedings of the 1st International IBM Cloud Academy Conference*, pp. 1–9, Raleigh, North Carolina, USA, April 2012.

[4] D. Contractor and D. Patel, "Accountability in cloud computing by means of chain of trust," *International Journal on Network Security*, vol. 19, pp. 251–259, 2017.

[5] N. J. Navimipour, A. M. Rahmani, A. H. Navin, and M. Hosseinzadeh, "Job scheduling in the Expert Cloud based on genetic algorithms," *Kybernetes*, vol. 43, p. 12, 2014.

[6] S. Mehmi, H. K. Verma, and A. Sangal, "Simulation modeling of cloud computing for smart grid using CloudSim," *Journal of Electrical Systems and Information Technology*, vol. 4, no. 1, 2016.

[7] W. Kong, Y. Lei, and J. Ma, "Data security and privacy information challenges in cloud computing," *International Journal of Computational Science and Engineering*, vol. 16, no. 3, pp. 215–218, 2018.

[8] S. Chenthara, K. Ahmed, H. Wang, and F. Whittaker, "Security and privacy-preserving challenges of e-health solutions in cloud computing," *IEEE Access*, vol. 7, Article ID 74382, 2019.

[9] A. Qasim, A. Sadiq, A. Kamaludin, and M. Al-Sharafi, "E-learning models: the e_ectiveness of the cloud-based E-learning model over the traditional E-learning model," in *Proceedings of the 2017 8th International Conference on Information Technology (ICIT)*, IEEE, Piscataway, NJ, USA, May 2017.

[10] N. S. Aldahwan and M. S. Saleh, "Developing a framework for cost-benefit analysis of cloud computing adoption by higher education institutions in Saudi arabia," in *Proceedings of the 2018 International Conference on Smart Computing and Electronic Enterprise (ICSCEE)*, pp. 1–9, Selangor, Malaysia, July 2018.

[11] H. Ding, X. Li, and C. Gong, "Trust model research in cloud computing environment," in *Proceedings of the 2015 International Symposium on Computers & Informatics*, Beijing, China, January 2015.

[12] D. Talia, "Clouds meet agents: toward intelligent cloud services," *IEEE Internet Computing*, vol. 16, no. 2, pp. 78–81, 2012.

[13] S. Goyal, "Public vs. private vs. hybrid vs. community - cloud computing: a critical review," *International Journal of Computer Network and Information Security*, vol. 6, no. 3, pp. 20–29, 2014.

[14] C. C. Rao, M. Leelarani, and Y. R. Kumar, "Cloud: computing services and deployment models," *International Journal of Engineering and Computer Science*, vol. 2, no. 12, pp. 3389–3392, 2013.

[15] G. Conway and E. Curry, "Managing Cloud Computing - A Life Cycle Approach," in *Proceedings of the 2nd International Conference on Cloud Computing and Services Science CLOSER*, pp. 198–207, Porto, Portugal, April 2012.

[16] V. Gonçalves and P. Ballon, "Adding value to the network: mobile operators' experiments with Software-as-a-Service and Platform-as-a-Service models," *Telematics and Informatics*, vol. 28, no. 1, pp. 12–21, 2011.

[17] H. A. S. Ahmed, M. H. Ali, L. M. Kadhum, M. F. Zolkipli, and T. A. Alsariera, "A review of challenges and security risks of cloud computing," *Journal of Telecommunication, Electronic and Computer Engineering*, vol. 9, pp. 87–91, 2017.

[18] K. A. Rodrigues de Castro, "Feasible community cloud architecture for provisioning infrastructure as a service in the government sector," in *Proceedings of the 20th Annual International Conference on Digital Government Research*, pp. 35–40, Dubai, United Arab Emirates, June 2019.

[19] K. Dubey, M. Y. Shams, S. C. Sharma, A. Alarifi, M. Amoon, and A. A. Nasr, "A management system for servicing multi-organizations on community cloud model in secure cloud environment," *IEEE Access*, vol. 7, Article ID 159546, 2019.

[20] O. A. Wahab, J. Bentahar, H. Otrok, and A. Mourad, "Misbehavior detection framework for community-based cloud computing," in *Proceedings of the 2015 3rd International Conference on Future Internet of Things and Cloud*, pp. 181–188, IEEE, Rome, Italy, August 2015.

[21] S. Yokoyama and N. Yoshioka, "A distributed cloud architecture for academic community cloud," *Communications in Computer and Information Science*, vol. 512, pp. 169–186, 2015.

[22] R. Baig, F. Freitag, and L. Navarro, "On the sustainability of community clouds in guifi.net," *Economics of Grids, Clouds, Systems, and Services*, vol. 9512, pp. 265–278, 2016.

[23] A. Kawa and M. Ratajczak-Mrozek, "Cloud community in logistics e-cluster industry clusters and e-clusters as a network structure," *Intelligent Information and Database Systems. ACIIDS*, vol. 8398, pp. 495–503, 2014.

[24] Y. Zhang, F. Patwa, R. Sandhu, and B. Tang, "Hierarchical secure information and resource sharing in OpenStack community cloud," in *Proceedings of the 2015 IEEE International Conference on Information Reuse and Integration*, pp. 419–426, Hamburg, Germany, September 2015.

[25] M. D. Ös and G. Bressan, "A community cloud for a real-time financial application - requirements, architecture and mechanisms," *Algorithms and Architectures for Parallel Processing*, in *Proceedings of the International Conference on Algorithms and Architectures for Parallel Processing*, pp. 364–377, Dalian, China, August 2014.

[26] S. Valluripally, M. Raju, C. Prasad et al., "Community cloud architecture to improve use accessibility with security compliance in health big data applications," in *Proceedings of the 20th International Conference on Distributed Computing and Networking*, pp. 377–380, Bangalore, India, January 2019.

[27] Y. Wu, M. Su, W. Zheng, K. Hwang, and A. Y. Zomaya, "Associative big data sharing in community clouds: the MeePo approach," *IEEE Cloud Computing*, vol. 2, no. 6, pp. 64–73, 2015.

[28] F. Baiardi and D. Sgandurra, "Securing a community cloud," in *Proceedings of the 2010 IEEE 30th International Conference on Distributed Computing Systems Workshops*, pp. 32–41, IEEE, Genoa, Italy, June 2010.

[29] S. Filiposka and C. Juiz, "Community-based complex cloud data center," *Physica A: Statistical Mechanics and Its Applications*, vol. 419, pp. 356–372, 2015.

[30] M. Selimi and F. Freitag, "Towards application deployment in community network clouds," in *Proceedings of the International Conference on Computational Science and Its Applications*, pp. 614–627, Springer, Guimaraes, Portugal, July 2014.

[31] M. Selimi, F. Freitag, R. P. Centelles, and A. Moll, "Distributed storage and service discovery for heterogeneous community network clouds," in *Proceedings of the 2014 IEEE/ACM 7th International Conference on Utility and Cloud Computing*, pp. 204–212, IEEE, Guimaraes, Portugal, July 2014.

[32] D. Kovachev, R. Renzel, R. Klamma, and Y. Cao, "Mobile community cloud computing: emerges and evolves," in *Proceedings of the 2010 Eleventh International Conference on Mobile Data Management*, pp. 393–395, IEEE, Kansas City, Missouri, USA, May 2010.

[33] A. Adimabua Ojugo, "Dependable community-cloud framework for smartphones," *American Journal of Networks and Communications*, vol. 4, no. 4, pp. 95–103, 2015.

[34] R. Baig, F. Freitag, and L. Navarro, "Cloudy in guifi. net: establishing and sustaining a community cloud as open commons," *Future Generation Computer Systems*, vol. 87, pp. 868–887, 2018.

[35] H. M. Alsaghier, S. K. Udgata, and L. S. S. Reddy, "A secure and lightweight protocol for mobile DRM based on DRM community cloud (DCC)," in *Advances in Intelligent Systems and Computing*, pp. 475–483, Springer, Singapore, 2017.

[36] K. Ahmad, A. Wahid, M. P. Quadri, and A. Fathima, "Parallel virtualization in IaaS in community cloud," in *Proceedings of the 2015 Fifth International Conference on Communication Systems and Network Technologies*, pp. 1071–1075, IEEE, Gwalior, MP, India, April 2015.

[37] A. M. Khan, F. Freitag, S. Gupta, V. Muntès-Mulero, J. Dominiak, and P. Matthews, "On supporting service selection for collaborative multi-cloud ecosystems in community networks," in *Proceedings of the 2015 IEEE 29th International Conference on Advanced Information Networking and Applications*, pp. 634–641, IEEE, Gwangju, Korea, March 2015.

[38] S. Wen, J. Yang, G. Chen, J. Tao, X. Yu, and A. Liu, "Enhancing service composition by discovering cloud services community," *IEEE Access*, vol. 7, pp. 32472–32481, 2019.

[39] P. Zhao and X. Yang, "Joint optimization of admission control and rate adaptation for video sharing over multirate wireless community cloud," *China Communications*, vol. 13, no. 8, pp. 24–40, 2016.

[40] I. Petri, J. Diaz-Montes, O. Rana, M. Punceva, I. Rodero, and M. Parashar, "Modelling and implementing social community clouds," *IEEE Transactions on ServicesComputing*, vol. 10, no. 3, pp. 410–422, 2015.

[41] O. Sus, M. Stengel, S. Stapelberg et al., "The Community Cloud retrieval for CLimate (CC4CL) - Part 1: a framework applied to multiple satellite imaging sensors," *Atmospheric Measurement Techniques*, vol. 11, no. 6, pp. 3373–3396, 2018.

[42] H. Luo, X. Liu, and J. Liu, "Queueing theory based service replica strategy for business process efficiency optimization in community cloud," in *Proceedings of the 2014 International Conference on Cloud Computing and Big Data*, pp. 83–90, Alaska, USA, July 2014.

[43] W. Li, "A Community Cloud Oriented Workflow System Framework and its Scheduling Strategy," in *Proceedings of the 2010 IEEE 2nd symposium on web society*, pp. 316–325, IEEE, CA, USA, October 2010.

[44] J. P. Barraca, A. Matos, and R. L. Aguiar, "User centric community clouds," *Wireless Personal Communications*, vol. 58, no. 1, pp. 31–48, 2011.

[45] S. L. Mohan, Y. R. Reddy, and G. R. Gangadharan, "Compac—a pricing model for community cloud," in *Proceedings of the 2017 International Conference on Advances in Computing, Communications and Informatics (ICACCI)*, pp. 2033–2039, IEEE, Manipal, Mangalore, India, September 2017, þ.

[46] F. Shirazi and A. Qbal, "Community clouds within M-commerce: a privacy by design perspective," *Journal of Cloud Computing*, vol. 6, no. 1, 2017.

[47] R. E. Yoro and A. A. Ojugo, "An intelligent client-trusted and dependable security framework to ease smartphone portability on community cloud-computing," *Journal of Computer Networks*, vol. 6, no. 1, pp. 1–7, 2019, þ.

[48] R. Baig, F. Freitag, A. Moll, L. Navarro, R. Pueyo, and V. Vlassov, "Cloud-based community services in community networks," in *Proceedings of the 2016 International Conf on Computing, Networking and Communications (ICNC)*, pp. 1–5, IEEE, Kauai, Hawaii, USA, February 2016.

[49] R. Baig, F. Freitag, and L. Navarro, "Fostering Collaborative Edge Service Provision in Community Clouds with Docker," in *Proceedings of the 2016 IEEE International Conference on Computer and Information Technology (CIT)*, pp. 560–567, Helsinki, Finland, August 2017.

[50] F. Hao, D. S. Park, J. Kang, and G. Min, "A two-layer multi-community-cloud/cloudlet social collaborative paradigm for mobile edge computing," *IEEE Internet of Things Journal*, vol. 6, no. 3, pp. 4764–4773, 2018.

[51] M. Giacobbe, M. Scarpa, R. Di Pietro, and A. Puliafito, "An Energy-Aware brokering algorithm to improve sustainability in community cloud," in *Proceedings of the SMARTGREENS - 6th International Conference on Smart Cities and Green ICT Systems*, pp. 166–173, Porto, Portugal, April 2017.

[52] F. Hao, G. Min, J. Chen et al., "An optimized computational model for multi-community-cloud social collaboration," *IEEE Transactions on Services Computing*, vol. 7, no. 3, pp. 346–358, 2014.

[53] S. Bruque-Cámara, J. Moyano-Fuentes, and J. M. Maqueira-Marín, "Supply chain integration through community cloud: effects on operational performance," *Journal of Purchasing and Supply Management*, vol. 22, no. 2, pp. 141–153, 2016.

[54] T. M. Al-Mashat, F. A. El-Licy, and A. I. Salah, "Semantic cloud community framework for services provision," in *Proceedings of the International Conference on Advanced Intelligent Systems and Informatics 2017*, pp. 222–231, Springer, Cairo, Egypt, September 2017.

[55] A. M. Khan, F. Freitag, and L. Rodrigues, "Current trends and future directions in community edge clouds," in *Proceedings of the 2015 IEEE 4th International Conference on Cloud Networking (CloudNet)*, pp. 239–241, IEEE, Niagara Falls, ON, Canada, IEEE, October 2015.

[56] N. Apolónia, R. Sedar, F. Freitag, and L. Navarro, "Leveraging low-power devices for cloud services in community networks," in *Proceedings of the 2015 3rd International Conference on Future Internet of Things and Cloud*, pp. 363–370, IEEE, Rome, Italy, August 2015.

[57] J. Li, Z. Lu, W. Zhang et al., “SERAC3: smart and economical resource allocation for big data clusters in community clouds,” *Future Generation Computer Systems*, vol. 85, pp. 210–221, 2018.

[58] Y. Liu, V. Vlassov, and L. Navarro, “Towards a community cloud storage,” in *Proceedings of the 2014 IEEE 28th International Conference on Advanced Information Networking and Applications*, pp. 837–844, IEEE, Victoria, BC, Canada, May 2014.

[59] B. Saovapakhiran and M. Devetsikiotis, “Enhancing computing power by exploiting underutilized resources in the community cloud,” in *Proceedings of the 2011 IEEE International Conference on Communications (ICC)*, pp. 1–6, IEEE, Kyoto, Japan, June 2011.

[60] G. Garlick, “Improving resilience with community cloud computing,” in *Proceedings of the 2011 Sixth International Conference on Availability, Reliability and Security*, pp. 650–655, IEEE, Vienna, Austria, August 2011.

[61] S. Ren and M. V. D. Schaar, “Efficient resource provisioning and rate selection for stream mining in a community cloud,” *IEEE Transactions on Multimedia*, vol. 15, no. 4, pp. 723–734, 2013.

[62] C. W. Keung, “A conceptual model of cloud-based virtual community for BIM innovation and promotion,” in *Proceedings of the 21st International Symposium on Advancement of Construction Management and Real Estate*, pp. 45–52, Springer, Singapore, 2018.

[63] A. M. Khan, X. Vilaça, L. Rodrigues, and F. Freitag, “Towards incentive-compatible pricing for bandwidth reservation in community network clouds,” in *Proceedings of the International Conference on the Economics of Grids, Clouds, Systems, and Services*, pp. 251–264, Springer, Napoca, Romania, September 2015.

[64] F. Shirazi, “An intelligent interactive home care system: an MPLS-Based community cloud,” in *Human Interface and the Management of Information. Information and Interaction for Health, Safety, Mobility and Complex Environments*, pp. 207–216, Springer, Berlin, Heidelberg, 2013.

[65] T. Mullins, A. Bagula, S. Rhekis, and N. Boudriga, “Service provisioning for lightweight community cloud infrastructures,” *CONF-IRM*, vol. 21, Cape Town, South Africa, May 2016.

[66] J. Jiménez, R. Baig, P. Escrich et al., “Supporting cloud deployment in the Guifi. net community network,” in *Proceedings of the Global Information Infrastructure Symposium-GIIS 2013*, pp. 1–3, IEEE, Madrid, Spain, October 2013.

[67] H. Zhao, X. Liu, and X. Li, “Towards efficient and fair resource trading in community-based cloud computing,” *Journal of Parallel and Distributed Computing*, vol. 74, no. 11, pp. 3087–3097, 2014.

[68] B. D. Deebak and F. Al-Turjman, “A Novel Community-Based Trust Aware Recommender Systems for Big Data Cloud Service Networks,” *Sustainable Cities and Society*, vol. 61, 2020.

[69] Y. Levy, “A systems approach to conduct an effective literature review in support of information systems research,” *Informing Science: The International Journal of an Emerging Transdiscipline*, vol. 9, pp. 181–212, 2006.

[70] S. E. Group, “Guidelines for performing systematic literature reviews in software engineering,” *Technical Report, EBSE Technical Report*, 2007.

[71] B. Kitchenham, O. Pearl Brereton, D. Budgen, M. Turner, J. Bailey, and S. Linkman, “Systematic literature reviews in software engineering - a systematic literature review,” *Information and Software Technology*, vol. 51, no. 1, pp. 7–15, 2009.

[72] J. Webster and R. T. Watson, “Analyzing the past to prepare for the future: writing a literature review,” *MIS Quarterly*, vol. 26, no. 2, 2002.

[73] I. Odun-Ayo, R. Goddy-Worlu, J. Yahaya, and V. Geteloma, “A systematic mapping study of cloud policy languages and programming models,” *Journal of King Saud University - Computer and Information Sciences*, vol. 33, no. 7, pp. 761–768, 2021.

[74] M. Sharma, R. Gupta, and P. Acharya, “Analysing the Adoption of Cloud Computing Service: A Systematic Literature review,” *Global Knowledge, Memory and Communication*, vol. 70, no. 1-2, pp. 114–153, 2020.

[75] N. S. Aldahwan and M. S. Ramzan, “Factors affecting the organizational adoption of secure community cloud in KSA,” *Security and Communication Networks*, vol. 2021, Article ID 8134739, 8 pages, 2021.

[76] F. Casino, T. K. Dasaklis, and C. Patsakis, “A systematic literature review of blockchain-based applications: current status, classification and open issues,” *Telematics and Informatics*, vol. 36, pp. 55–81, 2019.

[77] P. K. Senyo, E. Addae, and R. Boateng, “Cloud computing research: a review of research themes, frameworks, methods and future research directions,” *International Journal of Information Management*, vol. 38, no. 1, pp. 128–139, 2018.

Hindawi
Scientific Programming
Volume 2022, Article ID 5649363, 11 pages
https://doi.org/10.1155/2022/5649363

Research Article

IoT Communication for Grid-Tie Matrix Converter with Power Factor Control Using the Adaptive Fuzzy Sliding (AFS) Method

A. Suresh Kumar[1], **S. Jerald Nirmal Kumar**[2], **Subhash Chandra Gupta**[3], **Anurag Shrivastava**[4], **Keshav Kumar**[5] and **Rituraj Jain**[6]

[1]*Department of Computer Science and Engineering, Graphic Era (Deemed to be University), Dehradun, India*
[2]*School of Computing Science and Engineering, Galgotias University, Greater Noida, Delhi NCR, India*
[3]*Department of CSIT, KIET Group of Institutions, Ghaziabad, India*
[4]*Lakshmi Narain College of Technology and Science, Indore 453111, Madhya Pradesh, India*
[5]*University Institute of Computing, Chandigarh University, Chandigarh, Punjab, India*
[6]*Department of Electrical and Computer Engineering, Wollega University, Nekemte, Ethiopia*

Correspondence should be addressed to Rituraj Jain; jainrituraj@wollegauniversity.edu.et

Received 7 January 2022; Revised 17 February 2022; Accepted 4 March 2022; Published 29 March 2022

Academic Editor: Punit Gupta

In this work, we propose and encourage the sending of an IoT-based domestic systems conditions small scale programmable framework for grid-tie matrix converter that can efficiently be executed with low-control equipment plan with quick execution capacity. The proposed framework for matrix grid-tie converter has been performed based on an adaptive fuzzy sliding technique and furthermore monitors the grid status through an IoT server. The adaptive fuzzy sliding method was connected to the framework, and a unity power factor was fulfilled alongside the wanted sinusoidal input and output results. The proposed AFS-based matrix converter has been validated through simulation using MATLAB software. The control clock signals are generated for the positive and negative clock pulses of the sequence. Here the sinusoidal reference signal is compared with the switching frequency of the triangular carrier frequency. The hardware results were also verified to validate the simulation. When diverged from other standard techniques, the proposed AFS technique has achieved 97.23% efficiency in full load conditions.

1. Introduction

The Internet of Things (IoT) is a system and a perspective that contemplates the inevitable closeness in nature of an impressive proportion of things/objects. The remote and wired affiliations and exceptional tending to plans can interface with one another and take part with various things or articles to grow new applications/organizations and accomplish shared goals. The essential purpose of the IoT is to be an engaging part to be related whenever, wherever, with anything and anyone, ideally used in any case and any organization. The Internet of Things is another transformation of the Internet. Things make themselves apparent, and they obtain learning by settling on or enabling setting-related decisions because of the way that they can give information about themselves. Existing projects with connected grid systems that use the grid conversion take into consideration the breeze turbine or power age system. The network converter generator terminal voltage is predicted to be lower the frame voltage list because the matrix bin converter is a down-stage converter. The network converter's FRT function is tough to grasp. Both observers changed their opinion on the grid converter scarcity ride method. They can get information that has been gathered by various means, or they can be sections of cutting-edge organizations. Shrewd urban communities are requesting conditions where a few zones of advancement meet to enhance socioeconomic improvement and personal satisfaction considerably.

The smart grid (SG) tie matrix converter, the intelligent power grid, could be viewed as the unique instantiation of the

IoT organization in the next future. The whole power grid chain, from the power control plant generation to the power buyers (houses, buildings, mechanical offices, open lighting, electric vehicles, splendid machines, etc.). Counting transmission and dispersion control frameworks will be stacked with information and two-way correspondence abilities to screen and control the power organize wherever, at a brilliant granularity and high precision. For instance, smart houses will be equipped with smart meters and sharp contraptions, while control generators and electric transmission and movement frameworks will be outfitted with various sensors and actuators. The SG join matrix converter hopes to keep an even harmonic between power generation and use by permitting a fine-grained watch and control over the power chain because of the unique number of two-way signals passing on smart objects. The Internet of Things (IoT) will use a more quick-witted lattice to empower more data. Through the IoT, customers, producers, and utility suppliers will reveal better approaches to oversee gadgets, last ration assets, and spare cash by utilizing keen meters, home entryways, brilliant fittings, and associated machines. In this way, the bright lattice grid-tied converter likewise requires the accompanying ability besides the FRT prerequisites.

In the interim, a grid converter has likewise been pulled into numerous considerations as a superior AC-AC converter. The lattice tie network converter is depended upon to achieve higher capability, smaller size, and longer lifetime compared to a standard back-to-back structure. The entire power grid chain is involved houses, buildings, mechanical offices, open lighting, electric vehicles, splendid machines. Counting, transmitting, and dispersing control frameworks will be combined with data and two-way communication capacities to monitor and regulate the power arrangement wherever it is, with incredible granularity and accuracy. Because the identifier of two-way was passed on to smart objects, the SG join matrix converter aims to maintain an equal harmonic between power generation and usage by allowing fine-grained monitoring and control over the power chain. The breeze turbine, or power age system, is taken into account in existing projects with tied grid systems using the grid converter. But since the matrix bin converter is a down-stage converter, the network converter generator terminal voltage is expected to be lower than the frame voltage list. The FRT operation for the network converter is difficult to comprehend.

The grid converter scarcity ride strategy was revised by both observers. It is proposed to reach a standard FRT control protocol with (1) a steady FRT operation, (2) a matrix-reacting current control, and (3) the generator torque control in the middle of the voltage fall in a short period of time. The limitation of IoT devices is that cybercriminals could be accessible to the network and acquire private data. Because we are connected to so many gadgets on the network, there seems to be a possibility that our data may be exploited. They are completely dependent on the Internet and therefore are unable to function properly without it. There are numerous ways for systems to fail due to their complexity. We will lose control of our lives and become completely dependent on automation. However, it is important to comply with this control scheme since the current generator adequacy is simply regulated, and the receptive power (d-axis) is retained at zero. The device converter cannot, however, meet the FRT specifications for structure current at more than 43% voltage drop due to the suppression of the generator current.

This paper proposes an AFS technique for extending the fastening grid converter FRT operation. The current q-axis is constrained by the snubbed mechanism, and the current d-axis is sent to a voltage source inverter of a frame converter on the network circuit. The proposed technology keeps the q-axis current and creates a d-pivot current to expand the engine current. This helps to raise the grid current obtained to prolong the FRT process. This research paper is organized into four sections: Section 1 describes the introduction, the research background is described in Section 2, Section 3 describes the result and discussion, and finally, the conclusion part is described in Section 4.

2. Research Background

Several documents based on open winding topology based on the matrix converters. This topology comprises a total of 18 22 switches (that is, 36 IGBT and diodes) and is organized point by point in the data with the simplest output voltage of 1.5 times the voltage [1]. As the double matrix converter framework is shown, a control unit was suggested for reduced mode voltage in the storage terminals [2, 3]. The V/F approval engine's open-circle control scheme will display exploratory results. In a modulation method, [4, 5] is expressed in order to decrease the CMV and tests are carried out with a particular resistive load. Moreover, the dual matrix converter conspire has been widely considered for applications in multiphase open-end AC winding drives. For instance, a topology parallel matrix converter [6] 3–5, a total of 60 power gadgets are required, and a switching technique for reducing CMV is being proposed. The structure was experimentally tested with a 5 kW, 5-arrange recorder motor. In the same vein [7], the proposed adjective technique should take the CMV out and expand it to a selection method stack with a double matrix converter configuration of 3–7 (96 IGBTs and diodes required).

The structure consists of an asynchronous PM machine (EM) that is related straight to the internal consumer diesel engine. The active neutral point converter (ANPC) on the EM is connected with a bidirectional DC/DC interlaced multiarrange converter that interfaced with the dc battery [8]. The DC/DC converter is interconnected [6]. The architecture of the electric drive, the control subjects, and the power converter are expressed in this work. The reproduction of a hybrid structure includes a prototype test location consisting of two external magnet-synchronous magnet rotor devices at the same speed and connected to the same shaft [9]. A concept research scale based on proliferation and testing, used as the building square, are two or three difficult voltage restorer converters and the vector transform converter (VeSC) (DVR). They discuss their work aspirations and suggest diminishing exhibits. Effects have been introduced on limited models [10]. The device's key function is the creation of a wireless sensor network in various regions and multiple converters [11]. Wireless sensor networks are commonly used in domestic computerization, process monitoring, and wellness management systems. If the controller lacks the network harmonic voltage, the interval transition is constant and thus the FCM is calculated. This can be done if the controller [12] uses a well-designed phase loop (PLL) or if the controller has a short bandwidth. It fulfills this requirement. The leading matrix approach is based on the IoT approach, which allows active multiport network matrices to be expanded. Multi-inverter and multiconverter realization are only feasible for operational amplifiers $(n + m)$, [13].

All the systems mentioned above have a problem with grid-tie matrix converters, so this work proposes a novel AFS method-based grid-tie matrix converter module to solve all the issues. The topology uses two modules for specific and autonomous grouping voltage synthesis [14]. Therefore, the roundabout matrix converter proposed here can make up for adjusted and additionally lopsided voltage hangs/swells. Every module is acknowledged as utilizing a vector-switching matrix converter [15]. The whole topology is vitality storage free, and every module is beat width regulated using straightforward DC duty proportions. This work gives points of interest in the indirect matrix converter modeling, identical circuit, and feedback controller plan.

The general architecture of the proposed convertor system is shown in Figure 1. The AC input source has been taken, and it can be associated with a bidirectional rectifier for control of the indirect matrix converter. From that load, the particular parameters are ascertained and put away by utilizing distributed computing [16]. By using closed-loop control, the IoT benefit has been associated with PC and server, so we can see/observe the parameters esteems on the web or by utilizing a cell phone [17]. The Internet of Things gives plans for the coordination of information advancement, which suggests hardware and software computer programs are being utilized to store, recoup, and process data that joins electronic structures used for collaboration between individuals or social events. Since the AFS voltage exchange proportion of the IMC employing the PWM strategy is expanded, it brings about a decrease of THD and enhanced productivity.

2.1. IM Converter Circuit Design. The proposed indirect matrix converter circuit diagram is shown in Figure 2. The LC filter, bidirectional rectifier, and clamp circuits are the main components of this circuit [18]. A clamp circuit compared to film capacitor Cc, third harmonic current injection, fast recovery DC response, and voltage source converter. Three bidirectional switches, an inductor, and bridge legs response are comprised of current third harmonic injection. Under ordinary operation conditions, just a single of the three two-way switches is swung on to infuse the harmonic current into the corresponding input stage. As indicated by the prerequisites of the load, the voltage source converter provides variable frequency, amplitude, and three-phase output results. The clamp circuit is utilized to retain the power put away in the spillage inductance of the load when the framework shuts down.

2.2. IM Working Principles. The working standards of IMC are portrayed as being based on for the switches As+, Bs+, and Cs+ of the rectifier, the change joined to the info stage with the most noteworthy voltage is put away; for the switches As−, Bs−, and Cs−, the change associated with the information stage with the least vitality is continued. The switches Ys+ and Ys− in the third-symphony current infusion circuit are controlled to frame the third-consonant current iy coursing through the inductor Ly.

The bidirectional switch associated with the input organizes with the most diminished preeminent voltage keeps on implanting the third-symphony current. For instance, when the data voltages satisfy ua > ub > UC, switches As+ and Cs− in the rectifier and the bidirectional switches Bys and Bsy in the harmonics current implantation circuit are turned on, as shown in Figure 3, and whatnot. Like this, sinusoidal three-phase input streams and controllable power factors are practical.

2.3. AFS Algorithm Design for Proposed Converter. The AFS system uses neural network architecture to optimize the membership function of the adaptive fuzzy logic controller. Figure 4 illustrates AFS controller with two inputs; error $(e\,(k))$ and change by mistake $(\Delta e\,(k))$ is modeled as follows:

$$\begin{aligned} e\,(k) &= i_{ref} - i_f, \\ \Delta e\,(k) &= i_{ref} - i_f, \end{aligned} \tag{1}$$

where i_{ref} = reference current, i_f = filter output, $e(k)$ = error, and $\Delta e\,(k)$ = error corrected result.

The training membership function is obtained using the proposed AFS controller. The inputs are switched into linguistic variables [19]. In this case, five adaptive fuzzy membership functions are defined; NB, NS, Z, PS, and PB. The membership functions utilized for previously, then after the fact, training is shown in Figure 5.

Figure 5 plots the AFS set of the error and change error data which has triangular interests. The proposed AFS picks the change in control concerning voltage to supplant the dedication cycle of the pulse width modulation (PWM) to increase to decrease the voltage until the point that the point when the power is most remarkable, as it appears in Figure 3. AFS has two wellsprings of data, which are: botch and the modification in error; and one output managing the pulse width direction to control the DC-to-DC converter. The two AFS input factors, error E and change of error CE, at inspected times k described by

$$\begin{aligned} \text{Error}\,(k) &= \frac{P\,(k) - P\,(k-1)}{V\,(k) - V\,(k-1)}, \\ \text{Change\_Error}\,(k) &= \text{Error}\,(k) - \text{Error}\,(k-1), \end{aligned} \tag{2}$$

where $P(k)$ = power of energy generator and Error (k) = load operation point.

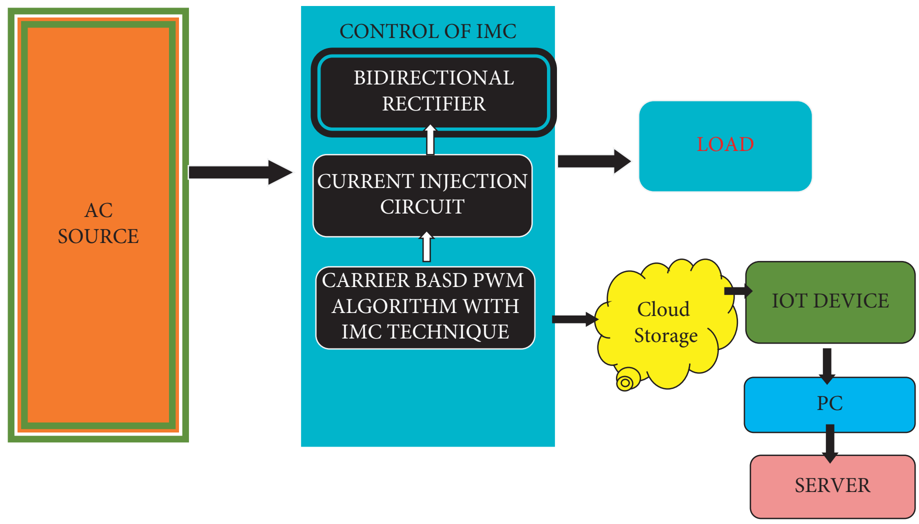

Figure 1: General architecture of proposed converter system design.

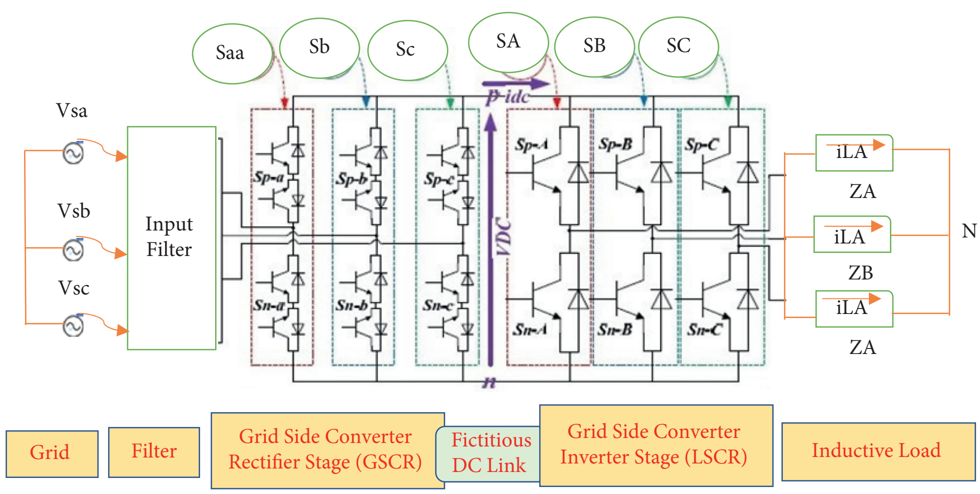

Figure 2: Proposed indirect matric converter topology.

While the moving direction of the point expresses the change of the input error, the AFS consists mainly of three blocks: fuzzification, fuzzy rule, and defuzzification.

Figure 6 represents the AFS set of the Iref output with triangular memberships. The surmising mechanism is assessed from the arrangement of errors by utilizing control rules.

Table 1 demonstrates the desired connection between the input and output factors regards to the membership functions.

2.4. Working Procedure of Adaptive FUZZY Sliding (AFS)

(1) At the start, the introduction of the info factors called the parameters is done, which is in a parallel shape, and the information factors are a fuzzy field.

(2) After information fuzzification, output fuzzification is finished by applying fuzzy administrators like AND or OR administrators.

(3) Membership capacities are characterized and are figured to track the given info/output information.

(4) The parameters related to the enrollment work changes through the learning procedure.

(5) Fuzzy principles are made based on the information yield relationship of the framework.

(6) After making rules, the accumulation of different yields is done, and afterward, the resulting capacities are defuzzified to get an ideal yield.

(7) The gathered output is then prepared by applying it to the neural system through the following propagation strategy.

(8) The error is diminished by performing different emphases in the neural system, and we get a streamlined yield.

(9) The suggested framework for matrix grid-tie converters are based on an adaptive fuzzy sliding approach and also monitors grid status through an IoT

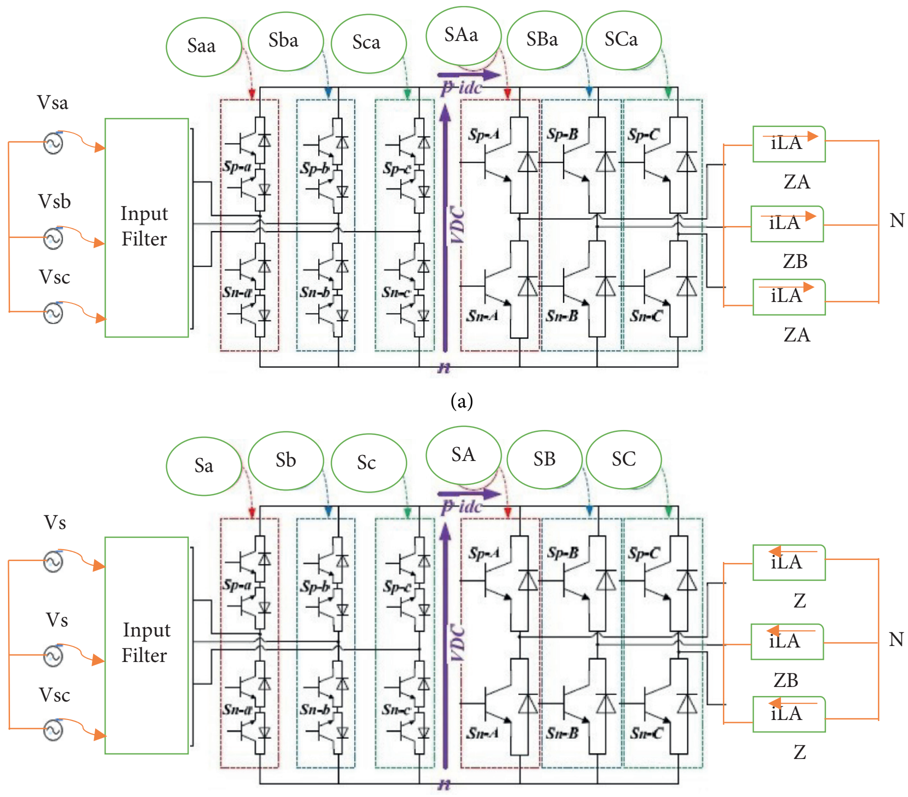

FIGURE 3: Equivalent circuit diagram of indirect matrix converter: (a) forward flow control and (b) reverse flow control.

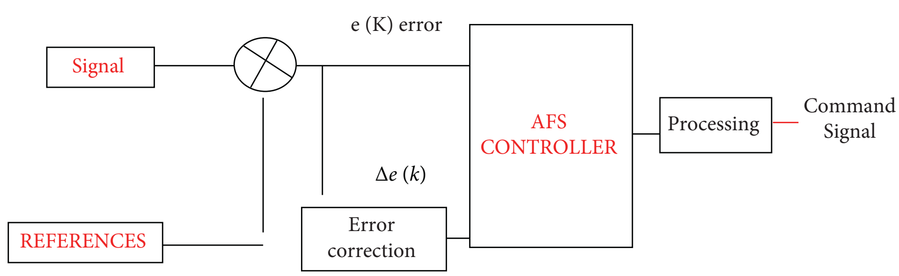

FIGURE 4: AFS controller.

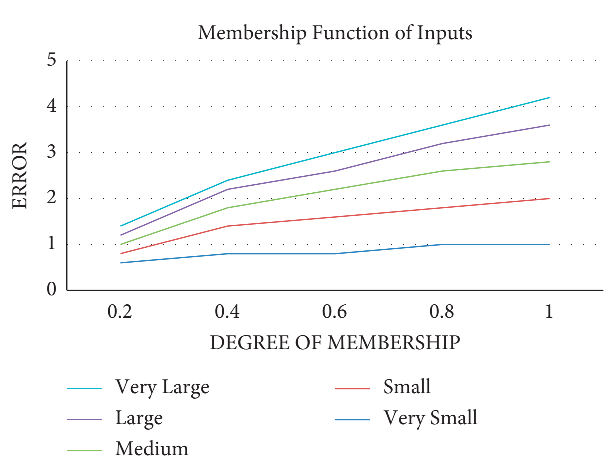

FIGURE 5: Membership function of inputs.

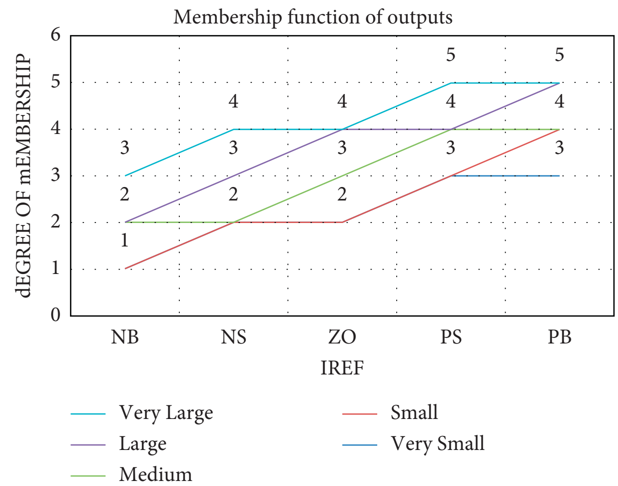

Figure 6: Membership function of output.

Table 1: AFS rules.

C_E	Very small	Small	Medium	Large	Very large
Very small	**ZO**	**NS**	**PS**	**PS**	**NS**
Small	**NB**	**ZO**	**PS**	**PS**	**NS**
Medium	**PB**	**PB**	**ZO**	**NS**	**NS**
Large	**PB**	**PB**	**NB**	**ZO**	**NS**
Very large	**NB**	**NB**	**NB**	**ZO**	**NS**

server. The framework was coupled to the adaptive fuzzy sliding approach, and a unity power factor was achieved along with the desired sinusoidal input and output outcomes.

2.5. Pseudo Code for IM Converter

2.6. AFS Algorithm for Cloud Server Side. This section discusses how neighborhood information is obtained and the stacking of indirect parameters of the matrix converter in the IoT. In addition, the proposed AFS strategy is given. When the proposed AFS technique is shown to the various centers differently from existing traditional systems such as PID, FUZZY, and ANFIS, the data collection speed and the logical outcome are high. Two and three IoT units represent a parameter, and this benchmark quantifies the IoT contractual qualities of the groups squeezed from the sender near the zone, bunch inaction in the senders near the zone, and the IoT unit differentiation into the goal unit. The probabilities of shift for the relationships can be found for these characteristics. These attributes are objectively presented as follows:

Through linking the electrical power supplied to the IMC and the mechanical energy supplied to the whole device, the IMC dependent on AFS can be tested. The above-listed algorithms have ideal results for an indirect matrix converter unit power factor.

3. Results and Discussion

Simulation is performed using SIMULINK/MATLAB as shown in Figure 4. The SIMULINK library incorporates inbuilt models of numerous electrical and electronic segments and gadgets, for example, diodes, MOSFETs, capacitors, control supplies, etc. The circuit components are associated according to outline without error, the parameters of all parts are designed according to prerequisites, and reproduction is performed.

The above Figure 7 demonstrates the SIMULINK model of an indirect matrix converter utilizing an AFS controller. The hardware points of interest of the proposed framework converter particulars are given in Table 2 and equipment setup is shown in Figure 7.

Figure 8 above shows the current source and the quick reactive power, both with reactive and reactive power. At first, the weighting factor C is set to zero, with the goal of preventing active control. The upper load current THD is 2.37% satisfied by this result, while the lower load current THD is 2.23%. The transitory reactive power minimization is performed, and the actual THD source is 21.73%.

The hardware structure of the proposed matrix converter topology is seen in Figure 9. MOSFETs are used for both optional and low voltage switches. High-voltage side switches are identified by IGBTs. Programmable system-on-chip (PSoC) for the transmission of PWM signals and changes in the final goal for the two-fold platform converter, taking into account the voltage and current recognized. The deliberate forms of the wave show separately.

Figure 10 shows the GUI window, which is the controller module, where the data is changed over to the extraordinary regard using increment factors and a while later shows the characteristics and processed adequacy. In fact, even with the

Input: a source of the indirect matrix converter.
Output: motor.
Begin
Every pattern of power Pi from IMC
V_{out} = every pattern generation (P_{i}).
Source voltage $Vs = \sum_{i=1}^{\text{size}(cp)} V_{\text{out}} P_i$
End
To select the maximum power
$\text{Power}(P) = \text{Max}(\forall(V_i(V_S)))$
Activate the designated MOSFET M_{i}.
$$\text{Pattern generation}(PS) = \{M_i, \{C1, C2, Cn\}, \{V1, V2, V3 \ldots Vn\}, Vi\}$$
Perform pattern generation
$CP = \sum P_i(CP) + P_S$
Stop.

Algorithm 1: Pseudo code for IM converter.

Input: indirect matrix converter's values
Output: load M
Input voltage = V_{in}
Begin
Load 9val hi, h20
  If h2 = null
return h1
else
    return xmeld (h1, h2);
end
Procedure return xmeld (val h1, h2);
IF $h1$ = null
return h2;
If item(h1) > item (h2)
H1 ↔ h2
(**1child** (h1), rchild (h1) ← (xmeld(rchild(h1), h2), 1child(h1));
return h1;
Stop.

Algorithm 2: AFS algorithm for cloud server side.

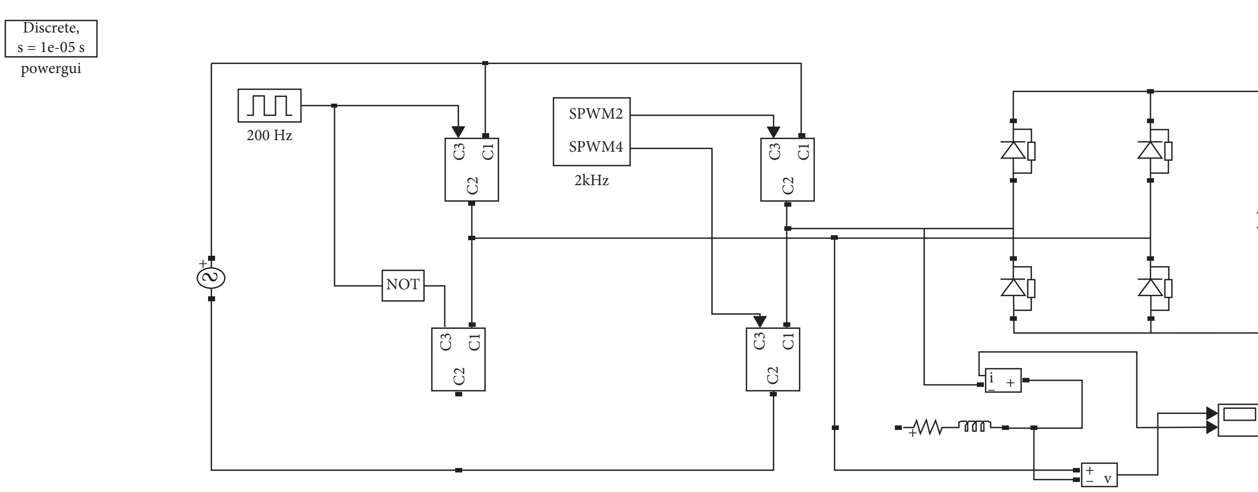

Figure 7: Simulation diagram of indirect matrix converter.

Table 2: Design parameters.

Parameters	Symbols	Value
Input voltage range	V_{in}	20 V
Output voltage	V_o	440 v AC
Output power	P_o	1.29 KW
Magnetizing inductance	L_m	310 μH
Leakage inductance	L_{ik}	15.8 μH
Quality factor		0.61
Resonant frequency	F_r	3.84 KHz
Switching frequency	F_s	3.84 KHz
Resonant capacitor	C_r	1.09 μH
Snubber capacitor	CT1, CB1	6.8 nF

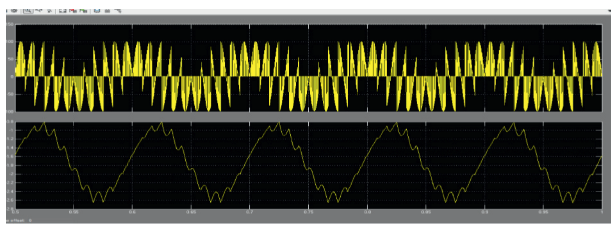

Figure 8: IM converter voltage and current.

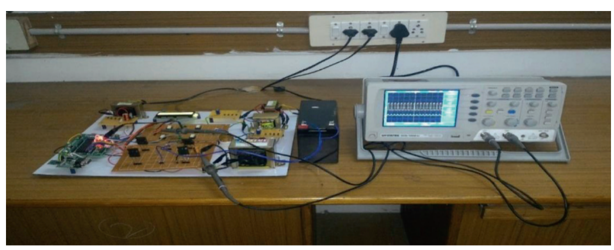

Figure 9: Hardware setup.

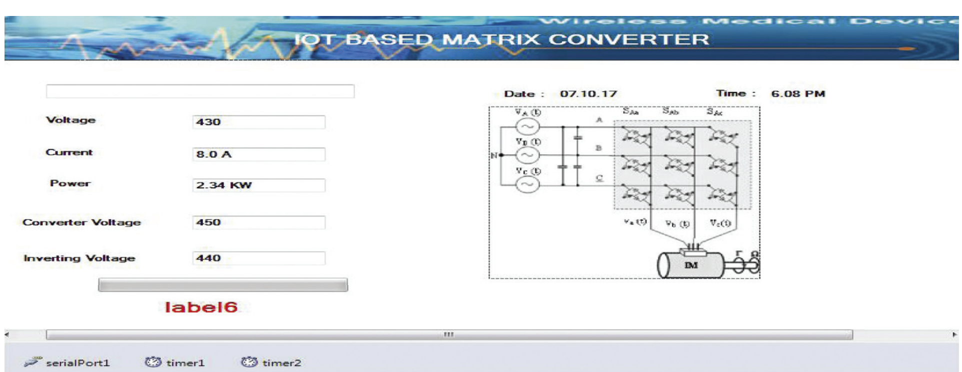

Figure 10: GUI snapshot of the cloud server.

issues in data transmission utilizing the WSN in a couple of circumstances, the structure will have the ability to convey supportive watching information, since all getting ready is done over the framework. The going with deficiency examination is used as a piece of the arranged solicitation, like voltage, current, suffering state error, FFT, and THD checking.

Figure 11 shows that the sophisticated and adaptive, fluid sliding control approach has made it powerful to carry out inquiries into various algorithms rather than different techniques.

Figure 12 illustrates a cloud-based safety evaluation using multiple methods, and it shows beyond question that

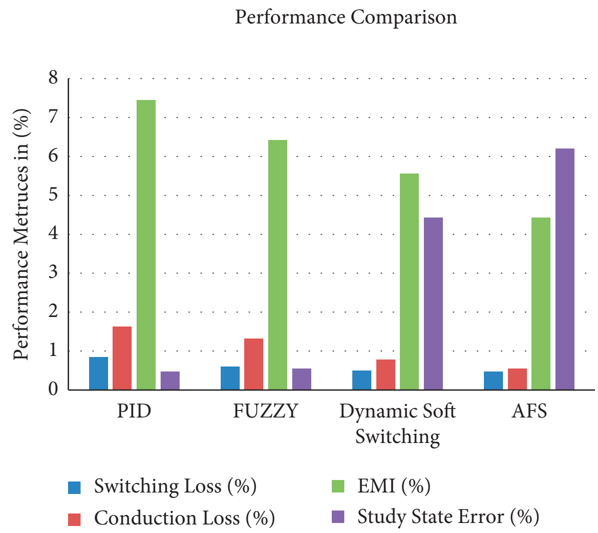

Figure 11: Performance comparison.

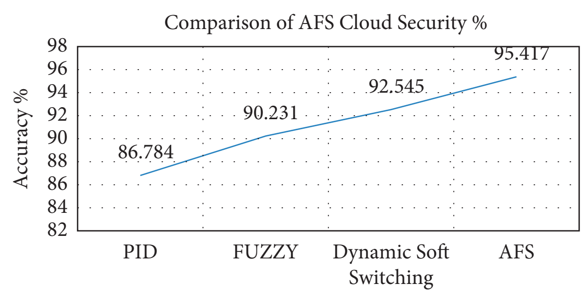

Figure 12: Cloud security comparison.

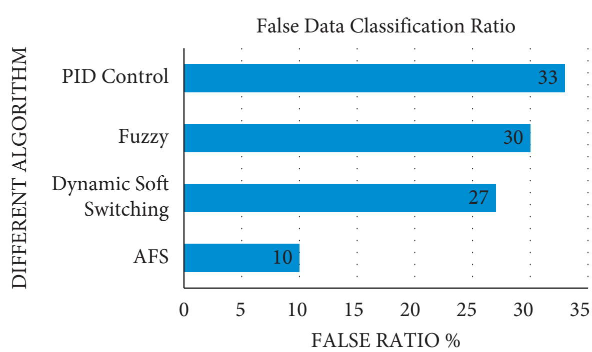

Figure 13: Comparison of various methods in false ratio.

Table 3: Comparison of features from different algorithms.

Compared features	PI control	FUZZY	Dynamic soft switching	AFS
Cost	High	High	Medium	Low
Physical structure	Big	Big	Small	Small
Resistance to work environment	High	High	Medium	Low
Finding fault	Difficult	Difficult	Easy	Very easy
Communication	Difficult		Difficult	Very easy
Production planning	Difficult	Moderate	Easy	Very easy
Security	Low	Moderate	Low	High
Monitoring data	Unavailable	Moderate	Difficult	Very easy

AFS has improved its precision compared with other techniques.

Figure 13 shows the correlation of results obtained from the execution of the different techniques for data classification in the IoT server. When contrasted with other regular techniques, the proposed AFS strategy has a lower false classification rate.

The above Table 3 analyzes the correlation features of a different algorithm. When contrasted with other conventional methods, the proposed system gives a perfect result. From the most basic assessment played out, the proposed AFS procedure has been surveyed with various parameters and has conveyed precision when compared with another customary methodology.

4. Conclusion

In this work, we proposed an indirect matrix converter that has the collective focal points of voltage control ability from an indirect matrix converter utilizing adaptive fuzzy sliding methods of IoT, including in nature interleaved operation, wide direction extend, low part focus, little output swell, adaptable pick-up augmentation, and high effectiveness. The proposed topology has decreased the multiple-faceted design that is suitable for large-scale output mix, relative to other customary developments such as the tapped inductor approach, multi-inductor transfer strategy, or transforming strategy. The proposed AFS-based matrix converter has been validated through simulation using MATLAB software. The control clock signals are generated for the positive and negative clock pulses of the sequence. Here the sinusoidal reference signal is compared with the switching frequency of triangular carrier frequency. The hardware results were also verified to validate the simulation. As compared to other conventional methods, the proposed AFS technique has achieved 97.23% efficiency in full load conditions.

Data Availability

The data used in this study will be made available on request.

Conflicts of Interest

The authors declare that they have no conflicts of interest.

References

[1] Y. N. Hassan, G. Ramanathan, and M. Kovatsch, “Demo: developing smart environments in the internet of things with the semantic IDE,” in *Proceedings of the 2015 5th International Conference on the Internet of Things (IoT)*, pp. 1-2, Seoul, Korea, October 2015.

[2] X. Wang, H. Lin, H. She, and B. Feng, “A research on space vector modulation strategy for matrix converter under abnormal input-voltage conditions,” *IEEE Transactions on Industrial Electronics*, vol. 59, no. 1, pp. 93–104, 2012.

[3] J. Rodriguez, J. Espinoza, M. Rivera, F. Villarroel, and C. Rojas, “Predictive control of source and load currents in a direct matrix converter,” in *Proceedings of the 2010 IEEE International Conference on Industrial Technology*, pp. 1826–1831, Via del Mar, Chile, March 2010.

[4] M. Hamouda, F. Fnaiech, K. Al-Haddad, and H. Kanaan, “Matrix converter control: a sliding mode approach,” in *Proceedings of the IEEE IECON*, vol. 3, pp. 2295–2300, Busan, Korea, November 2004.

[5] H. Hojabri, H. Mokhtari, and L. Chang, “A generalized technique of modeling, analysis, and control of a matrix converter using SVD,” *IEEE Transactions on Industrial Electronics*, vol. 58, no. 3, pp. 949–959, Mar 2011.

[6] B. Metidji, F. Tazrart, A. Ahmed, N. Taib, and T. Rekioua, “A new fuzzy direct torque control strategy for induction machine based on indirect matrix converter,” *International Journal of Research and Reviews in Computing Engineering*, vol. 1, no. No. 1, pp. 18–22, 2011.

[7] L. I. Zheng, “Simulation on matrix converter fed induction motor DTC drive system,” in *Proceedings of the IEEE Conference On Intelligent Systems And Application (ISA)*, pp. 1–4, Wuhan, China, May 2009.

[8] B. Cai and J. Zhu, “Direct torque control for induction machine based on space vector modulated matrix converters,” in *Proceedings of the IEEE International Workshop On Database Technology And Applications (DBTA)*, pp. 1–4, Wuhan, China, November 2010.

[9] C. Venugopal, “Fuzzy logic based DTC for speed control of matrix converter fed induction motor,” in *Proceedings of the IEEE conference on power and energy (PECON)*, pp. 753–758, Kualamampur, Malaysia, December 2010.

[10] V. Faraji, M. Aghasi, D. A. Khaburi, and M. Kalantar, “Conductance matrix approach to the synthesis of active resistive N - port networks,” in *Proceedings of the IEEE Conference On Electrical, Electronics And Computer Engineering(ELECO)*, pp. 309–314, May 2013.

[11] V. Faraji and D. A. Khaburi, “A new approach to DTC-ISVM for induction motor drive system fed by indirect matrix converter,” in *Proceedings of the 2nd Power Electronics, Drive Systems, And Technologies Conference*, pp. 367–372, Tehran, Iran, February 2011.

[12] H. F. Abdul Wahab and H. Sanusi, “Simulink model of direct torque control of induction machine,” *American Journal of Applied Sciences*, pp. 1083–1090, 2008.

[13] Y. Li and W. Liu, “A novel direct torque control method for induction motor drive system fed by two-stage matrix converter with strong robustness for input voltage,” in *Proceedings of the 2nd IEEE conference on industrial electronics and applications(ACIEA)*, pp. 698–702, Harbin, China, May 2007.

[14] D.-Fa Chen, C.-W. Liao, and K.-C. Yao, “Direct torque control for a matrix converter based on induction motor drive systems,” in *Proceedings of the 2nd IEEE conference on innovative computing, information, and control(ICICI)*, pp. 101–104, Kumamoto, Japan, September 2007.

[15] P. Baroni, P. Pillai, V. W. C. Chook, S. Chessa, A. Gotta, and Y. F. Hu, “Wireless sensor networks: a survey on the state o-+f the art and the 802.15.4 and ZigBee Standards,” *Computer Communication*, vol. 30, no. 7, pp. 1655–1695, 2007.

[16] F. Salvadori, M. de Campos, P. S. Sausen et al., “Monitoring in industrial systems using wireless sensor network with dynamic power management,” *IEEE Transactions on Instrumentation and Measurement*, vol. 58, no. 9, pp. 3104–3111, 2009.

[17] V. C. Gungor and G. P. Hancke, “Industrial wireless sensor networks: challenges, design principles, and technical

approaches," *IEEE Transactions on Industrial Electronics*, vol. 56, no. 10, pp. 4258–4265, 2009.

[18] H. Wei, Y. Chen, J. Tan, and T. Wang, "Sambot: a self-assembly modular robot system," *IEEE*, vol. 16, no. 4, pp. 745–757, 2011.

[19] J. Takahashi, T. Yamaguchi, K. Sekiyama, and T. Fukuda, "Communication timing control and topology reconfiguration of a sink-free meshed sensor network with mobile robots," *IEEE*, vol. 14, no. 2, pp. 187–197, 2009.

Hindawi
Scientific Programming
Volume 2022, Article ID 4208749, 12 pages
https://doi.org/10.1155/2022/4208749

Research Article

Optimization of Electronic Data Investigation Mode Based on Intelligent Perception and Positioning Technology

Xin Zhang [1,2] and Chao Cheng [3]

[1] College of Law, JiLin University, ChangChun, JiLin, China
[2] Law Department, Jilin Police College, ChangChun, JiLin, China
[3] School of Computer Science and Engineering, Changchun University of Technology, Changchun 130012, China

Correspondence should be addressed to Xin Zhang; xinz16@mails.jlu.edu.cn

Received 21 December 2021; Revised 19 January 2022; Accepted 31 January 2022; Published 25 March 2022

Academic Editor: Punit Gupta

The exploration reported here is aimed at obtaining the geographic information and ecological information of the user's specific location to understand the real-time needs of the user and provide users with accurate and timely services. Firstly, intelligent sensing and positioning technology is introduced under the background of big data. Then, the Geographic Information Systems (GIS) and Location-Based Service (LBS) technology are sketched out. Besides, an environmental intelligent perception and positioning model is proposed based on the GIS technology, LBS technology, and visible light propagation model. Finally, the proposed model is verified by experiments. The research results demonstrate that the environmental intelligent perception and positioning model can improve the positioning ability and efficiency of the users' location and significantly enhance the accuracy of the location of the target. The positioning accuracy of the positioning system based on GIS combined with LBS reaches more than 80%, meeting the positioning requirements in daily life. Therefore, the research reported here provides a new perspective and new method for intelligent perception, makes a guarantee for further improving the efficiency of user work and life, and sets an example for future research.

1. Introduction

With the further expansion of China's urban scale, the increasing population, and the continuous development of various electronic information technologies, the emergence of diverse intelligent technologies and equipment has completely changed the life and learning style of people. Smart devices carried by device users and the growing popularity of Internet of Things (IoT) facilities can not only connect to the Internet anytime and anywhere, but also feel the user's movements and changes in the environment at any time. When the smart device can obtain the user's movements and the changes of the surrounding geographical environment and ecological environment, it can help users to improve their limited perception range [1, 2] and help users to expand their perception.

Big data technology refers to the application of big data to solve problems. Big data denotes a large-scale data collection that greatly exceeds the capabilities of traditional database software tools in terms of acquisition, storage, management, and analysis [3]. It has four major characteristics, namely, massive data scale, fast data circulation, diverse data types, and low value density. Intelligent perception involves visual, auditory, tactile, and other perceptual abilities. Both humans and animals can interact with nature through various intelligent perception abilities. For example, autonomous vehicles obtain intelligent perception ability by sensing equipment like laser radar and other artificial intelligence algorithms [4]. Machines have more advantages than humans in perceiving the world, since human beings perceive the surroundings passively, but machines can perceive the environment actively, such as laser radar, microwave radar, and infrared radar. Either a sensing robot like Big Dog or an autonomous vehicle takes full advantage of neural network technology and big data, and consequently the machine has become increasingly close to humans in terms of perceptual intelligence [5, 6].

Geographic Information System (GIS) [7], also known as geographic information science, refers specifically to a fixed and vital spatial information system. GIS is a special system for the collection, analysis, and management of partial or overall Earth surface information with the support of computer technology and various computational detection methods. Location Based Services (LBS) [8] technology is a means of using various positioning technologies to obtain the location information and the basic services of the mobile network. For intelligent systems, spatial positioning software can capture and collect location information and other spatial and attribute information, automatically extract the information of interest from the data, and display the information to users in the form they want. Mobility, distribution, individual perception, and popularization are the most fundamental characteristics of this system.

The different luminance and angle of visible light in different spaces are analyzed based on the visible light propagation model. Besides, the GIS technology is combined with LBS technology to establish an environmental intelligent perception and positioning model. Finally, the model is verified by experiments. The research reported here enriches the development of intelligent perception and positioning technology in China from a new perspective and provides more convenient behavioral guidance for the majority of users. The positioning system combining LBS and GIS reported here can provide high-precision positioning, and the positioning accuracy in a complex environment is also about 80%. These outcomes lay a solid foundation for the rapid development of urbanization and the planning research of urbanization in China in the future.

2. Construction of the Intelligent Perception and Positioning Model

2.1. Big Data and IoT Technology

2.1.1. Big Data Technology. Big data refers to the data set that cannot be captured, managed, and processed by conventional software tools within a certain period. It is a massive and diversified information asset with high growth rate that requires a new processing model for stronger abilities of decision-making, insight, and optimization [9, 10].

Here are the multiple advantages of big data:

(a) Better decision-making: big data analysis can provide business decision-makers with the data-driven insight they need to help enterprises compete and develop their business and improve productivity. In addition, the insights gained from these analyses often enable organizations to improve productivity more widely throughout the company and reduce costs.

(b) Improve customer service: social media and customer relationship maintenance systems can provide enterprises with much information about their customers. Naturally, they will use these data to serve these customers better.

(c) Fraud detection: another common use of big data analysis is fraud detection, especially in the financial services industry. One advantage of big data analysis systems that rely on machine learning is that they are excellent in detection.

(d) Increasing revenue: when organizations use big data to improve decision-making and customer service, increasing revenue is usually a natural result, improving flexibility.

(e) Better innovation: innovation is another general interest of big data.

The most prominent feature of big data is the huge size beyond the analysis capability of traditional data processing software such as Excel and MySQL. This also means that in the big data era there will be completely different processing technologies for either data storage or data processing, such as Hadoop and Spark. Within the enterprise, data experiences various processing processes from production, storage, analysis, to application, and interrelates with each other, forming the overall architecture of big data. Figure 1 illustrates the basic architecture of big data [11].

For big data technology, there are usually the following processing steps for data before the finalizing data report or algorithmic prediction by data:

(a) Data acquisition: it refers to the synchronization of data and logs generated by the application into the big data system.

(b) Data storage: massive amounts of data need to be stored in the system to facilitate the next use of queries.

(c) Data processing: the original data needs to be filtered, spliced, and converted to be finally applied, collectively called data processing. Generally, there are two types of data processing. One is offline batch processing, and the other is real-time online analysis.

(d) Data application: the processed data can provide services to the outside world, such as generating visual reports, providing interactive analysis materials, and providing training models for recommendation systems.

2.1.2. IoT. The IoT technology is an emerging information service architecture based on the Internet and recognition technology and communication technology, which was proposed in 1999 at Massachusetts Institute of Technology in the United States. This architecture aims to enable the information technology infrastructure to provide safe and reliable commodity information through the Internet, and to create an intelligent environment to identify and determine commodities to facilitate information exchange within the supply chain. The increasingly booming IoT technology at present has brought changes to all aspects of human life, but also brought a series of urgent technical and ethical issues,

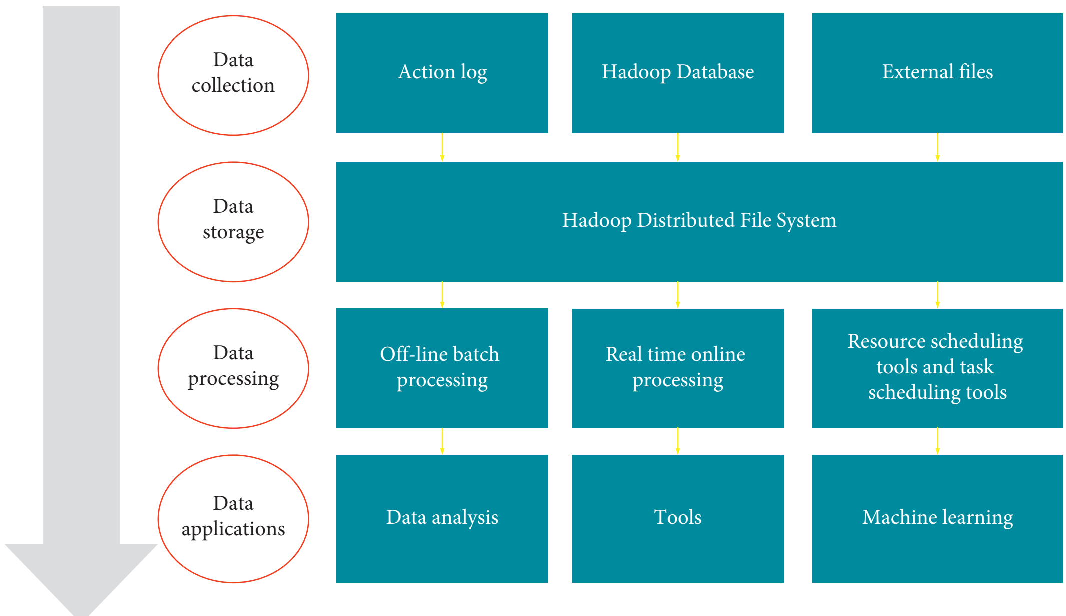

Figure 1: Basic architecture of big data.

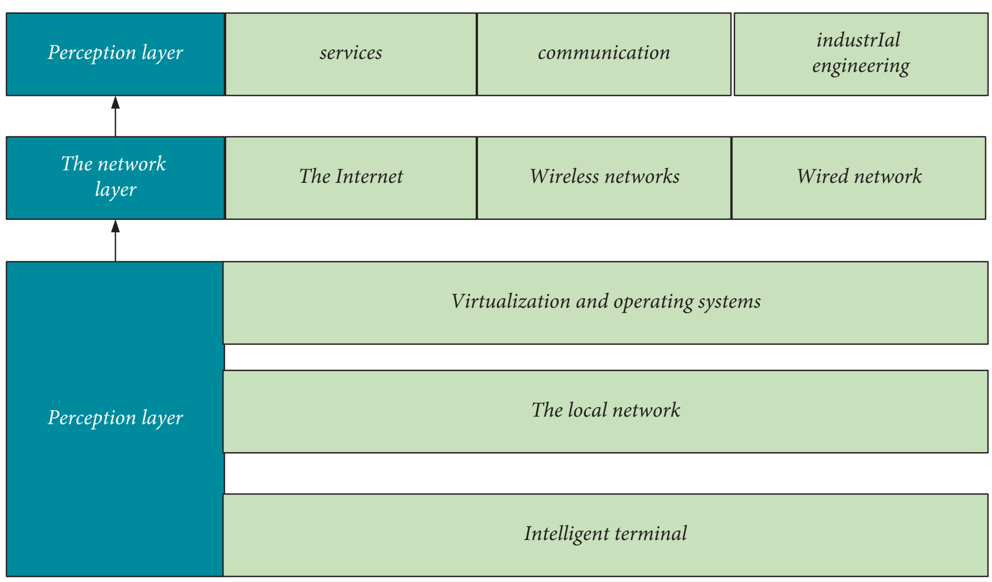

Figure 2: Architecture of IoT.

security issues, and legal issues to be addressed. The IoT on the user side is usually deployed in the device domain, network domain, data domain, and application domain, which empowers the device with the ability of intelligent perception, automatic assembly connection, and deployment strategy. Besides, IoT devices can solve the problem of data concentration and provide local business logic and intelligent service [2, 12]. Figure 2 reveals the architecture of IoT.

Through Figure 2, the IoT architecture is primarily composed of three layers, namely, two perception layers and a network layer. The perception layer consists of intelligent terminals, local networks, virtualization, and operating systems. The network layer mainly contains networks, wireless networks, and wired networks. The last perception layer is a port mainly responsible for communication and service. The first perception layer transmits information to the relevant perception layer through the network layer, thus forming the universal interconnection of IoT.

Big data technology and IoT technology complement each other. The IoT is the “Internet of things connected to each other.” The perception layer of IoT generates massive data, greatly promoting the development of big data. Similarly, big data applications also play the value of the IoT, which in turn stimulates the use demand of IoT. The intelligent perception and positioning technology studied here cannot be separated from the support of IoT and big data

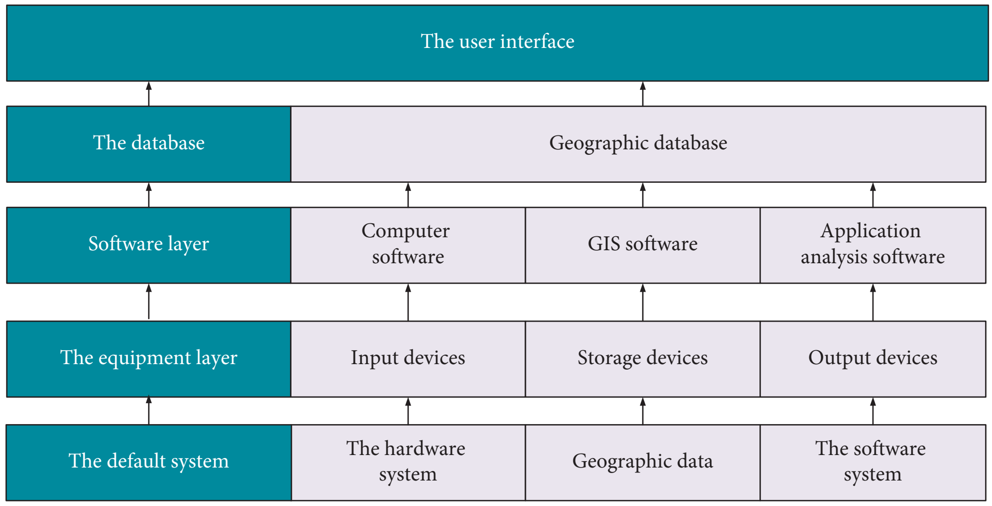

Figure 3: Structure of the GIS system.

technology. Big data technology provides abundant data resources for intelligent perception. The accurate positioning of an object can be easily determined according to data, which not only realizes intelligent perception but also provides convenience for the demanders. Similarly, the IoT technology can integrate all resources, including relevant positioning data, through its own broad channels, to meet the various needs of the masses. The IoT technology and big data can provide impetus for the rapid development of intelligent sensing and positioning technology. In turn, intelligent sensing and positioning technology can enrich the field of IoT, and they complement each other.

2.2. Positioning Technology and Behavior Perception System Based on GIS and LBS. The system design follows the following principles: (1) security: system security and confidentiality mainly refer to the security of system operation, data security, and confidentiality; (2) practicability: the practicability of the system is the premise of system maintenance and operation and benefit creation, and the primary goal of system construction; (3) advanced nature: the system must have advanced solid nature, including system design, operation platform, development tools, database selection, and hardware equipment selection, all of which should conform to the mainstream technology development direction; (4) friendliness: the friendliness of the system refers to the unified style, beautiful, and convenient use of the interface.

2.2.1. GIS Positioning. GIS is a comprehensive discipline combining geography, cartography, remote sensing, and computer science, which has been widely used in different fields. It is also a computer system for inputting, storing, querying, analyzing, and displaying geographic data. GIS is a computer-based tool that can analyze and process spatial information (in short, it maps and analyzes phenomena and events on the Earth). GIS technology integrates the unique visual effect and geographic analysis function of maps with general database operations such as query and statistical analysis. Figure 3 shows the structure of the GIS system [13, 14].

The GIS system can be divided into the following sections: (a) developers, the most important part of the GIS system. Before using the GIS system, developers need to define the various types of data and tasks in the GIS system, and write relevant programs. Therefore, high-level developers are particularly important for the GIS system; (b) data: the accuracy of data will directly affect the query results; (c) hardware: the performance of computer hardware also directly affects computing power and the speed of data processing; (d) software: the software includes the system software of, database, and GIS software of the computer; (e) process: the GIS system needs to clearly define tasks to generate testable results.

2.2.2. LBS Positioning Technology. LBS positioning technology uses mobile terminals to connect the wireless communication network or Global Positioning System [15], to find the corresponding coordinate data of the user in the database. Then, the user's geographic coordinate information is combined with other information around the user to provide location-related peripheral service information [16, 17]. Figure 4 provides the fundamental structure of LBS positioning technology.

2.2.3. Behavior Perception System. The positioning technology can be used to obtain the real-time physical state of current equipment users, but the intelligent perception technology is the foundation of the subsequent understanding of user information and surrounding information. The perception of the surrounding information is completed by GIS system and LBS system, while the user behavior perception requires the user perception system of the device. The sensor installed in the corresponding position of the device is utilized to collect the user's current state data and analyze the data. The processed data is compared with the

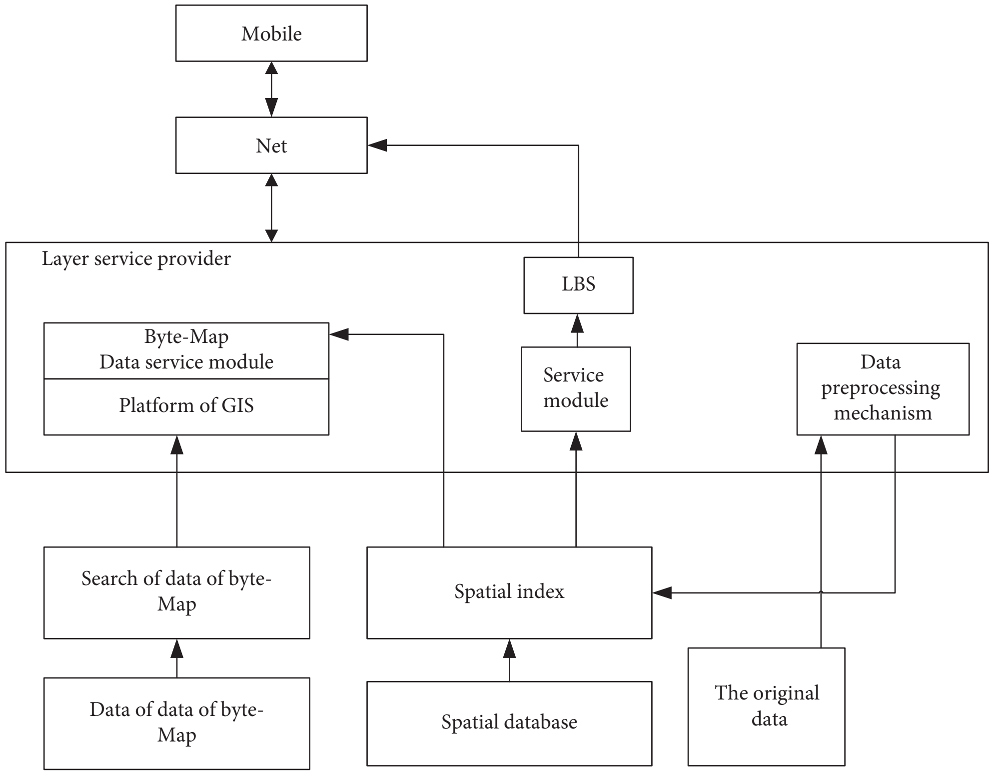

Figure 4: Fundamental structure of LBS positioning technology.

user's behavior data set to obtain accurate services for different users [18].

The system is mainly divided into the data layer, business layer, transmission layer, and display layer. The data layer contains the server data layer and terminal data layer server. The data layer is mainly responsible for storing spatial data, attribute data, and map data, while the terminal data layer is responsible for storing system pictures. The business layer is responsible for data reading, transformation, analysis, and requests and responses to client data. The transport layer is responsible for data transfer, mainly via the mobile Internet. The display layer is responsible for displaying attribute data, spatial data, data operation, etc. Figure 5 reveals the structure of this system.

2.3. Indoor Perception and Positioning Model Based on Visible Light

2.3.1. Module Composition. System A is designed as an indoor positioning system based on visible light, which is composed of several modules shown in Figure 6. Table 1 indicates the operation flow of System A [19, 20].

In addition, the corresponding protection mechanism is set up, since the environment of the system application is relatively complex and changeable. When the environment in which the device is deployed changes (such as communication equipment falling from the height or being loaded into the container by the user), the system operation will be disturbed. Then, the protection mechanism with excellent system stability and robustness will first determine the obtained data to exclude the input value obtained under abnormal conditions. If it is the output value obtained under abnormal conditions, the system will adjust the weight of the particles. Otherwise, the system will run according to the previous process.

2.3.2. Visible Light Receiving Model. The direction of the user's handheld device significantly impacts the visible light intensity. This paper uses the mobile camera as the visible light receiving device. The visible light intensity is significantly affected by the orientation of the device held by the user. Therefore, when the device is laterally twisted or yawed, there is an appreciable impact on the light intensity received by the device. However, the horizontal rotation has little effect on the light intensity received by the device, so the following model is obtained [21–23]. Figure 7 is the light incidence diagram.

In Figure 7, ϕ represents the radiation angle of the light source, θ denotes the incident angle of the light source, and d refers to the distance from the light source to the device receive. Among them, two variables are fixed to test the relationship between the third variable and the received light intensity. Hence, the propagation of basic visible light can be described as follows:

$$J = L_0 \frac{\cos\phi \cdot e^{-(\theta/2)^2}}{d^2}. \quad (1)$$

In (1), when L0 equal to the received light intensity $\theta + 0$, $d = 1$ m, and $J = 1$.

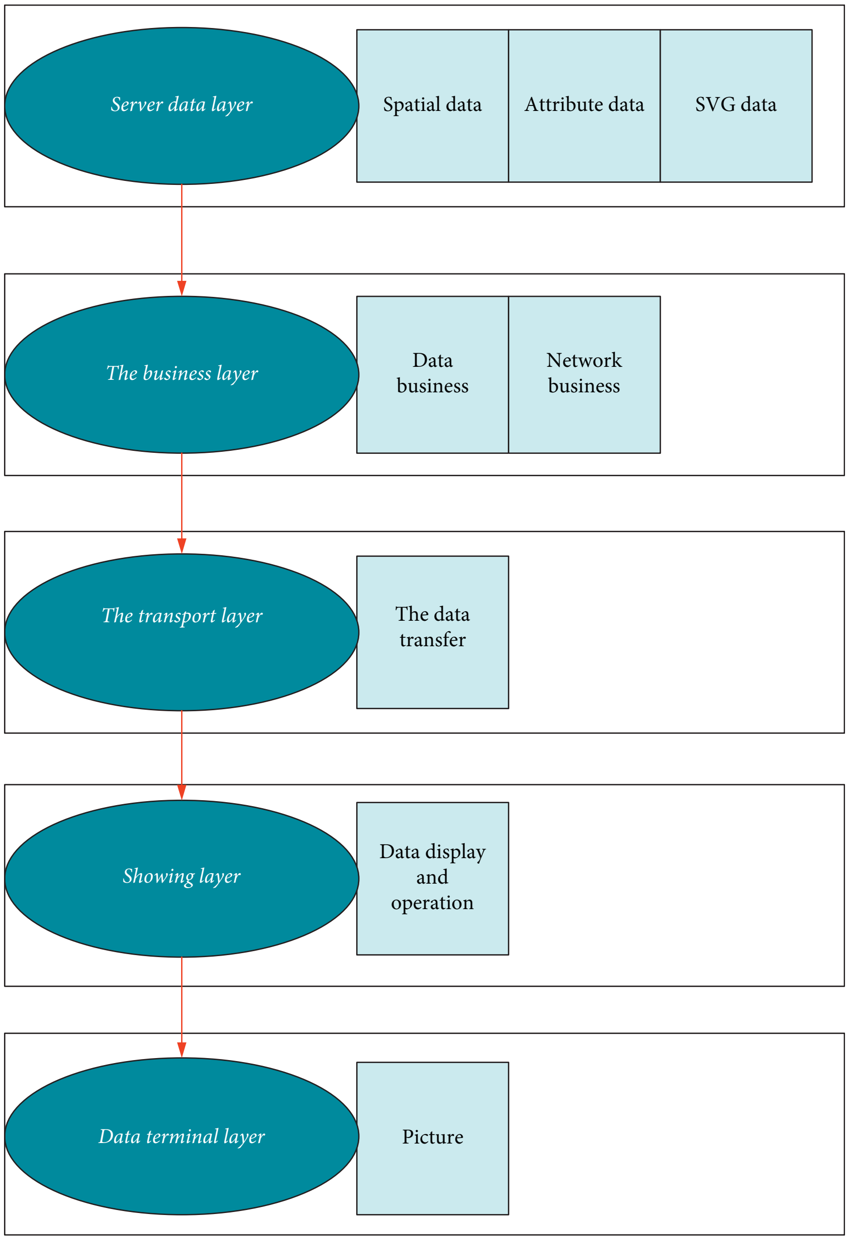

Figure 5: Behavior perception system based on LBS combined with GIS.

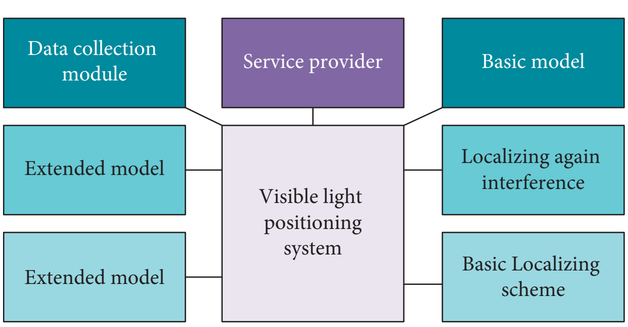

Figure 6: Indoor visible light positioning system.

Considering the robustness of the device, it is necessary to simulate and set up a defense mechanism for various interferences. For example, consider the following:

(a) Different devices have different efficiencies in their light collectors, which will result in pronounced differences between the light data sequences collected by different devices even if the user's actions and routes are identical. Therefore, the received light intensity values here are normalized and transformed it into the closed region [0, 1]. Then, the system can use the dynamic time warping algorithm to normalize the collected light data.

(b) Obstacles blocking light: since obstacles will make the light intensity data collected by the light sensor different from the actual value, a function $b(l)$ is set to describe this. If the light is not covered, $b(l) = 1$. Otherwise, $b(l) = 0$.

(c) The condition of multiple light sources: when there are multiple light sources in a scene, which are

Table 1: Operational process of indoor positioning system based on visible light.

Step	Module	Operation
1	Visible light sensor	Collect received light intensity
2	System	Collect the corresponding acceleration sensor data and gyroscope sensor data
3	Positioning module	A series of candidate positions are generated according to the current scene, or candidate particles are selected in a particle filter
4	Pedometer	The RLS sequence collected in this step, the corresponding acceleration sampling sequence, and the gyroscope sampling sequence are packed as the input of the positioning module
5	Positioning module	The received light intensity of each candidate particle is calculated by the designed visible light propagation model
6	System	By comparing the received light intensity calculated by RLS and visible light propagation model, the system gives each candidate particle different weights. Particles with weak weight and those violating scene restrictions will be deleted. Further, the system checks whether the remaining particle sets meet the convergence requirements. If it is satisfied, the system outputs the best candidate particle and constantly updates its location for real-time tracking. Otherwise, the system is ready to accept the user's next data input. In this process, the last round of surviving candidate particles is taken as candidate particles of the current calculation round

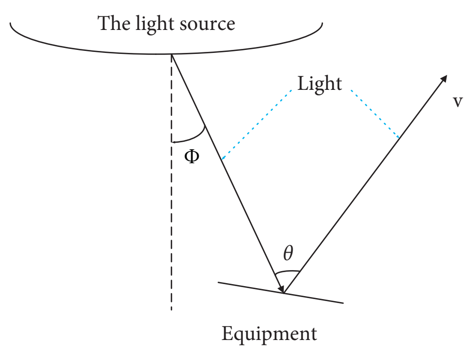

Figure 7: Incidence of light.

distributed densely, the received light intensity is likely to be affected by multiple light sources. At this moment, it is insufficient to only consider the influence of a single light source. Therefore, the following theoretical model is used for analysis: set a region containing n light sources, and the received light intensity data at m position are collected, as shown in the following equations:

$$J_j = \sum_{i=1}^{n} L_{sij}, \tag{2}$$

$$J_j = \sum_{i=1}^{n} L_{0i} \cdot p_{ij}, \tag{3}$$

$$p_{ij} = \frac{e^{-\left(\theta_{ij}^2/\delta^2\right)} \cos \phi_{ij}}{d_{ij}^2}. \tag{4}$$

Among the above three equations, ϕ_{ij} represents the radiation angle of the light source i, θ_{ij} signifies the incident angle of the light source i, and d_{ij} denotes the relative distance of the light source i. Meanwhile, $L0_i$ is the matrix, which is calculated according to

$$\left[J_i\right] = \left[p_{ij}\right]\left[L_{0i}\right]. \tag{5}$$

(6) describes the complete visible light model, and (7) illustrates the three-dimensional position of the light source i. Moreover, (8) indicates the position vector of the equipment, while (9) shows the direction vector of the equipment. Among them, d_i, ϕ_i, and θ_i are the radiation angle, incidence angle, and relative distance of the light source i.

$$J(c, v) = \sum_{\substack{i\in[1,n] \\ b(Li)=1}} L_{0i} \frac{e^{-\left(\theta_{ij}^2/\delta^2\right)} \cos \phi_{ij}}{d_{ij}^2}, \tag{6}$$

$$l_i = \left(l_{ix}, l_{iy}, l_{iz}\right), \tag{7}$$

$$c = \left(c_x, c_y, c_z\right), \tag{8}$$

$$v = \left(v_x, v_y, v_z\right), \tag{9}$$

$$d_i = \left|l_i - c\right|. \tag{10}$$

2.3.3. Positioning Scheme. The principle of the positioning module is to use the movement of the device holder to weaken or even eliminate the error caused by the single light-source receiving system, to obtain the current specific location information of the user. Therefore, $L(t)$ is denoted as the receiving light intensity of the light source at the time t, and $G(t)$ represents the gyroscope parameters of the collected equipment. Besides, $D(t)$ denotes the rotation matrix data of the collected equipment, and $V(t)$ shows the direction of the equipment. The step number of the equipment owner is indirectly calculated by collecting the acceleration of the equipment. Therefore, the data input of the positioning module contains $L(t)$, $G(t)$, $D(t)$, and $V(t)$. After operation, the system outputs real-time position information and the three-dimensional coordinate position, step size, and moving direction of the user. The steps of the positioning scheme are as follows [24].

a. Initialization. Firstly, numerous particles are distributed discretely in the three-dimensional space. The i-th scattered particle is denoted as $P(i)$. Moreover, for each single particle in the space, $p \in P(i)$, and the state of the particle is represented by

$$p_i = f(\omega, c, s, o). \tag{11}$$

In (11), ω refers to the possibility that this particle locates in the same position with the device holder, while c denotes the three-dimensional coordinates of the device holder, and s stands for the possible step size of the device user. Besides, o stands for the orientation vector of the device user. Due to the uniform distribution of particles in the space, the positioning perception system must select c, s, and o uniformly and randomly and add different weights to the three parameters, respectively. The weight is calculated according to (12), where $|p(i)|$ is the number of particles in the space system.

$$\omega = \frac{1}{|p[0]|}. \tag{12}$$

The mobility of the device holder leads to the iteration calculation of the system in the case of the original initial particle distribution, as the basis of the calculation of the next state. The state of the newly generated particles is calculated according to the particle distribution in the previous state and the motion state of the device holder during this period. Hence, the particles generated by a single iteration are called sub-generations, represented by p_c. The original particle in a single iteration is called parent generation, denoted as p_m. The single iteration time of the system increases from t_i to t_{i+1}, during which the particle state can be expressed as (13) and (14).

The owner of the device has a mobility feature that allows particles to operate continuously. The state of newly generated particles is calculated from the distribution of particles in the previous state and the motion state of the current device holder. Therefore, the particles generated by a single iteration are called sub-generations, which are represented by the symbol P_c.

$$p_m = p[i-1], \tag{13}$$

$$p_c = p[i]. \tag{14}$$

When the solution of p_c converges to a single particle and its position, or the number of iterations passes a certain threshold, the iteration will stop and the system outputs the particle p_{best} of p_c with the maximum weight. So the single parent particle state for the parent particle set $p(m)$ can be written as, and the single sub-generation particle state can be presented as (16).

$$p(m) = (\omega_m, c_m, s_m, o_m), \tag{15}$$

$$p_c = p[i]. \tag{16}$$

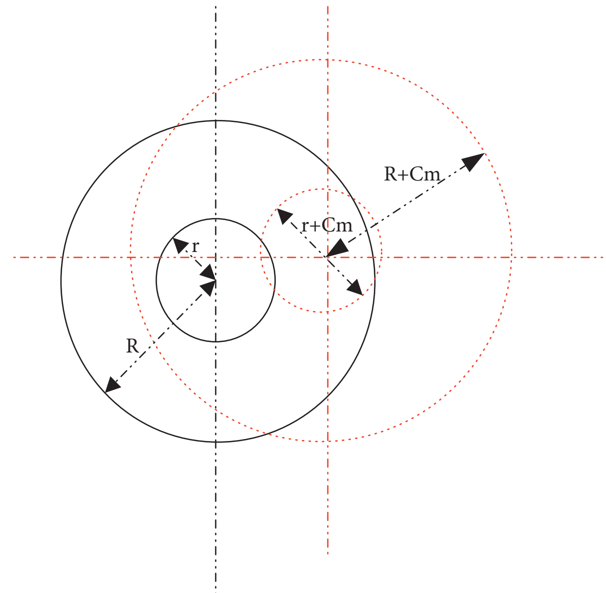

Figure 8: The normal distribution interval of the particle.

According to the above equations, the step size of the device holder is controlled in an annular range of $r \le s \le R$. Figure 8 displays the distribution of the walking interval of particles to more vividly illustrate the dispersion interval of particles [25].

The sub-generation particle $p(c)$ should fall into a ring range $r \le |c_c - c_m| \le R$, but if the particle $p(m)$ falls outside this range, $p(c)$ needs to be removed from the sub-generation set $p(m)$.

After the i-th step, the time increases from t_i to t_{i+1}. In this process, it is necessary to obtain the new received light intensity data to update the weight ω_c of the sub-generation particle set $p(c)$. The collected light intensity data is represented by the set $\{L\}$, and the light intensity data calculated by the visible light propagation model is represented by the set $\{H\}$.

There need to be $2|\{L\}|$ spatial locations for the parent particles and sub-generation particles generated during the iteration time increasing from t_i to t_{i+1}, to obtain the smooth data of set $\{H\}$. Each spatial position is denoted as ς_k, and H_k denotes the light intensity corresponding to each position ς_k. The corresponding occurrence time T_k of each position is shown in

$$T_k = t_i + \frac{k}{2|\{\varsigma_k\}|} \cdot (t_{i+1} - t_i). \tag{17}$$

A large weight represents a high possibility of the user to appear in the position, so when a position has the highest particle weight, it is most likely to be the position of the user. The dynamic time warping (DTW) is in the established system as the similarity detection method, with the relatively simple purpose to measure the similarity of two time series of different lengths. DTW is also applied widely, mainly in template matching, such as speech recognition of isolated words (recognition of whether the two voices represent the same word), gesture recognition, data mining, and

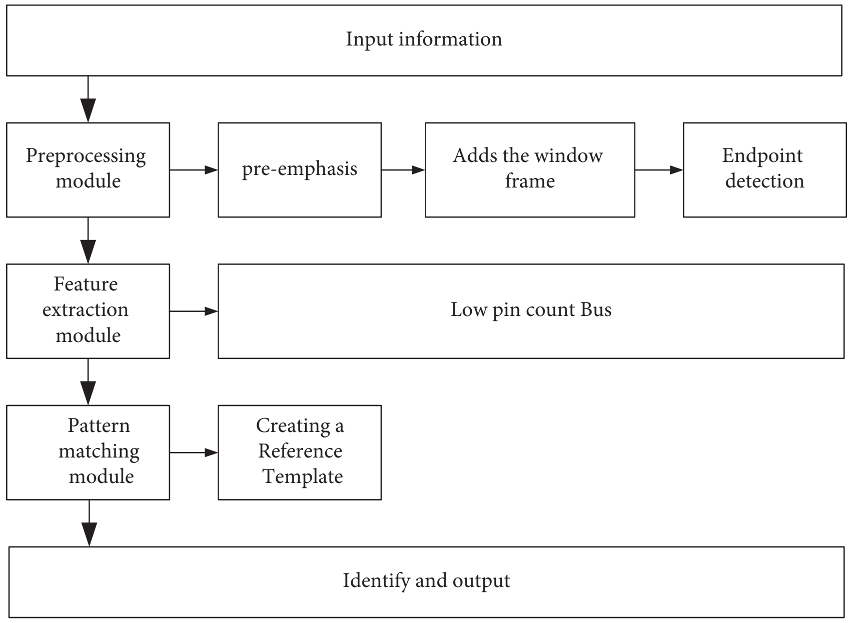

Figure 9: The basic principle of DTW.

information retrieval. The basic principle of DTW is shown in Figure 9, and the weight is expressed as (18).

When a location has a large particle weight, the user is more likely to appear here. A new DTW algorithm is established here, which is a method to measure the similarity of two time series with different lengths. It has an extensive application range, such as isolated word speech recognition, and gesture recognition. Figure 9 reveals the fundamental principle of DTW algorithm, and (18) describes the weight [26].

$$\omega_c = \exp\left[-\frac{\mathrm{DTW}(\{L\},\{H\})}{K}\right]. \quad (18)$$

2.4. Verification Experiment of the Visible Light Intelligent Perception and Positioning Model. The received light intensity calculated by the model is compared with the true value of the received light intensity in the experiment to verify the validity of the proposed model. Firstly, the gyroscope carrying the illumination test equipment is used for illumination tests. The light intensity data is collected by rotating the gyroscope into multiple angles and keeping it at multiple specific positions near the light source. The exponential model is expressed as the traditional EXP model. The light propagation model is expressed as the EXT model, and the real model is expressed as the TRUE model. The mean square error is calculated according to

$$\mathrm{MSE}(\overline{\theta}) = E(\overline{\theta} - \theta)^2. \quad (19)$$

In (19), $\overline{\theta}$ denotes the point estimate, and θ represents the true value of parameters.

The experiment is carried out on the proposed model with one male and one female. Due to the height, the average step lengths of the two subjects are different. The average step length of the male is 0.88 meters, and the average step length of the female is 0.56 meters. Twenty indoor points are selected as the starting point of the test, and 30 outdoor points are selected as the starting point for walking [27].

2.5. Optimization and Classified Modeling for Heterogeneous Training Sets. In data acquisition, various reasons lead to category errors of detection objects, such as artificial interpretation and evaluation of stratigraphic lithology errors. When using these data with potential anomalies for modeling, it is necessary to detect and correct the abnormal categories of these data to improve the recognition accuracy of the established model and enhance the generalization ability of the model. Data analysis on massive data often requires relatively high hardware and time costs. This paper chooses to implement data analysis on the Hadoop platform, a flexible structure to deal with different types of data quality problems. One or more modules handle each type of data quality problem. Hadoop is a distributed system infrastructure making full use of the power of the cluster for high-speed computing and storage. Users can develop distributed programs without understanding the underlying details of the distribution. Hadoop implements a distributed file system with high fault tolerance and deploys it on low-cost hardware; moreover, it provides high throughput to access applications' data, suitable for applications with a large data set. It can access data in the file system as streams.

The interactive module in the system provides an input interface for both the files to be cleaned and the requirements of cleaning data. The result display module provides the download link of cleaning data and compares dirty data and cleaned data. The entity recognition and truth-value discovery module is used to eliminate redundancy. Entity recognition clusters tuples pointing to the same real-world entity, and truth-value discovery is responsible for finding

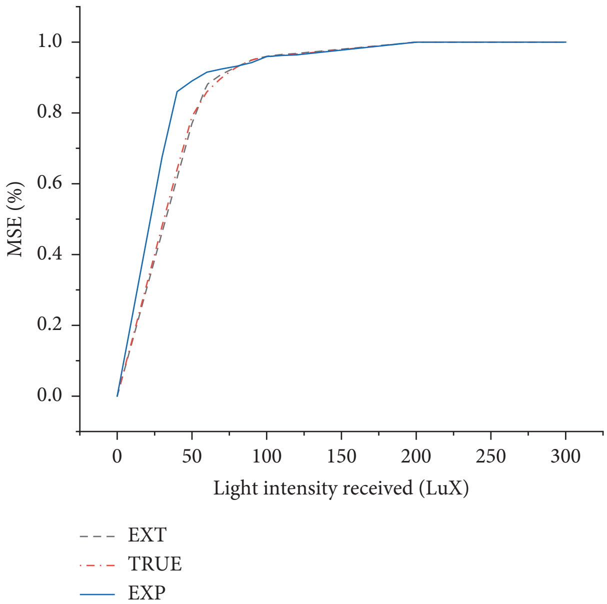

Figure 10: Comparison of the mean square error of the light intensity test.

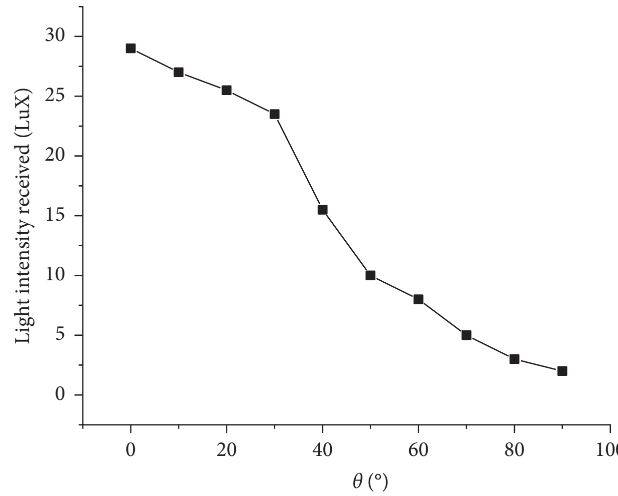

Figure 11: Deviation between the calculated value and real value of received light intensity.

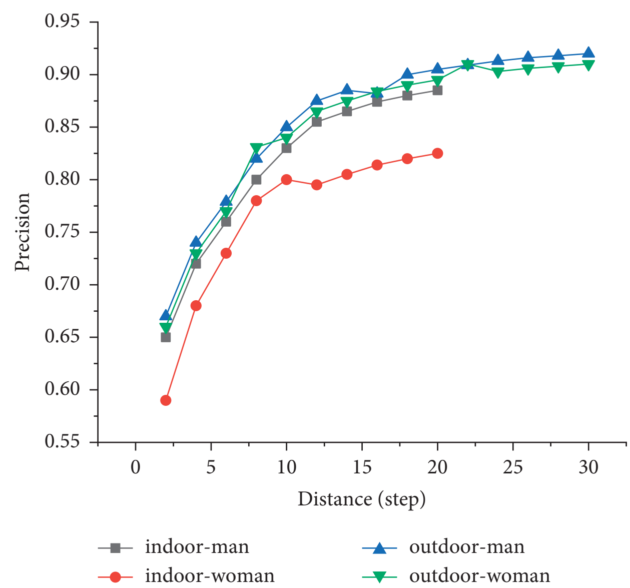

Figure 12: Overall positioning accuracy of the model indoors and outdoors.

the real value in the conflict. The inconsistency detection module finds the data part that violates the dependency rules and repairs the data to the state that meets the rules. The numerical filling part detects the missing part of the data and fills it. It can select an appropriate module to deal with the encountered data quality problems to optimize the data quality and improve the quality of the constructed data set. Due to the characteristics of the MapReduce programming model, a problem is often decomposed into many simple tasks, and a MapReduce round implements each task. This "decomposition" is excessive in most cases, resulting in redundant MapReduce. This paper appropriately merges the convergent tasks and meets the conditions such as reducing the number of MapReduce rounds and times of the original system without changing the algorithm complexity and iteration terminability of the original system to achieve the optimization purpose.

3. Experimental Results of the Visible Light Perception and Positioning Model

3.1. Visible Light Intensity Test. The test of intelligent perception and positioning model is inseparable from the test of visible light intensity. To verify the scientificity of the environmental intelligent perception and positioning model, comparative analysis is conducted on the test errors of light intensity and the received light intensity at different incident angles of several different models. Figures 10 and 11 provide the comparison results and the deviation between simulation values and real values.

As shown in Figure 10, the mean square error of the model increases with the continuous growth of light intensity. However, compared with the EXP model, the calculated value of the proposed model is closer to the true value, so the detection effect of the model is better than that of the traditional EXT model. In Figure 11, with the increase of incident angle, the deviation between the real light intensity and the received light intensity detected by the model is getting smaller and smaller. Besides, there is 50% probability that the error of calculated received light intensity is within 10 LuX, and there is 95% probability that the error keeps within 50 LuX. The purpose of this experiment is to intelligently perceive objects according to the light intensity of visible light. The light intensity test proves that the error of the visible light test is getting smaller and smaller, indicating that the selected model is effective.

3.2. Positioning Accuracy Test. The precision of positioning detection is the research focus in this experiment. Relevant data such as gender and indoor and outdoor positioning

Table 2: Comparison between positioning point coordinates and actual coordinates.

Anchor name	Anchor point coordinates	Actual coordinates
A	(110.545451, 30.292760)	(110.545472, 30.292781)
B	(110.544021, 30.290873)	(110.543998, 30.291272)
C	(110.543012, 30.285766)	(110.542971, 30.286001)
D	(110.526177, 30.266101)	(110.526159, 30.266105)
E	(110.501073, 30.201130)	(110.501059, 30.201164)

precision is collected and studied to further improve the effectiveness of the experiment. The results are presented in Figure 12.

From Figure 12, the overall positioning accuracy in the indoor is not as good as the overall positioning accuracy in the outdoor, and with the increase of the step number, the positioning accuracy increases gradually. When the experimenter walks within 10 steps, the accuracy increases fast, but after 10 steps, the accuracy increases rate of positioning decreases. Furthermore, after 20 steps, the accuracy increases slowly. Since step size of the male tester is larger, the distance of male tester moving each step increases faster, which is more conducive to the positioning accuracy. Therefore, the overall positioning accuracy of the male tester is always higher than that of the female tester. The radio frequency identification technology and Ultra Wide Band technology mentioned previously have limitations at that time, cannot be implemented in a large area, and do not have communication ability. In contrast, the environmental intelligent perception and positioning model presented here is not affected by space, so it can move indoors or outdoors for free.

3.3. Comparison of Positioning Accuracy. The analysis of many matching results shows in Table 2 that the positioning accuracy on the straight road is very high, reaching more than 80%. At intersections and more complex sections, the positioning accuracy is not very good, caused by the great randomness of the travel direction at intersections and the low prediction accuracy of steam travel direction and speed. Increasing sample training and adding auxiliary parameters may improve the prediction accuracy. In the case of rugged roads, the position prediction algorithm can accurately locate the travel trajectory. Besides, the positioning error does not change much over time. In addition, because the interruption time of the positioning signal is generally short, the position prediction algorithm can achieve more accurate positioning in a short time.

4. Conclusion

A visible light positioning model based on the combination of IoT intelligent perception system with GIS and LBS technology is established to change the traditional intelligent perception and positioning technology for electronic data investigation modes. Firstly, the intelligent perception and positioning technology under the background of big data is introduced. Then GIS technology and LBS technology are adapted to propose the indoor perception and positioning model based on GIS technology, LBS technology, and visible light propagation model. Meanwhile, the front-end perception of positioning work is used to achieve comprehensive data collection. Finally, the proposed model is experimentally verified. The experiment proves that the intelligent perception and positioning technology based on GIS and LBS can improve the ability and efficiency of location positioning for users, significantly ameliorate the accuracy of location positioning for targets, and further improve the efficiency of electronic data investigation.

The vigorous development of mobile computing and the upgrading of intelligent devices have revolutionized the lifestyle of modern human beings. Obviously, the traditional intelligent sensing positioning technology is inaccurate to electronic data reconnaissance. An environmental intelligent perception and positioning model is constructed based on GIS technology, LBS technology, and visible light propagation model. Through relevant experiments, the following conclusions are drawn. (1) By comparing the light intensity of the model reported here with that of the EXP model and EXT model, the proposed environmental intelligent perception and location model can not only provide results closer to the real light, but also achieve the data with decreasing error. (2) In indoor and outdoor positioning precision experiments found that the positioning precision indoors is not as good as outdoors.

Although the original expected research objectives have been basically reached, and some valuable research conclusions have been obtained, due to the limited academic literacy, there are still some deficiencies in the research work. The conclusions may be limited by the following two factors. (1) The positioning accuracy of the model and the intersection becomes lower under the condition of weak light. (2) Due to the problems of personal privacy regulations, many practical application cases cannot be found for analysis. Therefore, it is worth improving the model from the following two aspects in future research. (1) Develop weak light recognition patterns and use more intersection location data sets for model training. (2) More volunteers will be recruited for consultation and practical testing.

Data Availability

The data that support the findings of this study are available from the corresponding author upon reasonable request.

Conflicts of Interest

The authors declare that they have no conflicts of interest.

References

[1] S. Sawyer, "The Internet of things," *Journal of the American Society for Information Science and Technology*, vol. 70, no. 6, pp. 638-639, 2019.

[2] A. Hany, W. Robert, and W. Gary, "Fog computing and the Internet of things: a review," *Big Data & Cognitive Computing*, vol. 2, no. 2, pp. 10-11, 2018.

[3] B. Tao, Z. Gong, H. Wu, H. Ding, and Z. Yin, "An RFID-based mobile robot localization method combining phase difference and readability," *IEEE Transactions on Automation Science and Engineering*, vol. 18, no. 3, p. 123, 2020.
[4] P. Wu and D. Wu, "Positioning information system of indoor food delivery robot based on," *UWB Journal of Physics: Conference Scries IOP Publishing*, vol. 1, no. 1732, Article ID 012129, 2021.
[5] A. Singh, S. Garg, K. Kaur, S. Batra, N. Kumar, and K.-K. R. Choo, "Fuzzy-folded bloom filter-as-a-service for big data storage in the cloud," *IEEE Transactions on Industrial Informatics*, vol. 15, no. 4, pp. 2338–2348, 2019.
[6] A. R. Opotowsky and G. D. Webb, "Small defects, small effects, big data, big anxiety: our evolving understanding of low-risk congenital heart disease," *Circulation. Cardiovascular interventions*, vol. 13, no. 6, pp. 79–82, 2020.
[7] M. Kafil and M. Albaji, "Selecting wastewater sites using analytical hierarchy and geographic information system," *Proceedings of the Institution of Civil Engineers - Municipal Engineer*, vol. 171, no. 2, pp. 86–92, 2018.
[8] Z. Li, W. Li, F. Gao et al., "New blind filter protocol: an improved privacy-preserving scheme for location-based services," *The Computer Journal*, vol. 63, no. 12, pp. 1–4, 2020.
[9] W. Xu, H. Zhou, N. Cheng et al., "Internet of vehicles in big data era," *IEEE/CAA Journal of Automatica Sinica*, vol. 5, no. 1, pp. 19–35, 2018.
[10] M. Huda, A. Maseleno, P. Atmotiyoso et al., "Big data emerging technology: insights into innovative environment for online learning resources," *International Journal of Emerging Technologies in Learning*, vol. 13, no. 1, pp. 23-24, 2018.
[11] L. Mann, "Left to other peoples' devices? A political economy perspective on the big data revolution in development," *Development and Change*, vol. 49, no. 1, pp. 3–36, 2018.
[12] J. H. Pikul and H. Ning, "Powering the Internet of things," *Joule*, vol. 2, no. 6, pp. 1036–1038, 2018.
[13] D. E. Nejjary, F. Pinet, and M.-A. Kang, "Modeling and computing overlapping aggregation of large data sequences in geographic information systems," *International Journal of Information System Modeling and Design*, vol. 10, no. 1, pp. 20–41, 2019.
[14] T. B. Richards, C. M. Croner, and G. Rushton, "Geographic information systems," *The Journal of the American Board of Family Medicine*, vol. 23, no. 4, pp. 109–120, 2020.
[15] M. P. Peter, A. T. Choko, E. L. Webb et al., "Development and validation of a global positioning system–based "map book" system for categorizing cluster residency status of community members living in high-density urban slums in blantyre, Malawi," *American Journal of Epidemiology*, vol. 177, no. 10, pp. 1143–1147, 2013.
[16] P. Asuquo, H. Cruickshank, J. Morley et al., "Security and privacy in location-based services for vehicular and mobile communications: an overview, challenges and countermeasures," *Internet of Things Journal*, vol. 1, no. 6, pp. 1-2, 2018.
[17] G. Song and G. Mai, "Mobile GIS and location-based services," *Comprehensive Geographic Information Systems*, vol. 2, no. 4, pp. 384–397, 2018.
[18] X. Tao, Z. Shi, and X. Li, "A new IntelliSense strategy based on artificial immune system for multi-robot cooperation," *Journal of Robotics and Mechatronics*, vol. 30, no. 1, pp. 128–137, 2018.
[19] M. Maier, A. Ebrahimzadeh, S. Rostami, and A. Beniiche, "The Internet of No things: making the Internet disappear and see the invisible," *Communications Magazine*, vol. 99, no. 1, pp. 2–8, 2020.
[20] V. Abraham and Y. Poria, "A research note exploring socially visible consumption in tourism," *Tourism Management*, vol. 70, no. 8, pp. 56–58, 2019.
[21] S. A. Oktaria, N. Iskandar, M. Syafii, and Y. Yennita, "Effect of using the light refraction experiment device for student's learning outcomes in junior high school," *Jurnal Geliga Sains: Jurnal Pendidikan Fisika*, vol. 7, no. 2, pp. 71-72, 2020.
[22] P. R. Bhattacharjee and P. Ranjan, "Dispersive power of prism and grating in the light of the refined unambiguous angles of incidence, refraction and the unambiguous angle of diffraction," *Optik*, vol. 155, no. 1, pp. 344–350, 2018.
[23] J. Bhattachar and P. Ranjan, "Brewster's law in the light of the refined unambiguous angles of incidence, reflection, and refraction," *Journal for Light-and Electronoptic*, vol. 14, no. 2, pp. 324–328, 2018.
[24] R. F. Betzel and D. S. Bassett, "Specificity and robustness of long-distance connections in weighted, interareal connectomes," *Proceedings of the National Academy of Sciences of the United States of America*, vol. 115, no. 21, pp. 232–236, 2018.
[25] C. O. S. Kato, K. Shimizu, K. Kamiya, H. Ishikawa, and A. Igarashi, "Effects of brimonidine tartrate 0.1% ophthalmic solution on the pupil, refraction, and light reflex," *Entific reports*, vol. 8, no. 1, pp. 9003–9904, 2018.
[26] K. Lüders and R. O. Pohl, "The relation between absorption, reflection and refraction of light," *Pohl's Introduction to Physics*, vol. 4, no. 25, pp. 491–515, 2018.
[27] M. V. Gorkunov, I. V. Kasyanova, V. V. Artemov et al., "Superperiodic liquid-crystal metasurfaces for electrically controlled anomalous refraction," *ACS Photonics*, vol. 7, no. 11, pp. 3096–3105, 2020.

Hindawi
Scientific Programming
Volume 2023, Article ID 9780749, 1 page
https://doi.org/10.1155/2023/9780749

Retraction

Retracted: A Global Optimization Algorithm for Intelligent Electromechanical Control System with Improved Filling Function

Scientific Programming

Received 8 August 2023; Accepted 8 August 2023; Published 9 August 2023

This article has been retracted by Hindawi following an investigation undertaken by the publisher [1]. This investigation has uncovered evidence of one or more of the following indicators of systematic manipulation of the publication process:

(1) Discrepancies in scope
(2) Discrepancies in the description of the research reported
(3) Discrepancies between the availability of data and the research described
(4) Inappropriate citations
(5) Incoherent, meaningless and/or irrelevant content included in the article
(6) Peer-review manipulation

The presence of these indicators undermines our confidence in the integrity of the article's content and we cannot, therefore, vouch for its reliability. Please note that this notice is intended solely to alert readers that the content of this article is unreliable. We have not investigated whether authors were aware of or involved in the systematic manipulation of the publication process.

Wiley and Hindawi regrets that the usual quality checks did not identify these issues before publication and have since put additional measures in place to safeguard research integrity.

We wish to credit our own Research Integrity and Research Publishing teams and anonymous and named external researchers and research integrity experts for contributing to this investigation.

The corresponding author, as the representative of all authors, has been given the opportunity to register their agreement or disagreement to this retraction. We have kept a record of any response received.

References

[1] S. Zhang, K. Srividya, I. Kakaravada et al., "A Global Optimization Algorithm for Intelligent Electromechanical Control System with Improved Filling Function," *Scientific Programming*, vol. 2022, Article ID 3361027, 10 pages, 2022.

Hindawi
Scientific Programming
Volume 2022, Article ID 3361027, 10 pages
https://doi.org/10.1155/2022/3361027

Research Article

A Global Optimization Algorithm for Intelligent Electromechanical Control System with Improved Filling Function

Shuguang Zhang,[1] **Kode Srividya**,[2] **Ismail Kakaravada**,[2] **Dimitrios A. Karras**,[3] **Vishal Jagota**,[4] **Inamul Hasan**,[5] **and Abdul Wahab Rahmani**[6]

[1]*Institute of Applied Mathematics, Jiaozuo Normal College, Jiaozuo Henan 454000, China*
[2]*Department of Mechanical Engineering, Prasad V. Potluri Siddhartha Institute of Technology, Vijayawada, Andhra Pradesh, India*
[3]*National and Kapodistrian University of Athens (NKUA), School of Science, Dept. General, Athens, Greece*
[4]*Mechanical Engineering Department, Madanapalle Institute of Technology and Science, Madanapalle, AP, India*
[5]*ACS College of Engineering, Bangalore, Karnataka, India*
[6]*Isteqlal Institute of Higher Education, Kabul, Afghanistan*

Correspondence should be addressed to Shuguang Zhang; shuguangzhang371@126.com and Abdul Wahab Rahmani; ab.wahab.professor@isteqlal.edu.af

Received 18 January 2022; Revised 8 February 2022; Accepted 11 February 2022; Published 22 March 2022

Academic Editor: Punit Gupta

To improve the speed of global optimization algorithm, a class of global optimization algorithms for intelligent electromechanical control system with improved filling function is proposed. By attaching the intelligent managing system improving algorithm and the filling function procedure, the algorithm can stand out from the current particular optimal solution, avoid the phenomenon of falling into the local favorable solution in the process of algorithm iteration, make the algorithm find a better solution, and improve the efficiency of solving the multiextremum global improving problem. Multiextremum-seeking is an optimal control technique that works with unknown conditions while assuming that measurements of the plant's input and output signals are accessible. The presented work is for an electromechanical system which will handle the low accuracy and untimely tendency of conventional systems which are used in various practical applications. Few learning algorithms have been developed to explicitly optimize mean average precision (MAP) due to computational constraints. The outcomes show that the convergence of the test functions F6 and F7 is not good when the MAPID algorithm is only used for optimization. The MAPID_FF algorithm not only ensures the convergence and optimization precision of the two test functions, but also reduces the optimization time compared with the filling function method. Compared with the filling function method, the improved algorithm has higher accuracy and faster speed, and it is not simple to fall into the local optimum, so the global optimal value is more accurate.

1. Introduction

Since the 1990s, smart building technology has grown in popularity. This innovation serves a wide range of study fields, including space vehicles, aviation, train and car systems, robots, heavy machinery, and medical equipment. Noise and vibration are two examples of use. Common components include a host structure, actuators, and sensors, and a CPU that analyses data signals, a control law for changing the structure's characteristics, and integrated power electron signals, a control law to adjust the structure's features, and integrated power electronics [1, 2]. Optimization is a powerful tool to solve practical problems, which can be widely applied in many fields such as engineering, production, and science. At the early stage of the development of optimization theory, the research on it mainly focuses on the method and application of local optimization, and abundant theories and solutions have been obtained in the research of local optimization. However, with the rapid development of computing science and technology, more practical problem is modeled as an optimization model required to the global optimal solution rather than the local optimal value, which makes the global optimization become the hotspot in the academic field, and global optimization is becoming increasingly wide in the actual application and in many fields, such as molecular biology, neural network, and environmental engineering. It has been extended to many important fields such as economy, science, national defense. It is an indispensable numerical technique to calculate the global optimal solution of the corresponding optimization problem. Therefore, industrial departments, scientific research institutions, and government departments pay high attention to the research on the relevant theories and solving methods of global optimization problem, and the in-depth research on it has far-reaching application significance [3].

Due to the low accuracy and untimely tendency of conventional particle swarm optimization, the reactive power optimization control of an electromechanical system based on fuzzy particle swarm optimization approach was proposed. Working within the constraints of the operating environment is the idea. The network device loss was reduced by changing the voltage and reactive transmission lines of the system, and a static reactive power optimization mathematical model of the electromechanical system was created. A control law for changing the structure's characteristics and integrated power electronics for singnals was described in [4, 5]. The control system optimization algorithm uses the idea of "feedback" of the feedback control system. In the closed-loop control system, the output of the system is constantly approaching the set value of the system. If the iterative process of the optimization algorithm can be continuously approaching the global optimal, then the algorithm can successfully converge to the global optimal solution of the objective function. The controller of the feedback control system generally adopts the incremental PID control strategy. At this time, the three parameters k_p, k_i, and k_d need to be set manually. Combining the neural network technology with the traditional PID control, it can solve the traditional PID controller to a certain extent, which makes it not easy for it to carry out online real-time parameter tuning and other defects, and give full play to the advantages of PID control [6]. The proportional-integral-derivative (PID) control approach is the most often used and is well known in industrial control. The attractiveness of PID controllers originates in part from their resilience in a wide range of operating settings, as well as their functional simplicity, which allows engineers to run them in a straightforward and basic manner [7, 8]. This forms the neural network PID, referred to as PIDNN. Inspired by the idea of particle swarm parallel computing and group learning, the optimization algorithm of PIDNN was improved, and the optimization algorithm of intelligent control system MPIDNN was proposed (multiple control systems compute in parallel and learn from each other, which has the characteristics of "intelligence"). Because the global minimum value of the objective function is not clear at the beginning of the algorithm design, it is difficult to give an appropriate system value. If the initial values of Kp, Ki, Kd, and other parameters are not appropriate, the algorithm may not converge to the global minimum of the objective function or the optimization accuracy of the algorithm is very low. The filling function method is a transformation function method, which can solve the problem of initial parameter setting and precocious convergence of the optimization algorithm of intelligent control system. Combining the optimization algorithm of intelligent control system with the filling function method can not only reduce the difficulty of parameter setting of the optimization algorithm of intelligent control system, but also shorten the optimization time compared with the filling function method alone [9]. In recent years, several diagnostic and prognostic models based on statistical, artificial intelligence (AI), and soft computing (SC) techniques have been proposed and get satisfactory results. In this work, we apply the DE to optimize the control parameter by reducing the mechanical friction of the worm gear and reducing the fault occurrence due to friction in the electromechanical control [10, 11]. PIDNN controllers have recently been one of the most preferred approaches for controlling complicated systems. Several robust and auto-tuning options for improving the PIDNN controller's control and robust performance have been provided. An adaptive PIDNN controller was presented. To improve the convergence speed and prevent weights from being stuck in local optima, the neural network was initialized using the particle swarm optimization (PSO) technique. The utility of the proposed method is proved by actual evidence. The PSO approach, on the other hand, requires a long time to initialize the weights [12, 13]. Shi Dongwei et al. proposed an efficient global algorithm for solving quadratic programs with quadratic constraints. In this algorithm, we propose a new linearization method to solve the linear programming relaxation problem of quadratic programs with quadratic constraints. The proposed algorithm is integrated with the global optimal solution of the initial problem, and numerical experiments show the computational efficiency of the proposed algorithm [14]. Metaheuristics can help policymakers and decision-makers get the greatest results by lowering the cost function. In this research, an improved grasshopper optimization algorithm (GOA) was proposed with a novel starting approach to balance GOA's search capacity. The new method is known as the Improved Grasshopper Algorithm (IGOA). GOA is based on grasshopper swarms and mimics their natural behavior [15, 16]. Yue and Zhang proposed a GOA algorithm combining two strategies, namely, a new variant of PCA-GOA. First, using principal component analysis (PCA) strategies to obtain grasshoppers with small correlated variables can improve GOA's development capacity. Then, a new inertial weight is proposed to balance exploration and exploitation in an intelligent way, which gives GOA a better search capability. In addition, the performance of PCA-GOA was evaluated by addressing a number of baseline functions. Experimental results show that PCA-GOA provides better results than basic GOA for most functions and other most advanced algorithms, which indicates the superiority of PCA-GOA [9].

With its efficiency and simplicity, the grasshopper optimization algorithm (GOA), one of the most recent metaheuristic algorithms, has a wide range of applications. The fundamental GOA, on the other hand, offers plenty of space for development. As a result, a novel variation GOA algorithm is suggested that combines the two techniques, called PCA-GOA. To begin, the principal component analysis approach is used to get grasshoppers with minimum correlated variables, which can increase the GOA's exploitation capabilities [17, 18]. Based on this, the control system parameter adaptive adjustment and multisystem parallel computation are adopted to improve the control system optimization algorithm, and the global optimization algorithm of intelligent control system is proposed, which is called MAPID (Multisystem Adaptive EPID). In the algorithm of intelligent control system, the setting of the given value of the system is a troublesome problem. It is limited by the global minimum value of the unknown objective function, and it is difficult for the objective function with complex characteristics to use PID control strategy to achieve high precision optimization results.

The presented work is a global optimization algorithm approach for electromechanical system to handle the low accuracy and untimely tendency of conventional systems which are used in various practical applications. It possesses higher accuracy and faster speed and therefore its global optimal value is more accurate. In addition, the setting of initial parameters in the control decision will affect the optimization result and the optimization speed. For this reason, the filling function method is introduced to improve the optimization algorithm of intelligent control system, which is called MAPID_FF. In the simulation experiment, the results of 7 standard test functions show that MAPID_FF is superior to MAPID in optimization precision and superior to the filling function method in optimization speed [19]. Therefore, machine learning is often used to improve ranked retrieval systems. Despite its widespread application in evaluating such systems, few learning algorithms have been developed to explicitly optimize mean average precision (MAP) due to computational constraints. Existing MAP optimization approaches either fail to find a globally optimal solution or are wasteful in terms of computation [20, 21].

The practical application of the model has multidimensional aspects. These machines employ switches and relay circuitry to do sophisticated calculations. They may discover system faults and offer retry commands based on the programmed. Almost all moving equipment is powered by an electromechanical mechanism. These systems are found in the majority of electric motors, solenoids, and mechatronics. Most of the equipment we use in our everyday lives, from automotive electric windows and seats to dryers, rely on these systems. The novel approach of the algorithm is that it not only ensures the convergence and optimization precision of the two test functions, but also reduces the optimization time compared with the filling function method. Few learning algorithms have been developed to explicitly optimize mean average precision (MAP) due to computational constraints.

2. Research Methods

2.1. Global Optimization Algorithm of Intelligent Control System

2.1.1. Iterate Formula Definition. The model of the single-loop closed-loop control system is shown in Figure 1. The controlled object is the optimized objective function, R is the given value of the system, and the control strategy adopts PID algorithm. The global optimization problem is to solve the minf(x) problem, where $x \in R^n$. In order to simplify the design of the control strategy, the commonly used PID algorithm is adopted, and the parameter values in the PID algorithm adopt the method of self-adaptive adjustment. Therefore, this control strategy is called adaptive PID control strategy (APID).

Definition 1. According to the APID algorithm, the iteration formula of the independent variable x in the iteration process is defined as shown in equations (1)~(4):

$$\begin{aligned}
\Delta^2 \mathrm{E}(k) &= \mathrm{E}(k) - 2 \times \mathrm{E}(k-1) + \mathrm{E}(k-2),\\
\Delta \mathrm{E}(k) &= \mathrm{E}(k) - \mathrm{E}(k-1),\\
\mathrm{E}(k) &= R - f(k),\\
x(k+1) &= \begin{matrix} \omega \cdot x(k) + k_p \cdot \Delta \mathrm{E}(k) + \\ k_i \cdot \mathrm{E}(k) + k_d \cdot \Delta^2 \mathrm{E}(k) \end{matrix}.
\end{aligned} \tag{1}$$

Among them: k_p, k_i, k_d are the parameters of PID algorithm, ω is the inertia coefficient, and these four parameters are vectors of the same dimension as the independent variable x [22].

To prevent the calculation of a single system from falling into the local minimum, the parallel calculation method of multiple control systems is adopted, inspired by the parallel calculation of particle swarm optimization algorithm. The model of multisystem parallel computing is shown in Figure 2. The given value of each system is R, and the control strategy is PID algorithm, but the starting point of iterative calculation of each system is different. In each iteration, each system should not only learn from its own optimal value, but also learn from the optimal value of all systems.

Definition 2. After adopting the multisystem parallel computing method, equations (1)~(4) are replaced by equations (5)~(8):

$$\begin{aligned}
x(i,k+1) &= \omega(i) \cdot x(i,k) + k_p(i) \cdot \Delta \mathrm{E}(i,k) + k_i(i)\\
&\quad \cdot \mathrm{E}(i,k) k\ d(i) \cdot \Delta^2 \mathrm{E}(i,k) +\\
&\quad \cdot r_1(i) \cdot c_1(i) \cdot (x_\mathrm{best}(i) - x(i,k)) + r_2(i)\\
&\quad \cdot c_2(i) \cdot (x_\mathrm{allbest} - x(i,k)).\\
\mathrm{E}(i,k) &= R - f(i,k),\\
\Delta \mathrm{E}(i,k) &= \mathrm{E}(i,k) - \mathrm{E}(i,k-1),\\
\Delta^2 \mathrm{E}(i,k) &= \mathrm{E}(i,k) - 2 \cdot \mathrm{E}(i,k-1) + \mathrm{E}(i,k-2).
\end{aligned} \tag{2}$$

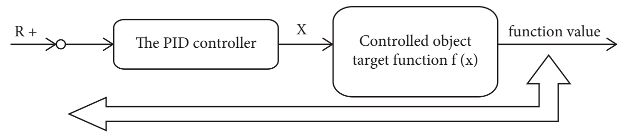

Figure 1: Single-loop control system model.

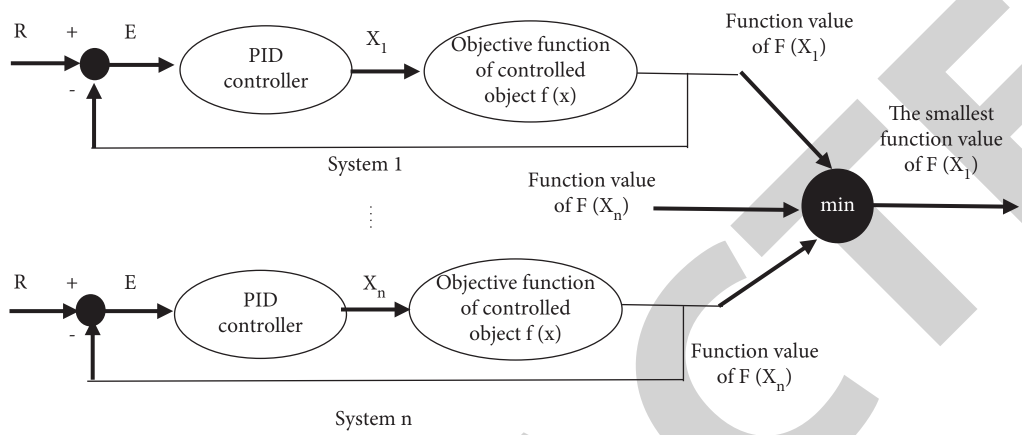

Figure 2: Multisystem parallel computing model.

It is assumed that there are n independent control systems in the multisystem ($n=5$ for the simulation parts); in the above formula, $x(i,k)$ represents the value of the KTH iteration independent variable x of the ith system; r_1, r_2 are adjustable parameters and often take the constant of 0~1; c_1, c_2 are vectors of the same dimension as the independent variable x, which are usually random values of -0.5~0.5. X_best (I) is the best position of the ith system in the iteration process, and AA is the best position of all systems in the iteration process [23].

2.1.2. Parameter Adjustment Mechanism. The optimization algorithm of the intelligent control system adopts APID control strategy, and the parameters of the strategy adopt the adaptive adjustment method. To ensure that equation (1) converges during iteration, Theorem 1 is given. To make the objective function $f(x)$ converge in the iterative process, the adaptive adjustment formulas of ω, k_p, k_i, k_d are shown in equations (9)-(12):

$$\omega(k+1) = \omega(k) - \eta \cdot \frac{\partial f(x)}{\partial x} \cdot x(k), \tag{3}$$

$$k_p(k+1) = k_p(k) - \eta \cdot \frac{\partial f(x)}{\partial x} \cdot \Delta \mathrm{E}(k), \tag{4}$$

$$k_i(k+1) = k_i(k) - \eta \cdot \frac{\partial f(x)}{\partial x} \cdot \mathrm{E}(k), \tag{5}$$

$$k_d(k+1) = k_d(k) - \eta \cdot \frac{\partial f(x)}{\partial x} \cdot \Delta^2 \mathrm{E}(k) \tag{6}$$

Prove that

$$\frac{\partial f(x)}{\partial t} = \frac{\partial f(x)}{\partial x} \cdot \frac{\mathrm{d}x}{\mathrm{d}t} = \frac{\partial f(x)}{\partial x} \cdot \left(\frac{\partial x}{\partial \omega} \cdot \frac{\mathrm{d}\omega}{\mathrm{d}t} + \frac{\partial x}{\partial k_p} \cdot \frac{\mathrm{d}k_p}{\mathrm{d}t} + \frac{\partial x}{\partial k_i} \cdot \frac{\mathrm{d}k_i}{\mathrm{d}t} + \frac{\partial x}{\partial k_d} \cdot \frac{\mathrm{d}k_d}{\mathrm{d}t} \right). \tag{7}$$

Obviously, $\partial f(x)/\partial t < 0$ ensures that the objective function converges during iteration. If any of the following equations (14)-(17) are true, $\partial f(x)/\partial t < 0$ must be true

$$\frac{d\omega}{\mathrm{d}t} = -\frac{\partial f(x)}{\partial x} \cdot \frac{\partial x}{\partial \omega}, \tag{8}$$

$$\frac{dk_p}{\mathrm{d}t} = -\frac{\partial f(x)}{\partial x} \cdot \frac{\partial x}{\partial k_p}, \tag{9}$$

$$\frac{dk_i}{\mathrm{d}t} = -\frac{\partial f(x)}{\partial x} \cdot \frac{\partial x}{\partial k_i}, \tag{10}$$

$$\frac{dk_d}{\mathrm{d}t} = -\frac{\partial f(x)}{\partial x} \cdot \frac{\partial x}{\partial k_d}. \tag{11}$$

Based on equation (1), we can get

$$\frac{\partial x}{\partial \omega} = x, \frac{\partial x}{\partial k_p} = \Delta \mathrm{E}, \frac{\partial x}{\partial k_i} = \mathrm{E}, \frac{\partial x}{\partial k_d} = \Delta^2 \mathrm{E}. \tag{12}$$

After discretization of equations (14)-(17):

$$\Delta\omega = -\eta \cdot \frac{\partial f(x)}{\partial x} \cdot x(k), \tag{13}$$

$$\Delta k_p = -\eta \cdot \frac{\partial f(x)}{\partial x} \cdot \Delta \mathrm{E}(k), \tag{14}$$

$$\Delta k_i = -\eta \cdot \frac{\partial f(x)}{\partial x} \cdot \mathrm{E}(k), \tag{15}$$

$$\Delta k_d = -\eta \cdot \frac{\partial f(x)}{\partial x} \cdot \Delta^2 \mathrm{E}(k) \tag{16}$$

where η is the iteration step size adjusted by parameters ω, k_p, k_i, k_d. Based on equations (19)-(21), the adaptive adjustment formula of equations (19)-(21) as parameters can be obtained. Theorem 1 is proved [24].

2.1.3. The Initial Position. There exists the problem of selecting the initial position of each system in multisystem parallel computing. The first step in adopting the Latin square method is to determine an appropriate Latin square. For example, if 5 systems are parallel and the independent variable x is of 10 dimensions, then the Latin square v5,10 is

$$v_{5,10} = \begin{bmatrix} 1 & 2 & 3 & 4 & 5 & 1 & 2 & 3 & 4 & 5 \\ 2 & 3 & 4 & 5 & 1 & 2 & 3 & 4 & 5 & 1 \\ 3 & 4 & 5 & 1 & 2 & 3 & 4 & 5 & 1 & 2 \\ 4 & 5 & 1 & 2 & 3 & 4 & 5 & 1 & 2 & 3 \\ 5 & 1 & 2 & 3 & 4 & 5 & 1 & 2 & 3 & 4 \end{bmatrix}. \tag{17}$$

The initial position o_{ij} can be calculated from (18), where $x \in [l, u]$, I represents the ith system, and n is the number of parallel systems.

$$o_{ij} = l + \frac{2v_{ij} - 1}{2n}(u - 1). \tag{18}$$

Let us say $x \in [-10, 10]$; then we have

$$o_{5,10} = \begin{bmatrix} -8 & -4 & 0 & 4 & 8 & -8 & -4 & 0 & 4 & 8 \\ -4 & 0 & 4 & 8 & -8 & -4 & 0 & 4 & 8 & -8 \\ 0 & 4 & 8 & -8 & -4 & 0 & 4 & 8 & -8 & -4 \\ 4 & 8 & -8 & -4 & 0 & 4 & 8 & -8 & -4 & 0 \\ 8 & -8 & -4 & 0 & 4 & 8 & -8 & -4 & 0 & 4 \end{bmatrix}. \tag{19}$$

Thus, there is a way to pick the initial position.

In this paper, an optimization algorithm of intelligent control system (MAPID) is proposed.

2.2. A Class of Improved Filling Function Algorithm Construction

2.2.1. Algorithm Design of a Class of Improved Filling Functions. According to the ideas of the filled function method and basic implementation steps, the algorithm in the feasible region is directly from any initial point $f(x)$. In the process of minimising the objective function, find a local minimum point. As the dimension of optimization increases, so will the iteration algorithm and the number of function evaluations. This will increase the calculation amount of the algorithm, thus affecting the efficiency of the algorithm. Based on the idea of selecting a better initial point to improve the search ability of the algorithm, a new local search strategy is firstly introduced. This local search method defines the neighborhood of the current initial point, uniformly selects several points in the neighborhood, and then gets the probability value of each point in the neighborhood according to the calculation and normalizes the value. That is, the sum of the probability values of the points in the calculated neighborhood to be selected is 1; then the higher the value of the objective function is, the larger the corresponding calculated value is, and the higher the probability of this point to be selected is. This method is briefly known as PLSM (Probability-selected Local Search Method). Theoretically, the PLSM method may be used to screen out a better point near the current initial point as a new initial point minimization function, which can improve the speed of the algorithm in finding the local minimum [25]. The steps of PLSM method are shown in Table 1.

Based on Table 1, PLSM, and new filled function (C2.5), design a new filled function with one parameter algorithm (A New Filled Function Algorithm: NFFA); the specific algorithm is described as follows: NFFA algorithm.

I. Initialization Steps:

(1) Admissible error $0 < \varepsilon < 1, e.g.\varepsilon{:} = 1.0e - 5$ of local minimization algorithm.

(2) Make $k = 1, f(x^*_{k-1}) = +\infty$.

(3) A large constant C is given as the upper bound on the number of iterations k.

(4) Choose a positive real number R0, as large as possible.

II. Main Steps:

(1) $s * n$ points within the feasible region X are uniformly selected to form $Y = \{y_1, y_2, \ldots y_{sn}\}$, according to the probability value $P(y_p)$, $\quad p \in \{1, 2, \ldots, sn\}$ of each point calculated in Table 1; the set $\overline{Y} = \arg\max \{P(y_p)\}_{y_p \in Y, p \in \{1,2,\cdots,sn\}}$ is obtained; pick any $x_k \in \overline{Y}$ as the starting point.

(2) Use PLSM to minimize $f(x)$ from x_k to obtain the local minimum point x^*_k, turn 5°;

(3) Construct filling function $P(x, x^*_k)$ at x^*_k.

(4) Let $x = x^*_k + \xi_i$ be the starting point, where $\xi > 0$ is a small constant, e_i is the unit coordinate vector, and $i = 1, 2, \ldots, 2n$, use PLSM to minimize $P(x, x^*_k)$ and find a local minimum x' of $P(x, x^*_k)$, let $x_{k+1} = x$, $k = k + 1$, and then rotate by 2 degrees.

(5) (Stop criterion) if $k < \mathrm{C}$ and it satisfies $|f(x^*_k) - f(x^*_{k-1})| \le \varepsilon$, or $k > \mathrm{C}$, the algorithm terminates; at this point, $x^* = x^*_k$ is the global minimum of $f(x)$, and $f(x^*)$ is the global minimum; otherwise, make $r \coloneqq 10 \cdot r$, increment: and turn 3°.

Table 1: Implementation steps of PLSM method.

Input: select an initial point x_k at random in the feasible region $X = [a,b] = \{x \mid a \le x \le b, a, b \in R^n\}$ and output local minimum point x_k^*
1. Uniformly select $s * n$ points in the neighborhood $U = [x_k - ((b-a)/m), x_k + (b-a)/m]$ of x_k , put in the set $Y = \{y_1, y_2, \ldots, y_{sn}\}$, where, n is the dimension of the problem variable, s is the number of points selected in each dimension, and m>a, and 1 is a positive integer.2. Find the set $\overline{y}$ of the points in Y with the highest probability of being selected:(1)To calculate $P(y_p) = [1 - (f(y_p)/\sum_{j=1}^{sn} f(y_j))]/s, p = 1, 2, \ldots, sn$(2) 令 $\overline{P} = \{P(y_p)\}, \overline{Y} = \arg\max(\overline{P})$ (3) $Z = \underset{x_k y e U x_k}{\arg\max} \{p(x_k), p_y\}$ is the set of initial points. Select any $z_k^0 \in Z$ to minimize $f(x)$ to obtain the local minimum point set $Z' = \{z_k^*\}$ and local minimum sequence $F = \{f(z_k^*)\}$ 4. Make $f(x_k^*) = \min(F)$; the local minimum point x_k^* is obtained

Note: (1) In this paper, $f(x)$ and $P(x, x_k^*)$ are minimized. The selected local minimization method is "FMINCON" in MATLAB. (2) In 5°, when r is sufficiently large in theory, a solution that is better than the current local optimal solution can be found.

2.2.2. Fill Function Method. The filling function method is a transformation function method, that is, using auxiliary functions from a certain point of the objective function to find another local minimum point better than the current point (the new local minimum point has a smaller objective function value). Therefore, the filling function method is actually a combination of local optimization algorithm and constructor method to achieve the purpose of global optimization. The realization process is mainly divided into three steps: firstly, the local optimization algorithm is used to find a local minimum X_1 of the objective function; then, an auxiliary function C is constructed at point X_1, and local optimization algorithm is used to conduct local optimization on function C with X_1 as the initial point, and a local minimum point X_2 of C is obtained. Finally, the local optimization algorithm is used to optimize the objective function with X_2 as the initial point, and a new local minimum point X_3, where $f(X_3) < f(X_1)$, is obtained. Repeat the above three steps until you find the global minimum of the objective function $f(x)$, as follows:

$$C(X, a) = -[f(X) - F(x_1)] \cdot \left(\|X - X_1\|^2 + \frac{1}{2}\right)^a, \qquad (20)$$

where $f(x)$ is the objective function, X_1 is a local minimum point of the objective function, which is a positive number, and $C(X, a)$ is the filling function constructed at the point X_1. Figure 3 reflects the characteristics of the constructed filling function. The objective function $f(x) = x\sin(x), x_1 = 4.9132$ in the figure is constructed by taking $a = 0.3$ and $a = 0.5$, respectively. It is clear from Figure 3 that, at $a = 0.3$, the function value increases. At $a = 0.5$, the function value increases to the maximum and the curve gets almost flattened.

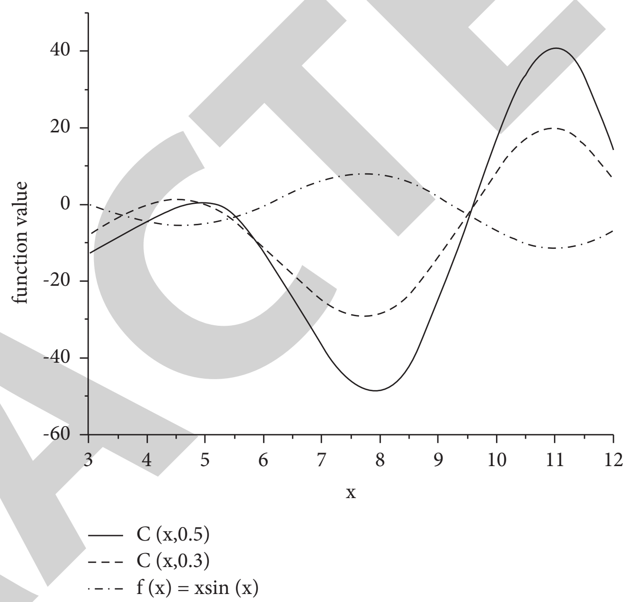

Figure 3: Characteristic diagram of filling function C(x).

2.3. Improved Optimization Algorithm of Intelligent Control System. The filling function optimization method starts from a local minimum point of the objective function and gradually converges to the global minimum point of the objective function. In each step, the corresponding local optimization algorithm should be called twice (once for the objective function and once for the filling function). This may lead to a longer optimization time, especially for the multimodal objective function. The specific idea of the improved intelligent control system optimization algorithm is as follows: (1) Use the optimization algorithm of the intelligent control system to optimize the objective function, stop after reaching the set number of iterations, and write down the best advantage obtained by searching; (2) the optimal advantage obtained by the optimization algorithm of the intelligent control system is used as the starting point and the filling function method is used to optimize, to obtain the global minimum value of the objective function. Combining the optimization algorithm of intelligent control system with the filling function method can not only reduce the difficulty of parameter setting of the optimization algorithm of intelligent control system, but also shorten the optimization time compared with the filling function method alone.

The concrete implementation steps of the improved optimization algorithm of the intelligent control system using the filling function method are as follows:

Step 1. Latin square is used to set the initial position of X (5 systems are used in parallel in the experimental part), set the initial value of ω, k_p, k_i, k_d, and determinate the number of iteration steps and the initial values of $f(x)$, error E, $(\partial f(x)/\partial x)$, f_best, and f_allbest.

Step 2. Use equation (5) to update the position of X and judge whether X has crossed the feasible region. If it has crossed the feasible region, the optimal position of the current five systems will be assigned to the current system X (that is, $X = X\_\text{AllBest}$). This method has achieved very good results in the experiment.

Step 3. Update the objective function $f(x)$, error E, $(\partial f(x)/\partial x)$, and f_best and determine the best of the five f_best values (that is, updates f_allbest).

Step 4. Adjust the value of ω, k_p, k_i, k_d with equations (9)~(12).

Step 5. Judge whether the number of iteration steps has been reached. If the number of iteration steps has been reached, the value of F_ALLBEST will be recorded as the optimization result of this part and transferred to Step 6; otherwise, the value of F_ALLBEST will be transferred to Step 2.

Step 6. Set the initial value of $X_0, a, \xi, M_t, f_{\min}$, where $X_0 = x\_\text{allbest}$, A is a positive number, ξ is a number greater than 1, and M_t is the upper limit of M ($f_{\min} < f\_\text{allbest}$).

Step 7. M sets zero to enter the first stage of the filling function method. Local optimization algorithm was used (FMINUNC function in MATLAB optimization toolbox was used in the experiment part) to optimize the objective function $f(x)$; the starting point is X_0. Obtain the local minimum point X_1; if $f(X_1) \leq f_{\min}$, then assign $f(X_1)$ to $f_{\min}$; otherwise, the $a = \xi \cdot a$.

Step 8. Enter the second stage of the fill function method. Use X_1 to construct the filling function C.

Step 9. Generate an appropriate random number $(e_1, e_2, \ldots, e_n)$ of the same dimension as X_1, and use $X_1 = (x_{11}, x_{12}, \ldots, x_{1n})$ to construct $X = (x_{11} + e_1\beta, x_{12} + e_2\beta, \ldots, x_{1n} + e_n\beta)$, where β is the linear search step size in the second stage. The search direction S is defined as $(X - X_1)/\|X - X_1\|$. Let $M = M+1$; take X_1 as the starting point and S as the search direction to search for the optimal linear search of C function.

Step 10. Continue the linear search until you reach point X.

(A) If X crosses the feasible region, jump to Step 11.

(B) If $f(X) < f(X_1)$, set $X_0 = X$; then jump to Step 6; otherwise go to Step 9.

(C) If X is a local minimum of function c, let $X_0 = X$ jump to Step 6; otherwise go to Step 9.

Step 11. If $M < M_t$, skip to Step 7; otherwise, the optimal point found is taken as the global minimum point of the objective function, and the algorithm stops. Steps 1~5 are the implementation of the optimization algorithm of intelligent control system (MAPID), and Steps 6~11 are the implementation of the filling function (FF) method.

3. Result Analysis

To show that the performance of the improved optimization algorithm of intelligent control system by using the filling function method has been improved, a comparative experiment was conducted with the filling function method and the optimization algorithm of intelligent control system. This part adopts a total of 7 standard test functions from F1 to F7. The hardware environment of the experiment is IntelPentiumM 1.70 GHz processor and 512 MB memory, and the software environment is Windows operating system and Matlab7.0 version, respectively.

The seven standard test functions are as follows:

$$F1 = \sum_{i=1}^{n}\left(x_i^2 - 10\cos(2\pi x_i) + 10\right),$$

$$F2 = -20\exp\left(\sqrt[-0.2]{\frac{1}{n}\sum_{i=1}^{n} x_i^2}\right) - \exp\left(\frac{1}{n}\sum_{i=1}^{n}\cos(2\pi x_i)\right) + 20 + \exp(1),$$

$$F3 = \frac{1}{4000}\sum_{i=1}^{n} x_i^2 - \Pi_{i=1}^{n}\cos\left(\frac{x_i}{\sqrt{i}}\right) + 1,$$

$$F4 = \frac{\pi}{n}\left\{10\sin^2(\pi y_1) + (y_n - 1)^2 + \sum_{i=1}^{n-1}(y_i - 1)^2 \cdot \left[1 + 10\sin^2(\pi y_{i+1})\right]\right\}, y_i = 1 + \frac{1}{4}(x_i + 1),$$

$$F5 = \frac{1}{n}\sum_{i=1}^{n}\left(x_i^4 - 16x_i^2 + 5x_i\right),$$

Table 2: Providing basic information about the test functions.

Test functions	The feasible region	Global optimal value	Dimension
F1	$[-5\cdot 12, 5\cdot 12]^n$	0	30
F2	$[-32, 32]^n$	0	30
F3	$[-600, 600]^n$	0	30
F4	$[-50, 50]^n$	0	30
F5	$[-5, 5]^n$	−78.33236	30
F6	$[-5, 10]^n$	0	30
F7	$[-5, 5]^n$	$3.0749E-4$	4

Table 3: Experimental results.

Test functions	MAPID		FF		MAPID-FF	
	The minimum value	CPU time (s)	The minimum value	CPU time(s)	The minimum value	CPU time(s)6
F1	$9.18E-11$	0.250	0	3.078	0	0.270
F2	$6.79E-10$	3.140	$5.16E-9$	45.890	$1.25EE-10$	4.470
F3	$7.08E-13$	0.235	0	0.453	0	0.265
F4	$1.92E-22$	6.687	$1.42E-16$	1.500	$5.28E-18$	1.375
F5	−78.3323	1.390	−78.3323	3.703	−78.3323	2.578
F6	28.0032	0.203	$6.7658E-24$	10.593	$4E-27$	9.500
F7	0.0215	0.219	$3.0749E-4$	0.562	$3.0749E-4$	0.204

$$
\begin{aligned}
F6 &= \sum_{i=1}^{n-1}\left[100\left(x_i^2 - x_{i+1}\right)^2 + \left(x_i - 1\right)^2\right],\\
F7 &= \sum_{i=1}^{11}\left[a_i - \frac{x_1\left(b_i^2 + b_i x_2\right)}{b_i^2 + b_i x_3 + x_4}\right]^2,\\
a &= [0\cdot 1957, 0\cdot 1947, 0\cdot 1735, 0\cdot 1600, 0\cdot 0844, 0\cdot 0627, 0\cdot 0456, 0\cdot 0342, 0\cdot 0323, 0\cdot 0235, 0\cdot 0246],\\
b &= \left[4, 2, 1, \frac{1}{2}, \frac{1}{4}, \frac{1}{6}, \frac{1}{8}, \frac{1}{10}, \frac{1}{12}, \frac{1}{14}, \frac{1}{16}\right].
\end{aligned} \tag{21}
$$

Table 2 is the basic information of the 7 standard test functions, including the dimension and feasible region of independent variables, as well as the standard global optimal value of the objective function. Table 3 is the average results of 10 experiments of 7 standard test functions, in which the optimization results and CPU time of the intelligent control system optimization algorithm (MAPID), the filling function (FF) method, and the improved intelligent control system optimization algorithm (MAPID_FF) are listed, respectively. As can be seen from Table 3, MAPID_FF algorithm is clearly superior to MAPID algorithm in optimization accuracy and superior to FF method in CPU consumption. When MAPID algorithm is only used for optimization, the convergence of test functions F6 and F7 is not good. After MAPID_FF algorithm is used, the convergence and optimization precision of these two test functions are guaranteed, and the optimization time is shortened compared with the filling function method. Therefore, MAPID_ FF algorithm proves out to be the better suit for electromechanical system to handle low accuracy and untimely tendency of conventional systems which are used in various practical applications. It imparts higher accuracy and faster speed and thus its global optimal value is more accurate.

4. Discussion

Because the model's practical applicability involves several dimensions, due to computational restrictions, only a few learning algorithms have been created that explicitly optimize mean average precision (MAP). The work given here is for an electromechanical system that will manage the low precision and unreliability of traditional systems utilized in a variety of practical applications. The convergence of test functions F6 and F7 is poor when the MAPID technique is utilized only for optimization. The convergence and optimization precision of these two test functions are ensured when the MAPID-FF technique is applied, and the optimization time is reduced when compared to the filling function approach, turned proven to be superior. As a result, the MAPID_ FF algorithm appears to be a better fit for electromechanical systems to manage the low precision and untimely inclination of conventional systems employed in a variety of real applications. It provides more precision and faster speed, resulting in a more accurate global ideal value.

5. Conclusions

Global optimization problems have multiple local optimal solutions and make the algorithm easy to fall into local optimum in the iterative process of defects, the intelligent control system of the optimization algorithm were studied, according to the basic ideas of fusion algorithm, by designing a class of filled function algorithms and blending intelligent control system optimization algorithm, then a global optimization algorithm for intelligent electromechanical control system with improved filling function is proposed. Compared with the optimization algorithm of intelligent control system, the algorithm has an obvious improvement in the precision of searching, and the initial point closer to the local optimal solution can be selected in the process of the algorithm, so that the convergence speed of the algorithm to the global optimal solution can be improved. The work given here is for an electromechanical system that will manage the low precision and unreliability of traditional systems utilized in a variety of practical applications. Due to computational restrictions, only a few learning algorithms have been created that explicitly optimize mean average precision (MAP).

Data Availability

The data pertaining to this study are in the article itself.

Conflicts of Interest

The authors declare that there are no conflicts of interest regarding the publication of this paper.

References

[1] S. Meri Al Absi, A. Hasan Jabbar, S. Oudah Mezan, B. Ahmed Al-Rawi, and S. Thajeel Al_Attabi, "An experimental test of the performance enhancement of a Savonius turbine by modifying the inner surface of a blade," *Materials Today Proceedings*, vol. 42, pp. 2233–2240, 2021.

[2] G. Verma and R. Chakraborty, "A hybrid privacy preserving scheme using finger print detection in cloud environment," *Ingénierie des Systèmes d'Information*, vol. 24, no. 3, pp. 343–351, 2019.

[3] Z. Deng and E. Hu, "Error minimization with global optimization for the difference of convex functions," *Discrete & Continuous Dynamical Systems*, vol. 12, no. 4&5, pp. 1027–1033, 2019.

[4] M. Singh, S. Maharana, A. Yadav et al., "An experimental investigation on the material removal rate and surface roughness of a hybrid aluminum metal matrix composite (Al6061/sic/gr)," *Metals*, vol. 11, no. 9, p. 1449, 2021.

[5] M. Demkah and D. Bhargava, "Gamification in education: a cognitive psychology approach to cooperative and fun learning," in *Proceedings of the 2019 Amity International Conference on Artificial Intelligence (AICAI)*, pp. 170–174, IEEE, Dubai, UAE, 2019, February.

[6] Y. Li, Y. Zhao, and J. Liu, "A Levy flight sine cosine algorithm for global optimization problems," *International Journal of Distributed Systems and Technologies*, vol. 12, no. 1, pp. 49–66, 2021.

[7] S. Saralch, V. Jagota, D. Pathak, and V. Singh, "Response surface methodology based analysis of the impact of nanoclay addition on the wear resistance of polypropylene," *The European Physical Journal - Applied Physics*, vol. 86, no. 1, Article ID 10401, 2019.

[8] Y. Xiao and J. Bhola, "Design and optimization of prefabricated building system based on BIM technology," *International Journal of System Assurance Engineering and Management*, pp. 1–10, 2021.

[9] X. Yue and H. Zhang, "Grasshopper optimization algorithm with principal component analysis for global optimization," *The Journal of Supercomputing*, vol. 76, no. 3, pp. 1–27, 2020.

[10] C. Li, "Hybrid optimization algorithm for cable design of electromechanical products based on A and genetic algorithm," *International Journal of Mechatronics and Applied Mechanics*, no. 5, pp. 165–178, 2019, https://ijomam.com/wp-content/uploads/2019/07/pag.-165-178_hybrid-optimization-algorithm-for-cable-design-of-electromechanical-products.pdf.

[11] T. P. Banerjee, S. Das, and A. Abraham, "Design of an optimized intelligent controller of electromechanical system in aerospace application," in *Proceedings of the 2011 11th International Conference on Hybrid Intelligent Systems (HIS)*, pp. 50–54, IEEE, Melacca, Malaysia, 2011, December.

[12] Y. Sun, H. Li, M. Shabaz, and A. Sharma, "Research on building truss design based on particle swarm intelligence optimization algorithm," *International Journal of System Assurance Engineering and Management*, pp. 1–11, 2021.

[13] P. Kumar, L. Kansal, G. S. Gaba, M. Mounir, A. Sharma, and P. K. Singh, "Impact of peak to average power ratio reduction techniques on Generalized Frequency Division Multiplexing for 5th generation systems," *Computers & Electrical Engineering*, vol. 95, Article ID 107386, 2021.

[14] D. Y. Shi, J. Yin, and C. Bai, "An effective global optimization algorithm for quadratic programs with quadratic constraints," *Symmetry*, vol. 11, no. 3, p. 424, 2019.

[15] B. Wang, X. Yao, Y. Jiang, C. Sun, and M. Shabaz, "Design of a real-time monitoring system for smoke and dust in thermal power plants based on improved genetic algorithm," *Journal of Healthcare Engineering*, vol. 2021, Article ID 7212567, 10 pages, 2021.

[16] A. Sharma and R. Kumar, "Service-level agreement-energy cooperative quickest ambulance routing for critical healthcare services," *Arabian Journal for Science and Engineering*, vol. 44, no. 4, pp. 3831–3848, 2019.

[17] R. K. Garg, J. Bhola, and S. K. Soni, "Healthcare monitoring of mountaineers by low power Wireless Sensor Networks," *Informatics in Medicine Unlocked*, vol. 27, Article ID 100775, 2021.

[18] V. Jagota and R. K. Sharma, "Wear volume prediction of AISI H13 die steel using response surface methodology and artificial neural network," *Journal of Mechanical Engineering and Sciences*, vol. 14, no. 2, pp. 6789–6800, 2020.

[19] P. Dhabe and P. S. V. Nataraj, "A gpu parallel Bernstein algorithm for polynomial global optimization," *International Journal of System Assurance Engineering and Management*, vol. 11, no. 1, pp. 21–44, 2020.

[20] M. K. Loganathan, P. Goswami, and B. Bhagawati, "Failure evaluation and analysis of mechatronics-based production systems during design stage using structural modeling," *Applied Mechanics and Materials*, vol. 852, pp. 799–805, 2016.

[21] D. Bhargava and S. Vyas, "Agent based solution for dining philosophers problem," in *Proceedings of the 2017*

Hindawi
Scientific Programming
Volume 2022, Article ID 7625465, 12 pages
https://doi.org/10.1155/2022/7625465

Research Article

COVID-19 Shocks, Monetary Policy, and Real Estate Price Volatility: Analysis Based on a Dynamic Stochastic General Equilibrium Perspective

Zhe Hou,[1,2] Yu Song ,[1] and Wen Xin[2]

[1]*School of Business, Macau University of Science and Technology, Macau 999078, China*
[2]*School of Finance and Trade, Zhuhai College of Science and Technology, Zhuhai 519000, China*

Correspondence should be addressed to Yu Song; ysong@must.edu.mo

Received 30 December 2021; Accepted 26 January 2022; Published 11 March 2022

Academic Editor: Punit Gupta

The COVID-19 pneumonia epidemic in early 2020 severely affected all sectors of the Chinese economy, with economic growth plummeting but the property market continuing to heat up after a brief contraction. How to formulate an effective monetary policy in the face of the COVID-19 shock to achieve stable economic growth while curbing excessive real estate price inflation has become a pressing issue for Chinese policymakers today. To this end, this paper focuses on the impact of two types of monetary policy, price-based and quantity-based, on macro-economic variables such as real estate prices and aggregate output by developing a multi-sectoral DSGE model incorporating the COVID-19 shock and comparing them. The analysis finds that both monetary policy rules can achieve the objective of dampening real estate prices. Nevertheless, while causing the same magnitude of real estate price contraction, quantity-based monetary policy leads to greater volatility in variables such as aggregate output, while other economic variables are less volatile under the price-based monetary policy.

1. Introduction

In the first quarter of 2020, the COVID-19 outbreak resulted in a nationwide shutdown to combat the epidemic and negative GDP growth for the first time in over 40 years. The government introduced a series of macro-economic policies, including active fiscal policy and flexible monetary policy, to counter the impact of the epidemic. Proactive fiscal policy promoted production recovery in tax and fee cuts and increased market capitalization to help enterprises ease their difficulties and resume production. Promoting demand recovery through flexible monetary policy, the People's Bank of China implemented a series of accommodative monetary policies, such as lowering refinancing rates and lowering the reserve requirement ratio to drive the economy back to life. Under this policy, the Chinese economy as a whole showed a steady recovery, but structurally, there was a clear divergence between different economic sectors. In 2020, China's disposable income, consumption, and manufacturing investment as a whole showed negative growth, while real estate investment bucks the trend. In 2021, as China's economy as a whole continues to pick up, real estate investment gets a further boost in the first half of this year, with commercial property sales growing at a much faster rate than before the outbreak, while real estate prices also show an upward trend. However, concerns about the impact of the epidemic are likely to continue, and pressure for continued slow growth in China's economy remains in the future.

Affected by the epidemic, the deep adjustment of the world economic and political landscape, and the deep overlap of domestic conflicts, the uncertainty of China's economy has increased. The Fifth Plenary Session of the 19th CPC Central Committee clearly proposed to "maintain financial security and guard the bottom line of no systemic risk." Furthermore, real estate is an important source of financial risk in China. Since the housing reform in 1998, the real estate market has experienced more than 20 years of booming development, and real estate prices have continued to rise, which has seriously affected residents' spending power. High prices characterize the real estate industry, high leverage, and high financialization, which has exacerbated distortions in the real estate market, spawned price bubbles, and generated a great shock to economic and financial stability. Against this realistic background, effectively curbing real estate prices, defusing real estate risks, and maintaining macro-economic stability through policy implementation have become a common concern for future policy researchers and policymakers.

Since 2012, China has repeatedly regulated the real estate market through macro-control measures, but the changes in real estate prices have not been satisfactory. From 2012 to 2013, the growth rate of real estate prices was basically stable; from 2014 to 2016, the growth rate of real estate prices rose to 10.1%. In the second half of 2016, the government's regulation and control efforts escalated again. Restrictions on purchasing and lending policies were introduced, raising policy interest rates in all provinces and cities. In 2017, General Secretary Xi Jinping proposed the policy of "housing is for living in, not speculation" in the report of the 19th National Congress, which brought the momentum of the rapid rise in real estate prices under control to some extent. However, since the outbreak of COVID-19, the real estate market has again seen the momentum of price increases. Although each regulation has played a role in stabilizing housing prices in the short term, housing prices have fallen into the strange circle of more and more adjustments in the medium and long term. It is not difficult to find that the real estate development investment accounted for the proportion of the total social fixed asset investment from 12.5% in 1998 to 27.26% the real estate industry after 20 years of rapid development in 2020 with depth analysis. The real estate industry has penetrated all fields of the national economy and become an important part of driving economic growth, promoting employment, and government revenue. China's economic development has entered a new normal with significant downward pressure on the economy in recent years. Loose macro-policies have effectively eased some of the pressure while tightening policies will inevitably add to the downward pressure on the economy. Therefore, the market generally expects that the tightening policy will not last, so there is a tendency for real estate prices to continue to rise in the medium to long term. Therefore, under the current complex and changing the background of domestic economic development, establishing a balance between the real estate market and economic development, i.e., regulating the real estate market and ensuring the smooth operation of China's economy, has become a major problem for policymakers and academics.

Because of this, this paper attempts to construct a DSGE model incorporating COVID-19 shocks, real estate market, and financial frictions based on the latest monetary policy theory research in the context of the current reality of global epidemic shocks and the new normal of China's economy. By studying the monetary policy transmission mechanism and its effectiveness, this paper examines the impact of different monetary policies on the real estate market and the macro-economy. Based on the analysis results, it selects the optimal policy conducive to calming housing prices and stabilizing economic development.

2. Related Literature

2.1. COVID-19 Shock and Monetary Policy. Since 2020, the catastrophic impact of COVID-19 on the global economy has become the focus of attention of macro-economic scholars at home and abroad. Studies on the impact of COVID-19 on the economy can be broadly divided into two categories [1]; one is from a micro-perspective, examining the impact of the epidemic shock on the behavior of micro-subjects and industrial structure through survey data information and other methods [2–4]. Another part of scholars establishing DSGE models from a macroperspective for the characteristics of the epidemic examine the impact of the epidemic shock on the macroeconomy and try to propose relevant policies to mitigate the negative impact of the epidemic.

While earlier literature on catastrophe shocks mainly deals with natural disasters such as earthquakes and floods, COVID-19 is significantly different from other catastrophic events in terms of the scope, magnitude, and duration of impact [5]. At present, it seems that the impact of COVID-19 on the global economy is comprehensive, from the internal circulation of economies to external exchange and from the demand side of the macro-economy (residential consumption, etc.) to the supply side (enterprise production, etc.) being seriously affected. On the demand side, from the perspective of household production, the COVID-19 shock brings more uncertainty by affecting the decision-making behavior of residents, such as consumption, leading to a decline in consumption [6, 7]. It forces households to restructure their assets and increase their holdings of lower-risk assets, resulting in the supply side of the economy also being affected, with investment and output trending downwards [8]. Zhu et al. proposed a characteristic of COVID-19 that distinguishes it from other disasters, namely, the sudden quiescence of the labor force, and introduced the labor force trilogy into the DSGE model [5]. However, as far as the current economic data are concerned, the impact of sudden labor force quiescence on the overall economy is not significant (with the rise of online offices, the Internet economy has defused this impact to some extent). Chen and Zhong combined the contagion (SIR) model with the DSGE model to depict the changes in aggregate supply and aggregate demand in the Chinese economy under the influence of COVID-19 and analyzed the impact of monetary policy under the interest rate rule [9]. However, the impact of quantitative monetary policy and mixed monetary policy is not discussed in depth.

In summary, although some of the literature analyzes the COVID-19 shock economy and the corresponding policy choices for domestic and international studies on the epidemic, there is no specific discussion on the optimal choice of multiple monetary policies under COVID-19 shocks. Examining optimal monetary policies based on the COVID-19 context to mitigate macro-economic volatility and quantitatively analyzing the impact of COVID-19 on the effectiveness of traditional monetary policies are still topics less covered in current studies. In addition, the possible real estate price volatility triggered by COVID-19 has been even less explored.

2.2. Real Estate Price Volatility and Monetary Policy. In recent years, many scholars at home and abroad have studied the relationship between real estate prices, monetary policy, and economic fluctuations, mainly using DSGE model analysis. However, different scholars have different views on the impact of monetary policy on the real estate market. Most of the early literature concluded that monetary policy need not respond to real estate price volatility and that monetary policy regulations that dampened asset price volatility reduced output volatility, albeit marginally. However, this led to more dramatic inflationary fluctuations and did not stabilize the economy [10, 11]. After an in-depth analysis of the above literature, it is not difficult to find that their models have the following two common features. First, incremental changes in assets such as real estate are not considered separately, which is clearly not in line with the current economic reality, where the real estate firms have become an important pillar of the national economy in many important economies. Second, many important financial market frictions were not attended to, which may lead to biased policy transmission paths and ultimately yield expected results inconsistent with reality. Therefore, later scholars continued their research to address the above issues by adding the real estate market as an important productive sector to the model for analysis. As the uncertainty of the economy increased after the subprime mortgage crisis, more scholars introduced financial frictions such as credit constraints and monetary policy shocks into the DSGE model. They began to focus on the financial stirrup effect and various types of shocks on the macro-economic regulation effect. It has been found that the inclusion of heterogeneous production sectors can better model the transmission path of monetary policy and multiple shocks to the real economy, and real estate prices have become an important transmission medium for monetary policy shocks [12–14]. This view gradually gained influence after 2008, with a growing literature affirming the role of monetary policy on asset prices and its macro-economic implications.

They analyzed the U.S. real estate market by building a DSGE model that includes credit constraints and found that real estate price volatility has a significant impact on the cyclical fluctuations of the economy [15]. Others focused on two frictions, asset collateral and external financing premium, and argued that negative fluctuations in asset prices lead to homogeneous fluctuations in investment and output, exacerbating negative fluctuations in the economy [16]. Real estate mortgages have a significant financial stirrup effect in economies where the macro-economic impact of real estate price volatility is more dramatic and that this spillover effect is more pronounced in countries with more developed real estate financial markets [17]. Some scholars obtained similar conclusions from their analysis in the context of the Chinese economy: price-based monetary policy shocks are a key determinant of real estate price volatility, and excessive real estate price increases can be curbed through the formulation of appropriate monetary policies [18]. The shocks such as mortgage rate shocks and preference shocks to real estate have a significant impact on macro-economic fluctuations in China [19]. Monetary policy shocks affect consumption and real estate demand through the medium of nominal interest rates, ultimately leading to fluctuations in real estate prices and aggregate demand [20, 21]. The government can use monetary policy and financial shock effects to achieve stability in the real estate market. Therefore, some scholars argue that expectations affect cyclical fluctuations in the real estate market and even the macro-economy [22]. Active use of monetary policy tools such as lending rates can effectively reduce the volatility of household debt and aggregate consumption and GDP. There are significant effects in dampening expectation-driven cyclical fluctuations in the real estate market and the macro-economy [23]. Starting from the correlation between real estate prices and variables such as interest rates, exchange rates, and financing size, scholars have also argued that monetary policy is significantly effective in smoothing real estate prices as well as stabilizing the macro-economy and have discussed the linkage mechanism between these three [24].

It is clear from the review of the above literature that while most early scholars and policymakers did not advocate intervention in asset price volatility with the help of monetary policy, the mainstream view changed significantly after the 2008 crisis. Using DSGE models that incorporate financial frictions, many scholars have affirmed the moderating role of monetary policy on real estate prices as well as macro-economic stability. Since most of the studies mentioned above discuss the impact of a single type of monetary policy on real estate prices, few articles compare and analyze the impact of different monetary policies. Therefore, there is no uniform analysis on the choice of the optimal monetary policy.

3. The DSGE Model

3.1. Model Frame. Compared with previous models, this paper constructed a DSGE model including COVID-19 shocks, the real estate market, and financial frictions. The model includes multiple macro-economic sectors, such as households, firms, commercial banks, and central banks. We try to compare and analyze the impact of different monetary policies. As seen in the 2020 Chinese and global economic data and related reports, the COVID-19 shock triggers a reduction in the rate of technological upgrading, human resource mismatch, and different proportions of original stock capital accumulation in each sector of production firms, and the overall performance of the economy is severely affected by the level of output. The impact of COVID-19 on the economy is similar to previous disasters in that it causes a reduction in the level of output in the economy and a decline in capital accumulation. However, the impact of this epidemic is much broader, and its negative impact is no less than that of any previous disaster. Consequently, the model in this paper will introduce variables u_s^t for COVID-19 shocks in the real estate firms, the consumer goods sector, and household capital accumulation, which result in sectoral total factor productivity and capital stock being affected, as shown in Figure 1.

3.2. Households. Drawing on Iacoviello's model setup, heterogeneous household characteristics are introduced in the household sector, considering the differences between Chinese and U.S. households: savings-type households and loan-type households [11]. The discount factor $\beta\prime$ is larger for savings-type households than for loan-type households $\beta\prime\prime$. When making utility maximization choices, loan-type households are more inclined to consume than savings-type households, while savings-type households are more inclined to save for investment. Thus, saving households accumulate physical capital through investment and save in commercial banks. In contrast, loan-based households do not accumulate physical capital and borrow from commercial banks as collateral for their only real estate asset that has a collateral function. Therefore, a financial stirrup mechanism is introduced in the model. The proportion of saving households is denoted as α and the proportion of loan households is $1-\alpha$.

3.2.1. Savings-Type Households. Saving-type households' discount factors β' is saving-type households' discount factor. Subjecting to the budget constraints, saving-type households rationally choose consumption C_t', housing H_t', labor N_t', assets: physical assets, and financial assets (including monetary M_t', deposits b_t', etc.) subject to budget constraints. Maximizing household lifetime utility:

$$\max E_t \sum_{t=0}^{\infty} (\beta')^t \left(\ln C_t' + J_t \ln H_t' + \ln M_t' - \frac{(N_t')^{1+\phi}}{1+\phi} \right), \quad (1)$$

where ϕ is the inverse of the real wage elasticity and J_t is a housing preference shock that obeys the AR(1) process $\ln J_t = \rho_t \ln J_{t-1} + \upsilon_{j,t}\ (\upsilon_{j,t} \sim N(0, \sigma_j^2))$(Exogenous shocks in the text take the same setting, i.e., they obey the first-order autoregressive process.). The labor supply of a saving household is the sum of its labor supply in the real estate and consumer goods sectors, assuming that labor supply is invested according to this equation:

$$N_t' = \left[(N_{ct}')^{1+\tau} + (N_{ht}')^{1+\tau} \right]^{1/1+\tau}, \quad (2)$$

where τ is the elasticity of substitution of labor inputs between sectors and N_{ct}' and N_{ht}' represent the household's labor supply in the consumer goods and real estate firms. The saving household faces the following budget constraint:

$$C_t' + b_t' + M_t' + Q_t H_t' = N_{ct}' W_{ct}' + N_{ht}' W_{ht}' + \frac{M_{t-1}'}{\Pi_t} + \frac{r_{t-1}^b b_{t-1}'}{\Pi_t} + Q_t (1-\delta_h) H_{t-1}', \quad (3)$$

where δ_h is the depreciation rate of real estate, W_{ct}' and W_{ht}' represent the level of real wages in the consumer goods sector and the real estate firms, Π_t is the inflation rate, r_t^b is the interest rate on bank deposits, and Q_t is the level of real estate prices.

3.2.2. Loan-Type Households. Loan-type households have a discount factor of $\beta\prime\prime$. Loan-type households have no capital holdings and mortgage their homes b_t'' (to commercial banks). Maximizing process lifetime utility:

$$\max E_t \sum_{t=0}^{\infty} (\beta'')^t \left(\ln C_t'' + J_t \ln H_t'' + \ln M_t'' - \frac{(N_t'')^{1+\phi}}{1+\phi} \right). \quad (4)$$

Similar to the saving-type household, the labor supply of the loan-type household is invested according to this equation:

$$N_t'' = \left[(N_{ct}'')^{1+\tau} + (N_{ht}'')^{1+\tau} \right]^{1/1+\tau}. \quad (5)$$

The budget constraints faced by loan-based households are as follows:

$$C_t'' + \frac{r_{t-1}^b b_{t-1}''}{\Pi_t} + M_t'' + Q_t H_t'' = N_{ct}'' W_{ct}'' + N_{ht}'' W_{ht}'' + \frac{M_{t-1}''}{\Pi_t} + b_t'' + Q_t (1-\delta_h) H_{t-1}'', \quad (6)$$

where r_t^b is the bank's lending rate. Loan-type households prefer to consume and use home mortgages, so they face the following credit constraints ($m\prime\prime$ is the mortgage rate):

$$b_t'' = m\prime\prime E_t \left[\frac{Q_{t+1}(1-\delta_h) H_t'' \Pi_{t+1}}{r_t^{b''}} \right]. \quad (7)$$

3.3. Labor Supply and Wage Setting. These two household sectors are the only labor supply sectors in the economy, providing labor for the real estate and consumer goods sectors. Assume a Calvo-type stickiness setup for households: assume that the proportion of households with adjustable wages in each period is $1-\theta_w$. θ_w is the wage stickiness index, i.e., the larger θ_w is, the stickier the wage is. In period t, households that can adjust their wages choose the actual optimal wage W_t^*. For households that cannot adjust their wages, wages are indexed to the inflation rate of the previous period (inflation inertia) and set to $W_{t-1}\Pi_{t-1}$ (the fully indexed setting) [25].

A large and competing class of labor integration agents in the economy adds up the heterogeneous labor supplied by each household i into homogeneous labor and supplies it to other sectors. ε_w can be understood as the wage elasticity of labor demand.

$$W_{(c,h),t} = \left[\int_0^1 \left(W_{(c,h),t}^i \right)^{1-\varepsilon_w} \mathrm{d}i \right]^{1/1-\varepsilon_w}, \quad (8)$$

where $W_{(c,h),t}$ denotes the real wage index for both sectors, assuming that the labor demand function faced by the first representative household is defined as

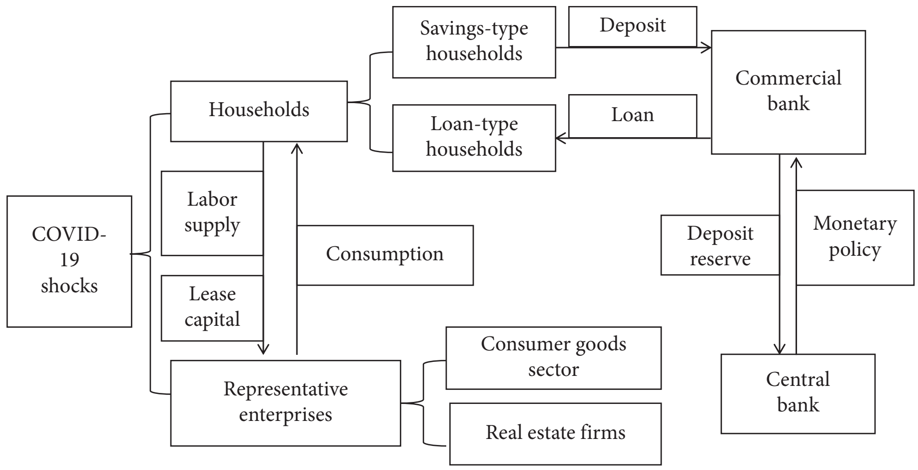

Figure 1: Model structure diagram.

$$N^{i}_{(c,h),t} = \left(\frac{W^{i}_{(c,h),t}}{W_{(c,h),t}}\right)^{-\varepsilon_w} N_{(c,h),t}, \tag{9}$$

where $N_{(c,h),t}$ is the aggregate demand in the labor market for both sectors. Solving the problem of setting the household optimal wage yields the real wage inflation equation for the household sector:

$$\begin{aligned}\widehat{W}_{(c,h),t} &= \frac{\beta\prime}{1+\beta\prime}E_t\left(\widehat{W}_{(c,h),t+1}+\widehat{\Pi}_{t-1}\right)\\ &\quad - \widehat{\Pi}_t + \frac{1}{1+\beta\prime}E_t\left(\widehat{W}_{(c,h),t+1}+\widehat{\Pi}_{t-1}\right)\\ &\quad - \frac{\left(1-\beta\prime\theta_w\right)\left(1-\theta_w\right)}{\theta_w\left(1+\beta\prime\right)\left(1+\varepsilon_w\phi\right)}\left(\widehat{W}_{(c,h),t}-\phi\widehat{N}_{(c,h),t}-\widehat{C}_t\right).\end{aligned} \tag{10}$$

3.4. Representative Enterprises

3.4.1. Real Estate Firms. The real estate firm produces housing, referring to the setting in the article by Wang and Hou [26]. The real estate firm is assumed to consist of monopolistically competitive manufacturers continuously distributed on the interval [0,1], with homogeneous and divisible products and non-sticky housing prices. Real estate manufacturers produce by hiring labor, renting capital from savers, and providing land. The manufacturer's production function can be expressed in the following form:

$$Y_{ht} = L_t\left(K_{h,t-1}\right)^{\alpha_h}\left(N'^{\alpha}_{ht}N''^{1-\alpha}_{ht}\right)^{1-\alpha_h}. \tag{11}$$

The COVID-19 shock has hit the global economy since the beginning of 2020. As shown in the Chinese and global economic data for 2020 and related reports, the COVID-19 shock triggered a reduction in the rate of technological upgrading, human resource mismatch, and a different proportion of the original stock of capital accumulation in production enterprises in various sectors, resulting in an overall severe shock to the output level of the economy. The shock of COVID-19 on the economy is similar to that of previous catastrophes in that both have caused a decline in output levels and capital accumulation in the economy. However, the shock of the COVID-19 was more widespread and caused as much negative shock as any of the previous catastrophes. Therefore, in two production sectors, namely, the real estate sector and the consumer goods sector, a variable u^s_t representing a COVID-19 shock is introduced to denote the probability of a COVID-19 shock occurring in period t [27]. This shock leads to a decrease in total factor productivity by a proportion s_{yh}. Since this COVID-19 shock has a greater impact than other previous catastrophic shocks, it can be distinguished by adjusting the size of the impairment proportion s_{yh}. Then, the above equation can be rewritten as follows:

$$Y_{ht} = \left(1-u^s_t s_{yh}\right)L_t\left(K_{h,t-1}\right)^{\alpha_h}\left(N'^{\alpha}_{ht}N''^{1-\alpha}_{ht}\right)^{1-\alpha_h}. \tag{12}$$

Assume that wages are non-differentiable within the same sector, i.e., $(N'^{\alpha}_{ht}N''^{1-\alpha}_{ht})$. Here the land supply directly affects the output of the vendor, assuming that the vendor faces a representative land supply shock L_t. Since the wages of labor in the real estate firms are non-differentiable, $W'_{ht} = W''_{ht} = W_{ht}$. From the vendor cost minimization problem, the real marginal cost function of the vendor is obtained.

$$\begin{aligned}MC_{ht} &= \frac{1}{L_t}\frac{1}{1-u^s_t s_{yh}}\left(\frac{1}{\alpha}\right)^{\alpha\left(1-\alpha_h\right)}\left(\frac{1}{\alpha_h}\right)^{\alpha_h}\left(\frac{1}{1-\alpha_h}\right)^{1-\alpha_h}\\ &\quad \left(\frac{1}{1-\alpha}\right)^{(1-\alpha)\left(1-\alpha_h\right)}R^{\alpha_h}_{ht}W^{1-\alpha_h}_{ht}.\end{aligned} \tag{13}$$

It is assumed above that prices in the real estate firms are not sticky, i.e., all real estate vendors can re-price each period. Therefore, it is assumed that vendors use the marginal cost-plus method for pricing and thus

$$Q_t = \frac{\varepsilon_h}{\varepsilon_h - 1} MC_{ht}, \tag{14}$$

where $\varepsilon_h/\varepsilon_h - 1$ is the price plus ratio and ε_h is the price elasticity coefficient of housing demand.

3.4.2. Consumer Goods Sector. Referring to some of the assumptions of the real estate firms, the production of goods in the consumer goods sector requires the input of capital and labor to produce and supply its products to other economic agents. Like the real estate firms, considering that the epidemic shock also impacts TFP (total factor productivity), the production function is defined in the following form:

$$Y_{ct} = \left(1 - u_t^s s_{yc}\right) A_t \left(K_{c,t-1}\right)^{\alpha_c} \left(N_{ct}^{'\alpha} N_{ct}^{''1-\alpha}\right)^{1-\alpha_c}. \tag{15}$$

Here the technology shock A_t directly affects the level of output of the vendor. Solving the vendor cost minimization problem yields the real marginal cost function of the vendor.

$$MC_{ct} = \frac{1}{A_t} \frac{1}{1 - u_t^s s_{yc}} \left(\frac{1}{\alpha}\right)^{\alpha(1-\alpha_c)} \left(\frac{1}{\alpha_c}\right)^{\alpha_c} \left(\frac{1}{1-\alpha_c}\right)^{1-\alpha_c} \left(\frac{1}{1-\alpha}\right)^{(1-\alpha)(1-\alpha_c)} R_{ct}^{\alpha_c} W_{ct}^{1-\alpha_c}. \tag{16}$$

Since this paper sets the existence of price stickiness in the consumer goods sector, the current price stickiness characteristics refer to the Calvo stochastic price adjustment model [28]. Assume that the proportion of manufacturers who can adjust prices in each period is $1 - \theta_c$, and θ_c is the price stickiness index. The NK Phillips curve for the consumer goods sector can be obtained as follows.

$$\widehat{\Pi}_t = \frac{\beta\imath}{1+\beta\imath} E_t\left(\widehat{\Pi}_{t+1}\right) + \frac{1}{1+\beta\imath}\widehat{\Pi}_{t+1} + \frac{\left(1-\beta\imath\theta_c\right)\left(1-\theta_c\right)}{\theta_c\left(1+\beta\imath\right)} \widehat{MC}_{ct}. \tag{17}$$

3.5. Capital Accumulation and Investment Decisions. It is assumed that saving households, as owners of capital goods, invest their holdings in various production sectors and achieve capital accumulation through investment decisions in each period [29]. The COVID-19 shock introduced in the model can lead to an impairment of the capital stock by a percentage. The capital accumulation of saving households in each sector satisfies the following equation.

$$\begin{aligned} K_{ct} &= \left(1 - u_t^s s_{kc}\right)\left[(1-\delta_k)K_{c,t-1} + I_{ct}\left(1 - \frac{\psi_c}{2}\left(\frac{I_{ct}}{I_{ct-1}} - 1\right)^2\right)u_t^I\right], \\ K_{ht} &= \left(1 - u_t^s s_{kh}\right)\left[(1-\delta_k)K_{h,t-1} + I_{ht}\left(1 - \frac{\psi_h}{2}\left(\frac{I_{ht}}{I_{ht-1}} - 1\right)^2\right)u_t^I\right]. \end{aligned} \tag{18}$$

δ_k is the capital depreciation rate. Assuming that the saving household does not separate ownership and operation of the firm, the household makes its choice of capital along with its choice of investment, ψ_c and ψ_h are the sensitivity coefficients of the capital adjustment costs of the two sectors, respectively, and u_t^I is the investment shock. Then, the saving household makes its investment decision through the following optimization problem.

$$\max E_t \sum_{t=0}^{\infty} (\beta\imath)^t \lambda_t'\left(K_{c,t-1}R_{ct} + K_{h,t-1}R_{ht} - I_{ct} - I_{ht}\right). \tag{19}$$

3.6. Commercial Bank. Considering the model consistency and solution problems, the commercial bank sector in the model is set to be highly simplified compared to the behavioral characteristics of commercial banks in practice. The profit sources of commercial banks are deposit and loan spreads, which are obtained by taking deposits from saving households and then extending loans to the real estate firms and lending households to maximize profits. In the course of their operations, commercial banks are subject to the required legal deposit reserve $RR_t = b_t' f_t^{RR}$, of which f_t^{RR} is the legal deposit reserve ratio. Thus, the asset-liability structure of commercial banks can be expressed as follows:

$$RR_t + b_t'' = b_t'. \tag{20}$$

Commercial banks need to consider liquidity issues while generating profits. Referring to the loan stock adjustment problem proposed by Atta and Dib, banks adjust the number of deposits and loans according to various requirements such as capital adequacy ratio in their operations [30]. This adjustment cost is assumed to be $\psi_b/2\,(b_t''/b_{t-1}'' - 1)^2 b_{t-1}''$, where b_t'' denotes the total amount of loans and ψ_b is the loan stickiness parameter. Solving the bank's profit maximization problem yields the first-order condition as

$$\begin{aligned} & r_t^{b} - \frac{r_t^b}{1 - f_t^{RR}} - \psi_b\left(\frac{b_t''}{b_{t-1}''} - 1\right) \\ & = \beta\imath\left[\frac{\psi_b}{2}\left(\frac{b_{t+1}''}{b_t''} - 1\right)^2 - \psi_b\left(\frac{b_{t+1}''}{b_t''} - 1\right)\frac{b_{t+1}''}{b_t''}\right]. \end{aligned} \tag{21}$$

3.7. Central Bank. There is no uniform conclusion on the applicability of monetary rules in China, and Huang and Xu conducted a policy analysis using a Taylor rule with additional interest rate stickiness and obtained good fitting results [31]. In contrast, others argued that a quantity rule based on monetary supply regulation is more representative of China's macro-policy practice [32, 33]. Given the above literature, in the following analysis, the model settings are considered separately for both interest rate and quantity rules, which are commonly used in the literature.

3.7.1. Interest Rule. Assuming that the lending rate is the main operating instrument of the central bank [26], the monetary policy rule takes the form of the promoted Taylor rule:

$$\frac{r_t^b}{r_{ss}^b} = \left(\frac{r_{t-1}^b}{r_{ss}^b}\right)^{\rho_b} \left[\left(\frac{\Pi_t}{\Pi_{ss}}\right)^{\varphi_\Pi} \left(\frac{Y_t}{Y_{ss}}\right)^{\varphi_Y} \left(\frac{Q_t}{Q_{ss}}\right)^{\varphi_Q}\right]^{1-\rho_b} u_t^r, \quad (22)$$

where r_t^b denotes the lending rate, ρ_b is the interest rate smoothing coefficient, which is set to avoid the impact of large fluctuations in interest rates on the economy and allows for some inertia in the adjustment of interest rates, φ_Π, φ_Y, φ_Q denote the response coefficients of output gap, inflation, and real estate prices, and u_t^r is the monetary policy shock.

3.7.2. Quantity Rule. Under the quantity rule, the monetary supply becomes the main operating tool of the central bank. According to the model setting of this paper, the monetary aggregate is $M_t = M_t' + M_t'' + b_t'$ [33], the monetary growth rate can be expressed as $g_{mt} = M_t/M_{t-1}$, and the monetary policy rule is as follows:

$$\frac{g_{mt}}{g_{mss}} = \left(\frac{g_{mt-1}}{g_{mss}}\right)^{\rho_m} \left[\left(\frac{\Pi_t}{\Pi_{ss}}\right)^{-\varphi_\pi} \left(\frac{Y_t}{Y_{ss}}\right)^{-\varphi_y} \left(\frac{Q_t}{Q_{ss}}\right)^{-\varphi_q}\right]^{1-\rho_m} u_t^g, \quad (23)$$

where ρ_m is the smoothing factor that regulates the monetary supply, allowing for some inertia in the adjustment of the monetary supply, and u_t^g is the monetary policy shock at this point.

3.8. Equilibrium. The clearing conditions of the whole system, including the commodity market, are

$$\begin{aligned} Y_t &= Y_{ct} + Q_t Y_{ht}, \\ Y_{ct} &= C_t' + C_t'' + I_{ct} + I_{ht}, \\ Y_{ht} &= \left[H_t' - (1-\delta_h)H_{t-1}'\right] + \left[H_t'' - (1-\delta_h)H_{t-1}''\right], \\ b_t' &= \frac{b_t''}{\left(1 - f_t^{RR}\right)}, \end{aligned} \quad (24)$$

where Y_t denotes real GDP. The equilibrium conditions of the above-mentioned economic agents and production sectors and the exogenous shock processes together construct an economic dynamical system.

4. Parameter Calibration and Estimation

4.1. Parameter Calibration. When calculating the steady state, it is necessary to calibrate the relevant parameters to determine the steady state. In this paper, the data related to the Chinese economic variables are matched to the relevant parameters in the steady-state model and are summarized in Table 1.

Among them, s_y, s_k are estimated based on the estimation method of Barro using Chinese real GDP per capita growth rate data [35]. Figure 2 shows China's real GDP per capita growth rate indicators during 1953–2020. The average value of the nine negative values is taken as the percentage of total factor productivity loss due to disaster shocks in China, and the estimated percentage of total factor productivity loss is 0.0678. Therefore, the above percentage of loss is set to 0.0678.

4.2. Parameter Simulation. There are seven external shocks included in the model. This paper selects relevant data from seven primary data such as consumer price index, total retail sales of consumer goods, fixed asset investment, gross domestic product, average price of commercial housing (calculated from sales of commercial housing/area of commercial housing sales), and monetary and quasi-monetary (M2) supply to estimate the model. The data sample period is from the first quarter of 2000 to the fourth quarter of 2020. Since the model variables are all real values, the above nominal data are processed and converted to real values. Quarterly data are used for all data characterized by seasonal fluctuations, except for the monetary supply and interest rates, which do not have significant seasonal characteristics. Therefore, X12 is used to adjust these data seasonally. Next, the natural logarithm of the above-adjusted data was taken, and finally, HP filtering was applied to remove long-term trends from the data and convert them into observable variable information.

The parameters to be estimated by the model were estimated using Bayes methods to compare the posterior estimates under the price-based rule and the quantity-based rule, as shown in Table 2.

5. Impulse Response Analysis

This paper compares the impulse response results of monetary policy shocks of two rules, price-based and quantity-based (the dynamic responses of each variable in the figure are shown as percentage deviations from the steady state), to analyze the different impacts of the two monetary policy shocks on China's macro-economic fluctuations in terms of both the magnitude of fluctuations and the duration period and further analyzes the applicability of the two monetary policy rules in China.

Table 1: Parameter calibration.

Calibration	Meaning	Calibration value	Basis for taking values
$\beta\prime$	Savings-based household discount factor	0.988	Iacoviello and Neri [15]
$\beta\prime\prime$	Loan-based household discount factor	0.95	
δ_k	Elasticity of substitution between labor inputs in each sector	1	Wang and Hou [26]
ϕ	Quarterly depreciation rate of real estate	0.8%	
τ	Capital depreciation rate (quarterly)	2.5%	Xu and Liu [33]
δ_h	The inverse of the real wage elasticity of labor	1	Bernanke et al. [10], Peng and Fang [39]
$m\prime\prime$	Mortgage ratio	0.7	According to the current lending policy in China, the downpayment ratio for the first suite is usually 30%
ε_h	Elasticity of output with respect to capital for the real estate firms	0.5	Iacoviello and Neri [15]
α_h	Elasticity of output of the consumer goods sector with respect to capital	0.5	
α_c	Price elasticity of demand for housing	6	Iacoviello [11]
φ_Π	Inflation under the interest rate rule	0.15	
φ_Y	Output gap under the interest rate rule	1.5	
φ_Q	Real estate price response coefficient under the interest rate rule	1.5	Hou and Gong [18]
φ_π	Interest rate smoothing coefficient	0.8	
φ_y	Inflation under the quantity rule	0.5	
φ_q	Output gap under the quantity rule	1.5	
ρ_b	Real estate price response coefficient under the quantity rule	1.5	Xu and Liu [33]
ρ_m	Monetary supply smoothing coefficient	0.8	
s_y	Proportion of TFP declines in both sectors due to epidemic shocks	0.0678	Estimation based on Barro [35] estimation method with actual data from China.
s_k	Proportion of capital stock impaired due to epidemic shocks	0.0678	Chen et al. [34]

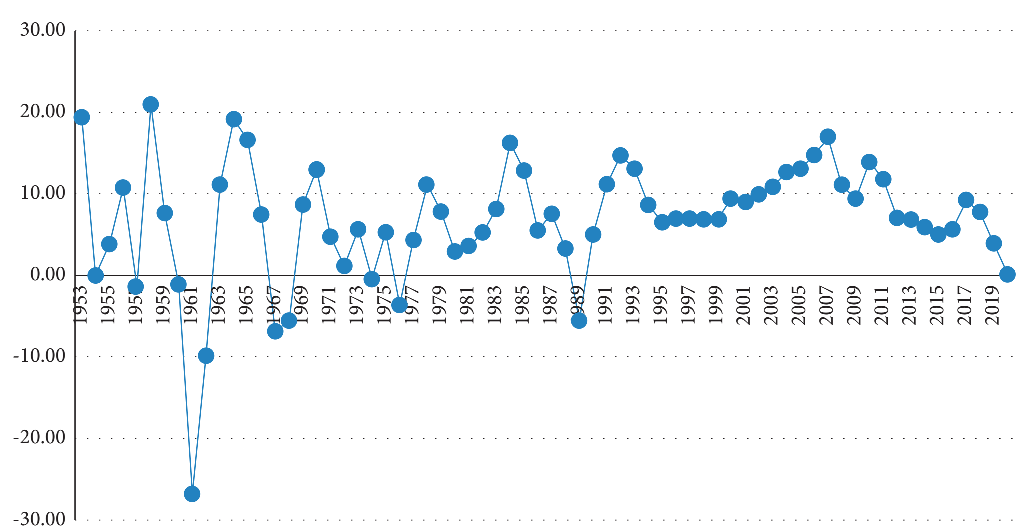

Figure 2: Trends in real GDP per capita growth rates(Data source: Calculated based on data from the official website of the National Bureau of Statistics.).

5.1. COVID-19 Shock. Figure 3 shows in comparison the dynamic impact of COVID-19 shock on macro-economic variables under both models. The simulation results above show that the onset of the epidemic has a significant short-term impact on the real estate market and the economy as a whole. Real estate prices contract more significantly under the epidemic shock but for a shorter duration. Aggregate output and consumption also fall sharply in a short period, which confirms the market performance since 2020, and the household sector does not experience post-disaster panic

Table 2: Bayes estimation results of the model.

Parameter	Prior distribution		Interest rule		Quantity rule	
	Distr.	Mean	Posterior mean	Confidence interval	Posterior mean	Confidence interval
ρ_j	Beta	0.8	0.7662	(0.7633, 0.7686)	0.8386	(0.7320, 0.9502)
ρ_u^I	Beta	0.7	0.9193	(0.9158, 0.9226)	0.8313	(0.8151, 0.8439)
ρ_u^s	Beta	0.8	0.7455	(0.7445, 0.7465)	0.8447	(0.8319, 0.8563)
ρ_l	Beta	0.8	0.9973	(0.9951, 0.9993)	0.8972	(0.8809, 0.9180)
ρ_a	Beta	0.8	0.8218	(0.8197, 0.8238)	0.4369	(0.4063, 0.4737)
ρ_f^{RR}	Beta	0.8	0.9152	(0.9117, 0.9181)	0.8700	(0.8295, 0.9208)
ρ_u^r/ρ_u^g	Beta	0.8	0.9991	(0.9986, 0.9998)	0.8471	(0.8145, 0.8770)
σ_j	Inv.Gamma	0.1	0.0059	(0.0026, 0.0092)	0.0078	(0.0024, 0.0139)
σ_u^I	Inv.Gamma	0.1	0.0070	(0.0060, 0.0079)	0.2996	(0.2453, 0.3526)
σ_u^s	Inv.Gamma	0.1	0.0017	(0.0015, 0.0020)	0.2346	(0.1774, 0.3195)
σ_l	Inv.Gamma	0.1	0.0019	(0.0018, 0.0020)	0.0929	(0.0778, 0.1081)
σ_a	Inv.Gamma	0.1	0.2271	(0.2142, 0.2409)	0.1476	(0.0832, 0.1789)
σ_f^{RR}	Inv.Gamma	0.1	0.1827	(0.1715, 0.1911)	0.0079	(0.0022, 0.0135)
σ_u^r/σ_u^g	Inv.Gamma	0.1	0.0057	(0.0050, 0.0065)	0.0355	(0.0290, 0.0418)

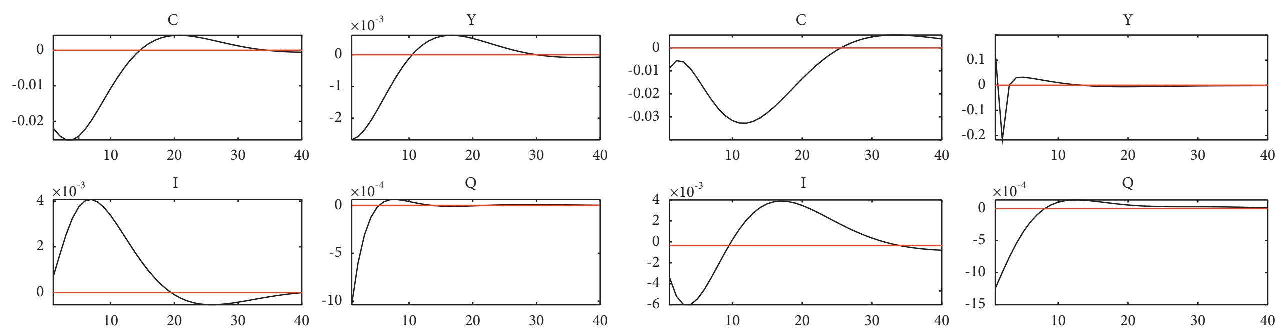

Figure 3: Impulse responses to COVID-19 shock. The figure on the left shows the interest rate rule model and that on the right is the quantity rule model.

consumption. As can be seen, the impact of the epidemic shock on real estate prices and aggregate consumption and investment is similar in magnitude in both models, but the volatility of output is more pronounced in the quantity-based model. Hence, the price-based model effectively regulates real estate prices and stabilizes the economy under an epidemic shock. In contrast, the quantity-based model can achieve the objective of regulating real estate prices but may cause drastic fluctuations in the total economy in the short run, which is not conducive to stabilizing economic development.

5.2. Monetary Shock. Figure 4 shows the dynamic effects of different monetary policy shocks on macro-economic variables. In the model, including the impact of the epidemic, real estate prices show a significant increase and a long duration when a positive interest rate shock occurs. Aggregate output and aggregate investment show varying degrees of decline, and aggregate consumption shows a rise followed by a decline. When a positive monetary growth rate shock hits the economy, real estate prices show a more pronounced rise and last longer. Aggregate output, aggregate investment, etc. show varying degrees of increase, and aggregate consumption shows a tendency to fall and then rise.

From the above simulation results, it can be seen that a tight monetary policy can be more effective in curbing the overheated development of real estate prices, but it also has a dampening effect on the total output of the economy, and the impact is relatively long-lasting. Thus, in the face of a pandemic shock, raising interest rates will dampen real estate prices in the short run, but it will also cause a certain degree of economic contraction. When using this type of monetary policy, attention needs to be paid to the negative effects on the economy. An accommodative quantitative monetary policy shock can positively impact investment and output, with real estate prices tending to rise and the impact having a high degree of permanence. However, the side effects of the policy are also evident, leading to persistent and significant inflation.

5.3. Investment Shock. Figure 5 compares the macro-economic dynamics of investment shocks in the two models. As can be seen, both models exhibit similar results when subjected to investment shocks, both affecting aggregate consumption in the short run and having some dampening effect on real estate prices. However, as higher interest rates reverse the dampening effect on investment, a slight rebound in housing prices ensues. The volatility of aggregate investment suggests that the long-run impact of

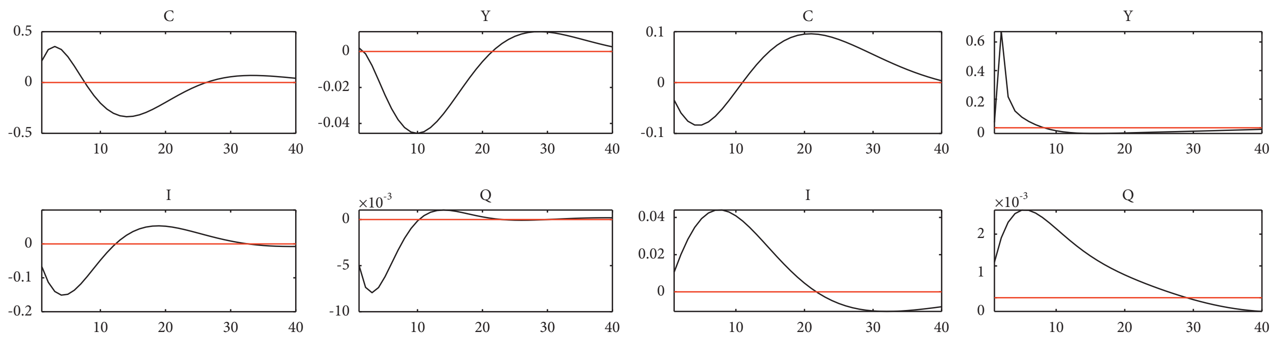

Figure 4: Impulse responses to monetary shock.

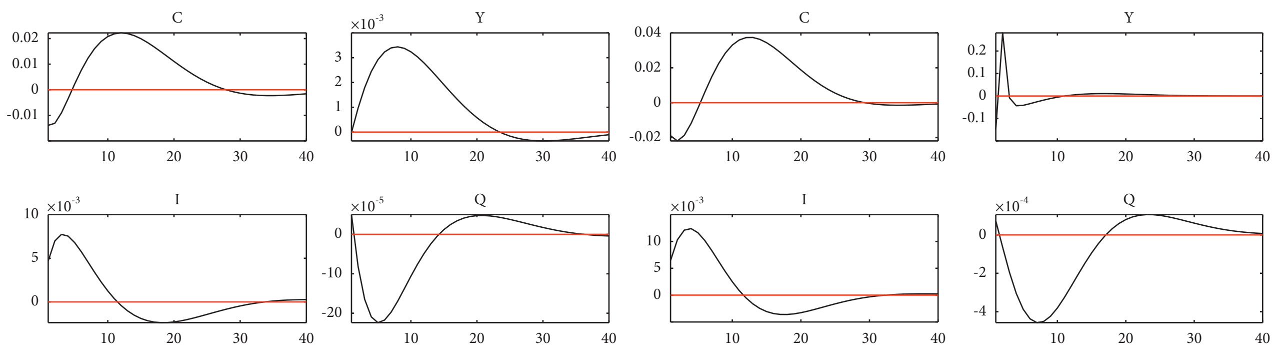

Figure 5: Impulse responses to investment shock.

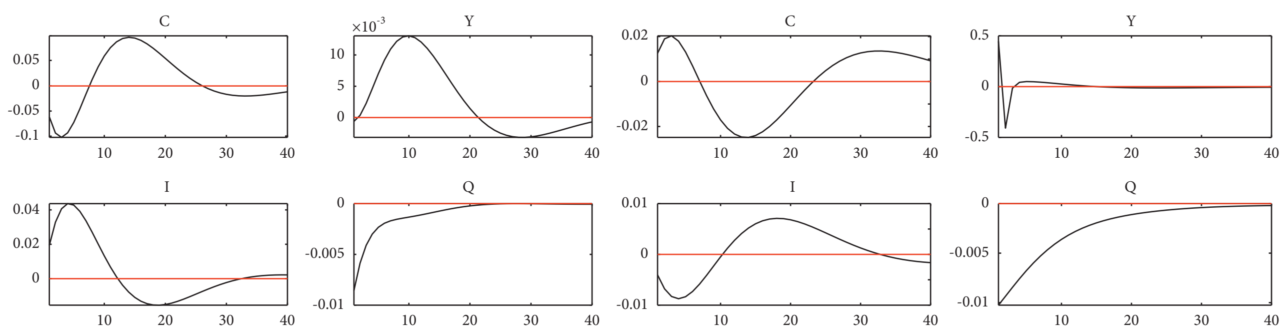

Figure 6: Impulse responses to land supply shock.

the current positive investment shock is poor and may be dragged down by the subsequent decline in aggregate social investment, which creates an awkward situation of early use, leading to a subsequent slippage in aggregate output as well.

5.4. Land Supply Shock. As can be seen from the simulation results below, a positive land supply shock effectively suppressed real estate prices over a longer period in both models. It also has a strong, persistent effect on all variables, which positively affects the overall adjustment of the economy. However, the drawback is also evident in that it causes inflation to remain at a high level for a longer period, which in the long run must prevent the economy from overheating, as shown in Figure 6.

In summary, in terms of stabilizing the real estate market as well as macro-economic fluctuations, the above shocks of both price-based and quantity-based rule models have produced certain effects on achieving real estate price regulation and stabilizing the economy, but the effects of each shock on aggregate output are more drastic under the quantity-based rule. Therefore, in practice, it is necessary to choose the optimal regulation instruments according to the current economic development and macro-economic regulation objectives in different periods while paying attention to the abnormal fluctuations of other variables.

6. Conclusions

Since the outbreak of COVID-19, the economies of various countries have been hit to varying degrees, and the recent rapid heating of the real estate market has drawn the attention of scholars. In this context, regulating the real estate market while stabilizing the economy has become a key problem faced by China's policy makers. This paper focuses on the effects of two types of monetary policies, price-based and quantity-based, on variables such as real estate prices and aggregate output by building a multi-sectoral DSGE model that includes COVID-19 shocks. The following conclusions are drawn.

First, price-based monetary policy is more effective in regulating real estate prices and stabilizing the economy. The analysis finds that both monetary policy rules achieve the goal of curbing real estate prices to some extent, but variables such as aggregate output are more volatile under the quantity-based rule, which is detrimental to economic stability. In contrast, in the model with the price-based rule, other variables such as aggregate output are less volatile under the same degree of real estate price volatility. Price-based monetary policy can curb real estate prices while having a milder impact on the overall economy.

Second, the COVID-19 shock dampened real estate prices in the short run but simultaneously had serious effects on other parts of the Chinese economy, and the effects lasted longer. Impulse response analysis finds that the impact of the epidemic shock on real estate prices lasts only about 4 periods, while the impact on aggregate consumption, aggregate investment, and aggregate output lasts more than 10. This finding is supported by economic reality, as China's real estate market heated up rapidly in the first quarter of the year, with real estate prices and volumes rising in many places, while the rest of the economy recovered more slowly.

Third, investment and land supply shocks can effectively curb real estate prices while not having much negative impact on other economic variables and can better cope with the current situation. While aggressive monetary policy can effectively stimulate the economy in the short run, it may lead to further increases in real estate prices. In contrast, investment and land supply shocks can stabilize the economy while dampening real estate prices in response to the epidemic.

This paper puts forward the following policy recommendations based on the above findings. First, given that the effects of COVID-19 are still ongoing, it is more appropriate to choose price-based monetary policies for macro-economic control at this time. Both types of monetary policies can effectively curb the rise of real estate prices under normal circumstances. However, in the face of a special period like COVID-19, the monetary authorities should minimize the impact on economic fluctuations in their policy operations to curb real estate prices. Obviously, at this time, price-based monetary policy is more effective and can achieve real estate price regulation while having a more moderate impact on the economy. Second, regulating real estate prices in the context of COVID-19 requires appropriate monetary policy and the coordination and cooperation of various other sectors better stabilize real estate prices in the long run, for example, stimulating investment through relevant policies and targeted increases in land supply by local governments at all levels.

Data Availability

The datasets used and/or analyzed during the current study are available from the corresponding author on reasonable request.

Conflicts of Interest

The authors declare that they have no potential conflicts of interest with respect to the research, authorship, and/or publication of this article.

References

[1] W. X. Zhu, P. Zhang, P. F. Li, and Z. Y. Wang, "Firm crisis, government support and policy efficiency under the epidemic shock: evidence from two waves of questionnaire on SMEs," *Management World*, vol. 36, no. 4, pp. 13–26, 2020.

[2] T. A. Hassan, S. Hollander, L. Lent, M. Schwedeler, and A. Tahoun, *Firm-level Exposure to Epidemic Diseases: COVID-19, SARS, and H1N1*, National Bureau of Economic Research, Cambridge, MA, USA, 2020.

[3] S. J. Liu, Y. Han, and D. W. Wang, "An impact path analysis of COVID-19 outbreak in China and policy response," *Management World*, vol. 36, no. 5, pp. 1–12+51+263, 2020.

[4] W. Liu, "Economic recovery from and the monetary policy response to the covid-19 shock," *Economic Perspectives*, vol. 8, no. 7, pp. 21–27, 2020.

[5] J. Zhu, S. C. Zhong, and J. Q. Li, "Economic effect and fiscal policy assessment of COVID-19 outbreak," *Review of Economy and Management*, vol. 36, no. 3, pp. 21–32, 2020.

[6] S. R. Baker, N. Bloom, S. J. Davis, K. Kost, M. Sammon, and T. Viratyosin, "The unprecedented stock market reaction to COVID-19," *The Review of Asset Pricing Studies*, vol. 10, no. 4, pp. 742–758, 2020.

[7] P. Xie, J. M. Zhang, and Y. X. Liu, "The routine response to COVID-19 epidemic: macro-hedging and collaborative governance," *Journal of Industrial Technological Economics*, vol. 39, no. 10, pp. 38–46, 2020.

[8] Z. F. Ding and C. Y. Kong, "The income distribution effect of hazard risks and structural fiscal policy," *Finance & Trade Economics*, vol. 41, no. 12, pp. 53–67, 2020.

[9] L. F. Chen and Y. T. Zhong, "Macroeconomic effects of covid-19 shocks under dynamic stochastic general equilibrium," *South China Finance*, vol. 23, no. 1, pp. 20–29, 2021.

[10] B. S. Bernanke, M. Gertler, and S. Gilchrist, "Chapter 21 the financial accelerator in a quantitative business cycle framework," *Handbook of Macroeconomics*, vol. 1, pp. 1341–1393, 1999.

[11] M. Iacoviello, "House prices, borrowing constraints, and monetary policy in the business cycle," *The American Economic Review*, vol. 95, no. 3, pp. 739–764, 2005.

[12] B. S. Bernanke, "Monetary policy and the housing bubble," in *Proceedings of the Speech at the Annual Meeting ofthe American Economic Association*, Atlanta, GA, USA, January 2010.

[13] C. Carvalho, "Heterogeneity in price stickiness and the real effects of monetary shocks," *Frontiers of Macroeconomics*, vol. 2, no. 1, 2006.

[14] E. Nakamura and J. Steinsson, "Monetary non-neutrality in a multisector menu cost model," *Quarterly Journal of Economics*, vol. 125, no. 3, pp. 961–1013, 2010.

[15] M. Iacoviello and S. Neri, "Housing market spillovers: evidence from an estimated DSGE model," *American Economic Journal: Macroeconomics*, vol. 2, no. 2, pp. 125–164, 2010.

[16] M. Gertler and P. Karadi, "A model of unconventional monetary policy," *Journal of Monetary Economics*, vol. 58, no. 1, pp. 17–34, 2011.
[17] A. Calza, T. Monacelli, and L. Stracca, "Housing finance and monetary policy," *Journal of the European Economic Association*, vol. 11, no. s1, pp. 101–122, 2013.
[18] C. Q. Hou and L. T. Gong, "Should monetary policy respond to housing price fluctuations an analysis based on a two-sector dynamic stochastic general equilibrium model," *Journal of Financial Research*, vol. 21, no. 10, pp. 15–33, 2014.
[19] Q. He, Z. X. Qian, and J. J. Guo, "Does real estate drive China's economic cycle?" *Economic Research Journal*, vol. 50, no. 12, pp. 41–53, 2015.
[20] L. F. Chen, "Financial shocks and housing price fluctuations in China: analysis based on dynamic stochastic general equilibrium model," *West Forum*, vol. 26, no. 1, pp. 61–73, 2016.
[21] Y. N. Liu, "credit constraints, real estate collateral and financial accelerator: a dsge framework," *Finance & Economics*, vol. 15, no. 2, pp. 12–24, 2017.
[22] L. Lambertini, C. Mendicino, and M. T. Punzi, "Expectations-driven cycles in the housing market," *Economic Modelling*, vol. 60, no. 60, pp. 297–312, 2017.
[23] Y. N. Liu and Y. T. Xu, "Credit collateral constraints, asset prices, and the duality paradox--analysis based on DSGE model in an open economy," *Studies of International Finance*, vol. 22, no. 8, pp. 25–34, 2019.
[24] C. Garriga, R. Manuelli, and A. Peralta-Alva, "A macroeconomic model of price swings in the housing market," *The American Economic Review*, vol. 109, no. 6, pp. 2036–2072, 2019.
[25] L. J. Christiano, M. Eichenbaum, and C. L. Evans, "Nominal rigidities and the dynamic effects of a shock to monetary policy," *Journal of Political Economy*, vol. 113, no. 1, pp. 1–45, 2005.
[26] P. Wang and C. Q. Hou, "Expectation shocks, real estate price volatility and economic volatility," *Economic Research Journal*, vol. 52, no. 4, pp. 48–63, 2017.
[27] F. Gourio, "Disaster risk and business cycles," *The American Economic Review*, vol. 102, no. 6, pp. 2734–2766, 2012.
[28] G. A. Calvo, "Staggered prices in a utility-maximizing framework," *Journal of Monetary Economics*, vol. 12, no. 3, pp. 383–398, 1983.
[29] L. J. Christiano, R. Motto, and M. Rostagno, "Risk shocks," *The American Economic Review*, vol. 104, no. 1, pp. 27–65, 2014.
[30] J. Atta-Mensah and A. Dib, "Bank lending, credit shocks, and the transmission of Canadian monetary policy," *International Review of Economics & Finance; Greenwich*, vol. 17, no. 1, p. 159, 2008.
[31] Z. G. Huang and W. Xu, "Housing market fluctuation and the effectiveness of macroeconomic policies," *Economic Research Journal*, vol. 52, no. 5, pp. 103–116, 2017.
[32] Y. Ma and Y. N. Tan, "Regime switch of financial variables and monetary policy reaction," *The Journal of World Economy*, vol. 42, no. 3, pp. 27–46, 2019.
[33] Z. W. Xu and J. F. Liu, "Income uncertainty, asset allocation and monetary policy choice," *Economic Research Journal*, vol. 54, no. 5, pp. 30–46, 2019.
[34] G. J. Chen, J. F. Chao, X. L. Wu, and X. Q. Zhao, "Rare disaster risk and macroeconomic volatility in China," *Economic Research Journal*, vol. 49, no. 8, pp. 54–66, 2014.
[35] R. J. Barro, "Rare disasters and asset markets in the twentieth century," *Quarterly Journal of Economics*, vol. 121, pp. 823–866, 2006.

Hindawi
Scientific Programming
Volume 2022, Article ID 6438331, 11 pages
https://doi.org/10.1155/2022/6438331

Research Article

Securing E-Healthcare Images Using an Efficient Image Encryption Model

Jaishree Jain [1,2] and Arpit Jain [3]

[1]*Computer Science & Engineering, TMU, Moradabad, India*
[2]*Department of Computer Science and Engineering, AKGEC, Ghaziabad, India*
[3]*Computer Science & Engineering, TMU, Moradabad, India*

Correspondence should be addressed to Jaishree Jain; jaishree3112@gmail.com

Received 5 December 2021; Revised 2 January 2022; Accepted 11 January 2022; Published 8 March 2022

Academic Editor: Punit Gupta

With the advancements in e-healthcare services, it is possible to provide remote medical services to patients and swifter first aid. Medical images play an essential role in e-healthcare applications for providing quick and better remote diagnosis and treatment to patients. Medical images generally comprise secret details about the patients and are therefore prone to various security threats during their transmission over public networks. Thus, it is required to secure these images prior to their communication over public networks. But due to distinctive properties of medical images, like higher correlation and redundancy among the pixels, and larger size, it is required to design an efficient encryption model to resist against various security threats. In this paper, an efficient encryption model for medical images is proposed. To obtain the secret keys, six-dimensional hyperchaotic map (SDHM) is proposed. Firstly, plain medical image is divided into three channels such as red, green, and blue. Secret keys are used to diffuse these channels. Lastly, encrypted channels are concatenated and final encrypted medical image is obtained. Extensive experiments are drawn by considering the benchmark medical images. Also, comparisons are performed among the proposed SDHM and competitive techniques by considering various performance metrics. Comparative analysis reveals that the proposed SDHM achieves remarkably good performance than the existing encryption models.

1. Introduction

With the advancements in multimedia applications, images are playing very crucial role in various applications. One of the most important applications is e-healthcare. Due to digitalization, the communication among the doctors and patients becomes very easy. The doctors from distant areas can collaborate and work together. The e-health has wide range of applications such as drug-synergy prediction, disease diagnosis, digital surgery, telemedicine, and telehealth. Generally, healthcare data are transmitted over public networks which may cause various security threats. In this paper, we focused only on medical images. The communication and storage of medical images over the public networks is not secure. The primary concerns of medical images are authentication, confidentiality, and integrity. The security vulnerabilities of medical images can pose various threats that further restrict the development of mobile healthcare applications [1, 2]. Therefore, it is required to protect the medical images while communication and storage. Image encryption is one the information security models that can be utilized to protect the medical images.

Many researchers have used chaotic maps to protect the medical images. The strength of the encryption model always lies on the secret keys. To produce secret keys, chaotic maps are extensively utilized. In [1], logistic map, cubic map, and sine map were used to secure the medical images. In [3], edge and chaotic maps were used to encrypt the medical images. In [4], secret key was obtained using double humped (DH) logistic map to encrypt the medical MRI and X-ray images. In [5], logistic-sine chaotic map was used to permute the original image. Then, image was divided into blocks, and the blocks were encrypted using hyperchaotic map. In [6], medical images were encrypted using the ElGamal cryptosystem. The secret key was obtained using Mersenne Twister pseudo-random number generator. In [7], sine map and Rossler dynamical systems were utilized to secure the medical images.

Chaotic encryption models come under spatial-domain models. In spatial-domain models, operations are directly applied on the plain image. To make medical image encryption models more secure, many researchers combined spatial and frequency domain models. In [8], cosine number transform was applied to protect the medical images. In [9], fuzzy chaotic map was used to encrypt the images along with discrete wavelet transform (DWT). In [10], medical images were protected using cosine number transform. In [11], edge maps and DWT were used to encrypt the medical images. In [12, 13], integer wavelet transform (IWT), DNA, and 3D Lorenz chaotic map were utilized to secure the medical images over public networks.

There are many other concepts which have been utilized to protect the medical images. One of them is homomorphic encryption. It allows to perform the operations on medical images stored in cloud storage without compromising the confidentiality [14]. However, the use of homomorphic encryption is computationally expensive. The combination of encryption and watermarking models was also applied to improve the security and reliability [15, 16]. The concept of optimization is also utilized by many researchers in the field of image encryption. The optimization algorithms help in selection of optimized encrypted image [17–19]. However, the selection of optimization algorithm and fitness function is very challenging. Along with this, optimization algorithms are very time consuming. The concept of compression was also used to reduce the processing time [20]. Compression may reduce the quality of medical images that is not acceptable in medical field where minute details are very important [21–23].

It is found that the medical images generally comprise secret details about the patients and are therefore prone to various security threats during their transmission over public networks. Thus, it is required to secure these images prior to their communication over public networks. But due to distinctive properties of medical images, like higher correlation and redundancy among the pixels, and larger size, the existing encryption models are unable to achieve high security. Therefore, they are unable to resist various security attacks. Thus, the main objective of this paper is to design an efficient image encryption model that can develop significantly complex secret keys.

The main contributions of this paper are as follows:

(1) An efficient image encryption model is proposed to encrypt e-healthcare images.

(2) To obtain the secret keys, six-dimensional hyper-chaotic map (SDHM) is proposed.

(3) Efficient permutation-diffusion-based encryption approach is proposed to encrypt the biomedical images.

The rest of the paper is organized as follows. Literature review is presented in Section 2. Section 3 discusses the proposed model. Section 4 presents the experimental analysis. The conclusion is presented in Section 5.

2. Literature Review

Every day many healthcare related images are transmitted over public networks. These images contain potential secret information related to patients. But these healthcare images are suspectable to numerous security attacks [24–26]. Therefore, many medical image encryption models have been implemented. In [27], Ding et al. designed a deep learning-based medical image encryption model. Cycle-generative adversarial network (CGAN) was used to encrypt the images. In [28], Khedr and Glenn implemented a GPU-accelerated homomorphic encryption model. This model can provide encryption results at a rapid speed. In [29], Liu et al. designed a verifiable multi-keyword search (VMKS) encryption model. It has utilized anonymous key generation for medical images. Convergence key was utilized to scramble electronic health records.

In [30], Yi et al. utilized Paillier and ElGamal cryptosystems (PECs) to implement statistical analysis on the healthcare data without compromising the patients' privacy. In [31], Haddad et al. presented a joint watermarking encryption approach so called JJL for medical images. Bit substitution watermarking modulation with JPEG-LS was also used to encrypt the data. In [32], Qiu et al. designed a secure communication model by using a selective encryption model (SET) combined with fragmentation and dispersion. In [33], Jiang et al. utilized somewhat homomorphic encryption (SHE) for homomorphic evaluation over single instruction multiple data. It can encrypt data with lesser number of overheads. In [34], Bao et al. designed a revocable, privacy-preserving fine-grained data sharing method with keyword search to encrypt the healthcare data. For data authenticity, a pseudo-identity-based signature approach was also used. In [35], Wang designed a blind batch encryption model to encrypt the healthcare data. It has been found that this model can resist six typical attacks. In [36], Zeng et al. studied that attribute-based encryption can ensure data confidentiality and user privacy in healthcare environment. Partially policy-hidden and large universe-based encryption model was also used.

In [37], Sara et al. used permutation and substitution framework to encrypt the medical images. Images were divided into blocks and these blocks are permutated using zigzag pattern. Logistic map was applied to obtain the secret keys and perform the substitution operation. In [38], Shafique et al. proposed a medical image encryption scheme using DWT, logistic map, and bit-plane extraction system. In [39], Ravichandran et al. protected the medical images by using chaotic maps and deoxyribonucleic acid (DNA). Multiple chaotic maps were applied to create random keys further used in permutation, encoding, and substitution processes to carry out the encryption. In [40], Ibrahim et al. designed an encryption scheme using chaotic maps and S-boxes to secure the medical images. In [41], Belazi et al. used DNA and chaotic maps to encrypt the medical images. SHA-256 was also used to obtain the initial values for secret keys. In [42], Wang et al. encrypted the medical images based on Galois field. In [43], Shankar et al. used adaptive grasshopper optimization algorithm to select the optimal secret key to encrypt the medical images.

From the literature, it is observed that the development of efficient encryption approach for e-healthcare is a challenging problem. Increasing the key space size is desirable. Therefore, high-dimensional hyperchaotic map can be designed to increase the key size.

3. Proposed Model

In this section, the proposed encryption model is presented for healthcare data. A SDHM is used to obtain the secret keys. These keys are then used to diffuse the medical images. The proposed SDHM is mainly divided into three parts: key generation, encryption process, and decryption process. The proposed encryption model is illustrated in Figure 1.

3.1. Six-Dimensional Hyperchaotic Map. To obtain the secret keys, a SDHM is used. It is more complex and dynamic than low-order dimensional chaotic maps. Due to this, it becomes difficult to guess the secret keys without the knowledge of initial values. It improves the security as well as robustness of the model. It is defined as [44, 45]

$$\left.\begin{aligned} w_1' &= \lambda_1 (w_2 - w_1) + w_4 + \lambda_2 w_6,\\ w_2' &= p w_1 - w_2 - w_1 w_3 + w_5,\\ w_3' &= -v w_3 + w_1 w_2,\\ w_4' &= f w_4 - w_1 w_3,\\ w_5' &= -b w_2 + w_6,\\ w_6' &= u_1 w_1 + u_2 w_2, \end{aligned}\right\} \quad (1)$$

where w_1, w_2, w_3, w_4, w_5, and w_6 are initial state variables of SDHM. λ_2, b, u_1, u_2, and h are the control parameters. λ_1, v, and p are the constant parameters. f is the coupling parameter. In this proposed SDHM, seven secret keys are used, and seventh secret key (w_7') is obtained as

$$w_7' = z w_1 \oplus f w_4, \quad (2)$$

where z is the constant parameter. The hyperchaotic nature of SDHM with attributes $\lambda_1 = 9$, $f = 2$, $b = 8.7$, $v = 7/2$, $\lambda_2 = 2, u_1 = 2, p = 31, u_2 = 3$, and $z = 1$ is shown in Figure 2. It can be seen that SDHM is dynamic in nature and provides more complexity that is needed for security of medical images.

3.2. Encryption Process. Algorithm. 1 represents various steps to encrypt the medical images. Firstly, plain image (P_{mg}) is divided into red (P_r), green (P_g), and blue (P_b) channels. The six keys w_1', w_2', w_3', w_4', w_5', and w_6' are obtained using equation (1). Another key, i.e., w_7', is computed by utilizing the XOR $(\oplus)$ (see equation (2)). P_r is diffused using w_1' and $\oplus$ operation and obtains P_r''. Similarly, P_g and P_b are diffused as P_g' and P_b' using w_2' and w_3', respectively. The diffused channels P_g' and P_b' are further diffused as P_g'' and P_b'' using P_r'' and P_g', respectively. To increase the complexity and strength of the secret keys, keys are further modified. w_5' is modified using w_4' and $\oplus$ operation as w_5''. w_6' is modified using w_4' and $\oplus$ operation as w_6''. w_7' is modified using w_4' and $\oplus$ operation as w_7''. The diffused channels P_r'', P_g'', and P_b'' are encrypted using w_5'', w_6'', and w_7'' with encryption factor E_f. The obtained resultant encrypted channels are C_r, C_g, and C_b. Finally, encrypted image (C_{mg}) is obtained by concatenating the ciphered channels C_r, C_g, and C_b (Algorithm 1).

3.3. Decryption Process. Decryption process converts the encrypted image back into original image. Algorithm. 2 shows the various steps to decrypt the encrypted image. Before starting the decryption, the algorithm needs parameters such as initial values of $w_1, w_2, w_3, w_4, w_5, w_6, w_7$, $\lambda_1, \lambda_1, b, v, f, u_1, u_2, z$, and p to obtain the secret keys using equations (1) and (2) and encryption factor E_f to perform the decryption. Decryption algorithm is identical to encryption algorithm, but in reverse order (Algorithm 2).

4. Experimental Analysis

The proposed method is implemented on MATLAB2021a with 16GB RAM on i7 processor. The proposed SDHM is compared with existing models such as CGAN, VMKS, PEC, JJL, SET, and SHE to assess the performance. Five colored medical images such as CT of ascites (CTA) [46], brain MRI (BMRI) [47], dermoscopy (DM) [48], fundus (FS) [49], and ultrasound (US) [50] are taken for testing. Figure 3 shows the visual analysis of the proposed medical image encryption. Figure 3(a) shows the plain medical images which are used for encryption. The histograms of the plain images are shown in Figure 3(b). The encrypted images and their respective histograms are shown in Figures 3(c) and 3(d), respectively. Here, we can see that the histograms of encrypted images are uniform which means that it does not reveal any statistical information to attackers. Figure 3(e) shows the decrypted images that exactly look like plain images.

4.1. Performance Parameters. To assess the performance of the proposed medical image encryption model, various parameters such as peak signal to noise ratio, entropy, and correlation coefficient are utilized.

4.1.1. Peak Signal to Noise Ratio. Peak signal to noise ratio (PSNR) is utilized to quantify the quality of decrypted images [51]. It can be computed as

$$\mathrm{PSNR} = 10 \times log_{10}\frac{255^2}{\mathrm{MSE}}. \quad (3)$$

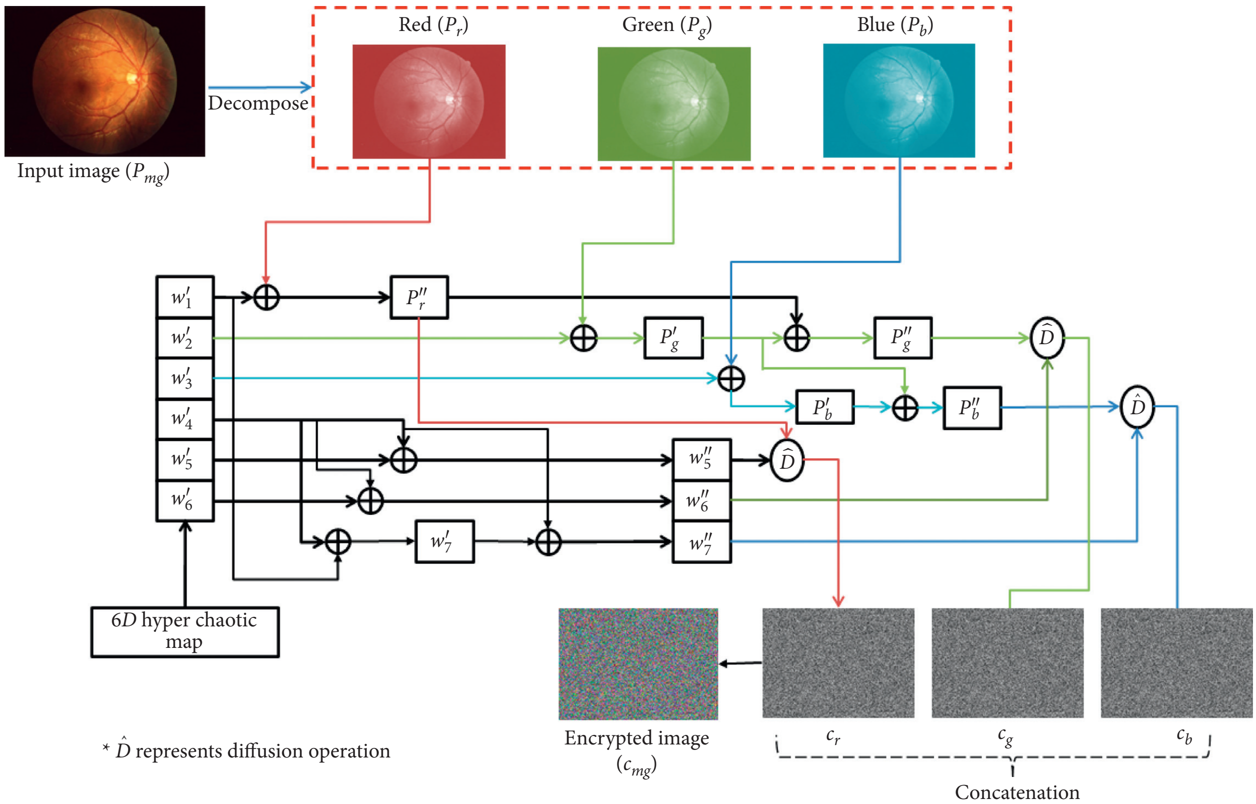

Figure 1: Proposed encryption scheme.

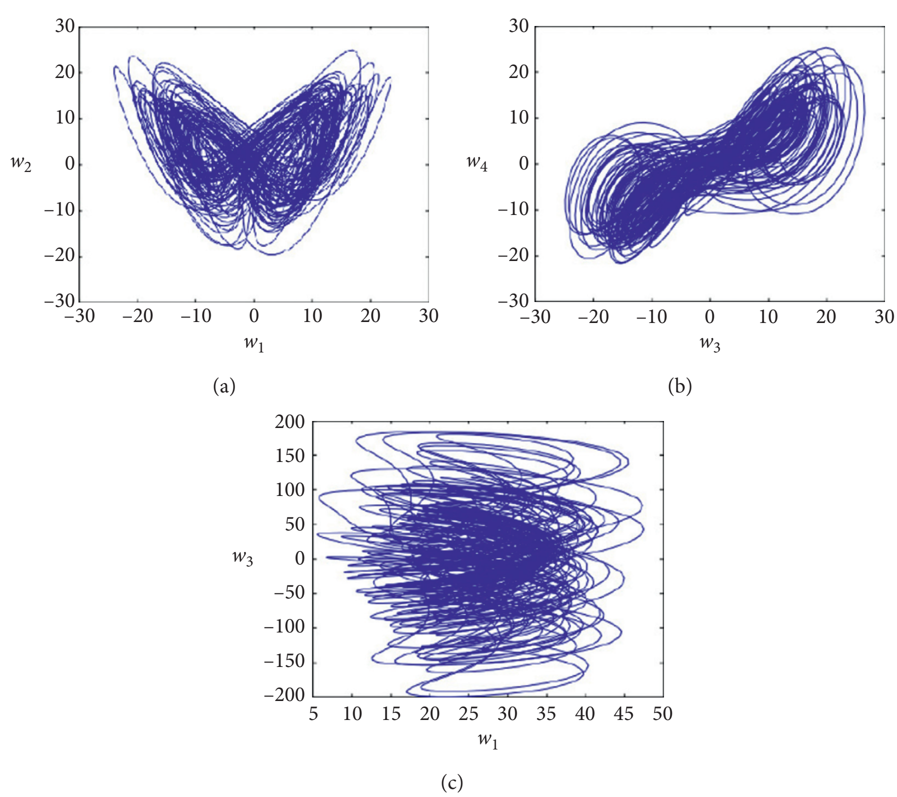

Figure 2: Chaotic attractors of SHM: (a)$w_1 - w_2$ plane, (b)$w_3 - w_4$ plane, and (c)$w_1 - w_3$ plane.

```
Input: plain image (P_mg)
Output: encrypted image (C_mg)
/* Decompose P_mg into red (P_r), green (P_g), and blue (P_b) matrices.*/
P_r = P_mg (:,:, 1)
P_g = P_mg (:,:, 2)
P_b = P_mg (:,:, 3)
   obtain secret key w'_i, with i = 1, . . . , 7 utilizing equations (1) and (2)
//Diffuse color channels using w'_1, w'_2, and w'_3
   P''_r = mod(P_r⊕w'_1, 256)
P_g ' = mod(P_g⊕w'_2, 256)
P''_g = mod(P'_g⊕P_r ", 256)
P'_b = mod(P_b⊕w'_3, 256)
P''_b = mod(P'_b⊕P_g ', 256)
   //Modify keys w'_5, w'_6, and w'_7 by considering w'_4
w_5 " = w'_5⊕w'_4
w_6 " = w'_6⊕w'_4
w_7 " = w'_7⊕w'4
//Diffuse P_r ", P_g ", and P_b " utilizing w''_5, w_6 ", and w_7 "
C_r = mod(w_5 " ×P_r " + (1 − E_f) × w_5 ", 256)
C_g = mod(w_6 " ×P_g " + (1 − E_f) × w_6 ", 256)
C_b = mod(w_7 " ×P_b " + (1 − E_f) × w_7 ", 256)
//Obtain an encrypted image by concatenating scrambled channels
C_mg = cat(C_r, C_g, C_b)
return C_mg
```

Algorithm 1: Proposed encryption algorithm for medical images.

```
Input: keys w_1, w_2, w_3, w_4, w_5, w_6, w_7, λ_1, λ_1, b, v, f, u_1, u_2, z, p, and E_f
Output: D_mg
//Decompose C_mg to red C_r, green C_g, and blue C_b channels
C_r = C_mg (:,:, 1)
C_g = C_mg (:,:, 2)
C_b = C_mg (:,:, 3)
obtain keys w'_1, w'_2, w'_3, w'_4, w'_5, w'_6, and w'_7 using equations (1) and (2)
//modify keys w'_5, w'_6, and w'_7 by w'_4
w''_5 = w'_5⊕w'_4
w''_6 = w'_6⊕w'_4
w''_7 = w'_7⊕w'_4 //Decrypt C_r, C_g, and C_b by w''_5, w''_6, and w''_7
P''_r = (C_r - (1-E_f) ×w''_5)/ E_f
P''_g = (C_g - (1-E_f) ×w''_6)/ E_f
P''_b = (C_b - (1-E_f) ×w''_7)/ E_F
//Decrypt P''_r, P''_g, and P''_b by considering w'_1, w'_2, and w'_3
P_r = P''_r⊕w'_1
P'_g = P_r⊕P''_g
P_g = P'_g⊕w'_2
P'_b = P''_b⊕P''_g
P_b = P'_b⊕w'_3
//Obtain original image by concatenating the decrypted channels
D_mg = cat(P_r, P_g, P_b)
return D_mg
```

Algorithm 2: Decryption algorithm.

Here, mean squared error (MSE) can be computed as

$$\mathrm{MSE} = \frac{1}{mn} \sum_{i=0}^{m-1} \sum_{j=0}^{n-1} \left[P_{mg}(i,j) - C_{mg}(i,j)\right]^2. \qquad (4)$$

Here, P_{mg} shows input image. C_{mg} shows encrypted image. (i, j) denotes pixel coordinates. mandn shows size of the input image.

Table 1 shows the performance evaluation of the proposed SDHM in terms of PSNR among decrypted and actual

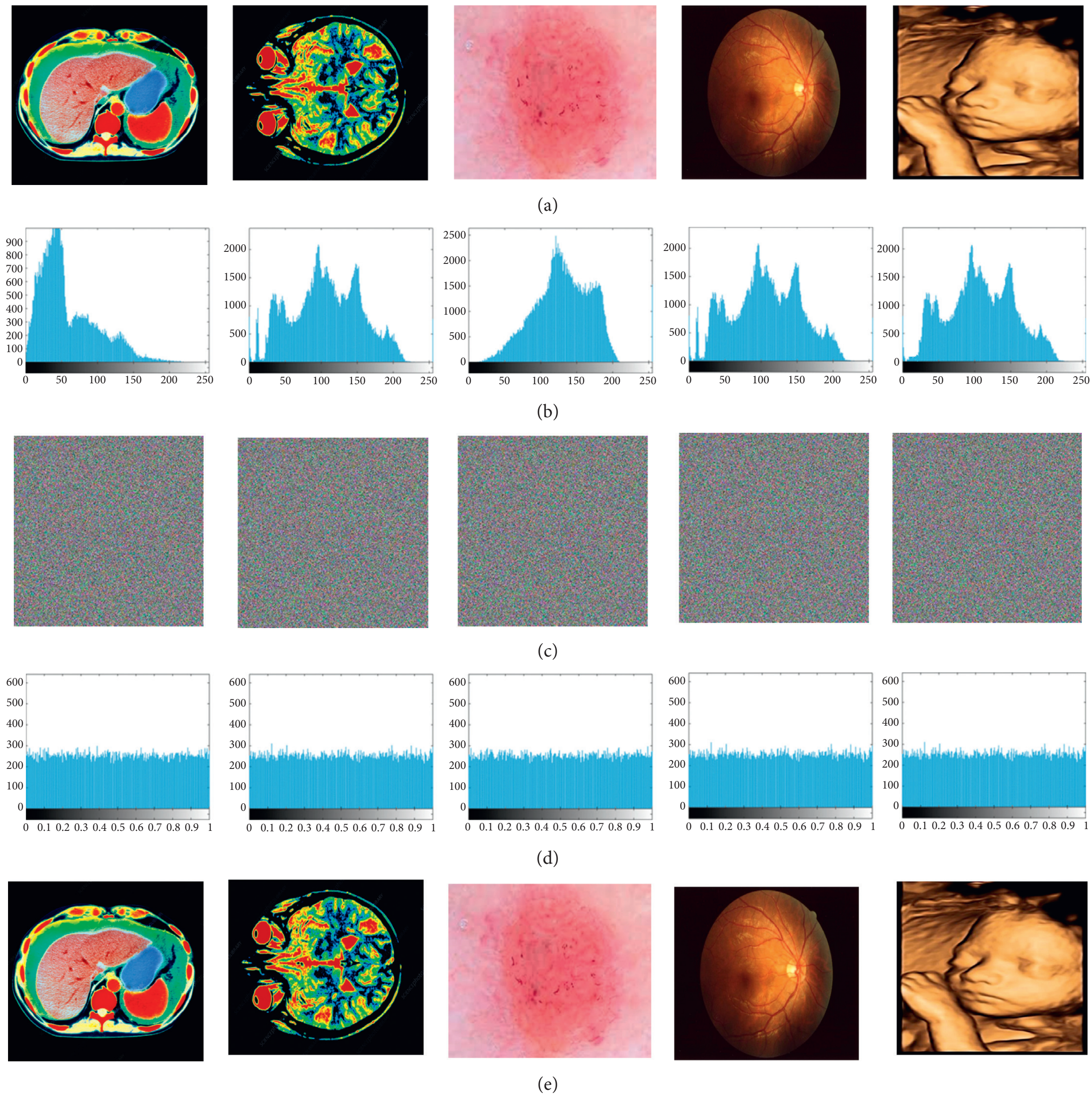

Figure 3: Visual analysis. (a) Plain medical images. (b) Histograms of plain images. (c) Encrypted medical images. (d) Histograms of encrypted images. (e) Decrypted images.

Table 1: Performance evaluation of color image in terms of PSNR between actual and decrypted images.

Technique	CTA	BMRI	DM	FS	US
CGAN [27]	56.62	47.31	40.16	51.86	50.59
VMKS [29]	56.52	43.77	47.51	52.99	52.81
PEC [30]	44.37	50.18	59.02	57.04	54.18
JJL [31]	58.21	52.55	51.12	59.32	53.92
SET [32]	57.12	56.94	43.53	57.02	57.41
SHE [33]	56.76	48.92	45.59	59.22	51.25
Proposed	**59.41**	**58.14**	**60.22**	**60.52**	**58.65**

images. PSNR among decrypted and actual images is desirable to be maximum. It is clearly found that the proposed SDHM achieves remarkably better PSNR values than the existing models. The proposed SDHM shows an average improvement in terms of PSNR as 3.4587%. Bold values indicate the high performance.

Table 2: Performance evaluation of color image in terms of PSNR between actual and encrypted images.

Technique	CTA	BMRI	DM	FS	US
CGAN [27]	6.18	4.25	2.44	3.73	4.27
VMKS [29]	4.32	5.12	2.17	2.42	5.27
PEC [30]	4.57	4.55	6.58	3.61	4.04
JJL [31]	1.64	3.45	5.99	3.55	1.75
SET [32]	5.05	6.92	4.61	4.32	4.44
SHE [33]	3.29	4.94	5.31	2.08	4.89
Proposed	**1.44**	**2.25**	**1.97**	**1.88**	**1.55**

Table 3: Performance evaluation of color image in terms of entropy.

Technique	CTA	BMRI	DM	FS	US
CGAN [27]	7.76	7.26	7.54	7.6	7.05
VMKS [29]	7.51	7.59	7.45	7.39	7.19
PEC [30]	7.21	7.72	7.5	7.07	7.31
JJL [31]	7.65	7.37	7.03	7.43	7.12
SET [32]	7.6	7.7	7.52	7.53	7.56
SHE [33]	7.16	7.53	7.55	7.14	7.12
Proposed	**7.59**	**7.53**	**7.38**	**7.43**	**7.39**

Table 2 demonstrates the performance evaluation of the proposed SDHM in terms of PSNR among encrypted and actual images. PSNR among encrypted and actual images is desirable to be minimum. It is clearly observed that the proposed SDHM obtains remarkably minimum PSNR values than the existing models. The proposed SDHM shows an average reduction in terms of PSNR as 1.6478%.

4.1.2. Entropy. Entropy is a well-known measure which indicates the degree of randomness in the image [52]. Entropy values of encrypted images are desirable to be 8. Entropy (m) of an image can be computed as

$$m = \sum_{i=0}^{m-1} p(m_i)\log 2 \frac{1}{p(m_i)}. \tag{5}$$

Here, m_i shows the probability values of corresponding pixels.

Table 3 shows the performance evaluation of the proposed SDHM in terms of entropy of encrypted images and it should be maximum. It is clearly observed that the proposed SDHM attains remarkably better entropy values than the existing models. The proposed SDHM shows an average improvement in terms of entropy as 0.8978%.

4.1.3. Correlation Coefficient. The attackers sometimes explore the relation among the adjacent pixels of an image for statistical attacks. Actually, the adjacent pixels of the plain image are highly correlated to each other in all three directions such as horizontally (H_C), vertically (V_C), and diagonally (V_C) [53]. This relation should be minimum so that no statistical information should be disclosed to the attackers. The relation among the adjacent pixels can be calculated as follows:

$$r = \frac{\sum (x_i - \mu_x)(y_i - \mu_y)}{\sqrt{\sum (x_i - \mu_x)^2 (y_i - \mu_y)^2}}. \tag{6}$$

Here, r is the correlation coefficient. x and y represent the adjacent pixels. μ_x and μ_y are the means of x and y, respectively. For this experiment, we randomly selected 3000 pairs of adjacent pixels (x, y) from plain and encrypted images. US image is taken for this test.

Figure 4 shows the inter-pixel correlation of US image. Horizontal (H_C), vertical (V_C), and diagonal (D_C) correlations between the pixels of plain red channel are presented in Figures 4(a), 4(b), and 4(c). Here, it shows that pixels of plain image are highly correlated. Figures 4(d), 4(e), and 4(f) show H_C, V_C, and D_C among the pixels of encrypted red channel. Here, it can be seen that pixels are random in nature and show no relation among the pixels.

The inter-pixel correlation of green channel is shown in Figure 5. H_C, V_C, and D_C between the pixels of plain green channel are shown in Figures 5(a), 5(b), and 5(c), respectively. Figures 5(d), 5(e), and 5(f) show H_C, V_C, and D_C among the pixels of encrypted green channel. It can be seen that pixels are loosely correlated to each other. Similarly, Figure 6 shows the correlation among the pixels of plain and encrypted blue channels. Figures 6(a)–6(c) show the relation between the pixels of plain blue channel. Figures 6(d)–6(f) show the relation among the pixels of encrypted green channel. It can be observed that pixels are not correlated to each other. Table 4 shows H_C, V_C, and D_C among the adjacent pixels

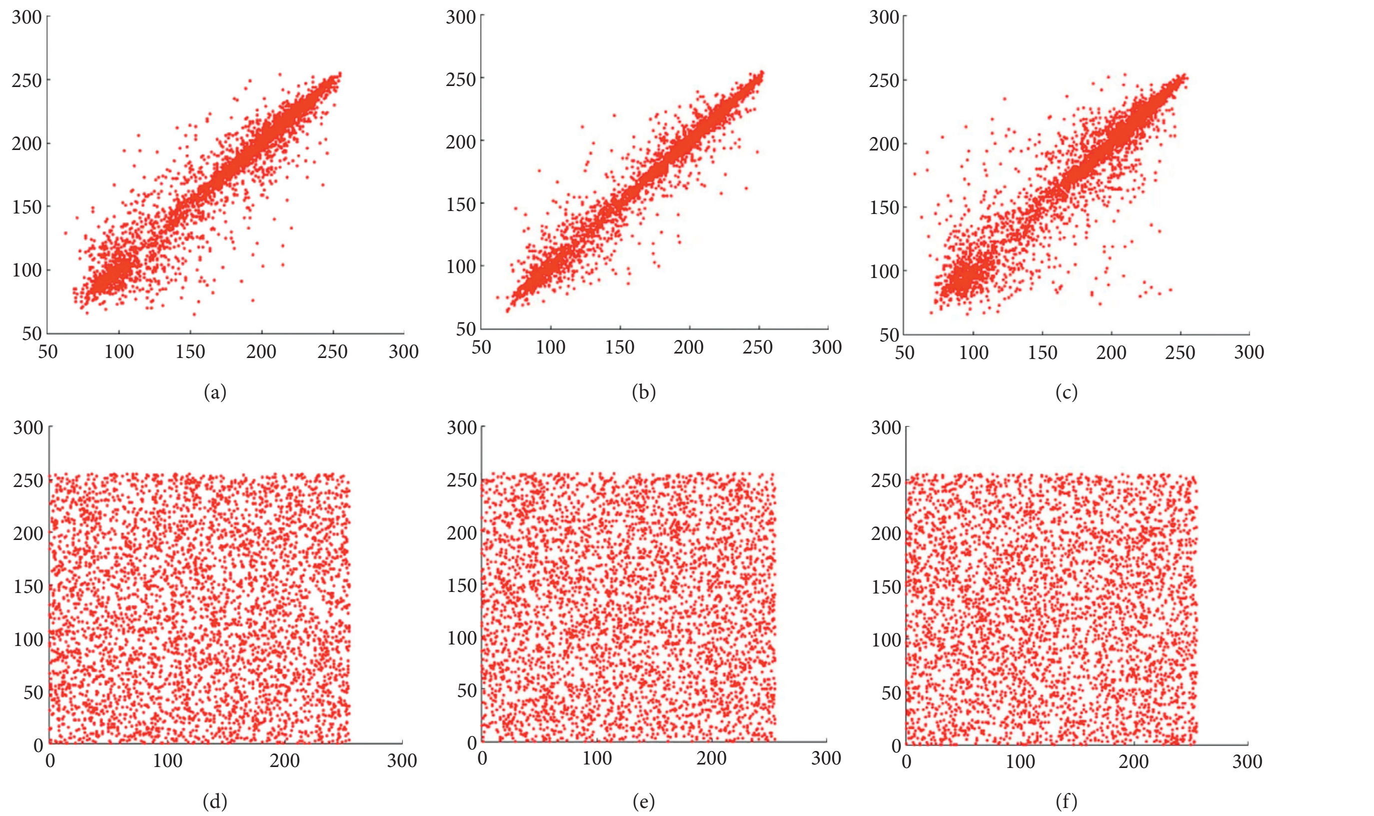

Figure 4: Correlation analysis of red channel of US image: (a)H_C, (b)V_C, and (c)D_C among the pixels of plain red channel and (d)H_C, (e)V_C, and (f)D_C among the pixels of encrypted red channel.

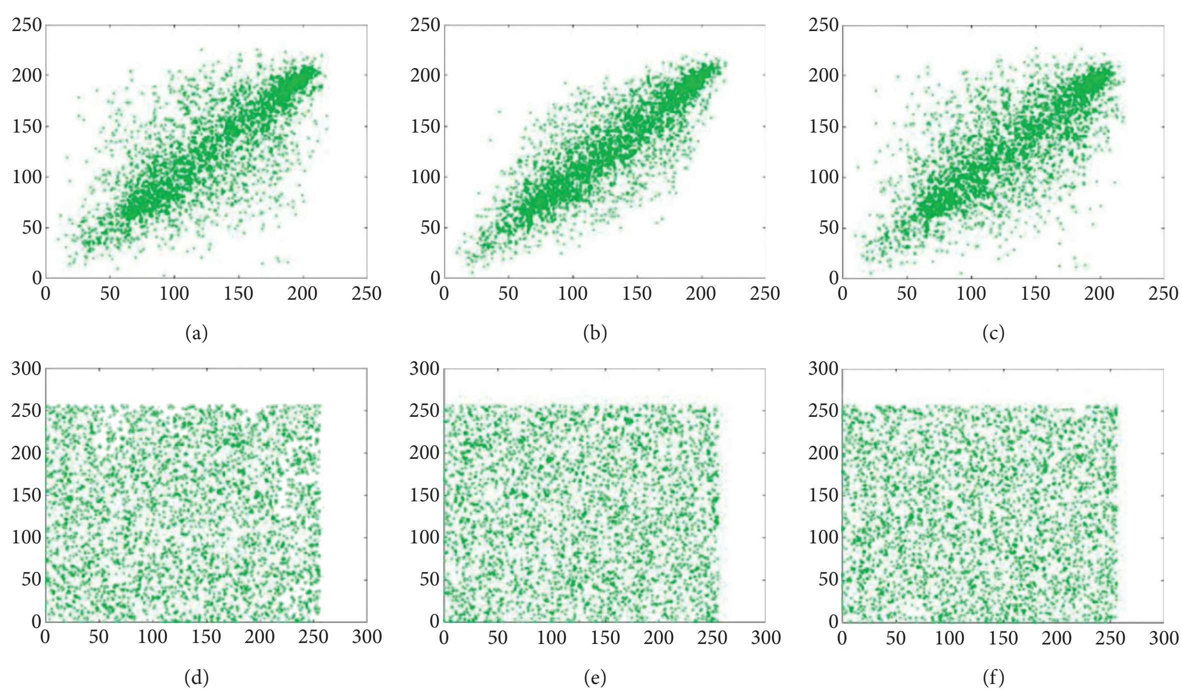

Figure 5: Correlation analysis of green channel of US image: (a)H_C, (b)V_C, and (c)D_C among the pixels of plain green channel and (d)H_C, (e)V_C, and (f)D_C among the pixels of encrypted green channel.

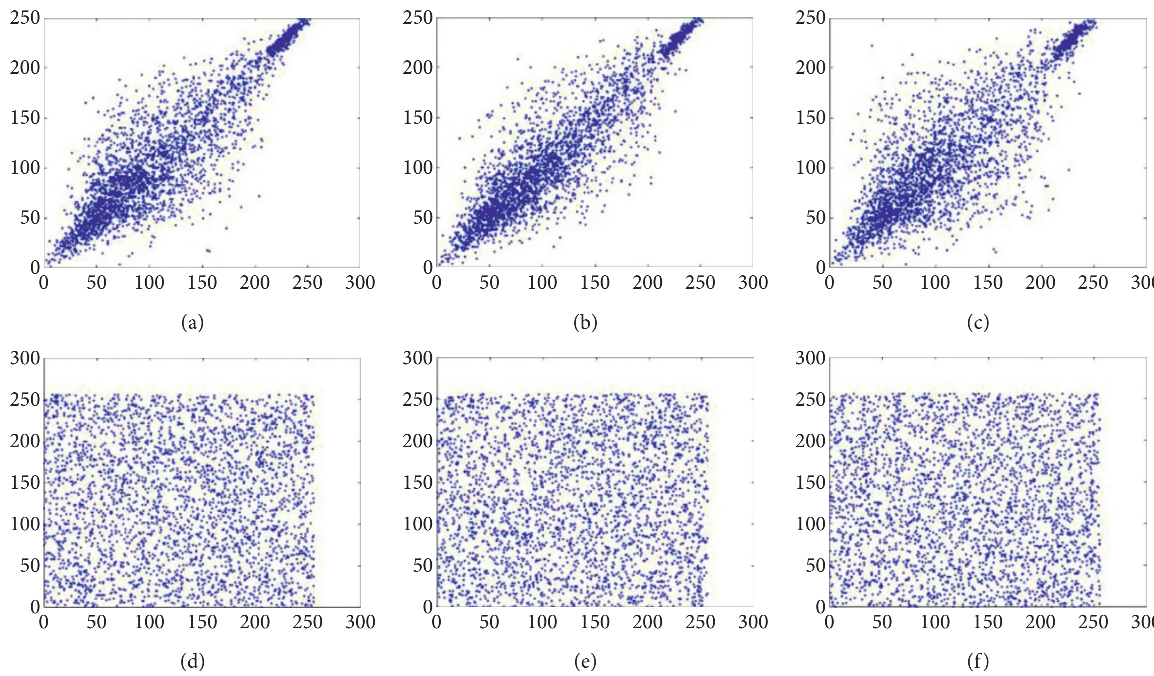

Figure 6: Correlation analysis of blue channel of US image: (a)H_C, (b)V_C, and (c)D_C among the pixels of plain blue channel and (d)H_C, (e)V_C, and (f)D_C among the pixels of encrypted blue channel.

Table 4: Correlation coefficient of encrypted medical images.

Technique	H_C	V_C	D_C
CTA	0.0076	0.0052	0.0049
BMRI	0.0051	0.0059	0.0045
DM	0.0021	0.0072	0.0015
FS	0.0065	0.0037	0.0032
US	0.0006	0.0027	0.0062

of encrypted medical images. From the values, it can be seen that there is no relation among the adjacent pixels of the encrypted medical images. Hence, attackers cannot discover any kind of statistical information to recover the information.

5. Conclusion

An efficient image encryption approach for medical images was proposed. Six-dimensional hyperchaotic map was utilized to obtain the secret keys. Firstly, plain medical image was divided into three channels such as red, green, and blue. Secret keys were used to diffuse these channels. Lastly, encrypted channels were concatenated and final encrypted medical image was obtained. Comparative analysis revealed that the proposed SDHM achieves remarkably good performance than the existing encryption models. The proposed SDHM has significantly increased the key size. Therefore, the proposed SDHM can resist various security attacks. Extensive experimental analysis revealed that the proposed SDHM outperforms the competitive models in terms of entropy, correlation coefficient, and PSNR by 1.7483%, 1.7483%, and 1.8325%, respectively.

In near future, we will utilize some soft-computing techniques to increase the size of secret keys. Additionally, more security attacks will be implemented to evaluate the performance of the proposed model.

Data Availability

The used datasets are freely available from the following: CT (https://www.kaggle.com/kmader/siim-medical-images); dermoscopy (https://www.kaggle.com/sergio814/dermoscopy-images); fundus (https://www.kaggle.com/andrewmvd/ocular-disease-recognition-odir5k); brain MRI (https://www.kaggle.com/mateuszbuda/lgg-mri-segmentation); ultrasound (http://femonum.telecom-paristech.fr/download.html).

Conflicts of Interest

The authors declare that they have no conflicts of interest.

References

[1] S. A. Banday, A. H. Mir, and S. Malik, "Multilevel medical image encryption for secure communication," in *Advances in Computational Techniques for Biomedical Image Analysis*, D. Koundal and S. Gupta, Eds., Academic Press, Cambridge, MA, USA, pp. 233–252, 2020.

[2] B. Gupta, M. Tiwari, and S. S. Lamba, "Visibility improvement and mass segmentation of mammogram images using quantile separated histogram equalisation with local contrast enhancement," *CAAI Transactions on Intelligence Technology*, vol. 4, no. 2, pp. 73–79, 2019.

[3] W. Cao, Y. Zhou, C. P. Chen, and L. Xia, "Medical image encryption using edge maps," *Signal Processing*, vol. 132, pp. 96–109, 2017.

[4] S. M. Ismail, L. A. Said, A. G. Radwan, A. H. Madian, and M. F. Abu-Elyazeed, "Generalized double-humped logistic map-based medical image encryption," *Journal of Advanced Research*, vol. 10, pp. 85–98, 2018.

[5] X. Chen and C.-J. Hu, "Adaptive medical image encryption algorithm based on multiple chaotic mapping," *Saudi Journal of Biological Sciences*, vol. 24, no. 8, pp. 1821–1827, 2017.

[6] A. Banik, Z. Shamsi, and D. S. Laiphrakpam, "An encryption scheme for securing multiple medical images," *Journal of Information Security and Applications*, vol. 49, Article ID 102398, 2019.

[7] V. Sangavi and P. Thangavel, "An exotic multi-dimensional conceptualization for medical image encryption exerting rossler system and sine map," *Journal of Information Security and Applications*, vol. 55, Article ID 102626, 2020.

[8] V. Lima, F. Madeiro, and J. Lima, "Encryption of 3d medical images based on a novel multiparameter cosine number transform," *Computers in Biology and Medicine*, vol. 121, Article ID 103772, 2020.

[9] C. Lakshmi, K. Thenmozhi, J. B. B. Rayappan, and R. Amirtharajan, "Encryption and watermark-treated medical image against hacking disease—an immune convention in spatial and frequency domains," *Computer Methods and Programs in Biomedicine*, vol. 159, pp. 11–21, 2018.

[10] J. Lima, F. Madeiro, and F. Sales, "Encryption of medical images based on the cosine number transform," *Signal Processing: Image Communication*, vol. 35, pp. 1–8, 2015.

[11] S. Jeevitha and N. A. Prabha, "Novel medical image encryption using dwt block-based scrambling and edge maps," *Journal of Ambient Intelligence and Humanized Computing*, vol. 12, no. 3, pp. 3373–3388, 2021.

[12] A. Banu S and R. Amirtharajan, "A robust medical image encryption in dual domain: chaos-dna-iwt combined approach," *Medical, & Biological Engineering & Computing*, vol. 58, no. 7, pp. 1445–1458, 2020.

[13] D. Jiang, G. Hu, G. Qi, and N. Mazur, "A fully convolutional neural network-based regression approach for effective chemical composition analysis using near-infrared spectroscopy in cloud," *Journal of Artificial Intelligence and Technology*, vol. 1, no. 1, pp. 74–82, 2021.

[14] A. Vengadapurvaja, G. Nisha, R. Aarthy, and N. Sasikaladevi, "An efficient homomorphic medical image encryption algorithm for cloud storage security," *Procedia Computer Science*, vol. 115, 2017.

[15] D. Bouslimi, G. Coatrieux, and C. Roux, "A joint encryption/watermarking algorithm for verifying the reliability of medical images: application to echographic images," *Computer Methods and Programs in Biomedicine*, vol. 106, no. 1, pp. 47–54, 2012.

[16] Y. Xu and T. T. Qiu, "Human activity recognition and embedded application based on convolutional neural network," *Journal of Artificial Intelligence and Technology*, vol. 1, no. 1, pp. 51–60, 2021.

[17] H. Nematzadeh, R. Enayatifar, H. Motameni, F. G. Guimarães, and V. N. Coelho, "Medical image encryption using a hybrid model of modified genetic algorithm and coupled map lattices," *Optics and Lasers in Engineering*, vol. 110, pp. 24–32, 2018.

[18] H. S. Basavegowda and G. Dagnew, "Deep learning approach for microarray cancer data classification," *CAAI Trans. Intell. Technol.*vol. 5, no. 1, pp. 22–33, 2020.

[19] C. Thirumarai Selvi, J. Amudha, and R. Sudhakar, "A modified salp swarm algorithm (ssa) combined with a chaotic coupled map lattices (cml) approach for the secured encryption and compression of medical images during data transmission," *Biomedical Signal Processing and Control*, vol. 66, Article ID 102465, 2021.

[20] M. K. Abdmouleh, A. Khalfallah, and M. S. Bouhlel, "A novel selective encryption scheme for medical images transmission based-on jpeg compression algorithm," *Procedia Computer Science*, vol. 112, pp. 369–376, 2017.

[21] I. Ahmad and S. Shin, "A novel hybrid image encryption-compression scheme by combining chaos theory and number theory," *Signal Processing: Image Communication*, vol. 98, Article ID 116418, 2021.

[22] G. Hu, S.-H. K. Chen, and N. Mazur, "Deep neural network-based speaker-aware information logging for augmentative and alternative communication," *Journal of Artificial Intelligence and Technology*, vol. 1, no. 2, pp. 138–143, 2021.

[23] S. Ghosh, P. Shivakumara, P. Roy, U. Pal, and T. Lu, "Graphology based handwritten character analysis for human behaviour identification," *CAAI Trans. Intell. Technol*, vol. 5, no. 1, pp. 55–65, 2020.

[24] W. Cao, Y. Zhou, C. P. Chen, and L. Xia, "Medical image encryption using edge maps," *Signal Processing*, vol. 132, pp. 96–109, 2017.

[25] X. Chen and S. Zou, "Improved wi-fi indoor positioning based on particle swarm optimization," *IEEE Sensors Journal*, vol. 17, no. 21, pp. 7143–7148, 2017.

[26] H. Kwok and W. K. Tang, "A fast image encryption system based on chaotic maps with finite precision representation, Chaos," *Solitons & Fractals*, vol. 32, no. 4, pp. 1518–1529, 2007.

[27] Y. Ding, G. Wu, D. Chen et al., "Deepedn: a deep-learning-based image encryption and decryption network for internet of medical things," *IEEE Internet of Things Journal*, vol. 8, no. 3, pp. 1504–1518, 2021.

[28] A. Khedr and G. Gulak, "Securemed: secure medical computation using gpu-accelerated homomorphic encryption scheme," *IEEE Journal of Biomedical and Health Informatics*, vol. 22, no. 2, pp. 597–606, 2018.

[29] X. Liu, X. Yang, Y. Luo, and Q. Zhang, "Verifiable multi-keyword search encryption scheme with anonymous key generation for medical internet of things," *IEEE Internet of Things Journal*1 page, 2021.

[30] X. Yi, A. Bouguettaya, D. Georgakopoulos, A. Song, and J. Willemson, "Privacy protection for wireless medical sensor data," *IEEE Transactions on Dependable and Secure Computing*, vol. 13, no. 3, pp. 369–380, 2016.

[31] S. Haddad, G. Coatrieux, A. Moreau-Gaudry, and M. Cozic, "Joint watermarking-encryption-jpeg-ls for medical image reliability control in encrypted and compressed domains," *IEEE Transactions on Information Forensics and Security*, vol. 15, pp. 2556–2569, 2020.

[32] H. Qiu, M. Qiu, M. Liu, and G. Memmi, "Secure health data sharing for medical cyber-physical systems for the healthcare 4.0," *IEEE Journal of Biomedical and Health Informatics*, vol. 24, no. 9, pp. 2499–2505, 2020.

[33] L. Jiang, L. Chen, T. Giannetsos, B. Luo, K. Liang, and J. Han, "Toward practical privacy-preserving processing over encrypted data in iot: an assistive healthcare use case," *IEEE Internet of Things Journal*, vol. 6, no. 6, Article ID 10177, 2019.

[34] Y. Bao, W. Qiu, P. Tang, and X. Cheng, "Efficient, revocable and privacy-preserving fine-grained data sharing with keyword search for the cloud-assisted medical iot system," *IEEE Journal of Biomedical and Health Informatics*, p. 1, 2021.

[35] Z. Wang, "Blind batch encryption-based protocol for secure and privacy-preserving medical services in smart connected

health," *IEEE Internet of Things Journal*, vol. 6, no. 6, pp. 9555–9562, 2019.

[36] P. Zeng, Z. Zhang, R. Lu, and K.-K. R. Choo, "Efficient policy-hiding and large universe attribute-based encryption with public traceability for internet of medical things," *IEEE Internet of Things Journal*, vol. 8, no. 13, Article ID 10963, 2021.

[37] S. T. Kamal, K. M. Hosny, T. M. Elgindy, M. M. Darwish, and M. M. Fouda, "A new image encryption algorithm for grey and color medical images," *IEEE Access*, vol. 9, Article ID 37855, 2021.

[38] A. Shafique, J. Ahmed, M. U. Rehman, and M. M. Hazzazi, "Noise-resistant image encryption scheme for medical images in the chaos and wavelet domain," *IEEE Access*, vol. 9, Article ID 59108, 2021.

[39] D. Ravichandran, P. Praveenkumar, J. B. B. Rayappan, and R. Amirtharajan, "Dna chaos blend to secure medical privacy," *IEEE Transactions on NanoBioscience*, vol. 16, no. 8, pp. 850–858, 2017.

[40] S. Ibrahim, H. Alhumyani, M. Masud et al., "Framework for efficient medical image encryption using dynamic s-boxes and chaotic maps," *IEEE Access*, vol. 8, Article ID 160433, 2020.

[41] A. Belazi, M. Talha, S. Kharbech, and W. Xiang, "Novel medical image encryption scheme based on chaos and dna encoding," *IEEE Access*, vol. 7, Article ID 36667, 2019.

[42] N. Wang, G. Di, X. Lv et al., "Galois field-based image encryption for remote transmission of tumor ultrasound images," *IEEE Access*, vol. 7, Article ID 49945, 2019.

[43] K. Shankar, M. Elhoseny, E. D. Chelvi, S. K. Lakshmanaprabu, and W. Wu, "An efficient optimal key based chaos function for medical image security," *IEEE Access*, vol. 6, Article ID 77145, 2018.

[44] Q. Yang, D. Zhu, and L. Yang, "A new 7d hyperchaotic system with five positive lyapunov exponents coined," *International Journal of Bifurcation and Chaos*, vol. 28, no. 05, Article ID 1850057, 2018.

[45] S. Osterland and J. Weber, "Analytical analysis of single-stage pressure relief valves," *International Journal of Hydromechatronics*, vol. 2, no. 1, pp. 32–53, 2019.

[46] Kaggle, "siim-medical-images," 2017, https://www.kaggle.com/kmader/siim-medical-images.

[47] Kaggle, "lgg-mri-segmentation," 2019, https://www.kaggle.com/mateuszbuda/lgg-mri-segmentation.

[48] Kaggle, "dermoscopy-images," 2019, https://www.kaggle.com/sergio814/dermoscopy-images.

[49] Kaggle, "ocular-disease-recognition-odir5k," 2020, https://www.kaggle.com/andrewmvd/ocular-disease-recognition-odir5k.

[50] femonum.telecom-paristech, "Femonum telecom paristech," 2018, http://femonum.telecom-paristech.fr/download.html.

[51] M. Kaur and D. Singh, "Multiobjective evolutionary optimization techniques based hyperchaotic map and their applications in image encryption," *Multidimensional Systems and Signal Processing*, vol. 32, no. 1, pp. 281–301, 2021.

[52] M. Kaur, D. Singh, V. Kumar, B. Gupta, and A. A. Abd El-Latif, "Secure and energy efficient based e-health care framework for green internet of things," *IEEE Transactions on Green Communications and Networking*, vol. 5, 2021.

[53] M. Kaur, D. Singh, K. Sun, and U. Rawat, "Color image encryption using non-dominated sorting genetic algorithm with local chaotic search based 5d chaotic map," *Future Generation Computer Systems*, vol. 107, pp. 333–350, 2020.

Hindawi
Scientific Programming
Volume 2022, Article ID 7134983, 11 pages
https://doi.org/10.1155/2022/7134983

Research Article

Study on Risk Analysis and Decision-Making of Small- and Medium-Sized Enterprises on BP Neural Network Algorithm

Yongyi Li ,[1,2] Jing Lu ,[3] Quankun Jiao,[1] and Kexin Cao[1]

[1]*College of Information Science and Engineering, Guilin University of Technology, Guilin 541006, China*
[2]*Qinzhou Key Laboratory of Big Data Resource Utilization, College of Electronic and Information Engineering, Beibu Gulf University, Qinzhou 535011, China*
[3]*Beibu Gulf University, Faculty of Science, Qinzhou 535011, China*

Correspondence should be addressed to Jing Lu; 1627199668@qq.com

Received 27 December 2021; Accepted 22 January 2022; Published 3 March 2022

Academic Editor: Punit Gupta

Artificial neural network algorithm has strong nonlinear mapping function. BP neural network algorithm is the representative of artificial neural network algorithm. Due to the relatively small scale of small, medium, and micro enterprises and lack of mortgage assets, the biggest market risk they usually face is credit risk. In order to avoid huge economic losses for banks, the impact of risk analysis on credit decision-making is the key. Therefore, the establishment of a scientific and complete credit risk assessment system has become the primary task. This paper mainly uses BP neural network algorithm to analyze the risk of small and medium-sized enterprises and solve the problem of credit decision-making. First, analyze the various influencing factors that cause credit risk, and layer the factors according to the degree of risk; secondly, use the fuzzy comprehensive evaluation method in mathematical modeling to rank each factor; then, use the fuzzy analytic hierarchy process to calculate the weight of each indicator factor as calculated by establishing the risk value function, using the function expression of the annual interest rate and the total credit formula to calculate the total credit, which solves the problem of the loan line of each enterprise, and use the optimal linear programming to give priority to the selection of the line and the interest rate. Enterprises: finally, for enterprises that do not have a credit rating, reasonable adjustments are made to the quota by establishing lending qualification expression, taking into account the impact of unexpected external factors, establishing an improved annual interest rate function, and achieving an optimized credit strategy through the establishment and solution of the model. The goal of optimizing credit strategy has been achieved.

1. Introduction

In practice, due to the relatively small scale of small, medium, and micro enterprises and lack of collateral assets [1], banks usually rely on credit policies, corporate transaction bill information, and the influence of upstream and downstream companies to provide companies with strong strength and stable supply-demand relations and provide loans and give preferential interest rates to companies with high reputation and low credit risk. Banks first evaluate the credit risk of small, medium, and micro enterprises based on their strength and reputation and then determine whether to lend and credit strategies such as loan limits, interest rates, and maturity based on factors such as credit risk.

A certain bank has a loan amount of 100,000 to 1 million yuan to an enterprise that is determined to lend; the annual interest rate is 4% to 15%; and the loan period is 1 year. Relevant data include the relevant data of 123 companies with credit records, the relevant data of 302 companies without credit records, and the 2019 statistics on the relationship between loan interest rates and customer churn rates. Then, how to establish a model to study the credit strategy for small, medium, and micro enterprises based on the actual situation and the data information in the attachment has become a key issue in bank lending.

For the bank's credit strategy, the following three issues need to be addressed:

(1) Quantify the credit risk of the 123 companies in Annex 1 and give the bank's credit strategy for these companies when the total annual credit is fixed.

(2) On the basis of question 1, conduct a quantitative analysis of the credit risk of the 302 companies in Annex 2 [2] and give the bank's credit strategy for these companies when the total annual credit is 100 million yuan.

(3) The production and operation and economic benefits of enterprises may be affected by some sudden factors, and sudden factors often have different effects on different industries and different types of enterprises. Considering the credit risk of each company in Annex 2 and the impact of possible sudden factors (such as the novel coronavirus epidemic) on each company, the bank's credit adjustment strategy when the total annual credit is 100 million yuan is given.

2. Problems Analysis

In response to question 1, we are required to quantify customer credit risk. The first problem is to find out the key factors that affect credit risk. We can consider the fuzzy analytic hierarchy process [3] to establish systematization and hierarchy. In a structured system, the elements in the system are compared in pairs, and a matrix is generated for quantitative analysis. After determining the collective evaluation (level) of the credit risk factors (indicators) of 123 companies, the fuzzy priority relationship matrix is obtained through custom data, and the fuzzy judgment matrix is calculated through the formula, then the weight of each factor level is determined, and the priority is judged. The most important risk factors can be obtained.

In response to problem 2, the goal is to solve the problems of credit risk quantification, loan interest rates, and bank credit optimal strategies. Because of the relevant data and loan interest rates of 302 companies with no credit records, the risk value cannot be calculated based on the reputation rating and default. Therefore, the relationship between the average profit rate and the risk is mainly considered, and the function is obtained by fitting the data in Annex 1. This problem can be solved; use the function of problem 1 to get the annual interest rate of 203 companies; use the formula of problem 1 to calculate the quota of each enterprise, and then use the combination optimization program and planning method to adjust the credit limit.

In response to question 3, focus on the sudden factors that affect the production and operation and economic benefits of the enterprise, and use the data in Annex 2 as the basis for analysis. Several questions are mainly considered. First, why are many companies operating negatively? Second, what is the reason why the corporate credit line is not within the scope of the bank's requirements? Third, how to reduce customer churn rate? In view of the above problems, the model designed in question 1 and question 3 can be improved.

3. Credit Strategy Based on Risk Quantitative Analysis

For question 1, it is necessary to find the credit factors to quantify the risk. Because the company has historical records, the fuzzy evaluation method can be considered; if the influencing factors can be determined, consider using the multiweight relationship [4] to calculate the risk value. From the risk value, the annual interest rate can be obtained by using a piecewise function or a fitting method; combined with the annual interest rate, on the basis of calculating the credit limit, linear programming and optimization methods can be used to select the optimal credit strategy.

3.1. Rating of Credit Factors. The first problem of question 1 is to find the important factors of credit evaluation. In order to select the factors that affect the credit of small and micro enterprises, the fuzzy comprehensive evaluation method is used to evaluate the credit decision, comprehensively considering various factors related to credit risk and based on indicators. The selection principle finally determines the level of the indicator system for corporate credit risk evaluation. The specific evaluation indicator structure is shown in Table 1.

Find the weights of the pairwise comparison matrix between the criterion layer and the target layer [5].

First, the criterion layer compares the target pair by pair and establishes the priority relationship matrix $G = (g_{ij})_{n\times n}$, with $g_{ij} = (1, 0.5, 0)$ to establish a priority matrix:

$$\begin{vmatrix} A_1 & B_1 & B_2 & B_3 & r_1 \\ B_1 & 0.5 & 1 & 1 & 2.5 \\ B_2 & 0 & 0.5 & 1 & 1.5 \\ B_3 & 0 & 0 & 0.5 & 0.5 \end{vmatrix}. \tag{1}$$

According to formula (2), the fuzzy judgment matrix is calculated, and then the square root method formula (3) is used to calculate the weight of the level index.

$$r_{ij} = \frac{r_i - r_j}{2n} + 0.5, \tag{2}$$

$$w_i = r_i \sum_{i=1}^{m} \overline{r_i}\ (i = 1, 2 \ldots\ldots m), \tag{3}$$

$$r_i = \sqrt[n]{\prod_{i=1}^{n} r_{ij}}\,(j = 1, 2 \ldots\ldots m). \tag{4}$$

Second, the criterion layer establishes a fuzzy consistent judgment matrix for the target:

$$\begin{vmatrix} A_1 & B_1 & B_2 & B_3 & W_1 \\ B_1 & 0.50 & 0.67 & 0.83 & 0.430 \\ B_2 & 0.33 & 0.50 & 0.67 & 0.316 \\ B_3 & 0.17 & 0.33 & 0.50 & 0.200 \end{vmatrix}. \tag{5}$$

Table 1: The structure of corporate credit evaluation indicators.

	First level indicator	Secondary indicators
Causes of corporate credit risk A1	Enterprise's own reasons B1	Reputation level C1
		Number of violations C2
		Bill information C3
		Upstream and downstream companies influence C4
	Bank's own reasons B2	Industry risk C1
		Professionalism of assessors C2
		Enterprise size C3
		Credit strategy C4
	Macro factor B3	Government administrative intervention C1
		National legal system C2
		National economy C3
		Vicious struggle between banks C4

Find the weight coefficient of the pairwise comparison matrix of the plan layer to the target layer.

First, the priority comparison matrix corresponding to the enterprise's own factor criteria is

$$\begin{vmatrix} B_1 & C_1 & C_2 & C_3 & C_4 & r_1 \\ C_1 & 0.5 & 1 & 1 & 1 & 3.5 \\ C_2 & 0 & 0.5 & 0 & 1 & 1.5 \\ C_3 & 0 & 1 & 0.5 & 1 & 2.5 \\ C_4 & 0 & 0 & 0 & 0.5 & 0.5 \end{vmatrix}. \quad (6)$$

Second, the company's own factor criteria establish a fuzzy consistent judgment matrix:

$$\begin{vmatrix} B_1 & C_1 & C_2 & C_3 & C_4 & W_2 \\ C_1 & 0.5 & 0.75 & 0.625 & 0.875 & 1.420 \\ C_2 & 0.25 & 0.5 & 0.375 & 0.375 & 0.768 \\ C_3 & 0.375 & 0.625 & 0.5 & 0.75 & 1.149 \\ C_4 & 0.125 & 0.625 & 0.25 & 0.5 & 0.663 \end{vmatrix}. \quad (7)$$

Then, the priority comparison matrix corresponding to the bank's own factor criteria is

$$\begin{vmatrix} B_2 & C_1 & C_2 & C_3 & C_4 & r_3 \\ C_1 & 0.5 & 1 & 1 & 1 & 3.5 \\ C_2 & 0 & 0.5 & 1 & 1 & 2.5 \\ C_3 & 0 & 0 & 0.5 & 1 & 1.5 \\ C_4 & 0 & 0 & 0 & 0.5 & 0.5 \end{vmatrix}. \quad (8)$$

Then, the fuzzy consistent judgment matrix corresponding to the bank's own factor criterion is

$$\begin{vmatrix} B_2 & C_1 & C_2 & C_3 & C_4 & W_3 \\ C_1 & 0.5 & 0.625 & 0.75 & 0.875 & 0.894 \\ C_2 & 0.375 & 0.5 & 0.625 & 0.75 & 0.723 \\ C_3 & 0.25 & 0.375 & 0.5 & 0.625 & 0.976 \\ C_4 & 0.125 & 0.25 & 0.375 & 0.5 & 1.404 \end{vmatrix}. \quad (9)$$

In addition, the priority comparison matrix corresponding to the macro factor criterion is

$$\begin{vmatrix} B_3 & C_1 & C_2 & C_3 & C_4 & r_4 \\ C_1 & 0.5 & 0.5 & 0 & 0 & 1 \\ C_2 & 0.5 & 0.5 & 0.5 & 0 & 1.5 \\ C_3 & 1 & 0.5 & 0.5 & 0 & 2.0 \\ C_4 & 1 & 1 & 1 & 0.5 & 3.5 \end{vmatrix}. \quad (10)$$

Finally, the fuzzy discriminant matrix corresponding to the macro factor criterion is

$$\begin{vmatrix} B_3 & C_1 & C_2 & C_3 & C_4 & W_4 \\ C_1 & 0.5 & 0.4375 & 0.375 & 0.1875 & 0.535 \\ C_2 & 0.5625 & 0.5 & 0.4375 & 0.25 & 1.130 \\ C_3 & 0.625 & 0.5625 & 0.5 & 0.3125 & 1.307 \\ C_4 & 0.8125 & 0.75 & 0.6875 & 0.5 & 1.027 \end{vmatrix}. \quad (11)$$

From the above calculation and analysis, it can be seen that the more weighted factors are C2 and C4 in B2; that is, the credit risk is mainly determined by the credit rating and bill information of the company's own factors, and C1 (national economy) is also affected by B3 (macro factor) [6] and other factors.

$$V_{ij} = w_i \times w_{ij}. \quad (12)$$

From formula (12), it can be concluded that the ranking of the influence of each factor on the credit decision of the enterprise is shown in Table 2.

3.2. Calculation of Risk Value Based on Multiweight Relationship. The quantitative analysis of the credit risk G of the 123 companies in Annex 1 is as follows.

First, construct the weight term sum risk value function, as shown in

$$G = P \times P_3 + D \times P_1 + W \times P_2, \quad (13)$$

$$P = \frac{S - C}{4}, \quad (14)$$

Table 2: Weights of corporate credit evaluation indicators [7].

	First level indicator	Secondary indicators	Weight w
Causes of corporate credit risk A1	Own cause B1	Reputation level C1	1.420
		Number of violations C2	0.768
		Bill information C3	1.149
		Upstream and downstream companies influence C4	0.663
	Bank's own reasons B2	Industry risk C1	0.894
		Professionalism of assessors C2	0.723
		Enterprise size C3	0.976
		Credit strategy C4	1.404
	Macro factor B3	Government administrative intervention C1	0.535
		National legal system C2	1.130
		National economy C3	1.307
		Vicious struggle between banks C4	1.027

$$D = \begin{cases} 0.9 & C_1 = A \\ 0.7 & C_1 = B \\ 0.5 & C_1 = C \\ 0 & C_1 = D \end{cases}, \tag{15}$$

$$W = \begin{cases} 0 & \text{breach of contract} \\ 1 & \text{no breach of contract} \end{cases}. \tag{16}$$

Among them, formula (14) is to calculate the average annual profit rate.

Then, use Excel to calculate the profit of each company = total expenditure (tax included)-total income (after tax). The total expenditure (including tax) here = SUMIFS (input invoice information! $G$2:$G$210948, input invoice information! $A$2:$A$210948, A2, input invoice information! $H$2:$H$210948, "Valid invoice"), Total income (after tax) = SUMIFS (output invoice information! $E$2: $E$162486, output invoice information! $A$2: $A$162486, A2, output invoice information! $H$2: $H$162486, "Valid invoice").

Finally, by using formulas (13)–(16) to calculate, finally calculate the risk Y. Specific data are shown in Table 3.

3.3. Calculate the Annual Interest Rate. After calculating the risk value in Annex 1, the evenly distributed risk value range is [0, 9.21]. According to the data in Annex, the value difference of the annual interest rate is 0.004. Therefore, the corresponding value of the risk value and the annual interest rate is obtained as shown in Table 4.

Perform data fitting on the data in Table 1 to obtain the calculated annual interest rate function, as shown in formula (22), and the specific annual interest rate is shown in Table 5.

$$Z = E + Q, \tag{17}$$

$$E = \frac{Y \times (1 - Y_2)}{I}, \tag{18}$$

$$G_2 = \frac{R - J}{J}, \tag{19}$$

$$I = T - U, \tag{20}$$

$$Q = E \times P_i, \tag{21}$$

$$y = 1E - 05x^2 - 0.0122x + 0.1505. \tag{22}$$

Calculate the total credit Z of the enterprise by formulas (17)–(21).

Use goal planning [8] to judge whether to lend to enterprises under the condition of maximizing the interests of banks:

$$E(x) = \max \sum_{i=1}^{n} Y_i x_i (1 + Y_i) M_i. \tag{23}$$

Among them,

$$M_i = \begin{cases} 0 & \text{credit rating is D} \\ 1 & \text{the credibility level is atleast C} \end{cases}, \quad 10 \le Y_i x_i \le G_i \le 0.15. \tag{24}$$

3.4. Calculate the Credit Limit of Each Company. x_i represents the loan amount, corporate credit line = last year's sales revenue × (1-previous year's sales profit rate) × (1 + estimated sales revenue growth rate)/number of capital turnover. Among them, the number of turnover = accounts receivable turnover days-accounts payable turnover days, the credit limit in 2021 is determined by calculating the 19–20 income growth rate and the number of capital turnover [9]. The specific data is shown in Table 6.

Through the above quantification of credit risk, the annual credit interest rate and credit limit can be calculated, and then the target planning model analysis can be used to obtain the credit strategy. First, if the bank wants to insure the collection, it can consider giving priority to mortgage

Table 3: Sample table of enterprise risk value data.

Enterprise code	Company name	Reputation rating	Rank weight	Breach of contract	Default weight	Average annual profit rate	Risk
E1	***Electric Appliance Sales Co., Ltd.	A	0.9	No	1	−0.3874844	0.688335602
E2	***Technology Co., Ltd.	A	0.9	No	1	2.63621849	2.182256471
E3	***Electronics (China) Co., Ltd. *** Branch	C	0.5	No	1	9.52389829	5.341012428
E4	***Development Limited Liability Company	C	0.5	No	1	6.22735183	3.71228772
E5	***Supply Chain Management Co., Ltd.	B	0.7	No	1	−0.1086503	0.703979141
E6	***Decoration Design Engineering Co., Ltd	A	0.9	No	1	0.14092075	0.949404716
E7	***Home Appliances Co., Ltd. *** Branch	A	0.9	No	1	7.07898782	4.377295512

Table 4: Corresponding value of risk value and annual interest rate.

Value at risk	Annual interest rate	Value at risk	Annual interest rate	Value at risk	Annual interest rate
9.21	0.04	5.920714286	0.0785	2.631428571	0.1185
8.881071429	0.0425	5.591785714	0.0825	2.3025	0.1225
8.552142857	0.0465	5.262857143	0.0865	1.973571429	0.1265
8.223214286	0.0505	4.933928571	0.0905	1.644642857	0.1305
7.894285714	0.0545	4.605	0.0945	1.315714286	0.1345
7.565357143	0.0585	4.276071429	0.0985	0.986785714	0.1385
7.236428571	0.0625	3.947142857	0.1025	0.657857143	0.1425
6.9075	0.0665	3.618214286	0.1065	0.328928571	0.1465
6.578571429	0.0705	3.289285714	0.1105	0	0.15
6.249642857	0.0745	2.960357143	0.1145		

Table 5: Sample table of corporate annual interest rate data.

Enterprise code	Company name	Reputation rating	Rank weight	Breach of contract	Default weight	Risk	Annual interest rate
E1	***Electric Appliance Sales Co., Ltd.	A	0.9	No	1	0.688335602	0.142107044
E2	***Technology Co., Ltd.	A	0.9	No	1	2.182256471	0.123924093
E3	***Electronics (China) Co., Ltd. *** Branch	C	0.5	No	1	5.341012428	0.085624913
E4	***Development Limited Liability Company	C	0.5	No	1	3.71228772	0.105347901
E5	***Supply Chain Management Co., Ltd.	B	0.7	No	1	0.703979141	0.14191641
...	...	...	...	...	...	...	...

Table 6: Sample table of corporate credit line data.

Enterprise code	Company name	Risk	2020 income (after tax)	2020 profit margin	19–20 revenue growth rate	Turnover	2021 quota
E1	***Electric Appliance Sales Co., Ltd.	0.688335602	73231470	−0.2228772	−0.95	94	48151.8
E2	***Technology Co., Ltd.	2.182256471	49935565	4.35035404	−0.81	−700	45669.9
E3	***Electronics (China) Co., Ltd. *** Branch	5.341012428	15380416.5	20.3692017	−0.89	335	97897.7

loans for enterprises with low risk. Choose companies with high annual interest rates; second, if banks want to maximize their benefits, they can expand credit lines or regulate annual interest rates for companies with high credit risks to maximize their annual returns.

4. Credit Strategy for Companies with No Credit History

For problem 2 the main solution is to carry out risk quantification, loan interest rate and bank credit optimal strategy for enterprises without credit records.

4.1. Quantify the Credit Risk of Companies with No Credit History. Because of the relevant data and loan interest rates of 302 companies with no credit records, the risk value cannot be calculated based on the credit rating and default or not. Therefore, the relationship between the average profit rate and the risk is mainly considered [10]; by fitting the data in Annex 1, the derived function can solve the problem.

First, determine the annual interest rate according to the method in question 1. The process is as follows.

First, use formula (25) and formula (26) to calculate the total expenditure (including tax) and total income (after tax) of each enterprise, then calculate the profit, and finally, use formula (27) to calculate the average profit of each enterprise rate.

$$Z(i) = \sum_{j=1}^{k} Q(i)(j). \tag{25}$$

Among them, $i = E124, E125, \ldots, E425$, Q is the amount of the input invoice, and j is the serial number of the input invoice of the i enterprise.

$$S(i) = \sum_{j=1}^{m} G(i)(j). \tag{26}$$

Among them, $i = E124, E125, \ldots, E425$, G is the total fare tax on output, and j is the serial number of the output invoice of enterprise i.

$$A(i) = \frac{G(i)(j) - Q(i)(j)}{Q(i)(j)/n}. \tag{27}$$

Among them, $i = E124, E125, \ldots, E425$, and n is the number of effective operating years.

Second, from the data relationship between the annual profit rate and the risk value in Annex 1, the risk value function is fitted by fitting: $y = -8E - 09x^2 + 0.4941x + 0.6467$, and the specific risk value is shown in Table 6 and Table 7.

4.2. Calculate the Annual Interest Rate. Using problem 1 function $y = 1E - 05\hat{x}2 - 0.0122x + 0.150$ to get the annual interest rate of 203 companies, the data sample table is shown in Table 8.

4.3. Credit Line Adjustment Strategy. Calculate the quota of each enterprise using the formula for calculating quota in question 1, and then adjust the quota according to the total amount of 100 million.

Strategy 1: select the legal limit range (100,000 to 1 million) and companies with purchase and sales data in 2020. Companies with low risk and high returns are preferred. Use the C# program to obtain the business portfolio and its credit line according to the conditions, and get the total amount of loans. The total income is 3497942.5 yuan, and the total income is 383611.8845 yuan. The specific data is shown in Table 9. This strategy minimizes the risk of repayment and maximizes the income of the lending bank, but it cannot meet the condition of a total loan of 100 million yuan.

Strategy 2: choose a company with purchase and sales data in 2020, with low risk and high return priority. In order to solve the problem of strategy 1, expand the scope of the line, use the C# program to obtain the business portfolio and its credit line according to the conditions, and get the total loan amount of 83966019.96. The total income is 919,9847.981 yuan. The specific data is shown in Table 10. This strategy expands the quota range to 10,000~40,000,000 yuan, minimizes the risk of repayment, and maximizes the income of the loan bank. According to the optimal linear programming method [11], run the C# program to achieve the goal of the total loan amount closest to 100 million.

5. Improvement of Credit Strategy Based on Emergencies

Question 3 needs to consider the unexpected factors that affect the company's production and operation and economic benefits. By calculating the purchase and sales invoice data of each company in Annex 2, we found the following problems:

(1) Affected by the new crown virus epidemic in 2020, many companies will experience negative growth in their operations
(2) The credit line of the enterprise is not within the range required by the bank
(3) Excessive annual corporate credit interest rates may cause serious loss of customers

In view of the above analysis, these problems can be solved through strategies such as focusing on assessing the changes in the company's purchase and sales invoice data in 2019, adjusting the credit limit, and improving the calculation method of the annual interest rate.

5.1. Reassessment of Companies That Have No Record of Purchase and Sales Invoices in 2020. Focus on assessing the data of purchase and sales invoices in 2019, and calculate the profit growth rate from 2018 to 2019. This is the credit reference for 2021. The formula in Excel changes to: =COUNTIFS(output invoice information! $A $2:$A$162486, A2, output invoice information!$H$2:$H$162486, "valid invoice", output invoice information!I$2:

Table 7: Sample table of process data for calculating Annex 2 risk value.

Enterprise code	Company name	Risk	Total expenditure	Total income	Average annual profit rate
E124	Self-employed E124	0.586753595	844202797.2	741780368	−0.1213244
E125	Self-employed E125	0.617094302	1001201809	941211364	−0.0599184
E126	Self-employed E126	2.149774437	128818723.6	520691098	3.04204516
E127	Self-employed E127	182.5994278	1765558.94	651937955	368.253011

Table 8: 203 corporate annual interest rate data sample table.

Enterprise code	Company name	Risk	Annual interest rate
E124	Self-employed E124	0.586753595	0.143345049
E125	Self-employed E125	0.617094302	0.142975258
E126	Self-employed E126	2.149774437	0.124318967

Table 9: 203 corporates' loan strategy data.

Enterprise code	Company name risk	Risk	Annual interest rate	2021 quota	Income
E149	***Construction labor Service Co., Ltd.	78.6259881	0.04	140987.6	5639.5052
E176	***Technology Co., Ltd.	8.778604263	0.044171667	157082.4	6938.5915
E144	***Labor Service Co., Ltd.	5.662303789	0.081740511	220474.2	18021.67
E392	***Technology Co., Ltd.	5.461949443	0.084162546	146091.3	12295.419
E234	***Mechanical and Electrical Equipment Trading Co., Ltd.	4.086490945	0.100811805	378987.4	38206.4
E303	***Book Distribution Co., Ltd.	3.486049648	0.10809172	886724.1	95847.533
E243	***Technology Co., Ltd.	3.392272855	0.109229346	207823.5	22700.43
E407	***Decoration Engineering Co., Ltd.	2.374062469	0.1215928	238903.3	29048.921
E302	***Electromechanical Equipment Co., Ltd.	1.476475579	0.132508798	275226.5	36469.927
E307	***Communication Engineering Co., Ltd.	1.091490391	0.137195731	128036.2	17566.024
E313	***Logistics Co., Ltd.	0.955389312	0.138853378	122741.0	17043.004
E232	***Investment Development Co., Ltd.	0.784912808	0.140930225	594865.0	83834.46

Table 10: 203 corporates' loan strategy 2 data.

Enterprise code	Company name	Risk	Annual interest rate	2021 quota	Income
E343	***Hardware Tools Business Department	1501.178169	0.04	14834298.2	593371.9
E359	***Kitchen Supplies Business Department	1050.753956	0.04	2924976.0	116999
E375	***Electrical Department	870.0656293	0.04	302790.5	12111.62
E382	***Education Information Consulting Co., Ltd. *** Branch	335.911581	0.04	935355.9	37414.23
E215	***Construction Engineering Co., Ltd.	139.7314732	0.04	57732.1	2309.285
E149	***Construction Labor Service Co., Ltd.	78.6259881	0.04	140987.6	5639.5052
E422	***Children's Clothing Store	14.05858053	0.04	125885.8	5035.43
E399	***Decoration Engineering Co., Ltd.	10.98344746	0.04	237148.3	9485.9306
E176	***Technology Co., Ltd.	8.778604263	0.044171667	157082.4	6938.5915
E144	***Labor Service Co., Ltd.	5.662303789	0.081740511	220474.2	18021.67
E392	***Technology Co., Ltd.	5.461949443	0.084162546	146091.3	12295.419
E413	***Stone Crafts Co., Ltd.	5.357296826	0.085427985	99596.6	8508.336
E254	***Equipment Installation Engineering Co., Ltd.	5.238550658	0.086864106	1193160.7	103642.8
E362	***Building Materials Co., Ltd.	4.730884788	0.093007018	2039255.1	189665
E210	***Construction Engineering Co., Ltd.	4.443812652	0.09648296	25676.5	2477.342
E234	***Mechanical And Electrical Equipment Trading Co., Ltd.	4.086490945	0.100811805	378987.4	38206.4
E398	***Medical Management Consulting Co., Ltd.	3.936529644	0.102629301	160134.2	16434.462
E303	***Book Distribution Co., Ltd.	3.486049648	0.10809172	886724.1	95847.533
E243	***Technology Co., Ltd.	3.392272855	0.109229346	207823.5	22700.43
E415	***Advertising Design Service Department	2.494874076	0.12012478	40176.9	4826.241
E315	***Tire Co., Ltd.	2.465996416	0.120475655	15648.5	1885.268
E407	***Decoration Engineering Co., Ltd.	2.374062469	0.1215928	238903.3	29048.921
E409	***Plastic Co., Ltd.	2.304318966	0.122440407	14148.8	1732.382
E406	***Tendering Agency Co., Ltd.	2.227985901	0.123368211	4772155.3	588732.3
E250	***Plastic Factory	1.82336773	0.12828816	48162.6	6178.688
E354	***Advertising Co., Ltd.	1.803160504	0.128533956	10605.9	1363.223

Table 10: Continued.

Enterprise code	Company name	Risk	Annual interest rate	2021 quota	Income
E372	***Auto Repair Co., Ltd.	1.779281527	0.128824424	26574.1	3423.388
E276	***Sports Facilities Engineering Co., Ltd.	1.555535584	0.131546663	18595.4	2446.165
E298	***Electrical Maintenance Service Co., Ltd.	1.547518376	0.131644224	13606.4	1791.204
E302	***Electromechanical Equipment Co., Ltd.	1.476475579	0.132508798	275226.5	36469.927
E256	***Materials Co., Ltd.	1.393742208	0.13351577	94308.9	12591.72
E305	***Labor Service Co., Ltd.	1.360741454	0.13391747	8349441.3	1118136
E355	***Carpet Business Department	1.264860734	0.135084698	38700704.4	5227873
E171	***Quality Inspection And Testing Station	1.256349819	0.135188316	27279.9	3687.92
E393	***Commercial And Trade Limited Company	1.186267081	0.136041614	892782.4	121455.6
E307	***Communication Engineering Co., Ltd.	1.091490391	0.137195731	128036.2	17566.024
E347	***Stainless Steel Material Co., Ltd.	1.084168799	0.137284895	2967322.6	407368.6
E249	***Construction Engineering Co., Ltd.	1.054026283	0.137651989	64464.9	8873.723
E313	***Logistics Co., Ltd.	0.955389312	0.138853378	122741.0	17043.004
E335	***Excavator Leasing Operation Department	0.900990849	0.139516029	1112123.0	155159
E397	***Hairy Crab Business Department	0.878407001	0.139791151	118020.2	16498.186
E361	***Survey And Design Engineering Co., Ltd.	0.878205611	0.139793604	13616.8	1903.548
E169	***Architectural Design Co., Ltd.	0.867856955	0.139919677	29880.3	4180.849
E160	***Steel Structure Engineering Co., Ltd.	0.800656764	0.140738398	13465.4	1895.099
E232	***Investment Development Co., Ltd.	0.784912808	0.140930225	594865.0	83834.46
E279	***Environmental Packaging Co., Ltd.	0.755090716	0.141293595	28942.8	4089.433
E334	***Mechanical Technology Co., Ltd.	0.743188632	0.141438622	76938.9	10882.13
E297	***Construction Machinery Leasing Co., Ltd.	0.723080704	0.141683644	32156.6	4556.064
E300	***Construction Engineering Co., Ltd.	0.720388899	0.141716445	30338.3	4299.442
E293	***Materials Co., Ltd.	0.596137139	0.143230681	20606.9	2951.545

Table 11: Growth rate of revenue of some enterprises in 2020.

Enterprise code	Company name	Risk	Annual interest rate	2020 expenditure (tax included)	2020 income (after tax)	2020 profit margin	19–20 revenue growth rate
E186	***Construction Labor Service co., Ltd.	13.29270342	0.04	1	1	0	−1.00
E128	Self-employed E128	12.94731484	0.04	1	1	0	−1.00
E166	***Construction Engineering Co., Ltd.	12.17331368	0.04	1	1	0	−1.00

Table 12: Credit lines calculated by certain companies based on revenue growth rates in 2019.

Enterprise code	Company name	Risk	Annual interest rate	2020 expenditure (tax included)	2020 income (after tax)	2020 profit margin	19–20 revenue growth rate	Turnover	2021 quota
E186	***Construction Labor Service Co., Ltd.	13.29270342	0.04	1	1	0	−1.00	−181	4078933.0
E128	Self-employed E128	12.94731484	0.04	1	1	0	−1.00	−561	11635616.4
E166	***Construction Engineering Co., Ltd.	12.17331368	0.04	1	1	0	−1.00	692	1171434.3

I$162486, 2019)-COUNTIFS(input invoice information!$A$2: $A$210948, A2, input invoice information! $H$2:$H$210948, "valid invoice", input invoice information! $I$2:$I$210948, 2019). The specific data comparison is shown in Tables 11 and 12.

5.2. Adjust Credit Limit. For some corporate credit lines, macrocontrol can be implemented in accordance with policies. The credit line can be increased if the credit line is less than 100,000, and the credit line can be reduced if the credit line is greater than 1 million.

5.3. Improve Annual Interest Rate. According to the data analysis, if the annual interest rate is too high, it will lead to a sharp increase in the customer churn rate. Therefore, in order to ensure that the customer churn rate is less than 50%,

Table 13: Annex 1 correspondence between corporate risk value and annual interest rate.

Reputation rating	Risk	Interest rate	Reputation rating	Risk	Interest rate	Reputation rating	Risk	Interest rate
B	0.308035	0.0785	B	0.870827	0.0627	A	2.106037	0.0498
C	0.43323	0.0782	C	0.885318	0.0621	A	2.182256	0.0494
C	0.602095	0.0775	A	0.921991	0.0616	A	2.211497	0.049
C	0.613443	0.0769	A	0.949405	0.0611	C	2.259863	0.0485
C	0.650022	0.0762	B	0.996121	0.0606	B	2.406582	0.0481
C	0.650045	0.0756	A	1.00881	0.06	B	2.416484	0.0477
C	0.652995	0.0749	B	1.017842	0.0595	A	2.423647	0.0473
A	0.688336	0.0743	B	1.023288	0.059	B	2.588746	0.0469
C	0.690585	0.0737	A	1.059018	0.0585	B	2.671114	0.0465
B	0.692255	0.073	B	1.108265	0.058	C	2.807199	0.0461
B	0.700992	0.0724	A	1.124168	0.0575	C	3.125604	0.0457
B	0.703979	0.0718	A	1.12627	0.0571	B	3.303712	0.0453
B	0.714014	0.0712	A	1.158062	0.0566	B	3.576327	0.045
A	0.724354	0.0706	A	1.19084	0.0561	C	3.685514	0.0446
B	0.727404	0.07	C	1.206253	0.0556	C	3.712288	0.0442
B	0.738483	0.0694	C	1.209741	0.0551	C	3.856233	0.0438
B	0.753467	0.0688	C	1.312666	0.0547	B	4.048533	0.0435
C	0.755346	0.0682	C	1.360376	0.0542	A	4.377296	0.0431
B	0.757424	0.0676	A	1.398631	0.0538	A	5.00316	0.0427
B	0.760574	0.0671	B	1.421465	0.0533	C	5.164616	0.0424
B	0.781265	0.0665	A	1.426184	0.0528	C	5.341012	0.042
A	0.805959	0.0659	C	1.533839	0.0524	B	5.782902	0.0416
A	0.810297	0.0654	B	1.721949	0.052	B	6.10317	0.0413
C	0.828054	0.0648	A	1.824604	0.0515	A	6.381905	0.0409
A	0.830954	0.0643	B	1.832157	0.0511	C	6.990441	0.0406
B	0.853665	0.0637	C	2.018004	0.0506	B	8.842854	0.0402
B	0.867381	0.0632	B	2.078559	0.0502	B	9.211668	0.04

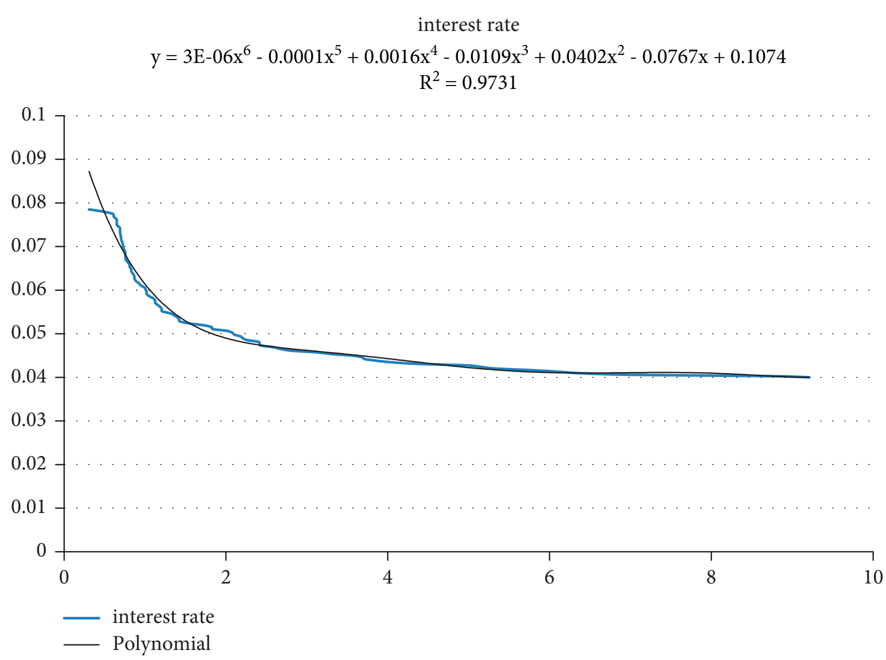

Figure 1: Improved annual interest rate function fitting effect diagram.

the annual interest rate can be controlled within 0.0785. For this, we renew the annual interest rate. The function is refitted. Redivide the data in Annex 1 as shown in Table 13.

Use Excel to perform trending fitting and get an improved annual interest rate function:

$$y = 3E - 06\hat{x}5 + 0.0016\hat{x}4 - 0.0109\hat{x}5 + 0.0402x\hat{\ }2 - 0.0767 + 0.1074.$$

The fitting effect is shown in Figure 1.

Through the calculation and comparison of the two functions ($y = 1E - 05\hat{x}2 - 0.0122x + 0.150$, $y = 3E - 06\hat{x}5 + 0.0016\hat{x}4 - 0.0109\hat{x}5 + 0.0402\hat{x}2 - 0.0767 + 0.1074$),

Table 14: Comparison of annual interest rate data before and after the improvement.

Enterprise code	Company name	Risk	Annual interest rate	Improve annual interest rate
E418	***Marketing Planning Co., Ltd.	4.446935282	0.096445142	0.077741233
E210	***Construction Engineering Co., Ltd.	4.443812652	0.09648296	0.077639054
E151	***Road & Bridge Engineering Co., Ltd.	4.421320197	0.096755374	0.076911235
E236	Self-employed E236	4.305518904	0.098158044	0.073384643
E353	***Tax Accountant Firm Co., Ltd.	4.204064239	0.099387158	0.070582929
E234	***Mechanical And Electrical Equipment Trading Co., Ltd.	4.086490945	0.100811805	0.067647979
E408	***Air Conditioning Refrigeration Co., Ltd.	3.959225983	0.102354198	0.064819217

the annual interest rate of some companies has been reduced, which has achieved the effect of reducing the customer churn rate. The specific data sample table is shown in Table 14.

During the experiment, BP neural network model, Fisher model, and logistic model are used to predict the risk of small and medium-sized enterprises [12]. According to the experimental results, compared with the other two models, the prediction accuracy of the model based on BP neural network (compared with the actual situation) is higher, which can ensure the prediction results and accuracy to a certain extent.

6. Conclusion

For the article's model design ideas for small, medium, and micro enterprises' credit decision-making, analysis is carried out according to the characteristics of the attached data provided by the title. First, use the fuzzy evaluation method to find the three factors that affect credit risk: reputation rating, default or not, and average profit rate, and use the addition of factor weights to get the function to calculate the credit risk value; secondly, find the function based on the risk value. The annual interest rate is used to calculate the credit limit of each enterprise through a function. According to the linear programming optimization theory, the program is used to find the best mortgage credit enterprise portfolio and provides an effective credit strategy; finally, based on the analysis of the data, analyze the operation of many enterprises. The reasons for negative growth, corporate credit lines not within the scope of bank requirements, and severe customer churn have been proposed to solve the above problems by changing the data changes in the invoicing and sales invoices of the assessed companies in 2019, adjusting the credit lines, and improving the calculation method of annual interest rates. The main advantages are as follows:

(1) The fuzzy evaluation method can prepare to find out the key factors affecting credit risk.
(2) The calculation methods of credit risk value, annual interest rate, credit line, etc. are scientific, and the result data is reasonable and reliable.
(3) Fitting based on the data in Annex 1 to ensure the accuracy of the related questions of the calculation question 2 and question 3.
(4) The mathematical model is combined with Excel to ensure the scientificity and accuracy of the model, and the C# program is used to realize the combination problem [13], which solves the batch data that cannot be processed manually.
(5) When the sample size of the data set increases significantly, compared with other models, the accuracy of enterprise risk prediction based on BP neural network model is higher.

After many experiments, it was found that there are deficiencies.

The large amount of data in the invoicing and sales invoices of enterprises and the excessive number of combinations result in a relatively long time for data processing. Some programs may cause problems such as memory overflow due to excessive data volume, and the degree of program optimization needs to be improved.

Data Availability

The datasets used and/or analyzed during the current study are available from the corresponding author on reasonable request.

Conflicts of Interest

The authors declare that they have no conflicts of interest.

Acknowledgments

The authors acknowledge Guangxi Higher Education Undergraduate Teaching Reform Project (2019JGB271), Natural Science Foundation of Guangxi in 2016 (2016GXNSFAA380102), Natural Science Foundation of Guangxi in 2016 (2016GXNSFAA380188), Junior Middle School Teacher's Basic Ability Promotion Project of Guangxi in 2017 (2017KY0797), and National Social Science Foundation in 2019 (19XJY015).

References

[1] R. Zhang, "The exploration and practice of the credit loan model of technology-based small, medium and micro enterprises," *China Business Forum*, vol. 30, no. 16, pp. 135–137, 2021.

[2] Z. Wang, Z. Wang, and H. Wan, "Decision-aid model based on quantitative analysis of credit risk," *Information and Computer (Theoretical Edition)*, vol. 33, no. 10, pp. 52–56, 2021.
[3] M. Sun and H. Wang, "Application of fuzzy analytic hierarchy process to the economic evaluation of composite wood structure buildings," *Journal of Northeast Forestry University*, vol. 49, no. 7, pp. 111–115, 2021.
[4] W. Tao and Y. Gui, "Model research on factors affecting the high-quality development of foreign trade from the perspective of spatial measurement," *Mathematics in Practice and Knowledge*, vol. 51, no. 15, pp. 113–122, 2021.
[5] Z. Dong and S. Mou, "Matrix factorization recommendation algorithm based on user rating weight," *Journal of Jilin Teachers College of Engineering and Technology*, vol. 37, no. 5, pp. 92–94, 2021.
[6] H. Su and W. Guo, "Optimization of credit risk evaluation indexes for banks' small and micro enterprises," *Finance and Accounting Monthly*, vol. 41, no. 1, pp. 27–32, 2020.
[7] Y. Yu and X. Wang, "Construction of the evaluation index system for the credit ability of private enterprises——based on a survey questionnaire of 12 industries and 300 enterprises in Guangdong Province," *Mathematics in Practice and Knowledge*, vol. 50, no. 8, pp. 307–315, 2020.
[8] X. Zhang, N. Li, and H. Fan, "Research on the credit decision of small, medium and micro enterprises based on multi-objective planning," *Contemporary Economics*, vol. 37, no. 6, pp. 24–29, 2021.
[9] Y. Gu, L. Huang, C. Lin, and C. Cao, "Research on the credit model of small, medium and micro enterprises based on risk level," *Software Engineering*, vol. 24, no. 7, pp. 56–59+55, 2021.
[10] W. Meng, "Interest rate risk management of commercial banks in interest rate marketization," *Oriental Corporate Culture*, vol. 7, no. 18, p. 207, 2010.
[11] Y. Zhang, "Research on the calculation method of the compromise optimal solution of the multi-level linear programming process," *Journal of Lanzhou University of Arts and Science (Natural Science Edition)*, vol. 34, no. 4, pp. 23–27, 2020.
[12] Y. Cheng, "Application of BP neural network in financial early warning of urban investment company," *Modern business*, vol. 16, no. 22, pp. 25–27, 2021.
[13] Y. Qin, "Application of an improved heuristic algorithm in solving combinatorial optimization problems," *Journal of Anhui Vocational College of Electrontcs and Information Technology*, vol. 20, no. 1, pp. 19–24, 2021.

Hindawi
Scientific Programming
Volume 2022, Article ID 6249065, 6 pages
https://doi.org/10.1155/2022/6249065

Research Article

Real Estate Development Strategy Based on Artificial Intelligence and Big Data Industrial Policy Background

Yu Liu

School of Management, Harbin Institute of Technology, Harbin, Heilongjiang 150006, China

Correspondence should be addressed to Yu Liu; liuyu_vip@outlook.com

Received 14 December 2021; Accepted 20 January 2022; Published 2 March 2022

Academic Editor: Punit Gupta

In recent years, as one of the pillar industries of the national economy, the real estate industry has achieved unprecedented development. Since the 1990s, my country's real estate industry has experienced three decades of rapid development. The average annual growth of commercial housing area is nearly 20%, and the average annual growth of housing prices in second-tier cities is 11.87%. However, in the rapid development, there are also many problems. For example, there are more and more phenomena such as unreasonable development, serious environmental pollution, and shortage of resources. At the same time, artificial intelligence has made great achievements in the development process in recent years, and it has continued to grow with technological progress and social demand. At present, China is in a transitional period of economic and social development, and the real estate industry is also facing huge challenges. In this context, research and development of traditional Chinese cities is very necessary and important. Therefore, how to effectively control and coordinate the real estate development behavior in the big data environment is one of the major problems that China is facing and needs to be solved urgently. This article uses questionnaire surveys and data analysis methods to understand the elements of real estate development strategies and analyze consumer purchase intentions through questionnaires. Randomly select 120 citizens of P city as the survey objects, and carry out a questionnaire survey. According to the survey results, most of the interviewees believe that the resource integration strategy occupies an important position in the real estate development strategy, and the big data management strategy also exerts its advantages. Most people believe that internal demand motivation is the most important, followed by the characteristics of real estate. It can be seen that real estate development must fully consider the actual needs of consumers and improve the development process to highlight the characteristics of real estate.

1. Introduction

The rapid development of artificial intelligence technology has brought earth-shaking changes to human life. As a new real estate development model under the background of the big data industry policy, smart real estate projects have become a current research hotspot at home and abroad. Under such circumstances, China has begun to vigorously promote smart housing, smart cities, and green buildings. How to effectively control and coordinate the real estate development behavior in the big data environment is one of the major problems that China is facing and needs to be solved urgently. Therefore, in the context of artificial intelligence and big data industrial policies, it is very necessary to carry out relevant research on real estate development strategies.

At present, the research results on the application of artificial intelligence and big data to real estate development are relatively rich. For example, Shi pointed out that China has been committed to the research and development of artificial intelligence, and the rapid rise and continuous development of big data technology have been widely used in various fields [1]. Luo analyzed the combination of big data technology and management accounting work, discussed the main points of management accounting work after the application of big data technology in real estate enterprises, and provided useful references and learning lessons for the same industry [2]. Jin and Li believed mastering residential property development and management strategies, developing commercial properties, maximizing the benefits of commercial property development and construction, and grasping the correct direction of commercial real estate development, so as to promote the development of urban commercial real estate [3]. Therefore, this article combines artificial intelligence and big data industrial policies to conduct research on real estate development strategies.

This research is based on the questionnaire survey method; through data analysis and arrangement, it draws suggestions for the development of the real estate market. This article mainly discusses these aspects. First of all, it elaborates on artificial intelligence and its related content. Then, it also introduces the big data industry and its policies and carries out related research. In addition, it discusses real estate development and strategies. Finally, a questionnaire survey is launched, and relevant survey results and analysis conclusions are drawn. The development of the research will not only help alleviate the troubled situation of my country's real estate development and promote the sustainable development of the industry but also help to better promote the integration of the real estate industry with information technology and fill the gaps in related research.

2. Related Theoretical Overview and Research

2.1. Artificial Intelligence. The research of artificial intelligence is to explore and imitate the intelligence that exists in the natural world and apply it to real life. And artificial intelligence can also be called an automated, programmed machine. Artificial intelligence is a subject, and its research fields mainly include biotechnology, computer simulation, and industrial automation. For example, people use artificial intelligence to perform speech recognition, breaking through the barriers to sound signal reception. In medicine, machines can also be used instead of people to perform some pathological or other disease diagnosis works [4, 5].

The development of artificial intelligence has gone through three stages. In the first stage, computer technology and sensor technology are combined to form an intelligent system. One is to simply complete tasks, and the other is to automatically process and detect information. In the second stage, the combination of "big data" technology and AI has formed a new model that provides conditions for human-computer interaction. The third stage is the transition from the researchers beginning in the direction of robot learning to the real realization of automated production processes, such as intelligent equipment and robots.

Artificial intelligence is an emerging technology, which has the following basic characteristics. One is intelligence. The robot runs and controls the computer system. The second is simple operation. It can change its own functions and performance according to changes in external conditions, and at the same time, it can self-learn and improve artificial intelligence through programs to make it continuously adapt to the external environment [6, 7].

2.2. Big Data Industry Policy and Related Research. With the advent of the Internet era and the continuous emergence of new technological revolutions such as cloud computing and information science, it has had a profound impact on social and economic development, and at the same time, it has provided more convenient services to humans in life. The big data industry is an emerging research field, which is based on cloud computing, the Internet of Things, and mobile internet, and relies on information processing technology.

Big data is not only innovation and technological progress but also has greatly changed the path of social development. At the same time, big data has become a weapon to lead the global economic and social transformation and promote the modernization of traditional industries. However, this is precisely because they belong to emerging industries, and their development trends are more difficult to grasp. Therefore, countries all over the world are actively adopting new big data strategies, actively promoting the development of the big data industry, and grasping the development trend [8, 9]. Table 1 shows the development index of China regional big data industry.

The big data industry is inseparable from the support of big data. Big data has become an important driving force and is developing into an emerging industry dominated by technology and information services. Therefore, data and big data technologies provide prerequisites for the emergence of the big data industry, and the application of big data drives the development of the big data industry.

Behind the vigorous development of the big data industry, there are also many hidden dangers such as talent and technology, weak industrial foundation, insufficient innovation and application, and imperfect laws and regulations. The existence of these problems severely restricts the future development of China's big data industry. Nowadays, more and more countries realize the importance of the big data industry and implement industrial policies one after another.

The big data industrial policy is an organic whole, which organically integrates various specific industrial policies, in which various components cooperate and interconnect with each other. After the development of the big data industry has gone through the initial exploration and start-up stages, the development of the big data industry has moved from the understanding of the theoretical basis to the industrial construction, promotion, and acceptance of big data technology and applications. With the gradual maturity of the society, the entire industry has developed rapidly, and the scope of the industry has gradually expanded [10, 11].

The big data industry policy has played an effective role in promoting the development of the big data industry. It can be summarized into four aspects, namely, the technology policy, structural policy, layout policy, and organizational policy of the big data industry. The big data industry is an important driving force for future social and economic development, and the structural policy of the

Table 1: Big data industry development index by region.

Development index	Eastern area	Western area	Middle area	Northeastern area
2017	471.324	346.533	186.714	83.612
2018	510.241	386.412	230.772	100.231
2019	590.783	457.561	298.134	178.424

big data industry is also an important part of the big data industry policy.

In response to the development of China's big data industry, the introduction of big data industry layout policies can promote the integration and concentration of data resources. The inequality in the development of big data industries in different regions and different industries can help promote each region. Each region also adopts different big data industry layout guidelines based on its own regional advantages and the status quo of the big data industry. Optimizing the big data industry organization policy is one of the important tasks to promote the development of China big data industry. It can better regulate the relationship between enterprises, maintain normal market order, and promote effective competition [12, 13]. Figure 1 shows the relationship between the main elements of the big data industry and the big data industry policy.

2.3. Real Estate Development and Strategic Research. Although there have been several bubbles during the development of the real estate industry, the real development of the real estate industry was after the abolition of the subsystem.

Real estate development is a comprehensive project that involves a wide range of areas, requires consideration of many factors, and is affected by multiple conditions throughout the process. Therefore, real estate projects have obvious particularities. From the preliminary investigation, planning, design, and construction of the project to the completion and acceptance, they are closely related to the land.

If real estate wants to develop and operate better, it is necessary to avoid the impact of residential real estate as much as possible and to find a fit for a commercial real estate development model with Chinese characteristics in accordance with the law of real estate development. Therefore, if commercial real estate wants to develop better, it needs to clarify the relevant theoretical basis first, and at the same time, it is necessary to learn a lot of advantages of Western developed countries in the commercial real estate development and operation process for reference. Solve various problems encountered in the development of China commercial real estate, and provide reference for the development of commercial real estate [14, 15].

There are three main branches of real estate development theory. The first is the theory of market analysis, which analyses and compares consumer needs, buying behavior, and sales methods with real estate companies as the research object and grasps the product life cycle through changes in the consumption environment and conditions. The second is the economic income hypothesis, which mainly includes two parts, population growth and per capita disposable income, as well as new benefits brought about by technological progress. The third is the theory of social structure, which refers to various production factors formed in the history of human society.

Real estate development strategy usually refers to the methods or means adopted by an enterprise in order to gain a competitive advantage and create greater and more profits within a certain range. From an economic perspective, strategic management theories can be divided into three types. The first is the combination strategy, the second is the overall policy, and the third is the external environment strategy. Real estate development projects generally have the characteristics of large scale and wide distribution. Therefore, reasonable planning and design of corresponding engineering schemes are required to improve their economic benefits and social impact effects. This is also one of the important goals implemented by developers [16, 17].

In addition, companies must fully investigate the current status of real estate development before formulating development strategies. Choose the right project and operating model not only to reduce the debt ratio and solve the problem of tight cash flow but also to obtain sales revenue in the shortest possible time.

The entire operation process of real estate is complex, including land development in the early stage and sales and promotion in the middle and later stages. Only by ensuring the smooth completion of each link can the entire project run smoothly. The real estate development process is shown in Figure 2.

3. Questionnaire and Research

3.1. Questionnaire Design Process. The questionnaire survey selected the citizens of city P, including consumers, real estate developers, and real estate sales staff. Through the issuance of online questionnaires or paper questionnaires, the collection and quantitative analysis of the information filled in by users are carried out to draw conclusions of the questionnaire.

(1) In the preliminary preparation of the questionnaire, the number of questions should be as concise as possible to avoid fatigue of the interviewees.

(2) The questionnaire is released. Questionnaires were distributed through online questionnaires, on-site questionnaires, and inviting friends to help ask friends and students around them. A total of 140

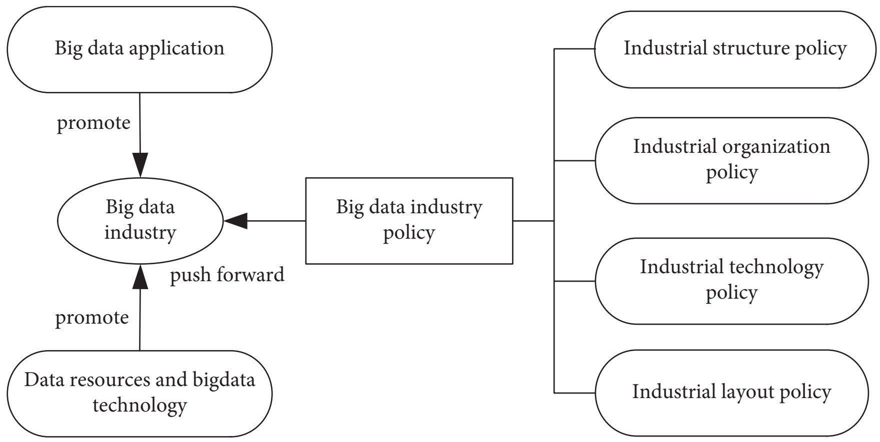

Figure 1: Relationship between the main elements of the big data industry and the policy.

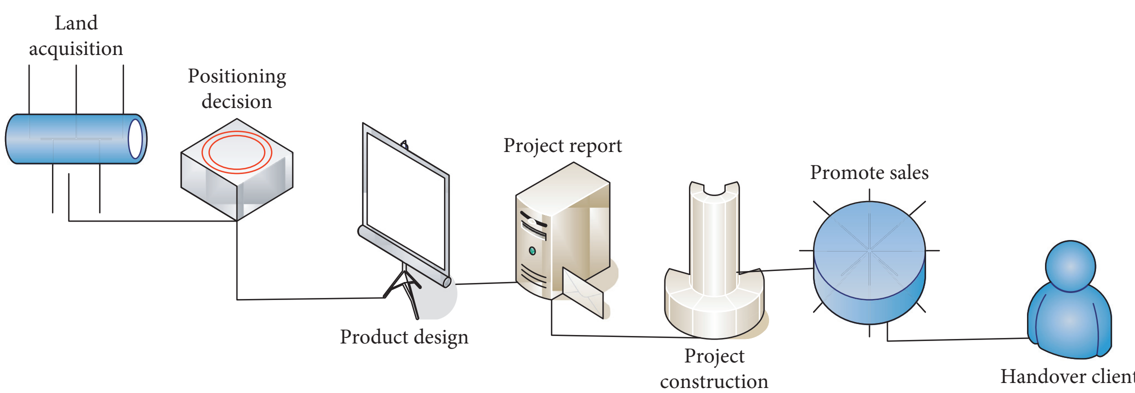

Figure 2: Real estate development process.

questionnaires were distributed, 120 valid questionnaires were returned, and the questionnaire recovery rate was 85.71%. The questionnaire distribution method and the results of the collection are shown in Table 2.

(3) Questionnaire analysis: organize the collected questionnaire information to get the required information data. Analyze the results of the questionnaire, including analysis of real estate development strategies and consumer purchase intentions. Some of the results obtained from the questionnaire are as follows.

3.2. Analysis of the Reliability and Validity of the Questionnaire. Reliability and validity testing is a very important link in the process of empirical research and is used to ensure the quality of questionnaires used in survey research [18, 19]. Only when the measurement tool (i.e., questionnaire) meets the reliability and validity requirements, the research results can be convincing [20, 21]. The specific calculation method is shown in formulas (1) and (2):

$$\lambda_d = \frac{\left(\sum \theta\right)^2}{\left[\left(\sum \theta\right)^2 + \sum (\theta)\right]}, \tag{1}$$

$$\lambda_e = \frac{\left(\sum \theta^2\right)}{\left[\left(\sum \theta^2\right) + \sum (\sigma)\right]}. \tag{2}$$

Among them, λ_d is the combined reliability, λ_e is the average extraction variance, θ is the standardized factor, and σ is the measurement error variance of the observed variable [22, 23].

3.3. Questionnaire Survey Content. The first part is the selected 120 citizens of city P, including consumers, real estate developers, and real estate sales staff, to investigate real estate development strategies in terms of resource integration, consumer experience, e-commerce integration, and big data management [24, 25].

The second part is to sort out the information collected by the questionnaire and investigate and analyze consumers' purchase intentions in terms of personal characteristics, internal

Table 2: Questionnaire distribution method and collection results.

Questionnaire distribution method	Number of questionnaires issued	Number of questionnaires returned	Recovery rate (%)
Internet questionnaire	45	41	91.1
On-site questionnaire	57	52	91.23
E-mail	38	27	71.05

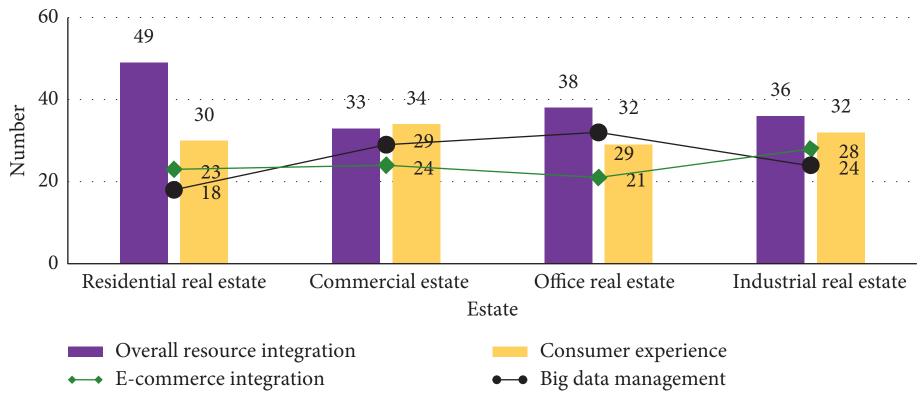

Figure 3: Survey results on the real estate development strategy.

Table 3: Survey results of consumer purchase intentions.

Project	Consumer	Real estate developer	Real estate sales staff
Personal characteristics	28	27	24
Internal demand motivation	34	35	39
Property characteristics	30	35	36
Social environment	25	26	21

demand motives, real estate characteristics, and social environment. Part of the questionnaire survey results is as follows.

4. Analysis and Discussion

4.1. Analysis of the Real Estate Development Strategy. This questionnaire survey launched a survey on real estate development strategies, including residential real estate, commercial real estate, office real estate, industrial real estate, agricultural real estate, and other uses of real estate, with regard to resource integration, consumer experience, e-commerce integration, big data management, etc. The survey results are shown in Figure 3.

As can be seen from Figure 3, of the 120 respondents, 49 people think that the overall resource integration strategy in residential real estate is the first priority, followed by consumer experience, while in office real estate, 38 people think the overall resource integration strategy is the first priority. It is a big data management strategy. It can be seen that most of the interviewees believe that the resource integration strategy occupies an important position in the real estate development strategy, and the big data management strategy also exerts its advantages.

4.2. Analysis of Consumers' Purchase Intention. This questionnaire survey will investigate and analyze consumers' purchase intentions in terms of personal characteristics, internal demand motives, real estate characteristics, and social environment. The survey results are shown in Table 3.

It can be seen from Table 3 that, among the 120 interviewees, including consumers, real estate developers, and real estate sales staff, 34, 35, and 39, respectively, believe that internal demand motivation is the most important, followed by real estate characteristics. It can be seen that real estate development must fully consider the actual needs of consumers and improve the development process to highlight the characteristics of real estate.

5. Conclusion

Starting from 2020, the Chinese government has stepped up its macrocontrol of the real estate market. Some real estate companies that rely on disorderly expansion have fallen into a quagmire, and the development of real estate companies has entered a state of stagnation. The development of this research provides a new idea for the development of the real estate market so that it can better grasp the actual market demand with the help of information technology, so as to formulate a more scientific development strategy. With the application of artificial intelligence in various fields, it has had a huge impact on various industries, especially the real estate industry. At present, China is in the era of big data, and the opportunities and challenges of real estate development coexist. Therefore, it is necessary to combine the support of artificial intelligence and big data industrial policies to break through the bottleneck of real estate development. Therefore, this article combines artificial intelligence and big data industrial policies to carry out research on real estate development strategies, which has important practical significance and research value. Research shows that the resource integration strategy plays an important role in the real estate development strategy, and the big data management strategy also exerts its advantages. At the same time, real estate development should fully consider the actual needs of consumers and improve the development process to highlight the characteristics of real estate.

Data Availability

The datasets used and/or analyzed during the current study are available upon reasonable request to the author.

Conflicts of Interest

The author declares no conflicts of interest.

References

[1] Y. Shi, "The countermeasures of management accounting for real estate enterprises under the background of big data," *Shangxun*, vol. 198, no. 8, pp. 55-56, 2020.
[2] W. Luo, "Strategic research on the perfect combination of artificial intelligence and big data," *Housing and Real Estate*, vol. 565, no. 6, p. 269, 2020.
[3] X. Jin and X. Li, "Development and strategic planning of commercial real estate in the era of Internet consumption," *Business and Economic Research*, vol. 22, no. 20, pp. 125–127, 2016.
[4] D. Xie, "Business strategy of real estate development enterprises under the new economic situation," *China International Finance and Economics (Chinese and English)*, vol. 31, no. 17, pp. 151-152, 2017.
[5] K. Fai, H. Lo, and Y. Huai, "Robust public-private partnerships for joint railway and property development," *Frontiers of Engineering Management*, vol. 4, no. 4, pp. 437–450, 2017.
[6] L. Ren, Q. Guo, and H. Wang, "Visual analysis of artificial intelligence literature big data based on CiteSpace," *Computer Systems & Applications*, vol. 27, no. 6, pp. 20–28, 2018.
[7] X. Su and Y. Dai, "Practice of innovative management accounting talent training model under artificial intelligence and big data environment," *The Journal*, vol. 45, pp. 116–118, 2021.
[8] G. Chen, L. I. Jing, and H. Chen, "Research progress of artificial intelligence technology in agriculture in the era of big data," *Journal of Jilin Agricultural University*, vol. 40, no. 4, pp. 502–510, 2018.
[9] Y. Zou, "Big data and artificial intelligence: a new vision for the inference of post-mortem interval[J]," *Journal of Forensic Medicine*, vol. 36, no. 1, pp. 86–90, 2020.
[10] J. Wang, "New financial thinking under the background of artificial intelligence and big data era," *The Journal*, vol. 17, pp. 195-196, 2021.
[11] S. Huang, L. Chen, and Z. Yin, "Research on systematic identification of strategic risks of real estate development enterprises," *The Journal*, vol. 25, pp. 90-91, 2021.
[12] K. Zhou, "Risk management of real estate development," *Economic Journal*, vol. 37, no. 2, pp. 341-342, 2016.
[13] J. Lu, "The interactive relationship between Chinas real estate development investment and GDP," *Real Estate Guide*, vol. 28, no. 24, p. 252, 2016.
[14] W. Cui, "Research on engineering management of real estate development and operation," *Urban Construction Theory Research (Electronic Edition)*, vol. 46, no. 8, p. 2071, 2016.
[15] L. Wang, "Cost optimization control of real estate development projects," *Commodity and Quality*, vol. 33, no. 46, pp. 49-50, 2016.
[16] S. Wang, "Cost control of real estate development projects," *Engineering Technology: Digest Edition*, vol. 16, no. 3, Article ID 00173, 2016.
[17] S. Guo, "Countermeasures for real estate development enterprises to strengthen cost management," *Engineering Technology*, vol. 27, no. 5, Article ID 00194, 2016.
[18] L. Wang, "Factors affecting real estate economic development and solutions," *Real Estate*, vol. 18, no. 7, pp. 0039-0040, 2021.
[19] Z. Li, "Double carbon" strategy redefines the real estate development model," *China Real Estate Finance*, vol. 29, no. 7, p. 1, 2021.
[20] S. Lin, "Discuss how the real estate market can promote the development of real estate economy," *Modern Enterprise*, vol. 11, no. 10, p. 2, 2021.
[21] A. Zhang, "Analysis on the influence and development of real estate economy in the new era," *Market Weekly·Theory Edition*, vol. 21, no. 4, p. 2, 2021.
[22] Ye Fan, "Application of target cost method in cost management of real estate development projects," *Low Carbon Real Estate*, vol. 32, no. 19, pp. 189-190, 2016.
[23] Q. Zhang, "Engineering cost control of real estate development enterprises," *Citation version: Engineering Technology*, vol. 43, no. 5, p. 33, 2016.
[24] W. Wang and Z. Lu, "How to prevent "grey rhinoceros" - a mirror of real estate development from the United States, Japan, and Germany and China's policy recommendations for preventing systemic risks," *China Economic Report*, vol. 34, no. 2, p. 11, 2021.
[25] X. Cai and N. Lin, "Research on the coordinated development path of new urbanization and real estate industry in Fujian Province," *The Journal*, vol. 15, pp. 147–152, 2016.

Hindawi
Scientific Programming
Volume 2022, Article ID 7358354, 15 pages
https://doi.org/10.1155/2022/7358354

Research Article

A Conceptual Model for Blockchain-Based Agriculture Food Supply Chain System

Ibtisam Ehsan,[1] Muhammad Irfan Khalid ,[1] Laura Ricci,[2] Jawaid Iqbal,[3] Amerah Alabrah,[4] Syed Sajid Ullah ,[5] and Taha M. Alfakih [6]

[1]*Department of Information Technology, University of Sialkot, Sialkot, Pakistan*
[2]*Department of Computer Science, University of Pisa, Pisa, Italy*
[3]*Department of Software Engineering, Capital University of Science and Technology, Islamabad, Pakistan*
[4]*Department of Information Systems, College of Computer and Information Sciences, King Saud University, Riyadh 11543, Saudi Arabia*
[5]*Department of Information and Communication Technology, University of Agder, N-4898 Grimstad, Norway*
[6]*Faculty of Engineering and Information Technically, Aljanad University for Science and Technology, Taiz, Yemen*

Correspondence should be addressed to Syed Sajid Ullah; syed.s.ullah@uia.no and Taha M. Alfakih; talfakih@just.edu.ye

Received 28 December 2021; Accepted 1 February 2022; Published 28 February 2022

Academic Editor: Punit Gupta

In agriculture supply chain management, traceability is a crucial aspect to ensure food safety for increasing customer loyalty and satisfaction. Lack of quality assurance in centralized data storage makes us move towards a new approach based on a decentralized system in which transparency and quality assurance is guaranteed throughout the supply chain from producer to consumer. The current supply chain model has some disadvantages like a communication gap between the entities of the supply chain and no information about the travel history and origin of the product. The use of technology improves the communication and relation between various farmers and stakeholders. Blockchain technology acquires transparency and traceability in the supply chain, provides transaction records traceability, and enhances security for the whole supply chain. In this paper, we present a blockchain-based, fully decentralized traceability model that ensures the integrity and transparency of the system. This new model eliminated most of the disadvantages of the traditional supply chain. For the coordination of all transactions in the supply chain, we proposed a decentralized supply chain model along with a smart contract.

1. Introduction

Agriculture is a need for the majority of people worldwide to survive [1]. Improvements in agriculture productivity and quality, adequate marketing infrastructure, and assistance, and efficient food management are all prerequisites for agriculture growth [2]. Food safety appears to be an essential aspect that both producers and consumers are concerned about. Transparency in supply chains helps to improve the procedures engaged in manufacturing [3]. Traceability is also crucial as it allows us to determine the product's origin, including data such as the producer, harvesting and production dates, and so on. To meet the growing demands, the agricultural system has to be vastly improved [4]. To address the complicated agricultural issues, advanced technologies are being developed. Blockchain is the most recent addition to these technologies. A cryptographic hash is the base of blockchain technology. It is a transaction ledger system that is decentralized and immutable [5]. This guarantees that the user's transactions and identity can never be affected. If a forged transaction takes place, the decentralized mining mechanism will prevent it from entering the encrypted chain [6]. The supply chain logistics industry is the most visible implementation of blockchain technology [7]. In the field of logistics, blockchain moves ahead with a lot of options regarding the shipment of data. Every product or item can be tracked, which helps in precautions for any possible delay in shipment [8]. Internet of things can be utilized with blockchain to track the supply of perishable goods. Blockchain has various trading applications as well. The transaction in agriculture supply chain management includes the data about raw material and quantity etc. and blockchain technology can maintain various crop insurance schemes with the help of proof of records for a claim during the loss of crop in any case. The use of smart contracts is helpful for settling transactions and eliminates intervene of any third party, and this could be considered the main advantage of blockchain technology [9].

2. Literature Review

In this particular section, we review the work related to blockchain in the agriculture supply chain found in the literature. Blockchain has gained massive popularity in the banking and finance industry, but it is growing steadily in agriculture. In [10], the authors proposed a hazard analysis and critical control points based agriculture food supply chain traceability model with the collaboration of blockchain and IoT. A use case of tracking a product from producer to consumer is implemented through hyper-ledger, and Ethereum is presented in [11]. Moreover, the authors introduced a traceability solution for the food value chain. The authors discussed how to apply blockchain technology in the agriculture food supply chain and also raise the trust, security, and integrity issues in [12]. In [13], the authors reviewed the Agri-ICT concept in blockchain and presented an improved model of ICT in the agriculture blockchain. For increasing efficiency in smart contracts and DLT, an approach is introduced in [14]. Furthermore, the authors highlighted the challenges and barriers while adopting blockchain technology in agriculture. In [15], researchers introduced an efficient blockchain agriculture food-management supply chain with smart contracts. Potential risks and challenges while adopting blockchain in the food supply chain are discussed in [16]. In [17], the authors proposed a new blockchain approach that is based on an IPBFT algorithm to optimize trading for food supply chain buyers. In [18], researchers presented an approach to measure the grain quality using blockchain smart contract. Authors explored in [19] how to blockchain-based systems promote value transfer in small-scale agricultural farms. To increase transparency and automate the process of blockchain in agriculture, authors in [20] introduced an advanced prototype. The authors studied challenges in the implementation of blockchain in the dairy industry in [21]; moreover, they introduced a hyper-ledger-based solution for blockchain-based traceability. As seen by the linked study, there is a strong trend toward using blockchain technology in food and agricultural supply chains to improve information security, transparency, and verification of different criteria [22]. The literature demonstrates how blockchain and smart contracts can provide supply chains with an efficient, trustworthy, safe, and decentralized trace and track. Table 1 describes the proposed methods and their attributes by various researchers.

3. Challenges

(i) There is no way to change or update data in a blockchain if, at any step, someone makes a mistake. The immutability of blockchain is one of the major advantages. However, as opposed to traditional database systems, blockchains are hard to amend or manipulate.

(ii) A verified transaction cannot be altered by security schemes.

(iii) Using smart contracts, the system can be controlled and the steps can be automated. Smart contracts cannot be modified after they are deployed.

(iv) The blockchain environment will require some money during its initial setup.

(v) It is possible for IoT devices to be hacked.

(vi) The acquisition of data requires IoT devices. Data collection can be affected if devices are damaged.

4. Traditional and Centralized Supply Chain

As shown in Figure 1, supply chains have a traditional structure. A central database containing data regarding all processes is created by using this approach. An administrator manages the database. Several limitations apply to this approach. This system uses a server to manage the database. Therefore, if that server fails, the entire system will go down. An administrator who is dishonest could change the data without the stakeholder's knowledge [4]. Those manipulations are inadmissible to trackback. Thus, this centralized approach is opaque and untraceable as well. Among the major challenges of the traditional supply chain ecosystem are traceability of products, transparency of stakeholders, and trust in collaborative systems. In the traditional approach, there are a lot of intermediaries, causing trust problems and performance problems [7]. Various supply chain entities include farmers, distributors, retailers, etc. Consequently, any outbreak involving food products will be extremely difficult to trace [10]. It is essential to examine the functional impact, social impact, and economic impact of emerging technologies in the supply chain ecosystem. Furthermore, the traditional supply chain ecosystem is highly centralized. This leads to trust issues when multiple organizations collaborate. A centralized process makes it easy to manipulate data without the knowledge of other stakeholders. Any carelessness in the food supply chain may put the lives or health of people at risk [8]. This is a big concern when it comes to traceability. Trust issues within the supply chain can result in significant losses for companies. Companies put the utmost effort into creating trust among consumers. Providing access to data while protecting it from being altered by others should resolve these issues. By utilizing emerging technologies in the supply chain, we can resolve these issues. With blockchain technology, supply chain performance can be improved, and issues can be eliminated. Furthermore, it has some features that make it useful for addressing supply chain concerns beyond its use of distributed ledger technology. As a result of its immutability

Table 1: Literature proposed methods and their attributes.

Papers	Provide system implementation	Traceability	Control over the system (smart contract)	Customer decision-making made easier	Getting real-time data	Fraud reduction	Eliminating third parties	Price transparency
[23]	No	Yes	Yes	Yes	Yes	Yes	Yes	No
[24]	Yes	Yes	Yes	Yes	No	No	Yes	No
[25]	No	Yes	No	Yes	Yes	Yes	Yes	No
[17]	No	Yes	No	No	Yes	Yes	Yes	No
[26]	Yes	No	Yes	No	Yes	Yes	No	No
[10]	Yes	Yes	Yes	No	No	Yes	Yes	No
[1]	No	Yes	Yes	No	Yes	Yes	Yes	Yes
[27]	No	Yes	Yes	No	No	No	Yes	No
[28]	Yes	Yes	Yes	Yes	No	Yes	Yes	No
[12]	Yes	Yes	Yes	No	No	Yes	Yes	No

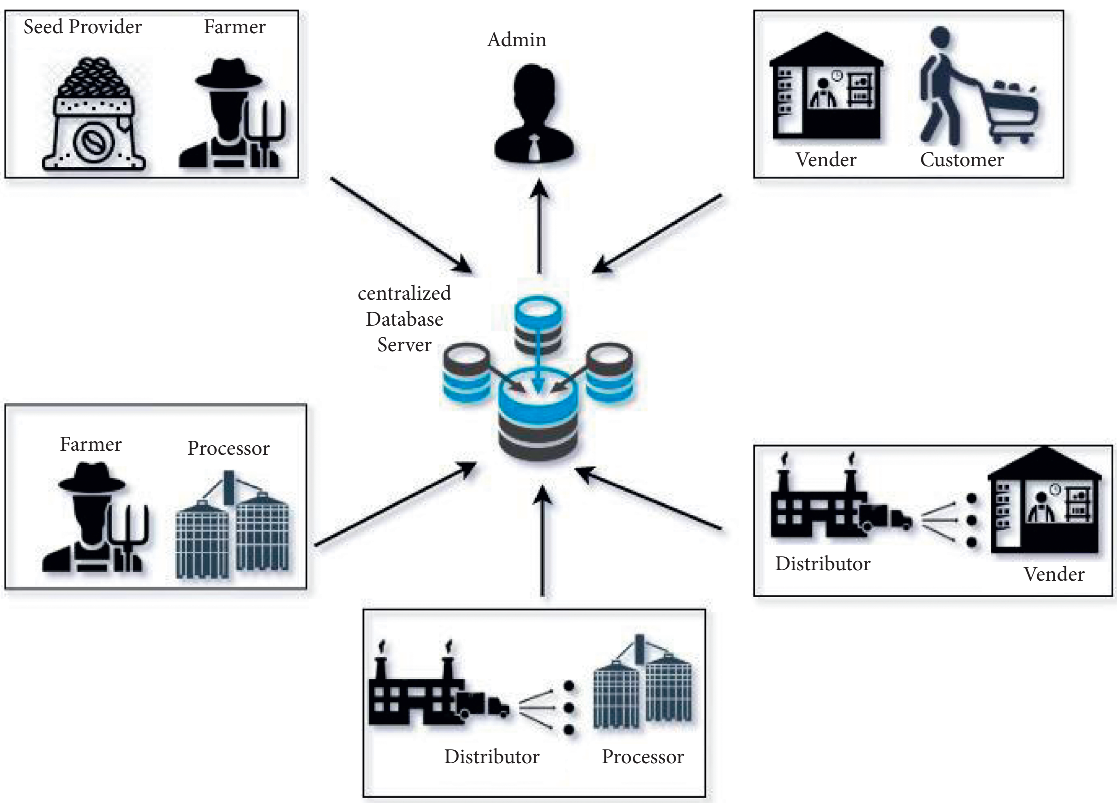

Figure 1: Centralized food supply chain.

and distributed nature, it provides a secure and reliable record that cannot be altered or altered. Food supply chain ecosystems can be improved by transparency and the use of emerging technologies [14].

5. Blockchain in the Agri-Food Supply Chain

Many difficulties have plagued agriculture and food (agri-food) supply chains, including a lack of traceability, poor visibility, and inefficiency [27]. These challenges have a direct and considerable impact on management efforts to ensure agri-food production compliance, enhance food safety and quality, reduce food waste, and decrease supply chain operation expenditures [29]. The advancement of a traditional supply chain becomes imperative in the case of unexpected growth of a product's demand [30]. Moreover, customer satisfaction can be improved with the help of supply chain management. A supply chain comprises operations such as product flow, information, and product travel history. Figure 1 portrays a traditional food supply chain that includes producers, suppliers, manufactures, distributers, and retailers working in a chain to deliver products from producer to consumer. Traditional supply chains based on centralized systems lacks traceability, transparency resulting in data loss, data tempering, and security threats. There are the following drawbacks of a traditional supply chain:

(i) No traceability and transparency.

(ii) No details of product origin.

(iii) No food safety is assured at any stage.

(iv) No record of any transaction in the whole supply chain.

The upper stated issues can be solved by blockchain technology; over distributed networks, it acts as a public ledger and overcomes information maintenance issues like verification and validation. Blockchain technology provides security, maintains temper proof record, avoids any kind of the third party of middle man in transactions, helps to reduce the overall cost of trans-action, and improves the product quality. The cryptographic approach followed here develops user confidence, resulting in increasing the product's demand [31]. Cryptocurrency-related encryption methods assist in the validation and verification of users and new blocks; that is why each block in the blockchain network contains the details of the transaction. The chain contains a ledger from the beginning to the creation of a new genesis block [32]. Each block has a reference to the preceding block due to a hash value. The peer-to-peer network assists in the verification of new transactions and users [33]. Among the emerging technologies, blockchain technology is likely to have a significant impact on many areas of collaboration. By using distributed ledger technology, entities can communicate without a middleman in a peer-to-peer network. By virtue of its numerous features, it promotes trust and transparency in cooperative environments. The decentralized nature of its operation means that it is not controlled by a single party or entity. A consensus refers to an agreement reached between all parties regarding how to carry out a transaction. This feature permits the traceability of any transaction. Whenever a transaction is made, the distributed ledger is updated so that all nodes can see it. One of the most important features of immutability is that it makes it impossible to tamper with [34]. Unlike traditional databases, the distributed ledger cannot be modified or deleted once it has been written. Smart contracts can also be implemented on the distributed ledger. These are computer programs used to specify the logic of a contract between two or more parties. After the contract is executed, certain conditions must be satisfied.

5.1. Provenance Tracking. Blockchain technology can be useful to resolve discrepancies in transactions when historical information is required. The blockchain-based solution can track the provenance of transactions. Transactions can be tracked from when they were initiated.

5.2. Transparent Procurement. A company looks for a middleman every time it is in the procurement process. It is almost impossible to track the exact volume or quantity between partnership firms, subsidiaries, etc., using the traditional approach. With the blockchain, this process can be automated. With the blockchain, virtually all transactions are visible and continually updated. Companies can check their orders by using distributed ledgers. Auditing employees are usually hired just for the auditing process [26]. As a result of blockchain, auditing will become much easier and faster without involving so many people.

5.3. Transacting Immutably. Authorized nodes can execute multiple transactions. Attackers cannot delete or modify the transactions. Transactions in the blockchain cannot be altered or deleted once they are recorded in the decentralized ledger since they are immutable [5]. It is impossible to delete or update transactions that have already been executed, not even the administrator. As part of blockchain technology, the hash function is used, which means modifying the data can affect the hash.

5.4. No Rogue Frauds. There is a decentralized ledger shared by all connected nodes on the blockchain. Each node's ledger reflects these transactions. Rogues who try to execute transactions for their own benefit are doomed to failure [21]. Each transaction must be approved by all stakeholders due to the consensus feature of blockchain. Table 2 illustrates the major challenges that exists with the agri-food supply chain system, apart from that all those challenges which currently opted supply chain process in the agri-food.

6. Use of Smart Contracts for Blockchain-Based Agriculture Supply Chain

The blockchain allows us to eliminate intermediaries, but the promises and trust boundaries between the contributing parties typically require something called a smart contract. In the same way that traditional contracts regulate trust between the parties, smart contracts provide organizational terms and conditions that govern trust within the scope of the contract. A smart contract is only different because it is coded in a programming language [7]. Using controlled coding, the rules, terms, and conditions reflected in the agreement are implemented exactly as agreed by all parties. A smart contract concept has existed since the 1980s, but all it lacked was the removal of intermediaries. Smart contracts were introduced in 1996 by Nick Szabo [35]. A smart contract embeds the contractual terms within a combination of hardware and software, making it difficult for them to be breached, and making them cost-prohibitive. As such, smart contracts increase safety by reducing attacks. Ethereum blockchain popularized the notion of smart contracts and its implementation in real life in 2016. The Ethereum network combines a decentralized Turing-complete blockchain with a smart contract environment and integration tools. Figure 1 shows the steps involved in building a smart contract. In other words, a smart contract automates processes in blockchain technology. By storing the contract within the blockchain, we can potentially use blockchain in other real-world situations. To automate the steps involved in the system, the authors in [18] use smart contracts as their core technology. Real-time tracking of products in a supply chain and a comprehensive view of the process are both part of the automation. Using a smart contract, [7] incorporates

Table 2: Challenges and opportunities while adopting block chain in agriculture.

Opportunities and potential benefits	Challenges and barriers
Food-borne disease risks are reduced when items are of higher quality	Platforms for education and training are limited
User friendly for farmers	Market fluctuations and ambiguity
Fewer number of frauds due to transparent transactions	Small businesses lack of competence
Financial transaction facilitation for every entity in the supply chain	New users may be unable to access marketplaces due to a lack of information infrastructure
Enhanced sustainability and reduction of waste	As the technology ahead forms trigonal methods, SMEs have various issues and difficulties while adopting
A valuable platform for reducing emissions	Understanding issues among policymakers and technical support staff
Pricing is more equitable across the whole value chain	Requirements of IoT/computing equipment
Purchase decisions are made by well-informed consumers	Digital gap between developing and developed countries
Consumers are well informed about what they are purchasing	Cryptocurrencies market share is dwindling, and there is a lot of volatility (reputation issues)
Less reliance on intermediates and third parties	Open technological questions and scalability problems for example transactions latency
Insurance policies and financial aids for rural area farmers	Limited flexibility in design decisions [19]
Traceability and transparency in value chains	Some food quality factors, particularly environmental indicators, cannot be assessed using objective analytical methods

industrial spare parts traceability research to implement the necessary functions, modifiers, and events to implement the logical flow mechanism to automate the entire process. By securing contracts within the blockchain, smart contracts can satisfy the fundamental need for trust between parties. The paper [2] proposes implementing an IoT-based automobile insurance ecosystem known as CAIPY, which implements step-by-step processes and communicates with tamper-proof IoT devices in order to monitor a car's condition. Smart contracts can be used for intellectual property rights management. Paper [36] presents BMCProtector, a music copyright management platform using blockchain and smart contracts. From song creation until royalty distribution, their smart contract system implements all the necessary functionality. It is nearly impossible to alter a smart contract that has been distributed within a blockchain because they are distributed inside the block chain, so you need to deploy them within a blockchain environment for maximum security. When coding smart contracts, you will frequently come across terms like attribute, function, event, and modifier. Here is an explanation of these terms.

Attribute: a variable that holds a value in memory is an attribute. Various primitive data types are supported in solidity: integers, chars, strings, doubles, and mappings, addresses, and enumerators.

Function: in a system, functions represent mechanisms and tasks. If a function is called, the task it contains will be executed.

Modifiers: actors or components have access power through modifiers. Although the contract owner has ultimate control over modifications, other actors or components can be granted some specific rights to modify or gain access.

Event: a blockchain transaction log stores anything that happens as part of an event. In the transaction logs of the blockchain, in response to an event taking place or being emitted, any argument that is passed along with that event gets recorded. This mechanism allows for the subsequent retrieval of historical information about the system. The system is auditable through this mechanism.

Smart contracts are computer programs that run when certain conditions are met and recorded on a blockchain [15]. They are often utilized to automate the execution of a contract so that all parties are instantly in-formed of the results, without the need for any middlemen or time waste. Traditional contracts are no longer efficient for blockchain technology [15]. The traditional supply chain also contains a huge amount of paperwork and documents which is not a good approach for tracking and records proofs. Smart contracts are automatically executed and triggered when preset criteria are fulfilled, can assist to address these drawbacks of transparency, efficiency, security, and tracking, and eliminate the role of a mediator [18]. These auto-executed code-based contracts enable agreed-upon activities (such as payments) to occur quickly upon the completion of the terms of the contract. This is a major function that differentiates blockchain from Ethereum. For example, when a client verifies their shipment, according to the instructions a smart contract will transfer money to the carrier. Smart contracts are unique in that they allow you to write code that executes itself without the need for a third party, which helps to save a lot of money, time, and effort, also no chance of errors or frauds. In comparison to a traditional contract, a smart agreement between two parties participating in a transaction holds each participant responsible for their participation in the transaction and also ensures that the contract is implemented. Smart contracts increase a supply chain's transparency, traceability, and efficacy, allowing it to be more flexible in establishing connections between partners. A unique address is assigned to every smart contract. This address never changes one of the contracts deployed in the blockchain. User transactions can only send to a contract address. Every consensus node in the network will execute the transaction to achieve a consensus on its output. The two forms of smart contracts are deterministic and non-deterministic smart contracts [29]. A deterministic smart contract executes without the need for any information from a third party. A non-deterministic smart contract relies on third-party data (database). A smart contract works by following simple "if/when . . . then . . ." statements which are written into the blockchain code.

An action is executed by a network of computers when certain conditions have been met and verified. A blockchain is then created to record the transaction. Parties who have already been granted permission are the only ones who can see the results of a transaction unless permission is granted [37]. The participants in a smart contract can specify as many conditions as necessary to ensure a successful outcome. By defining how transactions and their data will be represented on the blockchain, establishing the "if/when. . .then. . . rules" that will govern the transactions, exploring all alternative possibilities, and establishing the dispute resolution framework, participants are in the process of setting the conditions as shown in Figure 2. Supply chain management is expected to benefit from blockchain technology to reduce the number of coordination challenges [38]. Smart contracts can handle multiple transactions between parties, which reduces complexity, enables greater transparency across the supply chain, and enhances the trust-less verification process. The supply chain will be streamlined and made more flexible, and stronger partnerships will be fostered [39]. Considering the above discussion of the use of blockchain and smart contract in various fields and use cases, it is quite clear that the combination of blockchain and smart contract results in an automated, highly secure, and ingenious system. Rather than storing and tracking data in a blockchain, smart contracts implement the business logic and control access to the data.

7. Benefits of Smart Contract over the Traditional Supply Chain

7.1. Transparency. Through smart contracts, the provenance of goods can be recorded, enhancing supply chain transparency. The blockchain stores information such as the date, location, and quality, which are helpful in verifying a product's origin. Consumers will have more confidence that they are purchasing good products, and manufacturers will have the assurance that their raw material comes from a reliable source [40]. Smart contracts can also be used to enable transparent credentialing among supply chain partners by creating and storing digital forms of identification. With this system, parties can easily verify that other parties have the requisite certifications to be able to do their duties [41]. Blockchain technology can also be used to manage reputations and reliability.

7.2. Traceability. Using smart contracts, traceable inventory can be tracked from its raw material source to its delivery to its end-user, which can improve supply chain traceability. A serial number, RFID tag, or smart sensor can be used to accomplish this. In addition to location and environmental data, smart sensors can provide information about product quality (especially for perishable goods). The ability to make better and faster decisions will be improved with real-time information and updates about product status. In this case, it is easier to activate a reserve batch of goods midway through the supply chain process rather than to wait until the bad batch arrives before making a decision. As a result, delays can be reduced, and the supply chain can remain agile [35]. Natural disasters, factory strikes, and delivery accidents will also be dealt with well by the organizations. With the increase of product competition, ensuring continuity of supply can significantly enhance a brand's image among consumers.

7.3. Efficiency. A smart contract can improve the efficiency of the supply chain from both an operational and cost perspective. Using distributed ledgers to perform smart contracts simplifies multi-party supply chains, improving process efficiency. Because smart contracts execute themselves automatically, they can automatically execute "contractual rights and obligations, including payment and delivery terms" [42]. Reduced processing time and work are the results of reducing paperwork. Cost reduction is another way to enhance efficiency. As contractual agreements are executed using trusted computer code that can easily be customized, fewer physical documents need to be created and maintained by each party's purchasing, accounting, or legal departments. By eliminating physical records, a great deal of manual work can be reduced [43].

8. Process of Blockchain Implication in Agriculture

Consumer-to-provider solutions provide a database including an efficient structure as well as a public ledger that holds digital data about items, persons, and events that can be viewed or examined by a large number of people in the blockchain [44].

Using blockchain technology in supply chain management, we can overcome issues like the following:

(i) Overall management of the system.
(ii) System errors.
(iii) Product delay.
(iv) Transparency.
(v) Traceability.
(vi) Improving communication between all entities in the supply chain.
(vii) Increasing the trust between consumer and supplier.

Improvement in the supply chain is needed to tackle the changing and increasing demand of customers. Also, we can normalize the use of blockchain in the food supply chain to

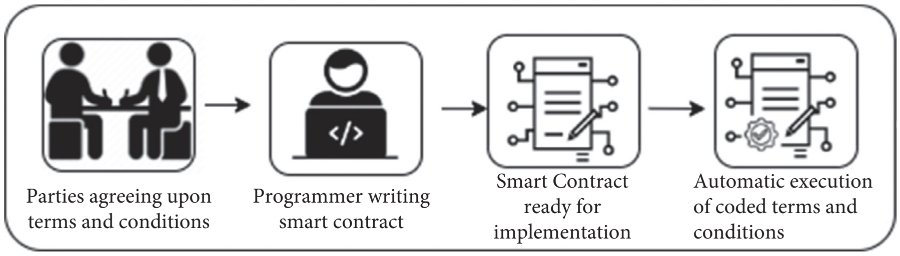

Figure 2: Smart contract building steps.

make a better marketing environment. The food product's data, such as its harvesting date and price, is uploaded by the supplier and then an RFID chip is embedded in the product as shown in Figure 3 [5]. These tags consist of an antenna and a microchip. Special printers are used to print identifying information on tags. The information on tags can be utilized for a variety of purposes. When RFID scanners scan a product, information from the tag is read, which might include essential information for preserving the item and managing the supply chain, such as the following:

(i) Components of product.
(ii) Product ID number.
(iii) Location history.
(iv) Order status.
(v) A serial number of an individual product.

Figure 3 illustrates how RFID receiver can be used to update and send this information and the data is not restricted to only containing serial numbers and ID. As the goods pass through warehouses and vehicles, the information provided by RFID will be linked to the system automatically tracking shipping and stock positions. By incorporating RFID into these systems, it is possible to verify the correct items and quality of products. Product information could be tracked throughout the whole shipping process and storage with the collaboration or IOT that increases accountability and accuracy. Supply chain networks fully utilizing RFID can detect the location of the goods, allowing theft and other unlawful actions to be found and punished instantly. After tagging by the supplier, the manufacturer gathers product information and adds a QR code to the package [41]. The product then moves towards the distributor, who is automatically notified of the arrival of food goods. Then, based on completely accessible data on customers, like delivery dates, and other user information, distributors select a suitable 3PL (Third Party Logistics) [45]. The origin and destination of food goods are then communicated to 3PL. It optimizes network flows flexibly. The product now transferred to the retailer uses machine intelligence to anticipate sales and also provides a mobile application to customers. The product is now ready for sale. Product information remains the same throughout the chain [17]. The store provides full transparency on delivery time. Each company now scans the RFID at each step of the manufacturing process and updates the information on the blocks in the cloud using a mobile app [6]. As a result, the cloud plays an important role in storing blocks. The app or website is used for verification, validation, and transactions, among other things [12]. A communication plat-form is provided through a website and a mobile app. When the genesis block is formed, the information is saved in it, and the very first transaction is carried out, and the blockchain technology begins to operate. Customers may access product data such as origin, aging, duration, and expiry by scanning the QR code using an app.

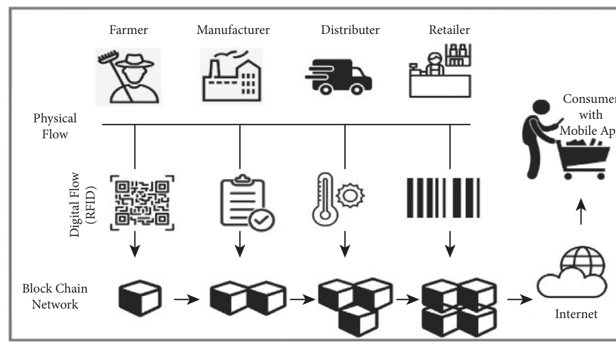

Figure 3: Traditional food supply chain.

9. Blockchain-Based Proposed Model for Agriculture Supply Chain Using Smart Contracts

In this paper, a new model for tracking and traceability is presented. Block chain smart contract is involved in this proposed model to coordinate traceability of food in the agriculture supply chain. The implementation of this model improves the traditional blockchain-based supply chain. There are 4 layers in this model. In the first layer, the producer agent manages all the operations that come in their domain like buying materials and selling products. The next layer deals with processor agents who process the products like sorting, packaging, and processing. In the transport layer, all the tasks regarding transport between whole supply chains are managed by transport agents. In the next layer, the retailer agent purchases a product from the processor agent and sells it further to customers. All the entities in the whole supply chain are interconnected in a decentralized blockchain with a smart contract. And every transaction in the whole system can be traced through blockchain network. Everyone in the whole supply chain can trace the product as portrayed in Figure 4.

A consumer can check the origin and processing of the product. This new supply chain model enables the agricultural industry to gigantically grow [24]. The use of blockchain enables the consumer to trace all the products from origin to delivery. The main benefit of this model is the confidence of the final consumer that will increase the sales a lot. Figure 5 shows the sequence diagram for the proposed model.

10. Outcomes of the Proposed Model

After having examined enough literature survey and experiments from numerous researchers, we proposed our conceptual model that has components that are being used in the manual/current agri-food supply chain processes and the other which would be a blockchain-based model. We have constructed a detailed Table 3 that explains the possible outcomes of the blockchain-based system and how this system can ensure transparency, traceability, security, and immutability in the entire agri-food supply chain process.

11. System Flow Analysis

Consider the supply of rice from the farmer to the consumer. The farmer first purchases seeds from seeds suppliers. The seeds are grown on the farmer's farm. After harvesting the crops, he uploads the detail document to the network, which contains information about the seeds, the seed suppliers, and the crops. The blockchain will record the transactions relating to this document. After reviewing all the details of a farmer's seeds and crops, the rice processor can place a purchase order directly with him. Unprocessed rice is sent to the processor with a document containing details about the processing. After the processor receives the order, the distributor oversees the contract. The distributor then inspects the retailer's buy order. Upon completion, the distributor ships the orders to the retailer [46]. A document with the shipment information is uploaded by the distributor. Upon receiving the rice from the distributor, retailers sell it to consumers. All information about the rice, from its starting date to its end process, can be viewed by the customer. Smart contracts permit communication between two entities. Proof of authority is established using a consensus mechanism in this model. The consensus determines which nodes are permitted to validate transactions. For example, an entity sending the data to the validator node for validation will be notified by the validator node [43]. A notification will be sent to the validator node once the transaction is complete. A transaction is approved by them if it is deemed legitimate. When a validator finds that a transaction is not authentic, it can be declined. The information flow of whole system is presented in Figure 6.

Apart from that, the diagram of the entity relationships is depicted in Figure 7. These depictions are for the reference of our system's work flow and events occurring at any stage of the whole process.

12. Contribution

In this paper, we have proposed a permissioned blockchain model that is essentially validated with the Ethereum blockchain. The blockchain supply chain model is full

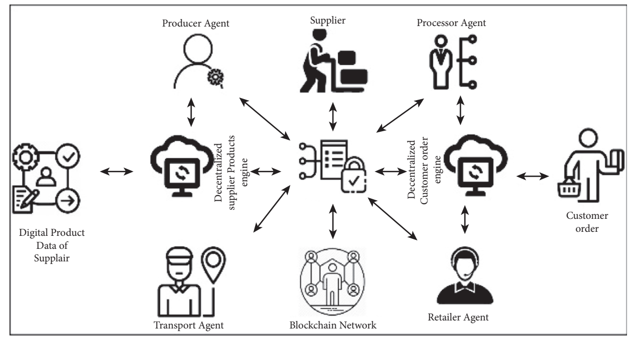

Figure 4: Decentralized smart contract-based supply chain.

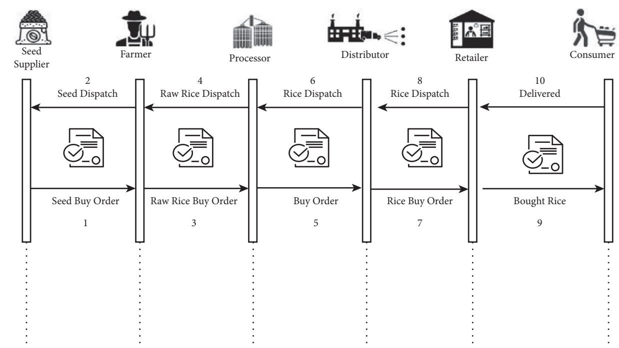

Figure 5: Sequence diagram of food supply chain.

decentralized model, in which we have introduced certain concepts that are vital for the effective process of supply chain using novel technologies like blockchain.

13. Validation of the Model by Ethereum Blockchain Smart Contact

Although we have studied and researched theoretical aspects of using smart contracts, still we are giving a testing and validation of the proposed model. Validation can also be performed by having an experiment with those stake holders who are currently using these systems. But here we are going to have some smart-contract-based technical validations. In order to give some sort of validation for our proposed model, we have used Ethereum blockchain and wrote a simple smart contract which has shown the possibility of using blockchain technology and its relevant tools for the innovation of the current agri-food supply chain process; our validation helps to identify the potential of blockchain technology. Below are a few shots of the smart contract and how that smart contact got compiled. Figure 8 shows the first part of our smart contract that we wrote for the validation of our proposed model.

Figure 9 depicts the smart contract for the proposed activity of supply chain process of agri-food process.

Figure 10 is again a representation the functions declarations and their calls for the specified events.

Figure 11 is for the reports that would be the ultimate source of transparency and through which we can have a detailed track of our supply chain procedure. Figure 12 is the last part of our smart contract.

Table 3: Outcomes of the proposed blockchain-based agri-food supply chain system.

Attributes	BC-based proposed system	Traditional method
Immutability	The information in a transaction cannot be changed even by the admin	Information can be easily manipulated by the admin
Consensus	Stakeholder agreement is taken into account	No consensus available
Provenance	Transaction histories are available	No history, no information record
Structure	Fully decentralized	Centralized
Trust	Increasing trust in a collaborative environment	Centralized approaches impose trust issues
Storage	Distributed storage	Centralized

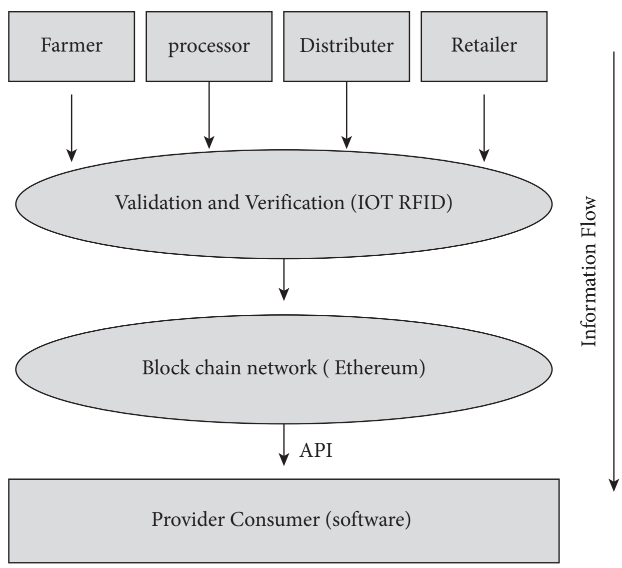

Figure 6: Information flow throughout the system.

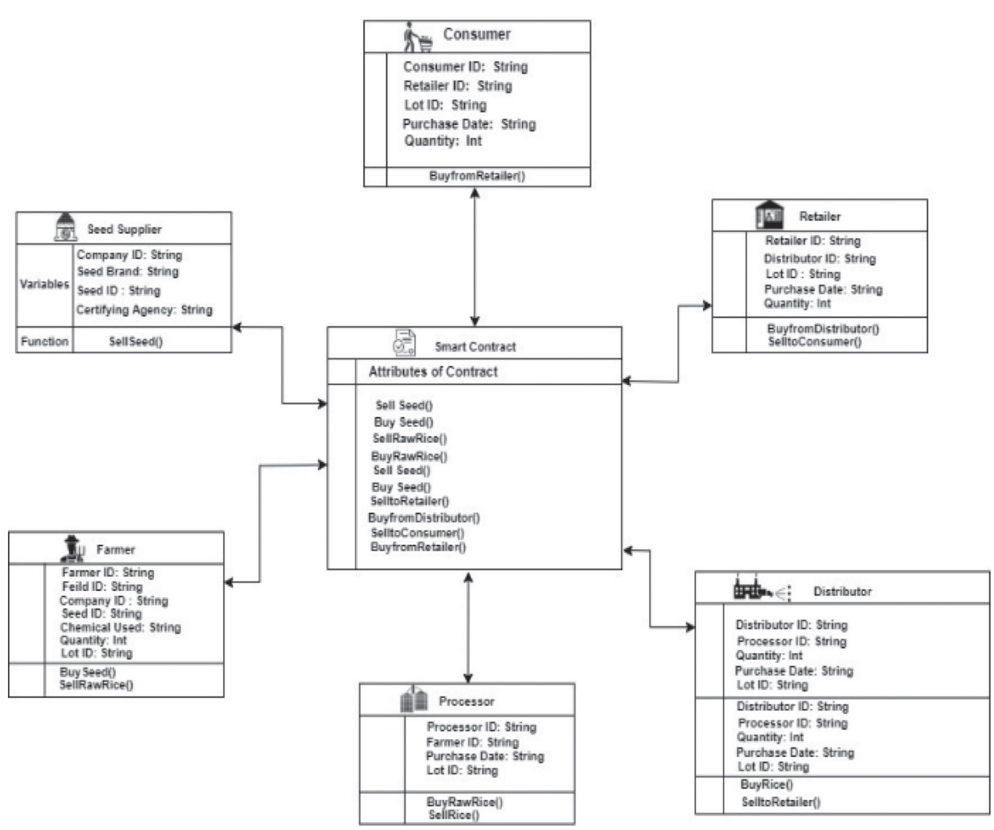

Figure 7: Entity relationship diagram of proposed model.

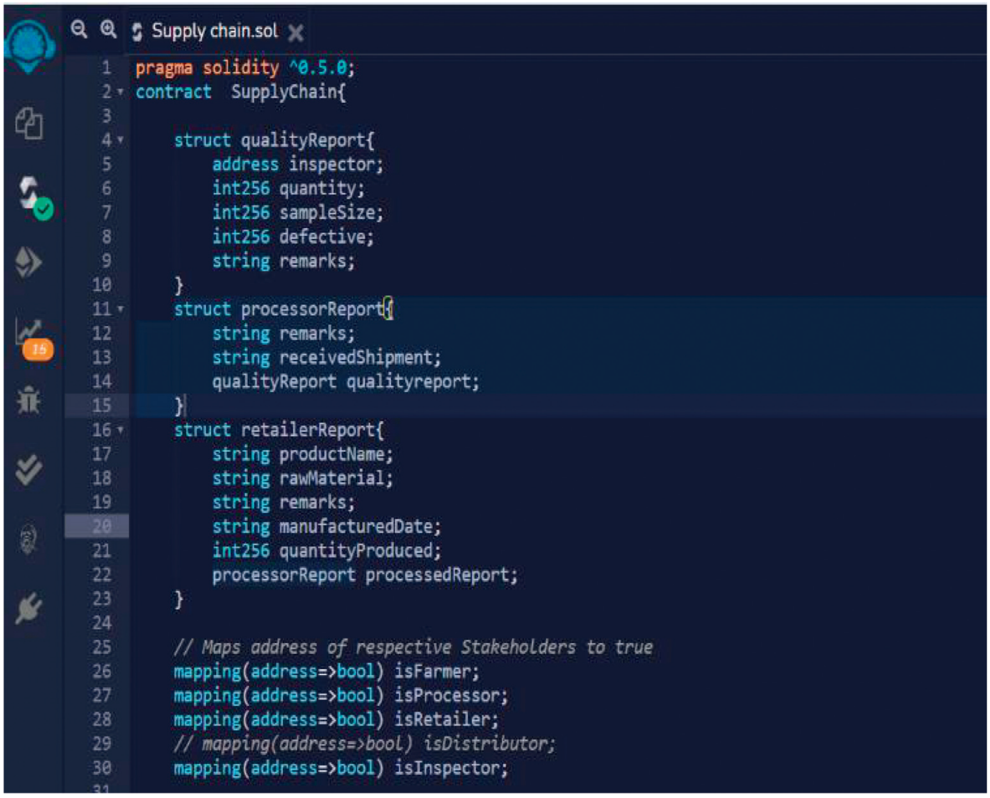

Figure 8: Part 1 of the smart contract.

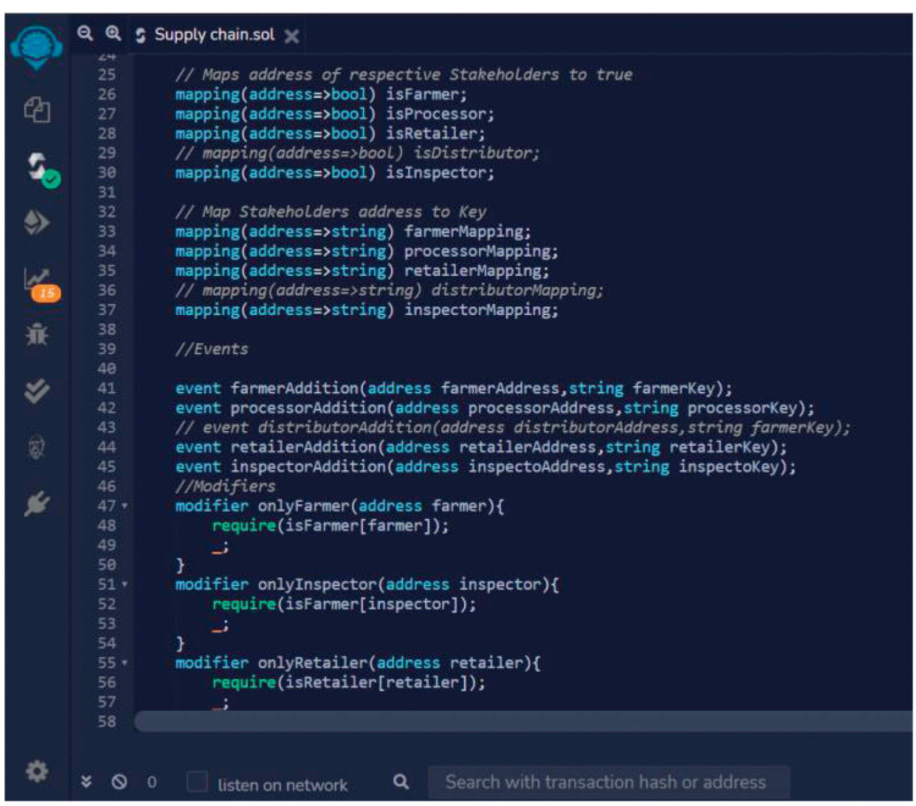

Figure 9: Part 2 of the smart contract.

```
// modifier onlyDistributor(address distributor){
//     require(isDistributor[distributor]);
//     _;
// }
mapping(address=>mapping(string=>qualityReport)) qualityReports; // mapping of farmers address to lotNumber and report
mapping(address=>mapping(address => mapping(string=>processorReport))) processorReports;
mapping(string => string) lotToBatch;
mapping(address=>mapping(string=>retailerReport)) retailerReports;

function addFarmer(address _farmer,string memory _farmerKey) public {
    isFarmer[_farmer] = true;
    farmerMapping[_farmer] = _farmerKey;
    emit farmerAddition(_farmer,_farmerKey);
}
function addProcessor(address _processor,string memory _processorKey) public {
    isProcessor[_processor] = true;
    processorMapping[_processor] = _processorKey;
    emit processorAddition(_processor,_processorKey);
}
```

Figure 10: Part 3 of the smart contract.

```
function getProcessorReport(address _processor,address _farmer,string memory _lotNumber) public view returns(
    string memory _remarks,
    string memory _receivedShipment
    ){
    _remarks = processorReports[_processor][_farmer][_lotNumber].remarks;
    _receivedShipment = processorReports[_processor][_farmer][_lotNumber].receivedShipment;
}
function BatchtoLot(string memory _batchNumber,string memory _lotNumber) public{
    lotToBatch[_batchNumber] = _lotNumber;
}
function addRetailerReport(address _retailer, address _processor, address _farmer,
    string memory _remarks,
    string memory _rawMaterial,
    string memory _productName,
    string memory _manufacturedDate,
    int256 _quantity,
    string memory _batchNumber
) public {
    retailerReports[_retailer][_batchNumber].productName = _productName;
    retailerReports[_retailer][_batchNumber].remarks = _remarks;
    retailerReports[_retailer][_batchNumber].rawMaterial = _rawMaterial;
    retailerReports[_retailer][_batchNumber].manufacturedDate = _manufacturedDate;
    retailerReports[_retailer][_batchNumber].quantityProduced = _quantity;
    retailerReports[_retailer][_batchNumber].processedReport = processorReports[_processor][_farmer][lotToBatch[_batchNumber]];
}
```

Figure 11: Part 4 of the smart contract.

```
function addInspector(address _inspector,string memory _inspectorKey) public {
    isInspector[_inspector] = true;
    inspectorMapping[_inspector] = _inspectorKey;
    emit inspectorAddition(_inspector,_inspectorKey);
}
function addRetailer(address _retailer,string memory _retailerKey) public {
    isRetailer[_retailer] = true;
    retailerMapping[_retailer] = _retailerKey;
    emit retailerAddition(_retailer,_retailerKey);
}
function addQualityReport(address _farmer,address _inspector,string memory _lotNumber,string memory _remarks,int256 _sampleSize,int256
    qualityReports[_farmer][_lotNumber].inspector = _inspector;
    qualityReports[_farmer][_lotNumber].remarks = _remarks;
    qualityReports[_farmer][_lotNumber].sampleSize = _sampleSize;
    qualityReports[_farmer][_lotNumber].defective = _defective;
    qualityReports[_farmer][_lotNumber].quantity = _quantity;
}
function getQualityReport(address _farmer,string memory _lotNumber) public view returns(
    string memory _remarks,
    address _inspector,
    int256 _sampleSize,
    int256 _defective,
    int256 _quantity
    ){
```

Figure 12: Part 5 of the smart contract.

While checking the issues in the deployed smart contract, we have then complied it with the available Ethereum test network and this can be seen in Figure 13.

Figure 14 shows the real-time working mechanism of the deployed smart contract where all the defined instances of the smart contracts are being called and executed.

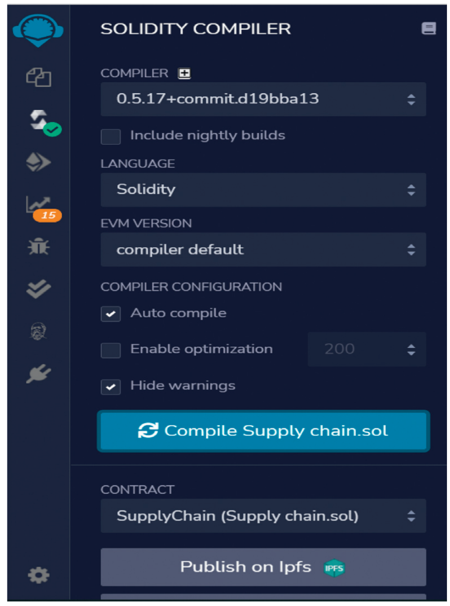

Figure 13: Part 6 of the smart contract.

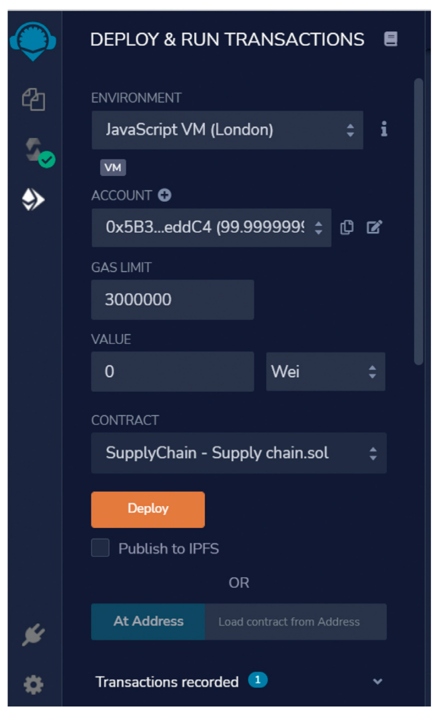

Figure 14: Part 7 of the smart contract.

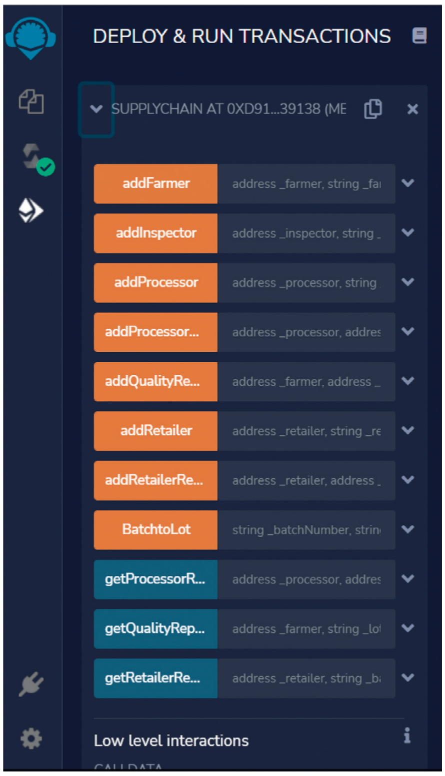

Figure 15: Part 8 of the smart contract.

The last part of the validation section is Figure 15; this part shows all the sections, i.e., the components of the assumed blockchain-based agri-food supply chain system, and how this can be tested with the help of Ethereum test networks.

14. Conclusion and Future Work

Researchers are trying hard to develop such systems that can bring innovation in the current scenarios. Blockchain technology is one of the developing and emerging technologies nowadays as this technology is disrupting every field and also it can make a lot of revolutionary changes in the agriculture field by improving the supply chain and ensuring the integrity, security, and traceability of data. It has the potential to improve the country's economic situation by lowering corruption and improving producer and customer satisfaction. Blockchain establishes an efficient and transparent system by eliminating the middleman in supply chain management. In this paper, we introduce an advanced blockchain approach to enhance the traditional supply chain. For managing the whole supply chain efficiently, we use a multi-agent system with smart contracts because they eliminate intermediaries, allowing the circular economy market to thrive. Our methodology is automated; it can be used to optimize any supply chain, resulting in increased security and efficiency. Utilizing blockchain technology, we give robust security characteristics to the agriculture system. Origin of product can be verified, shipment of product can be monitored, and proof of all transactions can be saved with this model. Agents who verify that both parties are following the terms and conditions of smart contact are another novelty of this study. Fine or penalties are imposed if the agent detects that a participant does not fulfill the conditions. This makes our models more reliable and efficient compared to other models; furthermore it can also track and authenticate orders. Apart from that, we have developed a smart contract in solidity using Ethereum blockchain to validate our model. Researchers can test this kind of proof of concepts as well as model using hyper ledger fabric composer or multi-chain tools that are exclusively designed to work with the permissioned blockchain where all the entities are known. The article addresses two main research questions. We first examine some of the most important issues of the traditional supply chain ecosystem, and then we explore how blockchain technology can be used to resolve these issues. This was done by looking at published research articles in the field. Our second question required an analysis of the benefits of integrating blockchain technology with supply chains. In conjunction with Ethereum's blockchain and the proof of authority consensus algorithm, an interplanetary file system is used. In smart contracts, payments can be processed directly and without intermediaries, which improves performance. An overview of the proposed smart contract model is presented in this paper, together with entity-relationship diagrams, sequence diagrams, and practical implementations. With the immutable nature of block chain technology, trust, transparency, and security can be enhanced within the supply chain. It is possible to adapt this model to a wide variety of supply chains in various domains.

Data Availability

The data used to support the findings of this study are available from the corresponding author upon request.

Conflicts of Interest

The authors declare no conflicts of interest.

Acknowledgments

This research was supported by the Researchers Supporting Project Number (RSP2022R476), King Saud University, Riyadh, Saudi Arabia.

References

[1] S. Umamaheswari, S. Sreeram, N. Kritika, and D. R. Jyothi Prasanth, "BIoT: blockchain based IoT for agriculture," in *Proceedings of the 2019 11th International Conference on Advanced Computing (ICoAC)*, pp. 324–327, IEEE, Chennai, India, 18 December 2019.

[2] J. Xu, S. Guo, D. Xie, and Y. Yan, "Blockchain: a new safeguard for agri-foods," *Artificial Intelligence in Agriculture*, vol. 4, pp. 153–161, 2020.

[3] J. Duan, C. Zhang, Y. Gong, S. Brown, and Z. Li, "A content-analysis based literature review in blockchain adoption within food supply chain," *International Journal of Environmental Research and Public Health*, vol. 17, no. 5, p. 1784, 2020.

[4] G. Mirabelli and V. Solina, "Blockchain and agricultural supply chains traceability: research trends and future challenges," *Procedia Manufacturing*, vol. 42, pp. 414–421, 2019.

[5] S. F. Wamba and M. M. Queiroz, "Blockchain in the operations and supply chain management: benefits, challenges and future research opportunities," *International Journal of Information Management*, vol. 52, no. xxxx, Article ID 102064, 2020.

[6] M. D. Borah, V. B. Naik, R. Patgiri, A. Bhargav, B. Phukan, and S. G. M. Basani, *Supply Chain Management in Agriculture Using Blockchain and IoT*, Springer, Singapore, 2020.

[7] P. Dutta, T.-M. Choi, S. Somani, and R. Butala, "Blockchain technology in supply chain operations: applications, challenges and research opportunities," *Transportation Research Part E: Logistics and Transportation Review*, July, vol. 142, , p. 102067, 2020.

[8] O. Bermeo-Almeida, M. Cardenas-Rodriguez, T. Samaniego-Cobo, E. Ferruzola-Gómez, R. Cabezas-Cabezas, and W. Bazán-Vera, "Blockchain in agriculture: a systematic literature review," *Communications in Computer and Information Science*, vol. 883, pp. 44–56, 2018.

[9] M. Torky and A. E. Hassanein, "Integrating blockchain and the internet of things in precision agriculture: analysis, opportunities, and challenges," *Computers and Electronics in Agriculture*, vol. 178, no. April, p. 105476, 2020.

[10] K. Salah, N. Nizamuddin, R. Jayaraman, and M. Omar, "Blockchain-based soybean traceability in agricultural supply chain," *IEEE Access*, vol. 7, no. c, pp. 73295–73305, 2019.

[11] A. Vangala, A. K. Das, N. Kumar, and M. Alazab, "Smart secure sensing for IoT-based agriculture: blockchain perspective," *IEEE Sensors Journal*, vol. 21, no. 16, pp. 17591–17607, 2021.

[12] A. Shahid, A. Almogren, N. Javaid, F. A. Al-Zahrani, M. Zuair, and M. Alam, "Blockchain-based agri-food supply chain: a complete solution," *IEEE Access*, vol. 8, pp. 69230–69243, 2020.

[13] S. Madumidha, P. S. Ranjani, U. Vandhana, and B. Venmuhilan, "A theoretical implementation: agriculture-food supply chain management using blockchain technology," in *Proceedings of the 2019 TEQIP III Sponsored International Conference on Microwave Integrated Circuits, Photonics and Wireless Networks (IMICPW)*, pp. 174–178, IEEE, Tiruchirappalli, India, 22 May 2019.

[14] M. A. Ferrag, L. Shu, X. Yang, A. Derhab, and L. Maglaras, "Security and privacy for green IoT-based agriculture: review, blockchain solutions, and challenges," *IEEE Access*, vol. 8, pp. 32031–32053, 2020.

[15] V. S. Yadav and A. R. Singh, "A systematic literature review of blockchain technology in agriculture," in *Proceedings of the Int. Conf. Ind. Eng. Oper. Manag.*, pp. 973–981, 2019.

[16] H. Kim and M. Laskowski, *Sustainable Solutions for Food , Farmers , and Financing*Blockchain Res. Inst., Canada, 2018, https://ssrn.com/abstract=3028164.

[17] J. Lin, A. Zhang, Z. Shen, and Y. Chai, "Blockchain and IoT based food traceability for smart agriculture," in *Proceedings of the ACM Int. Conf. Proceeding Ser.*, pp. 1–6, ACM, Singapore, 28 July 2018.

[18] M. Creydt and M. Fischer, "Blockchain and more - algorithm driven food traceability," *Food Control*, vol. 105, pp. 45–51, 2019.

[19] S. H. Awan, S. Ahmed, A. Nawaz et al., "BlockChain with IoT, an emergent routing scheme for smart agriculture," *International Journal of Advanced Computer Science and Applications*, vol. 11, no. 4, pp. 420–429, 2020.

[20] G. Zhao, S. Liu, C. Lopez et al., "Blockchain technology in agri-food value chain management: a synthesis of applications, challenges and future research directions," *Computers in Industry*, vol. 109, pp. 83–99, 2019.

[21] M. H. Ronaghi, "A blockchain maturity model in agricultural supply chain," *Information Processing in Agriculture*, vol. 8, no. 3, pp. 398–408, 2021.

[22] A. Kamilaris, A. Fonts, and F. X. Prenafeta-BoldÚ, "The rise of blockchain technology in agriculture and food supply chains," *Trends in Food Science & Technology*, vol. 91, pp. 640–652, 2019.

[23] F. Feng Tian, "A supply chain traceability system for food safety based on HACCP, blockchain & Internet of things," in *Proceedings of the 2017 International Conference on Service Systems and Service Management*, 16-18 June 2017.

[24] M. P. Caro, M. S. Ali, M. Vecchio, and R. Giaffreda, "Blockchain-based traceability in Agri-Food supply chain management: a practical implementation," in *Proceedings of the 2018 IoT Vertical and Topical Summit on Agriculture - Tuscany (IOT Tuscany)*, pp. 1–4, IEEE, Tuscany, Italy, 8 May 2018.

[25] M. Kim, B. Hilton, Z. Burks, and J. Reyes, "Integrating blockchain, smart contract-tokens, and IoT to design a food traceability solution," in *Proceedings of the 2018 IEEE 9th Annual Information Technology, Electronics and Mobile Communication Conference (IEMCON)*, vol. 1, pp. 335–340, Vancouver, BC, Canada, 1 November 2018.

[26] M. Shyamala Devi, R. Suguna, A. S. Joshi, and R. A. Bagate, *Design of IoT Blockchain Based Smart Agriculture for Enlightening Safety and Security*, Vol. 985, Springer, , Singapore, 2019.

[27] S. S. Kamble, A. Gunasekaran, and R. Sharma, "Modeling the blockchain enabled traceability in agriculture supply chain," *International Journal of Information Management*, vol. 52, pp. 101967–102016, November 2020.

[28] D. Bumblauskas, A. Mann, B. Dugan, and J. Rittmer, "A blockchain use case in food distribution: do you know where your food has been?" *International Journal of Information Management*, vol. 52, no. September, pp. 102008–102010, 2020.

[29] L. Hang, I. Ullah, and D.-H. Kim, "A secure fish farm platform based on blockchain for agriculture data integrity," *Computers and Electronics in Agriculture*, vol. 170, Article ID 105251, 2020.

[30] K. Demestichas, N. Peppes, T. Alexakis, and E. Adamopoulou, "Blockchain in Agriculture Traceability Systems: a Review Featured Application: the paper elaborates on the applicability of blockchain technology in traceability systems of agri-food products," *Applied Sciences*, vol. 10, 2020, http://www.mdpi.com/journal/applsci.

[31] A. Scuderi, V. Foti, and G. Timpanaro, "The supply chain value of pod and pgi food products through the application of blockchain," *Qual. - Access to Success*, vol. 20, no. S2, pp. 580–587, 2019.

[32] S. V. Akram, P. K. Malik, R. Singh, G. Anita, and S. Tanwar, "Adoption of blockchain technology in various realms: opportunities and challenges," *Security and Privacy*, vol. 3, no. 5, pp. 1–17, 2020.

[33] P. W. Khan, Y.-C. Byun, and N. Park, "IoT-blockchain enabled optimized provenance system for food industry 4.0 using advanced deep learning," *Sensors*, vol. 20, no. 10, pp. 2990–3024, 2020.

[34] B. M. A. L. Basnayake and C. Rajapakse, "A Blockchain-based decentralized system to ensure the transparency of organic

food supply chain," in *Proceedings of the 2019 International Research Conference on Smart Computing and Systems Engineering (SCSE)*, pp. 103–107, IEEE, Colombo, Sri Lanka, 28 March 2019.

[35] V. S. Yadav and A. R. Singh, "Use of blockchain to solve select issues of Indian farmers," in *Proceedings of the 1St International Conference on Advances in Mechanical Engineering and Nanotechnology (Icamen 2019)*, vol. 2148, AIP, 3 September 2019.

[36] P. Patil, M. Sangeetha, and V. Bhaskar, "Blockchain for IoT access control, security and privacy: a review," no. 1815, , 2020.

[37] J. Taskinsoy, "Blockchain: an unorthodox solution to reduce global warming," *SSRN Electronic Journal*, pp. 1–14, 2019.

[38] U. Bodkhe, S. Tanwar, P. Bhattacharya, and N. Kumar, "Blockchain for precision irrigation: opportunities and challenges," *Transactions on Emerging Telecommunications Technologies*, pp. 1–30, 2020.

[39] V. S. Yadav, A. R. Singh, R. D. Raut, and U. H. Govindarajan, "Blockchain technology adoption barriers in the Indian agricultural supply chain: an integrated approach," *Resources, Conservation and Recycling*, vol. 161, no. April, Article ID 104877, 2020.

[40] R. Casado-Vara, J. Prieto, F. D. la Prieta, and J. M. Corchado, "How blockchain improves the supply chain: case study alimentary supply chain," *Procedia Computer Science*, vol. 134, pp. 393–398, 2018.

[41] F. Antonucci, S. Figorilli, C. Costa, F. Pallottino, L. Raso, and P. Menesatti, "A review on blockchain applications in the agri-food sector," *Journal of the Science of Food and Agriculture*, vol. 99, no. 14, pp. 6129–6138, 2019.

[42] G. Rathee, M. Balasaraswathi, K. P. Chandran, S. D. Gupta, and C. S. Boopathi, "A secure IoT sensors communication in industry 4.0 using blockchain technology," *Journal of Ambient Intelligence and Humanized Computing*, vol. 12, no. 1, 545 pages, 2020.

[43] O. Alfandi, S. Khanji, L. Ahmad, and A. Khattak, "A survey on boosting IoT security and privacy throuagh blockchain Exploration , requirements , and open issues," *Cluster Computing*, vol. 24, no. 1, pp. 37–55, 2020.

[44] L. I. Frameworks, "PoAh: a novel consensus algorithm for fast scalable private blockchain for PoAh: a novel consensus algorithm for fast scalable private blockchain for large-scale IoT frameworks," 2020, https://arxiv.org/abs/2001.07297.

[45] S. Homayoun, A. Dehghantanha, R. M. Parizi, and K.-K. R. Choo, "A blockchain-based framework for detecting malicious mobile applications in app stores," in *Proceedings of the 2019 IEEE Canadian Conference of Electrical and Computer Engineering (CCECE)*, no. Ccece, 5 May 2019.

[46] R. Xu, S. Y. Nikouei, D. Nagothu, A. Fitwi, and Y. Chen, "BlendSPS: a BLockchain-ENabled decentralized smart public safety system," *Smart Cities*, vol. 3, no. 3, pp. 928–951, 2020.

Hindawi
Scientific Programming
Volume 2022, Article ID 6842388, 5 pages
https://doi.org/10.1155/2022/6842388

Research Article

Implementation of the Teaching of Economic Management Specialty in the Background of Internet+ Based on Smart Agent

Chao Zhang[1] and Xiaoyu Hang[2,3]

[1]*Economics and Business Management School, Tianjin Sino-German University of Applied Sciences, Tianjin 300350, China*
[2]*Department of Economics and Trade, Tianjin University of Commerce Boustead College, 300384 Tianjin, China*
[3]*School of Finance, Central University of Economics and Finance, 102206 Beijing, China*

Correspondence should be addressed to Xiaoyu Hang; xh21@caa.columbia.edu

Received 26 October 2021; Revised 11 November 2021; Accepted 20 December 2021; Published 27 February 2022

Academic Editor: Punit Gupta

Today is the age of information and networks. In the context of the Internet, our country's economy is growing rapidly. However, given the current state of economic governance, traditional courses and educational models can no longer be applied. It is necessary to combine the content of teaching materials, the needs of social development, and the current situation of students to carry out reforms and innovations to deepen and promote the overall development of basic education in our country. This article mainly introduces how to refer to literature surveys, analysis-level processes, and questionnaire survey. In this article, we will use Internet+ to study the application of specialized education in economic management and create possible mathematical models. The model is resolved through a process in the analysis hierarchy, the application and research status of economic management education is evaluated, and the accuracy of assessing the implementation status of economic management education is evaluated. Results show that the process of analytical hierarchy increased the effectiveness of conducting economic management education by 13% and reduced the rate of false positives. Finally, the system explains the impact of Internet+ on the implementation of economic management by comparing the analysis of problems existing in the education of economic management courses on the Internet with the analysis of the satisfaction level of practical education of economic management courses. The survey results show that the professional practice research of comprehensive professional training and compulsory professional courses needs improvement.

1. Introduction

Education is the foundation of national revitalization. To achieve sustainable development of our economy, we must strengthen the quality of education [1], encourage the abilities and skills of all students, increase their enthusiasm and motivation, and lay the foundation for the sound development of the national economy [2, 3]. Teaching an economic management course is very important in today's information society and knowledge economy [4]. From a scientific point of view, rationalization can only be achieved by understanding this knowledge and continuously developing the latest courses [5]. Combining student experience can improve science, for example, the development of professional talent, the innovation of science and technology, and the contribution to the economic development of the country [6, 7]. A large amount of data was collected in this study to evaluate the framework of this study. This case study demonstrates the importance of Internet+ for implementing economic management education and system implementation [8, 9]. However, the process of collecting messages is so complex that the results of the data are not very accurate. Based on research on the application of economic management training in the context of Internet+, educational applications for key parts of economic management are being studied via Internet+. A method has been established for calculating procedures in the analytical hierarchy combined with a bibliographic.

2. Implementation Research Methods of Economic Management Professional Teaching under the Background of Internet+

2.1. AHP. Mathematical methods are used to convert the relative importance of each index into weights and classify the various decision shapes to find the best decision shape. We then proceed to normalize the importance of each evaluation factor, that is, the range of functions required to classify weight values [10, 11]. The test uses the following formula:

$$Q_A = \gamma_{\max} A, \tag{1}$$

where $\gamma_{\max}$ is the largest feature root of Q_A and W is the normalized feature vector corresponding to $\gamma_{\max}$.

The randomization rate of the table is represented by EI. The general index of the evaluation table is represented by M.

$$\mathrm{EI} = \frac{(\gamma_{\max} - M)}{(M-1)}. \tag{2}$$

The basic principle of analytic hierarchy process is that analytic hierarchy process systematically absorbs research material and makes decisions based on variations, comparisons, evaluations, and complex thinking [12]. This method is especially useful for evaluating unstructured systems and for systems with multiple properties, multiple criteria, and time periods. Not only is this method suitable for high-level statistics but it also focuses on powerful, high-quality models for processing behaviors, thoughts, concepts, and complex systems to coordinate human thinking advancement. This method is combined with accepting and adjusting various practical, general, and difficult scenarios, which are difficult to compare with decisions on many issues at the same level. The calculations are easy, and the results found are easy for decision makers to understand.

2.2. Investigation and Research Method. This article conducts a comprehensive investigation, analysis, synthesis, comparison, and summary of the current situation and reasons for the formation of party member ideology and policies in the traditional and new media era. The large amount of data collected through the survey can improve the professional teaching of how to comprehensively construct and deeply understand business management in the Internet era.

3. Implementation Research Experiment of Economic Management Professional Teaching under the Background of Internet+

3.1. Experimental Design of Practical Teaching System for Economic Management Majors. Economics and management belong to the applied research disciplines of applied economics and management. Students should have basic knowledge and basic professional theories and be able to use the knowledge gained in practice to improve their practical ability. Therefore, how to enhance and improve the level of practical education of financial management graduates has become an important issue of current university development. In order to determine the system of professional financial management practice, the research team visited relevant companies and investigated employment trends.

In the questionnaire, the professional management system of professional management skills is divided into four levels: professional basic knowledge, professional operation skills, professional comprehensive training, and professional research skills. These four levels are progressive, so students can be trained at various levels. Through training, students establish a sound economic management professional knowledge system and gradually increase comprehensive professional skill and will eventually develop into excellent economic management professionals.

3.2. Experimental Data Collection of Practical Teaching System for Economic Management Majors. For effective performance analysis, this article studies positions in commercial banks, securities companies, companies, and manufacturing and processing companies. Through seminars and other methods, 200 undergraduates and students in the field of economic management were organized. After this study identified the skills students need to stay in the workplace, we opened courses to improve the knowledge of each skill. After analyzing the results, it is said that the useful research results obtained are comparable to the results of interviews with economic and administrative leaders. The data results are shown in Table 1.

It can be seen from Table 1 that the average scores of professional basic knowledge, professional operating skills, professional comprehensive training, and professional research and practice before graduation are 10, 9, 6, and 5 points higher than the exam results after graduation, which shows that the four aspects of professional basic knowledge, professional operating skills, professional comprehensive training, professional research and practice are of great significance to economic management. Professional students are very important. For students majoring in economics and management after graduation, it reflects that basic professional knowledge, professional operating skills, professional comprehensive training, professional research and practice are indispensable skills among many skills. To help the readers better understand the three relationships, the results are shown in Figure 1.

It can be seen from Figure 1 that the four majors necessary for economic management students are professional basic knowledge, professional operating skills, professional comprehensive training, and professional research practice. Before and after graduation, students' cognition of these four skills has changed from shallow to deep, which shows that the implementation of the teaching of economics and management majors needs to improve students' ability to have the skills necessary for the major deep knowledge.

Table 1: Statistics on the ability of economic management students.

Grading	Professional basic knowledge/point	Professional operation skills/point	Professional comprehensive training/point	Professional research practice/point
Test average score before graduation	78	88	79	86
Test standard deviation before graduation (X0.01)	25	32	14	24
Test average score after graduation	88	97	85	91
Test standard deviation after graduation (X0.01)	12	31	12	20

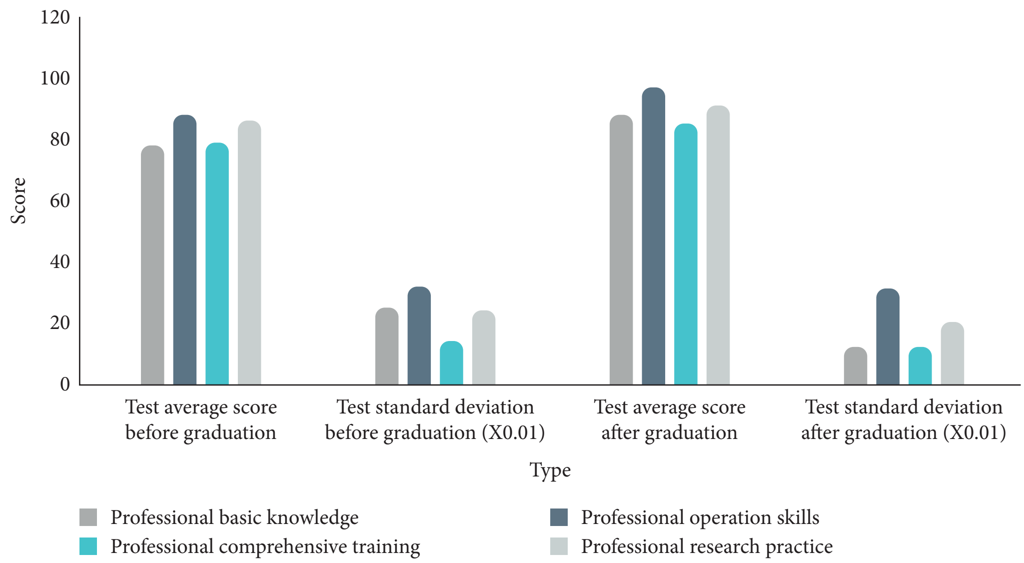

Figure 1: Statistics chart of ability data of economic management majors.

4. Implementation of Economic Management Teaching under the Background of Internet+

4.1. Problems Existing in the Teaching of Economics and Management Courses under the Background of the Internet. Under the influence of traditional thinking, the mentality of most teachers has not changed, and insight cannot be stimulated in this learning process. Direct teaching improves the quality of economic management skills training. In addition, in the curriculum, the teacher-centered way of thinking needs to be changed. Keeping an open mind should be a key part of the classroom so that they can actively participate in learning and use their theme initiatives and creativity to maximize the impact of classroom learning. At the same time, economics and management need to combine theory with practice, while the lack of economic research talents requires more in-depth improvement and innovation.

4.2. Satisfaction Analysis of Economic Management Courses Teaching Practice Arrangement. Courses analyzed include basic knowledge of business and management-students, business, accounting management, marketing, human resource management, operational skills, professional training in business management, business management and school environment, network marketing, e-commerce economic management, property evaluation, international regulations, and other practical training. management; property evaluation; international regulations and other practical training. Through management types, sales management, project management, and business consulting courses, we teach students risk management and management skills and renew outdated business skills. Through the financial field training experience and manual operation enabled by the advanced educational financial sand table platform, the students can practice management skills of managing enterprises.

So far, this article has evaluated the satisfaction of education provided in economic management courses, the satisfaction of extensive training, and the satisfaction of practical research. The data results are shown in Table 2.

From Table 2 ,in response to the question “Are you satisfied with the order of the official’s practical courses?”, 65% of the students believe that full-time job training is the objective of the required courses, while 75% of the students believe that the selected courses are not according to the intermediate training activities. Only 2% of students are dissatisfied with the vocational practice of learning required vocational courses, while the remaining 21.33% of students think it is appropriate and satisfactory. In other words, in the teaching system of practical courses, the number of satisfied students has not yet reached half of the total number of students surveyed. The analysis is shown in Figure 2.

Table 2: Data of satisfaction with the arrangement of practical teaching courses for this major.

Course setting and implementation	General compulsory course (%)	General elective course (%)	Major required courses (%)	Professional elective (%)
Professional comprehensive training satisfaction	65	75	78	73
Professional practice research satisfaction	78	88	65	81
Course schedule satisfaction	86	95	83	72

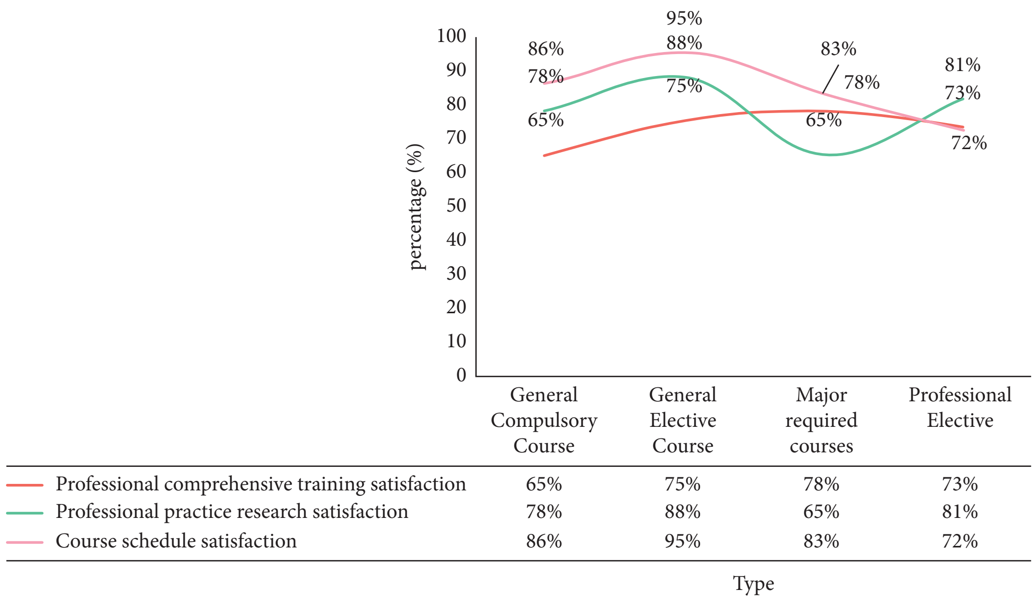

Figure 2: Data graph of satisfaction with the arrangement of practical teaching courses for this major.

From Figure 2, it can be seen that the professional comprehensive training satisfaction of general compulsory courses, the professional comprehensive training satisfaction of general elective courses, the satisfaction with the professional practice research of the compulsory professional courses, and the curriculum arrangement of the professional elective courses are the lowest. From then on, it can be seen that the economic management course teaching practice curriculum is set and implemented in the professional comprehensive training of the general compulsory courses and the general elective courses. The professional practice research of comprehensive professional training and compulsory professional courses needs improvement.

5. Conclusions

In this article, we did some research on bibliographic reference research methods, analytical hierarchical procedures, and research methods, but they still have many drawbacks. There are also many comprehensive results and research methods on the implementation of financial education and management on the Internet. Therefore, we can learn from existing methods when studying financial education and management. The system explains the impact of the Internet+ on the implementation of economic management by comparing the analysis of problems existing in the education of economic management courses on the Internet with the analysis of the satisfaction level of practical education of economic management courses. The survey results show that the professional practice research of comprehensive professional training and compulsory professional courses needs improvement.

Data Availability

No data were used to support this study.

Conflicts of Interest

The authors declare that they have no potential conflicts of interest with respect to the research, authorship, and/or publication of this article.

Acknowledgments

This study was supported in part by Tianjin Technical Expert Project (19JCTPJC44000), Tianjin Municipal Education Commission 2019 Scientific Research Project (2019SK123), and Tianjin Municipal Education Commission 2020 Scientific Research Project (2020SK142).

References

[1] N. Bilan, "The research of the motivation sphere of future electric power engineers to study foreign language," *Professional Education: Methodology, Theory and Technologies*, vol. 10, no. 10, pp. 9–24, 2019.

[2] L. Yaroshevska, "Civic education of youth by means of musical art by V. Sukhomlinsky," *Scientific Visnyk V.O. Sukhomlynskyi Mykolaiv National University. Pedagogical Sciences*, vol. 65, no. 2, pp. 373–377, 2019.

[3] O. S. Pankrateva, Y. V. Yurova, P. K. Krylov, E. V. Zinoviev, D. O. Vagner, and L. M. Likhonos, "Errors in differential diagnosis of burn injury at the prehospital stage," *Russian Sklifosovsky Journal "Emergency Medical Care"*, vol. 9, no. 4, pp. 659–665, 2021.

[4] S. Sarvepalli, D. Kumar, M. Lie et al., "S1235 pilot implementation of video telehealth for gastrointestinal sub-specialty care to veterans during the COVID-19 pandemic," *American Journal of Gastroenterology*, vol. 115, no. 1, Article ID S620, 2020.

[5] A. Tsyrulnik, K. Goldflam, R. Coughlin et al., "Implementation of a physician assistant emergency medicine residency within a physician residency," *Western Journal of Emergency Medicine*, vol. 22, no. 1, pp. 45–48, 2020.

[6] S. A. Rehman Khan, Y. Zhang, M. Anees, H. Golpîra, A. Lahmar, and D. Qianli, "Green supply chain management, economic growth and environment: a GMM based evidence," *Journal of Cleaner Production*, vol. 185, no. 1, pp. 588–599, 2018.

[7] W. Wu and C. Huang, "Research on the CAD/CAM technology teaching of the mechanical specialty of applied undergraduate university in the background of intelligent manufacturing," *Science and Education*, vol. 417, no. 3, pp. 50–52, 2018.

[8] O. Pylypenko and O. A. Yurchenko, "Improving the professional education of accountants for the effective operation of the economic security system at company level," *Statistics of Ukraine*, vol. 89, no. 2-3, pp. 148–154, 2020.

[9] Q. Wu and F. Yin, "Research on the construction of practical teaching system—a case study of management specialty in application-oriented university," *Journal of Changchun Institute of Technology (Social Science Edition)*, vol. 17, no. 3, pp. 128–131, 2016.

[10] L. Ivanova and E. Lukomskaya, "On the implementation of the communicative approach in foreign language teaching of students in non-linguistic universities," *Scientific Research and Development Modern Communication Studies*, vol. 9, no. 1, pp. 47–52, 2020.

[11] L. Song, "On the implementation of experience teaching in "The Outline of Modern History of China"," *Science and Education*, vol. 369, no. 11, pp. 26–28, 2016.

[12] B. Behforouz and A. D. Frumuselu, "The reflection of vocabulary implementation through educational texting on EFL learner's reading skill," *International Journal of Interactive Mobile Technologies (IJIM)*, vol. 15, no. 1, Article ID 88, 2021.

Hindawi
Scientific Programming
Volume 2022, Article ID 4905190, 5 pages
https://doi.org/10.1155/2022/4905190

Research Article

Network Clustering Algorithm Based on Fast Detection of Central Node

Ziruo Jia [1] and Fuqiang Qi [2]

[1] *China-France Joint Research Center of Applied Mathematics for Air Traffic Management, School of Economics and Management, Civil Aviation University of China, Tianjin, China*
[2] *School of Economics and Management, Civil Aviation University of China, Tianjin, China*

Correspondence should be addressed to Ziruo Jia; zrjia@cauca.edu.cn

Received 25 December 2021; Revised 31 December 2021; Accepted 11 January 2022; Published 25 February 2022

Academic Editor: Punit Gupta

Based on scale-free and density-based complex networks and numerical clustering algorithm, a graph clustering algorithm based on fast detection of central nodes is proposed. Through the calculation of local density and comprehensive clustering of nodes in the network, the clustering center in the network can be found quickly and noncentral nodes can be divided into the clustering center according to the nearest neighbor principle, thus avoiding parameter limitations such as the number of clustering to be set in advance using conventional classic social network detection algorithm. The experimental comparison and analysis in the real network indicate that the graph clustering algorithm based on fast detection of the central node is highly effective and efficient.

1. Introduction

The detection of social structure is vitally important to understand topology structure and the interaction between nodes in the network. With the development of application of graph clustering algorithm in different scientific fields, researchers have attached great importance to graph clustering algorithm and conducted researches and improvements. In recent years, graph clustering algorithm has been extensively used as the module maximization and spectral clustering algorithm. Module maximization transforms graph clustering into a problem of realizing module maximization and spectral clustering algorithm applies spectrum analysis technology in graph theory to graph clustering, thereby minimizing cutting. Furthermore, agglomeration algorithm and splitting algorithm as two common hierarchical clustering techniques [1, 2] have their respective advantages, which both require prior information such as network clustering number under great constraints. Although density clustering algorithm is not restricted by the condition to test the clustering of any shape, the general density clustering algorithm is only used for numerical clustering, not for network clustering [3–6].

Density-based clustering algorithm is the crucial direction of clustering analysis. The classic density-based clustering algorithm is DBSCAN algorithm, which divides high-density areas into multiple clusters. Although it can find clusters of arbitrary shapes in spatial data with noise, it cannot reflect changes in high-dimensional data and data density [7]. Therefore, researchers improved the algorithm and proposed OPTCIS algorithm, which can be used for multidimensional spatial data clustering. The current algorithm improvements are based on DBSCAN and OPTICS. In recent years, the CFSDP based on density clustering algorithm proposed by Alex et al. is popular with the main idea of adhering to the following two principles in the selection of clustering center: firstly, the density of the clustering center itself is greater than the density of adjacent points; secondly, the distance between the clustering center and other clustering center is relatively long. Based on CFSDP algorithm in combination with scale free of complex networks, the clustering algorithm for fast detection of central nodes proposed in this paper has the advantages of high efficiency of density-based numerical clustering algorithm and no need to set clustering quantitative parameters in advance [8].

2. Methodology

2.1. Density-Based Clustering Algorithm. Density-based cluster is a dense region separated by sparse regions in the data space, and the density in any cluster is higher than that in other noisy regions. Each core point requires for no fewer than MinPts points adjacent to radius Eps, that is, the density of the neighborhood must exceed a certain threshold. Let D be the data space containing all data points, and density-based cluster definition assumes that the distance function of a pair of points is $\text{dist}(p,q)$, and NEps (p), the esp-neighborhood of p, can be expressed as $\text{NEps}(p)=\{q\in D|\text{dist}(p,q)\leq \text{Eps}\}$. If $p\in \text{NEp}(q)$ and $|\text{NEp}(q)|\geq \text{MinPts}$, p is directly accessible from q. If there is a set of sample points $p1, p2, \ldots, pn$, $p1=q$, $Pn=q$ so that $Pi+1$ is directly accessible from Pi to p and q, and the density accessibility is given by the transitive closure of direct density accessibility, that is, the specification extension of direct density accessibility. Since the secondary relation is transferred, if there is a point o that makes both p and q accessible from the density of o, then the density of p is related to the density of q.

Density-based clustering is the maximum set of data points connected by density. If a cluster C is a nonvoid subset of D, then

(1) $\forall p, q$, if $p\in C$ and p from q can access to density, $q\in C$ (maximum)

(2) $\forall p$, $q\in C$, p, and q has density connection (connectivity)

Let $C_1 \ldots C_k$ be the clustering of data space D. Noise is the set of points in D that do not belong to any clustering C_i, that is, noise $=\{p\in D|\forall i\text{: } p\notin D\}$.

Density-based clustering distinguishes three different types of points: the core points with dense neighboring points, the boundary points that belong to the same clustering but not densely neighboring points, and the noise points not belonging to any clustering.

2.2. Graph Clustering Algorithm Based on Fast Detection of Central Node. An unweighted network is represented by $G=(V,E,W)$. V is the set of vertices, E is the set of edges, W_{ij} represents the weight of nonitemized edges connected to node V_i and V_j, and W_{ij} represents the distance and proximity between node V_i and V_j in the graph clustering algorithm. According to the central idea of graph clustering algorithm based on fast detection of center node, the network is divided into k disjoint subgraphs, with dense edge connections inside and sparse edge connections between each other. In the k subgraph, each subgraph contains a cluster center. When clustering, the cluster center should be identified first, and then the noncluster central nodes are divided into appropriate clusters. Therefore, graph clustering algorithm based on fast detection of central node needs to solve three core problems: (1) how to define the density and distance of a node; (2) how to determine the clustering center; (3) noncluster center clustering strategy.

In scale-free network, the degree distribution of nodes follows the power-law distribution, that is, the probability that a node is connected to k, other nodes $P(k)$ satisfy $P(k)\sim k-r$ (r is a constant.) Obviously, the fewer the nodes, the higher the degrees. In addition, these nodes are surrounded by denser nodes, allowing the importance of nodes to be described and all clustering centers in the network to be found. In order to describe the importance of nodes, the concept of local density is introduced, and the local density Pi of node I is defined as

$$\begin{aligned} \rho_i &= \sum_j X\left(d_{ij}-d_c\right), \\ d_{ij} &= \min \sum_{z=i}^{j-1} W_{z(z+1)}. \end{aligned} \tag{1}$$

If $X\leq 0$, $X(x)=1$, otherwise $X(x)=0$, d_{ij} represents the shortest distance between node i and j, and d_c is the truncation distance. ρ_i is equal to the number of adjacent points whose distance from node i is less than d_c. However, since the local density of nodes cannot determine the clustering center, for quick identification of the clustering center, the comprehensive distance i of node i should be introduced to represent the shortest distance weighted value from node i to nodes with higher local density:

$$\begin{aligned} \beta_i &= \delta_i\left(\varphi_i+1\right), \\ \delta_i &= \min_{j:\, \rho_j>\rho_i} d_{ij}. \end{aligned} \tag{2}$$

δ_i represents the minimum distance between node i and any other node with high density, φ_i is the median centrality of node i, which is the weight factor used to control the influence of node, and C is the constant. If node i has the highest density, set δ_i equal to 0.3 times the diameter of the network.

Obviously, only the nodes whose local density is the local or global maximum value has a much larger comprehensive distance than their neighboring points. Therefore, the clustering center is the node with abnormally large ρ_i and β_i and the network graph can be depicted by the local density of node ρ and the comprehensive distance β, thereby identifying the network clustering center quickly.

2.3. Algorithm Description. In the network $G=(V,E,W)$, to calculate the local density ρ of each node in the network G and the comprehensive distance β, the network G decision graph should be drawn on the basis of the ρ and β to determine the clustering center rapidly. After the cluster center is determined, the number of network clustering can be determined, and the noncluster central node can be divided into the cluster where the cluster center is located.

Firstly, through Algorithm 1, graph clustering algorithm, based on fast detection of central node, the input is network G and the output contain k clustering C.

(i) Input: undirected unweighted graph G $G = (V, E, W)$
(ii) Output: k clustering $C = \{C_1, C_2, \ldots, C_k\}$
(1) Calculate the local density ρ and the comprehensive distance β of the node in figure G
(2) Detect the clustering center by identifying the clustering center algorithm
(3) Divide the noncluster centers into appropriate clusters by nonclustering central node algorithm
(4) Return the clustering result $C = \{C_1, C_2, \ldots, C_k\}$

Algorithm 1: Graph clustering algorithm based on fast detection of central node (CFCN).

(i) Input: undirected unweighted graph $G = (V, E, W)$, local density ρ, and comprehensive distance β
(ii) Output: k clustering $C = \{c_1, c_2, \ldots, c_k\}$
(1) Determine the threshold *thrho* and *thbeta* by characterizing the local density ρ with the integrated distance β decision graph
(2) $k = 0$
(3) For each vertex i in G, perform
(4) If $\rho_i >$ *thrho* and $\beta_i >$ *thbeta,* then
(5) $k = k + 1$
(6) Set node i as the clustering center c_k
(7) End if
(8) End for
(9) Return Cen $= \{c_1, c_2, \ldots, c_k\}$

Algorithm 2: Clustering center algorithm.

Then, find the clustering center by Algorithm 2: the clustering center algorithm finds out the clustering center, specifically as shown in Algorithm 2.

In Algorithm 2, the input is network G and the local density ρ and the comprehensive distance β of node i in Algorithm 1. The output is the Cen of clustering central node. In Algorithm 2 (1), the thresholds *thrho* and *thbeta* of ρ and β are determined by characterizing the decision graph. From (3) to (8), find all nodes with local density greater than *thrho* and comprehensive distance greater than *thbeta*. Through Algorithm 2, the clustering center algorithm can find the clustering center in the network only by traversing the nodes in the network once. Nonclustering center node clustering algorithm is used to cluster other nonclustering central nodes (Algorithm 3).

The input is network G, local density of all nodes and comprehensive distance β, nonclustering central node U, and clustering center Cen; the output is K clustering C. In Algorithm 3, from (4) to (6), divide v into the cluster with the closest clustering center in Cen. In (7), remove the nonclustering central node that has been clustered from U and determine whether the clustering is completed by judging whether U is an empty set.

3. Results and Discussion

3.1. Data. Through its application on real networks (Karate; Lesmis; Polbook; Netscience; and Metabolic) and comparing module maximization algorithm (GN), spectral clustering algorithm (Spectral), and early density–based graph clustering algorithm (SCAN), the network clustering algorithm based on the rapid detection of the central node can be evaluated, and the main comparison indexes are selection method ($F1$_score), module degree (Q), and performance (Performance). The algorithm is implemented in Python and in order to avoid randomness, perform the runs 10 times. Details are as shown in Table 1.

3.2. Comparison and Analysis. Firstly, apply CFCN algorithm to Karate network to verify that CFCN algorithm does not need to set the number of clustering before clustering. Figure 1 shows the network topology and social network structure. Set the truncation distance dc = 1, calculate the local density ρ_i of each node i and the comprehensive distance β_i, and visualize it as the decision graph (Figure 2). Nodes i and 34 in the decision graph are outliers, which have greater local density and comprehensive distance compared to other nodes, so they can be determined as the clustering center. In the practical application of Algorithm 2, clustering center algorithm, the threshold values *thrho* and *thbeta* need to be determined. The threshold value range of clustering centers 1 and 34 and other nodes can be determined by the decision graph. Finally, Algorithm 3, nonclustering center node algorithm, is applied to cluster other nonclustering center nodes. As shown in Figure 3, the same shape (colour) has the same clustering. Through the above examples, it is found that the number of clustering is only related to the network topology, with no need for setting in advance.

Secondly, apply the CFCN algorithm, GN algorithm, and spectral algorithm to real social networks for comparative testing and evaluate clustering quality through the performance and module degree Q to verify the higher efficiency of CFCN algorithm. Set the parameter dc = 1; Table 1 shows the comparison of the modularity and performance of CFCN algorithm and other algorithms in social networks with different structures. It can be found that although the GN

```
Input: undirected unweighted graph G G = (V, W, W), local density ρ and comprehensive distance β, nonclustering central node U,
    and clustering center Cen = {c_1, c_2, . . ., C_k}
Output: clustering result C = {C_1, C_2, . . ., C_k}
Add ck to Ck
While U ≠ ϕ, perform
            v = a vertex in U
            For each c ∈ Cen, perform
Join node v into the cluster to connect closer c
            End for
            Remove node v from U
Return C
```

Algorithm 3: Nonclustering central node clustering algorithm.

Table 1: Data statistics.

Network	Number of nodes	Number of edges	Average degree	Number of clusters
Karate	34	78	4.589	2
Lesmis	75	252	6.595	4
Polbook	106	442	8.413	3
Netscience	378	912	4.827	8
Metabolic	453	2041	9.005	11

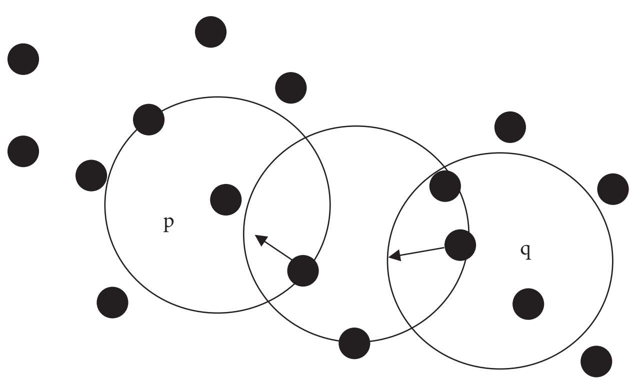

Figure 1: Clustering results.

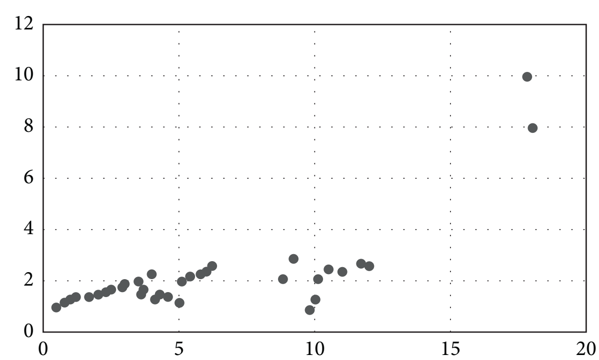

Figure 3: Density-reachable.

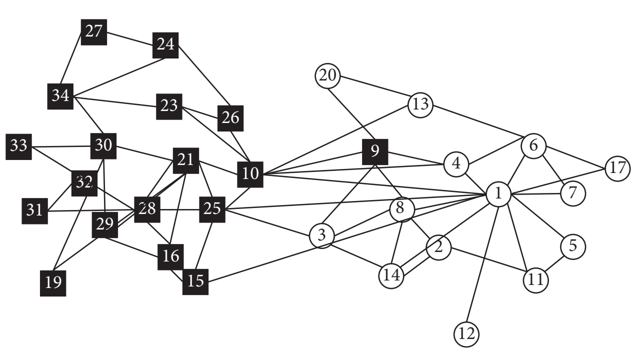

Figure 2: Decision-making.

algorithm in Polbook network module is better than CFCN algorithm, spectral algorithm in Metabolic network performance is better than CFCN algorithm, CFCN is superior to other algorithms overall.

4. Conclusion

This paper conducted an experimental research on graph clustering algorithm based on fast detection of central node. The following conclusions can be drawn from this research.

Through the calculation of local density and comprehensive clustering of nodes in the network, the clustering center in the network can be found quickly and noncentral nodes can be divided into the clustering center based on the nearest neighbor principle, thus avoiding parameter limitations such as the number of clustering to be set in advance in the conventional classic social network detection algorithm.

The experimental comparison and analysis in the real network indicate that the graph clustering algorithm based on the fast detection of the central node is highly effective and efficient.

Data Availability

The datasets used and/or analyzed during the current study are available from the corresponding author on reasonable request.

Conflicts of Interest

The authors declare no potential conflicts of interest with respect to the research, authorship, and/or publication of this article.

Acknowledgments

This research was supported by the National Natural Science Foundation of China under No. 51904313.

References

[1] H. Jeong, B. Tombor, R. Albert, Z. N. Oltvai, and A.-L. Barabási, "The large-scale organization of metabolic networks," *Nature*, vol. 407, no. 6804, pp. 651–654, 2000.

[2] F. Murtagh and P. Contreras, "Algorithms for hierarchical clustering: an overview," *WIREs Data Mining and Knowledge Discovery*, vol. 2, no. 1, pp. 86–97, 2012.

[3] E. Ahmadi, M. Zandieh, M. Farrokh, and S. M. Emami, "A multi objective optimization approach for flexible job shop scheduling problem under random machine breakdown by evolutionary algorithms," *Computers & Operations Research*, vol. 73, no. 9, pp. 56–66, 2016.

[4] M. Aladeemy, S. Tutun, and M. T. Khasawneh, "A new hybrid approach for feature selection and support vector machine model selection based on self-adaptive cohort intelligence," *Expert Systems with Applications*, vol. 88, no. 9, pp. 118–131, 2017.

[5] I. Skrjanc, J. A. Iglesias, A. Sanchis, D. Leite, E. Lughofer, and F. Gomide, "Evolving fuzzy and neuro-fuzzy approaches in clustering, regression, identification, and classification: a Survey," *Information Sciences*, vol. 490, no. 6, pp. 344–368, 2019.

[6] J. J. Whang, D. F. Gleich, and I. S. Dhillon, "Overlapping community detection using neighborhood-inflated seed expansion," *IEEE Transactions on Knowledge and Data Engineering*, vol. 28, no. 5, pp. 1272–1284, 2016.

[7] A. Rodriguez and A. Laio, "Clustering by fast search and find of density peaks," *Science*, vol. 344, no. 6191, pp. 1492–1496, 2014.

[8] M. Hajjar, G. Aldabbagh, N. Dimitriou, and M. Z. Win, "Relay selection based clustering techniques for high density LTE networks," *Wireless Networks*, vol. 25, no. 5, pp. 2305–2314, 2019.

Hindawi
Scientific Programming
Volume 2022, Article ID 7257564, 11 pages
https://doi.org/10.1155/2022/7257564

Research Article

A New Variant of JM Software Reliability Model

Kuldeep Singh Kaswan,[1] Sunita Choudhary,[2] Santar Pal Singh,[3] Anil Audumbar Pise,[4] and Simon Karanja Hinga[5]

[1]*School of Computing Science & Engineering, Galgotias University, Greater Noida-203201, India*
[2]*Department of Computing Science, Banasthali Vidyapith, Vanasthali, Rajasthan-304022, India*
[3]*Department of Computer Science & Engineering, Thapar Institute of Engineering and Technology, Patiala-147004, India*
[4]*School of Computer Science and Applied Mathematics, University of the Witwatersrand, Johannesburg-2000, Gauteng, South Africa*
[5]*Department of Electrical and Electronic Engineering, Technical University of Mombasa, Mombasa, Kenya*

Correspondence should be addressed to Simon Karanja Hinga; kahinga@tum.ac.ke

Received 27 November 2021; Accepted 21 January 2022; Published 25 February 2022

Academic Editor: Punit Gupta

Software reliability is the probability of failure-free operations of software in a specific environment in a given time period. Various software reliability models have been designed by the researchers, but the JM model is the first influential model. The JM model was developed with the basic assumption that the faults are independent in this model and the debugging process is perfect. But practically, all debugging processes may not be perfect, especially when the faults are dependent; in this case, the fault that is actually to have been removed may also remove more than one fault and cause it to add some new faults. To handle this behavior of faults mutual dependency, we need a new model which may be less reliable or the result accuracy of the model may be lower than that of the existing ones, but it can handle more practical situations in the fault removal process. In this paper, we proposed a new software reliability model with the same assumption that at whatever time a failure is detected, it is not completely eradicated and there is a possibility of raising some new faults because of wrong analysis or inaccurate modifications in the software or the removal of the existing fault may also remove some other faults. The proposed model is more practical than the existing ones.

1. Introduction

Software reliability models are used to find the faults in a software product, and for the prediction of faults, these models predict and estimate the number of faults in the build. On behalf of this, one can take the decision whether this product has to be released or corresponding changes have to be made to improve the quality. Nowadays, due to the usage of software in real-time applications, even a single fault in the software becomes very critical, and it may result in the loss of life and other consequences. So, researchers are putting their best efforts in developing and improving the software reliability models so that it may help to provide more reliable software and better-quality software. Several software reliability models were proposed, but still the industry crept around the faults and unstable software. The JM model states that faults are independent of each other and equally likely to cause a failure during a test. The detected fault is eliminated immediately without the detection of any new fault. But these assumptions are not realistic. In our proposed work, we have extended the JM model by replacing these assumptions with the new assumptions that the faults are dependent and not equally likely to cause a failure in the test, and whenever a failure occurred, the identified faults are removed with probability p, and it may result in the removal and generation of some other faults, from the total number of faults, with random probabilities r, such that $p > r$, respectively.

This paper is organized into the following sections. Related work is given in Section 2. JM model, its assumptions, and the mathematical formulation are described in Section 3. In Section 4, we have proposed a new variant of the JM model. Results and discussions are given in Section 5. Finally, Section 6 concludes the work.

2. Related Work

The first reliability model was reported in 1967 using the Weibull distribution of time between failures [1]. After this, in 1972, the first influential software reliability model [2] with initial N bugs was reported [2]. A similar Jelinski–Moranda (JM) model was developed in 1975 [3, 4]. Some researchers designed the first nonhomogeneous Poisson process model [5]. In 1983, Meinhold and Singpurwalla proposed a Bayesian software reliability model which was a variant of the JM model that used the prior distributions to the parameters [6]. Jewell used the Meinhold and Singpurwalla model to derive a new model that provides Bayesian analysis of the software reliability model of JM [7]. Tohma proposed a new software reliability model [8] for estimating the number of residual software faults based on the hypergeometric distribution [8, 9]. Brocklehurst improved reliability predictions by a process of recalibration [10]. Sahinoglu uses the probability density estimation of failures in the clustering event of the software failures [11]. Campodonico and Singpurwalla proposed a Bayesian approach using the logarithmic Poisson model to predict the number of failures in a software system [12]. Chen and Arlat proposed a fault correction history-based input domain reliability growth model [13]. A software reliability model using enhanced nonhomogeneous Poisson process (ENHPP) approach was reported in the literature [14]. Some authors considered the phenomena of failure correlation to develop a software reliability model framework [15]. Tian described a model for homogeneous failure intensities by grouping data into clusters [16]. Huang estimated the reliability with the unified scheme of some nonhomogeneous Poisson process models [17]. Some researchers proposed a model for individual component-based software reliability and the architecture of the system [18]. Advanced chaos theory to the stochastic models, an alternative approach of software reliability, is also there in the literature [19].

Raj Kiran and Ravi group different models to accurately forecast software reliability [20]. Jun-Gang proposed an RVM (relevance vector machine)-based model for software reliability prediction [21]. Some researchers addressed the issue of optimal selection of software reliability growth models [22].

An improved additive model to reliability estimation of modular structure-based software is there to study [23]. Inoue and Yamada discussed discrete software reliability measurement based on a discredited (NHPP) model [24]. Kiyoshi Honda prosposed a stochastic process based software reliability model [25], and Kim HeeCheul proposed a comparative problem of a reliability model for Lomax and Gompertz distribution property [26]. Shinji Inoue proposed a new software reliability model with the effect of a change point for the Markovian software reliability model having an imperfect debugging environment [27]. This proposed model shows that the observed time-dependent behavior of the expected number of failures occurred after the change point has more practical situations compared to the other existing models. Kwang Yoon Song proposed a new nonhomogeneous Poisson process (NHPP) software reliability model [28]. An explicit mean value function solution for the proposed model is presented. Jinyong Wang and Xiaoping Mi proposed a new software reliability model [29] considering the decreasing trend of fault detection rate. This model has better predictive performance and better fitting than the previous existing models in this field. Yoshinobu Tamura and Shigeru Yamada proposed a deep learning-based scheme for the optimal selection of a software reliability model [30]. As model selection affects the optimal release time and total software cost, in this paper we also discussed these two criteria for the selection of a software reliability model. Subhashis Chatterjee and Ankur Shukla developed a new software reliability method with the imperfect debugging phenomenon [31]. A new ranking method has been proposed to improve the accuracy of model ranking. Da Hye Lee proposed a software reliability model based on NHPP [32]. The proposed model has the same mean value functions and the testing coverage, but it considers the environment that is uncertain. There are unexpected variables like syntax error considered in the proposed model. Shozab Khurshid designed a generalized framework to develop an effort-based software reliability model [33] with fault reduction factor (FRF), change point, and error generation. Yunlu Zhao, Tadashi Dohi, and Hiroyuki Okamura proposed a nonhomogeneous binomial processes (NHBPs)-based framework [34] for test-run reliability modeling. This paper also demonstrates that Poisson binomial distribution has a vital role in reliability modeling. Barack and Huang [35] proposed software reliability growth models (SRGMs) to assess and predict the reliability of a mobile application. Through the analysis of bug reports, four software reliability models are used to assess the dependability of an open-source mobile application. Sun and Li [36] proposed a new nonhomogeneous Poisson process (NHPP) based on fault severity considerations. We categorise software faults into three levels based on their complexity: Level I denotes a simple fault, Level II a general fault, and Level III a severe fault. Raghuvanshi et al. [37] proposed a time-variant software reliability model (SRM) that takes fault detection and the highest number of faults in software into account. The time-variant genetic algorithm process is used to evaluate the SRM parameters. The proposed model is based on a nonhomogeneous Poisson process (NHPP) and includes fault-dependent detection, software failure intensity, and unremoved error in the software. Van Driel et al. [38] predict the software reliability in agile testing environments and attempt to model this way of working by extending the Jelinski–Moranda model to a "stack" of feature-specific models, assuming that bugs are labelled with the feature to which they belong.

3. Jelinski–Moranda (JM) Model

The Jelinski–Moranda (JM) model [4] is a Markov model, and this model has strongly influenced many later models.

Numerous software reliability models have been proposed by assuming this model as the base model.

Characteristics of the JM model are as follows:

(1) It is a binomial type model
(2) It is probably the first and definitely one of the well-recognized black-box models
(3) This model always produces an overoptimistic reliability prediction
(4) JM model follows a perfect debugging process

3.1. Model Assumptions. The assumptions considered in the JM model are given as follows:

(i) There are unknown numbers of faults in the software initially and these fault counts are fixed and constant
(ii) The faults are not dependent on each other and equally likely to cause a failure during a test
(iii) There are independent time intervals among the occurrences of failures, exponentially distributed random variables
(iv) The software failure rate remains constant over the intervals between fault occurrences
(v) The failure rate is directly proportional to the number of faults that linger in the software
(vi) A detected fault is eliminated immediately, and no new faults are initiated during the elimination of the detected fault
(vii) When a failure occurs, the corresponding fault is removed with certainty

3.2. Mathematical Formulation of the JM Model

(i) Software fault rate: it is defined as the faults per unit time

$$\lambda(t_i) = \phi[N - (i-1)] \quad \text{where } i = 1, 2, \ldots, N, \tag{1}$$

in which ϕ is a constant of proportionality representing the failure rate contributed by each fault, N is the initial number of faults in the software, and t_i is the time between $(i-1)$ th and ith failure.

(ii) Failure density function: it is the function that assigns to each number the probability that the random variable takes a value less than or equal to the given number.

It is defined as the derivative of the failure probability.

$$f(t_i) = \phi[N - (i-1)]\exp(-\phi[N-(i-1)]t_i). \tag{2}$$

(iii) Distribution function is given as follows:

$$F_i(t_i) = 1 - \exp(\phi[N-(i-1)]t_i). \tag{3}$$

(iv) Reliability function at the ith failure interval is given by

$$R(t_i) = 1 - F_i(t_i) = \exp(-\phi[N-(i-1)]t_i). \tag{4}$$

(v) MTTF for the ith failure $= 1/\phi[N-(i-1)]$.

4. Proposed Model

The assumptions (ii) and (vi) of the JM model states that faults are independent of each other and equally likely to cause a failure at some point in a test. The detected fault is removed immediately without the detection of any new fault. But these assumptions are not realistic. We extended the JM model by replacing the assumptions (ii) and (vi) with the new assumptions that the faults are dependent and not equally likely to cause a failure during a test, and whenever a failure occurred, the detected faults are eliminated with probability p, and it may result in the removal and generation of some other faults, from the total number of faults, with random probabilities r, such that $p > r$, respectively.

4.1. Model Assumptions of the Proposed Model. The assumptions in the proposed model include the following:

(i) to (v) Assumptions (i) to (v) are the same as of the JM model

vi) Whenever a failure occurred, the detected faults are removed with some probability and it may result first in the removal of some other faults with the random probability p and second in the generation of some other new faults with the random probability r, such that $p > r$.

4.2. Mathematical Formulation of the Proposed Model

(i) Failure rate:

$$\lambda(t_i) = \Phi\left[N - (i-1)\left\{\frac{\sum_{j=i}^{N} pj}{N-(i-1)} - \frac{\sum_{k=1}^{m} rk}{m}\right\}\right], \tag{5}$$

where φ is the proportionality constant representing the failure rate contributed by each fault, N is the initial no. of faults in the software, t_i is the time between $(i-1)$th and ith failure, p_j is the random probability to remove the faults, r_k is the random probability to add some new faults, and m is the number of faults added such that $p_j > r_k$ and $m < N-(i-1)$.

(ii) Failure density is defined as "at any point in the life of a system, the incremental change in the number of failures per associated incremental change in time"

$$f(t_i) = \Phi\left[N-(i-1)\left\{\frac{\sum_{j=i}^{N} pj}{N-(i-1)} - \frac{\sum_{k=1}^{m} rk}{m}\right\}\right]\exp\left[-\Phi\left(N-(i-1)\left\{\frac{\sum_{j=i}^{N} pj}{N-(i-1)} - \frac{\sum_{k=1}^{m} rk}{m}\right\}\right)t_i\right]. \tag{6}$$

The failure distribution function is the integral of the failure density function.

(iii) Distribution function (cumulative density function):

$$F_i(t_i) = 1 - \exp\left[-\Phi\left(N-(i-1)\left\{\frac{\sum_{j=i}^{N} pj}{N-(i-1)} - \frac{\sum_{k=1}^{m} rk}{m}\right\}\right)t_i\right] \tag{7}$$

or

$$F_i(t_i) = 1 - \exp[-\lambda_i t_i]. \tag{8}$$

(iv) The mean time to failure (MTTF) is the average time between observed failures: MTTF = $1 - F_i(t_i)$.

(v) Reliability function:

$$R(t_i) = 1 - F_i(t_i) = \exp\left[-\Phi\left(N-(i-1)\left\{\frac{\sum_{j=i}^{N} pj}{N-(i-1)} - \frac{\sum_{k=1}^{m} rk}{m}\right\}\right)t_i\right]. \tag{9}$$

4.3. Parameter Estimation. We have to estimate the number of remaining faults N' and the constant of proportionality Φ. Our proposed model parameters are estimated using the maximum likelihood estimation method.

(i) Parameter estimation:

$$\begin{aligned}&\sum_{i=1}^{n}\frac{1}{N'-(i-1)\left[\sum_{j=i}^{N} pj/N-(i-1)-\sum_{k=1}^{m} rk/m\right]}\\&=\frac{n}{N'-\left(1/\sum_{i=1}^{n} tn\right)\left[\sum_{i=1}^{n}(i-1)\left\{\sum_{j=i}^{N} pj/N-(i-1)-\sum_{k=1}^{m} rk/m\right\}t_i\right]},\end{aligned} \tag{10}$$

$$\Phi = \frac{n}{\sum_{i=1}^{n} N'-(i-1)\left[\sum_{j=i}^{N} pj/N-(i-1)-\sum_{k=1}^{m} rm/m\right]t_i}. \tag{11}$$

We have obtained maximum likelihood estimation N' by solving the equation (10) and put this value into (11) to obtain the maximum likelihood estimation Φ.

A program has been implemented in MATLAB to find the value of N' from (5) (Algorithm 1)

$$\begin{aligned}f(N') = &\sum_{i=1}^{n}\frac{1}{N'-(i-1)\left[\sum_{j=i}^{N} pj/N-(i-1)-\sum_{k=1}^{m} rk/m\right]}\\&-\frac{n}{N'-\left(1/\sum_{i=1}^{n} tn\right)\left[\sum_{i=1}^{n}(i-1)\left\{\sum_{j=i}^{N} pj/N-(i-1)-\sum_{k=1}^{m} rk/m\right\}t_i\right]}.\end{aligned} \tag{12}$$

Now find the reliability for the next time interval.

(i) Reliability:

```
(1) for n = 3 to 136
      begin
(2)     for N′ = 3 to 150
          begin
(3)         r = f(N′)
          end
(4) Find the minimum value of r and print N′ for that value.
      end
```

Algorithm 1: Algorithm to estimate N' from equation (5).

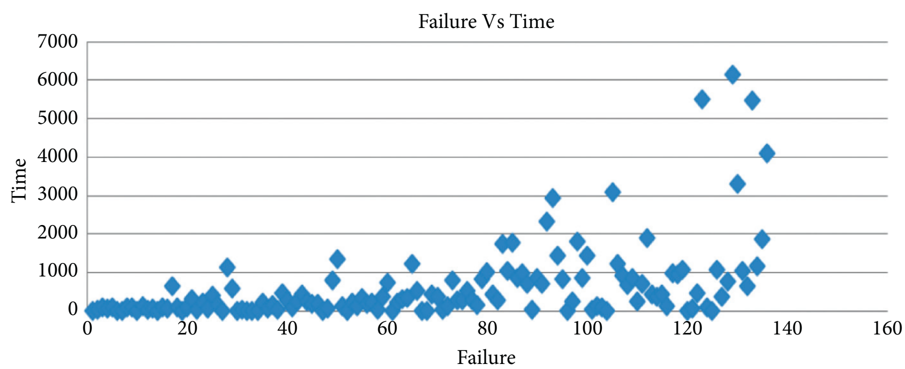

Figure 1: Failure vs. time.

Table 1: Proposed model vs. JM model.

N	t_n	JM model					Proposed model				
		N'	ϕ	λ	MTTF	$R = 1 - f(t)$	N'	ϕ	λ	MTTF	$R = 1 - f(t)$
1	3	1	0.333300	0.000000	∞	1.000000	1	0.333333	0.333333	3	0.367879
2	30	2	0.055600	0.000000	∞	1.000000	2	0.036263	0.059414	16.831049	0.168230
3	113	3	0.016500	0.000000	∞	1.000000	3	0.009324	0.018380	54.406556	0.125311
4	81	4	0.009800	0.000000	∞	1.000000	4	0.004840	0.014483	69.0432864	0.309382
5	115	6	0.004600	0.004600	218.600000	0.959700	6	0.002671	0.011844	84.430767	0.256131
6	9	11	0.002100	0.010500	95.233300	0.979200	6	0.002871	0.011980	83.469009	0.897785
7	2	∞	0.000000	0.019800	50.428600	0.164600	7	0.002838	0.013825	72.332568	0.972728
8	91	28	0.000742	0.014800	67.368800	0.189700	8	0.002414	0.012989	76.983480	0.306642
9	112	16	0.001400	0.009900	100.746000	0.861700	11	0.001567	0.012004	83.300114	0.260660
10	15	46	0.000424	0.015300	65.505600	0.121600	12	0.001471	0.012387	80.726542	0.830429
11	138	20	0.001100	0.009800	102.181800	0.613000	NaN	NaN	NaN	NaN	NaN
12	50	27	0.000756	0.011300	88.216700	0.417800	12	0.001353	0.009844	101.574951	0.611251
13	77	29	0.000695	0.011100	89.932700	0.765800	13	0.001233	0.010802	92.573668	0.435278
14	24	61	0.000300	0.014100	70.835900	0.217700	14	0.001175	0.010457	95.6241495	0.778035
15	108	39	0.000494	0.011800	84.416700	0.352600	15	0.001079	0.009997	100.022048	0.339676
16	88	38	0.000509	0.011200	89.335200	0.000600	16	0.000978	0.009748	102.584017	0.424079
17	670	18	0.001400	0.001500	686.235300	0.839600	17	0.000665	0.007561	132.245087	0.006305
18	120	20	0.001200	0.002300	429.944400	0.941300	18	0.000554	0.006507	153.677753	0.458014
19	26	23	0.000899	0.003600	278.236800	0.663800	22	0.000463	0.007150	139.855327	0.830351
20	114	25	0.000782	0.003900	255.740000	0.280600	20	0.000515	0.006244	160.132492	0.490705
21	325	24	0.000844	0.002500	395.047600	0.870000	21	0.000458	0.005896	169.592304	0.147141
22	55	27	0.000684	0.003400	292.281800	0.436900	23	0.000408	0.005975	167.343635	0.719884
23	242	28	0.000639	0.003200	312.773900	0.804600	25	0.000363	0.006200	161.274074	0.223007
24	68	31	0.000541	0.003800	263.910700	0.202100	24	0.000377	0.005658	176.711764	0.680581
25	422	29	0.000608	0.002400	410.950000	0.645300	30	0.000281	0.005879	170.070077	0.083631
26	180	31	0.000538	0.002700	372.084600	0.973500	28	0.000290	0.004883	204.750312	0.415148
27	10	35	0.000439	0.003500	285.060200	0.017900	27	0.000304	0.005190	192.65184	0.949417

Table 1: Continued.

N	t_n	JM model N'	ϕ	λ	MTTF	$R = 1 - f(t)$	Proposed model N'	ϕ	λ	MTTF	$R = 1 - f(t)$
28	1146	30	0.000576	0.001200	867.339300	0.500700	28	0.000249	0.004452	224.595888	0.006081
29	600	31	0.000529	0.001100	944.913800	0.984300	29	0.000208	0.003817	261.922210	0.101189
30	15	33	0.000462	0.001400	721.477800	0.951300	34	0.000175	0.003886	257.306309	0.943370
31	36	35	0.000412	0.001600	606.540300	0.993400	31	0.000197	0.004052	246.749856	0.864246
32	4	38	0.000354	0.002100	471.322900	1.000000	35	0.000180	0.004712	212.192154	0.981325
33	0	41	0.000312	0.002500	400.609800	0.980200	39	0.000166	0.004508	221.801057	1
34	8	46	0.000259	0.003100	321.838200	0.493900	34	0.000196	0.004231	236.344719	0.966717
35	227	47	0.000251	0.003000	331.804800	0.822100	40	0.000167	0.004566	219.000994	0.354685
36	65	52	0.000215	0.003400	290.074700	0.545100	36	0.000186	0.004050	246.873528	0.768516
37	176	54	0.000204	0.003500	287.804500	0.817500	37	0.000182	0.004212	237.414285	0.476484
38	58	60	0.000176	0.003900	258.077800	0.170200	44	0.000154	0.004847	206.272099	0.754890
39	457	55	0.000200	0.003200	313.152200	0.383700	46	0.000143	0.004333	230.744445	0.137993
40	300	56	0.000194	0.003100	322.792200	0.740400	NaN	NaN	NaN	NaN	NaN
41	97	60	0.000175	0.003300	300.445400	0.416700	41	0.000155	0.004072	245.535290	0.673642
42	263	61	0.000171	0.003200	308.000000	0.230500	51	0.000124	0.004525	220.977867	0.304171
43	452	58	0.000185	0.002800	360.924000	0.493400	53	0.000155	0.004254	235.032626	0.146147
44	255	60	0.000175	0.002800	357.265600	0.576100	52	0.000155	0.004091	244.438673	0.352323
45	197	62	0.000167	0.002800	352.882400	0.578700	46	0.000129	0.003872	258.217142	0.466301
46	193	65	0.000155	0.002900	339.527500	0.982500	47	0.000126	0.003811	262.382299	0.479233
47	6	71	0.000137	0.003300	304.892700	0.771700	50	0.000120	0.004016	248.944067	0.976186
48	79	77	0.000122	0.003500	282.576900	0.055700	48	0.000127	0.003553	281.394045	0.755220
49	816	67	0.000149	0.002700	373.731300	0.026900	49	0.000118	0.003763	265.736415	0.046388
50	1351	59	0.000183	0.001600	607.193300	0.783700	52	0.000100	0.003386	295.265642	0.010300
51	148	61	0.000173	0.001700	578.515700	0.964400	51	0.000098	0.003147	317.685879	0.627589
52	21	65	0.000155	0.002000	497.463000	0.626000	56	0.000091	0.003221	310.373974	0.934577
53	233	67	0.000147	0.002100	485.574100	0.758800	53	0.000096	0.003241	308.498330	0.469883
54	134	70	0.000137	0.002200	456.072900	0.457100	54	0.000095	0.003194	312.990824	0.651728
55	357	71	0.000134	0.002100	466.751100	0.661300	NaN	NaN	NaN	NaN	NaN
56	193	74	0.000125	0.002300	443.803600	0.587600	56	0.000090	0.003282	304.614060	0.530683
57	236	76	0.000120	0.002300	438.064600	0.931700	NaN	NaN	NaN	NaN	NaN
58	31	81	0.000109	0.002500	398.967800	0.396600	58	0.000087	0.003455	289.420777	0.898426
59	369	81	0.000109	0.002400	416.571600	0.166000	70	0.000072	0.003446	290.145967	0.280333
60	748	78	0.000116	0.002100	481.008300	1.000000	60	0.000082	0.002949	339.070155	0.110136
61	0	82	0.000107	0.002200	444.750200	0.593500	72	0.000067	0.003388	295.134138	1
62	232	85	0.000101	0.002300	429.852700	0.464100	62	0.000079	0.002638	379.051733	0.542236
63	330	86	0.000099	0.002300	437.323000	0.434000	69	0.000070	0.003359	297.657092	0.330001
64	365	87	0.000098	0.002200	445.354600	0.064300	65	0.000074	0.003250	307.669056	0.305336
65	1222	81	0.000109	0.001700	572.519200	0.387300	65	0.000070	0.002786	358.894706	0.033210
66	543	81	0.000109	0.001600	610.210100	0.983700	66	0.000066	0.002768	361.168940	0.222361
67	10	85	0.000101	0.001800	551.660000	0.971400	67	0.000066	0.002500	399.861661	0.975301
68	16	89	0.000094	0.002000	508.892200	0.353600	68	0.000065	0.002919	342.534350	0.954363
69	429	89	0.000094	0.001900	534.642800	0.492200	69	0.000064	0.002675	373.720337	0.242804
70	379	90	0.000092	0.001800	543.980000	0.922300	70	0.000062	0.002393	417.854376	0.403727
71	44	94	0.000086	0.002000	506.655200	0.775200	71	0.000062	0.002759	362.371404	0.885659
72	129	98	0.000080	0.002100	478.508000	0.184000	NaN	NaN	NaN	NaN	NaN
73	810	95	0.000084	0.001900	538.806400	0.583800	73	0.000059	0.002668	374.698345	0.115124
74	290	97	0.000082	0.001900	532.678600	0.569400	74	0.000058	0.002778	359.874367	0.446713
75	300	99	0.000079	0.001900	527.241700	0.366700	75	0.000057	0.002715	368.299667	0.442836
76	529	99	0.000079	0.001800	550.189400	0.600100	76	0.000055	0.002621	381.517830	0.249931
77	281	101	0.000077	0.001800	544.009700	0.745200	77	0.000054	0.002564	389.939847	0.486448
78	160	105	0.000072	0.001900	514.758800	0.200200	78	0.000054	0.002684	372.443989	0.650772
79	828	102	0.000075	0.001700	576.648300	0.173200	79	0.000052	0.002524	396.126421	0.123657
80	1011	99	0.000079	0.001500	664.027600	0.511600	80	0.000050	0.002304	433.903508	0.097294
81	445	101	0.000076	0.001500	654.198100	0.636100	81	0.000048	0.002689	371.789765	0.302125
82	296	103	0.000074	0.001600	643.633600	0.065400	82	0.000047	0.002356	424.331389	0.497794
83	1755	98	0.000081	0.001200	827.210400	0.276300	83	0.000045	0.002230	448.354358	0.019954
84	1064	97	0.000082	0.001100	935.631900	0.148700	NaN	NaN	NaN	NaN	NaN
85	1783	95	0.000086	0.000856	1168.300000	0.479000	85	0.000040	0.001948	513.315339	0.031008
86	860	96	0.000084	0.000836	1195.900000	0.439600	NaN	NaN	NaN	NaN	NaN

Table 1: Continued.

N	t_n	JM model N'	ϕ	λ	MTTF	$R=1-f(t)$	Proposed model N'	ϕ	λ	MTTF	$R=1-f(t)$
87	983	96	0.000084	0.000754	1326.000000	0.586700	NaN	NaN	NaN	NaN	NaN
88	707	97	0.000082	0.000738	1354.900000	0.975900	88	0.000035	0.001920	520.822995	0.257311
89	33	100	0.000077	0.000845	1183.700000	0.480300	92	0.000034	0.001999	500.222704	0.936158
90	868	100	0.000077	0.000770	1298.200000	0.572500	94	0.000033	0.002061	485.139850	0.167098
91	724	101	0.000075	0.000755	1325.000000	0.173200	NaN	NaN	NaN	NaN	NaN
92	2323	100	0.000077	0.000615	1625.800000	0.164900	99	0.000029	0.001955	511.391098	0.010646
93	2930	99	0.000079	0.000471	2123.100000	0.502500	105	0.000026	0.001861	537.187177	0.004277
94	1461	99	0.000079	0.000394	2539.200000	0.717500	94	0.000028	0.001583	631.710908	0.098986
95	843	101	0.000075	0.000448	2233.200000	0.994600	104	0.000024	0.001666	599.918456	0.245320
96	12	102	0.000073	0.000439	2275.400000	0.891600	96	0.000027	0.001485	673.395806	0.982337
97	261	104	0.000070	0.000489	2044.300000	0.414600	116	0.000022	0.001836	544.648991	0.619273
98	1800	104	0.000070	0.000420	2382.100000	0.695500	121	0.000021	0.001641	609.064039	0.052060
99	865	106	0.000067	0.000466	2145.700000	0.512300	99	0.000021	0.001656	603.577182	0.238562
100	1435	106	0.000067	0.000401	2495.100000	0.988000	NaN	NaN	NaN	NaN	NaN
101	30	108	0.000064	0.000447	2236.700000	0.938100	116	0.000021	0.001310	762.984731	0.961443
102	143	110	0.000061	0.000490	2042.500000	0.948500	110	0.000022	0.001477	677.017482	0.809595
103	108	112	0.000059	0.000529	1890.100000	1.000000	103	0.000024	0.001442	693.326793	0.855755
104	0	114	0.000057	0.000566	1766.100000	0.171900	134	0.000018	0.001799	555.814849	1
105	3110	113	0.000058	0.000461	2169.600000	0.562800	105	0.000023	0.001441	693.594304	0.011289
106	1247	114	0.000056	0.000451	2215.900000	0.653400	106	0.000022	0.001402	712.758614	0.173853
107	943	115	0.000055	0.000443	2259.600000	0.733600	131	0.000017	0.001575	634.876873	0.226428
108	700	116	0.000054	0.000435	2301.000000	0.683700	108	0.000021	0.001388	720.189902	0.378338
109	875	118	0.000052	0.000469	2134.000000	0.891500	109	0.000020	0.001355	737.558886	0.305334
110	245	119	0.000051	0.000462	2166.700000	0.714300	110	0.000020	0.001413	707.414134	0.707277
111	729	121	0.000049	0.000493	2028.800000	0.392600	121	0.000018	0.001203	830.853083	0.415857
112	1897	121	0.000049	0.000444	2252.900000	0.820000	112	0.000019	0.001380	724.616992	0.072953
113	447	123	0.000047	0.000475	2106.100000	0.832500	118	0.000018	0.001553	643.567841	0.499291
114	386	124	0.000047	0.000468	2137.400000	0.811700	NaN	NaN	NaN	NaN	NaN
115	446	126	0.000045	0.000497	2014.000000	0.941200	115	0.000019	0.001209	826.530574	0.582978
116	122	128	0.000044	0.000524	1908.000000	0.595200	116	0.000019	0.001299	769.428084	0.853372
117	990	129	0.000043	0.000516	1938.900000	0.613300	117	0.000018	0.001422	702.849012	0.244496
118	948	131	0.000041	0.000539	1854.200000	0.557900	118	0.000019	0.001006	993.772526	0.385220
119	1082	132	0.000041	0.000531	1884.200000	0.988400	119	0.000018	0.001129	885.207957	0.294548
120	22	134	0.000040	0.000555	1802.500000	0.959200	120	0.000020	0.001302	767.619405	0.971746
121	75	136	0.000039	0.000578	1731.300000	0.757000	121	0.000018	0.000978	1021.98930	0.929241
122	482	138	0.000037	0.000598	1672.000000	0.037100	122	0.000018	0.001441	693.576499	0.499100
123	5509	134	0.000040	0.000436	2292.400000	0.957300	123	0.000017	0.001153	866.636866	0.001734
124	100	136	0.000038	0.000461	2169.400000	0.995400	124	0.000016	0.001434	697.121298	0.866366
125	10	138	0.000037	0.000485	2063.700000	0.595100	125	0.000016	0.000697	1433.87795	0.993050
126	1071	139	0.000037	0.000477	2094.700000	0.837700	126	0.000016	0.001357	736.891254	0.233773
127	371	141	0.000036	0.000499	2004.600000	0.674300	127	0.000016	0.001108	902.406476	0.662905
128	790	143	0.000035	0.000518	1929.700000	0.041300	NaN	NaN	NaN	NaN	NaN
129	6150	139	0.000037	0.000367	2723.300000	0.295400	129	0.000015	0.000894	1118.172980	0.004086
130	3321	139	0.000037	0.000330	3031.000000	0.708400	130	0.000014	0.001045	956.790792	0.031086
131	1045	140	0.000036	0.000325	3079.800000	0.810300	159	0.000011	0.001370	729.439350	0.238685
132	648	141	0.000036	0.000320	3125.400000	0.172900	NaN	0.000008	NaN	NaN	NaN
133	5485	140	0.000036	0.000253	3953.600000	0.745700	206	0.000004	0.001080	925.678922	0.002670
134	1160	141	0.000036	0.000249	4020.900000	0.629000	373	0.000004	0.001466	681.741222	0.182405
135	1864	142	0.000035	0.000244	4094.400000	0.365900	NaN	NaN	NaN	NaN	NaN
136	4116	142	0.000035	0.000209	4777.000000	0.000000	NaN	NaN	NaN	NaN	NaN

$$R(tn+1) = 1 - Fn + 1(tn+1)$$
$$= \exp\left(-\Phi\left[(N-n)\left\{\frac{\sum_{j=i}^{N} pj}{N-n} - \frac{\sum_{k=1}^{m} rk}{m}\right\}\right]tn+1\right). \tag{13}$$

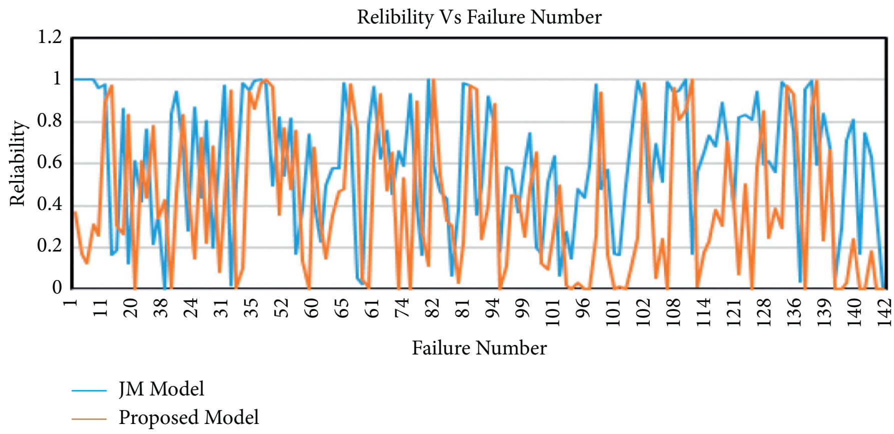

Figure 2: Reliability vs. failure number.

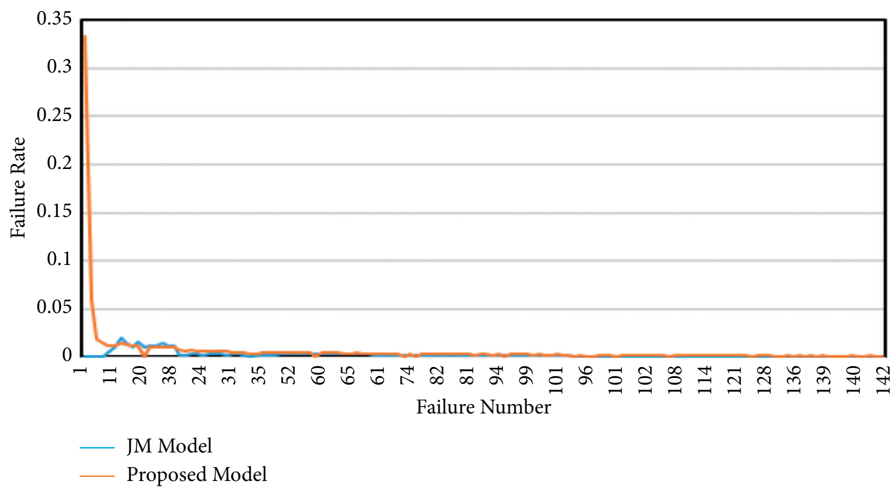

Figure 3: Failure rate vs. failure number.

5. Results and Discussion

In this paper, we proposed and implemented a new variant of the JM model. The failure vs. time graph based on the dataset used by Musa [9] is shown in Figure 1.

We estimate the parameters (ϕ, λ). With the help of these parameters, we calculate the mean time to failure (MTTF) and the reliability for the JM model and the proposed model using MATLAB R 2015a.

The model validation is given in Table 1.

It is concluded from this table that the reliability of the proposed model is not as expected as the JM model. But the proposed model assumptions are more realistic and will act as a new approach for software reliability estimation.

A response graph has been used to show the effect of individual input failure parameters on selected responses. The effect of the following one factor graphs (Figures 2–4) was studied on output.

(a) Reliability vs. failure number

(b) Failure rate vs. failure number

(c) Failure rate vs. MTTF

In Figure 2, we have compared the software reliability with the failure numbers. The result shows that the proposed model exhibits almost similar behavior as the JM model, and the proposed model is found to be more practical than the JM model. Figure 3 shows that the failure rate for the proposed model is greater than that for the JM model, as the proposed model is for imperfect debugging. Figure 4 compares MTTF and failure rate, and at some point, MTTF for the proposed model is less than that for the JM model.

We have compared the proposed model and the JM model in terms of average MTTF and the average reliability of the system and the results are shown in Figures 5–6.

From Figure 5, it has been found that the average mean time to failure (MTTF) for the proposed model is less than that for the JM model. This shows that, using the proposed model, we have improved the system.

From Figure 6, it has been found that the average reliability for the JM model is more than that for the proposed model, but the proposed model is more practical and has a better real-world approach.

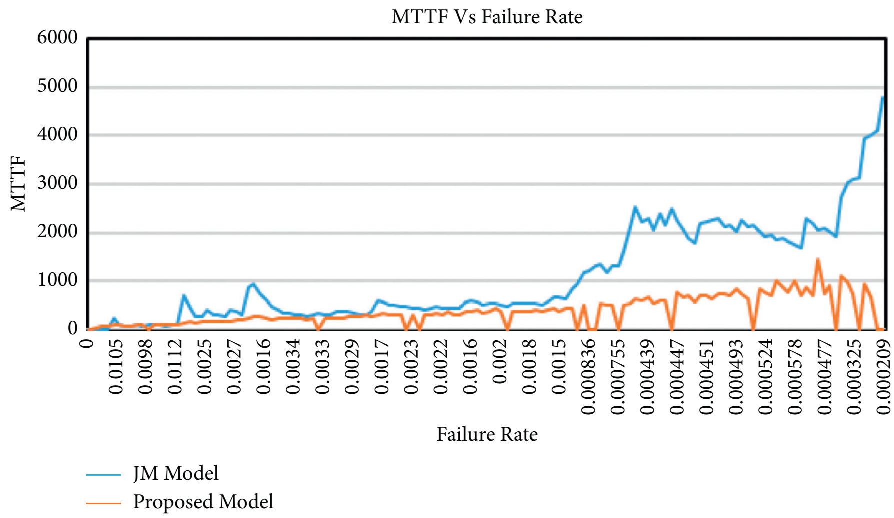

Figure 4: MTTF vs. failure rate.

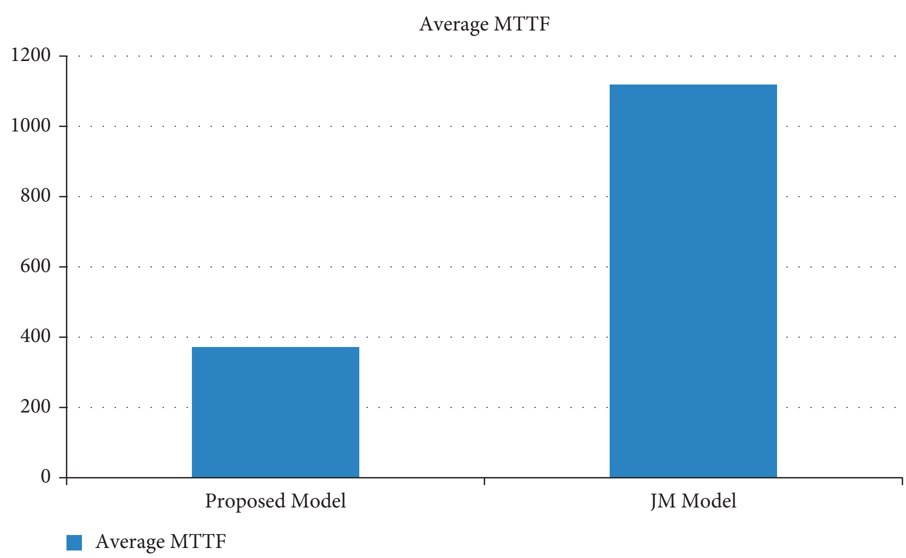

Figure 5: Comparison of the proposed model MTTF with the JM model MTTF.

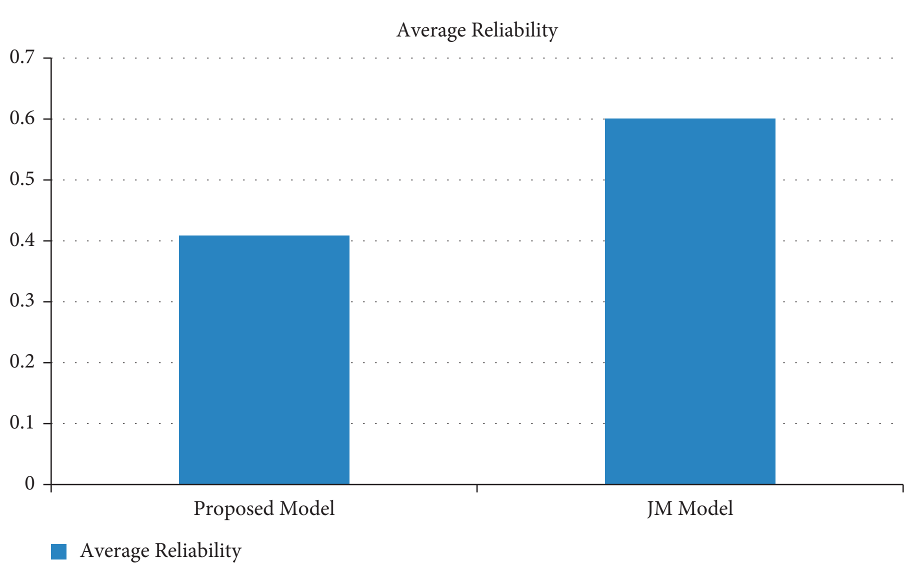

Figure 6: Comparison of the average reliability of the proposed model with the JM model reliability.

6. Conclusion

The proposed model is an imperfect debugging process model with fault dependency. In this model, the removal of the existing fault can also remove some other faults with the random probability of an individual and it may also generate some new faults with some probability. Reliability for the JM model and the proposed model is 0.6 and 0.4, respectively. The mean time to failure (MTTF) for the JM model and the proposed model is 1118.596 and 371.5370972, respectively. Experimental results indicate that MTTF for the proposed model is found to be better than that for the JM model. But the reliability of the proposed model is not as good as the JM model, but it has a more real-world approach and practical nature.

Data Availability

The data that support the findings of this study are available on request from the corresponding author.

Conflicts of Interest

The authors declare that they do not have any conflicts of interest.

References

[1] G. R. Hudson, "Program error as a birth and death process," ReportNo. SP-3011, System Development Corporation, Santa Monica, CA, USA, 1967.

[2] Z. Jelinski and P. Moranda, "Software reliability research," in *Statistical Computer Performance Evaluation*, W. Freiberger, Ed., Academic Press, New York, NY, USA, pp. 465–484, 1972.

[3] M. L. Shooman, "Software reliability: measurement and models," in *Proceedings of the Annual Reliability and Maintainability Symposium*, pp. 485–491, Washington, DC, USA, January 1975.

[4] J. D. Musa, "A theory of software reliability and its application," *IEEE Transactions on Software Engineering*, vol. SE-1, no. 3, pp. 312–327, 1975.

[5] A. L. Goel and K. Okumoto, "Time-dependent error-detection rate model for software reliability and other performance measures," *IEEE Transactions on Reliability*, vol. R-28, no. 3, pp. 206–211, 1979.

[6] R. J. Meinhold and N. D. Singpurwalla, "Bayesian analysis of a commonly used model for describing software failures," *The Statistician*, vol. 32, no. 1/2, pp. 168–173, 1983.

[7] W. S. Jewell, "Bayesian extensions to a basic model of software reliability," *IEEE Transactions on Software Engineering*, vol. SE-I1, no. 12, pp. 1081–1091, 1985.

[8] Y. Tohma, K. Tokunaga, S. Nagase, and Y. Murata, "Structural approach to the estimation of the number of residual software faults based on the hyper-geometric distribution," *IEEE Transactions on Software Engineering*, vol. 15, no. 3, pp. 345–355, 1989.

[9] J. D. Musa, "Data," Data & Analysis Center for Software, 1980, http://www.dacs.dtic.mil/databases/sledfswrel.shtml.

[10] S. Brocklehurst, P. Y. Chan, B. Littlewood, and J. Snell, "Recalibrating software reliability models," *IEEE Transactions on Software Engineering*, vol. 16, no. 4, pp. 458–470, 1990.

[11] M. Sahinoglu, "Compound-Poisson software reliability model," *IEEE Transactions on Software Engineering*, vol. 18, no. 7, pp. 624–630, 1992.

[12] S. Campodonico and N. D. Singpurwalla, "A bayesian analysis of logarithmic-Poisson execution time model based on expert opinion and failure data," *IEEE Transactions on Software Engineering*, vol. 20, no. 9, pp. 677–683, 1994.

[13] Y. Chen and J. Arla, "An Input Domain-Based Reliability Growth Model and its Applications in Comparing Software Testing Strategies," LAAS Report No.95105, LAAS-CNRS, France, 1995.

[14] S. S. Gokhale and K. S. Trivedi, "A time/structure-based software reliability model," *Annals of Software Engineering*, vol. 8, no. 1/4, pp. 85–121, 1999.

[15] K. G. Popstojanovaand, K. S. Trivedi, Failure correlation in software reliability models," *IEEE Transactions on Reliability*, vol. 49, no. 1, pp. 37–48, 2000.

[16] J. Tian, "Better reliability assessment and prediction through data clustering," *IEEE Transactions on Software Engineering*, vol. 28, no. 10, pp. 997–1007, 2002.

[17] C. Y. Huang, M. R. Lyu, and S. Y. Kuo, "A unified scheme of some nonhomogenous Poisson process models for software reliability estimation," *IEEE Transactions on Software Engineering*, vol. 29, no. 3, pp. 261–269, 2003.

[18] J.-H. Lo, C.-Y. Huang, I.-Y. Chen, S.-Y. Kuo, and M. R. Lyu, "Reliability assessment and sensitivity analysis of software reliability growth modeling based on software module structure," *Journal of Systems and Software*, vol. 76, no. 1, pp. 3–13, 2005.

[19] S. Dick, C. L. Bethel, and A. Kandel, "Software-reliability modeling: the case for deterministic behavior," *IEEE Transactions on Systems, Man, and Cybernetics - Part A: Systems and Humans*, vol. 37, no. 1, pp. 106–119, 2007.

[20] N. Raj Kiran and V. Ravi, "Software reliability prediction by soft computing techniques," *Journal of Systems and Software*, vol. 81, no. 4, pp. 576–658, 2007.

[21] J. G. Lou, J.-H. Jiang, C. Y. Shuai, R. Zhang, and A. Jin, "Software reliability prediction model based on relevance vector machine," in *Proceedings of the IEEE Int. Conf. on Intelligent Computing and Intelligent Systems*, pp. 229–233, Shanghai, China, November 2009.

[22] K. Sharma, R. Garg, C. K. Nagpal, and R. K. Garg, "Selection of optimal software reliability growth models using a distance based approach," *IEEE Transactions on Reliability*, vol. 59, no. 2, pp. 266–276, 2010.

[23] S. Chatterjee, S. Nigam, J. B. Singh, and L. N. Upadhyaya, "An improved additive model for reliability analysis of software ,with modular structure," *J. Appl. Math. Informatics*, vol. 30, pp. 489–498, 2012.

[24] S. Inoue and S. Yamada, "A bootstrapping approach for software reliability measurement based on a discretized NHPP model," *Journal of Software Engineering and Applications*, vol. 6, no. 4, pp. 1–7, 2013.

[25] K. Honda, H. Washizaki, and Y. Fukazawa, "A generalized software reliability model considering uncertainty and dynamics in development," in *Proceedings of the Int. Conf. on Product Focused Software Process Improvement*, pp. 342–346, Trondheim, Norway, November 2016.

[26] H. C. Kim, "A performance analysis of software reliability model using Lomax and Gompertz distribution property," *Indian Journal of Scienec and Technology*, vol. 9, no. 20, pp. 1–6, 2016.

[27] S. Inoue and S. Yamada, "Software reliability modeling with imperfect debugging and change of test environment," in

Proceedings of the Sixth International Conference on Reliability, Infocom Technologies and Optimization Trends and Future Directions, pp. 128–131, ICRITO), Noida, India, September 2017.

[28] K. Y. Song, I. H. Chang, and H. Pham, "An NHPP software reliability model with S-shaped growth curve subject to random operating environments and optimal release time," appl," vol. 7, no. 12, Article ID 1304, 2017.

[29] J. Wang and X. Mi, "Open-source software reliability model with the decreasing trend of fault detection rate," *The Computer Journal*, vol. 62, no. 19, pp. 1301–1312, 2019.

[30] Y. Tamura and S. Yamada, "Software reliability model selection based on deep learning with application to the optimal release problem," *Journal of Industrial Engineering and Management Science*, vol. 2016, no. 1, pp. 43–58, Article ID 3, 2016.

[31] S. Chatterjee and A. Shukla, "A unified approach of testing coverage-based software reliability growth modeling with fault detection probability, imperfect debugging, and change point," *Journal of Software: Evolution and Process*, vol. 30, 2018.

[32] D. H. Lee, I. H. Chan, H. Pham, and K. Y. Song, "A software reliability model considering the syntax error in uncertainty environment, optimal release time, and sensitivity analysis," *Applied Science*, vol. 8, Article ID 1483, 2018.

[33] S. Khurshid, A. K. Shrivastava, and J. Iqbal, "Effort based software reliability model with fault reduction factor, change point and imperfect debugging," *International Journal of Information Technology*, vol. 13, 2019.

[34] Y. Zhao, T. Dohi, and H. Okamura, "Software test-run reliability modeling with non-homogeneous binomial processes," in *Proceedings of the 2018 IEEE Twenty Third Pacific Rim International Symposium on Dependable Computing*, pp. 145–154, PRDC), Taipei, Taiwan, December 2018.

[35] O. Barack and L. Huang, "Assessment and prediction of software reliability in mobile applications," *Journal of Software Engineering and Applications*, vol. 13, no. 9, pp. 179–190, 2020.

[36] X. Sun and J. Li, "Simulation of software reliability growth model based on fault severity and imperfect debugging," in *Proceedings of the Simulation Tools and Techniques, Twelveth EAI International Conference*, SIMUtools, Guiyang, China, August 2020.

[37] K. K. Raghuvanshi, A. Agarwal, K. Jain, and V. B. Singh, "A time-variant fault detection software reliability model," *SN Applied Sciences*, vol. 3, no. 18, 2021.

[38] W. D. Van Driel, J. W. Bikker, and M. Tijink, "Prediction of software reliability," *Microelectronics Reliability*, vol. 119, Article ID 114074, 2021.

Hindawi
Scientific Programming
Volume 2022, Article ID 3798734, 13 pages
https://doi.org/10.1155/2022/3798734

Research Article

An Online Kernel Adaptive Filtering-Based Approach for Mid-Price Prediction

Shambhavi Mishra,[1] **Tanveer Ahmed**,[1] **Vipul Mishra**,[1] **Sami Bourouis**,[2] **and Mohammad Aman Ullah**[3]

[1]*School of Engineering and Applied Sciences, Bennett University, Greater Noida 201310, India*
[2]*Department of Information Technology College of Computers and Information Technology, Taif University, Taif 21944, Saudi Arabia*
[3]*Department of Computer Science and Engineering, International Islamic University Chittagong, Chittagong, Bangladesh*

Correspondence should be addressed to Mohammad Aman Ullah; aman_cse@iiuc.ac.bd

Received 30 August 2021; Revised 25 October 2021; Accepted 27 November 2021; Published 15 February 2022

Academic Editor: Punit Gupta

The idea of multivariate and online stock price prediction via the kernel adaptive filtering (KAF) paradigm is proposed in this article. The prediction of stock prices is traditionally done with regression and classification, thereby requiring a large set of batch-oriented and independent training samples. This is problematic considering the nonstationary nature of a financial time series. In this research, we propose an online kernel adaptive filtering-based approach for stock price prediction to overcome this challenge. To examine a stock's performance and demonstrate the work's superiority, we use ten different KAF family of algorithms. In this paper, we take on this challenge and propose an approach for predicting stock prices. To analyze a stock's performance and demonstrate the work's superiority, we use ten distinct KAF algorithms. Besides, the results are analyzed on nine-time windows such as one day, sixty minutes, thirty minutes, twenty five minutes, twenty minutes, fifteen minutes, ten minutes, five minutes, and one minute. We are the first to experiment with several time windows for all fifty stocks on the Indian National Stock Exchange, to the best of our knowledge. It should be noted here that the experiments are performed on stocks making up the main index: Nifty-50. In terms of performance and compared to existing methods, we have a 66% probability of correctly predicting a stock's next upward or downward movement. This number clearly shows the edge that the proposed method has in actual deployment. Furthermore, the experimental findings show that KAF is not only a better option for predicting stock prices but that it may also be used as an alternative in high-frequency trading due to its low latency.

1. Introduction

Time-series prediction is prevalent in economics and investment research. Stock price prediction is one of the most popular applications of time-series prediction. Its success stems from its ability to reduce asset management costs, market impacts, and volatility risks [1]. It is a commonly held notion that stock markets are complex, volatile, and chaotic [2]. The markets, in our perspective, are made up of a variety of factors that influence stock movement. Predicting stock's value at any given time in the future is, therefore, an important problem of academia and industry. Previous studies [3] have shown that the prediction of stock prices, particularly with the nonstationary and the nonlinear nature of the underlying asset, is challenging. In this regard, several models have been proposed, but the problem is nowhere near its end [4], and a substantial improvement is required. In addition, studies have also extended the problem by predicting option prices, volatility [5], and so on. This significant body of work demonstrates that stock price prediction remains a significant issue requiring solutions to a wide range of problems.

As discussed in the previous paragraph, stock price prediction is a significant challenge. In this regard, a plethora of techniques have been used for predicting stock prices, such as neural network (NN), support vector machine (SVM), genetic algorithm, fuzzy logic, and Bayesian model [6]. However, getting an optimal solution is still a long way to go. During our literature review, we discovered that current research has overlooked kernel adaptive filtering (KAF) and has not thoroughly investigated this paradigm for financial time-series forecasting, especially stock prediction. Although there are a few introductory studies [7], a large-scale comprehensive evaluation lacks literature. With this shortcoming in mind, we would like to emphasize that KAF can be an effective stock prediction tool. The following observations serve as the foundation for our argument: first, KAF-based algorithms have a faster convergence rate; that is, the algorithm requires fewer iterations. Second, KAF has demonstrated excellent performance in nonstationary time-series prediction [8]. Third, KAF algorithms exhibit universal function approximation properties useful in highly dynamic environments [9]. Lastly, KAF has been used extensively in chaotic time-series prediction [10, 11]. Hence, it is also worth exploring the idea in financial time-series prediction. Therefore, in this article, we use the concept of KAF to examine and comprehend the real-time movement of stock prices. In addition to KAF being one of the largest unexplored paradigms in stock prediction, the literature review revealed one more issue. It contains one of the problems related to batch learning. We believe that sequential learning is the best tool rather than batch learning for financial time-series forecasting. This is mainly because a financial time series is nonstationary. We further argue that expecting a model trained on offline samples to perform excellently in a real situation is a slippery slope. The rationale here is supported by the work presented in the literature, which claims that online learning is the best way to understand and interpret nonstationary data behavior [12]. Consequently, studies have shown that online learning can be an effective method [13]. It is based on the concept of sequential measurement (training is performed sample-by-sample and in real time). Various scenarios can easily be added, and the algorithm adjusts the weight vector to provide accurate predictions. As a result, in order to solve the issue stated in the article, we enhance the KAF idea with online learning.

With respect to the challenges and the ideas discussed in this section, we present an online KAF algorithms to predict the price of stock. The use of KAF techniques to stock price prediction is still limited [7, 14]. However, the concept is based upon this study is precedent and builds upon it to extend the application of KAF to a broader range of environments and contexts. With data taken from Nifty-50, the Indian Stock Index, we first build our dataset consisting of prices collected at a time window of one day, sixty minutes, thirty minutes, twenty five minutes, twenty minutes, fifteen minutes, ten minutes, five minutes, and one minute. These windows are chosen as they are some of the most common windows looked at by day traders. It should be noted here that the prices are collected for a total of fifty companies (they make up the main index: Nifty-50). Subsequently, we apply the ideas on each of the time windows and predict the next potential number for the "mid-price" of the stock. With comprehensive numerical investigation, we have found that the proposed trading algorithm has an extra 16% edge in the field, thereby making it an effective method capable of generating good returns in the long run. The following are the paper's key contributions:

(1) A novel KAF-based online method for forecasting a stock's mid-price is introduced. We look at two situations in which the mid-price is measured as (high + low)/2 and (open + close)/2, respectively. The main motivation for looking into mid-price was that mid-price time series is less noisy than close-price time series.

(2) With a comprehensive investigation performed on nine different time windows. We discover the best window for predicting stock prices. In the literature, several authors have focused on predicting daily prices [15, 16]. We, however, show that focusing efforts on other time windows could also be optimal.

(3) In this article, ten different KAF algorithms are used, and a detailed analysis is presented to validate the work. To the best of our knowledge, an investigation of this magnitude eludes literature.

The following section has been divided into sections. The methods proposed by various researchers in the subject of stock prediction are discussed in Section 2. Proposed methodology is described in Section 3. The experiments performed with different KAF algorithm, and their results are included in Section 4. Finally, in Section 5, the conclusions and future scopes are described.

2. Related Work

The work of other authors in the field of stock prediction is discussed in this section. Predicting stock has remained one of the nontrivial issues of the literature [17]. Previous studies have shown that the prediction of stock prices is difficult due to the inherent nonstationary behavior in the data [18]. Several studies [5] have shown that stock prediction is challenging and noisy. Various linear techniques such as correlations, discriminating analysis, autoregressive models, and moving averages have also been studied in the past [19]. Machine learning (ML) has been a popular field in time-series prediction in recent years. ML-based techniques are explored heavily as they can recognize complex patterns in stock prices [20]. Due to the nonlinear and time-varying nature of time-series, there has recently been a surge in demand for online prediction algorithms [21]. Online algorithms use the sequential calculation to achieve reliable and faster outcomes [13]. In this regard, several techniques have been developed, such as online support vector regression (SVR), NN [8], and KAF algorithms [10]. NN methods take a lot of processing power and have a slow convergence rate [22]. SVR provides superior applicability; however, it is not appropriate for huge datasets. Furthermore, the multifilter neural network (MFNN) is investigated, and it is discovered that MFNN outperforms SVR, random forests, and other neural network-based approaches. The use of convolutional neural networks (CNN) has also been explored to predict the next-day prices [23]. CNN outperformed for multimodality images in the biomedical domain [24, 25]. Furthermore, for stock price prediction, long short-term memory (LSTM) is applied [26]. The authors used an LSTM network with a single layer and 200 nodes in [27]. Furthermore, the network employs a single-layer LSTM with 140 nodes [28]. In contrast to using a deep architecture with four LSTM layers and 96 nodes in the hidden layers, each LSTM layer was further followed by a dropout layer [29].

Adaptive filtering has been proven to be a preferable choice for streaming data having nonstreaming behavior [11, 30, 31]. For sequential stock prediction, KAF can be used by exploiting market interdependence. Fast convergence, low computational complexity, and nonparametric behavior make KAF a preferable choice [10, 32]. One research [33] focuses on adaptive asynchronous differential evolution with trigonometric mutation modified mutation operation, and adaptive parameters modified the convergence speed and diversity. In [34], the authors proposed meta-cognitive recurrent kernel online learning for multistep predictions of stocks. Although these studies show the potential that KAF has, KAF has not been investigated thoroughly in the context of stock price prediction. Though there are few studies in literature focusing on the area, large-scale investigation eludes literature. Nevertheless, we must point that the work presented in [14] proposes a two-phase method for stock prediction. First, sequential learning using KAF was applied to learn the underlying model for each stock separately. In the second phase, to improve prediction, real time models are learned from different stock. In [7], the authors proposed the idea of multikernel adaptive filters for online options trading. The method was applied to Taiwan composite stock index. Garcia-Vega et al. [35] presented a multikernel learning approach to overcome the two primary concerns with KAF: kernel size and step size. Despite the fact that these papers concentrate on using the KAF paradigm to forecast stock prices, none of them validates the paradigm's effectiveness on a large-scale dataset. Moreover, the impact of multiple time windows is not considered. In our opinion, testing the method on multiple time windows that are often looked at by traders is of prime importance.

3. Methodology

3.1. Brief Discussion on KAF. We work with online learning-based KAF techniques, as discussed in Section 1. The purpose of KAF is to learn with well-known input-output mapping $f\colon S \longrightarrow R$, and it contains sequence of data such as $((s_1, d_1), (s_2, d_2), \ldots, (s_i, d_i))$, where, $S \subseteq R^L$ is the input space, s_i, $i = 1, \ldots, n$, is the system input at sample time, and d_i is known as desired response. In reproducing kernel Hilbert space (RKHS) F, KAF transforms the data into a set of points. Inner products can then be used to solve the problem. There is no need to do expensive computations in high-dimensional space, owing to the famous "kernel trick." In KAFs, generally, the computation involves the use of a kernel. The following equation is an example of a kernel:

$$\kappa < s, s' > \; = \exp \frac{\left(\left\| s - s' \right\|^2 \right)}{\sigma^2}, \tag{1}$$

where σ represents the kernel width.

3.2. Kernel Adaptive Filtering Algorithms. In this subsection, we briefly describe the ten different KAF methods.

3.2.1. Least Mean Square (LMS). The LMS algorithm, according to [36] employs a finite impulse response (FIR) filter, also known as a traversal filter, whose output is based on a linear combination of the input presented in the following equation:

$$y_i = \varpi^T_{(i-1)} s_i, \tag{2}$$

where $\varpi_{(i-1)}$ represents the weight vector at iteration $(i-1)$. The following equation contains the main idea of the LMS algorithm:

$$\begin{aligned} \varpi_0 &= 0, \\ e_i &= t_i - \varpi_{(i-1)} s_i, \\ \varpi_i &= \varpi_{(i-1)} + \eta e_i s_i, \end{aligned} \tag{3}$$

where η and e_i stands for step size and prior error. The weight-update equation findings were represented in the following equation:

$$\varpi_i = \eta \sum_{i=1}^{N} e_i s_i, \tag{4}$$

The following equation represents the inner product:

$$\begin{aligned} t = \varpi_i(s) &= \eta \sum_{i=1}^{n} e_i < s_i, s >, \\ e_i &= t_i - \eta \sum_{i=1}^{n-1} e_i < s_i, s >. \end{aligned} \tag{5}$$

3.2.2. Kernel Least Mean Square (KLMS). To derive KLMS [36], the input (s_i) is converted into F as $\phi(s_i)$. Using LMS, we can now rewrite the input and output mapping as follows:

$$\begin{aligned} \varpi_0 &= 0, \\ e_i &= d_i - \varpi^T_{(i-1)} \phi(i), \\ \varpi_i &= \varpi_{(i-1)} + \eta e_i \phi(i), \end{aligned} \tag{6}$$

where e_i is represented as the prediction error, η is the size of every step, and $\phi(s_i)$ is defined as the transformed filter input at a certain point in time or iteration i. Equation (7) compute the result, where we can use the famous kernel tricks. Consequently, the model now becomes

$$f_0 = 0,$$
$$e_i = d_i - f_{i-1}(s_i), \quad (7)$$
$$f_i = f_{i-1} + \eta e_i \kappa < s_i, . >.$$

In KLMS, a new unit of the kernel is assigned to all new samples points with ηe_i as the coefficient value. Following the radial basis function (RBF) described in this section, the system is represented as follows:

$$f_i = \sum_{j=1}^{i} o_j(i) \kappa < s_j, . >. \quad (8)$$

The coefficients $o(i)$ and the centers $C(i) = \{s(j)\}_{j=1}^{i}$ are saved inside the storage during the training process.

3.2.3. Kernel Affine Projection Algorithm (KAPA). KAPA [37] is used where we want to improve the performance owing to the gradient noise. In KAPA, we estimate using the weight vector ϖ and minimise the cost function with the sequences $\{d_1, d_2\}$ and $\{\phi(1), \phi(2)\}$ as shown below

$$\min_{\varpi\text{emp}} \left| d - \varpi^T \phi(s) \right|^2. \quad (9)$$

We replace the concept of covariance and cross variance matrix-vector by local approximation directly from the data using stochastic gradient descent summarized in

$$\varpi_i = \varpi_{(i-1)} + \eta \psi(i) \left[d(i) - \psi(i)^T \varpi_{(i-1)} \right], \quad (10)$$

where $\psi(i) = [\phi(i - K + 1), \ldots, \phi(i)]$ and K is the observation and regressor.

3.2.4. Leaky Kernel Affine Projection Algorithm (LKAPA). LKAPA [37] is the extension of KAPA as discussed in Section 3.2.3.Based on the selected kernels, the feature space can be infinitely dimensional, where the weight updation task is difficult. In the common consideration, the solution is the modification in equation (10) as follows.

The weight vector in Equation (11) is calculated using the following criteria:

$$\varpi_i = \sum_{j=1}^{i} o_j(i) \phi(i), \quad \forall_i \geq 0. \quad (11)$$

Equation (12) is used to reduce the following objective function from the perspective of empirical risk minimization:

$$\min_{\varpi\text{emp}} \left| d - \varpi^T \phi(s) \right|^2 + \Lambda \|\varpi\|^2. \quad (12)$$

Then, we get the updated weight, and it is shown in

$$\varpi_i = (1 - \Lambda\eta) \varpi_{(i-1)} + \eta \psi(i) \left[d(i) - \psi(i)^T \varpi_{(i-1)} \right], \quad (13)$$

where $\psi(i) = [\phi(i - K + 1), \ldots, \phi(i)]$.

Finally, coefficient $o_\kappa(i)$ is updated as

$$o_\kappa(i) = \begin{cases} k = i, \eta \left(d_i - \sum_{j=1}^{i-1} o_j(i-1) k_{i,j} \right) \\ \text{for}\{i - K + 1 \leq k \leq i - 1\} (1 - \Lambda\eta) o_k(i-1) + \eta \left(d(k) - \sum_{j=1}^{i-1} o_j(i-1) \kappa_{k,j} \right). \\ 1 \leq k < i - K + 1 (1 - \Lambda\eta) o_k(i-1) \end{cases} \quad (14)$$

3.2.5. Normalized Online Regularized Risk Minimization Algorithm (NORMA). Similarly, the LKAPA [37] extension comes in NORMA, and also it is related to KAPA discussed in Section 3.2.3. It also includes the regularization and nonfunctional approaches.

3.2.6. Quantized Kernel Least Mean Square Algorithm (QKLMS). Quantization techniques are used in various applications such as digitization, data compression, speech, and image coding. QKLMS is a famous algorithm proposed in [11], which deals with the issue of data redundancy. The computational complexity of QKLMS and KLMS is nearly identical. The main difference between the two algorithms is that QKLMS uses redundant data to update the coefficient of closest centre in real time. The following equation represents the main idea using the quantization operator:

$$\varpi_0 = 0,$$
$$e_i = t_i - \varpi_{(i-1)}^T \phi(i), \quad (15)$$
$$\varpi_i = \varpi_{(i-1)} + \eta e_i \mathcal{Q}[\phi(i)],$$

where $\mathcal{Q}[.]$ signifies the quantization in feature space F. The following equation summarises the learning rule for QKLMS:

$$f_0 = 0,$$
$$e_i = t_i - f_{i-1}(s_i), \quad (16)$$
$$f_i = f_{i-1} + \eta e_i \kappa(Q[s_i]).$$

3.2.7. Fixed Budget Quantized Kernel Least Mean Square Algorithm (FBQKLMS). The FBQKLMS [38] deals with the increasing popularity of online kernel approaches. The suggested algorithm uses a significance measure-based pruning criterion based on the weighted contribution of existing data centres.

3.2.8. Kernel Adaptive Filtering with Maximum Correntropy Criterion (KMCC). The fundamental goal of the method is to maximise the crossentropy between the desired d_i and actual output y_i [39]. Using the MCC technique [39] and SGD, the algorithm can be written as follows:

$$\begin{aligned}
\varpi_0 &= 0,\\
\varpi_{(i+1)} &= \varpi_i + \eta \frac{\partial \kappa_\sigma\left(t_i, \varpi_i^T \phi(s_i)\right)}{\partial \varpi_i}; = \varpi_i + \eta\left[\left(\exp \frac{\left(-e_i^2\right)}{2\sigma^2}\right) e_i \phi(i)\right],\\
\ldots &= \eta \sum_{i=1}^{n}\left[\left(\exp \frac{\left(-e_i^2\right)}{2\sigma^2}\right) e_i \phi(i)\right],\\
y_i &= \eta \sum_{i=1}^{n}\left[\left(\exp \frac{\left(-e_i^2\right)}{2\sigma^2}\right) e_i \kappa < s_i, s_n > \right], e_i = d_i - y_i,
\end{aligned} \tag{17}$$

where η is the step size and σ is the kernel width. The entire amount of error and prediction calculation can be summarized in equation (17).

3.2.9. Multikernel Normalized Least Mean Square (MKNLMS). According to [30], the KNLMS algorithm is used to create dictionaries based on the coherence requirement. Here, we explore at KNLMS through the perspective of MKNLMS-CS (multi-kernel normalised least mean square algorithm with coherence-based sparsification). Consider the empty dictionary at the initial stage represented as ($\mathcal{J}_0^{cs} := \varnothing$), by which the H_0 is shown as an empty matrix as M^*. Consider the Hilbertian unit for simplification of $\kappa(s,s) = 1, \forall_s \in s$, which is satisfied by the Gaussian kernel. n is added into $\mathcal{J}_n^{cs}$ in the case when the defined condition holds in the proposed methodology presented in equation (18)

$$\|\kappa\|_{\max} := \max_{m \in \mathcal{M}} \max_{j \in \mathcal{J}_n^{cs}} \left|\kappa_m\left(s_n, s_j\right)\right|, \leq \phi, n \in N, \tag{18}$$

where $\eta \in [0,2]$ and $\Lambda > 0$ denotes the step size and regularization parameter, respectively. $\delta > 0$ is the threshold.

Considering

If equation (18) is satisfied, $\mathcal{J}_{n+1}^{cs} := \mathcal{J}_n^{cs} \cup \{n\}$. If equation (18) is not satisfied, $j_{n+1}^{cs} := j_n^{cs} \cup \{n\}$:

$$\begin{aligned}
H_{n+1} &:= \overline{H}_n + \eta \frac{t_n - < \overline{K}_n, \overline{H}_n >}{\left\|\overline{K}_n\right\|^2 + \Lambda} \overline{K}_n,\\
H_{n+1} &:= H_n + \eta \frac{t_n - < H_n, K_n >}{\left\|K_n\right\|^2 + \Lambda} K_n,
\end{aligned} \tag{19}$$

where $\overline{H}_n := [H_n 0]$ and $\overline{K}_n := [K_n \overline{k}_n]$ with $\overline{k}_n := [\kappa_1 (s_n, s_n), \kappa_2 (s_n, s_n), \kappa_3 (s_n, s_n), \ldots \kappa_M (s_n, s_n)]^T$ where $0 \in\in R^M$ is the zero vector. The value of M for KNLMS is 1.

3.2.10. Probabilistic Least-Mean Square Filter (PROB-LMS). PROB-LMS [31] gives adaptable step-size to the LMS algorithm in Section 3.2.1. and also applied in the stationary and nonstationary environment. The LMS filter can be approximated effectively using a probabilistic approach. It includes a step-size LMS algorithm that may be modified as well as a measure of estimation uncertainty. It also maintains the standard LMS's linear complexity.

3.3. Problem Formulation. Our main objective, is to predict the stock's mid-price as stated in Section 1. The motive of stock price prediction is to calculate stock's future values depending on historical values. For this, we measured the percentage change in mid-price. As a result, we used the concept of order n auto-regression to predict future stock price changes. The sample regression equation is shown in Table 1. Multivariate financial time-series estimation often employs this formulation [40, 41] to predict future values of a time series. The formulation shown in Table 1 is done by considering daywise mid-prices. It should be noted here that the same procedure was used for all time windows. As a result, the problem was rephrased as follows: autoregression-based next percentage prediction. The exact mid-price of the stock may therefore be easily calculated using the percentage change. Figure 1 depicts the proposed approach's overall methodology. The Nifty-50 dataset was used in the experiments. We consider two different aspects for the mid-price prediction: (i) (high + low)/2 and (ii) (open + close)/2. As a result of this calculation, we created the dataset and preprocessed it using nine prediction windows (one-minute, five-minutes, ten-minutes, fifteen-minutes, twenty-minutes, twenty-five minutes, thirty-minutes, sixty-minutes, and one day). Further, the percentage change was calculated for each time windows, and min-max normalization was applied. The selection of embedding dimension (M) is a difficult task. We choose different $M \in \{2, 3, 4, 5, 6, 7\}$ and set the maximum dictionary size for required algorithms to 500 with Gaussian

Table 1: A one-day time frame (Stock-TITAN).

Day	High price	Low price	(high + low)/2	Change in price
1 day	1573	1555.95	1564.475	−0.765 4
2 days	1567	1538	1552.5	0.430 0
3 days	1576.85	1541.5	1559.175	2.079 6
4 days	1621.35	1561.85	1591.6	−2.456 6
5 days	1570	1535	1552.5	−0.908 2
6 days	155.3	1521.5	1538.4	NA

If we choose $M = 3$, then **Input** = [{−0.765 4, 0.430 0, 2.079 6}.], **Output** = [{−2.456 6}].

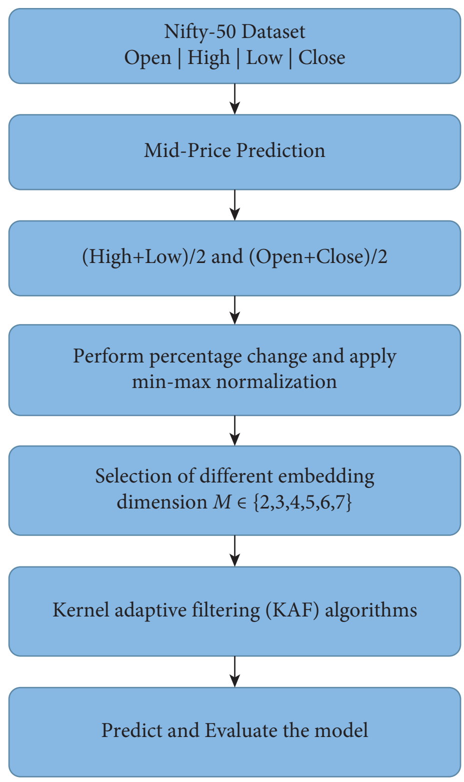

Figure 1: Proposed mid-price prediction framework.

kernel for each time window. In Table 1, we have shown an example considering the time window of 1 day (Stock-TITAN). The error estimation was performed with the help of ten different KAF algorithms for each time window. For example, the performance of each algorithm is analyzed to find which embedding dimension produces the best result. After getting the best embedding dimension for each algorithm, the embedding dimension that produces the best result and the corresponding algorithm is selected.

4. Experiments and Results

4.1. Dataset Description. This section explores into the specifics of the dataset that was used to test the applicability of the proposed method. For this study, we used data from the National Stock Exchange of India. The main index of NSE, Nifty-50, has 50 stocks. Based on the average and total daily turnover for equity shares, Nifty-50 is India's largest stock exchange. We collected data between January 01, 2021, and May 31, 2021, from 9:15 a.m. to 3:30 p.m. In addition, experimentation data are available at https://shorturl.at/lnvF2. The original data included open, high, low, and close (OHLC) prices and were available for one minute. The original data consisted of OHLC prices and were available for one minute. The dataset is generated and preprocessed in accordance with the nine prediction windows (one minute, five minutes, ten minutes, fifteen minutes, twenty minutes, twenty five minutes, thirty minutes, sixty minutes, and one day). Data samples range is different according to their time window. As pointed out in Section 1, we are trying to predict the mid-price with two different scenarios: (high + low)/2 and (open + close)/2. For this, firstly we calculated the percentage change of mid-price. All data values were normalized between zero to one range. Ten different KAF algorithms were used to the final preprocess data and each stock and analyse the comparative performance.

4.2. Evaluation Criterion. To measure and analyse the efficacy of various KAF algorithms, standard assessment criteria are used. In Table 2, y_i and d_i represent the actual and predicted output. n is the time step, and

$$D_i = \begin{cases} 0, & \text{otherwise}, \\ 1, & (y_i - y_{i-1})(d_i - d_{i-1}) \geq 0, \end{cases} \quad (20)$$

Calculating the evaluation metrics with Nifty-50.

(1) The parameter listed in Table 3 were tuned manually. The parameter description for ten different algorithms are presented in Table 3. These values were found after multiple rounds of experimentation.

(2) For the error values, we applied the methods to all stocks and tried to quantify the predictive performance via the metrics discussed in this section. In total, we get 50×3 (one for each stock) error values for MSE, MAE, and DS, respectively.

(3) Then, for each of the 50 stocks, error estimation was performed using nine different prediction windows for ten different KAF algorithms.

(4) Finally, we used the average of all fifty-error metrics for a single time window and a single stock to reach the final value, which is presented in Tables 4 and 5. On all 50 stocks, the provided number represents the models' overall predictive capacity.

4.3. Prediction, Convergence, and Residual Analysis. In this subsection, we examined prediction, converge and residual analysis with the help of KAF algorithms. Regarding this, we have shown the prediction graphs with the KAPA algorithm (discussed in Section 3.2.3) for one stock (TITAN). Figure 2 shows the results for (high + low)/2, while Figure 3 shows the results for (open + close)/2. The predictive curve suits well against the original curve, as can be seen from the prediction graphs. It is worth noting that we have only given results for one prediction window (thirty-minutes) with one stock (TITAN). However, we must note that other stocks in the dataset produced similar result. The prediction graphs clearly show that the predictions are not exact, although they are close. To be precise, the numbers for MSE and MAE are presented in Tables 4 and 5. We must point out that getting accurate value in financial time series forecasting is tough. The goal has always been to get close enough values. Therefore, the result that we achieved shows the good predictive capability of the work. Figures 4 and 5 show the convergence graph for mid-price for (high+low)/2, (open+close)/2, respectively. We have provided the results using the KAPA algorithm with only one prediction window (thirty minutes) and one stock (TITAN), similar to the prior scenario. The algorithm converges quickly, as evidenced by the graphs, at the 1000th data point. We can see in KAF algorithms capacity to adapt and converge quickly. One more important point to note from the convergence graphs is that although there is some fluctuation in the graphs, it is nevertheless acceptable. This is because there will be noise in the new data and minor changes are inevitable. In addition to the results discussed so far, we have complemented the analysis by presenting the distribution of error residuals in Figures 6 and 7. It can be seen from the figures that residuals follow a normal distribution. Moreover, the outliers are also less. Furthermore, the residual's variance is low, demonstrating the KAF algorithm's superior prediction capability and potential in predicting the next immediate, mid-priced occurrence. Directional symmetry is used to determine the continuity of actual and expected prices in terms of stock movement. It is a measure for determining a model's ability to predict a stock's direction. We examined the ten different algorithms mentioned in Section 3 to better understand the actions of a stock's movement. The experiment revealed that using KNLMS, we have a 66% percent chance of accurately predicting the next up or down movement. This is shown in Table 5. The best result is obtained at the window of ten minutes, and the worst result is obtained at the one-minute window. From the table, it is also visible that there is a big difference in the number obtained for the one minute window and that for the rest of the windows. This is expected as there is much noise in a minute, which indeed affects prediction. It should be noted here that literature often ignores looking at these different time windows. Work mostly focuses on predicting daily prices [42, 43]. We discovered the perfect balance by playing with various time windows. Furthermore, when trading, it is recommended to strike a balance between error minimization and directional symmetry.

4.4. Comparative Evaluation of KAF Algorithms. Since we have used ten algorithms in our experimentation, it becomes essential to compare their performance. In this context, we present the topic in two separate situations. First, we analyze the results considering mid-price as (high + low)/2 to find the best algorithm. In the next scenario, we tried mid-price using (open + close)/2. Tables 4 and 5 show the outcome of this experiment. In terms of MSE and MAE, the tables show that KAPA outperforms other algorithms. When it comes to directional symmetry, we can see a contradiction. In directional symmetry, we see a conflict. Here, NORMA and KNLMS give the best performance.

4.5. Comparison with Methods of a Similar Kind. We have also compared the result with other existing techniques such as [28, 29] and [44]. These are some of the most recent deep learning (DL)-based algorithms for predicting stock prices. It should be noted here that these methods were trained and tested using 80:20 splits for 25 epochs. The time taken to train and make prediction was recorded. Specifically, these methods [28, 29] and [44] were reimplemented based on the architecture details and hyper-parameters setting found in the respective papers. The Nifty-50 dataset was used to train all of the methods. To ensure consistency across different methods for experimentation, we use sixty-minute time periods, for fifty stocks. All of the methods' results were then compared to the proposed method. Table 6 contains the

Table 2: Evaluation metrics.

MSE	MAE	DS
$\sum_{i=1}^{n} (y_i - d_i)^2$	$(1/n) \sum_{i=1}^{n} \lvert y_i - d_i \rvert$	$(1/n) \sum_{i=1}^{n} D_i$

Table 3: Parameter description of KAF techniques for NSE-50 dataset for mid-price.

Parameter	KAPA	KLMS	KMCC	KNLMS	FBQKLMS	LKAPA	LMS	NORMA	PROB-LMS	QKLMS
(σ)	5.0	7.0	4.0	7.0	5	6	—	3	—	4
(η)	1.5	1.7	1.7	1.7	0.2	0.03	—	—	—	0.2
(ϵ)	1E-4	—	—	1E-4	0.4	—	—	1.5	—	0.5
(β)	—	—	—	—	0.85	—	—	—	—	—
(Λ)	—	—	—	—	—	1E-2	—	1E-2	0.4	—
($\sigma_2 n$)	—	—	—	—	—	—	—	—	2	—
($\sigma_2 d$)	—	—	—	—	—	—	—	—	3	—
mu0	0.2	—	—	2	—	—	0.2	—	—	—
(P)	20	—	—	—	—	20	—	—	—	—
τ	—	—	—	—	—	—	—	5000	—	—
tcoff	—	—	—	—	—	—	—	4	—	—

σ = kernel width, $\sigma_2 n$ = variance of observation noise, $\sigma_2 d$ = variance of filter weight diffusion, η = step-size, ϵ = regularization parameter, Λ = Tikhonov regularization, tcoff = learning rate coefficient, τ = memory size (terms retained in truncation), mu0 = coherence criterion threshold, P = memory length, nu = approximate linear dependency (ALD) threshold, and β = forgetting factor for influence.

Table 4: Result in terms of MSE, MAE, and DS for mid-price (high + low)/2.

Time window	MSE	Best algorithms out of ten discussed (according to MSE)	MAE	Best algorithms out of ten discussed (according to MAE)	DS	Best algorithms out of ten discussed (according to DS)
1 day	0.030 6	KAPA	1.412 9	KAPA	0.537 8	NORMA
60 minutes	0.009 1	KAPA	0.509 6	KAPA	0.559 2	NORMA
30 minutes	0.005 3	KAPA	0.359 5	KAPA	0.555 8	PROB-LMS
25 minutes	0.004 7	KAPA	0.331 4	KAPA	0.557 8	NORMA
20 minutes	0.003 8	KAPA	0.290 9	KAPA	0.555 0	NORMA
15 minutes	0.003 0	KAPA	0.253 4	KAPA	0.555 6	NORMA
10 minutes	0.002 1	KAPA	0.201 9	KAPA	0.547 2	NORMA
5 minutes	0.001 2	KAPA	0.144 7	KAPA	0.534 2	PROB-LMS
1 minute	0.000 27	KAPA	0.059 0	KAPA	0.549 6	NORMA

Table 5: Result in terms of MSE, MAE, and DS for mid-price (open + close)/2.

Time window	MSE	Best algorithms out of ten discussed (according to MSE)	MAE	Best algorithms out of ten discussed (according to MAE)	DS	Best algorithms out of ten discussed (according to DS)
1 day	0.032 4	KAPA	1.298 9	KAPA	0.597 0	NORMA
60 minutes	0.009 0	KAPA	0.454 1	KAPA	0.636 7	NORMA
30 minutes	0.004 8	KAPA	0.316 8	KAPA	0.654 7	NORMA
25 minutes	0.004 1	KAPA	0.290 3	KAPA	0.659 2	NORMA
20 minutes	0.003 3	KAPA	0.254 3	KAPA	0.658 0	NORMA
15 minutes	0.002 6	KAPA	0.219 8	KAPA	0.665 2	KNLMS
10 minutes	0.001 7	KAPA	0.174 7	KAPA	0.666 6	KNLMS
5 minutes	0.000 9	KAPA	0.122 4	KAPA	0.662 8	KNLMS
1 minute	0.000 25	KAPA	0.055 2	KAPA	0.601 8	KNLMS

results. The table's data clearly demonstrate the proposed method's superiority over a number of other ways

4.6. Effect of Different Kernels. In Table 7, we can see the effect of different kernel methods. For this test, we used a thirty-minute time window (Stock-TITAN) with the algorithm KAPA and analyzed the best performance of RBF kernel in terms of MSE. That is why, we have chosen RBF kernel (gauss) for each algorithm.

4.7. Experimentation with Dictionary Size. We also conducted experiments with various dictionary sizes. The result for this test is shown in Table 8. For this test, we used a thirty-minute time window with the algorithm KMCC. It is visible

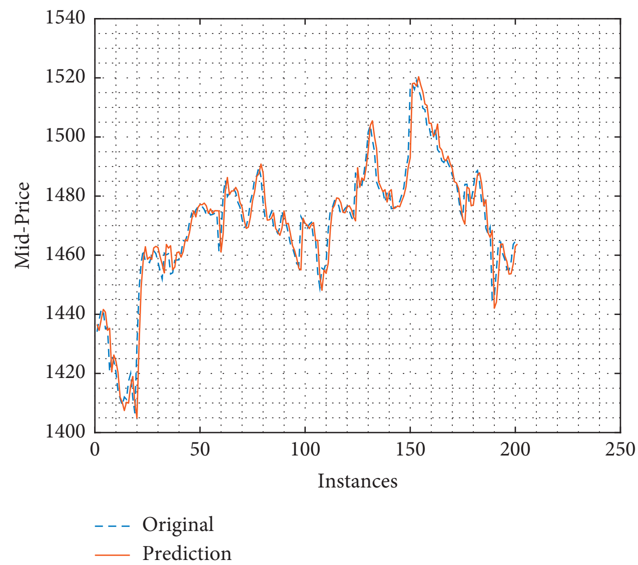

Figure 2: Prediction for one stock (TITAN) using KAPA (high + low)/2.

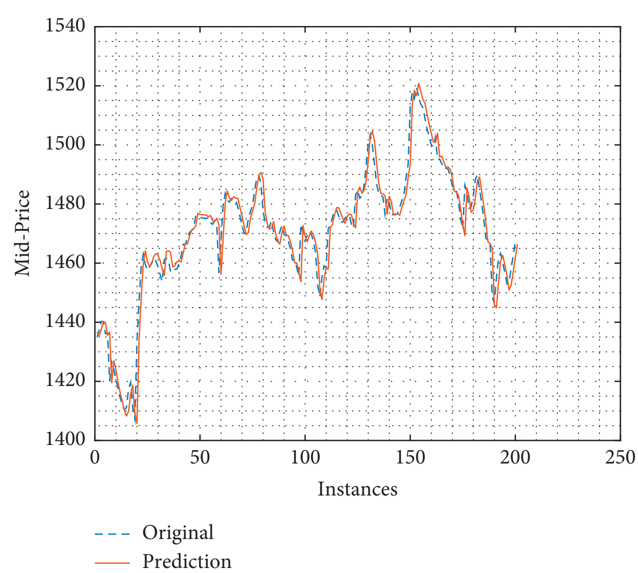

Figure 3: Prediction for one stock (TITAN) using KAPA (open + close)/2.

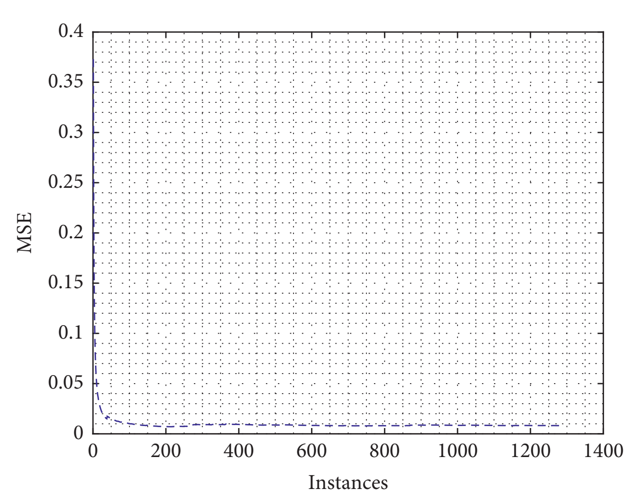

Figure 4: Error convergence for one stock (TITAN) using KAPA (high + low)/2.

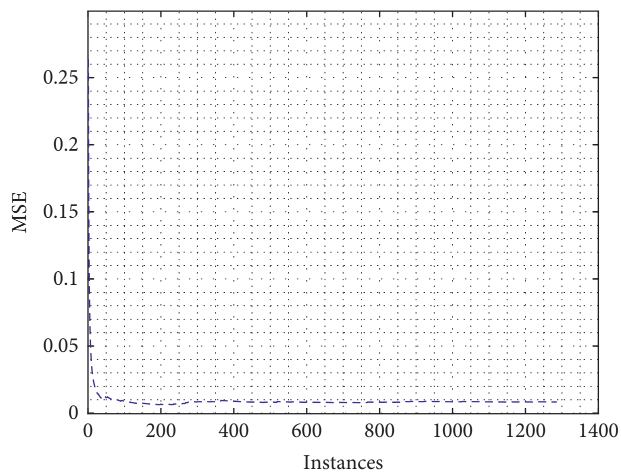

Figure 5: Error convergence for one stock (TITAN) using KAPA (open + close)/2.

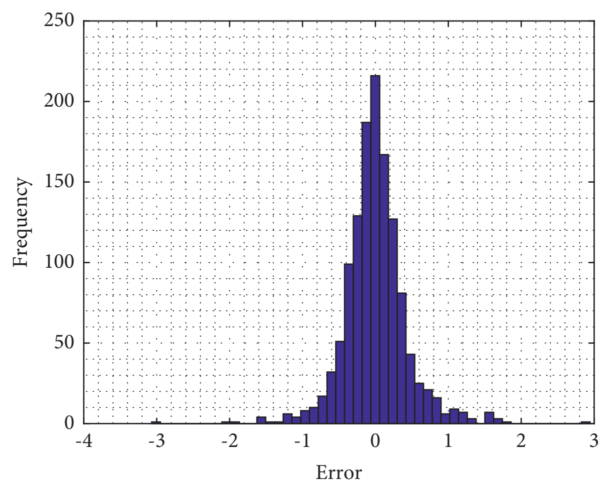

Figure 6: Error residuals for one stock (TITAN) using KAPA (high + low)/2.

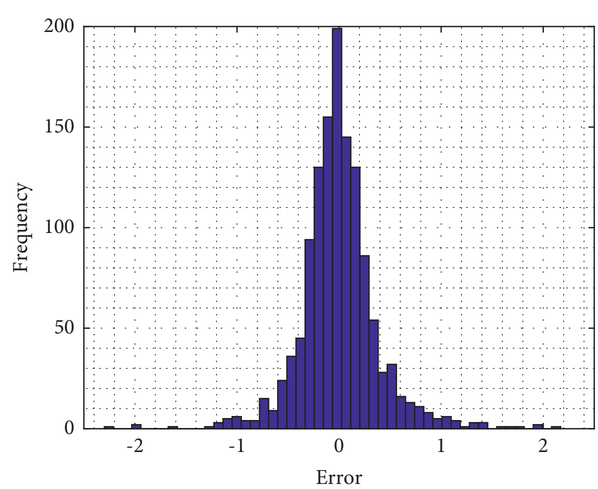

Figure 7: Error residuals for one stock (TITAN) using KAPA (open + close)/2.

Table 6: The proposed research is compared to different state-of-the-art stock prediction approaches.

Method	MSE	Execution time (s)
LSTM [28]	0.683 1	256.16
LSTM [29]	0.681 7	945.09
LSTM [44]	0.682 4	1770.40
KAPA (proposed method)	**0.009 1**	2.132

Table 7: Effect of different kernel methods on time window of thirty minutes (Stock-TITAN) using KAPA for (high + low)/2.

	(High + low)/2			(Open + close)/2		
Kernel function	MSE	MAE	DS	MSE	MAE	DS
RBF kernel (Gauss)	0.008 120	0.298 57	0.534 21	0.008 27	0.260 47	0.531 88
Anisotropic RBF kernel (Gauss-anis)	0.019 19	0.406 17	0.515 55	0.025 35	0.348 68	0.579 31
Laplace kernel (Laplace)	0.008 128	0.298 72	0.533 43	0.008 28	0.260 61	0.531 10

Table 8: The influence of dictionary size.

Dictionary size	MSE	MAE	DS	Execution time (s)
500	0.014 8	0.368	0.545 8	0.820 2
1000	0.032 3	0.530 2	0.614 3	0.853 3
5000	0.011 37	0.308 0	0.644 6	1.314

The algorithm chose KMCC (30 minutes).

from Table 8 that increasing the dictionary size leads to an improvement in the system's performance. It should be noted here that when the size is 1000, the performance has fallen. The reason for this behavior could be the erratic behavior of the stock, the presence of noise, or too much irrelevant data. The exact reason is unknown. However, it is worth noting that with a dictionary size of 500, for forecasting a single stock, execution time is 0.82 seconds. This low number clearly shows the advantage one can achieve in high-frequency trading.

4.8. Important Note: Error Minimization and Profitability. We obtain an MSE of 10^{-4} as the lowest error. We can observe from Tables 4 and 5 that KAPA gives best results in terms of MSE and MAE. It is important to note that, in the one-minute time window, we reached a minimum error value. From Tables 4 and 5, we can also see that going down the column (for MSE and MAE only), the results are improving with the one-minute time window giving the best figures. However, because the time window is one minute, the volatility is low enough that decreasing error will not result in too much benefit. Moreover, there is too much noise while trading at one-minute window. To look at it another way, one-minute volatility is lower, resulting in very close predictions. However, in a low-volatility environment, the chances of taking a position and making a highly profitable trade are also low.

5. Conclusion and Future Work

This paper focuses on predicting a stock's mid-price. Predicting a financial nonstationary time series is an open fundamental and a nontrivial problem of literature. To address this, we proposed a framework based on online learning-driven KAF algorithms. In the proposed work, ten different KAF algorithms were evaluated and analyzed on Indian National Stock Exchange (Nifty-50). In contrast to the existing methods, experiments are performed on nine different time windows. This was done keeping in mind the method's applicability in intraday and swing trading. Previous studies often underestimated the importance of intraday time windows. We, therefore, tried to bridge this gap through the work presented here. The experimental results show the superiority and predictive capabilities of the work. The KAF class of algorithms was also discovered to be not only efficiently working in execution time but also providing best results of error minimization, demonstrating their importance in high-frequency trading. The goal of the research was to propose a KAF-based method for the prediction of stock's mid-price. The empirical results on Nifty-50 dataset show that the proposed method achieved superior performance over existing stock prediction methods. On voting schema KAPA shown better prediction performance with all-time windows, NORMA & KNLMS gave the best performance in terms of directional symmetry. It is worth noting that every KAF-based algorithm is hyperparameter-sensitive. As a result, in the future, we will experiment with various hyper-parameter optimization approaches in order to enhance the framework's predictive capabilities.

Data Availability

The data used to support the findings of this study are available from the corresponding author upon request.

Conflicts of Interest

The authors declare that there are no conflicts of interest regarding the study.

Acknowledgments

The authors would like to thank Taif University Researchers Supporting Project, Taif University, Taif, Saudi Arabia (no. TURSP-2020/26).

References

[1] Y. S. Abu-Mostafa and A. F. Atiya, "Introduction to financial forecasting," *Applied Intelligence*, vol. 6, no. 3, pp. 205–213, 1996.

[2] A. Abraham, N. S. Philip, and P. Saratchandran, "Modeling chaotic behavior of stock indices using intelligent paradigms," 2004, https://arxiv.org/ftp/cs/papers/0405/0405018.pdf.

[3] M. P. Clements, P. H. Franses, and N. R. Swanson, "Forecasting economic and financial time-series with non-linear models," *International Journal of Forecasting*, vol. 20, no. 2, pp. 169–183, 2004.

[4] M. Kumar and M. Thenmozhi, "Forecasting stock index movement: a comparison of support vector machines and random forest," in *Proceedings of the Indian institute of capital markets 9th capital markets conference paper*, Mumbai, India, January 2006.

[5] R. Singh and S. Srivastava, "Stock prediction using deep learning," *MultimedForecasting stock index movement: a comparison of support vector machines and random forestdia Tools and Applications*, vol. 76, no. 18, pp. 18569–18584, 2017.

[6] M. Vijh, D. Chandola, V. A. Tikkiwal, and A. Kumar, "Stock closing price prediction using machine learning techniques," *Procedia Computer Science*, vol. 167, pp. 599–606, 2020.

[7] S.-C. Huang, C.-C. Chiou, J.-T. Chiang, and C.-F. Wu, "A novel intelligent option price forecasting and trading system by multiple kernel adaptive filters," *Journal of Computational and Applied Mathematics*, vol. 369, p. 112560, 2020.

[8] M. Han, S. Zhang, M. Xu, T. Qiu, and N. Wang, "Multivariate chaotic time series online prediction based on improved kernel recursive least squares algorithm," *IEEE transactions on cybernetics*, vol. 49, no. 4, pp. 1160–1172, 2018.

[9] W. Liu, J. C. Principe, and S. Haykin, *Kernel Adaptive Filtering: A Comprehensive Introduction*, vol. 57, John Wiley & Sons, New Jersey, United States, 2011.

[10] W. Weifeng Liu, I. Il Park, and J. C. Principe, "An information theoretic approach of designing sparse kernel adaptive filters," *IEEE Transactions on Neural Networks*, vol. 20, no. 12, pp. 1950–1961, 2009.

[11] B. Chen, S. Zhao, P. Zhu, and J. C. Príncipe, "Quantized kernel least mean square algorithm," *IEEE Transactions on Neural Networks and Learning Systems*, vol. 23, no. 1, pp. 22–32, 2011.

[12] J. Q. Candela and O. Winther, "Incremental Gaussian processes," *Advances in Neural Information Processing Systems*, pp. 1025–1032, 2003.

[13] J. Pardo, F. Zamora-Martínez, and P. Botella-Rocamora, "Online learning algorithm for time series forecasting suitable for low cost wireless sensor networks nodes," *Sensors*, vol. 15, no. 4, pp. 9277–9304, 2015.

[14] S. Garcia-Vega, X.-J. Zeng, and J. Keane, "Stock returns prediction using kernel adaptive filtering within a stock market interdependence approach," *Expert Systems with Applications*, vol. 160, Article ID 113668, 2020.

[15] X. Zhong and D. Enke, "Forecasting daily stock market return using dimensionality reduction," *Expert Systems with Applications*, vol. 67, pp. 126–139, 2017.

[16] S. Jeon, B. Hong, and V. Chang, "Pattern graph tracking-based stock price prediction using big data," *Future Generation Computer Systems*, vol. 80, pp. 171–187, 2018.

[17] J. Eapen, D. Bein, and A. Verma, "Novel deep learning model with cnn and bi-directional lstm for improved stock market index prediction," in *Proceedings of the 2019 IEEE 9th annual computing and communication workshop and conference (CCWC)*, pp. 0264–0270, IEEE, Las Vegas, NV, USA, January 2019.

[18] N. Zhang, A. Lin, and P. Shang, "Multidimensionalk-nearest neighbor model based on EEMD for financial time series forecasting," *Physica A: Statistical Mechanics and Its Applications*, vol. 477, pp. 161–173, 2017.

[19] M. Kumar and M. Thenmozhi, "Forecasting stock index returns using arima-svm, arima-ann, and arima-random forest hybrid models," *International Journal of Banking, Accounting and Finance*, vol. 5, no. 3, pp. 284–308, 2014.

[20] Y. Qiu, H.-Y. Yang, S. Lu, and W. Chen, "A novel hybrid model based on recurrent neural networks for stock market timing," *Soft Computing*, vol. 24, pp. 1–18, 2020.

[21] K. George and P. Mutalik, "A multiple model approach to time-series prediction using an online sequential learning algorithm," *IEEE Transactions on Systems, Man, and Cybernetics: Systems*, vol. 49, no. 5, pp. 976–990, 2017.

[22] T. Choudhary, V. Mishra, A. Goswami, and J. Sarangapani, "A comprehensive survey on model compression and acceleration," *Artificial Intelligence Review*, vol. 53, no. 7, pp. 5113–5155, 2020.

[23] E. Hoseinzade and S. Haratizadeh, "CNNpred: CNN-based stock market prediction using a diverse set of variables," *Expert Systems with Applications*, vol. 129, pp. 273–285, 2019.

[24] M. Kaur and D. Singh, "Multi-modality medical image fusion technique using multi-objective differential evolution based deep neural networks," *Journal of Ambient Intelligence and Humanized Computing*, vol. 12, no. 2, pp. 2483–2493, 2021.

[25] H. Kaushik, D. Singh, M. Kaur, H. Alshazly, A. Zaguia, and H. Hamam, "Diabetic retinopathy diagnosis from fundus images using stacked generalization of deep models," *IEEE Access*, vol. 9, pp. 108276–108292, 2021.

[26] C. Sang and M. Di Pierro, "Improving trading technical analysis with tensorflow long short-term memory (lstm) neural network," *The Journal of Finance and Data Science*, vol. 5, no. 1, pp. 1–11, 2019.

[27] M. Nabipour, P. Nayyeri, H. Jabani, A. Mosavi, E. Salwana, and S. Sahab, "Deep learning for stock market prediction," *Entropy*, vol. 22, no. 8, p. 840, 2020.

[28] P. Gao, R. Zhang, and X. Yang, "The application of stock index price prediction with neural network," *Mathematical and Computational Applications*, vol. 25, no. 3, p. 53, 2020.

[29] A. Moghar and M. Hamiche, "Stock market prediction using lstm recurrent neural network," *Procedia Computer Science*, vol. 170, pp. 1168–1173, 2020.

[30] M. Yukawa, "Multikernel adaptive filtering," *IEEE Transactions on Signal Processing*, vol. 60, no. 9, pp. 4672–4682, 2012.

[31] J. Fernandez-Bes, V. Elvira, and S. Van Vaerenbergh, "A probabilistic least-mean-squares filter," in *Proceedings of the 2015 IEEE International Conference on Acoustics, Speech and Signal Processing (ICASSP)*, pp. 2199–2203, IEEE, South Brisbane, QLD, Australia, April 2015.

[32] S. Garcia-Vega, X.-J. Zeng, and J. Keane, "Stock price prediction using kernel adaptive filtering within a stock market

interdependence approach," *SSRN Electronic Journal*, vol. 160, p. 113668, 2020.
[33] V. Yadav, A. K. Yadav, M. Kaur, and D. Singh, "Trigonometric mutation and successful-parent-selection based adaptive asynchronous differential evolution," *Journal of Ambient Intelligence and Humanized Computing*, pp. 1–18, 2021.
[34] Z. Liu, C. K. Loo, K. Pasupa, and M. Seera, "Meta-cognitive recurrent kernel online sequential extreme learning machine with kernel adaptive filter for concept drift handling," *Engineering Applications of Artificial Intelligence*, vol. 88, Article ID 103327, 2020.
[35] S. Garcia-Vega, X.-J. Zeng, and J. Keane, "Learning from data streams using kernel least-mean-square with multiple kernel-sizes and adaptive step-size," *Neurocomputing*, vol. 339, pp. 105–115, 2019.
[36] W. Liu, P. P. Pokharel, and J. C. Principe, "The kernel least-mean-square algorithm," *IEEE Transactions on Signal Processing*, vol. 56, no. 2, pp. 543–554, 2008.
[37] W. Liu and J. C. Príncipe, "Kernel affine projection algorithms," *EURASIP Journal on Applied Signal Processing*, vol. 2008, pp. 1–12, 2008.
[38] S. Zhao, B. Chen, P. Zhu, and J. C. Príncipe, "Fixed budget quantized kernel least-mean-square algorithm," *Signal Processing*, vol. 93, no. 9, pp. 2759–2770, 2013.
[39] S. Zhao, B. Chen, and J. C. Principe, "Kernel adaptive filtering with maximum correntropy criterion," in *Proceedings of the 2011 International Joint Conference on Neural Networks*, pp. 2012–2017, IEEE, San Jose, CA, USA, June 2011.
[40] S. K. Ahn and G. C. Reinsel, "Estimation for partially nonstationary multivariate autoregressive models," *Journal of the American Statistical Association*, vol. 85, no. 411, pp. 813–823, 1990.
[41] T. Ouyang, H. Huang, Y. He, and Z. Tang, "Chaotic wind power time series prediction via switching data-driven modes," *Renewable Energy*, vol. 145, pp. 270–281, 2020.
[42] A. H. Moghaddam, M. H. Moghaddam, and M. Esfandyari, "Stock market index prediction using artificial neural network," *Journal of Economics, Finance and Administrative Science*, vol. 21, no. 41, pp. 89–93, 2016.
[43] M. R. Hassan, "A combination of hidden Markov model and fuzzy model for stock market forecasting," *Neurocomputing*, vol. 72, no. 16-18, pp. 3439–3446, 2009.
[44] M. Nikou, G. Mansourfar, and J. Bagherzadeh, "Stock price prediction using deep learning algorithm and its comparison with machine learning algorithms," *Intelligent Systems in Accounting, Finance and Management*, vol. 26, no. 4, pp. 164–174, 2019.

Hindawi
Scientific Programming
Volume 2022, Article ID 5377984, 9 pages
https://doi.org/10.1155/2022/5377984

Research Article

Green and Environmental Protection Recycled Concrete in Road Engineering

Yulong Ma,[1] Yongcheng Ji ,[1] and Lei Jin[2]

[1]*College of Civil Engineering, Northeast Forestry University, Harbin 150040, China*
[2]*College of Economics and Management, Tianjin University, Tianjin 300000, China*

Correspondence should be addressed to Yongcheng Ji; yongchengji@nefu.edu.cn

Received 11 December 2021; Revised 3 January 2022; Accepted 21 January 2022; Published 15 February 2022

Academic Editor: Punit Gupta

In response to a series of national strategic guidelines for green and sustainable development, recycled concrete is used as a recyclable resource. First, the mechanical properties, workability, and durability of recycled concrete are briefly introduced, and the benefit and necessities of research on recycled concrete are described from environmental, economic, and social perspectives. Second, the mixing method and molding process of recycled concrete are described in detail, and the influence of vibration molding and compression molding on the performance of recycled concrete is analyzed. It is found that the compressive strength first increases and then decreases with the increase of molding pressure. In addition, porosity decreases as molding pressure build-up. Therefore, it is recommended that the molding pressure of recycled concrete be generally controlled between 600 and 800 N. Then, the influence of the water-cement ratio on recycled concrete's fluidity and mechanical properties is discussed. It is found that with the increase of the water-cement ratio, the compressive strength first increases and then decreases and the optimum water-cement ratio is proposed to be 0.2. Finally, the application status and problems of recycled concrete in road engineering are briefly described, and relevant suggestions for construction technology are put forward. Based on the fire safety and reliability requirements of concrete structures, the performance of high-performance concrete structures after fire can be restored to the initial level or even improved through the processes and measures of building structure design, repair, and reinforcement; the strength and crack healing of high-performance concrete after fire can be gradually restored by applying or soaking repair agent and water curing; the recovery of pH value of concrete after fire and the reduction of carbonation depth can be realized by using electrochemical realkalization technology; using carbon fiber to strengthen the components after fire can restore the bearing capacity, but the degree of stiffness recovery is low; and beam side steel plate reinforcement and steel bonding reinforcement can realize the recoverability of bearing capacity, stiffness, and ductility of members after fire.

1. Introduction

For decades, China's economic development has made remarkable achievements, and people's basic survival needs have been satisfied already. Since then, people have begun to pay more attention to the quality of life and pursue green development and a healthy lifestyle. Energy conservation, environmental protection, and sustainable development have become the focus of society in this context. However, much construction waste will be generated in traditional road construction, and abandoned concrete is one of them. This phenomenon is contrary to the concept of environmental protection and sustainability, taken seriously by the industry and the country. Therefore, a technology for making green and environmental-friendly recycled concrete from abandoned concrete and reusing it for road engineering construction has been widely studied and applied [1].

The research shows that the demand for recycled coarse aggregate exceeds the supply of waste concrete, indicating that the market prospect of recycled coarse aggregate is broad [2]. Huang et al. [3] studied the effect of recycled coarse aggregate gradation on the shear behavior of recycled concrete and found that the shear strength of well-graded recycled coarse aggregate is greater than that of poorly graded and discontinuous graded recycled coarse aggregate.

Xiong et al. [4] studied the mechanical properties of recycled concrete with different coarse aggregate substitution rates and put forward the prediction formula of compressive strength. Liang et al. [5] studied the effect of different coarse aggregate substitution rates on hysteretic energy and found that hysteretic energy increased with the coarse aggregate substitution rate increase. Wajeeha et al. [6] studied the durability of recycled concrete with different replacement rates of recycled coarse aggregate in a chloride environment. Through the pull-out test, it is found that 30% of natural coarse aggregate concrete can be used as structural concrete in Pakistan's construction sector. Zhang et al. [7] studied the mechanical properties of recycled concrete with the replacement rate of a recycled coarse aggregate of 0%, 25%, 50%, 75%, and 100%, respectively. The results show that with the increase of the replacement rate of recycled coarse aggregate, the mechanical properties of concrete show a linear downward trend. Therefore, it is concluded that the amount of recycled coarse aggregate in road construction should not exceed 50%, considering the dry shrinkage and temperature shrinkage test results. Xie et al. [8] studied cast-in situ recycled aggregate concrete's mechanical properties and durability under chemical sulfate attack, prepared concrete cylinders with recycled concrete aggregates of 0%, 30%, 50%, and 100%, respectively. They found that recycled concrete aggregates have a significant impact on the mechanical properties of concrete. Marian et al. [9] prepared recycled concrete with the replacement rate of a recycled coarse aggregate of 50% and 100%, respectively. Three specimens with different curing periods (7, 14, and 28 days) were tested. The results show that with the increase of recycled aggregate content, the compressive strength and flexural strength of all recycled concrete decrease, while the density is slightly affected. Kashkash saied et al. [10] prepared four mixtures using recycled concrete aggregate and recycled crushed aggregate as natural coarse aggregate substitutes with different replacement percentages. A series of tests were carried out to study the characteristics of fresh and hardened concrete samples prepared from mixtures of various components. The results show that recycled concrete with recycled aggregate instead of 50% natural coarse aggregate can have sufficient fresh and hardening properties. Although the compressive strength of recycled concrete is higher than that of conventional concrete, the workability of recycled concrete mix proportion decreases significantly.

All of above studies are conducted. However, the benefits and properties of recycles concrete are not clear. The procedure and methodology of recycled concrete construction need to be further investigated.

2. Property Characteristics of Green and Environmental-Friendly Recycled Concrete

Although green recycled concrete is economically and environmentally friendly, its relevant property cannot be comparable to that of ordinary concrete due to the process of rebuilding after crushing abandoned concrete and is one grade worse than that of ordinary concrete. Therefore, before road engineering application, it is necessary to study its property characteristics in detail. Furthermore, the preparation process of green recycled concrete should be selected according to different requirements in specific road construction [11].

2.1. Mechanical Properties. The application characteristics of concrete material in road engineering require that concrete material have a specific bearing capacity, mainly reflected by its mechanical properties. The mechanical properties of green environmental-friendly concrete are related to its breaking method of recycled aggregate, the strength of abandoned concrete, water-cement ratio, and specific construction environment [12]. According to the research, the strength of recycled concrete is inversely proportional to the replacement rate of recycled aggregate, positively proportional to the water-binder ratio, and positively proportional to the strength of abandoned concrete. The smaller the replacement rate of recycled aggregate, the greater the strength; the higher the water-binder ratio, the stronger the strength, and the stronger the abandoned concrete is, the stronger the recycled concrete will be.

2.2. Workability. The workability of green recycled concrete is related to the replacement rate of recycled aggregate and the water-binder ratio. Compared with ordinary concrete, recycled concrete is made of abandoned concrete after crushing, and the surface of recycled aggregate is so rough that the water absorption performance is more significant than ordinary concrete. Consequently, the slumps of recycled concrete are smaller than that of ordinary concrete with similar conditions. Specifically, the slumps of recycled concrete are inversely proportional to the content of recycled concrete and are positively proportional to its water-binder ratio, that is, the less recycled aggregate, the greater the slumps of recycled concrete; and the smaller the water-binder ratio is, the smaller the slumps of recycled concrete is [13].

2.3. Durability. For all concrete materials, durability is a crucial property index, which determines the severity of the application environment of concrete materials and the service life of the concrete. Under normal circumstances, compared with two kinds of concrete materials with similar conditions, recycled concrete has better crack resistance, but its freeze-thaw resistance and permeability resistance are not as good as ordinary concrete materials [14]. For recycled concrete, its permeability resistance can be improved by adding fly ash, and its freeze-thaw resistance can be improved by reducing its water-binder ratio. However, improving the property of recycled concrete will inevitably lead to the increase of its preparation cost, which requests the engineers to select the optimal balance point according to the application requirements of road engineering and the comprehensive consideration of cost.

3. Benefits of Recycled Concrete Applied in Road Engineering

3.1. Environmental Benefits. At present, the abandoned concrete generated in the construction of domestic road engineering is mostly stacked in the open air, occupying many land resources, which pollutes the urban environment and harms the urban landscape, and causes a massive waste of resources. In addition, during the handling and stacking of abandoned concrete, problems such as dust raising will occur, aggravating environmental pollution. Therefore, recycling abandoned concrete during road construction can save resources, protect the environment, and significantly contribute to China's energy saving and environmental protection.

3.2. Economic Benefits. In the construction of a new road project or road widening and rebuilding project, many concrete materials are generally required. Stone concrete is one of the indispensable materials. However, stones are often unavailable locally and need to be transported from tens of kilometers, resulting in higher transportation costs, which directly increases the production cost of concrete materials. At this point, the economic value of recycled concrete and be highlighted. In road engineering construction, if the abandoned concrete is reused and processed into concrete aggregate, it can reduce the transportation cost of stone and reduce the material cost of stone, thus reducing the cost of concrete. Furthermore, it is worth noting that a large amount of abandoned concrete will be generated when repairing the pavement of a high-grade highway, which has few impurities and can be used for processing and making concrete aggregate instead of stone. In a word, the recycling of abandoned concrete in road engineering can reduce the cost of concrete to a great extent and has significant economic value.

3.3. Social Benefits. The Chinese government has paid much more attention to energy conservation, environmental protection, and resource reuse in recent years. In this context, recycled concrete in road engineering construction is a reform and innovation of road construction technology and can promote the sustainable development of China's basic transportation construction.

4. Study on Preparation Technology of Recycled Concrete

Unlike ordinary concrete, recycled concrete is a uniquely functional building material with a porous structure composed of a layer of cement slurry on the surface of coarse aggregates. The improper preparation process will result in uneven pore distribution and an increased proportion of discontinuous pores in concrete [15]. Therefore, unique methods and techniques should be adopted during mixing, molding, and maintaining.

4.1. Research on the Mixing Process. The mixing process of ordinary concrete usually adopts a mixing method, which is easy enough to operate. However, recycled concrete belongs to stiff concrete, and there is no ball effect produced by fine aggregate during the mixing process. Therefore, the high resistance and the coarse aggregates are very vulnerable to crushing. Moreover, improper mixing sequence and charging sequence will result in slurry aggregation, significantly reducing the proportion of connected porosity of recycled concrete. Consequently, it is of great significance to study the mixing process of recycled concrete.

The mixing method in this paper refers to the wrapped slurry process, which significantly improves the property of recycled concrete by changing the order of raw materials' charging sequence and significantly increases the proportion of connected porosity in concrete on the premise of the high strength of recycled concrete. Specific steps are as follows: First, add all the coarse aggregates and 50% water into the mixer and stir for 30 seconds, which can clean the aggregate surface and avoid forming weak areas between the cement slurry and the coarse aggregates. Moreover, wetting the surface can increase the bonding effect with the cement; second, 100% cement, water, and additives are added and stirred for 180 seconds. In this way, the aggregate surface is evenly coated with a high flow slurry, which can significantly reduce the friction between the aggregate, thus preventing the crushing of coarse aggregate due to excessive resistance. Moreover, the slurry is evenly wrapped on the surface of coarse aggregate, making it further spheroid [16]. The spheres bond with each other from point to point and surface to surface. As a result, the proportion of concrete-connected porosity is significantly increased under the premise of the high strength of recycled concrete.

4.2. Research on the Molding Process. Coarse aggregates account for about 60% of the recycled concrete, and the friction between them is so great that the compactness of the structure cannot be satisfied only by rodding. On the other hand, standard molding methods mainly include vibration molding and compression molding. Therefore, it is essential to study the influence of the mentioned two methods on the property of recycled concrete.

4.2.1. Influence of Vibration Molding on Properties of Recycled Concrete. Recycled concrete was prepared from coarse aggregate with a single-particle size of 9.5–16 mm, with a water-cement ratio of 0.20 and a cement-aggregate ratio of 1/6. The fresh concrete is loaded in three layers into the mold of $100 \times 100 \times 100 \mathrm{mm}^3$, and the thickness of each layer should not be more than 5 mm, inserting from all sides to the center screw for at least 15 times with the 25 mm ramming rod. Then, the connected mold of the specimen was placed on the vibration table for 0–SC, respectively, and put into the standard curing room later. After 1 day, the specimen was demolded and put back into the stand curing room for 3 days and 28 days. The strength and porosity of recycled concrete with different vibration times are tested, respectively [17].

Figures 1 and 2 show the influence of vibration time on recycled concrete's compressive strength and porosity. It can be seen that with the increase of vibration time, the porosity of recycled concrete gradually decreases, while the strength first increases and then decreases. When the time remains about 8s, the strength reaches its maximum value. It is mainly because of the increase of vibration time. The aggregates become more and more compact from the loose deposit under the vibration. Moreover, the aggregate is bonded point to point and surface to surface, producing an effect of mechanical bit [18], so the compressive strength is obviously higher than that of nonvibration recycled concrete. However, with the accumulation of the vibration time, the cement slurry wrapped in the aggregate surface slides and densely distributes at the bottom of the concrete. As a result, the slurry volume on the concrete upper part and the bonding area between the aggregates decreases, which leads to the decline of the overall compressive strength of recycled concrete. The cement slurry concentrated at the bottom of concrete forms a dense layer (shown in Figures 1 and 2), which seriously affects the connectivity between the upper and lower layers of recycled concrete. However, the vibration time is related to the water-cement ratio and the amount of slurry used, so the specific engineering test should determine the specific vibration time.

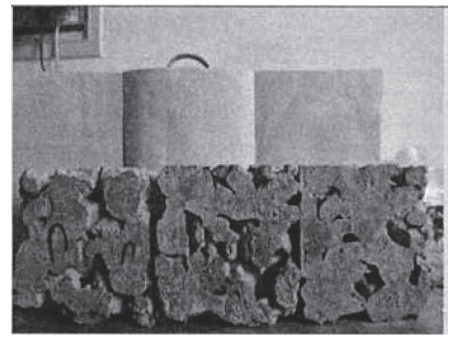

Figure 1: Overlong vibration time.

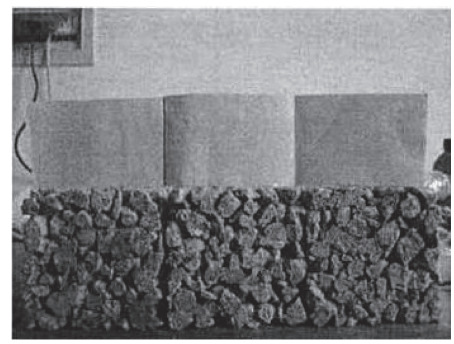

Figure 2: Proper vibration time [17].

4.2.2. Influence of Compression Molding on Properties of Recycled Concrete. Due to the high viscosity of fresh mixed recycled concrete, it cannot be fully compacted by mechanical vibration only. Therefore, in addition to vibration molding, compression molding is mainly used in China. After the fresh concrete is loaded in three layers into the mold of $100 \times 100 \times 100 mm^3$, pressure is applied to the surface to promote the compactness of the whole structure of recycled concrete [19]. The raw materials and mix ratio used in this test are the same as that of vibration molding, but the molding pressure is changed to 400N–1000 N during the molding process, lasting for 5 seconds. The test results are shown in the following figure.

Figures 3 shows the influence of molding pressure on recycled concrete's compressive strength and porosity. It can be seen from Figure 4 that the relationship between molding pressure and compressive strength is not simply linear. With the increase of molding pressure, the compressive strength increases first and then decreases, while the porosity decreases continuously with the accumulation of molding pressure. It is mainly due to the volume compression of the loose concrete after the press pours ramming at the beginning. As a result, the volume of recycled concrete changes, the porosity is constantly reduced, and the aggregate is more closely combined, so the compressive strength shows a rising trend. However, when the molding pressure increases to a certain extent, the aggregate is in closed contact with each other, and the volume of recycled concrete cannot be further reduced. At this time, a continuous increase of pressure may cause damage to the contact point or aggregate, leading to the decline of the compressive strength. Therefore, the molding pressure of concrete is generally controlled between 600 and 800N [20].

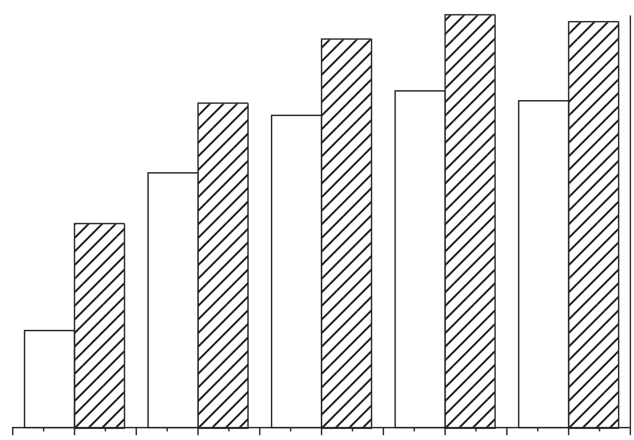

Figure 3: Effect of molding pressure on compressive strength.

Improper selection of molding technology is likely to cause uneven pore distribution and an increase of discontinuous pore in concrete. In order to verify the rationality of the combined molding process of vibration molding and compression molding [21], a cylindrical recycled concrete specimen with a size of 110 mm × 150 mm was prepared with 9.5–16 mm single-particle aggregates in this test. The axial plane porosity distribution of recycled concrete when vibration time is 8 seconds, and molding pressure remains 800N combined with CT scanning technology.

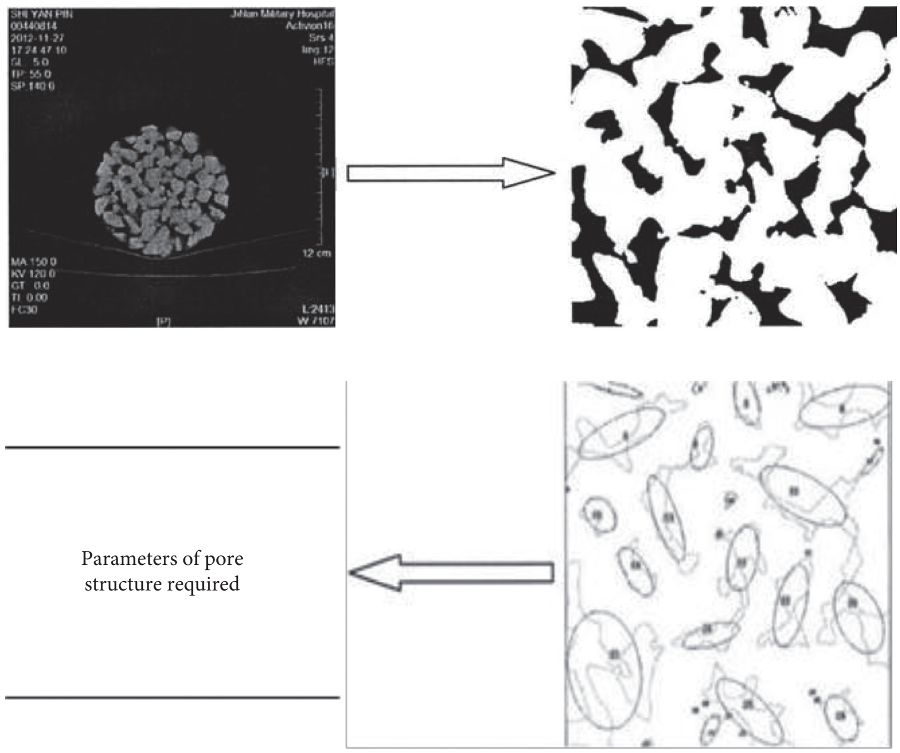

Figure 4: Scanned image processing schematic diagram [18].

5. Influence of Water-Cement Ratio on Properties of Recycled Concrete

The water-cement ratio is an essential parameter for recycled concrete, which determines the workability of the concrete and has a specific influence on its compressive strength, pore structure, and permeability performance. The appropriate water-cement ratio is the first step to prepare recycled concrete successfully [22]. So far, there is no specific method to determine the water-cement ratio in China. The crushed basalt with a 9.5–16 mm particle size was selected in this test to prepare the recycled concrete with the cement-aggregate ratio of 1/6 and the water-cement ratio of 0.18–0.24 [23]. Moreover, standard maintenance is carried out by artificial ramming, vibration, and compression. The influence of water-cement ratio on recycled concrete's compressive strength and porosity for 3 and 28 days is discussed. The results are shown in the table below.

It can be seen from Table 1 that for a particular cement, there is an optimum water-cement ratio under the same aggregate gradation, cement-aggregation ratio, and molding curing process. The compressive strength of recycled concrete shows an upward trend when the water-cement ratio increases from 0.18 to 0.20. This is mainly due to the low water-cement ratio, easy agglomeration of slurry, and uneven wrapping of aggregate surface, so that the friction between them increases significantly, and the strength is relatively low because of insufficient stirring. While the water-cement ratio is more than 0.20, the slurry will slide off the aggregate and deposit at the bottom of the concrete due to its own gravity during the preparation of recycled concrete. This not only results in a significant reduction of the cementing materials on the upper part of concrete, different compactness of test block on the upper and lower sides, and a reduction of overall compressive strength but also enriches cement slurry on the bottom of recycled concrete [24], forming a dense cement slurry layer, which seriously affects the connectivity of pore. When the water-cement ratio is 0.20, the fluidity of cement slurry is moderate, and the aggregate surface is evenly coated with a layer of slurry. Therefore, the overall structure is stable enough. Moreover, the compressive strength for 3 days and 28 days of concrete is 12.46 MPa and 13.85 MPa, respectively.

The influence of fluidity on mechanical properties and porosity of recycled concrete was discussed by measuring the slurry fluidity under different water-cement ratios with reference to test method for fluidity of cement mortar (GB2419) [25]. It can be seen from Table 1 and Figure 5 that the water-cement ratio determines the fluidity of slurry, whereas the fluidity determines the uniformity of concrete aggregate coating. When the water-cement ratio is less than 0.18, the slurry fluidity is less than 170 mm, and the slurry is rugged and easy to agglomerate. Moreover, the aggregate cannot be evenly wrapped. As a result, the fresh concrete is loose, dry, and dull. When the water-cement ratio is 0.18–0.22, the fluidity of slurry is between 170 mm and 220 mm, and the appearance of freshly mixed concrete is improved, with the slurry of good cohesion. However, when the water-cement ratio is more than 0.22, the fluidity is more than 220 mm, and the fresh concrete slurry flows, with the aggregate of poor cohesion. At this time, the slurry will settle to the bottom of the specimen due to its own weight, which will result in partial or complete blockage of the

Table 1: Effect of water-cement ratio on slurry fluidity and porous ecological concrete properties.

Water-cement ratio	Mortar fluidity (Imm)	Cement-aggregate ratio	Aggregate size (mm)	Compressive strength for 28 d (MPa)	Porosity (%)
0.18	168.3	1/6	9.5–16	6.16	28.57
0.20	207.5	1/6	9.5–16	12.46	28.01
0.22	219.6	1/6	9.5–16	9.89	27.44
0.24		1/6	9.5–16	7.33	27.13

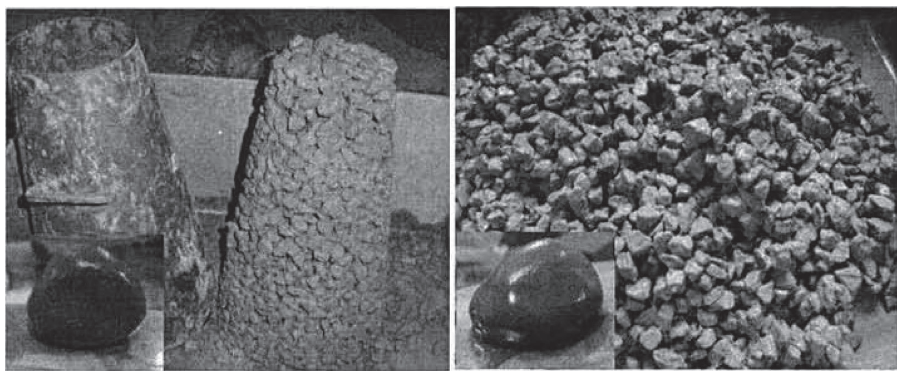

(0.20) (0.24)

Figure 5: Slurry coating aggregate when water-cement ratio is 0.20 and 0.24, respectively [25].

pore at the bottom of the concrete, and the permeation coefficient will be greatly reduced. Therefore, the water-cement ratio of recycled concrete can be determined by measuring the fluidity of slurry in the mix design so that recycled concrete with both porosity and mechanical properties can be prepared. The water-cement ratio of sulphoaluminate brine slurry selected in this test should be controlled between 0.20 and 0.22, and it is the best at 0.20 [26].

6. Application Status and Existing Problems of Recycled Concrete in Road Engineering

6.1. Application Status of Recycled Concrete in Road Engineering. Concrete is the most widely used material in road engineering construction. With the robust construction of highway projects and municipal road projects in China, many problems in natural resources, sustainable development, and environmental protection have arisen. Recycled concrete can be used in road construction requires two main premises: a. the continuous construction of road engineering needs a large number of concrete materials, which will inevitably consume a large number of natural resources and b. when widening and rebuilding the existing roads, there will be many abandoned concrete. This abandoned concrete occupies a considerable space in the processing but also causes some pollution to the environment. The above phenomena are not consistent with the basic policy of green and sustainable development in China, which leads to the imperative of using recycled concrete in road engineering to ensure the sustainable development of road engineering.

Nowadays, more and more road projects use recycled concrete in the construction process. However, when the road engineering pavement exceeds a specific operating time, the mechanical properties of bituminous concrete or cement concrete will deteriorate accordingly. Moreover, when traffic volume on the road exceeds its design level, the road surface will be more or less damaged. Therefore, in terms of the concrete pavement repair [27], the original concrete surface needs to be generally broken first, and then the base is repaired, and finally resurfaces the concrete by paving and rolling.

6.2. Problems Existing in the Application of Recycled Concrete in Road Engineering

6.2.1. The Insufficient Research Depth of Recycled Concrete. At present, green recycled concrete has not become a large-scale application. One of the key reasons is that the current technical research depth is so insufficient that it cannot play a substantial role in supporting its engineering application from a technical perspective. After all, for practical engineering applications, the technology used must be rigorously and carefully verified to ensure the maturity and reliability of the technology. As for recycled concrete, due to the lack of investment in this area, related technical is problematic, resulting in the current technical research and engineering application of recycled concrete has not reached the depth of engineering application. This is also one of the essential bottlenecks hindering the rapid development of recycled concrete.

6.2.2. The Insufficient Standards Followed by the Application. So far, although some laws and regulations have given specific guidance and requirements for applying recycled concrete in road engineering construction, there are still some problems. On the one hand, to meet the laws and regulations of the quality and reliability, some technical details have to be too conservative due to its overall technology immaturity, resulting in an unavoidable cost waste. However, on the other hand, these laws and regulations are not systematic enough, and there is no clear and complete description and requirements for any technical problems in the practical application of recycled concrete. Therefore, it will result in the engineers being afraid to use it without precise specification [28]. Moreover, the investor is unwilling to use recycled concrete for the safety of its investment due to its immature technology.

6.2.3. The Limited Bearing Capacity of Recycled Concrete. In addition to the problems mentioned above, the limitations of properties are also one of the critical reasons that restrict the application range of recycled concrete. From the performance characteristics of recycled concrete in the previous section, it can be seen that under similar conditions, the properties of recycled concrete are generally worse than that of ordinary concrete. This weakness determines the upper limit of the practical application of recycled concrete in engineering, which is destined to be narrower than ordinary concrete. Many researchers are committed to promoting recycled concrete's performance and successfully generating some with strength and properties. However, in general, recycled concrete still has some limitations, restricting its wide application in road engineering.

7. Construction of Recycled Concrete

7.1. Preparations.

(a) Make a comprehensive investigation of the site environment before the construction begins and remove all obstacles that may hinder the normal construction, such as trees and isolation belts.

(b) Damages on the original pavement that this reconstruction cannot repair shall be effectively pretreated before it begins, and different types of damages should resort to different treatment methods:

   (a) In terms of crushed and loose damage, if the depth is greater than the maximum depth of reconstruction, it is necessary to be dug and repaired
   (b) In terms of deformation, based on the construction depth, if the depth reaches more than 30 cm, it needs to be milling before reconstruction
   (c) In terms of cracks, the causes should be figured out first, and the cracks should be properly handled before reconstruction if they are determined to have an impact

(c) Use the milling planer to drive the existing expansion joint. The front and rear ends are milled for 1-2 meters and 2–5 meters, respectively. The milling depth is consistent with the maximum depth of reconstruction, and then, the new mixture shall be used for paving.

(d) Before formal construction, the feasibility should be determined through the construction of the test section, which should be more than 200 meters long, and representative. The construction scheme should be adjusted appropriately accordingly to the results of the test section to ensure the effect of reconstruction.

7.2. Pavement Sweeping and Lining. The pavement surface should be carefully swept before construction to avoid debris and garbage mixed into the mixture. Then draw lines outside the edge of the reconstruction. Of course, the original road surface edge can also be directly used as the baseline of the reconstruction to ensure the aesthetics and straightness of the edge.

7.3. Heating of the Original Road Surface. The original road surface must be heated before the reconstruction. Otherwise, the aggregate will be damaged in raking, thus affecting the quality of construction. At the same time, it is also necessary to prevent the asphalt from aging in advance caused by very high heating temperature. The specific temperature is determined according to previous experience. Moreover, the width of heating needs to be widened by 20 centimeters on both sides, respectively, based on the milling range [29].

7.4. Raking of the Original Road Surface. The depth should be kept uniform while raking. However, if the depth must change, it shall change suddenly but not dramatically. By raking, the roughness of the surface is better, which can create good conditions for subsequent reconstruction. Moreover, it should be noted that the surface temperature should reach over 70°C when the raking is finished.

7.5. Spraying the Rejuvenation Agent. The rejuvenation agent should be sprayed with a particular device. Its walking needs to be linked with the remixer and realize the automatic control. It needs to be sprayed accurately according to the dose determined by design. Apart from that, the rejuvenation agent should also be heated before spraying to improve its fluidity and make it thoroughly fused with asphalt. The temperature needs to be controlled by the limited temperature that does not destroy its function. In addition, the actual amount of rejuvenation agent should be adjusted according to milling depth and its change [30].

7.6. Mixing and Paving. After completing the spraying of the rejuvenation agent and confirming that it meets the requirements of the remixer, use the machine to keep the mixture homogeneous. Then use a paver to spread the mixture evenly with a constant speed of 1.5–5.0 m/min. It is necessary to ensure the uniformity of the surface to prevent segregation, cracks, and galling. In addition, during construction, a particular person should be arranged to track and inspect the paving situation, and once problems are found, they should be dealt with immediately. Properly adjust the power of the screed according to the thickness of the reconstruction layer, make the paved mixture reach a good initial density, and reduce heat loss through the vibration of the screen. During paving, the temperature shall be strictly controlled within the range of 120–150°C.

7.7. Rolling. After the paving is completed, a roller should be applied. There are two main types of rollers, including double-drum roller and pneumatic tyred roller. No matter what kind of roller is chosen, it should be closely followed by the paver in front, but pay attention to prevent collision with the paver. When the double-drum roller is used, appropriate amount of water can be sprayed on the surface in order to avoid that the mixture is bonded with the wheel. But the amount of water should be controlled, not too much to cause accumulation. However, while rolling by pneumatic tyred roller, spraying is generally not required [21]. And where large roller cannot reach, small machines and tools can be used for compaction manually.

7.8. Traffic Opening and Traffic Control. The mixture after compaction can be opened for traffic after natural cooling. However, attention should be paid to maintenance and management in that process, and personnel or vehicles are not allowed to enter. Otherwise, it will cause displacement, make the surface of the reconstruction layer uneven, and affect the subsequent application.

8. Conclusion

Engineering construction is developing continuously, and green environmental protection will be one of its essential requirements and characteristics. Three properties and benefits of green and environmentally friendly recycled concrete are summarized. First, the preparation technology of recycled concrete and the effect of the water-cement ratio are discussed. Then, the procedure of recycled concrete construction is presented after considering the application status and existing problems in recycled concrete road engineering. Thus, it is necessary to study recycled concrete technology to support road engineering construction's green, energy-saving, and sustainable development and accelerate its large-scale application in road engineering.

Data Availability

All data generated or analysed during this study are included in this published article.

Conflicts of Interest

The authors declare that they have no conflicts of interest.

References

[1] J. Song, "Discussion on the application of energy saving and environmental protection road recycled concrete," *Green Environmental Protection Building Materials*, vol. 19, no. 9, 2016.

[2] H. N. Han, I. Tomonori, R. Kubota et al., "Financial and economic evaluation of construction and demolition waste recycling in Hanoi, Vietnam," *Waste Management*, vol. 131, 2021.

[3] Y. Huang, J. Wang, M. Ying, J. Ni, and M. Li, "Effect of particle-size gradation on cyclic shear properties of recycled concrete aggregate," *Construction and Building Materials*, vol. 301, 2021.

[4] B. Xiong, D. Cristoforo, J. Xu, S. Alessandra, M. G. Carlo, and X. Yan, "High-strain rate compressive behavior of concrete made with substituted coarse aggregates: recycled crushed concrete and clay bricks," *Construction and Building Materials*, vol. 301, 2021.

[5] C. Liang, J. Xiao, C. Wang, and Z. Ma, "Hysteretic energy and damping variation of recycled aggregate concrete with different cyclic compression loading levels," *Journal of Building Engineering*, vol. 44, 2021.

[6] W. Mahmood, A. Khan, and T. Ayub, "Mechanical and durability properties of concrete containing recycled concrete aggregates," *Iranian Journal of Science and Technology*, vol. 6, 2021.

[7] J. Zhang, Li Cheng, Le Ding, and Li Jian, "Performance evaluation of cement stabilized recycled mixture with recycled concrete aggregate and crushed brick," *Construction and Building Materials*, vol. 296, 2021.

[8] F. Xie, J. Li, G. Zhao, C. Wang, Y. Wang, and P. Zhou, "Experimental investigations on the durability and degradation mechanism of cast-in-situ recycled aggregate concrete under chemical sulfate attack," *Construction and Building Materials*, vol. 297, 2021.

[9] M. Sabău and J. R. Duran, "Prediction of compressive strength of general-use concrete mixes with recycled concrete aggregate," *International Journal of Pavement Research and Technology*, vol. 15, 2021.

[10] K. Saied, O. Zoltan, and C. Oliver, "The influence of utilizing recycled and reclaimed coarse aggregates in producing concrete for structural applications," *Tehnički Vjesnik*, vol. 28, no. 3, 2021.

[11] C. Du, J. Luo, and L. Jia, "Review on the application of recycled concrete," *Shanxi Architecture*, vol. 42, no. 7, pp. 109-110, 2016.

[12] J. Guo, S. Liang, Q. Zhang, and Z. Xiao, "Study on factors influencing the dry shrinkage performance of low alkalinity sulphate aluminate cement," *China Cement*, vol. 1, no. 1, pp. 8–11, 2010.

[13] Z. Xie, Z. Li, and J. Lu, "Research status and development suggestions of green concrete," *Recyclable Resources and Circular Economy*, vol. 12, no. 2, pp. 36–39+44, 2019.

[14] L. Song and D. Yang, "Discussion on the application of recycled coarse aggregate in low strength grade concrete," *Guangdong Building Materials*, vol. 9, no. 9, pp. 47–49, 2017.

[15] T. Wang, S. Cheng, and F. Xu, "Discussion on shrinkage and creep performance of recycled concrete in different aggregate grades," *Metallurgical Collections*, vol. 3, no. 1, p. 13, 2017.

[16] R. Li, *Study on Preparation and Performance of Vegetated Ecological Concrete*South China University of Technology, Guangzhou, China, 2009.

[17] E. A. B. Koenders, *Simulation of Volume Changes in Hardening Cement-Based materials*, pp. 97–99, Delft University Press, Delft, Netherlands, 1997.

[18] Z. Meng, Z. Wu, and J. Qian, "Alkalinity of pore fluid of high-addition flyash concrete," *Journal of Chongqing Jianzhu University*, vol. 21, no. 1, pp. 24–27, 1999.

[19] L. Liang, H. Yu, and Z. Pan, "Actual mesostructure-based three-dimensional reconstruction of porous concrete," *Journal of Hohai University (Natural Sciences)*, vol. 38, no. 4, p. 427, 2010.
[20] Y. Zhou, "Determination and calculation of specific surface area of concrete aggregate," *Concrete*, vol. 2, pp. 48–51, 1984.
[21] Y. Li and X. Hu, "Designing of previous concrete mixture proportion by surrounding spherical model," *Concrete*, vol. 227, no. 9, pp. 29–32, 2008.
[22] N. Feng, *New Practical Concrete Collection*, Science Press, Beijing, China, 2005.
[23] X. Pan, *Study on Preparation Method and Properties of Porous Cement Concrete Pavement Materials*Chang'an University, Xi'an, China, 2010.
[24] L. Mao, *The Mechanics Analysis of Vegetation Root in Ecology Slope Protection*, Wuhan University of Technology, Wuhan, China, 2007.
[25] J. Dong, Y. Pei, and L. Wang, "Research and practice of environmental friendly greening concrete," *Jilin Water Resources*, vol. 2, no. 2, pp. 1–4, 2002.
[26] Z. Liu and C. Lu, *Study on the Cementitious Materials with Low Alkalinity for Environmentally Friendly Concrete*Nanjing Hydraulic Research Institute, Nanjing, China, 2004.
[27] J. Wei, "Study on application of ecological concrete technology," *Communications Science and Technology Heilongjiang*, vol. 4, no. 4, pp. 1-2, 2010.
[28] W. Tian, "Reflect over composition of comprehensive harness plan for soil and water conservation on road construction programme," *Bulletin of Soil and Water Conservation*, vol. 20, no. 3, pp. 31–34, 2000.
[29] Z. Xu, R. Liao, and C. Lou, "Control measures of non-point source pollution in urban river areas," *Beijing Water*, vol. 5, no. 5, pp. 26–28, 2005.
[30] W. Liang, A. Chen, and C. Yu, "Performance research and engineering application of recycled aggregate oncrete," *Guangdong Building Materials*, vol. 8, no. 8, pp. 18–20, 2017.

Hindawi
Scientific Programming
Volume 2022, Article ID 2626868, 9 pages
https://doi.org/10.1155/2022/2626868

Research Article

Wheat Seed Classification: Utilizing Ensemble Machine Learning Approach

Ajay Khatri [1] **Shweta Agrawal,** [2] **and Jyotir M. Chatterjee** [3]

[1] *CSE, SAGE University, Indore 452001, India*
[2] *CSE, SAGE University, Indore 452001, India*
[3] *Lord Buddha Education Foundation, Kathmandu 44600, Nepal*

Correspondence should be addressed to Jyotir M. Chatterjee; jyotirchatterjee@gmail.com

Received 19 October 2021; Accepted 13 January 2022; Published 2 February 2022

Academic Editor: Punit Gupta

Recognizing and authenticating wheat varieties is critical for quality evaluation in the grain supply chain, particularly for methods for seed inspection. Recognition and verification of grains are carried out manually through direct visual examination. Automatic categorization techniques based on machine learning and computer vision offered fast and high-throughput solutions. Even yet, categorization remains a complicated process at the varietal level. The paper utilized machine learning approaches for classifying wheat seeds. The seed classification is performed based on 7 physical features: area of wheat, perimeter of wheat, compactness, length of the kernel, width of the kernel, asymmetry coefficient, and kernel groove length. The dataset is collected from the UCI library and has 210 occurrences of wheat kernels. The dataset contains kernels from three wheat varieties Kama, Rosa, and Canadian, with 70 components chosen at random for the experiment. In the first phase, K-nearest neighbor, classification and regression tree, and Gaussian Naïve Bayes algorithms are implemented for classification. The results of these algorithms are compared with the ensemble approach of machine learning. The results reveal that accuracies calculated for KNN, decision, and Naïve Bayes classifiers are 92%, 94%, and 92%, respectively. The highest accuracy of 95% is achieved through the ensemble classifier in which decision is made based on hard voting.

1. Introduction

In many developing nations, farming is the most significant economic sector. Most of the tasks are carried out without the use of modern technology. Seed categorization is usually done based on human understanding. The purification of seeds plays an important role in this process and must be enhanced. Manually determining the type of wheat needs expert judgment and takes time. When an array of seeds appears so similar, manually distinguishing them becomes a challenging process [1–4].

A quality evaluation method for wheat crops is required with the evolution of the grain chain [5]. The goal is a high-quality wheat product in greater quantities. Tests on seed germination are required for seed labeling [6]. The seeds were tested for pureness test, which is required to ascertain a seed sample's physical and varietal purity. The genetic integrity of the original wheat cultivar may be compromised by mechanical mixing and improper labeling [7].

Classification testing is accomplished via a taxonomic categorization method and nondestructive grain feature analysis [8, 9]. Seed tester classifies seeds on two levels: species level and varietal level for varietal purity. The varietal level may be challenging due to the great degree of resemblance in the characteristics of different kinds of wheat seeds. The growth circumstances may also affect the grain's properties [5]. The actual classification test procedure is still a low-throughput process, and its correctness is contingent on the expert's performance and cumulative experience.

Machine learning techniques are now the subject of study in a variety of disciplines, particularly with the expansion of the Internet and the usage of bigger datasets [4]. Without specific tools or automatic software procedures, it is difficult for a human operator to interpret or handle such data. Machine learning is frequently used in various applications such as categorization, regression, and forecasting to meet these demands [10]. The use of a single classifier for the objects which has a very minute difference in physical characteristics such as color, texture, and morphology does not give better accuracy [11]. To address this problem, ensemble approach is used in the present work. By combining many models into a single, highly reliable model, ensemble methods seek to increase model prediction. The most common ensemble approaches are boosting, bagging, and stacking. Ensemble techniques are particularly well suited to regression and classification, where they minimize bias and variance while increasing model accuracy. The major findings of this paper are as follows:

(1) An optimized classifier is designed for wheat seed classification by utilizing an ensemble machine learning approach with bagging

(2) The model is compared with three machine learning classifiers: K-nearest neighbors (KNN) classifier, decision tree classifier (CART), and Gaussian NB (NB).

(3) The highest achieved accuracy is 95%, which is with the ensemble method

2. Related Work

Seed categorization using machine algorithms has been the subject of research. These studies employed a variety of machine classifiers and achieved a high degree of accuracy in their work. Machine learning techniques had previously been successfully applied in a variety of production chains for seed and cereals classification [12–14]. In [15], the study shows the capability and possibilities of machine vision for shapes, sizes, and varietal types using well-trained multilayer neural network classifiers. They utilized Weka classification tools such as function, Bayes, meta, and lazy approaches to categorize the seeds. In [16], the authors proposed a fuzzy theory-based approach for recognizing wheat seed types that take into account the features of the seed. The tabu search technique was used. In [17], the authors have used an artificial neural network for classifying wheat seeds based on VLC and obtained an accuracy of 92.1 percent and 85.72 percent, respectively. In [18], authors have discussed morphological, color, and textural characteristics of the seed. If there is a very minute difference in morphological features, then seed classification is very difficult. Cereal yield is determined by the number of grains per ear and the size of the grains. Counting seeds and morphometry by sight is time-consuming. As a result, different ways for effective grain morphometry employing image processing techniques have been proposed [19, 20].

In [21], the authors created a workstation to aid in grain analysis for classification, and a video colorimetry approach is presented to support in determining cereal grain color. The categorization of chickpea seed varieties was done based on the morphological characteristics of chickpea seeds, using 400 samples from four types: Kaka, Piroz, Ilc, and Jam [22]. According to the commercial point of view, a machine vision built of existing neural network models may be utilized for rice quality assessment [23]. In this, it uses neural networks to categorize rice varieties, using a total of nine separate varieties of rice. The authors employ seed image acquisition to classify these variations. They also created a method for extracting 13 morphological features, 6 color features, and 15 texture features from color photographs of seeds. Their model has produced an overall classification accuracy of 92%. The k-nearest neighbors classifier necessitates storing the entire training set, which can be prohibitively expensive when the set is huge, and several researchers have attempted to eliminate the training set's redundancy to relieve this problem [24, 25].

For plant categorization, the authors have utilized deep learning models [26]. Two tendencies may be seen in the current state of the art. The first is linked to high-throughput phenotyping and plant identification, as evidenced by Ubbens and Stavness' work in this area [27]. The second problem is plant disease identification and monitoring [28, 29]. In [30],the authors present many voting techniques for testing ensembles of classifiers learned using the bagging approach. Multilayer perceptron is used as classifiers. Using groups of classifiers rather than individual ones is one option. Bagging [31] and boosting [32] are two of the most well-known ensemble techniques, in which many classifiers are combined to generate a single, more accurate result. In [33], the authors studied the performance of several voting techniques, with bagging being utilized for the reconciliation model, which is a process of merging classification models. Table 1 contains various features considered in machine vision systems for food grain quality evaluation.

3. Methodology

The methodology adopted for this work includes the collection of datasets, features identification, data augmentation, classification using machine learning algorithms like KNN, Naive Bayes, and CART implementation, implementation of ensemble approach for better accuracy with fine-tuning, and comparison of results.

3.1. Dataset. In the study, the seed dataset was received from the UCI library [42]. There are 210 occurrences of wheat kernels in the collection. In addition to the class attribute, each instance contains 7 other attributes. All the samples share the same 7 characteristics (area, perimeter, compactness, kernel length, kernel width, asymmetry coefficient, and kernel groove length). All of the characteristics are constant. Figure 1 shows the features of the dataset number of classes presented and selected machine learning algorithms.

The examined set contained kernels from three wheat varieties: Kama, Rosa, and Canadian, with 70 components. To perceive high-quality picturing of the interior kernel construction, a soft X-ray method is employed. It is less abrasive and more affordable than other sophisticated imaging techniques such as scanning microscopy or laser technology. Images are recorded on X-ray KODAK plates

Table 1: Features considered in machine vision systems for food grain quality evaluation.

S. no.	Features	Application	Grain	References
1	Morphology	Variety-based classification	Rice	[34–36]
2	Color	Identification of microbial infection	Popcorn	[37]
3	Morphology + color	Variety-based classification	Chickpea	[38, 39]
4	Morphology	Variety-based classification	Wheat	[40, 41]

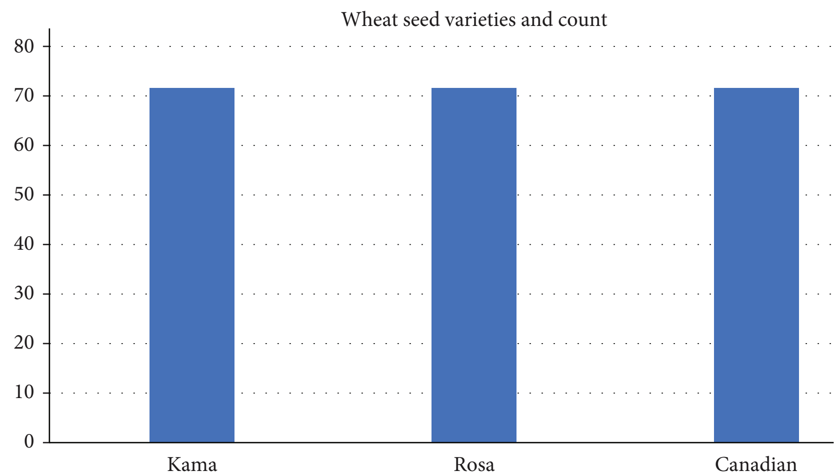

Figure 1: Count of different wheat seed varieties.

measuring 13×18 cm. At the Institute of Agrophysics of the Polish Academy of Sciences in Lublin, studies were supplemented by association harvested wheat grain patenting from experimental fields. In Table 2, classes represent 3 varieties of wheat which are Kama (1), Rosa (2), and Canadian (3).

3.2. Machine Learning Models

K-nearest neighbor: a k-nearest-neighbor algorithm is a data categorization method that predicts how likely a data point belong to one of two groups based on which group the data points closest to it belong to [43]. Any common method can be used to determine the distance. A Euclidean distance is an example of a distance. After that, we collect a certain feature value from all the training set in the immediate vicinity. We categorize our fresh testing data using most of this number as a prediction [44].

Classification and regression trees (CART): CART is a nonparametric supervised learning method [45, 46]. The objective is to build a model of the value of a target variable by learning basic decision rules from data characteristics. A piecewise constant is approximated by a tree. Nonstatisticians can analyze CART quite well [45, 47].

Gaussian Naïve Bayes: A basic approach for Naive Bayes is Bayes decision theory. The likelihood is used to make this classification decision. The posterior probability is calculated using the likelihood, prior probabilities, and evidence. Evidence is merely a scalar that ensures that posterior probability equals one. Resultant classes for the given test data are chosen based on the category with the highest posterior probability.

Ensemble methods: ensemble methods are strategies for increasing the accuracy of model outputs by integrating many models rather than utilizing just one. The integrated models greatly improve the accuracy of the outcomes. The popularity of ensemble techniques in machine learning has risen because of this. When dealing with enormous amounts of data or a lack of appropriate data, ensemble-based solutions can be unexpectedly effective. When the quantity of training data is too enormous to train a single classifier, the data can be divided into smaller groups deliberately. After that, each division may be used to train a distinct classifier, which can then be merged using a suitable combination algorithm. If there is not enough data, bootstrapping may be used to train alternative classifiers using distinct bootstrap samples of the data, each of which is a random sample of the data taken with replacement and handled as if it were drawn independently from the underlying distribution [48].

Bagging is one of the oldest, more obvious, and most likely simplest ensemble-based methods, and it has very maximum performance. Bootstrapped copies of the training data are used to obtain the diversity of classifiers in bagging such that different chunks of training data are arbitrarily chosen from the entire training dataset, with substitution. Each subset of training data is utilized to train a particular sort of classifier. Individual classifiers are then merged using a simple majority vote. By resampling the data, boosting also produces an ensemble of classifiers, which are subsequently

Table 2: Sample from wheat seed dataset.

Area of wheat	Perimeter of wheat	Compactness	Kernel length	Kernel width	Asymmetry coefficient	Kernel groove length	Classes
18.55	16.22	0.8865	6.153	3.674	1.738	5.894	2
19.15	16.45	0.889	6.245	3.815	3.084	6.185	2
14.11	14.1	0.8911	5.42	3.302	2.7	5	1
20.88	17.05	0.9031	6.45	4.032	5.016	6.321	2
11.84	13.21	0.8521	5.175	2.836	3.598	5.044	3
11.87	13.02	0.8795	5.132	2.953	3.597	5.132	3
15.78	14.91	0.8923	5.674	3.434	5.593	5.136	1

merged by majority vote. Resampling, on the other hand, is used deliberately in boosting to give the most useful training data for each subsequent classifier.

We applied a hard voting classifier, which means that the forecasted output class is the one that obtains the most votes. Three classifiers predicted the output wheat classes Kama, Rosa, and Canadian, and most of them anticipated Kama wheat variety as the result. As a result, the ultimate forecast will be Kama wheat.

3.3. Experimental Setup. Python3 libraries such as NumPy, SciPy, scikit-learn, Keras, pandas, and Matplotlib are utilized to perform the categorization through ML models. Scikit-learn appears to be the most user-friendly and reliable machine learning library [49, 50]. The foundations of this package are NumPy, SciPy, and Matplotlib. The results of the dataset analysis, as well as the model's training and testing using numerous feature extractions are presented in this section. Figure 2 shows the classification process.

3.4. Performance Evaluation Matrix. To measure the effectiveness of the classifier, a confusion matrix is required, which provides the number of accurate and wrong predictions based on known true values. It shows true positive (TP): actual value is true and model predicted it true, true negative (TN): both actual value and predicted value are false, false positive (FP): actual value is false but model predicted it true, and false negative (FN): actual value is true but model predicted it as false.

Accuracy: accuracy is the measure of how often a model has predicted the right value as per the given input. But it does not give detailed information regarding FP and FN. For some applications where FP and FN are considerable, $F1$-score and recall play a very important role. Accuracy is calculated by

$$\text{accuracy} = \frac{\text{true positive} + \text{true negative}}{\text{true positive} + \text{true negative} + \text{false positive} + \text{false negative}}. \tag{1}$$

Precision: this evaluation parameter tells how frequently a model predicts true positive. The low value of precision infers high false positives. Formula for calculating precision is as follows:

$$\text{precision} = \frac{\text{TP}}{\text{TP} + \text{FP}}, \tag{2}$$

Recall: this parameter gives information regarding how often a model predicts false negatives. The low value of recall means the model predicted high false negatives. Formula for calculating recall is as follows:

$$\text{recall} = \frac{\text{TP} + \text{TN}}{\text{TP} + \text{FN}}. \tag{3}$$

$F1$-score: the $F1$-score is calculated by combining both precision and recall. That is, a high F1 score indicates a low number of false positives and false negatives, which infers that the model is accurately detecting actual threats and are not bothered by false alarms. The formula for calculating the F1 score is

$$\text{F1} - \text{score} = 2 * \frac{\text{precision} * \text{recall}}{\text{precision} + \text{recall}}. \tag{4}$$

4. Result

Results present the evaluation of considered four ML models: KNN, Naive Bayes, CART, and ensemble method. For evaluating models, we have divided the collected data into 70% for the training set and 30% for the testing set. The wheat classes Kama, Rosa, and Canadian have been assigned numbers 1, 2, and 3, correspondingly. The results of all considered algorithms are evaluated based on recall, precision, F1-score, and accuracy. Tables 3–7 show the value of these parameters for KNN, Naive Bayes, CART, and ensemble method, respectively. Figures 3–6 show the confusion matrix for KNN, Naive Bayes, CART, and ensemble method, respectively. The accuracy determined for KNN, decision, and Naive Bayes classifiers is 92 percent, 94 percent, and 92 percent, respectively, according to the data. Ensemble classifier, which makes decisions based on hard voting, has the best accuracy of 95 percent.

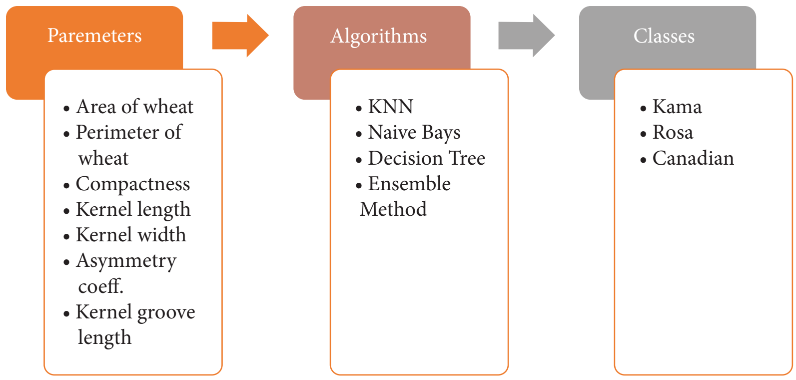

Figure 2: The block diagram of the classification process.

Table 3: Result of wheat seed classification using KNN.

Class	Precision	Recall	*F*1-score	Support
1	0.9	0.86	0.88	22
2	0.92	0.96	0.94	23
3	0.94	0.94	0.94	18
Avg/total	0.92	0.92	0.92	63

Table 4: Result of wheat seed classification using CART.

Class	Precision	Recall	*F*1-score	Support
1	0.91	0.91	0.91	22
2	0.96	0.96	0.96	23
3	0.94	0.94	0.94	18
Avg/total	0.94	0.94	0.94	63

Table 5: Result of wheat seed classification using NB.

Class	Precision	Recall	*F*1-score	Support
1	0.87	0.91	0.89	22
2	1	0.91	0.95	23
3	0.89	0.94	0.92	18
Avg/total	0.92	0.92	0.92	63

Table 6: Hard voting in ensemble method.

S. no.	KNN	CART	Naive Bayes (NB)	Ensemble method
1	1	3	1	1
2	3	2	3	3
3	2	2	3	2
4	3	3	1	3

Table 7: Result of wheat seed classification using ensemble method.

Class	Precision	Recall	*F*1-score	Support
1	0.91	0.95	0.93	22
2	1	0.96	0.98	23
3	0.94	0.94	0.94	18
Avg/total	0.95	0.95	0.95	63

5. Discussion

To implement the KNN, we use the scikit-learn K-neighbors classifier. As an input parameter, the approach requires the number of neighbors. We can determine the wheat seed category by simply changing the number of neighbors. With this procedure, 92% accuracy is attained. The accuracy of building a CART using the scikit-learn is 94 percent. We used the scikit-learn Gaussian NB classifier and 92% accuracy is attained. We

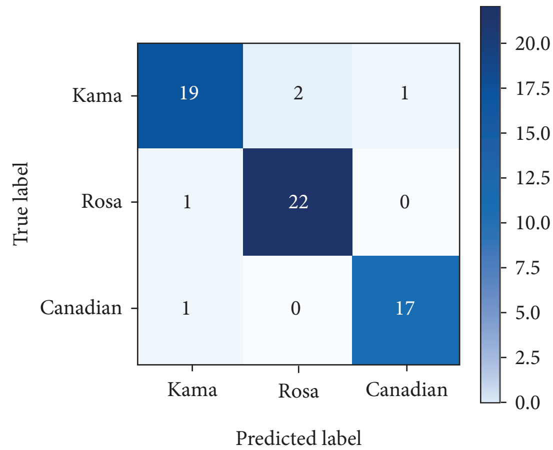

Figure 3: Confusion matrix (KNN).

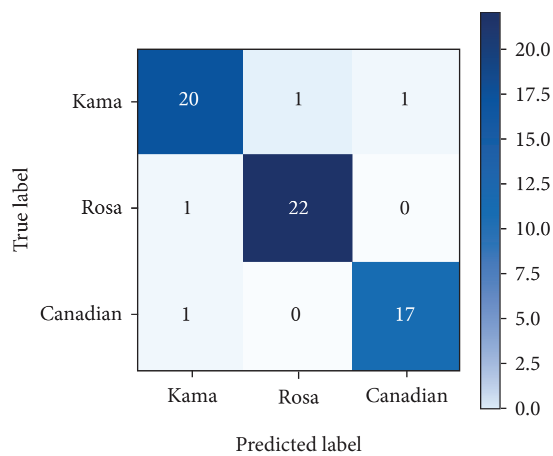

Figure 4: Confusion matrix (CART).

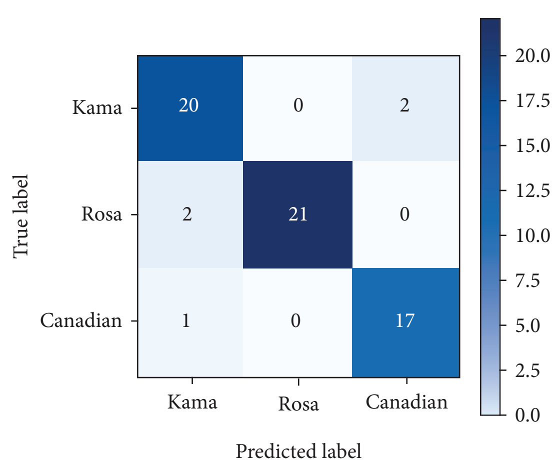

Figure 5: Confusion matrix (NB).

have achieved 95% accuracy using the ensemble method. Based on machine learning, a model for predicting determining factors of seeds has been created. The precision, recall, and F1 score of wheat seed dataset categorization using K-neighbors classifier (KNN), classification and regression trees (CART), Gaussian NB (NB), and

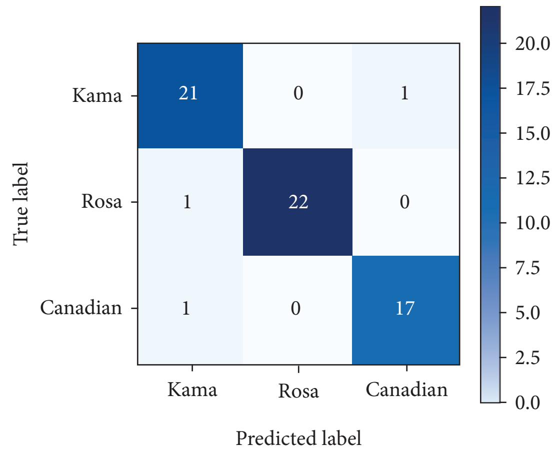

FIGURE 6: Confusion matrix (ensemble method).

TABLE 8: Comparison between precision, recall, and F1-score

Classifier	Precision	Recall	$F1$-score
KNN	0.92	0.92	0.92
CART	0.94	0.94	0.94
NB	0.92	0.92	0.92
Ensemble	0.95	0.95	0.95

TABLE 9: Summary of various classifiers accuracy.

Classifier	Accuracy (%)
KNN	92
CART	94
NB	92
Ensemble	95

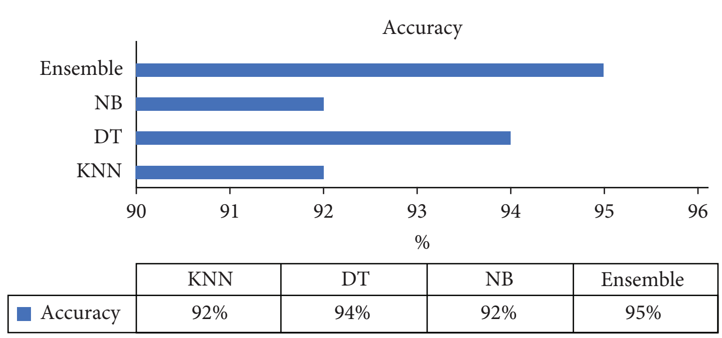

FIGURE 7: Summary of various classifier accuracy.

ensemble method are compared in Table 8. Table 9 shows the summary of various classifiers accuracy. A chart is also presented to compare the accuracy of various methods in Figure 7 which shows the summary of various classifier accuracy.

6. Conclusion

Machine learning approaches in grain seed analysis and classification are playing a very important role. The major challenge in seed classification is the very minute difference between different categories of seeds. The accuracy of predictions with this challenge is improved by utilizing the concepts of ensemble learning. Wheat seed classification by considering seven independent features area, perimeter, compactness, kernel length, kernel width, asymmetry coefficient, and kernel groove length is presented in the paper. The ensemble machine learning approach with bagging and hard voting is utilized to best fit the classifier. Three machine learning algorithms K-nearest neighbors classifier (KNN), classification and regression trees (CART), and Gaussian NB (NB) are also implemented to compare the results. The results reveal that the accuracy calculated for KNN, decision, and Naïve Bayes classifiers are 92%, 94%, and 92%, respectively. The highest accuracy 95% is achieved through the ensemble classifier in which the decision is made based on hard voting. In the future, we can use other classification algorithms to improve accuracy.

Data Availability

Datasets related to this article can be found at "https://archive.ics.uci.edu/ml/datasets/seeds," an open-source online data repository hosted at UCI Machine Learning Repository [42].

Conflicts of Interest

The authors declare that they have no conflicts of interest.

References

[1] R. Tandon, D. S. Agrawal, and D. P. Goyal, "Sequential convolutional neural network for automatic breast cancer image classification using histopathological images," *J. Crit. Rev.*vol. 7, no. 15, p. 14, 2020.

[2] H. S. H. Chitra, S. Suguna, and S. N. Sujatha, "A survey on image analysis techniques in agricultural product," *Indian Journal of Science and Technology*, vol. 9, no. 12, 2016.

[3] M. R. Siddagangappa and A. P. A. H. Kulkarni, "Classification and quality analysis of food grains," *IOSR Journal of Computer Engineering*, vol. 16, no. 4, pp. 1–10, 2014.

[4] S. Agrawal and S. K. Jain, "Medical text and image processing: applications, issues and challenges," in *Machine Learning with Health Care Perspective*, V. Jain and J. M. Chatterjee, Eds., vol. 13, pp. 237–262, Cham: Springer International Publishing, Manhattan, NY, USA, 2020.

[5] C. Wrigley, "Cereal-grain morphology and composition," in *Cereal Grains*, C. Wrigley, I. Batey, and D. Miskelly, Eds., pp. 55–87, Woodhead Publishing, Cambridge, UK, 2nd edition, 2017.

[6] S. G. Elias, L. O. Copeland, M. B. McDonald, and R. Z. Baalbaki, *Seed Testing: Principles and Practices*, East Lansing: Michigan State University Press, East Lansing, MI, USA, 2012.

[7] S. Matthews, "Copeland, L.O. and McDonald, M.B. Principles of seed science and technology. 4th edn," *Annals of Botany*, vol. 89, no. 6, p. 798, 2002.

[8] W. S. Meyer and H. D. Barrs, "Non-destructive measurement of wheat roots in large undisturbed and repacked clay soil cores," *Plant and Soil*, vol. 85, no. 2, pp. 237–247, 1985.

[9] J. Acer, *Rules Proposals for the International Rules for Seed Testing*, Vol. 47, International Seed Testing Association, Switzerland, Europe, 2019 edition, 2019.

[10] M. Agrawal and S. Agrawal, "A systematic review on artificial intelligence/deep learning applications and challenges to battle against COVID-19 pandemic," *Disaster Advances*, vol. 14, no. 8, pp. 90–99, 2021.

[11] N. S. Visen, J. Paliwal, D. S. Jayas, and N. D. G. White, "AE-automation and emerging technologies," *Biosystems Engineering*, vol. 82, no. 2, pp. 151–159, 2002.

[12] D. I. Patrício and R. Rieder, "Computer vision and artificial intelligence in precision agriculture for grain crops: a systematic review," *Computers and Electronics in Agriculture*, vol. 153, pp. 69–81, 2018.

[13] P. Vithu and J. A. Moses, "Machine vision system for food grain quality evaluation: a review," *Trends in Food Science & Technology*, vol. 56, pp. 13–20, 2016.

[14] C.-J. Du and D.-W. Sun, "Learning techniques used in computer vision for food quality evaluation: a review," *Journal of Food Engineering*, vol. 72, no. 1, pp. 39–55, 2006.

[15] T. Tujo, "A predictive model to predict seed classes using machine learning," *Int. J. Eng. Tech. Res.*, vol. 6, pp. 334–344, 2019.

[16] L. Li and S. Liu, "Wheat cultivar classifications based on tabu search and fuzzy C-means clustering algorithm," in *Proceedings of the 2012 4th International Conference on Computational and Information Sciences*, pp. 493–496, Chongqing, China, August. 2012.

[17] R. Choudhary, S. Mahesh, J. Paliwal, and D. S. Jayas, "Identification of wheat classes using wavelet features from near infrared hyperspectral images of bulk samples," *Biosystems Engineering*, vol. 102, no. 2, pp. 115–127, 2009.

[18] S. V. Neeraj Singh Visen, J. Jitendra Paliwal, D. Digvir Jayas, and N. D. G. White, "Image analysis of bulk grain samples using neural networks," *Canadian Biosystems Engineering/Le Genie des biosystems au Canada*, vol. 46, 2003.

[19] T. Tanabata, T. Shibaya, K. Hori, K. Ebana, and M. Yano, "SmartGrain: high-throughput phenotyping software for measuring seed shape through image analysis," *Plant Physiology*, vol. 160, no. 4, pp. 1871–1880, 2012.

[20] E. Komyshev, M. Genaev, and D. Afonnikov, "Evaluation of the SeedCounter, A mobile application for grain phenotyping," *Frontiers of Plant Science*, vol. 7, 2017.

[21] M. R. Neuman, E. Shwedyk, and W. Bushuk, "A PC-based colour image processing system for wheat grain grading," in *Proceedings of the 3rd International Conference on Image Processing and its Applications, 1989*, pp. 242–246, Warwick, UK, July 1989.

[22] S. Salah Ghamari, "Classification of chickpea seeds using supervised and unsupervised artificial neural networks," *African Journal of Agricultural Reseearch*, vol. 7, no. 21, 2012.

[23] C. Silva and U. Sonnadara, "Classification of rice grains using neural networks," *Proceedings of Technical Sessions*, vol. 29, 2013.

[24] M. Kubat and J. R. Martin Cooperson, "Voting Nearest-Neighbor Subclassifiers," in *Proceedings of the 17th International Conference on Machine Learning*, pp. 503–510, San Francisco, CA, USA, January. 2000.

[25] E. Alpaydin, "Voting over Multiple Condensed Nearest Neighbors," in *Lazy Learning*, D. W. Aha, Ed., Springer Netherlands, Dordrecht, The Netherlands, 1997.

[26] A. Kamilaris and F. X. Prenafeta-Boldú, "Deep learning in agriculture: a survey," *Computers and Electronics in Agriculture*, vol. 147, pp. 70–90, 2018.

[27] J. R. Ubbens and I. Stavness, "Corrigendum: deep plant phenomics: a deep learning platform for complex plant phenotyping tasks," *Frontiers of Plant Science*, vol. 8, p. 2245, 2018.

[28] M. Brahimi, K. Boukhalfa, and A. Moussaoui, "Deep learning for tomato diseases: classification and symptoms visualization," *Applied Artificial Intelligence*, vol. 31, no. 4, pp. 299–315, 2017.

[29] K. P. Ferentinos, "Deep learning models for plant disease detection and diagnosis," *Computers and Electronics in Agriculture*, vol. 145, pp. 311–318, 2018.

[30] M. Van Erp, L. Vuurpijl, and L. Schomaker, "An overview and comparison of voting methods for pattern recognition," in *Proceedings of the 8th International Workshop on Frontiers in*

Handwriting Recognition, Niagara on the Lake, pp. 195–200, Niagra-on-the-Lake,ON, Canada, August 2002.
[31] L. Breiman, "Bagging predictors," *Machine Learning*, vol. 24, no. 2, pp. 123–140, 1996.
[32] R. E. Schapire and Y. Singer, "Improved boosting algorithms using confidence-rated predictions," in *Proceedings of the 11th annual conference on Computational learning theory - COLT' 98*, pp. 80–91, Madison, WI, USA, July 1998.
[33] K. T. Leung and D. S. Parker, "Empirical comparisons of various voting methods in bagging," in *Proceedings of the ninth ACM SIGKDD international conference on Knowledge discovery and data mining - KDD '03*, p. 595, Washington, DC, USA, August 2003.
[34] S. J. MousaviRad, F. Akhlaghian Tab, and K. Mollazade, "Application of imperialist competitive algorithm for feature selection: a case study on bulk rice classification," *International Journal of Computer Application*, vol. 40, no. 16, pp. 41–48, 2012.
[35] N. A. Kuchekar and V. V. Yerigeri, "Rice grain quality grading using digital image processing techniques," *Journal of Electronics and Communication Engineering*, vol. 13, 2018.
[36] M. M. Agrawal and D. S. Agrawal, "Rice plant diseases detection & classification using deep learning models: a systematic review -," *J. Crit. Rev.*vol. 7, no. 11, pp. 4376–4390, 2020.
[37] O. Yorulmaz, T. C. Pearson, and A. EnisÇetin, "Detection of fungal damaged popcorn using image property covariance features," *Computers and Electronics in Agriculture*, vol. 84, 2021.
[38] O. Díaz, T. Ferreiro, J. Rodríguez-Otero, and Á. Cobos, "Characterization of chickpea (cicer arietinum L.) flour films: effects of pH and plasticizer concentration," *International Journal of Molecular Sciences*, vol. 20, no. 5, p. 1246, 2019.
[39] S. Sankaran, M. Wang, and G. J. Vandemark, "Image-based rapid phenotyping of chickpeas seed size," *Engineering in Agriculture, Environment and Food*, vol. 9, no. 1, pp. 50–55, 2016.
[40] K. Laabassi, M. A. Belarbi, S. Mahmoudi, S. A. Mahmoudi, and K. Ferhat, "Wheat varieties identification based on a deep learning approach," *Journal of the Saudi Society of Agricultural Sciences*, vol. 20, no. 5, pp. 281–289, 2021.
[41] A. Bhande and D. S. V. Rode, "Quality identification of wheat by using image processing," *International Journal of Engineering Science and Computing*, vol. 6, 2016.
[42] UCI Machine Learning Repository, "UCI Machine Learning Repository: Seeds Data Set," 2021, https://archive.ics.uci.edu/ml/index.php.
[43] G. Guo, H. Wang, D. Bell, and Y. Bi, "KNN Model-Based Approach in Classification," in *Proceedings of the OTM Confederated International Conferences On the Move to Meaningful Internet Systems*, Amantea, Italy, October 2004.
[44] D. Agrawal and P. Dahiya, "Comparisons of classification algorithms on seeds dataset using machine learning algorithm," *Compusoft*, vol. 7, pp. 2760–2765, 2018.
[45] H. H. Patel and P. Prajapati, "Study and analysis of decision tree based classification algorithms," *International Journal of Computer Science and Engineering*, vol. 6, no. 10, pp. 74–78, 2018.
[46] B. G. Priya, "A comparison of various machine learning algorithms for wheat seed data set classification," *An international journal of advanced computer technology*, vol. 7, no. 5, 2019.
[47] R. Lewis, "An Introduction to Classification and Regression Tree (CART) Analysis," in *Proceedings of the 2000 Annual Meeting of the Society for Academic Emergency Medicine*, San Francisco, CA, USA, January 2000.
[48] T. N. Rincy and R. Gupta, "Ensemble learning techniques and its efficiency in machine learning: a survey," in *Proceedings of the 2nd International Conference on Data, Engineering and Applications (IDEA)*, pp. 1–6, Bhopal, India, February. 2020.
[49] X. Wei and Y. Cao, "Automatic counting method for complex overlapping erythrocytes based on seed prediction in microscopic imaging," *Journal of Innovative Optical Health Sciences*, vol. 9, no. 5, Article ID 1650016, 2016.
[50] D. Saravagi, S. Agrawal, and M. Saravagi, "Opportunities and challenges of machine learning models for prediction and diagnosis of spondylolisthesis: a systematic review," *International Journal of Engineering Systems Modelling and Simulation*, vol. 12, no. 2/3, pp. 127–138, 2021.

Hindawi
Scientific Programming
Volume 2022, Article ID 1877282, 7 pages
https://doi.org/10.1155/2022/1877282

Research Article

Discussion on the Teaching Method of Using Cloud Computing Technology to Improve the Stability Training of the Trunk Pillar in College Physical Education Curriculum

Yongan Wang [1,2] and Yun Feng [2]

[1]Graduate School, Capital University of Physical Education and Sport, Beijing 100191, China
[2]The Faculty of Physical Education, China West Normal University, Nanchong 637009, Sichuan, China

Correspondence should be addressed to Yun Feng; fengyun1991@cwnu.edu.cn

Received 5 October 2021; Revised 15 November 2021; Accepted 24 November 2021; Published 29 January 2022

Academic Editor: Punit Gupta

This work is to develop an effective trunk support stability training program, thereby improving the quality of college physical education. First, the advantages and characteristics of trunk support stability training are analyzed under the physiological basis and biomechanical basis of trunk support stability training. Then, the trunk support stability training program is developed to train the stability, strength, and balance of the sprint athletes' shoulder, trunk, and buttocks musculature, as well as the control ability of the limbs. Twenty undergraduates in the track and field sprint special class of Xi'an Physical Education University are recruited and rolled into experimental group and control group, each with 10 students, and trained for 8 weeks. Finally, functional movement screen (FMS), postshot throw, level-ten stepping tests, and sprint tests (30 m, 60 m, and 100 m) are performed. The results show that before the start of the experiment, there is no considerable difference in the score comparison between experimental group and control group in different test items ($P > 0.05$). After the experiment, the test scores of level-ten stepping, postshot throw, and 30 m, 60 m, and 100 m sprint of experimental group are remarkably different within the group ($P < 0.05$). In addition, the level-ten stepping and 60 m and 100 m sprint scores of experimental group and control group have great differences between the groups, indicating that the trunk support stability training program formulated in this work has a notable effect on college physically educated students.

1. Introduction

With the rapid development of society, economy, and science and technology, the continuous progress of competitive sports has been promoted, which has led to the formation of fierce competition among many sports [1]. Under the combined action of many factors, the competitive level of sports athletes has also been continuously improved, and the dynamic performance of many athletes is basically close to the limit of human beings. It is because of the need for the comprehensive development of athletes' competitiveness. Moreover, higher and higher requirements for special sports capabilities are also important reasons, which are very important influencing factors [2, 3]. Through scientific training, athletes strive to achieve excellent results in sports competitions, but they must also avoid physical injury as much as possible [4]. Based on the basic theory of modern sports function training, the performance of athletes is attributed to different sports techniques, and the basis of controlling body posture and ensuring sports quality is the stability of trunk support [5].

The concept of trunk support stabilization first appeared in Europe and was first used in the medical field to treat low back pain and chiropractic. Researchers first proposed that the components of the trunk supports were the spine, thoracic-abdominal cavity, and erector spinal muscles. The erector spinae can absorb external forces to maintain the elasticity of the spine and its central position. The benign feedback can maintain the stability of the trunk supports and avoid low back pain [6]. At the end of the twentieth century,

Table 1: Advantages of trunk support stability training.

Advantages	Main content
Status advantage	It focuses on the activation and training of deep muscles under unstable conditions
Theoretical advantage	The power chain theory is taken as the theoretical basis.
Dimensional advantage	It makes multidimensional connections, optimizes the transmission of strength, and improves the coordination between body muscles

the theory of trunk support stability was used in sports rehabilitation and competitive sports. The strength of football players' trunk supports was tested, and different parts of the trunk were affected by the training intensity. The strength of the torso pillar played a vital role in promoting the action performance of football players [7]. The key to athletes' ability to transmit power and performance smoothly is having a strong and stable core. Trunk support stability training was an indispensable training method for athletes [8]. In China's competitive sports, teams such as the national team and the provincial team will conduct trunk support and stability training. Through this training, remarkable results have been achieved in swimming and track and field. Some researchers pointed out that more muscle fibers could be generated through training to solve unstable factors of the trunk, and the nervous system could also be trained to react quickly and obtain precise control capabilities. However, under normal circumstances, trunk support and stability training are difficult. Even advanced athletes need to train step by step to improve their ability. Trunk support stability training can promote the acquisition of special sports skills [9]. At present, there are relatively few research studies on sprint athletes' trunk support and stability training in the field of track. There are only studies on the accelerated running technology of sprint athletes but very little research on the special abilities of sprint athletes.

The physiological and biomechanical basis of trunk support stability training is analyzed, and a special trunk support stability training program for college sports students is innovatively formulated. Moreover, it is compared with the traditional trunk strength training program, to verify the feasibility and effectiveness of the program and provide experimental basis for improving the quality of college physical education.

2. Methods

2.1. The Scientific Mechanism of Trunk Support Stability Training. The core function of trunk support and stability training is to improve the strength, balance, and stability of the muscles between the shoulders and buttocks. The main feature is that it can maintain the stability and erection of the athlete's spine and pelvis and improve the stability and balance of the body, thereby greatly improving the efficiency of energy transfer from the trunk to the limbs. In addition, it can prevent physical injuries in sports and improve the sports performance of athletes [10]. The main purpose of this study is improving the subjects' basic abilities such as stability, strength, balance, and speed, as well as gradually improving the relationship between the trunk muscles and the limbs, thus enhancing the motor function of the limbs. The advantages of trunk support stability training compared with traditional waist and abdominal muscle strength training are shown in Table 1.

According to the main idea of sports training, the training method of trunk support stability is an actual practice method based on the stability and flexibility of human body function [11]. In a specific sports environment, practice methods should be selected according to the characteristics of the athlete's core muscle tissue, and special techniques that adapt to specificity should be developed under the development of stable balance ability. Studies pointed out that trunk support stability training can improve balance and stability, but it cannot improve running balance and stability [12], which meant that in the trunk support and stability training, the training program should be matched with special techniques.

The physiological basis of trunk support stability training includes three parts: skeletal ligament system, muscle power system, and nerve control system. The functions of each system are shown in Table 2.

To develop an efficient trunk support stability training program, it is necessary to analyze its biomechanical mechanism. In strength training, the muscles at both ends of the bones tend to work in the middle. If one end is fixed, the energy formed by the work at the other end will gradually approach it [13]. Therefore, to avoid the occurrence of redundant movements, athletes need to arrange training content reasonably and effectively and train the proximal muscles fixedly, letting the distal muscles cooperate and produce activities, so that the muscles contract faster. To realize such effect and state, the coach must be able to accurately grasp and control the content of the exercise during the training process [14]. If there is no scientifically formulated plan, it will cause other muscles to participate in the activity, forming a compensation effect and causing the athlete to make redundant movements. The human body consumes too much energy, which affects the normal performance of athletes' sports skills and causes sports injuries [15].

Trunk support stability training on sprint athletes can gradually increase the strength of the athlete's trunk support, stabilizes the center of gravity, improves running posture, enhances energy efficiency, and ultimately improves sports performance [16]. The imbalance of the body is adjusted by improving the muscle strength of weak parts of sprint athletes so as to prevent sports injuries.

2.2. Trunk Support Stability Training Plan Formulation. The sprint special trunk support and stability training are aimed at the stability, strength, and balance of sprint athletes'

Table 2: Physiological basis of trunk support stability training.

Different systems	Main functions
Bone ligament system	The spine is made up of 26 vertebrae that are connected to ligaments around the spine to maintain stability in physical activity. When the body moves, its weight and external momentum are transferred from the spine to the extremities. The soft tissue between the vertebrae increases the flexibility of the spine, thereby increasing the range of motion of the entire spine.
Muscle strength system	Controlling the range of motion and stability of the spine can produce great force. Performing centripetal movement activates muscles and helps control the angle and stability of the spine.
Neural control system	Constantly improving the body's adaptations can improve control of the limbs. The nerves of the human body can control the adjustment of the trunk muscles in the unstable state and tend to stabilize, thus speeding up the nervous system activity and improving the motor ability.

Table 3: Training plan of experimental group and control group.

Time	Group	Content
Monday	Experimental group	Basic (5 min) ⟶ jogging + stretching + sprint + targeted exercise (25 min) ⟶ trunk support stability training (20 min) + sprint training (30 min) ⟶ static stretching (5 min).
	Control group	Basic ⟶ running + stretching + sprint + targeted exercises ⟶ traditional trunk strength training + sprint training ⟶ static stretching; the training time is the same as experimental group.
Wednesday and Friday	Experimental group	Basic (5 min) ⟶ jogging + stretching + sprint + targeted exercise (40 min) ⟶ trunk support stability training (30 min) + sprint training (45 min) ⟶ jogging + static stretching (10 min).
	Control group	Basic ⟶ jogging + stretching + sprint + targeted exercises ⟶ traditional trunk strength training + sprint training ⟶ jogging + static stretching, the same time as experimental group.

shoulder, trunk, and hip musculature, as well as the control ability of the limbs [17]. Studies show that when athletes hear a gun, they respond quickly through nerve conduction and start into the acceleration stage. The first starting steps are particularly important, requiring the extent of the torso to lean forward in the process of running. Therefore, it focuses on the ability of the nervous system to mobilize and control deep muscles and improve the coordination ability of sprint athletes with multimuscle groups and multiplanar joints [18]. The subjects selected in the experimental plan are 20 undergraduates in the track and field sprint special class of Xi'an Physical Education University, which are rolled into an experimental group and a control group, with 10 students each. There are eight weeks of training, three times a week (Monday, Wednesday, and Friday), and the three-day training plan is shown in Table 3.

(1) The trunk support strength training of experimental group includes hip training (gluteal bridge training, kneeling hip abduction, and Swiss ball-clip ball to hip), spine and lumbar training (push bridge, side bridge, and Russian rotation), and shoulder training (Bosu ball-push-ups and combined stretching).

There are three kinds of hip training. First is gluteal bridge training. Subjects lie on their back with their knees bent 90 degrees and then lift their hips, hips, waist, lower back, and midback in turn. Shoulders and upper back touch the ground, and upper side of upper body tilts and stabilizes. When the subject has mastered the weight, he can increase the amount and strength of the weight by reducing the support point, raising the other leg to straighten or bend the leg, and adding unstable equipment. Second is kneeling position hip abduction. The body is in the shape of a four-legged stool, kneeling, and hooked feet, with the left leg bent and the knee 90 degrees. With the toe abduction, it returns to the starting position. Then, right leg is slowly lifted to the right so does the left leg. As the subject improves, the bent leg can be changed into a straight leg to increase the power of the movement. Third is Swiss ball-pinch ball hip turn. The subject should lie on the back, clamp the Swiss ball between heel and hamstring, clamp the ball between left hip, and return to starting position clamp the ball between right hip.

There are three kinds of spinal and lumbar training. First is bending bridge. The feet and elbows are on the ground, front feet are on the ground, and back of the body is on a plane. After the subjects master the static position, the load can be gradually increased. Second is side bridge. The elbow and feet are on the ground, hips are off the floor, and body is in a diagonal line. After the subject has mastered the static side bridge movement, the difficulty and strength can be increased by raising the upper arms and legs or adding unstable equipment such as balance pads and Bosu balls. Third is the Russian twist. The subject should lie on the Swiss ball with his legs bent 90 degrees and his shoulder blades touching the ball. He should straighten the arms, keep hands together, tighten the abdominal muscles, and keep torso and thighs parallel to the floor. Then, turn right until the hands are parallel to the floor and return to the starting position and work backwards.

Shoulder training includes Bosu ball-push up (push up with Bosu ball support) and combination stretch (feet are shoulder-width apart, knees bent, arms in T-Y-W-L position, the instability equipment is increased as appropriate, and the strength is gradually increased).

The limbs are trained for the vertical throw (lifting the ball over the head and dropping it vertically to the ground), side throw (holding the ball in both hands and throwing it

Table 4: Basic Information for control students.

Stature	Weight	Age	Years of exercise
179	83	24	4
176	70	23	4
184	80	23	5
174	65	24	5
185	75	25	6
178	68	21	5
181	73	20	5
177	69	21	5
175	63	22	4
172	61	23	5

Table 5: Basic information of students in the experimental group.

Stature	Weight	Age	Years of exercise
181	83	20	5
176	67	21	6
177	75	22	5
174	67	24	5
183	69	23	4
173	63	23	5
175	66	24	4
179	83	25	5
178	70	21	4
182	80	20	5

sideways against the wall with toe forward), and squatting with weight on one leg (with left leg standing, right leg bent, right foot lifted back on the Swiss ball, the barbell is held with both hands and squat on the knees, and the tasks are alternately completed).

(2) The traditional trunk strength training methods in control group include sit-ups, supine alternating leg lifts, flexion and straight leg abdominal tucks, barbell high turns, and side bends of the weight bearing body.

2.3. Experimental Testing and Data Analysis Tools. (1) Test indicators in the experiment are as follows. The first is FMS test [19], which is used to evaluate the quality of the action mode. The subjects' ability to control and stabilize their movements is observed through seven basic action modes. The second is postshot throw and level-ten stepping, which reflect the unique strength qualities of sprint athletes, the continuous explosive ability of the lower limbs, and the strength of the upper limbs. In addition, they also reflect the upper and lower limb coordination ability and power chain transmission ability [20]. The third is the sprint test (30 m, 60 m, and 100 m), which reflects the subjects' starting ability, acceleration ability, and sprint conversion ability.

(2) SPSS 26.0 is employed to input and analyze experimental data. Paired sample T test is performed to compare the differences within group before and after the experiments. Independent sample T test is used to compare between groups, expressed by mean and variance. $P < 0.05$ represents statistical significance.

3. Results and Discussion

3.1. Application Effect Evaluation

3.1.1. Research Subject

(1) Experimental Group. 10 subjects are selected for trunk support strength training. See Table 4 for the specific information.

(2) Control Group. 10 subjects are selected for traditional trunk strength training. See Table 5 for the specific information.

3.1.2. Research Methods. FMS test, postshot throw, level-ten long jump test, and sprint test are performed on the subjects in experimental group and control group.

3.1.3. Mathematical Statistics Method. In this paper, experimental data were input and statistically analyzed using SPSS17.0, and paired sample T test was used for the pre- and posterior comparisons of the same group and independent sample T test for the comparison between the two groups. The results are expressed as mean and variance (M sergeant SD) and are statistically significant as $P < 0.05$.

3.2. Experimental Results

3.2.1. Comparison of Test Indicators between the Two Groups before the Experiment. Before the experiment, FMS, postshot throw, level-ten long jump, and sprint tests are performed on the subjects in experimental group and control group. The results are shown in Figure 1.

Figure 1 shows that before the experiment, the scores of the experimental group and the control group in the FMS (a) test were 17.78 ± 1.48 and 18.01 ± 1.78, respectively. In the FMS (b) test, the scores were 16.78 ± 2.35 and 17.94 ± 1.83, respectively. There was no significant difference between the two groups ($P > 0.05$). The scores of the two groups were (29.55 ± 1.38 and 28.28 ± 1.46) and (15.16 ± 1.23 and 14.98 ± 1.02), respectively, with no significant difference ($P > 0.05$). In sprint test C, the speeds of the experimental group and the control group in the 30 m test were 3.87 ± 0.08 and 3.89 ± 0.09, respectively. In the 60 m test, the speeds were 6.97 ± 0.22 and 6.99 ± 0.09, respectively. In the 100 m test, the velocities were 11.22 ± 0.18 and 11.33 ± 0.15, respectively, with no significant difference ($P > 0.05$).

3.2.2. FMS Test Results of the Two Groups before and after the Experiment. FMS test results of experimental group and control group are compared before and after the experiment. The results are shown in Figure 2.

Figure 2 shows that the left FMS test score of subjects in experimental group increases from 17.78 to 19.61, with an increase of 1.83 points, and there is dramatical difference in comparison ($P < 0.01$). The right FMS test scores of subjects in experimental group increase from 16.78 to 19.44, with an

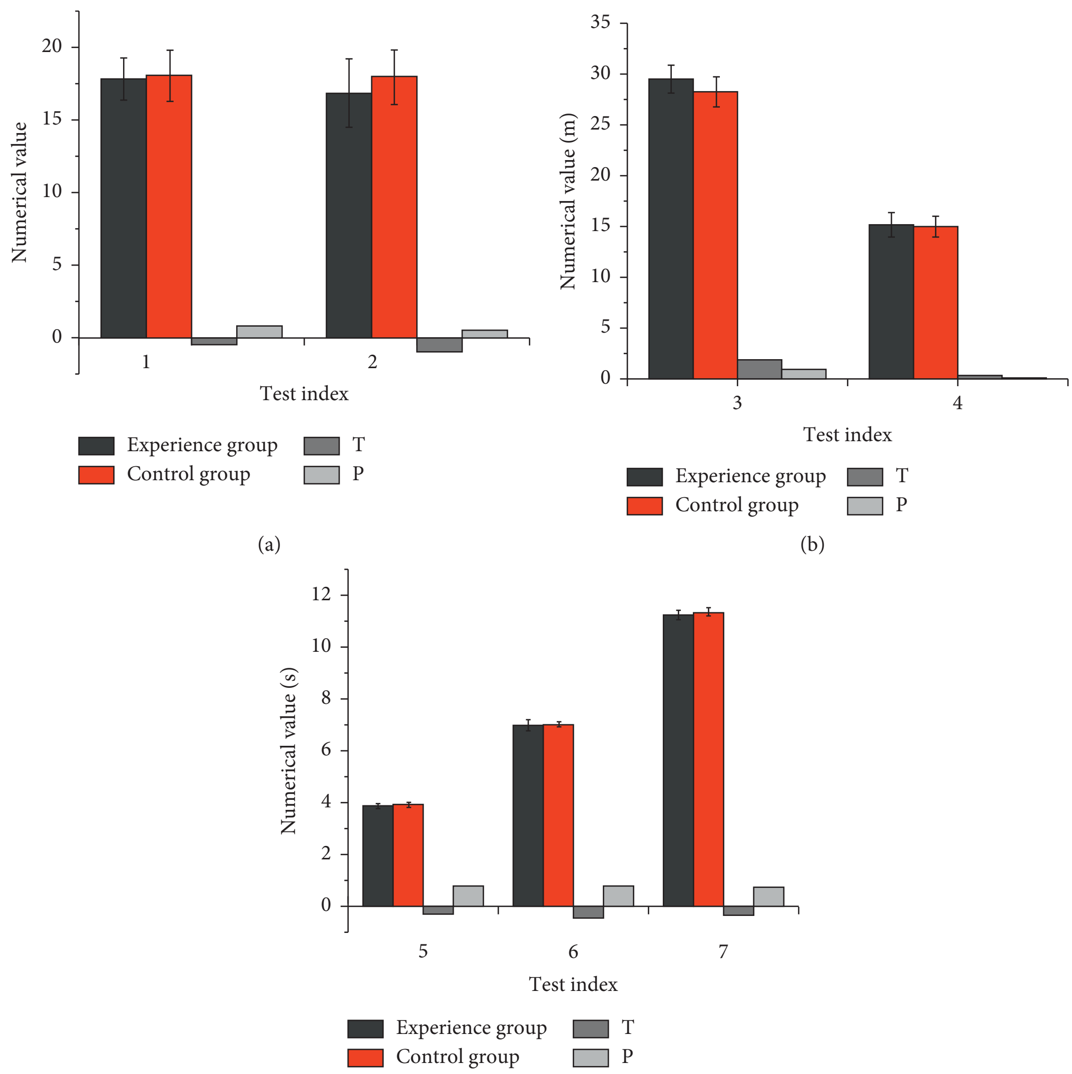

Figure 1: Comparison of the test results between the experimental group and the control group before the experiment. (a) FMS: 1: left, 2: right; (b) 3: level-ten long jump, 4: shoot; (c) 5 : 30 m, 6 : 60 m, 7 : 100 m.

increase of 2.66, with obvious difference ($P < 0.01$). The left FMS test score of control group increases from 18.01 to 18.72, and the right FMS test score of the control subjects increases from 17.94 to 18.78, with substantial difference ($P < 0.01$). It means that both trunk support and stability training and traditional trunk strength training can improve subjects' FMS performance. The difference between the two groups is not great ($P > 0.05$), but the improvement of experimental group is obviously greater than that of control group.

3.2.3. The Strength Test Results of the Two Groups before and after the Experiment. The level-ten stepping and postshot throw test results of experimental group and control group are compared, and the results are shown in Figure 3.

Figure 3 shows that for the subjects in experimental group, the level-ten stepping increases from 28.55 ± 1.34 to 29.15 ± 1.23, and the contrast is notably different ($P < 0.05$). The postshot throw increases from 14.01 ± 1.97 to 14.77 ± 1.72, and the contrast is greatly different ($P < 0.05$). For the subjects in control group, the level-ten stepping increases from 27.28 ± 1.46 to 27.66 ± 1.29, and there is no remarkable difference ($P > 0.05$). The postshot throw increases from 14.01 ± 0.95 to 14.25 ± 1.15, without considerable difference ($P > 0.05$). In addition, there is dramatical difference in the level-ten stepping results between the two groups ($P < 0.05$).

3.2.4. Speed Test Results of the Two Groups before and after the Experiment. The sprint (30 m, 60 m, and 100 m) test results of experimental group and control group are compared, as shown in Figure 4.

After the subjects are trained according to the formulated plan, the sprint scores of subjects in experimental group (30 m, 60 m, and 100 m) increase from 3.87 to 3.72 s, from 6.97 to 6.87 s, and from 11.21 to 11.09 s, respectively

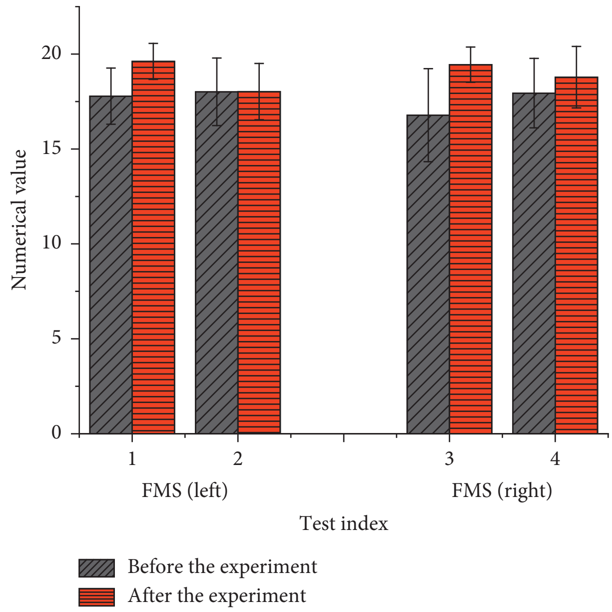

Figure 2: FMS test results of experimental group and control group before and after the experiment (1 and 3 represent before the experiment; 2 and 4 represent after the experiment).

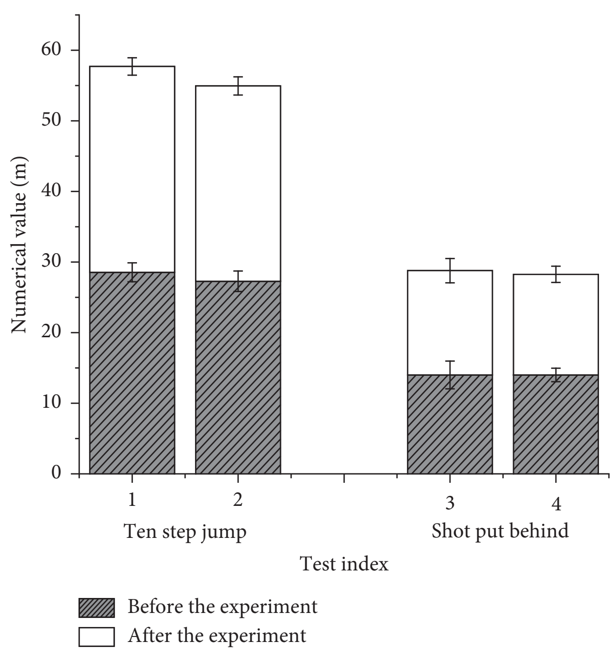

Figure 3: Level-ten stepping and postshot throw test results of experimental group and control group (1 and 3 represent before experiment; 2a and 4 represent after experiment.).

(Figure 4). There is a notable difference in comparison ($P < 0.05$). Under the traditional training program, experimental group and control group only have a remarkable difference in the 30 m training performance ($P < 0.05$), and there is no great difference in the 60 m and 100 m performance ($P > 0.05$). However, for the comparison between the

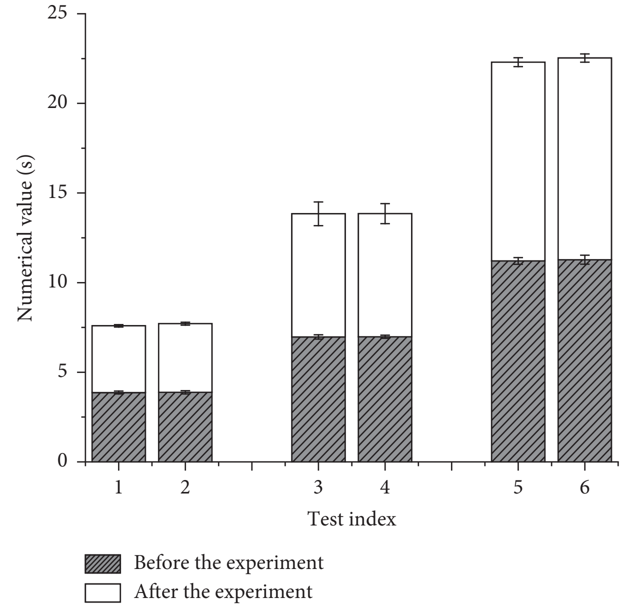

Figure 4: Test results of sprint (30 m, 60 m, and 100 m) of experimental group and control group (1, 3, and 5 represent before the experiment and 2, 4, and 6 represent after the experiment.).

two groups, there is a considerable difference between the 60 m and 100 m scores ($P < 0.05$).

4. Conclusion

The scientific mechanism of trunk support stability training is analyzed in this work so do the advantages of trunk support stability training, the physiological basis of trunk support stability training, and its biomechanical mechanism. Moreover, a trunk support stability training program is developed for sprint athletes, which focuses on the stability, strength, and balance of sprint athletes' shoulder, trunk, and buttocks musculature, as well as the training of limb control ability. Then, the test results of trunk support stability training are compared with those of traditional trunk strength training. From the results, both trunk support and stability training and traditional trunk strength training can improve subjects' FMS performance. There is no substantial difference between the two groups, but the improvement of experimental group is better relative to control group. For the strength test of subjects, only the level-ten stepping contrast between groups has a considerable difference, and the value of postshot throw before and after the experiment is very obvious. The speed difference between the two groups of subjects is very obvious, especially the 60 m and 100 m sprints. However, this work also has certain shortcomings. The experimental plan has a short period, and most of the students in sports colleges are national second-level athletes, which makes the results fail to reflect the actual situation of high-level athletes, and it needs to be analyzed in the follow-up research plans.

Data Availability

Data sharing is not applicable to this article as no datasets were generated or analyzed during the current study.

Conflicts of Interest

The author(s) declare that there are no conflicts of interest with respect to the research, authorship, and/or publication of this article.

References

[1] M. Timme, J. M. Steinacker, and A. Schmeling, "Age estimation in competitive sports," *International Journal of Legal Medicine*, vol. 131, no. 1, pp. 225–233, 2017.

[2] J. S. Hamilton, N. S. Schutte, G. M. Moyle, and R. Brown, "The relationships between mindfulness, sport anxiety, pessimistic attributions and flow in competitive cyclists," *International Journal of Sport Psychology*, vol. 47, no. 2, pp. 103–121, 2016.

[3] N. Mascret, J. L. Falconetti, and C. Franois, "Conceptions of sport ability and practice of sport: an implicit measure," *International Journal of Sport Psychology*, vol. 47, no. 2, pp. 122–132, 2016.

[4] I. Mujika, A. P. Sharma, and T. Stellingwerff, "Contemporary periodization of altitude training for elite endurance athletes: a narrative review," *Sports Medicine*, vol. 49, no. 11, pp. 1651–1669, 2019.

[5] C. Paquette, E. Franzén, and F. B. Horak, "More falls in cerebellar ataxia when standing on a slow up-moving tilt of the support surface," *The Cerebellum*, vol. 15, no. 3, pp. 336–342, 2016.

[6] Z. F. Zheng, Y. S. Liu, X. Min, J. B Tang, H. W Liu, and B. Cheng, "Recovery of sympathetic nerve function after lumbar sympathectomy is slower in the hind limbs than in the torso," *Neural Regeneration Research*, vol. 12, no. 007, pp. 1177–1185, 2017.

[7] D. Wafa, B. Dugue, L. Vinches et al., "Cooling during exercise enhances performances, but the cooled body areas matter: a systematic review with meta-analyses," *Scandinavian Journal of Medicine & Science in Sports*, vol. 29, no. 11, pp. 1660–1676, 2019.

[8] S. Y. Xia, Q. Zhan, and A. Rahmani, "ZMP based motion stability analysis of a wheeled humanoid robot with bending torso," *Applied Mechanics and Materials*, vol. 851, pp. 497–502, 2016.

[9] P. Zhou, H. Cai, and C. Yang, "Stabilization of the unstable equilibrium points of the fractional-order BLDCM chaotic system in the sense of Lyapunov by a single-state variable," *Nonlinear Dynamics*, vol. 84, no. 4, pp. 2357–2361, 2016.

[10] J. L. RoryM Cc, A. J. Chambers, A. Daftary, and M. S. Redfern, "Torso kinematics during gait and trunk anthropometry in pregnant fallers and non-fallers," *Gait & Posture*, vol. 76, pp. 204–209, 2019.

[11] V. K. Tjong, B. M. Devitt, M. L. Murnaghan, D. J. O. Harris, and J. S. Theodoropoulos, "A qualitative investigation of return to sport after arthroscopic bankart repair: beyond stability," *The American Journal of Sports Medicine*, vol. 43, no. 8, pp. 2005–2011, 2016.

[12] L. Stanciu, "Financial stability - fundamental pillar of macroeconomic balance and stability," *International Conference Knowledge-Based Organization*, vol. 25, no. 2, pp. 93–97, 2019.

[13] F. Giesche, J. Wilke, T. Engeroff et al., "Are biomechanical stability deficits during unplanned single-leg landings related to specific markers of cognitive function?" *Journal of Science and Medicine in Sport*, vol. 23, no. 1, pp. 82–88, 2020.

[14] A. Gayed, B. T. Bryan, K. Petrie et al., "A protocol for the HeadCoach trial: the development and evaluation of an online mental health training program for workplace managers," *BMC Psychiatry*, vol. 18, no. 1, p. 25, 2018.

[15] J. B. Farley, L. M. Barrett, J. W. L. Keogh, C. T. Woods, and N. Milne, "The relationship between physical fitness attributes and sports injury in female, team ball sport players: a systematic review," *Sports Medicine - Open*, vol. 6, no. 1, p. 45, 2020.

[16] L. Pereira, C. Winckler, C. C. C. Abad et al., "Power and speed differences between brazilian paralympic sprinters with visual impairment and their guides," *Adapted Physical Activity Quarterly*, vol. 33, no. 4, pp. 311–323, 2016.

[17] M. I. Khan, V. Santamaria, J. Kang et al., "Enhancing seated stability using trunk support trainer (TruST)," *IEEE Robotics and Automation Letters*, vol. 2, no. 3, pp. 1609–1616, 2017.

[18] I. Aoi, I. Aya, M. Saori, K. Aya, E. Kumiko, and F. Satoshi, "Comparison of site-specific bone mineral densities between endurance runners and sprinters in adolescent women," *Nutrients*, vol. 8, no. 12, p. 781, 2016.

[19] S. B. Ju and G. D. Park, "Effects of the application of ankle functional rehabilitation exercise on the ankle joint functional movement screen and isokinetic muscular function in patients with chronic ankle sprain," *Journal of Physical Therapy Science*, vol. 29, no. 2, pp. 278–281, 2017.

[20] M. Jeon, A. Jeon, and J. H. Lee, "Differences in body composition of upper and lower limbs in elite taekwondo athletes," *International Journal of Morphology*, vol. 38, no. 2, pp. 265–272, 2020.

Hindawi
Scientific Programming
Volume 2022, Article ID 3065780, 16 pages
https://doi.org/10.1155/2022/3065780

Research Article

An Algorithm Tool for Atom Decomposition and Interaction: AD Visualiser

Xiaobo Liu

School of Computer Science, University of Manchester, Manchester M13 9PL, UK

Correspondence should be addressed to Xiaobo Liu; xiaobo.liu@sxgkd.edu.cn

Received 25 October 2021; Accepted 8 December 2021; Published 28 January 2022

Academic Editor: Punit Gupta

With the rapid development of software-defined network and network function virtualization technology, the scale of infrastructure and the number of available resources in cloud platforms continue to grow. It is also be used in AD Visualiser. AD is a visualisation tool for displaying the atomic decomposition (AD) of OWL ontologies. As the size of ontologies increases, ontology engineers become more difficult to understand and reuse ontologies. Atomic decomposition (AD) is a modular structure to help ontology engineers modularly manage ontologies. It decomposes ontologies into sets of atoms, with dependency, based on modules that provide strong logical guarantees (such as locality-based modules). This paper describes the design and implementation process of AD Visualiser and discusses its usability for ontology engineers in their daily work. For example, using AD Visualiser, ontology engineers avoid choosing signatures and determining the extraction results. They can extract modules very simply and faster. Besides, the graph of AD's modular structure should be helpful for engineers to intuitively explore and comprehend ontologies.

1. Introduction

In recent decades, ontologies have progressively attracted the attention of researchers and engineers due to their unique knowledge expression in their field or industry [1]. Ontologies are widely used in many application fields, such as agent systems [2], knowledge management systems [3], and e-commerce platforms [4]. They can produce natural language, integrate intelligent information, and provide semantic-based access to the web. Additionally, they can also be used to extract data from texts in addition to many other applications to declare the knowledge embedded in them explicitly [5]. Besides casual ontology users, ontology experts even have been challenged to deal with the tasks of design, maintenance, reuse, and integration of complex ontologies. For example, in the medical industry, Systematized Nomenclature of Medicine – Clinical Terms (SNOMED CT) [6], Foundational Model of Anatomy (FMA) Ontology [7], and Gene Ontology (GO) are famous large ontologies. Their size also increases with the expansion of knowledge, which makes them difficult to comprehend, edit, and use. For example, FMA contains a large amount of knowledge that is irrelevant to a particular application area, such as anatomy. In this case, an increasing number of methodologies and tools have been developed to support ontology-related work.

When creating ontologies, designers may be experts in one field but is not familiar with other fields. Especially for medium and large ontologies, such problems are more common. Take the FMA ontology as an example; when expanding the knowledge related to body structure, if the creator only knows the bones but not the skin, then the most straightforward and cheapest method is to obtain a subset of the skin from existing ontologies. In addition, when using FMA ontology, the dermatologist may not need orthopaedic-related knowledge. The fastest and direct method is to extract a subset of the dermatological knowledge from the original ontology. Therefore, both in the process of creating and using an ontology, it is helpful for ontology engineers to extract a subset of knowledge about a specific term from the existing ontology. In order to complete this task better, the module extraction of ontologies have been explored in recent years [8]. Syntactic locality-based module extraction

(ME) [9] is a module extraction algorithm. Its module extraction time linearly depends on the size of the ontology. However, for medium and large ontologies, there are some disadvantages in extracting modules directly from the ontology [10]. First, loading the file into the memory for subsequent ME will cause much delay. For example, GO's OWL file exceeds 200 MB, and pre-loading it into the main memory will cause a great burden on the memory. Second, the conventional ME algorithm checks the relevance of every piece of knowledge in the ontology, which wastes lots of time. Third, it is difficult to determine the content of the extracted module. For example, the user only uses the term bone to extract the module from FMA ontology through ME. The result is unpredictable and may be different from the user's wishes. One way to solve this problem is modularisation of ontologies.

Atomic decomposition (AD) is a fine-grained, well-connected, and easily computable modular structure based on modules that provide strong logical properties, such as locality-based modules (LBMs) [11]. In the case that AD of an ontology shows in text form, people uneasy directly discover the internal connection between the overall structure and the decomposition results. Intuitively, displaying AD in graphical forms can make it more straightforward and more accessible for people to understand the structure and internal relations of the results [12]. However, displaying only graphical AD is less likely to display complete information or directly help people extract modules. Therefore, in order to improve the usability of tools, it is essential to add features allowing users to explore and interact with images. So far, it has been challenging to find an AD visualisation tool that meets the assumptions aforementioned, so we decided to develop such software called AD Visualiser to fill the gap.

2. Background

2.1. Description Logics. Description logics (DLs) are a family of knowledge depiction languages that describe a specific domain's knowledge in a well-structured and easy-understood form [13]. Generally, a DL is a decidable fragment of first-order logic (FOL) [14]. FOL is a standard for the formalising of mathematics into first-order formulas (named axioms). Then, it can be said that the DL is a syntactically restricted subset of axioms in which truth is computable. From the perspective of knowledge representation, DLs typically contain two main parts of domain knowledge: a terminological part called the TBox (T) and the assertional part called the ABox (A). The union of these two is called a knowledge base (K) [13]. Among them, the TBox represents knowledge about the structure of the domain (similar to the schema in JSON, XML, or database), while the ABox is about a concrete scenario (akin to the data in JSON, XML, or database).

Example 1 shows the knowledge base of the juice domain (1–14 from ABox and 15 and16 from TBox).

Example 1

Juice = { $\alpha 1$: Apple $\sqsubseteq$Fruit,

$\alpha 2$: Orange $\sqsubseteq$Fruit,

$\alpha 3$: Adult $\sqsubseteq$Person,

$\alpha 4$: Child $\sqsubseteq$Person,

$\alpha 5$: Carrot $\sqsubseteq$ Vegetable,

$\alpha 6$: Tomato $\sqsubseteq$ Vegetable,

$\alpha 7$: NamedJuice$\sqsubseteq$Juice,

$\alpha 8$: ChildJuice $\sqsubseteq$NamedJuiceH∃hasTagetPerson.Child,

$\alpha 9$: FruitJuice $\sqsubseteq$ JuiceH∃hasIngredient.Fruit,

$\alpha 10$: AppleJuice $\sqsubseteq$ FruitJuice H∃hasIngredient.Apple,

$\alpha 11$: OrangeJuice $\sqsubseteq$ FruitJuice H∃hasIngredient.Orange,

$\alpha 12$: VegetableJuice $\sqsubseteq$ JuiceH∃hasIngredient.Vegetable,

$\alpha 13$: CarrotJuice $\sqsubseteq$ VegetableJuice H∃hasIngredient.Carrot,

$\alpha 14$: TomatoJuice $\sqsubseteq$ VegetableJuice H∃hasIngredient.Tomato,

$\alpha 15$: Bobby: Child,

$\alpha 16$: (Bobby, ChildJuice):: likes

}

To the semantics of DL is defined in terms of an interpretation I = ("21600" o:spt = "75" o:preferrelative = "t" path = "m@4@5l@4@11@9@11@9@5xe" filled = "f" stroked = "f"> Δ^I, $\cdot^I$). The interpretation domain Δ^I is a nonempty set, and an interpretation function $\cdot^I$ that maps each atomic concept **A** to a subset $\mathbf{A}^I$ of Δ^I, each atomic role **r** to a binary relation $\mathbf{r}^I$ on $\Delta^I \times \Delta^I$, and each individual a to an element $a^I \in \Delta^I$ [13].

Different DL languages use different sets of constructors, which distinguish and limit the expressive power of this DL. The two main DLs cited throughout this project are $\mathcal{ALC}$ and *SROIQ*. The constructors allowed in the language, their syntax, and their semantics are described in Table 1, where $\mathbf{C}^I$ is the extension of **C** in I and $b \in \Delta^I$ is an **r**-filler of a in I if $(a, b) \in \mathbf{r}^I$.

The logic-based semantics of DLs make each statement to be well-defined and easy to share, so it is easy to judge whether a knowledge base entails a piece of knowledge. DLs use the standard entailment symbol "$|=$" because the semantics of entailment in DL coincides with FOL [13]. Entailment is a deduction or implication, that is, some axioms are logically derived from or implied by other axioms.

2.2. Ontology. In computer science, the term ontology typically represents a formal, explicit specification of a conceptual model specified using some ontology languages [15]. To be more specific, the ontology denotes a computer-processable and well-defined knowledge description form about concepts and their interrelationships. Previous ontology languages are generally based on semantic networks and frames. In contrast, recently, a majority of ontology languages is based on DLs [16]. An ontology can be viewed as a knowledge base. Therefore, an ontology can be regarded as a finite set of axioms. So we can call Example 1 juice ontology.

Table 1: DLs semantics.

Language	Name	Syntax	Semantics
$\mathscr{A}LC$	Top	$\top$	Δ^I
	Bottom	$\perp$	$\varnothing$
	Intersection	$\mathbf{C}\sqcap\mathbf{D}$	$\mathbf{C}^{I\cap}\mathbf{D}^I$
	Atomic negation	$\mathbf{A}$	$\Delta^I\setminus\mathbf{A}^I$
	Limited		
	Existential		
	Quantification value	$\exists r$	$\{a \in \Delta^I \mid \exists b \cdot (a,b) \in r^I\}$
	Restriction	$\forall r.C$	$\{a \in \Delta^I \mid \forall b.(a,b) \in r^I \longrightarrow b \in \mathbf{C}^I\}$
SROIQ	Union	$\mathbf{C}\sqcup\mathbf{D}$	$\mathbf{C}^{I\cup}\mathbf{D}^I$
	Negation	$\mathbf{C}$	$\Delta^I\setminus\mathbf{C}^I$
	Role chain	$\circ$	$\mathbf{r}\circ\mathbf{s}\sqsubseteq\mathbf{t}$
	Nominal	$\{a\}$	$\{a\}^I\subseteq\Delta^I$ with# $\{a\}^I = 1$
	Inverse		
	Role	$\mathbf{r}^-$	$\{(a,b) \in \Delta^I\wedge\Delta^I \mid (a,b) \in \mathbf{r}^I\}$
	Unqualified	$\geq n\mathbf{r}$	$\{a \in \Delta^I \mid \#\{\text{bin}\Delta^I \mid (a,b) \in \mathbf{r}^I\} \geq n\}$
	Number	$\leq n\mathbf{r}$	$\{a \in \Delta^I \mid \#\{\text{bin}\Delta^I \mid (a,b) \in \mathbf{r}^I\} \leq n\}$
	Restriction	$= n\mathbf{r}$	$\{a \in \Delta^I \mid \#\ \text{bin}\ \Delta^I \parallel (a,b) \in \mathbf{r}^I\} = n\}$
	Qualified	$\geq n\mathbf{r}.\mathbf{C}$	$\{a \in \Delta^I \mid \#\{b \in \mathbf{C}^I\} \geq n\}$
	Number	$\leq n\mathbf{r}.\mathbf{C}$	$\{a \in \Delta^I \mid \#\{b \in \mathbf{C}^I\} \leq n\}$
	Restriction	$= n\mathbf{r}.\mathbf{C}$	$\{a \in \Delta^I \mid \#\{b \in \mathbf{C}^I\} = n\}$

The backbone of ontology entails a generalization/specialization hierarchy of concepts, such as taxonomy. This example can be described in lots of ontology languages. In particular, the most concerned language in this project is Web Ontology Language (OWL), a state-of-the-art semantic web language standardized by the World Wide Web Consortium (W3C). OWL uses its own grammar to explain the grammar in DL, but such a grammatical sentence is too long and complicated. In order to facilitate users to understand the meaning of the content, AD Visualiser uses Manchester syntax, which is a user-friendly compact syntax of OWL ontologies. It is frame-based, contrary to other axiom-based syntaxes of OWL. This project involves these three kinds of syntaxes in total. Example2.2.1 borrows the DL syntax. The OWL syntax is mostly used in OWL files. For the convenience of users to read and understand, the software uses the Manchester syntax on the user interface. The comparison of the DL, OWL, and Manchester syntaxes is shown in Table 2.

2.3. Module. Given a seed signature Σ, a module M is a subset of the ontology O. Therefore, for all axioms with terms only from the signature, we have M $|= a$ if O $|= a$. As the usability of OWL ontology continues to improve, some of them already contain thousands of concepts. Medium to large ontologies generally contains more than 30,000 axioms (such as gene ontology, including 558,760 axioms [17]). As a result, these posed some major challenges to the entire development process of the ontology, such as understanding, editing, and debugging. As a subset of ontology, modules can be used to share and reuse parts of ontology. In recent years, several approaches to ontology module extraction and ontology modularisation have been explored. For these tasks, the most fundamental question is which module to choose as the basis. This project focuses on locality-based modules (LBMs), a family of logical modules that provide strong logical guarantees. Compared with other module types, they are proved to be more suitable for module extraction [8]. The reasons are that they are easy to obtain, are computationally efficient, and has been implemented and used to extract modules [18]. Besides, LBMs are as expressive as SROIQ: they provide necessary and unique features (called logical guarantee), such as coverage, self-contained functions, and exhaustive functions, which make the axioms locality. In other words, for each axiom, whether it is included in the module or not, it must be independent of other axioms. They strike a perfect balance between the computable and the minimal. This means that given the seed signature, although the LBM extracted from the ontology possibly contains axioms that are not relevant to the signature, the extraction time is truly short.

2.4. Atomic Decomposition. Atomic decomposition (AD) is a method of decomposing ontology into modules and offering a modular structure. Using LBMs as the basis, AD divides an ontology into numerous portions, called atoms, which have a dependency relationship in pairs. An atom is a set of axioms that always cooccur in a module. Thus, any Σ −module either contains all axioms in the atom or does not contain any axioms. Dependency relation means that all modules containing atom a must also contain atom b, meaning that atom a depends on atom b.

All atoms of the ontology are represented as A(O); then each atom in A(O) is disjoint with any another one. Atoms are maximal subsets of axioms that are not separated by any Σ −module. The definition of the genuine module is that a Σ −module that cannot be decomposed as the union of two or more incomparable modules. Therefore, every module can be obtained as the union of suitable genuine modules. In this sense, atoms are genuine modules; thus, a new module can be obtained with the union of atoms.

Table 2: Comparison of syntaxes.

DL	OWL	Manchester
T	owl:Thing	owl:Thing
⊥ ConceptnameRole name	owl:Nothing Class	owl:Nothing
C ¬ **C**	Object property	Class
D *H***D**	ObjectComplementOf(C)	Object property
*H***D**	ObjectUnionOf(C D)	notC
∃ **r** . **C**	ObjectIntersectionOf(C D)	C or D
∀ **r** . **C**	ObjectSomeValuesOf(C D)	C and D
(≥*n* **r** . **C**)	ObjectAllValuesFrom(r C)	r some D
(≤*n* **r** . **C**)	ObjectMinCardinality(n r C)	r only C
(=*n* **r** . **C**)	ObjectMaxCardinality(n rC)	r min nC
	ObjectExactCardinality(n rC)	r max nC
		r exactly n C

The definition of dependency is a binary relation between atoms in terms of cooccurrence in modules. The relation is a partial order: if both a depends on b, and b depends on a hold, consequently a = b. We use > for the strict partial order underlying ≤. We can use the standard notions of a principal ideal (a downwards closed subset of a partially ordered set) and an antichain:

(1) The poset (A(O), >) is denoted as atomic decomposition (AD) of O.
(2) The principal ideal of an atom a ∈ A(O) is the set ↓ a: = {b|a ≤ b}.
(3) An antichain of atoms is a set B ⊆ O such that a Ç b for any two distinct.

An ontology's modular structure is determined by all modules and interrelations of the ontology or at least a suitable subset thereof [11]. This modular structure is based on two fundamental notions: (a) an atom of the input ontology O is a maximal subset of axioms that are never separated by any module of O and (b) the dependency relation between atoms of O captures a further kind of cohesion and allows for a natural definition of basic modules of O. Consequently, the atoms of O are O's highly cohesive and low-couple subsets, and the number of axioms in O bounds that of atoms. Because AD is based on LBMs, it also has three types corresponding to the notions of locality (⊥ bot, ⊥ top, and T⊥∗ nested).

2.5. Existing Ontology Visualisers. A number of software provides developers with a standard ontology development environment, such as Prote´ge´ [19], SWOOP [20], and OntoTrack [21]. These tools can assist users in completing ontology-related work in the text form. For humans, however, the text is not as intuitive as images. Hence, with the rise of ontology, ontology visualisation software has received widespread attention as a method of giving information well-defined meaning.

In the last couple of years, with the popularity of ontologies, a variety of ontology visualisation tools have been developed. There are mainly two ways to realise them: a plug-in of the ontology editor Prote´ge´ and a standalone web application. But visual tools for AD of ontologies are still scarce, one of which is a tiny visual tool for AD; it is a part of Nicolas Matentzoglu's framework, named Katana [22]. It only illustrates the AD as a graph without any further operation or information. However, the image gives viewers an insight to consider the structure of ontologies. Since AD is a modular structure of an ontology, the characteristics of the visible results of the software and the overall design concept of the software can be learned and referenced in the AD visualisation tool. The following are three representative software.

2.5.1. Graph Visualisation of Ontologies. The graphs are typically laid out in force-directed, radial or hierarchical way, which usually produce appealing visualisations. However, only a few visualisations show complete ontology information. For example, KC-Viz [23], OWLViz [24], and OntoGraf [25] show merely the class hierarchy of ontologies. Numerous works provide more comprehensive graph visualisations that represent all critical elements of ontologies. For example, TGViz [26] and NavigOWL [27] use easy to understandable node-link diagrams where all nodes and links are in different colours. Other than that, 3D-graph visualisations for ontologies, such as OntoSphere and Onto3DViz, provide users with a multidimensional sight to view ontologies.

2.5.2. UML-Based Ontology Visualisations. Unified Modelling Language (UML) is not new to most software engineers. The benefits of presenting ontology information in that language form are obvious: engineers can easily understand and have familiarity with the tools. However, its disadvantages cannot be ignored: on the one hand, it is unfriendly to users who are not familiar with UML as some basic knowledge of UML is required. On the other hand, it is designed to associate objects in the field of software engineering, and there are some limitations when it comes to the knowledge presentation domain. For example, ontology focuses on the description of relationships between classes, while software engineering focuses on the description of properties and methods of objects themselves.

2.5.3. Symbol-Based Ontology Visualisations. The OWLGrEd Ontology Visualiser (OWLGrEd) [28] is an online visualiser for OWL ontologies using a compact UML-based notation. OWLGrEd provides a "bird's-eye view" of the ontology to help developers debug ontologies. The notation of OWLGrEd is UML-style diagrams that most software engineers are familiar with and easy to use. OWLGrEd map OWL features to UML concepts, that is, OWL classes to UML classes, data type properties to class attributes.

Using defined symbols to explicit splitting rules, symbol-based ontology visualiser specifies different elements in the graph. The visual representation of OWL ontology is a visual language for ontology representation. It defines the graphical descriptions of most elements of OWL, and these are represented as forced graph layouts of visual ontologies that replace text.

The Visual Notation for OWL Ontologies (VOWL) [29, 30] is a type of visual language for the user-oriented ontologies representation. It provides graphical representations for elements of the OWL Web Ontology Language. Not only domain experts but also beginners have the ability to understand the content of OWL ontology with clearly specified symbols.

3. Design and Implementation

3.1. Design. This project aims to create an atomic decomposition visualiser (AD Visualiser) for ontology engineers to express the AD of large- and medium-sized ontology intuitively and comprehensively. AD Visualiser focuses on two parts of the visual representation: one part is the hierarchical structure of classes and object attributes, and the other part is the atoms and their relationships. The functional design of AD Visualiser is mainly based on the three ontology-related tasks mentioned in Section 3, to help users complete tasks-related tasks. AD Visualiser can parse and display a graph for the AD of an OWL ontology in an interactive way. For medium and large ontology, the way to visualise AD is more direct and objective than using other edit tools such as Prote´ge´, and it offers a method to find the module related to a signature faster. Users can expeditiously browse the ontology in a modular structure to find and extract the modules they need. In the reasoning result, users can quickly see classes, object property hierarchy, and graphical AD. Users can detect the atom's information efficiently in the tool. They can recognise the notion of the modular structure of an ontology, which has the potential to help users comprehend, share, and maintain ontology. Users can use it to guide their extraction choices, to understand its topicality, connectedness, structure, unnecessary parts, or differences between actual and intended modelling. For example, ontology designers can inspect the modular structure and observe unconnected parts that are intended to be connected and modelled parts of their ontology.

Figure 1 depicts the system flow chart. It illustrates the possible results and corresponding logic of all operations that the user may perform from the start of the software. In addition, it also reveals how the tool guides users to explore the ontology, and what functions the tool provides for users to interact with the ontology.

3.2. Basic Building Blocks of AD Visualiser. AD Visualiser uses the OWL API to underpin all ontology management tasks, including loading, decomposing, and saving ontologies. Then, it uses Gephi API to draw the graph.

3.2.1. User Interface. Figure 2 shows the user interface (UI) prototype diagram of AD visualiser that includes the menu bar, search bar, classes (and object property) hierarchy, and graphical AD.

The visualisation of AD is one of the most significant tasks of AD Visualiser. When displaying image-based AD, in order to retain and display as many AD functions as possible, we set the following information conversion method from text to image. The features of AD determine the structure of its graphical result. In the graph, each node corresponds to an atom in the AD, and each arrow line between a pair of nodes corresponds to a dependency relationship between two atoms. Moreover, the graph layout depends on the source data structure so that the graph of AD can be easily generated. The reason is that the result of AD is a partial set, so the graph of AD is the type of directed acyclic graph (DAG).

In an AD, an atom has many attributes. For example, an atom's size is determined by the number of its axioms; an atom may be top or bottom atom according to its position (an atom only have dependents may be at the bottom, and the atom only have dependencies may be at the top); an atom may have many types of labels (positive Boolean formula (PBF) label is used in this project, which is a representation of all seed signatures of the atom's module with the only union and intersection constructors). In the program of AD Visualiser, every node is an object with multiple attributes to represent the relevant atom's attributes. This system defines a set of visual language systems to help users understand AD in a visual language way. For example, the node's size is relevant to the atom's size; the node's position shows the atom's position in the AD; the node's label corresponds to the atom's label; and much more. The features of nodes in a graph are more intuitive and easy to understand than the information of atoms in textual AD.

Algorithm 1 shows the process of drawing DAG in AD Visualiser.

Another important component in AD Visualiser is hierarchy trees of classes and object properties.

Algorithm 2 shows the process of building a classes tree.

3.3. Colour Scheme. Colours play a significant role in beautifying user interfaces. For example, in graphical AD, colours are important from differentiating nodes' positions to finding the target node to identifying a module. Besides, elements in the background and foreground of a screen have to be different colours. If their colours are the same, it is difficult to identify the foreground elements immediately. Hence, colours that distinguish with each other are also meaningful.

Figure 3 illustrates that even the colours of the small square and background are different, it is still ugly, and people may feel uncomfortable when looking at them. The

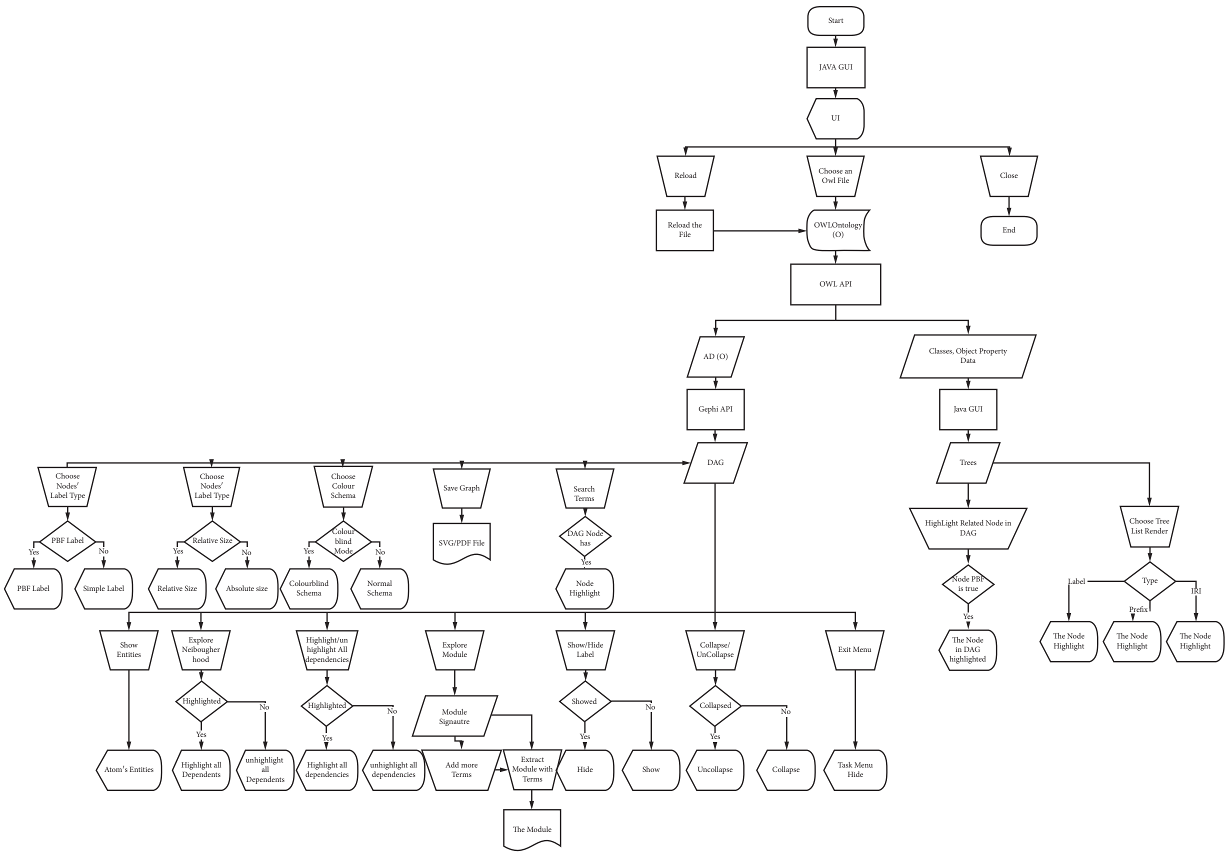

Figure 1: The system flow chart.

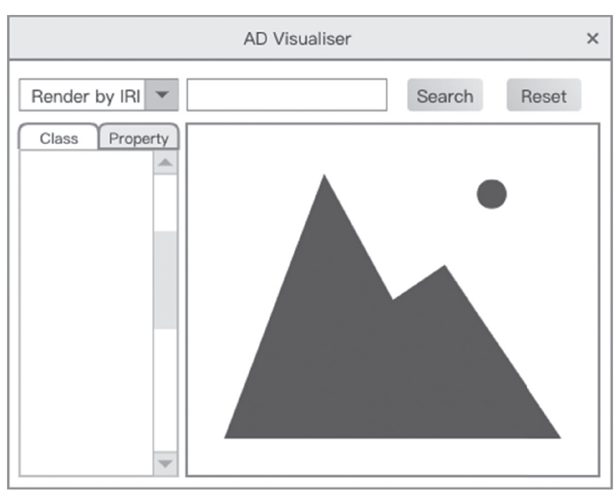

Figure 2: User interface design.

reason is that the contrast ratio for the two colours is smaller than 4.5:1 [31].

If the contrast ratio is higher, the screen looks more legible and readable. Moreover, human beings may have different experiences with the same colour. Some of us have defects in vision, called colour blindness, which is defined as the inability to distinguish the same colour differences (the most common ones are red and green or blue and yellow). It is estimated that 1 in 12 men and 1 in 200 women have such an unusual colour experience [31]. In order to make these people have a better experience, AD Visualiser provides a colour blind mode for users to choose. The solution for these users is still to increase the contrast of colours. By using high-contrast colours, they can distinguish these colours no matter what actual colours are used. Following these colour matching rules, the colour scheme of this project is shown in Table 3.

```
Input: An Ontology O
Output: A DAG g
ad←AtomicDecomposition(O);
g←DirectedGraph(ad);
graphNodes←0/;
topAtoms←topatoms ∈ ad
dep(atom)←atoms ∈ dependenciesofatom
foreachatom ∈ topAtoms do
graphNodes ← graphNodes ∪ atom;
end for
repeat
 if atom/graphNodes then
graphNodes ← graphNodes ∪ atom;
endif
if dep(atom) = 0/then
for eachatomChild ∈ dep(atom)do
if atomChild/graphNodes then
graphNodes ← graphNodes ∪ atomChild;
endif
endfor
endif
until add all the atoms in graphNodes of ad
repeat
if ad.getDependencies(atom).size()! = 0then
foreachatomChild ∈ ad.getDependencies(atom)do
g.addEdge(atom, atomChild);
endfor
endif
until draw all the edges
show the result g;
```

ALGORITHM 1: DAG drawing algorithm.

```
Input: An OntologyO
Output: A DAGgraph
supperClass ← owl: Thing;
supper ← Node sup perClass;
repeat
if subClasses (supperClass) ≠∅&& owl :  Nothing ∉ subClasses (supperClass)
then
foreachsubClass ∈ subClasses(supperClass)do
subNode ← subClass
supperNode.addSubNode(subNode);
supperClass ← subClass;
endfor
endif
until add all the classes as nodes in the tree
show the result tree;
```

ALGORITHM 2: Tree building algorithm.

In this project, many types of highlights are used to distinguish the target nodes from others. The author shows people's possible different experiences with colours in the picture below. These include deuteranopia (Figure 4; lack of green affects about 5% of men), protanopia (Figure 5; red defects affect about 2.5% of men), tritanopia (Figure 6; blue defect affects about 0.5% of men), and grayscale (Figure 7; luminance-preserving grayscale simulation).

3.4. Functionality Introduction. Users can view a graphical AD of an OWL file and then explore the AD around or target to their interested module with a signature. As mentioned before, a module is a principal ideal of an atom a; each atom is a unique set of axioms; and each node in the graph corresponds to an atom. To quickly find a, every atom has two types of labels,

The simple label containing all terms in the atom and positive Boolean formula (PBF) label. Given the terms, the

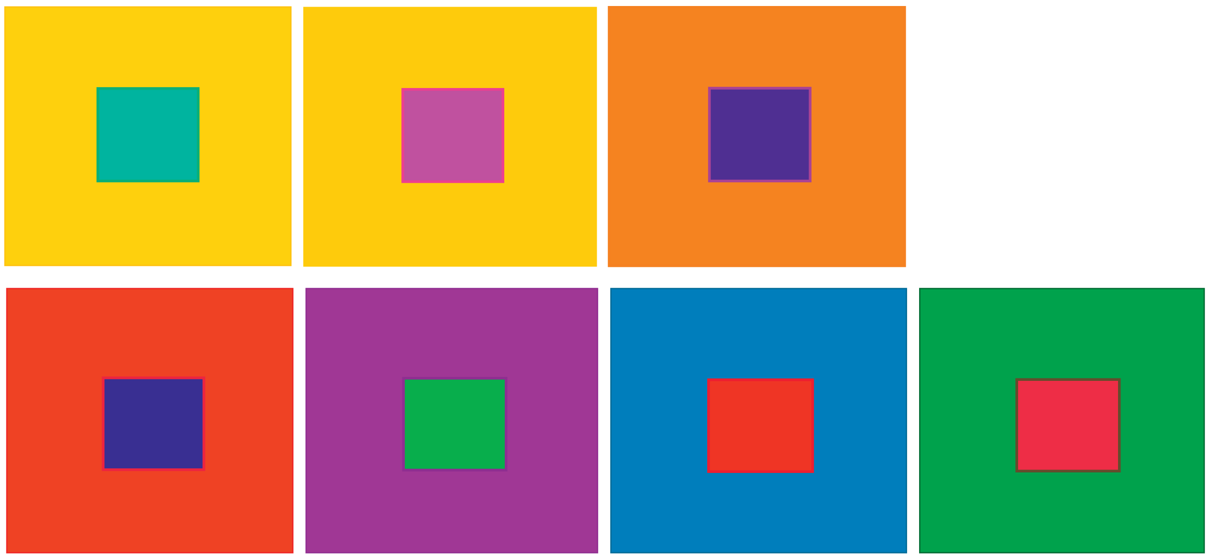

Figure 3: Colour contrast [31].

Table 3: Colour schema.

Name	Colour	Application
Green		Nodes below connected to a node
Cyan		Nodes direct connected to a node
Blue		Nodes have hidden subnodes
Yellow		Nodes are not bottom nodes
Grey		Nodes are bottom nodes
Red1		Nodes contain one term
Red2		Nodes contain two terms
Red3		Nodes contain three terms
Red4		Nodes contain four terms
Red5		Nodes contain five terms
Red6		Nodes contain more than five terms

tool calculates each atom's PBF label and then highlights true-result corresponding nodes. With a, users can explore the genuine module and extract it until they feel satisfied.

These are three solutions to tasks mentioned in Section 3.2:

(i) Ontologists not only have a bird's-eye view of an ontology with a modular structure but also can focus on a small part of an ontology. Additionally, they have the opportunity to check each atom's information. Hence, we suppose this tool is helpful for them to refine ontologies.

(ii) A feasible way to merge ontologies is to import other ontologies from the web. After merging, designers can find, and the term may be involved in many small ontologies to check whether or not they are intended in the final big ontology. Consequently, we suppose this tool should be useful for ontology merging.

(iii) Developers have the opportunity to explore an ontology with terms and extract their interesting modules from an ontology in AD Visualiser.

That is pretty helpful for them to reuse the ontology flexibly.

3.5. Implementation

3.5.1. User Interface. Figure 8 depicts the layout of AD Visualiser's user interface. It depends on the GridBagLayout [32], a type of flexible layout manager provided by the Java platform.

Figure 9 displays the grid for the user interface. As shown in the screenshot, the grid has two rows and four columns. All the components are in the grid except the menu bar fixed at the top of the window. Particularly, the panel in the lower right corner spans three columns.

Using juice ontology as an example, Figure 10 shows how the DAG looks like in AD Visualiser in which grey nodes are bottom nodes and the others are yellow.

Name	Colour	Application
Green		Nodes below connected to a node
Cyan		Nodes direct connected to a node
Blue		Nodes have hidden subnodes
Yellow		Nodes are not bottom nodes
Grey		Nodes are bottom nodes
Red1		Nodes contain one term
Red2		Nodes contain two terms
Red3		Nodes contain three terms
Red4		Nodes contain four terms
Red5		Nodes contain five terms
Red6		Nodes contain more than five terms

Figure 4: Deuteranopia.

Name	Colour	Application
Green		Nodes below connected to a node
Cyan		Nodes direct connected to a node
Blue		Nodes have hidden subnodes
Yellow		Nodes are not bottom nodes
Grey		Nodes are bottom nodes
Red1		Nodes contain one term
Red2		Nodes contain two terms
Red3		Nodes contain three terms
Red4		Nodes contain four terms
Red5		Nodes contain five terms
Red6		Nodes contain more than five terms

Figure 5: Protanopia.

Name	Colour	Application
Green		Nodes below connected to a node
Cyan		Nodes direct connected to a node
Blue		Nodes have hidden subnodes
Yellow		Nodes are not bottom nodes
Grey		Nodes are bottom nodes
Red1		Nodes contain one term
Red2		Nodes contain two terms
Red3		Nodes contain three terms
Red4		Nodes contain four terms
Red5		Nodes contain five terms
Red6		Nodes contain more than five terms

Figure 6: Tritanopia.

Name	Colour	Application
Green		Nodes below connected to a node
Cyan		Nodes direct connected to a node
Blue		Nodes have hidden subnodes
Yellow		Nodes are not bottom nodes
Grey		Nodes are bottom nodes
Red1		Nodes contain one term
Red2		Nodes contain two terms
Red3		Nodes contain three terms
Red4		Nodes contain four terms
Red5		Nodes contain five terms
Red6		Nodes contain more than five terms

Figure 7: Grayscale.

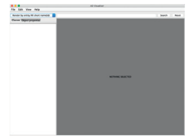

Figure 8: UI of AD Visualiser.

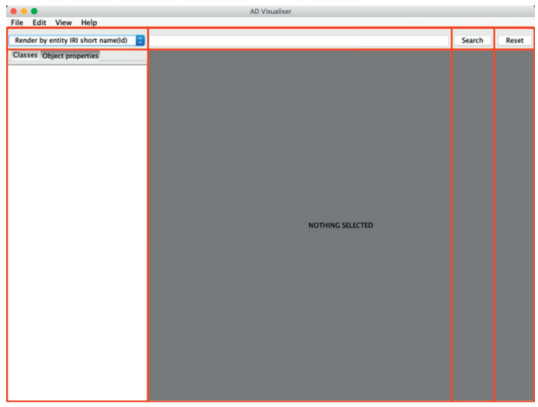

Figure 9: GridBagLayout.

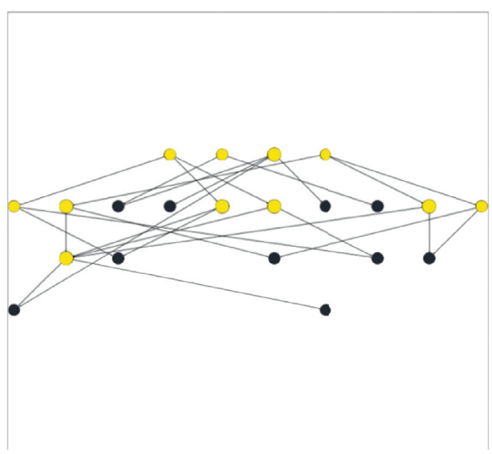

Figure 10: DAG of juice ontology.

3.5.2. Search Terms. Figure 11 shows the feedback from AD Visualiser to users when searching the term carrot.

3.5.3. The Node Menu in Graphical AD. As shown in Figure 12, the implementation of the functions in the menu bar is as follows:

(i) *Show Entities*. Figure 13 shows the entities of the highlighted node.

(ii) *Explore Neighbourhood*. As shown in Figure 14, the neighbours of the chosen node are cyan.

(iii) *Explore All Dependencies*. As shown in Figure 15, the subnodes (all descendants) pointed to by the selected node are in green.

(iv) *Explore Module*. As shown in Figure 16, the "Module Signature" is the signatures obtained through the seed signature pre-extraction module. Related signature uses the characteristics of the directed graph to extract the signatures contained in the atoms corresponding to the node that is connected to the selected node and the arrow points to the selected node. When the user adds an atom to the module, the author uses the same method to add the signatures of its related atoms to a table, which is convenient for users to view and operate.

(v) *Show or Hide a Node Label*. The label of a node shows or hides.

(vi) *Collapse and Uncollapse a Node Chain through Exploring All Dependencies*. Nodes connected below the selected node are obtained. As shown in Figure 17, hiding these nodes can remove these nodes from the graph.

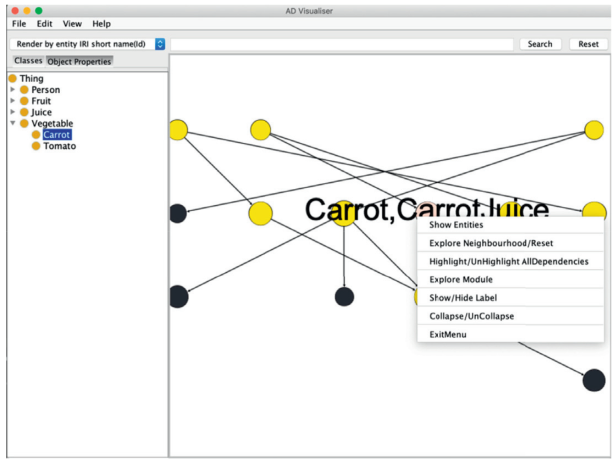

Figure 11: Search carrot.

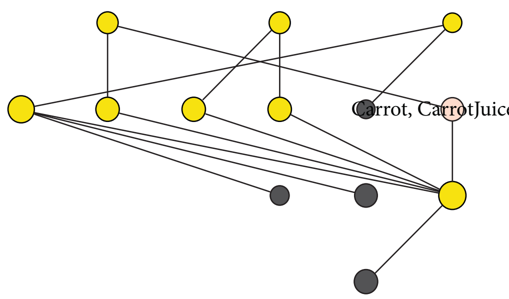

Figure 12: Node menu.

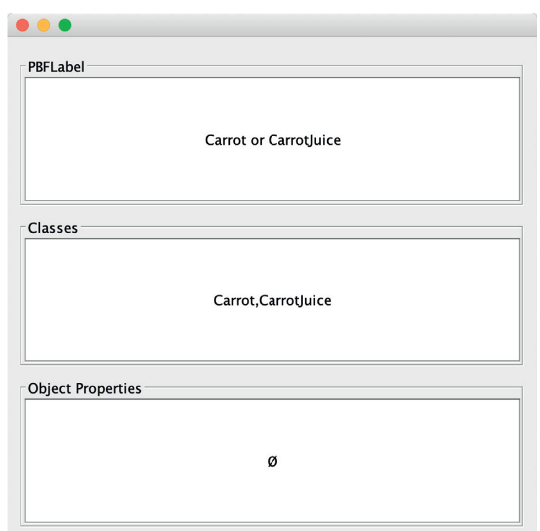

Figure 13: Show entities.

4. Testing and Evaluation

In the later stages of program development, testing and evaluation are critical to measuring and improving system performance. For this project, software testing is divided into two parts. The first part is the self-testing of the software performance: whether it meets the functional requirements mentioned in Section 3, the operating speed, and efficiency of the software. The second part is to invite experts to try the software and then give the trial experience and opinions.

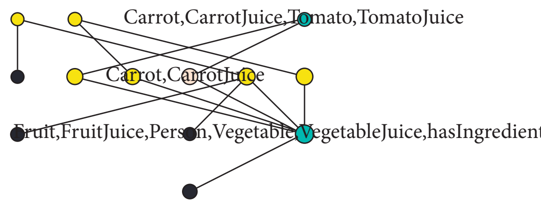

Figure 14: Explore neighbourhood.

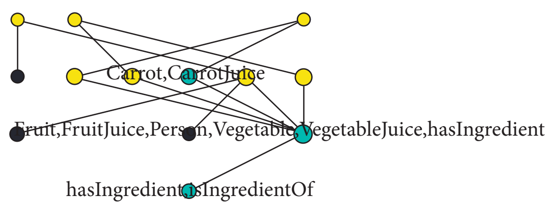

Figure 15: Highlight all dependencies.

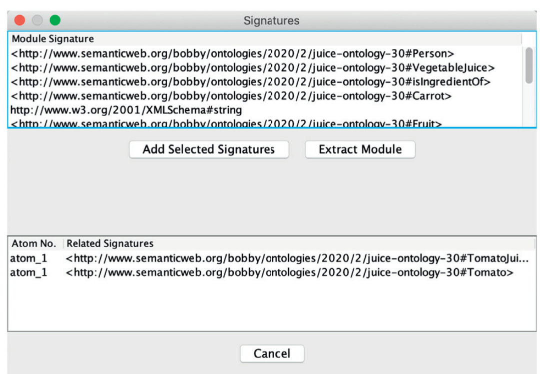

Figure 16: Explore module.

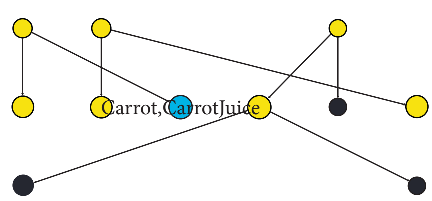

Figure 17: Collapse a node chain.

4.1. Test Design and Implementation. Test Cases Selection. Since AD is more dependent on logical axioms, the author deliberately selected some small (including 1,000 logical axioms), medium (including 1,000 to 20,000 logical axioms), and large ontologies (including more than 20,000 logical axioms) for testing. Through this method, it is possible to test the visual results and functional support of AD Visualiser for ADs of different sizes ontologies.

Influence Factors. The length of time to parse the advertisement depends on the OWL API. Chiara Del Vescovo, the inventor of AD theory, had tested 357 ontologies; the computing time for half of the ontologies spend less than 1 second; 95% spend within 2 minutes; and 99% spend no more than half and 1 hour. Besides, the length of time for Gehpi API drawing graphical AD and JTree drawing hierarchy trees depends on Algorithms 1 and 2, respectively. The author tested six small ontologies, one medium ontology, and two large ontologies and individually recorded the time spent in each stage before the image was displayed. Table 4 illustrates the performance of the AD visualiser when processing these ten ontologies. Figure 18 shows the visualisation result of pizza ontology as a representative of small ontologies. Figure 19 presents the visualisation result of wbphenotype as a representative of medium ontologies, and Figure 20 displays the visualisation of gene ontology as a representative of large ontologies.

Table 4: Processing time.

Name	Axioms	TBox	Atoms	Type	AD (s)	DAG (s)	Tree (s)	Total (s)
			BOT	13	0.047	1.235	0.074	2.170
juice	53	33	TOP	1	0.008	1.001	0.12	1.062
			STAR	13	0.018	1.008	0.009	1.065
			BOT	75	0.080	1.159	0.124	2.183
gfo-basic	479	212	TOP	2	0.010	1.002	0.032	1.126
			STAR	90	1.090	0.039	1.019	1.290
			BOT	29	0.012	1.012	0.007	1.076
Biblio	332	219	TOP	197	0.17	1.014	0.009	1.233
			STAR	99	0.022	1.017	0.009	1.090
			BOT	283	0.010	2.019	0.022	2.127
asdphenotype	1,434	283	TOP	77	0.012	1.004	0.030	1.094
			STAR	283	0.010	1.007	1.078	
			BOT	89	0.045	2.030	0.220	2.380
pizza	801	322	TOP	1	0.011	1.002	0.145	1.215
			STAR	91	0.088	2.023	0.118	2.286
			BOT	154	0.135	2.051	0.469	2.821
gist	664	384	TOP	5	0.019	1.010	0.472	1.559
			STAR	159	0.165	2.075	0.645	2.968
			BOT	2581	6.355	31.417	5.471	45.149
wbphenotype	20,255	3,939	TOP	348	286.78	4.823	5.876	40.353
			STAR	2774	8.348	25.168	5.179	39.438
			BOT	8281	47.143	216.667	190.65	285.153
fission-yeast	35,968	27,602	TOP	20	6.282	1.975	30.7178	
			STAR	10464	70.385	475.906	182.37	565.964
			BOT	20058	185.54	441.972	122.22	475.740
cell-culture	53,297	33,235	TOP	5	7.416	1.606	378.45	48.226
			STAR	27481	38.209	435.993	42.804	518.325
			BOT	43652	1058.634	535.129	2004.321	
gene	558,760	103,676	TOP	1	8.766	1.390	441.792	465.306
			STAR	63311	669.733	948.899	478.616	2112.548

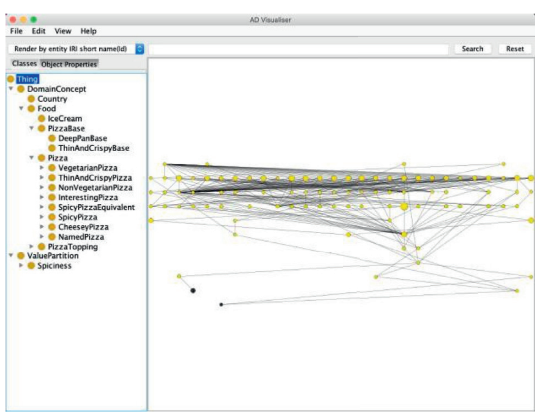

Figure 18: The test of pizza ontology.

5. Results and Analysis

AD Visualiser fully supports small ontologies; the visualisation results are clear; and various functions are fully supported. For medium-sized ontologies, the graphical ADs are relatively clear, and users may have a little difficulty in finding the highlighted nodes. However, users can view nodes' information and explore their neighbourhood at will, and AD Visualiser is also very smooth to use. Moreover, for large ontologies, the visualisation results are very poor. Users may have a clear sense of lag in use, and users can hardly find the highlighted nodes.

Table 4 depicts that the processing time of AD Visualiser on the ontology increases as the number of logical axioms (TBox in Table 4 points at the number of ontology's logical axioms) in the ontology increases. They are approximately linearly related. Over the first 15 minutes, Uli Sattler introduced the origin and principle of the theory of AD. Then the author spent some time introducing and showing how to use AD Visualiser to the audiences. Dave McComb asked the

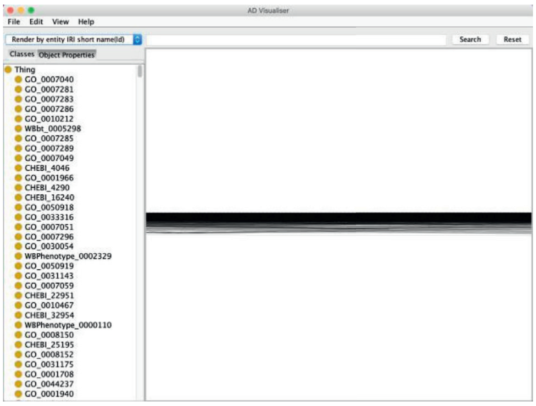

Figure 19: The test of wbphenotype on-tology.

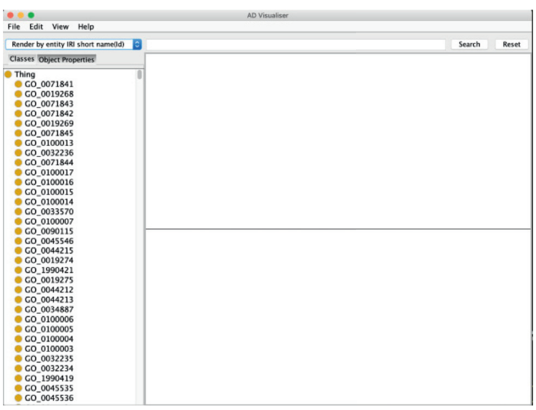

Figure 20: The test of gene ontology.

author to extract a module about the term Person. Then, we checked the person module in Protege. The details are shown in Figures 21 and 22.

The result of module extraction surprised all of the audiences. Even though they are designers and makers of gist ontology, they have never thought that so many terms are related to the term person, and then heated discussions began. To their surprise, they even wondered that if the author opened the correct module just extracted. Haoruo Zhao discovered that the module contains 41 disjoint axioms, which may be the possible reason for retaining some much knowledge perhaps, which is attributed to logical guarantees. They thought disjoint is a common and important relation between axioms, but they were not convinced that this relation has such a powerful influence on the term or the ontology.

Dave McComb, the president and cofounder of Semantic Arts, believes the visualisation of AD is less useful for him. Instead, the important thing is obtaining a suitable module from an ontology. He said "the presentation helped me think a lot in this respect, it did not occur to me until this that there would have to be some 'explain' function that could explain why a given concept or axiom got included." In terms of the task of ontology reusing, he said most existing ontologies are not reusable. As every OWL ontology has a domain and range, once the module is extracted out from ontologies'

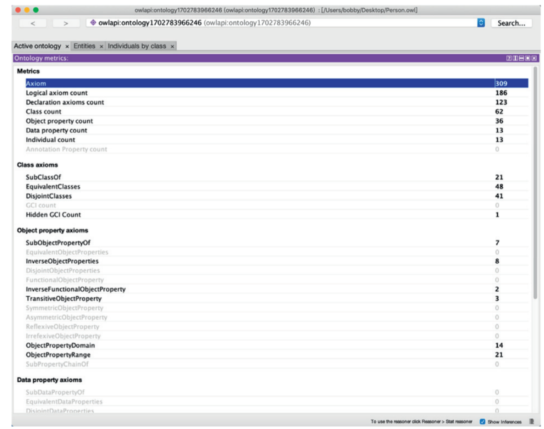

Figure 21: Ontology metrics of person module.

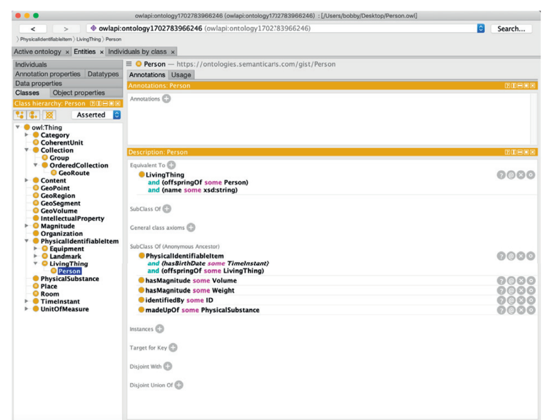

Figure 22: Classes hierarchy of person module.

original context, they are not compatible with others. Sometimes, ontologists even need to trim the module down to make it compatible with new ontologies. He supposed such a complex operation could not be accomplished by a tool or algorithm automated.

Peter Winstanley, an ontologist in the Semantic Arts and cochair of the W3C Dataset Exchange Working Group, said AD Visualiser had stimulated a more in-depth revision of an ontology, such as gist ontology. Its development tends to be organic and driven by many stakeholders. He thought AD Visualiser provides a new insight for his colleagues and him for their daily work.

Michael Uschold, a senior ontology consultant at Semantic Arts, is an internationally recognised expert with more than two decades of experience in developing and transitioning semantic technology from academia to industry. He pointed out that AD Visualiser cannot be used immediately in his daily work. This is because the super-granularity makes the graphics huge, and then it is not easy to see at a glance. Such a case is a significant obstacle to the effective use of images. In this regard, he suggested that images can be cut into small pieces so that users can see a magnified view of a specific area. Regarding the functional requirements of the tool, he hopes that the tool can achieve excellent support for the input of a specific ontology with hundreds of classes and object properties. After proper processing, the output is a subset of the gist that should have everything they need, and nothing else is superfluous.

More than dozens of people attended this online conference, and they are all experienced engineers working on ontology. Most of them are rather interested in AD Visualiser and its functionality. For Dave's negative feedback, it may be because the author only focuses on introducing the functionality of the tool in a short period and neglected to introduce the characteristics of visualisation. For example, users can intuitively see the size of the atom and the relationship between atoms, quickly find the top and the bottom atoms and explore more simply and quickly to extract modules.

6. Conclusion and Discussion

This project is to develop a Java-based tool called AD Visualiser to visualise OWL ontology in a modular structure based on AD theory. Unlike other existing ontology visualisation tools that focus on displaying ontology content with image symbols, AD Visualiser pays more attention to assisting users in completing ontology-related tasks. AD Visualiser allows users to interact with graphical AD in a variety of ways, such as finding nodes related to terms, obtaining detailed information about the terms contained in a node, and viewing the dependency relationship of a node corresponding to the atom. Its functional design is based on three tasks related to ontology: ontology refinement, ontology merging, and original use. At present, it has achieved two specific functions. One of them is the visualisation of AD that better supports medium-sized ontology (including 1,000 to 20,000 axioms). The ultrafine granularity of AD causes that when the body is too large, the number of atoms in the imaged AD and the dependence between atoms are too much, so the current AD Visualiser's display effect of its imaged AD is not good. Another is the support of module extraction with some terms from the ontology. This module is encapsulated, which means that it contains all the knowledge about terms and is independent of the original body.

The limitations have been identified and discussed in Section 5 based on expert feedback. In the next version of AD Visualiser, modifications and upgrades will be made based on these issues.

First of all, it is most important to change the display mode of the graphical AD. On the one hand, the author plans to display AD containing less than 100 atoms directly. For larger AD, take bottom AD as an example. In the beginning, the graphical AD only displays bottom atoms and then displays related nodes (including terms and the PBF result is true), and all its dependencies based on the terms are searched by the user. Besides, they can also explore the neighbourhood of any node. In this way, AD Visualiser can support the visualisation of large ontology AD. Users can focus on the modules related to terms or freely explore AD from the bottom to up. At the same time, it can also greatly reduce the computer's memory consumption and computing time. On the other hand, in the graphical AD, the user will be able to hide all the nodes above and connect to a node. In this case, users can hide information they do not care about. Additionally, a scale will be added to the lower left of the graphical AD to assist users in zooming in and out.

Next, optimise the colour matching of the software user interface to enhance the user's visual experience. The author plans to convey the information using as few colours as possible. The nodes in the graphical AD are in yellow except the bottom nodes that are in grey. When the user locates a node related to the terms, the related nodes are in red. The more the terms contained, the darker the red. When exploring the neighbourhood of a node, it and its neighbours are in blue. At the same time, nodes with unshown neighbourhoods are no longer in blue. When the node explored by the user has no neighbours, AD Visuliser will prompt with a symbol and a red text message next to it. In order to facilitate users to understand the meaning of different colours, the author plans to record the colour information in the colour schema item in the help column of the menu bar for users.

Then, optimise the details of the interface display during the user module extraction process. When the user selects terms in the hierarchy trees of classes or object properties or searches for terms in the search bar, the colour of the icons of the selected nodes in the hierarchy trees changes to red to show that they are selected. When the user explores the module according to any node, the user is allowed to go back and cancel the current operation after adding a piece of content.

The author also plans to improve the user experience of AD Visualiser. One of them is to display a loading bar between user operations to remind users of the estimated waiting time, for example, when the user opens an OWL file and waits for the image to load, when the user locates the relevant node in the map through terms to refresh the image content, when the user saves the explored module, and when the user saves the image of the graphical AD. Although many tasks will be completed within a few seconds, the flashing loading bar can also display a kind of feedback to the user's operation.

In addition to optimising the existing functions, AD Visualiser will add new functions to meet user needs (ontology refinement, ontology merging, and original use). AD Visualiser distinguishes the AD atoms of each ontology referenced by the four colour map theorem with different colours. Among them, the atoms belonging to multiple bodies are in colour as a result of colour mixing. This function can help users view the status of each component ontology in the merged ontology. In the future, AD Visualiser may be used as a plug-in for Protege to help more ontology engineers.

Data Availability

All data, models, and code generated or used during the study appear in the submitted article.

Conflicts of Interest

The author declares that there are no potential conflicts of interest with respect to the research, authorship, and/or publication of this article.

References

[1] N. F. Noy, *Tools for Mapping and Merging Ontologies*, Springer, Berlin, Germany, 2004.

[2] M. Obitko and V. Marik, "Adding owl semantics to ontologies used in multi-agent systems for manufacturing," in *Proceedings of the International Conference on Industrial Applications of Holonic & Multi-Agent Systems*, Prague, Czech Republic, September 2003.

[3] D. Fensel, "Ontology-Based Knowledge Management," *IEEE Computer Society Press*, vol. 35, no. 11, 2002.

[4] C. C. Albrecht, D. L. Dean, and J. V. Hansen, "An ontological approach to evaluating standards in e-commerce platforms," *IEEE Transactions on Systems, Man and Cybernetics, Part C (Applications and Reviews)*, vol. 37, no. 5, pp. 846–859, 2007.

[5] S. Staab and R. Studer, "Handbook on ontologies," *International Handbooks on Information Systems*, Springer, vol. 2, pp. 227–255, Berlin Germany, 2004.

[6] K. A. Spackman, K. E. Campbell, and R. A. Cote, "Snomed rt: a reference terminology for health care," *Proceedings A Conference of the American Medical Informatics Association*, vol. 4, pp. 640–644, 1997.

[7] C. Rosse and J. L. V. Mejino, "A reference ontology for biomedical informatics: the foundational model of anatomy," *Journal of Biomedical Informatics*, vol. 36, no. 6, pp. 478–500, 2003.

[8] B. Cuenca Grau, I. Horrocks, Y. Kazakov, and U. Sattler, "Modular reuse of ontologies: theory and practice," *Journal of Artificial Intelligence Research*, vol. 31, no. 1, pp. 273–318, 2008.

[9] R. Kontchakov, L. Pulina, U. Sattler et al., "Minimal module extraction from dl-lite ontologies using qbf solvers," in *Proceedings of the 21st International Joint Conference on Artificial Intelligence IJCAI*, vol. 9, pp. 836–841, Pasadena, CA, USA, July 2019.

[10] P. Klinov, C. Del Vescovo, and T. Schneider, *Incrementally Updateable and Persistent Decomposition of Owl Ontologies*, OWLED, 2012, http://webont.org/owled/2012/papers/paper_7.pdf.

[11] C. Del Vescovo, B. Parsia, U. Sattler, and T. Schneider, "The modular structure of an ontology: atomic decomposition," in *Proceedings of the Twenty-Second International Joint Conference on Artificial Intelligence*, Barcelona, Spain, July 2011.

[12] V. Geroimenko and C. Chen, "Visualizing the Semantic Web," *Xml-Based Internet and Information Visualization*, Springer, London, UK, 2006.

[13] F. Baader, I. Horrocks, C. Lutz, and U. Sattler, *Introduction to Description Logic*, Cambridge University Press, Cambridge, UK, 2017.

[14] C. Del Vescovo, "The modular structure of an ontology: atomic decomposition and its applications," PhD Thesis, University of Manchester, Manchester, UK, 2013.

[15] T. R. Gruber, "A Translation Approach to Portable Ontology Specifications," *Knowledge Acquisition*, vol. 5, no. 2, 1993.

[16] F. Baader, D. Calvanese, D. L. Mcguinness, D. Nardi, and P. F. Patelschneider, "The description logic handbook," *Theory, Implementation, and Applications*, Cambridge University Press, Cambridge, UK, 2nd edition, 2007.

[17] M. A. Harris, J. Clark, A. Ireland et al., "The gene ontology (go) database and informatics resource," *WCB/McGraw-Hill*, vol. 32, 2004.

[18] U. Sattler, T. Schneider, and M. Zakharyaschev, "Which kind of module should i extract?" in *Proceedings of the International Workshop on Description Logics*, Oxford, UK, July 2009.

[19] H. Knublauch, R. W. Fergerson, N. F. Noy, and M. A. Musen, *The Protege Owlplugin: An Open Development Environment for Semantic Web Applications*, Springer, Berlin, Germany, 2004.

[20] A. Kalyanpur, B. Parsia, E. Sirin, B. C. Grau, and J. Hendler, "Swoop: A web ontology editing browser," *Journal of Web Semantics*, vol. 4, no. 2, pp. 144–153, 2014.

[21] T. Liebig and O. N. Ontotrack, "A semantic approach for ontology authoring," *Web Semantics: Ence, Services and Agents on the World Wide Web*, vol. 3, no. 2, pp. 116–131, 2011.

[22] N. Matentzoglu, "Module-based Classification of Owl Ontologies," Thesis, University of Manchester, Manchester, UK, 2016.

[23] E. Motta, S. Peroni, J. M. Go´mez-Pe´rez, M. D'Aquin, and N. Li, *Visualizing and Navigating Ontologies with KC-Viz*, Springer, Berlin, Germany, 2012.

[24] M. Horridge, "Owlviz," 2020, https://protegewiki.stanford.edu/wiki/OWLViz.

[25] S. Falconer, "Ontograf," 2020, https://protegewiki.stanford.edu/wiki/OntoGraf.

[26] H. Alani, "Tgviz," hhttps://protegewiki.stanford.edu/wiki/TGViz, 2020.

[27] K. L. Ajaz Hussain and A. T. Rextin, "Navigowl," 2020, https://protegewiki.stanford.edu/wiki/NavigOWL.

[28] R. Liepins, M. Grasmanis, and U. Bojars, "Owlgred ontology visualizer," in *Proceedings of the 2014 International Conference on Developers*, vol. 1268, pp. 37–42, Riva del Garda, Italy, October 2014.

[29] S. Lohmann, S. Negru, F. Haag et al., "Visualizing ontologies with vowl," *Semantic Web*, vol. 7, no. 4, pp. 399–419, 2016.

[30] D. M. M. Uschold, "Introduction to gist," 2020, https://iaoa.org/isc2014/uploads/Whitepaper-Uschold-IntroductionToGist.pdf.

[31] P. Pierce, "How to boost usability with intelli- gent color choices," 2020, https://www.sitepoint.com/how-to-boost-usability-with-intelligent-color-choices/.

[32] J. Zukowski, *Java AWT Reference*, OR´eilly & Associates, Inc., Sebastopol, CA, USA, 1997.

Hindawi
Scientific Programming
Volume 2022, Article ID 1361226, 8 pages
https://doi.org/10.1155/2022/1361226

Research Article

Optimized Algorithm Analysis of Factors Affecting the Effectiveness of English Teaching under the New Curriculum Concept

Lu Zhang

School of English Language and Literature, Xi'an Fanyi University, Xi'an 710105, Shaanxi, China

Correspondence should be addressed to Lu Zhang; zl_8583@163.com

Received 29 October 2021; Accepted 14 December 2021; Published 24 January 2022

Academic Editor: Punit Gupta

The purpose is to explore the influencing factors in English teaching under the new curriculum concept. Teachers and students in a representative middle school in a city are taken as the research object. First, classroom observations are employed to have a preliminary understanding of the teaching mode of English reading. Then, a questionnaire survey is conducted to analyze teachers' and students' opinions about English reading education. Besides, some interviews are given to the teachers and the students for deep study. Subsequently, the results of the survey are analyzed to summarize the factors that affect the effectiveness of English reading education under the new curriculum concept. The results show that the influencing factors of the teaching effect include teachers, students, and teaching materials. Finally, the corresponding strategies are put forward in response to the relevant problems, and they have a positive effect on promoting the English teaching research. The research content provides a reference for middle school English teaching, solves the problems in English teaching, and makes a contribution to improving teachers' teaching ability in the senior high school.

1. Introduction

After the *New Curriculum Standard on Students' Education in China* was issued, senior high school education made some progress and achieved development. With the continuous advancement of the new curriculum standard, the problems in senior high school teaching have gradually emerged, and English teaching is no exception [1]. Due to the further development of English education, English teaching becomes particularly important, which constitutes the main part of teaching in senior high school [2]. The purpose is to find out the problems in English teaching and then try to explore and discuss the subjective and objective factors that affect students' ability in English teaching with some experienced teachers, thereby putting forward some valuable opinions and suggestions on middle school English teaching from a new perspective.

The existing problems in English teaching are as follows. English class is still teacher-centered, and there is no definite teaching goal; students spend much time doing endless exercises to improve their scores temporarily; students' psychological development as well as students themselves is ignored by teachers [3]. There is no long-term effective feedback mechanism in class, and students only want to score higher by doing exercises, rather than out of interest; they cannot employ learning strategies flexibly and do not have good reading habits; the reading materials offered are not moderate, and they are boring for students [4, 5]. According to the students' actual needs, teachers should help them develop good reading habits, pay attention to students' personality and psychological development, and strive to treat them as individuals and help each one achieve their full potential [6]. In addition, teachers should work in teams, and each team should be assigned a task. For example, one team is asked to hold teaching and research meetings; another collects and sorts reading materials, gradually forming a test database suitable for their students [7]. Middle school students in cities are more representative with uneven scores and receive more education than those in rural areas, and middle school English is the most basic, so it is convenient to study the factors that affect the English teaching effect under the new curriculum concept.

English teachers and students of a senior high school in a city are selected as the research objects, and the factors influencing English teaching are studied and analyzed. The methods involve a questionnaire and an interview, and the following three questions are put forward to realize the research purpose. The questions are as follows. (1) What is the current situation of high school English teaching? (2) What are the factors that affect high school English teaching? (3) What are the teaching strategies based on the factors? After the data are collected, sorted, and analyzed, the current situation of teaching is informed, the factors that affect English teaching are explored, and the corresponding suggestions to improve high school English teaching are discussed.

2. English Teaching Design Based on New Curriculum Concept

2.1. Research Issues. Years of teaching convinces us that there are some problems in senior high school English teaching. In recent years, China has issued and implemented the new curriculum standards, but the problems are not solved fundamentally [8]. The survey shows that students in English class have no interest in reading, and the major obstacles in doing exercises are narrow vocabulary, complicated grammar structures, and difficult contents, which make them flinch when the students have trouble in English learning, and the students' self-motivated language practice activities are rare [9]. In addition, some open classes also show that teachers tend to pay attention to students with good performance, neglecting the ones with poor basic knowledge of English. Therefore, the research content is as follows: the current situation of middle school English teaching is analyzed; the factors that affect middle school English teaching are explored; and the strategies that improve the effect of middle school English teaching are proposed.

2.2. Research Objects. The investigated objects are some students and teachers. 300 students from a middle school in a city are taken as the research object, and each class has 50 students. There are three types of classes in middle school, and they are rocket class, experimental class, and ordinary class. Before the experiment, two classes of each type are selected. Also, 20 English teachers in the third grade of senior high school are surveyed. According to the researchers, 30 is the minimum sample number, and it makes sense to have more than 30 samples; the number of the collected data that is less than 30 cannot form a normal distribution. The student's questionnaires are 300, while the number of teachers is less than 30. Therefore, teacher's English teaching survey is mainly conducted by interviews, supplemented by questionnaires. 320 students and English teachers are investigated, and 288 valid questionnaires are collected, with a percentage of 90%.

2.3. Data Collection. The first step is to find the right questionnaire. According to the relevant principles of questionnaire preparation, the existing questionnaires are reviewed to determine the form of the questionnaire, and then the questionnaire is carefully prepared and designed by combining the actual situation of high school English teaching. The second is measurement. To ensure the effective recovery of the questionnaire, a survey is carried out in a representative senior high school. The face-to-face questionnaire is helpful for the respondents to understanding the problems in time and winning their cooperation. The third step is to sort out the test results. The collected questionnaires are carefully and strictly reviewed, and invalid questionnaires are eliminated to make the research effective and scientific [10]. English teachers should strengthen the learning of English teaching theories at home and abroad, combine classroom practice, change the traditional teaching mode, and fully mobilize the enthusiasm of students. The present situation of traditional grammar teaching method should be appropriately changed, the communicative method should be combined with the situational teaching method, and the teacher-centered absolute teaching mode should be changed into the student-centered new teaching mode to ensure the accuracy of data.

2.4. Classroom Observation. Classroom observations are undertaken, and the main tasks are observing student's vocabulary, their reading proficiency, and teachers' teaching strategies. The results show that teachers pay more attention to enlarging student's vocabulary and emphasize the spelling and meaning of the new words. In terms of students' mastery of word meanings, teachers usually make spot checks in the classroom and just play the role of supervision. Moreover, they do not pay enough attention to the connotations of vocabulary and seldom provide appropriate polysemy exercises to help students master the deep meaning of vocabulary and its less common usage in context. As for reading comprehension, teachers' discourse awareness is not strong enough to cultivate students' text sense effectively. Besides, the reading texts are rarely classified according to different topics, which is not conducive to improving students' reading efficiency. Students lack the communicative environment necessary to consolidate and internalize language knowledge. Students have few opportunities to use English outside the classroom. This is not only true in schools with good conditions for small classes but also worse in large classes with poor conditions. Students rely on very limited opportunities for classroom English communication. In addition, the students' cultural background knowledge reserve is seriously insufficient, and most of what they understand is the knowledge reflecting Chinese society and culture and the college life under this background.

3. Data Analysis

3.1. Analysis of the Results of the Survey on Teachers. The results of the survey on in-service teachers are shown in Figure 1.

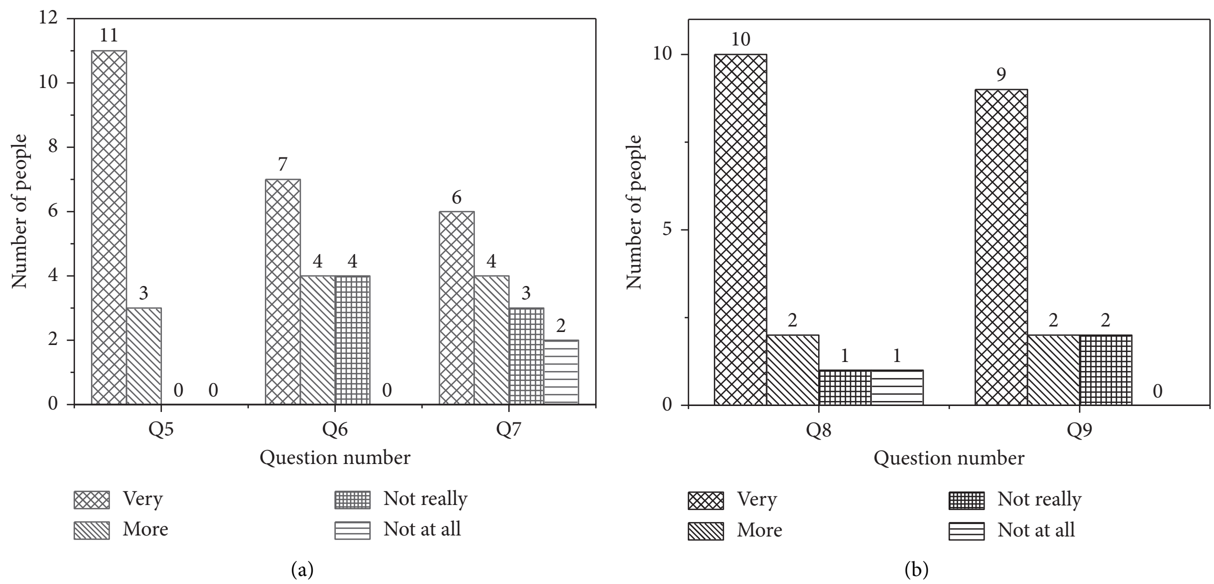

Figure 1: Survey results of teachers' teaching concepts. (a) Teachers' teaching strategies. (b) Teachers' teaching theories.

The survey on teacher's English teaching strategies shows that 11 teachers hold the idea that appropriate strategies can improve students' learning ability, while 7 teachers argue that the importance of learning should be focused on, rather than the strategies. Some teachers disagree to emphasize the importance of English teaching, and they assume that if the basic knowledge is developed, their performance will be improved naturally. Also, they think that the teaching theory has no practical use. In terms of teacher's English teaching theory, 10 teachers hold that they should often employ relevant teaching theories to guide students to read, and 9 teachers attach importance to nonverbal knowledge like cultural background.

The survey on teachers' requirements for students' exercise training is shown in Figure 2.

The survey on teachers' requirements for students' exercise training shows that 10 teachers think that the reading materials in class are limited and the students need to read more extracurricular materials as a supplement. About 40% of the teachers argue that there is no need for training on reading methods. In the interview, the teachers also expressed their concern that the reading task could not be completed in class, leading to some reading problems that cannot be solved by students themselves. Therefore, a lot of factors have to be taken into consideration in the implementation of the teaching plan.

The survey on teachers' attitude towards reading is shown in Figure 3.

The following can be inferred from Figure 3. Most teachers thought much concern should be given to the text structure analysis of reading materials, followed by teaching students' reading strategies. Half of the teachers assumed that the biggest problem is lack of reading materials. To make the research results more scientific and comprehensive, interviews are applied for more data.

3.2. Result Analysis of the Survey on Students. The results of the focus of the teaching content and question-answering skills are shown in Figure 4.

Figure 4(a) shows that in the process of teaching, vocabulary and phrases are the ones that teachers think about the most, followed by grammar. The skills and training of reading strategies receive little attention from the students. Only six students thought that teachers focused on cultural background in English teaching. Figure 4(b) indicates that the teachers give some guidance to the students' answering skills, which includes guessing the meaning of words according to the context, grasping the key sentences, and paying attention to the turning words. They are the three most commonly used in answering questions. It is noticed that only 19 students chose the option of "all of the above," which shows that the teachers give students reading strategy guidance in reading education, but the guidance is inadequate.

The interaction between teachers and students in teaching class and students' interest in English reading are shown in Figure 5.

In terms of the interaction in English class, 53% of the students hold that there is little interaction between teachers and students in reading education, 31% think that teachers occasionally interact with students, and only 14% think that teachers often interact with students. As for students' interest and attitude towards English reading, only 30 students are very interested in reading, accounting for only about 10%. More than 20% of the students are interested in reading. However, more than 40% of the students are not interested in reading.

The attitude towards English learning and the students' learning motivation are shown in Figure 6.

As for the students' attitude towards English learning, 107 think that learning English is boring, and they

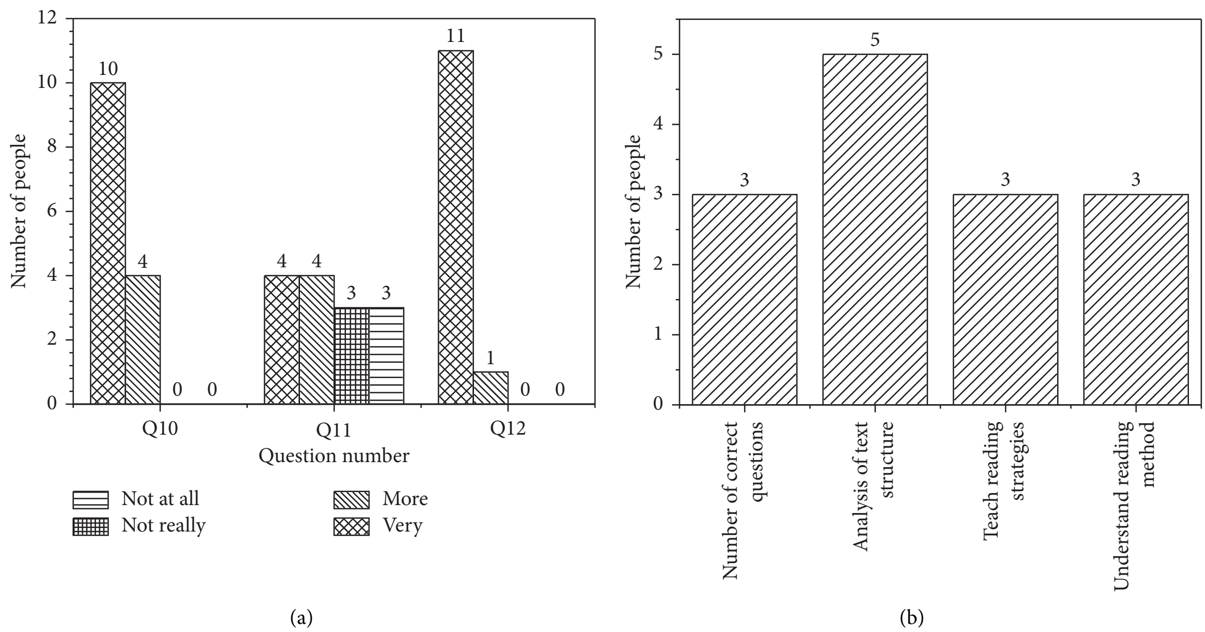

Figure 2: Teachers' requirements. (a) Teachers' English exercise requirements. (b) Teachers' attitude towards English teaching.

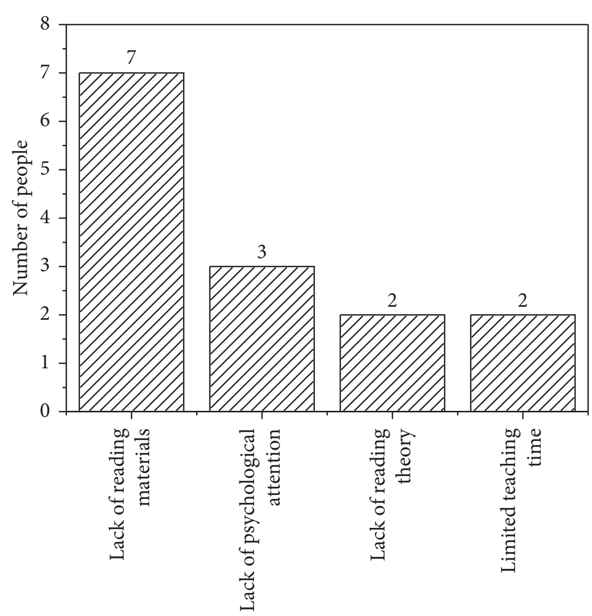

Figure 3: Results of teachers' attitude towards reading.

chose the option casually. 74 students did not finish answering the questions on the questionnaire. Only 34 students actively read, wanted to expand their knowledge, and did extra exercises for ability training. According to the results of the motivation for learning English, 160 students hope to improve their reading ability and test scores through practice, while only 26 students want to do exercises for the improvement of their reading ability, which is opposite to the original educational objective.

The results of the survey on students' habit and the obstacles in the learning process are shown in Figure 7.

About 13% of the students chose "no such habit," and 23% read or read with the help of the moving nib. 34% said that they first translated the reading content into Chinese and then thought about the questions; 30% said that they repeated their reading back and forth in the process of reading without missing any words. The results of the survey on English learning obstacles prove that more than one-third of the students thought that they have narrow vocabulary and poor grammar knowledge, which are the biggest obstacles in English learning. The second option is "lack of effective reading strategies," and the option wins about 30% students; the third is "having no interest in reading," and about 18% students chose it. The fourth is "insufficient background knowledge," and it was chosen by 9% students. The last one is "having no interesting and easy to read materials," with a percentage of 7% students.

The results of the survey on the level of the difficulty of the reading materials and the number of English reading materials are shown in Figure 8.

The following can be inferred from Figure 8. 35% of the students thought that most of the reading materials are too difficult, which reduced their confidence in continuing the reading; 52% argued that the level of the difficulty of reading materials is moderate and acceptable; 13% of the students thought that the reading materials are too simple to improve their ability. This proves that almost all the students are not satisfied with reading materials. 25% of the students assumed that the reading materials suitable for them are abundant; 32% said that they are little; 43% thought that it is difficult to find appropriate reading materials.

3.3. Influencing Factors and Strategies. In English teaching, the main factors that affect the teaching effect include teachers, students, and teaching materials. The influencing

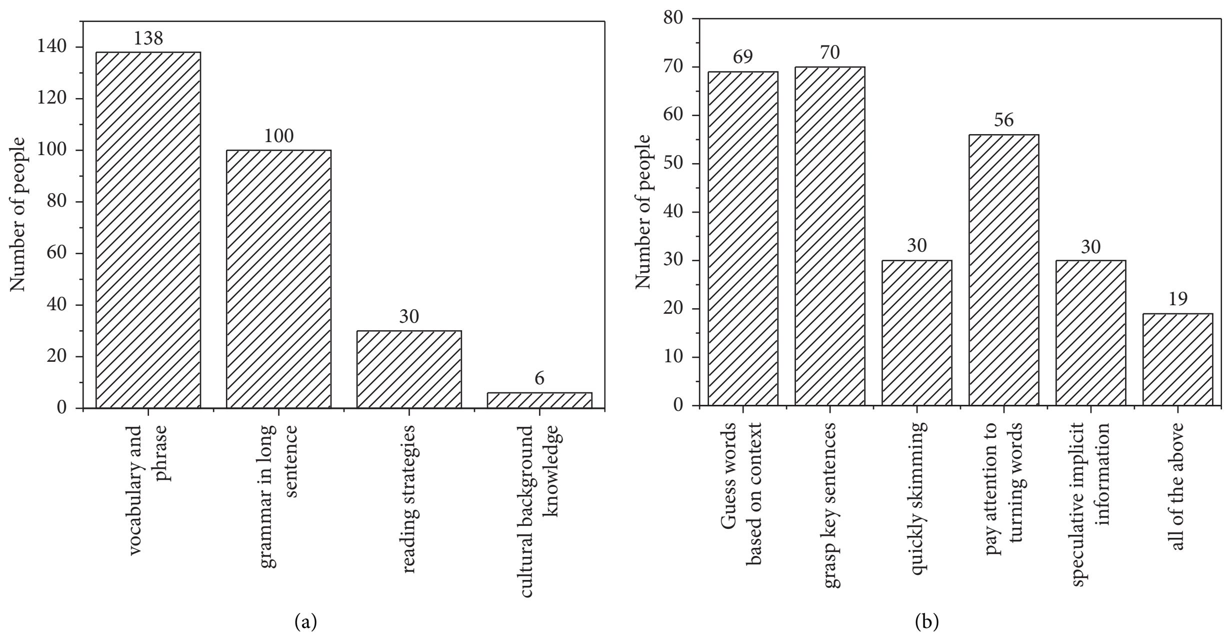

Figure 4: Results of the survey on teaching strategies. (a) The focus of teaching content. (b) Question-answering skills.

factors of teachers include three aspects. The first one refers to teachers' teaching ideas, which directly affect teaching methods, teaching focus, and teaching effect. If a teacher pays more attention to vocabulary and grammar, students emphasize them accordingly. The second one refers to teachers' achievements. A knowledgeable teacher with excellent English listening, speaking, reading, and writing ability can cultivate the talents of students as outstanding as he/she is, which has a positive impact on students. The last one refers to teaching strategies. In the process of English reading education, teachers should consciously introduce the corresponding reading skills and strategies, so that students can benefit a lot from English reading [11].

Three factors affect students' English teaching. The first one refers to students' reading motivation and attitude. Only when students have correct learning motivation and a positive attitude can teaching achieve the expected goal. This is mentioned in relevant literature [12, 13]. The second one refers to reading ability and strategies. In the process of English reading, students should consciously learn and use certain reading skills and strategies, such as skimming, searching, guessing new words, reasoning, judging, predicting, and summarizing. These strategies greatly affect the effect of reading education, which is consistent with the literature [14, 15]. The third one refers to personality and psychological factors. Students' psychological factors include anxiety, inhibition, empathy, classroom communication, and cross-cultural awareness, and teachers should have insight into students' personality and psychological activities and carry out targeted reading education [16].

The best materials come from textbooks. The arrangement and the level of difficulty of textbooks directly affect the teaching effect. Therefore, the textbook should be carefully designed and the content should be based on the syllabus, in which vocabulary and syntax knowledge are the foci of the college entrance examination [17]. It is very appropriate to use the content of the textbook as the reading materials because textbooks have a great influence on teaching and they are the key to the implementation of curriculum standards, the main basis for teachers to design and carry out teaching activities, and also the core content of students' learning. Reading materials in English textbooks account for a large proportion in each unit, and there are many language points [18]. The learning degree of the reading materials in English textbooks determines their English achievements. However, the reading materials are too few in the textbooks, and extracurricular reading materials need to be supplemented.

In view of these factors, the corresponding teaching strategies are put forward for teachers. Teachers should update their teaching concepts and apply them to the teaching practice, which can enhance teachers' sense of achievement and change their teaching strategies. The feasible teaching strategies are cultivating students' good reading habits, arousing their enthusiasm, and changing their attitude towards reading [19]. The teachers should also develop students' habit of thinking in English and the habit of reading with a time limit and increase the students' reading volume. Reading education should be based on students' personalities and psychology. With regard to the teaching materials and extracurricular reading materials, it is hoped that relevant foreign language research institutions should pay attention to the natural cohesion and difficulty in transition of senior high school teaching materials, so that teachers can select them according to students' learning progress [20].

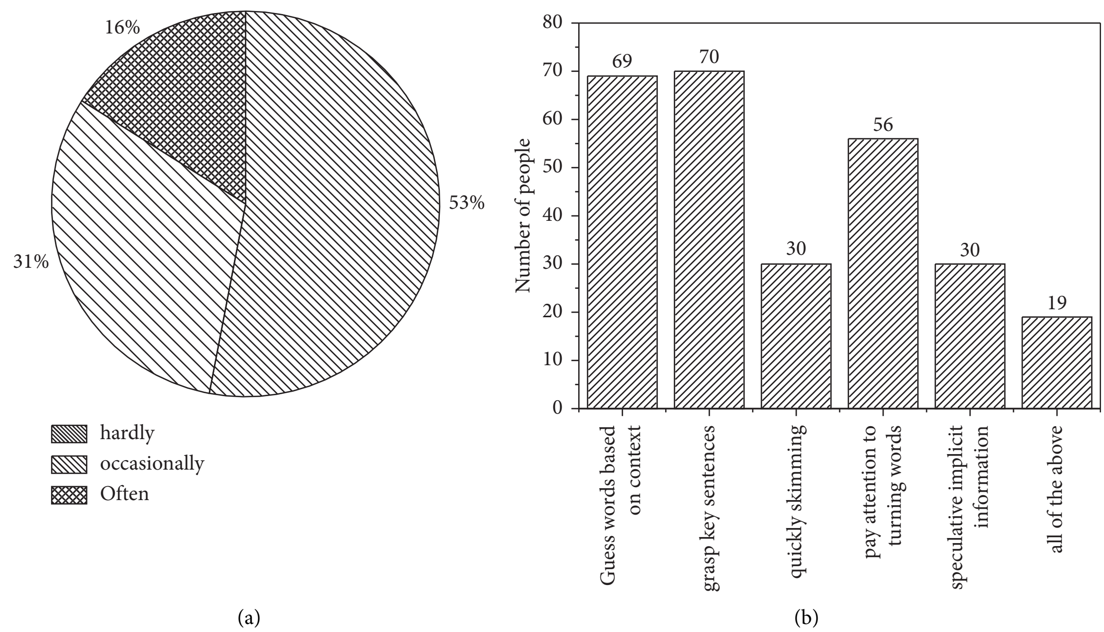

Figure 5: Interaction between teachers and students and students' interest in reading. (a) Frequency of teacher-student interaction. (b) Students' interest in reading.

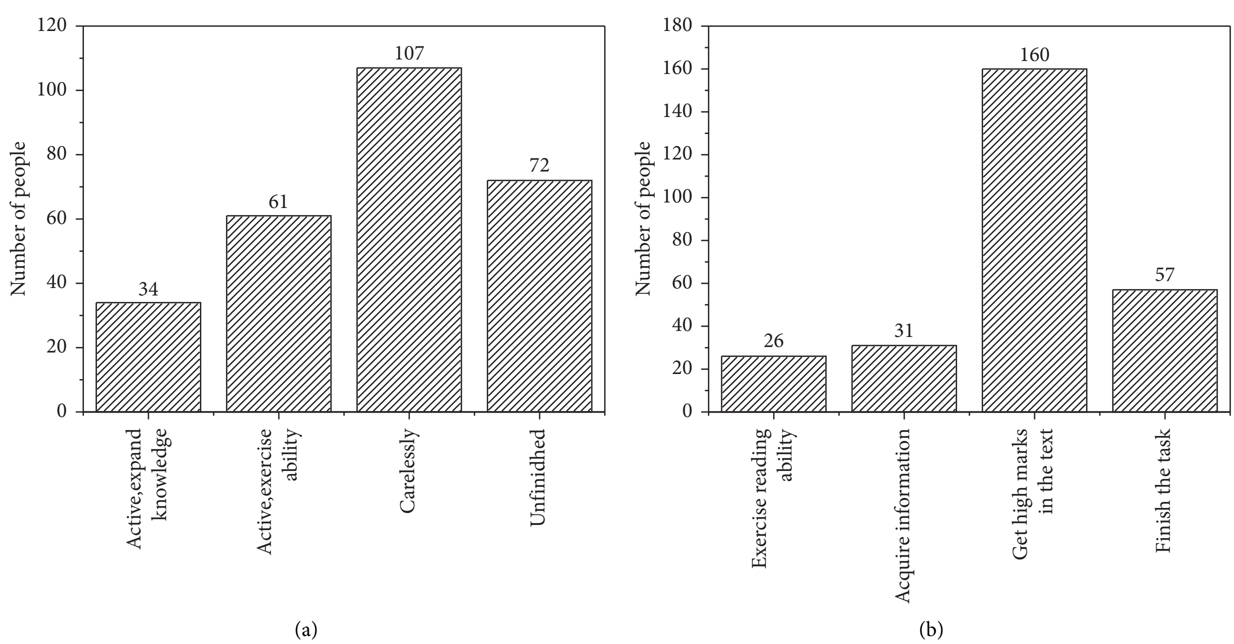

Figure 6: Attitude towards English learning and the students' learning motivation. (a) Attitude towards English learning. (b) Motivation of learning English.

4. Discussion

The results of the surveys show that English teachers in senior high schools are under the pressure of examination. Most of the English reading teaching modes are established to serve for the college entrance examination. In this case, English classes should be diversified and flexible to arouse students' interest in learning and improve their learning ability. It is found that half of the teachers usually require the students to complete the exercise on their workbooks and just check whether they complete the exercise or not, ignoring the correct probability. This shows that the effect of English teaching is affected by the heavy teaching loads, the teachers' limited time, and the lack of supervision and evaluation of English practice. Half of the teachers chose the English materials that are not only in line with the level of the difficulty and themes of the college entrance examination but also original. Other teachers chose the teaching materials

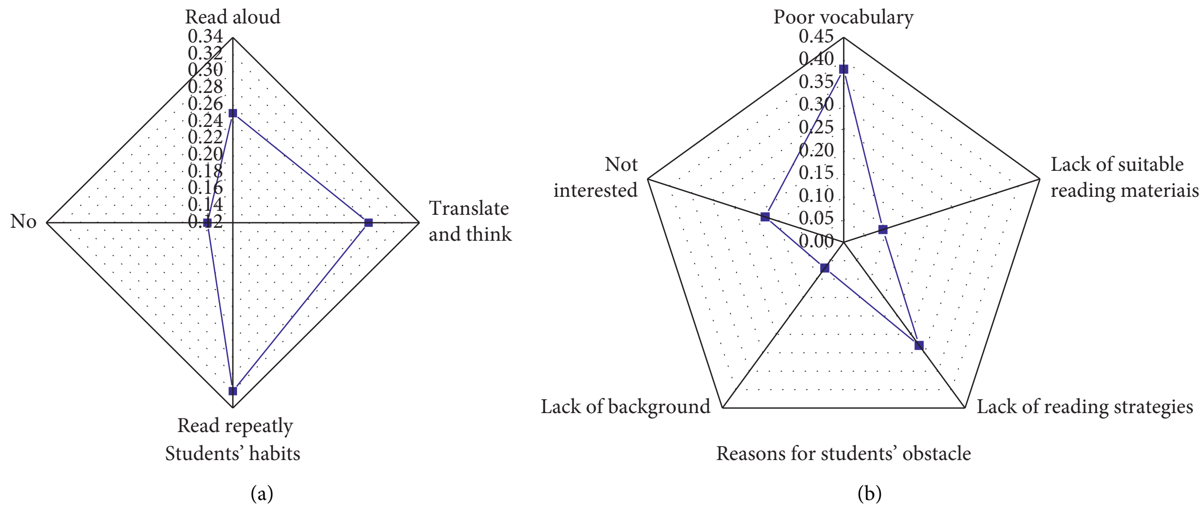

Figure 7: Habits and obstacles in learning English. (a) Habits in learning English. (b) Obstacles in learning English.

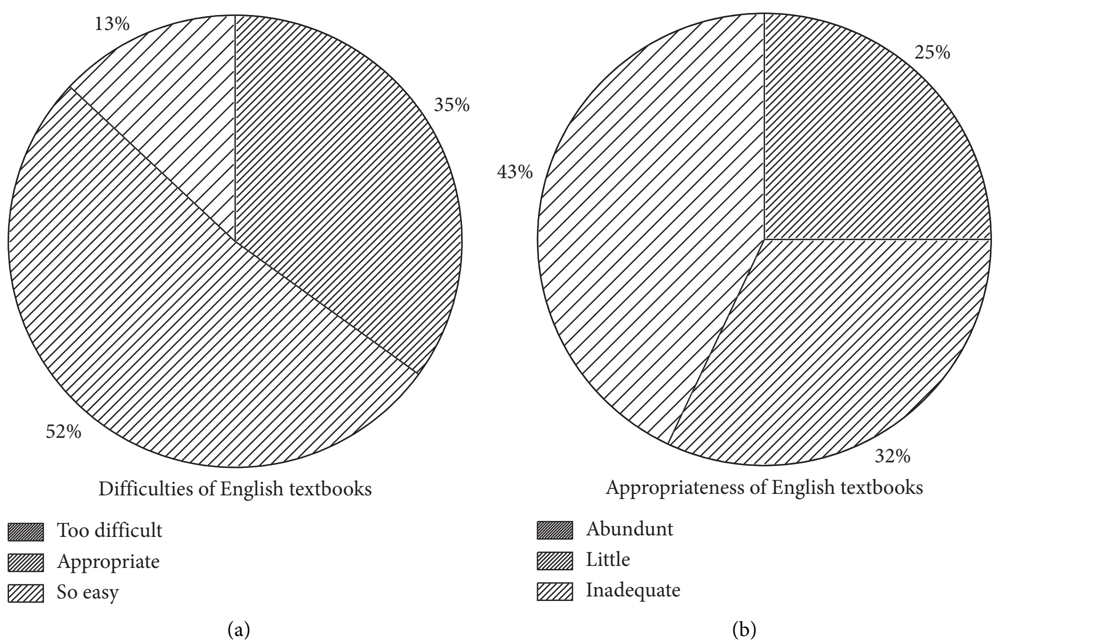

Figure 8: Reading materials and reading volume. (a) Difficulties of English textbooks. (b) Appropriateness of reading volume.

with rich background knowledge, novel ideas, and a sense of the times. Nearly two-thirds encourage the students to read *21st Century Teens*, which is considered to be effective, interesting, and practical. Teachers tend to pick up the materials with rich content to make the students concentrate and stimulate their desire for reading. As a result, the primary basis for teachers to choose materials is whether they meet the requirements of the level of the difficulty and topics of the college entrance examination, and the second is whether the content is rich and the intention is novel, which is limited by the college entrance examination.

Concerning English reading under the new curriculum standard, teachers participating in the survey agree that English teaching becomes the main source of information and an important channel to acquire knowledge. In the new situation, it helps students to broaden their horizons and have access to more information timely, laying a solid foundation for the overall development of students' English learning ability. In teaching, teachers should guide the students to acquire knowledge and skills, develop their emotions, and have the correct attitude. Learning strategies and cultural awareness can help students develop their talents. Since teachers play a leading role in teaching, their teaching ideas and decisions directly affect reading education. In the classroom, although the guidance of teachers is very important to the teaching effect, the role of students cannot be ignored, and they also play an important role in the process of English teaching.

5. Conclusion

Based on the investigation and study of the main problems in senior high school English reading education, both teachers' teaching and students' learning in English reading education have problems to be solved. Under the new curriculum concept, three factors affect the effectiveness of English classroom teaching: teachers, students, and teaching materials. According to the new curriculum standard, the current situation of the senior high school English teaching is investigated and it is found that there are many problems in English teaching, which should be improved. The corresponding teaching strategies are put forward to solve the relevant problems. This study has a positive effect on promoting English teaching under the new curriculum concept and provides a research direction for future English curriculum reform. It is expected that more scholars will conduct more comprehensive and in-depth research on English teaching, so that English teaching under the new curriculum standard will gradually become mature, realizing the perfect integration of English learning and practice.

Data Availability

No data were used to support this study.

Conflicts of Interest

The author declares that there are no conflicts of interest.

References

[1] N. Oeamoum and C. Sriwichai, "Problems and needs in English language teaching from the viewpoints of pre-service English teachers in Thailand," *Asian Journal of Education and Training*, vol. 6, no. 4, pp. 592–601, 2020.

[2] X. Wei, "Research on the development strategy of cross-cultural ecological education in English translation teaching at colleges," *Ekoloji*, vol. 28, no. 107, pp. 1665–1669, 2019.

[3] S. C. Chien, "Writing for scholarly publication in English for Taiwanese researchers in the field of English teaching," *Sage Open*, vol. 9, no. 3, Article ID 2158244019870187, 2019.

[4] Y. Du, "Discussion on flipped classroom teaching mode in college English teaching," *English Language Teaching*, vol. 11, no. 11, pp. 92–97, 2018.

[5] U. Sulistiyo, "Factors affecting English language learning in English as a foreign language (EFL) context: a literature review study," *IJER (Indonesian Journal of Educational Research)*, vol. 3, no. 1, pp. 20–24, 2018.

[6] F. Huang, T. Teo, and M. Zhou, "Factors affecting Chinese English as a foreign language teachers' technology acceptance: a qualitative study," *Journal of Educational Computing Research*, vol. 57, no. 1, pp. 83–105, 2019.

[7] M. M. Rahman, A. Pandian, and M. Kaur, "Factors affecting teachers' implementation of communicative language teaching curriculum in secondary schools in Bangladesh," *Qualitative Report*, vol. 23, no. 5, pp. 1104–1126, 2018.

[8] Y. You, "The seeming 'round trip' of learner-centred education: a 'best practice' derived from China's New Curriculum Reform," *Comparative Education*, vol. 55, no. 1, pp. 97–115, 2019.

[9] A. M. Songbatumis, "Challenges in teaching English faced by English teachers at MTsN Taliwang, Indonesia," *Journal of foreign language teaching and learning*, vol. 2, no. 2, pp. 54–67, 2017.

[10] M. Geuens and P. De Pelsmacker, "Planning and conducting experimental advertising research and questionnaire design," *Journal of Advertising*, vol. 46, no. 1, pp. 83–100, 2017.

[11] M. Mohammadi and A. Amini Faskhodi, "Modeling AMO factors affecting English teachers' performance using system dynamics," *Language Teaching Research Quarterly*, vol. 16, pp. 22–39, 2020.

[12] K. Andi and B. Arafah, "Using needs analysis to develop English teaching materials in initial speaking skills for Indonesian college students of English," *The Turkish Online Journal of Design, Art and Communication (TOJDAC)*, pp. 419–436, Special Edition, 2017.

[13] T. Teo, M. Zhou, A. C. W. Fan, and F. Huang, "Factors that influence university students' intention to use Moodle: a study in Macau," *Educational Technology Research & Development*, vol. 67, no. 3, pp. 749–766, 2019.

[14] M. J. Nelson, R. Voithofer, and S.-L. Cheng, "Mediating factors that influence the technology integration practices of teacher educators," *Computers & Education*, vol. 128, pp. 330–344, 2019.

[15] M. Abrar, A. Mukminin, A. Habibi, and A. Fadhil, "If our English isn't a language, what is it?" Indonesian EFL Student Teachers' Challenges Speaking English," *Qualitative Report*, vol. 23, no. 1, pp. 129–145, 2018.

[16] S. Wang and S. Seepho, "Facilitating Chinese efl learners' critical thinking skills: the contributions of teaching strategies," *Sage Open*, vol. 7, no. 3, pp. 2158244017734024–2158244017734031, 2017.

[17] P. A. Jennings, J. L. Brown, J. L. Frank, and B. Joshua, "Impacts of the CARE for Teachers program on teachers' social and emotional competence and classroom interactions," *Journal of Educational Psychology*, vol. 109, no. 7, Article ID 1010, 2017.

[18] O. Sert, "Transforming CA findings into future L2 teaching practices: challenges and prospects for teacher education," *Classroom-based Conversation Analytic Research: Theoretical and Applied Perspectives on Pedagogy*, Springer, Sweden, pp. 259–279, 2021.

[19] M. Gamboa Á, "Reading comprehension in an English as a foreign language setting: teaching strategies for sixth graders based on the interactive model of reading," *Folio*, vol. 45, pp. 159–175, 2017.

[20] X. Wei, "Optimization design of teaching strategies for English teaching achievement improvement based on original algorithm," *Wireless Personal Communications*, vol. 102, no. 2, pp. 1191–1201, 2018.

Hindawi
Scientific Programming
Volume 2022, Article ID 5615353, 9 pages
https://doi.org/10.1155/2022/5615353

Research Article

Application of Computer Simulation in Innovation and Entrepreneurship Teaching Reform of Economics and Management Specialty

Li Liu,[1] Cuifang Zhang ,[2] and Tong Wu[3]

[1]*School of Economics and Management, Wuchang Institute of Technology, Wuhan 430065, Hubei, China*
[2]*School of Economics, Guangzhou College of Commerce, Guangzhou 511363, Guangdong, China*
[3]*Business School, University of New South Wales, Kensington, NSW 2052, Australia*

Correspondence should be addressed to Cuifang Zhang; z5381962@ad.unsw.edu.au

Received 13 September 2021; Revised 26 December 2021; Accepted 30 December 2021; Published 17 January 2022

Academic Editor: Punit Gupta

Innovation is the source and power of national development. Innovation and entrepreneurship education is the top priority of social construction and development and has become an important part of entrepreneurs. With the rapid development of economy, the society's demand for talents with innovation ability and practical ability is more urgent. Therefore, the teaching reform of blazing new trails and starting an undertaking for economics and management majors has become the top priority. The economics and management major should conform to the social era and the development of education and carry out blazing new trails and starting an undertaking teaching reform. On the foundation of broad research and analysis, according to the teaching situation of the economics and management major, this article carries out the blazing new trails and starting an undertaking teaching reform of the economics and management major. This study first puts forward the idea of blazing new trails and starting an undertaking education and computer simulation teaching model, then designs the educational method of blazing new trails and starting an undertaking education reform for college students, then constructs an entrepreneurial model for economics and management majors, and finally uses computer simulation technology to simulate it to understand the evaluation of various operating strategies of the teaching system. Through the questionnaire survey experiment, this study makes statistics on the current situation of students majoring in economics and management participating in blazing new trails and starting an undertaking activity and their views on the reform of blazing new trails and starting an undertaking education. For the experiment, first economics and management is understood, the experiment is designed, a digital model of the teaching process is constructed, a statistics of the experimental data is made, and the obtained data to verify the model are used. After collecting and analyzing the results of the questionnaire, the effective rate of the questionnaire was 97.4%. Under the idea of blazing new trails and starting an undertaking education, the teaching reform of economics and management specialty in colleges should be carried out according to the situation of students in different grades and construct computer simulation experiment teaching through simulation technology, which is conducive to the innovative talent training.

1. Introduction

As the Belt and Road Initiatives grow with each passing day, the demand for professional talents in various industries continues to increase. This has brought new reform requirements for the personnel training in colleges. In the context of current social development, mass blazing new trails and starting an undertaking have become an unchangeable trend. As a discipline whose main work is to cultivate talents in economics and financial fields, the teaching innovation reform of economics and management specialty is also imminent [1]. In teaching, teaching reform is one of the effective ways to improve the learning ability and interest of college students, and it also guides the main direction of teachers' teaching. Therefore, it is necessary to speed up the research progress in the direction of economics teaching reform and management majors based on the idea of blazing new trails and starting an undertaking education, to provide the country and society with appropriate talents. Therefore, students majoring in economics and management can better help them understand professional courses through simulation experiments in computer and economics and management professional courses, rather than just accepting knowledge from textbooks. Furthermore, blazing new trails and starting an undertaking education can also find suitable methods for students according to some of their needs and provide them with special training and education, thereby improving their practical and social skills [2].

2. Literature Review

Sievidova I A analyzed the basic mechanism of the formation of blazing new trails and starting an undertaking idea system and listed the factors that affect the teaching reform of economics and management in colleges and universities. This determines the importance and necessity of teaching reform to adapt to the concept of blazing new trails and starting an undertaking development. He summarized the problems existing in the transformation of teaching model, updating of teaching goals, and display of teaching results and integrated blazing new trails and starting an undertaking concept into the relevant directions of the reform of economics and management majors, but his research focuses too much on the theoretical aspects, which is not conducive to the substantial reform of the teaching direction [3]. Magnus et al. introduced the development of experimental teaching platform in the teaching system of economics and management. The platform is composed of a simulation teaching system, which is responsible for the parameterization of the regulator so that the system can operate effectively [4]. The main contribution of Srinivasa et al.'s research is to provide experimental verification for the digital model of the experimental teaching platform in the economics and management professional teaching system, to optimize the control design and parameterization. The real platform he provides helps to improve students' learning level, professional level, and practical ability. However, his project research cost is relatively high, which is not suitable for university development and use [5]. Gilbert studied educational programs with intergenerational influence. He found that the factors that lead to the development of children's achievement orientation are affected by the parents of the same period by studying the structural equation model based on 422 triples. However, this effect is also variable [6].

The innovation of this study lies in the following: in the process of research, the main problem is the innovative teaching of economics and management and the main concrete manifestation of the change in teaching methods. For this reason, (1) three reform experimental teaching schemes are designed, including case teaching, experiential teaching, and heuristic teaching; (2) the hierarchical teaching model is analyzed and established for different grades, different knowledge, and different abilities of economics and management majors; and (3) it is committed to exploring the reform of the experimental teaching model on economics and management under the computer simulation environment, the problems and shortcomings in the current experimental teaching model are analyzed, and the ideas in the reform of the teaching model of computer simulation experiments are put forward.

3. Methods of Teaching Reform in Economics and Management Specialty Based on Innovation and Entrepreneurship

3.1. Current Situation of Innovation and Entrepreneurship Education. As a scientific theory, the educational concept of blazing new trails and starting an undertaking economics and management also requires a complete set of scientific theoretical systems in line with its own characteristics [7, 8]. Students can improve their comprehensive ability and prepare for entering society. However, China's blazing new trails and starting an undertaking education have just started, and its theoretical system is not mature. The root causes include the following two aspects [9]. On the one hand, the theoretical system of blazing new trails and starting an undertaking education lacks depth in content. At present, in the aspect of blazing new trails and starting an undertaking education, many domestic scholars focus on the analysis and discussion of the surface and related issues of blazing new trails and starting an undertaking education, but not the substantive and fundamental issues such as the goal, practice system, and evaluation system of blazing new trails and starting an undertaking education. On the other hand, the teaching method of the current innovation and starting an undertaking theory system is relatively single, and it is difficult to apply it to normal teaching [10]. In fact, most of the domestic research on blazing new trails and starting an undertaking education theory in China stays in theoretical research, and few scholars use practical methods for research, and empirical research is even less [11]. This situation restricts the rapid development of theoretical research. In this social environment, schools can introduce theoretical teaching methods and gradually realize teaching innovation [12]. In addition, combined with some advanced foreign experience and technology, it has laid a good foundation for China's modernization theory [13].

Judging from the current situation, my country's economic system is not perfect, and an economic system suitable for domestic social development has not yet been formed [14, 15]. Judging from the current situation, if you want to develop blazing new trails and starting an undertaking education, higher education institutions should investigate and screen the current socioeconomic contradictions and problems, find out the root causes of the problems, and find solutions to these contradictions after careful analysis [16, 17]. On the other hand, institutions must accurately analyze and grasp the development of the market economy on the basis of in-depth analysis of the market, understand the law of market development, and promote the achievements of market system innovation and technological innovation [3, 18]. Institutions should explore the combination of social and market needs, education, and scientific research and closely integrate with blazing new trails and starting an undertaking education [19, 20].

3.2. Insufficiency and Problems of Innovation and Entrepreneurship Education Teaching Reform

3.2.1. Blazing New Trails and Starting an Undertaking Education Model Have Not Yet Been Formed. In some colleges, leaders do not pay much attention to blazing new trails and starting an undertaking education, and the relevant courses set by the school are less, so it is difficult to form a certain atmosphere of blazing new trails and starting an undertaking education; for students, they may be more prepared for the national civil servant examination or postgraduate entrance examination or directly participate in work. These may make the blazing new trails and starting an undertaking education model of some universities difficult to form [21].

3.2.2. Few Courses. Many colleges and universities lack systematic, comprehensive, and detailed blazing new trails and starting an undertaking education course, and most of them stay in theoretical teaching and lack practical operation. Students only understand textbook knowledge and theory, but do not learn how to put textbook knowledge into practice. In addition, there are some problems such as the lack of clear positioning and training objectives in some colleges and universities [22].

3.2.3. Lack of Experienced Teachers. Teachers in some local colleges and universities usually work mainly on teaching, and they invest less energy and time in scientific research. As we know, very few teachers have rich experience and innovative ability. It is necessary to restrict blazing new trails and starting an undertaking teacher to the students' blazing new trails and starting an undertaking guidance experience.

3.2.4. Lack of Practical Platform. Blazing new trails and starting an undertaking education need the support of human, material, and financial resources. Not only should there be an experimental base on campus, but also there should be a corresponding practice base outside the school. However, no university can withstand this pressure for the establishment of entrepreneurship parks and entrepreneurial bases. What is more, even the entrepreneurship experimental base on campus cannot provide students with it.

3.3. Methods of Teaching Reform of Economics and Management Majors

3.3.1. Literature Retrieval. Through famous paper websites such as CNKI, a large number of documents are retrieved, classified, summarized, and analyzed. The development situation, knowledge demand, and training model of economics and management major teaching reform under the concept of economics and management teaching reform in recent years are consulted, and the training programs of excellent colleges and universities are carefully studied; then, it analyzes the innovation of foreign literature. This article reviews the historical evolution and current situation of the educational reform of economics and management and uses relevant experience to provide a research foundation and theoretical basis. Research on education reform in economics and business management is based on the idea of blazing new trails and starting an undertaking education.

3.3.2. Text Analysis. This method is expected to select six well-known universities in North China, East China, West China, and Central China and conduct a text analysis of the reform and training programs of the economics and management majors of these six universities, to understand and learn from the relevant experience of excellent colleges on the teaching innovation reform of economics and management majors under the idea of blazing new trails and starting an undertaking education.

3.3.3. Questionnaire Survey. The article selects 6 well-known colleges and universities participating in this research to receive blazing new trails and starting an undertaking education and the college's own teachers as the questionnaire survey objects. Through the questionnaire survey of teachers and students, the reform and cultivation of blazing new trails and starting an undertaking education in economics and management majors are understood, and statistical analysis on unreasonable suggestions in the training process and problems in the teaching practice is conducted.

3.4. Teaching Reform Experiment of Economics and Management Majors

3.4.1. Economics and Management Teaching Reform Design. China's higher education is basically a unified teaching model, a single teaching plan, and so on, almost ignoring the personality of students. Among them, the blazing new trails and starting an undertaking education mainly adopt the single indoctrination method and tend to teach and assess the theoretical knowledge. If we want to make the blazing new trails and starting an undertaking education of economics and management students to achieve effective results, we must reform the single teaching method in the classroom, adopt a variety of methods, and create a new teaching atmosphere. The blazing new trails and starting an undertaking teaching design process are shown in Figure 1.

The purpose of this research tends to teach and evaluate theoretical knowledge, so that the blazing new trails and starting an undertaking education of economics and management students can achieve practical results.

(1) Case Teaching Design. Case teaching design is through one or several unique and representative blazing new trails and starting an undertaking practice typical case as the teaching content, using vivid forms to give people the feeling

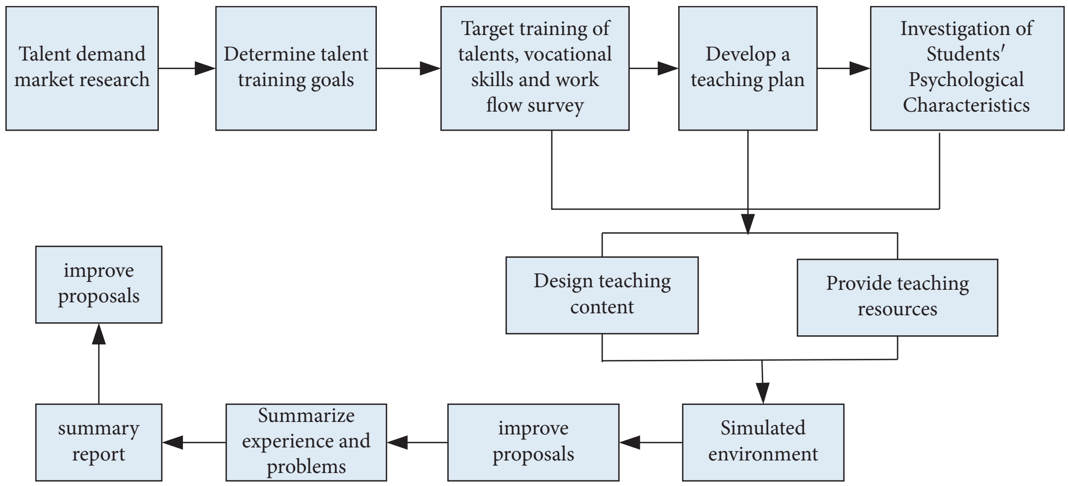

Figure 1: Innovative entrepreneurship teaching design flowchart.

of being in the scene, and it is convenient for students to understand and study the course. Instead of talking to themselves in class, teachers need to learn how to organize teaching by citing cases, master the progress of the course and guide the direction of discussion, and discuss problems with students. Students can increase their knowledge by understanding and being familiar with other people's entrepreneurial experience, show real examples to students, and analyze market economy laws using cases, to realize the development of ideas and stimulate students' interest in blazing new trails and starting an undertaking.

(2) Experiential Teaching. The purpose of experiential teaching is to cultivate students' self-improvement, self-reliance, innovation, and other qualities and stimulate students' love of learning, and it is possible to stimulate their personal teaching method. In the teaching process, we should mobilize students' learning enthusiasm, make the learning of double innovation education become the subjective things that students want to do, integrate the cognitive process of students with the emotional experience process, and let students learn the relevant knowledge in the experiential teaching. The core of experiential teaching design is to stimulate students' emotion and interest. It is a teacher-led and student-centered teaching model. Teachers design a mode of experience to guide students out of the complex environment and uncertain risks, and this can increase students' interest in innovation, entrepreneurship, and innovative thinking, thereby cultivating their creative thinking.

(3) Heuristic Teaching Design. The advantage of heuristic education is that it can guide students to acquire knowledge according to various methods of teachers. Then, teachers provide hypothesis of problems based on the actual situation of students, take inspiring students' thinking as the core, to mobilize students' learning enthusiasm, inspire students to think independently, find problems, and finally solve practical problems, to cultivate college students' practical ability of analysis, decision-making, operation, and management. Some educators have said that "the most effective learning method is to let students learn in the process of experience and creation, which is more obvious than the cramming teaching method. Without pressure, students can learn happily in the experience atmosphere, enable students to gradually develop the habit of serious study."

3.4.2. Interview Design. The whole process of investigation can be composed of two aspects: the first part is the basic information of the interviewee and the second part is the content of the questionnaire. This article aims to analyze the overall status quo of blazing new trails and starting an undertaking education in domestic colleges and the atmosphere of economics and management education including the statistics of the collected data and the integration of the current situation of education. Then, where the problem lies is found out, an in-depth analysis of it is conducted, and finally detailed measures for reform are obtained.

(1) Subject of Investigation. The survey objects of this questionnaire are the students who accept blazing new trails and starting an undertaking education in six famous colleges and universities in the North, East, West, and Central China, as well as the blazing new trails and starting an undertaking teacher set up by the colleges. The selected teachers are senior teachers of the college and have a long teaching experience. They have a deep understanding of the development of blazing new trails and starting an undertaking education in the college and have personally participated in the formulation of education reform plan for economics and management majors; the students selected in the questionnaire survey are students of economics and management major, covering all grades.

(2) Questionnaire Survey Content. For teachers, the questionnaire content includes age, professional title, education background, subject background, management department, full-time and part-time teachers, teaching or work category, whether they have relevant qualification certification,

whether they have enterprise management experience or entrepreneurial experience, whether they have presided over or participated in research on blazing new trails and starting an undertaking, working hours, and the largest number of teachers in the education process. For students, the questionnaire includes gender, age, grade, whether they have participated in blazing new trails and starting an undertaking association, whether they have participated in blazing new trails and starting an undertaking competition, do they have work experience, working hours, and whether they are interested in entrepreneurship.

(3) Questionnaire Survey Statistics. The SO JUMP matches with the conventional questionnaire investigation, and it has the assets of precise data, high confidence level, simplicity of manipulation, and perfect statistical function, and therefore, it has been broadly used in university study. This investigation adopted the method of online random sampling. 100 questionnaires were issued to teachers, 100 were returned, and the effective rate was 100%; 500 questionnaires were issued to students, and 487 were returned, and the effective rate was 97.4%. The sample size of the questionnaire survey was 100 questionnaires for teachers and 500 questionnaires for students. 87 valid questionnaires were obtained for teachers and 412 for students. The questionnaire is distributed randomly.

3.4.3. Computer Simulation Teaching. The teaching of economics and management is more theoretical and lacks reasonable practical teaching. For this reason, this study proposes computer simulation teaching. The preparation of the computer simulation teaching system mainly includes the collection of pictures, audio and video materials, and the design of the network teaching platform. The teaching center has carried out this design and experiment in previous teaching activities and has certain experience. The teachers should be communicated before simulation teaching, and preparations for simulation teaching are made. IEE generally refers to the British Institute of Engineering and Technology.

The teachers of the teaching group prepared lessons collectively, visited and inspected the site, communicated and cooperated with each other, and discussed the whole process of the teaching design. The layout design of the simulated teaching scene, the teaching content, and the preparations that students should make are discussed. Particular attention should be paid to communicating with teachers and discussing the use and cooperation of multimedia, computer, and simulation teaching.

(1) The simulation of corporate competition conforms to the learning theory of constructivism. To make good decisions, students have to consider many factors. There is no simple formula to follow. Students put themselves in a simulated situation to think, analyze the external environment and internal factors of the enterprise, communicate, exchange, argue, and negotiate with their peers, and seek satisfactory decision-making plans. A good enterprise competition simulation software should leave enough room for imagination and a stage for students to display their decision-making ability, so that students can develop their inherent potential under the strong encouragement of competition.

(2) Economics and management students and business managers have a strong interest in this teaching and training method. Competitiveness, interest, and practicality of competitive simulation are unmatched by other classroom teaching methods. We admit that case teaching is an effective teaching method for many years. Compared with case teaching, competition simulation is more antagonistic, the application of knowledge is more comprehensive, and the students' enthusiasm appears higher.

3.5. Teaching Reform of Economics and Management Majors

3.5.1. Survey of Teachers. According to the results of the questionnaire survey, the content of the questionnaire survey is mainly focused on the survey of relevant information such as age, academic qualifications, and teaching subjects. The basic situation of teachers is obtained and drawn into a table, as shown in Table 1,

The analysis of blazing new trails and starting an undertaking is mainly based on the statistics of the survey process of entrepreneurial experience in the survey process in Table 1. According to Table 1, the proportion of teachers with master's degree is 62%, the percentage of doctoral degree is 26%, and that of bachelor's degree is 12%. This shows that most innovative and entrepreneurial teachers in most famous universities have high education, which can better guide students to conduct blazing new trails and starting an undertaking activity using knowledge and experience; from the perspective of teaching sector, 59% of teachers lead the study. Students carry out practical activities, which can make students experience blazing new trails and starting an undertaking more quickly; the disadvantage is that, from the perspective of the working years of teachers, most teachers have less years of education, and the experience may be relatively insufficient.

3.5.2. Survey of the Students Majoring in Economics and Management. Through the analysis of the data in the figure, the cognition and willingness of students of different grades in these colleges and universities can be obtained and drawn, as shown in Table 2.

According to the analysis in Table 2, it can be concluded that the economic and management students who have participated in the entrepreneurship and innovation association are more inclined to start a business, while the economic and management students who have not participated in the entrepreneurship and innovation association do not want to start a business; in addition, the number of students who participated in the entrepreneurship and innovation competition was significantly less than the number of students who did not participate. To better observe and compare, the table is drawn into a graph, and we see Figure 2.

Table 1: Basic situation of teachers.

Statistical items		Number	Percentage (%)
Age	30 and under	11	11
	31 to 40	52	52
	41 to 50	34	34
	51 to 60	3	3
Educational background	Doctor	26	26
	Master	62	62
	Bachelor	12	12
Teaching section	Theory teaching	41	41
	Practical teaching	22	22
	Theory + practice	37	37
Entrepreneurial experience	Yes	24	24
	No	76	76
Project research	Yes	44	44
	No	56	56
Working years	1 to 5	68	68
	6 to 10	16	16
11	11 to 15	11	11
	15 and above	5	5

Table 2: Basic information of students majoring in economics and management.

Statistical items	Number of students	Percentage (%)
Join the club	284	56.8
Have not participated in the club	216	43.2
Participated in the competition	167	33.4
Have not participated in the competition	333	66.6
Want to start a business	259	51.8
Not want to start a business	241	48.2

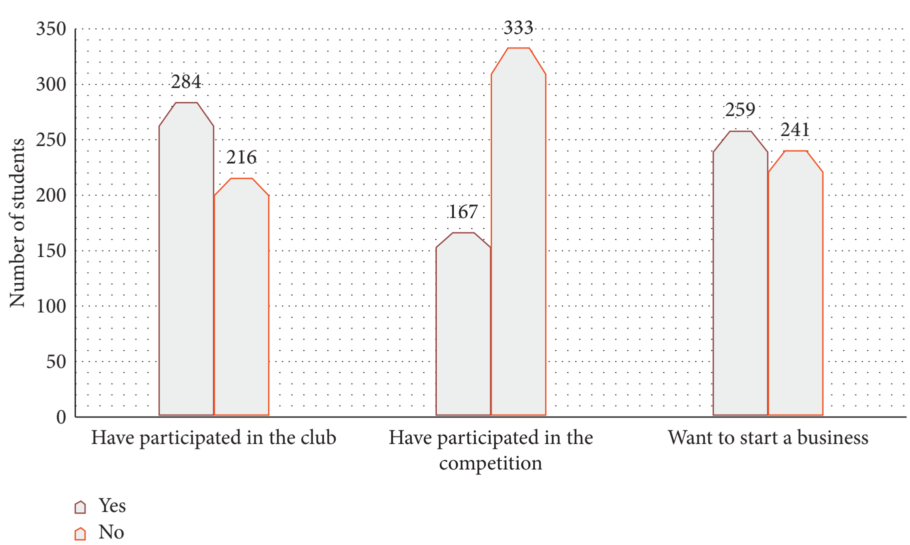

Figure 2: Basic information of students majoring in economics and management.

According to Figure 2, the biggest gap among the selected economics and management majors is whether they have joined the double creation competition, with a total difference of 166, The problems of blazing new trails and starting an undertaking education in colleges and universities can be inferred that the lack of experimental bases and less practical activities lead to the gap. To promote students' performance and practice of activities, colleges and universities proposed to accelerate the reform of economics and management disciplines.

3.5.3. Teaching Model of Economics and Management Majors under the Idea of Blazing New Trails and Starting an Undertaking Education. In the process of the questionnaire survey, the statistical data show that they are not similar in the past experience of different grades of college students majoring in economics and management. The specific differences reveal in Figure 3.

In addition, during the questionnaire survey, the support rate of different grades of students majoring in economics and management for the teaching reform of the professional courses under the concept of blazing new trails and starting an undertaking was statistically analyzed, as shown in Figure 4.

Under the idea of blazing new trails and starting an undertaking education, the purpose of teaching economics and management is to cultivate applied talents with innovative thinking and entrepreneurial abilities. It is especially important to establish a training model based on different levels, different abilities, and different knowledge to carry out the teaching of the right medicine to the case.

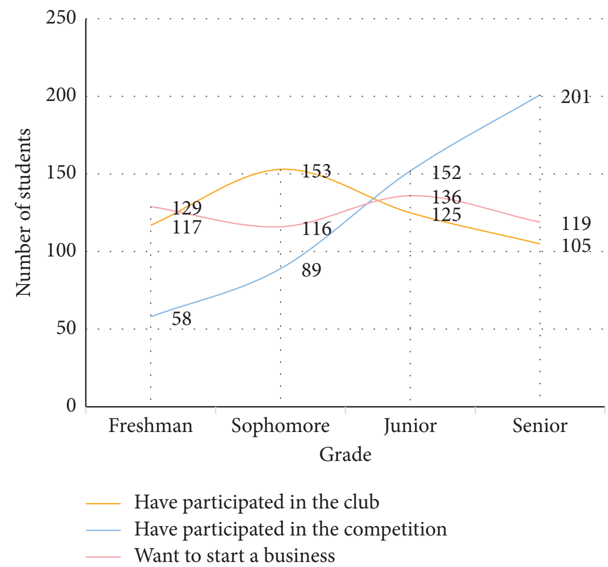

Figure 3: Blazing new trails and starting an undertaking experience of students of different grades.

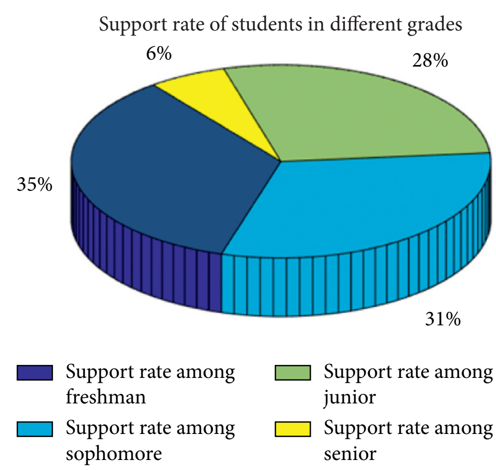

Figure 4: Support rate of students in different grades.

(1) Teaching and Training of Economics and Management Majors under the Idea of Blazing New Trails and Starting an Undertaking Education for Freshmen. Generally speaking, college freshmen have not been exposed to the idea of blazing new trails and starting an undertaking education and have little knowledge of blazing new trails and starting an undertaking education. Colleges and universities must offer blazing new trails and starting an undertaking education courses, such as learning college students' blazing new trails and starting an undertaking education, college students' career planning, and entrepreneurship management. Universities should actively carry out various forms of blazing new trails and starting an undertaking knowledge lectures, or introduce some outstanding companies to students for internships, to understand the development process of these enterprises and encourage freshmen's innovative thinking and entrepreneurial consciousness. In addition, colleges and universities should organize a variety of community activities, so that students with strong ability in blazing new trails and starting an undertaking can drive the relatively weak students forward. Only in this way can freshmen at different levels promote each other. In addition, through the campus broadcast, campus newspaper, campus network, and other campus culture publicity, the blazing new trails and starting an undertaking spirit are rooted in the students' hearts, to achieve the purpose of encouraging students' learning progress.

(2) Blazing New Trails and Starting an Undertaking Education for Sophomores. Although sophomores have formed the awareness of blazing new trails and starting an undertaking, they still do not know the specific implementation methods. Therefore, it is very important to improve their thinking and innovation ability. Therefore, through the guidance of some experienced teachers, a series of innovative and entrepreneurial projects can be established to improve the students' personal qualities and the collective sense of honor of the class. For students with a highly innovative and entrepreneurial spirit, students are guided to complete experimental projects independently, and research papers based on experimental results are published, which are combined in various magazines. In addition, universities must also encourage students to create and invent. When formulating a training plan for entrepreneurial spirit, it is necessary to formulate an appropriate training plan according to the personality of various students. At the same time, the theory of blazing new trails and starting an undertaking must be strengthened. The school also needs to actively organize students to participate in internships in experimental bases and affiliated companies inside and outside the school to improve students' practical ability and innovation and entrepreneurial ability. Moreover, universities need to combine blazing new trails and starting an undertaking education with community activities and improve students' innovative thinking and entrepreneurial ability. To mobilize enthusiasm, the association should

organize various training activities and competitions to improve their blazing new trails and starting an undertaking capability.

The economics and management course takes blazing new trails and starting an undertaking education as the goal and as the main purpose to create a strong entrepreneurial cultural atmosphere in the university. Through the enlightenment of entrepreneurial content, we feel that we can continuously improve and cultivate good business behavior habits in the training, departments, and activities provided in various fields of the school. Conclusions inspired by entrepreneurship, we can provide training for school students and let students establish a good corporate awareness. Let students broaden their vision of connecting with business leaders through campus activities and establish a systematic training system.

4. Conclusions

This study analyzes the education status of some universities and the basic situation of blazing new trails and starting an undertaking students majoring in economics and business through student statistics and various guidance methods such as design case education and experience education. Humanized education provides some new ideas for studying economics and business education reform based on the idea of blazing new trails and starting an undertaking education.

Then, we use computer simulation and simulation experiments to teach economics and management courses, which are closely combined with the learning concept of "discovery-oriented learning and research-oriented learning," providing students with valuable educational resources. An experimental and step-by-step education model is created within students to effectively cultivate students' innovative practical ability. The computer simulation teaching experiment mentioned in the article is mainly a simulation of the current concept, not a real experiment. Computer simulation teaching experiment has built a new experimental education model adapted to the information age and created a step-by-step internal experimental teaching method for basic learning, which can effectively cultivate students' practical and innovative abilities. Under the idea of blazing new trails and starting an undertaking education, the teaching reform of economics and management majors in colleges and universities should be carried out according to the conditions of students of different grades. The use of simulation technology to construct computer simulation experiment teaching is conducive to the cultivation of innovative talents.

Through the investigation and analysis of the basic situation of all levels of students majoring in economics and management in colleges, it is transformed into establishing a hierarchical training model based on different grades, different knowledge, and different abilities. In addition, professional training plans for various abilities have been developed. If it is a senior student, it is necessary to develop a project plan. To provide financial support, track and guide projects, and help superior experts to innovate and entrepreneurs to develop economy and management, we will recommend related projects to superiors.

Data Availability

The data that support the findings of this study are available from the corresponding author upon reasonable request.

Disclosure

The authors received no financial support for the research, authorship, or publication of this article.

Conflicts of Interest

The authors declare that they have no conflicts of interest.

References

[1] T. S. Kishore and M. Sanapala, "Towards self-reliant renewable power generation: techno-economic analysis of an educational institute based hybrid power system," *Water and Energy International*, vol. 61, no. 7, pp. 31–37, 2018.

[2] M. Judge, "Large-scale laboratory teaching for first-year EEE undergraduates," *International Journal of Electrical Engineering Education*, vol. 55, no. 1, p. 88, 2018.

[3] I. A. Sievidova, "Factors affecting the economic management efficiency of agricultural enterprises in Ukraine," *Problems and Perspectives in Management*, vol. 15, no. 2, pp. 203–210, 2017.

[4] D. Magnus, L. Carbonera, L. Pfitscher, D. Bernardon, A. Tavares, and C. Scharlau, "Experimental and educational platform for operation tests and parameterization of power system regulators and stabilizers," *IEEE Latin America Transactions*, vol. 17, no. 01, pp. 54–62, 2019.

[5] K. G. Srinivasa K G, B. J. Sowmya Bj, A. Shikhar, R. Utkarsha, and A. Singh, "Data analytics assisted internet of things towards building intelligent healthcare monitoring systems," *Journal of Organizational and End User Computing*, vol. 30, no. 4, pp. 83–103, 2018.

[6] C. Gilbert, "Creating educational destruction: a critical exploration of central neoliberal concepts and their transformative effects on public education," *The Educational Forum*, vol. 83, no. 1, pp. 60–74, 2018.

[7] W. Wu, Y. Liu, C. H. Wu, and S. B. Tsai, "An empirical study on government direct environmental regulation and heterogeneous innovation investment," *Journal of Cleaner Production*, vol. 254, Article ID 120079, 2020.

[8] A. Schmitz, D. Urbano, M. Guerrero, and G. A. Dandolini, "Activities related to innovation and entrepreneurship in the academic setting: a literature review," *Innovation, Technology, and Knowledge Management*, vol. 13, no. 2, pp. 1–17, 2016.

[9] M. A. Cusumano, "The puzzle of Japanese innovation and entrepreneurship," *Communications of the ACM*, vol. 59, no. 10, pp. 18–20, 2016.

[10] G. Sharma, "Innovation and entrepreneurship research in India from 2000 to 2018: a bibliometric survey," *The Journal of Management Development*, vol. 38, no. 4, pp. 250–272, 2019.

[11] S. Sysoieva and O. Protsenko, "Implementation of the continuing education concept in the european educational area: regulatory provision," *Continuing Professional Education: Theory Into Practice*, no. 2, pp. 78–84, 2020.

[12] J. Petrovic, "The influence of Dewey's educational concept on Serbian pedagogues in defining education," *Godisnjak Pedagoskog fakulteta u Vranju*, no. 7, pp. 153–168, 2016.

[13] O. M. Herasymenko, "Risk identification as a tool for economic security for risk-oriented approach to business

management," *Cherkasy University Bulletin: Economics Sciences*, vol. 2018, no. 4, pp. 22–33, 2018.
[14] M. Hamid, A. Mohsen, and A. Reza, "Reconfigurable rapid prototyping platform for power electronic circuits and systems for research and educational purposes," *IET Power Electronics*, vol. 11, no. 7, pp. 1314–1320, 2018.
[15] J. T. Mortimer, L. Zhang, C.-Y. Wu, J. Hussemann, and M. K. Johnson, "Familial transmission of educational plans and the academic self-concept," *Social Psychology Quarterly*, vol. 80, no. 1, pp. 85–107, 2017.
[16] J. Mutale, "Educational challenges: issues with power engineering education [in my view]," *IEEE Power and Energy Magazine*, vol. 16, no. 5, pp. 120–117, 2018.
[17] I. S. Leushina, A. A. Temerbekova, and A. A. Temerbekova, "Analysis of the main approaches to definition of the concept universal educational actions»»," *Tomsk State Pedagogical University Bulletin*, vol. 1, no. 1, pp. 28–32, 2017.
[18] M. Zhou, Y. Wang, Y. Liu, and Z. Tian, "An information-theoretic view of WLAN localization error bound in GPS-denied environment," *IEEE Transactions on Vehicular Technology*, vol. 68, no. 4, pp. 4089–4093, 2019.
[19] S. Fedulova, V. Dubnytskyi, V. Komirna, and N. Naumenko, "Economic development management in a water-capacious economy," *Problems and Perspectives in Management*, vol. 17, no. 3, pp. 259–270, 2019.
[20] T. V. Morozova, T. Polyanskaya, and V. E. Zasenko, "Economic analysis in the financial management system," *International Journal of Applied Business and Economic Research*, vol. 15, no. 23, pp. 117–124, 2017.
[21] P. Partlova, J. Strakova, J. Vachal, F. Pollak, and J. Dobrovic, "Management of innovation of the economic potential of the rural enterprises," *Marketing and Management of Innovations*, no. 2, pp. 340–353, 2020.
[22] C. Xiang and L. Dehua, "Exploration on projectized-teaching reform of "crushing and grinding technology" in higher vocational education," *World Nonferrous Metals*, vol. 000, no. 19, pp. 224–226, 2018.

Hindawi
Scientific Programming
Volume 2022, Article ID 6557374, 10 pages
https://doi.org/10.1155/2022/6557374

Research Article

The Innovative Practice of Artificial Intelligence in the Inheritance of Chinese Xiangjin Art

Zhao Wenji, Cui Rongrong, and Niu Li

School of Design, Jiangsu Intangible Cultural Heritage Base, Jiangnan University, Wuxi 214122, China

Correspondence should be addressed to Zhao Wenji; 7180306008@stu.jiangnan.edu.cn

Received 14 December 2021; Accepted 3 January 2022; Published 17 January 2022

Academic Editor: Punit Gupta

This paper attempted to study the cultural characteristics and intelligent inheritance of Chinese Xiangjin brocade. Qualitative data was collected by in-depth interview method, and more than 1000 pieces of Xiangjin brocade of Suzhou Archives in China were measured for analyzing artistic features of their pattern design, color matching skills, and weaving technology, the study of which illustrated artistic features of modern Xiangjin brocade in detail and provides an important reference for its cultural and weaving inheritance. In addition, the artificial intelligence (AI) and the inheritance of Xiangjin art characteristics are integrated, the traditional handicrafts and digital art are docked, and the corresponding digital art protection mode is selected according to the characteristics of traditional handicrafts. The intelligent inheritance of cultural heritage not only changes the way of inheriting the artistic characteristics of Xiangjin, but also changes people's general cognition of the cultural characteristics of Xiangjin. As a result, the integrity, authenticity, reliability, and comprehensiveness of the technological process of Xiangjin can be inherited, the patterns of Xiangjin can be preserved and applied, and the craft culture of Xiangjin can be inherited, protected, and developed.

1. Introduction

Xiangjin brocade is a kind of traditional Chinese silk-woven portraits and landscape paintings, whose carriers are screens, wall hangings, bookmarks, and calendars. Its main content is human image, landscape photography, Chinese painting, oil painting, calligraphy, commemorative activities, and poster art. Xiangjin brocade, as a valuable art work for collection, is mainly used as a souvenir for tourism, as an interior decoration, and as a gift for interpersonal communication and national exchanges. Due to its unique aesthetic value, Xiangjin brocade has been used as gifts for G20 leaders and soft decoration in the venue. Although European countries, Japan, and other countries started earlier in textile production, they did not form a large scale. With rich cultural deposits and superb traditional weaving technology, Chinese Xiangjin brocade has taken the lead and become a unique category of silk-weaving products, selling well in domestic and abroad markets for nearly a century. Arguably, Xiangjin brocade is not only the representative of innovative products in China's silk industry, but also a successful model of inheriting and developing Chinese silk culture.

The authors participated a cooperative project "Cataloguing and Studying of Xiangjin Brocade in Silk Archives of Suzhou, China" on December 1st, 2020, to January 15th, 2021. Altogether, the authors measured each Xiangjin brocade and catalogued more than 1000 pieces in Silk Archives of Suzhou from the period of The Republic of China, the founding of People's Republic of China, and opening and reform period. With the theme of inheriting silk culture and spreading silk art, the authors not only collected data on structural characteristics, drawing technique, size, color collocation, and area comparison of Xiangjin brocade, but also focused on the emergence, development, and technology in cataloging process.

Domestic researches on Xiangjin brocade are summarized as follows: (a) the introduction of Xiangjin brocade from the aspect of art and weaving skills. They are Yuan Xuan-ping's Inheritance and innovation of modern Chinese brocade art, Yuan Xuan-ping and Xu Zheng's Hangzhou weaved photograph, He Yunfei's The artistic features of Du Jinsheng brocade, Liu Kelong's master thesis The flower of oriental art—the art of Du Jinsheng brocade, and Peng Zeyi's

History of handicraft industry in modern China (1840–1949). The making of Xiangjin brocade can be found in the third chapter of Peng's book, which involves the development of new products and the employment of new machine. The researchers mentioned above have studied the weaving process of Chinese brocade, Xiangjin brocade and West Lake brocade. (b) The introduction of Xiangjin brocade factories and Du Jinsheng brocade from the perspective of industrial development and management experience. They are represented by historical data for industry and commerce edited by Research Committee of Cultural and Historical Data of the CPPCC National Committee, Xie Mu and Wu Yongliang's China time-honored brand, Wang Xiang's The story of old brand, Yi Gan's Swaying ship: national industry and commerce (1900–1994), Li Gangyuan's An entrepreneur's innovative spirit and his cultural accumulation and world vision: A case analysis of Du Jinsheng and his Brand, and Hu Dan-ting's Survey of Hangzhou silk's reputation. Guo Xingmei takes brand as her research topic to scrutinize rough stages of introduction, digestion and innovation of modern Chinese silk technology. Taking three modern Chinese textile enterprise brands, i.e., "Shenxin Renzhong," "Meiya Silk," and "Wuhe Epai" as case examples, Guo explores how enterprises build up brand images and improve brand values by technology development, cultural exploration, and operation management. Then, Guo discusses the bottlenecks of contemporary textile enterprises and their brand development from the perspective of textile machinery innovation so as to offer some referential suggestions to the building of Chinese contemporary textile brands. (c) The introduction of Xiangjin brocade from the perspective of local history and brocade history. The representative works include Hangzhou in the Republic of China edited by Zhou Feng, Hangzhou local chronicles edited by Local Chorography of Hangzhou, New centennial chronicles of Zhejiang Province edited by Research Committee of Cultural and Historical Data of Zhejiang CPPCC, History of silk weaving industry in Jiangnan area in modern times edited by Xu Xinwu, and History of China modern textile edited by Editorial Committee of Modern Textile History of China. Besides, few scholars in other countries mentioned Chinese brocade when studying silk history, for example Japanese scholar Nuru Ono's Silk industry in Hangzhou. Although some Chinese scholars have introduced Du Jinsheng brocade from different perspectives, few of them combine Chinese brocade weaving techniques with modern textile design in practice. Other relevant researches can refer to the literature [1–5].

However, as the traditional brocade art design, Xiangjin brocade is attached to the specific cultural space and survival soil, is facing the plight of cultural disruption and lack of successors, and is gradually depressed and even going to decline. The inheritance of traditional Xiangjin brocade weaving skills is mainly family inheritance, industrialization inheritance, and so on. These inheritance methods are carried out under the relatively conservative and established space-asking mode, which is subject to many restrictions both in terms of the audience and the way of teaching. With the loss of time, it is not difficult to see that, due to the limited scope and space of inheritance and the excessive emphasis on specific groups, the traditional inheritance method has been difficult to maintain the survival of traditional crafts. Therefore, the selection of suitable technical means under the existing skill inheritance mode, especially the novel and unique artificial intelligence technology, can proceed from a unique artistic perspective. In order to develop a new concept of thinking to inherit, protect, and develop the traditional Xiangjin brocade skills. Since the advent of artificial intelligence, especially the wide application of "intelligent art," automatic art creation and performance appreciation have become a reality. It also has important practical application value in the fields of computer graphics, pattern design, light industry, and textile, as well as the inheritance of artistic features.

In order to protect this non-material cultural heritage, i.e., Chinese Xiangjin brocade, this paper adopts field survey method (visit Du Jinsheng Museum, Suzhou Chinese Silk Archives, and Xiangjin brocade enterprises) and market survey method to interpretate artistic characteristics of Chinese Xiangjin brocade in details, studies the application of Xiangjin brocade in modern textile design, especially in decorative crafts, and puts forward the suggestion of carrying on the intelligent inheritance of Xiangjin culture; that is, the artificial intelligence and the inheritance of Xiangjin art characteristics are integrated, the traditional handicrafts and digital art are docked, and the corresponding digital art protection mode is selected according to the characteristics of traditional handicrafts. The intelligent inheritance of cultural heritage not only changes the way of inheriting the artistic characteristics of Xiangjin, but also changes people's general cognition of the cultural characteristics of Xiangjin.

2. Artistic Features of Chinese Xiangjin Brocade

Chinese Xiangjin brocade has its unique artistic skills, such as artful color matching, delicate composition, vivid model, and profound meaning. It has beauty in both form and pursuit of elegant taste. It not only follows the scattered point penetration method of traditional literati paintings, but also draws on the western focus perspective method. In the long-term process of artistic development, it absorbs the excellent traditional elements of all periods, both ancient and modern time, China and foreign countries, developing its traditional and unique artistic features.

2.1. Exquisite Traditional Craftsmanship. As a pioneer of mechanized and large-scaled production in modern brocade industry in China, Xiangjin brocade took the lead in the innovation of traditional brocade in key processes such as craftsmanship, design and jacquard [6] and opened up a new era of brocade from manual weaving to industrial manufacture. It is of great significance in the history of Chinese silk weaving. Compared with paper products, it is tough and strong and more suitable to reveal the poetic charm of the original painting. Having artistic beauty and natural beauty, it is the perfect combination of painting, calligraphy art, and traditional brocade art.

2.1.1. Colored Tapestry: Special Processing Technology. In the coloring process, the artisan workers use small script pens or eyebrow pens to paint different watercolors and art requirements on the black-white landscape brocade according to the picture's theme [7]. They should first have a handle on picture theme, coloring, small samples before coloring process, and then follow the principle of light color at first and deep after, far things at first and close things after, buildings at first and plants after. This can also be done flexibly according to the picture, that is, using less color to display painting content. In Figure 1, the coloring technique of the local pavilions built in Spring Dawn at Su Causeway of West Lake can make audience better appreciate the life-like scenery of lakes and hills. Compared with black-white Xiangjin brocade, the rich colors of the Imperial Monument Pavilion, lake, and boats break through the traditional planar layout expression, enabling audience to be more deeply impressed.

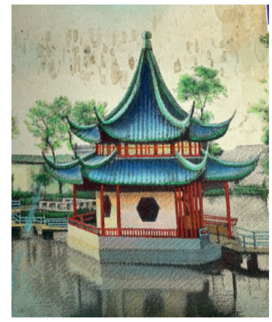

Figure 1: Colored Xiangjin brocade (archive collection, photos taken by the authors on Dec. 16th, 2020).

2.1.2. Multicolored Xiangjin Brocade: Perfect Technique. The coloration of multicolored Xiangjin brocade is mainly done through the ups and downs of the weft line. As a result, it is just like the photo itself, in which all the powder comes from the painter's hand. Though it keeps pace with Hunan brocade, the price is only the latter's one-twelfth, so it is cheap and cheerful. This kind of brocade is made of two groups of warps and multiple wefts interwoven into the multiple weft textile. One group of warps is the ground warp, while the other group is to press the floating weft tightly to connect the warp. In Figure 2, the multicolored Xiangjin brocade in the museum "Finch Plum" breaks through the traditional planar layout expression.

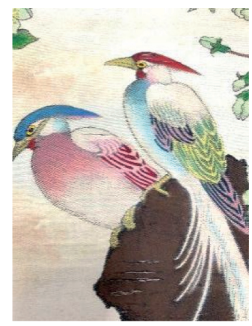

Figure 2: Multicolored Xiangjin brocade (archive collection, photos taken by the authors on Dec. 16th, 2020).

2.1.3. Painting Xiangjin Brocade: Reproduction of Masterpieces. Painting brocade is mainly woven with silk thread to manifest fine brushwork, freehand brushwork, and Chinese painting that combines fine brushwork with freehand brushwork. In this way, it has not only ink painting's quiet and elegant decorative effect, but also silk's natural and unrestrained charm. In addition to the use of color gradation to reveal shadow change, this multi-weft colorful Xiangjin brocade mainly uses the floating and sinking color of weft threads to form the color of the scene [8]. In Figure 3, the typical scenes that can best illustrate the heroine's personality in *Zhaojun Goes Beyond the Great Wall as a Bride* are meticulously colored to show the heroine's facial texture and emotional expression, including her clothing, hair on her temples, accessories, flowers, and pavilions.

2.1.4. Practical Xiangjin Brocade: Life-Oriented Technique. How to make Xiangjin brocade have both aesthetic taste and practical value? In order to increase the sales and practicability of silk-woven products, a practical Xiangjin brocade whose quality is far superior to that of Nanjing brocade was designed on the basis of multi-colored brocade.

It is the combination of painting, decoration, and art of living with character, landscape, and flowers as themes. Compared with traditional brocade, the most striking feature of Xiangjin brocade is its life-oriented technique. The main use of traditional brocade like Sichuan brocade, Yun brocade, or Song brocade is for making clothes, while Xiangjin brocade is mainly used for decoration from the date of its birth. As *West Lake Expo Daily* introduced, "Xiangjin brocade can be used for hall hanging, study ornament, orchid boudoir enjoyment, elegant and pleasant" [9]. Business Monthly also reported, "one important art invention which can be used for gift-giving and decoration." The two-warp-multi-weft structure of practical brocade becomes one-warp-three-weft structure, in which one group of warps interweave weft to form ground tissue, while another two groups of wefts weave flowers on ground tissue. Practical brocade includes silk fan, back cushion, bedspread, and handbags. Handbags are made of fabric scraps of raw materials so they can save cost and increase output, rather popular with customers at home and abroad. It is a true novelty in silk industry. In Figure 4, it is a Xiangjin brocade made from the Western classic drawing "reading" for hanging in bedroom.

2.2. Elegant Color: Affection for the East. Inheriting the main colors of Chinese traditional brocade, Xiangjin brocade is often colored with warm colors like red, yellow, and green. Unlike quiet, elegant, and simple style of Chinese traditional brocade, it uses gorgeous, rich, and chunky colors to reflect its strong and unrestrained artistic features. Regarding color matching skills, it employs the traditional "color change"

Figure 3: Painting Xiangjin brocade (archive collection, photos taken by the authors on Dec. 16th, 2020).

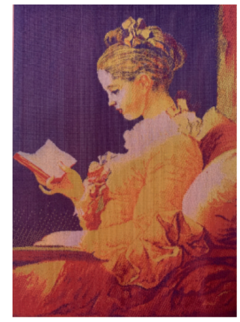

Figure 4: Practical Xiangjin brocade (archive collection, photos taken by the authors on Dec. 16th, 2020).

skills to make the picture natural, harmonious, and unified, while reducing the visual stimulation that chunky color produces. In Figures 5 and 6, "Comprehensive Painting Indicating Five Norms" that is themed with two gorgeous peacocks and a pair of cranes is the most representative. On the right, the green leaves and wild pines match with white willow warbler, while on the lower left, there is a pair of intimate mandarin ducks. Rich warm colors like red, yellow, and green match with black, white, and gray, which present a vibrant, lively, lovely, and harmonious decorative effect.

2.2.1. Sights of the West Lake Copied Vividly on Xiangjin Brocade. The well-known folk artist Zhang Daoyi mentioned in his work *Folk Art in China*, "Characterized by diversity, practicality and appreciation, Chinese folk arts have a strong local color" [10]. Japanese technologist Yanagi Souetsu argued, "All the handicrafts in history that are closely related to local history and culture have striking local features" [11]. Chinese Xiangjin brocade is indigenous to Hangzhou, and West Lake Xiangjin brocade is the most typical one, so it has distinct cultural characteristics of the West Lake. Xiangjin brocade takes photos as negatives and absorbs the strong points of photographic art through the form of brocade paintings. Thus, it has multiple styles of traditional national painting, western photographic art, and modern oil painting. Its silk weaving paintings with the same effect as photos are exquisite, vivid, and lifelike, so it blends inheritance with innovation.

2.2.2. Profound Implications of Oriental Charm. K'o-ssu, embroidery craft, and double-weft brocade craft are often utilized to weave silk articles based on Chinese paintings and calligraphic works. With the development of pattern jacquard technology, Xiangjin brocade employs different colors and weaving points with brightness to represent traditional Chinese oriental element; thus the color change becomes soft. Figures 7 and 8 are part of yarn-dyed and color-filled silk Chinese painting "Wu Guandai's Landscape Painting" (27×98 cm). They have the following features. First, black, white, and light-yellow rayon are utilized to treat weft color. Triple-weft structure which is more complex than the black-white double weft is employed to the weave the textile. Second, color filling method is used on the basis of yarn-dyed knitting. For example, painted color techniques are employed to make red, yellow, blue, green, and ochre on the picture. Third, it is very rare that Du Jinsheng trademark, factory's name, and four Chinese characters "Wu Cai Jin Xiu" are weaved on the bottom of the picture at the same time. Fourth, this work is rather grand, whose weft width is 27 cm, the number of jacquard needles is more than 2000, and the number of grain plates is more than 8000. This technology took the lead in the 1930s, which made near objects and distant landscape in the painting have rich levels, trees, houses and figures have strong three-dimensional sense, fully demonstrating the unique taste of silk paintings of landscape and figures.

2.2.3. Multivariate Utility of Intrinsic Value. As an important member of folk art, the themes of Xiangjin brocade are mostly derived from real life, which truly record the West Lake landscape culture, garden culture, architecture culture, folk culture, and religious culture, helping later generations intuitively appreciate scenery of the past. The themes include moral customs, humanistic education, and psychological concepts. Since its birth, a series of works such as Xiangjin brocade cushion, hanging scroll, wall calendar, and table cloth with great spirits has been innovated. In Figures 9 and 10, accompanied by a red maid, the legendary Goddess Avalokitesvara stands bare-footed on the lotus stage. She dresses in white clothes, smiling to an innocent infant beside her. This brocade shows people's high respect for Avalokitesvara, expressing Chinese nation's strong wish for reproducing offspring; thus it has a good educational effect.

2.3. Innovative Practice of Xiangjin Brocade in Modern Textile Design: Take Du Jinsheng Brocade as an Example. Chinese Xiangjin brocade is not only a product, but also a work of art, representing the peak of the development of contemporary Chinese brocade. With regard to brocade objects, there are not only fabric pattern paintings, but also large-scale paintings, which harmoniously display flat and three-dimensional paintings, especially vividly record different historical and cultural forms. In terms of painting performance, it inherits techniques of traditional Chinese paintings, religion paintings, New Year pictures, print makings, classical oil paintings, and western contemporary paintings.

Figure 5: Crane in comprehensive painting indicating five norms (archive collection, photos taken by the authors on Jan. 6th, 2021).

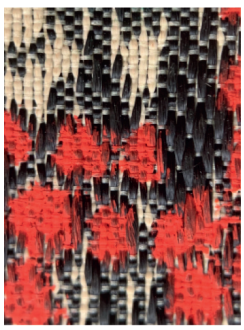

Figure 6: Hand coloring of comprehensive painting indicating five norms (archive collection, photos taken by the authors on Jan. 6th, 2021).

Figure 7: Part of Wu Guandai's landscape painting (archive collection, photos taken by the authors on Jan. 6th, 2021).

Figure 8: Hand coloring of Wu Guandai's landscape painting (archive collection, photos taken by the authors on Jan. 6th, 2021).

Its artistry exceeds the most precious "double brocade" hanging scroll in Ming and Qing dynasties. In the aspect of decorative brocade for daily necessities, rayon square table blanket, rayon round table blanket, and broad blessing table blanket have been successively produced.

2.3.1. Social Investigation of Innovative Practice of Xiangjin Brocade. In recent decades, there are different kinds of Xiangjin brocade products with different prices. To know the present situation of Xiangjin brocade in Chinese market, the authors used "Xiangjin brocade," "brocade," "traditional handicraft," "the intangible cultural heritage," "traditional textiles," "China's time-honored brand," and "Du Jinsheng" as key words to search information of Xiangjin brocade on three Chinese online platforms "Taobao," "Joy Buy," and "Tmall." The information included brocade brand, style, price, category, comment, and target population. Altogether, 1300 pictures were screened out.

Then, 13 famous brands of silk industry in Chinese market were selected, whose information was compared with that of products sold on the Internet to find out the dissimilarities between the two. Orange software was employed to analyze the collected data and position the present situation and dilemma of Chinese Xiangjin brocade.

Third, a survey was made on which kind of Xiangjin brocade customers prefer through closed Interview questions.

It can be seen from Table 1 and Figure 10 that more than half of the participants know something about the technique of Chinese Xiangjin brocade. Although online sales are booming at present, branded Xiangjin brocade enterprises are accepted by most consumers, for they can better represent Chinese brocade culture. More than half of the consumers do not accept the high price of Xiangjin brocade. Most interviewees pay more attention to the branded Chinese brocade handicrafts, including HSDP, Wensli, Hangsilian, Fuhua, Hongluo, and Jinyuan, among which Du Jinsheng brocade is the most popular one.

2.3.2. Innovative Practice of Du Jinsheng Brocade. As the representative of Hangzhou brocade, Du Jinsheng brocade came into being in 1921, including Xiangjin brocade, decorative brocade, and brocade for clothing whose more than 1640 varieties have become China's representative brocade [12]. According to different customers, traditional theme was made into patterns of different levels through mud floor, skimming silk, arrangement shadiness, and side shadiness. With regard to manifestation, free and irregular composition have replaced the traditional balanced and single composition. Du Jinsheng brocade have made three biggest textile works, i.e., hanging Xiangjin brocade, Xiangjin brocade carpet, landscape Xiangjin brocade. Among them, the Xiangjin brocade Ten Thousand Li of Rivers and Mountains (42×1125 cm) is known as the longest silk weaving picture in the world. One of them was hung in the hall of Swedish parliament in Stockholm.

Paying much attention to the market, Du Jinsheng brocade not only produced blanket and back cushion, but

Figure 9: Hanging scroll South China Sea Avalokitesvara (collection in Du Jinsheng Museu, photos taken by the authors on Jan. 5th, 2021).

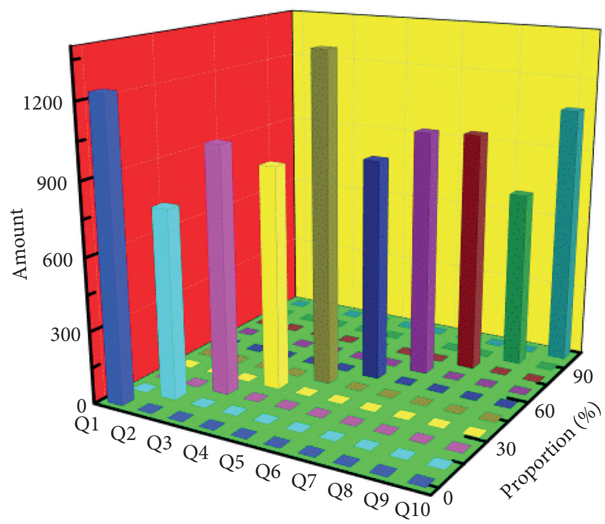

Figure 10: Questionnaire results.

Table 1: Interview questions.

No.	Interview questions	Choices (Y/N)	Amount	%
1	Do you know the technique of Chinese Xiangjin brocade?	Y	1233	61.65
		N	767	38.35
2	Can you give two artistic features of Xiangjin brocade?	Y	784	39.20
		N	1216	60.80
3	Do you think Xiangjin brocade can be applied in modern society?	Y	1021	51.05
		N	979	48.95
4	Do you anticipate the application of Xiangjin brocade in modern textile design?	Y	923	46.15
		N	1077	53.85
5	Do you pay more attention to Xiangjin brocade with a famous brand?	Y	1364	68.20
		N	636	31.80
6	Can you accept Xiangjin brocade with a price of ¥ 1000–2000?	Y	921	46.05
		N	1079	53.95
7	Do you know some brands of Chinese Xiangjin brocade?	Y	1012	50.60
		N	988	49.40
8	Do you like some innovative design of Chinese Xiangjin brocade?	Y	1001	50.05
		N	998	49.95
9	Do you think branded Xiangjin brocade can represent Chinese textile culture?	Y	738	36.90
		N	1262	63.10
10	Do you think Chinese traditional textile industry need some improvement?	Y	1078	53.90
		N	922	46.10

also designed Xiangjin brocade bedspread and silk-wool curtain, which are washable and bright colored and have strong senses of relief, so it has both practical value and ornamental value [13]. The brocade silk bags made in China that ladies of various countries held in G20 Hangzhou Summit can be regarded as the most representative and influential innovative works of Du Jinsheng brocade (see Figure 11). The inspiration came from glacier frostwork whose beautiful lines indicate the fantastic dreamy scenery of nature. Against elegant purple, the frostworks with conch divergent crystalline lines are pure and clear, classic and fashionable, and very pleasing to the eye. Theme pattern "fantastic frostwork" employs modern positioning yarn-dyed jacquard technology, natural reactive dyes, platform floral printings, biological enzyme finishing technology to make its color uniformly bright. Silk bags match with perfect leather piping, grand and elegant, exactly reflecting the excellent quality of national gifts. Figure 12 shows Du Jinsheng brocade back cushion that is themed with the Bronze Sparrow Terrace.

Meanwhile, through collation and analysis, we can classify more than 1000 Xiangjin brocade fabrics collected from Suzhou Archives in China; that is, they can be divided into four categories: landscape brocade, figure image brocade, painting brocade, and practical brocade from different perspectives of fabric theme, expression method, organizational structure, and use function. Furthermore, through the above analysis, we can restore the artistic characteristics and timeliness of the brocade industry in different periods and take history as a mirror to examine its value and significance to the contemporary textile industry and product design.

3. Results and Discussion

From the above statement, we have collected and sorted out the technological process, the implication of the pattern, and the cultural connotation of the Xiangjin brocade and deeply analyzed the artistic design, customs, and religious beliefs reflected behind the elephant of the Xiangjin brocade. And through the comparative study of the brocade ways of different regions and different cultures in the same period, taking the technological characteristics of Xiangjin brocade as a starting point, this paper summarizes the existing inheritance problems of Xiangjin brocade craftsmanship.

The inheritance of traditional Xiangjin brocade skills mainly includes family inheritance, industrialization inheritance, and so on, but with the passage of time, due to the limited scope and space of inheritance, too much emphasis on specific groups, the traditional way of inheritance has been difficult to maintain the survival of traditional technology. Therefore, the selection of appropriate technical means under the existing skill inheritance mode, especially the novel and unique artificial intelligence technology, can form a new idea to inherit, protect, and develop the traditional Xiangjin brocade skills. With regard to the application of artificial intelligence technology in the inheritance of cultural heritage, there are already some achievements, such as the literature [14–16].

3.1. Segmentation of Xiangjin Brocade Image Based on DeepLabv3+. Image semantic segmentation is a technology that enables computers to understand images, and it can realize object category recognition and high-precision image segmentation simultaneously in a network. In recent years, this technology has achieved remarkable results in the semantic segmentation of visible images [17–19], while the research on the scene understanding of Xiangjin brocade images is still in the blank stage. In this paper, the Xiangjin brocade image of Suzhou Archives is used as the training sample, and DeepLabv3+ network is used as the training model [20]. In order to improve the precision of final segmentation, the whole image of Xiangjin brocade was segmented from the complex background, and the semantic segmentation results were postprocessed by combining image morphology method. At the same time, it also lays a foundation for finding regions of interest, feature extraction, and state classification.

With the advent of full convolutional networks (FCN), Long [21] et al. replaced the full connection layer in mainstream classification networks such as AlexNet, VGGNet, and GoogLeNet into the convolutional layer. Finally, transpose convolution is added to restore the feature graph to its original size [22], so that the spatial location features of image pixels can be retained and semantic segmentation has a breakthrough development. In this paper, DeepLabv3+, which has the highest score in MIoU tests in public data sets in recent years, is used as a network to train the semantic segmentation model of images of Xiangjin brocade. The image segmentation results of Figures 2 and 3 are obtained in Figures 13 and 14. Figures 13 and 14 show the exploration of artificial intelligence technology in the cultural inheritance of Xiangjin brocade fabrics. Their significance lies in the more detailed analysis and inheritance of Xiangjin brocade images in the form of digital pictures. It allows people to segment the whole Xiangjin image from the complex background, so as to improve the final segmentation accuracy, narrow the target object analysis scope for searching the region of interest, and carry out feature extraction and state classification.

3.2. Intelligent Inheritance of Cultural Characteristics of Chinese Xiangjin Brocade. The application of artificial intelligence can expand the channels of inheriting the artistic characteristics of Xiangjin, from the previous family inheritance and industrialization inheritance to the current digital, VR image preservation, and other ways, so that the cultural heritage like Xiangjin, which is limited by time and space and is not easy to inherit, has been caught on the express train of "the development of the times." Specifically, the existing Xiangjin brocade fabrics can be digitally preserved and a digital museum of Xiangjin brocade can be established. Even if the years wear out the real thing, people can learn the whole picture of Xiangjin brocade fabric with the help of digital platform. Specifically, the 360-degree panoramic VR technology can be used to record the skills of the current inheritors of the brocade through audio, video, and animation. Through stories like those told in Xiangjin brocade and VR graphic tutorials, people can immerse themselves in the virtual world across time and space. The teaching of VR techniques can make the successors learn systematically and make them master the skills of Xiangjin brocade knitting skillfully. VR pattern tutorials can also enable successors to learn the pattern tutorials left by the older generation of tapestry masters through pattern

Figure 11: Pattern of fantastic frostwork Xiangjin brocade handbag and its front.

Figure 12: Pattern of bronze sparrow terrace Xiangjin brocade back cushion and its front.

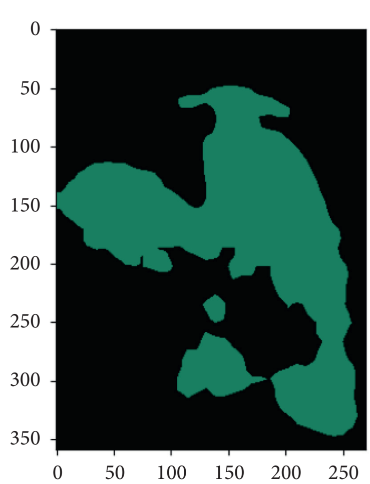

Figure 13: Segmentation diagram of DeepLabv3+ in Figure 2.

classification, so as to avoid the loss of skills as much as possible. For another example, we can use AR technology to develop a Xiangjin brocade experience game like "Happy Farm." In the web page promotion of Xiangjin brocade, scenes such as

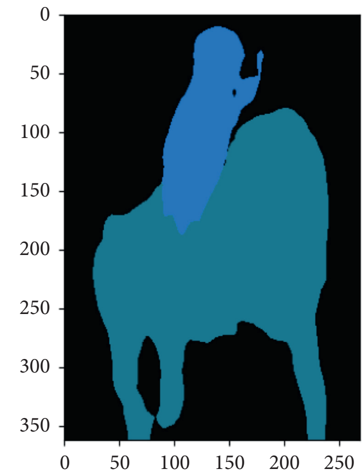

Figure 14: Segmentation diagram of DeepLabv3+ in Figure 3.

planting mulberry, rewinding, knitting, and packing are added to let the experiencers make guided virtual production through Mini Program. Then, the background will record the user's entire production process and make it manually, which can be sent home by express delivery after the user has paid for it. In this way, users can not only experience the charm of traditional Xiangjin culture, but also learn the production process of Xiangjin, which is extremely beneficial to the inheritance of Xiangjin culture. Artificial intelligence makes people know more about Xiangjin culture through sensory interaction, which not only enhances people's immersive experience, but also effectively makes up for the lack of communication between the two sides. Therefore, the integrated development of VR technology and the inheritance of the characteristics of Xiangjin brocade art not only changes the way of inheritance of the characteristics of brocade art, but also changes people's general cognition of the characteristics of brocade culture. In addition, the methods of machine learning and in-depth learning can also be applied to the inheritance of the artistic characteristics of Xiangjin brocade. There are some relevant literature as [23–29]. The comprehensive application of the two fully reflects the role of innovation in inheriting traditional culture such as Xiangjin brocade, so that the integrity, authenticity, reliability, and comprehensiveness of the technological process of Xiangjin brocade can be inherited, and the patterns of Chinese Xiangjin brocade can be preserved and applied.

In short, combined with literature and image data, this paper investigates the evolution of Xiangjin brocade and the changes of silk culture on the basis of regional characteristics. It is of great practical significance to systematically and scientifically research and study the different development periods of Xiangjin brocade.

4. Conclusion

Chinese Xiangjin brocade draws on the essence of Sichuan brocade, Yun brocade, and Song brocade and also dissolves the wit and beauty of Hangzhou brocade at the same time, so it forms its own unique artistic style, well-known as "the flower of oriental art." In this paper, we summarized and analyzed the artistic modeling characteristics of Chinese Xiangjin brocade and demonstrated that the aesthetics contained in Xiangjin brocade is consistent with the contemporary public way of life and summarized and analyzed the inherent deficiency of Chinese Xiangjin brocade in inheritance. Therefore, in order to make the process of Xiangjin brocade complete, real, reliable, and comprehensive to inherit, and the pattern of Xiangjin can be preserved and applied, we should adopt the new technology of artificial intelligence. This can not only change the way of inheriting the artistic characteristics of Xiangjin, but also change people's general cognition of the cultural characteristics of Xiangjin. The comprehensive application of the two can fully reflect the role of innovation in inheriting traditional culture like Chinese Xiangjin brocade. However, due to the regional limitations of sample collection, the scope of application of the conclusions is limited. At the same time, the technology of artificial intelligence is also developing rapidly, such as machine learning methods and deep learning methods, which can become new tools for us to study the cultural heritage of Chinese Xiangjin brocade.

Data Availability

The datasets used and/or analyzed during the current study are available from the corresponding author on reasonable request.

Conflicts of Interest

The authors declare no potential conflicts of interest with respect to the research, authorship, and/or publication of this article.

Acknowledgments

The authors acknowledge the Key Project of Philosophy and Social Science Research in Colleges and Universities (2018SJZDA130) and the "333 Project" of Jiangsu Province for Young and Middle-aged Leading Talents at the Second Level (BRA2016366).

References

[1] R. A. Bentley and M. J. O'Brien, *The Acceleration of Cultural Change: From Ancestors to Algorithms*, MIT Press, Cambridge, MA, USA, 2017.

[2] K. Chen, D. Lu, Z. Jin, M. Su, and J. Jin, "Song brocade in the ming and qing dynasties," *Clothing and Textiles Research Journal*, vol. 38, no. 4, pp. 285–297, 2020.

[3] A. Filomeno, "Application of the western art form based on artificial intelligence," *Cultural Communication And Socialization Journal*, vol. 1, no. 1, pp. 16-17, 2020.

[4] Z. Hongxia and L. Y. U. Zhijia, "Textiles design idea based on transboundary reference," *Cotton Textile Technology*, vol. 49, no. 597, 2021.

[5] X. Hu, "Usability evaluation of E-Dunhuang cultural heritage digital library," *Data and Information Management*, vol. 2, no. 2, pp. 57–69, 2018.

[6] N. Ibrahim and N. M. Ali, "A conceptual framework for designing virtual heritage environment for cultural learning," *Journal on Computing and Cultural Heritage*, vol. 11, no. 2, pp. 1–27, 2018.

[7] H. Kuang and J. Wu, "Survey of image semantic segmentation based on deep learning," *Computer Engineering and Applications*, vol. 55, no. 19, pp. 12–21, 2019.

[8] C. Li, *Du Jinsheng Brocade*, Donghua University Press, Shanghai, China, 2009.

[9] G. Li, *The Silk King Du Jinsheng*, Tianjin People's Publishing House, Tianjin, China, 2011.

[10] S. Li and Z. Wang, "Mural art in the context of new media: a new "crossover" of mural art driven by artificial intelligence," in *Proceedings of the 2nd International Conference on Language, Art and Cultural Exchange (ICLACE 2021)*, pp. 530–533, Atlantis Press, Dali, China, January 2021.

[11] K. Liu, *The Flower of Oriental Art—The Art of Du Jinsheng Brocade*, Hangzhou Normal University, Zhejiang, China, 2011.

[12] X. Liu, "Artistic reflection on artificial intelligence digital painting," *Journal of Physics: Conference Series. IOP Publishing*, vol. 1648, no. 3, Article ID 032125, 2020.

[13] J. Long, E. Shelhamer, and T. Darrell, "Fully convolutional net-works for semantic segmentation," in *Proceedings of the IEEE Conference on Computer Vision and Pattern RecoRuiriou*, pp. 3431–3440, Boston, MA, USA, June 2015.

[14] C. Lv, *Hangzhou Time-Honored Brand*, Hangzhou Publishing House, Hangzhou, China, 1998.

[15] S. Minaee, Y. Y. Boykov, F. Porikli, A. Plaza, N. Kehtarnavaz, and D. Terzopoulos, "Image segmentation using deep learning: a survey," *IEEE Transactions on Pattern Analysis and Machine Intelligence*, 2021.

[16] R. Pierdicca, M. Paolanti, F. Matrone et al., "Point cloud semantic segmentation using a deep learning framework for cultural heritage," *Remote Sensing*, vol. 12, no. 6, p. 1005, 2020.

[17] F. G. Rivera, E. Brolin, A. Syberfeldt, D. Högberg, A. Iriondo, and E. P. Luque, "Using virtual reality and smart textiles to assess the design of workstations," in *Proceedings of the SPS2020: Swedish Production Symposium*, vol. 13, p. 145, IOS Press, Jönköping, Sweden, October 2020.

[18] J. Tan, L. Shao, N. Y. K. Lam, A. Toomey, and L. Ge, "Intelligent textiles: designing a gesture-controlled illuminated textile based on computer vision," *Textile Research Journal*, 2021.

[19] S.-K. Tan, H.-H. Lim, S.-H. Tan, and Y.-S. Kok, "A cultural creativity framework for the sustainability of intangible cultural heritage," *Journal of Hospitality & Tourism Research*, vol. 44, no. 3, pp. 439–471, 2020.

[20] S.-K. Tan, S.-H. Tan, Y.-S. Kok, and S.-W. Choon, "Sense of place and sustainability of intangible cultural heritage - the case of George Town and Melaka," *Tourism Management*, vol. 67, pp. 376–387, 2018.

[21] C. Wang, *Research on Infrared Image Semantic Segmentation Technology Based on Deep learning*, University of Chinese Academy of Sciences (Shanghai Institute of Technical Physics, Chinese Academy of Sciences), Shanghai, China, 2017.

[22] West Lake Expo Ed, "West lake expo daily," 1929.

[23] Y. Xiao and J. Hu, "The inheritance and spreading of confucianism in modern China and South Korea," in *Proceedings of the 2019 5th International Conference on Social Science and Higher Education (ICSSHE 2019)*, pp. 1061–1064, Atlantis Press, Xiamen, China, January 2019.

[24] S. Yanagi, *Handicraft Culture*, Guangxi Normal University Press, Guangxi, China, 2006.

[25] M. Yuan, H. Huang, and C. Zhou, "Research progress of image semantic segmentation based on fully supervised learning," *Computer Engineering and Applications*, vol. 57, no. 4, pp. 43–54, 2021.

[26] N. Yun, "Research on manufacturing technology and cultural connotation of guangxi rongshui miao brocade strap," *Journal of Sociology and Ethnology*, vol. 3, no. 1, pp. 18–22, 2021.

[27] D. Zhang, *Zhang Daoyi's Comments on Folk Arts*, Shandong Fine Arts Publishing House, Shandong, China, 2008.

[28] J. Zhu, *The History of Du Jinsheng Brocade*, p. 36, China Social Sciences Publishing House, Beijing, China, 2014.

[29] W. Zhang, J. Pang, K. Chen, and C. C Loy, "K-net: towards unified image segmentation," *Advances in Neural Information Processing Systems*, p. 34, 2021, https://arxiv.org/abs/2106.14855.

Hindawi
Scientific Programming
Volume 2022, Article ID 6825228, 9 pages
https://doi.org/10.1155/2022/6825228

Research Article

Artificial Intelligence as a Service for Immoral Content Detection and Eradication

Fadia Shah,[1] Aamir Anwar,[2] Ijaz ul haq,[3] Hussain AlSalman,[4] Saddam Hussain,[5] and Suheer Al-Hadhrami[6]

[1]*Department of Computer Science, Shaheed Zulfiqar Ali Bhutto Institute of Science and Technology, Islamabad, Pakistan*
[2]*School of Computing and Engineering, University of West London, London W5 5RF, UK*
[3]*Faculty of Education, Psychology and Social Work, University of Lleida, Lleida 25003, Spain*
[4]*Department of Computer Science, College of Computer and Information Sciences, King Saud University, Riyadh 11543, Saudi Arabia*
[5]*School of Digital Science, Universiti Brunei Darussalam, Jalan Tungku Link, Gadong BE1410, Brunei Darussalam*
[6]*Computer Engineering Department, Engineering College, Hadhramout University, Hadhramout, Yemen*

Correspondence should be addressed to Saddam Hussain; saddamicup1993@gmail.com and Suheer Al-Hadhrami; s.alhadhrami1@gmail.com

Received 19 November 2021; Accepted 27 December 2021; Published 17 January 2022

Academic Editor: Punit Gupta

Social media is referred to as active global media because of its seamless binding thanks to COVID-19. Connecting software such as Facebook, Twitter, WhatsApp, WeChat, and others come with a variety of capabilities. They are well-known for their low-cost, quick, and effective communication. Because of the seclusion and travel constraints caused by COVID-19, concerns, such as low physical involvement in many possible activities, have arisen. Depending on their information, knowledge, nature, experience, and way of behavior, various types of human beings have diverse responses to any scenario. As the number of net subscribers grows, inappropriate material has become a major concern. The world's most prestigious and trustworthy organizations are keenly interested in conducting practical research in this field. The research contributes to using Artificial Intelligence (AI) as a service (AIaaS) for preventing the spread of immoral content. As software as a service (SaaS) and infrastructure as a service (IaaS), AIaaS for immoral content detection and eradication can use effective cloud computing models to leverage this service. It is highly adaptable and dynamic. AIaaS-based immoral content detection is mostly effective for optimizing the outcomes based on big data training data samples. Immoral content is identified for semantic and sentiment evaluation, and content is divided into immoral, cyberbullying, and dislike components. The suggested paper's main issue is the polarity of immoral content that can be processed using an AI-based optimization approach to control content proliferation. To finish the class and statistical analysis, support vector machine (SVM), selection tree, and Naive Bayes classifiers are employed.

1. Introduction

Connecting various people, the Internet has no longer most effectively aided the folks around the arena, ultimately, a huge extent of users can specify their perspectives. It is not acquainted as a city village by way of [1] insisted that despite the range of software applications have their procedures, nevertheless, the public voice is heard to share their views. Shah [2] mentioned big variations in lives. There are various factors, and COVID-19 has remote human beings from social lifestyles. Plentiful people are distantly related to society. COVID-19 has badly reshaped the lives of people, and now, nearly every research-based domain is actively exploring its consequences by various means. Shan [3] referred that this has made humans specific to their opinions on the Internet because the most effective manner for growth is to be truly mingled. The most popular social media platforms are YouTube, Facebook, TikTok, Twitter, etc.

Omar et al. [4] found that community-based software utilities encompass famous systems like Table 1 suggests the number of users improved in any type of social network from the last decade. The contemporary research directs that billions of users are connected through social media organizations. Because of the pandemic, the users prefer the Internet to live participation. Huynh [5] elaborated that the number of customers is countlessly accelerated. Several platforms are providing their specialized services to communiqué because physical presence is not obligatory. Furthermore, because of the hurdles of personal participation, the priority of human beings is the Internet because of its availability, easiness, and fast response. However, it is sometimes a problem to find the relevant information from the results provided by the Internet.

Another problem of these social platforms is that the use of these remote platforms is not always productive. Always, a certain group of people is responsible for creating trouble, humiliating, and wasting others' time. It is mentioned by researchers like [6] who elaborated that using these platforms creates troubles for a large number of users. Because of the community boom, this most probably these boards. The problem is crucial since it is now feasible for users to avail the message delivery to the rest of the users after simply signing into the system. The person who is a consumer of the software product can attain the attention of the other users by initiating a hot topic and involving several users. The comments can be used in two ways; constructively for the learning and problem-solving mode; or the manipulated and exaggerated theme by involving comments like racism, extremism, political dispute, or specific objectives.

The researchers like [7–9] are those examples, including [10] quantified linguistic behavior o the communication method. The techniques of effective communication are verbal exchange and nonverbal communication. If the primary purpose is met, the communication is effective. The receiver understands exactly what the sender wants to say. While verbal communication is not always effective, it indicates that the sender is saying something the receiver does not understand. As virtual communication lacks physical engagement, there is a lack of body language, such as the tone of voice, eye contact, and others, which can lead to misleading impressions. Hu [11] said that this false impression creates conflicts. Because of this, aggressive and abusive language initiates. Even though there are various elements worried. It includes a lack of records, and the distinction makes it hard enough to make it understand. It creates doubts and many other problems. When an individual wants to win the comment, the individual can go up to any level of exchange of comments. Those are the types of individuals who do not hesitate to harass others. Often, the annoyed candidates annoy others with their remarks, scripts, and responses on shared media.

The further study is consistent with that of the academician [12]. Harassment is identified by offensive stated material. Mankind's isolation is more usually found in

Table 1: Increase in the number of people using social media each year.

year	Users in millions
2010	95
2011	120
2013	148
2015	210
2017	245
2019	280
2020	294
2021	326

immoral stuff, which is a serious problem. It is increasing daily. Immoral content is produced by a specific group of individuals. It includes a common mentality from a specific period, gender, reputation, education, and religion. It is a problem that a large number of clients on social media are dealing with. Almost every social structure provides some sort of venue for recording or avoiding immoral content [13]. Reporting this person may result in a warning or, in the worst-case scenario, a permanent ban. Toxic information can be quite hazardous to even the most innocent minds.

The big populace browsing the net has a variety of kids who are new to the worldwide village. They are studying and making their minds apprehensive of the sector. A few researchers [14] are still looking into the content, while a few girls are housewives who spend their leisure time working on websites. The Immoral depend is being managed by social media web-based systems in a completely professional manner. There is a unique mechanism in place to deal with this type of information. The assessment committee and the concerned personnel are constantly on the lookout for complaints and inquiries. The pathetic content displayed on the Internet can be refined using an information technology architecture.

Oppressive language character is not just about as basic as a lump of cake. Sorting out exploitative substance material is a difficult task, especially when it needs to be extracted from large data. Oppressive language is of several kinds. The sentence structure is made up of a variety of expressions. The character of hazardous words in this series surely necessitates a handful of particular strategies. Table 1 illustrates that the number of net clients is steadily increasing. With a larger population, there are more opportunities to obtain diverse measures.

Governmental concerns have been raised, and strategies are being explored in every impacted district around the world to develop new mechanisms to restore normalcy and control coronavirus. Because the Coronavirus has boosted web traffic, determining the text's sequence is crucial. The prevalence of web material can be spread, and false content can be eliminated. Savelev et al. [15] expressed with regards to quick data sharing and spread that the web is the main source to associate, and similar data is divided among different clients. Some of the time the worry isn't about unwavering quality, however, individuals share content unexpectedly to make their darlings update about the ongoing occurring. Boksova et al. [16] referenced that individuals are classified as web clients and nonclients.

Gao et al. [17] made an intensive report on assessment investigation and the utilization of online media content. Social substance investigation is prevalently broken down by opinion examination. The different strategies of opinion examination are utilized, including deceptive substances. There are various methods, such as determining the uniqueness of senders, messages, and recipients. Krzewniak [18] reported that web-based clients have access to all data on the Internet, however, this might put the information of clients in grave danger. There has been research on how scientists have used information mining processes to characterize data in the past. Rule-based frameworks, solo learning procedures, administered learning strategies, and other well-known ways are examples of this dynamic. As shown in Table 1, the number of informal community clients is increasing every year. Gianfredi et al. [19] Table 2 shows the most well-known exercises [20] and the level to which they were carried out by individuals in the global information media status report.

The table above shows how frequently people use Internet hotspots for various activities in their daily lives. The web is considered the backbone by the majority of the dynamic. Considering these characteristics to be of top priority, the suggested research paper identifies two common issues. The first is the assurance of deceptive content from online media (utilizing AI classifiers). The subsequent issue is the assignment of classifications to untrustworthy substances based on their power degree, including simulated intelligence, to the point where the most dreadful class should be acknowledged for special arrangements.

The plausibility of the review is that the web cannot separate the moral and exploitative substance. The valid and bogus assertions cannot be recognized. [21] If questionable data is halted to engender and its ubiquity can be diminished, there are opportunities to guarantee the web is dependable. Likewise, there are opportunities to decrease the consuming circumstance and lead the course toward the quiet circumstance as the consistently famous substance is not a dependable substance as well. Man-made intelligence is so stretched out in different applications that now it is not only utilized for consistent programming but also as a policymaker and a device. Shrewd frameworks (K. Ghosh, 2019) for web-based media are fundamental these days for quality assistance arrangement.

2. Related Work

The major purpose of the research is to create text-mining algorithms for detecting immoral content on social networking sites [22]. Elareshi et al. [23] have discussed and evaluated several areas of aspect mining using text in depth. Text mining is the process of analyzing content using a variety of machine learning algorithms established by experts [24]. Supervised learning, unsupervised learning, rule-based learning, pattern-based learning, and so on are common learning methodologies. As a result, there are three categories of literature on this subject.

Table 2: Proportion of Internet users activities.

Sr. No	Utility	Proportion
1	In contact with friends/Family	48.6
2	Spare time usage	36.3
3	News updates	35.2
4	Entertainment	30.9
5	Information in the air	29.3
6	Products browsing	26.1
7	Opinion sharing	24.9
8	Live stream watch	23.7
9	Make new contacts	23.6
10	Content browsing from favorite brands	22.9
11	Work-related networking and research	22.7
12	Finding communities and interests	22
13	Favorite sports	21.1
14	Celebrities & stuff	20.7

2.1. Artificial Intelligence as a Service (AIaaS). Artificial intelligence is a concept that refers to the scientific studies and practices aimed at improving the efficiency with which robots make decisions. The term “intelligence” encompasses a wide range of concepts. It includes factors, such as addressing the problem in a short amount of time, solving the problem correctly, providing the best answer, and so on, according to the experts [25]. Computers are used to efficiently solve complex problems. Machine learning, with or without the assistance of a person, strives to solve issues using computations and create proper outcomes (Jiwon Kang). Several machine learning techniques exist that combine great computational capabilities with low computing expenses. Li et al. [26] reported that supervised, unsupervised, and reinforcement learning are among the machine learning approaches employed. Shah and Li [27] AI’s effects on jobs and society [25] management and strategic challenges associated with AI [25]. They all use different approaches, however, the end goal is the same: to find the most effective solution. AI is utilized as a third party because it strives to deliver better/improved reasoning. The computed results are employed as a third party, and the data is communicated and evaluated using these results in many research and technology domains. Machine learning and artificial intelligence are employed in a variety of platforms. It is for this reason that it is known as third-party evaluation. Artificial intelligence and machine learning have a big impact on information and communication systems in general. The machine is being programmed to calculate the solution automatically.

As a result, the ideal solution is not only quick but also offers precise results. The year Takeuchi and Yamamoto [28]. The more capable a system is of delivering accurate results, the more it is called a smart system [29]. It also offers the capability of halting processing in the event of an error or autonomously rectifying processing before output without contacting an external entity. The term “agents” is used to refer to intelligent systems. Agent decision-making has been a prominent issue in research for years, and now it can be used as a service to run a variety of systems.

Several analysts [30] devised various ways to incorporate AI into their projects to improve the quality and efficiency of their work. Real-time frameworks are those that initiate their actions at a specific interval or timeframe. Social media content is derived from a variety of sources. The majority of the design is built on a dispersed framework layout. The cloud underpins all-encompassing interfacing of workstations in various regions, linked through organized topologies, and ensures error-free data transfer. Such systems are well-prepared so that sending data from one source to a few kilometers away arranged recipient takes only a few seconds.

The Internet of Things (IoT) is a connected example of a socially connected distributed system. Gianfredi et al. [19] articulated around the data generated by a variety of devices and disseminated through social media applications. Because Yang et al. [31] is like mimicking human insights in information translation and applying a clever decision-making framework, it can be used as a supplement to circumvent social media's forceful content. An intelligent degree for social media substance isn't too brutal rough substance; rather, there should be distinguishing proof of brutal substance and destruction of that smudged stuff some time lately increasing it to various systems. Here, we use AIaaS for immoral content detection and eradication can use effective cloud computing models to leverage this service. It is highly adaptable and dynamic. AIaaS-based immoral content detection is mostly effective for optimizing the outcomes based on big data training data samples.

2.2. Machine Learning. Text mining techniques, which are applied under the platform of machine learning techniques, help identify immoral content material. Machine mastery for medically-linked textual material polarity is also based on strategies that are a systematic manner to apply some algorithms by teaching a computer to decide for itself.

Unsupervised, supervised, and reinforcement learning is used to apply machine learning-based text mining strategies. In addition to labeled datasets, the supervised learning-based skilled models [32] emphasized text mining in the biomedical dataset. The impacts already understood are included in the supervised learning of facts. The outcomes are evaluated using a supervised learning-based approach model. The data set was used for prediction by using a support vector machine (SVM) decision tree.

His ideality was a topic for churn, and he developed a neural network for audience-related literary material with the help of [33]. However, the findings of a survey-based dataset linear regression, which are well-known supervised researching approaches for determining immoral text, have been spectacular. The goal of this study is to use supervised learning to identify the outcomes from the data.

The application of supervised learning to understand the use of the SVM algorithm was originally done by [34]. It was previously multilingual and employed seven languages, as well as a variety of bootstrap sentiment analysis methodologies.

Once, a progressive B4MSA polarity classification was utilized. Forman, et al. [35] and Heri [36] introduced a the detection of negative consequences of publicly publishing humiliating content material on social media. Other multilingual sentiment assessment models employed were SENTIPOLC′14, SemEval'15–16, and TASS′15. It determined the harshness and disrespectfulness of the words. For classification-based tasks, the results were environmentally favorable.

2.3. Big Data, A Source of Unethical Content. Social media platforms are the sources of revenue gains for various regions. Various small and medium financial industries are now applying technology as a mandatory component of their procedures. Shan et al. [37] emphasized the vitality of platforms for data reforms for the future growth of a region. The increase in data during the last decade is increasing, however, the pandemic since 2019 has isolated the social activities of mankind. Technically, domestic isolation has raised behavioral complications. The vitality of the content generated during a pandemic is more polluted with the combination of less ethical and more unethical statements. People found no other way to communicate, For online social networking applications, where it is recommended to proceed with all the activities while staying at home, people have no alternative ways to establish social networking activities [38]. Only the online social media platforms facilitate them to meet new people virtually. Platforms such as Twitter, Facebook, Netflix, Yahoo, Whatsapp, Wechat, and similar applications can help one to find new people and discuss his ideas fearlessly.

Another research by [39] illustrated the sufferings raised because of more use of gadgets, especially by the youngsters. Big data is saturated with more impact of poor communication, inappropriate words, lack of belief, and particularly, it is saturated with the impact of cyberbullying impression. He used the classification approach for unethical text determination. Most of the platforms justify there are more proportions of immoral content. The proposed study emphasizes more on Twitter data set because of its diversity in the same domain, availability, and rapid user interactions.

2.4. Datasets. The dataset is made of Twitter, Kaggle, and survey-based information. There was no uniformity in the columns, information format, or aesthetic style because the data was acquired from a variety of sources. Although this unstructured data had previously been in text format, it was no longer appropriate for the next stage of processing. To advance to the next level, the authors converted heterogeneous data into homogeneous data with a standardized form. Twitter also offers an API (Twitter Stream API) that may be used to retrieve data from the website, such as tweets, comments, and likes, but only with authentication.

In social networks, the detection of abusive content, cyberbullying, and harassment is typically framed as a classification problem. The homogeneity of the data set was not the only concern. There was also the issue of multiclass imbalanced datasets, which resulted in a varied distribution of situations into instances.

Using the approach of oversampling, the problem was attempted to be minimized up to the lowest stage. Rapidminer is used to process the records to simulate models quickly and accurately.

2.5. Model. The primary goal of the proposed study is to determine which records contain immoral content. The aggregated records have been reduced to a set of documents containing 13,000 tuples and seven features. AI's utility is machine learning. After consolidation, the factual units were in a homogeneous state. This data was once sophisticated enough to be used as input in the mannequin. The flowchart of the AIaaS-based model for immoral content detection and eradication is shown in Figure 1.

The figure indicates there are two sections of the proposed system. The top approach of the flow chart shows the processing of data from the initial stage till the identification of unethical content. The process continues for the entire data chunks. It is sure that if the data set is big enough, the methodology is applicable for the data segments until the entire data is examined. The results are stored and the same logic is applied as service-based architecture. It can be possibly achieved for cloud architecture. The dedicated unethical content identification cache can encounter the text with segmentwise results calculation until the condition is stable. Both types, i.e., semantic and sentiment analysis, are possible in the above model.

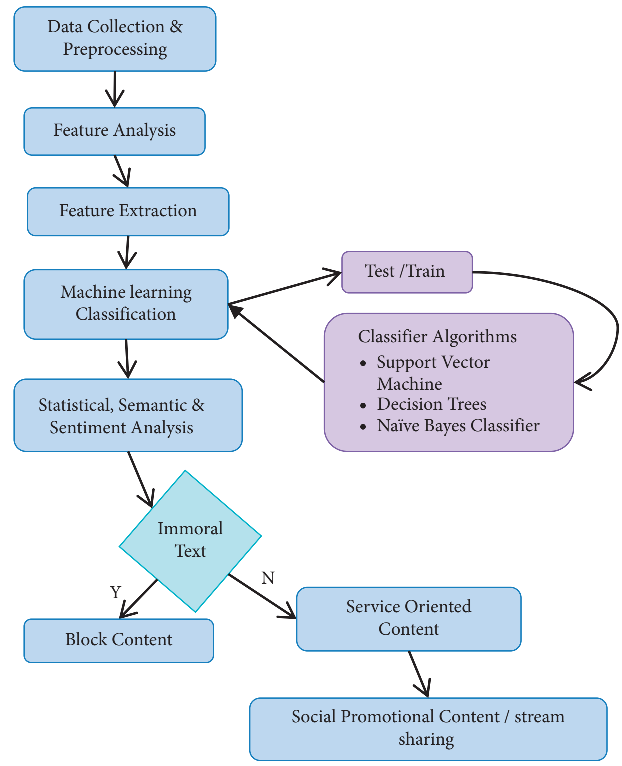

Figure 1: A flowchart of AIaaS-based model for immoral content detection and eradication.

2.6. Data Preprocessing. The preprocessing of records is the initial stage in the suggested paradigm. The facts collection is heterogeneous with little homogeneity and a large number of information elements. The preprocessing of facts is usually the first stage for each mannequin. It is utilized to turn it into a more homogeneous state. The information that has resulted is now of high quality. Data preparation is required to remove noise from the data and to improve the accuracy of the effects purchased once purified records have been utilized for mannequin training.

There were numerous abnormalities in our dataset, including incomplete records with missing values, incorrect values, and special data sorts for a variety of attributes. The information gathered from a variety of sources was also incorrect. It is critical not to remove any useful information from the content while preparing the data. Anomalies were present in the data sets used in our research.

It is important that often preprocessing and data cleansing deletes the missing and abnormal or incorrect values. However, in the proposed study, preprocessing is applied to the data items that contain minimum null values. The missing values were replaced with the most possible/nearly estimating possible values. The impure data was found to be approximately 0.002%, which is quite less in proportion. The problem of overfitting and underfitting were carefully observed so that the data quality should be consistent. The data after preprocessing is quality-oriented.

2.7. Opinion Mining NLP. The data set is ideal for linguistic research. The discoveries that are reached following the information analysis are referred to as features. The two most important types of features are determined in this study. The facts are a collection of social behavior statistics. In this study, two categories of points are specifically examined. Sentiment points and semantic characteristics are what they are called. In the model for detecting abusive language, feature extraction is crucial. These considerations will aid in the detection of abusive phrases and context-based abuse. Preprocessed data aids in the extraction of particular elements, such as sentiment features, semantic features, unigram features, and pattern features, to detect abuse and subtypes, such as aggression, dislike, misbehavior, cyberbullying, and vulgar language in the material. The sentiment feature determines whether a tweet or remark has a sentiment thing, whereas the semantic feature aids in the detection of contextual base abuse by the usage of a specific letter, symbol, or word in the tweet.

2.7.1. Semantic Analysis. Semantic analysis is used to determine the relationship between the sentences. It can distinguish the sentence's class. It is the type of sentence that is employed in the sentence. It can distinguish the sentence's class. It is the type of sentence that is employed in the sentence which means the clear theme of the context is expressed in terms of semantic analysis [40]. Particularly, it is the comment on the expression's context. The planned research also assesses whether the statement is straightforward or contains some hidden meaning. In semantic analysis, the selection of words and closures is critical. It is used for approximation analysis in machine learning. The theme of predicate information analysis is used to complete it. The proposition is a collection of predicates and quantifiers. These assertions are used to complete a sentence's structure. A minimum of one item of information should be included in each proposal. They result in variables, which are then utilized to form a variety of functions that provide useful data to the systems. When analyzing a sentence for semantic analysis, the same common sense is employed. In semantic analysis, letters, symbols, and quantifiers are used.

2.7.2. Sentiment Analysis. Another feature is sentiment evaluation, which is the determination of the sentence's polarity. It is utilized for opinion mining, with the ability to look at things in three ways: positively, negatively, or neutrally. It can tell whether the text is polarised in a very positive, positive, neutral, negative, or extremely poor way. Doaa Mohey El-Din Mohamed Hussein, 2021 identified issues in analyzing social media content (Shambhavi Dinakar). The texts utilized for sentiment analysis include a variety of languages (Rastislav Krchnavy) and negative and slang phrases, hashtags, and emoticons (Dr.Pappu Rajan). A lot of lookup scholars have extended this kind of view for herbal language processing. Microblog textual content analysis (Fotis Aisopos).

Table 3 states that out of 4458 tuples of datasets 1,2 and three The category of kind of content is decided by sentiment and semantic analysis. Hence, the classification of subcategories is made viable to in addition follow the model.

2.8. Feature Extraction. The facts set consisted of 12 features. The computation was once processed by way of using.

The key function of function extraction is to determine the most influential features that take part in result generation. In the chosen information set, the aspects that conclude their content as immoral, cyberbullying, or dislike text were text, content, category, and …… Particularly, the reachable information units have awesome facets called textual content and effects as two foremost chosen facts.

2.9. Optimization and Training. This section includes the model optimization and training for the dataset so that the results could be precise and valid.

2.10. Classification. Additionally, divide the dataset into a teach or look at dataset to train a model for detecting abusive language. As the mannequin is trained using a 70% dataset, the records set is partitioned into the educated and check-facts sets. The proposed lookup is classified using the supervised computer to get to know the method [41]. The ramifications of the statistics units are already recognized in this case. The ability to classify data is such that the results of trained statistics sets can be compared to the outcomes of checking out records.

Table 3: Opinion mining classification.

	Semantic data	Sentiment data	Total
Data set 1	2517	1941	4458
Data set 2	1375	1433	2808
Data set 3	1341	2307	3648
Tuples	5233	5681	10,914

There are a variety of classifiers [42]. Classification techniques are even important on encrypted data [43] and [44]. The accuracy measurement determines the overall performance of the mannequin. The three classes that are the consequence of categorization are immoral, cyberbullying, and hatred [45]. The classification process is divided into three stages. The classification is done by three classes. It incorporates binary classification, which divides the records into two categories. The outcome of binary categorization distinguishes the two major groups. Binary categorization has the advantage of displaying the straightforward distribution of statistics into two main groupings.

Ternary classification is the next step after categorizing the statistics into binary labeled results. As the proposed study identifies three classes, namely immoral, cyberbullying, and dislike, the tertiary classification is used. The research completes its classification, however, if it needs to be extended to more than three classes, a multivalued classification is used.

The three most common and popular classifiers used in this study were Naive Bayes, SVM, and Decision Tree, which were used to divide the content material into categories, such as aggression, misbehaving, dislike, cyberbullying, vulgar message, and ordinary. In Table 4, the categorization consequences are discussed. The commonplace class represents natural language. If a tweet or remark is not harsh, it will be listed here. By modifying these factors, the optimal parameter will help improve the overall performance of classifiers. The accuracy of each classifier will be displayed one by one for each class in the result. This accuracy will exhibit how precisely to discover the abusive language from the content. The exponential growth of big data might increase the chance of abusive and unethical content compared to ethical content [46]. The proportion of neutral content is much less than the other components. Thus, there are more aspects the people behave unethically over the Internet. It may be because of reasons, such as their identity being unknown and them being remotely available, or concerns, such as they can approach various platforms free of cost and they have freedom of speech. However, there are more traces of nonvaluable text.

3. Result and Discussion

The binary classification process produces two main lessons and has a 91.2 percent accuracy rate. The third category is considered neutral. Hence, if one runs the classification model on these three instructions, one gets an accuracy of 85.70%.

Table 5 indicates the accuracy of the proposed approach. It means the identification of unethical content via machine

Table 4: Sentiment analysis classification.

	Immoral	Dislike	Cyberbullying	Neutral	Total
Data set 1	1257	1327	794	1080	4458
Data set 2	736	1434	43	595	2808
Data set 3	1454	1324	462	408	3648
Tuples	3462	3354	2965	1133	10,914

Table 5: Social dataclassification

	Sentiment analysis			Semantic analysis		
	Precision	Recall	F1 score	Precision	Recall	F1 score
Immoral	0.57	0.32	0.46	0.42	0.71	0.46
Cyberbullying	0.43	0.41	0.53	0.43	0.12	0.36
Dislike	0.41	0.31	0.41	0.44	0.31	0.32

learning algorithms is promising, particularly for the datasets that are of larger size. The sentiment analysis and semantic analysis evaluations provide noticeable results. This approach can be applied for the larger data sets by selecting the segments of huge chunks of data, and the repetition of the process at various intervals can be deterministic for the data available.

3.1. Content Oriented AI as a Service. After passing through the model's elements, the outcomes disclose three key parameters. The statistical output is once again used as a source for hospitality analysis [47]. From banking transactions [48]. For content show processing, the impacts obtained after sentiment and semantic analysis are critical. Instead of displaying before the readers, items that are more infected with traces of immoral, cyberbullying, and dislike classes with high accuracy (meaning are more corrupt) can be prevented. Low-accuracy communications may provide a risk of displaying content material on the Internet. The most situation column in Table 1 has a high F1 score. In any event, the recall, precision, and F1 rating factors would no longer be prioritized.

3.2. AI Influencial Content Control. The content material with excellent polarity is ideal for displaying in front of the reviewers. Negative polarity and a poor F1 score are the examples of material with negative impact. Alternatively, if the content material is displayed, it may harm the users. After the model has been applied, the cumulative results can be separated into different labels and the time stamp can be lowered. If the content is very obnoxious, it may be prohibited at an early stage. The dreadful effect can be mitigated in this way. This method is ideal for websites that have a great reputation and only provide excellent service. These social media platforms are often at high popularity.

4. Conclusion

The suggested investigation is completed to find and remove immoral content from social media networks. Misbehaving, cyberbullying, and use of immoral language; in the statement is unethical content. Textual content mining is done using a supervised learning approach. To obtain reliable results, firstly, unethical content identification is done. Then, based on these results, the content containing illegal text can be prevented. The use of a multiclass imbalanced dataset is refined with resampling, undersampling, and oversampling techniques. Then, sentiment and semantic analysis methods are applied to find the severity of immoral content. Decision Tree, SVM, and NaveBayes are used for classification. The content polarity and unethical sensitivity are determined. The negative content is limited to the social media display. The feasibility of this study is extremely important for better text-based component decision-making. New policies pushed decision-making, social content delivery, and display, as well as the permissibility and prohibition of ethical writing on reputable and genuine websites. The proposed study's social advantages are measured in terms of the amount of content that can be exhibited, regional characteristics from the community, and many more.

Data Availability

The data used to support the findings of this study are available from the corresponding author upon request.

Conflicts of Interest

There are no conflicts of interest associated with publishing this paper.

Acknowledgments

This research was supported by the Researchers Supporting Project number (RSP-2021/244), King Saud University, Riyadh, Saudi Arabia.

References

[1] C. Forman and N. van Zeebroeck, "Digital technology adoption and knowledge flows within firms: can the Internet overcome geographic and technological distance?" *Research Policy*, vol. 48, no. 8, p. 103697, 2019.

[2] N. Shah, "From global village to global marketplace: metaphorical descriptions of the global Internet," *International Journal of Media and Cultural Politics*, vol. 4, no. 1, pp. 9–26, 2008.

[3] Y. Shah, Y. Liu, Y. Liu, F. Shah, and F. Shah, "Challenges of small- and medium-sized businesses in Pakistan due to COVID-19 pandemic," *R-ECONOMY*, vol. 6, no. 3, pp. 222–226, 2020.

[4] H. Omar, S. Haggag, J. Grundy, and M. Abdelrazek, "COVID-19 vs social media apps: does privacy really matter," in *Proceedings of the 2021 IEEE/ACM 43rd International Conference on Software Engineering: Software Engineering in Society (ICSE-SEIS) 2021*, IEEE, Madrid, ES, May 2021.

[5] G. T. T. Huynh, N. T. B. Chung, and T. T. Phung, "How to purchase an order from brick and mortar retailers during COVID-19 pandemic? A rise of crowdshipping," *International Journal of Data and Network Science*, pp. 439–450, 2021.

[6] M. Han, X. Y. Tan, R. Lee, J. K. Lee, and R. Mahendran, "Impact of social media on health-related outcomes among

older adults in Singapore: qualitative study," *JMIR Aging*, vol. 4, no. 1, p. e23826, Article ID e23826, 2021.
[7] P. Walaski, "Social media: powerful tools for SH&E professionals," *OnePetro*, pp. 40–49, 2013.
[8] Y. Katz, "Social media is powerful, but can it change policies of institutionalized organizations such as the Israeli army?" *International Journal of Humanities and Social Sciences*, vol. 6, no. 6, pp. 29–34, 2017.
[9] D. R. Admane, "**Social media powerful way to bring positivity during the covid-19 pandemic**," *Social media during covid-19 pandemic*, vol. 8, no. 1s, 2021.
[10] D. G. Taylor, "Putting the "self" in selfies: how narcissism, envy and self-promotion motivate sharing of travel photos through social media," *Journal of Travel & Tourism Marketing*, vol. 37, no. 1, pp. 64–77, 2020.
[11] W. Hu, "Innovative university subject teaching mode under the information technology environment," *Panyapiwt international conference on social sciences and management*, vol. 81, pp. 571–578, 2020.
[12] N. Peimani and H. Kamalipour, "Online education and the COVID-19 outbreak: a case study of online teaching during lockdown," *Education Sciences*, vol. 11, no. 2, p. 72, 2021.
[13] F. Shah, J. Li, J. D. Khan, F. Shah, and Y. Shah, "Hybrid compression for medical big data," *ICCWAMTIP*, vol. 2018, 2018.
[14] S. Raj Sangwan et al., "D-BullyRumbler: a safety rumble strip to resolve online denigration bullying using a hybrid filter-wrapper approach," *Multimedia Systems*, 2021.
[15] A. O. Savelev, A. Y. Karpova, D. V. Chaykovskiy et al., "The high-level overview of social media content search engine," *IOP Conference Series: Materials Science and Engineering*, vol. 1019, no. 1, p. 012097, Article ID 12097, 2021.
[16] J. Boksova, M. Bokša, J. Horák, K. Pavlica, J. Strouhal, and S. Saroch, "E-government services and the digital divide," *Journal of Telecommunications and the Digital Economy*, vol. 9, no. 1, pp. 27–49, 2021.
[17] Z. Gao, S. Fujita, N. Shimizu et al., "Measuring public concern about COVID-19 in Japanese internet users through search queries: infodemiological study measuring public concern about COVID-19 in Japanese," *Internet Users Through Search Queries: Infodemiological Study*, vol. 7, no. 7, Article ID e29865, 2021.
[18] D. Krzewniak, "Selected elements of the internet users' information security culture," *Roczniki Nauk Społecznych*, vol. 13(49), no. 2, pp. 121–140, 2021.
[19] V. Gianfredi, S. Provenzano, and O. E. Santangelo, "What can internet users' behaviours reveal about the mental health impacts of the COVID-19 pandemic? A systematic review," *Public Health*, vol. 198, pp. 44–52, 2021.
[20] B. Carlson, "Indigenous internet users: learning to trust ourselves," *Australian Feminist Studies*, vol. 36, no. 107, pp. 9–25, 2021.
[21] Y. Song, K. H. Kwon, Y. Lu, Y. Fan, and B. Li, "The "parallel pandemic" in the context of China: the spread of rumors and rumor-corrections during COVID-19 in Chinese social media," *American Behavioral Scientist*, vol. 65, no. 14, pp. 2014–2036, 2021.
[22] S. Chen, X. Guo, T. Wu, and X. Ju, "Exploring the online doctor-patient interaction on patient satisfaction based on text mining and empirical analysis," *Information Processing & Management*, vol. 57, no. 5, p. 102253, Article ID 102253, 2020.
[23] M. Elareshi, A.-K. Ziani, and A. Al Shami, "Deep learning analysis of social media content used by Bahraini women: WhatsApp in focus," *Convergence: The International Journal of Research Into New Media Technologies*, vol. 27, no. 2, pp. 472–490, 2020.
[24] D. Antons, E. Grünwald, P. Cichy, and T. O. Salge, "The application of text mining methods in innovation research: current state, evolution patterns, and development priorities," *R & D Management*, vol. 50, no. 3, pp. 329–351, 2020.
[25] M.-H. Huang and R. T. Rust, "A strategic framework for artificial intelligence in marketing," *Journal of the Academy of Marketing Science*, vol. 49, no. 1, pp. 30–50, 2021.
[26] M. Li, D. Yin, H. Qiu, and B. Bai, "A systematic review of AI technology-based service encounters: implications for hospitality and tourism operations," *International Journal of Hospitality Management*, vol. 95, p. 102930, 2021.
[27] F. Shah and J. P. Li, "Broad big data domain," in *Proceedings of the 2017 4th International Conference on Systems and Informatics (ICSAI)*, IEEE, Hangzhou, China, Nov. 2017.
[28] H. Takeuchi and S. Yamamoto, "Method for assessing the applicability of AI service systems," *Human Centred Intelligent Systems*, vol. 189, pp. 323–334, 2021.
[29] X. Lv, Y. Liu, J. Luo, Y. Liu, and C. Li, "Does a cute artificial intelligence assistant soften the blow? The impact of cuteness on customer tolerance of assistant service failure," *Annals of Tourism Research*, vol. 87, p. 103114, 2021.
[30] S. Robinson, C. Orsingher, L. Alkire et al., "Frontline encounters of the AI kind: an evolved service encounter framework," *Journal of Business Research*, vol. 116, pp. 366–376, 2020.
[31] Y. Yang, L. Li, and J. Jiang, "The impact of COVID-19 pandemic on emerging country stock markets: evidence of the value effect," *Emerging Markets Finance and Trade*, vol. 58, no. 1, pp. 70–81, 2021.
[32] U. Naseem, I. Razzak, M. Khushi, P. W. Eklund, and J. Kim, "COVIDSenti: a large-scale benchmark twitter data set for COVID-19 sentiment analysis," *IEEE Transactions on Computational Social Systems*, vol. 8, no. 4, pp. 1003–1015, 2021.
[33] J. Mell, S. Jang, and S. Chai, "Bridging temporal divides: temporal brokerage in global teams and individual performance," *Academy of Management Proceedings*, vol. 2020, no. 1, p. 13037, Article ID 13037, 2020.
[34] C. P. D. Cyril, J. R. Beulah, N. Subramani, P. Mohan, A. Harshavardhan, and D. Sivabalaselvamani, "An automated learning model for sentiment analysis and data classification of Twitter data using balanced CA-SVM," *Concurrent Engineering*, vol. 29, no. 4, pp. 386–395, 2021.
[35] C. Forman, A. Goldfarb, and S. Greenstein, "How did location affect adoption of the commercial Internet? Global village vs. urban leadership," *Journal of Urban Economics*, vol. 58, no. 3, pp. 389–420, 2005.
[36] H. Heri, E. D. Minarti, and L. Linda, "Mathematical difficulties of 7th grade MTs students analysis in online learning based on the realm bloom's taxonomy," *Journal of Medives: Journal of Mathematics Education IKIP Veteran Semarang*, vol. 5, no. 2, p. 201, 2021.
[37] F. Shah, fnm au, Y. Liu, Y. Shah, and F. Shah, "Influence of shareholder equity on trade credit demand: the study of non-financial firms in Pakistan," *R-Economy*, vol. 7, no. 1, pp. 61–67, 2021.
[38] P. Xhelili, E. Ibrahimi, E. Rruci, and K. Sheme, "Adaptation and perception of online learning during COVID-19 pandemic by Albanian university students," *International Journal on Studies in Education*, vol. 3, no. 2, pp. 103–111, 2021b.
[39] N. Radwan, *Big Data Ethics*, vol. 19, no. 1, 2021.

[40] X. Yang et al., “Frontline encounters of the AI kind: an evolved service encounter framework,” *Journal of Business Research*, vol. 116, pp. 366–376, 2020.

[41] O. FYFY, fnm au, A. JET et al., “Supervised machine learning algorithms: classification and comparison,” *International Journal of Computer Trends and Technology*, vol. 48, no. 3, pp. 128–138, 2021.

[42] S. B. Kotsiantis, I. D. Zaharakis, and P. E. Pintelas, “Machine learning: a review of classification and combining techniques,” *Artificial Intelligence Review*, vol. 26, no. 3, pp. 159–190, 2006.

[43] C. Buffington, J. Fields, and L. Foster, “Measuring the impact of COVID-19 on businesses and people: lessons from the census bureau’s experience,” *Aea papers and proceedings*, vol. 111, pp. 312–316, 2021.

[44] S. M. Weiss and I. Kapouleas, “An empirical comparison of pattern recognition, neural nets, and machine learning classification methods,” *Proceedings of the 11th international joint conference on Artificial intelligence*, vol. 1, 1989.

[45] D. Michie, D. J. Spiegelhalter, and C. Taylor, “Machine learning, neural and statistical classification,” *Does acute artificial intelligence assistant soften the blow? The impact of cuteness on customer tolerance of assistant service failure*, vol. 37, no. 4, 1994.

[46] Bo Pang, L. Lee, and S. Vaithyanathan, “Sentiment classification using machine learning techniques,” *Proceedings of EMNLP*, vol. 79, 2002.

[47] M. Mariani and M. Borghi, “Customers’ evaluation of mechanical artificial intelligence in hospitality services: a study using online reviews analytics,” *International Journal of Contemporary Hospitality Management*, vol. 33, no. 11, pp. 3956–3976, 2021.

[48] E. H. Manser Payne, A. J. Dahl, J. Peltier, and J. Peltier, “Digital servitization value co-creation framework for AI services: a research agenda for digital transformation in financial service ecosystems,” *The Journal of Research in Indian Medicine*, vol. 15, no. 2, pp. 200–222, 2021.

Hindawi
Scientific Programming
Volume 2022, Article ID 1092880, 5 pages
https://doi.org/10.1155/2022/1092880

Research Article

Study on the High Accuracy and Fast Acquisition of Satellite Signals Based on the Blind Source Separation Technique

Bo Li, [1] **Kan Xie**, [1,2] **Yulei Bai**, [1,3] **Zongze Wu**, [1,4] **and Shengli Xie** [1,5]

[1] *School of Automation, Guangdong University of Technology, Guangzhou, China*
[2] *Key Laboratory of Intelligent Information Processing and System Integration of IoT (GDUT), Ministry of Education, Guangzhou, China*
[3] *111 Center for Intelligent Batch Manufacturing Based on IoT Technology (GDUT), Guangzhou, China*
[4] *Guangdong Key Laboratory of IoT Information Technology (GDUT), Guangzhou, China*
[5] *Guangdong-HongKong-Macao Joint Laboratory for Smart Discrete Manufacturing (GDUT), Guangzhou, China*

Correspondence should be addressed to Kan Xie; kxie@gdut.edu.cn

Received 14 October 2021; Revised 22 November 2021; Accepted 27 December 2021; Published 17 January 2022

Academic Editor: Punit Gupta

To address the problems of slow acquisition speed and low accuracy faced by existing grid search-based satellite acquisition methods in complex scenarios, this study proposes a high accuracy and fast satellite signal acquisition method based on blind source separation. The proposed method first adopts wavelet threshold denoising to reduce the noise in the overlapped satellite signal received by the receiver so as to improve the signal-to-noise ratio of the satellite signal. On this basis, a subspace estimation method is introduced to construct a blind acquisition algorithm for satellite signals, which achieves high accuracy and fast solution for the Doppler frequency shift and code phase shift of satellite carrier signals and is able to recover the unobservable individual source signals. The effectiveness of the proposed method is verified through experiments and compared against the traditional grid search type acquisition method, which confirmed that the method is suitable for the acquisition requirements of weak signals and has a good engineering application value.

1. Introduction

Satellite signal acquisition is an important part of the receiver baseband signal processing, which is a prerequisite for tracking and positioning. The performance of the acquisition algorithm directly affects performance metrics such as the receiver acquisition speed and accuracy [1, 2]. For a particular GPS satellite signal, signal acquisition is the estimation of the carrier frequency and code phase of the satellite signal [3–5]. Previous research has proposed to use a parallel search algorithm for Doppler frequency and code phase on a two-dimensional grid [6]; however, as finer grid divisions are required to improve acquisition accuracy, while coarser grid divisions are required to improve acquisition speed, this method cannot simultaneously optimize both the acquisition speed and accuracy. Cui et al. [7] also proposed a matched filter coarse acquisition and linear frequency modulation Z-transform fine acquisition method that improves the acquisition speed while maintaining a certain degree of satellite signal acquisition accuracy; however, the method has a relatively high complexity and has poor acquisition performance in complex scenarios where the signal-to-noise ratio is low. Although many studies on satellite signal acquisition techniques have been performed, no method to date can achieve both fast and accurate satellite signal acquisition in complex scenarios.

Based on the existing research, this study proposes a high accuracy and fast acquisition method for satellite signals based on blind source separation [8, 9]. The proposed method first introduces the wavelet denoising method to reduce the background noise of the satellite signal. Subsequently, the blind source separation model of the satellite signal is constructed by frequency multiplication sampling, and the subspace estimation theory is introduced to resolve and compute the Doppler frequency shift and code phase shift. Finally, the acquisition performance of the proposed method is evaluated based on actual GPS satellite signals and compared against that of the traditional parallel search method.

2. Methodology

2.1. Blind Acquisition Model of Satellite Signals. The satellite signal received by the receiver contains 3 aspects: the carrier wave, the pseudo-random code, and the data code. Each satellite corresponds to a unique pseudo-random code, i.e., the C/A code. The C/A code and the data code are modulated into a combination code, and the low code rate combination code is secondarily modulated using spread spectrum communication techniques to form the final satellite signal as follows:

$$r(t) = \sum_{i=1}^{N} A_i \cdot C_i(t) \cdot D_i(t) \cdot \cos\left[2\pi \cdot \left(f_{IF} + f_i\right) \cdot t + \theta_i\right] + n(t). \tag{1}$$

In the above equation, N is the total number of satellites received by the receiver, time t denotes the continuity of the satellite signal, $A_i$is expressed as the amplitude of the i^{th} satellite's carrier signal, $C_i(t)$ corresponds to the C/A code of the i^{th} satellite, f_{IF} represent the carrier frequency, f_i and θ_i are, respectively, the Doppler frequency shift and initial phase of the i^{th} satellite's carrier signal, the solution involving these two parameters corresponds to the acquisition of the satellite, $D_i(t)$ is the i^{th} satellite's navigation data code, and $n(t)$ is the background noise.

The solution of Doppler frequency shift and code phase shift in equation (1) can be reduced to a single-channel blind source separation problem, i.e., separating each satellite carrier signal from the mixed carrier signal received by the receiver and then solving for the Doppler frequency shift and code phase. However, without any a priori knowledge, the single-channel blind source separation is a pathological computational problem. As such, this study converts the satellite signal into an aliased sinusoidal sampled signal with multichannel output through frequency multiplication sampling. The sampling points of each channel are different during the sampling process, ensuring that there is variability in the information observed by each channel, thus adding new observational information. Because C/A codes and navigation data codes are digitally coded signals, when sampling is sufficiently dense, the values of C/A codes and navigation data codes are constant across different channels for a given point in time. Based on this train of thought, considering only a particular sampling point and assuming an evenly spaced distribution of sampling points between channels for a given point in time, the satellite signal reception model after channel serialization can obtained as

$$r(\rho) = \sum_{i=1}^{N} A_i \cdot P_i \cdot \cos\left[2\pi \cdot F_i \cdot \frac{t_M}{M-1} \cdot (\rho - 1) + \theta_i\right] + n(\rho), \tag{2}$$

where $P_i = C_i(t)\, D_i(t)$ and $F_i = f_{IF} + f_i$, $j = 1, 2, \ldots, M$ are the sampling channels, and t_M is the sampling time corresponding to the M^{th} sampling channel. Rewriting equation (2) in matrix form by means of Euler's formula,

$$\begin{aligned}
&\mathbf{r} = \mathbf{A} \cdot \mathbf{x} + \mathbf{n},\\
&\mathbf{A} = \begin{bmatrix}
1 & 1 & \cdots & 1 \\
\exp\left(j \cdot 2\pi F_1 \cdot \frac{t_M}{M-1}\right) & \exp\left(-j \cdot 2\pi F_1 \cdot \frac{t_M}{M-1}\right) & \cdots & \exp\left(-j \cdot 2\pi F_N \cdot \frac{t_M}{M-1}\right) \\
\exp\left(j \cdot 2\pi F_1 \cdot \frac{2t_M}{M-1}\right) & \exp\left(-j \cdot 2\pi F_1 \cdot \frac{2t_M}{M-1}\right) & \cdots & \exp\left(-j \cdot 2\pi F_N \cdot \frac{2t_M}{M-1}\right) \\
\vdots & \vdots & \cdots & \vdots \\
\exp\left(j \cdot 2\pi F_1 \cdot t_M\right) & \exp\left(-j \cdot 2\pi F_1 \cdot t_M\right) & \cdots & \exp\left(-j \cdot 2\pi F_N \cdot t_M\right)
\end{bmatrix}_{M\times 2N},\\
&\mathbf{x} = \left[\frac{A_1 P_1}{2} \cdot \exp\left(-j \cdot \theta_{1,0}\right) \;\; \frac{A_1 P_1}{2} \cdot \exp\left(j \cdot \theta_{1,0}\right) \;\; \cdots \;\; \frac{A_N P_N}{2} \cdot \exp\left(j \cdot \theta_{N,0}\right)\right]_{1\times 2N}^{H},\\
&\mathbf{n} = \left[n(1) \;\; n(2) \;\; \cdots \;\; n(M)\right]_{1\times M}^{T},
\end{aligned} \tag{3}$$

where $\mathbf{r}$ is the satellite signal after channel serialization, and $F_N = f_{IF} + f_N$ is the coefficient in matrix $\mathbf{A}$; the unknown parameters A_N and $\theta_{N,0}$, contained within the column vector $\mathbf{x}$, are the satellite carrier signal intensity and initial phase, respectively. Equation (3) is the blind source separation model of the satellite signal constructed in this study by simulating multiple channels through frequency multiplication sampling. The acquisition process is the separation of matrix $\mathbf{A}$ and vector $\mathbf{x}$ from $\mathbf{r}$.

2.2. Blind Source Separation of Satellite Signals. To perform blind source separation on equation (3), the satellite carrier signal needs to be first denoised. Since threshold denoising is conceptually simple and computationally inexpensive, this study uses wavelet threshold denoising to perform noise reduction on the satellite signal. The main implementation steps of this process are outlined in the following sentences. First, wavelet transform with layer number 5 is performed on noisy signal r to obtain the wavelet coefficients corresponding to the fine details b_k, and soft thresholding is then applied to b_k to obtain the estimated wavelet coefficients w_k. Finally, wavelet reconstruction is performed using $b_k w_k$ to obtain the signal after noise reduction as the reconstructed signal [10, 11].

Using the reconstructed signal as the input signal $\mathbf{r}$ for the blind source separation model, simultaneously finding the autocorrelation matrix for both sides, and combining the frequency invariance of the sinusoidal signal's correlation function, the autocorrelation matrix $Q = E(r - r^H)$ is obtained. Decomposing the matrix Q into two parts, namely, the signal subspace and the noise subspace, and performing the eigenvalue decomposition,

$$\mathbf{Q} = \mathbf{U} \sum \mathbf{U}^H = \mathbf{U}_X \sum \mathbf{U}_X^H + \mathbf{U}_N \sum \mathbf{U}_N^H, \tag{4}$$

where the matrix $\mathbf{Q}$ has $2N$ large eigenvalues and $M - 2N$ small eigenvalues after mathematical decomposition. $\mathbf{U}_X$ is the signal subspace spanned by the eigenvectors corresponding to the large eigenvalues; $\mathbf{U}_N$ is the noise subspace spanned by the eigenvectors corresponding to the small eigenvalues. The signal subspace and the noise subspace are mutually orthogonal; using the orthogonality of the two subspaces, the spatial spectral function can be constructed as

$$P = \frac{1}{\mathbf{A}^H \mathbf{U}_N \mathbf{U}_N^H \mathbf{A}}. \tag{5}$$

By optimizing the above spatial spectral function, the sought Doppler frequency shift of the satellite signal is obtained as the frequency corresponding to the extremum value. Finally, the matrix least squares method is used to obtain a blind estimate of the initial phase of the satellite carrier signal: $\mathbf{X} = \mathbf{A}^{\dagger}\mathbf{r}$, where $\mathbf{A}^{\dagger}$ is the pseudoinverse matrix of matrix $\mathbf{A}$. Thus, the initial phase of the carrier can be solved as follows.

$$\theta = \arctan\left[\frac{\mathrm{Im}(\mathbf{x})}{\mathrm{Re}(\mathbf{x})}\right], \tag{6}$$

where Im ($\mathbf{x}$) and Re ($\mathbf{x}$) represent the imaginary and real parts of the complex numbers $\mathbf{x}$, respectively. The acquisition of the satellite signal is completed once both the Doppler frequency and phase of the satellite carrier signal have been obtained.

3. Results and Discussion

The dataset used consists of actual GPS signals collected by the University of Colorado Boulder and is named "GPSdata-Discrete Components-fs38_192-if9_55.bin." The GPS signal is quantized with 8 bit, IF signal frequency of 9.548 MHz, sampling frequency of 38.192 MHz, carrier frequency of 1.023 MHz, C/A code length 1023, and downsampling factor of 11. The signal consists of 8 channels, from which 32 satellites may be acquired. The signal acquisition threshold is set to 2.5. Figure 1 shows the results of satellite acquisition based on the blind source separation method. The PRN number represents the GPS satellite serial number. From figure, we can see that the method proposed in this study resulted in the successful acquisition of the signal from 8 visible satellites, for which the acquisition peaks are all greater than the preset threshold of 2.5. The remaining satellite signals with correlation peaks less than 2.5 were not acquired. The acquired satellite Doppler frequency and code phase parameters are accurate, with both the frequency error and code phase error being controlled within the allowable limits to meet the requirements of subsequent tracking.

In the following paragraphs, satellite PRN21 is used as an example to analyze the acquisition accuracy of the method proposed in this study and the parallel code phase search based on fast Fourier transform (FFT). Figure 2(a) shows the acquisition results obtained using the parallel search algorithm, and Figure 2(b) shows the results obtained using the acquisition algorithm proposed in this study. The Doppler frequency shift can be evaluated by subtracting the IF signal frequency result from 9.548 MHz, which can be used for quantifying the algorithm performance. From figures, it can be seen that the IF signal frequency obtained by the parallel code phase search algorithm is 9.54743 MHz, which has a Doppler frequency shift of −570 Hz in comparison with the actual IF signal frequency. The IF signal frequency estimated by the acquisition algorithm in this study is 9.54825 MHz, which has a Doppler frequency shift of −250 Hz. Hence, it can be seen that the algorithm proposed in this study has a more accurate estimation of the Doppler frequency shift.

The execution times of the algorithms proposed in this study and the parallel search algorithm were statistically tested under the same environment for a total of 10 measurements. The average values were calculated, and the results obtained are given in Table 1. As given in Table 1, the execution time of the acquisition algorithm proposed in this study is much smaller than the execution time of the traditional parallel acquisition algorithm; thus, the acquisition speed of the algorithm proposed in this study is fast.

To verify the sensitivity of the acquisition algorithm, signals with different signal-to-noise ratios need to be acquired for testing. Since the flexible control of the signal-to-noise ratio cannot be realized on physically acquired data, the software Matlab was used to generate simulated GPS signals as the test signals. The simulation generates the No. 6

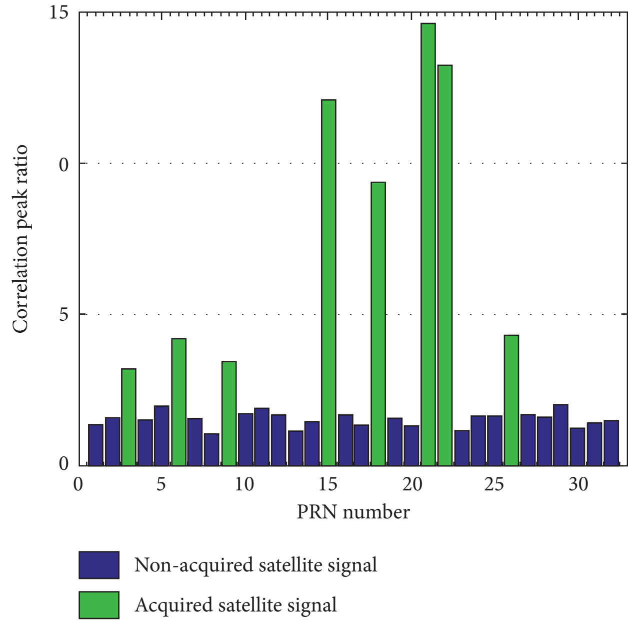

Figure 1: Signal acquisition results on actual collected GPS signals.

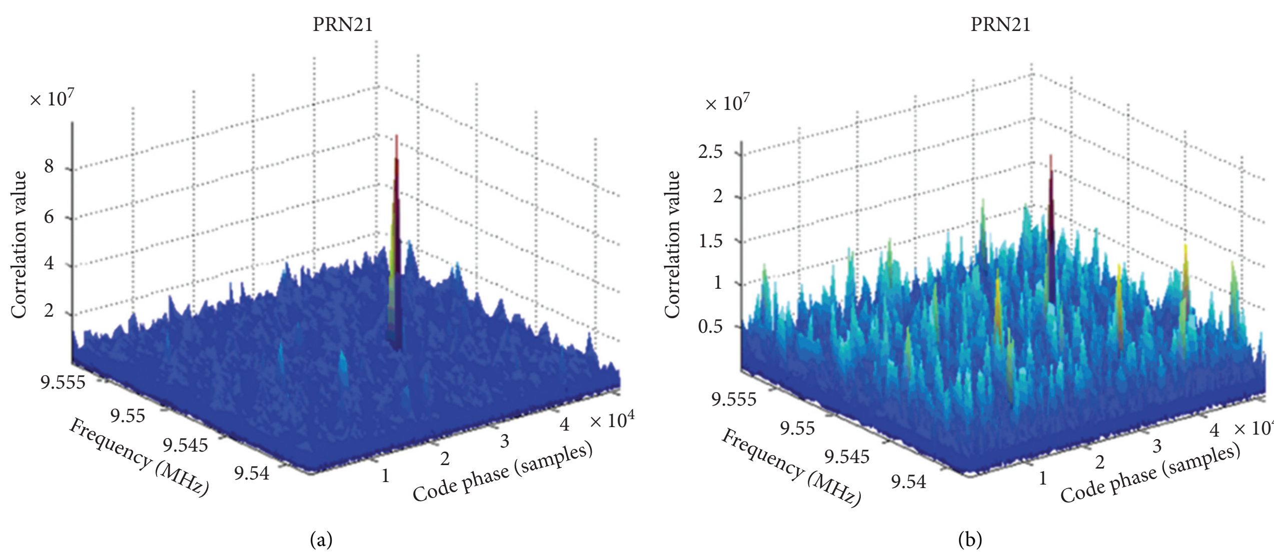

Figure 2: Acquisition results (a) for the parallel search and (b) for the proposed method.

Table 1: Comparison of algorithm execution times.

Frequency search step (Hz)	Parallel search (s)	Proposed method (s)
1000	10.415	0.256
500	19.783	0.598

GPS satellite signal with a data length of 100 ms, randomized navigation message data, signal frequency of 4 MHz, sampling frequency of 16 MHz, and initial signal phase of 0. The signal is combined with additive zero-mean Gaussian white noise with noise variance $\sigma_2 = 1$. Figure 3 shows the performance comparison of using the parallel code phase search acquisition algorithm using the acquisition algorithm proposed in this study to acquire the simulated GPS satellite signal.

As shown in figure, the probability of a correct acquisition increases with the increase of signal-to-noise ratio for both algorithms; however, compared with the traditional parallel acquisition algorithm, the acquisition performance of the proposed algorithm is better and more sensitive for any given signal-to-noise ratio. For the probability of correct acquisitions to reach 90%, the traditional parallel acquisition algorithm requires a signal-to-noise ratio of −41 dB or more, while the acquisition algorithm used in this study requires a signal-to-noise ratio of only −44 dB. This demonstrates that

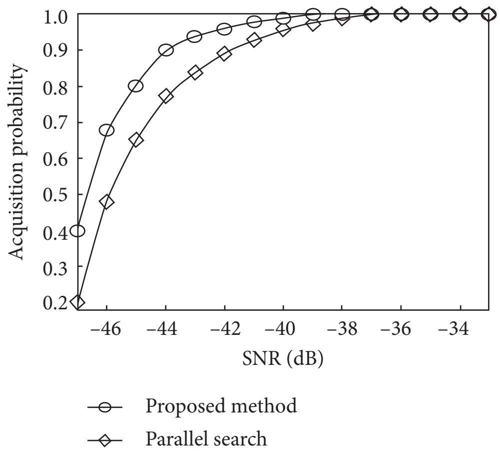

Figure 3: Performance comparison of acquisition algorithms.

the acquisition algorithm used in this study is more suitable for the acquisition of weak signals as compared to the traditional algorithm.

4. Conclusion

In order to meet the requirement of precise navigation in a real time, the compromise between acquisition speed and acquisition accuracy needs to be addressed. In this work, we proposed a new method to capture the satellite with both high accuracy and fast satellite signal acquisition. Unlike the traditional algorithm, e.g., parallel searching based on Fourier transform, the proposed method employs an idea of signal optimization where the Doppler frequency can be analytically calculated. Based on the mixture signal from multiple satellites and the time-dependent amplitude, we implemented the frequency multiplication sampling to generate the standard sinusoidal signal and then established the signal acquisition model according to blind source separation. After that, the signal background noise is reduced by introducing the wavelet denoised method where a wavelet threshold is preset. This can enhance the signal-to-noise ratio, thereby improving the acquisition performance of the satellite receiver. Finally, the subspace-based estimation algorithm was used to blindly estimate the Doppler frequency and phase of the satellite signal so as to overcome the technical limitations faced by existing acquisition methods, using which a simultaneously fast and accurate acquisition of satellite signals cannot be achieved. The experimental results from GPS satellite signal acquisition demonstrate that, as compared with the traditional acquisition methods, the new acquisition algorithm proposed in this study can achieve high accuracy and fast acquisition of the satellite signal. Furthermore, it can effectively acquire weak signals, making it more suited for high-sensitivity software receivers.

Data Availability

The datasets used and/or analyzed during the current study are available from the corresponding author upon request.

Conflicts of Interest

The authors declare that they have no conflicts of interest.

Acknowledgments

The authors acknowledge the National Natural Science Foundation of China (61973087) and the Key Research and Development Program of Guangdong Province (2019B010141001).

References

[1] D. Kaplan and J. Hegarty, *Understanding GPS: Principles and Applications*, Artech House, London, UK, 1996.

[2] Y. Rubinpur and S. Toledo, *Signal Processing for a Reverse-GPS Wildlife Tracking System: CPU and GPU Implementation Experiences*, Concurr. Comp-Pract. E., NJ, USA, 2021.

[3] K. Vasudevan, “Coherent detection of turbo-coded OFDM signals transmitted through frequency selective Rayleigh fading channels with receiver diversity and increased throughput,” *Wireless Personal Communications*, vol. 82, no. 3, pp. 1623–1642, 2015.

[4] M. A. Farhad, M. R. Mosavi, A. A. Abedi, and K. Mohammadi, “Increasing the resistance of GPS receivers by using a fuzzy smart estimator in weak signal conditions,” *Journal of Navigation*, vol. 73, no. 5, pp. 991–1013, 2020.

[5] S. Jing and W. Zhang, “Fast and precise acquisition of GPS signal optimized by improved orthogonal search,” *Laser and Optoelectronics Progress*, vol. 57, no. 13, Article ID 131206, 2020.

[6] S. F. Ahamed, G. S. Ganesh, and L. Gabeshc, “Fast acquisition of GPS signal using FFT decomposition,” *Procedia Computer Science*, vol. 87, pp. 190–197, 2016.

[7] H. Cui, Z. Li, and Z. Dou, “Fast acquisition method of GPS signal based on FFT cyclic correlation,” *International Journal of Communications, Network and System Sciences*, vol. 10, no. 8, pp. 246–254, 2017.

[8] Y. Xie, K. Xie, and S. Xie, “Underdetermined blind separation of source using lp-norm diversity measures,” *Neurocomputing*, vol. 411, pp. 259–267, 2020.

[9] J. Henríquez and W. Kristjanpoller, “A combined Independent Component Analysis-Neural Network model for forecasting exchange rate variation,” *Applied Soft Computing*, vol. 83, Article ID 105654, 2019.

[10] J. Li, Y. Li, Y. Li, and Z. Qian, “Downhole microseismic signal denoising via empirical wavelet transform and adaptive thresholding,” *Journal of Geophysics and Engineering*, vol. 15, no. 6, pp. 2469–2480, 2018.

[11] Q. Peng, T. Yu, W. Luo et al., “An adaptive iteratively weighted half thresholding algorithm for image compressive sensing reconstruction, communications signal processing and systems,” in *Proceedings of the 2018 CSPS*, Dalin, China, July 2018.

Hindawi
Scientific Programming
Volume 2022, Article ID 1892836, 14 pages
https://doi.org/10.1155/2022/1892836

Research Article

Bike-Sharing Fleet Allocation Optimization Based on Demand Gap and Cycle Rebalancing Strategies

Jianhua Cao,[1,2] **Weixiang Xu**,[1] **and Wenzheng Wang**[3]

[1]*School of Management, Zhejiang University of Technology, Hangzhou, China*
[2]*School of Management Science and Engineering, Anhui University of Technology, Maanshan, China*
[3]*Shanghai Pudong Development Bank, Hefei, China*

Correspondence should be addressed to Jianhua Cao; jhcao_74@ahut.edu.cn

Received 23 November 2021; Revised 10 December 2021; Accepted 17 December 2021; Published 13 January 2022

Academic Editor: Punit Gupta

In Bike-Sharing System (BSS), the initial number of bikes at station will affect the time interval and the amount of rebalancing, which is usually empirically determined and does not reflect the characteristics of consumer demand in finer time granularity, thus possibly leading to biased conclusions. In this paper, a fleet allocation method considering demand gap is first proposed to calculate the initial number of bikes at each station. Then, taking the number of demand gap periods as the decision variable, an optimization model is built to minimize the total rebalancing amount. Furthermore, the research periods are divided into multiple subcycles, the single-cycle and multicycle rebalancing strategies are presented, and the additional subcycle rebalancing method is introduced to amend the number of bikes between subcycles to decrease the rebalancing amount of the next subcycle. Finally, our methods are verified in effectively decreasing the rebalancing amount in a long-term rebalancing problem.

1. Introduction

In recent years, the rapid expansion of motorized transportation system in cities has made the urban environment deteriorate rapidly and traffic congestion seriously, posing a serious threat to the health and travel convenience of urban residents [1]. Today's petroleum-based mobility system is making transportation systems face unprecedented pressure. Especially in the past decades, with the accelerated pace of globalization, urbanization, and motorization in the world, energy shortage and environmental pollution are common problems faced by many developed and developing countries [2]. According to official statistics, traffic jams caused urban Americans to travel an extra 8.8 billion hours and purchase an extra 3.3 billion gallons of fuel for a congestion cost of $166 billion. In particular, we can see many cities all over the world sunk in heavy smokes in the winter threatening the health of citizens. Consequently, the search for low-consumption and low-emission transports has become an urgent issue that many researchers and practitioners are willing to challenge. To our relief, many exciting advancements in transportation appear, such as the station-base bike-sharing which is not only a green and healthy way to travel, but also a traffic mode of energy saving and emission reduction. After the first Bike-Sharing System (BSS) appeared in Amsterdam, the Netherlands, the system quickly spread around the world because of its flexibility, economy, and convenience [3]. Compared to motorized transport, BSS provides an alternative to short distance travel, effectively addresses the last mile travel problem, significantly reduces traffic accidents and congestion [4].

In BSS, bikes and empty docks are arranged at fixed stations available for users to ride when and where they require. The station has capacity limitations, representing the maximum number of bikes or empty docks at a station. When people require, they rent from the nearest station and, after a short ride, return them to the station closest to their destination. However, when BSS runs, people usually start and finish their riding at two different stations, which often lead to the imbalance of system. The imbalance here means that the bikes or empty docks of a station cannot meet its customer demand, which not only increases economic losses of operators, but also decreases the service quality, thus affecting the normal operation and sustainable development of BSS. An effective solution to this issue is the operators using vehicles to transfer bikes from excessive stations to deficient ones, which is called a bike-sharing rebalancing problem or bike-sharing repositioning problem (BRP).

In parallel with the explosion of BSS worldwide, in addition to BRP, experts and scholars have been concerned about the fleet allocation optimization of BSS, such as how many bikes are required for each station during BSS planning stage and how many bikes are configured for each station during rebalancing responding to customer demand for renting and returning bikes, in addition to the extent to which the fleet allocation affects the rebalancing operation and so on.

Martinez et al. [5] designed a mixed integer linear program, while Saharidis et al. [6] introduced a pure integer linear program, both of which optimize the station locations, fleet size, and bicycle relocation activities in daily operations. With the deepening of research, Yan et al. [7] developed four planning models for leisure-oriented public bicycle rental systems under deterministic and stochastic demands, respectively. Chen et al. [8] formulated two mathematical programming models to determine the number of bikes maximizing the time interval between repositioning events and the satisfaction of demands. formulated two-stage and multistage stochastic optimization models to determine the optimal number of bikes to assign to each station at the beginning of the service. Vishkaei et al. [9] determined the station capacity and fleet size, taking into account a constraint for the fleet size of the system, then formulated a model using the Jackson network, and developed a genetic algorithm to obtain the proper amounts of variables to balance the inventory of the system.

Once station configuration has been determined, the capacity of each station, i.e., the maximum number of bikes and empty docks, is difficult to change in the short term, but the consumer demand for renting and returning bikes is constantly changing over time. Rebalancing is the best option to solve this problem, which is more efficient and economical than replacing the facilities.

The vast majority of BRP studies belong to the operator-based BRP, and the objectives of BRP considered in the existing literature are diverse. Most of them are intended to minimize the total rebalancing cost or time from the operator' s point of view to improve the effectiveness and efficiency of BSS [10, 11]. In addition to these objectives, many of the literature also target customer satisfaction or service level [12]. In recent years, the user-based BRP has received some attention and several incentive strategies have been proposed to encourage users to relocate the bikes among stations [13].

The fleet size of the station has a great influence on the rebalancing amount, but only a few scholars have explored their comprehensive optimization; for example, Yuan et al. [14] proposed a unified mixed integer linear programming (MILP) model to provide an integrated solution for the number, location, capacity of bicycle stations, total fleet size design, depot location design, and rebalancing and maintenance plans. Sayarshad et al. [15] proposed a mathematical model which attempted to optimize a BSS by determining the minimum required bike fleet size in order to minimize unmet demand, unutilized bikes, and the need to transport empty bikes between rental stations. Frade and Ribeiro [16] formulated maximal covering models and took the available budget as a constraint to determine the location of new stations, station capacity, number of bikes, and rebalancing quantity. Chen et al. [8] studied how to determine the number of bikes that need to be deployed at stations to maximize the time interval or the satisfaction of demands within a fixed time interval during rebalancing. modeled the evolution of the number of vehicles at each station as a stochastic process and proposed a rebalancing strategy iteratively to solve a chance-constrained optimization problem in order to find a rebalancing schedule ensuring no service failures in the future with a given level of confidence. Being different from previous studies, proposed a framework to obtain the optimal bike fleet size and rebalancing strategy from the life cycle's perspective.

We study how to achieve guaranteed service availability in such systems. Specifically, we are interested in determining (a) the fleet size and (b) a vehicle rebalancing policy that guarantees that (a) every customer will find an available vehicle at the origin station and (b) the customer will find a free parking spot at the destination station. We model the evolution of the number of vehicles at each station as a stochastic process. The proposed rebalancing strategy iteratively solves a chance-constrained optimization problem to find a rebalancing schedule that ensures that no service failures will occur in the future with a given level of confidence. We show that such a chance-constrained optimization problem can be converted into a linear program and efficiently solved.

This article seeks answers to two major questions:

(i) How can the fleet allocation (i.e., the initial number of bikes at each station) be determined?

(ii) Are the research periods considered as a cycle (single cycle) or divided into multiple subcycles (multicycle) to rebalance?

Then, a series of questions are derived from them, such as whether and to what extent does the initial number of bikes of stations influence the rebalancing interval and amount? Which is better, the single-cycle rebalancing or the multicycle rebalancing? At the same time, if the research periods are divided into subcycles, how is the initial number of bikes of each subcycle determined?

Aiming at the above problems, this paper focuses on the fleet allocation and cycle rebalancing of BSS. First, considering the demand gap, a fleet allocation method is proposed to determine the initial number of bikes. Secondly, an optimization model with the objective of minimizing the total rebalancing amount is established. Then, the research periods are divided into subcycles, and a multicycle rebalancing strategy (MCRS) is presented, in which the single-cycle rebalancing strategy (SCRS) is introduced to rebalance in each subcycle and an additional subcycle rebalancing method (ACRM) is proposed to decrease the rebalancing amount of the latter subcycle. Thirdly, a fleet allocation optimization algorithm embedded in the fleet allocation and cycle rebalancing strategy is designed to solve the problem. Finally, the effectiveness of our methods is verified by a large number of experiments.

The key contributions of this article are as follows:

(i) A fleet allocation method for determining the initial number of bikes is proposed, which considers the demand gap in finer time granularity.

(ii) A mathematical model is formulated, which takes the number of demand gap periods as decision variables and aims at the objective of minimizing the total rebalancing amount.

(iii) Based on cycle division, a multicycle rebalancing strategy (MCRS) is presented, including a sing-cycle rebalancing strategy (SCRS) and an additional subcycle rebalancing method (ACRM). The cycle division method can give full play to the effect of the fleet allocation method in reducing the rebalancing amount.

2. Problem Description and Model Formulation

2.1. Problem Description. In order to reveal the effect of the initial number of bikes on the rebalancing interval and amount, we set up two scenarios which have the same daily customer demands, choosing two stations 1 and 2 with different initial number of bikes in the two scenarios, and a datum period of one day, as shown in the table in the upper left of Figure 1.

In scenario 1, more bikes were rented from station 1 than were returned on days 1 and 2, resulting in a steady decline in the number of bikes, so that no bikes were available for renting the third day. Similarly, there will be no empty docks at station 2 for customers to return their bikes on that day. Therefore, a rebalancing is required. Furthermore, customers cycle 18 times from station 1 to station 2 and 12 times from station 2 to station 1, resulting in a demand gap of 18−12 = 6 at station 1, meaning that station 1 needs at least 6 bikes to meet the customer demands. Instead, the demand gap at station 2 is −6, standing that station 2 requires 6 empty docks to meet the customer demands of that day. Therefore, at the end of the second day, 6 bikes had to be transported from station 2 to station 1 to meet the customer demands on the third day.

During the study periods, more bikes are rented from station 1 than returned each day, so at the beginning of scenario 2, 25 bikes are placed at station 1. In contrast to scenario 1, the rebalancing is delayed by one day to the third day and the rebalancing amount is only 1. Therefore, the use of the demand gap to determine the initial number of bikes at a station can extend the time interval until the next rebalancing and reduce the rebalancing amount. However, existing studies determining the initial number of bikes at stations tend to base on station capacity percentage [17] or the ratio of rental demand to returning demand [18], ignoring the demand gap, which is often subjective and arbitrary.

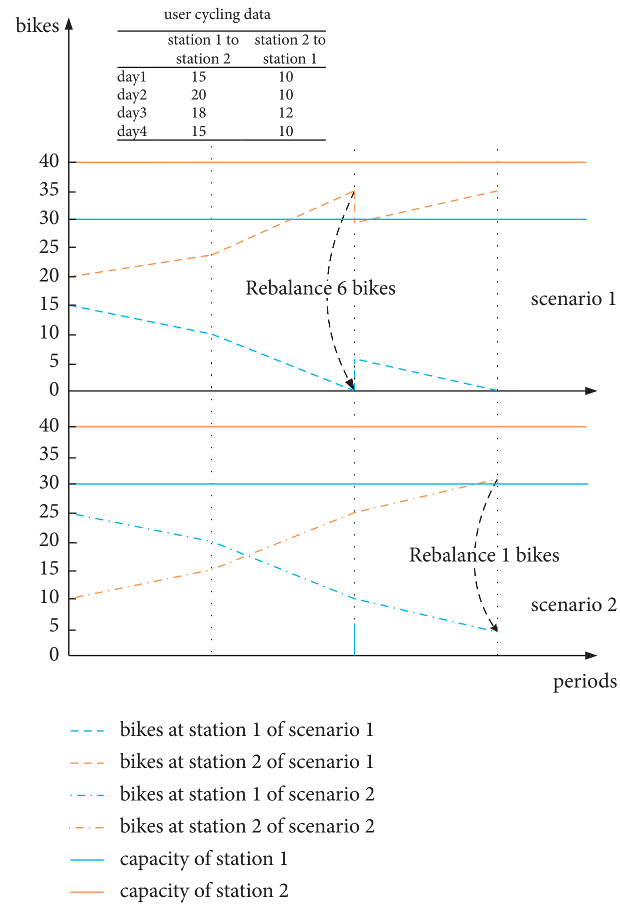

Figure 1: The influences of setting different number of bikes at the initial moment on rebalancing.

When the initial number of bikes or empty docks of a station plus the demand gap is within its station capacity, this means that the station can meet its customer demand and is defined in this paper as a normal station without having to rebalance. Otherwise, the station is called a problem station and needs to be rebalanced. If the initial number of bikes or empty docks of a station plus multi-period demand gaps remains within its station capacity, it stands that the station can meet its customer demand for all these periods without having to rebalance. Here the multiperiod demand gaps are defined as a cumulative demand gap value based on how many periods are used to determine the initial number of bikes, called demand gap periods. Problem stations can be further divided into loading and unloading stations. As the name implies, the loading station is a station without enough bikes to meet the rental demand, while the unloading station means that its empty docks are not sufficient to cover the returning demand.

In addition, effective rebalancing strategies should also be developed, including the stations that need to be rebalanced, the rebalancing amount of each station, and the route of rebalancing, all of which have a profound impact on the rebalancing.

Here is an example, assume that there are four stations in BSS, as can be seen in Figure 2. The three figures above a station represent the capacity, the initial number of bikes, and the demand gap of the station, respectively. For instance, at station 1, its capacity and initial number of bikes are 30 and 25, respectively. The demand gap −10 means 10 empty docks are needed to meet its customer demand for the next day, while there are only 5 empty docks currently; thus, 5 bikes are needed to be loaded from station 1. Similarly, stations 2 and 3 can meet their customer demand, while station 4 is required to unload 10 bikes to meet its customer demand the following day. According to the definition of station, stations 1 and 4 are problem stations, further station 1 is loading station and station 4 is unloading station, and stations 2 and 3 are normal stations.

The two rebalancing strategies are then compared, one of which is the traditional strategy of selecting the closest station to participate in the rebalancing and then extending it from the near to the far stations, regardless of whether they are normal or problem stations. Another is to give priority to rebalance between problem stations, more specifically, between the loading and unloading stations; when one of these types of station disappears, problem stations still exist; then the rebalancing will continue between problem stations and normal stations. The processes of these two rebalancing strategies are shown in Figure 2. Obviously, the rebalancing amounts in two strategies are 15 and 10, respectively, indicating that strategy 2 can greatly reduce the rebalancing amount.

From the analysis and discussion above, the preliminary conclusions can be easily drawn: (i) setting the appropriate initial number of bikes at stations can reduce the rebalancing amount and increase the interval between rebalances and (ii) effective rebalancing strategy can reduce the rebalancing amount and the workload of operators, while improving customer satisfaction.

2.2. Mathematical Model. As mentioned above, demand gap can reflect the customer demand over periods. Considering multiperiod demand gaps to determine the initial number of bikes can effectively extend the time interval of rebalancing and reduce the rebalancing amount. Therefore, the number of demand gap periods needs to be first determined, and the cumulative demand gap value of these periods should be calculated; then rebalancing is performed. In this section, an optimization model is proposed which takes the number of demand gap periods as decision variables and aims at minimizing the total rebalancing amount, which calculates the optimization objective value based on the cumulative rebalancing amount of all periods. The main reason for this is that BRP is a multiple periods problem, if taking a day as found and reducing the total rebalancing amount in multiple periods is of great significance to reduce the rebalancing amount and cost of rebalancing and improve the overall operating efficiency of BSS.

2.2.1. Assumptions.

(1) Take one day as a basic period and perform rebalancing at 24 : 00 every night

(2) The daily demand of each station is known

2.2.2. Sets.

S is the set of stations, indexed by i and j where $i, j = \{1, 2, \ldots, n\}$

T is the set of time periods, indexed by t where $t = \{1, 2, \ldots, m\}$

2.2.3. Decision Variables.

b_{it} is the number of bikes at station i $(i \in S)$ at the beginning of period t $(t \in T)$

r_{ijt} is the number of bikes rebalanced from station i $(i \in S)$ to station j $(j \in S)$ at the ending of period t $(t \in T)$

z_i is the number of demand gap periods of station i $(i \in S)$

2.2.4. Parameters.

c_i is the capacity of station i $(i \in S)$

α is the initial bike availability rates

f_{it} is the rental demand of station i $(i \in S)$ during period t

g_{it} is the returning demand of station i $(i \in S)$ during period t

M is the number of periods

Based on the above notations, the following mathematical model can be formulated:

$$\min \quad \sum_{t\in T}\sum_{i\in S}\sum_{j\in S} r_{ijt}. \tag{1}$$

S.t.

$$b_{i1} = \alpha \times c_i + \sum_{t=1}^{z_i}\left(f_{\mathrm{it}} - g_{\mathrm{it}}\right) \quad \forall i \in S, \tag{2}$$

$$b_{i1} = \begin{cases} 0, & \text{if } b_{i1} < 0 \\ c_i, & \text{if } b_{i1} > c_i \end{cases} \quad \forall i \in S, \tag{3}$$

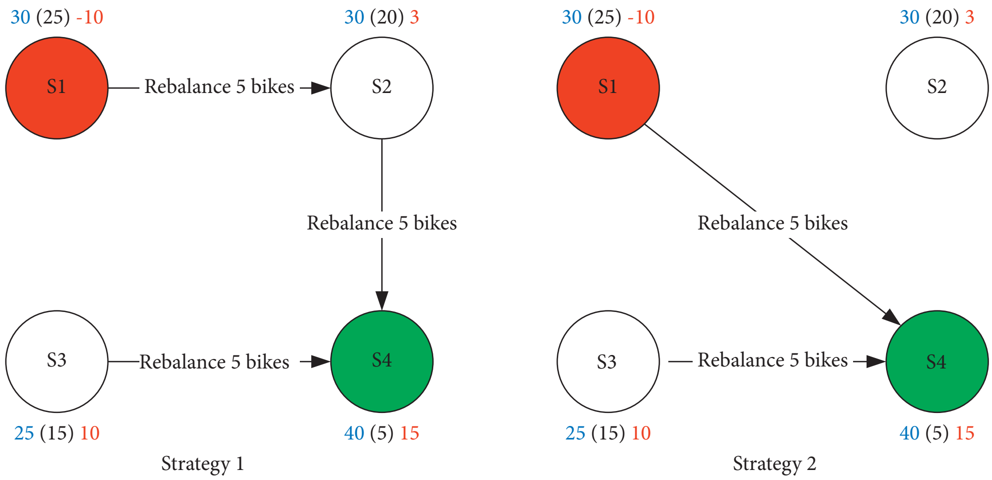

FIGURE 2: Comparison of different rebalancing strategies on rebalancing amount.

$$b_{\mathrm{it}} = b_{i(t-1)} + g_{i(t-1)} - f_{i(t-1)} + \sum_{j\in S} r_{ji(t-1)} - \sum_{j\in S} r_{ij(t-1)} \quad \forall i \in S,\ j \in S,\ t \in T, \tag{4}$$

$$0 \le b_{it} \le c_i \quad \forall i \in S,\ t \in T, \tag{5}$$

$$1 \le z_i \le M \quad \forall i \in S, \tag{6}$$

$$b_{\mathrm{it}} \ge f_{it} - g_{\mathrm{it}} \quad \forall i \in S,\ t \in T, \tag{7}$$

$$c_i - b_{it} \ge g_{\mathrm{it}} - f_{\mathrm{it}} \quad \forall i \in S,\ t \in T, \tag{8}$$

$$\sum_{j\in S} r_{ijt} \le b_i \quad \forall i \in S,\ t \in T, \tag{9}$$

$$\sum_{j\in S} r_{jit} \le c_i - b_{\mathrm{it}} \quad \forall i \in S,\ t \in T, \tag{10}$$

$$b_{\mathrm{it}}, r_{ijt} \in N \forall i \in S, \forall j \in S, \forall t \in T. \tag{11}$$

The objective function (1) minimizes the total accumulative rebalancing amount of BSS. Constraint (2) is to determine initial number of bikes at station i. Constraint (3) modifies the initial number of bikes at station i. Constraint (4) defines the number of bikes of station i at the beginning of period t, which is the number of bikes at the beginning of period t–1 plus the customer demand of period t–1 plus the rebalancing amount of period t–1. Constraint (5) defines that the number of bikes of station i at the beginning of period t is within the station capacity c_i. Constraint (6) defines the demand gap within the longest period. Constraint (7) defines that station i must have enough bikes to meet the rental demand at period t. Constraint (8) defines that station i must have enough empty docks to meet the returning demand at period t. Constraint (9) defines that the number of bikes rebalance from station i is within the station capacity bit. Constraint (10) defines that the number of bikes rebalance to station i is within the station capacity c_i-bit. Constraint (11) restricts the domain of the decision variables.

3. A Fleet Allocation Optimization Algorithm Based on Demand Gap and Cycle Rebalancing Strategy

In this paper, a day is taken as a basic period instead of an hour, mainly because hourly user demand is constantly changing; in particular, there are morning and evening rush hours during the working day that are difficult to track. Furthermore, rebalance is usually carried out at night when the number of bike-sharing used is very low, so that the impact of changes in user demand on the rebalancing can be largely ignored.

Based on demand gap periods, an optimization method determining the initial number of bikes for each station is first proposed in this section. Then, the research periods are divided into multiple subcycles and a multicycle rebalancing strategy (MCRS) is presented, in which a single-cycle rebalancing strategy (SCRS) is introduced to rebalance in each subcycle and an additional subcycle rebalancing method (ACRM) is also developed to amend the rebalancing amount between subcycles.

3.1. A Fleet Allocation Method considering Demand Gap (FAMDG). We propose a method to determine the initial number of bikes at each station using demand gap periods, referred to as FAMDG, which can reflect changes in customer demand of each station in future periods. Start with determining the basic number of bikes at station i referring to the percentage capacity [17]; α is the percentage of capacity c_i, as shown in the following equation:

$$b_{i1} = \alpha \times c_i. \tag{12}$$

The demand gap of station i is the difference between the rental amount and returning amount, as shown in the following equation:

$$G_{\text{it}} = f_{\text{it}} - g_{\text{it}}. \tag{13}$$

Then, the initial number of bikes at station i in the first period b_{i1} is calculated by the basic number of bikes at station i plus the demand gap of station i in the first period, as shown in (14). If b_{i1} is still within the capacity of station i, it means that b_{i1} determined in this way can meet the customer demand and station i without requiring rebalancing.

$$b_{i1} = \alpha \times c_i + \left(f_{i1} - g_{i1}\right). \tag{14}$$

By the same token, the initial number of bikes of station i in multiple periods is still within the station capacity, that denotes b_{i1} determined in this way can meet the multiperiod customer demands without having to rebalance, as seen in equation (2). However, the multiperiod demand gaps at a station change over time and they either exceed the station capacity or are negative. So, it is not the more the demand gap periods, the more optimal the initial number of bikes. Therefore, the number of demand gap periods should be optimized. At the same time, in order to prevent the initial number of bikes from exceeding the station capacity, equation (3) is used to correct it, i.e., if the initial number of bikes obtained by equation (2) exceeds the station capacity, it will be set to the station capacity, and if it is less than 0, to zero.

3.2. Cycle Rebalancing Strategy

3.2.1. The Single-Cycle Rebalancing Strategy. We treat the research periods as one cycle and propose the single-cycle rebalancing strategy (SCRS). In SCRS, the rebalancing is conducted at the end of each period except for the last, and the number of rebalancing operations is the periods minus 1.

Now let b_{it}' represent the number of bikes at the end of period t, which equals the number of bikes b_{it} at the beginning of period t plus the demand gap G_{it} of period t, seen in equation (15), and $G_{i(t+1)}$ represents the demand gap of period $t+1$; then Z_{it} represents station classification value which equals b_{it}' plus $G_{i(t+1)}$, as can be seen in equation (16). According to Z_{it}, all stations can be divided into problem stations and normal stations, and problem stations can also be further divided into loading and unloading stations. If $Z_{it} < 0$, it means that bikes need to be loaded to station i in period t to meet its customer rental demand, which is defined as loading station, and the number of bikes to be loaded is referred to as loading amount; if $0 < Z_{it} < c_i$, it means that bikes or empty docks of station i in period t can meet its customer rental and returning demand, which is defined as normal station; if $Z_{it} > c_i$, it means that station i does not have enough empty docks to meet its customer returning demand; thus, bikes need to be unloaded from it, which is referred to as unloading station and the number of bikes to be unloaded is defined as unloading amount, as shown in the following equation:

$$b_{\text{it}}' = b_{\text{it}} + G_{\text{it}}, \tag{15}$$

$$Z_{\text{it}} = b_{\text{it}}' + G_{i(t+1)}, \tag{16}$$

$$\begin{cases} \text{if } Z_{\text{it}} < 0, & \text{then station } i \in \text{the set of loading stations } I, \\ \text{if } Z_{\text{it}} > c_i, & \text{then station } i \in \text{the set of unloading stations } E, \\ \text{if } 0 < Z_{\text{it}} < c_i, & \text{then station } i \in \text{the set of normal stations } N. \end{cases} \tag{17}$$

Then calculate the rebalancing amount e_{it} of problem station i in period t. If station i is a loading station, its rebalancing amount is 0 minus Z_{it}, and if station i is an unloading station, its rebalancing amount is Z_{it} minus C_i, seen in (18). Moreover, according to e_{it} of each station, the rebalancing between loading and unloading stations is carried out in order from near to far, mainly according to the actual distance to judge.

$$e_{\text{it}} = \begin{cases} 0 - Z_{\text{it}}, & \text{if } i \in I, \\ Z_{\text{it}} - c_i, & \text{if } i \in E. \end{cases} \tag{18}$$

At the end of the rebalancing between problem stations, once the $b_{i(t+1)}$ of problem station i is within its capacity, it becomes a normal station. If there still are problem stations, rebalancing is done between problem stations and normal stations until all stations become normal stations.

The pseudocode of SCRS during period t is shown as Algorithm 1.

3.2.2. The Multicycle Rebalancing Strategy. In this section, the research periods are divided into multiple subcycles and a multicycle rebalancing strategy (MCRS) is proposed. Note that, in each subcycle, the initial number of bikes is calculated by FAMDG and SCRS is conducted. The main purpose of dividing subcycle is to make full use of FAMDG in each subcycle. However, the initial number of bikes at stations in each subcycle is determined based on the cumulative demand gaps of all periods in the subcycle, and the number of bikes at the end of the subcycle is obtained through SCRS. Obviously, the numbers of bikes at the end of one subcycle and the beginning of the next are determined in different ways, so the two numbers are usually not equal. If the former is adjusted to the latter between the two subcycles, the effect of the fleet allocation on rebalancing can be applied to each subcycle. Therefore, this paper proposes an additional subcycle rebalancing method (ACRM) to rebalance between subcycles.

The ACRM begins with the loading and unloading stations being redefined at the end of each subcycle. If the number of bikes of a station at the end of a subcycle is less than the number of bikes calculated based on demand gap periods for the next subcycle, it is redefined as an unloading station; otherwise, it is redefined as a loading station. The number of bikes calculated based on demand gap periods in the next subcycle is then used as a reference value, and then rebalancing is conducted between loading and unloading stations in order to bring the number of bikes at the end of the previous subcycle close to the reference value until one of the sets of loading and unloading stations is empty.

Algorithm 2 is a pseudocode flowchart of MCRS.

3.3. Algorithm Flow. Compared with traditional optimization algorithms, genetic algorithm starts from the string set of the solution rather than from a single solution, which has a large coverage and is advantageous to global optimization. In order to reduce the complexity of the problem, a single-cycle rebalancing strategy and a multicycle rebalancing strategy are embedded in the single-cycle and multicycle rebalancing problem, and a fleet allocation method taking into account demand gap is proposed that can further improve the search speed of the algorithm and find better solutions.

3.3.1. Encoding. In this paper, each cell on a chromosome represents the cumulative demand gap periods at a station. Figure 3 is an example of a chromosome structure consisting of six stations, each location representing a station and the figure denoting the cumulative demand gap periods at the station. Therefore, the cumulative demand gap periods of the six stations are 3, 4, 2, 7, 5, and 3, respectively. For instance, 3 is the cumulative demand gap periods of the first station, similarly as 4, 2, 7, 5, and 3.

3.3.2. Initialization. Initialization is the first step in genetic algorithm [19] and the first population is generated during initialization. The value of each cell in the chromosome is randomly generated within the range [1, m], of which m is the maximum value of periods. When M chromosomes are generated, the initialization ends.

3.3.3. Function Fitness. According to equations (2) and (3), the initial number of bikes is calculated by the demand gap periods optimization (DGPO). Then, perform rebalancing by SCRS or MCRS. Once the SCRS or MCRS is executed, the total cumulative rebalance amount can be obtained. At the same time, the minimum rebalancing amount is regarded as the objective function; see equation (1); therefore, the reciprocal of the objective function is selected as the adaptive evaluation function f_i.

3.3.4. Selection. This section uses roulette wheel strategy for selection, and the general steps of the strategy are as follows:

(1) The fitness value f_i of an individual in population is superimposed to obtain the total fitness value $F = \sum_{i=1}^{N} f_i$, where N is the number of individuals in the population.

(2) The fitness value of each individual is divided by the total fitness value to determine the probability of the individual being selected $p_i = f_i/F$.

(3) Calculate the cumulative probability of individuals to construct a roulette wheel.

(4) Roulette selection: generate a random number at intervals of [0,1]. If the random number is less than or equal to the cumulative probability of an individual i and is greater than the cumulative probability of individual i-1, the individual is selected to enter the next offspring population.

3.3.5. Crossover. This section uses a unified crossover strategy which exchanges the intersection point on the patrilineal individual based on probability to generate two new individuals. The general steps of this strategy are as follows:

(1) Two individuals are randomly chosen from parents

(2) Crossover points are swapped according to probability

The process of unified crossover is shown in Figure 4.

3.3.6. Mutation. The strategy has two purposes: one is to make the genetic algorithm have the ability of local stochastic searching and the other is to make the genetic algorithm maintain the diversity of the population to prevent

Input: The number of bikes at the end of period t of station $i\{b_{it}'\}_{i=1}^{n}$, Demand gap of period $t+1$ of station $i\{G_{i(t+1)}\}_{i=1}^{n}$, Station capacity $\{c_i\}_{i=1}^{n}$
Output: Rebalancing amount $\sum_{i\in S}\sum_{j\in S} r_{ijt}$
for $i = 1$ to n **do**
  station classification $Z_{it} = b_{it}' + G_{i(t+1)}$
  if $Z_{it} > c_i$ **then**
    the unloading amount at station i is $e_{it} = Z_{it} - c_i$, station i belongs to the set of unloading stations E
  else if $Z_{it} < 0$ **then**
    the loading amount at station i is $e_{it} = 0 - Z_{it}$, station i belongs to the set of loading stations I
  else
    station i belongs to the set of normal stations N
end
Conduct rebalancing amount r_{ijt} between problem stations in sequence from near to far;
for $i = 1$ to n **do**
  if $0 \le Z_{it} + \sum_{j\in I} r_{jit} - \sum_{j\in E} r_{ijt} \le c_i$ **then**
    station i belongs to the set of normal stations N
end
while E *or* I is not empty set **do**
  Conduct rebalancing amount r_{ijt} between problem stations and normal stations in sequence from near to far
end
return $\sum_{i\in S}\sum_{j\in S} r_{ijt}$

Algorithm 1: The single-cycle rebalancing strategy.

Input: Number of data periods l, Number of bikes at station i at the beginning of a cycle $c\{b_{ic}^{8}\}_{i=1}^{n}$, Rental demand of period $t\{f_{it}\}_{i=1}^{n}$, Returning demand of period $t\{g_{it}\}_{i=1}^{n}$, Station capacity $\{c_i\}_{i=1}^{n}$
Output: Rebalancing amount $\sum_{t=1}^{m}\sum_{i=1}^{n}\sum_{j=1}^{n} r_{ijt} + \sum_{c=1}^{q-1}\sum_{i=1}^{n}\sum_{j=1}^{n} r_{ijc}^{e}$ Divide l periods into q subcycles, each cycle has $z = l/q$ periods;
for $c = 1$ to q **do**
  for $d = 1$ to z **do**
    Implement SCRS
  end
  if $c \ne q$ **then**
    get the number of bikes of station i at the end of cycle $c\, b_{ic}^{e}$;
    if $b_{ic}^{e} > b_{i(c+1)}^{8}$ **then**
      the unloading amount at the station i is $e_{ic} = b_{ic}^{e} - b_{i(c+1)}^{8}$; station i belongs to the set of unloading stations E
    else if $b_{ic}^{e} < b_{i(c+1)}^{8}$ **then**
      the unloading amount at station i is $e_{ic} = b_{i(c+1)}^{8} - b_{ic}^{e}$; station i belong to the set of normal stations I
    else
      station i belongs to the set of normal stations N
    Conduct rebalancing amount r_{ijt}^{e} between problem stations in sequence from near to far;
    if $b_{ic}^{e} + \sum_{j\in I} r_{jic}^{e} - \sum_{j\in E} r_{ijc}^{e} = b_{i(c+1)}^{8}$ **then**
      station i belongs to the set of normal stations N
    end
    while E *or* I is not empty set **do**
      Conduct rebalancing amount r_{ijc} between problem stations and normal stations in sequence fron near to far
    end
  end
end
return $\sum_{t=1}^{m}\sum_{i=1}^{n}\sum_{j=1}^{n} r_{ijt} + \sum_{c=1}^{q-1}\sum_{i=1}^{n}\sum_{j=1}^{n} r_{ijc}^{e}$

Algorithm 2: The multicycle rebalancing strategy.

3	4	2	7	5	3

Figure 3: An example of a chromosome structure.

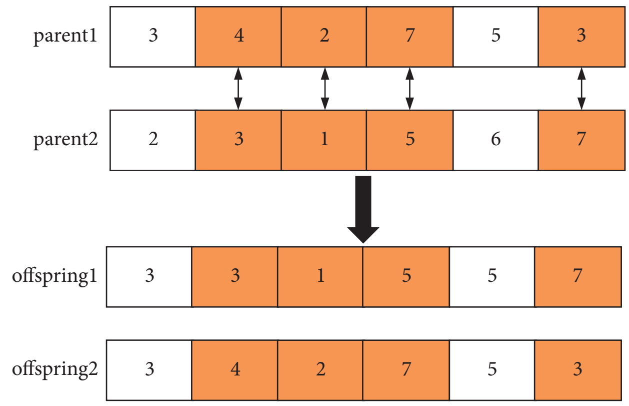

Figure 4: The process of uniform crossing.

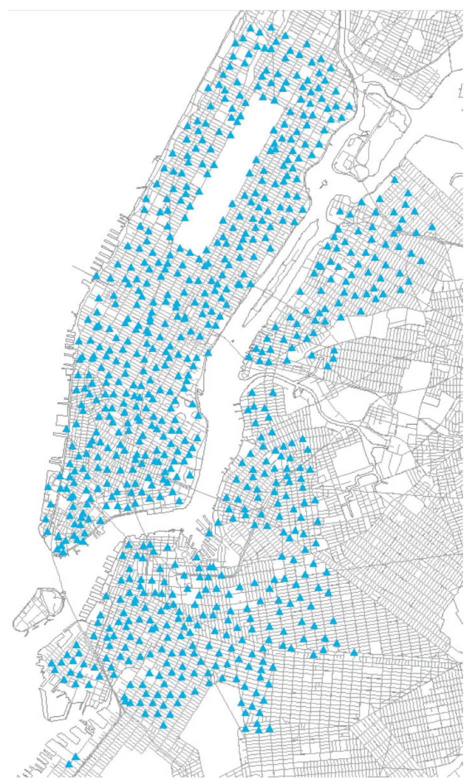

Figure 5: The distribution of Cite Bike stations in New York City.

immature convergence. In this paper, a unified variation method is used to replace each gene value in an individual with a lower probability of random numbers within the range of $[1, m]$.

4. Computational Experiment and Analysis

4.1. Data Source and Data Setting. The case data used in this paper are obtained from https://s3.amazonaws.com/tripdata/201903-citibike-tripdata.csv.zip, which is the Citi Bike System data in March 2019, and the system is the first bike-sharing project in New York, USA. Due to its low data missing and good universality after preprocessing, the system data is favored by many experts and scholars and used in the research of bike-sharing. Citi Bike System adopts the mode of docking stations, with an initial launch of 6,000 bikes and 300 stations. It then expanded rapidly, with 12,000 bikes and 770 stations by March 2019. All experiments are performed with Python 3.6 and implemented on an Intel(R) Core(TM) i7-7700HQ CPU @2.80 GHz, 8 GB computer equipped with Windows10 system.

To visually describe data, we used ArcGIS 12.0 to visualize station information, as shown in Figure 5, which shows the distribution of Cite Bike stations in New York, with each blue triangle indicating the location of a station. At the same time, we obtain partial travel data of Citi Bike System, each row of which is a piece of customer travel data including the time, the id, latitude, and longitude of

Table 1: The partial travel data of Citi Bike System.

Start time	End time	Start station id	Start station latitude	Start station longitude	End station id	End station latitude	End station longitude
2019/3/1 0:00	2019/3/1 0:24	319	40.711066	−74.009447	347	40.728846	−74.008591
2019/3/1 0:00	2019/3/1 0:05	439	40.726280	−73.989780	150	40.720873	−73.980857
2019/3/1 0:00	2019/3/1 0:12	526	40.747659	−73.984907	3474	40.725255	−74.004120

Table 2: The rental and returning amount of station id 72 from March 1 to 7.

Station id	Date	Rental amount	Returning amount
72	3.1	56	62
72	3.2	34	32
72	3.3	29	32
72	3.4	64	41
72	3.5	68	66
72	3.6	94	116
72	3.7	107	109

Note that, under different parameters, convergence of genetic algorithm is different, as shown in Figure 6. Under the conditions of the crossover rate $p_r = 0.8$, mutation rate $p_m = 0.01$, a relatively best result can be obtained, which may be used in experiments of this paper.

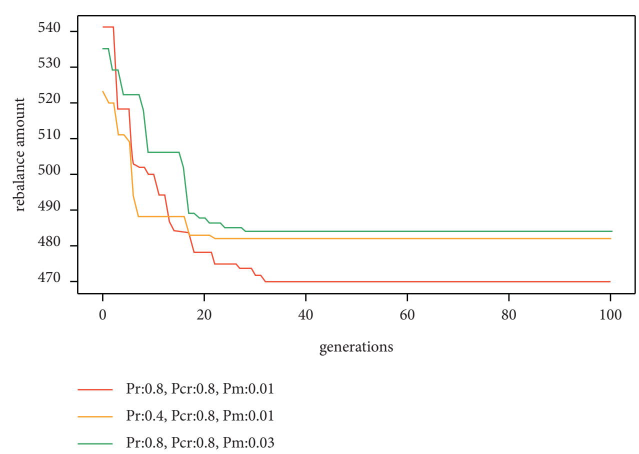

Figure 6: The convergence of genetic algorithm with different parameters.

departure and terminal stations, as shown in Table 1. Based on these data, it is possible to calculate the rental and returning amount of each station at any given period.

The experimental data are the travel data of Citi Bike in March 2019 with a total of 1,327,960 travel records, of which 769 stations are processed for travel data. To further clarify the format and structure of the data, we choose the station of *id* 72 and give its rental and returning amount of March 1 to 7, as shown in Table 2.

4.2. Single-Cycle Experiment Results. The validities of DGPO and SCRS in the 7-day cycle are verified by comparing with the methods commonly used in existing literatures. First, the initial number of bikes calculated based on DGPO is compared with the other three methods, namely, station capacity percentage, ratio of rental demand to returning demand, and uniform demand gap period which is defined as using the same demand gap periods. Secondly, SCRS is compared with traditional strategies, which tends to rebalance between problem stations preferentially, while the latter tends to rebalance station to station depending on the distance.

The experimental results show the total accumulative rebalancing amounts from March 1 to 7, which are obtained through eight experiments using four methods determining the initial number of bikes and two rebalancing strategies, as shown in Table 3.

Start with the traditional strategies, the initial numbers of bikes are calculated using the four methods, and the corresponding total accumulative rebalancing amounts are 2646, 2487, 996, and 980, respectively. Clearly, with an approach considering the demand gap, either the uniform demand gap period or DGPO is preferable to the other

Table 3: The experiment results of single cycle from March 1 to 7.

	The traditional strategy	SCRS
The station capacity percentage (50%)	2646	1468
Ratio of rental demand to returning demand	2487	1346
Uniform demand gap period (6 days)	996	520
ODGP	980	470

Table 4: Daily cumulative rebalancing amount and station number of participating in rebalancing under different methods.

Periods	The station capacity percentage (50%)	The ratio of rental demand to returning demand	The uniform demand gap period (6 days)	ODGP
Day 1	32 (6)	23 (5)	24 (11)	19 (6)
Day 2	69 (15)	55 (11)	41 (21)	30 (16)
Day 3	148 (46)	122 (30)	70 (29)	60 (26)
Day 4	291 (124)	240 (98)	102 (35)	92 (32)
Day 5	590 (247)	513 (191)	172 (45)	162 (42)
Day 6	969 (464)	869 (392)	303 (75)	292 (70)
Day 7	1468 (686)	1346 (625)	520 (129)	492 (125)

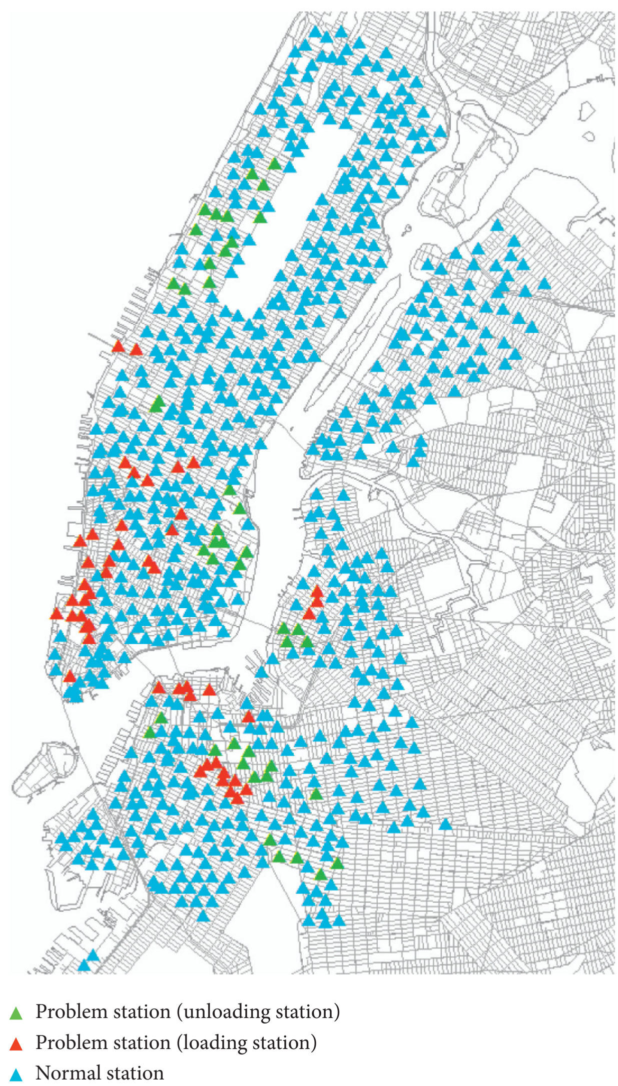

Figure 7: Distribution of problem and normal stations at the end of the 20th day.

Table 5: Comparison of experimental results of different rebalancing strategies.

Rebalancing strategy	Total rebalancing amount
Citi Bike official data	22280
SCRS, 28 days as single cycle	16743
MCRS, 7 days as subcycle	16732
MCRS, 14 days as subcycle	15463

Table 6: The results of MMCRS, MCRS and SCRS.

Cycle	Period	MMCRS		MCRS		SCRS	
		Cumulative rebalancing amount	Daily rebalancing amount	Cumulative rebalancing amount	Daily rebalancing amount	Cumulative rebalancing amount	Daily rebalancing amount
First subcycle	Day 1	19	19	19	19	211	211
	Day 2	30	11	30	11	371	160
	Day 3	60	30	60	30	513	142
	Day 4	92	32	92	32	642	129
	Day 5	162	70	162	70	743	101
	Day 6	292	130	292	130	930	187
	Day 7	492	200	492	200	1171	241
	ACRM	2358	1866	4326	3834		
Second subcycle	Day 8	2469	111	4350	24	1580	409
	Day 9	2675	206	4437	87	1954	374
	Day 10	2765	90	4454	17	2120	166
	Day 11	2944	179	4560	106	2447	327
	Day 12	3238	294	4766	206	2956	509
	Day 13	3575	337	4978	212	3522	566
	Day 14	4078	503	5380	1054	4309	787
	ACRM	6947	2869	9595	4215		
Third subcycle	Day 15	7225	278	9660	65	5223	914
	Day 16	7611	386	9753	93	6297	1074
	Day 17	7883	272	9813	60	7016	719
	Day 18	8098	215	9946	133	7739	723
	Day 19	8439	341	10214	268	8473	734
	Day 20	9031	592	10650	436	9381	908
	Day 21	9534	503	11036	386	10191	810
	ACRM	12266	2732	15147	4111		
Fourth subcycle	Day 22	12481	215	15249	102	10870	679
	Day 23	12688	207	15291	42	11705	835
	Day 24	12953	265	15362	71	12534	829
	Day 25	13175	222	15461	99	13504	970
	Day 26	13505	330	15688	227	14317	813
	Day 27	14045	540	16109	421	15473	1156
	Day 28	14800	755	16732	623	16743	1270

methods, and the latter is superior. Then, SCRS still uses four methods to determine the initial number of bikes, with a cumulative rebalancing of 1,468, 1,346, 520, and 470. Obviously, SCRS has done better than the traditional strategy in decreasing the total accumulative rebalancing amount. The effectiveness of the proposed DGPO and SCRS has been fully demonstrated and they are highly competitive compared with other methods.

To further illustrate this point, a comparative experiment is conducted, in which 7 periods are selected as a cycle and SCRS is used to calculate the total cumulative rebalancing amount under the four different methods to determine the initial number of bikes, as shown in Table 4. Note that the figure in brackets is the number of stations participating in rebalancing. Obviously, both the uniform demand gap period and DGPO have been effective in reducing rebalancing amount, as well as the number of stations involved in rebalancing, especially as periods increase, compared to the other two methods. In particular, DGPO is more superior to the uniform demand gap period.

4.3. Multicycle Experiment Results. Select the data from March 1 to 28 for multicycle experiment, and the distribution of problem and normal stations at the end of the 20th period is shown in Figure 7.

Assuming 7 or 14 days as a subcycle, 28 days can be correspondingly divided into four or two subcycles to execute MCRS, and in particular 28 days are also regarded as a single cycle to execute SCRS. The initial number of bikes of

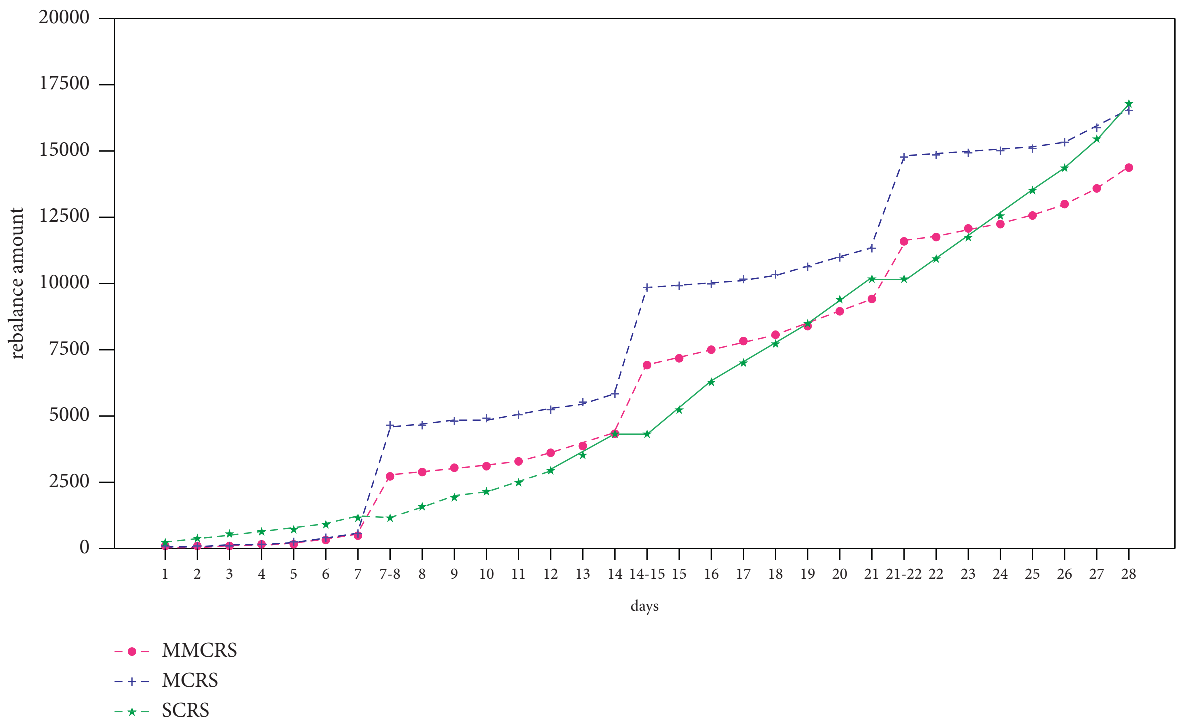

Figure 8: The results of MMCRS, MCRS, and SCRS.

each cycle is still determined based on DGPO. The Citi Bike official data comes from Citibank Monthly Bike Report of March 2019, with a rebalancing amount of 22280. Then, comparative experiments in the four cases mentioned above are carried out, and the results are shown in Table 5.

Obviously, compared with Citi Bike official data, the rebalancing strategies we have proposed are very helpful in reducing the total rebalancing amount. Of these results, regarding 14 days as a subcycle and performing MCRS yield the best result. Notably, both SCRS and MCRS have significantly reduced the rebalancing amount and the latter is superior in situation of excessive periods.

Another issue deserving special attention is that ACRM is modified to rebalance targeting only those stations with a rebalancing amount greater than the threshold value 40, namely, MMCRS. The validity of MMCRS and MCRS is also verified by experiments. The data of 28 days are still selected as experiment data, which is divided into four cycles with 7 days for each subcycle, and the initial number of bikes of each subcycle is calculated based on DGPO. The compared experiment results are shown in Table 6 and Figure 8.

The experimental results show that MMCRS is superior to MCRS in reducing the rebalancing amount. At the end of the first subcycle, the cumulative rebalancing amount using the two methods is the same as 492, as ACRM has not yet been applied. Starting with the second cycle, the cumulative repositioning amount of each subcycle calculated by MMCRS is lower than that calculated by MCRS in subsequent subcycles, as only problem stations with reposition amount greater than 40 need rebalancing in MMCRS, unlike the case of MCRS, in which all problem stations require rebalancing.

In addition, compared with SCRS, since ACRM is first carried out between the first and second subcycles, MMCRS and MCRS generate more cumulative rebalancing amount than SCRS at the end of the first subcycle; however, both of them declined significantly the daily rebalancing amount within subcycles. As periods increase, the advantages of MRCS and ACRM become more apparent, especially for MMCRS, where the rebalancing amount of each period is lower than that of the SCRS.

5. Conclusions and Future Work

Aiming at the problems of the fleet allocation determining and the research periods division, this paper proposes a fleet allocation method based on demand gap and a cycle division method which can give full play to the effect of the fleet allocation method in reducing the rebalancing amount. The initial number of bikes is calculated by the demand gap periods optimization (DGPO). Based on cycle division, a multicycle rebalancing strategy (MCRS) is presented, including a sing-cycle rebalancing strategy (SCRS) and an additional subcycle rebalancing method (ACRM). The fleet allocation optimization algorithm embedded in demand gap and cycle rebalance strategy is designed to solve the problem. The effectiveness of DGPO and SCRS has been fully demonstrated and they are highly competitive compared with other methods. Both of MCRS and ACRM decline significantly the daily rebalancing amount within subcycles, and with periods increasing, the advantages of MRCS and ACRM become more apparent.

The proposed methods are available for the planning and configuration at stations and the repositioning problem of

BSS for operators, meanwhile enriching the literature and providing references for researchers in related field. However, this paper assumes that customer demand is known and, in fact, tends to fluctuate over time, so we will reasonably predict the future customer demand with more accurate time granularity. In addition, the rebalancing objective in this paper is only one, but the multiobjective model is more adaptable. Therefore, we can establish the multiobjective function to further research.

Data Availability

The data that support the findings of this study are available with the identifier(s) at the private link. (https://s3.amazonaws.com/tripdata/201903-citibike-tripdata.csv.zip).

Disclosure

The authors declare that the work described was original research that has not been published previously and is not under consideration for publication elsewhere, in whole or in part.

Conflicts of Interest

The authors declare that they have no conflicts of interest.

Authors' Contributions

Jianhua Cao conceptualized the study, developed methodology, provided software, validated the study, responsible for formal analysis, wrote original draft, and visualized and supervised the study. Weixiang Xu provided resources, reviewed and edited the manuscript, and was responsible for project administration. Wenzheng Wang investigated the study, provided resources, and reviewed and edited the manuscript.

Acknowledgments

This work was partially supported by the National Natural Science Foundation of China (Grant no. 71774145).

References

[1] M. Börjesson and J. Eliasson, "The value of time and external benefits in bicycle appraisal," *Transportation Research Part A: Policy and Practice*, vol. 46, no. 4, pp. 673–683, 2012.

[2] M. Muratori, P. Jadun, B. Bush et al., "Exploring the future energy-mobility nexus: the transportation energy & mobility pathway options (TEMPO) model," *Transportation Research Part D: Transport and Environment*, vol. 98, Article ID 102967, 2021.

[3] G. Aifadopoulou, G. Tsaples, J. M. G. Salanova, I. Mallidis, and N. Sariannidis, "Management of resource allocation on vehicle-sharing schemes: the case of Thessaloniki's bike-sharing system," *Operational Research*, vol. 1–6, 2020.

[4] E. A. A. Abdellaoui and S. C. T. Koumetio, "Intelligent management of bike sharing in smart cities using machine learning and Internet of Things," *Sustainable Cities and Society*, vol. 67, Article ID 102702, 2021.

[5] L. M. Martinez, L. Caetano, T. Eiro, and F. Cruz, "An optimisation algorithm to establish the location of stations of a mixed fleet biking system: an application to the city of Lisbon," Edited by V. Aguilera, N. Bhouri, N. Farhi, F. Leurent, and R. Seidowsky, Eds., in *Proceedings of the Ewgt 2012 -Fifteenth Meeting of the Euro Working Group on Transportation*, vol. 54, pp. 513–524pp. 513–, Paris, France, September 2012.

[6] G. K. D. Saharidis, A. Fragkogios, and E. Zygouri, "A Multi-Periodic Optimization Modeling Approach for the Establishment of a Bike Sharing Network: A Case Study of the City of Athens," in *Proceedings of the International Multi-Conference of Engineers and Computer Scientists*, S. I. Ao, O. Castillo, C. Douglas, D. D. Feng, and A. Lee Jeong, Eds., Hong Kong, China, March 2014.

[7] S. Yan, J. R. Lin, Y. C. Chen, and F. R. Xie, "Rental bike location and allocation under stochastic demands," *Computers & Industrial Engineering*, vol. 107, pp. 1–11, 2017.

[8] Q. Chen, M. Liu, and X. Liu, "Bike fleet allocation models for repositioning in bike-sharing systems," *IEEE Intelligent Transportation Systems Magazine*, vol. 10, no. 1, pp. 19–29, 2018.

[9] B. M. Vishkaei, I. Mahdavi, N. A. Mahdavi, and E. Khorram, "Balancing public bicycle sharing system using inventory critical levels in queuing network," *Computers & Industrial Engineering*, vol. 141, pp. 1–10, Article ID 106277, 2020.

[10] B. P. Bruck, M. I. C. Fábio, and A. Subramanian, "The static bike sharing rebalancing problem with forbidden temporary operations," *Transportation Science*, vol. 53, no. 3, pp. 882–896, 2019.

[11] F. Cruz, A. Subramanian, B. P. Bruck, and M. Iori, "A heuristic algorithm for a single vehicle static bike sharing, rebalancing problem," *Computers & Operations Research*, vol. 79, pp. 19–33, 2017.

[12] S. C. Ho and W. Y. Szeto, "Solving a static repositioning problem in bike-sharing systems using iterated tabu search," *Transportation Research Part E: Logistics and Transportation Review*, vol. 69, pp. 180–198, 2014.

[13] G. Xu, T. Xiang, Y. Li, J. Li, and Q. Guo, "A mixed rebalancing strategy in bike sharing systems," *Engineering Optimization*, pp. 1–18, 2021.

[14] M. Yuan, Q. Zhang, B. Wang, Y. Liang, and H. Zhang, "A mixed integer linear programming model for optimal planning of bicycle sharing systems: a case study in Beijing," *Sustainable Cities and Society*, vol. 47, Article ID 101515, 2019.

[15] H. Sayarshad, S. Tavassoli, and F. Zhao, "A multi-periodic optimization formulation for bike planning and bike utilization," *Applied Mathematical Modelling*, vol. 36, no. 10, pp. 4944–4951, 2012.

[16] I. Frade and A. Ribeiro, "Bike-sharing stations: a maximal covering location approach," *Transportation Research Part A: Policy and Practice*, vol. 82, pp. 216–227, 2015.

[17] J. C. García-Palomares, J. Gutiérrez, and M. Latorre, "Optimizing the location of stations in bike-sharing programs: a GIS approach," *Applied Geography*, vol. 35, no. 1, pp. 235–246, 2012.

[18] J. X. Cao, C. C. Xue, M. Y. Jian, and X. R. Yao, "Research on the station location problem for public bicycle systems under dynamic demand," *Computers & Industrial Engineering*, vol. 127, pp. 971–980, 2019.

[19] Y. Feng, L. Cheng, B. Bruno, L. Fenu, and T. Zordan, "Cable optimization of a cable-stayed bridge based on genetic algorithms and the influence matrix method," *Engineering Optimization*, vol. 54, pp. 1–20, 2020.

Hindawi
Scientific Programming
Volume 2022, Article ID 1712929, 8 pages
https://doi.org/10.1155/2022/1712929

Research Article

The Path of Film and Television Animation Creation Using Virtual Reality Technology under the Artificial Intelligence

Xin Liu [1] and Hua Pan [2]

[1] *School of Art and Design, Lanzhou Jiaotong University, Lanzhou, China*
[2] *Lanzhou Echo Creative Culture Communication Co., Ltd., Lanzhou, China*

Correspondence should be addressed to Xin Liu; marcliu@lzjtu.edu.cn

Received 19 November 2021; Revised 9 December 2021; Accepted 27 December 2021; Published 13 January 2022

Academic Editor: Punit Gupta

The purpose is to provide a more reliable human-computer interaction (HCI) guarantee for animation works under virtual reality (VR) technology. Inspired by artificial intelligence (AI) technology and based on the convolutional neural network—support vector machine (CNN-SVM), the differences between animation works under VR technology and traditional animation works are analyzed through a comprehensive analysis of VR technology. The CNN-SVM gesture recognition algorithm using the error correction strategy is designed based on HCI recognition. To have better recognition performance, the advantages of depth image and color image are combined, and the collected information is preprocessed including the relations between the times of image training iterations and the accuracy of different methods in the direction of the test set. After experiments, the maximum accuracy of the preprocessed image can reach 0.86 showing the necessity of image preprocessing. The recognition accuracy of the optimized CNN-SVM is compared with other algorithm models. Experiments show that the accuracy of the optimized CNN-SVM has an upward trend compared with the previous CNN-SVM, and the accuracy reaches 0.97. It proves that the designed algorithm can provide good technical support for VR animation, so that VR animation works can interact well with the audience. It is of great significance for the development of VR animation and the improvement of people's artistic life quality.

1. Introduction

Virtual reality (VR) technology is making continuous progress with the continuous development of science and technology, providing a new production method for animation creation [1]. The change of the new VR animation' production mode leads to the corresponding change of the final work experience mode [2]. Among them, the most prominent is the audience's participation in the works, and the plot development of the works is closely related to the interaction of the audience. Human-computer interaction (HCI) technology under artificial intelligence (AI) needs to be further discussed to provide more possibilities for animation creation under VR technology [3].

In a VR environment, strong online perception ability and interactive feedback ability are needed, and gesture interaction is included in the abilities. Gesture interaction generally includes static gesture recognition and dynamic gesture recognition. The static recognition has gradually changed from the artificial feature extraction method to the mainstream convolutional neural network (CNN) feature extraction method, which has a more efficient recognition ability. On this basis, scholars have proposed gesture recognition using a neural network as a classifier. This method is to use edge detection to obtain the gesture features and then recognize the gesture through the neural network, while its accuracy is not satisfactory [4, 5]. Therefore, scholars have introduced the contour descriptor based on the depth projection map after continuous exploration. It is generally used to obtain the hand shape and structure information in depth image. The recognition accuracy has been improved through support vector machine (SVM) classification. Gesture recognition is used more in interaction, so related research is very crucial. The existing gesture recognition mostly uses CNN to build the relevant model of gesture recognition, which can greatly reduce the subjectivity and limitations caused by manual feature extraction. On this basis, the convolutional neural network—support vector machine (CNN-SVM) makes the model more robust [6]. The disadvantage is that the model has no relevant means to correct the wrong gesture when there is a recognition error.

In response to the shortcomings of previous algorithms, a new classification estimation error correction strategy is proposed based on the gesture recognition of CNN-SVM, and CNN-SVM is optimized to improve the final effect of the model. The innovation is to improve the recognition accuracy of similar gestures. The optimized CNN-SVM is designed to achieve the final effect of the optimization model. Later, the necessity of image preprocessing is discussed through experiments, and the recognition accuracy of the optimized CNN-SVM is compared, which proves that the accuracy of the designed gesture recognition algorithm is good enough. Thus, it provides reliable algorithm support for VR technology animation production and is of great significance to the development of art forms.

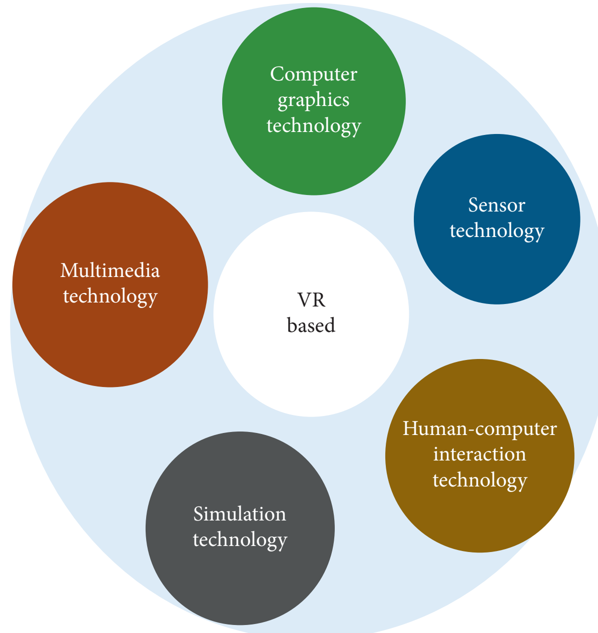

Figure 1: Technical basis of VR.

2. Materials and Methods

2.1. Differences between VR and Traditional Animation. VR technology is what people often call VR. This technology is a comprehensive new technology composed of various platforms established based on computer media [7]. Figure 1 shows its main technical basis.

The main function of VR is to create a simulated simulation environment to achieve very realistic effects like real life. In the process of realizing this environment [8], it is essential to build an image and sound in a three-dimensional (3D) space. Moreover, the simulated simulation environment also needs the ability of online perception and interactive feedback, such as vision, hearing, touch, and orientation. From the perspective of perception, it mainly records and analyzes people's relevant actions and other physical activity data, uses the computer to analyze the corresponding perception signals online, and transmits them to the perception equipment for people to perceive. The accuracy and timeliness of computer data processing are the most core in this process [9].

Making animation through VR technology is generally enriched at the perceptual level and added interactive mode. Animation has developed from hand drawing to computer drawing. Then, the 3D rendering of the image by computer has gradually matured, making the image have the level of 3D feeling and depth of field. The previous audience group of animation was relatively passive for the picture in animation, and there were almost no interaction and feedback with the relevant elements in the picture [10]. Present VR technology makes it possible for the groups watching animation to participate in the development of the plot. In daily life, there are various forms of interaction between people's subjective initiative and multiple elements in the real environment. People will also receive various forms of feedback in this process, that is, people's interaction in real life, which can also exist in a VR environment. The previous animation had no interaction in any form, so there was no way for people's subjective behavior to change the plot in animation, and there was no feedback link in any form [11].

It should be noted that the emergence of VR technology does not mean that the traditional form of animation will disappear from people's vision. The form of animation will exist in diversified forms for a long time. There are two reasons for this. One is that traditional animation has established a relatively perfect theoretical system; the other is that the art shown by traditional animation has a unique beauty, which is difficult to disappear over time. Traditional animation may not have much freshness for viewers from the form of expression, but it still does not affect people's acceptance of it. More mature forms of expression and the addition of more high-quality content can still exert a great influence. A typical case is that many traditional animations launched in Japan have achieved strong influence in multiple countries. Different types of animation can meet people's different spiritual needs. The development research path of animation based on VR technology mainly includes the following three lines (Figure 2) [12].

The development path of VR animation is based on the above content. A brief analysis is given as follows:

(1) The transformation from "plane" to "stereo" vision: the production of traditional animation is hand-drawn by relevant workers. It is to draw the motion track of the image very carefully, arrange it on the drawing paper in order, and then use the camera and other shooting tools to shoot in the corresponding order, followed by the rewashing work. Finally, the sample film is made. On this basis, fine editing work is conducted. In the animation production a long time ago, the animation workers first faced a piece of

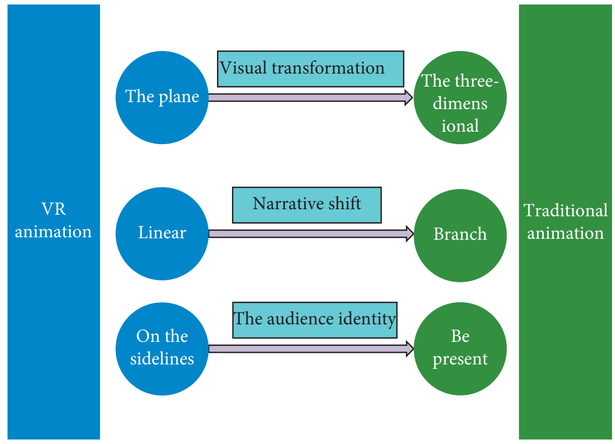

Figure 2: Research path of VR animation development.

white paper, and the core technology was the workers' painting skills. After the computer appeared, the computer monitor replaced the paper. The later 3D animation develops on this basis. However, it is still difficult to show a 3D feeling because it cannot get rid of the computer screen and cannot be said to be 3D. Later, this defect can be made up by wearing relevant equipment. 3D glasses are the most widely used equipment in daily life (Figure 3) [13].

However, the visual range is fixed, and the perceived "3D" has great limitations. The use of VR technology has greatly changed the previous creation methods, and the vision has changed from "plane" to "3D." The produced animation works are presented to the audience in a form without any dead corner, which gets rid of the previous screen and creates a 3D and realistic space. The whole animation production process is to use software to realize the whole process automation, greatly reducing the workload compared with the previous manual method [14].

(2) Narrative transformation from "linear" to "branch": VR technology can reflect the feedback ability of animation, which is why it has "vitality." Figure 4 shows the change of narrative mode.

The continuous development and evolution of the whole plot of traditional animation are similar to the form of storytelling. It generally has a complete time-plot of the beginning, development, climax, and end of things, which is often referred to as the "linear" development structure. The audience is more passive to accept the whole story and has no impact on the development of the whole story. VR technology itself has the characteristics of interactivity, which has brought different narrative forms to the development of the whole story. A "branch" is added at a certain point in the story to make the structural change of a line become a "branch" structure. The audience chooses different branches according to their own preferences to make the story develop towards different endings and exert an important impact on the development and change of the whole story [15].

(3) The transformation from "watching" to "being present": in the past, when watching animation, the audience, as an independent individual, is a "bystander," just watches quietly, and has no relationship with any element in the animation. To make the audience feel immersive to the greatest extent, movie players will try their best to create a dark and quiet viewing environment during the screening. However, no matter how optimized the environment is, it cannot be denied that the audience is still a bystander [16]. VR technology provides a different viewing form from the past because the immersion characteristics of the technology itself will enable the audience to participate in the interaction in the animation from the first perspective, and interactive feedback is added in the animation production process, so that the audience can change from "watching" to "being present."

2.2. Principle of SVM Classifier. The lifelike effect of interactive feedback is very dependent on the development of HCI technology. Among them, AI technology provides crucial technical support. The gesture recognition method studied is the CNN-SVM hybrid model. In this hybrid model, SVM uses different kernel functions to transform the samples that cannot be divided into low-dimensional input space into high-dimensional feature space, so that it can be linearly divided. Its theoretical basis is to minimize institutional risk, form the best hyperplane in the feature space, and obtain the structured information of data distribution, so as to reduce the requirements for data scale and data distribution [16] and reduce the error of independent test set. The effect of the SVM classifier is affirmed by many people. SVM is evolved from the optimal classification surface in the separable state. The optimal classification surface needs to classify accurately and maximize the classification interval. If the training sample $(\vec{x}_1, y_1), \ldots, (\vec{x}_i, y_i)$, $\vec{x}_i \in R^m$, $i = \{1, 2, \ldots, l\}$ needs a

FIGURE 3: 3D glasses based on the principle of the binocular angle difference.

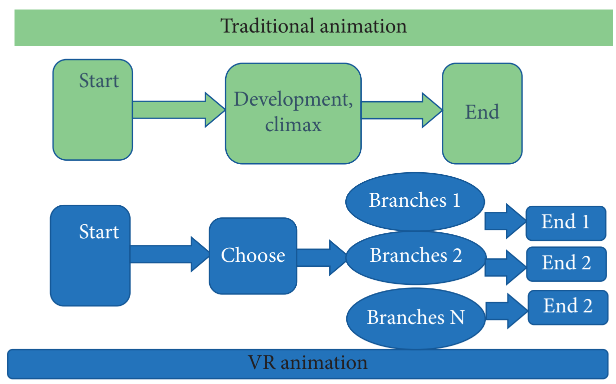

FIGURE 4: Change of VR animation narrative mode.

hyperplane with the largest interval so that the training set can be linearly separable (where $\vec{x}_i$ is the eigenvector and y_i is the relevant label), the problem of finding a hyperplane can be transformed into the following problem:

$$\min: P\left(\vec{w}^T, b, \vec{\xi}\right) = \frac{1}{2}\vec{w}^T \cdot C\sum_{i}^{1}\xi_i$$
$$\text{s.t}\begin{cases} y_i\left(\vec{w}^T\phi(\vec{x}_i)+b\right) \geq 1-\xi_i \\ \xi_i \geq 0,\ i=1,2,\ldots l, \end{cases} \tag{1}$$

where $\vec{w}$ is an m-dimensional vector, b is a scalar, and $\vec{\xi}$ is a relaxation variable. C is a penalty factor, which greatly affects the balance between edge maximization and classification error minimization. The training data $\vec{x}_1$ are mapped to a higher dimensional space by using function $\phi(\cdot)$ [17].

Chih-jen Lin developed a library for support vector machines (LIBSVM) that is used to build SVM. LIBSVM, as a software package for efficient classification and regression [18], can solve multiple classification problems. It uses a one-to-one method in the process of solving, which is to build $k(k-1)/2$ classifiers. Each classifier uses two types selected from k-type data in the training set [19]. The problems to be solved read:

$$\min: P\left(\vec{w}^{ij}, b^{ij}, \vec{\xi}^{ij}\right) = \frac{1}{2}\left(\vec{w}^{ij}\right)^T \cdot \vec{w}^{ij} + C\sum_{n}\xi_n^{ij}$$
$$\text{st}\begin{cases} \left(\vec{w}^{ij}\right)^T\phi(\vec{x}_n)+b^{ij} \geq 1-\xi_n^{ij} & y_n = i \\ \left(\vec{w}^{ij}\right)^T\phi(\vec{x}_n)+b^{ij} \leq -1+\xi_n^{ij} & y_n \neq i \\ \xi_n^{ij} \geq 0 & n=1,\ldots,k\dfrac{(k-1)}{2}, \end{cases} \tag{2}$$

where i and j refer to type i training data and type j training data. When making classification decisions, LIBSVM uses the maximum winning algorithm. Each classifier will vote on the category it determines, and the final classification result will be qualified by the category with a higher number of votes. LIBSVM can classify the classification results and provide classification probability information for different test samples. SVM is used for classification results with prediction probability during training. The probability of classification results will be used in gesture error correction to judge whether the classification results can be used [20].

2.3. Principle of CNN Classifier. CNN is a deep feedforward neural network, which generally has two parts: an automatic feature extractor and a trainable classifier [21]. It can make the deep CNN structure automatically obtain the high-level features of the image, so as to reduce the artificial design or selection of features. It transmits the obtained features to the classifier in the fully connected layer for classification processing. In this process, it will use supervised learning to optimize the weight between each layer in detail and later obtain a model with better robustness and accuracy [22].

Caffe framework is adopted to build CNN and identify and learn the model. Alex Krizhevsky network (AlexNet) is taken as the training network model. Figure 5 displays its network structure.

Figure 5 shows that the AlexNet network has 8 layers, including 5 convolution layers and 3 fully connected layers. The last fully connected layer outputs a 9-dimensional softmax to represent the prediction of 9 categories [23].

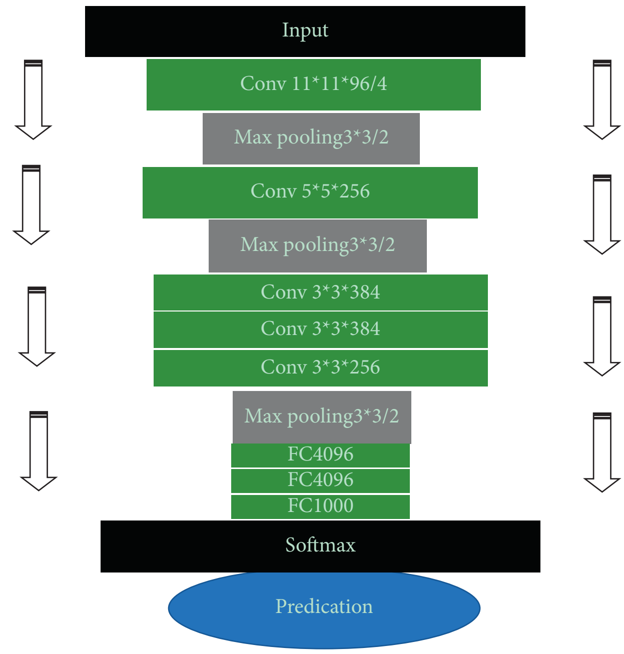

Figure 5: Model structure of AlexNet.

2.4. Error Correction Strategy Based on CNN-SVM Hybrid Model. CNN-SVM hybrid model is to replace the last output layer in CNN with SVM. The replacement process is as follows. First, the unprocessed image needs to be transmitted to the input layer for learning and training in CNN until convergence or the number of iterations is sufficient. Then, the images of the training samples are transmitted to the trained CNN training model, and 2048 dimensional training samples are obtained. The obtained sample feature vector is defined as the training set to train the SVM classifier, so as to obtain the CNN-SVM hybrid model [24].

In the following prediction results, LIBSVM estimates the probability that each sample is divided into a certain category. Finally, the most likely one will be selected as the classification conclusion. There is a problem of N classification in the decision-making process of LIBSVM. The similarity between the two classes is generally represented by distance. The absolute value of the prediction probability difference is used to represent the distance. The smaller the distance is, the smaller the gap between the two is. In the error correction strategy, the threshold M_{ij} represents the average distance between class i and class j. The threshold equation is as follows:

$$M_{i,j} = \frac{1}{s_{i,j}} \sum_{n=0}^{n=S_{i,j}} \left(P_n(i) - P(j)\right). \tag{3}$$

In equation (3), it should be noted that $P_n(i) \langle P_n(j)$. $P_n(i)$ is the probability of predicting that the nth test sample is class i, and it is the maximum value in the prediction results. $P_n(j)$ is the class j corresponding to the submaximum probability value; S_{ij} refers to the sample whose prediction result is class i, and it should meet that the submaximum value is class j. When the distance is lower than $M_{i,j}$, it shows that classification error is probable between the two classes. When the classification prediction meets the following conditions, the category corresponding to the maximum value is changed to the category corresponding to the maximum value.

$$\text{s.t}\begin{cases} W_n(i,j)M_{i,j} \\ \dfrac{1}{1+e^{-p_{i,j}/w_n(i,j)}}\text{rand}(0,1), \end{cases} \tag{4}$$

where $w_n(i,j)$ is the distance between the maximum value of possibility prediction and the submaximum value in the nth sample, that is, the value is $P_n(i) - P_n(j)$. $p_{i,j}$ is the probability that the predicted result is i, and the true rate is j. Small $w_n(I,j)$ and large $p_{i,j}$ indicate that the probability of errors in class i and class j will increase.

2.5. Data Preprocessing. Figure 6 shows the model running environment.

At present, multiple machine vision gesture databases are collected and obtained based on Kinect. Figure 7 shows the Kinect structure.

The data and images used in this experiment are the relevant gesture images of 400 college students' left hands 2 meters in front of Kinect, a total of 4000 depth images, and 4000 color images. The data need to be processed before use to improve the accuracy of the experiment.

Although the gestures made by people in color images can be recognized easily, it is still difficult to recognize them quite accurately. The reason is that gestures are affected by complex background conditions such as appearance and shape. The depth information in the depth image will not be disturbed by the environment such as light. Therefore, the

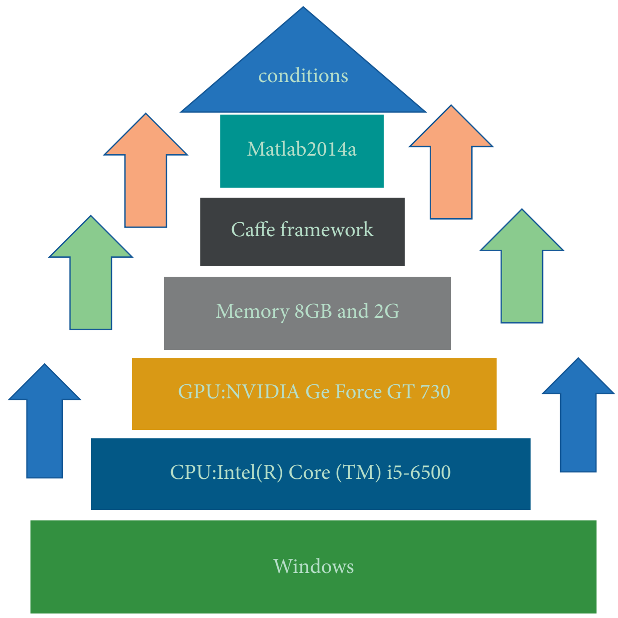

Figure 6: Model running environment.

Figure 7: Kinect structure.

depth image can well preserve the structural features of the human hand. The hand depth image is segmented, and then, the gesture range of the color image is segmented, so as to reduce the background interference of the color image. Figure 8 shows a specific preprocessing flow.

The main process of image preprocessing consists of three steps, which are explained in detail below. First, the collected depth image needs to be stored as a grayscale depth image with a pixel value of [0–255]. After the gray value 125 is used as the threshold, a binary image related to the gesture area will be obtained and then defined as a mask image. Then, the defined mask image and color image are calculated to obtain the gesture area image with low accuracy. The depth image and color image acquired by Kinect have the disadvantage of the inconsistent resolution, which will lead to the influence of other pixels near the acquired gesture area. Finally, the acquired gesture region needs skin color segmentation, and the final gesture region image is obtained through Bayesian skin color model. Figure 9 shows a depth gesture image after segmentation.

The interference of complex backgrounds and other environments is effectively eliminated. Later, the use of the Bayesian skin color model can also well preserve the useful information in the gesture area, so that the later recognition training has the support of data information.

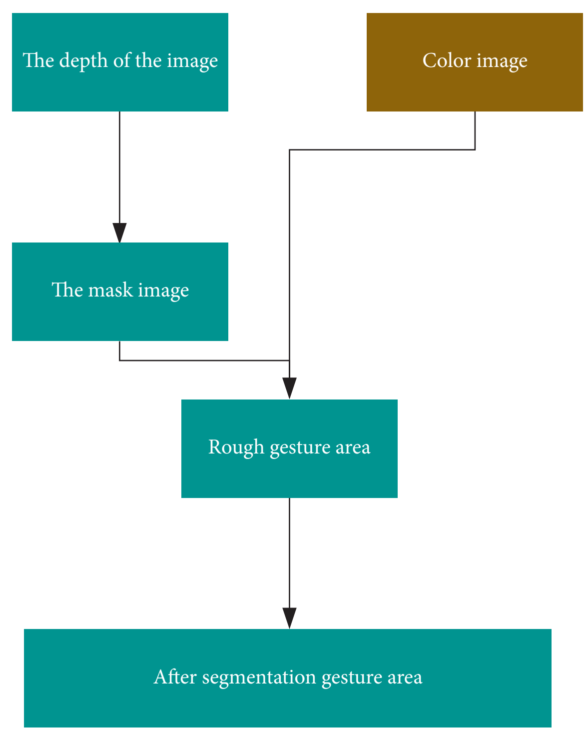

Figure 8: Preprocessing flow of image segmentation.

2.6. Case Analysis. In the following experimental link, the gesture image above will be segmented into 30000 images for the experimental dataset, among which 26000 images are used for model training and 4000 images are used for testing. On this basis, experiments will be conducted on the relationship between iteration times and the accuracy of different images. Besides, the accuracy of the designed optimized CNN-SVM recognition method, AlexNet, and CNN-SVM is tested, so as to evaluate their performance. The

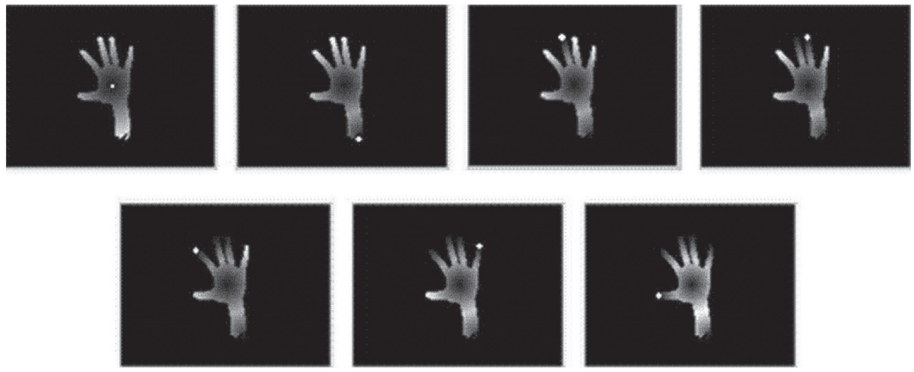

Figure 9: Depth gesture image after segmentation.

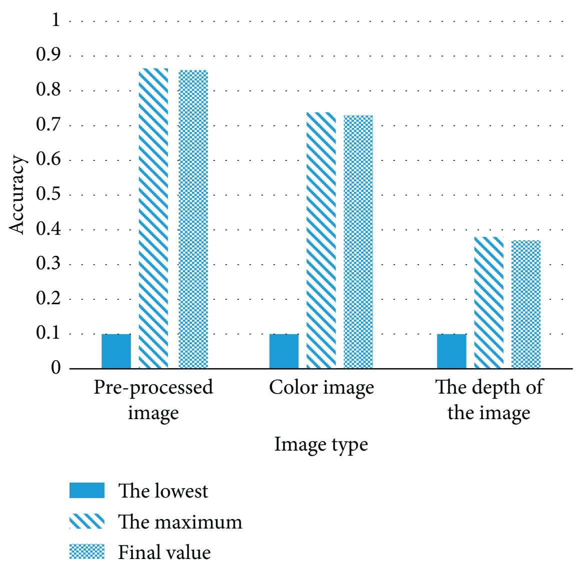

Figure 10: Accuracy of different images.

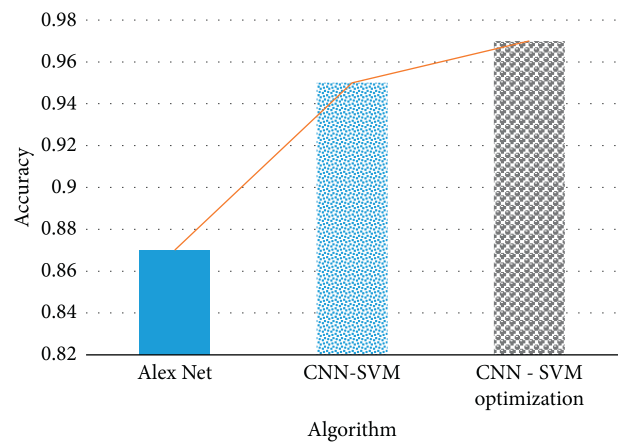

Figure 11: Accuracy of different methods on the test set.

accuracy and performance of the algorithm are plotted by using Excel 2020 software.

3. Results

3.1. Relationship between Iteration Times and Accuracy of Different Image Training. The relationship between the number of iterations and accuracy of different images is obtained through unilateral CNN network training on 26000 processed images (the number of iterations is specified as 3000), as shown in Figure 10.

Figure 10 shows that when the number of iterations is 3000, the highest accuracy of the color image is only 0.37, the highest accuracy of the depth image is 0.73, and the highest accuracy of the preprocessed image is 0.86. Therefore, the gesture after preprocessing and segmentation can effectively reduce the influence of complex background and other interference factors, so that CNN network learning can obtain richer and more accurate features.

3.2. Accuracy of Different Methods on the Test Set. The accuracy of the optimized CNN-SVM, AlexNet, and CNN-SVM recognition methods is tested on the test set of 4000 images. Figure 11 shows the test results.

Figure 11 shows that the accuracy of the optimized CNN-SVM is higher than that of the original CNN-SVM. From the numerical comparison, the optimized CNN-SVM has a recognition accuracy of 0.97, which is better than the other two algorithms. It provides excellent algorithm support for HCI and provides more reliable technical conditions for VR animation creation.

4. Conclusion

With the continuous development of science and technology, VR is also making continuous progress. It provides a new production method for animation creation. The animation works based on VR need the support of a reliable human-computer interaction technology when they are in use. Inspired by AI, a CNN-SVM gesture recognition algorithm with the error correction strategy is proposed. Based on CNN-SVM, the differences between animation works under virtual reality technology and traditional animation works are analyzed based on VR, and the CNN-SVM gesture recognition algorithm based on the error correction strategy is discussed from the perspective of human-computer interaction. The advantages of depth images and color images are combined, and the collected information is preprocessed to make the algorithm have better recognition performance. After experiments, the image preprocessing steps are summarized, and the recognition accuracy of the optimized CNN-SVM is compared with that of other algorithms. The comparison results show that the optimized algorithm is superior to others. It plays an important role in improving the ability of interactive feedback of VR and enhancing the interactive ability of films and television animation works. However, the size of the data is small, and it will be expanded in the follow-up study, making the research conclusions more convincing. The study promotes the development of VR and improves people's living standards.

Data Availability

The datasets used and/or analyzed during the current study are available from the corresponding author on reasonable request.

Conflicts of Interest

The authors declare that they have no conflicts of interest.

References

[1] L.-H. Ho, H. Sun, and T.-H. Tsai, "Research on 3D painting in virtual reality to improve students' motivation of 3D animation learning," *Sustainability*, vol. 11, no. 6, p. 1605, 2019.

[2] B. Gan, C. Zhang, Y. Chen, and Y. C. Chen, "Research on role modeling and behavior control of virtual reality animation interactive system in Internet of Things," *Journal of Real-Time Image Processing*, vol. 18, no. 4, pp. 1069–1083, 2021.

[3] Q. Wang, C. Li, Z. Xie et al., "The development and application of virtual reality animation simulation technology: take gastroscopy simulation system as an example," *Pathology and Oncology Research*, vol. 26, no. 2, pp. 765–769, 2020.

[4] A. Cannavò, C. Demartini, L. Morra, and F. Lamberti, "Immersive virtual reality-based interfaces for character animation," *IEEE Access*, vol. 7, Article ID 125463, 2019.

[5] H. Liang, S. Deng, J. Chang, and J. J. Zhang, "Semantic framework for interactive animation generation and its application in virtual shadow play performance," *Virtual Reality*, vol. 22, no. 2, pp. 149–165, 2018.

[6] L. Zhang, "Application research of automatic generation technology for 3D animation based on UE4 engine in marine animation," *Journal of Coastal Research*, vol. 93, no. SI, pp. 652–658, 2019.

[7] W. Chujitarom and P. Piriyasurawong, "Animation augmented reality book model (AAR book model) to enhance teamwork," *International Education Studies*, vol. 10, no. 7, pp. 59–64, 2017.

[8] J. Lee, "A Study on effective directive technique of 3D animation in Virtual Reality-Focus on Interactive short using 3D Animation making of Unreal Engine," *Cartoon and Animation Studies*, vol. 6, pp. 1–29, 2017.

[9] M. J. Blanchard, M. Reisch, and Y. V. Mejia, "Swing: 2D and 3D animation in virtual reality work-in-progress," *Frame*, vol. 2, no. 1, p. 12, 2020.

[10] J. Qi, G. Jiang, G. Li, Y. Sun, and B. Tao, "Intelligent human-computer interaction based on surface EMG gesture recognition," *Ieee Access*, vol. 7, Article ID 61378, 2019.

[11] B. K. Chakraborty, D. Sarma, M. K. Bhuyan, and K. F. MacDorman, "Review of constraints on vision-based gesture recognition for human–computer interaction," *IET Computer Vision*, vol. 12, no. 1, pp. 3–15, 2018.

[12] A. Haria, A. Subramanian, N. Asokkumar, S. Poddar, and J. S. Nayaka, "Hand gesture recognition for human computer interaction," *Procedia Computer Science*, vol. 115, pp. 367–374, 2017.

[13] J. Singha, A. Roy, and R. H. Laskar, "Dynamic hand gesture recognition using vision-based approach for human–computer interaction," *Neural Computing & Applications*, vol. 29, no. 4, pp. 1129–1141, 2018.

[14] G. Li, H. Wu, G. Jiang, S. Xu, and H. Liu, "Dynamic gesture recognition in the internet of things," *IEEE Access*, vol. 7, Article ID 23713, 2018.

[15] T. H. Tsai, C. C. Huang, and K. L. Zhang, "Design of hand gesture recognition system for human-computer interaction," *Multimedia Tools and Applications*, vol. 79, no. 9, pp. 5989–6007, 2020.

[16] C. Linqin, C. Shuangjie, X. Min, and Y. Jimin, "Dynamic hand gesture recognition using RGB-D data for natural human-computer interaction," *Journal of Intelligent and Fuzzy Systems*, vol. 32, no. 5, pp. 3495–3507, 2017.

[17] Y. Xu and Y. Dai, "Review of hand gesture recognition study and application," *Contemporary Engineering Sciences*, vol. 10, no. 8, pp. 375–384, 2017.

[18] W. Lv, "Gesture recognition in somatosensory game via Kinect sensor," *Internet Technology Letters*, p. e311, 2021.

[19] P. S. Negi, R. Pawar, and R. Lal, "Vision-based real-time human–computer interaction on hand gesture recognition," in *Micro-Electronics and Telecommunication Engineering, Lecture Notes in Networks and Systems*, D. K. Sharma, V. E. Balas, L. H. Son, R. Sharma, and K. Cengiz, Eds., vol. 106, Singapore, Springer, 2020.

[20] S. Hazra and A. Santra, "Robust gesture recognition using millimetric-wave radar system," *IEEE sensors letters*, vol. 2, no. 4, pp. 1–4, 2018.

[21] S. Ahmed, K. D. Kallu, S. Ahmed, and S. Cho, "Hand gestures recognition using radar sensors for human-computer-interaction: a review," *Remote Sensing*, vol. 13, no. 3, p. 527, 2021.

[22] J. Li, J. Wang, and Z. Ju, "A novel hand gesture recognition based on high-level features," *International Journal of Humanoid Robotics*, vol. 15, no. 2, Article ID 1750022, 2018.

[23] X. Yu and Y. Yuan, "Hand gesture recognition based on faster-RCNN deep learning," *Journal of Computers*, vol. 14, no. 2, pp. 101–110, 2019.

[24] K. A. Smith, C. Csech, D. Murdoch, and G. Shaker, "Gesture recognition using mm-wave sensor for human-car interface," *IEEE sensors letters*, vol. 2, no. 2, pp. 1–4, 2018.

Hindawi
Scientific Programming
Volume 2022, Article ID 1846254, 10 pages
https://doi.org/10.1155/2022/1846254

Research Article

Modeling and Simulation of Consumer Preference Decision for Commercial Complex Location Based on System Dynamics

Bin Guo,[1,2] **Bing Zhang**,[1] **and Yang Li**[2]

[1]*School of Management, Xi'an University of Architecture and Technology, Xi'an, China*
[2]*School of Public Administration, Xi'an University of Architecture and Technology, Xi'an, China*

Correspondence should be addressed to Yang Li; liyang@live.xauat.edu.cn

Received 28 October 2021; Accepted 14 December 2021; Published 10 January 2022

Academic Editor: Punit Gupta

The influencing factors of consumer shopping behavior play a key role in the later performance of commercial real estate enterprises. On the basis of analyzing the influence factors of customer patronage and the influence factors of commercial complex site selection decision and their relationship, a causal relationship graph and a system dynamic model are established, which can describe the influence of customer preference on commercial complex site selection decision. And introducing customer subjective factors optimize the original pure objective factors site selection decision model. The model is implemented by using the system dynamics modeling tool Vensim. At the same time, the model is verified by using the data of the first-hand investigation. The results show that the calculated data of the model is in good agreement with the actual data. The results show that the system dynamics method can effectively simulate the influence of various factors on the decision-making of the commercial complex. As the forecast of the model, the key indexes of the decision-making of the city commercial complex are discussed, and the measures to be taken are put forward, which can provide reference for the decision-making of the location.

1. Introduction

With the development of social economy and the increasing income of urban residents, consumer's consumption demand is also gradually becoming rich and diversified. More and more preference is given to the large commercial complex, which integrates commerce, hotel, culture and entertainment, catering, and office. This demand strongly promotes the rapid development of commercial complex. Site selection has great influence on the business operation and development in the later stage of the commercial complex. The decision-making of commercial complex is a complicated process, and it is immutable and irreversible. Whether the decision-making of location can be made scientifically is the precondition and necessary condition for the success of the business. But, in practice, most of the objective factors, such as regional economic level, population distribution, business circle, and traffic, are taken as the decision-making factors of location. But factors of consumer subjective that influence the location of commercial complex are rarely considered. Therefore, this paper from the perspective of consumer preference decision is of more practical significance.

The study of site selection for commercial complex has been strongly promoted. In 1929, Hotelling published a study on the location of two competing ice cream vendors on a straight line. The first study of competitive location is carried out [1]. The Hotelling model is the basic research model of competitive location. The paper studies the location of two competitive stores in a line and brings together the economic, geographical, and game theory. On this basis, many scholars put forward the competition location model from different angles. At present, the research on competitive site selection domestically and abroad has been mature, which is divided into three main types: competitive site selection, static competition site selection, and dynamic competition site selection, and the mature competition site selection theory and related model are formed [2–5].

In practice, after the commercial complex site selection, construction and start of business, the location, transportation convenience, the level of regional economic development, natural resource conditions and operational level, and other factors will have a major impact on the consumer's willingness. Besides the level of operation, these major factors, all in the site selection decision-making phase have been determined, and it is difficult to change again. Competitive location of the largest market share must be based on commercial complexes that attract the largest range of consumers. Most of the research methods of domestic and foreign scholars on the site selection of commercial complexes are based on objective factors, such as location, population distribution, business circle, and traffic conditions, while few subjective studies are conducted on consumers' intention of patronage and behavioral differences. The fuzzy analytic hierarchy process, analytic hierarchy process, comprehensive evaluation model, cluster analysis, and SEM analysis are adopted to minimize the risk of site selection decision by determining the index evaluation system of commercial complex site selection. Some scholars use GIS and consider using spatial analysis methods to process spatial data and find the optimal location for shopping malls. The consumer patronage intentions of this research are introduced into the study of the commercial complex's site selection. Through the analysis and identification of the main factors influencing the consumer patronage intentions to guide commercial complex site selection, site selection in decision-making phase will increase the consumer patronage intentions to maximize market share factors, which were fully considered. Location decision is regarded as a complex system composed of many elements.

Therefore, based on the analysis of the influence factors and their relationship between the decision-making system and the decision-making system of the commercial complex, this paper considers the decision-making system as a whole according to the rational behavior theory and the planning behavior theory and establishes a system dynamic model, which can describe the influence of the decision-making of the commercial complex, and verifies the validity of the model through simulation.

2. Analysis of Location Decision System for Patronage and Commercial Complex

2.1. Analysis of Influencing Factors of Patronage. The primary premise of studying the consumers' patronage is to identify the key factors that affect the patronage, and it is necessary to identify the key factors that influence the consumers' patronage.

2.1.1. Regional Stereotypes. Stereotypes are the cognition of a certain thing formed in people's activities and interactions. The later people's understanding is based on the foundation of the former and is vulnerable to subjective restrictions, making the later awareness of the constraints [6]. Regional stereotype is a cognitive structure that covers the individual's recognition and expectation in a certain region [7]. Because of the difference of living environment and culture, there are differences in the perception of the individual in different regions for a long time. The perception of the individual has "specificity" and "regionality," which are embodied in the special geographic imprint of the region, the values, and the sense of belonging of the individual.

2.1.2. Consumer Behavior Patterns. Consumers gradually form a specific lifestyle under the influence of their internal and external factors. This unique way of life can create a demand and desire that match consumers. And these needs and desires need to be met by specific consumer behaviors. Some consumers turn to a commercial complex to buy a product or service, which is often called a utilitarian consumer. Other consumers who favor a commercial complex are not just shopping or consuming, and they view the commercial complex as a form of leisure or entertainment [8].

2.1.3. Traffic Convenience. The shopping trips of consumers are always aimed at the lowest cost, and the time cost spent in traffic is one of the main factors that affect consumers' preference for commercial complexes, and due to the homogeneity of business complexes, consumers rarely "go closer" for shopping or consumption [9].

2.1.4. Regional Natural Conditions. A good natural environment will have an impact on consumer demand, consumption structure, consumption level, and mode of consumption [10]. Abundant natural, human landscape resources and clean surrounding environment will create a sense of pleasure to boost consumption, and if a commercial complex is built around parks or tourist attractions, it will increase consumers' willingness to go [11].

2.1.5. Regional Economic Conditions. If the industrial structure of the urban areas is reasonable, the foundation is good, the population density is large, the economic development is better, the urban public supporting resources will be better, and the consumption level of surrounding residents will be correspondingly higher. In those areas with backward industries and no other advantages such as transportation, the economic development is relatively poor, and the consumption level of the surrounding residents is relatively low [12]. Regions with good economic development are more attractive to groups with high academic level, high income, and high consumption.

2.1.6. Operational Level. The operational level of the commercial complex usually includes the variety of goods, shopping environment, service level, and so on. And even the light, color, and smell of the complex will influence the consumer's willingness. If it can have obvious advantages in the commercial form, service level, internal environment, and price compared with other commercial complexes in the same city later, or it can provide personalized services which are not available in other commercial complexes [13], it will attract more consumers.

2.2. Analysis of the Influence Factors of Business Complex Decision. The urban commercial circle represents the level of economic development of a city to a certain extent. The development of commercial circle can attract more commercial complex projects, which further promote the development of urban commercial circle and are interdependent and mutually promoted. Based on the theoretical analysis of regional growth pole, the factors affecting the decision-making of commercial complex site include economy, politics, culture, location, environment, and other five categories, covering the urban development, policy, consumer culture, location, transportation, natural environment, and other aspects of the content. A comprehensive table of factors affecting the decision-making of commercial complex site is presented.

Twelve experts with senior experience were selected from senior practitioners in institutions of higher learning and industries. Based on the theoretical analysis of regional growth pole theory and the five-force theory, the paper puts forward a table of factors influencing the business complex site selection decision and asks experts to judge the influence of the selected index factors on the business complex site selection decision on a scale of one to five according to their experience. After the first round of the survey was completed, the findings were recycled, inconsistent information was fed back to the experts, and then, the second round of the survey was launched. On this basis, the weight of each index is analyzed by using the analytic hierarchy process, and finally the influencing factors and the weight of each index are determined, as shown in Table 1.

3. Patronage Affects the Decision-Making of Commercial Complex

3.1. System Dynamics Model. System dynamics is based on system theory, supplemented with feedback theory and information theory to study information feedback science. The theory was founded in 1956 by Professor Jay W. Forrester of MIT in the United States, and the core of the theory is the system dialectical view, from the point of view of the whole, connection, movement, and development, to study the problem and emphasize the use of qualitative and quantitative methods to analyze the system [14, 15].

The system dynamics has the following characteristics, which makes it better to study the consumer's preference for decision-making of commercial complex location decision. (1) The research of system dynamics is mainly aimed at the social and economic system, which has a good pertinence to the research of this paper. (2) The system dynamics adopts the combination of quantitative analysis and qualitative analysis, which breaks the deficiency of the traditional research, and can more truly simulate the characteristics of the business complex preferential system. (3) It can clearly reflect the various internal feedback, including implicit and intuitive. The decision-making factors of commercial complex location are complex, and the system dynamics can be used to express these circuits, and the relationship between various factors and internal and external systems can be clarified.

3.2. Causal Relationship of Site Selection for Commercial Complex. Based on the research results of the previous paper, the content boundary of the system includes six aspects: regional stereotypes, consumer behavior patterns, traffic facilitation, natural environment, regional economic development, and operation level, and six subsystems corresponding to them are formed.

Regional stereotypes have an impact on consumers' regional identity, values, and sense of community ownership. The extent to which consumers have a geographical impression of the region where the business complex is located is directly proportional to their willingness to benefit. Consumers are affected by their own values such as preferences and believe that the sense of group belonging gained by the commercial complex consumption in different regions will be different. The stronger the sense of group belonging is, the higher the chance of generating the willingness to favor [16–18] will be.

Consumer behavior patterns can be influenced by a variety of factors, among which consumers have strong personal attributes such as gender, age, and income [19]. In addition, the personalized differences of consumer behavior patterns are mainly affected by the factors such as the income level, occupation, educational background, age, family structure, and external factors, such as social class and social culture [20]. The chances of a consumer getting a high income are positively correlated with education, and the higher the income, the stronger the purchasing power. And the growth of consumer age will change the structure of the family. External factors mainly refer to the group and class of consumers and the consumption environment [21].

In this paper, the dynamic analysis of traffic factors is performed according to four aspects, namely, time, reliability, selection, and comfort. The preference for business complexes decreases with increasing travel time, reflecting consumers' preference for business complexes, which is less time-consuming in traffic. The distance between the commercial complex and the consumer, the geographical situation around the commercial complex, and the convenience of transportation will affect the time spent by the consumer [22]. Moreover, the safety of traffic and the selectivity of transportation also matter to the consumers when they produce preferential behavior, showing positive correlation.

The natural environmental factors and environmental quality of the region will have a great influence on the location of the commercial complex [23]. Consumers are more inclined to favor those areas with relatively flat terrain, unique natural landscape, historical and cultural relics, and other resources, and factors such as regional ecological indicators, air quality, and road cleanliness will also affect consumers' preference. Consumers usually have multiple objectives when traveling, and consumers will give priority to those areas with relatively complete public support.

The level of urbanization is a measure of the level of development of a regional economy that can attract more potential consumers. At the same time, the improvement of regional infrastructure with high level of economic development can attract more talents, and there is a clear positive relationship between the level of economic development and

Table 1: Factors affecting the site selection of commercial complexes.

Target layer	Criterion layer	Secondary indicator	Weight
A commercial complex site selection decision	B1 politics	U11 government policy	0.14
		U12 medium- and long-term urban development plan	0.07
	B2 economy	U21 level of economic development	0.07
		U22 population	0.05
		U23 disposable income per capital	0.04
		U24 industrial structure	0.02
		U25 development potential	0.03
	B3 culture	U31 consumer culture	0.11
	B4 location	U41 traffic facilitation	0.11
		U42 infrastructure facilities	0.08
		U43 business district	0.15
		U44 level of competition	0.05
	B5 others	U51 surrounding natural resources and environment	0.04
		U52 topography	0.02
		U53 geological conditions	0.02

the location of commercial complex [24]. Regions with high economic development levels can attract more investors to build a commercial complex, thus forming a "business circle" within a certain geographic scope, increasing the attractiveness of the whole region to consumers.

The business type, service level, shopping environment, and price level of the commercial complex are also the main factors that influence the customer's preference. The trade form is the quantity of the commodity which can be provided by the commercial comprehensive carrier for the consumer to choose, and its abundance is directly related to the consumer's willingness to favor. Consumers prefer to consume in the commercial complex where the shop assistants can provide high quality service, besides women's private parking spaces, special room for mother and infant, women's exclusive floors, and so on. Consumers prefer commercial complexes that offer good shopping environments such as indoor air flow, pleasant smell, clear signs, light and soft lighting, and relaxing background music. There is a clear positive correlation between the business complexes and the consumer, which means the more they are focused on hot topics and create a good internal and external atmosphere, the more attractive it is to consumers [25].

Through the previously mentioned analysis, the causality diagram of the influence of various factors on the site selection of commercial complex can be constructed (see Figure 1).

3.3. System Dynamics Flowchart. Based on the previously mentioned analysis, a stock map of the location of the commercial complex can be drawn as shown in Figure 2.

4. Model Simulation

As Xi'an is a central city in China, it has a good economic and population foundation and is less affected by the network of neighboring cities than the eastern coastal cities, so it has the foundation for the independent analysis of the impact of commercial site selection in large cities in this study. This paper uses the system dynamics modeling software Vensim to implement the model, based on the indicators and data Xi'an City Statistics Bureau published, as well as the business complex A project data, to verify the model. Since the business complex A of this study started to operate in December 2008, the simulation time of this study is set to 2008–2018, and the simulation step is one year, with a total of 10 years.

4.1. Simulation Result Analysis. In order to quantify the preference of consumers, consumers are divided into groups with preference and groups without preference, and the growth rate of preference is used as the rate variable to generate the preference of the population as the stock. The growth rate of preference is mainly affected by regional stereotypes, consumer behavior patterns, traffic convenience, natural resources, regional economic development, and operation level. Through system dynamics simulation, the final preference of simulation results is obtained (Figure 3).

As can be seen from the simulation results, the final willingness to patronize in the simulation period presents three stages of change: steady phase, slow growth phase, and rapid growth phase. In the early development of business complex, the infrastructure and service level are at the primary level, and the customer groups coming to the complex are less, so the development is relatively stable. With the improvement of transportation and other infrastructures, the continuous improvement of the service level, and the impact of word of mouth, the number of consumers who will purchase in the commercial complex gradually increase. The later business complex will form its own fixed customer group, and the fixed customer will lead to the surrounding potential consumers, therefore showing a trend of rapid growth.

Compared with the ultimate preference, the total income of the commercial complex has a more obvious trend of change. For example, in Figure 4, the early commercial complex needs to increase the publicity, promotion, and early-stage investment. The customer experience and the level of employee service are low, so the total income is low

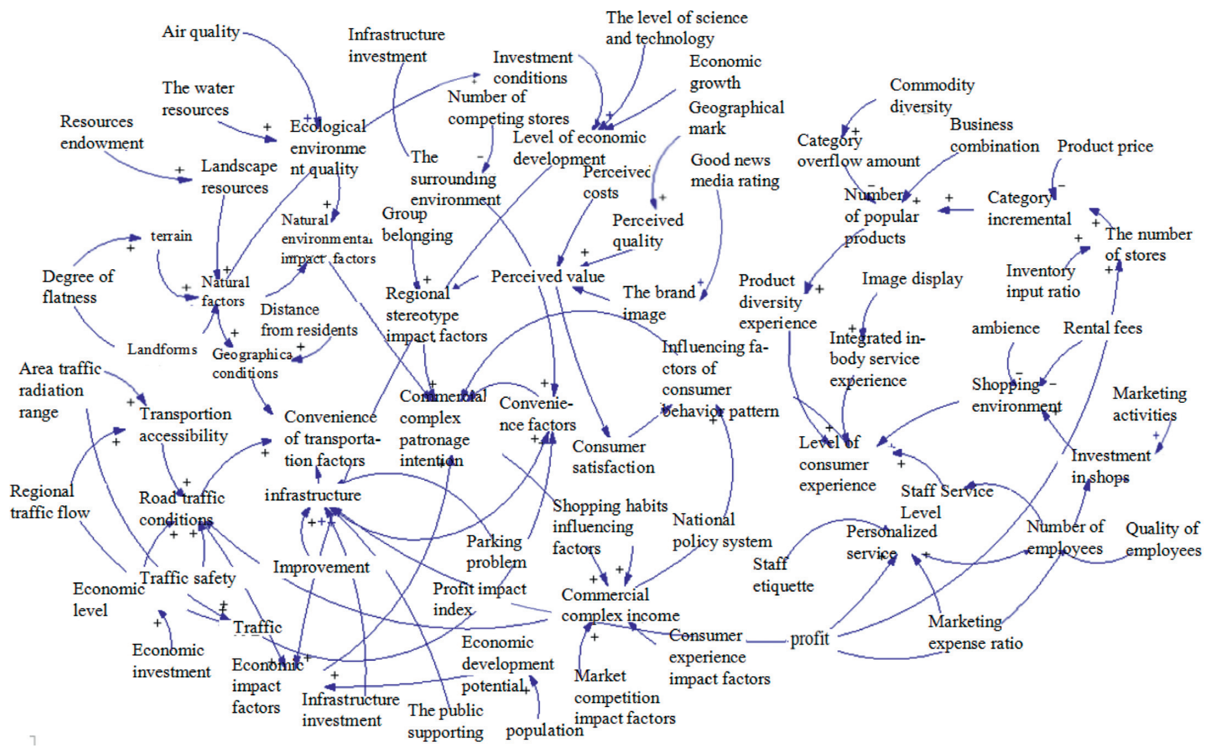

FIGURE 1: Causal relationship diagram for the location of commercial complex site selection.

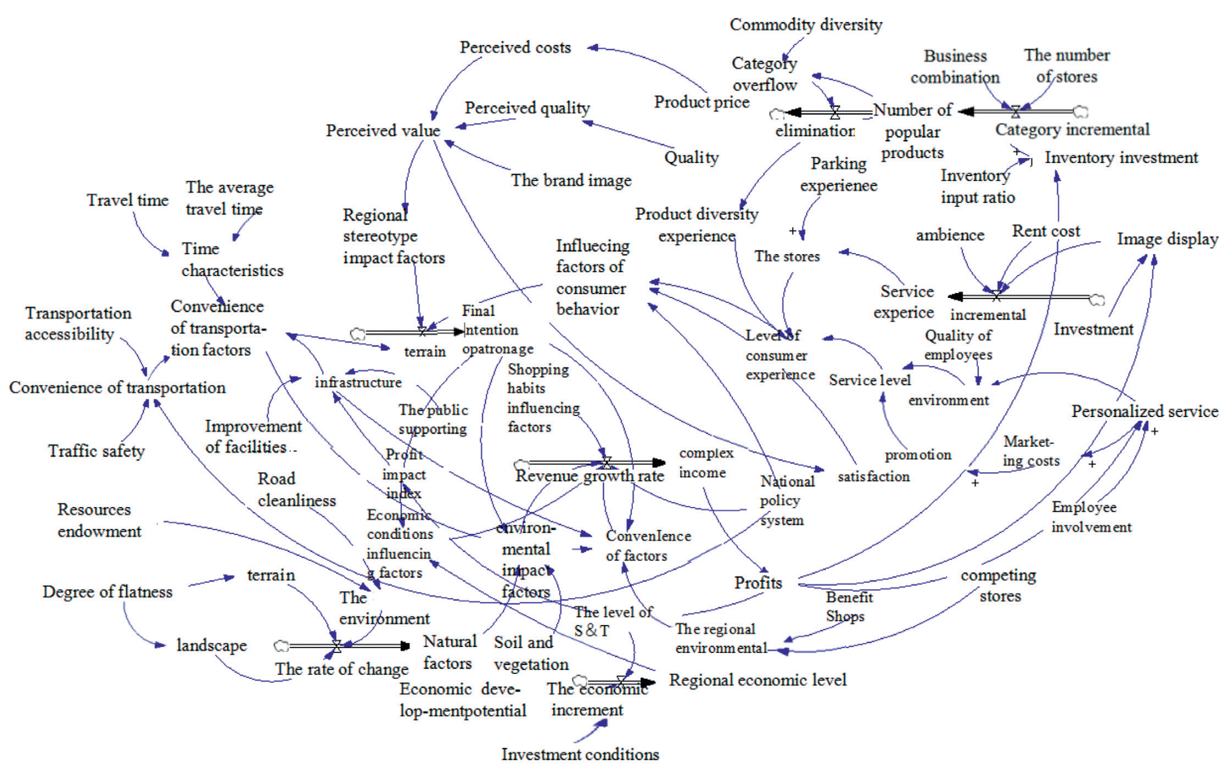

FIGURE 2: Flow stock map for the location of commercial complexes.

and the increase is small. The later increase in income was added. Although the increase was relatively significant, there was room for improvement.

4.2. Comparative Analysis on Site Selection Optimization of Commercial Complex. By adjusting the influence factors of regional stereotypes, consumer behavior patterns, traffic

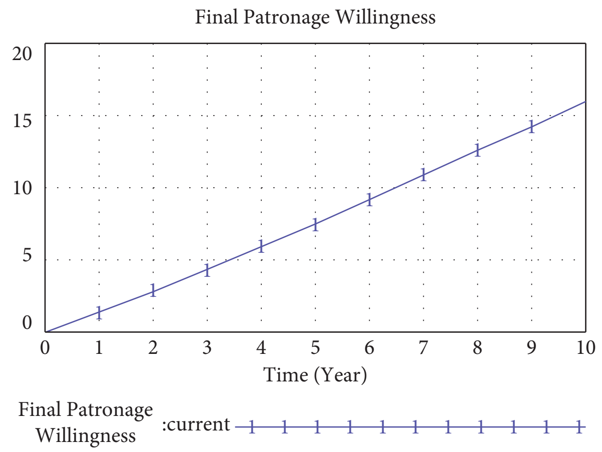

Figure 3: Simulation diagram of final patronage willingness.

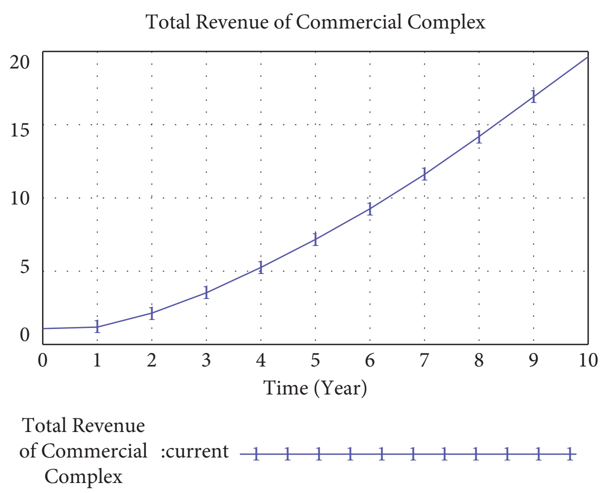

Figure 4: Simulation diagram of total revenue of commercial complex.

conditions, natural environment, regional economy, and operation level in the dynamic model of the system, the changes of consumers' preferences and the profits of commercial complexes were observed (see Figures 5–16).

Based on the previously mentioned comparison, this paper gives the following suggestions on the commercial complex location decision-making from six aspects of influencing factors of consumer's preference.

Regional Stereotypes. Before planning the business district or commercial complex project, the government planning department should fully understand the regional stereotypes of the area where the plot is located as far as possible to avoid planning the commercial complex land in the more negative imprint areas. If the land use planning is indeed restricted by some conditions that cannot be changed artificially, the planning department should take into consideration the planning conditions, such as volume rate AND construction withdrawal, and provide hardware support for the later change of these negative seals by the development enterprise.

Consumer Behavior. Before bidding for land, real estate development enterprises should conduct sufficient investigation and demonstration on the relevant information of the target consumers in the region. Project positioning shall be based on the regional consumption level and consumption capacity, and the project positioning shall not be too advanced or significantly higher than the regional consumption level and consumption capacity. At the same time, it is necessary to complement each functional section and pay attention to controlling the volume of commercial.

Transportation Convenience. Real estate development enterprises must fully understand the mid- and long-term planning of the public transport. The project should be actively integrated into the function of the city when it is located in the decision-making stage. During the construction design stage, the project should be connected with the site of the active and public transport on the building form, function, and dynamic line. Through the design method, the project of commercial complex becomes a kit of the city; for example, the entrance and exit of the subway directly connected to the interior of the commercial complex and the bus station setup near the entrance and exit of the commercial complex.

Regional Natural Conditions. The real estate development enterprises shall carry out the commercial theme positioning and function positioning according to the regional climate characteristics and landscape resource conditions, combine the theme and function with the surrounding historical culture and natural landscape as far as possible, and provide consumers with different consumption experiences, thus avoiding the dilemma of being in the same competition with other comprehensive projects.

Regional Economic Conditions. Real estate development enterprises should fully understand the total amount of regional economy, per capita disposable income and other basic information, and at the same time, they should also understand the regional future development planning, including the industrial layout, government fiscal and taxation policies, infrastructure construction, and so on.

Operational Level. Commercial complex projects are usually managed and operated by professional operating companies after the construction of real estate developers is completed. In reality, many projects in the operation team take over only to find that there is a big problem in the volume, function and dynamic line, which brings a lot of inconvenience to the late operation, so the operation team in the location decision-making stage should intervene, dividing business format and planning the internal business dynamic line according to the project positioning. In the construction stage, the operation team should put action to attract business, including the main stores, the secondary main stores, the various brands, and the merchants.

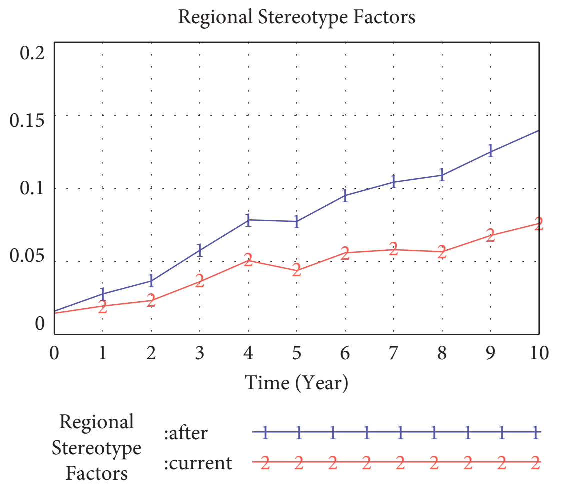

Figure 5: Comparison of regional stereotype optimization.

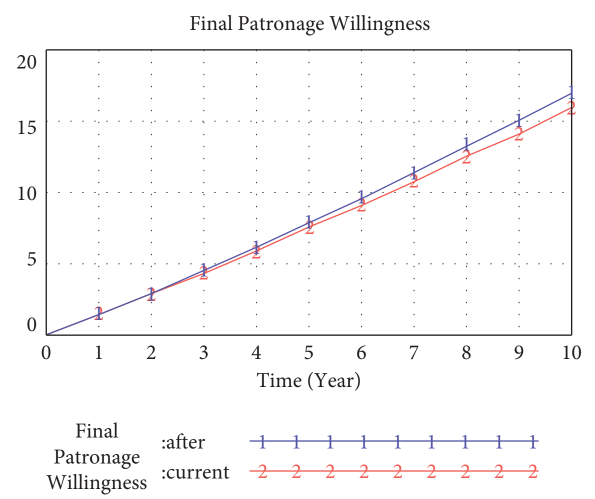

Figure 6: Comparison of optimization of patronage growth.

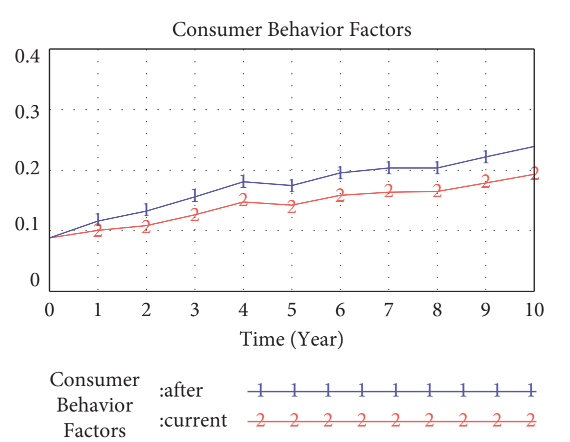

Figure 7: Comparison of consumer behavior factors after optimization.

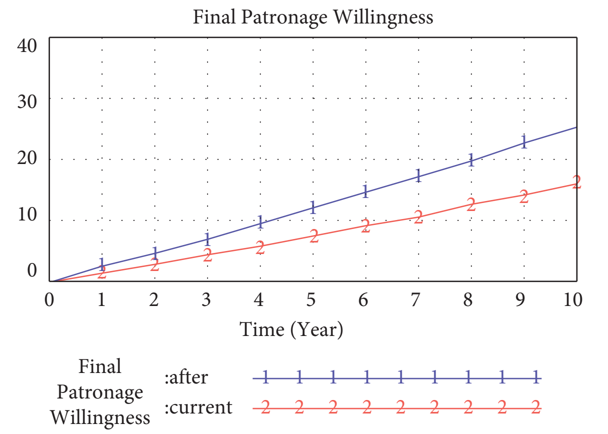

Figure 8: Comparison chart of optimization of growth rate of patronage willingness.

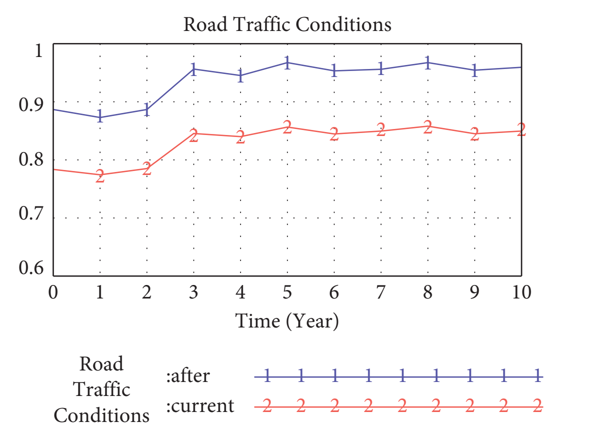

Figure 9: Optimization and comparison of factors affecting traffic convenience.

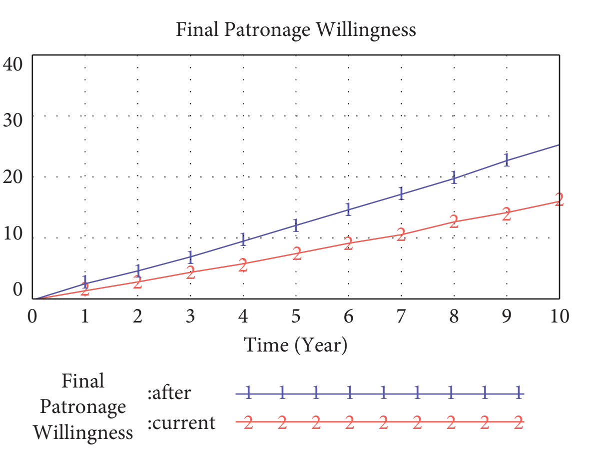

Figure 10: Comparison of final patron intention optimization.

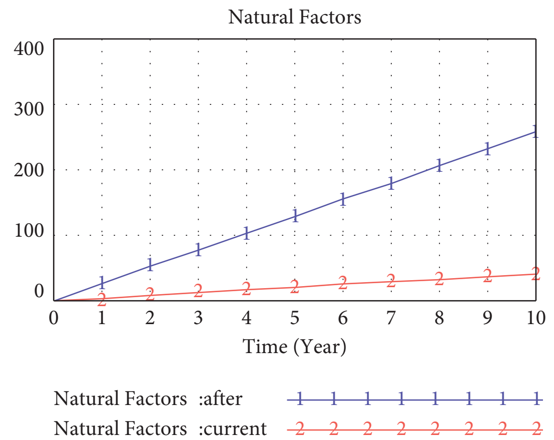

Figure 11: Comparison of natural factors optimization.

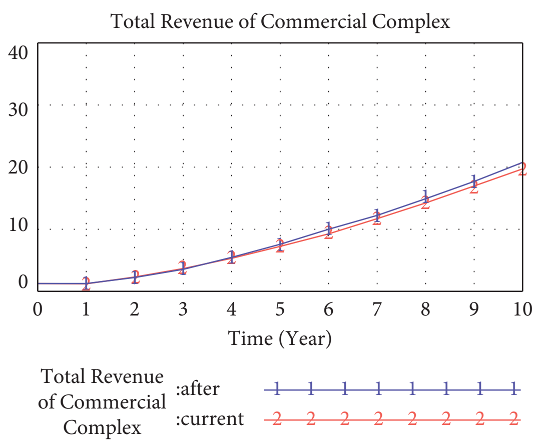

Figure 12: Comparison of comprehensive commercial income.

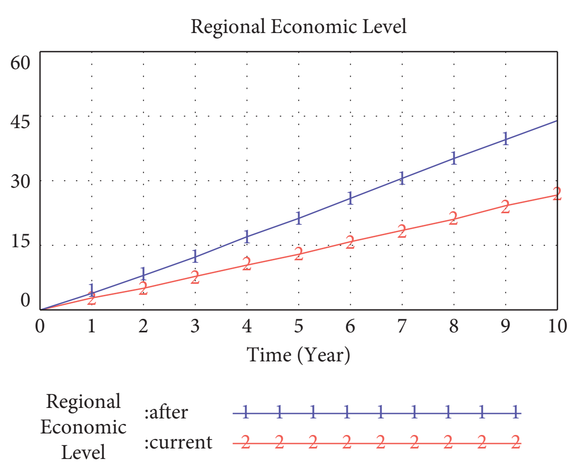

Figure 13: Comparison of regional economic level optimization.

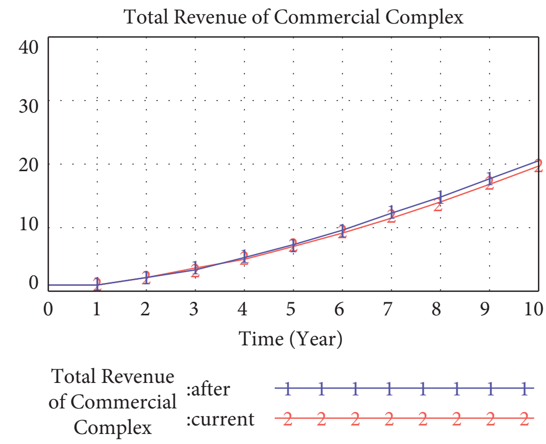

Figure 14: Comparison of total revenue optimization of commercial complexes.

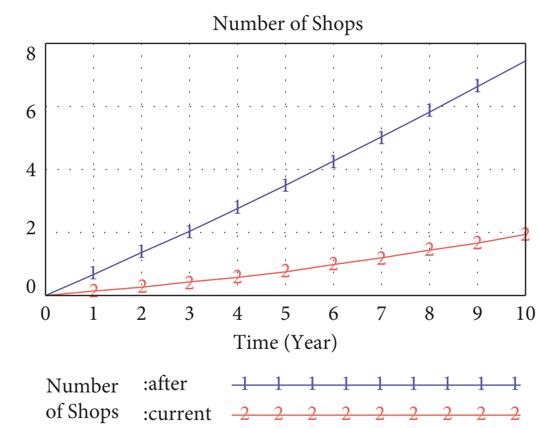

Figure 15: Comparison of optimization of the number of shops.

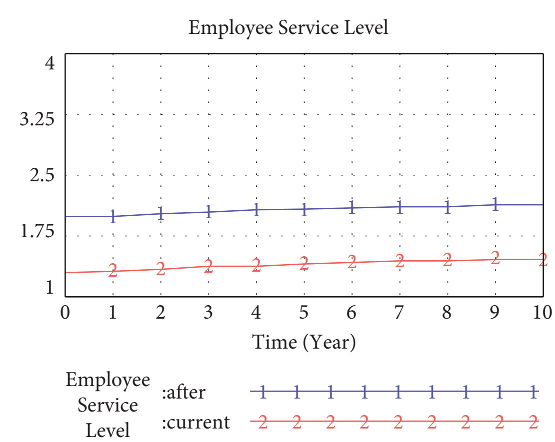

Figure 16: Comparison of employee service level optimization.

5. Conclusion

This paper studies the influencing factors of consumers' preference and the influencing mechanism of various factors on the decision-making of commercial complex location and establishes the decision-making model of commercial complex location based on consumers' preference. Through the questionnaire data combined with statistical software, the model of this paper is tested. The empirical test provides the scientific basis for the decision-making of commercial complex location through the simulation and optimization analysis of commercial complex location.

This study has the following innovations. First, this paper introduced the customer's patronage intention, which has a decisive influence on the later operating income, to further optimize the site selection decision model. This paper fully considered the possibility of diversified selection of subjects caused by the development of the times, respecting the validity of the traditional commercial complex site selection decision model based on objective factors. Second, based on the theory of consumer planned behavior and the theory of customer perceived value, the paper analyzes the influencing factors of consumers' patronage intention to commercial complex, which enriches the research of patronage intention to the location decision of commercial complex. Third, the site selection decision-making index system of commercial complex based on consumer patronage intention is constructed to expand the research scope of site selection of commercial complex. Fourth, the system dynamics model of the commercial complex site selection decision is constructed, and the dynamic simulation of the commercial complex site selection decision is carried out, which enhances the explanatory ability of the influence of patronage intention on the commercial complex site selection decision. All these efforts make the decision result more in line with the actual demand to improve the rationality of site selection.

Data Availability

The datasets used and/or analyzed during the current study are available from the corresponding author on reasonable request.

Conflicts of Interest

The authors declare no potential conflicts of interest with respect to the research, authorship, and/or publication of this article.

References

[1] H. Hotelling, "Stability in competition," *The Collected Economics Articles of Harold Hotelling*, Springer, New York, NY, USA, pp. 50–63, 1990.

[2] G. Faltings, "The proof of Fermat's last theorem by R. Taylor and A. Wiles," *Notices of the American Mathematical Society*, vol. 42, no. 7, pp. 743–746, 1995.

[3] S. L. Hakimi, "Optimum locations of switching centers and the absolute centers and medians of a graph," *Operations Research*, vol. 12, no. 3, pp. 450–459, 1964.

[4] R. Hassin, A. Levin, and D. Morad, "Lexicographic local search and the p-center problem," *European Journal of Operational Research*, vol. 151, no. 2, pp. 265–279, 2003.

[5] R. C. Rosen, J. Catania, and L. Pollack, "Male sexual health questionnaire (MSHQ): scale development and psychometric validation," *Urology*, vol. 64, no. 4, pp. 777–782, 2004.

[6] M. A. Qian-Li and T. L. Huang, "Analysis of and study on the difficulties in the fire protection design of large commercial complex," *Procedia Engineering*, vol. 11, pp. 302–307, 2011.

[7] X. U. Jie and L. Jun, "ROPPONGI HILLS:urban Re-development commercial complex," *Time + Architecture*, vol. 2, 2005.

[8] R. G. Dugan, J. J. Clarkson, and J. T. Beck, "When cause-marketing backfires: differential effects of one-for-one promotions on hedonic and utilitarian products," *Journal of Consumer Psychology*, vol. 31, pp. 1–19, 2021.

[9] K. P. Koller and A. Pennington-Cross, "The density of convenience retail and the type of traffic—commuting, local and retail," *Journal of Real Estate Research*, vol. 41, no. 2, pp. 319–346, 2019.

[10] Z. Liang, "Relationship between commercial complexes and urban space," *Journal of Hefei University of Technology*, vol. 29, no. 9, pp. 1166–1168, 2006.

[11] T. Hall and H. Barrett, *Urban Geography*, Routledge, Oxfordshire, UK, 2018.

[12] C. C. Williams, "The contribution of regional shopping centres to local economic development: threat or opportunity?" *Area*, vol. 24, pp. 283–288, 1992.

[13] S. Prashar, C. Parsad, and T. S. Vijay, "Segmenting young Indian impulsive shoppers," *Journal of International Consumer Marketing*, vol. 29, no. 1, pp. 35–47, 2017.

[14] J. W. Forrester, "Industrial dynamics:A majior breakthrough for decision makers," *Harvard Business Review*, vol. 36, no. 4, pp. 368–385, 1958.

[15] J. W. Forrester, "Urban dynamics," *IMR; Industrial Management Review (pre-1986)*, vol. 11, no. 3, p. 67, 1970.

[16] A. Raymond, A. James, E. Jacob, and J. Lyons, "Influence of perceptions and stereotypes of the nursing role on career choice in secondary students: a regional perspective," *Nurse Education Today*, vol. 62, pp. 150–157, 2018.

[17] M. Hřebíčková, S. Graf, T. Tegdes, and I. Brezina, "We are the opposite of you! Mirroring of national, regional and ethnic stereotypes," *The Journal of Social Psychology*, vol. 157, no. 6, pp. 703–719, 2017.

[18] Y. Wu and D. Ding, "An analysis on the factors affecting the activation and applications of stereotype in interpersonal cognition," *Science of Social Psychology*, no. 1, pp. 101–105, 2007.

[19] Yu Tian, "Analysis of Chinese consumer purchasing behavior pattern and marketing countermeasure," *Enterprise Economy*, no. 3, pp. 67–70, 2007.

[20] H. Xiao, J. Zhou, and Z. Liu, "On the change of consumption idea and its effect," *Consumer Economics*, no. 2, pp. 50–52, 1986.

[21] R. F. Gordon, M. O. C. Jorge, and B. P. Rafael, "Consumer behavior analysis and the marketing firm: measures of performance," *Journal of Organizational Behavior Management*, vol. 41, pp. 1–27, 2021.

[22] L. Xuxun, J. Zhicai, and N. Anning, "Review of reliability of urban network transportation system," *Application Research of Computers*, vol. 29, no. 8, pp. 2817–2820, 2012.

[23] J. A. Ortega-García, F. A. López-Hernández, M. L. A. Funes, M. F. Sánchez Sauco, and R. Ramis, "My partner and my neighbourhood: the built environment and social networks' impact on alcohol consumption during early pregnancy," *Health & Place*, no. 61, Article ID 102239, 2020.

[24] Z. Chen, "Study on the relationship between store image customer satisfaction and customer patronage intention," *Review of Economy and Management*, vol. 30, no. 6, pp. 76–81, 2014.

[25] G. Zhuang, M. Zhu, and Z. Liu, "The reason, intention, and action of customers' direction complaint: an empirical study based on the experiences of customers dissatisfied to electronic applause in China," *Chinese Retail Research*, vol. 1, no. 1, pp. 1–19, 2009.

Hindawi
Scientific Programming
Volume 2022, Article ID 6422442, 9 pages
https://doi.org/10.1155/2022/6422442

Research Article

Algorithmic Study on Position and Movement Method of Badminton Doubles

Yu Xie,[1] **Xiaodong Xie**,[1] **Huan Xia**,[1] **and Zhe Zhao**[2]

[1]*Physical Education Institute, Hunan University, Changsha 410082, China*
[2]*Physical Education Institute, Hunan Normal University, Changsha 410012, China*

Correspondence should be addressed to Zhe Zhao; 16334@hunnu.edu.cn

Received 27 September 2021; Accepted 16 December 2021; Published 10 January 2022

Academic Editor: Punit Gupta

The algorithms used by schedulers depend on the complexity of the schedule and constraints for each problem. The position and movement of badminton players in badminton doubles competition is one of the key factors to improve the athletes' transition efficiency of offense and defense and the rate of winning matches and to save energy consumption. From the perspective of basic theory, the author conducts research on the position and movement of badminton doubles. Based on the numerical analysis method, the optimal model of standing position and direction composed of 7 nonlinear equations is established. In addition, the final of 10 matches of the super series of the world badminton federation in 2019 was selected as the sample of speed parameters. With the help of MATLAB mathematical analysis software, the numerical model established by the least square method was adopted to optimize the specific standing position and walking model. Ultimately, the optimal solution has been obtained, which can be represented on a plane graph. The optimal position of the attack station should be the blocking area (saddle-shaped area) and the hanging area (circular arc area in the middle). The optimal defensive positioning should be left defensive positioning area (left front triangle area) and right defensive positioning area (right front triangle area), which is consistent with our current experience and research results. The research results use mathematical tools to calculate the accurate optimal position in doubles matches, which has guiding significance to the choice of athletes' position and walking position in actual combat and can also be used as a reference for training, providing a certain theoretical basis for the standing and walking of badminton doubles confrontation. The data collection and operation methods in this study can provide better calculation materials for artificial intelligence optimization and fuzzy operation of motion displacement, which is of great significance in the field of motion, simulation, and the call of parametric functions.

1. Introduction

As a sport of both recreational fitness and competition, the amount of exercise of badminton can be independently chosen by the participants according to their own conditions, and the requirements for equipment and venues can be high or low. And because the noncontact confrontation reduces the possibility of injury and physical requirements, it has been widely popularized in all parts of the world and has become an Olympic competition [1]. According to the number of participants, the badminton events can be divided into singles, doubles, and three against three. The singles events have high physical requirements [2–4], while the doubles events emphasize more on tactics [5, 6], which is essentially an accelerated version of doubles.

In badminton doubles tactics, standing and walking are the basis, which are related to the cooperation between two people and the reasonable distribution of areas [7]. Athletes' technique ability not only needs to have their own characteristics but also must keep strong backcourt tactics ability before, during, and at the same time [8] because, in the game, every detail might affect the competition results; it also makes athletes need to have strong ability of details. The footwork of badminton is an important part of the players' technical and tactical abilities, among which backtracking is the last step of the footwork of badminton, and backtracking connects with the starting link of the next footwork [9]. Reasonable positioning and walking in doubles make the division of labor of teammates clear, makes the preparation of athletes more reasonable, reduces the unnecessary running of athletes in the confrontation, saves physical energy, and increases the efficiency of scoring. Quite a few scholars [8–13] have carried out research and discussion on the positions and moves of doubles and reached some consensus. Gawin [10] analyzed the match data and made statistics on what kind of movement mode in doubles is beneficial to gain the advantage in the serve. Zhu qiang et al. [14] used the method of literature review, observation and interview, etc., to discuss the position of attack and defense switch in badminton doubles. Lin [15] also used similar research methods to analyze and discuss Yang wang Xiao li's position in 10 doubles matches from 2013 to 2014.

It can be seen that, in addition to forming some empirical consensus, there have also been some relevant studies on the positioning and movement of doubles. Partial least squares correlation analysis (PLSCA) (Abdi and Williams, 2013; Weaving et al., 2019) [16] was used to investigate the composite relationship between perceived wellness status and technical-tactical performance for both the forwards' and backs' positional groups as per previous methods [17] (Emmonds et al., 2020). However, the conclusions of these studies are all qualitative and empirically based, which may be practical but not rigorous. In order to scientifically optimize the positioning of doubles in training and actual combat, it is very important to model and analyze the positioning of doubles, theoretically explore the most reasonable positioning and movement of doubles, and avoid the existing errors. Therefore, based on the mathematical model [16–19], the following research is carried out on the optimization of badminton doubles' position and movement, in order to provide some theoretical basis on this issue.

2. The Positioning Model of Doubles Based on the Analytic Method

2.1. The Basic Idea of Model Building. In a badminton match, when a player of his own side hits the ball, the time it takes for the ball to fly from his own field to the field of his opponent is the time for the player of his own side to stand. Similarly, after the opponent hits the ball, the time for the ball to fly from his court to his opponent's court is the time for his opponent to start and hit the ball. This is the basic rhythm of badminton.

As can be seen from Figure 1, the time required for the ball to fly from one side of the field to different areas of the opposite side of the field is different, that is, the time from starting to hitting is different for the incoming ball from different landing points. For example, the split lob is faster and shorter than the high ball, so the player who wants to catch the ball should start and run to the right hitting area in a shorter time. Of course, there is a certain difference between the running speed of the players' forward net footwork and the running speed of the players' backward retreats' footwork. To sum up, ignoring the secondary influencing factors, the players should have a corresponding optimal positioning point for the position of the ball when facing the opponent's shot. From this positioning point, it should be equally difficult for them to return several furthest corners of the area they are responsible for. In order to get this position, the emphasis is on the evaluation of the difficulty of connecting each ball at the farthest corner. As the ball travels from the opposing field to each of these farthest corners, it corresponds to the distance the player must run and the time he has to start to hit the ball, which is the amount of speed the player must put into catching the ball. The magnitude of this required speed is a measure of difficulty. So, the optimal positioning should allow the player at that point to run at the two farthest corners of the net at the same speed. The two farthest corners of the baseline should run at the same speed. Moreover, the running speed towards the furthest corner of the net and the furthest corner of the baseline should satisfy the proportional relation between the running speed of the net footwork and the running speed of the back-and-back footwork.

2.2. Badminton Court Coordinate System Creation. In order to calculate the distance better, an optimization model is established based on the analytical method in this paper. Therefore, the analytical coordinate system of the site should be built first to obtain the coordinate values of each key point. One end of the center line of the net is taken as the origin of the coordinate system. The X-axis is along the long side of the court, while the Y-axis bisects the opposite side of the court along the direction of the net, as shown in Figure 2.

In Figure 2, the X-axis represents the longitudinal distance in the direction of the badminton court sideline, the Y-axis represents the transverse distance in the direction of the center line, and the intersection of one side sideline and the middle is the origin. Doubles position is the end of the movement to the position, the starting point to hit the ball, and the basis of other doubles tactics. Therefore, each position corresponds to the position of the ball when an opponent hits the ball. In order to better illustrate the optimization process, the ball is located at the corner of the opponent's baseline (G spot in Figure 2) as an example; see Figure 2, for the coordinates of the two players' position points (points J and K on Figure 2) and the farthest corner points (points A, B, C, D, E, and F on Figure 2) in the area they are responsible for (CD is the dividing line of the area). Considering that when the opponent hits the ball from the baseline and ignores the situation that the ball rolls over the net with a small probability, the ball should not fall into the area surrounded by the two sideline of the line AE, the field, and the net line (Y-axis), so there is no distribution of points needing to catch the ball in this area. At this point, there are seven unknown coordinate parameters, including the two-axis coordinates $x1$ and $y1$ at point J, the two-axis coordinates $x2$ and $y2$ at point K, the two-axis coordinates m and n at point C, and the y-coordinate p at point D, where the coordinates $x1$ and $y1$ and $x2$ and $y2$ of J are exactly the coordinate values to be obtained.

2.3. Optimization Model Creation. As shown in Figure 2, the ball falls from point G to A, B, or C. Points B, D, and F correspond to the point where the ball clicks back from G. The horizontal component of the average flying speed of the

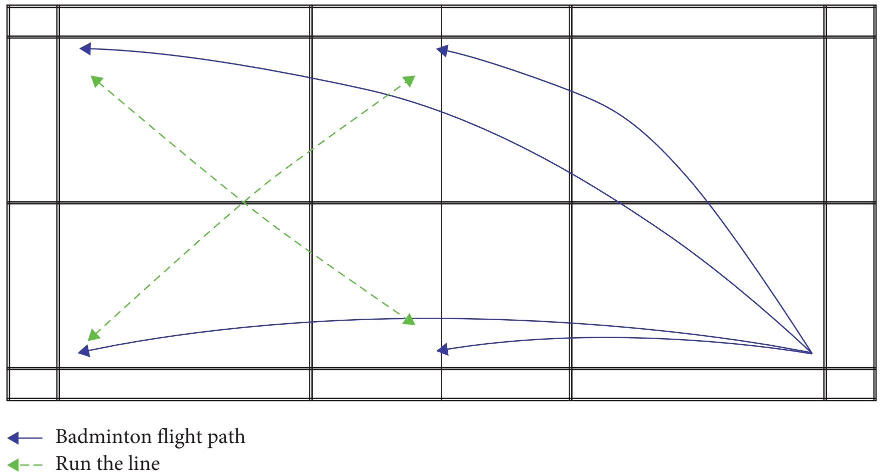

Figure 1: Badminton flight and running circuit diagram.

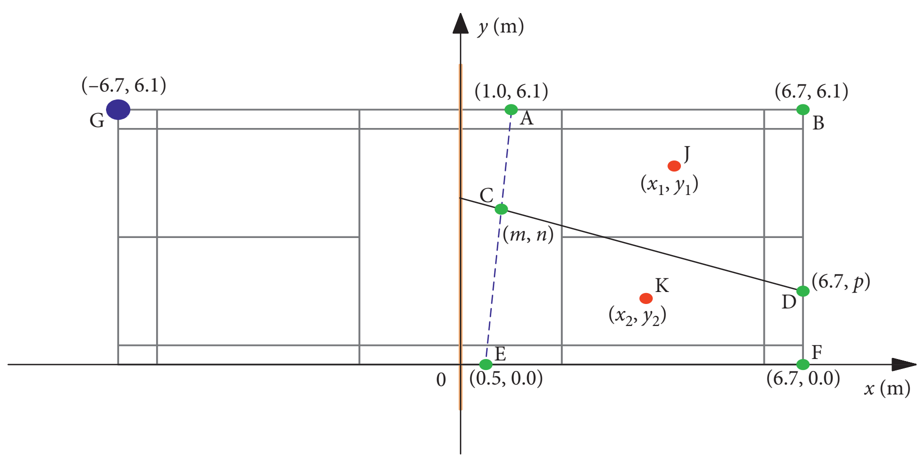

Figure 2: Analytical coordinate system of badminton doubles court and station.

ball when hitting the ball is m/s. The average speed of returning the ball after receiving the ball is m/s. According to the physical relationship between flight distance, flight speed, and flight time, the time (unit: s) of the ball from point G to points A, B, C, D, E and F is

$$t_{\mathrm{GA}} = 7.7/\overline{V_{\mathrm{ds}}}, \quad (1)$$

$$t_{\mathrm{GB}} = 13.4/\overline{V_{\mathrm{hc}}}, \quad (2)$$

$$t_{\mathrm{GC}} = \frac{\sqrt{(6.7+m)^2 + (6.1-n)^2}}{\overline{V_{\mathrm{ds}}}}, \quad (3)$$

$$t_{\mathrm{GD}} = \frac{\sqrt{13.4^2 + (6.1-p)^2}}{\overline{V_{\mathrm{hc}}}}, \quad (4)$$

$$t_{\mathrm{GE}} = \frac{\sqrt{7.2^2 + 6.1^2}}{\overline{V_{\mathrm{ds}}}} = \frac{9.4}{\overline{V_{\mathrm{ds}}}}, \quad (5)$$

$$e\,w\,t_{\mathrm{GF}} = \frac{\sqrt{13.4^2 + 6.1^2}}{\overline{V_{\mathrm{hc}}}} = \frac{14.7}{\overline{V_{\mathrm{hc}}}}. \quad (6)$$

Assuming that the opponent hits the ball at the exact time when the receiver starts, then according to the physical relationship between running distance, running speed, and running time, the running speed required by the player at point J to catch the ball at A, B, C, and D is

$$V_{\mathrm{JA}}^{n} = \frac{\sqrt{(x_1-1.0)^2 + (6.1-y_1)^2}}{t_{\mathrm{GA}}}, \quad (7)$$

$$V_{\mathrm{JB}}^{b} = \frac{\sqrt{(6.7-x_1)^2 + (6.1-y_1)^2}}{t_{\mathrm{GB}}}, \quad (8)$$

$$V_{\mathrm{JC}}^{n} = \frac{\sqrt{(x_1-m)^2 + (y_1-n)^2}}{t_{\mathrm{GC}}}, \quad (9)$$

$$V_{\mathrm{JD}}^{b} = \frac{\sqrt{(6.7 - x_1)^2 + (y_1 - p)^2}}{t_{\mathrm{GD}}}. \quad (10)$$

The running speeds required by players at point K to catch the ball at four points C, D, E, and F are

$$V_{\mathrm{KC}}^{n} = \frac{\sqrt{(x_2 - m)^2 + (n - y_2)^2}}{t_{\mathrm{GC}}}, \quad (11)$$

$$V_{\mathrm{KD}}^{b} = \frac{\sqrt{(6.7 - x_2)^2 + (p - y_2)^2}}{t_{\mathrm{GD}}}, \quad (12)$$

$$V_{\mathrm{KE}}^{n} = \frac{\sqrt{(x_2 - 0.5)^2 + y_2^2}}{t_{\mathrm{GE}}}, \quad (13)$$

$$V_{\mathrm{KF}}^{b} = \frac{\sqrt{(6.7 - x_2)^2 + y_2^2}}{t_{\mathrm{GF}}}. \quad (14)$$

In order to simplify the calculation, at the same time, according to the split in the following section hanging ball when the average speed of horizontal component of the ball when the ball hits the back of the level of the average speed component, athletes do back to the bottom line of footwork when running with speed and athletes to the net do online gait as running speed of the related research (specific data discussed in Section 3), the ratio of discovery can be approximately considered as the constant value, which is

$$\frac{\overline{V_{\mathrm{hc}}}}{\overline{V_{\mathrm{ds}}}} = K_1, \quad (15)$$

$$\frac{V^n}{V^b} = K_2. \quad (16)$$

According to the basic idea in Section 2.1, when the athletes at point J and at point K meet the requirements of equation (16), the speed required to catch the ball at the farthest corner point should be in the optimal position:

$$V_{\mathrm{JA}}^{n} = K_2 V_{\mathrm{JB}}^{b} = V_{\mathrm{JC}}^{n} = K_2 V_{\mathrm{JD}}^{b}, \quad (17)$$

$$V_{\mathrm{KC}}^{n} = K_2 V_{\mathrm{KD}}^{b} = V_{\mathrm{KE}}^{n} = K_2 V_{\mathrm{KF}}^{b}. \quad (18)$$

By substituting equations (1)~(15) into equations (17) and (18), we can obtain

$$13.4\sqrt{(x_1 - 1.0)^2 + (6.1 - y_1)^2} = 7.7K_1K_2\sqrt{(6.7 - x_1)^2 + (6.1 - y_1)^2}, \quad (19)$$

$$\sqrt{(x_1 - 1.0)^2 + (6.1 - y_1)^2} \cdot \sqrt{(6.7 + m)^2 + (6.1 - n)^2} = 7.7\sqrt{(x_1 - m)^2 + (y_1 - n)^2}, \quad (20)$$

$$\sqrt{(x_1 - 1.0)^2 + (6.1 - y_1)^2} \cdot \sqrt{13.4^2 + (6.1 - p)^2} = 7.7K_1K_2\sqrt{(6.7 - x_1)^2 + (y_1 - p)^2}, \quad (21)$$

$$9.4K_1K_2\sqrt{(6.7 - x_2)^2 + (p - y_2)^2} = \sqrt{(x_2 - 0.5)^2 + y_2^2} \cdot \sqrt{13.4^2 + (6.1 - p)^2}, \quad (22)$$

$$9.4\sqrt{(x_2 - m)^2 + (n - y_2)^2} = \sqrt{(x_2 - 0.5)^2 + y_2^2} \cdot \sqrt{(6.7 + m)^2 + (6.1 - n)^2}, \quad (23)$$

$$14.7\sqrt{(x_2 - 0.5)^2 + y_2^2} = 9.4K_1K_2\sqrt{(6.7 - x_2)^2 + y_2^2}. \quad (24)$$

Since point C is located on the point line AE, it should be satisfied:

$$n = 12.2m - 6.1. \quad (25)$$

3. Model Parameters and Solutions

3.1. Model Parameters: Speed Parameters. In order to simplify and solve the established optimization model, this paper tests the horizontal component of the average flying speed of the ball when splitting the crane, the horizontal component of the average flying speed of the ball when hitting the backcourt ball, the running speed when the player makes a backward step to the In this paper, and the final videos of 10 matches of the world badminton federation super series in the recent year were selected as the statistical space to conduct sample statistics of various speed parameters. The source of the matches is shown in Table 1. A total of 668 effective sum ratio data and 382 effective sum ratio data were obtained, and their distribution is shown in Figure 3.

Through fitting, it can be approximated to a fixed value of 0.7657 and a fixed value of 1.3026. In equations (19)~(25) of the optimization model, it is always multiplied, so it can be regarded as a parameter.

3.2. Model Solution. Models (19)–(25) are for nonlinear equations, and the equation number equals the number of variables (which can be regarded as known quantity), so a

Table 1: Model data source statistics table.

Event name	Category	Contestant	The number of data
Yubo Cup Final 2018	Women's doubles	Yuki Fukushima Katsuka Hiroda vs. Zonko pan Ravinda	69
2018 World Championships	Men's doubles	Li Junhui/Liu Yuchen vs. Jiamura Kenshi/Yueda Qigu	77
2018 World Championship Final	Women's doubles	Yoshiyuki Fukushima/Hiroda Katsuhwa vs. Maayu Matsumoto Naga	66
2018 World Badminton Final	Women's doubles	Takahashi Lihua/Matsuomi Sasaki vs. Li Shaoxi/Shen Shengzan	65
2019 Sudiman Cup Final	Men's doubles	Li Junhui/Liu Yuchen vs. Watanabe Yuda/Endo Dayou	72
2018 World Badminton Final	Women's doubles	Takahashi Lihua/Matsuomi Sasaki vs. Li Shaoxi/Shen Shengzan	65
2019 World Championship Final	Men's doubles	Setiawan/Ahsan vs. Tomoki Zhuo/Kobayashi	59
2018 World Championship Final	Women's doubles	Yoshiyuki Fukushima/Hiroda Katsuhwa vs. Maayu Matsumoto/ Naga	66
2019 World	Women's doubles	Badminton final Mayou Matsumoto/Nagawara vs. chen Morin/Jia Yifan	64
2019 World Championship Final	Women's doubles	Mayou Matsumoto/Nagawara/Yuki Fukushima/Kohwa Hiroda	71

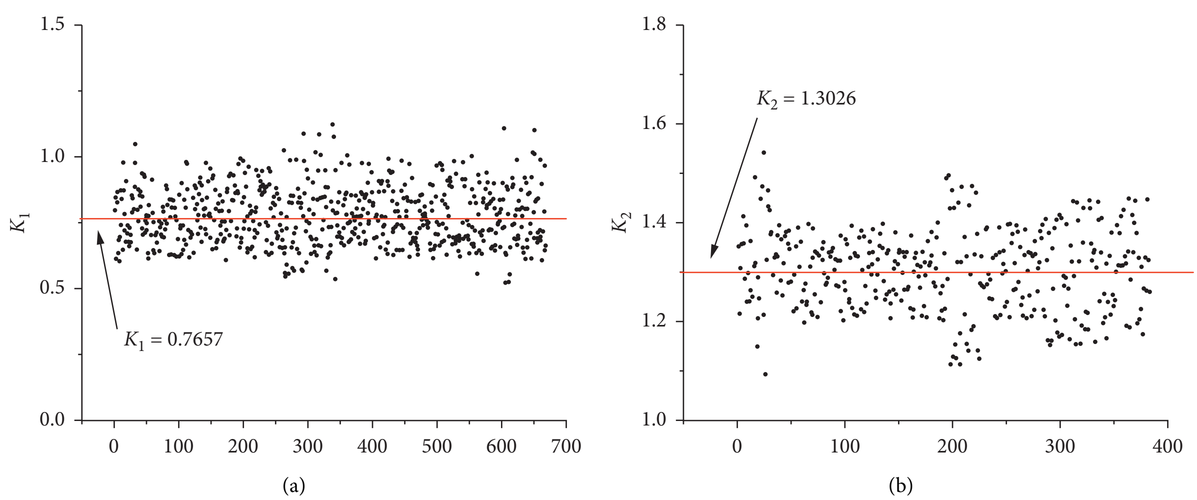

Figure 3: Velocity parameter distribution diagram. (a) K_1 distribution diagram. (b) K_2 distribution diagram.

given interval may have a solution. Now, the fsolve function of MATLAB mathematical software is used for trial calculation and solution. According to the help file of MATLAB, the fsolve function is to use the least square method to solve the nonlinear equations, and the general solution formula is

$$X = \mathrm{FSOLVE}\,(\mathrm{FUN}, \mathrm{X0}, \mathrm{OPTIONS}), \tag{26}$$

Where FUN is the nonlinear system of equations requiring solution. For this paper, equations (19)~(25) are the nonlinear system and the initial value of the variable. Because the solution process has a certain dependence on the numerical value, in this paper, the understanding range is roughly calculated according to the experience. Then, we set the initial value. OPTIONS represents the structure created for OPTIMSET, which is the default value for this optimization parameter.

Table 2: Results obtained from equations (19)~(25) (unit: m).

	x_1	y_1	x_2	y_2	m	n	p
Results	2.8661	4.6844	2.6353	1.9088	0.7839	3.4636	2.9784

In the input equations (19)~(25) and the estimated initial values of each parameter, the number of cycles is set to 1000 generations. The final results of each parameter are shown in Table 2. The various errors corresponding to the solutions obtained through numerical iteration are shown in Table 3.

Put the result back into the field map, and Figure 4(a) can be obtained. The point of the left field is the position of the ball when the opponent hits the ball. The point on the right side of the field is the optimal station point of the two players of the team based on the optimization of analytical method. By the same method, the optimal solution of the position required by

Table 3: Errors of equations (19)~(25) corresponding to solutions.

Equation	(19)	(20)	(21)	(22)	(23)	(24)	(25)
Error	−8.74*E*-07	−1.18*E*-07	−9.76*E*-07	8.91*E*-07	−1.37*E*-07	−9.30*E*-07	8.26*E*-14

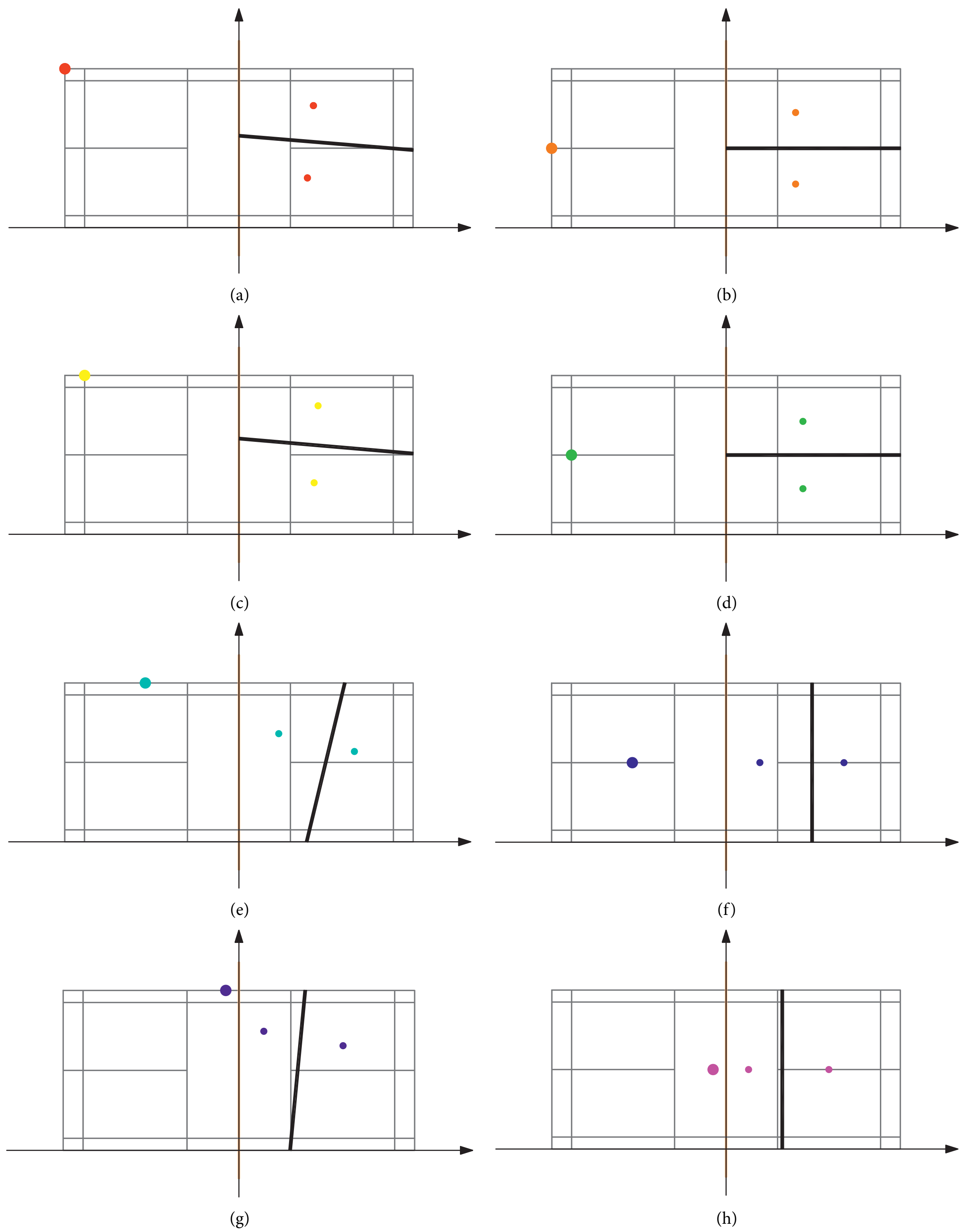

Figure 4: Results of optimal positioning when the ball is at each key point in the opposite side field area. (a) Scenario 1. (b) Scenario 2. (c) Scenario 3. (d) Scenario 4. (e) Scenario 5. (f) Scenario 6. (g) Scenario 7. (h) Scenario 8.

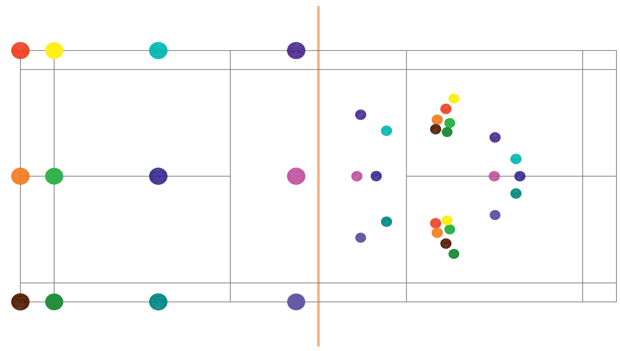

Figure 5: Summary of optimized station positioning results.

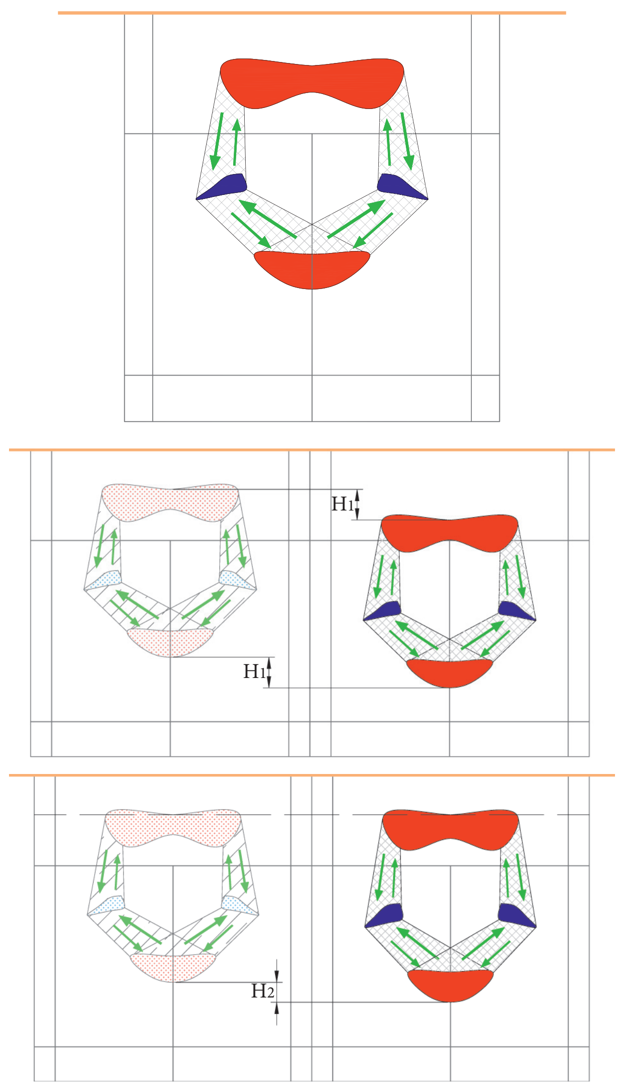

Figure 6: Station area and rotation path.

the opponent when the ball is at the other key points of the opponent's court can be calculated, as shown in Figures 4(b)~4(h). All the obtained optimized station positions and the results obtained according to the symmetry relation are collected in the same figure, as shown in Figure 5. The points in the left and right field areas of the same color correspond to the position of the ball and the corresponding relationship between the positions of the square and the station.

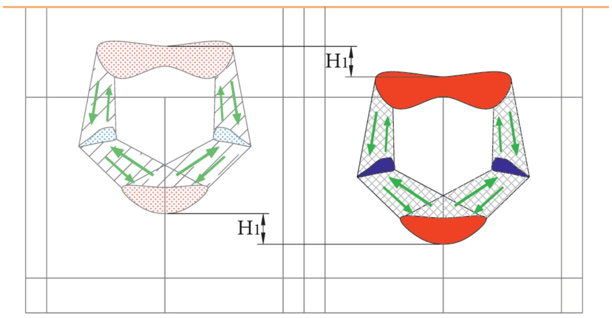

(a) Backward translation (b) Longitudinal lengthening

Figure 7: Conjecture of running circle results when more factors are considered. (a) Backward translation. (b) Longitudinal lengthening.

4. Analysis and Discussion

In Figures 4 and 5, the X-axis represents the longitudinal distance in the direction of the badminton court sideline, the Y-axis represents the transverse distance in the direction of the center line, and the intersection of one side sideline and the middle is the origin. The different color dots sign the footfall dots and the directions. Three spline curves were used to connect the stations of each side in the center and right field in Figure 4 to obtain two offensive areas (red area) and two defensive areas (blue area), as shown in Figure 6.

There are two offensive areas; one is in the front of the field, in the actual combat process, which should be responsible for the front of the net, so it can be called the net position area; the other is in the back court, in the actual combat process, which should be responsible for the back court attack, so it can be called the killing and hanging station area. The two defensive areas are located in the left and right field, respectively, which can be called the left guard area and the right guard area (in real combat rotation, players should try their best to move in a straight line to reduce the distance of moving, so they should use a straight line to connect the boundaries of the offensive area and the defensive area). The rotation path in Figure 6 can be obtained. In the actual combat process, the so-called offensive to defensive and defensive to offensive are the two players who continue to choose a reasonable position between the offensive zone and the defensive zone through these paths. Based on the analytical method, we obtain Figure 6, which is obtained by the optimization study of such a stance area and rotary path graph; you can connect the attack area and defensive area and their rotary path as a special "movement." Using the running circle, we can guide the positioning and walking training of doubles players and even put the running circle on the field, so as to develop the fixed thinking and concept of positioning and field of doubles players. In this way, the possible errors of positioning or moving can be reduced due to panic in high-speed doubles competition.

This study is based on the mathematical analysis method to optimize the position of doubles, and a running circle is preliminary calculated. For example, consider that, in practice, when players hit the ball at the baseline, they often choose to kill the ball vigorously instead of hitting it to the far corner of their own side. When the player receives the ball in front of the court, he can use a certain arm span and racket length; the center of gravity does not move to the position of the ball. It also takes time for the athlete to start the turn from the position. Taking the secondary influencing factors into account will be the next step for more deepening the research on the optimization of the target on the basis of the overall train of thought. It is assumed that when the above factors are taken into account, the resulting running circle may be the result of a backward shift (as shown in Figure 7(a)) or a longitudinal stretch (as shown in Figure 7(b)) compared with the current one. These assumptions need to be further studied to confirm whether they are reasonable. This kind of data has the position characteristics of relatively optimized fuzzy algorithm. These features can provide reference for data collection and feature analysis of subsequent sports competitions of multiple athletes. After collecting the location data of multiple multievent competitions, the database can optimize the multipoint fuzzy computing of computer cloud, so as to obtain a better model.

5. Conclusion

Based on the analytical method, this paper establishes the optimal model of badminton doubles position, obtains the relevant speed parameters through statistical analysis, then solves the model by numerical method, and draws the following conclusions.

(1) Based on the analytical method, an optimization model is established. By inputting reasonable speed-related parameters, the specific points of the optimal positions of the two players in badminton doubles can be solved.

(2) The specific distribution of these optimal stations constitutes four regions, namely, the area of net closing (the saddle-shaped area in the front), the area of killing and hanging (the circular arc area in the middle), the area of left guard (the triangle area in the left front), and the area of right guard (the triangle area in the right front).

(3) The rotation path can be obtained by connecting the boundary between the offensive zone and the defensive zone. The two players can constantly choose a reasonable position between the offensive zone and the defensive zone through the rotation path to realize the switch from offense to defense and from defense to offense.

(4) The offensive zone and the rotation paths that connect them combine to form a running circle, which can be used to guide doubles players in positioning training.

(5) As a model of multiplayer sports, this study can provide more detailed data and statistics. The research also provides a reference model for the collection and calculation of multievent and multiproject secretaries of subsequent cloud

computing, to obtain the optimization of algorithm and model.

Data Availability

The datasets used and/or analyzed during the current study are available from the corresponding author upon reasonable request.

Conflicts of Interest

The authors declare that there are no conflicts of interest with respect to the research, authorship, and/or publication of this article.

References

[1] J. Y. Guillain, *Badminton: An Illustrated History-From Ancient Pastime to Olympic Sport*, Editions Publibook, France, 2012.

[2] M. K. Chin, A. S. Wong, R. C. So, O. T. Siu, K. Steininger, and D. T. Lo, "Sport specific fitness testing of elite badminton players," *British Journal of Sports Medicine*, vol. 29, no. 3, pp. 153–157, 1995.

[3] P. Majumdar, G. L. Khanna, V. Malik, S. Sachdeva, M. Arif, and M. Mandal, "Physiological analysis to quantify training load in badminton," *British Journal of Sports Medicine*, vol. 31, no. 4, pp. 342–345, 1997.

[4] O. Faude, T. Meyer, F. Rosenberger, M. Fries, G. Huber, and W. Kindermann, "Physiological characteristics of badminton match play," *European Journal of Applied Physiology*, vol. 100, no. 4, pp. 479–485, 2007.

[5] D. Cabello Manrique and J. J. Gonzalez-Badillo, "Analysis of the characteristics of competitive badminton," *British Journal of Sports Medicine*, vol. 37, no. 1, pp. 62–66, 2003.

[6] M. Blomqvist, P. Luhtanen, and L. Laakso, "Comparison of two types of instruction in badminton," *European Journal of Physical Education*, vol. 6, no. 2, pp. 139–155, 2001.

[7] M. Blomqvist, *Game Understanding and Game Performance in Badminton: Development and Validation of Assessment Instruments and Their Application to Games Teaching and Coaching*, University of Jyväskylä, Jyväskylä, Finland, 2001.

[8] H. Abdi and L. J. Williams, "Partial least squares methods: partial least squares correlation and partial least square regression," *Methods in Molecular Biology*, vol. 27, pp. 549–579, 2013.

[9] D. Bates, M. Mächler, B. Bolker, and S. Walker, "Fitting linear mixed-effects models using lme4," *Journal of Statistical Software*, vol. 67, no. 1, 2015.

[10] W. Gawin, C. Beyer, H. Hasse, and D. Büsch, "How to attack the service: an empirical contribution to rally opening in world-class badminton doubles," *International Journal of Performance Analysis in Sport*, vol. 13, no. 3, pp. 860–871, 2013.

[11] D. Jin-Biao, "Analysis on the application of technique and tactics in badminton men's doubles," *Journal of Shanghai institute of sport*, vol. 22, no. 2, pp. 36–40, 1998.

[12] li Cheng, *Comparative Analysis on Technique and Tactics of Mixed Doubles Badminton between China and Foreign Countries*, Chengdu Institute of Physical Education, China, 2013.

[13] T. Zhao, *Analysis on the Technical and Tactical Characteristics of the World's Outstanding Badminton Men's Doubles Players*, Beijing Sport University, Beijing, China, 2010.

[14] Q. Zhu and Y. Tang, "On the skills of defense and attack conversion in badminton doubles," *Contemporary sports science and technology*, vol. 4, no. 16, pp. 41-42, 2014.

[15] Q. Lin, *Analysis and Research on Coordination Position in Women's Badminton Doubles*, Shandong institute of physical education, Shandong, China, 2016.

[16] R. Kager, Q. W. Ma, and J. L. Wang, *Optimality Theory*, Cambridge University Press, Cambridge, United Kingdom, 1999.

[17] J. J. McCarthy, *A Thematic Guide to Optimality Theory*, Cambridge University Press, Cambridge, United Kingdom, 2002.

[18] B. Tesar, *Learnability in Optimality Theory*, Mit Press, Cambridge, Massachusetts, United States, 2000.

[19] D. Archangeli, *Optimality Theory*, John Wiley & Sons, New York, NY, USA, 2006.

Hindawi
Scientific Programming
Volume 2022, Article ID 9117981, 11 pages
https://doi.org/10.1155/2022/9117981

Research Article

Artificial Intelligence in the Protection and Inheritance of Cultural Landscape Heritage in Traditional Village

Xin Wang

School of Art & Design, Lanzhou Jiaotong University, Lanzhou, Gansu 730070, China

Correspondence should be addressed to Xin Wang; wangxin@mail.lzjtu.cn

Received 15 November 2021; Revised 7 December 2021; Accepted 16 December 2021; Published 7 January 2022

Academic Editor: Punit Gupta

To continue to protect and inherit the cultural landscape heritage of traditional villages, starting from the perspective of artificial intelligence (AI), literature review methods are used, and related theories are collected. Then, Wuyuan County in Jiangxi Province in the traditional villages is taken as the research object. By analyzing the tourism income of this place from 2016 to 2020, the overall income of this county is relatively good. In fact, due to the weak protection of traditional villages in Wuyuan County, the lack of supervision awareness, the implementation of the "immigrant and relocation" policy, and the backward thinking of residents, the cultural landscape of traditional villages has collapsed and destroyed. Up to now, there are 113 ancient ancestral temples, 28 ancient mansion houses, 36 ancient private houses, 187 ancient bridges, and only 12 ancient villages. Finally, AI technology is applied to the cultural landscape of traditional villages. Through image restoration technology, traditional villages can be restored to a certain extent. Intelligent positioning and radio frequency (RF) technology can also realize real-time monitoring of traditional villages from the perspective of weather and service life to achieve the purpose of protecting cultural landscape heritage. Therefore, AI technology is applied in the protection and inheritance of traditional village cultural landscape heritage, which has great reference significance for the management of various historical and cultural heritage.

1. Introduction

As China enters a new stage of transformation and development, it is the new requirements of this new stage to promote the great development and prosperity of socialist culture, promote the excellent traditional Chinese culture, and enhance the self-confidence of the national culture. Traditional villages are important carriers of traditional culture. Protecting the cultural landscape of traditional villages and promoting the development of traditional village tourism functions are important ways to inherit and promote traditional Chinese culture. Meanwhile, the cultural landscape heritage is the epitome of the development of different eras and the manifestation of the continuous progress of human civilization. However, there are some problems in the cultural landscape protection and tourism development of traditional Chinese villages. The rapid development of artificial intelligence (AI) has been widely used in robotics, economic and political decision-making, control systems, and simulation systems. Similarly, AI technology can also be applied to the protection and inheritance of the cultural landscape heritage of traditional villages. The cultural landscape heritage is diverse. As a major country of cultural landscape heritage, the Chinese nation must not only continue to carry forward its cultural spirit but also consider how to protect and inherit this cultural landscape heritage [1–3].

Qiu (2018) combined cultural landscape with ecological economics and studied how to realize the common development of cultural ecological landscape and human beings under the premise of ecological protection [4]. He emphasized that human beings should make a scientific plan for tourism development from multiple perspectives, multiple aspects, and multiple fields, combining the actual situation. Roger (2018) established Canada's geographic information positioning technology by Canada's regional location. Later, after researching with experts and scholars, he introduced the positioning technology to the protection of cultural landscape heritage, and the restoration technology of images slowed the disappearance of cultural landscapes to a certain extent [5]. Livio (2019) proposed to use image information analysis technology in the artificial neural network model to establish a modern digital network operation platform. In addition, he also integrated Augmented Reality (AR) with traditional villages, striving to use image information analysis technology to design more vivid traditional villages. Finally, he analyzed and summarized the future development of traditional villages [6]. Li (2019) researched traditional Chinese villages by consulting literature on cultural landscape heritage. He used 3D digital technology to display cultural landscape heritage in a digital museum. Although the traditional village no longer exists, after entering the digital museum, people can be immersed and enjoy the local customs at that time [7]. Peter (2018) proposed a new traditional village protection method in his published paper. He emphasized ecological balance, advocated the preservation of different cultural elements, and opposed cookie-cutter styles, styles, and colors. In addition, he also proposed that while protecting the traditional villages, the roads, facilities, and buildings around the villages should be harmonious and consistent to avoid the emergence of overly exaggerated scenes [8]. Scholars have expounded on the related theories of traditional village cultural landscape heritage from different angles. However, their research fields are relatively single, and they do not start from a global perspective. Meanwhile, some necessary analysis tools and technologies require more funds. In practical applications, funding issues need to be considered.

In this context, Wuyuan County in Jiangxi Province is taken as the research object. Firstly, data to understand the development status of traditional villages in Wuyuan County are collected. Then, artificial intelligence (AI) technology is used to realize the restoration of the cultural landscape heritage of traditional villages and the protection of cultural landscape heritage of traditional villages by smart sensing technology and radio frequency (RF) identification technology. This has far-reaching reference significance for the inheritance and protection of the cultural landscape of traditional villages. The first section is the introduction. The background of traditional village cultural landscape heritage, the status quo of domestic and foreign research, and the significance of research are introduced. The second section is the theory and method. Cultural landscape heritage, AI technology-related theories, research methods, and traditional villages in Wuyuan County, Jiangxi Province, are summarized. The third section is the results and analysis. Through the collection of relevant data, the current situation of the development of tourism and traditional village cultural landscape heritage in Wuyuan County is analyzed from different perspectives. Finally, AI technology is applied in the protection and inheritance of traditional villages. The fourth section is the conclusion. Through analysis, relevant conclusions are drawn, and future directions for improvement are proposed.

2. Construction of Traditional Village Cultural Landscape Using AI

2.1. AI Model Construction by Cultural Landscape Research. Cultural landscape generally refers to the human landscape familiar to the public, which is the result of the cocreation of nature and mankind. These cultural landscapes can reflect the unique cultural heritage and connotation of the region from the side [9–11]. The cultural landscape can be embodied in many ways, including clothing, architecture, religion, and food. Cultural landscapes mainly include the following types: (1) landscapes designed and constructed intentionally by humans, such as Suzhou gardens in Suzhou, the Great Wall of China, and Xidi Hong village; (2) organically evolved landscapes, including various fossil landscapes and rocky landscapes; (3) relevant cultural landscapes, including the Leshan Giant Buddha in Sichuan. Cultural landscape heritage refers to the rare and irreplaceable cultural landscape recognized by the United Nations Educational, Scientific, and Cultural Organization (UNESCO) and the World Heritage Committee (WHC). It is recognized by all mankind as a "common work of nature and mankind" with outstanding significance and universal value [12]. The villages in the cultural landscape heritage area are an important part of the cultural landscape [13, 14]. The specific composition of the World Heritage Site is shown in Figure 1.

Villages mainly refer to large-scale settlements or groups formed by multiple settlements. This group is mainly by the primary industry agriculture as the main production and lifestyle [15–18]. As a relatively primitive way of living in groups, villages are formed earlier, mostly retaining traditional material and nonmaterial forms, and carrying a certain local culture [19].

AI is a technical science used to simulate human intelligence theory methods and application systems [20, 21]. There are two different ways to realize AI on the computer: one is the engineering method, and the other is the simulation method [22]. Artificial Neural Network (ANN) is a simulation method. Its operating principle is to simulate certain human learning behaviors through corresponding computer technology. The specific ANN model is shown in Figure 2.

In Figure 2, a1, a2, a3, and a4 represent the input signal of the neuron. The calculation method of the relationship between output and input is as follows:

$$A = z\left(\sum_{i=1}^{4} a_i b_i + c\right), \tag{1}$$

where z represents an activation function, a_i represents the input information of the neuron, b_i represents the weight value corresponding to the neuron information element, and c represents the intercept.

According to equation (1), the weighted sum of neurons can be obtained, and the specific calculation method is as follows:

$$H_i = \sum_{j=1}^{n} b_{ij} a_j + c_j, \tag{2}$$

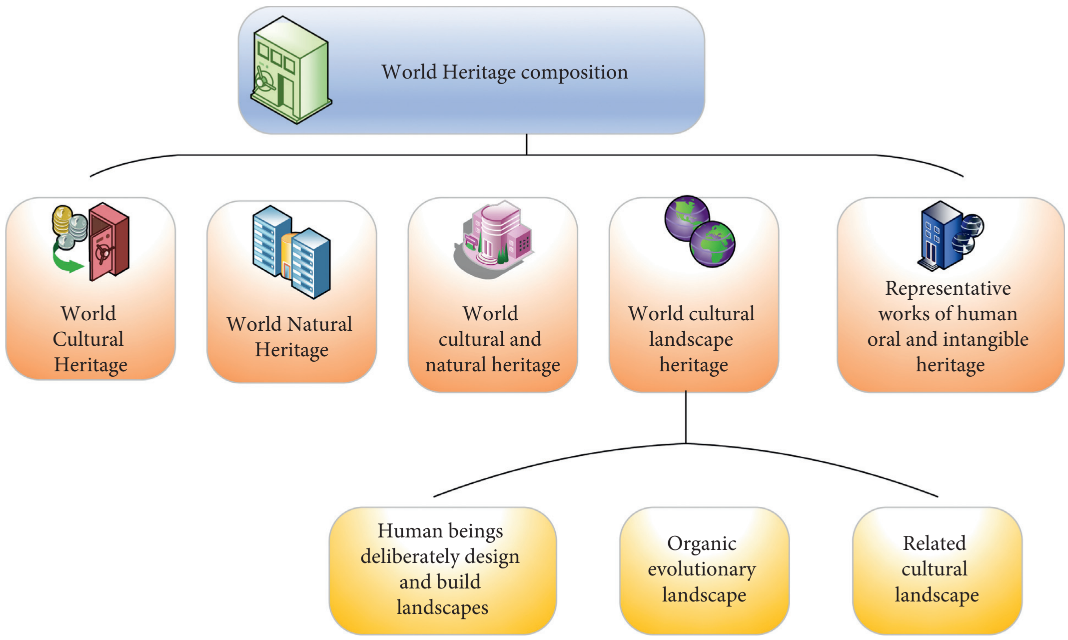

Figure 1: Composition of world heritage.

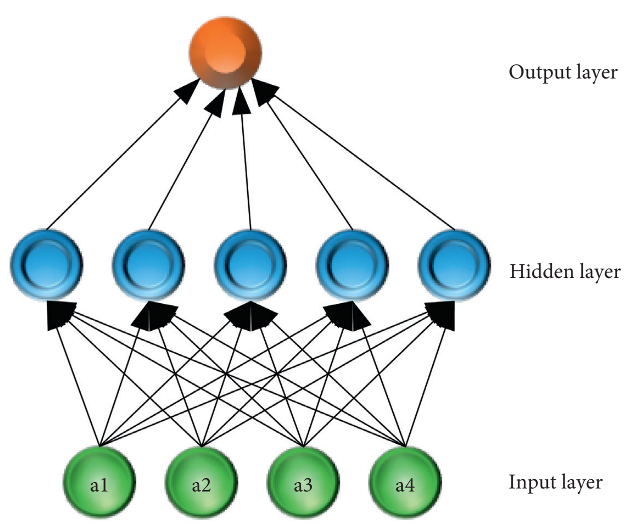

Figure 2: ANN model.

where H_i represents the weighted sum of neurons, j represents the j-th neuron information element, b_{ij} represents the i-th weight value corresponding to the j-th neuron information element, and a_j represents the input information corresponding to the j-th neuron information element. c_j represents the intercept corresponding to the j-th neuron.

The activation value of the neuron is obtained according to equation (2), and the specific calculation method is as follows:

$$e_i = z(H_i), \tag{3}$$

where e_i represents the activation value of the i-th neuron, z represents an activation function, and H_i represents the weighted sum of neurons.

The backpropagation algorithm is an important algorithm for neural network training. But before using this algorithm, a cost function needs to be set. The specific cost function calculation method is as follows:

$$J(b,c) = \left[\frac{1}{n}\sum_{i=1}^{n}\left(\frac{1}{2}\left\|h_{b,c}\left(x^{(i)} - y^{(i)}\right\|^2\right)\right] + \frac{\lambda}{2}, \tag{4}$$

where J represents the cost function, b represents the weight value corresponding to the neuroinformation element, c represents the intercept, n represents the number of layers, $x^{(i)}$ and $y^{(i)}$ represent a different training set, λ represents random, and h represents the magnitude of the weight. According to equation (4), the gradient descent algorithm can be used to update the network parameters, and the specific calculation method is as follows:

$$b_{ij} = b_{ij} - \beta \frac{1}{b_{ij}} J(b, c), \tag{5}$$

where the specific meanings of b, J, and c are the same as equation (4), i and j represent different neurons, and β represents the learning rate.

$$c_i = c_i - \beta \frac{1}{c_i} J(b, c). \tag{6}$$

where c_i is the intercept corresponding to the i-th neuron information element, and the meanings of the remaining letters are the same as equation (5).

The partial derivatives of equations (5) and (6) are calculated, and the result is shown as follows:

$$J(b, c) = \left[\frac{1}{n} \sum_{i}^{n} J\left(b, c; x^{(i)}, y^{(i)}\right)\right] + \lambda b_{ij}. \tag{7}$$

In equation (7), the meaning of the letters is the same as equation (6).

$$J(b, c) = \frac{1}{n} \sum_{i=1}^{n} J\left(b, c; x^{(i)}, y^{(i)}\right). \tag{8}$$

In equation (8), the meaning of the letters is the same as equation (7).

Meanwhile, the calculation method for the neuron residual of the output layer is shown as follows:

$$\begin{aligned} \eta_i &= \frac{1}{2}\left\| y - h_{b,c} \right\|^2 \\ &= -\left(y_i - a_i\right). \end{aligned} \tag{9}$$

where η represents the residual, y represents the training set, a represents the input information, and the meanings represented by the remaining letters are the same as those represented by equation (8).

The partial derivatives of equations (8) and (9) are calculated, and the result is shown as follows:

$$J(b, c; x, y) = a_j \cdot \eta_i. \tag{10}$$

In equation (10), the meaning of letters is the same as equation (9).

$$J(b, c; x, y) = \eta_i. \tag{11}$$

2.2. Research Methods. (1) Comparative analysis method: it refers to the multiparty comparison of two or more research objects to explore the similarities and differences between them. The purpose of analyzing and learning good methods is to continue to inherit the cultural landscape heritage of the village [23–25]. (2) Case study method: through the collection of data, the representative cultural heritage of traditional villages in society has been found. Take them as analysis cases, combine various problems existing in current social reality, establish a corresponding research framework, and make the paper more scientific [26]. (3) Expert interview method: by visiting experts in this area of cultural landscape heritage management, they will be invited to interview. And these experts will be asked about their views on the current status of cultural landscape heritage management in society in recent years. Additionally, continue to listen to experts' suggestions and opinions in this regard to increase the scientific and rationality of the paper [27, 28]. (4) Document method: due to writing needs, firstly, use CNKI, Google Scholar, Wanfang Data, and other channels for data query. Secondly, there are many articles and works from columnists and related Internet information. In addition, some journals and books related to the paper in the school library, *Into the World of Cultural Landscape Heritage*, *Illustrated Chinese Geography Encyclopedia*, and *Protection of Rural Heritage in the Perspective of Cultural Landscape*, have also been inquired and reviewed. Through the collection and summary of this series of data, it provides a favorable theoretical basis for research ideas and methods [29]. The data used comes from the website of the Wuyuan County Government in Jiangxi Province. The relevant parameters in the ANN model are shown in Table 1.

2.3. Introduction to Traditional Villages in Wuyuan County, Jiangxi Province. Wuyuan County is in Shangrao City, Jiangxi Province, and is one of the birthplaces of Huizhou culture in China [30, 31]. The historical and cultural heritage of this place is very profound, and it is one of the typical traditional village cultural landscape heritages. Wuyuan County currently retains many traditional villages. The traditional villages here are very different from other villages (such as Xidi Hong village). It retains the most primitive Huizhou architectural style in ancient times, and it pursues the harmony between man and nature [32–34]. In addition to traditional villages, there are also many cultural sites, memorial halls of famous people, "ghost dances," and so on [35, 36]. The specific list of cultural landscape heritage of Wuyuan County is shown in Figure 3.

3. Analysis of the Application Results of AI Technology by the Protection and Inheritance of Cultural Landscapes

3.1. Status Quo of Tourism Development in Wuyuan County. Wuyuan County is a representative of the cultural landscape heritage of traditional villages, and tourism is also a pillar industry in the area. By using the method of document collection, the tourism income of the place from 2016 to 2020 is found. The specific data results are shown in Figure 4.

In Figure 4, the comprehensive tourism income of Wuyuan County in 2016 was 5.63 billion yuan. Among them, ticket revenue was 431 million yuan, catering revenue was 821 million yuan, and entertainment project revenue was 1.029 billion yuan. In 2017, Wuyuan County's comprehensive tourism revenue was 6.21 billion yuan. Among them, ticket revenue was 592 million yuan, catering revenue was 1.195 billion yuan, and entertainment project revenue was 1.201 billion yuan. In 2018, the comprehensive tourism

Table 1: ANN parameter settings.

Parameter	Meaning	Setup
Maxlen	Text length, greater than this length, truncated, less than filled	300
Embedding_size	Embedding word vector dimension	300
Kernel_size	Size of the convolution kernel	2
Filters	Number of convolution kernels	412
Batch_size	The number of samples required for one training in gradient descent	156
Dropout_rate	Dropout ratio	0.1
Verbose	Log display	1

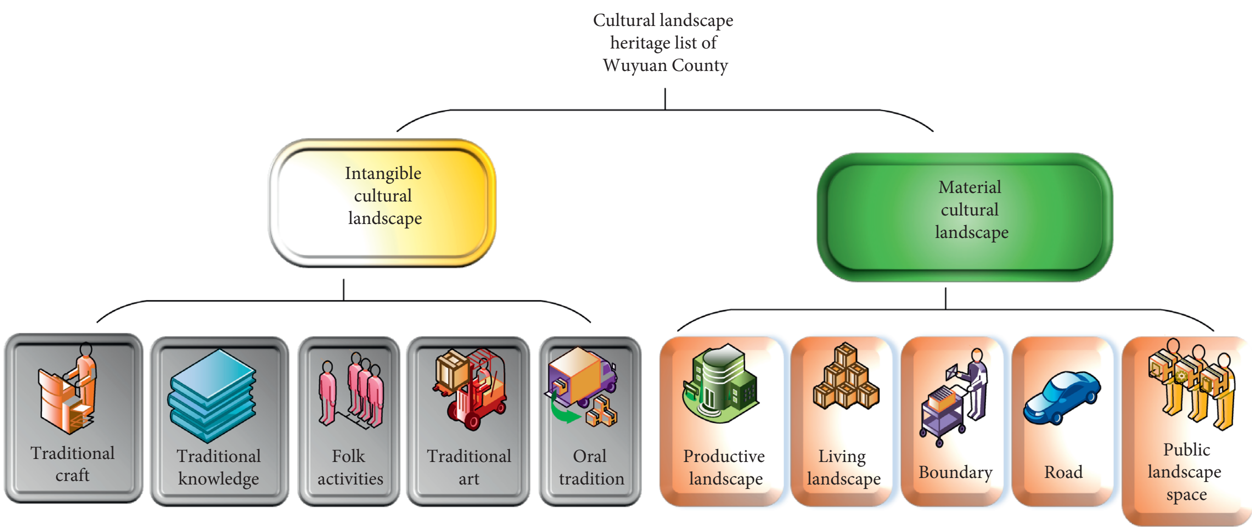

Figure 3: List of cultural landscape heritage of Wuyuan County.

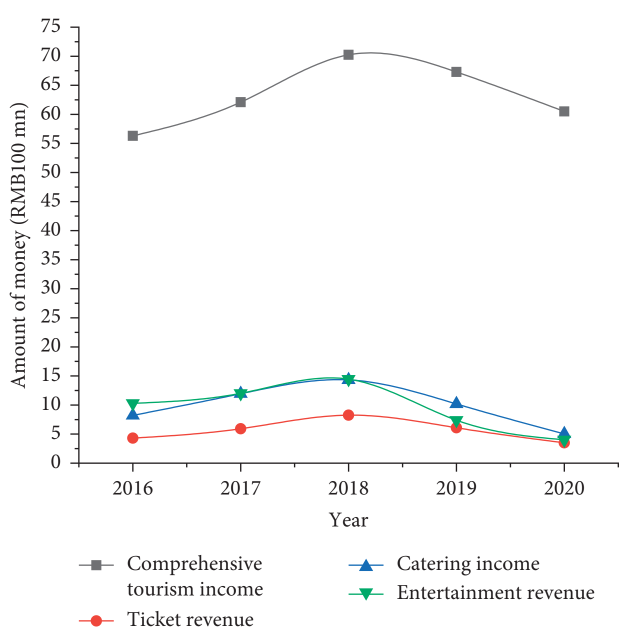

Figure 4: The tourism income of Wuyuan County from 2016 to 2020.

income of Wuyuan County was 7.25 billion yuan. Among them, ticket revenue was 826 million yuan, catering revenue was 1.433 billion yuan, and entertainment project revenue was 1.446 billion yuan. The comprehensive tourism income of Wuyuan County in 2019 was 6.73 billion yuan. Among them, ticket revenue was 610 million yuan, catering revenue was 1.018 billion yuan, and entertainment project revenue was 739 million yuan. This shows that, from 2016 to 2018, whether it is ticket revenue, catering revenue, or entertainment revenue, Wuyuan County has been on a rising trend. But since 2019, tourism revenue has declined. Compared to 2019, the village's tourism income has experienced the largest decline in 2020. The reason for this phenomenon has a lot to do with the Corona Virus Disease 2019 (COVID-19) epidemic that broke out at the end of 2019. The advent of the epidemic has brought a crisis to the development of tourism in Wuyuan County.

From 2016 to 2020, the number of tourists and the income of local farmers in Wuyuan County are shown in Figure 5.

Figure 5 shows that, in 2016, Wuyuan County had 11.236 million tourists, and the per capita income of farmers was 7086 yuan. In 2017, the number of tourists in Wuyuan County was 12.634 million, and the per capita income of farmers was 7,502 yuan. In 2018, the number of tourists in Wuyuan County was 13.988 million, and the per capita income of farmers was 8,011 yuan. In 2019, the number of tourists in Wuyuan County was 13.504 million, and the per capita income of farmers was 7631 yuan. In 2020, Wuyuan County had 11.201 million tourist trips, and the per capita income of farmers was 7,203 yuan. In the three years from 2016 to 2018, the number of tourists in Wuyuan County and

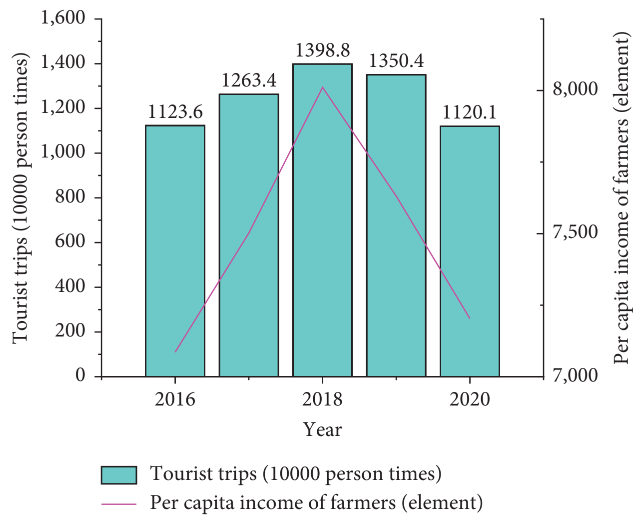

FIGURE 5: The number of tourists and farmers' income in Wuyuan County from 2016 to 2020.

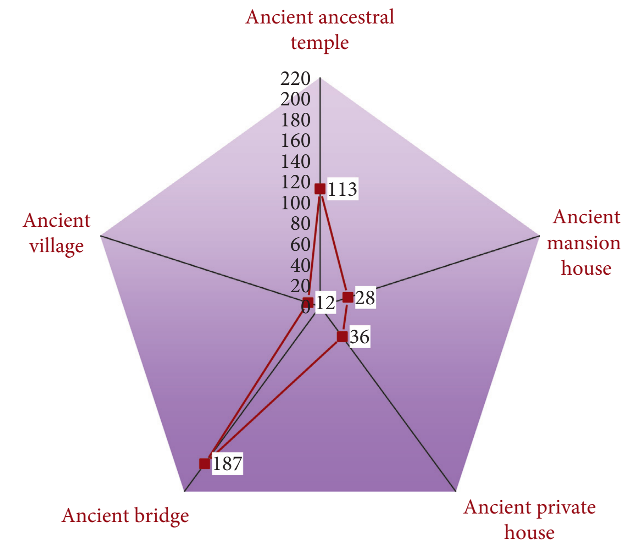

FIGURE 6: The number of existing cultural landscape sites in Wuyuan County.

the per capita income of local farmers have been increasing. However, since 2019, the number of tourist arrivals has declined. The reason for this situation in the local tourism industry is that it has been hit hard by the COVID-19 epidemic.

From the above data results, the unique cultural landscape of traditional villages in Wuyuan County can attract many tourists to a certain extent. So, the local landscape heritage must be protected and inherited.

3.2. Status Quo of the Development of Cultural Landscape Heritage in Wuyuan County. From the perspective of tourism income and the number of tourists, the tourism industry in Wuyuan County continued to develop steadily from 2016 to 2020. However, according to relevant research records, the local traditional village cultural landscape sites are slowly disappearing over time. This is mainly reflected in the following aspects: (1) The protection is not strong. Up to now, the specific situation of the existing ancient village ruins in Wuyuan County is shown in Figure 6.

In Figure 6, there are currently 113 ancient ancestral temples, 28 ancient mansion houses, 36 ancient private houses, 187 ancient bridges, and only 12 ancient villages. Although there are a lot of cultural landscape sites, many villages, ancient mansion houses, and so on have disappeared compared to before. Traditional Huizhou buildings are dominated by civil structures, and the longer they exist, the slower they will collapse. With the continuous development of the social economy, more and more people choose to live in cities, leading to many traditional villages being abandoned. In addition, some old houses are demolished and destroyed, new modern houses are built on the land, and so on. These actions are destroying monumental architectural sites. (2) There are few records of traditional villages in Wuyuan County. Since there are few recorded documents and architectural design drawings, this has brought difficulties for the use of modern AI technology to restore cultural landscape sites. The original houses are now asking residents, and they are built on what they remember. The house built in this way lacks a certain degree of authenticity. (3) The "immigrant relocation" policy hinders the development of the cultural landscape of traditional villages in Wuyuan County. According to the results of the Seventh National Census, the current permanent population of Wuyuan County is only about 300,000. The massive evacuation of residents has left more traditional villages abandoned, changing the original development goals. The ancient towns, ancient private houses, and ancient ancestral temples are short of people to manage and clean them. (4) There is a lack of innovative spirit. At present, Wuyuan County is still developing in accordance with the traditional tourism model, which will undoubtedly be eliminated by the times. To a certain extent, intangible cultural heritage can complement the cultural landscape of traditional villages. The specific list of intangible cultural heritage is shown in Table 2.

Table 2 shows that there is a total of eight intangible cultural heritages in Wuyuan County. Among them, there are five traditional skills and three folk customs. However, due to the traditional ideology of the residents, the customs of "passing on men but not women" have caused some intangible cultural heritage to gradually withdraw from people's vision, such as tea art, ghost dance, paper umbrellas, and carving techniques in Wuyuan County.

3.3. Application of AI in the Protection and Inheritance of Traditional Villages. The cultural landscape of traditional villages in Wuyuan County has been damaged to a certain extent by the outside world. To continue to inherit the cultural landscape of the place, AI technology is needed to restore the damaged buildings. The specific operation steps are shown in Figure 7.

Table 2: List of intangible cultural heritage of Wuyuan County.

Type	Serial number	Name
Traditional skills	1	Wuyuan pineapple lacquerware making technology
	2	Wuyuan emblem embroidery technique
	3	Traditional refining techniques of Wuyuan camellia oil
	4	Wuyuan huiweimingcheng secret spicy sauce making technology
	5	Traditional making techniques of Wuyuan rice spoon
Name and custom	1	Zhu Zi's family motto
	2	Wuyuan Wengong sacrifice
	3	Wuyuan Zhan family motto

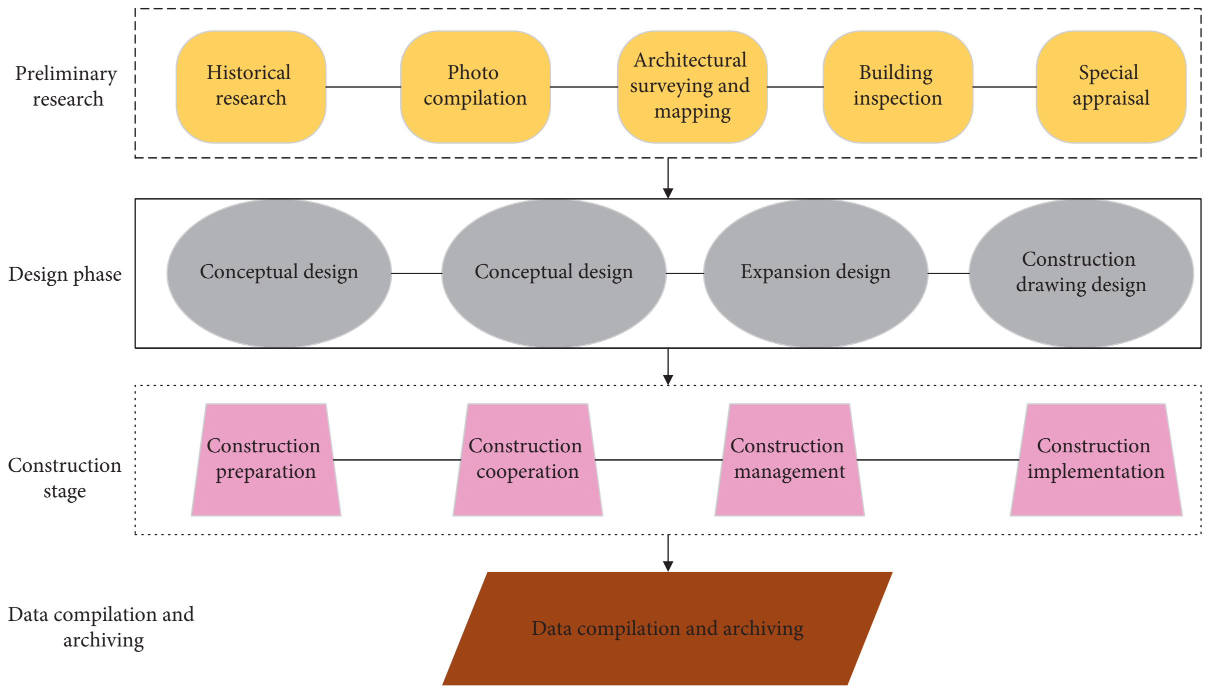

Figure 7: Restoration steps of traditional village cultural landscape.

Figure 7 shows that the restoration of the traditional village cultural landscape needs to go through four stages: preliminary investigation, design stage, construction stage, and data compilation and filing. These four stages are indispensable, and problems in any of these stages will have a serious impact on the restoration of the following traditional villages. The results of the design stage have important implications for the restoration of the entire traditional village, which means that the design stage is the most important of these four stages.

Meanwhile, the restoration of the cultural landscape of traditional villages is inseparable from the research and analysis of village images. The analysis mainly involves traditional village similarity detection, village-style classification, selection of the main color of the village, automatic image sorting, and automatic recognition and restoration of image damage. The specific operation method is shown in Figure 8.

Figure 8 shows that there are many projects involved in image analysis research. The neural network model calculation method in the AI algorithm is also used. In the entire image research and analysis, in addition to the analysis of the image of the traditional village, there is also the study of drawing and restoration. AI technology is of great significance to the inheritance of cultural landscape heritage.

In addition, after analyzing the images of traditional villages, it is necessary to manually review the images before entering the next stage. In the scene of manual review processing, ANN technology is needed to realize the recognition of pictures. ANN technology mainly reviews the following aspects of pictures: (1) The angle of picture drawing should be consistent with the angle of traditional village construction. (2) The style of picture drawing should be consistent with the style of the original traditional village. (3) The color of the drawn picture should also be like the original village's tone as much as possible, there should not be too much difference, and so on. If there is any discrepancy, it will be deleted. The implementation of ANN technology for image review is shown in Table 3.

Table 3 shows that there is a total of six neural layers. Each layer has its unique functions to ensure the normal operation of the image review program. Similarly, each layer cannot be replaced or deleted.

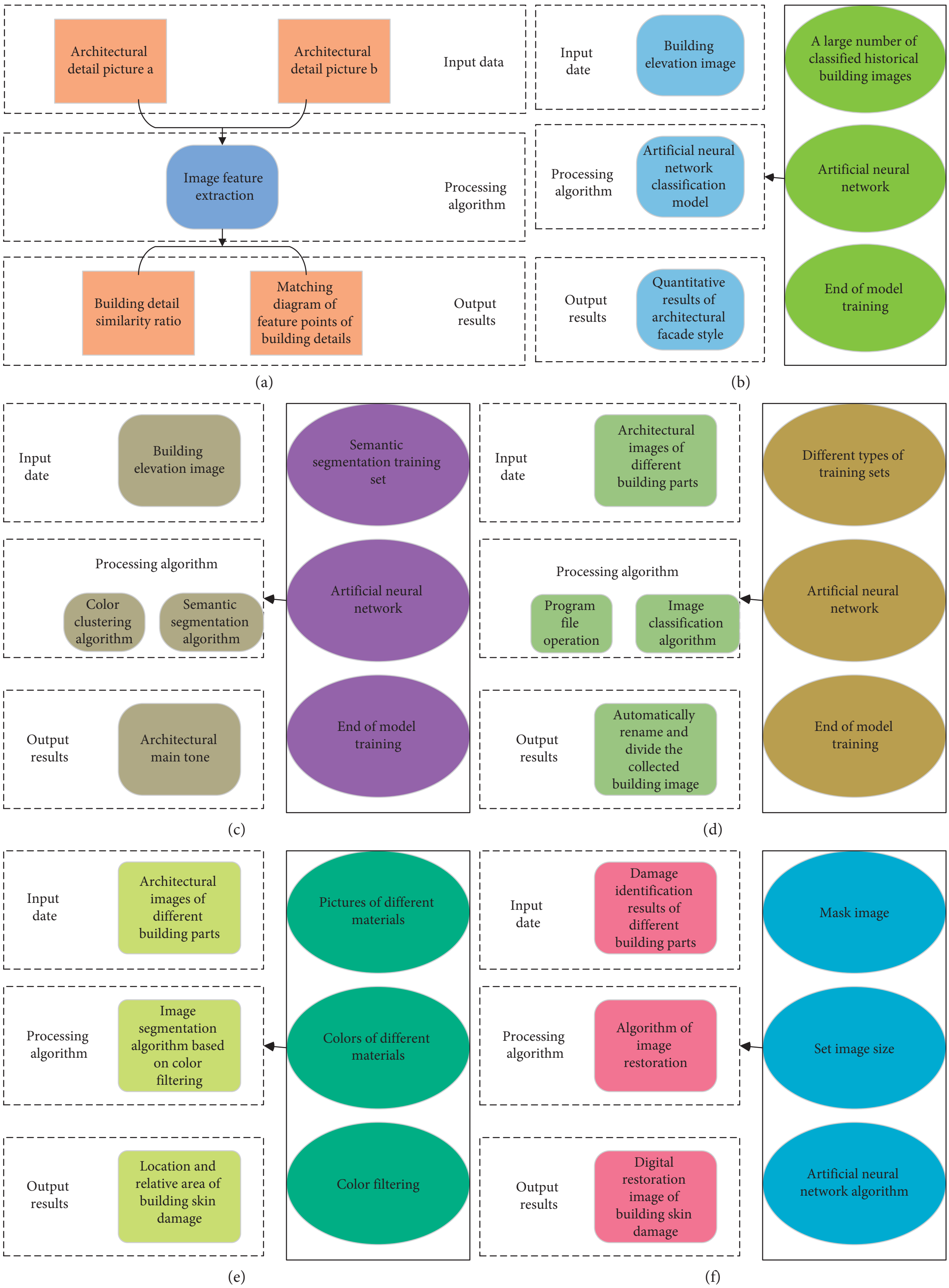

Figure 8: Analysis of images in the restoration of traditional village cultural landscape. (a) The similarity detection of traditional villages, (b) the classification of traditional village styles, (c) the selection of the main colors of traditional villages, (d) the automatic image collation, (e) the automatic recognition of image damage, and (f) the automatic restoration of the image.

Table 3: Functions of each layer of ANN in image review.

Nerve layer	Function
Input layer	Preprocess the input image data for subsequent calculation
Convolution layer	Different convolution kernels are used to filter the image data and obtain the feature set of the image
Active layer	The above linear calculation operation is transformed into a nonlinear calculation
Pool layer	It is usually placed between and continuous convolution layers to compress the image
Full connection layer	It is usually located at the last level of the neural network and connects the above-extracted feature set
Output layer	Output the classification result of image recognition

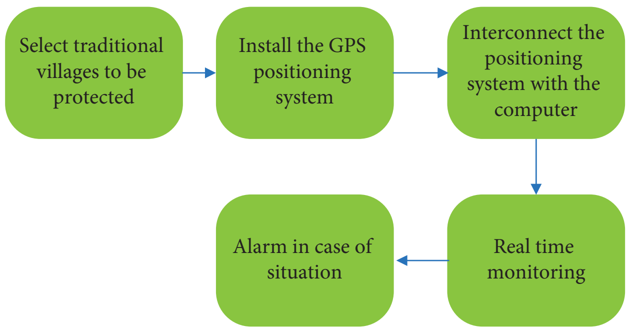

Figure 9: The application method of intelligent sensing technology in the protection of cultural landscape.

The cultural landscape of traditional villages in Wuyuan County must not only be inherited but also be protected. In the protection of cultural landscapes, intelligent perception and RF identification technology can be applied. The specific application method is shown in Figure 9.

Figure 9 shows that the first step is to select the traditional villages that need to be protected. After selecting the village, the Global Positioning System (GPS) is installed. After the installation is complete, the system will be associated with the computer, and then the system will transmit the required data to the computer in real time, including weather, temperature, existing age, and the service life of the building. In this way, it is possible to learn various specific data information without the need for relevant management personnel to arrive at the site of the traditional village. If the building is damaged or there is a risk of collapse, the system will also issue an alarm to remind the management staff. AI technology plays an important role in the protection of the cultural landscape of traditional villages.

4. Conclusion

Applying AI technology to the protection and inheritance of the cultural landscape heritage of traditional villages, the following conclusions can be found: (1) taking Wuyuan County in Jiangxi Province as the research object in the traditional villages from 2016 to 2018, tourism income shows a rising trend. However, due to the outbreak of the epidemic in 2019, tourism revenue has declined to a certain extent. (2) Although Wuyuan County's tourism income has been relatively optimistic in recent years, in fact, the traditional villages in this area have gradually disappeared, and the protection of traditional villages is not strong. Due to these reasons and the implementation of the "Immigration and Relocation" policy, Wuyuan County has lost its previous "vitality." (3) Applying AI technology to traditional villages can roughly restore traditional villages by previous images. In the restoration process, the involved stages are particularly important. Not only must the image be drawn and repaired, but also the drawn image must be reviewed and processed by ANN. (4) The application of intelligent perception and RF identification technology in traditional villages can monitor and analyze cultural landscapes in real time and realize the protection of traditional villages. AI technology is used in the protection and inheritance of traditional village cultural landscape heritage. This provides a basis for further analysis and resolution of problems in heritage protection. Mainly literature collection methods such as the literature analysis method and questionnaire survey method are used. AI technology can not only draw images of traditional villages but also restore existing cultural relics. This has great reference significance for the management of various historical and cultural heritages.

Due to limited energy, there are certain limitations in data acquisition, leading to deviations in some analysis of related data. The application of AI technology to the inheritance and protection of traditional village cultural landscape heritage has not been discussed in terms of economic investment. The follow-up research can conduct benefit evaluation according to the specific situation so that this technology can bring certain beneficial effects to the protection and inheritance of the traditional village cultural landscape heritage in the future.

Data Availability

The datasets used and/or analyzed during the current study are available from the corresponding author upon reasonable request.

Conflicts of Interest

The authors declare that they have no conflicts of interest.

References

[1] E. A. Bilgin, T. V. Arslan, and S. Durak, "Physical changes in World heritage sites under the pressure of tourism: the case of cumalıkızık village in bursa," *European Journal of Sustainable Development*, vol. 8, no. 2, pp. 249–260, 2019.

[2] P. K. Awah, M. Mvetumbo, T. Oishi, and N. T. Marlene, "The persistence of spleen sickness culture in Cameroon: a comparison between a remote village in the Eastern Region and an urban," *Area of the Central Region*, vol. 458, no. 10, pp. 459-460, 2020.

[3] L. T. Tan, R. Q. Hu, and L. Hanzo, "Twin-timescale Artificial intelligence aided mobility-aware edge caching and computing in vehicular networks. Vehicular technology," *IEEE Transactions on*, vol. 789, no. 456, pp. 152–155, 2019.

[4] R. Qiu, "Assessing Disease activity in ulcerative colitis using artificial intelligence: can "equally good" Be seen as "better"?" *Gastroenterology*, vol. 159, no. 4, pp. 785–790, 2018.

[5] T. Roger, "Artificial intelligence for sex determination of skeletal remains: application of a deep learning artificial neural network to human skulls," *Journal of Forensic & Legal Medicine*, vol. 56, no. 11, pp. 245–250, 2018.

[6] T. Livio, "Artificial intelligence for interpretation of segments of whole MRI in CNO: pilot study comparing radiologists versus machine learning algorithm," *Pediatric Rheumatology Online Journal*, vol. 18, no. 45, pp. 362–365, 2019.

[7] Y. Li, "Incidental cerebral aneurysms detected by a computer-assisted detection system by artificial intelligence: a case series," *Medicine*, vol. 99, no. 43, pp. 215–220, 2019.

[8] Z. Peter, "AIRSENSE-TO-ACT: a concept paper for COVID-19 countermeasures by artificial intelligence algorithms and multi-sources," *Data Processing*, vol. 486, no. 752, pp. 56–60, 2018.

[9] W. L. Lu, X. Chen, L. Wang, and H. Li, "The combination of an artificial intelligence approach and laser tweezers Raman spectroscopy for microbial identification," *Analytical Chemistry*, vol. 78, no. 45, pp. 89-90, 2020.

[10] Y. Lu, N. Vincent, C. Y. Suen, and P. S. P. Wang, "Guest editorial: special issue on the international conference on pattern recognition and artificial intelligence (ICPRAI 2020)," *International Journal of Pattern Recognition and Artificial Intelligence*, vol. 96, no. 452, pp. 789–800, 2021.

[11] P. Ström, K. Kartasalo, H. Olsson et al., "Artificial intelligence for diagnosis and grading of prostate cancer in biopsies: a population-based, diagnostic study," *The Lancet Oncology*, vol. 21, no. 2, pp. 222–232, 2020.

[12] J. Licato and Z. Zhang, "Correction to: evaluating representational systems in artificial intelligence," *Artificial Intelligence Review*, vol. 52, no. 4, p. 1, 2019.

[13] F. Riguzzi, K. Kersting, M. Lippi, and S. Natarajan, "Editorial: statistical relational artificial intelligence," *Frontiers in Robotics and AI*, vol. 6, no. 6, pp. 68–70, 2019.

[14] D. Marina, L. Codari, O. Simone et al., "Artificial intelligence for breast mri in 2008-2018: a systematic mapping review," *Air American Journal of Roentgenology*, vol. 369, no. 456, pp. 78–80, 2019.

[15] C. Niu and L. He, "Research on athlete recognition by image feature extraction and artificial intelligence classification," *Journal of Ambient Intelligence and Humanized Computing*, vol. 723, no. 5, pp. 48–55, 2021.

[16] P. Guha, "Spatiotemporal analysis of COVID-19 pandemic and predictive models by artificial intelligence for different states of India," *Journal of The Institution of Engineers (India) Series B*, vol. 753, no. 8, pp. 742–750, 2021.

[17] S. Doki, S. Sasahara, D. Hori et al., "Comparison of predicted psychological distress among workers between artificial intelligence and psychiatrists: a cross-sectional study in Tsukuba Science City, Japan," *BMJ Open*, vol. 11, no. 6, pp. 265–270, 2021.

[18] C. Macdonald, M. Yang, S. Learn, R. Hugo, and S. Park, "Liquid pipeline rupture detection using multiple artificial intelligence classifiers during steady-state and transient operations 2020 13th," *International Pipeline Conference*, vol. 485, no. 56, pp. 90–100, 2020.

[19] M. Mohamed-Seghir, A. Krama, S. S. Refaat, and M. Trabelsi, "Artificial intelligence-based weighting factor Autotuning for model predictive control of grid-tied packed U-cell inverter," *Energies*, vol. 13, no. 12, pp. 85–100, 2020.

[20] T. Lui, K. Wong, L. Mak et al., "Feedback from artificial intelligence improved the learning of junior endoscopists on histology prediction of gastric lesions," *Endoscopy International Open*, vol. 789, no. 45, pp. 478–500, 2020.

[21] M. P. Mehr and E. Solgi, "Investigation of artificial intelligence approaches (ANN-MLP, CAFIS) for the daily prediction of winter air pollutants (CO2, SO2, NOx, O3) in," *Hamedan city using meteorological data*, vol. 489, no. 103, pp. 756–780, 2020.

[22] H. Sun, "Historic town as cultural landscape——the relationship between historic town, traditional village and urban archaeological site," *Journal of Human Settlements in West China*, vol. 520, no. 423, pp. 78–100, 2019.

[23] N. Dwijendra and I. Paramadhyaksa, "The complexity of orientation in traditional village architecture in bali, Indonesia," *Humanities Diliman*, vol. 18, no. 1, pp. 99–117, 2021.

[24] W. Li, Z. Wu, L. Liu, and W. Chen, "Relationship embedding, knowledge acquisition and tourism innovation intention of traditional village under resource constraints: a case study from the perspective of community tourism participation and case comparison," *Geography and Geo-Information Science*, vol. 569, no. 452, pp. 452–460, 2019.

[25] H. Ono and H. Shimizu, "6062 A tendency of the traditional village structure and development of the village in the limestone soil of the Okinawa southern part Shimajiri area: case study of the Itoman-City villages//Architectural Institute of Japan," *Architectural Institute of Japan*, vol. 236, no. 489, pp. 789–800, 2019.

[26] B. X. Tran, G. T. Vu, C. A. Latkin et al., "Characterize health and economic vulnerabilities of workers to control the emergence of COVID-19 in an industrial zone in Vietnam," *Safety Science*, vol. 129, no. 452, Article ID 104811, 2020.

[27] Z. Bai, S. Fang, J. Gao et al., "Could vegetation index be derive from synthetic aperture radar? – the linear relationship between interferometric coherence and NDVI," *Scientific Reports*, vol. 10, no. 1, pp. 723–750, 2020.

[28] E. E. Jones, M. B. Krause, C. R. Watson, and G. N. O'Saile, "Economic and social interactions in the piedmont village tradition-mississippian boundarylands of southeastern north America, AD 1200-1600," *American Antiquity*, vol. 85, no. 1, pp. 72–92, 2020.

[29] D. Fang, S. Pan, Z. Li et al., "Large-scale public venues as medical emergency sites in disasters: lessons from COVID-19 and the use of Fangcang shelter hospitals in Wuhan, China," *BMJ global health*, vol. 5, no. 6, pp. 281–290, 2020.

[30] X. Wang, G. Chen, M. Cui, and D. Liu, "Analysis of public cognition on traditional village landscape environmental planning and design—taking hetian area as an example," *IOP Conference Series: Materials Science and Engineering*, vol. 780, no. 11, pp. 72–131, 2020.

[31] D. U. Sen and X. Dong, "Research on the development of traditional villages by the protection of earthen sites——taking mogou village, lintan county," *Gansu Province as an Example*, vol. 47, no. 2, pp. 489–500, 2019.

[32] B. Wei, M. Yang, and X. U. Wenfang, "An analysis on the characteristics and protection strategies of Korean traditional villages——taking bailong village as an example," *Research on Heritages and Preservation*, vol. 78, no. 856, pp. 523–530, 2019.

[33] X. Wang and T. Chai, "Study on the protection, development and utilization of trench-cave-type traditional villages in

wangbian village of southern hebei Province under the rural revitalization strategy," *Architecture & Culture*, vol. 486, no. 10, pp. 486–500, 2019.

[34] N. Jaffar and N. Z. Harun, "Preserving cultural landscape: Malaysia's east coast traditional Malay settlement in change," *Asian Journal of Behavioural Studies*, vol. 4, no. 16, pp. 49-50, 2019.

[35] B. V. Ciorua, A. L. Pop, and M. Coman, ""Dimitrie gusti" national village museum - short philatelic history review," *Asian Journal of Education and Social Studies*, vol. 41, no. 40, pp. 1–17, 2020.

[36] T. Hue, V. T. Hien, N. Ha, and N T A. Hang, "Water quality in Thanh Luong rice vermicelli and fresh noodle craft village, Thanh Oai district, Hanoi, Vietnam," *IOP Conference Series: Earth and Environmental Science*, vol. 266, no. 896, pp. 120–130, 2019.

Hindawi
Scientific Programming
Volume 2022, Article ID 6588777, 7 pages
https://doi.org/10.1155/2022/6588777

Research Article

Research on Fast Face Retrieval Optimization Algorithm Based on Fuzzy Clustering

Xiajun Dong, Bin Huang, and Yuncai Zhou

College of Computer Science, Yangtze University, Jingzhou 434023, Hubei, China

Correspondence should be addressed to Bin Huang; jonsen@yangtzeu.edu.cn

Received 11 November 2021; Accepted 8 December 2021; Published 7 January 2022

Academic Editor: Punit Gupta

Aiming at the problem of long retrieval time for massive face image databases under a given threshold, a fast retrieval algorithm for massive face images based on fuzzy clustering is proposed. The algorithm builds a deep convolutional neural network model. The model can be used to extract features from face photos to obtain a high-dimensional vector to represent the high-level semantic features of face photos. On this basis, the fuzzy clustering algorithm is used to perform fuzzy clustering on the feature vectors of the face database to construct a retrieval pedigree map. When the threshold is passed in for database retrieval of the target face photos, the pedigree map can be quickly retrieved. Experiments on the LFW face dataset and self-collected face dataset show that the model is better than the commonly used K-means model in face recognition accuracy, clustering effect, and retrieval speed and has certain commercial value.

1. Introduction

In recent years, due to the rapid development of image recognition technology, face recognition technology is also developing rapidly [1]. The face recognition [2, 3] model based on deep learning keeps refreshing records on the open-source dataset, such as LFW [4], MegaFace [5], and other datasets. Many cameras have implemented deep learning algorithms in the camera in order to realize the real-time face recognition function just using the camera. This type of face recognition camera can easily complete the frame-by-frame analysis of the captured video and extract the face from the video. The face captured by the camera is transmitted to the server for storage. In the field of security [6], the facial recognition cameras deployed by county-level units upload 5 million facial photos to the server every day. Each face photo uploaded to the server needs to be compared with a locally constructed blacklisted face database in real time to determine whether the person is a person on the blacklist controlled by the police.

The face comparison process of the large dataset contained in the above scenario has great social value in the security field. Face comparison under the large face dataset faces the following challenges:

(1) The face database has a huge number of faces. In most scenarios, its quantity can reach tens of millions or even hundreds of millions.

(2) There are a lot of face photos collected by the same person, such as person's ID photos, front-grabbing photos, side-grabbing photos, and so on. This will double the size of the face database and make the comparison more difficult.

(3) The number of samples of each type of face is not balanced, resulting in different comparison times in the same class. Due to the short board effect, the final comparison speed is dragged down by the samples with a large number of samples.

In 2018, Li et al. used the deep feature clustering algorithm to optimize the problem of massive face retrieval [7] and achieved good results because they used the K-means clustering algorithm to cluster the face features. Unbalanced distribution of features will lead to serious missed detection.

In 2019, Dubey improved the discrimination of face image descriptors by using the decoder concept of multichannel decoded local binary pattern over the multifrequency patterns. In this paper, a frequency decoded local binary pattern (FDLBP) is proposed with two decoders. This can greatly improve the accuracy of face retrieval, but when the number of faces is huge and the number grows dynamically, it cannot meet the requirements of high real time [8].

This paper is based on the deep learning model for feature extraction of face photos, combined with feature fuzzy clustering algorithm for fuzzy clustering of face feature vectors. Using Caltech 10 k Web Faces Dataset as the training set, clustering of face photos on the LFW face dataset and the face dataset collected from the Internet has achieved good results.

2. Design of Face Image Retrieval Model Based on Fuzzy Clustering

The model structure of the facial image retrieval algorithm based on fuzzy clustering is shown in Figure 1. The face image retrieval model mainly includes two parts. The first part uses the deep convolutional neural network model [9, 10] to extract features from the face image [2, 3] to obtain a 256-dimensional face feature vector $v_i\{v_1, v_2, \ldots, v_n\}$. Each component in the feature vector (v_i) is a floating-point type data, and it keeps 4 decimal places. The formula for calculating the similarity of the feature vectors of two people's faces is defined as shown in formula (1). If the value of Similar_{ij} tends to 1, then the face photos represented by feature vectors v_i and v_j are more similar.

$$\begin{aligned} &\text{Similar}_{ij} = \sum v_i \times v_j,\\ &\text{Similar}_{ij} = 1, \text{IF}\left(\text{Similar}_{ij} > 1\right),\\ &\text{Similar}_{ij} = 0, \text{IF}\left(\text{Similar}_{ij} < 0\right). \end{aligned} \tag{1}$$

Algorithms commonly used to calculate image similarity, such as Euclidean distance, cosine distance, hamming distance, and so on, have their own advantages and disadvantages. In formula (1), we use an algorithm that approximates the Euclidean distance to calculate the similarity of two face images. This algorithm is closer to the calculation method of matrix multiplication and can perform $N:N$ face similarity calculations at the same time. GPU is best at matrix operations, so this algorithm can maximize the performance of GPU.

The second part is to perform fuzzy clustering on the eigenvectors in the face database to be compared to obtain the similarity matrix of the pairwise eigenvectors S_{ij} and to draw a pedigree map P for the cluster $\left\{C_1, C_2, \ldots, C_j\right\}$. The next step is to calculate the center point of each cluster in the pedigree graph to get the cluster center point $\{\mu_1, \mu_2, \ldots, \mu_n\}\max(n) = 256$. After extracting the features of the face image to be searched, perform further retrieval according to the cluster center points in the pedigree diagram.

2.1. Face Feature Extraction-Deep Convolutional Neural Network Structure Design. The deep learning model used in this article is mainly based on the convolutional neural network(CNN), and the structure of the convolutional neural network is fine-tuned to satisfy the effective feature extraction of face photos. Considering that the feature information of face photos will lose part of the information during the global pooling operation, resulting in incomplete expression of face features, the maximum pooling method is used in the structural design. The input of the deep convolutional neural network is a face picture, and the output is a one-dimensional vector of 256 dimensions. This vector is used to represent the characteristics of the face, which we call the feature vector of the face.

The structure design of the face feature extraction model based on the deep convolutional neural network is shown in Figure 2. The network is called FFEDN (Face-Feature Extract Dense Net) in this article, and the Stack Conv* structure in the model is the structure shown in Figure 3.

2.2. Design of Face Image Retrieval Process. The design of the face image retrieval process is shown in Figure 4. The face photos to be searched are processed into pictures with $W \times H \times C$ pixels in the system. We use $128 \times 128 \times 3$ pixels in this model. Then, we can get a 256-dimensional vector through the FFEDN model. The next step is to calculate the similarity between this vector and the cluster center point vector. After this step, we can get the most similar clusters. Then, search within this cluster until you get the most similar leaf node. Finally, return all face photos in this cluster in descending order of similarity.

In the public security application scenario, when performing face retrieval, the 100 most similar face images are often screened out, namely, top100. Therefore, fuzzy clustering can avoid the problem of missing the most similar face due to inaccurate determination of K value when using K-means clustering [10].

3. Face Image Retrieval

3.1. Feature Vector Extraction Method for Face Photos. The face photos to be searched need to be processed into a three-dimensional tensor structure $F(I)$: $W_I \times H_I \times C_I$. In this structure, C_i represents the number of channels of the color picture, and this article takes the three channels of the picture, namely, $C_i = 3$, W means the picture width, H means the picture height, and the model will process the picture into a dimension of 128×128, that is, $W = 128$; $H = 128$. That is, the face image needs to be processed as a tensor with $128 * 128$ pixels and a channel of 3.

The calculation process of tensor in the deep neural network structure shown in Figure 2, and the calculation of the convolutional layer is defined as follows:

$$X_{W,b}^{m(l)} = f\left(b^{m(l)} + \sum_n W^{mn(l)} * X_{W,b}^{m(l-1)}\right), \tag{2}$$

where $X^{m(l)}$ represents the mth channel of layer l, $W^{mn(l)}$ and $b^{m(l)}$ are the corresponding convolution kernel filters and bias terms, and $*$ is the convolution operator.

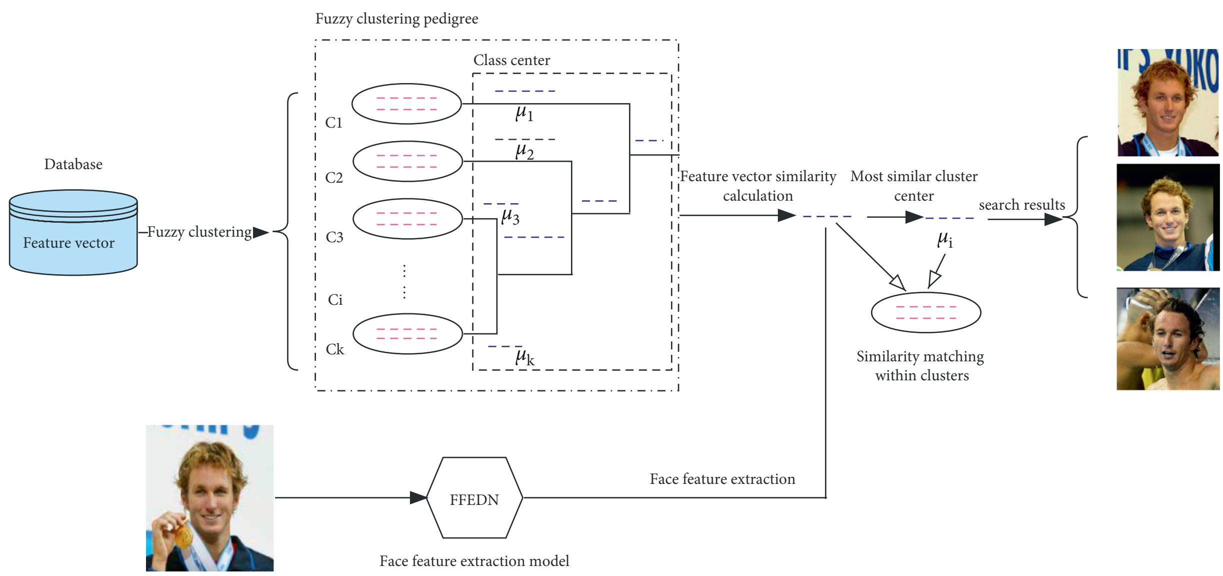

Figure 1: Face image retrieval model structure.

In order to avoid inaccurate feature expression caused by overfitting, this model structure uses a local maximum pooling (max-pooling) method to process the output of the convolutional layer.

$$X^{m(l)}_{(i,j)} = \max_{\forall (p,q)\in\Omega(i,j)} \left\{X^{m(l)}_{(p,q)}\right\}, \quad (3)$$

where $\Omega_{(i,j)}$ is the specific area of index (i, j) and (p, q) is the index of the specific position on Ω. The last layer of the network is a fully connected layer, and finally a 256-dimensional 1D vector is obtained to represent the characteristics of the face.

3.2. Fuzzy Clustering of Facial Feature Vector. According to formula (1), calculate the correlation coefficient matrix (r^*_{ij}) between the feature vectors of two people's faces.

Use formula (4) to perform matrix transformation on the correlation coefficient matrix, so that the value in r^*_{ij} is converted to the interval [0,1], thereby forming a fuzzy matrix $R = (r_{ij})$.

$$r_{ij} = \frac{1 + r^*_{ij}}{2}. \quad (4)$$

Perform a convolution operation on the fuzzy matrix: $R \longrightarrow R^2 \longrightarrow R^3 \longrightarrow \cdots \longrightarrow R^n$. After a finite number of convolution operations, make $R^n \bullet R = R^n$, where "$\bullet$" represents the convolution operator. When $R^n \bullet R = R^n$, R is the final correlation coefficient matrix. Sort the correlation coefficient values λ_{ij} in the correlation coefficient matrix in descending order, intercept the values λ_{ij} >0.75 to construct the pedigree diagram, and finally obtain the pedigree diagram. The threshold 0.75 is a commonly used value for face recognition, that is, when $\text{Similar}_{ij} > 0.75$, it can be considered that the two persons are the same person or people with high similarity.

3.3. Building a Pedigree Map and Searching within Clusters in the Pedigree Map. In Section 3.2, after the fuzzy matrix is calculated, the fuzzy matrix is sorted in reverse order according to the value λ_{ij} of the fuzzy matrix, and the same values are classified into the same cluster according to the result of the sorting, thereby constructing a clustering pedigree diagram. Next, calculate the center point of the eigenvectors of each pedigree graph, and the calculation formula (5) is as follows:

$$\text{circle} = \frac{\sum_{i=1}^{n} r(i)}{256} n = 1, 2, \cdots, 256. \quad (5)$$

In the face retrieval process, set the given similarity threshold to threshold = 0.75. First calculate the similarity with the nodes in the pedigree graph, and the similarity calculation formula is shown in formula (1). Select nodes with similarity >0.75 to perform intranode branch search, and the judgment condition is still whether the similarity is greater than the threshold. Finally, the same similarity calculation method in the cluster can be used to calculate the face similarity, and the final results are returned in descending order.

4. Experimental Process and Result Analysis

The CPU of the server used in the experiment is Intel(R) Core(TM) Xeon-5600 series. The memory of the server is 128 G. The GPU uses NVIDIA Ti-Tan. The operating system uses Centos 7.4. This experiment is based on the TensorFlow framework.

4.1. Face Recognition Dataset. In this paper, the Caltech Web Faces Dataset is used to train the model, and the LFW dataset and some datasets collected from the Internet are used as the model's test dataset. The total dataset contains 1000 samples and about 600,000 face photos. Some of the datasets are shown in Figure 5.

4.1.1. Training Dataset. The training set used in this article is Caltech 10 k Web Faces Dataset, which was released in 2007

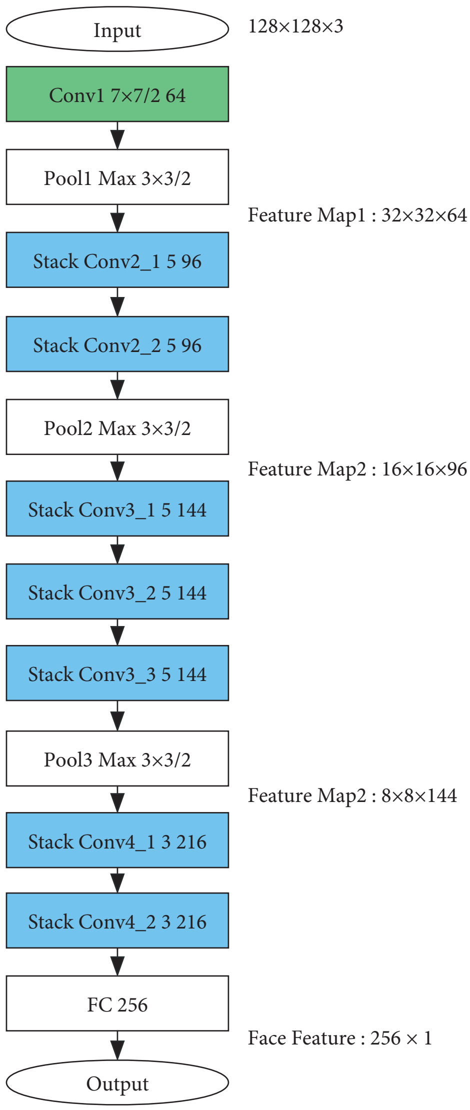

Figure 2: Deep convolution facial feature extraction neural network structure diagram.

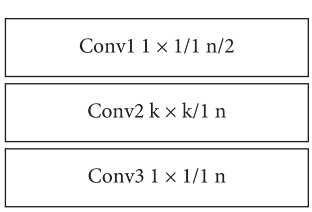

Figure 3: Model convolutional layer structure diagram.

and is obtained by crawling Google search engine with keywords. This dataset provides the center coordinates of the front eyes, nose, and mouth in each picture. The dataset has 10,524 pictures with different resolutions. Before the formal model training, we perform basic processing on the picture: face alignment, face cropping, and face cropping. The size after face cropping is 128×128 pixels.

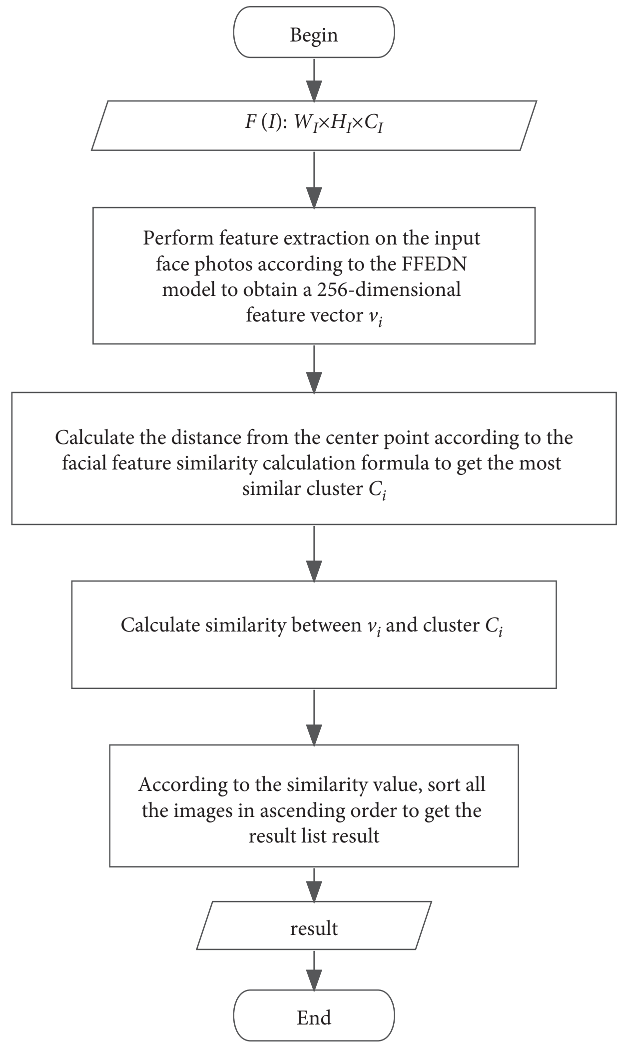

Figure 4: Face image retrieval process design.

4.1.2. Test Dataset. The test set LFW (Labeled Faces in the Wild dataset) is used in this article. This dataset contains 13,233 face photos of 5749 different people. At the same time, a search engine was used to collect face image datasets of 100 celebrities, with about 200 photos of each celebrity, and a total of 16,846 face photos were collected. The image collection process is as follows:

(1) Determine the list of names of people to be crawled.

(2) Use the Java HTTP component framework to call the search engine to search for pictures based on the names of the characters and download the pictures and save them in the designated folder.

(3) Invoke its own face comparison algorithm and cloud face recognition SDK [2] to compare the collected face photos to identify as the same person as possible, and at the same time, delete poor quality pictures, such as severely occluded and blurred pictures.

(4) Rotate, align, and crop the collected pictures, and the final picture size will be 128×128 pixels.

(1) Caltech Web Faces partial face data

(2) LFW partial face data

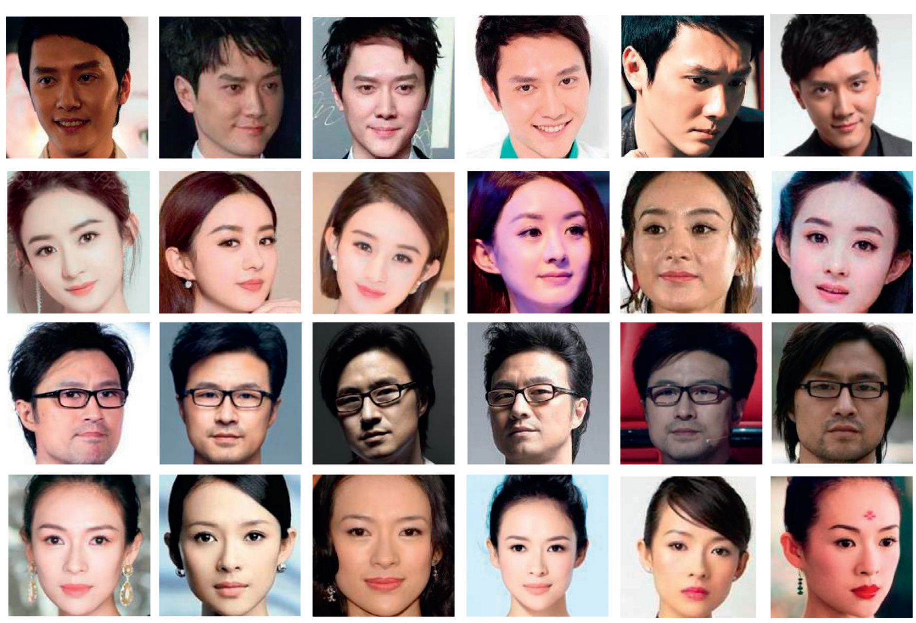

(3) Collect some facial data from the Internet

Figure 5: Training data used in the experiment (some face image data). (a) Caltech web faces partial face data. (b) LFW partial face data. (c) Some facial data from the Internet.

Table 1: Comparison of results between K-means clustering algorithm and fuzzy clustering algorithm based on LFW test dataset.

Algorithm/evaluation method	LFW			
	F_1 measurement	Cluster/node	LSR	Time/s
K-means	0.328	5749	0.232	367.86
Based on fuzzy clustering	0.824	5869	0.046	168.45

Table 2: Comparison of the results of K-means clustering algorithm and fuzzy clustering algorithm on the star test dataset.

Algorithm/evaluation method	Self-collected star dataset			
	F_1 measurement	Cluster/node	LSR	Time/s
K-means	0.828	100	0.02	321.16
Based on fuzzy clustering	0.964	100	0.00	134.28

In summary, the test dataset has two sets of data and 5949 face photos of 30079 different people, of which 4,069 people contain only one photo. Before the test, the face photos in all test groups were also aligned and cropped.

4.2. Clustering Algorithm Evaluation Method. In order to better evaluate the clustering ability and retrieval effect of the face clustering algorithm, this paper uses the F_1 metric to evaluate the clustering results, as shown in the following formula:

$$F_1 = \frac{2 \times P_{\text{pair}} \times R_{\text{pair}}}{P_{\text{pair}} + R_{\text{pair}}}, \tag{6}$$

where P_{pair} is called the pairwise precision and R_{pair} is called pairwise recall (pairwise recall). When each sample is clustered into a single cluster, a high accuracy rate will be obtained, but the recall rate will be very low. On the contrary, when all samples are clustered into a cluster, a very low accuracy will be obtained. Therefore, the F_1 metric combines the accuracy rate and the recall rate. Only when the accuracy rate and the recall rate are both high, the F_1 metric can get a higher value.

In the actual application process of face retrieval, it is often necessary to return face pictures whose similarity is higher than a certain threshold in descending order of similarity for practical application. Under normal circumstances, the full database of faces is compared for similarity, and it is enough to return face photos greater than the threshold, but after clustering, due to different clustering effects, there will be no face photos with high similarity to the retrieval target. The clusters are not retrieved, so this article defines a new index to comprehensively evaluate the retrieval effect after clustering. The index is named LSR (lost search ratio), and the index formula is expressed as follows:

$$\text{LSR} = \frac{S_p}{R_p}, \tag{7}$$

where S_p is the number of retrieved faces whose similarity is greater than the threshold and R_p is the total number of faces in the library whose similarity is greater than the threshold. In this paper, the average value of the missed detection rate LSR obtained from 100 random searches is taken as the evaluation index.

4.3. Analysis of Face Clustering Algorithm. In this paper, the two algorithms based on K-means clustering and fuzzy clustering, which are widely used, are compared experimentally, and the clustering effect and retrieval effect are comprehensively evaluated. The results are shown in Table 1. On the LFW dataset, the LSR value based on fuzzy clustering is 0.046. It can be seen that compared to the K-means algorithm, fuzzy clustering can more accurately retrieve similar faces greater than the threshold. At the same time, it can be seen from the result that fuzzy clustering has faster clustering speed. Judging from the distribution of fuzzy cluster clusters/nodes, its clustering is also very close to the true cluster value.

Since the number of face photos of the same person in the LFW dataset is skewed, it can be seen from the previous description of the test set that there are 4,069 people with only one photo in the face database. Therefore, in order to make the test results more reliable, this article uses the collected star dataset to test the model again. The test results are shown in Table 2. Table 2 shows that the performance of the K-means algorithm on the star data set is better than that on the LFW data set. It can be seen from the results in Table 2 that if the data samples in the face database are balanced, the performance based on fuzzy clustering is still better than the performance of the algorithm based on K-means clustering.

Experiments show that, when performing face retrieval under a given threshold, the clustering algorithm based on fuzzy clustering is more suitable for scenes with large amounts of data, multiple categories, and skewed samples.

5. Conclusion

Aiming at the problem of clustering and fast retrieval of face data with large amount of data, multiple categories, and inclined samples, this paper proposes a face database clustering method based on fuzzy clustering and a face retrieval method under a given threshold. First, deep learning is used to extract the feature of the face photos in the face database to obtain the feature vector of the face photo, then fuzzy clustering is performed to obtain the pedigree map, and the center point feature vector of the node is calculated and stored in the pedigree map. When searching, the score can be compared according to the similarity of the nodes in the pedigree graph, and only the threshold with the comparison score within the threshold range can be used, greatly reducing the number of comparisons.

This paper conducts experiments on LFW and self-collected star datasets. By analyzing the clustering effect, the LSR indicator of the missed detection rate, and the clustering time indicator, it shows that the fuzzy clustering algorithm can be used in large-scale datasets and face samples. In the case of fast clustering, given a specific threshold for face retrieval, there is a greater advantage.

Data Availability

The datasets used and/or analyzed during the current study are available from the corresponding author upon reasonable request.

Conflicts of Interest

The authors declare that they have no potential conflicts of interest with respect to the research, authorship, and/or publication of this article.

References

[1] A. Krizhevsky, I. Sutskever, and G. E. Hinton, “ImageNet classification with deep convolutional neural networks,” in *Proceedings of the 25th International Conference on Neural Information Processing Systems*, pp. 1097–1105, ACM Press, New York, 2012.

[2] O. M. Parkhi, A. Vedaldi, and A. Zisserman, “Deep face recognition,” in *Proceedings of the British Machine Vision Conference*, September 2015.

[3] F. Schroff, D. Kalenichenko, and J. Philbin, “FaceNet: a unified embedding for face recognition and clustering,” in *Proceedings of the 2015 IEEE Conference on Computer Vision and Pattern Recognition(CVPR)*, Boston, MA, USA, June 2015.

[4] G. B. Huang, M. Matter, and T. Berg, “Labeled faces in the wild: a database for studying face recognition in unconstrained environments,” https://vis-www.cs.umass.edu/lfw/lfw.pdf.

[5] I. Kemelmacher-Shlizerman, S. M. Seitz, D. Miller, and E. Brossard, *The Mega Face Benchmark: 1 Million Faces for Recognition at Scale*CVPR, Seattle, Washington, 2016.

[6] X. F. Li, “Development status and changes of the face recognition market,” *China Security*, vol. Z1, pp. 39–42, 2020.

[7] Z. Li, Y. Zhong, B. Zhang, and D. Cao, “Mass face image retrieval based on deep feature clustering,” *Journal of Harbin Institute of Technology*, vol. 50, no. 11, pp. 101–109, 2018.

[8] S. R. Dubey, “Face retrieval using frequency decoded local descriptor,” *Multimedia Tools and Applications*, vol. 78, no. 12, pp. 16411–16431, 2019.

[9] A. Krizhevsky, I. Sutskever, and G. Hintonge, “ImageNet classification with deep convolutional neural networks,” *Advances in Neural Information Processing Systems*, p. 1097, Curran Associates Inc., Long Beach, 2012.

[10] Z. Simonyank, “Very deep convolutional networks for large-scale image recognition,” ArXiv Preprint ArXiv: 1409.1556, 2014.

Hindawi
Scientific Programming
Volume 2022, Article ID 5945117, 16 pages
https://doi.org/10.1155/2022/5945117

Research Article

Recognition of Gurmukhi Handwritten City Names Using Deep Learning and Cloud Computing

Sandhya Sharma,[1] Sheifali Gupta,[2] Deepali Gupta,[2] Sapna Juneja,[3] Gaurav Singal,[4] Gaurav Dhiman,[5] and Sandeep Kautish[6]

[1]*Chitkara University Institute of Engineering and Technology, Chitkara University, Solan, Himachal Pradesh, India*
[2]*Chitkara University Institute of Engineering and Technology, Chitkara University, Patiala, Punjab, India*
[3]*KIET Group of Institutions, Delhi, Ghaziabad, India*
[4]*Netaji Subhash University of Technology, Delhi NCR, India*
[5]*Govt. Bikram College of Commerce, Patiala, Punjab, India*
[6]*LBEF Campus, Kathmandu, Nepal*

Correspondence should be addressed to Sandeep Kautish; dr.skautish@gmail.com

Received 19 October 2021; Accepted 13 December 2021; Published 4 January 2022

Academic Editor: Punit Gupta

The challenges involved in the traditional cloud computing paradigms have prompted the development of architectures for the next generation cloud computing. The new cloud computing architectures can generate and handle huge amount of data, which was not possible to handle with the help of traditional architectures. Deep learning algorithms have the ability to process this huge amount of data and, thus, can now solve the problem of the next generation computing algorithms. Therefore, these days, deep learning has become the state-of-the-art approach for solving various tasks and most importantly in the field of recognition. In this work, recognition of city names is proposed. Recognition of handwritten city names is one of the potential research application areas in the field of postal automation For recognition using a segmentation-free approach (Holistic approach). This proposed work demystifies the role of convolutional neural network (CNN), which is one of the methods of deep learning technique. Proposed CNN model is trained, validated, and analyzed using Adam and stochastic gradient descent (SGD) optimizer with a batch size of 2, 4, and 8 and learning rate (LR) of 0.001, 0.01, and 0.1. The model is trained and validated on 10 different classes of the handwritten city names written in Gurmukhi script, where each class has 400 samples. Our analysis shows that the CNN model, using an Adam optimizer, batch size of 4, and a LR of 0.001, has achieved the best average validation accuracy of 99.13.

1. Introduction

Cloud computing is equipped with good solutions to meet the increasing demand of data storage. It has provided users with various benefits, thereby reducing the efforts to manage the data in an efficient and effective manner. The cloud relies mainly on the data centers, and the data centers, which are located far away from the user, are further linked together to build data center networks. So, the next generation cloud computing architectures have made it possible to process the data closer to the user instead of processing it at the data center. These emerging paradigms of cloud computing generate huge amount of data. But there is the possibility that this huge data may not be analyzed to uncover the new information [1]. Various algorithms can be applied for the analysis of data. Performance of traditional algorithms decreases when the amount of data increases. But, the performance of these deep learning algorithms improves when the amount of data increases. Deep learning is the subset of machine learning, and it has gained the attention of various researchers due to its strength of handling huge amount data. This is the reason why applications of deep learning in the emerging paradigms of cloud computing are also gaining the attention of research community. These days, all the information in our lives is being processed through electronic devices. As computers are involved in every field, there is a requirement to transfer all the information between humans and computers with the help of some efficient and fast algorithms. So, there exists text recognition, which helps in providing an interface, so that humans and computers can interact with each other. An example of such systems lies in the digitization of documents images, which may be handwritten or printed. Such systems are relevant in many applications like automatic form processing, postal automation, cheques processing, preservation of historical documents, etc. In this proposed work, recognition of city names that are written in Gurmukhi script is implemented and is one of the application research areas of postal automation. As manual sorting of mails is a cumbersome as well as labor-intensive task due to the high labor cost involved in the process. So, it is required to develop a postal automation system that can read all the necessary fields of the postal document and can help in reaching the document to its destination. Gurmukhi script is the Punjab state's official language, which is used by the Punjab state's government officials to communicate their documents. An example of such a document is shown in Figure 1, in which the address field of the document to be posted is written in Gurmukhi [2] script, and the city name "Mohali" is also highlighted.

Several researchers are already working in the field of postal automation, and research is already going on for the recognition of various scripts like Devanagari, Bangla, English, Russian, etc., but still no postal automation system exists for Gurmukhi script. This proposed work aims to employ a deep learning technique based on CNN for the recognition of Gurmukhi handwritten city names. Out of various deep learning techniques, CNN is widely used for the purpose of text recognition [1]. The most important challenge for the recognition of Gurmukhi script is its cursive writing style, and the characters are so closely written, which makes their segmentation a difficult task. So, this paper has proposed the recognition technique using a segmentation-free approach, which is known as the Holistic approach. Figure 2 is showing the sample of handwritten Gurmukhi script.

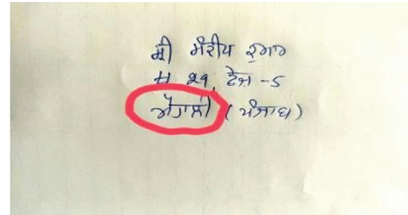

Figure 1: Postal document with city name written in Gurmukhi.

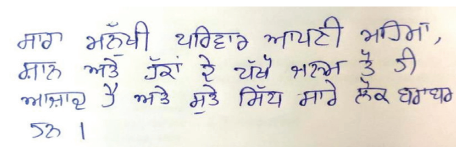

Figure 2: Sample of Gurmukhi script.

2. Related Work

Emerging cloud computing paradigms have helped the user by generating data at the edge of the network without being transferred at the far cloud center. In this section, a literature survey is given on the use of ConvNet in the emerging cloud computing architectures. Huang et al. [3] have proposed a ConvNet model using edge computing algorithm for the classification of various mosquitoes. A device was developed for the detection of mosquitoes and preprocessing of videos before sending them to data center. Later, a ConvNet model is employed for the classification of mosquitoes. Similarly, Liu et al. [4] have also proposed a CNN based ConvNet model for the recognition of food. A server equipped with the centos 7.0 was used at the cloud. Later, again, the CNN based model ConvNet is implemented for the purpose of identification and classification of food images. Azimi et al. [5] have used ConvNet for the diagnosis of heart diseases. For the reading of files, a local Wi-Fi is programmed and for the uploading POST request to the edge device, a machine with Apache server is used. Hosain et al. [6] have proposed ConvNet model using edge cloud computing, in which data is sent to the center using radio access technology. For the formation of edge cloud, a MEC server is used, and later, a CNN based ConvNet is used for the classification. Similarly, in the field of postal automation, i.e., for the recognition of various fields like city name, pin code, and street name, a huge amount of data is required. This huge data can be processed efficiently by deep learning algorithms. Among the relevant works, recognition of such fields is done in various scripts using character-level recognition, in which the word is segmented into individual characters before recognition (analytical approach) or word level recognition, which is segmentation-free approach (holistic approach). Pal et al. [7] have employed character-level recognition using machine learning for the recognition of multilingual script-based city names for Indian postal automation. Similarly, Thadchanamoorthy et al. [8] have proposed a technique for the recognition of Tamil city names. The accuracy obtained is 96.89%. Some have worked on the recognition of pin codes only, which are written in different scripts like English, Bangla, etc. One such example is Vajda et al. [9], where the authors have recognized pin codes written in Bangla as well as in English script using a nonsymmetric half-plane hidden Markov model and achieved an accuracy of 94.13% and 93%, respectively. Sahoo et al. [10] have implemented a holistic approach for the recognition of city names written in Bangla script using shape-context features, while multiclassifiers are employed for the classification purpose. The datasets used here are the large datasets that are stored on the cloud. There are some other examples where authors have implemented only a holistic approach for the recognition of various scripts like English, Bangla, and Arabic and achieved an accuracy of 90.3%, 83.64%, and 63% [11–13]. Manchala et al. [9] have used NN for the recognition of English script using the Holistic approach. Similarly, Bhowmik et al. [10] have proposed a technique for the recognition of Bangla script.

Wahbi et al. [11] have worked on the recognition of Arabic script again by holistic approach, and the model employed for the recognition is hidden Markov model. Few other authors have also used the holistic approach for the recognition of text, in which features are manually extracted [14, 15], while others have used CNN for character recognition, in which features are automatically extracted [16]. The aim of this proposed work is to employ CNN with the holistic approach for the recognition of Gurmukhi handwritten city names. All these techniques have been employed on huge datasets, which are stored on cloud.

2.1. Contributions of the Proposed Work

(i) A dataset having 4000 samples of the handwritten images in the Gurmukhi script for the 10 city names has been generated.

(ii) A CNN model for the automation of postal system for the recognition of Gurmukhi handwritten city names has been prepared. The model can recognize all the 10 city names with an average validation accuracy of 99.13%.

3. Present Work

In this proposed work, a dataset of 4000 Gurmukhi handwritten city names is created for 10 different classes (city names), where each class is having 400 samples that can be fed to the model. As manual sorting of postal documents is a labor-intensive task, so, recognition of city names will help in the automation of postal system for the state of Punjab. Finally, the designed model has predicted various parameters for the recognition of city names. The methodology followed for the recognition is shown in Figure 3.

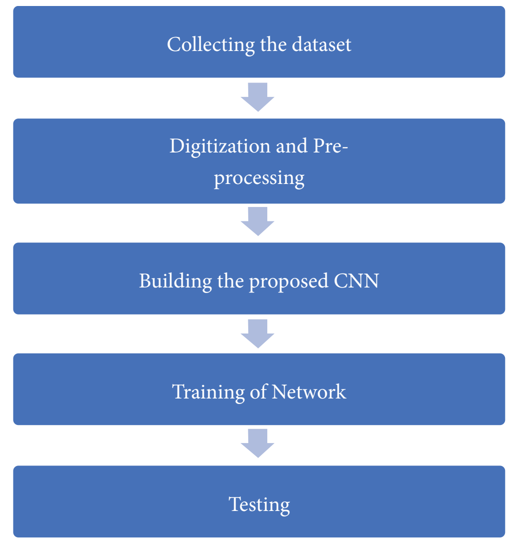

Figure 3: Methodology of the proposed work.

3.1. Dataset. For the preparation of dataset, each sample is written 10 times by 40 different writers generating 4000 samples. For collecting the dataset, two sheets were given to each writer to write each word five times on each sheet, generating total 10 samples for each word from both sheets. So, each writer generated 100 samples. Writers were selected from different age groups, educational levels, and different dialects. Writers were free to use any colored pen.

3.2. Digitization and Preprocessing of Dataset. For the digitization of collected samples, a scanner with 300 dpi was used to scan the collected sheets containing samples. For the preprocessing of dataset, each scanned sheet is converted into gray scale image, and later, normalization is performed. Further, brightness adjustment, contrast adjustment, and intensity level adjustment are performed to improve the quality of the image before cropping the word samples from the digitized sheets. Adobe Photoshop is used for the purpose of contrast adjustment, brightness adjustment, intensity level adjustment, and cropping of images. Later, cropped samples were placed in their respective folders that were named as per the city name. Later, the prepared dataset is stored on the cloud as it has to be accessed using the deep learning network.

Once the preprocessing is done, the dataset is divided into training and validation dataset [17, 18]. 80% of the data is kept for training the model, and 20% is kept for validating the performance of the model. Table 1 below is showing the city name and its corresponding handwritten digitized image in the Gurmukhi script.

3.3. Data Augmentation. Data augmentation is the technique that helps in increasing the available data. So, available data is further increased by flipping or rotating the images, and data augmentation is the inbuilt function of the proposed model. Rotation of city name "Amritsar" is shown in Figure 4.

3.4. Model Design. To build the CNN model, three layers are required: (i) convolution layer; (ii) pooling layer; (iii) output layer. The primary function of the first convolution layer is to apply the predefined filter weight to derive the features from an image. Based upon the weighting filter used, the number of feature maps is produced. The complexity of the extracted features keeps on increasing with the increasing model depth, while the last convolution layer of the model generates the feature maps, which are much closer to the required recognition task. The next layer is the pooling layer, and the most commonly used pooling technique is max pooling. This further helps in preserving the features by selecting the maximum value as this has the closest similarity to the required features. The pooling layer also helps in reducing the size of the image by getting rid of the features, which are not important. The last layer is the fully connected layer, and from here, the output classes are obtained. The proposed CNN model is shown in Figure 5.

The first convolution layer used in this proposed work has 32 filters of size 3 * 3 with a stride of 1 * 1, 32 feature maps are derived from this, and the convolution layer is

Table 1: Ten city names with their corresponding handwritten digitized image in Gurmukhi.

S. no.	City name	Written by "writer 1"	Written by "writer 2"
1	Amritsar		
2	Fazilka		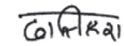
3	Hoshiarpur	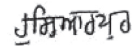	
4	Jalandhar	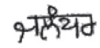	
5	Ludhiana	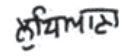	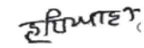
6	Mansa	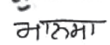	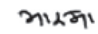
7	Mohali	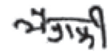	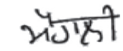
8	Muktsar	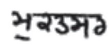	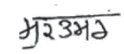
9	Pathankot	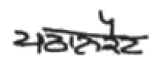	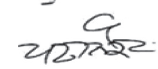
10	Patiala		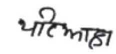

(a) (b) (c)

Figure 4: Augmentation. (a) Actual image. (b) Rotated by 60°deg. (c) Rotated by 180°deg.

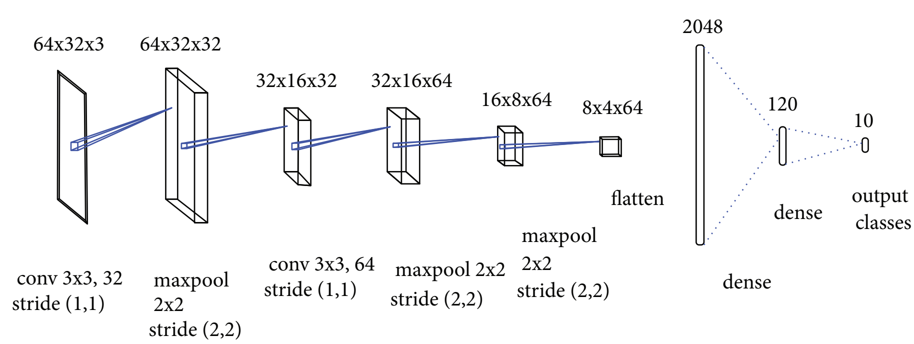

Figure 5: Proposed CNN model.

followed by the ReLU activation function. The obtained feature maps are then passed to the max pooling layer of 2 * 2 filter size and a stride of 2 * 2, which means that the pooling layer has reduced the size of the feature map by a factor of 2. The obtained pooled feature maps are passed to the next convolution layer, which has 64 filters with a size of 3 * 3 and a stride of 1 * 1, which is again followed by max pooling layer of size 2 * 2 and a stride of 2 * 2, which is further followed by another max pooling layer of the same size. Lastly, a fully connected layer is introduced with the SoftMax activation function, having 2048 neurons in the input layer, then 120 neurons in the middle layer, and 10 neurons in the last, which is the output layer. The fully connected layer transforms the obtained feature maps to the 10 classes. Rectified linear unit (ReLu) is used as the activation function for all the layers in the model, except for the pooling layers.

4. Experiments and Results

The proposed model is implemented on the dataset of 4000 images using Python with the help of Keras and Tensorflow, which are machine learning libraries.

4.1. Experimental Setup and Performance Metrics Used. The efficiency of the model is impacted by various parameters, but in this paper, three important parameters are considered: the optimizer, LR, and the batch size of the model. The optimizer is used to update the network weights; also, the choice of optimizer means good results in minutes, hours, or days. LR tells how rapidly the neuron weights will be adapted, while the batch size tells the number of samples that are processed before the model is being updated. The proposed model is analyzed using two different optimizers, Adam and stochastic gradient descent (SGD), three different LRs, 0.001, 0.01, and 0.1, and the batch size: 2, 4, and 8. It is known that the batch size is an important hyperparameter for deep learning systems. Large batch size helps in speeding up the computation, but it leads to poor generalization [19]. So, it is always preferable to use a small batch size. This proposed model has given good generalization with batch size of 2, 4, and 8 only, while the accuracy drastically reduced when the batch size is further increased. Response time for the training and validation of the model varies from model to model, depending on the dataset to be trained, batch size, and LR, and it also depends on the hardware of the system used like CPU, GPU, RAM, etc. [20]. To evaluate the proposed CNN model, various parameters are calculated like training and validation loss, validation accuracy [21, 22], precision, and recall also. All these parameters are calculated using the different metrics of the confusion matrix, which are true positive (TP), false positive (FP), true negative (TN), and false negative (FN). The parameters are defined as follows:

4.1.1. Accuracy. Accuracy is defined as the ratio of the number of correct predictions made by the model to the total number of predictions made as shown in

$$\text{Accuracy} = \frac{(\text{TP} + \text{TN})}{(\text{TP} + \text{TN} + \text{FP} + \text{FN})}. \tag{1}$$

4.1.2. Precision. It is a metric that tells about the proportion of cases that report true and are actually true as shown in

$$\text{Precision} = \frac{\text{TP}}{(\text{TP} + \text{FP})}. \tag{2}$$

4.1.3. Recall (Sensitivity). The recall measures the ability of the designed model to detect positive samples. It is calculated as the sum of true positive across all classes divided by the sum of true positive and false negative across all classes as shown in

$$\text{Recall} = \frac{\text{TP}}{(\text{TP} + \text{FN})}. \tag{3}$$

4.2. Results Obtained Using Adam Optimizer with a Batch Size of 4. In this section, various parameters are obtained on three different LRs, while the Adam optimizer is used with a batch size of 4.

4.2.1. Results Obtained with a LR of 0.001. Table 2 shows the values of various parameters obtained with the LR of 0.001, while the optimizer used is Adam with a batch size of 4. Maximum obtained validation accuracy on the validation dataset is 99.8% with a minimum validation loss of 0.01, and the average obtained validation accuracy is 99.13%.

Figure 6 shows the different parameters convergence plots for the training dataset, as well as for the validation dataset. Y-axis is showing the particular value obtained, while the X-axis is the number of epochs, for which the model is trained. Validation accuracy is the main parameter; while checking the model's performance for the recognition of text, it can be observed that the accuracy plot is almost increasing after the run of few epochs. The maximum validation accuracy obtained is 99.8%. The value of loss should be less, and the minimum value of the loss obtained is 0.01 and 0.07 for the validation and training dataset. Values of other parameters are approaching 1, which shows that the designed model is reasonably good.

Results can also be analyzed by plotting the confusion matrix. Figure 7 is showing the plot of the confusion matrix for multiclassification results obtained in Figure 6. On the X-axis, the predicted labels are depicted, while on the Y-axis, true labels are depicted. The confusion matrix tells the information about the actual (true) and the predicted classification done by the designed classification model. The highlighted value in blue boxes represents the true positive values, which tell how much the designed model has correctly predicted the positive classes as positive [23]. For example, for the city Amritsar, the designed model has correctly predicted all the 80 samples, while, for the city Fazilka, the model has correctly predicted 78 samples and incorrectly predicted 2 samples as Ludhiana, which can be observed in Figure 7.

4.2.2. Results Obtained with a LR of 0.01. Now, the LR is changed to 0.01, while the optimizer used is Adam. Table 3 shows the outcomes of various parameters, when the LR is changed from 0.001 to 0.01, while other parameters are kept the same. From the obtained results, it can be observed that the LR of the model impacts the accuracy results. The validation accuracy obtained on 10^{th} epoch is 99%, and the values of training loss, validation loss, validation precision, and validation recall are 0.11, 0.01, 0.99, and 0.99, respectively. The average obtained validation accuracy is 96.95%, which is less than the average validation accuracy obtained, with the LR of 0.001, which was 99.13%. Figure 8 shows the parameters convergence plot, and the confusion matrix for the same is shown in Figure 9, where it has misclassified 4 classes. It can be observed from Figure 8 that the obtained plots are not so linear as compared to the plots obtained in Figure 6, while linearity can be observed in the last few epochs only [24].

4.2.3. Results Obtained with a LR of 0.1. Table 4 shows the outcomes of various parameters, when the LR is further changed from 0.01 to 0.1, while other parameters are kept the same. On the 10^{th} epoch, maximum validation accuracy obtained is 99.3%. The obtained values for training loss, validation loss, validation precision, and validation recall are 0.10, 0.00, 0.99, and 0.99. The average obtained validation accuracy is 98.17%, which is less than the average validation accuracy obtained with the LR of 0.001, which was 99.13%. Figure 10 shows the parameters convergence plot, and the

Table 2: Results obtained with a LR of 0.001 by employing Adam optimizer.

Epoch	Training loss	Validation loss	Validation accuracy (%)	Validation precision	Validation recall
1	0.49	0.08	98.5	0.98	0.97
2	0.19	0.07	98.3	0.98	0.97
3	0.13	0.05	99.2	0.99	0.99
4	0.12	0.04	99.1	0.99	0.98
5	0.09	0.02	99.3	0.99	0.98
6	0.09	0.01	99.5	0.99	0.99
7	0.09	0.03	99.6	0.99	0.98
8	0.09	0.02	99.6	0.99	0.99
9	0.09	0.02	99.8	0.99	0.99
10	0.07	0.01	99.8	0.99	0.99

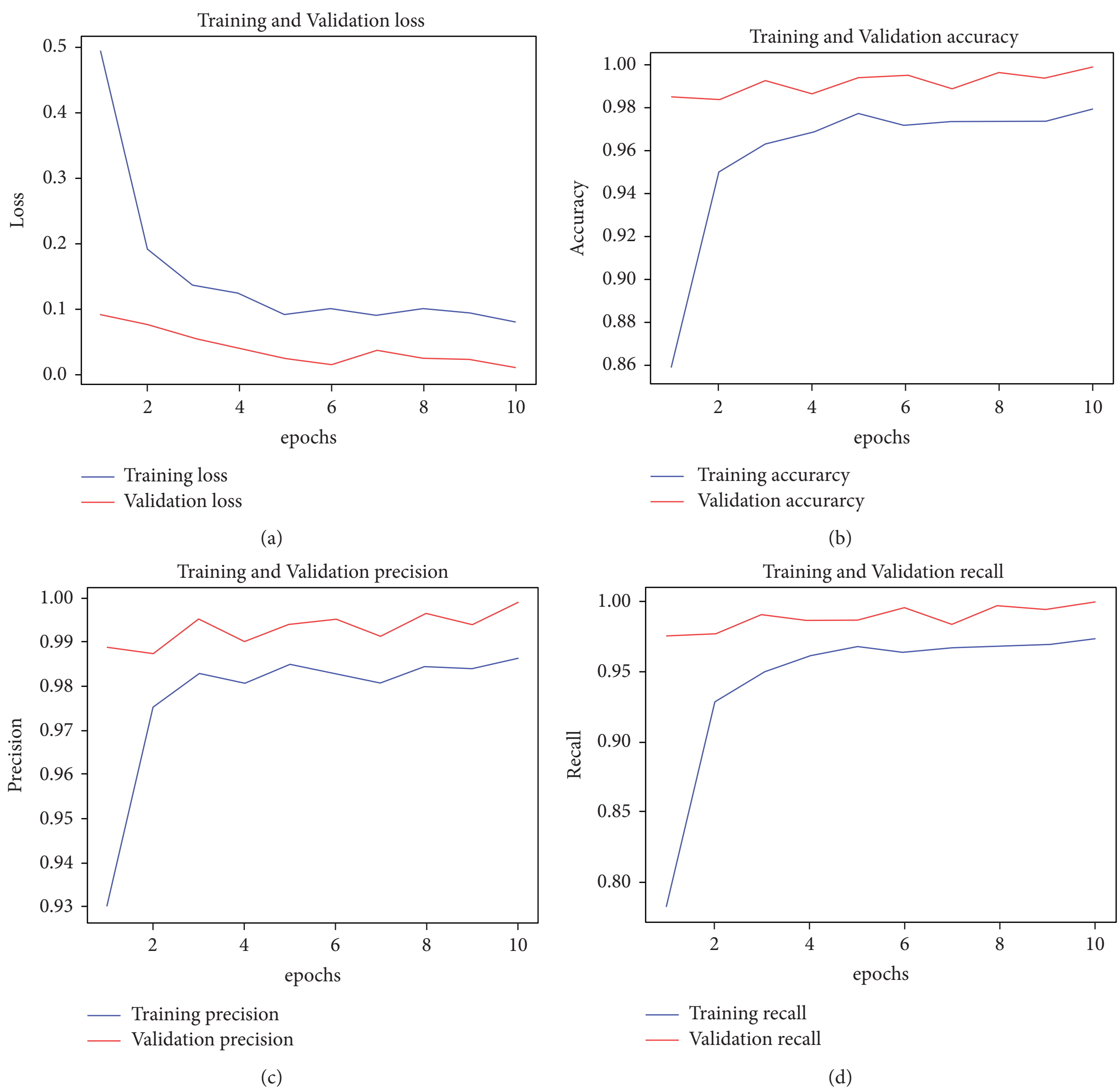

Figure 6: Plots obtained with a LR of 0.001 by employing Adam optimizer. (a) Training and validation loss plot. (b) Training and validation accuracy plot. (c) Training and validation precision plot. (d) Training and validation recall plot.

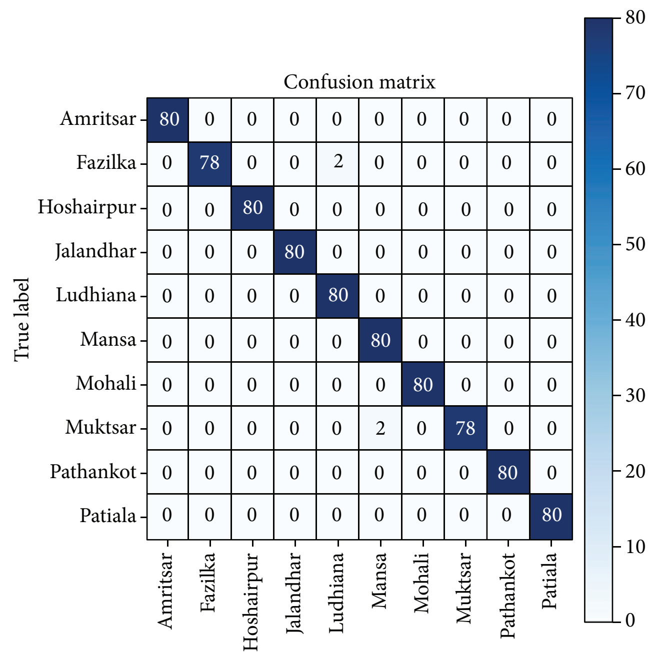

Figure 7: Confusion matrix for LR 0.001.

Table 3: Results obtained with a LR of 0.01 by employing Adam optimizer.

Epoch	Training loss	Validation loss	Validation accuracy (%)	Validation precision	Validation recall
1	0.58	0.12	95	0.95	0.95
2	0.28	0.74	90	0.90	0.89
3	0.18	0.19	97	0.97	0.97
4	0.15	0.04	98	0.98	0.98
5	0.12	0.25	94	0.95	0.94
6	0.14	0.38	97	0.96	0.96
7	0.10	0.49	99	0.99	0.99
8	0.14	0.32	98	0.98	0.98
9	0.10	0.24	99	0.99	0.99
10	0.11	0.01	99	0.99	0.99

confusion matrix for the same is shown in Figure 11. In Figure 10, all the plots are linearly varying, the loss plot is almost decreasing, and other plots are approaching to 1.

From Figure 11 of confusion matrix for LR 0.1, it can be observed that the proposed model has misclassified few more classes as compared to the previous confusion matrix. 56 samples of the city "Fazilka," 73 samples of the city Hoshiarpur, 78 of Jalandhar, and so on are correctly predicted.

It can be observed from Tables 2, 3, and 5 that the LR of the model impacts the accuracy results obtained for recognition. A LR of 0.001 has generated the average validation accuracy of 99.13%, which is highest as compared to the validation accuracies obtained by other LRs.

4.2.4. Optimal LR Selection with Adam Optimizer. Analysis of the validation accuracy obtained from Tables 2, 3, and 5 is done in Figure 12. It shows that the Adam optimizer with a LR of 0.001 has performed better for the available dataset. Figure 12 shows the validation accuracy obtained on 10 epochs for all the three LRs. Y-axis shows the validation accuracy obtained, while the X-axis shows three different LRs on 10 epochs. It can be observed on the 10^{th} epoch that the validation accuracy obtained with a LR of 0.001 is the highest as compared to the LR of 0.01 and 0.1. It can also be observed that the validation accuracy is high for most of the epochs using LR of 0.001. Figure 13 shows some of the misclassified results obtained by Adam optimizer. City name "Ludhiana" is misclassified as "Patiala" in Figure 13(a), while city "Fazilka" is misclassified as "Ludhiana" in Figure 13(b).

From the above discussions of the accuracy results obtained using Adam optimizer with a LR of 0.001, 0.01, and 0.1, it can be observed that the proposed model has achieved the best validation accuracy with a LR of 0.001, as the proposed model has also misclassified few images. Results for the same are shown in Figure 13.

4.3. Results Obtained Using Adam Optimizer: LR of 0.001 on Different Batch Sizes. It has been analyzed from Figure 12 that LR of 0.001 has achieved better validation accuracy as

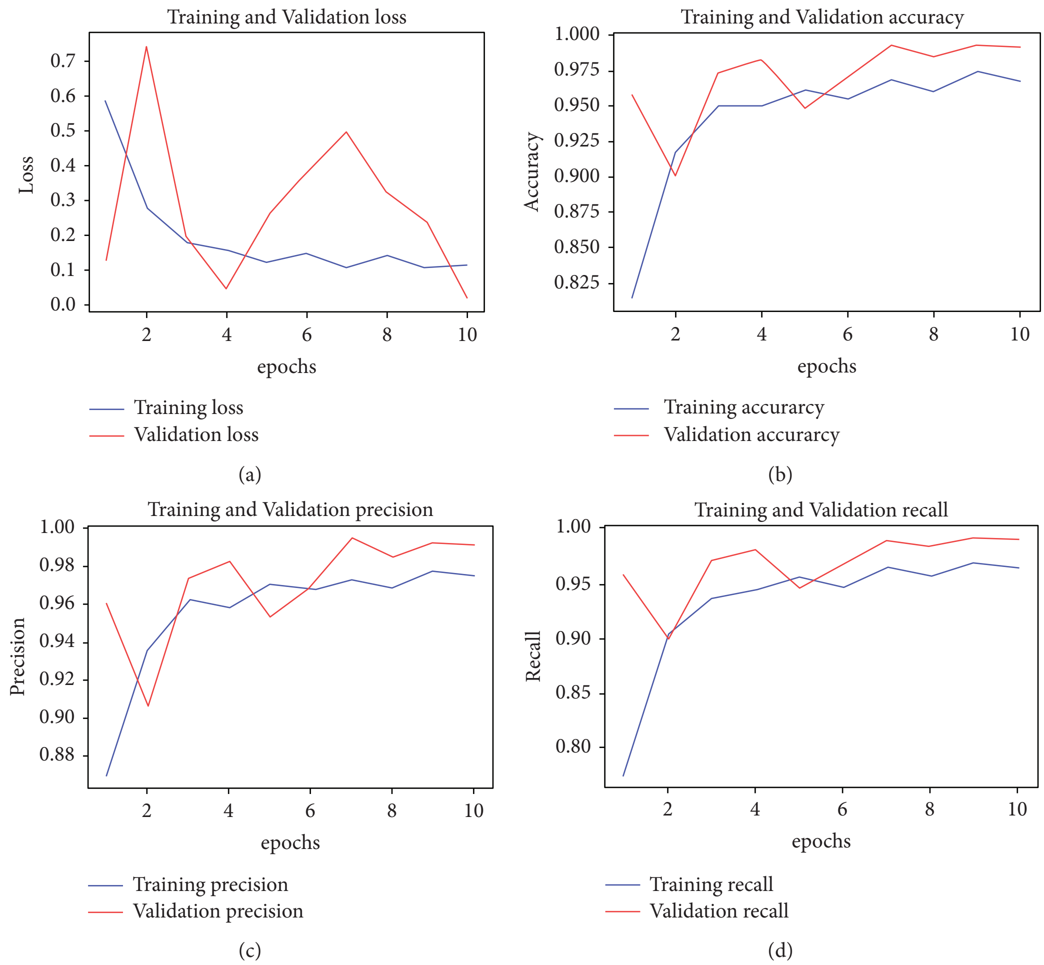

Figure 8: Plots obtained with a LR of 0.01 by employing Adam optimizer. (a) Training and validation loss plot. (b) Training and validation accuracy plot. (c) Training and validation precision plot. (d) Training and validation recall plot.

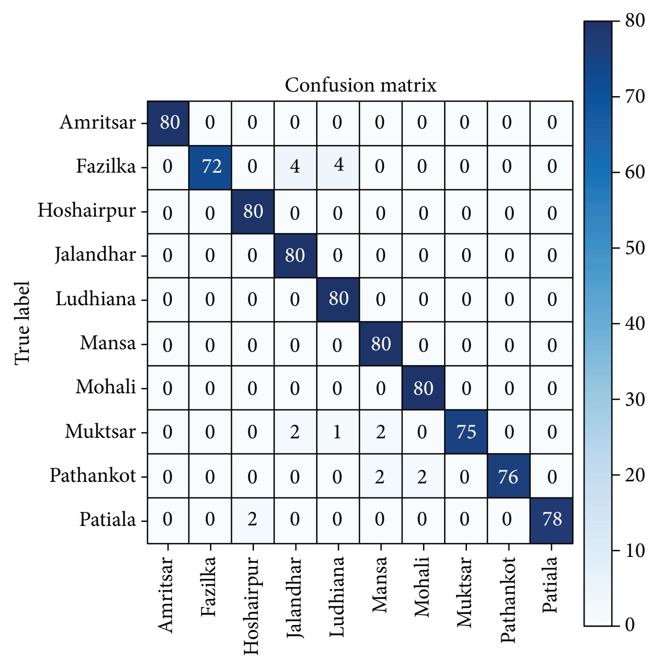

Figure 9: Confusion matrix for LR 0.01.

Table 4: Results obtained with a LR of 0.1 by employing Adam optimizer.

Epoch	Training loss	Validation loss	Validation accuracy (%)	Validation precision	Validation recall
1	1.12	0.17	93.5	0.94	0.92
2	0.32	0.05	98.3	0.98	0.98
3	0.21	0.01	98.5	0.99	0.99
4	0.18	0.11	99	0.99	0.99
5	0.10	0.02	99.5	0.99	0.99
6	0.14	0.00	99.6	0.99	0.99
7	0.11	0.01	99.5	0.99	0.99
8	0.11	0.02	99.1	0.99	0.98
9	0.09	0.02	99.4	0.99	0.98
10	0.10	0.00	99.3	0.99	0.99

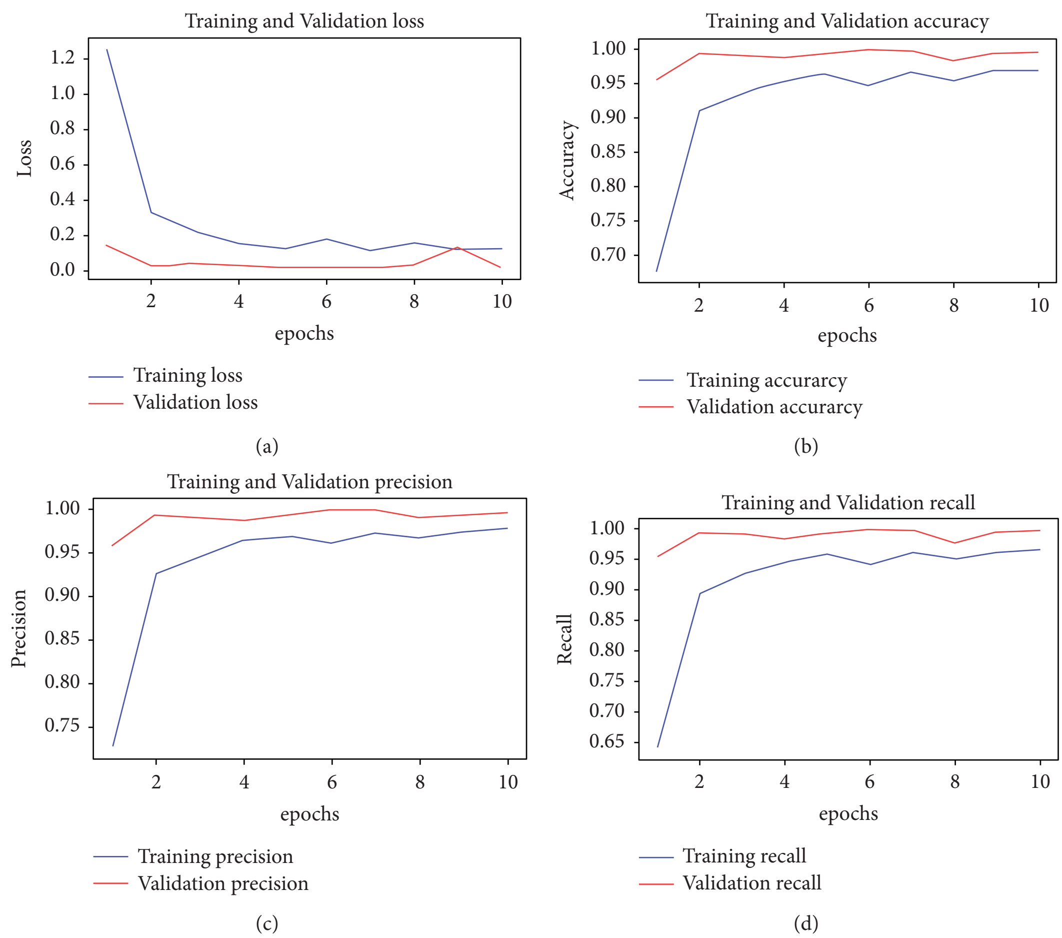

Figure 10: Plots obtained with a LR of 0.1 by employing Adam optimizer. (a) Training and validation loss plot. (b) Training and validation accuracy plot. (c) Training and validation precision plot. (d) Training and validation recall plot.

compared to the LR of 0.01 and 0.1. It has been observed that the batch size of the model also impacts the accuracy results [25]. Now, the model is analyzed using three different batch sizes (2, 4, and 8) with Adam optimizer and a LR of 0.001. Table 6 shows the various results obtained by changing the batch size, while the LR of 0.001 is used. It can be observed from the table that batch size of 4 has given good accuracy results as compared to batch size of 2 and 8. The best average validation accuracy achieved is 99.13% when the batch size is kept at 4, while it is 97.24% and 92.07% with a batch size of 8 and 2 with a LR of 0.001.

4.3.1. Comparison of Three Different Batch Sizes Using Adam with a LR of 0.001. It can be observed from Figure 12 that LR of 0.001 has given good results as compared to LR of 0.1 and 0.01. In Table 4, various parameters are obtained using three different batch sizes. Average validation accuracy obtained

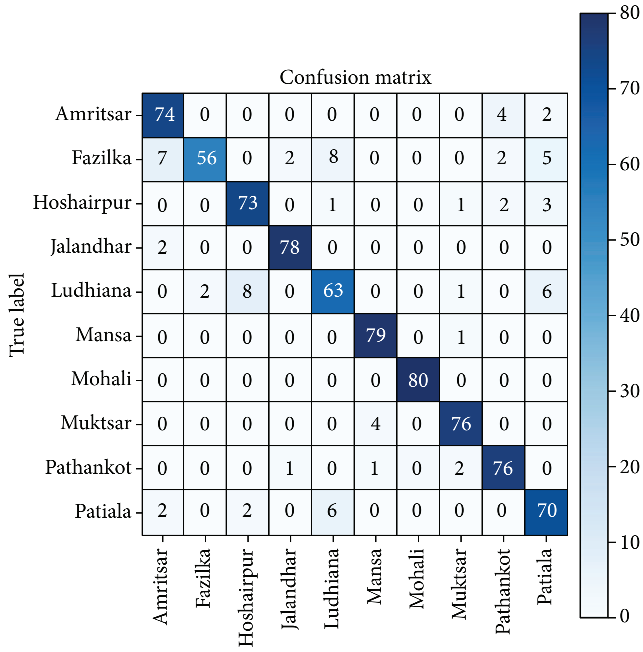

Figure 11: Confusion matrix for LR 0.1.

Table 5: Layered architecture for each layer.

Layers	Input image size	Filter size	No of filters	Activation function	Output without padding	Parameters
Input image	64 * 32 * 3					
Convolution	64 * 32 * 3	3 * 3	32	ReLU	64 * 32 * 32	896
Max Pooling	64 * 32 * 32	Pool size (2 * 2)	—	—	32 * 16 * 32	0
Convolution	32 * 16 * 32	3 * 3	64	ReLU	32 * 16 * 64	18496
Max Pooling	32 * 16 * 64	Pool size (2 * 2)	—	—	16 * 8 * 64	0
Max Pooling	16 * 8 * 64	Pool size (2 * 2)	—	—	8 * 4 * 64	0
Flatten	8 * 4 * 64	—	—	—	1024	—
Dense	1024	120	—	ReLU	120	123000
Dense	120	—	—	SoftMax	10	1210

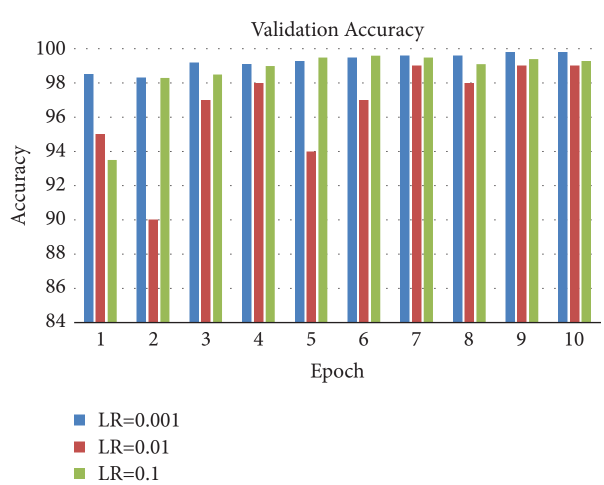

Figure 12: Analysis of validation accuracy on three different LRs using Adam Optimizer.

by batch size 2 is 92.07%, batch size 4, 99.13%, and batch size 8, 97.24%. Now, validation accuracy obtained on 10 different epochs of Table 4 is compared in Figures 14 and 15 by three different batch sizes. In Figure 14, Y-axis is representing the validation accuracy obtained, while the X-axis is representing the three different batch sizes on 10 epochs and in

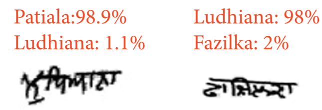

(a) (b)

Figure 13: Misclassification results. (a) “Ludhiana” is misclassified as “Patiala.” (b) “Fazilka” is misclassified as “Ludhiana.”

Table 6: Results obtained for different batch sizes.

Batch size	Epochs	Training loss	Validation loss	Validation accuracy (%)	Average validation accuracy
2	1	1.59	0.70	80.2	92.07%
	2	1.22	0.39	85.1	
	3	1.08	0.31	92.4	
	4	0.92	0.30	92.5	
	5	0.91	0.16	94.2	
	6	0.76	0.24	93.5	
	7	0.78	0.11	95.4	
	8	0.76	0.43	92.6	
	9	0.73	0.10	97.1	
	10	0.68	0.08	97.5	
4	1	0.49	0.08	98.5	99.13%
	2	0.19	0.07	98.3	
	3	0.13	0.05	99.2	
	4	0.12	0.04	99.1	
	5	0.09	0.02	99.3	
	6	0.09	0.01	99.5	
	7	0.09	0.03	99.6	
	8	0.09	0.02	99.6	
	9	0.09	0.02	99.8	
	10	0.07	0.01	99.8	
8	1	0.23	0.54	78.6	97.24%
	2	0.03	0.02	99.1	
	3	0.02	0.03	98.5	
	4	0.01	0.00	99.2	
	5	0.01	0.00	99.2	
	6	0.03	0.04	97.8	
	7	0.02	0.02	99.1	
	8	0.01	0.02	99.7	
	9	0.00	0.01	99	
	10	0.00	0.01	99	

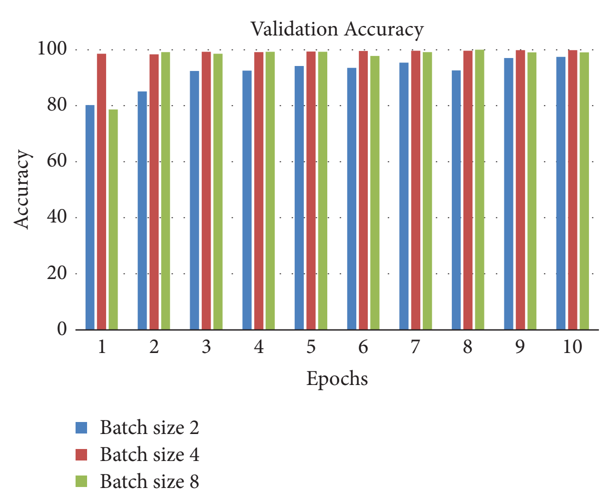

Figure 14: Comparison of validation accuracy using batch sizes 2, 4, and 8 for Adam optimizer and with a LR of 0.001.

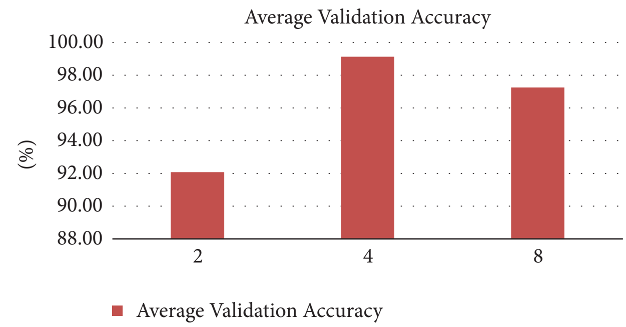

FIGURE 15: Comparison of average validation accuracy using batch sizes 2, 4, and 8 for Adam optimizer and with a LR of 0.001.

TABLE 7: Results obtained using SGD optimizer with a LR of 0.001.

Epoch	Training loss	Validation loss	Validation accuracy (%)	Validation precision	Validation recall
1	1.4	1.08	65.1	0.84	0.42
2	0.60	0.23	94.1	0.95	0.91
3	0.38	0.15	95.7	0.96	0.94
4	0.33	0.13	96	0.97	0.94
5	0.27	0.11	97.3	0.97	0.96
6	0.25	0.07	99.0	0.99	0.98
7	0.22	0.07	99.0	0.99	0.98
8	0.19	0.07	99.0	0.98	0.98
9	0.18	0.07	98.8	0.98	0.98
10	0.17	0.07	98.8	0.98	0.98

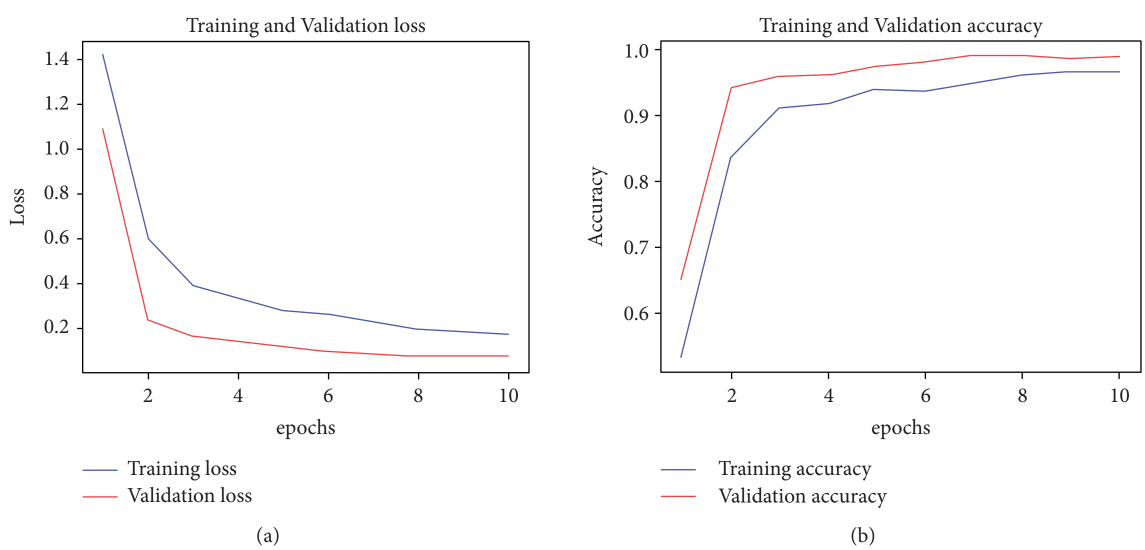

FIGURE 16: Continued.

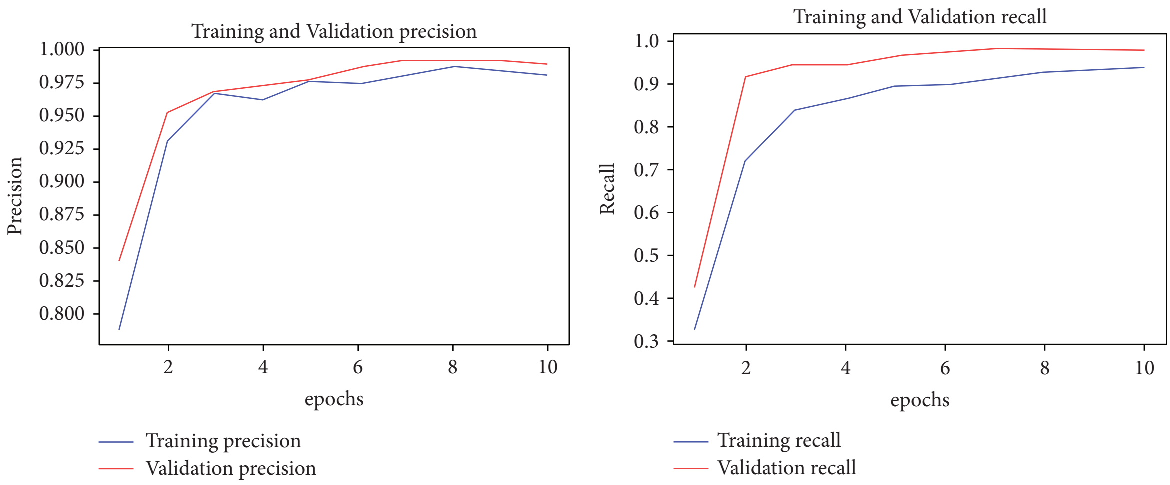

(c)

(d)

Figure 16: Plots obtained with a LR of 0.001 by employing SGD optimizer. (a) Training and validation loss plot. (b) Training and validation accuracy plot. (c) Training and validation precision plot. (d) Training and validation recall plot.

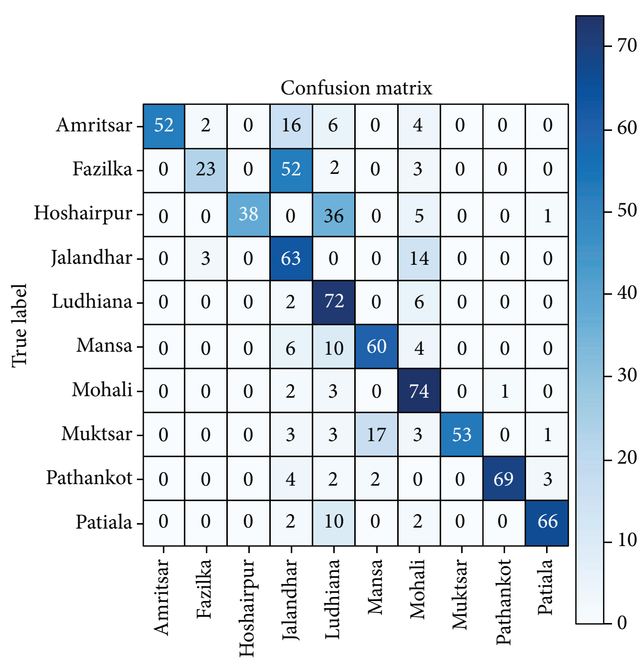

Figure 17: Confusion Matrix for SGD optimizer with a LR of 0.001.

Figure 15, Y-axis is representing the average validation accuracy obtained, while the X-axis is representing the batch sizes 2, 4, and 8. It can be observed from Figure 14 that batch size 4 has given higher accuracies as compared to other batch sizes, while Figure 15 shows that the high average validation accuracy is given by a batch size of 4.

4.4. Results Obtained Using SGD Optimizer with a LR of 0.001 and Batch Size of 4. The optimizer employed in CNN model also affects the accuracy obtained. In this section, the results are obtained using SGD optimizer with a LR of 0.001 and a batch size of 4. LR of 0.001 and batch size of 4 are chosen based upon the best accuracy results obtained by them in the previous sections. Table 7 shows the results for various parameters obtained using SGD optimizer, while Figure 16 shows the parameters convergence plot, and Figure 17 shows the confusion matrix for the same. Figure 16 shows that the plots are almost linear for all the parameter values obtained in Table 7. The plot in Figure 16(a), training and validation loss, is approaching value “0” with each epoch, while plots in Figures 16(b)–16(d) for training and validation accuracy, precision, and recall are approaching “1.” The maximum validation accuracy obtained in the last epoch is 98.8%,

Table 8: Comparison of SGD optimizer with three different batch sizes.

Batch size	Epochs	Training loss	Validation loss	Validation accuracy	Average validation accuracy
2	1	1.96	1.11	63.2	87.6%
	2	1.51	0.84	76.1	
	3	1.25	0.83	75.3	
	4	1.08	0.31	91.1	
	5	1.03	0.30	90.7	
	6	0.85	0.26	93.6	
	7	0.88	0.21	95.0	
	8	0.78	0.10	98	
	9	0.68	0.10	97.2	
	10	0.71	0.10	97.6	
4	1	1.4	1.08	65.1	94.18%
	2	0.60	0.23	94.1	
	3	0.38	0.15	95.7	
	4	0.33	0.13	96	
	5	0.27	0.11	97.3	
	6	0.25	0.07	99.0	
	7	0.22	0.07	99.0	
	8	0.19	0.07	99.0	
	9	0.18	0.07	98.8	
	10	0.17	0.07	98.8	
8	1	1.1	0.99	64.3	93.31%
	2	0.37	0.28	92.12	
	3	0.24	0.15	95.3	
	4	0.17	0.15	96.5	
	5	0.13	0.13	96.3	
	6	0.11	0.11	96.7	
	7	0.10	0.09	97.0	
	8	0.09	0.09	98.5	
	9	0.08	0.08	98.2	
	10	0.07	0.08	98.3	

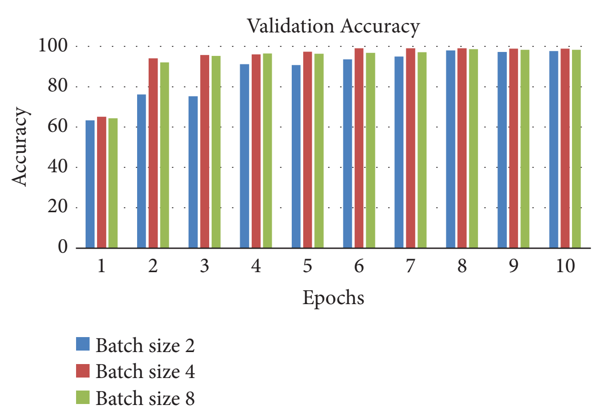

Figure 18: Comparison of validation accuracy using batch sizes 2, 4, and 8 for SGD optimizer with a LR of 0.001.

which is less than the best accuracy obtained by Adam optimizer.

4.4.1. Comparison of Three Different Batch Sizes Using SGD Optimizer with a LR of 0.001. The comparison of SGD optimizer on three different batch sizes is carried out in this section. Training loss, validation loss, validation accuracy, and average validation accuracy are compared using 10 epochs. The average validation accuracy obtained by batch size 2 is 87.6%, batch size 4, 94.18%, and batch size 8, 93.31%. It can be observed from Table 8 that the highest average validation accuracy is obtained by batch size 4. Figure 18 shows the comparison plot for validation accuracy using batch sizes 2, 4, and 8 for SGD optimizer with a LR of 0.001, while Figure 19 shows the comparison plot for average validation accuracy for the same. It can be concluded that, here, also batch size of 4 has worked better for the available

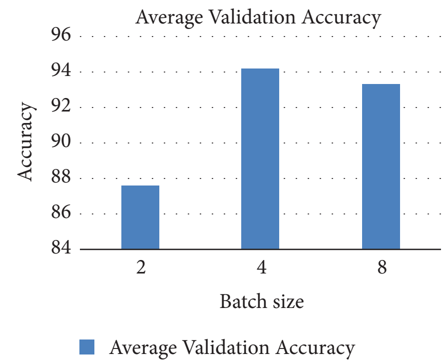

FIGURE 19: Comparison of average validation accuracy using batch sizes 2, 4, and 8 for SGD optimizer with a LR of 0.001.

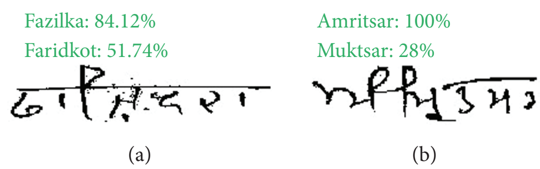

FIGURE 20: Testing of images. (a) Fazilka image. (b) Amritsar image.

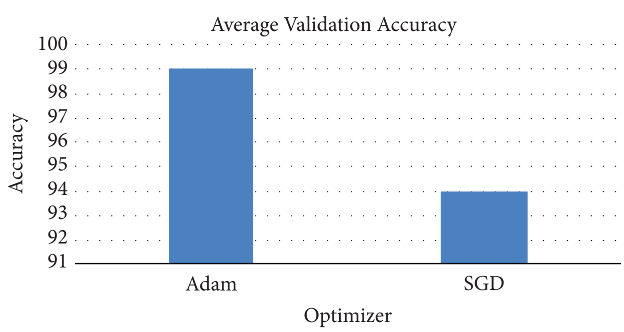

FIGURE 21: Analysis plot of average validation accuracy obtained by Adam optimizer and SGD optimizer.

dataset using SGD optimizer although the achieved validation accuracy is less than the validation accuracy achieved by Adam optimizer.

5. Testing of Some Images

In this section, some randomly selected images are given to the CNN model, which has employed Adam optimizer with a LR of 0.001 and BS of 4. Figure 20(a) shows that the image of city name "Fazilka" has been recognized with an accuracy of 84.12%, while the image of city name "Amritsar" has been recognized 100% correctly.

6. Analysis

It can be analyzed from Tables 4 and 7 that Adam optimizer with a LR of 0.001 and batch size of 4 has given the good results in terms of average validation accuracy. The best average validation accuracy obtained by Adam is 99.13%, while best average validation accuracy obtained by SGD optimizer is 94.18%. Analysis plot of average validation accuracy obtained by Adam optimizer and SGD optimizer is shown in Figure 21. It can be concluded that Adam with a LR of 0.001 and batch size of 4 has performed much better as compared to SGD optimizer using the same LR and batch size.

7. Conclusion

Deep learning is the machine learning, which is applied to the large datasets. Deep learning requires huge amount of data to train the network, which can be stored on cloud. Therefore, cloud computing helps in making deep learning accessible and easier in handling large amount of data, and also, the training of algorithms can be easily done on the distributed hardware. It also helps in providing the access to configurations of various hardware such as FPGAs, GPUs, and high performance computing systems. It can be concluded that the emerging paradigms of cloud computing work very well with the deep learning algorithms instead of traditional algorithms. The performance of the deep learning model depends on various hyperparameters like the LR, batch size, choice of optimizers, and so on. In Tables 2, 3, and 5, various parameters are obtained using an Adam optimizer with a LR of 0.001, 0.01, and 0.1, and the obtained average validation accuracies are 99.13%, 96.9%, and 98.17%. Table 4 has also obtained the average validation accuracy by changing the batch size of 2, 4, and 8, while the LR is kept fixed at 0.001. Results are also analyzed by changing Adam optimizer to SGD optimizer for the LR of 0.001. Average validation accuracy obtained for SGD optimizer using batch size of 2, 4, and 8 is 87.6%, 94.18%, and 93.31%, while the best average validation accuracy obtained by Adam and SGD is 99.13% and 94.18%, respectively. From the above experimentation, it has been observed that Adam optimizer with a batch size of 4 and a LR of 0.001 has achieved the best average validation accuracy of 99.13%. In the future, this model can be implemented for word recognition for other scripts also.

Data Availability

The data will be available from the author upon request (sandhya.sharma@chitkara.edu.in).

Conflicts of Interest

The authors declare that they have no conflicts of interest.

References

[1] P. Zhang, Q. Zhao, J. Gao, W. Li, and J. Lu, "Urban street cleanliness assessment using mobile edge computing and deep learning," *IEEE Access*, vol. 7, pp. 63550–63563, 2019b.

[2] S. Dargan, M. Kumar, M. R. Ayyagari, and G. Kumar, "A survey of deep learning and its applications: a new paradigm to machine learning," *Archives of Computational Methods in Engineering*, vol. 27, no. 4, pp. 1071–1092, 2020.

[3] L.-p. Huang, M. Hong, C. Luo, S. Mahajan, and L. Chen, "A vector mosquitoes classification system based on edge computing and deep learning," in *Proceedings of the 2018 Conference on Technologies and Applications of Artificial Intelligence*, pp. 24–27, TAAI, Taichung, Taiwan, December 2018.

[4] C. Liu, Y. Cao, Y. Luo, G. Chen, V. Vokkarane, and M. Yunsheng, "A new deep learning-based food recognition system for dietary assessment on an edge computing service infrastructure," *IEEE Transactions on Services Computing*, vol. 11, no. 2, pp. 249–261, 2018.

[5] I. Azimi, J. Takalo-mattila, A. Anzanpour, and M. Rahmani, "Empowering healthcare iot systems with hierarchical edge-based deep learning," in *Proceedings of the International Conference on Connected Health: Applications, Systems and Engineering Technologies*, pp. 63–68, IEEE/ACM, Washington, DC, USA, September 2018.

[6] M. S. Hossain, G. Muhammad, and S. Umar, "Improving consumer satisfaction, in smart cities using edge computing and caching: a case study of: date fruits classification improving consumer satisfaction in smart cities, using edge computing and caching: a case study of date fruits classification," *Future Generation Computer Systems*, vol. 88, pp. 333–341, 2018.

[7] U. Pal, R. K. Roy, and F. Kimura, "Multi-lingual city name recognition for Indian postal automation," in *Proceedings of the International Conference on Frontiers in Handwriting Recognition, Bari*, pp. 169–173, Bari, Italy, September 2012.

[8] S. Thadchanamoorthy, N. D. Kodikara, H. L. Premaretne, U. Pal, and F. Kimura, "Tamil handwritten city name database development and recognition for postal automation," in *Proceedings of the 12th International Conference on Document Analysis and Recognition*, pp. 793–797, IEEE, Washington, DC, USA, August 2013.

[9] S. Vajda, K. Roy, U. Pal, B. B. Chaudhuri, and A. Belaid, "Automation of Indian postal documents written in Bangla and English," *International Journal of Pattern Recognition and Artificial Intelligence*, vol. 23, no. 8, pp. 1599–1632, 2009.

[10] S. Sahoo, S. K. Nandi, S. Barua, S. Malakar, and R. Sarkar, "Handwritten Bangla city name recognition using the shape-context feature," in *Intelligent Engineering Informatics*, pp. 451–460, Springer, Singapore, 2018.

[11] S. Y. Manchala, J. Kinthali, K. Kotha, K. S. Kumar, and J. Jayalaxmi, "Handwritten text recognition using deep learning with TensorFlow," *International Journal of Engineering Research & Technology*, vol. 9, no. 5, pp. 594–600, 2020.

[12] S. Bhowmik, S. Malakar, R. Sarkar, S. Basu, M. Kundu, and M. Nasipuri, "Off-line Bangla handwritten word recognition: a holistic approach," *Neural Computing & Applications*, vol. 31, no. 10, pp. 5783–5798, 2019.

[13] T. M. Wahbi and M. E. Musa, "Holistic approach for Arabic word recognition," *International Journal of Computer Applications Technology and Research*, vol. 5, no. 3, pp. 141–146, 2016.

[14] N. Sharma, A. Sengupta, R. Sharma, U. Pal, and M. Blumenstein, "Pincode detection using deep CNN for postal automation," in *Proceedings of the International Conference on Image and Vision Computing New Zealand (IVCNZ)*, pp. 1–6, IEEE, Christchurch, New Zealand, December 2017.

[15] J. Dasgupta, K. Bhattacharya, and B. Chanda, "A holistic approach for Off-line handwritten cursive word recognition using directional feature based on Arnold transform," *Pattern Recognition Letters*, vol. 79, pp. 73–79, 2016.

[16] U. Jindal, S. Gupta, V. Jain, and M. Paprzycki, "Offline handwritten gurumukhi character recognition system using deep learning," in *Advances in Bioinformatics, Multimedia, and Electronics Circuits and Signals*, pp. 121–133, Springer, Singapore, 2020.

[17] S. Bansal, M. Kumar, and M.. Garg, "A New approach for Handwritten city name recognition," in *Proceedings of the International Conference on Advances in Engineering and Technology(ICAET)*, pp. 106–109, Roorkee, India, May 2014.

[18] U. Pal, R. K. Roy, and F. Kimura, "Handwritten street name recognition for Indian postal automation," in *Proceedings of the 2011 International Conference on Document Analysis and Recognition*, pp. 483–487, IEEE, Beijing, China, September 2011.

[19] I. Kandel and M. Castelli, "The effect of batch size on the generalizability of the convolutional neural networks on a histopathology dataset," *ICT express*, vol. 6, no. 4, pp. 312–315, 2020.

[20] Q. Abbas, M. E. Ibrahim, and M. A. Jaffar, "A comprehensive review of recent advances on deep vision systems," *Artificial Intelligence Review*, vol. 52, no. 1, pp. 39–76, 2019.

[21] Y. Wen, Y. Lu, and P. Shi, "Handwritten Bangla numeral recognition system and its application to postal automation," *Pattern Recognition*, vol. 40, no. 1, pp. 99–107, 2007.

[22] K. Roy, S. Vajda, U. Pal, and B. B. Chaudhuri, "A system towards Indian postal automation," in *Proceedings of the Ninth International Workshop on Frontiers in Handwriting Recognition*, pp. 580–585, IEEE, Kokubunji, Japan, October 2004.

[23] S. Juneja, M. Gahlan, G. Dhiman, and S. Kautish, "Futuristic cyber-twin architecture for 6G technology to support internet of everything," *Scientific Programming*, vol. 20217 pages, 2021.

[24] S. Sharma, S. Gupta, and N. Kumar, "Holistic approach employing different optimizers fortheRecognition ofDistrict names using CNN model," *Annals of RSCB*, vol. 25, no. 3, pp. 3294–3306, 2021.

[25] S. Juneja, S. Jain, A. Suneja et al., "Gender and age classification enabled blockschain security mechanism for assisting mobile application," *IETE Journal of Research*, pp. 1–13, 2021.

Hindawi
Scientific Programming
Volume 2022, Article ID 2079880, 26 pages
https://doi.org/10.1155/2022/2079880

Research Article

A Comprehensive Formalization of AADL with Behavior Annex

Yu Tan,[1] **Yongwang Zhao**,[2] **Dianfu Ma**,[3] **and Xuejun Zhang**[1]

[1]*Beijing Institute of Control and Electronic Technology, Beijing 100038, China*
[2]*College of Computer Science and Technology, School of Cyber Science and Technology, Zhejiang University, Hangzhou 310058, China*
[3]*State Key Laboratory of Software Development Environment, School of Computer Science and Engineering, Beihang University, Beijing 100191, China*

Correspondence should be addressed to Xuejun Zhang; ty138686@sina.com

Received 20 October 2021; Revised 22 November 2021; Accepted 8 December 2021; Published 4 January 2022

Academic Editor: Punit Gupta

In safety-critical fields, architectural languages such as AADL (Architecture Analysis and Design Language) have been playing an important role, and the analysis of the languages and systems designed by them is a challenging research topic. At present, a formal method has become one of the main practices in software engineering for strict analysis, and it has been applied on the tools of formalization and analysis. The formal method can be used to find and resolve the problems early by describing the system with precise semantics and validating the system model. This article studies the comprehensive formal specification and verification of AADL with Behavior annex by the formal method. The presentation of this specification and semantics is the aim of this article, and the work is illustrated with an ARINC653 model case study in Isabelle/HOL.

1. Introduction

In safety-critical domains such as avionics, aerospace, automotive, and defence, a latent software error even can give rise to catastrophic consequences. Such systems have to be carefully designed and analyzed according to some strict standards such as DO-178C [1], which stipulates analysis, testing, and certification activities. Formal methods have become the recommended practice in the safety-critical fields. Formal methods are special techniques based on mathematics and are suitable for the description, development, and verification of software and hardware systems. By applying formal methods to software and hardware designs, it is hoped that, like other engineering disciplines, appropriate mathematical analysis can be used to improve the reliability and robustness of designs. In the design of computer software systems, formal verification means that mathematical methods can be used to prove their correctness or incorrectness according to one or some formal specifications or attributes.

Theorem proving, program analysis, and model checking are the main branches of formal verification. To be formally verified, systems should be firstly specified with a specific formalism. AADL (Architecture Analysis and Design Language) [2] is a modeling standard used in safety-critical software engineering to describe the structure of systems, such as a package of software components, which is mapped on an execution platform. AADL adopts formal modeling concepts for the description of software and hardware architecture, so that it is often used to design and analyze the software and execution platform of real-time embedded systems. The operation of these systems depends strongly on meeting nonfunctional requirements such as availability, reliability, responsiveness, throughput, safety, and security. As a supplement of runtime environment in terms of distinct components and their interactions, the standard AADL Behavior annex [3] represents a behavioral extension for AADL, which allows a more detailed specification of the software behavior. Using AADL with its Behavior annex, the complete models can be designed in a way that large information about data models, timing, and communication behaviors is available at the modeling phase, and it is especially effective for the model-driven design of complex embedded real-time systems. AADL is standardized by the SAE, and its second version was published in 2009 and revised in 2017; for its analyzability and extensibility, AADL has become one of the popular languages within architectural modeling in the industry [4]. AADL has been studied in several projects for different modeling, analysis, simulation, compilation, extension, and formal verification. Moreover, the AADL semantic can be extended via user-defined properties and annexes.

However, AADL cannot be directly generated into the executable code, which is reliably used in safety-critical systems. So how to compile AADL to the C code is our final goal. Although there is not any comprehensive compiler or method from AADL to C on the open-source platform so far, there is some existing related work about the verified compiler or transformation of model languages like Lustre [5], CompCert [6]. As we do, proving the correctness of general-purpose compilers is undeniably a related problem, and fortunately, this work [7] encourages us and presents the possibility of development based on the model-driven design in prover tools. We aim at exploring a formal method of compiling AADL to C-like language, so we firstly limit our survey to work that focuses on the particularities of AADL.

The AADL provides a sufficient syntax and semantic to describe an embedded real-time system based on software/hardware components and their relations. Dealing with such rich models accentuates the need for model analysis and verification. Unfortunately, AADL is a textual and graphical language, which means it is a semiformal modeling language. It lacks formal specification and semantics, and this severely limits both unambiguous communication among model developers, and the development of simulators and formal analysis tools, so itself cannot be directly used for formal verification. In this work, we choose Isabelle/Isar/HOL [8], a tool suite (within its functional language) that gathers specification, validation, and verification of AADL and models, and also the code generation towards AADL runtime C-like language for the future work. The Isabelle/Isar language provides a readable grammar and a convenient way to produce the proofs.

In this article, we provide an approach for the formal verification of behavioral AADL models. In detail, this article makes the following contributions:

(i) Different from transforming AADL into other formal model languages, our work takes an approach by formally specifying AADLs, its corresponding models of definitions, lemmas, and proof structures necessary to verify the model, providing a blueprint for performing similar work in any prover tool. Also we can state and prove a correctness relation between the source and target semantic models, and even directly build on the compilation project in Isabelle/HOL as our future work.

(ii) We consider the AADL focusing on safety-critical software, so our work mostly covers the whole AADL elements including components, communication among components, and Behavior annex defined inside, and also supports the key features and properties. The considered AADL subset consists of both software and hardware AADL components with complex state transitions being comprehensive and that can be used in more realistic applications.

(iii) We perform formal validation and verification of the AADL model and specify the critical properties. Specifically, we (1) analyze and summarize the description for the AADL standard defined by the SAE republished in 2016 and take 47 significant details into account as the grammar rules in Isabelle/HOL; (2) exploit the comprehensive semantics including Behavior annex, Thread, Process, and System, and then integrate them into a whole model execution semantics; and (3) perform formal instantiation, validation, and verification of three realistic AADL models.

In this context, we aim at the comprehensive formal specification and verification of AADL core language (software part) with its Behavior annex. The remainder of this article is organized as follows: in Section 2, we describe the concept of AADL along with its Behavior annex and Isabelle/HOL, and also present the strength of Isabelle/HOL and its specification language to justify why we choose it to model AADL and Isabelle/HOL to perform formal analysis; Section 3 overviews our approach including the AADL elements we selected; in Section 4, we present the syntax of our selection and the validation rules for grammar in Isabelle/HOL; In Section 5, we present the semantics of selection and the verification, and in addition, we present the semantics of Behavior annex; Section 6 then presents a case study; and Section 7 gives the conclusions and future directions.

2. Background

2.1. AADL and Its Behavior Annex. AADL is a textual and graphical language used to model, specify, and analyze architectures (included software and hardware part) of safety-critical and real-time embedded systems, and it has been studied in several projects for different purposes analysis, code generation, extensions, and formal verification. AADL is based on a component-centric model, and it defines the system architecture as a set of interconnected components that hierarchically describes the interfaces, the implementations, the properties, and the channels among components. It describes a system as a hierarchy of software and hardware components and offers a set of predefined component categories as follows:

(i) Software components: data, subprogram, subprogram group, Thread, Thread group, Process, and their types, implementations, features, connections, properties

(ii) Execution platform components (hardware components): processor, memory, bus, and device

(iii) System composites: they represent composite sets of software and execution platform components

(iv) Annex subclauses: they allow annotations expressed in a sublanguage to be attached to the component and contain Behavior Annex, Error Annex, Data Annex, etc

According to the component categories, AADL software component elements are composed and synchronized to form the whole software system. Figure 1 gives an overview of the AADL software components containing essential constructions.

2.2. Isabelle/HOL Notations. Isabelle/HOL (the full name is Isabelle/Isar/HOL, Isabelle is often for short) is a generic interactive theorem prover for implementing logical formalisms of a specification and verification, and it is the specialization of Isabelle for HOL (higher-order logic) [9]. Isabelle is implemented in ML [10]. This has influenced some of Isabelle/HOL's concrete syntax Isabelle/Isar [11], an extension of Isabelle, which hides the implementation language almost completely. Based on a small (meta)-logical inference kernel, Isabelle's LCF-style architecture ensures very high confidence about its soundness as a theorem prover. Since our whole work focuses on the verification of formalization and the output, moreover, also will invoke the theorem prover's code generator and run the test suite on the C-like code generated by itself in the future, Isabelle is used to prove the methodology in this work. This work mainly restricts itself to the core of Isabelle (simply typed Lambda calculus with ML-style polymorphism and inductive datatypes). The main notations used in this work are explained as follows:

theories, working with Isabelle means creating theories. Roughly speaking, a theory is a named collection of types, functions, and theorems, much like a module in a programming language or a specification in a specification language. In fact, theories in HOL can be either. The general format of a theory T is

theory T

imports $B_1 \ldots B_n$

begin

Declarations, definitions, and proofs

end

where $B_1 \ldots B_n$ are the names of existing theories that T is based on and declarations, definitions, and proofs represent the newly introduced concepts (types, functions, etc.) and proofs about them.

lemma, this command starts the proof and gives the lemma a name. As a result of that final done, Isabelle/HOL associates the lemma just proved with its name. Lemma, theorem, and rule are used interchangeably for propositions that have been proved.

base types, in particular bool, the type of truth values, and nat, the type of natural numbers.

type variables, denoted by 'a, 'b, etc., like in ML.

datatypes, the general form of a datatype definition looks like this:

da tatype $('a_1, \ldots, 'a_n)t = C_1$ " $\tau_1, 1$" ..."τ_1, n_1"

| ...

$|C_k$ " $\tau_k, 1$ " ..." τ_k, n_k"

It introduces the constructors $C_1 : : \tau_1, 1 \Longrightarrow \ldots \Longrightarrow \tau_1, n_1 \Longrightarrow ('a_1, \ldots, 'a_n)t$ and expresses that any value of this type is built from these constructors in a unique manner.

records, introduces a new record-type scheme by specifying its fields, which are packaged internally to hold up the perception of the record as a distinguished entity. A record of Isabelle/HOL covers a collection of fields, with select and update operations. Here is a simple example:

record point = Xcoord:: int

Ycoord:: int

In this work, we choose a deep embedding method, which does not try to directly represent elements of the language as expressions of the target language (in this case: Isabelle/HOL), but rather encodes them.

3. Approach Overview

The general methodology of our work is given as follows: at first, we select a comprehensive core AADL with its Behavior annex and a policy for modeling as 3.1.1 and 3.1.2 presented; secondly, we define a specification from AADL in Isabelle/HOL and model an example; next, we determine some significant rules about AADL grammar from AADL official standard manual and transform them into the model-checking functions, and then, we present a validation by using these functions; finally, we present the semantics of the comprehensive core AADL and verify some properties (reachability, trace refinement, etc.) by the semantics in Isabelle/HOL. The main idea of our methodology is illustrated in Figure 2.

3.1. Selection of AADL

3.1.1. Selection of Core AADL in This Work. In this article, our work focuses on the specification and analysis of the software components of systems, and most of execution platform components in AADL (virtual processors, memory, buses, virtual buses and devices, etc.) are not under consideration except the processor (simply discussed). Moreover, the group, prototype, and refinement are regarded as a set element, and mainly for the reusability of the AADL code, software systems can be modeled even without these elements; therefore, they are not accounted in this work. This selection of AADL core elements is comprehensive and sufficient to specify and model an embedded system on the software side.

A component can be a subcomponent of the other component. Thus, the following components are supported: *processor*, *data*, *subprogram*, *thread*, *process*, *system*, and thread's *Behavior annex*. A processor component is an abstraction of hardware and software that is responsible for scheduling and executing threads that are bound to it. A data component represents a data type and also static data in the

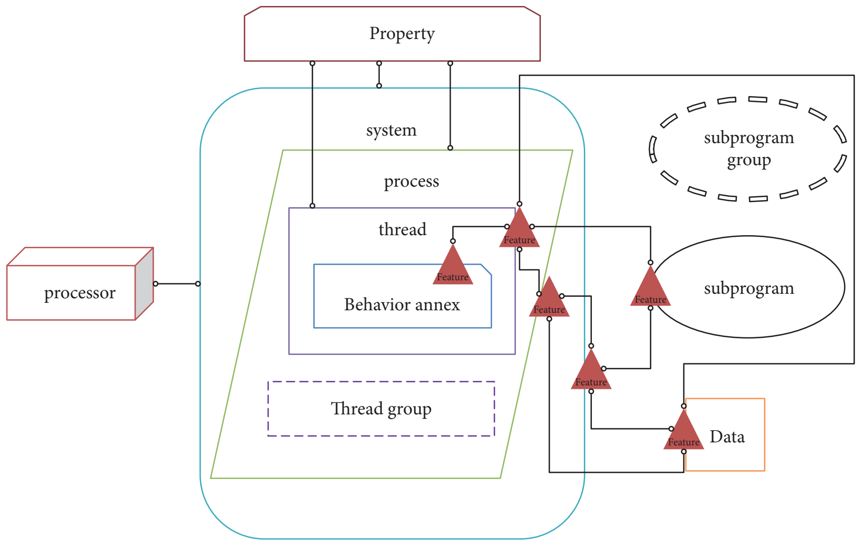

Figure 1: AADL software component elements.

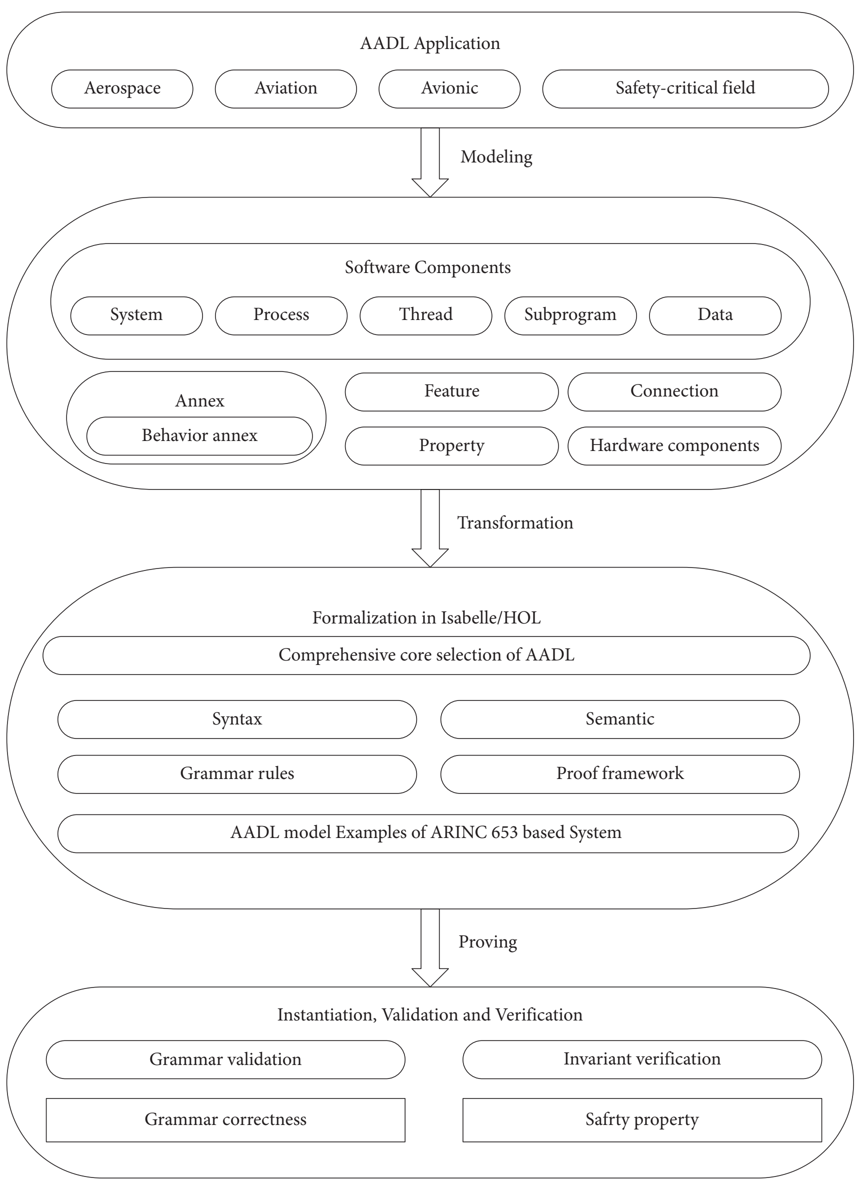

Figure 2: Approach overview.

source text. A subprogram component represents sequentially executed source text that is called with parameters. A thread component is a schedulable unit that is declared within a process component and can be executed concurrently with other threads. A process component represents its virtual address space, and a software system represents an assembly of interacting application software.

A feature is a part of a component definition that specifies how that component interfaces with other components in the system. Features consisted of *port*, *access,* and *parameter* in our work. In addition, features can be combined with properties, and our work can support some temporal and queuing properties, such as Dispatch_Protocol (periodic, sporadic, timed), Period, Queue_Processing_Protocol (FIFO, LIFO), Queue_Size, Elapsed_Time, Execution_Time, and Scheduling_Protocol.

A connection is a linkage between features of two components representing communication of data and control between components. Our work supports connections between *port connections*, *parameter connections*, *dataaccess connections*, and *subprogramaccess connections*.

A property provides information about model elements, and it has a name, a type, and a value. Each property has a value or list of values that is associated with the named property in a given specification. Our work focuses on the indispensable properties, which depend on the specific components.

3.1.2. Selection of AADL Behavior annex. The Behavior annex document provides a standard sublanguage extension to allow behavior specifications to be attached to AADL components. It is an important part of AADL, as it split a whole system model into several single composable components to make design and analysis easier. The Behavior annex of a Behavior annex instance is defined on the vocabulary consisting of its private variables behavior_variable, its states behavior_state, and ports of its parent component. Its transition system is the union of the transitions specified by a behavior_transition. A Behavior Annex specification of a thread contains *variables*, *states*, and *transitions*. The states may be *initial*, *complete*, *execution*, or *final*.

Our work can support the Behavior annex with its specification to enrich the running model. The aim of the Behavior annex is to refine the implicit behavior specifications that are specified by the core of the language. Yet we practically state that behavior specification subclauses can only be added in a thread, and the behavior specification subclauses describe the thread that the behavior specification subclause belongs to, since the execution of the whole system at one processor is actually the execution of one thread.

3.2. Related Work. AADL lacks formal specification and semantics; therefore, it cannot be directly used for formal verification and it is often transformed into several formal model languages to be adopted with existing formal analysis tools. We study several formal approaches on AADL. According to the transformation method and the consideration of the AADL model with or without Behavior annex, these are grouped into three categories.

The first category is often based on model transformation into different languages without (or barely with) Behavior annex such as Petri nets [12], Timed automata [13], TLA+ [14], Lustre [15], Fiacre [16], and CSP [17,18]. These approaches are contented with the AADL semantic described in its standard, which is enough to formally simulate the system and verify a set of behavioral properties. The second category represents work about the model transformation of AADL with its Behavior annex such as BIP [19], Signal [20], TASM [21, 22], and Ocarina [23]; for example, Ref. [19] defines a transformation into the BIP language, and then, the BIP model is transformed into nontimed models to enable model checking and simulation with the BIP framework. The third category almost only specializes in behavior and analysis by using and mapping AADL behavioral models such as IF [24] and real-time Maude [25]. Such a mapping allows the analysis of the performance and the dependability.

These AADL formal approaches mainly consider different AADL subsets (with or without annexes) and carry on formal verification with existing tools such as UPPAAL, Tina, and Polychrony. They often define a model transformation to implement whole AADL model certification instead of AADL itself. Moreover, a formal proof of the semantics preservation of the transformation has not been considered by them. Our work considers several resource information in the transformation, and the theorem prover is used to prove the methodology, that is, the correctness of the translation. The comparisons of the above-related works are listed in Table 1.

These works focus on a subset of the AADL, and most of the related works only consider a small subset of Behavior annex. For AADL elements, our work supports Behavior annex and components, in which variables, states, state transitions of Behavior annex and connections, features, and software components of components are represented by a "+". For the aspect of verified properties, our work considers more types of properties by Isabelle, for example, grammar, reachability, and trace refinement.

The main goal of our work is to contribute to a better integration of the formal techniques in a compilation process. So this article is full of formal approaches revolving around the AADL, and we choose Isabelle/Isar/HOL [8], a tool suite (within its functional language) that gathers specification, validation, and verification of AADL and models, and also the code generation towards AADL runtime C-like language for the future work. Besides the tool suite that can be used as stand-alone compiler, the Isabelle/Isar language provides a readable grammar and a convenient way to produce the proofs.

4. Abstract Syntax and Validation

4.1. Presentation of Abstract Syntax in Isabelle/HOL. This section describes those aspects of components that are common to all AADL component categories. Our work provides the abstract syntax of the considered AADL in

Table 1: Comparison of related AADL formal approaches.

Works	Specification language	Verification tool	Elements covered						Support for transformation correctness verification
			Behavior annex	Components				Safety	
				Thread	Process	System	Others		
Gina et al.	Petri Nets	ADAPT	−	++	−	−	−	−	−
Johnsen et al.	Timed Automata	UPPAAL	+	+++	+	−	+++	+	−
Jean-Francois et al.	TLA+	TLC	−	+	−	−	−	−	−
Jahier et al.	Lustre	Lurette, Lesar	−	++	+	−	−	+	−
Berthomieu et al.	Fiacre	Tina	+	+++	−	−	−	+	−
Yang et al.	CSP	FDR	−	++	−	−	+	++	−
Chkouri et al.	BIP	BIP framework	++	++	−	−	−	+	−
Besnard et al.	Signal	SynDEx	+	+	−	−	−	−	−
Yang et al.	TASM	TASM, UPPAAL	+	+++	+	−	+++	+	−
Mkaouar et al.	LNT	Ocarina	−	+	+	−	+++	+	−
Abdoul et al.	IF	IFx framework	Its own behavioral language	+	−	−	−	++	−
Ölveczky et al.	Real-time Maude	Maude	++	++	−	−	−	+	−
Ours	Isabelle/Isar	Isabelle/HOL	+++	+++	+	+	+++	++	+

Isabelle/HOL: an AADL model contains several software subcomponents (like threads), several features (like ports), and Behavior annex specification. Each Behavior annex can belong to a thread, and each thread with its Behavior annex belongs to a process. In this article, to keep the article reasonably concise, some structural elements and model attributes are expressed in a uniform abstract syntax. In addition, at the whole system level, a system is viewed as a set of processes, and a process is viewed as a set of threads in communication through port and access connections. According to the selection of AADL and its Behavior Annex, the classification of main syntax is discussed in the following subsections.

4.1.1. Features and Connections. Features are a part of component type definition that specifies how that component interfaces with other components in the system. Features are specified as *port*, *access*, and *parameter*. Two components are connected between features by a linkage called connections, and connections can be the transmission of control and data in components' implementation. AADL supports connections between *port*, *access*, and *parameter connections*.

The details of Features and Connections are much more than we have space to present here, and some of them are defined in Figures 3 and 4, and the code snippets are shown in Figures 5 and 6.

4.1.2. Type and Implementation Base. Components represent some hardware or software entity that is part of a system being modeled in AADL. A component has a component type, and zero or more component implementation, which defines a functional interface and realization. The component type acts as the specification of a component that other components can operate against, and the component implementation specifies the realization of a component variant. A component type and implementation instance are presented in Figures 7 and 8.

By default, we consider one component *Type* has only one component *Implementation* to avoid the complexity of the actual modeling arisen from polymorphism. To reduce code redundancy, some basic elements of *Type* and *Implementation*, like *Features* and *Subcomponents*, are declared as the datatypes as the type_base, impl_base, and their own *Properties* to add in the respective components later. Their syntaxes in Isabelle/HOL are presented in Figures 9 and 10.

```
feature ::=  port | data_access
             | subprogram_access | parameter
```

Figure 3: The syntax of Feature.

```
connection ::=  connection_identifier
                ( port_connection | access_connection | parameter_connection)
                [ '{' { property_association } + '}' ]
                [ in_modes_and_transitions ]
```

Figure 4: The syntax of Connection.

```
datatype ('Port, 'Dataaccess, 'Subpaccess, 'Parameter) Feature =
FPort 'Port | FDataaccess 'Dataaccess | FSubpaccess 'Subpaccess |
FParam ‘Parameter
```

Figure 5: The code of Feature in Isabelle/HOL.

```
datatype Connection-cate = PORT | PARAMETER |
DATA-ACCESS | SUBP-ACCESS

record ('Port, 'Dataaccess, 'Subpaccess, 'Parameter, 'Data,
'Subprogram, 'Thread, 'Process, 'System) conn-conf =
cc-name :: string
cc-cate :: Connection-cate
cc-endp-src :: ('Port, 'Dataaccess, 'Subpaccess, 'Parameter, 'Data,
'Subprogram, 'Thread, 'Process, 'System) Connection-ref
cc-endp-des :: ('Port, 'Dataaccess, 'Subpaccess, 'Parameter, 'Data,
'Subprogram, 'Thread, 'Process, 'System) Connection-ref
cc-direction :: Connection-dir
cc-timing-type :: Timing-type option
cc-trans-type :: Transmission-type option
```

Figure 6: The code of Connection in Isabelle/HOL.

```
type_base ::=   [ type_name ]
                [ features { feature } + ]
```

Figure 7: The syntax of component type base.

```
subcomponent ::=   basic_type | data | subprogram
                   | thread | process | system
impl_base ::=      impl_name
                   [ connections { connection } + ]
                   [ subcomponents { subcomponent
                   } + ]
```

Figure 8: The syntax of component implementation base.

```
record ('Port, 'Dataaccess, 'Subpaccess, 'Parameter) type-base =
type-features :: ('Port, 'Dataaccess, 'Subpaccess, 'Parameter) Feature
set
type-name :: string
```

Figure 9: The code of component type base in Isabelle/HOL.

```
record ('Connection, 'Data, 'Subprogram, 'Thread, 'Process,
'System) impl-base =
impl-subcomps :: ('Data, 'Subprogram, 'Thread, 'Process, 'System)
Subcomponent set
impl-conns :: 'Connection set
impl-name :: string
```

Figure 10: The code of component implementation base in Isabelle/HOL.

4.1.3. Software Subcomponents. Software subcomponents represent the components contained within another software component. They can be the instantiations of component implementations if they are contained in their own subcomponents. As the statement of the core AADL selection in Subsection 3.1.1, the software subcomponents are specified as Data, Subprogram, Thread, Process, and System. Their instances are presented in Figure 11.

```
data_type :: =          type_base [data_properties]
data_impl :: =          impl_base [data_properties]
subprogram_type :: =    type_base [subprogram_properties]
subprogram_impl :: =    impl_base [subprogram_properties] [subprogramcalls]
thread_type :: =        type_base [thread_properties] [behavior_annex]
thread_impl :: =        impl_base [thread_properties]
                        [subprogramcalls] [behavior_annex]
process_type :: =       type_base [process_properties]
process_impl :: =       impl_base [process_properties]
system_type :: =        type_base [system_properties]
system_impl :: =        impl_base [system_properties]
```

Figure 11: The syntax of Subcomponents.

We consider that there is only one system as a parent component in a practically running model. This results in a component containment hierarchy that ultimately describes the whole actual system as a system instance. This section defines the following categories of software subcomponents: data subcomponent, subprogram subcomponent, thread subcomponent, process subcomponent, and system component. Their code snippets in Isabelle/HOL are presented as Figures 12–16.

4.1.4. Behavior Annex. As discussed in Subsection 3.1.2, a behavior specification subclause is a part of a thread, and it describes the thread that the Behavior annex belongs to. The Behavior annex is composed of variable set, state set, transition set, and its private information (like its name and ports of its parent component), and its elements are united by its transitions. A behavior_annex instance is presented in Figure 17.

The transitions can describe the behavior as a state-transition system linked with *guards* by some conditions and *actions*. The behavior_transition defines a relation from a source state to a destination state and represents a sequence of actions within a thread, which can be executed once its condition is satisfied. A behavior_transiton consists of its name, source state, destination state, guard condition, and actions. The actions associated with transitions are action block. A transition instance is presented in Figure 18.

The guards combined of conditions are in the transitions, which are explicitly classified as dispatch conditions and execution conditions. A dispatch condition is a Boolean expression that specifies the trigger of events. An execution condition is a logical expression on the inputs, outputs, values, and properties, or any other execute conditions. A transition instance is presented in Figure 19.

The actions can be classified as basic actions and action blocks in the transitions. The basic actions can be defined as empty (marked as NULL), assignment actions, communication actions, or timed actions. The action blocks are in the

```
record data-properties =
dt-access-right :: Access-right option
dt-concurrency-control-protocol :: Concurrency-Control-Protocol
option

record ('Port, 'Dataaccess, 'Subpaccess, 'Parameter) data-type =
('Port, 'Dataaccess, 'Subpaccess, 'Parameter) type-base +
dt-properties :: data-properties option

record ('Connection, 'Data, 'Subprogram, 'Thread, 'Process,
'System) data-impl = ('Connection, 'Data, 'Subprogram, 'Thread,
'Process, 'System) impl-base +
dt-properties :: data-properties option
```

Figure 12: The code of data in Isabelle/HOL.

```
record subprogram-properties =
sp-urgency :: int option
sp-compute-exetime :: TimeRange option
sp-compute-deadline :: Time option
sp-call-type :: Call-type option

record ('Port, 'Dataaccess, 'Subpaccess, 'Parameter)
subprogram-type =
('Port, 'Dataaccess, 'Subpaccess, 'Parameter) type-base +
sp-properties :: subprogram-properties option

record ('Connection, 'Subprogramcalls, 'Data, 'Subprogram,
'Thread, 'Process, 'System) subprogram-impl =
('Connection, 'Data, 'Subprogram, 'Thread, 'Process, 'System)
impl-base +
sp-spcalls :: 'Subprogramcalls set
sp-properties :: subprogram-properties option
```

Figure 13: The code of subprogram in Isabelle/HOL.

```
record ('Port, 'Data, 'Subprogram, 'Thread, 'Process, 'System)
thread-properties = thd-stack-size :: Size option
thd-initialize-entrypoint :: ('Data, 'Subprogram, 'Thread, 'Process,
'System) Subcomponent option
thd-period :: Time option
thd-deadline :: Time option
thd-priority :: int option
thd-resumption-policy :: Resumption-policy list option
thd-deactivation-policy :: Deactivation-policy option
thd-dispatch-protocol :: Dispatch-protocol option
thd-dispatch-trigger :: 'Port list option
thd-dispatch-deadline :: Time option
thd-dispatch-offset :: Time option
thd-schedule-policy :: Schedule-policy option
thd-initialze-deadline :: Time option
thd-activate-deadline :: Time option
thd-deactivate-deadline :: Time option
thd-compute-deadline :: Time option
thd-recover-deadline :: Time option
thd-finalize-deadline :: Time option
thd-dispatch-time :: TimeRange option
thd-compute-time :: TimeRange option
thd-recover-time :: TimeRange option

record ('Port, 'Dataaccess, 'Subpaccess, 'Parameter, 'Data,
'Subprogram, 'Thread, 'Process, 'System, 'BehaviorAnnex)
thread-type = ('Port, 'Dataaccess, 'Subpaccess, 'Parameter)
type-base +
thd-properties :: ('Port, 'Data, 'Subprogram, 'Thread, 'Process,
'System) thread-properties option
thd-ba :: 'BehaviorAnnex option

record ('Port, 'Connection, 'Subprogramcalls, 'Data, 'Subprogram,
'Thread, 'Process, 'System, 'BehaviorAnnex) thread-impl =
('Connection, 'Data, 'Subprogram, 'Thread, 'Process, 'System)
impl-base +
thd-spcalls :: Subprogramcalls set
thd-properties :: ('Port, 'Data, 'Subprogram, 'Thread, 'Process,
'System) thread-properties option
thd-ba :: BehaviorAnnex option
```

Figure 14: The code of Thread in Isabelle/HOL.

form of sequences or sets. Every single action block is like imperative language and can be defined as conditionals and loops. Both assignment actions and communication actions consist of expressions; moreover, communication actions can reference for the events of initiating or freezing the parameters. Timed actions are a kind of predefining computation action. An action instance is presented in Figure 20.

The expressions consist of logical expressions, relational expressions, and arithmetic expressions. The values of expressions can be variables, constants, or the result of another expression, and the constants expression values can be Boolean, numeric or string literals, property constants, or property values. The presentation of this part is omitted as they are totally the same like the expression of imperative language.

According to all the related works above contributed to the formal specification, we define the syntax of the Behavior annex in Isabelle/HOL, and some parts are presented in Figure 21.

Notice: dispatcher is a predefined type, and it describes the hardware expression language used in the annex and is not given here; 's is a state set describing all possible values stored in ports; the action language of the annex is abstracted as a function computing outputs from the value of its input ports. The time consumption of an action is directly modeled as a time attribute.

4.1.5. Whole Model. In our work, we aim at a running model for the next formal verification in a development. For this end, we define a whole system, which is described with a set of mapping between the datatypes and the configuration records in practice, and the whole system model syntax is presented in Figure 22.

4.2. Validation Rules for Grammar. AADL is a standard defined by the SAE, and its reversion was published in 2016. There are numerous methods and rules of description for AADL in the new version, and they cover syntax, naming rules, legality rules, consistency rules, and standard properties, and also several discrete and temporal semantics. However, none of current tools have integrated these methods and rules to check the AADL model comparatively at present, even they do not take these rules into account, especially the rules.

record process-properties = pro-period :: Time option
pro-priority :: int option
pro-resumption-policy :: Resumption-policy option
pro-deactivation-policy :: Deactivation-policy option
pro-load-exe-time :: TimeRange option
pro-load-deadline :: Time option
pro-startup-exe-time :: TimeRange option
pro-startup-deadline :: Time option

record (*'Port, 'Dataaccess, 'Subpaccess, 'Parameter*) *process-type* =
(*'Port, 'Dataaccess, 'Subpaccess, 'Parameter*) *type-base* +
pro-properties :: process-properties option

record (*'Connection, 'Data, 'Subprogram, 'Thread, 'Process, System*) *process-impl* = (*'Connection, 'Data, 'Subprogram, 'Thread, 'Process, 'System*) *impl-base* +
pro-properties :: process-properties option

Figure 15: The code of process in Isabelle/HOL.

record *system-properties = sys-period :: Time option*
sys-priority :: int option
sys-resumption-policy :: Resumption-policy option
sys-startup-deadline :: Time option

record (*'Port, 'Dataaccess, 'Subpaccess, 'Parameter*) *system-type* =
(*'Port, 'Dataaccess, 'Subpaccess, 'Parameter*) *type-base* +
sys-properties :: system-properties option

record (*'Connection, 'Data, 'Subprogram, 'Thread, 'Process, 'System*) *system-impl* = (*'Connection, 'Data, 'Subprogram, 'Thread, 'Process, 'System*) *impl-base* +
sys-properties :: system-properties option

Figure 16: The code of system in Isabelle/HOL.

```
behavior_annex ::=   [ variables { behavior_variable }+ ]
                     [ states { behavior_state }+ ]
                     [ transitions { behavior_transition }+ ]
```

Figure 17: The syntax of Behavior annex.

```
behavior_transition ::= [ trans_identifier [ [ trans_priority ] ] : ]
source_state_identifier { , source_state_identifier }+
                 –[ guard_condition ] →
    destination_state_identifier [ action_block ] ;
```

Figure 18: The syntax of Transition.

```
guard_condition ::= execute_condition
                  | dispatch_condition
execute_condition ::= logical_expression
                    | no_others
dispatch_condition ::= ondispatch [ trigger_condition ]
                       [ frozen ( frozen_ports ) ]
```

Figure 19: The syntax of guard.

```
action_block ::= "{" actions "}"
actions ::= action | action_sequence | action_set
action ::= basic_action
         | if ( logical_expression ) actions
             [ else actions ] end if
         | while ( logical_expression ) "{" actions "}"
         | for ( element_identifier in element_values )
             "{" actions "}"
basic_action ::= NULL
               | assignment_action
               | communication_action
               | timed_action
action_sequence ::= action { ; action }+
action_set ::= action{ & action }+
```

Figure 20: The syntax of Action.

Our work integrates the rules into the theorem prover Isabelle/HOL, which come to having a partial mapping from concrete syntax to abstract model. In this section, for the next formal verification built on the firmer trust basis, our work makes a link of the validation for the AADL model in Isabelle/HOL. Firstly, since some of all the rules are mandatory and others are recommended, our work determines 47 significant rules on account of AADL selection and they are considered to be compulsive. These rules cover software components, features, connections, and Behavior annex from the grammar perspective. Secondly, these rules R are specified as the definitions or functions by the functional language Isabelle/Isar in Isabelle/HOL as the properties needed to be validated. We specify the constraints as properties by using the function definition aim at guaranteeing the correctness of the built AADL model. And then, we abstract the element e of a realistic AADL model into Isabelle and instantiate all elements together into a concrete model M. It is mapped as a parameter of these rules definitions. Lastly, we identify the lemmas of these rule definitions and integrate into a comprehensive lemma about grammar. The correctness of the validation pass hinges on a lemma that shows the assertion:

M ⊨ grammar_validate (R e)

For the given lemma *grammar_validate*, the correctness of the validation pass is simple to state. Due to the space constraints, the segmental validation rules and definition code for grammar are classified as syntax, naming, and others (including legality, consistency, and stand properties), which are shown in Tables 2–4.

5. Formal Semantics and Verification

Formal semantics is a kind of mechanism based on strict and mathematical logic, which is especially important for describing safety-critical systems. Model's correctness and valid execution can be guaranteed by formal semantics. Although the AADL standard has depicted some execution semantics by natural language, it is the absence of precise dynamic semantics and even has no formal semantics at present. In addition, the AADL model cannot be executed directly because it is just an abstract description of the

```
datatype Behavior-state-kind = INITIAL | COMPLETE | FINAL |
EXECUTION
type-synonym BA-state = string × ( Behavior-state-kind set )
type-synonym 's bexp = 's set

datatype ('s, 'Port, 'Dataaccess, 'Subpaccess, 'Parameter, 'Data,
'Subprogram) BA-action = Skip
| Basic-Assign 's ⇒ 's
| Basic-CommunSend ('Port, 'Dataaccess, 'Subpaccess, 'Parameter)
Feature 's ⇒ Data Message
| Basic-CommunRecv ('Port, 'Dataaccess, 'Subpaccess, 'Parameter)
Feature 'Data Message ⇒ 's
| Basic-CommunFreeze
| Basic-CommunInisend
| Basic-CommunCallsp 'Subprogram 's ⇒ 's
| Seqs ('s, 'Port, 'Dataaccess, 'Subpaccess, 'Parameter, 'Data,
'Subprogram) BA-action ('s, 'Port, 'Dataaccess, 'Subpaccess,
'Parameter, 'Data, 'Subprogram) BA-action
| Sets ('s, 'Port, 'Dataaccess, 'Subpaccess, 'Parameter, 'Data,
'Subprogram) BA-action ('s, 'Port, 'Dataaccess, 'Subpaccess,
'Parameter, 'Data, 'Subprogram) BA-action
| If 's bexp ('s, 'Port, 'Dataaccess, 'Subpaccess, 'Parameter,
'Data, 'Subprogram) BA-action ('s, 'Port, 'Dataaccess, 'Subpaccess,
'Parameter, 'Data, 'Subprogram) BA-action
| While 's bexp ('s, 'Port, 'Dataaccess, 'Subpaccess, 'Parameter,
'Data, 'Subprogram) BA-action

datatype ('s, 'Dispatcher, 'Port, 'Subpaccess) Behavior-Condition =
DispatchCond 'Dispatcher
| DispatchCond-TriggerLogicExp ('Dispatcher option × 'Port) set
| DispatchCond-Subpaccess 'Dispatcher option × 'Subpaccess
| DispatchCond-Stop 'Dispatcher × Event
| DispatchCond-Timeout 'Dispatcher × Time option
| ExecuteCond-LogicExp 's bexp
| ExecuteCond-Timeout Time option

record ('s, 'Dispatcher, 'Port, 'Dataaccess, 'Subpaccess, 'Parameter,
'Data, 'Subprogram) BA-transition = src-state :: BA-state
des-state :: BA-state
condition :: ('s, 'Dispatcher, 'Port, 'Subpaccess) Behavior-Condition
option
actions :: ('s, 'Port, 'Dataaccess, 'Subpaccess, 'Parameter, 'Data,
'Subprogram) BA-action list

record ('Data, 'Subprogram, 'Thread, 'Process, 'System) BA-var =
var-name :: string
```

Figure 21: The code of Behavior annex in Isabelle/HOL.

system architecture. This not only restricts the possibility of formal analysis of AADL models, but cannot conduct model checking and verification. It is necessary to propose a way to specify AADL models with formal models. However, AADL is mainly a mathematical model, which cannot be used to automatically verify properties of a given AADL model. In order to provide evidence of model checking and enable the proof of semantics preservation of system running, the informal execution semantics of AADL formalized directly in Isabelle/HOL are considered an operational semantics.

In this article, the AADL semantics is given an operational semantics, which is delivered from the AADL informal execution semantics and can be compared with the informal one. The main benefit with operational semantics is that it is based on a rigorous mathematical foundation and is built on the same principles as functional programming languages. Such benefits determined us to define an underlying operational semantics for AADL and its Behavior Annex, and consequently implement the verification in Isabelle/HOL.

```
AADL_model ::=   { features }
                 { connections }
                 { subprogramcalls }
                 { data_type }
                 { data_impl }
                 { subprogram_type }
                 { subprogram_impl }
                 { thread_type }
                 { thread_impl }
                 { process_type }
                 { process_impl }
                 { system_type }+
                 { system_impl }
                 { behavior_annex }
```

Figure 22: The syntax of the model.

5.1. Semantics of Behavior Annex. The AADL model is completed with behavioral descriptions using the Behavior annex, like computation and communication for threads. Thus, there is a relation between the AADL execution model and the Behavior annex. The execution model specifies when the Behavior annex is executed and on which data it is executed, while the Behavior annex acts in a thread (or a subprogram) and describes behaviors more precisely. For this purpose, the semantic specifications given as above will be enriched by the Behavior annex. Since the behavior is explicitly expressed by atomic transitions, the operational semantics of the Behavior annex is defined based on the refinement of the rule of each transition in the Behavior annex, and the execution semantics of the Transition is based on the semantics of the Actions in itself. This section begins by describing how to formalize the meaning of Behavior annex using automaton. And then, the constituents of the Behavior annex and their semantics are defined (including transition system, action and expression language, etc.).

5.1.1. Formalization of Behavior Annex by Automaton. We present the formalization of a Behavior annex by using an incomplete automaton AM with several variables. The AM is used to interpret the meaning of the whole Behavior annex, and $AM = (S, s0, V, P, B, T, C)$ is defined as

(i) S: the states set of AM.
(ii) $s0$: the initial state, $s0 \in S$.
(iii) V: the local variables set of AM.
(iv) P: the ports set of AM (including the input set IP and the output set OP, $P = IP \cup OP$).

Table 2: Description and code of syntax rules.

Description	Code in Isabelle/HOL
(N1) The defining identifier for a component type must be unique in the namespace of the package within which it is declared.	definition type_name_valid:: "('s, 'Dispatcher, 'Port, 'Dataaccess, 'Subpaccess, 'Parameter, 'Subprogramcall, 'Subprogramcalls, 'Connection, 'Data, 'Subprogram, 'Thread, 'Process, 'System, 'BehaviorAnnex) AADL_model ⇒ bool" where "type_name_valid m ≡ (∀dt1 dt2. (data_tp m)≠None ∧ dt1≠dt2 ⟶ (type_name (the (data_tp m) dt1))≠(type_name (the (data_tp m) dt2))) ∧ (∀sp1 sp2. (subprogram_tp m)≠None ∧ sp1≠sp2 ⟶ (type_name (the (subprogram_tp m) sp1))≠(type_name (the (subprogram_tp m) sp2))) ∧ (∀thd1 thd2. (thread_tp m)≠None ∧ thd1≠thd2 ⟶ (type_name (the (thread_tp m) thd1))≠(type_name (the (thread_tp m) thd2))) ∧ (∀pro1 pro2. (process_tp m)≠None ∧ pro1≠pro2⟶ (type_name (the (process_tp m) pro1))≠(type_name (the (process_tp m) pro2))) ∧ (∀sys1 sys2. sys1≠sys2 ⟶ (type_name ((system_tp m) sys1))≠(type_name ((system_tp m) sys2)))"
(N1) A component implementation name consists of a component type identifier and a component implementation identifier separated by a dot ("."). The first identifier of the defining component implementation name must name a component type that is declared in the same package as the component implementation, or name an alias to a component type in another package.	definition impl2type_name_valid:: "('s, 'Dispatcher, 'Port, 'Dataaccess, 'Subpaccess, 'Parameter, 'Subprogramcall, 'Subprogramcalls, 'Connection, 'Data, 'Subprogram, 'Thread, 'Process, 'System, 'BehaviorAnnex) AADL_model ⇒ bool" where "impl2type_name_valid m ≡ (∀dt. (data_im m)≠None ∧ (data_tp m)≠None ∧ (the (data_im m) dt)≠None ⟶ (get_prename_impl_dt m dt)=(type_name (the (data_tp m) dt))) ∧ (∀sp. (subprogram_im m)≠None ∧ (subprogram_tp m)≠ None ∧ (the (subprogram_im m) sp)≠None ⟶ (get_prename_impl_sp m sp)=(type_name (the (subprogram_tp m) sp))) ∧ (∀thd. (thread_im m)≠None ∧ (thread_tp m)≠None ∧ (the (thread_im m) thd)≠None ⟶ (get_prename_impl_thd m thd)=(type_name (the (thread_tp m) thd))) ∧ (∀pro. (process_im m)≠ None ∧ (process_tp m)≠None ∧ (the (process_im m) pro)≠None ⟶ (get_prename_impl_pro m pro)=(type_name (the (process_tp m) pro))) ∧ (∀sys. (system_im m)≠None ∧ (the (system_im m) sys)≠ None ⟶ (get_prename_impl_sys m sys)=(type_name ((system_tp m) sys)))"
......	......

(v) B: the Boolean formulas set of AM (these multisorted logical formulas are defined over the vocabulary available in the lexical scope of a Behavior annex: AADL value constants, port, state, and variable names, $B = S \cup V \cup P$).

(vi) T: the transition function set defines the transition system of AM, $T \in F \times S \longrightarrow F \times S$. Each specified transition has its quadruple (s, g, a, d) which defines the source state s, guard formula g, action formula a, and destination state t. includes the guard g and the action a.

(vii) g denotes the source formula of a transition defined on V and I.

(viii) a represents the target formula of a transition defined from V and P.

(ix) C: the constraint set of AM, which denotes the invariants (properties, requirements) of the denoted AADL object and denoted by the multisorted logical formulas, $C \in B$. It must always equal 0.

If the thread is in dispatch status, the states (initial, complete, final) of Behavior annex can be observed, as these states are specified in a transition and they can be mapped to the execution of the outside components. If the thread is under execution, the detail of states cannot be observed, as their execution states are just held in a running thread and they are the internal states related to the processor in the whole Behavior annex. So our work defines the formal execution semantics of Behavior annex as two parts: one is about transitions, and the other is about Actions in transitions. These two parts are described by big-step semantics through a global state (shared variables), and they can be recombined to the integrated semantics of whole Behavior annex. Furthermore, the Action semantics can be mapped to some imperative language in the future work, and its formal semantics would make the preservation more clear.

Table 3: Description and code of naming rules.

Description	Code in Isabelle/HOL
(N1) The defining identifier for a component type must be unique in the namespace of the package within which it is declared.c	definition type_name_valid:: "(′s, ′Dispatcher, ′Port, ′Dataaccess, ′Subpaccess, ′Parameter, ′Subprogramcall, ′Subprogramcalls, ′Connection, ′Data, ′Subprogram, ′Thread, ′Process, ′System, ′BehaviorAnnex) AADL_model ⇒ bool" where "type_name_valid m ≡ (∀dt1 dt2. (data_tp m)≠None ∧ dt1≠dt2 ⟶ (type_name (the (data_tp m) dt1))≠(type_name (the (data_tp m) dt2))) ∧ (∀sp1 sp2. (subprogram_tp m)≠None ∧ sp1≠sp2 ⟶ (type_name (the (subprogram_tp m) sp1))≠(type_name (the (subprogram_tp m) sp2))) ∧ (∀thd1 thd2. (thread_tp m)≠None ∧ thd1≠thd2 ⟶ (type_name (the (thread_tp m) thd1))≠(type_name (the (thread_tp m) thd2))) ∧ (∀pro1 pro2. (process_tp m)≠None ∧ pro1≠pro2⟶ (type_name (the (process_tp m) pro1))≠(type_name (the (process_tp m) pro2))) ∧ (∀sys1 sys2. sys1≠sys2 ⟶ (type_name ((system_tp m) sys1))≠(type_name ((system_tp m) sys2)))"
(N1) A component implementation name consists of a component type identifier and a component implementation identifier separated by a dot ("."). The first identifier of the defining component implementation name must name a component type that is declared in the same package as the component implementation, or name an alias to a component type in another package.	definition impl2type_name_valid:: "(′s, ′Dispatcher, ′Port, ′Dataaccess, ′Subpaccess, ′Parameter, ′Subprogramcall, ′Subprogramcalls, ′Connection, ′Data, ′Subprogram, ′Thread, ′Process, ′System, ′BehaviorAnnex) AADL_model ⇒ bool" where "impl2type_name_valid m ≡ (∀dt. (data_im m)≠None ∧ (data_tp m)≠None ∧ (the (data_im m) dt)≠None ⟶ (get_prename_impl_dt m dt)=(type_name (the (data_tp m) dt))) ∧ (∀sp. (subprogram_im m)≠None ∧ (subprogram_tp m)≠ None ∧ (the (subprogram_im m) sp)≠None ⟶ (get_prename_impl_sp m sp)=(type_name (the (subprogram_tp m) sp))) ∧ (∀thd. (thread_im m)≠None ∧ (thread_tp m)≠None ∧ (the (thread_im m) thd)≠None ⟶ (get_prename_impl_thd m thd)=(type_name (the (thread_tp m) thd))) ∧ (∀pro. (process_im m)≠None ∧ (process_tp m)≠None ∧ (the (process_im m) pro)≠None ⟶ (get_prename_impl_pro m pro)=(type_name (the (process_tp m) pro))) ∧ (∀sys. (system_im m)≠None ∧ (the (system_im m) sys)≠ None ⟶ (get_prename_impl_sys m sys)=(type_name ((system_tp m) sys)))"
...	...

5.1.2. Semantics of Transition in Behavior Annex. Actually, the transition system, which is described by three sections (variable declarations, state declarations, and transition declarations mentioned in Section 4.1.4), is a refinement of the AADL Behavior annex, and it is created by linking two states using a guarded automaton. A transition ($Si-$ [conditions] $\longrightarrow Sj${actions}) specifies the behavior as a state change from a source state Si to a destination state Sj, which can be guarded by conditions (dispatch or execution). In this section, we specify the meaning of the elements in transition and use them to express the semantics of transition.

(1) Variables: The variables, which are temporary through the whole Behavior annex subclause, declare the identifiers that represent local variables and record intermediate results within the scope of the whole Behavior annex subclause. They can be used to hold the values of out parameters on subprogram calls and also can hold input from incoming port queues or values read from data components in the AADL specification.

(2) States: The states, which may be mapped to the various thread states, are categorized as initial, complete, final, or execution state. The initial state means thread state halted, the complete state means thread state awaiting for dispatch (suspend or resume), the final state means thread state stopped, and the execution state means the rest of thread states (running) that are not be observable.

(3) Transitions: The transitions define an execution automaton in a thread. They may be guarded by dispatch or execute conditions, and the sequence of actions within each transition can be executed atomically when their conditions are satisfied. Dispatch conditions explicitly specify dispatch trigger conditions out of a complete state to another state. Execute conditions specify transition conditions out of an execution state. Actions can be subprogram

Table 4: Description and code of other rules.

<table>
<tr><th>Description</th><th>Code in Isabelle/HOL</th></tr>
<tr><td>(1) A thread models a concurrent task or an active object, that is, a schedulable unit that can execute concurrently with other threads. Each thread represents a sequential flow of control that executes instructions within a binary image produced from the source text. One or more AADL threads may be implemented in a single operating system thread. A thread always executes within the virtual address space of a process; that is, the binary images making up the virtual address space must be loaded before any thread can execute in that virtual address space. Threads are dispatched; that is, their execution is initiated periodically by the clock or by the arrival of data or events on ports, or by the arrival of subprogram calls from other threads.</td><td>definition thread_thread2system_valid:: "('s, 'Dispatcher, 'Port, 'Dataaccess, 'Subpaccess, 'Parameter, 'Subprogramcall, 'Subprogramcalls, 'Connection, 'Data, 'Subprogram, 'Thread, 'Process, 'System, 'BehaviorAnnex) AADL_model ⇒ bool"
where "thread_thread2system_valid m ≡ ∀sys. ∃sc1 sc2. (if ((system_im m)≠None ∧ (the (system_im m) sys)≠None ∧ (impl_subcomps (get_sysimpl m sys))≠{})
then (sc1∈(impl_subcomps (get_sysimpl m sys))
⟶ (case sc1 of SCThd _ ⇒ True
| SCPro pro ⇒ (if ((process_im m)≠None ∧ (the (process_im m) pro)≠None ∧ (impl_subcomps (get_proimpl m pro))≠{})
then (sc2∈(impl_subcomps (get_proimpl m pro)) ⟶
(case sc2 of SCThd _ ⇒ True
| _ ⇒ False))
else False)
| _ ⇒ False))
else False)" definition thread_thread2process_valid:: "('s, 'Dispatcher, 'Port, 'Dataaccess, 'Subpaccess, 'Parameter, 'Subprogramcall, 'Subprogramcalls, 'Connection, 'Data, 'Subprogram, 'Thread, 'Process, 'System, 'BehaviorAnnex) AADL_model ⇒ bool"
where "thread_thread2process_valid m ≡ ∀pro. ∃sc. (if ((process_im m)≠None ∧ (the (process_im m) pro)≠None ∧ (impl_subcomps (get_proimpl m pro))≠{})
then (sc∈(impl_subcomps (get_proimpl m pro)) ⟶ (case sc of SCThd _ ⇒ True
| _ ⇒ False))
else False)"</td></tr>
<tr><td>...</td><td>...</td></tr>
</table>

calls, receiving of input and sending of output, assignments to variables, read/write to data components, or other activities.

We describe a transition as a series of atomic operation in Behavior annex, and a series of Transitions are composed into a whole behavior. As a transition is mainly supported to complete the thread component with behavior handling inputs and outputs in order to enrich the communication mechanism, so in some sense, talking about the semantics of whole transitions is about Behavior annex actually. Our work defines the semantics of Behavior annex by the operational big-step semantics presented by the automaton AM as T=(s, g, a, d), and they are defined inductively as follows:

T: 's BA_Transition

s, d: State

a: Actions

g: Conditions

The core state space is denoted in terms of states by the type 's different from the state of transitions, it is polymorphic, and its semantics is augmented with control flow information in Isabelle/HOL as follows.

Where the type variable state 's is regarded as a set of variable states and related to the variable state in Actions when the execution is in a normal state Normal s. Besides, 's can hold the value of variables on inputs or outputs, and it is attached to the receiving or sending events as a message Msg s as an option.

Moreover, a transition is guarded by conditions, and conditions can be either dispatch conditions or execution conditions as shown in Figure 19. We consider a dispatch condition g of T formed by clock c as its dispatch trigger; it means the dispatch condition is presented as time trigger. An execution condition g of T is considered logical value expressions. The semantic of transition is defined inductively by the rules in Isabelle/HOL as shown in Figure 23.

5.1.3. Semantics of Action in Behavior Annex. This section defines the semantics of Actions by the operational big-step semantics. Actions of the Behavior annex define actions performed during transitions. Actions associated with transitions are action blocks that are presented in Figure 20, where the single action can be defined as control structures such as basics, conditionals, and loops. The action_sequence means it is executed in order, while action_set can be executed in any order.

The basic_action can be empty, assignment, communication, or time-consuming. The assignment_action is reference for the value assignment. The communication_action is reference for receiving and sending data, event, or event data on the inputs and outputs. The Timed_action is predefined computation actions.

Since this section should be related to the semantics of transitions and be a part of it, the semantics of Action is defined as $\Gamma : : \langle s, a \rangle \Rightarrow d$, which means in the procedure environment Γ execution transforms the source state s to the destination state d. Actually, the destination state d is the

```
type-synonym  ('s, 'Dispatcher, 'Port, 'Dataaccess, 'Subpaccess,
'Parameter, 'Data, 'Subprogram, 'Thread, 'Process, 'System,
BehaviorAnnex) BA-body
                              = 'BehaviorAnnex ⇒ ('s, 'Dispatcher, 'Port,
'Dataaccess, 'Subpaccess, 'Parameter, 'Data, 'Subprogram, 'Thread,
'Process, 'System) behavior-annex-conf option

inductive
     BA-bigstep :: [('s, 'Dispatcher, 'Port, 'Dataaccess, 'Subpaccess,
'Parameter, 'Data, 'Subprogram, 'Thread, 'Process, 'System,
'BehaviorAnnex) BA-body,
                           ('s, 'Dispatcher, 'Port, 'Dataaccess, 'Subpaccess,
'Parameter, 'Data, 'Subprogram) BA-transition,
                                  ('s, 'p, 'f, 'Dispatcher, 'Port, 'Dataaccess,
'Subpaccess, 'Parameter, 'Data, 'Subprogram, 'Thread, 'Process,
'System, 'BehaviorAnnex) AADL-state,
                                  ('s, 'p, 'f, 'Dispatcher, 'Port, 'Dataaccess,
'Subpaccess, 'Parameter, 'Data, 'Subprogram, 'Thread, 'Process,
'System, 'BehaviorAnnex) AADL-state] ⇒ bool
                  (-⊢⟨-,-⟩→- [93,92,94,94] 95)
                                         for  BA-BODY :: ('s, 'Dispatcher, 'Port,
'Dataaccess, 'Subpaccess, 'Parameter, 'Data, 'Subprogram, 'Thread,
'Process, 'System, 'BehaviorAnnex) BA-body
where
Tran-ini2com: [[BA-BODY BA = Some ba-conf ;
                ba-tran ∈ (ba-trans ba-conf );
                ba-var ∈ (ba-vars ba-conf );
                (snd (src-state ba-tran)) = INITIAL;
                (snd (des-state ba-tran)) = COMPLETE;
               (snd ((ba-st s) BA)) = INITIAL ∧ (fst (src-state ba-tran))
= (fst ((ba-st s) BA));
                     (snd ((ba-st t) BA)) = COMPLETE ∧ (fst (des-state
ba-tran)) = (fst ((ba-stt) BA));
                (condition ba-tran) = None
                ∨ (the (condition ba-tran) = DispatchCond -)
             ∨ (the (condition ba-tran) = DispatchCond-TriggerLogicExp
{(-,-)})
                   ∨ (the (condition ba-tran) = DispatchCond-Subpaccess
(-,-))
                ∨ (the (condition ba-tran) = DispatchCond-Stop (-,-))
                ∨ (the (condition ba-tran) = DispatchCond-Timeout (-,-))
                 ∨ ((the (condition ba-tran) = ExecuteCond-LogicExp be)
∧ (case s1 of Normal s' ⇒ s' ∈ be));
                              acts=(actions-block ba-tran);
                s1=((ba-var-st s) ba-var);
                s2=((ba-var-st t) ba-var);
                ACT-BODY⊢⟨acts,s1⟩ ⇒ s2]]
               =⇒BA-BODY⊢⟨ba-tran, s⟩ →t
......
```

Figure 23: Big-step semantics of transition in Isabelle/HOL.

destination state d of its transition. To connect with the automaton T, we refinement a in the automaton T as a new automaton A and reconstitute the automata T'=(s, g, true, t) ∪ A and A=(t, true, a, d) where a in A and a in the previous T are not same, and the former is the detailed implementation of the latter. T' and A are defined by the case on Actions as follows:

(i) Action sequence is a list type of executions. For example, action_sequence a = [a1; a2] separates A=(t, true, a, d) into A1=(t, true, a1, t') and A2=(t', true, a2, d) by introducing an intermediate state t', and then, T'=(s, g, true, t) ∪ A1 ∪ A2 by the union of them.

(ii) Action set is a disorderly combination of executions. For instance, action_set a = [a1 & a2] makes that A =(A1 × A2), which the composed elements are A1 = (t1, true, a1, d1), A2 = (t2, true, a2, d2), t=(t1, t2), and d=(d1, d2).

(iii) Empty_action of basic_action NULL can be represented as an invalid operation to the states and defined by SKIP.

(iv) Assignment_action of basic_action v\coloneq e represents a variable state transition and it is defined by A = (t, true, v' = e, d) where v' represents the successor state of v.

(v) Communication_action of basic_action is divided into the output port action port!(e) and the input port action port?(v). The output can be defined by A=(t, true, port = e, d). The input can be defined by A=(t, true, v' = port, d) where v' represents the successor state of v.

(vi) Timed_action of basic_action computation(t1. . .tN) represents the execution time of the action block. It is specified as two ports—pb (port begin) and pe (port end), and defined by A = {(s, true, pb, i), (i, pe, true, d)}, where i is an intermediate state as a complete state and timed constraint Val(pb + t1) ≤ Val(pe + tN).

(vii) Conditional_action, for instance, if(exp) a1 else a2 end if can be defined by T' = {(s, g, true, t1), (s, g, true, t2)} ∪ A1 ∪ A2 which A1 = (t1, true, a1, d), A2 = (t2, true, a2, d), and the guard g is corresponding to the logical expression exp in conditional_action.

(viii) While_loop_action, for instance, while(exp) { a } can be defined by T' = {(s, g, t g, true, d), (t2, g, true, t1), (t2, g, true, d)} ∪ A, where the guard g is corresponding to the logical expression exp in while_loop_action and A=(t1, true, a, t2).

(ix) For_loop_action, for instance, for(I in e) { a } can be translated by the action sequence [a1; . . .; an], where ai results from the substitution of i by the i_th element value of e in a.

The semantic of Action is defined inductively by the rules in Isabelle/HOL as shown in Figure 24. The procedure environment *act-body* denotes the static procedure declarations as mapping from subprogram names to actions programs of Behavior annex and defines the execution of command c that transforms the initial state s to the final state t under *act-body*.

5.1.4. Semantics of Expressions in Behavior Annex. Expressions consist of logical expressions, relational expressions, and arithmetic expressions like the expressions of imperative language. Values of expressions can be variables, constants, or the result of another expression. In AADL, expressions are used as logical conditions of guards in transitions or logical expressions in conditional actions, or as values for basic actions. Values of variable expression are evaluated from inputs, local variables, and data subcomponents. Values of constant expression are Boolean, numeric or string literals, and property values. In our work, expressions are defined by the type variables's as a set of states in Isabelle/HOL and related to the variable state in Actions.

5.2. Semantics of AADL Components. There are a great number of components that can be used to build hierarchical models in AADL, and it makes AADL have a great capacity of expression. In our work, the AADL model is viewed as a set of concurrent tasks scheduled by a processor and asynchronously interacted. Generally, we consider the following components: data, thread, process, and processor. These components are connected through AADL port connections, completed with a set of standard properties, and finally grouped in the system component. However, in a running system model, a process component represents the virtual address space and scheduled by the processor. Indeed, a thread component is the minimum schedulable unit under execution, and then, they are concepts that require detailed attention as they include the behavior of AADL. What's more, our goal is to verify system behavior, so in this section, we focus our experimentation on software components in the software model and thread management. Besides, the mode semantics is not yet completely stabilized in the standard so we take no account of mode management, and our work highlights several constructions(like Global_Timer, Dispatcher, and Scheduler) to make the AADL system model running and also its semantics of components more coherent.

According to the AADL standard, the running model of software components can be described by execution automaton; the following paragraph describes that the software components are applied to the execution automaton and the management of communication (Figure 25).

5.2.1. Semantics of Thread Component Execution Model. First of all, the necessary Thread execution model elements are currently specified according to the AADL running models by two points—dispatching and scheduling, and they both can be expressed by an automaton as shown in Figure 26.

```
type-synonym ('s, 'Port, 'Dataaccess, 'Subpaccess, 'Parameter,
'Data, 'Subprogram) act-body = 'Subprogram ⇒ ('s, 'Port,
'Dataaccess, 'Subpaccess, 'Parameter, 'Data, 'Subprogram)
BA-action option
inductive
BA-action-bigstep :: [('s, 'Port, 'Dataaccess, 'Subpaccess, 'Parameter,
'Data, 'Subprogram) act-body,
                        ('s, 'Port, 'Dataaccess, 'Subpaccess, 'Parameter,
'Data, 'Subprogram) BA-action, 's vstate, 's vstate] ⇒ bool
                     (-⊢⟨-,-⟩ ⇒ -[97,96,98,98] 99)
                  for ACT-BODY :: ('s, 'Port, 'Dataaccess, 'Subpaccess,
'Parameter, 'Data, 'Subprogram) act-body
where
SKIP: ACT-BODY⊢⟨Skip, Normal s⟩ ⇒ Normal s
| Assign: ACT-BODY⊢⟨Basic-Assign ba, Normal s⟩ ⇒ Normal (ba
s)
| CommunSend: ACT-BODY⊢⟨Basic-CommunSend bcs, Msg m⟩ ⇒
Msg (bcs m)
| CommunRecv: ACT-BODY⊢⟨Basic-CommunRecv bcr, Normal s⟩ ⇒
Normal (bcr s)
| CommunFreeze: ACT-BODY⊢⟨Basic-CommunFreeze, Normal s⟩ ⇒
Normal s
| CommunInisend: ACT-BODY⊢⟨Basic-CommunInisend, Normal s⟩ ⇒
Normal s
| CommunCallsp: [[ACT-BODY sp=Some baact;
                ACT-BODY⊢⟨Basic-CommunCallsp sp paras, Normal s⟩ ⇒
Normal (paras s);
                ACT-BODY⊢⟨baact,Normal (paras s)⟩⇒t]]
              =⇒ ACT-BODY⊢⟨Basic-CommunCallsp sp paras, Normal
s⟩ ⇒ t
| Seqs: [[ACT-BODY⊢⟨a1, Normal s⟩⇒s';
         ACT-BODY⊢⟨a2, s'⟩ ⇒ t]]
        =⇒ ACT-BODY⊢⟨Seqs a1 a2, Normal s⟩ ⇒ t
| Sets: [[ACT-BODY⊢⟨a1, Normal s⟩ ⇒ t;
         ACT-BODY⊢⟨a2, Normal s⟩ ⇒ t]]
        =⇒ ACT-BODY⊢⟨Sets a1 a2, Normal s⟩ ⇒ t
| IfTrue: [[s∈be; ACT-BODY⊢⟨a1, Normal s⟩ ⇒ t]]
          =⇒ ACT-BODY⊢⟨If be a1 a2, Normal s⟩ ⇒ t
| IfFalse: [[s∉be; ACT-BODY⊢⟨a2, Normal s⟩ ⇒ t]]
            =⇒ ACT-BODY⊢⟨If be a1 a2, Normals⟩⇒t
| WhileTrue: [[s∈be;
              ACT-BODY⊢⟨a, Normal s⟩ ⇒ s';
              ACT-BODY⊢⟨While be a, s'⟩ ⇒ t]]
            =⇒ACT-BODY⊢⟨While be a, Normal s⟩ ⇒ t
| WhileFalse: [[s∉be]]
              =⇒ ACT-BODY⊢⟨While be a, Normal s⟩ ⇒ Normal s
```

Figure 24: Big-step semantics of Action in Isabelle/HOL.

The dashed box represents Thread_Computation state, and in the Thread_Computation of the execution automaton, the Thread internal behavior is carried out according to the behavior expression, which was described in Section 5.1. In order to integrate all the Thread execution states in one Thread, the other execution states are generated for each Thread. Every Thread execution states transition is managed by its previous states, its parent Process, and System execution state. They also are both decided by the next state of the Transition in Behavior annex, so the semantics of Transition are embedded in this part for connecting with Thread_Computation. In the case of execution Initialize, the

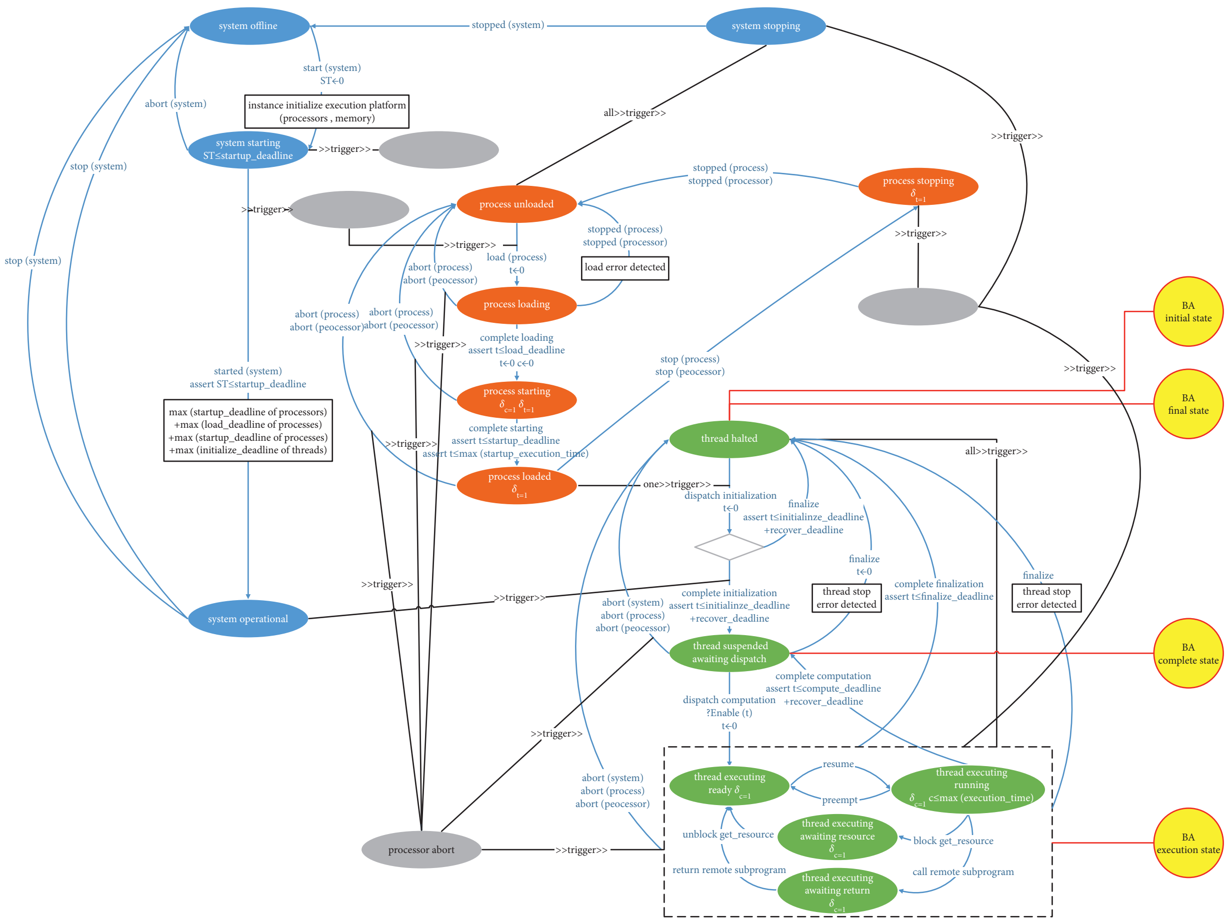

FIGURE 25: Whole execution automaton.

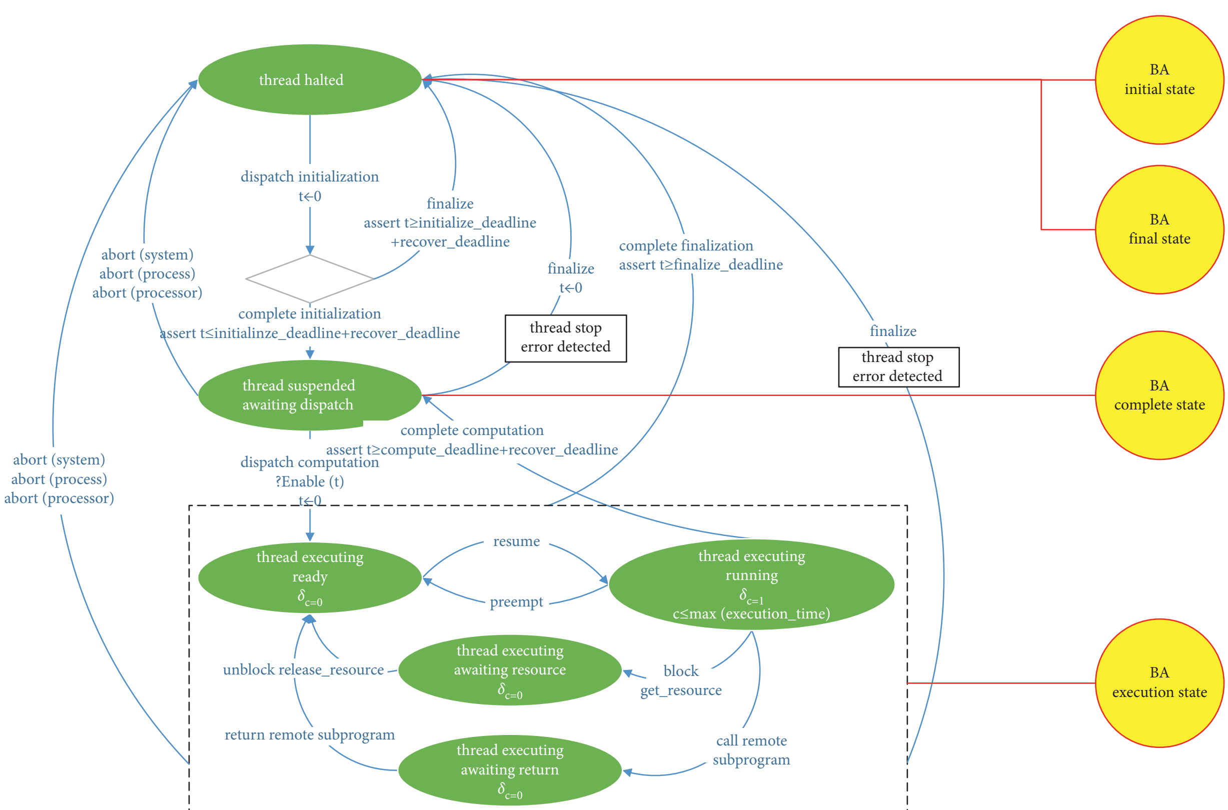

FIGURE 26: Thread execution automaton.

code of state conditions management part in Isabelle/HOL is shown in Figure 27.

In the transitions automaton, the execution time, the elapsed time, and waiting time are controlled by the creation of the global clock and the various Deadline (initialize_Deadline, compute_Deadline, recover_Deadline, etc.), and they provide the possibility to manage several kinds of Thread including periodical, aperiodic, and sporadic ones. In the case of execution Initialize, the code of temporal part in Isabelle/HOL is shown in Figure 28.

To support sending and receiving messages (data, event, and data_event) between components, the Connections provide the communication mechanism to manage messages from the source to the destination point. They are typed with Access_Connections and Port_Connections. The Access_Connections type is used to model the data flow shared by access between components like Subprogram_Access and Data_Access, and the Port_Connections type is used to model transfer of data or events between ports. All types also include the Parameter_Connections, which models a data flow representing the parameter of subprogram included in a Thread, but this type is not managed in our transformation on account of the practical frequency.

Now, we focus our presentation on the Port_Connection type. It deals with the processing of the sent and received messages and the properties describe several behavioral features (like the Queue_Size, Queue_Processing_Protocol, and some other properties) to define a queue of messages associated with a port. The processing of the messages received by Thread is carried out when it is in the execution state Thread_Computation. This state is reached after the dispatch of Thread. Unfortunately, these necessary concepts are not described explicitly in the AADL standard, so we should take into account an execution model definition.

In our work, several processing conditions are added on the Thread semantic to specify the Connection model. For example, the port queue state is estimated and the messages on the queue are handled by a dispatch mechanism. This mechanism is dedicated to detach the internal behavior of a Thread and the message consumption. In the Thread execution model, the dispatch action is performed on the transition between the state Thread_Suspend_Waiting_Dispatch and Thread_Computation. Generally, the message once arrives on the ports will be copied in variables in the Behavior of the Thread through the dispatch. In the execution state of Thread_Computation, the Thread handles its behavior with data and event copies. So, we combine the state of the Behavior and add the definitions "is_port_queue_empty" and "handle_port" to specify and to conceptualize the Connections based on the AADL standard properties. In the case of execution Initialize, the code in Isabelle/HOL is presented in Figure 29. For these additions, they are mainly used at a design level for code generation and they also make the semantics of Behavior add into the model execution semantics to be a whole complete and continuous semantics.

5.2.2. Semantics of Process Component Execution Model. A process represents a virtual address space at runtime, so the Process execution model is driven by the processor mainly and it works on the state to affect its own Thread execution model inside in effect. We consider that the Process execution model is managed by the clock and express its parent System execution state as an automaton as shown in Figure 30.

In the transitions automaton, the execution time, the elapsed time, and waiting time are controlled by the creation of the global clock and the various Deadline (load_Deadline, startup_Deadline, etc.), and also the prestate and poststate must be satisfied. In the case of execution Load, the code of the process execution Load part in Isabelle/HOL is shown in Figure 31.

5.2.3. Semantics of System Component Execution Model. A system represents the runtime architecture of an actual system that consists of application software components and execution platform components, and it is the top hierarchy of the whole execution model, so the System execution model is only driven by the processor and it works on the state to affect its own Process and Thread execution model inside in effect. Same as the Process execution model, the system execution model is managed by the clock and it is presented as an automaton as shown in Figure 32.

In the case of execution Start_Complete, the code of the System execution Start_Complete part in Isabelle/HOL is shown in Figure 33.

5.3. Formal Verification for AADL

5.3.1. Proof system Framework. The calculation of the AADL execution model is actually a sequence of transitions. The computations set for whole executions with static information Σ is defined as $\Gamma(\Sigma)$. We use function $\Gamma(\Sigma, \rho, s, e)$ to present the computations of an execution system ρ starting up from an initial state s and execution e. A configuration of computation is defined as a triple $\delta = (\theta, s, e)$ where θ is specified as transition rules in execution model systems, which have the form $\Sigma \vdash (\theta_n, s_n, e_n) \longrightarrow (\theta_{n+1}, s_{n+1}, e_{n+1})$.

A specification in the proof system is a tuple $\langle pre, pst \rangle$, where *pre* is short for the precondition, and *pst* stands for the postcondition. For each computation $\delta \in \Gamma(\Sigma, \rho, s, e)$, the configuration at index i is denoted by δ_i, and we use θ_{δ_i}, s_{δ_i} and e_{δ_i} to signify the element inside $\delta_i = (\theta, s, e)$. We use A and C to denote assumption and commitment functions, respectively.

process ∈ (*get-pros-bysys m system*);
thread ∈ (*get-thds-bypro m process*);
port ∈ (*get-ports-bythd m thread*);
subpaccess ∈ (*get-subpaccesses-bythd m thread*);
dataaccess ∈ (*get-dataaccesses-bythd m thread*);
ps1=((*port-st s*) *port)* ∧ *spaccs1*=((*spacc-st s*) *subpaccess*);
(*pr-state* ((*pr-st s*) *process*))=*PRO-LOADED* ∧ (*pr-state* ((*pr-st t*) *process*))=*PRO-LOADED;*
(*th-state* ((*th-st s*) *thread*))=*HALTED;*
(*th-state* ((*th-st t*) *thread*))=*SUSPENDED-WAITING-DISPATCH;*
(*snd* ((*ba-st s*) *th-ba*))=*INITIAL* ∧ *fst* ((*ba-st s*) *th-ba*) = *fst* (*src-state th-ba-tran*);
(*snd* ((*ba-st s*) *th-ba*))=*INITIAL* ∧ *fst* ((*ba-st s*) *th-ba*) = *fst* (*src-state th-ba-tran*);
(*snd* ((*ba-st t) th-ba*))=*COMPLETE* ∧ *fst* ((*ba-st t*) *th-ba*) = *fst* (*des-state th-ba-tran*);
if ((*is-port-queue-empty s port*)=*False*)
  then ((*ps2*=*handle-port s port*) ∧ (*spaccs2*=*spaccs1*))
  else ((*spaccs2*=*handle-spaccess s subpaccess*) ∧ (*ps2*=*ps1*));
((*port-st t*) *port*) = *ps2* ∧ ((*spacc-st t*) *subpaccess*) = *spaccs2*;
(*BA-BODY th-ba*) = *Some th-ba-conf;*
BA-BODY⊢⟨*th-ba-tran, s*⟩ → *t*

Figure 27: The state conditions management of Thread execution Initialize semantic.

gt = (*cur-time s*);
(*begin-time* ((*th-st s) thread*)) = (*cur-time s*);
(*action-begin-time* ((*th-st s*) *thread*)) = (*cur-time s*);
(*elapsed-time* ((*th-st t*) *thread*)) ≤ (*the* (*thd-initialze-deadline* (*the* (*thread-type.thd-properties* (*the* (*thread-tp m*) *thread*)))))+(*the* (*thd-recover-deadline* (*the* (*thread-type.thd-properties* (*the* (*thread-tp m*) *thread*)))));
(*cur-time t*) = (*cur-time s*) + (*elapsed-time* ((*th-st t*) *thread*));
(*cur-time t*) = (*action-begin-time* ((*th-st s*) *thread*)) + (*elapsed-time* ((*th-st t*) *thread*));
(*exe-time* ((*th-st t*) *thread*)) ≤ (*elapsed-time* ((*th-st t*) *thread*));

Figure 28: The temporal part of Thread execution Initialize semantic.

if ((*is-port-queue-empty s port*)=*False*)
then ((*ps2*=*handle-port s port*) ∧ (*spaccs2*=*spaccs1*))
else ((*spaccs2*=*handle-spaccess s subpaccess*) ∧ (*ps2*=*ps1*));
((*port-st t*) *port*) = *ps2* ∧ ((*spacc-st t*) *subpaccess*) = *spaccs2;*

Figure 29: The connection part of Thread execution Initialize semantic.

$$\begin{aligned} A(\Sigma, pre) &\equiv \left\{\rho \mid s_{\delta_i} \in pre \wedge \left(\forall i < (\text{length}\,(\delta) - 1) \cdot (\Sigma \vdash \delta_i \longrightarrow \delta_{i+1}) \longrightarrow \left(s_{\delta_i}, s_{\delta_{i+1}}\right)\right)\right\}, \\ C(\Sigma, pst) &\equiv \left\{\rho \mid \left(\forall i < (\text{length}\,(\delta) - 1) \cdot (\Sigma \vdash \delta_i \longrightarrow \delta_{i+1}) \longrightarrow \left(s_{\delta_i}, s_{\delta_{i+1}}\right)\right) \wedge \left(\theta_{\text{last}\,(\delta)} = \lfloor \bot \rfloor \longrightarrow s_{\delta_n} \in pst\right)\right\}. \end{aligned} \tag{1}$$

We define validity of specification for executions as

$$\Sigma \vDash \rho \,\text{sat}\, \langle \text{pre}, \text{pst} \rangle \equiv \forall s, x. \Gamma(\Sigma, \rho, s, e) \cap A(\Sigma, \text{pre}) \subseteq C(\Sigma, \text{pst}). \tag{2}$$

It represents that the set of computations ω, which starts at the configuration (θ, s, e), with $s \in pre$ and a computation $\delta \in \omega$. If an execution terminates, then the final states belong to *pst*.

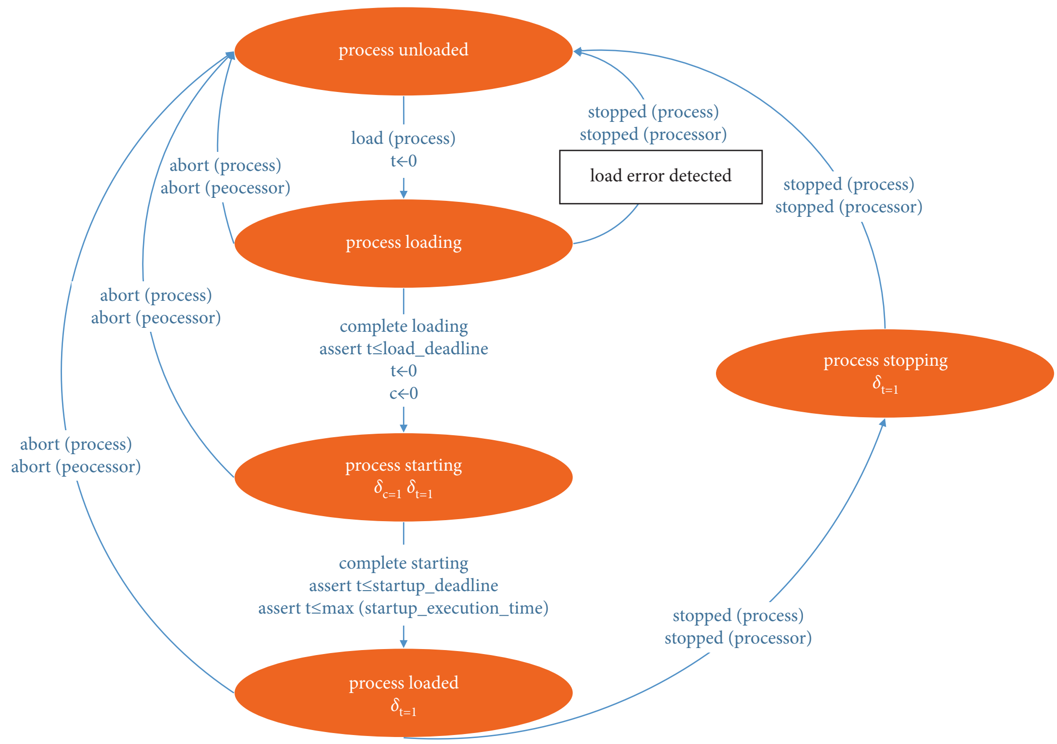

FIGURE 30: Process execution automaton.

sy-state ((sy-st s) system))=SYS-OPERATIONAL;
process∈ (get-pros-bysys m system);
(*pr-state ((pr-st s) process))=PRO-UNLOADED*;
(*pr-state ((pr-st t) process))=PRO-LOADING*;
gt = (*cur-time s*);
(*begin-time* ((*pr-st s*) *process*)) = (*cur-time s*);
(*action-begin-time* ((*pr-st s*) *process*)) = (*cur-time s*);
(*cur-time t*) = (*cur-time s*) + (*elapsed-time* ((*pr-st t*) *process*));
(*cur-time t*) = (*action-begin-time* ((*pr-st s*) *process*)) + (*elapsed-time*
((*pr-st t*) *process*));
(*exe-time* ((*pr-st t*) *process*)) ≤ (*elapsed-time* ((*pr-st t*) *process*))

FIGURE 31: The process execution Load semantic.

5.3.2. Invariant Verification. The core of the correctness proof shows the invariance of states between components generated from it. The proof proceeds by induction on the former, and actually, it is long and contains many technicalities. In many cases, we would like to show that the AADL execution model preserves certain data invariants. Since the Behavior annex may not be a closed system; that is, a state may be changed by its environment or conditions. So that the reachable states of Behavior annex depend on both the initial states and the environment. A Behavior annex with static information Σ is defined as follows:

$$\forall s_0, x_0 \delta \cdot \delta \in \Gamma(\Sigma, \rho, s_0, e_0) \cap A(\Sigma, \text{inits}) \longrightarrow \left(\forall i < \text{length}(\delta) \cdot \text{invars}\left(s_{\delta_i}\right)\right). \quad (3)$$

The above formula demonstrates that it starts up from a set of initial states *init*, and it will preserve an invariant *inv* if its reachable states satisfy the predicate.

In this definition, δ denotes an arbitrary computation of ρ from a set of initial states *inits* and under an environment R. It requires that all states in δ satisfy the invariant *invars*.

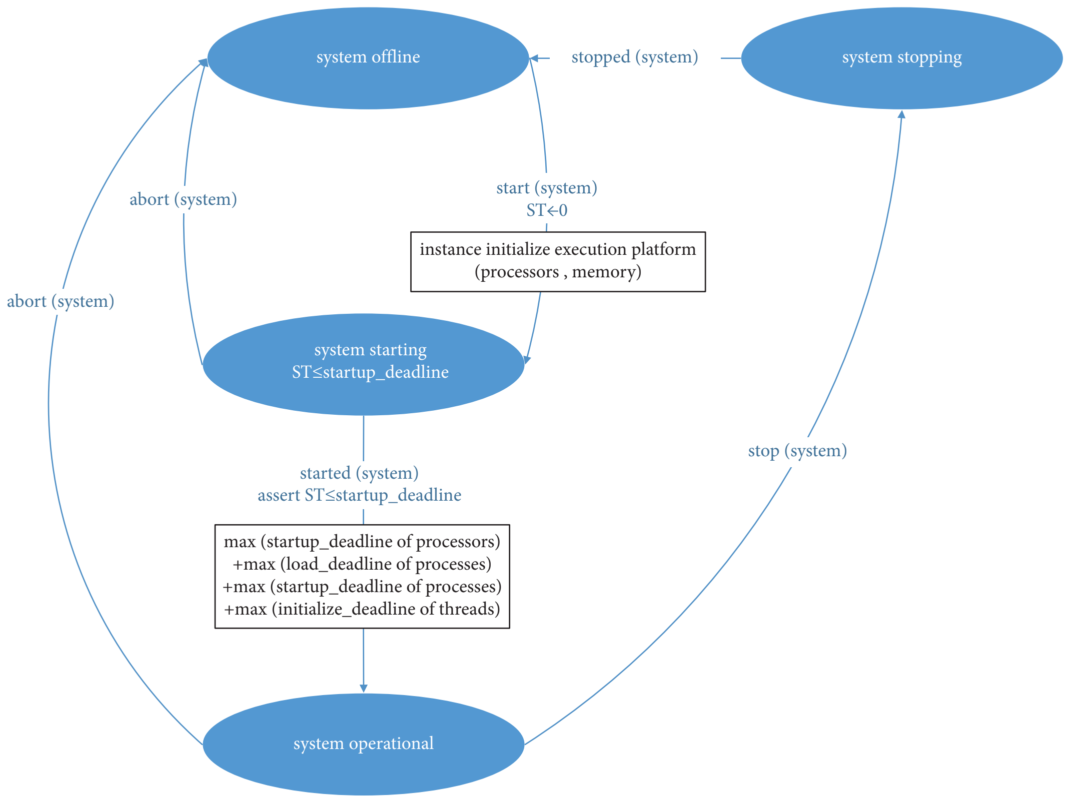

Figure 32: System execution automaton.

(processor-state s) = PCOR-STARTED;
(sy-state ((sy-st s) system))=SYS-STARTING;
(sy-state ((sy-st t) system))=SYS-OPERATIONAL;
process∈(get-pros-bysys m system);
gt = (cur-time s);
(cur-time s) = 0;
(begin-time ((sy-st s) system)) = (cur-time s);
(action-begin-time ((sy-st s) system)) = (cur-time s);
(cur-time t) = (cur-time s) + (elapsed-time ((sy-st t) system));
(cur-time t) = (begin-time ((sy-st s) system)) + (elapsed-time ((sy-st t) system));
(cur-time t) = (action-begin-time ((sy-st s) system)) + (elapsed-time ((sy-st t) system));
(exe-time ((sy-st t) system)) ≤ (elapsed-time ((sy-st t) system));
(elapsed-time ((sy-st t) system)) ≤ (get-pro-loaddeadline-max m (get-pros-bysys m system))
+ (get-pro-startupdeadline-max m (get-pros-bysys m system))
+ (get-thd-initialzedeadline-max m (get-thds-bypro m process));
(elapsed-time ((sy-st t) system)) ≤ (the (sys-startup-deadline (the (system-type.sys-properties ((system-tp m) system)))))

Figure 33: The System execution Start_Complete semantic.

To show that *invars* is preserved by a system ρ, and it suffices to show the invariant verification theorem as follows. This theorem indicates that (1) the system satisfies its specification $\langle \text{inits}, \text{post} \rangle$, (2) *invars* initially holds in the set of initial states, and (3) each action transition as well as each environment transition preserves *invars*. Later, by the proof system, invariant verification is decomposed to the verification of individual executions.

Theorem 1. *(Invariant Verification). For formal specification ρ and Σ, a state set inits, and invars, if*

(i) $\Sigma \vdash \rho$ *sat* $\langle inits, post \rangle$.

(ii) $inits \subseteq \{s \cdot invars(s)\}$,

then invars is preserved by ρ, inits.

6. Case Study: Formalization of an ARINC653-Based System

Our work aims at the formal specification and verification in a system development based on the AADL, so we apply the proof system for the specification, the validation, and the verification of an ARINC653-based System. In Figure 34, we provide an example, which is based on the ARINC653 OS platform using AADL with its Behavior Annex specification. This example is adapted from the ARINC653 annex document for the AADLv2 and shows a system with two partitions. It shows the components involved in the modeling of the ARINC653 system and illustrates the mapping of ARINC653 concepts to the AADL.

In fact, the architecture is described as the client thread “a_client” for calls and communication of action: either do not need to wait on the calculation of long distance calls and finished to send, or due to server for HSER subroutine call and waiting for the results to the values, send the results and return to continue to wait for the next execution among them, the thread a data port connection between tasks, each thread internal use behavior to define its specific behavior, describe the action to perform with state systems conditions and order.

6.1. Formal Transformation of AADL into Isabelle/HOL. We define several modeling rules of model transformation from the AADL model into Isabelle/HOL specification for the next step about formal validation and verification. The model transformation rules of AADL are specified with a set of corresponding rules between AADL and Isabelle/HOL in a way to obtain a modular specification, and a part of the transformation rules is described as follows.

6.1.1. Transformation of Components and Connections. Transform components and connections to datatypes in Isabelle/HOL.

6.1.2. Transformation of Properties and Features. Transform properties and features of components to the predefined records type as definitions in Isabelle/HOL. Notice that, if there is any subcomponent as a existed component in the other component, it is considered an abbreviation instead of secondary definition.

6.1.3. Transformation of Behavior Annex. Transform Behavior annex specification comprises some sophisticated procedures, and transformation rules are as follows:

(i) Transform variables in a Behavior annex to the predefined records type as definitions in Isabelle/HOL.

(ii) Transform states in a Behavior annex corresponding to initial, complete, and final states to denote the current state.

(iii) Transform transitions in Behavior annex as the predefined records type, and transform guards and actions in a transition to conditions and actions list as definitions. Assemble the elements representing transitions to one compositional definition, which comprise all the state transitions of a behavior specification.

As depicted in Figure 35, we show the segmental transformation code for the example thread in Figure 34.

6.2. Formal Instantiation, Validation, and Verification in Isabelle/HOL. This section introduces the next formal steps of the example model after transformation into Isabelle/HOL as well as the validation and verification with its proof system. In this section, we use the instantiation of the AADL example to formally specify and verify the properties of the system model.

6.2.1. Instantiation. The basic transformation rules have been listed in Section 6.1, and we can use it to abstract an example of AADL model (see Figure 34) in Isabelle/HOL. In the implementation of AADL in Isabelle/HOL, we use record to create the framework, where components of AADL are represented as parameters and assumptions of record. Records are the Isabelle/HOL’s approach for dealing with parametric datatype. Every component of the same type inside the system model can be mapped and encapsulated into an instantiation by Isabelle/HOL specification, and the component type and implementation are instantiated. In the last stage of modeling, we can integrate datatype to type variable as parameter and get the concrete AADL model code in Isabelle/HOL. For instance, the instantiation of the process type is implemented by the mapping function as follows:

primrec *process-type-map*: *ExProcess* (ExPort; ExDataaccess;

‘Subpaccess; ‘Parameter) process-type

where *pro-tp1: process-type-map partition1-process =*

partition1-process-type |

pro-tp2: process-type-map partition2-process =

partition2-process-type

6.2.2. Validation. The part of rules for grammar have been listed in Section 4.2, and we rewrite the validation rules as 47 definitions in Isabelle/HOL. After the formal description of rules, we reach the validation phase to check the grammar of the AADL model above. In our work, we use the validation rules code to check whether the model from the

```
thread a_server
features
  long :  provides subprogram access long_computation
     { Behavior_Properties :: Subprogram_Call_Protocol => LSER; };
  short :  provides subprogram access send_result
     { Behavior_Properties :: Subprogram_Call_Protocol => HSER; };
properties
  Dispatch_Protocol => timed;
  Period => 100 ms ;
end a_server;
thread implementation a_server . i
subcomponents
  local_result : data result_type . i;
 connections
  cnx1: data access  local_result -> local_result.result;
  cnx2: data access  local_result -> short.result;
annex behavior_specification {**
  states
    s0 :  initial complete final state;
    s1 :  complete state;
    s2 :  complete state;
  transitions
    s0 -[  on dispatch  long ] -> s1;
    s1 -[  on dispatch  ] -> s2  timeout 60ms;
    s1 -[  on dispatch timeout  ] -> s2 { local_result.status : = 0 };
    s2 -[  on dispatch  short ] -> s20 { send_result! (local_result, local_result) };
**};
end a_server . i;
```

Figure 34: AADL example of the ARINC653-based system: a typical thread with Behavior annex.

transformation satisfies a given property specified with temporal logic. Since the lemmas of validations are consistent with the integrating model, the proof obligations for the validation rule are proven immediately after unfolding the definitions of the precondition, postcondition, and relations. After applying the conditional and the grammar rules on the components, only the proof of the verification of each lemma body is left. Using these auxiliary lemmas, the postcondition is proven immediately by applying the properties over multisets. All the lemmas of validations are similarly proven, we omit the details here and the interested reader can refer to the Isabelle/HOL sources. We present an example of validation 7th as follows.

6.2.3. Safety Verification. Safety represents "nothing bad will happen," which comprises reachability or properties expressed in the form of finite state automata by invariance. After transforming the AADL abstract model to a target concrete model, we use the proof system (see Section 5.3) to verify its trace refinement and reachability properties.

Trace refinement checks "whether the abstract behavior trace of an implementation satisfies its abstract behavior trace of a specification." For instance, an assertion for trace refinement compares the whole abstract behaviors of a given action with another action, that is, whether there is a succeed relationship. For one of actions, the refinement analysis of actions is executed as follows.

Reachability refers to the ability to get from one state to another with one or multiple events. For instance, definition action-reach state shows the concrete state's reachability of the action for Behavior annex:

Only with thread inputs and outputs without interior actions, the above definitions are used to verify whether all abstract behaviors refine the outside abstract behaviors, and whether the system reaches the goal of state.

```
datatype ExThread = a-client | a-server
datatype ExBehaviorAnnex = ba-a-client | ba-a-server
definition long-a-server-conf :: (ExData, ExSubprogram, Ex-
Thread, ExProcess, ExSystem) subpaccess-conf
  where long-a-server-conf ≡ (|spac-name = ''long'',
                          spac-dir=PROVIDES,
                          spac-right =None,
                          spac-queueprotocol =None,
                          spac-queuesize =None,
                          spac-queue =None,
                          spac-obj =Some (SCSubp long-computation)|)
abbreviation local-result ≡ result-type
definition ba-a-server-conf :: ('s, 'ExDispatcher, 'Port, ExDataac-
cess, ExSubpaccess, ExParameter, ExData, ExSubprogram, Ex-
Thread, ExProcess, ExSystem) behavior-annex-conf
        where ba-a-server-conf ≡ (|ba-states={s0-ba-a-server,
s1-ba-a-server, s2-ba-a-server},
                          ba-trans={tran1-ba-a-server,tran2-ba-a-server,
tran3-ba-a-server,tran4-ba-a-server},
                         ba-vars={},
                         ba-name=''Dispatcherehavior-specification''|)
definitiona-server-impl :: (ExConnection, 'Subprogramcalls, ExDa-
ta, ExSubprogram, ExThread, ExProcess, ExSystem, ExBehaviorAn-
nex) thread-impl
  where a-server-impl ≡ (|impl-subcomps= {SCData local-result},
                       impl-conns = {cnx1-a-server, cnx2-a-server},
                       impl-name = ''a-server.i'',
                       thd-spcalls={},
                       thread-impl.thd-properties=None,
                       thread-impl.thd-ba=Some ba-a-server|)
```

FIGURE 35: The segmental code of Thread in Isabelle/HOL.

7. Evaluation and Conclusion

Our work presents a method of the description of AADL and a methodology of model transformation from a comprehensive subset of AADL to Isabelle/HOL. To specify this transformation, a preliminary analysis and comprehension of AADL and Isar/Isabelle/HOL languages are necessary and reveal the need to take into account the various parts of the language: structural, execution model, and its semantics description. Then, we use Isabelle/HOL as the specification, instantiation, validation, and verification system to conduct proofs against the properties of grammar and semantic in the structured proof language Isar, allowing for proof text naturally understandable for both humans and computers.

7.1. Evaluation Results. All derivations of our proofs have passed through the Isabelle/HOL proof kernel. The total development of our framework has $\approx$ 1280 lines of Isabelle/HOL specification and proof (LOSP). The concrete syntax of AADL consists of $\approx$ 630 LOSP, and the semantic of AADL consists of $\approx$ 650 LOSP. The two parts of specification and proof are completely reused in AADL . We use $\approx$ 750 LOSP to develop our validation system and $\approx$ 500 LOSP to develop the verification system including the formalization of 47 grammar rules. Finally, we develop $\approx$ 3300 LOSP for three case studies of AADL system model, which is ARINC653-based. We find two grammatical mistakes in the second case study and summarize that the instantiation in Isabelle/HOL has $\approx$ 3 times as much code as the lines of the AADL model.

7.2. Conclusion and Future Works. Different from the majority of AADL formal approaches above, our proposition aim at defining a formal executable semantics of a comprehensive AADL subset to allow the instantiation, validation, and verification of behavioral and temporal properties. Besides, the considered AADL subset consists of both software and hardware AADL components with a significant set of temporal and queuing AADL properties. The considered subset covers fundamental features that can be used in more realistic applications rather than "without behavior" and "model transformation into other languages" approaches. Our experience is encouraging, but much more works remain ahead. First, increasingly larger AADL subsets should be considered to face complex applications such as shared variables by several threads with subprogram access, complex scheduling, etc. in the future works. Second, we need more complex industrial applications to examine our theory and the toolset, adjust our schema, and revise the technical architecture and implementation details, so as to realize our object that increase the confidence of safety-critical software. We plan to extend the AADL in Isabelle/HOL to support more structures and stepwise refinement. Third, we need to verify more properties like the rules of model transformation conforms to semantics equivalence, the satisfaction of the noninfluence, etc. And the following important perspective concerns are compilation aspect from AADL to C language as our next step.

Data Availability

Data sharing is not applicable to this article as no datasets were generated or analyzed during the current study.

Conflicts of Interest

The authors declare no potential conflicts of interest with respect to the research, authorship, and/or publication of this article.

Acknowledgments

The part of previous work on formal specification has been published at IOP Science as a conference paper [26]; the whole work of this article is based on and improved on it. This research was supported (in part) by the formal verification project for the microkernel operating system.

References

[1] RTCA and EUROCAE, "Software Considerations in Airborne Systems and Equipment Certification," *RTCA DO-178*, 2011.

[2] SAE, "Architecture Analysis & Design Language (AADL)," *AS 5506C-2017, Version 2.2*, 2017.

[3] SAE, "Architecture Analysis & Design Language (AADL) Annex," *AS 5506/2-2011*, vol. 2, 2011.

[4] I. Malavolta, L. Patricia, M. Henry, P. Patrizio, and T. Antony, "What industry needs from architectural languages: a survey," *IEEE Transactions on Software Engineering*, vol. 39, pp. 869–891, 2013.

[5] T. Bourke, L. Brun, P. E. Dagand, X. Leroy, M. Pouzet, and L. Rieg, "A formally verified compiler for Lustre," *Acm Sigplan Notices*, vol. 52, pp. 586–601, 2017.

[6] X. Leroy, "Formal verification of a realistic compiler," *Communications of the ACM*, vol. 52, no. 7, 2009.

[7] R. Krebbers, X. Leroy, and F. Wiedijk, *Formal C semantics: CompCert and the C standard. Interactive Theorem Proving*, Springer International Publishing, Berlin, Germany, 2014.

[8] N. Tobias, M. Wenzel, and L. Paulson, *Isabelle/HOL: A Proof Assistant for Higher-Order Logic*, Springer-Verlag, Berlin, Germany, 2002.

[9] T. Nipkow and G. Klein, *Concrete Semantics*, Springer Publishing Company, New york, NY, USA, 2014.

[10] L. C. Paulson, *ML for the Working Programmer*, Cambridge University Press, Cambridge, UK, 2nd edition, 1996.

[11] M. Wenzel, "The Isabelle/Isar reference manual.," 2021, https://isabelle.in.tum.de/doc/isar-ref.pdf.

[12] A. E. Rugina, K. Kanoun, and M. Kaaniche, "The ADAPT tool: from AADL architectural models to stochastic petri nets through model transformation," in *Proceedings of the European Dependable Computing Conference (EDCC)*, Kaunas, Lithuania, May 2008.

[13] A. Johnsen, K. Lundqvist, P. Pettersson, and O. Jaradat, "Automated verification of AADL-specifications using UPPAAL," in *Proceedings of the 2012 IEEE 14th International Symposium on High-Assurance Systems Engineering*, Omaha, NE, USA, October 2012.

[14] R. Jean-Francois, B. Jean-Paul, F. Mamoun, C. David, and T. Dave, "Modes in asynchronous systems," in *Proceedings of the IEEE International Conference on Engineering of Complex Computer Systems IEEE*, Belfast, UK, March 2008.

[15] E. Jahier, N. Halbwachs, P. Raymond, X. Nicollin, and D. Lesens, "Virtual execution of AADL models via a translation into synchronous programs," in *Proceedings of the 7th ACM & IEEE International Conference on Embedded Software*, pp. 134–143, ACM, Salzburg Austria, September 2007.

[16] B. Bernard, J. P. Bodeveix, C. Chaudet, and S. D. Zilio, "Formal verification of AADL specifications in the topcased environment," in *Proceedings of the 14th Ada-Europe International Conference on Reliable Software Technologies (Ada-Europe '09)*, pp. 207–221, Springer-Verlag, Brest, France, June 2009.

[17] C. Yang, D. Yunwei, Z. Fan, A. Ehsan, and G. Bin, "Formal semantics of AADL models with machine-readable CSP," in *Proceedings of the IEEE/ACIS 11th International Conference on Computer and Information Science IEEE*, Shanghai, China, June 2012.

[18] Z. Feng, Z. Yongwang, M. Dianfu, and N. Wensheng, "Formal verification of behavioral AADL models by stateful timed CSP," *IEEE Access*, vol. 5, 2017.

[19] M. Y. Chkouri, B. Marius, S. Joseph, and R. Anne, *Translating AADL into BIP - Application to the Verification of Real-Time Systems*, Models in Software Engineering Springer-Verlag, Toulouse, France, 2009.

[20] L. Besnard, B. Adnan, G. Thierry et al., "Timed behavioural modelling and affine scheduling of embedded software architectures in the AADL using Polychrony," *Science of Computer Programming*, vol. 106, pp. 54–77, 2015.

[21] Z. Yang, "From AADL to timed abstract state machine: a certified model transformation," *Journal of Systems & Software*, vol. 93, no. 2, pp. 42–68, 2014.

[22] K. Hu, T. Zhang, Z. Yang, and W. T. Tsai, "Exploring AADL verification tool through model transformation," *Journal of Systems Architecture*, vol. 61, no. 3-4, pp. 141–156, 2015.

[23] H. Mkaouar, Z. Bechir, J. Mohamed, and H. Jérôme, "An ocarina extension for AADL formal semantics generation," in *Proceedings of the 33rd Annual ACM Symposium on Applied Computing*, pp. 1402–1409, New York, NY, USA, April 2018.

[24] T. Abdoul, "AADL execution semantics transformation for formal verification," in *Proceedings of the Engineering of Complex Computer Systems, 2008. ICECCS 2008. 13th IEEE International Conference on IEEE*, Washington, DC, USA, March 2008.

[25] P. C. Ölveczky, A. Boronat, and J. Meseguer, "Formal semantics and analysis of behavioral AADL models in real-time Maude," in *Formal Techniques for Distributed Systems. FMOODS 2010, FORTE 2010. Lecture Notes in Computer*

Science, J. Hatcliff and E. Zucca, Eds., vol. 6117, Berlin, Germany, Springer, 2010.

[26] Yu Tan, D. Ma, and L. Qiao, "Towards formal specification for AADL with behavior annex in Isabelle," *IOP Conference Series: Earth and Environmental Science*, vol. 769, no. 4, Article ID 42016, 2021.

Hindawi
Scientific Programming
Volume 2021, Article ID 3688300, 11 pages
https://doi.org/10.1155/2021/3688300

Research Article

Research on Danjiang Water Quality Prediction Based on Improved Artificial Bee Colony Algorithm and Optimized BP Neural Network

Jian'qiang He [1,2], Naian Liu [3], Mei'lin Han [1], and Yao Chen [1,2]

[1] *Electronic Information and Electrical College of Engineering, Shangluo University, Shangluo 726000, China*
[2] *Shangluo Artificial Intelligence Research Center, Shangluo 726000, China*
[3] *College of Communication Engineering, Xi'an University of Electronic Science and Technology, Xian 710126, China*

Correspondence should be addressed to Jian'qiang He; hejianqiang@slxy.edu.cn

Received 12 November 2021; Accepted 8 December 2021; Published 29 December 2021

Academic Editor: Punit Gupta

In order to ensure "a river of clear water is supplied to Beijing and Tianjin" and improve the water quality prediction accuracy of the Danjiang water source, while avoiding the local optimum and premature maturity of the artificial bee colony algorithm, an improved artificial bee colony algorithm (ABC algorithm) is proposed to optimize the Danjiang water quality prediction model of BP neural network is proposed. This method improves the local and global search capabilities of the ABC algorithm by adding adaptive local search factors and mutation factors, improves the performance of local search, and avoids local optimal conditions. The improved ABC algorithm is used to optimize the weights and thresholds of the BP neural network to establish a water quality grade prediction model. Taking the water quality monitoring data of Danjiang source (Shangzhou section) from 2015 to 2019 as the research object, it is compared with GA-BP, PSO-BP, ABC-BP, and BP models. The research results show that the improved ABC-BP algorithm has the highest prediction accuracy, faster convergence speed, stronger stability, and robustness.

1. Introduction

The Party Central Committee, State Council, Provincial Committee, and Provincial Government attach great importance to the work of ecological environment protection in Qinling area. General Secretary Xi Jinping emphasized: "No one can destroy the natural ecological beauty of the Qinling Mountains." The Danjiang River originates from the southern foot of the Qinling Mountains in the northwestern part of Shangluo, Shaanxi Province, and flows through Shaanxi Province, Henan Province, and Hubei Province. It is injected into Danjiangkou Reservoir in Danjiangkou City of Hubei Province and intersects with the Han River [1]. The total length of the mainstream is 390 km, which is the longest tributary of the Hanjiang River. The basin area is 17300 square kilometers, accounting for 10% of the total area of the Hanjiang River Basin [2]. The Danjiang River is an important water source for the Middle Route Project of the "South-to-North Water Diversion". In recent years, Shangluo City has fully implemented the circular development strategy to protect the water sources, built ecological Shangluo, and ensured that "a river of clean water is supplied to Beijing and Tianjin." However, with the advancement of the resettlement project and social economic development, more and more domestic sewage is discharged to the Danjiang River, which directly affects the water quality of the Danjiang River Basin. Therefore, by predicting the water quality of the Danjiang River Basin, a scientific decision-making basis can be provided for the protection and management of the water environment.

The currently used common methods for water quality prediction include the GM model, artificial neural network, and SVM. In the literature [3], the gray prediction method is used for water quality prediction. This method is only suitable for short-term prediction. There is also the disadvantage that the larger the gray level of the data, the lower the prediction accuracy. Literature [4] and Literature [5] proposed a water quality prediction model based on the weighted combination, combined exponential smoothing method, and water quality prediction model of GM (1,1) model. Compared with the literature [3], the prediction accuracy of this method has been improved to a certain extent, but there is a problem of excessive error, which cannot be solved. Literature [6] and Literature [7] proposed an improved water quality prediction model based on the gray GM(1,1) model, which is much better than the traditional gray GM(1,1) model. The BP neural network has the advantages of self-learning and fault tolerance, which is widely used in water quality prediction. In the literature [8], BP neural network was applied to the study of water quality evaluation and temporal-spatial evolution trend of water quality. The results showed that the evaluation results of this method were more objective and the evaluation process was more convenient. Aiming at the problem of low prediction accuracy of small sample data and easy to fall into local optimum of BP neural network, a water quality prediction model of double hidden layer BP neural network based on artificial bee colony algorithm is proposed in the literature [9], the initial weights and thresholds of BP neural network are optimized by the ABC algorithm, and the prediction accuracy is improved. However, the BP neural network with double hidden layers has overfitting, which easily leads to the decrease of the generalization ability of the prediction model.

Aiming at the problems existing in the current water quality prediction model, this paper improves the local and global search ability of the ABC algorithm by adding adaptive local search factors and mutation factors. The improved ABC algorithm is used to optimize the weights and thresholds of the BP neural network, and the improved ABC-BP hybrid neural network model is obtained. Taking the water quality monitoring data of the source of Dan River (Shangzhou District) from 2015 to 2019 as the research object, compared with GA-BP, PSO-BP, ABC-BP, and BP models. The results show that the algorithm has the highest prediction accuracy and faster convergence speed.

2. Principle of BP Neural Network

BP neural network is mainly composed of input layer, hidden layer (one or more layers), and output layer [10]. The neurons in the same layer are not interconnected, and the neurons in the adjacent layer are connected by weights, and the output of each layer of nodes only affects the input of the nodes of the lower layer. The BP neural network model structure is shown in Figure 1. The learning process of the BP neural network is mainly composed of two parts: forward propagation of signal and backpropagation of error. In the forward propagation process of the signal, after the input signal passes through the network weight, threshold, and neuron transfer function, an output signal can be obtained in the output layer. If the error between the output value and the expected value is greater than the specified amount, then the error will be entered The backpropagation process of the error, that is, through the error return layer by layer, the error is “allocated” to the neurons of each layer, and the weight is self-adjusted until the error between the output data value of the output layer and the expected data value reaches the preset range, then the training of the network is completed.

Suppose the number of nodes in the input layer, hidden layer, and output layer of the BP neural network is n, m, and l, respectively; the weights between the input layer and the hidden layer and the weights between the hidden layer and the output layer are w_{ij} and w_{jk}, respectively; the thresholds of the hidden layer and the output layer are t_j and t_k, respectively; f is the transfer function; the expected output of the output layer is d_k.

The output of the hidden layer node and the output layer node is

$$\begin{aligned} y_j &= f\left(\sum_{i=1}^{n} w_{ij}x_i - t_j\right) = f\left(net_j\right), \\ o_k &= f\left(\sum_{j=1}^{m} w_{jk}y_j - t_k\right) = f\left(net_k\right). \end{aligned} \tag{1}$$

The error between the output value and the expected output is

$$\begin{aligned} E &= \frac{1}{2}\sum_{k=1}^{l}\left(d_k - o_k\right)^2 \\ &= \frac{1}{2}\sum_{k=1}^{l}\left(d_k - f\left\{\sum_{j=1}^{m} w_{jk} f\left(\sum_{i=1}^{n} w_{ij}x_i - t_j\right) - t_k\right]\right\}^2. \end{aligned} \tag{2}$$

It can be seen from the error formula that the error E can be changed by adjusting the weights w_{ij} and w_{jk}, and the weight adjustment is proportional to the drop of the error gradient, then for the output layer and the hidden layer

$$\begin{aligned} \Delta w_{jk} &= -\eta\frac{\partial E}{\partial w_{jk}} = -\eta\frac{\partial E}{\partial n\ et_k}\frac{\partial n\ et_k}{\partial w_{jk}} = \eta\delta_k y_j, \\ \Delta w_{ij} &= -\eta\frac{\partial E}{\partial w_{ij}} = -\eta\frac{\partial E}{\partial n\ et_j}\frac{\partial n\ et_j}{\partial w_{ij}} = \eta\delta_j x_i, \end{aligned} \tag{3}$$

where η is the learning rate,

$$\begin{aligned} \delta_k &= -\frac{\partial E}{\partial net_k} = \left(d_k - o_k\right) f'\left(net_k\right) \\ &= \left(d_k - o_k\right) o_k\left(1 - o_k\right), \\ \delta_j &= -\frac{\partial E}{\partial net_j} = f'\left(net_j\right)\left(\sum_{k=1}^{l}\delta_k w_{jk}\right) \\ &= \left(\sum_{k=1}^{l}\delta_k w_{jk}\right) y_j\left(1 - y_j\right). \end{aligned} \tag{4}$$

Among them, the transfer function $f(x) = (1 + e^{-x})^{-1}$, then $f'(x) = f(x)[1 - f(x)]$.

BP weight adjustment formula is

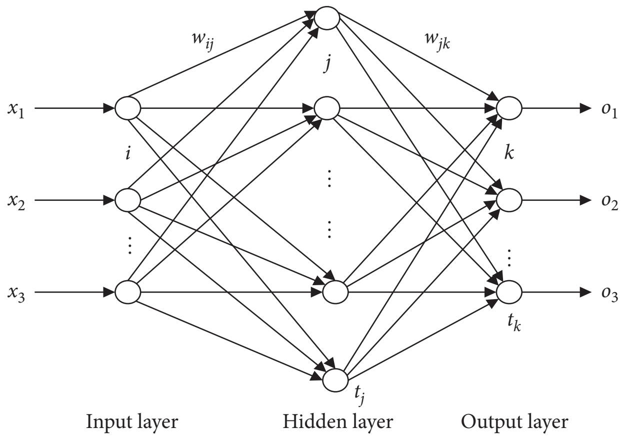

Figure 1: BP neural network model structure diagram.

$$\Delta w_{jk} = \eta (d_k - o_k) o_k (1 - o_k) y_j,$$
$$\Delta w_{ij} = \eta \left(\sum_{k=1}^{l} \delta_k w_{jk} \right) y_j (1 - y_j) x_i. \tag{5}$$

Since the BP neural network has slow convergence speed and low prediction accuracy, it cannot meet the performance requirements of water quality prediction. Therefore, this paper uses an improved artificial bee colony algorithm to optimize the weights and thresholds of the BP neural network to improve its water quality prediction performance.

3. Artificial Bee Colony Algorithm

In order to solve the problem of multivariate function optimization, Karaboga proposed the artificial bee colony (ABC) algorithm model in 2005, which simulates the honey-collecting behavior of bees to search for global optimization goals [11, 12].

3.1. Basic Artificial Bee Colony Algorithm. Artificial bee colony algorithm is a swarm intelligence optimization algorithm that simulates the process of bees searching for the best quality and the largest number of nectar sources in nature. The algorithm contains three types of bee colonies: collecting bees, observing bees, and investigating bees. The nectar source is a possible solution in the solution space. Assuming that the algorithm is solved in the K-dimensional space, the total amount of nectar source is N, and the initial position formula is .

$$x_{ij}^{new} = x_{\min,j} + rand\left(x_{\max,j} - x_{\min,j}\right), \tag{6}$$

where x_{ij}^{new} is the position of the initial solution, $x_{\min,j}$ and $x_{\max,j}$ are the upper and lower bounds of j dimension, $i = 1, 2, 3 \cdots, N$; $j = 1, 2, 3 \cdots, K$; And both i, j are randomly generated and are not equal to each other; *rand* is a randomly generated number between 0 and 1.

Suppose the probability of finding a new high-quality nectar source and being selected is

$$p_i = \frac{\text{fit}_i}{\sum_{n=1}^{N} \text{fit}_n}. \tag{7}$$

In the formula, fit_i represents the i^{th} nectar source, that is, the fitness value of the solution. If the fitness of the new solution is higher than the original solution, it will be replaced by the new solution.

$$fit_i = \begin{cases} \dfrac{1}{1 + f_i}, f_i > 0, \\[2ex] \dfrac{1}{1 + abs(f_i)}, f_i < 0, \end{cases} \tag{8}$$

where f_i is the objective function value of the i^{th} solution.

When falling into the local optimum, the honey bee will abandon the nectar source and become a scout bee. According to formula (9), a new nectar source position will be randomly generated to replace the corresponding position in the initially marked nectar source to determine the final nectar source. According to this, iteration is carried out repeatedly until the termination condition of the algorithm is reached [13].

$$v_{ij} = x_{ij} + r\left(x_{ij} - x_{tj}\right). \tag{9}$$

In the formula, $j = 1, 2, 3 \cdots, K$; $t = 1, 2, 3 \cdots, N$, and t is not equal to i, both t and j are randomly generated; r is a randomly selected value between [1,−1].

3.2. Improved Artificial Bee Colony Algorithm. In order to enhance the global optimization and local search capabilities of the algorithm, adaptive local search factors and mutation factors are added to improve the ABC algorithm to avoid premature phenomena [14].

3.2.1. Adaptive Search Factor. In the initial search stage of the algorithm, an adaptive local search factor ω is introduced to prevent falling into local optimization. The local search is enhanced by adaptively adjusting the population update step size, and the global and local search capabilities of the algorithm are balanced. That is, equation (9) is updated to

$$v_{ij} = \omega x_{ij} + r\left(x_{ij} - x_{tj}\right). \tag{10}$$

In the formula, x_{ij} is the previous worst source of nectar.

The introduction of ω can speed up the algorithm convergence speed and avoid premature maturity. The change of ω is

$$\omega = \omega_{\min} + \left(\omega_{\max} - \omega_{\min}\right) \times \frac{T_{\max} - c}{T_{\max}}, \tag{11}$$

where $\omega_{\max}$ and $\omega_{\min}$ are the maximum and minimum values of inertia weight; $T_{\max}$ is the maximum number of maximum mixing iterations between the subpopulations; c represents the total number of iterations of the current subpopulation.

3.2.2. Variation Factor. In order to improve the global optimization ability and accuracy of the algorithm, the mutation factor Levy is introduced. Compared with other operators (such as the Gaussian operator, etc.), the mutation factor can greatly improve the global optimization ability of the algorithm and prevent the algorithm from emergence of precocious puberty. The introduction of the Levy mutation factor enhances the global optimization capability of the algorithm based on the adaptive factor. The specific implementation is to add the Levy mutation operator to equation (3) and update it to the following equation:

$$v_{ij}^{new} = \left[\omega x_{ij} + r\left(x_{ij} - x_{tj}\right)\right] \times L_{\mathrm{j}}(t)\oplus. \tag{12}$$

In the formula, $L_{\mathrm{j}}(t)$ is a random number that obeys the Levy distribution.

After introducing the adaptive mutation factor, the local update method of the ABC algorithm is shown in equations (13) and (14):

$$x_{ij}^{new} = \left[\omega x_{ij} + r\left(x_{ij} - x_{tj}\right)\right] \times L_{\mathrm{j}}(t), \tag{13}$$

$$x_{tj} = x_{tj} + x_{ij}. \tag{14}$$

4. Improved Water Quality Prediction Model of ABC-BP Algorithm

In this paper, a water quality prediction model is established by improving the ABC-BP algorithm. The input of the BP neural network is ammonia nitrogen (NH3–N), dissolved oxygen (DO), chemical oxygen demand (COD), permanganate index (I_{Mn}), and total phosphorus, six water quality evaluation indicators of total nitrogen and total nitrogen, and the output is the water quality grade. The water quality prediction model is shown in Figure 2, and the algorithm flow chart is shown in Figure 3.

Step 1. Take 6 indicators of NH3–N, DO, COD, I_{Mn}, total phosphorus, and total nitrogen as the input of the BP network for training.

Step 2. Optimize the weights $(\omega_{ij}, \omega_{jk})$ and (t_j, t_k) thresholds trained by the BP network.

Step 3. Determine whether the output data O and the error value meet the requirements, if the requirements are met by the formula (6), the optimal solution is the output, and the optimal weight and threshold are obtained.

Step 4. If the requirements are not met, the search bee will find a new nectar source according to formula (13) and output the value of the solution.

Step 5. Repeat the loop, and finally get the optimal solution.

Step 6. If the number of calculations exceeds the set maximum number of iterations, the training ends, otherwise the function of formula (7) is returned.

Step 7. Obtain the optimal solution, and verify the BP neural network according to the weight and threshold.

5. Experimental Analysis

5.1. Data Source. In order to verify the reliability and effectiveness of the improved ABC-BP algorithm for water quality prediction, the water quality measurement data from the six monitoring points in the Shangzhou section of Shangluo City in the Danjiang River Basin from 2015 to 2019 was used as the research object for experimental research. The geographical distribution and latitude and longitude information of water quality monitoring points are shown in Figure 4 and Table 1, respectively.

5.2. Water Quality Evaluation Index. Water quality evaluation is the process of determining the water quality level of the sampled water sample based on the various index values of the sampled water sample and the water quality evaluation standard, combined with a certain mathematical model [15]. Since there are many indicators for water quality analysis [16], combined with surface water environmental quality standards, the water quality evaluation indicators used in this article are DO, NH3–N, COD, I_{Mn}, total phosphorus and total nitrogen [17], which correspond to The water quality grades and content standards are shown in Table 2.

5.3. Data Preprocessing and Evaluation Indicators. In order to improve the accuracy of the predicted data, use formula (15) to normalize the data and convert the data to the range of [−1, 1].

$$y = \frac{2\left(X_i - X_{\min}\right)}{X_{\max} - X_{\min}} - 1. \tag{15}$$

In the formula, X_i represents the original water quality data, $X_{\max}$ is the maximum value in the original data sequence, $X_{\min}$ is the minimum value in the original data sequence, and y represents the data after the normalization transformation, which can reduce the difference between the result and the actual value The deviation. In order to facilitate the comparison of water quality grade evaluation of different evaluation methods, formula (16) is used as the evaluation index of water quality grade evaluation:

$$C = \frac{TN}{N} \times 100\%. \tag{16}$$

In the formula, C represents the accuracy of evaluation; N is the total number of samples; TN is the number of samples correctly classified.

5.4. Experimental Results and Analysis. The water quality measured data from 2015 to 2019 in the Shangzhou section of Shangluo city in the Danjiang River basin was selected as the research object. After sorting, the measured data was divided into two parts: a training set and a test set. The training set was mainly used to establish a Danjiang water quality prediction model, the test set is mainly used to test

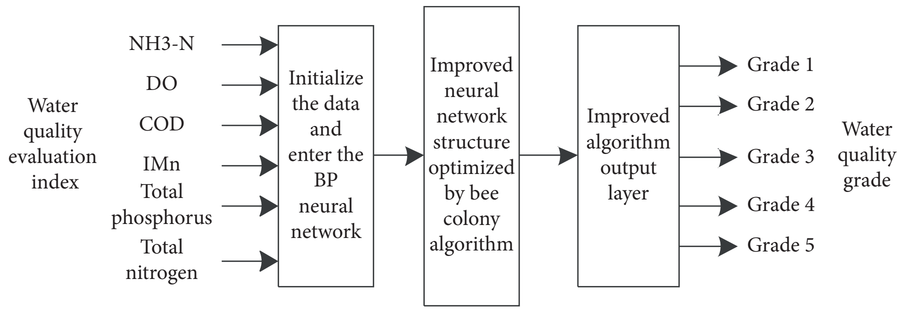

Figure 2: Water quality prediction model.

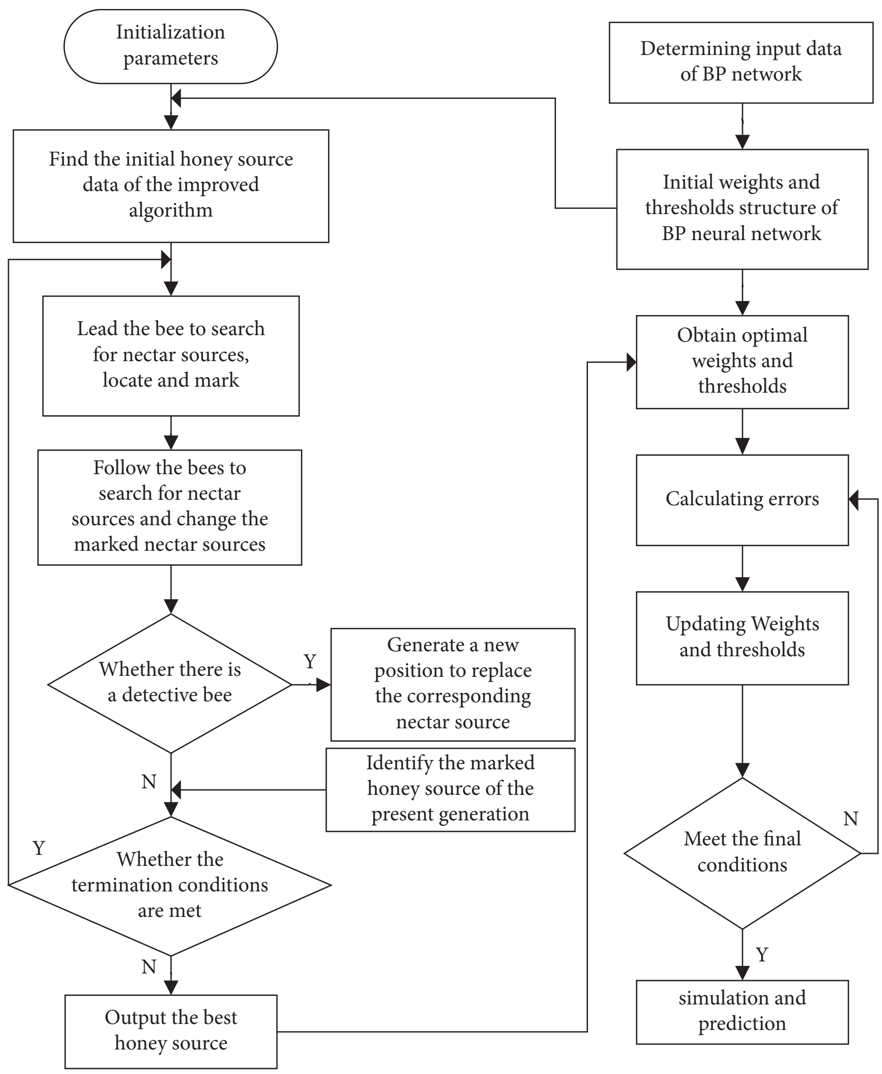

Figure 3: Algorithm flow chart.

the pros and cons of the built model. In order to verify the superiority of the improved ABC-BP algorithm, it is compared with GA-BP, PSO-BP, and ABC-BP algorithms.

Six indicators of NH3–N, DO, COD, I_{Mn}, total phosphorus, and total nitrogen were used as the input of the improved ABC-BP model, and the water quality grade was used as the output of the improved ABC-BP model to establish the improved ABC-BP water quality evaluation model [18, 19]. This article sets the number of input layer nodes of the BP network inputnum = 6, the number of hidden layer nodes hiddennum = 20, the output layer node outputnum = 5, the hidden layer transfer function is the purelin function, the output layer transfer function is the logsig function, and the training function is the trainlm

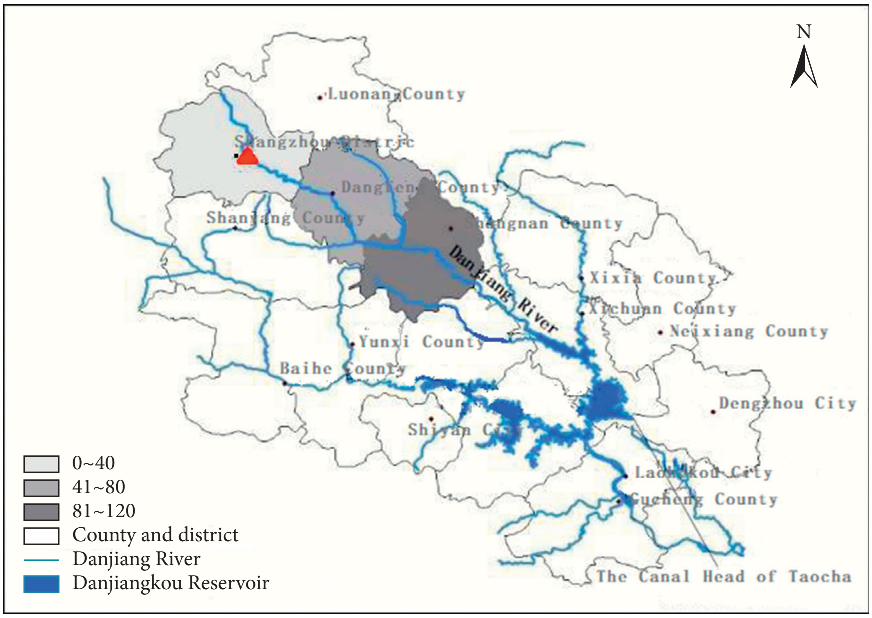

Figure 4: Geographical distribution map of water quality monitoring points.

Table 1: Site name and latitude and longitude information.

Monitoring point number	Site name	Longitude (degrees)	Latitude (degrees)
Monitoring point 1	Gouyu bridge	110.02176	33.88903
Monitoring point 2	Wangyuan bridge	109.92283	33.87804
Monitoring point 3	Jinyuan water bank	109.93153	33.86736
Monitoring point 4	Overpass	109.93836	33.86604
Monitoring point 5	Rainbow bridge	109.95553	33.86311
Monitoring point 6	Renyuan bridge	109.97052	33.85894

Table 2: Water quality content grades and classification standards.

Taxon description	Class 1	Class 2	Class 3	Class 4	Class 5
NH3–N/mg $\bullet$ L^{-1}	0–0.15	0.15–0.50	0.5–1.0	1.0–1.5	1.5–2.0
DO/mg $\bullet$ L^{-1}	7.5–6.0	6.0–5.0	5.0–4.0	4.0–2.0	2.0–0
COD/mg $\bullet$ L^{-1}	0–10	10–15	15–20	20–30	30–40
I_{Mn}/mg $\bullet$ L^{-1}	0–2.0	2.0–4.0	4.0–6.0	6.0–10	10–15
Total phosphorus/mg $\bullet$ L^{-1}	0–0.02	0.02–0.10	0.10–0.20	0.20–0.30	0.30–0.40
Total nitrogen/mg $\bullet$ L^{-1}	0–0.20	0.20–0.50	0.50–1.0	1.0–1.5	1.5–2.0

function, The maximum number of training times is set to 1000 times, and the learning accuracy target is 0.0001. Different algorithms are run independently for 10 times, and the average of the 10 water quality prediction results is used as the final evaluation result. The population size of GA-BP, PSO-BP, and ABC-BP algorithms are all set to 10, the maximum number of iterations is 100, the search interval is [−1,1], the algorithm runs 10 times independently, and the results of 10 water quality predictions The average value is used as the final evaluation result [20]. The results are shown in Table 3, Figures 5 and 6.

From the comparison results of the evaluation accuracy in Table 3, it can be seen that in the training set and test set, the optimal accuracy rate of improved ABC-BP is the highest, 96.58% and 97.32%, respectively, and the accuracy rate is higher than that of GA-BP, PSO-BP, and ABC-BP; compared with the ABC-BP, the optimal accuracy rate is increased by 3.64% and 3.28%, respectively; compared with the PSO-BP, the optimal accuracy rate is increased by 3.90 and 4.07%, respectively; compared with the GA-BP, the optimal accuracy rates were increased by 3.86% and 3.99%, respectively, indicating that the improved ABC-BP can effectively improve the accuracy of water quality evaluation.

On the training set and test set, the worst and average accuracy rates of the improved ABC-BP algorithm are higher than those of GA-BP, PSO-BP, and ABC-BP, which shows that the improved ABC-BP algorithm has better stability and robustness.

Figures 7 and 8 are the simulation comparison diagrams between the single BP neural network algorithm, the

Table 3: Comparison of water quality evaluation accuracy.

Method	Training set accuracy (%)			Test set accuracy (%)		
	Optimal	Worst	Average value	Optimal	Worst	Average value
GA-BP	92.72	91.68	92.2	93.24	92.17	92.70
PSO-BP	92.68	92.19	92.43	93.16	92.39	92.77
ABC-BP	92.94	92.38	92.66	93.95	93.42	93.68
Improved ABC-BP	96.58	93.36	94.97	97.23	93.89	95.56

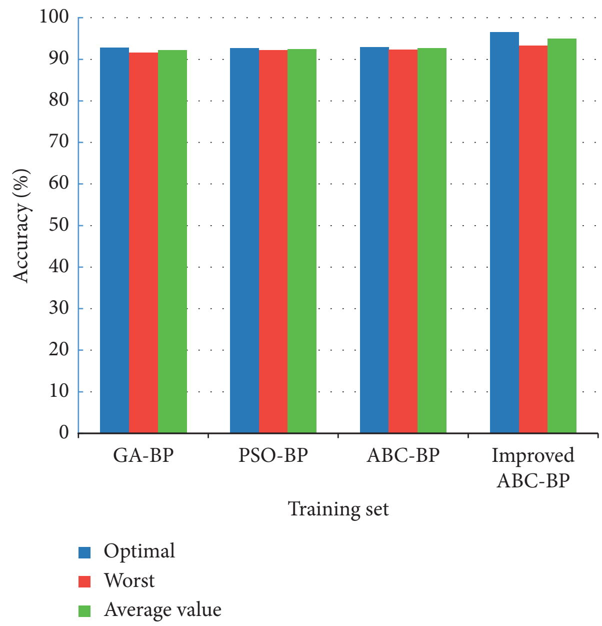

Figure 5: Training set.

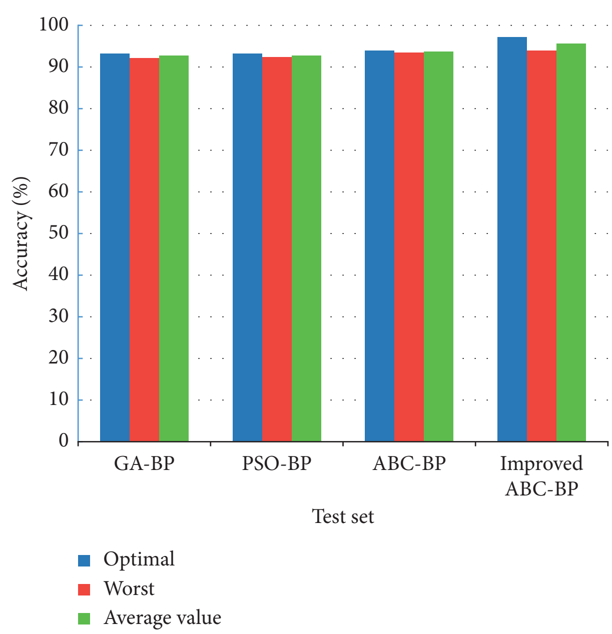

Figure 6: Test set.

improved ABC-BP algorithm, the standard ABC-BP algorithm iteration number, and the target error. From the figure, it can be seen that the improved ABC-BP algorithm, the number of iterations of the BP algorithm tending to the target error value is lower than that of the other two algorithms. When the standard ABC algorithm falls into the

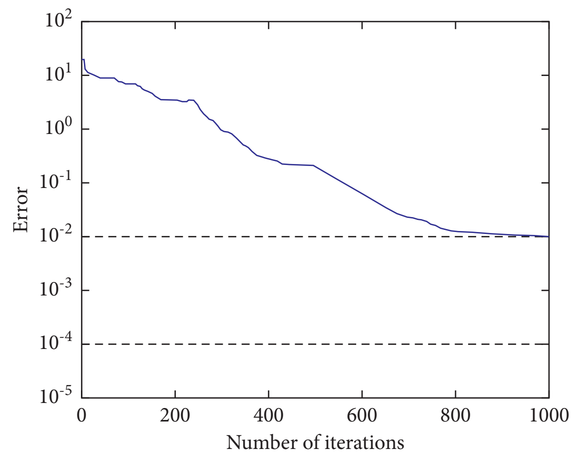

Figure 7: BP network simulation diagram.

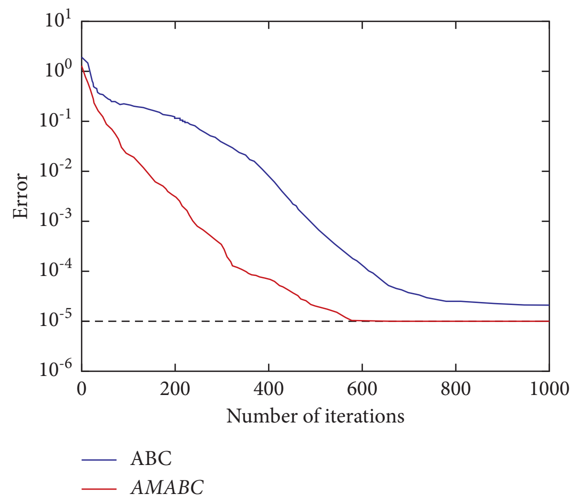

Figure 8: AMABC and ABC optimization comparison chart.

local optimization, the improved ABC-BP algorithm can jump out of the local optimization. Due to the addition of the levy factor and the adaptive factor, the prediction accuracy, convergence speed, and stability of the improved ABC-BP algorithm are greatly improved. Figure 9 is a fitting diagram of actual output and target output. It can be seen from the figure that the fitting is better, indicating that the improved ABC-BP algorithm has better convergence.

In order to compare and study the influence of different hidden layer node numbers, learning rate, and iteration number parameters on the water quality prediction and evaluation results, the accuracy rates of different parameters were compared, and the results are shown in Figure 10.

It can be seen from Figure 10(a) that the accuracy rate of the water quality evaluation model gradually increases with the number of hidden layer nodes. When the number of nodes is 20, the accuracy rate reaches the maximum, and when the number of hidden layer nodes increases, the accuracy rate gradually decreases, and the network complexity increases. Therefore, considering the prediction accuracy, network generalization ability, and complexity, the best number of hidden layer nodes of the BP neural network is 20. It can be seen from Figure 10(b) that as the learning rate increases, the accuracy of the water quality evaluation model gradually increases. When the learning rate is 0.05, the accuracy reaches the maximum, and after it exceeds 0.05, the accuracy gradually increases and then it reduces. It can be seen that when the learning rate is 0.05, the effect of the model is the best, and the generalization ability and accuracy rate reach the best state. It can be seen from Figure 10(c) that as the number of iterations increases, the accuracy of the water quality evaluation model gradually increases. When the number of iterations is about 500, the prediction accuracy is the highest. After more than 500, the accuracy increases with iterations. The increase in frequency gradually decreases. It can be seen that when the number of iterations is about 500, the local search ability and global search ability of the model are the best, and the accuracy rate is the highest. At the same time, the iteration time and prediction accuracy of GA-BP, PSO-BP, ABC-BP, and improved ABC-BP are compared, and the results are shown in Table 4. Analysis of the results shows that the improved ABC-BP algorithm has

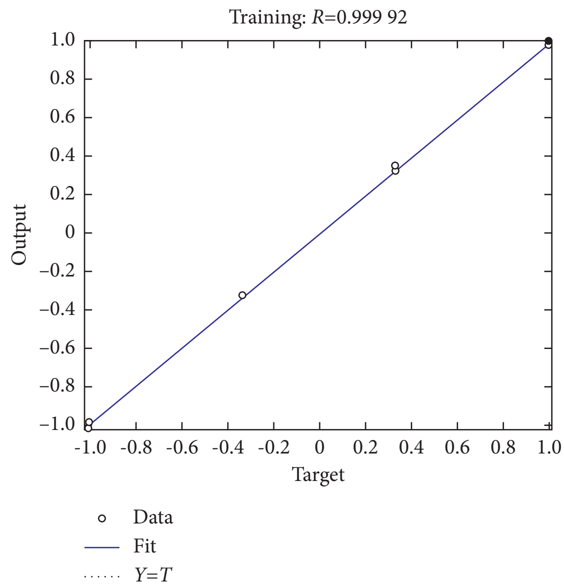

Figure 9: Fitting diagram of actual output and target output.

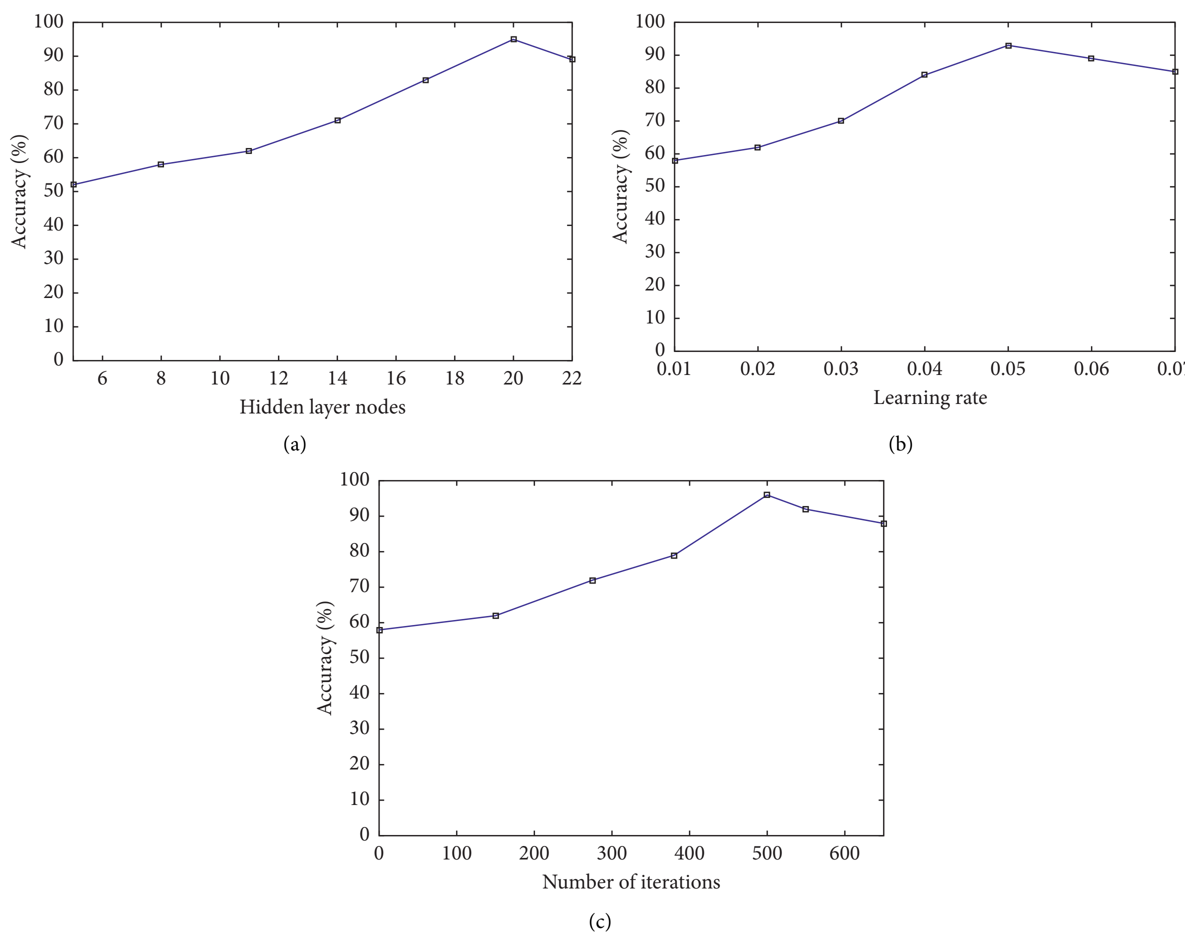

Figure 10: Relationship between different parameters and accuracy (a) Number of hidden layer nodes (b) Learning rate (c) Number of iterations.

Table 4: Comparison of optimization algorithms.

Algorithm name	Iteration time (ms)	Accuracy rate of water quality evaluation (%)
GA-BP	51.6	92.43
PSO-BP	49.8	92.87
ABC-BP	44.3	93.58
Improved ABC-BP	42.1	95.56

the shortest iteration time, the highest accuracy, and the best model. The above analysis lays the foundation for the construction of the later water quality evaluation model and the study of parameter selection.

6. Conclusion

In order to build a stable, reliable, and highly accurate water quality prediction model, an improved ABC-BP algorithm model is proposed. By adding the adaptive local search factors and mutation factors, the local and global search capabilities of the ABC algorithm are improved to improve the performance of local search and avoid local optimal conditions. The improved ABC algorithm is used to optimize the weights and thresholds of the BP neural network and establish a water quality grade prediction model. Taking the water quality monitoring data of Danjiang source (Shangzhou section) from 2015 to 2019 as the research object, compared with GA-BP, PSO-BP, ABC-BP, and BP models, the research results show that the improved ABC-BP algorithm has lower iterations, faster convergence speed, highest prediction accuracy, and has good engineering application and promotion value. Since there are fewer evaluation indicators that affect the water quality grade in this article, more water quality evaluation methods with more influencing factors will be studied later to further improve the applicability of the model.

Data Availability

The datasets used and/or analyzed during the current study are available from the corresponding author on reasonable request.

Conflicts of Interest

The author(s) declare no potential conflicts of interest with respect to the research, authorship, and/or publication of this article.

Acknowledgments

The authors acknowledge the National Natural Science Foundation of China (Grant: 61876143), Shaanxi Provincial Department of Education 2019 Special Scientific Research Plan Project (Grant: 19JK0261), Shaanxi Provincial Department of Science and Technology 2019 Scientific Research Plan Project (Grant: 2019JQ-541), and Special Project of Shangluo University Serving Local Scientific Research (Grant: 19FK002).

References

[1] L. I. Xiao-gang, B Qiao-hui, and P Jiang-li, "Grain size analysis and heavy metal pollution assessment of river surface sediments in Danjiang River basin," *Acta Agriculturae Jiangxi*, vol. 31, no. 4, pp. 93–98, 2019.

[2] Y. Cheng, G. Xu, L. I Peng, X.-J. Liu, T.-G. Zhang, and L. Fei-Fei, "Spatial variation characteristics of runoff nutrients in Dan River," *Journal of Northwest A&F University*, vol. 44, no. 4, pp. 93–99, 2016.

[3] L.-L. Guo, Z.-H. Zou, and A. N. Yan, "Study on water quality forecast based on GM(1,1) residual modification model," *Mathematics in Practice and Theory*, vol. 44, no. 19, pp. 176–181, 2014.

[4] D. Liu and Z. Zou, "Application of weighted combination model on forecasting water quality," *Acta Scientiae Circumstantiae*, vol. 32, no. 12, pp. 3128–3132, 2012.

[5] M. Xu, Y. Fu, Z. Liu, G. Li, and P. Qu, "Forecasting of water quality using grey GM(1,1) -wavelet-GARCH hybrid method in Songhua River Basin," *Transactions of the Chinese Society of Agricultural Engineering*, vol. 32, no. 10, pp. 137–142, 2016.

[6] C. Zhang, Y. Luo, and P. Lv, "Application of grey metablism GM(1,1) in the quality prediction of water in main stream yangtze river," *Environment and Ecology in the Three Gorges*, vol. 34, no. 4, pp. 11–14, 2012.

[7] Y. Ran, W. He, X. Lei, and H. Xia, "Application of GM(1,1) model and improved model to predict the water Quality of Weihe River in Tianshui section," *Journal of Water Resources &Water Engineering*, vol. 22, no. 5, pp. 88–91, 2011.

[8] Y. He, Y. Tang, L. Chen, Y. Li, A. Jing, and J. Xiao, "Evaluation of water quality based on BP neural network and study of the temporal and spatial evolution trend of water quality," *Environmental Protection Science*, vol. 44, no. 3, pp. 114–120, 2018.

[9] C. Su, N. Xiang, G. Chen, and F. Wang, "Water quality evaluation model based on artificial bee colony algorithm and BP neural network," *Chinese Journal of Environmental Engineering*, vol. 6, no. 2, pp. 699–704, 2012.

[10] J. I. Guang-yue, "Prediction of Xijiang River water quality based on improved particle swarm optimization and BP neural network," *CHINESE JOURNAL OF HYDRODYNAMICS*, vol. 35, no. 5, pp. 567–574, 2020.

[11] S Yan-xia, J. Chen, and W. U. Ding-hui, "A multi-objective artificial bee colony based on evolutionary knowledge integrated," *Control and Decision*, vol. 32, no. 12, pp. 2176–2182, 2017.

[12] Q. Liu, H. Xu, and C. Shi, "Research on power flow optimization based on multi-objective artificial bee colony algorithm," *Power System Protection and Control*, vol. 43, no. 8, pp. 1–7, 2015.

[13] W. Tan, Y. Wang, and S. Li, "Crack identification of asphalt pavement surface based on improved artificial bee colony algorithm and BP neural network," *Journal of Railway Science and Engineering*, vol. 16, no. 12, pp. 2991–2998, 2019.

[14] J. Wu, H. Ding, X. Ma, B. Yan, and X. Wang, "Application of improved adaptive bee colony optimization algorithm in transformer fault diagnosis," *Power System Protection and Control*, vol. 48, no. 9, pp. 174–180, 2020.

[15] X. Sun and X. Sun, "Study on water quality classification forecast based on MFOA-ELM," *Journal of Chinese Agricultural Mechanization*, vol. 40, no. 8, pp. 176–181, 2019.

[16] L. Zhu, Y. Wang, M. Han, Y. Zhu, H. Yu, and Y. Song, "Spatio-temporal distribution of water quality and source identification of pollution in Wushui River Basin," *Acta Scientiae Circumstantiae*, vol. 38, no. 6, pp. 2150–2156, 2018.

[17] L Bing, Y Gui-shan, W Rong-rong, L Bao-gui, D Xue, and X Chen, "Temporal variability of water quality in poyang lake outlet and the associated water level fluctuations:A water quality sampling revelation," *Resources and Environment in the Yangtze Basin*, vol. 26, no. 2, pp. 289–296, 2017.

[18] J. C. Casila, G. Azhikodan, and K. Yokoyama, "Quantifying water quality and flow in multi-branched urban estuaries for a rainfall event with mass balance method," *Water Science and Engineering*, vol. 13, no. 4, pp. 317–328, 2020.

[19] Y. Yang, Q. Xiong, C. Wu et al., "A study on water quality prediction by a hybrid CNN-LSTM model with attention mechanism[J]," *Environmental Science and Pollution Research*, vol. 28, no. 39, pp. 55129–55139, 2021.

[20] J. Sha, X. Li, M. Zhang, and Z.-L. Wang, "Comparison of forecasting models for real-time monitoring of water quality parameters based on hybrid deep learning neural networks," *Water*, vol. 13, no. 11, p. 1547, 2021.

Hindawi
Scientific Programming
Volume 2021, Article ID 2344527, 7 pages
https://doi.org/10.1155/2021/2344527

Research Article

Optimizing the Construction of Multidimensional System of Entrepreneurship Education from the Perspective of the Second Classroom

Meng-Xi Zhu,[1] **In-Jae Kim**,[2] **and Zhi-Quan An**[3]

[1]*Student Affairs Office, Beihua University, Jilin City, China*
[2]*Hoseo University, Asan, Republic of Korea*
[3]*School of Economics and Management, Beihua University, Jilin City, China*

Correspondence should be addressed to Zhi-Quan An; bh1702@126.com

Received 7 September 2021; Accepted 18 November 2021; Published 28 December 2021

Academic Editor: Punit Gupta

Construction of the entrepreneurial ability evaluation system based on the Communist Youth League's second class is presented in this paper. Drawing on the advanced experience of foreign countries and in accordance with the requirements of UNESCO, the objectives of innovation and entrepreneurship education should be integrated into school education and teaching objectives, and the content, curriculum, and atmosphere of social entrepreneurship education should be highlighted, with the effectiveness of entrepreneurship education as the focus of practice. Combining the characteristics and advantages of all disciplines and disciplines, we will create an innovative and pioneering education system that integrates interyear, interdisciplinary, interdisciplinary, and distinctive features and infiltrates the entire process of cultivating outstanding professionals in various fields. Through entrepreneurship education, general education courses to guide students to focus more on professional courses pay more attention to the latest developments in professional fields and innovation thus optimizing their knowledge structure and cultivating their innovative thinking, entrepreneurial awareness, and professional competence

1. Introduction

With the continuous promotion of the education authorities and universities, college students' entrepreneurship and entrepreneurship education have quickly become a hot spot in higher education. However, there are still many areas worthy of improvement and optimization in the environment for entrepreneurship and entrepreneurship education that mainly manifested in [1–3]: the tripartite linkage mechanism between local governments, universities, and individual students under the framework of entrepreneurship education has not yet been established, and policies supporting college students' entrepreneurship have not yet been implemented (Figure 1).

The core of the entrepreneurship is innovation. Entrepreneurship based on innovation is full of vitality and has only sustainable development. China's urban economic structure shows transition from a big manufacturing country to a strong manufacturing country. Therefore, the basic elements of an innovative city include management innovation, technological innovation, and the industrial innovation. The curriculum system is a comprehensive reflection of the goal of the personnel training and teaching philosophy. The curriculum system to a certain extent determines the students' knowledge structure and ability structure [4].

The research on the establishment of entrepreneurial education curriculum is not only the need of improving the theory of the entrepreneurship education but also the actual need of then carrying out the undertaking education activities. To combine the curriculum system of entrepreneurship education with successful entrepreneurs, we must have entrepreneurial consciousness, personality traits, core competence, and social knowledge structure.

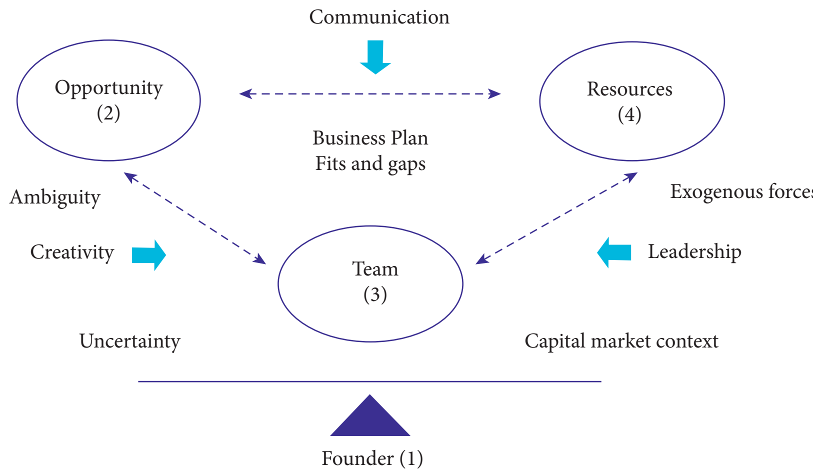

Figure 1: The entrepreneurial ability evaluation system framework.

The construction of the high-tech venture risk evaluation index system should also follow the following principles [5, 6]. (1) Scientific principle: the scientific principle is the basis of constructing the index system of high-tech venture risk. Its main performance indicators in the selection and design should have a theoretical basis, to grasp the regularity and creativity. (2) The principle of the development: enterprises of the same nature are faced with different risks in different periods, especially in the current market economy of our country. Because of the economic system, industrial policy, exchange rate policy, capital market, and other factors that have a significant impact on entrepreneurship are still not stable. High-tech entrepreneurship is facing a lot of uncertainty. (3) Systematic, targeted, and some operational principles: the various risks enterprises face in starting a business do not exist in isolation. They are interrelated and influence each other. In the construction of the index system, we should consider these risk factors as an organic system, analyze the risks that high-tech start-ups face, and at the same time pay attention to the measurability and accessibility of the indicators.

With the goal of cultivating outstanding professionals in various fields, a comprehensive and systematic course system of the innovation and entrepreneurship education and a first and second classroom interaction are set up. The comprehensive platform for interyear, interdisciplinary, and interdisciplinary entrepreneurship practice combines organic integration of general simulated exercises and actual exercises focusing on building a distinctive "one core, three platforms, and nine modules" innovation, and the entrepreneurship education system guides and helps college students change the employment concepts, broaden the entrepreneurial channels, cultivate innovative ability to create entrepreneurial talent, and through continuous exploration, gradually built into distinctive features, significant results, and demonstrative ability to drive the national or provincial college students innovation and entrepreneurship education demonstration base. In Table 1, we show the principles that should be considered [7].

2. Communist Youth League's Second Class

The second class transcript of the core Communist Youth League refers to the mechanism of the first class and combines the characteristics of the second class with the transcripts of students' participation in the second class activities in a manner similar to that of traditional university transcripts. The emergence of transcripts in the second class has led to the explicit display. As a forward front of ideological work, colleges and universities shoulder the important speech of the propaganda and general secretary series and new ideological and tactic strategies of governing state affairs and politics, nurturing and promoting the socialist core values and providing human resources protection for the realization of the Chinese dream of the great rejuvenation of the Chinese nation and intellectual support for the important task. Strengthening the ideological and political work in colleges and universities is a strategic project, a solid project, and a project of casting soul and is of great and far-reaching significance.

The "Transcripts of Second Class" of colleges and universities cover most of the tasks and responsibilities of CYL in colleges and universities. They guide, record objectively, scientifically evaluate, and promote the growth of students and systematically modularize and dataize students' participation in the second classroom. Students will be provided with a demonstration of self-evidence of some scientific evaluation systems as effectively leading students to take the initiative to integrate into the ideological and political education. In the analysis and research of some related cases, the author believes that the establishment of the second classroom transcript system can be developed from the "three-step" strategy:

(i) System and scientific assessment is the important link of the second class report card system. In order to then establish the system of the system, we can learn the pattern mechanism of the first class and combine the characteristics of the second classroom activity, such as attendance, ordinary performance, and final grade.

Table 1: The principles for the construction of the entrepreneurial ability evaluation system.

Principles	Details
Introduce the system of instructor and enhance the effectiveness of the system	Gradually establish a university venture research institutions. The sustainable development of college students' entrepreneurship education cannot be separated from the support of research work. Colleges and universities are the main front of scientific research activities. University teachers generally have some research ability.
Open entrepreneurship education public class and strengthen students entrepreneurship awareness education	In setting up the education curriculum system, we pay attention to the innovation and practicability of education, set up the education public course, and gradually build up a relatively perfect system of education courses with its own characteristics.
Professional knowledge embedded in innovation and entrepreneurship and education to play an active role in professional advantages and special talents	Curriculum teaching can accumulate and deepen students' entrepreneurial quality, add relevant contents of innovation and entrepreneurship, and promote innovation and entrepreneurship education in the whole process and individuation.

(ii) The establishment of the second class transcript system should pay attention to analysis, reflecting the needs of multiple analysis, and from the student's point of view, the second classroom transcript will be that students of the second classroom education were dominant Through the analysis of the results, on the one hand, students gain a sense of achievement; on the other hand, it also stimulates students to selectively participate in the weak links in the second class to think. From the perspective of schools, big data analysis is used to provide scientific data for school second class education reform on the one hand, and effective data for student personality development analysis on the other hand.

(iii) On the basis of their own reality and characteristics, colleges and universities can further clarify and conclude the second classroom activities types and establish a scientific second classroom curriculum system based on the practice of quality development practice.

The fundamental purpose of the personalized education is to enable students to develop their good personality, character, and specialty by providing personalized development goals, paths, models, and evaluations for different types of students. So that students' personal potential can be fully developed. Personalized education thought originated in the 1960s humanistic philosophy of education. As early as the 1980s, Europe and the United States started the pilot reform of the personalized education. Harvard professor Howard Gardner also wrote in 2009 that the era of personalized education is coming.

Personalized education has become an international trend of education. Individualized education is an inevitable requirement to adapt to the diversified talent structure in modern society. It is an inevitable choice to realize the smooth transition of the higher education. It reflects the true meaning of the education and the return of education essence. It is an important measure for CYL to acquire youth identity through its own advantages. Therefore, we should consider the following regulations:

(i) School material culture is the material carrier and guarantee of school spiritual culture. It is imperative to build a training base for students to cultivate their comprehensive qualities and at the same time strengthens the management of the characteristics of the community to then cultivate student sentiment, cultivate students' expertise, and enhance the employment competitiveness of students to lay the foundation.

(ii) Through the party branch's mass line education practice, service awareness and education awareness are raised. Through the mass line summary of education practice, improvement to participate in the students' cognitive ability, and actively guiding students to establish correct world outlook, the outlook on life, values, working for party, and government leadership attaches great importance to the basic campus culture construction attention responsible for the teacher correct guidance to participate in a strong situation of students' positive enthusiasm.

(iii) The work group of the Communist Youth League in Colleges and universities has a wide coverage and a good mass base. The campus culture activities carried out by the Communist Youth League activities are more vivid, and the leader role of student leaders is more effective.

Years of practical experience have proved that effective and high-quality social practice plays an important role in cultivating the comprehensive qualities of young people in relation to theory, innovative thinking, and social adaptability. In this sense, the second CYL education for the young people is an important guarantee for the all-round development of young people. Due to the change of the specific living environment and the continuous emergence of undesirable social phenomena in the transition period, the CYL must expand its relevant functions as needed to continuously innovate and improve the content and then form of the second class so as to provide assistance for the all-round development of young people as shown in Table 2.

3. The Construction of Entrepreneurial Ability Evaluation System

3.1. The Entrepreneurial Ability. Although there is a rapid development of our college students' innovation and basic entrepreneurship education, there are still some shortcomings and first teachers need to be strengthened urgently. Innovation and entrepreneurship education is a comprehensive quality education, not only to carry out innovation and entrepreneurship theoretical knowledge but also to pay attention to the stimulation of innovation and innovation and practical ability to improve. This requires that teachers not only have a wealth of the knowledge of innovative entrepreneurship but also have rich practical experience in innovation and entrepreneurship [8].

Broad sense of entrepreneurship refers to the post-entrepreneurial, and narrow sense of the general business only refers to the own business. Around the basic meaning of the innovation and entrepreneurship, colleges and universities should take the following countermeasures in cultivating students' ability of innovation and entrepreneurship [9, 10]. (1) Universities can organize a series of the innovation and entrepreneurship competition activities, cultivate students' innovative awareness, and improve students' innovation and entrepreneurship ability. Students are encouraged to actively participate in provincial, national innovation, and entrepreneurship competitions and academic activities. (2) The consciousness of innovation itself is a motive force and an accelerator of innovation. It dominates the creative ability of people and then promotes the cultivation and improvement of innovation ability. Cultivating students' consciousness of innovation and entrepreneurship is the basic goal of carrying out innovative and the entrepreneurial education in colleges and universities. The school publicises the innovation and entrepreneurship policies and successful entrepreneurs' experiences through the school magazine, the school radio station, the campus network, billboards, and other media to stimulate students' entrepreneurial enthusiasm. (3) Elective courses for innovation and entrepreneurship can include company law, modern enterprise system, innovative thinking, enterprise management, and entrepreneurship theory and practice. Students can choose appropriate courses and innovation and entrepreneurship practice activities according to their own interests and hobbies, so as to lay a good theoretical foundation for their own innovation and entrepreneurship. In Figure 2, we show the entrepreneurial ability and economic resources.

In terms of professional curriculum, there should combination with the characteristics of each professional and its key in basic conjunction with market, targeted to open innovation business-related courses and at the same time pay attention to the students' individual character development needs, according to their aptitude.

Colleges and universities should actively seek cooperation resources and establish multiple university-enterprise cooperation to create business incubators and gradually strengthen the university students innovative entrepreneurial atmosphere, kinds of innovation through entrepreneurship competition project to promote the practice of college students, through competition incentives to encourage the innovation of the college students entrepreneurship practice, provide students with more opportunities for innovation entrepreneurship practice, and promote the college students' innovative entrepreneurial ability of general ascension. The competitive situation in China's transition environment forces entrepreneurs to strengthen their learning to improve their own entrepreneurial ability, so as to improve the performance of new enterprises [11].

Although many scholars have emphasized the importance of the entrepreneurial learning to new company, existing research stays in the conceptual phase, and more entrepreneurial learning mechanism for new enterprises lack the corresponding empirical test. Teachers teach students ways to deal with the problems in the process of teaching, fully mobilize students involved in the actual teaching to let the students to use their own subjective initiative to solve the problem, and let the students in the learning process to realize their own sense of the accomplishment. After the students have achieved success, they have cultivated the correct learning method and cultivated a good attitude of learning [12, 13].

Students get a personal experience in learning and learn to create in the experience. Teachers use multimedia teaching instead of the traditional blackboard teaching, put forward corresponding problems, improve the classroom teaching atmosphere, improve students' practical ability, and guide the student to find problems in the learning process to solve. Students become masters of the learning in the process of solving problems, and teachers have some guidance around them, and the suggestions are listed as follows:

(i) Organization and management ability is the guarantee of business success and business development capacity relationship with the development of enterprise. On college students' entrepreneurs, business development capacity refers to have a keen sense of touch and the insight ability and able to capture the development trend of the industry. At the same time, it must have a strong ability to adapt and develop ability.

(ii) The improvement of college students' entrepreneurial ability requires the work of education, while the development of the education is more necessary for modern teaching methods, as well as the help of hardware facilities such as libraries, websites, and databases especially need to combine entrepreneurship education in colleges and universities practicality and other characteristics to establish a professional and advanced innovative entrepreneurial training department to let the students to fully experience the entrepreneurial practice under various scenarios.

(iii) Of course, our long-term exploration of the entrepreneurship education in the colleges and

Table 2: The communist youth league's second class suggestions.

Suggestions	Details
Stimulate wisdom and mobilize the enthusiasm of students	Each student has advantages such as fully exploiting its inherent potential and guiding them to participate actively in the second class of the Communist Youth League. This requires that the CYL must formulate a set of incentive policies that motivate students and teachers to participate and establish a way to encourage as many students as possible to participate in the second classroom activities and to maximize student motivation, initiative, and creativity.
To form a routine and ensure the smooth development of activities	To truly implement, we must establish the three-level management system from the school Youth League Committee, the Youth League Committee, and the class league branch. In this process, the guiding role of the teachers is very important. Under the guidance of professional teachers, the students' confusion period is shortened, and the enthusiasm of participating in the second class is also then improved.
All-round evaluation to promote the all-round development of students	It will improve teaching effectively and promote students' development and improvement to establish an evaluation system with multiple evaluation subjects and comprehensive evaluation contents and diversified evaluation methods.

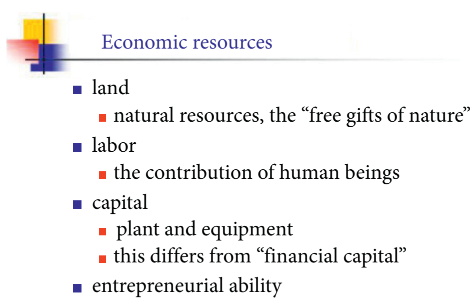

Figure 2: The entrepreneurial ability and economic resources.

universities has made some progress, but because the entrepreneurship education is still in the initial stage, the idea of education act too utilitarian and simple and entrepreneurship education has been in the job training and training work. In the current stage, self-employment education needs to be developed, so as to achieve the integration of the three aspects such as self-employment education, quality education, and regular education and deepen the educational reform.

3.2. The Business Evaluation Model. Through the research on evaluation and safeguard measures of entrepreneurship ability both at home and abroad, we can find that because college students start a business as a dynamic process, they need complex dynamic research and sequence analysis in methodology [14]. Many research studies tend to analyze the composition of entrepreneurial ability of the college students through questionnaire analysis to obtain the corresponding data as shown in Figure 3.

After the establishment of the index system and evaluation criteria of the internal performance evaluation control system of an enterprise, the final evaluation result needs to be quantified through the evaluation score method. The evaluation scoring method generally adopts a certain measurement model to unify the evaluation indexes of different types and types of systems and finally obtains the clear and definite evaluation results and then forms the evaluation conclusion and further completes the evaluation report. Because the interpersonal comprehensive ability is a comprehensive study of the interpersonal communication ability of the college students, in the face of complex entrepreneurial process, identification is conducive to college students to grasp the corresponding entrepreneurial opportunities and develop good executive ability as entrepreneurial project exercises, for college students venture to maintain good interest in order to effectively motivate students to start their own businesses, so the overall regression of these variables is more significant but also in line with the college students entrepreneurship theory and public awareness. In addition, full absorption of social human resources to make up for teachers hired successful entrepreneurs as visiting professors in entrepreneurship education, to carry out short-term teaching. Open lectures participate in case discussions to give students a professional guidance and evaluation of business plans but also pay attention to the professional growth of entrepreneurship teachers, to create more opportunities for teachers to enhance training. Through holding entrepreneurial teaching seminars, organizing teachers to attend the entrepreneurial academic conferences, and so on, special training for teachers is carried out to improve the quality of practitioners.

3.3. The Entrepreneurship System. Although we have given different explanations and choices about the concepts and curricula of the general education, the related theoretical research and practical exploration are also different [15]. However, the core concept always focuses on the all-round development of the "people" themselves. Therefore, we believe that general education is part of the nonprofessional education in college education. It is a "common education" that prepares students for any major study, aiming to cultivate social citizens with social responsibility, that sound personality, broad vision, and all-round development. The goal of the entrepreneurship education at three levels of the target orientation is as follows: first, on the whole, the basic goal of entrepreneurship education is to cultivate college students entrepreneurial awareness and entrepreneurial ability, to promote the practice of planning students; second, from colleges and universities, the goal of entrepreneurship

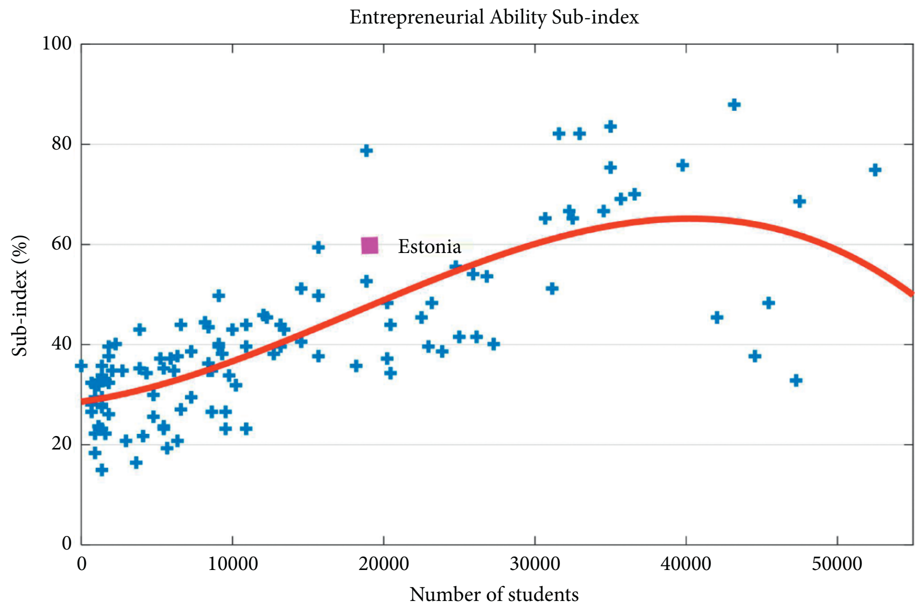

Figure 3: The business evaluation model simulation.

education is to cultivate the basic ability and pioneering personality of college students in different fields so that they have a good sense of entrepreneurship, entrepreneurial psychology, and entrepreneurial ability and form awareness and habits of initiative and research study; thirdly, from the perspective of individual students, the purpose of accepting startup education should be to cultivate their own professionalism and sense of responsibility, pioneering personality, the spirit of adventurousness, ability to work independently, and entrepreneurial ability to adapt to the changing social and professional environment, as well as the ability to coexist and collaborate with others.

After several years of practice, it is not hard to find that this model of entrepreneurship education did not rise to the level of concept guidance. There are some unavoidable problems, and without a clear distinction between the subject knowledge and the meaning of “creative” goals and the understanding of entrepreneurial talent, the sense of entrepreneurial entrepreneurship as well as the overall quality of entrepreneurship has not been truly cultivated. The knowledge structure needed by the students cannot be completely constructed. In the summary, we finalize the following suggestions. (1) In order to overcome the limitations of the traditional theory of classroom teaching to cultivate the real sense of entrepreneurial talent, entrepreneurship research needs to be actively carried out. Special entrepreneurship research institutions should be set up to carry out entrepreneurship education and entrepreneurship capacity building research. (2) Utilize favorable social resources, invite outside entrepreneurs, entrepreneurship successful people, and hold some business forums and lectures on a regular basis to tell students about the business process and share their entrepreneurial experience. Colleges and some universities should regularly carry out entrepreneurship competition plans to provide students with practice simulation opportunities. In addition, all-round guidance and support for the entrepreneurship students in schools should be given full play to the typical radiation role and a strong entrepreneurial atmosphere to promote the development of entrepreneurship education in higher education institutions. (3) College student startup education is the education that all college students should accept. It has the properties of the education. According to the basic idea of the general education in building the university entrepreneurship education curriculum system, popularize entrepreneurship education in ordinary colleges and universities as soon as possible, and the curriculum is the effective way to improve the quality of the entrepreneurship education in colleges and universities.

4. Conclusion

Construction of the entrepreneurial ability evaluation system based on the Communist Youth League’s second class is presented in this paper. The basic knowledge of entrepreneurship theory is the main focus of the school to promote innovation and entrepreneurship. According to the students’ essential knowledge, ability, and quality structure, they build up three modules and a three-dimensional foundation platform for entrepreneurship teaching. The cultivation of entrepreneurial talent’s comprehensive qualities requires that the students’ social adaptability and innovative ability be highlighted, and the limitation of professional adaptation in the past should be exceeded by one-sided emphasis on personnel training in higher education in which emphasis should be put on equally on both theory and practice, persistence in theory, and practice in personnel training.

Data Availability

The datasets used and/or analyzed during the current study are available from the corresponding author on reasonable request.

Conflicts of Interest

The authors declare that there are no conflicts of interest with respect to the research, authorship, and/or publication of this article.

Acknowledgments

This paper is a teaching and research project of Beihua University: Research on the construction of multidimensional teaching system of entrepreneurship education in colleges and universities (Grant xjyb20210001).

References

[1] M. Shahbani, A. Bakar, and A. Azmi, "Improving entrepreneurial opportunity recognition through web content analytics," *Journal of Telecommunication, Electronic and Computer Engineering*, vol. 9, no. 2-11, pp. 71–76, 2017.

[2] T. Nikraftar, E. Hosseini, E. Hosseini, and E. Hosseini, "Factors affecting entrepreneurial opportunities recognition in tourism small and medium sized enterprises," *Tourism Review*, vol. 71, no. 1, pp. 6–17, 2016.

[3] E. A. Wood, "Towards a perceptual model of corporate entrepreneurial activity: a focus on the South African financial sector (Doctoral dissertation)," 2016, https://www.semanticscholar.org/paper/Towards-a-perceptual-model-of-corporate-activity%3A-a-Wood/e97d62ee4979894e5d2fe7a30e138ede1e581ece.

[4] N. Rahmawati, S. Hartono, L. Rahayu, and Masyhuri, "Innovative and creativity as entrepreneurial ability of organic rice farmers in Bantul, DIY," in *Proceedings of the AIP Conference Proceedings*, vol. 1755, no. 1, p. 130002, September 2016.

[5] F. Hongyan, R. G. LianXiaojie, and L. Wei, "Explaining the relationship between entrepreneurial learning and entrepreneurial ability through knowledge management perspective among undergraduate students base on SEM-PLS," in *Proceedings of the Global Conference on Business and Economics Research (GCBER) 2017*, Universiti Putra Malaysia, Malaysia, August 2017.

[6] H. Jiang, W. Xiong, and Y. Cao, "Research on the mechanism of entrepreneurial education quality, entrepreneurial self-efficacy and entrepreneurial intention in social sciences, engineering and science education," *Eurasia Journal of Mathematics, Science and Technology Education*, vol. 13, no. 7, pp. 3709–3721, 2017.

[7] J. Haltiwanger, E. Hurst, J. Miranda, and A. Schoar, "Introduction to measuring entrepreneurial businesses: current knowledge and challenges," in *Measuring Entrepreneurial Businesses: Current Knowledge and Challenges*University of Chicago Press, Chicago, Illinois, United States, 2016.

[8] M. C. Bayon and Y. Vaillant, "International variations in the impact of perceived entrepreneurial ability and actual ability on entrepreneurial activities," *Strategic Change*, vol. 25, no. 2, pp. 131–150, 2016.

[9] B. Hynes, N. Kennedy, and J. Pettigrew, "The role of business schools in framing entrepreneurial thinking across disciplines: the case of allied health professions," in *Proceedings of the Innovative Business Education Design for 21st Century Learning*, pp. 75–91, Springer International Publishing, Switzerland, June 2016.

[10] A. M. B. Alizadeh, M. Abbaszadeh, and S. Hayati, *The Relationship between Social Intelligence with Entrepreneurial Ability Graduate Students of Tabriz University*, 2016.

[11] J. Liu, "Research on the competency model of innovative entrepreneurial team based on network information data mining technology," *RISTI (Revista Iberica de Sistemas e Tecnologias de Informacao)*, vol. E5, pp. 260–273, 2016.

[12] G. Anggadwita, B. S. Luturlean, V. Ramadani, and V. Ratten, "Socio-cultural environments and emerging economy entrepreneurship," *Journal of Entrepreneurship in Emerging Economies*, vol. 9, no. 1, pp. 85–96, 2017.

[13] M. Cook, "Essays on occupational choice and entrepreneurial ventures," *Publicly Accessible Penn Dissertations*, 2016, https://repository.upenn.edu/edissertations/1668.

[14] I. Kusumaningrum and H. Hidayat, "Learning outcomes in vocational education: a business plan development by production-based learning model approach," *International Journal of Environmental & Science Education*, vol. 11, no. 18, pp. 11917–11930, 2016.

[15] D. K. Panda, "Entrepreneurial orientation, intermediation services, microfinance, and microenterprises," *Managerial and Decision Economics*, vol. 39, 2017.

Hindawi
Scientific Programming
Volume 2023, Article ID 9828120, 1 page
https://doi.org/10.1155/2023/9828120

Retraction

Retracted: The Process and Model Innovation of Ideological Education Network Communication in Colleges and Universities Based on Cloud Computing

Scientific Programming

Received 8 August 2023; Accepted 8 August 2023; Published 9 August 2023

This article has been retracted by Hindawi following an investigation undertaken by the publisher [1]. This investigation has uncovered evidence of one or more of the following indicators of systematic manipulation of the publication process:

(1) Discrepancies in scope
(2) Discrepancies in the description of the research reported
(3) Discrepancies between the availability of data and the research described
(4) Inappropriate citations
(5) Incoherent, meaningless and/or irrelevant content included in the article
(6) Peer-review manipulation

The presence of these indicators undermines our confidence in the integrity of the article's content and we cannot, therefore, vouch for its reliability. Please note that this notice is intended solely to alert readers that the content of this article is unreliable. We have not investigated whether authors were aware of or involved in the systematic manipulation of the publication process.

Wiley and Hindawi regrets that the usual quality checks did not identify these issues before publication and have since put additional measures in place to safeguard research integrity.

We wish to credit our own Research Integrity and Research Publishing teams and anonymous and named external researchers and research integrity experts for contributing to this investigation.

The corresponding author, as the representative of all authors, has been given the opportunity to register their agreement or disagreement to this retraction. We have kept a record of any response received.

References

[1] H. Zhan, "The Process and Model Innovation of Ideological Education Network Communication in Colleges and Universities Based on Cloud Computing," *Scientific Programming*, vol. 2021, Article ID 7302877, 7 pages, 2021.

Hindawi
Scientific Programming
Volume 2021, Article ID 7302877, 7 pages
https://doi.org/10.1155/2021/7302877

Research Article

The Process and Model Innovation of Ideological Education Network Communication in Colleges and Universities Based on Cloud Computing

Haiyan Zhan [1,2]

[1]School of Marxism, Shaanxi Normal University, Xi'an 710119, Shaanxi, China
[2]School of Marxism, Shaanxi Institute of International Trade and Commerce, Xi'an 712046, Shaanxi, China

Correspondence should be addressed to Haiyan Zhan; longmahai@126.com

Received 13 September 2021; Accepted 28 November 2021; Published 26 December 2021

Academic Editor: Punit Gupta

The purpose is to improve the power and innovate the communication mode of mainstream I&P (Ideological and Political) education in C&U (Colleges and Universities). The opportunities and challenges that I&P education is facing or will face in media times are analyzed from three factors: the subjective, the mediator, and the environment, which affect the power of mainstream I&P in C&U. Educational means, carriers, resources, places and times, and the interactions between educators and the educated can bring opportunities for the improvement of the educational power of C&U. However, there are great challenges in all aspects of the mainstream ideology, such as education methods, education ideas, education content, education leadership and discourse power, and network public opinion control. Finally, a series of measures are proposed to improve the power of mainstream I&P education in C&U in media times, and they are updating the concept of media education, strengthening the ideological guidance, ensuring the direction of mainstream I&P education, and optimizing the media environment so that a more perfect innovative mode of I&P education is constructed. The research enriches and develops the theory of mainstream I&P education in C&U, innovates the methods of mainstream I&P education in C&U, and enhances the power of mainstream I&P education.

1. Introduction

In media times [1], improving mainstream I&P (Ideological and Political) education power in C&U (Colleges and Universities) [2] has great significance. First, the research on mainstream I&P education power in C&U is a response to the relevant policy and deployment of the party and the state [3]. The research can help communicate China's mainstream ideology to teachers, students, and even the whole society. Second, the research on the power of mainstream I&P education in C&U is a real demand for strengthening mainstream I&P education and responding to the challenges of mainstream I&P education in media times [4]. Third, it helps college students and staff to strengthen the mainstream ideology [5]. Fourth, it improves mainstream I&P education power of university staff [6].

At present, the academic circles make some achievements in the research of new media and ideology [7]. In terms of the above research, western scholars undertake earlier and make many theoretical achievements [8]. However, there are few concerning the ideas that college and university students hold in media times from the perspective of power education. Although the academic research involves the basic theoretical issues of idea construction in C&U in China [9], most of them are scattered in some papers and lack targeted research works. The main problems existing in the current research are: it is not thorough and comprehensive; most of the research suggestions are based on theory and do not combine with the actual needs of individuals and subjects; it is not from power effect, and specific measures are not proposed.

The purpose of ideological and political education network communication is very clear, in order to promote the overall development of college students. In a sense, on said, college students' ideological and political education is a communication process. It is to solve the spiritual and practical problems of college students, so that college students establish a correct world outlook, positive outlook on life, scientific values, and noble moral outlook, and promote their all-round development. In this educational process, communication is everywhere.

The methods adopted are the literature research method, interdisciplinary method, and induction method [10–12], and the corresponding solutions are summarized by sorting out the literature, referring to the related disciplines, and analyzing and inducting the problems so that the network communication process and innovation mode of mainstream I&P education for the new media era are established.

2. Influencing Factors of Idea Education and Network Communication in C&U

2.1. Subjective Factors. There are several views on the educational subject, such as single-subject theory, double-subject theory, and intersubjectivity theory [13], and the third is selected here. The main factors affecting idea communication in C&U are divided into two aspects: educators and the educated.

The ancients say, "a teacher is a model of a person." Teachers play an exemplary role in every aspect of life, including C&U. Teachers' words and deeds have a wide range of invisible mainstream I&P education power for students, and they influence students' thoughts, values, or political statement according to the teaching objectives, plans, and organizations, showing teachers' leading roles [14]. In the media age, resource sharing and equal communication have become the norm of education. However, compared with teachers, students lack the ability to dialectically absorb knowledge in mixed information. In this case, the main role of teachers as educators begins to play. According to the existing theories, teachers can use their cognitive and analytical ability in information management to make information choices and guide students to establish a healthy and positive ideology in the new era.

The educated are important participants in idea communication in C&U [15], and the purpose of mainstream I&P education and communication is to cultivate college students to form correct ideological concepts. Under the new media age, college students are receiving mainstream I&P education all the time. Meanwhile, they also restrict the publicity of mainstream I&P education. Their ideology and morals determine the goal setting, content selection, and educational links of idea education. The development of new media will undoubtedly show the collision between various ideologies. In such a complex new media environment, whether college students can adhere to the mainstream ideology appropriately is very important, and their ideological state can directly reflect the strength of college ideology.

Through the study of the network education platform based on cloud computing, the activities of teachers and students in the network education platform are optimized, and the channels for obtaining network teaching resources and network learning tools are broadened, so as to meet the needs of learners with various personalities.

2.2. Mediator Factors. Educational objectives, contents, methods, and carriers are important mediators that contribute to the interaction between educators and the educated [16], which is called educational mediators, and their importance is self-evident in mainstream I&P education and communication in C&U.

Having a specific educational goal is the premise of mainstream I&P education and communication because the goal shows the essence and direction, stipulates the content, and has a great influence on the methods and carriers. To deal with the more complicated problems in the new media times, the educational objective shows a trend toward mainstream I&P education for students, which includes the socialist ideological education, strengthening the scientific belief of Marxism, adhering to the leadership of the CPC (Communist Party of China), and reinforcing the political belief of socialism with Chinese characteristics. Also, other educational activities must focus on this goal, for it provides strong power for mainstream I&P education and communication. The key to mainstream I&P education and communication is whether this goal is achieved or not. Therefore, the educational goal is also an important reference to evaluate the results of mainstream I&P education and communication.

A comprehensive and systematic communication content of mainstream I&P education in C&U carries a good educational ability. A specific educational content, based on the objectives of I&P education, students' actual needs, and physical and mental development, is a major component of ideological education and communication, an important factor to achieve the goal of mainstream I&P education and communication, and also a reference for teachers and students to implement the mainstream ideology. In media times, there exists mixed ideology, and only more comprehensive and systematic ideological education content can help teachers to spread mainstream consciousness to students accurately and effectively, accordingly enhancing the attraction and affinity of mainstream consciousness.

Finally, the important conditions for the improvement of I&P education ability are methods and carriers. Methods are indispensable in mainstream I&P education and communication. The common educational methods that higher education employs are the practice method, the edification method, and the indoctrination method. In media times, the mainstream I&P education and communication in C&U must be innovative and developmental, and only in this way can the education and communication ability of the higher education improve. Besides, the realization of educational objectives, the construction of teaching content, and the application of the method are dependent on carriers, which includes classroom, activity, conference, and new media. The carrier can make other educational mediators play their roles.

2.3. Environmental Factors. The educational environment of ideology is a major factor affecting its communication [17], which is known as the environmental factors. The most important factor is the social environment, which is the macroenvironment for the formation of mainstream I&P education power, covering politics, culture, and social economy. The socialist economic system lays an economic foundation for the formation of ideology. A good economic environment is conducive for college students to better identifying with the mainstream ideology. Therefore, the development of the economic environment is essential for exchanging ideas. The political environment includes the current political system and the actual state of political development, which has a restrictive effect on mainstream I&P education. The continuous improvement of the education system, which possesses Chinese characteristics, is beneficial to the development of China's socialist ideology. In media times, only by strengthening the construction of socialist democracy and legal system, can its greatest superiority give full play and provide a good political environment for the education and communication of ideology. The cultural environment also plays an important role in the spread of mainstream I&P education. Without a good cultural atmosphere, people are easily lost in the complicated ideological flow in the new times.

The environment in C&U is the microenvironment. C&U are the main places for mainstream I&P education and communication [18]. The environment directly affects the formation of students' mainstream consciousness, and it includes the material environment, cultural environment, school system, and interpersonal communication. A harmonious campus environment can help students form a good sense of campus culture. Good infrastructure helps students learn effectively, campus culture leaves a deep impression for every student, and a harmonious interpersonal environment can form a good campus atmosphere. A warm and harmonious campus environment certainly contributes to the communication of mainstream I&P education in C&U in the new media times.

The virtual environment cannot be neglected. The new media era comes, and it changes people's lives [19] and the living space of students. The education and communication of ideology are deeply affected by it, forming a new environment for the education and communication of mainstream ideology. Its free and open characteristics greatly enhance the dominant position of students, meet the development requirements for students' free personality, and affect every aspect of their life and learning. Therefore, the new media has become an important environmental factor in the spread of mainstream I&P education.

The influencing factors of mainstream I&P education and network communication in C&U are shown in Figure 1.

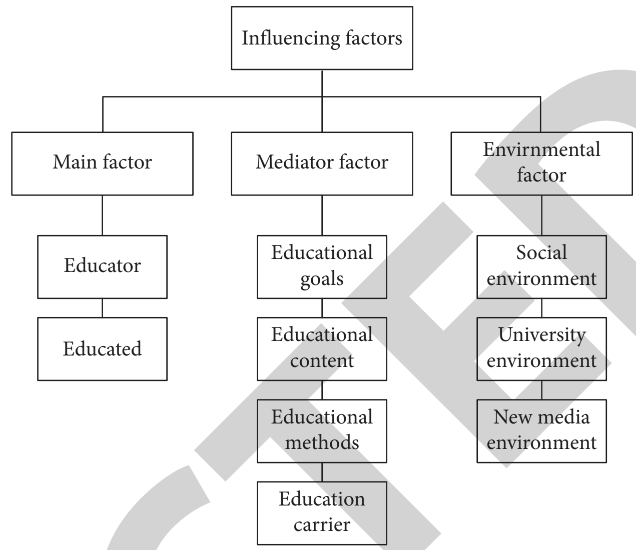

Figure 1: Influencing factors of mainstream I&P education and network communication in C&U.

2.4. Social Environmental Factors. The operation of cultural environment of ideological and political education outside the system is carried out under the contradiction between it and social environment and ideological and political education, thus entering two basic fields. First, it enters into the social environment system and exchanges information and energy with the economic and political environment. Second, it enters into the ideological and political education activities and forms a two-way construction with ideological and political education. Of course, the premise of ideological and political education is based on people in social reality, and "realistic people" become the logical starting point of ideological and political education.

3. Opportunities and Challenges of Mainstream I&P Education and Network Communication in C&U

3.1. Opportunities of I&P Education in C&U in Media Times. First, the new media enriches the means of education and expands the carrier of education. In the traditional education environment, mainstream I&P education in C&U mainly relies on teachers' unilateral knowledge transfer [20]. There is not much time for communication and interaction between educators and the educated, which leads to the education of mainstream ideology becoming a boring form of preaching. The after-class communication between educators and students is even little, and the problems encountered in students' life and learning are difficult to be understood by teachers. In the process of teaching, the carrier of education is single, and the enthusiasm of students is low. In media times, teachers can contact students anytime and anywhere, and the educational means change from offline mode to online and offline mode, strengthening the exchange between teachers and students. The application of multimedia, social tools, platforms, and various mobile terminals enriches the path of ideological education communication and enhances the effect of education communication.

Second, the educational resources should be rich and the educational content should be three-dimensional. In traditional I&P education and communication, the content is often prescribed in advance, most of which come from the national strategies [21]. Therefore, mainstream I&P

education is very conventional in the traditional education classroom. With the help of the carrier in the new times, I&P education classroom is not only lively, interesting, and humorous but also full of affinity and appeal. The network content is omnipresent, which greatly enriches the educational resources. Meantime, the resources are collected by online and offline parallel access so that teachers and students can have real-time, three-dimensional, and vivid ideological education and communication, having an all-round impact on students' behavior, habits, and ideas and making them feel the spread of mainstream ideology.

Third, it breaks space-time restrictions and strengthens the exchange between teachers and students. In the traditional way of education, I&P education is mostly limited to a fixed time and place [22], while the arrival of the new media times breaks this situation. First, under the advantage of network timeliness, mainstream I&P education can spread and interact in real time, to improve the timeliness of mainstream I&P education and expand the exchanging channels and influence of mainstream ideology. Besides, it also expands the space for education. Under the power of media, the exchange between educators and the educated is enhanced, and I&P education and communication are more affinities.

The opportunities of mainstream I&P education in C&U in modern times are shown in Figure 2.

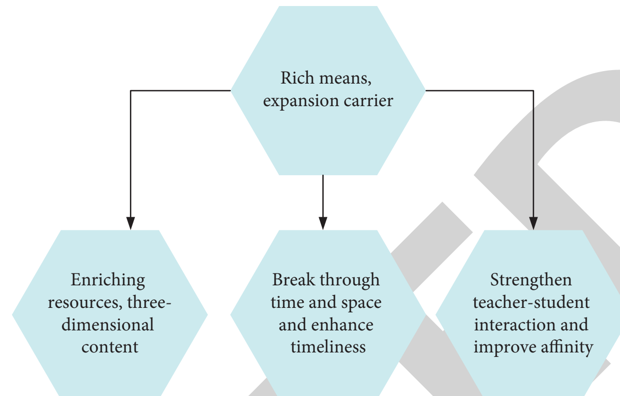

Figure 2: Opportunities of mainstream I&P education and communication in C&U in media times.

3.2. Challenges of the Communication of Mainstream I&P Education in C&U in Media Times. Everything has two sides, and opportunities come along with challenges. The old will be replaced by the new. If the traditional concept of education and teaching is not changed, it will take more risks. In media times, the unified education mode in C&U must comply with the development of the times; otherwise, the teaching effect is deeply affected. With the opening of information resources, the relationship between teachers and students is no longer a simple teacher-student, and it tends to equal communication. In this case, C&U should update their traditional education ideas. The new media environment helps to access a huge amount of information that cannot reach in traditional education, like the influx of western thoughts, which has a significant impact on the political beliefs of some college students. Besides, the virtual characteristics of the network environment weaken their sense of national identity and belonging, and consumerism brings impulsion and challenge to their correct values. What's more, the discourse power and leadership of the mainstream ideological education communication are also deeply challenged in modern times [23]. Based on all kinds of challenges, the difficulty of college network public opinion management and emergency response is increasing. Due to the influence of modern times, public opinions break the limitation of time and space. Anonymous participation makes it difficult for ideological educators to analyze public opinions. Also, it poses new challenges to the emergency handling of public opinions. Despite the difficulties, college and university management should be brave enough to actively meet the challenges, create a new mainstream I&P education and communication mode, figure out new countermeasures to keep pace with the times, and pave a way for the educational communication of mainstream ideology.

The opportunities and challenges of mainstream I&P education and network communication in C&U are shown in Figure 3.

3.3. Network Communication Subjects Initiate and Implement Communication. Finding the right time to initiate and implement network communication is the premise of good communication results. The network dissemination of ideological and political education for college students is a good opportunity for freshmen to enter the university. Many problems college students encounter in life, such as the development of intelligence, emotional vulnerability, and emotional instability, make them easy to accept communication from the main body of network communication.

The construction of network communication atmosphere should be combined with the specific goals of communication and the actual situation of college students. The main body of network communication should strive to create a democratic, equal, free. and lively communication atmosphere so that college students can actively realize the internalization and externalization of communication content in a good atmosphere.

Network communication is a two-way interactive process, due to the constant change of subjective and objective conditions, inevitably producing some deviations. Therefore, it is quite normal to adjust the progress, content, and methods of communication or even completely change the original communication process according to the actual effect of network communication. The subject of network communication flexibly adjusts the communication process on the premise of adhering to the overall goal so that it can maximize the realization of the communication goal and better adapt to the requirements of the network communication environment.

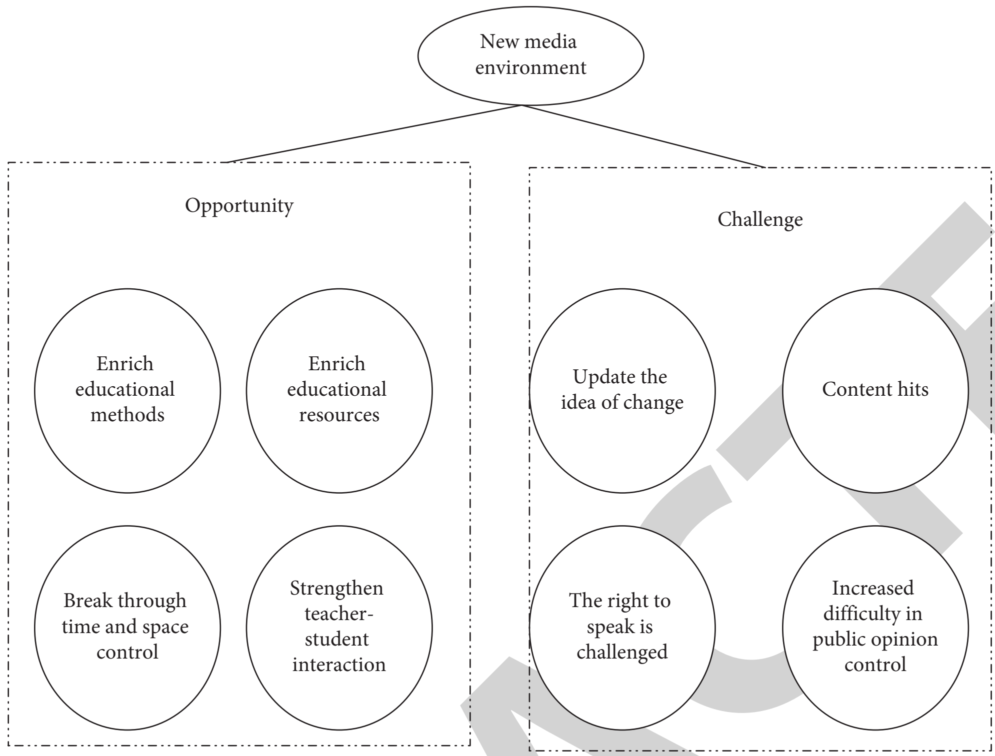

Figure 3: Opportunities and challenges of mainstream I&P education network communication in C&U.

4. Innovation of Network Communication Mode of Mainstream I&P Education

4.1. Cultivating Innovative Education Concept. Innovative ideas can maintain the advanced nature of education. The first step of innovating ideas is to build up the concept of joint education, which links the whole society through the new media of the Internet. I&P education and communication of college students are closely concerned with the whole society. Therefore, the educational concept of family, school, and society should be established, and their joint force of the three in education should be made full use. The joint role of traditional and new media communication as well as the joint efforts of traditional education methods and new media technology is also needed in mainstream I&P education and communication. Only by combining the old with the new, and the individual with the society, can higher education maximize the strength of all parties, promoting the communication of mainstream ideological education. The second step is to establish the educational concept of integrating education with entertainment. This concept aims to make use of new media technology, carrier, method, and environment to naturally store I&P education in digital images, entertainment games, and characters to increase the creativity, appeal, and influence of mainstream I&P education, carrying forward the spirit of the times and spreading the mainstream ideology. The third step is to establish the education concept, with students as the main body. As one of the main groups in the media environment, students enjoy full liberation and freedom. In the process of mainstream I&P education and communication, educators should respect students' subjectivity, change their roles, give enough guidance, provide help for students, and stimulate their study enthusiasm. C&U need to be in line with the law of students' growth, the law of mainstream I&P education, and the law of new media development and communication, and design appropriate teaching objectives and teaching plans.

The strategies of network communication mode of mainstream I&P education in C&U are shown in Figure 4.

I&P education direction under the new media is ensured by strengthening the ideological guidance, consolidating the ideological foundation and improving the mainstream I&P education power of C&U [24]. One of the ways to strengthen ideological guidance is to adhere to the guidance of Marxism and improve the ability of I&P education in C&U in media times. Marxism is the most basic theoretical guidance, and also the first theoretical thought of China's mainstream ideology [25], which diversifies the theoretical knowledge of college students' mainstream ideology and enables them to establish correct values and political beliefs, enrich the minds of college students, and ultimately make them unswervingly take the socialist road. The second is to adhere to the leadership of ideological work in C&U in modern times. The leadership of ideological work in the network field cannot be underestimated. Strengthening the leadership of ideological work can guide the I&P education in C&U, ensure its development direction, find out problems in time and solve them effectively, and deal with problems that violate the mainstream ideology. The third is to ensure the discourse power of the mainstream ideology in media times, which requires promoting the network of discourse mode and content, and actively occupying the network position of

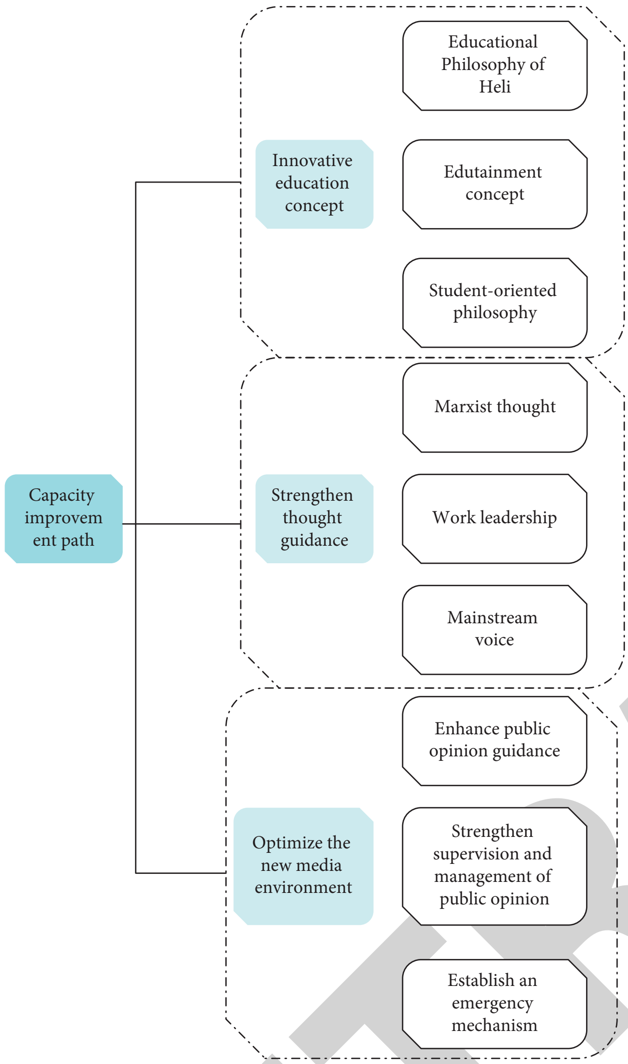

Figure 4: Strategies of network communication mode of mainstream I&P education in C&U.

the mainstream ideology in C&U, so that the mainstream ideology can be integrated into students' daily life and study.

4.2. Optimizing the New Media Environment. The new media era brings a new living space for human beings, namely virtual space [26], which has a tremendous impact on the global human society. During the process of innovating the mode of I&P education network communication in the new media era, much concern is given to virtual space. The first thing is to enhance the guidance of public thoughts in the media times. New media reflect the struggle of various ideological forces, follow the pace of the times, seize the high ground of network public opinion, strengthen the guidance of public opinion, and ensure the correct direction of network public opinion. Second, it is necessary to strengthen the supervision and regulation of the public thoughts of new media in C&U. Improving the supervision and management system of new media lays a foundation for strengthening management, and it helps to improve the organization and leadership system of new media. Also, the technical means

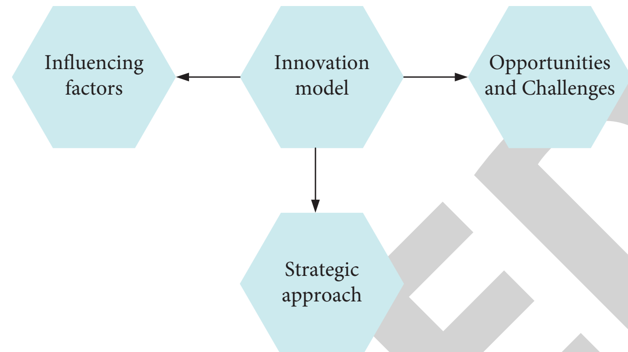

Figure 5: Innovation of the network communication mode of mainstream I&P education in C&U.

should be strengthened and a professional network monitoring system should be established. Finally, the emergency response mechanism of new media public opinion should be constructed in C&U because emergencies are inevitable. C&U should accurately analyze public opinions, master the golden rule of 24-hour handling emergencies, establish a rapid response mechanism, improve the relevant work programs and responsibilities of relevant departments, and ensure that they can respond quickly in the first time when emergencies occur, solving the problem properly and guiding the public opinion correctly.

The innovation of the network communication mode of I&P education in C&U is shown in Figure 5.

A series of measures are taken to improve the power of mainstream information processing education in the media era, update the concept of media education, strengthen ideological guidance, ensure the direction of mainstream information processing education, optimize the media environment, and build a more perfect innovation mode of information processing education.

5. Conclusions

According to the background of mainstream I&P education and network communication in media times, its influencing factors are analyzed in detail, and they include the main factor, mediator factor, and environmental factor. Taking the factors as the starting point, the opportunities and challenges experienced by mainstream I&P education and network communication are discussed. Challenges and opportunities often coexist. Therefore, challenges cannot be separated from opportunities and vice versa. Finally, in terms of the existing problems, the innovation mode is proposed, and it covers innovating educational ideas, strengthening thought guidance and other innovative ideas, and optimizing the environment of the media. The content can provide a theoretical basis and guidance for network communication and the mode of mainstream I&P education in C&U in the new times of media, helping C&U build a more perfect mainstream I&P education system, cultivate excellent talents, form a healthy mainstream consciousness, and finally contribute to the development of China under the socialist system.

Hindawi
Scientific Programming
Volume 2021, Article ID 5097003, 9 pages
https://doi.org/10.1155/2021/5097003

Research Article

Exploring Key Competencies and Professional Development of Music Teachers in Primary Schools in the Era of Artificial Intelligence

Xian Zhao, Zhenjie Guo, and Shanqin Liu

College of Education Science, Henan Institute of Science and Technology, Xinxiang, China

Correspondence should be addressed to Xian Zhao; 627079006@qq.com

Received 29 October 2021; Accepted 8 December 2021; Published 23 December 2021

Academic Editor: Punit Gupta

Artificial intelligence (AI) has introduced new era elements to the connotation of key competencies and professional development of music teachers in primary schools. The education management department in the AI era has flawed systems for the professional development of music teachers in primary schools. To assist music teachers in primary schools fulfill the development needs of the development of the times and enhance the quality of music education in primary schools, the status and income of music teachers in primary schools warrant improvement, and the system should be upgraded to promote the implementation of key competencies. Moreover, the related system construction of music teachers in primary schools should be reinforced by rationally arranging teachers, workload and creating a teacher learning community, in order to guide schools to provide a suitable environment for teachers, key competencies and professional development. Furthermore, methods like strengthening teachers, awareness of independent development and augmenting professional identity should be adopted to prompt teachers to comprehensively enhance their key competencies and professional development.

1. Background

Under the current background of artificial intelligence (AI) and "Internet +" and the deep integration of education and teaching [1, 2], key competencies [3, 4] and professional development [5–7] of music teachers in primary schools have garnered significant attention. AI is integrated through robust technology, resources and ideology into teachers, key competencies and professional development challenging teaching practice and professional development [8, 9]. Huang believed that AI education played a very important role in the basic stage of students, analyzed the components of key competencies content, designed relevant questionnaires, and finally drew the conclusion that AI courses can significantly improve students' key competencies ability [3]. Pomsta proposed that AI as a methodology for supporting teacher training and continuous professional development was of great help to enhance teachers' professional skills and professional practice [10]. Gunawan et al. described the competency enhancement program for science teacher that assisted by AI in designing higher-order thinking skills (HOTS)-based integrated science learning, which help to improve teachers' professional development [11]. Wu et al. proposed that video teaching reflection was the main method for teacher education and teachers' professional development. With the development of AI, information fusion between RGB video and bone information can improve the recognition accuracy and enhance teaching efficiency of teachers [12]. This study, conducts extensive research and practice by designing questionnaires (Sojump). Relevant data are plotted into graphs by combining Origin software, focusing on the understanding of key competencies of music education by music teachers in primary schools in the AI era and the methods of teachers, professional development of teachers in the AI era [13–15]. In addition, this study systematically explores the ways and methods of key competencies and professional development from the three aspects of education management departments, schools, and teachers in the AI era [16, 17]. Furthermore, smart learning resources for music teachers in primary schools are provided through the smart learning environment, which cultivate teachers, key competencies of teachers, and guides and promotes them to develop in a high-quality, professional and innovative direction [18–20].

2. Methodology

2.1. Research Objects. Xinxiang City is located in the northern part of Henan Province, which is one of the 18 prefecture-level cities in Henan Province. Xinxiang is a crucial industrial city in the north of Henan and is one of the significant cities that comprises the central Henan urban agglomeration. After years of urban development and growth, Xinxiang City has now become a key education, economy, culture and transportation city in Henan Province. Xinxiang City (District) has 186 primary schools and 274 music teachers which provided a large number of analysis samples for this study.

2.2. Experimental. This study primarily started from the basic condition of teachers, key competencies and professional development in the AI era, as well as considered the background of key competencies to examine the professional growth of some music teachers in primary schools in Xinxiang from multiple aspects. A total of 120 questionnaires were issued, among which 120 were returned and 112 were valid (effective rate = 93.3%). These data provided real data support for this study.

3. Results and Discussion

3.1. Basic Information. As shown in Figure 1(a), we surveyed 6 male and 106 female music teachers in primary schools, respectively, accounting for 5.36% and 94.64% of the total number of teachers surveyed, suggesting severe gender imbalance. This could be attributed to the fact that most college students majoring in musicology are females, making the main workforce of music teachers in schools. As shown in Figure 1(b), 63 teachers were in the age group of 20–30 years, 41 in the age group of 31–40 years, 8 in the age group of 41–50 years and none in the age group of 51–60 years respectively, accounting for 56.25%, 36.61%, 7.14% and 0% of the total number of teachers surveyed, suggesting that young and middle-aged teachers dominated the community of music teachers in primary schools in Xinxiang.

3.2. Understanding of Key Competencies of Music Education. To cultivate students, key competencies, it is essential to fortify the leadership of teachers, key competencies [21–23]. As shown in Figure 2(a), 15.18% and 80.36% music teachers in primary schools displayed good and a little understanding of key competencies respectively. When answering, "What do you think is included in key competencies of music education" (Figure 2(b)), most teachers believed that it should include aesthetic perception, artistic expression, and cultural understanding. Figure 2(c) shows that the ways for music teachers in primary schools to acquire key competencies of music education are training lectures (90.18%), peer exchanges (84.82%), online media (77.68%), and newspapers or books (59.82%), suggesting that key competencies have been documented in music teachers in primary schools to a certain extent. Nevertheless, some teachers did not fully comprehend the content of key competencies. By designing the question "What do you think of the relationship between three-dimensional goals and key competencies", 106 teachers (94.64% of the surveyed population) believed that the two were closely related and could promote each other, indicating that most teachers had a certain degree of awareness of the concepts and internal connections of these two things. However, a small number of teachers could not recognize the correlation between the two, which would compromise the implementation of key competencies in the process of primary school music teaching compromised.

Table 1 shows that 103 participants (91.96%) believe that key competencies are essential for music teachers' professional development. The data revealed that most teachers could recognize the significance of key competencies for their professional development. While answering "the understanding of connotation of key competencies of music education", 30.36% of teachers did not understand the concept of key competencies of music education very well, In addition, while answering, "Do you consciously improve your key competencies of music education", 33 teachers and 1 teacher, respectively occasionally and never intended to enhance their key competencies. We observed that, some music teachers in primary schools in Xinxiang City had an incomplete understanding of the connotation of key competencies of music education and lacked the awareness to actively advance their own music key competencies. Thus, the width of key competencies of music education in music education in primary schools warrants an extension. Furthermore, there remains much room for improving teachers' awareness of actively mastering key competencies of music education.

3.3. Conditions of Teachers, Professional Development in the AI Era. As shown in Figure 3(a), 63, 38, 11, and 0 teachers display strong, some, average and indifferent affection to their profession respectively, accounting for 56.25%, 33.93%, 9.82%, and 0% of the total number of surveyed teachers; this demonstrates that most teachers like their professions of being music teachers in primary schools, although some teachers that think that the profession is average that cannot stimulate more interest and enthusiasm in them, and who only consider this profession as one's own means of earning a living. Figure 3(b) shows that only 50% of teachers like their students to a great extent. In addition some teachers do not realize the precious creativity of their work, do not fully love their profession, and do not care for their students, which are not conducive to teachers' professional development under the background of key competencies.

While answering, "What is your teacher processional pursuit", 42.86% of teachers wanted to be national or provincial excellent teachers, 38.39% wanted to be municipal (district-level) excellent teachers, and 11.61% wanted to be

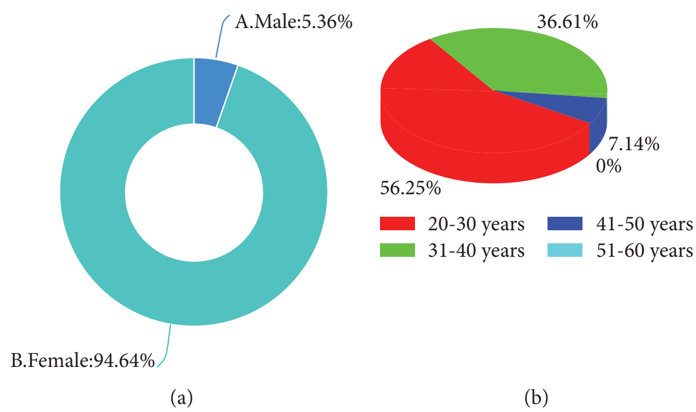

Figure 1: (a) Gender and (b) age of music teachers in primary schools.

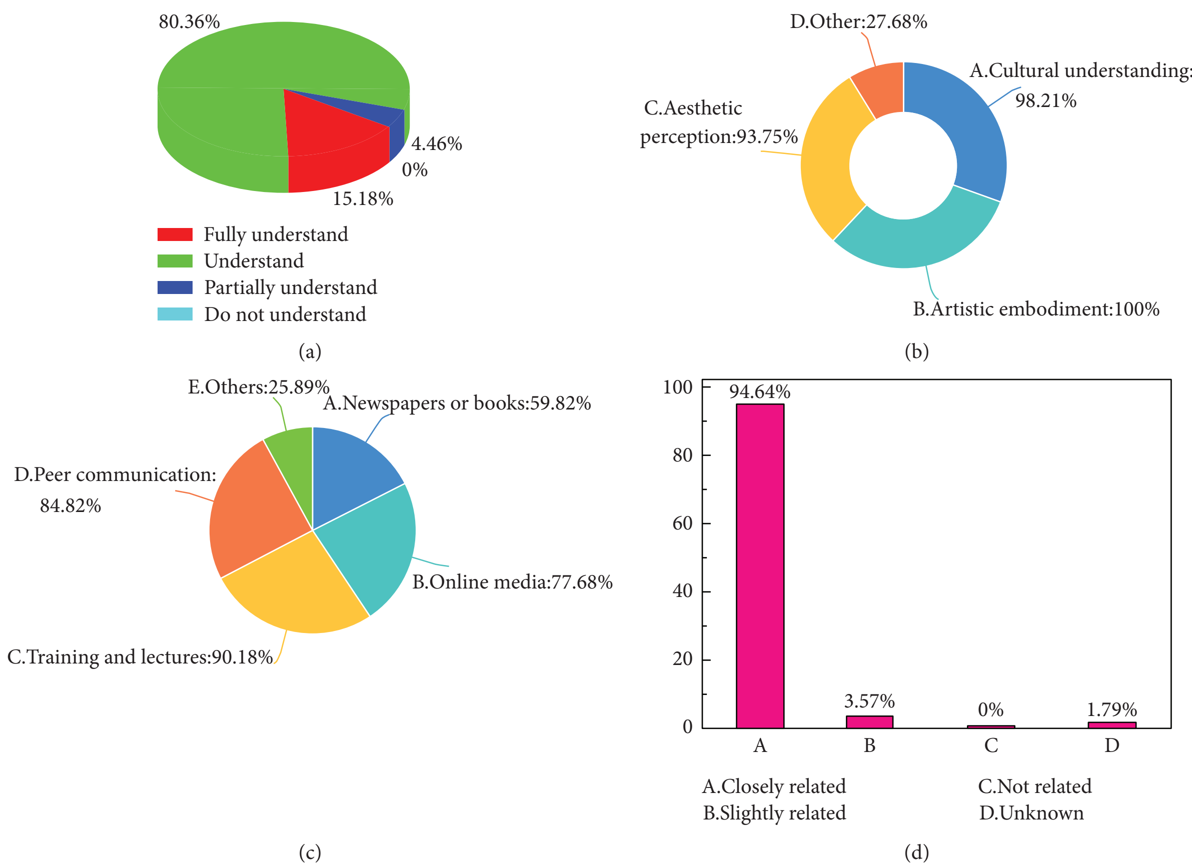

Figure 2: (a) Mastery of key competencies of music teachers in primary schools in the AI era; (b) reckoned contents included in key competencies of music education; (c) the understanding of the methods of key competencies of music education; (d) reckoned relationship between three-dimensional goals and key competencies.

school-level outstanding teachers. Only 7.14% of teachers wanted to be ordinary teachers (Figure 4(a)), showing that most teachers had lofty ideals and pursuits, but only a few of them had low professional pursuits and needed to be self-awakened or guided by others. Figure 4(b) shows that 36, 65, 11, and 0 music teachers have "seriously studied", "have some understanding", "heard of" and "no understanding" of professional standards, accounting for 32.14%, 58.04%, 9.82% and 0% of the total number of surveyed teachers, respectively. This demonstrated that there remain few teachers who have a deep understanding of professional standards, and the popularization of professional standards warrants further enhancement and extension.

3.4. Approaches and Methods of Teachers, Professional Development in the AI Era. When examining the motivation of music teachers in primary schools to promote their

Table 1: Connotation of influences of key competencies on professional development/key competencies of music education by music teachers in primary schools in the AI era, and whether they can consciously enhance their understanding of key competencies of music education.

	Option	Counts	Percentage
Influence of key competencies on professional music teachers,	Highly important	103	91.96
	Important	8	7.14
	Not important	0	0
	Not sure	1	0.89
Understanding of connotation of key competencies of music education	Fully understand	19	16.96
	Understand	65	58.04
	Partially understand	34	30.36
	Do not understand	0	0
Consciously mention improving key competencies of music education	Always	21	18.75
	Often	57	50.89
	Occasionally	33	29.46
	Never	1	0.89

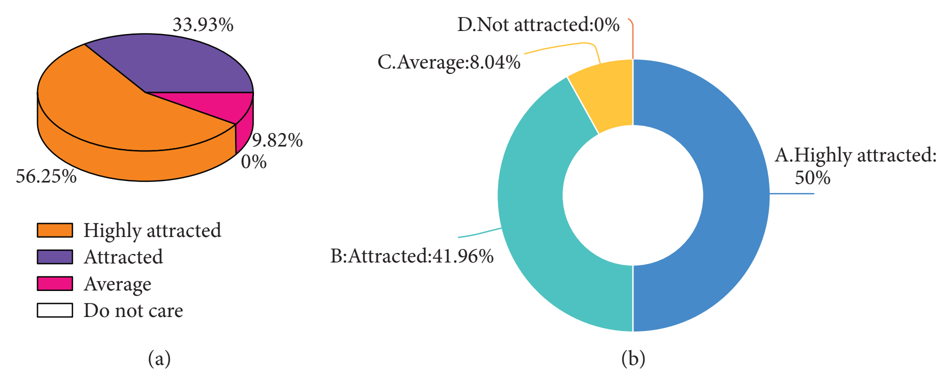

Figure 3: (a) Satisfaction with their profession of music teachers in primary schools in the AI era and (b) degree of preference for students of music teachers in primary schools in the AI era.

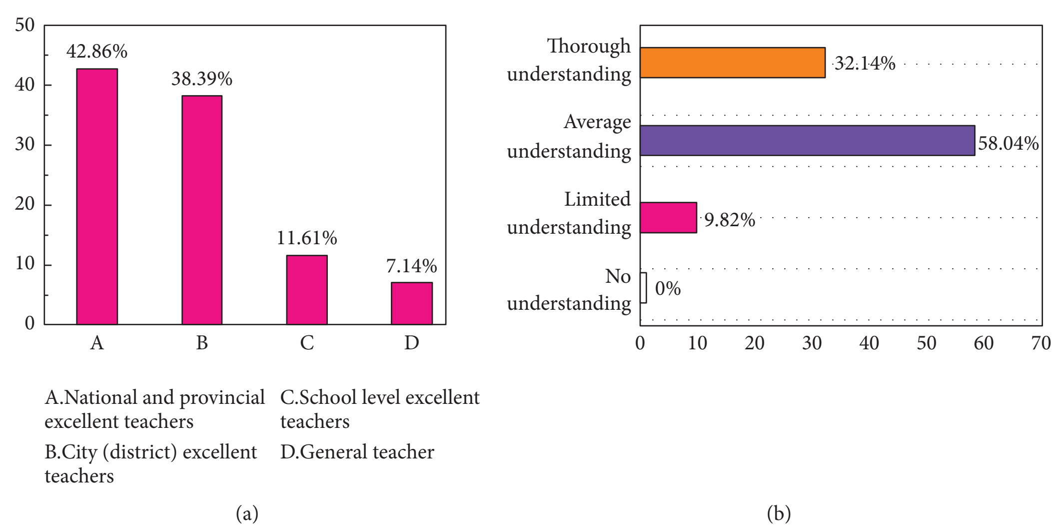

Figure 4: (a) Degree of pursuit for their professions of music teachers in primary schools in the AI era; (b) degree of mastery for professional standards of music teachers in primary schools in the AI era.

professional development (Figure 5(a)), 57 teachers considered it necessary for professional promotion, 99 thought that they could continuously enhance their quality and become better teachers, 65 thought it is the need of students, 81 claimed it is to adapt to the requirements of the times, and 43 thought it is for the schools' development. Although teachers' professional development has an internal and active professional improvement those with external and passive

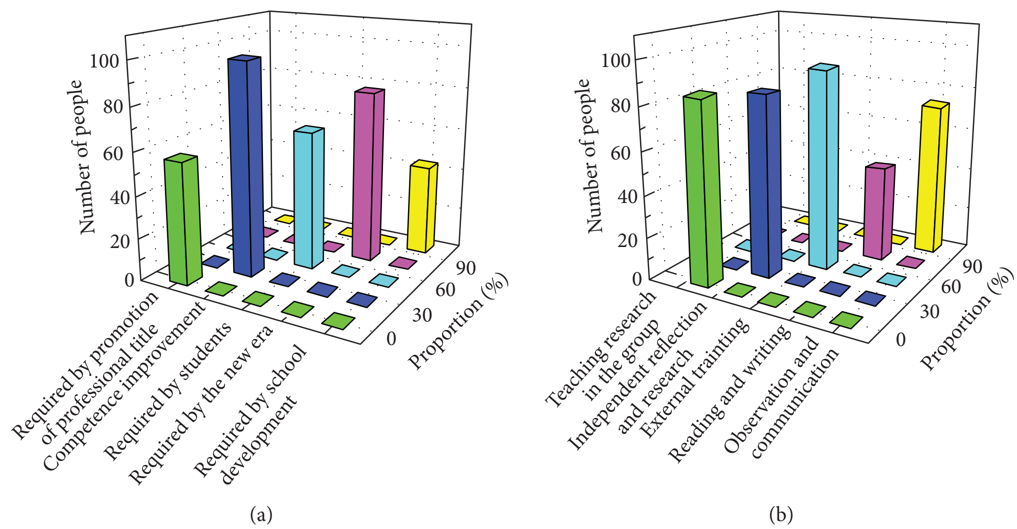

Figure 5: (a) Motivation diagram for promoting their professional development; (b) diagram for motivating the professional growth of music teachers in primary schools in the AI era.

Table 2: Training frequency and methods of music teachers in primary schools organized by schools.

	Option	Population	Proportion (%)
Whether the school organizes training for music teachers	Frequently	28	25
	Once or twice a semester	24	21.43
	Once or twice a school year	17	15.18
	Rarely	43	38.39
The methods of schools, organizing training for music teachers	In-school lectures, seminars	87	77.68
	Sending teachers out to study	78	69.64
	Expert lecture	51	45.54
	Remote teaching	49	43.75
	Other	22	19.64

professional improvement are also very common. While answering the question "What do you think are the professional growth paths of music teachers" (Figure 5(b)), 86, 85, 94, 45, and 73 teachers claimed that the improvement of their professional level could be attained by self-reflection and research, teaching and research within groups, outside training, reading and writing, and school teaching observation and communication methods respectively. Furthermore, most teachers claimed that the ways to promote their professional growth included outside training, independent reflection and research, and teaching and research within groups.

Teacher training is not only a crucial part of a teacher's role but also an essential way for teachers' professional development [24–26]. Table 2 shows that 25%, in terms of the frequency of training organized by schools, 21.43%, 15.18% and 38.39% of teachers think respectively that the school organizes training frequently, once or twice times a semester, once or twice a school year, and rarely organizes. In addition, 87, 78, 51, 49 and 22 teachers received training through in-school lectures and seminars, sending teachers to study abroad, expert lectures, remote lectures and other methods. The survey revealed that music teachers in primary schools had fewer opportunities to participate in training owing to the policy and funding reasons, and their participation methods were single, resulting in poor training effects and low enthusiasm of trainers, which is not conducive to teachers' professional development.

For training content desired by music teachers in primary schools (Figure 6(a)), 48, 27, 3, 32, and 2 teachers selected teaching skills, new ideas of education, information technology, professional knowledge and other methods to attain valuable training, accounting for 42.86%, 24.11%, 2.68%, 28.57% and 1.79% of the sample, respectively. In addition, the survey showed that music teachers in primary schools were more lacking in teaching skills and professional knowledge, and hoped to attain learning opportunities in these areas. When answering "What do you think are the factors restricting the professional development of music teachers" (Figure 6(b)), 91, 68, 52, 52, and 67 believed that these included reasons such as too many tasks, absence of attention from schools, absence of communication and collaboration among teachers, and absence of internal motivation and expert guidance. These findings revealed that most music teachers believe that the factor restricting their professional development is extensive workload. Hence, schools should arrange teaching tasks reasonably and provide room for the professional development of music teachers [27, 28].

Regarding the support provided by schools (Figure 7(a)), 72, 85, 70, 65, and 91 teachers believed that it included

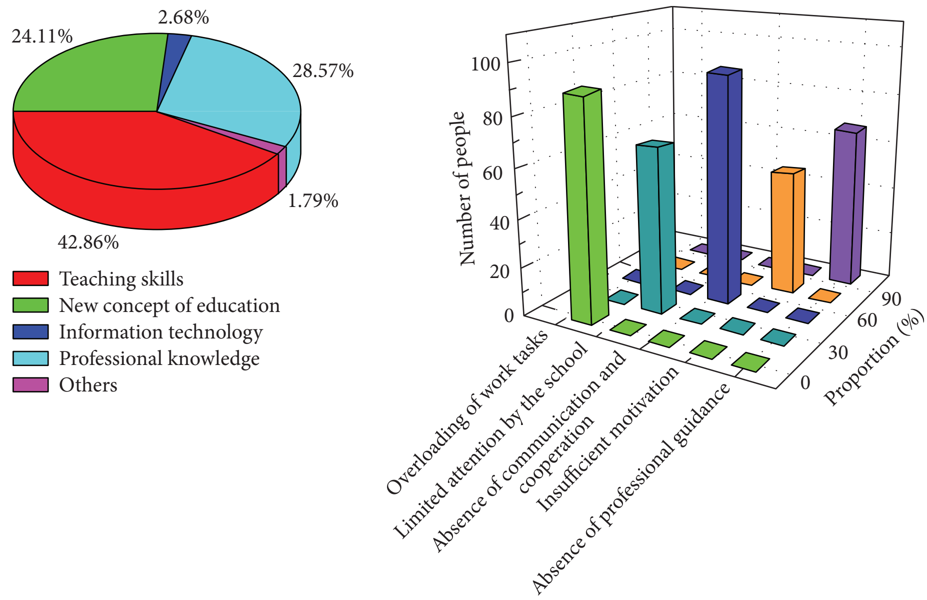

(a) (b)

Figure 6: (a) Diagram of the training content hoped to obtain; (b) Diagram of the factors that restrict professional development of music teachers in primary schools in the AI era.

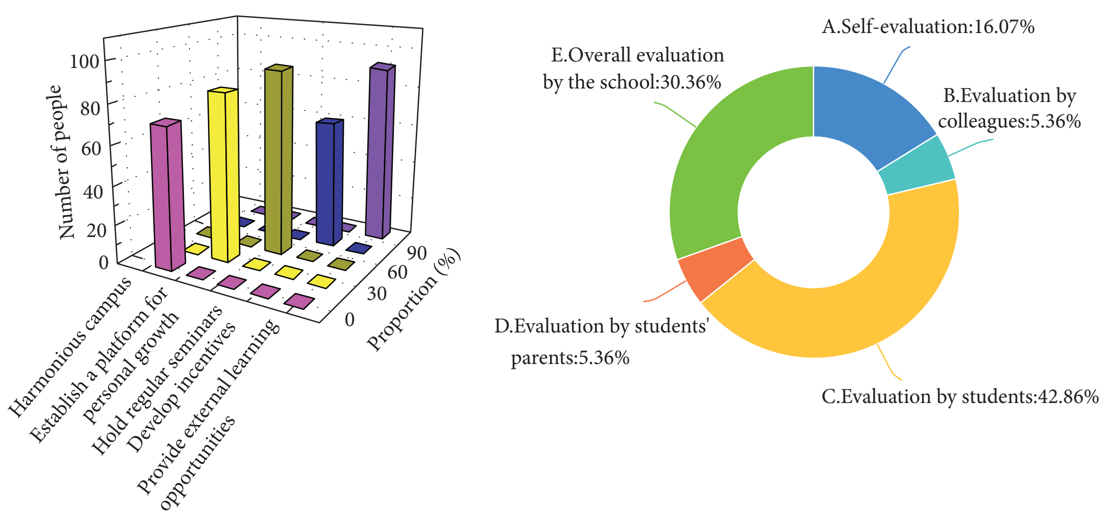

(a) (b)

Figure 7: (a) Diagram of desired support from schools; (b) diagram of reckoned sense of value achievement of professional development of music teachers in primary schools in the AI era.

construction of a supportive and harmonious campus environment, the establishment of a growth platform, regular teacher exchanges and discussions, the establishment of corresponding incentive policies, and the assistance of teachers' outside training respectively, this demonstrates that more teachers expected schools to provide opportunities to go out to learn, so as to promote their own professional development. While answering the question "What kind of evaluation do you think is the most valuable for teachers' professional development" (Figure 7(b)), it is considered self-evaluation, colleague evaluation, student evaluation, parent evaluation and school comprehensive evaluation by 18, 6, 48, 6 and 34 teachers, respectively. Overall, the findings revealed that teachers focus more on the evaluation of students, making it easier to disregard other effective evaluation methods.

Through the above investigation, it is found that the gender ratio of primary school music teachers is seriously unbalanced, and teachers' understanding of the core literacy of music subject is not deep. In the era of artificial intelligence, teachers should have higher career pursuit, and teachers' professional development approaches should be further diversified.

4. Methods and Countermeasures

4.1. The Education Management Department in the AI Era Should Strengthen the Construction of Relative Systems for the Professional Development of Music Teachers in Primary Schools

4.1.1. Improve the Status and Income of Music Teachers in Primary Schools. Evidently, the identity of music teachers in primary schools needs to be strengthened. Compared with teachers in major subjects of Chinese, mathematics and foreign languages, music teachers are at a disadvantage in the promotion of professional titles, and most are dissatisfied with their salaries. To handle the opportunities and challenges fronted by music teachers in primary schools in the context of key competencies, the education management department should enhance the protection mechanism of music teachers' professional development in primary schools and take real and practical action in terms of teacher identity, professional promotion, and salary so that music teachers can transfer more energy to music teaching and refining their qualifications.

4.1.2. Improve the Evaluation System to Promote the Implementation of Key Competencies. A scientific and effective management mechanism guarantee improvement of teachers' professional development. The education management department should establish a robust evaluation system for teachers to provide a basis for enhancing teachers' professional quality and promoting their professional development [29–31]. Thus, this study claims that the education management department should establish a special supervision group, which can regularly monitor the music class in primary schools and formulate corresponding evaluation standards. Schools that can effectively implement key competencies into the classroom should be commended, excellent music teachers should be rewarded, and notable lesson examples can be used as demonstration for publicity and learning. This not only improves the enthusiasm of teachers, but also promotes the development of students' key competencies.

4.2. A Good Environment Shall be Provided by Schools for the Professional Development of Music Teachers in Primary Schools in the AI Era

4.2.1. Reasonably Arrange the Workload of Teachers. School leaders should focus on the significance of the professional development of music teachers to the cultivation of key competencies of primary school students and the overall development of the school. It is essential to rationally arrange the workload of music teachers, allocate teaching tasks judiciously, and minimize other administrative tasks other than teaching tasks. Thus, music teachers can have adequate time and energy for professional learning and improve their professional development.

4.2.2. Form a Teacher Learning Community. In the AI era, key competencies need teachers to fortify professional exchanges and collaboration and enhance their professional development. Thus, schools must promote the establishment of teacher learning communities and create a win–win situation where teachers help each other and complement each other's advantages. The so-called "teacher learning community" is a learning group organized by teachers based on a shared goal and a sense of belonging to the subordinate team. In this group, teachers share their professional opinions and various learning resources, and complete specific tasks in the spirit of inquiry through equal communication, exchange and discussion, finally realizing the organizational form of their professional development.

4.2.3. Classify Training According to Needs. The Guiding Opinions on Deepening the Reform of the Training Model for Primary and Secondary School Teachers and Comprehensively Improving the Quality of Training states: training should be carried out per the needs of teachers at different stages of development, such as: pre-job training for new teachers, professional ability improvement training for in-service teachers, and advanced training for key teachers. Consistent with the requirements of the document, schools should understand the development needs of teachers from multiple viewpoints and arrange corresponding professional training based on different development stages. For example, for teachers new to the job and having a short teaching experience, some training on teaching design, class management, and after-school reflection, can be arranged; for teachers employed for 5–10 years, some training in aspects of innovative teaching methods and cutting-edge education theories can be arranged; for key teachers, some training on enhancing scientific research ability and educational research ability can be arranged. In the choice of training mode, schools should diversify training modes per the teachers' needs.

4.3. Music Teachers in Primary Schools in the AI Era Should Comprehensively Improve Their Professional Development

4.3.1. Enhance Professional Identity. Professional identity promotes teachers' self-confidence and is also a driving force for professional development. Music teachers in primary schools must identify with their profession, devote themselves to the career of music education in primary schools, and be responsible for educating students. Particularly in the development of key competencies under AI, teachers should continuously further their professional knowledge from various aspects, augment professional skills, and promote the all-round development of students. Currently, many music teachers in primary schools do not have precise professional positioning and feel that the subject they are teaching is a sub-subject. Thus, when exams approach, they tend to give up their class to Chinese, Math, and English teachers such deviation in understanding is not conducive to their professional development. Hence, music teachers in primary schools should enhance their professional identity, affirm the subject's professional value for themselves, love music from their heart, care for students, and continue to strive for music education as their own career.

4.3.2. Enrich Professional Knowledge. First, music teachers in primary schools must master knowledge of music subject, also known as ontological knowledge, it is an integral part of key knowledge of music teachers and a prerequisite for the development of music teaching activities. Music subject knowledge comprises music theory, sight-singing, ear training, harmony, song composition, vocal music, keyboards, dance, and folk music. Then, music teachers in primary schools must master professional theoretical knowledge of education, also known as conditional knowledge, including pedagogy and psychology. Teachers, as guides of students' learning, must master the theoretical knowledge of education. Only when teachers understand students' psychological characteristics and development rules can they start teaching according to the different stages of students from the actual situation. Moreover, music teachers in primary schools should reinforce the study of basic knowledge, also known as general knowledge, which typically implies that teachers should possess all the general cultural knowledge that is conducive to effective teaching.

4.3.3. Improve Professional Skills. Music teachers' professional skills in primary schools are primarily reflected in the control of classroom teaching, and students learn and understand key competencies of music education in music teaching activities. Thus, teachers should enhance their classroom teaching ability to better promote the cultivation of students' key competencies of music education.

Regarding lesson preparation, teachers can refer to the teacher's reference books, however, this does not imply that teachers can copy all of them. Lessons should be redesigned per the teaching content and students' characteristics. Then, in the course of teaching, teachers should focus on harnessing the corresponding skills of students based on different types of courses. Music classes in primary schools are primarily set up for two types of classes: (i) listening and appreciation classes, and (ii) singing and chorus classes. Together with a basic connotation of key competencies of music education, corresponding listening and appreciation classes primarily enhance students' aesthetic perception, while singing and chorus classes primarily improve students' artistic expression. Moreover, in terms of teaching evaluation and after-class reflection, teachers should focus on multiple evaluations and self-reflection consciousness. Regarding the evaluation of students, teachers should combine the training requirements of key competencies, as well as the evaluation of teachers, parents, and students themselves, to promote the overall development and improvement of students' overall quality.

5. Conclusions

With the advent of the AI era, education and teaching have undergone profound changes, presenting the topic of the times for the key competencies and professional development of music teachers in primary schools. Through a professional investigation platform combined with the AI analysis, this study methodically explored the problems of key competencies and professional development of music teachers in primary schools, demonstrating that the times require us to reorganize the system construction and development environment of music teachers in primary schools. It is crucial to summarize the experience in practice and accrue first-hand information to conduct more expensive research on key competencies and professional development of music teachers. Accordingly, teacher training programs that fulfill actual local conditions can be organized to guide teachers to consciously enhance their professional development, for improving the professional competencies of music teachers in primary schools and achieving the goal of nurturing key competencies in music for primary school students. Besides, it serves as a crucial reference for the comprehensive development of promoting the overall development of personality and capability of primary school students, thereby providing strong data support and an effective model for key competencies and professional development of music teachers in primary schools in China. This study will also provide better experimental methods and research models for key competencies and professional development of teachers in other disciplines.

Data Availability

The datasets used and/or analyzed during the current study are available from the corresponding author on reasonable request.

Conflicts of Interest

The author(s) declared no potential conflicts of interest with respect to the research, author-ship, and/or publication of this article.

References

[1] O. C. Santos, "Artificial intelligence in psychomotor learning: modeling human motion from inertial sensor data," *The International Journal on Artificial Intelligence Tools*, vol. 28, no. 33, Article ID 1940006, 2019.

[2] O. Z. Richter, V. I. Marín, M. Bond, and F. Gouverneur, "Systematic review of research on artificial intelligence applications in higher education-where are the educators?" *International Journal of Educational Technology in Higher Education*, vol. 16, no. 1, 2019.

[3] X. Huang, "Aims for cultivating students' key competencies based on artificial intelligence education in China," *Education and Information Technologies*, vol. 26, no. 5, pp. 5127–5147, 2021.

[4] L. Cañadas, M. L. S. Pastor, and F. J. Castejón, "Physicaleducation teachers' competencies and assessment in professional practice," *Apunts Educación Física y Deportes*, vol. 139, pp. 33–41, 2020.

[5] S. L. Chua and G. F. Welch, "A quantitative study of experiences impacting music teacher development," *Psychology of Music*, vol. 49, no. 3, pp. 445–461, 2019.

[6] M. Biasutti, S. Frate, and E. Concina, “Music teachers’ professional development: assessing a three-year collaborative online course,” *Music Education Research*, vol. 21, no. 1, pp. 116–133, 2018.

[7] A. Bautista, G.-Z. Toh, and J. Wong, “Primary school music teachers’ professional development motivations, needs, and preferences: does specialization make a difference?” *Musicae Scientiae*, vol. 22, no. 2, pp. 196–223, 2016.

[8] Y.-Z. Hsieh, S.-S. Lin, Y.-C. Luo et al., “ARCS-assisted teaching robots based on anticipatory computing and emotional big data for improving sustainable learning efficiency and motivation,” *Sustainability*, vol. 12, no. 14, 2020.

[9] G. Fang, P. W. K. Chan, and P. Kalogeropoulos, “Secondary school teachers’ professional development in Australia and shanghai: needs, support, and barriers,” *SAGE Open*, vol. 11, no. 3, Article ID 21582440211026951, 2021.

[10] K. P. Pomsta, “AI as a methodology for supporting educational praxis and teacher metacognition,” *International Journal of Artificial Intelligence in Education*, vol. 26, no. 2, pp. 679–700, 2016.

[11] K. D. H. Gunawan, L. Liliasari, I. Kaniawati, and W. Setiawan, “Implementation of competency enhancement program for science teachers assisted by artificial intelligence in designing HOTS-based integrated science learning,” *Jurnal Penelitian dan Pembelajaran IPA*, vol. 7, no. 1, pp. 55–65, 2021.

[12] D. Wu, J. Chen, W. Deng, Y. Wei, H. Luo, and Y. Wei, “The recognition of teacher behavior based on multimodal information fusion,” *Mathematical Problems in Engineering*, vol. 2020, Article ID 8269683, 8 pages, 2020.

[13] I. Bayram and F. Bıkmaz, “Implications of lesson study for tertiary-level efl teachers’ professional development: a case study from Turkey,” *SAGE Open*, vol. 11, no. 2, Article ID 215824402110237, 2021.

[14] K. Simoncini, B. Pamphilon, and H. Smith, “Learning from teachers like us: using video to move beyond ‘secret knowledge’ in Papua New Guinea elementary teacher professional development,” *Teachers and Teaching*, vol. 27, no. 1-4, pp. 48–63, 2021.

[15] M. Körkkö, M.-R. Kotilainen, S. Toljamo, and T. Turunen, “Developing teacher in-service education through a professional development plan: modelling the process,” *European Journal of Teacher Education*, vol. 1, pp. 1–18, 2020.

[16] A. Monteiro, A. Mouraz, and L. T. Dotta, “Veteran teachers and digital technologies: myths, beliefs and professional development,” *Teachers and Teaching*, vol. 26, no. 7-8, pp. 577–587, 2021.

[17] S. Dogan and A. Adams, “Augmenting the effect of professional development on effective instruction through professional communities,” *Teachers and Teaching*, vol. 26, no. 3-4, pp. 326–349, 2020.

[18] H. Li, “Modeling method of tax management system based on artificial intelligence,” *The International Journal on Artificial Intelligence Tools*, vol. 29, no. 7-8, pp. 1–15, Article ID 2040023, 2020.

[19] E. Seo, J. Ryu, and S. Hwang, “Building key competencies into an environmental education curriculum using a modified delphi approach in South Korea,” *Environmental Education Research*, vol. 26, no. 6, pp. 890–914, 2020.

[20] A. E. Wilson-Daily, M. Feliu-Torruella, and M. Romero Serra, “Key competencies: developing an instrument for assessing trainee teachers’ understanding and views,” *Teacher Development*, vol. 25, no. 4, pp. 478–493, 2021.

[21] R. D. Crick, “Key Competencies for education in a European context: narratives of accountability or care,” *European Educational Research Journal*, vol. 7, no. 3, pp. 311–318, 2008.

[22] L. Deng and P. Zhengmei, “Moral priority or skill priority: a comparative analysis of key competencies frameworks in China and the United States,” *Comparative Education*, vol. 57, no. 1, pp. 83–98, 2020.

[23] F. Caena and R. Vuorikari, “Teacher learning and innovative professional development through the lens of the personal, social and learning to learn european key competence,” *European Journal of Teacher Education*, vol. 1, pp. 1–20, 2021.

[24] S. E. A. Groothuijsen, G. T. Prins, and A. M. W. Bulte, “Towards an empirically substantiated professional development programme to train lead teachers to support curriculum innovation,” *Professional Development in Education*, vol. 45, no. 5, pp. 739–761, 2018.

[25] A. A. M. Abdelrahim and M. A. M. Abdelrahim, “Teaching and assessing metadiscoursal features in argumentative writing: a professional development training for EFL teachers,” *International Journal of Applied Linguistics*, vol. 30, no. 1, pp. 70–91, 2019.

[26] J. Frerejean, M. V. Geel, T. Keuning, D. Dolmans, J. J. G. V. Merriënboer, and A. J. Visscher, “Ten steps to 4C/ID: training differentiation skills in a professional development program for teachers,” *Instructional Science*, vol. 49, no. 3, pp. 395–418, 2021.

[27] A. Nawab, “Perceptions of the key stakeholders on professional development of teachers in rural Pakistan,” *SAGE Open*, vol. 10, no. 4, Article ID 2158244020982614, 2020.

[28] C.-M. Lam, “The impact of Philosophy for Children on teachers’ professional development,” *Teachers and Teaching*, vol. 27, no. 7, pp. 642–645, 2021.

[29] A. O. Adeogun, “Reconceptualizing the music teacher education curriculum for the colleges of education in Nigeria,” *SAGE Open*, vol. 5, no. 2, Article ID 2158244015585608, 2015.

[30] D. Sibanda and N. Amin, “The link between a mentorship programme for mathematics, science, and technology in-service teachers and professional development,” *SAGE Open*, vol. 11, no. 1, Article ID 2158244020988732, 2021.

[31] P. Hallinger and J. Kovačević, “A bibliometric review of research on educational administration: science mapping the literature, 1960 to 2018,” *Review of Educational Research*, vol. 89, no. 3, pp. 335–369, 2019.

Hindawi
Scientific Programming
Volume 2021, Article ID 9276457, 8 pages
https://doi.org/10.1155/2021/9276457

Research Article

Recreational Value Assessment of Urban Productive Landscape of Baguatian in Hangzhou Based on Contingent Valuation Method (CVM) and Cloud Computing

Jian-Guo Zhang ,[1] Jian Jiang,[2] and Rui Zhang[3]

[1]*School of Economics and Management, Huzhou University, Huzhou, Zhejiang 313000, China*
[2]*Corporate Management Department, Hangzhou Wahaha Group Co., Ltd, Hangzhou, Zhejiang 31009, China*
[3]*Shenzhen Zhongshan Industry Research Institute Co., Ltd, Shenzhen 518000, China*

Correspondence should be addressed to Jian-Guo Zhang; zhangjianguo2004@163.com

Received 2 September 2021; Accepted 2 November 2021; Published 17 December 2021

Academic Editor: Punit Gupta

Cloud computing has achieved rapid development in recent years, and the use of cloud platforms to carry various large-scale services has become the general trend of the development of the information industry. This study investigates WTP of Hangzhou residents for the recreational value of Baguatian productive landscapes based on CVM and cloud computing. In this study, we did the related analysis on the social and economic characteristics and WTP of interviewees and made the monetization assessment about the recreational value of its urban productive landscapes. The result shows 62.1% of interviewees have WTP and the average payment intention (WTP) is $40.74 per year. Besides, the total recreational value of Hangzhou Baguatian productive landscapes is 354 million yuan; the relatively accepted payment mode is tax-paying and cash payment; the educational degree, occupational background, and income are the main factors influencing the tourists' WTP and the correlation between interviewees' origin, permanent residence, and WTP is not apparent.

1. Introduction

With the social and economic development, the demands of urban residents on the public green land have increasingly shown the characteristics of content diversification and functions integration and the construction and application of urban productive landscapes have been more and more emphasized. The productive landscapes, as part of urban green land, as well as owning the main function of the traditional green land, can be an effective bearer of providing village landscape appreciation, agricultural knowledge dissemination, and farming activity experience [1, 2]. Objective understanding and quantitative evaluation on the recreational service value of urban productive landscape not only deepen the urban residents' understanding about the important functions of urban productive landscapes, but also help the city planning, construction, and managerial department fully recognize the important role of urban productive landscapes. The recreational value of urban productive landscapes belongs to the nonuse value and it can be evaluated with many methods, mainly including TCM (Travel Cost Method), REEM (Residential Environment Evaluation Method), and CVM (Contingent Valuation Method), etc., among which CVM is one of the most widely used methods [3, 4]. CVM mainly uncovers people's largest WTP aiming at the environment improvement or smallest WTA (willingness to accept) when the environment worsens by constructing the imaginary market and do the monetization assessment on the people's preference about the nonmarket goods so as to acquire all the use value and nonuse value related to the environmental goods [5]. Because there is no direct market deal about nonuse value, it cannot be measured with the market price method. The appearance of CVM has solved the difficult problem bothering people for a long time. As an agricultural science park and historical and cultural park, the Baguatian Scenic Area can produce fruits, vegetables, and food crops throughout the year. It has good economic and landscape benefits and attracts residents of Hangzhou and surrounding areas to enjoy the scenery and pick them, an urban productive landscape with typical and representative significance. Research into the existence value and meaning of Hangzhou Baguatian, a typical representative of urban productive landscapes, is of great reference significance for the following sustainable operation of urban productive landscapes of similar types. The paper adopts CVM to explore the urban residents' WTP and the influencing factors about the recreational value of productive landscapes [6], puts forward specific strategies and suggestions, and provides the scientific examples so as to offer the effective strategy and development suggestions about the development and preservation of productive landscapes in other cities and provinces and even the whole country.

2. Methodology

2.1. Questionnaire Design. The questionnaire is based on the related design principle of NOAA, pilot investigation results, and received feedback and after constant modifications and perfections, finally confirming the main content of the questionnaire, including three parts:

(1) Main social and economic characteristics of the interviewees, including the gender, age, occupation, education degree, origin, permanent residence, income, etc.

(2) The recognition degree, landscape preference, and satisfaction degree of the interviewees about Hangzhou Baguatian.

(3) The willingness to pay (WTP) of the interviewees about the productive landscape of Baguatian. A certain payment range is given to the interviewees to inquire about the amount of payment the interviewees would like to pay for the productive landscape leisure tourism function.

2.2. Investigation Process. The time period of this field questionnaire investigation is from March to April in 2018. The questionnaire is randomly handed out in different functional areas in Hangzhou Baguatian according to the research's characteristics and investigation content. To improve the effectiveness of the questionnaire investigation result and ensure that all the interviewees are fully aware of the investigation purpose and questionnaire content, the investigation method of communicating face to face before filling in the questionnaire is adopted [7]. 400 questionnaires are handed out to the tourists in the park and 400 questionnaires are collected on the site, thus making the recovery rate 100%. After deleting the fault questionnaire, 365 effective questionnaires are obtained, so the effective rate is 91.25%.

The size of samples directly affects the research cost, time, and reliability. According to the statistics theory, the sample number (n) of interviewed tourists can be calculated by Scheaffer sampling formula:

$$n = \frac{N}{(N-1)\sigma^2 + 1}. \tag{1}$$

In the formula, n is the number of sampling samples; N is the annual reception number of recreation site; σ is the sampling error, which is usually 6%. Hangzhou Baguatian Park mainly provides the recreational function for the city residents and the total population of Hangzhou is 8.7 million in 2017; therefore, through the calculation by the above formula, the sample number of research questionnaire in the study should be 278. After reserving 25% scrap rate, at least 371 questionnaires should be issued.

2.3. Calculation Method. CVM allows for the possibility of evaluating the use value of ecological environmental resources, but as this method is based on the virtual market, the result is likely to subjective, different investigation modes and places will cause huge differences, and meanwhile, during the investigation process, the discrepancies of the interviewees' social and economic characteristics and psychology will appear. For example, part of interviewees is likely to make the positive answers due to the consideration of satisfying the investigators, thus causing the deviation. The research adopts the median calculation method, which chooses payment quota of 50% accumulated frequency as the annual WTP value per person, through some rectification, and multiplies the total number in a certain range so as to get the recreational value of Hangzhou Baguatian productive landscapes [8] and uses SPSS19.0 to do the correlation and sensitivity analysis on the factors such as WTP value, the gender, age, occupation, educational degree, and income.

3. Statistics and Analysis on the Investigation Result

3.1. Sample Characteristics Statistics.

(1) *Gender and Age Structure.* In the investigation samples, the males account for 44.9% and the females account for 55.1%. The investigation indicates that the ages of tourists are mainly between 21 and 40, and in this age section, there are 43.21% female tourists, which is far higher than that of the male tourists; the next age section is from 41 to 60, including 17.68% and 16.02% tourists, respectively. For female tourists, the age section below 40 accounts for 77.77%, which is obviously higher than the male percentage of 51% in that age section. In the age section above 41, the male tourists make up for 49%. The age section between 41 and 50 makes up 24% of the total, which is evidently higher than the percentage the females account for in that age section. We can see that the consumption preference of

young females for the leisure agriculture is higher than that of the average people and the females in the age group between 31 and 40 account for the highest consumption structure of leisure agriculture [9]. The middle-aged men are the main consumption group and their percentage is higher than that of the females. It can be learned that young females and intellectual and middle-aged men have the higher preference for the leisure agriculture.

(2) *Cultural and Occupational Background Structure*. The investigation shows that tourists visiting Hangzhou Baguatian productive landscapes are mainly those with higher education, stable career, and higher income. In the sample tourists, the percentage of tourists with college degree and above is 65%; the percentages of junior high school education and senior high school education are 12% and 23%, respectively. In addition to the percentage of people with bachelor's degree and above of 43%, the two cover about 70% in total. From that we can see that the interviewees can fully understand the investigation content. The composition of the occupations nearly covers all the careers in various levels and the percentage of ordinary company staffs is the highest, 31.7%.

(3) *Income Structure*. Tourists accounting for 27.6% are mainly those with monthly income of 4000~6000, 17.9% of tourists' monthly income is below 2000, 18.3% of tourists' monthly income is between 2000 and 4000, and 36.2% of tourists' monthly income is above 6000. These datum show that most of the tourists have a good income and can afford to bring the whole family to enjoy the village.

(4) *Origin and Permanent Residence Structure*. 72.6% residents living in Hangzhou belong to local people and more local people visit Baguatian mainly due to the landscape of Baguatian. Its nature is different from that of Hangzhou West Lake, which is a world-renowned landscape. Baguatian is like the backyard of Hangzhou people, where they can bring their family to enjoy the intense picking fun. 16.9% tourists come from the surrounding counties and cities and 10.5% tourists are from places far away from Hangzhou city outside Zhejiang Province (Table 1).

3.2. Analysis on WTP and the Amount of Payment of Tourists. As shown in Table 2, the tourists willing to pay for the preservation of Hangzhou Baguatian recreational resources account for 36.7%, and the largest amount of WTP is 1000 yuan per year and the smallest amount of WTP is 5 yuan per year. From the percentage of bidding value of tourists with WTP, 100 yuan per year accounts for the most (8.2%), followed by the percentage of tourists willing to pay 10 yuan per year (5.7). All in all, majority of people are willing to pay 200 and below and the percentage is 95.6%. These indicate that the percentage of tourists reduces with the increase of bidding value and it conforms to the actual payment psychology of common people. Regarding the annual average WTP value, there is still a heated debate about "whether to choose the median value or average value" in the current academic circle. Considering a series of potential problems such as the disperse tendency of interviewees' WTP and the changes of the average value caused by the effect of the extremes, the paper adopts the median value method commonly used in CVM and takes 50% of accumulated payment quota as the annual average personal WTP value. According to Table 2, the value closest to 50% is 49.9% and 63.3%, which is corresponding to WTP value of 40 and 50, respectively; therefore, the median value of accumulated quota is 40.74, meaning that personal WTP is 40.74 yuan per year [10].

There are 231 tourists who refuse to pay the recreational fee for protecting Hangzhou Baguatian. The reasons are shown in the analysis which shows that 3.2% interviewees think that protection work is the responsibility of the country instead of the ordinary residents; 11.2% tourists hold that the recreational resources of Hangzhou Baguatian are good enough and do not need their protection; 22.2% tourists believe that the recreational resources of Hangzhou Baguatian are not rare enough and it is not worth protecting. 19.9% tourists think their income is too low to pay the fee; 10.8% tourists say they are far from there and have no interest in protecting the park voluntarily; 15.5% tourists are worried that the fees they pay are not truly used for the voluntary protection of recreational resources; 17.2% tourists refuse to pay for other reasons. The detailed information is as shown in Table 2.

3.3. Payment Motivation of Tourists. The research into the payment motivation of use value, as one of the important parts to measure the nonuse value, can provide the further reference for scientific and reasonable managerial decisions of the government and the related managerial department. Carson recognizes the payment motivation of use value as value type and thinks the payment motivation of nonuse value includes heritage value, existence value, and option value, which adds up to the nonuse value [11]. The statistical result shows that, in the tourists willing to pay, 64.8% tourists want to ensure the permanent existence of Hangzhou Baguatian's recreational resources; 18.5% tourists want to leave Hangzhou Baguatian's recreational resources to the future generation as heritage; 16.7% tourists want to make themselves, the future generations, and others be able to use Hangzhou Baguatian's recreational resources selectively. We can see that existence value is the main form of Hangzhou Baguatian's recreational resources' nonuse value; the next is the heritage value and the last is option value. It means that only the permanent existence of Hangzhou Baguatian's recreational resources is ensured, making leaving it to the future generation and the future selective use be possible.

3.4. Analysis on Tourists Payment Mode. Since the WTP of interviewees is given based on the imaginary market, the deviation of overestimation or underestimation may appear,

Table 1: Basic information of samples.

Factors	Category	Frequency	Percentage	Factors	Category	Frequency	Percentage
Gender	Male	165	44.9	Occupational background	Administrative and public institutions	30	8.2
	Female	202	55.1		Enterprises (including state-owned enterprises, foreign enterprises, and private enterprises)	33	9.1
Age	20 and below	27	7.3		Other provinces in China	116	31.7
	21 to 40	204	55.5		Ordinary enterprise staffs	5	1.3
	41 to 60	106	28.8		Peasants	91	24.9
	61 and above	30	8.1		Freelancers	91	24.9
Educational background	Junior high school and below	32	8.7		Students	60	16.2
	Senior high school/college degree	82	22.3		The emeritus and retired	32	8.6
	Higher vocational college	122	33.3	Origin	Hangzhou city	265	72.6
	Bachelor's degree	104	28.4		Zhejiang Province	62	16.9
	Master's degree and above	27	7.3		Other provinces in China	38	10.5
Monthly income level	2000 and below	66	17.9		Abroad	0	0
	2001 to 4000	67	18.3	Residence	Urban	297	80.9
	4001 to 6000	101	18.3		Suburban	64	17.4
	6000 to 8000	55	14.9		Rural	6	1.6
	8000 to 10000	41	11.2				
	Above 10000	37	10.1				

Data source: investigation data.

Table 2: Frequency distribution of interviewees' willingness to pay (WTP).

Payment value of WTP (yuan/year)	Absolute frequency (people)	Relative frequency (%)	Adjusted frequency (%)	Accumulated frequency (%)
5	5	1.3	3.7	3.7
10	21	5.7	15.7	19.4
20	18	4.9	13.4	32.8
30	19	5.2	14.2	47
40	4	1.1	2.9	49.9
50	18	4.9	13.4	63.3
60	2	0.5	1.4	64.7
90	2	0.5	1.5	66.2
100	30	8.2	22.5	88.7
120	1	0.2	0.8	89.5
200	8	2.2	5.9	95.4
300	1	0.2	0.8	96.2
500	3	0.8	2.2	98.4
700	1	0.3	0.8	99.2
1000 and above	1	0.3	0.8	100.0
Refuse to pay	231	36.3		
In total	365	100.0	100.0	

but designing the reasonable payment mode can reduce such kind of deviation to some degree. Through the statistical analysis on the payment mode in the 134 "Willing to Pay" questionnaire, it shows (as shown in Table 3) that 13.2% tourists think that the protection fee should be delivered to the country for the unified allocation in form of paying taxes, and this percentage is the highest in all the payment modes. Besides, 15.9% and 4.4% tourists hold that protection fees should be paid in cash to the managerial institutions or to buy the environmental protection funds or lottery ticket and the proportion of paying to nongovernmental organizations in cash is the lowest (2.5%) [12].

Table 3: The modes of WTP.

Payment mode	Frequency (people)	Percentage	Effective percentage	Accumulated percentage
Give it to the country for the unified allocation in form of paying taxes	48	13.2	35.8	35.8
Pay the managerial institute in cash	58	15.9	43.3	79.1
Pay in the form of buying environmental protection funds or lottery ticket	16	4.4	43.3	79.1
Give it to the nongovernmental organizations in cash	9	2.5	6.8	97.8
Other modes	3	0.8	2.2	100.0

3.5. Analysis on Recreational Value. Take the WTP value of investigated tourists as the evaluation index of Hangzhou Baguatian recreational value and do the correlation analysis to WTP with SPSS software. Through the analysis, it can be seen that only 1 person chooses 1000 yuan and above, which is deleted due to its unrepresentative characteristics (Table 2). Use the accumulated frequency median valuation method of WTP in CVM principle to deal with the investigation datum of interviewees and the calculation shows that the average recreational value of Hangzhou Baguatian is 40.74 yuan/person. Take the latest population statistical result of Hangzhou in 2017 as the sample and the total population of Hangzhou is 8.7004 million, meaning that $M = 8.7004$ million. Therefore, the recreational value of Baguatian in 2017 is 354 million yuan through calculation [13].

The nonuse value of recreational resources includes option value, heritage value, and existence value. Existence value refers to the fee people would like to pay for the preservation and the permanent existence of Baguatian recreational resources; heritage value refers to the protection fee the contemporary people would like to pay with the aim of leaving the Baguatian recreational resources to the future generations so that they can benefit from them; option value refers to the future use of the resources' potential function by the individual and society, which means people would like to pay some fees to ensure themselves or others can explore and use the Baguatian recreational resources selectively. In the sample WTP, the payment motivations of tourists for the existence value, heritage value, and option value of the Baguatian recreational resources account for 48%, 25%, and 27%, respectively. Therefore, the existence value, heritage value, and option value of the Baguatian recreational resources in 2018 are 170 million yuan, 89 million, and 96 million yuan.

3.6. Analysis on the Correlation between the Various Samples' Social and Economic Characteristics and WTP and WTP Value. The important methods and key steps of verifying the effectiveness and dependability of CVM are to analyze the effect of all the factors of the total sample on WTP and WTP value according to the effect of personal basic condition of the interviewees on the nonuse value of recreational resources to some degree. Therefore, the paper uses the Pearson correlation analysis in SPSS software to verify the correlation between the social and economic characteristics of 365 interviewees and WTP and WTP value. According to the personal social and economic characteristics, assign the value in the SPSS software as follows (Table 4).

3.6.1. Analysis on the Correlation between the Samples' Social and Economic Characteristics and WTP. Seen from the analysis on the correlation between the samples' social and economic characteristics and WTP (Table 5), it can be concluded that there is no significant correlation between the interviewees' origin, permanent residence, and WTP while there is positive correlation between the occupational background, educational degree, and WTP. It shows the educational degree, occupational background, and monthly income are the main factors influencing the tourists' WTP. Tourists' gender, understanding degree about Hangzhou Baguatian Park, and the tourism-generating regions have little effect on WTP. The reasons are as follows: the interviewees in the study are mainly young adults and middle-aged men between 20 and 40, whose incomes become relatively stable as the age increases and WTP becomes stronger. In the meantime, it is found that, in the investigation, the higher the educational degree of the interviewees is, the stronger their willingness to protect the recreational resources will become; thus, WTP tends to go up. Besides, some tourists think that Hangzhou Baguatian recreational resources are preserved well and no extra protection fees need to be paid. The main reason is the dispersed responsibility caused by the fact that their residence is far from the Hangzhou Baguatian Park and besides, the gender, origin, and the permanent residence, etc., have no significant influence on WTP [14].

3.6.2. Analysis on the Correlation between the Samples' Social and Economic Characteristics and WTP Value. It can be seen from the analysis on the correlation between the sample's social-economic characteristics and WTP value (as shown in Table 5) that there is a significantly positive correlation between tourists' monthly income and WTP value, but the correlation between other factors and WTP value is not significant; therefore, paying capacity is the main factor influencing the tourists' WTP value. Because the higher the tourists' income is, the stronger the corresponding paying capacity is. As long as they are willing to pay, WTP value will be bigger. It is found in the investigation that some tourists want to pay, but they refuse because they are worried about the specific use of these fees and they are

Table 4: Setting of independent variables in SPSS software.

Independent variables	Variables and assignment
Gender	Male = 1; female = 2
Age	[-, 20] = 1; [20, 40] = 2; [41, 60] = 3; [60, -] = 5
Educational degree	Junior high school and below = 1; senior high school or college degree = 2; higher vocational college = 3; bachelor's degree = 4; master's degree and above = 5
Occupational background	Administrative and public institution = 1; enterprises (managerial level) = 2; ordinary company staffs = 3; peasants = 4; freelancers = 5; students = 6; the emeritus and retired = 7
Monthly income level	(-, 2000] = 1; (2001, 4000] = 2; (4001, 6000] = 3; (6001, 8000] = 4; (8001, 10000] = 5; (10000, -) = 6
Origin	Hangzhou city = 1; Zhejiang Province = 2; other provinces = 3; abroad = 4
Permanent residence	Urban = 1; suburban = 2; rural = 3

Table 5: The analysis on the correlation between each sample's social-economic characteristics and WTP.

	Gender	Age	Educational degree	Occupational background	Monthly income	Origin	Permanent residence
Correlation coefficient	−0.042	0.003	0.043	0.073	−0.025	0.013	−0.029
Level of significance	0.420	0.999	0.890	0.162	0.630	0.802	0.802

Note. ** means the correlation coefficient is significant at 0.01 level and * means the correlation coefficient is significant at 0.05 level.

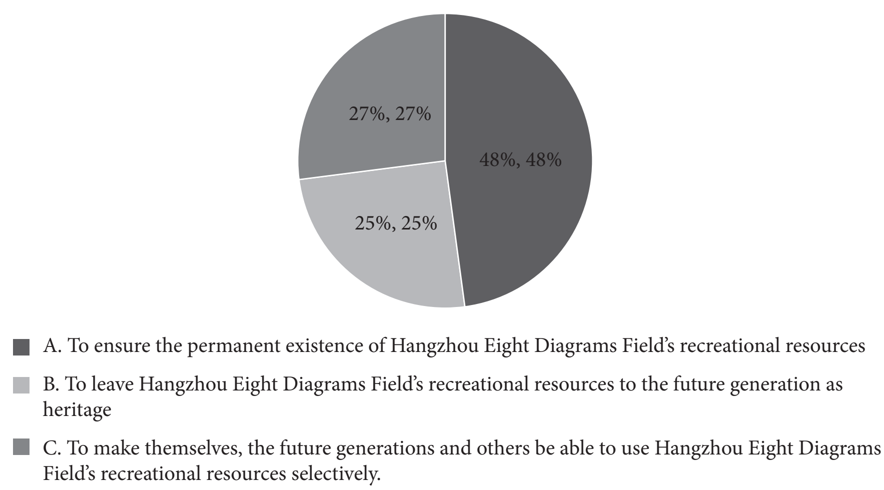

Figure 1: The selection of payment motivation.

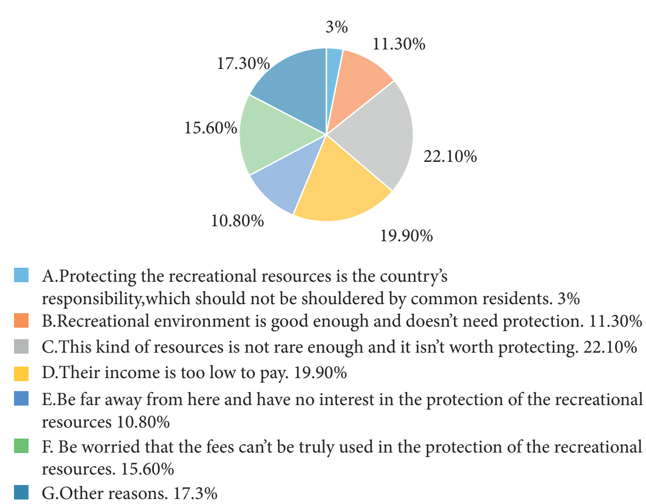

Figure 2: The reasons for refusing to pay.

Table 6: The analysis on the correlation between each sample's social-economic characteristics and WTP value.

	Gender	Age	Educational degree	Occupational background	Monthly income	Origin	Permanent residence
Correlation coefficient	−0.005	0.076	0.080	−0.073	0.124	−0.087	0.027
Level of significance	0.929	0.147	0.125	0.165	0.524	0.096	0.605

Note. * means the correlation coefficient is significant at 0.05 level.

unclear about the role of resources protection subjects (thinking that it is the country or the government's responsibility to protect the recreational resources, which should not be shouldered by the common residents, as shown in Figures 1 and 2). There is no significant correlation between the tourists' origin, permanent residence, and WTP value for Hangzhou Baguatian Park. With the development of modern society, the income gap between the male and the female is increasingly narrowing down; therefore, the gender difference does not have much effect on WTP value (Table 6).

4. Conclusion and Discussion

The paper adopts the internationally accepted CVM to evaluate the use value of Hangzhou Baguatian recreational resources and does the statistical analysis on the 365 effective questionnaires in the 400 investigation questionnaires and the following conclusions are obtained:

(1) 62.1% of the interviewed tourists are willing to pay for the recreational value of Hangzhou Baguatian Park, which indicates it is of great value significance to protect the recreational resources of Hangzhou Baguatian. The average WTP value is 40.74 yuan/person per year. In 2017, the recreational value of Hangzhou Baguatian Park is 354 million yuan, among which the existence value of 170 million yuan is the main form of the nonuse value of Hangzhou Baguatian, and next are the heritage value (89 million yuan) and option value (95 million yuan).

(2) 63.2% of tourists have no WTP and refuse to pay for the recreational value of Hangzhou Baguatian Park, mainly because they are unclear about the self-role of protecting the recreational resources. They are worried that the paid fees cannot be fully used for the protection of recreational resources or they are unable to pay the protection fees of Hangzhou Baguatian due to their terrible economic condition.

(3) In terms of payment mode, in the interviewees who are willing to pay, the highest percentage of tourists think that the protection fees should be handed in to the country for the unified allocation in the form of tax-paying (13.2%), the next are the percentages of tourists who hold that protection fees should be paid in cash to the managerial institutions or to buy the environmental protection funds or lottery ticket (15.9% and 4.4% respectively), and the proportion of paying to nongovernmental organizations in cash is the lowest (2.5%).

(4) Seen from the analysis on the correlation between the investigated samples' social and economic characteristics and their WTP and WTP value, there is no significant correlation between the interviewees' origin, permanent residence, and WTP and there is a positive correlation between occupational background, educational degree, and WTP, which means the educational degree, occupational background, and monthly income are the main factors influencing the tourists' WTP. Tourists' gender, the understanding degree about Hangzhou Baguatian Park, and the tourism-generating regions have little effect on tourists' WTP. There is a significantly positive correlation between the monthly income and WTP value and the correlation between other factors and WTP value is not significant, which means that the paying capacity is the main factor influencing the tourists' WTP value. The higher the income of the tourists is, the stronger their paying capacity will become; thus, as long as they are willing to pay, WTP value will be bigger.

CVM is the product under the pure market economic condition. The research on urban productive landscapes that cannot be fully marketized has certain limitations. The academic exploratory nature of its quantitative evaluation still has a certain value, and it needs to be continuously improved in the process of application. 365 samples in the paper are used to represent all the tourists of Hangzhou Baguatian, which will bring about certain deviation. Therefore, multiple methods should be combined to make the comparative analysis so as to make the evaluation result much closer to the actual value of research subjects and put forward a series of realistic suggestions and countermeasures aiming at the development and preservation of the productive landscapes similar to Hangzhou Baguatian to help promote the productive landscapes in the whole province and even the whole country [15].

Data Availability

The datasets used and/or analyzed during the current study are available from the corresponding author on reasonable request.

Conflicts of Interest

The authors declare no potential conflicts of interest with respect to the research, authorship, and/or publication of this article.

Acknowledgments

The authors acknowledge the Agricultural Project of Zhejiang Province Science and Technology Agency Nonprofit Technology Research (2016C32017) and Zhejiang Province NSFC Program (LY16C160008).

References

[1] H. Shi, X. L. Zhang, and J. G. Zhang, *Foreign Productive Landscape Theory Research and Application Condition*, pp. 352–355, Zhejiang A&F University, Zhejiang China, 2015.

[2] D. Han and J. G. Zhang, "Research into the urban productive landscape tourism experience based on the web text analysis---taking Hangzhou baguatian scenic spot for example," *China Forest Products Industry*, vol. 44, no. 12, pp. 54–58, 2017.

[3] T. Y. Zhao, P. Cao, Z. Y. Liu, Z. Jiang, and T. Jin, "Landscape leisure tourism value assessment of jinzhou city paddy field ecological system based on CVM," *Resources and Environment in the Yangtze Basin*, vol. 24, no. 3, pp. 499–503, 2015.

[4] X. J. Wang and C. B. Zhong, "The vague assessment model of haitu wetland ecological service value," *Acta Ecologica Sinica*, vol. 21, no. 4, pp. 466–471, 2018.

[5] Y. P. Liu and J. X. Jin, "The domestic application research characteristics and research trend of CVM---the literature publicly published in the domestic publications in 20 years," *Ecological Economy*, vol. 30, no. 2, pp. 23–29, 2014.

[6] M. Zhao, J. Zhang, J. Xie, and M. Zhang, "Empirical study on recreation suitability evaluation of suburban forest park - a case study of baiyun forest park in lishui city, China," *Applied Ecology and Environmental Research*, vol. 17, no. 2, pp. 3499–3512, 2019.

[7] Z. M. Ding, X. J. Huang, and J. J. Zhu, "Content validity verification of forest scenic spot recreational value based on CVM---taking fuzhou national forest park for example," *Issues of Forestry Economics*, vol. 37, no. 3, pp. 46–50, 2017.

[8] X. Y. Xiao, Q. D. Yu, Y. L. Zhang, J. Liu, and J. S. Guan, "Research into the tourism related resources value assessment general range expansion method," *Journal of Natural Resources*, vol. 28, no. 9, pp. 1623–1636, 2013.

[9] X. B. Lin, Y. Y. Yan, Q. W. Min et al., "Analysis on the agricultural cultural heritage non-use value evaluation and its influencing factors---taking fuzhou jasmine flowers' plantation and tea culture heritage for example," *Resources Science*, vol. 36, no. 5, pp. 1089–1097, 2014.

[10] W. J. Peng, S. B. Yao, and Y. Feng, "Recreational resources value assessment based on TCIA and CVM----taking taibaishan national forest park for example," *Economic Geography*, vol. 34, no. 9, pp. 186–192, 2014.

[11] W. Y. Feng, Y. H. Wang, J. K. Tanui, and X. Y. Li, ""Economic value assessment of tea culture tourism resources based on suzhou dongting biluochun tea," *Journal of Tea Science*, vol. 32, no. 4, pp. 353–361, 2012.

[12] Y. Xiao, S. Chen, Z. Q. Cao, T. Xia, and L. X. Hao, "Value assessment of shandong marine protection zone ecological system diversity maintenance service based on CVM," *Acta Ecologica Sinica*, vol. 36, no. 11, pp. 3321–3328, 2016.

[13] F. Su, Y. P. Zheng, L. N. Kan, and S. Cai, "Urban public green land service value evaluation based on CVM investigation method---taking western capital city for example," *Resources and Environment in the Yangtze Basin*, vol. 27, no. 1, pp. 2434–2441, 2018.

[14] M. O. Chen, *Value Assessment of Shennongjia Geopark Tourism Resources Based on TCM and CVM Method*, Hubei University, Wuhan, Hubei, China, 2016.

[15] J. G. Zhang and Z. Pang, "Research on evaluation index system construction of urban river scenic spots development suitablity," *Journal of Environmental Protection and Ecology*, vol. 19, no. 3, pp. 1215–1224, 2018.

Hindawi
Scientific Programming
Volume 2021, Article ID 4648814, 9 pages
https://doi.org/10.1155/2021/4648814

Research Article

The Influence of Information Interaction Behavior on Value Co-Creation Business Model of Online Education Enterprises Performances from the Perspective of Supply Chain

Jingjing Lv,[1] Nan Wang ,[1] and Shaoxin Xiang[2]

[1]*School of Economics, Guangdong Ocean University, Zhanjiang, Guangdong 524088, China*
[2]*Yunnan Normal University, Kunming, Yunnan 650500, China*

Correspondence should be addressed to Nan Wang; wang1023nan@gdou.edu.cn

Received 26 October 2021; Accepted 29 November 2021; Published 17 December 2021

Academic Editor: Punit Gupta

This paper analyzes the impact of information interaction ability on the value co-creation business model of online education enterprises from the perspective of supply chain. Integrate the perspective of supply chain and summarize the content of supply chain capability and performance. This paper analyzes the connotation and shortcomings of information interaction ability, combines the connotation of value co-creation to maximize the advantages of information interaction, assumes the impact of information interaction on value co-creation through questionnaire survey method, uses software to analyze the reliability and validity of data, and proves that the data are reasonable. Information interaction has a positive impact on the value co-creation business model of online education enterprises.

1. Introduction

Online education enterprise is a new teaching mode booming in the past two years. Under the current Internet environment and market economy environment, it has great development space. Although online education is mainly for the convenience of students to receive education at home, it is still a commercial organization with profit as the ultimate goal in the final analysis. Under the current business model, if an online education platform wants to be long term, it is necessary to create commercial value [1–3]. At present, online education in China is still in the initial stage. In order to attract more customers to accept online education, many enterprises have reduced their interests to the minimum, and more business value has not been highlighted. In order to achieve value co-creation, online education enterprises are also trying to explore and develop a value co-creation business model. For online education enterprises, the use of a co-creation value model can help enterprises create effective value [4]. At present, online education enterprises are facing the competitive pressure of huge student groups and schoolwork. Under the fierce competition market environment, independent online education enterprises cannot occupy the dominant market [5]. Only by information interaction, sharing industry information, and market situation can they achieve a win-win situation. Establishing and deepening the information exchange ability between online education enterprises and reducing the information isolation between enterprises can change the confusion encountered by enterprises in independent operation (there is a certain resource information dependence between online enterprises, and the information interaction ability can enhance their symbiosis) and solve the work content that enterprises cannot complete in independent operation [6]. Under the market economy, the competition among the same enterprises is becoming more and more fierce, and the related enterprises are gradually aware of this situation and are more willing to strengthen contact and share industry information with the enterprises of the same level and the same business model [7–9].

The supply chain is a network chain structure formed in the process of commodity circulation, aiming at the final receiving of goods by users. Some famous experts have expounded in their own works the fact that in today's market economy, enterprises are no longer the main body, but the supply chain is the main body. In the whole market, the competition among enterprises is no longer the competition to seize the market, but the competition between supply chains [10]. It can be seen that in the current situation of the increasing shortage of resources, the competition of supply capacity reflects the competition of the supply chain, and the results of supply competition are presented through the results of supply chain performance. From the perspective of the supply chain, this paper studies the evolution and development of the value co-creation business model of online education enterprises under the influence of information interaction ability and takes actual enterprises as the research object to carry out the case study.

2. Basic Concepts of Supply Chain

2.1. Integration from the Perspective of Supply Chain

2.1.1. The Meaning of Supply Chain Integration. The whole process of a product from production to sales involves many aspects of interest, among which the main roles include the producer responsible for the realization of the product, the supplier responsible for providing raw materials, the distributor responsible for the large-scale sales of goods, and the retail retailer responsible for the small-scale sales of goods. It is these businessmen who play different roles that form a closely linked and comprehensive economic network to realize the overall operation of the supply chain. Ordering, production, and transaction are all important parts of supply chain operation [11].

The fundamental purpose of online education enterprises using a supply chain is to ensure that they can not only obtain profits but also meet the basic needs of consumers. Only by meeting the needs of consumers can enterprises obtain the profit in the target. The fundamental operation purpose of each link in the supply chain is to meet the needs of consumers. Although the seller, supplier, and manufacturer are the key components, if subdivided, it also includes the most critical consumer, warehousing, transportation, and other branches. Consumers are the most critical link in the whole supply chain. It is precise because consumers have a demand for goods that drives the reasonable operation of the supply chain. From this level, it can be said that consumers are the inexhaustible power to drive the supply chain from one end to the other. Consumers send out their own demand for goods, and suppliers and manufacturers receive such requests, making production behavior, and the transportation department should give full play to the convenience of transportation, realize the supply of goods to consumers through retailers or distributors, and improve the bottom-up supply chain structure.

2.1.2. Supply Chain Integration. The integration of supply chain content can be divided into two parts, namely, external and internal integration. For the internal integration of the supply chain, it mainly focuses on the internal activities of online education enterprises, in order to achieve significant cooperation between suppliers and enterprises, and at the same time, online education enterprises meet the needs of consumers, coordinate and synchronize the activities of different departments in the enterprise; the external integration of online education enterprises is to build an alliance between external partners and online education enterprises, realize the common business strategic objectives of several enterprises, unify and coordinate the business operation process and cooperative operation process of each enterprise, and realize the unity of cooperation strategy. It is through this internal and external supply chain integration to improve the upper and lower ends of the supply chain management process and business model, and effectively improve the business performance of enterprises.

The purpose of integrating the supply chain is to improve the strategic cooperation ability and information sharing ability of online education enterprises in the operation stage. After the adjustment, the enterprises in each link of the supply chain cooperate with each other for common interests and operation purposes and work together for the strategic goal, so we should strengthen the deep cooperation of similar online education enterprises. At the same time, the deep integration of online education enterprise's supply chain is also to integrate and strengthen the internal and external business processes. Through the integration of the supply chain, the interests of the cooperative online education enterprises are maximized to enhance the value of each enterprise.

Through the above analysis, it can be seen that each node in the supply chain realizes the top-down integrated connection through the integration and adjustment of the supply chain. Through the integration and optimization of the supply chain, it realizes the closely connected supply chain structure, ensures that each associated enterprise can add value in the connection of the whole supply chain, obtains effective income, and, to a certain extent, ensures the close connection between production and consumption, so as to achieve the goal of all in one service. This kind of supply chain adjustment improves the overall economic benefits and soft power of enterprises, promotes the overall development of affiliated enterprises, and also improves China's comprehensive soft power to a certain extent.

2.2. Capability and Performance of Supply Chain. Logistics circulation ability and managers' decision-making ability and management ability in the process of supply chain operation are the embodiment of supply chain ability. In previous studies, it has been found that when defining the internal capability of the supply chain, the concept is composed of multiple dimensions, and this multidimensional problem is also involved in the above supply chain integration. As long as it includes production, storage, transportation, sales, and other links, these links together constitute the overall process of the supply chain, and the process also includes two levels of supply chain capabilities [12]. One of them is the basic ability of the supply chain; that is, the enterprise at each end of the supply chain completes the part of the work that the enterprise needs to be responsible for according to its own work content and division of labor content. Every link of the enterprise is concerned about the goal of profit as the goal; the main work is to ensure that the enterprise can work normally, so the basic ability of the supply chain is the ability of the basic work of the supply chain. The ability of the second level is the service ability that the supply chain can carry. This level needs the supply chain to have higher ability. The so-called service ability is the ability that each enterprise in each link of the supply chain can make the best response in the increasingly fierce market economy. The actual operation is more difficult, so once it starts, it will become a unique ability [13, 14]. The availability of these two levels of capabilities reflects the management of supply chain operation, which is related to the performance of supply chain operation.

Although the management and operation process of the supply chain is clear, it is an extremely complex process to form a complete and effective supply chain. Therefore, it is necessary to evaluate the operation performance of the supply chain. The relationship between the supply chain and the enterprise is both exterior and interior, and also, they affect each other. It has a strong guiding role to obtain the evaluation and analysis results between the enterprise and the supply chain. When evaluating the performance of the supply chain, it takes the cost, quality, delivery time, and other indicators as the standard, to modify the indicators appropriately according to the actual situation and research needs of the enterprise, and establish an index system to evaluate the performance of the supply chain.

3. Description of Information Interaction Ability

By using the mode of information interaction, enterprises can realize the information sharing and knowledge commonality of enterprises at each end of the supply chain, master the user needs and production standards, and have a unified understanding of the laws and regulations related to the production and transportation of related products, so as to promote enterprises to realize value co-creation. If online education enterprises want to develop for a long time, they need effective management and information interaction means to ensure the healthy competition. Information interaction can improve financial performance and supply chain performance and significantly increase user perception and emotional commitment.

One of the advantages of information interaction in promoting enterprise value co-creation is the transformation from information interaction resources to information interaction ability. The detailed process of this transformation ability is shown in Figure 1.

Online education enterprises use new information technology to build information interaction facilities to ensure the smooth and stable operation of online education, so as to improve the interaction efficiency and lay a good foundation for other content of subsequent information interaction; talents with the ability of information interaction constitute the human resource reserve of online education enterprises, bringing advanced technology and work experience to the enterprises. Combined with the current high, refined, and cutting-edge information technology, the enterprise's information interaction resources are formed. It is precisely because of the integration of these different functions that the values of enterprises can be created together.

Researchers in various fields have made preliminary achievements in the research of information interaction, but in the current form, there are still some problems in the research of interactive information.

3.1. The Object of Interaction Is Unknown. The key point of information interaction is the information interaction between enterprises at each end of the supply chain, but this excessive attention ignores the information interaction among information networks (companies at each end of the supply chain), value networks (between customers and enterprises), and customer networks (between customers).

3.2. The Scope of Interaction Is Unknown. Although, simply speaking, the relationship between the enterprises at each end of the supply chain is information interaction, the detailed interaction content is extremely extensive. In addition to the interaction of customer information, information interaction also needs to realize the interaction of production technology, new learning technology, and the interaction between scientific and technological means and users. These interactions are complex and changeable. There are many contents involved, and the boundary is often unclear in practical research [15].

3.3. The Level of Interaction Is Chaotic. At present, the interaction of basic production information and sales information between enterprises is a relatively basic content in the research field, but the most profound and core information is needed to achieve the healthy development of enterprises. In recent years, with the rapid development of cloud technology, Internet technology, and big data technology, a lot of information content can be obtained without going out of the house. This form has changed the traditional way of human communication and the management and distance between people, people and things, and things and things, breaking through the traditional restrictions. There are huge differences between the transmission frequency and privacy of information.

In the actual operation process of enterprises, in addition to the basic way of information interaction, continuous and in-depth information characteristics are all new characteristics of information interaction. It can be seen that the study of information interaction needs to start from the overall perspective of the enterprise. From the current research perspective and from the perspective of supply chain, information interaction is not only a simple technical ability, but also a core ability from the perspective of overall strategy. The application of information interaction in the value co-creation business model of online education enterprises will bring great benefits to the development of enterprises.

This section studies the basic concept of information interaction in detail; that is to say, under the background of

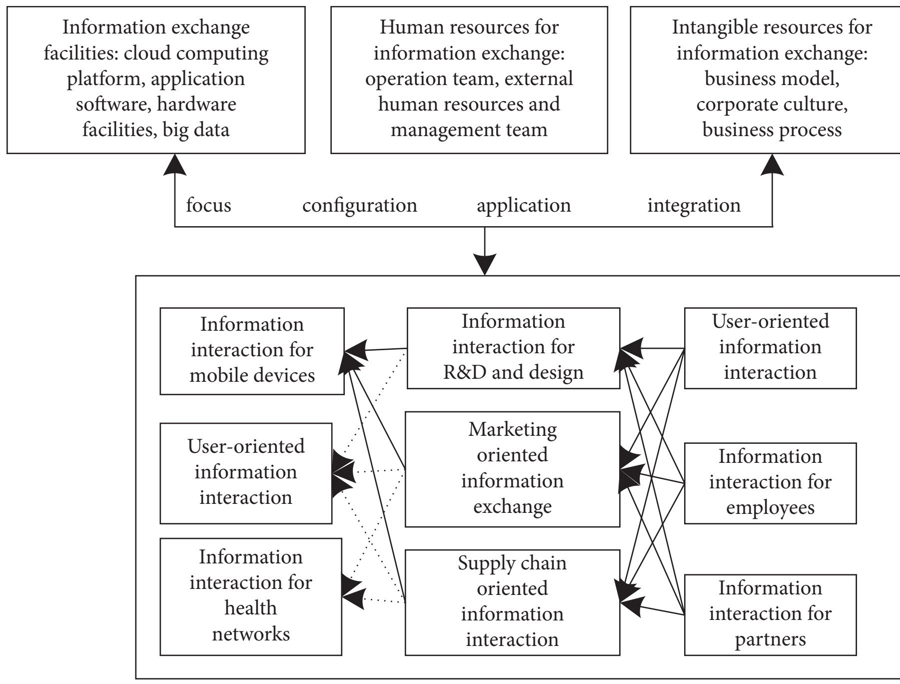

Figure 1: The transformation process from information interaction resources to information interaction capabilities.

the new economic environment, enterprises adjust and apply the content of information interaction. The fundamental purpose of interaction is to realize the value of enterprises, co-create business models, and help enterprises gain more competitive advantages in the fierce competitive environment. The communication principle of information interaction is shown in Figure 2.

Information interaction capability includes various concepts. Firstly, information interaction technology can provide more massive information interaction technology to online education enterprises under the rapid development of emerging information technology, so as to build more reasonable information interaction tools, help enterprises obtain more benefits in the business process, lay a favorable foundation for online education enterprises to achieve business value co-creation, and provide a reference for online education enterprises. The competitive development of enterprises brings necessary material resources support [16]. The other is that the guiding goal of information interaction is the value co-creation of enterprises. In recent years, the rapid development of all kinds of new information technology has led to the surplus of information resources in most online education enterprises. When the value co-creation is directly related to the user experience, the advantages of these new information technologies can be brought into full play.

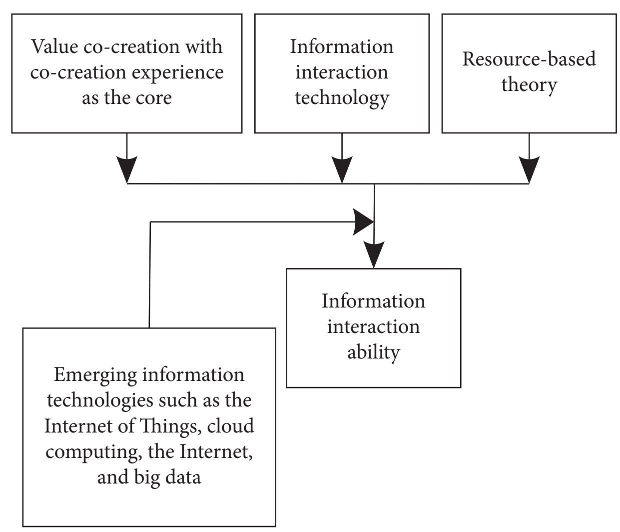

Figure 2: Principle of information interaction and transmission.

4. Connotation and Classification of Value Co-Creation Model

4.1. Connotation of Value Co-Creation Model. Taking the individual as the center is a new means of value creation under the perspective of market economy and supply chain. The creation of this kind of value is no longer solely dependent on the creation of enterprises but needs the joint creation of enterprises and customers. Value co-creation business model and information interaction share the enterprise's work tasks with customers who buy goods. The identity of customers has changed significantly. That is to say, under the same supply chain, customers and suppliers and manufacturers and sellers form a direct connection, which is also one of the links of enterprise value pursuit [17]. Customers not only create their own value, but also help enterprises reduce the consumption of human costs and create more value for enterprises. This proves that, from the perspective of supply chain, co-creation of value is not created by enterprises, but by customers' participation.

From the perspective of supply chain, enterprises and customers are closely connected in each link. Customers change from passive consumption to active participants in interest activities. There is an interactive and cooperative relationship between them, and the value is created together. In other words, under the information interaction technology, in order to achieve the common goal, customers and enterprises continuously transfer information and exchange their own resources so as to ensure customers' good consumption experience and obtain more information content, realizing the common creation of interests with enterprises. To study the specific performance of this kind of value co-creation is that customers participate in product design, or directly carry out consumer behavior to bring value to enterprise development, which is the most intuitive interaction and value co-creation between the two.

From the above research and analysis, we can see that the cooperation between enterprises and customers is mainly the demand for each other's resources. That is to say, customers need the products produced by enterprises, while enterprises need the demand information of users. Such resources need to cooperate between customers and enterprises under the information interaction technology so as to obtain a lot of information and make rational use of it to maximize benefits. Generally speaking, information interaction is the basis of value co-creation, and value acquisition is the ultimate goal of value creation from both the perspective of customers and enterprises. The key point of value co-creation is to realize the value experience of customers and enterprises. It can be seen that enterprises at each end of the supply chain are not the main body to obtain value, and customer participation is also the key step to realize value co-creation. The closer the relationship between customers and enterprises is, the more harmonious the value can be maximized, and this kind of information interaction runs through all links of the supply chain in every step of every enterprise.

4.2. Value Co-Creation Classification. For value co-creation, previous studies have divided it into two categories in detail, one of which is the value jointly generated by the enterprise and the customer, with the enterprise as the leading and the customer as the cooperator; the other is the value creation method with the enterprise and the customer as the main body, with the customer as the leading, and the enterprise as the cooperator. The following is the specific analysis process.

4.2.1. Production Field. In the field of production, the value co-creation of online education enterprises is carried out from the perspective of enterprises. From the perspective of supply chain, each end enterprise puts its own type resources and intangible information into the value creation system. Customers put forward value requirements according to their own needs and mix the resources invested by customers so as to integrate the resources of customers and enterprises in the supply chain and cooperate with each other to create business value. This kind of value co-creation can effectively improve the performance and business performance of each enterprise, create a good business image for the enterprise to a certain extent, inject fresh blood into the enterprise, enable the enterprise to continuously create new value, and ensure that a more harmonious relationship can be built between the enterprise and customers. Although under this classification, customers are not the main body of value production, they still play an important role in the process of value co-creation: because customers put forward demands for their own needs, enterprises can make a way conducive to value co-creation according to their needs; as a crucial link in the supply chain, customers also invest their own resources in information interaction, which enriches the level of resources and helps enterprises achieve value creation faster and better; customers and enterprises actively interact with each other to help each other and create business value together [18]. The value co-creation of any commodity in the field of production is dominated by the enterprise, which provides space for customers and takes the enterprise as the leading role. It is necessary to grasp the value creation and production all the time, and at the same time, it is also necessary to improve the level of enterprise management.

4.2.2. Consumption Field. In the field of consumption, if we want to realize the value co-creation, we need to take the customer as the main body, the customer fully considers their own interests, put their own information and knowledge resources into the information interaction, readjust and match the resource information, and use the interactive way to connect the customer and the enterprise so that the resources of the two can be effectively integrated and infiltrated into each other. It is the realization of value co-creation between enterprises and customers. In other words, when customers have demand for goods, enterprises will put forward their own value proposals according to the needs of enterprises. If customers are satisfied with this proposal, they will reach a consensus on value. With the assistance of information interaction, resources can be exchanged, and value co-creation between enterprises and customers can be realized under the supply chain. In order to realize the stable value co-creation, enterprises also need to make support to ensure the realization of value co-creation. It is because of the realization of value co-creation that customers can get good business experience and meet their demand for goods. The main focus of value co-creation under the category of consumption field is the integration of resources between enterprises and customers. Customers take themselves as the main body to create business value, but also need to invest their own resources and make an accurate evaluation of the value created.

The above two kinds of value co-creation classification are from the perspective of different subjects, mainly aiming at the particularity of different subjects to explain co-creation value. Although enterprises and customers have different performance in value pursuit, the demand for value maximization is consistent. Under the information interaction technology, both of them integrate their own information content. However, whether it is production or consumption, the pursuit of value co-creation is consistent. Customers and enterprises in the supply chain make their own contributions to the realization of value co-creation.

5. Case Analysis

This paper takes an online education enterprise as a case sample to analyze the impact of the company's enterprise development from the perspective of supply chain and the value co-creation business model of school education enterprise under the influence of information interaction technology. Detailed analysis of practical examples is carried out by using the information interaction technology and the basic theory of value co-creation introduced.

5.1. Research Methods and Strategies. There are still many deficiencies in the research of information interaction. In this paper, the research is carried out from the perspective of supply chain. Information interaction technology has the characteristics of organization and strategy. This paper focuses on the analysis of the impact of the use of information interaction technology on the co-creation business model of enterprises. Therefore, specific research is carried out for the enterprises that have made remarkable achievements in the field of online education. This paper analyzes the reasons behind the achievements of the enterprise. In this paper, we believe that information interaction technology can bring high-quality value co-creation effect for enterprises and ensure enterprises to obtain absolute enterprise advantage in similar enterprises. The detailed theoretical framework is as follows:

(1) The resources in the process of information interaction mainly include three aspects: intangible resources, human resource information, and basic information. These three types of information will be generated and applied in the normal business process of enterprises, but not all types of enterprises can be used in general. Online education enterprises use this kind of interactive form to complete information interaction and realize enterprise value co-creation.

(2) In fact, value co-creation is not a specific concept. Generally, related activities are used to carry out this abstract concept, so if it is needed to carry out the research of value co-creation, the perspective of components should be used.

(3) In the process of research, it needs to pay attention to the measurement of enterprise competitiveness. The research dimension includes two aspects, namely, long-term and short-term competitive advantage. The detailed indicators will be studied in the following.

5.2. Case Overview. The example selected in this paper is the enterprise that has achieved considerable results in the current online education enterprise: enterprise A. The enterprise started early for online education, and also, it plays an important leading role in the industry. In this field, the enterprise has been in a leading position. It is precisely because of the excellent business situation of the enterprise the use of information interaction technology can achieve good value and co-create efficiency. The enterprise was founded in 2010 and has developed rapidly in the past decade, which has a great influence in the industry and related industries.

5.3. Data Analysis. The questionnaire survey method is used to collect the data of the online education enterprise, that is, the hypothesis of the impact of information interaction on enterprise value co-creation. The analysis software SPSS 22.0 is used to analyze the data, and the observation variables are set. The content of the scale includes value co-creation, partnership, service concept, and service complexity. On this basis, the reliability and validity of the scale are analyzed, as well as other data. The results are as follows.

5.3.1. Reliability Analysis. The reliability and validity of each scale are evaluated and analyzed. Internal stability, internal consistency and equivalence are the indicators to measure the reliability of waiting room. The purpose of evaluation is to verify the reliability of measurement. In order to avoid the problem of measurement similarity, Cronbach's coefficient α is used to express the degree of homogeneity. 0-1 distribution interval is the value range of Cronbach. α-value of 0.64–0.69 is acceptable; that is, the value is reliable. If α value is 0.69–0.79, the reliability is moderate. If α value is above 0.79, the reliability is excellent.

The reliability analysis of information interaction influencing value co-creation is shown in Table 1.

It can be seen from Table 1 that the reliability analysis of the scale of value co-creation shows that each value is above 0.79. The results of reliability analysis show that the internal consistency of the scale is very high, which indicates that the scale constructed in this paper has good reliability. At the same time, it also shows that information interaction has a positive impact on the business model of value co-creation of online education enterprises.

5.3.2. Validity Analysis. Validity analysis is recognized as a factor to measure the quality of the sample scale in research. The scale used in this study belongs to the high maturity scale, so its validity is acceptable. The composite reliability (greater than 0.69), mean variance (greater than 0.49), and standardized factor (greater than 0.49) are used to measure the aggregate validity of the scale. The results of variable factor analysis are shown in Table 2.

It can be seen from Table 2 that the aggregation effect of the scale is good. It can be concluded that each variable factor has reached the specified range, which indicates that the scale constructed in this paper has good reliability. At the same time, it further indicates that information interaction has a positive impact on the value co-creation business model of online education enterprises.

The purpose of data analysis is to verify the impact of information interaction on the value co-creation business

Table 1: Reliability analysis of the scale.

Project	Content	Correlation with the total score	The coefficient of α
Signal communication	Information exchange between enterprises	0.855	0.883
	The upstream enterprises of the supply chain can clearly understand the opinions of the downstream enterprises	0.848	
	Information exchange between enterprises and customers	0.842	
To obtain	Ensure that customers receive detailed product information	0.851	0.895
	Customers can obtain the information of commodities through the Internet and other ways	0.813	
	Customers are able to accept goods from enterprises along the supply chain	0.757	
Risk-taking	Inform customers of possible risks of the product through information exchange	0.742	0.831
	The customer shares the risk with the enterprise	0.817	
Transparency	Companies do not use information asymmetry to deceive customers	0.852	0.831
	Customers have absolute trust in the enterprise and ensure the transparency of information between them	0.677	
	There is no information deception between enterprises and between enterprises and customers	0.759	
Information interaction enterprise relationship quality	Companies do not harm each other's interests	0.868	0.889
	Aim to maximize profits	0.862	
	Consistent cultural strategies between enterprises and between enterprises and customers	0.839	
Cooperative innovation performance	Improve product quality through innovation	0.813	0.855
	Accelerate the commercialization of goods	0.788	
	Businesses make profits from the sale of goods	0.818	

Table 2: Variable factor analysis.

Project	Content	Normalized factor coefficient	The mean	The standard deviation	T-statistic
Signal communication	Information exchange between enterprises	0.853	0.858	0.044	25.719
	The upstream enterprises of the supply chain can clearly understand the opinions of the downstream enterprises	0.848	0.851	0.053	19.881
	Information exchange between enterprises and customers	0.864	0.866	0.045	24.894
To obtain	Ensure that customers receive detailed product information	0.869	0.869	0.042	27.582
	Customers can obtain the information of commodities through the Internet and other ways	0.888	0.881	0.042	28.888
	Customers are able to accept goods from enterprises along the supply chain	0.918	0.918	0.028	47.677
Risk-taking	Inform customers of possible risks of the product through information exchange	0.865	0.867	0.031	28.584
	The customer shares the risk with the enterprise	0.898	0.898	0.035	36.748
Transparency	Companies do not use information asymmetry to deceive customers	0.784	0.798	0.076	12.273
	Customers have absolute trust in the enterprise and ensure the transparency of information between them	0.923	0.921	0.038	34.113
	False information of all units	0.886	0.887	0.039	30.862
Information interaction enterprise relationship quality	Companies do not harm each other's interests	0.828	0.3827	0.045	24.331
	Aim to maximize profits	0.789	0.789	0.059	16.599
	Consistent cultural strategies between enterprises and between enterprises and customers	0.821	0.821	0.054	19.118
Cooperative innovation performance	Improve product quality	0.812	0.763	0.085	12.342
	Accelerate the commercialization of goods	0.873	0.866	0.052	21.158
	Product revenue	0.811	0.788	0.054	18.932

Table 3: Comparison of information interaction behavior and value co-creation.

Compare the content of	To create value	Information interaction
The initial stage	The general needs of customers and enterprises are met	There is information distortion
Prerequisite for	Transparency, communication, and risk-taking	Information interaction infrastructure, information interaction resources
Process	Enterprise value co-creation management, interactive experience	Content optimization
The results of	Both the enterprise and the customer achieve a high-quality experience	Effective and high-level presentation of information

model of online education enterprises from the perspective of supply chain. Through the above data analysis, this paper obtains the verification results through a series of analysis methods such as questionnaire survey, proving that information interaction has a positive impact on enterprise's value co-creation.

From the perspective of supply chain interpretation, online education enterprises use information interaction in many aspects to achieve value co-creation between enterprises and between enterprises and similar enterprises. Table 3 shows the comparative analysis results of the two.

From the perspective of supply chain, online education enterprises use information interaction to continuously optimize and improve the content, reduce the possibility of information distortion, enhance the value of information interaction, effectively realize enterprise's value co-creation, meet the needs of enterprise development, ensure the consistency of production information and enterprise production information, and reduce the information gap between enterprises and customers caused by poor communication.

6. Conclusion

This paper analyzes the impact of information interaction ability on the value co-creation business model of online education enterprises from the perspective of supply chain. Through the research, the following conclusions can be obtained:

(1) For the scale of value co-creation, the reliability analysis is carried out, and each α value reaches more than 0.79. The reliability analysis results show that the internal consistency of the scale is very high, which shows that the reliability of the scale constructed in this paper is good. At the same time, it also shows that information interaction has a positive impact on the value co-creation business model of online education enterprises.

(2) The verification results are obtained by a series of analysis means, such as questionnaire survey. The data analysis results show that information interaction has a positive impact on the value co-creation business model of online education enterprises.

(3) From the perspective of supply chain, online education enterprises continuously optimize and improve the content when using information interaction, reduce the possibility of information distortion, enhance the value of information interaction, effectively realize enterprise value co-creation, meet the needs of enterprise development, ensure the consistency between production information and enterprise production information, and reduce the information gap between enterprises and customers caused by poor communication.

Data Availability

The datasets used and/or analyzed during the current study are available from the corresponding author on reasonable request.

Conflicts of Interest

The authors declare no potential conflicts of interest with respect to the research, authorship, and/or publication of this article.

Acknowledgments

This study was supported by The impact of information interaction ability on value co-creation business model from the perspective of supply chain—based on the competitiveness of online education enterprises, General Social Science Project of Guangdong Department of Education (230419073).

References

[1] J. Zhang, K. Schmidt, H. Xie, and H. Li, "A new mixed approach for modelling and assessing environmental influences to value co-creation in the construction industry," *International Journal of Production Research*, vol. 54, no. 21, pp. 6548–6562, 2018.

[2] M. Rafiei and L. A. R. Sandoval, "New frontiers, challenges, and opportunities in integration of design and control for enterprise-wide sustainability," *Computers & Chemical Engineering*, vol. 132, no. 4, pp. 106610.1–106610.18, 2020.

[3] C. Wang, Z. Wang, R.-Y. Ke, and J. Wang, "Integrated impact of the carbon quota constraints on enterprises within supply chain: direct cost and indirect cost," *Renewable and Sustainable Energy Reviews*, vol. 92, no. 9, pp. 774–783, 2018.

[4] T.-M. Choi, Y.-J. Cai, and B. Shen, "Sustainable fashion supply chain management: a system of systems analysis," *IEEE Transactions on Engineering Management*, vol. 66, no. 4, pp. 730–745, 2019.

[5] R. B. Gonzalo, O. M. Hurtado, C. Lunerti et al., "Biometric systems interaction assessment: the state of the art," *IEEE*

Transactions on Human-Machine Systems, vol. 49, no. 5, pp. 397–410, 2019.

[6] D. Priharsari, B. Abedin, and E. Mastio, "Value co-creation in firm sponsored online communities," *Internet Research*, vol. 30, no. 3, pp. 763–788, 2020.

[7] Y. Ma, K. Rong, Y. Luo, Y. Wang, D. Mangalagiu, and T. F. Thornton, "Value co-creation for sustainable consumption and production in the sharing economy in China," *Journal of Cleaner Production*, vol. 208, no. 16, pp. 1148–1158, 2019.

[8] L. Li, Q. Huang, K. Yeung, and Z. Jian, "Human-computer interaction and value co-creation in electronic service," *Industrial Management & Data Systems*, vol. 118, no. 1, pp. 218–235, 2018.

[9] L. Lei, T. Chi, T. Hao, and Y. Tao, "Customer demand analysis of the electronic commerce supply chain using big data," *Annals of Operations Research*, vol. 268, no. 1-2, pp. 113–128, 2018.

[10] H. Zhang, S. Gupta, W. Sun, and Y. Zou, "How social-media-enabled co-creation between customers and the firm drives business value? the perspective of organizational learning and social capital," *Information & Management*, vol. 57, no. 3, Article ID 103200, 2019.

[11] Y. Zhao, Y. Chen, R. Zhou, and Y. Ci, "Factors influencing customers' willingness to participate in virtual brand community's value co-creation: the moderating effect of customer involvement," *Online Information Review*, vol. 43, no. 3, pp. 440–461, 2018.

[12] Z. P. Dong, Q. G. Xu, and L. Ren, "Simulation of supply chain equilibrium optimization management in multi-layer logistics storage facilities," *Computer Simulation*, vol. 35, no. 3, pp. 361–364, 2018.

[13] B. Partida, "Sales order automation benefits the supply chain," *Logistics Management*, vol. 57, no. 9, pp. 22–24, 2018.

[14] H. K. Chan, J. Griffin, J. J. Lim, F. Zeng, and A. S. F. Chiu, "The impact of 3d printing technology on the supply chain: manufacturing and legal perspectives," *International Journal of Production Economics*, vol. 205, no. 11, pp. 156–162, 2018.

[15] Adrienne and Selko, "Why can't the supply chain get rid of abuse," *Material Handling & Logistics*, vol. 73, no. 1, p. 32, 2018.

[16] M. Hamelink and R. Opdenakker, "How business model innovation affects firm performance in the energy storage market," *Renewable Energy*, vol. 131, no. 2, pp. 120–127, 2019.

[17] M. Langenus and M. Dooms, "Creating an industry-level business model for sustainability: the case of the european ports industry," *Journal of Cleaner Production*, vol. 195, pp. 949–962, 2018.

[18] P. Lloyd and A. Oak, "Cracking open co-creation: categories, stories, and value tension in a collaborative design process," *Design Studies*, vol. 57, no. 7, pp. 93–111, 2018.

Hindawi
Scientific Programming
Volume 2021, Article ID 6492009, 8 pages
https://doi.org/10.1155/2021/6492009

Research Article

The Teaching Optimization Algorithm Mode of Integrating Mobile Cloud Teaching into Ideological and Political Courses under the Internet Thinking Mode

Yipei Jiao [1] and Yu Liu [2]

[1] *Affiliated Hospital of North Sichuan Medical College, Nanchong 637000, Sichuan, China*
[2] *School of Control Engineering, Chengdu University of Information Technology, Chengdu 610000, Sichuan, China*

Correspondence should be addressed to Yu Liu; liuyu123@cuit.edu.cn

Received 21 August 2021; Accepted 3 November 2021; Published 10 December 2021

Academic Editor: Punit Gupta

The purposes are to use the Internet technology to innovate the ideological and political (IAP) classroom teaching mode, take full advantage of the mobile platform under big data (BD), improve the effectiveness of IAP education, and deeply grasp the internal needs of students for the IAP classroom. First, the specific meaning and implementation process of mobile cloud teaching (MCT) under the Internet are deeply studied, as well as the connotation of the IAP course. Second, some suggestions are proposed. A theoretical analysis of the synergy between MCT and IAP classroom is conducted, and the teaching situation of cloud teaching classroom from the basic construction and operation mode of MCT platform is discussed. Finally, a case study on blue-ink cloud class is carried out. The results show that to realize the innovation of the IAP classroom teaching mode, it is considered that the IAP classroom has a strong dependence on the information. The MCT platform has wide access to information, which can well connect with the IAP classroom. The teaching methods of the cloud teaching platform tend to be diversified and interesting, and the overall teaching pattern is different from the traditional classroom teaching mode. The teaching effect is greatly improved based on the MCT platform. To achieve the synergy of the Internet and the MCT platform, the advantages of the cloud teaching platform should be expanded, the online communication between teachers and students should be strengthened, and the channels for information acquisition should be opened up. Blue-ink cloud class fully utilizes the advantages of the cloud teaching platform, which provides a great reference for IAP classroom teaching. Its flexible teaching method and intelligent management are helpful to the reform of IAP classroom teaching in the future.

1. Introduction

The world enters big data (BD), and Internet technology greatly affects people's learning, work, thinking mode, and so on. With the development of Internet technology, the teaching of teachers extends from classroom to network, from students to all who want to receive education, expanding the scope of work and the target being able to work according to their own interests and hobbies, free from time and place constraints, free from development space constraints. Through search engine technology, screening on the network of words, sounds, images: through hypertext, hyperlinks technology, and effective access to information and use. Self-centered information acquisition is more accurate and timely, which greatly improves learning and work efficiency. On the web, people can switch between tasks at any time, reading, writing, watching videos, and chatting and making friends at the same time. People can enter keywords and get all kinds of information through search engines; people are not only the receiver of information but also the sender and disseminator of information, which makes people become the media of information, and they are in the network of information without a center and edge. In the network age, people's thinking mode must also have the "nonlinear" characteristic of hypertextualization. Meantime, a series of reforms are carried out in various fields, such as artificial intelligence, smart city, cloud computing, and cloud teaching [1]. "Cloud teaching" with its rich educational resources, convenient use, diversified information content, and unique and fashionable education methods wins the favor of the vast majority of students [2], which also apparently impacts the thinking mode of contemporary students [3]. The rapid development of Internet technology around the world has changed the way of thinking again, and people have put forward the concept of "network thinking." As the latest form of the modern mode of thinking, the network thinking mode has the above "openness," "diversity" and "creativity." At the same time, it has made new breakthroughs in the horizontal, vertical and spatial structure, with an unprecedented "divergence." With the gradual growth of the students, the traditional teaching mode is unable to attract the students who live in the diversified information environment: (1) the teacher-centered school education will ignore the existence of students as learning subjects; (2) school education focuses on books, and teachers will only faithfully implement textbooks, which will become an obstacle to students' creation and innovation; (3) the teaching method of schools is monotonous, and teachers only treat students as containers to receive knowledge; and (4) in the learning process, students have problems such as single method, single goal, single problem, single evaluation, single process, and so on. Building a multidimensional learning environment with pictures and texts through the "cloud teaching" mode will be welcomed by more students [4]. Ideological and political (IAP) education is correlated with the future of the motherland and social development, and it is a compulsory course for every student in all growth stages. Therefore, how to carry out IAP education is a very important issue for schools [5]. Especially during the two sessions in 2019, national leaders make important instructions on school IAP theory, that is, the tradition of IAP work advantages and information technology are highly integrated to enhance the sense of the times and attractiveness. This fully reflects that the Party attaches the importance to IAP education, points out the direction for the reform of IAP curriculum, and provides an action guide for the construction of information classroom [6]. The combination of IAP education and Internet technology adapts to the development trend of the times, uses the thinking mode of the Internet to deepen the effectiveness of IAP education, strengthen educational achievements, and improves the overall level of IAP education [7]. In the "Internet" era, the acquisition of knowledge is no longer limited to the classroom as it used to be. Diversified information channels make it easier for knowledge to be learned. However, the focus of IAP education is not on knowledge, but on the cultivation of students' psychological quality [8]. Search, recommendation, and advertising are the three most important ways to obtain information in the Internet age. Search, recommendation, and advertising are essentially solving the problem of information overload. The means and goals are different, and they are born in different stages of the product life cycle so that the system realization is different. The issues are that the academic circle concerns are how to guide students to study actively through the Internet-based MCT and help them establish a correct outlook on life, values, honor and disgrace [9], becoming worthwhile members of the society while realizing their values.

To realize the substantial innovation of the IAP classroom teaching mode in the Internet era, the cloud teaching platform is analyzed and discussed by searching for the literature, combination of practice and theory, and case analysis, especially the analysis of the teaching advantages and development potential of the blue-ink cloud class, which has great significance to the current IAP education in schools.

2. Cloud Teaching and IAP Course

2.1. Overview of MCT. In a broad sense, MCT is a kind of behavior of learning activities anytime and anywhere through mobile electronic devices [10]. The emergence of cloud teaching brings interest to learning, enriches the channels to acquire knowledge, liberates students from the boring classroom, makes up for the shortcomings of offline learning, and improves the efficiency of learning. In recent years, with the large-scale popularization of smartphones, MCT gradually develops and matures. It optimizes the course content and opens up practical functions, like online question answering and real-time interaction. With diversified tutoring materials such as short videos, audios, graphics, and PPT, students' interest in learning is greatly aroused [11]. In addition, there are abundant course resources, all stored in the cloud for the different needs of students. Moreover, they can directly connect with teachers. Open topics can also be discussed in groups. This learning mode stimulates the enthusiasm of students, promotes the interaction between teachers and students, and greatly improves the teaching quality [12]. Its speed is fast and clear, to avoid a large number of teachers not only save a lot of classroom teaching time, increase the amount of classroom information, and the teaching content is lively and lively, improve the efficiency of classroom teaching efficiency. It not only enriches the teaching content but also broadens the knowledge scope of the students.

MCT is a modern education method based on Internet technology and mobile devices for network information teaching. It skillfully combines mobile devices with BD, and establishes a cloud teaching platform with cloud storage, cloud computing, cloud data and cloud website. Through the visual teaching mode, the mobile cloud constructs a platform to transform students' thinking mode and guide the students to learn autonomously [13,14]. The basic structure of cloud teaching is shown in Figure 1:

The MCT platform based on Internet BD promotes the reform of the teaching mode. Besides, in the process of establishing the platform, the platform aims to facilitate students to quickly grasp the operation methods of the platform and master various functions. Hence, it starts from students and centers on serving students to meet students' need and enhance the ability and the effectiveness of cloud teaching.

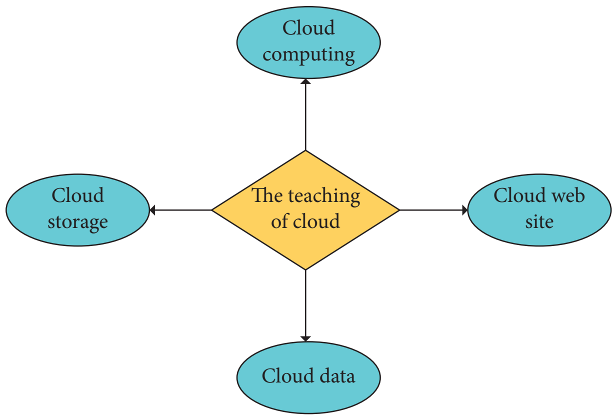

Figure 1: The basic structure of the cloud teaching.

2.2. Overview of the IAP Course. The content of the IAP course mainly includes the introduction to the basic principles of Marxism, the outline of modern Chinese history, the Mao Zedong Thought, and the theoretical system of socialism with Chinese characteristics, ideological and moral cultivation and legal basis, and formal policies [15]. It is the embodiment of the national core values, and a vital part of the national ideological and spiritual civilization construction. Every student needs to understand the theoretical system of socialism with Chinese characteristics and establish correct core values [16]. The IAP course has a lofty mission that other courses do not have to cultivate students' patriotic feelings, be loyal to the party and the country's beliefs, be good at using a dialectical perspective to look at problems, be good at observing the essence of things through phenomena, do well in grasping the main contradictions of things, always care about national affairs, devote themselves, repay the society, and grasp the direction of life in the tide of the times to realize the value of life. Because the IAP courses is extraordinary important, it is not easy to do a good job in IAP education. Although for many years, the party and the state emphasizes the construction of IAP education, often organize educators to carry out seminars on IAP education, and give targeted guidance [17]. However, as the science and technology and economy develop fast, the traditional IAP classroom is gradually unable to meet the needs of contemporary students. A new teaching mode should be established to optimize IAP class and improve students' interest in learning. In March 2019, national leaders hold a forum for teachers of IAP theory course in Beijing, which points out the need to "innovate classroom teaching" and realize "all staff, whole process and all-round" education.

2.3. Innovation of the Teaching Mode of the IAP Course under the Internet. The IAP course helps students understand themselves, society, and the world and establish a healthy and positive attitude toward life. The IAP course is a compulsory course for every student. Under BD, the diversity and explosive information resources of the Internet promotes the innovation and development of IAP education. As for how to realize the perfect combination of the Internet and the IAP classroom, the problems to be considered are as follows: first, the IAP classroom is highly dependent on information and needs information with high authenticity and timeliness as the basic content; second, the essential characteristic of the Internet is the fast speed of information dissemination, and it has a more intuitive and broad vision to excavate information. The Internet utilizes media to represent social problems and ideology, which is the most advanced function currently, and needs to establish a good connection with IAP education; second, the Internet combined with mobile devices can achieve learning activities anytime and anywhere. Compared with traditional classroom learning, the cloud teaching mode has several prominent characteristics: (1) the teaching methods tend to be diversified and interesting; the teaching pattern is completely different from the traditional classroom teaching; and it includes language form, the content, learning media [18]. The effect of IAP education is improved based on Internet technology. The key concepts and the overall pattern of cloud teaching are shown in Figure 2:

(2) The Internet technology deepens the communication between teachers and students, and their relationship is closer. Online answering and discussion make the learning effect significantly improved, achieve the objectives of strengthening IAP education, and fully show the Internet's connectivity function. (3) Through the mobile platform, students can fully express their ideas and opinions, and teachers can be informed of the specific learning situation of students and teach them in accordance with their aptitude. (4) Internet technology contributes to the centralized management of students, which is a very convenient management method for schools, teachers and students. In general, Internet technology provides a new teaching mode for IAP education and is vital in improving the effectiveness of IAP education [19].

2.4. Synergy of MCT and the IAP Classroom. The Internet-based cloud teaching system and the IAP teaching system need to cooperate with each other to produce synergy. Only in this way can the advantages of cloud teaching give a full play and optimize the IAP classroom greatly.

2.4.1. Magnifying the Advantages of MCT. Education is a process of value embodiment and the value output of educators to learners. The traditional teaching mode only focuses on the output form of educators and neglects the acceptance of knowledge by learners. The establishment of the mobile platform and the use of Internet technology can analyze BD and make the IAP educators fully understand students' dynamics, interests, problems, and opinions on the course. Thus, they can have a deep understanding of students' learning needs and guide students to form a right-thinking mode and correct their learning methods.

2.4.2. Increasing Online Communication between Teachers and Students. The inheritance of knowledge is a process of mutual recognition, and the MCT platform strengthens the interaction between teachers and students through the real-

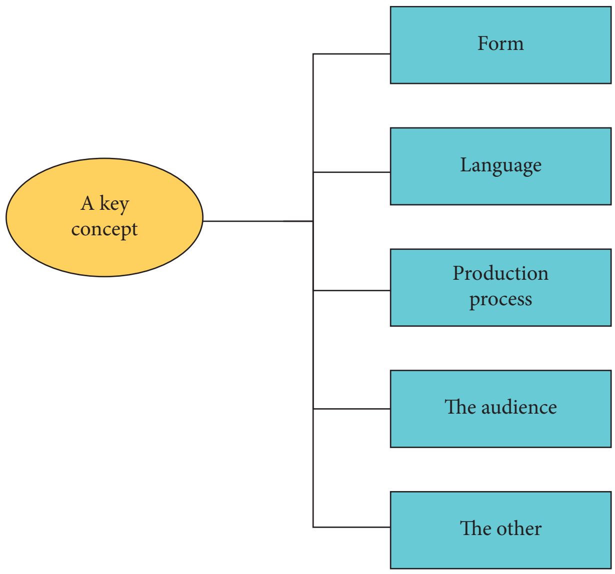

Figure 2: Key concepts and the overall pattern of the cloud teaching.

time teaching mode and one-to-one online answering. It takes individual students as the center; promotes the contact between teachers and students, teachers and parents, between students, and between teachers; and helps establish a comprehensive teaching system on a quid pro quo basis. The system can make teachers get feedback on students' learning status at the first time, and help them select the teaching content and make a teaching plan for the next period, improving the teaching quality.

2.4.3. Opening Up Information Access Channels. The biggest advantage of the MCT platform is its wide range of information sources. However, this information is highly fragmented and inconsistent, which posts an obstacle for students to collect more professional information.

2.4.4. Strengthening the Integration of Cloud Teaching and the IAP Education Classroom. The teaching mode is in line with the development of the times, which is a new experience for both students and teachers. The content of the classroom teaching becomes rich and interesting because of the diversity of media. The most important difference between the mobile platform and the traditional teaching method is that each student is the main body of the classroom, and students can seize the initiative of the classroom by sending barrage, comments, and praise. In addition, the interaction between teachers and students is conducive to grasping the rhythm of the classroom for teachers because teachers can appropriately add the beginning and ending, which makes the teaching process more complete [20].

2.4.5. Grasping the Core Idea and Making the Collaborative Progress. In the new era, with the development of the country and society, the demand for talents is increasing. While imparting knowledge, educators also need to pay special attention to students' IAP education. Schools and teachers must cultivate students' socialist core values and patriotism and guide students to have the right self-understanding, realize their values and have a lifelong goal. This requires that the MCT classroom must maintain a serious and lively style and does not put the cart before the horse while adding interesting elements to the learning process. The original intention of intelligent teaching is to educate students to have a correct worldview, values, and philosophy.

2.5. Significant Advantages of MCT

2.5.1. Diversified Teaching Methods. The MCT platform based on the Internet has the potential to improve the teaching mode of IAP courses because it has unique and wide dissemination of information, rich information access channels, and interactive platform. It conforms to the divergent and open characteristics of the IAP classroom. With the universality of mobile intelligent devices in society, more and more colleges and universities utilize its advantages of fast-speed and wide-coverage to strengthen their IAP teaching. The MCT enriches the traditional teaching modes, and students can get the latest information anytime and anywhere and learn knowledge from practice instead of learning from books alone, making them profoundly understand the knowledge. The knowledge acquisition channels of cloud teaching are major social platforms, such as MicroBlog and WeChat, official websites, various professional knowledge forums, academic papers, and journals database. Furthermore, some of these resources are interactive and still some can be shared with each other, which meet the demand for more information resources and extend the in-class knowledge to the practice, greatly improving the learning efficiency, imperceptibly guiding students to form a right-thinking mode [21].

2.5.2. Digitalization of the Teaching Process. The advantage of the MCT platform lies in the application of data cloud disk. On the one hand, it is reflected in the acquisition and update of teaching resources. The powerful functions of BD and cloud disk enable the platform to obtain massive resources anytime and anywhere, truly realize mobile teaching, and break the limitations of traditional classroom and knowledge database. Especially for the IAP classroom, the acquisition of real-time resources can cultivate students' habit and ability to pay attention to national affairs, strengthen students' ability to analyze and capture hot issues, guide students to treat things objectively, calmly and correctly in real life, and change their thinking mode imperceptibly. Besides, through the storage function of cloud disk, the course can be broadcasted or replayed, and they can review the key points and difficult knowledge repeatedly, which greatly improves the efficiency of the classroom and solves the problem of students' uneven ability level, so that every student can get a full education. On the other hand, online learning belongs to face-to-face teaching. Students and teachers can interact in real-time, which is convenient for teachers to know students' learning situations, and is conducive to creating a lively classroom atmosphere. More importantly, based on the digital teaching and management mode, students' learning situations can be intelligently evaluated and tested, and the targeted training and intelligent management can greatly help improving the effectiveness of classroom teaching. Specifically, students' classroom performance can form historical data to upload to the cloud, and the cloud system can make timely feedback, aided by strong support BD analysis and Internet intelligent computing technology. Each student's learning ability is intelligently graded. This reduces the burden on teachers, and the results are accurate and effective. The MCT platform collects and analyzes the collected student data, continuously optimizes and upgrades the curriculum, brings more perfect curriculum and teaching experience for teachers and students, promotes the organic unity of teaching and learning, and improves the teaching quality in the process of continuous integration of cloud teaching and IAP classroom [22].

2.6. Case Analysis. Currently, there are MCT platforms with similar functions in the market, and their operation modes are almost the same, but they have their advantages in teaching mode and operation management mode. The blue-ink cloud class is selected because it has research value. It is a MCT platform developed by the Beijing Blue-Ink Big Data Technology Research Institute, and its core competitiveness lies in the teachers' groups-building and students' participation in the class. Students can watch the content released by the teacher in each group for the preview before the class. Since the launch of the blue-ink cloud class, its powerful mobile teaching function wins the unanimous praise of teachers and students and is widely recognized by many scholars. Nearly 10 million teachers and students benefit from the blue-ink cloud class. To further investigate the real use of blue-ink cloud class, a satisfaction questionnaire is designed and 500 copies are randomly distributed to primary and secondary school students in a city. The results of the questionnaire are shown in Tables 1 and 2.

3. Analysis of the Teaching Mode of the Blue-Ink Cloud Class

3.1. Analysis of the Results of the Survey on Satisfaction of the Blue Ink Cloud Class. The results of the questionnaire are shown in Figure 3:

According to the results of the questionnaire, 72% of the students are very satisfied with the use of blue-ink cloud class, 14% of the students are basically satisfied, and also 14% of the students are not satisfied. Therefore, the satisfaction of the blue-ink cloud class is high, but it still needs continuous improvement. In terms of the operation mode of the blue-ink cloud class, 57% of the students think that the classroom teaching mode is the most attractive, and 22% of the students hold the idea that its after-class management is advanced, and its online clock out and comprehensive evaluation functions can improve the management efficiency; finally, 68% of the students argue that they will introduce the use of the blue-ink cloud class APP to their friends, which shows the APP has strong attraction and user stickiness, and the classroom effectiveness is guaranteed as well.

3.2. The Realization of the Teaching Mode. The classroom teaching mode of the blue-ink cloud class is very innovative. It is mainly divided into three parts: before-class, in-class, and after-class. The learning modes of different parts are shown in Figure 4:

3.2.1. Autonomous Learning before Class. Teachers assign preview tasks and send them to the cloud system of blue-ink cloud class in the form of computer files, and students download and complete the tasks on their mobile devices to understand the core content of the course in advance.

3.2.2. Teacher-Student Interaction in Class. The teacher divides the difficult points according to the content of the course. For the more important knowledge points, the multifunctional equipment can be used for teaching. Besides, the teacher can solve the problems with the students through questions, tests and other interactive links, grasp the rhythm of the classroom, reassign study enthusiasm, and ensure that the students actively participate in the classroom. The specific implementation of the interaction with students in class is shown in Figure 5.

Generally, interactive teaching can be divided into three modules:

The first is the "questioning." Teachers set questions based on the course content to guide students to think and answer, using the "Questionnaire" function of the blue-ink cloud class.

The second is "communication." The teacher inspires the students around the difficulties and key points of the course, divides the students into groups and discusses them separately. Through the "Question answering and discussion" function of the blue-ink cloud, the discussion results of each group are summarized and analyzed to understand the students' thoughts, which then guide and correct them pertinently.

The third is "evaluation." Before class, the teacher registers the students' attendance through the "blue-ink assistant." In class, the teacher checks the students' understanding and memory of knowledge through the classroom test provided by the cloud class. Finally, the results of the group discussion are added and summarized for comprehensive evaluation. In addition, other functions, like questionnaire surveys and extracurricular videos, can be used to get grade the growth value and acquire the attributions.

3.2.3. Sharing after Class. The function of "brainstorming" is set up after the end of the course in the blue-ink cloud class. The purpose is to guide students to actively discuss the problems that students encounter in the learning process and suggestions about the course and extend them to

Table 1: Basic information of samples.

Grades	Primary school	Junior middle school	Senior high school
Distributed number of the questionnaire	200	200	100

Table 2: Questions on the questionnaire.

Questions	Options
Frequencies of using the APP of blue-ink classroom teaching	A. Never B. Occasionally C. Often
Satisfaction with the APP of the blue-ink classroom teaching	A. Not satisfied B. General C. Very satisfied
Favorite module in the APP of blue-ink classroom teaching	A. Classroom teaching B. After-class management C. Others
The intention to introduce the blue-ink classroom	A. Not B. Maybe C. Definitely

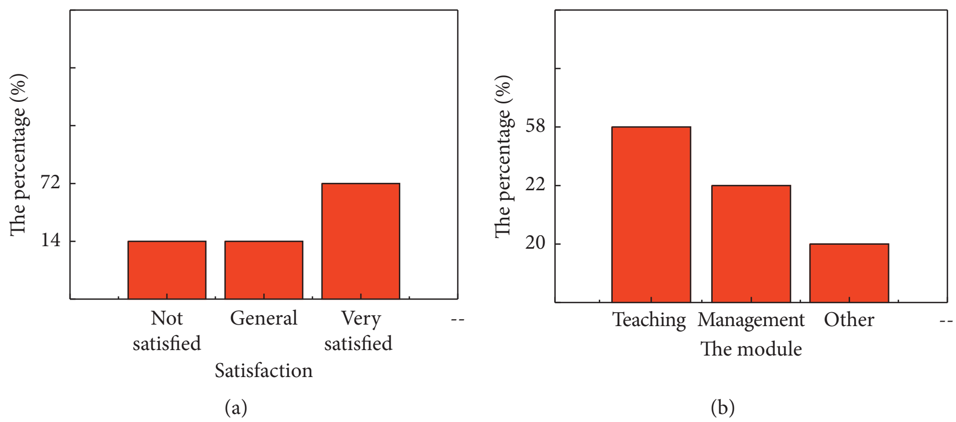

Figure 3: Results of the questionnaire of the blue-ink cloud class: (a) user satisfaction (b) the attraction of different modules to users.

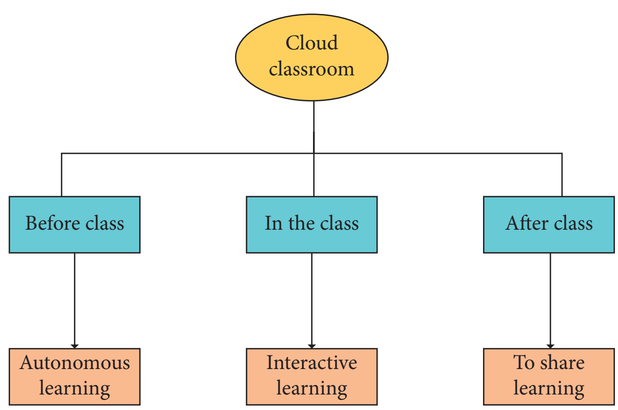

Figure 4: The teaching mode of the blue-ink cloud class.

extracurricular knowledge application to realize the collision of thinking sparks, improve students' independent thinking ability and finally, share the completion of the course to the social platform to gain learning experiences.

3.3. Advantages and Potentials. The advantages of the blue-ink cloud class teaching mode over the traditional teaching mode in the teaching practice are shown in Table 3:

The first is the acquisition of rich learning resources: with the help of blue-ink cloud mobile database, it can provide rich and diverse massive materials for classroom teaching; the second is the optimization of teaching methods: blue-ink cloud class adheres to the actual needs of teachers and students, strives to create a lively and relaxed classroom atmosphere, sets up a scientific and reasonable multifunctional classroom management mode, and realizes the transformation of the teaching mode from the traditional "a teacher to the whole classroom" to "face-to-face," which promotes the interaction between teachers and students; third, it is close to life, convenient and fast: it breaks the traditional way of learning in schools, realizes the learning anytime and anywhere, helps students break through the restrictions, and enhances students' sense of achievement and acquisition.

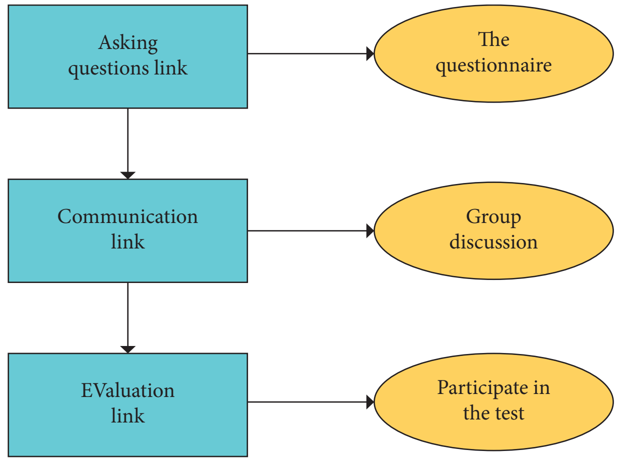

Figure 5: The specific implementation of cloud class teaching.

Table 3: Comparison between the blue-ink cloud class and traditional teaching mode.

Teaching mode	Traditional	Blue-ink cloud class
Learning content	Textbooks only	A number of learning materials and extracurricular resources
Teaching methods	Teachers' explanation	Face-to-face interactions between teachers and students
Learning places	In schools	Anytime and anywhere

4. Conclusion

The rise of MCT platforms based on the Internet is the need of the development of the times, and it also meets the needs of students and teachers. With the popularity of electronic devices, mobile teaching is gradually becoming one of the main teaching methods. Especially in the classroom of IAP education, real-time data updates and cloud data resources storage make IAP education no longer as dull as before. In addition, the synergy of MCT and the IAP classroom arouses students learning enthusiasm, reduces their addiction to mobile phones and also changes students' thinking and learning methods, promoting the integration of IAP courses and cloud teaching.

The shortcomings are as follows: the MCT platforms have their advantages and disadvantages, and only the blue-ink cloud class platform is selected, neglecting other MCT platforms. The advantages and potentials of cloud teaching still need further research. The Internet-based MCT platform possesses the capacity for development. The problems need to be further studied: how to correctly guide students to transform from "passive learning" to "active learning"; how to transform teaching structure from "teacher-centered" to "teacher-student centered"; how to make full use of the diverse teaching functions to achieve effective collaboration with modern teaching technology and IAP classroom; and how to improve the teaching effect with new teaching methods, which has great significance for reforming the teaching methods of IAP education.

Data Availability

No data were used to support this study.

Conflicts of Interest

The authors declare that there are no conflicts of interest.

Acknowledgments

This study was supported by the General Project of Open Problems of Si Chuan Network Culture Research Center in 2017 (WLWH17-11).

References

[1] L. Wang, "Research on the teaching mode of Internet + mobile cloud class," *Contemporary Education Practice and Teaching Research*, vol. 5, no. 656, pp. 15-16, 2017.

[2] Y. Yao, "Application of mixed teaching model based on mobile cloud platform in ideological and political theory course in higher vocational colleges," *Youth*, no. 22, pp. 221–224, 2019.

[3] Y. Liu, "Empirical research on learning situation data analysis based on mobile cloud teaching platform–taking dynamic website design course of independent college as an example," *Computer Engineering and Science*, vol. 41, no. 1, pp. 119–123, 2019.

[4] J. Zhou, "On blended teaching model of college English reading course based on blue-ink cloud class," *Literature Review*, no. 16, pp. 132-133, 2017.

[5] T. Tang, "Teaching reform of higher vocational professional courses in the "Internet +" era–taking E-commerce as an example," *Electronic Commerce*, vol. 3, no. 3, p. 79, 2017.

[6] Y. Wang and Y. Wang, "Transformation of teaching mode supported by intelligent education service," *Chinese Journal of Medical Education Technology*, vol. 33, no. 6, pp. 37–41, 2019.

[7] X. Liu and Y. Zhao, "Research on the effective English teaching model and strategy of blue-ink cloud class based on

mobile cloud teaching," *Think Tank Times*, vol. 168, no. 52, pp. 151–159, 2018.

[8] Y. Demchenko, A. Belloum, W. Los, T. Wiktorski, and S. Brewer, "EDISON data science framework: a foundation for building data science profession for research and industry," in *Proceedings of the IEEE International Conference on Cloud Computing Technology and Science*, vol. 40, no. 34, pp. 160–162, Luxembourg, Luxembourg, December 2017.

[9] T. E. Smith, P. S. Rama, and J. R. Helms, "Teaching critical thinking in a ge class: a flipped model," *Thinking Skills and Creativity*, vol. 28, no. 7, p. 17, 2018.

[10] A. R. Rao and R. Dave, "Developing hands-on laboratory exercises for teaching STEM students the internet-of-things, cloud computing and blockchain applications," in *Proceedings of the 2019 IEEE Integrated STEM Education Conference (ISEC)*, vol. 20, no. 2, pp. 37–34, Princeton, NJ, USA, March 2019.

[11] J. Amantha, V. Kumar, M. A. Sanmugam, and S. Osman, "Mobile applications for learning: exploring information technology undergraduates' preference in Malaysia," *Journal of Computational and Theoretical Nanoscience*, vol. 17, pp. 1113–1116, 2020.

[12] K. F. Mwakisole, M. M. Kissaka, and J. S. Mtebe, "Feasibility of cloud computing implementation for eLearning in secondary schools in Tanzania," *International Journal of Education and Development Using Information and Communication Technology*, vol. 6, no. 14, pp. 23–33, 2018.

[13] L. I. Jie and S. O. Business, "Research on cloud classroom teaching practice of insurance practice based on mobile terminal," *Journal of Zhejiang Fashion Institute of Technology*, vol. 39, no. 10, p. 223, 2018.

[14] T. Germain-Williams, "Teaching children to love problem solving (a reference from birth through adulthood)," *Developing Toddler Thinking*, vol. 10, no. 104, p. 15, 2017.

[15] X. U. Ding-Hua, Z. B. Luo, X. U. Xiao-Hong et al., "Research on internet plus medical image teaching model based on the online interactive cloud teaching platform," *Medical Education Research and Practice*, vol. 33, no. 2, p. 17, 2019.

[16] J. V. Biljon and V. Ronell, "Trends, drivers and barriers influencing Cloud Computing Services for mobile interactions in teaching and learning//Conference on," *Information Communications Technology & Society*, vol. 24, no. 1, p. 7, 2018.

[17] X. Huiying and M. Qiang, "College English cross-cultural teaching based on cloud computing MOOC platform and artificial intelligence," *Journal of Intelligent and Fuzzy Systems*, vol. 23, no. 14, pp. 1–11, 2020.

[18] J. A. Kumar, S. Rajamanickam, and S. Osman, "Exploring the use of mobile apps for learning: a case study on final year engineering undergraduates in Malaysia," *ASM Science Journal*, no. 3, pp. 63–67, 2020.

[19] P. Janardhana, K. Reddy, and G. Singaravelu, "Augmented reality (AR): the new trend in transforming teaching and learning in education," *International Journal of Analytical and Experimental Modal Analysis*, vol. 12, no. 4, pp. 620–626, 2020.

[20] O. Debauche, M. Sad, and S. A. Mahmoudi, "Internet of things: learning and practices. Application to smart city," in *Proceedings of the IEEE International Conference on Cloud Computing Technologies and Applications*, vol. 10, no. 33, p. 17, Brussels, Belgium, November 2019.

[21] B. N. Anderson, "When learning sinks in: using the incubation model of teaching to guide students through the creative thinking process," *The Gifted Child Today*, vol. 42, no. 13, p. 6, 2019.

[22] H. Rezk, A. E. Amin, and D. Maha, "E-management educational system based on mobile cloud computing," *International Journal of Computer Applications*, vol. 181, no. 50, pp. 15–20, 2019.

Hindawi
Scientific Programming
Volume 2021, Article ID 9265238, 6 pages
https://doi.org/10.1155/2021/9265238

Research Article

Application of Cloud Computing in the Optimization of College Calisthenics Teaching Mode

Huafeng Wang [1] **and Rong Huang** [2]

[1] *Ma'anshan Teachers' College, Ma'anshan, China*
[2] *Anhui Ma'anshan Industry School, Hefei, China*

Correspondence should be addressed to Huafeng Wang; 312557293@qq.com

Received 23 September 2021; Accepted 16 November 2021; Published 9 December 2021

Academic Editor: Punit Gupta

Informatization teaching has become an important method of physical education. Especially with the support of big data and cloud computing technology, physical education teaching pays more attention to the use of information technology to provide rich data information, focusing on the development of physical education under the rich virtual reality environment, targeted scene atmosphere layout, and abundant learning resources. The reform and practical research of college aerobics teaching mode has gradually become an important topic in college aerobics teaching and research, and it has gradually attracted wide attention from teachers and students in colleges and universities. This article explores the status quo of sports aerobics teaching under the conditions of informationizization and explores the application methods and methods of information technology in aerobics teaching, practically applies microclass and MOOC resources to physical education, and strives to organize and develop sports teaching intelligence with the help of information technology. In order to improve the quality of physical education and training with the help of information technology, it can meet the needs of students' independent learning and growth and optimize the efficiency of physical education.

1. Introduction

With the development of society, the degree of informatization is getting higher and higher, and people have a new understanding of information resources. Sports information resources in colleges and universities are an important part of the information resource database, covering new directions for the development of sports science at home and abroad, new achievements in sports scientific research, new technologies for training competitions, and so on. In addition, the comprehensive level of college sports is closely related to the collection and management of sports information resources to some extent. The rapid development of information technology has brought new opportunities and challenges to the construction of college sports information resources. The emergence of cloud computing technology has opened up new ways for the management and utilization of sports information resources. With the increase in the application of cloud computing, with the help of cloud computing technology, less investment can be used to solve the current problems to further improve the capacity of resource construction and information resource services and to promote sports teaching, sports promotion, sports scientific research, and other activities. This article is about the construction of sports information resources in colleges and universities. The current situation is analyzed, and new ideas for the construction of college sports information resources under the cloud computing environment are put forward. The innovation and change of teaching mode are the key to the college aerobics education meeting the needs of today's social development. The development of college aerobics education also needs to rely on the innovation and reform of the teaching mode to provide inexhaustible motivation. With the introduction of aerobics projects into the teaching of college physical education, aerobics began to be loved by college students, and the number of students participating in aerobics elective courses is increasing every year. The application of innovative education in the teaching of aerobics in colleges is conducive to promoting students to fully seize the techniques and skills of aerobics and improving the overall teaching quality and efficiency. Judging from the current status of aerobics teaching in colleges [1, 2], the curriculum resources and curriculum system are not perfect. Different schools have different teaching equipment. Some schools even do not invite professional aerobics teachers, but are replaced by physical education teachers. In this case, the resources invested by colleges cannot satisfy the teaching needs of aerobics, causing many students to learn passively. In order to change this situation, colleges must keep up with the times, actively use the Internet, and integrate traditional teaching with the Internet. On the basis of building a network teaching platform, more network teaching resources have been developed [3–5]. In the era of Internet +, the aerobics teaching reform should make use of Internet technology, strengthen the integration of aerobics information teaching and traditional teaching, satisfy the actual learning needs of students, solve the problems in traditional teaching methods, and make the integrated education form of "Internet + education" play a greater role [6]. Under the circumstances of "Internet +," in-depth analysis of the effective countermeasures of network aerobics teaching in colleges is of great importance to promote the development of aerobics teaching in colleges and stimulate the students' sports potential.

2. Characteristics of Aerobics Teaching Mode

In college aerobics teaching activities, the existing teaching problems are mainly concentrated in the following several aspects. First, the students' enthusiasm for participating in aerobics is not high. Because the teaching content of aerobics is relatively boring, and the teaching knowledge is mainly based on movements, students must practice basic movements again and again, coupled with the similarity of each movement, leading to a gradual decrease in the initiative of college students to participate in aerobics. Under this teaching mode, aerobics teachers do not attach great importance to students' learning interests and learning needs, resulting in students passively accepting knowledge for a long time [7], which greatly affects the play of students' subjective initiative and even leads to the gradual loss of students' innovation ability and creativity, and a sense of weariness for aerobics learning. Under the influence of cramming teaching form, many students believe that aerobics and broadcast gymnastics have the same nature and their movements are basically the same, so they do not have enthusiasm for aerobics registration in the process of physical education course selection. First of all, some teachers are deeply influenced by the traditional teaching philosophy and still use the traditional thinking to teach in the aerobics practice course [8–10]. They one-sidedly emphasize the essentials of movements and the smooth completion of movements and ignore the coordination of students' limbs and the difficulty of some movements. This greatly affects the cultivation of students' innovative thinking and innovative ability. Secondly, in the teaching process, much concentration is paid to teaching, and the teaching method is too simple. Because the aerobics course is extra-curricular teaching, it is difficult for some students to concentrate in class when teaching. At the same time, for some students who are far away from the teacher [11], it is difficult to hear the teaching content of the teacher, so it is difficult to attract students' concentration.

In the process of carrying out teaching activities, teachers' teaching concepts can influence their understanding and choice of new teaching methods to a large extent. At present, most aerobics teachers in colleges in my country generally have the problem that their teaching concepts are too old. They still have obvious conservative psychology in the attempts of new teaching methods. They cannot adapt and accept the new teaching form well, which is bound to produce their teaching process, as shown in Figure 1. Although aerobics teaching in my country's colleges has comprehensively promoted the reform and innovation in recent years, the traditional teaching concepts and methods have not been completely abandoned. In order to gain the goal of teaching reform, aerobics teachers will focus on improving the teaching form and regard it as the core content of aerobics teaching [12, 13]. However, in the actual teaching practice process, teachers still take demonstration teaching as the leading factor. Teachers' teaching concepts have not kept pace with the development of the times, which makes it difficult for students to fully exert their dominant position in the classroom teaching process. In the teaching content, teachers often pay attention to the cultivation of students' aerobics skills. Therefore, teachers carry out teaching in strict accordance with the content of the textbook and require students to exercise in their spare time to ensure that the task is completed on time. Because teachers only teach knowledge in class but do not let students practice in class, students cannot achieve better results in learning, and there is no chance to express their ideas and innovation of aerobics, which leads to the phenomenon that the teachers teach the course content unilaterally and do not interact with the students effectively [14, 15]. Secondly, in the teaching process, teachers usually teach students the essentials and basic movements of this lesson, and then let students practice by themselves [16]. They pay less concentration to the continuity and standard of students' movements, which leads to the problems of students' nonstandard movements and differences in movement order, which greatly affects students' cooperative learning.

Although some colleges in our country use the network teaching form in aerobics teaching, they usually only evaluate some traditional indicators in the process of investigating the teaching situation [17]. Therefore, for students, only through the traditional way of learning, they can successfully complete the learning task. The current network teaching evaluation of aerobics in colleges is mainly based on the students' examination results, and less concentration is paid to other factors, so the application of network teaching form is greatly limited [18]. Most of the time, it is not the teachers' outdated teaching concept, but the traditional teaching form has to be adopted because of the constraints of

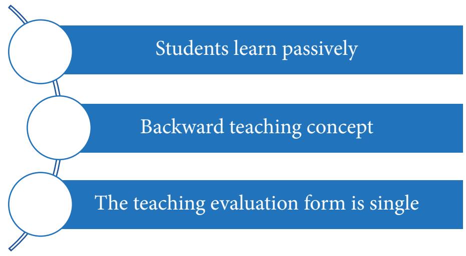

Figure 1: The current problems in college aerobics teaching mode.

teaching evaluation form and exam-oriented education mechanism. Therefore, in the process of using the network teaching form in aerobics teaching, most teachers do not combine the actual situation of students to carry out truly effective application, resulting in that their teaching form still does not really get rid of the shackles of traditional teaching form, and it is difficult to give full play to the advantages of network teaching form.

3. Cloud Computing in Aerobics

Efficient sports information resources are integrated based on cloud computing technology. The aerobics education is placed on the system client through cloud computing technology for system users to manage and integrate sports information resources. The spatial structure of the cloud computing technology of the system is shown in Figure 2. The application of innovative education in college aerobics teaching is conducive to promoting students to master aerobics technology and skills and improving the overall teaching quality and efficiency. In the current teaching process, there are still some problems such as backward teaching concept, passive learning, and low teaching efficiency. The main reason is that the lack of innovation in curriculum teaching leads to low interest in learning, which affects the practical effect of aerobics teaching in colleges. Therefore, the application of innovative education to promote the reform and development of college aerobics teaching is of great significance.

Cooperative teaching is one of the critical forms of physical education classroom teaching; aerobics teaching can also make full use of this teaching measure. Teachers can choose the way of cooperative learning. This not only can better enrich the training methods of aerobics but also can effectively stimulate students' enthusiasm in aerobics training. In the specific training, we can first create the situation, according to the actual situation of students, provide sports situation and reasonable grouping, maintain the similarities and differences between groups, and carry out heterogeneous grouping in the way of helping and guiding, so as to stimulate the atmosphere of classroom activities, as shown in Figure 3, and then carry out diversified interactive teaching; the teaching of "practice before teaching" should start from the form of cooperation and interaction and stimulate students' enthusiasm for participation in the classroom in the form of rich sports. Most students like interactive activities. At this time, teachers can make full use of everyone's needs to carry out cooperative

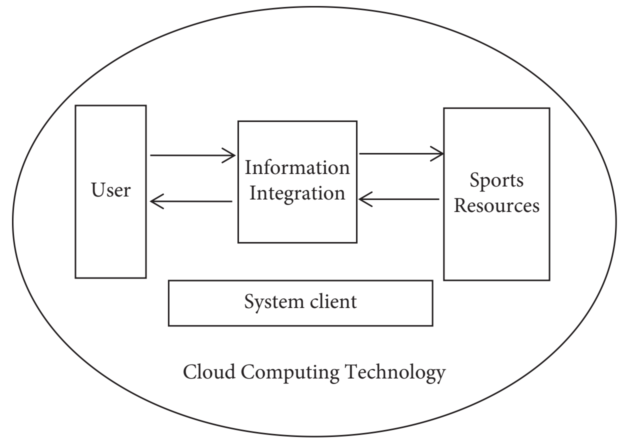

Figure 2: System space composition of the cloud computing technology.

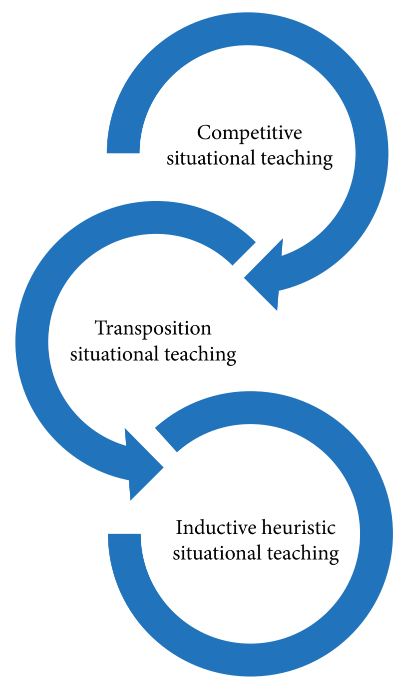

Figure 3: The construction of innovative teaching mode of aerobics in colleges.

teaching in the way of demonstration, group confrontation, pass test, and group evaluation, so as to enhance students' enthusiasm for classroom participation. In view of the lack of cooperative learning atmosphere for students, colleges need to build a strong cooperative learning atmosphere and create a good learning environment. According to the teaching content, online teachers can upload the relevant teaching materials of the course to the online teaching platform, clarify the learning tasks, and require students to study independently in groups. Offline can further enhance the relevant teaching equipment required for the course development and create good conditions for students' cooperative learning. For example, we can add the pedal, fitness, and other equipment for exercise. At the same time, teachers should be aware of the importance of students' cooperative learning. In specific teaching, students can be required to practice in groups and supervise each other, so as to promote students to maintain a high enthusiasm for learning. Teachers can also use collective training to give students more opportunities to play freely, so as to digest what teachers teach.

In the practical application of innovative education in college aerobics teaching, the most critical problem is to change the traditional education concept. If the teaching of aerobics in colleges still adheres to the conventional education concept, pays attention to the coordination and standardization of aerobics movements, and takes the traditional teaching materials as the overall teaching framework and all teachers use the same teaching system and each student needs to master the same teaching content, then the innovation education will not be able to achieve the ideal effect in the teaching of aerobics in colleges. Therefore, the teaching of aerobics in colleges must innovate the traditional education concept, truly integrate into the concept of talents, realize the transformation from exam-oriented education to quality-oriented education, construct innovative teaching mode, guide students from traditional passive receiving knowledge to active discovery and exploration, and strive to cultivate College students' innovative awareness of aerobics. Aerobics teachers must have the ability to develop and create and tap the individual value of students. Aerobics has the characteristics of diversity and complexity. Students have more freedom in the learning process, which can reflect the students' physical function and learning ability in real time and lay a solid foundation for carrying out innovative education. Aerobics teachers must abandon the teaching idea of teaching material as the core and have the teaching ability of teaching students in accordance with their aptitude.

"Online" teaching resources should be purposefully prepared, the content should be vivid, clear, and easy to understand, should be in line with the teaching content of each class, and make good preparation so that students can easily and happily accept the online knowledge of each class and fully prepare for the "offline" class psychologically. "Online" teaching can adopt heuristic teaching methods and they can independently think about problems and find solutions to problems in the stage of students' preparation for learning. At the same time, "online" discussion and evaluation are also a critical means to consolidate students' mastery of aerobics. Through "offline" learning and practice, questioning, discussion, summary, and evaluation are the sublimation of "online" and "offline" learning in each class. Figure 4 shows the innovative construction of teaching form of aerobics in colleges. From "preparation process result," teachers teach clearly and students learn clearly, which realizes the optimization of teaching. In general, colleges will not arrange too many class hours for aerobics teaching, and most students will not spend time to exercise after class. This phenomenon is mainly due to the lack of full mobilization of students' enthusiasm. Therefore, in order to better cultivate and enhance students' ability of independent thinking and independent innovation, teachers should make more efforts in the arrangement and design of homework after class. Students can arrange their own time and homework design,

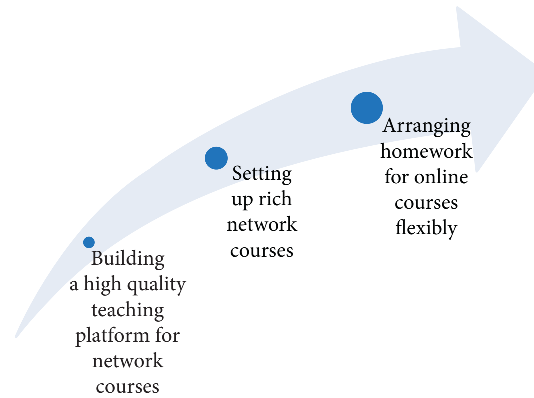

Figure 4: Practical application of aerobics network course construction in the era of Internet +.

and teachers are only responsible for reviewing the specific feasibility and results of the design. In this way, students can not only master specific theoretical knowledge more deeply in practice but also play a positive role in improving students' independent thinking ability and innovation ability. In the daily teaching process of aerobics, we should pay concentration to the cultivation of students' enthusiasm. We should not only enhance students' innovative consciousness and curiosity but also be good at discovering students' advantages and enhancing students' self-confidence so that each student's thinking ability can be greatly developed. In the process of implementing aerobics teaching, teachers need to consider the students' needs of dynamic development and make reasonable innovation from the aspect of evaluation. Teachers should actively practice the incentive teaching idea, conduct in-depth research on students' learning needs in aerobics, give students effective emotional incentives, and praise and affirm excellent students so that the students can have self-confidence in their own sports performance and show more vitality and enthusiasm in the process of participating in aerobics training in the future. At the same time, in the process of evaluation, teachers can emphasize that students actively participate in it, communicate with each other on the matters needing concentration in football through interactive communication, and also promote the effective sharing of experience between each other. In the evaluation, teachers need to strengthen the implementation of innovation from the specific level of technology carrier and give play to the role of microclass in guiding and guiding students' self-correction in the evaluation field. According to the specific presentation in the microvideo, teachers should guide students to think, promote the in-depth implementation of reflective learning, and let students make progress in reflection and grow up in error correction.

4. Results

For the integration of sports information resources, the application of cloud computing technology to design a sports information resource integration system based on cloud computing can not only effectively integrate and manage sports information resources but also ensure that sports information can be shared in cloud computing and improve actual sports information. The quality of resource integration management and active application value are worthy of popularizing and applying this technology in practice. Aerobics teaching in colleges, as a vital physical education discipline, has a positive significance for college students to strengthen their physique and realize the development of physical and mental health. Under the circumstances of “Internet +” era, the development and construction of aerobics network course in colleges are not only the realistic need of aerobics teaching reform but also the objective requirement of meeting the students’ diversified learning needs. Colleges in the construction of aerobics network course should be close to the aerobics teaching reform and the practical needs of college personnel training. Teachers should actively apply the network teaching form, promote students to better learn aerobics knowledge, enhance students’ sports comprehensive quality, and promote students to achieve all-round development.

5. Conclusion

In order to continually enhance the teaching quality of aerobics in colleges, teachers must reasonably apply and innovate the teaching skills of aerobics. According to the actual learning situation of students, teachers should adopt various effective teaching strategies to build an experiential teaching concept. In view of the current situation of students’ sports, teachers can design the aerobics education system and teaching links and use multimedia technology in the classroom teaching of physical education and constantly enhance the comprehensive learning effect of college students so that the sports ability of college students can be sustainable development.

To integrate innovative education into college aerobics teaching practice, we can innovate education environment, create a high-quality sports atmosphere, innovate education concept, strengthen the cultivation of innovative ability, innovate education objectives, carry out hierarchical and classified teaching, innovate education methods, enrich curriculum organization form, innovate education evaluation, and realize comprehensive teaching assessment. These ways can achieve the breakthrough of traditional aerobics teaching mode and promote the healthy and sustainable development of aerobics teaching.

Data Availability

Data sharing is not applicable to this article as no datasets were generated or analyzed during the current study.

Conflicts of Interest

The authors declare no potential conflicts of interest with respect to the research, authorship, and/or publication of this article.

Acknowledgments

This paper was supported by Provincial Teaching and Research Project of Colleges and Universities in Anhui Province “Research on the Reform of Aerobics Teaching in Colleges and Universities from the Perspective of Sports Power” (2017jyxm0622) and University-Level Key Scientific Research Project “Comparative Research on Sports Social Organizations and Other Social Organizations: A Case Study of Anhui Province” (2017xjzdky01).

References

[1] H. Lian, “Research on the application of the function of computer management system in college aerobics teaching,” *Journal of Physics: Conference Series*, vol. 1744, no. 3, 2021.

[2] C. Jia, “Research on the application of aerobics training methods in colleges,” *Boxing and fighting*, vol. 23, no. 3, pp. 94-95, 2021.

[3] J. Wang, “Research on the development of college aerobics network teaching resources,” *Research and practice of innovation and entrepreneurship theory*, vol. 4, no. 3, pp. 84-85, 2021.

[4] F. Meili, “Problems and countermeasures of cooperative learning in aerobics teaching,” *Sports science and technology literature bulletin*, vol. 29, no. 2, pp. 154-155, 2021.

[5] M. Yang and Z. Zhu, “Exploring the theory and practice of aerobics teaching reform in colleges,” *Contemporary sports science and technology*, vol. 11, no. 3, pp. 101-102, 2021.

[6] J. Wang and X. Su, “Innovation and reform of aerobics teaching mode in colleges,” *Contemporary sports science and technology*, vol. 11, no. 2, pp. 1-2, 2021.

[7] C. Shan, Z. Liu, J. Ge, W. Hai, and C. Wang, “Application of wechat platform in aerobics teaching under new media environment,” *Contemporary sports science and technology*, vol. 11, no. 1, pp. 1-2, 2021.

[8] L. Wang and K. Jin, “Research on the effectiveness of online and offline mixed teaching mode in improving students’ learning ability--taking aerobics teaching as an example,” *Contemporary sports science and technology*, vol. 11, no. 01, pp. 188–190, 2021.

[9] C. Lu, “Research on the innovation of aerobics teaching mode in colleges,” *Heilongjiang science*, vol. 11, no. 23, pp. 98-99, 2020.

[10] C. Huang, “On the problems and countermeasures of aerobics teaching in colleges,” *Contemporary sports science and technology*, vol. 10, no. 33, pp. 142-143+146, 2020.

[11] J. Yin, “The application of online and offline integration teaching mode in aerobics teaching in colleges,” *Research on ice and snow sports innovation*, vol. 4, no. 22, pp. 42-43, 2020.

[12] J. Yao, “The current situation and optimization path of aerobics teaching in colleges from the perspective of online class,” *Science and education guide (first ten issues)*, vol. 11, no. 31, pp. 152-153, 2020.

[13] C. Ting, “Research on the construction measures of the integration mode of aerobics teaching and training in colleges in China,” *Contemporary sports science and technology*, vol. 10, no. 30, pp. 169-170, 2020.

[14] L. Wang, “Teaching mode reform of college aerobics course based on MOOC,” *Xueyuan*, vol. 13, no. 28, pp. 24-25, 2020.

[15] J. Yang, "The feasibility of applying flipped classroom to aerobics teaching in colleges," *Science and education guide (next issue)*, vol. 45, no. 27, pp. 108-109, 2020.
[16] H. Wang, X.-M. Zhang, G. Tomiyoshi et al., "Association of serum levels of antibodies against MMP1, CBX1, and CBX5 with transient ischemic attack and cerebral infarction," *Oncotarget*, vol. 9, no. 5, pp. 5600–5613, 2017.
[17] J. Yao, L. Wang, K. Liu et al., "Evaluation of electrical characteristics of biological tissue with electrical impedance spectroscopy," *Electrophoresis*, vol. 41, no. 16-17, pp. 1425–1432, 2020.
[18] W. Gaihua, Z. Tianlun, D. Yingying, L. Jinheng, and C. Lei, "A serial-parallel self-attention network joint with multi-scale dilated convolution," *IEEE Access*, vol. 9, no. 5, pp. 71909–71919, 2021.

Hindawi
Scientific Programming
Volume 2021, Article ID 2218044, 16 pages
https://doi.org/10.1155/2021/2218044

Research Article

A Hybrid Intelligent Model for Urban Seismic Risk Assessment from the Perspective of Possibility and Vulnerability Based on Particle Swarm Optimization

Jinlong Chu,[1,2] Qiang Zhang,[1] Ai Wang ,[1,2] and Haoran Yu[1,2]

[1]*School of Architecture and Planning, Anhui Jianzhu University, Hefei 230022, China*
[2]*Anhui Urbanization Development Research Center, Hefei 230022, China*

Correspondence should be addressed to Ai Wang; 296712074@qq.com

Received 22 October 2021; Revised 9 November 2021; Accepted 16 November 2021; Published 7 December 2021

Academic Editor: Punit Gupta

Assessing seismic risk is an essential element of urban risk management and urban spatial security work. In response to the issues posed by the complexity and openness of urban systems, the nonlinearity of driving factors, and sudden changes in geological processes that affect urban seismic research, this paper is based on a variety of intelligent algorithms to develop a hybrid intelligent model that integrates probability and vulnerability to evaluate and quantify the difference in the urban spatial units distribution of earthquake risk. We applied this model to Hefei, one of the few superlarge provincial capital cities on the "Tancheng-Lujiang" fault zone, one of the four major earthquake zones in China, which suffers frequent earthquakes. Our method combined the genetic algorithm (GA), particle swarm optimization (PSO), and backpropagation neural network methods (BP) to automatically calculate rules from inputted data on known seismic events and predict the probability of seismic events in unknown areas. Then, based on the analytic hierarchy process (AHP), spatial appraisal and valuation of environment and ecosystems method (SAVEE), and EMYCIN model, an urban seismic vulnerability was evaluated from the four perspectives of buildings, risk of secondary disasters, socioeconomic conditions, and urban emergency response capabilities. In the next step, the overall urban seismic risk was obtained by standardizing and superimposing seismic probability and vulnerability. Using the hybrid intelligent model, earthquake probability, seismic vulnerability, and overall seismic risk were obtained for Hefei, and the spatial characteristics of its overall seismic risk were examined. This study concludes that areas with very high, high, low, and very low earthquake risk in Hefei account for 8.10%, 31.90%, 40.94%, and 19.06% of its total area, respectively. Areas with very high earthquake risk are concentrated in the old city, the government affairs district, Science City, and Xinzhan District. This study concludes that government authorities of Hefei should target earthquake safety measures consisting of basic earthquake mitigation measures and pre- and postearthquake emergency measures. In the face of regional disasters such as earthquakes, coordinating and governing should be strengthened between cities and regions.

1. Introduction

The Center for International Earth Science Information Network of Columbia University found that 450 of the world's 633 megacities are exposed to at least one disaster risk [1]. Earthquakes, which occur suddenly and are hugely destructive, involve a series of chain reactions, resulting in secondary disasters and induced seismicity [2–4]. They seriously impact the development of cities and the safety of urban residents. China is located at the intersection of the circum-Pacific and Alpide seismic belts, which means it is subject to highly frequent and intense seismic activity. China accounts for 7% of the world's landmass, but it has the most severe earthquakes in the world, having suffered 33% of the world's recorded strong earthquakes [5, 6]. With the acceleration of urbanization in China, urban economic output and structures are becoming increasingly complex, which means urban seismic risk is increasing exponentially [7, 8]. Strengthening our ability to appraise the overall risk of urban seismic activity and explore the spatial characteristics of that risk holds important practical significance for determining the social and economic impacts of earthquake damage, improving resilience in urban construction, and achieving sustainable urban development.

Due to the nonlinear nature of earthquake related factors and the complexity of geological processes, seismic research has long been an important and active topic among scholars [9, 10]. Past research has largely focused on analyzing the probability of earthquake occurrence and assessing the vulnerability of cities to earthquakes and the overall earthquake risks.

(1) Analyzing probability to earthquake: After the establishment of the California Earthquake Authority in 1994, the UCERF3 earthquake rupture forecast model was built, which has been continuously optimized and upgraded since. It integrates the time independent model for calculating long-term seismicity, the time-dependent model for calculating the probability of an earthquake considering the elapsed time since an earthquake, and the epidemic-type aftershock sequence spatiotemporal cluster model [10, 11]. Due to the shortcomings of the UCERF3 model, other scholars have researched earthquake probability forecasting. For example, Wang et al. (2019) calculated the long-term occurrence rate of earthquakes of different magnitudes by collecting seismic geology, geodesy, and seismology data in the Sichuan-Yunnan area [12]. Khan et al. (2018) proposed a practical event-based probabilistic seismic hazard assessment method that uses data on measured seismicity, available historical seismicity, and geological structure to simulate and predict the probability of earthquakes in regions where limited data is available [13]. Murray et al. (2015) proposed a new deep learning method called Focal Mechanism Network, which learns global waveform characteristics from theoretical data to predict the source focal mechanism [14]. Alarifi et al. (2012) proposed the application of an artificial intelligence prediction system to predict the magnitude and probability of earthquakes in various regions through adjustments to the neural network structure and different configurations of parameters [15].

(2) Assessing vulnerability to earthquakes: Earthquake vulnerability refers to the vulnerability of a city's society, economy, and physical environment to seismic activity [16, 17] (Rashed et al., 2003; Han et al., 2021). Noriega et al. (2012) explored the variations in demographics and socioeconomic characteristics associated with earthquake losses taking into consideration natural systems, the socioeconomic system, the built environment, and geospatial processes [18]. Joseph and Jacquleen (2013) constructed a seismic vulnerability assessment model of urban spatial, social, and economic systems [19]. After comparing the limitations of the different evaluation methods, Khan (2012) proposed a method to explore internal factors and mechanisms of earthquake vulnerability and, based on this, proposed relative solutions [20]. Mosen et al. (2018) on the other hand used Analytical Network Process (ANP) and Artificial Neural Network (ANN) models to construct a vulnerability index to measure the vulnerability of urban social and economic systems, geological conditions, and physical environments [21].

(3) In disciplines such as economics, engineering, and disaster science, the definition of risk mainly focuses on the possibility and consequences of a disaster [22, 23]. Therefore, the risk of an earthquake can be represented by the expected value of consequences, that is, the probability and scope of the occurrence of an earthquake, and whether the earthquake's intensity will exceed a city's safety threshold [24]. Based on analysis of the randomness and intensity of earthquakes, Zhong and Yu proposed a method of predicting earthquakes as a fuzzy random event [25]. Davidson et al. proposed the earthquake disaster risk index, which can measure the earthquake disaster risk in major cities and describes the relative contributions of various factors to overall earthquake risk [26]. Jena et al. (2020) developed an integrated model using the artificial neural network-hierarchy process (ANN-AHP) model to quantify urban population caused by impending earthquakes [27]. Mili et al. (2018) developed a model for assessing urban earthquake risk based on probability, vulnerability, and response capacity to explain the safety level of urban structures about earthquakes and assess the impacts of preventive measures on risk [28].

Scholars have conducted useful research on seismic risk, using various methods and models, including mathematical modeling, spatial analysis, and quantitative evaluation. Given the complexity and openness of urban systems, the nonlinearity of driving factors, and sudden changes that can occur to geological processes, however, existing models and algorithms, as well as assessment methods, need to be more rigorous. As for the measurement and quantification of earthquake risk, it is affected by different disciplines and the scale of the research object. Its evaluation indicators are limited to the level of regional elements, engineering facilities, or building units, without considering the interinfluencing factors at different scales, mutual feedback relationship. In particular, quantify the level of earthquake risk unilaterally based on the probability of earthquake occurrence or vulnerability assessment.

Because of this, this paper proposes a hybrid intelligent model and empirically applied it to Hefei, one of the few superlarge provincial capital cities on the "Tancheng-Lujiang" fault zone, one of the four major earthquake zones in China. Multiscale nested evaluation indicators and models are constructed from the three scales of Hefei City area, central city area, and block, as well as possibility and vulnerability. The model is based on the existing evaluation path system in the existing disaster science, urban management, computer engineering, and other disciplines [29, 30]. It combines the perspectives and advantages of multiple disciplines and is more targeted and adaptable to the complex nonlinearities of earthquakes. The hybrid intelligent model includes three aspects: First is to create a better GA-PSO-BP neural network model to predict the possibility of earthquakes by automatically calculating rules from data on known earthquake events to forecast earthquakes in unknown areas. Second, given the complex nonlinear characteristics of urban seismic vulnerability, an AHP-SAVEE-EMYCIN integrated algorithm is introduced to evaluate vulnerability to earthquake damage from four aspects: building vulnerability, risk of secondary disasters, socioeconomic vulnerability, and urban emergency response capabilities. In the next step, the overall urban seismic risk was obtained by standardizing and superimposing seismic probability and vulnerability. Third, the possibility of earthquake and the vulnerability of earthquake damage are unified and standardized to obtain the comprehensive urban earthquake risk, and the difference in the distribution of earthquake risk in urban spatial units is discussed, which provides new ideas for earthquake risk assessment and earthquake prevention management.

2. Materials and Methods

2.1. Study Area. Hefei is the provincial capital of Anhui Province. The city has experienced sustained social and economic development thanks to rapid urbanization, optimization of its industrial structure, and continuous infrastructure construction. Between 2009 and 2019, Hefei's urbanization rate and GDP growth rate both ranked first in China. Population growth and improvements to its industrial structure and infrastructure have promoted the peripheral expansion of the city, and Hefei's urban framework has continued to expand. Urban space has expanded from a small circle around the city and three wings to a multicenter city cluster, with an increasingly complex economy [31]. Hefei's rapid development has elevated it from among the middle and lower ranks of Chinese provincial capitals to among the top ten most successful, becoming a subcenter of the Yangtze River Delta City Cluster and home to one of China's four comprehensive national science centers.

Hefei is located in the hilly region between the Yangtze and Huai rivers, which is a complex geological environment [32]. The Tancheng-Lujiang fault zone in which Hefei City is located is the largest fault zone in eastern China, spanning 2,400 km of central Anhui Province (Figure 1(a)). The fault zone has undergone intensive transformations as a result of many tectonic movements over a long period and across a large area, leading to its current complex structural pattern. The Tancheng-Lujiang fault zone has experienced one earthquake of magnitude 8.5, six earthquakes of magnitude 7 or higher, and three earthquakes of magnitude 5 or higher in Anhui Province, as well as frequent smaller earthquakes. Hefei and its surrounding areas entered a new period of seismic activity in the 1990s. In 1996 and 2006, the State Council identified Hefei as a key national earthquake monitoring and defense city and noted that Hefei faces a great threat from earthquakes [33]. Because of the rapid development of Hefei and its location in the Tancheng-Lujiang fault zone, the city must pay attention to the danger of earthquakes. This paper selects the city of Hefei as its study area (Figure 1(b)), with the aim of comprehensively and systematically assessing the risk of an earthquake disaster and providing important support for improving the city's disaster prevention and mitigation capabilities, improving urban resilience, and building a high-quality human settlement.

2.2. Materials. The research data for this study largely relates to two areas: earthquake disasters and urban earthquake vulnerability. Hefei's earthquake disaster data consists of information on historical earthquakes, topography, and tectonics. The historical earthquake information includes the location and alignment of faults and the time, location, and magnitude of previous earthquakes. This is taken from the website of the Hefei Geological Bureau (http://dzj.hefei.gov.cn), and ArcGIS was used to carry out Euclidean distance analysis and kernel density analysis on seismic points and fault zones, giving the distribution of historical earthquakes in Hefei. Urban topography data is mainly from the geospatial data cloud (http://www.gscloud.cn), with analysis of slope and aspect in the elevation data revealing the topography of Hefei. Plate tectonic information includes peak ground acceleration (PGA) and rock and soil stability, which is obtained from the China Earthquake Administration (https://www.cea.gov.cn).

Earthquake vulnerability data includes building conditions, location of secondary disasters, socioeconomic conditions, and urban emergency response capabilities. Data on building conditions includes the profiles and heights of buildings in 2020 obtained from Baidu Maps, as well as building structures and ages obtained from historical satellite images and on-site investigations. Secondary disaster data mainly consists of information on floods, fires, pollutant leakages, and landslides caused by earthquakes. Data on fires and pollution sources are mainly from obtaining the geographic coordinates of gas stations, chemical plants, and heavily polluting factories and then performing Euclidean distance analysis. Data on flood disasters is based on the danger posed by large reservoirs on the north side of Hefei and low-lying places along rivers, which was combined with digital elevation models and reservoir water capacity information to conduct flood inundation analysis. Landslide data is based on the analysis of areas with a slope greater than 20°. Socioeconomic conditions include population distribution and economic strength. Population data is based on the number of people in each city district and total building area taken from the Hefei Statistical Yearbook, which was used to deduce overall population distribution. The distribution of the vulnerable population is based on Euclidean distance analysis of nursing homes, primary and middle schools, and elderly apartments using Python. Economic intensity is measured using NPP-VIIRS nighttime light data. Light data is from the Group on Earth Observations, with noise reduction performed and monthly data for 2020 combined into composite annual images. The city's emergency response capability is mainly based on the number of

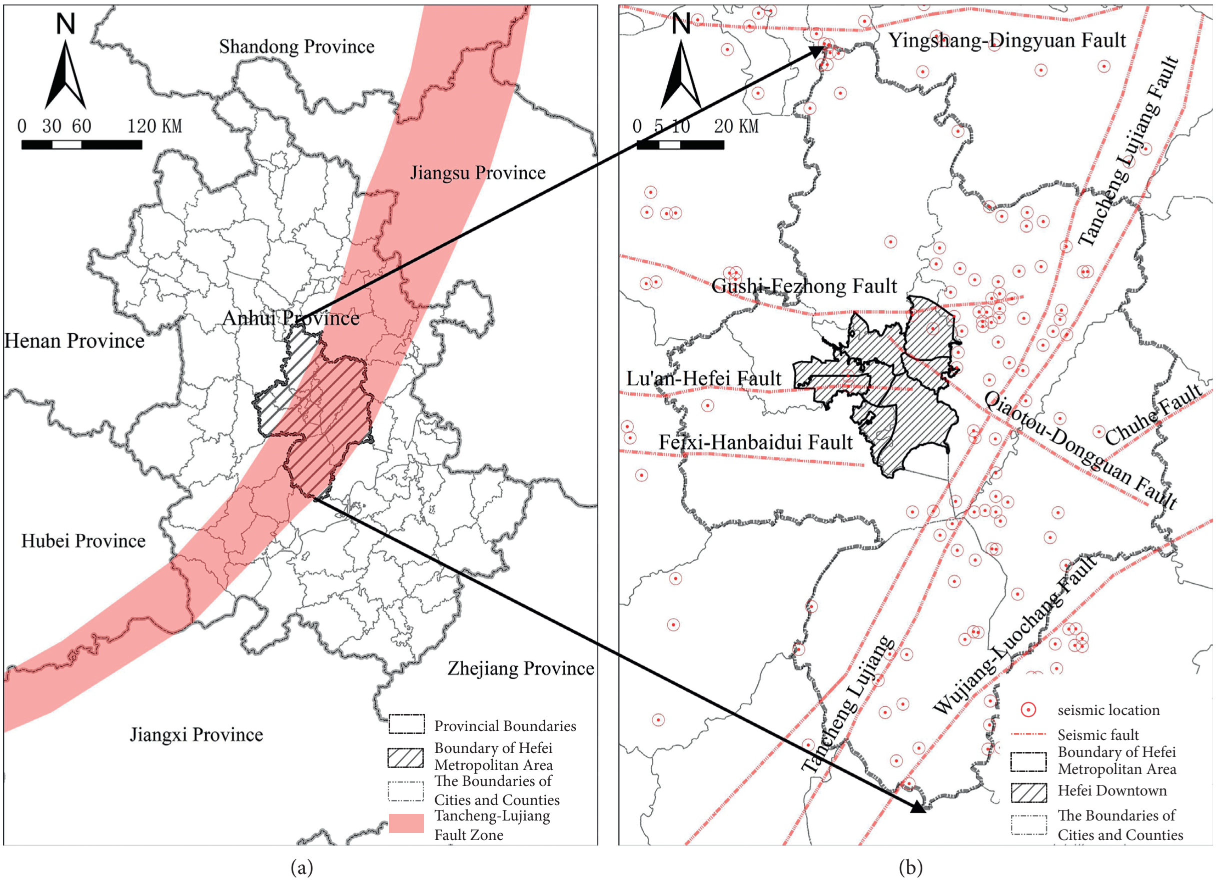

FIGURE 1: The location and earthquake situation of the study area. (a) Anhui Province; (b) Hefei metropolitan area.

fire stations, hospitals, and shelters it has. This data was used to gather geographic coordinates using Baidu Maps. After collecting data on earthquake disasters and urban seismic vulnerability, preprocessing including vectorization, standardization, and normalization of relevant data was completed using ArcGIS to create an earthquake disaster database.

3. Methods

3.1. A Hybrid Intelligent Model. Given the complexity and openness of urban systems, the nonlinearity of driving factors, and sudden changes in geological processes involved in urban seismic research [10, 34], this paper develops a hybrid intelligent model that integrates probability and vulnerability by integrating multiple intelligent algorithms (Figure 2).

The probability of urban seismic activity was evaluated based on the GA-PSO-BP neural network model. The main steps were as follows: First, seismic probability research in China and overseas was systematically sorted, selecting data in the three areas of earthquake history, topography, and geology. Data was then collected, vectorized, and preprocessed to create an earthquake disaster database for Hefei. The study area was divided into grids using ArcGIS, and the values of various factors were extracted to grid points to establish a data set. Based on historical seismic data, four known points of very high, high, low, and very low seismic probability were identified and imported into MATLAB as initial samples. Repeated training and simulation of the GA-PSO-BP integrated model were conducted and laws were automatically obtained from known earthquake events that could predict the probability of earthquakes in other areas. Finally, we simulated the probability of earthquakes in the entire study area.

An urban seismic vulnerability was evaluated using the AHP-SAVEE-EMYCIN method. The main steps were as follows: (1) Indicators that reflect the essential characteristics of vulnerability, such as the state of urban buildings, the risk of secondary disasters, socioeconomic conditions, and urban emergency response capabilities were selected, collected, and preprocessed to establish the Hefei earthquake disaster vulnerability database. (2) Based on the AHP method, an evaluation system from the perspective of vulnerability influencing factors and evaluation objectives was established, and the average weights of several experts were calculated. (3) The SAVEE algorithm was applied to standardize the value of factors and convert all values to between -1 and 1. (4) Using the EMYCIN formula, an evaluation result of urban seismic vulnerability was obtained by combining the value of influencing factors. Finally, the urban seismic probability and urban seismic vulnerability results were normalized and superimposed to obtain the final urban seismic risk result.

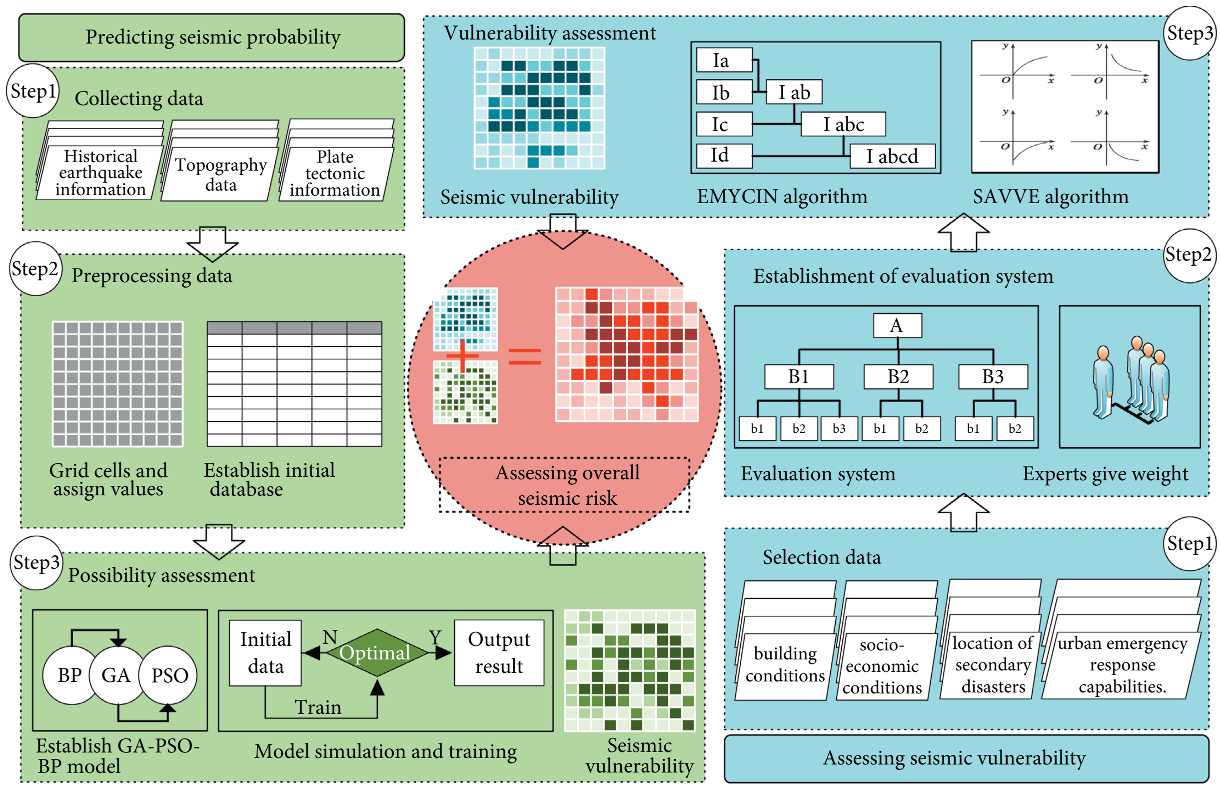

Figure 2: Research method.

3.2. Forecasting Model of Seismic Probability Based on GA-PSO-BP

3.2.1. Algorithms. Earthquakes are huge, complex systems, and the relationship between each influencing factor is intricate, with extremely significant spatial nonstationarity. The backpropagation (BP) neural network model is a nonlinear dynamic system with strong nonlinear mapping ability, high fault tolerance and robustness, and a strong ability to deal with nonlinear problems. Using the BP neural network algorithm, laws are automatically generated from the entered data of known earthquake events, and the possibility of earthquakes in other areas can be predicted based on quantitative analysis of those laws as well as statistics and probability theory, which avoids errors caused by human predictions of seismic events [35]. Particle Swarm Optimization (PSO) is a population-based stochastic optimization technique in which population particles continuously evolve to find their optimal position and speed [36]. A genetic algorithm (GA) is an iterative optimization algorithm for solving search problems [37]. GA converts spatial parameters of a problem into strings of binary digits called chromosomes and performs techniques inspired by natural evolution, such as selection, inheritance, crossover, and mutation, using an iterative method to evaluate the quality of chromosomes in the new population and finally screen the best chromosomes.

The learning process of the BP algorithm involves optimization and learning the two types of parameters of network connection weights and thresholds. If the initial BP parameters are not properly selected, the BP algorithm can fall into a local optimal solution, and the default gradient descent iterative algorithm tends to slow the convergence speed of the neural network. This study used the mapping ability of the BP neural network in a nonlinear model and combines the learning ability of the GA and PSO-optimized parameter models to create an integrated GA-PSO-BP algorithm (Figure 3). The integrated algorithm uses GA to determine the initial parameters of the BP network and uses PSO to change the connection weights and thresholds in the training iterations, thereby accelerating the convergence speed of the network.

$$\begin{aligned} VC_{i\,d} &= w^{*}VC_{i\,d} + C_1\text{rand}_1\left(P_{i\,d} - Z_{i\,d}\right) \\ &\quad + C_2\text{rand}_2\left(P_{g\,d} - Z_{g\,d}\right), \\ Z_{i\,d}(t+1) &= Z_{i\,d}(t) + VC_{i\,d}(t+1). \end{aligned} \tag{4}$$

3.2.2. Algorithm Steps

(1) Collecting and preprocessing data: In terms of influencing factors and assessment objectives of earthquake probability, we selected data from the three areas of seismic history, topography and geomorphology, and tectonics. Historical seismic data includes fault zone density, fault zone distance, earthquake density, and distance to the epicenter. Given the prolific nature of earthquakes, seismic activity is likely to occur repeatedly near the epicenter [38]. Topography and geomorphology, including elevation, slope, and tortuosity, are closely

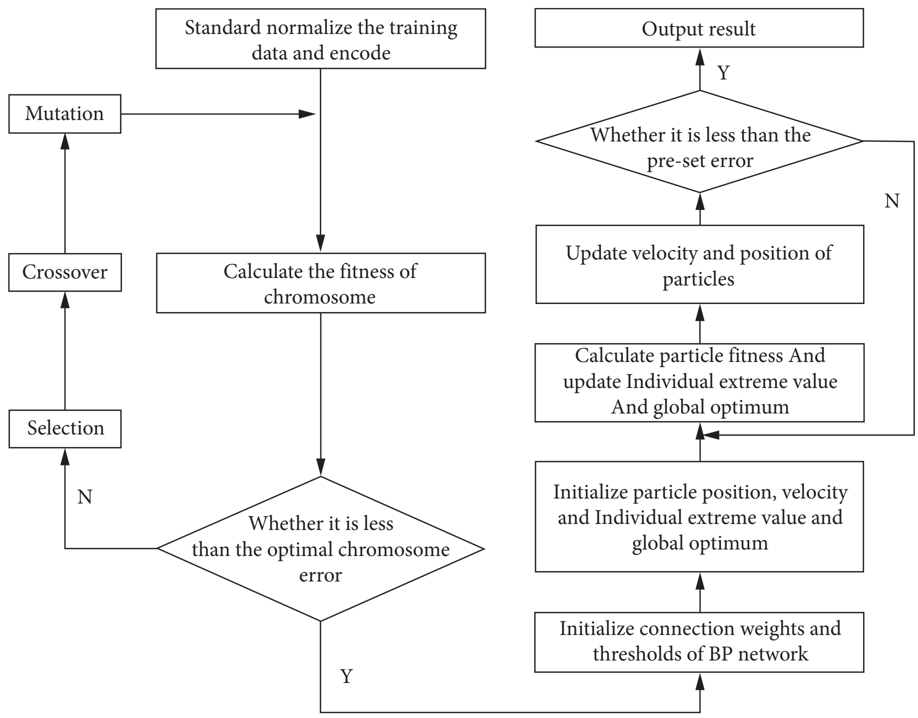

Figure 3: Operational flowchart of GA-PSO-BP.

related to earthquake disasters and are the main causes of secondary geological disasters [39]. Tectonics include peak ground acceleration and rock and soil stability, which reflect the exposure of cities to earthquakes and are the material basis for determining the development of earthquakes [38, 40]. ArcGIS created a grid and extracted various standardized factor values. Four known probability points (very high, high, low, and very low) were selected from historical seismic data and imported into MATLAB as the initial sample.

(2) Determining the structure of the initialized BP neural network: The next step is to determine the number of neurons in the input layer, hidden layer, and output layer. Nine neural units $x1$–$x9$ were set as the input layer n, corresponding to nine influencing factors, including the density of the fault, distance from the fault, earthquake density, distance from the epicenter, stability of rock and soil, and elevation. The output layer m was set as four neural units $y1$–$y4$, corresponding to the four levels of earthquake probability: very high, high, low, and very low.

(3) Calculating the initial connection weights and thresholds based on GA: After GA model training, maximum personal accommodation can be determined. Each component is then decoded into corresponding parameters, that is, the initial connection weights and thresholds of the network. It is then determined whether optimal fitness has been reached. If it is reached, the chromosome undergoes related calculations in the next step; otherwise, further selections, crossovers, and mutations are performed.

(4) Using PSO to calculate optimal connection weights and thresholds: In the iterative process, PSO is used to update the initial connection weights and thresholds obtained in the third step. Using the PSO algorithm, we set the population size to 30 and the maximum number of iterations to 100. Determine whether the new particle swarm generated by the iteration has reached optimal fitness to determine whether the algorithm has reached the preset error or reached the maximum number of iterations. If optimal fitness is reached, the global optimal solution is generated, and the simulation result of the probability of an earthquake in Hefei is obtained. The relevant formulas involved in the calculation process are as follows.

Fitness function: This affects the convergence speed of the genetic algorithm and judges whether the optimal solution is reached, wherein E_t is the sum of the errors of each unit, C_k^t is the actual output, y_k^t is the target output, and T is the number of test samples. The smaller the value of the objective function, the larger the fitness function.

$$E_t = \frac{1}{2}\sum_{k=1}^{m}\left(C_k^t - y_k^t\right)^2,$$

$$E = \frac{1}{2}\sum_{t=1}^{T}\sum_{k=1}^{m}\left(C_k^t - y_k^t\right)^2 \qquad (1)$$

$$= \sum_{t=1}^{T} E_t.$$

Designing the crossover operators: The two crossover operators are set as h_A^i and h_B^i, and crossover operations are performed on them, and two new individual sums $h_A^{(i+1)}$ and $h_B^{(i+1)}$ are created; a is random number distributed between 0 and 1.

$$\begin{aligned} h_A^{(i+1)} &= ah_B^i + (1-a)h_A^i, \\ h_B^{(i+1)} &= ah_A^i + (1-a)h_B^i. \end{aligned} \tag{2}$$

Designing the mutation operator: The mutation operator adopts a unified mutation strategy. Set an individual to $H = h_1 h_1 \ldots h_k h_j$, wherein h_k is the mutation point, and its value range is $(H_{\text{man}}^k - H_{\min}^k)$. After uniform mutation of H at this mutation point, a new individual $H = h_1 h_1 \ldots h_k' h_j$ is obtained. The new gene value of the mutation point is h_k', where β is a random number distributed between 0 and 1.

$$h_k' = H_{\min}^k + \beta\left(H_{\text{man}}^k - H_{\min}^k\right). \tag{3}$$

Update the velocity and position of the particles: XX and XX are the speed and position of the particles, respectively, which represent the best position of each particle, and rand() is a random number between (0, 1).

3.3. Urban Seismic Vulnerability Measurement Model Based on AHP-SAVEE-EMYCIN

3.3.1. Relevant Algorithms. The analytic hierarchy process (AHP) is a multiobjective decision-making analysis method that combines qualitative and quantitative analysis. It can help decision-makers observe and analyze problems and goals. It is widely used in urban operation management, disaster risk analysis, site selection, and other applications [41, 42]. The spatial appraisal and valuation of environment and ecosystems (SAVEE) methodology is a comprehensive method of evaluating value from multiple perspectives, which can reflect the influences of multiple driving factors. It features simple measurement analysis and strong operability. It is widely used in many fields, such as land valuing, landscape ecology, and natural resource planning [43, 44]. The EMYCIN algorithm is a model used to iteratively calculate the value of influencing factors and is an extension of reasoning under uncertainty based on the concepts and practical methods of probability theory [41]. Urban seismic vulnerability refers to the overall impact of an earthquake's intensity exceeding the safety threshold that the city can bear, which involves multidimensional influences such as the natural environment, engineering conditions, and social and economic activities.

Due to the spatial imbalance of urban seismic vulnerability, this article attempts to build an AHP-SAVEE-EMYCIN integrated model that combines the AHP, SAVEE, and EMYCIN formulas. The integrated algorithm uses the AHP method to establish the evaluation system and index weights, the SAVEE algorithm to standardize the values of influencing factors, and the EMYCIN calculation to superimpose the roles of various factors to obtain seismic vulnerability.

3.3.2. Calculation Steps

(1) Establish an evaluation system: Having studied previous seismic research by Chinese and overseas scholars, we selected evaluation indicators that reflect the essential features of seismic vulnerability and created a logical evaluation system that considers influencing factors and evaluation goals. The initial system consisted of 17 initial evaluation indicators, which were revised and improved following interviews and surveys with experts. Finally, we created a comprehensive vulnerability assessment index for urban seismic activity (Table 1) consisting of 13 evaluation indicators in the four criteria categories of building vulnerability, secondary disaster risk, socioeconomic vulnerability, and urban emergency response capabilities [45–49].

The vulnerability of buildings is largely a reflection of a city's exposure to earthquakes. Casualties and property losses caused by the collapse of buildings account for most of the total losses of an earthquake. The risk of secondary disasters, which include floods, fires, pollutant leakages, and landslides, mainly reflects the sensitivity of a city to an earthquake, which often causes losses that are several-fold higher than the initial earthquake. Compared with rural areas, secondary disasters and induced seismicity in urban areas are more serious. Socioeconomic vulnerability also reflects the sensitivity of a city to an earthquake and refers to the likelihood of seismic activity causing long-term damage such as social and psychological burdens as well as paralysis of the economic structure. It is mainly connected to the overall density of the urban population, the distribution of vulnerable populations, and the pattern of urban economic strength. Urban emergency response capabilities are mainly related to a city's own defense and resilience after an earthquake to meet the needs of residents for postdisaster emergency relief as well as rescue and treatment.

(2) Use AHP to calculate indicator weights: The relationship between the factors in the evaluation system is analyzed to establish a systematic hierarchical structure and compare the importance of each pair, and a consistency test is conducted to obtain the indicator weights of experts. To make the index weights of urban seismic vulnerability evaluation indicators even more rational, this study invited three experts in the fields of natural disasters, urban planning and management, and construction engineering safety to undergo interviews and provide scores, and the average weights of the three experts were used as the final weights (Table 1).

(3) Standardize the element values using the SAVEE algorithm: To assess the seismic vulnerability of Hefei, the SAVEE algorithm can be used to perform different standardized equation calculations on various types of seismic vulnerability influencing factors. For negative seismic vulnerability factors that increase as x

Table 1: Seismic vulnerability evaluation index.

Objective	Criteria	Factor	Weight
Evaluation of urban earthquake vulnerability	Building vulnerability 0.3300	Building age	0.0646
		Building structure	0.1628
		Building height	0.1026
	Secondary disaster risk 0.3300	Flood risk	0.0982
		Fire risk	0.0927
		Pollution leakage risk	0.0581
		Landslide risk	0.0810
	Socioeconomic vulnerability 0.1404	Population distribution	0.0436
		Vulnerable pop. dist.	0.0693
		Economic strength	0.0275
	Emergency response capability 0.1996	Fire station coverage	0.0499
		Hospital coverage	0.0499
		Shelter coverage	0.0998

increases, such as the coverage of fire stations, hospitals, and shelters, the standard calculation is carried out using formula (5), and the boundary value (A) is 1000 m. Positive vulnerability factors that increase as x increases, such as population distribution density, vulnerable population distribution, building age, and building height, are calculated using formula (6), and the boundary value is 2000 m. For positive vulnerability factors that decrease as x increases, such as flood risk, fire risk, and pollution leakage risk, formula (7) is used, and the boundary value is 2000 m. For negative vulnerability factors that decrease as x increases, formula (8) is used. The formula for the SAVEE algorithm is as follows:

$$V = -\left[\exp\left(\frac{-(x+1)}{|A|}\right)\right]^5, \quad x \le A, \ -1 \le V \le 0, \tag{5}$$

$$V = 1 - \left[\exp\left(\frac{-(x+1)}{|A|}\right)\right]^5, \quad x \le A, \ 0 \le V \le 1, \tag{6}$$

$$V = \left[\exp\left(\frac{-(x+1)}{|A|}\right)\right]^5, \quad x \le A, \ 0 \le V \le 1, \tag{7}$$

$$V = \left[\exp\left(\frac{-(x+1)}{|A|}\right)\right]^5 - 1, \quad x \le A, \ -1 \le V \le 0, \tag{8}$$

where in V is the standardized value of seismic vulnerability; x is the value of each influencing factor, and A is the boundary value.

(4) Calculate seismic vulnerability with the EMYCIN model: EMYCIN is an extension of reasoning under uncertainty based on the concepts and methods of probability theory. Based on evaluation data from the SAVEE model, the iterative algorithm is used to calculate the various pairwise standardized seismic vulnerability driving factors, until all the factors are analyzed and the seismic vulnerability of the study area is obtained. This will provide a visualization of seismic vulnerability at the spatial level. The EMYCIN formula is as follows:

$$\begin{aligned} I_{ab} &= I_a + I_b - I_a \times I_b, \quad I_a > 0,\ I_b > 0, \\ I_{ab} &= I_a + I_b + I_a \times I_b, \quad I_a < 0,\ I_b < 0, \\ I_{ab} &= \frac{(I_a + I_b)}{\left(1 - \min\left[|I_a|, |I_b|\right]\right)}, \quad \text{else}. \end{aligned} \tag{9}$$

I_a and I_b are the standardized values of seismic vulnerability of influencing factors a and b, and I_{ab} is the superimposed value of factors a and b.

4. Results

Earthquake risk assessment has become an effective means of government disaster risk management and resilient city construction. In order to predict and analyze earthquake disasters more accurately, scholars have conducted a lot of discussions, mainly using expert scoring method, multivariate statistical method, geostatistics, time series analysis, fuzzy comprehensive evaluation method, gray system theory, analytic hierarchy process, complex system theory, backpropagation (BP) neural network, and other methods [22–28]. Geographic Information System (GIS) technology is widely used because it can objectively reflect the distribution characteristics of earthquake risk. However, how to choose a reasonable earthquake risk assessment model has become an urgent problem to be solved. In order to solve the abovementioned difficulties and shortcomings, this paper proposes a hybrid intelligence model from the perspective of possibility and vulnerability. The evaluation results and the superiority of the algorithm are as follows.

4.1. Predicting Seismic Probability. The rapid development of computer technology represented by machine learning provides new ideas for the detection of seismic events. The main content of machine learning research is to let the machine generate a model from the input data, that is, a learning algorithm, and the generated model can provide corresponding judgments when facing new data. Machine learning and seismic historical data can help us further improve the detection accuracy under the premise of existing computing capabilities and algorithms and maximize the capabilities of the algorithm. For example, Jiang and Ning (2019) will combine features selected by manual experience with support vector machines [50], and Liu et al. (2020) combined Taiwan array strategy with deep learning [51]. The combination of multiple algorithms is also a new idea. For example, Witsil and Johnson (2020) combined GAN with K-Means [52], and Mousavi et al. (2019) combined CNN with LSTM network [53]. Semisupervised and unsupervised learning can avoid problems such as insufficient manual labeled data sets. Therefore, this paper proposes the GA-PSO-BP neural network model, which combines historical seismic data and geological plate conditions to predict the possibility of earthquakes.

Given the accuracy of prediction results and the limited earthquake related data for downtown Hefei, this paper expanded the scope of its earthquake probability assessment to the Hefei metropolitan area. ArcGIS was used to create a 500 m*500 m fishnet that divided Hefei into 45,745 grids. Various data was extracted into the grids, which was imported into MATLAB as the initial sample for simulation and prediction using the GA-PSO-BP integrated algorithm. The prediction results of earthquake probability in the metropolitan and downtown urban areas of Hefei were depicted using ArcGIS (Figures 4(j) and 4(k)). The analysis results show the following: Areas within the city with high earthquake probability are mainly concentrated in Feidong County and Lujiang County, with a few also in Hefei City, Feixi County, and Chaohu City. The reasons for their higher seismic probability are the high density of faults and epicenters, short distance to active faults and epicenters, poor geological stability, and complex topography. Areas of Changfeng County, Feixi County, and Chaohu City have lower earthquake probability. Of Hefei's main urban areas, the High-Tech Zone in the east, southern Shushan District, central Yaohai District, and northeastern Luyang District, as well as northern and southern parts of Xinzhan District, have a higher earthquake probability, whereas, Baohe District, the Economic Development Zone, the northern part of Shushan District, central Luyang District, and central Xinzhan District have lower earthquake probability.

Due to the advantages of the BP algorithm for solving nonlinear problems, GA was used to calculate the initial connection weights and thresholds, and PSO was used to optimize the connection weights and thresholds in each iteration, which eventually provided the seismic probability assessment result and algorithm efficiency for each grid in the Hefei metropolitan area. The performance index of neural network training is the average error between its predicted output value and the expected output value. The smaller the average error and the smaller the fitness value, the smaller the system error of the neural network. The GA model has the highest individual fitness value after 3 stop iterations. The GA-PSO-BP model has the lowest fitness after 25 stop iterations. The PSO model has 25 stop iterations, and its fitness is in between the other two (Figure 5(a)). Of the three earthquake probability prediction models, the GA-PSO-BP model has the highest prediction accuracy, with a rate of 82.50%; GA has a prediction accuracy rate of 81.25%, and PSO has a prediction accuracy rate of 79.37% (Figure 5(b)). It can be seen that the GA-PSO-BP integrated model combines the advantages of multiple algorithms and benefits from fewer calculations, fast convergence, and good global convergence.

4.2. Assessing Seismic Vulnerability. The AHP-SAVEE-EMYCIN is a method of reasoning under uncertainty that uses mathematical formulas and models to express various probabilistic reasoning. It can transform qualitative descriptions of influencing factors into quantitative values and combines the two in the assessment, making it useful in determining spatial imbalances in urban seismic vulnerability. The AHP method was used to determine the index system and weights. The SAVEE method standardized the impact factors of each type of seismic vulnerability (Figures 6(a)–6(m)), and pairwise iterations were performed using the iterative EMYCIN equation until all factors were in the calculation, which finally produced the results of the seismic vulnerability assessment for downtown Hefei (Figure 6(n)).

Areas with high seismic vulnerability are mainly concentrated in the old city, the area around Hefei West Railway Station, the government affairs district, Science City, and the East New Center. They are also distributed on a small scale in Xinzhan District, Gangji Town Industrial District, the Economic Development Zone, and Binhu New District outside the city's second ring road. These are areas of Hefei with more complex social and economic activities, higher building-related risks, more secondary disasters, and higher sensitivity and exposure to earthquakes. Low fire risk areas include Shushan Park, the Economic Development Zone, Science City, and the disused Luogang Airport, which are mainly used for scientific research and ecological and recreational functions, and their seismic vulnerability is low.

4.3. Assessing Overall Seismic Risk. Seismic risk is a combination of the probability of an earthquake and the effect of an earthquake that exceeds the safety threshold that a city can bear. Using ArcGIS, the seismic probability and vulnerability were superimposed after being standardized, and the composite result of the two provided overall seismic risk results (Figure 7(a)). Areas with high, higher, lower, and low seismic risk in Hefei accounted for 8.10%, 31.90%, 40.94%, and 19.06% of its total area, respectively. High risk areas are mainly concentrated in the old city, government affairs district, Science City, and Xinzhan District. These areas are closer to the seismic belt and are more vulnerable to earthquake damage. Low and lower risk areas include the disused Luogang Airport, the urban periphery, Gangji Town, Hefei Station, and Science City.

To investigate the differences in seismic risk in various areas of downtown Hefei, statistical analysis was carried out to determine the proportions of various levels of risk by land area and the proportions of various levels of risk by building

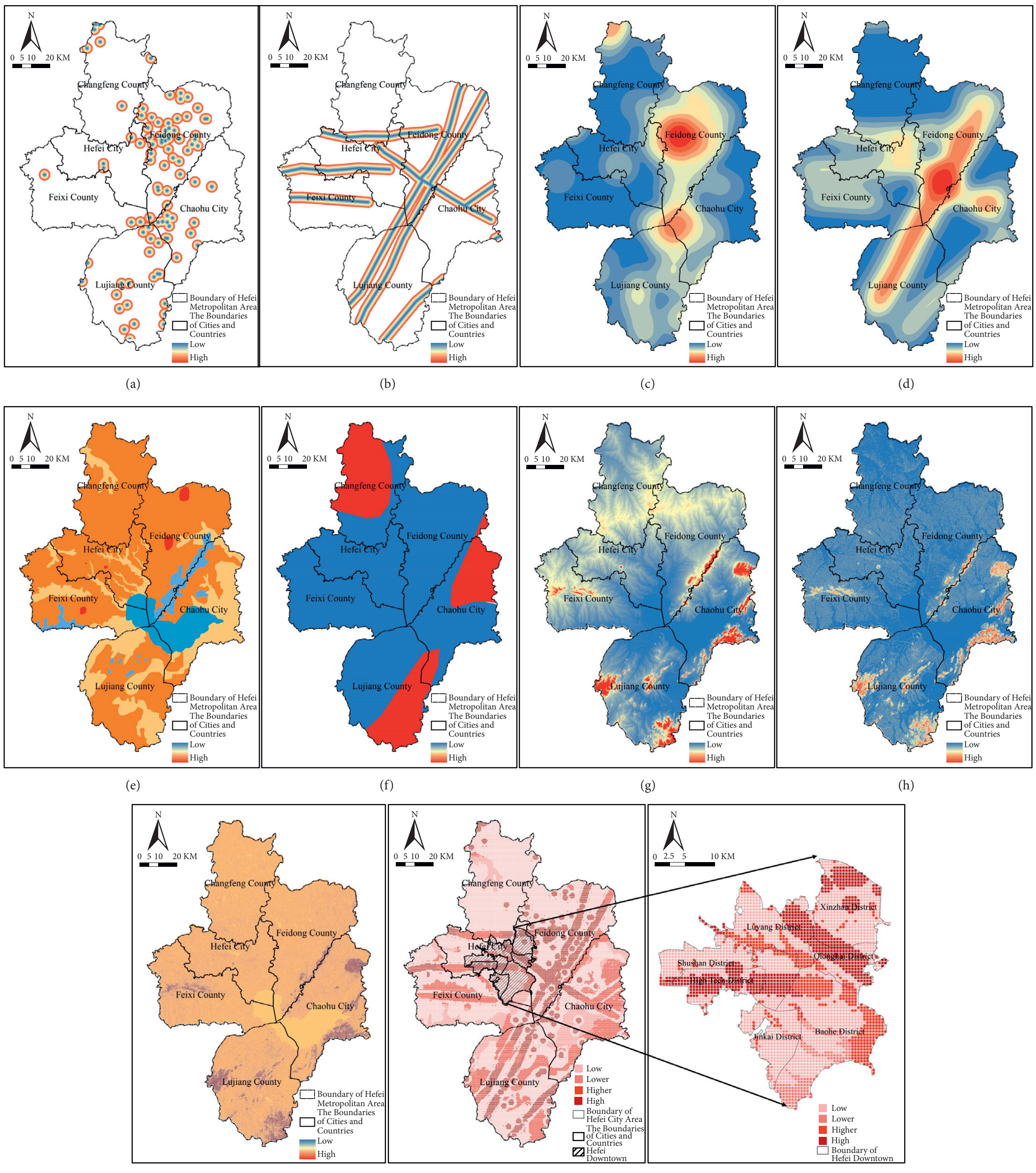

Figure 4: Predicting seismic probability. (a) Distance to epicenter. (b) Distance to fault zone. (c) Earthquake density. (d) Fault zone density. (e) Rock and soil stability. (f) Peak ground acceleration. (g) Elevation. (h) Slope. (i) Tortuosity. (j) Probability of earthquake in Hefei metro area. (k) Probability of earthquake in downtown Hefei.

area (Figures 7(b) and 7(c)). The area proportions reflect the overall seismic risk levels of each geographical area. The High-Tech Zone and Luyang District have the largest proportions of high risk areas, followed by Luyang District, Shushan District, and Xinzhan District, whereas, the Economic Development Zone and Baohe District have the smallest proportions. The Economic Development Zone has the lowest overall seismic risk, and Yaohai District and the High-Tech Zone have the highest overall seismic risk. The proportions of risk by building area reflect the level of seismic risk to a district's social and economic activities. The High-Tech Zone and Yaohai District have the largest proportions of high risk areas, followed by Luyang District, Shushan District, and Xinzhan District. The Economic Development Zone and Baohe District have the smallest proportions of high risk areas. The Economic Development Zone has the lowest building earthquake risk, and Yaohai District has the highest building earthquake risk.

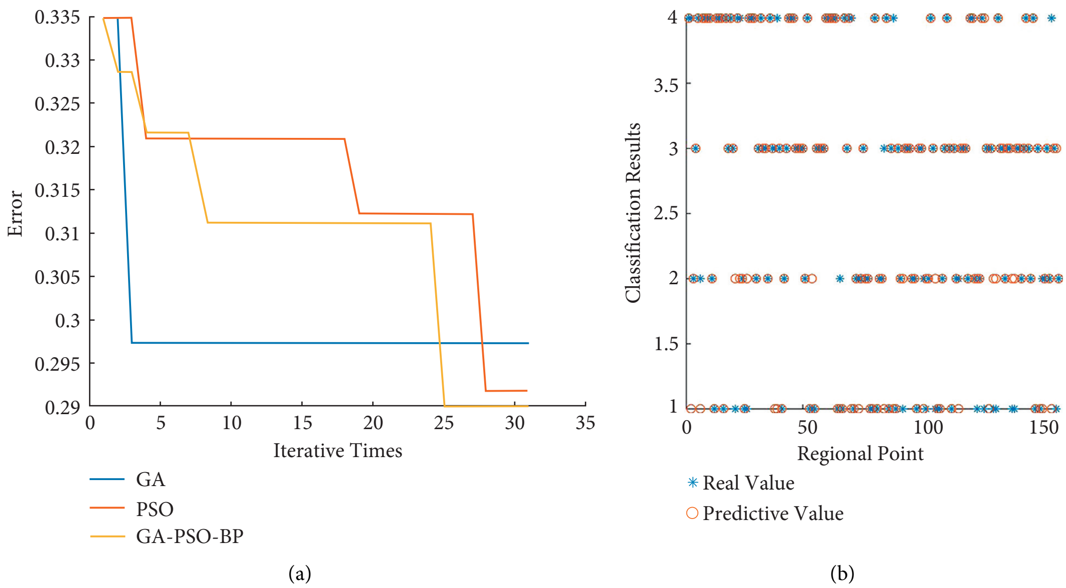

Figure 5: Algorithm efficiency. (a) Comparison chart of predictive values and real values. (b) Fitness curves of different models.

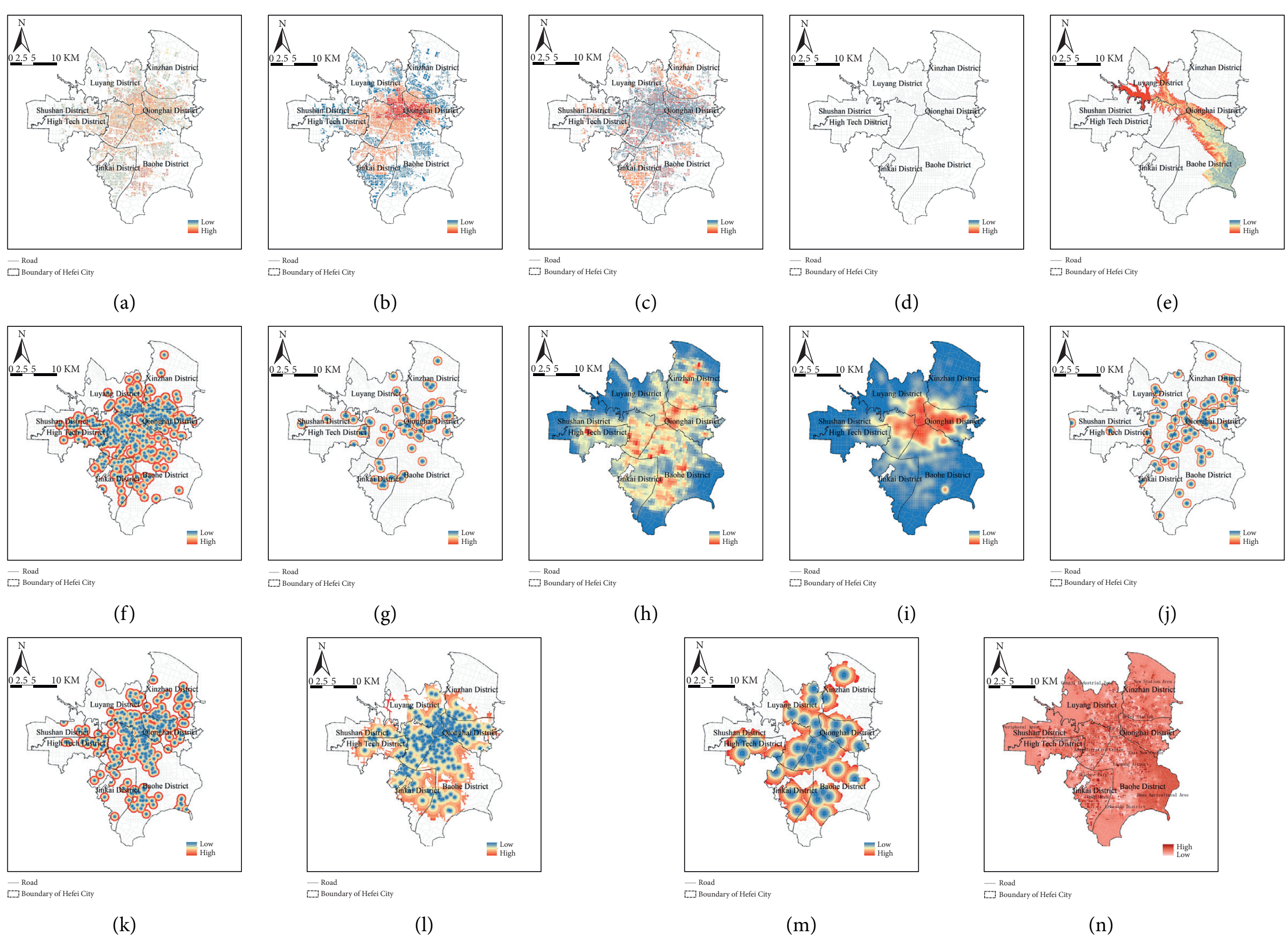

Figure 6: Assessing seismic vulnerability. (a) Building height. (b) Building age. (c) Building structure. (d) Landslide. (e) Flood. (f) Fire. (g) Pollution leakage. (h) Economic strength. (i) Population distribution. (j) Vulnerable population. (k) Shelter coverage. (l) Hospital coverage. (m) Fire station coverage. (n) Seismic vulnerability.

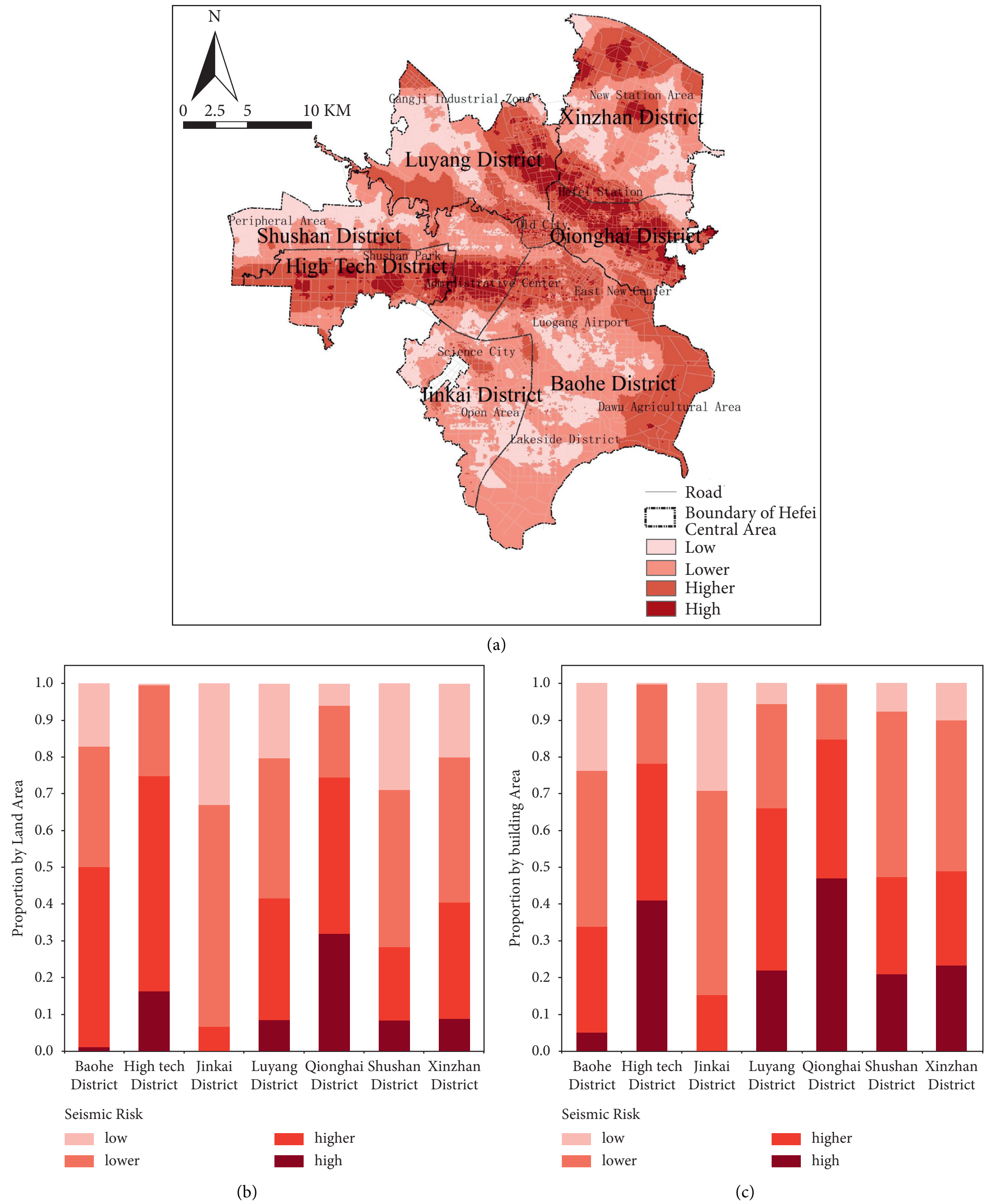

Figure 7: Assessing overall seismic risk. (a) Distribution of seismic risk. (b) Proportions by land area. (c) Proportions by building area.

Comparative analysis of the proportions of various risk levels by land area and building area shows that the High-Tech Zone and Yaohai District have high proportions of high risk districts by land area and by building area, so earthquake risk prevention measures in those districts should be strengthened to reduce potential losses caused by earthquakes. Hefei's future development should be concentrated in areas with lower seismic risk.

5. Discussion

5.1. Innovation and Application Scope of Urban Earthquake Risk Assessment Model. Established under the existing evaluation system in the disciplines of disaster science, construction engineering, and urban management, the hybrid intelligent model integrates the perspectives and advantages of multiple disciplines [22–24]. This model is more suited and adaptable to the complex nonlinearity of earthquakes. The hybrid intelligent model includes three parts: a GA-PSO-BP integrated algorithm to predict the probability of earthquakes; an AHP-SAVEE-EMYCIN integrated algorithm to measure urban vulnerability during earthquakes, and an assessment of overall seismic risk after earthquakes occur. (1) The GA-PSO-BP algorithm used GA to determine the initial parameters of the BP network and used PSO to change the connection weights and thresholds in the training iterations, thereby speeding up the convergence of the network and avoiding falling into the local optimal solution. GA-PSO-BP automatically generated laws from inputted data on known earthquake events, and the possibility of earthquakes in other areas was predicted based on quantitative analysis of those laws as well as statistics and probability theory, which avoided errors caused by human predictions of seismic events. (2) The AHP-SAVEE-EMYCIN algorithm used the AHP method to establish an evaluation system and index weights. The SAVEE algorithm standardized the value of the impact factors, and the EMYCIN iterative calculation superimposed the roles of various factors to obtain seismic vulnerability. The AHP-SAVEE-EMYCIN is a method of reasoning under uncertainty that uses mathematical formulas and models to express various probabilistic reasoning. It can transform qualitative descriptions of influencing factors into quantitative values and combines the two in the assessment, making it useful in determining spatial imbalances in urban seismic vulnerability. (3) In the next step, earthquake probability and vulnerability were unified and standardized using ArcGIS and then superimposed to obtain a composite result of the two, namely, overall seismic risk, which can provide new ideas for seismic risk assessment and urban earthquake prevention and management.

The hybrid intelligent model focuses on measuring a relative value of risk and comparing the spatial distribution characteristics of earthquake risk in different areas of cities, to guide government prioritization of disaster prevention and mitigation measures. This model is not only suited to assessing seismic risk in Hefei. The parameters of the intelligent model and its related weights can be adjusted according to the characteristics of a study area and the differentiation of a problem so that it is suitable for areas and cities with similar conditions.

5.2. Strengthen the Innovation of Cloud and Fog Computing in Earthquake Risk Assessment. From an analytical point of view, the hybrid intelligence still has limitations, including the need for high-quality data, a time-consuming process, and the need for the integrated model to perform a large volume of probability mapping training data points. Seismology is a data-driven science, and research progress and breakthroughs often come from observations by seismic stations [27, 28]. In addition, the basic data in the existing seismic business system has a wide variety and huge amount, and the model and the organization relationship between the models are complicated. The establishment of an earthquake disaster loss assessment system requires the purchase and establishment of a spatial geographic database and an earthquake basic data database and the development of corresponding technical systems to achieve other specific functions. In recent years, the development of cloud computing and fog computing can solve the waste and idleness of a large number of resources caused by repeated construction.

According to the definition of the National Institute of Standards and Technology (NIST), cloud computing is a computing model that uses the Internet to realize anytime, anywhere, on-demand, and convenient access to a shared resource pool [54]. Through cloud computing and fog computing, users can quickly obtain services that meet their own business needs, improving service quality while reducing operation and maintenance costs. As a major innovation in the information industry, the cloud and fog computing have been widely recognized by industry and academia. Through cloud computing and fog computing, software and hardware resources and seismic information can be shared, providing various users with different levels of services, enabling users to quickly customize their own services on demand, thereby overcoming the problems of long construction period and high cost of seismic business systems in the past.

5.3. Discussion on Strengthening the Seismic Risk Management System under Different Scales. Existing research on earthquake risk measurement and quantification is affected by different disciplines, research object scales, historical disaster data, and index data availability, etc. The evaluation indicators are too simplified to select individual indicators to characterize or are limited to areas, engineering facilities, or the level of the building itself, without considering the interrelationship and influence between different scale factors [29]. In addition, in urban disaster risk research, the accuracy of small scale index data such as streets and communities will also affect the rigor of the final risk assessment results.

Factors of different scales do not exist independently but are interrelated and influenced and are related to the characteristic boundary of a specific area [30]. This paper constructs a multiscale evaluation system from the three aspects of Hefei's metropolitan area, downtown, and neighborhoods. Among them, the city scale mainly uses historical seismic data, topography, and geological plate conditions to construct earthquake probability prediction models; the central city scale and block scale are used to evaluate the vulnerability of the city, and the central scale includes the city's secondary disasters, social economic strength, and urban emergency response capabilities, etc.; block scale main design and building vulnerability conditions such as building height, structural strength, and construction year. This article only draws on the concept of multiscale from the perspective of earthquake risk assessment and should emphasize the multiscale coordinated management of disaster risk.

In recent years, following the orderly advancement of China's urban agglomeration planning, metropolitan area strategy, regional integration, and other policies, the development of various cities and regions has become increasingly interwoven. Nevertheless, regional public crises often occur unexpectedly and can seriously damage the interests of society and individual citizens. Seismic fault zones often span multiple cities and even provinces, and differences in magnitude and focal depth of earthquakes mean that potential economic losses and social trauma are extremely difficult to estimate [4, 5]. The complexity and interconnectivity of crises caused by earthquakes these days are increasing, so the degree of coordination between government and social entities has a direct bearing on the effectiveness of earthquake crisis management [55, 56]. Follow-up research can explore the diverse ways social entities can participate in governance from the perspective of disaster management at multiple scales, including clarifying rights and responsibilities, strengthening policies and regulations, and optimizing the development environment of social entities, to build empirical and efficient mechanisms for coordinating and governing diverse entities during regional public crises.

For Hefei, the case of this paper, the seismic risk results from the hybrid intelligent model can be combined to implement earthquake defenses in two areas: basic measures to mitigate urban earthquake damage and emergency measures before and after earthquakes. Basic measures include moving essential infrastructure, such as energy, transportation, and communication facilities, away from areas with higher seismic risk; improving earthquake resistance or proofing in areas with higher earthquake risk; developing areas with less harmful construction, including more open spaces and protecting ecological spaces; seismic reinforcement of new construction projects as well as seismic retrofitting of old structures; and ensuring the city develops with earthquake resistance and disaster prevention in mind. Emergency measures mainly consist of accommodating Hefei's existing conditions by adopting temporary remedial measures and rationally deploying and organizing disaster relief to reduce losses and casualties caused by earthquakes.

6. Conclusions

The preearthquake risk assessment to determine the possible scope and spatial distribution of the earthquake can effectively promote the disaster prevention and mitigation work of the city against the earthquake and its induced disasters. This article aims to develop a new urban earthquake risk assessment model and conduct an empirical study on Hefei. Combining the definition of risk and the attributes of natural disasters, through the composite result of earthquake probability and urban vulnerability, the earthquake risk is quantitatively described, and the spatial distribution of urban earthquake risk is obtained. Our main conclusions are as follows.

The GA-PSO-BP model has an accuracy rate of 82.5% in predicting the probability of earthquakes. The model has the advantages of fewer calculations, fast convergence, and good global convergence. The simulation results indicate that areas with higher earthquake probability within the municipal area of Hefei are mainly in Feidong County and Lujiang County, with a small number scattered throughout Hefei City, Feixi County, and Chaohu City. These areas have a higher probability because they are located near the seismic fault and plate stability is poor. The High-Tech Zone, southern Shushan District, central Yaohai District, northeast Luyang District, and northern and southern parts of Xinzhan District have a relatively high probability of seismic activity.

The AHP-SAVEE-EMYCIN method was used to evaluate vulnerability to earthquake damage from four aspects: building vulnerability, secondary disaster risk, socioeconomic vulnerability, and emergency response capabilities. Our research showed that areas with high seismic vulnerability are mainly concentrated in the old city, the area around the Hefei West Station, the government affairs district, Science City, and the Hefei East New Center. These are large areas of Hefei with complex social and economic activities, higher building risks, more secondary disasters, and higher sensitivity and exposure to earthquakes.

Earthquake probability and vulnerability were standardized and then superimposed, to obtain a composite result of the two, which we call overall seismic risk. The areas with very high, high, low, and very low overall seismic risk accounted for 8.10%, 31.90%, 40.94%, and 19.06% of the total area of Hefei, respectively. Very high risk areas are mainly located in the old city, the government affairs district, Science City, and Xinzhan District. These areas are close to the seismic belt and are more vulnerable to earthquakes. In the future, targeted earthquake protection measures are required in the following two areas: basic measures to mitigate urban earthquake damage and emergency measures for before and after earthquakes.

Data Availability

The datasets used and/or analyzed during the current study are available from the corresponding author on reasonable request.

Consent

Not applicable.

Conflicts of Interest

The authors declare no conflicts of interest.

Authors' Contributions

Conceptualization was done by Q.Z. and A.W.; methodology was done by Q.Z., H.Y., and A.W; software was done by Q.Z. H.Y. and J.C.; writing—original draft preparation was done by Q.Z., J.C., and A.W.; writing—review and editing was done by Q.Z. and A.W.

Acknowledgments

This research was funded by the National Natural Science Foundation of China (Grant no. 51678001); the Natural Science Foundation of Anhui Province (Grant no. 2008085QE241); Anhui Provincial University Natural Science Research Key Project (KJ2019A0752); Anhui Provincial Quality Engineering Project (2020yjsyljc035).

References

[1] H. Brecht, U. Deichmann, and G. H. A. Wang, *Global Urban Risk Index. Policy Research Working Paper*, The World Bank Publication, Washington D C, USA, 2013.

[2] S. Tesfamariam and M. Saatcioglu, "Seismic vulnerability assessment of reinforced concrete buildings using hierarchical fuzzy rule base modeling," *Earthquake Spectra*, vol. 26, no. 1, pp. 235–256, 2010.

[3] M. Ouyang, L. Dueñas-Osorio, and X. Min, "A three-stage resilience analysis framework for urban infrastructure systems," *Structural Safety*, vol. 36-37, pp. 23–31, 2012.

[4] V. Lambert, N. Lapusta, and S. Perry, "Propagation of large earthquakes as self-healing pulses or mild cracks," *Nature*, vol. 591, no. 7849, pp. 252–258, 2021.

[5] Y. Wang, Q. Lin, and P. Shi, "Spatial pattern and influencing factors of landslide casualty events," *Journal of Geographical Sciences*, vol. 28, no. 3, pp. 259–274, 2018.

[6] J. Yang, C. Cheng, C. Song, S. Shen, T. Zhang, and L. Ning, "Spatial-temporal distribution characteristics of global seismic clusters and associated spatial factors," *Chinese Geographical Science*, vol. 29, no. 4, pp. 614–625, 2019.

[7] S. Zhou, G. Zhai, Y. Shi, and Y. Lu, "Urban seismic risk assessment by integrating direct economic loss and loss of statistical life: an empirical study in Xiamen, China," *International Journal of Environmental Research and Public Health*, vol. 17, no. 21, p. 8154, 2020.

[8] Y. Liu, W. Zhang, Z. Zhang, Q. Xu, and W. Li, "Risk factor detection and landslide susceptibility mapping using geo-detector and random forest models: the 2018 hokkaido eastern i earthquake," *Remote Sensing*, vol. 13, no. 6, p. 1157, 2021.

[9] J. Gomberg, P. A. Reasenberg, P. Bodin, and R. A. Harris, "Earthquake triggering by seismic waves following the Landers and Hector Mine earthquakes," *Nature*, vol. 411, no. 6836, pp. 462–466, 2001.

[10] M. T. Page, N. Van der Elst, T. H. Jordan, A. J. Michael, B. E. Shaw, and M. J. Werner, "A spatiotemporal clustering model for the third uniform California earthquake rupture forecast (UCERF3-ETAS): toward an operational earthquake forecast," *Bulletin of the Seismological Society of America*, vol. 107, no. 3, pp. 1049–1081, 2017.

[11] E. H. Field, T. E. Dawson, K. R. Felzer, and A. D. Frankel, "Uniform California earthquake rupture forecast, version 2 (UCERF 2)," *Bulletin of the Seismological Society of America*, vol. 99, no. 4, 2009.

[12] P. Wang, Z. Shao, Q. Liu, W. X. Wei, and X. F. Yin, "Probabilistic forecasting of earthquakes based on multidisciplinary physical observations and its application in Sichuan and Yunnan," *Chinese Journal of Geophysics*, vol. 62, no. 9, pp. 3448–3463, 2019.

[13] S. A. Khan, K. Pilakoutas, I. Hajirasouliha, and R. Garcia, "Seismic risk assessment for developing countries: Pakistan as a case study," *Earthquake Engineering and Engineering Vibration*, vol. 17, 2018.

[14] J. R. Murray, J. O. Langbein, S. E. Owen, T. H. Heaton, R. A. Iannucci, and D. L. Hauser, "Crowdsourced earthquake early warning," *Science Advances*, vol. 1, no. 3, Article ID e1500036, 2015.

[15] A. S. N Alarifi, N. S. N. Alarifi, and S. Al-Humidan, "Earthquakes magnitude predication using artificial neural network in northern Red Sea area," *Journal of University-Science*, vol. 24, no. 4, pp. 301–313, 2012.

[16] T. Rashed and J. Weeks, "Assessing vulnerability to earthquake hazards through spatial multicriteria analysis of urban areas," *International Journal of Geographical Information Science*, vol. 17, no. 6, pp. 547–576, 2003.

[17] J. Han, A. Nur, M. Syifa, M. Ha, and C. Lee, "Improvement of earthquake risk awareness and seismic literacy of Korean citizens through earthquake vulnerability map from the 2017 pohang earthquake, South Korea," *Remote Sensing*, vol. 13, no. 7, p. 1365, 2021.

[18] G. Noriega and L. Ludwig, "Social vulnerability assessment for mitigation of local earthquake risk in Los Angeles County," *Natural Hazards*, vol. 64, no. 2, pp. 1341–1355, 2012.

[19] J. Joseph, "Measuring vulnerability to natural hazards: a macro framework," *Disasters*, vol. 37, no. 2, pp. 185–200, 2013.

[20] S. Khan, "Vulnerability assessments and their planning implications: a case study of the Hutt Valley, New Zealand," *Natural Hazards*, vol. 64, no. 2, pp. 1587–1607, 2012.

[21] A. Mosen, N. Ibrahim, H. Mazlan, and P. Biswajeet, "A hybrid analytic network process and artificial neural network (ANP-ANN) model for urban earthquake vulnerability assessment," *Remote Sensing*, vol. 10, no. 6, p. 975, 2018.

[22] U. N. E. P. Global, *Outlook 3: Past, Present and Future Perspectives*, Earthscan Publications Ltd., London, UK, 2002.

[23] UNISDR, *Terminology on Disaster Risk Reduction*, UN Publications, Geneva, Switzerland, 2009.

[24] G. D. Bathrellos, H. D. Skilodimou, K. Chousianitis, A. M. Youssef, and B. Pradhan, "Suitability estimation for urban development using multi-hazard assessment map," *Science of The Total Environment*, vol. 575, pp. 119–134, 2017.

[25] Z. Zhong and J. Yu, "Prediction of earthquake damages and reliability analysis using fuzzy sets," in *Proceedings of the International Symposium on Uncertainty Modeling & Analysis. IEEE*, College Park, MD, USA, December 1990.

[26] R. Davidson and H. C. Shah, "A multidisciplinary urban earthquake disaster risk index EERI annual student paper award a multidisciplinary urban earthquake disaster risk index," *Earthquake Spectra*, vol. 13, no. , 2, pp. 211–223, 1997.

[27] R. Jena, B. Pradhan, G. Beydoun et al., "Integrated model for earthquake risk assessment using neural network and analytic hierarchy process: Aceh province, Indonesia," *Geoscience Frontiers*, vol. 11, no. 2, pp. 613–634, 2020.

[28] R. Robat Mili, K. Amini Hosseini, and Y. O. Y. Izadkhah, "Developing a holistic model for earthquake risk assessment and disaster management interventions in urban fabrics," *International Journal of Disaster Risk Reduction*, vol. 27, pp. 355–365, 2018.

[29] S. Curceac, P. M. Atkinson, A. Milne, L. Wu, and P. Harris, "An evaluation of automated GPD threshold selection methods for hydrological extremes across different scales," *Journal of Hydrology*, vol. 585, 2020.

[30] B. Yatsalo, T. Sullivan, V. Didenko, and I. Linkov, "Environmental risk management for radiological accidents: integrating risk assessment and decision analysis for remediation at different spatial scales," *Integrated Environmental Assessment and Management*, vol. 7, no. 3, 2011.

[31] A. Wang, Q. Zhang, L. Lu, H. R. Yu, and C. W. Huang, "Urban fire risk assessment and planning response based on multi-source data," *Science Journal*, vol. 31, no. 3, pp. 148–155, 2021, in chinese.

[32] F. Nie, Y. Shi, Z. Zhang, and J. Wang, "The initial time of the Tan-Lu wrench fault: In the view of geochronological data of the basement rocks, northern Anhui Province," *Chinese Science Bulletin*, vol. 60, pp. 2315–2326, 2015.

[33] Y. Li, S. Wu, W. Han, and Y. Zhang, "A study on geophysical features of deep structures of the Hefei Basin and the southern Tan-Lu fault zone," *Chinese Journal of Geophysics*, vol. 49, no. 1, pp. 115–122, 2006.

[34] T. Uchide, "Focal mechanisms of small earthquakes beneath the Japanese islands based on first-motion polarities picked using deep learning," *Geophysical Journal International*, vol. 223, no. 3, pp. 1658–1671, 2020.

[35] D. E. Rumelhart, G. E. Hinton, and R. J. Williams, "Learning representations by back-propagating errors," *Nature*, vol. 323, no. 6088, pp. 533–536, 1986.

[36] J. H Holland, *Adaptation in Natural and Artificial Systems: An Introductory Analysis with Applications to Biology, Control, and Artificial Intelligence*, University of Michigan Press, Ann Arbor, MI, USA, 1975.

[37] J. Kennedy and R. Eberhart, "Particle swarm optimization," *International Proceedings of the IEEE International Conference on Neural Networks*, vol. 4, no. 2, pp. 1942–1948, 1995.

[38] A. Huo, H. Zhang, L. Zhang, and M. Hou, "A sampled method of classification of susceptibility evaluation unit for geological hazards based on GIS," *Applied Mathematics & Information Sciences*, vol. 6, pp. 19–23, 2012.

[39] E. Zebardast, "Constructing a social vulnerability index to earthquake hazards using a hybrid factor analysis and analytic network process (F'ANP) modelConstructing a social vulnerability index to earthquake hazards using a hybrid factor analysis and analytic network process (F'ANP) model," *Natural Hazards*, vol. 65, no. 3, pp. 1331–1359, 2013.

[40] L. Chen, W. Wang, and W. Zhang, "Risk evaluation of regional collapses geological hazard based on DS evidence theory–a case study of Haiyuan active fault belt in Ningxia Province," *Energy Procedia*, vol. 16, pp. 371–376, 2012.

[41] M. W. Van, E. H. Shortliffe, and B. Buchanan, *EMY-IN: A Knowledge Engineer's Tool for Constructing Rule-Based Expert Systems*, pp. 249–263, Pergamon- lnfotech State of the Art Report on Machine Intelligence, Maidenhead, UK, 1981.

[42] M. Panahi, F. Rezaiee, and S. A. Meshkani, "Seismic vulnerability assessment of school buildings in Tehran city based on AHP and GIS," *Natural Hazards and Earth System Sciences*, vol. 1, no. 5, pp. 4511–4538, 2014.

[43] D. K. Loh and Y. T. C. Hsieh, *AI Applications: Natural Resources, Agriculture and* no. 1, , pp. 29–40.

[44] D. K. Loh, D. R. Holtfrerich, and S. E. P. Van Stipdonk, "Automated construction of rulebases for forest resource planning," *Computers and Electronics in Agriculture*, vol. 21, no. 2, pp. 117–133, 1998.

[45] D. F. D'Ayala, A. Carriero, F. Sabbadini et al., "Seismic vulnerability and risk assessment of cultural heritage buildings in istanbul, Turkey," in *Proceedings of the 14th WCEE*, vol. 3, Beijing, China, January 2008.

[46] W. Yang, X. Zhang, and P. Luo, "Transferability of convolutional neural network models for identifying damaged buildings due to earthquake," *Remote Sensing*, vol. 13, no. 3, p. 504, 2021.

[47] P. Guerrero-Miranda and A. G. González, "Responsibility, Social responsibility, sustainability, and public policy: the lessons of debris management after the manabí earthquake in Ecuador," *International Journal of Environmental Research and Public Health*, vol. 18, no. 7, p. 3494, 2021.

[48] J. Yin, S. Xu, Y. Jing, Z. Yin, and B. Liao, "Evaluating the impact of fluvial flooding on emergency responses accessibility for a mega-city's public services: a case study of emergency medical service," *Journal of Geographical Sciences*, vol. 73, no. 9, pp. 1737–1747, 2018.

[49] L. Ceferino, J. Mitrani-Reiser, A. Kiremidjian, G. Deierlein, and C. Bambarén, "Effective plans for hospital system response to earthquake emergencies," *Nature Communications*, vol. 11, no. 1, p. 4325, 2020.

[50] Y. R. Jiang and J. Y. Ning, "Automatic decision of semic body-wave phases and dermination of their arrival times based on support vector machine," *Chinese Journal of Geophysics*, vol. 62, no. 1, pp. 361–373, 2019, in Chinese.

[51] F. Liu, Y. Jiang, J. Ning, J. Zhang, and Y. Zhao, "An array-assisted deep learning approach to seismic phase-picking," *Chinese Science Bulletin*, vol. 65, no. 11, pp. 1016–1026, 2020.

[52] A. J. C. Witsil and J. B. Johnson, "Analyzing continuous infrasound from Stromboli volcano, Italy using unsupervised machine learning," *Computers & Geosciences*, vol. 140, Article ID 104494, 2020.

[53] S. M. Mousavi, W. Zhu, Y. Sheng, and G. C. Beroza, "CRED: a deep residual network of convolutional and recurrent units for earthquake signal detection," *Scientific Reports*, vol. 9, no. 1, 2019.

[54] P. Mell and T. Grance, *The NIST Definition of Cloud Computing*, National Institute of Standards and Technology, Gaithersburg, MD, USA, 2011.

[55] W. M. P. Klein, A. K. Boutté, H. Brake et al., "Leveraging risk communication science across US federal agencies," *Nature Human Behaviour*, vol. 5, no. 4, pp. 411–413, 2021.

[56] D. Lee, "The expertise of public officials and collaborative disaster management," *International Journal of Disaster Risk Reduction*, vol. 50, no. 6, Article ID 101711, 2020.

Hindawi
Scientific Programming
Volume 2023, Article ID 9804737, 1 page
https://doi.org/10.1155/2023/9804737

Retraction

Retracted: Research on the Optimization Strategy of Innovation Behavior and Entrepreneurship Intention in Entrepreneurship Teaching

Scientific Programming

Received 8 August 2023; Accepted 8 August 2023; Published 9 August 2023

This article has been retracted by Hindawi following an investigation undertaken by the publisher [1]. This investigation has uncovered evidence of one or more of the following indicators of systematic manipulation of the publication process:

(1) Discrepancies in scope
(2) Discrepancies in the description of the research reported
(3) Discrepancies between the availability of data and the research described
(4) Inappropriate citations
(5) Incoherent, meaningless and/or irrelevant content included in the article
(6) Peer-review manipulation

The presence of these indicators undermines our confidence in the integrity of the article's content and we cannot, therefore, vouch for its reliability. Please note that this notice is intended solely to alert readers that the content of this article is unreliable. We have not investigated whether authors were aware of or involved in the systematic manipulation of the publication process.

Wiley and Hindawi regrets that the usual quality checks did not identify these issues before publication and have since put additional measures in place to safeguard research integrity.

We wish to credit our own Research Integrity and Research Publishing teams and anonymous and named external researchers and research integrity experts for contributing to this investigation.

The corresponding author, as the representative of all authors, has been given the opportunity to register their agreement or disagreement to this retraction. We have kept a record of any response received.

References

[1] J. Huang, J. Wu, B. Deng, and S. Bao, "Research on the Optimization Strategy of Innovation Behavior and Entrepreneurship Intention in Entrepreneurship Teaching," *Scientific Programming*, vol. 2021, Article ID 4872108, 6 pages, 2021.

Hindawi
Scientific Programming
Volume 2021, Article ID 4872108, 6 pages
https://doi.org/10.1155/2021/4872108

Research Article

Research on the Optimization Strategy of Innovation Behavior and Entrepreneurship Intention in Entrepreneurship Teaching

Jieqi Huang,[1] **Jun Wu**,[1] **Baijun Deng**,[1] **and Shuqin Bao**[2]

[1]*School of Innovation and Entrepreneurship, Guangzhou Panyu Polytechnic, Guangzhou, China*
[2]*Guangdong University of Technology, Guangdong, China*

Correspondence should be addressed to Shuqin Bao; 15205511072@163.com

Received 14 October 2021; Revised 4 November 2021; Accepted 20 November 2021; Published 3 December 2021

Academic Editor: Punit Gupta

Entrepreneurial intention is a necessary prerequisite for prospective entrepreneurs to start a new business, and today's college students are the potential entrepreneurs of the future. How to improve students' willingness to start a business is an important topic that a large number of scholars continue to pay attention to. The purpose of this work is to disentangle how college students' previous innovative behavior affects their entrepreneurial intention from the view of social psychology. Survey data from a vocational college in China indicate that college students' previous innovative behavior facilitates flow, which in turn affects their entrepreneurial intention. Our empirical findings flourish the research on antecedents of college students' entrepreneurial intention, make contributions to the research on flow in entrepreneurship, and provide useful recommendations and suggestions in entrepreneurship teaching.

1. Introduction

One of the most significant factors of economic growth is the creation of new enterprises [1]. A considerable consensus exists about the significance of accelerating entrepreneurship to technological innovation and employment generation [2, 3]. It is not surprising that entrepreneurship has received more attention in emerging economies. To be specific, in China, with the advent of the new era of "mass entrepreneurship, mass innovation," entrepreneurship among college students is actively encouraged and supported by the state and local governments at all levels because today's students are tomorrow's aspiring entrepreneurs. According to the 2019 College Student Entrepreneurship Report survey, more than 75% of the surveyed college students have entrepreneurial intention, and more than 25% of them have a strong entrepreneurial intention.

How to improve students' commitment to start a business is an important topic that a large number of scholars continue to pay attention to. There has been a lot of research done on entrepreneurial intention. Existing studies on the antecedents of college students' entrepreneurial intention focus on individual traits, demographic characteristics, and environmental factors [4–6]. According to our observation in practical teaching over the past few years, students' entrepreneurial intention could be influenced by their previous innovation behavior to some extent. However, there is little research being done on it. Besides, previous studies mostly used cross-sectional data to verify the relationship between antecedents and entrepreneurial intention, while longitudinal studies are still lacking.

To address the limitations mentioned above, the present research adopts longitudinal research to investigate the relationship between college students' previous innovative behavior and entrepreneurial intention and introduces the flow as a mediator from the social psychology perspective to disclose the "black box" of how students' innovative behavior affects their entrepreneurial intention (see Figure 1). Combined, we offer two main and novel contributions to the existing literature. First, we enrich the research on the antecedents of college students'

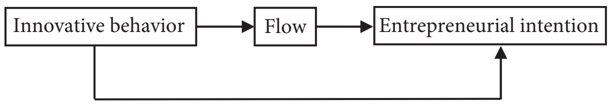

Figure 1: Research framework.

entrepreneurial intention. Second, we expand our knowledge of the role that flow shaping plays in affecting entrepreneurial intention.

2. Experimental Details

2.1. Literature Review

2.1.1. Entrepreneurial Intention. Entrepreneurial intention is "a self-acknowledged conviction by a person that they intend to set up a new business venture and consciously plan to do so at some point in the future." [7]. This has been viewed as the first step of entrepreneurship since new venture creation stems from this variable [8]. It is also the most appropriate predictor of entrepreneurial behavior [9, 10]. Existing studies on the antecedents of college students' entrepreneurial intention pay more attention to individual traits, demographic characteristics, and environmental factors. Rasli et al. [11] demonstrate that gender, work experience, conviction, education environment, and general attitude are positively related to college students' entrepreneurial intention. Furthermore, Gelard and Saleh [12] reported that structural, educational support, and formal and informal networks affect university students' entrepreneurial intentions. However, there is little research on the relationship between college students' previous innovative behavior and their entrepreneurial intention.

2.1.2. Innovative Behavior. According to Scott and Bruce, innovative behavior is a process of value creation supported by the generation of new thoughts, solutions, and applications [13]. Konermann also defined innovative behavior as a process that incorporates the following components: generation, development, application, execution, and modification of novel ideas to improve the performance of an organization [14]. In other words, innovation behavior is a complex process that includes the generation, promotion, and practice of thoughts.

Based on social cognitive theory, college students' previous innovative behavior helps to improve their analytical ability and identification ability. That is, innovative behavior would have a positive impact on opportunity identification. Low and MacMillan [15] concluded that the ability to identify opportunities is one of the main psychological characteristics that influence entrepreneurial intention. It can be seen that college students' innovative behavior has a critical influence on their entrepreneurial intentions with the improvement of their own ability in recognizing opportunity. Hence, we propose the first hypothesis:

Hypothesis 1: innovative behavior is positively related to entrepreneurial intention

2.1.3. Flow. Csikszentmihalyi, an American psychologist, found that when an individual is engaged in his favorite work, he is completely immersed in it, even forgetting to eat and sleep. This unique psychological experience produced by an individual is defined as flow [16]. On this basis, Bakker [17] developed the concept of work-related flow, referring to an individual's flow experience while working, which mainly includes three elements: absorption, work enjoyment, and intrinsic work motivation. The flow has been studied in a variety of fields, but entrepreneurship has received less attention.

Flow, as a positive emotion, can motivate individuals to pursue more challenging goals to constantly improve their abilities and ultimately achieve substantial personal growth. Different from traditional extrinsic motivation, flow is an internal self-motivation mechanism that enables individuals to immerse themselves in tasks over and over again and maximize their talents and abilities. A number of studies have shown that intrinsic motivation contributes to more creativity, greater cognitive resilience, and improved well-being as compared to extrinsic motivation [18]. The complexity and challenge of innovation bring them a unique mental experience, known as flow. A continuous flow state resulted from innovation behavior makes individuals want to be more innovative in many regards, which consolidates an individual's positive attitude towards entrepreneurship and thus improves the level of entrepreneurial intention. That is, an individual has entrepreneurial enthusiasm and vitality [19]. Therefore, we believe that the key mediator in accounting for the relationship between college students' innovative behavior and their entrepreneurial intention is flow. Hence, we put forward the second hypothesis:

Hypothesis 2: the positive relationship between innovative behavior and entrepreneurial intention is mediated by flow

2.2. Sample and Data Collection. To test the proposed hypotheses, we carried out a questionnaire survey of 226 students at a vocational university in China. We designed the questionnaire based on the previous measurements which have been proved to have high reliability and validity [9, 13, 17]. In order to ensure the representativeness of the sample, we selected research teams with different academic backgrounds. The questionnaire was filled out separately by the respondents in three rounds (before, during, and after class) to avoid the influence of common method variance. Firstly, each interviewee filled in and described his or her previous innovation experience and entrepreneurial intentions. Secondly, teachers were asked to evaluate the entrepreneurial intention and flow state of team members one by one, and then, the relevant researchers collected the information directly on the spot. Thirdly, according to the questionnaires filled by the research members, we asked the corresponding team members to evaluate their entrepreneurial intention and mental state, i.e., flow, and these finished questionnaires were also collected by the researchers. Finally, these paired questionnaires were sorted out and counted. We established dynamic panel data. Table 1 shows the characteristics of research sample.

Table 1: Characteristics of research sample ($N = 226$).

		Frequency	Percentage
Gender	Male	104	46.0
	Female	122	54.0
Class	Architectural engineering	36	15.9
	Finance	28	12.4
	Municipal administration	80	35.4
	Investment	82	36.3
Weeks	1 week	75	33.2
	6 weeks	68	30.1
	12 weeks	83	36.7

2.3. Measurements. We used back-translation to render them in Chinese because the items were originally written in English and applied a 5-point Likert scale for the measures (1 = strongly disagree; 5 = strongly agree). We adopted the entrepreneurial intention scale developed by Krueger et al. [9] (alpha = 0.901, CR = 0.903, and AVE = 0.699). For innovation behavior, we followed the six items measurement from Scott and Bruce [13] (alpha = 0.943, CR = 0.944, and AVE = 0.736). We assessed flow from three dimensions including absorption (alpha = 0.884, CR = 0.891, and AVE = 0.673), work enjoyment (alpha = 0.961, CR = 0.962, and AVE = 0.964), and intrinsic work motivation (alpha = 0.914, CR = 0.916, and AVE = 0.687) with a scale developed by Bakker [17].

We controlled for gender, class, and weeks because of their potential effects on entrepreneurial intention. Table 2 shows the constructs and measurements in this study.

3. Results

3.1. Reliability and Validity. We used SPSS 26.0 and Mplus 7 to check construct reliability and validity. All of the constructs' Cronbach's α surpassed the recommended minimum of 0.70, suggesting adequate reliability [20–22]. As shown in Table 2, our scale also has good construct reliability and sufficient convergent validity because the composite reliability and average variance extracted were, respectively, greater than 0.60 and 0.50 [23]. Meanwhile, all factor loadings were greater than 0.70 [24]. Each construct's "square root" of AVE was higher than the correlations among the constructs, indicating that the three constructs had strong discriminant validity [24]. Table 3 shows the descriptive statistics and correlations of all key variables.

3.2. Hypothesis Testing. To verify our hypotheses, we used hierarchical regression analysis. Before the regression analysis, we made several relevant checks. When VIFs exceed 10.0 or even 5.0, the model may have a multicollinearity problem [25]. So we calculated the average VIF, and it was 1.12. Besides, the maximum of VIFs was lower than 2.0, indicating that multicollinearity was not evident in our research. We looked for violations of normality assumptions and outliers as well, and no distinct violation was found, so the data could be used for regression analysis. Table 4 presents our regression results.

H1 proposed that college students' innovative behavior is positively related to entrepreneurial intention. As shown in Model 4, the coefficient is positively significant ($\beta = 0.786$, $p < 0.01$). Thus, H1 is strongly supported. To test the flow as a mediator between innovative behavior and entrepreneurial intention, we conducted Baron and Kenny's [26] three-stage multiple regression analysis. In the first stage (model 5), innovative behavior is positively related to entrepreneurial intention ($\beta = 0.786$, $p < 0.01$), while in the second stage (model 2 and model 6), innovative behavior is positively related to flow ($\beta = 0.772$, $p < 0.01$) and flow is positively related to entrepreneurial intention ($\beta = 0.736$, $p < 0.01$). In the last stage (model 7), innovative behavior is significantly related to entrepreneurial intention ($\beta = 0.641$, $p < 0.01$). Our results suggest that flow plays a partial mediator between innovative behavior and entrepreneurial intention. Therefore, H2 is supported.

4. Discussion

This study examined the relationship between college students' innovative behavior and entrepreneurial intention. Most studies on the antecedents of college students' entrepreneurial intention focus on individual traits, demographic characteristics, and environmental factors [4–6]. According to our observation in practical teaching over the past few years, students' entrepreneurial intentions could be influenced by their previous innovation behavior. However, there is little research on it.

We propose that college students' innovative behavior is positively related to their entrepreneurial intention. In detail, this study adopted longitudinal research and tested the mediating mechanism of flow from the view of social psychology. The empirical findings from 226 college students support our hypotheses, which suggest that innovative behavior does not directly lead to entrepreneurial intention. Instead, flow acts as a partial mediator that transforms students' previous innovative behavior into entrepreneurial intention. In the state of flow, an individual's actions are integrated with their consciousness. That is, they are in a state of positive psychological and emotional experience. Based on intrinsic motivation theory, this state can continuously consolidate the individual's positive attitude towards entrepreneurship so as to keep improving their entrepreneurial intention.

The findings make a contribution to literature in two aspects. First, this study examined the relationship between college students' prior innovative behavior and their entrepreneurial intention. It enriches the existing research on

Table 2: Constructs' measurements, reliability, and validity.

Constructs and measurements	Cronbach's α	Loading	AVE	CR
Flow			0.822	0.932
Absorption	0.884	0.781	0.673	0.891
When I take entrepreneurship classes, I think about nothing else		0.771		
I get carried away by my entrepreneurship classes		0.716		
When I take entrepreneurship classes, I forget everything else around me		0.837		
I am totally immersed in my entrepreneurship classes		0.941		
Work enjoyment	0.961	0.942	0.864	0.962
My entrepreneurship classes give me a good feeling		0.874		
I take my entrepreneurship classes with a lot of enjoyment		0.941		
I feel happy during my entrepreneurship classes		0.961		
I feel cheerful when I am taking entrepreneurship classes		0.939		
Intrinsic work motivation	0.914	0.984	0.687	0.916
I would still take entrepreneurship classes, even if I received less pay		0.907		
I find that I also want to consider entrepreneurship classes in my free time		0.727		
I take entrepreneurship classes because I enjoy them		0.893		
When I am taking entrepreneurship class, I am doing it for myself		0.760		
I get my motivation from the entrepreneurship class itself and not from the reward for it		0.843		
Innovation behavior	0.943		0.736	0.944
I always search out new technologies, processes, techniques, and/or product ideas		0.826		
I always generate creative ideas		0.874		
I always promote and champion ideas to others		0.898		
I always investigate and secure funds needed to implement new ideas		0.863		
I always develop adequate plans and schedules for the implementation of new ideas		0.839		
Generally, I am a person with innovative spirit		0.846		
Entrepreneurial intention	0.901		0.699	0.903
I think I will start my own business in the future		0.892		
I once considered running my own company		0.822		
If I have the opportunity and I have the freedom to make a decision, I will choose to start my own business		0.852		
Considering my current real situation and various limitations (such as lack of funds), I will still choose to start my own business		0.775		

Note: AVE refers to average variance extracted; CR refers to composite reliability.

Table 3: Means, standard deviations, and correlations ($N = 226$).

Variables	Means	SD	1	2	3
1. Innovative behavior	3.645	0.855	0.858		
2. Flow	3.786	0.816	0.813**	0.907	
3. Entrepreneurial intention	3.434	0.963	0.629**	0.703**	0.836

Note: $^{*}p < 0.05$; $^{**}p < 0.01$; $n = 226$.

Table 4: Regression results.

Variables	Flow		Entrepreneurial intention			
	M1	M2	M4	M5	M6	M7
Control variables						
Gender	0.177	0.097	0.276**	0.195**	0.146	0.177
Class	0.039	0.018	0.064	0.042	0.035	0.039
Weeks	−0.017	−0.009	−0.008	0.000	0.004	0.001
Independent variable						
Innovative behavior		0.772***		0.786***		0.641***
Mediator						
Flow					0.736***	0.187*
ΔR^2	0.014	0.006	0.014	0.009	0.011	0.011
R^2	0.016	0.665	0.022	0.505	0.404	0.514
F	1.186	109.696	1.631	56.447	37.485	46.501

Note: $N = 249$; $^{***}p < 0.01$, $^{**}p < 0.05$, and $^{*}p < 0.1$.

the antecedents of college students' entrepreneurial intention. Second, introducing the flow as a mediator variable not only helps further analysis of the "black box" of innovation behavior affecting entrepreneurial intention, but also serves as a supplement and breakthrough to the existing research on flow.

5. Conclusion

In conclusion, the main purpose of this research is to figure out the relationship between college students' prior innovative experience and their entrepreneurial intention from the view of social psychology. The study results show that students' innovative behavior is positively related to entrepreneurial intention and that flow mediates the positive relationship between innovative behavior and entrepreneurial intention.

This study has two potential practical implications. First, universities could set more relevant innovative and entrepreneurial courses, and companies could offer more internship opportunities to college students to inspire and promote their innovative behavior, which facilitates increasing their entrepreneurial intention. Second, our findings provide useful guidance to recognize students who are potential entrepreneurs.

However, there are two research limitations that point to prospective research directions to some extent. First, the diversity of this research sample needs to be improved. There are some differences between the characteristics of universities and enterprises [27]. This study especially chose vocational college students as our research sample to solve this problem to some extent. How to further promote the quality education of higher vocational college students? Let the students have the ability to adapt the modern production structure and the fast pace of enterprise competition, which is an important topic that a large number of colleges, experts, and scholars are exploring continuously. Thus, vocational college has a close connection with enterprises in many regards [28]. After all, the complexity of the real context in enterprises cannot be reflected by students in vocational colleges. Future research should continue to collect enterprise samples to verify the effectiveness of this model and increase the diversity of samples to increase the external validity of research conclusions.

Second, our empirical findings suggest that there is a partial mediating impact between students' innovative behavior and entrepreneurial intention. However, innovative behavior may have different influences on entrepreneurial intention for different individual traits, which indicates that there may be other possible mechanisms at work. Future studies could investigate other mediating mechanisms from different perspectives to further explain the relationship between students' innovative behavior and their entrepreneurial intention.

Data Availability

The datasets used and/or analyzed during the current study are available from the corresponding author on reasonable request.

Conflicts of Interest

The authors declare no potential conflicts of interest with respect to the research, authorship, and/or publication of this article.

Acknowledgments

This work was supported by Innovation and Entrepreneurship Education Research Project of Guangzhou Education Bureau (2019PT102).

References

[1] J. Schumpeter and U. Backhaus, *The Theory of Economic Development*, pp. 61–116, Joseph Alois Schumpeter. Springer, Boston, MA, USA, 2003.

[2] P. D. Reynolds, "New firms: societal contribution versus survival potential," *Journal of Business Venturing*, vol. 2, no. 3, pp. 231–246, 1987.

[3] S. A. Zahra, "The changing rules of global competitiveness in the 21st century," *Academy of Management Perspectives*, vol. 13, no. 1, pp. 36–42, 1999.

[4] D. Turker and S. S. Selcuk, "Which factors affect entrepreneurial intention of university students," *Journal of European Industrial Training*, vol. 32, 2009.

[5] S. Kristiansen and N. Indarti, "Entrepreneurial intention among Indonesian and Norwegian students," *Journal of Enterprising Culture*, vol. 12, no. 1, pp. 55–78, 2004.

[6] X. F. Tong, D. Y. K. Tong, and L. C. Loy, "Factors influencing entrepreneurial intention among university students," *International Journal of Social Sciences and Humanity Studies*, vol. 3, no. 1, pp. 487–496, 2011.

[7] E. R. Thompson, "Individual entrepreneurial intent: construct clarification and development of an internationally reliable metric," *Entrepreneurship: Theory and Practice*, vol. 33, no. 3, pp. 669–694, 2009.

[8] S. H. Lee and P. K. Wong, "An exploratory study of technopreneurial intentions: a career anchor perspective," *Journal of Business Venturing*, vol. 19, no. 1, pp. 7–28, 2004.

[9] N. F. Krueger, M. D. Reilly, and A. L. Carsrud, "Competing models of entrepreneurial intentions," *Journal of Business Venturing*, vol. 15, no. 5-6, pp. 411–432, 2000.

[10] I. Ajzen, "The theory of planned behavior," *Organizational Behavior and Human Decision Processes*, vol. 50, no. 2, pp. 179–211, 1991.

[11] A. Rasli, S. U. R. Khan, S. Malekifar, and S. Jabeen, "Factors affecting entrepreneurial intention among graduate students of Universiti Teknologi Malaysia," *International Journal of Business and Social Science*, vol. 4, no. 2, 2013.

[12] P. Gelard and K. E. Saleh, "Impact of some contextual factors on entrepreneurial intention of university students," *African Journal of Business Management*, vol. 5, no. 26, pp. 10707–10717, 2011.

[13] S. G. Scott and R. A. Bruce, "Determinants of innovative behavior: a path model of individual innovation in the workplace," *Academy of Management Journal*, vol. 37, no. 3, pp. 580–607, 1994.

[14] J. Konermann, "Teachers' work engagement: a deeper understanding of the role of job and personal resources in relationship to work engagement, its antecedents, and its outcomes," Ph D thesis, University of Twente, Enschede, Netherlands, 2012.

Hindawi
Scientific Programming
Volume 2021, Article ID 5421668, 7 pages
https://doi.org/10.1155/2021/5421668

Research Article

Optimization Research of Artificial Intelligence and Wireless Sensor Networks in Smart Pension

Liqing Li, Linli Jiang, and Zixuan Liu

College of Public Management&Law, Hunan Agricultural University, Changsha, China

Correspondence should be addressed to Linli Jiang; linlij1997@163.com

Received 15 October 2021; Accepted 19 November 2021; Published 30 November 2021

Academic Editor: Punit Gupta

As a new generation of information technology, artificial intelligence and wireless sensor network are of great significance in promoting the development of "smart pension" and improving the quality of life of the elderly. This paper expounds the application of existing relevant artificial intelligence and wireless sensor network in smart pension, including the daily life of the elderly, health care, and spiritual comfort. This study further puts forward corresponding improvement measures for the existing problems in order to provide ideas for the application of wireless sensor network in smart pension and improve the quality of life of the elderly.

1. Introduction

Internationally, the population aged 65 and over accounting for 7% of the total population is generally regarded as the country's entry into an aging society, and China's population structure has moved towards an aging society since the 1990s [1]. Since the 21st century, the problem of population aging in China has become more and more serious. Figure 1 shows the trend of the number and proportion of the elderly population in China from 2013 to 2019. According to the survey data of the National Bureau of Statistics in 2020, the population aged 60 and over in China reached 240.9 million, accounting for 17.3% of the total population in China; China's population aged 65 and over is 158.31 million, accounting for 11.4% of China's total population [2]. According to the prediction of China's population development report, in 2050, China's elderly population aged 60 and over will reach 35% of the total population, while the empty-nest elderly population will account for more than 54% of the total elderly population [3]. These figures show that the degree of population aging in China is becoming more and more intense, and the trend is very serious.

Under the background of China's aging society, traditional pension is difficult to meet the severe situation. Smart pension has become an important measure to alleviate China's population aging. Artificial intelligence and wireless sensor network are of great significance in promoting the development speed of "smart pension" and improving the quality of life of the elderly. This paper expounds the application of existing relevant artificial intelligence and wireless sensor network in smart pension, uses artificial intelligence and wireless sensor network to obtain the needs of the elderly at different levels (mainly including the daily life, health care, and spiritual comfort of the elderly), and gives corresponding feedback in time through information processing. It is superior to the traditional pension mode in efficiency and accuracy. This study further puts forward corresponding improvement measures for the existing problems in order to optimize the application of artificial intelligence and wireless sensor network in smart pension, further optimize resource allocation, reduce resource waste, and improve the quality of life of the elderly.

2. Traditional Pension and Smart Pension

2.1. Traditional Pension Conceptualization. Maslow's hierarchy of needs theory was proposed by Maslow in 1943, including the five-level model of human needs. From low level to high level, human beings can be divided according to five needs: physiological needs, security needs, social needs,

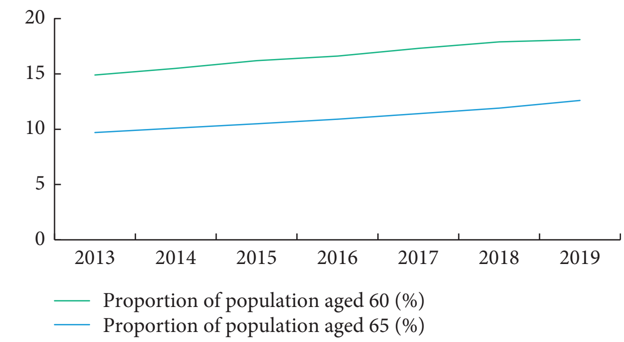

Figure 1: Trend of proportion of elderly population in China from 2013 to 2019 (http://www.stats.gov.cn/).

respect needs, and self-realization needs. Physiological needs and safety needs are the primary-level needs of human beings and the most basic needs of human beings for the safety of themselves and the surrounding environment. Social needs, respect needs, and self-realization needs are human's high-level needs, including human's high-level spiritual needs such as social emotion, social self-esteem, and self-realization. After the primary level needs are met, the high-level needs will become the main needs of individuals.

China's traditional way of providing for the aged has improved the material living conditions of the elderly, which also ensures the primary-level needs of the elderly population. However, the government and society often ignore the senior-level needs of the elderly population at a certain level. For example, due to children's work, family contradictions, age generation gap, and other reasons, children are unable to take care of the elderly 24 hours. Most children give economic subsidies to the elderly at home to meet the needs of the primary level. In addition, a large number of disabled elderly in China can only meet the needs of primary level by means of institutional pension and need 24-hour care workers. According to Huang's survey data, there is an imbalance between supply and demand in China's home-based elderly care and social institutional elderly care, and there is still a gap in meeting the primary-level needs of the elderly population under the traditional elderly care [4].

There is a phenomenon of empty nests in some areas of China. Children tend to send their parents to social pension institutions for care, which leads to the shortage of social pension institutions. In some rural areas, the phenomenon of family empty nest is more serious, but because the elderly care services and elderly care knowledge are not fully popularized, the vast majority of rural elderly can only provide for the elderly at home, which leads to the oversupply of social elderly care institutions. In addition, the current social pension institutions also have problems such as poor service quality and poor structure, such as the inability to meet the daily needs of the elderly, the inability to respond in time to emergencies, the direct inability of society, children, and the elderly to form a channel for timely information sharing and feedback, and the problems of low quality and untimely information transmission in the traditional way of pension [5]. The aging situation of China's social population is very serious, which has brought great unprecedented challenges to China's economic and social security. The traditional way of providing for the aged has been difficult to deal with the problem of aging. It is urgent to develop new ways of providing for the aged.

2.2. Smart Pension Conceptualization. The Fifth Plenary Session of the 19th CPC Central Committee put forward the "implementation of the national strategy to actively respond to population aging," which is closely related to the establishment of the national sustainable development strategy and is related to the harmonious development of people's society. We should deeply understand and implement the directive. Smart pension is a new type of pension service by introducing emerging information technology into the traditional pension mode to connect living homes, communities, and even pension institutions [6]. Using emerging information technologies such as the wireless sensor network to improve the quality of life of the elderly is one of the important measures to alleviate the problem of population aging in China [7]. With the development of artificial intelligence and wireless sensor network technology, its application has also been integrated into the life of the elderly. By improving the quality of elderly care services and the supervision efficiency of elderly care services, it not only improves the quality of life of the elderly but also promotes the continuous development of related technologies. At this stage, the continuous accumulation and development of emerging information technology provides a driving force for various industries. The development speed of artificial intelligence and wireless sensor network technology is accelerating. The traditional pension mode is embedded in emerging information technology. Smart pension is the general trend of pension in the future [8].

3. Wireless Sensor Network (WSN) Conceptualization

Based on the development of wireless network, hardware, and sensing equipment, Bill Gates first put forward the concept of wireless sensor network in 1995 [9]. In the subsequent development of the wireless sensor network, it underwent the naming of standardized definition bodies such as IFFF, ITU, 3GPP, and IETF. Ultimately, the wireless sensor network is defined as "a technology by which things or devices can provide users with richer value through their connection to the Internet". In short, the wireless sensor network realizes the information interconnection between things and between people and things through sensors, control chips, action mechanisms, wired or wireless networks, and relevant platform software. Specifically, the wireless sensor network is a network that connects any item with the Internet for information exchange and communication through information sensing equipment such as radio-frequency identification, infrared sensor, Global Positioning System, and laser scanner according to the agreed protocol, so as to realize intelligent identification, positioning, tracking, monitoring, and management. The architecture and key technologies of the wireless sensor network mainly include RFID technology, sensor technology, network communication technology, and cloud computing. The basic characteristics of the wireless sensor network can be summarized as comprehensive perception, reliable transmission, and intelligent processing. Through the wireless sensor network technology, objects become intelligent, which can realize the transmission of information with users and provide corresponding services [10] (see Figure 2 for details).

Many Chinese scholars divided China's pension model into family pension, institutional pension, and community pension. At the same time, most scholars believe that the traditional pension service has limitations. The supply methods of artificial intelligence and wireless sensor network in smart pension applications include home life, communities, elderly care institutions, and social organizations. The rapid development of wireless sensor network and other technologies will bring new ideas to traditional elderly care and elderly care services [11]. With the development and application of emerging information technology, artificial intelligence and wireless sensor network will generate a new industrial chain and bring a lot of market value. The informatization level of China's traditional elderly care service system is relatively backward as a whole, but the elderly care service system platform based on artificial intelligence and wireless sensor network technology uses wireless sensor network technology to collect data through terminal equipment and upload relevant information data to the cloud, so as to make the daily life of the elderly in a remote monitoring state. On the one hand, this technology can reduce the cost of elderly care; on the other hand, it can make intelligent elderly care more accurate [12].

4. AI and WSN in Smart Pension

4.1. In Daily Life. With the development and shaping of intelligent elderly care, artificial intelligence and wireless sensor network technologies have made the elderly, families, and society enjoy the greatest dividends [13]. China's wireless sensor network technology is used in the daily life of intelligent elderly care, mainly focusing on intelligent home, community service, positioning system, and other services, as shown in Figure 3.

Since the 21st century, in order to enable the elderly to enjoy intelligent services at home, the introduction, development, and application of smart home in China have been maturing. At present, it mainly includes intelligent electrical appliances, lighting control, and other intelligent electrical equipment. The audio and behavior of the elderly are collected through the intelligent terminal device, these data are uploaded to the cloud for analysis and processing by wired or wireless network, and then the feedback information is transmitted to the client. Smart home can also actively monitor and adjust the environmental indicators of the elderly, create an optimal environment for the elderly to live, and reduce the health risk of the elderly.

In the community, artificial intelligence and wireless sensor network technology are used to monitor the information data of the elderly in the community in real time through wearable terminal devices or residential installed terminal devices, upload the data to the network environment for analysis and processing, and provide community door-to-door service or remote service through the feedback information to solve the problems of the elderly in the daily life of the community [14]. For example, installing environmental monitoring devices at home and using wireless sensor network technology to transmit real-time monitoring information with the network environment can ensure the home safety of the elderly on the one hand and provide corresponding feedback through identification information on the other hand. When there is abnormal information such as water leakage, air leakage, and fire at home, the information is uploaded to the network processing system and fed back to the client in real time and the elderly are provided timely assistance through alarm and relevant personnel. At the same time, in case of abnormal data such as water fee, electricity fee, and network fee at home, the information can be fed back to the client for online payment and other convenient services.

The positioning system is mainly to timely and accurately capture the location and behavior information data of the elderly, which is of great help to the elderly group with memory decline and behavioral impairment. At present, the location of the elderly is located in real time through portable intelligent terminal equipment, and the collected location information is uploaded to the network environment. When the environment of the elderly is abnormal and lost, the abnormal data can be analyzed and processed and fed back to the client, and the location of the elderly can be found in time. When an elderly is suspected of falling down, his mobile phone or wearable device or monitoring device can quickly identify whether he has fallen and can automatically complete the call for an ambulance and notify his family.

4.2. Health Care. The empty nest of families and the imbalance between supply and demand of elderly care institutions put the health of the elderly at great risk. The integration of resources in families, medical institutions, and other aspects through artificial intelligence and wireless sensor network technology can reduce the probability of the elderly falling into health risk. China's artificial intelligence and wireless sensor network technologies are used for health care in intelligent elderly care, mainly for real-time self-monitoring of the body, disease, and living environment. Intelligent terminal devices are used to collect the body, living condition, disease, and other information data of the elderly in real time, then the data are uploaded to the network environment for analysis and processing, and finally the information data are fed back to the client [15] (see Figure 4 for details).

Through the terminal equipment, the health data of the elderly are monitored in real time and uploaded to the network environment for analysis and processing. When the health data of the elderly are abnormal, they are fed back to the client, enabling timely dialing 120, notifying children in the form of information, and providing community door-to-door rescue and other services. For example, a portable wrist

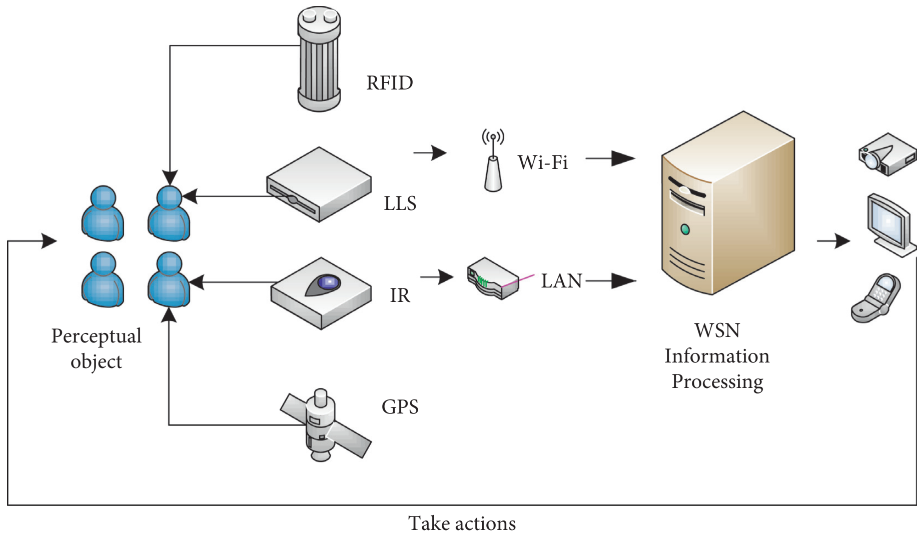

Figure 2: Basic framework of wireless sensor network system.

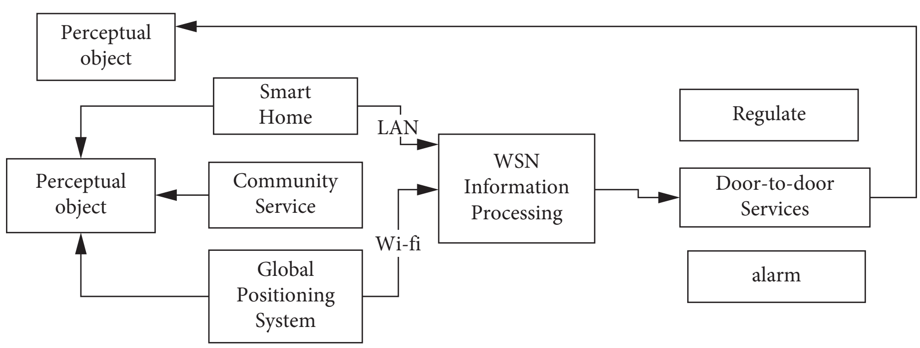

Figure 3: AI and WSN in daily life of the elderly.

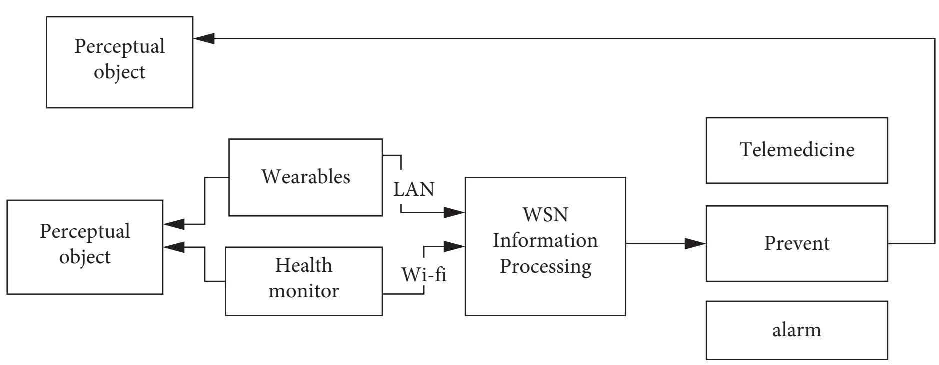

Figure 4: AI and WSN in health care of the elderly.

watch has built-in infrared pulse sensor, 3D gravity sensor, and GPS sensor. The collected data are transmitted to the network through wired or wireless network for data processing and analysis, and the feedback results are sent to the client.

In medical institutions, wireless sensors are installed in the living environment of the elderly, the video images and audio of the elderly are monitored in real time and uploaded to the network environment for processing and analysis, and a remote care system is established. Once the collected data are abnormal, they will be warned in time. Especially for the elderly suffering from heart disease, hypertension, and other diseases, they can get the remote escort of medical staff and timely treatment, so as to ensure the health status of the elderly and realize the accurate implementation of medical treatment [16].

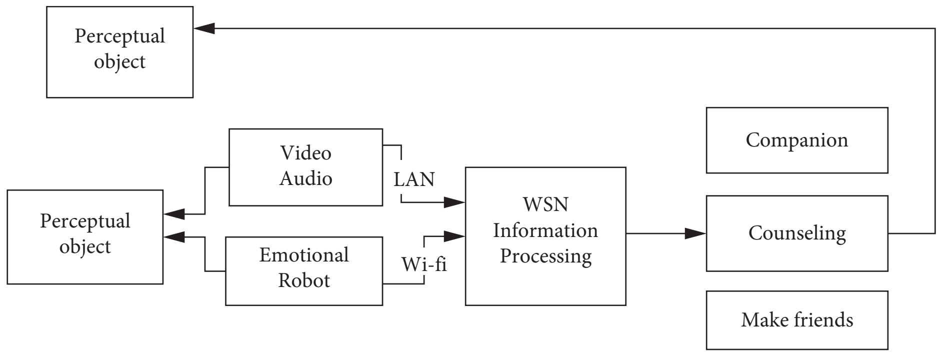

Figure 5: AI and WSN in spiritual comfort of the elderly.

4.3. Spiritual Comfort. Empty nests of families have appeared in some areas of China. Due to living habits, intergenerational education, children living in different places, and other reasons, the elderly lack spiritual comfort. China's artificial intelligence and wireless sensor network technologies are used for spiritual comfort in intelligent elderly care, mainly through the elderly and psychological counseling, chatting, promoting hobbies, making friends, contacting children, etc., as shown in Figure 5.

The audio and behavior of the elderly are identified through the intelligent terminal equipment, and the collected information data are uploaded to the processing system for analysis and processing. The processing system should input the emotional algorithm in advance, so as to feed back the corresponding information to the elderly, including chatting with the elderly, psychological consultation, and promoting their hobbies and making friends. The intelligent device has the ability to continuously learn, continuously input the emotional behavior information of the elderly, and learn psychological knowledge, so as to facilitate real-time and accurate spiritual comfort. For example, the smart speaker in our life is an intelligent terminal device, which can send feedback by identifying audio. However, as a special vulnerable group, the elderly need a more targeted identification and feedback system. At present, the spiritual comfort of artificial intelligence and wireless sensor network technology applied to intelligent elderly care is generally based on face recognition and audio recognition. First, face and audio information is collected and uploaded to the processing system with similar thinking mode to human beings, emotional information is analyzed and processed, and finally the emotion needed by the elderly is fed back to the elderly. At the same time, the processing system needs to constantly learn new knowledge, store more useful emotional information of the elderly, and train repeatedly to improve the accuracy [17].

5. Discussion and Conclusion

China's living standards and medical standards are gradually improving, and the average life expectancy of the people is also increasing. Under this background, the aging of the population has become a serious social problem. The traditional way of providing for the aged is difficult to meet the severe situation. Intelligent elderly care has become an important measure to alleviate China's population aging. This paper expounds the application of artificial intelligence and wireless sensor network in intelligent elderly care, uses artificial intelligence and wireless sensor network technology to obtain the needs of the elderly at different levels, gives corresponding feedback in time through information processing, which is superior to the traditional elderly care methods in efficiency and accuracy, further optimizes resource allocation, and reduces resource waste. Although the application of artificial intelligence and wireless sensor network technology in intelligent elderly care is conducive to alleviate the tense situation under the background of China's aging population, open up a new market for intelligent elderly care, and improve the quality of life of the elderly population, there are still some deficiencies.

(1) In the daily life of the elderly, intelligent home, community service, and positioning system are the main ways in which artificial intelligence and wireless sensor network technology are applied to intelligent elderly care. Real-time monitoring is carried out through positioning, home feedback, community service feedback, and emergency help. However, the positioning system is easily affected by other signals. As long as it is disturbed by other signals, real-time positioning monitoring will have errors. In the real-time monitoring of the daily life of the elderly, the model used by the positioning system cannot achieve 100% accuracy, which makes the cloud unable to give the most efficient and accurate feedback when the elderly live at home and encounter individual actions and emergencies. This needs to complement with a variety of positioning models in order to achieve the highest accuracy.

(2) In the health care of the elderly, artificial intelligence and wireless sensor network technology are applied to intelligent elderly care, mainly for real-time self-monitoring of the body, living conditions, disease and other information data of the elderly in real time, for uploading them to the network environment for analysis and processing, and to feed back the information data to the client. However, health monitoring depends on the performance of the terminal sensor.

The sensor has some problems, such as time loss, and the elderly cannot maintain it, which will lead to errors in health monitoring. This requires the use of high-performance sensors in the intelligent terminal health monitoring equipment and the provision of regular door-to-door maintenance services, so as to ensure the accuracy of the information and data collected by the intelligent terminal health monitoring, so as to achieve accurate health and medical feedback. At the same time, in terms of health monitoring, the whole process of government supervision shall be implemented to make medical and nursing services transparent and open, so as to protect the rights and interests of the elderly.

(3) In the emotional comfort of the elderly, artificial intelligence and wireless sensor network technologies are mainly through collecting video images and audio from the elderly, and then the recognition system converts them into data that the system can understand. Finally, the emotion recognition system generates corresponding images and voice according to the emotion preference algorithm and outputs them to the elderly. However, due to the unclear emotional expression of the elderly, especially the disabled elderly, there are some difficulties in identifying the emotional behavior and action information of the elderly by artificial intelligence products, and there are also difficulties in analyzing and processing the emotional action information of the elderly in the cloud. This requires regular input of the daily information of the elderly in the processing system of artificial intelligence products. At the same time, combined with the knowledge of psychology to comprehensively analyze the emotional state of the elderly, intelligently communicate with the elderly, so that the elderly has a better grooming effect and chaperoning effect on the spirit. With the further development of technology, the realization will be more and more accurate for the recognition of emotion, language, expression, and other states of the elderly and finally reach the machine and the elderly to communicate without difficulty.

Under the background of the increasingly serious problem of aging in China and the guidance and encouragement of national policies, we should optimize AI and WSN to maximize its effectiveness in smart pension, constantly improve the smart pension service mechanism, and improve the quality of life of the elderly.

Data Availability

Figure 1 related data belong to public databases National Bureau of Statistics. Users can download relevant data for free for research and publish relevant articles, http://www.stats.gov.cn/tjsj/.

Conflicts of Interest

The authors declare that they have no conflicts of interest.

Acknowledgments

This study was supported by the National Social Science Fund Major Project (XSP21ZDA001) and Hunan Postgraduate Research Innovation Funding Project (QL20210160).

References

[1] M. Zhu and M. Yan, "Population aging and goverrnment expenditure structure: evidence from China based on SD analysis," *Journal of Statistics and Information*, vol. 34, no. 11, pp. 50–58, 2019.

[2] X. Wang and X. Zhang, "An explanation of China's experience in eliminating absolute poverty and the orientation of relative poverty governance in the post-2020 era," *Chinese Rural Economy*, vol. 434, no. 2, pp. 2–18, 2020.

[3] China Development Research Foundation, "China development report2020:development trends and policies of China's population aging," 2020.

[4] X. Huang, "A mode research on "artificial intelligence Pension"Service," *Journal of Xi'an University of Finance and Economics*, vol. 33, no. 5, pp. 35–42, 2020.

[5] D. Sui and X. Liu, "Artificial intelligence home care service modelconstruction," *Chongqing Social Sciences*, vol. 7, pp. 6–19, 2020.

[6] H. Zheng, X. Ran, S. Xu, L. Yang, and X. Wang, "Application of artificial intelligence technology in elderly care," *Application of IC*, vol. 38, no. 9, pp. 184-185, 2021.

[7] J. Zhu, *Intelligent Old-Age with the Enablment of Wireless Sensor network*, C-Enterprise Management, vol. 411, no. 7, pp. 74–76, 2021.

[8] H. Hu and K. Cai, "Analysis on the development of healthy pension industry driven by artificial intelligence," *Chinese Medical Ethics*, vol. 33, no. 2, pp. 147–152, 2020.

[9] C. Amardeo and J. G. Sarma, "Identities in the future wireless sensor network," *Wireless Personal Communications*, vol. 32, no. 49, pp. 353–363, 2009.

[10] Z. Xing, "Research on community smart elderly service models and key technologies under the empowerment of artificial intelligence," *Chinese Nursing Research*, vol. 35, no. 9, pp. 1573–1579, 2021.

[11] Y. Luo, W. Shi, and Y. Xiao, "Change Trends,Existing problems and countermeasures of the modes of endowment for urban residents——based on the survey of the modes of the endowment for the aged urban residents in Xi'an," *Journal of Xi'an Jiaotong University*, vol. 33, no. 1, pp. 78–84, 2013.

[12] S. Miao and P. Peng, "A research of community endowment management system based on wireless sensor network technology," *Journal of Guangdong Polytechnic Normal University*, vol. 35, no. 3, pp. 15–20, 2014.

[13] K. Tang, "The future development prospect so fartificial intelligence," *People's Tribune*, vol. 582, no. 2, pp. 24-25, 2018.

[14] A. Alberdi Aramendi, A. Weakley, A. Aztiria Goenaga, M. Schmitter-Edgecombe, and D. J. Cook, "Automatic assessment of functional health decline in older adults based on smart home data," *Journal of Biomedical Informatics*, vol. 81, pp. 119–130, 2018.

[15] L. Liu, E. Stroulia, I. Nikolaidis, A. Miguel-Cruz, and A. Rios Rincon, "Smart homes and home health monitoring technologies for older adults: a systematic review,"

International Journal of Medical Informatics, vol. 91, pp. 44–59, 2016.

[16] W. W. Jiazy and C. Wang, “Application and development of wearable devices in medical field,” *China Medical Devices*, vol. 32, no. 2, pp. 96–99, 2017.

[17] R. Bellman, *An Introduction to Artificial Intelligence: Can Computers Think?*, Boyd & Fraser PubCo, San Francisco, CA, USA, 1978.

Hindawi
Scientific Programming
Volume 2023, Article ID 9804141, 1 page
https://doi.org/10.1155/2023/9804141

Retraction

Retracted: Retrospection of the Optimization Model for Designing the Power Train of a Formula Student Race Car

Scientific Programming

Received 29 August 2023; Accepted 29 August 2023; Published 30 August 2023

This article has been retracted by Hindawi following an investigation undertaken by the publisher [1]. This investigation has uncovered evidence of one or more of the following indicators of systematic manipulation of the publication process:

(1) Discrepancies in scope
(2) Discrepancies in the description of the research reported
(3) Discrepancies between the availability of data and the research described
(4) Inappropriate citations
(5) Incoherent, meaningless and/or irrelevant content included in the article
(6) Peer-review manipulation

The presence of these indicators undermines our confidence in the integrity of the article's content and we cannot, therefore, vouch for its reliability. Please note that this notice is intended solely to alert readers that the content of this article is unreliable. We have not investigated whether authors were aware of or involved in the systematic manipulation of the publication process.

Wiley and Hindawi regrets that the usual quality checks did not identify these issues before publication and have since put additional measures in place to safeguard research integrity.

We wish to credit our own Research Integrity and Research Publishing teams and anonymous and named external researchers and research integrity experts for contributing to this investigation.

The corresponding author, as the representative of all authors, has been given the opportunity to register their agreement or disagreement to this retraction. We have kept a record of any response received.

References

[1] M. N. Kumar, V. Jagota, and M. Shabaz, "Retrospection of the Optimization Model for Designing the Power Train of a Formula Student Race Car," *Scientific Programming*, vol. 2021, Article ID 9465702, 9 pages, 2021.

Hindawi
Scientific Programming
Volume 2021, Article ID 9465702, 9 pages
https://doi.org/10.1155/2021/9465702

Research Article

Retrospection of the Optimization Model for Designing the Power Train of a Formula Student Race Car

M. Naveen Kumar[1], **Vishal Jagota**[1], **and Mohammad Shabaz**[2,3]

[1]*Department of Mechanical Engineering, Madanapalle Institute of Technology & Science, Madanapalle, AP, India*
[2]*Arba Minch University, Arba Minch, Ethiopia*
[3]*Department of Computer Science Engineering, Chandigarh University, Mohali, Punjab, India*

Correspondence should be addressed to Mohammad Shabaz; mohammad.shabaz@amu.edu.et

Received 9 October 2021; Revised 8 November 2021; Accepted 15 November 2021; Published 29 November 2021

Academic Editor: Punit Gupta

This article describes the power train design specifics in Formula student race vehicles used in the famed SAE India championship. To facilitate the physical validation of the design of the power train system of a formula student race car category vehicle engine of 610 cc displacement bike engine (KTM 390 model), a detailed design has been proposed with an approach of easing manufacturing and assembly along with full-scale prototype manufacturing. Many procedures must be followed while selecting a power train, such as engine displacement, fuel type, cooling type, throttle actuation, and creating the gear system to obtain the needed power and torque under various loading situations. Keeping the rules in mind, a well-suited engine was selected for the race track and transmission train was selected which gives the maximum performance. Based on the requirement, a power train was designed with all considerations we need to follow. Aside from torque and power, we designed an air intake with fuel efficiency in mind. Wireless sensors and cloud computing were used to monitor transmission characteristics such as transmission temperature management and vibration. The current study describes the design of an air intake manifold with a maximum restrictor diameter of 20 mm.

1. Introduction

SUPRA SAE India is an annual national level Student Formula Category car competition conducted by Society of Automobile Engineers India (SAE India) with support from Maruti Suzuki. It is a global platform for undergraduate and postgraduate students to demonstrate their technical skills and talent by applying their engineering skills and competing with other institute participants in developing a student formula category vehicle according to defined instructions and safety precautions. The vibration decoupling rate and frequency of the powertrain mounting system are investigated utilizing rigid body dynamics and energy techniques to improve the powertrain mounting system's vibration isolation capabilities, with the powertrain of a front wheel drive car as the research object [1, 2]. The subsystem transmits the power developed by the engine or motor of automobiles to the wheels of the motor vehicle to move the motor vehicle forward or backward. Power train is also called drive train/transmission. It consists of a group of components in a vehicle that delivers power to the driving wheels. Components present in the motor vehicle are engine, clutch, gear box, drive shaft, differential, axles, and cooling system. Connection of these components involves physical linking which may be present between the two ends of the vehicle, so it requires long drive connections (propeller shaft/drive shaft). The speed of the engine and wheels are different, so it must be matched with the appropriate gear ratio. A vehicle could be front wheel drive (FWD) or rear wheel drive (RWD) depending on which axle is given power from the engine. It impacts the BHP and torque figures according to different conditions [3, 4].

The vehicle's reliability was improved as a result of the power train simulation in this study. After knowing the requirements of the power train system, looking at both advantages and disadvantages of different parts, with the careful selection of the engine platform, KTM 390 was selected. Fuel efficiency is also a key role in racing events for that design of air intake with the restrictor diameter of 20 mm. The purpose of designing the power train without compromising the driver safety precautions is achieved and the power train of formula student race cars has been designed by following the SAE International rules. The sequence of design procedure followed for the same is given in Figure 1.

2. Design Considerations of Engine

The heart of a vehicle is the engine, which converts chemical energy (fuel energy) into mechanical energy [5]. According to the competition regulations, the engine used to power the automobile must be a four-stroke cylinder with a displacement of no more than 610 cc per cycle. If more than one engine is utilized, each engine's displacement must be less than 610 cc, and all engines' intake air must flow via a single air intake restrictor. Two-wheeler motorcycle engines such as the KTM390, CBR600, and Royal Enfield 350 are available for engine choice.

In the proposed paper for the design of power train, various parameters were taken into consideration. As per the rules of SAE, engine was selected on the basis of high-power output under 610 cc segment considering less about the torque Figure 2. Speed transmissions have been selected for the gear, train, and RPM and torque was evaluated for different gears and accordingly. There are multiple mechanisms available like belt, pulley drive, direct mesh gear system, and chain drive. Various drags such as aerodynamic drag as well as friction resistance were taken into consideration and their empirical relations according to the aerodynamics of the vehicle were evaluated. Apart from torque and power, the fuel efficiency factor was considered and the air intake runner was designed accordingly.

2.1. Comparison of Engines. The comparative details and specification of the various engines have been presented in Table 1 above.

Although these two engines have more power compared to other engines, the performance of engines purely depends on air-fuel mixture, so the design of air intake could definitely affect the performance. As a first time participating in Race Events (SUPRA SAEINDIA and Formula Bharath), we did not make complications. Yamaha YZF R6 contains 4 cylinders arranged in a line, we have ruled that air should go through a single intake and that the diameter should be within 20 mm. Keeping this in mind, making an air intake with four runners is complicated. Moreover, for Yamaha YZF R3, it consists of 2 cylinders, and the design of a single air intake with two runners is complicated. Another factor is considering the availability cost of the engine, we did not opt for these two engines. We know that Royal Enfield will produce more torque than power, but for racing events we need more power than torque. Engine displacement is more compared to the remaining three engines, but the output power is low when compared to KTM RC390. Honda CBR250R &Yamaha WR250R, these two engines contain a single cylinder, but the output power and torque are low compared to KTM RC390.

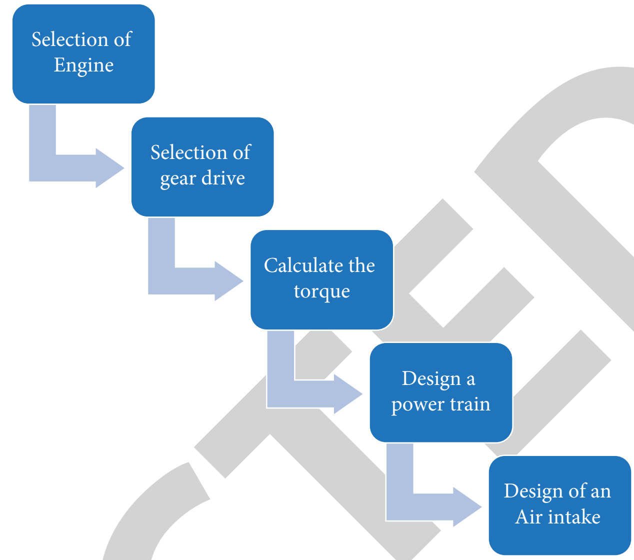

Figure 1: Block diagram for the design procedure for power train.

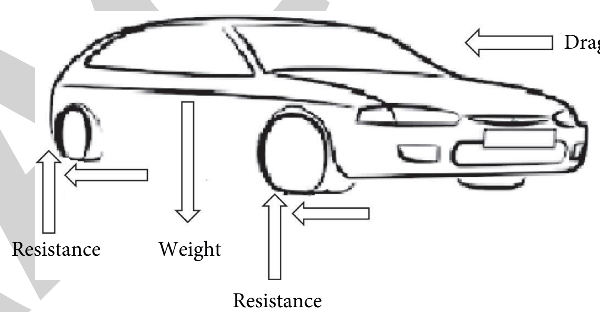

Figure 2: Total tractive force acting on the vehicle.

2.2. Reasons behind Selection of KTM RC 390. By considering the budget and availability of spare parts for better maintenance of the engine, the engine displacement is under 610 cc, which will satisfy the rule. It contains a single cylinder, so it may not be that much complicated in the design of air intake. KTM390 cc engine is an oversquare engine, so it produces more power compared to the torque which is required in racing conditions. The KTM RC 390 model is a sports bicycle made by KTM. In this form, sold from the year 2020, the dry weight is 149.0 kg (328.5 pounds) and it is outfitted with a single-chamber, four-stroke engine. The motor delivers the extreme pinnacle yield force of 44.00 HP (32.1 kW)) and a greatest force of 35.00 Nm (3.6 kgf-m or 25.8 ft. Lbs). With this drive train, the KTM RC 390 is equipped for arriving at the extreme maximum velocity of. About case attributes, liable for street holding, taking care of conduct and ride solace, the KTM RC 390 has a steel lattice outline, and powder covered edges with front suspension being WP topsy turvy Ø 43 mm and at the back, it is outfitted with WP Monoshock. Stock tire sizes are 95/75-R17 on the front and 115/75-R17 on the back. Concerning the halting force, the KTM RC 390 stopping mechanism incorporates single plate; ABS; four-cylinder callipers; size 320 mm (12.6 inches) at the front and single circle; ABS; coasting plate; single-cylinder calliper; size 230 mm (9.1 inches) at the back. KTM RC390 engine specifications as per manufacturer have been given in Table 2.

Table 1: Comparative analysis of various combustion engines.

Year	2020	2015	2014	2011	2010	1989
Engine model	Yamaha YZF R6	Yamaha YZF R3	KTM RC390	Honda CBR250R	Yamaha WR250R	Royal enfield 500
No. of cylinders	Inline 4	2	1	1	1	1
Displacement	599 cc	321 cc	373.3 cc	249.66 cc	249 cc	499 cc
Stroke	42.5 mm	44.1	60	55 mm	53.6 mm	90 mm
Bore	67 mm	68	89	76 mm	77 mm	84 mm
C.R	13.1 : 1	11.2 : 1	14.5 : 1	10.7 : 1	11.8 : 1	8.5 : 1
Transmission	6 speed	6 speed	6 speed	6Speed	6 speed	5 speed
Torque	61.7 Nm @10500 rpm	29.6 Nm @9000 rpm	35.3 Nm @7000 rpm	22.9 Nm @7000 rpm	23.7 Nm @8000 rpm	41.3 Nm @4000 rpm
Power	63.9 kW @14500 rpm	42 kW @10750 rpm	32 kW @9500 rpm	19.4 kW @ 8500 rpm	22.6 kW @10000 rpm	20.2 kW @5250 rpm
Cooling system			Liquid cooling			Air cooled
Fuel supply			Fuel injection			

Table 2: KTM RC390 engine specifications as per manufacturer.

Model	KTM RC390
Engine	Four-stroke, single cylinder
Capacity	373.4 cc
Bore × stroke	89 × 60 mm
Cooling system	Liquid cooled
Spark plug	Bosch VR 5 NE
Ignition	Fully electronic ignition system
Starting	Electric
Maximum power	32 kw/43.5 HP @9500 rpm
Maximum torque	35.3 Nm/26 ft-lb @7000 rpm
Clutch	Wet multidisc clutch

2.3. Selection of Gear System and Drive System. We selected KTM 390 cc engine in which the gear box is inbuilt with 6 speed transmission. There are multiple mechanisms available like belt, pulley drive, direct mesh gear system, and chain drive. The transmission system has been integrated with temperature and vibration sensors for monitoring purposes. These sensors wirelessly transfer real-time data of the transmission sections, temperatures, and vibrations monitored by a mobile-based app during the transmission operations. Nowadays, the use of sensors in automobiles has grown from the safety point of concern of the driver [6, 7].

2.4. Comparison of Different Drive Systems. Drive system is critical from the design point of view. The comparative details of the different drive systems have been presented in Table 3.

By observing from Table 3, the chain drive has been selected to make our transmission more efficient and reliable, i.e., driver sprocket, driven sprocket, and a chain.

3. Design and Results

3.1. Calculation of Forces. Let us assume the mass of the vehicle(M) is 350 kg (total weight of the vehicle including driver), wheel radius is 0.26 m, velocity of the vehicle (v) is 60kmph (assumption), and rolling resistance coefficient (f_r) is 0.02, this varies based on the type of road and tire, gradient angle (α) is 25° (maximum gradient angle in Formula Race Tracks) depends on the road, drag coefficient (C_d) is 0.7 (typical values for formula 1 car in range 0.7–1.1) depends on the car, frontal area (A) is 0.617 m^2 (calculate from design), density of air (ρ) is 1.225 kg/m^3, and gravity (g) is 9.81 m/s^2. Typical values of rolling resistance coefficient have been presented in Table 4.

3.1.1. Forces Calculation. We know that in a vehicle several forces are pulling on it. The vehicle motion can be completely determined by analyzing the forces acting on it. The different powers pulling up on a vehicle are shown in Figure 3.

3.1.2. Aerodynamic Drag. When a vehicle is travelling at a particular speed, the forward motion of a vehicle encounters an air force opposing its motion [8, 9]. This force is called aerodynamic drag. Observe Figure 3. Streamlined drag majorly affects the consistent state Vmax execution as it is the significant power to defeat at extremely high velocity and it is for the most part seen to be correspondingly significant for forceful track driving. The outcomes show that, for a 10% increment in drag coefficient, the warm impact around the Nurburgring is irrelevant with an expansion of just 0.2°C in liquid temperature and 0.5 s for lap time. There are two purposes behind this. Initially, the normal speed around the Nurburgring for the vehicles considered is around 85 mph and there are not many spots where the speed surpasses 120 mph. Indeed, even on the long straight where the drag turns out to be considerable, the speed is typically restricted (not by drag) to 155 mph. Furthermore, the vehicles are considered to have up to 500 hp accessible, so the drag power at the normal speed requires just a little extent of force accessible (around 10–15%), a large portion of which is utilized to defeat vehicle inactivity power during the speed increase. For lower fueled vehicles, which would spend a substantial extent of the lap at a speed restricted by drag, the impact would be a lot more noteworthy. Figure 4 shows how the drag force effects the motion of vehicle.

Aerodynamic drag force can be defined mathematically F_d: $1/2 * C_d * A * \rho * v^2 = 73.424$ N, whereas C_d is the coefficient of drag, A is the frontal area (m^2), ρ is the density of air (kg/m^3), and v is the speed of vehicle (m/s).

Table 3: Comparison of different drive systems.

S. No	Belt drive	Gear drive	Chain drive
1	Main element are pulleys and belt	Main element gears	Main element sprockets, chain
2	Chances of slip	No-slip	No-slip
3	Used for large centre distance	Used for the short centre distance	Used for the moderate centre distance
4	More space required	Less space required	Moderate space required
5	Simple in design and manufacturing	Complicated in design and manufacturing	The simplest in design and manufacturing
6	Failure in belt does not damage machine	Failure in gear may cause serious break down in the machine	Failure in a chain may not seriously damage the machine
7	Life time is less	More life time	Moderate life time
8	Lubrication not required	Requires proper lubrication	Lubrication required
9	Mainly used for low-velocity ratio	Mainly used for high velocity ratio	Mainly used for moderate velocity ratio
10	Low installation cost	High installation cost	Moderate installation cost

Table 4: Rolling resistance coefficient.

C- rolling resistance coefficient value for different conditions	
0.006–0.01	Truck tire on asphalt
0.01–0.015	Ordinary car tires on concrete, new asphalt, cobbles small new
0.02	Car tires on tar or asphalt
0.02	Car tires on gravel-rolled new
0.03	Car tires on cobbles-large worn
0.04–0.08	Car tire on solid sand, gravel loose worn, soil medium hard
0.2–0.4	Car tire on loose sand

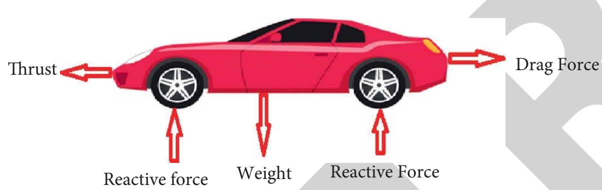

Figure 3: Different forces on the vehicle.

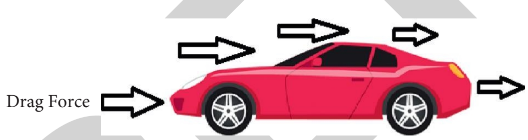

Figure 4: Drag force effects on the motion of the vehicle.

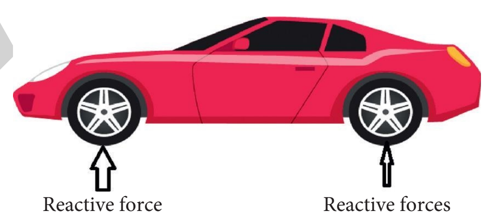

Figure 5: Gradient forces effect motion of vehicle.

3.1.3. Gradient Force. The resistance force acts on a vehicle when a vehicle drives over gradient. It depends on the weight of the vehicle and the angle of road inclination. It always acts towards down. Observe Figure 5 to see how the gradient forces effect the motion of vehicle.

In short, moving obstruction is the power needed to keep your vehicle's tires moving at a given speed. Tire makers evaluate it by moving a tire against a considerable tube-shaped drum and estimating the power in question. The outcome is the tire's moving opposition coefficient (RRC). Tires change shape as they pivot, and the piece of the tire in touch with the street is distorted before it gets back to its casual state. The energy needed to misshape a tire is more noteworthy than what has expected to return it to its unique shape: a wonder known as "hysteresis." This energy is disseminated as warmth, and this warmth assumes a significant part in the moving opposition. In the event that you have at any point when accelerating a bike on an underinflated tire, you have first-hand involvement in hysteresis. To voyage at a consistent speed, you need to place more mechanical energy into the framework, accelerating more earnestly than if the tire had been expanded to its legitimate level. That is on the grounds that underinflated tires have heaps of hysteresis, making seriously moving opposition. Things being what they are, with the chance that underinflated tires have high moving obstruction, why not just overinflate them to decrease their moving opposition? If that works, however, there is a cost to pay. For a certain something, the ride quality endures, turning out to be progressively cruel as tire pressures rise. All the more critically, the higher the pressing factor, the more modest the "impression," which is the contact fixed between your tires and the street surface. A more modest contact fix can mean less foothold, which means diminished slowing down and cornering execution, particularly on wet surfaces.

Gradient force can be defined mathematically F_g: Mg $\sin\alpha = 1451.05$ N, whereas M is the mass of the vehicle (kg), g is the gravity (m/s^2), and α is gradient angle.

3.1.4. Rolling Resistance. The force resisting the motion of the vehicle when it is moving on a road is called rolling resistance. Rolling resistance is also called rolling friction. Observe Figure 6 to see how the rolling friction acts on tire.

Rolling resistance can be defined mathematically F_r: f_rMg = 68.67 N, whereas f_r is the rolling resistance coefficient, M is the mass of the vehicle (kg), and g is the gravity (m/s^2).

Mathematical formulas used to calculate the forces are:

Drag force: $F_{d:}$ $1/2 * C_d * A * \rho * v^2$.

Drag force is the force acting on the front side. A is the frontal area on which air drags, ρ is the air velocity, and v is the velocity of air. All factors depend on each other.

Gradient force F_g: Mg sinα.

Gradient force is depending on the road angle. M is the mass of the vehicle, α is the gradient angle, and g is the gravity. Every factor is related to others.

Resistance force F_r: f_rMg

Resistance force is the force between tires and road. Mass of the vehicle and gravity are related to road.

With the addition of all forces, we will get all forces acting on the vehicle.

3.1.5. Total Tractive Force. The amount of total force applied by the drive wheels to the ground is called total tractive force and has been shown in Figure 2.

Total tractive force is defined as the sum of all forces $F_d + F_g + F_r = 1593.144$ N.

Torque at the wheels can be calculated by using the below mathematical formula.

Torque at wheels = total tractive force ∗ wheel radius ∗ resistance factor = 463.92 Nm.

3.2. Gear Ratio Calculation. Gear ratio helps us to find the desired output of power and torque [10, 11]. By considering each primary drive ratio in the engine gear box from the manufacturer and the secondary drive ratio (chain gear ratio), we calculated the torque and power.

Primary drive ratio: 30 : 80 = 2.66 : 1.

Secondary drive ratio: 15 : 45 = 3 : 1.

Overall gear ratio = secondary drive ratio ∗ primary drive ratio ∗ individual gear ratio.

3.2.1. Overall Gear Ratio. In Table 5, we mentioned the individual and overall gear ratio for different gears. With the help of the below equation, we will find the overall gear ratio.

Overall gear ratio = primary drive ratio ∗ secondary drive ratio ∗ individual gear ratio.

3.2.2. RPM and Torque at Different Gear Ratios. Below the comparison of RPM and torque are the actual engine crankshaft RPM (engine speed) and torque. Output RPM here is an engine RPM not vehicle RPM. Usually, the engine torque increases with the increase of RPM. This torque can be compromised with speed by shifting gears. In the 1st gear, we get RPM around 2648, whereas the torque is 93.3 N-M, and RPM increases from 1st gear to 6th gear, whereas the torque increases from 1st gear to 2nd gear and decreases from 3rd to 6th gear. You can clearly observe this relation in Figure 7. In Figure 7 we can observe clearly that the torque increases from gear 1 to gear 2 in addition to a gradual decrease from gear 2 to gear 6. We know that the torque at 2 ng gear is more when compared to all gears. Torque and RPM were inversely proportional. If we clearly observe between gear 1 and gear 2, there is a sudden decrease in the RPM and a sudden increase in torque. From gear 2 onwards, there is a gradual increase in RPM and a gradual decrease in torque. By observing this, we can clearly understand that there is an inverse proportion between torque and RPM.

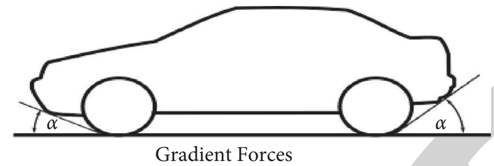

Figure 6: Rolling friction acts tire.

Table 5: Individual and overall gear ratio at different gears.

Gears	Individual ratios	Overall gear ratios
1st	2.6666	21.22
2nd	1.8571	14.81
3rd	1.4211	11.34
4th	1.1428	09.11
5th	0.9565	07.63
6th	0.8400	06.70

Torque for each individual gear can be calculated by using the below mathematical formula.

$$\text{Torque} = \text{maximun engine torque} * \text{Overall gear ratio}. \tag{1}$$

After calculating the torque from the above equation, at 1st gear, the torque is high whereas moving towards higher gear torque reduces. In the 1st gear, the torque is around 750 N-m and in the 6th the gear is around 240 N-m. Observe the comparison to see how the torque decreases when we move towards the higher gear in Figure 8.

Revolutions per minute can be calculated for each gear by using the following mathematical formula:

$$\text{RPM} = \frac{\text{Engine rpm}}{\text{overall gear ratio}}. \tag{2}$$

Vehicle RPM is low at the 2nd gear because we get more torque at the 2nd gear, the RPM of the vehicle gradually increases from 2nd gear to the final gear, but it decreases from 1st gear to 2nd gear. You can see the theoretical values from Table 6. Theoretical values for Engine RPM. Overall gear ratio and gear RPM.

3.2.3. Acceleration Calculation. We can calculate the acceleration for each gear by using the following mathematical formula:

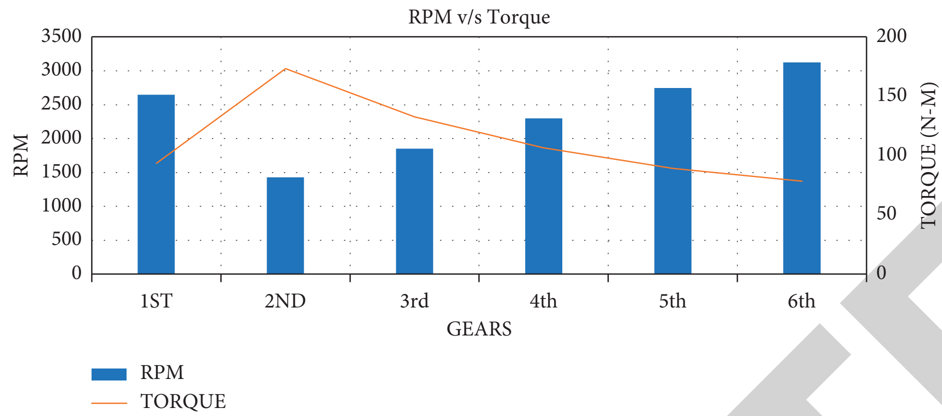

Figure 7: The RPM and torque values for differential gear.

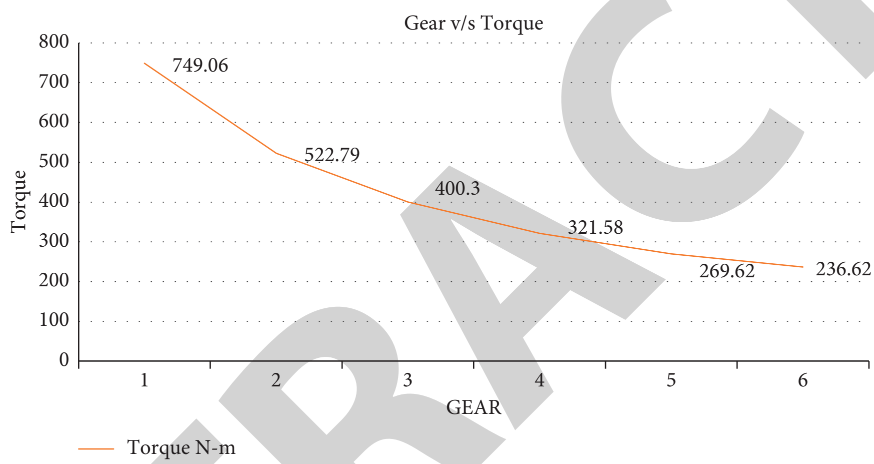

Figure 8: Torque ratios for differential gear systems.

Table 6: Theoretical values for engine RPM. Overall gear ratio and gear RPM.

Engine rpm	Overall gear ratios	Gear rpm
2625	21.22	123
1413	14.81	95
1849	11.34	163
2297	09.11	252
2745	07.63	359
3126	06.70	466

$$\text{Acceleration} = \frac{\text{torque}}{(\text{wheel radius} * \text{mass of vehicle})}. \quad (3)$$

Acceleration is decreasing when we start shifting to higher gears and at 1^{st} gear acceleration is 8.231 m/s^2 whereas at top gear it is 2.6 m/s^2. Observe the relation between torque v/s acceleration at different gears given in Figure 9. From Figure 9, we came to know the relation between the torque and acceleration. With the help of the diagram, we can observe that at initial gear both torque and acceleration are more. With the increase of gears, both torque and acceleration are decreases. Least torque and acceleration at top gear and more torque and acceleration are available at the 1st gear.

From Figure 10, we can observe how the acceleration decreases while we are moving towards higher gear.

3.3. Transmission Design

3.3.1. Sprocket Calculations. By taking consideration of the gear ratio 3 : 1 and the sprocket of the KTM390 engine with (driver sprocket) 15 teeth, the number of teeth in the rear sprocket (driven sprocket) is

$$3 * 15 = 45 \cdot \text{teeth}. \quad (4)$$

Sprocket diameter is calculated by the standard diameter of roller chain sprockets [12]. Details of driver and driving sprocket are given in Table 7.

3.3.2. Differential Specifications. Usually in such competitions it is preferable to use a chain differential as the power is transmitted to the axles by chain drive. We manufacture a sprocket made of 7075 aluminium and die steel with teeth of 45. The real-time monitoring of temperature and vibration data by cloud computing and mobile platform app has shown that during the transmission operations the temperature and vibrations were well between the safe limits of operation.

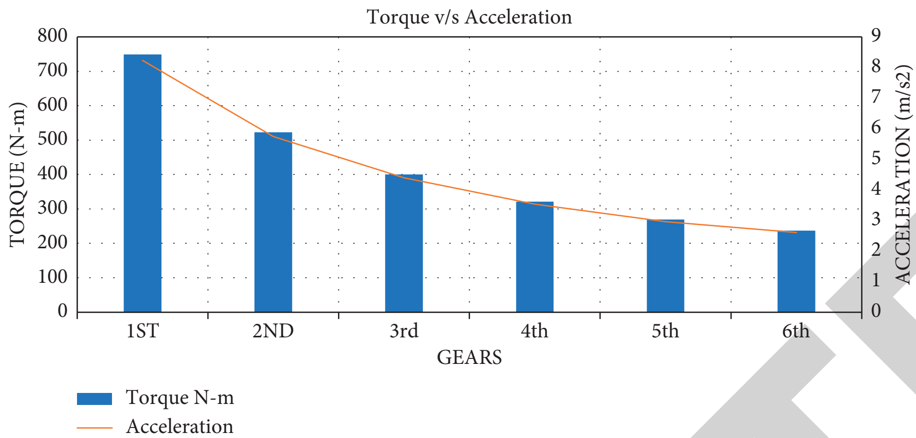

Figure 9: The relation between torque v/s acceleration at different gears.

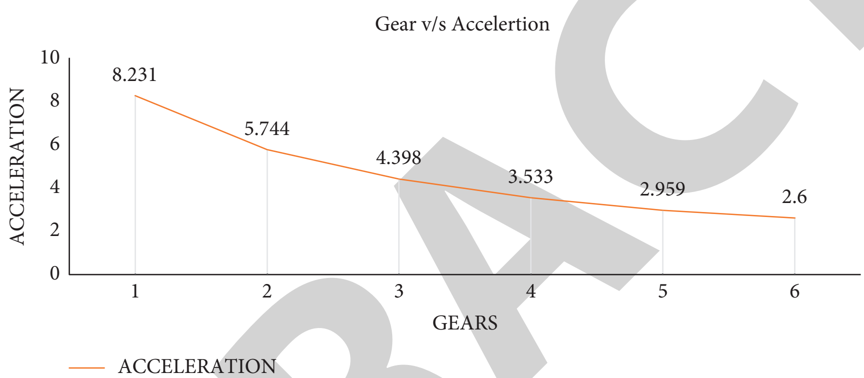

Figure 10: The relation between acceleration and different gears.

Table 7: Details of driver and driving sprocket.

Sprocket	Number of teeth	Outside diameter	Pitch diameter	Calliper diameter
Driver sprocket	15	3.315	3.006	2.590
Driven sprocket	45	9.313	8.960	8.554

3.4. Design of Air Intake

3.4.1. Consideration of Rules for Air Intake. Design of power train involves a lot of observations like to implement a system which moves the vehicle. The torque delivered by the engine is not sufficient to move the vehicle because the engine is designed for two-wheeler, while it is used for 4-wheeler. We will calculate the torque required to move our vehicle. Torque required is more when compared to the torque delivered by engine. Power train is designed to match the torque that requires moving the vehicle. To pass air into the cylinder, we design the air intake with the restrictor diameter of 20 mm. While designing the air intake, we need to be careful in the design of plenum and runner because the air intake is the combination of restrictor, runner, and plenum. Design of one part affects the dimensions of other parts.

A rarefaction wave flows upstream from the intake valve to the intake runner because there is low pressure downstream when it opens. From the open end, this wave reflects as a compression wave and returns to the pipe. When the intake valve opens, the rarefaction wave begins, and the compression wave must arrive precisely before the valve closes [13]. Maximum restrictor diameter is 20 mm, any portion of the air intake should be covered for side and back sway crashes, and any piece of the air consumption framework that is under 350 mm (13.8 inches) over the ground. The whole intake runner (Figure 11) has been divided into three pieces, two of which are located within the engine block and one of which is constructed. The fabricated intake portion goes within the engine block from upstream to downstream [14].

3.4.2. Restrictor. Given that the diameter of the restrictor (Figure 12) is maximum 20 mm, the diameter at the inlet portion is 46 mm, which is the diameter of the throttle body of KTM 390 cc, and the diameter at the outlet is depending on our design of plenum, converging, and diverging angles of the restrictor, if we observe the restrictor clearly, we have two sections named as converging section and diverging section. Mostly used converging angle is 12 degrees whereas diverging angle is 6 degrees.

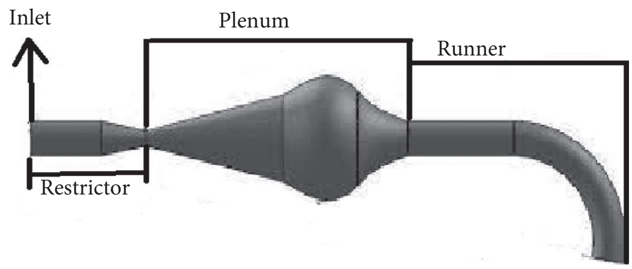

Figure 11: Diagram of intake runner.

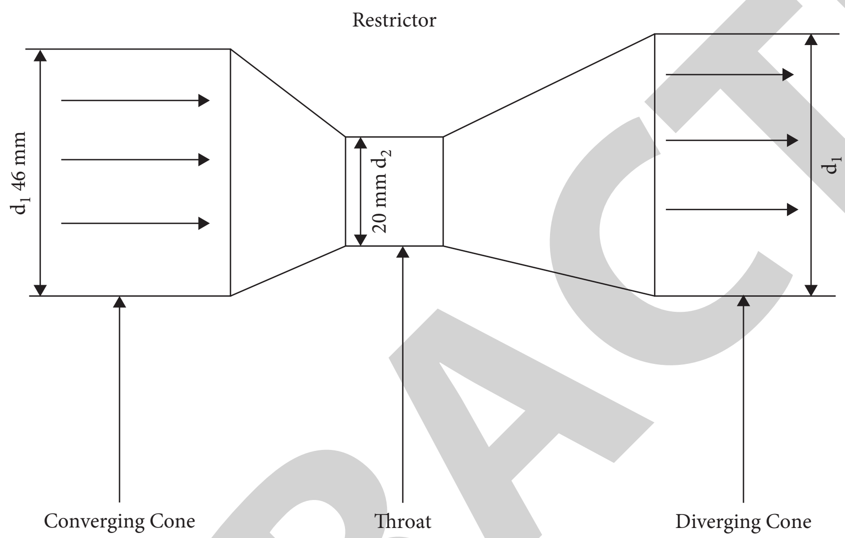

Figure 12: Diagram of restrictor.

3.4.3. Plenum. Plenum is a large cavity at the top of runner. It acts as a reservoir and stores air until it is ready to send to the cylinders. The main advantage over the usage of the plenum is evenly distributing the air into the runner. It is mostly preferable for Multi cylinder engines [15]. The volume of the plenum is almost 3 times the volume of the engine. Engine performance impact is based on the volume of the plenum.

3.4.4. Runner. Runner is the connection between the plenum and the engine cylinder. If the engine contains more than one cylinder, then runners are used to equally distribute the air into the plenum. The length of the runner is depending on the speed of the pressure wave and the cam duration, and the bending angle of the runner depends on the pressure wave.

3.5. Analysis. The method which was used while designing the power train is a conventional method, but all selections from engine selection to final drive follows certain technical rules, economically low, efficient and our availability. In any project one need to consider initially technical ways then efficient is important after that it should be economical cheaper then finally the part should be available. A power train was designed for formula student vehicle with KTM 390 engine. The final gear drive ratio is 3 : 1 (Driven: Drive) and chain differential was selected, because in FSAE Competitions we will transfer power through chain drive. To pass air into the engine we used air intake with restrictor diameter of 20 mm and plenum volume should be three time the engine volume. The diameter of air intake at engine end should be 46 mm because the diameter of KTM 390 engine throttle is 46 mm.

4. Conclusion

The vehicle's reliability was improved as a result of the powertrain simulation in this study. Most of the engineering student has a dream of designing powertrains with less weight-to power ratio. Selection of engine plays a major role in the power train; a square engine which produces more power compared to torque was selected. Power is the main important for race cars when compared to torque. After knowing the requirements of the power train system, look both advantages and disadvantages of different parts. With the careful selection of the engine platform, KTM 390 was selected as the best engine in the segment. It is certainly due to that the power required is more compared to the torque. Power is the main important for race cars when compared to torque. Along with the power, fuel efficiency also matters along with the medium to transfer the power. Power loss is reduced by selecting the chain drive. It appears sensible to continue research into improving the car's reliability and

Hindawi
Scientific Programming
Volume 2021, Article ID 6397786, 10 pages
https://doi.org/10.1155/2021/6397786

Research Article

A Fine-Grained Horizontal Scaling Method for Container-Based Cloud

Chunmao Jiang and Peng Wu

School of Computer Science and Information Engineer, Harbin Normal University, Harbin, Heilongjiang 150025, China

Correspondence should be addressed to Peng Wu; 864782389@qq.com

Received 26 September 2021; Revised 5 November 2021; Accepted 9 November 2021; Published 27 November 2021

Academic Editor: Punit Gupta

The container scaling mechanism, or elastic scaling, means the cluster can be dynamically adjusted based on the workload. As a typical container orchestration tool in cloud computing, Horizontal Pod Autoscaler (HPA) automatically adjusts the number of pods in a replication controller, deployment, replication set, or stateful set based on observed CPU utilization. There are several concerns with the current HPA technology. The first concern is that it can easily lead to untimely scaling and insufficient scaling for burst traffic. The second is that the antijitter mechanism of HPA may cause an inadequate number of onetime scale-outs and, thus, the inability to satisfy subsequent service requests. The third concern is that the fixed data sampling time means that the time interval for data reporting is the same for average and high loads, leading to untimely and insufficient scaling at high load times. In this study, we propose a Double Threshold Horizontal Pod Autoscaler (DHPA) algorithm, which fine-grained divides the scale of events into three categories: scale-out, no scale, and scale-in. And then, on the scaling strength, we also employ two thresholds that are further subdivided into no scaling (antijitter), regular scaling, and fast scaling for each of the three cases. The DHPA algorithm determines the scaling strategy using the average of the growth rates of CPU utilization, and thus, different scheduling policies are adopted. We compare the DHPA with the HPA algorithm under different loads, including low, medium, and high. The experiments show that the DHPA algorithm has better antijitter and antiload characteristics in container increase and reduction while ensuring service and cluster security.

1. Introduction

The rapid growth of container technology requires effective deployment and management strategies for containerized applications while addressing their runtime adaptability. In addition, the ability of cloud computing to provide resources on demand encourages the development of elastic applications that can accommodate changes in working conditions (e.g., variable workloads). Horizontal elasticity allows increasing (scaling-out) and decreasing (scaling-in) the number of application instances (e.g., containers) [1]. Most of the existing horizontal scaling methods explore resilience, which respond quickly to small load changes [2–4]. In this study, we build fine-grained horizontal scaling to cope with sudden load peaks.

As two crucial quantitative metrics, response time and resource utilization are essential measurements for various load variations under dynamic environmental conditions [2]. Container-based virtualization technology can improve application performance and resource utilization more efficiently than virtual machines (VM). Many existing scaling mechanisms employ fixed thresholds, which are based on cloud platform metrics, in general, such as CPU utilization. In contrast, such an approach is widely used, including Amazon's EC2, a virtual machine-based cloud platform. However, for applications that are constantly changing their requirements for CPU, memory, and other resources, their performance and resource utilization decrease significantly [5–7].

The adaptation of advanced metrics and dynamic thresholds may respond more finely to fluctuations in the workload, so it can improve application performance and get higher resource utilization. Therefore, we hope to develop a new dynamic autoscaling approach that automatically adjusts the thresholds based on the state of the execution environment observed by the monitoring system. In this way, the monitoring information, including infrastructure and application-specific metrics, will help the service provider to accomplish a satisfactory adaptation mechanism to various operational states. Furthermore, fine-grained scalability thresholds and degrees of scalability can better improve resource utilization and better cope with dynamic workload variations.

Therefore, this study aims to develop a new fine-grained dynamic scaling method based on the thought of granular computation. The major contributions of this study are as follows: first, we classify the container scaling events into three categories by establishing two thresholds, i.e., scale-out, neither scale-out nor scale-in, and scale-in. Second, we further subdivide the scaling strength into three levels for the scaling events, i.e., no scaling (to prevent jitter), regular scaling, and fast scaling. Third, the scalability metric applied in this study considers not only CPU utilization but also the growth rate of CPU utilization. We validate the algorithm's effectiveness by simulation under low load, medium load, and high load scenarios, respectively. The results show that the proposed algorithm in this study can resist high load and jitter well and effectively guarantee the cluster's quality of service (QoS).

The remainder of this study is organized as follows. Section 2 reviews the horizontal scaling mechanism of container clouds and presents the limitations that currently exist in Kubernetes. In Section 3, we present the DHPA algorithm, which is a dual-threshold horizontal scaling algorithm. And then, a specific example is given to illustrate the idea and process of the DHPA algorithm. Section 4 gives the experiment result and analysis. Finally, we conclude this study and prospective future studies in Section 5.

2. Related Work

Kubernetes [8–10] offers Horizontal Pod Autoscaler (HPA) [11–13], a built-in horizontal scaling controller, which automatically scales the ReplicaSet controller, deployment controller, or pod quantity based on statistical CPU utilization (or other custom metrics). This section presents the Kubernetes' horizontal scaling technique, including the acquisition of HPA metrics, how it works, and its limitations.

2.1. Horizontal Pod Autoscaler. HPA is a cyclic control process. The controller manager queries resource utilization during each cycle based on the metrics specified in each Horizontal Pod Autoscaler definition.

The controller manager can retrieve data from the following sources: (1) gather CPU utilization and memory usage data from Heapster, (2) use the Resource Metrics API to collect data from the Metrics Server that contains resource metrics for each pod in the cluster, and (3) the Custom Metrics Adapter provides the data collected by third-party plug-ins such as Prometheus to the Custom Metrics API, which the cluster then uses to fetch the data. In the latest version of Kubernetes, the cluster introduces a new data reporting channel—aggregation layer, an abstract data reporting interface that third-party plug-ins or administrators can use to implement this interface themselves. The approach of HPA to acquire data is shown in Figure 1.

2.2. How HPA Works. The principle of HPA is to poll resources of each pod every 30 seconds to determine whether the number of copies of the target pod needs to be adjusted by statistically analyzing the changes in the load of the target pod. There are two approaches to HPA to calculate the number of targets that the pod needs to scale-out or scale-in.

2.2.1. CPU Utilization Percentage. CPU utilization percentage represents the average CPU utilization of all copies of the current pod. A Pod's CPU utilization is the Pod's current CPU usage divided by the Pod Request value [14]. The calculation of the target number of pods for a scaling capacity is given by

$$\mathrm{ER} = \mathrm{ceil}\left[\mathrm{cR} * \left(\frac{\mathrm{cV}}{\mathrm{dV}}\right)\right], \tag{1}$$

where ER (expect replicas) represents the expected number of pods needed for expansion. The cR (current replicas) represents the number of pods in the current state. The cV (current value) represents the metrics that are currently be detected, such as memory usage, CPU utilization, and HTTP request traffic. The dV (desired value) represents the threshold for scaling up or scaling down, and Ceil represents the value, which is the nearest integer that is greater than or equal to the dV. Suppose the value of CPU utilization percentage exceeds 80% at a given moment. In that case, it means that the current number of pod copies is likely insufficient to support more subsequent requests, and dynamic scaling is required. When the request peak passes, the CPU utilization of Pod drops again, and HPA will reduce the number of pod copies to a reasonable level.

2.2.2. Application-Based Defined Metrics. CPU utilization percentage is implemented by the Heapster plug-in when calculating the CPU usage of the Pod, but adding a plug-in increases the complexity of the system while decreasing the efficiency of HPA's scaling. Kubernetes supports using custom metrics as metrics starting with version 1.2, which requires the given properties such as the metric units and how the metrics data are obtained. This mechanism is not widely used yet. The HPA control is illustrated in Figure 2.

The workflow of HPA can be summarized as follows. HPA will fetch the metrics data in the cluster every 30 seconds. Suppose the fetched metrics exceed the initial threshold. In that case, the HPA starts counting the number of target pods, and the HPA controller sends a command to the corresponding controller of the pods (ReplicaSet and deployment). The controller recycles or scales out the number of pods according to the number of target pods. After the operation of the pod is completed, the service layer

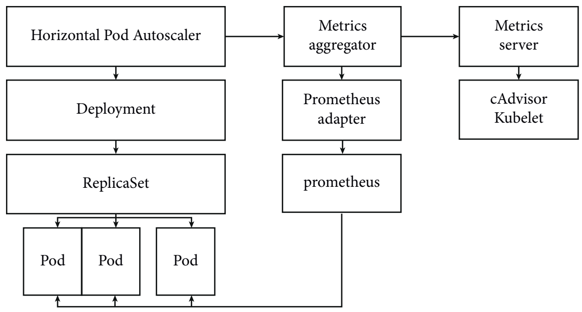

Figure 1: Flowchart of HPA collective data.

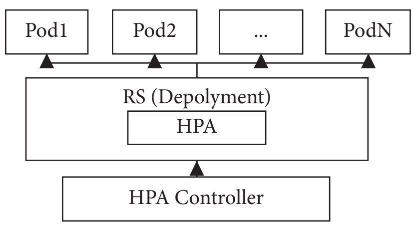

Figure 2: HPA system.

inside Kubernetes will automatically perform load balancing operations for the scaled-up or scaled-down pods. At this point, HPA has completed the entire horizontal scaling operation, and the scaling flowchart is shown in Figure 3.

2.3. Limitations Analysis of HPA. By analyzing the Kubernetes source code, we found that the HPA system implementation is relatively simple and has some limitations.

(1) The algorithm used by HPA for expansion and contraction is based on equation (1), which is simple to implement and inflexible. For example, suppose there are many network requests instantaneously. In that case, HPA will scale out, but it needs time and resources to start a pod service. Suppose the scale-out is not timely, or the number of scale-out is insufficient. It may seriously crash service and even threaten the cluster's security.

(2) Due to HPA's antijitter mechanism, the cluster will not be rescaled within 3 minutes after an expansion, which may result in an inadequate expansion. The number of containers cannot meet the subsequent service requests. The quality of service will be severely degraded or even collapse, which significantly affects the user experience and even cluster security. Simultaneously, there will not be any scaled operations within 5 minutes. If the scale occurs when traffic peaks to arrive again, the pod copy is not enough, which will eventually lead to a decline in the quality of service, cluster crash, and other issues.

(3) HPA fixes the time of data sampling to save resource consumption. The data reporting interval is the same during regular and high load periods, seriously affecting the cluster's access to information about the entire load during high load. The mechanism makes the cluster unable to correctly estimate the current pod load, prone to untimely and inadequate capacity expansion.

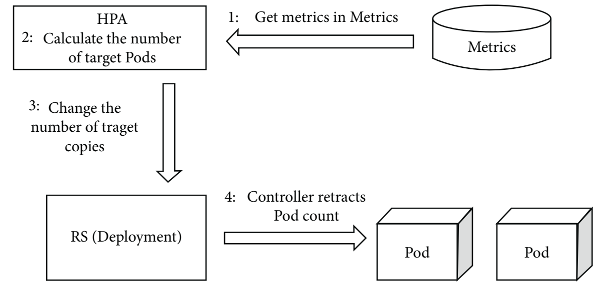

Figure 3: HPA flow chart.

A summary of the related work is shown in Table 1.

3. Dual-Threshold Horizontal Scaling Algorithm

In this section, we present a dual-threshold-based scaling algorithm (DHPA) and analyze the algorithm through an example.

3.1. The Basic Idea of DHPA. The basic idea of the DHPA algorithm is to divide the container scaling into finer granularity by introducing the idea of granular computation. First, a threshold is set for scale-out and scale-in, respectively, and the two thresholds divide a scaling event into three parts: scale-out, no scale-in, and scale-in. The scaling strength is also subdivided as follows: no scale-out, normal scale-out and scale-in, and fast scale-out and scale-in. This fine-grained division of the container scale-out and scale-in capacity problems can be an excellent solution to the problems mentioned above, and the algorithm implementation steps are as follows:

(1) In the DHPA algorithm, there will be no longer mechanisms such as no more expansion within 3 minutes and no more expansion within 5 minutes of shrinkage. DHPA will use dynamic antijitter measures in place with the original static antijitter mechanism.

(2) The DHPA algorithm dynamically adjusts the reporting time of cluster monitoring pod data, which is subdivided into three granularities, i.e., at low load, the reporting time is 30 seconds. For medium load, it is 10 seconds. For high load, the data uptime is once every 1 second. This mechanism improves the mastery of the pod load situation of this algorithm under different load cases, allowing for better control of the system's scaling operations.

(3) The DHPA algorithm dynamically adjusts the pod's expansion by triangulating the pod expansion situation. It performs no expansion operation when the fluctuation of the pod load changes little. When the fluctuation variation is moderate, it performs the regular expansion operation. If the pod's load

Table 1: Overview of various HPA for container.

Virtualization	Basis	Metrics	Method	Ability
Container	CPU and memory	Time and throughput	Control theory	Dynamic
Container	CPU	Nothing	Rule-based	Static
VM and container	CPU and bandwidth	Application throughput	Rule-based	Static
VM and container	CPU	Nothing	Rule-based	Static
Container	CPU, memory, and bandwidth	Time and throughput	Rule-based	Dynamic

fluctuation varies sharply, the algorithm will perform a robust expansion operation to meet the pod's load demand. This case will reduce the number of expansion resources wasted because of jitter and fully consider the expansion under different load conditions.

(4) During capacity reduction, the DHPA algorithm also dynamically adjusts the capacity reduction range of pods. It can effectively reduce the frequent expansion and reduction problems caused by the sudden increase in the load after the load drop and reduce the business crash caused by the antijitter problem.

3.2. Scheduling Algorithm

Definition 1. (base threshold). Let α and β represent two thresholds, which are used to adjust the capacity of provided pods.

When the DHPA monitors the current pod's CPU utilization U over α, it changes the monitoring time from 30 seconds to 10 seconds and starts the capacity expansion judgment. If the CPU utilization U of the monitored pod exceeds β, we change the refresh rate to 1 second.

Definition 2. A pod's CPU utilization queue is set, where n is customizable and in this study is provisionally defined as 3. The larger the value, the better the antijitter effect, but the more stringent the scaling conditions will be.

Definition 3. Two thresholds δ and β are defined, satisfying $0.1 < \delta < \beta$, and c and d are the two critical granularity thresholds used by the DHPA algorithm to determine the strength of the expansion and contraction. We suggest that a and b take 40% of their range of values, while d and e are suggested to be 70% of their range of values. The developer can determine the most appropriate threshold value by conducting experiments in their cluster.

Let $\Delta_n = (x_n - x_{n-1})/x_{n-1}$ be the growth rate between two neighboring CPU utilization rates in the CPU utilization queue. $\varphi_n = (\Delta_2 + \Delta_3 + \cdots + \Delta_{n-1} + \Delta_n)/n$ is the average of the growth rate of CPU utilization. The DHPA algorithm as follows addresses the above scaling problem and formulates scheduling algorithms for each of the three granularities in the scaling case.

The process of scaling up a container can be outlined as follows. For a given CPU utilization history queue $P = \{x_1, x_2, \ldots, x_n\}$, we first compute each item Δ_i in queue P, if not all of Δ_i are greater than δ, or one x_i is not greater than α, i.e., $\exists\Delta_i < \delta$ or $\exists x_i < \alpha$; then, the cluster will not be scaled up because the algorithm will determine it to be a normal jitter for pod services. If each Δ_i is greater than δ, but there is one Δ_i is not greater than α, or each utilization x_i in the queue is greater than α, i.e., $\forall\Delta_i < \delta$ and $\exists\Delta_i < \varepsilon$ or $\forall x_i > \alpha$, then the DHPA algorithm determines it as a normal cluster load rise and performs the normal scaling up, and the number of scaled-up pod copies is computed according to the following equation:

$$\mathrm{ER} = \mathrm{ceil}\left[\mathrm{cR} * \left(\frac{\mathrm{cV}}{\alpha}\right)\right]. \tag{2}$$

If the growth rate of each is greater than ε, and each xi in the queue is greater than α, that is, $\varepsilon < \Delta_2 < \Delta_3 < \ldots < \Delta_{n-1} < \Delta_n$, $\forall\Delta_i < \varepsilon$, and $\forall\Delta_i < \alpha$, then the algorithm determines that the traffic peak is about to come; therefore, this strategy adopts emergency expansion. The number of needed to expansion copies of the pod according to equation is as follows:.

$$\mathrm{ER} = \mathrm{ceil}\left[\mathrm{cR} * \left(\frac{\mathrm{cV}}{\alpha}\right) * \left|\varphi_n\right| * 10\right]. \tag{3}$$

The scaling-up strategy of the DHPA algorithm is summarized in the following equation:

$$\begin{cases} \exists\Delta_i < \delta, \quad \text{or}, \ \exists x_i < \alpha & \text{no expansion} \\ |\forall\Delta_i > \delta, \quad \text{and}, \ \exists\Delta_i < \varepsilon, \quad \text{or}, \ \forall x_i > \alpha & \text{normal expansion} \\ \varepsilon < \Delta_2 < \Delta_3 < \ldots < \Delta_n, \quad \text{and}, \ \forall\Delta_i < \varepsilon, \quad \text{and}, \ \forall x_i > \alpha & \text{rapid expansion} \end{cases} \tag{4}$$

Similarly, we give the following procedure for container scaling down. If there is a Δ_i that is greater than 0, or there is a Δ_i greater than $-\delta$, i.e., $\exists\Delta_i > -\delta$ or $\exists\Delta_i > 0$, the algorithm determines that this is a normal cluster load fluctuation and does not perform a scale-down operation. If each Δ_i is less than $-\delta$, there is one Δ_i that is greater than $-\varepsilon$, or each utilization x_i in the queue is less than α, i.e., $\forall\Delta_n < -\delta$ and $\exists\Delta_n > -\varepsilon$ or $\forall x_i < \alpha$. The algorithm determines that this is a normal cluster load drop and performs a normal scaling-down operation, and the number of shrunken pods is calculated according to the following equation:

$$\mathrm{ER} = \mathrm{ceil}\left[\mathrm{cR} * \left(\frac{\mathrm{cV}}{\alpha}\right)\right]. \tag{5}$$

If each of Δ_i is less than $-\varepsilon$, and at the same time each x_i in the queue is less than α, that is, at this point, the cluster load drops faster, this time you can do a quick scaling down, in order to save resources, scaling down the number of copies of the pod according to the following equation:

$$\mathrm{ER} = \mathrm{ceil}\left[\mathrm{cR} * \left(\frac{\mathrm{cV}}{\alpha}\right) * \left|\varphi_n\right| * 10\right]. \tag{6}$$

The time complexity of the DHPA algorithm is mainly focused on the polling step of the cluster load. Suppose the n represents the number of copies of each pod in the container cluster and u represents the cluster load at each moment. In the scaling process, each time needs to traverse the n copies of the cluster, so the time complexity of the DHPA algorithm is $O(N)$. The DHPA algorithm has a CPU utilization list and a pod list, each with a finite number of internal objects, so the space complexity of the DHPA algorithm is $O(N)$.

3.3. An Illustrative Example. This section gives an example of the DHPA algorithm. In the example, we use sin function to simulate the CPU utilization of a set of pods per second as shown in equation

$$U_{\mathrm{t}} = 200 * \sin(t), \tag{7}$$

where t represents the times (second), the entire experiment lasts 180 seconds $t = \{1, 2, \ldots, 180\}$, and then, the utilization for each second is $U_t = \{0, 3, \ldots, 200\} \cup \{200, \ldots, 3, 0\}$, thus simulating the trend of the pod's CPU utilization. Suppose $\alpha = 50$ and $\beta = 70$; these two basic thresholds are used to dynamically adjust the data reporting time of CPU utilization. Suppose $\delta = 0.1$ and $\varepsilon = 0.3$; these two granularity thresholds are used to determine the increase or decrease in the CPU utilization queue to determine the scaling effort. The RT can be used to represent the cluster data reporting interval. $p = \{x_1, x_2, \ldots, x_n\}$ represents the queue that holds the CPU utilization history. Then, $n = 3$ in this case.

(1) The experiment starts from 1 second, and $U_t = 3.49$ according to equation (7). According to the algorithm, we derive the current CPU utilization data reporting time $RT = 30$, which U_t is not reached α at this time, and the historical rate of change in the utilization has not reached δ or ε, therefore, not scaling up and scaling down.

(2) After an interval of 30 seconds, $U_t = 99$, and $P = \{3.49, 99.9\}$, the CPU utilization exceeds α, but the rate of change of the historical CPU utilization has not yet reached δ or ε, so do not perform a capacity scaling up. The RT is modified by 1 because$U_t = 99 > \beta$.

(3) At 31 seconds, $U_t = 103$, and $P = \{3.49, 99.9, 103\}$, the CPU utilization exceeds α, but the rate of change of the historical CPU utilization in the middle has not reached δ or ε, so do not perform a capacity scaling up.

(4) At 32 seconds and $P = \{99.9, 103, 105\}$, the CPU utilization has exceeded α, but the rate of change in the historical CPU utilization has not reached ε, so normal expansion. According to equation (2), the approach to calculate the number of copies of the pod should be expanded to 3, and then expansion starts.

(5) Since it takes 5 seconds to expand a container, the container is expanded to 3 copies at 42 seconds, so the expansion operation is completed.

(6) At 150 seconds, $U_t = 99$, and $P = \{105, 103, 99\}$, the CPU utilization is over α, but the rate of change in CPU utilization is less than 0, so the normal shrink operation is performed at this time according to equation (5). The number of copies of the shrink pod should be 2.

(7) Since it takes 5 seconds to shrink one container, at 160 seconds, the container will be shrunk to two, at which point the shrink operation is completed.

4. Experiments and Data Analysis

This section conducts comparative experiments on the DHPA algorithm's effectiveness in low, medium, and high load cases. The number of containers produced by the DHPA algorithm is compared with the number of containers produced by the HPA algorithm and the number of containers theoretically required to analyze the actual performance of the DHPA algorithm in the three load cases.

The experiment was conducted based on a simulator program written in Java. The specific environment was as follows: operating system Windows 10 1909 version, JDK version 1.8, data analysis program using Python language for writing, the data analysis tool Matplotlib version 3.1.1, and NumPy version 1.16.5. In the simulation experiments, the CPU utilization of a single pod was simulated using the sin function as the base data and multiplied by the corresponding multiplier to simulate the CPU utilization under different pressures. Ten experiments were performed for each of three cases, and the average of the experimental data was taken as a sample value.

4.1. Analysis of Experimental Data under Low Load Conditions. This experiment carries out a comparison by simulating the DHPA algorithm and Kubernetes' own HPA algorithm under low load, simulated node 4, node CPU cores for 4 cores, single-core processing power of 2,252 MIPS, node RAM of 16 GB, hard disk capacity 1 T, bandwidth 1,000 MB/s. In this experiment, CPU utilization ranges between 0% and 200%. We set that every second the CPU utilization of the pod is

$$U_t = 200 * \sin(t), \tag{8}$$

where t is the number of seconds, the whole experiment lasts 180 seconds, and the initial number of pods is set to 1. Part of the experimental data is shown in Table 2, where field time represents the time, BeforeUtil represents the real-time CPU utilization, CalPod represents the theoretical calculation of the number of pods, RealPod represents the actual number of pods after the expansion of the algorithm, AfterUtil represents the expansion of the calculation, and IsBreak represents whether the cluster crashes or not (a single pod crashes if its CPU utilization exceeds 100%).

It can be seen from Table 2 that the DHPA algorithm can perform expansion and contraction operations efficiently at all time points under low load.

The simulated experimental data for HPA are shown in Table 3. The HPA algorithm has a gap between the number of pods and the number of computed pods in most of the time points under low load and cannot promptly perform the scaling operation.

As shown in Figure 4, most of the time, the actual number of pods for the HPA algorithm is lower than the number of pods required, and this problem is largely due to the inadequate prediction of the HPA algorithm at the time of capacity expansion and the cooldown time after the expansion and contraction operation. The DHPA algorithm can efficiently expand and contract capacity after a short delay, which is very close to the theoretical number of pods needed by the cluster, which shows that the DHPA algorithm has a great advantage over the HPA native algorithm low load situations.

4.2. *Analysis of Experimental Data under Low Load Conditions.*

In the medium load experiment, we assume that the number of nodes is 20, the number of CPU cores per node is 4, the single-core processing power of 2,252 MIPS, node RAM is 16 GB, hard disk capacity 1 T, and bandwidth 1,000 MB/s. We expand the multiples of the sin function to simulate the CPU utilization of the pod. The experimental CPU utilization ranges between 0% and 1,000%. We set the CPU utilization per second as follows:

$$U_t = 200 * \sin(t), \tag{9}$$

where t is the number of seconds, the entire experiment lasts 360 seconds, the initial pod number is set to 10, and some of the experimental data are shown in Table 4.

There is a small difference between the number of pods scaled by the DHPA algorithm and the theoretical number of pods under medium load, proving that the DHPA algorithm also has good performance under medium load. As shown in Table 5, the HPA algorithm scales out the number of pods that are needed under medium load and the total number of pods that are needed.

From Figure 5, it can be seen that HPA algorithm has a large gap between the number of pods and the actual number of pods needed, so there were several cluster crashes, which show that the HPA algorithm has a large defect in scaling up and scaling down under medium load.

Table 2: Experimental data of the DHPA algorithm under low load.

Time (s)	BeforeUtil	CalPod	RealPod	AfterUtil	IsBreak
30	100	2	2	50	False
60	173	4	4	43	False
90	200	4	4	50	False
120	173	4	4	43	False
150	100	2	3	33	False

Table 3: Experimental data of the HPA algorithm under low load.

Time (s)	BeforeUtil	CalPod	RealPod	AfterUtil	IsBreak
30	100	2	1	100	False
60	173	4	3	58	False
90	200	4	3	67	False
120	173	4	3	58	False
150	100	2	3	33	False

The number of pods produced by the DHPA algorithm is very similar to the actual number of pods needed, so it can be seen that DHPA algorithm performs relatively well in scaling under medium load.

4.3. *Analysis of Experimental Data under High Load Conditions.*

In the high load experiment, we assume that the number of nodes is 40, the number of CPU cores per node is 4, the single-core processing power of 2,252 MIPS, node RAM is 16 GB, hard disk capacity 1 T, and bandwidth 1,000 MB/s. We expand the multiples of the sin function to simulate the CPU utilization of the pod. The experimental CPU utilization ranges between 0% and 2,000%. We set the CPU utilization per second as follows.

$$U_t = 1000 * \sin(t), \tag{10}$$

where t is the number of seconds, the entire experiment lasts 360 seconds, the initial pod number is set to 15, and some of the experimental data are shown in Table 6.

As seen in Table 6, under high load, the DHPA algorithm falls short of the actual number of pods needed because of the container expansion time limit. However, there is a high overlap with the actual number of pods in the overall expansion and contraction trend.

Table 7 shows that the antijitter delay mechanism still constrains the HPA algorithm, and the number of pods scaled out differs significantly from the theoretical number of pods, thus leading to multiple cluster crashes.

As shown in Figure 6, on the one hand, the DHPA algorithm has a lag in the trend of scaling-down capacity compared to the theoretical pod curve, but the overall trend remains consistent. The HPA algorithm, on the other hand, always maintains a lower number of pods, much lower than the actual number of pods needed. Hence, the DHPA algorithm still has a more significant scheduling advantage over HPA in high load situations and can properly schedule the number of containers to ensure the regular operation of the cluster.

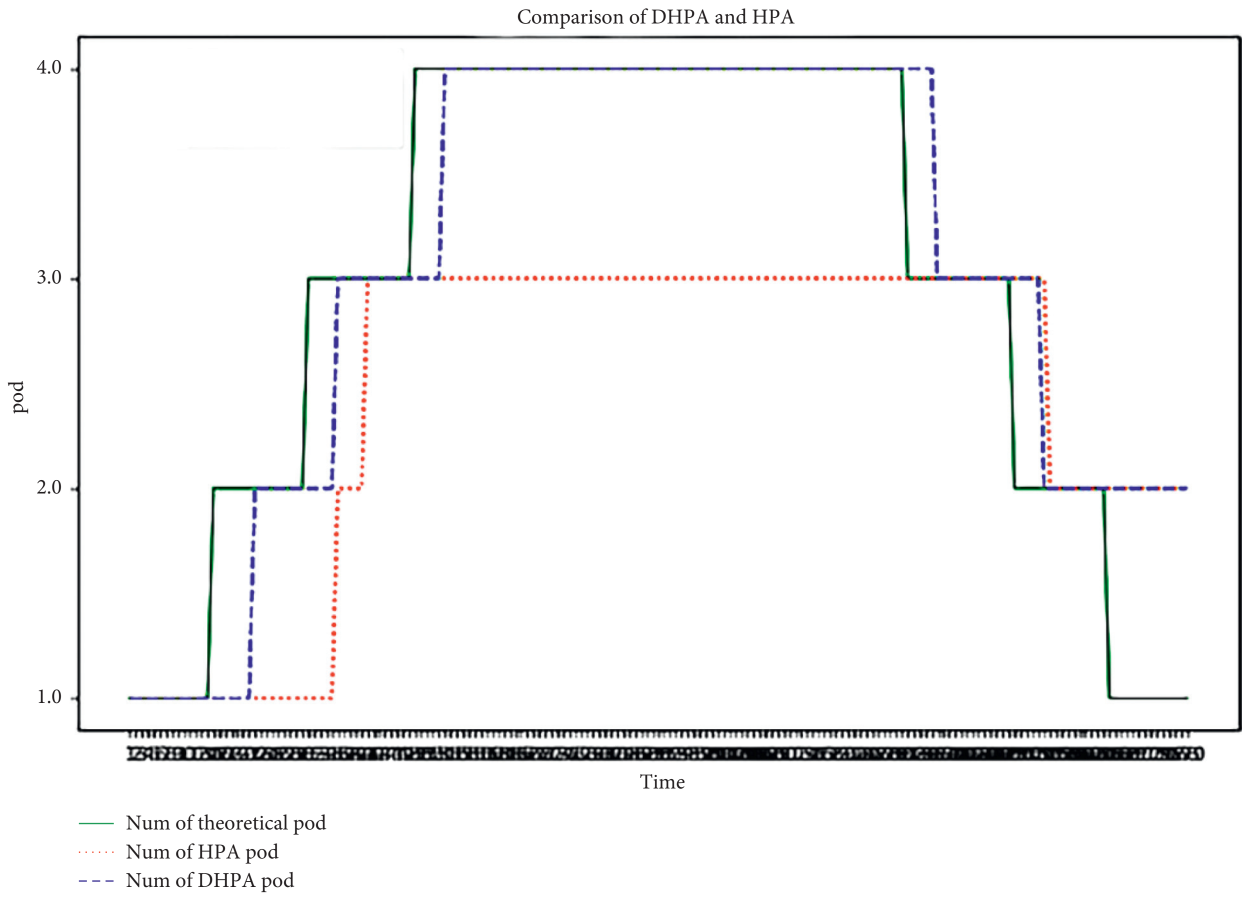

Figure 4: Comparison of the DHPA and HPA algorithms.

Table 4: Experimental data of the DHPA algorithm under medium load.

Time (s)	BeforeUtil	CalPod	RealPod	AfterUtil	IsBreak
60	866	18	16	54	False
100	984	20	21	21	False
160	342	7	11	31	False
230	766	16	11	69	False
280	984	20	21	46	False

Table 5: Experimental data of HPA algorithm under medium load case.

Time (s)	BeforeUtil	CalPod	RealPod	AfterUtil	IsBreak
60	866	18	9	96	False
100	984	20	9	109	Ture
160	342	7	9	38	False
230	766	16	4	191	Ture
280	984	20	4	246	Ture

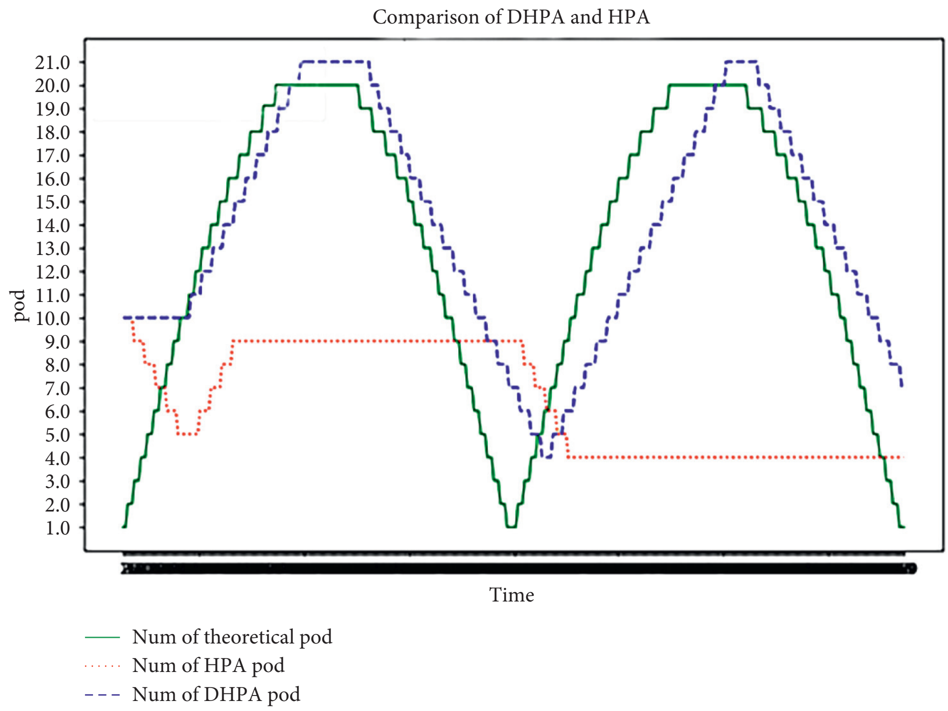

Figure 5: Comparison of the DHPA and HPA algorithms.

Table 6: Experimental data of the DHPA algorithm under high load.

Time (s)	BeforeUtil	CalPod	RealPod	AfterUtil	IsBreak
60	1732	35	22	78	False
100	1969	40	30	65	False
160	684	14	30	22	False
230	1509	31	22	68	False
280	1969	40	32	61	False

Table 7: Experimental data of HPA algorithm under high load conditions.

Time (s)	BeforeUtil	CalPod	RealPod	AfterUtil	IsBreak
60	1732	35	10	173	Ture
100	1969	40	15	131	Ture
160	684	14	15	45	False
230	1509	31	7	215	Ture
280	1969	40	32	281	Ture

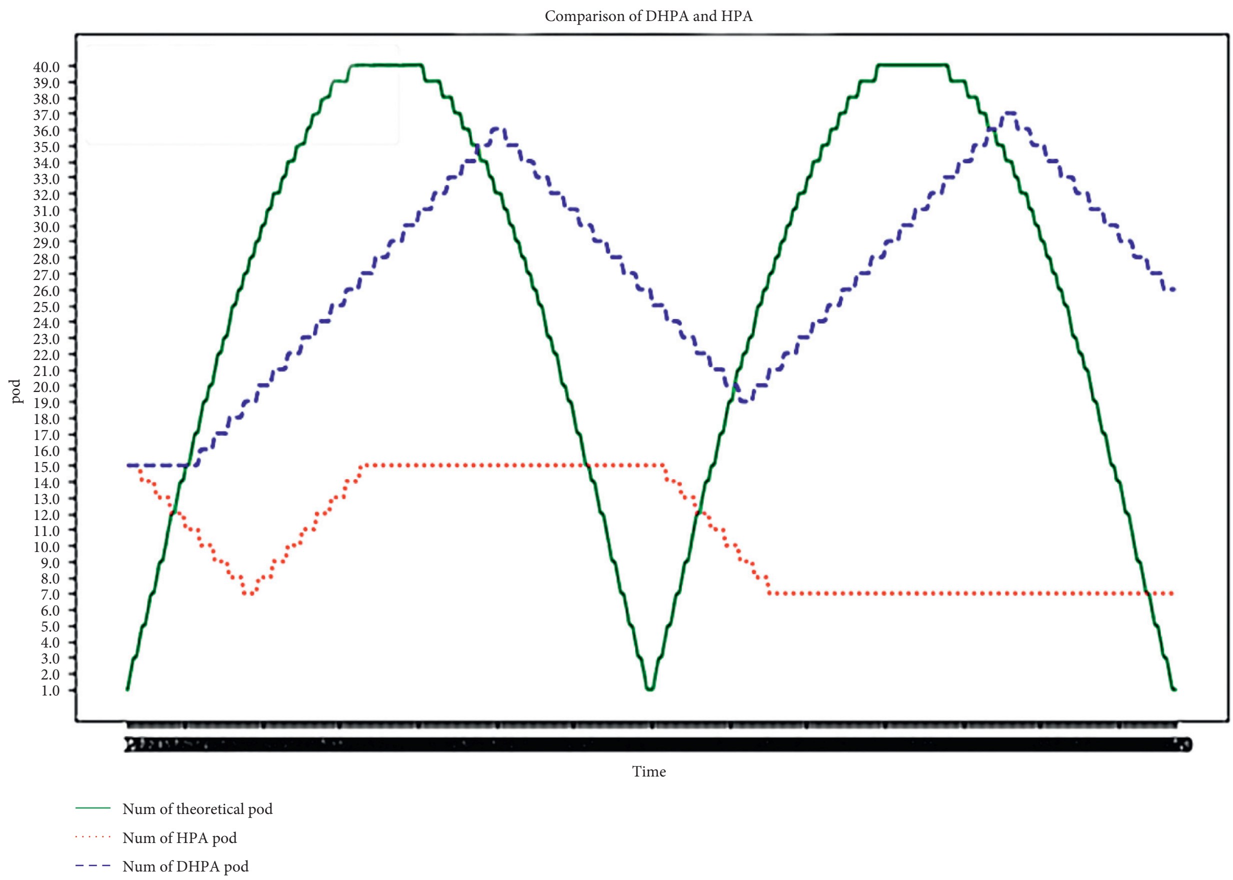

Figure 6: Comparison of the DHPA and HPA algorithms.

5. Conclusions

For highly dynamic workloads in cloud environments, this study proposes a fine-grained horizontal scaling mechanism that can apply dynamic rules to automatically increase or decrease the total number of compute instances to adapt to different workloads. The expansion and contraction operations of the DHPA algorithm are in a dynamic equilibrium state. Because of the pod expansion and contraction time lag, the queue cannot be updated in real time. Each time it scales, it is placed inside the message queue as a single task, so the number of pods dispatched by the algorithm deviates somewhat from the theoretical calculation, but the overall balance is dynamic.

The original HPA algorithm counts how many pods the entire cluster has each time and determines whether to expand or shrink based on the calculated expected pod value. This approach consumes many system resources. In this study, the proposed DHPA algorithm's expansion or contraction operation is based on calculating the growth rate of CPU utilization and on whether the CPU utilization exceeds the threshold to decide by introducing the idea of granularity calculation. Therefore, the DHPA algorithm is to traverse all pods each time in the cluster after calculating whether expansion is needed or not. If there is no expansion or contraction at this point, then there is no need for further operations, which nicely reduces the cluster's performance pressure with each poll. Simultaneous use of two metrics to comprehensively control the expansion and contraction trigger has better stability. The experiments also show that the DHPA algorithm has better antijitter performance in container spreading and shrinking capacity, ensuring the cluster's quality of service and security. In the future, we will try to extend the proposed approach to multi-instance architectures and high-level service customization.

Data Availability

All data used during the study are available in a repository or online in accordance with funder data retention policies (https://archive.ics.uci.edu/ml/datasets.php and http://cs.uef.fi/sipu/datasets/).

Conflicts of Interest

The authors declare that they have no known competing financial interests or personal relationships that could have appeared to influence the work reported in this paper.

Acknowledgments

This work was supported in part by the Natural Science Foundation of Heilongjiang Province (LH2020F031).

References

[1] A. J. Younge, G. Von Laszewski, L. Wang, S. Lopez-Alarcon, and W. Carithers, "Efficient resource management for cloud computing environments," in *Proceedings of the International Conference on Green Computing*, pp. 357–364, IEEE, Chicago, IL, USA, August 2010.

[2] F. Al-Haidari, M. Sqalli, and K. Salah, "Impact of cpu utilization thresholds and scaling size on autoscaling cloud resources," in *Proceedings of the IEEE 5th International Conference on Cloud Computing Technology and Science*, pp. 256–261, Bristol, UK, December 2013.

[3] D. Merkel, "Docker: lightweight Linux containers for consistent development and deployment," *Linux Journal*, vol. 2014, no. 239, p. 2, 2014.

[4] D. Bernstein, "Containers and cloud: from LXC to docker to Kubernetes," *IEEE Cloud Computing*, vol. 1, no. 3, pp. 81–84, 2014.

[5] D. Jaramillo, D. V. Nguyen, and R. Smart, "Leveraging microservices architecture by using docker technology," in *Proceedings of the SoutheastCon 2016*, pp. 1–5, IEEE, Norfolk, VA, USA, April 2016.

[6] F. Rossi, M. Nardelli, and V. Cardellini, "Horizontal and vertical scaling of container-based applications using reinforcement learning," in *Proceedings of the 2019 IEEE 12th International Conference on Cloud Computing (CLOUD)*, pp. 329–338, IEEE, Milan, Italy, July 2019.

[7] K. M. Patel, R. Kandula, B. R. Vempati, H. M. Negalaguli, and P. Chandana, "System and method for elastic scaling using a container-based platform," US Patent 9,462,427, 2016.

[8] E. Casalicchio and V. Perciballi, "Auto-scaling of containers: the impact of relative and absolute metrics," in *Proceedings of the 2017 IEEE 2nd International Workshops on Foundations and Applications of Self ∗ Systems (FAS ∗ W)*, pp. 207–214, IEEE, Tucson, AZ, USA, September 2017.

[9] E. A. Brewer, "Kubernetes and the path to cloud native," in *Proceedings of the Sixth ACM Symposium on Cloud Computing*, p. 167, Kohala, HI, USA, August 2015.

[10] Z. Zhong and R. Buyya, "A cost-efficient container orchestration strategy in kubernetes-based cloud computing infrastructures with heterogeneous resources," *ACM Transactions on Internet Technology*, vol. 20, no. 2, pp. 1–24, 2020.

[11] T. Menouer, "KCSS: Kubernetes container scheduling strategy," *The Journal of Supercomputing*, pp. 1–27, 2020.

[12] T.-T. Nguyen, Y.-J. Yeom, T. Kim, D.-H. Park, and S. Kim, "Horizontal pod autoscaling in Kubernetes for elastic container orchestration," *Sensors*, vol. 20, no. 16, p. 4621, 2020.

[13] S. K Lin, U. Altaf, G. Jayaputera et al., "Auto-scaling a defence application across the cloud using docker and kubernetes," in *Proceedings of the 2018 IEEE/ACM International Conference on Utility and Cloud Computing Companion (UCC Companion)*, pp. 327–334, IEEE, Zurich, Switzerland, December 2018.

[14] F. Rossi, V. Cardellini, and F. L. Presti, "Hierarchical scaling of microservices in Kubernetes," in *Proceedings of the 2020 IEEE International Conference on Autonomic Computing and Self-Organizing Systems (ACSOS)*, pp. 28–37, IEEE, Washington, DC, USA, August 2020.

Hindawi
Scientific Programming
Volume 2021, Article ID 3667252, 7 pages
https://doi.org/10.1155/2021/3667252

Research Article

Online Education Optimization Based on Edge Computing under the COVID-19 Pandemic

Huiling Wang [1] **and Jiasheng Wang** [2]

[1] *Chongqing City Management College, Chongqing 401331, China*
[2] *Chongqing Electric Power College, Chongqing 400053, China*

Correspondence should be addressed to Jiasheng Wang; wjscqu@cqu.edu.cn

Received 10 August 2021; Revised 15 September 2021; Accepted 18 October 2021; Published 27 November 2021

Academic Editor: Punit Gupta

The COVID-19 pandemic has strongly affected education in China, even if education departments and corresponding schools took a series of measures to manage online education of the school's new semester in China, including maneuver, learning platform allocation, and teacher training. In this paper, edge computing is used to optimize online education, and a task offloading algorithm is designed to minimize the computing delay of terminal tasks. Through preparation, practice, and reflection of this online education, this study aims to comprehensively demonstrate the learning condition of online education in China and present the real adjustment impact based on the problems encountered during the process. Although several schools gradually reopened to students in 3 months, several improvements are warranted in various ways. This study proposes the construction of education infrastructure, the adjustment of teaching organization, and the learning methods of teachers and students, providing a clear guiding significance for the development and enhancement of online education in the future.

1. Foreword

In mid-to-late January 2020, colleges, middle schools, and elementary schools in China were transitioning from the winter vacation when the COVID-19 virus outbreak, with acute infectious characteristics and asymptomatic incubation period, erupted and soon became a pandemic [1]. Based on its experience of handling the SARS pandemic of 2003, the Chinese government soon took a series of countermeasures, such as regulating population movements and decreasing population aggregation, especially in schools [2]. Considering the upcoming new semester, the Ministry of Education proposed an online education model to substitute the traditional face-to-face teaching model for governing the teaching progress under large-scale developed Internet construction in China. Consequently, some time was taken to prepare for the new semester, such as commissioning the teaching platform, persuading teachers and students to use the platform, and tapping and allocating educational resources—all of which are currently proceeding regularly. During the pandemic, China had 518,800 schools at various levels and types, 16.673 million full-time teachers, and 276 million students. It was unprecedented for the education system to conduct large-scale, nationwide online education for hundreds of millions of students during the pandemic prevention and control period.

Online education paves a new way of life, work, and learning across time and space by applying information and Internet technology. Thus, the way of knowledge acquisition has endured a fundamental alteration [2]. Indeed, in October 2019, the Ministry of Education of China, along with 11 departments, jointly proposed that the infrastructure construction level of online education would be markedly enhanced by 2020; modern information technology, such as the Internet, big data, and artificial intelligence, will be more extensively used in the education field, and the online education model will be rendered more extensively perfect, with abundant resources and services [3]. During the COVID-19 pandemic, it is time to accrue experience for this education reform, which is an opportunity to further augment the quality and depth of online education.

After the lockdown of Wuhan City on January 23, 2020, Chongqing Municipal Education Commission and several colleges and universities adopted a predictive management model and established an "emergency leadership group" to handle the upcoming large-scale development of online education. During the winter vacation and the Chinese Spring Festival, the schools' management staff communicated with students and their parents in advance and introduced them to what might occur in the teaching mode after the holiday. During the COVID-19 pandemic, China's Internet reached an equitably mature and stable stage, and several conditions of online education, such as teaching platforms, microclasses, and teaching resources, were relatively adequate. Besides, this pandemic proved to be the best test of all aspects, providing sound guidance and inspiration for online education in the future.

2. Online Education Foundation and Higher Education in China

2.1. Online Education: A Crucial Supplement to Education. With the advancement of information technology, online education preserves a stable development trend around the globe. Online education originated in the United States. Almost all top American colleges and universities have already launched online education. The majority of colleges and universities consider online education as a long-term development strategy. In addition, over half of the colleges and universities provide online degrees, all of which have become an integral part of the education system. With the assistance of the online platform independently developed by universities, the online education system in the United States has garnered numerous learners from all over the world [4, 5]. Of note, the online education objective is open to the world and crosses the social, family, economic, time, space, physiological, and other impediments. Thus, it can relax educational inequality in China, which comprises a large population and regional development differences. In recent years, the State Education Commission of China has guided and endorsed online education development, making it a vital part of the education system. Consequently, it has made remarkable successes as shown in Figure 1. A study reported that the online education market in China would reach 387 billion yuan in 2019 and 433 billion yuan in 2020 [6].

2.2. Premanagement and Countermeasures of Online Education. Based on the response experience accrued during the SARS outbreak in China, several education departments did corresponding research and decided to prioritize online office and conference, thereby progressively introducing "online education." Meanwhile, based on the situation during the pandemic, various large education platforms, such as New Oriental and Tomorrow Advancing Life (TAL), have taught lessons through online education. First, the regular management procedure and the implementation of teaching affairs, such as meetings and program operations, will be executed by the Internet, and project application is paperless through the Internet. As a supplement, full-time personnel are hired on duty for specific major projects, which warrant actual participation. Second, the teaching departments launched multiple online projects such as microclass production, online education, and high-quality e-textbooks before the pandemic. However, the coverage of all courses and involvement of all students in China and online education, which will replace the traditional one, were not considered. Third, considering the large scale of students in China, the education committees and schools at all levels explored several online education platforms, including TAL, massive open online courses of China Universities (MOOC), teaching cloud platform, and intelligent vocational education. Consequently, they promoted an online platform of open courses of Chongqing universities, experimental space (National simulation platform). Simultaneously, numerous corresponding teaching platforms are available such as Tencent Classroom and Tencent learning group for backup. Finally, some professionals were recruited to appease students and their parents in mental health care.

2.3. Requirements of Online Education and Adjustment Mechanism. Roger [7] reported that the adaptability of innovation in an organization depends on the following three factors: (i) the relevant features of organizational members; (ii) the innovation itself; and (iii) the pertinent information dissemination. Based on the analysis provided above, teaching in China has conditions of large-scale online education. First, the Internet has undergone significant progress in China, and there exist numerous large local multinational enterprises, such as Huawei, Zhongxing Telecom Equipment, and Tencent, since 2000. Currently, China has advanced information technology and Internet speed. Second, China's online education has also exhibited significant progress after 20-year development and has become a significant supplement of the education system gradually; indeed, the teaching impact of some courses can reach or even exceed the traditional teaching model. Finally, China has a broad base of Internet users, and the network has become one of the most crucial media in the country. Besides, it has already had the full use of the network to disseminate information and corresponding teaching conditions. Thus, large-scale online education offered fundamental support in China, and the COVID-19 pandemic also provided an opportunity to promote and perfect it. In the atypical period, the Internet helped us realize the preaching, receiving employment, and addressing queries between teachers and students.

3. Practice, Adjustment, and Impact of Large-Scale Online Education

After the beginning of the new semester, educational administration and teaching were processed online, and the corresponding teaching model was adjusted and perfected in practice.

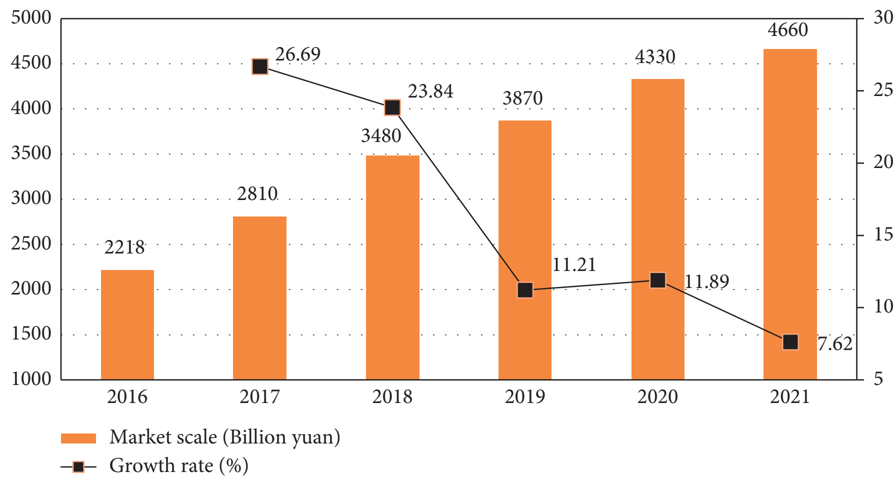

Figure 1: The 2016–2021 China online education market scale and forecast. Note: the data were obtained from Ref. [5], and the data were collected in 2019.

3.1. The High Efficiency of Teaching Administration. With the high-speed Internet access, the efficiency of school conference management improved markedly, the participation rate of the meeting was high, and the cost was significantly reduced; timeliness of information transmission was significantly improved and guaranteed; without time and space constraints, the school meeting was notified 1 hour in advance, and the participants could be in place during the COVID-19 pandemic. Fortunately, a relatively stable network exists in China, including mobile, telecommunications, and cable TV networks. Typically, teachers can enter a meeting as soon as possible, and the meeting time is also relatively short. During the pandemic, more emergency meetings were commenced in schools, which were relatively timely and reliable. Conversely, there were more school administrative meetings and academic meetings in the non-pandemic period. If the organizers could optimize the conference configuration and select the appropriate meeting by the Internet, the work efficiency of teachers and students would be significantly enhanced.

During the pandemic, many universities launched large-scale online job fairs, where candidates could complete the interview online. For example, Tsinghua University, Harbin University of Technology, Chongqing University, and other universities took the remote defense mode for numerous doctoral candidates. Some international competitions, such as the finals of the 2020 Future Problem Solving Program International Chinese National Competition, were also launched online on March 28, and the team members attained the goal through Tencent Meeting and completed the competition content. Although there is no close contact, the students can still feel that this is a game. Furthermore, some elementary school students created study groups online to jointly complete the homework assigned by teachers.

3.2. Miscellaneous Platforms and Mismatched Teaching Resources. In the last few years, several multinational enterprises have materialized online office, and the number of people working remotely online has risen dramatically. During the COVID-19 pandemic, the number of telecommuting personnel surged, which led to some congestion in the network. Thus, when all students participate in online learning, network congestion is inevitable. Although the education department conducted various tests during the winter vacation, the teachers performed well in advance. After the semester began, on February 17, 2020, universities, middle school, and primary schools started classes in stages, and students took online classes by the public online platform. Nevertheless, several online education platforms collapsed, such as MOOC, teaching cloud platform, and intelligent vocational education, and live teaching of most courses failed because of severe network congestion. To handle such problems, the education department arranged classes in more detailed stages and decentralized network traffic; nonetheless, network congestion prevails. Consequently, many teachers and students selected the self-media platform Tencent to complete teaching.

Meanwhile, the education department and school teachers prudently prepared and contacted some public online platforms, which then actively responded. However, some schools and teachers did not keep their promise and refused to provide public resources with multiple excuses during the policy implementation. Likewise, jamming during Internet traffic peak is standard on many public online platforms in China. Hence, most teachers and students selected the Tencent platform. However, online platforms, such as TAL and VIPKID, which are charging platforms, were relatively smooth, highlighting deficient technical handling and management of several public platforms. Usually, some private or charging platforms were worried about losing their customers, and they appeased users from management and commercial communication and augmented their technology to make their platforms smooth. During the adjustment process, the private and charging platforms added class interaction and function module, making the platforms more attractive and effective. Finally, teachers of public online platforms, such as MOOC, vocational education cloud, and cloud platform, selected the Tencent platform.

In the first large-scale online education, teaching software, network facilities, computer equipment, and other hardware differed from teachers and students, causing differences in teachers' proficiency and also affecting the class quality. Meanwhile, students varied from regions and family backgrounds, for example, some students in rural areas had low network signal, and they often disconnected during live teaching, while some students even had no computer at home.

3.3. Less Interactive Support and Low Concentration in Class. As a large number of participants in online education came from different family backgrounds, many had different perspectives toward online education. Indeed, some students even had no essential concept, let alone listening to online classes. Through the census, several rural students were relatively poor in teaching resources and had no progress management in classes. In the real process, several students did not wholly participate in online education and complete homework. Hence, numerous schools prompted students to return to classrooms as soon as possible and rearranged the process test. For the first large-scale online education, the educated group itself had a broad range, and it was challenging for teachers to monitor or supervise the process entirely, especially for imperfect platform modal and learning condition. Meanwhile, requiring an enhancement in teaching quality was unrealistic too.

Certainly, the growing age of students is clearly defined. For example, elementary school students are relatively weak in self-discipline and get easily distracted; thus, they need to be more restrained in class. Middle school students have higher relative self-control ability; however, they need to be reminded or interacted in some places. College students, on the other hand, are basically self-study based on purpose. All these warrant educators to study individual characteristics judiciously. At the beginning of online education, several students listened more intensively; however, with time, students became bored with such education. In teaching, if no interaction occurs between teachers and classmates, students tend to lose interest and become inattentive gradually. Students who want to learn will promote their progress through continuous interaction, whereas those who do not want to learn will often choose games to escape, and the impact of online learning would decline significantly over time.

3.4. Low Recognition of Online Education Quality. Owing to varying teaching conditions, the type of teaching organization will also change; after all, it is the bridge between teaching and learning and will reorganize and arrange teaching activities based on the teaching specific ideas, goals, content, and subjective and objective conditions [8]. There exists a complete lack of essential exploration and experimentation in the teaching organization for the abruptness of the pandemic outbreak. It is highly challenging for teachers to break the limitation in time and space and effectively combine the enormous contrast between online education and the traditional model; this change warrants very high personal organization and the learning ability of teachers. If a teacher is in a hurry to adjust teaching, the adjustment of teaching methods commands high requirements for students. After all, different children's family backgrounds and educational methods ascertain different understanding, and understanding bias can be eliminated only by face-to-face interaction. In the absence of objective conditions (language and behavior), online education lacks communication and integration, inevitably leading to the disapproval of teaching quality.

The typical online education is targeted at students, and its teaching organization has been optimized for a small student range in the online charging platform. With time, the scale of online education proliferates, and its teaching organization cannot be enhanced in a short time; thus, its online class quality is hard to fulfill the expected requirements. Online education quality is the fundamental condition for the continued existence and development of emerging online education. The focus of this research is how to ensure and enhance the quality of online education. In China, for example, the quality of several teaching materials is low, and even the knowledge in the teaching materials is misleading. All these problems need teachers to explain in class.

4. Enlightenment of Online Education Practice

Against the backdrop of China's fight against the COVID-19 pandemic, education departments have gone all out and attained certain teaching results; however, online education still needs significant enhancements.

4.1. Resource Support and Deployment

4.1.1. Online Education Foundation: Facility Construction. Online education is an integral cog in the construction of fundamental Internet. As of June 2019, the number of Internet users in China reached 854 million, the Internet penetration rate was 61.2%, and the number of broadband access users >100 million, accounting for 77.1% of the total Internet access [9]. Thus, China's high-speed Internet has not been wholly popularized yet. For regions where the Internet has not yet been connected to broadband or the capacity is inadequate, regular online education is affected markedly. Besides the interruption of video and live broadcasts, net jams also occur in cities, and many students are even squeezed out during class. On the other hand, several technical and management issues warrant improvement. Although the Tencent platform also experienced net jamming at the beginning of the new semester, the jam gradually vanished, and even many interaction models were added to enhance the platform after continuous optimization and improvement. Consequently, several teachers and students finally flocked to Tencent. The change is also vividly reflected in the charging platform TAL. Initially, TAL was blocked; however, its technicians adopted switching lines for winning time and optimized its platform until the jam was eliminated. Besides, the improved platform is more interactive between teachers and students. Hence, TAL not only retains its original customers but also attracts some customers from other platforms. Conversely, some charging platforms lack technology and creativity owing to the loss of customers during the pandemic.

Based on the students' characteristics in the region, the education departments will establish a corresponding platform for the corresponding student groups. The enhancement of the education platform also should be upgraded after the network technology matures. If the platform advances quickly, it increases the requirements for users and facilities. Besides, it can increase technical maintenance, which is also a crucial part; it can gather the platform information in real time, optimize the platform environment, and assist with the administration when necessary. During the COVID-19 pandemic, Facebook decreased the clarity of its software images to reduce network traffic, enabling people who need it more to use the Internet. Likewise, China also adopted measures like staggered surfing, effectively alleviating net jamming.

4.1.2. Enrichment and Enhancement of Educational Resources. In primary and secondary schools, uniform textbooks are present in China, and the relative error rate is low. However, many university textbooks are recommended by teachers. Due to the lack of supervision, the quality of these books is relatively low and often cannot meet the teaching requirements [10]. Currently, to seize the teaching textbook market, several publishing houses let textbooks go unsupervised, resulting in low quality. Second, some publishing houses did not open their textbooks to students during the pandemic, and some students had no textbooks in class. In traditional classrooms, teachers can correct errors in textbooks by direct communication; it is hard to deal with such problems in online education; at least, it would take some time to find suitable methods to perfect it. If online education is to be promoted on a large scale, textbook and teachers' quality should be improved markedly.

In April, after several students returned to school in China, even more students took online classes on the charging platform than before the outbreak. First, the habit of students taking online classes was shaping gradually. Second, the platforms ensured the improvement of teaching quality; their teachers graduated from famous universities at home and abroad, such as Zhejiang University and Peking University, besides excellent textbooks compiled by the platform teachers. Finally, good management was essential; over tens of thousands of students were studying in a TAL class, and these students were divided into many small classes to complete their homework, all of which was taken care of by some ordinary teachers. Furthermore, the charging was cost-effective for students and teaching quality and recommended books were good.

For large-scale online education, the education department must first reinforce control over the teachers' quality. If a teacher is unqualified, it will harm students [11]. Meanwhile, teaching textbook quality must be enhanced; after all, learning in class only is transient, and reinforcement and upgrading based on textbooks after class is the most crucial part [12]. Although China's education department has undertaken the construction of several planning teaching materials, excellent resource sharing courses, majors, and national teaching achievement awards, the actual impact has not reached a high level in terms of operability and quality at all.

4.2. Changing Participants' Attitude toward Online Education. At the beginning of the pandemic, online education was not accepted by most Chinese people because of long-time dominated traditional offline education. Compared with traditional education, online education has demonstrated its advantages during the pandemic to everyone, including students, students' parents, and teachers, which is also extensive marketing for online education. Despite several problems, online education has also played its advantages in several aspects, especially for time and efficiency, and there remains considerable room for improvement. Nowadays, educators and the educated consider more time efficiency in an era of knowledge explosion and fierce competition. Traditional education is a systematic framework; however, online education can replace these educational methods and fulfill the requirements of parents and students themselves. This is also the charm of the tremendous progress of online education at home and abroad in recent years. Likewise, several charging online platforms provide various online public classes such as Chinese, mathematics, physics, chemistry, and so on. Besides, these platforms provide excellent textbooks, teachers, and cheap fees for students.

Of note, the development of online education is inevitable. Thus, teachers and parents must harness their ability in online education and knowledge appraisal as well as guide students to effectively use online resources to enhance learning efficiency [13]. After the pandemic, the ability training of online education would become a major area. The online application can be indorsed in primary and secondary schools early and can implant professional classes; the requirement can augment the integration of students and teachers in advance. It is imperative to guide students to use the Internet to obtain resources correctly and effectively [14]. Second, parents should have a correct attitude toward online education, and they must be capable of identifying its advantages and disadvantages. Under such a situation, parents can exercise supervision and guide children's learning effectively at home. After all, online education is a live broadcast and open to the public; the fundamental application skills of online education and the preparation of professional courses are more demanding for a teacher.

4.3. The Application of Information Technology as an Educational Tool. Previously, schools and parents in China kept students away from computers and mobile phones to prevent them from playing games. The pandemic has also made schools and parents realize the significance of information technology courses and online education. Based on the effect of online education in the pandemic, the education department can implant more information technology courses into standard teaching in advance [15]. Meanwhile, it is also feasible to augment regular management and educational activities through the Internet. Of note, the security of the campus Internet must be strengthened; however, ordinary meetings can be adopted online, which is not suitable for large-scale work meetings involving confidentiality. If one intends to open a meeting in this area, you can use the internal lines of the campus network.

In addition, the operation of online education has highlighted several problems during the pandemic. First, students and teachers did not adapt to online education. Teachers were nervous or helpless in class, while students had relatively weak Internet knowledge. For students of colleges or universities, student's backgrounds differed, and their adaptability to online education varied markedly. The answer to this problem lies in unhinged education development. Thus, the online education department can standardize the frequently used functional modules and promote it in schools at all levels. Likewise, introducing some interactive links can be implanted in a public platform, such as group discussion and answering, which would assist students and teachers at all levels to provide online education purposefully. Besides, it is feasible to develop a self-grading platform for students, such as embedded algorithms like roll call, sign-in, interactive question answering, and homework, which can automatically serve as the general evaluation and can effectively decrease the teachers' workload. In preventing net jamming, an optimized algorithm can be used, or an optimized guarantee strategy can be adopted at the beginning of construction.

4.4. Teaching Management and Quality Improvement. Students, parents, and teachers had a difficult adjustment section toward online education because the teaching methods and habits of online education differed significantly from traditional education. Despite having reservations about the quality of education during the pandemic, participants and guardians only had this one option to choose from. Nonetheless, learning efficiency has always been a primary concern of online education practitioners. As an upcoming teaching mode, the form of online teaching organization should be changed considerably to enhance its efficiency.

In the traditional offline classes in China, teachers are the mainstay, and students are supplementary, whereas the essential positioning of the teacher-student role in online education is "learner-centered." Teachers are more often "assistants," the builders of "scaffolding" in the growth of students' thinking and innovation ability. In addition, curriculum design is a major concern, such as how to prevent students from distracting themselves or loss of vision during online class; all these can be effectively evaded through teaching organization. Regarding curriculum design, no matter how good online education is, several students still cannot achieve perfect communication. The new teaching organization will make students participate in the class as fully as possible and learn independently. From this perspective, the pandemic has provided more people with new thinking about online education; perhaps, China's forms of education would also become diversified in the future.

The curriculum can be created in different levels by the characteristics of students (e.g., primary school, junior high school, high school, and university) and the course itself. Unquestionably, it also can be the principle of combining online and offline education; part of the theory is taught online, while the offline part mostly focuses on practical. From the standpoint of large-scale teaching, there are tens of thousands or even hundreds of thousands of students (basic mathematics or Chinese) in an online class (TAL net class or some famous scholars' class), whereas teachers can teach one-to-one online or offline for challenging courses.

A general survey of online education revealed that students' learning effect is not good. Encountering the ever-increasing number of online courses, how to construct a comprehensive, objective, and instructive quality evaluation system is a pressing problem in China, which can not only give full play to the traditional advantages of China's education and teaching but also promote the benign development of large-scale online education courses in China.

5. Conclusions

The development and optimization of online education in China is an inevitable trend with the development of network technology. In addition, the pandemic offered an excellent opportunity for the education department to optimize online education continuously in practice. For instance, the quality of textbooks, teaching organization forms, and several specialized reforms are on the road for teachers and students, whereas China's 5G network is built, and public platforms are also optimized.

Moreover, parents and students can now fully realize the advantages of online education after experiencing the initial maladjustment of the pandemic. Even after the schools reopened, many students still opted for online education in many classes; this is the driving force of substantial growth in online students after the schools reopened compared with before the pandemic.

Furthermore, the online education platforms seized the catalyst of the "pandemic" to constantly innovate and tap their potential, which also won the trust of their customers. Besides, parents and children also affirmed this online education model during this period. Going forward, the map of the education industry will be reshuffled in the future, and online education will change from a supplementary method of traditional teaching to a mainstream method.

Data Availability

No data were used to support this study.

Conflicts of Interest

The authors declare that they have no conflicts of interest.

Acknowledgments

This study was supported by the Special Research Project of One Belt, One Road Education International Cooperation in 2019 (no. 19YDYL10), Chongqing Education Planning Project (no. 2020-GX-384), and Research Project of Chongqing City Management College (no. B-2).

References

[1] Y. Pan, D. Zhang, P. Yang, L. M. P. Leo, and Q. Wang, "Viral load of sars-cov-2 in clinical samples," *The Lancet Infectious Diseases*, vol. 20, no. 4, 2020.

[2] C. Chen, X. Zhu, and L. I. Xueru, "Campus management in the crisis of SARS," *Higher Education Exploration*, no. 2, pp. 2–8, 2020, (in Chinese).

[3] xinhuanet, "The level of infrastructure construction for online education will be greatly improve in China," 2019, http://www.xinhuanet.com/politics/2019-10/02/c_1125068451.htm(in Chinese).

[4] Y. H. Zhu, X. B. Han, J. Yang, and J. G. Cheng, "Irreversible online development of higher education:systematic analysis of 11-year sloan consortium report series on online education in the US," *Tsinghua Journal of Education*, no. 4, pp. 92–100, 2014, (in Chinese).

[5] I. Consultation, "China's Online Education Market Will Reach 387 Billion Yuan in 2019," 2019, https://www.iimedia.cn/c1061/65338.html.

[6] L. Peng and L. Zhou, "Reflections on the quality of online education by consulting," *JOURNAL OF HIGHER EDUCATION RESEARCH*, vol. 29, no. 3, pp. 66–68, 2006, (in Chinese).

[7] M. D. Byrd, "Back to the future for higher education," *The Internet and Higher Education*, vol. 4, no. 1, pp. 1–7, 2001.

[8] M. A. Xiaoqiang and D. U. Liping, "The evolution of organizational form of instruction and network-based teaching [J]," *Educational Research*, vol. 23, no. 4, pp. 49–51, 2002, (in Chinese).

[9] China Internet Network Information Center, "The 44th statistical report on China's Internet development," 2019, http://www.cac.gov.cn/2019-08/30/c_1124938750.htm(In Chinese).

[10] Z. Chen, "Research on online education development strategy of publishing industry under the concept of teaching resource sharing," *China Publishing Journal*, no. 12, pp. 29–32, 2017.

[11] X. Yang and X. Zhou, "Research on current situation and development trend of online education in China: from analysis of NetEase open class and other 16 online education platforms," *E-education Research*, vol. 38, no. 8, pp. 63–69, 2017, (in Chinese).

[12] J. Shen, "Challenges, problems and trends of textbook construction in the new era," *Curriculum, Teaching Material and Method*, no. 9, pp. 7–9, 2019, (in Chinese).

[13] L. Wang, "The Lates t development of MOOCs in the USA and its implications to Chinese higher education: based on an interpretation of sloan report series," *Journal for Higher Education Management*, no. 5, pp. 34–40, 2014, (in Chinese).

[14] J. Yang, "Science teaching focuses on guiding students to explore independently," *China Educational Technique & Equipment*, no. 13, 2011.

[15] Q. Yang and Y. U. Liang, "Analysis of the connotation, characteristics and core elements of "internet + education"," *The Chinese Journal of Ict in Education*, no. 3, pp. 25–30, 2018, (in Chinese).

Hindawi
Scientific Programming
Volume 2021, Article ID 2257415, 12 pages
https://doi.org/10.1155/2021/2257415

Research Article

A Data-Driven Optimization Model of Important Multidimensional Factors Affecting College Students' Cognitive Engagement in Ideological and Political Theory Course

Liangliang Wang [1,2]

[1]School of Marxism, Northwestern Polytechnical University, Xi'an 710072, Shaanxi, China
[2]School of Marxism, Xi'an Shiyou University, Xi'an 710065, Shaanxi, China

Correspondence should be addressed to Liangliang Wang; celiawong@mail.nwpu.edu.cn

Received 11 August 2021; Accepted 5 November 2021; Published 26 November 2021

Academic Editor: Punit Gupta

The optimization of important multidimensional factors is conducive to cognitive engagement, which is a crucial dimension of student engagement and plays a significant role in college students' learning of the Ideological and Political Theory Course. However, because there are many influencing factors associated with cognitive engagement, the influence mechanism and analysis strategy of this kind of model are relatively complex. In order to solve this research gap, this paper establishes an optimization model affecting Chinese college students' cognitive engagement in IPTC on the basis of sample collection and investigation. In this process, 4,700 questionnaires were distributed to 47 colleges and universities across the country, and copies were effectively recovered ($N = 3992$); the effective recovery rate was 84.94%. Cronbach's alpha of 0.759 indicates that the scale has high reliability and Pearson's correlation coefficient $P \leq 0.001$ shows that the scale has good validity. The KMO value of 0.703 in the Bartlett sphere test also shows that the scale is suitable for factor analysis. Firstly, according to the method of factor analysis, there are six important factor dimensions affecting college students' cognitive engagement in the IPTC, namely, attention and motivation factor dimension, behavior and value attainment factor dimension, interest and practicality factor dimension, personality and will factor dimension, evaluation and time factor dimension, and knowledge and strategy factor dimension. Then, through descriptive analysis, it is found that personality and will factor dimension ($M = 6.5837$) plays a relatively major role while knowledge motivation dimension ($M = 6.3505$) has a weak impact on cognitive engagement. Finally, from linear regression analysis, there is a significant positive correlation between cognitive engagement and other variables. In addition, undergraduates are slightly lacking motivation in the learning of the course, and vigorously strengthening college students' cognitive engagement is still necessary, so as to effectively enhance the effectiveness of the IPTC in the future.

1. Introduction

Students' degree of cognition toward things determines their choice of direction when encountering difficulties, which further affects the individual's learning efficiency and development. In China, the Ideological and Political Theory Course (IPTC) is considered to be a course that is a key to implementing the fundamental task of moral education [1]. Only by fully understanding the content of the Ideological and Political Course and its significance can we better solve the fundamental problem of whom to train and how to train [2]. Only with full cognition of these things can college students understand the relationship between subject and object, develop good learning emotions, invest in mental endeavors, and transform all of those merits into positive actions.

1.1. Cognitive Engagement as a Part of Student Engagement. Tyler, an American educator, first used the concept of "student engagement" in the 1930s and 1940s [3] and it consists of two parts, namely, engagement in learning and learning time. Tinto argued that student engagement is the integration of society and study [4]. Astin put forward the student engagement theory, revealing the main content of student engagement from five aspects. The main content mainly includes the relationship between the time and quality of a student's investment in school life, as well as learning outcomes [5]. Scholars, such as Christenson et al., gain an understanding of student engagement through conceptual decomposition. According to the classification method, student's engagement can be divided into four aspects: academic engagement (refers to a student's involvement in learning tasks, credit growth, and time spent completing assignments), behavioral engagement (refers to a student's attendance, participation, and preparation for the course), cognitive engagement (refers to value relationships, etc.), and emotional engagement (refers to a student's understanding and sense of belonging to the school) [6]. Recently, student engagement has been measured by participation in online courses [7].

Cognitive engagement can affect the degree and quality of a student's efforts in classroom activities. Although researchers have emphasized psychological engagement in learning, the focus of each researcher has also been different. Corno and Mandinach formerly proposed that cognitive engagement was a dimension of student engagement and believed that self-regulated learning was a representative form of cognitive engagement, which can guide students to a higher level of reflection [8]. Connell and Wellborn concluded that the concept of cognitive engagement included problem-solving flexibility, hard work, and active response in the face of failure [9]. Newmann et al.[10] and Wehlage et al. [11] have emphasized the engagement of internal psychological quality in the learning process. As can be clearly seen, the study of cognitive engagement is typically accompanied by the study of learning strategies and self-regulation. Regardless of which aspect they focus upon, students will use metacognitive strategies to plan, monitor, and evaluate their cognition when completing a learning task [12]. Students will consciously use certain learning strategies to help themselves, and they will also use persistence or suppress interference to maintain their cognitive participation [13]. In short, students definitely use a variety of cognitive strategies in their learning, thereby reflecting a high degree of integration of various psychological connections. The essence of cognitive engagement lies in students' level of self-regulation level in learning [14]. Generally, with a higher level of cognitive engagement, students can use deeper cognitive strategies, develop a stronger thirst for knowledge, and engage in more active and in-depth thinking. On the contrary, students with relatively low levels of cognitive engagement typically mechanically memorize information in the form of superficial engagement. Cognitive engagement, therefore, refers to a student's degree of engagement in learning and the use of strategies [15, 16].

1.2. The Meaning of Cognitive Engagement in IPTC. Cognitive engagement in the IPTC means paying attention to the IPTC itself and comprehensively recognizing the IPTC from the perspective of Marxism. Once this occurs, the cultivation of college students' values and motivations can be strengthened. The IPTC has a far-reaching effect on soul cultivation and education among college students [17]. Only when college students have sufficient and comprehensive "cognition" of the IPTC can the actual meaning of the IPTC be achieved and thus further strengthen the development and innovation. Only by continuously enhancing college students' theoretical literacy and thinking ability and then directing them to establish a scientific worldview, methodology, and values can college students enhance their sense of gain [18]. First of all, college students must realize the importance of setting up the IPTC. From the perspective of our national strategy, the IPTC is an important course in terms of realizing the great goal of modernizing education, building a strong and well-educated country, and providing satisfactory education for the people [19]. To achieve democracy in this country as well as national prosperity and a peaceful work-life balance for the people, our citizens must first fundamentally understand this country and establish the ideal of working hard for the country. The IPTC is exactly intended to assume this responsibility and help the country prepare for the cultivation of builders and successors of the socialist cause. Secondly, college students should recognize the content of the different IPTC. Compared with other learning phases, the college IPTC is indeed different in terms of curriculum goal planning, curriculum system adjustment, curriculum content coordination, and textbook system compilation. Therefore, student engagement is critical to students' learning, especially in the IPTC. It is also necessary to highlight the characteristics of the course and to establish a dialectical Marxist worldview and methodology through theoretical study, in order to understand the world and then transform the world. Finally, college students should recognize how to practice the IPTC. In the classroom teaching of the IPTC, theoretical teaching is the main teaching form. However, relying solely on theoretical teaching is not nearly enough to make education effective, useful, and deeply rooted in the hearts of the people as the college classroom become more and more complex, and there are more interested parties [20]. Practical teaching is an important and useful supplement. This type of teaching is not only able to combine theory and practice, classroom and society, and learning and research but also helps students learn how to think and analyze, by linking theory with practice.

1.3. Cognitive Engagement Benefits Other Dimensions of Student Engagement in IPTC. In the course of IPTC teaching, paying attention to students' engagement can improve the effectiveness of IPTC as student engagement consists of cognitive engagement, affective engagement, conation engagement, and behavioral engagement. In this way, teachers can enhance these four aspects of engagement to jointly improve the overall student engagement level. Cognitive engagement of IPTC is college students' understanding and recognition of the rich content of IPTC. Affective engagement is the attitude of love and hate advocated and propagated by college students to the courses. Conation engagement helps college students to realize the responsibility and obligation given by society and take conscious and unremitting efforts. Behavioral engagement is the performance of the content of IPTC in action based on cognitive engagement, emotional engagement, and conation engagement. In this process, the four dimensions of engagement seem to be relatively independent, but it is an integration process of mutual connection, mutual influence, mutual penetration, and mutual promotion. Among them, cognitive engagement is the foundation, which guides, controls, and regulates emotional input, conation engagement, and behavioral engagement. In IPTC teaching, students' engagement can generally be carried out in the order of improving cognitive engagement, cultivating emotional engagement, exercising mental engagement, and practicing behavior engagement. Because there is no rule about which dimension comes first and which is last, it is acceptable for all four dimensions to proceed sequentially or in leaps. Through cognitive engagement of IPTC, college students enhance the cultivation of noble sentiment, cultivate strong revolutionary will behavior, and have stronger expressive force, indicating that cognitive engagement is more important.

2. Methods

2.1. Sample Collection and Investigation Process. By referring to many research questionnaires in the field of students' cognitive engagement [21–25], this study formed the National Survey of Student Engagement in Ideological and Political Theory Course (NSSE-IPTC), allowing us to carry out research on college students' cognitive engagement with the IPTC. The cognitive engagement scale is a subscale of the Student Engagement Scale. When using the scale, students participating in this study were required to give different scores, according to their degree of agreement with each question. From disagreement to agreement, there are 1 to 10 points, respectively. The range of scores indicates the different degrees of cognitive engagement in processing information and answering questions.

Forty-seven universities were randomly sampled nationwide. Through open questionnaires, the cognitive engagement of different groups of students learned that the IPTC was investigated. The issuance of the questionnaire took into account multiple factors, such as region and school category. A total of 4700 questionnaires were actually distributed, and 4331 were recovered. After invalid questionnaires and incomplete waste papers were manually removed, 4115 valid questionnaires were recovered. After the data were input into the statistical software in the later period, another 123 nonconforming questionnaires were filtered out by high and low score grouping. Finally, 3992 questionnaires were available to be tested, so the effective rate of the questionnaire scale was 84.94%. The questionnaire was analyzed statistically with the help of Epidata and SPSS17.0 statistical software. The composition of the subject group is shown in Table 1.

Table 1: Participant composition frequency statistics.

	Frequency	Percentage
Gender		
Male	2115	53
Female	1877	47
Nationality		
Han	3940	98.7
Other	52	1.3
Student position		
Classroom cadre	471	11.8
Student union cadre	40	1
Other	3481	87.2
University type		
Project 985 University	1021	25.6
Project 211 University	866	21.7
Non-985 and non-211 project university	2019	50.6
Third batch of undergraduate	86	2
Student grade		
Freshman	702	17.6
Sophomore	1393	34.9
Junior	1672	41.9
Senior	225	5.6
Other	0	0
Major		
Liberal arts	1588	39.8
Science	2404	60.2
Family		
Only child	1449	36.3
Nononly child	2543	63.7
Join clubs		
Participation	846	21.2
No participation	3146	78.8
Religious		
None	3864	96.8
Buddhism	64	1.6
Christianity	43	1.1
Catholicism	21	0.5
Mother's occupation		
National party and Mass organization	527	13.2
Technical staff	317	7.9
Clerk	842	21.1
Business and service industries	385	9.6
Agriculture, forestry, animal husbandry, etc.	317	7.9
Other	1604	40.3
Father's occupation		
National party and Mass organization	83	2.0
Technical staff	617	15
Clerk	370	9.0
Business and service industries	623	15.1
Agriculture, forestry, animal husbandry, etc.	286	7.0
Other	2013	51.9

As can be seen from Table 1, the following information was explained:

(1) *Gender*. The gender ratio of male and female students was 53% and 47%, respectively, and the gender distribution was basically balanced. There is no uneven proportion distribution caused by departments, majors, and other reasons, so as to reduce the potential error as much as possible and ensure that the measurement results are not different due to gender differences.

(2) *Major*. In the survey, 1588 valid scales were from liberal arts students, accounting for 39.8% of the total number of surveys. Science students had 2,404 questionnaires, accounting for 60.2%. The majority of respondents were science students.

(3) *Nationality*. This study does not deliberately consider the proportion of ethnic minority students in IPTC, so the nationality of Han students accounts for 98.7%, while other ethnic groups only account for 1.3%. The reason is that most of the scales are distributed by the researcher's teachers, classmates, and friends, all of whom are from the Han nationality. As a result, the scales distributed to Han students account for a large proportion in the process of information collection, so that the scales do not pay special attention to the differences of ethnic minorities.

(4) *Family Members*. Since the subjects were post-1995 undergraduate students, the only one-child accounted for 36.3%, while other families with two or more kids accounted for 63.7%.

(5) *Student Positions*. In the survey, there were 471 student leaders, accounting for 11.8% of the surveyed students. Student union members are relatively small, 40 undergraduates, accounting for 1%. 87.2% did not hold the position of student position.

(6) *Join Clubs*. Of the respondents, 21.2% of students said they had participated in school clubs, while 78.8% had not.

(7) *University Type*. A total of twelve "985 universities," ten "211 universities," other 24 universities, and 1 tertiary university were investigated. In the study, 22 universities were included in the "double First-class," accounting for 47.3% of the subjects. The uniform distribution at the college level has achieved the sampling effect.

(8) *Religious*. 3.2% of college students have religious beliefs, among which 1.6% are Buddhism and 1.1% are Christianity, and only 0.5% are Catholicism. Other college students are not involved.

(9) *Grade of Students*. In the sampling, the factor of college students' grades is considered, because the IPTC has different contents in different grades. But there is an exception that some students finish IPTC in other grades because of other factors such as retaking and suspension. Every subject of IPTC is in a unity and unified set. Only when all courses are completed completely by students can the overall education and teaching effect be shown.

(10) *Parents' Occupation*. According to the research, 59.7% of college students expressed their mothers' occupation while 40.3% did not specify their mothers' occupation. Accordingly, 48.1% of the college students made a specific distinction about their father's occupation while 51.9% of the other students did not explain their father's occupation.

2.2. Reliability and Validity Test. This research uses Cronbach's alpha to test the reliability of the scale indicators. The degree of intersection refers to the degree of accuracy of the measurement result, that is, the degree of closeness between the measurement result and the object to be measured. The higher the correlation coefficient, the better the criteria of the questionnaire. From Table 2, Cronbach's alpha of college students' cognitive engagement in IPTC is 0.759, which performs well, thereby indicating that the scale has high credibility and is suitable for the factor analysis. A correlation analysis is to determine the statistical correlation between two or more variables. Then, the strength and direction of the correlation must be analyzed.

3. Optimization Model Analysis

3.1. Factor Analysis

3.1.1. The Basic Principle of Factor Analysis. When C. Sparman put forward factor analysis, it has been widely used in many fields [26]. That is, through the correlation study of many variables, many original variables are condensed into a few imaginary factor variables, so that these factor variables have stronger analytical power. The general model of factor analysis is as follows:

$$\begin{cases} X_1 = a_{11}F_1 + a_{12}F_2 + \cdots + a_{1m}F_m + \varepsilon_1, \\ X_2 = a_{21}F_1 + a_{22}F_2 + \cdots + a_{2m}F_m + \varepsilon_2, \\ \cdots \\ X_p = a_{p1}F_1 + a_{p2}F_2 + \cdots + a_{pm}F_m + \varepsilon_p. \end{cases} \tag{1}$$

$X_1, X_2, \ldots, X_p$ is the measured variable; $a_{ij}\,(i = 1, 2, \ldots, p; j = 1, 2, \ldots, m)$ is the factor load; $F_j\,(j = 1, 2, \ldots, m)$ is the common factor; $\varepsilon_i\,(i = 1, 2, \ldots, p)$ is a special factor. In the case that each factor is not correlated, the factor $loada_{ij}$ is the correlation factor between the i original variable and the j factor variable, that is, the relative importance of X_i on the j common factor variable. Therefore, the larger the load is, the closer the relationship between the i variable and the j factor is. The smaller the load is, the more distant the relationship between the i variable and the j factor is. In high-dimensional space, they are mutually perpendicular coordinate axes. However, the special factor is actually the residual between the measured variable and the estimated value. If the special factor is zero, the principal component analysis is performed. In order to make the principal factors found easier to explain, it is often necessary to rotate the factor loading matrix, and the most commonly used rotation method is the maximum variance rotation method Varimax. The purpose of factor rotation is to differentiate the square value of factor load in the factor load matrix toward 0 and 1, so that the large load is bigger and the small load is smaller. Therefore, factor scores need to be calculated. Since the common factor can reflect the relevant information of the original variable, it is sometimes more beneficial to describe the characteristics of the research object when the common factor is used to represent the original variable. Therefore, it is often necessary to express

Table 2: Reliability statistics.

Cronbach's alpha	No. of items
0.759	14

the common factor as a linear combination of variables (or samples) in reverse, namely,

$$F_j = \beta_{j1}X_1 + \beta_{j2}X_2 + \cdots + \beta_{jp}X_p; \quad j = 1, 2, \ldots, m. \quad (2)$$

Factor scoring function (2) is used to calculate the common factor score for each sample. Since the number of equations m is less than the number of variables p in the factor score function, the factor score cannot be calculated accurately, and only the factor score can be estimated. The usual estimation methods include the weighted least square method and regression method.

3.1.2. KMO and Bartlett Sphere Test. A Kaiser-Meyer-Olkin (KMO) test is used in research to determine the sampling adequacy of data that are to be used for factor analysis. Social scientists often use factor analysis to ensure that the variables they have used to measure a particular concept are measuring the concept intended [27]. The KMO test shows the data are suitable to run a factor analysis and therefore determine whether we have set out and what we intended to measure. Before conducting factor analysis, a KMO and Bartlett sphere test was performed. As shown in Table 3, the KMO value of the cognitive engagement scale for IPTC is 0.703 (greater than 0.5). This finding indicates that the variables have a strong correlation, and the data are suitable for factor analysis.

3.1.3. Principal Component Extraction and Factor Rotation. Suppose random variables $X = \{X_1, X_2, \ldots, X_p\}$, the normalized variable $x = \{x_1, x_2, \ldots, x_p\}$, its correlation matrix $R = (r\_ij)$, its $k\,(k \le p)$, and nonzero characteristic roots are $\lambda_1, \lambda_2, \ldots, \lambda_k$. The corresponding eigenvector is l_{ij}; then, the principal component estimation of the factor load of the j factor F_j is the product of the square root of the corresponding Eigen root and the corresponding eigenvector:

$$a_{ij} l_{ij} \sqrt{\lambda_j}, \quad i = 1, 2, \ldots,\ j = 1, 2, \ldots, k. \quad (3)$$

Factor load is the correlation coefficient between the common factor and index variable. The larger the load is, the closer the relationship between the common factor and index variable is. When determining the number of common factors, the number of factors equal to the number of original variables is first selected, the total variance of factors is calculated, and then, the factor whose eigenvalue is greater than 1 after rotation is taken as the common factor. Therefore, the change of six common factors of principal components after dimensionality reduction is selected to describe the change of the original index set.

3.1.4. Calculated Factor Score. Since the index variable X meets the orthogonal factor model, the common factor F can also be expressed as a linear combination of variable X, from which the model can calculate the comprehensive evaluation value, ranking the evaluation value from large to small, and ranking the cognitive input factors from high to low that can be given.

For cognitive engagement, there are only 6 equations and 14 variables, so it can only be estimated in the sense of least squares. The regression method is used to calculate the scores of factors F_1, F_2, F_3, F_4, F_5, and F_6, and the comprehensive score of each factor Q_t is shown in

$$Q_t = \frac{\sum_{i=1}^{33} \lambda_i F_i}{\sum_{i=1}^{33} \lambda_i}, \quad t = X_1, X_2, X_3, \ldots, X_{13}, X_{14}. \quad (4)$$

From formula (4), where λ_i is the eigenvalue corresponding to the correlation matrix of X, after several repetitions of the exploratory factor analysis on the scale, the total variance table explained by the factor components was obtained through the principal component analysis method [28].

As shown in Table 4, when the second component is reached, the 14 questions can explain 45.459% of the total variation. Also, six factors with an eigenvalue of greater than 1 can be determined, so the six common factors should be extracted. According to the component factors of the rotate on matrix, the first factor contains questions 2 and 12, the second factor contains questions 3 and 5, the third factor contains questions 13 and 14, the fourth factor contains questions 7 and 11, the fifth factor contains questions 6 and 9, and the sixth factor contains questions 4 and 10.

As can be seen from Figure 1, the eigenvalues of the first six factors are all greater than 1, and the inflection point appears from the seventh factor. Therefore, the first six factors were selected. According to the characteristics of college students, by combining literature with questionnaire items, a reasonable factor analysis of college students' cognitive engagement in IPTC was formed.

As shown in Table 5, there are six important factor dimensions affecting college students' cognitive engagement in the IPTC, namely, attention and motivation factor dimension, behavior and value attainment factor dimension, interest and practicality factor dimension, personality and will factor dimension, evaluation and time factor dimension, and knowledge and strategy factor dimension.

3.2. Descriptive Analysis of College Students' Cognitive Engagement. Descriptive statistics is a method of sorting out and analyzing data through graphs or mathematical methods and then estimating and describing the relationship between data distribution, digital features, and random variables[29]. Through descriptive statistics, the minimum and maximum estimates are solved; the other data are outliers. However, a logical outlier can be retained if it actually exists.

As shown in Table 6, for the attention and motivation dimension, the maximum value is 10, the minimum value is 4, and the mean value is 6.4701. For the behavior and value attainment dimension, the maximum value is 10, the minimum value is 4, and the mean value is 6.5153. For the

Table 3: KMO and Bartlett sphere test.

KMO sampling appropriateness measurement		0.703
Bartlett sphere test	Approximate chi-square	97.947
	Degrees of freedom	91
	Significance	0.291

Table 4: Explanation of the total variance of students' cognitive engagement in IPTC.

Initial eigenvalue				Extraction sums of squared loadings			Rotation sums of squared loadings
Component	Total	Variance percentage	Cumulative (%)	Total	Variance percentage	Cumulative (%)	Total
X_1	1.109	7.919	7.919	1.109	7.919	7.919	1.082
X_2	1.081	7.725	15.643	1.081	7.725	15.643	1.071
X_3	1.059	7.567	23.211	1.059	7.567	23.211	1.061
X_4	1.053	7.522	30.733	1.053	7.522	30.733	1.059
X_5	1.041	7.436	38.169	1.041	7.436	38.169	1.048
X_6	1.021	7.290	45.459	1.021	7.290	45.459	1.043
X_7	0.996	7.117	52.576				
X_8	0.988	7.056	59.632				
X_9	0.978	6.984	66.616				
X_{10}	0.961	6.865	73.481				
X_{11}	0.946	6.757	80.238				
X_{12}	0.934	6.672	86.910				
X_{13}	0.929	6.633	93.544				
X_{14}	0.904	6.456	100.000				

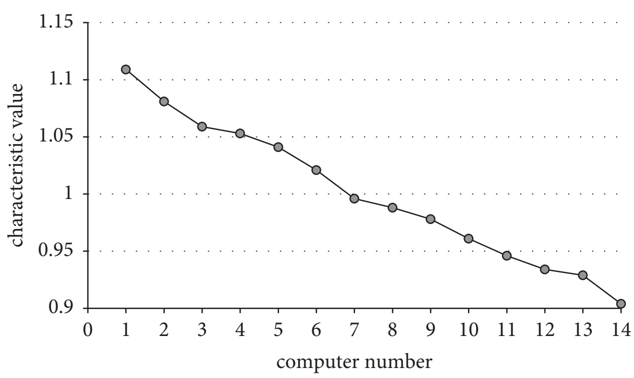

Figure 1: Gravel figure of effect factor.

interest and practicality dimension, the maximum value is 10, the minimum value is 4, and the mean value is 6.5435. For personality and will dimension, the maximum value is 10, the minimum value is 4, and the mean value is 6.5837. For evaluation and time dimension, the maximum value is 10, the minimum value is 4, and the mean value is 6.4696. For the knowledge and strategy dimension, the maximum value is 10, the minimum value is 4, and the mean value is 6.3505. This set of data shows no abnormal values, and all the mean values are between the minimum and maximum values. The scores of attention and motivation dimension, behavior and value attainment dimension, interest and practicality dimension, personality and will dimension, evaluation and time dimension, and knowledge strategy factor dimension are all greater than 6, indicating good overall evaluation. "Personality and will dimension" has the highest score ($M = 6.5837$), while the knowledge and motivation factor dimension has the joint lowest score ($M = 6.3505$). This finding indicates that personality and will dimension plays a relatively major role among the factors influencing college students' cognitive engagement in IPTC, while the knowledge motivation dimension has a weak impact on cognitive engagement.

3.3. Linear Regression Analysis of College Students' Cognitive Engagement. A Pearson's correlation coefficient can be used to measure the correlation between two fixed distance and fixed ratio variables, which is a parametric test [30]. From Table 7, one can see that the correlation is significant at 0.01 level (two-tailed) and the correlation is significant at the 0.05 level (two-tailed), which means that there is a significant positive correlation exists between cognitive engagement and other variables according to Pearson. The attention and motivation factor dimension, behavior and value attainment factor dimension, interest and practicality factor dimension, personality and will factor dimension, evaluation and time factor dimension, and knowledge and strategy factor dimension are all correlated with each other, which mean that the scale has structural validity. Through the correlation test, one can understand the correlation between the factors that influence cognitive engagement.

A linear regression analysis is a method used to study the influence relationship. The essence of such an analysis is to study the impact of one or more independent variables X on a dependent variable Y (quantitative data) [31]. A regression analysis is made on the basis of a correlation analysis and is used to study whether an influence relationship exists because a correlation may exist sometimes; there is not necessarily a regression influence relationship. As can be seen from Table 8, $R^2 = 0.719$, $F = 1699.351$, and $P \leq 0.001$. This indicates that attention and motivation dimension, behavior

Table 5: Factors influencing college students' cognitive engagement in IPTC.

Item	Index	Factor naming: Attention and motivation factor	Behavior and value attainment	Interest and practical factors	Personality and will factors	Evaluation and time factor	Knowledge and strategic factors
X_1	Attitude						
X_2	Attention	0.473					
X_3	Value attainment		0.444				
X_4	Knowledge acquisition						0.574
X_5	Behavior gain		0.43				
X_6	Teacher evaluation					0.441	
X_7	Personality				0.51		
X_8	Learning plan						
X_9	Learning time					0.405	
X_{10}	Learning strategy						0.414
X_{11}	Will				0.484		
X_{12}	Motivation	0.407					
X_{13}	Interest			0.488			
X_{14}	Practicality			0.629			

Table 6: Descriptive statistics of college students' cognitive engagement.

	N	Minimum	Maximum	Mean	Standard deviation
Attention and motivation	3992	4.00	10.00	6.4701	1.17031
Behavior and value attainment	3992	4.00	10.00	6.5153	1.04270
Interest and practicality	3992	4.00	10.00	6.5435	1.24626
Personality and will	3992	4.00	10.00	6.5837	1.19115
Evaluation and time	3992	4.00	10.00	6.4696	1.23148
Knowledge and strategy	3992	4.00	10.00	6.3505	1.18869
Number of valid cases (in a row)	3992				

Table 7: Correlation of college students' cognitive engagement.

		Cognitive engagement	Attention and motivation	Behavior and value attainment	Interest and practicality	Personality and will	Evaluation and time	Knowledge and strategy
Cognitive engagement	Pearson correlation	1	0.328**	0.323**	0.412**	0.380**	0.369**	0.361**
	Sig. (Two-tailed)		.000	.000	.000	.000	.000	.000

**At 0.01 level (two-tailed), the correlation is significant. *At the 0.05 level (two-tailed), the correlation is significant.

and value attainment dimension, interest and practicality dimension, personality and will dimension, evaluation and time dimension, and knowledge and strategy factor dimension all play a positive predictive role in college students' cognitive engagement. Of these factors, attention and motivation dimension has the highest influence weight (eigenvalue = 0.05), while knowledge and strategy dimension has the lowest influence weight (eigenvalue = 0.01).

4. Discussion

As seen from the statistical analysis, the following factors are important aspects that affect college students' cognitive engagement in IPTC.

4.1. Attention and Motivation Dimension. The relationships between the child-parent reading behaviors and the children's cognitive attainment were identified [32]. In the cognitive process of IPTC, both teachers' and students' cognition of attention are usually specific, sensible, and easiest to show. In teaching situations, attention is the first to be recognized and manifested. In a state of attention, a student's consciousness and psychological activities will be oriented to and focused on the learning content, in such a way that the consciousness content or object is clear and definite. The consciousness process is tense and orderly, and the individual's behavior and activities are finally controlled by consciousness. In the IPTC learning process, college students always differentiate their attention levels,

Table 8: Linear analysis of cognitive engagement.

	Model	Nonstandard coefficient		Standard coefficient	t	Significance	Collinearity statistics		R^2	F
		B	Standard error	Beta			Eigenvalue	VIF		
1	(Constant)	1.35	0.05		26.68	0.00	6.84		0.719	1699.351
	Attention and motivation	0.09	0.00	0.2	22.42	0.00	0.05	1.40		
	Behavior and value attainment	0.15	0.00	0.33	39.05	0.00	0.04	1.01		
	Interest and practicality	0.15	0.00	0.40	47.84	0.00	0.03	1.00		
	Personality and will	0.15	0.00	0.37	44.33	0.00	0.03	1.00		
	Evaluation and time	0.15	0.00	0.39	46.18	0.00	0.02	1.00		
	Knowledge and motivation	0.10	0.00	0.25	25.09	0.00	0.01	1.40		

depending on the degree of effort and whether or not there is the presence of a learning purpose. If one tries to use vivid pictures to illustrate the scenes of major events, the virtues of historical figures, or the tragedy of war, using modern media technology to give students strong sensory stimulation and thereby attract their attention, the students will naturally positively participate in learning these things. Motivation is the power and thought that triggers a person to engage in certain behavior. Motivation directly refers to the special psychological state and willingness to meet various specific needs. It is the internal stimulation or power that directly drives an individual's activities. The IPTC has been implanted in the lives of college students for a long time, due to the course's particularities. College students are not unfamiliar with these particularities. Therefore, the pressure on these students is quite small, leading to weakened learning motivation. This is precisely why students' level of cognitive engagement in the IPTC is not high.

4.2. Behavior and Value Attainment Dimension. There are some observable aspects, for example, time-on-task, class participation, and completion of homework [33] related cognitive engagement. But, most of them are often extracted from teachers' observations of students' behavior in the classroom [34]. In fact, the IPTC is a discipline that teaches theories and expounds on the value of thought so that learners pursue the course in the spirit of truth-seeking. However, such ideological value is not a rootless duckweed but must be rooted in the vastness of real life and must be dissolved in the melting pot of the times, which makes the behavior and value attainment dimension extremely important. College students' overall perception of the value of the IPTC is relatively satisfactory. Almost all of the college students who participated in the survey have an accurate understanding of the importance of the IPTC, and they believe that the IPTC is important for their entire lives. However, there are also college students who weaken the value of the IPTC when making important choices in their lives, in such a way that the course fails to display unique value. That is, compared with skill-based courses, the IPTC is not effective in students' decision-making.

4.3. Interest and Practicality Dimension. It has been argued that if teachers and schools could support students' academic behavioral skills, they could benefit from the engagement and then increase students' academic performance [35], from which the interest and practicality of students are important facts. In their learning of the IPTC, college students currently pay more attention to the maintenance of individual interests. In the IPTC, one can better understand this structure by studying students' psychological engagement, their interests and learning strategies, and especially their learning strategies related to self-regulation. College students show a clear goal orientation toward the IPTC, which reflects a certain extent that they need to input their stable individual interests into the IPTC learning process. By doing so, they can pay more attention to the course and learn more deeply. In the learning process, students may develop a great interest in a certain discipline or a certain class, due to various factors, such as teachers and individual psychology. However, as factors like environmental change, such situational interest may partially or even completely disappear. In the end, as seen from the overall course acquisition process, college students' cognitive engagement is not high. Such unstable states exist in different colleges, different majors, and different groups. In view of this, the course's application should be strengthened, so that college students will not turn the IPTC into a course of memorizing knowledge points under the pressure of coping with exams. That approach will ignore the existence value of the IPTC and will also ignore the course's role in deep-seated value guidance for college students.

4.4. Personality and Willing Dimension. Personality is a general feature that an individual exhibits in the face of real-life situations. However, recent research has demonstrated that personality is not substantially correlated with cognitive ability [36]. Intellectual characteristics, on the other hand, are the main components of a psychological feature that an individual displays in cognitive activities. In the cognitive engagement in the IPTC, effectively guiding and utilizing the personality and will factor of college students is an important way to increase the effectiveness of the IPTC. It is not difficult to understand that, in IPTC classrooms, most teachers will use fascinating situational introduction methods to arouse college students' interest. The teachers analyze college students' personality characteristics based on the overall judgment of the class, and they display certain inspiration and clue guidance through their words when students raise questions and express opinions. In essence,

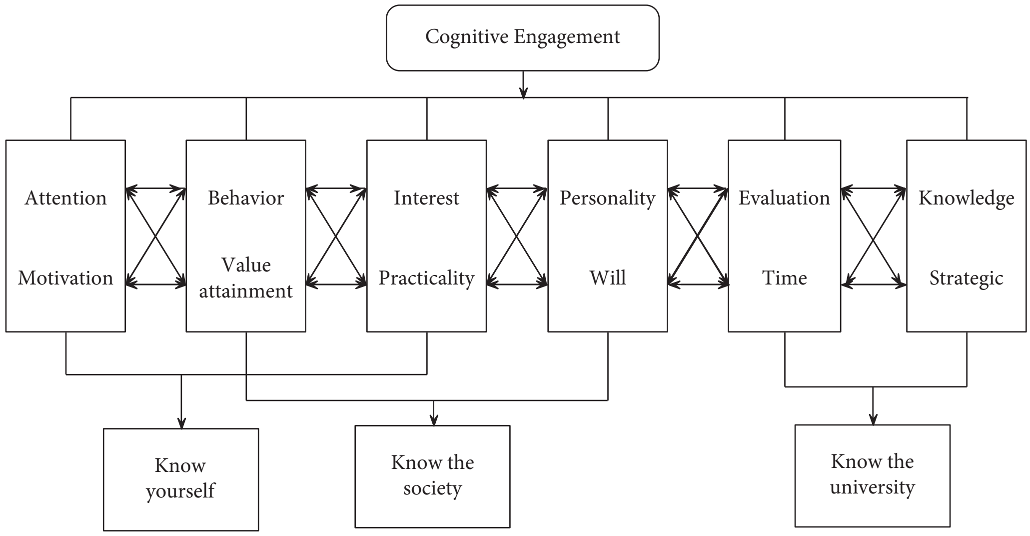

Figure 2: Important factors affecting cognitive engagement multidimensional optimization model.

teachers actively direct students to participate in the overall classroom organization from their aspects. This also means that teachers should discover and observe students' individual performance in learning materials in a timely manner. The teachers should use vivid language to give thinking space to those students who choose to listen and affectionate gazes to encourage students who are eloquent and willing to express and share their views.

4.5. Evaluation and Time Dimension. Recently, more and more students start their IPTC learning online, which has been explained to promote students engagement [37]. When the assessment of the IPTC is an important method to guide students to conscious learning, it may stimulate their enthusiasm for learning. However, the traditional ideological and political education evaluation model focuses on assessing students' theoretical knowledge. This model reduces college students' interest in learning ideological and political education courses and fails to comprehensively evaluate students' actual ideological and political consciousness. Optimizing the course assessment system and giving scientific student evaluations would inevitably improve the traditional evaluation model of ideological and political education; this approach would also construct a new, diversified three-dimensional evaluation model. With the rapid development of our society, social wealth has increased dramatically and people's lives have become more prosperous. Nonetheless, it is undeniable that some social phenomena have also existed (and even worsened) in our society during this transition period, such as the gap between the rich and the poor, social injustice, extravagance, and waste. The contradictions reflected in these phenomena are very inconsistent with the values and social civilization advocated by the IPTC. The impact on some college students will arouse irrational cognition, causing these students to become ambivalent and unwilling to invest their time and energy in the IPTC learning. Also, this situation will put the study of the IPTC in an awkward position.

4.6. Knowledge and Strategy Dimension. Strategies could help optimize the work environment in terms of affordable job demands and sufficient job resources as well as increase personal resources, such as optimism, self-efficacy, and self-esteem [38]. Subsequently, in the cognitive engagement of the IPTC, political, ideological, academic, and professional nature must be closely linked. Such a theoretical and highly professional curriculum will inevitably involve the influence of learning strategies, which will create an interactive influence between college students and teachers, students and learning content, and among students themselves. Research has demonstrated that the course could strongly support students in training interest and the role of self-efficacy for the course of study for task experiences and knowledge development [39]. In the process of cognitive engagement, teachers must actively adopt teaching strategies, while students should respond with active learning strategies. All parties should make their own adjustments, expand their thinking, and flexibly use autonomous learning strategies and goal-oriented strategies.

5. Conclusions

Through the investigation and statistical analysis of this research, the following conclusions can be drawn:

(1) The six fact dimensions affect college students' cognitive engagement. Although college students' cognition can be measured in different ways, compared with emotional and behavioral engagement, cognitive engagement is not so easily observed and captured; cognitive engagement is actually relatively hidden. Among the six multidimensional factors through principal component analysis and factor analysis methods, attention and motivation dimension, behavior and value attainment dimension, interest and practicality dimension, personality and will dimension, evaluation and time dimension, and knowledge and strategy dimension are important

factors that influence college students' participation in the learning process of the IPTC. College students lack motivation in IPTC learning. Some students show a helpless state in their studies; they are unwilling to devote their time and energy to learning, and they lack understanding of the learning process. College students have insufficient cognitive engagement and motivation in the subject. Some college students attach great importance to the beneficial value of the course, and these students focus on the benefits that the course brings to them. If the course has many benefits, the enthusiasm for learning is strong; otherwise, the enthusiasm is not high. Such serious individualism and utilitarianism exist.

(2) Through the descriptive statistical analysis method, the scores of the six factor dimensions are all greater than 6, indicating there is good overall evaluation, in which the score of "personality and will dimension" is the highest ($M = 6.5837$) and the score of "knowledge and motivation dimension" is the lowest ($M = 6.3505$). This finding indicates that the "personality and will dimension" plays a relatively important role among the factors influencing college students' cognitive engagement in IPTC, while the "knowledge and motivation dimension" has a weak impact on cognitive engagement. Teacher self-efficacy predicted later work satisfaction via engagement and their initial work satisfaction predicted later teacher self-efficacy via engagement too [40]. Compared with teachers' self-efficacy beliefs, engagement, and satisfaction directly and indirectly, the degree of college students' cognitive engagement in the IPTC also determines the different senses of self-efficacy. For example, the motivation dimension scores of learning engagement are significantly higher among students of "Project 985" and "Project 211" universities than those of ordinary colleges. At the same time, the scores of some "non-985" and "non-211" universities in this aspect are significantly lower than those of "Project 985" and "Project 211" universities. The key majors of some colleges and universities have also affected students' cognitive engagement. Students with a strong sense of professional superiority have a higher degree of recognition toward the IPTC, and vice versa. During the learning process of the IPTC, some students have relatively low expectations of learning, which also leads to a lower sense of self-efficacy. When it comes to choosing learning tasks and making learning plans, most students can arrange their time to learn the most important content first. Meanwhile, some students will skip the difficult content and only master the content within their capability, leading to different senses of information interaction efficacy among students. Those with a high overall evaluation of ideological and political learning activities will, overall, have a higher sense of efficacy in learning.

(3) Through correlation analysis and linear regression analysis, there is a significant positive correlation between cognitive engagement and other variables, and the data $R^2 = 0.719$, $F = 1699.351$, and $P \leq 0.001$ show that the six variables play a positive role in college students' cognitive engagement. Factors such as grade, status, and social experience will affect students' cognitive engagement in the IPTC. As far as grades are concerned, senior students have superior cognition and identification than those of lower grades. In terms of identity, student party members and student cadres have significantly superior cognition and identification than ordinary students. In terms of social experience, students with rich experience in social practices have superior cognition and identification than students who do not participate in social practices. The reasons behind these findings are worth reflection. In addition, in the cognitive engagement of the IPTC, individual goals do not play a sufficient role in the course; the learners' goals typically depend on whether they believe they can change the status.

(4) A multidimensional optimization model of important factors affecting college students' cognitive engagement in IPTC has been built.

From Figure 2, one can see that a multidimensional optimization model on important factors affecting cognitive engagement has been built in the paper. To improve the effectiveness of the IPTC and enhance college students' sense of acquisition in the IPTC in terms of both future education and teaching, teachers should adopt various effective ways to continuously strengthen and reinforce college students' cognitive engagement in the IPTC. Most important, teachers and universes should let college students know themselves and society. In this way, the uniqueness of the IPTC should be reflected, and the basic principles of Marxism should be used to arm college students' thinking. There is a necessity to combine students' cognitive feelings with the learned contents in a timely manner so as to achieve ideological enlightenment and guidance and to enable methodological improvement. In this way, one can increase college students' learning initiative and enthusiasm, integrate relevant educational resources, and make the IPTC a course that directly hits the hearts of college students and truly displays the effect of soul cultivation and education.

Data Availability

The data used to support the findings of this study are included within the article.

Conflicts of Interest

The author does not have any possible conflicts of interest.

Acknowledgments

This work was supported by the Shaanxi Association of Higher Education 2019 Higher Education Scientific

Research Project (XGH19080) and Northwestern Polytechnical University Degree and Graduate Education Research Fund Project (2019-2020). Also, the author would like to sincerely thank and appreciate Prof. Mingfang Fan for his suggestions and encouragement.

References

[1] Z. Su, "Casting soul and Educating people: the lifeline of ideological and political theory teaching," *Studies in Ideological Education*, vol. 320, no. 2, pp. 8–13, 2021.

[2] S. Huang, Y. Wei, and B. Li, "Three dimensions to strengthen the construction of ideological and political theory course in the new era," *Leading Journal of Ideological & Theoretical Education*, vol. 1, pp. 109–112, 2020.

[3] M. Harvey and I. Solomonides, "Peer review in a foundations in learning and teaching program," in *Peer Review of Learning and Teaching in Higher Education. Professional Learning and Development in Schools and Higher Education*, J. Sachs and M. Parsell, Eds., vol. 9, pp. 137–149, Springer, Dordrecht, Netherlands, 2014.

[4] V. Tinto, *Leaving College Rethinking the Causes and Cures of Student Attrition*, University of Chicago Press, Chicago, 2nd edition, 1993.

[5] A. W. Astin, "Student involvement: a developmental theory for higher education," *Journal of College Student Personnel*, vol. 99, no. 40, pp. 297–308, 1984.

[6] S. L. Christenson, A. L. Reschly, J. J. Appleton, S. Berman, D. Spanjers, and P. Varro, *Best Practices in School Psychology*pp. 45–57, National Association of School Psychologists, MD, USA, 5th edition, 2008.

[7] D. Marcia, "Measuring student engagement in the online course: the online student engagement scale (OSE)," *Online Learning*, vol. 19, no. 4, 2015.

[8] L. Corno and E. B. Mandinach, "The role of cognitive engagement in classroom learning and motivation," *Educational Psychologist*, vol. 18, no. 2, pp. 88–108, 1983.

[9] J. P. Connell and J. G. Wellborn, "Competence, autonomy, and relatedness: a motivational analysis of self-system processes," in *Proceedings of the Minnesota Symposium On Child Psychology*, pp. 23–36, University of Chicago Press, Hillsdale, MI, USA, October 1991.

[10] F. Newmann, G. G. Wehlage, and S. D. Lamborn, "The significance and sources of student engagement," *Student Engagement and Achievement in American Secondary Schools*, pp. 11–39, Teachers College Press, NY, USA, 1992.

[11] G. G. Wehlage, R. R. A. Rutte, G. A. Smith, N. L. Lesko, and R. R. Fernandez, *Reducing the Risk: Schools as Communities of Support*, pp. 78–114, Farmer Press, Philadelphia, PA, USA, 1989.

[12] P. R. Pintrich and E. V. De Groot, "Motivational and self-regulated learning components of classroom academic performance," *Journal of Educational Psychology*, vol. 82, no. 1, pp. 33–40, 1990.

[13] B. J. Zimmerman, "Self-regulated learning and academic achievement: an overview," *Educational Psychologist*, vol. 21, pp. 3–17, 1993.

[14] L. Corno, "The best-laid plans," *Educational Researcher*, vol. 22, no. 2, pp. 14–22, 1993.

[15] J. D. Finn, J. Folger, and D. Cox, "Measuring participation among elementary grade students," *Educational and Psychological Measurement*, vol. 51, no. 2, pp. 393–402, 1991.

[16] J. I. Rotgans and H. G. Schmidt, "Cognitive engagement in the problem-based learning classroom," *Advances in Health Sciences Education*, vol. 16, no. 4, pp. 465–479, 2011.

[17] G. Xiao, "On the institutionalization of ideological and political theory course in the New Era," *Leading Journal of Ideological & Theoretical Education*, vol. 4, pp. 98–104, 2021.

[18] L. Zhang, "Ideological and political theory course: the main channel of 'Three Views'education," *Social Sciences in Chinese Higher Education Institutions*, vol. 1, pp. 42–46, 2007.

[19] Z. Xie and Y. Shao, "The practice teaching of ideological and political course cultivates the system self-confidence of college students," *The Party Building and Ideological Education in Schools*, vol. 8, pp. 50–52, 2021.

[20] L. Wang, M. Fan, and F. Zhang, "Applying fuzzy fault tree method to evaluate the reliability of college classroom," *Front. Psychol.- Educational Psychology*, vol. 12, Article ID 593068, 2021.

[21] J. D. Finn and K. S. Zimmer, "Student Engagement: What Is it? Why Does it Matter?" *Handbook Of Research on Student Engagement*, Springer, NY, USA, pp. 97–131, 2012.

[22] J. J. Appleton, S. L. Christenson, D. Kim, and A. L. Reschly, "Measuring cognitive and psychological engagement: validation of the student engagement instrument," *Journal of School Psychology*, vol. 44, no. 5, pp. 427–445, 2006.

[23] C. R. Pace, *Measuring Outcomes of College: Fifty Years of Findings and Recommendations for the Future*, Jossey-Bass, San Francisco, CA, USA, 1979.

[24] C. Derouesné, C. Dealberto, M. J. Boyer, P. Lubin, and S. Sauron, "Empirical evaluation of the 'Cognitive Difficulties Scale' for assessment of memory complaints in general practice: a study of 1628 cognitively normal subjects aged 45–75 years," *International Journal of Geriatric Psychiatry*, vol. 8, no. 7, pp. 599–607, 1993.

[25] M. Csikzentmihalyi, "The flow experience and its significance for human psychology," *Optimal Experience*, pp. 15–35, Cambridge University Press, Cambridge, UK, 1998.

[26] R. J. Sternberg, "The geographic metaphor," in *Metaphors of Mind: Conceptions of the Nature of Intelligence*, R. J. Sternberg, Ed., pp. 85–111, NY: Cambridge, 1990.

[27] B. A. Cerny and H. F. Kaiser, "A study of a measure of sampling adequacy for factor-analytic correlation matrices," *Multivariate Behavioral Research*, vol. 12, no. 1, pp. 43–47, 1977.

[28] M. Awang, B. Singh, and I. Dzulkarnain, "An analysis of the relationship between effective teaching and effective learning at UTP," *Procedia - Social and Behavioral Sciences*, vol. 56, pp. 594–601, 2012.

[29] V. A. Profillidis and G. N. Botzoris, "Statistical methods for transport demand modeling," *Modeling of Transport Demand*, Elsevier, Amsterdam, Netherland, pp. 163–224, 2019.

[30] C. Sotos, A. Elisa, S. Vanhoof, V. Noortgate, and O. Patrick, *The Non-transitivity of Pearson' S Correlation Coefficient: An Educational Perspective*, International Statistical Institute, Voorburg, Netherlands, 2007.

[31] D. L. Gilstrap, "Understanding persistence of at-risk students in higher education enrollment management using multiple linear regression and network analysis," *The Journal of Experimental Education*, vol. 88, no. 3, pp. 470–485, 2019.

[32] K.-H. Cheng and C.-C. Tsai, "Children and parents' reading of an augmented reality picture book: analyses of behavioral patterns and cognitive attainment," *Computers & Education*, vol. 72, pp. 302–312, 2014.

[33] J. J. Appleton, S. L. Christenson, and M. J. Furlong, "Student engagement with school: critical conceptual and methodological issues of the construct," *Psychology in the Schools*, vol. 45, no. 5, pp. 369–386, 2008.

[34] J. D. Finn and K. S. Zimmer, "Student engagement: what is it? Why does it matter?," in *Handbook of Research on Student Engagement*, S. L. Christenson, A. L. Reschly, and C. Wylie, Eds., pp. 97–131, Springer Science + Business Media, 2012.

[35] F. Siddiq, P. Gochyyev, and O. Valls, "The role of engagement and academic behavioral skills on young students' academic performance—a validation across four countries," *Studies In Educational Evaluation*, vol. 66, Article ID 100880, 2020.

[36] D. Rozgonjuk, F. Schmitz, C. Kannen, and C. Montag, "Cognitive ability and personality: testing broad to nuanced associations with a smartphone app," *Intelligence*, vol. 88, Article ID 101578, 2021.

[37] S. L. Chan, C. C. Lin, P. H. Chau, N. Takemura, and J. T. C. Fung, "Evaluating online learning engagement of nursing students," *Nurse Education Today*, vol. 104, Article ID 04985, 2021.

[38] A. B. Bakker, "Strategic and proactive approaches to work engagement," *Organizational Dynamics*, vol. 46, no. 2, pp. 67–75, 2017.

[39] L. K. Fryer, A. Shum, A. Lee, and P. Lau, "Mapping students' interest in a new domain: connecting prior knowledge, interest, and self-efficacy with interesting tasks and a lasting desire to reengage," *Learning and Instruction*, vol. 75, Article ID 101493, 2021.

[40] H. Granziera and H. N. Perera, "Relations among teachers' self-efficacy beliefs, engagement, and work satisfaction: a social cognitive view," *Contemporary Educational Psychology*, vol. 58, pp. 75–84, 2019.

Hindawi
Scientific Programming
Volume 2021, Article ID 1894768, 9 pages
https://doi.org/10.1155/2021/1894768

Research Article

A Prognostic Three-Axis Coordination Model for Supply Chain Regulation Using Machine Learning Algorithm

Hariprasath Manoharan,[1] Yuvaraja Teekaraman,[2] Ramya Kuppusamy,[3] Arun Radhakrishnan,[4] and Mohamed Yaseen Jabarulla[5]

[1]*Department of Electronics and Communication Engineering, Panimalar Institute of Technology, Chennai 600123, India*
[2]*Mobility, Logistics, and Automotive Technology Research Centre, Faculty of Engineering, Vrije Universiteit Brussel, Brussel 1050, Belgium*
[3]*Department of Electrical and Electronics Engineering, Sri Sairam College of Engineering, Bangalore City 562 106, India*
[4]*Department of Electrical & Computer Engineering, Jimma Institute of Technology, Jimma University, Ethiopia*
[5]*School of Electrical Engineering and Computer Science, Gwangju Institute of Science and Technology, Gwangju 61005, Republic of Korea*

Correspondence should be addressed to Yuvaraja Teekaraman; yuvarajastr@ieee.org and Arun Radhakrishnan; arun.radhakriahnan@ju.edu.et

Received 23 September 2021; Revised 14 October 2021; Accepted 3 November 2021; Published 25 November 2021

Academic Editor: Punit Gupta

In this article, data processing of a supply chain management system has been monitored using the Internet of Space (IoS) which can be able to create possessions for managing the business process. In modern circumstances, many business inventiveness are trading and exporting products on their possession, but in many cases, information on such manufactured products is not monitored in an effective manner. To overcome the abovementioned issue, a precise model of monitoring several distributed products in supply chain management has been introduced with high sustainability error reduction. The framed model in the management process has been integrated with the boosting algorithm, a type of machine learning algorithm where training dataset has been introduced appropriately. This variation in the incorporation of the boosting optimization process not only increases the efficiency of the proposed model but also attempts to prove the success strategy under five different scenarios, where after sequential tests IoS model delivers high improvement in the distribution process for an average percentile of 67% than the existing methods.

1. Overview on Internet of Space (IoS) in Supply Chain Management

In day-to-day existence, the contrivance of data transfer is varying, and more amount of storage space is needed for the management process. Even after integration, most of the online cloud storage applications can be able to provide low storage whereat next period revitalization is necessary, which is a high cost optimization development model. If all these storage capabilities are lesser, then the sustainability rate of the technological process is lesser at high error rate. If such low susceptible methods are introduced in the supply chain management process, then it becomes very difficult to detect the movement of goods as it is a distribution process. Even in the supply chain management process, the distributed process can be monitored using the image-based technique, and they can be collected at different locations. But the major substance in the supply chain management process will be a new resource, which is framed in a natal mode at low storage capability.

In the exploration of guileless, it has been deliberated that IoS can be able to monitor the distribution of goods using existing antennas without high installation cost. Furthermore, IoS is used for analyzing significant data where lasers are pointed in free space, thus providing good communication in the management process. Even IoT can be used for the implementation of complex processes in supply chain applications. But low cost of implantation is not guaranteed, and error will be much higher, which leads to inadequate susceptible process. To avoid such inadequate process, old infrastructure can be converted to new detecting and data transfer techniques using IoS. Moreover, this IoS can be used as a backbone of any intelligent system as sudden propagations can be stopped at short period of time. Therefore, for a faultless distribution monitoring system, IoS has been integrated which even provides high-quality communication signals at remote locations shown in Figure 1.

1.1. Correlated Applications. In this section, all interconnected works on Internet of Space (IoS) applications have been discussed, which provides central ideas for the formation of the proposed work. However, the application of IoS has been updated from the Internet of Things (IoT), which provides high standard solutions to all problems addressed in the supply chain management process [1]. For providing solutions to an IoT process, big data analysis has been made, and solutions are based on the simulation model with a high variety of modifications with a new mathematical setup model. The solutions of the supply chain management monitoring process have been well defined in this collaborative model as high efficiency is observed with the minimization of risk in supply chain disturbance. By using the basic mathematical model, big data analysis has been further developed for analyzing the behavior of every consumer [2]. This type of model integrates regression analysis with the high forecast in demand, and at the same time, it minimizes the cost of installation. Also, a metaheuristic analysis on big data has been made using different algorithms which opens the path for innovative investigation in the areas of the supply chain monitoring process. Furthermore, the integration process is expanded by analyzing the approach of the data transfer technique which is referred to as the sustainable processing capability [3]. In such viable conditions, the parametric conditions such as the sustainability of data transfer to a receiver should be checked in a way that the integrated method should solve long-term problems that exists in real-life situation. The central system that provides support for the viable supply chain management process can be further classified with different adaptive mechanisms that ensemble in the area of high technological features.

Since an adaptive mechanism provides efficient solutions, it is also integrated for analyzing the effect of the smart grid process [4], where the nonlinear programming model is encoded for the optimization process. Even though the process aims to provide quick solutions to all prosumers, only implementation cost is observed with the distribution process. Moreover, this type of distribution is assimilated with the neural network which provides a solution to hidden grid terminals on a large scale, and this type of network is reliable to a greater extent. Another application that exists in the field of IoS is monitoring the emission of carbon-dioxide that is present in all industrial processes with central data distribution [5]. In this type of monitoring, authors have suggested an effectual model by considering multiple objectives, which reduces the effect of greenhouse gas, but there is no vital indication on the implementation cost. Conversely, case studies have been conducted in the Pareto frontier for defining the best model that is suitable in the real-time implementation process. Additionally, a review in the area of IoS is explored in analyzing the set of scales for Industry 4.0 where a diverse variable application has been enhanced [6]. While analyzing the each set of scales, the visibility level should be checked in a sensible manner, where data should be interrupted correctly. The abovementioned approaches differ from existing [1–5] methods in the absence of RFID tags which is a cost-saving process in the optimum method of creation of tags.

The importance of IoT has been further deliberated by considering 800 different journals which are developed as bibliometric analyses [7]. Most of the mechanisms implement the process of co-concurrence procedure which is specifically designed for industries and retail technology. By comparing different conventional procedures in the supply chain management process, more number of productions can be detected using IoS. One major entity that needs to be considered in IoS design is low-power networks [8] where, in wireless networks with low power, more amount of data should be transmitted at a short period of time. For every time period, the number of transmitted data will be updated as the process carried out using IoT by following the set of designed protocols. The procedure implemented in the low-power wireless networks uses the Global Positioning System (GPS) as an enhancement module for monitoring the goods in the management process. But after comprehending that GPS can be replaced with advanced systems, a review on machine learning technique [9] which provides high-end automation for the supply chain management system has been deliberated. By using machine learning algorithms, all monitored data will be updated in the central server; therefore, all users can open the server with appropriate encoded keys.

Still apprising instruments are required for providing smart solutions in the supply chain management process; hence, high-end instruments are designed, which can be alleged as a smart model for the monitoring process [10]. Even if high amount of data is present in this kind of smart model, all information on trailing goods is provided. A separate numerical analysis has been carried out for establishing a coordination model that forms a new design strategy for future enhancing techniques [11], where single and multiple objective cases are considered. Subsequently, foundations on different algorithms are analyzed to model all networks, thus calculating the aggregate percentage of probable decisions that are observed in real time [12]. As a final point, it is essential to find the tractability of the supply chain management process to be implemented in real time; thus, two different types of flexibility are designed such as organization and product [13, 14]. These two types enable the uses of the cost that provides an increase in the globalization of industries with optimal investments in IoS, thereby ensuring efficient worldwide operations.

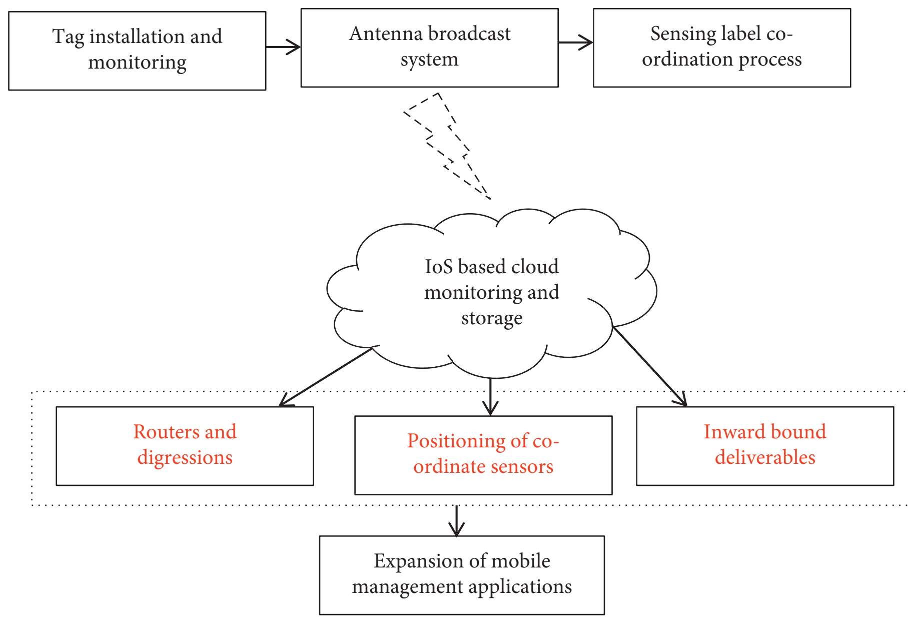

Figure 1: Schematic depiction of the proposed model using IoS.

1.2. Research Gap. Most of the existing methods describe only the impact of big data analysis using IoT for the supply chain management process by monitoring the changes in the distribution process. However, it has been witnessed that most of the methods are only experimental case studies, and even if implemented in real time, the distribution process cannot be monitored with changes at implemented locations. Even for storage capacity, a cloud-based monitoring system is not assimilated, which provides an abundant drawback. Moreover, it has been identified that meta-heuristic examination has been carried out with high-efficient algorithms, but due to the lack of the distribution process, very low efficiency is delivered.

1.3. Proposed Methodology. Therefore, to overcome the abovementioned gaps and problems, a research problem has been formulated using a new technique which is termed as "IoS". The major motive of implementing IoS is that there is no prerequisite of the external cloud storage system, and all distribution processes can be easily monitored using the three-axis coordinate system. This diversity of changes is motivated from settlement-based systems that exploit wireless technology, and even it can be extended for sixth-generation systems. If a three-axis coordinate system is framed, then the supply chain management process can be monitored without any involvement in the human recognition activity, and goods of all individual people can be examined at remote locations. Since synchronization is essential, an optimization data transfer approach which is termed as "boosting algorithm" is included, and efficiency is tested offline using MATLAB.

1.4. Objectives. The new flanged examination strategy on the application of the supply chain management process to analyze the movement of the distribution process will focus primarily on the following three major objectives:

(i) To implement an IoS-based three-axis coordinate system in all industrial applications for monitoring the distribution process

(ii) To formulate a control strategy for detecting the association of goods with the secured data transfer process

(iii) To integrate boosting algorithm with the three-axis system for detecting the sustainability and pseudorange of the optimization process

2. Mathematical Model of IoS for the Supply Chain Management

This section describes the mathematical model of the Internet of Space for monitoring the supply chain management process, where, in the first segment, fundamental equations that are related to IoS are formulated using a defined pseudo range model where the satellite images will be monitored periodically for 30-second interval with a common reference clock. This type of measurement model can be framed as given in the following equation:

$$\vartheta_i = \sum_{i=1}^{n} \left(R_{\text{in}} - R_s\right) * \text{speed of light}, \tag{1}$$

where R_{in} and R_s denote the interpretation of reading and receiver clocks, respectively.

Equation (1) indicates that the difference between two different clocks should be maintained within the pseudorange limits, and it should be multiplied with the speed of light which is equal to 299792458 m/s. However, equation (1) can be simplified using three different coordinate systems with unknown positions as modeled in the following equation:

$$\vartheta_i(R_{\text{in}}, R_s) = \sum_{i,j,k=1}^{n} \sqrt{\left(i^s(\tau^s) - i(\tau) - j^s(\tau^s) - j(\tau) - k^s(\tau^s) - k(\tau)\right)}, \quad (2)$$

where i^s, j^s, and k^s denote the corresponding satellite positions, i, j, and k represent the receiver position that moves with respect to satellite systems, and τ^s and τ denote the bias clock and reference clock that are changed in a periodic manner.

Since there is a necessity to determine linear equations, actual observations of different time intervals are modeled in the mathematical form and are given in the following equation:

$$O_i = \vartheta_i(R_{\text{in}}, R_s) + n_i, \quad (3)$$

where n_i denotes the amount of noise that is present in monitoring IoS system.

Equation (3) denotes that, original observations should be present with the low noise correlation capability where the positioning problem is solved with the exact linear observation model. In real time, it is not guaranteed that equation (3) will provide exact results; therefore, to reduce the error, the covariance matrix will be modeled as given in the following equation:

$$E_i = \begin{pmatrix} \sigma^2 & \cdots & 1 \\ \vdots & \ddots & \vdots \\ 1 & \cdots & \sigma \end{pmatrix}. \quad (4)$$

Since in IoS a rotation clock is implemented, it is necessary to use a rotational matrix by considering latitude and longitude constraints with the local coordinate system as given in the following equation:

$$\Delta r_i = RE_i \Delta_{ijk}, \quad (5)$$

where RE_i denotes the rotation matrix that is varied with respect to equation (3). Δ_{ijk} represents the normalized error of all three coordinate systems.

Once the error matrix is found in the subsequent segment, the process of control operation should be incorporated that follows an integral technique with a dynamic system performance improvement. The control formulation for a dynamic supply chain management system can be framed as

$$C(i) = \frac{1}{2}\int_{-\tau}^{+\tau} \in(i) + \in(j) + \in(k), \quad (6)$$

where $\in(i, j, k)$ denotes the corresponding elements in all three reference points.

Equation (6) indicates that integrative elements in all corresponding points should be reduced to half for monitoring the supply chain management process. In equation (6), the input needs to be entered, and the integral value of the management system should be within each state limits. Another important parameter for limiting the control process is the energy consumption that is monitored during supply chain management system, and it can be mathematically given in the integral form as

$$\rho(i) = \frac{1}{2}\int_{0}^{\tau} e^2 \mathrm{d}e, \quad (7)$$

where e denotes the total energy consumed by each node.

The major reason for incorporating IoS in the supply chain management system is to check the level of variation in the capacity and rate of production involved in the process. The aforementioned parameters can be modeled using the following equation:

$$\mu_i \frac{\partial I_i}{\partial \mu} = -\varphi_i \frac{\partial I_i}{\partial \varphi}, \quad (8)$$

where μ and φ denote the corresponding capacity and production rate.

In the proposed method, IoS is incorporated for a product management where the cost of implementation depends on the changing capacity rate, and it can be calculated using the following equation:

$$\operatorname{cost}(i) = \sum_{i=1}^{n} \frac{g(ijk)}{\varphi_i} \ \forall\, \text{IoS}, \quad (9)$$

where $g(ijk)$ denotes the average number of goods that are measured at three reference points using IoS.

Equations (1)–(9) represent all basic formulations for the integration of IoS with the supply chain management application process. All abovementioned equations are formulated based on a control technique mechanism, thus providing global solutions in terms of production rate and capacity. Thus, the objective function can be framed using equations (1)–(9) as

$$\operatorname{obj}(i) = \min \sum_{i=1}^{n} \rho(i) E_i C(i). \quad (10)$$

The above equation indicates the minimization problem where a triobjective case study has been formed using minimized values of error, controller, and energy values. If all the parameters in triobjective functions are minimized, then the three-axis coordinate system can be implemented in real time with a great advantage of outpost-based images. Moreover, in equation (10), cost terms can also be added for the minimization process, which is much needed for mortality.

3. Optimization Algorithm

In this section, a precise optimization algorithm for managing the supply chain process in industries has been selected where all feature predictions can be made much easier using the boosting algorithm. This type of boosting algorithm is a type of machine learning algorithm where all estimated values in different regions can be integrated in a suitable manner. For any given input, the CatBoost algorithm [15–17] provides an accurate output by solving a different set of features where high loss can be controlled.

Also, real-world application problems of the machine learning algorithm have been conferred for enhancing the intelligent process [16]. More quantities of data have been grouped where the data-driven approach for effective solutions has been secured for all industry authorities. With this review process, the secured mechanism is extended for detecting heart disease with big data on medical applications [17]. Even early detection is possible with the continuous observation of transience rate in humans, and the same approach can be extended for different applications which include supply chain management process. Since in the supply chain management process data are provided in different categories, this algorithm supports different category data such as text and numerical. In addition, fraud data can be detected, and it will be released in the next loop category; thus, the time of implementation is reduced. Also, training results in this type of boosting algorithm will be much higher using different command-line interfaces. In the starting segment of gradient boosting, constant values must be provided which provides high step implementation for further stages because 80 percent of the training set should be divided and 20 percent of the dataset should be provided initially. The process of initiating constant values in stage 1 can be framed as follows:

$$\theta(i) = \sum_{i=1}^{n} \pi_i, \quad \forall\, i \exists n, \tag{11}$$

where π_i indicates the constant indicator function for all values that exist in all different stages between i and n.

If equation (11) is integrated, then binary values should be indicated that provides the training data information for the boosting process. This can be framed using the following equation:

$$\pi_i = \begin{cases} 1, & \text{if } i \in n, \\ 0, & \text{otherwise.} \end{cases} \tag{12}$$

If the condition in (12) is gratified, then approximation can be made with reduction of losses in overall network. Furthermore, to simplify the equations, an approximate function should be derived by combining equation (11) as

$$Z_i = \sum_{i=1}^{n} \pi^t, \tag{13}$$

where π^t indicates the sum of different approximations in corresponding time intervals.

Equation (13) provides valuable information on periodic time changes that are provided at different time periods. Since more number of datasets are represented, it is necessary to consider Time Division Multiple Access (TDMA) in this type of boosting algorithm. Furthermore, the update for every dataset can be represented using the following equation:

$$|\widehat{A}(i)| = \frac{\min_i e_i^t}{e_i^{t-1} - e_i^{t+1}}, \tag{14}$$

where e^t, e^{t-1}, and e^{t+1} represent the current, preceding, and next time samples for exchanging periodic information.

Once the dataset has been updated, this algorithm has to be integrated with the pseudorange model using the residual function as follows:

$$\vartheta_i = \frac{\partial(R_{\text{in}}, Z_i)}{\partial(R_s)}. \tag{15}$$

The above equation indicates that the partial derivative of the reading clock and time period of each sample should be integrated for all corresponding pseudofunctions that are provided in three different coordinate systems. The step-by-step implementation of the CatBoost algorithm is provided in Figure 2, where it starts with the initialization of constant set values and the output will be based on exact prediction.

4. Results and Discussions

In this section, all formulated problems will be implemented with the projected algorithm, which in turn provides valuable solution for all monitored parametric values. This process is usually processed with the communication module which is termed as "transceiver," one important block for dispensation of hardware components. Since IoS is involved for monitoring all manufacturing equipment in the supply chain management process, an efficient hardware platform with a satellite-based system is needed for calculating the values with conventional objective functions. Furthermore, in this mechanism, there is no requirement for using different codes that are used as a reference purpose for identification. The abovementioned process is carried out to avoid misperception in all cases and the training set is initialized for detecting five different scenarios.

Scenario 1: control formation with error reduction

Scenario 2: limpidity on periodic intervals

Scenario 3: time of scale sustainability

Scenario 4: intensification of data security

Scenario 5: cost of implementation

Scenario 6: estimation on competence utility

For all five different scenarios, monitoring is carried out in both online and offline analyses, where, to understand the results in real time, the grids are plotted using MATLAB. Moreover, in MATLAB, all calculated component values are combined and only graphs are plotted, but all outcomes are observed in real time at periodic times in manufacturing industries. In the residual section, a detailed explanation about different scenarios is delivered.

4.1. Scenario 1. In this scenario, satellite systems are installed, and they are varied at different frequencies for the establishment of control information. If control information is established at an initial stage, then errors can be reduced in phase 1; else, errors will transpire through all phases under different paths, and as a result, due to high error values, the observed parametric values will rise above the threshold limit. Therefore, the control information is designed for all three coordinate axes using equations (1) and (2), where the reliability of the communication system is tested at two

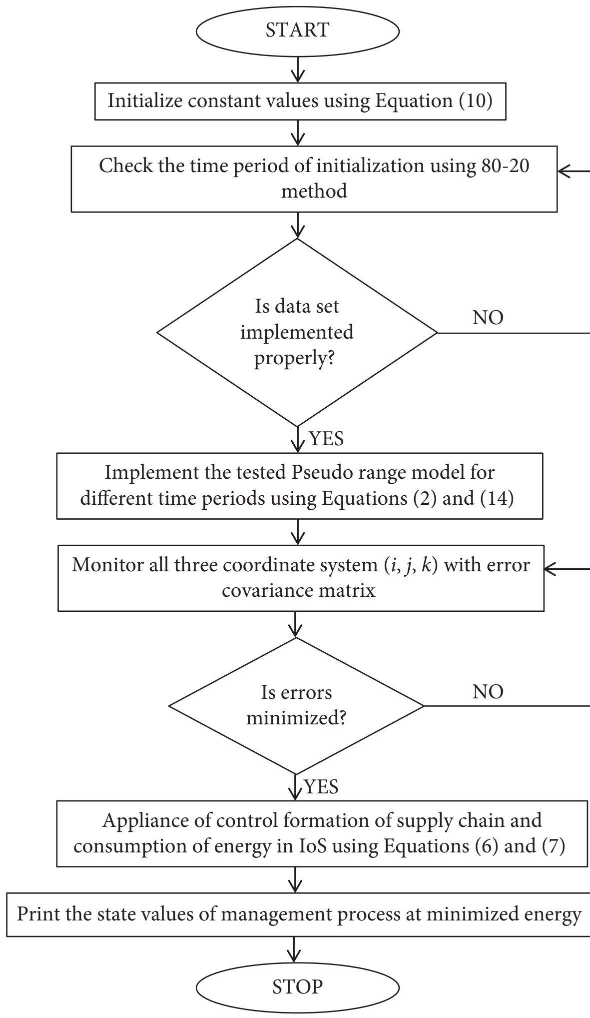

Figure 2: IoS for the supply chain management system.

different levels such as bit- and packet-level systems. In these two levels, if any failure is observed in equipped instruments, then a request will be directed to the central fault-tolerant system to delineate the probable limits. Thus, after observing the error values for different ranges of frequencies, Figure 3 is plotted using decibel values.

From Figure 3, it can be observed that a high degree of protection is assured for the proposed method when compared to existing methods [1]. To observe the parametric error values, frequency ranges are varied from 10 to 10000 Radians per second, and for each variation, error values are observed between −7 and −86 decibels for both proposed and existing methods. From offline analysis, it is much clear that an indicated marker for frequency of 1000 Radians per second provides an abundant difference in the error values of the existing method, as the proposed method delivers only low error values which is equal to −18 decibels. Since a high degree of accuracy is assured, the proposed method with the boosting algorithm can be integrated in real time with efficient control formation techniques.

4.2. Scenario 2. If error values are reduced in phase 1, then transparency values for periodic times are calculated since the values are observed directly from the universe with three different axes. This scenario is considered primarily for monitoring all public organizations as the number of instruments is higher, and they are positioned using mobility nodes. Since the nodes are moving at different scales, transparency will be varied and a high amount of percentage values determines the efficient method. In case if the demand for different utensils rises, then a communication tool can be installed at an isolated subdivision to provide solutions for all raising issues with different constraints. For providing comprehensible results, the periodic time values are plotted in Figure 4.

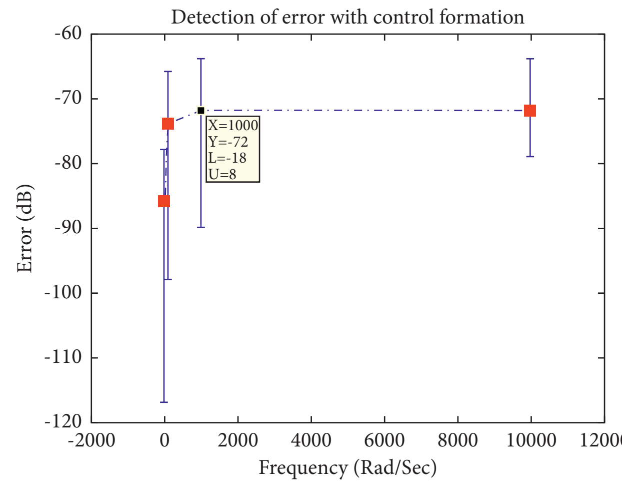

Figure 3: Observed error values for variation in frequency.

From Figure 4, it can be perceived that, for different time periods, the percentage of transparency is calculated at a growing self-sufficiency mode. For monitoring the proposed mechanism, the time period is considered between 60 and 360 seconds, and it is found that the percentage of transparency is maintained at a constant rate when the proposed method is integrated with the boosting algorithm as the training dataset is implemented in a precise manner. If the training set is varied, then the transparency level will also vary, but in case if training dataset is not included, then error values will rise, and as a result, it will affect the transparency values. Furthermore, Figure 4 provides a clear indication that the transparency value of the existing method [1] is maintained only at 65 to 75 percentage whereas, for the proposed method, the transparency values are conserved at 92 to 96 percentage, which is much higher than that of the existing methods.

4.3. Scenario 3. This scenario evaluates the amount of maintainable rate that can be handled by IoS modules. Since the lifetime of the proposed method should be at least 10 years, it is necessary to arrange for an appropriate power supply subsystem. The major need for this power supply module is that the data-centric process will work efficiently when the power supply is designed in a precise manner. Also, sustainability can be evaluated based on different time periods, but in the first stage battery, life time should be improved for sustainable operation. Furthermore, the

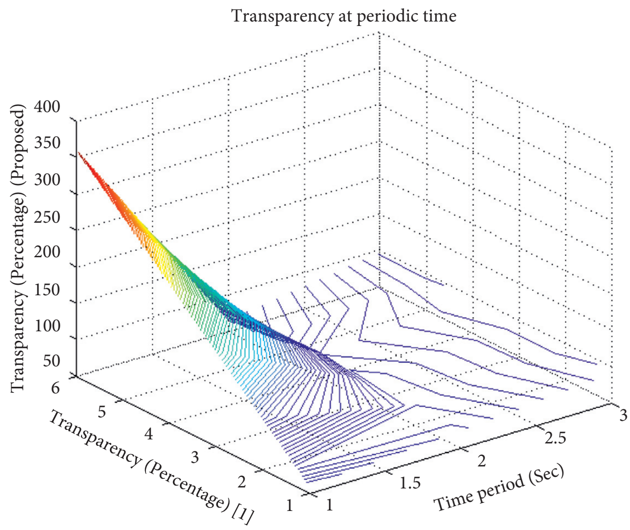

Figure 4: Percentage of transparency at periodic time interval.

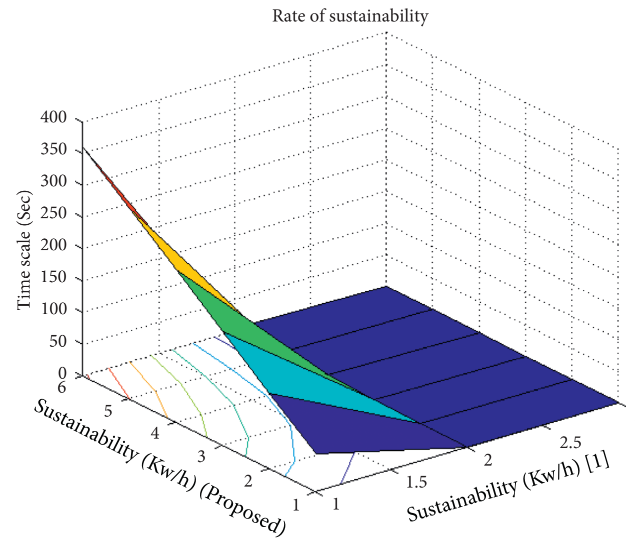

Figure 5: Rate of sustainability at periodic time scale.

central station should be designed using both transmitter and receiver modules that will be integrated using sufficient constraints. In the proposed method, three-axis coordinate systems are provided; therefore, a high sustainability rate should be observed which prevents the failure of the data-centric process. The observed sustainability rate is plotted in Figure 5.

From Figure 5, it can be detected that sustainability which is expressed in Kilo Watts per hour is determined in a varying rate using different time scales. For the small-time period monitoring, the time scales are taken between 60 and 360 seconds, and for each period, the rate of sustainability is maintained. Moreover, it is sensible that if the sustainability rate is maintained within 1 Kw/h, then the efficient operation of IoS is assured. This is possible in the proposed method because for a periodic time, the IoS is sustainable at 0.8 Kw/h, but with the same time period, the existing method [1] is sustainable at 4.3 Kw/h. This proves that the proposed method can able to sustain at low power and at low frequency.

4.4. Scenario 4. The foremost constraint for any IoS model is to check the percentage of data that will be secured during the data transfer stage. The security of data is calculated based on the average percentage received from all coordinate axes; hence, if more amount of encryption keys is added, the data can be secured further. But the main challenging task in this type of application is due to the implementation of the wireless medium, and low security measures are provided for all fundamental operations. However, in the proposed method, since directional antennas are used, signals will be transferred in all directions; therefore, high security threats are present. Thus, the percentage of data security is measured and is plotted in Figure 6.

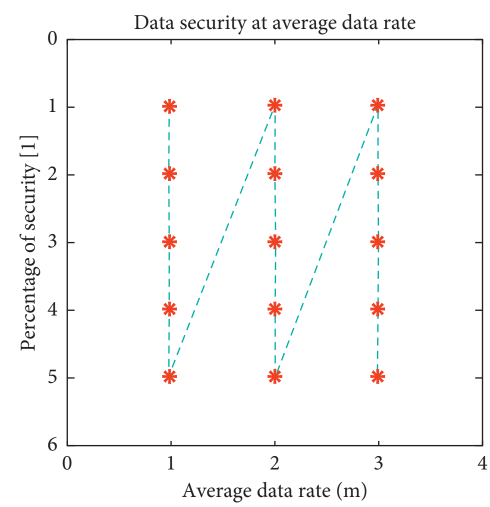

Figure 6: Security measures at average data rate.

Figure 6 provides sufficient solutions for the average percentage of data that is integrated with the boosting algorithm. In the proposed method, the average data is considered between 2000 and 10000 meters, where for each meter, data security at all three axes is calculated. In case if the average data rate is considered as 6000 meters, then the security of data for the existing method will be 68 percentage, whereas, for the proposed method, 85 percentage of data is secured. Moreover, for all average data rates, the proposed method secures the data for more than 80 percentage, thus resulting in achieving efficient safeguard of data.

4.5. Scenario 5. In the proposed method using IoS, the cost of implementation will not be much similar to the basic IoT mechanism as three coordinate axes need to be designed with satellite installation. Therefore, the cost of implementation will be higher when compared to IoT, but monitoring performance will be higher. Thus, the cost parameter for installation can be contented to some extent of available resources. In the proposed method, the cost of implementation is calculated based on the capacity rate of

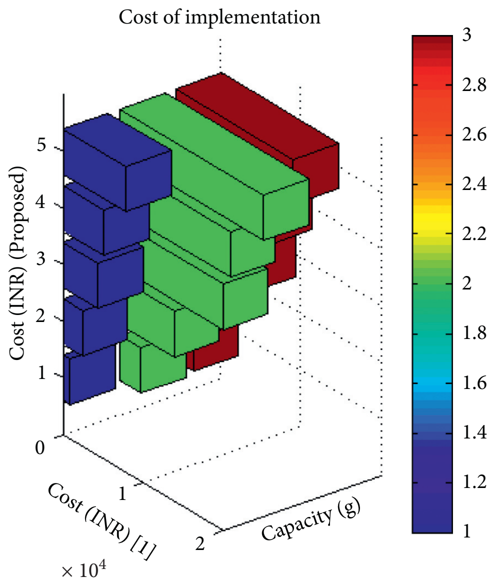

Figure 7: Implementation cost: proposed vs. existing.

available resources. The analyzed value for the implementation of the cost parameter is shown using a three-dimensional bar graph in Figure 7.

Figure 7 indicates the installed capacity in grams which is varied from 800 to 7800, and for these varying capacities, the cost of installed units is calculated. It is evident from the horizontal bar that the cost of installation of the more number of units in the proposed method is much lesser than that in the existing method. For example, if the capacity of installed units is 5000 grams, then the cost of installation is 13765 INR for the proposed method, whereas, with the same amount of capacity, the existing method implements a cost of 11378 INR which is one percentage higher than the existing methods. This indicates that the performance of the proposed method is higher at low cost of installation.

4.6. Scenario 6. In this scenario, the best fitness function is calculated by varying the number of variables, where depending on the weight of each integrated outposts, further the values will be maximized at the output. Every value of the fitness score is denoted for each variable; hence, a separate value is assigned, and an individual model is created using equation (10). In addition, for the modeled scenario, a time-based solution is provided which makes multiple tasks to be performed at the same time. Also, a three-axis coordinate system which specifies a Boolean representation is made with the help of historic data in the optimization problem. After integrating the projected objective with different case studies, the fitness function is evaluated in MATLAB and is deliberated in Figure 8.

From Figure 8, in the first stage, it can be seen that the number of generations is observed per second and a subsequent variable design is made. In the next stage, depending on the designed variables, fitness function is observed where in the proposed method values are found to be less than 0.5 which indicates a best fitness function is achieved at low

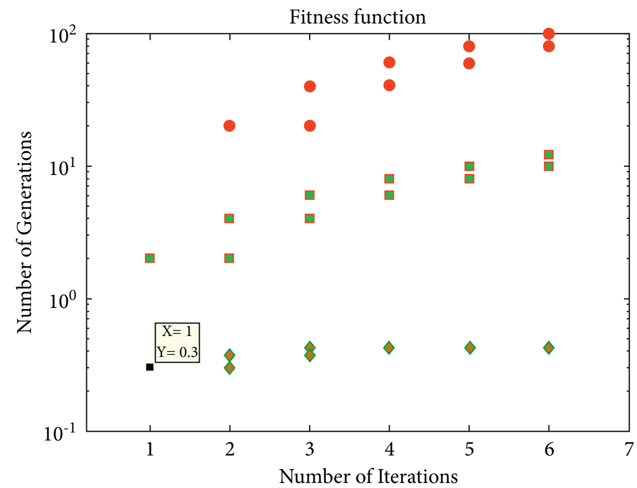

Figure 8: Effective fitness function of the proposed model.

generated values with 100. Moreover, a unique model has been designed for achieving this fitness function, and an unrestricted mode is switched on at different dynamic positions. At the final stage, the generated process is encoded with different values where it will be converted from outpost values to normally generated values.

5. Conclusions

Based on the awareness of supply chain management in the distributed system, an IoS procedure for the system model has been introduced in this article. In the proposed method, a new measurable model for the supply chain management process has been deliberated where all imports and exports can be monitored with the help of a three-axis coordinate system. However, this type of system can be established, and they can be able to monitor the abovementioned management parameters since the method has been extended from IoT. But the major demand is controlling the error during such monitoring process in public administrations as a small error will cause the system to obscure. Therefore, exertions have been taken for reducing the error of measurement at periodic intervals, and the percentage of sustainability has been extended by installing the IoS route with the boosting algorithm. By comparing the proposed method with the existing one, the investigation has been extended with several new parameters, and in addition, the proposed method has not only stopped in the stage of monitoring. This proves that the projected technique is implemented not only for monitoring, but also to solve real-time problems, efforts have been taken, and after comparing five different scenarios with the existing method, the proposed method proves to be much efficient in terms of sustainability and error reduction.

Data Availability

The data used to support the findings of this study are available from the corresponding author upon request.

Conflicts of Interest

The authors declare that they have no conflicts of interest.

References

[1] W. Jiang, "An intelligent supply chain information collaboration model based on Internet of Things and big data," *IEEE Access*, vol. 7, pp. 58324–58335, 2019.

[2] M. Seyedan and F. Mafakheri, "Predictive big data analytics for supply chain demand forecasting: methods, applications, and research opportunities," *Journal of Big Data*, vol. 7, no. 1, 2020.

[3] D. Ivanov, "Viable supply chain model: integrating agility, resilience and sustainability perspectives—lessons from and thinking beyond the COVID-19 pandemic," *Annals of Operations Research*, vol. 23, 2020.

[4] N. Saker and L. Kerbache, "Modeling smart grids using closed loop supply chain concepts," *International Journal of Smart Grid and Clean Energy*, vol. 15, pp. 8–14, 2014.

[5] F. Niakan, A. Baboli, V. Botta-Genoulaz, R. Tavakkoli-Moghaddam, and J. P. Camapgne, "A multi-objective mathematical model for green supply chain reorganization," *IFAC Proceedings Volumes (IFAC-PapersOnline)*, vol. 46, 2013.

[6] S. Ahmed, T. Kalsoom, N. Ramzan et al., "Towards supply chain visibility using Internet of Things: a dyadic analysis review," *Sensors*, vol. 21, no. 12, pp. 1–24, 2021.

[7] A. Rejeb, S. Simske, K. Rejeb, H. Treiblmaier, and S. Zailani, "Internet of Things research in supply chain management and logistics: a bibliometric analysis," *Internet of Things*, vol. 12, Article ID 100318, 2020.

[8] S. Yuvaraj and M. Sangeetha, "Smart supply chain management using Internet of things(IoT) and low power wireless communication systems," in *Proceedings of the 2016 IEEE International Conference on Wireless Communications, Signal Processing and Networking, WiSPNET 2016*, pp. 555–558, Chennai, India, March 2016.

[9] D. Jhala, "Review on smart supply chain management using IoT and machine learning," *International Journal of Innovative Research in Science, Engineering and Technology*, vol. 42, 2019.

[10] H. Elmesmary and A. S. Gamal Abd El-nasser, "Smart solutions for logistics and supply chain management," *International Journal of Recent Technology and Engineering*, vol. 8, no. 4, pp. 2996–3001, 2019.

[11] Y. H. Lee, P. Golinska-Dawson, and J. Z. Wu, "Mathematical models for supply chain management," *Mathematical Problems In Engineering*, vol. 2016, Article ID 6167290, 4 pages, 2016.

[12] S. Y. Barykin, I. V. Kapustina, S. M. Sergeev, and V. K. Yadykin, "Algorithmic foundations of economic and mathematical modeling of network logistics processes," *Journal of Open Innovation: Technology, Market, and Complexity*, vol. 6, no. 4, pp. 1–16, 2020.

[13] G. M. G. Farok, "Mathematical modeling for measures of supply chain flexibility," *Journal of Mechanical Engineering*, vol. 45, no. 2, pp. 96–117, 2016.

[14] P. Pourhejazy and O. K. Kwon, "The new generation of operations research methods in supply chain optimization: a review," *Sustainability*, vol. 8, no. 10, 2016.

[15] W. Liu, K. Deng, X. Zhang et al., "A semi-supervised tricatboost method for driving style recognition," *Symmetry*, vol. 12, no. 3, pp. 1–18, 2020.

[16] I. H. Sarker, "Machine learning: algorithms, real-world applications and research directions," *SN Computer Science*, vol. 2, no. 3, pp. 1–21, 2021.

[17] B. H. C. C. Priya and K. Viswavardhan Reddy, "Performance analysis of machine learning algorithms for disease prediction," in *Proceedings of the 2021 Grace Hopper Celebration India*, Bangalore, India, March 2021.

Hindawi
Scientific Programming
Volume 2021, Article ID 7880461, 9 pages
https://doi.org/10.1155/2021/7880461

Research Article

Algorithm of Ecocompensation in Sloping Land Conversion Program Based on Heckman's Two-Step Model

Haotian Wang[1], **Chen Ke**[1], **and Xiaojun Yang**[2]

[1]*Shenyang Agricultural University, Shenyang, Liaoning 110866, China*
[2]*School of Public Policy and Administration, Xi'an Jiaotong University, Xi'an, Shaanxi 710049, China*

Correspondence should be addressed to Haotian Wang; wangyucheng0107@126.com

Received 16 September 2021; Revised 12 October 2021; Accepted 19 October 2021; Published 24 November 2021

Academic Editor: Punit Gupta

In this paper, we broadly generalize the assignment auction algorithm to solve linear minimum cost network flow problems. It is significant to establish a market-based compensation mechanism by way of conservation auctions based on peasant households' willingness, which can promote the innovation of ecocompensation policies, green development, and balanced growth. Using the survey data collected from 453 households within 3 national pilot counties in ecologically fragile regions in northwest Liaoning for the Sloping Land Conversion Programme, measuring peasant households' willingness to accept ecocompensation through sealed auctions, we built a database through cloud computing to realize information collation and query and applied the Heckman's Two-Step Model to study the impact of risk preference, social capital, cognitive preference, land parcel characteristics, and family endowments on farmers' willingness to participate in protection auctions and their bid prices. The results reveal that the average bid price of peasant households in the ecologically fragile region in northwest Liaoning for the Sloping Land Conversion Programme is annually 274.5 yuan per mu and that risk preference and social capital have positive impacts on peasant households' willingness to participate in conservation auctions and on their bid prices, cognitive preference has a positive impact on peasant households' bid prices in conservation auctions, and land plot characteristics have a negative impact on peasant households' bid prices in conservation auctions. It is suggested that ecocompensation policies should be optimized with such methods as lowering peasant households' perception of high risks, setting role models for them to follow, and strengthening their perception of the environment, income, and property rights.

1. Introduction

Ecocompensation is a willingness-based transaction mechanism, where ecosystem service (ES) buyers/users/beneficiaries make direct and contractually agreed payments to ES providers [1]. Payment standards that influence incentive effects are always the core of policy design [2]. As a landmark project in the course of China's ecological conservation, research on ecocompensation standards for the Sloping Land Conversion Programme (SLCP) made by scholars with the ES value method [3, 4], contingent valuation method (CVM) [5, 6], choice experiment method (CE) [7], and opportunity cost approach (OCA) [8, 9] has been running through all the phases of programme implementation. Nondiscriminatory compensation standards based on opportunity costs for the SLCP have the advantages of openness, transparency, and easy operation, but they also have the problem of information asymmetry between ES providers and users [2], which leads to either insufficient compensations lower than ES providers' opportunity costs or inefficient overcompensation transactions. What is worse, recultivation in major grain producing areas and reclamation in barren areas occur even more frequently due to hidden action caused by moral hazard [10].

In order to reduce informational rents generated by heterogeneity in opportunity costs, Ferraro proposed three solutions: gathering information relevant to opportunity costs, revealing peasant types by screening contracts, and using conservation auctions [11]. As an effective market-based policy tool, the mechanism of conservation auction allows ES providers to express their opportunity costs actively through specific mechanism desig, and ultimately improve ES programs' fund use efficiency [12].

The mechanism of conservation auction was first used in ecocompensation practices in developed countries, including the BushTender Trial (BTT) in Australia and the Conservation Reserve Program (CRP) in the United States [13, 14]. Several cases of peasant households' participation in conservation auctions were also found in developing countries such as Indonesia, Malawi, and Kenya [15–17]. Thereafter, a few scholars in China started their research on conservation auctions [18–20].

An overview of key theoretical and laboratory studies on the mechanism of conservation auction by scholars at home and abroad reveals three problems that are worth noticing. First, there is a lack of theoretical research to reveal ES providers' opportunity costs. Second, there is currently little relevant research on unobservable factors featuring heterogeneity in ES providers [21]. Third, it still needs to be verified whether the mechanism of conservation auction can be used as an effective policy tool to solve environmental issues in developing countries.

To bridge the existing research gaps summarized above, this article takes the Sloping Land Conversion Programme, one of the biggest ecocompensation programs in the world at present, as an example to reveal peasant households' real opportunity costs through the mechanism of conservation auction, which is expected to provide a valuable reference for China's innovation of ecocompensation policies and its establishment of a long-term effective ecocompensation mechanism.

What makes this research innovative primarily lies in three aspects. First, the opportunity costs offered by peasant households for plots of land were taken as an essential indicator of ES provider heterogeneity to examine how peasant households' opportunity costs affect their participation in conservation auctions, which lays a foundation for the establishment of discriminatory ecocompensation standards. Second, based on Heckman's Two-Step Model, we study the impacts of unobservable factors including risk preference, cognitive preference, and social capital on peasant households' willingness to participate in conservation auctions, which is also innovative to some extent. Third, our study on SLCP ecocompensation with the conservation auction mechanism expands the range of applying the conservation auction mechanism in developing countries.

2. Research Design

2.1. Theories and Hypotheses. In 1997, Latacz-Lohmann and Van der Hamsvoort developed a hypothetical program to verify that the conservation auction mechanism can significantly promote the program's cost-effectiveness [12]. They concluded that an ES provider's bid price is formed based on a balance between net income and the probability of winning the bid, that the tender decision is made on the basis of the ES provider's expectation on the highest price acceptable to the government, and that the optimal bid price is the one that maximizes the expected utility or gain from the auction. Existing findings disclose several individual characteristics that affect an ES provider's tender decision, including his age, race, education, residence, etc. [21].

Risk preference is a key factor affecting SLCP peasant households' decision-making behavior [22]. When examining the issue of risk difference, Latacz-Lohmann and Van der Hamsvoort divided peasant bidders into two types: risk neutral and risk averse, arguing that risk averse bidders tend to lower their bids to increase the probability of winning the bid [12]. In reality, ES providers represented by peasant households are mostly the risk averse type, and there are even highly risk averse peasant households who refuse to participate in conservation auctions [23]. Cognitive preference also has impacts on SLCP peasant households [24]. When bidding in conservation auctions, those with relatively higher levels of environmental perception know better the importance of ecological services and therefore tend to increase their tender prices to earn informational rent [25]. According to *The Rational Peasant* by Schultz [26], peasant households' decision-making behavior is profit-driven, and the bid prices offered by peasant households in conservation auctions are positively correlated with their perception of income. As an important means to make external and public goods become internal and private, clarification of property rights is of positive significance to promote peasant households' management and conservation of natural resources [27]. Influenced by the endowment effect, peasant households having a better perception of property rights tend to offer higher tender prices [28]. As a sort of group characteristic, behavior, or outcome, social capital affects individual behavior or outcome [29]. Whether an individual possesses social capital or not decides his amount of right to speak or to make decisions. Therefore, participants with rich social capital tend to be in a more advantageous position in conservation auctions [30, 31]. Land is the most important means of production for peasant households, and plots of land are basic units for the SLCP. Peasant households make their bids based on the opportunity costs of land plots [25]. They tend to offer higher bid prices for good-quality land plots with higher opportunity costs. In this article, four hypotheses are summed up and proposed as follows:

H_1: peasant households' bid prices are positively correlated with their risk preference

H_{2a}: peasant households' bid prices are positively correlated with their perception of the environment

H_{2b}: peasant households' bid prices are positively correlated with their perception of income

H_{2c}: peasant households' bid prices are positively correlated with their perception of property rights

H_3: peasant households' bid prices are positively correlated with the social capital they own

H_4: peasant households' bid prices are positively correlated with the opportunity costs of their land plots

2.2. Data Sources. The Sloping Land Conversion Program is a major policy decision made by China to improve the ecological environment and build an ecological civilization

[32]. As one of the top ecologically sensitive zones in China, the ecologically fragile region in northwest Liaoning has finished one-fifth of Liaoning Province's SLCP work in the first round. The data of this article are sourced from the field survey made by the research team between 2019 and 2020 in 3 national SLCP pilot counties in the ecologically fragile region in northwest Liaoning, namely, Zhangwu, Beipiao, and Jianchang, involving 18 villages 6 townships. With the method of stratified sampling, the research team first selected 2 townships at random from each county and then selected 3 villages from each township at random for the survey. Ultimately, 480 households who participated in the first round of the SLCP were drawn as samples, and finally 453 valid questionnaires were sorted out, accounting for 94.4%.

2.3. Research Design. How conservation auctions are designed directly affects the effect of implementing the SLCP, which is supposed to reveal peasant bidders' real opportunity costs and avoid possible moral hazard caused by fraud [33]. Referring to the study by Han Hongyun and Yu Yonghong [7], this research is designed to adopt a sealed bid procurement auction to give peasant households continuous compensation for the SLCP. The use of a single-round auction permits a direct observation of the field experiment results of the conservation auction, which helps relieve participants' tiredness and cognitive load in the survey and meanwhile reduce the management and transaction costs of the auction [34, 35]. Auction payment rules mainly include discriminatory price auctions and uniform price auctions. Discriminatory pricing is closer to bidders' real costs, and its cost-effectiveness performs better on the whole [36, 37]. Before each auction, the researchers explain in detail the auction process to avoid abnormal bidders. The auction design in this article is shown in Table 1.

2.4. Research Methodology

2.4.1. Query of Farmers' Bidding Information under Cloud Computing. According to the bidding information resources, cloud computing technology is used to divide the integrated information resources into multiple subsets according to the attributes of the information relationship. After the division is completed, the database construction is completed in a bottom-up manner.

Adopt SQL SERVER 2000 database management system, call the distributed information integration function in the database, and coordinate the management of the database through cloud computing technology. Design four query methods:

(1) Uncertain query: In the database, there are two types. One is that the query information is stored on a certain node. When the word "query completed" appears, the query ends; the other is that the query information is stored on multiple nodes. Based on the first query, I want to continue to query and obtain information.

(2) Combined query: Divide the query information in more detail, and define query D as shown in the following formula:

$$D = d_1 \cup d_2 \cup \cdots \cup d_n. \tag{1}$$

In the formula, d_1, d_2, ...d_n represent atomic queries. Atomic query is to store all query results on a node, that is, to obtain the data at that point.

(3) Connect query: the connection query in the database is divided into two connection queries and multiple connection queries. In the first type, two connection queries, the query information is defined as follows:

$$D = d_1 \infty d_2. \tag{2}$$

In the formula, ∞ represents the connection symbol. There are three query results shown in the following formula:

$$TD \approx Td_1 \approx Td_2 \text{ or } TD \approx Td_1 \text{ and } TD > Td_2. \tag{3}$$

In the formula, T represents the record information; TD, Td_1, and Td_2, respectively, represent the record number of D, d_1, and d_2. The second is multi-connection query; the query information is defined as follows:

$$D = d_1 \infty d_2 \infty \cdots \infty d_n. \tag{4}$$

Reduce the redundant data in the database; at the same time, connect the atomic query with the node to complete the information query.

(4) Compound query: The composite result of the merge and join query is shown in the following formula:

$$D = F(d_1, d_2, \cdots, d_n). \tag{5}$$

In the formula, F represents the function composed of ∞ and $\cup$.

After completing the above steps, the database construction and information query can be realized.

2.4.2. Peasant Household Bidding Model. Supposing there are N peasant households participating in the government's compensation for the SLCP, the bid price and opportunity cost of Peasant Household i are, respectively, b_i and δ_i. Then, the objective function and the optimal strategy of Peasant Household i in the discriminatory auction are summed up as follows.

The objective function of Peasant Household i is

$$\max_{b_i} \prod_i = (b_i - \delta_i) E_i [P(b_i \le b_n)]. \tag{6}$$

The optimal strategy of Peasant Household i is

$$b_i^* = \delta_i - \frac{E_i [P(b_i \le b_n)]}{\partial E_i [P(b_i \le b_n)] / \partial b_i |_{b_i = b_i^*}}. \tag{7}$$

Table 1: Design of conservation auction.

Payment type	Discriminatory auction
Bid setting	A reserve price is set
Auction type	Sealed bid procurement auction
Auction budget	Unknown
Auction rounds	1 round (a trial before the formal experiment)
Number of bidders	Fixed
Bid unit	1 mu
Decision-making environment	Peasant households make individual decisions in their own places of residence, without any exchange of other information between households during the whole decision-making process

2.4.3. Heckman's Two-Step Model: The Mechanism Affecting Peasant Households' Bid Decision-Making. Referring to relevant research on Heckman's Two-Step Model [38], the current study divides peasant households' bid decision-making process into two steps in the current study. The first step is that peasant households make decisions on whether to participate in bidding and their willingness to do that is defined as a binary choice variable between 0 and 1; the second step is that peasant households who are willing to participate in bidding make decisions on their bid price, which is a continuous variable. The model is set as follows:

$$
\begin{aligned}
&Z_i = \begin{cases} 0, & Z_i^* \leq 0, \\ 1, & Z_i^* > 0, \end{cases} \\
&Z_i = a_0 + a_1 X_i + a_2 C_i + a_3 D_i + \varepsilon_i, \\
&Y_i = b_0 + b_1 X_i + b_2 C_i + b_3 \lambda + \mu_i \begin{cases} \text{unobservable}, & Z_i = 0, \\ \text{observable}, & Z_i = 1. \end{cases}
\end{aligned} \tag{8}
$$

Formulas (1) and (2) constitute the selection model for Heckman's first step, and formula (3) is the result model of Heckman's second step. In formula (1), Z_i^* is the latent variable of peasant households' willingness to bid. If $Z_i^* \leq 0$, then $Z_i = 0$; otherwise, $Z_i = 1$. In formula (2), X_i is the core explanatory variable affecting peasant households' bidding, C_i is the control variable, D_i is the identification variable, and ε_i is the error term. In formula (3), Y_i is the peasant household's bid price, λ is the inverse Mills ratio, and μ_i is the error term.

2.5. Variable Selection. In accordance with the research objectives, a peasant household's willingness to bid and bid price are chosen as explained variables, while a peasant household's risk preference, social capital, cognitive preference, and land plot characteristics are chosen as the core explanatory variables. According to theoretical research on behavioral economics, a peasant household's risk preference can be measured directly [39]. In this research, 2 indicators of risk preference, namely, planting risk and investment risk, are selected through combining the management characteristics of peasant households involved in the SLCP. Referring to the study made by Liao Peiling and other scholars [40], perception of the environment, perception of income, and perception of property rights are selected as 3 indicators of cognitive preference. Based on the research by Lv Qian and Wang Xin [41], social prestige, social network, and social participation are selected as 3 indicators of social capital. Referring to the proxy variables of ES opportunity costs proposed by Kosoy and other scholars [42], taking the ecological and economic benefits of a land plot into account, quality of the land plot, income of the land plot before conversion, and slop of the land plot are selected as 3 indicators of land plot characteristics. Control variables include low-income households, age of the head of household, health status of the head of household, education of the head of household, political status of the head of household, household labour, per capita annual income of household, proportion of the SLCP income, area of arable land, and area of converted land. According to the requirement of Heckman's Two-Step Model, identification variables should be chosen from the conditions that have significant impacts on willingness to bid but insignificant impacts on bid prices. To this end, proportion of SLCP peasant households in the village is selected as the identification variable due to two considerations: on one hand, peasant households are more likely to participate in conservation auction when there are higher proportion SLCP peasant households in the village; on the other hand, the proportion of SLCP peasant households in the village could not be likely affecting the individual peasant household's bid prices. The variables description and descriptive statistics are shown in Table 2.

3. Results and Analysis

3.1. Analysis of Results. Per capita income of household and income of the land plot before conversion are processed with logarithm to eliminate errors. Then, due to VIF, the two variables, income of the land plot before conversion (after logarithm) and soil quality, fail the test for multicollinearity. The first step is to construct the Probit regression model and calculate the inverse Mills ratio λ; the second step is to put the inverse Mills ratio λ into the least squares regression model with bid price as the dependent variable. The results show that the inverse Mills ratio λ is statistically significant at the 10% level, which implies sample selection bias exists and Heckman's Two-Step Model is applicable. Pseudo-R^2 of the Probit model is 0.424, and $R^2$of the OLS model is 0.505, which indicates a good fit between the two models. Results of the two regression models are shown in Table 3.

The estimated results of Heckman sample selection model are summarized as follows:

Table 2: Variable description and descriptive statistics.

Variables	Variable definition and description	Mean	Standard deviation	Minimum	Maximum
Explained variables					
Peasant household's willingness to bid	0 = unwilling to participate in bidding; 1 = willing to participate in bidding	0.786	0.411	0	1
Peasant household's bid price	Peasant household's bid price (yuan/mu)	274.535	125.824	50	650
Core explanatory variables					
Risk preference					
Planting rick	Willingness to plant new varieties of crops: very unwilling = 1, unwilling = 2, no opinion = 3, willing = 4, very willing = 5	2.980	1.359	1	5
Investment risk	Willingness to make high-risk investments: very unwilling = 1, unwilling = 2, no opinion = 3, willing = 4, very willing = 5	2.459	1.223	1	5
Social capital					
Social prestige	Is there any village cadre in the household: yes = 1, no = 0	0.099	0.299	0	1
Social network	Number of relatives in the village (households): 0~5 = 1, 5~10 = 2, 10~15 = 3, 15~20 = 4, >20 = 5	2.402	1.538	1	5
Social participation	Participation in village affairs: seldom = 1, occasionally = 2, sometimes = 3, often = 4, always = 5	2.461	1.190	1	5
Cognitive preference					
Perception of the environment	The SLCP helps improve the ecological environment: strongly disagree = 1, disagree = 2, no opinion = 3, agree = 4, strongly agree = 5	2.263	0.921	1	5
Perception of income	The SLCP helps improve household income: strongly disagree = 1, disagree = 2, no opinion = 3, agree = 4, strongly agree = 5	2.667	1.192	1	5
Perception of property rights	Management and conservation of the converted land each year (times): 0~20 = 1, 20~40 = 2, 40~60 = 3, 60~80 = 4, >80 = 5	1.782	1.216	1	5
Land plot characteristics					
Quality of the land plot	Soil quality: very bad = 1, bad = 2, medium = 3, good = 2, very good = 5	2.512	1.384	1	5
Income of the land plot before conversion	Net income of the land plot before conversion (yuan/mu)	309.117	134.714	50	680
Slope of the land plot	Slope of the land plot: flat slope (0°~5°) = 1, gentle slope (6°~15°) = 2, moderate slope (16°~25°) = 3, strong slope (26°~35°) = 4, very strong slope (>35°) = 5	1.962	1.158	1	5
Control variables					
Low-income household	Low-income household: yes = 1, no = 0	0.245	0.431	0	1
Age of the head of household	Actual age of the head of household (years)	54.731	8.457	25	70
Health status of the head of household	Good = 1, medium = 2, bad = 3	1.651	0.780	1	3
Education of the head of household	Illiterate = 0, primary = 1, junior high = 2, secondary and senior high = 3, junior college = 4, college and above = 5	2.645	0.764	1	5
Political status of the head of household	A party member or not: Yes = 1, No = 0	0.139	0.346	0	1
Household labour	Household labour within the 18–60 age range = 1, household labour below 18 and above 60 = 0.5, other cases = 0	1.961	1.095	0	5
Per capita annual income of household	≤5, 000 yuan = 1, 5,000–10,000 yuan = 2, 10,000–20,000 yuan = 3, 20,000–30,000 yuan = 4, >30,000 = 5	11987.385	9006.979	633.667	65075
Proportion of the SLCP income	Proportion of the income from the SLCP to the gross household income (%): 0~5 = 1, 5~10 = 2, 10~15 = 3, 15~20 = 4, >20 = 5	1.647	1.290	1	5
Area of arable land	Area of arable land owned by the household: mu	12.996	16.036	0	115
Area of converted land	The area of converted land owned by the household: mu	5.268	5.278	0.5	46
Identification variable					
Proportion of SLCP households	Proportion of households participating in the SLCP to the total number of households in the village (%)	0.364	0.029	0.269	0.427

(1) Risk preference: Although only investment risk significantly affects the probability of peasant households' willingness to participate in the conservation auction, both planting risk and investment risk are positively correlated with peasant households' bid prices at 5% significance level. This suggests that more risky peasant households are more willing to participate in conservation auctions and choose higher bid prices at the cost of reducing the probability of winning the bid.

(2) Social capital: Social prestige is positively correlated with peasant households' willingness to make a bid in conservation auctions at 5% significance level, which indicates village cadres are more willing than common peasant households to accept the policy design of taking conservation auctions as a means of ecocompensation payment; social participation has a positive impact on peasant households' bid prices at 5% significance level, which suggests that rural capable people who participate more in social activities are willing to achieve higher bid prices by making use of the resources and information in hand.

(3) Cognitive preference: The perception of the environment, income, and property rights, passing the 5% level, 10% level, and 5% level significance test, respectively, is positively correlated with peasant households' bid prices, which indicates that peasant households' perception of the ecological and economic benefits of the SLCP significantly promotes their bid prices in the conversation auction and that peasant households are more willing to choose relatively high bid prices when engaging more in the management and conservation of land plots under conversion to forests due to the influence of their perception of property rights.

(4) Land plot characteristics: As an indicator with dual attributes of generating both ecological and economic profits attributes, slope, is negatively correlated with peasant households' bid prices at 5% significance level, which indicates the stronger the slope of an SLCP land plot is, the less income it generates from planting before the implementation of the SLCP and the lower bid prices peasant households tend to offer when considering its opportunity costs.

(5) Control variables: The age of the head of household has a significantly negative impact on a peasant household's willingness to bid and bid prices, passing the 5% level and 1% level significance test, respectively. That suggests, with their ages growing and out of consideration for stable income, the peasants tend to lose their enthusiasm for participating in conservation auctions and choose relatively low bid prices for higher probabilities of winning the bid. The health and political status of the head of household are positively correlated with his willingness to bid, passing the 5% level significance test. The results indicate that a good health is the basic guarantee of peasants' participation in bid auctions and fulfillment of auction contracts and that peasant households with Party members are more active in participating in conservation auctions. The area of arable land has a negative impact on peasant households' willingness to bid but a positive impact on their bid prices, which suggests SLCP peasant households with rich arable land resources are not very willing to participate in conservation auctions but they are driven by economies of scale to choose relatively high bid prices.

(6) Identification variables: The proportion of SLCP peasant households has a positive relationship with peasant households' willingness to bid, passing the 1% level significance test, which indicates peasant households in the villages with higher proportions of households engaged in the SLCP are more willing to participate in conservation auctions. But this ratio has no significant impact on bid prices, which suggests the identification variable has been selected appropriately.

3.2. Suggestions on Optimizing Ecological Compensation. Strengthen the information publicity of ecological compensation policy, make the incentive policy open and transparent, reduce farmers' awareness of the high risk of ecological compensation, improve farmers' enthusiasm for participation through incentive policy, set up property right knowledge lectures, and enhance farmers' awareness of property rights. At the same time, it is best to establish ecological compensation projects in the surrounding areas, so that farmers can understand the relevant information of ecological compensation in the surrounding areas, deepen their understanding of ecological compensation, and enhance their willingness to participate in ecological compensation.

The diversification of farmers' income sources will also promote the implementation of ecological compensation policy. With the development of information society, farmers' demand for labour transfer is increasing day by day. They often struggle between continuing farming and going out to work. Generally speaking, the higher the education level, the faster the ability to accept new things. Therefore, for farmers with higher education, their vision and thinking are also broader. They are more able to look at the ecological compensation policy from an objective perspective, which can often play a role model and drive other farmers to participate. At the same time, the government should increase support for sideline and migrant work other than farming, based on the necessary help of farmers, which is also conducive to increasing farmers' confidence in the government, so as to improve farmers' participation in ecological compensation policies. In the process of implementing the ecological compensation policy, we can also vigorously support the development of organic agriculture, improve the protection of the ecological environment, develop low-carbon organic agriculture, fundamentally

Table 3: The estimated results of Heckman sample selection model.

	Probit regression			OLS regression		
	Coefficient	Standard error	z-score	Coefficient	Standard error	t-value
Core explanatory variables						
Risk preference						
Planting risk	0.096	0.087	1.11	15.251**	5.168	2.95
Investment risk	0.214**	0.108	1.97	20.489***	5.769	3.55
Social capital						
Social prestige	1.526**	0.543	2.81	30.771	19.256	1.60
Social network	−0.055	0.061	−0.91	1.583	3.479	0.45
Social participation	0.139	0.092	1.51	9.837**	4.914	2.00
Cognitive preference						
Perception of the environment	0.071	0.106	0.67	16.958**	5.982	2.83
Perception of income	−0.015	0.082	−0.18	8.040*	4.824	1.67
Perception of property rights	0.075	0.089	0.84	29.016***	4.304	6.74
Land plot characteristics						
Slope	0.037	0.076	0.49	−10.550**	4.795	−2.20
Control variables						
Low-income households	−0.150	0.191	−0.79	−4.367	12.808	−0.34
Age of the head of household	−0.043**	0.013	−3.27	−4.628***	0.668	−6.93
Health of the head of household	−0.246**	0.117	−2.09	−6.780	8.182	−0.83
Education of the head of household	−0.085	0.123	−0.69	−3.217	7.043	−0.46
Political status of the head of household	0.767**	0.296	−2.59	−6.502	18.263	−0.36
Household labour	0.035	0.082	0.43	−4.351	4.978	−0.87
Proportion of SLCP income	0.083	0.097	0.86	0.856	4.789	0.18
Area of arable land	−0.015**	0.007	−2.25	0.800**	0.343	2.34
Area of converted land	0.002	0.023	0.09	0.932	1.005	0.93
Identification variables						
Proportion of SLCP peasant households	31.794***	4.832	6.58			
Inverse Mills ratio (λ)				35.716*	21.327	1.67
Constant variable	−10.625***	2.368	−4.49	321.800***	82.631	3.89

*, **, and ***represent the estimated coefficient is statistically significant at the 1% level, at the 5% level, and at the 10% level, respectively.

improve the agricultural economic benefits, and promote the sustainable development of economy and society through the ecological compensation policy.

4. Conclusion and Discussion

Our results show that the average bid price of peasant households in the ecologically fragile region in northwest Liaoning for the Sloping Land Conversion Programme is annually 274.5 yuan per mu, close to the net income of 309.1 yuan per mu before the SLCP and also close to the compensation standard of 300 yuan per mu for the new-round SLCP [32]. It is 3.05 times the subsidies for the consolidation period of the first-round SLCP. As the important subjects to implement and manage the SLCP, 78.6% of peasant households are willing to participate in conversation auctions, which indicates means of compensation based on the willingness of peasant households are easier to be accepted, among them, the query function constructed by cloud computing provides convenience for farmers to obtain information to a large extent. Risk preference and social capital have positive effect on peasant households' willingness to bid in conservation auctions as well as on their bid prices; cognitive preference has positive effect on bid prices in conservation auctions; land plot characteristics have negative effect on bid prices in conservation auctions; of the factors of family endowment, the age of the head of household has significantly negative effect on peasant households' willingness to bid and on their bid prices, the health and political status of the head of household has positive effect on the peasant household's willingness to bid, and the area of arable land has negative effect on peasant households' willingness to bid but positive effect on their bid prices. According to these findings, it is advised to improve ecocompensation policy design following peasant households' willingness, lower SLCP peasant households' risk perception, give play to the leading and exemplary role of the village Party branch, the village committee, village cadres, and active management participants, strengthen peasant households' perception that the SLCP helps improve the environment and income, and encourage peasant households' management and conversion of the converted land through the design of conservation auction contracts.

This paper uses protective auction mechanism to solve the problem of information asymmetry. At the same time, it is innovative to use cloud computing to establish a database, realize information query, facilitate farmers, and establish an ecological compensation standard based on farmers' real opportunity cost. However, this paper only selects the information of 453 farmers in three national pilot counties in western Liaoning as the data sample, which has limitations. Therefore, in the next research, more data will be used for statistics and supplemented with more sample data for research and analysis, so as to make the application of distribution auction algorithm in the operation of ecological compensation more persuasive and referential, make the ecological compensation standard based on farmers' protection auction mechanism more perfect, and lay a good foundation for extensive promotion in the future.

Data Availability

Data sharing is not applicable to this article as no datasets were generated or analysed during the current study.

Conflicts of Interest

The authors declare no potential conflicts of interest with respect to the research, authorship, and/or publication of this article.

Acknowledgments

This paper was supported by General Projects of National Social Science Fund in 2020 "Study on the impact of collective forest land use control on the welfare of farmers and ecological compensation system in Nature reserves" (20BGL173), China National Natural Science Foundation "Research on Ecological Public Welfare Forest Compensation Mechanism from the Perspective of Farmer Behavior Response: Based on the Empirical Study of Framed Field Experiments and Follow-up Investigation" (72073029), Soft Science Research Project of Department of Science and Technology of Shaanxi Province (2021KRM040), and Key Scientific Research Project of Education Department of Shaanxi Province (20JT049).

References

[1] S. Wunder, *Payments for Environmental Services: Some Nuts Andbolts*, CIFOR Occasional Paper, Center for International Forestry Research, vol. 42, pp. 3–8, Jakarta, Indonesia, 2005.

[2] L. Di, H. Zhentong, and J. Leshan, "A review of the analysis framework of ecological conservation compensation," *Acta Ecologica Sinica*, vol. 38, no. 2, pp. 380–392, 2018.

[3] G. Huimin and W. Wukui, "Spatial distribution of compensation funds for the conversion of farmland to forests based on opportunity costs: taking Zhangjiakou as an example," *Science of Soil and Water Conservation*, vol. 13, no. 4, pp. 137–143, 2015.

[4] M. Y. Hou, S. B. Yao, Y. J. Deng et al., "Spatial-temporal evolution pattern and differentiation of ecological service value in Yan'an city at the grid scale based on sloping land conversion program," *Journal of Natural Resources*, vol. 34, no. 3, pp. 539–552, 2019.

[5] Wang, H. G. Hao, R. X. Zhai, and S. F. Liu, "Determinants of farm households'ecological compensation expectation to the grain for green project: an empirical analysis based on Haba Lake National Nature Reserve and Liupanshan Mountain National Nature Reserve," *Journal of Arid Land Resources and Environment*, vol. 31, no. 8, pp. 69–75, 2017.

[6] P. Jie, C. Zongling, and J. Leshan, "Research on the willingness of peasant households with heterogeneous resources to be compensated for the conversion of farmland to forests and its influencing factors—based on the survey data of 2 counties in Yunnan province," *Rural Economy*, vol. 38, no. 1, pp. 104–111, 2020.

[7] H. Hongyun and Y. Yonghong, "Research on ecological compensation for the conversion of farmland to forests—cost Basis, acceptance willingness or ecological value standards," *Issues in Agricultural Economic*, vol. 35, no. 4, pp. 64–72, 2014.

[8] Q. Yanhong and K. Muyi, "The compensation standards for peasant households' participation in ecological construction based on opportunity costs: taking peasant households' participation in the Conversion of farmland to forests in Wuqi County as an example," *China Population, Resources and Environment*, vol. 21, no. 12, pp. 65–68, 2011.

[9] S. Hanyu and L. Guoping, "The impact of ecological benefits and economic rents on the willingness to be compensated for ecological conservation," *China Population, Resources and Environment*, vol. 28, no. 11, pp. 91–101, 2018.

[10] C. Xie, K. Zhang, W. Peng et al., "Policy trends and demand during the alternating phase of conversion of cropland to forests program—the main results of 2014 social economic M&E of conversion of cropland to forests program," *Forestry Economics*, vol. 37, no. 6, pp. 16–22.

[11] P. J. Ferraro, "Asymmetric information and contract design for payments for environmental services," *Ecological Economics*, vol. 65, no. 4, pp. 810–821, 2008.

[12] L. U. Latacz and H. C. Van der, "Auctioning conservation contracts: a theoretical analysis and an application," *American Journal of Agricultural Economics*, vol. 79, no. 2, pp. 407–418, 1997.

[13] G. Stoneham, V. Chaudhri, A. Ha, and L. Strappazzon, "Auctions for conservation contracts: an empirical examination of Victoria's BushTender trial," *The Australian Journal of Agricultural and Resource Economics*, vol. 47, no. 4, pp. 477–500, 2003.

[14] R. Claassen, A. Cattaneo, and R. Johansson, "Cost-effective design of agri-environmental payment programs: U.S. experience in theory and practice," *Ecological Economics*, vol. 65, no. 4, pp. 737–752, 2008.

[15] B. K. Jack, B. Leimona, and P. J. Ferraro, "A revealed preference approach to estimating supply curves for ecosystem services: use of auctions to set payments for soil erosion control in Indonesia," *Conservation Biology*, vol. 23, no. 2, pp. 359–367, 2010.

[16] K. Kawasaki, T. Fujie, K. Koito, N. Inoue, and H. Sasaki, "Conservation auctions and compliance: theory and evidence from laboratory experiments," *Environmental and Resource Economics*, vol. 52, no. 2, pp. 157–179, 2012.

[17] B. Leimona, B. K. Jack, B. Lusiana, and R. Pasha, "Designing a procurement auction for reducing sedimentation: a field experiment in Indonesia," *EEPSEA Research Report*, vol. 113, no. 6, pp. 1265–1267, 2010.

[18] D. Xiaohong and X. Zhongmin, "The application of auctions with participants having different risk preferences to ecological compensation: taking the conversion of grazing land to grassland in Sunan County as an example," *Systems Engineering-Theory and Practice*, vol. 32, no. 11, pp. 2412–2418, 2012.

[19] X. Wang, J. Bennett, J. Xu, and H. Zhang, "An auction scheme for land use change in Sichuan Province, China," *Journal of Environmental Planning and Management*, vol. 55, no. 10, pp. 1269–1288, 2012.

[20] Z. Liu, J. Xu, X. Yang, Q. Tu, N. Hanley, and A. Kontoleon, "Performance of agglomeration bonuses in conservation auctions: lessons from a framed field experiment,"

Environmental and Resource Economics, vol. 73, no. 3, pp. 843–869, 2019.
[21] S. G. M. Schilizzi, "An overview of laboratory research on conservation auctions," *Land Use Policy*, vol. 63, pp. 572–583, 2017.
[22] Z. Chaohui, "An analysis of the influencing factors of peasant households' risk perception in the new round of conversion of farmland to forests: based on survey data in Aksu, Xinjiang," *Resources Science*, vol. 40, no. 7, pp. 1387–1396, 2018.
[23] İ. Unay-Gailhard and Š. Bojnec, "Sustainable participation behaviour in agri-environmental measures," *Journal of Cleaner Production*, vol. 138, no. 1, pp. 47–58, 2016.
[24] S. Hengtong, W. Zhengyu, and Y. Liang, "The impact of ecological perceptionon peasant households' behavior in conversion of farmland to forests—based on the theory of planned behavior and multi-group structural equation model," *China Land Science*, vol. 33, no. 3, pp. 42–49, 2019.
[25] T. N. Cason, L. Gangadharan, and C. Duke, "A laboratory study of auctions for reducing non-point source pollution," *Journal of Environmental Economics and Management*, vol. 46, no. 3, pp. 446–471, 2003.
[26] T. W. Schultz, *Transforming Traditional Agriculture*, Translated by Liang Xiaoming, Commercial Press, Beijing, China, 1987.
[27] A. Y. Banana and W. Gombya-Ssembajjwe, "Successful forest management: the importance of security of tenure and rule enforcement in Ugandan forests," *People and Forest*, vol. 30, no. 7, pp. 87–98, 2000.
[28] J. Dijk, E. Ansink, and D. P. Van Soest, "Conservation auctions, collusion and the endowment effect," *SSRN Electronic Journal*, no. 93, pp. 1–20, 2018.
[29] A. Portes, "Social capital: its origins and applications in modern sociology," *Annual Review of Sociology*, vol. 24, no. 24, pp. 1–24, 1998.
[30] C. A. Holt and S. K. Laury, "Risk aversion and incentive effects," *The American Economic Review*, vol. 92, no. 5, pp. 1644–1655, 2002.
[31] G. J. Kits, *The Impacts of Social Capital andLeadership on Conservation Auctions*, University of Alberta, Canada, 2011.
[32] National Forestry and Grassland Administration, *China's Conversion of Farmland to Forests and Grasses for Twenty Years (1999–2019)*, 2020.
[33] U. Latacz-lohmann and S. Schilizzi, "Auctions for conservation contracts: a review of the theoretical and empirical literature," *Inorganic Chemistry*, vol. 49, no. 3, pp. 943–951, 2005.
[34] B. K. Jack, "Private information and the allocation of land use subsidies in Malawi," *American Economic Journal: Applied Economics*, vol. 5, no. 3, pp. 113–135, 2013.
[35] K. D. Messer, P. J. Ferraro, and W. Allen, "Behavioral nudges in competitive environments: a field experiment examining defaults and social comparisons in a conservation contract auction," in *Proceedings of the AAEA &WAEA Joint Annual Meeting*, Anaheim, CA, USA, July 2015.
[36] T. N. Cason and L. Gangadharan, "Auction design for voluntary conservation programs," *American Journal of Agricultural Economics*, vol. 86, no. 5, 2004.
[37] S. Schilizzi and U. Latacz-Lohmann, "Evaluating conservation auctions with unknown bidder costs: the Scottish fishing vessel decommissioning program," *Land Economics*, vol. 88, no. 4, pp. 658–673, 2012.
[38] J. J. Heckman, "Sample selection bias as a specification error," *Econometrica*, vol. 47, no. 1, pp. 153–161, 1979.
[39] J. M. E. Pennings and R. Leuthold, "The role of peasant households' behavioral attitudes and heterogeneity in futures contractsusage," *American Journal of Agricultural Economics*, vol. 82, no. 4, pp. 908–919, 2000.
[40] P. L. Liao, X. J. Li, M. L. Bi, and X. L. Xia, "Impact of family endowment and cognitive preferences on farmers' willingness to manage, maintain and invest in the achievement of grain for green project—based on the survey data of 554 households in Shan-Gan-Ning region," *Journal of Arid Land Resources and Environment*, vol. 33, no. 5, pp. 47–53, 2019.
[41] L. Qian and W. Xin, "An overview and analysis framework of social capital," *Commercial Research*, no. 2, pp. 141–145, 2012.
[42] N. Kosoy, M. Martinez-Tuna, R. Muradian, and J. Martinez-Alier, "Payments for environmental services in watersheds: insights from a comparative study ofthree cases in Central America," *Ecological Economics*, vol. 61, no. 2/3, pp. 446–455, 2007.

Hindawi
Scientific Programming
Volume 2021, Article ID 6787406, 11 pages
https://doi.org/10.1155/2021/6787406

Research Article

Secured Insurance Framework Using Blockchain and Smart Contract

Abid Hassan,[1] **Md. Iftekhar Ali**,[1] **Rifat Ahammed**,[1] **Mohammad Monirujjaman Khan**,[1] **Nawal Alsufyani**,[2] **and Abdulmajeed Alsufyani**[2]

[1]*Department of Electrical and Computer Engineering, North South University, Bashundhara, Dhaka 1229, Bangladesh*
[2]*Department of Computer Science, College of Computers and Information Technology, Taif University, P.O. Box 11099, Taif 21944, Saudi Arabia*

Correspondence should be addressed to Mohammad Monirujjaman Khan; monirujjaman.khan@northsouth.edu

Received 9 October 2021; Accepted 6 November 2021; Published 24 November 2021

Academic Editor: Punit Gupta

Traditional insurance policy settlement is a manual process that is never hassle-free. There are many issues, such as hidden conditions from the insurer or fraud claims by the insured, making the settlement process rough. This process also consumes a significant amount of time that makes the process very inefficient. This whole scenario can be disrupted by the implementation of blockchain and smart contracts in insurance. Blockchain and innovative contract technology can provide immutable data storage, security, transparency, authenticity, and security while any transaction process is triggered. With the implementation of blockchain, the whole insurance process, from authentication to claim settlement, can be done with more transparency and security. A blockchain is a virtual chain of data blocks that is a decentralized technology. Any transaction or change in the blocks is done after the decentralized validator entity, not a single person. The smart contract is a unique facility stored on the blockchain that gets executed when the predetermined conditions are met. This paper presents a framework where smart contracts are used for insurance contracts and stored on blockchain. In the case of a claim, if all the predetermined conditions are met, the transaction happens; otherwise, it is discarded. The conditions are immutable. That means there is scope for alteration from either side. This blockchain and intelligent contract-based framework are hosted on a private Ethereum network. The Solidity programming language is used to create smart contracts. The framework uses the Proof of Authority (PoA) consensus algorithm to validate the transactions. In the case of any faulty transaction request, the consensus algorithm acts according to and cancels the claim. With blockchain and smart contract implementation, this framework can solve all the trust and security issues that rely on a standard insurance policy.

1. Introduction

Insurance is an agreement in which an individual or institution receives financial protection or compensation from an insurance provider in the event of a loss, represented by a policy. Insurance is a widely practiced method of security all over the world. According to a statistical report, the global insurance market is valued at over 5050.3 billion US dollars for 2021 [1]. There are various types of insurance policies for health, business, and vehicles. These policies are prevalent in developed countries around the world. In much of Europe, Latin America, Canada, Australia, and Japan, national health insurance schemes are in existence through national policies [2]. Though insurance policies are prevalent, settling claims is not always a fault and a hassle-free procedure. There are often situations when insurance companies refuse to pay the insured by misrepresenting conditions and terms. Again, false claims are another set of problems that are troubling the insurance companies. Conventional contractual methods are not fault-proof. These contracts lack transparency and have loopholes. These loopholes lead to exploitation in many cases by both insurers and insureds. These conditions can be disrupted using smart contracts on the blockchain, as it reduces the need for trust and financial risk in existing agreements and provides legal clarity.

This research applies the method of creating a conceptual framework using blockchain and smart contracts to applications in insurance. Its primary goal is to use blockchain and smart contracts to ensure secure, insurance fraud-free transactions. This framework covers client registration, issuing a policy, and refund settlement activities using blockchain technology, making the whole insurance system more robust.

A blockchain is an accumulation of blocks that hold data. Each block contains the previous block's cryptographic key [3], timestamp, and transaction information. This technology has been prevalent for a series of applications. Since Satoshi introduced the Bitcoin platform based on the blockchain system in 2009 [4], blockchains have been attracting attention with various applications in various fields. Till now, the most accepted usage of blockchain technology has happened in Bitcoin's distributed transactions [5]. However, researchers have found other practical applications of blockchain in the government's public services [6]. IOT [7] and the most important financial and banking sector [8] are two major fields where the proper usage of blockchain technology can bring more productivity. Blockchain technology has several unique properties that make it ideal for financial transaction applications. The main characteristics of the blockchain are decentralized, consensus, provenance, immutability, and finality. Decentralized means no single most potent entity controls the whole blockchain, and it is a crucial feature of the blockchain. The whole system runs on the standard agreement of its participants. This standard agreement is called consensus. Again, consensus is one of the most important characteristics of the blockchain. When all the participants of a blockchain network agree on a transaction, the transaction gets executed.

A typical agreement is a must for a transaction on a blockchain. These consensus characteristics make the system very trustworthy among the participants [9]. The provenance feature ensures the traceability of data blocks. In the blockchain, each block's whereabouts are traceable. Suppose an item is sold on a blockchain system. In that case, every aspect of its development must be recorded in its blocks, from the moment it was built to the previous owner's information. When a valid transaction is completed and recorded in the specific block, no one in the network can change or alter it. This immutable nature of the blockchain makes it very secure compared to other transactional methods. All these immutable blocks are linked in one single ledger. In a blockchain system, there is only one ledger with one common truth [10]. There is a whole system that has one policy that operates everything. For any query about the transaction, the blockchain ledger is the only information hub. In general, there are three types of blockchain: public (or unauthorized), private (or permitted), and consortium (or allowed). Due to the general uniqueness of the network's geographic region, each one has its distinct features [11].

Smart contracts are simple scripts that are enforced when forethought conditions are fulfilled and are recorded on a blockchain [12]. They are frequently used to automate the implementation of an agreement so that all parties are guaranteed a timely conclusion without the need for any middlemen or wasted time. They can also automate a workflow by initiating the following step when certain circumstances are fulfilled [13]. A generic smart contract's life cycle begins with the parties entering the conditions of a contract on a distributed ledger. Then they connect to internal or external databases and systems. The contract waits for predefined conditions to be evaluated by external variables. Finally, the contract self-executes when criteria are met via triggers. The ease with which smart contracts may be deployed on public blockchains, also known as public smart contracts, has sparked a slew of business uses [14]. Using smart contracts for insurance can be very useful for claim settlements.

Several research studies have shown the possible disruption of the insurance industry by using blockchain and smart contracts. In this paper [15], the researchers concentrated on developing a blockchain-based infrastructure for processing insurance-related transactions. They created a prototype using Hyperledger Fabric, an open-source permissioned blockchain architecture platform. Researchers in [16] used blockchain in a user-based insurance model for vehicle insurance. They presented an application of blockchain to the Pay as You Drive (PAYD) and Pay How You Drive (PHYD) insurance schemes. Pay As You Drive (PAYD) is a common type of usage-based insurance. The insurance premium is determined by the number of kilometers driven in the vehicle throughout the covered period.

Customers who drive less get a lower insurance rate. The insurance duration can be tailored to the customer's specific needs. Pay How You Drive (PHYD) is a type of usage-based insurance that is quickly gaining popularity in the industry because of its numerous advantages. PHYD calculates insurance rates depending on how the vehicle is driven, rather than the vehicle's type and model, the driver's age, employment, or other factors. Because the driving pattern is a significant predictor of how likely the user is to make a claim, this evaluation method is more suitable. A reckless driver, for example, is more likely to be involved in an accident and, as a result, to submit a claim. As this information is stored using a blockchain, it is immutable. In [17], researchers predict that, when fully implemented, blockchain might pose a threat to the existing insurance business model since it suggests substantial cost reductions. However, by pooling resources and collaborating with these new players, this danger may be mitigated. However, there are also different views. In [18], the authors state that blockchain smart contracts are not fully secured. Smart contracts are regularly targeted by hackers, with devastating results in certain situations. This element may pose a particular danger to peer-to-peer insurance policies, which rely heavily on smart contracts for governance. In [12], the authors mention that the "ordinary user's" engagement with the blockchain is still complicated. Understanding the fundamentals of wallets, transactions, mining, and other related concepts necessitates some technical knowledge. At the same time, Bitcoin has been linked to a pyramid scheme or a scam on several occasions. As a result, there is still much misunderstanding about blockchain. The authors state that blockchain technology is still not mature enough for insurance applications yet. However, the authors also mentioned that the technology would gain more acceptance among insurance consumers with time. As of 2021, Bitcoin is more accepted all over the world than at any time in history. In [19], the authors discussed the influence of blockchain on the payments sector and the technology's disruptive nature. Based on these findings, they looked into how blockchain influences important areas of radical innovation and developed contributions from innovation management. Blockchain technology can provide immutable security for payments in banks, Equated Monthly Installment (EMIs), installments, or regular billing. In [20], the authors discuss that blockchain has the ability to innovate and drastically disrupt the insurance industry as we know it by providing cryptographically secure forms of distributed records. In [21], the authors presented a secured blockchain-based data exchange platform that can fight against fraudulent activities regarding insurance. Though blockchain technology is comparatively new in fintech, blockchain as a technology has the potential to disrupt the insurance sector by promoting honesty and openness, as well as influencing consumer risk perceptions, which might impact how insurers promote mutualization. The authors of [22] present a survey of blockchain disruption in various domains, most notably blockchain and how blockchain can improve the insurance domain by eliminating fraud, automating claims, analyzing data with the Internet of things, and preserving reinsurance.

The above research works present blockchain and smart contracts for use or, in some cases, the possibility of future use in the insurance industry with increased security, immutability, and accountability. With blockchain implementation, the traditional insurance industry can be disrupted and accountable to both insurers and the insured. This paper presents a secure framework for insurance using blockchain technology and smart contracts. The whole framework is implemented on a private Ethereum network. Smart contracts for the system are developed using the Solidity language. The framework covers all the expectations for insurance, client registration, client query, policy initialization, issuing, claiming, and refund.

Problem Statement: General people get registered for insurance policies to use the insurance money in case of any danger. On the other hand, insurance companies are an excellent money-making business that creates jobs and pays taxes like any other business. So, whether it is a claim settlement for the insured or a false claim causing trouble for the insurance companies, none is expected. So, it is crucial to have a fast and fraud-proof settlement process. The insurance industry is going through various settlement and trust issues in the traditional method of insurance. Implantation of blockchain in insurance can be a robust solution to the security and trust issues related to these problems.

Motivation: Blockchain technology uses a decentralized, secure authentication process to store data in blocks. For any transaction or change in the blocks, the transaction request has to pass through an established consensus algorithm that makes any unauthorized change virtually impossible. Also, it encrypts data during the transaction and puts time stamp blocks that make the whole transaction process secure and immutable. The whole process is made more efficient by the introduction of smart contracts that are transparent and very secure. Suppose the test cases match transaction requests' triggers and eventually get executed by passing through a consensus algorithm. Implementing this whole process for insurance makes the whole insurance structure more trustworthy, efficient, and secure for both stakeholders, the insured and the insurer.

The introduction of the paper is presented in section one, and section two describes the method and materials. The results and analysis of this paper are provided in section three. Section four discusses the conclusion.

2. Method and Materials

The methods and materials utilized to achieve the goal are discussed in this section. The goal is to create an insurance ecosystem using blockchain technology. The main idea is to deploy the whole execution and storage of the contract. Its conditions and logic for execution will be structured as smart contracts and written using the Solidity programming language. The deployment of these contracts will be on a blockchain-enabled distributed platform, in our case, Ethereum. The first subsection here presents a basic system model for the framework. The following parts present the characters involved, mechanism of the framework for insurance, network platform, consensus algorithm, blockchain blocks, smart contracts, and framework components and algorithm. Section 3 presents the results and analysis of the framework. Finally, in Section 4, the whole framework is concluded.

The major contribution of this proposed system is the implementation of blockchain technology in the field of all kinds of insurance processes. It also includes the use of a specific consensus algorithm (in this case: Proof of Authority) in the system and the detailed algorithm and the explanation of the whole process.

2.1. Outline of Full System. Figure 1 shows the whole system model diagram of the proposed framework. It indicates that the client will be able to register and issue a policy, claim, and refund with the help of their corresponding agent. With the help of the corresponding agent, the information gets placed into the Ethereum private network. The agent is fully responsible for submitting all client requests within the network. When the transaction happens, the validators are responsible for validating the transactions.

It is to be noted that it is supposed to be a framework for an insurance company. Thus, the diagramed model is only of the members and clients of the company. The blockchain network in this case is the private Ethereum network. The validators are previously selected and will validate transactions per the rules of the Proof of Authority algorithm.

2.1.1. Authentication. Though the system is mainly a proposed algorithmic framework, it has a barebones frontend which includes the authentication process as well for the

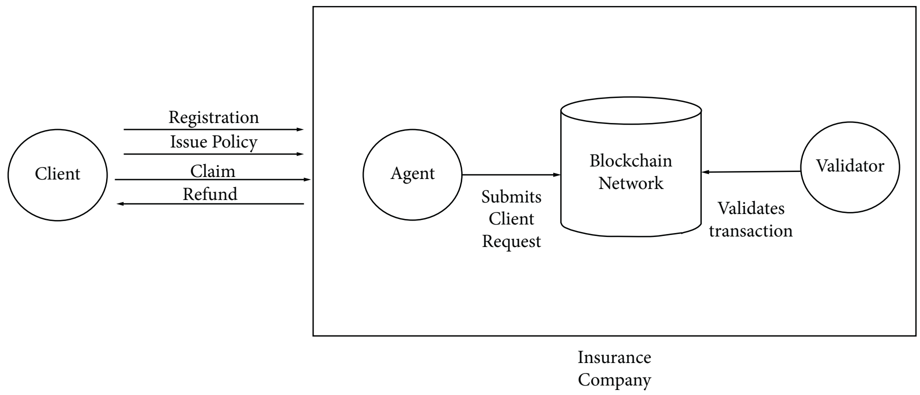

Figure 1: Full system diagram.

stakeholders involved in the system. Figures 2(a)-2(b) show the authentication User Interface (UI) for the system. The authentication is maintained by Google's Firebase system. The same login is used for both the client and the authority. A hard coded filter is enabled to filter the client and the authority after being logged in. The authority members are registered manually as it has to be private and discreet inside the agency. So, the sign-up serves a purpose for the clients only.

2.1.2. Agent Panel. Whether a desktop, console, or Web application, the agent panel is essential as it is the vital stakeholder of the system. They control important features like policy issuing, policy initializing, and different client queries. The agent and the validator have the same portal, because in some cases, the agency can select one for both roles. Figure 3 shows the agent panel interface where he can control all the features, including looking into clients' lists, the agency policy lists, the transaction history, etc.

2.2. Participation of Characters in This Model. The main character that is directly involved in the model is the client. He can register for the contracts, request insurance policies, submit claim requests, apply for a refund, and more. There is a middle man, an agent, who will process all clients' documents and demands and put them on the blockchain network. In the framework of some validators present in this system, they are responsible for verifying contract policies and transactions and storing the contracts in the ledger.

The stakeholders are as follows:

(i) Clients.
(ii) Insurance company authority
(iii) Agents
(iv) Validators

2.3. Mechanism of the Framework for Insurance. The client has to register with a unique id along with other necessary attributes as values. These IDs are to be stored in a DB. Previously, all policies and regulations would be written in the form of smart contracts. They are designed to be triggered when all the requirements or logics are met for the transactions. When a transaction is made, the record logs and execution results will be stored in a ledger in the blockchain network. In between the transactions, there is a set of endorsers and validators who verify the transaction and validate and store the transaction block in the blockchain ledger.

2.4. Network Platform. The whole network distribution is going to be deployed on a private Ethereum platform. This is an access-controlled blockchain. Participants are invited into this network by the insurance company authority. Based on access controls, this dedicated network will limit individuals who can participate in the network. Here, the network will allow the distribution of the ledger to a specific group of participants without making the transaction information public to all.

2.5. Consensus Algorithm Used in This System. This framework uses the Proof of Authority (PoA) consensus algorithm to validate and generate transaction blocks before adding them to the blockchain network. The validators will be preselected by the insurance company authority. Only those people who have proven their reliability as authorities get the right to generate new blocks or transaction logs. Once the validators are selected, they are allowed to make transaction logs and other monitoring stuff.

Figure 4 shows the flow diagram for the Proof of Authority algorithm in the specific use case of this research topic. The members of the authority are essentially the insurance authority. The algorithm has to go through the configuration option of the period. Then the transaction nodes or blocks, after being validated, are added to the Ethereum private network of the agency by the help of the issuing power of the insurance agent. Else, the block gets discarded.

On a broader perspective, the algorithm will be in need of configuration settings to work with the relevant system network. The configuration will have the chain-data, gaslimit, other relevant information, and so on. Now the authority members, in this case, the validators, when they receive a new block, will need to solve complex mathematical

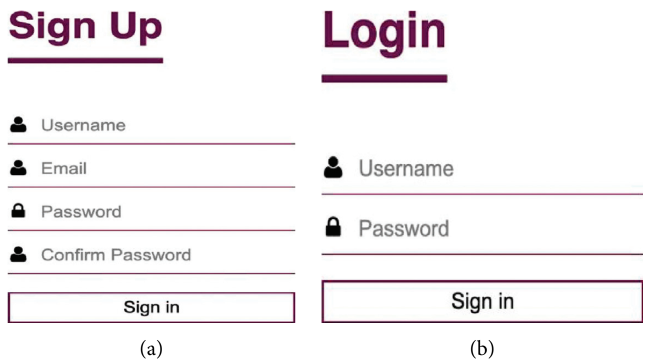

(a) (b)

Figure 2: Sign-up and login and interface.

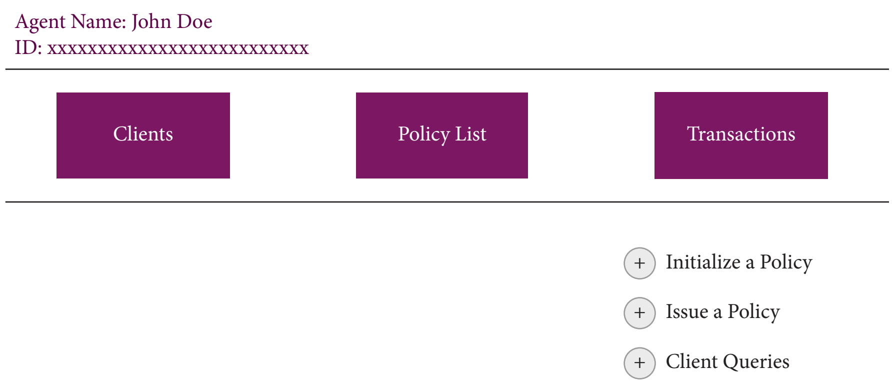

Figure 3: Agent panel.

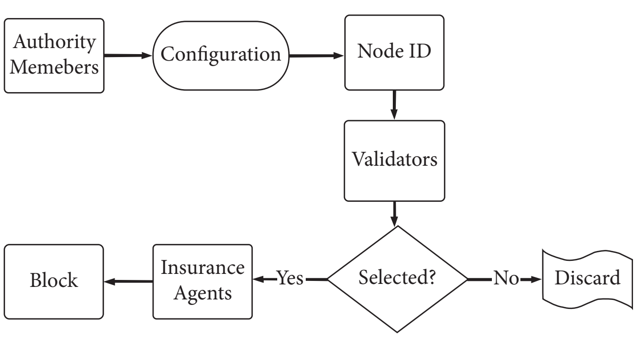

Figure 4: Proof of authority (PoA) flow diagram.

instructions to validate the block. When a validator has successfully mined the correct block, it will be selected to be added to the main blockchain network. The validator or the corresponding agents will be responsible for adding the block to the mainframe. Otherwise, the block will be stashed.

Figure 5 shows a genesis.json file, which is necessary for a PoA consensus-based network. The configuration ensures that all the known protocol changes are available. It also, importantly, configures the Clique Engine of PoA consensus.

2.6. Blockchain Blocks for Insurance. A blockchain is a chain consisting of blocks or data packages where a block consists of multiple transactions. The blockchain increases its length

Figure 5: Period configuration for a PoA network.

with every addition of the blocks. Figure 6 presents the structure for each block. Each block in the blockchain is validated by a specific validator before it is added or executed. Each block contains timestamps and hashes that allow it to be distinguished from the rest of the blockchains. Other than the hash and time stamp, there is information stored in blocks. This information varies according to the application needs. Below we have shown a generic block for any insurance application through the blockchain. Essential data

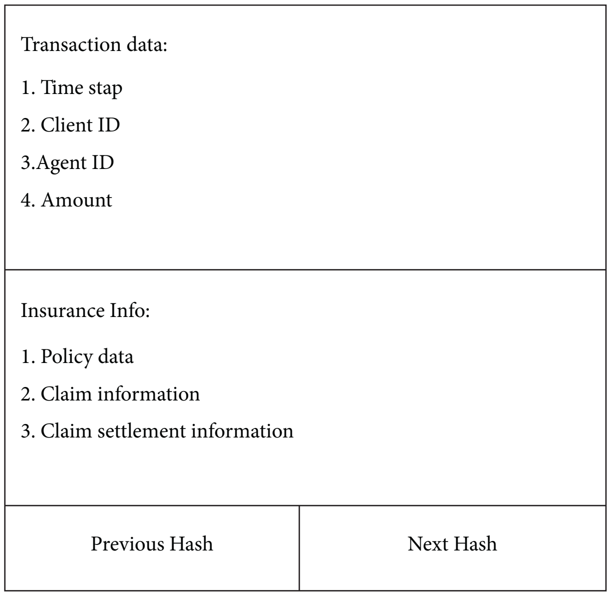

Figure 6: Structure of each block.

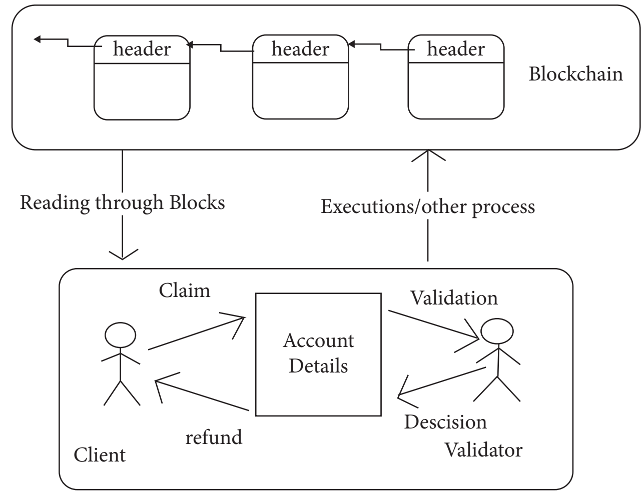

Figure 7: Structure of smart contract.

for insurance are , for example, Client ID, Agent ID, Amount, and essential insurance information.

2.7. Smart Contracts in Insurance. The blockchain containing insurance details will be contractualized on the Ethereum smart contract platform, where each peer or validator of the system will implement access control for its resources. Smart contracts are digital contracts between the client and service provider. As the contracts are well specified and transparent, there is a slight possibility to manipulate the contract conditions as the processing is done under the supervision of validators who have well-defined contract clarity.

In the insurance smart contract presented in Figure 7, when a client claims a refund, it sends account details to the validator. The validators check the contract details and send confirmation of their decision. Then it goes through the execution process and creates essential changes in the blockchain.

2.8. Framework Components and Algorithms. In this framework, maintaining and processing part of the insurance environment is done using blockchain technology. Blockchain technology ensures the security factor of false claims and the accountability of insurance.

Figure 8 shows the basic use case functionalities for the framework. These functionalities of an insurance policy are maintained through distributed smart digital contracts that are safe, reliable, and almost temper proof. Smart contracts will register the client and policy details as an object in a database. By taking a look, it can be seen that the client has the ability to register and to apply for the policy initialization, claiming, and refund. Agents and validators are internal personnel of the insurance company. The agents will be the direct interactors with the clients. They will help the client or have access to the registration and perform client queries, policy initializing, and issue. The validators have access to policy claiming, refund, and transaction block validation.

2.8.1. Client Registration. With the help of smart contract, clients get registered with the insurance system. To initialize a client, a client object structure ($\text{Struct}_{\text{OC}}$) is created in the database. The client object contains attributes like a unique id, name, age, contact, history, etc. To register that client object, a composite key (C_{key}) is created by an agent and the client object (O_C) is created using the C_{key}. (Algorithm 1).

2.8.2. Client Query. After a client is registered, his information with all the attributes is stored in the blockchain network. Now, to retrieve any specific client details, the insurance agent has to create a composite key (Algorithm 2).

2.8.3. Policy Initialization. The smart contract will contain the policy issuance, claims, refunds, etc. To initialize a policy ($\text{Struct}_{\text{OP}}$) and policy-client ($\text{Struct}_{\text{OPC}}$), their structures are created in the database. The policy structure is going to have its id, name, premium, reimburse, and term information. The policy-client structure will have its id, policy id, amount claimed, claim acceptance indicator, claim submission date, etc. (Algorithm 3).

2.8.4. Policy Issuing. To issue a policy, a client chooses a policy from the available policy (Policy_id) in the database. After choosing the policy, the client submits a premium to the agent. If the transaction passes all the verification and checks, a corresponding policy-client object ($\text{Object}_{\text{Policy-Client}}$) is made and stored in the database (Algorithm 4).

2.8.5. Policy Claiming. To process a claim, the client submits his credentials to his corresponding agent. All the necessary conditions go through verification, and the refund is initiated accordingly (Algorithm 5).

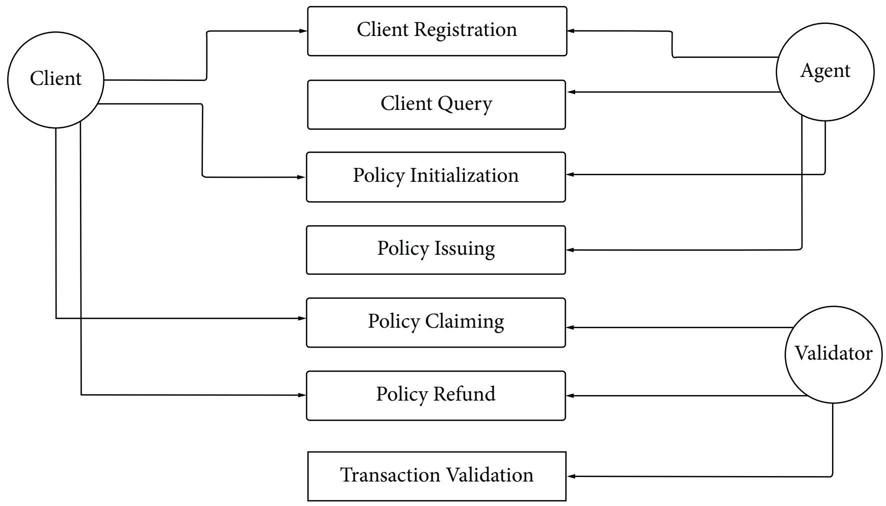

Figure 8: Use case diagram for the framework.

(1) *Struct*$_{OC}$ ← *(id, name, age, contact, history)*;
(2) *Database* ← *Struct*$_{OC}$;
(3) C_{key} ← *f (Agent_id, Client_id)*;
(4) *Store (*C_{key}*, Object*$_{Client}$*) in theDatabase;*

Algorithm 1: Client registration.

(1) C_{key} ← *f (Agent_id, Client_id)*;
(2) *Search (*C_{key}*) in the Database*;
(3) *If(exists) retrieve desired Object*$_{Client}$ *Else return Error;*

Algorithm 2: Client query.

(1) *Struct*$_{OP}$ ← *(Policy_id, Policy_name, Policy_Premium, Policy_Reimburse, Policy_Term)*;
(2) *StructOPC* ← *(Policy_id, Client_id, Amount, Acceptance, Date)*;
(3) *Store the structures in the Database;*

Algorithm 3: Policy initialization.

(1) *Check if the Object*$_{PolicyClient}$ *already exists*;
(2) *Check Client Smart Contract if Client with an id is registered to an Agent;*
(3) *Check if Client Premium matches Policy Premium*;
(4) *CkeyPolicyClient* ← *f (Agent_id, Client_id, Policy_id)*;
(5) *Object*$_{PolicyClient}$ ← *new Struct*$_{OPC}$*(Client_id, Policy_id, 0, yes, date);*
(6) *Store (Ckey*$_{PolicyClient}$*, Object*$_{PolicyClient}$*) in the Database;*

Algorithm 4: Policy issuing.

(1) $Ckey_{PolicyClient} \leftarrow f$ *(Agent_id, Client_id, Policy_id)*
(2) *Check if the Object*$_{PolicyClient}$ *exists using the Ckey*$_{PolicyClient}$
(3) *If Object*$_{PolicyClient}$ *exists, check acceptance in Object*$_{PolicyClient}$*;*
(4) *if (acc==Yes) then*
if amt + Client_Reimburse <= Policy_Reimburse then
Refund(Agent_id, Client_id, Policy_id, Client_Reimburse)
else
Refund(Agent_id, Client_id, Policy_id, Policy_Reimburse–amt)
end;

Algorithm 5: Policy claiming.

2.8.6. Policy Refund. The refund process is initiated from the earlier claim process. Here, the client's total claimed amount in the policy-client object is updated in the database (Algorithm 6).

3. Result and Analysis

This chapter analyzes the result of the framework from the point of view of outputs, security, and scalability. The potential threats and their corresponding prevention along with the used consensus algorithm are analyzed here. Also, it points out the average response time per size of blocks.

3.1. Transactions and Outputs. The transactions in the blockchain stay like a chain. To get it like a printed list output, here one transaction block is shown in Figure 9. The list itself is an array of transaction block objects. The first property is its index number. Secondly, there is the previous hash property, one of the main important concepts of the blockchain technology. The proof here is the Proof of Authority (PoA). There is a timestamp property which is the time the transaction happened. Next on the list is the transaction array. It is the combination of the above information and the client-agent information, along with the transaction cost amount. Finally, the list includes the corresponding policy data for that particular transaction block.

The transaction array in that block is very vital. Figure 10 breaks down the transaction array and shows the properties inside. The first property is the amount, which indicates the number of times the agent sends and receives a separate unique number for each transaction. Next is the client_id. To keep it simple and agent-friendly, the id is simply a string which is the id_name of the client. The last property is the sender or agent hash_id. This whole transaction array is also linked to that certain timestamp of the block. During transactions, the consensus protocol helps to agree on the list contents, which guarantees the integrity of the blocks and transaction. If validated, then the blocks get added to the main blockchain. These transactions depend on the hash and their values. If fraud or any suspicious block gets detected, it will easily get detected and will not be added.

The whole test-development phase ran inside the Rinkeby testnet. It is an Ethereum test network that allows the development testing phase to be done, before being deployed on the main network. As the research's target network is the Ethereum private network, this testnet has been pretty useful in the test phase. The corresponding transactions took place on the testnet, and the data could be retrieved for that network. Figure 11 shows the retrieved transaction data from the testnet. The retrieved data includes the transaction's both parties, the transaction hash, gas values, and so on. The data is safe and secure.

3.2. Security of the Proposed Framework. Table 1 indicates the potential threats to the framework and how it is going to prevent them. Though the blockchain network is already secured with its immutable design, the table further indicates how different malicious activities can harm the framework. Unwanted modification and deletion of client data will be handled by our chosen Proof of Authority (PoA) consensus algorithm. The endorsement and other policies will be scripted in the smart contract on the Ethereum network, so any kind of wrong endorsement will be noticeable and can be figured out as well.

3.3. Consensus Algorithm Analysis. The PoA algorithm suits the purpose of this framework pretty well. Proof of Authority (PoA) consensus is used in permissioned blockchain platforms. The consensus mechanism works on permissionless and permissioned platforms. In the permissionless ones, anyone can become a node. Meanwhile, in the permissioned one, all the nodes and validators are preselected, enabling the system to be more secure. PoA is a type of consensus that is super fault-tolerant and able to achieve high performance.

In this algorithm, only the nodes that have proven their reliability as authorities get the right to generate new blocks or transaction logs. Once the validators are selected, they are allowed to make transaction logs and other monitoring stuff. Unlike all other consensus algorithms we have seen here, the validators do not need to stack their coins or spend money on expensive storage or hardware; all they have to do is to use their reputation to get the right to validate and generate the blocks. Proof of Authority is based on the trust of the selected validators. This algorithm suits both private and public networks, where trust is distributed.

3.4. Scalability Analysis. Figure 12 shows the performance of the system with the response time for storage requests on the y axis and the peers (block size 20) on the x axis. The results

(1) $Ckey_{PolicyClient} \leftarrow f\,(Agent\_id,\ Client\_id,\ Policy\_id)$
(2) *Check if the* $Object_{PolicyClient}$ *exists using the* $Ckey_{PolicyClient}$
(3) *Update* $amt = amt + reimburse_{client}$ *in* $Object_{PolicyClient}$

Algorithm 6: Policy refund.

Figure 9: Genesis blocks and their properties.

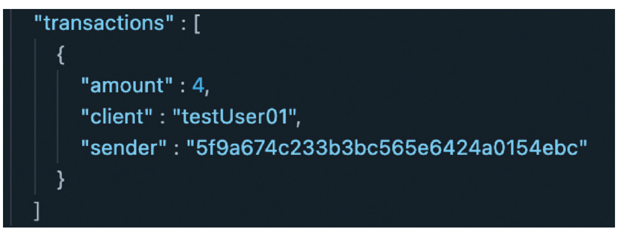

Figure 10: Transaction array.

Figure 11: Retrieved transaction data from Rinkeby.

Table 1: Potential threats and prevention.

Potential threat	Prevention
Modify/delete client data	PoA consensus algorithm
Word endorsement	Endorsement policy
Wrong auditing result	PoA consensus algorithm

show that the response is greater as the number of peers increases. 50 peers can have less than 20 ms response time in average, which could easily be used in real time applications using blockchain.

The chain code of the smart contract is written in Solidity and all the tests are written in plain Javascript as the network is a private Ethereum network. The experiment was carried out on a system with a core i7 (2.60 GHz) with 8 Gigabytes (GB) of ram, running Windows 10.

3.5. Comparison with Existing Papers. Table 2 analyzes the comparison and difference between this paper and other existing papers. The table's comparison context is mainly the

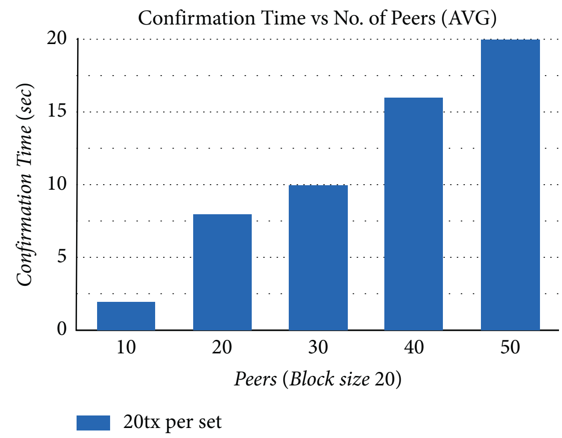

Figure 12: Average confirmation time vs. no. of peers (batch timeout: 2 sec).

Table 2: Comparison table with this paper and other papers.

Points of this paper	Points of other papers
1. This paper implements the Proof of Authority (PoA) consensus algorithm and uses the Ethereum private network to run the system.	1. There is no mention of a consensus algorithm and the system uses Hyperledger Fabric network to run the system [15].
2. This paper shows a generalized approach for all types of insurance.	2. A usage-based insurance model for cars is presented in the paper [16].
3. As this paper uses a private Ethereum network, it is solely for the authorized peers. Proof of Authority consensus needs the control of 51% of peers to attack the blockchain smart contracts, which is virtually impossible. So, it is secured.	3. This paper presents concerns about the security of smart contracts at a period of time when the Proof of Authority consensus algorithm was not established [18].
4. This paper presents a full framework for implanting blockchain technology into insurance.	4. Blockchain technologies' possibility of disrupting sectors like the insurance sector is only being discussed [19].

consensus algorithm, the network platform, methods, and so on. Apart from the differences between them, there are also several advantages and expanding scopes of this proposed system.

This paper is a novel work in the field of insurance, as it introduces some processes that were not used earlier in the corresponding field. This proposed system also has several impacts and advantages in the field of its use. It is basically a generalized approach to all types of insurance. Other existing research on this technology is pretty much focused on a small or distinguished part. This system also introduces the use of the Proof of Authority consensus running in the core. As an insurance process mainly works within a closed circle or an authority, Proof of Authority is a very good choice in this case. This research also specifies the network system used for this whole system, a private Ethereum network. Overall, it is a complete framework for implementing blockchain technology into insurance.

In some cases, some papers did not mention or talk about their consensus algorithm. In this paper, the consensus algorithm is briefly discussed along with its config file and diagrams. Proof of Authority has been used here, which makes it unique in terms of being used in an environment like this. There are some papers in the table which did not talk about their internal feature workflow. Here in this paper, the corresponding feature algorithms are highly focused. The flowchart and use case of the system are discussed briefly in this paper. A paper talked about the smart contracts vulnerability. On the other hand, this paper solves the confusion with the use of the Proof of Authority algorithm. Also, it is considered as a whole new framework. The other papers were domain and field specific, whereas this paper focused on a generalized approach for all types of insurance.

4. Conclusion

The goal of this research is to present an insurance framework using blockchain and smart contracts. The insurance transaction process gets executed in a secure private Ethereum based decentralized system that increases security to a great extent. The usual contracts for insurance are made using smart contracts in this framework. This framework's decentralized Solidity smart contracts eliminate the complexities regarding claim settlements and insurance by their immutable nature. The use of the PoA algorithm in this framework saves a lot of storage and money. So, the framework provides an efficient and secure solution to insurance operations and functionalities.

The framework presented in this paper is not a domain-specific one. It focuses on a standard approach for standard insurance policies. For any specific kind of insurance, this framework is also prevalent with customization in the smart contract. This framework provides a secure procedure to execute the whole process with security and transparency from registration to refund in insurance. In this framework, the scalability is tested by increasing the number of peers for a fixed block size of 20. It is shown that the confirmation time increases as there are more peers. Though the confirmation process gets slower with more peers, the security increases significantly with more validators.

The proposed system framework has plenty of room for improvement in the future. It is basically implemented as a central solution to all kinds of insurance processes. If it is thought to be a specific case like the IOT-based Car Insurance Process, or other insurance processes, or fields similar to supply chain, and so on, they can be implemented easily based on the proposed framework. Thus, it has plenty of opportunities to expand.

Data Availability

No data were utilized to support this research's findings.

Conflicts of Interest

The authors declare that they have no conflicts of interest to report regarding the present study.

Acknowledgments

The authors are thankful for the support from Taif University Researchers Supporting Project (TURSP-2020/115), Taif University, Taif, Saudi Arabia.

References

[1] "Estimated Size of the Global Insurance Market 2020, with Forecasts up until 2025," 2020, https://www.statista.com/statistics/1192960/forecast-global-insurance-market/.

[2] E. M. Immergut, "Health policy," in *International Encyclopedia Of the Social & Behavioral Sciences*, pp. 6586–6591, Elseiver, Amsterdam, Netherlands, 2001.

[3] A. Narayanan, J. Bonneau, E. W. Felten, A. Miller, and S. Goldfeder, *Bitcoin and Cryptocurrency Technologies: A Comprehensive Introduction*, Princeton University Press, Princeton, NJ, 2016.

[4] "Bitcoin.org," https://bitcoin.org/bitcoin.pdf.

[5] M. Lischke and B. Fabian, "Analyzing the bitcoin network: the first four years," *Future Internet*, vol. 8, no. 4, p. 7, 2016.

[6] Government Office for Science, "Distributed ledger technology: beyond block chain," in *Government of United Kingdom*, https://www.gov.uk/government/news/distributed-ledger-technology-beyond-block-chain, 2016.

[7] K. Christidis and M. Devetsikiotis, "Blockchains and smart contracts for the Internet of things," *IEEE Access*, vol. 4, pp. 2292–2303, 2016.

[8] W. Tsai, R. Blower, Y. Zhu, and L. Yu, "A system view of financial blockchains," in *Proceedings of the 2016 IEEE Symposium On Service-Oriented System Engineering (SOSE)*, pp. 450–457, Oxford, UK, March 2016.

[9] D. Mingxiao, M. Xiaofeng, Z. Zhe, W. Xiangwei, and C. Qijun, "A review on consensus algorithm of blockchain," in *Proceedings of the 2017 IEEE International Conference on Systems, Man, and Cybernetics (SMC)*, pp. 2567–2572, Banff, Canada, October 2017.

[10] J. Ellul and G. Pace, "Blockchain and the common good reimagined," 2019, https://arxiv.org/abs/1910.14415.

[11] O. Alfandi, S. Otoum, and Y. Jararweh, "Blockchain solution for iot-based critical infrastructures: byzantine fault tolerance," in *Proceedings of the NOMS 2020 - 2020 IEEE/IFIP Network Operations and Management Symposium*, Budapest, Hungary, April 2020.

[12] V. Gatteschi, F. Lamberti, C. Demartini, C. Pranteda, and V. Santamaría, "Blockchain and smart contracts for insurance: is the technology mature enough?" *Future Internet*, vol. 10, no. 2, 2018.

[13] H. Luo, M. Das, J. Wang, and J. C. P. Cheng, "Construction payment automation through smart contract-based blockchain framework," in *Proceedings of the 36th International Symposium on Automation and Robotics in Construction (ISARC 2019)*, pp. 1254–1260, Banff Alberta, Canada, May 2019.

[14] S. N. Khan, F. Loukil, C. G. Ghedira, E. Benkhelifa, and A. H. Bani, “Blockchain smart contracts: applications, challenges, and future trends,” *Peer-to-PeerNetworking and Application*, vol. 14, pp. 1–25, 2021.

[15] M. Raikwar, S. Mazumdar, S. Ruj, S. G. Sen, A. Chattopadhyay, and K. Y. Lam, “A blockchain framework for insurance processes,” in *Proceedings of the 2018 9th IFIP International Conference On New Technologies, Mobility And Security (NTMS)*, pp. 1–4, Paris- France, February 2018.

[16] P. K. Singh, R. Singh, G. Muchahary, M. Lahon, and S. Nandi, “A blockchain-based approach for usage-based insurance and incentive in its,” in *Proceedings of the TENCON 2019 - 2019 IEEE Region 10 Conference (TENCON)*, pp. 1202–1207, Kochi, India, October 2019.

[17] K. Sayegh, *Blockchain Application in Insurance and Reinsurance*, 20 pages, SKEMA Business School, Lille, France, 2018.

[18] N. Atzei, M. Bartoletti, and T. Cimoli, “A survey of attacks on ethereum smart contracts (SoK),” in *Proceedings of the International Conference on Principles of Security and Trust*, pp. 164–186, Uppsala, Sweden, April 2017.

[19] F. Holotiuk, F. Pisani, and J. Moormann, “Radicalness of blockchain: an assessment based on its impact on the payments industry,” *Technology Analysis & Strategic Management*, vol. 31, no. 8, pp. 915–928, 2019.

[20] P. Tasca, “Insurance under the blockchain paradigm,” in *Business Transformation Through Blockchain*, pp. 273–285, Springer International Publishing, Cham, Switzerland, 2019.

[21] Nath, “Data exchange platform to fight insurance fraud on blockchain,” in *Proceedings of the 2016 IEEE 16th International Conference on Data Mining Workshops (ICDMW)*, pp. 821–825, Barcelona, Spain, December 2016.

[22] W. Chen, Z. Xu, S. Shi, Y. Zhao, and J. Zhao, “A survey of blockchain applications in different domains,” in *Proceedings of the 2018 International Conference On Blockchain Technology And Application - ICBTA 2018*, Xi’an, China, December 2018.

Hindawi
Scientific Programming
Volume 2021, Article ID 9031150, 5 pages
https://doi.org/10.1155/2021/9031150

Research Article

Optimizing Kenmi Manipulation Courses of High School Sports Based on CDIO Model under the Background of Cloud Computing

Luosha Liu

Harbin University, Harbin 150086, China

Correspondence should be addressed to Luosha Liu; lls19740130@163.com

Received 30 August 2021; Accepted 3 November 2021; Published 19 November 2021

Academic Editor: Punit Gupta

Cloud computing is an increase, use, and delivery model of Internet-based services. It usually involves the provision of dynamic transactions and often virtualized resources through the Internet and provides the most reliable and secure data storage center. Therefore, cloud computing technology has features of cost saving and scalability. In view of this, the design and research of an autonomous learning platform based on the CDIO concept can make full use of cloud computing technology. The CDIO teaching model is a combination of theory and practice, closely linking the cultivation of knowledge, abilities, and personal qualities, subverting the previous education methods. Although it is an engineering field, it is based on an open system. Penetrating into all fields of education, the teaching methods of aerobics in colleges and universities are as practical as the CDIO teaching model and must be applied to practice. The independent learning ability, critical thinking, and team cohesion emphasized by the CDIO teaching model are also involved in the teaching of aerobics. CDIO is a key issue that needs to be solved urgently in talent training. CDIO is just a platform and framework. Under this framework, different schools and majors can integrate their own teaching systems and teaching content as needed. The reform of aerobics courses is guided by the educational framework and philosophy of CDIO and designed in accordance with the standards of CDIO. It is very important to plan the system and training of this course. This paper researches and analyzes the application of CDIO teaching mode in college sports aerobics under the background of cloud computing.

1. Introduction

With the engineering education concept of "integrated teaching plan," CDIO attaches importance not only to the cultivation of students' professional quality and basic theory but also to the improvement and development of students' sense of teamwork, communication skills, and innovative practical capabilities. It also attaches importance to the cultivation of students' comprehensive ability of system conception, design, implementation, and operation. CDIO is an open educational concept. Each school or educational institution can reform it according to its own actual situation, thereby optimizing educational resources and seeking its own development. The CDIO engineering education model is one of the new achievements of the international engineering education reform, which was first initiated and implemented by the Department of Aeronautics and Astronautics of the Massachusetts Institute of Technology (MIT). The concept of CDIO engineering education is based on the whole life cycle of conception (conceive), designing (design), realization (implement), and operation (operate). Cultivate students' basic knowledge, engineering practice ability, independent learning ability and teamwork ability from four aspects to achieve expected goals [1, 2]. Based on the training goals of applied talents, the CDIO model has been widely used in major universities. Liu and Zhang [3] studied cloud computing technology and application courses based on the concept of CDIO; Dai Xu et al. [4] proposed a software engineering application talent training program based on the concept of CDIO under the background of new engineering; Donghui et al. [5] proposed Research on the Flipped Classroom Teaching Model of CDIO Engineering Education Concept. CDIO engineering education concepts and blended teaching as emerging teaching concepts and methods provide useful reference and breakthroughs for the reform and improvement of teaching quality in universities. The requirements of enterprises for talents have also changed from "single discipline, independent work" to "interdisciplinary, teamwork." Enterprises require graduates to have engineering professionalism and good team coordination ability [6].

Starting in the 1970s, China began to introduce aerobics courses. Through continuous development, aerobics courses have also become an important part of Chinese university education courses as one of the well-known courses. According to the investigation and research on the effects of aerobic exercise, it is found that aerobics can be integrated with very rich aesthetic elements and matched with dance. After a unique arrangement, aerobics can show the aesthetics of the human body. Therefore, it is also called "dance on the playground" in the western sports world. In 1982, Darly Siedentop, a well-known American sports scholar, proposed a sports education model at the Brisbane Federal Sports Conference in Australia. In the "Several Opinions of the Ministry of Education and Other Departments on Further Strengthening the Practice Education Work of Colleges and Universities," the practice education work is regarded as a reference for colleges and universities. It is also one of the important indicators of school quality and level evaluation [7–9]. The rapid development of today's society has created higher requirements for talent training. The new era requires high-quality talents with strong self-learning ability, cooperation ability, innovation ability, and strong critical thinking. The training of high-quality talents needs to update our traditions. Teaching concepts and teaching methods should abandon the old methods and introduce advanced teaching concepts into teaching to cultivate students' comprehensive abilities [10, 11]. Chinese students lack practical experience in participating in projects and teamwork. Some developed countries in Europe and the United States have already walked ahead of us. The teaching concepts and methods used in these countries are worthy of our reference and research. Using CDIO's educational framework and concepts to guide the reform of aerobics education in colleges and universities and designing and planning the curriculum system and training plan of this course in accordance with CDIO standards have certain significance for colleges and universities to improve students' abilities and system expansion.

2. Existing Problems

The new curriculum reform requires teachers to pay more attention to the development of students and cultivate all-round new talents that adapt to modern society. The university is an important stage in shaping all-round talents. In this stage, teachers should not only pay attention to students' professional knowledge and cultural courses but also pay attention to students' health and fitness. For this reason, in addition to regular and necessary health checks, in order to improve the physical fitness of students, schools should also develop appropriate physical fitness courses. Aerobics is a very good choice. With the deepening of China's higher education reforms, the emphasis on students' physical quality education has been strengthened in higher education, which has led to an increase in the proportion of sports courses in the curriculum. However, in the face of the teaching of a new type of aerobics, the existing teaching model still has many problems. Many teachers are still limited to traditional teaching thinking, only emphasizing the compulsory inculcation of skills, while ignoring students' experience and interest in the sport. There is a lack of effective interaction between teachers and students, teachers cannot grasp the students' personal physical conditions and psychological conditions in a timely manner, and students' acceptance of courses cannot be effectively fed back to teachers. The emergence of these problems is prompting college educators to reflect.

There are also problems of insufficient teachers and limited teachers' level, which objectively affects the teaching effect of bodybuilding classes. The lack of effective professional communication between limited professional teachers makes it difficult to promote each other's professional improvement, which exacerbates this problem. We still cannot get rid of the traditional teaching mode, which means that students are not the leaders of the classroom. At present, teachers still dominate the classroom, focusing on teachers "teaching" students and "learning." Students learn passively. Teachers teach in order to complete their teaching tasks. They do not pay much attention to whether students participate in teaching or whether students are autonomous learning. Teachers should try their best to let the students explore the problems that students can solve through their own efforts. For the content that must be explained, teachers should use the most essential language and the least time to complete the teaching and ultimately achieve the goal of improving the efficiency of college aerobics teaching.

The unity of teaching content restricts the use of the autonomous learning teaching mode. Aerobics is a sport that emphasizes continuity and collectiveness. Now, the teaching content of most colleges and universities is relatively simple and has no sense of rhythm, which cannot arouse students' interest in learning. In addition, teachers are mostly used in the classroom to demonstrate students' imitation and follow standard movements. There is no fresh activity in the classroom, which makes students tired of taking aerobics classes. Among college students, most of the students who prefer aerobics are female students. They hope to build a perfect body by learning aerobics. However, for some male students, they think that aerobics is not suitable for boys to learn. Aerobics must be learnt to keep fit. Students should always keep their views up to the pace of the times, so as not to derail with the times.

3. Advantages of the CDIO Teaching Mode

Table 1 is obtained by analyzing two teaching modes.

It can be seen from Table 1 that, in a short period of time, aerobics teaching allows students to accept new movements and master the learning content, which does not meet the requirements of the times for students' all-round development. Integrating the CDIO teaching model into college

Table 1: Comparison of the CDIO teaching mode and traditional teaching mode.

	Teaching method	Teaching objectives	Teaching philosophy	Teaching subject
Traditional teaching mode	Explain, teach, directly inject dhamma, etc	Pay attention to students' technical movements and ignore students' interest in learning	Focus on theory and light on practice, and on knowledge and light on ability	Teacher is the subject and core
CDIO teaching mode	Inquiry learning method, class and team learning system, etc	Pay attention to students' practice and ability training, and cultivate students' basic ability	Advocate the integrated teaching concept of "teach, learn and do" and develop in an all-round way	Focus on students and advocate cooperation between teachers and students

aerobics classes provides students with the following three aspects of value: lasting learning motivation, multidimensional learning effects, and a relaxed learning environment. Learning motivation stimulates students' interest in learning and then stimulates and maintains students' learning behavior. The learning effect of students with long-term motivation is better than that of students with long-term motivation. Incorporating the CDIO teaching model into the aerobics classroom can make the originally monotonous, boring, and tasteless classroom full of vitality and mobilize the enthusiasm and initiative of students in learning, thereby inspiring students' interest in aerobics learning and students' lasting learning motivation and eliminating students who are tired of learning aerobics; in this learning motivation, students enjoy learning and reduce boring emotions in the learning process, and students can well achieve the teaching goals set by the teacher.

Taking 300 female students in an optional course of aerobics in a university as the research object, the two groups of students were taught in the same school year with the same equipment, the same progress, and the same content, and the same assessment methods were used for assessment. The teaching method of the experimental group adopts the CDIO teaching method, and the teaching method of the control group adopts the traditional teaching method.

It can be seen from Table 2 that the learning attitude of students in the experimental group is far better than that of the control group. This fully shows that, through the CDIO education model, students have a greater change in their attitude towards college aerobics, and they are more active. The learning environment is one of the external factors that affect learners' learning. It is an external condition that promotes learners to actively construct knowledge and promote ability generation. This teaching mode is student-centered, the subjectivity of students is clearer, and students have more independence. The time for thinking and self-study is to ensure that students solve problems by themselves. The time for students' teamwork and class discussion is greatly increased. Students change from passive receivers of knowledge to active explorers, which is conducive to the digestion and absorption of knowledge and the cultivation of learning ability. Teachers can further emancipate their minds in higher education physical education, conduct teaching activities more calmly and effectively, and better cultivate modern talents.

As for aerobic exercise, we should pay special attention to the coordination of the students' limbs. Therefore, in the teaching process, attention should be paid to cultivating the flexibility of students' bodies and joints. Because female students have better flexibility than boys, female postural aesthetics should also be reflected in the design of aerobics movements. Only when the aesthetics is embodied, students can be inspired to participate in aerobic exercises. Students' autonomous learning must not only ensure sufficient time but also have the correct guidance of the teacher. For example, when the student learns aerobics, the teacher tells the students that you do a good job and are very standard, which is great for the students. Students who need your encouragement will be more confident and easier to find the direction of their efforts. Based on the needs of students, reasonable and rich teaching activities are designed. Contemporary college students are more receptive to new things. Teachers must use innovative teaching to make them attracted to the classroom. When students encounter difficulties, teachers will not. Instead of giving answers directly, students can further explore by setting the same situation or asking key questions, using appropriate guidance to stimulate students' curiosity and thirst for knowledge, stimulate students' thinking, and obtain information purposefully. Students play their own strengths and characteristics in a team and motivate each other, which is conducive to students' independent learning.

4. Apply the CDIO Education Model to College Aerobics

The CDIO outline divides students' abilities into four parts: basic knowledge ability, personal skills and work attitude, teamwork ability and communication ability, and systematic conception-design-implementation-application ability. The four abilities correspond to the four teaching goals. First, let students master the basic knowledge of aerobics in theory, and combined with specific practice, explain the principles, methods and steps of creating aerobics, and how to choose appropriate music and appropriate movements. Secondly, explain some basic music theory knowledge in the classroom, instruct students how to choose music in the process of arranging and exercises, and emphasize the integrity of the music and the complete set of movements, as well as the consistency of the phrase, rhythm, and movement, and help students understand the rhythm of the music. Through the coordination of music power and action power, the unity of music rhythm and action style is achieved. Teachers will further highlight the difficulties and key points of teaching.

Table 2: Comparison of students' learning attitudes.

	Control group		Test group	
	Number of people	Proportion (%)	Number of people	Proportion (%)
Interested in aerobics	80	53.3	138	92.0
Think learning is joyful	76	56.6	143	95.3
Learned to learn independently	47	31.3	140	93.3
Actively cooperate with teachers	127	84.6	140	93.3

Only in this way, they can distinguish between primary and secondary. Aerobics teaching can be conducted on campus or in the form of clubs. By cooperating with some clubs in society, more students can participate in club extracurricular activities, which will improve their sense of identity with aerobics teaching and sports and also improve their physical fitness.

The principle of "talk one, practice two, and do three": the main difference between the current domestic college physical education model and internationalization is that foreign countries are "speaking one practice, two doing three," while we are "teaching three, practicing two, and doing one." The education model of "speaking three, practicing two, and doing one" cannot fully trap students' self-learning ability and innovation ability and even seriously hinders the development of talents. And, this link just implements the principle of "speaking one, training two, and doing three," giving full play to the leading role of students. As students become familiar with the teaching mode and role-playing, they will have more creative choices for movements during the aerobics season. The main body of the competition will get greater play, and more time will be spent on the creation of the action formation and the competition. Through the creation of action formations, students' creativity, imagination, organization, and communication skills are fully stimulated. Through the competition, students can deepen their understanding of the operation of each link of the competition, improve their sports skills and tactical abilities in practice, and allow students to experience the fun of this sport in an all-round way. The cultivation of humanistic care and sports culture runs through the entire teaching process. The education model contains the following keywords: cooperation, competition, creation, celebration, awards, slogans, mascots, oaths, etc. Behind each keyword, the students have a unique cultural experience of aerobics. The all-round experience enhanced the students' sports cultural awareness and attracted more students to participate.

Teachers can play aerobics videos to allow students to enjoy performances and competitions of different levels, different projects, and different styles, so that students have an overall impression of aerobics performances. Then, divide the whole class into several groups according to the natural class, and each group has its own name (for example: Hyun Dance Team, Big Dipper, etc.), and each team carries out aerobics action combination, formation arrangement, modeling design, etc., according to its own characteristics. Music production and performance costume design: perform team program presentations in turn, record them on-site, and make them into CDs. This link fully demonstrates and excavates the students' personality and expressiveness and cultivates the students' sense of competition, spirit of collaboration, collective honor, and sense of accomplishment. Choose wonderful programs outside of class to participate in performances or competitions inside and outside the school to improve students' on-the-spot performance ability. Movement learning and creation: under the CDIO teaching mode, students' preclass learning is purposeful, principled, level-based, and guided by the teacher's specific learning methods. It is a good way for students to improve their learning ability. Teachers arrange in advance through the Internet, video, etc. Preclass tasks allow students to use all available resources and learning methods to complete part of the learning tasks.

5. Results

Teaching evaluation has the functions of improvement, feedback, value judgment, motivation, and guidance. Effective and scientific teaching evaluation is conducive to the implementation of the CDIO education model in college aerobics teaching. Learning evaluation is no longer an isolated behavior, and the evaluation content is more comprehensive. It not only emphasizes the evaluation of learning emotions, learning habits, learning attitudes, learning motivation, learning interest, and quality of will but also emphasizes the examination of learning ability and skills; secondly, pay more attention to integration and students' other evaluations, self-evaluations, and teacher evaluations. Teachers will give students more encouraging, instructive, and diagnostic comments during the evaluation, focusing on encouragement and reducing direct criticism; thirdly, it is necessary to achieve a variety of evaluation methods. The diversification of evaluation methods promotes the comprehensive training of teachers and students' abilities and is conducive to the establishment and improvement of the evaluation system and the exploration of a more advanced learning evaluation system. The DIO teaching model eliminates the disadvantages of traditional teaching evaluations such as focusing on knowledge, neglecting ability, focusing on results, and neglecting process in the assessment stage at the end of teaching, thereby optimizing students' learning methods and teachers' teaching methods and greatly improving teaching effects.

6. Conclusion and Discussion

The effective integration of the CDIO engineering education concept and the new teaching model derived from it into the online teaching process based on the low-cost and scalable operating platform of the cloud computing environment provides a good platform for China's online learning. The development and application can change the current situation of China's online teaching and promote the rapid development of China's online teaching. CDIO education model is not only a teaching practice model but also a value pursuit and an idea. Improving the effectiveness of college aerobics teaching has long been the common pursuit of the majority of college physical education teachers. It has become the fundamental requirement and key link in deepening the reform of college physical education elective courses. Compared with the traditional teaching model, it has more advantages. The application of aerobics teaching has lasting learning motivation, multidimensional learning effects, and a relaxed learning environment. Colleges and universities should actively exert creativity, explore and innovate in the teaching methods of aerobics, continuously innovate the teaching guiding ideology, introduce advanced CDIO teaching concepts, and be based on the aerobics major and not limited to this major.

Data Availability

No data were used to support this study.

Conflicts of Interest

The author declares no conflicts of interest.

References

[1] H. Dai and H. Da, "The software based on CDIO concept under the background of new engineering research on the training program for application-oriented talents in software engineering," *Computer Education*, vol. 64, no. 1, pp. 64–67, 2020.

[2] Z. Hu, S. Ren, and Z. Chen, "Engineering undergraduate talent training program project and its optimization: based on the concept of CDIO-CMM," *Advanced Engineering Educational Research*, vol. 36, no. 6, pp. 20–28, 2010.

[3] Y. Liu and N. Zhang, "Cloud computing technology and application based on the concept of CDIO research on curriculum teaching reform," *Computer Age*, vol. 21, no. 12, pp. 75–78, 2019.

[4] D. Xu, G. Liu, and W. Guo, *Based on CDIO Engineering Education*, Sanlian Bookstore, Shanghai, China, 2017.

[5] "Research on the flipped classroom teaching model of nian," *Education and Teaching Forum*, vol. 20, no. 13, pp. 316–318, 2020.

[6] J. Zhao and X. Gao, "About the implementation of undergraduate education with "students as the center" thinking of academic reform," *China Higher Education Research*, vol. 35, no. 8, pp. 36–40, 2017.

[7] Y. Li, "Teaching practice of software technology courses in applied undergraduate colleges research," *Computer Education*, vol. 29, no. 12, pp. 117–121, 2019.

[8] *Study on the Difference of Cheerleading Management Systems in Universities in China and the United States*, Hubei Sports Science and Technology, Hubei, China, 2017.

[9] R. Gao, J. Zhang, and H. Gao, *Analysis on the Teaching Process Structure of Sports Education Model*, Sanlian Bookstore, Beijing, China, 2018.

[10] S. Sim and H. Choi, "A study on the service discovery support method in the IoT environments," *International Journal of Electrical Engineering Education*, vol. 57, no. 1, pp. 85–96, 2020.

[11] H. Wang, X.-M. Zhang, G. Tomiyoshi et al., "Association of serum levels of antibodies against MMP1, CBX1, and CBX5 with transient ischemic attack and cerebral infarction," *Oncotarget*, vol. 9, no. 5, pp. 5600–5613, 2017.

Hindawi
Scientific Programming
Volume 2021, Article ID 6536470, 6 pages
https://doi.org/10.1155/2021/6536470

Research Article

rmvPFBAM: Removing Primers from BAM Files Based on Amplicon-Based Next-Generation Sequencing and Cloud Computing When Analyzing Personal Genome Data

Yanjun Ma

Public Security Information Department, Liaoning Police College, Dalian, Liaoning, China

Correspondence should be addressed to Yanjun Ma; mayanjun0010@yeah.net

Received 23 September 2021; Accepted 1 November 2021; Published 16 November 2021

Academic Editor: Punit Gupta

Personal genomic data constitute one important part of personal health data. However, due to the large amount of personal genomic data obtained by the next-generation sequencing technology, special tools are needed to analyze these data. In this article, we will explore a tool analyzing cloud-based large-scale genome sequencing data. Analyzing and identifying genomic variations from amplicon-based next-generation sequencing data are necessary for the clinical diagnosis and treatment of cancer patients. When processing the amplicon-based next-generation sequencing data, one essential step is removing primer sequences from the reads to avoid detecting false-positive mutations introduced by nonspecific primer binding and primer extension reactions. At present, the removing primer tools usually discard primer sequences from the FASTQ file instead of BAM file, but this method could cause some downstream analysis problems. Only one tool (BAMClipper) removes primer sequences from BAM files, but it only modified the CIGAR value of the BAM file, and false-positive mutations falling in the primer region could still be detected based on its processed BAM file. So, we developed one cutting primer tool (rmvPFBAM) removing primer sequences from the BAM file, and the mutations detected based on the processed BAM file by rmvPFBAM are highly credible. Besides that, rmvPFBAM runs faster than other tools, such as cutPrimers and BAMClipper.

1. Introduction

Genomic variations are associated with the pathogenesis and treatment of many diseases, especially cancer. Identifying genomic variations of genetic biomarkers is important for the clinical diagnosis and treatment of cancer patients. Nowadays, there are several technologies to detect genomic variations, such as polymerase chain reaction (PCR), Sanger Sequencing, and next-generation sequencing [1]. Next-generation sequencing is the most effective way for detecting genomic variations because it can obtain hundreds of millions of bases of DNA molecules at one time.

Targeted sequencing is one commonly useful solution of next-generation sequencing focused on specific genomic regions [1]. Because targeted sequencing is cost-effective and could produce high-depth sequencing data which are able to detect low-frequency genomic variations, targeted sequencing is the most widely used approach in clinical cancer diagnosis [2]. There are two methods commonly used for targeted sequencing: capture hybridization-based sequencing and amplicon-based sequencing [3]. Amplicon-based sequencing uses multiplex PCR technology to generate thousands of amplicons for massively parallel sequencing and is one of the widely used targeted sequencing technology because of its easier operation and higher amplification efficiency [4–9]. However, during the primer amplification, false-positive mutations could be introduced in the primer region because of nonspecific primer binding and primer extension reactions [10]. So, it is necessary to remove the primers before executing the downstream analysis, such as detecting mutations.

The existing removing primer tools usually remove primers from FASTQ files, such as cutPrimers [11] and pTrimmer [12], and the only one tool removing primers from BAM (Binary sequence Alignment/Map) files is

BAMClipper [13]. There are some drawbacks of cutting primers from FASTQ files. For example, because the length of read is shorter after cutting the primer, the probability of the reads misalignment may be improved, and the shorter reads may lead to inaccurate detecting of copy number variation, even unable to use copy number variation tools such as ONCOCNV [14].

BAMClipper clips primers from BAM file by only modifying the CIGAR (Concise Idiosyncratic Gapped Alignment Report) value in BAM files instead of removing primers from reads. If downstream analysis such as detecting mutations was processed based on the cutting primer BAM file processed by BAMClipper, false-positive mutations existed in primer region can still be detected when using VarScan [15], that is, a classical tool for detecting mutations. So, we developed a tool removing primers based on the BAM file (rmvPFBAM) by creating a new BAM, and the tool is available at github (https://github.com/YanjunMasir/rmvPrimer). rmvPFBAM runs faster than the other tools, and mutations detected from rmvPFBAM's cutting primer BAM file are more accurate than those from BAMClipper's BAM.

2. Methodology

2.1. Datasets. For clinical research, the patient's surgical tissue can be collected to construct sequencing library that will be running on the sequencing machine, and the sequencing data will be produced after finishing running. The sequencing data are one input of rmvPFBAM, and the other input of rmvPFBAM is the primers used for capturing the target genomic region.

All reads and primers in the article are from the dataset of Ultradeep Targeted Sequencing of a set of Cancer Genes Project (SRP019940), presenting the molecular profile of 38 breast cancer species [16, 17]. This project used a panel of 47 genes involving 1,736 amplicons. The average length of the amplicon was 20 bp, and all reads were obtained by sequencing on matched normal and tumor tissues using Illumina MiSeq sequencer under a 150 bp long-paired reads protocol. For rmvPFBAM demonstration purpose, six patients from the SRP019940 were randomly selected to form the dataset (SRR866441, SRR866442, SRR866443, SRR866444, SRR866445, and SRR948507). The raw reads were downloaded from the European Nucleotide Archive datasets. Then, the reads were aligned using the BWA software [18]. rmvPFBAM and BAMClipper were executed based on the aligned BAM files, and cutPrimers was executed based on the FASTQ files.

2.2. Implementation. In target sequencing, each target region is covered by millions of reads (Figure 1). For pair-end reads, read 1 and read 2 contain the forward primer and reverse primer, respectively, but if the fragment is shorter than 150 bp, then read 1 contains part or whole of the reverse primer and read 2 contains part or whole of the forward primer (Figure 1). Due to the high error rate of base pairing during primer extension, the forward and reverse primer needed to be removed before processing the reads.

The rmvPFBAM workflow is implemented with python language and is available to Linux platform. The program rmvPFBAM uses BAM file and primer file as input. The primer file must contain the amplicon information, such as chromatin, amplicon's start position, amplicon's end position, front primer sequence, and reverse primer sequence. rmvPFBAM uses pysam package to process the BAM file and regex package to search primer sequences with regular expressions and multiprocessing for multithreading. Pysam is the most widely used python module that can manipulate mapped short read sequence data stored in SAM/BAM files. Because the primer files usually contain thousands of primers, rmvPFBAM splits the primers into several parts with each part containing hundreds of primers. Then, these several parts of primers are processed at the same time.

We compared our tool with already existing tools cutPrimers and BAMClipper. cutPrimers removed primers from FASTQ file instead of BAM file. BAMClipper removed primer sequences from BAM files, and it only modified the CIGAR value in the BAM file instead of modifying the BAM files, but rmvPFBAM not only modified the CIGAR value but also the BAM file. Examples of commands used for execution are available in Supplementary Material.

The flowchart (Figure 2) shows the details of processing one amplicon in the program. For one amplicon, all reads mapping to this amplicon were extracted. Then, for one primary mapping read, find the read pair of this read and remove the primer sequence from the reads only if the reads contain the primer sequence. After removing primer sequence, save the processed reads to one file and continue to process the next read mapping to this amplicon. Reads not containing the primer sequence are not allowed to save to the file.

3. Results

We performed comparative evaluation of the three programs using six samples from the SRP019940. Besides that, we also downloaded three datasets from the amplicon-based sequencing data [5] to compare rmvPFBAM, cutPrimers, and BAMClipper. The results were displayed in the Supplementary Material.

As cutPrimers remove primers from FASTQ files, only the runtime of this tool is compared with rmvPFBAM. Comparison of the functionality of rmvPFBAM, cutPrimers, and BAMClipper included the following parameters: (1) time of running, (2) no. of paired reads after cutting primer, (3) no. of target region reads after cutting primer, (4) no. of nontarget region reads after cutting primer, (5) no. of mutations detected based on the cutting primer BAM, and (6) no. of mutations based on the cutting primer BAM (falling in the target region). Results of the comparative analysis are presented in Table 1. We executed all processes on a personal computer (Intel(R)Xeon(R) CPU E5-2620 v2 2.10 GHz, 32 G RAM).

'No. of paired reads after cutting primers (%)' indicates the count of reads in the BAM file before cutting primers and

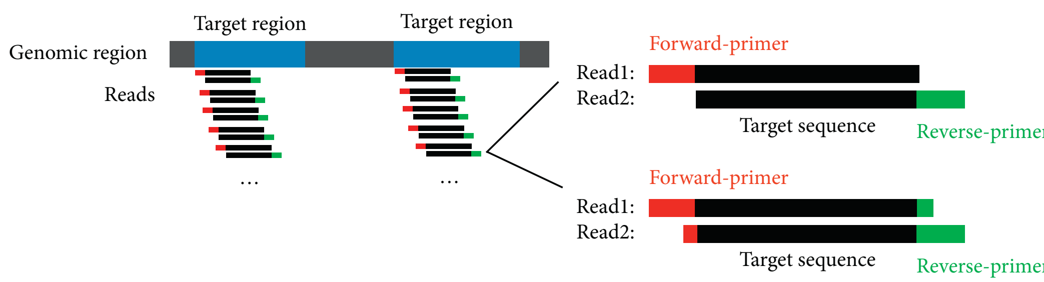

FIGURE 1: Scheme of the target sequencing by multiplex PCR. The blue region is the target region that we want to get the sequence of that and millions of reads are produced to cover it. For each read, the red sequence is the forward primer and the green sequence is the reverse primer. For each pair of read, read 1 contains forward primer (red) and read 2 contains reverse primer (green).

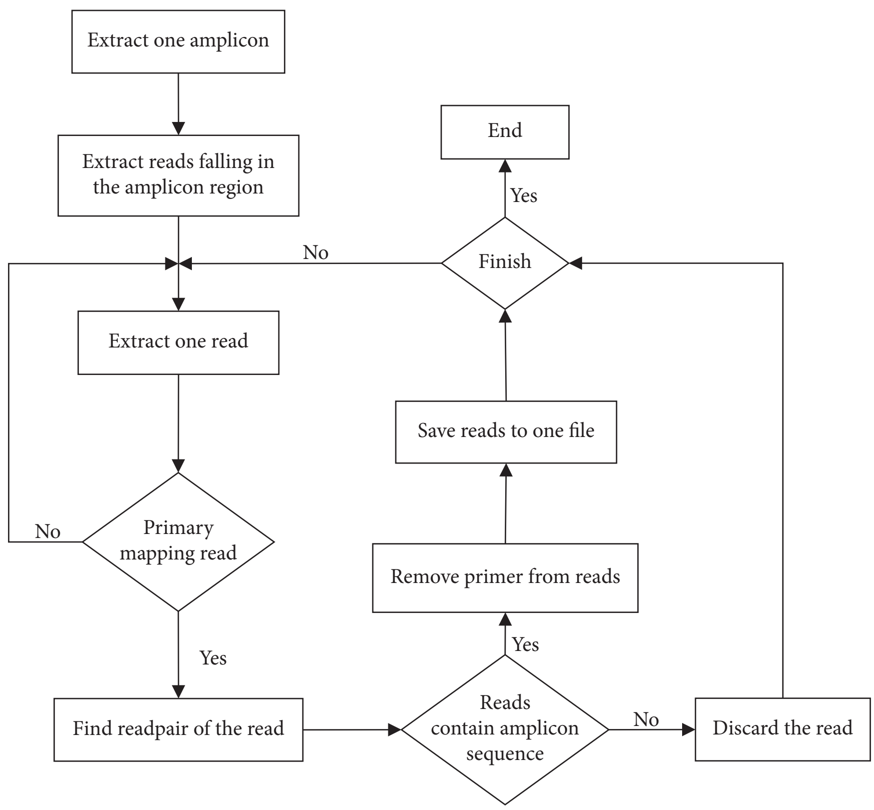

FIGURE 2: Workflow of rmvPFBAM.

the percent of those reads in the total reads. 'No. of target region reads after cutting primers (%)' indicates the reads falling in the target region and the percent of those reads in the total reads. 'No. of nontarget region reads after cutting primers (%)' indicates the reads falling in the nontarget region and the percent of those reads in the total reads. 'No. of mutations detected based on the cutting primer BAM' indicates the count of mutations detected by VarScan2 based on the cutting primer BAM file. 'No. of mutations based on the cutting primer BAM (fall in target region)' indicates the count of mutations falling in the target region based on the cutting primer BAM.

rmvPFBAM showed a much higher speed of processing reads than cutPrimers and BAMClipper in the six datasets (Figure 3(a)). The average running time of rmvPFBAM was 162 s, the cutPrimers was 526 s, and the BAMClipper was 1137 s. rmvPFBAM's running time was almost four or seven times that of the other two tools. Besides that, we compared the number of reads falling in the target region. Because BAMCliper only modifies the CIGAR value in the BAM file, the modified BAM by BAMClipper contains the same number of reads as the before modified BAM. However, the number of reads mapping to the target region is less different between rmvPFBAM and BAMClipper (Figure 3(b)).

Only reads mapping to the target region are useful for the downstream analysis, such as detecting mutations. So, we compared the number of mutations detected based on rmvPFBAM's and BAMClipper's BAM file. One classical tool for detecting mutations-Varscan2 was used to detect mutations from BAM files processed by BAMClipper and rmvPFBAM. About a third of mutations detected from the BAMClipper's BAM files were in the nontarget region

Table 1: Comparative data among the three tools by using six samples from amplicon-based next-generation sequencing data.

Sample (no. of paired reads)	Parameter	CutPrimers (err = 3, threads = 4)	BAMClipper (with −g)	rmvPFBAM (err = 3)
SRR866441 (2238436)	Time of running(s)	451	869	121
SRR866442 (2738246)		507	1135	159
SRR866443 (2628572)		485	1052	150
SRR866444 (3586450)		672	1467	229
SRR866445 (2760844)		513	1148	149
SRR948507 (2749834)		525	1149	164
SRR866441 (2238436)	No. of paired reads after cutting primers (%)	–	2238436(100)	1840262(82.2)
SRR866442 (2738246)			2738246(100)	2518726(92.0)
SRR866443 (2628572)			2628572(100)	2320172(88.3)
SRR866444 (3586450)			3586450(100)	3342890(93.2)
SRR866445 (2760844)			2760844(100)	2380948(86.2)
SRR948507 (2749834)			2749834(100)	2430968(88.4)
SRR866441 (2238436)	No. of target region reads after cutting primers (%)	–	1882305(84.1)	1840262(82.2)
SRR866442 (2738246)			2609012(95.3)	2518726(92.0)
SRR866443 (2628572)			2365634(90.0)	2320172(88.3)
SRR866444 (3586450)			3390685(94.5)	3342890(93.2)
SRR866445 (2760844)			2424973(87.8)	2380948(86.2)
SRR948507 (2749834)			2473225(89.9)	2430968(88.4)
SRR866441 (2238436)	No. of nontarget region reads after cutting primers (%)	–	269848(12.1)	0
SRR866442 (2738246)			103128(3.8)	0
SRR866443 (2628572)			186292(7.1)	0
SRR866444 (3586450)			161479(4.5)	0
SRR866445 (2760844)			254749(9.2)	0
SRR948507 (2749834)			221905(8.1)	0
SRR866441 (2238436)	No. of mutations detected based on the cutting primer BAM	–	981	676
SRR866442 (2738246)			527	329
SRR866443 (2628572)			584	398
SRR866444 (3586450)			544	349
SRR866445 (2760844)			847	515
SRR948507 (2749834)			793	488
SRR866441 (2238436)	No. of mutations based on the cutting primer BAM (fall in target region)	–	727	676
SRR866442 (2738246)			351	329
SRR866443 (2628572)			415	398
SRR866444 (3586450)			361	349
SRR866445 (2760844)			552	515
SRR948507 (2749834)			527	488

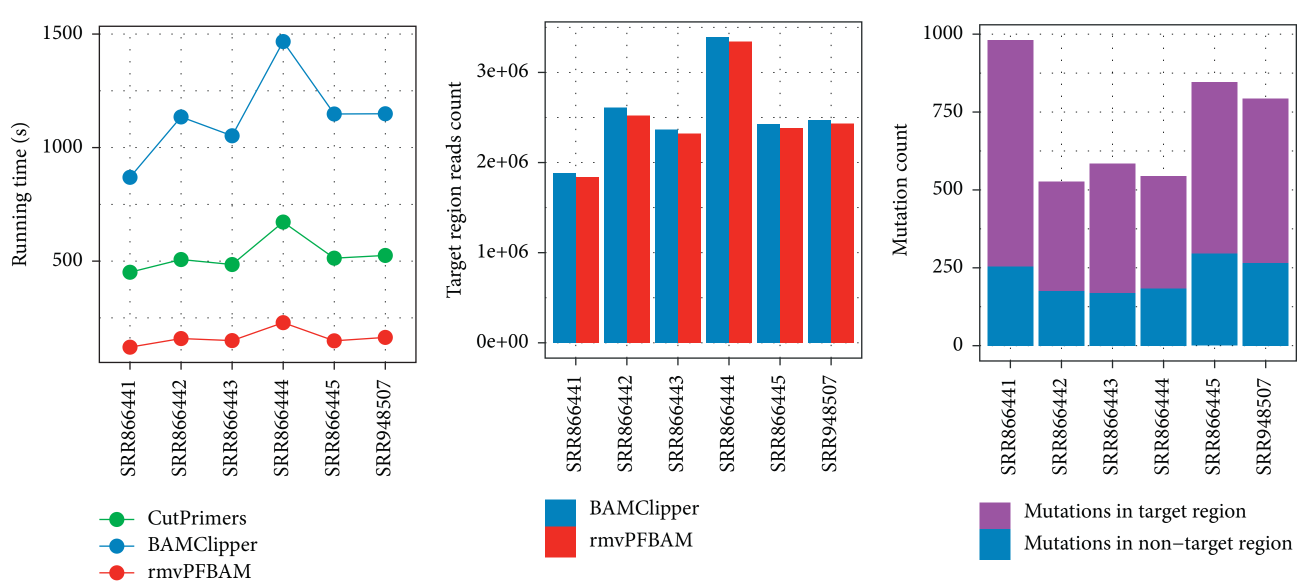

(a) (b) (c)

Figure 3: Continued.

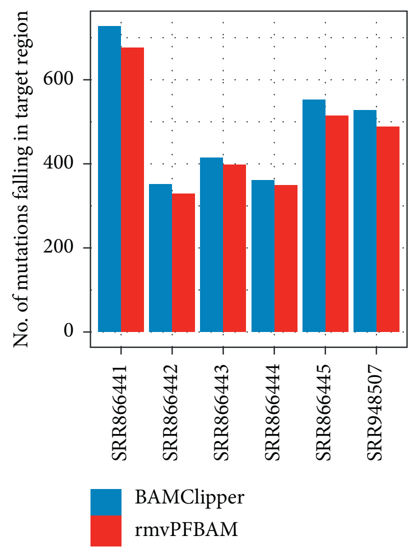

(d)

Figure 3: Comparative results of the three tools: (a) the running time of the three tools; (b) the target region reads count of BMAClipper and rmvPFBAM; (c) the counts of SNVs falling in the target region and nontarget region detected by BAMClipper; (d) the number of mutations falling in the target region detected by BAMClipper and rmvPFBAM.

(Figure 3(c)), and they were mostly like to be false-positive [8]. When only comparing mutations falling in the target region, the count of mutations from the BAM file processed by rmvPFBAM was almost the same as that of from BAMClipper (Figure 3(d)). So, the mutations detected from the rmvPFBAM's cutting primer BAM file mostly fall in the target region and show little false-positive mutations compared with BAMClipper.

4. Discussion

rmvPFBAM is one tool cutting primer sequences from the BAM file of amplicon-based next-generating sequencing. The processing speed of this tool is much faster than that of the other tools. Also, owing to its creation of a new BAM file instead of only modifying the CIGAR value of the BAM file, the downstream analysis based on rmvPFBAM's created BAM file is more accurate than from BAMClipper's BAM files.

Amplicon-based next-generation sequencing is widely used in the diagnosis of clinical cancer patients. Accurate and reliable detection of mutations could improve diagnostics and find new potential targets. Although there are many tools to remove primers, most tools remove primers from FASTQ files instead of BAM files. Removing primers from FASTQ file is simple to implement, but it is slightly limited for the downstream analysis. Nowadays, BAMClipper is the only published tool removing primers from BAM files. It processes the primers for a long time and only modified the CIGAR value of the BAM file so we developed rmvPFBAM. The processing speed of rmvPFBAM is much faster than that of BAMClipper, and it modified all the items in the BAM file including CIGAR and sequence. The result of downstream analysis such as detecting mutations is more accurate than BAMClipper. However, because rmvPFBAM applies a more strict strategy to remove primers from pair-end reads, about 10 percent of reads were discarded from the original BAM file. It is valuable to get more accurate results through the loss of 10 percent of the data.

Data Availability

Data sharing is not applicable to this article as no datasets were generated or analyzed during the current study.

Conflicts of Interest

The author declares that there are no conflicts of interest with respect to the research, authorship, and/or publication of this article.

Acknowledgments

The author acknowledges the Innovation Team Support Program of Liaoning Police College and the Soft Science Research Project of the Ministry of Public Security (Grant 2020LLYJLNST050).

Supplementary Materials

The supplementary file contains the "Commands that were used for tool execution" and the "Comparative data among the three tools by using six samples from amplicon-based next-generation sequencing data." (*Supplementary Materials*)

References

[1] S. Goodwin, J. D. McPherson, and W. R. McCombie, "Coming of age: ten years of next-generation sequencing technologies," *Nature Reviews Genetics*, vol. 17, no. 6, pp. 333–351, 2016.

[2] F. Bewicke-Copley, E. Arjun Kumar, G. Palladino, K. Korfi, and J. Wang, "Applications and analysis of targeted genomic sequencing in cancer studies," *Computational and Structural Biotechnology Journal*, vol. 17, pp. 1348–1359, 2019.

[3] S. S. Hung, B. Meissner, E. A. Chavez et al., "Assessment of capture and amplicon-based approaches for the development of a targeted next-generation sequencing pipeline to personalize lymphoma management," *Journal of Molecular Diagnostics*, vol. 20, no. 2, pp. 203–214, 2018.

[4] N. Guibert, Y. Hu, N. Feeney et al., "Amplicon-based next-generation sequencing of plasma cell-free DNA for detection of driver and resistance mutations in advanced non-small cell lung cancer," *Annals of Oncology*, vol. 29, no. 4, pp. 1049–1055, 2018.

[5] Y. Liao, Z. Ma, Y. Zhang et al., "Targeted deep sequencing from multiple sources demonstrates increased NOTCH1 alterations in lung cancer patient plasma," *Cancer Medicine*, vol. 8, no. 12, pp. 5673–5686, 2019.

[6] Y. Onda, K. Takahagi, M. Shimizu, K. Inoue, and K. Mochida, "Multiplex PCR targeted amplicon sequencing (MTA-Seq): simple, flexible, and versatile SNP genotyping by highly multiplexed PCR amplicon sequencing," *Frontiers of Plant Science*, vol. 9, p. 201, 2018.

[7] B. Snetsinger, C. K. Ferrone, and M. J. Rauh, "Targeted, Amplicon-Based, Next-Generation Sequencing to Detect Age-Related Clonal Hematopoiesis," *Methods Molecular Biology*, vol. 2045, pp. 167–180, 2019.

[8] E. Strengman, F. A. S. Barendrecht-Smouter, C. d. Voijs, P. d. Vree, and I. J. Nijman, "Amplicon-based targeted next-generation sequencing of formalin-fixed, paraffin-embedded tissue," *Methods in Molecular Biology*, vol. 1908, pp. 1–17, 2019.

[9] J. Tian, Y. Geng, D. Lv et al., "Using plasma cell-free DNA to monitor the chemoradiotherapy course of cervical cancer," *International Journal of Cancer*, vol. 145, no. 9, pp. 2547–2557, 2019.

[10] C. M. McCall, S. Mosier, M. Thiess et al., "False positives in multiplex PCR-based next-generation sequencing have unique signatures," *Journal of Molecular Diagnostics*, vol. 16, no. 5, pp. 541–549, 2014.

[11] A. Kechin, U. Boyarskikh, A. Kel, and M. Filipenko, "cutPrimers: a new tool for accurate cutting of primers from reads of targeted next generation sequencing," *Journal of Computational Biology*, vol. 24, no. 11, pp. 1138–1143, 2017.

[12] X. Zhang, Y. Shao, J. Tian et al., "pTrimmer: an efficient tool to trim primers of multiplex deep sequencing data," *BMC Bioinformatics*, vol. 20, no. 1, p. 236, 2019.

[13] C. H. Au, D. N. Ho, A. Kwong, T. L. Chan, and E. S. K. Ma, "BAMClipper: removing primers from alignments to minimize false-negative mutations in amplicon next-generation sequencing," *Scientific Reports*, vol. 7, no. 1, p. 1567, 2017.

[14] N. Rieber, R. Bohnert, U. Ziehm, and G. Jansen, "Reliability of algorithmic somatic copy number alteration detection from targeted capture data," *Bioinformatics*, vol. 33, no. 18, pp. 2791–2798, 2017.

[15] D. C. Koboldt, Q. Zhang, D. E. Larson et al., "VarScan 2: somatic mutation and copy number alteration discovery in cancer by exome sequencing," *Genome Research*, vol. 22, no. 3, pp. 568–576, 2012.

[16] O. Harismendy, R. B. Schwab, H. Alakus et al., "Evaluation of ultra-deep targeted sequencing for personalized breast cancer care," *Breast Cancer Research*, vol. 15, no. 6, p. R115, 2013.

[17] S. E. Yost, H. Alakus, H. Matsui et al., "Mutascope: sensitive detection of somatic mutations from deep amplicon sequencing," *Bioinformatics*, vol. 29, no. 15, pp. 1908-1909, 2013.

[18] H. Li and R. Durbin, "Fast and accurate long-read alignment with Burrows-Wheeler transform," *Bioinformatics*, vol. 26, no. 5, pp. 589–595, 2010.

Hindawi
Scientific Programming
Volume 2021, Article ID 2042158, 6 pages
https://doi.org/10.1155/2021/2042158

Research Article

An Experimental and Algorithm Research on the Influence of OTO Teaching Mode on College Students' PE Learning Interest Based on Cloud Computing

Shijun Wu,[1,2,3] **Jianghong Dai**,[3] **and Jiujiu Yang**[3]

[1]*School of Physical Education and Health, East China Normal University, Shanghai 200241, China*
[2]*Key Laboratory of Adolescent Health Assessment and Exercise Intervention of Ministry of Education, Shanghai 200241, China*
[3]*School of Physical Education, Hunan University of Humanities, Science and Technology, Loudi, Hunan 417000, China*

Correspondence should be addressed to Shijun Wu; wsj151978498@163.com

Received 26 August 2021; Accepted 6 October 2021; Published 9 November 2021

Academic Editor: Punit Gupta

Algorithm is a step of problem-solving, and algorithm can be defined as any special method for solving a certain type of problem. In computer science, algorithms are described in computer algorithm language and represent accurate and effective methods for solving a class of problems with computers. In order to verify the role of the OTO teaching mode from the perspective of cultivating learning interest and to provide a practical basis for the reform of physical education in colleges and universities, 107 second-year physical education majors in a common university were selected as experimental subjects and divided into an experimental group and a control group, and the two groups were intervened through a 16-week experiment. Multivariate covariance was used to analyze the influence of two teaching modes on college students' interest in sports learning. After excluding factors such as student gender, physical exercise behavior stage, football learning experience, and physical health, the groups have statistical significance in the four dimensions of positivity, skill learning, extracurricular activities, and negativity in sports learning interest. However, there is no significant difference in the influence of sports attention on sports learning interest. The research proves that the application of OTO teaching mode is conducive to promoting students' learning positivity, technical learning, and extracurricular activities and alleviating students' negative learning emotions. The degree of attention to sports in the interest of sports learning is not very significant. It is suggested that colleges and universities adopt the OTO teaching mode in the teaching of general football courses.

1. Introduction

Being interested in a certain sport activity can encourage people to devote more time and energy to it, generate lasting attention, and maintain a clear perception. Interest is caused by the needs of the individual, and a tendency to engage in a certain activity is produced under the interaction of the individual's subjective state and environmental characteristics. It is a guarantee of motivation to promote and maintain the individual to continue to engage in a certain activity [1]. PE learning interest is the psychological state generated by the interaction between the individual's subjective state and the physical learning environment [2], and it is an important driving force for acquiring sports and health knowledge and skills and promoting the physical and mental health of students. It affects the direction and intensity of specific activities of people participating in sports. For example, the Opinions on Strengthening School Sports to Promote the Comprehensive Development of Students' Physical and Mental Health promulgated by the General Office of the State Council in 2016 pointed out that students should cultivate interest, develop exercise habits, and master sports skills [3].

As the work of campus football enters the 2.0 era, China attaches significant importance to the development of campus football and has introduced a lot of policies. Football has also made considerable progress among young people. However, some problems have also appeared in the teaching of football courses in colleges and universities, such as backward sports concepts, traditional teaching methods, single teaching methods in football courses [4, 5], and lack of attention to physical education. These greatly reduce the students' positivity for participating in football and their interest and positivity for football. The study found that with the continuous deepening of the new curriculum reform, higher physical education is also facing higher and newer requirements. The traditional teaching model is more and more difficult to adapt to the requirements of higher education, and not only it is not obvious enough to improve the physical quality of students but also it is not conducive to cultivating students' interest in learning [6].

The OTO teaching mode was first proposed by Alex Rampell in the United States. "OTO" means "online and offline" in Chinese. Scholars believe that the OTO teaching mode is a hybrid teaching that combines traditional classroom teaching and modern online education in the mobile Internet, big data, and cloud computing environment and effectively combines online learning resources and online learning tools with student learning and teacher teaching [7–9].

Therefore, the OTO teaching mode is not just a type of teaching form, but a new teaching method that uses all the information and tools on the mobile Internet and the intelligent application of mobile terminals to conduct interactive teaching through the network. In the case of the huge impact of the COVID-19 pandemic on education and teaching, the Ministry of Education requires the online course platform to follow "suspension of classes without cessation of learning, suspension of classes without cessation of teaching" which means that no matter when the school resumes classes, we must first keep the children in a state of learning during the epidemic. Based on this, this study adopts the online and offline hybrid teaching mode combining Chaoxing Learning Platform + Tencent WeChat Group in the teaching of football general courses, mainly using the Chaoxing Learning Platform as a platform to integrate the syllabus, teaching plan, PPT courseware, and teaching content. The teaching videos, animations, and other related materials are uploaded to the Chaoxing Learning Platform, and a teaching model of "online teaching, offline training" is formed [10]. At the same time, the provincial high-quality football online courses that come with the platform provide excellent teaching resources for students to study on their own [11]. On this basis, exploring the impact of OTO teaching mode on college students' interest in sports learning has important practical significance to the reform of college physical education and teaching.

2. Research Objects and Methods

2.1. Research Objects. Students in the second year in four football classes of a university's physical education major were selected as experimental subjects, including 51 in the experimental group and 56 in the control group (Table 1). Among them, the experimental class adopts the OTO teaching mode for teaching and the control class adopts the traditional teaching mode for teaching. Before and after the experiment, focus on students' PE learning interests (including positivity, negativity, skill learning, extracurricular activities, and sports attention) and football skills (including bumping the ball, passing on the inside of the foot, shooting around the club, and kicking far) were analyzed.

2.2. Teacher Settings. The Jianghong Dai is a teacher in the experimental group, specializing in football, has ten years of college football teaching experience, and has implemented certain research on online and offline teaching modes. The teacher in the control group is an old teacher of college football special teaching with 20 years of teaching experience. The teaching method is relatively traditional. He has participated in the compilation of traditional teaching plans and is familiar with the teaching content and process. Both groups of teachers are specialized in football, with rich teaching experience, serious teaching attitude, and good teaching effect.

2.3. Intervention Programme. The teaching plan of the experimental group was compiled by the author according to the structure and characteristics of the OTO course teaching mode. The teaching plan of the control group was prepared by the teachers of the general football course based on the syllabus of the teaching syllabus. It has gone through four years of teaching practice.

2.3.1. Teaching Content Settings

(1) Teaching content of each semester: the overall teaching content of the experimental group and the control group is the same, including basic theories, basic techniques (inner foot pass, bump, 20M round shot, long kick), basic tactics (two-over-one cooperation, defensive counterattack), physical fitness (speed, strength, flexibility, bounce, agility), and examination (technical, quality examination). However, the design concept of the teaching schedule is not the same. The experimental group is based on the OTO teaching model, using software to learn and using online and offline teaching methods to design content. It is roughly divided into 4 stages. First, the basic stage includes learning and watching a relatively simple, basic combination of basic football moves, such as the combination of passing the ball on the inside of the foot and moving left and right. Second, the development stage includes learning and watching movement skills that are slightly more difficult, such as 20-meter circumnavigation and shooting. Third, the promotion stage includes combining the actions learned in the previous stage in the set competition. Fourth, the application stage includes using them in actual competitions. The control group is designed according to the difficulty of mastering technology or tactics and is roughly divided into 3 stages. First, the basic stage includes learning the basic skills of football. Second, the development stage includes learning basic tactics. Third, the application stage includes the competition application stage.

Table 1: Basic situation of experimental group and control group students (M±SD).

Class time	Group	Number	Height	Weight	Age
Tuesday (5-6)	Experimental	26	171. ± 6.05	70.3 ± 4.25	19.3 ± 1.01
Tuesday (7-8)	Experimental	25	170. ± 7.12	71.6 ± 5.18	19.5 ± 0.82
Total	Experimental	51	171. ± 6.58	70.9 ± 4.72	19.4 ± 0.91
Tuesday (5-6)	Control	28	170. ± 5.12	70.6 ± 5.23	19.3 ± 0.72
Tuesday (7-8)	Control	29	171. ± 6.21	70.7 ± 4.15	19.4 ± 0.63
Total	Control	57	170. ± 5.32	70.6 ± 4.69	19.3 ± 0.67

(2) Teaching content of each lesson: the teaching content of the experimental group is mainly on the inside of the foot to pass, bump the ball, 20M around the shot, and kick long. In addition, the learning pass software is used to record teaching videos and the learning pass software is then uploaded. Using flipped classroom, students learn the teaching content of this lesson through the learning software before the class. In the rest interval of classroom teaching, the teacher introduces the teaching content of this lesson in combination with the teaching video of the learning software. The teaching of the control group mainly adopts traditional teaching methods. For example, the teacher first explains the key points of the pass movement on the inside of the foot, as well as the key and difficult points, the teacher's demonstration, and the form of exercises by the students.

2.3.2. Teaching Process and Procedure Settings

(1) The teaching process of each lesson: the teaching process of the experimental group and the control group includes three parts, the preparation part, the basic part, and the end part and they are different. During the preparation period, the experimental group had previewed the teaching content of the class through Chaoxing Learning Platform, watched the teaching video, and had a preliminary impression of the teaching content in their minds. During the basic part, the teachers of the experimental group spent less time talking than those of the control group and the students were mainly asked to practice more, interspersed with re-review of the video during the period. Finally, after the course is over, homework will be assigned to the Chaoxing Learning Platform, such as uploading a video of after-school practice of what they have learned. The control group mainly used conventional teaching procedures.

(2) Teaching steps for each exercise: the experimental group adopts the OTO teaching mode to teach. The main steps are preclass preparation, participation in class consolidation after class, and assessment and evaluation (Figure 1).

Among the teaching steps, the main practice method adopted is the motor image learning method. Through the use of the Chaoxing Learning Platform, the learning content is studied before class and the teacher's explanation is combined with the content in the class to carry out structured learning. After class, the content of the class is practiced, a video is recorded, and it is uploaded to the Chaoxing Learning Platform.

The teaching steps of technical exercises in the control group are explanation, demonstration, exercises organization, cycle guidance, and teaching feedback. The teaching content of the second class is taken as an example (Table 2).

2.3.3. Teaching Method. The teaching methods adopted by the experimental group mainly include intuitive teaching method, discovery teaching method, heuristic teaching method, and competition teaching method. The teaching methods adopted by the control group mainly include the demonstration method, the intuitive teaching method, the complete method, and the decomposition method.

2.4. Experimental Steps

2.4.1. Pretest. The experimental group and the control group started teaching from the first week of the first semester of the 2020-2021 school year, two hours a week, and the teaching lasted for 16 weeks. In the first week, the students' interest in sports learning was tested through the PE learning interest scale and the technical evaluation standards were used to test the basic technical movements of football (passing on the inside of the foot, kicking far, bumping the ball, 20M shooting around the shot).

2.4.2. Intervention Content. In the process of experimental intervention, the control group used traditional teaching and activity schedules, that is, normal football teaching; the experimental class used the OTO teaching mode for football teaching.

The experimental group carried out a general football course intervention every week. In class, after finishing the preparatory activities, the teaching assistant will use the computer to hold a Tencent meeting and all the students will join the meeting. The assistant will explain the football teaching video online, and the video time is 10 minutes while explaining the technical actions offline. And, questions are asked randomly, for about 10 minutes.

Teaching process includes the following: watching football teaching video (teacher-assisted explanation), practicing without a ball (teacher- and assistant-guided teaching), and practicing with a ball (teacher- and assistant-guided practice).

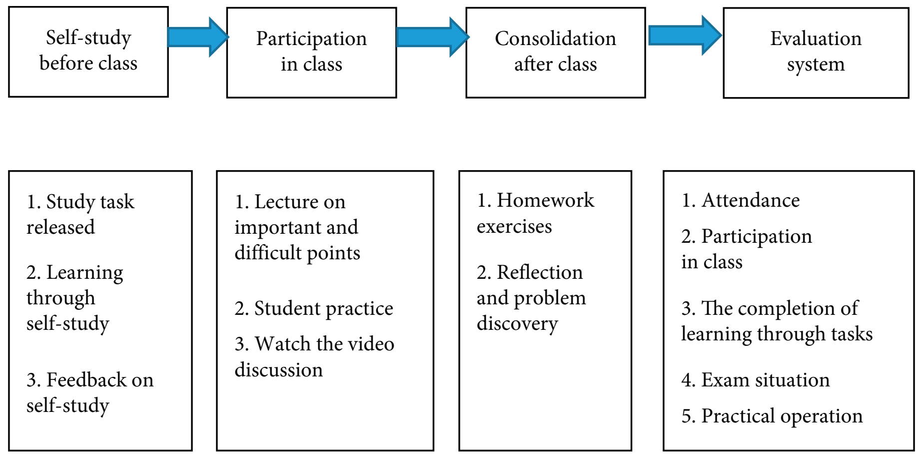

Figure 1: Teaching implementation steps.

Table 2: Comparison of the teaching steps of the inside of the football foot between the experimental group and the control group.

Experimental group	Control group
1. Preparation before class: the teacher uploads relevant learning materials such as the syllabus, teaching design, teaching-related videos, and animations to the Chaoxing Learning Platform course column for students to preview in advance. Teaching content videos are published through group mailboxes, QQ, WeChat, etc.	1. Explanation: the teacher introduces the concept of passing the ball on the inside of the foot, the action essentials, and the application of the game.
2. Classroom teaching: the teacher will give a brief explanation after the demonstration.	2. Demonstration: the teacher demonstrates the complete pass of the inside of the football foot.
3. Organizing student exercises: exercises are paired in groups of 2, exercises are paired on the move, and exercises are applied in the game.	3. Organizing student exercises: these include ball-free exercises and fixed ball exercises, exercises are paired in groups of 2, and exercises are paired on the move.
4. Teaching feedback: teacher inspection guidance and error correction.	4. Teaching feedback: teacher inspection guidance and error correction.
5. Homework: homework assigned to Chaoxing Learning Platform.	

2.4.3. Intervention Implementation and Control. The experimental intervention period of this study is from October 2020 to January 2021, a total of one semester, 16 weeks. At the same time, in order to reduce the impact of time, weather, and other reasons on students' football skills test and PE learning interest test, it is unified to conduct football skills and PE learning interest index tests for the experimental group and the control group in mid-October. Among them, the football skill test includes passing the ball on the inside of the foot, kicking the ball far, bumping the ball, and shooting 20M around the pole. The PE learning interest evaluation scale includes five indicators: positivity, negativity, skill learning, extracurricular activities, and sports attention. Through a one-semester intervention, in late January 2021, the students will be posttested on football skills and PE learning interests in the same venue, with the same test format and method. The authenticity of the two test data records must be guaranteed.

2.5. Research Tool. Using the "College Student Sports Learning Interest Evaluation Scale" compiled by Gu Haiyong and Jie Chao, the reliability coefficient of the scale is 0.925, which has very high reliability. The scale uses a 5-point scoring method, ranging from "completely disagree" to "completely agree." The larger the score is, the greater the influence on the behavior will be. The scale contains 5 dimensions:

(i) Positivity includes questions 1, 2, 3, 4, 5, and 6
(ii) Negativity includes questions 7, 8, 9, 10, 11, and 12
(iii) Skills learning includes questions 13, 14, 15, and 16
(iv) After-school activities include questions 17, 18, and 19
(v) Sports attention includes questions 20, 21, 22, 23, and 24.

3. Results

3.1. Before the Experiment, There Was No Significant Difference between the Experimental Group and the Control Group in the Results of the Physical Learning Interest Level Test Items. Before the experiment, the independent sample T-test results of students' PE learning interest level showed that there was no significant difference in the five dimensions of positivity, passivity, skill learning, extracurricular activities, and sports attention between the experimental group and the control group. (T positivity = −0.083, $P > 0.05$; T negativity = −0.237, $P > 0.05$; T skill learning = −0.213, $P > 0.05$; T extracurricular

Table 3: Before the experiment, the comparison and analysis table of the difference in students' PE learning interest level between the experimental group and the control group ($n = 107$).

Test items	Test index	Group	Number	Mean, M±SD	T	P
PE interest level	Positivity	Group 1	51	1.75 ± 1.02	−0.083	0.751
		Group 2	56	1.70 ± 1.04		
	Negativity	Group 1	51	3.74 ± 1.30	−0.237	0.506
		Group 2	56	3.79 ± 1.11		
	Skills	Group 1	51	4.01 ± 1.01	−0.213	0.278
		Group 2	56	4.05 ± 0.97		
	Activities	Group 1	51	3.78 ± 1.15	−1.044	0.428
		Group 2	56	4.0 ± 1.058		
	Attention	Group 1	51	3.8 ± 1.165	0.911	0.368
		Group 2	56	3.6 ± 0.936		

Note. Group 1: experimental group; Group 2: control group.

activities = −1.044, $P > 0.05$; T sports attention = 0.911, $P > 0.05$. See Table 3 for details.) This result shows that before the experiment, the students in the experimental group and the students in the control group basically show the same level of interest in sports learning.

3.2. Analysis on the Differences of Different Dimensions of Sports Interest between the Experimental Group and the Control Group after the Experiment. After the experiment, the independent sample T-test results of the students' PE learning interest level showed that there were significant differences in the four dimensions of the PE learning interest level of positivity, negativity, skill learning, and extracurricular activities between the experimental group and the control group. The P value of the dimension of sports attention is greater than 0.05, so there is no significant difference in sports attention. (T positivity = −2.473, $P < 0.05$; T negativity = 3.209, $P < 0.007$; T skill learning = 2.786, $P < 0.05$; T extracurricular activities = 2.934, $P < 0.01$; T sports attention = 1.119, $P > 0.05$. See Table 4 for details.) The results show that the online and offline teaching mode can effectively enhance students' interest in sports learning, but it has little effect on sports attention.

4. Discussion

The experimental results show that the PE learning interest of the experimental group is significantly higher than that of the control group and its negative interest is significantly lower than that of the control group. It can be concluded that the experimental results support some of the hypotheses put forward by the research. That is to say, the OTO teaching mode with football lessons as the carrier has obvious promotion effect on the positivity of college students' PE learning interest, skill learning, and extracurricular activities and alleviating the negativity of PE learning interest. The reason is that, first of all, compared with the traditional offline teaching action explanation, the OTO teaching mode is a new type of teaching mode. It integrates sound and picture, with high clarity and interest, and can be intuitive to students. The stimulus of the picture makes the students' interest in physical education to gradually increase, so that their learning positivity will be higher [12]. Second, in football teaching, the understanding and mastery of technical movements is the key. The teaching of football technical actions requires a lot of observation, imitation, feedback, and correction in the process of technical action and a lot of perceptual information besides proprioception, such as visual information and auditory information. Online teaching can integrate animations and assist teachers in providing students with various perceptions of three-dimensional space and conducting specific practical exercises offline to form a mixed teaching mode of "online teaching and offline training." In addition, due to factors such as the age and technical level of some teachers, it is impossible to demonstrate some difficult football skills. Multimedia production can solve it as well, and the actions can be decomposed in an orderly manner and displayed from different angles. These undoubtedly play a significant role in promoting the learning of skills. Third, the OTO teaching mode has expanded infinitely in terms of space and time. Students can study the teaching content without restriction before, during, and after class, without being restricted by time and space. Finally, the OTO teaching model can optimize the evaluation mechanism and build a hybrid evaluation mechanism of "online + offline." Online classroom can count student sign-in frequency and online learning time [10]. It provides a reference for the evaluation of the usual grades at the end of the term. A trinity comprehensive evaluation system of "student self-evaluation, student-student mutual evaluation, and teaching evaluation" is introduced offline to complement the online mode to promote the development of students' football skills, thereby enhancing students' interest in sports learning.

The OTO teaching mode also presents some shortcomings in practical application. First of all, the lag of online teaching facilities and technology affects the effect of online teaching. For example, network freezes occur during online teaching, football teaching video resources will have not formed a system, and echoes during the playback process often occur, which affect the effect of online teaching. Second, it is difficult to supervise online teaching, which mainly relies on the consciousness of students [13]. Although there are abundant resources online, due to the constraints of time and space, teachers cannot directly face students and it is difficult to comprehensively, accurately, and timely grasp the learning status of students, which affects the application effect of the OTO teaching mode.

Table 4: Comparison and analysis table of differences in football skill test scores between the experimental group and the control group after the experiment ($n = 107$).

Test items	Test index	Group	Number	Mean, $M \pm SD$	T	P
PE interest level	Positivity	Group 1	51	1.11 ± 0.313	−2.473	0.027*
		Group 2	56	1.45 ± 0.731		
	Negativity	Group 1	51	4.59 ± 0.524	3.209	0.007**
		Group 2	56	3.94 ± 1.024		
	Skills	Group 1	51	4.65 ± 0.501	2.786	0.014*
		Group 2	56	4.58 ± 0.968		
	Activities	Group 1	51	4.36 ± 0.529	2.934	0.005**
		Group 2	56	3.99 ± 0.948		
	Attention	Group 1	51	4.66 ± 0.544	1.199	0.280
		Group 2	56	4.45 ± 0.731		

Note. $^{*}P < 0.05$ has a significant difference; $^{**}P < 0.01$ has an extremely significant difference. Group 1: experimental group; Group 2: control group.

5. Conclusions and Suggestions

5.1. Conclusions

(1) The implementation of the OTO teaching mode can effectively stimulate the positivity of students' PE learning interest, skill learning, and extracurricular activities and alleviate the negativity of PE learning interest.

(2) The OTO teaching mode has little effect on sports attention in PE learning interest.

5.2. Suggestions

(1) All colleges and universities should actively adopt the OTO teaching mode in physical education, which is conducive to stimulating students' interest in physical education, improving teaching quality, and promoting the reform and development of college physical education courses.

(2) In the course of daily class, you should grasp the time of online class and allow enough time for students to practice.

(3) A diversified evaluation system of evaluation subject, evaluation content, and evaluation dimensions should be adopted in order to obtain more objective, comprehensive, and accurate evaluation results and more accurately reflect the learning situation of students.

Data Availability

Data sharing is not applicable to this article as no datasets were generated or analyzed during the current study.

Conflicts of Interest

The authors declare no conflicts of interest.

Acknowledgments

This work was supported by research grants from the 2020 Education Reform Project of the Hunan Provincial Department of Education (HNJG-2020-0962) and Provincial "Thirteenth Five-Year" Education Planning Project (XJK18BGD010).

References

[1] Z. Duan and Y. Tian, "Genetic analysis of learning interest," *Educational Science*, vol. 28, no. 3, pp. 33–37, 2012.
[2] S. Hidi, "Interest: a unique motivational variable," *Educational Research Review*, vol. 1, no. 2, pp. 69–82, 2006.
[3] General Office of the State Council, *Opinions on Strengthening School Sports to Promote the All-Round Development of Students' Physical and Mental Health*, General Office of the State Council of China, Beijing, China, 2016.
[4] X. Niu and J. Yang, "Research on single teaching mode of football," *Science and Technology Information*, vol. 15, no. 2, pp. 222-223, 2017.
[5] L. Yu, "Analysis of the application of MOOC method in the training of football teachers in vocational colleges," *Young people*, vol. 83, no. 10, 2019.
[6] L. Yang, "Thoughts on the application of open teaching mode in higher vocational physical education," *Journal of Science & Technology Economics*, vol. 27, no. 34, p. 157, 2019.
[7] Y. Xie and H. Hong, "Exploration and thinking on the guiding ideology of public physical education in ordinary colleges and universities," *Beijing Sport University News*, vol. 37, no. 1, pp. 94–99, 2014.
[8] Y. Ding, "Exploration of OTO teaching mode and management mechanism based on the concept of flipped classroom," *Higher Education Management*, vol. 10, no. 1, pp. 111–115, 2016.
[9] N. Wang, Y. Dong, L. Yang, and B. Han, "Exploration of college students' social practice management model based on OTO," *Modern Economic Information*, vol. 452, no. 22, 2015.
[10] M. Dai, H. Zhang, and Y. Liang, "Teaching exploration of online and offline hybrid advanced manufacturing technology training," *Laboratory Research and Exploration*, vol. 40, pp. 150–153, 2021.
[11] J. Gao, C. Yu, and M. Ma, "Exploration and practice of online teaching of medical immunology under the new coronary pneumonia epidemic," *Chinese Journal of Immunology*, vol. 36, no. 18, pp. 2200–2204, 2020.
[12] H. Tang and Z. Wang, "The influence of online and offline teaching methods on the learning of basketball special courses in colleges and universities," *Sports Science and Technology Literature Bulletin*, vol. 28, no. 3, pp. 6–8+ 12, 2020.
[13] Y. Liu, P. Shan, and M. Fan, "How is the "substantial equivalent" of online and offline teaching quality possible," *Journal of National Academy of Educational Administration*, vol. 3, pp. 67–75, 2021.

Hindawi
Scientific Programming
Volume 2021, Article ID 1198794, 11 pages
https://doi.org/10.1155/2021/1198794

Research Article

An Intelligent Scheduling Access Privacy Protection Model of Electric Vehicle Based on 5G-V2X

Cheng Xu [1], Hongjun Wu [1], Hongzhe Liu [1], Xuewei Li [1], Li Liu [2] and Pengfei Wang [3]

[1] *Beijing Key Laboratory of Information Service Engineering, Beijing Union University, Beijing, China*
[2] *Information Center, Yunnan Power Grid Co., Ltd., Kunming, China*
[3] *Communication and Information Center of Ministry of Emergency Management of the People's Republic of China, Beijing, China*

Correspondence should be addressed to Hongzhe Liu; liuhongzhe@buu.edu.cn

Received 20 August 2021; Revised 11 October 2021; Accepted 18 October 2021; Published 9 November 2021

Academic Editor: Punit Gupta

It is more and more important to optimize electric power system scheduling in the development of the Internet of Vehicles. How to improve the applicability and scientific nature of electric vehicle charging is an urgent problem to be solved. This paper proposes an intelligent scheduling access model for electric vehicles based on blockchain. Firstly, the layout simplification calculation is carried out for the layout of the traditional distributed power grid. Then, a data storage and consensus system is built using blockchain smart contracts to ensure that all historical data are not tampered with and are traceable. Finally, the model forms an electricity price guidance model in the intelligent scheduling and access of electric vehicles, optimizes the multivehicle line congestion in operation, and can dynamically schedule and correct the model. In terms of the experiment, 13 test electric vehicles were dispatched based on 12 real power station nodes and 36 test nodes of Yunnan Power Grid Co. Information Center for verification. The result analysis shows that the model can effectively and quickly solve the blocking and unblocking of the Internet of Vehicles and can develop a scheduling scheme conforming to the safety constraints of electric vehicles in a relatively short time.

1. Introduction

Electric vehicles (EVs) replacing traditional fuel cars are of great significance in alleviating urban air pollution. Compared with traditional fuel cars, electric vehicles are expensive, take longer to charge, and have a shorter range. In particular, the lack of charging piles greatly affected the promotion of electric vehicles. All countries are committed to the research and development of new energy vehicle key technologies, but the penetration rate is not high [1]. In the future, the proportion of electric vehicles on the Internet of Vehicles (IoV) or Internet of things (IoT) will be increasingly large, because of its great advantages; for example, logistics enterprises can provide a fixed charging station. Compared with fuel cars, electric trucks are environmentally friendly and cost-saving. At present, EV charging service has problems such as difficulty in finding a pile for charging users, difficulty in information connection between charging stations, and difficulty in charging transaction settlement [2, 3]. For example, the introduction of a central organization to manage charging services and charging transaction information can improve the current situation, but it requires high cost and risks of information leakage [4]. Therefore, we need to seek new charging service mode and transaction information management system. With the increasing level of digitalization and decentralization of energy systems, the need for reliable defense against cyberattacks in the IoV has increased dramatically. If properly applied, blockchain technology can fix vulnerabilities in networking and data communication. It can improve data confidentiality and privacy, so as to effectively defend against various threats from the inside and outside [5]. In terms of data communication vulnerability repair, blockchain technology can integrate the pricing and settlement functions of the wholesale power market into a secure blockchain system. It can greatly reduce the risk of fake data injection and price manipulation. It ensures that the dataset or communication series specified between the trading parties is immutable. At the same time, blockchain can improve data confidentiality and privacy. As digitally distributed systems become the norm in the energy sector and billions of energy-using devices are integrated into power systems, malicious attackers will see more opportunities to break into these systems and attempt to disrupt them [6].

Due to the wide network coverage, high data information transmission rate, low end-to-end latency, and support for massive connections, 5G networks are rapidly spreading [7]. As the underlying network communication technology, 5G can deeply empower upper-layer vertical applications. The integration of 5G and blockchain can cause them to empower each other. With its high speed and low latency, 5G helps the blockchain accelerate transactions (full network broadcasting), avoiding stalls and long-term unresponsiveness [8]. Moreover, because 5G drives V2X, it has spawned a lot of data and scenarios, which is conducive to the implementation of blockchain applications.

In this context, how to improve the applicability and scientific nature of electric vehicle charging is an urgent problem to be solved. In order to improve the scheduling optimization of EV in the development of IoV in the real environment, this paper proposes an intelligent scheduling access model for EV based on blockchain.

The rest of this paper is organized as follows. Section 2 explores the latest methods about blockchain, IoV, and intelligent contract. Section 3 presents the access model of intelligent scheduling of EV based on blockchain. Comparisons of experimental results with other works and discussion are provided in Section 4. Section 5 summarizes the paper and offers directions for future research.

2. Related Work

2.1. Blockchain Security in Power Grid Industry. The decentralization, openness, intelligence, and sharing of blockchain are in line with the ideas of the IoV and the energy Internet. They can be done by means of data encryption, timestamps, distributed consensus, and economic incentives. Point-to-point transaction, coordination, and collaboration can be realized based on decentralized credit in a distributed system where nodes do not need to trust each other [9]. The application of blockchain in IoV will effectively support the open interconnection of multitype systems and the extensive and deep participation of multiple users. It can not only solve network access, long-distance transmission loss, demand-side response, network security, and other problems, but also form some new models for the inherent market mechanism and business model of the power industry [10].

At the same time, in terms of power market transactions, blockchain can exist in three decentralized forms with different degrees of the public chain, private chain, and alliance chain. The internal finance of power grid adopts a private chain, which is conducive to the transparency of internal management universities and the improvement of clearing and auditing efficiency. Alliance chain, power plant, power grid, electricity selling company, and other subjects are adopted among the trading subjects in the power market to reach contract agreements, improve efficiency, and facilitate inquiry and statistics. The public link is adopted between the electricity selling company and users, and automatic meter reading, metering, and billing are adopted to improve transparency and credibility [11].

Blockchain has a natural network threat defense capability, which benefits from the following characteristics [12, 13]:

(1) Tamper-proof data: after proper application of blockchain, all calculations will be performed in hash form and will be tamper-proof when the data are generated, thus avoiding the risk of being tampered with in transmission.
(2) Complete data availability: blockchain can store data in a decentralized form through multiple nodes. Under such an architecture, even if some nodes or servers are hacked, the user can still get the complete dataset.
(3) Redundancy: the operation of blockchain has no central failure point, so this architecture is inherently highly reliable through redundancy.
(4) Privacy and control: blockchain users can choose which data are permanently transparent and which data are encrypted, so only the designated receiver can view the data content.
(5) Outsourcing calculation: the encrypted data can be sent to a third party for processing, and the data content will not be displayed in the whole process.

2.2. IoV in the Grid Intelligent Scheduling Algorithm. Vehicle scheduling problem was first proposed by Dantzig and Ramser [2]. The goal is under certain constraints, such as the limitation of vehicle load and the volume of the goods to seek the best assembly, also called the vehicle scheduling problem (VSP), or seek vehicles' best path, also called the vehicle routing problem (VRP), which makes the total distribution cost minimum. Therefore, the vehicle scheduling problem is a typical nondeterministic polynomial problem. When the electric vehicle is used for transportation, the problem is more difficult to solve due to the influence of charging and endurance. In recent years, the logistics scheduling problem based on new energy vehicles is collectively known as the green vehicle routing problem (GVRP). As GVRP is relatively new, there is not much classical research literature. Literature [6] summarizes the research status of EVRP before 2014. It summarizes the technical background of electric vehicles, including vehicle type and battery, cost comparison with traditional fuel car, vehicle grouping, route selection, and optimal route, and gives possible research directions.

In the past two years, representative research results included the following: vehicle scheduling problems under the constraints of time and charging station are widely concerned [9–11]. Literature [9] adopted a new hybrid heuristic algorithm to solve this problem. The new algorithm combined variable domain search and tabu search algorithm to test on the standard set and achieved good results. Literature [10, 11] studied the hybrid formation problem of different types of electric vehicles. In the model, the improved branch-and-price algorithm based on Adaptive Large Neighborhood Search was adopted to solve the problem with the constraints of transportation time, transportation cost, vehicle load, etc. The experiment showed that the algorithm was effective. Moreover, literature [12] studies the different trolley charging conditions under different scheduling paths under time constraints and uses branch-price-and-cut algorithms to determine whether there are multiple charging stations on each scheduling path and whether each charge must be filled to get 4 combinations. The study shows that in the case of 100 customers and 21 charging stations, all four combinations have solutions. The comparison of the four kinds of path planning reveals that multiple charging piles have more advantages than the other three cases without full charging. Literature [13] proposes a universal EVRP model, which takes minimum transportation time, minimum energy consumption, and minimum transportation vehicle as constraints and passes through each customer only once. Different from previous models, the problem of power consumption under different loads is considered in this modeling. In this model, the feasible solution space is not large, so the computer is used to solve it accurately. However, the above work did not solve the problem of electricity price optimization.

2.3. Intelligent Contract for Secure Access. As a new application technology of the new form of IoV, blockchain has the characteristics of weak centralization, distrust, and not being tampered with easily. It can realize the undifferentiated records of multiple nodes and promote the interconnection of information [5, 6]. Intelligent contracts can be widely used in various interconnection scenarios of energy transactions such as power market transactions and energy demand response [9, 10]. Literature [11] proposes to use blockchain technology to realize transparent and trust-based charging of public charging piles. Literature [12] proposed Ethereum EV charging transaction mode, in which EV users choose the best bidding charging station. Literature [13] proposed a charging pile sharing platform based on a lightning network, blockchain, and intelligent contract. Literature [14] proposed electric vehicle charging transaction based on a lightning network, which solved the possible security problems in a lightning network.

The above studies generally use the traditional bitcoin or Ethereum blockchain architecture, which requires tokens and public chain, which is not conducive to improving transaction efficiency and reducing transaction cost. Therefore, it is necessary to select a blockchain architecture more suitable for the performance requirements of EV charging transaction business. Many scholars use the weakly centralized alliance chain to improve the efficiency and security of EV transaction. In literature [15], multiple agent nodes are set up to manage the choice and transaction of user charging mode, but the implementation structure of a specific alliance chain is not mentioned. In [16], electric vehicle users and distributed energy operators were set up for the application scenario of microgrid. Literature [17] used an alliance chain to design charging and discharging transactions between electric vehicles and set up local aggregators to act as service nodes, without involving user transactions in different aggregators.

The sorting and analysis of the above research status show that blockchain can effectively improve the defects of grid security access and optimize the charging model of electric vehicles.

3. Intelligent Scheduling Access Model of EV

3.1. Electric Vehicle Charging Security Access Trading Design. EV charging trading system architecture can be divided into application layer, intelligent contract layer, consensus layer, network layer, and data layer [18]. The data layer stores the transaction data in LevelDB or CouchDB in the data structure of Merkle Bucket tree and blockchain list [19]. The network layer selects HTTP/2-based P2P protocol as the network transmission protocol and makes the node listen to verify whether the new block or new transaction of the broadcast is valid. The consensus layer adopts a practical Byzantine fault-tolerant algorithm. The intelligent contract layer encapsulates the electric vehicle charging trading intelligent contract written in Go language. The application layer supports EV charging applications with query charging stations and transfer transaction functions [20–24].

Figure 1 shows the network structure of EV charging transaction model. Participants include application, charging station nodes of charging operators and utility companies, sorting service nodes, and regulatory authorities of charging transaction market.

Each charging operator or utility serves as an organization in the transaction network structure, with multiple charging station nodes per organization. All nodes are accounting nodes, responsible for validating transactions and writing them into the books. On this basis, a node can also act as master node, anchor node, and endorsement node. The master node is the node responsible for communicating with the sorting service node, which receives the transaction containing the endorsement signature. It sorts unpackaged transactions, generates blocks, and broadcasts them to the billing node. Anchor nodes are nodes that can communicate with the nodes of other organizations. By running its installed smart contract, the endorsement node can sign and endorse the charging transaction proposal put forward by the client and feed back the result. The transaction model calculates the endorsement experience value M according to the endorsement times of the nodes and refers to this index in service evaluation, so as to encourage each charging station node to act as the endorsement node and maintain the stable operation of the blockchain platform. The expression of endorsement experience value M is

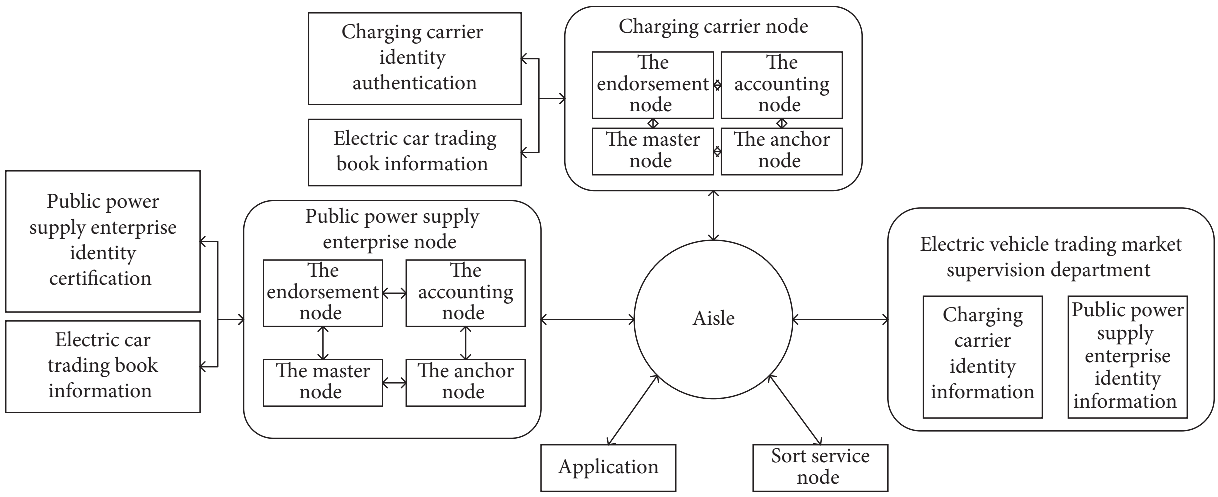

Figure 1: Network structure of EV charging transaction model.

$$M = \beta \frac{l_{c,n}}{L_n}, \tag{1}$$

where $l_{c,n}$ is the number of account updates of the charging station node as the endorsement node up to this transaction. L_n is the total number of ledger updates. β is the weight of the adjusted endorsement experience value.

Data exchange is realized by establishing a trading channel, which is a virtual channel of atomic broadcasting. The design of the trading channel makes it impossible for the nodes outside the channel to access the data inside the channel, which provides safe and efficient data exchange. The channel is managed by the regulatory department of the EV charging trading market and connects charging station nodes and sequencing service nodes of multiple companies. Users who register with any charging operator or utility can have the account authentication of the trading platform and deposit their wallet address, account balance, current credibility, certificate, and public/private key pair. Through the application, users can access all endorsement nodes in the channel and select charging services provided by multiple charging operators and utility companies.

3.2. The Process of Trading Electric Cars in IoV. The operational process of EV charging transaction model is based on practical Byzantine fault tolerance (PBFT) algorithm [25, 26]. PBFT is a copy replication algorithm for state machines that replicate on different nodes. The client sends a request to the master node to invoke the service operation, and upon receiving the request information, the master node enters the preparatory stage to broadcast to other nodes. After receiving the broadcast, other nodes simulate the transaction, generate the transaction result, generate the hash value of the new block according to the result information, and enter the preparation stage to carry out the broadcast within its scope.

As shown in Figure 2, the operation of EV charging trading mode is the process of transaction initiation, contract execution, and transaction verification by the trading subject under the consensus mechanism. Firstly, EV users select charging stations according to service rating and use the charging clients to send a request to the endorsement node in the channel and invoke charging service operation. After receiving the request message, the endorsement node verifies the client's identity, performs intelligent contract simulation transactions, and evaluates the charging service. The endorsement node outputs the result of the intelligent contract, that is, a set of key values read or written in the intelligent contract. The transaction request response with the endorsement signature is sent back to the client. The client broadcasts it to the sorting service node. The sorting service node passes ordered transactions as blocks to all nodes on the channel. Each node verifies that the execution result can be written to the ledger status database and notifies the client.

3.3. Smart Contract for EV Charging Trading Model. Smart contracts are programs that run on a ledger of blockchain data and are automatically executed by computers [27]. The main functions of the intelligent contract for EV charging transactions include EV charging charge settlement, charging service, user credit evaluation, and transaction order query from users, charging operators, utility companies, and other institutions.

Every time the owner completes the transaction settlement of electric vehicle, the credibility of the owner is evaluated, R_v, according to it transaction behavior, and the formula is

$$R_v = \frac{1}{J} \sum_{j=0}^{J} C_{vj}, \tag{2}$$

where C_{vj} is the integral reward that EV account v obtains or deducts after the j-th charging transaction is completed, and its value is set. Let its value meet the set $C_{vj} \in \{-1, +1\}$. When the user completes the correct payment of the previous charging service, it can get a bonus point. Otherwise, it can deduct a credit point. If the credit is lower than the

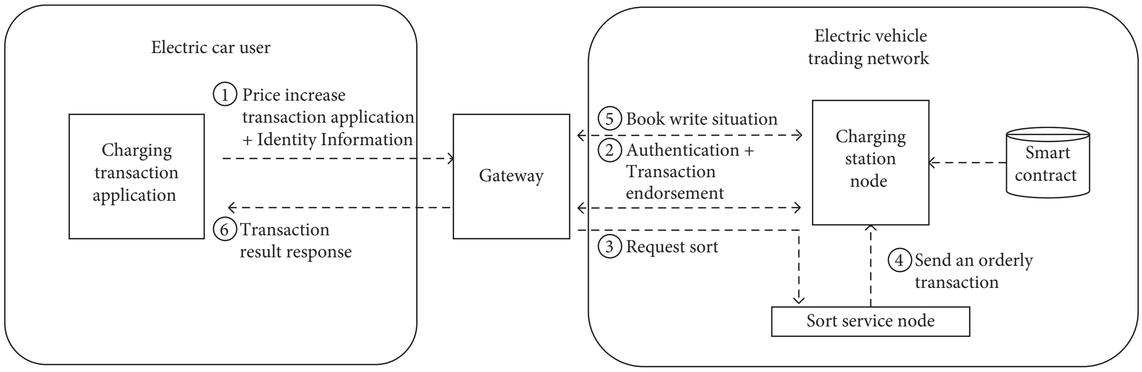

Figure 2: Operation process of EV charging transaction model.

minimum threshold set by the system, that is, $R_v < R_{v,\min}$, the user will not be able to use charging service normally. In this model, the initial value of credit and the threshold value are 0.

The transaction model recommends charging stations with high evaluation of nearby charging services to users with normal credibility for charging transactions. The charging service evaluation $R_{cs,n}$ of the charging station node is constantly updated with the increase of n times of transactions. The following equation calculates the charging service evaluation of the charging station according to the score given by users with different credibility and the endorsement experience value of the charging station node.

$$\begin{cases} R_{cs,n} = R_{cs,n-1} + \dfrac{1}{\alpha}(1+M)\phi\left(R_{cs,n-1}\right)R_v\left(W_n - E_n\right), \\ \phi\left(R_{cs,n-1}\right) = 1 - \dfrac{1}{1+e^{-\left(R_{cs,n-1}-D\right)/\sigma}}, \\ E_n = \dfrac{R_{cs,n-1}}{D}, \end{cases} \tag{3}$$

where $R_{cs,n-1}$ represents the $n-1$ transaction service evaluation of charging station node, and the adjustment parameter $\alpha > 1$ determines the speed of change of service evaluation after each transaction score. The value of α can be adjusted so that after the service capacity of charging station nodes with low evaluation is improved, the evaluation will not always be affected by the previous bad evaluation. M is the calculated endorsement experience value. W_n is the score made by users whose credit rating is higher than the minimum threshold, and in this paper $W_n = \{1, 2, 3, 4, 5\}$. The E_n is the expected score of the charging station node. The D is the highest level in service evaluation, and this model takes $D = 6$. The $\phi(R_{cs,n-1})$ is the damping function that makes the change of charging service evaluation value tend to be gentle. The σ is the acceleration factor in the damping function, and $\sigma = 0.7$.

In the calculation of charging service evaluation, the credibility of EV users and endorsement of charging station nodes are considered to make the evaluation value more reasonable. Moreover, they can stimulate charging station nodes to improve charging service level, contribute computing power, and maintain stable and efficient operation of the trading platform. A charging station is set up to provide charging service for EV. The charges that EV users need to pay to charging operators and utility power companies include electricity fee and service fee, and the formula is

$$\begin{aligned} F_{\text{charging}(v)} &= f_{\text{charging}(v)}\left(E_e - E_s\right), \\ F_{\text{sercice}(v)} &= f_{\text{service}(v)}\left(E_e - E_s\right), \end{aligned} \tag{4}$$

where E_s is the initial electric quantity of the electric vehicle. E_e is the power after charging. $f_{\text{charging}(v)}$ is the unit price of electricity charge. $f_{\text{service}(v)}$ is the service fee unit price. The total cost of charging an electric car v is

$$F_v = F_{\text{charging}(v)} + F_{\text{service}(v)} = f_{\text{charging}(v)}P_v t + f_{\text{service}(v)}P_v t, \tag{5}$$

where P_v is the charging power. t is the charging time.

The specific steps of the transaction fee settlement function are as follows. The first step is to receive the parameters including charging amount $E_{\text{charging}(v)}$; The second step is to apply the API of querying the ledger to get the balance of the charging station and EV account, as well as the unit electricity price corresponding to the period number. The third step is to complete the calculation of the charging transaction amount payment function according to the formula and transfer the corresponding amount in the EV account to the charging station account. If the balance of the electric vehicle account is lower than the threshold value, the credit points will be deducted and the bonus points will be increased. The fourth step is to write deals into the blocks.

Administrators of electric vehicle users and charging operators can query various data of charging bills through intelligent contracts, taking the function of bill inquiry by users as an example. The first step is to receive the EV number (EVID) from the client's SDK. The second step constructs the query string based on the EVID, sends the query string proposal to the ledger, and retrieves the query result. Query results include transaction time, charging cost, unit electricity price, charging station number, organization number of the user, and organization number of the charging station. The third step is to aggregate all query results and return them. Unlike other functions that need to be written into the ledger, such as invoking the transaction ledger function, the node runs the intelligent contract to access the status data and directly outputs the running results to the client without consensus.

4. Experiment and Analysis

4.1. The Experiment Platform. In terms of the experiment, the hardware platform includes 13 unmanned logistics vehicles, as shown in Figure 3, 12 charging nodes, laptop computers, and servers. The software platform includes 36 test nodes and blockchain based on alliance chain.

4.2. The Experiment Design. The experiment evaluates the computational efficiency of the model by using performance indicators of data throughput, response time, and latency. As shown in Figure 4, under the same node, when using the model in this article, it has better throughput and response time than the traditional model. Compared with the traditional model, the proposed model has more data throughput, shorter response time, and lower delay time under the same node. As shown in Figure 5, with the same number of vehicles, the number of nodes is gradually increased, and the performance of the model in this paper is better than the traditional model.

Under large-scale scheduling, the ratio of the warehouse's storage capacity to the vehicle's transportation capacity is an important index affecting scheduling. In this article, it is called the α coefficient, which is

$$\alpha = \frac{\sum_{i=1}^{n} Wi}{\sum_{j=1}^{m} Vj}, \tag{6}$$

where Wi stands for storage capacity and Vi stands for vehicle transportation capacity.

In this experiment, 13 vehicles are dispatched using 36 nodes. The proposed algorithm and the traditional scheduling algorithm are run 150 times each with different number of vehicles, and the average of the running results was applied for the comparison. As shown in Figure 6, under the same number of vehicles, the model in this paper has better data than traditional algorithms, which increases vehicle scheduling efficiency.

In order to test the safety of this model, the illegal vehicle ID packet was synthesized with the correct vehicle ID packet to try to link the charging device. When a blockchain-based charging device identifies an illegal data packet, it will give alarm and detect the average alarm time. As shown in Figure 7, the conventional model does not identify the illegal vehicle ID data packet several times; thus, the charging device starts to work. When using this experimental model, all illegal vehicle ID data packets are detected and an alarm is issued successfully. As shown in Figure 7, the detection time was significantly lower than the traditional model.

The transmission network includes load L1 and two large units G1 and G2. The distribution network is divided into two active distribution networks, ADN1 and ADN2. According to the line and geographical location, the ADN1 includes 1 wind turbine (W2), 2 tram stations (EV2 and EV3), 1 set (DG3), and 1 load node (L3). The ADN2 consists of 1 wind turbine (W1), 1 tram station (EV1), 2 units (DG1 and DG2), and 1 load node (L2). The unit information is shown in Table 1, where a, b, and c are the constant, primary, and secondary coefficients of the generation cost, respectively. The $P_{\min}$ and $P_{\max}$ are the minima and maxima of output, respectively. The optimal regulation of generating set is shown in Table 2.

4.3. The Experimental Analysis. In the experiment, a common algorithm without model optimization is firstly used to conduct vehicle scheduling and charging as a comparison item. After that, the distributed optimization algorithm and the dynamic adjustment model based on blockchain were adopted to conduct V2G optimization of the power grid, distribution network, and vehicle charging schedule; meanwhile, the dynamic constraint counting method was adopted for blocking management.

In the scheduling process, as shown in Table 3, power flow overload occurs in some nodes such as 15, 16, and 17. By adding the 3 modulation constraints into the constraint set, the traditional algorithm presents large information blocking, which makes the vehicle scheduling appear sluggish, and the charging efficiency is greatly reduced. After that, the proposed model was used for optimization. After the optimization, there was no longer the case of charging overload in statistics, so the results were in line with the optimal solution of security constraints. In the test, the traditional algorithm presented information blocking. Under the optimization of the proposed model, the interference is quickly eliminated, and the charging of multiple vehicles is not disturbed. Moreover, under the optimization model, the electricity price of charging is lower than that without optimization.

As shown in Figure 8, when blockchain is used in scheduling and charging transactions, the delay is greatly reduced. The increase of information throughput strengthens the optimization effect of the model and achieves a good experimental result.

The running time and cost after optimization are less than those without model optimization. The optimized optimal power flow distribution and the data are better than the data obtained without model optimization. It can be seen from the above results that when vehicle scheduling is carried out by using the proposed model, the charging efficiency of the vehicle is higher, the cost is lower, there is no information blocking, and it is safer and more efficient. The optimal scheduling scheme is developed in a short time to make the vehicle running and charging more reasonable. The proposed model enables logistics enterprises to make better profits and achieve higher logistics efficiency.

Figure 3: Unmanned logistics vehicles.

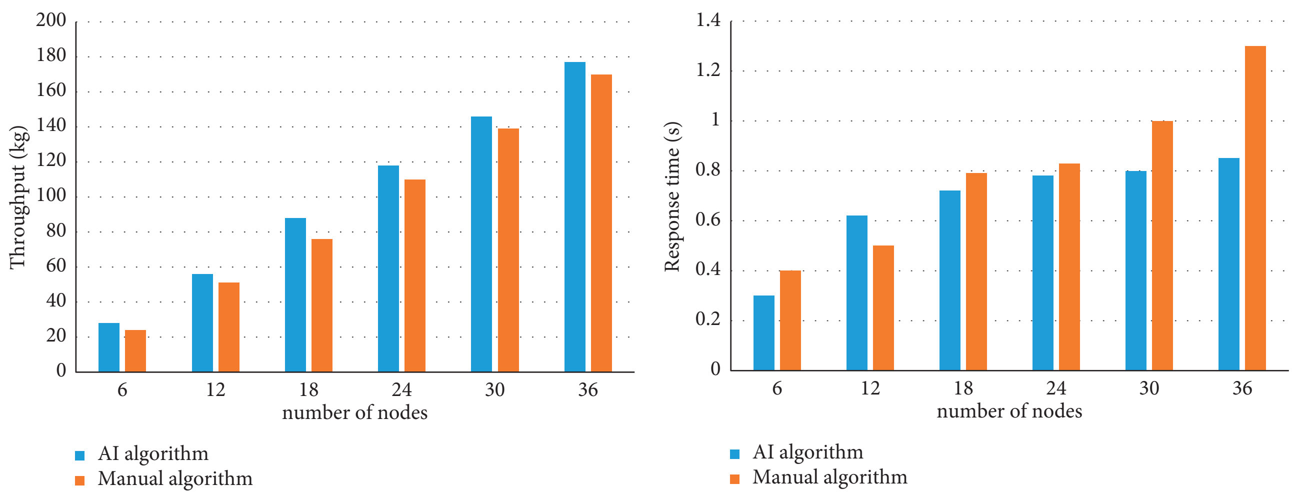

(a) (b)

Figure 4: Throughput (a) and response time (b) for the same number of nodes.

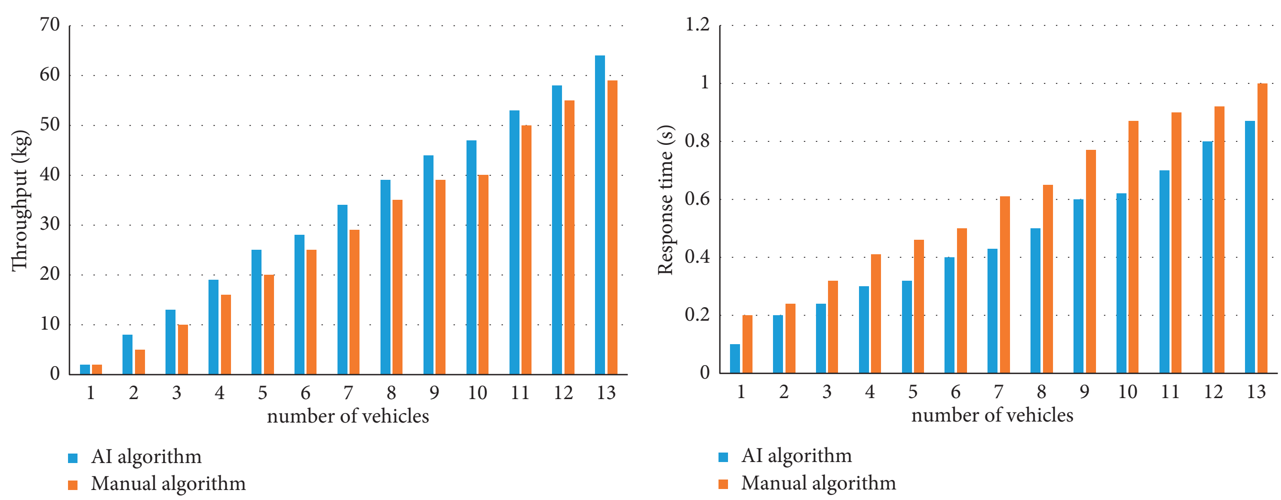

(a) (b)

Figure 5: Throughput (a) and response time (b) for the same number of vehicles.

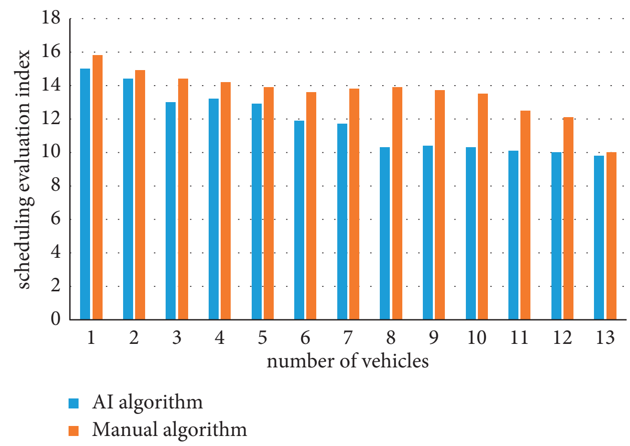

Figure 6: Scheduling evaluation index varying with number of vehicles.

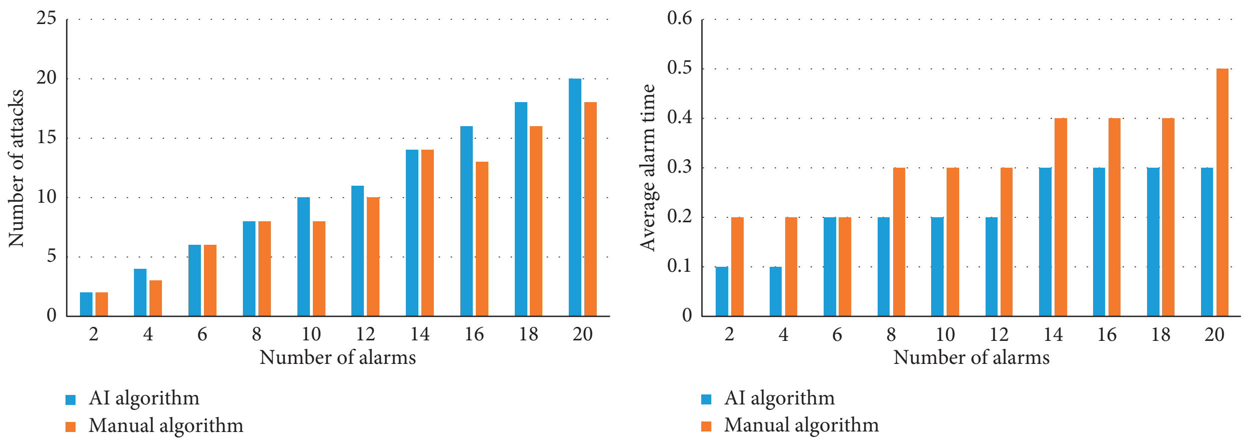

(a) (b)

Figure 7: Number of alarms (a) and average alarm time (b) with the same vehicle number.

Table 1: Generator information.

	P_{min}/MW	P_{max}/MW	a/yuan	b/yuan ∗ MW−1	c/yuan ∗ MW−2
G1	20	160	450	28	15
G2	10	130	330	20	25
DG1	0	45	450	23	15
DG2	0	30	360	29	20
DG3	0	45	360	17	15

Table 2: Optimal generating.

Time	DG1/MW	DG2/MW	DG3/MW	G1/MW	G2/MW
1	25.6	29.8	31.2	42.1	34.5
2	24.1	29.1	30.8	40.2	33.2
3	23.3	29.5	29.5	40.3	32.4
4	22.7	29.9	29.6	37.4	33.5
5	22.4	30.2	28.3	37.1	30.7
6	23.8	30.0	28.2	38.7	32.3
7	23.5	30.0	28.6	36.9	30.8
8	24.3	30.3	27.7	40.2	32.5
9	23.4	28.9	29.8	38.5	31.1
10	20.1	29.1	28.5	33.1	27.8

Table 2: Continued.

Time	DG1/MW	DG2/MW	DG3/MW	G1/MW	G2/MW
11	25.8	29.0	24.1	41.4	34.3
12	29.1	28.7	30.1	41.8	38.9
13	30.1	30.1	35.5	47.5	44.8
14	20.8	30.2	36.4	51.5	37.9
15	31.1	30.2	35.3	45.2	39.8
16	20.9	30.1	26.5	44.3	38.1
17	23.8	29.7	29.3	50.9	45.8
18	30.1	29.8	28.5	57.4	39.2
19	30.4	30.2	36.3	50.3	40.2
20	29.6	30.2	40.5	43.6	45.6
21	30.1	30.0	37.8	45.3	40.1
22	30.8	29.8	37.5	49.6	40.3
23	30.1	30.0	35.2	39.3	39.8
24	23.5	30.1	29.0	40.1	35.6

Table 3: Branch information.

Branch number	Outflow node	Injection node	Current limit/MW
1	1	3	60
2	1	10	60
3	2	21	80
4	3	26	70
5	4	25	65
6	5	26	65
7	3	34	65
8	11	30	65
9	12	31	65
10	16	35	65
11	2	22	70
12	6	21	70
13	6	20	70
14	7	9	70
15	9	8	70
16	13	6	70
17	15	2	70
18	19	1	60
19	23	23	60
20	22	28	60
21	28	27	60
22	26	31	80
23	26	31	80
24	29	34	75
25	34	35	75
26	33	25	65
27	36	22	65
28	30	10	65
29	16	9	65
30	18	9	65
31	11	7	60
32	34	5	60
33	30	2	60
34	31	17	60
35	29	15	60
36	28	11	60

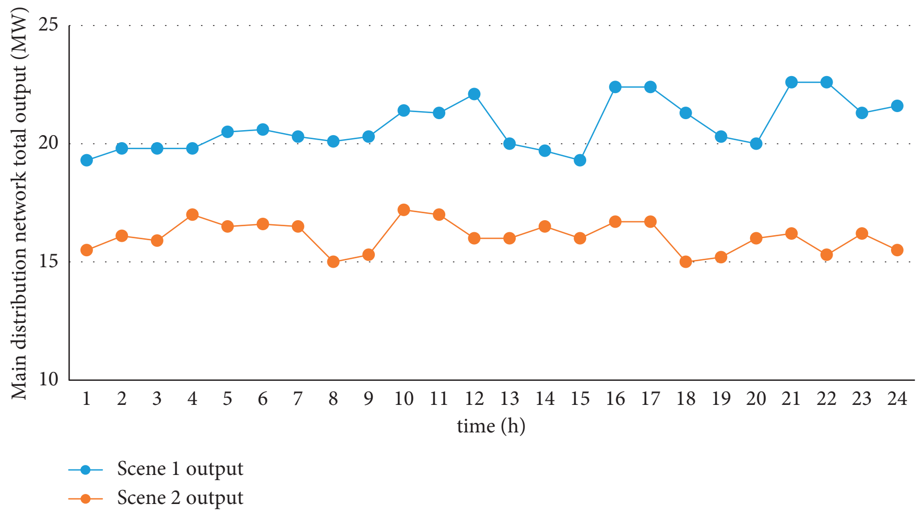

Figure 8: Sum generating of distribution and transmission grid.

5. Conclusion

In view of the fact that the current electric vehicle dispatching is mostly manual dispatching and its efficiency is low, we investigate how to improve the applicability and scientific problem of electric vehicle charging in the existing distributed grid layout. Based on blockchain and 5G technologies, the proposed intelligent vehicle dispatching model realizes the simplified calculation of the layout of the traditional distributed power grid. It uses smart contracts to build data storage and consensus systems to ensure that all historical data are not tampered with and is traceable. It forms the electricity price guidance model in the electric vehicle intelligent dispatching and access, optimizes the multivehicle line blocking in the operation, and dynamically adjusts the model scheduling. It has achieved good results in application, such as optimizing charging running time, saving power, and controlling cost. The simulation and actual test show that the model is feasible and correct. Compared with the traditional scheduling algorithm, the proposed intelligent vehicle dispatching model realizes the dynamic adjustment and correction and better optimizes the distributed power system to make up for the current electric vehicle. The future research will discuss the blockchain in more power nodes and multivehicle collaborative optimization problems.

Data Availability

The datasets used and/or analyzed during the current study are available from the corresponding author on reasonable request.

Conflicts of Interest

The authors declare that they have no conflicts of interest.

Acknowledgments

This work was supported by the Beijing Municipal Commission of Education Project (nos. KM202111417001 and KM201911417001), the National Natural Science Foundation of China (Grant nos. 62102033, 61871039, 62171042, 61906017, and 61802019), the Collaborative Innovation Center for Visual Intelligence (Grant no. CYXC2011), and the Academic Research Projects of Beijing Union University (nos. ZB10202003, ZK40202101, and ZK120202104).

References

[1] K. Kaur, G. Kaddoum, and S. Zeadally, "Blockchain-based cyber-physical security for electrical vehicle aided smart grid ecosystem," *IEEE Transactions on Intelligent Transportation Systems*, vol. 22, no. 8, pp. 5178–5189, 2021.

[2] R. Elshaer and H. Awad, "A taxonomic review of metaheuristic algorithms for solving the vehicle routing problem and its variants," *Computers & Industrial Engineering*, vol. 140, Article ID 106242, 2020.

[3] S. S. Fazeli, S. Venkatachalam, R. B. Chinnam, and A. Murat, "Two-stage stochastic choice modeling approach for electric vehicle charging station network design in urban communities," *IEEE Transactions on Intelligent Transportation Systems*, vol. 22, no. 5, pp. 3038–3053, 2020.

[4] B. Wang, D. Zhao, P. Dehghanian, Y. Tian, and T. Hong, "Aggregated electric vehicle load modeling in large-scale electric power systems," *IEEE Transactions on Industry Applications*, vol. 56, no. 5, pp. 5796–5810, 2020.

[5] I. Makhdoom, I. Zhou, M. Abolhasan, J. Lipman, and W. Ni, "PrivySharing: a blockchain-based framework for privacy-preserving and secure data sharing in smart cities," *Computers & Security*, vol. 88, Article ID 101653, 2020.

[6] G. Kumar, R. Saha, M. K. Rai, R. Thomas, and T.-H. Kim, "Proof-of-Work consensus approach in blockchain technology for cloud and fog computing using maximization-factorization statistics," *IEEE Internet of Things Journal*, vol. 6, no. 4, pp. 6835–6842, 2019.

[7] D. C. Nguyen, P. N. Pathirana, M. Ding, and A. Seneviratne, "Blockchain for 5G and beyond networks: a state of the art survey," *Journal of Network and Computer Applications*, vol. 166, Article ID 102693, 2020.

[8] G. Praveen, V. Chamola, V. Hassija, and N. Kumar, "Blockchain for 5G: a prelude to future telecommunication," *IEEE Network*, vol. 34, no. 6, pp. 106–113, 2020.

[9] C. Rus-Casas, G. Jiménez-Castillo, J. D. Aguilar-Peña, J. I. Fernández-Carrasco, and F. J. Muñoz-Rodríguez, "Development of a prototype for monitoring photovoltaic self-consumption systems," *Electronics*, vol. 9, no. 1, p. 67, 2020.
[10] V. Sharma, "An energy-efficient transaction model for the blockchain-enabled Internet of vehicles (IoV)," *IEEE Communications Letters*, vol. 23, no. 2, pp. 246–249, 2019.
[11] H. Wang, H. Qin, M. Zhao, X. Wei, H. Shen, and W. Susilo, "Blockchain-based fair payment smart contract for public cloud storage auditing," *Information Sciences*, vol. 519, pp. 348–362, 2020.
[12] A. Miglani, N. Kumar, V. Chamola, and S. Zeadally, "Blockchain for Internet of energy management: review, solutions, and challenges," *Computer Communications*, vol. 151, no. 1, pp. 395–418, 2020.
[13] J. Kang, Z. Xiong, D. Niyato, D. Ye, D. I. Kim, and J. Zhao, "Toward secure blockchain-enabled Internet of vehicles: optimizing consensus management using reputation and contract theory," *IEEE Transactions on Vehicular Technology*, vol. 68, no. 3, pp. 2906–2920, 2019.
[14] A. S. Almasoud, F. K. Hussain, and O. K. Hussain, "Smart contracts for blockchain-based reputation systems: a systematic literature review," *Journal of Network and Computer Applications*, vol. 170, Article ID 102814, 2020.
[15] G. Liang, S. R. Weller, F. Luo, J. Zhao, and Z. Y. Dong, "Distributed blockchain-based data protection framework for modern power systems against cyber attacks," *IEEE Transactions on Smart Grid*, vol. 10, no. 3, pp. 3162–3173, 2019.
[16] N. B. Truong, K. Sun, G. M. Lee, and Y. Guo, "GDPR-compliant personal data management: a blockchain-based solution," *IEEE Transactions on Information Forensics and Security*, vol. 15, pp. 1746–1761, 2020.
[17] T. Ding, Z. Zeng, J. Bai, B. Qin, Y. Yang, and M. Shahidehpour, "Optimal electric vehicle charging strategy with markov decision process and reinforcement learning technique," *IEEE Transactions on Industry Applications*, vol. 56, no. 5, pp. 5811–5823, 2020.
[18] Z. Zhou, B. Wang, M. Dong, and K. Ota, "Secure and efficient vehicle-to-grid energy trading in cyber physical systems: integration of blockchain and edge computing," *IEEE Transactions on Systems, Man, and Cybernetics: Systems*, vol. 50, no. 1, pp. 43–57, 2020.
[19] F. Ahmad, M. Khalid, and B. K. Panigrahi, "An enhanced approach to optimally place the solar powered electric vehicle charging station in distribution network," *Journal of Energy Storage*, vol. 42, Article ID 103090, 2021.
[20] L. Yin and S. Li, "Hybrid metaheuristic multi-layer reinforcement learning approach for two-level energy management strategy framework of multi-microgrid systems," *Engineering Applications of Artificial Intelligence*, vol. 104, Article ID 104326, 2021.
[21] U. Bac and M. Erdem, "Optimization of electric vehicle recharge schedule and routing problem with time windows and partial recharge: a comparative study for an urban logistics fleet," *Sustainable Cities and Society*, vol. 70, Article ID 102883, 2021.
[22] B. Zhou, J. Zou, C. Yung Chung et al., "Multi-microgrid energy management systems: architecture, communication, and scheduling strategies," *Journal of Modern Power Systems and Clean Energy*, vol. 9, no. 3, pp. 463–476, 2021.
[23] H. F. Atlam, M. A. Azad, A. G. Alzahrani, and G. Wills, "A review of blockchain in Internet of things and AI," *Big Data and Cognitive Computing*, vol. 4, no. 4, p. 28, 2020.
[24] P. Patil, M. Sangeetha, and V. Bhaskar, "Blockchain for IoT access control, security and privacy: a review," *Wireless Personal Communications*, vol. 117, no. 3, pp. 1815–1834, 2021.
[25] J. H. Chen, M. R. Chen, G. Q. Zeng, and J. S. Weng, "BDFL: a byzantine-fault-tolerance decentralized federated learning method for autonomous vehicle," *IEEE Transactions on Vehicular Technology*, vol. 70, no. 9, pp. 8639–8652, 2021.
[26] A. Yazdinejad, R. M. Parizi, A. Dehghantanha, Q. Zhang, and K.-K. R. Choo, "An energy-efficient SDN controller architecture for IoT networks with blockchain-based security," *IEEE Transactions on Services Computing*, vol. 13, no. 4, pp. 625–638, 2020.
[27] K. Yu, L. Tan, M. Aloqaily, H. Yang, and Y. Jararweh, "Blockchain-Enhanced data sharing with traceable and direct revocation in IIoT," *IEEE transactions on industrial informatics*, vol. 17, no. 11, pp. 7669–7678, 2021.

Hindawi
Scientific Programming
Volume 2021, Article ID 8946885, 8 pages
https://doi.org/10.1155/2021/8946885

Research Article

Two-Stage Channel Adaptive Algorithm for Unmanned Aerial Vehicles Localization with Cellular Networks

Chenxi Zeng,[1,2] **Zhongliang Deng**,[1] **Jiyang Ma**,[2] **and Shengsong Yang**[3]

[1]*Beijing University of Posts and Telecommunications, Beijing, China*
[2]*China Academy of Information and Communication Technology, Beijing, China*
[3]*University of Science and Technology Beijing, Beijing, China*

Correspondence should be addressed to Chenxi Zeng; 810920991@qq.com

Received 18 August 2021; Revised 17 October 2021; Accepted 25 October 2021; Published 8 November 2021

Academic Editor: Punit Gupta

Unmanned aerial vehicle (UAV) is regarded as a powerful tool to expand the existing ground wireless network into aerial space. Since high mobility is an essential characteristic for UAV, it is important to carry out an accurate, real-time, and high-precision localization in terms of safe operation and communication link maintenance. The cellular network-based localization technology has provided UAV a solution with both high coverage and seamless connection. However, the complex channel environment between the UAV and terrestrial base station (BS) would have weakened the localization performance. To solve this problem, a two-stage channel adaptive algorithm for cellular-connected UAV has been proposed. The first stage of the algorithm is to revise the observation error introduced by the complex channel environment using the model of DDPG. The second stage is to locate the UAV position with TDOA algorithm using the revised observation values. Simulation results have demonstrated that the proposed algorithm can achieve the channel adaptive effect by revising the observation errors and improve location performance greatly, especially for UAVs at a relative lower altitude.

1. Introduction

With the large-scale deployment and application of the fifth generation (5G) cellular system, researchers start to focus their studies on the sixth generation (6G) mobile communication network. Compared with 5G, the most impressive improvement of 6G network is the ability to provide an intelligent, seamless, and three-dimensional (3D) aerial access network connectivity with a data rate of several terabits per second (TBPs) and ultralow delay of sub-millisecond [1]. In order to fulfill the innovative objective in wireless communications for the coming 6G communication systems and provide an on-demand connectivity from the sky, new subjects such as satellites, high- and low-altitude platforms, drones, aircrafts, and airships are being included to take the role as aerial base stations. Among them, the unmanned aerial vehicles (UAVs) have been regarded as a powerful tool to expand the existing 5G wireless network into the aerial access network with its flexible on-demand deployment capability [2].

Since high mobility is an essential characteristic for UAVs, it is very important to carry out an accurate, real-time, and high-precision localization in terms of the safe operation and communication link maintenance. According to [3], GNSS (Global Navigation Satellite System), INS (Inertial Navigation System), and visual-based navigation are three technologies used by UAV localization. GNSS is the most widely used one for its global coverage; however the satellite signal is sensitive to obstacles and blockings, leading to accuracy drops in complex environments like city centers. INS does not rely on the satellite signal, but the relatively high cost of equipment makes it not suitable for small aircraft, and the accumulated offset error over time due to integral drift is an unsettled problem [4]. Visual-based localization depends on weather conditions; low visibility environments like dusty or smoking can damage the visual signal seriously, causing significant declines of accuracy [5]. Furthermore, visual-based localization demands large amount of image processing, which requires high computing capability and increases the system complexity.

As the rise of 6G, the aerial-terrestrial integration network has provided an alternative for UAV localization, namely, the cellular-connected UAVs localization solution [6–8]. 6G aerial network can provide cellular connectivity with ubiquitous accessibility for UAVs and not restricted by satellite signal attenuation and visual signal damage. Cellular-connected UAV can also be a research model of user experience for the high-altitude network as well to help improving the service quality of the aerial network [7, 9]. Furthermore, the existing wireless communication technologies such as massive MIMO and millimeter wave communication can also be exploited for UAV localization.

From 1G to 5G, various localization technologies have been designed and implemented [10]. Network topology information and radio signal from wireless network are the main information source for mobile network localization. According to the implementation principle, the location algorithm can be divided into five categories: proximity, angle of arrival (AOA), received signal strength (RSS), time of arrival (TOA)/time difference of arrival (TDOA), and hybrid method [11]. Among them, the proximity method depends on the density of the network transmitter, leading higher cost of the positioning equipment [12]; AOA is easily affected by the external environment, and the need of additional hardware makes it not suitable for the large-scale sensor networks respect to the hardware size and power consumption [13]; the RSS method shows good characteristics in the experimental environment, but its low robustness of the environment temperature, humidity, and propagation mode makes it difficult to implement in the practical world [14]; TOA-based positioning also has a relatively good performance on location accuracy, but it requires accurate time synchronization among all the nodes, which is very difficult to implement and requires a high cost [15]; TDOA is widely implemented in the current mobile network positioning technology, not only for it retains the advantages of TOA's small ranging error, but also for its no need of the strict time synchronization between nodes [16].

Related research like drone detection and tracking using technologies mentioned above has achieved positive results. In [17], authors have designed a system in order to detect the unlicensed small-sized drones in 5G mm wave cellular networks. Schloemann et al. [18] have investigated the application of cellular networks for localization of terrestrial mobile terminals with the theory of stochastic geometry. However, those studies have not considered the complex aerial environment UAV works in; the new emerging aerial users (such as cellular-connected UAVs) would have introduced much more complexity to the existing location model as well.

Generally, factors such as the three-dimensional mobility of UAVs, altitude-dependent channel characteristics (between BSs and UAVs), line of sight (LOS)/nonline of sight (NLOS) conditions, and the interference from the neighboring BSs contribute to the complex aerial environment. It is quite difficult to achieve a satisfied result by adjusting only one factor at a time for the coexistence and cooperation among parameters [19]. One creative way to solve this is to observe the problem from a global view instead of regional parts, oriented by factors affecting the localization performance other than reasons complicated UAV working environment. According to [18, 20], localization performance depends on three factors no matter which technology was used. These factors are as follows: number of participating BSs, accuracy of original observations, and relative distance between surrounding BSs and the target device. Among them, location observation is the only option with enough flexibility to be optimized; number of participating BSs and relative distance between BSs and the target device are related to the infrastructures which are relatively difficult to be modified.

To improve the quality of location observations from a global view, reinforcement learning (RF) is introduced to compensate the errors. RF is a machine learning algorithm trained by unlabelled data similar to the semisupervised learning. Since the dynamic aerial model is difficult to describe and the action of TDOA is a continuous behaviour, model-free policy optimization methods are good options under these circumstances. Policy optimization methods can solve problems of continuous behaviour space with controllable computational complexity using a dual neural network (actor-critical network). Gradient algorithm (VPG) [21], trust region policy optimization (TRPO) [22], proximity policy optimization (PPO) [23], and deep deterministic policy gradient (DDPG) [24] are typical policy algorithms. In [25], Zhang et al. used the PPO algorithm to correct the NLOS measurement error in AOA location and achieved good results. However, PPO uses online strategy which cannot take efficient usage of the historical data and increases the cost of training set. However, DDPG has skilfully combined the advantage of Q learning and policy algorithm by using experience playback and a duel-double network. That means DDPG can solve the problem of continuous action space and improve data utilization rate of TDOA at the same time.

In this paper, a channel adaptive algorithm for UAV localization by optimizing the location observations based on DDPG has been proposed. The proposed algorithm has included two stages: firstly, revise the location observations error introduced by the complex aerial channel environment by studying the historical data using DDPG model; secondly, calculate the location of target UAV using the TDOA algorithm. Since the observation values are revised by the learning model of the whole channel environment instead of each single variable, the complexity of the algorithm can be reduced while the location performance increased.

The organization of the paper is as follows: the channel propagation model of aerial environment UAV works in has been analysed in Section 2. The introduction of basic idea in DDPG, observation revised model, and TDOA procedure analysis have been constructed in Section 3. Simulation results have been illustrated in Section 4. Section 5 has concluded the whole paper and the future work plans.

2. Channel Model

Due to the complexity of the aerial wireless channel communication environment, the location observation value will be interfered by many factors such as three-dimensional mobility of UAVs, altitude-dependent channel characteristics between base stations (BSs) and UAVs, LOS/NLOS conditions, and interference from neighboring BSs, who will lead certain deviations to the final location accuracy. In this section, the wireless transmission channel model of location observation and the mathematical expression of error would be illustrated.

Assume that there are M transmitting antennas at the base station, N receiving antennas in the mobile receiving terminal, one wireless propagation path between the transmitting and receiving points. Then the signal received by the receiving antenna at time t can be expressed as follows [26, 27]:

$$y_j = \sum_{i=1}^{M} x_i(t) h_{i,j}^{l}(t) + n_{i,j}(t), \tag{1}$$

where $x_i(t)$ is the transmitted signal, y_j is the received signal, $h_{i,j}^{l}(t)$ is the channel model between transmitting antenna i and receiving antenna j at time t, and $n_{i,j}(t)$ is the noise.

Assume t_0 is the time delay caused by multipath propagation, so that each multipath subchannel model of MIMO system can be defined as

$$h_{i,j}^{l}(\tau - t) = h_{i,j}^{l}(t)\delta(\tau - t_0). \tag{2}$$

The propagation delay is usually caused by the signal reflection, refraction, and scattering introduced by the NLOS condition in the environment. Therefore, the observation values used in the location algorithm as input of the second stage will introduce certain errors to the location system. The mathematical expression of the error is shown as follows:

$$\alpha_{i,j} = \alpha_{0,i,j} + \alpha_{n,i,j} + \alpha_{e,i,j}, \tag{3}$$

where $\alpha_{0,i,j}$ is the location observation value in the ideal environment, $\alpha_{n,i,j}$ is the channel error caused by NLOS, $\alpha_{e,i,j}$ is the measurement error introduced by the complex environment, i is the number of transmitting antennas, and j is the number of receiving antennas. Our goal is to minimize the sum of $\alpha_{n,i,j}$ and $\alpha_{e,i,j}$ so that the value $\alpha_{i,j}$ is as close to $\alpha_{0,i,j}$ as possible.

3. Channel Adaptive Algorithm

3.1. Deep Deterministic Policy Gradient. DDPG is a combination of Q learning and policy gradient. There are four networks in DDPG, namely, the critic, actor, target critic, and target actor network. The critic network responses for the Q function updates using the loss function similar as DQN (deep Q network) [28], except that the action is calculated separately by the actor network. This operation makes DDPG possible to deal with complex and continuous actions. The actor network calculates an action result with the highest Q value according to the policy gradient used in DPG (deterministic policy gradient) [29]. It is deterministic since DDPG does not calculate the probability of every possible action but outputs only one deterministic action.

Since in many cases (for example, our localization scenery), targets keep changing while update values are calculated, which would lead in difficulties for update. Similar as DDQN (deep reinforcement learning with double Q learning) [30], DDPG has implicated the fix network technology to fix the target network before assigning the new parameters. The parameter assignment of the target network has taken usage of a soft update instead of the hard one to assure the stability of learning.

In order to avoid the correlation of samples and different feature unit, DDPG has introduced the replay buffer and batch normalization mechanism. The replay buffer stores a finite set of state, action, and reward pair.The actor and critic network take samples from the replay buffer to calculate the target at each time step. When the buffer is full, the oldest set would be discarded, leaving room for the new comings.

The core of the channel adaptive algorithm proposed here is to revise the location observation with the help of the DDPG model. Since the observation value is time-changing and needs a continuous revised action, it is quite suitable for taking use of DDPG. Once the observations are revised, the UAV location will be calculated using the revised observation value by the TDOA algorithm.

3.2. Location Observation Revise Model. Assume $\{N\text{Ideal}_i, i = 1, \ldots, N1\}$ are samples of $N1$ observation values under the real channel environment and $\{\text{Ideal}_i, i = 1, \ldots, N2\}$ are samples of $N2$ observation values under ideal channel environment. According to formula (3), the relationship is as follows:

$$N\text{Ideal}_i = \text{Ideal}_i + \alpha_{n,i} + \alpha_{e.i}. \tag{4}$$

Let $S = \{N\text{Ideal}_i, i = 1, \ldots, N1\}$ and $T = \{T\text{Ideal}_i, i = 1, \ldots, N2\}$; denote S as the initial state of the revise model and T as the training target. According to the DDPG algorithm, there are four networks in the system. During the initialization process, four networks and their caches would be assigned initialized values. The initialization process is as follows:

(i) Initialize the critic network $Q(s, a|\theta^Q)$ and actor network $\mu(s|\vartheta^\mu)$ randomly, with s representing the current state of two networks, a representing the action to be executed, θ^Q and θ^μ are network parameters.

(ii) Initialize the target networks Q' and target actor μ' randomly, with network parameters $\theta^{Qi} = \theta^Q$, $\theta^{\mu'} = \theta^\mu$.

(iii) Empty the replay buffer and denote it as R.

After initialization, for $i = 1, \ldots, M$, denote S to be the initial state set and perform the following steps at time $t = 1, \ldots, T$:

(i) Obtain action $a_t = \mu(s_t|\theta^\mu)$ in the policy network at state S,

where μ is a mapping from state to action with function approximators parameterized by θ^μ and s_t is the state action that a_t starts from.

(ii) Execute action a_t and obtain the new state s_{t+1} and reward r_t.

(iii) Store (s_t, a_t, r_t, s_{t+1}) into the replay buffer R.

(iv) Select N groups of variables $B = \{(s_i, a_i, r_i, s_{i+1})\}$ from R randomly and input B into the actor target network and critical target network, respectively.

(v) Calculate the next action a_{t+1} in the actor target network with

$$a_{t+1} = \mu'\left(s_{t+1} \mid \theta^{\mu'}\right), \tag{5}$$

where μ' is the mapping function of state and action at time $t+1$ whose function approximators parameterized by $\theta^{\mu'}$.

(vi) Calculate the target value y_i of Q in the critical target network:

$$y_i = r_i + \gamma Q'\left(s_{i+1}, \mu'\left(s_{i+1} \mid \theta^{\mu'}\right) | \theta^{Q'}\right), \tag{6}$$

where r_i is the reward at time step i, γ is a discounting factor with $\gamma \in [0,1]$, and $Q'(s_{i+1}, \mu'(s_{i+1}|\theta^{\mu'})|\theta^{Q'})$ represents the expected return after taking action a_{i+1} at state s_{i+1}. However, y_i is also dependent on $\theta^{Q\prime}$.

(vii) Calculate the loss function L of Q:

$$L = \frac{1}{N} \sum_i \left(y_i - Q\left(s_i, a_i | \theta^Q\right)\right)^2, \tag{7}$$

where N is the number of sets selected from the replay buffer.

(viii) Update the critical network by minimizing the loss function.

(ix) Update the actor network by the gradient back propagation algorithm of the neural network:

$$\nabla_{\theta^\mu} J \approx \frac{1}{N} \sum_i \nabla_a Q\left(s, a \mid \theta^Q\right)\Big|_{s=s_i, a=\mu(s_i)} \nabla_{\theta^\mu} \mu\left(s \mid \theta^\mu\right)\Big|_{s_i}. \tag{8}$$

This is the policy gradient calculation model, and the derivation process can be found in [27].

(x) Update critical target network parameters and actor target network parameters:

$$\begin{aligned} \theta^{Q'} &\longleftarrow \tau\theta^Q + (1-\tau)\theta^{Q'}, \\ \theta^{\mu'} &\longleftarrow \tau\theta^\mu + (1-\tau)\theta^{\mu'}, \end{aligned} \tag{9}$$

where τ is the soft update parameter with value of $\tau \in [0,1]$.

(xi) Complete the current iteration if s_{t+1} is the termination state, otherwise return the first step.

Figure 1 has illustrated the training process of the observation data using DDPG. In our model, action a_t is a continuous value that can make the location observation samples as close as the samples in the ideal environment. The

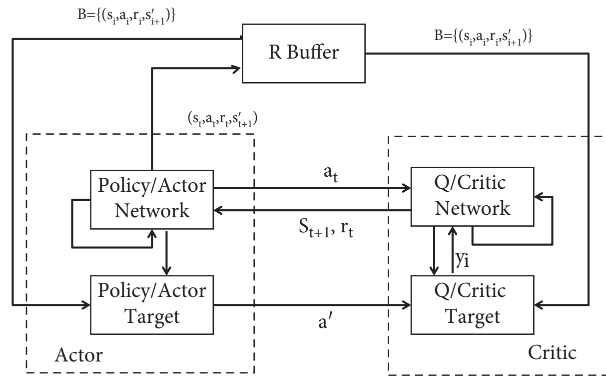

Figure 1: The training process of DDPG.

reward information r_t represents the quality of the location observation value of DDPG model, and the policy would adopt corresponding correction actions according to r_t, in order to maximize the reward value.

Since the concept of "Replay Buffer" is quoted in this paper, the data of the previous policy can be used for each training episode instead of only the current cycle, which would reduce the training data scale and improve the data utilization efficiency.

3.3. UAV Location with TDOA. In the location system of TDOA, once the observation value is determined, the distance between UAV and base station can be calculated. Several observation values could constitute a set of hyperbolic equations about the terminal position of the target, and the estimated position would be obtained by solving those equations.

Assume there are N base stations distributed in the three-dimensional (3D) space, the coordinate of the i-th base station is (x_i, y_i, z_i), the location of target UAV is (x, y, z), and the distance between target UAV and the i-th BS is R_i, where $i = 1, 2, 3, \ldots, M$. Then we got

$$R_i = \sqrt{(x-x_i)^2 + (y-y_i)^2 + (z-z_i)^2}. \tag{10}$$

Denote signal from BS1 as signal 1, and mark it as the reference signal. Record the time difference between signal i $(i \in m)$ and signal 1 as t_{i1} and the distance as R_{i1}; then

$$\begin{aligned} t_{i1} &= t_i - t_1, \\ R_{i1} &= c * t_{i1} \\ &= c\left(t_i - t_1\right) \\ &= R_i - R_1, \end{aligned} \tag{11}$$

where c is the propagation velocity of electromagnetic wave. After transposition, we got

$$\begin{aligned} R_i^2 - R_1^2 = {} & (x-x_i)^2 + (y-y_i)^2 + (z-z_i)^2 \\ & - (x-x_1)^2 - (y-y_1)^2 - (z-z_1)^2. \end{aligned} \tag{12}$$

After calculation, equation (12) can be presented as

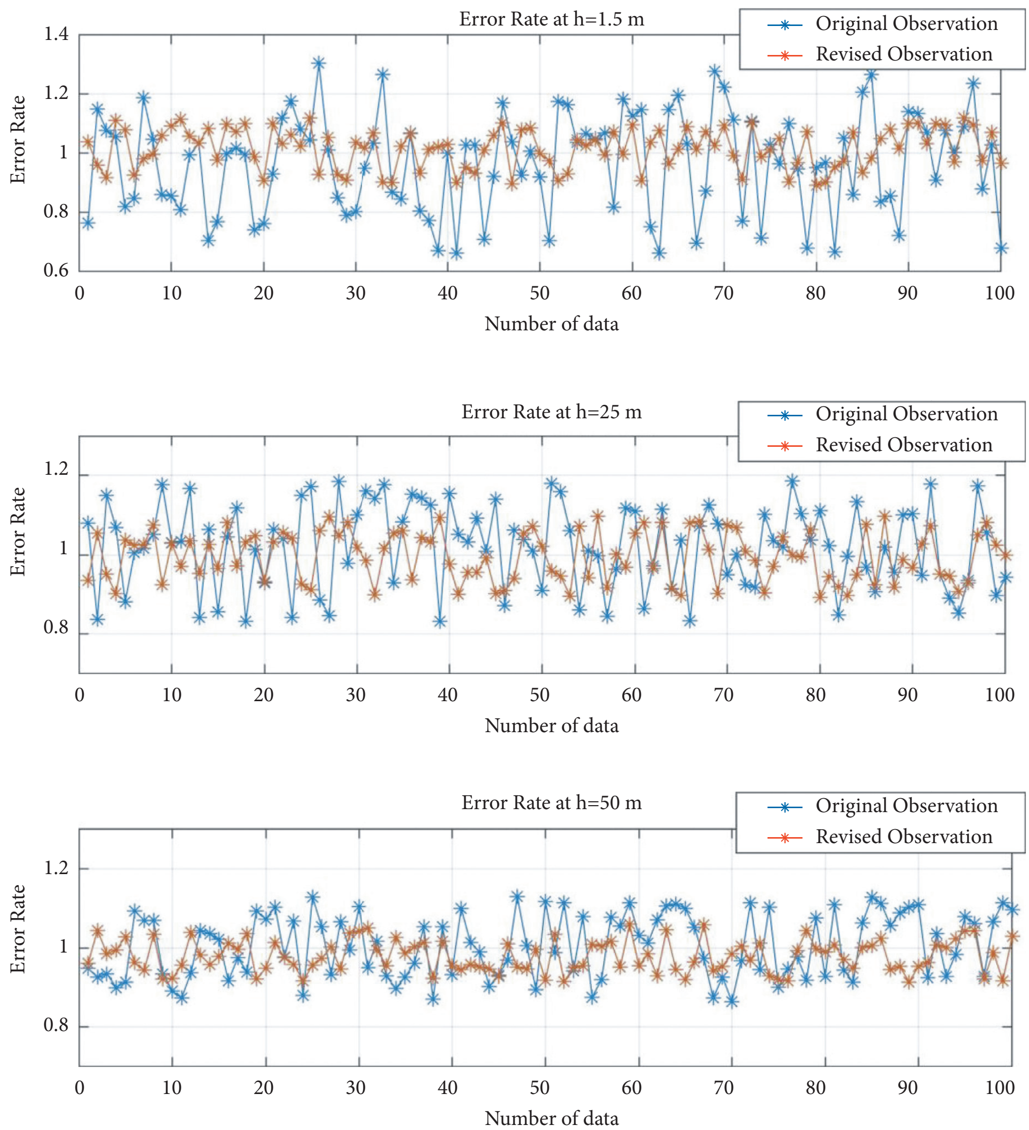

FIGURE 2: Error rates of the observation value before and after using the revised model at different UE altitude.

$$2(x_1 - x_i)x + 2(y_1 - y_i)y + 2(z_1 - z_i)z + \left(x_i^2 + y_i^2 + z_i^2\right) - \left(x_1^2 + y_1^2 + z_1^2\right). \tag{13}$$

Here, we denote

$$\begin{aligned} K_i &= x_i^2 + y_i^2 + z_i^2, \\ X_{i,1} &= x_1 - x_i, \\ Y_{i,1} &= y_1 - y_i, \\ Z_{i,1} &= z_1 - z_i. \end{aligned} \tag{14}$$

After simplification, we got

$$R_i^2 - R_1^2 = 2\left(X_{i,1} \quad Y_{i,1} \quad Z_{i,1}\right)\begin{pmatrix} x \\ y \\ z \end{pmatrix} + K_i - K_1. \tag{15}$$

When there are four base stations participating in the localization process successfully, at least three TDOA observations can be obtained. Assume R_1 is known, and the location of UAV can be calculated as

$$\begin{pmatrix} x \\ y \\ z \end{pmatrix} = -\begin{pmatrix} X_{2,1} & Y_{2,1} & Z_{2,1} \\ X_{3,1} & Y_{3,1} & Z_{3,1} \\ X_{4,1} & Y_{4,1} & Z_{4,1} \end{pmatrix} * \left[\begin{pmatrix} R_{2,1} \\ R_{3,1} \\ R_{4,1} \end{pmatrix} R_1 + \frac{1}{2}\begin{pmatrix} R_{2,1}^2 - K_2 - K_1 \\ R_{3,1}^2 - K_3 - K_1 \\ R_{4,1}^2 - K_4 - K_1 \end{pmatrix}\right]. \tag{16}$$

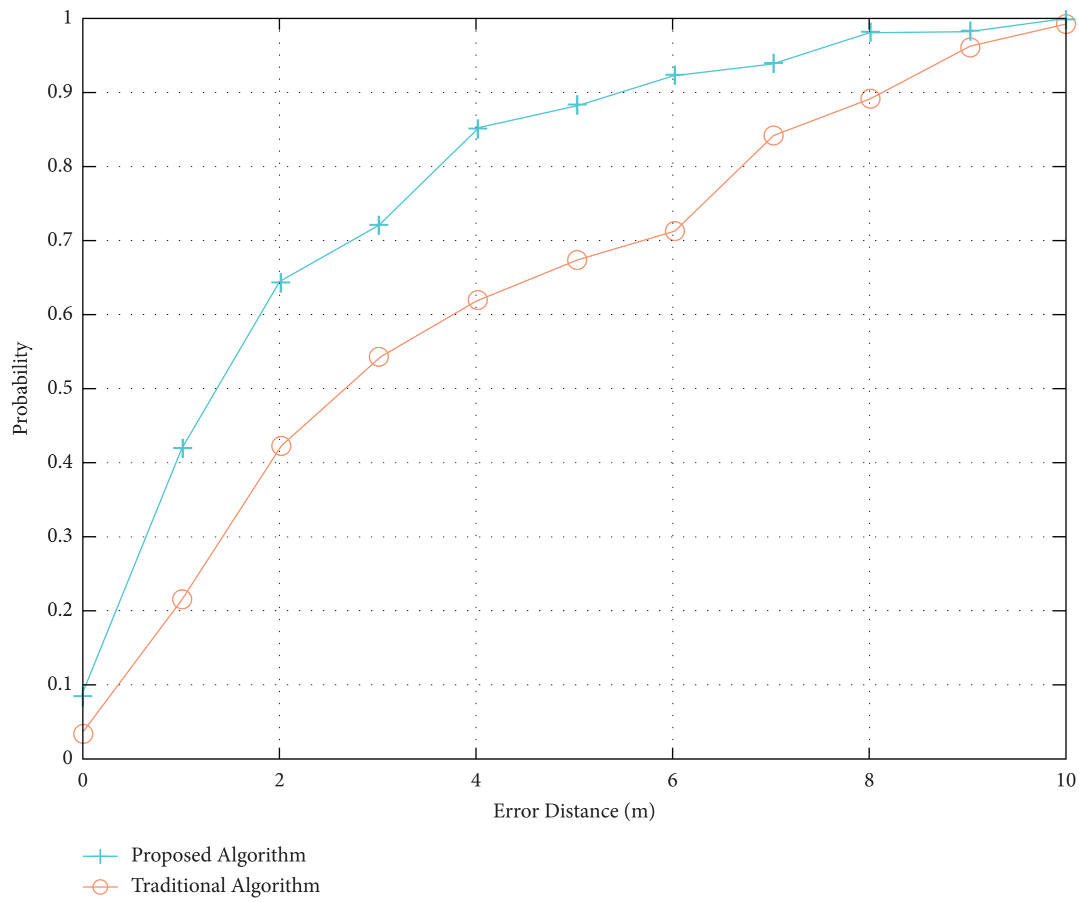

Figure 3: The cumulative distribution error of location accuracy of the proposed algorithm and traditionalTDOA.

This is the specific location information of the UAV to be measured. It can be seen that to localize an UAV with TDOA algorithm, at least four base stations are required to participate the localization. For simplification, we discussed only the four base stations case in this paper.

4. Simulation Results

4.1. Simulation Parameters. The 3GPP research project has studied three cellular-connected UAV scenarios, namely, urban-macro with aerial vehicles (UMa-AV), urban-micro with aerial vehicles (UMi-AV), and rural-macro with aerial vehicles (RMa-AV) [7]. The eNodeB antennas mounted above the rooftop levels of surrounding buildings in urban environment are UMa-AV scenarios. UMi-AV represents scenarios where eNodeB antennas are mounted below rooftop. eNodeB antennas mounted on top of towers of larger cells in rural environment are represented by RMa-AV [31]. In our simulation study, the 3GPP channel model of UMa-AV scenario for UAVs is considered.

The simulation environment is set by assuming the intersite distances of 500 m, and the height of BS is 25m [4]. The channel being used is with bandwidth of 10 MHz and the carrier frequency (fc) of 2 GHz. Variance of the shadowing is modelled as 4.64exp (−0.0066hUT) and 6 dB for LOS and NLOS conditions, respectively [4]. The transmitted power is taken as 46 dBm and the noise figure of the UAV as 9 dB.

4.2. Numerical Results. Since our proposed algorithm is a two-staged process, there are two parts of numerical results demonstrated in this section, that is, the observation revised results and the final UAV location accuracy analysis.

Before setting the error revised model, it is necessary to collect a set of reference data under the ideal environment to help training and evaluating the revised effect. Define error ratio as the ratio between observation value and the reference data. An error ratio of 1 indicates that the observed data are exactly the same as the reference data.That is, the closer the error ratio is to 1, the better the correction effect will be.

Figure 2 shows the error ratio of observation data of TDOA before and after using the revised model as the UAV working at different altitudes. It is obvious that the revised observations have smaller amplitude than the original ones, which means their error rates are better. This advantage becomes more pronounced when the UAV (UE) stays at a relatively lower altitude. This phenomenon is consistent with the probabilistic simulation results of LOS at different UE heights. The references [7, 20] have shown the same result.

For the location stage, the cumulative distribution of positioning error is used to measure the final location accuracy. The cumulative error of positioning accuracy represents the cumulative probability value of positioning results within a specific range. Within the same distance range, the higher the cumulative probability value is, the better the positioning accuracy is.

Figure 3 shows the cumulative distribution error of location accuracy obtained by the TDOA algorithm before and after optimization. The UAV's altitude (hUE) was set to 25 m here. It can be seen that the proposed algorithm has a probability of 64.4% that the location accuracy is within 2 m, and the probability of positioning error within 4m is 85.4%; compared with the results of using the original TDOA algorithm, the positioning accuracy within 2 m has been improved by 51.9%, and the positioning accuracy within 4m has been improved by 37.7%.

Simulation results shown in this chapter have demonstrated that the proposed algorithm can achieve the channel adaptive effect by revising the observation errors and improving location performance greatly, while the improved effect is especially noticeable for UAVs at a relative lower altitude.

5. Conclusions

In this paper, a two-stage channel adaptive algorithm for cellular-connected UAV has been proposed. The first stage of the algorithm is to revise the observation error introduced by the complex channel environment between UAV and base stations. The second stage is to locate the UAV position with TDOA using the revised observation values. Simulation results have demonstrated that the proposed algorithm can achieve the channel adaptive effect by correcting the observation errors and improving location performance greatly, especially for the UEs at a relatively lower altitude.

The future work would be concentrated on the following aspects: one is to replace the single TDOA algorithm in this paper by the hybrid algorithm composed of TDOA, AOA, or RSS to optimize the location algorithm itself; the second aspect is to introduce the random policy factor represented by the information entropy into the optimization algorithm, in order to improve the randomness of the system and avoid the problem of the local optimal trap. The third aspect is to expand the quality evaluation domain from single location accuracy to a diversified set by introducing other user experience target, leading the model closer to user experience.

Data Availability

Data sharing not applicable to this article as no datasets were generated or analysed during the current study.

Disclosure

The founding sponsors had no role in the design of the study; in the collection, analyses, or interpretation of data; in the writing of the manuscript; or in the decision to publish the results.

Conflicts of Interest

The authors declare no conflicts of interest.

Authors' Contributions

Chenxi Zeng conceived the main idea and the game theory model; all authors contributed to data analysis, simulations, and the writing of this paper.

References

[1] Z. Xiao and Y. Zeng, "An overview on integrated localization and communication towards 6G, signal processing," 2020, https://arxiv.org/abs/2006.01535.

[2] Y. Zeng, Q. Wu, and R. Zhang, "Accessing from the sky: a tutorial on UAV communications for 5G and beyond," *Proceedings of the IEEE*, vol. 107, no. 12, pp. 2327–2375, 2019.

[3] C. S. Y. C. S. Yoo and I. K. A. I. K. Ahn, "Low cost GPS/INS sensor fusion system for UAV navigation," *In IEEE Digital Avionics Systems Conference*, vol. 2, 2003.

[4] A. Nemra and N. Aouf, "Robust INS/GPS sensor fusion for UAV localization using SDRE nonlinear filtering," *IEEE Sensors Journal*, vol. 10, no. 4, pp. 789–798, 2010.

[5] J. P. Queralta, C. M. Almansa, F. Schiano, D. Floreano, and T. Westerlund, "UWB-based system for uav localization in gnssdenied environments: characterization and dataset," 2020, https://arxiv.org/abs/2003.04380.

[6] Y. Zeng, J. Lyu, and R. Zhang, "Cellular-connected UAV: potential, challenges, and promising technologies," *IEEE Wireless Communications*, vol. 26, no. 1, pp. 120–127, 2018.

[7] 3GPP, "Study on enhanced LTE support for aerial vehicles," Technical Report, 3GPP TR, Southwest of Nice, France, 2017.

[8] A. Azari, F. Ghavimi, M. Ozger, R. Jantti, and C. Cavdar, "Machine learning assisted handover and resource management for cellular connected drones," in *Proceedings of the 2020 IEEE 91st Vehicular Technology Conference (VTC2020-Spring)*, pp. 1–7, Antwerp, Begium, May 2020.

[9] M. M. Azari, F. Rosas, A. Chiumento, and S. Pollin, "Coexistence of terrestrial and aerial users in cellular networks," in *Proceedings of the 2017 IEEE Globecom Workshops (GC Wkshps)*, pp. 1–6, Singapore, December 2017.

[10] J. A. D. P. Rosado, R. Raulefs, J. A. L. O. Salcedo, and G. S. Granados, "Survey of cellular mobile radio localization methods: from 1G to 5G," *IEEE Communications Surveys & Tutorials*, vol. 20, no. 2, pp. 1124–1148, 2017.

[11] B. Brown and M. Aaron, "The politics of nature," in *The Rise of Modern Genomics*, J. Smith, Ed., Wiley, NY, USA, 3rd edition, 2001.

[12] C. Laoudias, A. Moreira, S. Kim, S. Lee, L. Wirola, and F. Carlo, "A. survey of enabling technologies for networklocalization, tracking, and navigation," *IEEE Communications Surveys & Tutorials*, vol. 20, no. 4, 2018.

[13] K. Doğançay and H. Hmam, "Optimal angular sensor separation for AOA localization," *Signal Processing*, vol. 88, pp. 1248–1260, 2008.

[14] Z. li, Z. Deng, F. Yang, and A. Hu, "The effect of temperature and humidity on finger print positioning," in *Proceedings of the China Satellite Navigation Conference, CSNC*, Harbin, China, 2018.

[15] J. S. Junyang, A. F. Molisch, and J. Salmi, "Accurate passive location estimation using TOA measurements," *IEEE Transactions on Wireless Communications*, vol. 11, no. 6, pp. 2182–2192, 2012.

[16] A. Dersan and Y. Tanik, "Passive radar localization by time di_ erence of arrival," in *Proceedings of the IEEEMilitary Communications Conference MILCOM*, vol. 2, pp. 1251–1257, IEEE, Anaheim, CA, USA, October 2002.
[17] D. Solomitckii, M. Gapeyenko, V. Semkin, S. Andreev, and Y. Koucheryavy, "Technologies for efficient amateur drone detection in 5G millimeter-wave cellular infrastructure," *IEEE Communications Magazine*, vol. 56, no. 1, pp. 43–50, 2018.
[18] J. Schloemann, H. S. Dhillon, and R. M. Buehrer, "Toward a tractable analysis of localization fundamentals in cellular networks," *IEEE Transactions on Wireless Communications*, vol. 15, no. 3, pp. 1768–1782, 2015.
[19] I. A. Meer, M. Ozger, and C. Cavdar, "On the localization of unmanned aerial vehicles with cellular networks," 2020, https://arxiv.org/abs/2003.04889.
[20] J. Schloemann, H. S. Dhillon, and R. M. Buehrer, "Localization performance in cellular networks," in *Proceedings of the IEEE International Conference on Communication Workshop (ICCW)*, pp. 871–876, London, UK, June 2015.
[21] R. Sutten, D. M. Allen, S. Singh, and Y. Mansour, "Policy gradient methods for reinforcement learning with function approximation, 2000-02," *Advances in Neural Information Processing Systems*, vol. 12, 2020.
[22] J. Schulman, S. Levine, P. Moritz, M. I. Jordan, and P. Abbeel, "Trust region policy optimization," 2017, https://arxiv.org/abs/1502.05477.
[23] J. Schulman, F. Wolski, P. Dhariwal, A. Radford, and O. Klimov, "Proximal policy optimization algorithms," https://arxiv.org/abs/1707.06347.
[24] T. P. Lillicrap, J. J. Hunt, A. Pritzel et al., "Continuous control with deep reinforcement learning," 2019.
[25] Y. Zhang, Z. Deng, and Y. Gao, "Angle of Arrival Passive Location Algorithm Based onProximal Policy Optimization," *Electronic*, vol. 8, no. 12, 2019.
[26] K. Lee, J. Oh, and K. You, "TDOA/AOA based geolocation using Newton method under NLOS environment," in *Proceedings of the 2016 IEEE International Conference on Cloud Computing and Big Data Analysis (ICCCBDA)*, pp. 373–377, ChengDu, China, July 2016.
[27] N. Aghaie and M. A. Tinati, "Localization of WSN nodes based on NLOS identification using AOAs statistical information," in *Proceedings of the 2016 24th Iranian Conference on Electrical Engineering (ICEE)*, pp. 496–501, Shiraz,Iran, May 2016.
[28] V. Mnih, K. Kavukcuoglu, D. Silver et al., "Human-level control through deep reinforcement learning," *Nature*, vol. 518, no. 7540, pp. 529–533, 2015.
[29] D. Silver, G. Lever, N. Heess, T. Degris, D. Wierstra, and M. Riedmiller, "Deterministic policy gradient algorithms," in *Proceedings of the 31st International Conference on Machine Learning (ICML 2014)*, Beijing China, June 2014.
[30] H. V. Hasselt, A. Guez, and D. Silver, "Deep reinforcement learning with double q-learning," 2015, https://arxiv.org/abs/1509.06461.
[31] S. D. Muruganathan, X. Lin, H. LiinaMaattanen, W. A. H. ZhenhuaZou, and S. Yasukawa, "An overview of 3gpp release-15 study on enhanced lte support for connected drones. networking and internet architecture (cs.ni)," 2019, https://arxiv.org/abs/1805.00826.

Hindawi
Scientific Programming
Volume 2021, Article ID 2592604, 14 pages
https://doi.org/10.1155/2021/2592604

Research Article

Novel Multidimensional Collaborative Filtering Algorithm Based on Improved Item Rating Prediction

Tongyan Li,[1] **Yingxiang Li**,[1] **and Chen Yi-Ping Phoebe**[2]

[1]*Chengdu University of Information Technology, Department of Communication Engineering, Chengdu 610225, China*
[2]*Department of Computer Science and Information Technology, La Trobe University, Melbourne, VIC 3086, Australia*

Correspondence should be addressed to Tongyan Li; sunny_cs061@163.com

Received 26 August 2021; Accepted 9 October 2021; Published 5 November 2021

Academic Editor: Punit Gupta

Current data has the characteristics of complexity and low information density, which can be called the information sparse data. However, a large amount of data makes it difficult to analyse sparse data with traditional collaborative filtering recommendation algorithms, which may lead to low accuracy. Meanwhile, the complexity of data means that the recommended environment is affected by multiple dimensional factors. In order to solve these problems efficiently, our paper proposes a multidimensional collaborative filtering algorithm based on improved item rating prediction. The algorithm considers a variety of factors that affect user ratings; then, it uses the penalty to account for users' popularity to calculate the degree of similarity between users and cross-iterative bi-clustering for the user scoring matrix to take into account changes in user's preferences and improves on the traditional item rating prediction algorithm, which considers user ratings according to multidimensional factors. In this algorithm, the introduction of systematic error factors based on statistical learning improves the accuracy of rating prediction, and the multidimensional method can solve data sparsity problems, enabling the strongest relevant dimension influencing factors with association rules to be found. The experiment results show that the proposed algorithm has the advantages of smaller recommendation error and higher recommendation accuracy.

1. Introduction

Recommendation algorithms are mainly divided into six categories: content-based filtering, collaborative filtering, recommendation based on association rules, recommendation based on utility, recommendation based on knowledge, and mixed recommendation [1, 2]. Collaborative filtering (CF) algorithms are the most widely used and classic because of their easy implementation, high accuracy, and high recommendation efficiency. However, in the era of big data, one typical feature is that the amount of data is huge but the information density is low, which can also be called information sparse data. Collaborative filtering algorithms are often ineffective when dealing with large amounts of sparse data. Furthermore, the complex data environment results in many factors affecting the recommendation. With the development of the mobile Internet, mobile devices can easily obtain more information about dimensions, such as location, weather, and social relationships. Under different external influences, the recommendation results will change greatly. However, most of the current collaborative filtering algorithms are based on a single dimension for recommendation.

In order to improve the performance of collaborative filtering recommendation algorithms, researchers resolve the problems from different perspectives and propose a variety of recommendation algorithms. Some researchers optimized the user scoring matrix using different methods [3–6], and others used fuzzy sets to efficiently represent user features [7, 8]. These methods all effectively alleviate the problem of sparse data. In order to find a neighbor set that is more similar to the target user's interest and improve the accuracy of recommendations, some researchers improved the similarity calculation method [7, 9, 10], and others used location information and trust relationship information, such as [11, 12]. The potential relationship between information mining users provides new ideas for finding neighbors. Researchers have also used demographic knowledge [13, 14] to achieve major breakthroughs, while some scholars used score ranking prediction methods to enhance recommendation performance such as [15–17], and others chose the genetic algorithm used in the prediction process to improve recommendation performance, such as [18, 19]. Context as a dynamic description of an item and a user's situation affects the user's decision-making process; hence, it is essential for any recommendation system in a big data environment [20–22].

These algorithms alleviate the problems caused by data sparsity to some extent, improve the accuracy of calculation similarity and recommendation quality with different methods, but the implementation of the algorithm depends on a large amount of user information and calculation, which can be due to high complexity and hard implementation.

In this paper, we focus on the recommendation algorithm of data in complex environments. Firstly, we study the traditional item rating prediction algorithm and make some improvements with adding the weight problem considering user score. We introduce the system error factor based on statistical learning for the user to develop a personalized rating prediction algorithm. Then, we propose a personalized rating prediction method that is combined with a classical collaborative filtering algorithm User-Inverse Item Frequency (User-IIF) [23] to develop a novel collaborative filtering algorithm. This method is based on both User-IIF and personalized rating prediction. Secondly, we focus on the impact of multidimensional factors and propose a novel multidimensional method, which can separate user groups based on context-aware dimensions combined with both user clustering and item clustering. Finally, we conduct a series of experiments to prove that our algorithms and methods are effective and efficient. The experiment results prove that our algorithms are easy to implement with low computational overhead. In addition, our algorithms can also process sparse data and improve the accuracy of recommendations.

The rest of the paper is organized as follows. The works related to our research and our novel methods to deal with multidimensional recommendation are proposed in Section 2, and the experiment results and discussion are presented in Section 3. Finally, the conclusion and suggestions for future work are given in Section 4.

2. Methodology

2.1. Proposed Item Rating Prediction Method. Traditional item rating prediction algorithms take the target user's average item historical score as the reference center and then use the similarity between similar neighbors to perform item rating prediction. When user data is sparse, the error rate of traditional item rating prediction algorithms increases and the accuracy rate decreases. This proposed method adds weights to consider user ratings and introduces systematic error factors based on statistical learning to improve traditional item rating prediction algorithms.

2.1.1. User Rating Weighting Factor. Traditional item rating prediction algorithms take the historical average score of the target user as the central value and rely on the neighbor's score to correct it. Traditional algorithms rely too much on the user's score and its anti-interference ability is ineffective when it is faced with data sparseness. For example, when a user has not scored many items, even if the average user score is close to 0, using the user's historical average score as the center value may result in inaccurate recommendation results. The item scoring prediction method proposed in this work considers the factors of public scoring, improves the algorithm using (1), introduces the weighting factor a of the user's score, and assigns the weight of the scoring $(1-\alpha)$ to the scoring of the item.

$$r_{ui} = a \cdot \overline{r_u} + (1-a) \cdot \overline{r_i} + \frac{\sum_{v \in s(u,K) \cap N(i)} \mathrm{sim}_{uv} \left(r_{vi} - \overline{r_v} \right)}{\sum_{v \in s(u,K) \cap N(i)} \left| \mathrm{sim}_{uv} \right|}. \tag{1}$$

2.1.2. Systematic Error Factor Based on Statistical Learning. A large number of studies show that there are errors in item rating prediction, which only a few algorithms have addressed by performing a statistical analysis calculation on each recommendation result. In order to achieve more personalized recommendations, it is necessary to establish a system error factor generated by the recommendation system for each user.

The system error ε_u generated by the recommendation of target user u is calculated by (2), where the actual score of user u on item i is represented as R_{ui}, and r_{ui} describes the predicted rating of user u generated by the system. $N_{I(u)}$ describes the number of items in the itemsets $I(u)$ that target user u adopts from the recommendation results. Through statistical learning, the system sets the error factor for each user, and then this is applied to the collaborative filtering algorithm to correct the item rating prediction, as shown in (3), for a more accurate personalized recommendation algorithm for the target user.

$$\varepsilon_u = \frac{\sum_{i \in I(u)} \left(R_{ui} - r_{ui} \right)}{N_{I(u)}}, \tag{2}$$

$$r_{ui} = a \cdot \overline{r_u} + (1-a) \cdot \overline{r_i} + \frac{\sum_{v \in s(u,K) \cap N(i)} \mathrm{sim}_{uv} \left(r_{vi} - \overline{r_v} \right)}{\sum_{v \in s(u,K) \cap N(i)} \left| \mathrm{sim}_{uv} \right|} + \varepsilon_u. \tag{3}$$

Based on the above calculations, this paper proposes a novel algorithm, namely, improved item-rating prediction (IIP) for user scoring. The main steps of IIP are shown in Figure 1(a). The basic idea is to form a set of error factors for

ALGORITHM 1: IIP (Improved Item-rating Prediction)

```
Input:  (1) R, user rating matrix (R[user][item]=rating);
        (2) U_R, user's average historical rating (U_R[user]=rating);
        (3) I_R, average rating of item (I_R[item]=rating);
        (4) S, user similarity matrix (S[user][sim_user]=sim);
        (5) A, user rating weighting factor (0<A<=1);
Output: P_R, predicted item-rating (P_R[user][item]=rating);

For each user in R do
{ N[user]←Number of items that user like;
  E[user]←The sum of the difference between the predicted rating and the true;
  AVGE[user]←E[user] / N[user];
  Set fz←Ø; fm←Ø;
  For each sim_user, sim in Top-K S[user] do
  { For each item in R[sim_user] do
    { If item not in R[user] then
      { fz.setdefault(item, 0.0); fm.setdefault(item, 0.0);
        fz[item]←fz[item]+sim*(R[sim_user][item])-U_R[sim_user]);
        fm[item]←fm[item]+sim;
      }
    }
  }
  For each item in fm do
    P_R[user][item]←A*U_R[user]+(1-A)*I_R[item]+fz[item]/fm[item]+AVGE[user];
}
```

(a)

ALGORITHM 2: cross-iterative biclustering

```
Input:  (1) U, user set;
        (2) I, item set;
Output: Adjusted cluster;

By K-means clustering method, get the initial user cluster UC ={uc_1, uc_2, ⋯, uc_k} and clustering center UCC ={ucc_1, ucc_2, ⋯, ucc_k}, the initial item cluster IC= {ic_1, ic_2, ⋯, ic_k} and clustering center ICC ={icc_1, icc_2, ⋯, icc_k };
Repeat;
For each user cluster uc_iUC do
{ For each user u_juc_i do
  { Calculat the correlation S_U(u_j, ucc_i) between u_j and clustering center ucc_i;
    If (S_U(u_j, ucc_i) > ε)
      continue;
    else
      Calculate the similarity between u_j and other cluster centers, and add it to the cluster with the most similarity;
  }
}
Recalculate the center of each cluster in UC and update to UCC;
For each item cluster ic_iIC do
{ For each item i_jic_i do
  { Calculat the correlation S_I(i_j, icc_i) between i_j and clustering center icc_i;
    If (S_I(i_j, icc_i) > η)
      continue;
    else
      Calculate the similarity between i_j and other cluster centers, and add it to the cluster with the most similarity;
  }
}
Recalculate the center of each cluster in IC and update to ICC;
Until clusters, the elements in the cluster are no longer separated or reach the set number of iterations.
```

(b)

ALGORITHM 3: Context similarity calculation

```
Input:  (1) I_R, average rating of item (I_R[item]=rating);
        (2) I, user rating and corresponding context information;
        (3) contexts X and Y;
        (4) current context t;
Output: S_xyi, similarity between contexts X and Y;

X_t←Standard deviation of context dimension X;
Y_t←Standard deviation of context dimension Y;
f←Ø;
For each user, item in I do
{ f.setdefault(item, 0.0);
  f←f+(I_xt[user][item]-I_R[item])*(I_yt[user][item]-I_R[item]);
}
S_xyi=f/( X_t* Y_t);
```

(c)

ALGORITHM 4: Multi-dimensional context-aware

```
Input:  (1) user, target user;
        (2) I, user rating and corresponding context information;
        (3) U_R, user's average historical rating (U_R[user]=rating);
        (4) S, user similarity matrix (S[user][sim_user]=sim);
Output: P_R, predicted item-rating (P_R[item]=rating);

For each u, i in I do
  // Apply the context similarity algorithm to calculate S(c,x,t);
  R[u][i] ←
Set fz←Ø; fm←Ø;
For each sim_user, sim in Top-K S[user] do
{ For each item in R[sim_user] do
  { If item not in R[user] then
    { fz.setdefault(item, 0.0); fm.setdefault(item, 0.0);
      fz[item]←fz[item]+sim*(R[sim_user][item])-U_R[sim_user]);
      fm[item]←fm[item]+sim;
    }
  }
}
For each item in fm do
  P_R[item]←U_R[user]+fz[item]/fm[item];
}
```

(d)

Figure 1: Multidimensional collaborative filtering algorithm based on improved item rating prediction. (a) Algorithm 1. (b) Algorithm 2. (c) Algorithm 3. (d) Algorithm 4.

each user through statistical learning, and then apply it to the collaborative filtering algorithm to correct the item rating prediction.

2.2. User Scoring Based on Multidimensional Context

2.2.1. User Similarity Calculation. The first step of our method is to get the user's neighbor cluster, which is obtained through the user's scoring matrix. Users in the user group whose interests are similar to each other can be selected as neighbor users. This paper utilizes Pearson's similarity [24] to measure the distance between users as shown in (4). Pearson's similarity is similar to cosine similarity in form. The average evaluation value of users is subtracted during calculation, which is to normalize the cosine similarity and unify the user's scoring standard. The range of Pearson's similarity is [−1, 1], which is more accurate than that of Jaccard's correlation coefficient and cosine similarity.

$$s_{u,v} = \frac{\sum_{i\in I_u\cap I_v}\left(r_{u,i}-\overline{r_u}\right)\left(r_{v,i}-\overline{r_v}\right)}{\sqrt{\sum_{i\in I_u\cap I_v}\left(r_{u,i}-\overline{r_u}\right)^2\sum_{i\in I_u\cap I_v}\left(r_{v,i}-\overline{r_v}\right)^2}}, \tag{4}$$

where $s_{u,v}$ represents the similarity value between target user a and its neighbor cluster user, I_u represents the set of items that target user u has scored, and I_v indicates the set of products scored by neighbor cluster user v. i represents the item that the target user u and neighbor cluster user v scored together. $r_{u,i}$ indicates the rating of item i by target user u, and $\overline{r_u}$ indicates the average rating of target user u. Following the same principle, $r_{v,i}$ is the score of neighbor cluster user v for item i, and $\overline{r_v}$ indicates the average rating of neighbor cluster user v. The traditional collaborative filtering algorithm uses the above formula to calculate the similarity between users.

A user will have different scoring standards under different contexts, such as the user's rating of a hotel when traveling on business and the rating criteria for a hotel when traveling privately. So after considering the context, it has nothing to do with the previous rating and is replaced by a new symbol, we use $\overline{r_{u,c}}$ instead of $\overline{r_u}$ and $\overline{r_{v,c}}$ instead of $\overline{r_v}$, where $\overline{r_{u,c}}$ represents the average rating of user u under context condition c. The range of c can be appropriately generalized or filtered as needed. The proposed improved method can be described as follows:

$$s_{u,v,c} = \frac{\sum_{i\in I_u\cap I_v}\left(r_{u,i}-\overline{r_{u,c}}\right)\left(r_{v,i}-\overline{r_{v,c}}\right)}{\sqrt{\sum_{i\in I_u\cap I_v}\left(r_{u,i}-\overline{r_{u,c}}\right)^2\sum_{i\in I_u\cap I_v}\left(r_{v,i}-\overline{r_{v,c}}\right)^2}}. \tag{5}$$

The improved user neighbor cluster similarity calculation formula takes into account the influence of context factors on the basic rating, making the calculation formula closer to the context recommendation environment. After considering the context, the user's similarity calculation (4) is improved to (5), and the influence of the context on the user's rating is taken into account when using the mean calibration error of the score.

2.2.2. User and Item Cross-Iterative Bi-Clustering. The cross-iterative bi-clustering method is used for cluster users and items separately. Due to the sparsity of the user-item matrix, the initial clustering is not accurate enough. Therefore, we use the cross-iterative method to adjust both user clustering and item clustering.

User clustering adjustment is calculated by (6), and item clustering adjustment is calculated by (7)

$$S_U(u_t,u_c) = \begin{cases} 1, & u_t = u_c, \\ \dfrac{1}{\sum_{k=1}^{n} r_{tk}\sum_{k=1}^{n} r_{ck}} \displaystyle\sum_{i_i\in I(u_t,u_c)}\ \sum_{i_j\in I(u_t,u_c)} \mathrm{sim}\left(i_i,i_j\right), & \text{else}, \end{cases} \tag{6}$$

where r_{tk} is the score of user u_t for each item and r_{ck} is the score of user u_c for each item. $I(u_t,u_c)$ is a collection of items that u_t and u_c have scored together, and $\mathrm{sim}(i_i,j_j)$ is the similarity between items i_i and j_j. Here, we also use Pearson's similarity to calculate this. If there are a lot of items that have been rated together, they can be considered as users with similar interests. If the obtained $S_u(u_t,u_c)$ is greater than a certain threshold ε, it can be kept in the cluster; otherwise, it will be separated from the current cluster. Then, we calculate the similarity between u_t and the other cluster centers. This is added to the cluster with the most similarity to complete the adjustment of the user cluster.

$$S_I(i_t,i_c) = \begin{cases} 1, & i_t = i_c, \\ \dfrac{1}{\sum_{k=1}^{m} r_{tk}\sum_{k=1}^{m} r_{ck}} \displaystyle\sum_{u_i\in U(i_t,i_c)}\ \sum_{u_j\in U(i_t,i_c)} \mathrm{sim}\left(u_i,u_j\right), & \text{else}, \end{cases} \tag{7}$$

where r_{tk} is the score of each user on item i_t and r_{ck} is the score of each user on item i_c. $U(i_t, i_c)$ is the set of users that i_t and i_c have scored together. $\mathrm{sim}(u_i, u_j)$ is the similarity between items u_i and u_j. Here, we use Pearson's similarity. If the obtained $S_I(i_t, i_c)$ is greater than a certain threshold η, the item will be kept in the cluster; otherwise, it will be separated from the current cluster. Then, we calculate the similarity between i_t and the other cluster centers. This is added to the cluster with the most similarity to complete the adjustment of the user cluster. Algorithm 2 is proposed for cross-iterative bi-clustering, as shown in Figure 1(b).

2.2.3. Context Similarity Calculation. When the scope of the context is very large, there are many different dimensions, such as time, place, surrounding people, etc. According to the characteristics of the dataset and the environment collection ability, the context dimension selected by the recommendation system will be different. As far as the time dimension is concerned, it can also be specifically subdivided into seasons, weeks, moments, holidays, and so on.

Assume that we select a system with z different dimensions, which is shown as $c = (c_1, c_2, \ldots, c_z)$, where $c_t\,(t = 1, \ldots, z)$ is a contextual dimension (such as time, location, weather, etc.). The similarity of the context between two score records x, y on dimension t can be recorded as $\mathrm{sim}_t(x, y)$. We use the degree of influence of the context dimension on the score to measure the similarity between the two context variables as follows:

$$\mathrm{sim}_t(x, y, i) = \frac{\sum_{u=1}^{n}\left(r_{u,i,x_t} - \overline{r_i}\right)\cdot\left(r_{u,i,y_t} - \overline{r_i}\right)}{\sigma_{x_t}\cdot\sigma_{y_t}}, \tag{8}$$

where u is the user and r_{u,i,x_t} describes the rating of item i under the context of x_t by user u. $\overline{r_i}$ is the average score of item i. Similarly, r_{u,i,y_t} is user u's rating of item i under context y_t, σ_{x_t} is the standard deviation of context dimension x_t, and σ_{y_t} is the standard deviation of context dimension y_t. This paper proposes a novel method to measure the similarity of context x and y, according to the influence degree of different contexts on the score of the same commodity i in the t dimension. Algorithm 3 is shown in Figure 1(c) to calculate context similarity efficiently.

2.2.4. The Proposed Multidimensional Context-Aware Based Method. In multidimensional recommendation, the addition of context results in a lot of interesting rules and mining high-frequency patterns between contexts and items can help discover the impact of different contexts on user decisions. In this paper, we select the multidimensional context from strong association rules with the algorithm FP-growth.

Generally, when determining the neighbor user group, the N-user with the largest similarity can be selected as the cluster neighbor of the target user according to the similarity calculation formula. The context can help the user to filter out some of the user score records that have a large difference in context from the current recommendation environment. Because some commodity decisions are closely related to a certain context factor, the context is called a hard context and must be considered and satisfied in the recommendation. Some score records that do not satisfy the current context can be filtered out preferentially and are not considered when calculating the similarity of neighbor clusters.

Due to the influence of the context, the user's rating record has its own context background, and the target user's current background is different, so the rating record in different contexts is different from the user in the current context. In order to distinguish the relevance of the rating record under the current context, we use the contextual similarity calculation method to calculate $\mathrm{sim}_t(x, y, i)$, which describes the similarity between context x and context y in the t dimension. The user rating predictions in a multidimensional context can be described as follows:

$$\begin{aligned} r_{u,i,c} &= \alpha\cdot\overline{r_u} + \beta\cdot\overline{r_i} + (1-\alpha-\beta)\cdot\overline{r_c} \\ &\quad + \frac{\sum_{v\in S(u,K)\cap N(i)}\mathrm{sim}_{u,v}\left(r_{v,i} - \overline{r_v}\right)}{\sum_{v\in S(u,K)\cap N(i)}\left|\mathrm{sim}_{u,v}\right|} + \varepsilon_u, \end{aligned} \tag{9}$$

where c is the context in which the target user is located and ε_u is the system error (the other symbols are described in the previous formula). It is well known that contexts can have many specific dimensions, depending on the data collection, such as time, location, and related personnel. The time dimension can be divided into seasons, weeks, moments, holidays, and so on.

After comprehensively considering the influence of context on the recommendation system, (10) can be replaced with (11). The basic clustering rating prediction formula is modified as follows:

$$R_{u,i,c} = k\sum_{x\in c}\sum_{c=1}^{z} r_{u,i,c}\cdot\mathrm{sim}_t(x, y, c), \tag{10}$$

$$P = \overline{r_{u,c}} + \frac{\sum_{v\in N_c}\left(R_{v,i,c} - \overline{r_{v,c}}\right)\times\mathrm{sim}(u, v, c)}{\sum_{v\in N_c}\mathrm{sim}(u, v, c)}. \tag{11}$$

Algorithm 4 shown in Figure 1(d) is proposed as the multidimensional context-aware based method. Using this algorithm, item scores can be obtained under multidimensional conditions.

3. Experiments and Results

3.1. Experimental Datasets and Environment. In order to verify the impact of a user's scoring weight on the recommendation results and to prove that the recommendation accuracy of the collaborative filtering algorithm based on the user and improved item scoring is more accurate, it is necessary to compare our proposed algorithm with traditional algorithms that are based on classical item scoring prediction methods.

These experiments were conducted under the following conditions: (1) CPU dual core i7-8750H with frequency 2.5 GHz; (2) main memory of 8 G; (3) Windows 10 64-bit operating system; (4) database software version MySQL 5.7. The proposed machine learning algorithms are implemented using an object-oriented dynamic type interpreted scripting language Python, including Python itself with some powerful libraries and third-party modules which cover scientific computing, database interfaces, etc., such as NumPy, pandas, etc. The integrated development environment is JetBrains PyCharm Professional 2018.2.5.

The experiments to improve user rating prediction utilize two datasets, MovieLens and Jester. The Jester dataset was developed by Ken Goldberg and his team at the Berkeley University of California. The Jesters dataset scored [−10, 10], the jester-dataset-1 comprises data from 24,983 users who have rated 36 or more jokes, a matrix of 24983×101; and jester-dataset-3 comprises data from 24,938 users who have rated between 15 and 35 jokes, a matrix of 24938×101 dimensions. The MovieLens dataset was organized by the Group Lens team at the University of Minnesota. The MovieLens 100K dataset comprises 100,000 ratings from 1000 users for 1,682 movies, rated between 1 and 5. The sparsity of the set is about 93.7%, and the data sparse problem is evident. In the experiment, in order to simulate datasets of different scales and different sparsity levels, the existing datasets were processed to generate four datasets as shown in Table 1. From this table, we can see that the datasets were randomly divided into training sets and test sets during the experiment, where the training set accounted for 80% of the entire dataset, and the test set accounted for the remaining 20%. When the Jesters dataset was processed, the score was formulated with the value 0 to 5 by $r^* = (r + 10)/4$.

The source of the experimental datasets for testing the multidimensional collaborative filtering algorithm is CARSKit (https://github.com/irecsys/CARSKit/), which is an open-source Java-based context-aware recommendation engine. We used two datasets: DePaulMovie [25] and TripAdvisor_v1 [26]. In the experiments, DePaulMovie kept its original shape, and TripAdvisor_v1 was filtered and adjusted. We used 70% of the dataset as the training set and 30% as the test set.

3.2. Evaluation Indicators of the Experiment Results. In order to study the performance of the improved recommendation algorithm, the experiment used four indicators, namely, precision, recall, mean absolute error (MAE), and root mean square error (RMSE).

Precision is an important indicator for evaluating the performance of a recommendation algorithm. It describes the proportion of the recommended items that the recommendation system makes for the user. The larger its value, the higher the accuracy of the system, and the better the system's recommendation. Precision is computed as shown in the following formula:

$$\text{precison} = \frac{\sum_u |R(u) \cap T(u)|}{\sum_u |R(u)|}, \quad (12)$$

where u is the target user who uses the system, $R(u)$ is the set of recommended items for the user, and $T(u)$ is the set of items in which the user is actually interested.

"Recall" describes how many of the products the user is interested in and how many are actually recommended to him by the system. Recall is computed as shown in the following formula:

$$\text{Recall} = \frac{\sum_u |R(u) \cap T(u)|}{\sum_u |T(u)|}. \quad (13)$$

The molecular weight of recall is the same as the molecule of the precision, which is the intersection of $R(u)$ and $T(u)$; however, their denominators are different. The denominator part of the accuracy rate is $R(u)$, which is the set of all items recommended to the user, and the denominator of the recall rate is $T(u)$, which is the collection of all the items of interest of the user. A larger recall corresponds to a better performance.

MAE avoids the problem where the errors cancel each other out and accurately reflects the actual prediction error. The calculation method is as shown as in formula (14), which averages the absolute value of the difference between the actual score and the predicted score.

$$\text{MAE} = \frac{1}{m}\sum_{i=1}^{m} \left|Y_i - y_i\right|, \quad (14)$$

where Y_i and y_i denote the original data and predicted data, respectively.

RMSE is used to measure the deviation between the observed value and the true value. The calculation method is shown in formula (15), that is, the ratio of the square of the difference between the predicted score and the actual score to the m number of observations squared.

$$\text{RMSE} = \sqrt{\frac{1}{m}\sum_{i=1}^{m} \left(Y_i - y_i\right)^2}. \quad (15)$$

The smaller the MAE and RMSE values, the better the recommended performance of the algorithm.

3.3. Experiment Results

3.3.1. Choosing the Best Value for the User Score Weighting Factor. Firstly, the optimal value for the user's score weighting factor a is determined for the collaborative filtering algorithm (U&IPRP-CF), based on the user and the improved item rating prediction. To ensure the accuracy of the experiment, the number of item recommendations N of the Jester-500-100, Jester-1000-100, and Jester-1000-200 datasets is set to a constant $N = 10$, meaning that 10 items are recommended to each target user. However, the number of items in the MovieLens dataset is large, and the number of recommended items N is set to a constant $N = 30$, meaning that 30 items are recommended to each target user. The K number of the most similar neighbors selected for each target user is a variable, and K is taken from 50, in increments of 10, and sequentially taken to 100, that is, [50, 60, 70, 80, 90, 100].

Each dataset was tested on a set of values of $a = 1, 0.9, 0.8, 0.7, 0.6, 0.5$ for a. The experiment results of the Jester-500-

Table 1: Dataset and related parameters.

Item	User number	Item number	Score	Sparseness
Jester-500-100	500	100	35,861	0.283
Jester-1000-100	1000	100	70,675	0.293
Jester-1000-200	1000	200	50,516	0.747
MovieLens	943	1,682	100,000	0.937

100 dataset are shown in Tables 2 and 3. The best value of a is around 0.9. The experiment results of the Jester-1000-100 dataset are shown in Tables 4 and 5. The best value of a is around 0.8 and 0.9. The experiment results of the Jester-1000-200 dataset are shown in Tables 6 and 7. The best value of a is around 0.7. The experiment results of the MovieLens dataset are shown in Tables 8 and 9. The best value of a is around 0.7. In summary, as the size of the dataset increases and sparsity increases, the optimal value of the user's score weighting factor a decreases.

After determining the best value of the user's score weighting factor, a comparative experiment is carried out, and the algorithms are first sorted and named, as shown in Table 10.

The algorithms are compared in Table 10. In order to ensure the accuracy of the experiment, the recommended number N of Jester-500-100, Jester-1000-100, and Jester-1000-200 datasets is a constant $N = 10$. The recommended N number of items in the MovieLens dataset is a constant $N = 30$. The K number of most similar neighbors selected for each target user is a variable. K has a value from 50 to 100 with an interval of 10, expressed as [50, 60, 70, 80, 90, 100].

The comparison results of the performance for different datasets are shown in Figure 2. The experiment results for the Jester-500-100 dataset are shown in Figures 2(a) and 2(b). The experiment results for the Jester-1000-100 dataset are shown in Figures 2(c) and 2(d). The experiment results for the Jester-1000-200 dataset are shown in Figures 2(e) and 2(f). The experiment results for the MovieLens dataset are shown in Figures 2(g) and 2(h). It can be seen that for the different datasets, the error generated by the U&IPRP-CF algorithm is smaller than the traditional algorithm, and it has obvious advantages in terms of the accuracy of recommendations.

In the three datasets Jester-500-100, Jester-1000-100, and Jester-1000-200, the U&URWFRP-CF algorithm does not reduce the recommendation error, whereas the recommendation error for the U&URWFRP-CF algorithm is reduced in the MovieLens dataset. This shows that when the dataset is small and sparse, the user's score is very reliable; otherwise, when the dataset is large and information sparse, the user's score is less likely to be referenced under a large base. In this situation, the weights of the user ratings need to be considered.

From these figures, it can be seen that when the scale and sparsity of the dataset are gradually increased, the recommendation error of the U&IPRP-CF algorithm is also reduced and the performance becomes increasingly better, which alleviates the data sparsity problem to some extent.

It can be seen from the experiment results that using the average score of the public to replace the average historical score weight of the user alone can enable the system to predict the user's score on the unrated item, resulting in less error, thus making more accurate recommendations. To reduce the error of score prediction, a systematic error factor is established for each user, and statistical learning is improved on each recommendation, which can effectively correct the error and improve the accuracy of recommendations.

In addition, combined with experiment 3.3.1, it can be seen that choosing the correct parameters is also key to improving the accuracy of recommendations. When the number of items recommended by item N, the number of neighbors of target user K, and the user's score weighting factor a are in a practical application, the recommendation system needs to compare and select appropriate values for the experiment.

3.3.2. Performance Comparison Experiments Using Different Algorithms. The experimental results were verified by DePaulMovie and TripAdvisor_v1 datasets published by GroupLens. Our paper compared four recommendation algorithms: CF, CF-AR, Multi-CF, Multi-CF-AR, CF-AR-IIP, and Multi-CF-AR-IIP, the latter two being the algorithms proposed in this paper. The algorithms are explained as follows:

(a) CF: classical user-based collaborative filtering recommendation algorithm
(b) CF-AR: user-based collaborative filtering recommendation algorithm combined with association rules mining
(c) CF-AR-IIP: user-based collaborative filtering recommendation algorithm combined with association rules mining and improved item-rating prediction, which is proposed in this paper
(d) Multi-CF: classical multidimensional context-aware user-based collaborative filtering algorithm
(e) Multi-CF-AR: multidimensional context-aware user-based collaborative filtering algorithm combined with association rules mining
(f) Multi-CF-AR-IIP: user-based collaborative filtering recommendation algorithm combined with association rules mining and improved item-rating prediction, which is proposed in this paper

In the experiments based on the DePaulMovie datasets, the top-K ($K = 10$, 15, 20, 25) neighbors with the highest similarity for each user and the top-N ($N = 10$, 15, 20) recommended items with the highest predicted rating for the target users are selected. The system has three context

Table 2: Comparison of MAE using Jester-500-100.

a	$K=50$	$K=60$	$K=70$	$K=80$	$K=90$	$K=100$
1	0.5791	0.5781	0.5985	0.5723	0.5539	0.5574
0.9	0.5530	0.5655	0.5591	0.5334	0.5480	0.5675
0.8	0.5411	0.5795	0.5710	0.5350	0.5597	0.5815
0.7	0.5754	0.5729	0.5903	0.5630	0.5356	0.5871
0.6	0.5632	0.5917	0.5917	0.5782	0.5618	0.5746
0.5	0.5747	0.6027	0.5973	0.5806	0.5712	0.5800

Table 3: Comparison of RMSE using Jester-500-100.

a	$K=50$	$K=60$	$K=70$	$K=80$	$K=90$	$K=100$
1	0.8860	0.8982	0.9618	0.9141	0.8662	0.8731
0.9	0.8710	0.8975	0.8942	0.8560	0.8542	0.8966
0.8	0.8529	0.9222	0.9120	0.8507	0.8922	0.9335
0.7	0.9032	0.9243	0.9456	0.8928	0.8469	0.9438
0.6	0.8928	0.9568	0.9396	0.9212	0.8770	0.9056
0.5	0.8976	0.9722	0.9466	0.9487	0.8865	0.9084

Table 4: Comparison of MAE using Jester-1000-100.

a	$K=50$	$K=60$	$K=70$	$K=80$	$K=90$	$K=100$
1	0.5091	0.5105	0.5528	0.5385	0.5199	0.5058
0.9	0.5029	0.5081	0.5366	0.5432	0.5195	0.5225
0.8	0.5006	0.5302	0.5191	0.5263	0.5233	0.5460
0.7	0.5090	0.5141	0.5289	0.5364	0.5377	0.5409
0.6	0.5330	0.5289	0.5572	0.5431	0.5429	0.5337
0.5	0.5417	0.5440	0.5647	0.5534	0.5509	0.5455

Table 5: Comparison of RMSE using Jester-1000-100.

a	$K=50$	$K=60$	$K=70$	$K=80$	$K=90$	$K=100$
1	0.8212	0.8322	0.8932	0.8659	0.8242	0.8212
0.9	0.8120	0.8372	0.8736	0.8865	0.8345	0.8332
0.8	0.8130	0.8713	0.8474	0.8692	0.8418	0.8788
0.7	0.8345	0.8543	0.8753	0.8832	0.8713	0.8722
0.6	0.8783	0.8707	0.9133	0.8792	0.8740	0.8590
0.5	0.8918	0.8885	0.9246	0.8993	0.8822	0.8667

dimensions, namely, $C=(C1, C2, C3)=$ (Time, Location, Companion), where $C1$ (Time) = (Weekday, Weekend), $C2$ (Location) = (Cinema, Home), and $C3=$ (Companion) = (Alone, Family, Partner).

In the experiments based on the TripAdvisor_v1 dataset, the top-K ($K=20$, 30, 40, 50) neighbors with the highest similarity for each user and the top-N ($N=10$, 15, 20) recommended items with the highest predicted rating for the target users are selected. The system has three context dimensions as follows: $C=(C1, C2, C3)=$ (USER_TIMEZONE, HOTEL_TIMEZONE, Trip Type), where $C1$ (USER_TIMEZONE) = (Eastern, Central, Pacific, Mountain, HI, AK), $C2$ (HOTEL_TIMEZONE) = (Eastern, Central, Pacific, Mountain), and $C3$ (Trip Type) = (1, 2, 3, 4, 5). Table 11 shows information on the related context dimensions selected for the datasets.

Figures 3(a) and 3(b) show the precision of the algorithms. Multi-CF-AR-IIP achieves the best precision, and Multi-CF-AR is the second best. Particularly when N is small, Multi-CF-AR-IIP has obvious advantages. As N increases, the precision of all the algorithms decreases, and the difference between the algorithms becomes increasingly smaller. This shows that the increase in the number of recommendations reduces the accuracy of the recommendation. Different algorithms will exhibit different characteristics in different datasets. Multi-CF has an advantage in DePaulMovie, but it does not work well in TripAdvisor_v1.

Figures 3(c) and 3(d) show the recall of the algorithms. The result is the same as for precision, where Multi-CF-AR-IIP achieves the best recall, and Multi-CF-AR is the second best. However, recall increases significantly as N increases. This is because the denominator of recall is the number of items in which the user is actually interested and its value is small.

Figures 3(e) and 3(f) show the MAE of the algorithms and Figures 3(g) and 3(h) show the RMSE of the algorithms. In DePaulMovie, except CF, the resulting errors of the other

Table 6: Comparison of MAE using Jester-1000-200.

a	$K = 50$	$K = 60$	$K = 70$	$K = 80$	$K = 90$	$K = 100$
1	0.4139	0.3714	0.2611	0.1727	0.2059	0.1799
0.9	0.3562	0.4590	0.2103	0.2422	0.1879	0.1815
0.8	0.2933	0.3235	0.2426	0.2472	0.1991	0.1999
0.7	0.2309	0.3507	0.1582	0.2160	0.2616	0.2489
0.6	0.3161	0.3401	0.2105	0.2445	0.2566	0.2718
0.5	0.2940	0.3113	0.2763	0.2415	0.2604	0.3213

Table 7: Comparison of RMSE using Jester-1000-200.

a	$K = 50$	$K = 60$	$K = 70$	$K = 80$	$K = 90$	$K = 100$
1	0.8962	0.6459	0.3511	0.3651	0.4679	0.3333
0.9	0.9843	0.5405	0.4266	0.3451	0.4401	0.3403
0.8	0.7912	0.6234	0.4295	0.3887	0.3769	0.3676
0.7	0.7718	0.4226	0.4382	0.5201	0.5442	0.4873
0.6	0.7545	0.5812	0.5336	0.4989	0.5547	0.5323
0.5	0.6692	0.5975	0.5068	0.5343	0.5589	0.6286

Table 8: Comparison of MAE using MovieLens.

a	$K = 50$	$K = 60$	$K = 70$	$K = 80$	$K = 90$	$K = 100$
1	0.2634	0.6377	0.7479	0.7883	0.7851	0.3524
0.9	0.1978	0.4791	0.4692	0.3977	0.0811	0.0249
0.8	0.2178	0.3709	0.3448	0.2918	0.0931	0.1255
0.7	0.2456	0.2994	0.3058	0.2271	0.1942	0.1589
0.6	0.3610	0.3881	0.3552	0.2668	0.1889	0.1499
0.5	0.4612	0.4560	0.3491	0.2803	0.2177	0.2261

Table 9: Comparison of RMSE using MovieLens.

a	$K = 50$	$K = 60$	$K = 70$	$K = 80$	$K = 90$	$K = 100$
1	0.7249	1.4619	1.5619	1.4962	1.5344	0.3524
0.9	0.6457	1.0449	1.0487	1.0665	0.3218	0.0249
0.8	0.6294	0.9029	0.8317	0.7804	0.3212	0.1255
0.7	0.6488	0.7891	0.7623	0.6921	0.4911	0.1589
0.6	0.8638	0.9174	0.8160	0.7339	0.5431	0.1499
0.5	0.9838	1.0053	0.7864	0.7406	0.5577	0.2261

Table 10: The names of the algorithms.

English abbreviation	Full name
COS&TPRP-CF	Collaborative filtering algorithm based on cosine and traditional item rating prediction
U&TPRP-CF	Collaborative filtering algorithm based on user and traditional item rating prediction
U&URWFRP-CF	Collaborative filtering algorithm based on user and user scoring weight factor rating prediction
U&IPRP-CF	Collaborative filtering algorithm based on user and improved item rating prediction (our algorithm)

five algorithms are almost similar. But the error gap in TripAdvisor_v1 is obvious, and the multidimensional algorithms produce a high number of errors. MAE and RMSE calculate the difference between the predict rating and the user's true rating, which aims to measure the difference between the recommended result and the user's true preference. The smaller the MAE and the RMSE, the more users like the recommended items. Association rule mining (ARM) improves the precision and recall of the recommendation, which means that it improves click volume and purchase amount. At the same time, it also makes it difficult for the recommender system to predict the rating, and the probability of the system recommending items that the user does not like is increased. From the experiment results, it can reduce MAE and RMSE with improved item-rating prediction (IIP) method.

In general, the fusion algorithm Multi-CF-AR-IIP has better recommendation performance than the others. It

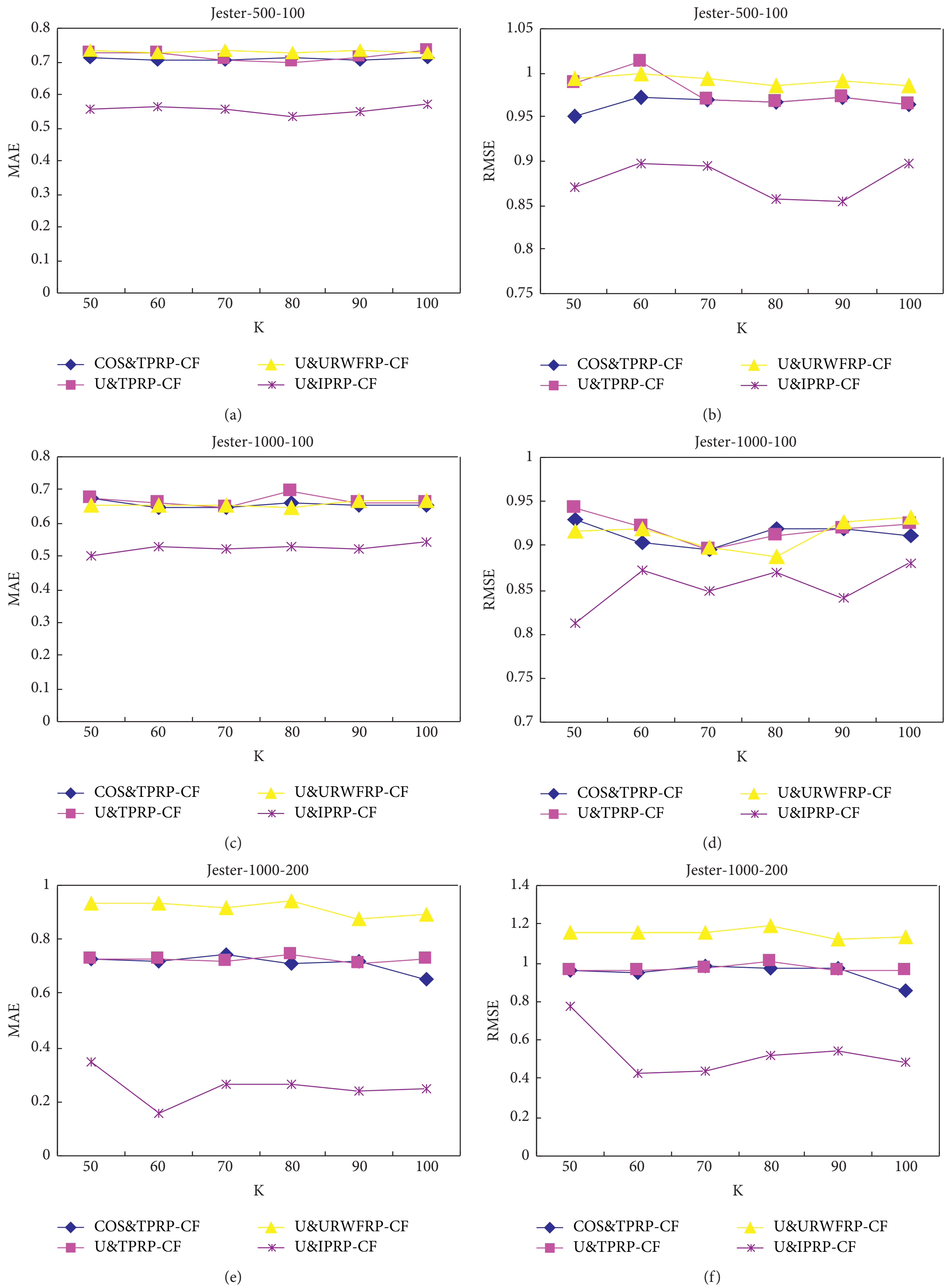

(a) (b) (c) (d) (e) (f)

FIGURE 2: Continued.

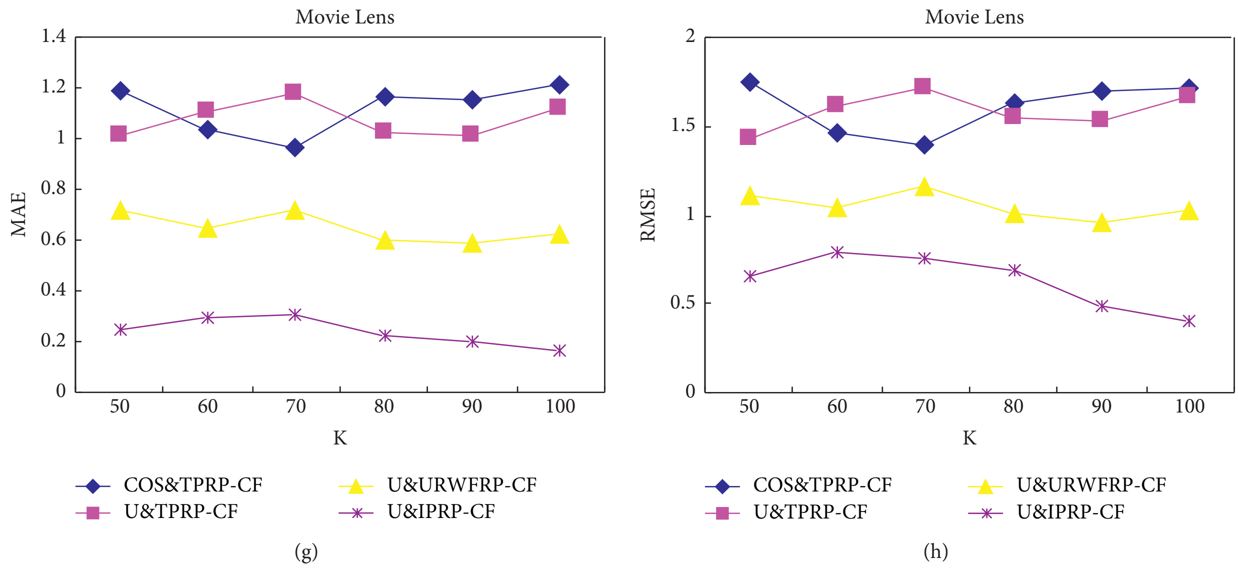

FIGURE 2: Comparison of the performance results for the different datasets. (a) Comparison of MAE for Jester-500-100. (b) Comparison of RMSE for Jester-500-100. (c) Comparison of MAE for Jester-1000-100. (d) Comparison of RMSE for Jester-1000-100. (e) Comparison of MAE for Jester-1000-200. (f) Comparison of RMSE for Jester-1000-200. (g) Comparison of MAE for MovieLens. (h) Comparison of RMSE for MovieLens.

TABLE 11: Information on the related context dimensions for the datasets.

DePaulMovie	Number	Users	Items	Ratings	Sparsity
		97	79	5043	0.3419
	Context dimension	Time	Location		Companion
		Weekday, weekend	Cinema, home		Alone, family, partner
TripAdvisor_v1	Number	Users	Items	Ratings	Sparsity
		1129	48	4669	0.9138
	Context dimension	USER_TIMEZONE	HOTEL_TIMEZONE		Trip type
		Eastern, central, pacific, mountain, HI, AK	Eastern, central, pacific, mountain		1, 2, 3, 4, 5

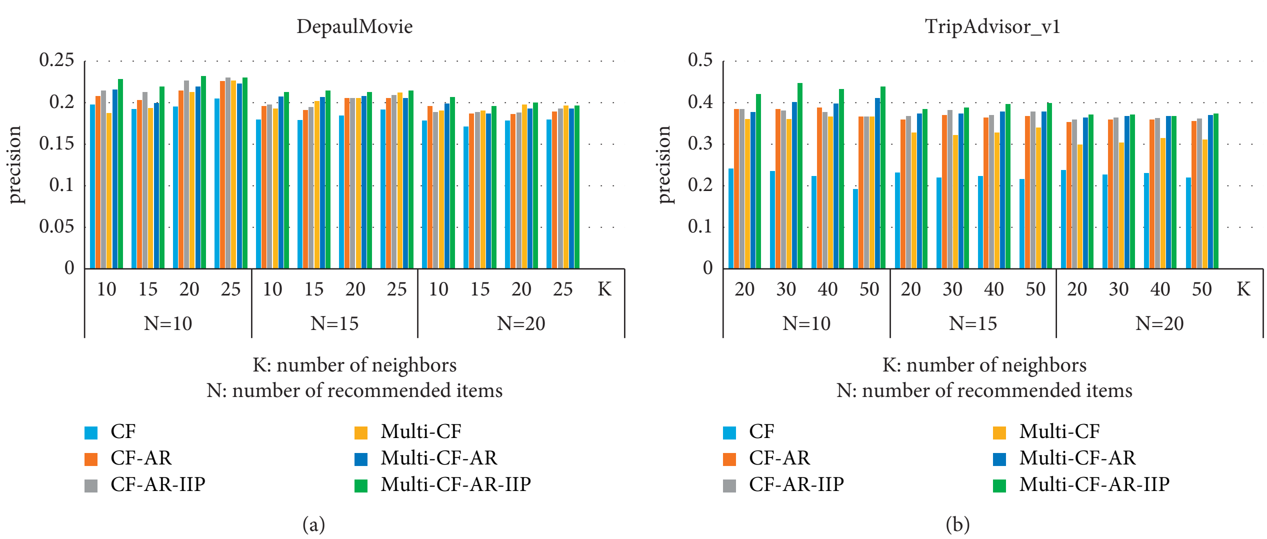

FIGURE 3: Continued.

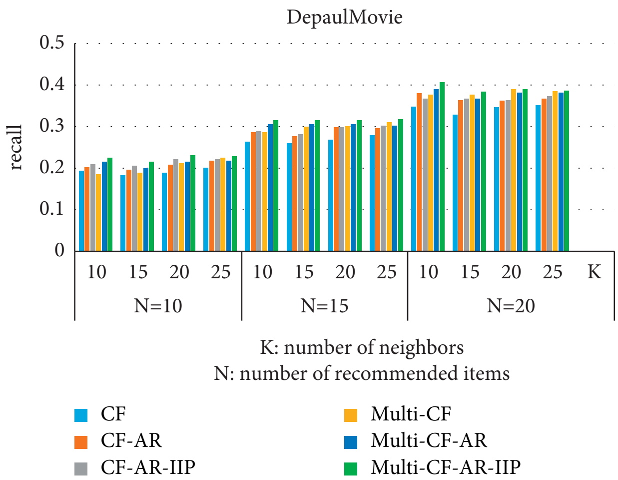

(c)

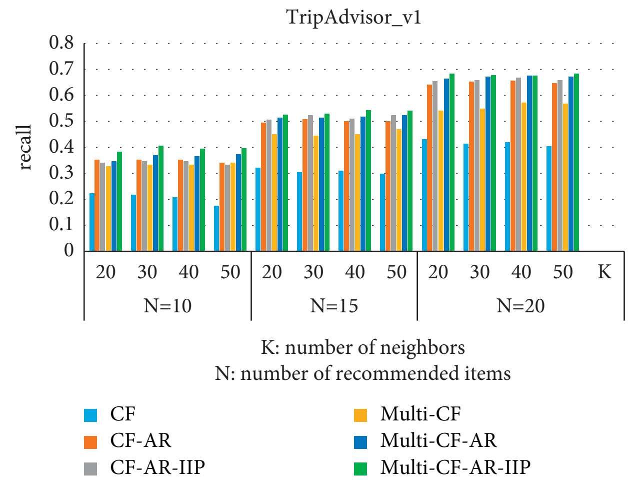

(d)

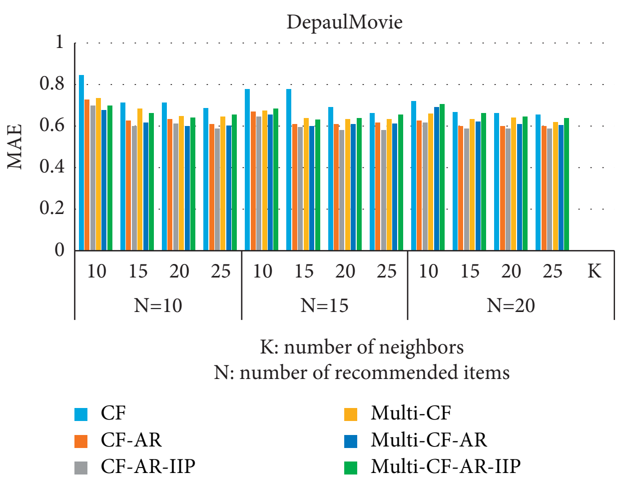

(e)

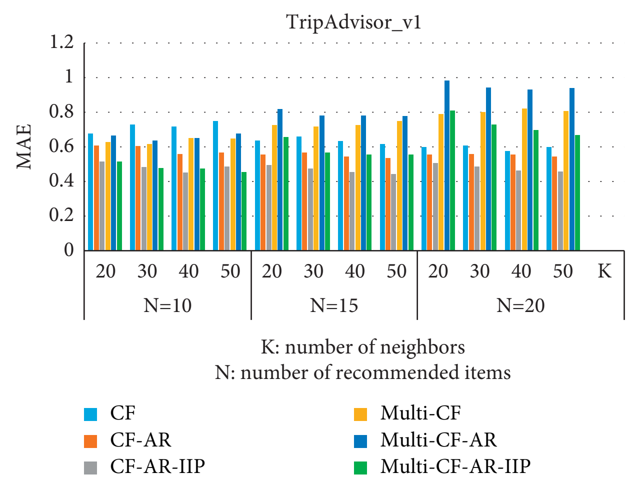

(f)

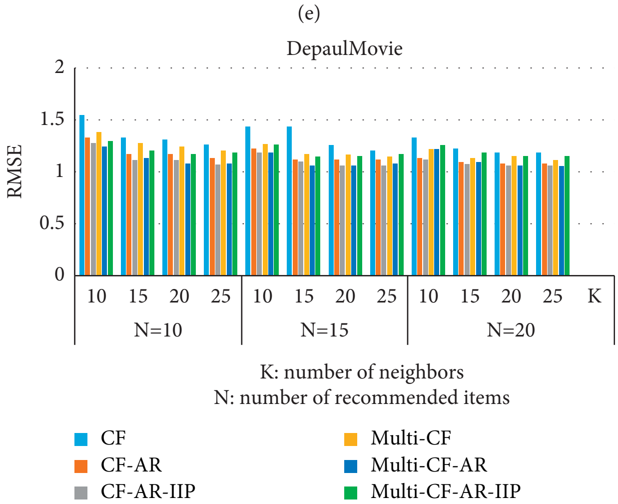

(g)

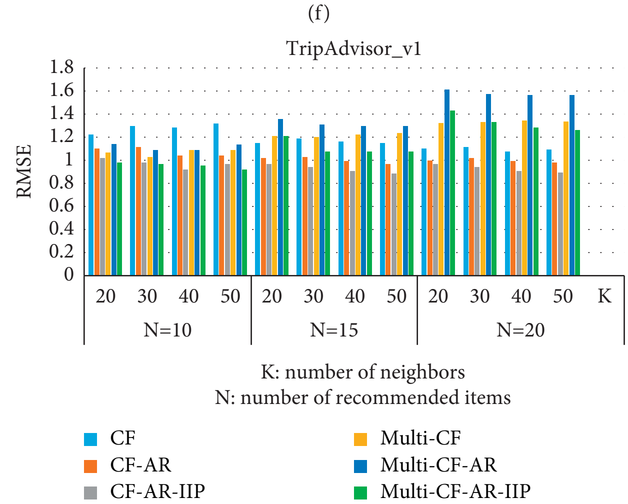

(h)

FIGURE 3: Performance comparison of algorithms based on different datasets. (a) Comparison of precision of algorithms based on DePaulMovie. (b) Comparison of precision of algorithms based on TripAdvisor_v1. (c) Comparison of recall of algorithms based on DePaulMovie. (d) Comparison of recall of algorithms based on TripAdvisor_v1. (e) Comparison of MAE of algorithms based on DePaulMovie. (f) Comparison of MAE of algorithms based on TripAdvisor_v1. (g) Comparison of RMSE of algorithms based on DePaulMovie. (h) Comparison of RMSE of algorithms based n TripAdvisor_v1.

recommends more diversified items to users by using multidimension context and AR and recommends items that users may prefer by using IIP.

4. Conclusion

In recent years, recommendation systems have been widely used in various fields. The accuracy and applicability of the recommendation system is very important. In this paper, we proposed a novel recommendation algorithm based on improved collaborative filtering with multidimensional context and association rules. Firstly, an improved cross-iterative bi-clustering based user scoring prediction method is proposed. Then, the multidimensional context-aware method is introduced into the traditional user collaborative filtering algorithm by using context-aware related information. In this method, a multidimensional context is used to filter the original data, the excess data is filtered to adjust the recommendation results, and the context data is integrated into the similarity calculation process of the user and the product to obtain more accurate recommendation results. In addition, in order to better compensate for the impact of data sparseness and increase the user's satisfaction, association rules can be used to find similar preferences between users with low similarity. By mining the context and the relevance of the user's selected items, we can find popular items with a high degree of contextual relevance to complement the algorithm's novelty and reliability. The algorithm proposed in this paper can enhance the user's experience on the recommendation platform and strengthen the connection between context and recommendation results. The algorithms we propose provide recommendations for users in a multidimensional context environment, which not only complements the omission of the collaborative filtering algorithm, but also improves the accuracy and efficiency of the recommendation results.

In the future, we will study high-dimensional clustering algorithms, which will help solve the problem of data sparsity and determine the decision-making of social groups. To establish a more personalized recommendation system, we must develop effective recommendation methods from multiple perspectives. Another new research direction is how to use recursive neural networks to provide personalized advice.

Data Availability

Data sharing is not applicable to this article as no datasets were generated or analysed during the current study.

Conflicts of Interest

The authors declare no potential conflicts of interest with respect to the research, authorship, and/or publication of this article.

Acknowledgments

This work was supported by Fund Item of the China Scholarship Council (CSC) and Key Laboratory Project of Sichuan University (QXXCSYS201705).

References

[1] A. K. Sahu and P. Dwivedi, "User profile as a bridge in cross-domain recommender systems for sparsity reduction," *Applied Intelligence*, vol. 49, no. 7, pp. 2461–2481, 2019.

[2] L. Xu, C. Jiang, Y. Chen, Y. Ren, and K. J. R. Liu, "User participation in collaborative filtering-based recommendation systems: a game theoretic approach," *IEEE Transactions on Cybernetics*, vol. 49, no. 4, pp. 1339–1352, 2018.

[3] T. Xiao and H. Shen, "Neural variational matrix factorization for collaborative filtering in recommendation systems," *Applied Intelligence*, vol. 49, no. 4, pp. 3558–3569, 2019.

[4] B. Loepp, T. Donkers, T. Kleemann, and J. . Ziegler, "Interactive recommending with tag-enhanced matrix factorization (TagMF)," *International Journal of Human-Computer Studies*, vol. 121, pp. 21–41, 2018.

[5] H. Luo, M. Li, S. Wang, Q. Liu, Y. Li, and J. Wang, "Computational drug repositioning using low-rank matrix approximation and randomized algorithms," *Bioinformatics*, vol. 34, no. 11, pp. 1904–1912, 2018.

[6] W. Wang, J. Chen, J. Wang, J. Chen, J. Liu, and Z. Gong, "Trust-enhanced collaborative filtering for personalized point of interests recommendation," *IEEE Transactions on Industrial Informatics*, vol. 16, no. 9, pp. 6124–6132, 2020.

[7] N. V. Dat, P. V. Toan, and T. M. Thanh, "Solving distribution problems in content-based recommendation system with Gaussian mixture model," *Applied Intelligence*, vol. 5, pp. 1–13, 2021.

[8] W. Zhang, X. Zhang, and D. Chen, "Causal neural fuzzy inference modelling of missing data in implicit recommendation system," *Knowledge-Based Systems*, vol. 222, no. 10, pp. 66–78, 2021.

[9] A. A. Amer, H. I. Abdalla, and L. Nguyen, "Enhancing recommendation systems performance using highly-effective similarity measures," *Knowledge-Based Systems*, vol. 217, Article ID 106842, 2021.

[10] M. Liu, W. Pan, M. Liu, Y. Chen, X. Peng, and Z. Ming, "Mixed similarity learning for recommendation with implicit feedback," *Knowledge-Based Systems*, vol. 119, no. 1, pp. 178–185, 2017.

[11] Z. Duan, W. Xu, Y. Chen, and L. Ding, "Etbrec: a novel recommendation algorithm combining the double influence of trust relationship and expert users," *Applied Intelligence*, vol. 2021, no. 3, 2021.

[12] X. Kong, F. Xia, J. Wang, A. Rahim, and S. k. Das, "Time-location-relationship combined service recommendation based on taxi trajectory data," *IEEE Transactions on Industrial Informatics*, vol. 13, no. 3, pp. 1202–1212, 2017.

[13] W. X. Zhao, S. Li, Y. He, L. Wang, J. Wen, and X. Li, "Exploring demographic information in social media for product recommendation," *Knowledge and Information Systems*, vol. 49, no. 1, pp. 1–25, 2015.

[14] Y. Wang and X. Li, "Study on improved clustering collaborative filtering algorithm based on demography," *Computer Science*, vol. 44, no. 3, pp. 63–69, 2017.

[15] S. Mandal and A. Maiti, "Deep collaborative filtering with social promoter score-based user-item interaction: a new perspective in recommendation," *Applied Intelligence*, vol. 51, pp. 1–26, 2021.

[16] Y. Pan, Y. Huo, J. Tang, Y. Zeng, and B. Chen, "Exploiting relational tag expansion for dynamic user profile in a tag-aware ranking recommender system," *Information Sciences*, vol. 545, no. 6, pp. 448–464, 2021.

[17] J. Gou, J. Guo, L. Zhang, and C. Wang, "Collaborative filtering recommendation system based on trust-aware and domain experts," *Intelligent Data Analysis*, vol. 23, no. S1, pp. 133–151, 2019.

[18] X. Y. Xu, L. H. Ren, and Y. S. Ding, "An improved D-S evidence theory based on genetic algorithm to VIP intelligent recognition and recommendation system," *Applied Mechanics and Materials*, vol. 347-350, pp. 2442–2446, 2013.

[19] J. Xiao, M. Luo, J.-M. Chen, and J.-J. Li, "An item based collaborative filtering system combined with genetic algorithms using rating behavior," *Lecture Notes in Computer Science*, vol. 9227, pp. 453–460, 2015.

[20] Y. Lin, P. Ren, Z. Chen, Z. Ren, J. Ma, and M. De Rijke, "Explainable outfit recommendation with joint outfit matching and comment generation," *IEEE Transactions on Knowledge and Data Engineering*, vol. 32, no. 8, pp. 1502–1516, 2018.

[21] A. Mcy, B. Ik, and B. Ksl, "Temporal context-aware task recommendation in crowdsourcing systems," *Knowledge-Based Systems*, vol. 219, Article ID 106770, 2021.

[22] Z. E. Yebdri, S. M. Benslimane, F. Lahfa, M. Barhamgi, and D. Benslimane, "Context-aware recommender system using trust network," *Computing*, vol. 2021, no. 103, pp. 1919–1937, 2021.

[23] J. S. Breese, D. Heckerman, and C. Kadie, "Empirical analysis of predictive algorithms for collaborative filtering," *Uncertainty in Artificial Intelligence*, vol. 98, no. 7, pp. 43–52, 2013.

[24] B. Hui, L. Zhang, X. Zhou, X. Wen, and Y. Nian, "Personalized recommendation system based on knowledge embedding and historical behavior," *Applied Intelligence*, vol. 2021, no. 7, 2021.

[25] Y. Zheng, B. Mobasher, and R. Burke, "CARSKit: a java-based context-aware recommendation engine," in *Proceedings of the 15th IEEE conference on Data Mining Workshops*, pp. 1668–1672, IEEE, Atlantic City, NJ, USA, Nov-2015.

[26] Y. Zheng, R. Burke, and B. Mobasher, "Differential context relaxation for context-aware travel recommendation," in *Proceedings of the 13th International Conference on Electronic Commerce and Web Technologies (EC-WEB 2012)*, pp. 88–99, Springer, Chicago City, IL, USA, Sep-2012.

Hindawi
Scientific Programming
Volume 2023, Article ID 9753907, 1 page
https://doi.org/10.1155/2023/9753907

Retraction

Retracted: Study on Resource Sharing Strategy of e-Commerce Innovation and Entrepreneurship Education Based on Cloud Computing

Scientific Programming

Received 8 August 2023; Accepted 8 August 2023; Published 9 August 2023

This article has been retracted by Hindawi following an investigation undertaken by the publisher [1]. This investigation has uncovered evidence of one or more of the following indicators of systematic manipulation of the publication process:

(1) Discrepancies in scope
(2) Discrepancies in the description of the research reported
(3) Discrepancies between the availability of data and the research described
(4) Inappropriate citations
(5) Incoherent, meaningless and/or irrelevant content included in the article
(6) Peer-review manipulation

The presence of these indicators undermines our confidence in the integrity of the article's content and we cannot, therefore, vouch for its reliability. Please note that this notice is intended solely to alert readers that the content of this article is unreliable. We have not investigated whether authors were aware of or involved in the systematic manipulation of the publication process.

Wiley and Hindawi regrets that the usual quality checks did not identify these issues before publication and have since put additional measures in place to safeguard research integrity.

We wish to credit our own Research Integrity and Research Publishing teams and anonymous and named external researchers and research integrity experts for contributing to this investigation.

The corresponding author, as the representative of all authors, has been given the opportunity to register their agreement or disagreement to this retraction. We have kept a record of any response received.

References

[1] Q. Cao, "Study on Resource Sharing Strategy of e-Commerce Innovation and Entrepreneurship Education Based on Cloud Computing," *Scientific Programming*, vol. 2021, Article ID 8268000, 8 pages, 2021.

Hindawi
Scientific Programming
Volume 2021, Article ID 8268000, 8 pages
https://doi.org/10.1155/2021/8268000

Research Article

Study on Resource Sharing Strategy of e-Commerce Innovation and Entrepreneurship Education Based on Cloud Computing

Qian Cao

Business Starting School, Yiwu Industrial and Commercial College, Jinhua 322000, China

Correspondence should be addressed to Qian Cao; caoq1982@126.com

Received 3 September 2021; Accepted 13 October 2021; Published 5 November 2021

Academic Editor: Punit Gupta

As a popular education major at present, e-commerce and innovation and entrepreneurship education are combined with research that has important strategic significance for talents. In the process of the coordinated development of the two, the sharing of educational resources is the core issue. For this reason, an e-commerce professional innovation and entrepreneurship education resource sharing platform has been constructed. The platform is divided into three hierarchical structures of resource layer, middle layer, and application layer, and detailed analysis is performed on the key modules in the construction of the educational resource sharing platform, including user login module, educational resource management module, system management module, and database design module; based on modular design, after logging in to the system, users can independently publish educational information and can also browse and retrieve shared resources. Experimental results show that the platform has a good operating effect, strong load capacity, rapid response of the system, and high safety performance, with a maximum safety of 97%.

1. Introduction

At present, the country vigorously advocates the spirit of innovation, strengthens the cultivation of innovative education and innovative talents in many aspects, and builds an innovative society in an all-round way, and the concept of innovative entrepreneurship education follows. Innovative entrepreneurship education takes creativity and innovation as the core content and improves students' comprehensive quality based on the combination of teaching and practice [1, 2]. By carrying out innovative entrepreneurship education, we can cultivate students' autonomy, reduce the shackles of traditional education on students' learning methods and ideas, deeply tap students' potential, cultivate students' ability to choose jobs and compete, and vigorously develop innovative entrepreneurship education. It not only is the demand for contemporary students' career development but also plays an important role in the construction of innovative country.

Innovation and entrepreneurship education is not a separate education, but it should be integrated into professional education and teaching, and the two should continue to integrate and practice, in order to truly play the role of innovation [3]. With the development of science and technology, e-commerce major has been developed and valued. The combination of e-commerce education and innovation and entrepreneurship education will greatly benefit the professional development of students and provide more ways for social employment development.

Many scholars have studied the concept of innovation and entrepreneurship education. The study in [4] points out the importance of the integration of industry and education. In view of the current lack of innovation ability of higher vocational e-commerce students, through extensive research and resource integration, this paper constructs an innovation and entrepreneurship ability training model. The authors of [5] put forward an innovative model of university, industry, and government, which has some shortcomings in resource sharing, cooperation mode, and so on. Therefore, this paper constructs a community of innovative entrepreneurship education in colleges and universities in order to change the cooperation model and establish a community of resource sharing and cooperation. The study in [6] puts forward the knowledge and ability structure requirements of cross-border e-commerce talent training and explores the cross-border e-commerce innovation and entrepreneurial talent training methods from the perspective of school-enterprise cooperation to meet the market demand. The work in [7] analyzes the ways of cultivating college students' innovative entrepreneurial ability in special poor areas, uses file inquiry to understand the current situation of local students, and implements them by perfecting the education system, developing new teaching models, and constructing management platforms to maximize the sharing of educational resources and improve the innovative entrepreneurial ability of college students in poor areas.

On the basis of the existing relevant research, we learn the importance of college students' innovation and entrepreneurship education resources, in order to improve college students' innovation and entrepreneurship ability, explore resource sharing strategies, and provide ways for the innovative development of e-commerce majors.

2. Related Work

Innovation and entrepreneurship education is an inevitable requirement for the development of higher education in the era of knowledge economy. As a new type of professional education, e-commerce major should establish the core curriculum of innovation and entrepreneurship, strengthen the sharing of educational resources, gather more innovation and entrepreneurship resources of e-commerce major, and further deepen the reform of the education system; it is a new direction to develop e-commerce education. During the development of innovation and entrepreneurship education, there will be huge data resources, which are widely distributed and difficult to concentrate. Therefore, the education resources in some regions cannot meet the teaching needs. Hence, how to provide a convenient and efficient way of resource sharing and make it play a greater role in education is an important problem to be solved.

In foreign research, the study in [8] put forward the way of sharing educational resources based on 5G network and FPGA system, studied the reform of the Wushu teaching system by the latest fifth generation technology, realized the experimental verification of FPGA system integration and equipment leasing system, and then realized the educational goal of comprehensive reform of the Wushu teaching system. It provides a theoretical reference for the new cooperative practice to require physical education planning, and the research of this method is relatively single. The work in [9] points out that resource sharing has become a key problem to be solved in the network environment. This paper studies the link prediction method in online education and establishes an appropriate model for online education. A neural network path-sorting algorithm based on the path-sorting method is proposed to realize the link prediction problem in online learning knowledge base, which provides support for educational resource sharing but has a long response time. The study in [10] explores and studies the network distance teaching and resource sharing system of higher education, comprehensively introduces the social needs, framework composition, main functions, and expected objectives of the system, analyzes the main problems and development bottlenecks in combination with teaching practice, and obtains a better method of resource sharing platform construction through practical application. The study in [11] designed an object-oriented statistical analysis platform for educational data to meet the needs of teaching resource sharing service business and analysed the problem of teaching resource sharing from the perspective of different school color users, but the research results are not deep enough.

There are also many studies in China. The study in [12] provides research support for e-commerce teaching and education from the perspective of concept consensus, but there is a problem of poor operation function of sharing mechanism. The work in [13] has studied the mechanism of innovative entrepreneurship education resources integration and put forward specific ways of resource integration from many levels, including the construction of the system, the platform, and the way to expand. The construction of the resource sharing platform is insufficient. The work in [14] suggests that in the construction of practical teaching resources between schools and enterprises, the problem of resource sharing is insufficient in demand and scope. Therefore, this paper studies the sharing strategy of teaching resources in detail in order to improve the sharing degree of teaching resources. This improves the use value, but the sharing efficiency is not good. In [15], taking innovative entrepreneurship education as the background, this paper expounds the necessity of resource sharing, starting with the establishment of resource sharing goal, the construction of shared service platform, the establishment of related mechanism, and the construction of talent team, and comprehensively analyzes the problem of resource sharing.

In view of the shortcomings of the existing research, this paper studies the e-commerce professional innovation and entrepreneurship education resource sharing strategy, constructs the education resource sharing platform, modularizes the design of the platform, divides it into three parts, resource layer, middle layer, and application layer, and focuses on the analysis of user management, education resource management, and system management; the running function, load, running performance, and system security of the platform are tested, and the feasibility of the platform is verified. Finally, combined with the platform construction, the paper puts forward the e-commerce professional innovation and entrepreneurship education resource sharing strategy from multiple perspectives, which provides support for e-commerce professional education.

3. Construction of the Resource Sharing Platform for Innovation and Entrepreneurship Education for e-Commerce Majors

In order to study an effective e-commerce professional innovation and entrepreneurship education resource sharing strategy, this paper constructs an education resource sharing platform based on computer intelligent analysis technology and hopes to provide more abundant and comprehensive innovation and entrepreneurship education resources for e-commerce specialty through the platform construction, so as to meet the needs of e-commerce professional teachers, students, and more users for innovation and entrepreneurship resources, promote the in-depth reform and development of e-commerce professional education, strengthen the cultivation of innovative talents, and provide talent strategic support for the construction of an innovative country [16, 17]. The framework of e-commerce innovation and entrepreneurship education resource sharing platform is given in Figure 1.

It can be seen from Figure 1 that this paper divides the educational resource sharing platform into three parts: resource layer, middle layer, and application layer. Each part is modularized, each module has strong independence, and different modules are connected by interface, which is convenient for the later maintenance of the system.

The resource layer is the basic layer of the platform, covering all kinds of hardware facilities. The middle layer mainly includes the data interface system and the shared resource processing system, which manages the interface by classification, connects the upper and lower layers for data transmission, realizes the information circulation, enhances the system flexibility, and analyzes and processes the transmitted data according to the user requirements of the application layer. The application layer is the task implementation layer, where users issue demand instructions, through the operation of the resource layer and the middle layer to complete the sharing of educational resources users need.

In order to fully meet the needs of users, in the design of e-commerce professional innovation and entrepreneurship education resource sharing platform, it is necessary to clarify the functional and nonfunctional requirements of the platform according to the user characteristics.

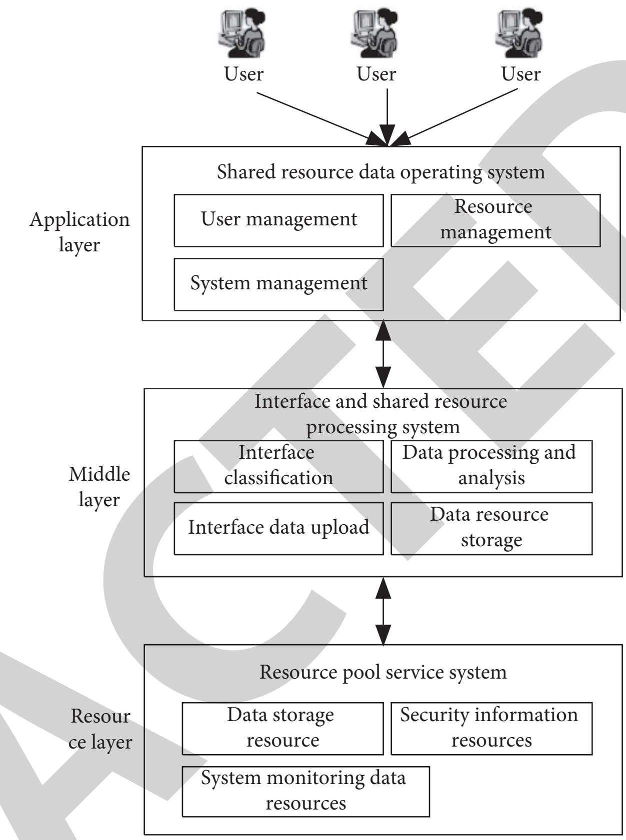

Figure 1: Sharing platform for e-commerce professional innovation and entrepreneurship education.

3.1. Functional Requirements. In the construction of e-commerce professional innovation and entrepreneurship education resource sharing platform, it mainly includes administrator and user roles, among which the user includes teachers, students, and so on. Users can publish new e-commerce professional education resources through the platform and also search the required resources from the platform. Unhealthy information needs to be reviewed and deleted one by one, so as to ensure the quality of e-commerce professional innovation and entrepreneurship education resources in the platform. At the same time, safety maintenance work needs to be carried out [18]. The structure of functional requirements is shown in Figure 2.

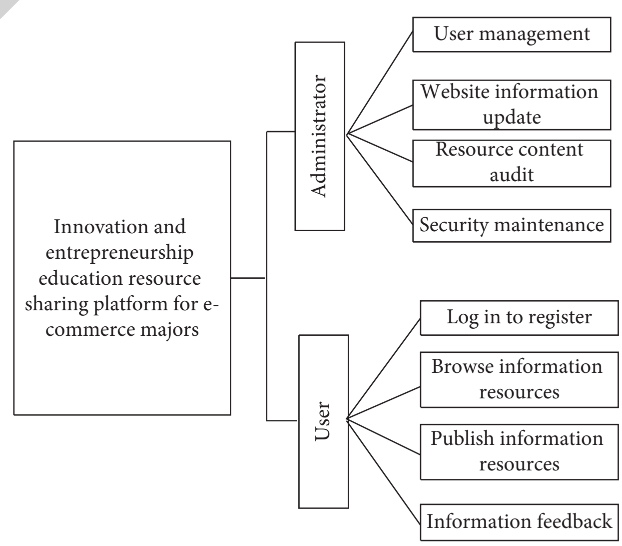

Figure 2: Functional requirements structure chart.

3.2. Nonfunctional Requirements. The nonfunctional requirements for running the E-commerce professional innovation and entrepreneurship education resource sharing platform include operational requirements and security requirements; operational requirements are usually relatively simple, and mastering the basic knowledge of computer use can complete the operation. The design of operation interface is usually more humanized [19].

Nonfunctional requirements specify the service level that the system must meet, the attributes of nonrunning time of the system, and the constraints that the system must comply with. Although nonfunctional requirements do not directly affect the system function, they have a great impact on the recognition of the information system by users and system support personnel. Nonfunctional requirements mainly include system constraints and assumptions, system availability, reliability, performance, scalability, etc.

The content of nonfunctional requirements is generally expressed by nonquantitative indicators. Indicators describe a range from which certain characteristics of the system can be measured. In this project, the system is required to adopt simple and friendly man-machine interface, so that users can apply it conveniently and quickly. Due to the limited computer application level of customer employees, it is required not to change the man-machine interface and operation habits of the client of the previous version of real-time cooperation system.

4. Analysis of Key Platform Modules

4.1. User Login Module. User registration and login are the basis of system operation and use. In order to ensure the high-quality and high-accuracy operation of the educational resource sharing platform and strengthen the security performance of platform operation, users must correctly select their identity after logging in with their user name and entering their password. They can log in to the system only after all verification is accurate; otherwise, they will be prompted to log in incorrectly, unable to enter the platform system. If you log in correctly, users with different identities will jump to the corresponding interface. Teachers and students have different permissions, and the accessible interface is not exactly the same. The user login process is shown in Figure 3.

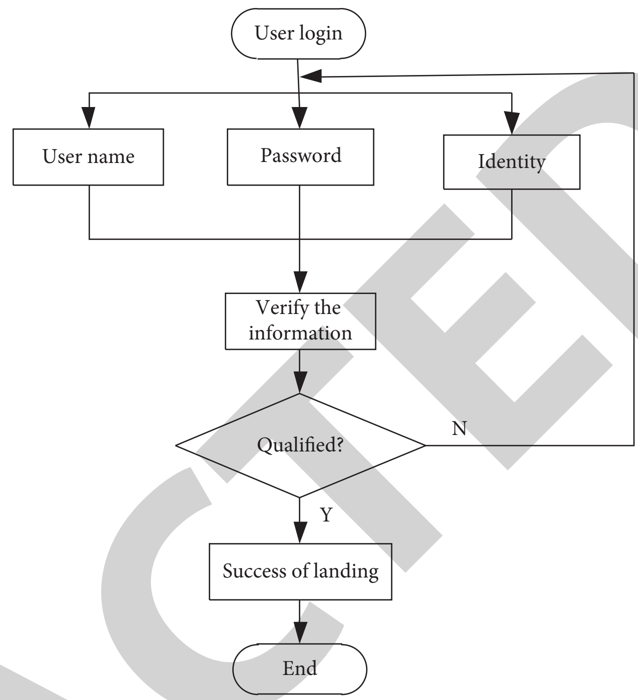

Figure 3: User login flowchart.

4.2. Education Resource Management Module. The main basis for the realization of educational resource sharing is that users can obtain the required resource information through website browsing. How to help users quickly and accurately obtain the required resources from the platform is a problem to be considered in the design of this module, so the design of educational resource management module is particularly important [20]. In this module, users with different roles can upload and download information related to e-commerce innovation and entrepreneurship education and administrators can delete resources in this module.

4.2.1. Resource Uploading. Considering the normative characteristics of educational resources, before uploading the resources related to innovation and entrepreneurship education of e-commerce major, administrators should first review the resources and relevant explanations themselves and then they can be released successfully after the completion of the audit. The main contents of the audit include the completeness of resource filling and the accuracy of resource classification. In addition, the modification function is also set to facilitate users to modify the content in time according to the feedback information of the system. After the modification is completed, the administrator will review it again. After the review, the information can be released successfully. The overall process of resource uploading is given in Figure 4.

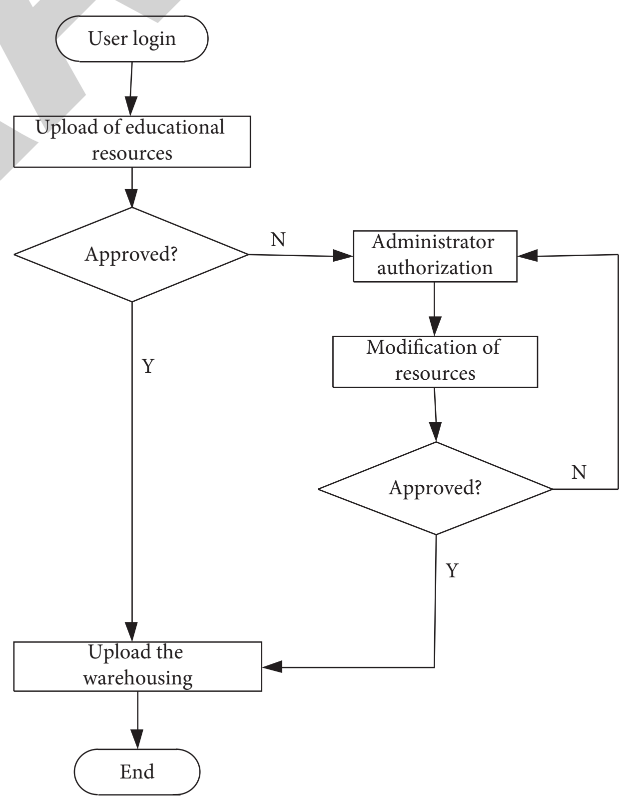

Figure 4: Resource uploading process.

4.2.2. Resources Downloading. After users log in to the platform and get the required educational resources through website and web browsing, they can download the resources after permission application. It is important to note that different users have different rights to download resources. Users can only download resources within their own permission. The specific flow is given in Figure 5.

4.2.3. Resource Deletion. Resource deletion is the exclusive authority of the system manager. During the normal operation and maintenance process of the platform system, the system administrator can delete invalid educational resources such as duplicate data, much old data, and so on according to maintenance needs.

4.3. System Management Module. After logging into the system, the administrator is mainly responsible for the operation and management of the user's general information and permissions and must timely audit the shared resources issued by the user, so as to prevent the spread of bad information and invalid information. In addition, daily maintenance of the system is needed to ensure the normal operation of the platform. The operation flow of system administrator is given in Figure 6.

4.4. Database Design Module. Traditional databases often use a single user server to complete data sharing, so this study uses cloud service technology to design the platform database, which allows multiple users to share and use the same database and centrally manage platform data [21]. The physical architecture of cloud database is given in Figure 7.

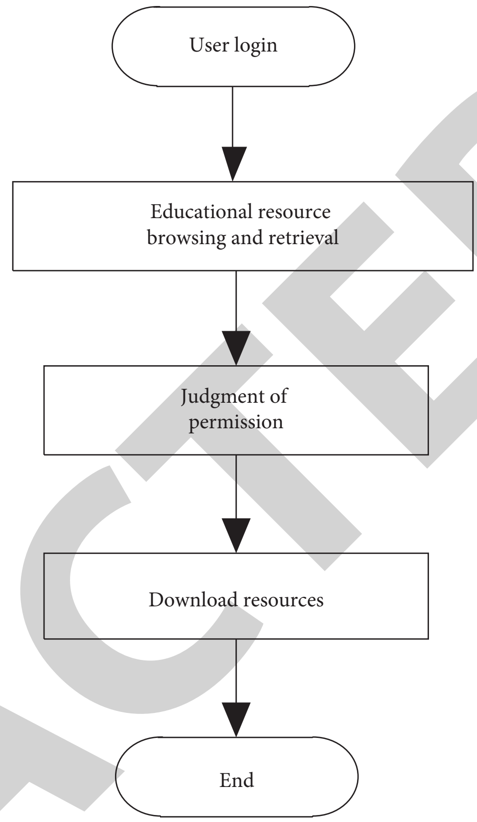

Figure 5: Resource downloading process.

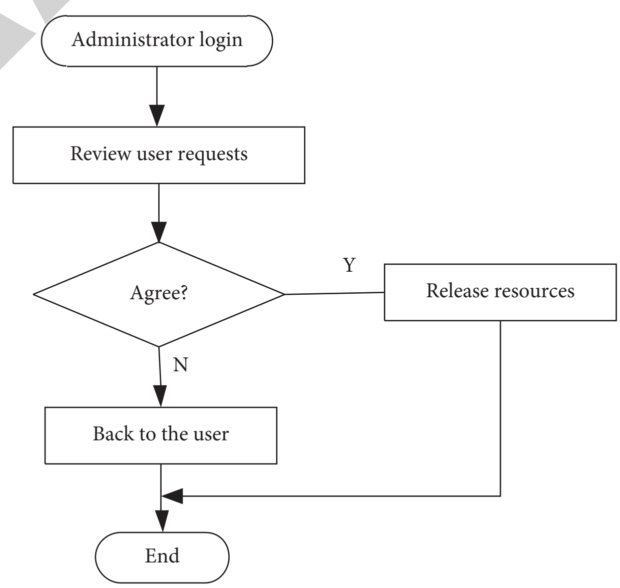

Figure 6: Flowchart of the system administrator.

5. Test Analysis of the Educational Resource Sharing Platform

After the construction of educational resource platform, the testing process is very important, which can find some problems in time and avoid unnecessary trouble. Taking the innovative entrepreneurial education resources of e-commerce major in a province as an example, the performance of this paper is tested. The data are from all colleges and universities in the province, and the time range is 2019–2020.

The software and hardware environments tested on the platform are given in Table 1.

In the test environment given in Table 1, the functions, performance, and security of the educational resource sharing platform are tested.

5.1. Functional Testing. The user login and administrator operation function are used to analyze and in many experiments to test whether the platform can successfully complete user login and administrator operations. The results are shown in Table 2.

As can be seen from Table 2, many tests show that the functional modules of the platform are running well.

5.2. Performance Testing. By selecting load capacity and response time as indicators, the performance of platforms of this paper and [9], [10], [14], and [15] is compared and tested. The response time refers to the time when the system makes the response when the user visits; the shorter the response time, which indicates that the higher the efficiency of the system, the higher the user experience. Load capacity refers to the response time of the system when the number of users is increasing. The shorter the response time is, the stronger the load bearing capacity of the system will be. The performance test results are shown in Figure 8.

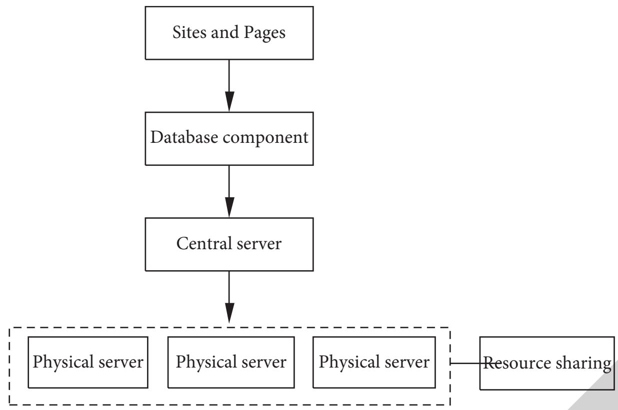

Figure 7: Physical architecture of the cloud database.

Table 1: Platform test environment.

Hardware environment		Software environment	
Name	Type	Name	Type
Operating system	Windows 10	Programming technology	JavaScript
Database server	MySQL	Programming language	Java
Central server	Web	Platform design framework	CI
Operating environment	Php5.6		

Table 2: Functional testing.

Number of experiments/times	User login function	Administrator action function
10	Good running	Good running
20	Good running	Good running
30	Good running	Good running

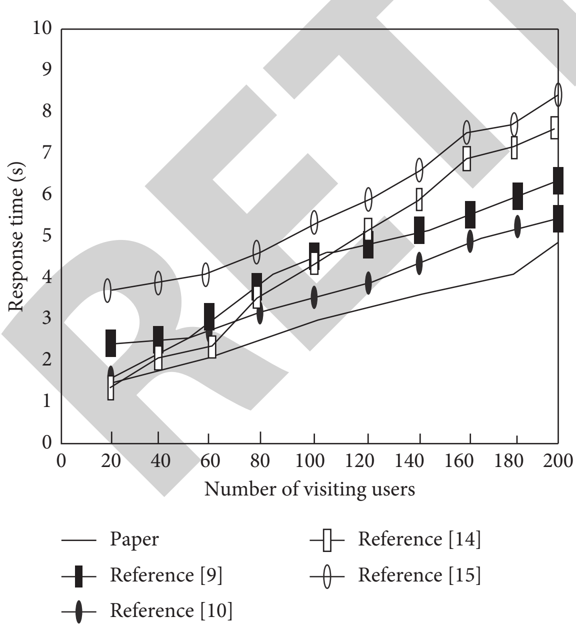

Figure 8: Performance test analysis of the platform.

By analyzing Figure 8, it can be seen that when the number of users is 100, the response time of the system in this paper is about 3 s and when the number of users is 200, the response time of the system in this paper is about 5 s, which can quickly respond to user operations. The study in [15] has the longest response time, up to 8 s when the number of users is 200. In terms of response time, the response time of the system in this paper is far lower than that in other references.

From the analysis of system load capacity, with the increase in access users, the response time curve of this paper's system and reference [10] system is relatively small, the curve of platforms in reference [14] and reference [15] is larger, and the increase in access users leads to the slowdown of the system. System load capacity is not strong. Comprehensive analysis found that the system has strong load capacity and running ability and its performance is better. The reason is that this paper adopts cloud service design platform database and centrally manages platform data, which enhances the efficiency of the system.

5.3. Safety Testing. Security is very important for educational resource platforms. Especially for confidential educational resources, security tests are required to prevent data leakage and system vulnerabilities. The test results are given in Table 3.

It can be seen from Table 3 that the security performance of different systems will decrease slightly under high load. The educational resource sharing platform in this paper can better cope with the system load. The security is high under

Table 3: Safety test analysis (%).

System	High load operation	Low load operation
Paper	93	97
Reference [9]	85	88
Reference [10]	80	83
Reference [14]	72	76
Reference [15]	75	79

high load and low load conditions, up to 97%. In other literature studies, the safety of system in reference [9] is relatively high and that of reference [15] is relatively low. The reason for the good security performance of the system in this paper is that during the construction of the platform, an access tool is designed to detect the security performance regularly and the administrator will also maintain the security of the system in daily operation, which improves the security of the platform built in this paper.

6. Discussion

Innovative entrepreneurship education is a new form and new concept of talent training and social innovation development in the new era. If e-commerce major wants to achieve great development, the cultivation of high-quality e-commerce talents is the key. In order to improve the quality of e-commerce talents and promote the smooth implementation of the innovation and entrepreneurship education reform of e-commerce specialty, we can put forward the strategy of sharing educational resources from the following aspects:

(1) Strengthen the understanding of innovation and entrepreneurship education. Set up advanced education ideas and improve the training standard of e-commerce professionals, to promote the concept of quality education in colleges and universities, to integrate innovative entrepreneurship education into the study plan of e-commerce major and to fully run through it, to deeply analyze the characteristics of e-commerce major, and to strengthen education in combination with professional characteristics. Improve students' understanding of innovative entrepreneurship education and strengthen students' innovative entrepreneurial ability. In evaluating the training quality of e-commerce professionals, colleges and universities should add the assessment of innovative entrepreneurial ability and gradually strengthen the importance of this index.

(2) It is the core to build a sharing platform for e-commerce innovation and entrepreneurship education resources. The platform has the corresponding mechanism of technical support and guarantee, can fully expand the e-commerce professional education knowledge base, gather high-quality education resources, can consult the required knowledge to students and teachers on the platform, can further understand innovation and entrepreneurship education, so as to enrich the educational form, can deeply tap the education needs, and can strengthen the e-commerce professional talent innovation and entrepreneurship learning. Through the construction and gradual application of the sharing platform of e-commerce innovation and entrepreneurship education resources, e-commerce education resources will continue to accumulate and strengthen gradually, so as to provide a good foundation for e-commerce talents training.

(3) Create an atmosphere for sharing educational resources. Build an organizational atmosphere of trust and respect, improve the willingness of teachers and students of e-commerce majors to share knowledge, and strengthen encouragement and support for students' innovative consciousness of e-commerce majors. Gradually, form a new mechanism to promote the development of innovative entrepreneurship education.

(4) Innovation and entrepreneurship education should be integrated into practical education. Combining theory learning with practice, the innovative entrepreneurship education resources will be integrated into e-commerce professional education, teaching content and teaching mechanism will be improved, the quality of professional talents and practical ability of entrepreneurship and employment will be continuously improved, and more efforts will be cultivated for the development of e-commerce education.

7. Conclusion

The innovation and development of e-commerce technology can ensure the security of network data. In order to highlight the effectiveness of e-commerce teaching, sharing teaching resources is an extremely effective means. In order to find an efficient education resource sharing strategy, this paper constructs an innovation and entrepreneurship education resource sharing platform for e-commerce specialty and modularizes the platform structure. Users can publish resources after logging in to the platform and can also obtain their own education resources on the platform. The construction of the platform can enrich the education content of e-commerce specialty, promote the education reform of e-commerce specialty, and provide favorable promotion for cultivating innovative and entrepreneurial e-commerce talents. In the future research work, we should improve the security of the platform to ensure that the information e-commerce teaching information will not be invaded or tampered with.

Data Availability

Data sharing not applicable to this article as no datasets were generated or analysed during the current study.

Conflicts of Interest

The author declares no conflicts of interest.

Hindawi
Scientific Programming
Volume 2021, Article ID 3902030, 15 pages
https://doi.org/10.1155/2021/3902030

Research Article

Computer Vision for Human-Computer Interaction Using Noninvasive Technology

Janarthanan Ramadoss,[1] J. Venkatesh,[1] Shubham Joshi ,[2] Piyush Kumar Shukla ,[3] Sajjad Shaukat Jamal ,[4] Majid Altuwairiqi,[5] and Basant Tiwari [6]

[1]*Center for Artificial Intelligence and Research, Chennai Institute of Technology, Chennai, Tamil Nadu, India*
[2]*Department of Computer Engineering, SVKM's NMIMS MPSTME Shirpur Campus, Savalade, India*
[3]*Computer Science & Engineering Department, University Institute of Technology, Rajiv Gandhi Proudyogiki Vishwavidyalaya, (Technological University of Madhya Pradesh), Bhopal 462033, India*
[4]*Department of Mathematics, College of Science, King Khalid University, Abha, Saudi Arabia*
[5]*College of Computers and Information Technology, Computer Science Department, Taif University, Taif, Saudi Arabia*
[6]*Department of Computer Science, Hawassa University, Institute of Technology, Hawassa, Ethiopia*

Correspondence should be addressed to Basant Tiwari; basanttiw@hu.edu.et

Received 17 July 2021; Revised 4 September 2021; Accepted 11 September 2021; Published 3 November 2021

Academic Editor: Punit Gupta

Computer vision is a significant component of human-computer interaction (HCI) processes in interactive control systems. In general, the interaction between humans and computers relies on the flexibility of the interactive visualization system. Electromyography (EMG) is a bioelectric signal used in HCI that can be captured noninvasively by placing electrodes on the human hand. Due to the impact of complex background, accurate recognition and analysis of human motion in real-time multitarget scenarios are considered challenging in HCI. Further, EMG signals of human hand motions are exceedingly nonlinear, and it is important to utilize a dynamic approach to address the noise problem in EMG signals. Hence, in this paper, the Optimized Noninvasive Human-Computer Interaction (ONIHCI) model has been proposed to predict human motion recognition. Average Intrinsic Mode Function (AIMF) has been used to reduce the noise factor in EMG signals. Furthermore, this paper introduces spatial thermographic imaging to overcome the conventional sensor problem, such as gesture recognition and human target identification in multitarget scenarios. The human motion behavior in spatial thermographic images is examined by target trajectory, and body movement kinematics is employed to classify human targets and objects. The experimental findings demonstrate that the proposed method reduces noise by 7.2% and improves accuracy by 97.2% in human motion recognition and human target identification.

1. Introduction

Nowadays, with the rapid development of information technology, human beings are trying to communicate with computers more naturally [1]. The conventional human-computer interaction input devices such as the mouse, keyboards, and remote devices lack flexibility, and there is no longer a natural way of interacting [2]. In general, voice commands and body language are natural ways for people to communicate with computers, including many online commercial products [3]. The interaction between humans and computers is the most important application of computer vision for autonomous structures [4]. It is essential to acquire precise data like shape, behavior, and motions for efficient human-computer interaction [5]. An effective characteristic analysis of these human targets can accurately recognize and identify the targets [6]. Human target identification and objects surrounding play a crucial role and pose many challenges before interaction between computers and humans [7]. We rapidly determine the number of important facts and qualities about each other during human-to-human interaction, including identification, age, facial expressions, and gestures. These visual cues/features have an impact on the content and flow of a conversation, and they provide contextual information such as situation and speech context. A gesture or a facial expression, for example, could be intended as a signal of understanding, or the gaze direction can be used to differentiate between the object referred to like this and the direction over there in speech. As a result, other communication channels such as speech and gestures are both coexpressive and complementary to the visual channel.

Conversely, conventional sensors do not deliver an acceptable field of view (FOV) to monitor various targets to examine human movement and body features [8]. The process of human movement identification needs sufficient space to map command gestures and different human targets [9]. It is significant to recognize the human targets and surrounding objects, and the computer aims to satisfy the requirements of the human interaction environment [10]. The user's gesture would be consistent with the physical space of the virtual world; i.e., the user's action should be matched with the gesture in the virtual field, and it is more appropriate to estimate the gesture for human-computer interaction [11]. A rich user experience and more effective and efficient interaction can be obtained by integrating visual information with other input modalities (such as keyboard and mouse). In addition to standard desktop computing, vision-based interaction could be beneficial in a variety of scenarios, including mobile, immersive, and ubiquitous computing.

Presently, sensor technology such as electromyographic (EMG) and signal processing has been extensively utilized in the field of human-computer interaction and multifunctional prosthetic hand control [12, 13]. Electromyographic (EMG) signal collects superficial muscle and nerve trunk activity bioelectric signals through electrodes on the surface of the skin and performs muscle processes evaluations and simulations via the recorded, filtered, amplified, transmitted, and feeding of the collected bioelectric signals [14, 15]. Since the EMG signaling of the human leg or hand movements during object usage easily interferes with noise [16]. The main problem to accomplish a difficult understanding of hand motion is successfully gathering signals, extracting features, and classifying diverse hand movements for human-computer interaction [17]. From the object's characteristics such as weight, size, and shape, it is possible to identify human targets/emotions [18].

In this paper, the Optimized Noninvasive Human-Computer Interaction (ONIHCI) model has been proposed to address gesture recognition and human target identification problems. The electromyographic (EMG) signal can represent the muscles' active conditions; the data of the neural activities can be determined [19]. The advantage of electromyographic is noninvasive; thus, it executes well in studying neurological rehabilitation, motion detection, and artificial control. Besides, the AIMF algorithm has been employed to reduce noise in the EMG signal. The present models focus on human-computer interaction, emphasizing a specific target or the behavioral analysis of a set of targets [20]. The spatial thermographic images for human motions are analyzed to explain the trajectory actions and the kinematics motion of the human and objects. Our approach defines human targets precisely and allows them to improve their restricted vision and overcome traditional methodological problems related to gesture recognition and human target identification [21]. Target trajectory examines human motion behavior in spatial thermographic images, and body movement kinematics is used to classify human targets and objects.

The rest of the paper is arranged as follows. Section 1 and Section 2 discussed the overview of computer vision for human-computer interaction and related works. In Section 3, the Optimized Noninvasive Human-Computer Interaction (ONIHCI) model has been suggested. In Section 4, the experimental results have been performed. Finally, Section 5 concludes the research paper.

2. Related Works and Features of This Research Article

Qi et al. [22] introduced the linear discriminant analysis and extreme learning machine (LDA-ELM) method for smart human-computer interaction based on surface EMG gesture recognition. The proposed method can minimize the useless data in Surface Electromyography (SEMG) signals and enhance identification accuracy and efficiency. This paper concentrates on time variances optimization in surface [23]. EMG pattern recognition and the numerical outcomes are advantageous to decreasing the time variances in gesture identification based on surface EMG. Chen et al. suggested the Motor Unit Spike Trains with Blind Source Separation Algorithm (MUST-BSSA). That is how well high-density EMG signals recognize motor unit movements during hand postures. They characterize the precision in recognition of motor unit actions during hand postures from high-density EMG signals. The results demonstrate the possibility of recognizing motors during the assigned motor operations and the high precision of hand gestures classification for human-computer interface perspectives [24].

Song et al. [25] discussed the Guidance framework for tracking by detection (GFTD) for hand detection based on the thermal image. They introduced an Adaptive Hand Detection (AHD) based automatic tracking-by-detection algorithm utilizing the Kernelized correlation filters tracker to enhance the performance of the proposed model. The proposed model detects hands in real time by decreasing calculation utilizing a single sensor instead of fusing manifold sensors, enables precise tracking, and enhances hand tracking precision. Xiao et al. [26] proposed the variational mode decomposition and composite permutation entropy index (VMD-CPEI) method to classify hand movements. The approach suggested in this paper uses the VMD procedure for decomposing the initial SEMG signal into multiple VMFs and measuring the related CPEI of each signal component. The model proposed can enhance the quality of life of amputees, disabled persons, and others.

Sekhavat et al. [19] introduced Affective User Interface Design and Evaluation (AFFUIDE) to evaluate the effect of using facial expressions emotions as a user interface (UI) and system input in virtual scenarios. The data suggests that the traditional usable user interface is the most useful and that the full affective user interface feels the best fun and user experience. Choudhary et al. [20] recognized someone even when they were not in a neutral condition or had any facial expression. Using a hidden Markov model with singular value decomposition, they could identify persons whose top half face is visible (HMM-SVD). Singular value decomposition parameters were used in this article to build a series of blocks for each picture of a face [21]. To cover the entire face, a seven-state HMM was employed. In this paper, the Optimized Noninvasive Human-Computer Interaction (ONIHCI) model has been proposed to address gesture recognition and human target identification [23]. This paper proposes a novel approach to determine the human targets in spatial thermographic images [24, 27] using vision perception. This system estimates the capacity of the human targets to view when they have restricted visualization and supports targets perceiving their surroundings by informing them about their condition through the visualization system [28, 29]. Identifying human targets is the main aim and, at the same time, recognizing the scenario for human targets. The signals of human hand motions have been gathered utilizing an EMG acquisition device [30, 31]. A motor unit classification-based gesture recognition method was proposed in [32]. MUSTs were first classified into 11 categories, one per motion. The averaged discharge timings of MUSTs in each group are then used to measure the activation level of the cerebral drive to each motion. By comparing the estimated activation levels of each motion, the output gesture class was determined. AIMF has been used to denoise the obtained real signs and feature sets for the hand movement classification process [22, 25, 33]. The proposed method is briefly described in the following section.

3. Optimized Noninvasive Human-Computer Interaction Model (ONIHCI)

In this paper, the Optimized Noninvasive Human-Computer Interaction (ONIHCI) model has been proposed to address gesture recognition and human target identification problems. The requirement for computer vision-based human-computer interaction and human movement recognition has been increased in fields like intelligent monitoring, security, and surveillance system. The most significant and common human movement is walking and running. Many studies aimed to develop a computer model of motion. The role of human movement recognition is a challenge in human-computer interaction. Motion analysis includes measuring, analyzing, and evaluating the motion functions associated with walking or running activity to determine the human target in an HCI system.

Case 1. Human kinematics analysis and trajectory analysis for human target identification

Solution 1. Analysis of human kinematics is the initial measure to determine a human in the course of its movement or static prospect. Human frames are extracted from the spatial thermographic image, and areas are calculated from dynamic targets to explore trajectories and kinematics to calculate the proposed approach. The key targets know the instructions and are in an upright position. This paper utilizes three human targets for the identification of human targets.

Figure 1 shows the human body kinematics analysis. The human body orientation around the arm region $[X_B Y_B Z_B]$, legs $[X_{L,R} Y_{L,R} Z_{L,R}]$, and head for the upper part of the targets spot $[X_V Y_V Z_V]$ is determined for every human.

Human Target 1 (G_1). The human body orientation around the arm region is denoted as $[X_{B_1} Y_{B_1} Z_{B_1}]$, left leg $[X_{L_1} Y_{L_1} Z_{L_1}]$, right leg $[X_{R_1} Y_{R_1} Z_{R_1}]$, and head target sport $[X_{V_1} Y_{V_1} Z_{V_1}]$

Human Target 2 (G_2). The human body orientation around the arm region is denoted as $[X_{B_2} Y_{B_2} Z_{B_2}]$, left leg $[X_{L_2} Y_{L_2} Z_{L_2}]$, right leg $[X_{R_2} Y_{R_2} Z_{R_2}]$, and head target sport $[X_{V_2} Y_{V_2} Z_{V_2}]$

Human Target 3 (G_1). The human body orientation around the arm region is denoted as $[X_{B_3} Y_{B_3} Z_{B_3}]$, left leg $[X_{L_3} Y_{L_3} Z_{L_3}]$, right leg $[X_{R_3} Y_{R_3} Z_{R_3}]$, and head target sport $[X_{V_3} Y_{V_3} Z_{V_3}]$

The human body provides a few signs of motion or static state disposition. The inclination for direction is extracted from the determination of the direction between these kinematics. If the legs and head position are open at a certain angle, the motion direction from the slope of the head is provided by the angle between the legs and head. Figure 1 shows the human body kinematics; here, the human target G_1 is being demonstrated with a running direction to the head and right sloped toward a similar direction. In the instance of a static condition of the target, body, legs, and head orientation comprising arms might be parallel to human targets G_2 and G_3. The interactive system point of view transferred kinematics is provided with G_W and the kinematics from the initial interactive system, $[X_G, Y_G, Z_G]$ are multiplied with orientation and translation, and the interactive systems and rotation between the interactive systems are expressed as

$$G_{W_1} = \begin{bmatrix} X_{G_1} & Y_{G_1} & Z_{G_1} \end{bmatrix} \begin{bmatrix} \cos\theta & -\sin\theta & 0 \\ \sin\theta & \cos\theta & 0 \\ 0 & 0 & 1 \end{bmatrix} + \begin{bmatrix} x_t & y_t & z_t \end{bmatrix}, \tag{1a}$$

$$G_{W_2} = \begin{bmatrix} X_{G_2} & Y_{G_2} & Z_{G_2} \end{bmatrix} \begin{bmatrix} \cos\theta & -\sin\theta & 0 \\ \sin\theta & \cos\theta & 0 \\ 0 & 0 & 1 \end{bmatrix} + \begin{bmatrix} x_t & y_t & z_t \end{bmatrix}, \tag{1b}$$

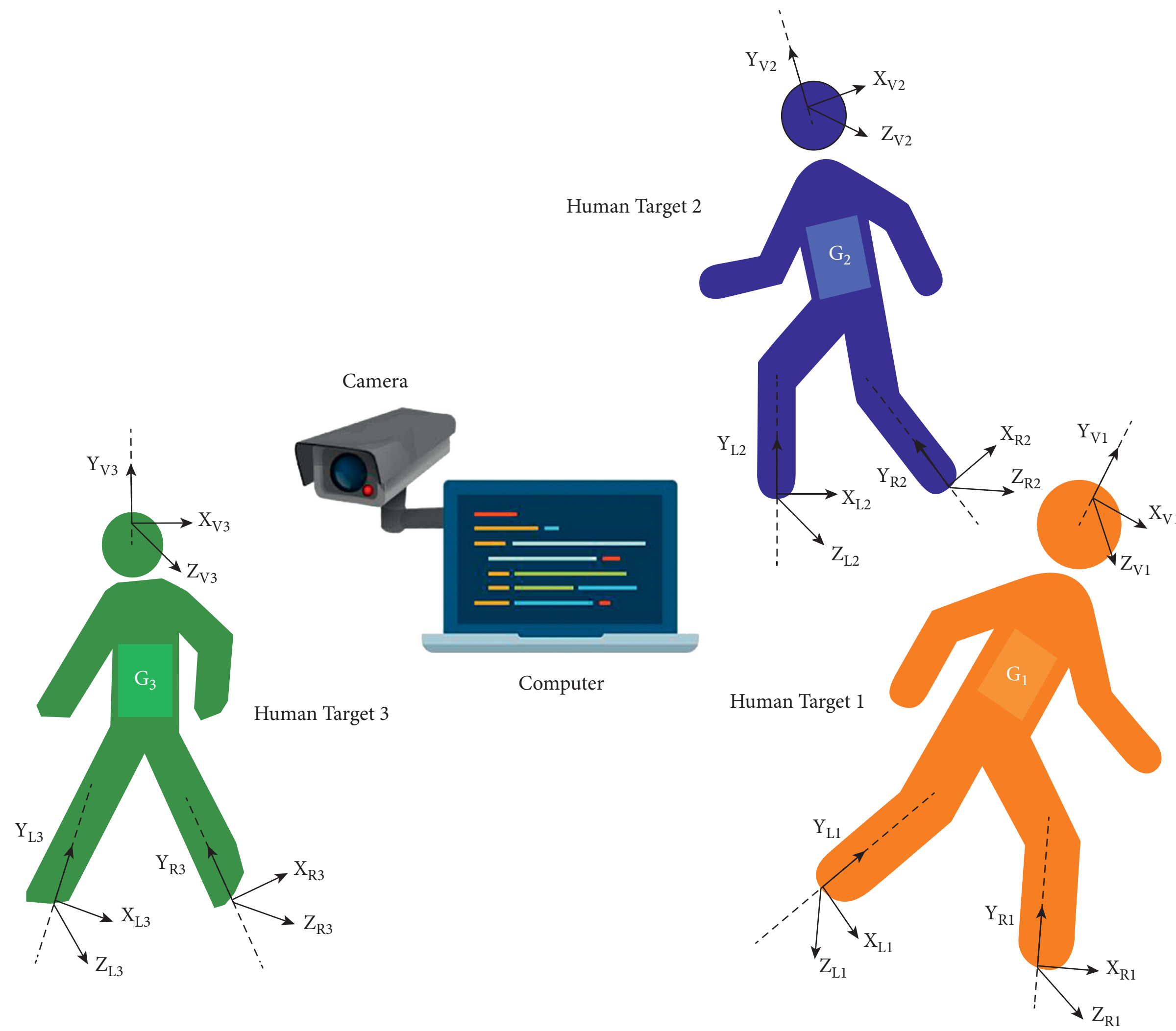

Figure 1: Human body kinematics analysis.

$$G_{W_3} = \left[\, X_{G_3} \;\; Y_{G_3} \;\; Z_{G_3} \,\right] \begin{bmatrix} \cos\theta & -\sin\theta & 0 \\ \sin\theta & \cos\theta & 0 \\ 0 & 0 & 1 \end{bmatrix} + \left[\, x_t \;\; y_t \;\; z_t \,\right]. \tag{1c}$$

As inferred from equations (1a), (1b), and (1c), the human body target rotation matrix, kinematics, and translation vector of the transformation vector can be computed. The relationship between two groups of kinematics can be utilized to choose the categorized targets from two interactive systems to connect similar targets in two various thermographic views.

Figure 2 shows the position data of every computer or interactive system T_t, and R_t is utilized to convert the human body kinematics of the other view direction. In Figure 2, the spatial thermographic interactive system coordinate system is denoted as $Q_{ST} = [X_{ST} Y_{ST} Z_{ST}]$, the single perspective interactive system is denoted as $Q_W = [X_W Y_W Z_W]$, and the interactive stereo system denoted is as $Q_{ST} = [X_Q Y_Q Z_Q]$. The rotation and translation between interactive systems are denoted as R_Q, T_Q and R_W, T_w. The human target trajectories are examined in the thermographic scene concerning the trajectory trend of the respective target's feature points. The height and width of the target area are evaluated for a ratio to determine the first data about the trajectory target trend. The ratio variations are reliant on the target alignment through the center rotation. The height and width variations for the target's backward and forward motion concern the interactive system.

In Figure 3, the backward and forward motion calculations and the magnitude and direction vector are provided for every interactive system denoted as dotted lines. The variations of ratios from every interactive systems perspective are presented in Figure 3. Stereo vision-based identification combines features extracted from two-dimensional stereo images with reassembled three-dimensional object features to sense humans in an interactive setting. The interactive stereo system is already monitoring the target G_1, the computer endowed perspective sensor; thermographic camera altered its direction to the absorbed target as a portion of the human-computer interaction task. The human target coordinate system is represented by the direction vector U_1, width s_w, and the height g_w; the ratio $(g_{q,1}/s_{q,1})$ indicates the target G_1 moving toward a single

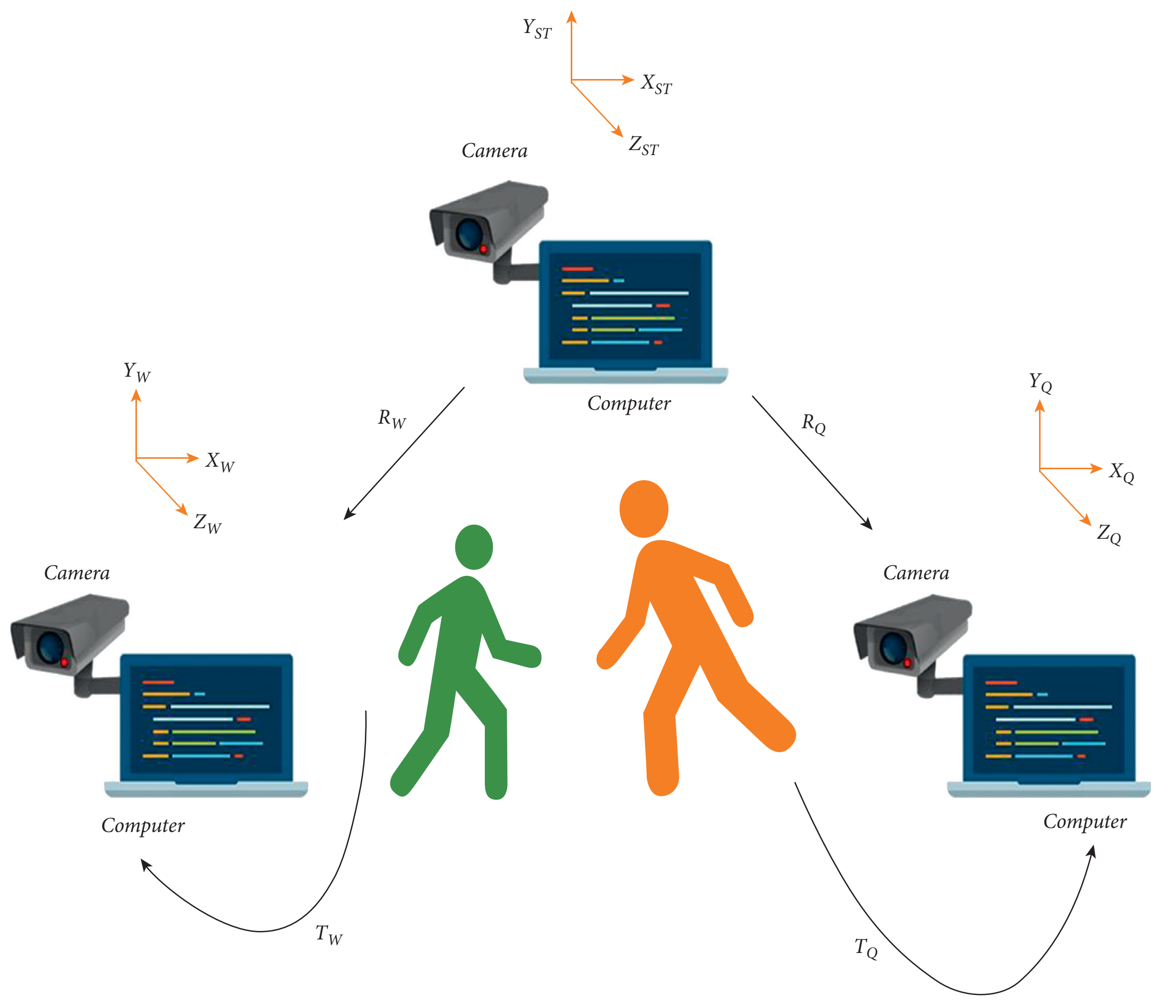

Figure 2: Three interactive systems equipped with a single thermal camera, stereo thermal sensor, and IR sensor. Rotation and translation between interactive systems are exposed with a corresponding spatial thermographic interactive system.

perspective interactive system. The ratio $(g_{w,1}/s_{w,1})$ indicates the target G_1 moving toward the interactive stereo system; c_s is the direction. The rotation and translation between interactive systems are denoted as R_Q, T_Q and R_W, T_W. These variations are noted during the movement of the target G_1 and updated for a time r by equation (2). To determine the method vector direction U_s, the height g_w and width s_w are utilized in the thermographic image.

$$U_s = \begin{cases} s_{w,r} - s_{w,r-1}, & \text{if}\left(\dfrac{g_w}{s_w}\right)_r - \left(\dfrac{g_w}{s_w}\right)_{r-1} = 0, \\ 0, & \text{if}\left(\dfrac{g_w}{s_w}\right)_r - \left(\dfrac{g_w}{s_w}\right)_{r-1} \neq 0. \end{cases} \quad (2)$$

As shown in equation (2), s_w denotes rotation width, g_w denotes rotation height, and (g_w/s_w) denotes the rotation ratio. If there is no variance between successive proportions, the direction vector U_s is acquired from the variance between the successive target's width in successive pictures. If the proportion is varying, let us think that the target is creating a rotation around itself.

The horizontal target motion is utilized for right and left directions in its trajectory. Let us assume the overall extracted feature point for this particular target is F and the feature extracted point for a particular target is x_f. The horizontal motion feature point x_f is followed after the evaluation of their mean coordinates until the overall number of F. The final horizontal position average at the time $r - 1$ is deducted from the present mean. This variation supports the determination of the direction and horizontal vector magnitude c_w from the next expression.

Condition 1:

$$c_w = \frac{\left(\sum_{f=1}^{F} x_{f,r}\right)}{F}. \quad (3a)$$

Condition 2:

$$c_w = \frac{\left(\sum_{f=1}^{F} x_{f,r-1}\right)}{F}. \quad (3b)$$

After computing

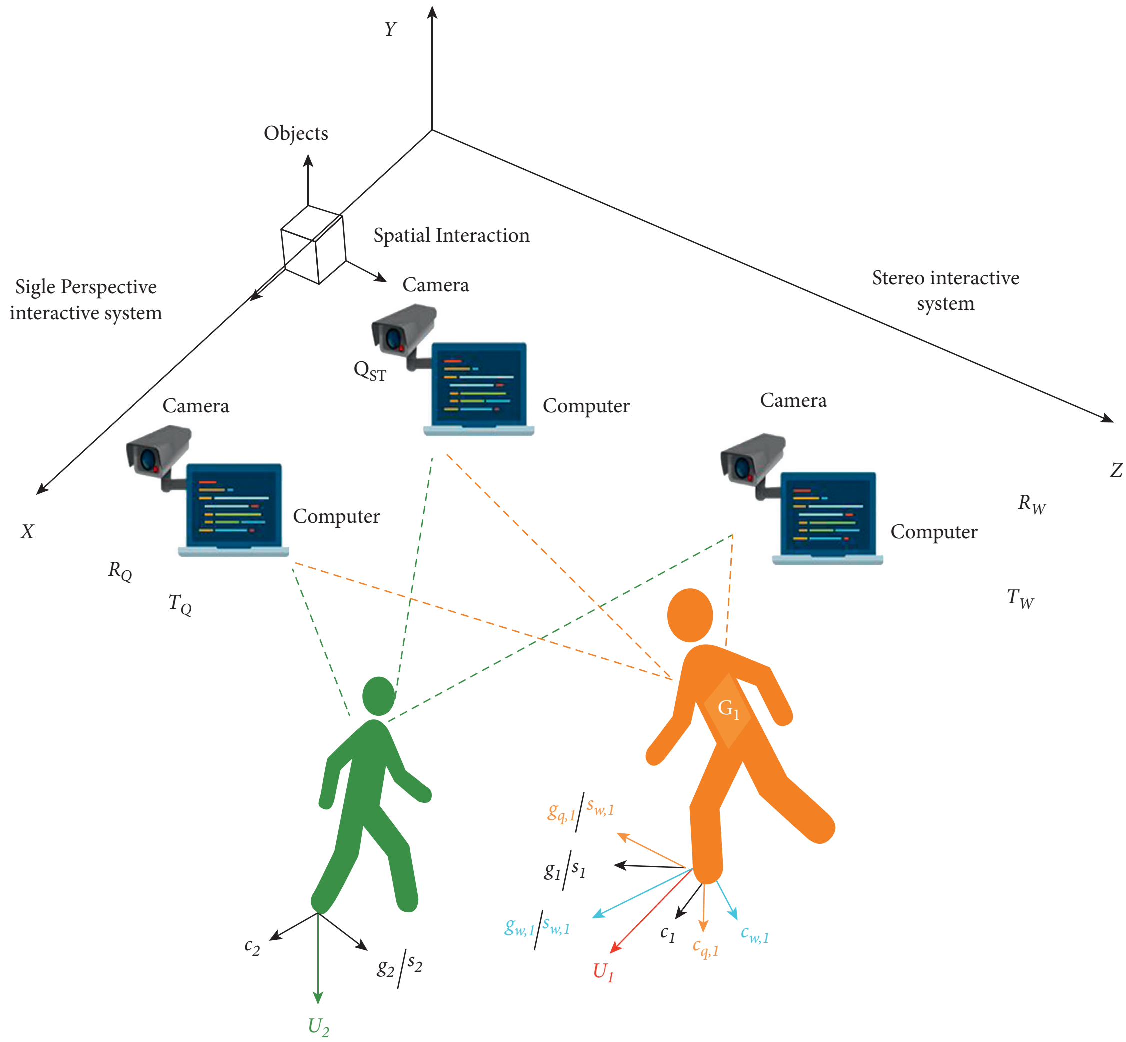

FIGURE 3: Interactive system identifying the trajectory vector for every target.

$$c_w = \frac{\left(\sum_{f=1}^{F} x_{f,r}\right)}{F} - \frac{\left(\sum_{f=1}^{F} x_{f,r-1}\right)}{F}, \tag{3c}$$

$$U_w = \sqrt{U_s^2 + c_w^2}. \tag{3d}$$

As discussed in equations (3a), (3b), and (3c) x_f denotes the extracted feature points for a particular target. F denotes the overall extracted features point for specific targets. The final horizontal position average at period $r-1$ is deducted from the present mean r. c_w denotes the direction and horizontal vector magnitude. U_w denotes the final trajectory vector. A trajectory trend is produced for every target in the spatial thermographic picture, and it is equated with another interactive system trajectory assessment. Every interactive system assessment utilizes a horizontal and method vector to determine the last trajectory vector.

The target areas identified are labeled with two criteria for their characteristics. The human target areas are identified and bounded by a rectangle frame. The frame is split into $W = (Ga/m_{\text{ver}})(Sa/m_{\text{hor}})$ number of cells to examine every segment distinctly. The number of cells in the horizontal direction m_{hor} and the vertical direction is provided with m_{ver}. The human target is chosen utilizing associated elements and distinct from added substances in the target frame. The pixels in each cell are added by equation (4), and the overall human target field is determined for the respective cell. Let us consider that w is the respective cell, A_w is the overall cell pixel value, and $G_a$and S_a are the height and width of the target frame, respectively. Each row and the cell column are added to a bird's eyesight and perception target spectrum as an added target indistinguishable signature:

$$A_w = \sum_{x=A_x}^{x_k} \sum_{y=A_y}^{x_k} q(x, y). \tag{4}$$

As shown in equation (4), A_w is the overall cell pixel value. Each pixel in a cell is provided with the pixel q, and the coordinates of this pixel in the cells are (x, y). The final pixel directs from the bottom and left of each cell can be evaluated from the subsequent expression:

$$(xy)_k = f\left((xy)_k\right) = \begin{cases} x_k, & \text{if } (m_{\text{hor}}) = A_x + w_x\left(\dfrac{S_a}{m_{\text{hor}}}\right), \\ \\ y_k, & \text{if } (m_{\text{ver}}) = A_y + w_y\left(\dfrac{G_a}{m_{\text{ver}}}\right), \end{cases} \tag{5a}$$

$$x_k = A_x + w_x\left(\frac{S_a}{m_{\text{hor}}}\right)y_k = A_y + w_y. \tag{5b}$$

Equations (5a) and (5b) show the thermographic image final pixel coordinates of each cell, where the number of cells in the horizontal direction m_{hor} and the vertical direction is provided with m_{ver}. G_a and S_a are the target frame height and width, respectively. The beginning coordinates of every cell A_x and A_y are determined from the present directs of the target frame and frame height and width from the resulting expression:

$$(A)_{xy} = f\left((A)_{xy}\right) = \begin{cases} A_x, & \text{if } (m_{\text{hor}}) = \dfrac{S_a}{m_{\text{hor}}}(w_x - 1), \\ \\ A_y, & \text{if } (m_{\text{ver}}) = \dfrac{G_a}{m_{\text{ver}}}\left(w_y - 1\right), \end{cases} \tag{6a}$$

$$A_x = \frac{S_a}{m_{\text{hor}}}(w_x - 1), \tag{6b}$$

$$A_y = \frac{G_a}{m_{\text{ver}}}\left(w_y - 1\right), \tag{6c}$$

As derived in equations (6a), (6b), and (6c), every cell index is evaluated from $w_y = [w - 1/m_{\text{ver}}] + 1$ utilizing floor function after division and $w_y = w - w_y m_{\text{hor}}$. After determining the kinematics for arm, leg, and head areas, corr chooses the relationship of these kinematics for each thermographic image of a similar target. Additional correlation outcome originates trajectories utilizing the human target trajectory directions $[X\ Y\ Z]$ with corr( ) to choose the last trajectory direction with the maximum association outcome. Human motion has been identified based on human body kinematics and target trajectory analysis; human activity has been identified accurately for the human-computer interaction process. With the collective thermographic images of pixel and edge variances, human motion detection has been performed. The spatial thermographic images have many noises, low image resolution, and low contrast to resolve these problems. AIMF algorithm has been proposed.

Case 2. EMG based human motion recognition.

Solution 2. A better human-computer interaction can be accomplished utilizing electromyographic (EMG) based human motion recognition. The signals of common human gestures have been gathered using the EMG acquisition device. Electrode's locations have been chosen in line with the musculoskeletal of these 5 muscles and definite by contractions of the muscle-specific, which involve physically repelled finger abduction and extension. EMG signals are bioelectrical reactions affected by muscle fiber movement during multiple muscle contractions.

Figure 4 displays the human-computer interaction procedure based on the EMG signal. Data acquisition, preprocessing, classification model, and feature extraction are the significant and main stages in human gesture classification. The gesture classification can identify discrete body gestures and cannot be utilized for control of the interactive system and, thus, continuous motion regression, which has assessments for more motion information. Compared to the EMG signal-based musculoskeletal model for gesture recognition, the mapping between EMG and angular acceleration, joint moment, joint angular velocity, and angle can be recognized. The commonly utilized feature can be primarily separated into a time-frequency domain feature and a frequency domain feature. The initial EMG signals gathered include a variety of noise signals, like electromagnetic noise, electrode noise, and pervasive noise, caused by an external environment and acquisition system. Therefore, reducing the noise of the real signal is necessary to generate actual and efficient information for the extraction of features.

As shown in Algorithm 1, the proposed AIMF algorithm with an adaptive time-frequency data analysis can be distinctly a time series into a finite number of elements, known as Empirical Mode Decomposition (EMD). For the self-adaptive decomposition, the data processing method is used for the nonstationary and nonlinear signals, where t is the acquisition channel, input $E(t)$ is the EMG signal, and output D_{IMF} is the intrinsic mode function. To reduce the noise in EMG signal, let us compute all the extreme points of $E(t)$; i.e., $K(t) = \{K_{\min}(j), K_{\max}(j)\}$. We fit the high points by interpolation approach: upper envelope represented as $K_{\max}(j) \longrightarrow O_{\max}(j)$ and lower envelope represented as $K_{\min}(j) \longrightarrow O_{\min}(j)$; subsequently, we compute average envelope value; i.e., $V(t) = (O_{\min}(j) + O_{\max}(j))/2$; after that, we obtain a stationary data sequence; $S(t) = E(t) - V(t)$. The algorithm decomposes the actual signal divides noise from the efficient signal with high time-frequency resolution and better adaptability in various intrinsic mode functions. Therefore, the collecting the features of the EMG signal, the AIMF algorithm is a perfect method for decreasing the EMG signal noise.

As shown in Algorithm 1, Empirical Mode Decomposition is executed on every EMG signal channel; a set of AIMF can be determined as

$$D(t) = \sum_{i}^{m} D_{\text{IMF}}(i) + \gamma_m. \tag{7}$$

As inferred from equation (7), γ_m denotes the residual of the actual EMG signal after extracting m AIMFs D. The data signal determined after noise reduction using Algorithm 1 guarantees the feature extraction of original motion signals.

Input: the actual data sequence of the EMG signal, $E(t)$, $(t = 1, \ldots, m)$
Output: intrinsic mode function, $D_{\mathrm{IMF}}(i)$;
Repeat
While $j < L$ **do**
for all j such as $1 \le j \le l$ **do**
Compute $E(t)$ i.e., $K(t) = \{K_{\min}(j), K_{\max}(j)\}$;
Obtain upper envelope: $K_{\max}(j) \longrightarrow O_{\max}(j)$,
Obtain lower envelop: $K_{\min}(j) \longrightarrow O_{\min}(j)$;
Compute average envelope value $V(t) = (O_{\min}(j) + O_{\max}(j))/2$;
Obtain a stationary data sequence, $S(t) = E(t) - V(t)$;
Update $t = t + 1$;
Until convergence

Algorithm 1: Average intrinsic mode function algorithm for electromyographic signal noise reduction.

Figure 5 shows the communication between interactive systems. Without loss of generalization, it is preassumed that the l th HCI system records data of K heterogeneous variable to be evaluated and I heterogeneous variable to interact, which produce a computation vector $c_l' = [c_{l,1}, \ldots, c_{w,I}']^T$ and communication vector $d_l' = [d_{l,1}', \ldots, d_{l,I}']^T$, where c_l' and d_l' are calculated values of the k th computation variable and i th communication variable at l th HCI system, respectively. As a reminder for computation, the interactive system engages itself in computing k th targeted function through the following equation:

$$p_k = f_k\left(\sum_{l=1}^{L} h_{l,k}\left(c_{l,k}\right)\right), \quad k = 1, \ldots, K. \tag{8}$$

As discussed in equation (8), p_k is the ideal computation output, and $h_{l,k}(\cdot)$ and $f_k(\cdot)$ denote the preprocessing function at the l th interaction system. Let us consider $d_l = [h_{l,k}(c_{l,k}), \ldots, h_{l,K}(c_{l,K})]^T$ indicating the preprocessed computation signal at the l th interaction system. For simplicity of exploration and without loss of generalization, let us preassume that the communication signals and computation signals are distributed with the unit norm; that is, $E\{d_l d_l^H\} = J$ and $E\{d_l' d_l'^H\} = 1$. Therefore, the l th interactive system builds the coded transmit EMG signal y_l as

$$y_l = S_l d_l + \sum_{i=1}^{I} u_{l,i} d_{l,i}'. \tag{9}$$

As inferred from equation (9), $S_l \in E^{N\times K}$ and $u_{l,i} \in E^{N\times 1}$ indicate the transmit beams for the communication and computation signal, respectively.

$$\|S_l\|_F^2 + \sum_{i=1}^{I} \|u_{l,i}\|^2 \le \frac{Z_l}{T/2}, \quad \forall l, i. \tag{10}$$

Thus, the received signal at the interactive system is expressed as

$$x = \sum_{l=1}^{L} H_l y_l + m = \underbrace{\sum_{l=1}^{L} H_l S_l d_l}_{\text{computation signal}} + \underbrace{\sum_{l=1}^{L}\sum_{i=1}^{I} H_l u_{l,i} d_{l,i}'}_{\text{communication signal}} + m. \tag{11}$$

As shown in equation (11), m is the noise vector with variances σ_m^2. Initially, the processing of the computation signals has been discussed. Because of the one-to-one mapping between $c = \sum_{l=1}^{L} c_l$ and $p = [p_1, p_2, \ldots, p_K]^T$ in equation (8), let us take a precise c at the interactive system as the targeted function signal. It is anticipated to execute a receive beam at the interactive approach to reduce the distortion of the targeted function signal affected by channel noise, fading, and interference. Therefore, the received signal for computation at the interactive system is expressed as

$$\hat{c} = V^L \sum_{l=1}^{L} H_l S_l d_l + V^L\left(\sum_{l=1}^{L} H_l \sum_{i=1}^{I} u_{l,i} d_{l,i}' + m\right). \tag{12}$$

As derived in equation (12), $V \in E^{M\times K}$ is a receive beam for computation outcomes at the interactive system. As a rule, the distortion of computation at the interactive system is calculated by the Root Mean Square Error (RMSE) between c and $\hat{c}$ which is stated as

$$\mathrm{RMSE}(d, \hat{d}) = Z\left\{tr\left((\hat{d} - d)(\hat{d} - d)^H\right)\right\}. \tag{13}$$

Replacing (12) into (13), the computation distortion can be calculated as the resulting RMSE function of transmitting and receiving beam:

$$\begin{aligned}\mathrm{RMSE}\left(V, S_l, u_{l,i}\right) = {} & \sum_{l=1}^{L} \left\|V^H H_l S_l - J\right\|_F^2 + \sigma_m^2 \|V\|_F^2 \\ & + \sum_{l=1}^{L}\sum_{i=1}^{I} \left\|V^H H_l u_{l,i}\right\|^2.\end{aligned} \tag{14}$$

Subsequently, communication signal processing has been discussed. The received EMG signal for communication at the interactive system can be evaluated as

$$x_{l,i}' = q_{l,i}^H H_l u_{l,i} d_{l,i}' + q_{l,i}^H \sum_{j=1,\, j\neq l}^{L} H_j \sum_{n=1,\, n\neq i}^{I} q_{j,n} d_{j,n}' + q_{l,i}^H \sum_{j=1}^{L} H_j S_j d_j + q_{l,i}^H m. \tag{15}$$

As inferred from equation (15), $q_{l,i} \in E^{M\times 1}$ indicates the receive beam vector for communication signal $c_{l,i}'$ at the interactive system. As a result, the received EMG signal to inference and noise proportion at the communication receiver system can be calculated using

$$\zeta_{l,i} = \frac{\left|q_{l,i}^H H_l u_{l,i}\right|^2}{\sum_{j=1,\, j\neq l}^{L} \sum_{n=1, m\neq i}^{I} \left|q_{l,i}^H H_j u_{j,n}\right|^2 + \sum_{j=1}^{L} \left\|q_{l,i}^H H_j S_j\right\|^2 + \sigma_m^2 \left\|q_{l.i}\right\|^2}. \tag{16}$$

Besides, the transmit signal of EMG relies on the energy beam sent by the human-computer interaction system.

EMG signal-based human motion recognition, Lyapunov exponent, is utilized to detect the numerical features in a complex system and denoted the system sensitivity to the first value as the parameter progress with a period t. The M-dimensional systems have M Lyapunov exponents, creating an exponential spectrum. Thus, it is broadly utilized in system fault diagnosis along with muscle activity and muscle contraction identification. It is stated as

$$\lambda_{\max} = \frac{1}{\Delta t} \sum_{p=1}^{N} \frac{L(t_p)}{L(t_{p-1})}. \tag{17}$$

As discussed in equation (17), $L(t_p)$ denotes the distance between two adjacent 0 points at the time t_p, Δt is the sampling time, and N indicates the overall step length. The distance between end-to-end paths is generally reproduced by the forecast fault on the log function to attain the Lyapunov exponent of the complete set of IMF. It is stated as

$$k(p) = \frac{1}{Mt} \sum_{m=1}^{M} 1a \frac{\Gamma_m(p)}{\Delta m}. \tag{18}$$

As shown in equation (18), Δm denotes the distance between phase points,E_{m+1} is the adjacent point to E_m, and $\Gamma_m(p)$ is the distance between E_m and E_{m+1} after p convolution step length time. M indicates the aggregate number of phase points. The two typical EMG signal features embedded in dimension and delay time are two essential variables for evaluating the Lyapunov exponent. The motion characteristics of the EMG signal have been chosen and represented using these two parameters. The delay time was calculated using the mutual information technique as follows:

$$B(\tau) = k(Y_m, Y_{m+\tau}) \ln \frac{k(Y_m, Y_{m+\tau})}{k(Y_m) k(Y_{m+\tau})}. \tag{19}$$

As shown in Figure 6 and equation (19) representing the delay time calculation, $B(\tau)$ denotes the EMG signal delay time and $k(Y_m)$, $k(Y_{m+\tau})$, and $k(Y_m, Y_{m+\tau})$ are likelihood values.

By Algorithm 1, the embedded dimension has been evaluated, which is stated as

$$O_1(n) = \frac{O(n+1)}{O(n)}. \tag{20}$$

As discussed in equation (20), $O(n+1)$ and $O(n)$ are the mean thresholds of the distance between every two adjacent neighbors in the recreated $n+1$ dimensional space and n-dimensional space, respectively.

The proposed AIMF algorithm reduces the EMG signal noise and obtains active human motion features for the human-computer interaction. Finally, the proposed Optimized Noninvasive Human-Computer Interaction (ONIHCI) model addresses the problems such as accurate gesture recognition and human target identification and reduces the noise in EMG signal for an effective HCI process. The following section briefly describes the experimental results.

4. Experimental Results and Discussion

The proposed Optimized Noninvasive Human-Computer Interaction (ONIHCI) model experimental results have been performed in a computer vision-based human-computer interaction environment. Different situations have been used analyzed using the training and testing dataset [21]. From the large dataset, a 70 : 30 ratio of training and testing data has been formed. A different dataset was randomly chosen among the testing data and observed various performance metric values. The following figure 7 and table 1 give the results observed from this analysis. Human targets are running, walking, and slow waving; the data is divided into multiperson and single-person behavior. The analysis of human trajectory and human kinematics has been discussed in this section. The human targets are detected in multiple thermographic images.

Furthermore, EMG-driven musculoskeletal model-based motion recognition has been utilized, to the map between EMG and joint angular velocity, angle, joint moment, or angular acceleration. The experimental results show that the HCI suggested method achieves lesser noise and enhances the accuracy in human motion recognition and identifying human targets with high performance. Simulation parameter has been used for the human motion recognition based on EMG signal acquisition with a simulation time of 4 seconds, and sampling frequency utilized is 25 kHz, muscle length is 200 mm, the number of electrodes used is 64, muscle radius is 20 mm, muscle fiber length is 45 mm, muscle fiber diameter is 35.77, and fiber length is 150 mm.

4.1. Root Mean Square Error (RMSE) Ratio Analysis

4.1. Root Mean Square Error (RMSE) Ratio Analysis. The Root Mean Square Error is often used in continuous motion prediction. It compares the actual values to the projected values. The conflict is squared to prevent canceling negative

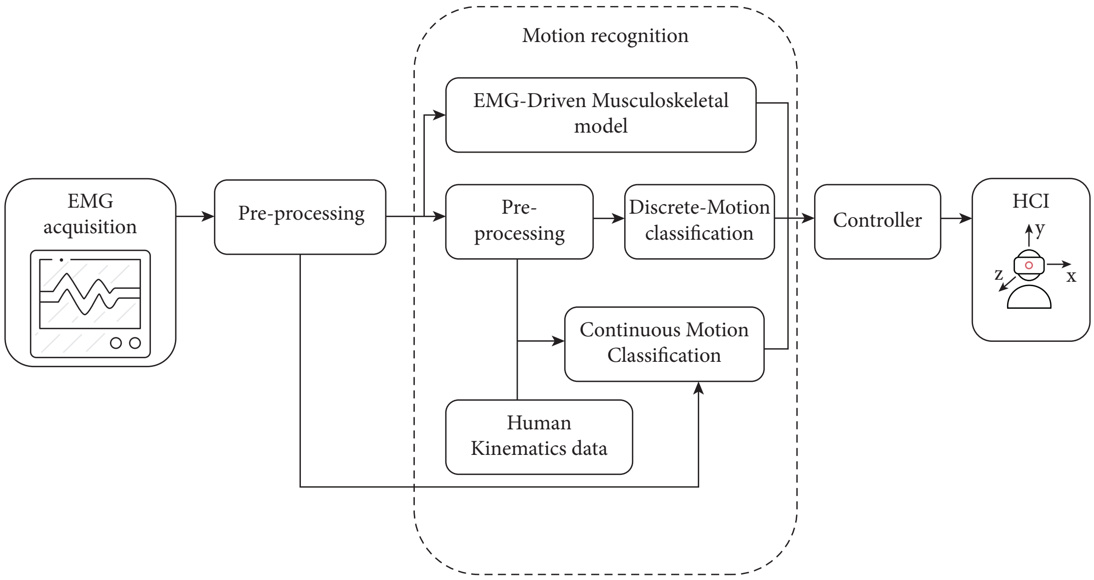

Figure 4: The process of EMG signal-based human-computer interaction.

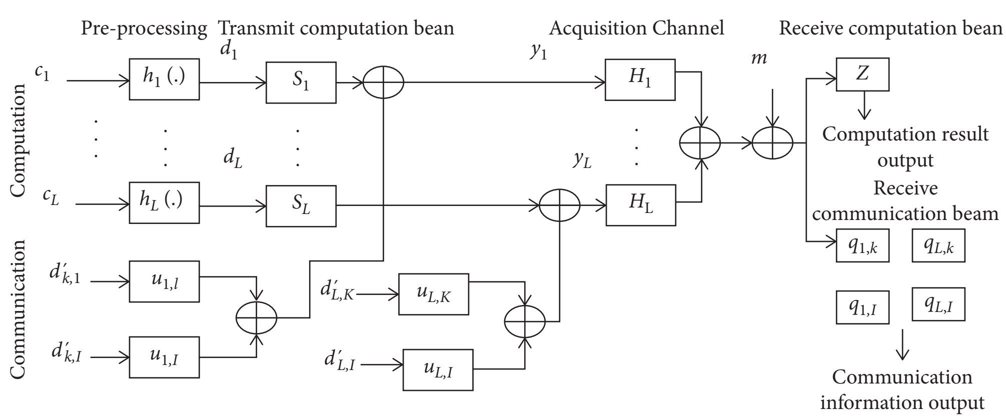

Figure 5: Communication between interactive systems.

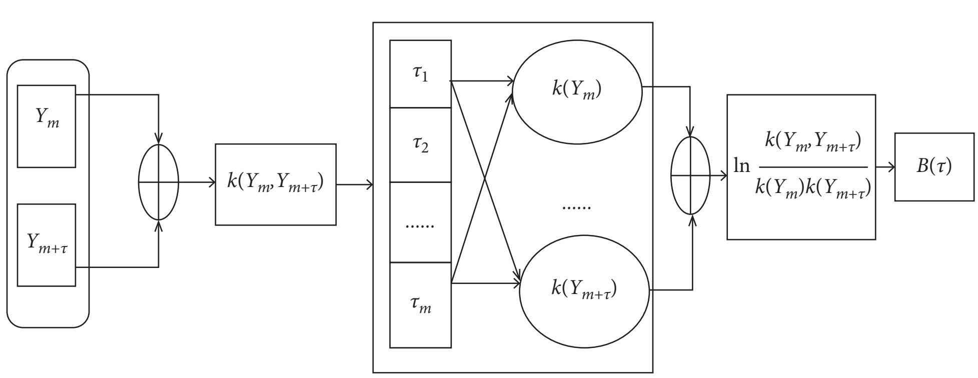

Figure 6: Delay time calculation.

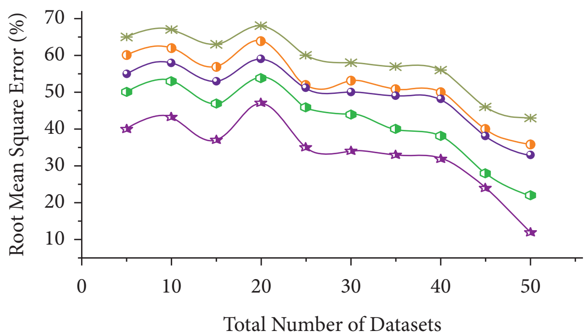

Figure 7: Mean square error ratio.

and positive values. The distortion of the computation at the interactive system is evaluated by the mean square error d and $\hat{d}$ which is stated as

$$\mathrm{RMSE}(d,\hat{d}) = Z\left\{tr\left((\hat{d}-d)(\hat{d}-d)^H\right)\right\}. \tag{21}$$

Replacing (12) into (13), the computation distortion can be calculated as the following RMSE function of receive and transmit beam:

$$\begin{aligned}\mathrm{RMSE}\left(V, S_l, u_{l,i}\right) &= \sum_{l=1}^{L} \left\|V^H H_l S_l - J\right\|_F^2 + \sigma_m^2 \|V\|_F^2 \\ &+ \sum_{l=1}^{L}\sum_{i=1}^{I} \left\|V^H H_l u_{l,i}\right\|^2.\end{aligned} \tag{22}$$

Therefore, the computation outcome should have a low RMSE. Figure 7 demonstrates the RMSE using the suggested system.

The performance ratio evaluation of the recommended ONIHCI system is shown in Table 1. To detect the movement of a human, it is necessary to track the body's motion throughout physical activity. Data processing to better portray such movement aids in the operation's detection, which helps this study effectively. Compared to other technologies, the human-computer interface performance based on human motion recognition findings is quite successful. Table 1 shows that the highest performance ratio of 95.4% by the proposed model outperforms the existing models in the literature survey. For all sets of data inputs, the ONIHCI gives the highest performance ratio.

4.2. Recognition Accuracy Ratio Analysis. The human thermographic view is examined for comprehending the trajectory behaviors and the motion kinematics during the target's movement. Humans are initialized using the kinematics system by features like the number of limbs, degrees of freedom, limb length, etc. Humans are represented as images, and personality traits like form or region are extracted and stored in the image model. The acknowledgment, as well as the complexity of the motion, can be determined effectively. The accuracy from every sensor is provided in Table 2 concerning every sensor's kinematics and trajectory analysis utilizing thermographic images. The simulation outcomes demonstrated that the suggested approach could assess the human target angle with high accuracy compared to other existing approaches. Figure 8 demonstrates the recognition accuracy ratio using proposed ONIHCI methods.

4.3. Delay Time Determination and Noise Reduction Ratio Analysis. In reflection of the nonlinear dynamic EMG signal, the actual EMG signal has been decomposed into a set of IMF when noise reduction, as demonstrated in Figure 9(b). The actual EMG signal $X(t)$ has been decomposed into $D_{\mathrm{IMF}}(i)$, $(i = 1, 2, \ldots, 6)$ and deviation γ_m. $D_{\mathrm{IMF}}(i)$ is an oscillation function with various frequencies and amplitudes. γ_m is a monotonic signal, denoting the drift element determined by deducting every $D_{\mathrm{IMF}}(i)$ from the actual signal, and $X(t)$ no longer meets the decomposition states. Embedded dimension and delay time are two significant constraints for the manipulative Lyapunov exponent. Moreover, the chosen delay time is too short and not advantageous to EMG signal optimization.

The two typical EMG signal features embedded in dimension and delay time are essential for evaluating the Lyapunov exponent. These two parameters are appropriate for depicting EMG gesture time sequence data; the motion features of the EMG signal have been selected and represented.

The mutual information approach has been utilized for calculating delay time which is stated as

$$B(\tau) = k\left(Y_m, Y_{m+\tau}\right)\ln\frac{k\left(Y_m, Y_{m+\tau}\right)}{k\left(Y_m\right)k\left(Y_{m+\tau}\right)}. \tag{23}$$

As shown in the above equation, $k(Y_m)$, $k(Y_{m+\tau})$, and $k(Y_m, Y_{m+\tau})$ are likelihood values.

Based on Algorithm 1, the embedded dimension has been evaluated, which is stated as

$$O_1(n) = \frac{O(n+1)}{O(n)}. \tag{24}$$

As discussed in the above equation, $O(n+1)$ and $O(n)$ are the mean thresholds of the distance between every two adjacent neighbors in the recreated $n+1$-dimensional space and n-dimensional space, respectively. Figure 9(a) shows the delay time using the proposed ONIHCI method.

The quality of the EMG signal measurement is demonstrated by the ratio of the EMG signal calculated to unwanted environmental noise inputs. A high-quality signal offers more information to predict the intention so that it increases prediction accuracy. Nevertheless, noises from various sources are possible, and the analysis of EMG signals may be contaminated. To maximize the signal-to-noise relation in this respect, amplifiers are designed and used to reject or eliminate noises. The accuracy of EMG signals is affected by noise and artifacts from various causes (including electric devices, power lines, and physiological factors),

Table 1: Performance ratio evaluation.

No. of datasets	LDA-ELM [22]	MUST-BSSA [32]	GFTD [25]	HMM-SVD [26]	ONIHCI (proposed approach)
5	54.2	56.1	67.1	77.7	80.1
10	51.3	53.3	60.4	67.8	63.5
15	63.9	56.5	78.4	87.9	52.4
20	76.2	77.6	78.5	73.7	72.3
25	83.1	54.7	56.9	76.5	77.1
30	54.7	50.8	53.8	57.4	81.2
35	43.9	44.4	46.7	47.3	82.2
40	51.8	54.3	56.7	60.2	89.2
45	65.3	65.2	76.6	77.1	90.3
50	67.2	66.1	77.5	87.2	95.4

Table 2: Precision ratio analysis.

No. of datasets	LDA-ELM	MUST-BSSA	GFTD	HMM-SVD	ONIHCI
5	32.1	34.1	35.7	37.7	70.1
10	53.3	54.3	69.4	67.8	61.5
15	64.9	54.5	79.4	87.9	42.4
20	77.2	72.6	72.5	73.7	72.3
25	82.1	44.7	53.9	76.5	77.1
30	53.7	42.8	54.8	57.4	79.2
35	42.9	49.4	45.7	47.3	82.2
40	51.8	59.3	56.7	60.2	77.2
45	64.3	67.2	76.6	77.1	92.3
50	68.2	62.1	77.5	87.2	96.4

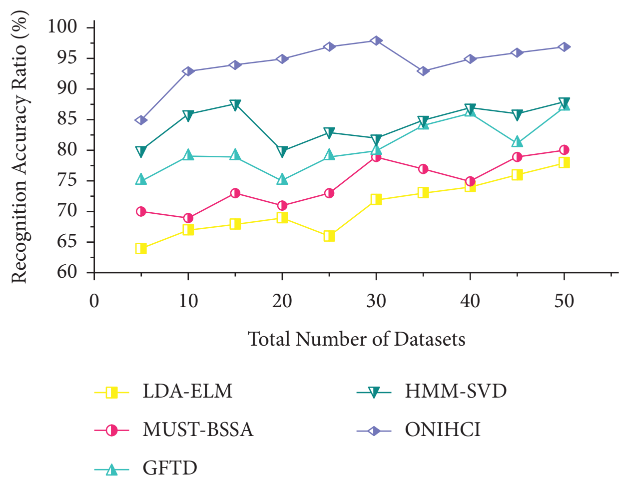

Figure 8: Recognition accuracy ratio analysis.

which may contribute to the inaccurate analysis of data or a misunderstanding of motion parameters. In the proposed ONIHCI method, the AIMF algorithm reduces the noise level seen in the raw EMG signal. Figure 9(b) shows the noise reduction ratio using the proposed method.

Table 2 shows the precision ratio using the proposed ONIHCI method. The present system implemented in this study is user-friendly compared to a command-based system or standard device and robust in detection and recognition. The proposed AIMF algorithm is extensively utilized in the classification and regression of HCI because of its simple execution, high precision, and antinoise capability.

4.4. Normalized Computation Error Evaluation. Normalized computation error is a statistical assessment utilized to compare proficiency testing outcomes where the uncertainty in the measurement outcomes is included. The cause for error with the spatial thermographic sensor has the minimal image size of the targets and unexpected changes. Single perspective and stereo sensors provided a benefit to decreasing the computation error with surplus views. The distance between the human target and interactive system positions at every degree of target force direction is averaged over a tracking cycle known as normalized tracking error. The proposed method has lesser

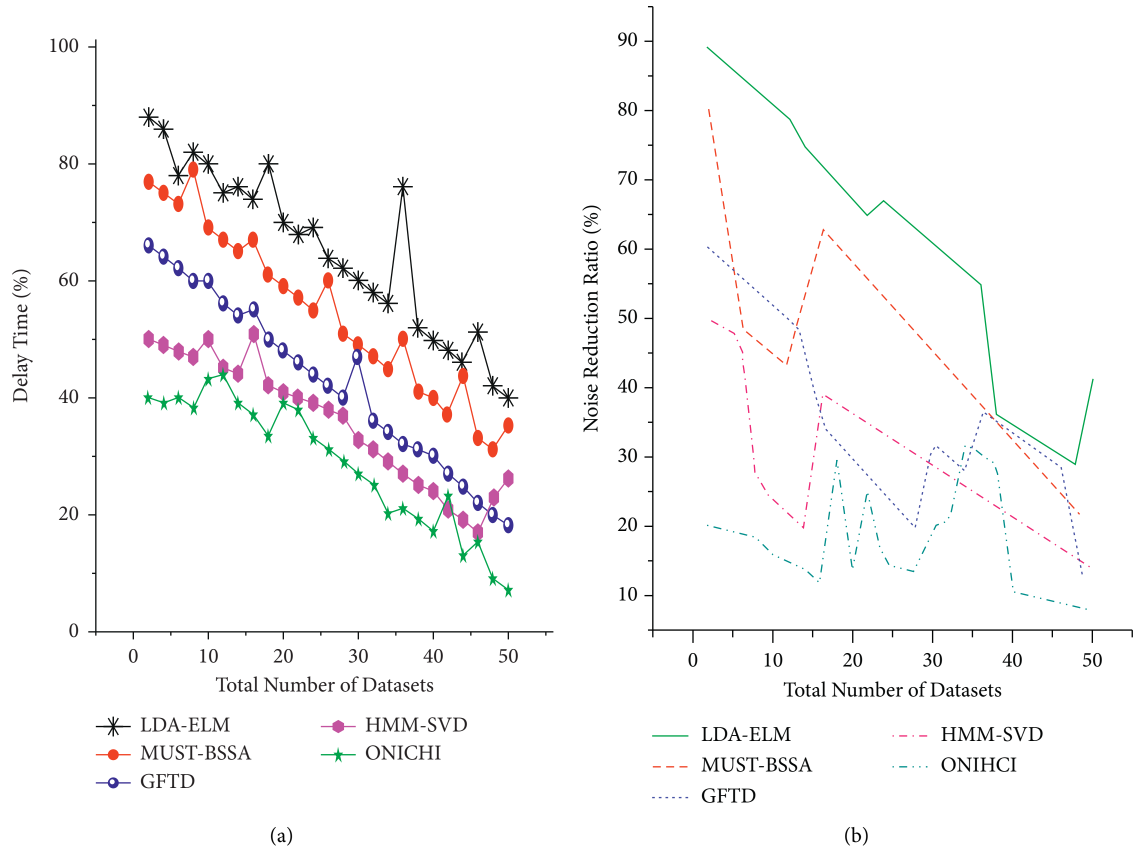

Figure 9: (a) Delay time determination. (b) Noise reduction ratio analysis.

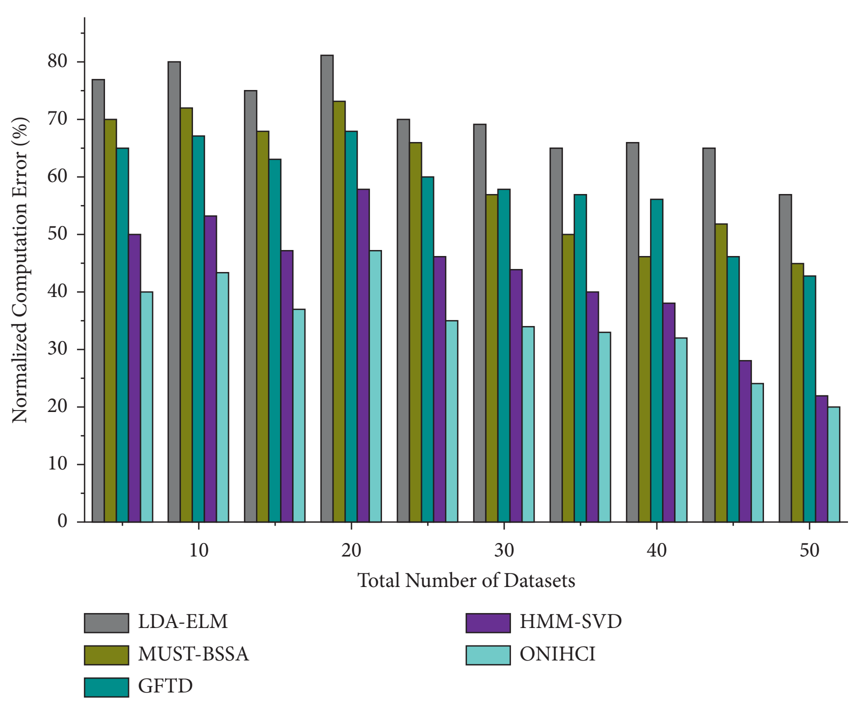

Figure 10: Normalized computation error evaluation.

computation error compared to other existing methods. Figure 10 shows the normalized computation error using the proposed ONIHCI method. The proposed Optimized Noninvasive Human-Computer Interaction (ONIHCI) model achieves high recognition accuracy and lesser delay time and noise when compared to other existing linear discriminant analysis and extreme learning machine (LDA-ELM) method, Motor Unit Spike Trains with Blind Source Separation Algorithm (MUST-BSSA), Guidance framework for tracking by detection (GFTD), and Hidden Markov Model and Singular Value Decomposition (HMM-SVD) methods.

5. Conclusion

This paper presents the Optimized Noninvasive Human-Computer Interaction model (ONIHCI) to address gesture recognition and human target identification problems. Human trajectory analysis and human kinematics analysis have been introduced, and the human targets are detected in the multitarget scenarios based on spatial thermographic images and using different sensors. Furthermore, EMG-driven musculoskeletal model-based human motion recognition has been utilized to map EMG and joint angular velocity, angle, joint moment, or angular acceleration for HCI. To reduce the noise in EMG signals, the AIMF algorithm has been introduced. The experimental findings demonstrate a lower noise ratio of the proposed system of 7.2% and enhance the accuracy ratio of 97.2% in human motion recognition, identifying human targets with high performance.

Data Availability

The data that support the findings of this study are available on request from the corresponding author.

Conflicts of Interest

The authors declare that they do not have any conflicts of interest.

Acknowledgments

The authors extend their gratitude to the Deanship of Scientific Research at King Khalid University for funding this work through research group program under grant number. R.G.P. 1/77/42.

References

[1] F. Zhang, T.-Y. Wu, J.-S. Pan, G. Ding, and Z. Li, "Human motion recognition based on SVM in VR art media interaction environment," *Human-centric Computing and Information Sciences*, vol. 9, no. 1, p. 40, 2019.

[2] N. R. Baek, S. W. Cho, J. H. Koo, N. Q. Truong, and K. R. Park, "Multimodal camera-based gender recognition using human-body image with two-step reconstruction network," *IEEE Access*, vol. 7, pp. 104025–104044, 2019.

[3] A. Brunetti, D. Buongiorno, G. F. Trotta, and V. Bevilacqua, "Computer vision and deep learning techniques for pedestrian detection and tracking: a survey," *Neurocomputing*, vol. 300, pp. 17–33, 2018.

[4] S. Khan, H. Rahmani, S. A. A. Shah, and M. Bennamoun, "A guide to convolutional neural networks for computer vision," *Synthesis Lectures on Computer Vision*, vol. 8, no. 1, pp. 1–207, 2018.

[5] J. Qi, G. Jiang, G. Li, Y. Sun, and B. Tao, "Surface EMG hand gesture recognition system based on PCA and GRNN," *Neural Computing & Applications*, vol. 32, no. 10, pp. 6343–6351, 2020.

[6] M. Oudah, A. Al-Naji, and J. Chahl, "Hand gesture recognition based on computer vision: a review of techniques," *Journal of Imaging*, vol. 6, no. 8, p. 73, 2020.

[7] J. Meng, P. Pan, Z. Yang et al., "Degradable and highly sensitive CB-based pressure sensor with applications for speech recognition and human motion monitoring," *Journal of Materials Science*, vol. 55, no. 23, pp. 10084–10094, 2020.

[8] K. Campbell, K. L. Carpenter, J. Hashemi et al., "Computer vision analysis captures atypical attention in toddlers with autism," *Autism*, vol. 23, no. 3, pp. 619–628, 2019.

[9] S. Coşar and N. Bellotto, "Human Re-identification with a robot thermal camera using entropy-based sampling," *Journal of Intelligent and Robotic Systems*, vol. 98, no. 1, pp. 85–102, 2020.

[10] Y. Xue, X. Ji, D. Zhou, J. Li, and Z. Ju, "SEMG-based human in-hand motion recognition using nonlinear time series analysis and random forest," *IEEE Access*, vol. 7, pp. 176448–176457, 2019.

[11] J. Imran and B. Raman, "Deep motion templates and extreme learning machine for sign language recognition," *The Visual Computer*, vol. 36, no. 6, pp. 1233–1246, 2020.

[12] S. Jiang, Q. Gao, H. Liu, and P. B. Shull, "A novel, co-located EMG-FMG-sensing wearable armband for hand gesture recognition," *Sensors and Actuators A: Physical*, vol. 301, Article ID 111738, 2020.

[13] A. Jaramillo-Yánez, M. E. Benalcázar, and E. Mena-Maldonado, "Real-time hand gesture recognition using surface electromyography and machine learning: a systematic literature review," *Sensors*, vol. 20, no. 9, Article ID 2467, 2020.

[14] W. Wei, Q. Dai, Y. Wong, Y. Hu, M. Kankanhalli, and W. Geng, "Surface-Electromyography-based gesture recognition by multi-view deep learning," *IEEE Transactions on Biomedical Engineering*, vol. 66, no. 10, pp. 2964–2973, 2019.

[15] H. Sun, X. Zhang, Y. Zhao, Y. Zhang, X. Zhong, and Z. Fan, "A novel feature optimization for wearable human-computer interfaces using surface electromyography sensors," *Sensors*, vol. 18, no. 3, p. 869, 2018.

[16] Y. Tan, W. Yan, S. Huang, D. Du, and L. Xia, "A motion deviation image-based phase feature for recognition of thermal infrared human activities," *Engineering Letters*, vol. 28, no. 1, 2020.

[17] Z. Zhang, K. Yang, J. Qian, and L. Zhang, "Real-time surface emg pattern recognition for hand gestures based on an artificial neural network," *Sensors*, vol. 19, no. 14, Article ID 3170, 2019.

[18] S. Maragliulo, P. F. A. Lopes, L. B. Osório, A. T. De Almeida, and M. Tavakoli, "Foot gesture recognition through dual channel wearable EMG System," *IEEE Sensors Journal*, vol. 19, no. 22, pp. 10187–10197, 2019.

[19] Y. A. Sekhavat, M. J. Sisi, and S. Roohi, "Affective interaction: using emotions as a user interface in games," *Multimedia Tools and Applications*, vol. 80, no. 4, pp. 5225–5253, 2021.

[20] P. Choudhary, A. Tripathi, A. K. Singh, and P. C. Vashist, "Upper half face recognition using hidden markov model and

singular value decomposition coefficients," in *Advances in Computational Intelligence and Communication Technology*, pp. 549–561, Springer, Singapore, 2021.

[21] https://www.rami-khushaba.com/electromyogram-emg-repository.html.

[22] J. Qi, G. Jiang, G. Li, Y. Sun, and B. Tao, "Intelligent human-computer interaction based on surface EMG gesture recognition," *IEEE Access*, vol. 7, pp. 61378–61387, 2019.

[23] A. Aggarwal, V. Sharma, A. Trivedi et al., "Two-way feature extraction using sequential and multimodal approach for hateful meme classification," *Complexity*, vol. 2021, Article ID 5510253, 7 pages, 2021.

[24] D. Singh and V. Kumar, "Image dehazing using Moore neighborhood-based gradient profile prior," *Signal Processing: Image Communication*, vol. 70, pp. 131–144, 2019.

[25] E. Song, H. Lee, J. Choi, and S. Lee, "AHD: thermal image-based adaptive hand detection for enhanced tracking system," *IEEE access*, vol. 6, pp. 12156–12166, 2018.

[26] F. Xiao, D. Yang, Z. Lv, X. Guo, Z. Liu, and Y. Wang, "Classification of hand movements using variational mode decomposition and composite permutation entropy index with surface electromyogram signals," *Future Generation Computer Systems*, vol. 110, pp. 1023–1036, 2020.

[27] D. Singh and V. Kumar, "A comprehensive review of computational dehazing techniques," *Archives of Computational Methods in Engineering*, vol. 26, no. 5, pp. 1395–1413, 2019.

[28] M. Agrawal, A. U. Khan, and P. K. Shukla, "stock price prediction using technical indicators:A predictive model using optimal deep learning," *International Journal of Recent Technology and Engineering*, vol. 8, no. 2, pp. 2297–2305, July 2019.

[29] P. Tiwari and P. Shukla, "Artificial neural network-based crop yield prediction using NDVI, SPI, VCI feature vectors," in *Information and Communication Technology for Sustainable Development*, M. Tuba, S. Akashe, and A. Joshi, Eds., vol. 933, Advances in Intelligent Systems and Computing, Springer, Singapore, 2020.

[30] X. Tang, F. Li, T. G. Seetharam, and C. C. Vignesh, "Internet of things-assisted intelligent monitoring model to analyze the physical health condition," *Technology and Health Care*, 2021.

[31] E. Benli, Y. Motai, and J. Rogers, "Visual perception for multiple human–robot interaction from motion behavior," *IEEE Systems Journal*, vol. 14, no. 2, pp. 2937–2948, 2019.

[32] C. Chen, Y. Yu, S. Ma et al., "Hand gesture recognition based on motor unit spike trains decoded from high-density electromyography," *Biomedical Signal Processing and Control*, vol. 55, Article ID 101637, 2020.

[33] R. Bhatt, P. Maheshwary, P. Shukla, P. Shukla, M. Shrivastava, and S. Changlani, "Implementation of fruit fly optimization algorithm (FFOA) to escalate the attacking efficiency of node capture attack in wireless sensor networks (WSN)," *Computer Communications*, vol. 149, pp. 134–145, 2020.

Hindawi
Scientific Programming
Volume 2021, Article ID 9261934, 10 pages
https://doi.org/10.1155/2021/9261934

Research Article

Research on the Evaluation and Optimization Method of the Impact of Chorus Education on University Culture Based on Coevolution Model in the Background of Artificial Intelligence

Qingna Lin and Lizheng Zhuo

International College, Krirk University, Bangkhen, Bangkok 10220, Thailand

Correspondence should be addressed to Lizheng Zhuo; 845902916@qq.com

Received 3 September 2021; Revised 23 September 2021; Accepted 13 October 2021; Published 31 October 2021

Academic Editor: Punit Gupta

The development of artificial intelligence technology is a field where all walks of life need to carry out in-depth research in the future, and the introduction of artificial intelligence technology in the field of university evaluation has become an inevitable trend. Through the collection and collation of the literature at home and abroad, the influence of chorus education on college culture in China has long remained in qualitative and experiential judgment and the significance and value of chorus education to colleges and universities are relatively single. Therefore, it is of great innovative value and practical significance to establish a scientific, systematic, and comprehensive evaluation mechanism for the impact of chorus education on university culture and to scientifically analyze key issues, establish evaluation criteria, and inject new research perspectives into the promotion of chorus education in colleges and universities in China, combining with the mature coevolution theoretical model of management science. It is of great innovative value and significance to combine the DEMATEL research method with the current practice of promoting chorus education in China's colleges and universities and to systematically and comprehensively construct the evaluation system and research paradigm in line with chorus education by using the qualitative and quantitative methods.

1. Introduction

Hegel, a famous philosopher, once said that imagination is the most outstanding skill in artistic creation. Einstein, a scientist, also pointed out in his treatise On Science that imagination is more important than knowledge, because knowledge is limited, while imagination summarizes everything in the world, promotes progress, and is the source of knowledge evolution [1]. Because of the sensibility of the evaluation method, it is often criticized by the academic circles, and the research on the subjective conjecture and experience summary of the cultivation of college students' personality, moral accomplishment, innovation ability, and imagination ability is seldom confirmed by authority. Therefore, the quantitative research on the impact of chorus education in colleges and universities is an important theoretical and practical innovation of chorus education research in colleges and universities and has important practical significance and value for enhancing the scientificity, systematicness, and integrity of the impact evaluation of chorus education in colleges and universities. Based on the coevolution theory of management, this paper constructs a comprehensive and systematic impact evaluation system for chorus education in colleges and universities. By combining qualitative and quantitative research methods, it objectively, systematically, and comprehensively demonstrates the overall situation of the development of chorus education in different colleges and universities and provides scientific suggestions and opinions for the development of chorus education in different types of colleges and universities in a holistic way. Because of the sensibility of the evaluation method, it is often criticized by the academic circles, and the research on the subjective conjecture and experience summary of the cultivation of college students' personality, moral accomplishment, innovation ability, and imagination ability is seldom confirmed by authority. Therefore, the quantitative research on the impact of chorus education in colleges and universities is an important theoretical and practical innovation of chorus education research in colleges and universities and has important practical significance and value for enhancing the scientificity, systematicness, and integrity of the impact evaluation of chorus education in colleges and universities. Based on the coevolution theory of management, this paper constructs a comprehensive and systematic impact evaluation system for chorus education in colleges and universities. By combining qualitative and quantitative research methods, it objectively, systematically, and comprehensively demonstrates the overall situation of the development of chorus education in different colleges and universities and provides scientific suggestions and opinions for the development of chorus education in different types of colleges and universities in a holistic way. Because of the sensibility of the evaluation method, it is often criticized by the academic circles, and the research on the subjective conjecture and experience summary of the cultivation of college students' personality, moral accomplishment, innovation ability, and imagination ability is seldom confirmed by authority. Therefore, the quantitative research on the impact of chorus education in colleges and universities is an important theoretical and practical innovation of chorus education research in colleges and universities and has important practical significance and value for enhancing the scientificity, systematicness, and integrity of the impact evaluation of chorus education in colleges and universities. Based on the coevolution theory of management, this paper constructs a comprehensive and systematic impact evaluation system for chorus education in colleges and universities. By combining qualitative and quantitative research methods, it objectively, systematically, and comprehensively demonstrates the overall situation of the development of chorus education in different colleges and universities and provides scientific suggestions and opinions for the development of chorus education in different types of colleges and universities in a holistic way.

2. Research Status of Chorus Education and College Culture at Home and Abroad

The research on chorus education and university culture has been carried out for many years at home and abroad. From the collation and research of various literature materials at present, we can see that the depth and breadth of the research are relatively comprehensive. There are many studies on chorus education in China in the fields of chorus creation, chorus history, chorus culture, chorus value and significance, chorus education methods and means, chorus development and management, and so on. In the study of the history of chorus, Chang has made a more in-depth discussion on the development of Chinese and Western chorus art, pointing out that both Chinese and Western chorus have gradually developed from monophonic to polyphonic and that Western chorus is mainly religious music, while Chinese chorus is mainly the source of "human" labor, life, and entertainment needs [2]. From the perspective of ancient Chinese music aesthetics, *Pan* made a more in-depth discussion on the origin and development of ancient Chinese chorus art and put forward that "the mainstream of ancient Chinese chorus is the thought of rites and music, pursuing the aesthetic thought of harmony between man and nature." In the second century BC, a monograph "On Music" in the early Western Han Dynasty pushed China's musical aesthetics to its peak [3]. Shao examined the origin of Western chorus from the perspective of Western music history and concluded that "the trinity of music, dance, and poetry is related to the participation of religious sacrificial groups, while the original performance of tragedy is mainly chorus [4]." From the perspective of the value and significance of chorus, Huang [5] proposed that chorus has important value and significance for stimulating the spirit of teamwork, collectivism and patriotism from the perspective of chorus creation, chorus lyrics, chorus culture, chorus context and chorus aesthetics. Li [6] put forward the role of chorus curriculum education in stimulating students' imagination, singing ability and innovation ability in the aspects of chorus foundation, culture, ideology and morality, national spirit, and command skills. Huaxia [7] and Sun [8] put forward the value and significance of chorus as a collective art form in students' aesthetic and moral education, discussed the role of chorus art and education, and put forward the role of chorus curriculum education in cultivating students' EQ. It also puts forward the process and ways of chorus education for the development of human personality. The research on chorus education from the perspective of professional development is an important aspect of chorus education and campus culture research. From the perspective of the development of modern campus music, Pan [9] explores how chorus can better realize the integration and promotion of aesthetic education and singing skills, innovation, and aesthetic ability, as a driving force for the development of chorus on campus. Guo [10] carried out research on chorus education from the perspective of non-art comprehensive universities and put forward suggestions and opinions for development. Liu [11] carried out higher education research on Liszt and Hungarian chorus education and explored the future development path of professional chorus education in China through the research on the development of chorus education in professional colleges and universities at home and abroad. Hu [12] starts from the educational significance of chorus education, understands the "human" bred in the development of chorus, and integrates its life attribute value. Zhang [13], Xu [14], Jin [15], and Wang [16] focus on the construction and management of chorus education in colleges and universities from different perspectives and put forward the corresponding campus cultural value and significance, so as to construct the management mode and brand value of chorus education in colleges and universities from the macro- and microperspectives. The above research paradigm has strong theoretical research value and practical significance for the current development of chorus education in China and has important guiding significance for promoting the development of chorus education in China and chorus education in colleges and universities.

There are many research paradigms and research methods in the world to carry out chorus education and chorus art research, which have formed a wealth of literature. The research perspective is different from the domestic research. In the research, we should combine film art, social life, psychotherapy, and other fields to study, while the relevant literature of pure theory, technology, practice, and management is not the focus of the research [17]. Through the analysis of the impact of film on commercial behavior and social consciousness, it mainly takes the film chorus as an example to analyze the value and significance of innovation, creation, and imagination by analyzing the relevant content of social consciousness in chorus films [18]. This paper analyzes the current situation of chorus education in primary and secondary schools, explores the optimal operation mechanism of chorus education, and scientifically plans and designs the future development of chorus education [19]. Combining chorus with dance art and exploring educational value in social interaction, the research content has practical value and significance [20]. The training methods of perceiving the world, experiencing life, and creative thinking in the training of a cappella in primary and secondary schools are applied to the educational concept of life, and in the process of practice and application, the combination of a cappella and social life is explored. In terms of literature research on the combination of chorus education, music education research, psychology, and medical research, the international community is very rich, in which a large number of qualitative and quantitative comprehensive studies are carried out by means of investigation, experiment, and questionnaire (Ahn et al. [21] and Jacob [22]). Through the experimental study of the volume of music and people's aesthetic point of view, the acceptance limit of music art is measured (Nilesh [23]). The students are put in music environment and the music content and memory they can bear in a day is measured through the method of experimental verification (García González et al. [24]), that is, through experiments and comparative studies, to determine the effects of prenatal music stimulation on fetal heart condition, neonatal physical measurement, and vital signs of pregnant women and to scientifically analyze the effects of music on human beings (Crickmore [25]). It is an effective measurement and research on the cultivation effect of music and chorus art on people's aesthetic taste and draws corresponding research conclusions (Tai et al. [26]). By using the method of questionnaire, this paper studies the effect of music education of parents and children in Hong Kong and draws the conclusion that parents are the important factors that effectively influence the value of children's music consciousness (Duarte et al. [27]). That is to say, through the questionnaire survey and measurement of the impact of music festival activities on the image of tourist destinations, the analysis proves that there is a positive correlation between them (Music [28]). It proves that chorus and music education are closely related to therapy and health, aesthetic concepts, life measurement, and new media (Barrientos-Fernández et al. [29]). By means of follow-up investigation, questionnaire, and experiment, the comprehensive ability, different types of intelligence (general intelligence, linguistic and nonlinguistic intelligence, and multiple intelligence), academic performance, and learning habits of students are effectively measured, which proves the relevance of music education (Shin and George [30] and Wesolowski [31]). Rasch measurement model is used to make a comprehensive qualitative and quantitative evaluation of music performance evaluation and music performance evaluation and to explore the attempt of scientific evaluation of music art (Das et al. [32]). From the analysis of scientific research, the influence of music on human brain, and the influence value of the change of music content on people's attention and concentration ability, the above qualitative and quantitative research combined with psychology and medicine is an exploration of the scientific research of music and chorus art education, which fully illustrates the influence of music and chorus art on people's cognition, imagination, innovation, aesthetics, morality, intelligence, and learning. This influence is invisible, but through scientific research, we can find its corresponding law of value. This is the research frontier of chorus education, art education, and music education in the future.

In recent years, domestic researchers have made great progress in theoretical exploration and practical research by combining qualitative and quantitative methods, but due to the difficulty of research and the interdisciplinary research background required by the research, there are still some limitations in the current talent cultivation in China. Therefore, at present, it is difficult to find the research materials that really combine qualitative and quantitative analysis by searching the literature. For the research in the field of chorus education, the most difficult thing is to evaluate the level of its educational development. The scientificity, comprehensiveness, subjectivity, and objectivity of the evaluation will directly affect the identification of the development of chorus education. It is of great research value and significance to scientifically and rationally formulate the development strategy of chorus education and to study the key factors affecting the development of chorus education. Pei put forward that "measurement and evaluation is the axis of the operation of art education [33]"; Zhu put forward the following: "To construct an objective evaluation system of chorus education in colleges and universities can not only measure and evaluate students' artistic level, but also guide and standardize students' chorus training [34]." The above scholars have also put forward many research ideas on the evaluation system and methods of chorus education. Zhou and Xu put forward that "evaluation" is to measure the value of people or things [35]. The scientificity and systematization of "evaluation" are one of the basic contents to complete the qualitative and quantitative research of chorus education. Therefore, it is of great research value and significance for the development of different types of colleges and universities to carry out scientific research on the impact of chorus education on college culture, scientifically analyze its development, establish a professional system for the development of chorus education in colleges and universities, and comprehensively analyze the internal and external complex factors affecting its development.

3. Analysis of Influencing Factors Based on Coevolution Theory

Coevolution [36] theory was first put forward by biologists Paul Erich and Peter Raven in 1964 in their paper entitled "Butterflies and Plants: A Study in Coevolution (Jazen [37], Norgaard [38], Eisenhardt [39], and Hodgson [40]). With the development of scholars, at the beginning of the twenty-first century, the theoretical system of coevolution has been basically established, and fruitful research results have been achieved in nonbiological fields, such as social economy, organization, management, and computer modeling [41]. It regards the evaluation and occurrence process of things as a complete whole, fully considers the relationship between various factors and elements that constitute the development process of things, and affirms their interaction in the development and change, which is of great value for analyzing the complex and changeable social environment and the laws that cannot be inferred by mathematics. It has a strong practical significance for the study of the development law of current organizational management, enterprise management, and other fields, for the analysis and study of the key factors and elements affecting the development of organizations and enterprises, and for the study of development law. The introduction of coevolution theory into the study of the influence of chorus education on university culture has important innovative value and significance for objectively judging the influencing factors and influencing factors of university chorus education and exploring the key influencing dimensions.

Based on systematic and holistic research, this paper constructs a model of the impact of chorus education on university culture, analyzes the corresponding development characteristics of different types of chorus education in universities, and explores its different development paths (see Figure 1). On the basis of respecting the relationship between each element and each factor, we must also consider the synergistic correlation between each element and each factor. The traditional research on the influence of chorus education on university culture only pays attention to the in-depth study of one aspect, while ignoring the influence of other factors. The theory of synergistic evolution is based on the research dimension of inside and outside, people and things. It fully affirms the correlation between the factors and breaks through the traditional thinking mode of one-way causality, so the model construction of this study has great exploratory and innovative value for the systematic and scientific research of chorus education. Based on systematic and holistic research, this paper constructs a model of the impact of chorus education on university culture, analyzes the corresponding development characteristics of different types of chorus education in universities, and explores its different development paths (see Figure 1). On the basis of respecting the relationship between each element and each factor, we must also consider the synergistic correlation between each element and each factor. The traditional research on the influence of chorus education on university culture only pays attention to the in-depth study of one aspect, while ignoring the influence of other factors. The theory of synergistic evolution is based on the research dimension of inside and outside, people and things. It fully affirms the correlation between various factors and breaks through the traditional thinking mode of one-way causality, so the model construction of this study has great exploratory and innovative value for the systematic and scientific research of chorus education. Based on the theory of coevolution, this paper constructs a set of influencing factors of chorus education on university culture. The influence of chorus education on university culture will not be a single form, but more an integrated display. Each factor has a close relationship and does not exist independently, so it should be carried out in a multi-level and multidimensional way of coevolution. The factors are more determined from the actual research and interviews, and at the same time, there are corresponding expert suggestions. This paper systematically studies the influence system of university culture from the two dimensions of people and things, external and internal, and establishes four quasi-lateral influence elements and sixteen element-level influence factors. It analyzes the mutual influence relationship from the four quasi-lateral elements of campus demand, campus organization, campus environment, and cultural products and comprehensively influences the change of campus demand from the needs of classmates, teachers, courses, and society. This paper analyzes the internal relevance of the external influence factors from the perspective of "people," analyzes the internal relevance of the internal influence factors from the perspective of "people" from the relationship between the school level, college level, community, and mass organizations, comprehensively affects the construction of campus organizations, and comprehensively studies the influence relevance affecting the construction of campus environment from the dormitory, classroom, activity, and social influence. From the construction of campus brand of courses, celebrities, works, and activities, the influence system of campus chorus education development of cultural products is constructed.

4. Empirical Analysis of Cases

From the model of the influence of chorus education on university culture constructed by the theory of coevolution, we can see the correlation between its elements and factors, but for the value and significance of its influence, there is a lack of intuitive reflection, which requires scientific calculus and valuation and the combination of subjective judgment and objective comprehensive analysis. After quantifying the judgment information of various influencing factors collected from various sources, we can comprehensively show the influence of chorus education on culture in colleges and universities, so as to better reflect the value and significance of its research. In this paper, through a comprehensive university of science and technology in southwest China, the school has not set up a music major, chorus education is

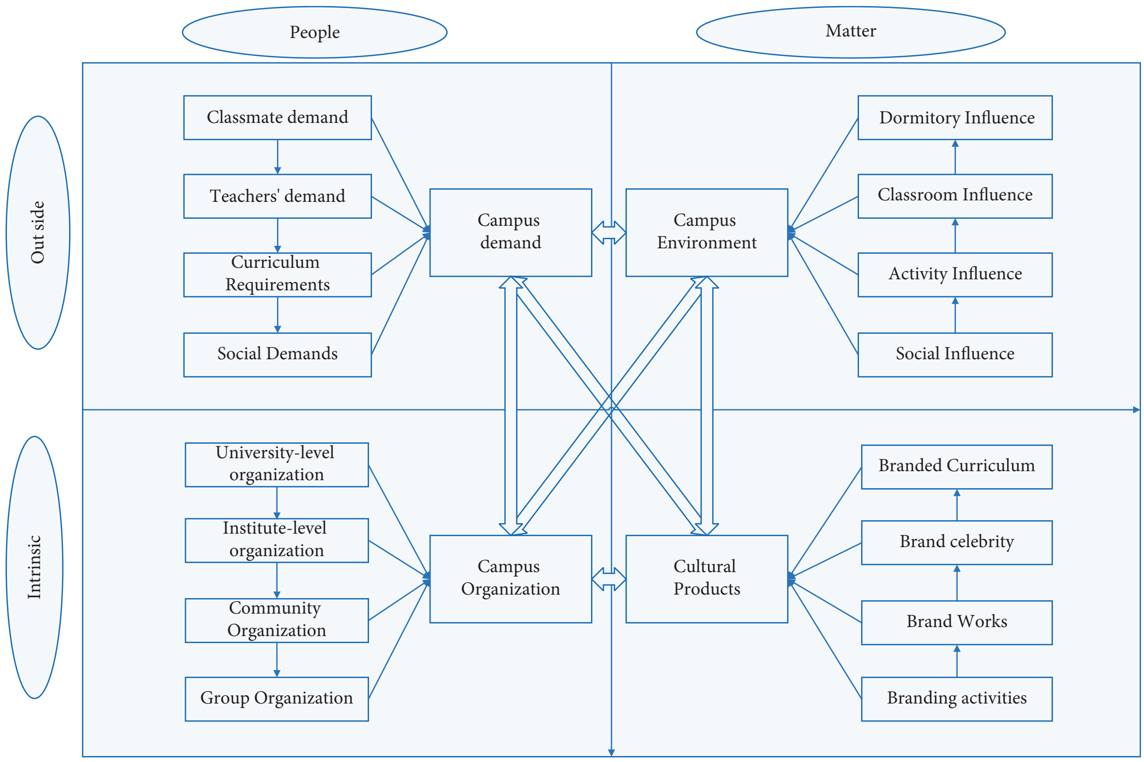

Figure 1: Model of the impact of chorus education on college culture.

mainly displayed in the form of courses and the establishment of university choirs, through the investigation of teachers and managers who participated in the management of choirs, as well as the investigation of some students who chose to study chorus courses, and a total of 20 samples were collected and interviewed: among them, one chorus conductor, two teachers from relevant management departments, five chorus cadres, two chorus members, five students who have taken chorus courses, and five students who have not taken chorus courses. In-depth interviews and questionnaires are combined to carry out relevant empirical research. The basis for selecting the relevant samples is mainly the management and participants of the chorus, mainly composed of instructors and relevant managers. In addition, the students who minor in related courses and those who do not minor in related courses make a certain differential choice, which is more objective to show the value of the study.

The method of DEMATEL (Decision Making Trial and Evaluation Laboratory) is used, which uses graph theory and matrix tools to objectively analyze the elements and factors and uses expert scoring method. Determine the logical relationship between the relevant elements in each dimension and construct the impact matrix, calculate the impact between each element and its impact, as well as the impact between other elements through the relevant formula, and finally form the impact analysis method of evaluation purpose [42]. DEMATEL comprehensive evaluation method attaches importance to the experience and knowledge of relevant experts and integrates the comprehensive judgment of experts and scholars on complex problems. "DEMATEL is a more effective evaluation method, especially for those systems with uncertain element relationships [43]." This method better integrates qualitative and quantitative research, is very suitable for the objective reality of this study, has certain adaptability for the analysis of the impact of chorus education on college culture, can objectively integrate the comprehensive opinions of experts, scholars, and students from different angles, and can effectively overcome the problem of inconsistent subjective opinions and judge the development of chorus education in colleges and universities. It provides a better research path and method to solve this problem and is more objective and close to the actual situation of chorus education in the development of colleges and universities.

4.1. Comprehensive Analysis and Construction of the Index System. Through the relevant influencing factors and elements in the model of the impact of chorus education on university culture constructed by the theory of coevolution, the analysis index system should be established, and the four elements of campus demand, campus organization, campus environment, and cultural products should be constructed as the criterion layers U1–U4 of the index system. Students' needs A1, teachers' needs A2, curriculum needs A3, social needs A4, school-level organizations A5, college-level organizations A6, community organizations A7, group organizations A8, dormitory influence A9, classroom influence A10, activity influence A11, social influence A12, brand courses A13, brand celebrities A14, brand works A15, brand activity A16 are taken as the element layer of the index system, and the evaluation and analysis system of the impact of chorus education on university culture is taken as the target layer, through the construction of a complete evaluation index system with three main levels of target layer, criterion layer, and element layer as shown in Table 1.

4.2. Basic Assumption and Operation Steps of Modeling. The first step is to design an evaluation interview questionnaire by combining the coevolution theory, the evaluation and analysis index system, and the DEMATEL research method and to establish a five-level evaluation system with five levels of 0, 1, 2, 3, and 4 as the strong and weak correlation, where 0 means no influence, 1 means slight influence, 2 means small influence, 3 means medium influence, and 4 means large influence. 20 people were interviewed, and the overall effectiveness of the survey was 100%.

The second step is to construct the direct impact matrix of element level and criterion level by collecting the comprehensive impact data obtained from interviews. Finally, Xd is obtained as shown in the following:

$$X^d = \begin{bmatrix} 0 & A_{1,2} & \cdots & A_{1,j} \\ A_{2,1} & 0 & \cdots & A_{2,j} \\ \vdots & \vdots & \vdots & \vdots \\ A_{i,1} & A_{i,2} & \cdots & A_{i,j} \end{bmatrix}. \tag{1}$$

Among $1 \le i \le n, 1 \le j \le n$, n is the total number of impact elements.

Step 3 is to calculate the normalized impact matrix. Through the direct impact matrix X^d, the sum of the elements in each row is calculated and the maximum value is taken. The sum of the elements in each row is calculated and the maximum value is taken; the maximum values in the row and column are compared to obtain the maximum values in the row and column, and in the impact matrix X^d of the comprehensive evaluation and analysis index system, each element is divided by the maximum value to obtain the standardized direct impact matrix X.

Step 4 is to calculate the comprehensive impact matrix T. According to the formula, the comprehensive influence matrix T is obtained from the direct influence matrix X. T_{ij} represents the degree of direct and indirect influence of element i on element j or element J.

The extent of the combined effect from element i is shown in the following:

$$T = X(1 - X)^{-1} = \left(t_{ij}\right). \tag{2}$$

Step 5 is to calculate the influence degree (R), the influenced degree (D), the centrality $(R + D)$, and the cause degree (R-D) in the comprehensive influence matrix. Centrality $(R + D)$ is the direct manifestation of the influence of the four factors. Cause degree >0 indicates that the element has a great influence on other elements, which is called cause element. The result element refers to the element whose cause degree is less than 0, which indicates that the element is greatly influenced by other elements and is called the result element as shown in the following:

$$R = \sum_{j=1}^{n} T_{ij} \, (1 \le i \le n, 1 \le j \le n), \tag{3}$$

$$D = \sum_{j=1}^{n} T_{ij} \, (1 \le i \le n, 1 \le j \le n). \tag{4}$$

The sixth step is to establish the weight ratio of the influence of chorus education on university culture. Because the centrality is used to calculate the comprehensive influence value of each criterion layer element on the whole, the comprehensive proportion is displayed comprehensively through the numerical value. "Therefore, the weight of the first-level index can be obtained by normalizing the centrality of each index [44, 45]." The comprehensive impact matrix index weight vector formula is shown in the following:

$$A = \left(a_n \Big| \sum_{n=1}^{4} a_n = 1, 0 \le a_n \le 1, n = 1, \cdots, 4 \right). \tag{5}$$

In the previous equation, a_{n} is the weight of the indicator, U_{n}.

4.3. Analysis of the Empirical Results of a University in Southwest China. Through the above calculation steps and the collected questionnaire evaluation ratings of relevant experts, scholars, students, and cadres, we assign them to the direct matrix of DEMATEL research method and finally calculate the comprehensive impact matrix T of chorus education on university culture in a southwest university, as shown in Table 2.

By calculating the influence degree, affected degree, centrality, and cause degree in the comprehensive influence matrix, the comprehensive influence relationship table of chorus education on university culture in a southwest university is formed, as shown in Table 3.

Through normalization processing, the weight vector of each criterion layer is finally obtained by integrating the relevant influencing factors of each element layer, as shown in Table 4.

4.3.1. Analysis of Empirical Results at the Element Level. Through the calculation of the relevant data of a university in southwest China, the above analysis results are finally calculated, so that the comprehensive evaluation results of the impact of chorus education on campus culture in a university in southwest China can be clearly judged, and the factors and results affecting chorus education in this university can be analyzed. Among the campus needs, social needs and students' needs are the main factors to promote the development of chorus education, and school-level organizations and mass organizations are the main driving forces to construct the organizational system of chorus education in a university in southwest China. Through investigation, research, and analysis, school-level organizations are mainly composed of school-level league organizations and mass organizations, and the mass

Table 1: Evaluation and analysis index system of the impact of chorus education on university culture.

Target layer	Criterion layer	Feature layer
Evaluation of the influence of chorus education on college culture	Campus demand U1	Classmate demand A1 Teacher needs A2 Course requirements A3 Social needs A4
	Campus organization U2	University-level organization A5 Institute-level organization A6 Community organization A7 Group organization A8
	Campus environment U3	Dormitory influence A9 Classroom influence A10 Event impact A11 Social influence A12
	Cultural products U4	Brand course A13 Brand celebrity A14 Brand work A15 Brand campaign A16

Table 2: Comprehensive impact matrix of chorus education on university culture in a southwest university.

	A1	A2	A3	A4	A5	A6	A7	A8	A9	A10	A11	A12	A13	A14	A15	A16
A1	0.32	0.71	0.76	0.42	0.00	0.00	0.00	0.00	0.00	0.00	0.00	0.00	0.00	0.00	0.00	0.00
A2	0.34	0.34	0.58	0.40	0.00	0.00	0.00	0.00	0.00	0.00	0.00	0.00	0.00	0.00	0.00	0.00
A3	0.45	0.56	0.46	0.50	0.00	0.00	0.00	0.00	0.00	0.00	0.00	0.00	0.00	0.00	0.00	0.00
A4	0.71	0.87	0.93	0.44	0.00	0.00	0.00	0.00	0.00	0.00	0.00	0.00	0.00	0.00	0.00	0.00
A5	0.00	0.00	0.00	0.00	0.12	0.44	0.40	0.20	0.00	0.00	0.00	0.00	0.00	0.00	0.00	0.00
A6	0.00	0.00	0.00	0.00	0.24	0.14	0.31	0.24	0.00	0.00	0.00	0.00	0.00	0.00	0.00	0.00
A7	0.00	0.00	0.00	0.00	0.13	0.15	0.09	0.13	0.00	0.00	0.00	0.00	0.00	0.00	0.00	0.00
A8	0.00	0.00	0.00	0.00	0.16	0.27	0.36	0.09	0.00	0.00	0.00	0.00	0.00	0.00	0.00	0.00
A9	0.00	0.00	0.00	0.00	0.00	0.00	0.00	0.00	0.29	0.45	0.36	0.20	0.00	0.00	0.00	0.00
A10	0.00	0.00	0.00	0.00	0.00	0.00	0.00	0.00	0.73	0.43	0.52	0.49	0.00	0.00	0.00	0.00
A11	0.00	0.00	0.00	0.00	0.00	0.00	0.00	0.00	0.64	0.54	0.36	0.47	0.00	0.00	0.00	0.00
A12	0.00	0.00	0.00	0.00	0.00	0.00	0.00	0.00	0.78	0.77	0.72	0.37	0.00	0.00	0.00	0.00
A13	0.00	0.00	0.00	0.00	0.00	0.00	0.00	0.00	0.00	0.00	0.00	0.00	0.72	1.11	1.04	1.11
A14	0.00	0.00	0.00	0.00	0.00	0.00	0.00	0.00	0.00	0.00	0.00	0.00	0.61	0.56	0.65	0.76
A15	0.00	0.00	0.00	0.00	0.00	0.00	0.00	0.00	0.00	0.00	0.00	0.00	0.78	0.89	0.63	0.89
A16	0.00	0.00	0.00	0.00	0.00	0.00	0.00	0.00	0.00	0.00	0.00	0.00	0.78	0.89	0.83	0.69

Table 3: Comprehensive impact of chorus education on university culture in a southwest university.

Factor		Degree of influence	Influenced degree	Centrality	Degree of cause	Factor attribute
Classmate demand A1	A1	2.21	1.83	4.03	0.38	Causal factor
Teacher needs A2	A2	1.67	2.48	4.15	−0.81	Result factor
Course requirements A3	A3	1.97	2.73	4.69	−0.76	Result factor
Social needs A4	A4	2.95	1.75	4.69	1.20	Causal factor
University-level organization A5	A5	1.17	0.65	1.82	0.52	Result factor
Institute-level organization A6	A6	0.92	1.01	1.93	−0.08	Result factor
Community organization A7	A7	0.50	1.16	1.66	−0.66	Result factor
Group organization A8	A8	0.88	0.65	1.53	0.22	Causal factor
Dormitory influence A9	A9	1.30	2.44	3.73	−1.14	Result factor
Classroom influence A10	A10	2.18	2.20	4.37	−0.02	Result factor
Event impact A11	A11	2.01	1.95	3.96	0.06	Causal factor
Social influence A12	A12	2.64	1.54	4.17	1.10	Causal factor
Brand course A13	A13	3.98	2.89	6.87	1.09	Causal factor
Brand celebrity A14	A14	2.57	3.44	6.02	−0.87	Result factor
Brand work A15	A15	3.19	3.15	6.33	0.04	Causal factor
Brand campaign A16	A16	3.19	3.44	6.63	−0.26	Result factor

Table 4: Weight ratio of chorus education to campus culture in a university in southwest China.

Factor	Campus demand U1	Campus organization U2	Campus environment U3	Cultural products U4
Centrality	17.57	6.94	16.25	25.85
Normalization processing	26.37%	10.42%	24.39%	38.81%

organizations here are mainly formed by the spontaneous development of school students, which reflects that the spontaneous love of students for chorus art in this university is an important force to promote the development of chorus education. The influence of activities inside and outside the school and the social influence are the causes of the influence of chorus education on the campus cultural environment of a university in southwest China, among which the social influence is the decisive value and the most important thing to promote the construction of campus culture. The social influence factors of campus chorus education in colleges and universities are far more important than the influence of activities. Therefore, when the social influence declines, it will certainly affect the comprehensive investment of colleges and universities in chorus education and ultimately affect the improvement of the whole level of chorus education. Among the cultural products, brand courses and brand works are the reasons for the influence of chorus education in a university in southwest China on university culture, which reflects the importance of the construction of brand courses in chorus education in universities. Courses are an important manifestation of meeting the needs of students and society, and works are a key factor in shaping social influence. The most important factor in promoting chorus education in comprehensive colleges and universities is the construction and shaping of brand courses and works, which will bring comprehensive effects to demand, organization, and environment. From the empirical calculation, we can see that dormitory influence, brand celebrities, and teachers' needs account for a higher proportion of the result factors, which is different from the perceptual cognition obtained from the survey and interview. In the perceptual cognition of students and teachers, it is generally believed that the construction of dormitory culture and the cultivation of teachers' ability are the key factors affecting the development of chorus education in colleges and universities. However, through comprehensive analysis and calculation, combined with feedback from all sides, it is found that these are not important factors, and how to further stimulate the needs of students, meet the needs of society, expand social influence, and develop brand courses are the key factors to promote the long-term development of school chorus education.

4.3.2. Analysis of Empirical Results at the Criterion Level. By normalizing the empirical results of the criterion layer, it can be clearly found that in the study of the impact of chorus education on university culture in a university in southwest China, the demand for cultural products on campus culture construction accounts for the highest proportion, which fully reflects that universities have invested more energy in this area. It can be found that the two elements of campus organization and campus environment account for a low proportion, of which the proportion of campus organization in colleges and universities is only 10.42%, reflecting the relative lack of organizational construction in the construction of chorus education in colleges and universities. After normalization, the relative mean of the four elements of the criterion layer can better reflect the balanced development trend of the school from the three levels of teachers, cadres, and students. From the overall analysis of the university, we can see that the unbalanced development of the school is more obvious, and the brand courses and works of the university are important factors affecting the overall development. Through research and empirical analysis, we can find that the university's cultural products play an important supporting role in meeting the needs of teachers, cadres, and students, which shows that the expectations of teachers and students for excellent courses and works are the key factors to promote the development of chorus education. Therefore, strengthening the construction of campus culture is the primary task of the construction of campus culture and improving the overall development level of the school, enhancing the overall competitiveness of the school, and promoting the overall development of the school. Therefore, from the study of the criterion level, it can be clearly seen that strengthening the development of organizational construction in school chorus education is the top priority of the current school chorus education and that schools need to enhance the influence of organizations at all levels on other elements and factors and improve the absorption and integration of school-level organizations and mass organizations, to provide a good development space and environment for the college and community organizations, to promote the comprehensive improvement of the influence of the result elements, and to strengthen the comprehensive coordination of the campus environment, campus cultural products, and other factors, so as to improve the overall influence of school chorus education in the construction of campus culture.

5. Conclusions and Recommendations

Through the in-depth study of this paper, we can see that it is wrong for many colleges and universities to rely more on the support of schools and the state when promoting chorus education in aesthetic education, without really facing the main group of students in education, and we need to change the original logic of campus chorus development, starting from the students' understanding and thinking of chorus. To find the development motivation from the cultivation of students' overall hobbies, we need to go deep into enterprises to understand the social needs and promote the development of campus chorus from the side incentive effect of the ability cultivation of students with comprehensive quality. In addition, we should rely on chorus education to continuously enhance the marketing power of the whole society and thus establish brand courses, improve curriculum content, form and method innovation, constantly promote the development of the overall chorus education, and stimulate the evolution of campus aesthetic education chorus education. It constantly updates and evolves its development logic from different dimensions, different needs, and different development perspectives to promote the innovative development of chorus education.

Based on the theory of coevolution, using DEMATEL research method, and combining qualitative and quantitative methods, this paper constructs an evaluation model of the impact of chorus education on university culture and makes a quantitative and qualitative study of the current situation of chorus education in a comprehensive and non-music major construction university in southwest China. It summarizes the qualitative analysis of different experts, scholars, students, teachers, and administrators on the current development of chorus education in the university. By collecting the key differences of different perspectives, different viewpoints, different thinking, and different values, we can scientifically and systematically quantify the opinions of all parties and identify the key factors affecting the development of schools in the general cognition. By synthesizing the opinions of all parties, we can scientifically form a cognitive judgment acceptable to the public, comprehensively analyze the current situation of the development of university chorus, evaluate and quantify the advantages and disadvantages of the development of university chorus, locate the key issues of concern, and facilitate the objective integration of consensus among decision makers. Construction methods are put forward scientifically, and reasonable strategic development plans and objectives are formulated. This research method takes the construction of a comprehensive and systematic research paradigm as the main innovation point, aiming to provide a new research method for the scientific and systematic development of the impact of chorus education on university culture and to provide new research ideas and paths for the deepening research of aesthetic education, humanistic training, value shaping, and other aspects of education in colleges and universities [31].

Data Availability

Data sharing is not applicable to this article as no datasets were generated or analyzed during the current study.

Conflicts of Interest

The authors declare no conflicts of interest.

References

[1] E. Albert, L. Xu, B. Li, Z. Zhao, and X. Li, *Einstein on Science and Education*, Commercial Press, vol. 4, p. 102, Beijing, China, 2016.

[2] Y. Chang, "The main forms of western choral music and its artistic presentation in teaching a review of an introduction to western choral music," *Science and Technology Management Research*, vol. 41, no. 13, p. 238, 2021.

[3] Q. Pan, "On the significance of mass chorus in the construction of mass culture," *The Artist*, vol. 9, pp. 120-121, 2020.

[4] Y. Shao, "On the current situation of mass chorus and counseling strategies," *Voice of Yellow River*, vol. 7, p. 174, 2020.

[5] Z. Huang and Z. Chen, "Research on diversified development and artistic innovation of chorus in the new era," *University of Electronic Science and Technology Press*, vol. 4, pp. 4–6, 2017.

[6] W. Li, *Research on Teaching Reform of Chorus and Conducting in Colleges and Universities*, p. 58, Suzhou University Press, Suzhou, China, 2017.

[7] Huaxia, "On the embodiment and cultivation of emotional quotient in chorus education," *Popular Technology*, vol. 17, no. 6, pp. 209-210, 2015.

[8] S. Fan, "Chorus education and art education," *Voice of Yellow River*, vol. 21, p. 35, 2013.

[9] M. Pan, "How to cultivate the chorus ability of middle school students," *Journal of Xiangnan University*, vol. 37, no. 1, pp. 86–90, 2016.

[10] Y. Guo, "On the teaching and training of college students' chorus of non-art majors," *Journal of Jiaozuo University*, vol. 30, no. 3, pp. 105–107, 2016.

[11] W. Liu, "Liszt and the study of Hungarian choral higher education," *Journal of Xinghai Conservatory of Music*, vol. 2, pp. 140–145, 2014.

[12] S. Hu, "How new teachers quickly lead the primary stage of the newly-built chorus thoughts on improving the effectiveness of chorus training," in *Proceedings of the National Teachers Research Fund Management Office. Scientific Research Achievements of National Teacher Research Fund 2019 (VII)*, p. 2, National Teacher Research Fund Management Office, USA, October 2019.

[13] J. Zhang, "On the brand management of university chorus," *Northern Music*, vol. 10, pp. 47-48, 2013.

[14] Q. Xu, "On the construction and development of college chorus," *Yihai*, vol. 10, pp. 84–86, 2014.

[15] R. Jin, "Macroscopic thinking on the construction and development of university chorus," *Journal of Heihe University*, vol. 7, no. 6, pp. 159-160, 2016.

[16] Z. Wang and S. Xin, "Construction and management of college chorus," *Arthritis Research*, vol. 1, pp. 196-197, 2017.

[17] A. Gorrochotegui, "El cine y la generación de conocimiento en la educación empresarial: estudio de caso con la película los coristas movies in the creation of knowledge in business education: case study with the film," *The Chorus*, vol. 6, no. 2, pp. 83–94, 2009.

[18] Y. SungWon, "An operational system design for chorus education in elementary and secondary schools," *Journal of Music Education Science*, vol. 14, no. 2, pp. 81–89, 2012.

[19] Anbihwa, "A study on chorus dance education for social communication," *Resach of Dance Education*, vol. 26, no. 2, pp. 19–33, 2015.

[20] H. Cho, "A study on utilizing plan of a cappella chorus in primary and secondary school for life-style education," *Broadcasting and Arts Research Institute*, vol. 2, no. 3, pp. 157–175, 2017.

[21] H. J. Ahn, J. Bahng, and L. J. H. Hee, "Measurement of acceptable noise level with background music," *Journal of audiology & otology*, vol. 19, no. 2, pp. 79–84, 2015.

[22] K. Jacob, "Scientific tests and measurements applied to musicâ," vol. 10, no. 5, pp. 30–32, 2016.

[23] N. J. Washnik, S. L. Phillips, and S. Teglas, "Student's music exposure: full-day personal dose measurements," *Noise and Health*, vol. 18, no. 81, pp. 98–103, 2016.

[24] J. García González, M. I. Ventura Miranda, F. Manchon García et al., "Effects of prenatal music stimulation on fetal cardiac state, newborn anthropometric measurements and vital signs of pregnant women: a randomized controlled trial," *Complementary Therapies in Clinical Practice*, vol. 27, 2017.

[25] L. Crickmore, "The measurement of aesthetic emotion in music," *Frontiers in Psychology*, vol. 8, p. 651, 2017.

[26] D. M. Tai, S. N. Phillipson, and S. Phillipson, "Hong Kong parents and their children's music training: measurement properties of the parental involvement in music training questionnaire," *Educational Psychology*, vol. 38, no. 5, 2018.

[27] P. Duarte, J. A. Folgado-Fernández, and J. M. Hernández-Mogollón, "Measurement of the impact of music festivals on destination image: the case of a womad festival," *Event Management*, vol. 22, no. 4, pp. 517–526, 2018.

[28] G.. Music, "Therapy and in daily life: health of musicians, concepts of aesthetics, measurement, and new media," *Nordic Journal of Music Therapy*, vol. 27, no. 4, 2018.

[29] A. Barrientos-Fernández, R. Sánchez-Cabrero, A. Arigita-García, L. Mañoso-Pacheco, F. J. Pericacho-Gómez, and M. Á. Novillo-López, "Measurement of different types of intelligence (general, verbal vs. non-verbal, multiple), academic performance and study habits of secondary students at a Music Integrated Centre," *Data in Brief*, vol. 25, 2019.

[30] O. P. Shin and E. George, "Examining rater judgements in music performance assessment using many-facets rasch rating scale measurement model," *Journal of Applied Measurement*, vol. 20, no. 1, 2019.

[31] B. C. Wesolowski, "Predicting operational rater-type classifications using rasch measurement theory and random forests: a music performance assessment perspective," *Journal of Educational Measurement*, vol. 56, no. 3, 2019.

[32] P. Das, S. Gupta, and B. Neogi, "Measurement of effect of music on human brain and consequent impact on attentiveness and concentration during reading," *Procedia Computer Science*, vol. 172, 2020.

[33] L. Pei, "Cognitive approach to the measurement and evaluation of musical achievement," *Chinese Music*, vol. 4, pp. 39–41 + 66, 2001.

[34] W. Zhu, "Theoretical research on the construction of the evaluation system of university chorus education," *Music Composition*, vol. 6, pp. 141–143, 2011.

[35] H. Zhou, *Educational Evaluation and Evaluation System*, Z. Xu, Ed., vol. 7, p. 1, Guangxi Education Press, Nanning, China, 1989.

[36] P. R. Ehrlich and P. H. Raven, "Butterflies and plants: a study in coevolution," *Evolution*, vol. 18, no. 4, pp. 586–608, 1964.

[37] D. H. Janzen, "When is it coevolution?" *Evolution*, vol. 34, no. 3, 1980.

[38] R. B. Norgaard, "Coevolutionary agricultural development," *Economic Development and Cultural Change*, vol. 32, no. 3, pp. 525–546, 1984.

[39] G. Eisenhardt, "Coevolving: at last, a way to make synergies work," *Harvard Business Review*, vol. 78, pp. 91–101, 2000.

[40] Hodgson, "Darwinism in economics: from analogy to ontology," *Journal of Evolutionary Economics*, vol. 12, pp. 259–281, 2002.

[41] C. Li and S. Xu, *60 Theories Commonly Used in Management and Organization Research*, vol. 03, pp. 21–25, Peking University Press, Beijing, China, 2019.

[42] H. Li, D. Zhou, and L. Zhang, "Improvement of AHP by using DEMATEL method and cross-reinforcement matrix method," *Statistics and Decision Making*, vol. 8, pp. 10-11, 2006.

[43] Y. Du and S. Wang, "Performance evaluation method of science foundation projects based on DEMATEL-fuzzy comprehensive evaluation," *Science Foundation in China*, vol. 2, pp. 161–169, 2018.

[44] L. Tang, J. Zhou, and G. Wang, "Research on integrated innovation evaluation of industry-university-research based on DEMATEL-ANP - - a case study of dalian double D port enterprises," *Science of Science and Management of Science and Technology*, vol. 12, pp. 89–96, 2013.

[45] W. Wang and W. Huaian, "Construction of evaluation index system of collaborative innovation capability - - an empirical study based on state key laboratory," *Science of Science Research*, vol. 3, pp. 471–480, 2016.

Hindawi
Scientific Programming
Volume 2021, Article ID 7678931, 9 pages
https://doi.org/10.1155/2021/7678931

Research Article

Housing Price Prediction Based on Multiple Linear Regression

Qingqi Zhang

The Hong Kong University of Science and Technology, Clear Water Bay, Kowloon, Hong Kong

Correspondence should be addressed to Qingqi Zhang; qzhangbs@connect.ust.hk

Received 24 August 2021; Accepted 18 October 2021; Published 29 October 2021

Academic Editor: Punit Gupta

In this paper, the author first analyzes the major factors affecting housing prices with Spearman correlation coefficient, selects significant factors influencing general housing prices, and conducts a combined analysis algorithm. Then, the author establishes a multiple linear regression model for housing price prediction and applies the data set of real estate prices in Boston to test the method. Through the data analysis and test in this paper, it can be summarized that the multiple linear regression model can effectively predict and analyze the housing price to some extent, while the algorithm can still be improved through more advanced machine learning methods.

1. Introduction

The real estate industry has been one of the leading researches focusing on modern economics, for its significant implications on relevant industries and fields such as construction, investment, and public welfare. In general, purchasing and investing in any real estate project will involve various transactions between different parties. Thus, it could be a vital decision for both households and enterprises. How to construct a realistic model to precisely predict the price of real estate has been a challenging topic with great potential for further research [1]. It is generally believed by academia that correctly predicting the special price for a specific real estate is impractical since it involves plenty of factors exerting influence on the eventual cost.

There is a well-known saying about the appraisal of real estate by Li Ka-Shing, the most famous property tycoon in Hong Kong: "Three major factors are determining the price of a property, the first one is location, the second one is location, and the third one is still location." His word does not seem to make much sense from a statistical research perspective. Nevertheless, as a successful businessman in the property industry, what makes him attach so much significance to some specific factors like location when appraising a property is crucial. To what extent a particular factor like location plays an essential role in pricing a property is worth exploring by adopting a statistical model in real estate economics research.

The appraisal of real estate is traditionally conducted by a licensed professional, who would carry out a holistic survey based on several factors such as location, surroundings, areas, and facilities of a real estate. Nevertheless, the manual appraisal would inevitably have the possibility to involve the appraisers' factors and vested interest. This potential risk would likely cause a biased or subjective evaluation of a particular real estate, bringing loss for investors or households [2]. Thus, constructing a feasible algorithm and automated model which could appraise the real estate impartially and objectively has critical significance for any potential parties participating in these transactions.

According to economics principles, the market price of properties is attained when the demand and supply curves intersect with each other, which is subject to various factors, both subjectively and objectively. It is doubtful in practice that the market price of a property will equal the market value, as the market for real estate has been too unpredictable and fluctuating to be considered as an ideal market [3]. Affected by many subjective factors, it is significantly crucial for real estate appraisers to figure out the objective factors that account most for the pricing of properties.

In modern research on the property industry, advanced research methods such as machine learning and artificial intelligence have been widely adopted in many aspects. Not only are they utilized in evaluating the price and value but also they are applied to figure out potential future applications and would-be challenges [4]. The comprehensive adoption of machine learning and artificial intelligence in the property industry has generally transformed this experience-driven industry with great arbitrage opportunities to an intelligent and data-driven enterprise [5].

Real estate appraisal has been divided into mainstreams at the current stage: mass appraisal and individual appraisal. The personal assessment is conducted when specific values are given for different characteristics of a given real estate. At the same time, mass appraisal adopts a systematic methodology to perform a precise assessment for a group of properties by adopting standardized procedures and rigorous testing in statistics [6]. Besides traditional techniques like the linear regression model, modern mass appraisal methodology has broadly incorporated computational intelligence approaches such as support vector machine (SVM), multilayer perceptron (MLP), and neural network. In practice, it has been widely employed in property appraisal for various purposes such as taxation and investment forecasting [4].

The current study of price modeling in real estate has mainly been based on the theory of hedonic prices, which was initiated by a famous economist Sherwin Rosen. His approach is generally regarded as feasible and could be applied to extensive research in the real estate field by academia. According to his theory, the property price could be characterized as a utility function of many relevant variables such as structural characters, neighborhoods, and the environment [7]. Based on this theory, pricing models for real estate are generally built through a multiple regression model, in which many general assumptions such as independence, homoskedasticity, and normal distribution of residuals must be fulfilled [8].

The definition of hedonic prices refers to the regression for the marginal contribution of properties and the neighborhood relations. This model and methodology have been widely adopted in property research since Rosen's research in 1974. A model was constructed to assess the value of properties and conducting urban analysis by considering many variables. This was seen as the initial development of the definition of the hedonic pricing model. As time went on, more statistical research and applications for Rosen's model have come into being. Stevenson, for example, has reexamined the heteroskedasticity in the hedonic price model, which, to a greater extent, consolidates the theory and veracity of the model [9]. By adopting modern information technology like Geographic Information System (GIS), Bin [10] has used precise geographical data to verify the preciseness of the model, proving that the semiparametric regression model is practical for both analyzing and predicting the property price [11].

In recent decades, unlike the hedonic regression model, artificial neural network (ANN) and fuzzy logic (FL) methodology have also been widely accepted. In Din et al.'s [12] research on the ANN method for property appraisal, it generally performs well and generates acceptable performance in some respects. Still, it also turns out that different input choices of variables would sometimes generate statistically different values of output, which indicates the instability and immaturity of the ANN methodology. In terms of fuzzy logic, it is widely believed to be a more promising and generic approach for evaluating properties. Liu et al. [13] have constructed a statistical model based on the fuzzy neural network prediction model, which incorporates the hedonic theory and a great database with relevant characteristics affecting the price of properties based on recently sold projects. The experimental outcome and analysis have shown that the fuzzy neural network prediction model has a promising ability for real estate price prediction given reliable input data with high quality. A comparative experiment has also revealed that multiple regression applications for property appraisal work well with given data [14].

However, theoretically, the models based on multiple regression seem to attach more significance to statistical inference rather than prediction due to its nature. For this reason, extensive research on this theory has put the focus on the significant factor that influences the model the most, evaluating the economic value of real estate with specific characteristics and identifies the causal effect relationship behind the regressors [3]. Despite the profound and far-reaching significance brought by this method, its potential for statistical prediction on the pricing of real estate has been in deficiency by its nature. The limit of the traditional hedonic regression model has a significant influence on the procedure of generating the model, making it hard to identify the appropriate variables to set up the eventual model. Therefore, adopting other methodologies to conduct rigorous and viable research to a different extent is indispensable.

2. Spearman Correlation Coefficient

With the development of technology, high-dimensional data have been widely adopted in various fields, including economics, finance, and engineering. High-dimensional data are an indispensable ingredient when processing relevant data and conducting research. In addition, Big Data is also a newly emerged concept, indicating the following two features: enormous sample size and high dimensions of data.

Spearman correlation coefficient has been a nonparametric rank statistic. It was initially designed as a measure of the strength of the association between two variables. As a significant measure of monotone association, it is widely adopted when the input distribution makes the ordinary Pearson's correlation coefficient misleading. Not a measure of the linear relationship between two variables, the Spearman correlation coefficient evaluates the extent that an arbitrary monotonic function can depict the relationship between two variables on the condition that there is no further assumption made about the frequency distribution. One advantage of the Spearman coefficient is that it does not require the linear assumption as Pearson's coefficient does. This significant advantage has made it widely adopted by many statisticians in analyzes.

The correlation coefficient is a measure to depict the association between variables, which can delineate the association for two variables co-occurring. The correlation coefficient has been widely used in the scientific research field. We will mainly discuss the Spearman correlation coefficient in this part.

We first assume two-dimensional random vectors:

$$(X_1, Y_1), (X_{2,} Y_2), (X_3, Y_3), \tag{1}$$

are identically independently distributed (i.i.d.). Its joint distribution function is defined as H, and marginal distribution functions are defined as G and H, respectively. Considering the covariance among those two-dimensional random vectors, the Spearman correlation coefficient can be defined as follows:

$$\begin{aligned}\rho_s = 3\big(P\{(X_1 - X_2)(Y_1 - Y_3) > 0\} \\ -P\{(X_1 - X_2)(Y_1 - Y_3) < 0\}\big).\end{aligned} \tag{2}$$

The outcome ρ will not be affected by substituting (X_2, Y_3) with (X_3, Y_2).

In another form for better calculation purposes, we can also offer a format for sampling for random samples:

$$\begin{aligned}&\{(X_i, Y_i), i = 1, \ldots, n\}, \\ &r = \frac{1/n\sum_{i=1}^{n}\left(RX_i - (n+1)/2\right)\left(RY_i - (n+1)/2\right)}{1/12\left(n^2 - 1\right)}.\end{aligned} \tag{3}$$

This equation can be viewed as a Euclidean distance for RX_i and RY_i. From a nonparametric point of view, it can be explained as follows: the smaller the distance is, the more likely X and Y will be positively correlated. The greater the distance is, the more likely X and Y are negatively correlated.

From the derivation above, it is apparent that the Spearman correlation coefficient is a rank correlation of coefficient. Therefore, it obtains some common merits of the rank correlation coefficient [15].

First of all, the Spearman correlation coefficient does not have a strict requirement for the sample normality as a nonparametric correlation coefficient. Thus, it has a more extensive adoption in statistical research.

Secondly, the Spearman correlation coefficient uses the rank of variables to compute the correlation between different variables. In this process, strict monotone transformation is employed so that the rank of variables will stay unchanged. Therefore, it has the merit of monotonousness. We can perform some transformation to generate various statistical models based on monotonousness, which extends this model to more variable filtering methods such as logistics model and box-cox transfer model.

Thirdly, the Spearman correlation coefficient can process discrete data practically. It will not be affected by dimension, which means it can precisely measure the correlation between different dimensions. Furthermore, the Spearman correlation coefficient is very unlikely to be affected by extreme values, which can minimize the negative impact of extreme values on our statistics.

Finally, the Spearman correlation coefficient can better depict some nonlinear relations. As pointed out by Lancaster, dependence or correlation measures indicate the strength of correlation, especially the mutually independent variables. Therefore, the correlation of variables does not necessarily mean the linear relationship between variables. It even cannot indicate a direct functional relation. In this sense, the Spearman correlation coefficient can better depict the correlation between variables when there exists nonlinearity [16].

3. Housing Price Prediction Based on Multiple Linear Regression

3.1. The Analysis of Main Factors Affecting Housing Price. Housing price is affected by multiple factors and features of a specific house. According to the previous research, some analysts have proposed several variables that significantly influence the overall housing price. According to Kusan et al. [9], these factors can be classified into three types: house factors, environmental factors, and transportation factors. Each factor and the effective primary mechanism are elaborated in the following text.

House factors can be divided into several types. The most influential type is residential factors, including residence, usability, and number of rooms. When people consider purchasing a house for living purposes, the factors above are the main determinants for the living quality. Buyers with family members would typically attach more importance to the essential feature of the house, like the living area and number of rooms, which have a significant impact on the overall living quality and experience in the house. Besides, the intangible features, like the view of residence and usability, also have a rather considerable influence on the housing price, through affecting buyers' experience on the house and willingness to pay.

The other influential types are the main factors related to building properties and floor factors. Building properties are mainly about hardware and basic facilities in the building, such as the elevator, generator, and garage. To depict an example of this, the number of containable cars within a garage is a rather important consideration. The rising trend of numbers of vehicles per household possessing generates a necessary demand for the quality and capacity of a garage in a house. Other affiliated facilities to the house like the swimming pool and backyard have also played an essential role in determining the housing price, as the demand for leisure and relaxation has been arising with the economic progress.

On the other hand, floor factors, like the number of floors, have also impacted the housing price significantly. Typically, household prefers the house with the number of the floors most suitable for their daily convenience. A family with children and elders tends to prefer a house with multifloor construction, which offers different family members separate living areas with appropriate privacy while living together.

Environmental factors mainly consist of two parts: regional environment and nearby pollution. Regional environment refers to the overall living conditions in the surrounding community. Sanitation, as a significant indicator of the living quality, has been given more importance in the recent decades. A community with comprehensive sanitation services tends to attract buyers to pay a higher price. In addition, natural scenery, as an objective feature of the community where the specific house is in, also influences the housing price through various channels. Purchasers with a preference for a house with a mountain view or lake view may be willing to pay a higher price for a house near the natural scenery. Even for those buyers who do not have a specific preference, a decent and beautiful view would add more weight for the specific house and community when purchasers are choosing from various options.

On the other hand, nearby pollution is also an environmental factor negatively related to the quality of the house. The most apparent factors are noise and air pollution. Noise is generally affecting the community through various channels such as the nearby factories, cars running in the central lane, and pedestrians crossing the community. Air pollution, compared with noise, is a somewhat measurable and quantifiable indicator of environmental pollution. The general measurement for air pollution and air quality is AQI, which stands for air quality index. Typically, houses located in a community with better air quality tend to attract buyers with a higher willingness to pay, thus generating higher housing prices in the market.

Transportation, as the principal channel for connecting the community with the outer areas, is worth our specific discussion when analyzing the external factors influencing the housing price. Transportation can influence housing via various aspects, including the distance to social and cultural centers, distance to trade and shopping centers, and distance to public transportation stations.

The distance to social and cultural centers can be a meaningful consideration for many household buyers. As children need to go schooling and enhance cultural and physical education, facilities such as libraries, schools, and sports complexes are the frequently visited places for those buyers, who has blended into their daily lifestyle. The commuting time is positively related to the distance between the house and the destination. Closer distance offers greater convenience for all the household members, thus contributing to a higher price when choosing various options.

Following the same logic, we can reasonably derive that the distance to the local shopping centers and public transportation stations is also crucial to the housing price. Shopping is one of the most frequent activities for daily lives in the United States. Residents tend to drive to the nearest supermarkets for daily consumption like grocery and to the comprehensive mall for higher-level consumption like clothing or luxuries. Public transportation, on the other hand, has been significant for residents as well. Although driving is the most common way of commuting in the United States, other ways like taking an airplane or metro are also important substitutes for transportation choices.

3.2. Multiple Linear Regression Model for Housing Price Prediction. Analyzing data is for extracting accurate estimation from basic information provided. The most important and common question is whether there is a statistical relationship between an explanatory variable (usually denoted by X_i) and a response variable (usually denoted by Y). To solve this problem, a typical way is to apply regression analysis to model and quantify this statistical relationship. Many types of regression are adopted in scientific research, depending on the feature and type of given data.

The most used model for conduction regression is called the linear regression model, which is used when the distribution of the response variable Y is continuous and approximately regular. Linear regression is the procedure that estimates the coefficients of the linear equation, with at least one independent variable that best predicts the value of a dependent variable. Our goal is to predict the outcome Y based on the given values of predictor variables X_i. The linear regression model allows us to evaluate the impact of multiple variables in the same model.

An appropriate model could be a straight line in an actual application, a higher degree polynomial, a logarithmic, or exponential. We may find a proper model by the forwarding method, in which we start by assuming a relatively simple straight line $Y = a + bX$. Next, we may find the most suitable estimator of the assumed model. If the model does not fit the data well, we may alternatively assume a more complicated model, like a second-degree polynomial model $Y = a + bX + cX^2$. On the other hand, the other method is called the backward method, in which we assume a complicated model first, and we then fit the model, trying to simplify it. Both methods could achieve the same goal for modeling the data appropriately, depending on the given situation and features of the data set [17].

A multivariate linear regression model is based on the assumption [18]:

$$y_i = \beta_0 + B' x_i + \varepsilon_i, \tag{4}$$

where $y_i = (y_{i1} \ldots, y_{id}, \ldots y_{iD})'$ and x_i are the D-dimensional vector of the output variables and the P-dimensional vector of the fixed regressor values for the i^{th} sample unit correspondingly. β_0 is a D-dimensional vector containing the intercepts for the D response; B is a matrix of the dimension $P \times D$ whose (p, d) element, β_{pd}, is the regression coefficient of the p^{th} regressor on the d^{th} response; eventually, ε_i symbolizes the D-dimensional random vector of the error terms corresponding to the i^{th} observation. The classical multivariate linear regression model also assumes that $\varepsilon_i (i = 1, \ldots, I)$ is the independently and identically distributed random vector. Its distribution is assumed to be multivariate Gaussian with a D-dimensional vector with mean value zero and a positive definite covariance matrix $\sum$ of dimension $D \times D$, which is

$$\varepsilon_i \sim \mathrm{MVN}\left(0, \sum\right). \tag{5}$$

The proposed multivariate linear regression model is based on the aforementioned assumption and

$$\varepsilon_i \sim \sum_{k=1}^{K} \Pi_k \mathrm{MVN}\left(\nu_K, \sum K\right), \quad (6)$$

where π_k represents positive weights that sum to 1 and ν_k represents D-dimensional mean vectors that satisfy the constraint:

$$\sum_{k=1}^{K} \pi_k \nu_k = 0. \quad (7)$$

4. Simulation

4.1. Spearman Correlation Coefficient Analysis. According to the reference research and our previous discussion in Section 2, an analysis for correlation coefficients of different variables with the housing price is conducted. With the data processing methodology using Python, Spearman correlation coefficients can be simulated as shown in Figure 1 using the housing price data set in Boston.

The Spearman correlation coefficients between the house price and variables in the data set are shown above. These factors vary from house factors to environmental factors, all contributing to the formation of the overall price. This coefficient analysis reveals the general trend and significant factors on the housing price. To elaborate more about the exact definition of each variable, we can refer to the description in Table 1.

4.2. Multivariable Regression Analysis. As the methodology discussed above indicates, an empirical analysis based on the Boston housing price data set is conducted to test multiple factors and their impact on the median housing price as a response variable.

In the first place, data analysis is conducted on housing price, in the sense that the influence of the number of rooms on the overall housing price is analyzed, which can be seen in Figure 2. In Figure 2, the horizontal axis represents the average number of rooms per house, while the vertical axis represents the median price of self-owned houses in that region, measured in 1,000 US dollars. From Figure 1, there exists a positive, upward-sloping relationship between the number of rooms and overall housing price. With more rooms, the house is more likely to be a superior residence with higher quality and market value. This empirical evidence and trend have been a consistency of our common sense, which indicates a property will generally sell at higher prices when it has more rooms and space for living purposes. This empirical result has cross verified the features and trends that we have discussed in Section 3.

Next, we regressed the weighted average distance from the property to 5 employment centers in Boston, and we got the scatter plot as shown in Figure 3, in which the horizontal axis represents the weighted average distance from the house to 5 employment centers in Boston. From Figure 2, it can be summarized that the housing price is more concentrated in the middle and lower level when the distance ranges from 0 to 5 kilometers in the area close to the employment center. From a geographical perspective, this trend also shows that the sample has a higher density near the city center, in the sense that houses in Boston are more concentrated in a central location with an appropriate price. On the other hand, it can also be concluded that the house price distribution will be more sporadic as the distance increases, in the sense that the price variation between different houses may grow as the distance is getting further from the employment center in the city, and the price may fall into different ranges when the houses are in suburban regions.

From the empirical analysis based on Spearman correlation coefficient in using the previous data set for housing price in Boston, these factors including the proportion of lower-income group in the region, proportion of property land area larger than 25,000 square feet, the average number of rooms, etc., are among the primary factors that influence the housing price.

In this empirical analysis, with the data set of Boston housing prices, a multiple linear regression model is constructed to analyze different factors' impact on the housing price and predict the corresponding housing price based on the given input.

A typical standardization process in data analysis for the raw data is first conducted after obtaining the major influencing factors from previous analysis based on the Spearman correlation coefficient. By definition, the standardized value here will range between 0 and 1:

$$\text{standardized value} = \frac{(\text{characteristic value} - \text{minimum of characteristic value})}{(\text{maximum of characteristic value} - \text{minimum of characteristic value})}. \quad (8)$$

In the next step, as a tradition for regression analysis, the whole data set is divided into 2 parts: the training set and the testing set. A further comparison is made between the regression result based on the training set with the modeling result based on the test set. By this means, it could efficiently evaluate the accuracy and efficiency of the model empirically.

In the training process, a quantitative tool named gradient descent optimizer is optimized to calculate the parameters of the training model. The goal of this optimizer is to minimize the loss function in this analysis to find the optimum. The value of the loss function is obtained as shown in Figure 4. The vertical axis represents the loss value for each epoch, while the horizontal axis represents the epoch, which is the time of iteration.

In the next step, we train 100 epochs on the model parameters using the training data until the loss function converged, as the general methodology of multiple linear

Table 1: Description of each variable.

Variable	Description
Lstat	The proportion of lower-income groups in the region
Indus	Percentage of nonretail business in the region
Nox	Nitric oxide concentration (per 10 million)
tax	Full property tax rate per 10,000 US dollars
crim	The average crime rate in the town
ptratio	The student-teacher ratio in the town
age	The proportion of the self-built property before 1940
rad	Radial accessibility index to highway
chas	Charles River (a dummy variable)
zn	The proportion of property land area larger than 25,000 square feet
dis	The weighted average distance from the property to 5 employment centers in Boston
rm	The average number of rooms per house

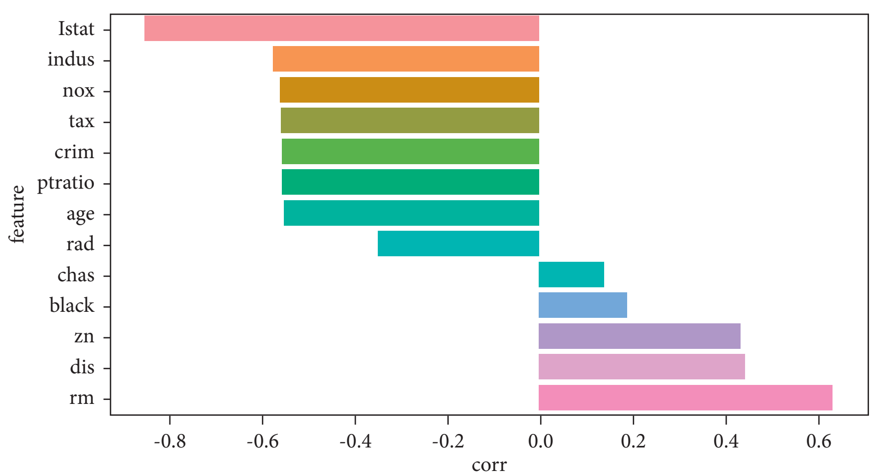

Figure 1: The correlation coefficients.

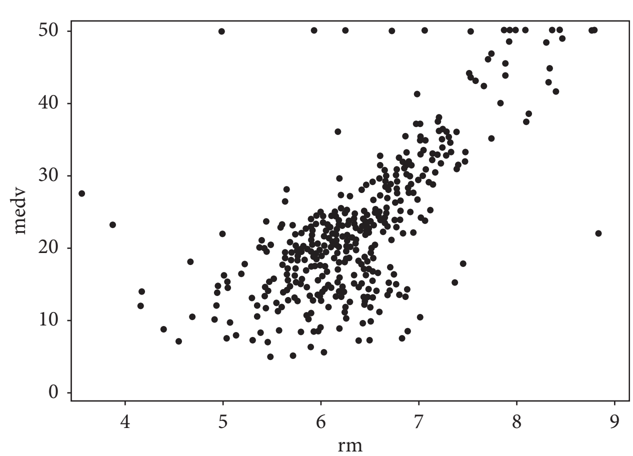

Figure 2: Housing price for the average number of rooms per house.

regression suggests. Based on this, the model parameters are used to forecast the housing price, and 100 samples are taken to obtain the prediction results, as shown in Figure 5.

As can be seen from Figure 5, the prediction results of the model are generally consistent with the trend of real value in the comparison set since the trend moves along the same direction with each other in most cases, and the overall deviation is generally acceptable in most cases. After training the model again for 500 epochs, the result is shown in Figure 6.

From Figure 6 result in the validation set, the prediction result is highly similar to that of Figure 5 in

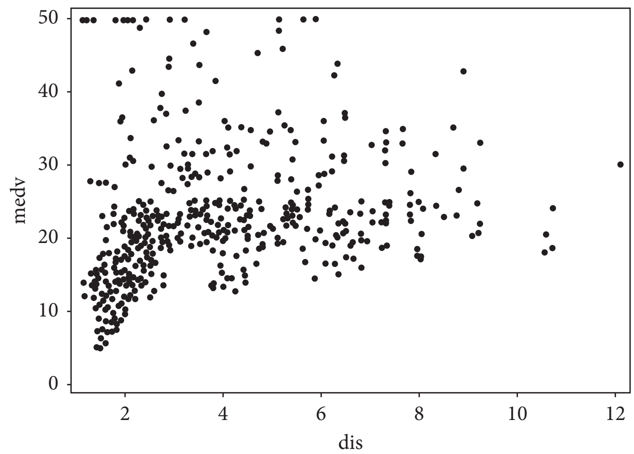

Figure 3: The house price distribution with different distances.

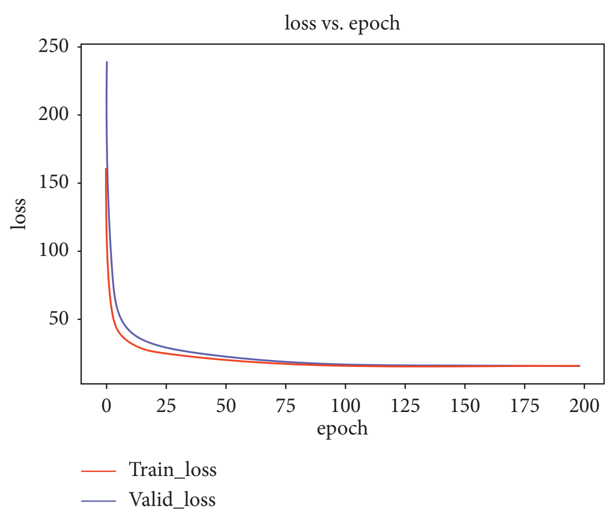

Figure 4: Loss function.

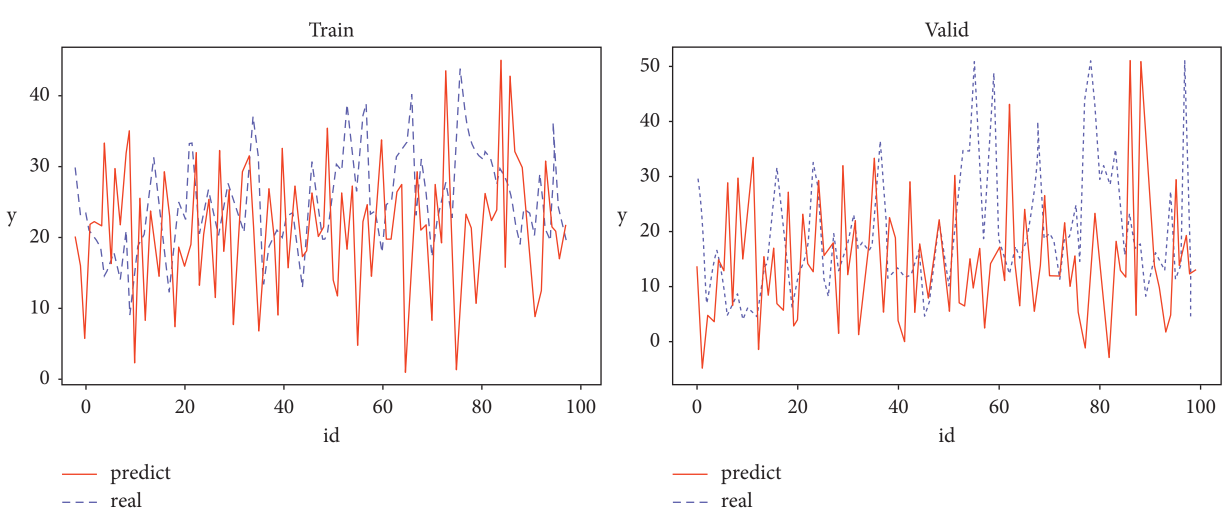

Figure 5: Prediction result.

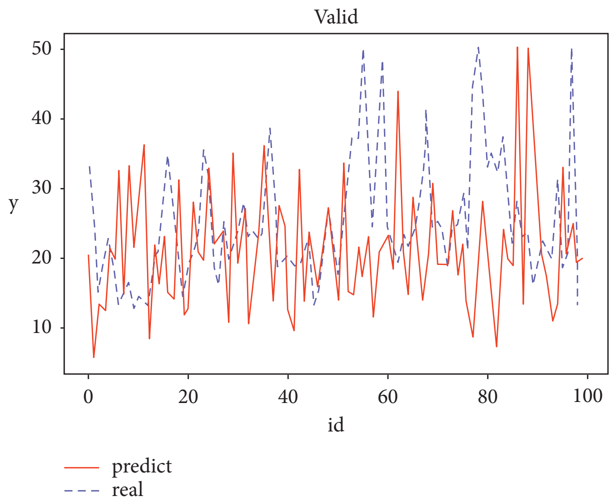

FIGURE 6: Prediction result.

general. This result can partially verify the accuracy and practicability of our empirical model constructed based on the Boston housing price data set. Therefore, with the analysis and discussion in this paper, it can be summarized that the multiple linear regression model can effectively predict and analyze the housing price to some extent. On the other hand, the prediction accuracy is still limited to some extent. In the further research, the application of machine learning algorithms and relevant methodologies in housing price prediction will be further optimized and widely researched.

5. Conclusion

The author constructs a fundamental algorithm based on the multiple linear regression method to predict housing prices and combines it with the Spearman correlation coefficient to determine the influential factors affecting housing prices. To train and test the parameters of this multiple linear regression model, the author applies the data set of the housing prices in Boston for model construction. From the simulation results shown above, it can be concluded that the proposed multiple linear regression model can effectively analyze and predict the housing price to some extent. Admittedly, the prediction accuracy is still limited at specific points, and the universality of the model still needs to be improved in further research. In further research into the corresponding models, the author will further study machine learning in the application of housing price prediction, as well as constructing a more robust algorithm based on a more advanced machine learning methodology.

Data Availability

The raw data sets used for this work are available upon request from the corresponding author.

Conflicts of Interest

The author declares that there are no conflicts of interest.

Acknowledgments

The author would like to express his deepest gratitude to his parents for supporting him in conducting the study and research. It is their spiritual and material support that contributes to the completion of this humble paper. The author would also like to extend his sincere gratitude to Dr. Owen HU for his assistance and guidance in the data processing part of this paper. His patient guidance enlightens the confidence and enthusiasm in conducting further research on this topic.

References

[1] S. Borde, A. Rane, G. Shende, and S. Shetty, "Real estate investment advising using machine learning," *International Research Journal of Engineering and Technology (IRJET)*, vol. 4, no. 3, p. 1821, 2017.

[2] B. Trawinski, Z. Telec, J. Krasnoborski et al., "Comparison of expert algorithms with machine learning models for real estate appraisal," in *Proceedings of the 2017 IEEE International Conference on INnovations in Intelligent SysTems and Applications (INISTA)*, Gdynia, Poland, July 2017.

[3] V. Kontrimas and A. Verikas, "The mass appraisal of the real estate by computational intelligence," *Applied Soft Computing*, vol. 11, no. 1, pp. 443–448, 2011.

[4] M. Woźniak, M. Graña, and E. Corchado, "A survey of multiple classifier systems as hybrid systems," *Information Fusion*, vol. 16, pp. 3–17, 2014.

[5] J. R. Barr, E. A. Ellis, A. Kassab, C. L. Redfearn, N. N. Srinivasan, and K. B. Voris, "Home price index: a machine learning methodology," *International Journal of Semantic Computing*, vol. 11, no. 1, pp. 111–133, 2017.

[6] W. J. McCluskey, M. McCord, P. T. Davis, M. Haran, and D. McIlhatton, "Prediction accuracy in mass appraisal: a comparison of modern approaches," *Journal of Property Research*, vol. 30, no. 4, pp. 239–265, 2013.

[7] S. Rosen, "Hedonic prices and implicit markets: product differentiation in pure competition," *Journal of Political Economy*, vol. 82, no. 1, pp. 34–55, 1974.

[8] E. Lughofer, B. Trawiński, K. Trawiński, O. Kempa, and T. Lasota, "On employing fuzzy modeling algorithms for the valuation of residential premises," *Information Sciences*, vol. 181, no. 23, pp. 5123–5142, 2011.

[9] H. Kusan, O. Aytekin, and I. Özdemir, "The use of fuzzy logic in predicting house selling price," *Expert Systems with Applications*, vol. 37, no. 3, pp. 1808–1813, 2010.

[10] O. Bin, "A prediction comparison of housing sales prices by parametric versus semi-parametric regressions," *Journal of Housing Economics*, vol. 13, no. 1, pp. 68–84, 2004.

[11] Y. Kang, F. Zhang, W. Peng et al., "Understanding house price appreciation using multi-source big geo-data and machine learning," *Land Use Policy*, vol. 2020, Article ID 104919, 2020.

[12] A. Din, M. Hoesli, and A. Bender, "Environmental variables and real estate prices," *Urban Studies*, vol. 38, no. 11, pp. 1989–2000, 2001.

[13] J.-G. Liu, X.-L. Zhang, and W.-P. Wu, "Application of fuzzy neural network for real estate prediction," *Advances in Neural Networks - ISNN 2006*, vol. 3973, pp. 1187–1191, 2006.

[14] I. V. Lokshina, M. D. Hammerslag, and R. C. Insinga, "Applications of artificial intelligence methods for real estate valuation and decision support," in *Proceedings of the In*

Hawaii international conference on business, Honolulu, Hawaii, USA, January 2003.

[15] J. Hauke and T. Kossowski, "Comparison of values of Pearson's and Spearman's correlation coefficients on the same sets of data," *QUAGEO*, vol. 30, no. 2, pp. 87–93, 2011.

[16] T. Oladunni and S. Sharma, "Hedonic housing theory - a machine learning investigation," in *Proceedings of the 2016 15th IEEE International Conference on Machine Learning and Applications (ICMLA)*, Anaheim, CA, USA, December 2016.

[17] L. Petrella and V. Raponi, "Joint estimation of conditional quantiles in multivariate linear regression models with an application to financial distress," *Journal of Multivariate Analysis*, vol. 173, pp. 70–84, 2019.

[18] G. Soffritti and G. Galimberti, "Multivariate linear regression with non-normal errors: a solution based on mixture models," *Statistics and Computing*, vol. 21, no. 4, pp. 523–536, 2010.

Hindawi
Scientific Programming
Volume 2021, Article ID 9534976, 6 pages
https://doi.org/10.1155/2021/9534976

Research Article

Research on the Impact Mechanism and Application of Financial Digitization and Optimization on Small- and Medium-Sized Enterprises

Qiuxia Li

Renmin University of China, 100872 Beijing, China

Correspondence should be addressed to Qiuxia Li; changfeng326@163.com

Received 2 September 2021; Accepted 12 October 2021; Published 29 October 2021

Academic Editor: Punit Gupta

Background. With the continuous advancement of digital technology and the accelerated development of digital finance, the rise of digital finance has had a vital impact on the true evolution of SMEs. The digital economy has a significant positive impact on the productivity of SMEs. *Method*. This article first analyzes the digital level of SMEs, studies the incentive effect of digital finance on the level of technological revolution of SMEs, and analyzes the mitigation effect of digital finance evolution on the financing constraints of SMEs. At the same time, it also studies how to develop the digital economy and achieve high-quality business evolution. *Result*. The digital economy can promote the growth of enterprise productivity through four indirect ways: scale economy effect, scope economy effect, technological revolution effect, and management benefit effect. *Conclusion*. The Financial Technology Optimization program helps financial leaders adopt new digital technologies to optimize financial processes while minimizing disruption.

1. Introduction

The deep incorporation of new generation of Internet of Things, big data, Tencent Cloud computing, artificial intelligence, blockchain, and traditional industries has made commercial and social evolution move towards networking, digitization, and intelligence and gradually formed a new form of digital economy. Digital finance has the attribute of low financing cost, high effectiveness, and free from time and space constraints, so it has attracted wide attention of the society. SMEs, with its unique volume advantage, are not only an important driving force for commercial growth but also the backbone of technological revolution. Financial technology has shown great evolution potential and space [1–3]. The rapid evolution of financial technology can alleviate information asymmetry and broaden the scope of financial services. All sectors of society in China are very concerned about the evolution of SMEs because SMEs can play an important role in promoting commercial growth, stimulating market vitality, promoting scientific and technological progress, and expanding employment. There has been a phenomenon that the concept is greater than action in the evolution of digital finance because digital inclusive finance is faced with global common problems such as high cost, low effectiveness, and unbalanced service [4, 5]. How to balance policy support and market evolution is quite difficult.

Digital finance refers to various and significant commercial activities that utilize digital knowledge and information as critical production factors, state-of-the-art information network as a critical carrier, and the effective use of information and communication technology as an important driving force for effectiveness improvement and commercial structure optimization. The impact of digital economy on productivity is closely related to the evolution of information technology. Digital finance can curtail the related costs, solve the problem of information asymmetry, and provide the ability to predict threats through the application of intelligent technologies such as computer technology, data communication, big data analysis, and cloud computing in the financial field. Compared with traditional nondigital services, digital finance can better provide appropriate and effective financial services for SMEs at affordable costs. With the continuous revolution of digital technology and the booming popularity of digital economy, digital finance has become the only way for financial evolution. Digital technology provides solutions to overcome financial difficulties. The digital platform can evaluate the credit threat of hundreds of millions of users through big data analysis technology, which greatly curtails the cost of customer threat control and improves the feasibility of inclusive financial evolution. Digital finance is the deepening of inclusive finance, and inclusive finance must develop in the direction of digital finance. Research on the evolution of digital finance has certain practical significance for the evolution of SMEs. The stability structure of China's financial science and technology has basically formed, the incorporation of underlying technologies has accelerated, and the application pilot has continued. The blockchain industry has ushered in a new round of growth, which provides a strong impetus for commercial evolution. Therefore, studying the conjunction between digital finance and SMEs has an important guiding role and practical significance for the government to innovate the local financial market environment and formulate the financial evolution strategy of SMEs.

2. Materials and Methods

The state attaches great importance to the evolution of revolution and entrepreneurship activities and has issued many policies to encourage the public to actively carry out revolution and entrepreneurship activities. However, since revolution and entrepreneurship require substantial financial support, most SMEs face varying degrees of financing difficulties in the early stages of entrepreneurship. In this context, the birth of digital finance has brought new hope to the financing of SMEs. By constructing the index of technological and financial evolution level of SMEs, it is found that financial technology can increase enterprise revolution by alleviating the financing constraints of SMEs and improve the revolution effect of government tax return. In the new era, the rapid incorporation of big data technology and financial activities and the deep incorporation of information technology and financial industry have promoted the evolution of financial science and technology, a new type of financial industry, greatly changed the traditional financial service mode, and broken many restrictions on traditional financial services. In the R&D stage of technological revolution in SMEs, enterprises will carry out research and evolution, test new technologies or new products with great uncertainty, face high technical threats, and need a lot of human capital and fixed equipment investment. Enterprises need the support of revolution threat capital, so at this stage, financing constraints will have a significant impact on technological revolution of SMEs [6–8]. The evolution of digital finance can alleviate the financing constraints of SMEs, and the level of commercial evolution and legal environment are important factors restricting digital finance to alleviate the financing constraints of SMEs. Digital finance can give full play to the advantages of low cost, high speed, and wide coverage through scenarios and data, curtail the threshold and cost of financial services, improve the financing environment of SMEs [9], and more effectively serve inclusive financial entities. The level of financial evolution is one of the key factors because in the underdeveloped financial market, enterprises will face higher external financing costs, and a good financial evolution environment will help ease the financing constraints faced by enterprises. Digital inclusive finance is the deepening of inclusive finance [10, 11]. The combination of data and financial revolution products more effectively curtails the information asymmetry between capital reservoir and demand and more significantly curtails the threshold and cost of financial services [12, 13]. Therefore, digital inclusive finance can ease the financing constraints of SMEs.

The impact mechanism of financial evolution on technological revolution: on the one hand, some scholars believe that financial evolution may encourage SMEs to achieve technological revolution by opening trade or reducing transaction costs, easing financing constraints of SMEs, and loosening R&D capital investment [14]. On the other hand, some scholars believe that the attribute of technological revolution projects, such as high investment and long cycle, make small- and medium-sized innovative enterprises have a strong dependence on external financing. Countries (regions) with a sound financial market system and high level of financial evolution will optimize the allocation of financial resources, reasonably guide the flow of funds, and curtail the problem of information asymmetry. The indirect mechanism of the influence of the digital economy on enterprise productivity is shown in Figure 1. With the commercial society moving from the industrial economy era to the digital economy era, the traditional way of achieving performance growth through factor expansion is difficult to meet the needs of high-quality evaluation of enterprises [15, 16]. Under this background, enterprises realize the automation and intelligence production and service through a digital transformation, curtail the dependence on labor, directly curtail the production cost, and improve the production effectiveness [17, 18]. The indirect mechanism of the digital economy on the productivity of small and medium enterprises is shown in Figure 1. At the same time, the data resources generated by the digital transformation of enterprises can not only participate in the production process as production factors together with capital, labor, and other resources, directly driving productivity growth, but also improve the utilization effectiveness and allocation effectiveness of traditional production factors such as capital and labor, thus improving the productivity of enterprises.

In the new era, the accelerated incorporation of big data technology and financial activities and the deep incorporation of information technology and financial industry have promoted the evolution of digital finance, a new type of financial industry, which has greatly changed the traditional financial service model and broken many limitations of traditional financial services. First of all, due to its own limitations, traditional financial institutions are generally difficult to penetrate into financially poor areas. As a product of the combination of digital technology and finance, digital

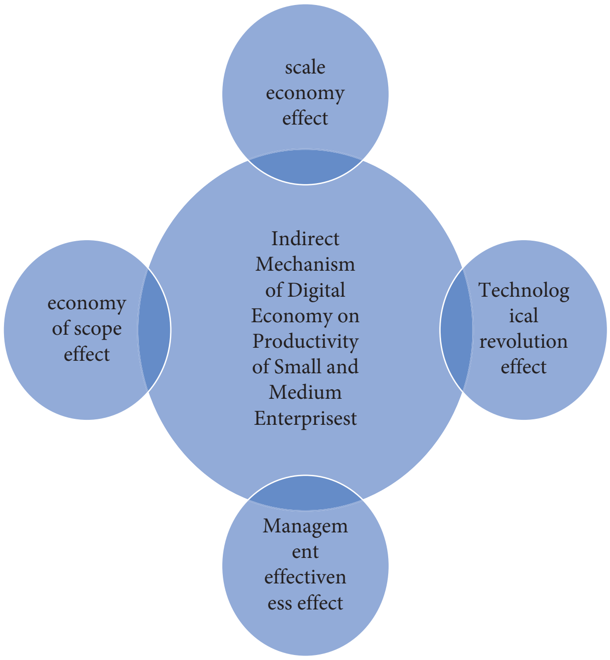

Figure 1: The indirect mechanism of the influence of digital economy on enterprise productivity.

finance has strong geographical penetration, breaks the time and space constraints, and can participate in financial activities anytime and anywhere to improve the availability of financial services. With the breakthrough evolution of science and technology revolution, the coverage of digital finance will be further expanded, which can curtail the financing cost of SMEs, greatly alleviate the financial exclusion faced by SMEs, and provide financial support for the technological revolution of SMEs. The influence mechanism of digital finance on small and medium enterprises is shown in Figure 2. Secondly, financial science and technology can fully understand SMEs based on big data analysis, improve enterprise information transparency, alleviate information asymmetry between financial institutions and SMEs, curtail adverse selection and moral hazard, transform resources in the market into effective reservoir, curtail resource, optimize resource allocation, and provide necessary conditions for improving technological revolution of SMEs. First, digital finance enables SMEs to obtain the same market opportunities as large enterprises, helps them establish market credit, and improves sales revenue. The third is to promote the internal information construction of enterprises, improve the standardization and effectiveness of management, and curtail the management cost of SMEs. The fourth is to make the revolution of products and services become the key to win the market competition and improve the revolution consciousness of SMEs. The increase and diversity of consumption create market opportunities for SMEs.

Digital finance can promote the technological revolution of SMEs by promoting e-commerce, affecting the total consumption and structure, easing financing constraints and technology spillover. The empirical results show that the evolution of digital finance in China significantly promotes the technological revolution of SMEs, and the influence mechanism is as follows: first, digital finance improves the profitability of enterprises by increasing sales revenue and reducing management costs. Second, by reducing the cost of borrowing and improving the structure of borrowing, digital finance makes the structure of enterprise borrowing long-term and eases the credit constraints of enterprises. Third, the payment, monetary fund, insurance, credit, and other business functions of digital finance have significantly promoted the technological revolution of enterprises. In addition, the classification study found that the evolution of digital finance in China is very uneven among regions, especially in the central and western regions.

3. Results

China's complete industrial system is supported by the industrial chain cluster composed of large- and medium-sized enterprises and small enterprises with meticulous division of labor, professional, and orderly. In the reservoir chain of the industrial chain cluster, it is inevitable that the core large enterprises monetize their dominant position in the market, such as extending the accounting period, which leads to the shortage of funds for SMEs. Digital finance focuses on the confirmation of core enterprise contracts or commercial bills in the reservoir chain. With the help of blockchain technology, it can cover the multilevel enterprises in the reservoir chain and solve the liquidity replenishment problem of some SMEs. The evolution of digital finance also makes it possible to build a public credit information platform for SMEs. The public credit information platform can not only get through all kinds of scene data but also cooperate with all kinds of financial institutions to develop models, investment, and loan linkage and provide SMEs with life-cycle training, guidance, and financing intermediary services, as shown in Figure 3. Digital technology improves the revolution ability of SMEs, and the improvement of technological revolution level is one of the main ways to improve productivity. In the R&D mode, the open digital R&D management system helps SMEs turn from the traditional closed revolution mode to the open revolution mode with the participation of all departments, even the whole industry chain and the whole society, so that R&D and design activities can be carried out in a multidimensional collaborative network, to realize integrated and networked revolution and improve enterprise revolution ability. In the R&D process, digital design tools such as digital twin and digital simulation can accurately simulate various physical parameters of physical entities and display them in a visual way, to achieve R&D revolution in a variety of scenarios in a dynamic and uncertain environment and improve the accuracy of R&D. Digital finance can provide financial basis for revolution activities and create more entrepreneurial opportunities. Information technology is an important factor to promote the evolution of business model. Internet big data technology has greatly weakened the cost in search, evaluation, transaction, and other aspects, making great changes in the traditional business model. Digital finance breaks the space limitation of traditional transactions, enables businesses and consumers to trade

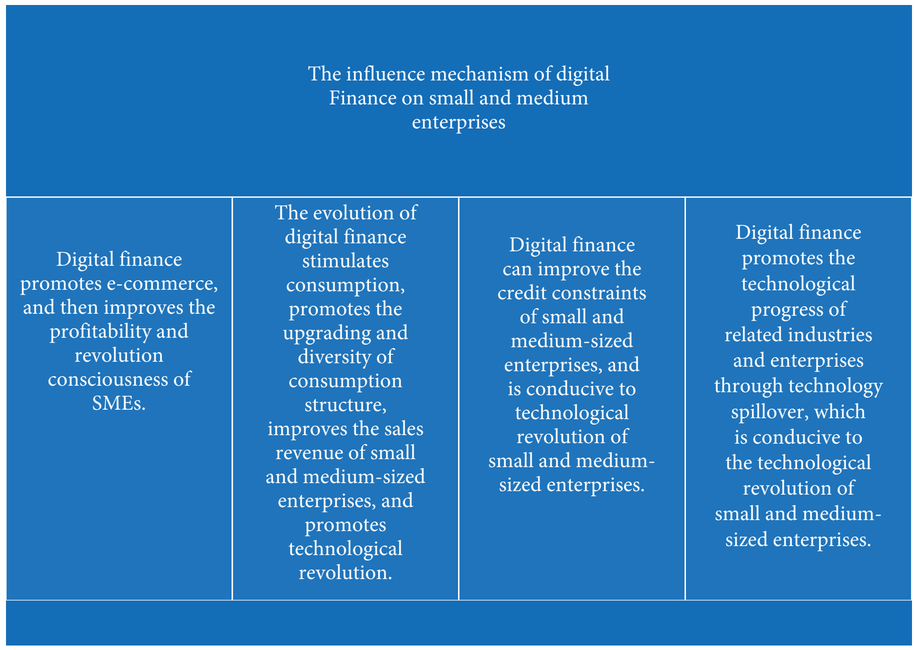

Figure 2: The influence mechanism of digital finance on small and medium enterprises.

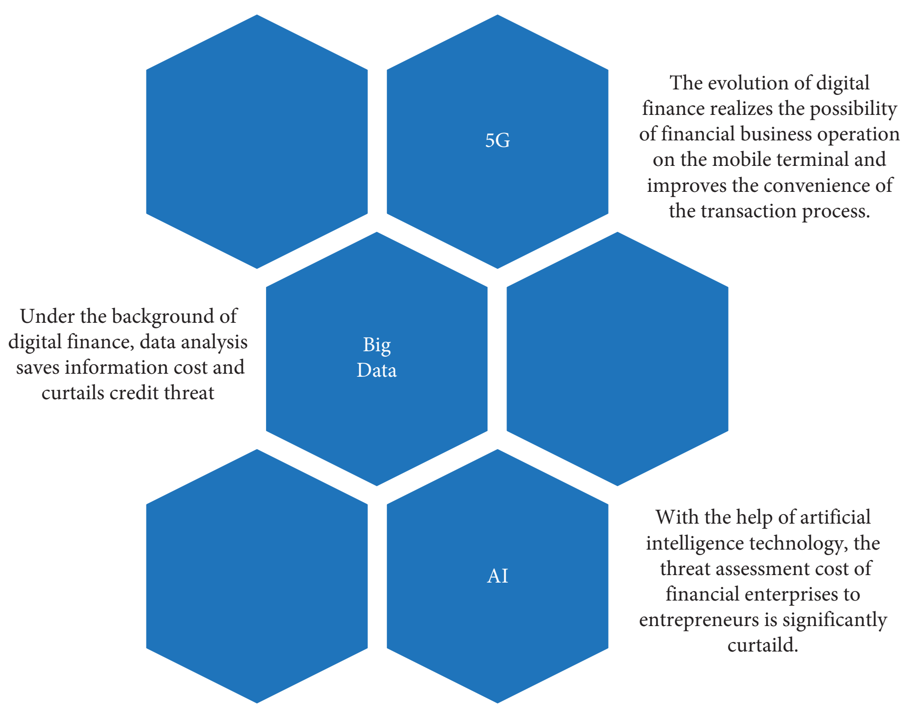

Figure 3: Some common technical applications of digital finance.

online, curtails the financial delivery link in the traditional business model, and improves the effectiveness of financial transactions. Similarly, taking Alipay as an example, the appearance of Alipay changed the way of payment and promoted the evolution of e-commerce. It laid the foundation for the transformation of traditional financial business. The evolution of online car hailing, bike sharing, and other fields all benefit from the evolution of digital payment technology. It can be seen that digital finance is of great significance to promote revolution and create employment opportunities for SMEs. The role of digital finance in promoting SMEs makes up for the problem that traditional financial institutions cannot take care of backward SMEs and self-employed households, which can affect the effective evolution of local revolution and entrepreneurship activities to a large extent. The transformation and upgrading of industrial chain not only needs the high-quality evolution of SMEs but also needs the coordinated evolution of industrial clusters. Therefore, it is necessary to build an "industrial digital finance" consortium, aggregate the real industry, finance, science, and technology, build an ecological community, based on the industrial chain and industrial ecology, relying on the industrial Internet platform and financial service platform, deeply integrate the industrial chain, revolution chain, and capital chain, and jointly serve and empower the industrial cluster. In this ecological community, finance should play the role of an accelerator. Based on various scenarios of the industrial chain, it should provide science and technology support, data penetration, financial matching for the industry, empower the entity enterprises, and realize the improvement of production effectiveness, product revolution, and service upgrading. For example, through bill settlement and payment settlement platform, digital finance can improve the effectiveness of capital turnover in industrial clusters and provide comprehensive financial services of "stock debt loan investment" for the scale expansion of core leading enterprises. Furthermore, we should provide SMEs in the chain with financing products such as "order loan" to solve the problem of capital turnover.

The high-quality evolution of SMEs is an important guarantee to promote high-quality commercial evolution. The central government attaches great importance to the revolution and evolution of SMEs and puts forward higher requirements for financial support to SMEs. In particular, facing the COVID-19 pandemic, protecting small and medium enterprises is to ensure employment. Protecting employment is to protect people's livelihood. SMEs need financial support. The emergence of digital finance provides new financing channels for the revolution and evolution of small and microenterprises and provides an effective means for small and microenterprises to balance revolution and evolution, prevent, and resolve financial threats.

4. Conclusion

In the critical period of the transformation of new and old kinetic energy, we should continue to strengthen the construction of relevant financial infrastructure, give certain policy support to SMEs, increase investment in 5G, big data, cloud computing, blockchain, and other fields, improve the ability of independent research and evolution of technology, and promote the integrated evolution of digital technology and financial market. At the same time, we should strengthen the precise support for SMEs and private enterprises, realize one-to-one docking, establish a diversified financial system, provide rich and high-quality financing channels, provide enterprises with lower cost and more convenient financial services, and fully release the vitality of financial technology to promote technological revolution and commercial growth. Digital finance has a significant role in promoting the financing of SMEs and individual entrepreneurs, which can effectively curtail the financing threshold and improve the financing availability of entrepreneurs. It also helps to curtail part of the financing cost and improve the utilization rate of resources. In order to further strengthen the application effectiveness of digital finance in the field of entrepreneurship, in addition to improving the corresponding laws and regulations, we should speed up the construction of a reasonable digital financial system, build professional entrepreneurial digital financial institutions, pay attention to the revolution of the market and the improvement of the order, and provide the most basic guarantee for the entrepreneurship of all kinds of main bodies in China.

Data Availability

Data sharing not applicable to this article as no datasets were generated or analysed during the current study.

Conflicts of Interest

The author declares no conflicts of interest.

References

[1] U. Marjanovic, S. Rakic, and B. Lalic, "Digital servitization: the next "big thing" in manufacturing industries," *IFIP Advances in Information and Communication Technology*, vol. 56, no. 11, pp. 510–517, 2019.

[2] S. D. Oliner, D. E. Sichel, and K. J. Stiroh, "Explaining a productive decade," *Journal of Policy Modeling*, vol. 30, no. 4, pp. 633–673, 2008.

[3] A. Philippe and H. Peter, "Joseph Schumpeter lecture appropriate growth policy: a unifying framework," *Journal of the European Commercial Association*, vol. 4, no. 2, pp. 269–314, 2006.

[4] H. Jiang and Y. Liu, "Digital finance, reservoir chain finance and corporate financing constraints: empirical evidence from listed companies on SME Board," *Research on technology economy and management*, vol. 3, pp. 73–77, 2021.

[5] F. Zhao, "Financial technology and high quality commercial evolution: evidence from provincial level," *Financial economy*, vol. 3, pp. 9–18, 2021.

[6] T. Wu and R. Wang, "Digital finance, bank competition and bank threat-taking: a study based on 149 small and medium-sized commercial banks," *Journal of Finance and commercials*, vol. 3, pp. 38–48, 2021.

[7] W. Huang, "Promoting industrial digital connection and building digital financial ecology -- thinking and practice of financial technology revolution of China Guangfa bank," *China financial computer*, vol. 3, pp. 20–22, 2021.

[8] S. Pan, D. Ye, and Y. Xian, "Is digital finance inclusive? empirical evidence from urban revolution," *Economist*, vol. 3, pp. 101–111, 2021.

[9] Q. Wu and Y. Zhu, "Research on the impact of digital inclusive finance on enterprise technological revolution - identification of stage mechanism and analysis of heterogeneity," *Industrial technology economy*, vol. 40, no. 3, pp. 143–151, 2021.

[10] J. Jia and Y. Liu, "Digital finance, executive background and enterprise revolution: empirical Evidence from listed companies on SME board and gem," *Finance and Trade Research*, vol. 32, no. 2, pp. 65–76 + 110, 2021.

[11] C. Du and Y. Zhang, "Research on the influence mechanism of digital economy evolution on enterprise productivity growth," *Securities market guide*, vol. 2, pp. 41–51, 2021.

[12] C. Cui and L. Zhao, "The evolution and influence of digital inclusive finance," *China's national conditions and strength*, vol. 2, pp. 8–10, 2021.

[13] L. Li and W. Tian, "Digital financial evolution, industrial structure transformation and regional commercial growth: an empirical analysis based on spatial durbin model," *Financial Theory and Practice*, vol. 2, pp. 8–16, 2021.
[14] A. Chinnasamy, B. Sivakumar, P. Selvakumari, and A. Suresh, "Minimum connected dominating set based RSU allocation for smartCloud vehicles in VANET," *Cluster Computing*, vol. 22, no. 5, pp. 12795–12804, 2019.
[15] H. Zou and Y. Huang, "Research on the effect of digital Inclusive Finance Evolution on regional revolution effectiveness," *Finance and economy*, vol. 1, pp. 48–55, 2021.
[16] Y. Zhou, "The role and Countermeasures of digital Inclusive Finance in promoting the evolution of small and micro enterprises," *Financial journal*, vol. 1, pp. 24–31, 2021.
[17] S. Feng and Q. Song, "The impact of digital finance evolution on the quality of life of Chinese residents," *Commercial and management review*, vol. 37, no. 1, pp. 101–113, 2021.
[18] Sivakumar, S. Prasanna, S. Hemalatha, and B. Sivakumar, "A harmonized trust assisted energy efficient data aggregation scheme for distributed sensor networks," *Cognitive Systems Research*, vol. 56, pp. 14–22, 2019.

Hindawi
Scientific Programming
Volume 2021, Article ID 4263981, 6 pages
https://doi.org/10.1155/2021/4263981

Research Article

Research on the Development of Innovation Path of Ideological and Political Education in Colleges and Universities Based on Cloud Computing and K-Means Clustering Algorithm Model

Juan Hong

Suzhou Industrial Park Branch of Jiangsu Union Technical Institute, Suzhou 215123, Jiangsu, China

Correspondence should be addressed to Juan Hong; hongjuan_edu@outlook.com

Received 10 September 2021; Revised 29 September 2021; Accepted 15 October 2021; Published 29 October 2021

Academic Editor: Punit Gupta

As a distributed computing technology, cloud computing has the characteristics of fast processing speed, large-capacity data processing, and high overall efficiency. With the continuous development of communication technology today, cloud computing technology has begun to be applied in various industries and has promoted the development and progress of the industry. As an important part of college education, ideological and political education in colleges and universities is also constantly developing. The integration of cloud computing and ideological and political education is the main trend in the future. At present, the application research of cloud computing and wireless communication technology in the ideological and political education of colleges and universities has obtained some results, but there are still some problems. Therefore, the research on innovative methods of ideological and political education is extremely important. At present, under the attention of all walks of life, scholars have strengthened the research on new paths of ideological and political education in colleges and universities, and they are also constantly experimenting with innovative methods. In this context, this paper studies the current situation of ideological and political education in colleges and universities through questionnaire surveys and analyzes the innovative mode of ideological and political education in colleges and universities in the context of cloud computing through the K-means clustering algorithm model.

1. Introduction

Cloud computing is a distributed computing that processes and analyzes data through a system composed of multiple servers [1]. Cloud computing has a variety of core advantages, enabling cloud computing technology to undertake important tasks in a variety of scenarios in the future [2]. Compared with the past, its advantages mainly lie in the fast processing speed, ability to perform large-capacity calculations, and high overall efficiency [3,4].

The current ideological and political education in colleges and universities is different from the previous single textbook model and the introduction of online teaching and online courseware. However, this change is simply the use of communication technology to achieve the digitalization of the teaching mode [5], and the main way for students to acquire knowledge is still through the combination of teacher dictation and PPT. This method does not make full use of the advantages of cloud computing technology.

Under the current high development of communication technology, some universities and enterprises have combined computer technology to develop an online course platform that can store courses. College students can improve their ideological and political knowledge by taking courses corresponding to famous teachers. However, although this teaching method is effective, it requires extremely high awareness of students, and some students will complete the learning tasks in a perfunctory manner [6].

At present, colleges and universities have used WeChat applets, Weibo, and various short video platforms to conduct comprehensive ideological and political education for students in their lives. This method belongs to self-media communication and has a certain degree of innovation. However, adding too many of these elements to the ideological and political teaching of colleges and universities may make students feel disgusted [7].

With the continuous development of communication technology, cloud computing technology continues to innovate. However, adopting today's popular university ideological education methods has not kept up with the pace of scientific and technological progress [8].

This paper obtains research data through questionnaire surveys and uses the K-means algorithm model for quantitative analysis. It points out the current problems of ideological and political education in colleges and universities and proposes a new path for ideological and political education in colleges and universities based on cloud computing [9].

2. Related Work

This article mainly uses the K-means clustering algorithm to study the development of the innovation path of ideological and political education in colleges and universities. It first introduced the K-means clustering algorithm model and method and then obtained data related to ideological and political education in colleges and universities through the questionnaire and finally analyzed the data according to the K-means clustering algorithm model to draw conclusions.

Authors such as Zhang Xiaoli studied the application of K-means clustering algorithm in education and teaching evaluation, but did not use K-means clustering algorithm to study specific subjects such as ideological and political education in colleges and universities. Deng Jingyan and others studied the innovative model of ideological and political education in colleges and universities under the background of big data, but they did not establish a model for quantitative analysis. Wu Xinghui et al. used the PERMA model to conduct quantitative research on ideological and political education, but the selection of the model was not optimal.

In short, although the abovementioned scholars have conducted research on the innovative development model of ideological and political education in colleges and universities, there are defects such as insufficient quantitative analysis and poor model selection. This research uses the optimized K-means clustering algorithm to study the innovative development path of ideological and political education in colleges and universities, which can solve these problems.

3. Algorithm Model and Method

3.1. K-Means Clustering Algorithm Model. K-means is a classic clustering algorithm, clustering according to the distance or dissimilarity between samples, classifying samples with similar characteristics into one category,] and dissimilar samples into different clusters. Compared with other algorithms of the same type, the K-means clustering algorithm is relatively fast, and at the same time, it has higher computational efficiency. It is very suitable for initial screening of large quantities of data.The main steps of the K-means algorithm are as follows:

(1) Select m samples from the training set $S = \{x1, x2, \ldots, xn\}$ as the initial cluster centers $C = \{c1, c2, \ldots, cm\}$.

(2) Calculate the distance from each sample xi to the initial center point of m samples in the data set and divide each sample into the class of the center point closest to it. The distance calculation is shown as follows:

$$f(x, C_i) = \sqrt{\sum_{j=1}^{m} \left(x_j - C_{ij}\right)^2}. \quad (1)$$

(3) Each cluster category is δi; recalculate the centroids of all samples in the cluster $\delta i \in Cj \sum Xj$. The calculation formula of the cluster center point is as follows:

$$C_i = \max\left\{D_j;\, j = 1, 2, \ldots, n\right\}, \quad (2)$$

$$D_j = \min\left\{f\left(x_j, C_i\right)\right\}. \quad (3)$$

(4) Repeat the above two steps, iteratively update until the change of the centroid of each type is less than the threshold or reaches the maximum number of iterations.

In short, it is to select the data center, calculate the distance, cluster, reselect the centroid of the data, and repeat until the data converge or reach the maximum number of iterations. The steps to select the training process are as follows:

(1) Train n k-dimensional data and randomly generate m k-dimensional points of the initial cluster center

(2) Find all the data points belonging to this cluster and calculate the centroid of this type

(3) Repeat the above steps until the centroid change of each type is less than the set threshold or reaches the maximum number of iterations

(4) Set the maximum number of features, set the group K value of the classification, and perform data analysis on the training feature data

Although the algorithm cannot guarantee convergence to the global optimum, it can be as close to the global optimum as possible by optimizing the training process. The specific optimization directions are reflected in the following aspects:

(1) Expand the scale of training data and reduce convergence deviations

(2) Filter all data points of the cluster and clean the meaningless edge data points

(3) Optimize the selection of K value to improve the analysis accuracy of training data

This paper filters and cleans the data, removes stop words, transforms it into a vector model, and uses the TF-IDF algorithm to calculate the weight of the word frequency.

TF is the word frequency, IDF is the inverse document frequency, and TF-IDF reflects the importance of a word in the text. Use the TFIDF transformer and count vectorizer methods of the sklearn module in *Python* to calculate the TF-IDF value, convert it into a space vector model, and select the K-means clustering algorithm to mine and analyze the data.

3.2. Questionnaire Survey

3.2.1. Survey Object. An online questionnaire survey was conducted among 600 students and teachers majoring in ideological and political education in 20 universities across the country. The questionnaire is anonymous, and the questions in the questionnaire have been fully designed and demonstrated. 600 questionnaires were distributed, 582 questionnaires were returned, and the questionnaire recovery efficiency reached 97%.

3.2.2. Investigation Method. Online questionnaire survey is a questionnaire survey conducted through the Internet, which is one of the most suitable methods for surveying contemporary college students. It cannot be restricted by region. It can not only increase the number of teachers and students participating in the questionnaire survey but also save time and increase the enthusiasm of teachers and students to participate. In terms of problem setting, in addition to drawing on the merits of existing research, it has also been optimized according to the actual situation of the survey subjects to make it more information-based one.

3.2.3. Design of the Questionnaire. It mainly investigates the current status of ideological and political education in colleges and universities, including students' attitudes towards ideological and political subjects, students' mental state, and teaching content. Attitudes to the ideological and political disciplines mainly include the following: do you think that the ideological and political discipline is an important subject? Are you interested in ideological and political subjects?

The mental state of students includes exercise time, sleep time, work and study efficiency, self-friendliness and universal humanity, mindfulness, self-criticism, overidentification, isolation, and other personal behavior factors.

The teaching content is mainly about students'recognition of ideological and political classroom teaching methods, including whether it is recommended to use communication technology completely, whether it is believed that 5G technology will have a qualitative impact on ideological and political teaching, whether it will cooperate with communication technology to teach, and whether 5G technology is expected. The details are shown in Table 1.

4. Results and Discussion

4.1. Insufficient Attention to Ideological and Political Courses. Judging from the actual situation in colleges and universities, although every school offers a Marxist ideological and political education course, students often treat it as a side course and fail to correctly understand its importance. Some students also completed ideological and political courses. The content of professional courses is just to get some play time after class. Some students think that ideological and political education is meaningless, and there are cases of not completing homework, skipping classes, and even cheating on exams [10]. Some college students are not interested in learning ideological and political content and do not usually pay attention to political development. They learn Marx only because they need party members and course credits; some students show that they blindly follow Western culture and ignore the study of ideological and political courses [10]. On the other hand, the ideological and political curriculum system in colleges and universities is relatively outdated, and a set of textbooks has been used for many years. The classroom teaching of ideological and political teachers is sticking to the old rules and lacks close contact with the contemporary. Various classical theories are readily available, but they cannot guide students to use them in the judgment of social phenomena, which makes students question the practicality of ideological and political courses.

4.2. The Student's Personal Mental State Is Poor, and the Study Is Not Concentrated. Keeping students in a good state of mind is the first step in effective ideological and political learning. According to reports, most contemporary college students have mental health problems, mainly due to the development of network technology, communication, and communication between people is mostly done through social software. Students may become addicted to mobile phones when using related software, even abandoning ideological and political courses because of playing online games. Statistics show that more than half of the students only go to bed early in the morning because they play on mobile phones. In this case, because of the lack of communication with others and staying up late, students are prone to mental health problems, which leads to ideological and political education courses, The mental state is not good, and the learning effect is poor. Some scholars have analyzed the data on the impact of sleep and isolation of college students on physical and mental health [11], including exercise time, sleep time, work and study efficiency, self-friendliness and universal humanity, mindfulness, self-criticism, overidentification, isolation, and other personal behavior factors. This article draws it into an intuitive display diagram, and the specific situation is shown in Figure 1.

4.3. The Actual Interaction between Students and Teaching Content Is Not Enough. The current ideological and political course education in colleges and universities is mainly because students sit side by side under the platform and receive the corresponding content dictated by the teacher. However, when this traditional teaching method is combined with the content of the ideological and political course itself, it will give some students a sense of irritability, mainly because this teaching method is the same as that of other courses, and there is not much communication in the whole course [12]. The author found through a survey of 500 students in a university that 39%

Table 1: Questionnaire survey theme design.

Attitudes towards ideological and political disciplines	Do you think that the subject of ideological and political is an important subject? Are you interested in ideological and political subjects?
Student mental state	Exercise time Sleep time Work and study efficiency Self-friendliness and universal humanity Over-identification Isolation and other personal behavior factors
Ideological and political teaching content	Is it recommended to use communication technology entirely Do you think 5G technology will have a qualitative impact on ideological and political teaching? Will it cooperate with the communication technology Do you expect 5G technology application teaching It is not recommended to use wireless communication technology It is not recommended to introduce 5G in college classrooms

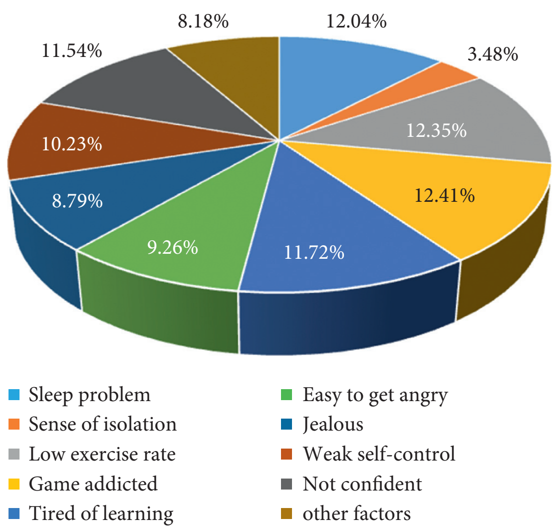

Figure 1: The relationship between sleep and isolation of college students and personal health.

Table 2: Students' recognition of ideological and political classroom teaching methods.

Option	Proportion
Fully use 5G technology	0.393
5G technology will revolutionize the classroom	0.147
Teaching with communication technology	0.682
Looking forward to 5G technology application	0.528
Do not use wireless communication technology	0.031
Not recommended to 5G	0.089

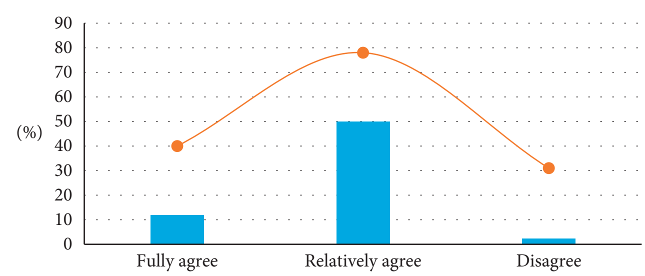

Figure 2: Visualization of the proportion of students' recognition of ideological and political classroom teaching methods.

of the students believe that the full use of advanced wireless communication technology in the classroom will make the classroom more active; 15% of the students believe that 5G technology will completely change the classroom teaching mode, and 68% of the students It is believed that video or documentary clips are interspersed in the class, and with communication technology equipment, the teacher will explain that the effect of this kind of teaching is better than simply listening to the teacher. 53% of the students expect 5G technology application to teach, only 3% of the students feel that the acceptance of teaching without using any wireless communication technology is good, 9% of students do not recommend the introduction of 5G technology in college classrooms. The details are shown in Table 2 and Figure 2.

From the data in the figure, it can be inferred that students expect the reform of classroom teaching methods for ideological and political education in colleges and universities. Because the teaching methods in colleges and universities are still the same as traditional teaching methods, students can only listen to the teachers in most cases. In college education, classroom resources are more stressful, usually two classes with more than 60 people in the class, students have fewer opportunities to participate in answering questions raised in the teacher's course, so a single duck-filling teaching is formed, no interaction or less interaction.

5. Innovation Path of Ideological and Political Education in Colleges and Universities under the Background of 5G and Wireless Communication

5.1. Build a 5G Data Platform for Students to Customize Learning Content. We often say that interest is the best teacher. For ideological and political courses, interest teaching should also be put first. Combining 5 G and wireless communication technology with the application of the latest technology can provide interactive immersive teaching experience, big data data analysis, and intelligent personalized learning content recommendation support for ideological and political education in colleges and universities, which can provide ideological and political learning for college students a source of great interest [13].

Through the analysis of the aforementioned problems and causes, it is found that students have a deviation in understanding of ideological and political education. The solution to this problem is to build a student 5G data platform and use the big data analysis method in the application of 5G communication technology to analyze students. Due to the fast speed of 5G communication, 5G communication is also more advantageous than 4G in big data analysis. It can recommend ideological and political learning content for students through recommendation algorithms, so that each student's ideological and political learning content is different. The same and they are all recommended content that the students are satisfied with. The personalized customized data can also be separately assigned to the students' ideological and political teachers and counselors through 5G and wireless communication, so that relevant teachers can pay attention to the current status of the students in time and grasp the recent personal information of the students [14]. The dynamic changes of thoughts and emotions and the specific content of the follow-up ideological and political education courses are arranged according to the emotional problems of the students, so that there will be no problems of cognitive deviation and misconduct.

5.2. Health Reminder Based on 5G and Wireless Communication Technology. In response to the current problems of college students who are personally addicted to social media and mobile games, 5G technology and wireless communication technology can be combined with personal wearable devices to remind students of their time management. Whenever students are addicted to games or short video software, they exceed the normal time. To remind or force the shutdown operation, 5G technology combined with wireless communication technology, the data transmission speed is extremely fast, allowing students to immediately end the current entertainment activities, long-term so that they can form a healthy work and rest habits, for the follow-up ideological and political. The course study maintains a good mental state, not only that 5G communication technology includes multiple personal privacy and security protection applications but also the use of 5G and communication technology for personal health management reminders does not have to worry about data leakage [15].

5.3. Explore Flexible Teaching Methods. In view of the current problem of no interaction between students and teaching content in ideological and political education in colleges and universities, it can be solved by the application of 5G communication technology. VR is one of the applications of 5G and wireless communication technology. It can be used to simulate real situations, such as using virtual reality (VR). Interactive technology simulates scene pictures to increase the interactivity of the classroom. VR requires higher image quality, so it also needs a higher data transmission speed; so, the high speed of 5G can just match the VR needs of most college students. First, colleges and universities can prepare the background VR images of the content of the ideological and political courses in the classroom, and then students can watch them live in the classroom or remotely participate in the viewing in the dormitory [16]. The specific content in VR is interactive. Students are interested in the ideological and political courses. The level of mastery is also evaluated in the context of VR use. If the evaluation fails, the device will record the results of the evaluation on the spot and determine the time for the next re-examination. This will increase the interest of students in learning ideology and politics while not forgetting the most fundamental teaching methods. On the other hand, college teachers can also make full use of the application of 5G and wireless communication technology to assist their own teaching and research work in the teaching process. For example, the big data analysis in 5G applications is used to determine whether the teaching content meets the needs of all students in the class. In this case, the actual interaction between college students and the ideological and political teaching content is sufficient, and there is no performance assessment problem.

6. Conclusion

Colleges and universities are the cradle of talents in the motherland, and political and ideological education in colleges and universities is an important link in the cultivation of talents in the motherland. Contemporary college students belong to the rebellious era of freshmen. The education that most students receive from childhood has cultivated them into people with independent thinking ability and at the same time makes their thinking more "elegant." They always think about problems from strange angles, and they are thinking about colleges and universities. Problems in ideological and political education are also prone to deviation or lack of interest. Only the latest 5G and wireless communication technologies can be fully applied to ideological and political education in colleges and universities, and various 5G-applied equipment and black technologies can be used to improve students' interest in learning and thinking ability can truly cultivate qualified contemporary college students.

As the implementers of education, most college teachers know best about the problems and needs of college education at this stage. In particular, teachers with a background in science and engineering know the many possibilities that 5G and wireless communication technology applications can bring to college ideological and political education. The ideological and political education in colleges and universities under the background of the current technological age can no longer be the same as the duck-filling education model in the old age. College administrators and college teachers should use new technologies in their daily education work to influence their understanding of ideological and political learning [17]. Students who are aware of deviations will eventually realize that all college students correctly accept the influence of ideological and political education and culture.

In general, under the current background of continuous deployment of wireless communication and 5G technology, colleges and universities have gradually begun to use the applications brought by these new technologies in ideological and political education. If colleges and universities want to give students good ideological and political education effects, they need to rely on students starting from needs, learn to walk into student life, think from the perspective of students, and use the latest communication technology to make obscure political principles easy to understand, so as to show the true meaning of ideological and political affairs and allow students to spontaneously establish learning ideas of political interest.

Data Availability

Data sharing not applicable to this article as no datasets were generated or analyzed during the current study.

Conflicts of Interest

The authors declare that they have no conflicts of interest.

Acknowledgments

This work was supported by the Specialized Project of Jiang'su Educational Science during the "13th Five-Year Plan": Study and Practice on "2P5E" Teaching Model of Ideological and Political Theory Courses in Secondary Vocational School under the background of "teaching is for not teaching" (YZ-b/2020/01) and the Educational Research Project on the Civilization of Vocational College Committee of Education Ministry of China in 2020: Research on the Process of Curriculum System Establishment Based on the Ideology of "Technology Plus Humanity" for Intelligent Manufacturing Major (2020 ZD 02).

References

[1] P. Li, "Analysis of the application of 5G mobile communication technology in the construction of "smart radio and television" networks," *Network Security Technology and Application*, vol. 11, no. 6, pp. 84-85, 2021.

[2] W. Hu, "Introduction of 5G network key technologies and exploration of industry application integration," *Management and Technology of Small and Medium-sized Enterprises (Late Issue)*, vol. 38, no. 6, pp. 193-194, 2021.

[3] J. Zhou, "Development and improvement of wireless communication technology," *Information/Communication*, vol. 27, no. 7, pp. 250-251, 2013.

[4] N. Niu, "Research on the precision communication of college students' ideological and political education under the new media environment—based on Laswell's "5W" communication model," *News Research Guide*, vol. 12, no. 7, pp. 251-252, 2021.

[5] F. Zhao, "Effective countermeasures for college students' ideological and political education under the new media environment," *Chinese and foreign corporate culture*, vol. 53, no. 3, pp. 152-153, 2021.

[6] L. Lu, "Research on the countermeasures of using new media to improve the quality of college students' ideological and political education," *Chinese and Foreign Corporate Culture*, vol. 26, no. 3, pp. 170-171, 2021.

[7] H. Wu, "Research on the ideological and political education of college students from the perspective of integration of knowledge and action," *Journal of Zhejiang Business Vocational and Technical College*, vol. 20, no. 1, pp. 47–50, 2021.

[8] G. Lu, "Innovation in the practice of ideological and political education in colleges and universities from the perspective of Internet + comment on research on the development of ideological and political teaching theory and practice in the horizon of Internet +," *News and Writing*, vol. 2021, no. 6, p. 115, 2021.

[9] J. Liu, X. Yu, and Y. Lu, "Thoughts on the innovation of mental health education in colleges and universities from the perspective of ideological and political education in the new era," *Journal of Heilongjiang Teachers Development Institute*, vol. 40, no. 5, pp. 107–109, 2021.

[10] H. Jiang, "On the innovation of ideological and political theory education in colleges and universities in the new era—comment on "principles of ideological and political education," *Journal of Tropical Crops*, vol. 42, no. 5, pp. 1541-1542, 2021.

[11] K. Wang, "Research on the innovation of ideological and political education in colleges and universities in the all-media era," *Popular Literature and Art*, vol. 19, no. 9, pp. 158-159, 2021.

[12] H. Wang, "The innovation of ideological and political education model in colleges and universities in the era of big data," *Forum on Industry and Technology*, vol. 20, no. 10, pp. 192-193, 2021.

[13] S. Liu and C. Xie, "Research on collaborative innovation of ideological and political education in colleges and universities based on big data," *Guangxi Social Sciences*, vol. 35, no. 4, pp. 167–171, 2021.

[14] S. Rong and Z. Mi, "Exploration of the innovation path of ideological and political education in colleges and universities under the Internet background," *Theoretical Research on Innovation and Entrepreneurship*, vol. 4, no. 7, pp. 156–158, 2021.

[15] H. Zhou and Q. Gong, "Analysis on the integration path of new media technology and ideological and political courses in colleges and universities," *Audio-visual Education Research*, no. 10, p. 24, 2020.

[16] M. Zhang, W. Xia, and Y. Jiang, "The influence of "micro era" on the teaching of ideological and political courses in colleges and universities and its countermeasures," vol. 26, no. 2019-1, pp. 62–64, 2021.

[17] D. Qi, "The predicament and resolution of the teaching mode combining micro-class teaching and special topic teaching——taking the ideological and political theory class in colleges and universities as an example," *Innovative Education Research*, vol. 8, no. 1, pp. 21–26, 2020.

Hindawi
Scientific Programming
Volume 2021, Article ID 6808521, 12 pages
https://doi.org/10.1155/2021/6808521

Research Article

Research on Multiperson Motion Capture System Combining Target Positioning and Inertial Attitude Sensing Technology

Yifei Wang [1] and Yongsheng Wang [2]

[1]*Faculty of Humanities, Shaanxi University of Technology, Shaanxi, China*
[2]*School of Art and Design, Lanzhou Jiaotong University, Gansu, China*

Correspondence should be addressed to Yongsheng Wang; wys_lz@126.com

Received 20 August 2021; Accepted 28 September 2021; Published 29 October 2021

Academic Editor: Punit Gupta

The purpose of this study is to solve the problems of multiple targets, poor accuracy, and inability to obtain displacement information in motion capture. Based on fusion target positioning and inertial attitude sensing technology, Unity3D is employed to create 3D scenes and 3D human body models to read real-time raw data from inertial sensors. Furthermore, a gesture fusion algorithm is used to process the raw data in real time to generate a quaternion, and a human motion capture system is designed based on inertial sensors for the complete movement information recording of the capture target. Results demonstrate that the developed system can accurately capture multiple moving targets and provide a higher recognition rate, reaching 75%~100%. The maximum error of the system adopting the fusion target positioning algorithm is 10 cm, a reduction of 71.24% compared with that not using the fusion algorithm. The movements of different body parts are analyzed through example data. The recognition efficiency of "wave," "crossover," "pick things up," "walk," and "squat down" is as high as 100%. Hence, the proposed multiperson motion capture system that combines target positioning and inertial attitude sensing technology can provide better performance. The results are of great significance to promote the development of industries such as animation, medical care, games, and sports training.

1. Introduction

Human motion capture is widely utilized in film and television production, somatosensory games, sports training, medical rehabilitation, and human behavior analysis. This technology plays a vital role in promoting the development of relevant industries [1]. In the film and television production industry, the shaping of many characters uses human motion capture technology. Characters in movies are 3D virtual actors designed using computers. The 3D virtual animation actors are driven by capturing the movements and facial expressions of real actors, thereby making the actions of the virtual animator the same as the real actors' actions [2]. In somatosensory games, electronic games can be operated by swinging the handle if inertial sensors are added so that people can obtain visual stimulation and feel the happiness brought by electronic games [3]. In sports training, the real-time monitoring and calculation of the athletes' limb movement process can help control the exercise amount of each athlete, achieving efficient and safe training [4]. In the medical rehabilitation field, human motion capture can provide accurate exercise programs by recording human body motion information for a long time, thereby assisting rehabilitation training for patients [5]. Therefore, human motion capture technology is a comprehensive interdisciplinary technology developed in recent years, involving computer graphics, ergonomics, communication technology, and other disciplines. It is currently a research hotspot in the field of human-computer interaction. However, the current human motion capture system faces problems such as more targets, poor accuracy, and inability to obtain displacement information, which severely restricts the development of related industries. Therefore, research on human motion capture technology plays a very important role in promoting the development of the industry.

Motion capture technology can accurately and in real time restore the human body's motion state in real life via a virtual 3D computer model [6]. Fusion methods are often utilized in motion capture. In China, research on the complexity of the fusion target positioning technology has started late. Also, the information processing level is low, which cannot reach the standard as a typical information fusion system. Valuable information fusion methods, such as compensation learning fusion method, active perception method, Mahle's random fusion method, the expert system method, physical model method, and parameter template method, are adopted [7]. The multiperson motion capture system often employs inertial sensor-based motion capture equipment, which can overcome the problem of insufficient light and shade in optical motion capture [8]. However, this device system faces a series of problems. The motion capture device based on inertial sensors needs to bind the inertial sensor nodes to the human joints to return the measurement information of the human joints during the movement in real time [9]. Besides, Xia et al. proposed that the inertial sensor's gyroscope could measure the angular velocity of the human body's joints relative to the human body coordinate system. The human body's current attitude could be obtained when the initial state of the human body was known. However, the gyroscope sensor chip had zero bias error, and long-term integration would cause the error to increase [10]. Liu et al. pointed out that as the time of the motion capture device increased, there would be zero offsets and drift. The system could not simultaneously capture multiperson motions [11].

Research significance: motion capture simplifies the human body into a multibody system, generally an articulated multirigid body system; input data are obtained by means of measurement or mode; the movement of the human body is simulated by describing the movement of the multibody system as the output result. The limitations of traditional motion capture (high price and restricted space) make the market urgently need affordable and portable motion capture equipment to be applied to various industries, such as improving the quality of physical education by capturing the sports characteristics of athletes and helping patients with rehabilitation by capturing normal human postures. Therefore, based on the existing motion capture methods, how to use a small number of sensors to accurately and stably capture motion has become one of the difficulties in this field.

Therefore, to solve the above problems, a multiperson motion capture system is designed and implemented using fusion target positioning and inertial attitude sensing based on analyzing relevant literature. Then, human behavior recognition is achieved on this basis. The innovative points are as follows: (i) the data of human inertial sensors are combined to generate quaternions, and the 3D human model is driven to precisely capture body movements. (ii) A multiperson motion capture solution combining target positioning and inertial attitude sensing is proposed. The fusion target positioning technology and inertial sensor positioning technology are combined to capture human spatial displacement information. (iii) Different equipment and parameters are employed for continuous optimization. Finally, a multiperson motion behavior capture system with a better actual operation and higher accuracy can be obtained.

2. Research Method

2.1. Multiperson Sensor Capture System. The human motion capture system based on inertial sensors consists of hardware and software. The hardware acquires human motion information and transmits data, while the software realizes the functions of 3D animation display and human behavior recognition. The system includes the inertial sensor, the 3D animation display, the human body displacement positioning technology, and human behavior recognition. The inertial sensor captures human body movement information in situ. The inertial sensor measures nine data pieces at the same time, including a 3D magnetic field meter, a 3D gyroscope, and a 3D acceleration. These nine data pieces need to be fused first, and then the human body posture can be calculated. Three-dimensional animation display is to present the captured motion animation in real time in the form of 3D virtual characters on the computer. The human body displacement positioning technology introduces positioning technology to measure the displacement of the human body in space. It also improves the positioning accuracy as much as possible to obtain human displacement information during the capture process. According to the human behavior data captured by the inertial sensor human motion capture system, the human behavior recognition recognizes human movements through data processing, feature extraction, and machine learning. The specific structure is shown in Figure 1.

The system hardware includes the inertial sensor node module, the information receiving module, and the positioning module. The inertial sensor node collects human body information; the information receiving module realizes the communication between the wireless inertial sensor node and the computer; the positioning module acquires human body displacement information. The inertial sensor node module is bound with human joints to collect human joint motion information in real time. The inertial sensor node module includes the nine-axis inertial sensor, Zigbee transmission module, and microprocessor and power circuit. The nine-axis inertial sensor module includes a three-axis magnetometer, a three-axis gyroscope, and a three-axis accelerometer. It collects the three-axis acceleration, three-axis magnetic force, and angular velocity generated by the human limbs in real time. The sensor nodes are wirelessly transmitted sending the collected data to the receiving module through the Zigbee transmission module. When the inertial sensor is bound to the human joints, elastic bands with Velcro are used. The elastic bands can be easily bound to the human joints. The Velcro is glued to the back of the inertial sensor nodes. During use, the elastic band is tied to the human body joint, and the inertial sensor node with Velcro is directly attached to the strap. The information receiving module realizes the communication between the wireless inertial sensor node and the computer. The

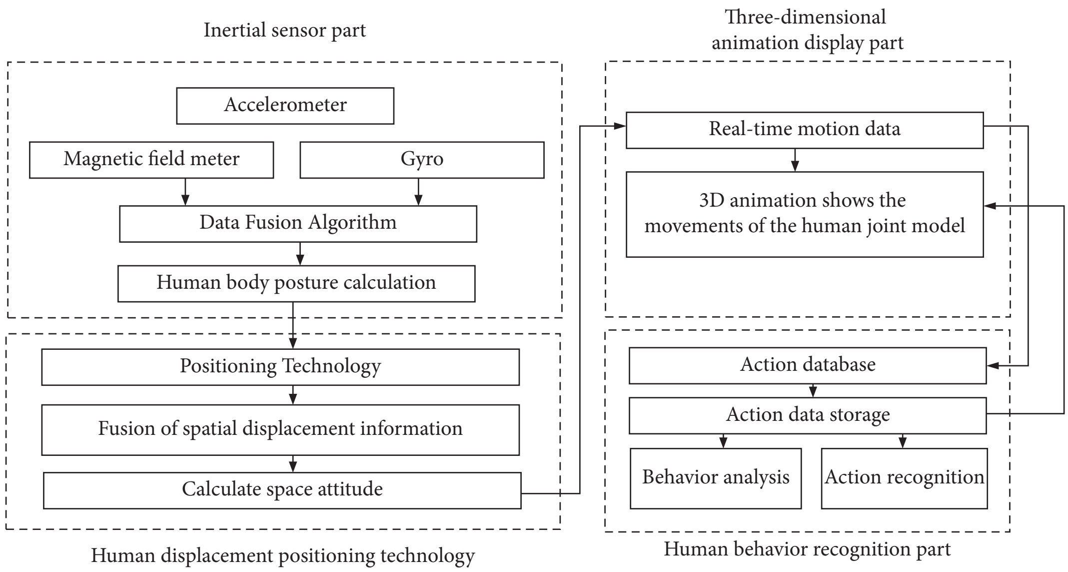

Figure 1: Overall design of the multiperson motion capture system.

information receiving module is connected to the computer through the USB interface. The information sent by the inertial sensor node is transmitted through the Zigbee wireless network, the information receiving module receives the node information and sends the received information to the computer through the serial port, and the data are processed in the computer.

The system software includes 3D scene creation, movement data storage, and human behavior recognition. Three-dimensional scenes are used for the reproduction of human motions; motion data storage stores captured human behavior data as files; human behavior recognition uses human motion information collected by inertial sensors and uses pattern recognition to identify human behaviors.

The process of reading data from the inertial sensor is displayed in Figure 2. After the information collection device is connected to the computer through the USB interface, the corresponding serial port is opened, and the baud rate is set to 115200. A thread for reading the inertial sensors and a thread for reading attitude data is created to solve the problem that the refresh rate of reading inertial sensor data does not match that of the human model animation.

The module of the inertial sensor node is bound to human joints for a real-time collection of human joint motion information. It includes human inertial sensors, Zigbee transmission, microprocessor modules, and power circuit modules. The principle of inertial sensor nodes is presented in Figure 3. The human body inertial sensor module includes a three-axis magnetometer, a three-axis gyroscope, and a three-axis accelerometer, which are used to collect the three-axis acceleration, three-axis magnetic force, and angular velocity generated by the movement of the human body in real time. The sensor node is wirelessly transmitted through the Zigbee transmission module and sends the collected data to the receiving module.

2.2. Inertial Attitude Sensing. The attitude is calculated by magnetometer and acceleration. Despite the poor dynamic response, it will not produce a cumulative error. Therefore, the gyroscope, magnetometer, and accelerometer have complementary characteristics in the frequency domain. Hence, using complementary filters to fuse these three types of data in the inertial sensor can improve the measurement accuracy of the inertial sensor and the dynamic response performance of the system. The calculation steps are illustrated in Figure 4. First, the quaternion is calculated according to the initial state of the inertial sensor when fusing the inertial sensor attitude data. The gravity vector and magnetic field lines are then deducted to obtain and normalize the accelerometer and magnetometer data. After the matrices are multiplied, they are summed, and the proportional-integral controller is used to adjust the data. Finally, the quaternion is updated.

The sensor network can obtain the motion data of different feature points of the human body. The human body is abstracted and divided. Every movement of a limb can be regarded as a limb movement relative to the joint of the parent node. Since the hip joint has a small motion range, it is selected as the root node of the entire joint tree. The model of the human body's principal joints is presented in Figure 5. The corresponding sensors are placed at each joint to form a sensor network. The central controller of human body attitude data is controlled by different control modules. It can

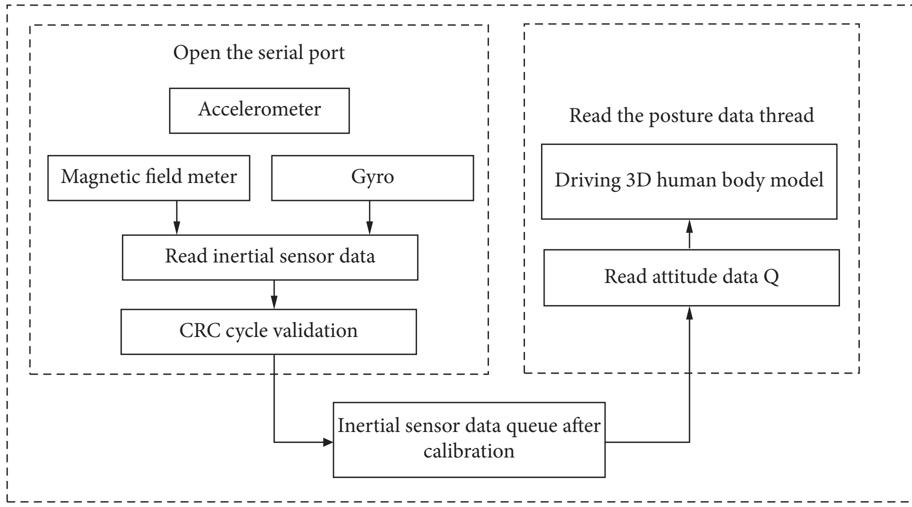

FIGURE 2: The flowchart of inertial sensor data reading.

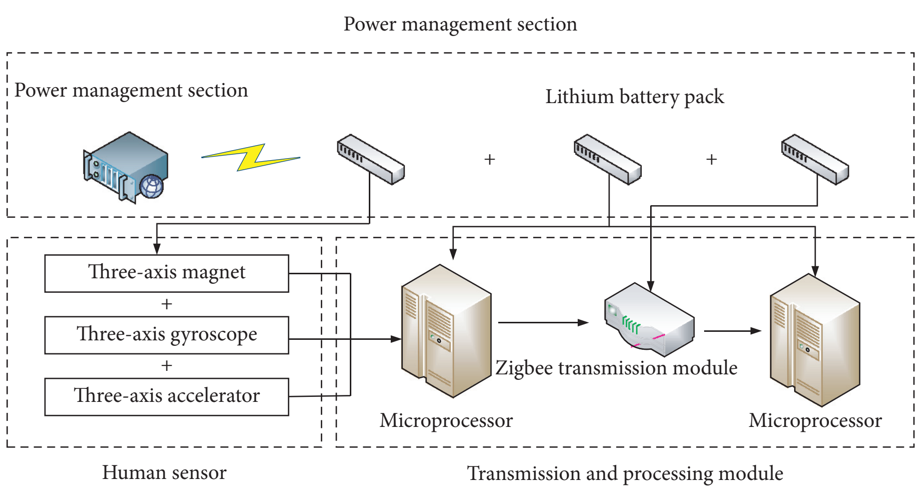

FIGURE 3: Inertial sensor nodes.

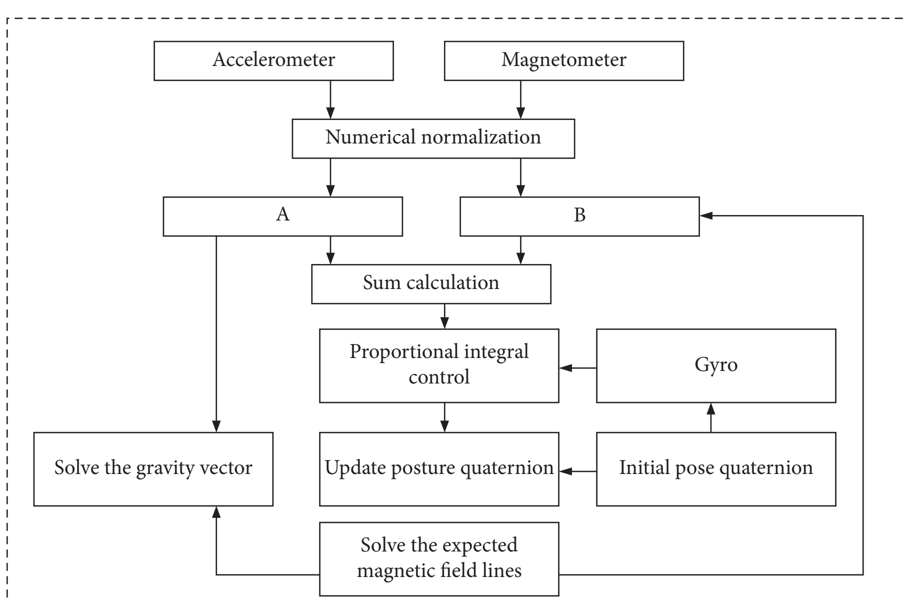

FIGURE 4: The flowchart of the attitude fusion algorithm.

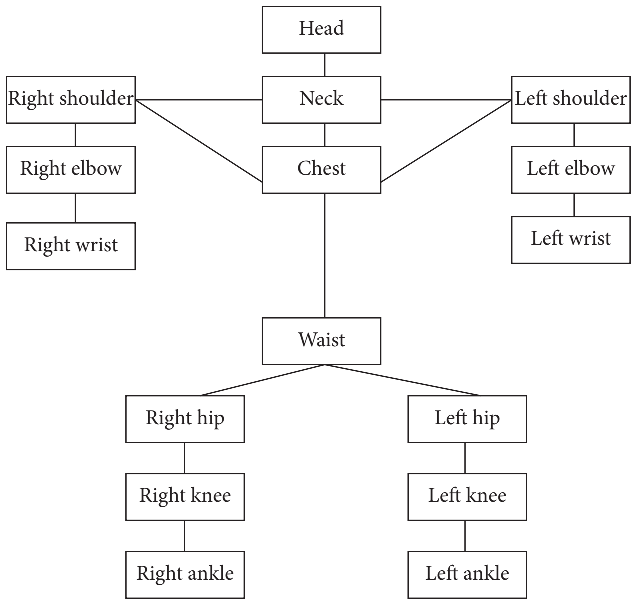

FIGURE 5: Human joint structure.

control different sensor nodes, obtain the data of the nodes, and integrate the wireless transmission module through programming to transmit the data wirelessly.

2.3. Human Posture Positioning. Because inertial sensor motion capture systems do not have an external reference point, they cannot directly obtain position information. Therefore, most inertial motion capture systems only estimate the posture of the human body in situ and cannot obtain accurate position information of the human body in global coordinates. Target positioning technology obtains the 3D position information of the captured target and records the complete movement information of the captured target through the data fusion algorithm. To solve the problem that inertial sensors cannot capture the displacement of the human body, researchers have proposed a variety of solutions, such as a Kalman filter-based inertial navigation system and radio frequency identification system tightly coupled method for indoor pedestrian positioning and navigation. A motion capture system that integrates inertial sensors, GPS, pressure sensors, cameras, and theodolites is employed to capture the 3D dynamics and kinematics information of the human body during alpine skiing competitions. The fusion target positioning technology and inertial sensor positioning technology are combined because the two sensors have good complementarity. In terms of indoor positioning, the fusion target positioning technology has higher positioning accuracy than other positioning methods. However, the fusion target positioning technology is easily affected by the nonline-of-sight effect during the positioning process. The nonline-of-sight effect is that two devices are blocked during the communication process, and the nonline-of-sight effect affects the positioning accuracy. The inertial sensors can make up for the shortcomings of ultra-wideband positioning technology, thereby improving the positioning accuracy in the human motion capture system.

The fusion target positioning technology fuses and merges multiple methods, including the fusion of sensors, image recognition algorithms, and feature algorithms, to accurately position target actions and behaviors [12]. The integral method is adopted to calculate the position $X_{\mathrm{SIM},n}$ of the human body at time step n in the x-dimension. The equation is as follows:

$$X_{\mathrm{SIM},n} = \begin{bmatrix} x_{\mathrm{SIM},n} \\ y_{\mathrm{SIM},n} \\ z_{\mathrm{SIM},n} \end{bmatrix} = X_{P,n} + \frac{\delta_{xP,n}}{\delta_{xP,n} + \delta_{\mathrm{IMU},n}} \left(X_{\mathrm{IMU},n} - X_{P,n} \right). \tag{1}$$

In (1), $x_{\mathrm{SIM},n}$, $y_{\mathrm{SIM},n}$, and $z_{\mathrm{SIM},n}$ refer to the 3D coordinates of the human body position at time step n, $X_{P,n}$ corresponds to the human body position coordinates at time step n in the x-dimension of the fusion target positioning, $\delta_{xP,n}$ represents the human body position coordinates of the inertial sensor in the x-dimension at time step n, $X_{\mathrm{IMU},n}$ stands for the standard deviation of fusion target positioning in the x-axis to provide position estimation, and $\delta_{\mathrm{IMU},n}$ denotes the standard deviation of the inertial sensor. Since it is difficult to predict the standard deviation of the inertial sensor, the three dimensions are all set to the same value. The following process is utilized to deal with the influence of the integration error. At time step n, if the currently estimated ultra-wideband (UWB) positioning standard deviation is less than the inertial sensor standard deviation of $n-1$, it is represented by

$$\delta_{k,P,n} < \delta_{\mathrm{IMU},n-1} \forall k \in \{x, y, z\}. \tag{2}$$

In (2), $\delta_{k,P,n}$ represents the position deviation of fusion target positioning at time step n, and $\delta_{\mathrm{IMU},n-1}$ denotes the standard deviation of the inertial sensor at time step $n-1$. Then the standard deviation of the inertial sensor will be reset to

$$\delta_{\mathrm{IMU}} = 0.05. \tag{3}$$

Otherwise, the standard deviation of the inertial sensor is set as

$$\delta_{\mathrm{IMU},n} = \frac{0.05}{\sec^2 \cdot t_{sr}^2}. \tag{4}$$

In (4), t_{sr}^2 refers to the sampling frequency of the inertial sensor. Therefore, according to the error standard deviation of fusion target positioning, the infinite increase in the error standard deviation of the inertial sensor is limited, and the integral error is reset under the visual distance condition. Under the condition of nonvisual distance, if the error caused by nonvisual distance is less than the integral error, the integral error is reset. The flowchart of the fusion algorithm is shown in Figure 6. The workflow is as follows.

Here, Unity3D is adopted as a development tool to create a 3D scene and a 3D human body model. Besides, the 3D

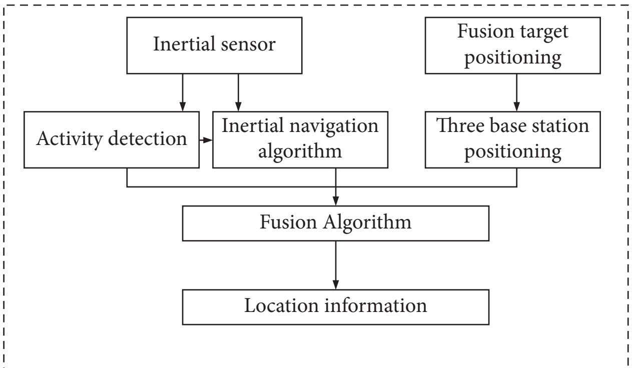

Figure 6: The flowchart of fusion target positioning algorithm.

human body model is employed to display the captured human movements in real time. Unity3D supports most mainstream 3D animation technologies and has a visual design environment, a scene editor that is easy to learn, and a convenient design process. Unity3D can well support 3D model files, saving the time of creating 3D scenes. The raw human motion data captured by the inertial sensor in real time is processed to generate an attitude quaternion. The motion parameters input to the virtual 3D human body model are quaternion data, and the quaternion data are converted into angle rotation parameter information in the bone pipeline.

Human body displacement positioning technology: there is no external reference point during human motion capture, and the spatial displacement information cannot be obtained because the inertial sensor is a self-contained system. Therefore, positioning technology is required to obtain the displacement information during human motion capture. Wireless positioning technology includes wide-area positioning technology and short-distance positioning technology [13]. Wide-area positioning is a large-scale technology, and the commonly used approaches include satellite positioning and mobile positioning. The short-range positioning technology has many kinds, including Wireless Local Area Network (WLAN), Radio Frequency Identification (RFID), Global Positioning System (GPS), UWB, Bluetooth, and ultrasonic. Table 1 summarizes the accuracy and scale of various positioning methods.

Ultra-wideband positioning technology is very different from traditional communication technology. Traditional communication technology uses carrier waves, while ultra-wideband positioning technology uses nanosecond-level narrow pulses with GHz-level bandwidth. Ultra-wideband positioning technology has been successfully applied to many fields, such as valuables storage positioning, mine personnel positioning, and parking lot positioning. Compared with other positioning technologies, ultra-wideband positioning technology has many advantages, such as strong penetration, low power consumption, resistance to multipath effects, and high positioning accuracy. As shown in Figure 7, the ultra-wideband positioning technology is used to obtain human body displacement information in the process of human body motion capture. To effectively improve the detection range and accuracy, a variety of positioning combinations are prepared in this project. The system of this project will first call different positioning modules according to the corresponding distance so that different calling distances can be positioned in real time.

2.4. Behavior Recognition and Display. The 3D animation display includes three parts: 3D scene creation, action data storage, and recognition. The 3D scenes are used for the reproduction of human actions. Human action recognition uses human action information collected by inertial sensors. By limiting the range of motion of each joint in the human joint model, the captured human motion can be more in line with normal human motion. When capturing human motion, the inertial sensor node is bound to the designated joint of the body first. It is determined according to which joint movements need to be collected. Increasing the number of inertial sensor nodes can improve the accuracy of motion capture and make the captured human movements more accurate. According to the principle that each joint of the human body exists independently and interacts, the motion properties of the human body are restricted by the joints, and the motion of the human body is composed of several key joints. Therefore, it is unnecessary to consider the part of the joint that has less impact during human movement. The main joint model of the human body adopts a tree-like hierarchical structure, and the entire joint model of the human body is called a joint tree. The entire joint tree consists of a root node and multiple leaf nodes to form a parent-child relationship. In the process of human movement, every movement of a limb can be regarded as a limb movement relative to the joint of the parent node. Because the hip joint has a relatively small range of motion, it is selected as the root node of the entire joint tree.

The common ways of storing motion data include motion file storage, video file storage, and database storage. Motion file storage generally stores the motion information saved by animation editor software. The database storage can store the captured motion information in the database system; the commonly used database systems include MySQL and Oracle. Table 2 presents a comparison of various motion data storage methods. According to the needs of this project, the storage of human motion capture data requires a small space occupation and a simple storage structure. Besides, the third-party database software is not adopted to make other software more convenient to call the stored motion information. Bounding Volume Hierarchy (BVH) files occupy a small space and are easy to read and store. The BVH file uses Euler angles to describe the rotation data of the bone and limb joints, and the human body model is displaced in 3D space by changing the parameters of the hip node.

Human behavior recognition module: the multiperson motion capture based on fusion target positioning and inertial attitude sensing technology is a new research field, which overcomes many shortcomings and limitations of traditional motion recognition based on video sequences and has higher operability and practicality. The human motion information collected by inertial sensors uses BVH

Table 1: Accuracy and positioning scale of various positioning methods.

Positioning methods	Positioning accuracy (m)	Positioning scale
GPS	About 10	Outdoor wide-area positioning
Mobile positioning	About 10	Outdoor wide-area positioning
RFID, infrared, ultrasonic	1~10	Outdoor local positioning
WLAN, Bluetooth	1~10	Indoor positioning
UWB	0.1~1	Indoor positioning

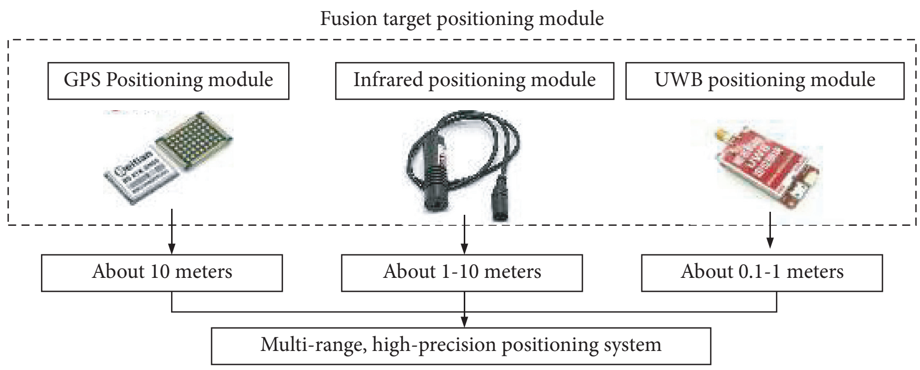

Figure 7: Human displacement positioning technology.

Table 2: Comparison of various motion data storage methods.

Storage methods	Storage types	Space occupation	Storage structure	Whether special software is required
BVH format	Motion file	Small	Simple	No
FBX format	Motion file	Small	Simple	Yes
Maya format	Motion file	Small	Simple	Yes
Database system	Database	Large	Complicated	Yes
Video format	Video	Large	Complicated	Yes

files to store human behaviors. Human behavior recognition preprocesses data and extracts features based on the data stored in BVH files. Moreover, it uses algorithms to recognize human behaviors. The process of human behavior recognition is to extract and select those feature vectors that have a large contribution to classification and recognition from BVH motion data. However, too many features will also cause redundancy between features and reduce the recognition accuracy. Hence, the principal component analysis is required. Finally, the appropriate motion classification algorithm is selected for behavior recognition.

2.5. Data Performance Comparison.

(1) Data source: data are read from the inertial sensor. After the information collection device is connected to the computer through the USB interface, the corresponding serial port is opened, and the baud rate is set to 115200. To solve the problem that the refresh rate of reading inertial sensor data does not match the refresh rate of the human body model animation, a thread for reading inertial sensor and a thread for reading posture data are created. The read inertial sensor thread realizes that the original data read from the inertial sensor consists of three parts, namely, a three-axis accelerometer, a three-axis magnetometer, and a three-axis gyroscope, and then uses CRC16 to check the data. After verification, the data fusion algorithm is used to fuse the data into posture data and then put it into the Queue; the read posture data thread reads the posture data from the Queue and uses the posture data to drive the 3D human body model.

(2) Experimental environment: the behavioral information of eight healthy school students is collected during the experiment. The participants in the experiment include four females and four males, with ages of 22–27 years, height of 158–180 cm, and weight of 45–80 kg. Each participant in the experiment performs 16 actions, which were required by the experimenter. The types of actions are divided into three parts: upper limbs, lower limbs, and trunk according to the human joints. Each action is composed of these three parts. The main types of movements can be determined according to different movements. For example, the movement of waving a hand is mainly the movement of the upper limbs, and the movements of the trunk and lower limbs are relatively simple; thus, this type of movement belongs to the type of upper limbs. Before the behavior

collection, the subject of the purpose of the collection action is informed, and the behavior is demonstrated to the subject. After the subjects put on the inertial sensors, the behavior collection begins. Each behavior is repeated four times, and each behavior is required to be completed within 5 to 15 seconds.

(3) Performance comparison: the method of [14] is used to conduct a comparative analysis to further verify the effectiveness of the proposed model. A motion capture system based on multiple cameras is developed in the literature. To improve the capture accuracy, the multicamera layout method is used as a motion capture system for various animals with significant differences in appearance characteristics and motion behavior. Motion capture determines the demand boundary based on the object's appearance type (shape and space volume) and behavioral characteristics, thereby deriving a typical matching principle. A multicamera system locked in a 3D force measurement platform is used, its semicircular layout model shows that the error of the system is only below 3.8%, and the capture deviation rates are 3.43% and 1.74%, respectively.

3. Results and Discussion

In the result section, the appropriate model kinematics method is determined first, and then the method is used to conduct experiments under different conditions to determine the performance of the model. The effectiveness of the method is further determined by analyzing the human body motion trajectory. To prove that the proposed method has better performance than other models, it is compared with the method in [14], and finally, a human body model for motion capture is given.

3.1. Model Kinematics Method Determination. The forward kinematics of the human body is the posture of the human body displayed when the rotation angle of each joint of the human body is known. The position of any joint of the human body can be calculated by the connection of the human body joint, the joint length, and the rotation angle. There is only one general forward kinematics solution. Human body inverse kinematics gives the parameters of each joint based on the known posture. Therefore, it is difficult to solve the problem of inverse kinematics, and the solution result is not unique. In the process of human motion capture, the legs have fewer joints, simple movements, and relatively small calculations. Therefore, it is more suitable. The inverse kinematics of the legs calculates all the joint variables corresponding to the limbs based on the position and posture of the limbs. In this movement, the foot is the end, and the trigonometric function can be used to calculate the movement data of the thigh and calf when the foot is moving. Because the motion range of the human foot joints is limited, the foot and calf are treated as a whole in the process of using inverse kinematics motion capture. The four-position movement is involved in the process of body rotation so that quaternary data are used for calculation. Figure 8 shows the analysis result of leg kinematics information data, and the left leg is stepped forward. Figure 8(a) shows the calculation result of quaternary data using inverse kinematics, and Figure 8(b) shows the fourth data of forwarding kinematics. In the meta-calculation results, as can be seen from the figure, the motion capture accuracy of inverse kinematics is higher than that of forwarding kinematics. In the same data image with different spatial coordinates, the highest model accuracy of inverse kinematics is 0.9178, and the highest model accuracy of inverse kinematics is 0.5562%. The two are quite different so that the inverse kinematics method is finally selected for image analysis.

3.2. Model Performance under Different Conditions. Figures 9(a)–9(f) display the results of the system capture distance under different line-of-sight algorithms. The positioning data of the X-axis and Y-axis fluctuate under the line-of-sight conditions; overall, however, they tend to be stable. Under the nonline-of-sight conditions, the model data without the fusion positioning algorithm fluctuates greatly. The fluctuation ranges of X and Y are [100–150] and [110–150], respectively. After the fusion algorithm is adopted, the fluctuation trend of positioning data is significantly reduced. The fluctuation ranges of X and Y are [125, 135] and [125, 140], respectively. Apparently, the maximum error of using fusion target positioning alone is 35 cm, while the error of fusion target positioning and the inertial sensor is 10 cm, a reduction of 71.24%. Moreover, the accuracy of model positioning is significantly improved.

3.3. Human Body Motion Trajectory Analysis. Figure 10 shows the results of the model positioning motion trajectories under different positioning systems.

Figure 10(a) presents the fusion target positioning system, and Figure 10(b) shows the method of combining fusion target positioning with inertial sensors. In the entire process, both methods can provide a clear positioning of the target. However, for the model without inertial sensors, the motion trajectory is narrower, showing a large gap with the actual moving process. In contrast, the fusion model can provide a higher positioning accuracy, and all the moving processes within the range can be shown.

3.4. Results of Human Gesture Recognition. Figures 11(a) and 11(b) display the comparison result of the proposed method and the classification algorithm of [14] on human behavior recognition. The behavior with the worst recognition effect is "draw X" and "draw circle," and the recognition result is 62.5%; the behavior with the best recognition effect is "wave," "throw," "crossover," "pick up," "walk," and "squat down," and the recognition result reaches 100%. In terms of the method in [14], the behavior with the worst recognition result is "draw X," "draw circle," and "forward," and the recognition result is 75%; the behavior with the best recognition result is "wave," "crossover," "triangle," "pick up," "run," "walk," and "squat down," and the recognition result reaches 100%. Both classification algorithms have the best recognition results for

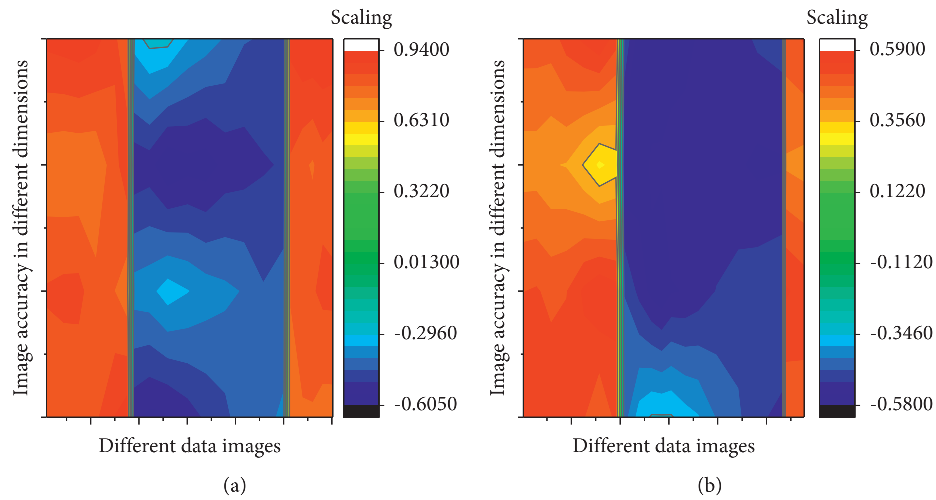

FIGURE 8: Different kinematic leg data information.

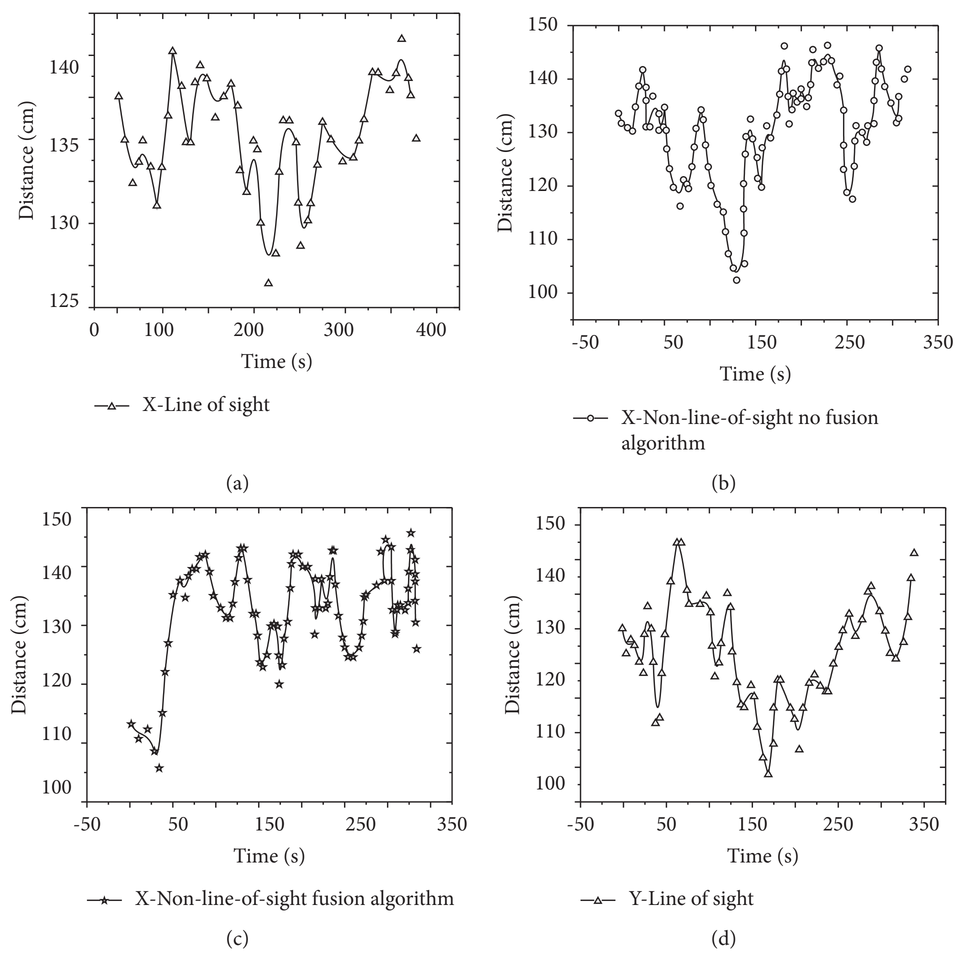

FIGURE 9: Continued.

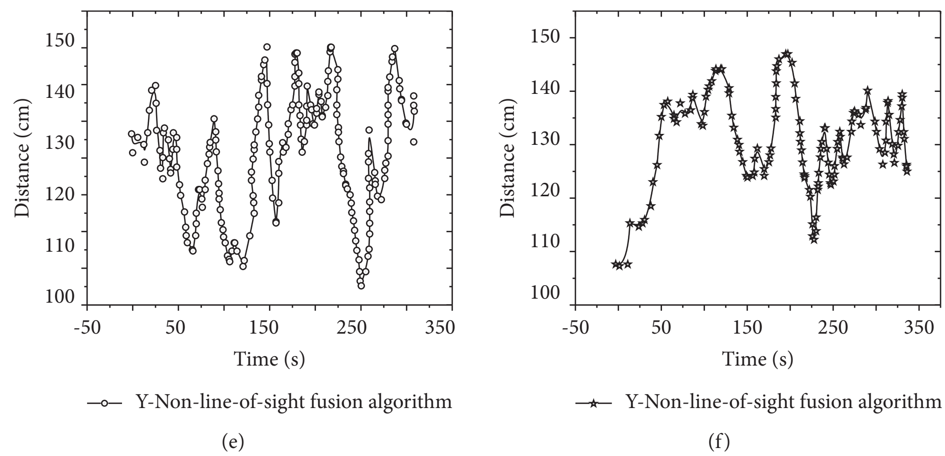

Figure 9: System capture distance results under different line-of-sight algorithms.

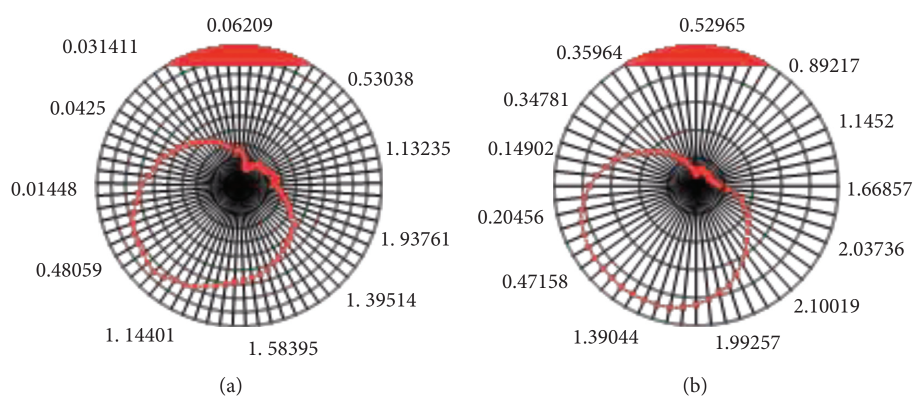

Figure 10: Model positioning motion trajectory results under different positioning systems.

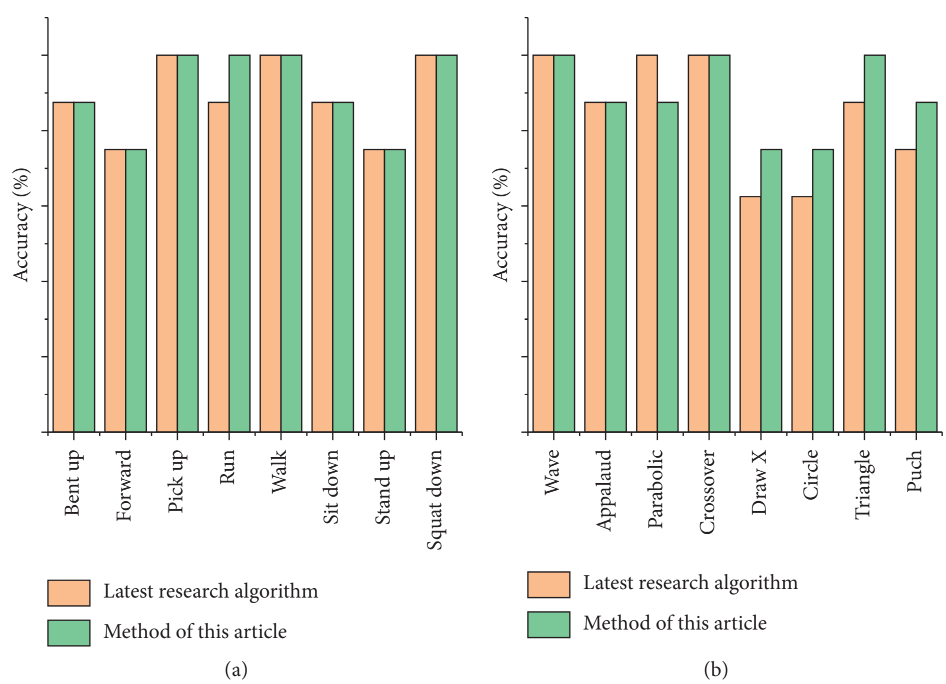

Figure 11: Different behavior recognition results.

Figure 12: Results of human motion capture.

the behaviors of "wave," "crossover," "pick up," "walk," and "squat down," and the recognition results for the behaviors of "draw X" and "draw circle" are the worst. On the whole, the classification result of [14] is better than the classification result of the method. This is because the collected behavior data samples are more balanced, and the classification needs to divide the behavior data into 16 groups, which is a multiclassification problem. Therefore, the classification result of the algorithm in [14] is better. According to the results of human behavior recognition, the behavior with a recognition rate of 100% has a larger motion range and is obviously different from other behaviors, such as "squat," "walk," and "pick up." The behaviors with low recognition rates are caused by other similar behaviors. For example, the behaviors of "draw circle" and "draw *X*" are very similar so that the recognition rate is low. Therefore, the design of the human body behavior recognition method can better recognize the behaviors with larger motion amplitude; besides, the motion is relatively single, and the recognition rate for behaviors with small changes in human joints is low.

3.5. Motion Capture Result Display. As shown in Figure 12, many experiments on the upper and lower limbs of the human body find that the motion attitude of the 3D human body model can capture the motion state of the upper and lower limbs of the human body in real time and accurately. Besides, the constructed model can capture the human body attitude in real time. In particular, complicated motions can also be effectively recognized. When the human body moves, muscles contract, and inertial sensors can also move joints through the jitter of nodes, proving the effectiveness of the proposed model.

4. Conclusion

The existing human motion capture systems based on inertial sensors and related research on human behavior recognition methods are studied. On this basis, a human motion capture system based on wireless inertial sensors is designed and implemented to recognize human behaviors. Moreover, a scheme that fuses inertial sensors and ultra-wideband positioning is proposed. The ultra-wideband positioning technology and inertial sensor positioning technology are combined together to capture human spatial displacement information. The captured human motion data are analyzed in depth based on motion capture. Experimental steps are designed, including human behavior data collection, human behavior data storage, dataset analysis, feature extraction, and pattern recognition. Based on the extracted feature parameters, different algorithms are used to recognize human behaviors. The algorithm has a recognition rate of 62.5%~100% for 16 human behaviors, which can better realize the recognition of human behaviors. Although a suitable multiplayer motion capture system has been constructed, there are still several shortcomings. First, in human motion recognition, the angular velocity is time-integrated to evaluate the angle of the joint. However, this is easily affected by the magnetic field and surrounding equipment. The algorithm of the fusion inertial sensor can be analyzed more profoundly to reduce unnecessary interference. Second, in the process of human behavior feature training, because there is no suitable dataset for training, the training data is less, and the accuracy of the model is not very high. In the following research, these two aspects will be analyzed and researched in depth to further improve the model of the multiperson motion capture system.

Data Availability

The datasets used and/or analyzed during the current study are available from the corresponding author on reasonable request.

Conflicts of Interest

The authors declare that they have no conflicts of interest.

Acknowledgments

This study was supported by Scientific Research Projects of Colleges and Universities in Gansu Province "Multiperson Real-Time Motion Capture Technology Fusing Optical Positioning and Attitude Sensing" (Item no. 2018D—11).

References

[1] E. van der Kruk and M. M. Reijne, "Accuracy of human motion capture systems for sport applications; state-of-the-art review," *European Journal of Sport Science*, vol. 18, no. 6, pp. 806–819, 2018.

[2] T. Y. Mou, "Keyframe or motion capture? Reflections on education of character animation," *Eurasia Journal of Mathematics, Science and Technology Education*, vol. 14, no. 12, pp. 1649–1669, 2018.

[3] B. Yang, H. Dong, and A. E. Saddik, "Development of a self-calibrated motion capture system by nonlinear trilateration of multiple Kinects v2," *IEEE Sensors Journal*, vol. 17, no. 8, pp. 2481–2491, 2017.

[4] J. A. Goldsmith, C. Trepeck, J. L. Halle et al., "Validity of the open barbell and tendo weightlifting analyzer systems versus the optotrak certus 3D motion-capture system for barbell velocity," *International Journal of Sports Physiology and Performance*, vol. 14, no. 4, pp. 540–543, 2019.

[5] Z. Yang, M. H. Rafiei, A. Hall et al., "A novel methodology for extracting and evaluating therapeutic movements in game-based motion capture rehabilitation systems," *Journal of Medical Systems*, vol. 42, no. 12, pp. 255–263, 2018.

[6] M. Yoshimura, M. Kitazawa, Y. Maeda, M. Mimura, K. Tsubota, and T. Kishimoto, "Smartphone viewing distance and sleep: an experimental study utilizing motion capture technology," *Nature and Science of Sleep*, vol. 9, pp. 59–65, 2017.

[7] G. Liu, L. Shi, J. Xun, S. Chen, L. Zhao, and Y. Shi, "An orientation estimation algorithm based on multi-source information fusion," *Measurement Science and Technology*, vol. 29, no. 11, Article ID 115101, 2018.

[8] A. Filippeschi, N. Schmitz, M. Miezal, G. Bleser, E. Ruffaldi, and D. Stricker, "Survey of motion tracking methods based on inertial sensors: a focus on upper limb human motion," *Sensors*, vol. 17, no. 6, pp. 1257–1265, 2017.

[9] M. Rigoni, S. Gill, S. Babazadeh et al., "Assessment of shoulder range of motion using a wireless inertial motion capture device-A validation study," *Sensors*, vol. 19, no. 8, pp. 1781–1793, 2019.

[10] S. Xia, L. Gao, Y.-K. Lai, M. Z. Yuan, and J. Chai, "A survey on human performance capture and animation," *Journal of Computer Science and Technology*, vol. 32, no. 3, pp. 536–554, 2017.

[11] Y. Liu, Y. Zhang, and M. Zeng, "Sensor to segment calibration for magnetic and inertial sensor based motion capture systems," *Measurement*, vol. 142, pp. 1–9, 2019.

[12] W. Zhao, S. Han, R. Q. Hu, W. Meng, and Z. Jia, "Crowdsourcing and multisource fusion-based fingerprint sensing in smartphone localization," *IEEE Sensors Journal*, vol. 18, no. 8, pp. 3236–3247, 2018.

[13] R. Bharadwaj, S. Swaisaenyakorn, C. G. Parini, J. C. Batchelor, and A. Alomainy, "Impulse radio ultra-wideband communications for localization and tracking of human body and limbs movement for healthcare applications," *IEEE Transactions on Antennas and Propagation*, vol. 65, no. 12, pp. 7298–7309, 2017.

[14] W. Zong, Z. Wang, Q. Xing et al., "The method of multi-camera layout in motion capture system for diverse small animals," *Applied Sciences*, vol. 8, no. 9, 2018.

Hindawi
Scientific Programming
Volume 2021, Article ID 2404997, 13 pages
https://doi.org/10.1155/2021/2404997

Research Article

A New Estimation Study of the Stress-Strength Reliability for the Topp–Leone Distribution Using Advanced Sampling Methods

Abdullah M. Almarashi,[1] Ali Algarni,[1] Amal S. Hassan,[2] M. Elgarhy,[3] Farrukh Jamal,[4] Christophe Chesneau,[5] Khudir Alrashidi,[1] Wali Khan Mashwani,[6] and Heba F. Nagy[2]

[1]*Faculty of Science, Department of Statistis, King Abdulaziz University, Jeddah, Saudi Arabia*
[2]*Faculty of Graduate Studies for Statistical Research, Cairo University, Giza 12613, Egypt*
[3]*The Higher Institute of Commercial Sciences, Al Mahalla Al Kubra 31951, Algarbia, Egypt*
[4]*Department of Statistics, The Islamia University of Bahawalpur, Punjab 63100, Pakistan*
[5]*Universit´e de Caen, LMNO, Campus II, Science 3, 14032, Caen, France*
[6]*Institute of Numerical Sciences, Kohat University of Science & Technology, Kohat 26000, Pakistan*

Correspondence should be addressed to Wali Khan Mashwani; mashwanigr8@gmail.com

Received 8 September 2021; Accepted 4 October 2021; Published 28 October 2021

Academic Editor: Punit Gupta

In this manuscript, we investigate the estimation of the unknown reliability measure $R = P[Y < X]$, in the case where Y and X are two independent random variables with Topp–Leone distributions. As the main contribution, various advanced sampling strategies are studied. The suggested strategies are simple random, ranked set, and median ranked set samplings. Firstly, based on the maximum likelihood, we give an efficient estimator of R when the observations of the two random variables are selected from the same simple random sample. Secondly, such an estimator is addressed when the observations of the two random variables are selected from the ranked set sampling method. Then, based on median ranked set sampling, the maximum likelihood estimator of R is addressed in all the four cases. When the observations from the two random variables are selected from the same set size, two cases are considered, while the other two cases are considered at different set sizes. A simulation research is developed to evaluate the behavior of the obtained estimates based on standard and median ranked set samplings with their simple random sampling equivalents. The ratio of mean square error is used to assess the effectiveness of these estimates.

1. Introduction

First and foremost, the simplified version of the Topp–Leone (TL) distribution is a bounded support one-parameter J-shaped distribution. It possesses a bathtub-shaped hazard rate (see [1]). For these reasons, it is very effective for modeling life-time tests. Mathematically, it is defined by a one-parameter probability density function (PDF) and a one-parameter cumulative distribution function (CDF) given, respectively, by

$$\begin{aligned} f(x) &= 2\alpha x^{\alpha-1}(1-x)(2-x)^{\alpha-1}, 0 < x < 1, \alpha > 0, \\ F(x) &= x^{\alpha}(2-x)^{\alpha}, 0 < x < 1, \alpha > 0. \end{aligned} \quad (1)$$

Hereafter, the TL distribution will be sometimes denoted by $\mathrm{TL}(\alpha)$ in order to highlight the parameter.

In recent years, the TL distribution and its model have obtained a lot of attention in the literature. For instance, the authors in [2] proposed an extension of the TL distribution. The authors in [3] examined several features of the TL distribution, including the failure rate (classical and reversed) and the mean residual life time. A bivariate generalization of the TL distribution was introduced in [4]. Two-side based version of the TL distribution was proposed in [5]. Estimation of the stress-strength (SS) model was discussed based on censored samples in [6]. The author in [7] derived some moments properties of order statistics associated to the TL distribution. Using record values, the authors in [8] discussed Bayesian and non-Bayesian estimation methods for the unique parameter of the TL distribution. The author in [9] examined admissible minimax estimates of the TL distribution.

On the other hand, the notion of ranked set sampling (RSS) has been presented in [10] as a sampling scheme for data collection. This scheme is a useful technique when it is hard to measure a large number of elements, but it is easier visually (without inspection) to rank some of them. The RSS scheme has evolved into a complex strategy for enhancing mean estimation accuracy. The mathematical foundations for RSS design have been provided in [11,12]. The RSS scheme has been effective in applied sciences, with impressive wins in agriculture and ecology. The selection of a RSS of size n entails the drawing of n random samples, each containing n units. Judgment is used to rank the n units in each sample. The first sample is used to measure the smallest rank unit, and the second sample is used to measure the second smallest rank unit, and so on. When the unit with rank n is chosen from the nth set, the first cycle is finished. It is worth noting that the n observations are dispersed randomly. Because n in the RSS is usually low, the following approach is used to create a sample of size (ns) by repeating its times or cycles.

Reference [13] suggested the median ranked set sampling (MRSS) scheme as another contribution to the RSS scheme. The MRSS method is easy to apply since only the middle of the sample is considered. The following is an outline of the MRSS method: We choose n^2 units randomly by using the simple random sampling (SRS) from the population, the n^2 randomly chosen units are divided into n sets, each of size n, and the units within each set are ranked according to a variable of interest. If the set size n is odd, the $((n+1)/2)$th lowest ranked unit in each set, which is the set's median, should be chosen for measurement. Furthermore, if n is even, the $(n/2)$th smallest lowest ranked units from the first $n/2$ sets should be chosen, followed by the $((n+2)/2)$th lowest ranked units from the second $n/2$ sets. To obtain ns units, the cycle can be repeated s times.

For several years, the SS models have attracted the attention of significant statisticians due to their applicability in distinct fields like economics, engineering, medicine, and quality control. To depict the life of a component with unpredictable strength and random stress, the SS model is utilized. The chance that the system will be able to sustain the stress placed on it is the reliability of the system, denoted by R. That is, $R = P(Y < X)$, where X and Y are continuous random variables (RVs) that are independent, modeling the random strength and stress, respectively. Applications of the SS model in medicine and engineering were provided in [14]. An outstanding review of the growth of the SS model up to 2003 was conducted in [15].

The problem of estimating R has been intensively used in the statistical literature under various sampling schemes. In this work, we give a review of RSS schemes; for instance, the authors in [16, 17] concerned with estimating R when X and Y are independent RVs with exponential distributions under the RSS. The authors in [18, 19] handled with the same problem but RR with Burr type XII distributions under some forms of RSS schemes. Also, the authors in [20] discussed the estimation of R when X and Y are independent RVs with Weibull distributions under some versions of RSS. In this setting, Lindley distributions were supposed in [21], and exponentiated Pareto distributions were discussed in [22], both based on RSS. Using MRSS, the authors in [23] considered this estimation problem with generalized inverse exponential distributions.

Although no author has yet examined the estimation of R for the TL model via ranking schemes and their modifications in the literature, we would like to point out that reference [6] contributed to this problem using censored schemes. So, in this manuscript, we use two different ranking schemes, namely, MRSS and RSS, as well as the traditional complete scheme, i.e., SRS, to converge on the estimation of R when $X \sim \mathrm{TL}(\alpha)$ and $Y \sim \mathrm{TL}(\beta)$ are independent. When both X and Y are selected from the same sample schemes (SRS, RSS, and MRSS), we get the ML estimator of R. Also, we obtain the ML of R when both X and Y are selected from various sampling schemes (MRSS with odd size or even sample size). To demonstrate the theoretical results, a simulation study is provided. The following is a summary of the manuscript. When the SRS is considered, Section 2 calculates the ML estimator of R. When the RSS is considered, the ML estimator of R is used in Section 3. When observed data from both X and Y are chosen from the MRSS with an even set size (MRSSE) or MRSS with an odd set size (MRSSO) or vice versa, Section 4 deals with the ML estimator of R. In Section 5, the simulation findings are discussed. In the last section, we wrap up the paper.

2. ML Estimation of *R* Based on SRS

Let $X \sim \mathrm{TL}\ (\alpha)$ and $Y \sim \mathrm{TL}\ (\beta)$ be independent. Then, with a standard integral development, the measure R of the SS model for the TL distribution is basically given by

$$R = P[Y < X] = 2\alpha \int_0^1 x^{\alpha-1}(1-x)(2-x)^{\alpha-1} x^{\beta}(2-x)^{\beta} \mathrm{d}x = \frac{\alpha}{\alpha+\beta}. \tag{2}$$

To get the ML estimator of R, we need to get the ML estimators for the unknown distribution parameters first. In this regard, suppose that $X_1, X_2, \ldots, X_{n^*}$ is a classical random sample from the distribution TL (α) and $Y_1, Y_2, \ldots, Y_{m^*}$ is a classical random sample from the distribution TL (β). The related observations are denoted as small $x_1, x_2, \ldots, x_{n^*}$ and $y_1, y_2, \ldots, y_{m^*}$, and this is consistent across all the paper. The joint likelihood function for the observed samples is as follows:

$$\ell = (2\alpha)^{n^*}(2\beta)^{m^*}\prod_{i=1}^{n^*} x_i^{\alpha-1}(1-x_i)(2-x_i)^{\alpha-1}\prod_{j=1}^{m^*} y_j^{\beta-1}(1-y_j)(2-y_j)^{\beta-1}. \tag{3}$$

The corresponding joint log likelihood (LL) function is obtained as follows:

$$\begin{aligned}\ln \ell = {} & 2(\ln n^*) + 2(\ln m^*) + n^* \ln \alpha + m^* \ln \beta + (\alpha-1)\sum_{i=1}^{n^*}\ln[x_i(2-x_i)] \\ & + \sum_{i=1}^{n^*}\ln(1-x_i) + (\beta-1)\sum_{j=1}^{m^*}\ln[y_j(2-y_j)] + \sum_{j=1}^{m^*}\ln(1-y_j).\end{aligned} \tag{4}$$

As usual, the ML estimators of α and β are produced by the maximization of LL with respect to the parameters, which is equivalent to differentiating the function in equation (4) and equating with zero, and we obtain

$$\begin{aligned}\hat{\alpha} &= \frac{-n^*}{\sum_{i=1}^{n^*}\ln[x_i(2-x_i)]}, \\ \hat{\beta} &= \frac{-m^*}{\sum_{j=1}^{m^*}\ln[y_j(2-y_j)]}.\end{aligned} \tag{5}$$

Thanks to the so-called invariance property, we deduce the ML estimator of R, denoted by $\hat{R}$; it is derived by directly substituting equation (5) in equation (2).

3. ML Estimation of R Based on RSS

Suppose that $\{X_{i(i)e},\ i=1,2,\ \ldots,\ n;\ e=1,2,\ \ldots s_x)$ is a RSS observed from the distribution TL (α), with sample size $n^* = ns_x$, where n is the set size and s_x is the number of cycles, and that $\{Y_{j(j)h}, j=1,2\ldots, m; h=1,2,\ldots s_y)$ is a RSS observed from the distribution TL (β), with sample size $m^* = ms_y$,where m is the set size and s_y is the number of cycles. In this setting, the following is the likelihood function ℓ_1 of the observed samples:

$$\begin{aligned}\ell_1 &= \prod_{e=1}^{s_x}\prod_{i=1}^{n} f_i(x_{i(i)e})\prod_{h=1}^{s_y}\prod_{j=1}^{m} f_j(y_{j(j)h}), \\ f_i(x_{i(i)e}) &= \frac{2\alpha n!\, x_{i(i)e}^{\alpha i-1}}{(i-1)!\,(n-i)!}(1-x_{i(i)e})(2-x_{i(i)e})^{\alpha i-1}\left(1-x_{x_{i(i)e}}^{\alpha}(2-x_{i(i)e})^{\alpha}\right)^{n-i}, x_{i(i)e}>0, \\ f_j(y_{j(j)h}) &= \frac{2\beta m!\, y_{j(j)h}^{\beta j-1}}{(j-1)!\,(m-j)!}(1-y_{j(j)h})(2-y_{j(j)h})^{\beta j-1}\left(1-y_{j(j)h}^{\beta}(2-y_{j(j)h})^{\beta}\right)^{m-j}, y_{j(j)h}>0.\end{aligned} \tag{6}$$

The LL function of ℓ_1 is as follows:

$$\begin{aligned}\ln \ell_1 \propto {} & s_x n \ln \alpha + s_y m \ln \beta + \sum_{e=1}^{s_x}\sum_{i=1}^{n}(\alpha i-1)\ln[x_{i(i)e}(2-x_{i(i)e})] + \sum_{e=1}^{s_x}\sum_{i=1}^{n}\ln(1-x_{i(i)e}) \\ & + \sum_{e=1}^{s_x}\sum_{i=1}^{n}(n-i)\ln\left(1-x_{i(i)e}^{\alpha}(2-x_{i(i)e})^{\alpha}\right) + \sum_{h=1}^{s_y}\sum_{j=1}^{m}(\beta j-1)\ln[y_{j(j)h}(2-y_{j(j)h})] \\ & + \sum_{h=1}^{s_y}\sum_{j=1}^{m}\ln(1-y_{j(j)h}) + \sum_{h=1}^{s_y}\sum_{j=1}^{m}(m-j)\ln\left(1-y_{j(j)h}^{\beta}(2-y_{j(j)h})^{\beta}\right).\end{aligned} \tag{7}$$

With regard to α and β, we have

$$\frac{\partial \ln \ell_1}{\partial \alpha} = \frac{n^*}{\alpha} + \sum_{e=1}^{s_x}\sum_{i=1}^{n} i \ln\left[x_{i(i)e}\left(2 - x_{i(i)e}\right)\right] - \sum_{e=1}^{s_x}\sum_{i=1}^{n} \frac{(n-i)\ln\left[x_{i(i)e}\left(2 - x_{i(i)e}\right)\right]}{x_{i(i)e}^{-\alpha}\left(2 - x_{i(i)e}\right)^{-\alpha} - 1}, \tag{8}$$

$$\frac{\partial \ln \ell_1}{\partial \beta} = \frac{m^*}{\beta} + \sum_{h=1}^{s_y}\sum_{j=1}^{m} j \ln\left[y_{j(j)h}\left(2 - y_{j(j)h}\right)\right] - \sum_{h=1}^{s_y}\sum_{j=1}^{m} \frac{(m-j)\ln\left[y_{j(j)h}\left(2 - y_{j(j)h}\right)\right]}{y_{j(j)h}^{-\beta}\left(2 - y_{j(j)h}\right)^{-\beta} - 1}. \tag{9}$$

Because the system "Equations (8) and (9) equal to zero" is difficult to solve analytically, we use an iterative technique to evaluate the ML estimators. Then, owing to the invariance property, the ML estimator of R follows by inserting these estimators into Equation (2).

4. ML Estimation of R Based on MRSS

In this section, we investigate the ML estimator of R based on MRSS in four situations. In the first and second situations, we estimate $R = P(Y_{\mathrm{MRSSO}} < X_{\mathrm{MRSSO}})$ and $R = P(Y_{\mathrm{MRSSE}} < X_{\mathrm{MRSSE}})$, i.e., when both stress and strength are of the same size. When both X and Y have different set sizes, we estimate R in the third and fourth situations.

4.1. Estimation with an Odd Set Size. Suppose that $X_{i(g)e}$ where $i = 1,\ldots,n$, $e = 1,\ldots,s_x$, and $g = [n + 1/2]$ is the MRSS with sample size $n^* = ns_x$, where n is the set size and s_x is the number of cycles, selected from the distribution TL (α), and that $Y_{j(k)h}$ where $j = 1,\ldots,m$, $h = 1,\ldots,s_y$, and $k = [m + 1/2]$ is the MRSS with sample size ms_y, where m is the set size and s_y is the number of cycles, selected from the distribution TL (β). The associated likelihood function ℓ_2 for the observed samples is given by

$$\begin{aligned}
\ell_2 &= \prod_{e=1}^{s_x}\prod_{i=1}^{n} f_g\left(x_{i(g)e}\right)\prod_{h=1}^{s_y}\prod_{j=1}^{m} f_k\left(y_{j(k)h}\right),\\
f_g\left(x_{i(g)e}\right) &= \frac{n!2\alpha x_{i(g)e}^{\alpha g-1}}{[(g-1)!]^2}\left(1 - x_{i(g)e}\right)\left(2 - x_{i(g)e}\right)^{\alpha g-1}\left(1 - x_{x_{i(g)e}}^{\alpha}\left(2 - x_{i(g)e}\right)^{\alpha}\right)^{g-1}, x_{i(g)e} > 0,\\
f_k\left(y_{j(k)h}\right) &= \frac{2m!\beta y_{j(k)h}^{\beta k-1}}{[(k-1)!]^2}\left(1 - y_{j(k)h}\right)\left(2 - y_{j(k)h}\right)^{\beta k-1}\left(1 - y_{j(k)h}^{\beta}\left(2 - y_{j(k)h}\right)^{\alpha}\right)^{k-1}, y_{j(k)h} > 0.
\end{aligned} \tag{10}$$

The LL function of ℓ_2 is as follows:

$$\begin{aligned}
\ln \ell_2 \propto{}& s_x n \ln \alpha + s_y m \ln \beta + \sum_{e=1}^{s_x}\sum_{i=1}^{n}(\alpha g - 1)\ln\left[x_{i(g)e}\left(2 - x_{i(g)e}\right)\right] + \sum_{e=1}^{s_x}\sum_{i=1}^{n}\ln\left(1 - x_{i(g)e}\right),\\
&+ \sum_{e=1}^{s_x}\sum_{i=1}^{n}(g-1)\ln\left(1 - x_{i(g)e}^{\alpha}\left(2 - x_{i(g)e}\right)^{\alpha}\right) + \sum_{h=1}^{s_y}\sum_{j=1}^{m}(\beta k - 1)\ln\left[y_{j(k)h}\left(2 - y_{j(k)h}\right)\right],\\
&+ \sum_{h=1}^{s_y}\sum_{j=1}^{m}\ln\left(1 - y_{j(k)h}\right) + \sum_{h=1}^{s_y}\sum_{j=1}^{m}(k-1)\ln\left(1 - y_{j(k)h}^{\beta}\left(2 - y_{j(k)h}\right)^{\beta}\right).
\end{aligned} \tag{11}$$

Again, the ML estimators of α and β are derived by maximizing $\ln \ell_2$. In this regard, the first partial derivatives of $\ln \ell_2$ with respect to the parameters are

$$\frac{\partial \ln\ \ell_2}{\partial \alpha} = \frac{n^*}{\alpha} + \sum_{e=1}^{s_x}\sum_{i=1}^{n} g\ \ln\left[x_{i(g)e}\left(2 - x_{i(g)e}\right)\right] - \sum_{e=1}^{s_x}\sum_{i=1}^{n} \frac{(g-1)\ln\left[x_{i(g)e}\left(2 - x_{i(g)e}\right)\right]}{x_{i(g)e}^{-\alpha}\left(2 - x_{i(g)e}\right)^{-\alpha} - 1}, \tag{12}$$

$$\frac{\partial \ln\ \ell_2}{\partial \beta} = \frac{m^*}{\beta} + \sum_{h=1}^{s_y}\sum_{j=1}^{m} k\ \ln\left[y_{j(k)h}\left(2 - y_{j(k)h}\right)\right] - \sum_{h=1}^{s_y}\sum_{j=1}^{m} \frac{(k-1)\ln\left[y_{j(k)h}\left(2 - y_{j(k)h}\right)\right]}{y_{j(k)h}^{-\beta}\left(2 - y_{j(k)h}\right)^{-\beta} - 1}. \tag{13}$$

By solving the system "Equations (12) and (13) equal to zero," we get the ML estimators of α and β. Hence, reliability estimator of R is produced by immediately by substitution of parameter's estimators in equation (2).

4.2. Estimation with an Even Set Size. Suppose $\{X_{i(q)e}, i=1,\ldots,q;\ e=1,\ldots,s_x\} \cup \{X_{i(q+1)e},\ i=q+1,\ldots,n;\ e=1,\ldots,s_x\}$, with even set sizes where $q = n/2$ be the observed MRSSE selected from the distribution TL (α). Also, suppose$\{Y_{j(v)h}, j=1,\ldots,v; h=1,\ldots,s_y\} \cup \{Y_{j(v+1)e}, j=\nu+1,\ldots,m; h=1,\ldots,s_y\}$, with even set sizes where $\nu = m/2$ be the observed MRSSE selected from the distribution TL (β). Therefore, the likelihood function ℓ_3 of the observed data is written as follows:

$$\begin{aligned}
\ell_3 &= \prod_{e=1}^{s_x}\prod_{i=1}^{q} f_q\left(x_{i(q)e}\right)\prod_{e=1}^{s_x}\prod_{i=q+1}^{n} f_{q+1}\left(x_{i(q+1)e}\right)\prod_{h=1}^{s_y}\prod_{j=1}^{\nu} f_\nu\left(y_{j(\nu)h}\right)\prod_{h=1}^{s_y}\prod_{j=\nu+1}^{m} f_{\nu+1}\left(y_{j(\nu+1)h}\right),\\
f_q\left(x_{i(q)e}\right) &= \frac{n!2\alpha x_{i(q)e}^{\alpha q-1}}{(q-1)!q!}\left(1 - x_{i(q)e}\right)\left(2 - x_{i(q)e}\right)^{\alpha q-1}\left(1 - x_{x_{i(q)e}}^{\alpha}\left(2 - x_{i(q)e}\right)^{\alpha}\right)^{q}, x_{i(q)e} > 0,\\
f_{q+1}\left(x_{i(q+1)e}\right) &= \frac{n!2\alpha x_{i(q+1)e}^{\alpha(q+1)-1}}{(q-1)!q!}\left(1 - x_{i(q+1)e}\right)\left(2 - x_{i(q+1)e}\right)^{\alpha(q+1)-1}\left(1 - x_{x_{i(q+1)e}}^{\alpha}\left(2 - x_{i(q+1)e}\right)^{\alpha}\right)^{q-1}, x_{i(q+1)e} > 0,\\
f_\nu\left(\left(y_{j(\nu)h}\right) &= \frac{m!2\beta y_{j(\nu)h}^{\beta\nu-1}}{(\nu-1)!\nu!}\left(1 - y_{j(\nu)h}\right)\left(2 - y_{j(\nu)h}\right)^{\beta\nu-1}\left(1 - y_{j(\nu)h}^{\beta}\left(2 - y_{j(\nu)h}\right)^{\beta}\right)^{\nu}, y_{j(\nu)h} > 0,\\
f_{\nu+1}\left(y_{j(\nu+1)h}\right) &= \frac{m!2\beta y_{j(\nu+1)h}^{\beta(\nu+1)-1}}{(\nu-1)!\nu!}\left(1 - y_{j(\nu+1)h}\right)\left(2 - y_{j(\nu+1)h}\right)^{\beta(\nu+1)-1}\left(1 - y_{j(\nu+1)h}^{\beta}\left(2 - y_{j(\nu+1)h}\right)^{\beta}\right)^{\nu-1}, y_{j(\nu+1)h} > 0.
\end{aligned} \tag{14}$$

The LL function of ℓ_3 for α and β based on MRSSE is

$$\begin{aligned}
\ln\ \ell_3 \propto{} & \sum_{e=1}^{s_x}\sum_{i=1}^{q}\left[(\alpha q - 1)\ln\left(x_{i(q)e}T_1\right) + \ln\left(1 - x_{i(q)e}\right)\right] + \sum_{e=1}^{s_x}\sum_{i=q+1}^{n}(\alpha(q+1) - 1)\ln\left(x_{i(q+1)e}T_2\right)\\
&+ s_x n\ \ln\ \alpha + s_y m\ \ln\ \beta + \sum_{e=1}^{s_x}\sum_{i=q+1}^{n}\left[\ln\left(1 - x_{i(q+1)e}\right) + (q-1)\ln\left(1 - x_{i(q+1)e}^{\alpha}{T_2}^{\alpha}\right)\right]\\
&+ \sum_{e=1}^{s_x}\sum_{i=1}^{q} q\ \ln\left(1 - x_{i(q)e}^{\alpha}{T_1}^{\alpha}\right) + \sum_{h=1}^{s_y}\sum_{j=1}^{\nu}\left[(\beta\nu - 1)\ln\left(y_{j(\nu)h}N_1\right) + \ln\left(1 - y_{j(\nu)h}\right)\right]\\
&+ \sum_{h=1}^{s_y}\sum_{j=\nu+1}^{m}(\beta(\nu+1) - 1)\ln\left(y_{j(\nu+1)h}N_2\right) + \sum_{h=1}^{s_y}\sum_{j=\nu+1}^{m}\left[\ln\left(1 - y_{j(\nu+1)h}\right) + (\nu-1)\ln\left(1 - y_{j(\nu+1)h}^{\beta}{N_2}^{\beta}\right)\right]\\
&+ \sum_{h=1}^{s_y}\sum_{j=1}^{\nu}\nu\ \ln\left(1 - y_{j(\nu)h}^{\beta}{N_2}^{\beta}\right),
\end{aligned} \tag{15}$$

where $T_1 = (2 - x_{i(q)e}), T_2 = (2 - x_{i(q+1)e}), N_1 = (2 - y_{j(\nu)h})$, and $N_2 = (2 - y_{j(\nu+1)h})$. Hence,

$$\begin{aligned}\frac{\partial \ln \ell_3}{\partial \alpha} &= \frac{n^*}{\alpha} + \sum_{e=1}^{s_x}\sum_{i=1}^{q} q \ln\left(x_{i(q)e}T_1\right) + \sum_{e=1}^{s_x}\sum_{i=q+1}^{n} (q+1)\ln\left(x_{i(q+1)e}T_2\right) \\ &\quad - \sum_{e=1}^{s_x}\sum_{i=1}^{q} \frac{q \ln\left(x_{i(q)e}T_1\right)}{x_{i(q)e}^{-\alpha}T_1^{-\alpha} - 1} + \sum_{e=1}^{s_x}\sum_{i=q+1}^{n} \frac{(q+1)\ln\left(x_{i(q+1)e}T_2\right)}{x_{i(q+1)e}^{-\alpha}T_2^{-\alpha} - 1},\end{aligned} \tag{16}$$

$$\begin{aligned}\frac{\partial \ln \ell_3}{\partial \beta} &= \frac{m^*}{\beta} + \sum_{h=1}^{s_y}\sum_{j=1}^{\nu} \nu \ln\left(y_{j(\nu)h}N_1\right) + \sum_{h=1}^{s_y}\sum_{j=\nu+1}^{m} (\nu-1)\ln\left(y_{j(\nu+1)h}N_2\right) \\ &\quad - \sum_{h=1}^{s_y}\sum_{j=1}^{\nu} \frac{\nu \ln\left(y_{j(\nu)h}N\right)_1}{y_{j(\nu)h}^{-\beta}N_1^{-\beta}} + \sum_{h=1}^{s_y}\sum_{j=\nu+1}^{m} \frac{(\nu-1)\ln\left(y_{j(\nu+1)h}N_2\right)}{y_{j(\nu+1)h}^{-\beta}N_2^{-\beta} - 1}.\end{aligned} \tag{17}$$

We solve "Equations (16) and (17) equal to zero" to take out the ML estimators. Further, we insert the obtained ML estimators in Equation (2) to have an estimator of R.

4.3. Estimation with an Odd Strength and Even Stress Sizes. Here, we get the ML estimator of R under the following configuration: based on the MRSSO, we select observed samples of X from the distribution TL(α); based on the MRSSE, we select observed samples of Y from the distribution TL(β).

Suppose that $X_{i(g)e}$, where $i = 1,\ldots,n$, $e = 1,\ldots,s_x$, $g = [(n+1)/2]$, with sample size ns_x, where n is the odd set size and s_x is the number of cycles, is the observed MRSSO from the distribution TL(α), and that $\{Y_{j(\nu)h}, j = 1,\ldots,\nu; h = 1,\ldots,s_y\} \cup \{Y_{j(\nu+1)e}, j = \nu+1,\ldots,m; h = 1,\ldots,s_y\}$, with even set sizes where $\nu = m/2$, is the observed MRSSE selected from the distribution TL(β). Therefore, the associated likelihood function ℓ_4 is

$$\ell_4 = \prod_{e=1}^{s_x}\prod_{i=1}^{n} f_g\left(x_{i(g)e}\right) \prod_{h=1}^{s_y}\prod_{j=1}^{\nu} f_\nu\left(y_{j(\nu)h}\right) \prod_{h=1}^{s_y}\prod_{j=\nu+1}^{m} f_{\nu+1}\left(y_{j(\nu+1)h}\right), \tag{18}$$

where the PDFs of $X_{i(g)e}$, $Y_{j(\nu)h}$, and $Y_{j(\nu+1)h}$ are as defined before. The LL of the observed data is

$$\begin{aligned}\ln \ell_4 &\propto s_x n \ln \alpha + s_y m \ln \beta + \sum_{e=1}^{s_x}\sum_{i=1}^{n} (\alpha g - 1)\ln\left[x_{i(g)e}\left(2 - x_{i(g)e}\right)\right] + \sum_{e=1}^{s_x}\sum_{i=1}^{n} \ln\left(1 - x_{i(g)e}\right) \\ &\quad + \sum_{e=1}^{s_x}\sum_{i=1}^{n} (g-1)\ln\left(1 - x_{i(g)e}^{\alpha}\left(2 - x_{i(g)e}\right)^{\alpha}\right) + \sum_{h=1}^{s_y}\sum_{j=1}^{\nu} (\beta\nu - 1)\ln\left(y_{j(\nu)h}N_1\right) \\ &\quad + \sum_{h=1}^{s_y}\sum_{j=1}^{\nu} \ln\left(1 - y_{j(\nu)h}\right) + \sum_{h=1}^{s_y}\sum_{j=\nu+1}^{m} (\beta(\nu+1) - 1)\ln\left(y_{j(\nu+1)h}N_2\right) + \sum_{h=1}^{s_y}\sum_{j=\nu+1}^{m} \ln\left(1 - y_{j(\nu+1)h}\right) \\ &\quad + \sum_{h=1}^{s_y}\sum_{j=1}^{\nu} \nu \ln\left(1 - y_{j(\nu)h}^{\beta}N_1^{\beta}\right) + \sum_{h=1}^{s_y}\sum_{j=\nu+1}^{m} (\nu-1)\ln\left(1 - y_{j(\nu+1)h}^{\beta}N_2^{\beta}\right).\end{aligned} \tag{19}$$

Maximizing $\ln \ell_4$ with respect to α and β, we obtain the ML estimators. The partial derivatives of $\ln \ell_4$ with respect to the parameters are given by

$$\frac{\partial \ln \ \ell_4}{\partial\alpha} = \frac{n^*}{\alpha} + \sum_{e=1}^{s_x}\sum_{i=1}^{n} g \ \ln\left[x_{i(g)e}\left(2 - x_{i(g)e}\right)\right] - \sum_{e=1}^{s_x}\sum_{i=1}^{n} \frac{(g-1)\ln\left[x_{i(g)e}\left(2 - x_{i(g)e}\right)\right]}{x_{i(g)e}^{-\alpha}\left(2 - \ x_{i(g)e}\right)^{-\alpha} - 1}, \tag{20}$$

$$\begin{aligned}\frac{\partial \ln \ \ell_4}{\partial\beta} &= \frac{m^*}{\beta} + \sum_{h=1}^{s_y}\sum_{j=1}^{\nu} \nu \ \ln\left(y_{j(\nu)h}N_1\right) + \sum_{h=1}^{s_y}\sum_{j=\nu+1}^{m} (\nu+1)\ln\left(y_{j(\nu+1)h}N_2\right) \\ &\quad - \sum_{h=1}^{s_y}\sum_{j=1}^{\nu} \frac{\nu \ \ln\left(y_{j(\nu)h}N_1\right)}{y_{j(\nu)h}^{-\beta}{N_1}^{-\beta} - 1} + \sum_{h=1}^{s_y}\sum_{j=\nu+1}^{m} \frac{(\nu-1)\ln\left(y_{j(\nu+1)h}N_2\right)}{y_{j(\nu+1)h}^{-\beta}{N_2}^{-\beta} - 1}.\end{aligned} \tag{21}$$

There appear to be no closed form solutions to Equations (20) and (21) when equal with zero. As a result, numerical techniques are used to find the solution.

4.4. Estimation with an Even Strength and Odd Stress Sizes. Here, the estimator of $R = P(Y_{\mathrm{MRSSO}} < X_{\mathrm{MRSSE}})$ is derived, where X is selected from the distribution TL (α) based on the MRSSE and Y is selected from the distribution TL(β) based on the MRSSO. Let $\{X_{i(q)e}, i = 1,\ldots,q; e = 1,\ldots,s_x\} \cup \{X_{i(q+1)e}, i = q+1,\ldots,n;\ e = 1,\ldots,s_x\}$, where $q = n/2$ and $Y_{j(k)h}$ where $j = 1,\ldots,m,\ d = 1,\ldots,s_y$, and $h = [(m+1)/2]$. The likelihood function ℓ_5 of the observed data is given by

$$\ell_5 = \prod_{e=1}^{s_x}\prod_{i=1}^{q} f_q\left(x_{i(q)e}\right)\prod_{e=1}^{s_x}\prod_{i=q+1}^{n} f_{q+1}\left(x_{i(q+1)e}\right)\prod_{h=1}^{s_y}\prod_{j=1}^{m} f_k\left(y_{j(k)h}\right). \tag{22}$$

Therefore, the LL function of ℓ_5 for observed data is

$$\begin{aligned}\ln \ \ell_5 &\propto s_x n \ \ln \ \alpha + s_y m \ \ln \ \beta + \sum_{e=1}^{s_x}\sum_{i=1}^{q}\left[(\alpha q - 1)\ln\left(x_{i(q)e}T_1\right) + \ln\left(1 - x_{i(q)e}\right)\right] + \sum_{e=1}^{s_x}\sum_{i=1}^{q} q \ \ln\left(1 - x_{i(q)e}^{\alpha}T_1^{\alpha}\right) \\ &\quad + \sum_{e=1}^{s_x}\sum_{i=q+1}^{n}\left[(\alpha(q+1) - 1)\ln\left(x_{i(q+1)e}T_2\right) + \ln\left(1 - x_{i(q+1)e}\right)\right] + \sum_{e=1}^{s_x}\sum_{i=q+1}^{n}(q-1)\ln\left(1 - x_{i(q+1)e}^{\alpha}T_2^{\alpha}\right) \\ &\quad + \sum_{h=1}^{s_y}\sum_{j=1}^{m}(\beta k - 1)\ln\left[y_{j(k)h}\left(2 - y_{j(k)h}\right)\right] + \sum_{h=1}^{s_y}\sum_{j=1}^{m}\ln\left(1 - y_{j(k)h}\right) + (k-1)\ln\left(1 - y_{j(k)h}^{\beta}\left(2 - y_{j(k)h}\right)^{\beta}\right).\end{aligned} \tag{23}$$

The ML estimators of both parameters are determined by maximizing ln ℓ_5. The first partial derivatives of α and β are represented by

$$\begin{aligned}\frac{\partial \ln \ \ell_5}{\partial\alpha} &= \frac{n^*}{\alpha} + \sum_{e=1}^{s_x}\sum_{i=1}^{q} q \ \ln\left(x_{i(q)e}T_1\right) + \sum_{e=1}^{s_x}\sum_{i=q+1}^{n}(q+1)\ln\left(x_{i(q+1)e}T_2\right) - \sum_{e=1}^{s_x}\sum_{i=1}^{q}\frac{q \ \ln\left(x_{i(q)e}T_1\right)}{x_{i(q)e}^{-\alpha}{T_1}^{-\alpha} - 1} \\ &\quad + \sum_{e=1}^{s_x}\sum_{i=q+1}^{n}\frac{(q-1)\ln\left(x_{i(q+1)e}T_2\right)}{x_{i(q+1)e}^{-\alpha}{T_2}^{-\alpha} - 1},\end{aligned} \tag{24}$$

$$\frac{\partial \ln \ \ell_5}{\partial\beta} = \frac{m^*}{\beta} + \sum_{h=1}^{s_y}\sum_{j=1}^{m} k \ \ln\left[y_{j(k)h}\left(2 - y_{j(k)h}\right)\right] - \sum_{h=1}^{s_y}\sum_{j=1}^{m}\frac{(k-1)\ln\left[y_{j(k)h}\left(2 - y_{j(k)h}\right)\right]}{y_{j(k)h}^{-\beta}\left(2 - \ y_{j(k)h}\right)^{-\beta} - 1}. \tag{25}$$

The ML estimators of the parameters are constructed by setting Equations (24) and (25) to zero and solving them numerically. Putting the ML estimator of α and β in Equation (2), we obtain the SS reliability estimator.

5. Simulation Results

The results of a simulation are compared with the performance of estimators based on RSS and MRSS. For a wide range of sample sizes and parameter settings, the absolute

TABLE 1: Numerical results for the considered sampling schemes, as well as their efficiency with regard to SRS for even set size for $s_x = s_y = 5$ cycles.

(n^*, m^*)	SRS			(n, m)	RSS			MRSS			Efficiency		
	$\widehat{R}$	AB	MSE		$\widehat{R}$	AB	MSE	$\widehat{R}$	AB	MSE	(R_{RSS}, R_{SRS})	(R_{MRSS}, R_{SRS})	(R_{MRSS}, R_{RSS})
$R = 0.6$, $(\alpha, \beta) = (3, 2)$													
(10,10)	0.58590	0.01410	0.00962	(2,2)	0.59378	0.0062	0.00721	0.58687	0.01313	0.00957	1.334	1.005	0.753
(20,20)	0.57552	0.02448	0.00419	(4,4)	0.59572	0.0043	0.00314	0.61566	0.01566	0.00257	1.334	1.630	1.222
(30,30)	0.58033	0.01967	0.00323	(6,6)	0.59456	0.00544	0.00166	0.60022	0.00022	0.00132	1.946	2.447	1.258
$R = 0.714$, $(\alpha, \beta) = (5, 2)$													
(10,10)	0.66237	0.05192	0.00828	(2,2)	0.71570	0.0014	0.00801	0.71802	0.00374	0.00327	1.034	2.532	2.450
(20,20)	0.67325	0.04103	0.00452	(4,4)	0.70793	0.0064	0.00246	0.70897	0.00531	0.00217	1.837	2.083	1.134
(30,30)	0.67316	0.04113	0.00348	(6,6)	0.71232	0.0020	0.00133	0.71331	0.00097	0.00096	2.617	3.625	1.385
$R = 0.833$, $(\alpha, \beta) = (5, 1)$													
(10,10)	0.77568	0.05765	0.00716	(2,2)	0.82910	0.0042	0.00366	0.83314	0.00020	0.00279	1.956	2.566	1.312
(20,20)	0.78243	0.05090	0.00437	(4,4)	0.83501	0.0017	0.00086	0.83006	0.00327	0.00114	5.081	3.833	0.754
(30,30)	0.78296	0.05037	0.00378	(6,6)	0.82980	0.0035	0.00055	0.82888	0.00445	0.00037	6.873	10.216	1.486
$R = 0.9$, $(\alpha, \beta) = (4, 0.4)$													
(10,10)	0.87219	0.03690	0.00317	(2,2)	0.89599	0.0131	0.00137	0.90395	0.00514	0.00087	2.314	3.644	1.575
(20,20)	0.86806	0.04103	0.00276	(4,4)	0.90907	0.00004	0.00034	0.90762	0.00147	0.00031	8.118	8.903	1.097
(30,30)	0.86770	0.04139	0.00230	(6,6)	0.90665	0.0024	0.00020	0.90703	0.00206	0.00014	11.500	16.429	1.429

Table 2: Numerical results for the considered sampling schemes, as well as their efficiency with regard to SRS for odd set size for $s_x = s_y = 5$cycles.

(n^*, m^*)	SRS			(n, m)	RSS			MRSS			Efficiency		
	$\widehat{R}$	AB	MSE		$\widehat{R}$	AB	MSE	$\widehat{R}$	AB	MSE	(R_{RSS}, R_{SRS})	(R_{MRSS}, R_{SRS})	(R_{MRSS}, R_{RSS})
$R = 0.6$, $(\alpha, \beta) = (3, 2)$													
(15,15)	0.57522	0.02478	0.00575	(3,3)	0.59414	0.00586	0.00496	0.59838	0.00162	0.00482	1.159	1.193	1.029
(25,25)	0.57902	0.02098	0.00353	(5,5)	0.59015	0.00985	0.00181	0.60097	0.00097	0.00172	1.950	2.052	1.052
(35,35)	0.57768	0.02232	0.00280	(7,7)	0.59967	0.00033	0.00107	0.60226	0.00226	0.00100	2.617	2.800	1.070
$R = 0.714$, $(\alpha, \beta) = (5, 2)$													
(15,15)	0.66754	0.04674	0.00635	(3,3)	0.71012	0.00417	0.00355	0.71037	0.00391	0.00309	1.789	2.055	1.149
(25,25)	0.67578	0.03850	0.00361	(5,5)	0.71080	0.00349	0.00158	0.71661	0.00233	0.00180	2.285	2.006	0.878
(35,35)	0.67205	0.04224	0.00339	(7,7)	0.71695	0.00267	0.00103	0.71468	0.00039	0.00063	3.291	5.381	1.635
$R = 0.833$, $(\alpha, \beta) = (5, 1)$													
(15,15)	0.78343	0.04990	0.00509	(3,3)	0.82827	0.00507	0.00175	0.82773	0.00560	0.00147	2.909	3.463	1.190
(25,25)	0.78392	0.04941	0.00390	(5,5)	0.83297	0.00036	0.00076	0.83259	0.00074	0.00074	5.132	5.270	1.027
(35,35)	0.78279	0.05054	0.00362	(7,7)	0.83553	0.00219	0.00044	0.83306	0.00028	0.00034	8.227	10.647	1.294
$R = 0.9$, $(\alpha, \beta) = (4, 0.4)$													
(15,15)	0.86426	0.04484	0.00306	(3,3)	0.90495	0.00414	0.00055	0.90883	0.00026	0.00054	5.564	5.667	1.019
(25,25)	0.86700	0.04210	0.00238	(5,5)	0.91048	0.00139	0.00030	0.90396	0.00513	0.00028	7.933	8.500	1.071
(35,35)	0.86929	0.03980	0.00205	(7,7)	0.90550	0.00359	0.00016	0.90809	0.00100	0.00012	12.813	17.083	1.333

Table 3: Numerical results for the considered sampling schemes, as well as their efficiency with regard to SRS under the following configuration: X and Y have odd and even set sizes, respectively, for $s_x = s_y = 5$cycles.

(n^*, m^*)	SRS			(n, m)	RSS			MRSS			Efficiency		
	$\widehat{R}$	AB	MSE		$\widehat{R}$	AB	MSE	$\widehat{R}$	AB	MSE	$(R_{\text{RSS}}, R_{\text{SRS}})$	$(R_{\text{MRSS}}, R_{\text{SRS}})$	$(R_{\text{MRSS}}, R_{\text{RSS}})$
$R = 0.6$, $(\alpha, \beta) = (3, 2)$													
(15,10)	0.57227	0.02773	0.00742	(3,2)	0.62347	0.02347	0.00737	0.55437	0.04563	0.00931	1.007	0.797	0.792
(15,20)	0.58160	0.01840	0.00478	(3,4)	0.58371	0.01629	0.00410	0.56015	0.03985	0.00528	1.166	0.905	0.777
$R = 0.714$, $(\alpha, \beta) = (5, 2)$													
(15,10)	0.67062	0.04367	0.00722	(3,2)	0.71808	0.00379	0.00435	0.67086	0.04342	0.00674	1.660	1.071	0.645
(15,20)	0.67184	0.04245	0.00512	(3,4)	0.70000	0.01428	0.00347	0.67416	0.04013	0.00419	1.476	1.222	0.828
$R = 0.833$, $(\alpha, \beta) = (5, 1)$													
(15,10)	0.77789	0.05545	0.00621	(3,2)	0.84215	0.00882	0.00230	0.79789	0.03545	0.00445	2.700	1.396	0.517
(15,20)	0.78283	0.05050	0.00477	(3,4)	0.82452	0.00881	0.00111	0.85350	0.02010	0.00130	4.297	3.669	0.854
$R = 0.9$, $(\alpha, \beta) = (4, 0.4)$													
(15,10)	0.86924	0.03985	0.00274	(3,2)	0.90086	0.00823	0.00064	0.89166	0.01743	0.00085	4.281	3.224	0.753
(15,20)	0.86250	0.04659	0.00398	(3,4)	0.91083	0.00173	0.00068	0.88869	0.02040	0.00164	5.853	2.427	0.415

Table 4: Numerical results for the considered sampling schemes, as well as their efficiency with regard to SRS under the following configuration: X and Y have even and odd set sizes, respectively, for $s_x = s_y = 5$cycles.

(n^*, m^*)	SRS			(n, m)	RSS			MRSS			Efficiency		
	$\widehat{R}$	AB	MSE		$\widehat{R}$	AB	MSE	$\widehat{R}$	AB	MSE	(R_{RSS}, R_{SRS})	(R_{MRSS}, R_{SRS})	(R_{MRSS}, R_{RSS})
$R = 0.6$, $(\alpha, \beta) = (3, 2)$													
(10,15)	0.54159	0.05841	0.00838	(2,3)	0.64139	0.04139	0.00733	0.64730	0.04730	0.00650	1.143	1.289	1.128
(20,15)	0.57654	0.02346	0.00499	(4,3)	0.61961	0.01961	0.00423	0.63700	0.03700	0.00460	1.180	1.085	0.920
$R = 0.714$, $(\alpha, \beta) = (5, 2)$													
(10,15)	0.66847	0.04582	0.00687	(2,3)	0.69401	0.02028	0.00557	0.74170	0.02740	0.00450	1.233	1.527	1.238
(20,15)	0.66813	0.04616	0.00557	(4,3)	0.72361	0.00933	0.00255	0.74160	0.02730	0.00270	2.184	2.063	0.944
$R = 0.833$, $(\alpha, \beta) = (5, 1)$													
(10,15)	0.77908	0.05426	0.00642	(2,3)	0.82359	0.00975	0.00195	0.85350	0.02020	0.00200	3.292	3.210	0.975
(20,15)	0.78587	0.04746	0.00413	(4,3)	0.84004	0.00671	0.00117	0.80703	0.02630	0.00226	3.530	1.827	0.518
$R = 0.9$, $(\alpha, \beta) = (4, 0.4)$													
(10,15)	0.87510	0.03399	0.00291	(2,3)	0.89599	0.01310	0.00137	0.91680	0.00770	0.00070	2.124	4.157	1.957
(20,15)	0.86658	0.04252	0.00294	(4,3)	0.91311	0.00402	0.00044	0.92150	0.01240	0.00040	6.682	7.350	1.100

bias (AB), mean square error (MSE), and relative efficiency (RE) criteria are used to investigate the estimated reliability. The following set sizes and number of cycles are taken into account when developing the simulation: (n, m)=(2, 2), (2, 3), (3, 2), (3, 3), (3, 4), (4, 3), (4, 4), (5, 5), (6, 6), (7, 7), and $s_x = s_y = 5$, respectively. As presented earlier, the sample sizes are given by $s_x n$ and $s_y m$ for the RSS and MRSS sampling schemes. Also, (n^*, m^*)=(10, 10), (10, 15), (15, 10), (15, 15), (15, 20), (20, 15), (20, 20), (25, 25), (30, 30), (35, 35) are selected as sample sizes for SRS. The parameter values are determined as (α, β)=(3, 2), (5, 2), (5, 1), (4, 0.4), giving $R = 0.600$, 0.714, 0.833, and 0.933, respectively. From the distributions TL(α) and TL(β), 1000 random samples are generated. In this setting, the definition of efficiency is as follows:

$$\begin{aligned}\text{efficiency}\left(R_{\text{RSS}}, R_{\text{SRS}}\right) &= \frac{\text{MSE}\left(R_{\text{SRS}}\right)}{\text{MSE}\left(R_{\text{RSS}}\right)},\\ \text{efficiency}\left(R_{\text{MRSS}}, R_{\text{SRS}}\right) &= \frac{\text{MSE}\left(R_{\text{SRS}}\right)}{\text{MSE}\left(R_{\text{MRSS}}\right)},\end{aligned} \tag{26}$$

$$\text{efficiency}\left(R_{\text{MRSS}}, R_{\text{RSS}}\right) = \frac{\text{MSE}\left(R_{\text{RSS}}\right)}{\text{MSE}\left(R_{\text{MRSS}}\right)}. \tag{27}$$

Furthermore, the absolute bias is defined by$\text{AB}\left(R_\delta\right) = |R - E\left(R_\delta\right)|, \delta = \text{SRS}, \text{RSS}, \text{MRSS}$.

The ABs and MSEs of the reliability estimates based on the SRS, RSS, and MRSS are summarized in Tables 1–4. They also show the efficiency of the RSS and MRSS-based reliability estimates with respect to the SRS, as well as the efficiency of the MRSS with respect to the RSS, for different sample sizes and distribution parameters.

We can deduce the following from Tables 1–4:

(i) For all scenarios, the reliability estimates under the RSS scheme outperform the corresponding ones under the SRS (see Tables 1–4)

(ii) The reliability estimates under the MRSS scheme outperform the corresponding ones under SRS in most situations, except when X has an odd set size and Y has even set sizes at $R = 0.6$ (see Tables 1–4)

(iii) The reliability estimates under the MRSS scheme outperform the corresponding ones under the RSS in most situations, except at $(n, m) = (2, 2)$ where $R = 0.6$ and at $(n, m) = (4, 4)$ where $R = 0.833$ (see Table 1)

(iv) The reliability estimates under the MRSS scheme outperform than the corresponding ones under the RSS in most situations, except at $(n, m) = (5, 5)$, where $R = 0.714$ (see Table 2)

(v) The reliability estimates under the RSS scheme outperform the corresponding ones under the MRSS for all cases (see Table 3)

(vi) The reliability estimates under the RSS scheme outperform the corresponding ones under the MRSS for all cases for $(n, m) = (2, 3)$ except at $R = 0.833$ while the reliability estimates under the MRSS scheme outperform the corresponding ones under the RSS for all of the situations at $(n, m) = (4, 3)$ except $R = 0.9$ (see Table 4)

6. Conclusions

In this manuscript, we have examined the estimation of the unknown reliability measure $R = P\,[Y < X]$, assuming that X and Y are modeled by independent identically distributed RVs from the TL distribution. We obtain the ML estimator of R in the setting of the SRS or RSS. In the MRSS design, we establish the reliability estimator of R in four situations. In the first and second situations, we obtain the reliability estimator when both X and Y have the same set size. The reliability estimator is derived in the third and fourth situations when the observed samples from the stress distribution have the MRSSO and the observed samples from the strength distribution have the MRSSE, and vice versa. We check the performance of different estimates through numerical studies.

Data Availability

The data are fully included in the article or the mentioned references.

Conflicts of Interest

The authors declare that there are no conflicts of interest.

Authors' Contributions

All authors have contributed equally to this work, and they read and agreed to the published version of the manuscript.

Acknowledgments

This project was funded by the Deanship of Scientific Research (DSR), at King Abdulaziz University, Jeddah, under grant no. KEP–PhD-69-130-42. The authors, therefore, acknowledge with thanks to DSR technical and financial support.

References

[1] S. Nadarajah and S. Kotz, "Moments of some J-shaped distributions," *Journal of Applied Statistics*, vol. 30, no. 3, pp. 311–317, 2003.

[2] S. Kotz and J. R. Van Dorp, *Beyond Beta: Other Continuous Families of Distributions with Bounded Support and Applications*, World Scientific, Singapore, 2004.

[3] M. E. Ghitany, S. Kotz, and M. Xie, "On some reliability measures and their stochastic orderings for the Topp-Leone distribution," *Journal of Applied Statistics*, vol. 32, no. 7, pp. 715–722, 2005.

[4] S. Nadarajah and S. Kotz, "The beta exponential distribution," *Reliability Engineering & System Safety*, vol. 91, no. 6, pp. 689–697, 2006.

[5] D. Vicari, J. R. Van Dorp, and S. Kotz, "Two-sided generalized Topp and leone (TS-GTL) distributions," *Journal of Applied Statistics*, vol. 35, no. 10, pp. 1115–1129, 2008.

[6] A. İ. Genç, "Estimation ofP(X>Y) with topp-leone distribution," *Journal of Statistical Computation and Simulation*, vol. 83, no. 2, pp. 326–339, 2013.
[7] S. M. T. K. MirMostafaee, "On the moments of order statistics coming from the Topp-Leone distribution," *Statistics & Probability Letters*, vol. 95, pp. 85–91, 2014.
[8] S. M. T. K. MirMostafaee, M. Mahdizadeh, and M. Aminzadeh, "Bayesian inference for the Topp-Leone distribution based on lower k-record values," *Japan Journal of Industrial and Applied Mathematics*, vol. 33, no. 3, pp. 637–669, 2016.
[9] H. A. Bayoud, "Admissible minimax estimators for the shape parameter of Topp-Leone distribution," *Communications in Statistics - Theory and Methods*, vol. 45, no. 1, pp. 71–82, 2016.
[10] G. McIntyre, "A method for unbiased selective sampling, using ranked sets," *Australian Journal of Agricultural Research*, vol. 3, no. 4, pp. 385–390, 1952.
[11] K. Takahasi and K. Wakimoto, "On unbiased estimates of the population mean based on the sample stratified by means of ordering," *Annals of the Institute of Statistical Mathematics*, vol. 20, no. 1, pp. 1–31, 1968.
[12] T. R. Dell and J. L. Clutter, "Ranked set sampling theory with order statistics background," *Biometrics*, vol. 28, no. 2, pp. 545–555, 1972.
[13] H. A. Muttlak, "Median ranked set sampling," *Journal of Applied Statistical Science*, vol. 6, pp. 245–255, 1997.
[14] R. A. Johnson, "3 Stress-strength models for reliability," *Handbook of Statistics*, vol. 7, pp. 27–54, 1988.
[15] S. Kotz, Y. Lumelskii, and M. Pensky, *The Stress-Strength Model and its Generalizations: Theory and Applications*, World Scientific, Singapore, 2003.
[16] S. Sengupta and S. Mukhuti, "Unbiased estimation ofP(X > Y) for exponential populations using order statistics with application in ranked set sampling," *Communications in Statistics - Theory and Methods*, vol. 37, no. 6, pp. 898–916, 2008.
[17] H. A. Muttlak, W. A. Abu-Dayyeh, M. F. Saleh, and E. Al-Sawi, "Estimating P (Y<X) using ranked set sampling in case of the exponential distribution," *Communications in Statistics - Theory and Methods*, vol. 39, no. 10, pp. 1855–1868, 2010.
[18] A. S. Hassan, S. Assar, and M. Yahya, "Estimation of R= P [Y<X] for Burr type XII distribution based on ranked set sampling," *International Journal of Basic and Applied Sciences*, vol. 3, no. 3, pp. 274–280, 2014.
[19] A. S. Hassan, S. Assar, and M. Yahya, "Estimation of P (Y<X) for Burr distribution under several modifications for ranked set sampling," *Australian Journal of Basic and Applied Sciences*, vol. 9, no. 1, pp. 124–140, 2015.
[20] F. G. Akgül and B. Şenoğlu, "Estimation of P (X<Y) using ranked set sampling for the Weibull distribution," *Quality Technology & Quantitative Management*, vol. 14, no. 3, pp. 296–309, 2017.
[21] F. G. Akgül, Ş. Acıtaş, and B. Şenoğlu, "Inferences on stress-strength reliability based on ranked set sampling data in case of Lindley distribution," *Journal of Statistical Computation and Simulation*, vol. 88, no. 15, pp. 3018–3032, 2018.
[22] A. Ibrahim Al-Omari, I. M. Almanjahie, A. S. Hassan, and H. F. Nagy, "Estimation of the stress-strength reliability for exponentiated Pareto distribution using median and ranked set sampling methods," *Computers, Materials & Continua*, vol. 64, no. 2, pp. 835–857, 2020.
[23] A. S. Hassan, A. Al-Omari, and H. F. Nagy, "Stress-strength reliability for the generalized inverted exponential distribution using MRSS," *Iranian Journal of Science and Technology Transaction A-Science*, vol. 45, no. 2, pp. 641–659, 2021.

Hindawi
Scientific Programming
Volume 2021, Article ID 3965247, 12 pages
https://doi.org/10.1155/2021/3965247

Research Article

Surface Defect Detection of Seals Based on K-Means Clustering Algorithm and Particle Swarm Optimization

Xiaoguang Li,[1] Juan Zhu ,[2] Haoran Shi,[3] and Zijian Cong[3]

[1]*Changchun Guanghua University, Changchun 130000, China*
[2]*Changchun University of Technology, Changchun 130000, China*
[3]*Changchun University, Changchun 130000, China*

Correspondence should be addressed to Juan Zhu; zhujuan@ccut.edu.cn

Received 7 September 2021; Accepted 18 October 2021; Published 28 October 2021

Academic Editor: Punit Gupta

As an important part of automobile, the quality and safety of automobile engine high-pressure oil circuit seal parts are an important indicator of the manufacturer's production process. In order to improve the detection accuracy and efficiency of seal parts in the traditional production process, the defect detection method on the surface of the seal was studied. A K-Means clustering image segmentation algorithm based on particle swarm optimization was proposed. To detect the surface defects of seals, first, preprocess the seal image. Then, use the SURF algorithm to extract the feature points of the seal image. Finally, according to the particle swarm fitness variance function, select the insertion point calculated by combining particle swarm optimization and K-Means algorithm. Through iteration, optimize the initial clustering center of K-Means algorithm. The efficiency of K-Means algorithm clustering iteration is improved. The test verifies the applicability of the algorithm in the actual process, and it can be used to accurately detect seals. Experimental results show that the detection accuracy rate reaches 98%, which is highly applicable to the actual production.

1. Introduction

As an important part of the automobile engine oil circuit, the high-pressure oil circuit seal of the automobile engine is very important for the entire driving process of the automobile to ensure the integrity of the seal. In the production process, it is of great significance to ensure the accuracy and efficiency of seal defect detection. With the development of industrial automation technology, the application range of machine vision technology has been continuously expanded, and it has achieved greater application and development in the application of industrial product inspection [1]. This article takes automotive engine high-pressure oil circuit seals as the research object and aims at the disadvantages of traditional observer visual inspection, inspector touch, and surface whetstone polishing stampings, which are labor-intensive, time-consuming, low detection accuracy, and efficiency [2]. A machine vision-based surface defect detection system for high-pressure oil circuit seals of automobile engines is established.

Surface defect detection based on machine vision is realized by pattern recognition of surface defect characteristic parameters through image processing algorithm. Pattern recognition includes supervised and unsupervised learning modes. The image features are classified and recognized by constructing a classifier. Zhang Hongjie et al. [3] used principal component analysis to eliminate the cross-correlation between image features. Build a solder joint quality classifier based on minimum risk Bayesian image recognition technology. Effectively evaluate the solder joint quality. In order to improve the reliability and stability of traditional hub defect detection based on X-ray image, Wang and Zhang [4] proposed an automatic hub defect recognition algorithm based on improved fuzzy pattern classification. Classify and grade hub defects. Wiltschi et al. [5] tested the surface quality of steel plate image based on the minimum distance. Pernkopf [6] constructed Bayesian network classifier. The likelihood calculation is completed by the coupled hidden Markov random field. The detection of billet surface defects is realized.

Through the collection and analysis of the seal image data samples, it is found that, during the production process in the factory, the process technology and the cutting and handling of the parts will cause defects such as scratches and melting points on the surface of the seal. Starting from the feature extraction, defect classification, and detection algorithm of the surface defects of the seal, this paper proposes a K-Means clustering image segmentation algorithm based on particle swarm optimization to detect surface defects of seals.

2. Design of the Visual Inspection System

The seal visual defect detection system described in this article mainly includes three modules: image acquisition, image processing, and image display. The functions of each module are shown in Figure 1. The main operation process of the inspection system is to collect the digital image of the seal through the image acquisition module and store the image in the computer memory through the conversion of the photoelectric signal to obtain the real-time image of the target part. Then the image is processed by the image processing software in the image processing module to detect the integrity of the target seal parts. Finally, through the image display module, the defect characteristics of the seal and the result image of the inspection are displayed on the human-computer interaction interface.

The specific experimental process is as follows:

(1) Image acquisition: the first is the construction of the experimental platform. The selected camera and light source are fixed through the bracket, and the height of the camera and the illumination angle of the light source are adjusted according to the designed lighting scheme, so that the camera can collect a clear seal within the field of view. Through the host computer processor, save the collected image data.

(2) Image processing: the image algorithm processing process of automobile engine oil circuit seals includes image preprocessing, image target area feature extraction, and defect area target segmentation. This paper analyzes the characteristics of the seal itself and the characteristics of surface defects and uses the operations of extracting RGB image components, image filtering, and background removal to achieve image preprocessing operations. After that, the SURF (Speeded-Up Robust Features) algorithm is used to extract the feature point data of the image surface, and the initial coordinate data set is established. According to the extracted image feature data, the initial center is optimized by the particle swarm optimization algorithm, and the image segmentation is realized by the K-Means clustering algorithm.

(3) Image display: in the process of experimental image acquisition, combined with the SDK development kit that comes with the camera, a human-computer interaction interface based on MFC is established, which displays the seal image under the camera lens in real time and can display the processed seal image and the processing result, to facilitate the statistics and analysis of experimental results. Figure 2 shows the structure diagram of the image acquisition system of the visual inspection system in this article and the physical picture of the laboratory.

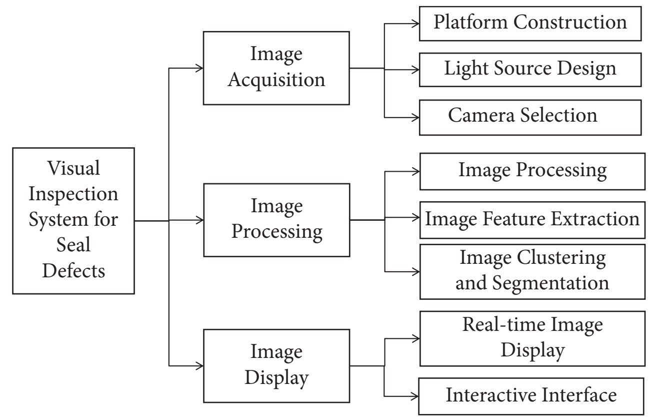

Figure 1: The overall architecture diagram of the visual inspection system.

2.1. Design of the Optical Scheme for Surface Defect Detection. The related hardware content design of the laboratory lighting scheme include the selection of cameras, lenses, and light sources. The specific design principles of the lighting scheme will be introduced below based on optical principles. Figure 3 shows the optical path principle diagram of the scratches on the surface of the seal and the melting point defect under the laboratory ring light.

In the schematic diagram in Figure 3 on the left, position A in the figure is the defect position, which is recessed downward for the complete surface. As shown in the route of light path 2 in the figure, the incident light enters the defect area, and there is a pit at A, making the incident angle change and enter the area of the camera lens photosensitive chip, and it receives a stronger signal and the brightness is stronger. The scratches on the surface of the collected seals have high brightness and obvious defect features. For the schematic on the right, point B in the figure is the melting point defect area. After being illuminated by the ring light source shown in the figure, the melting point of the defect in the image can make the light path reflect vertically into the lens area, and the melting point area is brighter.

2.2. Image Preprocessing. For seals under experimental illumination, light reflection is easily caused by the influence of their own metal properties, forming a bright area on the surface of the seal, which affects the detection of defect features. Therefore, the pixel value of the seal image is first transformed through the image inversion, and then the B color component of the RGB image of the seal is extracted to highlight the two defect features on the surface of the seal. The result is shown in Figure 4.

In order to effectively extract the characteristic information of the surface of the seal image, it is necessary to perform further filtering processing on the seal image to

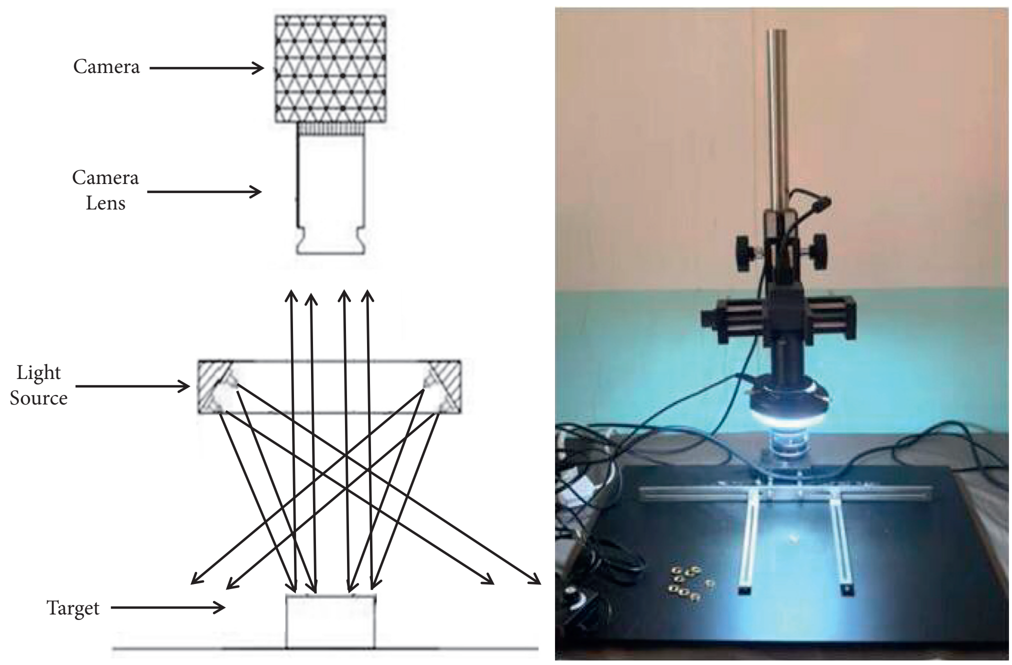

Figure 2: Schematic diagram and physical image of the image acquisition system.

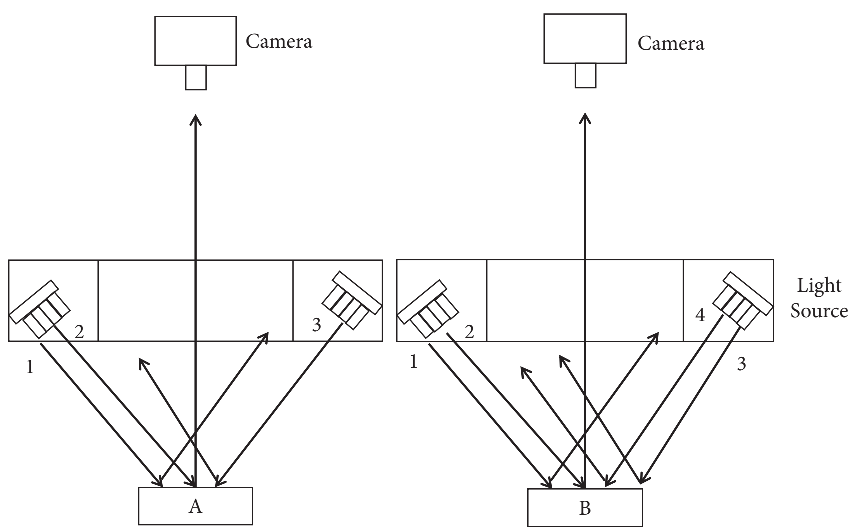

Figure 3: Schematic diagram of the defect lighting optical path.

Figure 4: B component image of the RGB image. (a) Scratches. (b) Melting point.

reduce the noise information introduced by the environment and the equipment itself as much as possible and obtain high-quality sample images. Comparing the advantages and disadvantages of several commonly used filtering operations, such as two linear filtering methods, mean filtering, and Gaussian filtering, the filtering operation of the target image is realized through the principle of averaging, which is easy to filter out the boundary information of the image. But it is not conductive to the image feature information extraction [7]. Therefore, consider the use of a nonlinear median filtering method. The filtered image is shown in Figure 5.

Generally, the quality of image filtering is evaluated by calculating the similarity before and after image processing. The parameters commonly used in image similarity calculation include mean absolute error (MAE), root mean square error (MSE), normalized mean square error (NMSE), signal-to-noise ratio (SNR), and peak signal-to-noise ratio (PSNR) [8]. This paper compares the filtering effects of the two templates of median filtering by calculating the values of the root mean square error (MSE), peak signal-to-noise ratio (PSNR), and signal-to-noise ratio (SNR) before and after image processing.

The root means square error (MSE) calculation formula of the image is shown as follows:

$$\mathrm{MSE} = \frac{1}{M \times N} \sum_{i=1}^{M} \sum_{j=1}^{N} \left(f(i,j) - g(i,j) \right)^2, \quad (1)$$

where $f(i,j)$ and $g(i,j)$, respectively, represent the original image before and after filtering and the image to be evaluated. M and N, respectively, represent the length and width of the two images before and after processing, and the length and width of the two images. The dimensions are the same.

The formula for calculating the peak signal-to-noise ratio (PSNR) is as follows:

$$\begin{aligned} \mathrm{PSNR} &= 10 \log_{10} \frac{Q^2 \; M \times N}{\sum_{i=1}^{M} \sum_{j=1}^{N} \left(f(i,j) - g(i,j) \right)^2} \\ &= 10 \log_{10} \frac{Q^2}{MSE} = 10 \log_{10} \frac{2^n - 1}{MSE}. \end{aligned} \quad (2)$$

Q is the gray level of the image pixel, generally 255; n is the binary digits used by a pixel, generally 8 bits.

The signal-to-noise ratio (SNR) formula is as follows:

$$\mathrm{SNR}(dB) = 10 \log_{10} \frac{\sum_{x=1}^{M} \sum_{y=1}^{N} f(x,y)^2}{\sum_{x=1}^{M} \sum_{y=1}^{N} \left(f(x,y) - g(x,y) \right)^2}. \quad (3)$$

Here, $f(x,y)$ is the sum of the original image $g(x,y)$ and the noise signal $e(x,y)$ the MSE, PSNR and SNR of Scratches and Melting point is shown in Table 1.

Compare the calculation results in the table, where the root mean square error calculates the mean square value of the image before and after the filtering process, and judge the degree of distortion of the processed image from this. The lower the root mean square error value, the smaller the difference between the corresponding two images, and the less the distortion of the image. The peak signal-to-noise ratio is calculated by the ratio of the maximum signal amount of the image to the noise intensity. The higher the value of the peak signal-to-noise ratio [9], the closer the quality between the two images before and after filtering. The signal-to-noise ratio is used to compare the qualities of the two images before and after the filtering operation. The larger the value of the signal-to-noise ratio, the better the image quality after filtering. Therefore, this paper selects a filter template with a size of 3×3 to filter the seal image.

2.3. Feature Extraction of the Seal Image Surface. The SURF algorithm is a local feature point detection and description algorithm, proposed by Herbert Bay. SURF is an improvement on the SIFT (Scale-Invariant Feature Transform) algorithm proposed by David Lowe in 1999. It improves the execution efficiency of the algorithm and provides the algorithm for its application in real-time computer vision systems [10, 11]. The basic steps of the SURF algorithm for extracting image feature points are the same as the SIFT algorithm, but the SURF algorithm proposes an improvement to the SIFT algorithm feature extraction and description method and adopts a more efficient method. The algorithm implementation process is as follows.

2.3.1. Construction of the Hessian Matrix to Generate the Feature Points of the Image. The construction process of the Hessian matrix is equivalent to the Gaussian convolution in the SIFT algorithm. The purpose is to generate a relatively stable feature point in the target image to prepare for the feature extraction below. The function is similar to that of Laplacian and Canny edge detection. *Edge Features*. The Hessian matrix is a square matrix composed of the second-order partial derivatives of a multivariate function. It describes the local curvature of the function. It was proposed by the German mathematician Ludwin Otto Hessian in the 19th century [12, 13].

Set an input digital image $f(x,y)$, and its Hessian matrix is as follows:

$$H(f(x,y)) = \begin{bmatrix} \dfrac{\partial^2 f}{\partial x^2} & \dfrac{\partial^2 f}{\partial x \, \partial y} \\ \dfrac{\partial^2 f}{\partial x \, \partial y} & \dfrac{\partial^2 f}{\partial y^2} \end{bmatrix}. \quad (4)$$

Construct a Hessian matrix for the image after Gaussian filtering and convolution, which is expressed as

$$H(x,\sigma) = \begin{bmatrix} L_{xx}(x,\sigma) & L_{xy}(x,\sigma) \\ L_{xy}(x,\sigma) & L_{yy}(x,\sigma) \end{bmatrix}. \quad (5)$$

When the discriminant of the Hessian matrix takes the local maximum, it means that the current point takes the extreme value among the pixels in the surrounding neighborhood, and the coordinates of the image feature points can be located. In the description of discrete digital images, the

(a) (b)

Figure 5: The filtered image. (a) Scratches. (b) Melting point.

Table 1: Comparison of the effects of the two templates of median filtering.

Defect category	Template size	MSE	PSNR	SNR
Scratches	3×3	291.6471	23.4822	22.5117
	5×5	284.5962	23.5885	22.6180
Melting point	3×3	100.9967	28.0877	27.0636
	5×5	149.3811	26.3878	25.3637

Table 2: Principles of image defect classification.

Characteristic parameters	Classification rules	Classification result
Dispersion and rectangularity	Dispersion <2.05 Rectangularity <7.17 Aspect ratio <6.05	Scratches
Rectangularity and aspect ratio	Rectangularity <3.56 Aspect ratio <2.28	Melting point

first derivative is defined as the gray level difference of adjacent pixels:

$$D_x = f(x+1, y) - f(x, y). \quad (6)$$

The second derivative is the second derivative of the first derivative:

$$\begin{aligned} D_{xx} &= [f(x+1, y) - f(x, y)] - [f(x, y) - (x-1, y)] \\ &= f(x+1, y) + f(x-1, y) - 2\times f(x, y). \end{aligned} \quad (7)$$

On the other hand, look at the discriminant of the Hessian matrix, which is actually the second-order partial derivative in the horizontal direction of the current point multiplied by the second-order partial derivative in the vertical direction and then the quadratic of the horizontal and vertical second-order partial derivatives of the current point:

$$\det(H) = D_{xx}\times D_{yy} - D_{xy}\times D_{xy}. \quad (8)$$

In order to improve the calculation speed, the Gaussian filter in the SIFT algorithm is approximately replaced by a box filter in the SURF algorithm, and a weighting coefficient ω is added to balance the error caused by the box filter approximation [14]. The value of ω is approximately 0.9.

$$\det(H) = D_{xx}\times D_{yy} - \left(0.9\times D_{xy}\right)^2. \quad (9)$$

The schematic diagrams of Gaussian filter and box filter are shown in Figure 6. Figure 6(a) shows the value of the second derivative of the Gaussian filter template in the vertical direction of the image D_{yy} and D_{xy}. Figure 6(b) shows the result of the approximate replacement of the box filter. The pixel value of each color area is shown in the figure.

2.3.2. Construction of Scale Space. Expressed by the algorithm pyramid, in the SIFT algorithm, the original image is continuously Gaussian smoothing and downsampling, and the Gaussian blur coefficient is gradually increasing. In the SIFT algorithm, the image of the next layer is highly dependent on the image of the previous layer, and the size of the image needs to be reset to half of the previous layer, but the image size in the same layer is the same, which makes the algorithm process more computationally expensive. SURF is the opposite. While keeping the original image unchanged, the template size and blur coefficient of the box filter gradually increase, as shown in Figure 7.

2.3.3. Precise Positioning of Feature Points. The steps of locating feature points in SURF algorithm and SIFT algorithm are the same. Add preset extreme points to filter feature points, and discard smaller feature points. In the detection process, the pixels processed by the Hessian matrix are compared with the remaining points in the own scale layer and the points in the upper and lower scale layers to

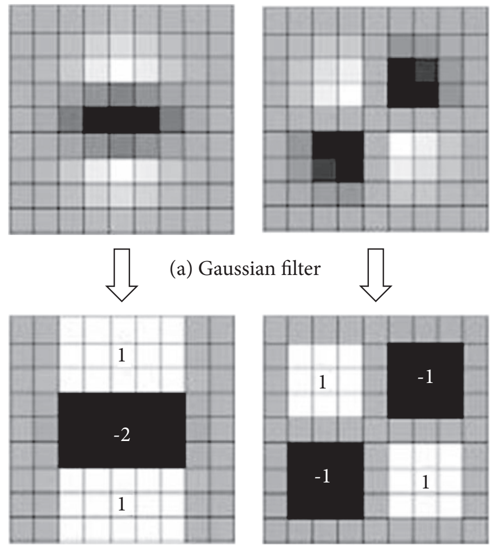

(a) Gaussian filter

(b) Box filter

Figure 6: Schematic diagram of Gaussian filter and box filter. (a) Gaussian filter. (b) Box filter.

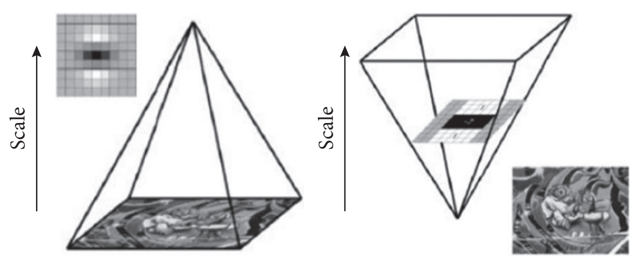

Figure 7: SIFT and SURF algorithm pyramid.

realize the preliminary positioning of the key points, and then screen the wrong and weaker key points, and get the final feature point. Figure 8 shows the detection principle of the 3×3 filter.

2.3.4. Determination of the Main Direction. In order to have rotation invariance, each feature point needs to be assigned a reproducible direction [15]. The SIFT algorithm uses the histograms of the directions near the feature points and selects the largest and occupies a larger proportion of the directions as the main direction. The SURF algorithm first counts the total amount of characteristic responses of Haar wavelets in the horizontal and vertical directions of all feature points in the 60-degree fan-shaped area, then rotates the fan-shaped area to count the characteristic responses of the Haar wavelet in the entire circular area, and finally selects the longest in the fan-shaped direction. The vector direction locates the main direction of the feature point [16]. The whole process is shown in Figure 9.

2.3.5. SURF's Feature Point Descriptor. First divide a rectangular area with a feature scale of 20 in the feature area, rotate it to the main direction of the feature point, then divide the rectangular area into 4×4 subareas along the main direction, and use the Haar template with a scale of 2 to calculate each subarea. Wavelet response values are within the range. Count the wavelet response values of $\sum dx, \sum |dx|, \sum dy, \sum |dy|$ as the feature vector of the subregion.

$$V_i = \left[\sum dx, \sum |dx|, \sum dy, \sum |dy|\right]. \tag{10}$$

Here, $\sum dx$ represents the sum of Haar wavelet features in the horizontal direction; $\sum |dx|$ represents the sum of absolute values of Haar wavelet features in the horizontal direction; $\sum dy$ represents the sum of Haar wavelet features in the vertical direction; $\sum dy$ represents the sum of absolute value of Haar wavelet features in the vertical direction [17]; and Vi represents the vector of each subregion. Since the square area contains $4*4$ subareas, the feature descriptors of SURF have a total of $4 * 4 * 4$ dimensional vectors, as shown in Figure 10.

The feature points on the surface of the seal are extracted by the SURF algorithm, as shown in Figure 11.

Figure 11(a) is the origin image of seal with scratch, Figure 11(b) is the feature of scratch, Figure 11(c) is the original image of seal with melting point, and Figure 11(d) is the feature of melting point. From the experimental result image, it can be seen that the feature points of the image area can be effectively extracted by the SURF algorithm, and the

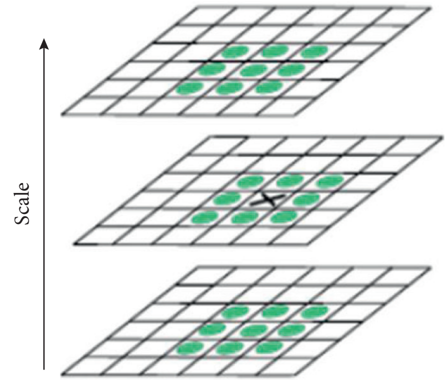

Figure 8: Feature point positioning.

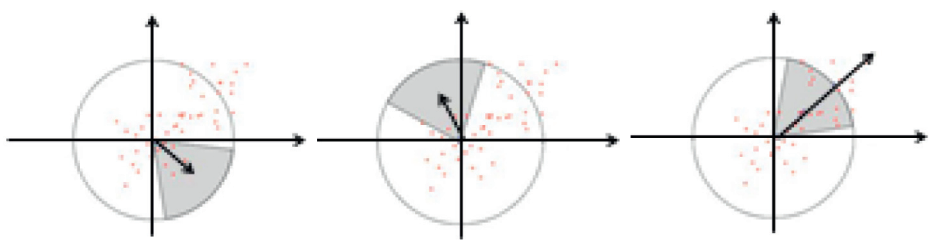

Figure 9: Determination of the main direction of feature points.

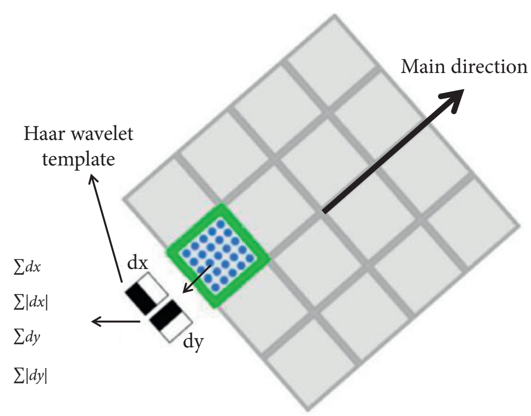

Figure 10: The structure of the SURF feature descriptor.

(a) (b) (c) (d)

Figure 11: Image feature point extraction based on SURF algorithm.

coordinate values of the feature points in the image can be obtained. Provide numerical values for the following particle swarm optimization, and select the initial clustering center of K-Means clustering image segmentation.

3. Research of Image Segmentation Algorithm

3.1. K-Means Clustering Algorithm. Under the experimental lighting of the seal, the pixel distribution on the surface of the collected seal image is uneven. Compared with the image segmentation method based on threshold and edge, the K-Means algorithm is a clustering algorithm based on partition, which calculates the distance between clustering objects. The Euclidean distance judges the similarity between cluster objects [18, 19]. The larger the Euclidean distance, the higher the similarity between cluster objects, and the easier it is to be classified into the same category; otherwise, the opposite is true. Therefore, this paper uses K-Means clustering and segmentation to realize the detection of the surface defect area of the seal.

Generally speaking, the K-Means algorithm process is as follows.

If we define the input sample set $D = \{x_1, x_2, \ldots x_m\}$, the number of clusters is k, and the maximum number of iterations is N; the output is the class division $C = \{C_1, C_2, \ldots C_k\}$:

(1) Randomly select k samples from the sample data set D as the initial k cluster center vectors: $\{\mu_1, \mu_2, \ldots, \mu_k\}$.

(2) For $n = 1, 2, \ldots, N$:

  (1) Initialize the class division C as $C_t = \varnothing$, $t = 1, 2, \ldots k$.

  (2) Let $i = 1, 2, \ldots, m$, calculate the distance between sample x_i and each cluster center vector $\mu_j\,(j = 1, 2, \ldots k)$:

$$d_{ij} = x_i - \mu_{j2}^{2}. \tag{11}$$

$$C_{\lambda_i} = C_{\lambda_i} \cup \{x_i\}. \tag{12}$$

  Mark the sample x_i with the smallest distance from the cluster center as d_{ij}, and its corresponding category is λ_i, and update the output category by

$$C_{\lambda_i} = C_{\lambda_i} \cup \{x_i\}.$$
$$\mu_j = \frac{1}{\left|C_j\right|} \sum_{x \in C_j} x. \tag{13}$$

  (3) Let $j = 1, 2, \ldots, k$, and divide all sample points in the output class C_j by formula (13) to recalculate new cluster centers:

$$\mu_j = \frac{1}{\left|C_j\right|} \sum_{x \in C_j} x. \tag{14}$$

  (4) If the cluster center vectors of all k samples have not changed, repeat step (3).

  Mark the sample x_i with the smallest distance from the cluster center as d_{ij}, and its corresponding category is λ_i, and update the output category by

$$C_{\lambda_i} = C_{\lambda_i} \cup \{x_i\}.$$
$$\mu_j = \frac{1}{\left|C_j\right|} \sum_{x \in C_j} x. \tag{15}$$

  (3) Let $j = 1, 2, \ldots, k$, and divide all sample points in the output class C_j by formula (13) to recalculate new cluster centers:

$$\mu_j = \frac{1}{\left|C_j\right|} \sum_{x \in C_j} x. \tag{16}$$

  (4) If the cluster center vectors of all k samples have not changed, repeat step (3).

  (3) Let $j = 1, 2, \ldots, k$, and divide all sample points in the output class C_j by formula (13) to recalculate new cluster centers:

$$\mu_j = \frac{1}{\left|C_j\right|} \sum_{x \in C_j} x. \tag{17}$$

  (4) If the cluster center vectors of all k samples have not changed, repeat step (3).

(3)Output the result of class division: $C = \{C_1, C_2, \ldots C_k\}$.

According to the process of the K-Means algorithm, the clustering process of the K-Means algorithm is easily affected by the initial cluster center, and it is easy to fall into the local optimum during the clustering iteration process. In order to improve the shortcomings of the K-Means algorithm, this paper introduces a particle swarm optimization algorithm to optimize the initial center and iterative process of the K-Means algorithm to improve the clustering accuracy and computational efficiency of the original algorithm.

3.2. Particle Swarm Optimization Algorithm. The basic idea of the particle swarm optimization algorithm is to simulate the migration and gathering behavior of a flock of birds in the process of foraging [20, 21]. Each individual in the flock of birds is regarded as a particle (particles have only two attributes: speed and position). The collection of individuals is the population. The specific calculation process is as follows:

(1) Initialization: at the beginning of the algorithm, each particle is given a random initial position and velocity to form an initial population.

(2) Find the individual extreme value and the global optimal solution: calculate the fitness value of each particle according to the defined fitness function, and

filter out a global value by comparing the fitness value corresponding to the historical best position, which is called the current iteration number, the optimal solution. Then, the iterative calculation process is repeated, compared with the previously recorded global optimal value, and the individual extreme value and the global optimal solution of the search space are updated.

(3) The formula for speed and position update is as follows:

$$\begin{aligned} V_{id} &= \omega V_{id} + C_1 \text{random}(0,1)\left(P\,\text{best}_{id} - X_{id}\right) \\ &\quad + C_2 \text{random}(0,1)\left(g\,\text{best}_d - X_{id}\right), \\ X_{id} &= X_{id} + V_{id}. \end{aligned} \tag{18}$$

Here, $\omega\,(\omega \geq 0)$ represents the inertia factor. When the value of ω is large, the local optimization ability and global optimization ability of the algorithm are stronger; when the value of ω is small, the local optimization ability of the algorithm is stronger. The global optimization capability is the opposite. Therefore, the local optimization performance and global optimization performance of the algorithm flow can be adjusted by adjusting the size of ω. C_1 and C_2 represent acceleration constants, C_1 represents the individual learning factor of each particle in the search space, and C_2 represents the social learning factor of each particle in the search space. Generally, take $C_1 = C_2 \in [0\ ,\ 4]$. Random (0,1) represents a random number on the interval [0,1], $P\,\text{best}_{id}$ represents the d-th dimension of the individual extreme value of the i-th variable, and $g\text{best}_d$ represents the d-th dimension of the global optimal solution. V_{id} and X_{id}, respectively, represent the d-th dimension component of the flight velocity vector and position vector of the iterated particle i.

Termination conditions are as follows:

(1) Reach the set number of iterations.

(2) The difference between the algebras satisfies the minimum limit

3.3. K-Means Clustering Algorithm Based on Particle Swarm Optimization. Comparing the calculation processes of the above two intelligent algorithms, in order to achieve a reasonable combination of the two algorithm principles to achieve efficient segmentation and recognition of seal images, a K-Means clustering image segmentation method based on particle swarm optimization is proposed. The algorithm principles are as follows.

First, by extracting the feature points on the surface of the seal image, the coordinate data of the feature points on the surface of the seal image is obtained, and the coordinates of all the feature points are regarded as a data set. The advantage of the particle swarm optimization algorithm is that it can search for the global optimal value in the entire image space. The particle swarm algorithm is used to optimize the calculation of the seal image feature coordinate data set, and the optimal value of the coordinate data of the surface defect area of the seal can be obtained, and the feature point data coordinate closest to the optimal solution is selected as the initial of the K-Means clustering algorithm. For the cluster center, the number of cluster categories is determined by the number of optimal solutions after the final optimization. At the same time, the clustering iteration process of the K-Means algorithm improves the shortcomings of the slower convergence speed of the particle swarm algorithm in the later stage and improves the computational efficiency of the algorithm in the later stage [20]. According to the relevant references, the particle swarm algorithm does not need to perform clustering operations during the global search process. It is necessary to start the clustering process of the K-Means algorithm when the particle swarm algorithm reaches the convergence of the initial data processing and start the local search. Among them, the starting point of particle swarm algorithm convergence needs to be judged based on the overall change of the fitness of all particles. The criterion function for evaluating the clustering effect of the K-Means algorithm is used as the fitness function for evaluating the particle position performance of the particle swarm optimization algorithm, and the fitness value is used to determine the quality of the k clustering centers corresponding to the particle position in the particle swarm optimization algorithm [22]. The fitness function $f(x)$ can be defined as

$$f(x) = \sum_{j=1}^{k}\left(\sum_{x_i \in c_j} x_i - z_j\right). \tag{19}$$

Here, $f(x)$ represents the value of the fitness function when the particle position is x, $C_j\,(1 \leq j \leq k)$ represents the jth class in the clustering calculation process, Z_j represents the cluster center of the cluster category C_j, and X_i represents the data sample in the feature data set. The smaller the fitness value, the tighter the combination of the data sample objects within the class, and the better the effect of the clustering algorithm. When the particle i is in the $t+1$th iteration, if $f(x_i(t+1)) < f(p_{\text{best}_i}(t))$, then $p_{\text{best}_i}(t+1) = x_i(t+1)$; otherwise, $p_{best_i}(t+1) = p_{\text{best}_i}(t)$. If $\min f(p_{\text{best}_i}(t+1)) < f(G_{\text{best}}(t))$, then $G_{\text{best}}(t+1) = p_{\text{best}_{\min}}(t+1)$; otherwise, $G_{\text{best}}(t+1) = G_{\text{best}}(t)$.

The overall fitness variance is defined as

$$\sigma^2 = -\sum_{i=1}^{n}\left(\frac{f_i - f_{\text{avg}}}{f}\right)^2. \tag{20}$$

Here, n is the number of particles; f_i is the fitness value of the i-th particle; f_{avg} is the current average fitness of the particle swarm. When $\sigma^2 < m < m$, m is a certain threshold (20-30), indicating that the particle swarm optimization algorithm has entered the convergence stage and can start to execute the subsequent K-Means clustering algorithm to achieve the target seal defect area segmentation. The processing effect of the seal image is shown in Figure 12. Figures 12(a) and 12(b) are the seals with scratch. Figures 12(c) and 12(d) are seals with melting point.

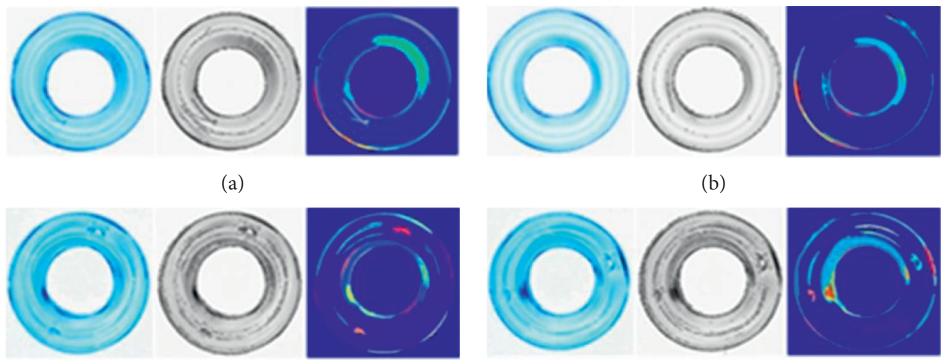

(a) (b)

(c) (d)

Figure 12: Image segmentation result image.

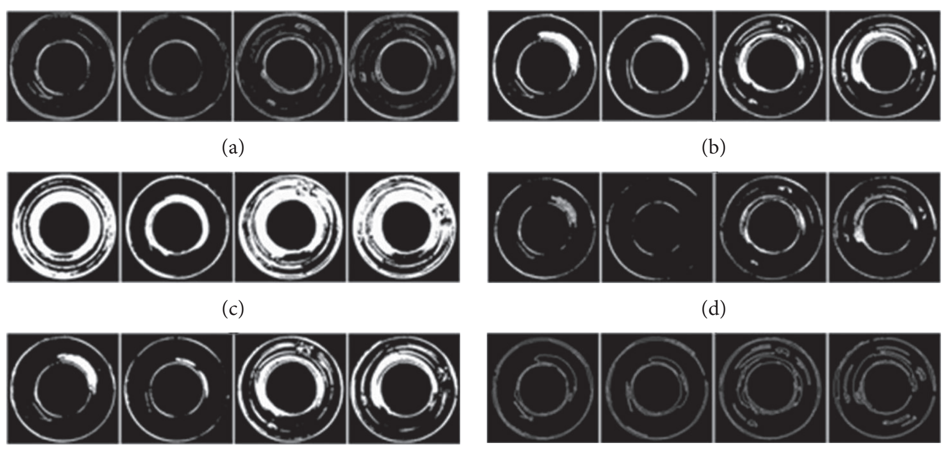

(a) (b)

(c) (d)

(e) (f)

Figure 13: Comparison of this algorithm with other image segmentation algorithms.

3.4. Comparison of Various Image Segmentation Algorithms. The image segmentation method proposed in this paper and several common image segmentation algorithms process the seal image as shown in Figure 13.

Figure 13(a) is scale morphological image segmentation; Figure 13(b) is histogram threshold segmentation; Figure 13(c) is OTSU threshold segmentation; Figure 13(d) is image segmentation based on neural network; Figure 13(e) is traditional K-Means clustering algorithm image segmentation; Figure 13(f) shows the K-Means clustering image segmentation method based on particle swarm optimization proposed in this paper. Combining the result image to analyze the advantages and disadvantages of several image segmentation algorithms, the segmentation algorithm proposed in this paper can accurately segment the defect area of the seal image and realize the defect detection of defective seal parts.

According to the comparison of the results of several image segmentation algorithms, different image segmentation algorithms have different advantages and disadvantages [23]. The scale morphology method is more accurate in the division and positioning of the feature area on the surface of the seal. The feature area is segmented obviously, but there are defects such as discontinuity in the segmentation area and more noise points; the histogram threshold segmentation is greatly affected by the threshold value, and the threshold difference is relatively large. Large area segmentation is more obvious, with less noise; OTSU threshold segmentation method extracts the outline of the entire image more complete, but it is not obvious to extract the surface defect feature of the seal, and the threshold range has a greater impact; image segmentation based on neural network has a greater impact on the image details. Feature segmentation is more obvious, which can separate the feature area of the seal surface defect separately, but it is greatly affected by the pixel value and neural network parameter settings, and some features cannot be recognized;

Figure 14: Defect inspection result image.

Table 3: Test and inspection situation of automobile engine oil circuit seals.

Type of defect	Number of inspections	Number of errors	Accuracy (%)	Time (s)
Scratches	50	1	98	6
Melting point	50	1	98	6

the traditional K-Means clustering segmentation algorithm is affected by the initial clustering center. The image segmentation algorithm proposed in this paper uses the particle swarm algorithm to optimize the selected initial clustering center and improves the convergence speed of the later calculation of the particle swarm algorithm through clustering iteration. The algorithm in this paper has good continuity, high integrity, and less noise in the segmentation of the surface feature area of the seal. It can clearly identify the defect area on the surface of the seal.

4. Analysis of Results

The K-Means clustering segmentation algorithm combined with particle swarm optimization divides the seal image into several independent regions with their own characteristics and uses colors to mark the different regions. Analyze the characteristic parameter attributes of seal defects (rectangularity, dispersion, and aspect ratio), extract the characteristic parameters of different color areas of the image after segmentation through the feature expression function, and screen out the defect characteristic areas of the seal that meet the defect judgment value to achieve defect sealing. The results of the inspection of parts are shown in Figure 14. Principles of image defect classification is shown in Table 2.

After the system platform based on the machine vision defect detection system is built, it is verified through experiments whether the various indicators of the vision detection system in this paper are in line with the actual production. In this test, 50 defect samples of seals, including scratches, melting point, oxidation, and edge contour defects, were selected. The sample test was carried out by mixing several types of defective seal parts. The results are shown in Table 3.

From the inspection results of the samples, the detection accuracy of the visual inspection system in this paper is 98% for the surface defects of the seals. The reasons for the error in the results are as follows: the image data of the collected test samples is poor, and when there are many bright areas on the surface of the seal under the influence of ambient light, it is easy to determine the scratches and melting point and the high light area on the surface of the seal for the defective part.

5. Conclusion

According to the characteristics of high-pressure oil circuit seals of automobile engines, this paper proposes a K-Means clustering algorithm image segmentation method based on particle swarm optimization for the scratches and melting point defects on the surface of the seals and realizes the image segmentation of the seals. *Detection of Defects*. By extracting the RGB image color component image of the seal and image filtering, the seal image is preprocessed; after that, the feature points of the seal image are extracted, and the algorithm ideas proposed in this paper are used to realize the identification of the surface defect area of the seal. After testing, the detection accuracy rate reaches 98%, which is highly applicable to actual production.

Data Availability

No data were used to support this study.

Conflicts of Interest

The authors declare that they have no conflicts of interest.

Acknowledgments

This work was supported by the Department of Science and Technology of Jilin Province (20200401134GX) and Development and Reform Commission of Jilin Province (2020C019-8 and 2020C018-3).

References

[1] X. Zheng and B. Liu, "Surface defect detection of aluminum die castings using machine vision," *Journal of Huaqiao University*, vol. 37, no. 2, pp. 139–144, 2016.

[2] W. Zhang, "The development of machine vision technology and its industrial application," *Infrared*, no. 2, pp. 11–17, 2006.

[3] H. Zhang, J. Zhang, and X. Sui, "Spot welding quality evaluation based on Bayesian image pattern recognition technology," *Journal of welding*, vol. 35, no. 1, pp. 109–112+118, 2014.

[4] Q. Wang and C. Zhang, "Research on defect detection technology of automobile hub casting based on pattern recognition," *Casting technology*, vol. 38, no. 12, pp. 2889–2891+2899, 2017.

[5] K. Wiltschi, A. Pinz, and T. Lindeberg, "An automatic assessment scheme for steel quality inspection," *Machine Vision and Applications*, vol. 12, no. 3, 2000.

[6] F. Pernkopf, "Detection of surface defects on raw steel blocks using Bayesian network classifiers," *Pattern Analysis & Applications*, vol. 7, no. 3, 2005.

[7] P. Hu, *Research on the Method of Judging Traffic Line Pressure Based on Machine Vision*, Xi'an University of Science and Technology, Xi'an, China, 2017.

[8] Z. Chen and Z. Hu, "Remote sensing image denoising based on improved wavelet threshold algorithm," *Bulletin of Surveying and Mapping*, vol. 0, no. 4, pp. 28–31, 2018.

[9] K. Zhang, *Research on Remote Sensing Image Fusion Algorithm Based on NSST Transform*, Northern University for Nationalities, Ningxia, China, 2018.

[10] H. Bay, T. Tuytelaars, and L. V. Gool, *SURF: Speeded up Robust features*, Springer-Verlag, Berlin, Germany, 2006.

[11] Q. Chen, M. Li, C. Luo, J. Zhou, P. Huang, and L. Lei, "Research on image feature point extraction and matching

algorithm in visual SLAM," *Modern Manufacturing Engineering*, no. 10, pp. 135–139+134, 2019.

[12] B. Xu, *Research on Region Recognition Based on UAV and Image Feature Extraction*, Tianjin University, Tianjin, China, 2018.

[13] Q. Zhang, "Application research of SURF feature matching in cloud base height measurement," *Shanxi Architecture*, vol. 45, no. 6, pp. 203–205, 2019.

[14] Z. Zhou, F. Yuan, K. Zhang, and Z. Wu, "Image matching method combining SURF and FLANN algorithm," *Intelligent Computers and Applications*, vol. 9, no. 6, pp. 160–163+167, 2019.

[15] L. Guo, J. Li, Y. Zhu, and Y. Ma, "Fast image matching algorithm based on multi-scale FAST-9," *Computer Engineering*, vol. 38, no. 12, pp. 208–210+217, 2012.

[16] Z. Lan, L. Zhan, and W. Li, "Research on lane image sequence mosaic based on SURF and best stitching line," *Journal of Chongqing Jianzhu University*, vol. 38, no. 10, pp. 13–18, 2019.

[17] L. Fan and F. Yu, "Human behavior recognition based on global and local features," *Progress in Laser and Optoelectronics*, vol. 57, no. 2, pp. 83–89, 2020.

[18] S. Bao, L. Sun, X. Zheng, and L. Guo, "Density peak clustering algorithm based on shared nearest neighbor similarity," *Journal of Computer Applications*, vol. 38, no. 6, pp. 1601–1607, 2018.

[19] Y. Cheng, *Research on Chinese Short Text Clustering Algorithm*, Jilin University, Jilin, China, 2016.

[20] F. Wang, *Self-organized Control of Multiple Drones Based on Particle Swarm Optimization Algorithm*, Nanjing University of Posts and Telecommunications, Jiangsu, China, 2019.

[21] H. Hao and T. Zhang, "Research on unit load optimization based on improved particle swarm algorithm," *Science and Technology Innovation Herald*, vol. 16, no. 28, pp. 106–108, 2019.

[22] X. Xie, *Research on Clustering Algorithm Based on Improved Particle Swarm Optimization Algorithm*, Guangxi University, Nanning, China, 2013.

[23] H. Yuran, *Research on Infrared Image Segmentation Based on Swarm Intelligence Algorithm*, North China University of Water Conservancy and Hydropower, Zhengzhou, China, 2019.

Hindawi
Scientific Programming
Volume 2021, Article ID 5166993, 5 pages
https://doi.org/10.1155/2021/5166993

Research Article

Artificial Intelligence Applications in the New Model of Logistics Development Based on Wireless Communication Technology

Shuaiqi Wang

School of Transportation, Southeast University, Nanjing 211189, China

Correspondence should be addressed to Shuaiqi Wang; wangshuaiqiuk@163.com

Received 3 September 2021; Accepted 10 October 2021; Published 27 October 2021

Academic Editor: Punit Gupta

With the continuous development of artificial intelligence technology, the supply chain logistics industry has shown new changes. The products of the intelligent era such as smart devices, big data computing, and Internet of Things technology have gradually become the transformation and innovation of logistics and supply chain enterprises. The important driving force of the logistics and supply chain industry will greatly improve the operational efficiency of the logistics and supply chain industry. *Methods*. This article studies the technical framework of artificial intelligence and explores the upgrading and transformation of supply chain logistics enterprises in logistics infrastructure, production tools, and logistics operation processes under the promotion of artificial intelligence technology, from warehouse location, inventory management, warehousing operations, transportation, and distribution. The data analysis and prediction analyze the impact of artificial intelligence on the supply chain logistics field and finally point out the problems in the intelligent development of the supply chain logistics field and put forward targeted suggestions to promote the modern supply chain logistics to become more intelligent. developThe new development trend of smart logistics is towards sharing economy, automation, service efficiency, and cost reduction. *Results*. In this context, if logistics companies want to achieve higher-quality development, they cannot do without business model innovation and larger-scale collaboration, transparency of logistics information, and more comprehensive information sharing. The new trend of the development of smart logistics is to develop in the direction of sharing economy, automation, service efficiency, and cost reduction. *Conclusion*. Intelligence and the Internet of Things are the inevitable trend of the development of smart logistics, which is mainly realized through the Internet of Things path in terms of visual information technology, intelligent robot operation, vehicle scheduling, and cargo traceability.

1. Introduction

In 2015, the government pointed out in the "Internet +" strategy that it is necessary to give full play to the optimization and integration role of the Internet in the allocation of production factors, deeply integrate the Internet and various fields of the economy and society, and enhance the innovation power of all fields of society. This strategic orientation accelerates the application of modern smart logistics information technology in China, and the overall development trend of the domestic and foreign logistics markets continues to improve, which has promoted the service integration demand of the logistics industry [1].

Affected by factors such as environment, terrain, and history, the development of the logistics industry varies from place to place [2]. Traditional logistics companies manage all kinds of small areas and are relatively small in scale. They cannot connect the entire logistics map. Therefore, how to realize the improvement of smart logistics integration capabilities and explore a new model of logistics development under the "Internet +" has become a key issue that needs to be resolved in the current industry. The impact of the Internet of Things on logistics will also be comprehensive. The revolutionary innovation of logistics information technology, the agile and intelligent supply chain transformation, the real-time traceable product distribution network, the traceable source of medicine and food, and so on all represent the era of smart logistics.

Under the background of "Internet +" in the new era, a new round of scientific and technological revolution has begun. It has promoted the in-depth integration of the Internet and the logistics industry. The introduction of information systems has changed the logistics, transportation, and warehousing links from no information exchange to communicative, and queryable smart logistics has also promoted the informatization and standardization of logistics networks to promote information sharing and interconnected communication [3]. The concept of smart logistics makes logistics people pay more attention to the balance of various logistics links, the optimization of logistics costs and logistics services in overall planning, and the use of modern information technology and functional equipment. The background of "Internet +" in the new era has become China's logistics. As a new driving force and opportunity for the high-quality development of enterprises, it is believed that under the development of information technology innovation, logistics enterprises will enter a new era of modernization and intelligence more quickly. And this article mainly discusses the new model of logistics development under the background of the Internet and modern logistics.

The application of artificial intelligence technology has a certain impact on the core competitiveness of logistics enterprises.

Influence. Hu Yue et al. (2020) based on AMOS software and structural equation model constructed "Artificial Intelligence+" from the three aspects of capital, human resources, and knowledge management [4–6]. The results of the study show that manual intelligent technology capital is the core competence that influences logistics enterprises based on artificial intelligence technology. Among them, the level of big data processing is the biggest factor affecting competitiveness. Human resources and knowledge management will also have a greater impact on the core competitiveness of logistics enterprises. The big impact is only slightly inferior to artificial intelligence technology capital.

2. Prospects and Innovations of the Logistics Industry Development under the Background of "Internet +"

With the development of science and technology and the mature Internet technology every day, there are more and more people online; at the same time, this model has also increased. People can carry out various activities through various modes such as online shopping. At present, people can buy goods without going out because of the increase in the number of express delivery and the rapid development of express delivery logistics systems. According to the China Logistics Data Information Center, China's total social logistics reached 229.7 trillion yuan in 2016 and 252.8 trillion yuan in 2017. Since 2010, the compound growth rate has been 10.53%, indicating the development of the logistics system. However, the current logistics system cannot meet people's expectations, so continuous intelligence transformation is required. Therefore, this is an important development trend in the world today. Consider the development of science and technology in the logistics industry, as well as logistics systems. Facing the increasingly severe trend of the information age, the logistics industry has applied the data model in the large-scale development process to enhance the construction of smart logistics, accelerate the efficiency of logistics system construction, improve the logistics level, and provide more satisfactory services to consumers [7].

3. Disadvantages Existing in Today's Logistics Industry

3.1. Incomplete Policies for Smart Logistics Industry. At present, China's laws and regulations on the development of smart logistics are not perfect, and it is difficult to provide guarantees for the development of logistics enterprises from the legal and policy levels. As a result, the independent development model of smart logistics has problems with high difficulties and major obstacles, in terms of legality and disputes. There are major hidden dangers. The problem of disorder and disorder in the logistics market still exists, and there is an urgent need for relevant national administrative units to formulate planning standards to create a high-quality environment for smart logistics for enterprises.

3.2. Decentralized Management and Contact Evacuation. Affected by factors such as environment, topography, and history, the development of the logistics industry varies from place to place. Traditional logistics companies manage various small areas and are relatively small in scale. They cannot make full use of the interconnection of the entire logistics landscape. A new type of logistics enterprise developed by science and technology, [8] due to excessive reliance on "Internet +", lacks relevant logistics experience, and logistics is a collective development industry, interconnected with each other; the two do not have good communication due to their own shortcomings. Lack of management experience cannot form a complete logistics industry network [9].

3.3. Lack of High-End Professionals with Logistics Concepts. Analyzed from the current number and quality of employees in the logistics industry, the industry lacks high-quality comprehensive logistics talents who understand that logistics business and communicate information technology, high-end professionals, and many small- and medium-sized logistics companies have limited investment capabilities and lack smart logistics technology operations. The new hardware equipment restricts the development of China's smart logistics. Although some large logistics companies have realized the application of smart logistics technology, they are still in the exploratory stage, and the concept of smart logistics has not yet been fully implemented, for the construction of logistics innovative talent training plan. For the management major under the Internet + background, a total of 500 questionnaires were issued to logistics management students and 415 valid questionnaires were restored. According to the questionnaire survey, the proportion of participating students is shown in Figure 1, and the gender ratio is shown in Figure 2.

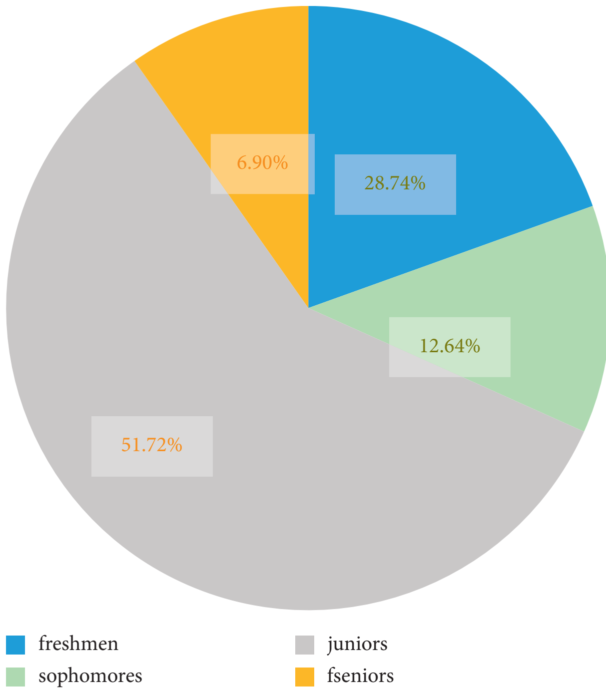

Figure 1: The proportion of students participating in the survey.

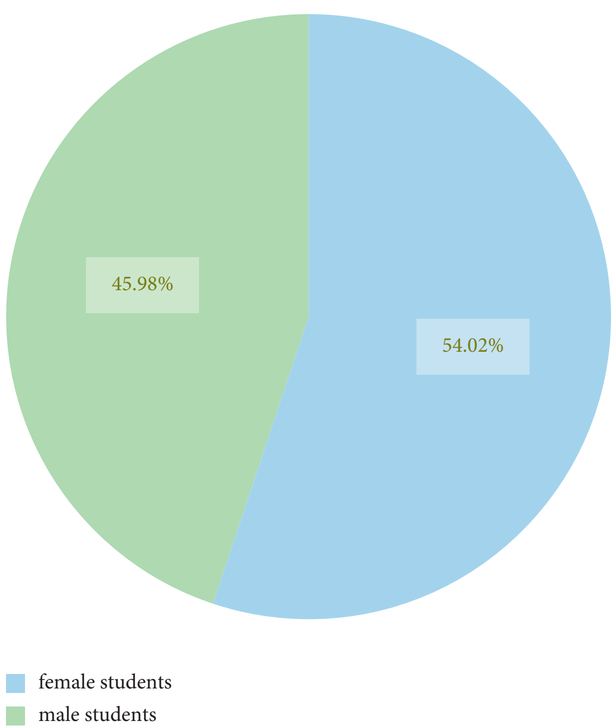

Figure 2: Gender ratio of students participating in the survey.

It can be seen from Figure 1 that among the students participating in the survey, 28.74% are freshmen, 12.64% are sophomores, 51.72% are juniors, and 6.9% are seniors. It can be seen from Figure 2 that the survey shows that boys account for 54.02% and girls account for 45.98%. Among the 415 valid questionnaires, 7.95% of the students were not satisfied with the courses provided by their current majors. The main reasons for their dissatisfaction are as follows: lack of technical courses; curriculum coverage is too wide, messy but not ideal; some courses offered are not related to majors; serious deviation from society; and so on.

3.4. There Are Also Many Constraints in the Development of Rural Logistics. The main disadvantages in the application of Internet information technology are the following three points. First, the rural logistics-related information platform has not been built and perfected, and some e-commerce logistics practitioners in rural areas have insufficient knowledge of network information, resulting in a lack of advanced information processing in rural logistics. With the support of transmission technology and management mode, the development of rural logistics is slow. Second, due to the fact that some rural areas, especially remote mountain villages, have not yet achieved network coverage and the logistics and transportation system is not sound, the advantages of Internet information technology are difficult to use, and there will be detours and secondary distribution during distribution, resulting in rural logistics timeliness. The poor performance also increases the cost of distribution. Third, due to the relatively slow development of China's Internet of Things, logistics, and information technology applications, the development of the e-commerce logistics industry is relatively lagging in the development of talents in China's Internet of Things, logistics, and information technology applications. However, due to the remoteness and backwardness of rural areas, relevant technical talents are extremely lacking, and most of the employees are less educated. The number of nonprofessionals also makes it difficult for Internet technology to truly play its due role in the rural logistics industry.

4. The Direction of Logistics Development under "Internet +"

4.1. Enterprises Leverage the "Internet + Logistics" Model. The integration, optimization, and configuration of social resources are realized through the establishment of information platforms, the sharing of logistics information is realized, the added value of logistics is increased, and the logistics interoperability between enterprises and industries is strengthened, thereby optimizing the operation mode of logistics enterprises and improving operating efficiency and profits [10–12]. The emergence of multi-industry linkage has also accelerated the development of logistics enterprises. Multi-industry linkage development can achieve resource integration and coordinated development between industries. It is an important means for the logistics industry and other industries to achieve a win-win situation and is related to the sustainability of national economic development [13–15]. It is also related to local economic growth. The development of enterprise logistics needs to be bigger and stronger, not just by doing it alone but also by cooperating with other enterprises in the supply chain. This is the advantage of the "Internet + logistics" operation model. For example, companies can unite with other companies in the supply chain through

“Internet + manufacturers,” “Internet +Suppliers,” “Internet + channel providers,” and so on to establish a common development model, establish mutually beneficial policies, and achieve common benefits. The base is strong.

4.2. Development of Rural Logistics. Modern logistics is highly dependent on Internet information technology. In view of the insufficiency of informatization in the development of rural logistics, rural areas should speed up the construction of logistics information platforms so that agricultural product sellers can grasp market information and sales channels in time, and production is marketable. Logistics development informatization can improve quality. And it also enables rural e-commerce logistics practitioners to implement effective supervision of logistics transportation, warehousing, distribution, and other links through the information platform terminal, which improves logistics efficiency while reducing cargo damage rate, greatly improving the service level of rural logistics, thereby accelerating construction of rural logistics information platform.

4.3. The Logistics Operation Mechanism Is Getting Better and Better. The difference between the “Internet + logistics” operation mode and the traditional logistics operation mode is not only its high efficiency and speed in information processing but also to a large extent that it is basically in a transparent state in terms of information processing. For materials, not only the sender can see the transportation status of the materials but the recipients and even some competitors can also see the transportation status of the materials through the network platform. The logistics and transportation work of enterprises is under the supervision of many eyes. Therefore, if an enterprise wants to satisfy its customers with its services and keep its customers from being snatched by competitors, it must improve the traditional logistics operation mechanism, so that the eyes of multiparty surveillance are impeccable.

4.4. Create a Green Logistics System. The green logistics system mainly includes green procurement, green processing, green packaging, green transportation, green warehousing, and green distribution. Logistics companies start to purchase equipment that has no impact on the environment. They should not blindly focus on how much they invest. They should be advocated by the state. The main purpose of the concept of environmental protection is to phase out old transportation vehicles that pollute the environment and purchase new vehicles, especially to encourage the use of energy-saving and environmentally friendly vehicles. The application of these methods can reduce the overall energy consumption of the logistics industry, and the use of new energy greatly reduces pollution, the total emission. The location of the logistics center should be set up in the links that must be stopped during transportation, such as short-distance road transportation to the airport, air transportation must be reloaded, appropriate circulation processing in the logistics center, and combined processing and distribution measures. In order to reduce the overall operating cost of logistics enterprises, the frequency of using standardized equipment is increased such as containers and pallets during transportation, which can improve the level of logistics handling and save transportation time. Constructing a green logistics base, realizing the sharing of vehicle information among various logistics enterprises, and the joint deployment of vehicles can improve the utilization rate of vehicles, reduce the consumption of vehicles in the operation process, save fuel and materials, and protect the environment. Logistics companies should focus on building high-standard, multifunctional automated three-dimensional warehouses, focus on improving the informatization level of storage facilities and equipment, effectively integrate the resources of various companies, and build energy-saving green warehouses with environmental protection as the starting point. The branches established by the logistics company are integrated at various locations to establish a common distribution site, and a unified distribution or common distribution logistics distribution model is adopted at the logistics distribution site to fully and efficiently mobilize the original limited distribution vehicles and redo route planning and personnel deployment, which can save resources and unnecessary waste to the greatest extent.

5. Conclusion

The logistics industry, as a stimulating industry under the background of the Internet + era, must always take the national development plan as the prerequisite for its own development, look to the future, start from the perspectives of theoretical basis, technological improvement, and social development, and establish a logistics industry suitable for the development of logistics industry. As an important technical resource in the twenty-first century, artificial intelligence can provide supply chain logistics with technical support that integrates big data, cloud computing, and the Internet of things. Artificial intelligence is a powerful driving force for the transformation of the logistics industry. For supply chain logistics companies, they should follow the current trend of intelligent development in all walks of life, vigorously promote the transformation of logistics infrastructure and production tools to intelligent, realize the construction of supply chain logistics operation processes in the direction of intelligence, and at the same time realize the supply chain resource sharing and sound system standards, increase the training of artificial intelligence professionals, and promote the integration and coordinated development of artificial intelligence and supply chain logistics.

Data Availability

Data sharing is not applicable to this article as no datasets were generated or analyzed during the current study.

Conflicts of Interest

The author declares that there are no conflicts of interest with respect to the research, authorship, and/or publication of this article.

References

[1] L. Zheng, "Jiangsu smart logistics enhances logistics integration capability under "Internet+" research on countermeasures," *Logistics Engineering and Management*, vol. 42, no. 8, pp. 21–24, 2020.

[2] A. Geetha and C. Subramani, "An idea for students project work: energy management in hybridization of energy sources for transportation application," *International Journal of Electrical Engineering Education*, vol. 57, no. 3, pp. 253–271, 2020.

[3] S. Wang and Z. Yang, "Research on the construction of smart logistics development system," *Business Economy Research*, no. 23, pp. 90-91, 2018.

[4] N. Liu and Z. Dou, "Talking about the letter of intelligent logistics warehousing in the 5G era information development," *Logistics Engineering and Management*, vol. 4, no. 41, pp. 25–29, 2019.

[5] X. Liu, "The transformation and upgrading of logistics enterprises in the era of artificial intelligence development trend," *Business and Economic Research*, vol. 3, no. 4, pp. 1–10, 2019.

[6] H. Han, "The impact and difference of artificial intelligence technology on the efficiency of the logistics industry analysis," *Business and Economic Research*, vol. 2, no. 22, pp. 33–42, 2020.

[7] Z. Xin-yong, "The realization of wisdom physical logistics based on the internet of things," *Journal of Changzhou Institute of Technology*, vol. 24, no. 5, pp. 46–48, 2011.

[8] Y. Pan, *Research on the Impact of Information Intervention on Internet Logistics Information Platform Users' Intention to Adopt Research*, Zhejiang Gongshang University, Hangzhou, China, 2015.

[9] H. Zhao, "The support body of my country's smart logistics development under the background of "Internet +" department research," *Journal of Changchun Normal University (Humanities and Social Sciences Edition)*, vol. 39, no. 3, pp. 65–67, 2020.

[10] R. Xu, C. Wang, X. Luo, and J. Li, "Based on the background of "internet +" research on deep intelligence of logistics real estate," *Logistics Technology*, vol. 40, no. 3, pp. 7–11, 2017.

[11] X. Wang, J. Zhou, and Y. Gu, "Smart logistics deployment in the context of new retail model study: taking ali hema xiansheng as an example," *Logistics Engineering and Management Li*, vol. 42, no. 1, pp. 22–25, 2020.

[12] X. Lan, "Thinking and practice in the era of intelligent logistics in the "Internet +" supply chain," *Modern Business*, no. 8, pp. 26-27, 2020.

[13] H. Wang, X.-M. Zhang, G. Tomiyoshi et al., "Association of serum levels of antibodies against MMP1, CBX1, and CBX5 with transient ischemic attack and cerebral infarction," *Oncotarget*, vol. 9, no. 5, pp. 5600–5613, 2017.

[14] J. Yao, L. Wang, K. Liu et al., "Evaluation of electrical characteristics of biological tissue with electrical impedance spectroscopy," *Electrophoresis*, vol. 41, no. 16-17, pp. 1425–1432, 2020.

[15] W. Gaihua, Z. Tianlun, D. Yingying, L. Jinheng, and C. Lei, "A serial-parallel self-attention network joint with multi-scale dilated convolution," *IEEE Access*, vol. 9, no. 5, pp. 71909–71919, 2021.

Hindawi
Scientific Programming
Volume 2021, Article ID 7555550, 8 pages
https://doi.org/10.1155/2021/7555550

Research Article

Current Status of Ceramic Industry and VR Technology Used in Ceramic Display and Dissemination

Xue Li [1] and Xiaobing Hu [2]

[1]*School of Art and Design, Jingdezhen Ceramic University, Jingdezhen 333000, Jiangxi, China*
[2]*Fine Art School, Anqing Normal University, Anqing 246001, Anhui, China*

Correspondence should be addressed to Xiaobing Hu; 315698886@qq.com

Received 16 August 2021; Accepted 9 October 2021; Published 26 October 2021

Academic Editor: Punit Gupta

With the deepening of reform and opening up, the development of China's ceramic industry has been rapidly improved, leading the world, and various ceramic varieties have also been greatly developed. However, as the growth rate of the global economy has gradually slowed down and structural imbalances have become more obvious, China's economy has gradually entered a new development trend. In the context of supply-side structural reforms, the severe macroenvironment and policy pressure to eliminate backward production capacity have further promoted the development of China's ceramic industry to face greater challenges. In the context of the rapid development of various high-tech technologies such as "Internet +" and intelligent manufacturing, this paper discusses the use of VR technology in the design of ceramics from the principles and characteristics of ceramic design and, according to the characteristics of virtual design of ceramics, demonstrates the feasibility of its shape, decoration, color matching, and so on. The ceramics are classified according to their use functions, and the characteristics of different types of virtual display of ceramics and their suitable virtual display methods are discussed. Finally, this paper combines panoramic image display technology and graphic VR display technology to create the best virtual display method suitable for different types of ceramic products, implements the interactive design in virtual software, and then performs virtual display.

1. Introduction

Over the past 30 years of reform and opening up, China's ceramic industry has developed rapidly. China has taken the forefront of ceramic development, becoming the center of ceramic manufacturing and the main producer of ceramics, with the first annual output and export. Chinese daily ceramics are about 70% of the world, 65% and about 50% of sanitary ceramics, and 64% of construction ceramics. Due to the obvious labor cost and resource advantages, the competitiveness of China's ceramic industry is also being rapidly improving, and its position in the world ceramic market is being rapidly improving.

In recent years, China's ceramic industry has grown rapidly at an average annual rate of more than 20%, is at the middle development level in all industries of the national economy, and far exceeds the growth rate of GDP. The ceramic industry has developed into one of the important industries to promote the sustainable, steady, and healthy development of China's national economy.

Despite the continuous improvement of the technology and development of China's ceramic industry, the domestic and foreign markets have grown rapidly and have achieved good results. However, as the global economic growth rate gradually slows down and the structural imbalance becomes more obvious, China's economy has gradually entered a new development trend. In the context of supply-side structural reform, the severe macroenvironment and the policy pressure of eliminating backward production capacity further promote the development of China's ceramic industry that is facing greater challenges. However, with the continuous improvement of Chinese residents consumption level, "Internet +," and intelligent manufacturing rapid development of various high-tech technology, as well as the rapid implementation of the development of ceramic industry special planning, China's ceramic industry ushered in a good development opportunity, supporting the development of China's ceramic industry in the future in a good and rapid direction.

This paper mainly analyzes the development status of China's ceramic industry in recent years in a narrative manner and combines the advantages of VR technology in the promotion and display of the ceramic industry to do research. Based on the application of VR technology in ceramics, some scholars have made some comments from different perspectives. These studies can be roughly divided into three categories. One is the analysis of the local kiln opening display from a case study [1], which focuses on the use of VR technology to display ancient cultural relics. The point of view is that the display of ancient cultural relics in the real scene is likely to cause damage to the artifacts, and not only can the use of VR technology satisfy people's appreciation of ancient cultural relics, especially in the post-epidemic era, but also people can display them in VR without leaving their homes. Feel the charm of ceramics in the virtual space. One is the use of VR technology in the design of ceramic products [2], mainly discussing how to apply cutting-edge VR technology to improve users' interactive virtual experience of products on e-commerce platforms. Solve the contradiction between mass production and individual differences in consumption; at the same time, it discusses how to use it to realize the reproduction, repair, and data storage of ceramic products and how to realize the construction of a virtual inspection and evaluation system for ceramic products; third class is the application of VR technology in modern ceramic display design [3]. The point of view is that the ceramic exhibition hall is a platform to showcase the ceramic culture and disseminate ceramic art to the audience. As the ceramic capital of millennia, Jingdezhen ceramic art has been promoted to a large extent Thanks to the development of exhibition art, with the development of technology, virtual reality technology is also promoting the development of ceramic exhibition halls. The current basic characteristics of immersion, interactivity, and sharing of virtual reality technology are designed for ceramic exhibition halls. Work brings new inspiration and vitality. The application of VR technology to the design of ceramic exhibition halls is bound to be the development trend of ceramic exhibition hall exhibition design in the future. The above-mentioned research results are to explain the application of VR technology in ceramics display and design in a small range, and the application methods and technical points of VR technology had not been involved in the analysis of China's ceramic industry; this will be the focus of this paper.

2. Ceramic Development Environment and Influence

2.1. Impact of the International Economic Environment on China's Ceramic Industry. After the outbreak of the US financial subprime crisis in 2008, the global scope further expanded, triggering a global financial crisis, and the global economy is gradually entering a period of deep adjustment. In the coming extraordinary period, global economic development will generally recover. Under this background, there will still be greater uncertainty and instability. The global trade environment has also become worse, and it is unlikely to improve in the short term. Moreover, with the introduction of the TPP trade agreement headed by the United States, China, as the world's largest producer and exporter of ceramic products, has also been excluded from the agreement. With the arrival of US President Donald Trump, the TPP agreement was canceled during this period, which is also a very rare opportunity for the development of China's ceramic industry.

At the same time, we also need to see that the overall trend of international economic development presents new opportunities. World economic development focus gradually shifted from the established developed countries to the current emerging markets and developing countries or economies, industrialization and urbanization space, may form huge demand for production and life, and will have a great impact on the development demand and regional distribution of Chinese ceramic products. Developing countries and emerging economies are also playing an increasing position in China's ceramic industry exports.

However, the international market demand for daily ceramics has a trend of slowing down under the environmental impact of the global economy. However, the demand for high-grade and quality daily ceramics is increasing year by year. This situation has caused the international manufacturers of daily ceramics to focus on the high-grade and cultural and artistic characteristics of ceramics; those products with collection value and gift value, good quality, full function, and novel decoration are gradually favored. This situation is an opportunity for Chinese producers. Since ancient times, the ceramic industry has had a profound cultural heritage, the ceramic products in each producing area are distinctive, and the whole can produce complementary utility to seize the international market. China is a large import country of ceramics between the United States and the EU, USD 22,222 billion from China, accounting for 38.56% of the total ceramic imports, and $1.698 billion from China in 2016, representing 43.67% of the total ceramic imports. From the total ceramic import output of the United States and the EU in 2016 (Figures 1 and 2), China has an obvious ceramic industry in these two regions.

2.2. Influence of the Domestic Economic Environment on the Ceramic Industry. As the Chinese market economy enters a structural slowdown, GDP slows from high development to medium development. China is also facing great downward pressure on the reverse of transformation and upgrading of economic structure. Under increasing economic downward pressure, decreasing marginal effect of monetary policy, increasing resource and environmental constraints, rising factor costs, and overcapacity industries, "three high" type pollution industries face "overcapacity," and the ceramic industry is also affected. Under the background of supply-side structural reform and development, the ceramic

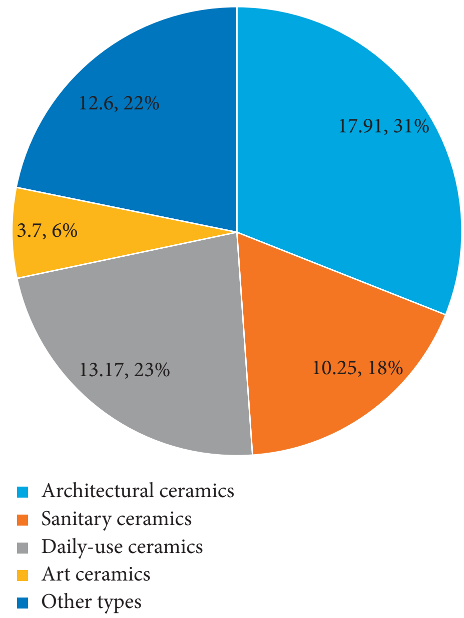

Figure 1: Import of American ceramics in 2016.

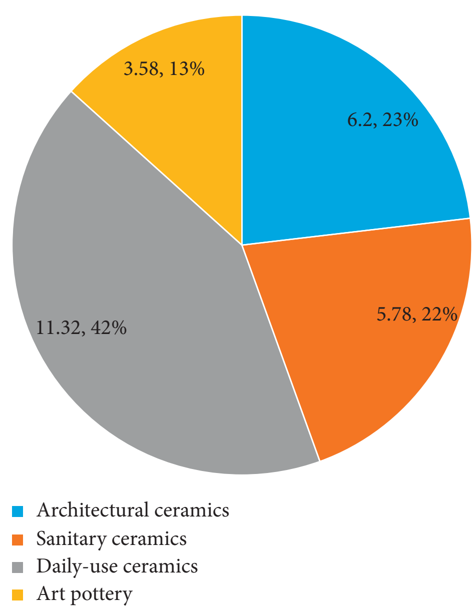

Figure 2: Import situation of EU ceramic products in 2016.

industry is bound to face the extremely severe market competition pressure and the huge constraints of the environment, and the transformation and upgrading will also become an inevitable choice for the ceramic industry in the future development process.

Over the years, the rapid growth of GDP has gradually become an important prerequisite for the stable growth of household income, covering the social security system of towns and villages, and specific consumption habits have also been initially formed. The current desire to upgrade consumption is extremely strong. In addition, in the context of accelerating the construction of new urbanization, new consumer demand has also created a new market for the transformation and upgrading of the ceramic industry. Based on the recovery of the real estate market, continue to promote the rapid recovery of the downstream building and health ceramics industry. During this period, new rigid demands and improved demands were also activated. The development of the ceramic industry is facing new development opportunities. The "Internet + ceramics" model has been continuously developed in the exploration of the modern market, which has promoted the rapid integration and development of the traditional ceramic industry and the emerging service industry and promoted the structural transformation and upgrading of the ceramic industry.

2.3. Development Environment and Technical Status in the Ceramic Industry. There are a large number of enterprises in the ceramic industry, and the average scale is relatively small, with weak research and innovation ability and low brand value. A series of problems have become very prominent at present, resulting in problems related to low-level repeated construction, unreasonable industrial layout, and the imbalance between supply and demand caused by the rapid growth of production capacity. In recent years, as the whole society has increased awareness of environmental governance, energy conservation, and emission reduction, the rapid increase of energy consumption and environmental protection costs restricts the development of the ceramic industry, because the problem has been "closed, stopped, merged, and transferred" production lines or those seeking pollution "haven" are gradually increasing. A large number of backbone enterprises with large scale, advanced technology, standardized management, strong brand awareness, and a strong sense of social responsibility in the industry have achieved good results in product quality, energy conservation, emission reduction, economic benefits, and many other aspects, and the industrial concentration degree has been gradually improved. However, as far as the overall operation and development level of ceramic enterprises, the number of enterprises that can participate in the whole industrial chain of the cooperation is not large. The market-oriented cooperation of the whole industrial chain still needs the further deepening and development of the ceramic industry. At the same time, China's ceramic industry has its typical disadvantages, mainly small and medium enterprises, difficult to quickly integrate into the global value chain. The competitive advantage is low factor cost and low tax incentives. Fusion positioning and homogenization of competition are very prominent; the low-level competitive advantage is prone to an antidumping investigation. In addition, small- and medium-sized ceramic exporters also have the risk of being replaced by lower-cost developing country enterprises, relying on low value-added products to support the industry's rapid growth model.

The technical environment of China's ceramic industry has been continuously improved, and the industrial technology research and development have basically entered a virtuous circle, but the intellectual property protection system still needs to be further improved. In the process of global competition, key technologies still need to be improved. In recent years, the construction of intellectual property protection system in China's ceramic industry has gradually tended to the overall benign development but is not ideal in intellectual property protection and law enforcement effect; the infringement still needs to be strengthened; the victim relief measures are still imperfect, resulting in the insufficient innovation motivation of small and medium-sized enterprises. "Promoting porcelain through science and technology" has gradually developed into a consensus of enterprises. Investment in research and development and technology promotion is constantly increasing, providing solid technical support for the transformation and upgrading of the industrial structure. To further improve the development quality and output efficiency of the building and healthy ceramic industry, prevent excessive growth, curb low-level repetitive construction, and promote the transformation and upgrading of the ceramic industry, relevant departments have also formulated or further revised a series of necessary development plans. Introduce the technical conditions for the development of smart ceramics and the basic conditions for its application. In addition to the various production technologies of the porcelain areas themselves, these technologies vigorously develop VR technology and AR technology, which are a more practical and scientific way to publicize and display Chinese ceramics in the world. Because VR technology does not need to work in the porcelain area and public display space, at home you can browse the representative ceramics in the virtual space with the Internet and computer, which effectively plays a role in promoting the publicity of Chinese ceramics.

3. VR Technology and Application Methods

3.1. VR Technology. VR technology is an advanced computer man-machine interface technology with basic features of immersion, interactivity, and conception, which integrates the science of human and information [4]. It comprehensively utilizes computer graphics, simulation technology, multimedia technology, artificial intelligence technology, computer network technology, parallel processing technology, and multisensor technology to simulate human vision, hearing, touch, and other sensory organ functions, so that people can be immersed in computer generation in the virtual realm and can interact with it in real time through natural means such as language and gestures, creating a humanized multidimensional information space. Users can not only experience the fidelity experienced in the objective object through the virtual reality system, so that people have a kind of "immersive" sense of reality, but also can break through the space, time, and other objective constraints and feel in the real world. Experience cannot be experienced personally [2].

Due to the main characteristics of VR technology such as immersion, interactivity, and conception, in the current society, especially in the postepidemic era, it has a very obvious advantage in the promotion and display of Chinese ceramics. In this process, companies use modern technological means of VR technology to achieve good interaction between users and products in the process of publicity and display in an effective way. Even under certain conditions, viewers can also use VR. Technology is involved in the design of ceramic products.

3.2. 3D Modeling of VR Technology Intervention Display. The interactive characteristics of VR video refer to the audience's subjective consciousness and the right to operate things existing in space; on the other hand, virtual reality space accordingly gives natural and reasonable feedback and interaction behavior. The generation of VR video interactivity requires some supporting equipment such as using VR glasses, VR helmets, and data gloves so that the audience can feel the same in the real world through natural contact. The quality of the interactive hardware device affects the content delivered. It is because of the interaction function that determines that the effect of video delivery varies from person to person. The implementation of audience interaction in VR video also reflects the nature of the current interaction. This is also an improvement of Internet interaction that implements interactive behavior. Real-time feedback improves the value of the interaction behavior [5, 6].

SolidWorks is the mainstream solid modeling software based on parametric geometric features. SolidWorks uses geometric features as the design unit and uses geometric features to build part models. Geometric features are the basic units that make up a 3D model. In SolidWorks, geometric features are divided into sketch features and directly generated features according to different production methods. Before designing the model, it is necessary to decompose the complex model, establish a general function sequence, and clarify how to determine the sketch and reference level of each function [7].

Entity modeling software requires users to have certain 3D reverse thinking and can split a complex 3D model into groups of sketch features or directly generate feature combinations. At the same time, in the process of creating the basic features, how to choose the benchmark plane and how to choose the sketch plane are a test of the user's ability and experience. Polygon modeling software requires users to have a strong sense of space and space sense, and reasonable structure control ability, reasonable wiring ability, 3D model structure control ability, and 3D model grid distribution ability are also an index [8] to distinguish the level of polygon modeling ability.

3.3. The Production Process of VR Technology Virtual Display Design. The need for the virtual display of ceramic products is mainly based on the virtual reality display technology of 3D modeling. The display principle can be embodied by the following design and production steps:

(1) According to the purpose and content of the display, the designer uses 3D MAX, MAYA, and other types of three-dimensional modeling software to construct the digital model and make related optimizations.

(2) Use the corresponding mechanism material materials to map or render the built ceramic product three-dimensional model, give the relevant scene lights in the virtual space, and then adjust the relevant parameters according to different space display requirements.

(3) Create animation effects after setting up the scene camera.

(4) After the first three parts are completed, save them in the corresponding format and then import them into the VR software for interactive design production, so that it has the function of the interactive operation. At the same time, multimedia information such as sound effects, text, and UI interface should be added.

(5) After the interactive production is completed, the output file can be used in practice according to the type of release.

The design process is shown in Figure 3.

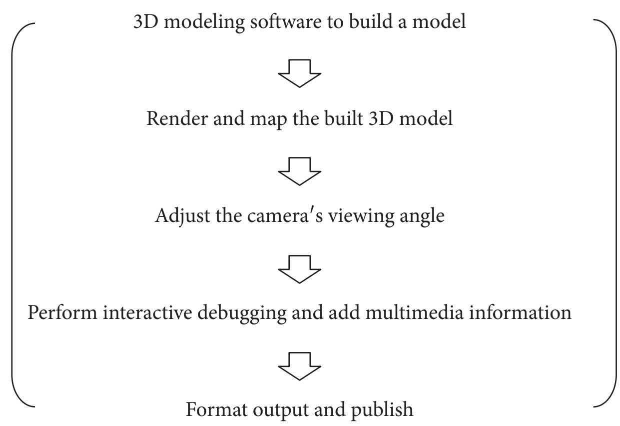

Figure 3: Diagram of the process of VR technology for display design.

3.4. Realization of VR Technology in Ceramic Display. The three-dimensional modeling design based on virtual reality display has its characteristics. Its rich display effect allows the audience to watch it. In addition to zooming in and out, it can also rotate at any angle, modify the selection of colors and patterns, and so on. The interactive performance is much better than the way of displaying panoramic video. Therefore, for the realization of VR technology in the display of ceramic products, we must first figure out how to encode and decode VR panoramic images. Among them, the process of encoding and decoding is essential to analyze and decode each frame for projection to realize panoramic video. We proceed as follows.

One is to decompose the panoramic video image into a single frame image. Since ceramic products are mostly three-dimensional, it is most appropriate to analyze the ceramic display with the principle of panoramic projection of geometric spheres as a case. First, perform different projection formats according to different geometric models [9]; then, according to the actual situation, expand the geometry module [10] and again rearrange the geometry by different layout methods module; finally, the spherical image is converted into more conventional flat rectangular images, and these images are regarded as panoramic frames and correspond to the two-dimensional flat frames.

Second, the sequence of two-dimensional plane frames is encoded and compressed to obtain a data stream for video storage or transmission.

After the above two processes, the panoramic video encoding is completed. For decoding, it is to reverse the sequence of the encoding process to achieve decoding.

Spherical panoramic images are generally represented by a three-dimensional sphere, and the coordinates on it are mostly following the rules of right-hand operation and are represented by a three-dimensional coordinate system. The points on the sphere can refer to the marking method of the three-dimensional scanner and perform punctuation on several latitudes and longitudes [11]. Longitude takes the x-axis as the coordinate direction and uses counterclockwise rotation, and the rotation angle value is positive. On the contrary, when the rotation angle is clockwise, the rotation angle is negative. The longitude value is represented by π, and the value range is $[-\pi, \pi]$. Taking the equator on the sphere as the coordinate, the latitude uses the Y-axis as the coordinate direction, the coordinate point moves toward the north pole, and the angle value is positive. On the contrary, if the coordinate point moves to the south pole, the angle value is negative. Therefore, the latitude value range is $[-\pi/2, \pi/2]$. The coordinates of a point on the unit sphere can be expressed by latitude and longitude coordinates $[\Phi, \theta]$ or by three-dimensional coordinates (X, Y, Y), which are expressed as follows:

$$\begin{aligned} &X \cos \varphi \cos \theta, \\ &Y = \sin \varphi, \\ &Z - \cos \varphi \sin \theta. \end{aligned} \tag{1}$$

Through the above analysis, the essence of panoramic image projection is to project the panoramic image frame and all pixels on the spherical texture in a certain way and then convert the 3D video image into a 2D plane video frame image. That is to say, to realize the VR technology to display the artifacts in the virtual space, it is necessary to establish a geometric model, map the coordinate points on the spherical surface to the surface of the geometric body, complete the spherical video projection to the two-dimensional plane [12], and transform and rotate the texture pixels on each surface of the geometry.

From another level, in the panoramic video image, the spherical panoramic image can also be realized according to the idea of equidistant cylindrical projection. The method is to use coordinate points of the same value to expand the latitude line data on the sphere and map it on a two-dimensional plane to obtain a rectangular video. In the unified plane coordinate system, the plane coordinate points use U and V to represent the values, and the range of values is (0,1). The latitude and longitude coordinate points on the spherical surface are (θ, Φ); thus, the spherical panoramic image to the plane image conversion, the corresponding method of its value, is obtained by a formula using the coordinates of the plane point (U, V) (formula (2)). Then, the three-dimensional point coordinates (X, Y, Y) on the spherical surface are calculated by formula (1).

$$\begin{aligned}\theta &= 2\pi \times (U - 0.5),\\ \theta &= \pi \times (0.5 - V).\end{aligned} \tag{2}$$

If any point (X, Y, Y) in the three-dimensional space is inversely converted into a two-dimensional plane point, the longitude and latitude values (Φ, θ) can be obtained by formula (1), and the value of the plane point (U, V) can be obtained by formula (2) [1].

3.5. Display Mode of the Ceramic Space Scene. VR technology is involved in the design of ceramic virtual exhibition space; one not only can feel the atmosphere of the scene but also can better observe the objects. This method is more suitable for ceramic products and artworks, allowing viewers to fully and profoundly reflect the performance of ceramic products in the space atmosphere. It can not only display ceramic products and artworks but also use other ceramic categories, such as architectural ceramics, industrial ceramics, and special ceramics. However, from the perspective of display purposes, ceramic products and artworks require a panoramic view, object body, and scene. Several display methods cooperate to realize viewing in virtual space. First of all, in the environment of panoramic display mode, the displayed objects are relatively fixed and can only be moved 360 degrees through the lens. During the movement of the lens, the viewer will appreciate the complete display space scene as the lens moves. Secondly, look around the 360-degree landscape from a height. Secondly, use the object display. In this display mode, the lens is relatively fixed. By rotating the object up, down, left, and right, the viewer can observe the object; the last is the scene display, which is both the object and the lens. Generate movement, such as setting multiple observation points; you can walk from one observation point to another; that is, you can watch the scene as well as the object, and you can feel the object from the atmosphere of the scene.

Regardless of the way of display, the show requires multiple observation points; through VR technology and interactive design in the virtual software with corresponding background music, the viewer can comfortably roam from one display scene in the virtual space to another display scene; in the virtual display space, the viewer can not only appreciate the whole object but also magnify the part of the object and appreciate the local details of the object; under the background music rendering, the viewer is completely immersed in the appreciation in the charming space of ceramics. At the same time, the viewer can zoom in and out, move up and down, watch from multiple angles, and change the glaze color or decorative style of the ceramics in the virtual design [1]. Especially in the postepidemic era, some public exhibition spaces such as museums have been affected by the epidemic, and the flow of people has been correspondingly restricted. The introduction of VR technology into the design and display of ceramic products effectively solves the limitation of not being able to go to the museum to watch the real scene but also narrates the distance between people and the objects and increases the enthusiasm of the public to participate in ceramic design.

4. Advantages of VR Technology for Chinese Ceramics Exhibition

4.1. VR Technology Used to Display Ceramic Products Helps Spread China's Ceramic Culture. China has a long ceramic culture and there are so many ceramic-producing areas in China. The audience cannot visit all the ceramic-producing areas for on-the-spot inspections to experience the characteristics of the utensils in different producing areas. In addition, the porcelain is fragile, which is displayed in the real space. The above brought certain difficulties, which made it difficult for Chinese ceramics to be accepted by the masses, resulting in the inadequate dissemination of ceramic culture. The emergence of VR technology provides a new way for the dissemination of ceramic culture, breaks through the limitations of traditional communication methods, and adds a boost to the dissemination of ceramic culture. Relevant units and social organizations can use VR technology to spread ceramic culture, make full use of the characteristics of VR technology, and display ceramic culture to the masses in a novel way so that ceramic culture can be better spread. The masses can also make full use of VR technology, VR cultural promotion center, or their VR equipment to understand the ceramic culture.

4.2. The Viewer Has a Diversified Sensory Experience for Ceramic Display under the VR Field of Vision. The traditional display method mainly adopts real-time display, which consumes a lot of manpower and material resources in the preparation process, and it is also easy to cause damage to the ceramics. In addition, the flow of people is often restricted during the exhibition, so that the viewer cannot get the sensory experience of the appointment. In the current era of information development, traditional display methods cannot meet the needs of the masses and therefore cannot meet the needs of ceramic display and ceramic culture dissemination. VR technology has unique advantages and strong interactivity, which can effectively strengthen the interaction between the experiencer and ceramic culture. The VR scene designer can construct virtual historical characters in the VR scene, interact with the experiencer, and enhance the experience of the experiencer. At the same time, VR technology can present sensory sensations such as hearing and touch, enabling the experiencer to obtain a diversified sensory experience.

4.3. VR Technology Makes the Audience Situation of Ceramics Exhibition Tend to Be Good. In recent years, with the strong support of the government and relevant departments, intangible cultural bases and ceramic industry inheritance centers have been established everywhere, and ceramics can be displayed and disseminated to the maximum extent. As

Figure 4: The bluish-white glazed phoenix head pot of Fanchang kiln.

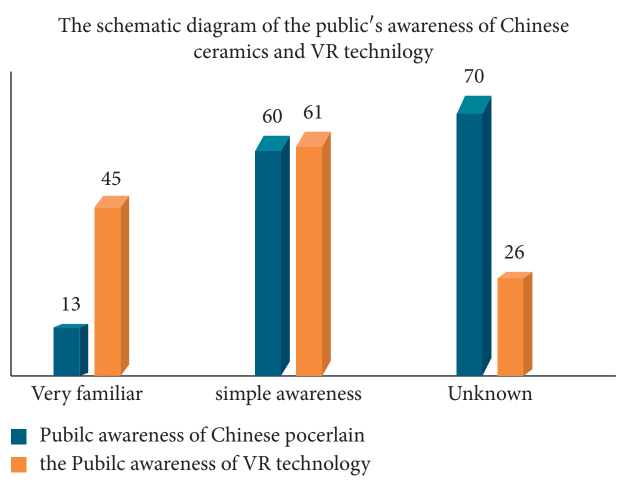

Figure 5: The cognitive comparison of the number of people.

the broad masses of the people, we have the responsibility and obligation to promote, protect, and inherit Chinese traditional culture. Compared with the encouraging, compulsory, and guiding propaganda methods adopted by the government and relevant departments, mass groups have the advantages of wide dissemination and high information openness. This result has made the public actively appreciate the sensory charm brought by ceramic culture and spontaneously join in the promotion of Chinese ceramic culture, becoming the main force of ceramic culture promotion. In the process of studying the bluish-white porcelain of Fanchang kiln, the author took the bluish-white glazed phoenix head pot (Figure 4) as the display object, explained the characteristics of the phoenix head pot in detail to the audience in the virtual scene of VR, and analyzed the main points of the design of the utensil. After obtaining this information, he quickly became a disseminator, making Fanchang kiln blue and white glaze a star display product. Based on this, to obtain audience data, the author publishes questionnaire information through his social circle, museum visitors, and student groups. As shown in Figure 5, among the 100 users, 40 are women, 40%, and 60 are men, accounting for 60%. Most of them are 21–40 years old, followed by 41–60 years old, under 20 years old, and 61 years old and above. The results show that the use of VR technology in the display of ceramic products has increased the number of audiences to a certain extent, and there is a tendency to increase.

5. Conclusion

With the development of science and technology, VR technology as a display medium provides an opportunity for the development of the ceramic product industry. The use of VR technology for display allows people to perceive products as if they have entered a real scene, and they can also interact with products in the scene at any time. This method not only plays a role in protecting ceramic products but also provides a superior path for the spread of ceramic culture. VR technology has realized the essential characteristics of different ceramic products and the physical functions of ceramic products. Take targeted solutions to explore the most suitable virtual display performance methods for different types of ceramic products, and accurately express the display content and display of different types of ceramic products. The key point is to realize the viewing and interaction of ceramic products from different angles, and the virtual display method can be applied to the production of the virtual display through the network and interactive projection. Let VR technology make up for the disadvantages of traditional exhibition halls. In terms of interactivity, both customers and merchants can obtain accurate information and promote the development of the ceramic industry.

Data Availability

Data sharing is not applicable to this article as no datasets were generated or analyzed during the current study.

Conflicts of Interest

The authors declare that they have no conflicts of interest.

Acknowledgments

This article was funded by the Anhui Province Outstanding Top Talent Project (gxbjZD2021005).

References

[1] X. Hu and L. Zhang, "VR technology in bluishwhite porcelain display design of Fanchang kiln," *IEEE Access*, Article ID 3019466, 2020.

[2] Y. Wang, Z. Zhao, and W. Song, "Virtual ceramic product design based on VR technology," *Packaging Engineering*, vol. 00, no. 12, pp. 209–211, 2007.

[3] Z. H. Wang, "Application of VR technology in modern ceramic display design," *Youth Era*, vol. 46, no. 22, pp. 47-48, 2018.

[4] Xi Tao, "On virtual reality technology (VR) leading the development of industrial design," *Packaging Engineering*, vol. 28, no. 7, pp. 124–126, 2007.

[5] M. C. Ward, "The 'new listening': richard wagner, nineteenth-century opera culture, and cinema theatres," *Nineteenth Century Theatre and Film*, vol. 43, no. 1, pp. 88–106, 2016.

[6] Y. Wang and X. Hu, "Wuju opera cultural creative products and research on visual image under VR technology," *IEEE Access*, vol. 8, pp. 161862–161871, 2020.

[7] W. Yanqun and L. Yanghua, "Design and practice of cultural creative product of Training Meilin opera," *Package Engineering*, vol. 38, no. 22, pp. 203–206, 2017.

[8] A. Karim, "Multi-layer masking of character data with a visual image key," *International Journal of Computer Network and Information Security*, vol. 9, no. 10, pp. 41–49, 2017.

[9] W. Liu, X. Meng, and J. Zhang, "Application research of panoramic roaming based on VR technology in ice and snow sculpture display design," *IPPTA: QuarterlyJournal of Indian Pulp and Paper Technical Association*, vol. 30, no. 6, pp. 360–363, 2018.

[10] M. Wang, X.-Q. Lyu, Y.-J. Li, and F.-L. Zhang, "VR content creation and exploration with deep learning: a survey," *Computational Visual Media*, vol. 6, no. 1, pp. 3–28, 2020.

[11] G. Xiao, M. Wu, Q. Shi, Z. Zhou, and X. Chen, "DeepVR: deep reinforcement learning for predictive panoramic video streaming," *IEEE Transactions on Cognitive Communications and Networking*, vol. 5, no. 4, pp. 1167–1177, 2019.

[12] W.-T. Lee, H.-I. Chen, M.-S. Chen, I.-C. Shen, and B.-Y. Chen, "High-resolution 360 video foveated stitching for real-time VR," *Computer Graphics Forum*, vol. 36, no. 7, pp. 115–123, 2017.

Hindawi
Scientific Programming
Volume 2021, Article ID 2039235, 6 pages
https://doi.org/10.1155/2021/2039235

Research Article

Music Education to Rescue Psychological Stress in Social Crisis Based on Fuzzy Prediction Algorithm

Jian Wang

Beihua University, Jilin, China

Correspondence should be addressed to Jian Wang; bhyy7777@126.com

Received 31 August 2021; Accepted 8 October 2021; Published 25 October 2021

Academic Editor: Punit Gupta

In order to alleviate human drowsiness in social crisis, it is necessary to predict the psychological rescue function of music education in social crisis and improve the accurate monitoring and analysis ability of the psychological rescue function of music education in social crisis; this paper puts forward a prediction model of psychological rescue function of music education in social crisis based on quantitative statistical analysis. The prediction and control model of the psychological rescue function of music education in social crisis is constructed, the fuzzy prediction algorithm is combined, the psychological rescue function characteristics of music education in social crisis are analyzed, and the descriptive statistical analysis model of the psychological rescue function of music education in social crisis is established. Through the fuzzy feature extraction method, the big data feature detection of the psychological rescue function of music education in social crisis is carried out, the statistical analysis model of the psychological rescue function of music education in social crisis is established, the dynamic analysis and prediction of the psychological rescue function of music education in social crisis are carried out by combining fuzzy information mining and adaptive learning methods, and the dynamic feature mining of the psychological rescue function of music education in social crisis is carried out by adopting the quantitative statistical feature analysis method. Statistical characteristics of the psychological rescue function of music education in social crisis are established, dynamic monitoring and feature prediction according to the analysis of the psychological rescue function of music education in social crisis are carried out, the ambiguity prediction and feature optimization judgment ability of the psychological rescue function of music education in social crisis are improved, and accurate prediction of the psychological rescue function of music education in social crisis based on the optimization statistical analysis results is carried out. The simulation results show that the statistical analysis ability and fuzzy judgment ability of using this method to predict the psychological rescue function of music education in social crisis are better, which improves the pertinence and effectiveness of music education.

1. Introduction

In music education, it is necessary to combine the social crisis for the relief and suppression analysis of the psychological rescue function of music education and establish a statistical analysis model of the psychological rescue function of music education in the social crisis. Combined with quantitative statistical analysis methods, the prediction and analysis of the psychological rescue function of music education in social crises are constructed, and the fuzzy detection analysis model of the psychological rescue function of music education in social crises is constructed [1]. Through the load dynamic analysis method, the dynamic analysis of the psychological rescue function of music education in social crisis is carried out. Combining the methods of dynamic statistical analysis and big data analysis, the improvement and fuzzy dynamic analysis of music education in social crisis is carried out, which improves the output stability of music education in social crisis [2]. Combined with the method of ambiguity analysis, the statistical analysis model of big data is used to predict and analyze the psychological rescue function of music education in social crisis. The dynamic big data joint analysis method is used to extract the dynamic feature quantity of the psychological rescue function of music education in social crisis. The prediction and dynamic evaluation of the psychological rescue function of music education in a social crisis have been carried out, which has improved the stability of the psychological rescue function of music education in a social crisis. The research on the rescue function prediction and big data analysis methods of music education has attracted great attention [3].

The prediction of the bailout function of music education is based on the big data collection and feature analysis of the psychological rescue function of music education. Among the traditional methods, the dynamic prediction methods for the rescue function of music education in social crisis mainly include fuzzy feature analysis methods, correlation dimension statistical analysis methods, and dynamic response feature detection methods. Reference [4] proposed a method for predicting the psychological rescue function of music education in social crisis based on the SSA-PPR model. It used the SSA-PPR model to build a big data statistical analysis model for the prediction of the psychological rescue function of music education in social crises and combined fuzzy information detection methods to achieve the psychological rescue function prediction of music education. This method improves the prediction accuracy of the rescue function of music education, but the prediction of the rescue function of music education by this method is ambiguous and has poor correlation. Reference [5] proposed a function prediction model based on descriptive statistical analysis and performed a change prediction and dynamic analysis of the psychological rescue function of music education in a social crisis. The dynamic feature quantity reflecting the psychological rescue function of music education in social crisis is extracted, and the method of correlation feature analysis is used to perform dynamic analysis and optimal scheduling of the psychological rescue function of music education in social crisis. This method has a relatively high degree of ambiguity in the dynamic analysis of the changes in the psychological rescue function of music education during social crises, and its ability to identify features is not good [6].

In order to solve the above problems, this paper proposes a prediction model for the psychological rescue function of music education in social crisis based on quantitative statistical feature analysis. The big data feature detection of the psychological rescue function of music education in social crisis is carried out by the method of fuzziness feature extraction. The quantitative statistical feature analysis method is used to mine the dynamic features of the psychological rescue function of music education in social crisis and establish the statistical feature quantity of psychological rescue function of music education in social crisis. In the simulation experiment, combined with the descriptive statistical analysis method, the rescue function prediction of music education in social crisis is realized.

2. Statistical Analysis of Big Data of the Rescue Function of Music Education in Social Crisis

2.1. Flow Sequence Modeling of the Rescue Function of Music Education in Social Crisis. In order to realize the prediction of the psychological rescue function of music education in social crisis, the SSA-PPR model is used to build a statistical analysis model of big data for the prediction of psychological rescue function of music education in social crisis. A descriptive statistical analysis method was used to establish the characteristic sequence distribution model of the psychological rescue function of music education in social crisis and to analyze the correlation feature of the psychological rescue function of music education in social crisis. The predictive feature quantity of the psychological rescue function of music education in social crisis is extracted, and a vertical topological analysis model of psychological rescue function of music education in social crisis is constructed. Through yield response control and fuzzy parameter identification methods, the longitudinal characteristics of the psychological rescue function of music education in social crisis are analyzed [7–9]. Combined with the fuzzy information correlation prediction method, the rescue function prediction model of music education in social crisis is obtained, and the longitudinal distribution sequence of rescue function of music education in social crisis is as follows:

$$A(x) = AJ(x)a(x) + B(1 - b(x)), \tag{1}$$

$$\begin{cases} \dot{m}_i(t) = -a_i m_i(t) + b_i(p_i(t-\sigma), p_2(t-\sigma), \cdots, p_n(t-\sigma)) \\ \dot{p}_i(t) = -c_i p_i(t) + d_i m_i(t-\tau) \end{cases}$$

is a set of dynamic distribution features of the psychological rescue function of music education in social crisis. $h(t) = H\sum_{m=1}^{M}\sum_{k=1}^{K(m)} \alpha_{mk}\delta(t - T_m - \tau_{mk})$ is the load intensity distribution set of the psychological rescue function of music education in social crisis. The attribute value of the psychological rescue function of music education in the social crisis of $V = \{v_1, v_2, \cdots, v_N\}$ is $(u, v) \in E$. In the prediction process of the psychological rescue function of music education in a social crisis, a directed graph analysis model $h(t) = H\sum_{m=1}^{M}\sum_{k=1}^{K(m)} \alpha_{mk}\delta(t - T_m - \tau_{mk})$ is used to represent the statistical distribution of the psychological rescue function of music education in a social crisis where V is the autocorrelation distribution set of the psychological rescue function of music education in social crisis, $V = \{v_1, v_2, \cdots, v_N\}$, and the vertical imbalance dynamic distribution set of the psychological rescue function of music education in social crisis is $q_i(t1) = [w1, x1, y1, z1]$ and $q_i(t2) = [w2, x2, y2, z2]$. Calculating the feature quantity of the plane motion state of the psychological rescue function of music education in the social crisis, the feature distribution set is $(u, v) \in E$, and $W = \{\omega_1, \omega_2, \cdots, \omega_m\}$ is the dynamic weight of the psychological rescue function of music education in a social crisis. Using high-dimensional phase space reconstruction technology to carry out spatial reorganization of the psychological rescue function sequence of music education in social crisis, the reconstructed phase space is as follows:

$$\mathbf{X} = [\mathbf{x}(t_0), \mathbf{x}(t_0 + \Delta t), \cdots, \mathbf{x}(t_0 + (K-1)\Delta t)] = \begin{bmatrix} x(t_0) & x(t_0 + \Delta t) & \cdots & x(t_0 + (K-1)\Delta t) \\ x(t_0 + J\Delta t) & x(t_0 + (J+1)\Delta t) & \cdots & x(t_0 + (K-1)\Delta t + J\Delta t) \\ \vdots & \cdots & \ddots & \cdots \\ x(t_0 + (m-1)J\Delta t) & x(t_0 + (1 + (m-1)J)\Delta t) & \cdots & x(t_0 + (N-1)\Delta t) \end{bmatrix}, \quad (2)$$

where $\mathbf{x}(t)$ is the dynamic feature distribution set of the psychological rescue function of music education in social crisis, J is the disturbance window function, m is the embedding dimension of the psychological rescue function of music education in social crisis, and Δt is the jump width of psychological rescue function of music education in social crisis. The probability density of the state distribution of the psychological rescue function state of music education in the social crisis is as follows:

$$w_{ij} = \beta \times w(e_p k_q)\,(\beta > 1), \quad (3)$$

where β is a positive definite periodic solution and $w(e_p k_q)$ is the fluctuation coefficient of the psychological rescue function of music education in a social crisis. Combined with the fuzzy prediction algorithm, the characteristic analysis of the psychological rescue function of music education in social crisis is carried out, and a descriptive statistical analysis model of the psychological rescue function of music education in social crisis is established. Through the fuzziness feature extraction method, the big data feature detection of the rescue function of music education in social crisis [10], the difference function is as follows:

$$\widehat{W} = \begin{cases} \operatorname{sgn}(W)(|W| - \alpha Ts) & |W| \geq Ts \\ 0 & |W| < Ts \end{cases}, \quad (4)$$

where α is the adaptive adjustment coefficient of the psychological rescue function of music education in social crisis and W is the steady-state feature solution for the prediction of psychological rescue function of music education in social crisis, and its value range is $0 \leq \alpha \leq 1$. Based on the above analysis, a time series distribution model of the psychological rescue function of music education in social crises is established, and a dynamic analysis is performed based on the psychological rescue function distribution of music education in social crises [11].

2.2. Statistical Analysis of the Rescue Function of Music Education. The PCA model is used to build a big data statistical analysis model for the prediction of the psychological rescue function of music education in a social crisis. The SSA-PPR model function is as follows:

$$\left.\begin{aligned} &\min_{w,b,\xi} \frac{1}{2}\|w\|^2 + C\sum_{j=1}^{l} u(x_j)\xi_j \\ &s.t.\ \ y_j((w \cdot x_j) + b) + \xi_j \geq 1 \\ &\xi_j \geq 0, j = 1, 2, \ldots, l \end{aligned}\right\}. \quad (5)$$

Taking the main component features of the psychological rescue function of music education in social crisis as the reference feature quantity, the fourth-order Runge–Kutta method is used to solve the longitudinal imbalance feature quantity of psychological rescue function of music education in social crisis [12]. The kernel function of the model distribution for the psychological rescue function of music education is $k(x_i, x_j)$. Then, the linear programming function of the psychological rescue function of music education in the social crisis is as follows:

$$\left.\begin{aligned} &\min_{\alpha} \frac{1}{2}\sum_{i=1}^{l}\sum_{j=1}^{l} y_i y_j \alpha_i \alpha_j K(x_i, x_j) - \sum_{j=1}^{l} \alpha_j \\ &s.t.\ \ \sum_{j=1}^{l} y_j \alpha_j = 0 \\ &0 \leq \alpha_j \leq u(x_j)C, \quad j = 1, 2, \ldots, l \end{aligned}\right\}. \quad (6)$$

The linear programming design of the psychological assistance function of music education in social crises uses the square programming algorithm [13]. The optimized function for predicting the psychological assistance function of music education in social crises is as follows:

$$h(t) = H\sum_{m=1}^{M}\sum_{k=1}^{K(m)} \alpha_{mk}\delta(t - T_m - \tau_{mk}). \quad (7)$$

To construct the topological distribution function of the psychological rescue function of music education in social crisis, the statistical analysis model of psychological rescue function of music education in social crisis is as follows:

$$\frac{\partial u_i}{\partial p_i} = \frac{Gh_i}{\sum_{j\neq i} h_j p_j + \sigma^2\left(1/1 + \gamma_i - \beta_{c_1}\right)}. \tag{8}$$

According to the results of statistical analysis, the characteristics of the psychological rescue function of music education in social crisis are decomposed, and the multidimensional scale feature distribution is obtained as follows:

$$\eta_{comm} = \frac{k_1 \cdot l}{E_{comm}} \cdot \left(1 - p_{drop}\right), \tag{9}$$

where p_{drop} is the SSA-PPR model parameter of the psychological rescue function of music education in social crisis. Through the fuzziness feature extraction method, the big data feature detection of the psychological rescue function of music education in social crisis is established to establish a descriptive statistical analysis model of the psychological rescue function of music education in social crisis [14].

3. Predictive Model of Rescue Function of Music Education in Social Crisis

3.1. Big Data Analysis of the Rescue Function of Music Education in Social Crisis. This paper proposes a method for predicting the psychological rescue function of music education in the social crisis based on the SSA-PPR model. By extracting the feature analysis of the psychological rescue function of music education in social crisis [15], the distribution set of the statistical characteristics of the two-way planning to analyze the psychological rescue function of music education in social crisis is as follows:

$$S_b = \sum_{i=1}^{c} p_i\left(\vec{m}_i - \vec{m}\right)\left(\vec{m}_i - \vec{m}\right)^T, \tag{10}$$

where $\vec{m} = \sum_{i=1}^{c} p_i \vec{m}_i$ is the autocorrelation adjustment component of the psychological rescue function of music education in social crisis. According to the correlation index of the psychological rescue function of music education in social crisis, n variables of the psychological rescue function of music education in social crisis are collected. Taking the feature decomposition to get the association rule set of the psychological rescue function of music education in social crisis, expressed by a_j, the template function of the psychological rescue function prediction of music education in social crisis is described as follows:

$$\begin{cases} G_1 = b_{11}a_1 + b_{12}a_2 + \cdots b_{1n}a_n \\ G_2 = b_{21}a_1 + b_{22}a_2 + \cdots b_{2n}a_n \\ \cdots \quad \cdots \quad \cdots \\ G_n = b_{n1}a_1 + b_{n2}a_2 + \cdots + b_{nn}a_n \end{cases} \tag{11}$$

Both G_j and G_k have a strong correlation. G_k represents the difference in the psychological rescue function of music education in social crisis. G_j is the main component characteristic quantity of the psychological rescue function of music education in social crisis. The template matching method is used to obtain the adaptive weighting coefficient of the psychological rescue function of music education in social crisis, and the fuzzy information weighting matrix is as follows:

$$B = \begin{bmatrix} b_{11} & b_{12} & \cdots b_{1n} \\ b_{21} & b_{22} & \cdots b_{2n} \\ \cdots & \cdots & \cdots \\ b_{n1} & b_{n2} & \cdots b_{nn} \end{bmatrix}. \tag{12}$$

Using adaptive learning methods, the fitting coefficient of the psychological rescue function of music education in social crisis is $S = \{(x_1, y_1, u(x_1)), \ldots, (x_l, y_l, u(x_l))\}$ where $x_j \in R^n$, $u(x_j) \in \{-1, 1\}$, $\sigma \leq u(x_j) \leq 1$, σ is the model parameter of the statistics of the psychological rescue function of music education in the social crisis and $u(x_j)$ is the psychological rescue function of music education in social crisis. The output of $(x_j, y_j, u(x_j))$ is the correlation $(j = 1, \ldots, l)$ of $y_j = 1$ (positive category) or $y_j = -1$ (negative category). Combined with fuzzy information mining and adaptive learning methods, the dynamic analysis and prediction of the psychological rescue function of music education in social crisis are carried out.

3.2. Rescue Function of Music Education. According to the analysis of the psychological rescue function of music education in social crises, dynamic monitoring and feature prediction are carried out to establish the statistical characteristic quantity of psychological rescue function of music education in social crises. This improves the ability of ambiguity prediction and feature optimization judgment of the psychological rescue function of music education in social crisis. The fuzzy output feature set of music education is $CH_i(i \in C_1)$. Combined with the optimized statistical analysis results, the psychological relief effect of music education in social crisis was predicted accurately, and, the output is as follows:

$$f(x) = \operatorname{sgn}\left\{\sum_{j=1}^{l} \alpha_j^* y_j K\left(x, x_j\right) + b^*\right\}, \quad x \in R^n, \tag{13}$$

where $b^* = y_i - \sum_{j=1}^{l} y_j \alpha_j K(x_j, x_i)$, $i \in \{i \mid 0 < \alpha_i^* < u(x_i)C\}$. The statistical feature quantity of the psychological rescue function of music education in social crisis is established, and dynamic analysis based on the fusion result of the psychological rescue function of music education in social crisis is performed. The characteristic quantity of ambiguity is as follows:

$$Y_k = \left[y_{k1}, y_{k2}, \cdots, y_{kj}, \cdots, y_{kJ}\right], \quad (k = 1, 2, \cdots, N), \tag{14}$$

where y_{kj} represents the unbalanced feature quantity of the psychological rescue function of music education in social crisis and N is the data length of psychological rescue

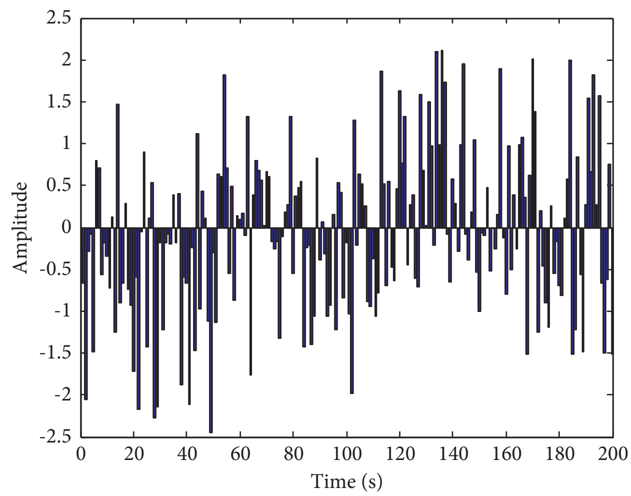

Figure 1: Time domain distribution of the psychological rescue function of music education in social crisis.

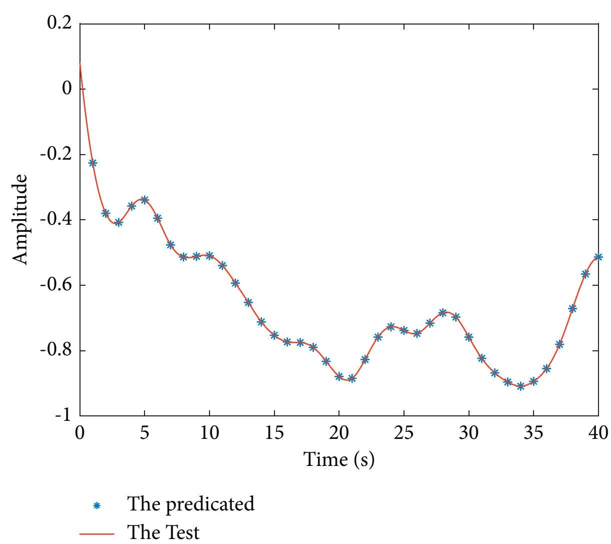

Figure 2: Rescue function index of music education in social crisis.

function of music education in social crisis. Through the association data mining, the optimization prediction and evaluation of the psychological rescue function of music education in social crisis are realized.

4. Simulation Test and Analysis

Through simulation experiments, the effectiveness of the method in this paper in realizing the prediction and quantitative analysis of the psychological rescue function of music education in social crisis is verified. The number of days of bailout guidance for social education in social crisis is 24 days, the length of the intermittent sample sampling is 1 h, the number of samples for statistical analysis of the psychological rescue function of music education is 500, the correlation coupling coefficient is 0.26, the ambiguity coefficient is 0.28, and the root mean square error is set to 0.25. According to the above parameter settings, the rescue function information of music education in social crisis is sampled, and the large data distribution of the sampled samples is shown in Figure 1.

According to the sampling results of the psychological rescue function information of music education in the social crisis in Figure 1, the changes in the psychological rescue function of music education in the social crisis are predicted. Using the SSA-PPR model to build a big data statistical analysis model for the prediction of the rescue function of music education in social crises, the rescue function index of music education in social crises is obtained, as shown in Figure 2.

It can be seen from Figure 2 that the method in this paper can effectively predict the rescue function of music education in social crisis, and the prediction has good convergence. The prediction accuracy test was conducted, and the comparison results are shown in Table 1. It can be obtained that the method proposed in this paper has a higher precision in predicting the psychological rescue function of music education in social crisis.

Table 1: Comparison of prediction accuracy of psychological rescue function of music education in social crisis.

Number of iterations	This paper method	Reference [3]	Reference [4]	Reference [6]
100	0.945	0.856	0.878	0.878
200	0.967	0.888	0.897	0.898
300	0.980	0.890	0.902	0.895
400	0.993	0.932	0.923	0.895

5. Conclusion

In order to construct an ambiguity detection and analysis model for the psychological rescue function of music education in social crises, this paper combines the method of ambiguity analysis and uses the big data statistical analysis model to predict and analyze the psychological rescue function of music education in social crisis. This paper proposes a prediction model of the psychological rescue function of music education based on quantitative statistical characteristics analysis. It uses high-dimensional phase space reconstruction technology to carry out the spatial reorganization of the psychological rescue function sequence of music education in social crisis. A descriptive statistical analysis model for the psychological rescue function of music education in social crises is established, and the big data feature detection of the psychological rescue function of music education in social crises is carried out by fuzziness feature extraction. And combined with fuzzy information mining and adaptive learning methods, the dynamic analysis and prediction of the psychological rescue function of music education in social crisis are carried out. The study shows that the accuracy of the rescue function prediction of music education in social crises in this paper is high, and the feature matching is good.

Data Availability

Data sharing not applicable to this article as no datasets were generated or analyzed during the current study.

Conflicts of Interest

The author declares that there are no conflicts of interest with respect to the research, authorship, and/or publication of this article.

Acknowledgments

This paper is the result of the project of Jilin Provincial Department of Education: The Construction of Jilin Provincial College Students' Growth Planning Platform (jjkh20200093sk) and Jilin Provincial Education Science Planning Project: Research on the Relief Function of Music in Social Crisis (gh20283).

References

[1] J. Sun, Y. Wu, G. Cui, and Y. Wang, "Finite-time real combination synchronization of three complex-variable chaotic systems with unknown parameters via sliding mode control," *Nonlinear Dynamics*, vol. 88, no. 3, pp. 1677–1690, 2017.

[2] X. Chen, T. Huang, J. Cao, J. H. Park, and J. Qiu, "Finite-time multi-switching sliding mode synchronisation for multiple uncertain complex chaotic systems with network transmission mode," *IET Control Theory & Applications*, vol. 13, no. 9, pp. 1246–1257, 2019.

[3] Y. Yu, Z. Y. Wang, and D. G. Xu, "Speed and current sensors fault detection and isolation based on adaptive observers for induction motor drivers," *Journal of Power Electronics*, vol. 5, no. 14, pp. 967–979, 2014.

[4] W. Zhang and Z. Wang, "Research on join operation of temporal big data in distributed environment," *Computer Engineering*, vol. 45, no. 3, pp. 20–25, 2019.

[5] Y. Goldberg, "A primer on neural network models for natural language processing," *Journal of Artificial Intelligence Research*, vol. 57, no. 1, pp. 345–420, 2016.

[6] H. Zhang, L. I. Chong, Y. Ke, and S. Zhang, "A distributed user browse click model algorithm," *Computer Engineering*, vol. 45, no. 3, pp. 1–6, 2019.

[7] D. Yu, X. Yuan, W. Zhang, and C. Wang, "Spatiotemporal crowdsourcing online task allocation algorithm based ondynamic threshold," *Journal of Computer Applications*, vol. 40, no. 3, pp. 658–664, 2020.

[8] T. S. Song, Y. X. Tong, L. B. Wang, and K. Xu, "Online task assignment for three types of objects under spatial crowdsourcing environment," *Journal of Software*, vol. 28, no. 3, pp. 611–630, 2017.

[9] U. ul Hassan and E. Curry, "Efficient task assignment for spatial crowdsourcing: a combinatorial fractional optimization approach with semi-bandit learning," *Expert Systems with Applications*, vol. 58, no. C, pp. 36–56, 2016.

[10] J. Wang, W. Liu, W. Xing, and S. Zhang, "Visual object tracking with multi-scale superpixels and color-feature guided kernelized correlation filters," *Signal Processing: Image Communication*, vol. 63, pp. 44–62, 2018.

[11] M. Danelljan, G. Häger, F. S. Khan, and M. Felsberg, "Discriminative scale space tracking," *IEEE Transactions on Pattern Analysis and Machine Intelligence*, vol. 39, no. 8, pp. 1561–1575, 2017.

[12] J. F. Henriques, R. Caseiro, P. Martins, and J. Batista, "High-speed tracking with kernelized correlation filters," *IEEE Transactions on Pattern Analysis and Machine Intelligence*, vol. 37, no. 3, pp. 583–596, 2015.

[13] D. S. Bolme, J. R. Beveridge, B. A. Draper et al., "Visual object tracking using adaptive correlation filters," in *Proceedings of the 2010 IEEE Conference on Computer Vision and Pattern Recognition*, pp. 2544–2550, IEEE, San Francisco, CA, June 2010.

[14] X. Zhang and Y.-H. He, "Modifid interpolatory projection method for weakly singular integral equation eigenvalue problems," *Acta Mathematicae Applicatae Sinica, English Series*, vol. 35, no. 2, pp. 327–339, 2019.

[15] Z. Zhang Chaohua, L. Li, and G. Yun, "Study on moving dislocations in decagonal quasicrystals," *Chinese Journal of Solid Mechanics*, vol. 38, no. 2, pp. 165–169, 2017.

Hindawi
Scientific Programming
Volume 2021, Article ID 6182824, 7 pages
https://doi.org/10.1155/2021/6182824

Research Article

Research on the Realization Path of College English Education Based on the SVM Algorithm Model under the Background of Cloud Computing and Wireless Communication

Lijuan Yang

Department for Candidates to Study Overseas, Xi'an International Studies University, Xi'an 710061, China

Correspondence should be addressed to Lijuan Yang; yanglijuan_edu@outlook.com

Received 27 August 2021; Accepted 12 October 2021; Published 22 October 2021

Academic Editor: Punit Gupta

The rapid development of cloud computing and wireless communication technology has brought a huge impact to traditional education methods, especially for college English education where the teaching mode is relatively simple and the impact is more than other disciplines. How to make full use of this information technology revolution and make it an opportunity for us to innovate in English education has become a topic that many scholars are paying attention to. Research on teaching innovation in the context of cloud computing and wireless communication has yielded fruitful results. This research wants to fully absorb the valuable experience of these research results, through the establishment of an optimized SVM algorithm model, and then conduct an online questionnaire survey of English majors in colleges and universities in Zhejiang Province in the form of a questionnaire survey. The design of the questionnaire mainly includes the following aspects: students' satisfaction with English education in the context of cloud computing and wireless communication, their own comprehensive English ability, and teacher's teaching ability. According to the data obtained from the questionnaire survey, combined with the SVM algorithm model for analysis, so as to optimize English teaching, the research results show that, in the context of cloud computing and wireless communication, college students are generally low in satisfaction with traditional English classroom teaching, but have a higher interest in the teaching innovation of cloud computing and wireless communication technology. This provides us with useful ideas for the realization of the path innovation of college English education at this stage.

1. Introduction

The development of cloud computing and wireless communication technology has caused violent turbulence in the traditional working mode of various industries. At this stage, people have become accustomed to life and work forms that once existed only in imagination, such as digital payment and mobile office. The influence of cloud computing and wireless communication has become more and more widespread in terms of geographical breadth and age level. In order to occupy a leading position in technology in the new era, many countries and regions have deployed and made efforts in this field. The changes brought by cloud computing and wireless communications to the education industry are also obvious [1, 2]. In addition to enriching the teaching content of the classroom, it can also promote education to a level of individualization and refinement through the construction and development of supporting applications. Therefore, whether it can actively respond to the changes brought about by the development of wireless communication technology will greatly affect the actual effect of teaching [3, 4].

English teaching has always been an area that is easily overlooked in the teaching reform of colleges and universities. On the one hand, the importance of English in nonprofessional colleges is decreasing, and on the other hand, teaching resources are limited. It is difficult for many schools to achieve innovation in teaching models through their own teaching power [5]. Under the comprehensive influence of these factors, it is difficult for college English teaching to play its due role in improving students' English ability. Xu Liangliang believes that cloud computing and wireless communication has achieved a large-scale expansion in application fields based on 5G technology. Reflected in the field of education, it is to innovate from the PPT and multimedia at the beginning of the 21st century to the current stage of network teaching and intelligent classrooms [6]. Zhang Jianhui pointed out that the development of cloud computing and wireless communication technology enables college English education to use network platforms to promote the transformation of innovative learning, and this transformation also conforms to the trend of demand for talents in the 5G era and, therefore, builds a full range of digital and intelligent English. The learning system has become an important support for college English education in the future [7]. Li Huahua believes that the English education system built on the basis of cloud computing and wireless communication technology will help teachers better arrange learning tasks according to the students' personal abilities. With the assistance of big data mining, teachers can conduct online analysis and real-time guidance of students' learning, which helps to realize the real-time communication and mutual communication between teaching subjects and objects and achieves the goal of precise teaching [8–10].

At the same time, the research results are not limited to the theoretical field. At the practical level, research on this subject is also widely carried out [10]. Some colleges and universities use cloud computing and wireless communication technology to record, broadcast, and replay English classroom content and teaching priorities, and some schools have formed a teaching resource-sharing platform to build English classrooms online so that the advantages of teaching resources can be shared [11, 12]. Teachers are only responsible for the teaching of a number of units. Teachers take turns to answer students' questions on the learning platform, avoiding the shortcomings of communication and communication between English teachers and students in colleges and universities in the past [13, 14]. The student office of some colleges and universities uses wireless intelligent assistants to remind students of English classes, sign in, etc., which not only strengthens the management of students but also reduces the workload of teachers so that they can devote all their energy to teaching [15]. In order to better transform the existing research results into practice, this research combines it with the results of the questionnaire survey to guide our follow-up teaching innovation. The SVM algorithm model is used to detect it, so as to build a college English teaching system that meets the needs of the times.

2. SVM Algorithm Model and Research Method

The SVM algorithm model has a good solution to machine learning problems with a relatively small sample size, can solve high-dimensional problems, and has a high resolution. Therefore, this paper chooses the SVM algorithm model to assist the research.

2.1. SVM Algorithm Model. The original intention of SVM is to solve the problem of binary classification, and it has a good effect on solving the problem of binary classification. The collected samples are classified in a certain way to expand the scope of the classification interval, and at the same time, the confidence interval is converged and reduced, and the empirical risk is reduced by improving the accuracy. Later, SVM introduced soft intervals to solve the nonlinear inseparable problem, through a series of kernel function transformations; the data were spatially mapped to solve the nonlinear classification problem. The architecture diagram of the SVM model is shown in Figure 1:

The optimized SVM algorithm model is as follows. When the classification is a binary classification, the output $x = \{0, 1\}$ is a binary function. The prediction function $g(k, a)$ is the discriminant function in pattern classification, and the loss function is shown in Formula (1). Among them, the loss function is $\oint F(x, g(k, a))$:

$$F(x, g(k, a)) = \begin{cases} 0, x = g(k, a) \\ 1, x \neq g(k, a) \end{cases}. \tag{1}$$

The loss function P is the loss caused by the error between the prediction function $g(k, a)$ and the real output x, where P stands for machine learning. A different P is composed of different loss functions:

$$P(a) = \oint F(x, g(k, a)) \mathrm{d}F(x, g). \tag{2}$$

2.2. Research Methods. In this paper, the method of questionnaire survey is used to obtain research data, and the sample size is calculated according to Formula (3), where Q is the sample size, M is the statistic, $M = 1.93$ when the confidence is 95% and $M = 1.67$ when the confidence is 90%, H is the error value, and U is the probability value:

$$Q = \frac{M^2 U (1 - U)}{H^2}. \tag{3}$$

2.2.1. Design of the Questionnaire. The main goal of the development of college English teaching behavior under the background of wireless communication is to improve the comprehensive ability of college students, especially non-English majors, in this field. Therefore, this questionnaire will also focus on this type of student group. In order to better eliminate the impact of students' own English ability on the survey results, the coverage of the colleges distributed by the online questionnaire of this survey is very wide. Among the 5 colleges, there are 985 colleges and ordinary undergraduate colleges. There are 30 questions in the questionnaire. The first 5 questions provide a simple understanding of the students. The remaining 25 questions can be divided into 5 aspects, namely, satisfaction with English courses, their own comprehensive ability in English, and the school's wireless communication, the application of technology, the teaching ability of English teachers, and the effectiveness of the school in teaching management. The questionnaire starts with the sixth question, and each question is set with 4 alternative answers, arranged in order

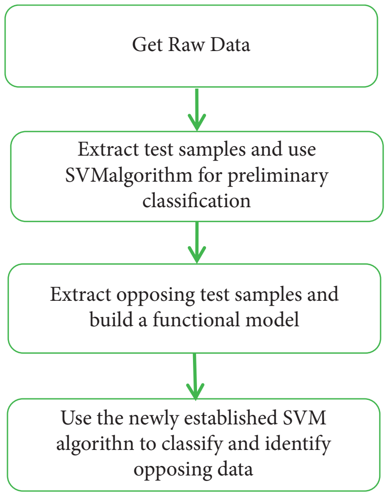

Figure 1: The architecture diagram of the SVM model.

from low to high, and are assigned values of 1–4. In order to make the calculation results more intuitive, all points are converted into a hundred-point system for horizontal comparison, as shown in Table 1.

2.2.2. Investigation Process. After the opening of each university in the first semester of 2021, one 985 university and 4 general undergraduate universities in Zhejiang Province were selected as the survey subjects. With the approval of the Academic Affairs Office of 5 universities, we loaded the questionnaire on the campus official website and invited non-English majors of grade 1–3 undergraduates to participate in answering. The questionnaire answers are valid for 2 months, and each ID is limited to one answer. A total of 1423 students participated in answering questions during the period. After screening for obviously unreasonable extreme values, there were 1298 valid questionnaires, with an effective rate of 91.2%.

It can be seen from Table 2 that the gender ratio of the students participating in the survey is relatively balanced, while the difference in grade distribution is relatively large. Sophomores accounted for more than half of the total number [16]. The second and third places were freshmen and junior students.

2.2.3. Experimental Process. Using the SVM algorithm to build a model, the first step is to preprocess various factors that affect the effect of college English classrooms and exclude specific and individual factors. Next is the extraction of general factors. It is based on the preprocessed dataset to extract information that is helpful for vector processing. Specifically, in this study, what factors can better improve the teaching effect and make it close to the ideal assignment?

3. Results and Discussion

3.1. Results. It can be seen from Figure 2 that, in the five main aspects covered by the questionnaire survey, except for the satisfaction with English courses and the English teacher's teaching ability score of nearly 80, the scores of the other three aspects are all below 70. Among them, in the school, the effectiveness score in teaching management just exceeded the passing line.

It can be seen in Figure 3 that there are certain gender differences in the respondents' responses to the questionnaire. In addition to the average score of girls in their own assessment of comprehensive English ability which is slightly higher than that of boys, the average scores of other four aspects are slightly lower than boys. It shows that girls demand for English teaching which is slightly higher than that of boys, and their comprehensive ability is also slightly higher than that of boys.

As shown in Figure 4, students' scores for the same question in this survey are also different in different grades. In addition to assigning average points in the assessment of their own comprehensive English ability, the average points assigned in the other four areas are all in the same grade as the increase in the response decreases. This reflects from the side that the enthusiasm of students in English is gradually weakening.

3.2. Discussion

3.2.1. The Characteristics of College English Courses in the Context of Cloud Computing and Wireless Communication. College English education in the context of wireless communication refers to the rapid development of wireless communication technology. College English has made a series of changes in order to conform to the trend of the times. This allows both teaching parties to get rid of the constraints of fixed learning locations and time to a large extent and achieve more efficient English teaching in the form of online teaching, video playback, and online exams. At this stage, a number of online classrooms and student management apps have been developed [17]. The former, such as Tencent conferences and Huihui classrooms, can achieve excellent teaching effects under wireless transmission; the latter includes the school treasure APP, curtain APP, and various question-making APPs. With the support of wireless communication technology, contemporary college English education has changed significantly from traditional teaching in terms of teaching mode and training goals.

(1) Professionalism: college English education at the current stage has gradually changed the past mode of unifying teaching content. Instead, in addition to public English, it has also tried to combine with the students' majors so that students can independently read the foreign literature of their majors.

(2) Practicality: under the background of wireless communication, English teaching in colleges and universities reflects higher practicability, and the teaching content can be closer to the learning needs of students and has a stronger practical value.

(3) Sustainability: although the system of linking English scores with degrees is cancelled at this stage, it does

Table 1: Thematic distribution of the questionnaire.

Title attribution	Number of questions
Basic student information	5
Satisfaction with English courses	3
Own comprehensive ability of English	4
School's application of cloud computing and wireless communication technology	7
English teacher's teaching ability	6
Effectiveness of the school in teaching management	5

Table 2: Basic information of students participating in the survey (only valid answers).

Category		Number
Gender	Boys	632
	Girls	666
Grade	Freshman	442
	Sophomore	658
	Junior	323

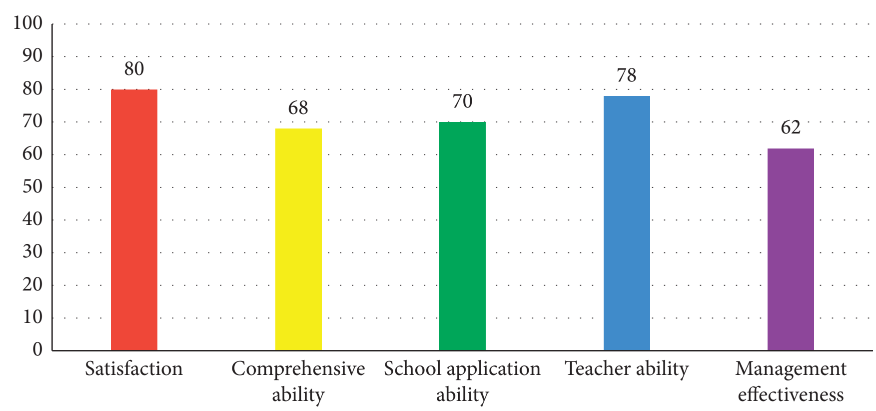

Figure 2: Distribution of average scores from questionnaire survey.

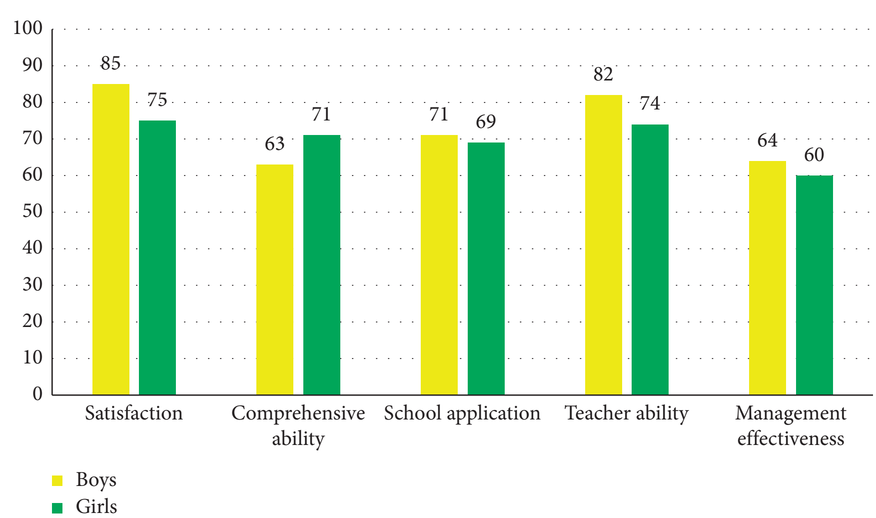

Figure 3: Analysis of the difference in scores between males and females in the questionnaire survey.

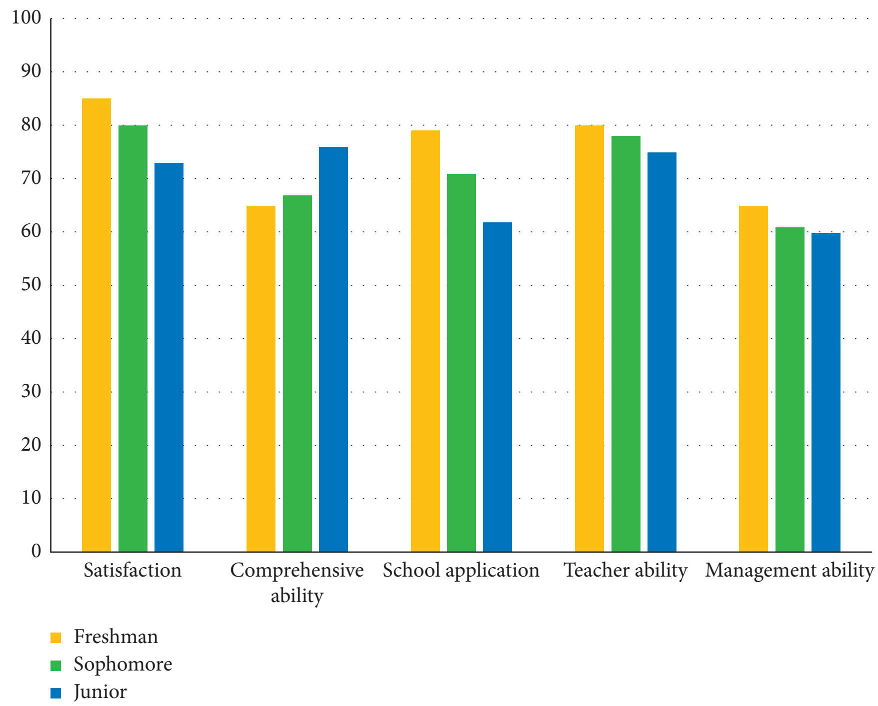

Figure 4: Analysis of the differences in the scores of students in each grade.

not mean that the "tradition" of students saying goodbye to English after taking the CET exam is still continuing. On the contrary, the continuity of English learning has been enhanced because the English that students learn has been transformed into a real boost to improve their professionalism.

(4) Changes in teaching objectives: the goal of developing college English education is to improve students' English proficiency so that students have better academic research and expression skills. This is very different from the one-sided focus on public English in the past and the emphasis on CET pass rate. In the past, most non-English major colleges and universities in my country only offered English courses in the freshman and sophomore years. Students basically say goodbye to English when they reach the third grade. Except for students who need postgraduate entrance examinations or going abroad, it can be said that they will not invest more in English and more in energy to learn. Today, with the rapid development of wireless communication technology, students have more opportunities and a broader platform to learn English, which provides a solid guarantee for the change of teaching goals.

3.2.2. The Changes Brought by Cloud Computing and Wireless Communication Technology to College English Education

(1) Enhance the richness of teaching resources: wireless communication technology enables all kinds of resources to be transmitted to students' information terminals more quickly and conveniently. On the basis that 5G has increased the transmission rate by nearly a hundred times, students can browse the educational resources designated by teachers almost at any time. In addition, with the transformation of the teaching objectives of contemporary college English teaching, more and more colleges and universities use actual simulation as an important means to improve the practicality of English teaching. This requires not only comprehensive resource integration but also human-computer interaction and other forms to stimulate students' enthusiasm. In this field, the advantages of wireless communication are enormous.

(2) Expanded the flexibility of teaching methods: the traditional college English classroom is almost in the same line as the middle and high school stages. Teachers follow the fixed process of "word recitation-text explanation-grammar focus" and review later. Effective interaction between the two parties is extremely limited. The development of wireless communication technology provides an excellent opportunity to change this model. Both parties can expand according to the content to be taught in the classroom and adopt flexible teaching methods.

(3) Promote students' understanding and absorption of what they have learned: in the past, the most important way for college students to learn English was by rote memorization, striving to pass the CET exam in the shortest time. Students rarely have a deep understanding of word methods and grammatical connotations. As a result, although some students

obtain high scores in the CET exam, their practical ability to use English is very limited, and they lack the favorable conditions for actual simulation. The reduction in tariffs and the increase in the rate brought about by the development of wireless communication technology have greatly increased the opportunities for students to communicate online, thereby deepening the students' understanding and absorption of what they have learned.

(4) Freedom of teaching space: the construction of college English teaching based on the highly developed wireless communication technology not only has obvious advantages in teaching content and teaching effects but also solves the fixedness of teaching space to a large extent. Teachers and students do not need to go to a fixed classroom to start teaching, but only need to participate in the teaching process through the wireless information terminal at the specified time. This not only saves time but also allows both teachers and students to interact in a more free and comfortable environment.

3.2.3. Current Problems in English Education

(1) English teachers still occupy the leading position in the classroom: on the one hand, students' enthusiasm in class is not high. Except for professional English colleges, English is just an ordinary public course in colleges and universities. Coupled with the recent cancellation of the CET test score and degree linkage system, students' enthusiasm for learning has greatly reduced. On the other hand, college English teachers must complete the teaching tasks specified by the Academic Affairs Office within a very limited class time and can only tell as much as possible in the classroom.

(2) Some students have a serious perfunctory mentality: based on wireless communication technology, many colleges and universities have developed or purchased APPs for students' English learning and uploaded corresponding learning resources in combination with the teaching plan. Students are required to check-in and complete a certain number of exercises every day. This idea is the scientific use of wireless communication technology. However, from the actual effect, many students have a serious perfunctory mentality, and some even spend money to hire classmates to complete their homework tasks. This not only failed to improve the ability but also caused a great waste of learning resources.

(3) Limited improvement in students' English application ability: the study found that the English application ability of college students has not been significantly improved due to the development of wireless technology. The main reason is that the current evaluation of the teaching ability of English teachers in colleges and universities still stays at the rigid indicator of the CET pass rate of the teaching class. Therefore, teachers have to focus on the students' test-taking ability in the teaching process. Although the application ability training has increased, in fact, the improvement of students' English application ability is very limited.

Therefore, colleges and universities should focus on improving students' enthusiasm for English learning and carry out targeted reforms in response to the abovementioned problems existing in traditional English teaching. Exams are important, but the ultimate goal of English learning is to enable students to express themselves in English flexibly. Colleges and universities should pay attention to improving students' English application ability.

4. Suggestions on the Realization Path of College English Education under the Background of Cloud Computing and Wireless Communication

4.1. Give Students More Room to Play. Although the CET is cancelled through the degree-linked system, it does not mean that English teaching should be ignored. This will make students misunderstand the importance of English. Teachers in colleges and universities can boldly adopt a variety of teaching modes, reduce the prescribed teaching tasks, and advocate increasing the guidance of students' language expression and appreciation of masterpieces.Conditional schools can investigate students' learning intentions and points of interest through the Internet, divide students into corresponding groups for learning, and open up the assessment methods [18]. Enable students to learn really because of interest.

4.2. Actively Adjust Students' Perfunctory Psychology. Combine institutional management and ideological education to guide students to change their perfunctory psychology in the field of English learning. For example, regular video scanning is performed when students are doing questions, and check-in is performed by fingerprint entry or face recognition technology [19]. For students who adopt employment, plagiarism, etc. in the course of homework, once discovered, the final grade will be judged as a failure, in order to enhance the students' emphasis on English learning.

4.3. Pay Attention to the Improvement of Students' English Ability. Colleges and universities should focus on building a comprehensive evaluation system, formulate and emphasize guidelines for the improvement of CET pass rate and application ability, and allow teachers to actively balance the proportion of test-taking ability and application ability training. Choose more scientific methods in written expression and oral language, invest more energy, and fully realize the instrumental nature of English. Efforts to enable students to improve their comprehensive abilities while passing the CET exam.

5. Conclusion

With the closer integration of cloud computing and wireless communication technology with college English education, traditional English classrooms have undergone tremendous changes, showing many new features from teaching models and teaching concepts to teaching goals. At the same time, due to the adjustment of the system, the enthusiasm of non-English majors in colleges and universities for English learning has been reduced. How to scientifically deal with the challenges brought about by the combined forces of these multiple factors is a key issue facing our college English education at this stage. Through experimental research, it can be seen that, due to differences in gender and grade, students have different attitudes towards English learning in the context of wireless communication. We should actively adjust and start with self-transformation. Integrate English teaching with the professional needs of students and, at the same time, have the courage to break through the limitations of teaching methods, and choose teaching methods that can more stimulate students' interest to serve teaching. With the help of the SVM algorithm, find out several key factors to improve the teaching effect. This points out the direction for us to continue in-depth research and also provides a scientific basis for the next step of carrying out differentiated experiments.

Data Availability

Data sharing is not applicable to this article as no datasets were generated or analysed during the current study.

Conflicts of Interest

The authors declare that they have no conflicts of interest.

Acknowledgments

This research was supported by the Shaanxi Provincial Social Science Foundation (Project no. 2016K014).

References

[1] J. Li and M. Wang, "Practical teaching problems and improvement strategies for English education majors in local colleges and universities," *University Education*, vol. 6, pp. 124–127, 2021.

[2] Z. Wang, "Analysis of the current situation of the influence of network teaching on college students' English ability," *Overseas English*, vol. 10, pp. 125-126, 2021.

[3] L. Cui, "The construction of an ecological model of college English education in the new era: a review of "cross-cultural communication research and the innovative exploration of college English teaching," *Chinese Journal of Education*, vol. 5, p. 130, 2021.

[4] Y. Han and F. Sun, "Thoughts on the design and implementation of open examinations in the reform of college English teaching," *Modern Communication*, vol. 6, pp. 177–179, 2021.

[5] Misha and N. He, "Innovation and practice of college English education and teaching in the new media era," *Food Research and Development*, vol. 42, no. 3, p. 235, 2021.

[6] L. Xu and W. Zhang, "Application of wireless communication technology in digitalization," *Electronic Technology and Software Engineering*, vol. 9, pp. 21-22, 2020.

[7] H. Pan and X. Ma, "Diversified needs and effective teaching of English education in colleges and universities: from the perspective of subject experts and students," *Foreign Languages in China*, vol. 17, no. 6, pp. 69–76, 2020.

[8] L. X. hua, "Research on the path of precision poverty alleviation in college English language education under the background of "internet +," *Microcomputer Applications*, vol. 35, no. 12, pp. 37–39, 2019.

[9] Y. Guo, "Innovative practice of multi-modal teaching mode in college English education and teaching practice," *High Education Journal*, vol. 13, pp. 22–24, 2019.

[10] S. Chen and X. Chen, "The reform of the "2+1" talent training model for English education majors in colleges and universities in the era of "internet +"-based on the perspective of credit banks," *Journal of Hubei University of Economics (Humanities and Social Sciences Edition)*, vol. 16, no. 5, pp. 154–157, 2019.

[11] Y. Dong, "Research on the influence of multicultural integration on contemporary college English teaching," *Food Research and Development*, vol. 20, 2020.

[12] M. Peng, "The changes brought about by the development of new media to college English teaching," *Chinese and Foreign Entrepreneurs*, vol. 673, no. 11, p. 212, 2020.

[13] Y. Ma, "Research on the development of college English teaching model from the perspective of \\"internet+," *Journal of Hubei Correspondence University*, vol. 032, no. 6, pp. 134-135, 2019.

[14] A. Elzamly, B. Hussin, S. A. Naser, and K. Khanfar, "A new conceptual framework modelling for cloud computing risk management in banking organizations," *International Journal of Grid and Distributed Computing*, vol. 32, no. 3, pp. 137–154, 2016.

[15] "Rethinking the meaning of cloud computing for health care: a taxonomic perspective and future research directions," *Journal of Medical Internet Research*, vol. 20, no. 7, pp. 216–226, 2018.

[16] Y. Wang, "Teaching practice of college English education under the mode of micro-classes-comment on "informative teaching reform of college English teaching and exploration of micro-class teaching mode," *Forest Products Industry*, vol. 58, no. 1, p. 110, 2021.

[17] X. Gao, "Analysis of the practical application of listening and speaking teaching theory in college English education and teaching-comment on "English classroom teaching mode," *Chinese Journal of Topical Crops*, vol. 42, no. 6, p. 1820, 2021.

[18] D. Liu, "Research on Chinese cultural identity in the development of English education in colleges and universities-comment on "the changes of Chinese modern college English education and the renaissance of Chinese culture," *Science and Technology Management Research*, vol. 41, no. 10, p. 234, 2021.

[19] Y. Li, "An analysis of college English education and teaching based on a multicultural perspective," *Shaanxi Education (Higher Education)*, vol. 8, pp. 43-44, 2021.

Hindawi
Scientific Programming
Volume 2021, Article ID 4520642, 9 pages
https://doi.org/10.1155/2021/4520642

Research Article

Research on the Involvement of Computer Graphics Algorithms in Systems for the Creation of Public Sculpture

Acheng Zhou and Chao Gao

School of Design, Jiangnan University, Wuxi 214122, Jiangsu, China

Correspondence should be addressed to Chao Gao; 1810012022@stu.jci.edu.cn

Received 14 September 2021; Accepted 9 October 2021; Published 21 October 2021

Academic Editor: Punit Gupta

Currently, there is less research on how to improve the efficiency of the application of computer graphics technology in the creation of public sculpture. Therefore, this paper will focus on how computer graphics algorithms can enable systems for the creation of public sculpture with the intervention of computer graphics technology to create more accurate and completed works of public sculpture. It will explore and analyze how computer image algorithms can help creators apply computer image technology to finish complete and accurate public sculptures, and individual studies, computer imagery, and model analysis are also used. In systems for the creation of public sculpture, the point cloud data of the model is obtained through 3D laser scanning technology; then the algorithm of the point cloud model is integrated and the Statistical Outlier Removal algorithm of the point cloud model intervention is processed. By this way, the point cloud model of the work is optimized, and then a more completed and accurate public sculpture work can be produced by 3D sculpting or 3D printing. The research shows that, in the creation of public sculptures with the intervention of computer graphics technology, the computer graphics algorithm acquires the basis of the high-definition public sculpture data model. The computer graphics algorithm improves the accuracy and completeness of the creator using computer graphics technology; it is also the key to transform the accurate enlargement and transformation of the sculptural model into the actual sculptural work.

1. Introduction

Up to now, specialized computer graphics techniques and tools for the creation of public sculpture, such as ZBrush, Mudbox, 3D-Coat, 3ds Max, Blender, and Maya, have become common means of creation for many artists because those techniques and tools can broaden the creative approach of creators [1]. In the planning, designing, implementation, displaying, and dissemination of public sculpture, especially in the process of creating public proper sculpture, computer graphics technology is playing a big and important role in the development of public sculpture [2]. Along with the development of computer graphics technology, computer graphics technologies such as 3D scanning, 3D printing, and 3D sculpting, as well as related materials and equipment, have emerged one after another. These techniques, materials, and equipment have been gradually involved in the creation of public sculpture and have great potential prospects for application. At the same time, some scholars in China have also begun to pay attention to this, for example, Liao Anshun's thesis on "*The Use of Computer Image Technology in Public Sculpture Design*" [3], Zhang Wang's thesis on "*The Application of Computer Image Technology in Modern Public Sculpture*" [4], and Zheng Miao and Deng Wei's thesis on "*A New Approach to Plastic Art—Talking about Digital Technology Intervention in Sculpture*" [5]; all the mentioned scholars and their papers have discussed this issue from different perspectives. The paper titled "*A New Approach to Plastic Art—Talking about Digital Technology Intervention in Sculpture Art*" by Zheng Miao and Deng Wei explores this issue from different perspectives. However, little research has been conducted on how to improve the integrity and accuracy of public sculptures created by creators using computer graphics technology.

In order to investigate how to make the public sculptures created by the public sculpture creation system with the intervention of computer graphics technology more accurate and complete, this paper will introduce some practical examples of public sculpture and analysis of relevant computer graphics algorithm formulas and models. Two questions will be mainly discussed in this paper: (1) What are the key points of computer graphics algorithms in systems for creation of public sculpture? (2) Which computer graphics algorithms and how can they be used to improve the accuracy and integrity of public sculptures created by computer graphics technology? These questions are explored in two separate sections: firstly, an analysis of the pathway for computer graphics algorithms to intervene in the creation of public sculpture and, secondly, an analysis of the specific ways in which computer graphics algorithms can intervene in the creation of public sculpture.

2. Pathways for the Intervention of Computer Graphics Algorithms in Systems for Creation of Public Sculpture

Computer image algorithms are the software systems that make computer image technology possible, and, in this perspective, computer image algorithms are also called digital image processing algorithms. The involvement of computer graphics algorithms in the creation of public sculpture is achieved through computer graphics technology. Therefore, a study of the path of computer graphics algorithms in systems for creation of public sculpture also needs to start with the way in which computer graphics technology intervenes in public sculpture creation systems.

Systems for creation of public sculpture are formed on the basis of urban master plans and therefore they do not have a fixed pattern [6]. In order to clearly understand the involvement of computer graphics algorithms in the creation of public sculpture, we can start by analyzing the involvement of computer graphics technology in the creation of public sculpture. On this basis, we can then explore the involvement of computer graphics technology in the creation of public sculpture itself, and, by this, the key points of the involvement of computer graphics algorithms in the creation of public sculpture can be clearly clarified.

2.1. Intervention in Public Sculpture Creation Process System through Computer Graphics Technology. In terms of the process of creating public sculpture, the system of creating public sculpture can be understood as follows: planning of public sculpture—creation of design—production of works—installation of works—display and dissemination. This creation system is the procedure for the creation of public sculpture and can therefore also be called the public sculpture creation process system. However, the steps in the public sculpture creation process system are not linear but have nonlinear characteristics. The path of computer graphics algorithms in the creation of public sculpture can be analyzed through the model of a public sculpture creation process system involving computer technology.

In order to help the creator to complete the creation of the public sculpture, different computer graphics technologies can be involved in each stage of the public sculpture creation process. In the planning stage of public sculpture, software and technologies such as planimetric mapping, 3D mapping, spatial analysis, and virtual reality can be involved; in the design stage, software and technologies such as 2D design, 3D modelling, and 3D scanning software can be involved; in the production stage, technologies and tools such as 3D printing, numerical control, and digital materials can be involved; in the installation stage, software and technologies such as planimetric mapping and 3D mapping can be involved; and, in the display and dissemination stage, software and technologies such as numerical control and multimedia can be involved. Software and technology can be involved in the installation stage of the work; in the display and dissemination stage, technology such as CNC, multimedia, and Internet technology can be involved.

In the process of creating public sculpture, computer graphics technology will also intervene in systems for creation of public sculpture as a means of artistic expression for the creator. Its intervention in the creation system of public sculpture is mainly manifested in two ways, namely, the method of using digital technology as a starting point and the method of using public sculpture as a starting point. The specific expressions are as follows: (i) the use of digital technology means related to information expressions such as lighting, sound, and three-dimensional images [7] and (ii) the use of traditional public sculpture languages such as materials, shapes, and contexts [8]. In general, the traditional language of public sculpture is the inner shell and the digital technology is the outer one, and both work together to make computer graphics technology reasonably effective in the creation of public sculpture.

In order to introduce computer graphics technology into the creation of public sculpture in a natural, dynamic, and scientific way, its involvement in the creation of public sculpture needs to be carried out under certain conditions and bases. [9] In other words, there are certain principles that need to be followed when computer graphics technology is introduced into the creation of public sculpture. Firstly, the basic characteristics of public sculpture must be followed and the concept of art for the public must be upheld [10]. Secondly, the public should be the main subject, and the relationship between the public, public sculpture, and public space should be well coordinated [11]. It is also necessary to follow the characteristics of digital technology and to grasp the intrinsic links between the various factors involved in the creation of public sculpture, so that it can give full play to creativity in the system [12]. In addition, the systemic and creative nature of the creation of public sculpture must be followed [13]. This means that the basic characteristics of public sculpture, the principle of the trinity of public, public sculpture, and public space, the characteristics of digital technology itself, and the principles of systemic and creative creation must be followed.

In other words, when computer graphics technology is intervened in public sculpture creation program system, the functions and themes to be achieved have to be considered, certain principles have to be obeyed, and relevant methods have to be used, so that all parts of the public sculpture creation process can be complementary, interrelated, and integrated into one [14]. The integration of computer graphics technology into the process of creating public sculpture allows for a high degree of integration between digital technology and the creation of public sculpture, optimizing the process of creation and greatly reducing the time and cost of production, as well as ensuring the accuracy, ease of installation, and safety of use of the work. In short, the involvement of computer graphics technology in the creation of public sculptures can make the creation of public sculptures more rational, systematic, and effective. A model of a public sculpture creation process involving computer graphics technology is shown in Figure 1.

The computer graphics algorithm, in short, is a computer graphics technology that intervenes in the "planning—creation—design—installation—display and dissemination" of public sculpture according to the functions and themes to be achieved, following certain principles and using relevant methods. The process of creating a public sculpture is based on the principles of planning—creating—designing—installing—displaying, and disseminating, and thus, it helps the creator to complete the public sculpture.

2.2. Intervention in the Ontological System of Public Sculpture Creation through Computer Graphics Technology. The creation process system of public sculpture contains a number of unit links, which can be regarded subsystems of the creation process system [15]. The process of creation, design, production, and installation is the process of creating the body of public sculpture, which can be called the ontological creation system of public sculpture. This ontological system of public sculpture creation determines the way in which public sculpture artworks exist, and its system composition has a close relationship with public space and audiences [16]. Therefore, it can be said that the ontological system of public sculpture creation is the core of the public sculpture creation process system. The effect of the intervention of computer graphics technology in the ontological system of public sculpture creation has a decisive impact on the quality of public sculpture.

The involvement of computer graphics technology in the creation of public sculpture is also based on the functions and themes to be achieved and on certain principles and methods. In addition, it is important to adhere to the concept of creation and to apply computer graphics technology on the base of the way in which the art exists. Besides, the significance and value of computer graphics technology in the creation of public sculpture should be considered. Moreover, it is necessary to analyze and study what kind of computer graphics technology should be involved, in what way, and in which system and link the concept and positioning of the creation to the various units of the system of ontological creation, so as to play the proper role of the system together [17]. For example, the Chinese artist Dong Shubing created the public sculpture "Son of the Earth" firstly acquiring the data model through 3D scanning of the sleeping baby and then enlarging the whole model to 15 metres long and dividing it into 40 cm square units, followed by sculpting the red sandstone material into solid units according to the content and size of the units through 3D sculpting technology and finally putting the units together. The solid units are then assembled and placed in a monumental size on the Gobi beach, conveying the idea of a sleeping child of the Earth lying in the arms of the sky and the Earth. The author has carried his concept through to the positioning of the infant figure and the ontology creation system through a series of steps such as 3D scanning to obtain the data model—analysis and refinement of the 3D data model—division of the 3D data model—sculpting of the divided data model units—installation of the work in a series of ontological creation systems (as shown in Figure 2). Throughout the creation system of this work, computer graphics technology strongly supports the author's creating process, creative ideas, and the realization of the artistic presence of the public sculpture [18].

Of course, the main way in which computer graphics technology is currently being used for creation is to combine it with manual creation. This, then, requires full consideration of the integration of digital technology with the manual shaping process. In the ontological creation of such public sculptures, the creation of small sculptural drafts is usually done manually, and then the small drafts are scanned through 3D scanning technology and tools; then the scanned data is processed and enlarged, and, next, the public sculptures are printed using 3D printing technology and tools and finally modified and refined by hand. For example, Chinese artist Sui Jianguo's public sculptures in the Handwriting series were created using a combination of 3D scanning and 3D printing technology. The sculptural forms of clay or plaster made by hand are scanned by the author using 3D scanning technology and then enlarged in a computer to show clearly the texture of the hand that remains in it, and then the enlarged forms are printed out in fine detail using 3D printing technology, and finally the work is finished by turning and installing (as shown in Figure 3). Through 3D scanning technology and 3D printing, presenting the creator's manuscript in a clear and complete enlargement becomes a quite possibility. Besides this, new connotation and meaning of the product are displayed.

In this type of ontology system, 3D scanning and 3D printing technologies allow the creator to have more space and possibilities for artistic expression. In this type of public sculpture, the accuracy of 3D scanning and 3D printing technology has a crucial impact on the degree of completion of the public sculpture [19]. Improving the accuracy of 3D scanning and 3D printing technologies and tools is therefore key to their efficient involvement in the creation of public sculptures.

In the process of creating a system of public sculpture with the involvement of computer graphics technology, 3D scanning is the process of acquiring model data and 3D

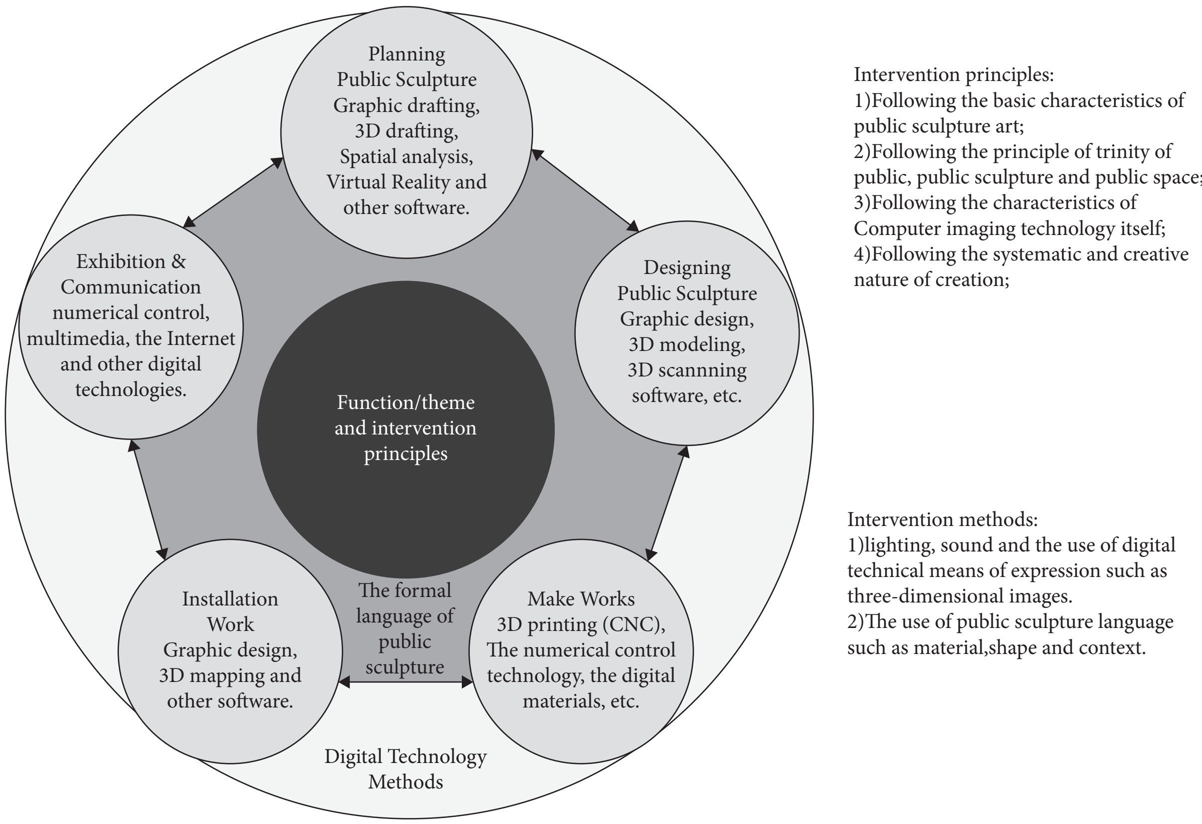

Figure 1: A model of a public sculpture creation system with the intervention of computer graphics technology.

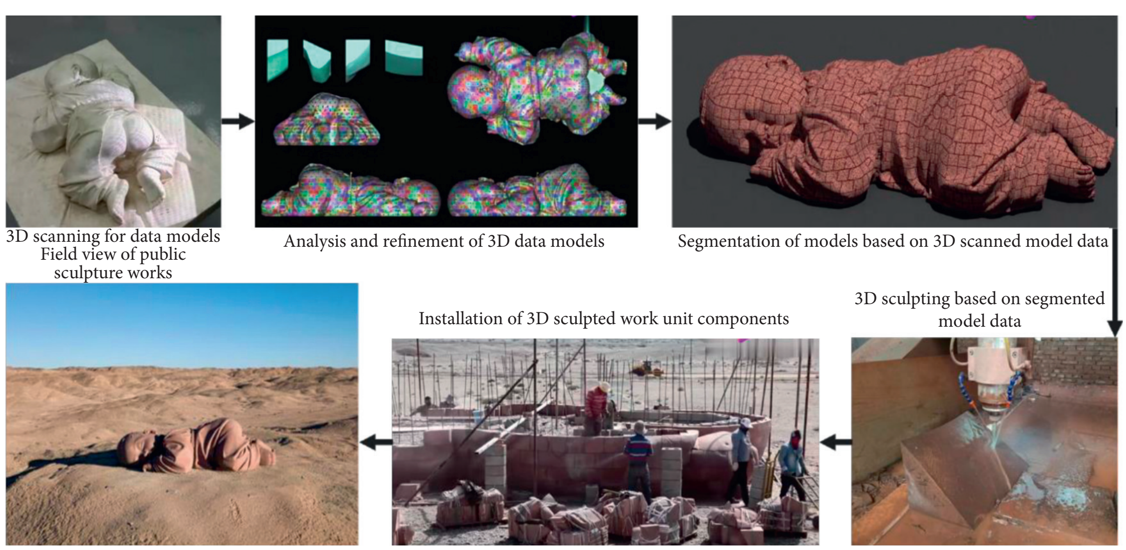

Figure 2: Intervention of computer graphics technology in the ontological system process of the creation of Children of the Earth.

printing or sculpting is the process of outputting the data [20]. The key to improving the accuracy of 3D printing or 3D sculpting techniques and tools lies in the process of improving the accuracy of the data model acquiring and outputting. In the process of acquiring data model and outputting it, with certain amount of 3D scanning equipment, the key to improving the accuracy of the acquired data lies in the processing of the acquired with a certain amount of 3D scanning equipment, and the key to improving the accuracy of the acquired data model lies in the processing of the acquired data model. That is to say, in the case of certain amount of 3D scanning equipment, after 3D scanning of the work model, the acquired 3D model data also needs to be processed to make the 3D data more accurate and complete, and then accurate and complete works can be produced through 3D printing technology. From this point of view, in the process of creating public sculptures with the involvement of computer graphics technology, the integrity and

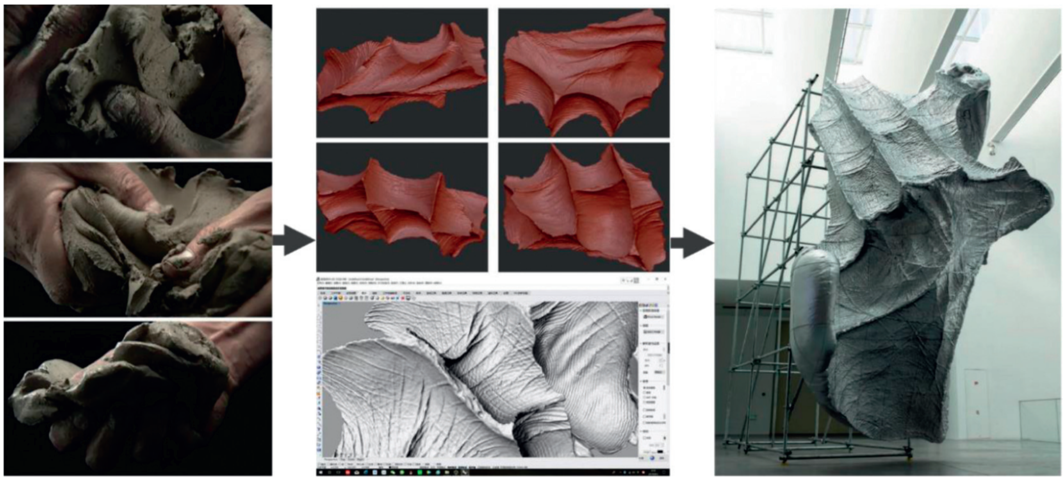

Some forms of the hand pinch Processing of data collecting by 3D scanning A 3D-printed sculpture

Figure 3: Computer graphics intervention in the making of the sculpture "Handwriting."

accuracy of the work depend on the collection and processing of the data of the public sculpture [21]. This requires the intervention of computer graphics algorithms, which are thus involved in the creation of public sculpture systems to help creators use computer graphics technology to create complete and accurate public sculptures. In short, the key to improving the accuracy of 3D scanning and 3D printing technologies and tools is the intervention of computer graphics algorithms.

3. Intervention Methods of Computer Graphics Algorithms in Systems for Creation of Public Sculpture

In systems for creation of public sculpture, since the intervention of computer graphics algorithm is the key to the creator's ability to create accurate and complete public sculptures through computer graphics technology, what kinds of computer graphics algorithms are used? How can they be used to help the creator to create accurate works? These questions are addressed in the following discussions: the computer graphics algorithms and their interventions in the collection, processing, and output of data from the model objects of public sculpture.

3.1. Collecting Data of Public Sculptural Works. In the practice of creating public sculptures, 3D laser scanning, also known as point cloud scanning, is the most common 3D scanning technique used to obtain data models of works. This technology is currently more mature and has a very high accuracy, for example, the 3D CaMega body scanner from Beijing Bovee Hengxin, with a measurement accuracy of 0.50 mm. Using 3D laser scanning technology based on harmless white light to scan the whole body, this scanner can obtain accurate 3D data of the human as quickly as several seconds [22].

Point cloud scanning technology incorporates photonics, computer graphics, and information processing and computer vision technologies. The principle is to obtain the spatial coordinate data of the object surface by scanning the spatial shape and structure of the object [23]. In order to obtain a point cloud model data of the object, the point cloud scanning technique takes a noncontact approach, scanning the spatial shape and structure of the object to obtain the spatial coordinates of the surface.

The 3D point cloud data model is formed using geometric data of the surface of the object obtained by scanning the target object using the 3D scanning tool, which has a customized 3D coordinate system (see Figure 4) consisting of three mutually perpendicular X-, Y-, and Z-axes, capable of indicating the point cloud coordinate data of the object. When the 3D point cloud scanner is used to acquire the point cloud data, a laser emitter sends a laser pulse to the target object, which is then diffusely reflected on the surface of the target object and the laser signal returns in an almost identical path, which is then received by the built-in receiver of the instrument, and then this instrument calculates the distance between the target point and the scanner. At the same time, the scanner detects and counts the transverse angular value α and the longitudinal angular value θ of the pulse signal [24]. From this, the point cloud coordinates of the target object can be calculated according to equation (1), which enables the point cloud coordinates to be calculated, thus obtaining the point cloud data of the object.

$$\begin{cases} X_P = S \cos \theta \cos a, \\ Y_P = S \cos \theta \sin a, \\ Z_P = S \sin \theta. \end{cases} \tag{1}$$

During the period of creating a public sculpture, the creator can use the 3D point cloud scanner to scan the model of the public sculpture or the solid object without contact and therefore without damage to the scanned object. Once the scanning of the model or solid object is completed, the point cloud data of the model or solid object can be obtained with the intervention of the cloud point 3D coordinate formula. For example, when the Chinese artist Dong

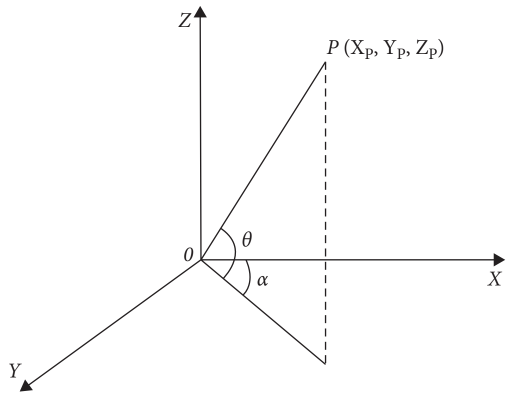

Figure 4: Diagram of the coordinate system in the 3D scanning tool.

Shubing created the work "'Children of the Earth," he used this scanning technique to scan a baby to obtain data of the model object; when the Chinese artist Sui Jianguo created the series "Handwriting," he used this scanning technique to scan a hand-crafted clay model to obtain data of the model object.

3.2. Processing of Data Models for Public Sculpture Works. In the creation of public sculpture, the quality of the point cloud model directly determines the accuracy and completeness of the public sculpture produced by 3D printing technology [25]. However, public sculptures are often complex, and it is difficult to obtain accurate and complete point cloud data from just one perspective. Therefore, in order to collect more accurate and complete point cloud data models, it is often necessary to use a multiangle scanning approach to obtain data of public sculptures in multiple directions. This then requires the processing of the collected point cloud data models in multiple orientations. The processing of the collected point cloud data models is an essential part of improving the quality of the point cloud models. The processing of the collected point cloud data models consists of two steps: integration of the point cloud data models and noise reduction of the point cloud data models.

3.2.1. Integration of Point Cloud Data Model. The point cloud data models of public sculptures obtained from different angles by 3D scanning equipment need to be integrated to form a complete point cloud model. This requires the point cloud data models from different angles to be converted into the same coordinate system, a process known as integration of point cloud data models [26].

When the same 3D scanning device is used to scan a model object of a public sculpture, the point cloud data models obtained from different angles have the same proportional relationship to each other and can be converted to a uniform coordinate system by simply translating or rotating the different point cloud data models when integrating them. That is to say, if the coordinates of the first set of point cloud data models (x_1, y_1, z_1) are transformed into the coordinates of the second set of point cloud data models (x_2, y_2, z_2), only three rotation parameters (α, β, γ) and three translation parameters $(\Lambda x, \Lambda y, \Lambda z)$ need to be transformed. Of course, if these six parameters are to be calculated, more than three points are required to be common to the different point cloud data models. The algorithm for the conversion of point cloud data model coordinates is given in equations (2) and (3) [27].

$$\begin{bmatrix} X \\ Y \\ Z \end{bmatrix} = R(a, \beta, \gamma) \begin{bmatrix} x \\ y \\ z \end{bmatrix} + \begin{bmatrix} \Lambda x \\ \Lambda y \\ \Lambda z \end{bmatrix}. \tag{2}$$

From equation (2),

$$R = \begin{bmatrix} \cos\beta\cos\gamma & \cos\beta\sin\gamma & -\sin\beta \\ -\cos\alpha\sin\gamma + \sin\alpha\sin\beta\cos\gamma & \cos\alpha\cos\gamma + \sin\alpha\sin\beta\sin\gamma & \sin\alpha\cos\beta \\ \sin\alpha\sin\gamma + \cos\alpha\sin\beta\cos\gamma & -\sin\alpha\cos\gamma + \cos\alpha\sin\beta\sin\gamma & \cos\alpha\cos\beta \end{bmatrix}. \tag{3}$$

There are two ways to integrate point cloud data model: the first way is feature-point-based integration and the second is non-feature-point-based integration [28]. The feature-point-based integration approach is to identify more obvious feature points between each point cloud data model to be integrated and then to integrate the coordinate parameters of these feature points to complete the integration of the point cloud data model. In public sculpture creation systems, the feature-point-based integration approach is more suitable for integrating the point cloud data models of public sculpture objects, because public sculptures usually have unique modelling characteristics.

The integration process based on feature points is as follows [29]:

(1) Find the feature points p_1, p_2, p_3 of the first set of point cloud data model and the corresponding feature points b_1, b_2, b_3 of the second set of point cloud data model.

(2) As the following vector: $(p_1 - p_2)$, $(p_3 - p_1)$, $(b_2 - b_1)$, $(b_3 - b_1)$, order $N_1 = p_2 - p_1$ and $M_1 = b_2 - b_1$.

(3) As the following vector: U_3 and M_3.

$$\begin{cases} U_3 = U_1 \times (p_3 - p_1), \\ M_3 = M_1 \times (b_3 - b_1). \end{cases} \quad (4)$$

(4) As the following vector: N_2 and M_2.

$$\begin{cases} U_2 = U_3 \times U_1, \\ M_2 = M_3 \times M_1. \end{cases} \quad (5)$$

(5) As the following unit vector:

$$\begin{aligned} u_1 &= \frac{u_1}{|u_1|}, \\ u_2 &= \frac{u_2}{|u_2|}, \\ u_3 &= \frac{u_3}{|u_3|}. \\ m_1 &= \frac{M_1}{|M_1|}, \\ m_2 &= \frac{M_2}{|M_2|}, \\ m_3 &= \frac{M_3}{|M_3|}. \end{aligned} \quad (6)$$

(6) Convert any point of $[n]$ to $[m]$ by the formula $P_i' = P_i R + T$.

(7) Since $[m] = [u]R$, the rotation matrix $R = [u]^{-1}[m]$ can be solved for.

(8) Let $P_1' = b_1$ and $P_1 = p_1$, and bring them into the formula $P_i' = P_i R + T$, then the translation matrix can be derived as follows:

$$T = b_1 - p_1 [u]^{-1} [m]. \quad (7)$$

(9) Based on the previous equations, the equation formula for integrating the point cloud data model for public sculptures can be rewritten as follows:

$$A\prime = A[u]^{-1}[m] - A_1 [u]^{-1}[m] + b_1. \quad (8)$$

Based on the above steps, the integration of different point cloud data models of the same public sculpture model object can be achieved with the intervention of the computer graphics algorithm formula; all these can make the point cloud model obtained by scanning the public sculpture model or solid object with the 3D scanning tool more accurate and complete.

3.2.2. Noise Reduction Processing by Point Cloud Model. When acquiring point cloud data models of public sculptures or solid objects through 3D scanning, the acquired point cloud data models may produce some noise in the point cloud data models due to the influence of the instruments or the working environment. In systems for creation of public sculpture, these noises in the point cloud model will have a negative impact on the main body of the point cloud model, which in turn will affect the quality of the public sculpture produced by the 3D printing technology. Therefore, in order to obtain a clearer and more detailed 3D model, the point cloud data model needs to be integrated and then noise-reduced.

Some noise can be easily noted, and it can be dealt with manually, while less obvious noise needs to be dealt with in an appropriate way. For the creation of public sculptures, the Statistical Outlier Removal method is more effective in dealing with noise in point cloud data models [30].

The Statistical Outlier Removal method was used to deal with the noise in the point cloud data model as follows [31]:

(1) Set the noise reduction region D of the point cloud model, where the number of point clouds is n. Starting from point P_i , the distance from P_i to all its neighbouring points is d_i; then, according to equation (9), the average distance δ and standard deviation σ_i can be solved.

$$\begin{aligned} \mu &= \frac{\sum_{i-1}^{n} d_i}{n}, \\ \sigma^2 &= \frac{\sum_{i-1}^{n} (d_i - \mu)^2}{n-1}. \end{aligned} \quad (9)$$

(2) Since the number of point clouds is n and the previous step needs to be repeated to obtain N that means the number of average distances and standard deviations, equation (10) can be used to calculate the average distance μ_o and standard deviation σ_o from the noise points to point P_i in the whole point cloud data model.

$$\begin{aligned} \mu_o &= \frac{\sum_{i-1}^{n} \mu_i}{N}, \\ \sigma_o^2 &= \frac{\sum_{i-1}^{n} (\mu_i - \mu_o)^2}{N-1}. \end{aligned} \quad (10)$$

(3) The average distance of all the noise points in the point cloud data model to point P_i is judged, and the standard deviation multiplier is positioned at k. If the average distance value is greater than $\mu_o + k\sigma_o$, then the noise points can be judged to be deleted.

In systems for creation of public sculpture, the Statistical Outlier Removal method is used to process the noise in the point cloud data model, resulting in a clearer point cloud data model of the captured public sculpture work model or solid object.

3.3. Output of Data Model for Public Sculpture Works. The process of exporting the point cloud data model is in fact the process of applying 3D printing technology and equipment to produce public sculptures based on the collected and processed data models. In a public sculpture creation system, the point cloud model data of the public sculpture model or solid object is collected and processed by 3D scanning, and then the public sculpture is produced by 3D printing technology [32].

There are two main types of 3D printing technology used in systems for creation of public sculpture: The first type is CNC (Computer Numerical Control Machine) numerical control sculpting technology, also often called 3D sculpting technology, which renders works by subtracting material [33]. The second is the 3D shaping technology by adding materials to render the work, which is commonly referred to as 3D printing technology. In all of these, CNC sculpting technology is used to manipulate the robotic arm by digital control to carve materials such as foam, stone, and wood into sculptural objects [34]. CNC engraving technology is less accurate than 3D shaping technology, and therefore it is less used in the production of highly refined public sculptures. However, it is often used in the production of large public sculptures that require a low degree of refinement. For example, in Chinese artist Dong Shubing's public sculpture "*Son of the Earth*," the physical presentation of the point cloud data model of the model object is completed by CNC engraving technology. The 3D shaping technology is a technique of stacking resin, plastic, and powdered metal materials into three-dimensional objects by means of layer-by-layer printing. In the process of creating public sculpture, 3D shaping technology can accurately restore the digital model collected and processed, enabling the digital model to be accurately converted into a public sculpture entity. For example, in the case of Chinese artist Sui Jianguo's public sculpture series "*Handwriting*," the point cloud data model of his work is physically shaped by 3D shaping technology.

In systems for creation of public sculpture involving computer graphics technology, the accuracy of the output of the point cloud data model of a public sculpture depends primarily on the obtaining and processing of the point cloud data model. In other words, the accuracy of the work is determined by the processing of the point cloud data model, whether it is achieved by subtracting material through 3D sculpting or adding material through 3D shaping. The effect of the processing of the point cloud data model lies in the intervention of appropriate computer graphics algorithms. The accuracy of public sculptures can be improved by the integration of feature-based algorithms and Statistical Outlier Removal algorithms into public sculpture creation systems.

4. Conclusion

Due to the paucity of relevant research, this paper draws on a limited number of sources and is therefore limited in the depth of what it can explore. The following conclusions can be drawn from an analysis of the ways and means by which computer graphics algorithms can intervene in the creation of public sculpture systems:

(1) The involvement of computer graphics algorithms in systems for creation of public sculpture is achieved through the involvement of computer graphics technology in the creation program system and the ontology system of public sculpture. The involvement of computer graphics algorithms in systems for creation of public sculpture is the key to the creation of accurate and complete public sculptures by the creator through computer graphics technology.

(2) The impact of computer graphics algorithms on public sculpture creation systems is mainly displayed in the process of extracting and processing the point cloud data model of a public sculpture, which is obtained by scanning with a 3D scanning tool and calculating the point cloud coordinate formula. In order to obtain a complete and clear point cloud data model of the public sculpture object, the point cloud data model conversion formula can be used to integrate the point cloud data models of different angles of the same object model, and then the Statistical Outlier Removal algorithm is used to process the noise in the point cloud data model.

(3) In the public sculpture creation system, the computer image algorithm is the basis for collecting, processing, and transforming the point cloud data of the public sculpture work with high definition. Its intervention in the public sculpture creation system improves the accuracy of the sculptor's using computer graphics technology when they create public sculptures. Besides, it plays a key role when the creator use computer graphics technology to accurately enlarge and transform public sculpture models into physical public sculptures.

Data Availability

Data sharing is not applicable to this article as no datasets were generated or analyzed during the current study.

Conflicts of Interest

The authors declare that they have no conflicts of interest.

References

[1] S. Zhu, "Opportunities of edges-prospect of sculpture under 5G," *Sculptre*, vol. 132, no. 4, pp. 22–26, 2019.
[2] W. He, "Public sculpture design strategy in the perspective of rural revitalization," *Journal of Anshan Normal University*, vol. 21, no. 6, pp. 78–81, 2019.
[3] A. S. Liao, "The use of computer imaging technology in the design of public sculpture," *Ceramics Science & Art*, vol. 73, no. 6, pp. 18–22, 2020.
[4] W. Zhang, "A discussion of computer imaging technology and public sculptures," *Architecture & Culture*, vol. 145, no. 10, pp. 21–23, 2015.
[5] M. Zheng, "A new approach to plastic art - digital technology intervention in public sculpture art," *Fine Art*, vol. 65, no. 4, pp. 75–77, 2017.
[6] J. Zhang, "A preliminary investigation of the content and methods of public art planning based on urban cultural construction," *Art Journal*, vol. 56, no. 5, pp. 103–108, 2018.
[7] W. Wang, "Research on digital media art under the characteristics of technicality," *Stage*, vol. 11, pp. 94–97, 2017.

[8] W. Liao, "Narrative analysis of sculptural language," *Qilu Realm of Arts*, vol. 115, no. 4, pp. 15–17, 2010.
[9] Xi-C. Zhang, "Reflection on the principle of publicness of urban cultural space and sculpture," *Creative Design Source*, vol. 121, no. 5, pp. 4–11, 2017.
[10] C. Wang, "Analysis of modern urban public art issues," *Urban Construction Theory Research*, vol. 35, no. 5, pp. 1610-1611, 2015.
[11] G. Zhang, "The convergence of diversity: the new media turn in public art," *Art and Design*, vol. 1, pp. 176–180, 2017.
[12] Z. Guo, "Analysis of the application and maintenance of digital fiber optic communication equipment," *Information/ Communication*, vol. 189, no. 9, pp. 255–258, 2018.
[13] W. Zhang, "Research on the application of digital technology in modern public sculpture," *Architecture & Culture*, vol. 115, no. 10, pp. 21–25, 2015.
[14] W. Luo, "Urban sculpture based on 3D scanning and 3D printing technology," *Art Panorama*, vol. 102, no. 8, pp. 107-108, 2020.
[15] J. Chen and K. Leng, "Public Sulpture Manufacturing System Based on Virtual Reality and 3D Printing," *Design*, vol. 201, no. 15, pp. 26-27, 2015.
[16] W. A. Zhang, "Discussion of digital technologies and publicsculptures," *Architecture & Culture*, vol. 145, no. 10, pp. 21–23, 2015.
[17] H.-C. Yang, "The logical structure of "artistry" in the creation of sculpture," *Fine Arts Literature*, vol. 33, no. 4, pp. 53–56, 2019.
[18] J.-Q. Cui, "Usion·Promotion·Development: design elements of the nowadays developing sculpture art region," *Sculpture*, vol. 5, pp. 66-67, 2015.
[19] D. Yan, "The application of 3D printing technology in the teaching of general technology," *Experimental teaching and instruments*, vol. 33, no. 1, pp. 37–44, 2016.
[20] L. Huang, "The utility of three-dimensional modeling technology in the display of silk road treasures," *Electronics*, vol. 10, pp. 163–165, 2020.
[21] W.-A. Luo, "Urban sculpture based on 3D scanning and 3D printing technology," *Art panorama*, vol. 96, no. 8, pp. 105–109, 2020.
[22] H. Wei, "Garment design and development based on 3D scanning technology," *Textile Guide*, vol. 103, no. 2, pp. 72–77, 2016.
[23] Y. Li, "Development of a 3D automatic measurement system for body dimensions," *Journal of Northwest Textile Engineering College*, vol. 15, no. 9, pp. 8–11, 2019.
[24] C. Liu, *Data Processing and Feature Extraction for Laser 3D Remote Sensing*, pp. 21–23, Science Publishing, Beijing, China, 2009.
[25] H. W. Zhou, *Ground-based 3D Laser Scanning Point Cloud Data Processing and Model Construction*, pp. 28–33, Kunming University of Technology, Kunming, China, 2011, Dissertation.
[26] Y. H. Ding, "Research on the alignment of ground-based 3D laser data," *Journal of Surveying & Mapping*, vol. 30, no. 2, pp. 57–59, 2017.
[27] Y. Xu, "3D laser scanning technology," *Mapping Information and Engineering*, vol. 36, no. 4, pp. 5-6, 2017.
[28] L. Cheng, "Ground-based 3D laser scanning data alignment methods," *Journal of Surveying & Mapping*, vol. 28, no. 12, pp. 80–85, 2017.
[29] X. Wang, *Ground-based 3D Laser Scanning Modelling and its Application in Building Mapping*, Dissertation, Central South University, Changsha, China, 2018.
[30] R. B. Rusu, Z. C. Marton, N. Blodow, M. Dolha, and M. Beetz, "Towards 3D Point cloud based object maps for household environments," *Robotics and Autonomous Systems*, vol. 56, no. 11, pp. 927–941, 2008.
[31] H. Luo, "Research on 3D model reconstruction technology based on terrestrial laser scanner,", Dissertation, East China University of Technology , 2016.
[32] C. Shi, "Discussion on mechanical engineering and automation," *Architectural Engineering Technology and Design*, vol. 20, pp. 38–42, 2017.
[33] Q. Mai, "Lab VIEW - based analysis and research of woodworking engraving machine spindle vibration," *Modern Electronics Technique*, vol. 37, no. 21, pp. 156–162, 2018.
[34] J. Wen, "Study on the application of handmade candles in mixed media decorative painting," *Construction Materials & Decoration*, vol. 21, pp. 51–56, 2019.

Hindawi
Scientific Programming
Volume 2023, Article ID 9810957, 1 page
https://doi.org/10.1155/2023/9810957

Retraction

Retracted: Construction of the Luxury Marketing Model Based on Machine Learning Classification Algorithm

Scientific Programming

Received 8 August 2023; Accepted 8 August 2023; Published 9 August 2023

This article has been retracted by Hindawi following an investigation undertaken by the publisher [1]. This investigation has uncovered evidence of one or more of the following indicators of systematic manipulation of the publication process:

(1) Discrepancies in scope
(2) Discrepancies in the description of the research reported
(3) Discrepancies between the availability of data and the research described
(4) Inappropriate citations
(5) Incoherent, meaningless and/or irrelevant content included in the article
(6) Peer-review manipulation

The presence of these indicators undermines our confidence in the integrity of the article's content and we cannot, therefore, vouch for its reliability. Please note that this notice is intended solely to alert readers that the content of this article is unreliable. We have not investigated whether authors were aware of or involved in the systematic manipulation of the publication process.

Wiley and Hindawi regrets that the usual quality checks did not identify these issues before publication and have since put additional measures in place to safeguard research integrity.

We wish to credit our own Research Integrity and Research Publishing teams and anonymous and named external researchers and research integrity experts for contributing to this investigation.

The corresponding author, as the representative of all authors, has been given the opportunity to register their agreement or disagreement to this retraction. We have kept a record of any response received.

References

[1] Q. Chen, S. Cai, and X. Gu, "Construction of the Luxury Marketing Model Based on Machine Learning Classification Algorithm," *Scientific Programming*, vol. 2021, Article ID 6511552, 11 pages, 2021.

Hindawi
Scientific Programming
Volume 2021, Article ID 6511552, 11 pages
https://doi.org/10.1155/2021/6511552

Research Article

Construction of the Luxury Marketing Model Based on Machine Learning Classification Algorithm

Qiaoshan Chen,[1] Shousong Cai ,[2] and Xiaomin Gu[3]

[1]*Shanghai Institute of Visual Arts, Shanghai 201620, China*
[2]*School of Business Administration, Shanghai Lixin University of Accounting and Finance, Shanghai 201209, China*
[3]*School of Financial Technology, Shanghai Lixin University of Accounting and Finance, Shanghai 201209, China*

Correspondence should be addressed to Shousong Cai; 20170111@lixin.edu.cn

Received 9 September 2021; Revised 27 September 2021; Accepted 9 October 2021; Published 19 October 2021

Academic Editor: Punit Gupta

China has become the world's largest luxury goods consumer market due to its population base. In view of the bright prospects of the luxury consumer market, major companies have entered and want to get a share. For the luxury goods industry, traditional mass marketing methods are not able to serve corporate sales and marketing strategies more effectively, and targeted marketing is clearly much more efficient than randomized marketing. Therefore, in this paper, based on consumer buying habits and characteristics data of luxury goods, the paper uses a machine learning algorithm to build a personalized marketing strategy model. And the paper uses historical data to model and form deductions to predict the purchase demand of each consumer and evaluate the possibility of customers buying different goods, including cosmetics, jewelry, and clothing.

1. Introduction

In recent years, with the rapid development of the economy, people's living standards have also risen. China has become the world's largest luxury goods consumer market due to its population base. The consumption of Chinese luxury consumers has increased year by year, accounting for 35% of the global luxury market. Some people expect that China's consumption will account for half of the world's market by 2025. In view of the bright prospects of the luxury consumer market, major companies have entered and want to get a share [1]. At this time, for enterprises, how to carry out effective marketing has become the key to the survival and even prosperity of enterprises. Specifically, how to collect and process the data, understand the user's needs, accurately find the target user group, and provide corresponding solutions so as to achieve enterprise profit and user experience win-win is in line with the trend of the times.

However, for the luxury goods industry, traditional mass marketing methods are not able to serve corporate sales and marketing strategies more effectively, and targeted marketing is clearly much more efficient than randomized marketing [2]. As we all know, the actual purchase behavior and past habits of customers in the past are the guides to future shopping behavior. In other words, it is accurate to infer customers' future consumption behavior according to their past consumption habits and behaviors. Therefore, enterprises can collect and save consumers' actual consumption records, search records, website clicks, and personal information and then utilize machine learning algorithms to accurately simulate consumer habits and behaviors so as to accurately locate the target customer group and realize the precise marketing of customers.

2. Machine Learning Classification Algorithm and Selection

There are two main technologies in the field of data mining: classification algorithm and clustering algorithm. The method of classification is to construct a classification function or a classification model according to the characteristics of data sets and map the samples of unknown categories to a given category with the model so as to achieve the effect of classification [3]. The classification algorithm process mainly consists of two steps: in the first step, create a model that describes the categories of known data sets, which is obtained by analyzing the data records in the database, and the columns of each record are descriptions of their attributes, and in the second step, the obtained model is used for the purpose of classification operation.

Classification algorithms are widely used, such as loan risk assessment, telecom customer classification, spam identification, potential user classification, consumer demand forecast analysis, and so on [4]. Different classification methods will produce different classifiers, the advantages and disadvantages of which directly affect the efficiency and accuracy of data mining. Therefore, when classifying data, it is important to choose the most efficient classification algorithm.

2.1. Artificial Neural Network Classification Algorithm. The artificial neural network (ANN) is a mathematical model that uses information similar to the structure of brain synaptic connections for information processing. The most basic component of neural networks is the neuron model [5]. Each neuron is connected to other neurons, and the neuron can receive input signals from n other neurons. From the computer point of view, we can ignore whether the neural network really simulates the biological nervous system but only need to regard a neural network as a mathematical model containing many parameters, which is composed of several functions [6].

The key point of the neural network classification algorithm is to construct a threshold logic unit. A logical unit is an object that can input a set of weighting coefficients and sum them. If the sum reaches or exceeds a certain threshold, an amount is output. Assume the following input values x_1, $x_2, \ldots, x_n$, and their weight coefficients are $w_1, w_2, \ldots, w_n$, summation calculation is $x_i \times w_1$, and the excitation layer is as follows:

$$a = (x_1 \times w_1) + (x_2 \times w_2) + \cdots + (x_i \times w_i) + \cdots + (x_n \times w_n). \tag{1}$$

Here, x_i is the frequency of occurrence of each record or other parameters and w_i is the weight coefficient obtained in the real-time feature evaluation model.

There are many types of neural network models, including RBF networks, ART networks, SOM networks, cascading related networks, and so on. In practical applications, it has been found that the advantages of artificial neural networks include high accuracy, strong parallel processing capability, strong distributed storage and learning ability, and the function of associative memory. However, it still has some shortcomings that neural networks require a lot of parameters as a hard-to-interpret "black box model," and it cannot observe the learning process [7].

2.2. Decision Tree Classification Algorithm. The decision tree is the most common classification algorithm. Decision tree is based on the structure of the tree for decision-making. Generally, a decision tree contains a node, several internal nodes, and several leaf nodes. The leaf nodes correspond to decision results, and each other node corresponds to a property test [8]. The sample set contained in each node is divided into child nodes according to the result of the attribute test. The node contains the complete set of samples, and the path from the node to each leaf node corresponds to a decision test sequence. The purpose of decision tree learning is to create a tree with strong generalization ability [9].

Currently, the most famous representative of the decision tree learning algorithm is ID3, CART, C4.5 (C5.0), Random Forest, and multivariate adaptive regression spline (MARS) algorithm. They have their own differences in the choice of techniques used to test attributes, the structure of the resulting decision tree, the method of pruning, timing, ability to handle large data sets, and so on. For example, C4.5 Rule is an algorithm that converts a C4.5 decision tree into a symbol rule. Each branch of the decision tree can be overridden by a rule, but the C4.5 Rule algorithm will perform rules preassembly and deletion operation during the conversion process, so the generalization performance of the final rule set may even be better than the original decision tree.

The advantages of a decision tree algorithm include easy understanding, simple data preparation, the ability to process both data and regular attributes, easy derivation of logical expressions, strong data source analysis capability, and so on [10, 11]. And its disadvantage is mainly that for data with inconsistent sample sizes for each category, in the decision tree, the results of the information gain are biased toward those with more values. In addition, a decision tree is difficult to deal with missing data, and sometimes, it would probably lead to overfitting problems.

2.3. K-Nearest Neighbor Classification Algorithm. K-nearest neighbor (KNN) classification algorithm was first proposed by Cover and Hart in 1968, and it has developed into a more mature method in theory. Its core idea is to judge the characteristics of data according to the nearest samples [12–15]. The specific idea of the KNN algorithm is: find out k training samples closest to the unknown sample x, determine which category most of the k samples belong to, and then categorize x into that category. KNN is similar in principle to the limit theorem, but it is only related to a very small number of adjacent samples in class decision-making. In addition, the KNN method is more suitable than other methods for the sample set with more overlaps because it mainly depends on the limited neighboring samples around, rather than the method of discriminating the class domain to determine the category.

The main applications of the KNN algorithm in the industry are as follows: customer churn prediction and loan fraud, Euclidean distance calculation, and so on. KNN algorithm is more suitable for the automatic classification of class domains with larger sample size, but it is easier to produce misclassification for those domains with smaller sample size.

KNN algorithm also has obvious shortcomings. Since the KNN algorithm is a lazy learning method, its accuracy will be affected naturally. KNN algorithm's category score is not standardized as a probability score, and the interpretability of output is not strong. In addition, one of the biggest problems of KNN is a large amount of calculation. At present, the commonly used solution is to remove samples that have little effect on classification beforehand.

2.4. Logistic Regression Classification Algorithms. Logistic regression is also a very common classification algorithm, especially in the field of enterprise management. The applications of logistic regression include analysis of the possibility of consumers buying goods, potential consumer forecasting, potential consumer forecast, precision decision-making of advertising placement, and so on.

Dependent variables of logistic regression can be bi- or multicategorized. But the former is more common and easier to explain, so the most commonly used in practice is bicategorized logistic regression.

The conventional steps of the logistic regression classification algorithm are as follows:

(1) Construct predictive function h. The general predictive function is in the following form:

$$h_\theta(x) = g\left(\theta^T x\right) = \frac{1}{1 + e^{-\theta^T x}}. \quad (2)$$

(2) Construct loss function J. The general loss function is in the following form:

$$J(\theta) = -\frac{1}{m} l(\theta). \quad (3)$$

(3) Try to minimize J function and get regression parameters (θ).

Generally, the advantage of logistic regression is that logistic regression models are usually more intuitive and easier to interpret. Since the algorithm can give a specific prediction probability for each target category, it is easy to compare between variables. The disadvantage of logistic regression is that the effect of processing high-dimensional data is not ideal.

2.5. Support Vector Machine Classification Algorithms. Support vector machine (SVM) algorithm is proposed by Vapnik in 1995. The SVM algorithm has relatively good performance indicators. The basic idea of SVM is based on training set D to find a dividing hyperplane in the sample space and separate the samples of different categories. The hyperplane can separate the data in the training set, and the distance from the class boundary is perpendicular to the direction of the hyperplane. Therefore, SVM algorithm is also called the maximum margin algorithm. The specific algorithm steps are as follows:

Given a kernel function K, training sample data set $X_{\text{traim}} = \{x_i, y_i\}_{i=1}^n$, construct a cost function Φ to minimize it as follows:

$$\Phi(w, \xi) = \frac{1}{2} w^t w + C \sum_{i=1}^n \xi_i^k. \quad (4)$$

The constraints are

$$y_i\left(w^T w + b\right) \geq 1 - \xi_i, \quad \xi_i \geq 0;\ i = 1, 2, \ldots, n, \quad (5)$$

where C is penalty factor, ξ_i is actual error, $k = 1$ or 2, w is classified interface vector, and b is intercept. According to the constraints, the Lagrangian function is as follows:

$$L_p = \frac{w^2}{2} + C \sum_{i=1}^n \xi_i^k - \sum_{i=1}^n \alpha_i \left[y_i\left(w^T x_i + b\right) - 1 + \xi_i \right] - \sum_{i=1}^n \mu_i \xi_i. \quad (6)$$

where $\alpha_i \geq 0$, $\mu_i \geq 0$, α_i, and μ_i are Lagrange multipliers. Finally, according to KKT conditions, we can obtain:

$$\begin{aligned} &\alpha_i \left[y_i\left(w^T x_i + b\right) - 1 + \xi_i \right] = 0 \quad i = 1, 2, \ldots, n, \\ &\left(C - \alpha_i\right) \xi_i = 0 \quad i = 1, 2, \ldots, n, \\ &C \geq \alpha_i \geq 0, \quad \sum_{i=1}^n \alpha_i y_i = 0. \end{aligned} \quad (7)$$

Determine the category of a new sample x as follows:

$$\operatorname{sgn}[f(x)] = \operatorname{sgn}\left[\sum_{i=1}^n \alpha_i y_i K(x_1, x_i) + b \right]. \quad (8)$$

In summary, the solution of the support vector machine is a convex optimization technique by means of the Lagrangian function. The advantages of the SVM classification algorithm include effective solution to machine learning problems, high-dimensional problems, nonlinear problems in small sample cases, and avoiding neural network structure selection and local minimum point problem. But its limitations are sensitive to missing data, and there is no universal solution to nonlinear problems.

2.6. Selection of Classification Algorithms for Luxury Marketing. The purpose of this paper is to use the classification algorithm model to analyze the most likely target populations of several high-end luxury goods in a certain region. We chose fragrance, makeup, and skincare for empirical analysis. We divided the sample set into two parts: the training set and the test set. The ratio of the number of samples in the training set to the test set is exquisite. Because if the training set is too small, the classifier obtained by the training must not be excellent enough; but if the training set is too large, the error rate estimate will be very low. The most common methods include resubstitution, retention, and cross-validation. Among them, the retention method is to use a part of the sample set as the training set and retain the remaining part as the test set. And the best ratio of the training set to test set is 7:3.

We used full sample data to construct model and then chose the optimal model through empirical analysis results. The empirical results of all the classification algorithms are shown in Table 1.

We can see that the accuracy of the five algorithms is over 0.9. Negative samples have high accuracy and recall rates, but positive sample accuracy and recall rates are generally low. The overall performance of decision trees, artificial neural networks, and support vector machines is relatively better. In practical applications, enterprises pay more attention to the accuracy of forecast results, that is, they pay more attention to which customers will buy products, and what kind of products will be purchased and do not pay attention to customers who will not buy; we should focus on analyzing the purchase crowd. We believe that the reason for this phenomenon is that the sample data is not too balanced, which greatly affects the accuracy of machine learning.

Through further analysis, we obtained the ROC curve of all the algorithms, as shown in Figure 1.

From the ROC curve of each algorithm, we can see the simulation results are not very good. Relatively, decision tree algorithm, artificial neural network, and support vector machine algorithm are better. The corresponding area under the curve of ROC (AUC) of the five model algorithms is summarized in Table 2.

We can conclude that the decision tree algorithm performs better, but it is not particularly noticeable. Logistic regression algorithm, decision tree algorithm, and KNN algorithm learn faster in the modeling process than ANN algorithm and SVM algorithm. But by comprehensively considering the classifier's fitness for data, the interpretability of the model, and the AUC value, since the decision tree algorithm has the advantages of simple data processing, strong interpretability, and intuitive visualization of the tree structure between variables, we choose decision tree algorithm for empirical research.

3. Construction of the Luxury Marketing Model

Here, we take the data of the luxury market in a certain area as an example and construct the marketing model to analyze potential buyers' purchase needs.

3.1. Case Background. In the field of cosmetics, especially in the high-end cosmetics field, which has been hot in recent years, the purchase demand of consumers is the most concerned issue of enterprises. Therefore, based on the theoretical research basis of the classification algorithm as above, this paper collects the sales data of luxury goods in a certain area and conducts the corresponding customer demand forecast analysis. We have chosen cosmetics, jewelry, and clothing, which are typical luxury consumer goods, to carry out empirical research on the marketing model. In the actual modeling process, the possibility that each consumer will purchase these three types of products will be predicted: 1 represents possible purchase, and 0 represents impossible purchase.

The specific research ideas are as follows: firstly, collect purchase data of related commodities from July 1, 2017, to March 31, 2018, and then the original data are processed to sort out the variables needed for modeling into three tables: cosmetics, jewelry, and clothing. Taking table jewelry as an example, we define that if there is a jewelry-purchasing record in the first nine months, as well as in the last three months, then the explanatory variable is marked as 1. If there is no purchase record in the last three months, then the explanatory variable is marked as 0. In the three tables, all variables except the explained variable are the same.

3.2. Data Preparation. According to the case background, we selected 16 variables from the database. Figure 2 displays model variables arrangement.

According to the above 16 variables, the consumption and quantity ratio of cosmetics, jewelry, and clothing is to be calculated. Together with other variables, which are quantified, we sorted out the data for modeling. Figure 3 presents model data processing.

3.3. Data Cleaning. When the variables are selected, the data needs to be cleaned, including outlier processing, missing value processing, and data standardization.

3.3.1. Outlier Processing. Since the outliers will produce errors in the estimation of the model parameters, we need to handle the outliers of the continuous variables in the dataset. In basic applied statistics, it is generally believed that values beyond three standard deviations are abnormal values. For the data set of this study, the data that may generate outlier is column AGE. We use SPSS software for processing as import data sets into SPSS, add a column ZAGE and then the values beyond three standard deviations, and finally mark the outliers of these data as NULL. We rechecked the data after marking and found that the minimum age is 10, while the maximum is 60. Considering that minors lack the ability to buy luxury goods, so we also marked 136 people aged 10 to 18 as NULL.

3.3.2. Missing Value Processing. There are many methods to deal with missing values, such as delete missing data, average filling missing data, K-nearest neighbor filling missing data, regression filling missing data, and so on. There are missing values in column AGE and GND_MEMO in the original data set. In this paper, the linear interpolation method is used to supplement the missing values, and the related operations are specifically carried out in SPSS.

3.3.3. Data Standardization. In machine learning, some algorithms need to standardize data, such as logistic regression algorithm, while some others do not, such as decision tree and artificial neural network algorithm. Since there are many algorithms involved in this paper, it is necessary to standardize the data. We use the deviation standardization method to linearly transform the raw data. The data normalized conversion function is as follows:

$$y_{ik} = \frac{x_{ik} - \min(x_k)}{\max(x_k) - \min(x_k)}. \tag{9}$$

Table 1: Empirical results of all classification algorithms.

Algorithm	Accuracy	Error	Precision (positive)	Recall (positive)	Precision (negative)	Recall (negative)	F1 measure
ANN	0.926	0.071	0.148	0.562	0.990	0.934	0.475
Decision tree	0.930	0.072	0.156	0.598	0.992	0.934	0.501
KNN	0.968	0.033	0.322	0.349	0.968	0.910	0.665
Logistic regression	0.927	0.071	0.689	0.003	0.927	1.001	0.008
SVM	0.922	0.779	0.198	0.443	0.979	0.941	0.550

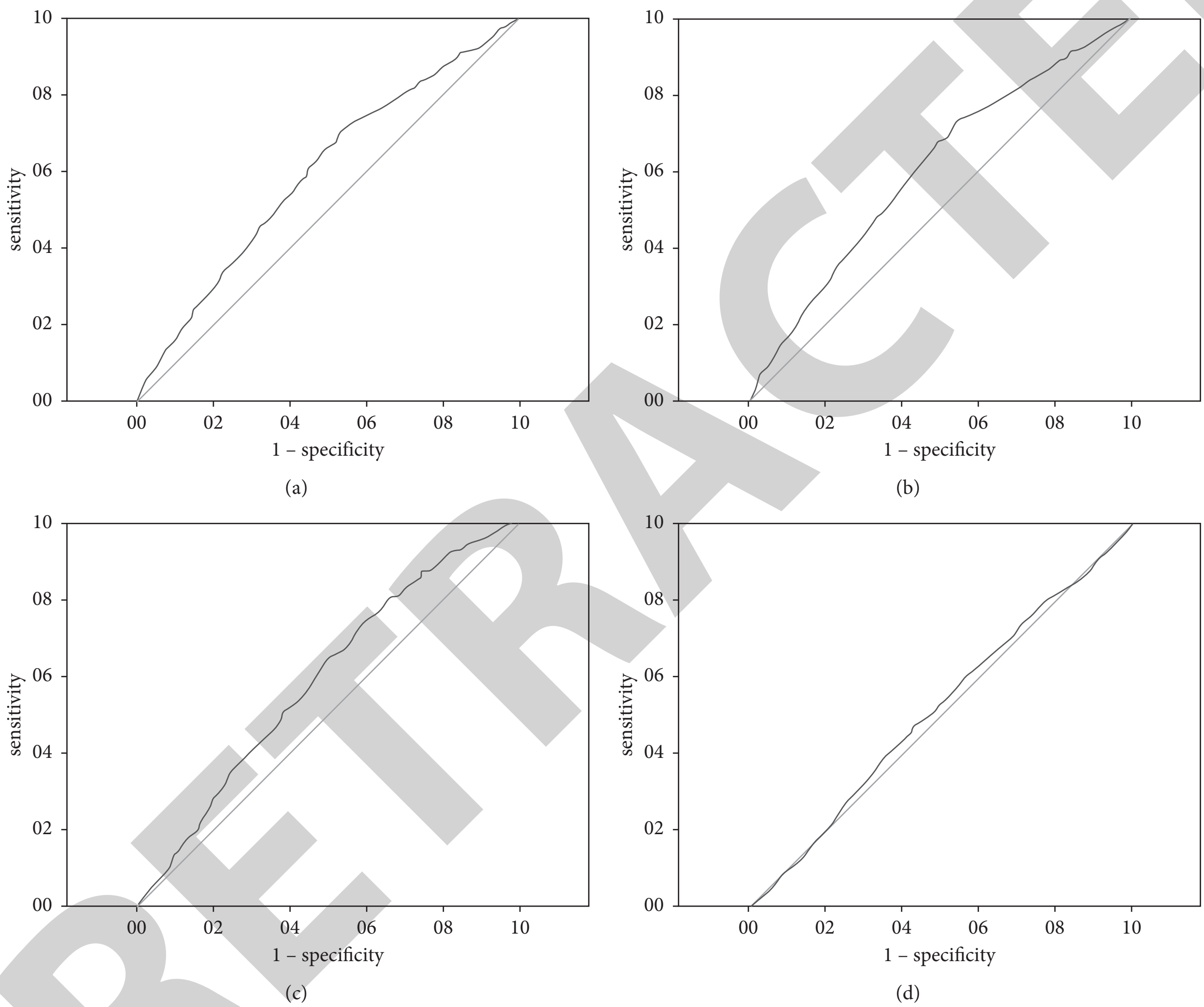

Figure 1: Continued.

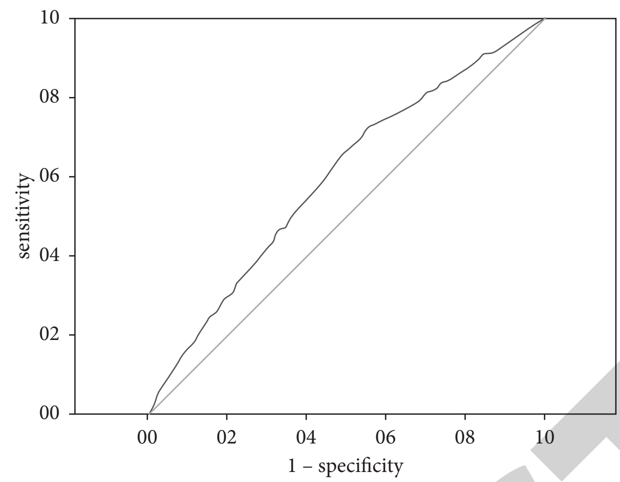

(e)

Figure 1: ROC curve of all the algorithms: (a) ANN algorithm, (b) decision tree algorithm, (c) KNN algorithm, (d) logistic regression algorithm, and (e) SVM algorithm.

Table 2: Evaluation parameters of all classification algorithms.

Algorithm	Calculation speed (s)	Classifier's fitness for data	Interpretability	AUC value
ANN	266.71	Data do not need to be standardized	Complex	0.597
Decision tree	206.81	Data need to be standardized	Strong	0.611
KNN	210.34	Data need to be standardized	Not strong	0.598
Logistic regression	187.79	Data need to be standardized	Strong	0.525
SVM	375.69	Data need to be standardized	Complex	0.605

	CTT_DESC	GND_MEMD	age	PUR_CST_ID	FREQ	TLL_FREQ	TTL_SPENDING	QTY	N_PROD	Fragranoe_sales	Make_Up_sales	Skin_Care_sales
1	Normal middle	Female	43	155150	1	3	2125.00	3	3	NULL	1400.00	725.00
2	Vip	Female	44	4579	2	3	148.00	3	3	NULL	670.00	810.00
3	Normal middle	Female	41	68685	1	2	1780.00	4	2	NULL	640.00	1140.00
4	Top Vip	Female	NULL	44170	7	18	25340.00	20	16	1240.00	2190.00	21910.00
5	Normal middle	Unknown	NULL	44253	1	4	2310.00	5	4	NULL	1890.00	420.00
6	Valuable middle	Female	49	59980	1	3	1505.00	3	3	NULL	1000.00	505.00
7	Top Vip	Female	34	25935	5	12	6925.00	13	12	3415.00	3510.00	NULL
8	Normal middle	Female	45	82659	1	1	320.00	1	1	NULL	320.00	NULL
9	Normal middle	Female	38	82791	1	1	600.00	1	1	NULL	600.00	NULL
10	Vip	Female	37	52526	1	1	350.00	1	1	NULL	350.00	NULL
11	Valuable middle	Female	NULL	62303	2	5	2860.00	5	4	690.00	2170.00	NULL
12	Vip	Female	34	83861	4	8	5960.00	8	8	NULL	2540.00	3420.00
13	Vip	Female	56	83910	4	5	1615.00	5	5	365.00	1250.00	NULL
14	Normal middle	Female	29	77060	1	1	320.00	1	1	NULL	320.00	NULL
15	Normal middle	Female	37	18081	1	1	1520.00	1	1	1520.00	NULL	NULL
16	Inactive	Female	53	83976	1	1	365.00	1	1	365.00	NULL	NULL

Figure 2: Model variables arrangement.

The data after standardization can be seen in Figure 4.

3.4. Data Descriptive Statistics. Before modeling, it is usually necessary to have a general understanding of the data, so descriptive statistical analysis of the data is very important. In order to understand the overall structure of data sets more clearly, descriptive statistical analysis can be carried out separately for numerical variables and classified variables.

pur_cst_id	age	ctt_desc	ghd_meno	percent_freq_fragrance	percent_freq_makeup	percent_freq_skincare	percent_spending_fragrance
3029250	22	3	0	0.5	0	0.5	0.67
3223716	22	2	0	0.25	0.25	0.25	0.49
3223731	40	2	0	1	0	0	1
3223733	30	3	0	0.29	0.43	0.14	0.52
3223750	46	2	0	0	1	0	0
1963347	46	3	0	0	0.2	0.2	0
3030005	22	2	1	0	0	0.5	0
3030082	28	2	0	0.25	0.25	0	0.69
3224337	23	2	0	0	1	0	0
3224339	52	2	0	0	0.5	0.5	0
3224348	33	2	0	0.5	0	0.5	0.47
3224373	28	3	0	0	0.33	0.33	0
3224380	29	2	0	0	1	0	0
3249469	23	2	1	0.33	0.33	0	0.61
3272986	31	2	0	0.33	0	0.33	0.34
3272999	39	2	0	1	0	0	1
3273001	29	2	0	1	0	0	1
3273018	25	2	0	1	0	0	1
3273035	25	3	0	0.13	0.38	0.25	0.18
3273050	26	3	0	0.33	0.33	0.33	0.69
3090232	29	3	0	0.67	0.33	0	0.94
3220258	43	2	1	0	0.67	0	0
3220273	24	2	0	0	1	0	0
3220288	28	2	0	0.17	0.33	0.17	0.34
3220290	31	2	0	0	0.17	0.17	0
3220307	33	2	1	1	0	0	1

Figure 3: Model data processing.

3.4.1. Descriptive Statistics of Numerical Variables. The typical numerical data in this paper include age, total consumption, total quantity, and total costs. The descriptive statistics of numerical variables are set out in Table 3.

3.4.2. Descriptive Statistics of Classified Variables. The frequency statistic result of customer level is displayed in Table 4.

We define the customer label of the original data set as lost and sleeping as 0; the customer label as normal new; valuable new as level 1; the customer label as inactive, normal middle; valuable middle as level 2; the customer label as top vip; and vip as level 3. The higher the customer level, the higher the customer value, and of course, the more targeted marketing is.

Similarly, the frequency statistic result of customer gender can be seen in Table 5.

We can see from Table 5 that women account for about 90.9% of customers. Therefore, it is necessary to specialize in marketing for women.

3.5. Model Establishment. Based on the comparison of the classification algorithms above, this paper selects the fast and high precision decision tree algorithm for modeling. For the three tables of cosmetics, jewelry, and clothing, the model is established with a full amount of 294,345 data. Table 6 compares the simulation result by the decision tree algorithm.

We can see from Table 6 that the model has high precision. However, the prediction accuracy of the three sets of data is as low as 16.9%, 21.8%, and 17.7%. The recall rates and F1 measure are also low.

3.6. Model Prediction. The model prediction results of table of cosmetics, jewelry, and clothing on the data set are set out in Figure 5.

From Figure 5, it can be seen that the gap between predictions 1 and 0 is large and the stability is high. In order to observe the prediction accuracy of the model, the ROC curve is shown in Figure 6.

From Figure 6, it can be seen that all the ROC curves are close to the longitudinal axis and far from the diagonal line.

pur_cst_id	age	ctt_desc	gnd_memo	fir_date	max_date
367166	0.166666666666667	0.333333333333333	0	0.0875912408759124	0.0875912408759124
436123	0.261904761904762	0.666666666666667	0	0.328497153284672	0.328467153284672
469439	0.571428571428571	0.666666666666667	0	1	0.452554744525547
126444	0.714285714285714	0.666666666666667	0	0.970802919708029	0.970802919708029
3678682	0.285714285714286	0.333333333333333	0	0.0693430656934307	0.0693430656934307
2360992	0.142857142857143	0.666666666666667	1	0.985401459854015	0.985401459854015
3514433	0.261904761904762	0.333333333333333	1	0.397810218978102	0.397810218978102
2058230	0.19047619047619	0.666666666666667	0	0.664233576642336	0.664233576642336
3304248	0.30952380952381	0.666666666666667	0	0.713868613138686	0.81368613138686
3444869	0.19047619047619	0.333333333333333	1	0.543795620437956	0.543795620437956
3408437	0.785714285714286	0.333333333333333	0	0.616788321167883	0.616788321167883
3643249	0.30952380952381	0.333333333333333	0	0.145985401459854	0.145985401459851
1344271	0.380952380952381	0.666666666666667	1	0.284971532846715	0.284671532846715
3386073	0.0714285714285714	0.333333333333333	0	0.656934306569343	0.251824817518248
3007858	0.214285714285714	0.666666666666667	0	0.967153284671533	0.576642335766423
3234344	0.30952380952381	0.666666666666667	0	0.948905109489051	0.9489051094489051
3654908	0.0476190476190476	0.333333333333333	0	0.12043795620438	0.12043795620438
2328688	0.30952380952381	1	0	0.412408759124088	0.222627737226277
3494111	0.404761904761905	0.333333333333333	1	0.437956204379562	0.437956204379562

Figure 4: Data standardization result.

Table 3: Descriptive statistics of numerical variables.

	N	Minimum	Maximum	Average	Standard deviation
AGE	294345	18	60	31.36	7.520
FREQ	294345	1	94	1.62	2.049
TTL_SPENDING	294345	−7346	172926	2341.95	4169.208
QTY	294345	−9	230	3.55	5.443
Effective	294345	—	—	—	—

Table 4: Frequency statistic result of customer level.

		Customer level			
		Frequency	Percentage	Effective percentage	Accumulated percentage
Effective	0	20	0.0	0.0	0.0
	1	114002	38.7	38.7	38.7
	2	139450	47.4	47.4	86.1
	3	40872	13.9	13.9	100.0
	Total	294345	100.0	100.0	—

Table 5: Frequency statistic result of customer gender.

		Customer gender			
		Frequency	Percentage	Effective percentage	Accumulated percentage
Effective	0	267635	90.9	90.9	90.9
	1	26710	9.1	9.1	100.0
	Total	294345	100.0	100.0	—

Table 6: Simulation result by decision tree algorithm.

Table	Accuracy	Error	Precision (positive)	Recall (positive)	Precision (negative)	Recall (negative)	F1 measure
Cosmetics	0.928	0.076	0.169	0.569	0.990	0.936	0.546
Jewelry	0.901	0.103	0.218	0.600	0.980	0.908	0.635
Clothing	0.935	0.066	0.177	0.518	0.985	0.947	0.524

	pur_cst_id	0	1
1	3224348	0.96747967	0.03252033
2	3224373	0.96747967	0.03252033
3	3224380	0.96747967	0.03252033
4	3249469	0.96747967	0.03252033
5	3272986	0.96747967	0.03252033
6	3272999	0.96747967	0.03252033
7	3273001	0.96747967	0.03252033
8	3273018	0.96747967	0.03252033
9	3273035	0.24038462	0.75961538
10	3273050	0.96747967	0.03252033

(a)

	pur_cst_id	0	1
1	3029250	0.96747967	0.03252033
2	3223716	0.96747962	0.75961538
3	3223731	0.96747967	0.03252033
4	3223733	0.96747967	0.03252033
5	3223750	0.96747967	0.03252033
6	1963347	0.96747967	0.03252033
7	3030005	0.96747967	0.03252033
8	3030082	0.96747967	0.03252033
9	3224337	0.24038467	0.03252033
10	3224339	0.96747967	0.03252033

(b)

	pur_cst_id	0	1
1	3256718	0.96747967	0.03252033
2	3256743	0.96747967	0.03252033
3	3256745	0.96747967	0.03252033
4	3256777	0.96747967	0.03252033
5	3163821	0.74431818	0.25568182
6	3163832	0.74431818	0.25568182
7	3163896	0.96747967	0.03252033
8	3163998	0.96747967	0.03252033
9	3164023	0.24038467	0.03252033
10	3164030	0.74431818	0.25568182

(c)

Figure 5: Model prediction results of three tables: (a) jewelry, (b) cosmetics, and (c) clothing.

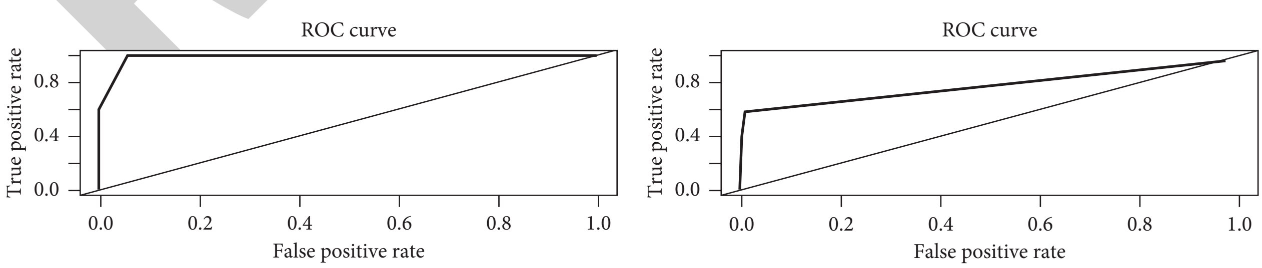

(a) (b)

Figure 6: Continued.

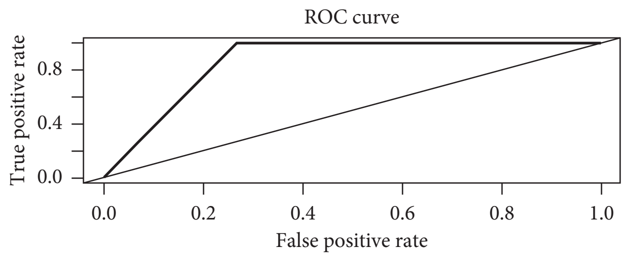

(c)

Figure 6: ROC curve of the three tables: (a) jewelry (b) cosmetics, and (c) clothing.

The AUC value of jewelry is predicted as 0.967, that of cosmetics is predicted as 0.821, and that of clothing is predicted as 0.855, all with high accuracy.

4. Conclusion

Through unbalanced treatment of interpreted variables, the accuracy of model prediction 1 has been significantly improved. Among them, the prediction accuracy of 1 in the table jewelry has been greatly improved to 80.6%, and prediction accuracy of clothing has been greatly improved to 86.5%. In this way, according to the predicted results, the merchants can count the different needs of each individual; integrate the cosmetics, jewelry, and clothing categories that consumers are interested in; carry out personalized marketing strategies for the customers who will buy these products; and ultimately improve marketing efficiency and customer satisfaction.

A personalized marketing strategy model can be applied not only in the luxury goods industry but also in many other Internet industries. For example, for music APP, according to the user's history of listening to songs, we can recommend songs that meet the user's preferences. The media can recommend interesting news to tourists according to their habit of browsing news. According to the characteristics of eating habits, the third-party ordering platform recommends restaurants that match the characteristics. You can even use investment preferences or sensational insights to recommend investment channels such as specific stocks. There is no doubt that personalized recommendations save people time and intimacy when using a variety of products.

Data Availability

The simulation experiment data used to support the findings of this study are available from the corresponding author upon request.

Conflicts of Interest

The authors declare that there are no conflicts of interest regarding the publication of this paper.

References

[1] J. S. Vickers and F. Renand, "The Marketing of Luxury Goods: an exploratory study-three conceptual dimensions," *The Marketing Review*, vol. 3, no. 4, pp. 459–478, 2003.

[2] R. Florez-Lopez and J. M. Ramon-Jeronimo, "Marketing segmentation through machine learning models," *Social Science Computer Review*, vol. 27, no. 1, pp. 96–117, 2009.

[3] M. M. A. Grau, M. Tajtakova, and D. A. Aranda, "Machine learning methods for the market segmentation of the performing arts audiences," *International Journal of Business Environment*, vol. 2, no. 3, pp. 356–375, 2009.

[4] C. Dhaoui, C. M. Webster, and L. P. Tan, "Social media sentiment analysis: lexicon versus machine learning," *Journal of Consumer Marketing*, vol. 34, no. 6, pp. 480–488, 2017.

[5] T. K. Mackey, J. Kalyanam, T. Katsuki, and G. Lanckriet, "Twitter-based detection of illegal online sale of prescription opioid," *American Journal of Public Health*, vol. 107, no. 12, pp. 1910–1915, 2017.

[6] Y. Wang, V. Chattaraman, H. Kim, and G. Deshpande, "Predicting purchase decisions based on spatio-temporal functional MRI features using machine learning," *IEEE Transactions on Autonomous Mental Development*, vol. 7, no. 3, pp. 248–255, 2015.

[7] H. Yi, "Secure social Internet of things based on post-quantum blockchain," *IEEE transactions on Network Science and Engineering*, p. 1, 2021.

[8] X. Lv and A. Wu, "The role of extraordinary sensory experiences in shaping destination brand love: an empirical study," *Journal of Travel & Tourism Marketing*, vol. 38, no. 2, pp. 179–193, 2021.

[9] Y. He, L. Dai, and H. Zhang, "Multi-branch deep residual learning for clustering and beamforming in user-centric network," *IEEE Communications Letters*, vol. 24, no. 10, pp. 2221–2225, 2020.

[10] Y. Zhang, F. Liu, Z. Fang, B. Yuan, G. Zhang, and J. Lu, "Learning from a complementary-label source domain: theory and algorithms," *IEEE Transactions on Neural Networks and Learning Systems*, pp. 1–15, 2021.

[11] C. Zhao, X. Liu, S. Zhong, K. Shi, D. Liao, and Q. Zhong, "Secure consensus of multi-agent systems with redundant signal and communication interference via distributed dynamic event-triggered control," *ISA Transactions*, vol. 112, pp. 89–98, 2021.

[12] G. Sun, Y. Cong, J. Dong, Y. Liu, Z. Ding, and H. Yu, "What and how: generalized lifelong spectral clustering via dual memory," *IEEE Transactions on Pattern Analysis and Machine Intelligence*, p. 1, 2021.

[13] G. Sun, Y. Cong, Q. Wang, B. Zhong, and Y. Fu, "Representative task self-selection for flexible clustered lifelong learning," *IEEE Transactions on Neural Networks and Learning Systems*, pp. 1–15, 2020.

[14] W. Yang, X. Chen, Z. Xiong, Z. Xu, G. Liu, and X. Zhang, "A privacy-preserving aggregation scheme based on negative

Hindawi
Scientific Programming
Volume 2023, Article ID 9821378, 1 page
https://doi.org/10.1155/2023/9821378

Retraction

Retracted: Enlightenment of Physical Education Teaching Experiment Based on Cloud Computing to the Current Physical Education Reform

Scientific Programming

Received 26 September 2023; Accepted 26 September 2023; Published 27 September 2023

This article has been retracted by Hindawi following an investigation undertaken by the publisher [1]. This investigation has uncovered evidence of one or more of the following indicators of systematic manipulation of the publication process:

(1) Discrepancies in scope
(2) Discrepancies in the description of the research reported
(3) Discrepancies between the availability of data and the research described
(4) Inappropriate citations
(5) Incoherent, meaningless and/or irrelevant content included in the article
(6) Peer-review manipulation

The presence of these indicators undermines our confidence in the integrity of the article's content and we cannot, therefore, vouch for its reliability. Please note that this notice is intended solely to alert readers that the content of this article is unreliable. We have not investigated whether authors were aware of or involved in the systematic manipulation of the publication process.

Wiley and Hindawi regrets that the usual quality checks did not identify these issues before publication and have since put additional measures in place to safeguard research integrity.

We wish to credit our own Research Integrity and Research Publishing teams and anonymous and named external researchers and research integrity experts for contributing to this investigation.

The corresponding author, as the representative of all authors, has been given the opportunity to register their agreement or disagreement to this retraction. We have kept a record of any response received.

References

[1] F. Wang, "Enlightenment of Physical Education Teaching Experiment Based on Cloud Computing to the Current Physical Education Reform," *Scientific Programming*, vol. 2021, Article ID 6607539, 11 pages, 2021.

Hindawi
Scientific Programming
Volume 2021, Article ID 6607539, 11 pages
https://doi.org/10.1155/2021/6607539

Research Article

Enlightenment of Physical Education Teaching Experiment Based on Cloud Computing to the Current Physical Education Reform

Feng Wang

School of Physical Education, Wuhan Business University, Wuhan 430056, Hubei, China

Correspondence should be addressed to Feng Wang; trainer_wong789@126.com

Received 27 August 2021; Accepted 30 September 2021; Published 18 October 2021

Academic Editor: Punit Gupta

Our country has a large land area, and the development of physical education is not balanced. In daily teaching activities, teachers and students use computers and networks to teach, which generates massive amounts of data. Schools are limited by funds and cannot meet the growing demand for storage of teaching resources. It is also unable to realize the sharing of teaching resources. In order to solve the problems existing in the existing education and teaching platform of the school, especially in the teaching reform, to meet the requirements of all parties facing physical education, the concept of cloud computing was proposed, and the services and methods provided by the cloud computing-based teaching resource platform were discussed. Through the questionnaire survey method of college students and teachers, statistical methods and logical analysis methods were used to analyze the data collected in the questionnaire. Summary and analysis are as follows. The survey results show that more than 50% of the people are dissatisfied with the current physical education and believe that it has not played its due role, and more than 70% of the people agree with the reform of physical education. The experimental results also show that interesting and diverse physical education courses can attract students to participate and increase their interest. From the overall survey results, the problem of college physical education courses is more serious, and it is urgent to optimize teaching from the cloud computing level. On the one hand, it is necessary to improve the relevant cloud computing and other technical platform facilities; on the other hand, it is necessary to improve the teaching level of teachers and change the current educational concept to make it livelier and more interesting.

1. Introduction

Teaching resources cannot be shared and fully utilized, which severely restricts the development of some sports schools. The development of network technology and the increasing maturity of "cloud computing" technology have given us a glimmer of light. Nowadays, "cloud computing" is the hottest topic, and "cloud" is everywhere. Its emergence will directly affect the way in which IT services are provided in the future and the way people use the network and obtain IT resources. The degree of integration between education and society is getting higher and higher, and naturally, it will be profoundly affected by "cloud computing" technology. Many schools at home and abroad have carried out research on the application of cloud computing and cloud computing itself and have achieved fruitful results.

Physical education teaching experiment is a school of physical education that has been highly praised in China, hoping to improve people's physical health. Therefore, different regions have different views on physical education curriculum. Although the national education policy has repeatedly advocated quality education and the all-round development of morality, intelligence, and physique, in the face of reality, especially due to the examination oriented education in China, which pays attention to scores, most students basically devote all their time to the course study, so as to strive for high marks in the examination. It is natural for them to ignore the physical education curriculum. In 2016, the purpose of Hiroaki's two consecutive documents was to promote the so-called learning and research path of cloud computing required to understand the nature of proof activities. They found that students are engaged in many proof activities through their own requirements, due to the teaching contract from the one identified in the ordinary math classroom to a completely different cloud computing platform. They also determined that the proof that these proof activities perform various functions is in the dialectics of the cloud computing environment [1]. In order to change this situation and improve students' interest in physical education curriculum, physical education curriculum in colleges and universities has been reformed for many times, and the slogan of letting students choose courses, time, and teachers independently has been put forward [2]. However, in practice, there are many difficulties and constraints in many aspects, such as teachers and curriculum arrangement, which cannot meet this requirement. Therefore, at present, most colleges and universities still adopt the original fixed time, fixed teachers, and fixed places for PE courses. Moreover, due to the tense curriculum and climate influence, many colleges and universities are still difficult to complete even if they are fixed courses. This is a blow to the enthusiasm of students, making students unwilling to take physical education courses.

Exercise can not only promote the development of brain and nervous system, but also help students improve their learning efficiency. The physical education curriculum is carried out in order to improve college students' personal memory, coordination, hand strength, and exercise of their reaction speed. Some studies have shown that a certain amount of exercise can not only improve people's physical fitness, but also improve their bad emotions. After a certain amount of exercise, the human body will secrete dopamine, endorphin, and other substances, which can relieve people's anxiety, depression, and other negative emotions and reduce pressure. In addition, students receive the most abundant knowledge of safety education in physical education courses, which can reduce the probability of students' safety accidents. College Physical Education Curriculum Optimization not only can attract more students to participate in sports and improve students' comprehensive quality, but also is very important to cultivate students' safety awareness.

Mr. Huang thinks that outward bound training can be added to the physical education curriculum in colleges and universities to form a brand-new physical education curriculum content to strengthen the quality training of students [3–5]; Xia et al. put forward the environmental behavior theory. They optimized the configuration of the physical education curriculum environment and provided students with a multichannel soft curriculum environment for participating in sports competitions through the development of the Internet + "the battle system" and the configuration of different levels of the competition environment [6]. Zhou explored the basic concepts of "innovation" and "development" of college physical education and the value of "innovation" constructed by the physical education curriculum system. In response to the new requirements for the reform of the college physical education curriculum system in the new era, he expanded his reform ideas and directions and conducted specific research [7]. Lin and Wang pointed out that physical education, as a compulsory course for talent training in colleges and universities, plays a very important role in the cultivation of college students' quality and daily life and study. However, there is a phenomenon that universities pay more attention to scientific research than teaching, which cannot well stimulate the enthusiasm of teachers in class and weaken the enthusiasm of physical education teaching. For this reason, they proposed to optimize the evaluation system of public physical education courses in colleges and universities, to stimulate the enthusiasm of the majority of physical education teachers to teach, and to improve the teaching level of the majority of physical education teachers [8].

On the one hand, these studies enrich our understanding of college sports, but on the other hand, the conclusions of the experiment are not completely reasonable. The sample size of the research is small, and the conclusion is not universal enough to be convincing. Using the method of literature analysis and questionnaire survey, this paper constructs a diversified evaluation system, in which the instructors of college physical education curriculum, namely, college teachers, and the receivers and subjects of college physical education curriculum, namely, students, jointly participate in the evaluation and survey system. Through the questionnaire survey, students and teachers think that there are problems in the current college physical education curriculum, and in view of these problems, the paper puts forward some suggestions. The relevant solutions can enrich the relevant scholars' research on the optimization of college physical education curriculum, which has certain theoretical research significance.

2. Physical Education and Teaching Methods

2.1. Physical Education Teaching Principles. Physical education is a course set up by colleges and universities to improve students' physique, and an important principle it needs to follow is the principle of safety education [9]. General safety education follows the following three principles [10, 11].

2.1.1. Safety First Principle. In the school teaching and living work, the first problem is the safety of school students. No matter the time is, the safety of school students should be put in the first place and given priority. Especially, when the safety work of school students conflicts with other work, priority should be given to the safety of school students. When school students are in danger, safety is the first priority; in the allocation of school resources, the allocation of expenses to ensure the safety of school students should be given priority to other expenses [12]; the publicity work of safety education should be prior to other work of the school; in the assessment of the school, safety education should occupy a certain proportion, so that schools, teachers, and students will firmly carry out safety education, keeping it in mind.

Protecting the life and property safety of students and teachers is the most basic and important attribute of the school. All teaching activities and teaching work of the school can be carried out on this basis. The principle of safety priority is the basis of normal teaching and related activities, and its position is unshakable [13–15].

2.1.2. Life First Principle. The principle of life first refers to putting the safety of students and teachers in the most important position in the production, life, and teaching work of the school. In short, when any person or thing threatens the life safety of teachers or students, the safety of teachers and students should be put in the first place [16], when the safety of students and teachers is different from others. When there is a conflict of interests, the safety of teachers and students should be the first protection goal. Nothing else can be compared with the life and health safety of teachers and students. Teachers and students are the most important wealth of the school [17].

2.1.3. Prevention First and Remedy Second. The principle of "prevention first, remedy second" means that, in the teaching and production activities of the school, the safety work should be found and solved in advance in the daily operation and maintenance. When the safety accident has not been found, the potential safety hazards should be eliminated. For the possible risks in the operation process of the school, the principle of proper handling in advance should be adhered to, so as to prevent the trouble in the bud [18]. The school is an important place for students and teachers to live in. The occurrence of safety accidents is a huge disaster for schools, teachers, and students. Therefore, we should adhere to the principle of prevention first and remedy as supplement and eliminate potential safety hazards in advance [19].

To enhance college students' sports ability and improve their physique, it is necessary to train students to exercise consciously, which requires joint efforts from various aspects, such as learning and students. Students should cultivate the awareness of self-use, and college teachers need to teach students' physical education courses according to the students' specific conditions, such as students' hobbies and specialties, and teach students in accordance with their aptitude, so that students can truly participate in sports and feel the charm of sports.

2.2. College Physical Education Curriculum. College physical education curriculum is set up to strengthen students' physique and exercise their related abilities through proper scientific and reasonable sports. With the continuous change of modern education concept, this course has been paid more and more attention.

College physical education curriculum is an independent subject, and related courses need scientific arrangement and research, putting in a lot of energy to study, in order to arrange the corresponding courses scientifically and reasonably. In the long run, the arrangement of college physical education curriculum should adhere to the concept of "reasonable, practical and healthy." Under the background of attaching importance to physical education in the new era, we should integrate relevant thoughts and promote the development of students' sports consciousness, so as to achieve the realization of students' self-worth and turn sports into college teaching in a real sense. Education is an indispensable part [20].

With the development of college physical education, people are more and more aware of the role of physical education. Scientific and reasonable physical education curriculum can not only improve students' sports level and physical quality, but also help them cultivate perseverance and pioneering spirit and enhance their collectivism and patriotism. As an independent subject, physical education also has corresponding philosophical content. From the current situation, the philosophical trend of college physical education can be roughly divided into two categories. The first ideology promotes competition; that is, physical education should focus on how to develop students' skills and tactics [21]. The second ideology advocates fitness and believes that sports should serve students' fitness and entertainment, which can improve students' physical quality. In today's era of advocating healthy diet and healthy life, the second concept of advocating fitness is more recognized by people. But in my opinion, these two ideas are not impossible to exist at the same time, they have a lot in common, and they can complement each other.

Reasonable and interesting physical education courses can attract students to actively participate in sports courses, form a good sports atmosphere, and improve students' skills and quality. Therefore, colleges and universities should formulate reasonable teaching plans according to their own teachers and students' specific conditions and relevant needs. They should not blindly follow the trend, but remember that the right ones are the best [22].

At present, there are some common problems in college physical education:

(1) The concept of physical education is not advanced. In the context of the current national sports, physical education teaching is also in the process of reform and optimization. However, the only change is the form of teaching; the corresponding teaching concept has not changed, and the use of the old set, in the process of education, ignoring the teaching should be student-centered, ignore the students' subjective initiative, and ignore the diversity of students, as well as subjective teaching plan, and it cannot achieve teaching, as well as the function of education, preaching, and teaching.

(2) Teaching mode is serious. The development time of physical education is not long, but with the passage of time, the requirements for the content of physical education curriculum are higher and higher, and its role is more and more important. However, in the current physical education teaching, the original backward set is still adopted, focusing on competitive sports, which greatly violates the original intention of carrying out efficient physical education curriculum and also makes the goal of college physical education difficult to achieve. In the long run, the teaching mode will inevitably lead to the teachers' unilateral teaching, but the students will be difficult to identify with and lose their interest in learning. Moreover, the students taught by the model teaching will have no personality and vitality.

(3) The investment in primary schools and schools does not attach importance to physical education. Although quality education is strongly advocated at present, examination oriented education still seriously covers the teaching of the school. The score of a

test paper will not only determine the fate and future of a student, but also affect the reputation and destiny of the school. In this mode, the investment of school for physical education curriculum is bound to shrink, and teachers, students, and related equipment cannot be guaranteed.

2.3. Resource Allocation and Cloud Computing. Resource allocation refers to the choice of resource allocation among various uses. Resources refer to the resources that can be collected and used in social activities, including human resources, material resources, and financial resources. Because there are too many things to do in production and life, if we do not carry out reasonable resource allocation but adopt the method of spreading cake, then all the goals may be difficult to achieve, because, in the social development, compared with the needs of people, the resources owned are always unable to achieve enough to meet all the things; this also requires people to focus on scientific and reasonable allocation of resources, in order to use the least consumption, achieve the most urgent goal, and obtain the maximum benefit.

Cloud computing is a more scientific technology for resource allocation. There are many definitions of cloud computing. This article tends to focus on virtual computing resources that can be self-maintained and managed on the Internet (large server clusters, including computing servers, storage servers, and broadband resources). A system implements network delivery of information services. Automatic management is realized by software, without human involvement, and services are distributed to end users with the help of modes such as IAAS. Its core concept is to reduce the processing burden of the user terminal by continuously improving the processing capacity of the "cloud," ultimately simplify the user terminal into a simple input and output device, and enjoy the powerful computing and processing capabilities of the "cloud" on demand. It can be a good guide to the reasonable allocation of resources.

Enterprises are market-oriented. Any fluctuation in the market will have an impact on the production of enterprises. Enterprises adjust their production and operation direction through the changes and fluctuations of market prices, so as to optimize the allocation of production resources. When the price of a commodity rises, it means that the number of such commodities in circulation in the market is insufficient, and they are in the seller's market, and the supply of goods is not suitable. At this time, enterprises will give priority to the allocation of resources and increase the output of such commodities. On the contrary, when the price of a certain commodity is cold, it indicates that there are too many unable to meet people's needs in the market for such goods. If the goods cannot be sold, the enterprise will reduce the production of such commodities or adjust the production direction to turn to the commodities in other seller's markets in order to maximize profits [23]. Making full use of the market's automatic adjustment function and rationally allocating resources are the main means for enterprises to maneuver in the market.

Therefore, the following function is used to describe the optimal allocation of fog resources:

$$T = \frac{1}{w_x} a_i b_i^2. \tag{1}$$

It is shown as follows:

$$T_n = \min \sum_{i=1}^{x} \frac{1}{w_x} a_i b_i^2. \tag{2}$$

Enterprises in the market operation and production will inevitably produce fierce competition; at this time, if enterprises cannot find their own positioning, strengthen management, improve efficiency, and create benefits in operation and management, it is bound to be swallowed up by other enterprises that do better. Finally, all the enterprises that can exist in the market are enterprises with high efficiency and can create profits, which encourages enterprises to continue in operation and management. The survival of the fittest is the survival of the fittest.

2.4. Teaching Optimization. Teaching optimization refers to the improvement of existing teaching methods or the addition of new teaching methods, so that students can quickly grasp the knowledge, skills, and methods they have learned and improve their physique. Through the optimization of teaching, students can have a preliminary understanding of the school's physical education content, physical education management, extracurricular sports activities, etc. The cultivation and exercise of working ability is also a comprehensive test of our school's education work, promoting the deepening of teaching reform and constantly improving the teaching quality of college physical education. The specific methods include the following.

And this kind of thing may happen on the local computer: when you are editing a file, the computer crashes, and then your file is lost. And if you are doing this work on the "cloud" side, there will be no such problems. There is a dedicated team of experts to help you manage this. Your data and files have multiple copies, which can basically prevent viruses and file loss. This is also an important aspect of improving teaching optimization.

(1) Improving teachers' teaching level: teachers' ability directly affects students' learning desire. Excellent teachers can directly promote students' learning; otherwise, it will damage students' learning enthusiasm. Therefore, it is necessary to increase the investment in professional talents, that is, teachers, to cultivate qualified teachers. Play the role of excellent teachers, through teachers to drive learning, and give play to the subjective initiative of students, to achieve the purpose of students who want to learn and are willing to learn [24].

(2) Changing teaching methods: with the change of science and technology, teachers' teaching methods are changing with each passing day, and teaching tools have also changed greatly. The original blackboard and a box of chalk have become a curtain and multimedia. These have greatly changed the way students learn but also make teaching methods vivid,

and multimedia teaching, distance teaching, and so on will become more and more three-dimensional [25].

(3) Reasonable arrangement of the corresponding courses: reasonable curriculum is the premise of the smooth progress of school physical education; the curriculum is the daily work of the school's command table, and a scientific and reasonable curriculum arrangement is an indispensable part of the smooth teaching, which requires that the school must proceed from its own reality and have a full understanding of its existing resources, teachers, and students, in order to be in the corresponding courses. Make the best use of the people in the arrangement. Only scientific and reasonable curriculum arrangement can enable students to learn what they are interested in the school physical education teaching and truly achieve what they have learned [26].

The optimization of college physical education curriculum can be improved on this basis. From the perspective of security, to optimize and improve the current college curriculum, it is necessary to solve the problems existing in college physical education curriculum, make scientific and reasonable arrangements for relevant courses, change teaching methods, improve teaching level, and optimize resource allocation.

For physical education in colleges and universities, the optimal value p is

$$P = \frac{6}{5\left(a_i + a_j\right)} \left[\frac{r_i r_j}{r_i + r_j}\right]^{1/2}. \tag{3}$$

Material parameters AI, AJ are

$$a_n = \frac{1 - t_n^2}{S_n}, \quad (n = i, j). \tag{4}$$

Physical education in colleges and universities: if there are no excellent physical education teachers to comprehensively promote school sports work, physical education curriculum and teaching reform are difficult to implement and grasp. The expansion of PE teaching skills, the improvement of PE teaching quality, the enhancement of PE teaching professional awareness, and the improvement of PE teaching quality can guarantee the normal learning of students and teachers.

The more a social occupation has the higher standard and higher difficulty compared with other occupations, the more it is respected and admired by people, and the more professional subjects can fully display themselves, improve themselves, and realize themselves. Some researchers have pointed out: "although the economic treatment and professional reputation of physical education teachers have not reached the status of doctors and lawyers, but with people's pursuit of physical health and increasing attention to the degree of physical health, the social reputation of physical education teachers will continue to improve with people's growing demand for sports."

3. Physical Education Experiment

3.1. Research Object. The purpose of this experiment is to optimize the physical education curriculum in colleges and universities, with empirical research as the main body, in order to obtain the basis of research; according to the basis of empirical research, put forward ideas for optimizing college physical education curriculum.

3.2. Research Basis. In the preliminary analysis of this study, using the literature research method, this method is mainly to collect literature, and through the collation of the existing literature to form a preliminary understanding of College Physical Education Curriculum Optimization, refer to the books about physical education in colleges and universities, the current situation of physical education courses in colleges and universities, the reform of physical education courses in colleges and universities, and the optimization direction of physical education courses in colleges and universities.

This study is based on the existing research results, using the existing model to design the scale, through the opinions and suggestions of experts and professors, testing and revision, and finally forming the questionnaire. This questionnaire survey adopts the combination of network questionnaire and field survey questionnaire. Through random sampling of 100 college students and 20 university teachers, this paper investigates the students' gender, grade, physical education curriculum frequency, related courses, satisfaction with the first college physical education curriculum, and the teachers' satisfaction with the college physical education curriculum and whether it is necessary. 200 questionnaires were distributed on the Internet to investigate the same problems.

According to the statistics of the number of questionnaires, as shown in Table 1, 100 questionnaires were distributed by the field survey group, and 100 were recovered, with the recovery rate of 100%; 200 questionnaires were distributed by the network survey group, and 180 questionnaires were recovered, with the recovery rate of 90%. 20 questionnaires were distributed to the teachers group, and 20 were recovered, with the recovery rate of 100%. A total of 320 questionnaires were sent out, and 320 were recovered, with a recovery rate of 100%.

3.3. Evaluation Criteria. In order to calculate the weight of physical education and ensure the objectivity of evaluation results, we use entropy weight method to determine the entropy value and entropy weight of each resource attribute.

$$\begin{aligned} t &= \frac{1}{\ln x} \sum_{n=1}^{1} f_{nm} * \ \ln f_{nm}, \\ r &= \frac{1 - t}{y - \sum_{m=1}^{m} t}, \end{aligned} \tag{5}$$

among

Table 1: Questionnaire survey.

Group	Number of copies issued	Number of copies recovered	Rate of recovery
Internet questionnaire group	100	100	100%
Field questionnaire group	200	200	100%
Teacher	20	20	100%

$$f_{mn} = \frac{z_{nm}}{\sum_{n=1}^{x} z_{nm}},$$
$$\sum_{m=1}^{x} w_m = 1. \tag{6}$$

Set objective weight:

$$d = \sqrt{\sum_{m=1}^{x} w_n * \left(r_{nm} - uq_m\right)^2},$$
$$d_n = \frac{1}{1 + d\left(r_n, uq\right)}. \tag{7}$$

Set the threshold of proximity, and the range is between [0, 1], from which the matching value Q can be obtained:

$$Q_\delta = \left\{r_n \middle| d\ \cos\left(r_n, uq\right)\right| \geq \delta\}. \tag{8}$$

The similarity between the resources in the matching resource set Q and the resources requested by users is calculated:

$$\cos\ m(r, uq) = \alpha *\ \cos(r, uq) + (1 - \alpha) * \frac{1}{m}\sum_{n=1}^{m} \delta_{ij}, \tag{9}$$

where a is the weight, and the range is between [0, 1]. The simulation parameters are calculated as follows:

$$F = \frac{\sum\left(q_{rp,rpn} - q_{rpm}\right)\left(q_{uq,uqn} - q_{uq}\right)}{\sum_{n=1}^{n}\left(q_r - q_{uq}\right)^2 \sqrt{\sum\left(q_{uq,uqm} - q_{uq}\right)^2}}. \tag{10}$$

4. An Analysis of Physical Education Experiment

4.1. Statistics of Survey Objects. The gender and grade of the respondents were statistically analyzed, as shown in Table 2. Besides teachers, there were 300 students in this survey, including 150 males and 150 females. There are 98 freshmen, 70 sophomores, 72 juniors, and 59 seniors. The details are shown in Table 2 and Figures 1 and 2.

4.2. Satisfaction of Physical Education Courses in Colleges and Universities. In 320 surveys, 295 people expressed dissatisfaction with the current physical education curriculum in colleges and universities. The main reasons are equipment and space problems, teachers' problems, occupation of physical education courses, few types of sports activities, too boring courses, etc. The details are shown in Figure 3.

For teachers' satisfaction with the current physical education curriculum in colleges and universities, we conducted a comprehensive survey on 10 teachers' satisfaction with the course content, curriculum effect, and classroom student management. The survey results are shown in Figure 4.

According to the research and statistics, the dissatisfaction degree of college students to the physical education curriculum has reached 90%, and the problems of equipment and space and physical education mode are prominent. According to the survey of teachers, they think that the main reasons for the current physical education curriculum are that the school does not pay attention to sports, the investment is insufficient, and the equipment aging brings security risks. In order to improve this situation, we must pay more attention to sports, increase investment, and improve the basic conditions. Physical education curriculum should be very dependent on equipment and venues. The quality of venues and equipment directly affects the treatment of courses. Under the background of comprehensive attention to sports, we should increase investment in sports, improve the infrastructure construction of related venues and equipment, and improve education Methods to adjust, so as to improve the quality of physical education courses in colleges and universities.

4.3. Attendance Rate of Physical Education Courses in Colleges and Universities. We have also made statistics on the number and rate of students attending physical education courses in recent five years. The statistical results are shown in Table 3.

As shown in Figures 5 and 6, more than 17% of students think that physical education teaching is boring, and they are not willing to take physical education. In view of this situation, we should update the teaching concept of physical education curriculum, adjust measures to local conditions, teach students according to different people, and enhance students' interest. Physical education curriculum is not a course for students' activities only. With the continuous change of sports concept, physical education curriculum has become a multiobjective and comprehensive course.

4.4. Impact of Physical Education Curriculum on Performance. Some schools think that physical education curriculum wastes students' time, delays their study, and will make students' performance retrogressive. We also through this questionnaire survey, the students' weekly physical education curriculum time, and performance survey, we get the relevant data. The specific statistics of the 300 students surveyed are shown in Table 4.

Table 2: Questionnaire population statistics.

	Boys	Girls	Freshman	Sophomore	Junior	Senior year
Field questionnaire	93	107	62	43	49	46
Internet questionnaire	57	43	36	28	23	13

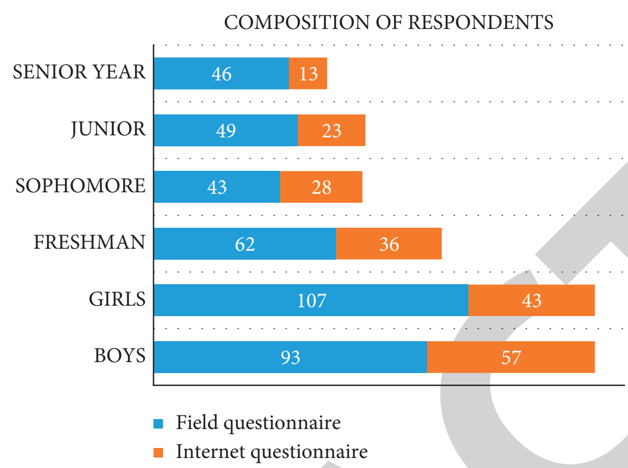

Figure 1: Composition of respondents.

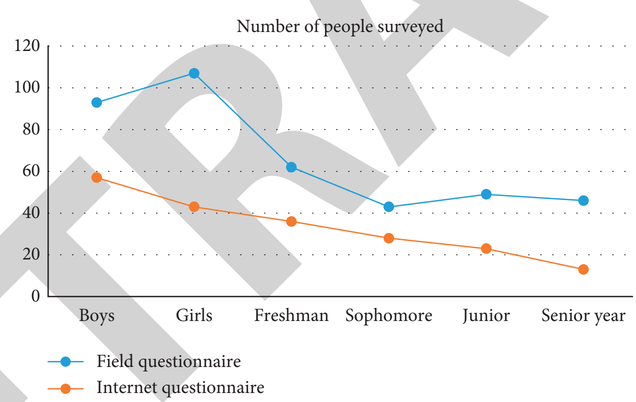

Figure 2: Number of people surveyed.

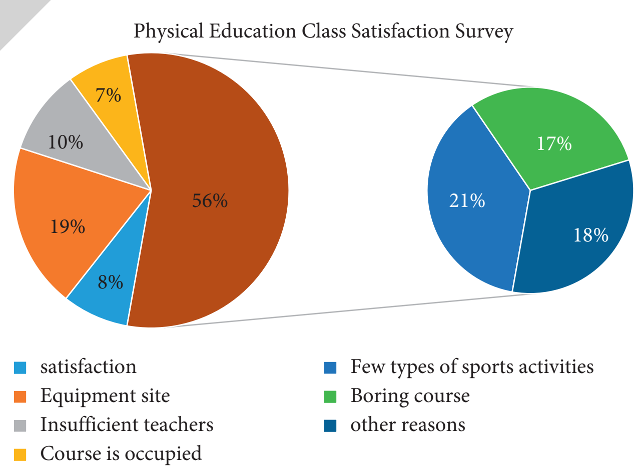

Figure 3: Reasons for students' dissatisfaction.

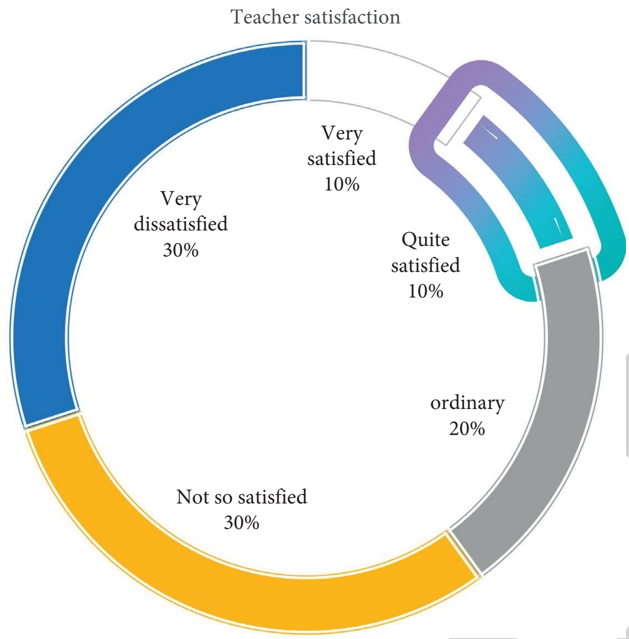

Figure 4: Reasons for teachers' dissatisfaction.

Table 3: Questionnaire population statistics.

	2015	2016	2017	2018	2019
Number of people to arrive	523	537	553	547	539
Actual number of people	517	514	529	519	507

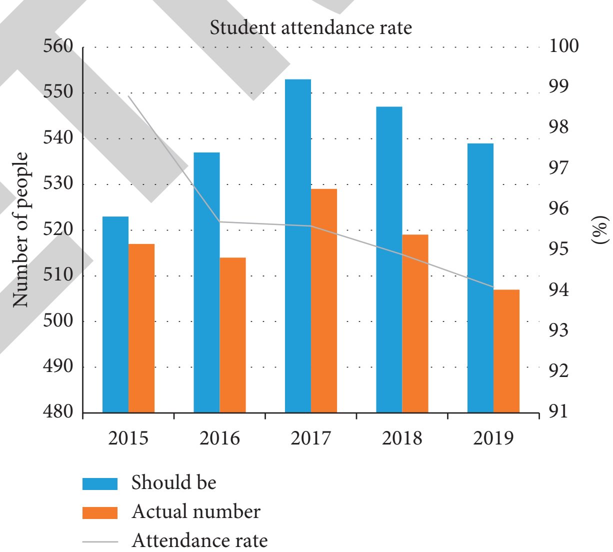

Figure 5: Reasons for teachers' dissatisfaction.

As shown in Figures 7 and 8, the overall score of the participants in the P.E. course was the highest in 76–100 divisions during the weekly and Tuesdays, and no one scored 0–60 points. Considering that the students' weekly PE courses were not uniform, the proportion of students whose scores were in the range of 76–100 was about 80%–84% of the students in the second level of physical education every week, while only 52% of the students do not attend physical education. Therefore, we can draw a conclusion that the physical education curriculum is not negatively correlated with the performance, or even positively correlated to a certain extent.

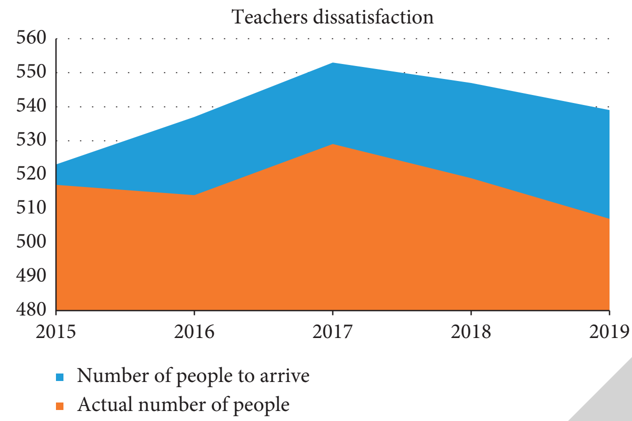

Figure 6: Reasons for teachers' dissatisfaction.

Table 4: Grades and physical education.

	0–60	61–75	76–90	91–100
No PE	5	12	23	1
One PE class	1	24	67	3
Two PE classes	0	26	77	7
Greater than two PE	0	18	32	4

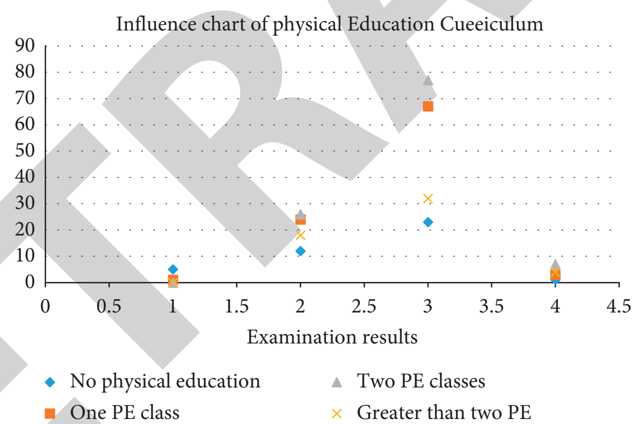

Figure 7: Grades and physical education.

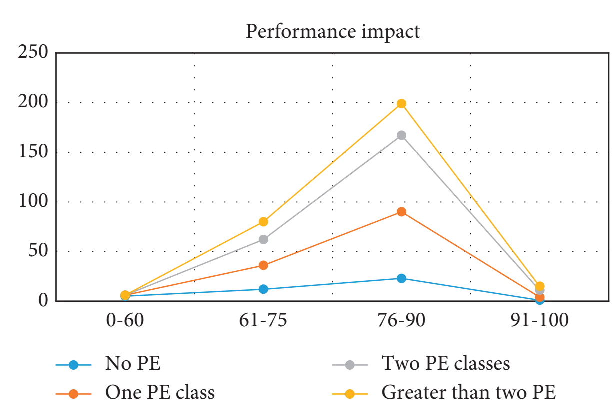

Figure 8: Influence of physical education on Performance.

5. Conclusion

A healthy body is the foundation of any activity we engage in. The basic purpose of setting up physical education course in colleges and universities is to cultivate and improve the overall quality of college students and improve their physical health. At present, the purpose of physical education curriculum cannot be achieved. China's physical education curriculum is still in the primary stage. The correct concept, method, and resource allocation of physical education curriculum have not been formed. In addition, due to the influence of examination oriented education for a long time, schools and society have not invested enough in Physical Education in colleges and universities and have not paid enough attention to it. College students and teachers are generally dissatisfied with the current college curriculum, so it is imperative to optimize the university curriculum. The emergence of cloud computing, the IAAS service level, and the "cloud" + "end" cloud service provision model have changed the development thinking of the entire IT industry. Physical education, of course, has also been affected by new technologies and new concepts, especially the core technology of cloud computing-"virtualization" and "distribution," which makes physical education face the problem of teaching resource management and laboratory management. The problem has a revolutionary solution.

In order to attract students, the most important thing is to change the relevant teaching content and change the original boring physical education curriculum into a relatively low difficulty, but diverse and entertaining sports. Secondly, it is necessary to change the existing concept of physical education curriculum. In the current college physical education curriculum, physical education curriculum is equipment, playground, and court. The physical education curriculum is limited to a small playground, far away from nature, has no connection with multimedia, and does not pay attention to sports news. These situations make students unable to integrate into sports, have no sense of identity with sports, and make the physical education curriculum stay not vivid.

Although the emergence of the "cloud" allows us to see the dawn of vocational education, all existing problems can be solved. With the passage of time, the maturity of cloud computing technology, the development of broadband networks, the popularization of information technology, the continuous upgrading of mobile terminals, and the development and improvement of cloud security technology, I believe that it is not only the private cloud for physical education that we proposed, but also a city, a province, and the whole of China's education will slowly begin in the near future. Let us open our arms to prepare for the magnificent education cloud era!

Data Availability

Data sharing is not applicable to this article as no datasets were generated or analyzed during the current study.

Conflicts of Interest

The author declares no potential conflicts of interest with respect to the research, authorship, and/or publication of this article.

Acknowledgments

This work was supported by 2018 Hubei Provincial Teaching Reform Research Project (no. 2018465).

References

[1] Hiroaki, Hamanaka, Koji, Otaki, Takeshi, and Miyakawa, "Proving activities in SRP based on the paradigm of questioning the world (II): through a teaching experiment for undergraduate students," *Journal of JASME: Research in Mathematics Education*, vol. 22, no. 2, pp. 59–72, 2016.

[2] B. Wen, "Research on the integration reform of college physical education curriculum in and out of class," *Contemporary Sports Science and Technology*, vol. 5, no. 21, pp. 245-246, 2015.

[3] Z. Chen, "Research on curriculum optimization of physical education in my country's colleges and universities——based on the perspective of kindergarten sports teacher demand," *Stationery & Sports Products & Technology*, vol. 3, no. 20, pp. 23–26, 2016.

[4] Y. Zhang, "Optimization of college physical education curriculum under the new curriculum teaching concept," *Xuezhou*, vol. 399, no. 15, pp. 20–23, 2019.

[5] F. Jiang, "Analysis of the optimization of college physical education under the new curriculum teaching concept," *Sports World (Academic Edition)*, vol. 785, no. 11, p. 146+152, 2018.

[6] D. Xia, D. Xie, and C. Qin, "Optimization of the curriculum environment of "integration of in class and out of class" in college physical education-a case study of Shenzhen university," *Journal of Physical Education*, vol. 13, no. 6, pp. 75–79, 2015.

[7] W. Zhou, "On the reform and structural optimization of college physical education curriculum system," *Heilongjiang Higher Education Research*, vol. 32, no. 1, pp. 168–170, 2015.

[8] Y. Lin and F. Wang, "Research on optimization of evaluation system of public physical education curriculum in colleges and universities ①," *Contemporary Sports Science and Technology*, vol. 239, no. 7, p. 113+115, 2017.

[9] Q. Chen, "Research on the optimization of "integrated" teaching mode in and out of college physical education," *Sports Boutique*, vol. 29, no. 11, pp. 40-41, 2019.

[10] H. Yu, "Discussion on the integration and optimization strategy of sports curriculum cultural resources in local colleges and universities in Hubei province," *Contemporary Sports Science and Technology*, vol. 8, no. 9, p. 77+79, 2018.

[11] T. Gao, "Internet plus" promotes the reform and innovation of physical education curriculum: taking the case library construction of capital institute of physical education as an example," in *Proceedings of the Summary of the 12th National Sports Information Technology Conference 2016*, p. 23+27, Harda, India, March 2016.

[12] L. Dan, "Reflections on several issues of college physical education reform," *Shanxi Youth*, vol. 1, no. 2, p. 244, 2018.

Hindawi
Scientific Programming
Volume 2021, Article ID 9054328, 11 pages
https://doi.org/10.1155/2021/9054328

Research Article

Reduction of Asymptotic Approximate Expansion of Navier–Stokes Equation and Solution of Inviscid Burgers Equation by Similarity Transformation

Farhad Ali,[1] **Wali Khan Mashwani**,[1] **Hamayat Ullah**,[1] **Ahmed Hussein Msmali**,[2] **Ikramullah Ikramullah**,[3] **and Zabidin Salleh**[4]

[1]*Institute of Numerical Sciences, Kohat University of Sciences and Technology, Kohat, Pakistan*
[2]*Department of Mathematics, Collage of Science, Jazan University, Saudi Arabia*
[3]*Department of Physics, Kohat University of Sciences and Technology, Kohat, Pakistan*
[4]*Department of Mathematics, Faculty of Ocean Engineering Technology and Informatics, Universiti Malaysia Terengganu, 21030 Kuala Nerus, Terengganu, Malaysia*

Correspondence should be addressed to Wali Khan Mashwani; mashwanigr8@gmail.com

Received 22 August 2021; Accepted 30 September 2021; Published 16 October 2021

Academic Editor: Punit Gupta

Symmetry methods for differential equations are a powerful tool for the solutions of differential equations. It linearizes nonlinear differential equations, reduces the order of differential equations, reduces the number of independent variables in partial differential equations, and solves almost all those differential equations for which the other analytic methods fail to solve them. Similarity transformation is a particular case of symmetries, but it is easy and often used to deal with differential equations. The similarity transformation can do all the aforementioned works. In this research, we use the similarity transformation to solve different nonlinear differential equations. Particularly, we will apply this transformation to the nonlinear Navier–Stokes partial differential equations to reduce them to ordinary differential equations. Ordinary differential equations are easy to deal with than partial differential equations. Some nonlinear physical examples of ODEs and PDEs are given to show that the similarity transformation solves those problems where the other analytic methods fail to work.

1. Introduction

Differential equations (DEs) are the dynamical equations, which describe the motion of particles. We have a dynamic world, everywhere anytime some dynamic phenomena occur. When mathematicians model a natural phenomenon, they put it in a mathematical system called DEs. DEs are broadly divided into ordinary differential equations (ODEs) and partial differential equations (PDEs). These DEs arise from many purely mathematical considerations, that is, the mathematician defines dependent and independent variables along with parameters corresponding to the given problem and put some constraints accordingly to model and put the given natural phenomenon in a beautiful and elegant short mathematical equation. There is a wide spectrum of different types of DEs, and various techniques and methods have been developed to deal with the quantitative and qualitative behavior of these equations. The field of fluid dynamics, for example, requires different constraints and techniques to model the fluid flow through different media and to make the computation of their solutions possible. The techniques which can handle linear PDEs such as integral transforms and Eigen functions can transform them into ODEs, which is comparably easy to solve. These techniques have some contributions in solving nonlinear PDEs [1]. There are numerous PDE systems that described natural phenomena. Some well-known systems are different types of wave and heat equations, Maxwell equations, Navier–Stokes equations, Schrodinger equation, Dirac equation, etc.

The majority of the natural phenomena are nonlinear in nature and are therefore modeled into different orders of nonlinear PDEs. Nonlinear PDEs [2, 3] are generally more complex and are therefore difficult to solve using well-established analytical and/or numerical techniques. Most of the time, nonlinear PDEs have no exact solutions. In such conditions, in the majority of the cases, we go for their qualitative behavior or at most solve them numerically. It is often very difficult to solve nonlinear PDEs analytically, such as equations of fluid mechanics and equations of plasma dynamics. [4, 5]. However, symmetry methods play an important role to deal with nonlinear DEs (ODEs and PDEs both). The similarity transformation (scaling symmetry) is a way that regroups the existing variables and defines new variables and puts the given harder nonlinear problem in the most simplest and easy form. In most cases, the problem becomes solvable or at least we reduce the order of ODE and the number of independent variables involved in the PDEs. In the case of two variables, PDEs become ODEs. The ODEs are easy to deal with as compared to PDEs.

This method was developed in the early twentieth century by Norwegian mathematician Sophus Lie, who observed that regrouping of variables is applicable in all types of DEs. The solutions obtained through similarity transformation are called similarity solutions, which mostly satisfy simpler equations than the real PDEs. The one-one correspondence between the solution space of the original and new solution space exists, and because of transformation, one can jump back and forth easily. The significance of similarity solutions lies in their simple calculation. We will apply the similarity conversion technique to PDEs to completely solve them or at least simplify them. This transformation decreases the number of autonomous (independent) variables of the system of PDE at least one less than that of the original equation [6]. Hussain et al. [7] recently studied the Hirota–Satsuma coupled system of KdV equations using OHAM with the addition of Daftardar–Jeffery polynomials. We also employ asymptotic expansion to the reduced Navier–Stokes equation. An asymptotic expansion is the series expansion that has the property of truncation after a finite number of terms and hence gives an approximate solution of the given problem. Power series is the most widely used form of an asymptotic expansion. Integral transforms such as Mellen and Laplace transforms and the Euler–Maclaurin summation formula generate such kinds of expansions. Here in this research, we are going to apply the similarity transformation to solve the nonlinear ODEs and PDEs. Specifically, we are interested in the solution of Burgers and Navier–Stokes equations.

Here in this research, we are going to apply the similarity transformation to solve nonlinear ODEs and PDEs. Specifically, we are interested in the solution of Burgers and Navier–Stokes equations. The organization of the present article goes in the following fashion: basic definitions related to Lie symmetries and similarity transformations are given in Section 2. Subsections 2.1–2.5 show the power of the similarity transformation that how this transformation solves the nonlinear ODEs and PDE. Burgers equations are solved by using appropriate similarity transformations in Section 3. Section 4 is devoted to the similarity solution of the inviscid Burgers equation. The system of Navier–Stokes equations of fluid dynamics is PDEs. By using the similarity transformations, these equations are converted into a system of ODEs, given in Section 5. The highlights of the investigation are concluded in the final Section 6.

2. Basic Definitions

In this section, we give some basic definitions related to Lie symmetries and solutions of DEs. The similarity symmetry transformation and similarity solution is a special case of the Lie symmetries. Our main concern in this paper is to use the similarity transformation for the solution of DEs. What is more special about the similarity transformation is that one can use it without the knowledge of symmetry methods. That is why we select the similarity transformation among others to handle some nonlinear natural phenomena.

2.1. Lie Symmetries and Their Uses. We have an n^{th} ordinary differential equation of the form

$$E(x, y, y' \ldots y^n) = 0. \tag{1}$$

A transformation,

$$\begin{aligned} X &= X(x, y, \varepsilon), \\ X(x, y, 0) &= x, \\ Y &= Y(x, y, \varepsilon), \\ Y(x, y, 0) &= y, \\ x &= x(X, Y, \varepsilon), \\ x(X, Y, 0) &= X, \\ y &= y(X, Y, \varepsilon), \\ y(X, Y, 0) &= Y, \end{aligned} \tag{2}$$

is said to be symmetry transformation of equation (1) if it remains invariant under this transformation, that is,

$$\begin{aligned} E(x, y, y' \ldots y^n) = E(X, Y, Y' \ldots Y^n) \\ = 0. \end{aligned} \tag{3}$$

An n^{th} order extended Lie symmetry generator is

$$\begin{aligned} \mathbf{L}^{[n]} = \xi(x, y)\frac{\partial}{\partial x} + \eta(x, y)\frac{\partial}{\partial y} + \eta_x(x, y, y')\frac{\partial}{\partial y'} \\ + \cdots + \eta_{\underbrace{xxx\ldots x}_{\text{ntime}}}(x, y, y' \ldots y^n)\frac{\partial}{\partial y^n}, \end{aligned} \tag{4}$$

where

$$\eta_k = \frac{d\eta_{k-1}}{dx} - y^k\frac{d\xi}{dx}, \tag{5}$$

where k is the order of differentiation. If equation (4) is the Lie symmetry generator of the differential equation (1), the Lie symmetry equation takes the form

$$\mathbf{L}^{[n]}E(x, y, y' \ldots y^n)|_{E=0} = 0. \tag{6}$$

The Lie differential equations corresponding to equation (6) are

$$\begin{aligned} &\frac{\mathrm{d}X}{\mathrm{d}\epsilon}|_{\epsilon\longrightarrow 0} = \xi(x, y), \\ &X(x, y, 0) = x\frac{\mathrm{d}Y}{\mathrm{d}\epsilon}|_{\epsilon\longrightarrow 0} = \eta(x, y), \\ &Y(x, y, 0) = y. \end{aligned} \tag{7}$$

The integration of Lie's equation gives the corresponding Lie symmetry transformation.

Example 1. Consider the first-order nonlinear ODE

$$\frac{\mathrm{d}y}{\mathrm{d}x} = \left(\frac{y^2}{x^3}\right) + x. \tag{8}$$

It admits the similarity symmetry generator

$$\mathbf{L} = x\frac{\partial}{\partial x} + 2y\frac{\partial}{\partial y}. \tag{9}$$

Using the Lie differential equation, we can find the corresponding Lie symmetry transformation

$$\begin{aligned} X &= e^{\epsilon}x, \\ Y &= e^{2\epsilon}y. \end{aligned} \tag{10}$$

The corresponding similarity transformation is

$$\begin{aligned} s &= x, \\ t &= \frac{x^2}{y}. \end{aligned} \tag{11}$$

The differential equation (8) in the similarity variables s and t takes the form

$$\frac{ds}{dt} = -\frac{1}{(t-1)^2}, \tag{12}$$

which is linear, the solution of which is

$$s = \frac{1}{t-1} + c. \tag{13}$$

The solution in the original coordinates takes the form

$$\ln(x) = \frac{y}{(x^2 - y)} + c. \tag{14}$$

The ODE given in equation (8) is nonlinear and none of the analytic methods will be applicable here, but we see that the similarity transformation converts it into linear and easily solvable equation. For PDEs, consider a function $v(x, t)$, the dependent and independent variables can be changed by a mapping $(x, t, v) \Longleftrightarrow (X, T, V)$, or more explicitly,

$$\begin{aligned} T &= T(t, x, v, \varepsilon), \\ T(t, x, v, 0) &= t \Longleftrightarrow t = t(T, X, V, \varepsilon), \\ t(T, X, V, 0) &= T, \\ X &= X(t, x, v, \varepsilon), \\ X(t, x, v, 0) &= x \Longleftrightarrow x = x(T, X, V, \varepsilon), \\ x(T, X, V, 0) &= X, \\ V &= V(t, x, v, \varepsilon), \\ V(t, x, v, 0) &= v \Longleftrightarrow v = v(T, X, V, \varepsilon), v(T, X, V, 0) = V, \end{aligned} \tag{15}$$

where T, X, V are smooth invertible functions of the parameter ϵ and the given variables [8, 9]. A PDE is transformed by symmetry transformations given in equation (15), if $V = V(T, X)$ is the solution of given PDE just like the solution $v(t, x)$. In other words, a symmetry transformation maps the solution set of the original PDE to the solution set of the target PDE and there is one correspondence between both the solution sets. Let us explain this by an example.

Example 2. The given PDE

$$v_t(t, x) = v(t, x)v_{xx}(t, x), \tag{16}$$

which admits the Lie symmetry generator

$$\mathbf{L}_p = t\frac{\partial}{\partial t} + \frac{x}{2}\frac{\partial}{\partial x}. \tag{17}$$

The corresponding similarity transformation takes the form

$$\begin{aligned} T &= e^{\varepsilon}t, \\ X &= e^{\varepsilon/2}x, \\ V &= v. \end{aligned} \tag{18}$$

Suppose the solution of the given PDE is $v(x, t)$; it is simple to check that $V(T, X) = v(e^{\varepsilon}t, e^{\varepsilon/2}x)$ is also the solution simply by putting it into the given PDE, that is,

$$\begin{aligned} \partial T\ V(T, X) &= e^{-\epsilon}\partial_t v(T, X) \\ &= V(T, X)\partial_{XX}V(T, X) \\ &= e^{(-\epsilon/2)-(\epsilon/2)}v(T, X)\partial_{xx}(v(T, X)) \\ &= e^{-\epsilon}v(T, X)v(T, X). \end{aligned} \tag{19}$$

From the above equation, we cancel the term $e^{-\varepsilon}$ from both sides and get

$$V(T, X)_T = V(T, X)V_{X,X}(T, X). \tag{20}$$

Hence, the symmetry transformation given in equation (18) does not change the structure of the given PDE. The PDE given in equation (16) also admit the similarity transformation

$$\begin{aligned} T &= t, \\ X &= \ln(x), \\ V &= \frac{v}{x^2}. \end{aligned} \tag{21}$$

This transformation reduces the PDE (11) to a first-order ODE

$$\frac{dV(T)}{dT} - 2V^2(T) = 0, \tag{22}$$

the solution of which is

$$V(T) = -\frac{1}{2T - C}. \tag{23}$$

The solution of the PDE given in equation (16) takes the form

$$v(t,x) = -\frac{x^2}{2t - c}. \tag{24}$$

We see that the PDE (11) is not solvable by another analytic method, but the similarity transformation given in equation (21) easily solved it.

Generally, we can define a similarity transformation for a system of PDEs in n independent variables $(x^1, x^2 \ldots x^n)$ and m dependent variables $u^j(x^1, x^2 \ldots x^n)$, $j = 1, 2, 3 \ldots m$, as

$$\begin{aligned} \overline{x}^i &= e^{\varepsilon a^i} x^i, \quad i = 1, 2, 3 \ldots n, \\ \overline{u}^j &= e^{\varepsilon b^j} u^j, \quad j = 1, 2 \ldots m, \end{aligned} \tag{25}$$

where ε is the parameter and a^i, b^j are constant to be determined correspondingly.

2.2. Similarity Transformation. The transformations which reduce the number of independent variables of a PDE (or a system of PDEs) at least one less than that of the original equation are designated as similarity transformations [10, 11].

Example 3. Consider the nonlinear PDE,

$$u_{tt}(t,x) - u_x^2(t,x) = 0, \tag{26}$$

admits the similarity Lie symmetry (scaling symmetry generator)

$$\mathbf{L} = t\frac{\partial}{\partial t} - 2u\frac{\partial}{\partial u}. \tag{27}$$

The corresponding similarity transformations is

$$\begin{aligned} T &= \ln(t), \\ X &= x, \\ U &= ut^2. \end{aligned} \tag{28}$$

2.3. Similarity Method. The method which searches for such a similarity transformation is known as similarity method. For example, the transformation given in equation (28) is the similarity transformation corresponding to the PDE given in equation (26).

2.4. Similarity Equations. When we transform a PDE or system of PDEs, $\Omega = 0$ (say), in n independent variables to a PDE, $\overline{\Omega} = 0$ in $n-1$ independent variables, then the equation is known as similarity equation or similarity representation of the system of Ω[12, 13]. Using the similarity transformation given in (19) in the PDE given in equation (26), we have the ordinary differential equation,

$$(U')^2(X) - 6U(X) = 0. \tag{29}$$

The similarity transformation given in equation (28) not only reduces the independent variables in the PDE given in (26) but also reduces the order of differentiation. We see that the ODE given in equation (29) is first-order ODE.

2.5. Similarity Solution. The solution which is obtained by employing the similarity transformations is known as similarity solution [14]. The nontrivial similarity solution of the reduced ODE given in equation (29) is

$$U = \frac{3}{2}(X - C_1)^2. \tag{30}$$

When we take the back transformation, the solution in the original coordinates become

$$u(t,x) = \frac{3}{2}\left(\frac{x - c_1}{t}\right)^2. \tag{31}$$

Thus, we solve a nonlinear PDE given in equation (26), with the help of similarity transformation, given in equation (28). The existing analytic methods other than symmetry methods will not be able to solve equation (26).

3. Solution of Burgers Equation by Similarity Transformation

Afterwards, we will use the similarity transformation to handle the problems. The detail calculation for finding the similarity transformation corresponding to each PDE is given. There is no need of the symmetry methods' knowledge for finding the similarity transformation. First, we consider the Burgers equation. In the universe, most of the physical phenomena are nonlinear, and the corresponding mathematical models are nonlinear PDEs. Burgers equation is one of the most celebrated PDEs, which models the fluid flow in a dissipative system given by [15–17]

$$\frac{\partial v(x,t)}{\partial t} + v(x,t)\frac{\partial v(x,t)}{\partial x} = \mu\frac{\partial^2 v(x,t)}{\partial x^2}, \tag{32}$$

where $v(x,t)$ is the velocity field, x is the spatial coordinate, t is the time, and μ is the viscosity parameter. The term v_{xx} models the diffusion and the vv_x models the convective flow, introducing the similarity transformations as

$$\begin{aligned} z_1 &= \varepsilon^{\alpha} x, \\ s &= \varepsilon^{\beta} t, \\ w &= \varepsilon^{\gamma} v, \end{aligned} \tag{33}$$

where ε is a positive parameter.

As

$$w = \varepsilon^{\gamma} v, \tag{34}$$

therefore

$$\frac{\partial v}{\partial t} = \varepsilon^{\beta-\gamma} \frac{\partial w}{\partial s}, \tag{35}$$

and

$$\frac{\partial v}{\partial x} = \varepsilon^{\alpha-\gamma} \frac{\partial w}{\partial z_1}. \tag{36}$$

Similarly,

$$\frac{\partial^2 v}{\partial x^2} = \epsilon^{2\alpha-\gamma} \frac{\partial^2 w}{\partial z_1^2}. \tag{37}$$

Putting (35), (36), and (37) in (32), we get

$$\begin{aligned} \varepsilon^{\beta-\gamma} \frac{\partial w}{\partial s} + \varepsilon^{-\gamma} w \varepsilon^{\alpha-\gamma} \frac{\partial w}{\partial z_1} &= \varepsilon^{2\alpha-\gamma} \frac{\partial^2 w}{\partial z_1^2}, \\ \varepsilon^{\beta-\gamma} \frac{\partial w}{\partial s} + w \varepsilon^{\alpha-2\gamma} \frac{\partial w}{\partial z_1} &= \varepsilon^{2\alpha-\gamma} \frac{\partial^2 w}{\partial z_1^2}. \end{aligned} \tag{38}$$

Equation (38) will be invariant under the similarity transformations, if

$$\begin{aligned} \beta - \gamma &= 0, \\ \alpha - 2\gamma &= 0, \\ 2\alpha - \gamma &= 0. \end{aligned} \tag{39}$$

Solving (39), we get

$$\begin{aligned} \frac{\alpha}{\beta} &= \frac{1}{2}, \\ \frac{\gamma}{\beta} &= -\frac{1}{2}. \end{aligned} \tag{40}$$

So, we take the solution of (47) of the form

$$\begin{aligned} v(x,t) &= t^{\gamma/\beta} g(\psi), \\ \psi &= x t^{-(\alpha/\beta)}, \\ v(x,t) &= t^{-(1/2)} g(\psi), \\ \psi &= x t^{-(1/2)}. \end{aligned} \tag{41}$$

Differentiating (41) with respect to t, we obtain

$$v_t = -\frac{1}{2} t^{-(3/2)} g(\psi) - \frac{1}{2} t^{-(3/2)} \psi g'(\psi). \tag{42}$$

Now, differentiating (41) twice with respect to x, we get respectively

$$v_x = t^{-1} g'(\psi), \tag{43}$$

$$v_{xx} = t^{-(3/2)} g''(\psi). \tag{44}$$

Putting (41), (42), (43), and(44) in (32), we obtain

$$\begin{aligned} & -\frac{1}{2} t^{-(3/2)} g(\psi) - \frac{1}{2} t^{-(3/2)} \psi g'(\psi) + t^{-(1/2)} g(\psi) t^{-1} g'(\psi) \\ & \quad = t^{-(3/2)} g''(\psi). \end{aligned} \tag{45}$$

After simplification, we get

$$g''(\psi) + \frac{1}{2} g(\psi) + \frac{1}{2} \psi g'(\psi) - g(\psi) g'(\psi) = 0. \tag{46}$$

Equation (46) can be written as

$$(g'(\psi))' + \left(\frac{\psi}{2} g(\psi)\right)' - \frac{1}{2}\left(g^2(\psi)\right)' = 0. \tag{47}$$

Integrating (47), we get

$$g'(\psi) + \frac{\psi}{2} g(\psi) - \frac{1}{2} g^2(\psi) = m. \tag{48}$$

Equation (48) is the Riccati-type equation, which has standard solution. Its solution is

$$g(\psi) = \frac{-2e^{-\psi^2/4}}{C + \sqrt{\pi} erf(\psi/2)}. \tag{49}$$

4. Solution of Inviscid Burgers Equation by Similarity Transformation

The inviscid Burgers equation [18, 19] for which $\mu = 0$ models the nondissipative flow which is given by

$$\frac{\partial v(x,t)}{\partial t} + v(x,t) \frac{\partial v(x,t)}{\partial x} = 0. \tag{50}$$

Introducing similarity transformations, we have

$$\begin{aligned} z &= \varepsilon^{\alpha} x, \\ s &= \varepsilon^{\beta} t, \\ u &= \varepsilon^{\gamma} v, \end{aligned} \tag{51}$$

where ε is a positive parameter.

As

$$u = \varepsilon^{\gamma} v, \tag{52}$$

therefore

$$\frac{\partial v}{\partial t} = \varepsilon^{\beta-\gamma} \frac{\partial u}{\partial s}, \tag{53}$$

and

$$\frac{\partial v}{\partial x} = \varepsilon^{\alpha-\gamma} \frac{\partial u}{\partial z}. \tag{54}$$

Putting (53) and (54) in (50), we get

$$\varepsilon^{\beta-\gamma}\frac{\partial u}{\partial s}+\varepsilon^{\alpha-2\gamma}u\frac{\partial u}{\partial z}=0. \tag{55}$$

Equation (55) will be invariant under the similarity transformations, if

$$\gamma=\alpha-\beta. \tag{56}$$

Therefore, we look for the solution of the form

$$\begin{aligned} v(x,t)&=t^{\gamma/\beta}g(\phi), \quad \phi=\frac{x}{t^{\alpha/\beta}},\\ &=t^{(\alpha/\beta)-1}g(\phi). \end{aligned} \tag{57}$$

Let $(\alpha/\beta)-1=m$, then $\alpha/\beta=m+1$; therefore, (25) becomes

$$v(x,t)=t^{m}g(\phi), \quad \phi=\frac{x}{t^{m+1}}. \tag{58}$$

Differentiating (58) with respect to t, we get

$$v_t=t^{m-1}\left[mg(\phi)-(m+1)\phi g'(\phi)\right], \quad \phi=\frac{x}{t^{m+1}}. \tag{59}$$

Now, differentiating (58) with respect to x, we get

$$v_x(x,t)=t^{m-1}g'(\phi)\frac{1}{t^{m}}. \tag{60}$$

Putting (60) and (59) in (54), we obtain

$$t^{m-1}\left[mg(\phi)-(m+1)\phi g'(\phi)\right]+g(\phi)g'(\phi)=0. \tag{61}$$

For $m=0$, (61) becomes

$$t^{-1}\left[-\phi g'(\phi)+g(\phi)g'(\phi)\right]=0, \tag{62}$$

since $t\neq 0$, therefore

$$-\phi g'(\phi)+g(\phi)g'(\phi)=0, \tag{63}$$

This gives

$$g(\phi)=\phi. \tag{64}$$

Therefore,

$$g(\phi)=\frac{x}{t^{\alpha/\beta}}, \quad \phi=\frac{x}{t^{\alpha/\beta}}. \tag{65}$$

As $(\alpha/\beta)-1=m$, but $m=0$, therefore $\alpha/\beta=1$. Now, equation (64) becomes

$$g(\phi)=\frac{x}{t}, \tag{66}$$

so

$$v(x,t)=t^{m}g(\phi). \tag{67}$$

Putting $m=0$ and $g(\phi)=x/t$, we have

$$v(x,t)=\frac{x}{t}, \tag{68}$$

which is a solution of the inviscid Burgers equation.

5. Reduction of Navier–Stokes Equations by Similarity Transformations

Fluid dynamics is a hot area of research and almost all dynamical equations that describe the motion of fluids are nonlinear. The basic ingredients of the fluid dynamics are the Navier–Stokes equations of fluid motion. The Navier–Stokes equations are nonlinear in nature and thus it is very difficult to find their exact/analytical solutions. Therefore, different constraint/assumptions are needed to approach the possible solutions of these equations. The analytic solution of the Navier–Stokes equations is possible only if we ignore the complexities and nonlinearities in the equations, or we proceed toward the possible solutions with numerical computation. But, these types of solutions not provide the actual picture of problem. The general compact form of the Navier–Stokes equations is

$$\begin{gathered} \frac{\mathrm{d}\rho}{\mathrm{d}t}+\rho(\nabla\cdot\mathbf{V})=0,\\ \rho\frac{\mathrm{d}\mathbf{V}}{\mathrm{d}t}=\rho\mathbf{g}-\nabla P+\mu\nabla^{2}\mathbf{V}. \end{gathered} \tag{69}$$

where $\rho(t)$ is the fluid density, $\mathbf{V}=(u,v,w)$ is the fluid velocity, $\mathbf{g}=(g_x,g_y,g_z)$ is the gravitational acceleration, P is the pressure of fluid, μ is the a constant, and

$$\begin{gathered} \nabla=\frac{\partial}{\partial x}\mathbf{i}+\frac{\partial}{\partial y}\mathbf{j}+\frac{\partial}{\partial z}\mathbf{k},\\ \frac{\mathrm{d}}{\mathrm{d}t}=\frac{\partial}{\partial t}+\dot{x}^{i}\frac{\partial}{\partial x^{i}}, \quad i=1,2,3. \end{gathered} \tag{70}$$

In more explicit form, the Navier–Stokes equation given (69) can be written as

$$\begin{aligned}
&\frac{d\rho}{dt} + \rho\left(\frac{\partial u}{\partial x} + \frac{\partial v}{\partial y} + \frac{\partial w}{\partial z}\right) = 0, \\
&\mathbf{i}\colon \rho\left(\frac{\partial u}{\partial t} + u\frac{\partial u}{\partial x} + v\frac{\partial u}{\partial y} + w\frac{\partial u}{\partial z}\right) = \rho g_x - \frac{\partial P}{\partial x} + \mu\left(\frac{\partial^2 u}{\partial x^2} + \frac{\partial^2 u}{\partial y^2} + \frac{\partial^2 u}{\partial z^2}\right), \\
&\mathbf{j}\colon \rho\left(\frac{\partial v}{\partial t} + u\frac{\partial v}{\partial x} + v\frac{\partial v}{\partial y} + w\frac{\partial v}{\partial z}\right) = \rho g_y - \frac{\partial P}{\partial y} + \mu\left(\frac{\partial^2 v}{\partial x^2} + \frac{\partial^2 v}{\partial y^2} + \frac{\partial^2 v}{\partial z^2}\right), \\
&\mathbf{k}\colon \rho\left(\frac{\partial w}{\partial t} + u\frac{\partial w}{\partial x} + v\frac{\partial w}{\partial y} + w\frac{\partial w}{\partial z}\right) = \rho g_z - \frac{\partial P}{\partial z} + \mu\left(\frac{\partial^2 w}{\partial x^2} + \frac{\partial^2 w}{\partial y^2} + \frac{\partial^2 w}{\partial z^2}\right).
\end{aligned} \tag{71}$$

For the steady flow of the fluid, the flow becomes time independent, in that case with $\mathrm{d}/\mathrm{d}t$ and $\partial/\partial t$ becoming zero, that is, the system (73) takes the form

$$\begin{aligned}
&\frac{\partial u}{\partial x} + \frac{\partial v}{\partial y} + \frac{\partial w}{\partial z} = 0, \\
&\mathbf{i}\colon \rho\left(u\frac{\partial u}{\partial x} + v\frac{\partial u}{\partial y} + w\frac{\partial u}{\partial z}\right) = \rho g_x - \frac{\partial P}{\partial x} + \mu\left(\frac{\partial^2 u}{\partial x^2} + \frac{\partial^2 u}{\partial y^2} + \frac{\partial^2 u}{\partial z^2}\right), \\
&\mathbf{j}\colon \rho\left(u\frac{\partial v}{\partial x} + v\frac{\partial v}{\partial y} + w\frac{\partial v}{\partial z}\right) = \rho g_y - \frac{\partial P}{\partial y} + \mu\left(\frac{\partial^2 v}{\partial x^2} + \frac{\partial^2 v}{\partial y^2} + \frac{\partial^2 v}{\partial z^2}\right), \\
&\mathbf{k}\colon \rho\left(u\frac{\partial w}{\partial x} + v\frac{\partial w}{\partial y} + w\frac{\partial w}{\partial z}\right) = \rho g_z - \frac{\partial P}{\partial z} + \mu\left(\frac{\partial^2 w}{\partial x^2} + \frac{\partial^2 w}{\partial y^2} + \frac{\partial^2 w}{\partial z^2}\right).
\end{aligned} \tag{72}$$

For incompressible fluid, the density of the fluid becomes independent of time, therefore we have $\mathrm{d}\rho/\mathrm{d}t = 0$. In that case, we have

$$\begin{aligned}
&\frac{\partial u}{\partial x} + \frac{\partial v}{\partial y} + \frac{\partial w}{\partial z} = 0, \\
&\mathbf{i}\colon \rho\left(\frac{\partial u}{\partial t} + u\frac{\partial u}{\partial x} + v\frac{\partial u}{\partial y} + w\frac{\partial u}{\partial z}\right) = \rho g_x - \frac{\partial P}{\partial x} + \mu\left(\frac{\partial^2 u}{\partial x^2} + \frac{\partial^2 u}{\partial y^2} + \frac{\partial^2 u}{\partial z^2}\right), \\
&\mathbf{j}\colon \rho\left(\frac{\partial v}{\partial t} + u\frac{\partial v}{\partial x} + v\frac{\partial v}{\partial y} + w\frac{\partial v}{\partial z}\right) = \rho g_y - \frac{\partial P}{\partial y} + \mu\left(\frac{\partial^2 v}{\partial x^2} + \frac{\partial^2 v}{\partial y^2} + \frac{\partial^2 v}{\partial z^2}\right), \\
&\mathbf{k}\colon \rho\left(\frac{\partial w}{\partial t} + u\frac{\partial w}{\partial x} + v\frac{\partial w}{\partial y} + w\frac{\partial w}{\partial z}\right) = \rho g_z - \frac{\partial P}{\partial z} + \mu\left(\frac{\partial^2 w}{\partial x^2} + \frac{\partial^2 w}{\partial y^2} + \frac{\partial^2 w}{\partial z^2}\right).
\end{aligned} \tag{73}$$

We consider the incompressible fluid in the xy plane, which flows steadily in the x direction [20–22]. For the asymptotic behavior of the fluid flow, an asymptotic term $U(x)(\mathrm{d}U/\mathrm{d}x) = \rho g_x - \partial P/\partial x$ is included in the dynamics which satisfy the given conditions. Our first aim is to find and use the similarity transformation and reduce the given nonlinear Navier–Stokes PDEs equations in ODEs equations. A step-by-step procedure for this conversion is given in the remainder of this paper.

$$\begin{aligned} &\frac{\partial u}{\partial x}+\frac{\partial v}{\partial y}=0,\\ &u\frac{\partial u}{\partial x}+v\frac{\partial u}{\partial y}=\frac{\partial^2 u}{\partial y^2}+U\frac{dU}{dx},\\ &u(x,0)=0,\\ &v(x,0)=0,\\ &u(x,\infty)=U(x). \end{aligned} \tag{74}$$

Introducing the following similarity transformation,

$$\begin{aligned} x' &= e^{\varepsilon a_1}x,\\ y' &= e^{\varepsilon b_1}y,\\ u' &= e^{\varepsilon c_1}u,\\ v' &= e^{\varepsilon p_1}v,\\ U' &= e^{\varepsilon q_1}U, \end{aligned} \tag{75}$$

from (75), we have

$$\frac{\partial u}{\partial x}=e^{\varepsilon(a_1-c_1)}\frac{\partial u'}{\partial x'}. \tag{76}$$

$$\frac{\partial u}{\partial y}=e^{\varepsilon(b_1-c_1)}\frac{\partial u'}{\partial y'}, \tag{77}$$

$$\frac{\partial v}{\partial y}=e^{\epsilon(b_1-p_1)}\frac{\partial v'}{\partial y'}, \tag{78}$$

$$\frac{\partial^2 u}{\partial y^2}=e^{\epsilon(2b_1-c_1)}\frac{\partial u'}{\partial y'}, \tag{79}$$

$$\frac{dU}{dx}=e^{\epsilon(a_1-q_1)}\frac{dU'}{dx'}. \tag{80}$$

Putting the above equations from (76) to (80) in (74), we get

$$\begin{aligned} &e^{\varepsilon(a_1-c_1)}\frac{\partial u'}{\partial x'}+e^{\varepsilon(b_1-p_1)}\frac{\partial v'}{\partial y'}=0,\\ &e^{\varepsilon(a_1-2c_1)}u'\frac{\partial u'}{\partial x'}+e^{\varepsilon(b_1-c_1-p_1)}v'\frac{\partial u'}{\partial y'}=e^{\varepsilon(2b_1-c_1)}\frac{\partial^2 u'}{\partial y'^2}\\ &\qquad+e^{\varepsilon(a_1-2q_1)}U'\frac{dU'}{dx'},\\ &u'(x',0)=0,\\ &v'(x',0)=0,\\ &u'(x',\infty)=U(x). \end{aligned} \tag{81}$$

In (81), dividing by the coefficients of the leading terms in each equation, we get the transformed equations as

$$\begin{aligned} &\frac{\partial u'}{\partial x'}+e^{\epsilon(b_1+c_1-a_1-p_1)}\frac{\partial v'}{\partial y'}=0,\\ &u'\frac{\partial u'}{\partial x'}+e^{\epsilon(b_1+c_1-a_1-p_1)}v'\frac{\partial u'}{\partial y'}=e^{\epsilon(2b_1+c_1-a_1)}\frac{\partial^2 u'}{\partial y'^2}\\ &\qquad+e^{2\epsilon(c_1-q_1)}U'\frac{dU'}{dx'},\\ &u'(x',0)=0,\\ &v'(x',0)=0,\\ &u'(x',\infty)=e^{\epsilon(c_1-q_1)}U(x). \end{aligned} \tag{82}$$

$$\begin{aligned} b_1+c_1-a_1-p_1&=0,\\ 2b_1+c_1-a_1&=0,\\ c_1-q_1&=0. \end{aligned} \tag{83}$$

Solving (83), we get

$$\begin{aligned} p_1&=\frac{(c_1-a_1)}{2},\\ b_1&=\frac{(a_1-c_1)}{2},\\ c_1&=q_1. \end{aligned} \tag{84}$$

Now, we have two arbitrary parameters a_1 and c_1; this gives flexibility in assigning specific values to these parameters. We assume that $c_1=ra_1$, where r is another parameter. Using this new parameter, (84) becomes

$$\begin{aligned} p_1&=\frac{(ra_1-a_1)}{2},\\ b_1&=\frac{(a_1-ra_1)}{2},\\ q_1&=ra_1. \end{aligned} \tag{85}$$

Expanding the exponentials in (75) by Taylor series and keeping the terms up to first order in ϵ and denoting the difference in transformed and original variables as differential, we have for the first term,

$$\begin{aligned} x'&=e^{\varepsilon a_1}x,\\ x'&=(1+\varepsilon a_1)x,\\ x'&=x+a_1\varepsilon x,\\ x'-x&=a_1\varepsilon x,\\ dx&=a_1\varepsilon x,\\ \frac{dx}{a_1x}&=\varepsilon. \end{aligned} \tag{86}$$

Similarly, the expansion of the other terms gives

$$\frac{\mathrm{d}y}{b_1 y} = \varepsilon. \tag{87}$$

$$\frac{\mathrm{d}u}{c_1 u} = \varepsilon. \tag{88}$$

$$\frac{\mathrm{d}v}{p_1 v} = \varepsilon. \tag{89}$$

$$\frac{\mathrm{d}U}{q_1 U} = \varepsilon. \tag{90}$$

Comparing (86), (87), (88), (89), and (90), we have

$$\begin{aligned}\frac{\mathrm{d}x}{a_1 x} &= \frac{\mathrm{d}y}{b_1 y}\\ &= \frac{\mathrm{d}u}{c_1 u}\\ &= \frac{\mathrm{d}v}{p_1 v}\\ &= \frac{\mathrm{d}U}{q_1 U}.\end{aligned} \tag{91}$$

Using the values of b_1, c_1, p_1, and q from (85) in (91), we obtain

$$\begin{aligned}\frac{\mathrm{d}x}{x} &= \frac{\mathrm{d}y}{((1-r)/2)y}\\ &= \frac{\mathrm{d}u}{ru}\\ &= \frac{\mathrm{d}v}{((r-1)/2)v}\\ &= \frac{\mathrm{d}U}{rU}.\end{aligned} \tag{92}$$

Using the method of characteristic to solve (92), the solution of

$$\frac{\mathrm{d}x}{x} = \frac{\mathrm{d}y}{((1-r)/2)y}, \tag{93}$$

is

$$\phi = yx^{(r-1)/2}. \tag{94}$$

Similarly, the solutions of the other equations in (92) are respectively given by

$$\begin{aligned}u &= x^r f(\phi),\\ v &= x^{(r-1)/2} g(\phi),\end{aligned} \tag{95}$$

$$U = kx^r. \tag{96}$$

Thus, we obtained the following similarity variable and functions:

$$\begin{aligned}\phi &= yx^{(r-1)/2},\\ u &= x^r f(\phi),\\ v &= x^{(r-1)/2} g(\phi),\\ U &= kx^r,\end{aligned} \tag{97}$$

where k is constant, using (97) to obtain the first- and second-order derivatives as in the following,

$$\begin{aligned}\frac{\partial u}{\partial x} &= rx^{r-1} f(\phi) + \frac{r-1}{2} x^{r-1} \phi f'(\phi),\\ \frac{\partial u}{\partial y} &= x^r \cdot x^{r-1/2} f'(\phi),\\ \frac{\partial^2 u}{\partial y^2} &= x^r \cdot x^{r-1} f''(\phi),\\ \frac{\partial v}{\partial y} &= x^{(r-1)} g'(\phi).\end{aligned} \tag{98}$$

Using these derivatives in (74), we get

$$\begin{aligned} &rf(\phi) + \frac{r-1}{2}\phi f'(\phi) + g'(\phi) = 0,\\ &\left(\frac{r-1}{2}\right)\phi f(\phi) f'(\phi) + rf^2(\phi) + g(\phi) f'(\phi) = f''(\phi) + rk.\end{aligned} \tag{99}$$

We have reduced the Navier–Stokes equation,

$$\begin{aligned} &\frac{\partial u}{\partial x} + \frac{\partial v}{\partial y} = 0,\\ &u\frac{\partial u}{\partial x} + v\frac{\partial u}{\partial y} = \frac{\partial^2 u}{\partial y^2} + U\frac{\mathrm{d}U}{\mathrm{d}x},\\ &u(x,0) = 0,\\ &v(x,0) = 0,\\ &u(x,\infty) = U(x),\end{aligned} \tag{100}$$

to ODEs using the proposed similarity transformations

$$\begin{aligned} &rf(\phi) + \frac{r-1}{2}\phi f'(\phi) + g'(\phi) = 0,\\ &\left(\frac{r-1}{2}\right)\phi f(\phi) f'(\phi) + rf^2(\phi) + g(\phi) f'(\phi) = f''(\phi) + rk,\\ &f(0) = 0,\\ &g(0) = 0,\\ &f(M) = k,\\ &M \longrightarrow \infty.\end{aligned} \tag{101}$$

6. Conclusion

In this research, we used the similarity transformation to solve completely or at least reduce the nonlinear PDEs to nonlinear ODEs. As the similarity transformations are the subclass of Lie symmetries, therefore some basic definitions related to Lie symmetry along with examples are given in Section 2. In the same section, we see the power of similarity transformation in solving the nonlinear ODEs and PDEs. Similarity transformation is a technique for solving complex and nonlinear DEs without the knowledge of Lie symmetry methods, that is, the main reason for using the similarity transformation in this research work. In this method, one takes a general similarity transformation, inserts it into the given equation (or system of equations), and solves for a particular similarity transformation. This procedure is shown in detail in Sections 3 and 4.

Generally, modeling fluid flow is a complex phenomenon due to its nonlinear nature. Burgers equation models the diffusion of the viscous fluid, whereas the inviscid Burgers equation is its special case by ignoring the viscous nature of the fluid. The mathematical model which described Burgers equation is nonlinear and cannot be solved analytically. We solve Burgers equation by using the similarity transformations. This technique reduced the number of independent variables in the equation and reduced the nonlinear PDEs to nonlinear ODEs. The similarity transformation transforms Burgers equation into Riccati-type equation, which has a standard solution. The detailed and step-by-step calculation of this work is given in Section 3.

The Navier–Stokes equations are second-order nonlinear PDEs that had been developed to model the compressible viscous fluid flow by adding the viscous term to the original Euler equations, which models the compressible friction-less flow. The general Navier–Stokes equations deal with compressible, viscous, nonsteady, and steady flow fluids. One can simplify these equations for his/her problem nature. For example, most of the fluids are incompressible, which implies that the density of the fluids does not depend on time, and equations become independent of the density derivative term. Similarly, for a steady flow, the velocity of the fluids becomes independent of time, which not only simplifies the equations but also helps in solving these nonlinear PDEs. The similarity transformation corresponding to the Navier–Stokes equations is given in Section 4. We reduced the nonlinear system of PDEs of the Navier–Stokes equations to nonlinear ODEs by using the similarity transformation. The quantitative and qualitative analyses of the transformed ODE system are the future works in which we will give the complete analysis of the fluid dynamics of the Navier–stokes equations.

Data Availability

No specific data were used to support this study.

Conflicts of Interest

The authors declare that they have no conflicts of interest to report regarding the present study.

References

[1] S. Dubljevic and P. D. Christofides, “Predictive output feedback control of parabolic partial differential equations (PDEs),” *Industrial & Engineering Chemistry Research*, vol. 45, no. 25, pp. 8421–8429, 2006.

[2] E.-G. Fan, “”Traveling wave solutions for nonlinear equations using symbolic computation,” *Computers & Mathematics with Applications*, vol. 43, no. 6-7, pp. 671–680, 2002.

[3] G. Adomian, “A new approach to nonlinear partial differential equations,” *Journal of Mathematical Analysis and Applications*, vol. 102, no. 2, pp. 420–434, 1984.

[4] D. A. Tarzia, “”A bibliography on moving-free boundary problems for the heat-diffusion equation,” *The Stefan and related problems, MAT-Serie A*, vol. 2, 2000.

[5] J. Hristov, “An approximate analytical (integral-balance) solution to a nonlinear heat diffusion equation,” *Thermal Science*, vol. 19, no. 2, pp. 723–733, 2015.

[6] M. Ali Aroon and M. A. Khansary, “Generalized similarity transformation method applied to partial differential equations (PDEs) in falling film mass transfer,” *Computers & Chemical Engineering*, vol. 101, pp. 73–80, 2017.

[7] K. Zawar Hussain, S. Khan, A. Ullah et al., “Extension of optimal homotopy asymptotic method with use of Daftardar–Jeffery polynomials to Hirota–Satsuma coupled system of Korteweg–de Vries equations,” *Open Physics*, vol. 18, no. 6, pp. 916–924, 2020.

[8] B. Fornberg and C. Piret, “A stable Algorithm for flat radial basis functions on a sphere,” *SIAM Journal on Scientific Computing*, vol. 30, no. 1, pp. 60–80, 2008.

[9] C. Sophocleous, “Transformation properties of a variable-coefficient Burgers equation,” *Chaos, Solitons & Fractals*, vol. 20, no. 5, pp. 1047–1057, 2004.

[10] Y. Cho and A. Aessopos, “Similarity transformation methods in the analysis of the two dimensional steady compressible laminar boundary layer,” *Term paper*, vol. 2, 2004.

[11] J. V. Lambers, “Derivation of high-order spectral methods for time-dependent PDE using modified moments,” *Electronic Transactions on Numerical Analysis*, vol. 28, pp. 114–135, 2008.

[12] S.-y. Lou, D.-f. Hang-yu-Ruan, D.-f. Chen, and W.-z. Chen, “Similarity reductions of the KP equation by a direct method,” *Journal of Physics A: Mathematical and General*, vol. 24, no. 7, pp. 1455–1467, 1991.

[13] S.-J. Liao, “A general approach to get series solution of non-similarity boundary-layer flows,” *Communications in Nonlinear Science and Numerical Simulation*, vol. 14, no. 5, pp. 2144–2159, 2009.

[14] E. C. Dauenhauer and J. Majdalani, “Exact self-similarity solution of the Navier-Stokes equations for a porous channel with orthogonally moving walls,” *Physics of Fluids*, vol. 15, no. 6, pp. 1485–1495, 2003.

[15] J. Doyle and M. J. Englefield, “Similarity solutions of a generalized burgers equation,” *IMA Journal of Applied Mathematics*, vol. 44, no. 2, pp. 145–153, 1990.

[16] E. Y. Rodin, “A Riccati solution for Burgers’ equation,” *Quarterly of Applied Mathematics*, vol. 27, no. 4, pp. 541–545, 1970.

[17] M. Nadjafikhah, “Classification of similarity solutions for inviscid burgers’ equation,” *Advances in Applied Clifford Algebras*, vol. 20, no. 1, pp. 71–77, 2010.

[18] E. R. Benton and G. W. Platzman, “A table of solutions of the one-dimensional Burgers equation,” *Quarterly of Applied Mathematics*, vol. 30, no. 2, pp. 195–212, 1972.

[19] M. Nadjafikhah, "Lie symmetries of inviscid burgers' equation," *Advances in Applied Clifford Algebras*, vol. 19, no. 1, pp. 101–112, 2009.

[20] H. Xu, Z.-L. Lin, S.-J. Liao, J.-Z. Wu, and J. Majdalani, "Homotopy based solutions of the Navier-Stokes equations for a porous channel with orthogonally moving walls," *Physics of Fluids*, vol. 22, no. 5, Article ID 053601, 2010.

[21] P. Lagerstrom and J. Cole, "Examples illustrating expansion procedures for the Navier-Stokes equations," *Indiana University Mathematics Journal*, vol. 4, no. 6, pp. 817–882, 1955.

[22] K. O. Friedrichs, "Asymptotic phenomena in mathematical physics," *Bulletin of the American Mathematical Society*, vol. 61, no. 6, pp. 485–505, 1955.

Hindawi
Scientific Programming
Volume 2021, Article ID 4120921, 8 pages
https://doi.org/10.1155/2021/4120921

Research Article

Research on Teaching Method and Class Evaluation for International Online Teaching

Min Qi [1,2] and Hongying Meng [3]

[1] School of Electronics and Information, Northwestern Polytechnical University, Xi'an, China
[2] National Engineering Laboratory for Integrated Aero-Space-Ground-Ocean Big Data Application Technology, Xi'an, China
[3] Department of Electronic and Computer Engineering, Brunel University London, Uxbridge, UK

Correspondence should be addressed to Min Qi; drqimin@nwpu.edu.cn

Received 28 July 2021; Accepted 21 September 2021; Published 13 October 2021

Academic Editor: Punit Gupta

The COVID-19 epidemic in 2020 posed a sudden and serious challenge to education where online teachings were adopted, and problems that people had not noticed before were exposed. Based on the experience of international online course and the study of online teaching, the paper focuses on the associated problems and puts forward some solutions. First, based on the performance of current software and hardware used in online teaching, the characteristics of commonly used teaching software have been analysed and compared. Then, efficient combinations of teaching software for complementary advantages are recommended to ensure a high-quality online teaching. Second, problems inside of class existing in online lecturing and learning are studied, and corresponding teaching methods have been explored including the aspects of class interaction design and implementation, alternative method for delivering essential video information, and online class management. Finally, some objective class evaluation criteria are studied in terms of coverage of class content, learning effect of specialized knowledge, and online class interaction. In the end, some feasible solutions are provided, and it can be served as a reference to improve the online teaching.

1. Introduction

At the beginning of 2020, a worldwide COVID-19 epidemic disrupted the orders of various fields including education. Universities, colleges, and schools had to close and stopped traditional face-to-face classes. The adoption of online teaching, which had developed for some time and adopted relatively infrequently before COVID-19 epidemic, had a sudden explosion. More than 650,000 teachers in China had introduced nearly 1.7 million online courses. Chinese Education Department had organized 22 online teaching platforms to provide free courses. The online teaching faced serious challenges, while also met a great opportunity to develop.

Online teaching or network teaching is a type of teaching model which relies on network technology. It completes the teaching process through the way of live course or recorded course using software including special online teaching platforms and some APP software used for teaching. With the sudden arrival of the COVID-19 epidemic, the number of online teaching customers increased dramatically, and the use of various software for teaching also increased greatly [1–4]. Some problems that were not found in online teaching in the past are now exposed. Pedagogical researches have studied these issues from the aspects of teaching methods [5–7], online teaching evaluation [8, 9], examination mode [10–13], and so on. It has greatly promoted the development of online teaching. Based on the teaching practice of international online course for overseas students and some Chinese students, this paper studies and summarizes the problems encountered in online teaching and gives corresponding valuable solutions.

2. Problems Existing in Online Teaching

2.1. Problems in Performance of Software and Hardware. The most important and basic challenge of online teaching is the strong dependence on software and network.

The logos of some well-known software for teaching are shown in Figure 1, such as Rain Classroom, DingTalk, QQ, Tencent Conference, Tencent Classroom, and WeChat. It includes online teaching platforms and APP software used in teaching. We call them teaching software in brief here. In the early design stage of software development, customer capacity was not properly assessed due to the limitation of previous network operation experience. So, during the development of teaching software, such explosive growth of customer capacity caused by emergencies was not taken into account. In this case, on the first day of university across the country in February 2020, all software encountered problems to varying degrees without exception. Paralysis, disruption, delay, and disconnection became the normal situation in the first time of online class. The fault of teaching platforms is generally very serious, and the fault of APP software is relatively minor. Obviously, faced with such a large number of network access during the sudden epidemic, online teaching software was not fully prepared.

In hardware respect, as a transmission medium of online teaching, the performance of network is undoubtedly very important and is the basic guarantee of online teaching. During the 2020 epidemic, most networks for teachers have good performance and can meet the requirements of online teaching due to the majority of universities having relatively strong network facilities. Sometimes, when there was delay phenomenon in wireless networks, the wired networks usually worked well for teaching activities. Network problems mainly occurred in students. All the students took online classes at home, who scattered across different provinces, cities, counties, and rural areas, and overseas students stayed outside China. The network performance in the student's location varied greatly, and usually, it was not as good as that of university networks. Also many students did not have computers at home and could only learn through their mobile phones which had much smaller screens and class interaction was not convenient. All these had a negative impact on students' learning. So the influence on students was greater than that on teachers. For example, video materials for teaching often could not be shared with students online because video signals could not be transmitted and received fast enough in some areas where students lived. The percentage of major problems encountered in online teaching and learning is shown in Figure 2.

2.2. Problems in Teaching and Learning. Before the outbreak of the 2020 epidemic, although the online teaching had been developing for quite a long time in China, the number of teachers who were familiar with online teaching was actually small. The majority of teachers did not have online teaching experience and never used the platform software. Face-to-face teaching in classroom was still the dominant form. When schools started during the epidemic, they faced a sudden change to an unfamiliar teaching mode, and both teachers and students felt difficult to adapt. Some problems emerged.

2.2.1. In terms of Teaching

(i) Online class is a special "no-one classroom." Although the teacher and students are in the same class, they are separated in space unlike traditional classroom teaching. Generally, to reduce network traffic and get better condition for smooth teaching, all cameras are turned off. In this case, facing the cold computer screen or mobile phone, teachers cannot get feedback from students' facial expressions. They are not clear about how students understand and master the knowledge.

(ii) It is inconvenient for teachers to manage the class. When teachers speak passionately during the class, they do not know whether the students can follow their ideas in time. This is easy to lead to the deviation in the rhythm of the lecture.

(iii) At the end of a course, many of the previous exam methods are no longer applicable.

2.2.2. In terms of Learning

(i) Students are also just facing a device screen. Instructional guidance from teacher declines and learning effect decreases obviously.

(ii) With the time extension of online teaching, the freshness of students for online courses gradually fades away, the enthusiasm of online learning is not high, and learning motivation is lacked. The phenomenon of being late for class and leaving early is much more than the traditional teaching in classroom. It even appeared that the students left the computer after he signed in for the class. This is one of the reasons that the online teaching effect is hard to be guaranteed.

(iii) Online class at home has a comfortable environment. Correspondingly, it is difficult to create a good learning atmosphere like that at school and is easily disturbed by family members.

According to the survey [14], the major problems of the online learning during the epidemic period include excessive learning interference, easy distraction, difficulty in-depth learning, and low learning efficiency. One student is often troubled by multiple problems. In addition, learning interests, learning methods, learning objectives, depth and breadth of learning, and whether to make learning plans also have certain impacts on learning. The percentage of each problem is given in Table 1.

3. Solutions to Problems of Online Teaching

Online teaching is an interactive activity between students and teachers, which depends heavily on online teaching conditions including hardware, software, and online teaching resources. It is a comprehensive process of interaction by students, teachers, online teaching conditions, online learning environment, and even other social factors as shown in Figure 3. Subjective and objective factors influence

Figure 1: The logos of some well-known software for teaching.

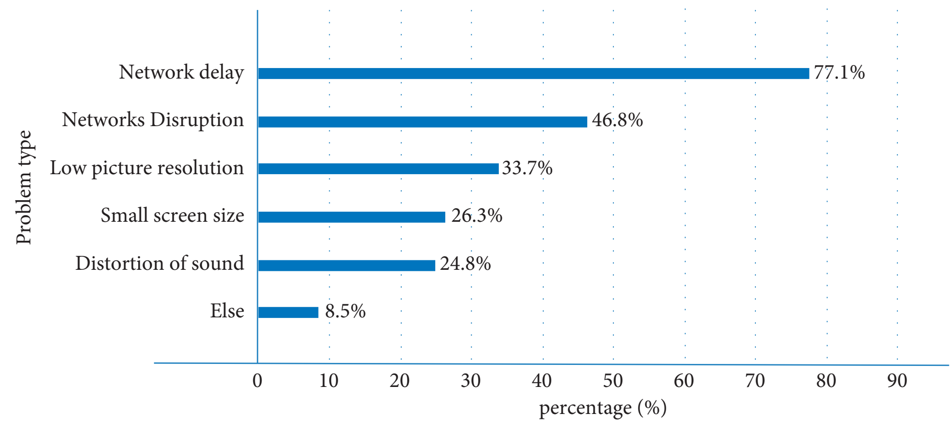

Figure 2: The percentage of major problems encountered in online teaching and learning.

Table 1: The proportion of problems with online learning.

SN	Problems with online learning	Proportion (%)
1	Excessive learning interference	60.98
2	Easy distraction	57.72
3	Difficulty in depth learning	46.34
4	Low learning efficiency	45.53
5	Learning interests	33.33
6	Learning methods	32.52
7	Learning objectives	29.27
8	Depth and breadth of learning	29.27
9	Whether to make learning plans	26.83

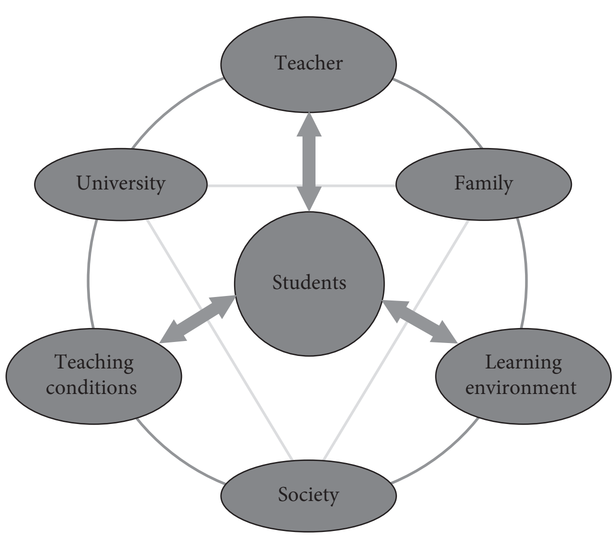

Figure 3: The interaction relationship among the factors of online teaching.

each other and cannot be clearly separated. Therefore, in view of the problems existing in the development of online teaching, we make a comprehensive analysis of them considering the subjective and objective factors together. Some solutions to improve the quality of online teaching are proposed as follows.

3.1. Using Multiple Teaching Software Comprehensively for Complementary Advantages. Although there are several kinds of online teaching software which are used by a large number of users because of their relatively good performance, in the special emergency situation of COVID-19 epidemic, none of the online teaching software can fully meet the requirements of a high-quality teaching. A piece of software usually shows prominent performances in some respects and obvious deficiencies in the other. The common phenomenon is that some kinds of online teaching software run stably and smoothly, but lack interactive functions needed in teaching; some kinds of software have powerful functions for teaching, but they crash very easily.

To ensure the online teaching effects under present network performance, teachers have made various explorations and attempts [15]. Using different software at the same time and combining their advantages together to complete the teaching task is a common attempt. This is an effective way at present to solve the aforementioned problems. Adopting two pieces of software is the most common approach at present, and they can make up for each other's shortcomings and sharing their strength. The following will summarize and analyse the main characteristics of several pieces of software commonly used in online teaching and then discuss some efficient combination modes.

3.1.1. Main Characteristics of Several Types of Software Commonly Used in Online Teaching. (1) QQ: In QQ, the "Share Screen" function is often used to show students PPT and other teaching materials, and the "Demo Whiteboard" function is used to show the content that the teacher writes impromptu in class. The transmission of picture, voice, and text information is very fast in QQ, and it can meet the needs of almost all the basic operation functions in teaching. At the same time, QQ has excellent fluency during the online class and rarely exhibits delay phenomenon. It is a very important advantage of QQ to meet both the common functional requirement and teaching fluency requirement.

(2) Tencent Conference: The APP system has high stability. When there are several opened files and windows on the desktop of the computer screen, it can choose any one to share online. Also, it has the whiteboard function for the teacher's writing in class. While, Tencent Conference has no function of group management and file transmission, this is very inconvenient for teaching.

(3) Tencent Classroom: Compared with QQ, Tencent Classroom is more stable when the number of students in class exceeds 100, and functions for teaching are powerful. However, both sound and graphics have a relatively large delay. Some details were not very good, such as the experience of mouse and display.

(4) DingTalk: The stability is basically the same as that of Tencent conference. It also has the problem of delay, and the interactive function of teaching is in the middle level.

(5) Rain Classroom: Rain Classroom has many good functions for teaching, such as various types of teaching interaction and class information statistics, which are incomparable to other software. However, when the number of users increases, the platform often crashes badly and the class cannot continue. This problem was very serious in the early days of online class when the COVID-19 broke out and the number of users increased dramatically, and it already resulted in the loss of a large number of users.

(6) WeChat: For the teaching requirement, the function of WeChat is too simple. It is not convenient for teaching and is relatively less used in class.

3.1.2. Efficient Combinations of Online Teaching Software. In order to ensure the class effect, it is an effective way to use different kinds of teaching software together. The following are several combination modes:

(1) Mode A: QQ and Rain Classroom are Used at the Same Time. In this case, Rain Classroom runs just on the teacher's computer. Students do not need to log in Rain Classroom. This helps to reduce network congestion. "Share Screen" function in QQ is used to show students the information displayed on the teacher's computer screen. In this mode, the rich and powerful interactive functions developed specifically for teaching in the Rain Classroom is maximized. All interactions can be displayed to students through QQ's "Share Screen". This approach reduces the crash probability of Rain Classroom and makes the best use of its excellent interactive function.

(2) Mode B: Tencent Conference and Rain Classroom are used at the Same Time. This is similar to Mode A. Tencent Conference also has excellent fluency. Under the important support, screen sharing function of Tencent Conference combining with the excellent interactive function of Rain Classroom can also achieve a satisfactory teaching effect.

(3) Mode C: QQ Runs on Computers and Mobile Phones to Meet Common Needs in Software Function for Teaching. In this mode, teachers need to use two devices: one computer and one mobile phone. On the computer, teachers can use QQ's "Share Screen" to show students PPT, and use "Demo Whiteboard" to write improvised ideas for students. At the same time, teachers can put forward questions to students and discuss them with students in QQ group by mobile phone. In this way, it is also easier for teachers to attract students' attention, and the proportion of students participating in class discussions is also high in this mode.

3.2. Exploring Teaching and Management Ways of Online Class. Characteristics of online teaching are different from face-to-face teaching in classroom. Some teaching methods can no longer be used and need to be adjusted to adapt the new teaching model. Several methods have been researched, and they have been proved to be feasible through teaching practice.

3.2.1. Class Organization Ways of Online Teaching. (1) New Ways of Class Interaction: In online teaching, students' microphones are usually off during the class to avoid noise from home or environment. Only the teacher can speak freely. In this case, face-to-face discussion way is no longer appropriate and needs to be adjusted. An alternative method is that the teacher asks questions and students type and send their answers to the discussion area of teaching software. This is obviously more difficult to communicate than face-to-face class when the issues are slightly complex. To improve the communication efficiency between teacher and students in the limited class time and realize a real-time discussion, we have explored and tried a way for online teaching. The key points are as follows:

(i) Decomposition of problems: When raising and discussing questions in class, divide the questions into several small questions of logical interlink. The level of decomposition is determined by the criterion that students can finish answers quickly.

(ii) Design of answers: There are two ways to answer questions: one is the choice mode, such as choosing the answer from "Yes/No", "1/0", or "A/B/C". The other is words mode. That means the question can be answered clearly in several words.

In this solution, students can instantly respond to the teacher's questions by typing. It can ensure the maximum degree of real-time interaction between the teacher and students in class. During the class, the teacher throws out each small question in turn, and students can respond rapidly without a break like that in face-to-face class.

According to students' feedback, the teacher can adjust his lecture content in time. Through this kind of interlocking rapid response, a complex discussion can be completed in a fluent and clear manner. The efficiency of class interaction has been greatly improved.

(2) Alternative Method for Efficient Presentation of Video Information: According to the analysis in Section 2.1, video materials cannot be played to students in real time in most cases under current network conditions. To convey the essential information of videos to students, it is an effective solution to extract the key frame images and make them into PPT. In class, this PPT will be presented to students accompanied by the teacher's supplementary explanations. Videos themselves can be sent to students and watched after class by downloading them locally. In this way, the main content of the course is almost unaffected, and it is also adapted to different situations of students.

3.2.2. Class Management Methods of Online Teaching. Both teaching at home and learning at home are subject to many restrictions, the management methods of online class need to change. According to the characteristics of online teaching, teachers can dig deeply into the functions of teaching software and use them to explore and develop flexible and diverse class management methods, such as sign in with hand gestures before class, random award-winning questions and answers in class, online brainstorming discussion, and after-class team video conference. These measures are conductive to effectively improve students' learning attention and interest in class. In addition, to ensure the attendance rate and learning effect of online teaching, some of the previous methods used in face-to-face class can still be adopted, such as supervisors' random attending class and randomly checking students' learning status.

4. Class Evaluation Criteria for International Online Teaching

Some representative class evaluation models are as follows: traditional expert model, Tyler's objective model, Sufflebeam's CIPP model, Stake's Countenance model, and ethnographic evaluation. These evaluation models have different features in the value orientation, method, and participant. Modern education theory considers that knowledge is a process and knowledge system is always in a state of flux. People must pay attention to the specific performance of students during the learning process and then implement a process evaluation.

There are three evaluation models in Chinese universities: expert evaluation, peer evaluation, and student secret ballot. Expert evaluation has limitation to accurately reflect teacher's teaching situation because of the limited amount of attending class of the expert. In addition, experts' personal teaching style, teaching habits, and thinking patterns also have an influence on the evaluation results. Peer evaluation is conducted in the form of faculty members from the department and the faculty listening to each other's lectures. This evaluation model may be influenced by the relationship between colleagues. For the secret ballot, students' cognitive ability is more in the perceptual stage, so the evaluation tends to be mixed with some random ego factors [16].

Problems of the three evaluation models are obvious. In addition, differences exist between online and offline class and also between lecturing in the native language and in foreign language. So, class evaluation of international online teaching is studied in this paper to achieve an objective result, in which evaluation criteria reflect the behaviour and learning effect of students in the learning process. The considerations are as follows:

(1) Percentage of class content to the syllabus
(2) Learning effect of specialized knowledge in online class taught in foreign language which is generally English
(3) Interactive activities of online class between learning and teaching

4.1. Percentage of Class Content to the Syllabus. In the course of online teaching, the interaction between teachers and students is affected to some extent because of space separation. For example, a discussion about a topic tends to take longer, so class contents may not be sufficient to meet the requirements of the syllabus in a time-limited class. This paper studies evaluation criteria to evaluate the class effect considering three respects: important contents, required contents, and understanding contents. For important contents, students are required not only to understand the concepts and principles but also have the ability to apply, analysis, and design. In required contents, students have an obligation to have a thorough understanding of concepts and principles. For understanding contents, students are only needed to understand the basic concepts.

First, to quantify the class contents into an objective value, formula (1) is designed for calculation:

$$S = \lambda_1 \sum_{i=1}^{N} I_i + \lambda_2 \sum_{i=1}^{N} M_i + \lambda_3 \sum_{i=1}^{N} E_i, \tag{1}$$

where i is the chapter number; N is the total number of chapters; I_i, M_i, and E_i are the numbers of important contents, required contents, and understanding contents of chapter i, respectively; λ_1, λ_2, and λ_3 are the weights of each item respectively and can be assigned different values to distinguish the importance of each item, such as 10, 3, and 1. S is the score of the class contents. On the syllabus: $I_i = I_{im}$, $M_i = M_{im}$, and $E_i = E_{im}$, that is, I_i, M_i, and E_i are all their maximums. In this case, $S = S_m$, which is the highest score of the class contents.

Then, the percentage of class contents to syllabus contents can be calculated by formula:

$$R_c = \frac{S}{S_m} \times 100\% = \frac{\lambda_1 \sum_{i=1}^{N} I_i + \lambda_2 \sum_{i=1}^{N} M_i + \lambda_3 \sum_{i=1}^{N} E_i}{S_m} \times 100\%, \tag{2}$$

R_c is called coverage of class contents. At this time, I_i, M_i, and E_i in formula (2) are the numbers of important contents, required contents, and understanding contents of chapter i that are actually taught in online class, respectively, so S is the score of actual taught contents. $R_c = 100\%$ indicates that all the contents required by syllabus have been completed. Among them, the understanding contents are often assigned to students for self-study.

4.2. Learning Effect of Specialized Knowledge in Online Class Taught in English. Due to the use of original English textbooks and the use of non-native language as teaching language, students have certain obstacles in thinking and lag in understanding. Therefore, more explanations are needed in the teaching process. However, the class time is bounded. Sometimes, some topics cannot be fully discussed, and students may not be able to comprehend them clearly. So, it is necessary to evaluate the effect of students' professional learning in time. Available methods include check students' mastery of specialized knowledge through flexible forms such as class discussions and quiz. The results are quantified by score, and it can compare to that of students who are taught in the native language of the same course. We assume that the whole knowledge consists of different knowledge points, and design formula (3) first evaluates the learning effect of students on knowledge point k:

$$P_k = \frac{1}{N}\sum_{i=1}^{N} s_i, \tag{3}$$

where N is the number of students, s_i is the score of the ith student for the knowledge point k, and P_k is the average score of all students on the knowledge point k. Assume that the average score of students taught in native language for the knowledge point k is P_{kn}, then the learning efficiency of students taught in English on knowledge point k can be obtained by

$$\eta_k = \frac{P_k}{P_{kn}} \times 100\%, \tag{4}$$

when $\eta_k < 1$, it indicates that students taught in English have lower learning effect on knowledge point k than those taught in native language. When $\eta_k > 1$, it indicates that students taught in English have better learning effect on knowledge point k. If student's score for all knowledge points is to be calculated, the overall learning efficiency η can be calculated as

$$\eta = \frac{P}{P_n} \times 100\% = \frac{1/C\left(1/N\sum_{i=1}^{N} s_i\right)_k}{P_n} \times 100\%, \tag{5}$$

where C is the total number of knowledge points and P_n is the average score of the students taught in native language for total knowledge. Similarly, when $\eta < 1$, it indicates that the overall learning efficiency of students taught in English is lower than that of students taught in native language. When $\eta > 1$, the overall learning efficiency of students taught in English is better than that of students taught in native language. η_k and η can reflect different levels of learning efficiency from some knowledge points to the whole knowledge.

4.3. Interactive Activities of Online Class between Learning and Teaching. Online teaching uses computer, network, mobile phone, and other hardware as carriers and relies on teaching software to realize long-distance and real-time teaching and learning. Online teaching makes students study different courses in front of the computer or mobile phone from morning to night every day. Students tend to feel sleepy when they use devices for a long time. In addition, studying at home, students cannot feel the restriction and learning atmosphere as that in the classroom. The lack of "presence" and "reality" leads to easy distraction. Interactive activities in online class have a significant effect on improving students' attention and learning interest.

In general, the more teaching interaction occurs in class, the better the class effect is. But too frequent interaction may slow down the teaching progress. Also, continuous intensive activities will make students unresponsive and easy to fatigue. At this time, interaction is easy to cause distraction instead. Considering the positive and negative effects, we study the teaching interaction incentive function to indicate the influence of teaching interaction on students' learning effect. The definition of teaching interaction incentive function is shown in

$$\xi_q = 1 + \sin\left(\frac{A_{qr}}{A_q}\pi\right), \tag{6}$$

where q represents the number of a teaching activity; ξ_q represents the incentive function value of the qth teaching activity; A_q is the total number of knowledge points in the qth teaching activity; and A_{qr} is the total number of knowledge points implemented with interaction in the qth teaching activities. $0 \le A_{qr} \le A_q$, and $1 \le \xi_q \le 2$. Assuming that the total number of teaching activities is N, the definition of the average teaching interaction incentive function ξ is as shown in

$$\xi = \frac{1}{N}\sum_{q=1}^{N}\xi_q = \frac{1}{N}\sum_{q=1}^{N}\left[1 + \sin\left(\frac{A_{qr}}{A_q}\pi\right)\right], \tag{7}$$

where the greater value of ξ means the greater incentive effect of interaction in the teaching activities. In typical cases, when there is no interaction in class, $A_{qr}/A_q = 0$ and ξ_q has a minimum value of 1, then ξ may have a minimum value of 1; when A_{qr} reaches half of A_{qr}, ξ_q has a maximum of 2, also ξ may have a maximum of 2. At this time, ξ_q represents that the class atmosphere is most active and the teaching effect is the best in the qth teaching activity, and ξ represents the same meaning for overall situation. When all the knowledge points are carried out with interaction, $A_{qr}/A_q = 1$ and ξ_q return to the minimum value of 1, also ξ may have the minimum value of 1. This implies that too much interaction will make negative effect counteract the positive effect. When $\xi > 1.9$, it indicates that the interaction effect in class reaches an ideal state.

4.4. Results and Discussion. The above three criteria provide the class evaluation ways for international online teaching from different aspects. In use, we can flexibly set a time period T to evaluate and examine the class effect for the desired time period. T can be set as the total time of a course or some credit hours of a course. The results can be used as the basis for improving the teaching method.

For coverage of class contents R_c, when T is set as some credit hours of a course, teachers just need to take the parameter values corresponding to the period T in formula (2). According to R_c, it will be convenient to check how much of the teaching plan has been completed in the period T. If there are problems, teachers will think about the reasons and solve them, then adjust their teaching progress in time. Another way to use criteria R_c is after a course is over. At that time, teachers can set T as the total time of the course to evaluate the class effect and obtain valuable information for the improvement of online teaching in the future.

Through the observation of overall learning efficiency η, teachers can see how well students are learning a course. It provides a useful hint for improving teaching in time to avoid the decline of students' learning effect. $\eta < 1$ is the most case, mainly because of the influence on understanding in non-native language teaching. For more detailed studies, one can further examine the learning efficiency η_k, and analyse and identify problems existing in certain knowledge points.

For the effect evaluation of class interaction, the mean teaching interaction incentive function ξ reflects the law that the incentive effect of class interaction increases from small to large and then decreases with the change of interaction from less to more. The range of ξ is [1, 2], and the larger the value, the better the incentive effect on class.

By comprehensively considering the aforementioned criteria about class contents, learning effect of specialized knowledge, and interactive activities of online class, an objective class evaluation of international online teaching can be achieved. Table 2 shows the evaluation results of applying three criteria to a course of "Introduction to Avionics systems" in its different stages. This is a 32-credit hour elective course which is taught in native language and English for different types of students. The course is taught for the first time in an online format after the outbreak of the new crown epidemic. We did an evaluation for the online English-taught course. Three criteria were used to evaluate the class when the first 16 credit hours of lecturing were completed, to check whether the teaching was going well, and to analyse and solve problems timely if there are. At the completion of the last 16 credit hours of lecturing, that was 17 to 32 credit hours of instruction, the class evaluation was done again to check whether the teaching had been improved and what problems still existed.

From the data in Table 2, it can be seen that the coverage of class contents R_c in the first 16 credit hours of the course was only 81%, which meant that the teaching progress was slow, and some teaching contents were not completed as planned. The overall learning efficiency η was 89.4% which is relatively low. Then observe the mean teaching interaction incentive function ξ whose value was 1.81, and its related parameter $A_{qr}/A_q = 0.70$ indicating that the number of class interaction was relatively high. The criteria indicated the problems existing in teaching. Through a review of the teaching process and a comprehensive analysis of these data, problems were found: since the online teaching was conducted for the first time, teachers could not adapt to the new teaching method immediately because they could not meet with students face to face, especially in terms of class interaction, some intuitive interactive information in the previous face-to-face teaching was no longer available, so teachers tried to adopt new interactive methods in online teaching to ensure the teaching effect. However, due to the lack of experience, the initial attempts were not efficient enough, the number of attempts was on the high side, and time control was not given enough attention, so that the teaching plan was not fully completed and the students' learning results were not good enough.

Table 2: Evaluation results of "Introduction to Avionics systems" in its different stages.

	R_c calculation		η calculation		ξ calculation	
T	$\lambda_1, \lambda_2, \lambda_3, \lambda_4, N$	R_c	P, P_n	η	A_{qr}/A_q	ξ
1–16 credit hours	10, 3, 1, 4	81%	76, 85	89.4%	0.70	1.81
17–32 credit hours	10, 3, 1, 4	100%	83, 87	95.5%	0.45	1.99

Based on the results of the above analysis, teachers used the solutions discussed in Section 3 to improve the online teaching method, focusing on optimizing the interaction ways to increase the efficiency of interaction while reducing the number of interactions so that the A_{qr}/A_q value was close to 0.5. Applying the improved teaching method to the last 16 credit hours of the course, the class effect was evaluated again at the end of the course, and it could be seen that R_c had been improved to 100%. That is, all teaching contents were completed. ξ was improved to 1.99, and the overall learning efficiency η was also improved to 95.5%. It could be seen that class evaluation method was effective. It was beneficial to understand the teaching effect and improve teaching method in time.

Class evaluation is one of important aspects that promote the improvement of international online teaching. The contribution lays a foundation for further exploring the class evaluation system of online teaching.

5. Conclusion

In view of the problems existing in current online teaching, we study the issue from several respects: (1) analyse and discuss the performance problems of software and hardware in present online teaching; (2) discuss the class problems in online teaching and learning; (3) recommend corresponding feasible solutions to discussed problems, including comprehensive use of multiple software for complementary advantages, class interaction design and implementation, alternative method for delivering video information and class management method; and (4) develop several class evaluation criteria for an objective class evaluation of international online teaching. A relatively complete online teaching operation system is formed. In the future, with the development of new technologies such as 5G, Big Data, Artificial Intelligence, and Internet of Things, online teaching might be gradually adapted more and more. The mode of online teaching might also become diverse, for example 5G live class, ultra HD video interaction, holographic live, VR live, and AI teacher. The study provides some valuable information for present online teaching research and practice and is also beneficial to its continuous development.

Data Availability

Data sharing is not applicable to this article as no data sets were generated or analysed during the current study.

Conflicts of Interest

The author(s) declare no potential conflicts of interest with respect to the research, authorship, and/or publication of this article.

Acknowledgments

The authors acknowledge the funding of the Key Project of Shaanxi Province Innovation Program, China (grant no. 2017ZDCXL-GY-11-02-02).

References

[1] C. Carrillo and M. A. Flores, "COVID-19 and teacher education: a literature review of online teaching and learning practices," *European Journal of Teacher Education*, vol. 43, no. 4, pp. 466–487, 2020.

[2] S. G. Wang, "Rain classroom: the wisdom teaching tool in the context of mobile Internet and big data," *Modern Educational Technology*, vol. 27, no. 5, pp. 26–32, 2017.

[3] X. Jin, "Application of computer in online teaching of professional courses," *International Journal of Emerging Technologies in Learning (iJET)*, vol. 15, no. 19, pp. 53–65, 2020.

[4] S. D. Chen, "Exploration of blended teaching mode," *Computer Era*, vol. 3, pp. 78–82, 2021.

[5] P. Zhang, F. D. Liu, and Z. Shan, "Thinking and practice of online teaching under COVID-19 epidemic," in *Proceedings of the 2nd International Conference on Computer Science and Educational Informatization*, pp. 165–167, Xinxiang, China, June 2020.

[6] S. Kasyadi, M. Lapasau, and V. Virgana, "Enhancing learning outcome in integral through online teaching based during COVID-19 pandemic," *Journal of Physics: Conference Series*, vol. 1663, no. 1, pp. 1–6, 2020.

[7] B. L. Cai, Q. Lin, G. Liang, Y. L. Shi, and H. C. Sun, "Study on the transformation of college students' learning style in online teaching environment: problems, trends and development paths," *Heilongjiang Researches on Higher Education*, vol. 12, pp. 140–144, 2020.

[8] M. Li and Y. Su, "Evaluation of online teaching quality of basic education based on artificial intelligence," *International Journal of Emerging Technologies in Learning (iJET)*, vol. 15, no. 16, pp. 147–161, 2020.

[9] Y. Zhao, Y. Tang, F. Liu et al., "Research and practice of online emergency teaching based on electronic information technology under the influence of COVID-19," *International Journal of Electrical Engineering Education*, Manchester University Press, Manchester, UK, Article ID 002072092098504, 2021.

[10] E. Dabbour, "Motivating engineering students by providing two midterm exams and dropping the lower mark," *Journal of Civil Engineering Education*, vol. 147, no. 1, Article ID 04020009, 2021.

[11] K. Butler-Henderson and J. Crawford, "A systematic review of online examinations: a pedagogical innovation for scalable authentication and integrity," *Computers & Education*, vol. 159, Article ID 104024, 2020.

[12] C. Eurboonyanun, J. Wittayapairoch, P. Aphinives, E. Petrusa, D. W. Gee, and R. Phitayakorn, "Adaptation to open-book online examination during the COVID-19 pandemic," *Journal of Surgical Education*, vol. 78, no. 3, pp. 737–739, 2021.

[13] H. Muranaka-Vuletich, "Effects of online language testing on final examination," *Education and Information Technologies*, vol. 26, no. 3, pp. 2795–2809, 2021.

[14] Y. B. Gao, Z. W. Li, F. Wang, and J. J. Yan, "Survey analysis of online learning of engineering college students during the COVID-19 epidemic," *Meitan Higher Education*, vol. 38, no. 4, pp. 36–43, 2020.

[15] J. Gong, "Teachers' need analysis of online teaching resources during the fight against novel coronavirus early 2020: based on an online survey among university teachers for German language," *The Science Education Article Collects*, vol. 495, pp. 186–188, 2020.

[16] Y. Liu, "The reconstruction of the teaching quality evaluation system of college teachers," *Heilongjiang Researches on Higher Education*, vol. 261, no. 1, pp. 59–61, 2016.

Hindawi
Scientific Programming
Volume 2021, Article ID 9683908, 7 pages
https://doi.org/10.1155/2021/9683908

Research Article

Image Network Teaching Resource Retrieval Algorithm Based on Deep Hash Algorithm

Guotao Zhao [1] and Jie Ding [2]

[1]*School of Foreign Languages, Hubei Engineering University, Xiaogan, China*
[2]*College of Technology, Hubei Engineering University, Xiaogan, China*

Correspondence should be addressed to Jie Ding; dingjie@hbeu.edu.cn

Received 30 July 2021; Accepted 27 August 2021; Published 11 October 2021

Academic Editor: Punit Gupta

In order to improve the retrieval ability of multiview attribute coded image network teaching resources, a retrieval algorithm of image network teaching resources based on depth hash algorithm is proposed. The pixel big data detection model of the multiview attribute coding image network teaching resources is constructed, the pixel information collected by the multiview attribute coding image network teaching resources is reconstructed, the fuzzy information feature components of the multiview attribute coding image are extracted, and the edge contour distribution image is combined. The distributed fusion result of the edge contour of the view image of the network teaching resources realizes the construction of the view feature parameter set. The gray moment invariant feature analysis method is used to realize information coding, the depth hash algorithm is used to realize the retrieval of multiview attribute coded image network teaching resources, and the information recombination is realized according to the hash coding result of multiview attribute coded image network teaching resources, thus improving the fusion. The simulation results show that this method has higher precision, better retrieval precision, and higher level of resource fusion for multiview coded image network teaching resource retrieval.

1. Introduction

With the continuous enrichment of multimedia network resources, it is necessary to build a fusion model of multiview attribute coded image network teaching resources under the conditions of multimedia environment, so as to improve the sharing level and retrieval ability of network teaching resources. Due to the increasing number of multiview attribute coding image network teaching resources, it is increasingly difficult to accurately retrieve and locate the multiview attribute coding image network teaching resources. In particular, under the condition of multiview attribute coding, the environmental distribution of image network teaching resources is more disturbed, and the search accuracy and completeness rates of multiview attribute coding image network teaching resource retrieval are not high [1]. An optimized multiview attribute coding image network teaching resource retrieval model needs to be constructed to realize the retrieval and sharing of multiview attribute coding image network teaching resources by combining the distribution characteristics of multiview attribute coding image network teaching resources [2].

Based on the multimedia image retrieval recognition distribution, a multiview attribute encoding image network teaching resource encoding and feature analysis model is established [3]. On the basis of feature extraction, the pixel feature analysis of multiview attribute encoded image web teaching resources is combined. The multiview attribute encoding image web-based teaching resources are realized by the semantic distribution of images. Among the traditional methods, the main methods for retrieval of multiview attribute encoded image web teaching resources are resource retrieval methods based on ontology information segmentation, multiview attribute encoded image web teaching resource retrieval methods based on Harris corner point location analysis, and multiview attribute encoded image web teaching resource retrieval methods based on evolutionary clustering analysis [4, 5]. A multiview attribute encoded image web teaching resource retrieval model based on similarity feature detection and semantic ontology fusion is proposed in [6]. He et al. constructed a parametric model for feature distribution of multiview attribute encoded image web teaching resources. It performs multiview attribute encoding image web teaching resource retrieval by fuzzy degree matching, but the accuracy of this method for multiview attribute encoding image web teaching resource retrieval is not high, and at the same time, the computational difficulty is high. An image resource retrieval method based on Harris corner point localization is proposed in [7]. The multiview attribute encoding image web-based teaching resource retrieval by corner point localization and parameter identification improves the localization ability of image retrieval, but the viewpoint discrimination of this method for image retrieval is not high.

To solve the above problems, this paper proposes an image network teaching resource retrieval algorithm based on deep hashing algorithm. Firstly, a pixel big data detection model of multiview attribute encoding image network teaching resources is constructed. Then, the retrieval of multiview attribute encoded image network teaching resources is achieved by deep hash algorithm [8]. Realize information reorganization according to the result of hash coding of multiview attribute encoding image network teaching resources, and improve the fusion and retrieval ability of multimedia image network teaching resources. Finally, the performance test of image network teaching resource retrieval is carried out by simulation test and constructive conclusions are obtained.

2. Multiview Attribute Encoding Image Web-Based Teaching Resource Distribution and Information Preprocessing

2.1. Multiview Attribute Encoding Image Web-Based Teaching Resource Fusion Processing. In order to realize multiview attribute coded image web teaching resource retrieval, a feature matching model for multiview attribute coded image web teaching resource retrieval is constructed by combining semantic feature analysis and fusion scheduling methods. According to joint feature detection, association rule fusion and similarity feature detection are used for data management of multiview attribute encoded image web teaching resource retrieval [9]. The overall structure model of multiview attribute encoding image web-based teaching resource retrieval is obtained as shown in Figure 1.

The cluster analysis method is used to obtain the cluster center of multiview attribute encoding image web teaching resource retrieval M_i with M_j. Using the method of rough set feature matching, the reliability matching degree of multiview attribute encoded image web teaching resource retrieval is obtained as $\mathrm{Clustdist}(M_i, M_j)$. The edge contour feature parameter set of multiview attribute encoded image web teaching resources is extracted, and the feature fusion process of multiview attribute encoded image web teaching resources is performed in the gradient pixel space. Based on Harris corner point localization, the set of regional pixels for multiview attribute encoding feature fusion is obtained as follows:

$$
\begin{aligned}
R_1(k) &= R_2(k)\exp\left(-j\omega_0 T_p/2\right), \quad k = 0, 1, \ldots, \frac{N-3}{2}, \\
R_2(k) &= A_k \exp\left(j\varphi_k\right), \quad k = 0, 1, \ldots, \frac{N-3}{2},
\end{aligned} \tag{1}
$$

where $R_2(k)$ is the multiview attribute encoding feature component, T_p is the sampling time interval of the multiview attribute encoding image, and $\omega_0 T$ is the joint component. Combining the semantic information detection of network teaching resources of multiview attribute-encoded images and the analysis results of invariant moment features of multiview attribute-encoded images, the teaching resource fusion parameters are obtained as

$$
\begin{aligned}
\varphi(X_k, t_i) &= G\left(\left\|X_k - t_i\right\|\right) \\
&= \exp\left(-\frac{1}{2\sigma_i^2}\left\|X_k - t_i\right\|^2\right) \\
&= \exp\left(-\frac{1}{2\sigma_i^2}\sum_{m=1}^{M}\left(x_{km} - t_{im}\right)^2\right),
\end{aligned} \tag{2}
$$

where $t_i = [t_{i1}, t_{i2}, \ldots, t_{iM}]$ is the discrete sequence to the multiview attribute encoding image web teaching resource retrieval and σ_i is the spatial distribution cost of multiview attribute encoding image web teaching resource retrieval.

2.2. Multiview Attribute Encoding Feature Analysis. The pixel information of the collected multiview attribute encoded image web-based teaching resources is structurally reorganized to extract the fuzzy information feature components of the multiview attribute encoded images [10]. The obtained distribution sequences of multiview attribute encoded image web-based teaching resources are denoted as

$$
\begin{aligned}
r_1(n) &= r_2(n)\exp\left(\frac{-j\omega_0 T_p}{2}\right), \quad n = 0, 1, \ldots, \frac{N-3}{2}, \\
r_2(n) &= A\exp\left[j\left(\omega_0 nT + \theta\right)\right], \quad n = 0, 1, \ldots, \frac{N-3}{2},
\end{aligned} \tag{3}
$$

where N is the sampling length of the image pixel sequence and ω_0 is the grayscale distribution interval.

Gradient pixel decomposition and information fusion techniques are used to construct a mean segmentation model of multiview attribute encoded image web-based teaching resources, denoted as

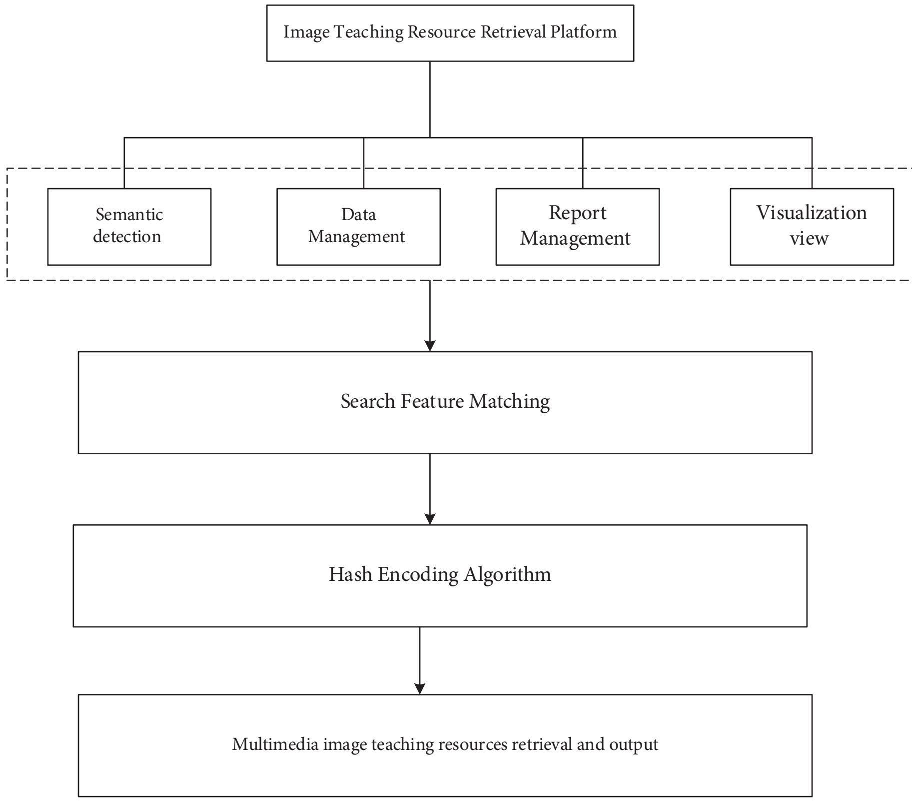

Figure 1: General structural model of multiview attribute encoding image web-based teaching resource retrieval.

$$\overline{x_T} = \frac{1}{T}\sum_{i=1}^{T} x_i, \quad (4)$$

where $x_1, x_2, x_3, \ldots, x_T$ is the edge profile deformation parameter of the multiview attribute encoded image and $_T$ is the mean sampling interval of the multiview attribute encoded image sampling.

A feature analysis model for multiview attribute encoding image web teaching resource retrieval is constructed. By feature decomposition, the RGB 3D reconstruction model of multiview attribute encoded image web teaching resource retrieval is constructed, and the RGB 3D feature detection component is obtained as N_l, whose calculation formula is

$$N_l = \begin{cases} 1, & l = 0, L, \\ \left[\dfrac{2\pi \cdot D/2 \cdot \sin \eta}{l_{\text{triangle}}}\right], & l = 1, \ldots, L-1, \end{cases} \quad (5)$$

where $l_{\text{triangle}} = \pi \cdot D/2L$ denotes the retinex corner point parameter value of the multiview attribute encoded image web-based teaching resource and L is the gray pixel intensity.

We combined the results of distributed fusion of edge contours of the view images of web teaching resources to achieve the construction of the view feature parameter set. Through the feature reconstruction and fuzzy mean clustering results [11], the comprehensive feature parameters of the web teaching resource view fusion are obtained as $k = 1, 2, \ldots, n$, $zk \in w^s$, $ak \in \{1, 2, \ldots, R\}$. The results of multiview attribute coding feature analysis are

$$\dot{\sigma_i} = \begin{cases} \mu \sin \dfrac{\pi e}{2\mu}, & |e_i| < \mu, \\ \mu, & |e_i| \geq \mu, \\ -\mu, & |e_i| \leq -\mu, \end{cases} \quad (6)$$

where σ_x, σ_θ, e_i denote the fitness covariates for the fusion of multiview attribute encoded image web teaching resources and μ denotes the detection statistical feature quantity of each pixel point, $\mu > 0$. This enables the fusion process of multiview attribute encoding image web-based teaching resources for multiview attribute encoding feature analysis [12].

3. Image Network Teaching Resource Retrieval Algorithm

3.1. Multiview Attribute Encoding Image Depth Hash Encoding. Let $y(n)$ be the amount of rough set features for multiview attribute encoded image web teaching resource retrieval, and according to the rough set feature matching results, the depth hash encoding algorithm is used to perform depth feature detection for multiview attribute encoded image web teaching resources [13]. The gradient value of each multiview attribute encoded image network teaching resource is calculated, and the depth hash coding convergence value is obtained as

$$P\left(\lim_{T\longrightarrow\infty}\overline{x_T}=K\right)=1, \tag{7}$$

where $\overline{x_T}$ denotes the correlation parameter between feature sets, K is the scale of feature vector encoding, and $Q(x_i, y_i)$ is the color moment of the training image and is the fusion result based on semantic information. When $(i \neq j, 1 \leq i \leq q, 1 \leq j \leq q)$, the joint feature generalization of the output of the multiview attribute encoded image web-based teaching resource retrieval is obtained as

$$\begin{aligned}F(t) &= X_p(u - v\sin a)\\ &= \frac{3}{(N+1)^2}x(N+1)x^3(N+1-\tau),\end{aligned} \tag{8}$$

where X_p is the source information of the semantic distribution of the multiview attribute encoded image web teaching resources, u is the joint distribution feature quantity of the multiview attribute encoded image web teaching resources, and v is the normative fuzzy detection basis function of the multiview attribute encoded image web teaching resources. Set $i=1$, the first multiview attribute coded image [14], and combined with the distribution of network teaching resources, the output of the depth hash code of the multiview attribute coded image network teaching resource is

$$\begin{cases} p_{th}^{(b_{\text{int}})} = C_t\sum_{x_i\in w}k\left(\|x_i\|\right)\delta\left(h(x_i)-b_{\text{int}}\right),\\ p_{te}^{(b_{\text{ine}})} = C_e\sum_{x_i\in w}k\left(\|x_i\|^2\right)\text{his}_{x_i}\delta\left(v_{x_i}-b_{\text{ine}}\right),\end{cases} \tag{9}$$

where $C_t = C_e = 1/\sum_{x_i\in w}k(\|x_i\|^2)$ denotes the depth information parameter of the multiview attribute encoding image web teaching resource aggregation and $b_{\text{ine}} \in [1, M]$ denotes the attribute category. In summary, the analysis is carried out to achieve deep hash encoding of multiview attribute encoded image network teaching resources [15].

3.2. Image Network Teaching Resource Retrieval Output. In order to obtain feature reconstruction and fuzzy mean clustering results, a gray invariant moment feature analysis method is used to achieve information encoding. A deep hashing algorithm is used to implement the retrieval of teaching resources for multiview attribute encoding image networks, and according to the depth feature weighting training [16], the weighted aggregation output function of teaching resources for multiview attribute encoding image networks is obtained and expressed as

$$E_{\text{Snake}} = \sum_{0}^{N-1}\left[E_{\text{int}}(vi)+E_{\text{ext}}(vi)\right], \tag{10}$$

where V_i is the morphological function for the weighted aggregation of multiview attribute encoded image web-based teaching resources and $i = 0, 1, \ldots, N-1$ is the set of pixel points. The multiview attribute encoding aggregation output is G.

$$G_t = AF_{t-1} + t. \tag{11}$$

$F_t = [x_t, y_t]^T$ is the associated pixel value of the tth frame of the multiview attribute encoded image teaching resource. The semantic association distribution model of multiview attribute encoded image web-based teaching resource retrieval is constructed to obtain the output retrieval trajectory distribution of

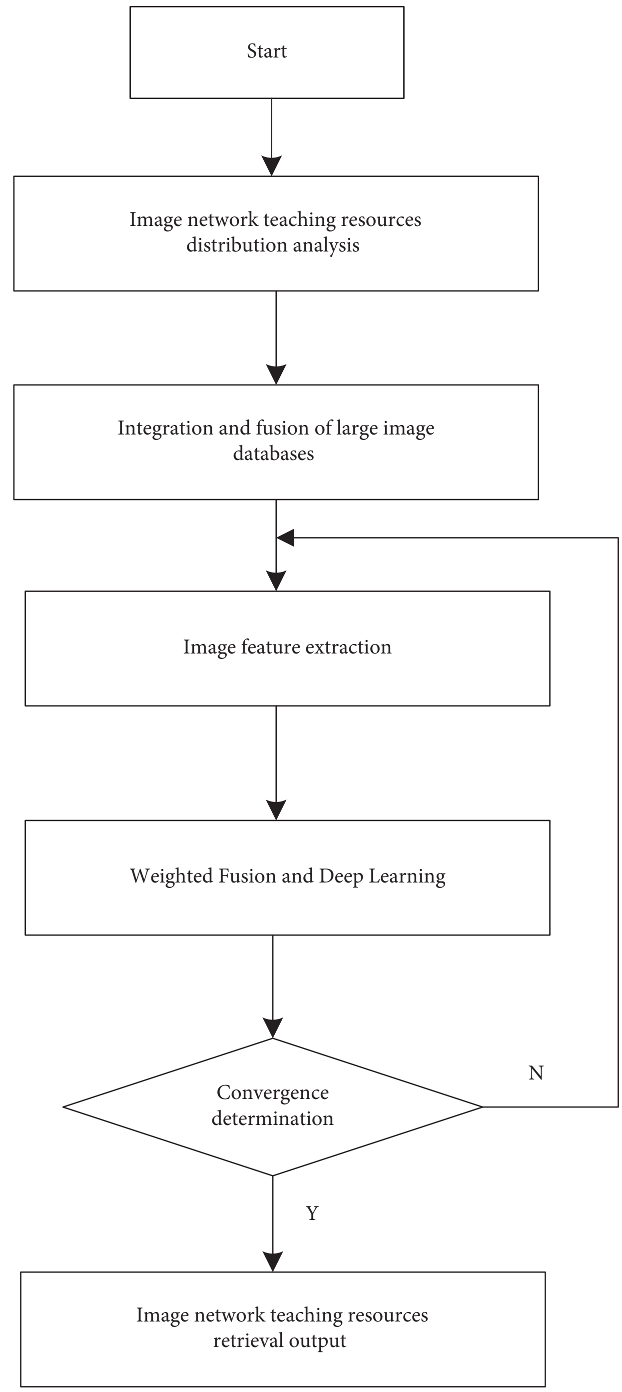

Figure 2: Algorithm optimization implementation flow.

Table 1: Image network teaching resource retrieval parameters.

Image samples	Pixel	Scale factor	Similarity
Rose	520.800	0.227	0.407
Plane	549.360	0.221	0.396
Bridge	514.080	0.218	0.391
Building	559.440	0.223	0.400
Elephant	500.640	0.231	0.415

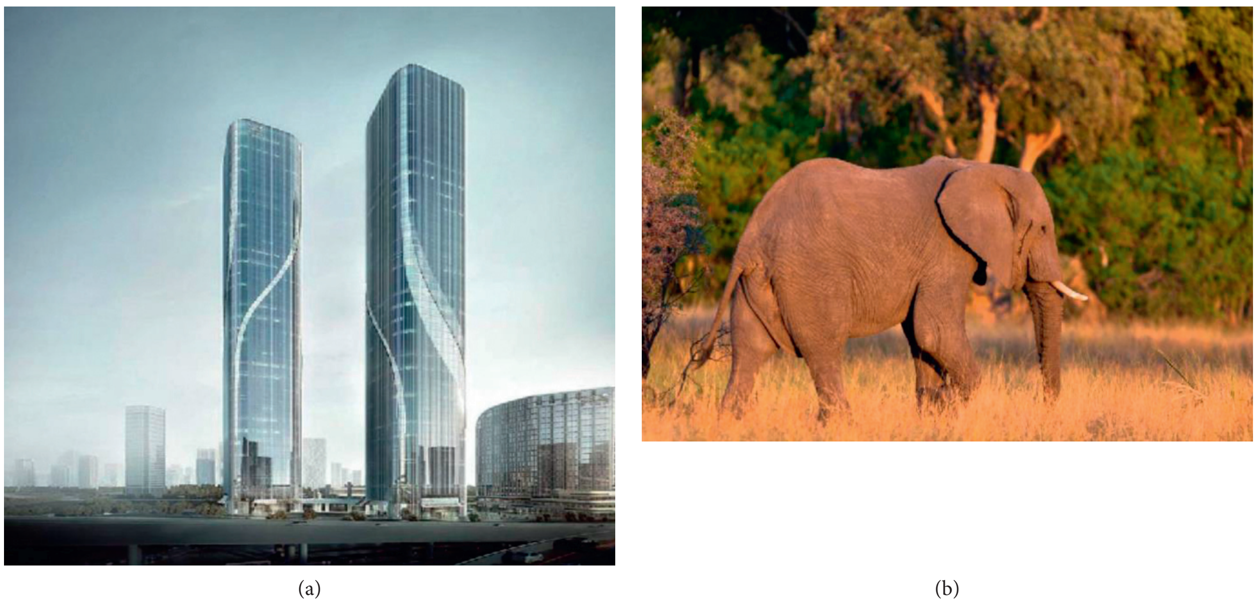

Figure 3: Sample multiview attribute encoded images. (a) Building. (b) Elephant.

$$\operatorname{trace}\left(x, y, \sigma^{(n)}\right) > \operatorname{trace}\left(x, y, \sigma^{(1)}\right), \quad l \in \{n-1, n+1\}, \tag{12}$$

where trace(.) denotes the fusion parameter of multiview attribute encoding image web teaching resource retrieval. The resulting iterative function for multiview attribute encoding image web-based teaching resource retrieval is

$$X_t = AX_{t-1} + t, \tag{13}$$

where $X = [x_t, y_t]^T$ is the training image set, and the output clustering matrix of the multiview attribute encoded image network teaching resource retrieval is obtained as

$$H = \begin{bmatrix} L_{xx}(x,\sigma) & L_{xy}(x,\sigma) \\ L_{xy}(x,\sigma) & L_{yy}(x,\sigma) \end{bmatrix}, \tag{14}$$

where $Lxx(x,\sigma)$ is the feature matching coefficient of multiview attribute encoded image web teaching resource retrieval and Lyy and Lxy are the pixel components of multiview attribute encoded image web teaching resource retrieval in different aggregation directions, respectively.

In summary, according to the analysis, the hash coding results of multiview attribute encoding image network teaching resources are realized to reorganize information and improve the multimedia image network teaching resource fusion and retrieval capability. The structure diagram of the implementation of the improved algorithm is shown in Figure 2.

4. Simulation Experiments and Result Analysis

In order to verify the application performance of this paper's method in implementing multiview attribute coding image network teaching resource retrieval, Matlab is used for simulation test analysis. The number of training samples for multiview attribute coding image network teaching resources is set to 4000, the test set is 490, the number of training iteration steps for deep hash coding is 240, the scale is 0.32, and other parameters are set as shown in Table 1.

According to the above parameter settings, multiview attribute encoded image web-based teaching resource retrieval is performed. Two sets of samples are taken, and the multiview attribute encoding image samples are obtained as shown in Figure 3.

The image of Figure 3 is used as the sample object to implement image depth hash coding, and the image hash coding fusion results are obtained as shown in Figures 4 and 5.

Analysis of Figures 4 and 5 shows that the method of this paper can effectively achieve the retrieval of multiview attribute encoded image web teaching resources. The performance of the retrieval output is good. The performance of multiview attribute coded image web teaching resource retrieval was tested, and the comparison results in terms of retrieval accuracy are shown

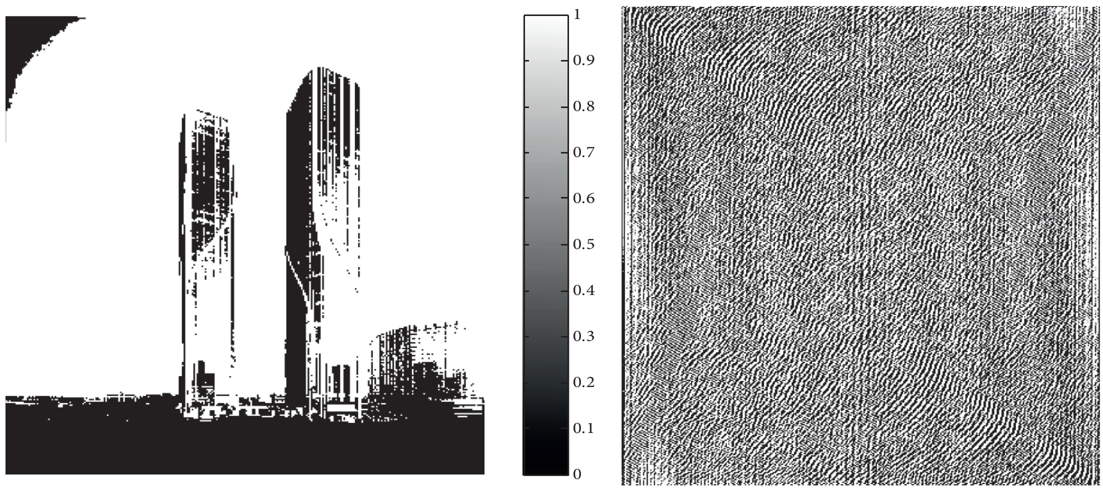

(a) (b)

Figure 4: Building image retrieval results. (a) Integration. (b) Deep hash encoding.

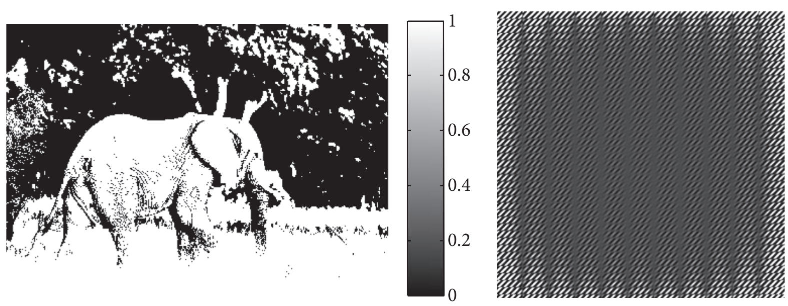

(a) (b)

Figure 5: Elephant image retrieval results. (a) Integration. (b) Deep hash encoding.

Table 2: Comparison of image web-based teaching resource retrieval performance.

Number of iterations	Methodology of this article	Wavelet transform	Spectrum detection
10	0.860	0.765	0.561
20	0.872	0.799	0.594
30	0.878	0.781	0.577
40	0.881	0.759	0.555
50	0.886	0.768	0.564
60	0.887	0.796	0.592
70	0.895	0.767	0.564
80	0.898	0.792	0.588
90	0.902	0.784	0.580
100	0.905	0.776	0.572
110	0.906	0.747	0.544
120	0.910	0.777	0.573
130	0.924	0.792	0.588
140	0.927	0.757	0.553
150	0.933	0.763	0.559

in Table 2, and the analysis of the results in Table 2 shows that the retrieval accuracy of multiview attribute coded image web teaching resource retrieval by this method is high.

5. Conclusion

An optimized multiview attribute encoding image network teaching resource retrieval model is constructed. Combined with the distribution characteristics of multiview attribute encoding image network teaching resources, the retrieval and sharing of multiview attribute encoding image network teaching resources are realized. This paper proposes the image network teaching resource retrieval algorithm based on deep hashing algorithm. The feature matching model for multiview attribute encoding image network teaching resource retrieval is constructed. Deep feature detection is performed for multiview attribute encoding image network teaching resources. The information reorganization is realized according to the hash coding results of multiview attribute encoded image network teaching resources, and the multimedia image network teaching resource fusion and retrieval capability is improved. The gradient value of each multiview attribute encoded image web teaching resource pixel is calculated. The deep hash encoding algorithm is used to realize the multiview attribute encoding image web teaching resource retrieval. It is learned that the method in this paper has a high rate of completeness and accuracy for multiview attribute encoding image web-based teaching resource retrieval.

Data Availability

No datasets were generated or analysed during the current study.

Conflicts of Interest

The authors declare that they have no conflicts of interest.

Acknowledgments

This study was supported by the Innovation Fund for Production, Study and Research of Chinese Universities of the Science and Technology Development Center of Ministry of Education, Innovation Project for New Generation's Information Technology (no. 2019ITA03027), Teaching Research Project of Hubei Provincial Department of Education (no. 2020806), and Teaching Research Project of College of Technology, Hubei Engineering University (no. 2020JY04).

References

[1] F. S. Wang, J. Wang, and B. Li, "Deep attribute learning based traffic sign detection[J]," *Journal of Jilin University (Engineering and Technology Edition)*, vol. 48, no. 1, pp. 319–329, 2018.

[2] J. Dai, Y. Li, and K. He, "R-FCN: Object Detection via Regionbased Fully Convolutionalnetworks," in *Proceedings of the 30th International Conference on Neural Information Processing Systems*, pp. 379–387, red Hook: Curran Associates Inc., Barcelona, Spain, December 2016.

[3] Q. L. Yao, X. Hu, and H. Lei, "Aircraft detection in remote sensing imagery with multi-scale feature fusion convolutional neuralnetworks," *Acta Geodaetica et Cartographica Sinica*, vol. 4810, pp. 1266–1274, 2019.

[4] J. Q. Wang, J. S. Li, X. W. Zhou, and X. Zhang, "Improved SSD algorithm and its performance analysis of small target detection in remote sensing images," *Acta Optica Sinica*, vol. 39, no. 6, pp. 73–382, 2019.

[5] Y. Jiang, J. W. Li, and Y. T. Zhang, "Ship object detection of SAR images based on feature reuse and semantic aggregation [J]," *Journal of Naval Aeronautical and Astronautical University*, vol. 34, no. 6, pp. 470–479, 2019.

[6] C. Szegedy, W. Liu, Y. Jia et al., "Going Deeper with convolutions," in *Proceedings of the 2015 IEEE Conference on Computer Vision and Pattern Recognition*, pp. 1–9, IEEE, Boston, MA, USA, June 2015.

[7] K. He, X. Zhang, S. Ren, and J. Sun, "Deep Residual Learning for Image recognition," in *Proceedings of the 2016 IEEE Conference on Computer Vision and Pattern Recognition*, pp. 770–778, IEEE, Las Vegas, NV, USA, June 2016.

[8] S. Li and Y. Guo, "Fast image retrieval based on hash algorithm in depth learning," *Computer & Digital Engineering*, vol. 47, no. 12, pp. 3187–3192, 2019.

[9] M. Everingham, S. M. A. Eslami, L. V. Gool, C. K. I. Williams, J. Winn, and A. Zisserman, "The pascal visual object classes challenge: a retrospective," *International Journal of Computer Vision*, vol. 111, no. 1, pp. 98–136, 2015.

[10] C. Xu, Z. Chen, and R. Hou, "Deep learning classification method of Landsat 8 OLI images based on inaccurate prior," *Journal of Computer Applications*, vol. 40, no. 12, pp. 3550–3557, 2020.

[11] D. S. Menashe, J. M. Gray, S. P. Abercrombie, and M. A. Friedl, "Hierarchical mapping of annual global land cover 2001 to present: the MODIS Collection 6 Land Cover product," *Remote Sensing of Environment*, vol. 222, pp. 183–194, 2019.

[12] V. F. G. Rodriguez, B. Ghimire, J. Rogan, M. O. Chica, and J. P. S. Rigol, "An assessment of the effectiveness of a random forest classifier for land-cover classification," *ISPRS Journal of Photogrammetry and Remote Sensing*, vol. 67, pp. 93–104, 2012.

[13] C. Zhang, I. Sargent, X. Pan et al., "An object-based convolutional neural network (OCNN) for urban land use classification," *Remote Sensing of Environment*, vol. 216, pp. 57–70, 2018.

[14] C. Homer, J. Dewitz, and L. Yang, "Completion of the 2011 national land cover database for the conterminous United States-representing a decade of land cover change information," *Photogrammetric Engineering & Remote Sensing*, vol. 81, no. 5, pp. 345–354, 2015.

[15] X. Hu, H. Guo, and R. Zhu, "Image super-resolution reconstruction based on hybrid deep convolutional network," *Journal of Computer Applications*, vol. 40, no. 7, pp. 2069–2076, 2020.

[16] M. F. Song, D. Z. Jia, and J. W. Guo, "A point cloud compression algorithm based on K-neighborhood cuboid," *Science Surveying and Mapping*, vol. 44, no. 10, pp. 93–100, 2019.

Hindawi
Scientific Programming
Volume 2021, Article ID 8715668, 14 pages
https://doi.org/10.1155/2021/8715668

Research Article

CBO-IE: A Data Mining Approach for Healthcare IoT Dataset Using Chaotic Biogeography-Based Optimization and Information Entropy

Manish Kumar Ahirwar,[1] **Piyush Kumar Shukla**,[1] **and Rakesh Singhai**[2]

[1]*Department of Computer Science and Engineering, UIT-RGPV, Bhopal 462033, India*
[2]*University Institute of Technology RGPV, Shivpuri, M.P. 473551, India*

Correspondence should be addressed to Piyush Kumar Shukla; pphdwss@gmail.com

Received 24 July 2021; Accepted 22 September 2021; Published 8 October 2021

Academic Editor: Punit Gupta

Data mining is mostly utilized for a huge variety of applications in several fields like education, medical, surveillance, and industries. The clustering is an important method of data mining, in which data elements are divided into groups (clusters) to provide better quality data analysis. The Biogeography-Based Optimization (BO) is the latest metaheuristic approach, which is applied to resolve several complex optimization problems. Here, a Chaotic Biogeography-Based Optimization approach using Information Entropy (CBO-IE) is implemented to perform clustering over healthcare IoT datasets. The main objective of CBO-IE is to provide proficient and precise data point distribution in datasets by using Information Entropy concepts and to initialize the population by using chaos theory. Both Information Entropy and chaos theory are facilitated to improve the convergence speed of BO in global search area for selecting the cluster heads and cluster members more accurately. The CBO-IE is implemented to a MATLAB 2021a tool over eight healthcare IoT datasets, and the results illustrate the superior performance of CBO-IE based on *F*-Measure, intracluster distance, running time complexity, purity index, statistical analysis, root mean square error, accuracy, and standard deviation as compared to previous techniques of clustering like K-Means, GA, PSO, ALO, and BO approaches.

1. Introduction

The big data [1, 2] is used and analyzed in several wireless applications by utilizing various characteristics like storage, processing, and maintenance of data. The preprocessing of a huge amount of data is performed before analysis to reduce the data redundancy with enhancing the data accuracy and efficiency [3–5]. The big data is processed by using various nature inspired optimization approaches like Genetic Algorithm (GA), Ant Colony Optimization (ACO), Ant Lion Optimization (ALO), and Particle Swarm Optimization (PSO) to perform optimal analysis [6].

The data mining [7–9] is a systematic procedure utilized for extracting the secret knowledge and model from an immense, multifaceted, and multidimensional dataset [10]. The association rule mining is one of the famous data mining approaches introduced with MapReduce concept to evaluate the relationship among data elements in a huge dataset [11]. These data relationships are recognized to generate maximum profit from marketing through IoT devices in industries. The time and security are crucial issues in business, which are frequently resolved by using data mining [12–14].

The data clustering [15] is a type of data mining, in which data components are divided into various sets or groups. The data are collected from various heterogeneous resources; after that time series clustering is applied on this huge amount of data to improve the data accessibility. The industry data are distributed more precisely and accurately by clustering to predict the future aspects of market [16]. The cybercrime data are analyzed after preprocessing to perform training and testing of clustering techniques. The nature of crime is easily understood and detected by clustering the similar type of crime patterns to reduce the crime ratio [17]. The healthcare data are also received by IoT devices in the form of data stream and divided into cluster by using stream clustering combining the cluster building and merging steps [18].

In above analysis, the clustering of data is an extremely challenging issue, while it creates baffling to select the optimal clustering strategy in nature. Additionally, it is to be an incredibly exigent attempt as every dataset is not expected to be consistent, allowing for the fact that infection form and previous medical circumstance area might differ immensely in training. Previously, having a meticulous prophecy scheme does not constantly offer a valuable height of exactness beneath entire healthcare application areas due to mostly depending on the situation utilized.

A lot of clustering algorithms are introduced on various datasets to enhance the data extraction. Several optimization approaches like GA, ALO, and PSO are also described for clustering. Although few clustering techniques realize an advanced output by means of a specified dataset, the efficiency of such clustering techniques might be complementary on other datasets. The nature of the clustering methods is steady by means of no-free-lunch theorem, but at hand no solitary clustering method survives which is able to be a cure for entire problems. This means all the problems are not resolved by any algorithm and convergence speed is also a major issue in optimization techniques, which are used for data clustering.

Here, a Chaotic Biogeography-Based Optimization approach using Information Entropy (CBO-IE) is implemented for clustering over healthcare IoT datasets, which is improved form of Biogeography-Based Optimization (BO) approach. In its place of basically performing a qualitative examination by utilizing a methodical mapping analysis regarding prior implemented works, this proposed work contributes on a quantitative examination of clustering strategy for healthcare dataset.

The contribution of implementing CBO-IE is as follows:

(1) The major intent of CBO-IE is to obtain accurate data point distribution in dataset by utilizing Information Entropy strategy and to give initial values of the population by utilizing chaos theory.

(2) Both Information Entropy and chaos theory are introduced to enhance the convergence speed of BO in exploration field globally for generating the cluster heads and cluster members more precisely.

(3) The CBO-IE is applied over eight healthcare IoT datasets and the outputs are evaluated on the basis of *F*-Measure, intracluster distance, running time complexity, purity index, statistical analysis, standard deviation, root mean square error, and accuracy as compared to previous techniques of clustering like K-Means, GA, PSO, ALO, and BO approaches.

The remainder of the paper is organized as follows: Section 2 explains the literature survey of data mining techniques, big data processing, and IoT dataset processing by utilizing numerous parameters. Section 3 describes the BO approach, and the proposed CBO-IE is explained in Section 4 briefly according to flowchart, algorithms, and preliminaries. The datasets, performance factors, and experimental results are illustrated in Section 5, and at last conclusions are given in Section 6.

2. Literature Survey

The IoT [19] is situated to transfigure entire future consequently for lives. The information extracted from the IoT systems will be explored to recognize and organize multifaceted surroundings about users, fitting superior decision creation, larger computerization, advanced effectiveness, efficiency, exactness, and prosperity production. This work explores the accessibility of multiple popular data mining approaches for IoT information. The results are evaluated over artificial intelligence and neural network with superior accuracy, efficiency, and velocity in comparison to prior techniques [20].

The K-Means approach is applied for processing the big data with the help of Hadoop platform over Internet of Things (IoT) aspects. The data from IoT devices are combined or distributed in several groups, known as clusters, which are used in various smart applications such as medical, disaster, and industries applications. The power expenses and traffic over communication network was reduced to use only necessary information, not whole raw data. In actuality, it supplies enormous flexibility, permitting the formation of clusters having millions of Hadoop illustrations [21].

This big data has raised the concept of space and time complexity due to storing and processing huge amount of data over mobile and dynamic network. The Extensible Mark-up Language (XML) and machine learning methods apply to big data processing like classification, clustering, and preprocessing of IoT information [22, 23]. Latest IoT applications and performances remain further on an intellectual indulgence of the surroundings from information extracted by means of assorted sensors and small machines. Here a framework combines an ontology dependent description of information dispensations by means of unusual logic for pretty beneficial incident recognition by seasoning the specific classification strategy of machine learning. A road and traffic examination is performed to verify the results of framework [24].

The personal data of users are digitally distributed over network through smart IoT devices and multiple artificial techniques are introduced to control the digitally transferred information following few rules and policies. An intellectual police examination strategy is introduced, discovering the contradictory policy or agreements of users over advocate platform. An intellectual decision-making method is applied with the help of fuzzy cognitive maps [25].

The business is directly or indirectly related to customer behaviour, evaluated by trust mining. The trust of sellers is evaluated by dynamic clustering, where data is modified day by day over huge network area. The quick development of online shopping details illustrates a growing issue for customers who are comprised to select faithful sellers and successful seller selections from numerous existing record beginning e-commerce usage areas to enhance the business. A dynamic clustering method is adopted to calculate the trust of customers and differentiate the buying equivalence of customers for predicting the customer behaviour. The real-time and artificial datasets are utilized to perform clustering and evaluate the results based on accuracy [26].

The medical field [27] also well utilizes the mining techniques like classification to identify the mental health and evaluate the risk to manage the system. This classification is done by decision trees to discover and classify the patients according to their mental health. Here, a relative calculation of a huge array classifier is associated with several areas like tree, group, neural, possibility, categorization, and policy dependent classifiers. The linear and random classifiers are introduced to perform disease classification [28].

The cancer disease in unstructured format is well classified to discover several types of cancer disease. It generates valuable results in terms of risk aspects, treatment, and management. The text mining is well exploited in cancer disease prediction like lung, breast, and ovarian cancer. The data about cancer patients is collected from several heterogeneous resources and text mining is performed to provide various cancer related information like survival, treatment, and risk of disease [29].

The geographical data is collected from several heterogeneous resources and data mining is initialized over the spatial data to manage the disaster. The natural hazards are previously identified before happening; this is achieved by spatial data mining over huge geographic information. The several geographical information such as soil, ocean, earth's crust, and air quality is used to employ the mining process with the help of PSO and fuzzy logics. The clusters are decided on the basis of spatial information and natural behaviours in environments [30].

The data mining based educational information extraction is a new era of research, in which distributed educational data is compiled and used for several purposes. The students, teachers, and other staffs have played an important role in educational data mining. The educational data is collected from several resources and saved in tabular format. These student data can be further analyzed by university and examined by data mining model to evaluate the results of students and maintain the records in appropriate manner [31].

The classification is also performed over data streams, combining the text, music, and video information with the help of decision trees and naive structure. These data streams also combined the human activities like movement of hands and legs [32, 33]. There are various key issues of classification like infinite size, perception development, and perception flow and characteristic assessment. Various researchers mainly solved the issues of infinite size and perception development, but the perception flow and characteristic assessment are not taken into consideration by researchers. Here, these two issues are removed in implementing a classification method over big data and parameters like error rate and running time are obtained to provide superior efficiency of the method [34].

3. The Biogeography-Based Optimization (BO) Approach

A Biogeography-Based Optimization (BO) is a metaheuristic approach based on island biogeography premise, which relates with the migration, evolution, and destruction of the castes in a habitat. A Habitat Suitability Index (HSI) is utilized to generate the best solution globally and share the characteristics with week habitat. The population is enhanced by taking the optimal solutions from prior iteration from emigrating [35] to immigrating habitats by using the migrating Suitability Index Variables (SIVs) in BO migrating process. A fresh characteristic is obtained in complete solution area using fitness function [36] and replaced every habitat's SIVs arbitrarily and stochastically to enhance the population [37] miscellany and searching strength in BO mutation process.

3.1. Migration Process

3.1. Migration Process. In migration stochastic process, several parents can be utilized for a particular offspring and every habitat (H_a) is modified by receiving the SIVs from a superior HSI habitat in population (P^S). The migration rates are straightly dependent on the caste number in a habitat for enhancing [38] the habitat miscellany and linear migration is evaluated by using the following equation:

$$H_a(\text{SIV}) = H_b(\text{SIV}), \tag{1}$$

where $H_b(\text{SIV})$ is a superior HSI b^{th} habitat (H_b) to transfer the SIV value to the a^{th} habitat (H_a).

The emigration rate (α) and immigration rate (β) are evaluated for c castes in habitat by using the two following equations:

$$\alpha_c = \frac{G_c}{N_{\text{maximum}}}, \tag{2}$$

$$\beta_c = M \times (1 - \alpha_c). \tag{3}$$

Here, G and M are highest emigration and immigration rates, respectively, and N_{maximum} is maximum realizable number of castes utilized by habitat.

There are six models developed for migration phase, out of which sinusoidal model performed superior migration as compared to the other five models. This model is evaluated for a^{th} habitat by using the two following equations:

$$\beta_a = \frac{M}{2}\left(1 + \cos\left(\frac{a\pi}{N_{\text{maximum}}}\right)\right), \tag{4}$$

$$\alpha_a = \frac{G}{2}\left(1 - \cos\left(\frac{a\pi}{N_{\text{maximum}}}\right)\right). \tag{5}$$

3.2. Mutation Process. A mutation is a stochastic operator enhancing the population miscellany to obtain optimal solution [39]. The mutation process is utilized for updating at least one arbitrary chosen SIV of a solution with the help of mutation rate (T_a) and the previous possibility of subsistence (S_a) by using the following equation:

$$T_a = T_{\text{maximum}}\left(1 - \frac{S_a}{S_{\text{maximum}}}\right), \tag{6}$$

where T_{maximum} is the highest mutation rate term illustrated by user and S_{maximum} is the highest possibility of castes count.

After that the mutation operator is improved by utilizing Cauchy model to provide optimal exploration strength of BO in huge searching area by reducing potential limitation of mutation strategy. The Cauchy distribution is evaluated with the help of probability density function, which is formulized by the following equation:

$$F(X; 0, 1) = \frac{1}{\pi\left(1 + X^2\right)}. \tag{7}$$

Hence, the Cauchy mutation equation is described by using the following equation:

$$\begin{aligned} H_a(\text{SIV}) = {} & \text{minimum}\left(H_a(\text{SIV})\right) + \left(\text{maximum}\left(H_a(\text{SIV})\right)\right. \\ & \left. - \text{minimum}\left(H_a(\text{SIV})\right)\right) \times \pi \times F\left(H_a(\text{SIV}); 0, 1\right), \end{aligned} \tag{8}$$

where $H_a(\text{SIV})$ is a^{th} habitat. $F(H_a(\text{SIV}); 0, 1)$ is Cauchy distribution (Algorithm 1).

4. The Chaotic BO Approach Using Information Entropy (CBO-IE)

An updated BO approach is proposed using the chaotic behaviour and Information Entropy. The BO approach is well suitable for exploration and exploitation in huge searching space and generates the efficient results for numeric optimization [40]. Still, the numeric optimization is reasonably different from data clustering mechanism. Here, some intrinsic characteristics are investigated and a chaotic BO is implemented using Information Entropy to apply the BO for data clustering.

4.1. Element Information Entropy. The data points are distributed in multidimensional area in data clustering strategy. The confusion degree of a probabilistic variable is calculated by utilizing Information Entropy; after that, this is utilized for elements measurements to calculate the distribution. The entropy (E_{a}) is evaluated to isolate the element values with estimation of every value to its closer integer by using the following equation:

$$E_a = -\sum_{b=\text{min}_a}^{\text{max}_a} R_b \log\left(R_b\right), \tag{9}$$

where E_a is the entropy of a^{th} element ($a = 1, 2, 3, \ldots, L$) and L is number of elements in dataset. min_a and max_a are lowest and highest integers after discretization of element values. R_{b} is b^{th} element integer percentage value.

The migration procedure of BO population is guarded by using element entropy; hence, maximum entropy is evaluated for every element in dataset by the following equation:

$$\text{maximum}\left(E_a\right) = -\log\left(\frac{1}{\text{max}_a - \text{min}_a + 1}\right), \tag{10}$$

where maximum (E_{a}) is maximum entropy of a^{th} element in dataset.

At last, the normalized entropy for every element is calculated by the following equation:

$$\text{nomalized}\left(E_a\right) = \frac{E_a}{\text{maximum}\left(E_a\right)}, \tag{11}$$

where normalized (E_a) is normalized entropy of a^{th} element in dataset.

Equation (11) is repeated for all data elements in dataset and normalized entropy set (normalized (E)) is generated as follows:

Normalized (E) = (normalized (E_1), normalized (E_2),…………, normalized (E_{L})).

4.2. Information Entropy-Based Migration Process in the BO Approach. Here, two mechanisms are introduced in migration to improve the performance of BO approach. The first one is original migration process of BO explained in the previous section. The second one is updated mechanism of original migration in which P particulars are elected arbitrarily from present population ($1 \le P \le P^S$) and the one optimal particular is assigned as reference particular (H_{ref}). The direction of migration is guided by H_{ref} and Information Entropy is utilized to provide equivalency between population miscellany and convergence speed. The higher Information Entropy of element indicates the maximum uncertainty, which slows down the convergence speed. Hence, the speed is enhanced for element by transferring it to the location based on reference particular, globally with maximum possibility, as compared to the least Information Entropy element.

4.3. Chaos-Based Population Selection of the BO Approach. The chaos method is extremely related to initial circumstances and successfully utilized for arbitrary number generation using logistic function. The chaotic system is used in the following equation:

$$\gamma_{f+1} = \mu \times \gamma_f \times \left(1 - \gamma_f\right), \tag{12}$$

where μ represents constants in the range of [1, 4]. γ represents variables ($\gamma \in [0, 1]$, $f = 0, 1, \ldots$).

The population of BO is initialized by utilizing chaos function (equation (12)), which has improved the efficiency of BO with proper use of huge solution area.

4.4. The Complete CBO-IE Approach for Data Mining. The Information Entropy-based migration and chaos-based population selection are combined in Chaotic Biogeography-Based Optimization using Information Entropy (CBO-IE) to solve the data mining, that is, data clustering in optimal way (Figure 1). Firstly, the population (P^S) of BO approach is initialized with the help of chaos function

START
Initialize the parameters $G = M = 1$, $T_{\text{maximum}} = 1$, P^S and Max_iteration
Initialize the populations (arbitrary group of habitats) H_1, H_2,........, H_P^s
Evaluate fitness value (HSI) for every habitat
WHILE (ending condition is not found)
  Evaluate α_a, β_a and T_a for every habitat
  Obtain a random $\in$ (0, 1)//**Migration**
  FOR every habitat (from minimum to maximum HSI values)
    Choose habitat H_a (SIV) stochastically proportional to β_a
    IF random $< \beta_a$ and H_a (SIV) choose, then
      Choose habitat H_b (SIV) stochastically proportional to α_a
      IF random $< \alpha_a$ and H_b (SIV) choose, then
        H_a (SIV) $= H_b$ (SIV)
      END IF
    END IF
  END FOR//MUTATION
  Choose H_a (SIV) with the help of mutation possibility proportional S_a
  IF random $< T_a$ then
    Arbitrary change the SIVs in H_a (SIV)
  END IF
  Evaluate HSI value
END WHILE
STOP

Algorithm 1: Biogeography-Based Optimization.

(equation (12)) and every particular is denoted as a vector with size $L_x = L \times K$ (L is number of elements in dataset, K is number of cluster centroids, and L_x is dimension of particulars). The K centroids locations are fixed into vector, in which 1st centroid relates with 1st L attributes, 2nd centroid relates to 2nd L attributes, and so on. The primary particular vector values are generated arbitrarily and consistently between lower and higher elements values in existing dataset within maximum number of iterations (Mi). Then, CBO-IE is applied to calculate the fitness values of entire particulars by using equations (1) to (8) (Algorithm 2).

5. Results and Analysis

In this section, the healthcare IoT datasets and performance factors for proposed CBE-IE approach are explained briefly. The entire approaches are implemented with the help of MATLAB 2021a tool using Core i3-3110M processor having Windows 8 operating system with 2 GB RAM and analyzed over 8 healthcare IoT datasets (Table 1). The proposed CBO-IE approach has evaluated the results for 500 iterations in terms of intracluster distance, purity index, standard deviation, root mean square error, accuracy, and *F*-Measure as compared to prior algorithms like K-Means, ACO, PSO, ALO, and BO over 30 independent runs.

5.1. Healthcare IoT Datasets. The proposed CBO-IE approach is applied on 8 dissimilar healthcare IoT datasets taken from UCI repository (Table 1). The datasets are thoracic surgery, breast cancer, cryotherapy, liver patient, heart patient, chronic kidney disease, diabetic retinopathy, and blood transfusion. The 470 instances of thoracic surgery dataset with 17 attributes are divided into 2 classes (survive and not survive), the 699 instances of breast cancer dataset with 10 attributes are distributed into 2 classes (benign and malignant), the 90 instances of cryotherapy dataset with 7 attributes are divided into 2 classes (success and failure), the 583 instances of liver patient dataset with 10 attributes are distributed into 2 classes (liver patient and not), the 299 instances of heart patient dataset with 12 attributes are divided into 2 classes (heart failure and not), the 400 instances of chronic kidney disease with 24 attributes are divided into 2 classes (disease found and not), the 1151 instances of diabetic retinopathy dataset with 18 attributes are distributed into 2 classes (diabetic retinopathy and not), and the 748 instances of blood transfusion dataset with 4 attributes are divided into 2 classes (donating blood and not).

5.2. Performance Factors. The performance of proposed CBO-IE approach is evaluated in terms of intracluster distance, purity index, standard deviation, root mean square error, accuracy, and *F*-Measure.

5.2.1. Intracluster Distance. Firstly, the distances between data points are evaluated within a cluster. After that, the average of these distances is generated representing an intracluster distance. The optimal clustering is achieved with least intracluster distance. For a cluster, the mean distance is evaluated between a centroid and total data points. This step is continuously performed for every cluster and at last mean value of entire clusters' intracluster distances is obtained.

Table 2 illustrates that the CBO-IE generates least intracluster distance value for all IoT datasets. The CBO-IE obtains 90% superior results than BO, 92% superior results

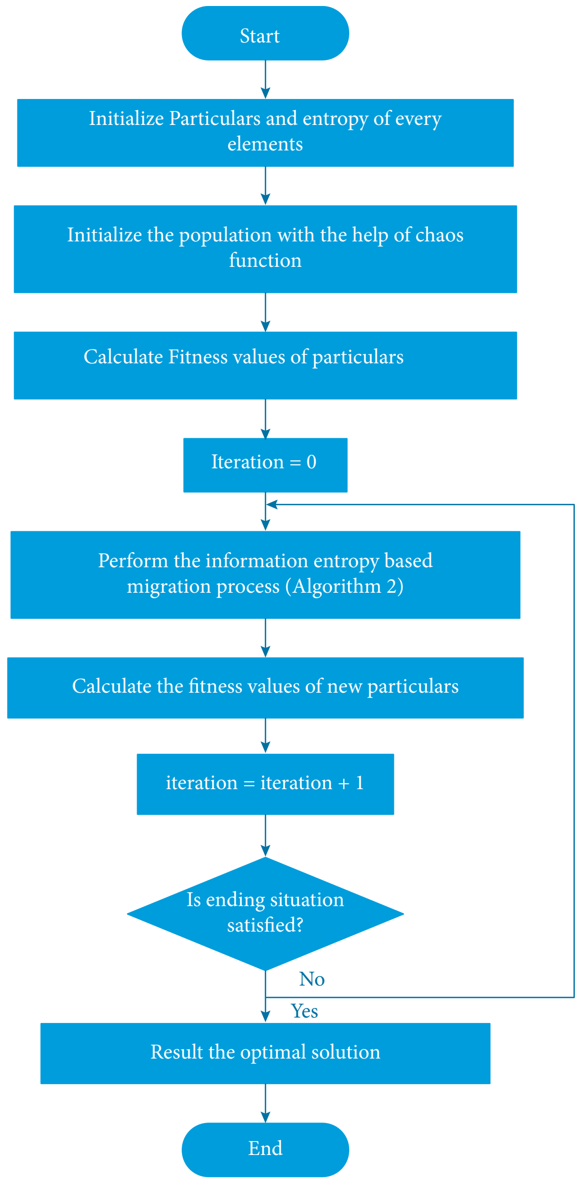

Figure 1: Flowchart of the CBO-IE approach.

than ALO, 94% superior results than PSO, 96% superior results than GA, and 98% superior results than K-Means in terms of intracluster distance for entire healthcare IoT datasets. The average ranking of all approaches is evaluated on the basis of minimum to maximum intracluster distance (from 1 to 6).

Figure 2 represents the better rank of proposed CBO-IE with least intracluster distance values against other approaches, K-Means, GA, PSO, ALO, and BO, for all IoT datasets.

5.2.2. Standard Deviation. The stiff data clustering in the region of average value is described by a numerical characteristic called standard deviation (D^S). The best clustering is achieved with less standard deviation, which is obtained by the following equation:

$$D^S = \sqrt{\frac{\sum (V - \overline{V})}{|H|}}, \tag{13}$$

where $|H|$ is dataset length, V is dataset values (points), and $\overline{V}$ is dataset average value.

Table 3 describes that the CBO-IE obtains less standard deviation value for all IoT datasets. The CBO-IE generates 93% better quality outcomes than BO, 95% better quality outcomes than PSO and ALO, 97% better quality outcomes than GA, and 98% better quality outcomes than K-Means in terms of standard deviation for entire healthcare IoT datasets.

Figure 3 shows the better standard deviation of proposed CBO-IE against other approaches, K-Means, GA, PSO, ALO, and BO, for all IoT datasets.

Algorithm	Number of Executions
START	
FOR a = 1 to P^S **DO**	(P^S+1)
Choose the optimal one from P arbitrary particulars as H_{ref}	P^S
FOR b = 1 to L_x **DO**	$P^S*(L_x+1)$
IF random < normalized (E_a) then	P^S*L_x
$H_a(SIV) = H_{ref}(SIV)$	
ELSE	
$H_a(SIV) = H_b(SIV)$	
END IF	
END FOR	
END FOR	
STOP	

Algorithm 2: Information Entropy-based migration process in the BO approach.

Table 1: Healthcare IoT datasets.

Sr. no.	Healthcare IoT dataset	No. of instances	No. of attributes	No. of clusters
1	Thoracic surgery	470	17	2
2	Breast cancer	699	10	2
3	Cryotherapy	90	7	2
4	Liver patient	583	10	2
5	Heart patient	299	12	2
6	Chronic kidney disease	400	24	2
7	Diabetic retinopathy	1151	18	2
8	Blood transfusion	748	4	2

Table 2: Average ranking of all algorithms based on intracluster distance.

Dataset	*K*-Means	GA	PSO	ALO	BO	CBO-IE
Thoracic surgery	3.364 (5)	0.7569 (4)	0.4256 (4)	0.2547 (3)	0.0657 (2)	0.00652 (1)
Breast cancer	26.265 (5)	0.8634 (4)	0.3126 (4)	0.2614 (3)	0.0874 (2)	0.00728 (1)
Cryotherapy	24.3640 (5)	0.4562 (4)	0.2864 (4)	0.2167 (3)	0.0725 (2)	0.00548 (1)
Liver patient	35.3245 (5)	0.5863 (4)	0.1567 (4)	0.1321 (3)	0.0635 (2)	0.00457 (1)
Heart patient	14.2366 (5)	0.9362 (4)	0.7265 (4)	0.6492 (3)	0.0623 (2)	0.00832 (1)
Chronic kidney disease	46.3625 (5)	0.5682 (4)	0.3568 (4)	0.2864 (3)	0.0742 (2)	0.00786 (1)
Diabetic retinopathy	0.3658 (5)	0.2526 (4)	0.1737 (4)	0.1421 (3)	0.0967 (2)	0.00758 (1)
Blood transfusion	0.6745 (5)	0.5684 (4)	0.2375 (4)	0.2068 (3)	0.0854 (2)	0.00852 (1)
Average ranking (AK_θ)	5	4	4	3	2	1

5.2.3. Purity Index. The correctness of clustering strategy is known as purity, in which accurate classification is performed over data elements. Hence, entire points of an isolated class can be accurately allocated to an isolated cluster. Purity index (I^P) is generated with the help of purity by equations (14) and (15). Maximum purity is achieved with maximum I^P value nearer to 1.

$$\text{purity}\left(R_z\right) = \frac{\text{maximum}\left(\left|R_{wz}\right|\right)}{\left|R_z\right|}, \tag{14}$$

$$I^P = \sum_{z=1}^{K} \frac{\left(\left|R_z\right|\text{Purity}\left(R_z\right)\right)}{|H|}, \tag{15}$$

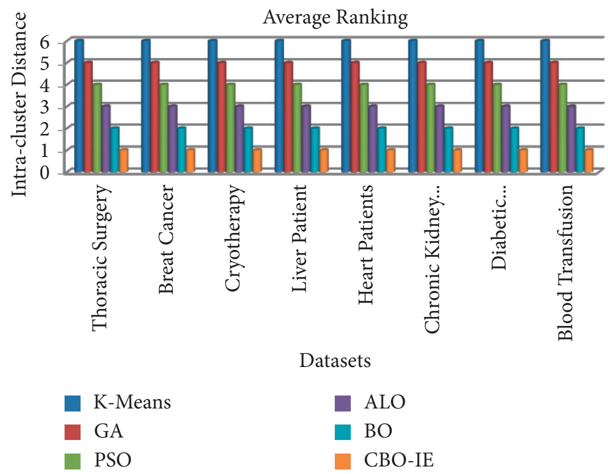

Figure 2: Average ranking based on intracluster distance.

Table 3: Standard deviation for entire IoT datasets.

Dataset	*K*-Means	GA	PSO	ALO	BO	CBO-IE
Thoracic surgery	0.116857	0.03984	0.012036	0.01452	0.007856	0.000524
Breast cancer	0.002578	0.168742	0.12542	0.15713	0.003657	0.000746
Cryotherapy	0.0025143	0.165875	0.001254	0.001674	0.001036	0.000845
Liver patient	0.256323	0.17589	0.147856	0.12312	0.096875	0.000986
Heart patient	0.212678	0.096852	0.042574	0.021563	0.003687	0.000251
Chronic kidney disease	0.020233	0.103625	0.09854	0.065214	0.006574	0.000865
Diabetic retinopathy	0.086574	0.186523	0.142657	0.102647	0.086478	0.0008657
Blood transfusion	0.213658	0.196875	0.185632	0.152461	0.010365	0.000236

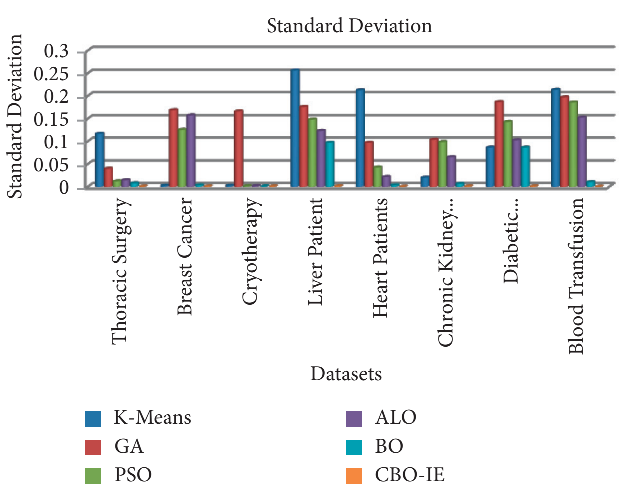

Figure 3: Standard deviation for all IoT datasets.

where Purity(R_z) is purity of z^{th} cluster. $|R_z|$ is z^{th} cluster length. $|R_{wz}|$ is the number of data elements of w^{th} class allocated to z^{th} cluster.

Table 4 explains that the CBO-IE generates maximum purity index value for all IoT datasets. The CBO-IE obtains 5% superior outputs than BO, 7% superior outputs than ALO, 8% superior outputs than PSO, 12% superior outputs than GA, and 15% superior outputs than K-Means in terms of purity index for entire healthcare IoT datasets.

Table 4: Purity index for entire IoT datasets.

Dataset	*K*-Means	GA	PSO	ALO	BO	CBO-IE
Thoracic surgery	0.83	0.86	0.89	0.89	0.91	0.93
Breast cancer	0.86	0.88	0.90	0.89	0.93	0.95
Cryotherapy	0.84	0.87	0.90	0.91	0.93	0.96
Liver patient	0.86	0.87	0.88	0.86	0.90	0.92
Heart patient	0.80	0.83	0.86	0.86	0.88	0.92
Chronic kidney disease	0.86	0.87	0.90	0.89	0.91	0.93
Diabetic retinopathy	0.88	0.90	0.91	0.91	0.93	0.95
Blood transfusion	0.76	0.78	0.81	0.83	0.86	0.88

Figure 4 represents the better quality purity index of proposed CBO-IE against other approaches, K-Means, GA, PSO, ALO, and BO, for all IoT datasets.

5.2.4. F-Measure. Firstly Precision (prsn) and Recall (rel) are evaluated to repossess the information by equations (16) and (17). After that, both are combined to formalize the *F*-Measure (FM) by utilizing equations (18) and (19).

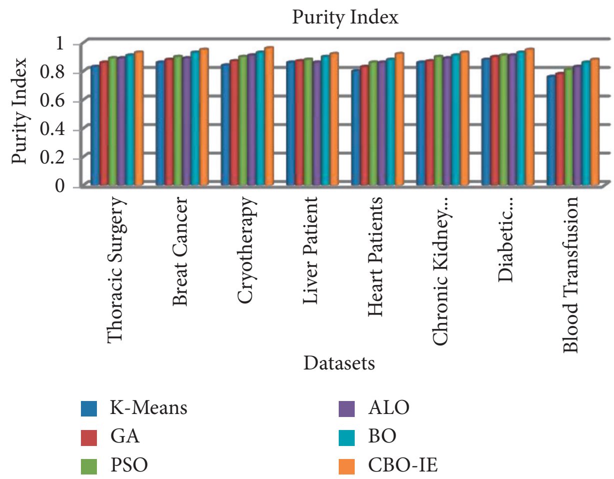

FIGURE 4: Purity index for all IoT datasets.

$$\mathrm{prsn}(w,z)=\frac{|R_{wz}|}{|R_z|}, \tag{16}$$

$$\mathrm{rel}(w,z)=\frac{|R_{wz}|}{|R_w|}, \tag{17}$$

$$\mathrm{FM}(w,z)=\frac{2\times\mathrm{prsn}(w,z)\times\mathrm{rel}(w,z)}{\mathrm{prsn}(w,z)+\mathrm{rel}(w,z)}, \tag{18}$$

$$FM=\sum_{w=1}^{K}\frac{|R_w|}{|H|}\text{maximum}\{FM(w,z)\}, \tag{19}$$

where $|R_w|$ is w^{th} class length.

Table 5 describes that the CBO-IE obtains higher *F*-Measure value for all IoT datasets. The CBO-IE generates 4% better outputs than BO, 7% better outputs than ALO, 8% better outputs than PSO, 13% better outputs than GA, and 16% better outputs than K-Means in terms of *F*-Measure for entire healthcare IoT datasets.

Figure 5 shows the better *F*-Measure of proposed CBO-IE against other approaches, K-Means, GA, PSO, ALO, and BO, for all IoT datasets.

5.2.5. Root Mean Square Error (RMSE). The RMSE is defined as a divergence between predicted values and experimental (calculated) values. The best clustering is achieved with minimum RMSE values of datasets. It is evaluated by utilizing the following equation:

$$\mathrm{RMSE}=\sqrt{\frac{1}{|H|}\sum_{j=1}^{|H|}\left(V_j-\widehat{V}_j\right)^2}, \tag{20}$$

where V_j is j^{th} element value in dataset and $\widehat{V}_j$ is j^{th} element predicted value in dataset.

Table 6 explains that the CBO-IE generates least RMSE value for all IoT datasets. The CBO-IE generates 8% better results than BO, 78% better results than ALO, 81% better results than PSO, 87% better results than GA, and 95% better results than K-Means in terms of RMSE for entire healthcare IoT datasets.

Figure 6 shows the better RMSE of proposed CBO-IE against other approaches, K-Means, GA, PSO, ALO, and BO, for all IoT datasets.

5.2.6. Accuracy. It evaluates the division of clusters that are accurate (i.e., it evaluates proportion of verdicts that are exact) and describes the portion of clusters in the prevailing group:

TABLE 5: *F*-Measure for entire IoT datasets.

Dataset	*K*-Means	GA	PSO	ALO	BO	CBO-IE
Thoracic surgery	0.81	0.84	0.87	0.87	0.89	0.91
Breast cancer	0.84	0.86	0.87	0.88	0.90	0.93
Cryotherapy	0.82	0.86	0.88	0.87	0.91	0.93
Liver patient	0.84	0.86	0.87	0.87	0.89	0.91
Heart patient	0.78	0.82	0.84	0.83	0.85	0.88
Chronic kidney disease	0.84	0.86	0.88	0.87	0.89	0.91
Diabetic retinopathy	0.86	0.89	0.90	0.91	0.92	0.94
Blood transfusion	0.74	0.77	0.79	0.82	0.85	0.87

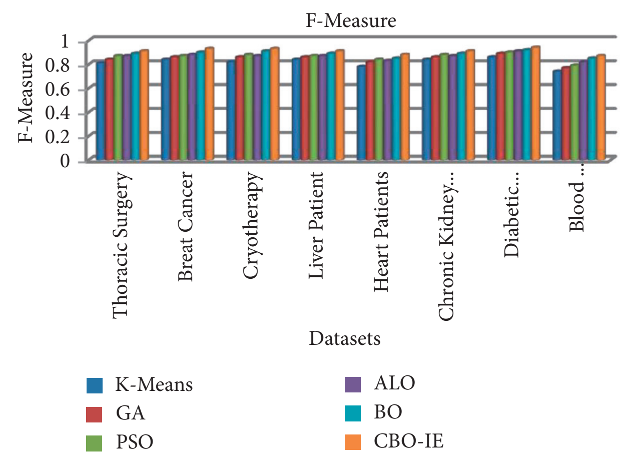

FIGURE 5: *F*-Measure for all IoT datasets.

TABLE 6: RMSE values for entire IoT datasets.

Dataset	*K*-Means	GA	PSO	ALO	BO	CBO-IE
Thoracic surgery	0.537	0.327	0.157	0.124	0.0124	0.0034
Breast cancer	0.567	0.386	0.168	0.264	0.0317	0.0075
Cryotherapy	0.621	0.374	0.234	0.364	0.0421	0.0066
Liver patient	0.437	0.361	0.261	0.213	0.0652	0.0054
Heart patient	0.537	0.412	0.201	0.186	0.0145	0.0063
Chronic kidney disease	0.610	0.422	0.341	0.267	0.0254	0.0047
Diabetic retinopathy	0.517	0.414	0.367	0.257	0.0374	0.0087
Blood transfusion	0.438	0.314	0.120	0.265	0.0451	0.0071

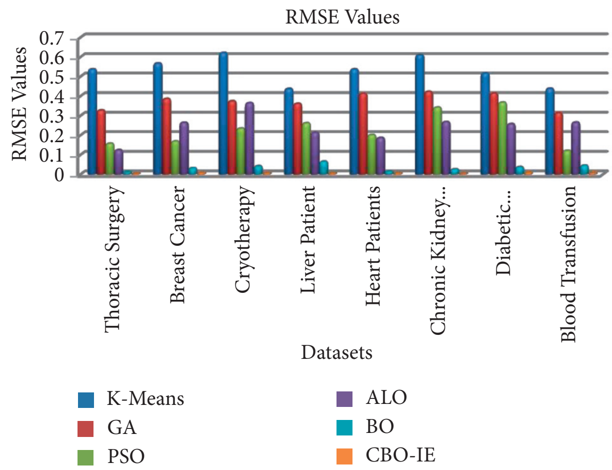

Figure 6: RMSE for all IoT datasets.

Table 7: Accuracy values for entire IoT datasets.

Dataset	*K*-Means	GA	PSO	ALO	BO	CBO-IE
Thoracic surgery	0.80	0.83	0.86	0.86	0.88	0.90
Breast cancer	0.83	0.85	0.86	0.87	0.89	0.92
Cryotherapy	0.81	0.85	0.87	0.86	0.90	0.92
Liver patient	0.83	0.85	0.86	0.86	0.88	0.90
Heart patient	0.77	0.81	0.83	0.82	0.84	0.87
Chronic kidney disease	0.83	0.85	0.87	0.86	0.88	0.90
Diabetic retinopathy	0.85	0.88	0.89	0.90	0.91	0.93
Blood transfusion	0.73	0.76	0.78	0.81	0.84	0.86

$$\text{accuracy} = \frac{\sum_{z=1}^{K} R_z}{|H|} * 100\%. \tag{21}$$

Table 7 represents that the CBO-IE obtains higher accuracy value for all IoT datasets. The CBO-IE has 3% superior outputs than BO, 5% superior outputs than ALO, 6% superior outputs than PSO, 9% superior outputs than GA, and 13% superior outputs than K-Means in terms of accuracy for entire healthcare IoT datasets.

Figure 7 represents the better accuracy of proposed CBO-IE against other approaches, K-Means, GA, PSO, ALO, and BO, for all IoT datasets.

The Information Entropy is used with BO approach for clustering to provide accurate and efficient distribution of data points in dataset. The chaos theory is utilized to initialize the population of BO to improve the searching capability of habitat, which helps in cluster member selection process more precisely. These two strategies, Information Entropy and chaos theory, have improved the performance of BO to provide the best selection of cluster heads and their members optimally. So, CBO-IE generates superior results than BO, ALO, PSO, GA, and K-Means clustering approaches.

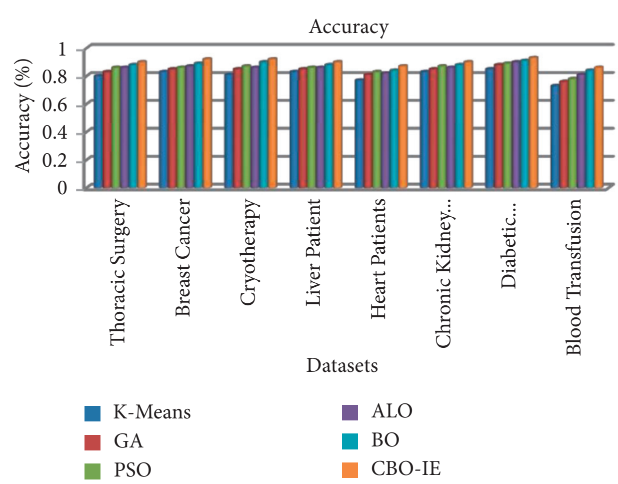

Figure 7: Accuracy for all IoT datasets.

5.3. Running Time Complexity of the CBO-IE Approach. The number of executions is directly related to time complexity of clustering approaches to run. The complexity is calculated by utilizing few circumstances as follows: P^S is population size, L is number of elements in dataset, L_x represents dimensions of particulars (elements), K is number of cluster centroids, and Mi represents maximum iterations. The cost of every execution is assumed as 1 unit. The Cost of all Executions (CE) is obtained to utilize Algorithm 3 by the following equations:

Algorithm	**Number of Executions**
START	
Initialize the parameters G=M=1, $T_{maximum} = 1$ and Mi	1
Calculate the information entropy for all elements and	
obtain the entropy vector normalized(E)	L
Initialize the population P^S of BO by using chaos function (eq. 8) and	
habitats symbolized as H_a $(1 \leq a \leq P^S)$	1
Evaluate fitness value (HSI) for every habitat	P^S
WHILE (ending condition is not found)	Mi+1
Evaluate α_a, β_a and T_a for every habitat	$Mi*P^S$
Obtain a $random \in (0, 1)$ //**Migration**	$Mi*P^S$
Perform the Information Entropy based Migration Process (Algorithm 2)	$Mi*(2*P^S*L_x+3*P^S+1)$
FOR every Habitat (from minimum to maximum HSI values)	$Mi*K*(P^S+1)$
Choose habitat H_a(SIV) stochastically proportional to β_a	$Mi*K*P^S$
IF random $< \beta_a$ and H_a(SIV) choose, then	$Mi*K*P^S$
Choose habitat H_b(SIV) stochastically proportional to α_a	
IF random $< \alpha_a$ and H_b(SIV) choose, then	$Mi*K*P^S$
$H_a(SIV) = H_b(SIV)$	
END IF	
END IF	
END FOR // **MUTATION**	
Choose H_a(SIV) with the help of mutation possibility proportional S_a	Mi*K*L
IF random $< T_a$ then	Mi*K*L
Arbitrary change the SIVs in H_a(SIV)	
END IF	
Evaluate HSI value	Mi*K*L
END WHILE	
STOP	

Algorithm 3: The complete CBO-IE approach.

Table 8: Holm strategy outputs.

J	Approaches	z value	p value	$(\lambda/(A^C - j))$	Hypothesis
1	K-Means	−6.3245	0.00001	0.020	Rejected
2	GA	−5.0596	0.00001	0.025	Rejected
3	PSO	−3.7947	0.0001	0.033	Rejected
4	ALO	−2.5298	0.0057	0.05	Rejected
5	BO	−1.3649	0.0861	0.10	Rejected

$$\begin{aligned} CE = {} & 1 + L + 1 + P^S + Mi + 1 + Mi \times P^S + Mi \times P^S + Mi \times \left(2 \times P^S \times L_x + 3 \times P^S + 1\right) \\ & + Mi \times K \times \left(P^S + 1\right) + Mi \times K \times P^S + Mi \times K \times P^S + Mi \times K \times P^S \\ & + Mi \times K \times L + Mi \times K \times L + Mi \times K \times L, \end{aligned} \tag{22}$$

$$CE = 2 \times Mi \times P^S \times L_x + 4 \times Mi \times K \times P^S + 3 \times Mi \times K \times L + 5 \times Mi \times P^S + Mi \times K + L + P^S + 2 \times Mi + 3. \tag{23}$$

Supposing that all circumstances are equal in equation (23) in worst case, equation (24) is generated as follows:

$$CE = 9n^3 + 6n^2 + 4n + 3. \tag{24}$$

The running time complexities of clustering approaches are O(n^3) for CBO-IE, O(n^3) for BO, O(n^3) for ACO, O(n^3) for PSO, O(n^3) for ALO, and O(n^2) for K-Menas in worst case. Hence, all are executable in polynomial time.

5.4. Statistical Examination Measurement. A statistical examination is functioned to obtain the extension of significance dissimilarities in the effectiveness of clustering techniques. Here, a nonparametric Friedman Examination (FE) is utilized to discover dissimilarities amid the group of serial appropriate variables. The entire clustering techniques provide equally effective explaining in the null hypothesis (Y_0).

The Friedman Examination (FE) is formulized by

$$FE = \frac{12 \times N^{DS}}{A^C\left(A^C + 1\right)} \left[\sum_{\theta=1}^{5} \left(AK_\theta\right)^2 - \frac{A^C \times \left(A^C + 1\right)^2}{4}\right], \tag{25}$$

where N^{DS} is number of datasets, AK_θ is average rank of θ^{th} approach, and A^C is number of clustering approaches.

The FE critical value is 2.04925 taken from F-distribution table [41] with (A^C-1) and (A^C−1)*(N^{DS}−1) freedom degree, which is obtained between (6–1) = 5 and (6-1)*(8-1) = 35 for applying 6 clustering approaches (A^C = 6) over 8 datasets (N^{DS} = 8) with λ = 0.10 (confidence stage). The calculated FE value is higher as compared to the critical value for null hypothesis (Y_0) rejection, if Y_0 is not accepted. The evaluated FE value is 17.14 for initiating 6 clustering approaches (A^C = 6) over 8 datasets (N^{DS} = 8) with λ = 0.10. Hence, the calculated FE is higher as compared to the critical FE, and then Y_0 is rejected. So, it is to be summarized that entire clustering approaches are not equally effective.

Therefore, a post hoc examination is performed using Holm strategy. The proposed CBE-IE is analyzed statistically against other clustering approaches in this examination. Firstly the z value is obtained from equation (24) and after that probability (p) is generated with the help of z value and normal distribution table [42]. At last, p_j value is analyzed with $(\lambda/(A^C - j))$ (Table 8):

$$Z = \frac{AK_j - AK_\theta}{\delta}, \tag{26}$$

where

$$\delta = \sqrt{\frac{A^C\left(A^C + 1\right)}{6 \times N^{DS}}}. \tag{27}$$

Table 8 illustrates that the $(\lambda/(A^C - j))$ value is higher as compared to p_j value; this indicates the hypothesis rejection for entire cases. Hence, the proposed CBO-IE is superior in clustering as compared to the K-Means, GA, PSO, and BO approaches according to the above analysis.

6. Conclusion

Various fields like medicine, education, and industries utilize data mining for their useful applications. The grouping of data is performed on data clustering, which is a specific task in data mining to examine the database efficiently. In this work, a Chaotic Biogeography-Based Optimization approach using Information Entropy (CBO-IE) is proposed to obtain data clusters for healthcare IoT datasets. The Information Entropy is introduced with a BO approach to generate a better distribution of data points in the dataset and chaos theory is utilized to initialize the population of BO approach. The Information Entropy and chaos theory are combined with BO approach to generate optimal cluster heads and cluster members with enhanced convergence speed of BO in huge search area. The MATLAB 2021a tool is used to implement the CBO-IE for eight healthcare IoT datasets and the outcomes describe the better quality efficiency of CBO-IE on the basis of F-Measure, intracluster distance, running time complexity, purity index, statistical analysis, standard deviation, root mean square error, and accuracy as compared to previous techniques of clustering like K-Means, GA, PSO, ALO, and BO approaches. The Friedman Examination and Holm strategy are introduced to perform statistical analysis of proposed CBO-IE against previous techniques of clustering like K-Means, GA, PSO, ALO, and BO approaches, which represent that the CBO-IE generates 90% accurate results. In future, the proposed technique will be anticipated to estimate and be authorized with huge databases under big data. Additionally, a cross-layer communication will be anticipated to be offered and legalized in IoT structural design in the future.

Data Availability

The data that support the findings of this study are available upon request from the corresponding author.

Conflicts of Interest

The authors declare that there are no conflicts of interest.

References

[1] A. Haque, L. Khan, and M. Baron, "SAND: semi-supervised adaptive novel class detection and classification over data stream," in *Proceedings of the 13th AAAI Conference on Artificial Intelligence (AAAI-16)*, pp. 1652–1658, Phoenix, AZ, USA, February 2016.

[2] N. Mishra, H. K. Soni, S. Sharma, and A. K. Upadhyay, "Development and analysis of artificial neural network models for rainfall prediction by using time-series data," *I. J. Intelligent Systems and Applications*, vol. 1, pp. 16–23, 2018.

[3] H. N. Dai, R. C. W. Wong, H. Wang, Z. Zheng, and A. V. Vasilakos, "Big data analytics for large scale wireless networks: challenges and opportunities," *ACM*, vol. 52, pp. 1–46, 2019.

[4] A. H. Sabry, W. Z. W. Hasan, M. N. Mohtar, R. M. K. R. Ahmad, and H. R. Harun, "Planter pressure repetability data analysis for health adult based on EMED system," *Malaysian Journal of Fundamental and Applied Sciences*, vol. 14, no. 1, pp. 96–101, 2018.

[5] A. Mensikova and C. A. Mattmann, "Ensemble sentiment analysis to identify human trafficking in web data," in *Proceedings of the ACM Workshop on Graph Techniques for Adversarial Activity Analytics (GTA)*, pp. 1–6, ACM, New York, Ny, USA, 2018.

[6] S. S. Gill and R. Buyya, "Bio-inspired algorithms for big data analytics: a survey, taxonomy and open challenges," *Big Data Analytics for Intelligent Healthcare Management*, Elsevier, Amsterdam, Netherlands, pp. 1–17, 2019.

[7] A. Verma, I. Kaur, and N. Arora, "Comparative analysis of informatio extraction techniques for data mining," *Indian Journal of Science and Technology*, vol. 9, no. 11, pp. 1–18, 2016.

[8] B. R. Manju, A. Joshuva, and V. Sugumaran, "A data mining study for condition monitoring on wind turbine blades using hoeffding tree algorithm through statistical and histogram features," *International Journal of Mechanical Engineering & Technology*, vol. 9, no. 1, pp. 1061–1079, 2018.

[9] I. Aytekin, E. Eyduran, K. Karadas, R. Akshan, and I. Keskin, "Prediction of fattening final live weight from some body measurements and fattening period in young bulls of crossbred and exotic breeds using MARS data mining algorithm," *Journal of Zoology*, vol. 50, no. 1, pp. 189–195, 2018.

[10] S. Ahmad and R. Varma, "Information extraction from text messages using data mining techniques," *Malaya Journal of Matematik*, vol. 5, no. 1, pp. 26–29, 2018.

[11] N. E. Oweis, M. M. Fouad, S. R. Oweis, S. S. Owais, and V. Snasel, "A novel mapreduce lift assiciation riule mining algorithm (MRLAR) for big data," *International Journal of Advanced Computer Science and Applications*, vol. 7, no. 8, pp. 1–7, 2016.

[12] C. W. Tsai, C. F. Lai, M. C. Chiang, and L. T. Yang, "Data mining for internet of things: a survey," *Communications Surveys and Tutorials, IEEE*, vol. 16, no. 1, pp. 77–97, 2014.

[13] F. Chen, P. Deng, J. Wan, D. Zhang, A. V. Vasilakos, and X. Rong, "Data mining for Internet of things: literature review and challenges," *International Journal of Distributed Sensor Networks*, vol. 2015, Article ID 365372, 14 pages, 2015.

[14] S. B. Patel, M. N. Patel, and S. M. Shah, "FEA-HUIM: fast and efficient algorithm for high utility item-set mining using novel data structure and pruning strategy," *National Conference on Advanced Research Trends in Information and Technologies (NCARTICT), IJSSET*, vol. 4, no. 2, pp. 1–7, 2018.

[15] S. Bhaskaran, R. Marappan, and B. Santhi, "Design and analysis of a cluster-based intelligent hybrid recommendation system for E-learning applications," *Mathematics, MDPI*, vol. 9, no. 107, pp. 1–21, 2021.

[16] D. Giordano, M. Mellia, and T. Cerquitelli, "K-MDTSC: K-Multi-Dimensional time-series clustering algorithm," *Electronics, MDPI*, vol. 10, no. 1166, pp. 1–21, 2021.

[17] R. Mothukuri and B. B. Rao, "Cluster Analysis of cyber crime data using R," *International Journal of Computer Science and Mobile Applications*, vol. 6, no. 2, pp. 62–70, 2018.

[18] A. N. Onaizah, "A novel data stream clustering algorithm in healthcare IoT," *International Journal of Research in Applied Natural and Social Sciences (IJRANSS)*, vol. 5, no. 6, pp. 51–60, 2017.

[19] R. Krishnamurthi, A. Kumar, D. Gopinathan, A. Nayyar, and B. Qureshi, "An overview of IoT sensor data processing, fusion, and analysis techniques," *Sensors, MDPI*, vol. 20, pp. 1–23, 6076.

[20] F. Alam, R. Mehmood, I. Katib, and A. Albeshri, "Analysis of eight data mining algorithms for smarter Internet of things (IoT)," in *Proceedings of the International Workshop on Data Mining in IoT Systems (DaMIS)*, pp. 437–442, Elsevier, London, UK, September 2016.

[21] A. M. C. Souza and J. R. A. Amazonas, "An outlier detect algorithm using big data processing and Internet of things architecture," in *Proceedings of the International Workshop on Big Data and Data Mining Challenges on IoT and Pervasive Systems (BigD2M)*, pp. 1010–1015, Elsevier, London, UK, June 2015.

[22] D. Gil, M. Johnsson, H. Mora, and J. Szymanski, "Review of the complexity of managing big data of the Internet of things," *Complexity*, vol. 2019, Article ID 4592902, 12 pages, 2019.

[23] M. S. Mahdavinejad, M. Rezvan, M. Barekatain, P. Adibi, P. Barnaghi, and A. P. Sheth, "Machine Learning for Internet of things data analysis: a survey," *Digital Communications and Networks*, vol. 4, pp. 161–175, 2018.

[24] M. Ruta, F. Scioscia, G. Loseto, A. Pinto, and E. D. Sciascio, "Machine learning in the Internet of things: a semantic-enhanced approach," *Semantic Web*, vol. 10, pp. 1–21, 2017.

[25] K. Demertzis, K. Rantos, and G. Drosatos, "A dynamic intelligent policies analysis mechanism for personal data processing in the IoT ecosystem," *Big Data And Cognitive Computing*, vol. 4, no. 9, pp. 1–16, 2020.

[26] N. Joseph and B. S. Kumar, “Top-K competitor trust mining and customer behavior investigation using data mining technique,” *Journal of Network Communications and Emerging Technologies (JNCET)*, vol. 8, no. 2, pp. 26–30, 2018.

[27] M. P. Dooshima, E. N. Chidozie, B. J. Ademola, O. O. Sekoni, and I. P. Adebayo, “A predictive model for the risk of mental illness in Nigeria using data mining,” *International Journal of Immonology*, vol. 6, no. 1, pp. 5–16, 2018.

[28] B. A. Tama and S. Lim, “A comparative performance evaluation of classification algorithms for clinical decision support systems,” *Mathematics, MDPI*, vol. 8, no. 1814, pp. 1–25, 2020.

[29] C. C. N. Wang, I. S. Chang, P. C. Y. Sheu, and J. J. P. Tsai, “Application of semantic computing in cancer on secondary data analysis,” in *Proceedings of the 2nd International Conference on Robotic Computing, IEEE*, pp. 407–413, Laguna Hills, CA, USA, February 2018.

[30] K. Ravikumar and A. R. Kannan, “Spatial data mining for prediction of natural events and disaster management based on fuzzy logic using hybrid PSO,” *Taga Journal*, vol. 14, pp. 858–878, 2018.

[31] B. M. M. Alom and M. Courtney, ““Educational data mining: a case study perspectives from primary to university education in Australia,” *International Journal of Information Technology and Computer Science*, vol. 2, pp. 1–9, 2018.

[32] S. Celik and O. Yilmaz, “Prediction of body weight of Turkish tazi dogs using data mining techniques: classification and regression tree (CART) and multivariate adaptive regression splines (MARS),” *Journal of Zoology*, vol. 50, no. 2, pp. 575–583, 2018.

[33] W. Ugulino, D. Cardador, K. Vega, E. Velloso, R. Milidíti, and H. Fuks, “Wearable computing: accelerometers data classification of body postures and movements,” in *Proceedings of the 21st Brazilian Symposium on Artificial Intelligence, Advances in Artificial Intelligence, Lecture Notes in Computer Science*, pp. 52–61, Springer, Stuttgart, Germany, September 2012.

[34] M. B. Chandak, “Role of big-data in classification and noval class detection in data streams,” *Journal of Big Data*, Springer, vol. 23, no. 5, pp. 1–9, 2016.

[35] M. Gupta, K. K. Gupta, and P. K. Shukla, “Session key based fast, secure and lightweight image encryption algorithm,” *Multimedia Tools and Applications*, vol. 80, pp. 10391–10416, 2021.

[36] H. S. Pannu, D. Singh, and A. K. Malhi, “Multi-objective particle swarm optimization-based adaptive neuro-fuzzy inference system for benzene monitoring,” *Neural Computing & Applications*, vol. 31, pp. 2195–2205, 2019.

[37] D. Singh, J. Singh, and A. Chhabra, “High availability of clouds: failover strategies for cloud computing using integrated check pointing algorithms,” in *Proceedings of the 2012 International Conference on Communication Systems and Network Technologies*, pp. 698–703, Rajkot, India, May 2012.

[38] D. Singh and V. Kumar, “A comprehensive review of computational dehazing techniques,” *Archives of Computational Methods in Engineering*, vol. 26, pp. 1395–1413, 2019.

[39] R. Gupta, “Performance analysis of anti-phishing tools and study of classification data mining algorithms for a novel anti-phishing system,” *International Journal of Computer Network and Information Security*, vol. 12, pp. 70–77, 2015.

[40] R. Bhatt, P. Maheshwary, P. Shukla, P. Shukla, M. Shrivastava, and S. Changlani, “Implementation of fruit fly optimization algorithm (FFOA) to escalate the attacking efficiency of node capture attack in wireless sensor networks (WSN),” *Computer Communications*, vol. 149, pp. 134–145, 2020, ISSN 0140-3664.

[41] F Distribution Table, http://www.socr.ucla.edu/applets.dir/f_table.html, 2018.

[42] Normal Distribution Table: http://math.arizona.edu/~rsims/ma464/standardnormaltable.pdf.

Hindawi
Scientific Programming
Volume 2021, Article ID 2466441, 12 pages
https://doi.org/10.1155/2021/2466441

Research Article

Reform of the Practice Teaching System of Entrepreneurship Education Based on 5G Fog Computing in Colleges and Universities

Feiping Liu [1,2] **Qiuling Gong** [3] **and Junjie Zhou** [4]

[1]School of Management, Wuhan University of Technology, Wuhan 430070, Hubei, China
[2]PE Department, Wuhan Institute of Technology, Wuhan 430215, Hubei, China
[3]PE Department, Zhongnan University of Economics and Law, Wuhan 430073, Hubei, China
[4]Department of Information Science and Technology, Wenhua College, Wuhan 4300074, Hubei, China

Correspondence should be addressed to Feiping Liu; 05090601@wit.edu.cn and Qiuling Gong; lfp9095@163.com

Received 21 August 2021; Accepted 21 September 2021; Published 6 October 2021

Academic Editor: Punit Gupta

Innovation is inevitable for economic development of the China and even the world, and entrepreneurship education is also an important topic for educators at home and abroad. It is an important issue for the sustainable development and effective operation of industry and education to establish an integrated support system of industry and education in universities. The purpose of this research is to analyze the reform of entrepreneurship education in the fusion of industrial education and university education and use the latest 5G fog computing technology. In this study, we select different types of universities and graduates as our subject. This study gathers the problems that exist in the academic view and measures of the integration of university production and education, education facilities, and entrepreneurship education through research, literature analysis, and interview methods. A corresponding solution is proposed in conjunction with an analysis model of student performance evaluation. The results show that 22% of teachers think that entrepreneurship education helps students develop in an all-round way, 42% of teachers interviewed think that entrepreneurship education is "graduation service," 13% of teachers think that entrepreneurship education is an organic supplement to professional education, and 23% of teachers interviewed say it is difficult to position it. 80.5% of university teachers think that the current school management system is not suitable for combination of production and learning, school enterprise cooperation, and development needs. It is concluded that the reform of entrepreneurship education system industry and education that are combined in this study has a good effect on improving the current employment problem, but the adaptation degree of colleges and universities is insufficient. This study contributes to the development of integrated model of new technology with entrepreneurship education.

1. Introduction

In the process of deepening entrepreneurship education in various universities, it is very important to cultivate large-scale entrepreneurship and innovation. However, as a new product of the times, there are many problems in entrepreneurship education. For example, the positioning of entrepreneurship education is vague. This is determined by the current situation of education in our country and the social background. In order to manage innovation and entrepreneurship, some local universities have joined the Youth League Committee as ideological and political work. For qualified teachers, the relevant courses are basically not part-time jobs of full-time teachers. Entrepreneurship education lacks profound development from recognition to action. These problems can be said to be accompanied by the disadvantages of practice, which require the optimization and promotion of entrepreneurship education.

5G fog computing is a new technology. In this mode, data, data processing, and applications are concentrated in devices at the edge of the network, instead of all remaining in the cloud. It is a derivative concept of cloud computing, which combines the new combining technology with traditional university education, this is very important to demonstrate the functions of the university and to improve social benefits. As far as the educational system is concerned, the main purpose of higher education reform characterized by reform and development is to promote the establishment of vocational education system in contemporary China, to realize the classification and management of universities, to improve higher education, and to educate the national economy.

In the research of entrepreneurship education and industry education integration, Zhang analyzed on the combination of production and learning, school enterprise cooperation, and the necessity of application-oriented personnel training mode. He summarized the innovation direction of application-oriented talent training mode, analyzed the characteristics of facility agricultural science, combined with engineering specialty, and discussed the related knowledge of facility agriculture teaching reform under the applied talent training mode of "combination of production and education, school enterprise cooperation." His method is out of date and inefficient [1]. Based on the spiral theory of three elements, Zizhou analyzes the functions of universities, enterprises, and government, namely, cultural function, economic function, and political function. His research focuses on promoting the development of regional innovation through the integration of industry, university, and research, making the three independent and complementary, forming a regional innovation network. His method is not practical [2]. Bullough et al. propose a framework for designing and implementing effective programs for women based on rich first-hand experience in entrepreneurship education and training programs and a comprehensive review of entrepreneurship and leadership literature related to entrepreneurship education and training. His framework provides the core factors that need to be considered to effectively achieve project goals: project elements, human factors, environment, and funding. Although his framework is generally applicable to entrepreneurial education and training projects, he has demonstrated its effectiveness by sharing first-hand examples with more than 20 female entrepreneurs in developing countries in the past 10 years. His method provides guidance to project managers who study entrepreneurship, leadership, business, and women in developing economies and provide entrepreneurial education and training programs. His method is not accurate enough [3]. Mandell's study analyzes the experimental entrepreneurship education programs in the top 25 undergraduate schools in the US. He is aware of the diversity and dynamism of entrepreneurship experienced in the United States. One of his goals is to investigate barriers to experienced entrepreneurship and determine affordable and viable options. He investigated the Dean of the School, the Rector, and the Undergraduate Project Director and evaluated and analyzed the experience gained from high-tech business creation projects. His research was aimed at entrepreneurship education researchers and business project managers, and his methods are not working [4].

The study first presents the basic elements of integration into production education, then six main characteristics of the integrated entrepreneurship education system. The study also describes concrete ways of promoting the development of entrepreneurship and use the latest 5G fog computing calculation to conduct in-depth research on the subject of this article. The main algorithms of the present study are the factor analysis models and Z standard fractions for the assessment of student performance. This study selected the different types of higher education institutions and of graduates from our province as a subject of study and carried out an experimental analysis of the reform of entrepreneurship education linked to productive education. Combining the results of the experiment with an analysis of the main problems is related to the integration of industrial research, to the practical orientation and reform of the teaching of innovative entrepreneurship, and to the integration of the teaching of innovative entrepreneurship and industrial research. The results of quantitative assessments are analyzed. The conclusion of this study is that the new educational reform may solve the current employment problems of some students.

2. 5G Fog Computing and Entrepreneurship Education Production Teaching Reform

2.1. 5G Fog Calculation. Fog computing is a newly proposed conceptual model in which data, data processing, and applications are concentrated in devices at the edge of the network instead of almost all stored data in the cloud. It is an extended concept of cloud computing. The concept of fog computing technology was proposed in 2011 and was defined in detail in 2012. Just like cloud computing, fog computing is also very vividly defined. "The cloud is high in the sky, very abstract, while the fog is close to the ground, with you and me." Fog computing does not have strong computing power, only some weak, scattered computing devices. Fog computing is not composed of powerful servers but is composed of computers with weaker and more scattered functions, which penetrates factories, automobiles, electrical appliances, street lights, and various supplies in people's material life. It mainly uses devices in the edge network, and data transmission has extremely low latency. Fog computing has a vast geographical distribution and a large-scale sensor network with a large number of network nodes. Fog computing is an extension of the concept of cloud computing. It mainly uses devices in the edge network, and data transmission has extremely low latency. Fog computing has a vast geographical distribution and a large-scale sensor network with a large number of network nodes. Fog computing has good mobility, mobile phones, and other mobile devices can communicate directly with each other, and the signal does not need to go to the cloud or even the base station to go around, supporting high mobility. Fog computing is not a powerful server, but is composed of computers with weaker and more dispersed functions. Fog computing is between cloud computing and personal computing and is a paravirtualized service computing architecture model. Emphasizing quantity, no matter how weak a single computing node is, it must play a role. Compared with cloud computing, the architecture adopted by fog computing is more distributed and closer to the edge of the network. Fog computing concentrates data, data processing, and applications in devices at the edge of the network, instead of storing almost all of them in the cloud like cloud computing, data storage, and processing rely more on local devices rather than servers. Fog computing is a new generation of distributed computing, in line with the "decentralized" characteristics of the Internet. Decentralization is the form of social relations and content generation formed during the development of the Internet and is a new type of network content production process relative to "centralization." Decentralization is not about avoiding the center, but letting nodes freely choose the center and freely determine the center. Simply put, centralization means that the center determines the node. The node must rely on the center, and the node cannot survive if it leaves the center. In a decentralized system, anyone is a node, and anyone can become a center. No center is permanent, but phased. No center is mandatory for nodes. Fog computing is completely different from cloud computing. Cloud computing is based on the services of IT operators and social public clouds. Fog computing wins by quantity, emphasizes quantity, and plays a role no matter how weak a single computing node is. Cloud computing emphasizes overall computing power, and calculations are generally completed by a bunch of concentrated high-performance computing devices. Fog computing expands the network computing model of cloud computing, extends network computing from the network center to the network edge, and thus is more widely used in various services. The country is vigorously developing the Internet of Things. The final result of the development of the Internet of Things is to interconnect all electronic devices, mobile terminals, household appliances, and so on. These devices are not only huge in number but also widely distributed. Only fog computing can satisfy the reality. Demand puts forward requirements for fog computing and also provides development opportunities for fog computing.

Cloud computing (cloud computing) technology is a type of distributed computing, which refers to the decomposition of huge data computing processing programs into countless small programs through the network "cloud," and then processing and analysis through a system are composed of multiple servers. These small programs get the results and return them to the user. "Cloud" is essentially a network. In a narrow sense, cloud computing is a network that provides resources. Users can obtain resources on the "cloud" at any time, use them as needed, and can be regarded as unlimited expansion, as long as you can pay for what you use. The "cloud" is like a water plant. We can receive water at any time and there is no limit. You can pay the water plant according to your own water consumption. Tracing back to the root of cloud computing, its emergence and development are closely related to the aforementioned parallel computing, distributed computing, and other computer technologies, which promote the growth of cloud computing. Virtualization technology must be emphasized that virtualization breaks through the boundaries of time and space and is the most significant feature of cloud computing. Virtualization technology includes application virtualization and resource virtualization. As we all know, there is no spatial connection between the physical platform and the application deployment environment, and it is through the virtual platform to complete the data backup, migration, and expansion of the corresponding terminal operations.

2.2. Basic Connotation of Industry Education Integration. Carrying out school-enterprise cooperation is an important part of the professional construction of vocational colleges and an important way for vocational colleges to demonstrate their school-running characteristics and improve teaching quality. The order-based talent training model is based on the three parties of schools, students, and enterprises. A cooperative school-running model established between schools and enterprises is based on cultivating student abilities and enterprise development. The unity of production and education is to realize the unity of production and education through the interaction between schools and enterprises. The detailed relationship between corporate production and education is combined with college education, higher education, corporate production, student quality improvement, scientific research and development, social services, and corporate management. The concept of combination of industry and education is to deepen the separation of education and employment, work, and learning, organically organise universities and businesses, form benign interactions and common development, and achieve the ideal benefits for each. The concept of industrial and educational combination is the combination of higher education and training skills and the need for quality employee training, changes between universities and businesses, and domestic industry. The advancement and innovation of traditional industries and technological progress in the enterprise have played an exciting role [5, 6].

2.3. Characteristics of the Integrated Entrepreneurship Education Curriculum System

2.3.1. Diversity. Diversity refers to the construction of each component of the curriculum system in a variety of forms, including the comprehensive consideration of each link, the diversity of target elements, the diversity of content elements, and the realization of good. The characteristics of interdisciplinary and interdisciplinary, for example, the goal elements must include the cultivation of entrepreneur consciousness, entrepreneur spirit quality, entrepreneur knowledge, entrepreneur ability, and so on. Elicitors must include entrepreneurial elements. Courses, basic knowledge courses of entrepreneurship, comprehensive courses of experts, entrepreneurship practice courses, other types of courses, various courses, and various talent training objectives are the key points [7].

2.3.2. Practicality. The course system remains a fundamental and important part of entrepreneurship education; therefore, the education system remains operational.

Entrepreneurship is an important factor for success in business. Entrepreneurship learning should build on the experience of entrepreneurship, so practice is one of the fundamental characteristics of a comprehensive entrepreneurship training program [8, 9].

2.3.3. School Wide. The basic principle of integrated entrepreneurship education curriculum system is to face the whole school. Teachers and other resources are provided by business schools to form a self-sufficient curriculum pattern. The merged curriculum system of entrepreneurship education breaks the boundary of focusing mode. The target of education will be extended to the whole school, integrating various resources of the government, society, and the school, so that college students of all majors have the opportunity to receive entrepreneurship education [10, 11].

2.3.4. Difference. Comprehensive entrepreneurship education curriculum system should not only focus on the construction of the whole school but also fully respect the independent choice of college students, that is, to reflect different characteristics. However, from an objective scientific point of view, not all college students want to train entrepreneurs and entrepreneurs. In order to become such a person, they are generally cultivating the awareness and spirit of entrepreneurs, on the basis of interest and enthusiasm of college students to realize the dream of entrepreneurs. Second, due to the different knowledge structure of different majors, the construction of curriculum system cannot ignore the difference of experts [12].

2.3.5. Continuity. The comprehensive entrepreneur education curriculum system fully considers the individual differences of college students, so the curriculum system is a continuous education process composed of multiple education stages, from shallow to deep, from popular to difficult, and from basic to professional experience. Moreover, the merged entrepreneur education curriculum system cannot be constructed without the basic principles of education and the basic laws of college students' personal development.

2.3.6. Innovation. Entrepreneurship education has a strong social character and is very sensitive to social, political, and economic development and change. Innovation is the life and soul of entrepreneurs. The merged entrepreneur education curriculum system must also recognize the importance of entrepreneurship innovation. Therefore, the various subsystems that constitute the curriculum system are always implemented and learning fields of professional knowledge such as the use of professional knowledge, the development of creative resources, the integration of resources, and the use of resources [13, 14]. Figure 1 shows the characteristics of the curriculum system of the integration of industry and education.

2.4. Specific Ways to Promote the Formulation of Laws and Regulations on the Integration of Industry and Education

2.4.1. Accelerating the Establishment of Domestic Restrictions. The combination of industry and education mainly uses various cooperation methods of universities, enterprises, and scientific research institutions. Because scientific research and technology cannot meet the requirements of enterprises, the method of "cooperative science education" implemented by education university aims at cultivating applied talents with innovative ability and high technology. On the basis of resource sharing, it cannot be mutually beneficial. Without the national macro policy and legal guarantee, all the beautiful "cooperative science and education" methods will not develop for a long time [15, 16].

2.4.2. Improving Industry and Regional Rules and Regulations. We should encourage the government to participate in the formulation of policies, regulations, and industry management. Through the use of laws, regulations, laws, and regulations, further restrict the rights and obligations of the government, enterprises, and industries and cultivate application-oriented talents in the integration of industries and education. In particular, the industries and enterprises that take part in the combination of industry and education determine the nature and status of applied talents participating in training. Specific provisions provide assurance of policies and regulations [17, 18].

2.4.3. Special Regulations on Promoting Education. The rights and obligations of the parties clearly define the rights and obligations of integration, the management modes, and the talent for industry and education [19, 20]. The training mode and the use of funds, the mechanisms of corresponding remuneration and punishment, and the government's liability and legal liability are very important. We need to establish a unified educational system. The characteristics of modern corporate talent development should be the establishment of a modern corporate education system, radiation exposure to a full employment access system, changing the current state of existing employment access systems, and establishing employment-level standards to improve employment access systems [21].

2.5. Factor Analysis Model of Student Achievement Evaluation. The model here is multiple and difficult to understand, but the problem is not big. I use many algorithms to describe this model in terms of algorithms, to show the accuracy of the analysis model.

2.5.1. Factor Analysis. Analysis techniques include regression analysis, causal analysis, grouping method, root cause analysis, prediction method (time series/scenario construction/simulation, etc.), failure mode and effect analysis (FMEZ), fault tree analysis, reserve analysis, trend analysis, earning value management, and difference analysis. Factor collection technology refers to the use of computer software

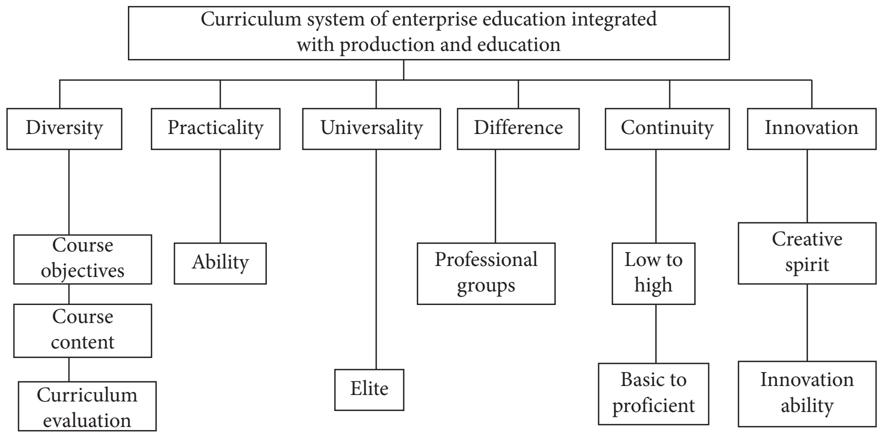

FIGURE 1: Characteristics of the curriculum system of enterprise education integration.

technology to conduct real-time information collection, extraction, mining, and processing for customized target data sources; extract unstructured information from a large number of web pages and save it in a structured database; and provide the entire process of data input for various information service systems.

The calculation steps of factor analysis are as follows:

(1) Raw data have been standardized to eliminate size order variables and size differences [22].
(2) Correlation matrix requirements to obtain standardized data.
(3) Determine the factors; let $f_1, f_2, f_3, \ldots, f_p$ be p factors, in which the total amount of information contained in the first C factors, that is, when the cumulative contribution rate mentioned above exceeds 80%, we can extract the first C factors to reflect the overall situation and reflect the original data.
(4) It is impossible to judge that the cumulative contribution rate of the extracted factor C is less than 80%, and the actual meaning of the formula cannot be determined, so it is necessary to transfer the fax.
(5) A linear combination of raw data variables to get points for each factor. Factor scores can be used for calculation: regression estimation and Thomson estimation [23, 24]:

$$F = \frac{\left(\lambda_1 f_1 + \lambda_2 f_2 + \lambda_3 f_3 + \cdots + \lambda_p f_p\right)}{\lambda_1 + \lambda_2 + \lambda_3 + \cdots + \lambda_p}, \tag{1}$$

where λ_i is the variance contribution rate of factors.
(6) Results ranking: the overall score is used to obtain the ranking list, which can be compared with the original data [25].

2.5.2. Mathematical Model of Factor Analysis. The factor analysis model is as follows: M original variables are $x_1, x_2, x_3, \ldots, x_m$. To find P factors $(P < m)$ as $f_1, f_2, f_3, \ldots, f_p$, the relationship between principal components and original variables is expressed as follows:

$$\begin{aligned} x_1 &= \partial_{11} f_1 + \partial_{12} f_2 + \partial_{13} f_3 + \cdots + \partial_{1p} f_p + \theta_1, \\ x_2 &= \partial_{21} f_1 + \partial_{22} f_2 + \partial_{23} f_3 + \cdots + \partial_{2p} f_p + \theta_2, \\ &\cdots \\ x_m &= \partial_{m1} f_1 + \partial_{m2} f_2 + \partial_{m3} f_3 + \cdots + \partial_{mp} f_p + \theta_m. \end{aligned} \tag{2}$$

The coefficient ∂_{ij} is the relationship between the ith variable and the P variable. A coefficient represents a linear combination of the original variable and a coefficient also known as a common coefficient. θ is a special factor and an influential factor other than the common one. The earlier equation can be described in matrix form as follows:

$$X = KF + \theta. \tag{3}$$

$F = (f_1, f_2, f_3, \ldots, f_p)^T$ is the common factor vector, that is, the main factor, $\theta = (\theta_1, \theta_2, \theta_3, \ldots, \theta_m)^T$ is the special vector factor, and $K = (\partial_{ij})_{m\times p}$ is the factor load matrix.

$$\begin{aligned} E(F) &= 0, \\ \operatorname{var}(F) &= I_p, \\ E(\theta) &= 0, \\ \operatorname{var}(\theta) &= D = \operatorname{diag}\left(\varepsilon_1^2, \varepsilon_2^2, \varepsilon_3^2, \ldots, \varepsilon_m^2\right), \\ \operatorname{cov}(F, \theta) &= 0. \end{aligned} \tag{4}$$

Based on the above assumptions, we clearly know that there is no relationship between common factors, there is a square identity matrix, there is no relationship between special factors, and there is no relationship between special factors and common factors.

Common measurement is

$$Z_i^2 = \sum_{j=1}^{m} \partial_{ij}^2, \quad i = 1, 2, \ldots, p. \tag{5}$$

The degree to which the information of variable x_i can be explained by P common factors is expressed by the variance contribution rate of P common factors to x_i I. Contribution rate of factor variance is

$$H_j^2 = \sum_{i=1}^{p} \partial_{ij}^2, \quad j = 1, 2, \ldots, m. \tag{6}$$

The variance sum of the jth common factor to variable x_i reflects the relative importance. In the factor analysis of students' scores, $X = (X_1, X_2, X_3, \ldots, X_n)^T$ can represent the m-dimensional random variable composed of n students' m-subject scores, while $F = (f_1, f_2, f_3, \ldots, f_p)^T$ cannot represent that p-dimensional random vector is a common factor. The actual significance of F still needs to be treated with specific problems.

2.5.3. Establishment Factor of Score Function. This function can be used to quickly establish the scoring function:

$$\begin{aligned} F_1 &= -0.326X_1 + 0.073X_2 - 0.390X_3 + 0.692X_4 \\ &\quad + 0.407X_5 + 0.344X_6, \\ F_1 &= 0.622X_1 + 0.220X_2 + 0.700X_3 - 0.462X_4 \\ &\quad - 0.130X_5 - 0.89X_6. \end{aligned} \tag{7}$$

From (7), you can calculate each student's fax score for free art and science faxes. The previous series of steps helps to save the new variables "fac1-1" and "fac2-1." Because we want to know more about the students' comprehensive scores after knowing their fax scores, we need to weigh the sum of the scientific factor $F1$ and the liberal factor $F2$, and the following equation is obtained:

$$F = \frac{43.139\% \times F_1 + 38.056\% \times F_2}{81.195\%}. \tag{8}$$

This is the comprehensive evaluation factor of students. According to the expression of the comprehensive evaluation factor, we can rank the students and compare them with the original data.

2.6. Standard Z-Score. The Z-score is also known as the standard score. The standard score formula is as follows:

$$Z = \frac{X - \theta}{\varepsilon}, \tag{9}$$

where x is the original score of a subject, that is, the specific score, θ is the average, ε is the standard deviation, and $X - \theta$ is the deviation from the average.

$$\begin{aligned} \theta &= \frac{1}{N} \sum_{i=1}^{N} X_i, \\ \varepsilon &= \sqrt{\frac{1}{N} \sum_{i=1}^{N} (x_i - \theta)^2} = \sqrt{\frac{1}{N} \sum_{i=1}^{N} X_i^2 - \left(\frac{1}{N} \sum_{i=1}^{N} \theta \right)^2}. \end{aligned} \tag{10}$$

The calculation method of frequency distribution table is

$$\theta = \frac{f_1X_1 + f_2X_2 + f_3X_3 + \cdots + f_mX_m}{f_1 + f_2 + f_3 + \cdots + f_m}, \tag{11}$$

where X_i represents the group median value of group I and f_i represents the frequency of group I.

$$\varepsilon = \sqrt{\frac{1}{N} \sum_{i=1}^{n} f_i X_i - \theta^2}, \tag{12}$$

where Z is the distance between the original score and the volume average of the matrix. It is calculated according to the standard deviation of the element. Because the Z score can reflect the distance between the score and the class average, you can get a better understanding of where you are now.

3. Teaching Reform Model Design of the Integration of Production and Education

3.1. Experimental Data Objects. A total of 296 respondents randomly selected the subjects for science, engineering, economics, business, and other major to advanced subjects. Thirty-three questions were invalid because they were not answered. A total of 263 valid questions were returned, and the actual recovery was 88.85%. The questionnaire is divided into six sides and has 17 questions. In other words, six dimensions are included, such as the intention of entrepreneur education, the development of entrepreneur education, the purpose of the curriculum, the teacher team, curriculum evaluation, and curriculum implementation.

3.2. Research Methods

3.2.1. Literature Analysis. The literature analysis method refers to the method that investigates the nature and status of the research object by studying the collected literature data and derives one's own views from it. It can help investigators to form a general impression about the research object, which is conducive to the dynamic grasp of the history of the research object and can also study research objects that are no longer accessible, such as people who have long died. The main content of the literature analysis method is as follows: (1) analyze and research the relevant archive materials found; (2) analyze and research the collected personal diaries, notes, and biographies; and (3) analyze and research the collected publicly published books and periodicals and other materials.

3.2.2. Questionnaire Survey. This study is based on a comprehensive understanding of the relationships between teachers and students in the area of entrepreneurial innovation, relationships with vocational education, teacher strength, educational programs, and practical platforms. The questionnaires were developed on their own initiative and the experts and part-time teachers used a simple method of random sampling. Student questionnaire survey the combination between innovation entrepreneurship education and professional education.

3.2.3. Semistructured Interview. In the survey, teachers and students can understand the combination of innovation, entrepreneur education, and professional education from the perspective of the questionnaire. Therefore, in this study, based on the five sides of the questionnaire, we create an interview and select the interview person by the simple random sampling.

3.3. Construction of the University Teaching System under the Guidance of Entrepreneurship Education Concept. In order to foster talented people with entrepreneurship, it is necessary to combine the research objectives of the school with current employment and economic development. The demand for existing professionals and markets is not necessarily the case. Based on the completion of the original training purpose of the technical college, focusing on the growth of expert spirit and entrepreneurship, the target training course provides a multilevel comprehensive content system for quality and capacity of the above and builds the intensity target system. Based on practical educational content, we increase entrepreneurship education and add various entrepreneurial knowledge, entrepreneurial content, and various entrepreneurial content, as well as pay attention to increasing lectures and courses on business operation and management, such as learning and practice in procurement, production, sales, and management systems.

4. Problems and Measures of Entrepreneurship Education Reform in the Integration of Industry and Education

4.1. Main Problems Related to the Integration of Motherhood

4.1.1. Construction of the University Management System Lags Behind. In recent years, the practice of "reform and development" of local universities in China has proved that the existing school-level system has basically retreated. The "reform measures" explored by secondary universities and scientific research institutions and the "existing system" at school level have reached all directions. "Fight" or "run into a brick wall" until many reform measures are difficult to achieve. Table 1 shows the statistics on the types of industry education integration system.

As can be seen from Table 1, more than four-fifths of teachers believe that the school has formulated a comprehensive system of production and education, while about one-fifth of teachers believe that there is no unified system of production and education. Not all teachers are familiar with this system. In addition, only 25 selected education, scientific research, finance, student management, personnel, and other five projects at the same time, accounting for 4.4% of the 574 valid questionnaires. There are very few newly established universities with unified production and education system. Mainly focus on logistics support and political party issues and other systems, fill in "other" interviewees. Table 2 shows the adaptation of school teaching management system and industrial research.

As shown in Table 2, the new undergraduate schools in China are establishing an integrated special education system; however, there is no support system in the fields of scientific research, finance, personnel, etc., of the integration of industrial research and cooperation between enterprises. Management system as to whether the system meets the requirements of productive integration and cooperative development, the 80.5% of secondary school teachers believe that the current teaching management system for the integration of production and education is "unsuitable" or "unsuitable" for codevelopment needs.

4.1.2. Legislation on the Integration of Production and Education Is Slow. In the process of merging industry and education, laws and regulations are insufficient. Due to the delay in the formulation of the legal provisions on the merger of industry and education, the legal responsibilities and rights of participants are irregular and cannot be obeyed. As shown in Table 3, main issues are related to the integration of industrial research in the different types of higher education institutions.

As shown in Figure 2, production education is integrated into higher education institutions.

The data shown in Table 3 and Figure 2 show that universities face many problems in integrating industry and education, such as lack of policy and regulatory support, lack of equipment investment, immature external environment, faced by universities in integrating industry and education. But the most significant problems are as follows: lack of support of the law; in general undergraduate colleges, 58.32% of them lack the support of laws and regulations, which is the most urgent problem among all the problems. At present, we have developed and implemented many policies for integrating research and development in the field of production, but they are neither perfect nor perfect. Industry, cooperation, and planning between universities and businesses are based mainly on verbal agreements rather than informal contracts. If either party violates the contract when tearing up the contract, it cannot rely on relevant policies, laws, and regulations to judge the correctness of the problem, and the oral agreement between the two parties is invalid.

4.1.3. Insufficient Investment. In my country, investments in research and development are increasing, but the rapid growth of GDP is far from sufficient. At the same time, it also developed the unified development of university industry and education in China. This is a very obvious gap and important obstacle as the ratio of R&D in GDP is very low. The ratio of R&D to GDP is very low. There is a serious shortage of funds for the integrated development of industrial education. Universities and enterprises cannot be guaranteed with funds, and the integrated development of industrial education is difficult. Table 4 shows China's R&D expenditure and the ratio of R&D to GDP in 2010–2019.

Table 1: Statistics on types of the industry education integration system.

System type	Teaching	Scientific research	Finance	Student management	Personnel matters	Other
Number	481	109	50	113	80	19
Percentage	83.7	19.0	8.6	19.6	13.9	3.2

Table 2: The adaptability of the teaching system to the integration of production and education.

	Very adaptable	Adaptable	More adaptable	Not very adaptable	Maladjusted
Number	22	36	57	378	86
Percentage	3.7	6.2	9.9	65.8	14.9

Table 3: Main issues related to the integration of industrial research in universities.

Main problems	All universities (%)	Research universities (%)	Teaching universities (%)	Vocational schools (%)
Regulatory support	60.58	47.07	58.33	76.33
Capital investment	60.11	50.99	41.69	61.19
External environment	52.08	45.11	50.09	63.17
Organizational guarantee	48.52	50.99	46.23	53.96
Coordinating body	20.35	11.77	21.02	21.72
Service sector	20.35	29.42	19.67	18.43
Other	2.65	0.00	2.87	3.30

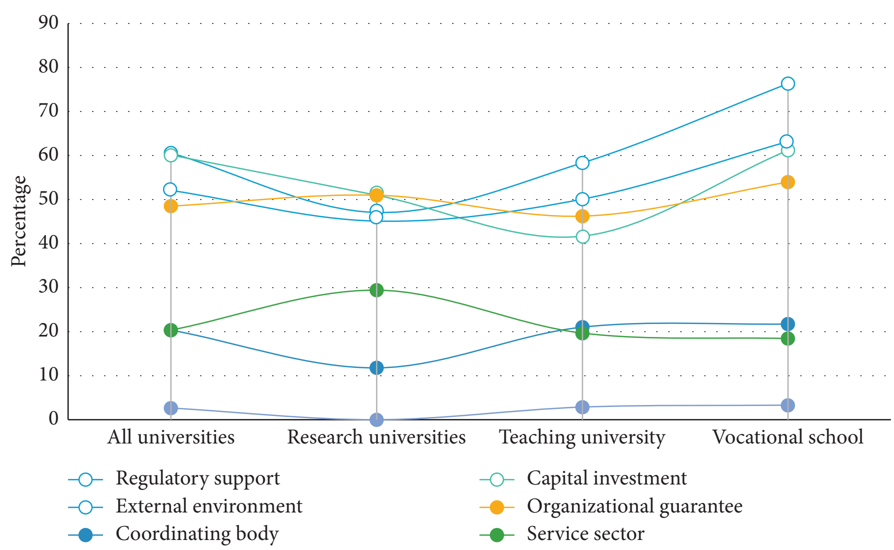

Figure 2: Integration of research and production in universities.

Table 4: Ratio of R&D expenditure and R&D to GDP in 2010–2019.

Particular year	Internal R&D expenditure/100 million yuan	Ratio of R&D to GDP (%)
2010	2449.98	1.35
2011	3003.11	1.43
2012	3710.25	1.45
2013	4616.03	1.55
2014	5802.12	1.71
2015	7062.59	1.77
2016	8687.02	1.85
2017	10241	1.99
2018	11848	2.09
2019	13401	2.11

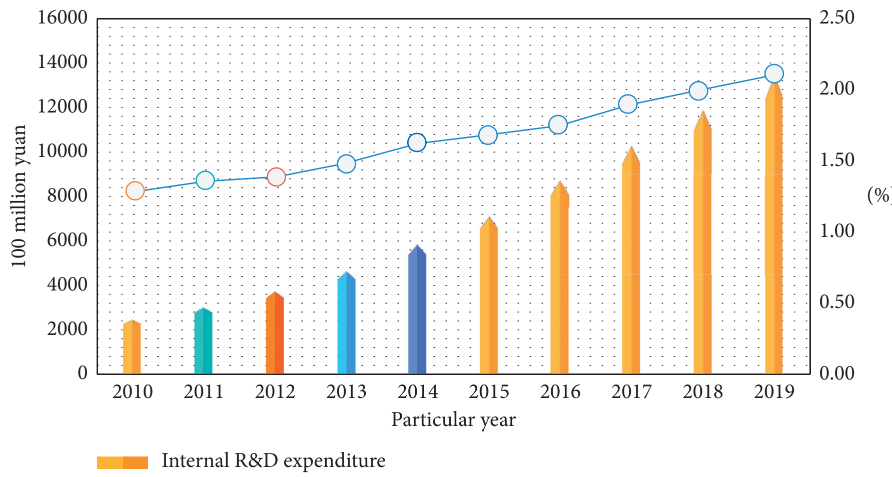

Figure 3: R&D expenditure and R&D% of GDP.

Figure 3 shows China's R&D expenditure and the percentage of R&D in GDP in recent years.

As shown in Table 4 and Figure 3, the state lacks financial support for the integration of industry and education. Therefore, it is difficult to balance the interests of enterprises and universities. Because of the liberation of research funds and development costs, expectations are quite different, and the desire of universities and research institutions to apply becomes lower. There is no guarantee that participants will be involved.

4.2. Practice Orientation and Teaching Reform. Education for entrepreneurship is relatively vague. Totally, 43% of students view entrepreneurial innovation as an "end of study activity" in higher education institutions. Thirty-one percent of students surveyed view innovation as a "student." Type of work; a few respondents (19%) felt that teaching entrepreneurship was complementary to vocational education. Seven percent of respondents considered education for innovative entrepreneurship to be an ideological and political activity. Statistics of student practice in teaching innovative entrepreneurship are shown in Figure 4.

Analysis of the questionnaires sent to teachers shows that 22% of teachers consider education for entrepreneurship to be an important element in the overall development of students, 42% consider education for innovative entrepreneurship as a "service." Thirteen% of teachers consider that entrepreneurial innovation is an "end of studies service." "I believe that the education of God is an organic complement to professional education." Twenty-three of one hundred teachers surveyed indicated that they were very happy to have trouble finding it. Statistics on the practice of teachers in teaching innovative entrepreneurship are shown in Figure 5.

Figures 4 and 5 reveal an ambiguity in the implementation of innovative entrepreneurship education from a

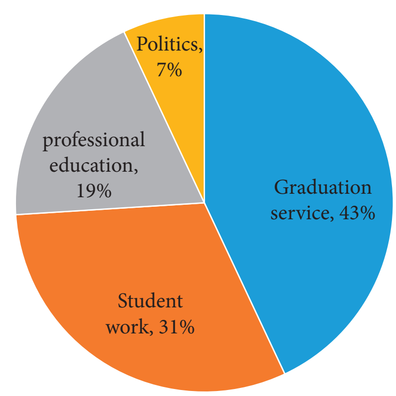

Figure 4: Statistics of students' practice on entrepreneurship education.

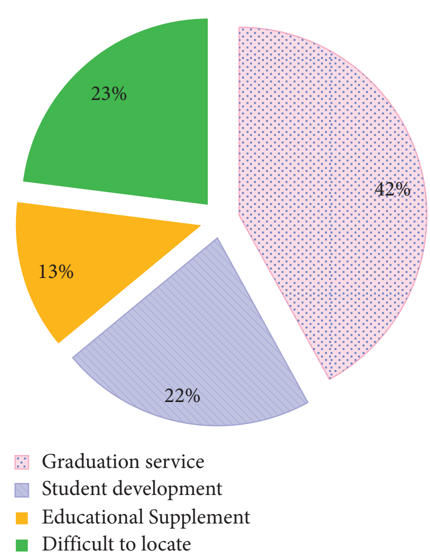

Figure 5: Statistics of teachers' practice on innovation and entrepreneurship education.

Table 5: Forms of innovation and entrepreneurship education expected by teachers and students.

	Teacher		Student	
	n	%	*n*	%
Required course	38	37	221	41.8
Elective course	50	49	251	47.4
Stratified teaching	58	57	262	49.5
Entrepreneurial mentor	57	56	189	35.7
Social practice	71	70	292	55.2
Competition	43	42	192	36.3
Other	3	2	54	10.1

Table 6: Opinion of teachers and students on entrepreneurship education program.

	Teacher		Student	
	n	%	*n*	%
Business orientation	76	75	396	74.9
Management	50	49	285	53.9
Practical learning	72	71	371	70.2
Professional theory	48	47	282	53.3
Operational capability	66	65	335	63.4
Social experience	56	55	328	62.0
Other	10	10	64	12.0

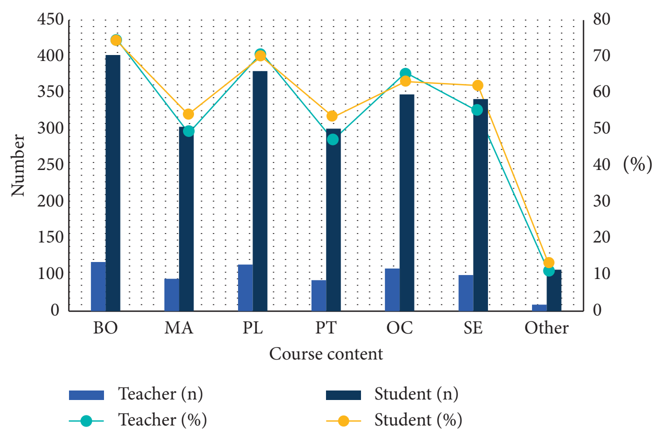

Figure 6: Curriculum content of innovation and entrepreneurship education.

higher education perspective. It is clear that innovative entrepreneurship education is not effective. However, the relationships between educational specialists, innovators, and educators have been neglected.

4.3. Innovation and Entrepreneurship Education and Industry Education Integration

(1) According to the survey results, most teachers and students believe that innovative entrepreneurship education programs should take the form of social practices. Most educational activities focus on teaching knowledge due to the traditional conception of education, local universities provide practical resources to students, and development of practical and practical skills of students requires appropriate practical skills and abilities. As shown in Table 5, teachers and students expect innovative education programs on entrepreneurship.

(2) Most teachers and students want to learn about entrepreneurship choice as part of entrepreneurship education programs, and when it comes to employment challenges, students want to better understand the spirit of entrepreneurship. Learning to innovate in entrepreneurship and laying the groundwork for future teacher and student views of entrepreneurship education programs, as shown in Table 6.

Figure 6 shows the content of entrepreneurship education courses for teachers and students.

As shown in Figure 6, although efforts are being made to integrate the current curriculum, it is not very focused; most of the courses are based on basic concepts and skills in entrepreneurship.

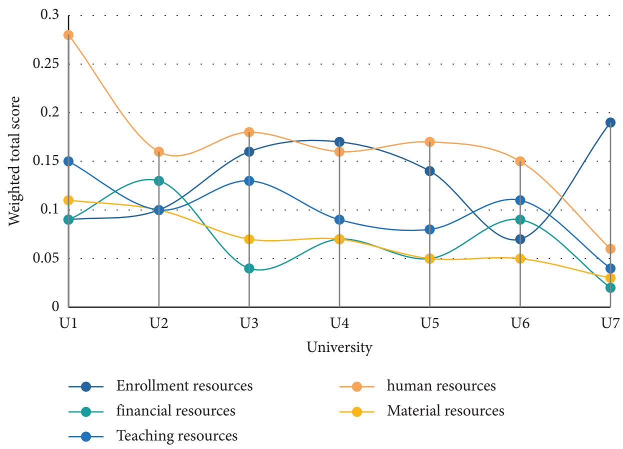

Figure 7: The result of quantitative evaluation of resource allocation of industry education integration in colleges and universities.

4.4. Quantitative Evaluation Results. By calculating the weight of the index, the size of the indicator system and the weight of each index are obtained. The standard value after the original data of the index is converted is weighted. After calculating the index scores of the two stages, the general situation is obtained for the quantitative evaluation score and ranking of educational resource allocation. The quantitative evaluation results of the allocation of integrated education resources of university production and education are shown in Figure 7.

As can be seen from Figure 7, universities in our province have the overall strongest advantage in the allocation of educational resources for education majors, ranking first in human resources, financial resources, material resources, and educational resources. The results of the quantitative evaluation of the allocation of professional education resources are in line with the assumption that the results of the quantitative evaluation of the allocation of educational resources of two or three new universities are relatively low.

5. Conclusion

The integration of research and development in the field of production is essential to meet the needs of social development and to adapt educational resources and social objectives. I know how to make a comprehensive evaluation of the above four industrial structures, the guarantee and guarantee of enterprise development, and the basic system of enterprise development and also understand how to establish a series of standardized standards and standardized cooperative relations to support the unified management system of university production and education. 5G fog computing is now a hot new technology. With the vigorous development of the Internet of Things, Big Data, 5G, and other technologies, various devices have begun to be interconnected. A large number of devices are not only numerous but also widely distributed. Only fog computing is required in order to meet its requirements. The combination of fog computing and entrepreneurial education in colleges and universities can allow students to understand the current hot technologies and development directions, which is very educational.

Through interviews and questionnaires with more than 800 graduates and graduate graduates, this study shows that teaching entrepreneurship in higher education institutions is poorly developed and students are poorly motivated. The theoretical path system of innovation entrepreneurship in college and education pattern is not flexible. School policies are not sufficiently supported, and there is no favorable climate for innovative entrepreneurship.

Our entrepreneurship education can neither blindly promote the "doctrine of usage" nor blindly imitate it. However, we should deepen the integration of the latest technologies such as 5G fog computing with entrepreneurship education and explore the entrepreneurship education with Chinese characteristics from those experiences in the integration of industry and education.

Data Availability

The data that support the findings of this study are available from the corresponding author upon reasonable request.

Conflicts of Interest

The authors declare no conflicts of interest with respect to the research, authorship, and/or publication of this article.

Acknowledgments

This work was supported by Social Sciences Research Project of Hubei Provincial Education Department in 2020 (project title: High-quality Development of Sports Industry in National Central Cities, Contract No. 20D052), supported by Social Science Foundation of Wuhan Institute of Technology and Teaching Research of Wuhan Institute of Technology in 2020 (project title: The Practice of Innovation and Entrepreneurship Talent Cultivation Innovative Model for Sports Graduate Students Based on the Integration of Education, Industry and Research), and 2019-2020 Education Research of Wuhan Institute of Technology (project title: Research on the Cultivation Effect of Interdisciplinary Talents in Sports Economics and Management, Contract No. 2020YB13).

References

[1] Y. Zhang, "Preliminary study on teaching reform of facility agriculture specialty under the model of "industry-education integration and school-enterprise cooperation," *International Journal of Social ence and Education Research*, vol. 2, no. 12, pp. 64–69, 2020.

[2] Y. Zizhou, "The main function of the integration of the production and education in the perspective of triple spiral," *Special Zone Economy*, vol. 12, no. 1, pp. 31–37, 2016.

[3] A. Bullough, M. S. De Luque, D. Abdelzaher, and W. Heim, "Developing women leaders through entrepreneurship education and training," *Academy of Management Perspectives*, vol. 29, no. 2, pp. 250–270, 2016.

[4] R. Mandel and E. Noyes, “Survey of experiential entrepreneurship education offerings among top undergraduate entrepreneurship programs,” *Education + Training*, vol. 58, no. 2, pp. 164–178, 2016.

[5] J. Radloff, “Elementary teachers’ positive and practical risk-taking when teaching science through engineering design,” *Journal of Pre-College Engineering Education Research (J-PEER)*, vol. 9, no. 2, p. 4, 2019.

[6] Y. Zhou, K. Su, and L. Shao, “Reform and exploration of virtual experiment teaching in the course of modern control system,” *Agro Food Industry Hi-Tech*, vol. 28, no. 1, pp. 1904–1908, 2017.

[7] W. Yi and X. Wei, “Suggestions and countermeasures of integration of production and education in higher vocational colleges,” *International Journal of Software Engineering and its Applications*, vol. 11, no. 5, pp. 109–114, 2017.

[8] L. Pittaway and J. Cope, “Entrepreneurship education,” *International Small Business Journal: Researching Entrepreneurship*, vol. 25, no. 5, pp. 479–510, 2016.

[9] A. D. Daniel, “Fostering an entrepreneurial mindset by using a design thinking approach in entrepreneurship education,” *Industry and Higher Education*, vol. 30, no. 3, pp. 215–223, 2016.

[10] S. G. Walter and J. H. Block, “Outcomes of entrepreneurship education: an institutional perspective,” *Journal of Business Venturing*, vol. 31, no. 2, pp. 216–233, 2016.

[11] M. Entrialgo and V. Iglesias, “The moderating role of entrepreneurship education on the antecedents of entrepreneurial intention,” *The International Entrepreneurship and Management Journal*, vol. 12, no. 4, pp. 1209–1232, 2016.

[12] V. B. Sánchez and C. A. Sahuquillo, “Entrepreneurial intention among engineering students: the role of entrepreneurship education,” *European Research on Management & Business Economics*, vol. 24, no. 3, pp. 53–61, 2018.

[13] A. Fayolle, C. Verzat, and R. Wapshott, “In quest of legitimacy: the theoretical and methodological foundations of entrepreneurship education research,” *International Small Business Journal: Researching Entrepreneurship*, vol. 34, no. 7, pp. 895–904, 2016.

[14] G. Nabi, A. Walmsley, F. Liñán, I. Akhtar, and C. Neame, “Does entrepreneurship education in the first year of higher education develop entrepreneurial intentions? the role of learning and inspiration,” *Studies in Higher Education*, vol. 43, no. 3, pp. 452–467, 2018.

[15] C. Thrane, P. Blenker, S. Korsgaard, and H. Neergaard, “The promise of entrepreneurship education: reconceptualizing the individual-opportunity nexus as a conceptual framework for entrepreneurship education,” *International Small Business Journal: Researching Entrepreneurship*, vol. 34, no. 7, pp. 905–924, 2016.

[16] C. W. Utami, “Attitude, subjective norms, perceived behavior, entrepreneurship education and self-efficacy toward entrepreneurial intention university student in Indonesia,” *European Research Studies*, vol. 20, no. 2, pp. 475–495, 2017.

[17] D. H. B. Welsh, W. L. Tullar, and H. Nemati, “Entrepreneurship education: process, method, or both?” *Journal of Innovation & Knowledge*, vol. 1, no. 3, pp. 125–132, 2016.

[18] S. A. Macht, S. Ball, and M. Mccracken, ““Authentic Alignment”–a new framework of entrepreneurship education,” *Education + Training*, vol. 58, no. 9, pp. 926–944, 2016.

[19] K. Fellnhofer and S. Kraus, “Examining attitudes towards entrepreneurship education: a comparative analysis among experts,” *International Journal of Entrepreneurial Venturing*, vol. 7, no. 4, pp. 396–411, 2017.

[20] W. W. Kirkley, “Cultivating entrepreneurial behaviour: entrepreneurship education in secondary schools,” *Asia Pacific Journal of Innovation and Entrepreneurship*, vol. 11, no. 1, pp. 17–37, 2017.

[21] T. Mets, I. Kozlinska, and M. Raudsaar, “Patterns in entrepreneurial competences as the perceived learning outcomes of entrepreneurship education,” *Industry and Higher Education*, vol. 31, no. 1, pp. 23–33, 2017.

[22] S. Farny, S. H. Frederiksen, M. Hannibal, and S. Jones, “A Culture of entrepreneurship education,” *Entrepreneurship & Regional Development*, vol. 28, no. 7-8, pp. 514–535, 2016.

[23] J. R. Cornwall and W. J. Dennis, “Peeling the onion: public policy in entrepreneurship education,” *Journal of Entrepreneurship & Public Policy*, vol. 1, no. 1, pp. 12–21, 2016.

[24] K. Bischoff, C. K. Volkmann, and D. B. Audretsch, “Stakeholder collaboration in entrepreneurship education: an analysis of the entrepreneurial ecosystems of European higher educational institutions,” *The Journal of Technology Transfer*, vol. 43, no. 1, pp. 20–46, 2018.

[25] J. Fox, L. Pittaway, and I. Uzuegbunam, “Simulations in entrepreneurship education: serious games and learning through play,” *Entrepreneurship Education and Pedagogy*, vol. 1, no. 1, pp. 61–89, 2018.

Hindawi
Scientific Programming
Volume 2021, Article ID 1538914, 11 pages
https://doi.org/10.1155/2021/1538914

Research Article

A Joint Optimization Framework of the Embedding Model and Classifier for Meta-Learning

Zhongyu Liu,[1] Xu Chu,[1] Yan Lu,[1,2] Wanli Yu,[3] Shuguang Miao,[4] and Enjie Ding[1]

[1]*National and Local Joint Engineering Laboratory of Internet Application Technology on Mine, China University of Mining and Technology, Xuzhou 221000, Jiangsu, China*
[2]*College of Information Engineering, Hainan Vocational University of Science and Technology, Haikou 570100, Hainan, China*
[3]*Institute of Electrodynamics and Microelectronics, University of Bremen, Bremen 28359, Germany*
[4]*School of Physics and Electronic Information, Huaibei Normal University, Huaibei 235000, Anhui, China*

Correspondence should be addressed to Enjie Ding; enjied@cumt.edu.cn

Received 29 July 2021; Accepted 8 September 2021; Published 1 October 2021

Academic Editor: Punit Gupta

The aim of meta-learning is to train the machine to learn quickly and accurately. Improving the performance of the meta-learning model is important in solving the problem of small samples and in achieving general artificial intelligence. A meta-learning method based on feature embedding that exhibits good performance on the few-shot problem was previously proposed. In this method, the pretrained deep convolution neural network was used as the embedding model of sample features, and the output of one layer was used as the feature representation of samples. The main limitation of the method is the inability to fuse low-level texture features and high-level semantic features of the embedding model and joint optimization of the embedding model and classifier. Therefore, a multilayer adaptive joint training and optimization method of the embedding model was proposed in the current study. The main characteristics of the current method include using multilayer adaptive hierarchical loss to train the embedding model and using the quantum genetic algorithm to jointly optimize the embedding model and classifier. Validation was performed based on multiple public datasets for meta-learning model testing. The proposed method shows higher accuracy compared with multiple baseline methods.

1. Introduction

The computing capacity of computers has recently developed and the amount of data has significantly increased. Deep learning has shown significant application in several tasks such as computer vision and natural language processing [1]. However, data collection and annotation of sample requires a lot of manual work, mainly data obtained from the industrial field, which is challenging to analyze [2]. Currently, the overfitting phenomenon appears easily with deep learning models based on supervised learning trained with small sample sizes [3]. Therefore, machine learning model design based on small samples has high application value. Small samples learning is also known as few-shot learning in the machine learning field. Notably, a machine learning model can achieve strong artificial intelligence [2].

Meta-learning is mainly used to model for few-shot learning problems. Meta-learning can learn new tasks quickly with the purpose of training the model to learn to learn. The traditional meta-learning methods can be divided into four categories including: methods based on data augmentation, methods based on metric learning, methods based on strong generalization of initialization, and methods based on parameter optimization. Their characteristics are explored in detail in the following section.

The method based on data augmentation is mainly used to expand the data volume and increase the number of samples. This process prevents the model from premature fitting in the training process and improves the generalization performance [4]. However, the number of samples for the deep neural network is often too large, and this method cannot meet the need of model training alone [5].

Therefore, the method is conjoined with other methods [6]. The metric-based method identifies small samples by calculating the feature vectors between samples and determining the feature distance between different samples [7]. This method mainly focuses on the designed similarity measurement [8]. Notably, the performance of the model is low if the samples have a close feature distance, mainly in the classification of fine-grained samples. The method based on external memory introduces the external memory module and achieves fast encoding of new information through the long-term and short-term memory functions. The main limitation of this model is that the efficiency of information filtering and classification storage is low and the number of external memory network parameters is too large, thus leading to an increase in training difficulty. The method based on initialization is mainly used to optimize the loss function which refers to the learning effect obtained by the expected gradient updating of a few steps. The training process comprises two parts: the inner cycle and the outer cycle [9]. Therefore, the model can quickly fit the distribution of multitask data and not the distribution of single task features. The gradient descent of the inner cycle in this method mainly depends on the setting of the learning rate and requires significant manual intervention.

In addition to the meta-learning methods described above, a new method was proposed and verified by [10]. This method comprises two stages. Firstly, a good feature embedding space is sought to map small samples to feature space. Second, a classifier is trained using these embedding features to quickly determine the feature distribution of samples and then achieve the inference of small samples.

The new method makes use of supervised learning to train a deep neural network to represent the features of the samples. In addition, it explores the performance of small samples embedded in different layers of the network on the classifier in the second stage of training. The characteristics of different layers of the deep convolutional neural network comprise different information. The bottom layer comprises high amounts of low-level visual information, whereas the top layer comprises semantic information [11, 12]. Low-level visual information and semantic information are important in visual recognition tasks. Therefore, the fusion of the features output by different layers of the CNNs (convolutional neural networks) is recommended for the effective embedding of the samples into the feature space. An adaptive hierarchical weighted loss training method of deep CNNs can optimize the feature representation of samples as presented in the current study.

The main contributions of the current study are presented as follows:

A joint optimization strategy of embedding model and meta-learner classifier is proposed. The embedding model is trained by adaptive multilevel loss, and the embedding model is optimized by combining results of the meta-learning classifier.

A quantum genetic algorithm is adopted to optimize the algorithm. The algorithm optimizes the weight of the hierarchical loss function of the embedding model and optimizes the joint feature expression for the classifier.

Experimental results based on multiple meta-learning datasets indicate that the proposed method is effective and reliable.

The study explores related studies and summarizes related methods of meta-learning. In addition, the proposed method is illustrated in detail. The method is then verified through experiments and the findings are presented.

2. Related Studies

2.1. Meta-Learning Based on Measurement. The goal of measurement of learning [13] is to obtain a paired similarity measurement function, in which similar sample pairs have a high similarity score, while dissimilar sample pairs have a low similarity score. Meta-learning methods adopt measurement learning strategies. Koch et al. [7] proposed a twin network that calculates the similarity between the query sample and all single-annotated samples. Hoffer and Ailon [14] designed a ternary network, which adopted positive and negative sample rules and predicted the category of the sample by calculating the distance between the query sample and the positive and negative samples. Vinyals et al. [15] designed a matching network based on memory and attention mechanisms, which can quickly learn the distribution of features of training samples. Snell et al. [16] used a prototype network to predict the category of the sample by learning the prototype points and then calculating the distance between the new sample and the prototype points. In addition, Sung et al. [17] proposed a relational network in 2018, in which the similarity between samples was calculated by embedding modules and relationship modules to complete the prediction of categories of new tasks.

2.2. Meta-Learning Based on Optimization. A previous study reported a meta-learning model based on optimization LSTM (Long Short-Term Memory) with hidden units in the method set as learners' parameters [18]. Meta-learners can adjust their learning rate based on the responses of different spatiotemporal models so as to train the spatiotemporal models faster. Deep learning usually adopts back-propagation and gradient descending methods to optimize massive parameters in the network. The feature expression performance of deep neural networks depends on a large amount of data. A meta-learning method based on the strong generalization of initialization parameters was previously reported [9]. The goal of the optimization of the network parameters of MAML (model-agnostic meta-learning) is to separate the gradient descent and back-propagation from the used data, thus obtaining better generalization performance. Several methods have been used to improve MAML, such as combining the hidden space method [19] and Bayesian prior [20] and optimizing the gradient descent process [21]. Moreover, MAML can be used for a series of models based on gradient descent, including classification, regression, and reinforcement learning owing to its openness and flexibility [22].

2.3. Meta-Learning Based on Data Expansion. A simple and general data enhancement framework called MetaGan was proposed previously [4]. This method mainly defined a tighter decision boundary for the model by distinguishing real data from virtual data with the aim of improving the feature extraction ability of the model. A previous study proposed a feature "analogy" method that divides the model into two parts: representation learning and small sample learning [23]. In the presentation learning stage, the learner extracts accurate feature representations on the base classes containing a large amount of data, whereas, in the small sample learning stage, the learner learns the classifier on the joint space of the new type containing a small amount of data and the previous base types. A data generation structure has been previously reported that mainly uses CycleGan as the generator of the new category of data and adds noise to the new data to make its distribution more diversified [24].

3. Methods

The current study reviews the meta-learning method based on feature embedding and then illustrates the algorithm framework proposed in the current work. The algorithm framework mainly comprises an adaptive hierarchical loss function optimization stage, an adaptive feature fusion stage, and the original classifier training evaluation and testing stage. The method is described in detail in the following section.

The datasets of meta-learning tasks can be divided into meta-training sets, meta-evaluation sets, and meta-testing sets. The traditional meta-learning method constructs the learning task based on the training set, which can be represented by a binary set $\{D^{\text{train},s}, D^{\text{train},q}\}$. The binary set then forms the support set and the query set. The support set and the query set normally have a few small samples, and this form is called N-way-K-shot. A basic learner is defined as follows: $\mathscr{A}$: $y_* = f_\theta(x_*)$, in which $*$ represents S and Q. $\mathscr{A}$ learns based on the training set $\{D^{\text{train},s}, D^{\text{train},q}\}$ to gain strong learning ability. A relative support set and query set should be constructed on the evaluation set or test set $\{D^{\text{val},s}, D^{\text{val},q}\}\{D^{\text{test},s}, D^{\text{test},q}\}$ to test the learning performance on the new task of $\mathscr{A}$. A new meta-learning method is proposed by a previous study [10], which defines an embedding mapping to map the features of samples into the embedding space. The training tasks of basic learners are then transformed into

$$\begin{aligned}\theta &= A\left(D_j^{\text{train}}, \phi\right)\\ &= \arg\min_\theta L^{\text{base}}\left(D_j^{\text{train}}; \theta, \phi\right) + R(\theta),\end{aligned} \tag{1}$$

where L represents the loss function and R represents the regular term. A good embedding model in the algorithm is aimed at high accuracy. The performance of the embedding model and meta-learners can be determined by finding the error between the two using the test datasets.

3.1. Algorithm Framework. The output features of different layers of CNNs have unique characteristics. The output in the top layer of CNNs comprises abundant semantic information, whereas the convolutional layer near the input comprises abundant low-level visual information. An embedding model and basic learner joint optimization algorithm are used to effectively fuse and utilize the information of the different layers. The algorithm framework is presented in Figure 1. The framework mainly comprises two parts: the optimization module of the adaptive hierarchical embedding model and the adaptive hierarchical feature fusion module. The optimization goal of the embedding model is the same as that of the feature fusion model, and both aim at the accuracy of meta test. Therefore, the optimization of the two models uses the same fitness function, which makes the modules of different stages evolve in the same direction. In addition, the optimization process of each embedding model is a supervised training process of a convolutional neural network. The training of the neural network usually takes a lot of time, so parallel programming is used to set the optimization process of each embedding model as a process. According to the graphics card equipped with the computer and its performance, n processes can be run at the same time, that is, n neural network models can be trained at the same time, which will greatly improve the efficiency of the algorithm. Compared with serial programming, it will effectively save a lot of time. The framework below describes the algorithm flow of the two modules in detail.

3.2. Quantum Genetic Algorithm. Encoding of chromosomes in the quantum genetic algorithm (QGA) uses the probability range of qubits in quantum physics, such that each chromosome represents multiple states. Quantum gates and revolving gates in quantum physics are used to update chromosomes to achieve the purpose of optimizing the population. An advantage of quantum genetic algorithm is its quantum parallelism, which improves the search ability of population size and increases the probability of obtaining the optimal solution compared with the traditional genetic algorithm [25].

Qubits are the basic storage units in quantum computing and are different from the bits referred to in existing computers; however, they are a two-state system. The two states in this case refer to two independent states in quantum computing: the 0 state and the 1 state. Borrowing the Dirac symbol "|>", $|0\rangle$ and $|1\rangle$ are used to represent the spin-down state (0 state) and the spin-up state (1 state), respectively. A quantum state is the superposition of these two states, which can be expressed as a linear combination of the two states as follows:

$$|\psi\rangle = \alpha|0\rangle + \beta|1\rangle, \tag{2}$$

where α and β represent the probability amplitudes of $|0\rangle$ and $|1\rangle$, respectively, and they must meet the conditions:

$$|\alpha|^2 + |\beta|^2 = 1, \tag{3}$$

where $|\alpha_i|^2$ indicates the probability of $|0\rangle$ state and $|\beta_i|^2$ indicates the probability of $|1\rangle$ state. This implies that when

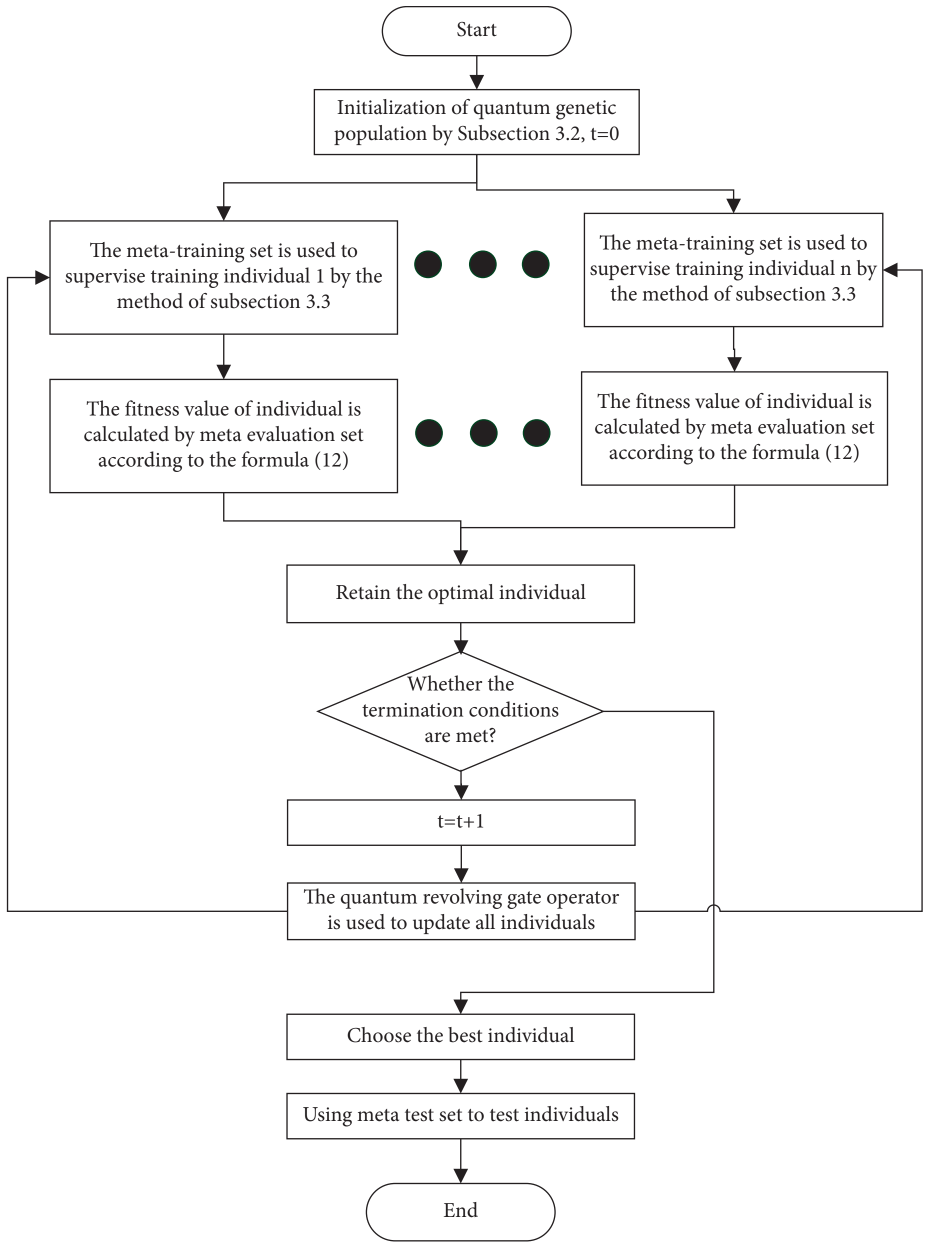

Figure 1: Joint optimization framework of the embedding model and classifier based on quantum genetic algorithm.

the probability of state 0 is 1, the probability of state 1 must be zero. Conversely, when the probability of state 1 is 1, the probability of state 0 is 0. The amplitude probability $[\alpha, \beta]^T$ represents the chromosome of the qubit. The set of all chromosomes is expressed as $P = \{p_1, p_2, \ldots, p_n\}$, where n represents the size of the total chromosomes. A quantum chromosome consisting of qubits can be described as follows:

$$p_i = \begin{bmatrix} \alpha_1 & \alpha_2 & \alpha_3 & \cdots & \alpha_m \\ \beta_1 & \beta_2 & \beta_3 & \cdots & \beta_m \end{bmatrix}, \tag{4}$$

where m represents the gene number of individual chromosomes.

To produce excellent individuals with a high probability in the iterative process of the population, the quantum genetic algorithm introduces a quantum revolving gate to realize the change of the population and abandons the selection, crossover, and mutation operations used in the genetic algorithm. The quantum revolving gate can increase the diversity of the population gene pool by adjusting the quantum state probability, such that the solution appears on the individuals with the highest adaptability. Therefore, the quantum revolving gate is very important in the quantum genetic algorithm. The expression of the quantum revolving gate is as follows:

$$R(\theta) = \begin{bmatrix} \cos\theta_i & -\sin\theta_i \\ \sin\theta_i & \cos\theta_i \end{bmatrix}. \tag{5}$$

The iterative process of the quantum revolving gate is expressed as follows:

$$\begin{bmatrix} \alpha_i' \\ \beta_i' \end{bmatrix} = R(\theta) \begin{bmatrix} \alpha_i \\ \beta_i \end{bmatrix}. \tag{6}$$

Here, $[\alpha_i, \beta_i]^T$ represents the $i-th$ qubit of the current chromosome, $[\alpha_i', \beta_i']$ indicates the state of the qubit after rotation, θ_i represents the rotation angle, and the direction and value of θ_i is set by adjustment strategy. The adjustment strategy is presented in Table 1.

$\theta_i = s(\alpha_i, \beta_i)\Delta\theta_i$ represents the angle of rotation, whereas $s(\alpha_i, \beta_i)$ represents the direction of rotation and $\Delta\theta_i$ represents the increment of rotation angle, to obtain convergence direction and convergence speed of the algorithm. In addition, in the adjustment strategy of the revolving gate, x_i represents the $i-th$ gene of the current chromosome and $f(x_i)$ indicates the fitness of the individual. b_i represents the $i-th$ gene in the current best chromosome, and $f(b_i)$ represents the fitness of the best individual. This method uses the fitness $f(b_i)$ of the best individual in the current population as a target value and compares the fitness $f(x_i)$ of the individuals in the population with it. If $f(x_i) > f(b_i)$, then the corresponding qubits in the individual are adjusted such that the probability amplitude (α_i, β_i) approaches x_i. Otherwise, if $f(x_i) < f(b_i)$, the corresponding quantum of the individual in the population bit is adjusted, such that the probability amplitude (α_i, β_i) approaches b_i.

3.3. Adaptive Hierarchical Loss Training Stage of the Embedding Model. The main purpose of the embedding model is to obtain the feature vector of the sample by mapping the original sample to the feature space. The meta-learner then learns the feature distribution of the sample based on the feature vector. Therefore, the performance of the embedding model is very important. The adaptive multilevel loss training method is adopted to train the embedding model to improve the feature representation performance of different layers of CNNs. The trained model is fused by a multiscale adaptive feature fusion algorithm. The framework of the adaptive multilayer loss training algorithm is shown in Figure 2.

The formal expression of the adaptive multilayer loss training algorithm is as follows: let F be any lightweight network, which normally has L stages. The output feature map from any intermediate stage is represented by $F^l \in \mathbb{R}^{H_l \times W_l \times C_l}$, where H_l, W_l, C_l represent the height, width, and number of channels of the feature map at $l-th$ stage, and $l = \{1, 2, \ldots, L\}$. The aim is to impose classification losses on the feature map extracted at different intermediate stages. The feature map of each stage performs the average pooling operation to obtain the feature vector f^l of the stage:

$$f^l = \mathrm{Pool}_{\mathrm{avg}}\left(F^l\right). \tag{7}$$

The Dot product similarity of the class prototype vector at this stage is then calculated to obtain the logits of the class, and finally, the loss function at this stage is obtained as shown in Figure 2:

$$\begin{aligned} \mathrm{loss}^l &= \ell^l{}_{\mathrm{Softmax}}\left(f^l\right) \\ &= -\log \frac{e^{f^l, y}}{\sum_{k=1}^{C} e^{f^l, k}}. \end{aligned} \tag{8}$$

Loss functions of all stages are weighted and summed to obtain the loss function of the network as follows:

$$\mathrm{loss} = \sum_{la=1}^{5} \omega^l \cdot \mathrm{loss}^l. \tag{9}$$

3.4. Meta-Evaluation and Meta-Test. The trained embedding model is used to extract the features of the samples in the meta-evaluation set and meta-test set. To make full use of the features of different layers of the embedding model, the method of feature fusion is used to represent the features of the samples. Several fusion methods have been explored. In the current study, the method of feature vector Mosaic was used as follows:

$$F^{\mathrm{fuse}} = \mathrm{concat}\left(\gamma^1 f^1, \gamma^2 f^2, \ldots, \gamma^n f^n\right). \tag{10}$$

The fused input classifier is trained or tested, and the calculation formula is expressed as follows:

$$z^{\mathrm{predict}} = \mathrm{classifier}\left(F^{\mathrm{fuse}}\right). \tag{11}$$

The fitness function of the quantum genetic algorithm is expressed as follows:

$$\begin{aligned} &\mathrm{fitness}(m_i) = g(x), \\ &g(x) = \frac{\#\text{ of correctly predicted samples}}{\text{total number of samples}} \times 100\%. \end{aligned} \tag{12}$$

All models are tested using the meta-test set when the optimization of the embedding model and feature fusion method is completed. The process of the meta-testing stage is the same as that of meta-evaluation. Formulas (10) and (11) are used for meta-testing. The algorithm flow is shown in Figure 3. The next section describes the details of meta-testing.

3.5. Meta-Classifier. Meta-learners are an important part of meta-learning. Meta-learners are referred to as meta-classifiers in the current study. Several models are available for classification tasks, such as nearest neighbor algorithm, linear regression, logistic regression, and support vector machine. The current study mainly uses the widely used logistic regression model for meta-classification. Logistic regression and linear regression are similar to the generalized linear model. Logistic regression assumes that the dependent variable y follows a Bernoulli distribution, whereas linear regression assumes that the dependent variable y follows a Gaussian distribution. Therefore, there are several similarities between logistic regression and linear regression. However, logistic regression introduces

Table 1: Quantum rotation gate adjustment strategy [26].

x_i	b_i	$f(x_i) \geq f(b_i)$	$\Delta\theta_i$	$s(\alpha_i, \beta_i)$			
				$\alpha_i\beta_i > 0$	$\alpha_i\beta_i < 0$	$\alpha_i = 0$	$\beta_i = 0$
0	0	False	0	—	—	—	—
0	0	True	0	—	—	—	—
0	0	False	δ	+1	−1	0	±1
0	0	True	δ	−1	+1	±1	0
1	0	False	δ	-1	+1	±1	0
1	0	True	δ	+1	−1	0	±1
1	1	False	0	—	—	—	—
1	1	True	0	—	—	—	—

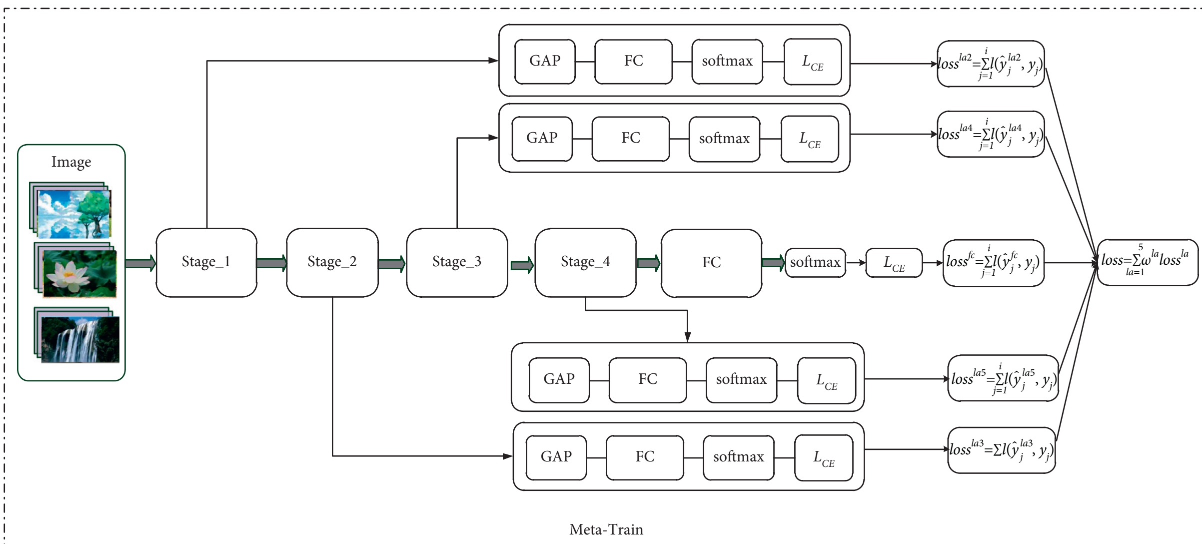

Figure 2: Adaptive hierarchical multistage loss training framework for the embedding model.

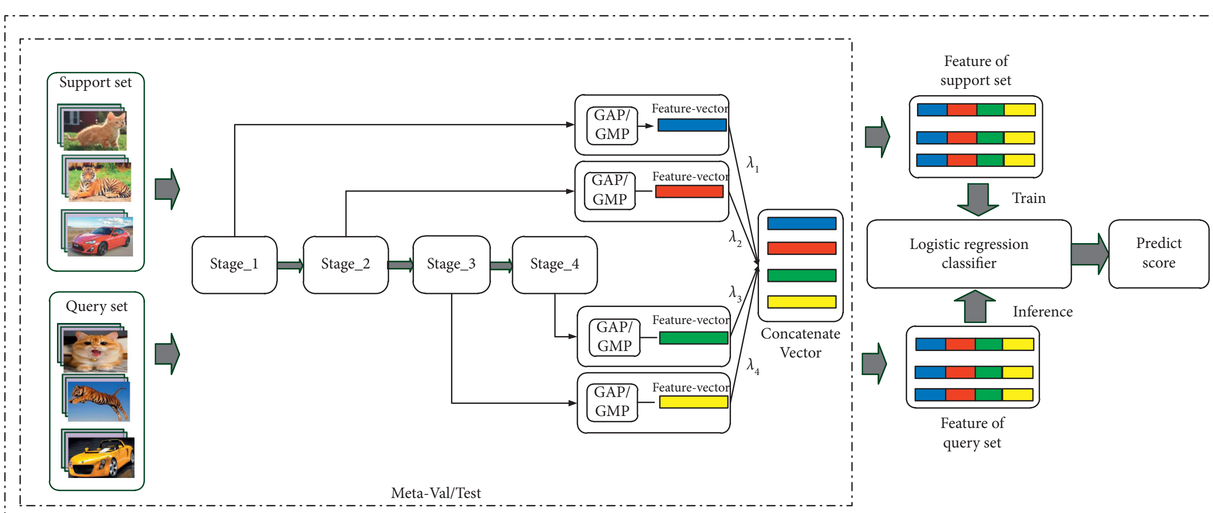

Figure 3: Adaptive hierarchical feature fusion method for meta-evaluation and meta-test.

nonlinear factors through the Sigmoid function; thus, it can easily handle the 0/1 classification problem. If the Sigmoid mapping function is removed, the logistic regression algorithm is similar to linear regression. This implies that logistic regression is theoretically supported by linear regression.

4. Experiments

4.1. Datasets. MiniImageNet: this is a dataset extracted from ImageNet by Vinyals et al. of the Google DeepMind team. This dataset contains a total of 100 categories and a total of 60,000 color images. Each category has 600 samples, and the size of each image is 84×84 pixels. The DeepMind team used the MiniImageNet dataset for small sample learning for the first time, and since then MiniImageNet has become the benchmark dataset for meta-learning and small sample research.

CIFAR-FS: the CIFAR-FS dataset refers to the CIFAR100 FEW-SHOTS dataset and is derived from the CIFAR100 dataset. It comprises 100 categories, 600 images per category, and a total of 60,000 images. For application purposes, it is divided into a training set (64 kinds), verification set (16 kinds), and test set (20 kinds) and the image size is unified as 32×32 pixels.

FC100: a few-shot CIFAR100 dataset. This dataset is similar to the CIFAR-FS dataset and is derived from the CIFAR100 dataset. It comprises 100 categories with 600 images for each category and a total of 60,000 images. The difference between CIFAR-FS and FC100 is that FC100 is not classified by category, but by Superclass. FC100 comprises 20 superclasses in total, including 12 superclasses in the training set, 4 superclasses in the verification set, and 4 superclasses in the testing set.

4.2. Setup. The PyTorch deep learning architecture was used to verify the performance of the proposed algorithms on meta-learning tasks [27]. The experiment was performed on an UltraLAB graphics workstation equipped with 192 GB memory and 8 NVIDIA GTX-2080 graphics processors, and each graphics card had 8 GB memory. The workstation was operated on Windows server operating system.

A ResNet-12 was chosen as the backbone. It included 4 residual blocks, and each block comprised 3 convolutional layers with 3×3 kernels. A 2×2 maximum pool layer was applied after the first 3 blocks. A global averaging pool layer is applied at the top of the fourth block to generate feature embedding. Drop-block was applied as a regularizer and the number of filters was varied from (64, 128, 256, 512) to (64, 160, 320, 640) as reported previously [28]. Consequently, the ResNet-12 presented in the current study is similar to that reported previously [28, 29]. The feature vectors of different layers were fused, and the feature fusion method and fusion weight were calculated based on formula (10) to obtain a good sample feature representation. Besides ResNet-12, SEResNet-12 is also used as the backbone network in the ablation experiments. The differences in residual block structure between the two backbone networks are shown in Figure 4 where (a) is the residual block of ResNet-12 and (b) is for the residual block of SEResNet-12. SEResNet-12 adds Squeeze and Excitation attention mechanism to ResNet-12, which is made up of two layers of full connection and one layer of pooling.

Optimization setup: SGD optimizer with a momentum of 0.9 and a weight decay of $5e-4$ was used in the current study. Each batch comprised 64 samples. The learning rate was initialized as 0.05 and decayed with a factor of 0.1 by three times for all datasets, except for miniImageNet where it only decayed twice as the third decay had no effect. A total of 100 epochs were trained for miniImageNet and 90 epochs for both CIFAR-FS and FC100.

Random clipping, color dithering, and random horizontal flipping were used to extend the data for training the embedding model on the converted meta-training dataset as reported previously [28]. In the current study, N-way logistic regression basis classifier was trained in the meta-test phase. The implementation was applied in Scikit-Learn.

4.3. Results and Discussion. Experiments were conducted using the miniImageNet dataset. ResNet-12 was used as the backbone network. The random seed number of the experiment was fixed to ensure repeatability of the experiment. The weight of the loss function in formula (9) and the fusion weight of formula (10) are optimized using the accuracy of the meta-evaluation set as the fitness function of the quantum genetic algorithm (Table 2). In the 1-shot strategy, the method proposed in the current study achieved similar results to MetaOptNet [29]. The proposed method in the current study achieved better performance in the 5-shot strategy compared with MetaOptNet (Table 2). These findings indicate that the proposed method is effective and reliable.

The proposed method was further verified on FC100 and CIFAR-FS. The fixed random seed number strategy was used to conduct the experiment to ensure the reproducibility of the experiment. The experimental results showed that the proposed method in the current study performed better compared with existing methods, especially when using the FC100 dataset (Table 3). The current method showed higher performance compared with existing methods. This indicated that the joint optimization of the embedded model and the classifier and use of feature fusion strategies improves the classification accuracy of the new task.

4.4. Ablation Study

4.4.1. Comparison of Different Classifiers. A variety of different classifiers were used to verify the two meta-learning datasets, FC100 and CIFAR-FC, to explore the effect of classifiers on the proposed method. Several kinds of algorithms are available for classification tasks. The current study mainly adopted three methods: the nearest neighbor, logistic regression, and support vector machine (Table 4). Logistic regression classifier showed the best performance in classification. The accuracy of the logistic regression classifier using the meta-test set of FC100 data and the current method was best. This accuracy was higher compared with that of the nearest-neighbor classifier which had the worst performance. Therefore, the logistic regression classifier was selected for subsequent analysis.

The current study proposes an adaptive hierarchical loss embedding model training method. An adaptive hierarchical loss training method was adopted to verify the effectiveness of the method developed in the current study; the model was

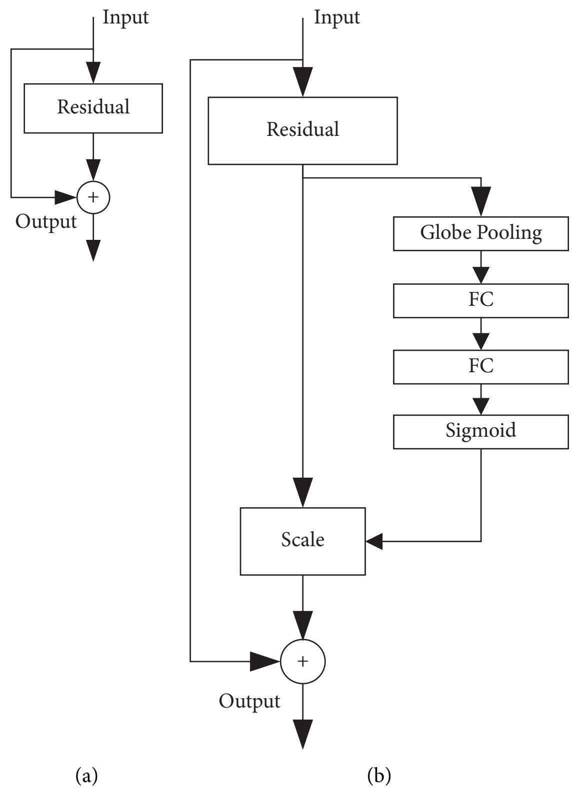

Figure 4: Comparison of residual block structure between ResNet-12 and SEResNet-12. (a) Residual block of ResNet-12. (b) Residual block of SEResNet-12.

Table 2: Experimental results using the miniImageNet dataset and comparison of the method developed in the current study with the existing classical methods.

Model	Backbone	MiniImageNet 5-way 1-shot	MiniImageNet 5-way 5-shot
MAML[9]	32-32-32-32	48.70 ± 1.84	63.11 ± 0.92
Matching Networks [15]	64-64-64-64	43.56 ± 0.84	55.31 ± 0.73
IMP [30]	64-64-64-64	49.2 ± 0.7	64.7 ± 0.7
Prototypical Networks [16]	64-64-64-64	49.42 ± 0.78	68.20 ± 0.66
TAML [31]	64-64-64-64	51.77 ± 1.86	66.05 ± 0.85
SAML [32]	64-64-64-64	$52.22 \pm$ n/a	$66.49 \pm$ n/a
GCR [33]	64-64-64-64	53.21 ± 0.80	72.34 ± 0.64
KTN [34]	64-64-64-64	54.61 ± 0.80	71.21 ± 0.66
PARN [35]	64-64-64-64	55.22 ± 0.84	71.55 ± 0.66
Dynamic Few-Shot [36]	64-64-128-128	56.20 ± 0.86	73.00 ± 0.64
Relation Networks [17]	64-64-128-128	50.44 ± 0.82	65.32 ± 0.70
AdaResNet [37]	ResNet-12	56.88 ± 0.62	71.94 ± 0.57
TADAM [38]	ResNet-12	58.50 ± 0.30	76.70 ± 0.30
Shot-Free [29]	ResNet-12	$59.04 \pm$ n/a	$77.64 \pm$ n/a
TEWAM [39]	ResNet-12	$60.07 \pm$ n/a	$75.90 \pm$ n/a
MTL [40]	ResNet-12	61.20 ± 1.80	75.50 ± 0.80
Variational FSL [41]	ResNet-12	61.23 ± 0.26	77.69 ± 0.17
MetaOptNet [28]	ResNet-12	62.64 ± 0.61	78.63 ± 0.46
Diversity w/Cooperation [42]	ResNet-18	59.48 ± 0.65	75.62 ± 0.48
LEO-trainval [19]	WRN-28-10	61.76 ± 0.08	77.59 ± 0.12
GEFS [10]	ResNet-12	62.02 ± 0.63	79.64 ± 0.44
Ours	ResNet-12	63.21 ± 0.78	81.55 ± 0.29

Average few-shot classification accuracies (%) with 95% confidence intervals on miniImageNet meta-test splits. a-b-c-d represents the size of the convolutional layer of the backbone network.

Table 3: Experimental results using CIFAR-FS and FC100 datasets and comparison of the current method with existing classic methods.

Model	Backbone	CIFAR-FC 5-way		FC100 5-way	
		1-shot	5-shot	1-shot	5-shot
MAML [9]	32-32-32-32	58.9 ± 1.9	71.5 ± 1.0	—	—
Prototypical Networks [16]	64-64-64-64	55.5 ± 0.7	72.0 ± 0.6	35.3 ± 0.6	48.6 ± 0.6
Relation Networks [17]	64-64-128-128	55.0 ± 1.0	69.3 ± 0.8	—	—
TADAM [38]	ResNet-12	—	—	40.1 ± 0.4	56.1 ± 0.4
Shot-Free [29]	ResNet-12	$69.2 \pm$ n/a	$84.7 \pm$ n/a	—	—
TEWAM [39]	ResNet-12	$70.4 \pm$ n/a	$81.3 \pm$ n/a	—	—
Prototypical Networks [16]	ResNet-12	72.2 ± 0.7	83.5 ± 0.5	37.5 ± 0.6	52.5 ± 0.6
MetaOptNet [28]	ResNet-12	72.6 ± 0.7	84.3 ± 0.5	41.1 ± 0.6	55.5 ± 0.6
GEFS [10]	ResNet-12	71.5 ± 0.8	86.0 ± 0.5	42.6 ± 0.7	59.1 ± 0.6
Ours	ResNet-12	72.62 ± 0.5	87.34 ± 0.6	45.18 ± 0.7	63.47 ± 0.6

Average few-shot classification accuracies (%) with 95% confidence intervals on CIFAR-FS and FC100. a-b-c-d represents the size of the convolutional layer of the backbone network.

Table 4: Ablation study on three benchmarks with ResNet-12 as the backbone network.

Model	CIFAR-FC 5-way		FC100 5-way	
	1-shot	5-shot	1-shot	5-shot
NN	69.58 ± 0.6	82.43 ± 0.6	43.3 ± 0.6	59.3 ± 0.6
LR	72.62 ± 0.5	87.34 ± 0.6	45.18 ± 0.7	63.47 ± 0.6
SVM	71.94 ± 0.6	84.57 ± 0.6	41.8 ± 0.7	59.6 ± 0.6

"NN" and "LR" represent the nearest neighbor classifier and logistic regression. "SVM" denotes support vector machine.

Table 5: Comparisons of different training strategies for the embedding model on CIFAR-FS and FC100.

Model	CIFAR-FC 5-way		FC100 5-way		MiniImageNet 5-way	
	1-shot	5-shot	1-shot	5-shot	1-shot	5-shot
Ours simple	72.38 ± 0.6	86.67 ± 0.85	44.1 ± 0.73	60.8 ± 0.6	62.49 ± 0.55	79.91 ± 0.40
Ours	72.62 ± 0.5	87.34 ± 0.6	45.18 ± 0.7	63.47 ± 0.6	63.21 ± 0.78	81.55 ± 0.29

Figure 5: Activation map of selected results on the miniImageNet dataset using ResNet-12 as the base model. From left to right: Column 1 is original images; Column 2 is Grad-CAM visualizations for the model trained with standard cross entropy; Column 3 indicates Grad-CAM visualizations for the model trained with the currently proposed method.

Table 6: Comparisons of different backbones on CIFAR-FS and FC100.

Model	CIFAR-FC 5-way		FC100 5-way	
	1-shot	5-shot	1-shot	5-shot
ResNet-12	72.62 ± 0.5	87.34 ± 0.6	45.18 ± 0.7	63.47 ± 0.6
SEResNet-12	72.91 ± 0.85	87.59 ± 0.7	45.47 ± 0.63	63.65 ± 0.6

then divided into loss training method and traditional training method for comparison. The dividing loss method was used to fix the loss weight of different layers, which is set as 1 in the current study. The traditional neural network training method was used to add the loss function in the last layer of the network. Cross entropy was used as the calculation method for the loss function of all layers. Experiments were conducted on three different datasets, and the results showed that the embedding model of adaptive hierarchical loss proposed in the current study was optimal by comparing with other methods (Table 5). These findings indicate that the hierarchical loss function can improve the shallow layer feature expression performance of the convolutional neural networ.

In addition, the feature map of the 4^{th} layer of ResNet-12 was visually visualized for adaptive hierarchical loss training. The visualization method used was CAM, which is used to visualize the feature map output by the convolutional layer in the neural network in the form of the heat map. The red area represents the response area of the neural network neurons in this layer. The findings showed that the embedding model of adaptive hierarchical loss function training proposed in the current study had a larger response area compared with that of the traditional method (Figure 5). This finding indicates the effectiveness of the current method.

4.4.2. Comparison of Different Network Backbones. In the above experiment, ResNet-12 was used as the backbone network to make fair comparisons with other methods. To verify the influence of the backbone network on the proposed algorithm, SEResNet-12 was also applied in the experiments. The experimental results are shown in Table 6. Notably, SEResNet-12 had a better representation of the sample characteristics.

5. Conclusion

This study presents a joint optimization method in which the embedding model and classifier are used for meta-learning. Specifically, we applied a quantum genetic algorithm to optimize the hierarchical multi-loss weight of the embedding model and the weight of feature fusion. The classification accuracy of the meta-learning evaluation set was used as the fitness function, which effectively combines the embedded model and classifier. The performance of the proposed method was tested on three well-known public meta-learning datasets. It was found that the performance of the proposed method was superior to that of most existing baseline meta-learning models. In the future, we plan to carry out studies on the joint optimization method of semisupervised or unsupervised embedding model and classifier. In addition, we shall explore more efficient evolution strategies to improve the efficiency of the joint optimization method.

Data Availability

The data used to support the findings of this study have been deposited in the Dropbox repository (https://www.dropbox.com/sh/6yd1ygtyc3yd981/AABVeEqzC08YQv4UZk7lNHvya?dl=0). The research uses public datasets, so readers can find resources online.

Conflicts of Interest

The authors declare that they have no conflicts of interest.

Acknowledgments

This research was funded by Research on Online Identification of Coal Gangue Based on Terahertz Detection Technology (Grant no. 52074273) and by the State Key Research Development Program of China (Grant nos. 2017 YFC0804400 and 2017YFC0804401). This work was also funded by the Key Natural Science Research Project for Colleges and Universities of Anhui Province (Grant no. KJ2020A0027).

References

[1] Y. LeCun, Y. Bengio, and G. Hinton, “Deep learning,” *Nature*, vol. 521, no. 7553, pp. 436–444, 2015.

[2] J. Vanschoren, “Meta-learning,” in *Automated Machine Learning*Springer, Berlin, Germany, 2019.

[3] A. Saxe, S. Nelli, and C. Summerfield, “If deep learning is the answer, what is the question?” *Nature Reviews Neuroscience*, vol. 22, no. 1, pp. 55–67, 2021.

[4] R. Zhang, T. Che, Z. Ghahramani, Y. Bengio, and Y. Sona, “MetaGAN: an adversarial approach to few-shot learning,” in *Proceedings of the Neural Information Processing Systems Conference*, p. 8, Montréal, Canada, December 2018.

[5] Y. Liu, Y. Zhou, X. Liu, F. Dong, C. Wang, and Z. Wang, “Wasserstein GAN-based small-sample augmentation for new-generation artificial intelligence: a case study of cancer-staging data in biology,” *Engineering*, vol. 5, no. 1, pp. 156–163, 2019.

[6] B. M. Lake, R. Salakhutdinov, and J. B. Tenenbaum, “Human-level concept learning through probabilistic program induction,” *Science*, vol. 350, no. 6266, pp. 1332–1338, 2015.

[7] G. Koch, R. Zemel, and R. Salakhutdinov, “Siamese neural networks for one-shot image recognition,” in *Proceedings of the ICML Deep Learning Workshop*, Lille, France, July 2015.

[8] X. Li, L. Yu, C.-W. Fu, M. Fang, and P.-A. Heng, “Revisiting metric learning for few-shot image classification,” *Neurocomputing*, vol. 406, pp. 49–58, 2020.

[9] C. Finn, P. Abbeel, and S. Levine, “Model-agnostic meta-learning for fast adaptation of deep networks,” in *Proceedings of the International Conference on Machine Learning*, pp. 1126–1135, PMLR, Sydney, Australia, August 2017.

[10] Y. Tian, Y. Wang, D. Krishnan, J. B. Tenenbaum, and P. Isola, “Rethinking few-shot image classification: a good embedding is all you need?” in *Proceedings of the Computer Vision–ECCV 2020: 16th European Conference*, Glasgow, UK, August 2020.

[11] W. Guo, W. Li, and W. Gong, “Extended feature pyramid network with adaptive scale training strategy and anchors for object detection in aerial images,” *Remote Sensing*, vol. 12, no. 5, 2020.

[12] T.-Y. Lin, P. Dollár, R. Girshick, K. He, B. Hariharan, and S. Belongi, “Feature pyramid networks for object detection,” in *Proceedings of the IEEE Conference on Computer Vision and Pattern Recognition*, pp. 2117–2125, Honolulu, HI, USA, July 2017.

[13] Q. Yang, P. Yan, Y. Zhang et al., "Low-dose CT image denoising using a generative adversarial network with Wasserstein distance and perceptual loss," *IEEE Transactions on Medical Imaging*, vol. 37, no. 6, pp. 1348–1357, 2018.

[14] E. Hoffer and N. Ailon, "Deep metric learning using triplet network," in *Proceedings of the International Workshop on Similarity-Based Pattern Recognition*, pp. 84–92, Springer, Copenhagen, Denmark, October 2015.

[15] O. Vinyals, C. Blundell, T. Lillicrap, K. Kavukcuoglu, and D. Wierstra, "Matching networks for one shot learning," in *Proceedings of the Advances in Neural Information Processing Systems*, vol. 29, pp. 3630–3638, Barcelona, Spain, 2016.

[16] J. Snell, K. Swersky, and R. Zemel, "Prototypical Networks for Few-Shot Learning," 2017, https://arxiv.org/abs/1703.05175.

[17] F. Sung, Y. Yang, L. Zhang, T. Xiang, P. Torr, and T. M. Hospedales, "Learning to compare: relation network for few-shot learning," in *Proceedings of the IEEE Conference on Computer Vision and Pattern Recognition*, pp. 1199–1208, Salt Lake City, UT, USA, June 2018.

[18] S. Ravi and H. Larochelle, "Optimization as a Model for Few-Shot Learning," in *Proceedings of the ICLR 2016*, San Juan, Puerto Rico, May 2016.

[19] A. A. Rusu, D. Rao, J. Sygnowski et al., "Meta-learning with latent embedding optimization," 2018, https://arxiv.org/abs/1807.05960.

[20] J. Yoon, T. Kim, and O. Dia, "Bayesian model-agnostic meta-learning," in *Proceedings of the32nd Conference on Neural Information Processing Systems (NIPS)*, Toronto, Canada, June 2018.

[21] A. Nichol, J. Achiam, and J. J. a. p. a. Schulman, "On first-order meta-learning algorithms," 2018, https://arxiv.org/abs/1803.02999.

[22] M. Al-Shedivat, T. Bansal, Y. Burda, I. Sutskever, I. Mordatch, and P. Abbeel, "Continuous adaptation via meta-learning in nonstationary and competitive environments," in *Proceedings of the ICLR 2017 Conference*, Toulon, France, April 2017.

[23] B. Hariharan and R. Girshick, "Low-shot visual recognition by shrinking and hallucinating features," in *Proceedings of the IEEE International Conference on Computer Vision*, pp. 3018–3027, Venice, Italy, October 2017.

[24] H. Gao, Z. Shou, A. Zareian, H. Zhang, and S. F. Chang, "Low-shot learning via covariance-preserving adversarial augmentation networks," in *Proceedings of the 32nd Conference on Neural Information Processing Systems (NIPS)*, Montréal Canada, December 2018.

[25] G. Zhang and H. Rong, "Real-observation quantum-inspired evolutionary algorithm for a class of numerical optimization problems," in *Proceedings of the 7th International Conference on Computational Science (ICCS 2007*, pp. 989–996, Beijing, China, May 2007.

[26] K. H. Han and J. H. Kim, "Genetic quantum algorithm and its application to combinatorial optimization problem," in *Proceedings of the 2000 Congress on Evolutionary Computation (CEC2000*, pp. 1354–1360, La Jolla, CA, USA, July 2000.

[27] N. Ketkar, "Introduction to pytorch," in *Deep Learning with Python*Springer, Berlin, Germany, 2017.

[28] K. Lee, S. Maji, A. Ravichandran, and S. Soatto, "Meta-learning with differentiable convex optimization," in *Proceedings of the IEEE/CVF Conference on Computer Vision and Pattern Recognition*, pp. 10657–10665, Long Beach, CA, USA, June 2019.

[29] A. Ravichandran, R. Bhotika, and S. Soatto, "Few-shot learning with embedded class models and shot-free meta training," in *Proceedings of the IEEE/CVF International Conference on Computer Vision*, pp. 331–339, Seoul, Korea, November 2019.

[30] K. Allen, E. Shelhamer, H. Shin, and B. J. Tenenbaum, "Infinite mixture prototypes for few-shot learning," in *Proceedings of the International Conference on Machine Learning*, pp. 232–241, PMLR, Long Beach, CA, USA, June 2019.

[31] M. A. Jamal and G.-J. Qi, "Task agnostic meta-learning for few-shot learning," in *Proceedings of the IEEE/CVF Conference on Computer Vision and Pattern Recognition*, pp. 11719–11727, Seoul, Korea, November 2019.

[32] F. Hao, F. He, J. Cheng, L. Wang, L. Cao, and D. Tao, "Collect and select: semantic alignment metric learning for few-shot learning," in *Proceedings of the IEEE/CVF International Conference on Computer Vision*, pp. 8460–8469, Seoul, Korea, November 2019.

[33] A. Li, T. Luo, T. Xiang, W. Huang, and L. Wang, "Few-shot learning with global class representations," in *Proceedings of the IEEE/CVF International Conference on Computer Vision*, pp. 9715–9724, Seoul, Korea, November 2019.

[34] Z. Peng, Z. Li, J. Zhang, Y. Li, G. J. Qi, and J. Tang, "Few-shot image recognition with knowledge transfer," in *Proceedings of the 2019 Ieee/Cvf International Conference on Computer Vision*, pp. 441–449, Seoul, Korea, November 2019.

[35] Z. Wu, Y. Li, L. Guo, and K. Jia, "PARN: position-aware relation networks for few-shot learning," in *Proceedings of the IEEE/CVF International Conference on Computer Vision*, pp. 6659–6667, Seoul, Korea, November 2019.

[36] S. Gidaris and N. Komodakis, "Dynamic few-shot visual learning without forgetting," in *Proceedings of the IEEE Conference on Computer Vision and Pattern Recognition*, pp. 4367–4375, Salt Lake City, UT, USA, June 201.

[37] T. Munkhdalai, X. Yuan, S. Mehri, and A. Trischler, "Rapid adaptation with conditionally shifted neurons," in *Proceedings of the International Conference on Machine Learning*, pp. 3664–3673, PMLR, Stockholm Sweden, July 2018.

[38] B. N. Oreshkin, P. Rodriguez, and A. Lacoste, "TADAM: task dependent adaptive metric for improved few-shot learning," in *Proceedings of the 32nd Conference on Neural Information Processing Systems (NIPS)*, pp. 124–137, Montréal Canada, December 2018.

[39] L. Qiao, Y. Shi, J. Li, Y. Tian, T. Huang, and Y. Wang, "Transductive episodic-wise adaptive metric for few-shot learning," in *Proceedings of the IEEE/CVF International Conference on Computer Vision*, pp. 3603–3612, Seoul, Korea, November 2019.

[40] Q. Sun, Y. Liu, T.-S. Chua, and B. Schiele, "Meta-transfer learning for few-shot learning," in *Proceedings of the 2019 Ieee/Cvf Conference on Computer Vision and Pattern Recognition*, pp. 403–412, Long Beach, CA, USA, June 2019.

[41] J. Zhang, C. Zhao, B. Ni, M. Xu, and X. Yang, "Variational few-shot learning," in *Proceedings of the IEEE/CVF International Conference on Computer Vision*, pp. 1685–1694, Seoul, Korea, October 2019.

[42] N. Dvornik, C. Schmid, and J. Mairal, "Diversity with cooperation: ensemble methods for few-shot classification," in *Proceedings of the IEEE/CVF International Conference on Computer Vision*, pp. 3723–3731, Seoul, Korea, October 2019.

Hindawi
Scientific Programming
Volume 2021, Article ID 7049857, 7 pages
https://doi.org/10.1155/2021/7049857

Research Article

An Efficient Teaching Model of International Cooperation Based on Artificial Intelligence

Meng Xiao[1] **and Haibo Yi**[2]

[1]*School of Management, Shenzhen Polytechnic, Shenzhen 518055, China*
[2]*School of Artificial Intelligence, Shenzhen Polytechnic, Shenzhen 518055, China*

Correspondence should be addressed to Haibo Yi; haiboyi@szpt.edu.cn

Received 28 July 2021; Revised 12 September 2021; Accepted 21 September 2021; Published 30 September 2021

Academic Editor: Punit Gupta

International cooperation in running schools has promoted the scale of higher education and trained a number of talents with international vision. However, there are many differences between domestic teaching and foreign teaching in the international cooperation in running schools. This makes it difficult for students to adapt to the teaching of foreign universities. Connecting domestic teaching with foreign teaching and solving the problem of differentiation has become an important issue in international cooperation in running schools. In order to improve the quality of international cooperation of high education, it is very urgent to design an efficient model of international cooperation. We exploit artificial intelligence to design a teaching model of international cooperation. We implement the effective model of international cooperation in logistics management and software technology, where the implementation results show that the model can provide learning suggestions of the foreign stage according to the learning situation of the domestic stage.

1. Introduction

In recent years, international cooperation in running schools has become a popular mode of higher education [1]. It is a common mode of international cooperation to study in domestic universities for 1–3 years and finish their studies in foreign universities in the remaining time.

In China, almost all universities have international cooperation programs. In the undergraduate colleges, "2 + 2" cooperative mode is usually adopted, where students complete the first two years of study in China and the second two years in foreign countries and obtain the diploma of foreign universities or domestic and foreign universities. In higher vocational colleges, "3 + 1" cooperative mode is usually adopted, where students complete the first three years of study in China and the last year in foreign countries and obtain a diploma from domestic universities and bachelor's degree from foreign universities.

International cooperation in running schools has promoted the scale of higher education and trained a number of talents with international vision. International cooperation in running schools has been widely concerned and accepted by many students and parents. Compared with direct study abroad, parents and students have lower learning costs in international cooperative education and can experience different types of higher education at home and abroad at the same time. International cooperation in running schools is very beneficial to the cultivation of interdisciplinary talents.

However, in the international cooperation in running schools, there are many differences between domestic teaching and foreign teaching. This makes it difficult for students to adapt to the teaching of foreign universities. Connecting domestic teaching with foreign teaching and solving the problem of differentiation has become an important issue in international cooperation in running schools.

In order to improve the quality of international cooperation of high education, it is very urgent to design an efficient model of international cooperation. Artificial intelligence technology is a very popular information technology in recent years, and the application of artificial intelligence in the field of education is gradually emerging [2–6]. Chiu and Chai proposed sustainable curriculum planning for artificial intelligence education [7]. Calvo et al. proposed a multidisciplinary PBL approach for teaching industrial informatics and robotics in engineering [8]. Marques et al. enhanced the student learning experience in software engineering project courses [9]. Aktan et al. applied distance learning to control engineering laboratories [10]. Graesser et al. proposed an intelligent tutoring system with mixed-initiative dialogue [11]. Hoic-Bozic et al. proposed a blended learning approach to course design and implementation [12]. The strong point of artificial intelligence technology is that it can model and analyze and predict according to the past data [13–20].

We exploit artificial intelligence to design a teaching model of international cooperation. Taking logistics management and software technology as examples, we analyze the learning situation of domestic students based on artificial intelligence and establish the training set of artificial intelligence model; then, based on artificial intelligence, we analyze the learning situation of foreign students and establish the labels of artificial intelligence model; finally, through artificial intelligence training, we build an effective model of international cooperation.

We implement the effective model of international cooperation in logistics management and software technology, where the implementation results show that the model can provide learning suggestions of the foreign stage according to the learning situation of the domestic stage. Compared with other models, the artificial intelligence-based model is more intelligent.

We present the rest of content in the following organization. Section 2 presents an overview of artificial intelligence. Section 3 proposes an efficient teaching model of international cooperation. Section 4 presents the results of implementation and comparison. Section 5 presents the conclusion of this paper.

2. Preliminaries

Artificial intelligence technology is a very popular information technology in recent years, and the application of artificial intelligence in the field of education is gradually emerging. The strong point of artificial intelligence technology is that it can model and analyze and predict according to the past data.

One of the main techniques of artificial intelligence is deep learning. Deep learning plays an important role in medical diagnosis and analysis. Klang proposed deep learning and medical imaging [21]. Haskins et al. proposed deep learning in medical image registration [22]. Ba proposed medical sports rehabilitation deep learning system of sports injury based on MRI image analysis [23]. Xu proposed a deep learning method to predict lung cancer from serial medical imaging [24]. Sourati et al. proposed intelligent labeling based on fisher information for medical image segmentation using deep learning [25].

In addition, deep learning also plays an important role in agriculture, industry, commerce, and other fields. Liu et al. proposed a new fluid factor and its application using a deep learning approach [26]. Hu et al. proposed deep collaborative learning with application to multimodal brain development study [27]. Asanuma et al. proposed deep learning applications to topology optimization of electric motor [28]. Al-Sharman et al. proposed deep learning-based neural network training for state estimation enhancement and application to attitude estimation [29]. Zhang et al. proposed deep learning-based mobile application isomorphic GUI identification for automated robotic testing [30]. Trivizakis et al. proposed extending 2D convolutional neural networks to 3D for advancing deep learning cancer classification with application to MRI liver tumor differentiation [31]. Yan et al. proposed soft sensor modeling method based on semisupervised deep learning and its application to wastewater treatment plant [32].

3. An Efficient Teaching Model of International Cooperation

3.1. Overview of the Scheme. In order to improve the quality of international cooperation of high education, it is very urgent to design an efficient model of international cooperation. Artificial intelligence technology is a very popular information technology in recent years, and the application of artificial intelligence in the field of education is gradually emerging. The strong point of artificial intelligence technology is that it can model and analyze and predict according to the past data.

We exploit artificial intelligence to design a teaching model of international cooperation based on artificial intelligence. In higher vocational colleges, "3 + 1" cooperative mode is usually adopted, where students complete the first three years of study in China and the last year in foreign countries and obtain a diploma from domestic universities and bachelor's degree from foreign universities.

We take "3 + 1" program of logistics management and software technology as examples.

(1) We analyze the learning situation of domestic students based on artificial intelligence and establish the training set of the artificial intelligence model, which is illustrated in Section 3.2.

(2) Based on artificial intelligence, we analyze the learning situation of foreign students and establish the labels of artificial intelligence model, which is illustrated in Section 3.3.

(3) Through artificial intelligence training, we build an effective model of international cooperation, which is illustrated in Section 3.4.

3.2. Collecting Training Data. We take "3 + 1" program of logistics management and software technology in higher vocational colleges as examples.

(1) We analyze the learning situation of domestic students based on artificial intelligence.

"3 + 1" cooperative mode is usually adopted in higher vocational colleges, where students complete the first three years of study in China and the last year in foreign countries and obtain a diploma from domestic universities and bachelor's degree from foreign universities.

Core courses of logistics management and software technology in higher vocational colleges include Python, Java, introduction to computer, computer network, data structure and introduction to logistics, logistics planning and design, procurement and supply management, procurement project management, and transportation management, which is summarized in Table 1.

(2) Based on the learning situation of domestic students, we establish the training set of artificial intelligence model.

We establish the training set based on the scores of the core courses of logistics management and software technology in higher vocational colleges. First, we convert all points that are not a percentage system to a hundred mark system. Second, we limit the range of data from 0 to 1 by dividing all fractions by 100. We illustrate the process of establishing training set in Table 2.

3.3. Labeling Training Data. Based on artificial intelligence, we analyze the learning situation of foreign students and establish the labels of artificial intelligence model.

In "3 + 1" cooperative mode, students complete the last year in foreign countries and obtain a diploma from domestic universities and bachelor's degree from foreign universities.

Courses of logistics management in foreign countries include warehouse management, distribution management, international logistics, international trade theory and practice, procurement process exercise, transportation technique, warehousing management practice, logistics distribution center design, international logistics practice, success study, innovation, quality development training, etc.

Courses of software technology in foreign countries include calculation method, compiling principle, software engineering, operating system principle, database system principle, network database, microcomputer principle and assembly language programming, web-based programming, software development technology, software testing technology, multimedia technology, network security technology, etc.

We label the training set based on the scores of the core courses of logistics management and software technology in the colleges of foreign countries. First, we convert all points that are not a percentage system to a hundred mark system. Second, we limit the range of data from 0 to 1 by dividing all fractions by 100. We illustrate the process of labeling training set in Table 3.

3.4. Building Model. Through artificial intelligence training, we build an effective model of international cooperation, which is depicted in Figure 1.

(1) Collecting training data and label: "3 + 1" cooperative mode is usually adopted in higher vocational colleges, where students complete the first three years of study in China and the last year in foreign countries and obtain a diploma from domestic universities and bachelor's degree from foreign universities. We take "3 + 1" program of logistics management and software technology as examples. We collect scores of core courses of logistics management and software technology in higher vocational colleges and foreign colleges as training data and labels.

(2) Selecting features of the model: we select ten core courses for logistics management and software technology in higher vocational colleges as the features, respectively. We use $l_1, l_2, \ldots, l_{10}$ to denote ten core courses for logistics management in higher vocational colleges and use $s_1, s_2, \ldots, s_{10}$ to denote ten core courses for software technology in higher vocational colleges.

(3) Designing model: we select ten core courses for logistics management and software technology in foreign colleges as the labels, respectively. We use $m_1, m_2, \ldots, m_{10}$ to denote ten core courses for logistics management in foreign colleges and use $t_1, t_2, \ldots, t_{10}$ to denote ten core courses for software technology in foreign colleges. Then, we need to find the relation between the training set and labels, i.e., training set $l_1, l_2, \ldots, l_{10}$, $s_1, s_2, \ldots, s_{10}$ and labels $m_1, m_2, \ldots, m_{10}$, $t_1, t_2, \ldots, t_{10}$.

We build an efficient model based on artificial intelligence. We build a five-layer architecture with the inputs of training set and the outputs of the labels. We take logistics management as an example and depict the architecture in Figure 2.

(4) Training model with the training data and label: we summarize the five-layer architecture in Table 4. The input layer represents the scores of the ten core courses for logistics management or software technology in higher vocational colleges. The output layer represents the scores of the ten core courses for logistics management or software technology in foreign colleges. Besides, we design three hidden layers, where each layer includes 100 nodes with full connections. In order to find the relation between inputs and outputs, we use the training set and label to train the model.

4. Result

4.1. Implementation. We implement the effective model of international cooperation in logistics management and software technology, where we use Python programming language with the version 3.6 and TensorFlow deep learning tool.

(1) We collect data based on "3 + 1" cooperative mode, which is usually adopted in higher

Table 1: Core courses of logistics management and software technology.

	Software technology	Logistics management
First year	Python, introduction to computer	Introduction to logistics
Second year	Java, computer network	Procurement project management
Third year	Data structure	Transportation management

Table 2: Establishing training set.

	Original score	First stage	Second stage
Python	A+	100	1
C++	A	95	0.95
Introduction to computer	B	85	0.85
Introduction to logistics	C	75	0.75
Java	D	65	0.65
Computer network	F	0	0
Procurement project management	100	100	1
Data structure	60	60	0.6
Transportation management	0	0	0

Table 3: Labeling training set.

	Original score	First stage	Second stage
Warehouse management	A+	100	1
International logistics practice	A	95	0.95
Distribution management	B	85	0.85
International logistics	C	75	0.75
Success study	D	65	0.65
Compiling principle	F	0	0
Software engineering	100	100	1
Operating system principle	60	60	0.6
Database system principle	0	0	0

Table 4: Five-layer architecture.

	Type	Nodes	Number of nodes
First layer	Input	$l_1, l_2, \ldots, l_{10}$	10
Second layer	Hidden	$h_{1,1}, l_{1,2}, \ldots, l_{1,100}$	100
Third layer	Hidden	$h_{2,1}, l_{2,2}, \ldots, l_{2,100}$	100
Fourth layer	Hidden	$h_{3,1}, l_{3,2}, \ldots, l_{3,100}$	100
Fifth layer	Output	$t_1, t_2, \ldots, t_{10}$	10

vocational colleges. Students complete the first three years of study in China and the last year in foreign countries and obtain a diploma from domestic universities and bachelor's degree from foreign universities. We take "3 + 1" program of logistics management and software technology as examples. We collect scores of ten core courses of logistics management and software technology in higher vocational colleges and foreign colleges as training data and labels.

(2) We convert all points that are not a percentage system to a hundred mark system. Then, we limit the range of data from 0 to 1 by dividing all fractions by 100.

(3) We build a five-layer architecture with the inputs of training set and the outputs of the labels.

(4) We collect testing data to test the architecture.

We summarize the implementation details in Table 5, where the accuracy of the model is 91.6%.

(1) A training set of 2000 samples is used in training the model.

(2) A testing set of 500 samples is used in testing the model.

(3) Inputs are $l_1, l_2, \ldots, l_{10}$, $s_1, s_2, \ldots, s_{10}$.

(4) Outputs are $m_1, m_2, \ldots, m_{10}$, $t_1, t_2, \ldots, t_{10}$.

The implementation results show that the model can provide learning suggestions of the foreign stage according to the learning situation of the domestic stage.

4.2. Comparison. We compared the traditional teaching mode with the AI-based teaching mode from four aspects: data-driven, subjectivity/objectivity, technology, and intelligence. The comparison results are summarized in Table 6. Compared with other models, the artificial intelligence-based model is more intelligent.

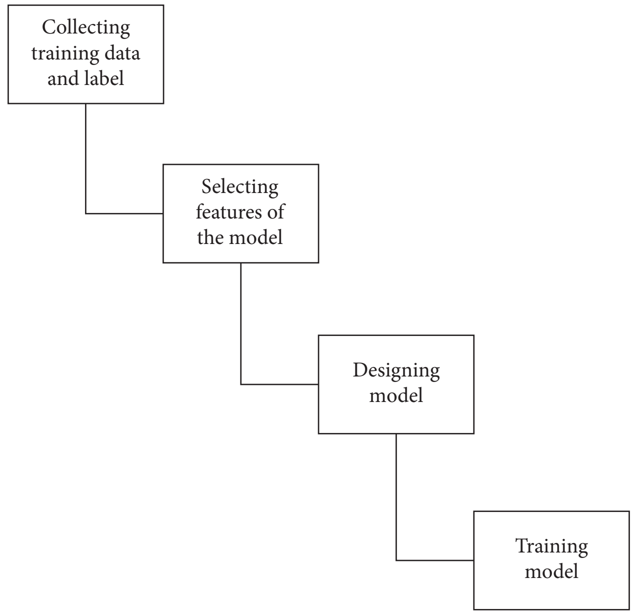

Figure 1: Building model.

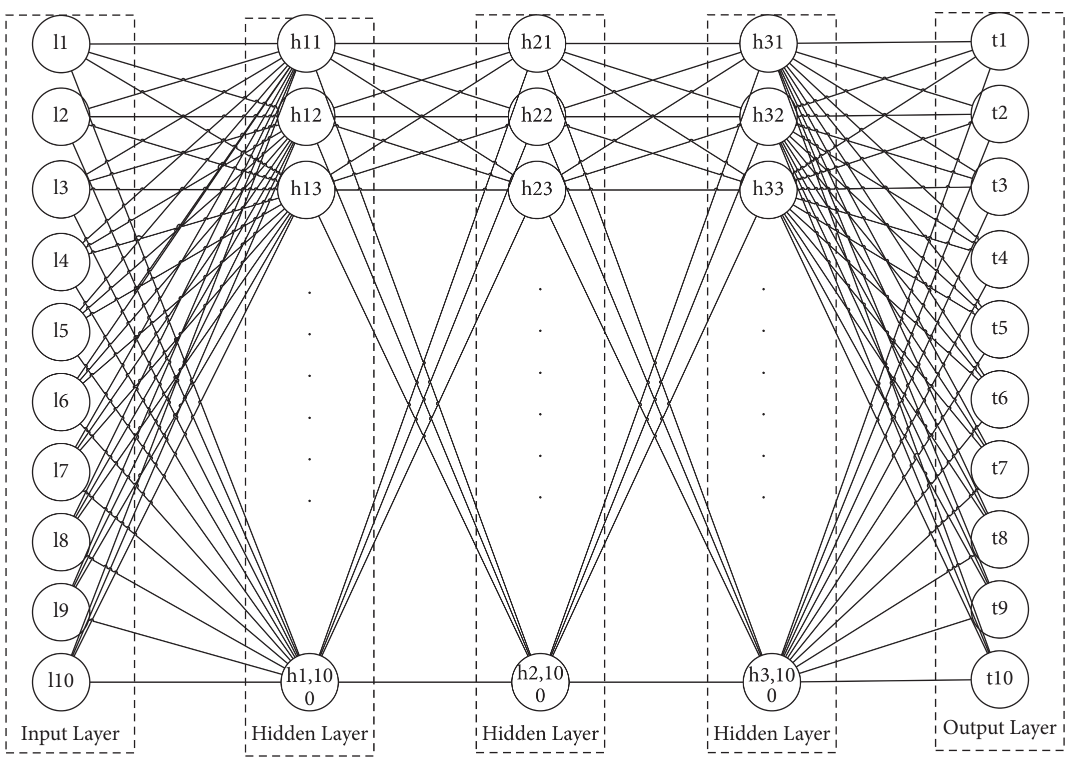

Figure 2: Five-layer architecture.

Table 5: Implementation results.

Training set	Testing set	Inputs	Outputs	Accuracy
2000	500	20	20	91.6

Table 6: Comparison results.

	Data-driven	Subjectivity/objectivity	Technology used	Model intelligence
Traditional teaching model	No	Subjectivity	Information technology	Low
AI teaching model	Yes	Objectivity	Artificial intelligence	High

5. Conclusions

In the international cooperation in running schools, there are many differences between domestic teaching and foreign teaching. In order to improve the quality of international cooperation of high education, it is very urgent to design an efficient model of international cooperation. Artificial intelligence technology is a very popular information technology in recent years, and the application of artificial intelligence in the field of education is gradually emerging. The strong point of artificial intelligence technology is that it can model and analyze and predict according to the past data. We exploit artificial intelligence to design a teaching model of international cooperation based on artificial intelligence. Taking logistics management and software technology as examples, we analyze the learning situation of domestic students based on artificial intelligence and establish the training set of artificial intelligence model; then, based on artificial intelligence, we analyze the learning situation of foreign students and establish the labels of artificial intelligence model; finally, through artificial intelligence training, we build an effective model of international cooperation.

We implement the effective model of international cooperation in logistics management and software technology, where the implementation results show that the model can provide learning suggestions of the foreign stage according to the learning situation of the domestic stage. Compared with other models, the artificial intelligence-based model is more intelligent.

Data Availability

No data were used to support this study.

Conflicts of Interest

The authors declare that they have no conflicts of interest.

Acknowledgments

The authors acknowledge Guangdong Province 2021 Educational Science Planning Project (no. DSYJ108), Shenzhen Science and Technology Program (grant no. 20200821082500001), and Teaching Research and Practice Project of Shenzhen Polytechnic (no. 7019310019J).

References

[1] L. Sisi, L. Baocun, and J. E. Aoun, "Robot-proof: higher education in the age of artificial intelligence," *Higher Education*, vol. 1, pp. 1–3, 2018.

[2] L. Deng, "Artificial intelligence in the rising wave of deep learning: the historical path and future outlook [perspectives]," *IEEE Signal Processing Magazine*, vol. 35, no. 1, pp. 180–177, 2018.

[3] Q. Zhang, L. T. Yang, Z. Chen, and P. Li, "A survey on deep learning for big data," *Information Fusion*, vol. 42, pp. 146–157, 2018.

[4] X. Sun, P. Wu, and S. C. H. Hoi, "Face detection using deep learning: an improved faster RCNN approach," *Neurocomputing*, vol. 299, no. 19, pp. 42–50, 2018.

[5] H. Chen, O. Engkvist, Y. Wang, M. Olivecrona, and T. Blaschke, "The rise of deep learning in drug discovery," *Drug Discovery Today*, vol. 23, no. 6, pp. 1241–1250, 2018.

[6] Q. S. Zhang and S. C. Zhu, "Visual interpretability for deep learning: a survey," *Frontiers of Information Technology & Electronic Engineering*, vol. 19, no. 1, pp. 27–39, 2018.

[7] T. K. F. Chiu and C.-s. Chai, "Sustainable curriculum planning for artificial intelligence education: a self-determination theory perspective," *Sustainability*, vol. 12, no. 14, p. 5568, 2020.

[8] I. Calvo, I. Cabanes, J. Quesada, and Q. Barambones, "A multidisciplinary PBL approach for teaching industrial informatics and robotics in engineering," *IEEE Transactions on Education*, vol. 61, pp. 1–8, 2018.

[9] M. Marques, S. F. Ochoa, M. C. Bastarrica, and F. J. Gutierrez, "Enhancing the student learning experience in software engineering project courses," *IEEE Transactions on Education*, vol. 61, pp. 1–11, 2018.

[10] B. Aktan, C. A. Bohus, L. A. Crowl, and M. H. Shor, "Distance learning applied to control engineering laboratories," *IEEE Transactions on Education*, vol. 39, no. 3, pp. 320–326, 2002.

[11] A. C. Graesser, P. Chipman, B. C. Haynes, and A. Olney, "AutoTutor: an intelligent tutoring system with mixed-initiative dialogue," *IEEE Transactions on Education*, vol. 48, no. 4, pp. 612–618, 2005.

[12] N. Hoic-Bozic, V. Mornar, and I. Boticki, "A blended learning approach to course design and implementation," *IEEE Transactions on Education*, vol. 52, no. 1, pp. 19–30, 2009.

[13] L. Li, Y. L. Lin, N. N. Zheng et al., "Artificial intelligence test: a case study of Intelligent vehicles," *Artificial Intelligence Review*, vol. 50, 2018.

[14] D. S. W. M. P. Dai, "Human intelligence needs artificial intelligence," *Sensors*, vol. 5855, no. 3, pp. 95–99, 2018.

[15] J. He, S. L. Baxter, J. Xu, J. Xu, X. Zhou, and K. Zhang, "The practical implementation of artificial intelligence technologies in medicine," *Nature Medicine*, vol. 25, 2019.

[16] C. Qi, A. Fourie, Q. Chen, and Q. Zhang, "A strength prediction model using artificial intelligence for recycling waste tailings as cemented paste backfill," *Journal of Cleaner Production*, vol. 183, no. 10, pp. 566–578, 2018.

[17] Y. Varatharajah, B. Berry, J. Cimbalnik et al., "Integrating artificial intelligence with real-time intracranial EEG monitoring to automate interictal identification of seizure onset zones in focal epilepsy," *Journal of Neural Engineering*, vol. 15, 2018.

[18] W. Pan and P. Suping, "A new scheme to improve the performance of artificial intelligence techniques for estimating total organic carbon from well logs," *Energies*, vol. 11, no. 4, p. 747, 2018.

[19] X. Zhang, Y. Wang, C. Liu, and Z. Chen, "A novel approach of battery pack state of health estimation using artificial intelligence optimization algorithm," *Journal of Power Sources*, vol. 376, no. feb.1, pp. 191–199, 2018.

[20] Y. Takefuji, "In the long run, the gap between the rich and poor will dramatically increase by artificial intelligence," *Science*, vol. 1, 2018.

[21] E. Klang, "Deep learning and medical imaging," *Journal of Thoracic Disease*, vol. 10, no. 3, pp. 1325–1328, 2018.

[22] G. Haskins, U. Kruger, and P. Yan, "Deep learning in medical image registration: a survey," *Machine Vision and Applications*, vol. 31, no. 1-2, 2020.

[23] H. Ba, "Medical sports rehabilitation deep learning system of sports injury based on MRI image analysis," *Journal of Medical Imaging and Health Informatics*, vol. 10, no. 5, pp. 1091–1097, 2020.

[24] Y. Xu, A. Hosny, R. Zeleznik et al., "Deep learning predicts lung cancer treatment response from serial medical imaging," *Clinical Cancer Research*, vol. 25, 2019.

[25] J. Sourati, A. Gholipour, J. G. Dy, X. Tomas-Fernandez, S. Kurugol, and S. K. Warfield, "Intelligent labeling based on Fisher information for medical image segmentation using deep learning," *IEEE Transactions on Medical Imaging*, vol. 38, no. 11, pp. 2642–2653, 2019.

[26] C. Liu, D. P. Ghosh, A. M. A. Salim, and W. S. Chow, "A new fluid factor and its application using a deep learning approach," *Geophysical Prospecting*, vol. 67, no. 1, pp. 140–149, 2019.

[27] W. Hu, B. Cai, A. Zhang, V. Calhoun, and Y.-P. Wang, "Deep collaborative learning with application to multimodal brain development study," *IEEE Transactions on Biomedical Engineering*, vol. 66, p. 1, 2019.

[28] J. Asanuma, S. Doi, and H. Igarashi, "Transfer learning through deep learning: application to topology optimization of electric motor," *IEEE Transactions on Magnetics*, vol. 56, no. 99, p. 1, 2020.

[29] M. K. Al-Sharman, Y. Zweiri, M. A. K. Jaradat, R. Al-Husari, and D. Gan, "Deep-learning-based neural network training for state estimation enhancement: application to attitude estimation," *IEEE Transactions on Instrumentation and Measurement*, vol. 69, pp. 1–11, 2019.

[30] T. Zhang, Y. Liu, J. Gao, L. P. Gao, and J. Cheng, "Deep learning-based mobile application isomorphic gui identification for automated robotic testing," *IEEE Software*, vol. 37, 2020.

[31] E. Trivizakis, G. C. Manikis, K. Nikiforaki et al., "Extending 2D convolutional neural networks to 3D for advancing deep learning cancer classification with application to MRI liver tumor differentiation," *IEEE Journal of Biomedical and Health Informatics*, vol. 23, p. 1, 2018.

[32] W. Yan, R. Xu, K. Wang, T. Di, and Z. Jiang, "Soft sensor modeling method based on semisupervised deep learning and its application to wastewater treatment plant," *Industrial & Engineering Chemistry Research*, vol. 59, no. 10, pp. 4589–4601, 2020.

Hindawi
Scientific Programming
Volume 2023, Article ID 9867894, 1 page
https://doi.org/10.1155/2023/9867894

Retraction

Retracted: Ice and Snow Sports Education Based on 5G Cloud Computing to Improve the Social Adaptability of Southern University Students

Scientific Programming

Received 31 October 2023; Accepted 31 October 2023; Published 1 November 2023

This article has been retracted by Hindawi following an investigation undertaken by the publisher [1]. This investigation has uncovered evidence of one or more of the following indicators of systematic manipulation of the publication process:

(1) Discrepancies in scope
(2) Discrepancies in the description of the research reported
(3) Discrepancies between the availability of data and the research described
(4) Inappropriate citations
(5) Incoherent, meaningless and/or irrelevant content included in the article
(6) Peer-review manipulation

The presence of these indicators undermines our confidence in the integrity of the article's content and we cannot, therefore, vouch for its reliability. Please note that this notice is intended solely to alert readers that the content of this article is unreliable. We have not investigated whether authors were aware of or involved in the systematic manipulation of the publication process.

Wiley and Hindawi regrets that the usual quality checks did not identify these issues before publication and have since put additional measures in place to safeguard research integrity.

We wish to credit our own Research Integrity and Research Publishing teams and anonymous and named external researchers and research integrity experts for contributing to this investigation.

The corresponding author, as the representative of all authors, has been given the opportunity to register their agreement or disagreement to this retraction. We have kept a record of any response received.

References

[1] D. Zhang and C. Xia, "Ice and Snow Sports Education Based on 5G Cloud Computing to Improve the Social Adaptability of Southern University Students," *Scientific Programming*, vol. 2021, Article ID 3828624, 12 pages, 2021.

Hindawi
Scientific Programming
Volume 2021, Article ID 3828624, 12 pages
https://doi.org/10.1155/2021/3828624

Research Article

Ice and Snow Sports Education Based on 5G Cloud Computing to Improve the Social Adaptability of Southern University Students

Donghui Zhang[1] and Chengqian Xia[2]

[1]*Department of Physical Education, Jinling Institute of Technology, Nanjing, Jiangsu 211169, China*
[2]*School of Sports Science, Nantong University, Nantong, Jiangsu 226019, China*

Correspondence should be addressed to Chengqian Xia; xiachengqian@ntu.edu.cn

Received 20 August 2021; Accepted 16 September 2021; Published 30 September 2021

Academic Editor: Punit Gupta

With the rapid development of the internet, the 5G cloud computing environment is gradually replacing the traditional computing environment. The social adaptation level of college students in this environment is an important indicator of whether college students can effectively integrate into the society. This article aims to study the design and reform of ice and snow sports education in the 5G cloud computing environment to enhance the social adaptability of college students. On this basis, in order to improve the social adaptability of southern university students, research on ice and snow sports education is proposed. This paper uses the literature method to study the characteristics of ice and snow sports education and the training model of social adaptability, constructs an experimental study on improving the social adaptability of southern college students, analyzes the overall impact of college students' participation in ice and snow sports education on social adaptability, and compares the situation with college students' participation in different sports to improve social adaptability. The social adaptability of college students from the lower grades to the upper grades is gradually enhanced, and the social adaptability score of boys is 35.8, the score of girls' social adaptability is 33.7, and the scores of boys are higher than those of girls.

1. Introduction

In today's society, competition is fierce, and everyone must adapt to this social environment. Strong social adaptability of students is the ladder and foundation to integrate well into the society. College students should effectively grasp this period and cultivate their social adaptability. The teaching method of physical education is different from other courses, and it has a good effect on the cultivation of students' social adaptability. Therefore, this article has very important significance and research value for the research of college physical education and the cultivation of college students' social adaptability.

Social adaptability is one of the basic qualities required by college students, and it is also an important part of higher-quality education for college students. Strong social adaptability is the ladder and foundation for students to integrate well into society. In university, cultivating strong social adaptability can help college students to enter society smoothly, cultivate good interpersonal relationships, and gradually lead to success in life. Ice and snow sports are an important part of sports in North China University. The introduction of ice and snow training courses strengthened the students' physique and stimulated the enthusiasm of college students. Rich and diverse teaching methods, strong competition, and entertainment are students' favorites. According to the current demand for economic and social development talents, Southern University has innovated the ice and snow education methods and methods based on physical and mental health, developed the characteristics of ice and snow sports teaching, actively implemented curriculum education reforms, and actively implemented students' social adaptation education and training that should be unified; in the ice and snow sports training, infiltrate high-quality education, antishock ability education, mental health education, innovation and entrepreneurship education, ideological and political education, etc. The practice of winter ice and snow sports makes the talents cultivated by the university have excellent social adaptability and better promotes economic and social development.

Yang is constantly advancing and deepening the reform of physical education in our country today. Innovative education has become a new development direction of education. School physical education urgently needs to carry forward the teaching method that integrates theory with practice and continuously innovate in teaching methods to cultivate more adaptability. High-quality compound sports talents needed by all sectors of society. Using literature analysis, logical induction, etc., it analyzes the creative concepts and challenges faced by physical education and proposes theoretical and practical innovations in physical education methods from the aspects of rationally determining the physical education process, implementing emotional physical education, and designing physical education classroom teaching. However, his research cannot fundamentally solve the current problems of physical education [1]. Van Tuan's adaptation to learning activities plays a very important role in the academic performance of first-year students. In order to have targeted solutions to improve the adaptability of first-year students to learning activities, it is necessary to find out influencing factors. This research aims to explore the factors affecting the learning adaptability of first-year students at the Vietnamese University of Labor and Social Affairs and to find ways to improve students' learning adaptability. Methods: this study adopts quantitative research methods, taking first-year students from Vietnam University of Labor and Social Affairs as the research object and surveying 300 students. Pearson's correlation coefficient test and linear regression analysis were performed on the research results. Main research results: the research results show that students' adaptability to learning activities is affected by many different factors; subjective factors such as motivation, learning methods, skills, etc., have a great impact on students' learning behavior. However, his research did not fully consider the combined influence of internal and external factors [2]. The development of Ardianto's e-sports education is not only playing games, but also various forms of education such as entrepreneurship, development, marketing, and scientific research for the purpose of training skills and providing knowledge. The opinions expressed by the public can take the form of support, criticism, and input. In order to distinguish between positive and negative sentiments, a large number of comments need to be accurately analyzed. This research aims to measure people's views on e-sports education or distinguish between positive and negative emotions in order to obtain valuable information from social media. The research was obtained through social media on Twitter. This research uses classification algorithms, naive Bayes and support vector machines. Through the comparison of the two algorithms, the prediction results show that the accuracy of the naive Bayes algorithm with SMOTE is 70.32%, and the AUC value is 0.954. The accuracy rate of SMOTE support vector machine is 66.92%, and the AUC value is 0.832. From these results, it can be seen that the naive Bayes algorithm has higher calculation accuracy. However, his educational research results cannot fully explain the actual application situation, nor has it changed the traditional e-sports education method [3].

The innovations of this article are as follows: (1) the combination of qualitative research and quantitative research, and adequate analysis of research data; (2) the combination of theoretical research and empirical research, based on the discussion of physical education theory, combined with ice and snow sports empirical investigation and analysis of the actual situation; and (3) innovatively adding ice and snow sports to the winter exercise courses of southern colleges and universities, providing a new alternative way to improve the social adaptability of college students.

2. Research Methods of Ice and Snow Sports Education on Improving the Social Adaptability of Southern College Students

2.1. Ice and Snow Sports Education. Universities in the north, especially those in the three northeastern provinces, have made full use of natural advantages, combined with specific geographical conditions, cold winter, long snowfall, and ice and snow characteristics and provided various ice and snow training courses [4]. For example, some universities provide educational content such as ice hockey, speed skating, ice dancing, skating, and snowball, and some schools provide courses such as durability skiing, curling, and ice and snow activities. Combining the characteristics of ice and snow, students have the opportunity to build themselves on ice and snow, cultivate self-confidence, show themselves, and fully grow [5].

Ice and snow sports education has the following characteristics:

(1) Adaptability: most of the ice and snow courses are conducted outdoors in the cold, and students must endure long-term low-temperature tests. As a result, the ability of students to adapt to harsh environments has been greatly improved, and students have the endurance and toughness that are not afraid of severe cold and difficulties [6].

(2) Exercise: most of the snow and ice routes provided by the university are outdoors with fresh air. Appropriate winter sports can promote the body's metabolism and improve the physical condition of students. In addition, outdoor aerobic exercise can concentrate students' energy and attention for a long time, and help students effectively improve their academic performance [7].

(3) Recreation: all kinds of ice and snow sports have a certain degree of entertainment and appreciation. For example, skating is a combination of aesthetics and sports elements, which brings people a happy mood. Students can not only appreciate the visual beauty brought by ice and snow in the first-class compulsory courses but also learn the ice and snow culture [8].

(4) Competitiveness: all sports are competitive, and ice and snow sports are no exception. In the education process, teachers can improve the effect of education and cultivate team spirit through competition. The spirit of cooperation and fair competition of college students can fully stimulate students' defying characteristics and teamwork ability [4].

(5) Educational: ice and snow training has the characteristics of humanitarian education. The ice-snow route combines local characteristic culture and modern elements to improve students' humanitarian literacy, cultivate outstanding personalities, adjust their psychological imbalances, and promote the overall development of college students.

(6) Normativeness: the normative characteristics of ice and snow sports, precisely under the strict ice and snow sports system and evaluation criteria, make ice and snow sports training very attractive and attractive [5].

Figure 1 shows the main features of ice and snow sports education.

Ice and snow sports are a kind of humanistic sports. They have a strong humanitarian atmosphere and characteristics that promote the development of people and society. The main target of ice and snow sports teaching is students, who cultivate and form characteristics in the learning process of students. If there is no student as the main body, then this kind of education will no longer exist. Ice and snow sports training must be based on the students' sports and social development needs [9]. In the process of ice and snow sports training, students gradually established the concept of humanitarianism to meet humanitarian needs [10]. The humanitarian value of ice and snow sports education refers to the importance and value of ice and snow sports education in the development of society and people. The human value of ice and snow education is not only related to the social status of ice and snow education in society, but also related to the development momentum of ice and snow education. Only through a correct understanding of the humane value of ice and snow sports education can the society and students' sports education needs be met [11].

In essence, sports are the pursuit of the organic unity of body and health, the pursuit of self-cultivation, and the common progress of physical function [12]. Ice and snow sports give full play to the functions of strengthening the body, alleviating emotions, promoting communication, and improving students' awareness of physical conditions. Improve your own comprehensive quality, nurture your own powerful strength to overcome the difficulties in life, strengthen the spiritual strength of students, cultivate students' innovative spirit, cherish the body, and enhance personality [9, 13]. In the training process of ice and snow sports, pay attention to the physical development of students, give full play to the main role of students, so that the physical and mental health of students can be well developed, and combine the physical and mental health of students to give full play to the infinite possibilities of students Through ice and snow sports education to guide students to learn to unite, learn to be a person, learn to adapt to society, and be a useful and valuable talent for society [14, 15].

2.2. Social Adaptability

2.2.1. Brief Description of Social Adaptability. Adaptation was first used in biology, which mainly refers to the purpose of adapting to the environment and survival by changing its own structure and function [16]. Later, this concept was introduced into the social environment, specifically referring to the process of human beings adapting to the social system of the natural and social environment. Some scientists have also put this concept that is called "debugging"; the common denominator is that the changes themselves to their own environmental action adaptation of the play interaction between people or groups [17].

In sociology, social adaptation refers to the process by which individuals or groups adjust their actions in order to adapt to the social environment. That is different from the process of biological adaptation to the natural environment. The new "social adaptation" education goal proposed in the "Outline" is to emphasize the social adaptation value of sports. The focus is on the way the individual enters the collective life-psychological adaptation in physical movement [18].

The process of social adaptation is the process of personal socialization, and social adaptation is not an empty abstract concept. The process of social adaptation is essentially a process of continuous socialization of individuals [11]. In order to become a social person, biologists must adapt to the social changes in which they live, gradually form concepts, adjust interpersonal relationships in communication and interaction with people, learn social roles and social relationships, and learn to experience various failures [19]. At the same time, we must realize that we must deal with various contradictions, learn to reconcile and adapt in the process of personal socialization, learn cooperation and competition, learn various rules and values, and accept various differences in society [20]. What is particularly important in the process of physical education is competition and adjustment, victory and defeat, the desire to win and the boundaries of rules, sensibility and rationality, and complex interactions. Contrary to the various characteristics of the educational process itself, sports promote socialization of the individual. It has an irreplaceable and unique effect in improving social adaptability [21].

The improvement of social adaptability is a natural person who consciously maintains social order through social education, values, and behavioral standards, starting with children and slowly learning social knowledge. Sports activities play an important role in improving people's social health and becoming social people. In sports, we must abide by the rules of the game and maintain the order of the game. This kind of awareness and action of interaction, cooperation, competition, and compliance with the rules of sports activities will be combined with daily social life and applied to study and work, which will help cultivate social adaptability.

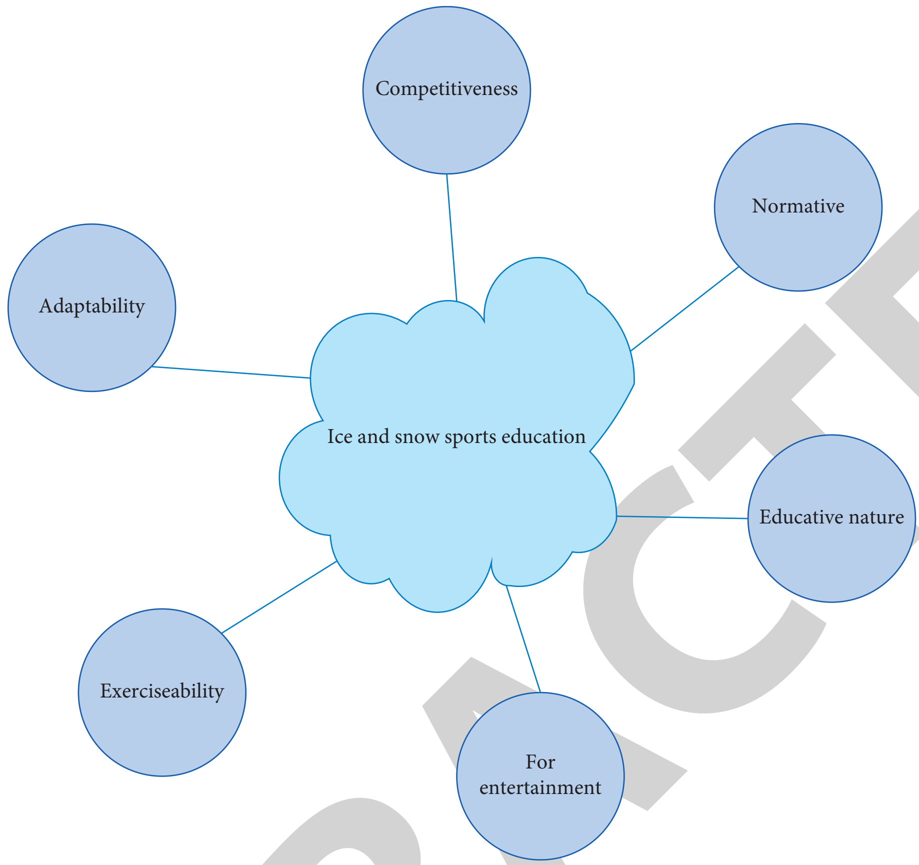

Figure 1: The main characteristics of ice and snow sports education.

2.2.2. The Relationship between Physical Exercise and Social Adaptability. Physical exercise helps to improve social adaptability. The role of sports in educating people is to take social responsibility. Society is an interactive part composed of political, economic, cultural, and other factors. Everyone plays one or more social roles. In society, in various situations, being connected with people of various identities, adapting to various social environments, and the ability to respond appropriately and quickly is an important manifestation of social responsibility. Sports activities can provide a higher environment and suitable conditions to teach people to learn to assume social roles. For example, in a basketball game, after a specific class is divided into groups, the various roles in the team, the wingers, center forwards, and guards of each group are in their respective positions, and mutual social relations are established through appropriate roles. In the social relationship created by sports, every role has the right to win, the right to win prizes, and the right to take technical actions in accordance with the rules. At the same time, it also has the obligation to comply with sports law, ethics, and technical regulations. Social role is to integrate social forms and individual actions necessary for social activities. Through the research on the role of sports, students realize that the role of society is a series of rules and obligations consistent with the role of sports. Action mode is people's expectation of individual actions with specific identities. This helps people understand the social concept of "what is like what" and lays an ideological foundation for their own work in order to adapt to the needs of various groups in society in the future. Through physical exercise, college students can play a variety of roles through personal efforts, and they can also experience an important method of changing social status and understanding social conditions through personal subjective efforts. This is especially important for modern young people.

Sports activities cultivate people's adaptability to social rhythms. With the further deepening of social opening up, the pace of economic growth has accelerated, and the pace of social movements has changed from slow to fast. From the perspective of increasing labor productivity, the average annual growth rate of primitive society is 1–2%, the average growth rate per 10,000 years of slave society and federal society is 4%, and the annual growth rate of capitalist society is 3%. Today's annual growth rate is 6–10% or more. The rapid increase in labor productivity and the continuous decrease in spare time will inevitably lead to the acceleration of work and life. The high-speed social rhythm not only brings material wealth and spiritual wealth to the society, but also brings people many health problems such as psychological stress and depression. Sports and recreational activities are important tools for people to adapt to the new rhythm of life. Some social experiments and studies have shown that athletes and people who regularly participate in sports have a strong ability to adapt to their own changes and able to master the rhythm of life well. This is because in sports activities, people have a variety of activity skills and quick action methods. It helps people avoid unnecessary activities and become out of control and complete various production and life activities correctly, coordinately, and quickly. Exercise can accelerate the operation of the human nervous system and cardiovascular system and can also improve the body's social adaptability. Decompression through sports can not only help relieve social pressure, reduce anxiety, and achieve the purpose of relaxation but also can stabilize the physical and mental emotions, enhance confidence, and improve social resilience in the long term.

2.3. Data Analysis Algorithm

2.3.1. The Principle of Logistics Regression and Zero-Width Space. The main idea of using logistics regression for classification is to establish a regression formula for the classification boundary line according to the existing data to classify. The term "regression" here comes from the best fit, which means to find the best fitting parameter set. The prediction function formula is

$$\sigma(z) = \frac{1}{1+e^{-z}}. \tag{1}$$

Cost function is

$$\sum_{i=1}^{m}\left(y^{(i)}\log h_{\theta}\left(x^{(i)}\right)+\left(1-y^{(i)}\right)\log\left(1-h_{\theta}\left(x^{(i)}\right)\right)\right). \tag{2}$$

The minimum value $J(\theta)$ obtained by the gradient descent method is

$$\theta_j \coloneqq \theta_j - \alpha\sum_{i=1}^{m}\left(h_{\theta}\left(x^{(i)}\right)-y^{(i)}\right)x_j^{(i)}, \quad (j=0,1,\ldots,n). \tag{3}$$

The process of training the classifier is to use the optimal algorithm to find the best fitting parameters. First of all, a suitable prediction function h is needed, which is also a classification function. It is used to predict the judgment result of the input data to construct a cost function (loss function), which represents the difference between the expected output (h) and the training data category (y). This may be the difference between the two (h-y). Fully consider the "loss" of all training data, that is, the total cost or average cost, and record it as a function $J(\theta)$. This represents the deviation of the estimated value of all training data from the actual category. Obviously, the lower the value of the function $J(\theta)$, the more accurate the prediction function (i.e., the more accurate the function h). Therefore, it is necessary to find the minimum value of the function $J(\theta)$ in this step [22].

2.3.2. Decision Tree. The decision tree is a tree structure (may be a binary tree or a nonbinary tree). Each nonleaf node represents a function test, each branch represents a range of specific function output values, and each drawing node stores a category. The process of using the decision tree to make a decision is to start from the root node, confirm the corresponding function of the classification item, select the output area according to the value, and use the category stored in the drawing node as the decision result.

Information gain:

$$I(x_i) = -\log_2 p(x_i). \tag{4}$$

Calculate entropy:

$$H = -\sum_{i=1}^{n} p\left|(x_i)\right|\log_2 p(x_i). \tag{5}$$

In the decision tree, let D be the division of training tuples by categories; then the entropy of D is expressed as

$$\operatorname{info}(D) = -\sum_{i=1}^{m} p_i \log_2(p_i). \tag{6}$$

Now, we assume that the training tuple D is divided by attribute A; then the expected information of A divided by D is

$$\operatorname{info}_A(D) = \sum_{j=1}^{v}\frac{|D_j|}{|D|}\operatorname{info}\left(D_j\right). \tag{7}$$

The information gain is the difference between the two:

$$\operatorname{gain}(A) = \operatorname{info}(D) - \operatorname{info}_A(D). \tag{8}$$

The advantage of this method is that the computational complexity is not high, the output result is easy to understand, it is not sensitive to the lack of intermediate value, and it can handle irrelevant feature data. It can be used for classification and regression.

$$P(A|B) = \frac{P(B|A)P(A)}{P(B)}. \tag{9}$$

Naive Bayes is not sensitive to missing data, and the algorithm is relatively simple, and it is often used for text classification.

Gaussian normal polynomial distribution:

$$P\left(X_1 = n_1, \ldots, X_k = n_k\right) = \left\{\frac{n!}{n_1!\cdots n_k!}p_1^{n_1}\cdots p_k^{n_k}, \quad \sum_{i=1}^{k} n_i = n, 0, \text{other wise.}\right. \tag{10}$$

Bernoulli distribution:

$$\frac{n!}{r!\,(n-r)!}p^{k}(1-p)^{n-k}. \tag{11}$$

3. Experimental Research of the Winter Sports Education to Enhance the Ability of the South Students of Social Adaptation

3.1. Physical Education Culture of Snow and Ice on the Ability to Adapt to College Students

3.1.1. Improve Students' Social Adaptability through Humanity Training. In the current course guidance process for college students, we should not only focus on cultivating students' high-quality education content, but also focus on cultivating students' humanistic qualities. The so-called humanized cultivation refers to the cultivation of human nature and society. In the guidance process of ice and snow sports courses, colleges and universities need to pay attention to improving students' comprehensive quality and learning awareness. For example, in a speed skating class, the content of speed skating can improve the learning ability of students, thereby forming a more challenging course teaching.

3.1.2. Realize the Humanized Mode of Teaching Methods. As an intuitive type of sports, ice and snow sports are rich in content, providing students with a good sports education experience. The creation of course content reflects the importance of students, emphasizes the student's dominant position, and converts traditional passive learning methods into active learning methods to create relaxing and comfortable education courses. Throughout the education implementation process, pay attention to the changes in student feelings over time. Consider the adaptability of students. At the same time, in the education process, physical education teachers must respect students, improve their learning awareness and self-improvement awareness, so that students can form an optimistic and self-confident mental state in the learning process and fully adapt to the development needs of students. Therefore, in the entire education process, the basic connotation of ice and snow sports must be emphasized to stimulate students' conscious desire to learn.

3.1.3. Establish a Humane Teaching Evaluation System. The humanized education evaluation system should fully consider students' autonomy and interest in learning in the course evaluation process and fully consider the quality of students, physical education, and personal development. Pay attention to students' learning achievements and implement differentiated and personalized education models. At the same time, in the course content evaluation process, students must fully integrate their daily academic performance and test results to establish a complete course evaluation model. Through the establishment of a humane teacher evaluation system, the differences between students can be found in a short time, laying a good foundation for the overall growth of students.

Figure 2 shows the research direction of ice and snow sports education on the cultivation of college students' adaptability.

3.2. Experimental Design to Enhance the Capacity of the South Students Study Social Adaptation of Snow Sports Education

3.2.1. Research Object. The research object selected in this article is based on the impact of ice and snow sports education on improving the social adaptability of southern college students. Affect the situation.

3.2.2. Research Methods

(1) *Literature Data Method*. This article has consulted a large amount of data and references, including CNKI, Wanfang Thesis Database, and Chinese Sports Journals, and organized a large amount of relevant information through the above channels.

(2) *Expert Interview Method*. The questionnaire survey in this article consulted many experts and scholars and revised and improved them under their guidance. In addition, I also consulted physical education experts in universities, communicated with them, absorbed their suggestions and opinions, combined with the actual situation, and completed the research of this article.

(3) *Questionnaire Survey Method*. According to the purpose of the research, a random sampling method is adopted to select some students from southern universities as the survey objects.

(4) *Mathematical Statistics*. Use mathematical methods, Excel software, sports statistics, and SPSS statistical software to analyze, classify, and organize data, and use graphs to reflect the survey results.

4. Research Situation of Ice and Snow Sports Education on Improving the Social Adaptability of Southern College Students

4.1. Status Quo of Domestic Research on Physical Education for Improving College Students' Social Adaptability. In order to understand the current status of domestic physical education research on the number of literatures on improving college students' social adaptability, this article selects the period from 2008 to 2018 as the time limit, selects "title" as the search term, and selects social adaptability as the "search topic." The full-text database and excellent paper database of Chinese journals, the search results show that a total of 1,692 papers have been published in China, including 1,494 papers, 4 doctoral papers, and 194 master papers. As shown in Table 1 and Figure 3, this paper compares the publication year of books and periodicals and the number of documents to form a distribution of the number of documents on

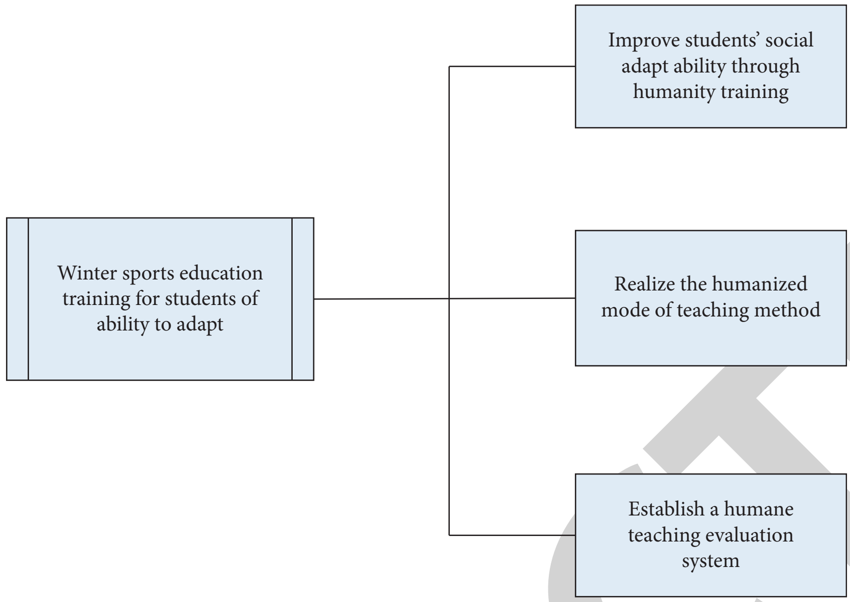

Figure 2: The research direction of ice-snow sports education on the cultivation of college students' adaptability.

Table 1: Research on the literature quantity of physical education for improving college students' social adaptability.

Years	Number of related literature studies	Growth ratio
2008	53	
2009	97	45.36
2010	98	1.32
2011	143	31.46
2012	173	17.34
2013	178	2.80
2014	217	17.97
2015	215	−0.93
2016	245	12.24
2017	235	−4.25
2018	267	11.98

physical education to improve the social adaptability of college students.

From Table 1 and Figure 3, it can be seen that the number of domestic physical education documents on improving college students' social adaptability is generally on the rise. The largest increase was in 2009, reaching 45.36%, and the highest number of documents in 2018 was 567, compared with the previous year. The increase of 11.98% shows that more and more researchers are concerned about the social adaptability of college students and hope to improve the social adaptability of college students through physical exercise.

4.2. Results of the Winter Sports Education to Enhance the Ability of Community College Students to Adapt to the Southern Analysis. It can be seen from Table 2 and Figure 4 that more women were interviewed than men, accounting for 83.9% of the total, and seniors accounted for 26.7%. According to the survey, boys' social adaptability is higher than that of girls, and the social adaptability of freshmen, sophomores, juniors, and seniors also increases with age. Comparing different majors, arts and sports students are slightly more socially adaptable than science and engineering students, and liberal arts students are slightly lower. It shows that the overall social adaptability of college students needs to be improved.

From Figure 5 and Table 3, it is found that 88.5% of the students who have received ice and snow physical education are mainly for physical fitness; in addition, 42.7% and 35.4% are for the purpose of shaping bodybuilding and promoting mental health. The proportion is also relatively large. The proportion of improving social adaptability is not high. The proportion of boys is 25.7% and the proportion of girls is 26.9%. This shows that college students' awareness of this aspect is not high enough, and colleges and universities need to give full consideration and guidance to help college students improve. It can be seen from this that, in the eyes of most students, the main purpose of receiving ice and snow physical education is to exercise, form a good body shape and maintain a healthy mental state.

This article divides sports venues into gymnasiums, school playgrounds, parks, and ski resorts. The exercise duration is divided into three time periods: less than 30 minutes, 30–60 minutes, and more than 60 minutes. From the data in Table 4, it can be seen that the proportion of people exercising on the school playground is the highest, reaching 38%, the proportion of people in the gym is 34%, and the proportion of people in the park is 28%. Most of the people who exercise on the school playground are college students, and their awareness of exercise is relatively high, and the school playground is a very convenient place for sports. The gym is mainly a place for young people to exercise. It can make friends widely, improve communication skills, and enhance social adaptability. As a professional sport, ski resorts need professional guidance. For Southern University students, setting up ski resorts for professional ice and snow sports education and training is not only a sense of

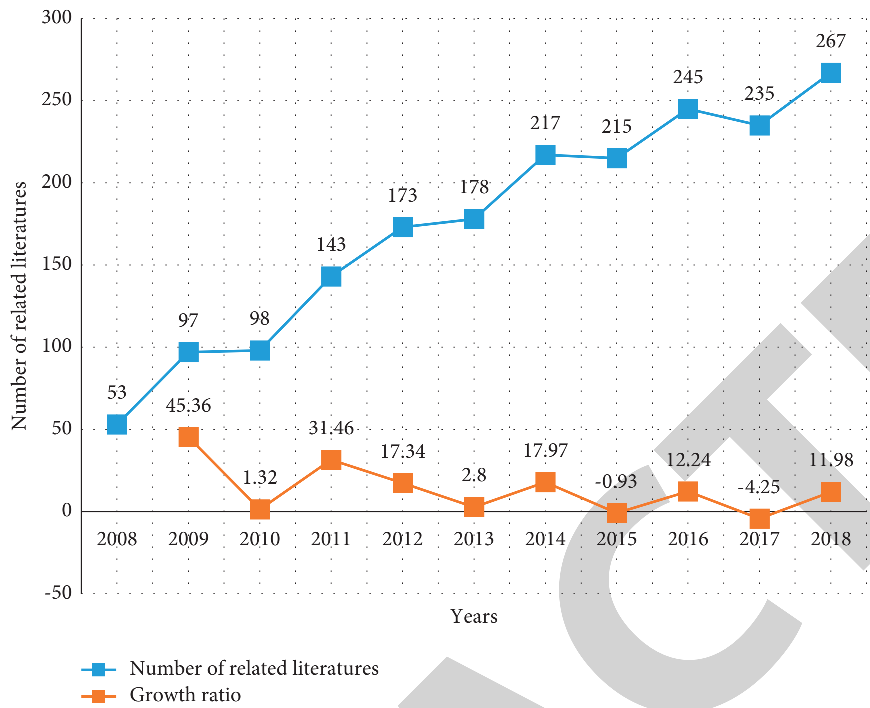

Figure 3: Research on the literature quantity of physical education for improving college students' social adaptability.

Table 2: An overall analysis of the influence of college students' participation in ice and snow sports on their social adaptability.

	Schoolboy	Girl student	Science and engineering	Sports art
Freshman	13.6	12.4	8.9	7.7
Sophomore	25.6	22.4	15.6	12.4
Junior	29.7	23.5	22.7	25.9
Senior	35.8	33.7	35.8	38.9
Population	98.7	83.9	84.9	87.3

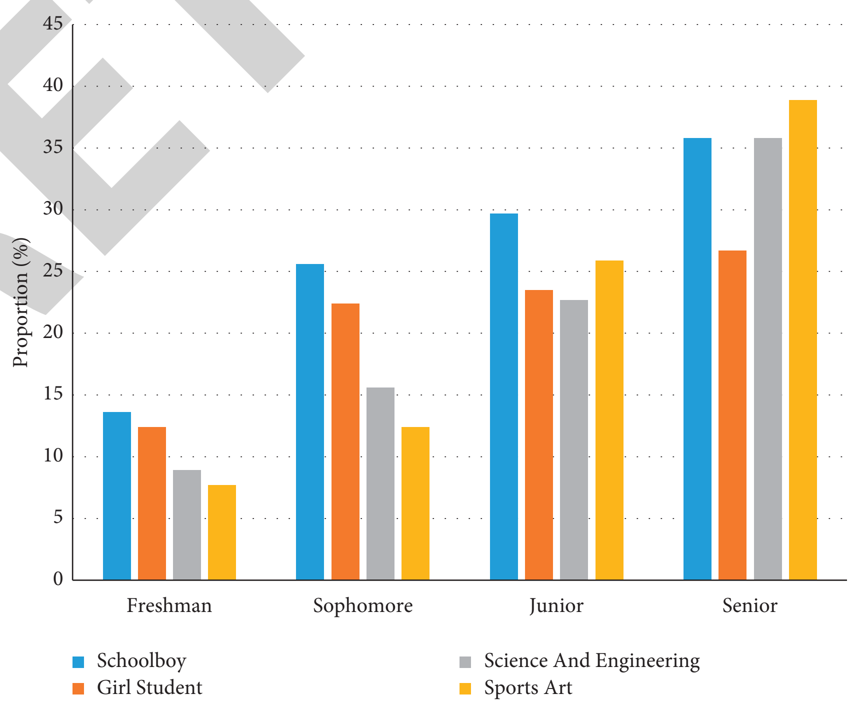

Figure 4: An overall analysis of the influence of college students' participation in ice and snow sports on their social adaptability.

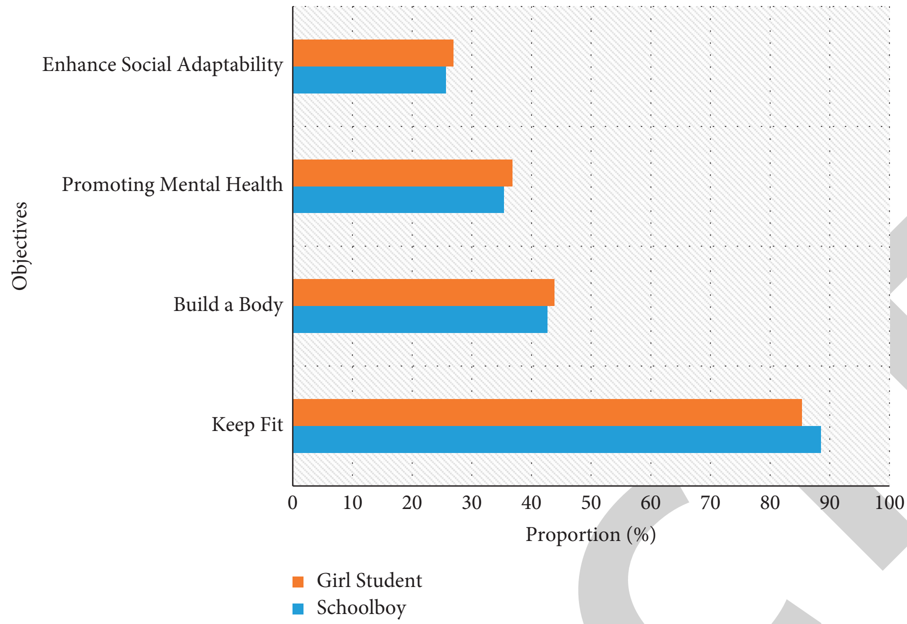

Figure 5: Analysis on the purpose of college students' participation in ice and snow sports education.

Table 3: Analysis on the purpose of college students' participation in ice and snow sports education.

Objective	Schoolboy	Girl student
Keep fit	88.5	85.3
Build a body	42.7	43.9
Promoting mental health	35.4	36.8
Enhance social adaptability	25.7	26.9

Table 4: The choice of sports time and sports place for college students.

Sports venues	Proportion of people (%)	Exercise duration (min)	Proportion of people (%)
Gym	34	Less than 30 minutes	15
		30–60	35
		Above 60	48
School playground	38	Less than 30 minutes	25
		30–60	46
		Above 60	12
Park	28	Less than 30 minutes	26
		30–60	33
		Above 60	13
Ski field	25	30–60	58

freshness, but also a sense of tension. 25% of students are willing to go to ski resorts to participate in ice and snow sports training. The course is set for 30–60 minutes, which can achieve the purpose of physical exercise and improve social adaptability. For Southern University students, they can better adapt to different situations. The external environment can also learn different exercise methods.

It can be seen from Figure 6 that 15% of the exercise time in the gym is less than 30 minutes, 35% of the time is 30–60 minutes, and 48% of the time is more than 60 minutes; regarding exercise in the school playground, the proportion of time less than 30 minutes is 25%, the proportion of time between 30 and 60 minutes is 46%, and the proportion of time exceeding 60 minutes is 12%; the proportion of fitness in the park is less than 30 minutes is 26%. The ratio of 30–60 minutes is 33%, and the ratio of more than 60 minutes is 13%. It can be seen from the data that gyms have the highest proportion of exercise time longer than 60 minutes, indicating that college students prefer professional sports venues. Therefore, setting up ice and snow sports teaching in colleges and universities can also greatly enhance students' interest and make students improve their social adaptability from ice and snow sports.

It can be seen from Figure 7 and Table 5 that group sports are more popular. This group of freshmen alone accounted for 59.6% of the total number; students who chose relatively independent programs accounted for 38.9%, and the remaining students who are uncertain in the lower part

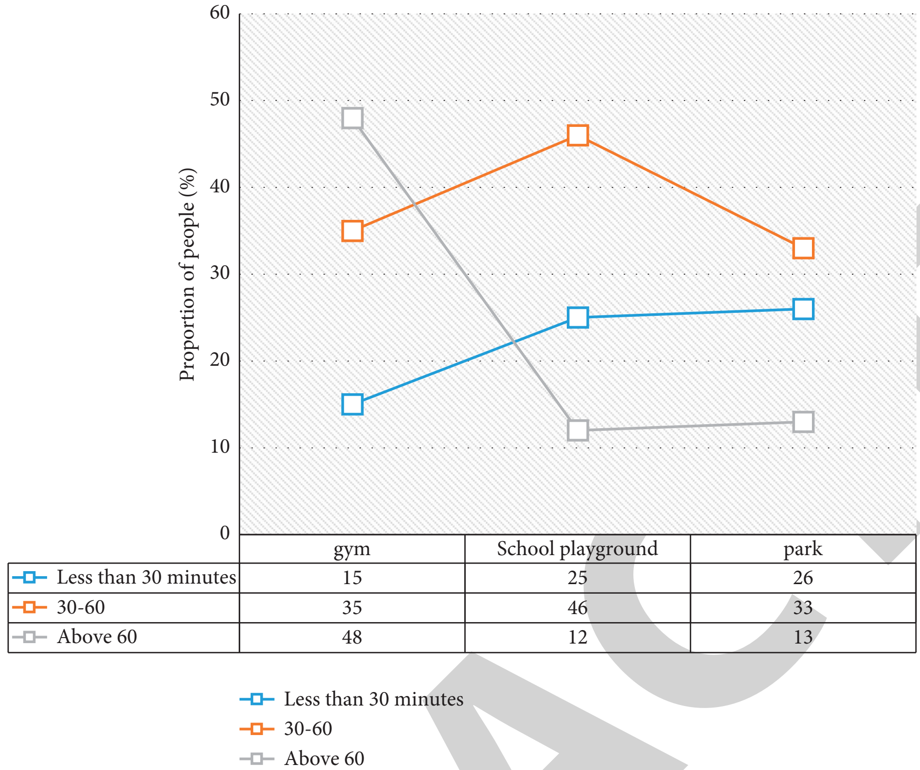

	gym	School playground	park
Less than 30 minutes	15	25	26
30-60	35	46	33
Above 60	48	12	13

FIGURE 6: Proportion of people's exercise time in different sports venues.

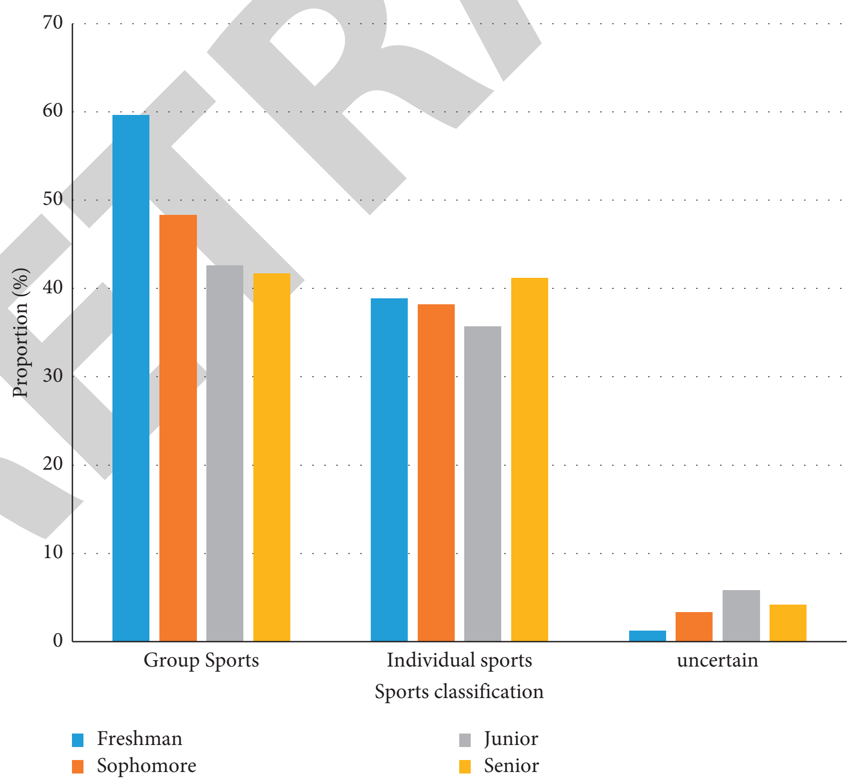

FIGURE 7: The influence of different forms of exercise on social adaptability.

account for less. Through summary analysis, it can be known that different forms of exercise can improve their own social adaptability to a certain extent, but the scores of social adaptability are quite different. Group sports are obviously higher than independent sports, which is uncertain. Students score higher than those of independence sports.

Table 5: The influence of different forms of exercise on social adaptability.

Sports classification	Freshman	Sophomore	Junior	Senior
Group sports	59.6	48.3	42.6	41.7
Individual sports	38.9	38.2	35.7	41.2
Uncertain	1.2	3.3	5.8	4.2

5. Conclusion

This article mainly focuses on the research of ice and snow sports education on improving the social adaptability of college students in southern China. It conducts in-depth research and discussion on ice and snow sports education and the social adaptability of college students through the method of literature data, questionnaire survey, and data analysis. This paper designs an experiment of ice and snow physical education to improve the social adaptability of college students in the south, analyzes the college students' exercise methods, exercise duration, and exercise venues, comprehensively contrasts and highlights the effect of ice and snow physical exercise on improving social adaptability, and through effective exercise methods. Let college students be more calm and calm in the face of the fierce external environment and deal with it safely.

The innovation of this article lies in the following points: first, combine qualitative research with quantitative research, and fully analyze the research data; second, combine theoretical research with empirical research, and combine it on the basis of discussing physical education theory. The actual situation in ice and snow sports is empirically investigated and analyzed. Third, the innovative addition of ice and snow sports to the winter exercise courses of southern colleges and universities provides a new alternative way to improve the social adaptability of college students.

This article suggests that major colleges and universities should combine the characteristics of their own schools to develop a socialization model suitable for physical exercise of college students in major colleges and universities and strengthen the explanation of the theoretical knowledge of students' sports health and social adaptation theory, so as to make a good foundation for their future adaptation to the society.

Data Availability

The data that support the findings of this study are available from the corresponding author upon reasonable request.

Disclosure

The authors confirm that the content of the manuscript has not been published or submitted for publication elsewhere.

Conflicts of Interest

The authors declare no conflicts of interest.

Authors' Contributions

All authors saw the manuscript and approved to submit it.

Acknowledgments

This work was supported by research results of educational reform at school level in Jinling Institute of Technology (JYJG2019-12) and Practical Research on Rural Sports Helping Precision Poverty Alleviation in the New Era (no. 18BTY108).

References

[1] Q. Yang, "A study of theories and practice of sports teaching methods based on Creative education concept," *Agro Food Industry Hi-Tech*, vol. 28, no. 1, pp. 3023–3025, 2017.

[2] P. Van Tuan, "Factors affecting the first-year students' adaptation to learning activities: a case study of a public university in Vietnam," *Humanities & Social Sciences Reviews*, vol. 8, no. 3, pp. 1422–1432, 2020.

[3] R. Ardianto, T. Rivanie, Y. Alkhalifi, F. S. Nugraha, and W. Gata, "Sentiment analysis on E-sports for education curriculum using naive Bayes and support vector machine," *Jurnal Ilmu Komputer dan Informasi*, vol. 13, no. 2, pp. 109–122, 2020.

[4] K. Alexander and J. Luckman, "Australian teachersí perceptions and uses of the sport education curriculum model," *European Physical Education Review*, vol. 7, no. 3, pp. 243–267, 2016.

[5] P. A. Hastie and T. Wallhead, "Models-based practice in physical education: the case for sport education," *Journal of Teaching in Physical Education*, vol. 35, no. 4, pp. 390–399, 2016.

[6] C. Evangelio, S. González-Víllora, J. Serra-Olivares, and J. C. P. Vicedo, "The sport education model in Spain: a review of state of the art and outlook," *Cuadernos de Psicología del Deporte*, vol. 16, no. 1, pp. 307–324, 2016.

[7] J. Patricios, "Sports medicine education: socrates, science and south Africa," *British Journal of Sports Medicine*, vol. 53, no. 10, pp. 585-586, 2019.

[8] F. Tian and L. Yang, "A brief talk on the development of student's social adaptability in junior school sports curriculum," *Science Education Journal*, no. 17, pp. 147-148, 2018.

[9] S. D. Fisher, J. L. Reynolds, and C. E. Sheehan, "The protective effects of adaptability, study skills, and social skills on externalizing student-teacher relationships," *Journal of Emotional and Behavioral Disorders*, vol. 24, no. 2, pp. 101–110, 2016.

[10] E. S. Chelsea, L. R. Jennifer, and D. F. Sycarah, "The protective effects of adaptability, study skills, and social skills on externalizing student-teacher relationships," *Journal of Emotional and Behavioral Disorders*, vol. 24, no. 2, pp. 101–110, 2016.

[11] R. Helens-Hart, "The employability self-assessment: identifying and appraising career identity, personal adaptability, and social and human capital," *Management Teaching Review*, vol. 4, no. 1, pp. 6–13, 2019.

[12] P. Hlao, L. Kvitkoviová, S. Jeek, and A. Hirschi, "Career adaptability and social support of vocational students leaving upper secondary school," *Journal of Career Assessment*, vol. 28, no. 3, pp. 478–495, 2020.

[13] K. L. Autin, R. P. Douglass, R. D. Duffy, J. W. England, and B. A. Allan, "Subjective social status, work volition, and career

Hindawi
Scientific Programming
Volume 2021, Article ID 7294206, 19 pages
https://doi.org/10.1155/2021/7294206

Research Article

An Intelligent Blockchain and Software-Defined Networking-Based Evidence Collection Architecture for Cloud Environment

Yunus Khan and Sunita Verma

Department of Computer Engineering, Shri G. S. Institute of Technology and Sciences Indore (RGPV), Bhopal, India

Correspondence should be addressed to Yunus Khan; yunuskhansgsits@gmail.com

Received 18 July 2021; Accepted 2 September 2021; Published 29 September 2021

Academic Editor: Punit Gupta

Cloud forensics is an extension of contemporary forensic science that guards against cybercriminals. However, consolidated data assortment and storage compromise the legitimacy of digital indication. This essay proposes an evolving modern algorithm automated forensic platform based on the blockchain idea. This proposes forensic structure design, evidence gathering, and storage on a blockchain that are peer to peer. Secure Block Verification Mechanism (SBVM) will protect unauthorised users. Secret keys are optimally produced using the cuckoo search optimization method. All data are saved and encrypted at the cloud authentication server for secrecy. Confidentiality-Based Algebraically Homomorphism, a new encryption method, is given to cryptosystem learning. Every data is assigned a block in the SDN controller, and the history is kept as metadata about data. Each block has a Secure Hash Algorithm version 3 of 512-bit hash-based tree. Our approach uses graph theory-based graph neural networks in Smart Contracts to track users' data (GNNSC). Finally, a blockchain-based evidence graph allows for evidence analysis. The experiments were run in a cloud environment with Python and network simulator-3.30 (for software-defined network). We achieved good results in terms of evidence response time, cloud evidence insertion time, cloud evidence verification time, computational overhead, hash calculation time, key generation times, and entire overall change rate of indication using our newly deliberated forensic construction using blockchain (FAuB).

1. Introduction

Cloud computing is an emerging technological concept that, through virtualization technology, provides users with physical resources. The cloud computing industry is growing with the benefit of allowing network accessing to a scalable and elastic combination of shared physical or virtual resources [1] with self-owned service provisioning and on-demand available services. There is also an enhancement in the number of cloud users using cloud computing because of these features. Security risks have begun to develop, however, with the rising cloud computing industry. Several security strategies for the cloud environment are being investigated with virtualization technologies, making it difficult to implement current digital forensic methods [2]. Access to certain system layers is restricted in Software-as-a-a-Service (SaaS) and Platform-as-a-a-Service (PaaS) [3] environments when the cloud environment is categorized according to the service model access to that layer which are regulated by Cloud Service Provider (CSP). It is therefore appropriate to supply the log data generated in the inaccessible layer to the CSP through agreement [4]. Investigators have complete control over the evidence in conventional digital forensics. In a cloud environment, however, data centers are geographically distributed; cloud service customers (CSCs) exchange physical infrastructure, unreliable data that disappear when the instance is shut down, virtual network, load balancing, and auto scaling to provide a smooth service environment [5]. Therefore, prior to a security incident for investigation, it is important not only to record data for cloud forensics but also to guarantee the truthfulness of the log data, while it is impossible for the investigator to directly capture the data and collect the data from the remote server. Forensic architecture is suggested for software-defined networking (SDN) using IoT [6] and blockchain. Blockchain's algebraic homomorphic encryption scheme is adapted here. Evidence data collection is performed in the presence of the SDN policy [7]. Digital evidence or stored on cloud using the data flow switches during the forensic examination. A (PDMS) data management system of provenance aware has been invented and built on the existing provenance monitoring framework [8]. Mchain [9] proposed an integrity management framework based on blockchain. Therefore, many analyses make an attempt that are distributed exploitation blockchain technology within the SDN cloud atmosphere [10]. During this analysis, within the cloud atmosphere, we tend to use the blockchain concept for cloud digital computer forensics. Forensic in cloud computing is an advancement of modern forensic science that protects against cyber criminals. Single centralize point compilation and storage of data, however, overcome the authenticity of digital evidence. In order to address this serious issue, this article suggests a modern automated forensic platform leveraging infrastructure as a cloud service (IaaS) based on blockchain concept. This proposed forensic architecture uses the blockchain technology to store the digital evidence and data are distributed among multiple peers. Secure Block Verification Mechanism (SBVM) is proposed to safeguarding the device from unauthorised users. Using the cuckoo search optimization algorithm for strengthening of the cloud environment, secret keys are optimally generated. On the bases of level of confidentiality, all data are stored and encrypted at cloud authentication server. Confidentiality-Based Algebraically Homomorphic Cryptosystems learning is presented with a fast-forwarding algorithm for encryption. A block in the SDN controller is created for every data, and information is stored in the cloud service provider, and the history is recorded as metadata about data. A hash-based tree is constructed in each block by the Secure Hash Algorithm version-3 of 512 bits. By implementing graph theory-based graph neural networks in Smart Contracts, our framework enables users to track their data (GNNSC). Finally, the construction of a Logical Graph of Evidence from blockchain data enables evidence analysis. Experiments were carried out in a Python for cloud and blockchain-integrated environment with network simulator-3.30 (for software-defined network). The proposed forensic architecture (FAuB) shows promising results in response time, evidence insertion time, evidence verification time, communication overhead, hash computation time, key generation time, encryption time, decryption time, and total change rate according to a comprehensive comparative study.

1.1. Research Contribution. In this article, the following contributions have been made to provide additional digital forensics research:

(1) In the case of cloud environment like infrastructure as a cloud service (IaaS), the digital forensics mechanism [11] design is constructed to collect, analyze, and release evidence. Blockchain technology is used to collect evidence.

(2) Evidence and information are secured against malicious users by using the Secure Block Verification Mechanism (SBVM) [12] driven by a cloud authentication server (CAS). The SBVM involves users who have completed successfully secure verification process by means of a globular logic and secret key (SK).

(3) Based on confidentiality level or the generation of digital signature [13] and encryption, the EL GAMAL algorithm is proposed. Key generation is done by the cuckoo search optimization algorithm in CB-EL GAMAL to generate strong secret keys. The main contribution of the Algebraically Homographic Cryptosystem algorithm based on confidentiality is that the proposed algorithm is based on the data level of sensitivity and adaptive in nature.

(4) Block was generated by control plane SDN and distributed across the blockchain network for all facts and statistics being deposited in the cloud-based server. For added security, a Secure Hashing-3 (SHA-3-512) algorithm has been proposed for blockchain accounts. By using neural network-based smart contracts (GNNSCs) on graph to track data activities throughout its life cycle, the data source is preserved.

2. Background

Siva Rama Krishna Tummalapalli [14] developed Bayesian fuzzy clustering and cluster search laid on support vector neural network-based intrusion detection mechanism simulator for clustering and two-level classifier working on cloud environment [15]. Saad Said Alkahtny developed a novel architecture to support forensic evidence collection and analysis of infrastructure as a service (IaaS) in cloud environment formally known as cloud forensic acquisition and analysis system without depending on cloud service provider and third party. This approach also provides the access of deleted data and overwritten data files which is not provided in existing forensic investigation techniques [5]. Zareefa and Mustafa found information obtained from the Zen Cloud Platform utilizing usable resources in the inquiry. Essentially the work focused on the three fields, such as adapting current techniques in the cloud world, gathering objects and data from the cloud, and assessing the interest of the information collected. In the near future, we will integrate existing tools of Platform-as-a-Service (PaaS) and Software-as-a-Service (SaaS) (or all service type frameworks in one framework) as part of the future path. Finally, this work centered on and retrieved XCP with file system- dependent storage repositories (SRS) dependent on LVM [16]. Throughout their research, Philip and Clark applied mostly exif metadata found in JPEG image files. In the near future, all research studies will be carried out in specific other file formats such as pdf, text, excel, ppt, and others [17]. Ramakrishnan addressed the big emerging developments in cloud computing protection and privacy concerns and often categorized security and privacy problems in security issues mainly, privacy issues mainly, and security issues intertwined [18]. In their work, Mhlupheki George and Sibiya explained the specifications for a cloud forensics framework and what standard procedures followed during the cloud forensic phase and how to build a cloud forensics system, as well as cloud forensics as a CFAAS architecture service [19].

In case of denial of service (DDoS), Alex and Kishore created a program that targets if the forensic management plane (FMP) gathers data regarding illegal forensic investigation activities. Throughout the immediate future, we should be able to execute the whole attack scenario throughout cloud platform [20, 21]. In their work, Ameer Pichan, Mihai Lazarescu, and Sie Teng Soh offered a systemic approach for examining cloud forensic problems, a potential answer for any process, and a description of forensic as a business model [22]. In their investigation, Vassil, Irfan, Andres, and Shane applied analysis and acquisition on SaaS and tested the results in their case studies. Kumodd: it is a tool used for the acquisition of cloud drives; Kumoocs: it is a tool for the acquisition and analysis of Google Docs; and Kumofs: it is a tool for remote previewing and cloud drive data screening [23].

Victor R Kebane built a cloud forensic preparation model as a test of the application software [7]. Grobler et al. suggested a six-dimensional virtual forensic approach to include the theory-based modern forensics solution [8]. Valjarevic and Ventor created a model consisting of three preparation phase assessments in the deployment and planning model. In ISO/IEC270 43 : 2015 [9], Valjarevic and Ventor built a model consisting of 3 preparation phase tests in the deployment and planning model [9]. Saad Said Alkahtny proposed a novel framework to assist IAAS cloud-based system (CFAAS) forensic discovery and analytics [10]. Alex and Kishore presented a forensic paradigm of denial of service (DDoS) assault for cloud storage and data processing utilizing forensic security plane (FMP) and FTK analyzer [11]. Emi Morioko, Mehdard S, and Sharbaf presented a method and algorithm for the procurement of Amazon Web Services (AWS) technical evidence [12]. Zareefa and Mustafa proposed a solution for accessing the recorded evidence value from the cloud and found an experimental result on Xen cloud platform [13]. Zachary, Katrina, and Kenji used snapshot submit Google Rapid Response (GRR) to plan and build automated forensic data acquisition system for forensic evidence collection [14]. In the cloud environment, Nhien An Le Khac, Michel Mollema, Robert Craig, and Steven Ryder are developing an innovative solution to data acquisition. We explain the legal context and address how to find the data center and deal with the actual job scenario of AWS [15]. Peng Xu, Yadong Zhang, and Kai Shuang deployed a modern streamlined data collection approach with hybrid data management review across the cloud logging (LOC) web service [24].

A cloud forensics tamperproof framework for cloud forensics is developed by the author that is available in a cloud environment that is untrusted and multitenancy. This framework relies on a forensic system based on the compressed multilayer counting filter [24], independent of daily cloud activity. No standard forensics preparedness model for cloud environments can be applied properly. A model for improving security [16] can be used in a cloud environment. Forensic preparedness is a way of maximizing the potential of an organization to respond to violations [17]. Figure 1 and Table 1 show that the number of papers published in various digital libraries like ACM, IEEE, ScienceDirect, Springer [16–23, 25–55], and Elsevier indicates that the lots of work have been done in the field of cloud forensics, and it is an active research area for the current cloud market.

Cloud logs will include useful data and information for the computer forensic investigation [18, 49], which is essential. Earlier designed logging systems have a few inconveniences to provide the cloud user with security. The existing system gives protection and security for user files that are either saved or uploaded by the user or authenticated [19] by the user. This paper secures logging by encrypting cloud logs using encryption techniques and identifying assaults on the cloud framework from DDoS (distributed denial of service) [25].

3. Evidence Collection

To classify and access forensic data from different parts and sources in the cloud world, the processing of evidence plays a critical role. Evidences are stored in one physical host, and data are split into another geographical region. Therefore, after an incident occurs, the evidence is very hard to find [26]. Proofs are obtained from different forensic origins such as switches, routers, servers, virtual machines, hosts, and browsers and from in-house storage content media such as hard disk drives, ram image files, and physical memory. The information is retrieved from multiple sources. Data collection from cloud servers, web browser objects [27], and physical memory analysis collects evidence.

3.1. Blockchain in Cloud Forensics. Blockchain is one of the overestimated breaking fields and has acquired significant consequences as an invention commonly used in numerous fields [20, 36]. The blockchain is known mostly as a billing book or digital distributed database [21]. The way blockchain interface, render device costs, monitor, and document transactions began to emerge as a revolutionary advance since its introduction in 2008. Blockchain [22] can be inexpensive, removing the do with to supervise and normalize transactions and communications [23] between various members of the central authorities. Other miners who have a record of the entire transaction history in a blockchain mark each move cryptographically [28, 50]. This renders time records that cannot be altered one by one safely, synchronized, and collective. Moreover, blockchain technology is considered IT and can be used in applications, industry, and industrial industries [29]. Figure 2 displays the blockchain design. The concept of blockchain consists of blocks like i to n numbers, current hash, and previous hash of the block; if hash value of any block is changed in blockchain network, it goes to invalid block and data tempering is detected.

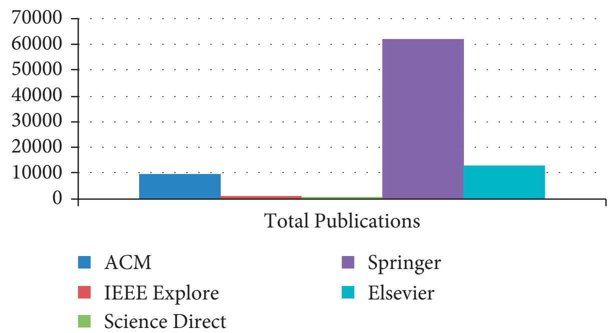

Figure 1: Year-wise analysis of research papers was published in digital libraries.

Table 1: Records of article types in various libraries on this topic.

	ACM	IEEE Explore	Science Direct	Springer	Elsevier
Journals	8994	209	197	683	506
Book chapters	469	3	17	60909	12551
Conference	70	698	3	509	80
Total publications	9533	910	217	62101	13137

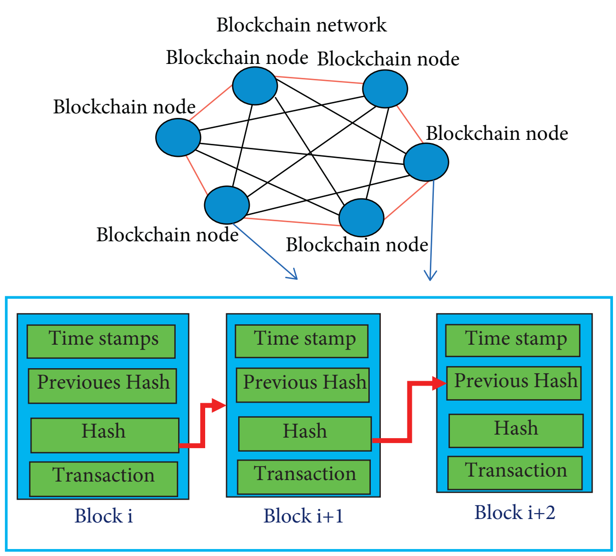

Figure 2: Architecture of blockchain technology.

4. Proposed Blockchain-Based Cloud Forensic (BCF)

The proposed forensic architecture, called blockchain-based forensics, is developed with the necessary algorithms in this section. The proposed forensic cloud uses software-defined network and blockchain concept collection of evidence and investigation.

4.1. Entities of the Architecture. The main objective of our experimental study is to acquire reliable proof or evidence in the cloud environment and to maintain the cloud provenance of data. The following entities comprise the overall forensic system:

(1) *Cloud Users (CU).* Cloud users (CU1, CU2, . . ., CUn) are included in our system "n" number. It is permissible for cloud users to save and access evidence at the server cloud.

(2) *Cloud Authentication Server (CAS).* At the start, the cloud clients are registered with CAS to deter unwanted access by users. Key generation and authentication are the major responsibilities of CAS.

(3) *Cloud Service Provider (CSP).* Cloud users store up all data in outer surface of their cloud on CSP hosted cloud servers. For every piece of data stored in CSP, a blockchain was developed.

(4) *Dataflow Open Switches (DFSs).* During this practice, a software-defined network is used to gather CSP data. We have therefore used many DFSs to relay CSP data to consumers. For data, the owned database flow regulations applied by the control plane to user DFSs may be mainly responsible. DFSs [R] only deploy and modify flow rules in the software-defined network control plane.

(5) *Software-Defined Networking Control (SDNC) Plane.* The software-defined networking control plane is responsible for applying network status data flow rules and for gathering all CSP evidence. The software-defined networking control plane manages blockchain for proof collection, and a block is generated for any CSP data. The complete machine architecture is seen in Figure 3.

Our forensic architecture's principal objective is to capture and conserve appropriate CSP data. We initially developed an efficient verification design to secure the device beginning unlicensed users. Data saved to the CSP are encrypted to ensure secrecy within the cloud setting. Decentralized data processing was planned based on blockchain technology.

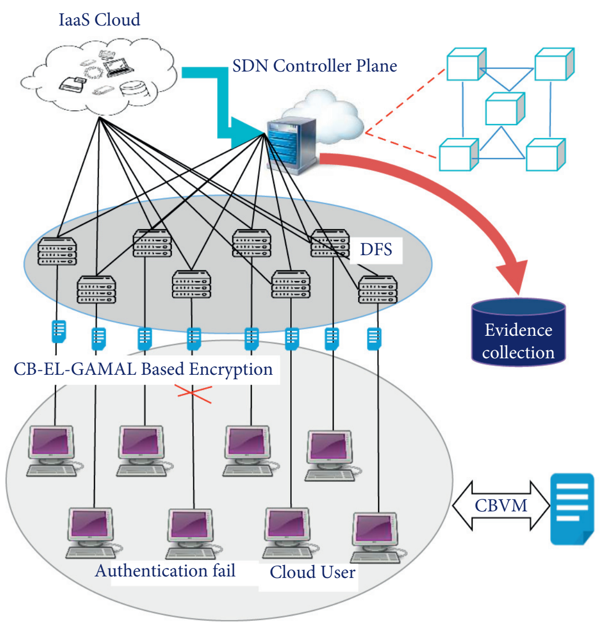

Figure 3: Blockchain-based cloud forensic (BCF) architecture.

Smart contracts can be used for the motto of recording and storing data history. For successful proof analyses, the graph-based research approach is recommended.

4.2. Cloud User Authentication. CAS is first registered with all cloud customers. User ID and password are user credentials that are taken into account when logging (PW). CAS produces a secret key (SK) for each documented CU by means of the cuckoo algorithm. Both users are valid at anywhere using the circular theorem's secret code (SC), SK, ID, and P.

4.2.1. Key Creation and Generation with the Help of Cuckoo Algorithm. The cuckoo search algorithm is a newly invented metaheuristic search optimization algorithm used to solve problems of optimization. This is a metaheuristic nature inspired algorithm focused on the brood parasitism of certain cuckoo birds, as well as spontaneous Levy flight walking. It has been carried out in a number of areas. The cuckoo algorithm is used in this research meant for the main generation of cryptography process.

The EL GAMAL equation is usually defined as follows. Alice:

$$\begin{aligned}\text{Choose the secret}1 \le a \le p-11 \le a \le p-1,\\ \text{Computer } A = \text{gamod}\,pA = \text{gamoda}.\end{aligned} \tag{1}$$

Alice sends the public key pk $= (p, g, A)$ pk $= (p, g, A)$ to Bob.

ElGamal is a public key cryptosystem dependent on the discrete logarithm issue for a gathering GG; for example, each individual has a key pair (sk, pk) (sk, pk), where sksk is the mysterious key and pkpk is the public key, and given just the public key, one needs to track down the discrete logarithm (take care of the discrete logarithm issue) to get the mysterious key. The cryptosystem is both an encryption plot (this part) which assists Alice and Bob with the issue of trading delicate data over an uncertain channel listened in by their enemy Eve and a computerized signature conspire (the following segment) which assists them with making advanced marks. The mark conspire is somewhat unique in relation to the encryption plot and different advanced mark plans; for example, the Schnorr signature plot and the digital signature algorithm (DSA) depend on ElGamal's unmistakable plan however with more limited keys. The public key created is as follows:

$$\text{Pu}(\text{SK}) = \text{Pr}(\text{SK}) \times P. \tag{2}$$

We may be capable of making out here the random generation of the private key (Pr(SK)) that attackers can crack quickly. The cuckoo algorithm is used to enhance the key generation process.

4.3. Cuckoo Search Explanations. Each egg is a solution in a nest, and a new solution is the cuckoo egg. The aim is to substitute not so nice nesting solutions with new and hopefully better solutions (cuckoos). The simplest shape of each nest is an egg [19]. The algorithm can be applied to more complex cases in which several eggs are present in each nest representing a set of solutions.

Three idealized rules are based on CS:

(1) Per cuckoo lays one egg on a single basis and dumps the egg into a randomly chosen nest.

The better nests with good egg content will hold the next generation.

(2) The number of available host nests is set, and host birds will possibly find the egg laid by a cuckoo.

(3) In this scenario, the host bird will throw away the egg/give up the nest and make a whole new nest.

For continuous nonlinear optimization, the cuckoo optimization algorithm is used. The lifestyle of the cuckoo family of birds is influenced by COA. This development optimization algorithm is based on the life style of these birds, their egg laying, and their breeding features. As other emerging approaches, a cuckoo optimization algorithm is introduced by an initial population. Here are two categories of cucumbers in various societies: mature cucumbers and larvae. The algorithm is based on the attempted survival. Any are discarded as they fight for life. The remaining cuckoos migrate to well again seats and begin raising and laying their eggs. Finally, the surviving cuckoos converge in such a way that there is a society of cuckoos with the same rate of profit.

To address the optimization issue, the variable values of the problem should take shape of an array. The "habitat" is called this array.

In an optimization problem, the next Nvar of a habitat will be a $1 \times$ Nvar array that shows the current living location of cuckoos. This array is described as follows:

$$\text{Habit} = [X_1, X_2 \ldots, X_n]. \tag{3}$$

The suitability (profit) of the current habitat is obtained by computing the function profit (p-f) in the habitat. Thus,

$$\text{profit} f \cdot b \cdot \text{(habit)} f.b[X_1, X_2 \ldots, X_n]. \tag{4}$$

To establish an optimization search algorithm, a habitat matrix of Npop ∗ Nvar size will be prepared and a random number of eggs will be allocated for each habitat.

Allowing for the number of eggs that every one cuckoo lays and as well as the space between the cuckoos and the current optimized zone, the laying radius will be calculated. After that, in that zone, the cuckoos start to lie. The laying radius is calculated as follows:

$$\text{ELR} = a \times \frac{\text{number of current cuckoos ggs}}{\text{total number of eggs}} \times (\text{Var}(hi) - \text{Var}(\text{low})). \tag{5}$$

Then, each cuckoo begins to lay her eggs in the nest within her ELR.

Thus, after each laying round, the less profitable percent of eggs (p%) (usually 10 percent) (their profit function is at the lower level) is destroyed. In the host nest, other chicks power up and develop.

4.3.1. The Cuckoo's Migration. While growing up and getting older, cuckoos live in their environments, but when the laying time comes, they migrate to superior habitats where the eggs have more chances to survive. The group with the best location will be targeted after composing the groups in different living locations in general (justified area or problem search space), and other cuckoos will migrate there.

When the cuckoos that are grown live all around the environment, it is not easy to determine which group belongs to each cuckoo. The cuckoos will be grouped by "K means" to solve this issue.

This method is actually a traditional method of grouping (finding a K between 3 and 5 is usually acceptable).

They do not travel the direct way when the cuckoos migrate to the target. With the deflection of (φ), they just travel (ƛ %, almost a percent) of the way.

These two parameters (φ) help cuckoos to explore a larger area. ƛ is a random number between 0 and 1, and φ is a number between (Algorithm 1):

$$-\frac{\mu}{6} + \frac{\mu}{6}. \tag{6}$$

In the method, the cuckoo algorithm selects an enhanced vector f(x) and is allotted to Pr (SK). Determining the secret key generated is difficult for cyber criminals because the cuckoo algorithm selects the random number more optimally.

4.3.2. Authentication Using Secure Block Verification Mechanism (SBVM). For those logged-in users, CAS produces secret keys and beginning points. For each operator of a particular circle, the root points are (Ox, Oy) co-ordinates. For each user in CAS, the respective credentials (ID, PW, and SC) are saved. In all stages of verification, all passwords are checked. The CAS key is a random code that makes it impossible for an attacker to invent the code for each user. By the following equation, a circle is defined as follows:

$$(Ax - Ox)^2 + (By - Oy)^2 = R^2. \tag{7}$$

Each user builds an SC consisting of origin points by using origin points (Ax, By). The user chooses an SC that follows the circle equation to effectively complete the authentication. While a client has to use the cloud, the client shall have each one ID and password along with the time stamp (TS).

Algorithms illustrate the method of SBVM-based authentication. A user who has legitimate passwords will complete the validation effectively. By making an allowance for SC next to TS, the protection level of the SBVM is increased. Although the SC differs over time, the attacker cannot split the SC. The attacker cannot use SC for the next authentication without being aware of the source points despite the SC being cracked at a time by the attacker.

4.4. Confidential Data Encryption. Users who have successfully completed the authentication process will enter the cloud computing environment in the planned forensic system. Within the cloud storage, users store their information in the form of ciphertext with extra security of digital signature. When mentioned in the prior paragraph, secret keys are produced by means of the cuckoo search algorithm. Data are translated into ciphertext by using the created strong secret key in the confidentiality encryption (CB- EL GAMAL) algorithm (Algorithm 2).

The EL GAMAL algorithm is paired through the CB-EL GAMAL algorithm probability and algebra. Algebraically homogenous crypto systems are a quick-release solution that is embedded in the decryption and encryption process across many unseen layers. The input layer of the homomorphic cryptosystem algorithm is used to encrypt, and Pu(SK) is initialized, and encryption is done on the secret layer. CB-EL GAMAL, however, is confidential and carries out the following data encryption procedures.

Algorithm 3 demonstrates the overall technique with an efficient hidden key for the CB-EL GAMAL algorithm [56]. By implementing graph theory-based graph neural networks in Smart Contracts, our framework enables users to track their data (GNNSC). The CB-EL GAMAL algorithm being proposed is shown in Figure 4. The neural network is used for the encryption process and calculating ciphertext in hidden layer for secret key generation, in which cryptosystems learning is a fast-forwarding method that is incorporated for the encryption and decryption process through multiple hidden layers [45].

Similarly, the input layer begins the ciphertext, and the output layer gets the original text when the data are decrypted. The participation in encryption of the Homographic Cryptosystems Algebraically algorithm [27] strengthens data security. To retain the documentation of possession, the data will be signed by the customer sooner than outsourcing to the cloud computing surroundings.

```
Start Function objective f (x), x = (x1), x2, . . ., XD) T;
Initial host nest population xi, I = 1, 2, . . ., n)
Duration or stop criterium (t < max generation)
  Get a cuckoo to Levy Flights by random means;
  Analyze Fi fitness
  Select a nest randomly between n (say j)
    If (Fi > Fj)
    Substitute j for the current result
    Finish If
  A fraction of the worst nests is deserted and new nests are created
  Maintain the right options (or quality solutions nests)
  Grading the solution and finding the right solution
  End for
  Posting and visualizing outcomes of processes
End Start
```

Algorithm 1: The Pseudo-code of Cuckoo Optimization Algorithm.

```
Input: password for users
Output: Status of authentication
Begin
For CU//Registration of Cloud User
  Register ID, Password ⟶ CAS
  CAS uses cuckoo algorithm to produce Secret Key (SK)
  CAS provides SKs; Origin Points ⟶ CU
End for//Registration completed by Cloud User
  If Ui requires on right to use cloud//Require validation
    Calculate secret code (SC) via equation (7)
    CUi submits IDi, Password, SC, TS ⟶ CAS
    CAS verifies User credentials
      If (User Credentials are correct match)
        Ui = Authorized user
        Else
        Ui = Unauthorized user
      End if
    Else
      End process
    End if
End
```

Algorithm 2: SBVM authorization mechanism (Pseudocode).

Digital signature using the EL GAMAL algorithm generates the same as mentioned, and the hash value is first created to sign the data as

$$HV = \mathrm{Hash}(D). \tag{8}$$

The digital signature is then created:

$$\text{signature} = \frac{HV + \Pr(SK).K2}{K1}, \tag{9}$$

where the random numbers are $k1$ and $k2$. The data have to be registered by the same data proprietor if data are updated or ownership

4.5. Efficient Collection of Evidence Using Blockchain Technology. In cybercrime, digital data are important source for analysis. The offenders will conceal their details and erase the evidence in a variety of parts of the infrastructure as a service cloud system. The key issue with the infrastructure as a service cloud infrastructure can be with the intention of data collection being spread on a wide scale. In comparison, cloud consumers monitor more than scholars, making it a difficult challenge to gather and preserve data. SDN and blockchain technologies are utilized in the proposed digital forensic infrastructure to gather and maintain cloud forensic data to combat all this issue. The evidence will be stored within the blockchain ledger under the control of the SDN control. In cloud forensics, some relevant meanings are as follows.

Evidence Integrity. Integrity of the evidence guarantees that the certificate reflects correctly the information contained in

```
Input: Public key and input data
Outputs: Ciphertext
 (1) Initialize public key (Pu(SK)) and Input data (d)
 (2)     If (d = Confidential)
 (3)     Split data d ⟶ d1 and d2
 (4)     For data d1
 (5)     Calculate ciphertext 1(c1) as,
 (6)     c1 = d1 φ d2
 (7)     End for
 (8)     For data d2
 (9)         Initiate Pu(SK), d2 at input layer
(10)         Calculate ciphertext 2 (c2) in hidden layer,
(11)         ca = k × P//k is a random number
(12)         cb = d2 + k × Pu(SK)
(13)         c2 = (ca, cb)
(14)         End for
(15)         Get ciphertext (c) as,
(16)         c = (c1, c2)
(17)     Else
(18)         For d
(19)             Repeat step number (8 to 13)
(20)         End for
(21)     End if
(21) End
```

Algorithm 3: CB- EL GAMAL (Pseudocode).

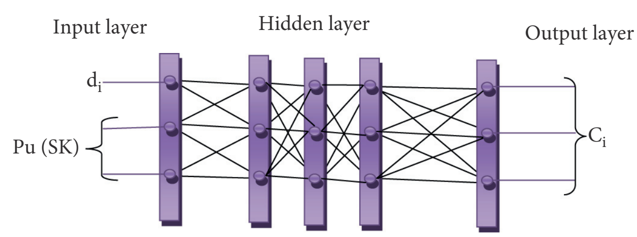

Figure 4: Neural network for encryption.

the PC. Several areas of the cloud influence knowledge respectfulness, but preserving integrity is a core component of the cloud crime scene investigation. The recognized technique to encrypt trustful information uses validated hash techniques, for example, MD5, SHA1, and SHA-256.

Data Origin. It is a form of authentication that corroborates a party as the (original) source of specified data generated in the past at some (typically unspecified) time.

Data Volatility. Unpredictability, after the power is switched off, memory or power failure of the material occurs. This is an important problem from a measurable standpoint since both memory and CPU procedures would vanish if the server crashes. If virtual computers are involved, these difficulties increase (VM). For ec IaaS, VM does not have permanent storage in this way; if the VM crashes, the volatile data may be lost.

Custody in Chain. The method of retaining and recording the chronological past of treating data as digital information can be represented. Data may be moved from the first responder, prosecutors (one or more), and judges to various layers of hierarchy of the automated forensics system. These provisional owners treat the proof during this lifetime. Because any evidence-based measure is held in the blockchain, our proposed work holds the custody chain.

Digital Evidence Ownership Proof. Digital evidence of ownership is defined here as the proof of existing digital proof of ownership. Multiple owners can manage the data during its lifespan. If the status of the data has shifted, the original owner must sign the data to retain the proof of cloud-based ownership. The patented evidence is retained in the framework as the transition in ownership is still preserved in the blockchain data history.

Graph Neural Network (GNN)-Based Smart Contracts. It is a computer program that tracks data history automatically. When the necessary conditions are met, the smart contract is activated and executed. To optimize smart contracts, graph theory algorithm rules are deployed in this work [56].

Data Lineage. It documents the history of possession and paper process throughout its entire life cycle. In other words, the record sequence showing the behavior taken from the data is known as a lineage or origin. With the aid of blockchain, we retain the data root; that is, in our work, any alteration made to the data is saved and traced by GNNSC in the blockchain.

The evidence has the hash value of the public ledger in the blockchain. We give a SHA-3-512 algorithm better in terms of security for hash value generation. The hash value in SHA-3 is determined accordingly for each block:

$$\text{hash} = \text{sponge}\left[g, pa\ d, q\right](T, L). \tag{10}$$

The hash unique value can be calculated here designed for input, that is, transaction (T) padding q, permutation g function, and output length L. The hash value is often created by the "sponge building" mechanism in SHA-3-512 as in EQATERY (10) rather than by the "sponge building" procedure. Accepting SHA-3-512 for hash calculations may bring various benefits over the current system with respect to time consumption and protection. Let us look at the $U1$ user's data $d1$ at time $t1$ in the cloud. After that, the block is formed by $d1$ and the hash value is created by SHA-3-512. Each transaction, i.e., the shift kept on $d1$, is based on the time the GNNSC block was installed in the system. Every update is processed and circulated as evidence in the blockchain network between the peers. The log contains the user name, IP address, time, and all other hardware information of the proof. The proof log, information history, is kept as the proof for each change found in detail in the blockchain. Past of data can involve lines that describe changes, ownership transition, and other behaviors on cloud-specific data. Algorithm 4 explains the method of collecting evidence. In favor of each single data residing within the cloud, the evidence can be gathered and preserved within the blockchain here. Furthermore, in the cloud environment, GNNSC tracks and wheels the ease of access of data stored by users.

During our initiative, we use smart contracts to alert cloud server when a graph theory law, which is often integrated as a proof record within the blockchain, is met. Many registered users will be able to the right of entry information contained in the cloud atmosphere. This thesis draws intelligent contracts from the graphology that functions on a secret stage of data. The smart contract is executed by means of the graph theory principles used in the framework. Figure 5 demonstrates GNNSC's pictorial representation. FSC presence tracks all big activities conducted under the data contained in the cloud server machine. Thus, any accurate evidence of the cloud server machine is gathered, and the correctness of evidence is conserved using blockchain technologies in our proposed forensic architecture.

Table 2 displays the laws of graph theory in GNNSC [57]. Because of these sets of laws, the statement is generated and saved like an evidence log. A modification of the data made after previous access is the previous danger. If the earlier hazard is restricted and information is nonconfidential, the log right of entry evidence will be overlooked and the report will not be produced. The produced statement is well thought out otherwise noteworthy and stored in the blockchain.

5. Cloud Forensic Investigation

If a cybercrime has been detected, the designated investigator (police and lawyers) must examine the digital evidence. CAS also authenticates the investigator prior to the inquiry. If a criminal enters an election voting room, his basic details, such as his Aadhar number and voter id, are kept in the election commission's database. If he tries to update or erase the evidence history by hacking the database, deleting, or modifying his entry into the voting space, he is attempting to upgrade or remove the evidence history.

Given that every one of the evidence record logs stored within a blockchain, we know that it is a distributed ledger and our suggested forensic architecture will be useful in this situation. It also passes the strong authentication before gaining access to the device. According to the investigator, the following steps should be taken when analyzing data.

5.1. Evidence Identification. The first step in a digital forensic investigation is to locate a possible evidence source of reliable evidence. As a result, the investigator must obtain legal consent from the relevant authority as shown in Table 3.

5.2. Evidence Acquisition. The investigator possibly will gather round all evidence log records of the blockchain by way of the consent of officially authorized authorities. The evidence log recorded inside the study contains mutual credentials of the user and evidence based on hardware. During this time, the investigators will have to adhere to court restrictions while also abiding by SLA agreements.

5.3. Evidence Analysis. The investigator then goes through all data logs and compiles a report on digital evidence. Logical graph with evidence for better research, this paper proposes a graph of proof. The evidence is used to build a graph of data with matching log attributes. If the perpetrator checks in at a polling site, submit the history of persons visited in the voting center, i.e., original details, just before the cloud to the administration of the election commission, i.e., a registered person. The evidence is currently being developed on blockchain for each one log record attribute (source_IP, timestamp, actions made, transaction hash, server of virtual machine, DFS_ID, and the like).

Think about the case where the suspect's check-in history was changed at $t2$. Then, in a subsequent block of log attributes, the next log is modified. Similarly, as soon as the hacker tries to access the information or erase it from the cloud, this should be treated as evidence and recorded in the subsequent block. The investigator must complete the following steps to create a graph of evidence:

(1) Sequentially arrange the evidence according to the timestamp

(2) Store each evidence through its attributes of log record

Input: cloud, user, data
Outcome: collected digital evidence
(1) Start
(2) For every CUi ϵ CU
(3)   Creates Cloud users with GNNSC
(4) End for
(5) For every data
(6) $U1$ stores $d1$ in Infrastructure as a Cloud Service
(7)   Create the block for $d1$
(8)   Calculate Hash value ($d1$) with the help of Equation (10)
(9)   Track $d1$ and modernize the evidence
(10) End for
(11) For every transaction on $d1$
(12)   Store Log timestamp, source or origin IP, Visual machine disk filetransaction hashdetails, Virtual Machine server, actions made, etc.
(13)   If (Graphtheoryrulesarenottrue)//GNNSC
(14)   Report Generation
(15)   Else
(16)   Do not produce the report
(17)   End of if
(18) End of for
(19) End

Algorithm 4: Efficient Evidence Collection Method (Pseudocode).

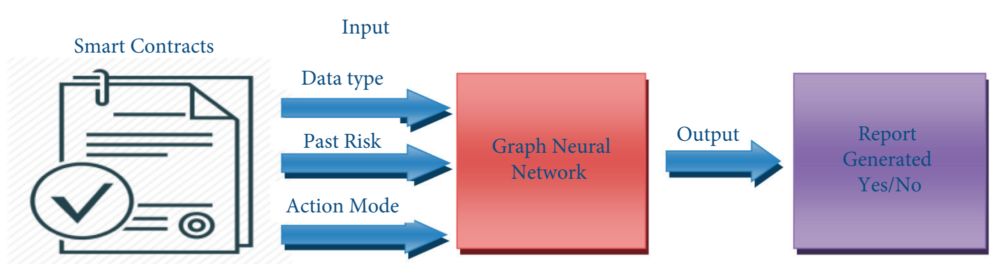

Figure 5: Pictorial representation of GNNSC.

Table 2: Attribute rules for GNNSC.

Data type	Past risk	Action performed	Report generation by GNNSC
Nonconfidential	Low	Read	No
Confidential	Low	Read	No
Nonconfidential	Low	Edit	No
Confidential	Low	Edit	Yes
Nonconfidential	Low	Delete	Yes
Confidential	Low	Delete	Yes
Nonconfidential	High	Read	No
Confidential	High	Read	Yes
Nonconfidential	High	Edit	No
Confidential	High	Edit	Yes
Nonconfidential	High	Delete	Yes
Confidential	High	Delete	Yes

Table 3: Evidence sample along with attributes.

Evidence identity (ID)	Different timestamps	IP_Source	Upload_User	Accessed user	Hash_Tn	Performed actions	Block hash	Location_Attribute	Virtual machine server	DFS
001	Ts1	192.168.10.xx	User A	User A	m-bits	Upload	n-bits	ZZZ	Pqrst	1
002	Ts2	192.168.10.xx	User A	User A	m-bits	Read	n-bits	ZZZ	Pqrst	2

Table 3: Continued.

Evidence identity (ID)	Different timestamps	IP_Source	Upload_User	Accessed user	Hash_Tn	Performed actions	Block hash	Location_Attribute	Virtual machine server	DFS
003	Ts3	192.168.10.xy	User A	User X	m-bits	Read	n-bits	ZZZ	Pqrst	3
004	Ts4	192.168.10.xx	User A	User X	m-bits	Edit	n-bits	zzz	pqrstklj	3
005	Ts5	192.168.10.xx	User A	User X	m-bits	Edit	n-bits	ZZZ	pqrstbvf	1
006	Ts6	192.168.10.xy	User A	User A	m-bits	Upload	n-bits	ZZZ	Pqrst	2
007	Ts7	192.168.10.xx	User A	User B	m-bits	Upload	n-bits	ZZZ	Pqrst	1
008	Ts8	192.168.10.xx	User A	User B	m-bits	Delete	n-bits	zzz	Pqrst	1

(3) Build an evidence graph according the evidence order and log record attributes

Table 2 shows properties of the survey evidence collection. A graph of evidence can be constructed using these data, as seen in Figure 6. The investigator can see from the graph of evidence that the suspect has edited (modified) the evidence (User *X*). However, the authorized user's location and IP addresses are different. Consider the case where the suspect's check-in history was changed at *t*2. Then, in a subsequent block of log attributes, the next log is modified. Similarly, when the suspect tries to hack these data or erase them from the cloud, this is treated as evidence and recorded in the subsequent block.

5.4. Reporting of Evidence. At the evidence review level, every one of the evidence within the graph of evidence is authenticated using a cryptographic digital signature that is kept together in the midst of the value of hash and data. Data should be signed earlier than being sent to the cloud according to our proposal. As a result, at what time an intruder could modify the evidence data, he or she should generate a digital signed signature.

For all evidence, the current transaction's hash value is stored at the blockchain. The hash significance of data stored in the cloud must match the Merkle tree root value of the block. The investigator compiles a report based on these findings and submits it to the court as a digital testimony. From acquisition to submission to juridictionary, algorithm, number 4 illustrates the collection process of evidence.

As a result, our designed architecture of cloud forensic, which incorporates blockchain and SDN technologies, allows for secure collecting evidence from the cloud. A strong authentication protocol stops unauthorised users from gaining access to the cloud environment, while a sensitivity aware encryption process improves data protection. Evidence storage using blockchain and SDN is an intellectual approach for distributed data protection. From evidence analysis to evidence reporting to the court, our designed architecture of cloud forensic facilitates the whole investigation.

5.5. Investigational Result Evaluation. Within this investigation result evolution, we compare the efficiency measurements of the designed architecture of cloud forensic with the earlier research contributions. We present our simulation environment in this section and at that time judge on our designed architecture of cloud forensic to the prior centralized log record process collection.

5.5.1. Configuration and Simulation. In a combined simulation platform, we configure our designed architecture for cloud forensic. Using CloudSim, we introduced an IaaS cloud environment in Python. Blockchain is the built data storage mechanism of IaaS cloud in Python Programming as described in the following Algorithm 5:

Both tests were run on Ubuntu OS by means of an Core-i7 Intel CPU running next to 2.80 GHz, 16 GB of RAM, and a 1000 GB SSD. The simulator version network 3.30 simulator, that is committed to network simulation for the software-defined networks, is also compatible with the cloud and blockchain environment. The Python platform's performance is merged by ns-3.30, in the direction to create a simulation environment.

The Ubuntu operating system underpins the entire work; we use NetBeans-8.2 for PYTHON blockchain setup, Network Simulator-3 for software-based network simulator, and CloudSim for IaaS cloud deployment.

Table 4 of our experiments explains the important parameters of simulation used in the direction of applying our designed architecture of cloud forensic. Prior to we get interested in the study, we will go through a real-world use of the proposed forensic scheme.

The Proof-of-Work principle is used by the miner to validate the blockchain. A corresponding block is generated for each piece of data that the user stores in the cloud environment and the stored hash values.

Use Case Diagram of Our Designed Architecture of Cloud Forensic Using Blockchain (FAuB). IaaS will be a cloud environment to be extremely versatile and can be used by any rising business. Many real-world implementations will benefit from our designed architecture of cloud forensic IaaS platform. In this paper, we look at one application of the proposed work in crime detection. Consider several voting centers that store their data such as voter records, financial information, maintenance information, personnel information, and surveillance information into IaaS cloud. Each data should be encrypted depending on top of the extent of data protection earlier than being outsourced to the cloud, as per our job. Furthermore, each voting center's administrator

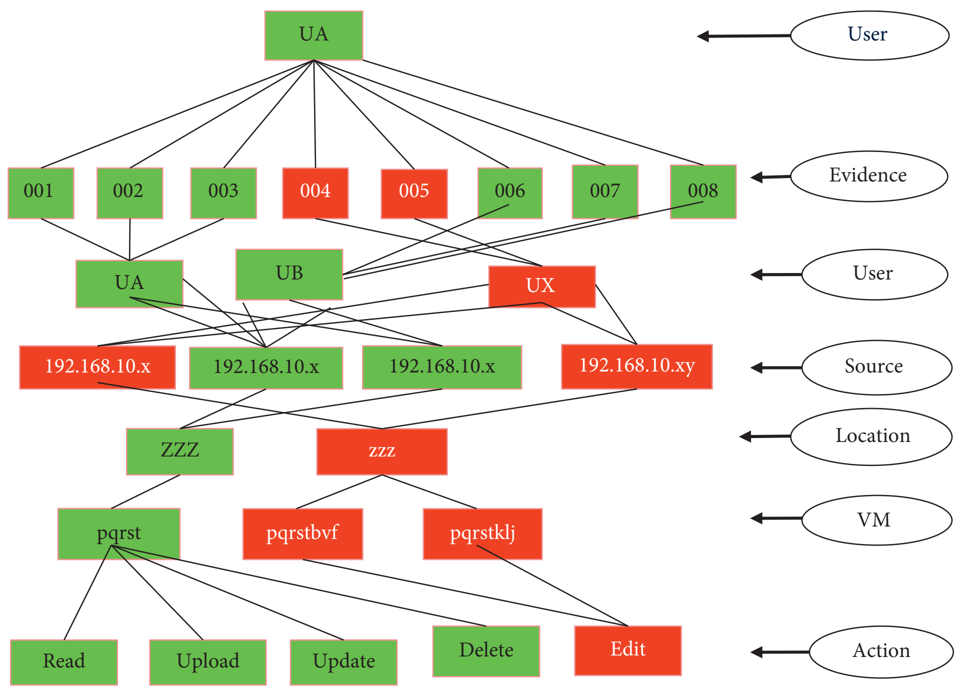

FIGURE 6: Evidence analysis scenario.

```
Evidence as: input
Evidence as: inputGraph of evidence as an: output
Begin
   Using the SBVM system, verify the investigator's identity.
   Determine the case's evidence.
   Collect evidence in the form of {Evidence_Identity, Time_stamp, IP_Source, uploaded_User, accessed_User,
Performed_Actions, Hash_Tn, Block Hash, Location_Attribute, virtual machine server, and OFS ID} from blockchain.
   Create an evidence graph by means of attributes of evidence.
   For every one of the evidence
      Ensure that {Block_Hash && IP_Source} are right and correct.
      If this is the case (Verification D True)
      Verify the signature//Validation of evidence
         If this is the case (Signature is valid)
            Collect reliable evidence
         Else
            Prepare illegitimate evidence
         End if
      End if
   End for
Prepare and share the copy of evidence with the jurisdictionary court.
End
```

ALGORITHM 5: For forensic investigation.

must be CAS-registered. The SDN controller collects evidence designed for every one of the data stored within the cloud atmosphere and stores it on a blockchain. Additionally, each admin may use GNNSC to monitor their data.

Figure 7 depicts an example of the anticipated use case. Consider the case of a suspect who voted for a few hours at the polling center A. The suspect's information will then be found in the voting center A's election record file. Furthermore, video of the perpetrator in the polling center will be used in the data obtained from security cameras. This could aid detectives in locating the suspect as soon as possible. Any change made to the voter registration database and surveillance data is recorded within the blockchain as evidence. The perpetrator will erase or change the register of the voter registry and the data of surveillance contained inside the cloud if we do not have a good forensics mechanism architecture. Every evidence is preserved in the blockchain, that is, a distributed block ledger, in our

Table 4: Simulation configuration setting.

Parameters		Value
Number of users		120
Number of OFSs		8
Number of controllers		1
Number of cloud authentication servers (CAS)		1
Number of keys generated		120
Cuckoo	Maximum iteration	120
EL GAMAL	Number of hidden layers	4
	Key size	256
SHA-3	Block size	576
	Word size	64 bits
	Number of rounds	24
	Customized contract	GNNSC
	Maximum handles	2048
Cloud	Number of virtual machines	35
	Average RAM	512 MB
	Average bandwidth	1000000 MB
Simulation time	100 ms	

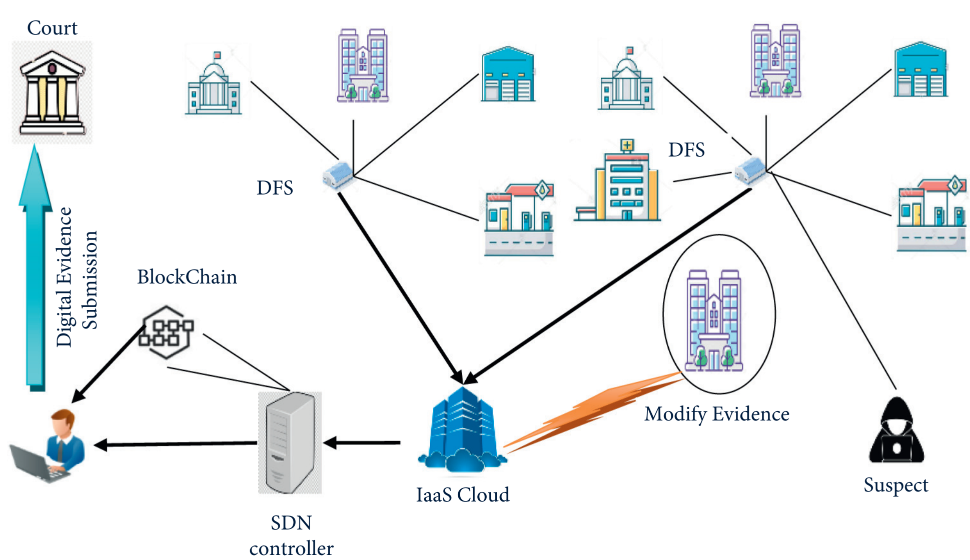

Figure 7: Digital forensic crime investigation case diagram.

proposed forensic architecture. We also store the VM logs in the blockchain as evidence. The investigator will obtain information from the blockchain even though the hacker changes and modifies the details on the cloud. Plotting an evidence graph with the collected data log will reveal whether there are any differences in the evidence. The investigator will pass the digital evidence from a CoC to the court based on the evidence obtained from blockchain.

5.5.2. Comparative Analysis. This section compares our designed architecture of cloud forensic to the current CFLOG [5] framework for safely collecting digital evidence. In CFLOG, the evidence is collected and stored in a centralized fashion, which is a major contrast between current forensic infrastructure and CFLOG. As mentioned in Section 3, this causes several problems. We designed an architecture of cloud forensic that collects in addition to storing digital information safely using SDN and blockchain technologies to overcome these challenges.

(1) Response Time Comparison. The time in use for users on the way to get a response to a data request is known as response time. The number of users interested in the forensic method validates this metric. In supplementary terminology, response time refers to the time it takes the forensic method to provide the necessary information or documentation to the users.

In Figure 8, the designed architecture of cloud forensic SDN-blockchain-based forensic framework is compared with the current CFLOG framework, which has a centralized framework. The numeral of requests of users increases by means of the increase inside the number of users in both works, so the response time steadily increases with the increasing user numbers. Still, for more user number, our designed architecture of cloud forensic responds to the requested users easily. That use of software-defined network technologies improves the ability of scaling or the ability to accommodate a large number of users at the same time. As a result, any cloud user can link to the server of the cloud instantly as well as download the data requested by users. Similarly, the prosecutor should be able to obtain information from the blockchain without having to wait for the SDN controller to respond.

As a result, the proposed forensic architecture reduces the time of response. CSP performs together data managing as well as evidence collection in a consolidated fashion in CFLOG, which increases the response time when there are a large number of users. The CFLOG system takes 100 ms to answer in the presence of 120 users, while the designed architecture of cloud forensic system takes 72 ms intended for the identical amount of user numbers. As a result, the designed architecture of cloud forensic outperforms the CFLOG system by 27%.

(2) Evidence Insertion Time Comparison. The point in the time it takes to (or create) insert digital data of evidence collected on a server of the cloud is known as evidence insertion time. It can know how to exist and describe at the same time as the time it takes SDN plane controller to generate a proof meant for the CSP's stored data inside our analysis.

The insertion of evidence period as a function of the different user numbers is shown in Figure 9. When the user number grows, so does the volume of data that must be alive stored and the number of pieces digital evidence that must be generated. As a result, the amount of time it takes to insert evidence increases as the number of users increases in all works. Every one of the evidence should be unruffled and stockpiled in a consolidated way beneath the supervision of CSP in the CFLOG process.

As a result, the centralized evidence collection procedure lengthens the time it takes to insert evidence. In addition, we protect the history of data in our work, which means that each change to data is treated as evidence and incorporated into the blockchain. The SDN controller, on the other hand, is in charge of creating and preserving documentation without the intervention of CSP. As a result, relative to previous work, evidence insertion in blockchain takes less time.

(3) Evidence Verification Time Comparison. The time it takes an investigator in the direction of collecting and validating the evidence commencing a blockchain is known as evidence verification time.

The time taken for verification of evidence within the CFLOG process and the proposed forensic system is compared in Figure 10. The proposed automated forensic technology achieves the shortest possible time for evidence verification. The investigator would use CSP to collect evidence in the CFLOG process, and the verification is done in the conventional method. Instead of CSP, the investigator in the suggested work aggregates all evidence from the controller. In addition, for the improved studies, evidence testing is carried out by creating a graph of evidence. Furthermore, we suggested SHA-3-based hash computation to maintain evidence consistency while reducing time consumption. As a result, we gain evidence integrity with the least amount of time spent on evidence verification.

In the presence of ten users, CFLOG takes 62 milliseconds to collect and validate digital evidence, while the planned digital forensics FAuB takes just 37 milliseconds, reducing the verification time by nearly half.

(4) Computational Overhead Comparison. The bandwidth amount used in the direction of executing a particular activity (transfer data, reading, update, generation of evidence, and verification of evidence) within the system of forensic is known as computational overhead.

Figure 11 depicts a comparison of computational overhead based on different user numbers. Because the amount of data on the way to be interpreted grows in tandem with the number of users, the computational overhead increases. The computational overhead is raised in the absence of blockchain technologies owing to centralized device administration. Both data and evidence collection in CFLOG occurs in CSP, which raises the overhead.

The suggested forensic method, on the other hand, keeps indication processing like collection, hash reckoning, and conservancy on the SDN controller, reducing the total computational overhead. Furthermore, incorporating SDN technology increases scalability without adding overhead. Thus, the proposed digital forensic infrastructure adds 8 KB of overhead for ten cloud customers, while the CFLOG framework adds 10 KB of overhead.

(5) Total Change Rate Comparison. The rate of total change is calculated by dividing the amount of evidence modification by total evidence existing within the forensic framework facing problems with the old CFLOG system as shown in Figure 12. When a hacker person changes data to organize on the way to destroy evidence, the net modification rate rises. The collected data must be accurate, and the evidence's accuracy must be maintained for an effective forensic method. Since only registered users are included in the proposed forensics scheme, any information along with data of unauthorised users is refused. Furthermore, we use blockchain technology based on top of the SHA-3 algorithm to maintain the credibility of evidence.

According to our findings, the proposed forensic method modifies 11.1% of the evidence. However, since we guarantee credibility, CoC, and PoO for evidence, this alteration is also registered as evidence in the blockchain. Because (i) centralized infrastructure ever since CSP can be able to be malicious, (ii) node single vulnerability (an attacker just wants to break CSP's), (iii) no credibility is protected, as well as (iv) interference to unauthorised user's accessing, approximately 60% of evidence is changed in the CFLOG process. We overcome all issues by means of the help of blockchain and SDN technologies that reduces the system's overall change total rate.

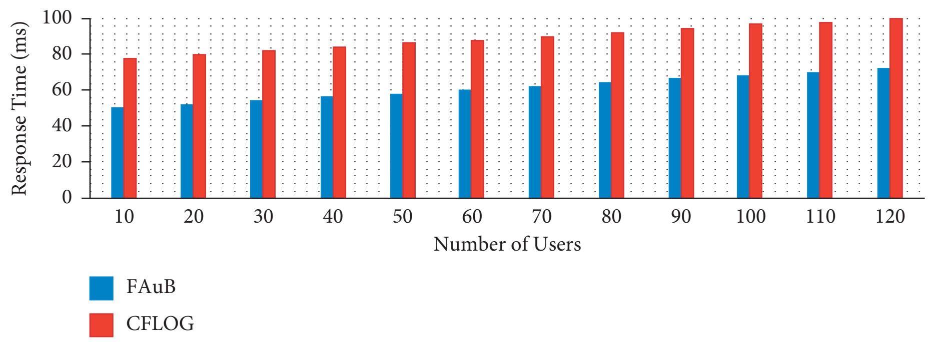

Figure 8: Response time comparison analysis.

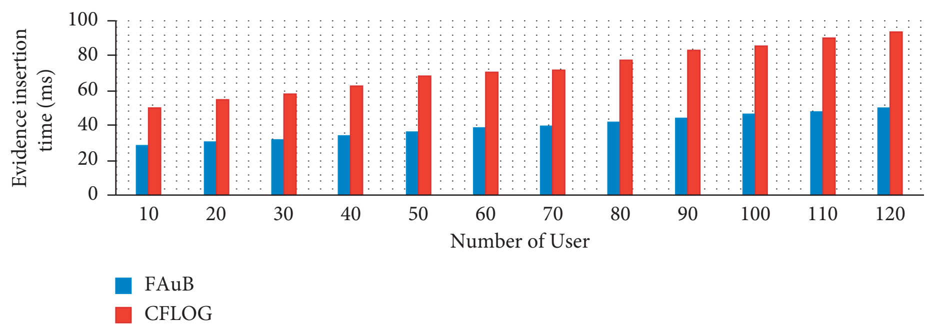

Figure 9: Evidence insertion time comparison analysis.

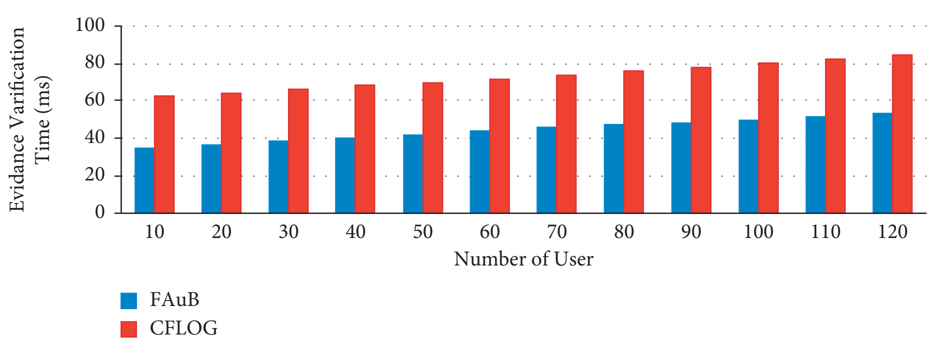

Figure 10: Evidence verification comparison analysis.

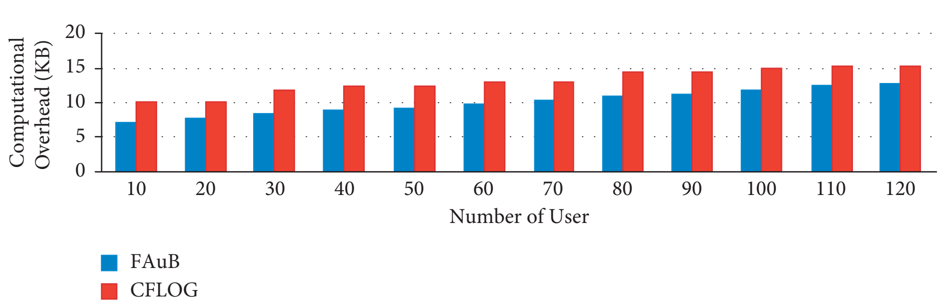

Figure 11: Computational overhead comparison analysis.

Table 5 compares the cumulative outcomes of the CFLOG process and the proposed forensic system in terms of performance measurements. We will see that each metric has improved with the proposed digital forensic FAuB architecture.

(6) Efficiency of CB-EL GAMAL with Cuckoo Algorithm. The elliptic curve cryptography (ECC) algorithm is regularly used design for digital signature concept in blockchain technology. On the other hand, there are

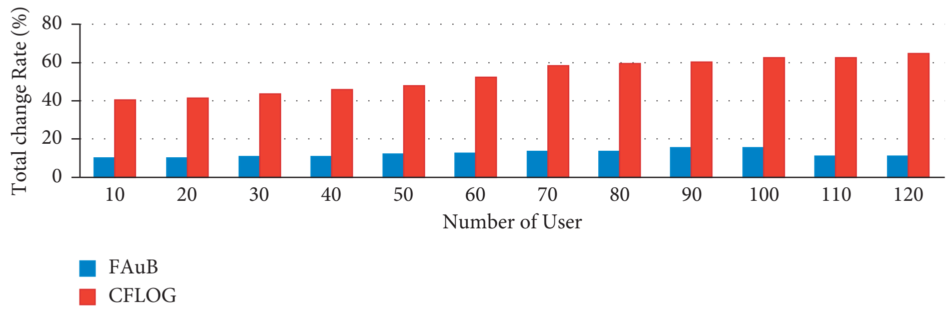

Figure 12: Total change rate comparison analysis.

several issues with key generation, encryption, and decryption. We suggested the CB-EL GAMAL algorithm with the cuckoo search optimization algorithm for key generation to improve the conventional ECC algorithm. As a result, we compare our proposed CB-EL GAMAL algorithm with the Paillier encryption algorithm proposed for blockchain technology using the cuckoo search optimization algorithm.

The suggested CB-EL GAMAL algorithm is examined in detail from Figures 13–16. For a stable blockchain architecture, the Paillier encryption algorithm is proposed. The Paillier encryption scheme, on the other hand, quickly improves key generation, encryption, and decryption times. The Paillier scheme consumes more time because it involves massive homomorphic computations.

On the other hand, data encryption is necessary in the environment of cloud and here the determination by several users. The algorithm of Paillier takes an average of 500 milliseconds to generate a key. Encryption and decryption, on the other hand, necessitate a significant amount of time, which is incompatible with the cloud environment.

The proposed CB-EL GAMAL algorithm, on the other hand, reduces the key generation time by using the cuckoo algorithm, which has a quick convergence time. Similarly, the CB-EL GAMAL algorithm's deep architecture reduces the time taken for encryption and decryption. As a result, the suggested SA-ECC algorithm outperforms the traditional algorithm in terms of increasing protection without increasing time consumption.

(7) SHA-3 Algorithm Efficiency. The most widely used hashing algorithm is used in blockchain technology. Hash computation in our proposed forensic scheme to increase the hash computation time and security standard is calculated by the SHA-3 algorithm.

Graph 10 compares the hash computation time of the proposed SHA-3 algorithm with that of the previous (SHA-256) 2 algorithm. In this review, SHA-3 reduces the calculation time of hash for 100 users to 16 milliseconds lacking sacrificing security. Inside general, SHA-3 outperforms SHA-256 against a variety of security threats, including length extension attacks. As a result, Merkle tree SHA-3 algorithm can construct a tree and increase protection without adding time to the process.

Overall, the proposed digital forensic FAuB architecture outperforms the current CFLOG scheme according to the report. The use of blockchain and SDN technologies increases the efficiency and scalability of the system.

Table 5: Analysis and comparison.

Performance analysis parameter	CFLOG	Proposed digital forensic architecture
Computational overhead time in KB	12.5	9.10
Evidence verification time in ms	70	42.1
Evidence insertion time in ms	71	44.2
Response time in ms	88.5	65.3
Total change rate in %	52	11.1

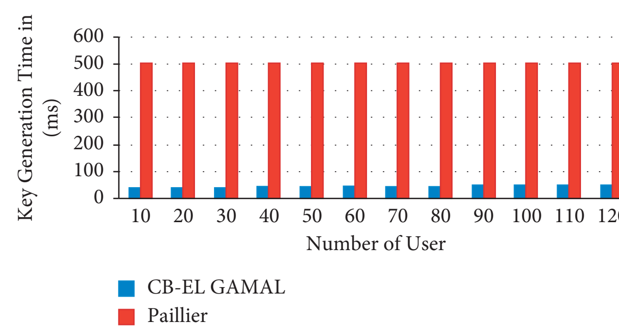

Figure 13: Key generation comparison analysis.

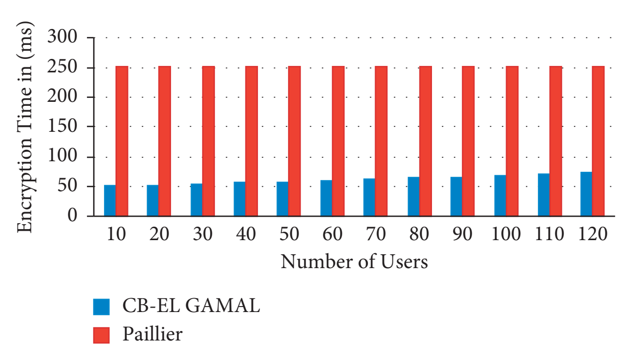

Figure 14: Encryption time comparison analysis.

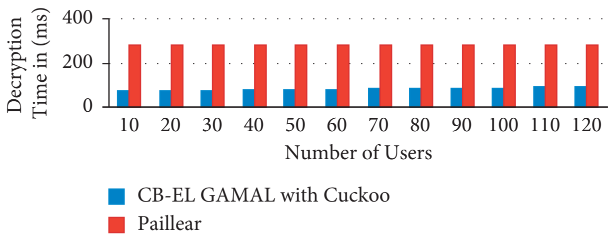

Figure 15: Decryption time comparison analysis.

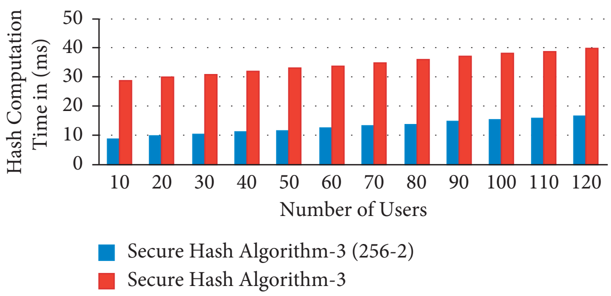

Figure 16: Hash computational time comparison analysis.

6. Conclusion

In this research work, with blockchain technology, a valuable architecture of digital forensic is proposed to gather and safeguard unfailing evidence from the substructure as a service cloud environment. Cloud authentication server CAS, with a secure verification mechanism known as the SBVM, authenticates all cloud users. The CB-EL GAMAL algorithm was proposed for data security. The cuckoo algorithm is proposed to generate secret key. A block in the controller is formed for every evidence stowed in the cloud. The integrity of evidence is ensured in every block by SHA-3-512-based hash tree building. All evidence is collected, and blockchain technology maintains evidence integrity, data origin, data link, digital evidence, ownership evidence, and custody chain. GNNSC is deployed in the system to trace data activities. The CB-EL GAMAL algorithm is proposed for data protection. The cuckoo algorithm generates optimum keys before that. At the controller, a block is spawned for each piece of cloud data. Merkle tree structure based on SHA-3 guarantees the consistency of evidence in each block. All documentation is collected, and the chain of custody and proof of ownership (CoC and PoO) are maintained using blockchain technology. GNNSC is installed in the system to monitor data events. Finally, the use of a graph for evidence analysis simplifies the evidence analysis. Overall, the forensic device is investigated using a Python and ns-3.30 simulation environment. Experimental findings suggest that the proposed forensic architecture outperforms the current unified forensic system. To improve the digital forensic infrastructure, we want to integrate network forensics in software-based networks as well as cloud forensics in the future [58–60].

Data Availability

The datasets generated during and/or analyzed during the current study are not publicly available but are available from the corresponding author who was an organizer of the study.

Conflicts of Interest

The authors declare that they have no conflicts of interest.

References

[1] A. A. Syed, M. Shahzad, and S. Farhan, "Analysis of cloud forensics techniques for emerging technologies," in *Proceedings of the International Conference on Computing, Networking, Telecommunications & Engineering Sciences Applications (CoNTESA)*, Tirana, Albania, December 2020.

[2] N. Kumar and I. Chana, "Load balancing and job migration techniques in grid: a survey of recent trends," *Wireless Personal Communications*, vol. 79, pp. 2089–2125, 2014.

[3] N. Rathore and I. Chana, "Job migration with fault tolerance based QoS scheduling using hash table functionality in social Grid computing," *Journal of Intelligent and Fuzzy Systems*, vol. 27, no. 6, pp. 2821–2833, 2014.

[4] A. Ahmed, F. A. Hany, and B. W. Gary, "Expert review of a cloud forensic readiness framework for organizations," *Journal of Cloud Computing*, vol. 8, p. 11, 2019.

[5] V. Sharma, R. Kumar, and N. Kumar Rathore, "Topological broadcasting using parameter sensitivity-based logical proximity graphs in coordinated ground-flying ad hoc networks," *Journal of Wireless Mobile Networks Ubiquitous Computing and Dependable Applications (JoWUA), SCOPUS indexed*, vol. 6, no. 3, pp. 54–72, 2015.

[6] A. K. Abdullahi, J. Aman, N. Y. Mohd, M. Aminu, K. I. Mohamad, and R. M. N., "Evidence collection and forensic challenges in cloud environment," *MACE Technical Journal (MTJ) MTJ*, vol. 1, no. 1, pp. 2710–6632, 2019.

[7] O. Akter, A. Arnisha, A. Akther, M. A. Uddin, and M. Manowarul Islam, "Cloud forensics: challenges and blockchain based solutions," *International Journal of Wireless and Microwave Technologies*, vol. 10, no. 5, pp. 1–12, 2020.

[8] N. Kumar, "Dynamic threshold-based load balancing algorithms," in *Wireless Personal Communication*, vol. 91, pp. 151–185, no. 1, Springer Publication, New-York, NY, USA, 2016.

[9] N. K. Rathore and I. Chana, "Job migration policies for grid environment," *Wireless Personal Communications*, vol. 89, no. 1, pp. 241–269, 2016.

[10] A. K. Samuel and J. Suhardi & Tutun, "Modeling cloud forensics readiness using MetaAnalysis approach," in *Proceedings of the IEEE, International Conference on Information Technology Systems and Innovation (ICITSI)*, Bandung, Indonesia, 2020.

[11] A. K. Haider, E. Gregory, and D. Herbert, "Blockchain for modern digital forensics: the chain-of-custody as a distributed ledger," in *Part of the Advanced Sciences and Technologies for Security Applications Book Series (ASTSA)*, Springer, Berlin, Germany, 2019.

[12] A. Akbarzadeh and E. Shadkam, "The study of cuckoo optimization algorithm for production planning problem," *International Journal of Computer Applications in Technology*, vol. 2, no. 3, 2015.

[13] N. K. Jain, N. K. Rathore, and A. Mishra, "An efficient image forgery detection using biorthogonal wavelet transform and improved relevance vector machine," *Wireless Personal Communications*, vol. 101, no. 4, pp. 1983–2008, 2018.
[14] N. Jain, N. Rathore, and A. Mishra, "An efficient image forgery detection using biorthogonal wavelet transform and improved relevance vector machine with some attacks," *Interciencia Journal*, vol. 42, no. 11, pp. 95–120, 2017.
[15] D. Choudhary and S. Malasri, "Machine learning techniques for estimating amount of coolant required in shipping of temperature sensitive products," *International Journal of Emerging Technology and Advanced Engineering*, vol. 10, no. 10, pp. 67–70, 2021.
[16] N. K. Rathore, D. Pandey, R. I. Doewes, and A. Bhatt, "A novel security technique based on controlled pixel based encryption of image blocks for sharing a secret image," in *Wireless Personal Communication,* Springer Publication, New York, NY, USA, 2021.
[17] E. H. Ezz and D. H. Manjaiah, "An efficient digital forensic model for cybercrime investigation in cloud computing," *Multimedia Tools and Applications*, vol. 80, pp. 14255–14282, Springer, Berlin, Germany.
[18] R. Neeraj and I. Chana, "Variable threshold-based hierarchical load balancing technique in Grid," *Engineering with computers*, vol. 31, pp. 597–615, 2015.
[19] K. Mndeep, K. Navreet, and K. Suman, "A literature review on cyber forensic and its analysis tools," *International Journal of Advanced Research In Computer And Communication Engineering*, vol. 5, no. 1, 2016.
[20] L. Pradeep and N. Rathore, "Load balancing algorithm in distributed network," *Solid State Technology*, vol. 63, no. 2s, 2020.
[21] N. Jain, A. Mishra, and N. Kumar, "Image forgery detection using singular value decomposition with some attacks," in *National Academy of Science Letters,* Springer Publication, Berlin, Germany, 2020.
[22] P. Srivastava and A. Choudhary, "Evolving evidence gathering process: cloud forensics," in *Proceedings of the International Conference on Big Data, Machine Learning and their Applications*, vol. 150, Springer Nature Singapore Pte Ltd., Allahabad, India, July 2021.
[23] N. Rathore, U. Rawat, and S. C. Kulhari, "Efficient hybrid load balancing algorithm," *National Academy of Science Letters*, Springer Publication, Berlin, Germany, 2020.
[24] M. G. Al-Thani, D. Yang, and D. y. Yang, "Machine learning for the prediction of returned checks closing status," *International Journal of Emerging Technology and Advanced Engineering*, vol. 11, no. 6, pp. 19–26, 2021.
[25] N. Kumar and P. K. Singh, "A comparative analysis of fuzzy based load balancing algorithm," *Journal of Computer Science*, vol. 5, no. 2, pp. 23–33, 2017.
[26] H. Singh and N. Kumar, "Analysis of grid simulators architechture," *Journal of Mobile Applications and Technologies (JMT)*, vol. 4, no. 2, pp. 32–41, 2017.
[27] N. Kumar, "A review towards: load balancing techniques," *Journal of Power Systems Engineering (JPS)*, vol. 4, no. 4, pp. 47–60, 2017.
[28] N. Kumar, "Efficient agent-based priority scheduling and load balancing using fuzzy logic in grid computing," *Journal of Computer Science*, vol. 3, no. 3, pp. 11–22, 2015.
[29] P. Liwen, L. Jing, and Li. Jin, "Information fusion-based digital forensics framework in cloud environment," in *Proceedings of the 3rd International Conference on Artificial Intelligence and Big Data (ICAIBD)*, IEEE, Chengdu, China, 2020.
[30] P. R. Brandao, "Computer forensics in cloud computing systems," *Budapest International Research in Exact Sciences (BirEx) Journal*, vol. 1, no. 1, pp. 71–86, 2019.
[31] N. Kumar, "Faults in grid," *International Journal of Software and Computer Science Engineering, MANTECH PUBLIATIONS*, vol. 1, no. 1, pp. 1–19, 2016.
[32] R. K. T. Siva and A. S. N. Chakravarthy, *Intrusion Detection System for Cloud Forensics Using Bayesian Fuzzy Clustering and Optimization Based SVNN*, Springer-Verlag GmbH Germany, part of Springer Nature, Berlin, Germany, 2020.
[33] R. Neeraj, "Installation of Alchemi.net in computational grid," *i-manager's Journal on Computer Science*, vol. 4, no. 2, pp. 1–5, 2016.
[34] R. A. Rahman, S. Masrom, S. Masrom, N. B. Zakaria, and S. Halid, "Auditor choice prediction model using corporate governance and ownership attributes: machine learning approach," *International Journal of Emerging Technology and Advanced Engineering*, vol. 11, no. 7, pp. 87–94, 2021.
[35] K. Neeraj, "Ethical hacking & security against cyber crime," *Journal of Information Technology*, vol. 5, no. 1, pp. 7–11, 2016.
[36] F. Khan and N. Rathore, "Internet of Things a review article," *Journal of Cloud Computing*, vol. 5, no. 1, pp. 20–25, 2018.
[37] N. Kumar and F. Khan, "Survey of IoT," *Journal of Cloud Computing, ManTech Publication*, vol. 1, no. 1, pp. 1–13, 2018.
[38] N. Rathore, "Map reduce architecture for grid," *Journal of Software Engineering*, vol. 10, no. 1, pp. 21–30, 2015.
[39] A. Nahar and S. Sharma, "Machine learning techniques for diabetes prediction: a Review, 2020," *International Journal of Emerging Technology and Advanced Engineering (ISSN 2250–2459)*, vol. 10, no. 3, pp. 28–34, 2020.
[40] N. Kumar, "Checkpointing: fault tolerance mechanism," *Journal of Cloud Computing*, vol. 3, no. 4, pp. 27–34, 2016.
[41] F. Ye, Y. Zheng, X. Fu, B. Luo, X. Du, and M. Guizani, "TamForen: a tamper-proof cloud forensic framework," in *Transactions on Emerging Telecommunications Technologies*, p. e4178, John Wiley & Sons, Hoboken, NJ, USA, 2020.
[42] N. Kumar and J. Rathore, "Efficient checkpoint Algorithm for distributed system," *International Journal of Engineering and Computer Science (IJECS), E-ISSN*, vol. 1, no. 2, pp. 59–66, 2019.
[43] I. Chana and N. Kumar, "Checkpointing algorithm in alchemi.NET, pragyaan: journal of information technology, IMS dehradun," *IEEE, CSI and MPCET*, vol. 8, no. 1, pp. 32–38, 2010.
[44] A. Goel and R. K. Bhujade, "A functional review, analysis and comparison ofposition permutation based image encryption techniques," *International Journal of Emerging Technology and Advanced Engineering*, vol. 10, no. 7, pp. 97–99, 2020.
[45] Neeraj, "GridSim installation and implementation process," *Journal of Cloud Computing*, vol. 2, no. 4, pp. 29–40, 2015.
[46] N. Kumar and I. Chana, "Report on hierarchal load balancing technique in grid environment," *Journal of Information Technology*, vol. 2, no. 4, pp. 21–35, 2013.
[47] S. Meshram, S. Kumar, and S. Shukla, "Enhanced robust and invisible of digital imageusing discrete cosine transform technique and binary shifting technique," *International Journal of Emerging Technology and Advanced Engineering*, vol. 10, no. 10, pp. 113–118, 2020.
[48] D. Pandey, U. Rawat, and N. Kumar Rathore, "Distributed biomedical scheme for controlled recovery of medical encrypted images," in *Innovation and Research in BioMedical Engineering,* Elsevier, Amsterdam, Netherlands, 2020.

[49] N. Rathore, "Performance of hybrid load balancing algorithm in distributed web server system," in *Wireless Personal Communication*, vol. 101, pp. 1233–1246, no. 4, Springer Publication, New York, NY, USA, 2018.

[50] N. Kumar Rathore, "Checkpointing: fault tolerance mechanism," *Journal of Cloud Computing*, vol. 3, no. 4, pp. 27–34, 2016.

[51] R. Bhatt, P. Maheshwary, P. Shukla, P. Shukla, M. Shrivastava, and S. Changlani, "Implementation of fruit fly optimization algorithm (FFOA) to escalate the attacking efficiency of node capture attack in wireless sensor networks (WSN)," *Computer Communications*, vol. 149, pp. 134–145, 2020.

[52] M. Saad Hamid, N. A. Manap, R. A. Hamzah, and A. F. Kadmin, "Stereo matching algorithm based on hybrid convolutional neural network and directional intensity difference," *International Journal of Emerging Technology and Advanced Engineering*, vol. 11, no. 6, pp. 87–96, 2021.

[53] D. Pathak and A. Verma, "Efficient and improved smart parking system based on IoT," *International Journal of Emerging Technology and Advanced Engineering*, vol. 10, no. 3, pp. 22–27, 2020.

[54] D. A. Pereira, R. R. Muñoz, and R. R. Muñoz, "Information system for integrated medical records with access via IOT technology," *International Journal of Emerging Technology and Advanced Engineering*, vol. 11, no. 4, pp. 6–17, 2021.

[55] E. D. Madyatmadja, T. R. Yulia, T. R. Yulia, D. J. M. Sembiring, and S. M. B. P. Angin, "IoT usage on smart campus: a systematic literature review," *International Journal of Emerging Technology and Advanced Engineering*, vol. 11, no. 5, pp. 45–52, 2021.

[56] K. Vijayalakshmi, "Comparitive approach of data mining for diabetes prediction and classification," *International Journal of Emerging Technology and Advanced Engineering*, vol. 10, no. 2, pp. 19–26, 2020.

[57] V. K. Gugulothu and S. K. Mohan Rao, "Classification of IRS LISS-III IMAGES by usingartificial neural networks," *International Journal of Emerging Technology and Advanced Engineering*, vol. 10, no. 4, pp. 24–31, 2020.

[58] Y. Peng and Z. Zheng, "Spectral clustering and transductive SVM based hyperspectral image classification," *International Journal of Emerging Technology and Advanced Engineering*, vol. 10, no. 4, pp. 72–77, 2020.

[59] N. R. Adytia and G. P. Kusuma, "Indonesian license plate detection and identification using deep learning," *International Journal of Emerging Technology and Advanced Engineering*, vol. 11, no. 7, pp. 1–7, 2021.

[60] R. Chakraborty, S. Sanyal, and P. Das, "IoT based thermal signature detector with alarm & e-mail notification with integrated social gathering screening using computer vision," *International Journal of Emerging Technology and Advanced Engineering*, vol. 10, no. 4, pp. 164–171, 2020.

Hindawi
Scientific Programming
Volume 2021, Article ID 4055281, 8 pages
https://doi.org/10.1155/2021/4055281

Research Article

Stock Prediction Based on Optimized LSTM and GRU Models

Ya Gao [1], Rong Wang [2], and Enmin Zhou [3]

[1] *School of Public Finance and Taxation, Central University of Finance and Economics, Beijing, China*
[2] *School of Computer Science and Technology, Xidian University, Xi'an, China*
[3] *School of Electronics and Information, Xi'an Jiaotong University, Xi'an, China*

Correspondence should be addressed to Ya Gao; 18737165379@163.com

Received 9 August 2021; Accepted 11 September 2021; Published 29 September 2021

Academic Editor: Punit Gupta

Stock market prediction has always been an important research topic in the financial field. In the past, inventors used traditional analysis methods such as K-line diagrams to predict stock trends, but with the progress of science and technology and the development of market economy, the price trend of a stock is disturbed by various factors. The traditional analysis method is far from being able to resolve the stock price fluctuations in the hidden important information. So, the prediction accuracy is greatly reduced. In this paper, we design a new model for optimizing stock forecasting. We incorporate a range of technical indicators, including investor sentiment indicators and financial data, and perform dimension reduction on the many influencing factors of the retrieved stock price using depth learning LASSO and PCA approaches. In addition, a comparison of the performances of LSTM and GRU for stock market forecasting under various parameters was performed. Our experiments show that (1) both LSTM and GRU models can predict stock prices efficiently, not one better than the other, and (2) for the two different dimension reduction methods, both the two neural models using LASSO reflect better prediction ability than the models using PCA.

1. Introduction

The financial market is quite volatile and experiences periods of contraction as well as expansion. The stock market, as a major financial market, is likewise highly volatile. The stock market has the characteristics of high return which has attracted the majority of investors and high risk which puts pressure on investors to sell out at the wrong time. In order to reduce unnecessary losses and obtain higher trading profits, the investors usually except to predict the stock price trend. As a result, stock market forecasting has been a major research topic in the financial area and attracts the attention of investors. In the stock market, the factors affecting the rise and fall of stock prices are complex and diverse. It includes not only the impact of economic factors such as price indicator, circulation indicator, activity degree, and economic uncertainty but also the impact of noneconomic factors such as traders' expectations, traders' psychological factors, and political environment. Therefore, the prediction of stock price has always been a challenging task.

According to the efficient market hypothesis [1], the stock price can be predicted according to the data of historical stocks. Furthermore, in recent years, since the increasing computing power and the decreasing data storage costs, especially the rise and development of innovative technologies such as big data, machine learning, reinforcement learning, and other optimization technologies, researchers have developed various models for predicting stock prices. Machine learning has been widely used in the capital market and plays an indispensable role in predicting future stock prices based on historical data. Traditional stock price forecasting models are mainly linear models, including autoregressive integrated moving average (ARIMA) model [2], multiple linear regression model, and exponential smoothing model [3, 4]. However, those (autoregressive integrated moving average,multiple linear regression model, and exponential smoothing model) linear models play an important role in promoting the progress and development of stock forecasting. Stock prices are typically noisy, fluctuating, and nonparametric, resulting in nonlinear and nonstationary characteristics in the stock market. The standard linear prediction model is unable to produce reliable stock predictions. With the development of deep learning methods, nonlinear neural networks are increasingly employed to predict the stock price for their higher accuracy.

The artificial neural network (ANN) includes MP neural network and back propagation (BP) neural network. However, the structure of ANN model is too single and there are some problems: (1) over fitting leads to the weak ability of the model generalization, (2) local extrema leads to the decline of the prediction ability of the model, and (3) the gradient disappears or explodes due to the excessive weight of neurons in the optimization process, resulting in the failure of prediction. Therefore, relevant scholars introduce deep neural networks (DNN), including convolutional neural network (CNN), recurrent neural network (RNN), long-term and short-term memory neural network (LSTM), and gated recurrent neural network (GRU), to improve the problems existing in the ANN model, so as to improve the accuracy and efficiency of prediction.

CNN is a type of neural network that has been increasingly popular in recent years. A one-dimensional CNN is a neural network that is designed to analyse image data efficiently. CNN can read and automatically extract the most significant features from the original input data for learning. This method feeds the network observed time series value as input and uses a multilayer network to predict the unobserved value. For example, Xu et al. [5] employed CNN to extract important stock features from stock market returns for forecasting stock market trends. Recurrent neural networks (RNN) such as long-term and short-term memory neural networks (LSTM) are another tool for predicting time series [6, 7]. LSTM accurately estimates time series data by using both the historical and the present stock data. In recent years, LSTM has been applied to stock market forecasting in different stock markets around the world. Chen et al. [8] used an LSTM model to predict China's Shanghai and Shenzhen stock markets. Li et al. [9] introduced the stock indicator with investor sentiment based on the LSTM model to predict the CS1300 index value, and the research results showed that the model was better than the support vector machine method in prediction accuracy. However, this model does not reduce the dimension of stock indicator. Jiawei and Murata [10] attempted to identify the influencing factors of stock market trend prediction through the LSTM model, which used a preprocessing algorithm to reduce the dimension of stock features and a sentiment analyzer to present financial news for stock trend prediction. However, only one dimension reduction method is used, and there is no comparison with other methods. Hu [11] reduced the dimension of stock technical analysis indicators by PCA and LASSO methods before using the LSTM model to predict. The results demonstrated that compared with the LASSO-LSTM model, the PCA-LSTM model can significantly reduce data redundancy and enhance prediction accuracy. Although this work used different dimension reduction methods, it only used one model and did not compare with other models.

Cho et al. [12] reduced the LSTM structure and created GRU, a new deep learning architecture that integrates long-term and short-term memory. GRU solves the problem of gradient disappearance and explosion in classic recurrent neural networks (RNNs) when learning long-term reliance. GRU has also been widely used in recent stock forecasting. Shen et al. [13] compared and predicted the trading signals of stock indicator based on the GRU model and SVM. The results demonstrated that the prediction accuracy of the two GRU models is higher than that of other models. However, the emotion indicator was not included in this study. Rahman et al. [14] used the stock data of Yahoo Finance mobile phone and GRU model to predict the stock price. The emotional indicators were not considered in this study, nor were compared with the performance of other models [15].

In this paper, we integrate a variety of technical indicators, such as investor sentiment indicators and financial data based on the Shanghai Composite Index data. We use LASSO and PCA methods to perform dimension reduction on the multiple influencing factors of the extracted stock price. The LSTM and GRU models are then utilized in this paper to forecast the stock price. Most importantly, by comparing the accuracy and stability of the LASSO-LSTM, LASSO-GRU, PCA-LSTM, and PCA-GRU models, the optimal forecasting model may be recommended.

2. Methodology

2.1. LASSO. In empirical analysis, in order to minimize the model deviation due to the lack of important independent variables, we set multidimensional variables. The models need to find the set of independent variables with the strongest explanatory power to the dependent variables. That is, the models need to improve the interpretability and prediction accuracy through independent variable selection (indicator selection and field selection). Indicator selection is an extremely important problem in statistical modelling. LASSO is an estimation method that can simplify the indicator set. It is a compressed estimation. It gets a more refined model by constructing a penalty function, which makes it compress some coefficients and set some coefficients to zero. Therefore, it retains the advantage of subset contraction and is a biased estimation for dealing with complex collinear data.

LASSO's basic idea is to minimize the sum of squares of residuals under the constraint that the sum of absolute values of regression coefficients is less than a constant, so as to produce some regression coefficients strictly equal to 0 and obtain an interpretable model. LASSO adds penalty term to the ordinary linear regression model, and the LASSO estimation of the ordinary linear model is

$$\begin{aligned} \widehat{\beta_{\text{Lasso}}} &= \arg\min_{\beta \epsilon R^d} \|Y - X\beta\|^2, \\ s.t. &\sum_{j=1}^{d} \left|\beta_j\right| \leq t, t \geq 0, \end{aligned} \tag{1}$$

which is equivalent to

$$\widehat{\beta_{\text{Lasso}}} = \arg\min_{\beta \epsilon R^d} \left(\|Y - X\beta\|^2 + \lambda \sum_{j=1}^{d} \left|\beta_j\right| \right), \tag{2}$$

where t and λ are said to be in one-to-one correspondence and they are the adjustment coefficients.

Let $t_0 = \sum_{j=1}^{d} |\widehat{\beta}_j(OLS)|$, and when $t < t_0$, some coefficients will be compressed to 0, so as to reduce the dimension of X and the complexity of the model. Finally, the variable selection can be realized by controlling the adjustment coefficient through the λ.

2.2. PCA. Principal component analysis (PCA) is a dimension reduction statistical method. With the help of an orthogonal transformation, it transforms the original random vector whose components are related into a new random vector whose components are not related. This is expressed algebraically as transforming the covariance matrix of the original random vector into a diagonal matrix and geometrically as transforming the original coordinate system into a new orthogonal coordinate system. Then, the multidimensional variable system is reduced, so that it can be transformed into low-dimensional variable system with a high accuracy, and the low-dimensional system can be further transformed into one-dimensional system by constructing an appropriate value function.

(1) Standardized collection of original indicator data p-dimensional random vector $x = (x_1, x_2, x_3, \ldots \ldots, x_p)^T$ and n samples $x_i = (x_{i1}, x_{i2}, x_{i3}, \ldots \ldots, x_{ip})^T$, where $i = 1, 2, \ldots, n (n > p)$. Then, we construct the sample array and carry out the following standardized transformation on the sample array elements: $Z_{ij} = x_{ij} - \overline{x_j}/s_j$, where $i = 1, 2, \ldots, n$, $j = 1, 2, \ldots, p$, $\overline{x_j} = \sum_{i=1}^{n} x_{ij}/n$, and $S_j^2 = \sum_{i=n}^{n} (x_{ij} - \overline{x_j})^2/n - 1$. Thus, the standardized matrix Z is obtained.

(2) Find the correlation coefficient matrix for the standardized matrix Z as

$$R = \left[r_{ij}\right]_{p\times p} = \frac{Z^T Z}{n-1}, \tag{3}$$

where $r_{ij} = \sum z_{kj}.z_{kj}/n - 1;\ i,\ j = 1, 2, \ldots, p$.

(3) Solve the characteristic equation of sample correlation matrix R by $|R - \lambda I_p| = 0$ to get p-characteristic roots, thus determining the principal component. Determine the value of m according to $\sum_{j=1}^{m} \lambda_j / \sum_{j=1}^{p} \lambda_j \geq 0.85$, so that the utilization rate of information can reach more than 85%. For each λ_j, $j = 1, 2, \ldots, m$, we solve the equation $Rb = \lambda_j b$ to obtain the unit eigenvector b_j^o.

(4) Convert the standardized indicator variable into the main component $U_{ij} = z_i^T b_j^o$, $j = 1, 2, \ldots, m$, where U_1 is called the first principal component, U_2 is called the second principal component, and so on. U_p is called the p principal component.

(5) Evaluate m principal components comprehensively. The final evaluation value is obtained by weighted sum of m principal components, and the weight is the variance contribution rate of each principal component.

2.3. LSTM and GRU. LSTM is a special type of recurrent neural network (RNN). The RNN neural network model can recycle the weight parameters of neurons and can effectively employ past data information for prediction. However, RNN can only deal with certain short-term dependence and is prone to gradient explosion and gradient disappearance, that is, long-term dependence on historical data. In order to solve these problems, LSTM was proposed by Hochreiter and Schmidhuber [6] and then improved and promoted by Graves [16]. It has been widely used in a variety of challenges and has yielded impressive outcomes.

Compared with the RNN model, the LSTM model introduces a cell state (C_t) and uses the input gate (i_t), forget gate (f_t), and output gate (O_t). The three gates are used to maintain and control information. At time t, x_t is the input data, h_t represents the current output, c_t is the value from the input gate, tan$h$ is hyperbolic tangent function, σ is the sigmoid function, W represents the matrix weight, and b is the bias. The operation formula of LSTM is as follows.

Forget gate:

$$f_t = \sigma\left(W_f * [h_{t-1}, x_t] + b_f\right). \tag{4}$$

Input gate:

$$\begin{aligned} i_t &= \sigma\left(W_i * [h_{t-1}, x_t] + b_i\right), \\ \widetilde{c}_t &= \tanh\left(W_c * [h_{t-1}, x_t] + b_c\right), \\ c_t &= f_t * c_{t-1} + i_t * \widetilde{c}_t. \end{aligned} \tag{5}$$

Output gate:

$$\begin{aligned} o_t &= \sigma\left(W_o * [h_{t-1}, x_t] + b_o\right), \\ h_t &= o_t * \ \tanh\left(c_t\right). \end{aligned} \tag{6}$$

The LSTM model is especially popular in the field of financial forecasting because it effectively deals with the redundancy of relevant information in historical data.

GRU is one of the variants of RNN which is introduced by Cho et al. [12]. By introducing gating structure, it solves the problem that RNN is difficult to deal with long-distance information acquisition. Compared with LSTM, GRU is simplified and only update gate (z_t) and reset gate (r_t) are introduced. In GRU, the update (or input) gate decides how much input (x_t) and previous output (h_{t-1}) to be passed to the next cell and the reset gate is used to determine how much of the past information to forget. The current memory content ensures that only the relevant information needs to be passed to the next iteration, which is determined by the weight W. The main operations in GRU are governed by the following formulae.

Update gate:

$$z_t = \sigma\left(W_z * [h_{t-1}, x_t]\right). \tag{7}$$

Reset gate:

$$r_t = \sigma\left(W_r * [h_{t-1}, x_t]\right). \tag{8}$$

After resetting the gate and updating the gate, the candidate status value of GRU unit is $\widetilde{h}_t$ and the final output status value is h_t:

$$\widetilde{h}_t = \tanh\left(W_{\widetilde{h}} * \left[r_t * h_{t-1}, x_t\right]\right),$$
$$h_t = \left(1 - z_t\right) * h_{t-1} + z_t * \widetilde{h}_t. \tag{9}$$

3. Experiment Settings and Results

3.1. Data Source and Indicator Selection. In this paper, the data of the Shanghai Composite Index (000001) from April 11, 2007, to August 3, 2021, are selected as the experimental data. The data comes from NetEase Finance and Economics website, with a total of 3,481 days. In order to evaluate the training effect of the model, we divide the experimental data into training set and test set, of which 80% are used as one training set to train the stock prediction model and the other 20% are used as test sets to verify the prediction effect of the model. In addition, we use Intel Core i9-9900K CPU with memory 64 GB to finish the experiments.

In the selection process of stock technical indicators, this paper considers the factors affecting the stock price as much as possible. Compared with other studies, this paper selects the open price, highest price, lowest price, trading volume, and other common technical indicators, such as OBV, KDJ, BIAS, RSI, CCI, and MFI, as well as other stock price judgment technical indicators and PSY indicators reflecting investors' psychological mood. These indicators comprehensively reflect the information affecting stock price fluctuations and have the strong explanatory power for stock price fluctuations. The selected indicators are described in detail in Table 1.

Table 1: Explanation of technical indicator variables.

Primary indicator	Secondary indicator	Variable
Momentum indicators	ADX	Z1
	ADXR	Z2
	BOP	Z3
	CCI	Z4
	DX	Z5
	MACD	Z6
	MACDEXT	Z7
	MACDFIX	Z8
	TRIX	Z9
	MFI	Z10
	MOM	Z11
	PPO	Z12
	ROC	Z13
	RSI	Z14
	WILLR	Z15
	DPO	Z16
	DMA	Z17
	EXPMA	Z18
	DMI	Z19
Volume indicator	OBV.OBV	Z20
	OBV.MAOBV	Z21
	ADOSC	Z22
Volatility indicators	ATR	Z23
	NATR	Z24
	TRANGE	Z25
Cycle indicators	HT_DCPERIOD	Z26
	HT_DCPHASE	Z27
	HT_ PHASOR	Z28
	HT_ SINE	Z29
Moving average indicator	BBI	Z30
	SMA	Z31
Overbought and oversold	KDJ.K	Z32
	KDJ.D	Z33
	KDJ.J	Z34
	BOLL	Z35
	BIAS.BIAS1	Z36
	BIAS.BIAS2	Z37
	BIAS.BIAS3	Z38
	WR.WR1	Z39
	WR.WR2	Z40
Volume price indicator	ASI	Z41
	EMV	Z42
Energy indicator	PSY	Z43
	MASS.MASS	Z44
	MASS.MAMASS	Z45
	MTM	Z46
	BRAR-BR	Z47
	BRAR-AR	Z48
	VR	Z49
Stock price basic type	Open price	Z50
	High price	Z51
	Low price	Z52
	Volume	Z53

3.2. Experimental Setup. Different superparameters have a significant impact on the prediction ability of LSTM and GRU models. Therefore, different superparameter data are set in the prediction to compare the prediction results. The number of neuron layers is set to 2 and 3, the number of neurons is set to 8, 16, and 32, the learning rate is usually set to 0.001, and the number of iterations is set to 1000. We can determine the most accurate prediction method by analyzing the prediction accuracy of the experimental results and the degree of fit of the trend between the predicted stock price and the historical stock price. The prediction accuracy is evaluated by mean square error function (MSE), root mean square error (RMSE), and mean absolute error (MAE) at different look-back values. The smaller the value of the three, the more accurate the forecast result is. The full specification of parameters used in these models is listed in Tables 2–5.

3.3. Experimental Results. The experimental results of stock prediction of four models are shown in Tables 2–5. Two different feature sets were obtained in this experiment. Set I is the data obtained from the LASSO dimension reduction method, and set II is the data obtained from the PCA dimension reduction method. These characteristic data are used to train LSTM and GRU models. In the experiment, different backtracking values were set. All parameter specifications used by the four models are shown in Tables 2–5. The results show that, through MAS, RMSE, and MAE indicators, both LSTM and GRU models can predict stock prices effectively, not one is more efficient than the other. However, for different dimension reduction methods, we find that all indicators (except the training time) show that

Table 2: Learning results of LASSO-LSTM.

Number of layers	Number of neurons	Look-back value	Train MSE	Train RMSE	Train MAE	Test MSE	Test RMSE	Test MAE	Train time
3	8	10	1904.5410	43.6410	29.6357	979.393	31.2953	23.7622	132.8780
3	8	20	1272.1884	35.6678	24.2016	904.9543	30.0825	22.6913	307.9990
3	8	30	2142.9192	46.2917	36.9945	957.2454	30.9394	22.6934	430.9928
3	8	40	4629.96388	68.0438	61.9541	5342.1396	73.0899	67.8341	576.7966
3	8	50	1214.7745	34.8536	23.3589	881.0265	29.6821	21.0112	766.2157
2	8	10	1248.6508	35.3363	23.4574	777.5208	27.8841	19.6554	95.1825
2	8	20	1608.0676	40.1007	27.8215	991.3244	31.4853	21.8147	213.3500
2	8	30	1251.1989	35.3723	22.9057	858.0669	29.2928	19.7988	320.6939
2	8	40	1202.1561	34.6721	23.1705	883.7101	29.7273	21.3382	411.6595
2	8	50	1206.7042	34.7376	23.1075	850.2483	29.1590	20.6415	490.2418
3	16	10	1031.0358	32.1097	21.8451	778.9459	27.9096	19.9938	376.8092
3	16	20	6555.5376	80.9663	75.5480	9468.3418	97.3054	93.4085	779.2415
3	16	30	1254.3915	35.4174	23.0273	733.8773	27.0902	18.6517	1189.4983
3	16	40	1015.5285	31.8674	21.3504	872.5764	29.5394	20.9425	1603.3826
3	16	50	984.6891	31.3798	22.6411	892.3263	29.8718	20.5884	2065.8919
2	16	10	1051.3169	32.4240	21.6973	786.5796	28.0460	19.8271	212.8883
2	16	20	1100.5430	33.1744	21.7411	734.0122	27.0927	18.7960	442.2047
2	16	30	1854.9745	43.0694	34.8938	1331.5276	36.4901	30.3015	725.7830
2	16	40	984.7316	31.3804	20.8187	803.8667	28.3525	20.9327	1080.9957
2	16	50	1006.7289	31.7290	21.1893	846.4849	29.0944	21.3891	1346.3720
3	32	10	787.5522	28.0634	20.2811	852.4590	29.1969	20.1759	306.4265
3	32	20	816.3383	28.5716	20.2925	1199.1475	34.6287	23.9940	636.0178
3	32	30	908.5170	30.1416	20.8915	1850.9948	43.0232	30.6120	970.8293
3	32	40	844.3165	29.0571	20.1408	2720.0981	52.1546	32.7257	1291.5366
3	32	50	1057.6416	32.5214	21.6094	2061.0061	45.3983	29.4876	1356.4536
2	32	10	1117.4025	33.4276	22.2174	799.0801	28.2680	19.8247	454.6504
2	32	20	919.8626	30.3292	21.2240	751.9146	27.4211	19.1840	929.6708
2	32	30	1096.1162	33.1076	23.0584	2220.7078	47.1244	31.1358	1358.4529
2	32	40	1124.6395	33.5356	23.5911	1125.7322	33.5519	25.2733	1385.7139
2	32	50	1442.5688	37.9812	29.5802	1449.2459	38.0690	29.8898	1497.0255

The number of epochs is 1000, learning rate is 0.001, and the activation function is *tanh*.

Table 3: Learning results of PCA-LSTM.

Number of layers	Number of neurons	Look-back value	Train MSE	Train RMSE	Train MAE	Test MSE	Test RMSE	Test MAE	Train time
3	8	10	1690.9171	41.1208	28.1397	10971.7773	104.7463	72.8242	94.6602
3	8	20	2939.5332	54.2175	36.5242	42278.7188	205.6179	176.8455	198.6585
3	8	30	3896.0701	62.4185	50.7139	5464.5537	73.9226	54.9697	286.6041
3	8	40	2811.6401	53.0249	35.2591	37730.9688	194.2446	160.7494	410.7228
3	8	50	2484.0608	49.8404	38.5345	30902.8711	175.7921	154.2262	541.6164
2	8	10	1619.0308	40.2372	27.5215	19627.638	140.0987	116.2432	60.6061
2	8	20	2298.5891	47.9436	34.5403	17482.4219	132.2211	102.2909	128.5815
2	8	30	2054.7803	45.3297	32.6867	24208.5762	155.5911	125.7793	191.2626
2	8	40	2300.3635	47.9621	34.4281	27250.1621	165.0762	143.2569	252.3014
2	8	50	1614.6926	40.1832	26.5031	27625.6934	166.2098	140.6607	313.6309
3	16	10	1022.4178	31.9753	23.6002	19104.1875	138.2179	105.8687	278.2536
3	16	20	1744.8813	41.7718	31.4407	100281.7656	316.6730	261.6820	543.4168
3	16	30	932.1148	30.5306	23.0709	5806.1943	76.1984	58.5185	846.4980
3	16	40	1688.8053	41.0951	31.0483	72460.7422	269.1853	225.7833	1090.1818
3	16	50	1101.5414	33.1895	25.5879	4054.6895	63.6764	42.8904	1654.7813
2	16	10	755.3936	27.4844	19.6168	7201.1304	84.8595	50.9353	93.1576
2	16	20	642.6140	25.3498	18.2508	3843.0637	61.9924	48.0259	207.6672
2	16	30	734.1151	27.0946	19.6506	13394.8955	115.7363	89.6245	311.5668
2	16	40	737.1022	27.1496	19.1860	5955.7412	77.1734	59.1523	427.4087
2	16	50	941.9175	30.6907	21.1289	4154.1406	64.4526	50.9237	666.0416
3	32	10	599.8295	24.4914	19.4298	35741.8242	189.0551	124.2747	514.5233

Table 3: Continued.

Number of layers	Number of neurons	Look-back value	Train MSE	Train RMSE	Train MAE	Test MSE	Test RMSE	Test MAE	Train time
3	32	20	594.4351	24.3810	18.6597	45484.7734	213.2716	169.4778	1064.2589
3	32	30	455.7460	21.3482	16.1783	17365.6328	131.7787	94.3915	1647.6020
3	32	40	805.4067	28.3797	23.0945	7770.9268	88.1529	58.4716	2789.5281
3	32	50	672.4887	25.9324	19.2775	91975.9453	303.2754	242.9042	2610.5209
2	32	10	495.8636	22.2680	16.6603	15152.0000	123.0935	90.1184	347.5115
2	32	20	627.7170	25.0543	18.4374	6696.0894	81.8296	50.5065	721.5676
2	32	30	454.6801	21.3232	15.7141	5454.8228	73.8568	51.7249	1089.6257
2	32	40	548.5927	23.4221	17.2341	17594.1758	132.6430	105.7155	1437.5246
2	32	50	407.0175	20.1747	14.6608	8100.0464	90.0003	66.1121	1808.6861

The number of epochs is 1000, learning rate is 0.001, and the activation function is *tanh*.

Table 4: Learning results of LASSO-GRU.

Number of layers	Number of neurons	Look-back value	Train MSE	Train RMSE	Train MAE	Test MSE	Test RMSE	Test MAE	Train time
3	8	10	1293.7802	35.9692	23.8084	831.7062	28.8393	20.3225	117.7369
3	8	20	1444.4125	38.0054	25.5757	910.9886	30.1826	21.6005	249.3114
3	8	30	1123.8232	33.5235	22.7495	826.1986	28.7437	20.0954	402.0947
3	8	40	1482.5836	38.5043	27.8070	943.8668	30.7224	20.9493	508.5391
3	8	50	1280.0657	35.7780	24.5826	978.3127	31.2780	24.1942	657.0113
2	8	10	1377.2985	37.1120	24.9828	834.2753	28.8838	20.0803	90.3936
2	8	20	1136.9731	33.7190	22.8381	799.1834	28.2698	19.5676	200.8435
2	8	30	1245.3809	35.2900	23.5962	864.6091	29.4042	20.8457	276.3479
2	8	40	1500.8726	38.7411	26.3263	1093.2498	33.0643	23.7652	350.2043
2	8	50	1239.8575	35.2116	23.4242	845.8825	29.0841	20.5453	431.4074
3	16	10	1138.9615	33.7485	22.0896	753.7004	27.4536	19.1470	378.2382
3	16	20	1192.8514	34.5377	24.7956	1015.7639	31.8711	23.3095	783.4717
3	16	30	985.8597	31.3984	21.1888	883.4285	29.7225	22.0179	1198.1594
3	16	40	1038.7191	32.2292	21.6453	802.5121	28.3286	19.8618	1622.0595
3	16	50	1116.0420	33.4072	22.7048	792.4473	28.1504	20.0095	2032.0963
2	16	10	1233.5467	35.1219	23.9346	833.0342	28.8623	19.9071	207.6725
2	16	20	1104.4722	33.2336	23.2089	869.4269	29.4860	21.8385	433.1125
2	16	30	1114.1602	33.3790	22.0850	796.8630	28.2288	20.7113	668.5479
2	16	40	1072.4717	32.7486	23.0368	802.4998	28.3284	19.7236	1073.6516
2	16	50	979.3882	31.2952	21.5892	844.8095	29.0656	19.7065	1373.0419
3	32	10	924.5891	30.4071	20.6728	831.0146	28.8273	20.2939	277.7194
3	32	20	862.2056	29.3633	20.4895	1081.1123	32.8803	24.4835	526.1457
3	32	30	907.1031	30.1182	21.2814	1127.4957	33.5782	23.5790	797.8424
3	32	40	847.7834	29.1167	21.0260	1012.2365	31.8157	21.7214	1066.6936
3	32	50	810.5232	28.4697	20.3346	1196.4927	34.5904	24.4721	1349.8547
2	32	10	969.9576	31.1441	20.7674	777.3851	27.8816	19.5336	367.9321
2	32	20	985.3215	31.3898	21.8014	829.0216	28.7927	20.1274	890.5871
2	32	30	861.6357	29.3536	20.5396	952.9534	30.8699	22.5985	1362.8664
2	32	40	1149.7027	33.9073	24.3771	821.3757	28.6597	20.0752	1392.1843
2	32	50	883.3071	29.7205	20.3320	833.8439	28.8764	20.4838	1596.1727

The number of epochs is 1000, learning rate is 0.001, and the activation function is *tanh*.

Table 5: Learning results of PCA-GRU.

Number of layers	Number of neurons	Look-back value	Train MSE	Train RMSE	Train MAE	Test MSE	Test RMSE	Test MAE	Train time
3	8	10	1369.6727	37.0091	27.3800	29235.9590	170.9853	152.2538	72.1253
3	8	20	2434.9895	49.3456	35.6683	12723.6592	112.7992	93.6385	168.9686
3	8	30	2101.9541	45.8471	33.8847	34108.7148	184.6854	166.6717	254.5802
3	8	40	2574.5256	50.7398	37.5205	21786.1641	147.6014	127.3568	333.7451
3	8	50	1194.8505	34.5666	25.1312	29938.3730	173.0271	151.4763	458.2760

Table 5: Continued.

Number of layers	Number of neurons	Look-back value	Train MSE	Train RMSE	Train MAE	Test MSE	Test RMSE	Test MAE	Train time
2	8	10	1196.4231	34.5893	23.0424	10500.0391	102.4697	82.4290	54.2256
2	8	20	2299.9802	47.9581	36.0542	29103.7676	170.5983	151.9113	112.4777
2	8	30	1426.4019	37.7677	26.6629	21631.0195	147.0749	121.6393	167.5188
2	8	40	1835.9618	42.8481	29.4047	9878.1016	99.3886	80.6860	225.1572
2	8	50	1503.7362	38.7780	26.7672	10440.7920	102.1802	86.5779	275.0539
3	16	10	943.2319	30.7121	21.8401	29209.2168	170.9070	148.9597	116.7384
3	16	20	816.0226	28.5661	20.8915	12768.4766	112.9977	99.0165	255.2906
3	16	30	965.2081	31.0678	23.1747	14524.5684	120.5179	99.9182	815.1597
3	16	40	980.0072	31.3051	22.1477	12230.3311	110.5908	84.3423	1096.2136
3	16	50	803.9420	28.3539	20.7994	9752.1914	98.7532	81.7505	1354.4110
2	16	10	776.4768	27.8653	19.3489	7601.5073	87.1866	74.7424	70.5103
2	16	20	784.2062	28.0037	21.0686	18093.4902	134.5120	119.4448	176.9984
2	16	30	747.7553	27.3451	20.0675	8023.9351	89.5764	77.0783	236.3435
2	16	40	720.6558	26.8450	19.3404	18241.6797	135.0617	117.5537	378.0467
2	16	50	713.9094	26.7191	19.0031	9412.2773	97.0169	79.6811	484.1664
3	32	10	453.6670	21.2995	15.6519	6122.3311	78.2453	61.3247	469.7184
3	32	20	456.4868	21.3656	15.9169	11951.0684	109.3209	90.6603	977.3712
3	32	30	626.6472	25.0329	19.3384	11865.4746	108.9288	86.8948	1483.5679
3	32	40	529.3604	23.0078	17.0553	9151.2109	95.6620	76.8583	1991.7930
3	32	50	504.7110	22.4658	16.9049	30787.4473	175.4635	153.6052	3289.7475
2	32	10	425.4210	20.6257	15.0201	6595.3359	81.2117	63.7287	268.0692
2	32	20	653.8412	25.5703	18.7442	10183.2344	100.9120	84.6054	539.5263
2	32	30	508.9430	22.5598	16.2366	6050.9692	77.7880	61.9705	856.6547
2	32	40	630.0575	25.1009	18.9956	7276.7456	85.3038	69.0245	1345.9522
2	32	50	623.7015	24.9740	18.0729	9594.8418	97.9533	80.5411	1678.2588

The number of epochs is 1000, learning rate is 0.001, and the activation function is *tanh*.

the prediction results of the two neural network models using LASSO dimension reduction are mostly better than those using PCA dimension reduction data. In other words, under the same network model, the prediction performance of LASSO-LSTM model is better than PCA-LSTM and the prediction performance of LASSO-GRU is better than PCA-GRU.

4. Conclusion

This study innovatively integrates a variety of technical indicators such as investor sentiment indicators and financial data and carries out dimension reduction on the multiple influencing factors of the extracted stock price through LASSO and PCA analysis approaches. This work carries out a comparison on the performances of LSTM and GRU for stock market forecasting under the different parameters. Our experimental results show that (1) both LSTM and GRU models can be used to predict stock prices effectively and (2) for different dimension reduction methods, the prediction results of the two neural network models using LASSO dimension reduction are mostly better than those using PCA dimension reduction data.

Data Availability

The experimental data used to support the findings of this study are available from the corresponding author upon request.

Conflicts of Interest

The authors declare that the research was conducted in the absence of any commercial or financial relationships that could be construed as potential conflicts of interest.

References

[1] E. F. Fama, "Efficient capital markets: a review of theory and empirical work," *The Journal of Finance*, vol. 25, no. 2, pp. 383–417, 1970.

[2] P.-F. Pai and C.-S. Lin, "A hybrid ARIMA and support vector machines model in stock price forecasting," *Omega*, vol. 33, no. 6, pp. 497–505, 2005.

[3] X. B. Huang, C. F. Wang, Z. M. Fang, and C. L. Xiong, "Detection of Chinese stock information based on hidden Markov model," *Syst. Eng.-Theory Pract*, vol. 32, no. 4, pp. 713–720, 2012.

[4] J. J. Shi and T. Song, "Analysis of long-term fluctuation trends and influencing factors in stock market-based on spline-GARCH model," *J. Appl. Stat. Manag*, vol. 34, no. 1, pp. 175–182, 2015.

[5] B. Xu, D. Zhang, S. Zhang, H. Li, and H. Lin, "Stock market trend prediction using recurrent convolutional neural networks," in *Proceedings of CCF International Conference on Natural Language Processing and Chinese Computing*, pp. 166–177, Hohhot, China, August 2018.

[6] S. Hochreiter and J. Schmidhuber, "Long short-term memory," *Neural Computation*, vol. 9, no. 8, pp. 1735–1780, 1997.

[7] H. Hewamalage, C. Bergmeir, and K. Bandara, "Recurrent neural networks for time series forecasting: current status and

future directions," *International Journal of Forecasting*, vol. 37, no. 1, pp. 388–427, 2021.

[8] K. Chen, Y. Zhou, and F. Dai, "A LSTM-based method for stock returns prediction: a case study of China stock market," in *Proceedings of the 2015 IEEE international conference on big data (big data)*, pp. 2823-2824, IEEE, Santa Clara, CA, USA, October 2015.

[9] J. Jiahong Li, H. Junjie Wu, and J. Wu, "Sentiment-aware stock market prediction: a deep learning method," in *Proceedings of the 2017 international conference on service systems and service management*, pp. 1–6, IEEE, Dalian, China, June 2017.

[10] X. Jiawei and T. Murata, "Stock market trend prediction with sentiment analysis based on LSTM neural network," in *Proceedings of the International Multi-Conference of Engineers and Computer Scientists (IMECS)*, pp. 13–15, Hong Kong, China, March 2019.

[11] Y. W. Hu, "Stock forecast based on optimized LSSVM model," *Computer Science*, vol. 48, no. S1, pp. 151–157, 2021.

[12] K. Cho, B. Van Merriënboer, C. Gulcehre et al., "Learning phrase representations using RNN encoder-decoder for statistical machine translation," arXiv preprint arXiv:1406.1078, 2014.

[13] G. Shen, Q. Tan, H. Zhang, P. Zeng, and J. Xu, "Deep learning with gated recurrent unit networks for financial sequence predictions," *Procedia computer science*, vol. 131, pp. 895–903, 2018.

[14] M. O. Rahman, M. S. Hossain, T. S. Junaid, M. S. A. Forhad, and M. K. Hossen, "Predicting prices of stock market using gated recurrent units (GRUs) neural networks," *Int. J. Comput. Sci. Netw. Secur*, vol. 19, no. 1, pp. 213–222, 2019.

[15] H. Wang, X.-M. Zhang, G. Tomiyoshi et al., "Association of serum levels of antibodies against MMP1, CBX1, and CBX5 with transient ischemic attack and cerebral infarction," *Oncotarget*, vol. 9, no. 5, pp. 5600–5613, 2017.

[16] A. Graves, *Supervised Sequence Labelling with Recurrent Neural Networks*, Springer, Berlin/Heidelberg, Germany, 2012.

Hindawi
Scientific Programming
Volume 2021, Article ID 4645596, 11 pages
https://doi.org/10.1155/2021/4645596

Research Article

An Approach to Study the Poverty Reduction Effect of Digital Inclusive Finance from a Multidimensional Perspective Based on Clustering Algorithms

Lu Zhou [1,2] and Huiling Wang [3]

[1] *College of Finance, Tianjin University of Finance and Economics, Tianjin 300222, China*
[2] *Tianjin Renai College, Tianjin 301636, China*
[3] *Chongqing City Management College, Chongqing 401331, China*

Correspondence should be addressed to Huiling Wang; 289672983@qq.com

Received 10 August 2021; Revised 7 September 2021; Accepted 21 September 2021; Published 29 September 2021

Academic Editor: Punit Gupta

The evaluation of clustering algorithms is intrinsically difficult because of the lack of objective measures. On the basis of the DIFI and China's Provincial Panel data, this study aims to test the poverty reduction effect of digital inclusive finance in three dimensions of income, education, and healthcare and further look at the transmission mechanism of digital inclusive finance in poverty alleviation. The results indicated that digital inclusive finance exerts a poverty reduction effect in three dimensions—medical poverty, income poverty, and education poverty. Of these, the coverage breadth significantly affects the alleviation of medical poverty, the use depth significantly affects the alleviation of income poverty and education poverty, and the digitization level affects the alleviation of poverty in three dimensions. The level of regional economic development plays an intermediary role in the poverty alleviation effect of digital inclusive finance. Compared with the western region, which is relatively backward in development, the poverty reduction effect of digital inclusive finance in the eastern region is more significant.

1. Introduction

Poverty alleviation has been placed in the important position of governing the country in China, and poverty eradication has become one of the fundamental tasks of building a moderately prosperous society in 2020. Over the past 40 years, people's living standards have continuously improved, and poverty alleviation has also attained remarkable results. When counting the number of poor people from 2015 to 2019, the score dropped from 55.75 million to 5.51 million, while poverty declined from 5.7% to 0.6%. Nevertheless, the work on poverty reduction in deep poverty-stricken areas still faces significant challenges. Per the endogenous growth theory, it is challenging for impoverished areas to get out of poverty because of the lack of funds and talents, which lead to economic activities producing low benefits. Financial support is an essential factor in poverty alleviation, and financial exclusion is predominantly evident in rural areas. Serious financing constraints have become a vital factor affecting poverty alleviation. The government work report in 2018 emphasized "supporting financial institutions to expand the inclusive financial business and increase efforts to get rid of poverty precisely." In 2019, the People's Bank of China issued guidance on carrying out a job effectively in financial targeted poverty alleviation from 2019 to 2020. In addition, it put forth specific requirements on optimizing the allocation of financial resources, innovating financial products and services, and enhancing the financial support for targeted poverty alleviation. Of note, alleviation of financial poverty plays a crucial role in targeted poverty alleviation. By constructing the financial system, financial services can be supplied for vulnerable groups and attain inclusive economic growth.

Owing to the limitation of the region or economic status, the poor groups have been unable to obtain sufficient financial services and have been in financial exclusion for a long time. Inclusive finance entails providing financial services to the excluded vulnerable groups and poor groups at an affordable cost, thereby ensuring that all social strata, including vulnerable and marginalized groups, can equally obtain the opportunities and it eventually benefits all people. With the improvement of financial inclusiveness, on the one hand, low-income groups will have access to financial services such that their consumption can be more stable and their production activities can be executed smoothly. Besides, insurance services can provide corresponding protection for them, decrease the risk of adverse impact, and thereby attain poverty alleviation. On the other hand, providing apposite financial services for low-income groups can promote an increase in their income and decrease the degree of income inequality.

Before the emergence of digital inclusive finance (DIF), customers could only handle business in the physical outlets of financial institutions. Owing to the limitation of geographical location or the level of economic development, financial institutions in poor areas set up very few outlets, and the financial products and services that residents could access were also minimal. To understand inclusive finance, that is, to increase financial availability, it is essential to enlarge the coverage of financial services. Under the traditional business model, the expansion of coverage certainly warrants the expansion of financial institutions' outlets, which requires considerable capital investment, which undoubtedly increases the operating cost of financial institutions, which would eventually be transformed into financial services. Although the expansion of financial institutions has accomplished geographical coverage, the enormous cost can completely offset the benefits of regional coverage. Digital inclusive finance can resolve this contradiction and decrease the increase in cost caused by the expansion of financial institutions' physical outlets to some extent and fill the gap in financial infrastructure. Digital inclusive finance overcomes the limitation of geographical location, shortens the distance between residents in poverty-stricken areas and finance, and improves access to financial services that were not available before. With the progress of information and communication technology, the internet penetration rate in China has been increasing year by year. It is estimated that the penetration rate of internet will reach 70.4% by the end of 2020, and the scale of mobile internet users will reach 989 million. Internet and smartphones have become an indispensable part of people's lives, and their high popularity strongly supports the development of digital inclusive finance. People can handle most of their financial businesses through the use of the internet and smartphones, which also provides the opportunity for the groups who are unable or inconvenient to handle financial business in the physical outlets of financial institutions to enjoy financial products and services. Speaking on a comparative basis, digital inclusive finance has the characteristics of a relatively lower operating cost and wide coverage, which means it can provide low-income groups with lower-cost financial products and services.

The blood transfusion poverty alleviation model is just like drinking poison to quench thirst; it can alleviate poverty in a short period, but is not conducive to the sustainable development of the region. Does the digital inclusive finance with wide coverage, fast information transmission, and low transaction cost support the regional economic growth? Has poverty alleviation been promoted? This study discusses and examines these problems.

2. Literature Review and Research Hypothesis

2.1. Literature Review. When the United Nations designated 2005 as the "International Year of Microcredit," it formally proposed the concept of inclusive finance, which aims to promote microcredit services, augment financial inclusiveness, and provide suitable financial services for the poor and vulnerable groups, which will help improve the status quo of the poor and vulnerable groups who have been in financial exclusion for a long time that will help alleviate and eventually eliminate poverty.

The demand for financial services of vulnerable groups cannot be met and also cannot match the financial services provided by financial institutions, which makes some groups and individuals incapable of entering the formal financial system [1] and acquire safe, appropriate, fair, and low-cost financial products and services from formal financial institutions [2]. To alter the status quo of financial exclusion, we need to promote the growth of inclusive finance. Inclusive finance can ensure that all groups can easily enjoy formal financial services [3] and also that the vulnerable groups have access to financial services and acquire adequate credit timely at an affordable cost [4]. Regarding the standards and methods of inclusive finance measurement, Honohan [5] developed a measurement index based on the proportion of access of the adult population to formal financial services [6] and created a comprehensive index to measure inclusive finance from multiple dimensions. Most scholars systematically created the inclusive finance index system from the aspects of geographical penetration, availability, and utility of financial services that will reflect the development level of inclusive finance.

With the proposal of the concept of "inclusive finance" and the expansion of inclusive finance practice, many scholars explored the economic impact of inclusive finance. Inclusive finance has a certain positive effect on finance stability. During the whole financial crisis, poor depositors and borrowers tended to maintain moderate financial behavior, pay off their loans on time, and deposit their deposits in a safe place [7]. Brune et al. [8] investigated the correlation between the expansion of bank branches and poverty reduction in India and reported that the expansion of rural bank branches helped cut down poverty, especially in rural areas without banks, and the decline in the poverty rate was more prominent. Beck et al. [9] claimed that, in the developed financial system, the income of the low-income group increases faster, the Gini coefficient declines faster, the proportion of the poor population decreases faster, and the cash flow constraints of enterprises are easier to resolve. Demirgüç-Kunt and Levine [10] deemed that financial development could promote economic activities, stimulate the labor demand, increase income, and provide more prosperous economic opportunities. In comparison to the higher-income groups and large companies, financial development exerted a greater positive impact on low-income groups, low-income families, and small enterprises. Allen et al. [11] found that the increase in commercial bank penetration positively and significantly affected the use of bank accounts and bank credit by Kenyan households, especially for families with no income or low income, and low education level. The increase in banking activities, especially the penetration of the microfinance business, would affect poverty and income inequality. Alvarez de la Campa [12] demonstrated that it is hard for the poor to accumulate savings to pay for health and education, and the lack of financing channels has gravely restricted the economic growth and poverty alleviation in the Middle East and North Africa. Pearce [13] highlighted that, despite the expansion of bank branches and microfinance institutions in some Middle East and North African countries, a large part of the population still has no access to financial services. Emara and Mohieldin [14] suggested that when people are included in the financial system, they could better improve their health, invest in education and business, and make choices beneficial to their entire family.

In addition, the crucial role of the development of information technology has been recognized in inclusive finance. Andrianaivo and Kpodar [15] utilized African countries as samples to explore the impact of ICT, especially the emergence of mobile phones, on economic growth. The research demonstrated that the growth of ICT, including mobile phones, promoted the development of inclusive finance and consolidated the impact on economic growth. The M-PESA system, designed and put to use in Kenya, allows money to flow electronically, thus letting the money flow to penetrate rural areas, thereby increasing income inflows for many rural residents. The G20 advanced principles of digital inclusive finance were proposed in 2016, which aimed to promote the growth of DIF, provided services for those who did not enjoy enough financial services, and resolved the "last mile" problem of financial services. Klapper et al. [16] claimed that digital payment—whether its healthcare, education, or other social safety nets—has crucial benefits for individuals. Moreover, it can enhance the efficiency of the government and aid agencies by decreasing transaction costs and leakage. Beck et al. [17] illustrated that the availability of mobile currency reduced the incidence of theft, thereby decreasing the output loss; however, it also alleviated the transaction friction between enterprises and suppliers, improved the value of trade credit, and had a positive impact on the growth of enterprises.

2.2. Research Hypothesis. The development of DIF decreases the degree of financial exclusion, provides various financial services, such as savings, insurance, credit, and payment, for the poor, expands the availability and payment convenience of financial services for the low-income groups, and enhances the ability of poor groups to resist risks. Poor groups are unable to get sufficient funds to support their labor production and venture capital in the environment of financial exclusion, which also bounds consumption growth [18]. In remote areas with poor conditions, there is generally a lack of financial institutions; this makes it hard for people in these areas to enjoy financial services. Digital inclusive finance overcomes the limitation of geographical conditions, provides convenient information transmission and financial transaction platform for the capital supplier and demander, breaks the barrier of financial exclusion, provides the poor groups with the funds needed for production and life, fulfills the investment needs of some poor groups, stimulates the innovation and entrepreneurship vitality of reform groups, and promotes the growth of the local economy. With the improvement in economic development, the employment situation and the level of income of the poor groups will be improved, which would drive the local consumption, and the improvement in the level of consumption would further drive the economic growth. In addition, low antirisk ability is a major feature of poor groups. Digital inclusive finance enhances the ability of poor groups to resist risks through credit, insurance, and other financial services. When poor groups fall into various unexpected challenging situations, such as diseases and disasters, the services offered by digital inclusive finance can help poor groups come out of such situations.

Digital inclusive finance not only overcomes geographical limitations but also decreases the cost of financial services. In China's poverty-stricken areas, with the continuous development of communication infrastructure, the application scope of digital technology continues to expand, which provides technical support for poverty-stricken areas to decrease the cost of various financial services and enjoy appropriate services. For one thing, it decreases the threshold of financial services by taking advantage of the wide coverage of the internet, as well as decreases the cost of construction and operation of financial institutions by combining face recognition, identity authentication, and other technologies. For another, the application of big data, cloud computing, and other technologies in the financial field accelerates information transmission and decreases market information asymmetry. Financial institutions can offer more accurate financial services for the poor, resolve the problem of financial mismatch to some extent, and enhance the efficiency of resource allocation. The establishment and improvement of the credit reference system improve the impact of risk control on financial institutions and decrease the cost of risk control. Moreover, DIF increases the transparency of information, intensifies the competition between financial institutions, promotes the reform of financial institutions, and is conducive to the innovation of financial products and the improvement of the service level. Furthermore, digital inclusive finance not only provides financial services to poor groups but also provides people with a channel to understand finance, which contributes to the improvement of financial literacy of poor groups.

The digital inclusive finance makes the poor people, who are separated from finance, avail the opportunity to enjoy the appropriate financial products and services. The poor areas can obtain low-cost credit funds, provide financial support for the industrial development of the poor areas, advance the economic growth of the area, and eventually abolish poverty. In addition, digital inclusive finance can facilitate more people to enjoy financial services, especially in remote rural areas, accumulate funds through savings and invest in poor areas, promote economic growth, create more employment opportunities, and improve the income level of people in poor areas. The increase in the level of income among people will lead to an increase in consumption, which will further promote the expansion of the local economy. The sustained economic growth not only increases people's income but also increases the education funds in the region, as well as provides student loans for poor families, thus helping to improve the education level of the children of poor families and amplifying their employment opportunities and work income. Likewise, sustained economic growth can increase medical and health expenditure, increase the investment in medical institutions and medical funds, and alleviate the medical poverty in the region. Furthermore, poor groups can use mobile terminals and internet platforms to choose the appropriate insurance or crowdfunding and other mutual aid ways to resist risks and alleviate medical poverty.

Accordingly, the following research hypotheses are proposed:

H1: the level of DIF is conducive to the alleviation of income poverty

H2: the level of DIF is conducive to alleviating educational poverty

H3: the level of DIF is conducive to the alleviation of medical poverty

3. Materials and Methods

3.1. Sample Selection and Data Sources. The DIF index is published by the Digital Finance Research Center of Peking University [19]. Since 2001, the Digital Finance Research Center of Peking University and Ant Financial Group have estimated the DIF index every year. Ant Financial Group provides inclusive financial services to the world. Based on the hundreds of millions of transaction account, DIF index reflects the overall development and trend of digital finance [20]. Other data were obtained from China's economic and social development (C/E/S/D) database, and other indicators were calculated through source data. The DIFI covered the period from 2011 to 2018; therefore, the selected samples were from 2011 to 2018.

3.2. Model Specifications and Variable Selection

3.2.1. Model Specifications. To validate hypotheses H1, H2, and H3, we employ fixed-effect models to examine the DIF effects on poverty reduction. Let $\mathrm{POV}_{i,t}$ indicate poverty indicators for province i in year t. The detailed model specifications are given as follows:

$$\mathrm{POV}_{i,t} = \beta_0 + \beta_1 \mathrm{DIFI}_{i,t} + \delta_i + \theta_t + \varepsilon_{i,t}, \tag{1}$$

where $\mathrm{DIFI}_{i,t}$ denotes the overall DIF index for province i in year t. For the estimations, we control for the fixed effects of the province and year, δ_i and θ_t in equation (1).

3.2.2. Variable Selection. The explained variable POV denotes income poverty, education poverty, and medical poverty, respectively, and is reflected by rural per capita disposable income, average number of junior high school students per 1,00,000 population, and diagnosis and treatment rate of township hospitals. The explanatory variable DIFI denotes the digital inclusive finance index. Based on the existing literature, income gap (THEIL), degree of opening up (IE), financial expenditure (FE), urbanization (UR), and inflation rate (CPI) were selected as control variables. This study further controlled the provincial fixed effect and year fixed effect. ε represents the random error. Table 1 shows the main variables and their definitions selected in this study.

3.3. Results and Analysis

3.3.1. Descriptive Statistical Analysis. The descriptive statistical results of the sample are shown in Table 2. The average values of POV1, POV2, and POV3 were 11,334.090, 3309.706, and 436.829, respectively, and their standard deviations were 4729.642, 936.138, and 151.169, respectively. The distributions of other variables were in a reasonable range.

3.3.2. The Impact of DIF on Poverty Alleviation. This study regressed the model and tested the impact of DIF on poverty alleviation. In order to ensure the robustness of the estimation results, the clustering robust standard error was used. Table 3 shows the specific results; columns (1) and (2) take income poverty (POV1) as the dependent variable, and column (1) only adds the independent variable digital inclusive finance index (DIFI) for regression, with the coefficient of 61.359 that is significant at the 1% level. This reveals that the higher the DIFI, the higher the per capita disposable income of farmers in this region, which alleviates the income poverty. Based on column (1), column (2) further adds other factors that affect poverty alleviation. The coefficient of the DIFI decreases to 50.467, but it is still significant at the 1% level. Columns (3) and (4) take education poverty (POV2) as the dependent variable, and column (1) only adds the independent variable digital inclusive finance index (DIFI) for regression, with a coefficient of 6.319 that is significant at the 5% level; this illustrates that the higher the DIFI, the more the average number of students per 100,000 junior high schools in the region; that is, the education poverty is alleviated. Based on column (3), column (4) further adds other factors affecting poverty alleviation. The coefficient of the DIFI becomes 7.823, which is still significant at the 5% level. Columns (5) and (6) take medical poverty (POV3) as the dependent variable, and column (5) only adds the

Table 1: Definition of main variables.

Variable	Definitions
POV1	Rural per capita disposable income
POV2	Average number of junior high school students per 100000 population
POV3	Number of patients in township hospitals/rural population ∗ 100
DIFI	Digital inclusive finance index
THEIL	Theil index
IE	Total import and export/GDP ∗ 100
FE	Fiscal revenue/total DGP ∗ 100
UR	Urban population/total population ∗ 100
CPI	Consumer price index

Table 2: Descriptive statistical analysis.

Variable	Sample size	Mean value	Median	Standard deviation	Minimum value	Maximum value
POV1	248	11334.090	10478.960	4729.642	3909.400	30374.730
POV2	248	3309.706	3292.000	936.138	1226.000	6146.000
POV3	232	436.829	413.743	151.169	146.163	827.775
DIFI	248	187.175	203.935	85.079	16.220	377.730
THEIL	248	5.091	4.435	2.691	2.660	21.168
IE	248	26.998	14.157	30.856	1.679	154.816
FE	248	28.082	22.705	21.215	11.027	137.916
UR	248	56.132	54.615	13.249	22.727	89.607
CPI	248	102.500	102.100	1.288	100.600	106.300

Table 3: Impact of the DIFI on poverty alleviation.

Variable	POV1		POV2		POV3	
	(1)	(2)	(3)	(4)	(5)	(6)
DIFI	61.359***	50.467***	6.319**	7.823**	2.117***	1.979***
	(3.66)	(3.70)	(2.15)	(2.72)	(3.04)	(2.67)
THEIL		406.567***		73.660***		3.211
		(5.72)		(2.94)		(1.09)
IE		−41.880***		0.642		−1.785***
		(−5.93)		(0.32)		(−3.12)
FE		−8.589		−2.580		−1.651
		(−0.36)		(−0.26)		(−1.25)
UR		103.430***		−23.665		1.322
		(2.85)		(−1.35)		(0.64)
CPI		395.344***		130.801***		6.462
		(3.34)		(4.15)		(1.01)
Constant	12734.97***	−28055.880**	1606.206***	−11809.76***	253.974***	−432.588
	(7.64)	(−2.41)	(5.31)	(−3.41)	(11.84)	(−0.60)
Year fixed effect	Yes					
Province fixed effect	Yes					
Number of samples	248	248	248	248	232	232
F	261.18	488.09	361.61	278.19	239.64	220.93
R^2	0.979	0.987	0.955	0.960	0.961	0.964

*, **, and *** indicate 10%, 5%, and 1% significance levels.

independent variable digital inclusive finance index (DIFI) for regression, with the coefficient of 2.117 that is significant at the 1% level. This demonstrates that the higher the DIFI, the higher the diagnosis and treatment rate of township hospitals in this region; that is, the medical poverty is alleviated. Based on column (5), column (6) further adds other factors affecting poverty alleviation. The coefficient of the DIFI drops to 1.979, but it is still significant at the 1% level.

3.3.3. Robustness Test. To enhance the reliability of previous empirical results, we tested the robustness from several aspects.

(1) In the benchmark regression of DIF on poverty alleviation, the impact variables of poverty alleviation were added one by one [21]. The direction and significance of the coefficient did not change, and the results were consistent with the existing conclusions.

(2) Considering the endogenous problem, two-stage least squares (2SLS) estimation was performed, and we used Li Muchen's method for reference [22], multiplied the spherical distance between each province and Zhejiang province with the corresponding digital inclusive finance index, and took the product as an instrumental variable. DIFI is based on the data provided by Ant Group. Although DIF plays a vital role in promoting financial services and financial products, its development is still influenced by the geographical space to some extent. Guo Feng and research from other people revealed that the development level of DIF reduces with the increase in distance from Hangzhou and, hence, slower is the development speed. Although distance affects the income level, education status, and medical conditions of each region, distance does not change with the change in the level of income, education status, and medical conditions. The distance between each province and Zhejiang province meets the two conditions of the instrumental variable; however, the distance variable does not change with time. Thus, the product of distance and the corresponding index was taken as an instrumental variable, and the control variable was added to the regression model, which also controlled the province and year. Table 4 shows the regression results. Using instrumental variables to control endogeneity, the coefficients of the digital inclusive finance index were statistically significant at the 1% level, and the results were consistent with the conclusions presented.

Instrumental variables pass the test of unrecognizability and weak instrumental variables.

Table 4: Impact of DIF on poverty alleviation.

Variable	POV1 (2)	POV2 (4)	POV3 (6)
DIFI	228.349***	28.666**	11.126***
	(4.46)	(2.41)	(3.51)
THEIL	486.967***	83.080***	10.027*
	(4.16)	(2.83)	(1.92)
IE	−2.538	5.252	−0.835
	(−0.14)	(1.40)	(−0.92)
FE	101.069*	10.270	4.179
	(1.79)	(0.75)	(1.27)
UR	82.914	−26.069	1.359
	(1.48)	(−1.31)	(0.39)
CPI	720.340***	168.882***	19.157*
	(3.27)	(4.39)	(1.65)
Constant	−86714.71***	−21812.69**	−432.588
	(−3.11)	(−2.34)	(−0.60)
Year fixed effect		Yes	
Province fixed effect		Yes	
Number of samples	248	248	232

3.4. Transmission Mechanism of DIF. The development of DIF realizes the poverty alleviation path by endorsing economic development. With the growth of digital technology, more residents have the opportunity to enjoy financial services [23]. The reduction in the cost of various services and the introduction of differentiated products help customers to participate in financial activities, select their own financial products and services, enhance transaction efficiency, and provide strong support for economic development. Digital inclusive finance has altered the payment habits of residents, decreased the demand for cash, increased savings, and is advantageous to the accumulation of small savings of residents. The accumulated savings are used for investment, which can further promote economic development and increase regional economic development. Per the "trickle-down effect" theory, with the improvement in the economic development level, the consumption expenditure will also increase. Simultaneously, it will provide more employment opportunities for low-income groups, improve the employment situation of the region, understand the income growth of low-income groups, and eventually eliminate poverty.

Based on the mediating effect test procedure of [24], the path model was set as follows:

$$\begin{aligned}
\mathrm{POV}_{i,t} &= a_0 + a_1\mathrm{DIFI}_{i,t} + \sum \mathrm{CTRL}_{i,t} + \delta_i + \theta_t + \varepsilon_{i,t}\ (\text{path a}),\\
\mathrm{EDL}_{i,t} &= b_0 + b_1\mathrm{DIFI}_{i,t} + \sum \mathrm{CTRL}_{i,t} + \delta_i + \theta_t + \varepsilon_{i,t}\ (\text{path b}),\\
\mathrm{POV}_{i,t+1} &= c_0 + c_1\mathrm{DIFI}_{i,t} + c_2\mathrm{EDL}_{i,t} + \sum \mathrm{CTRL}_{i,t} + \delta_i + \theta_t + \varepsilon_{i,t}\ (\text{path c}).
\end{aligned} \tag{2}$$

Among them, EDL denotes the intermediary variable, which represents the level of regional economic development, respectively. This study measured using per capita GDP. First, path "a" was used to analyze the impact of the DIFI on poverty alleviation without adding the intermediary variable EDL. If the coefficient a_1 was significant, it suggested that the total effect of the DIFI on poverty alleviation existed, which could be further analyzed. Second, path b was used to analyze the impact of the DIFI on the intermediary variable EDL. Third, path c was used to analyze the impact of the DIFI on the intermediary variable EDL on poverty alleviation. If the coefficient b_1 of path b and the coefficient c_2 of path c were significant, it implied that the mediating effect existed. If the coefficient c_1 was nonsignificant, it implied that the mediator played a complete mediating role. If the

Table 5: Impact of various financial services of digital inclusive finance on poverty alleviation: transmission mechanism test.

Path a (without mediators)	POV1 (1)	POV2 (2)	POV3 (3)
DIFI	50.467*** (6.03)	7.823*** (2.70)	1.979*** (3.92)
Control variable	Control	Control	Control
Year fixed effect	Control	Control	Control
Province fixed effect	Control	Control	Control
Number of samples	248	248	232
R^2	0.987	0.960	0.964
Path b (mediator)	EDL (4)	EDL (5)	EDL (6)
DIFI	324.893*** (7.03)	324.893*** (7.03)	324.893*** (7.03)
Control variable	Control	Control	Control
Year fixed effect	Control	Control	Control
Province fixed effect	Control	Control	Control
Number of samples	248	248	248
R^2	0.986	0.986	0.986
Path c (including mediators)	POV1 (7)	POV2 (8)	POV3 (9)
DIFI	16.693** (2.18)	4.771 (1.49)	0.804 (1.50)
EDL	0.104*** (9.99)	0.009** (2.16)	0.004*** (4.81)
Control variable	Control	Control	Control
Year fixed effect	Control	Control	Control
Province fixed effect	Control	Control	Control
Number of samples	248	248	232
R^2	0.991	0.961	0.968
P value of the Sobel test	≤0.001	0.039	≤0.001

*, **, and *** indicate 10%, 5%, and 1% significance levels.

coefficient c_1 was significant, it suggested that the mediator played a partial mediating role. If at least one of the coefficient b_1 of path b and the coefficient c_2 of path c was not significant, Sobel test was conducted to determine whether a mediating effect existed.

Table 5 presents the results of the intermediary test of the economic development level. Path a test showed that the DIFI coefficients were 50.467, 7.823, and 1.979, respectively, which were statistically significant at the 1% level. Path b test showed that digital inclusive finance was significantly positively correlated with economic development at the 1% statistical level. Path c test demonstrated that, after adding the mediating factor EDL, the coefficients of mediating factor EDL were significant at the 1% statistical level and also passed the Sobel test. For the three dimensions of poverty alleviation, DIFI's regression coefficient values declined. In addition, the impact of the digital inclusive finance index on income poverty alleviation was only significant at the 5% statistical level, while the impact on education poverty alleviation and medical poverty alleviation was not significant, suggesting that the level of economic development played a partial intermediary role in the impact of DIF on income poverty alleviation, and it has a complete mediating effect in the impact of digital inclusive finance on education poverty alleviation and medical poverty alleviation.

4. Additional Analysis

4.1. The Impact of Various Dimensions of Digital Inclusive Finance on Poverty Alleviation. Digital inclusive finance index includes three dimensions—coverage breadth, use depth, and digitization degree [25]. The coverage breadth of DIF is reflected in the coverage of financial services, including the number and scope of users who conduct financial transactions through digital means such as internet and mobile terminals. The wider coverage of digital inclusive finance illustrates that more groups benefit from digital finance, alleviates financial exclusion, and gives the groups, who cannot enjoy financial services owing to geographical restrictions, the opportunity to avail appropriate financial services [26]. Specifically, in terms of coverage areas, traditional financial services need to improve coverage by setting up institutional outlets, but the high cost of institutional outlets makes it difficult for traditional financial services to penetrate into economically backward areas [27]. The cross-border integration of digital technology and financial services overcomes this disadvantage. Even without bank outlets, ATM, and other hardware facilities in some areas, customers can still obtain the required financial services through computers, mobile phones, and other terminal devices. Compared with the situation that traditional financial institutions distribute their main resources in densely populated and commercial areas, digital finance makes financial services more direct and customer coverage wider. The product innovation of digital finance reduces the customer access threshold and makes the trend of popularization of financial services more obvious. The use depth of DIF is reflected in the types of financial services, including payment services, monetary fund services, credit services, insurance services, and investment services. Deeper the use of DIF, the more diversified the financial activities of digital financial service users through digital means. The digital degree of DIF depicts the influencing factors of users' use of digital financial services, including the degree of mobility, degree of affordability, degree of credit, and degree of convenience. The higher the digital degree of DIF, the lower the cost and higher the convenience of digital financial services.

We further tested the impact of the coverage, depth, and digitization degree of DIF on poverty alleviation. Table 6 shows the specific results. The results explain that the coverage breadth of DIF exerts no significant impact on the alleviation of income poverty and education poverty; however, the regression coefficient for the alleviation of medical poverty is 2.011, which is significantly positive at the 1% statistical level, suggesting that the higher the coverage breadth of DIF, the higher the diagnosis and treatment rate of township health centers, which affects the alleviation of medical poverty. The regression coefficients of the use depth of DIF to income poverty and education poverty were 18.625 and 3.750, respectively, which were significantly positive at the 1% statistical level, suggesting that the deeper the use depth of DIF, the greater the impact on the alleviation of income poverty and education poverty, while the impact on the alleviation of medical poverty was not significant. The regression

Table 6: Impact of coverage breadth, use depth, and digitization degree of DIF on poverty alleviation.

Variable	POV1			POV2			POV3		
	(1)	(2)	(3)	(4)	(5)	(6)	(7)	(8)	(9)
Breadth	−8.640			−4.240			2.011***		
	(−0.72)			(−1.01)			(3.42)		
Depth		18.625***			3.750***			0.549	
		(2.59)			(2.65)			(1.43)	
Digit			16.801***			2.542***			0.370*
			(4.49)			(2.95)			(1.77)
THEIL	365.257***	389.543***	301.995***	61.044***	71.289***	57.753**	6.006*	2.101	0.383
	(5.20)	(5.59)	(4.80)	(2.63)	(2.97)	(2.37)	(1.88)	(0.67)	(0.12)
IE	53.59***	43.402***	−49.662***	−1.360	0.853	−0.577	−1.919***	−1.721***	−2.131***
	(−6.88)	(−5.89)	(−7.57)	(−0.64)	(0.040)	(−0.28)	(−3.23)	(−2.82)	(−3.58)
FE	−42.076*	−31.479	−5.057	−8.568	−5.747	−2.160	−2.397*	−2.666**	−2.084
	(−1.87)	(−1.47)	(−0.22)	(−0.85)	(−0.58)	(−0.22)	(−1.94)	(−2.09)	(−1.53)
UR	104.369**	92.853**	92.876***	−25.159	−26.064	−25.240	2.510	1.050	0.918
	(2.37)	(2.41)	(2.87)	(−1.41)	(−1.50)	(−1.45)	(1.13)	(0.52)	(0.46)
CPI	289.168**	396.017***	249.008**	109.651***	135.208***	108.317***	7.723	6.281	1.278
	(2.14)	(3.19)	(2.16)	(3.48)	(2.65)	(3.68)	(1.25)	(0.99)	(0.22)
Constant	8699.576	24432.14*	−6546.353	−7897.916**	−11851.1***	−8493.508***	−589.443	−330.177	208.435
	(−0.58)	(−1.81)	(−0.52)	(−2.23)	(−3.34)	(−2.72)	(−0.84)	(−0.47)	(0.33)
Year fixed effect					Yes				
Province fixed effect					Yes				
Number of samples	248	248	248	248	248	248	232	232	232
F	664.58	455.27	494.23	284.45	312.09	252.82	198.91	174.00	163.28
R^2	0.985	0.986	0.988	0.959	0.960	0.961	0.963	0.962	0.962

*, **, and *** indicate 10%, 5%, and 1% significance levels.

coefficients of digital inclusive finance on income poverty and education poverty were 16.801 and 2.542, respectively, which were significantly positive at the 1% statistical level, suggesting that the deeper the digital degree of digital inclusive finance, the greater the impact on alleviating income poverty and education poverty, while the regression coefficient of medical poverty was 0.370, which was significantly positive at the 10% statistical level, suggesting that the digital inclusive finance positively affects alleviating income poverty and education poverty, while digital inclusive finance positively affects the alleviation of medical poverty.

4.2. The Impact of Various Financial Services of Digital Inclusive Finance on Poverty Alleviation. Currently, the types of financial services covered by China's digital inclusive finance primarily include payment business, insurance business, monetary fund business, investment business, and credit business [28]. Different types of service industries reflect the development of the use depth of digital inclusive finance business, and different depths exert different impacts on poverty alleviation.

This study further tested the impact of different types of financial services of digital inclusive finance on poverty alleviation. Tables 7–9 show specific results. The results indicate that payment business and insurance business have played a role in alleviating income, education, and medical poverty; monetary fund business affects alleviating education poverty, investment business affects alleviating income poverty and medical poverty, while credit business has no significant impact on alleviating poverty.

4.3. Regional Heterogeneity Test of Digital Inclusive Finance. There are great differences in the level of economic and social development in different regions of China. The economic development in the eastern region is relatively high, while economic development in the western region is relatively low [29]. Thus, per the division standard of the three zones of the International Bureau of Statistics, the sample was divided into three parts—the eastern part, the central part, and the western part. Table 10 shows the test results of regional heterogeneity of DIF. From the perspective of the alleviation effect of DIF on income poverty, the coefficients of the DIFI were 88.634 and 34.954 in the eastern and central regions, respectively, and were significant at the 1% statistical level, but in the western region, it is not significant, suggesting that the alleviation effect of DIF on income poverty was most obvious in the eastern region, whereas the impact on the central region was marginally decreased, with no significant effect on the western region. From the perspective of the alleviation effect of DIF on education poverty, the coefficient of the DIFI was 88.634 in the east, which was significant at the 1% statistical level, but in the central and western regions, it is not significant, suggesting that the alleviation effect of DIF on education poverty was obvious in the east, with no significant effect on the central and western regions. From the perspective of the alleviation effect of DIF on medical poverty, the coefficients of the digital inclusive finance index were 4.479 and 3.389 in the eastern and central regions, respectively, which were significant at the 1% statistical level, but not significant in the western region, suggesting that the alleviation effect of DIF on medical

Table 7: Impact of various financial services of digital inclusive finance on poverty alleviation: income poverty.

Variable	(1)	(2)	(3)	(4)	(5)	(6)
Payment	29.10***					
	(4.81)					
Insurance		4.651**				
		(2.33)				
Monetary			7.529			
			(1.03)			
Investment				21.440***		
				(6.14)		
Credit					−2.12	
					(−0.33)	
Credit investigation						−0.400
						(−1.30)
Control variable	Control	Control	Control	Control	Control	Control
Year fixed effect	Yes					
Province fixed effect	Yes					
Number of samples	248	248	186	155	248	124
F	417.58	353.21	221.76	201.38	344.98	106.12
R^2	0.988	0.983	0.988	0.994	0.985	0.993

*, **, and *** indicate 10%, 5%, and 1% significance levels.

Table 8: Impact of various financial services of digital inclusive finance on poverty alleviation: education poverty.

Variable	(1)	(2)	(3)	(4)	(5)	(6)
Payment	5.25***					
	(4.20)					
Insurance		1.157***				
		(2.85)				
Monetary			7.251***			
			(4.62)			
Investment				0.997		
				(0.90)		
Credit					−0.320	
					(−0.16)	
Credit investigation						0.429
						(1.09)
Control variable	Yes					
Year fixed effect	Yes					
Province fixed effect	Yes					
Number of samples	248	248	186	155	248	124
F	19.21	16.55	8.43	5.40	16.04	5.01
R^2	0.962	0.960	0.981	0.985	0.959	0.990

*, **, and *** indicate 10%, 5%, and 1% significance levels.

Table 9: Impact of various financial services of digital inclusive finance on poverty alleviation: medical poverty.

Variable	(1)	(2)	(3)	(4)	(5)	(6)
Payment	0.855**					
	(2.52)					
Insurance		0.219**				
		(2.16)				
Monetary			0.088			
			(0.28)			
Investment				0.559**		
				(2.09)		
Credit					−0.400	
					(−1.30)	
Credit investigation						−0.007
						(−0.06)
Control variable	Yes					

Table 9: Continued.

Variable	(1)	(2)	(3)	(4)	(5)	(6)
Year fixed effect			Yes			
Province fixed effect			Yes			
Number of samples	232	232	174	145	232	124
F	11.81	13.91	4.81	5.43	12.54	3.72
R^2	0.964	0.963	0.976	0.985	0.961	0.982

*, **, and *** indicate 10%, 5%, and 1% significance levels.

Table 10: Regional heterogeneity test of digital inclusive finance.

Variable	POV1 East (1)	POV1 Central section (2)	POV1 West (3)	POV2 East (4)	POV2 Central section (5)	POV2 West (6)	POV3 East (7)	POV3 Central section (8)	POV3 West (9)
DIFI	88.634***	34.954***	12.140	12.133**	0.417	0.977	4.479***	3.389***	−0.233
	(3.55)	(3.20)	(1.51)	(2.15)	(0.04)	(0.23)	(2.80)	(3.25)	(−0.38)
THEIL	1755.41***	178.769	101.900**	−229.363	−258.627	41.259	29.129	−23.618	−7.139*
	(3.16)	(0.52)	(2.02)	(−1.28)	(−1.07)	(1.36)	(0.75)	(−0.96)	(−1.94)
IE	−6.892	68.211*	−5.332	7.816***	−25.590	−2.733	1.613	6.569***	−0.954
	(−0.55)	(1.88)	(−0.56)	(2.78)	(−1.08)	(−0.55)	(1.53)	(2.73)	(−1.19)
FE	209.854**	−16.837	−9.237	5.513	−42.219	−0.690	0.487	4.742**	−1.425
	(2.60)	(−0.31)	(−0.51)	(0.31)	(−0.89)	(−0.06)	(0.10)	(1.32)	(−1.23)
UR	163.098**	−50.573	37.523	−6.198	26.581	−47.367**	1.19	−0.379	2.963
	(2.38)	(−1.34)	(1.05)	(−0.36)	(0.78)	(−2.29)	(0.25)	(−0.16)	(0.94)
CPI	236.027	322.331**	15.814	22.940	293.12***	45.147	9.377	16.932**	−14.542**
	(1.05)	(2.30)	(0.23)	(0.37)	(3.28)	(0.95)	(0.62)	(2.03)	(−2.35)
Constant	−37912.99	−26949.51*	1010.995	380.371	−26054.78**	1613.986	−1029.237	−1561.111*	1832.745***
	(−1.53)	(−1.76)	(0.13)	(0.06)	(−2.66)	(0.31)	(−0.59)	(−0.47)	(2.84)
Year fixed effect					Yes				
Province fixed effect					Yes				
Number of samples	88	64	96	88	64	96	72	64	96
F	164.14	811.80	358.28	2.76	9.14	15.31	9.45	23.82	6.78
R^2	0.987	0.994	0.990	0.960	0.950	0.959	0.938	0.989	0.951

*, **, and *** indicate 10%, 5%, and 1% significance levels.

poverty should be the most notable in the eastern region, with a marginal decline in the central region and no significant effect on the western region. Generally speaking, the groups with a higher education level are more eager and need to use digital information means to obtain more useful information and have corresponding information retrieval ability, information acquisition ability, and absorption and digestion ability, while the groups with a lower education level will appear poorer at the information level, resulting in the phenomenon of digital divide. The digital divide also leads to the difference of residents' utilization of digital inclusive finance in different regions.

5. Conclusions

The findings of this study are as follows: (1) digital inclusive finance exerts a poverty reduction effect in three dimensions of income, education, and healthcare. (2) The level of economic development plays a partial mediating role in the impact of DIF on income poverty alleviation, while it plays a complete mediating role in the impact of DIF on education poverty alleviation and medical poverty alleviation. (3) The coverage breadth of DIF exerts a significant impact on the alleviation of medical poverty, the use depth of DIF exerts a significant impact on the alleviation of income poverty and education poverty, and the digital degree of DIF exerts an impact on the alleviation of poverty in three dimensions. (4) The types of financial services also exert different effects on poverty alleviation. Generally, payment business and insurance business exert significant effects on the three dimensions of poverty alleviation. (5) The poverty reduction effect of DIF is the most notable in the eastern region, followed by the central region, but not significant in the western region.

Digital inclusive finance plays an evident role in poverty alleviation; however, from the perspective of use depth, the impact of credit business and investment business on poverty alleviation is not obvious. In future, we can appropriately increase the development of such financial business to alleviate the financial constraints of low-income groups. The economic development level of the western region and the construction of network infrastructure are relatively backward, which also affects the application of digital inclusive finance. In future, we can accelerate the construction and upgrading of communication network hardware in remote areas such that the residents can enjoy appropriate financial services and promote the expansion of DIF in the western region.

Data Availability

Data sharing is not applicable to this article as no datasets were generated or analyzed during the current study.

Conflicts of Interest

The authors declare no conflicts of interest.

Acknowledgments

This work was supported by Science and Technology Research Project of Chongqing Education Commission of China (KJQN201903304).

References

[1] A. Leyshon and N. Thrift, "Geographies of financial exclusion: financial abandonment in Britain and the United States," *Transactions of the Institute of British Geographers*, vol. 20, no. 3, pp. 312–341, 1995.

[2] R. Mohan, "Economic growth, financial deepening and financial inclusion," in *Proceedings of the Annual Bankers' Conference 2006*, Hyderabad, November 2006.

[3] M. Sarma, *Index of Financial Inclusion*, ICRIER Working Paper, Washington, DC, USA, 2008.

[4] Rangarajan Committee, *Report of the Committee on Financial Inclusion*, Government of India, South Asia, 2008.

[5] P. Honohan, "Cross-country variation in household access to financial services," *Journal of Banking & Finance*, vol. 32, no. 11, pp. 2493–2500, 2008.

[6] G. Amidžić, A. Massara, and A. Mialou, "Assessing countries' financial inclusion standing—a new composite index," *Journal of Banking and Financial Economics*, vol. 2, no. 8, 2017.

[7] A. Hannig and S. Jansen, *Financial Inclusion and Financial Stability: Current Policy Issues*, Working Paper, Washington, DC, USA, 2010.

[8] L. Brune, X. Giné, J. Goldberg, and D. Yang, "Commitments to save: a field experiment in rural Malawi," Working Paper, Washington, DC, USA, 2011.

[9] T. Beck, A. Demirgüç-Kunt, and R. Levine, "Finance, inequality and the poor," *Journal of Economic Growth*, vol. 12, no. 1, pp. 27–49, 2007.

[10] A. Demirgüç-Kunt and R. Levine, "Finance and inequality: theory and evidence," *Annual Review of Financial Economics*, vol. 1, no. 1, pp. 287–318, 2009.

[11] F. Allen, E. Carletti, R. Cull, J. Qian, L. Senbet, and P. Valenzuela, 2013.

[12] A. Alvarez de la Campa, *Increasing Access to Credit through Reforming Secured Transactions in the MENA Region*, Working Paper, Washington, DC, USA, 2010.

[13] D. Pearce, *Financial Inclusion in the Middle East and North Africa: Analysis and Roadmap Recommendations*, Working Paper, Washington, DC, USA, 2011.

[14] N. Emara and M. Mohieldin, "Financial inclusion and extreme poverty in the MENA region: a gap analysis approach," *Review of Economics and Political Science*, vol. 6, 2020.

[15] M. Andrianaivo and K. Kpodar, *ICT, Financial Inclusion, and Growth: Evidence from African Countries*, Working Paper, Washington, DC, USA, 2011.

[16] L. Klapper, M. El-Zoghbi, and J. Hess, *Achieving the Sustainable Development Goals: The Role of Financial Inclusion*, Working Paper,2016, Washington, DC, USA, 2016.

[17] T. Beck, H. Pamuk, R. Ramrattan, and B. R. Uras, "Payment instruments, finance and development," *Journal of Development Economics*, vol. 133, no. 7, pp. 162–186, 2018.

[18] H. Wang, X.-M. Zhang, G. Tomiyoshi et al., "Association of serum levels of antibodies against MMP1, CBX1, and CBX5 with transient ischemic attack and cerebral infarction," *Oncotarget*, vol. 9, no. 5, pp. 5600–5613, 2017.

[19] Digital Finance at Peking University and Ant Financial Services Group, "The peking university digital financial inclusion index of China, 2011–2018," *Institute of Digital Finance Peking University*, Index Report, Beijing, China, 2019.

[20] Q. Gong and X. Cheng, "Digital financial inclusion, rural poverty and economic growth," *Gansu Social Sciences*, vol. 6, pp. 139–145, 2018.

[21] H. Qian, Li Zheng, and X. De-ping, "Poverty reduction effect of digital inclusive finance and its transmission mechanism," *Reformation*, vol. 11, pp. 90–101, 2019.

[22] M. Li, S. Feng, and X. Xing, "Heterogeneity effects of digital inclusive finance on urban-rural income gap," *Journal of Nanjing Agricultural University*, vol. 20, no. 3, pp. 132–145, 2020.

[23] J. Li and X. Han, "The effect of financial inclusion on income distribution and poverty alleviation:policy framework selection for efficiency and equity," *Journal of Financial Research*, vol. 3, pp. 129–148, 2019.

[24] Z. L. Wen, L. Zhang, J. Hou, and H. Liu, "Testing and application of the mediating effects," *Acta Psychologica Sinica*, vol. 36, no. 5, pp. 614–620, 2004.

[25] J. Liu and C. Liu, "Rural poverty alleviation effect of digital inclusive finance: effects and mechanisms," *Collected Essays on Finance and Economics*, vol. 1, pp. 43–53, 2020.

[26] H. Luo and J. Luo, "Research on the influences of inclusive finance on rural poverty alleviation from a multidimensional perspective," *Contemporary Economic Management*, vol. 41, no. 3, pp. 80–88, 2019.

[27] H. Shao and K. Wang, "Poverty reduction effect and the mechanism of action in inclusive finance: empirical analysis based on cross-national panel data," *Financial Economics Research*, vol. 32, no. 6, pp. 65–74, 2017.

[28] W. Yang, L. Su, and M. Wang, "Digital financial inclusion and income of urban and rural residents: based on the intermediary effec of economic growth and entrepreneurial behavior," *Journal of Shanghai University of Finance and Economics*, vol. 22, no. 4, pp. 83–94, 2020.

[29] X. Zheng and Y. Zhu, "Inclusive Finance, Economic opportunity and poverty reduction," *World Economic Papers*, vol. 1, pp. 101–120, 2019.

Hindawi
Scientific Programming
Volume 2021, Article ID 6092792, 12 pages
https://doi.org/10.1155/2021/6092792

Research Article

Smart Supply Chain Management Using the Blockchain and Smart Contract

Manoshi Das Turjo,[1] **Mohammad Monirujjaman Khan**,[1] **Manjit Kaur**,[2] **and Atef Zaguia**[3]

[1]*Department of Electrical and Computer Engineering, North South University, Bashundhara, Dhaka 1229, Bangladesh*
[2]*School of Engineering and Applied Sciences, Bennett University, Greater Noida, India*
[3]*Department of Computer Science, College of Computers and Information Technology, Taif University, Taif 21944, Saudi Arabia*

Correspondence should be addressed to Mohammad Monirujjaman Khan; monirujjaman.khan@northsouth.edu

Received 23 July 2021; Accepted 20 September 2021; Published 28 September 2021

Academic Editor: Kashif Zia

The manufacture of raw materials to deliver the product to the consumer in a traditional supply chain system is a manual process with insufficient data and transaction security. It also takes a significant amount of time, making the entire procedure lengthy. Overall, the undivided process is ineffective and untrustworthy for consumers. If blockchain and smart contract technologies are integrated into traditional supply chain management systems, data security, authenticity, time management, and transaction processes will all be significantly improved. Blockchain is a revolutionary, decentralized technology that protects data from unauthorized access. The entire supply chain management (SCM) will be satisfied with the consumer once smart contracts are implemented. The plan becomes more trustworthy when the mediator is contracted, which is doable in these ways. The tags employed in the conventional SCM process are costly and have limited possibilities. As a result, it is difficult to maintain product secrecy and accountability in the SCM scheme. It is also a common target for wireless attacks (reply attacks, eavesdropping, etc.). In SCM, the phrase "product confidentiality" is very significant. It means that only those who have been validated have access to the information. This paper emphasizes reducing the involvement of third parties in the supply chain system and improving data security. Traditional supply chain management systems have a number of significant flaws. Lack of traceability, difficulty maintaining product safety and quality, failure to monitor and control inventory in warehouses and shops, rising supply chain expenses, and so on, are some of them. The focus of this paper is on minimizing third-party participation in the supply chain system and enhancing data security. This improves accessibility, efficiency, and timeliness throughout the whole process. The primary advantage is that individuals will feel safer throughout the payment process. However, in this study, a peer-to-peer encrypted system was utilized in conjunction with a smart contract. Additionally, there are a few other features. Because this document makes use of an immutable ledger, the hacker will be unable to get access to it. Even if they get access to the system, they will be unable to modify any data. If the goods are defective, the transaction will be halted, and the customer will be reimbursed, with the seller receiving the merchandise. By using cryptographic methods, transaction security will be a feasible alternative for recasting these issues. Finally, this paper will demonstrate how to maintain the method with the maximum level of safety, transparency, and efficiency.

1. Introduction

In today's global market, supply chain management (SCM) is critical. It has a significant influence on the global economy. SCM is often defined as the movement of goods from producer to consumer. It is divided into numerous phases, starting with the supply of raw materials and ending with the client, and includes the producer, distributor, and retailer. It is a global process in which components are sourced from a single location, packaged, and supplied globally. Traditional supply chain management serves a broad goal but falls short of full compliance. Giving the final customer the ability to reverse the transaction and assuring the quality of the items supplied has several limits. It usually corresponds to forward flows, or the flow of products from the sender to the recipient [1, 2]. Supporting the reverse flow of items and transactions for every consumer is also critical. The traditional supply chain management system might be disrupted by blockchain and smart contracts. The supply chain can benefit from the blockchain's transparency and immutability [3]. By offering a secure mechanism for collecting data and developing and running programmed scripts or applications known as smart contracts, the blockchain aids in the modernization of the supply chain [4]. Smart contracts can help supply chain managers track the origin and security of their products. We discussed the issues and came up with a solution.

The approach of developing a conceptual framework for a supply chain management system is included in this research. Its main objective is to leverage blockchain and smart contracts to provide safe transactions and high-quality products. It will allow any client to return a product and receive a refund for the money spent on it, resulting in a trustworthy worldwide market. Most significantly, under our paradigm, the whole SCM system will undergo a significant transformation.

A blockchain is a continuously growing list of logs known as cryptographically connected and secured blocks. The blocks are connected cryptographically. The bulk of the nodes check the blocks in the blockchain network. The block will then be added to the chain that all network nodes share when it has been verified. Handling a single piece of data necessitates thousands of instances, each of which requires a significant amount of work and time to avoid. Access to information is associated with higher quality in various blockchain systems. There are a few qualities that distinguish blockchain from other technologies. Data on the blockchain, for example, is immutable, tamper-resistant, and based on a decentralized network, and it can be hacked and encrypted. In general, three forms of blockchain exist: public or unauthorized, private or permitted, and consortium blockchain. Each one has specific characteristics because of the uniqueness of the network's geographic area [5, 6].

According to Nick Szabo, smart contracts are "a computerized transaction protocol that meets contract conditions." Smart contracts are pieces of code (software or scripts) written in a high-level programming language [7] like Java, C++, NodeJS, Python, Go, Solidity, and others. For smart contracts, many blockchain systems employ various high-level programming languages [7]. The Hyperledger manufacturing platform employs the programming languages NodeJS and Python. On the other hand, for their smart contracts, Ethereum employs a sound programming language [8]. Copies of intelligent contracts are available on the blockchain-based network for each peer. Scripts for smart contracts are run automatically, independently, and openly. It is always executed in a secure environment to guarantee that code and data integrity are maintained. [9, 10].

The essence of a cryptocurrency is that it may be exchanged through transactions and that it may be added to new blocks and mined by miners in the most secure way possible. There are three major levels in the crypto realm. Technology, currency, and tokens are the three. The coin is bitcoin, and the technology is blockchain (bitcoin is not just a currency). It is a set of rules. A protocol is a collection of rules that govern how individuals interact on a network. It determines how public keys and signatures should be used for authentication in bitcoin, ethereum, and other cryptocurrencies. The Coin is a built-in asset of the protocol that allows player interaction and is used to reward individuals for mining the blockchain and creating blocks. It is also used to let users buy stuff from other people. Smart contracts are used with tokens. There is a distinction to be made between a token and a coin. When someone invests in a coin, they are also investing in the underlying coin's protocol. They are investing in the concept behind what they are building if they invest in a token.

With the passage of time, the supply chain has evolved. As a result of the global market, SCM has become increasingly important in the current world. However, there are still some substantial challenges in supply chain management in numerous areas. Between the buyer and the seller, there must be trust. A trusted environment is required for transaction processing. However, in today's commercial world, there is no such thing as complete trust. In the transaction process, the intermediaries in a supply chain have a great deal of power. They can manipulate market value without telling genuine supply chain members, allowing them to benefit at the expense of the ultimate consumer. In today's supply chain, there is no encrypted mechanism to store people's private information in numerous businesses, hospitals, and other locations. This data will be vulnerable to cyberattacks, exposing the sensitive public and private information. Because of the supply chain's intermediaries, there is no price transparency. This will provide a direct link between the buyer and the vendor, making the transaction more transparent and trustworthy. Commodities flow in only one direction in today's supply chain management system. As a result, if a product is defective, the customer must bear the repercussions. He had no choice but to take the risk. There are several stages where paperwork must be manually filled out. In a global transaction, the monitoring mechanism is also based on humans. It is more susceptible to human mistakes, resulting in unjustified price rises and less chance to track down the source of the problem. As a result of the aforementioned factors, supply chain management has a significant impact on the worldwide market. The market is still shaky. There is no such thing as a flawless competition.

In this paper [11], it was proposed to do research on supply chain risk management finance using blockchain technology. We analyze the causes of their operational risks, trade authenticity risks, payback risks, and contingent risks in conjunction with blockchain technical characteristics and the supply chain finance business model and react to and track data in real time using physical sensors to improve supply chain risk control efficiency. Dwivedi et al. describe in this article [12] how the blockchain mechanism works in tandem with the existing pharmaceutical system to provide a more efficient supply chain management method. In the supply chain system, this paper offers a blockchain-based information sharing scheme that is safe and uses intelligent contracts and consensus methods. Using intelligent contract technology, the proposal also includes a way of securely providing the needed cryptographic keys to all parties. Alfonso-Lizarazo et al. investigated the usefulness of reverse logistics, or backward product flows and forward logistics, in the palm oil supply chain [13]. The authors presented a closed-loop system that considers "green operations." In both forward and backward flow, it attempts to maintain the environmental sustainability. The report also explains how statistical methods were used to perform mathematical modeling that resulted in a positive output across the supply chain. However, the implementation at the industrial level and data security and administration are not shown. In this essay, Yuan et al. looked at the supply chain management information system method and blockchain as significant technology [14]. From the perspective of blockchain, the process and consensus collaborative management approach is presented, which improves transaction process management and blockchain system consensus, accounting, and so on. Nehai and colleagues [15] present an innovative technique for smart contract validation. It uses a model-checking approach. The model investigates a number of rules for converting smart contracts into model checks. The method works on three levels to display the nature, logic, and execution of the smart contract. The NuSMV tool is used to develop and run programmed smart contract scripts. It is an excellent technique for confirming smart contracts, but IoT device interoperability and blockchain administration remain issues. Kshetri [16] discussed how blockchain may aid supply chain objectives such as speed, cost, risk, and product quality. It also looked into how IoT devices may be linked into a supply chain system based on blockchain. The application of blockchain technology in well-known supply chain use cases throughout the world, such as Alibaba and Maersk, has been extensively researched. It does not, however, provide the global oil supply chain with a full framework. Chang et al. [17] looked at how the pursuit of transparency and accountability across supply chain processes can potentially influence decentralization and automation. A comparative analysis of the current and proposed frameworks was conducted to support the core reasoning of this study. Ahmed and Dixit [18] have shown that consumers throughout India relied on these Kirana shops during the COVID-19 epidemic, which forced the closure of most other retail outlets. While COVID-19 created a new consumer affiliation for Kirana shops and offered new opportunities for these businesses to increase their client bases and product variety, it also exposed supply chain management flaws. Kamran et al. [19] discussed how he makes suggestions to key players in the logistics operations sector of the logistics business that is interested in using blockchain technology. Apart from the study's methodological limitations, system compatibility and layer configuration issues may cause possible difficulties when scaling up the implementation. Liu and Guo [20] discussed Matlab about the findings that indicate that blockchain technology may help propel the fresh food e-commerce supply chain to a greater level of management, coordination, and integration throughout the whole industrial chain. Investing in the blockchain system within a certain budget range may enhance not only product dependability but also the performance of each major component of the fresh food e-commerce supply chain, as well as overall performance. Yoo and Won [21] talked about a system that applies blockchain and smart contracts to the price-tracking component of supply chain management systems to ensure product distribution structure transparency. By increasing transparency in the SCM, this method enables businesses to monitor their transactions, preventing them from chasing excessive profits. By using Ethereum technology, the suggested reference model solves the shortcomings of current models. Furthermore, the researchers used the model to show its functionality in a real-time setting, which may serve as a model for future study. Compared with others, this paper progressively diminishes the participation of third parties in the supply chain system and makes data more secure. This will make the entire process more accessible, efficient, and time-efficient. Most importantly, individuals will feel more secure during the payment process. This paper has its own cryptocurrency with smart contracts to enable more secure dealings with products and put an end to their trust issues. This e-commerce website was secured in a highly secure way in this paper. Many blockchain papers are available on e-commerce websites. These are either peer-to-peer encrypted systems or smart contract embedded systems. In this study, however, it utilized a peer-to-peer encrypted system as well as a smart contract. There are a few other features as well. Because this paper utilized an immutable ledger, the hacker will be unable to get access to our system. Even if they get access to the system, they will be unable to alter any of the data. In the transaction procedure, this paper also utilized blockchain. If the goods are defective, the transaction will be halted and the customer will be reimbursed, with the merchandise being returned to the seller. In addition, the contract will be revised. As a result, the transaction process may be trusted. As a result, purchasers will be less likely to fall prey to fraud or other financial problems. As a result, our technology outperforms currently available e-commerce websites. It is safer and more dependable.

Blockchain and cryptocurrencies, as well as smart contracts, are briefly discussed in the first section. Section 2 gives an overview of the approach and materials utilized and a discussion of the concerns and a review of the literature. Section 3 depicts the design and outcomes of our efforts. The influence of the design is discussed in four sections. Finally, the work that can be done in the future and the conclusions expressed in Section 4 are reviewed.

1.1. Problem Statement. On a daily basis, supply chain management systems encounter problems, and nearly all of them require immediate attention and action. The degree and intricacy of these issues may vary. Easy data access, quality and sustainability, supplier management, and managing consumer expectations are just a few of them. The Supply Chain Management system confronts ever-increasing challenges year after year. And, with the emphasis on stability, these concerns are now front of mind. After all, supply chains are at the heart of effective business operations, and problems will inevitably have an influence on a company's bottom line.

1.2. Motivation. Blockchain technology validates and stores data using blockchain data structures, generates and updates data using distributed node consensus methods, uses encryption to guarantee data transmission and access security, and employs intelligent script code. It is a novel computer and distributed infrastructure paradigm for programming and manipulating data.

The transaction data produced by each participating entity is packed into a data block, which is then organized in chronological order to form a chain of data blocks in the blockchain system. The main body has the same data chain and cannot be tampered with unilaterally. Any changes to the information must be approved by a certain percentage of the topic, and only new material may be added. The old data cannot be changed or removed. The identification of each subject and the transaction information between entities are open and transparent and cannot be faked, thanks to information sharing and consistent decision-making.

2. Method and Methodology

This section delves into the many methods and materials used to achieve the goal. The modeling approach is based on the concept of the blockchain as a cyber SC chain of information services that represents the operational fulfillment of the physical SC. When transaction activities begin and conclude, the blockchain maintains an account of them. As a result, the operations of logistics companies may be viewed as information services that they provide to the blockchain architecture. Smart contract design, in this sense, may be thought of as the computation of start and completion timings for information services in a blockchain-driven cyber environment that mirrors real SC activities.

2.1. Outline of the Full System. This system proposes an abstract concept after briefly explaining and reflecting on current definitions of smart contracts. Because of the concept's novelty and its sophisticated technological foundation, there is no common definition of smart contracts at this time. Given the lack of agreement on nomenclature, it appears that providing an overview of existing techniques and refining an appropriate description is of the highest relevance.

In Figure 1, the whole structure of the blockchain and smart contract working mechanism is depicted. A variety of logistics service providers can take up some operations in the SC that are progressively arranged as flow-oriented activities (i.e., intermediates, carriers).

Different operations may be assigned to several logistics service providers. Assigning operations to logistics firms will

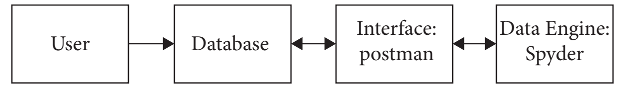

Figure 1: A minimal overview of the complete system.

result in a variety of work lead times and pricing because different logistics service providers operate at different times and at different rates. The process of creating smart contracts includes assigning logistics businesses to jobs and arranging their activities in the contracts, which results in a Blockchain design structure. The start and finish of the execution of the operations of the transaction will be recorded on the blockchain. As a result, the operations of logistics firms might be classified as information services provided by the blockchain architecture. In this sense, smart contract design may be described as the choice to start and stop information services in a blockchain-driven cyberspace that replicates physical SC activities.

For blockchain python, for smart contracts and cryptocurrency purposes, solidity was used in this new supply chain strategy. My ether wallet and Ganache were also used since virtual transactions were performed here for a more realistic outcome. The Spider IDE for implementing Python, the remix IDE for solidity, and nodejs for web pages are used in this system. Figure 2 is the entire process of the system, from the start of the seller's transaction.

Whenever any seller intends to buy any product, he has to do it on the website and there will be no involvement of any third party which can manipulate the payment method. After the buyer gets the product, he will unblock the payment that he has made and then the seller will get his payment. This transaction data will be autoupdated by the website. If, anyhow, the buyer gets a damaged product or becomes dissatisfied with the product he got, then he can return the product and take back his payment through the website. This will not cost any extra money to anyone. After they both make a clear statement review of the transaction, only then will the payment be updated.

Figure 3 is the diagram of the whole mechanism of this system. It will begin with the website receiving data from the user. After the transaction, the customer must approve if the goods are satisfactory or not. The administrator will be able to see the contents of this section.

It will expand in accordance with market circumstances. Any announcement may be made from here. All sales, customer information, and bounce rate data will be managed via this admin panel. The website will automatically update the transaction details. If the customer receives damaged goods or is unhappy with the product, he may return it and get a refund via the website. Nobody will have to pay any additional money as a result of this. Only when they have both completed a thorough statement review of the transaction can the payment be adjusted. Figure 4 is shown. This is the login page for the seller. The homepage features three web pages, which lead to three additional pages.

Another one of them is the login page for the seller. In order to log in, the seller will have to type in his e-mail address and password into his personal account. This page

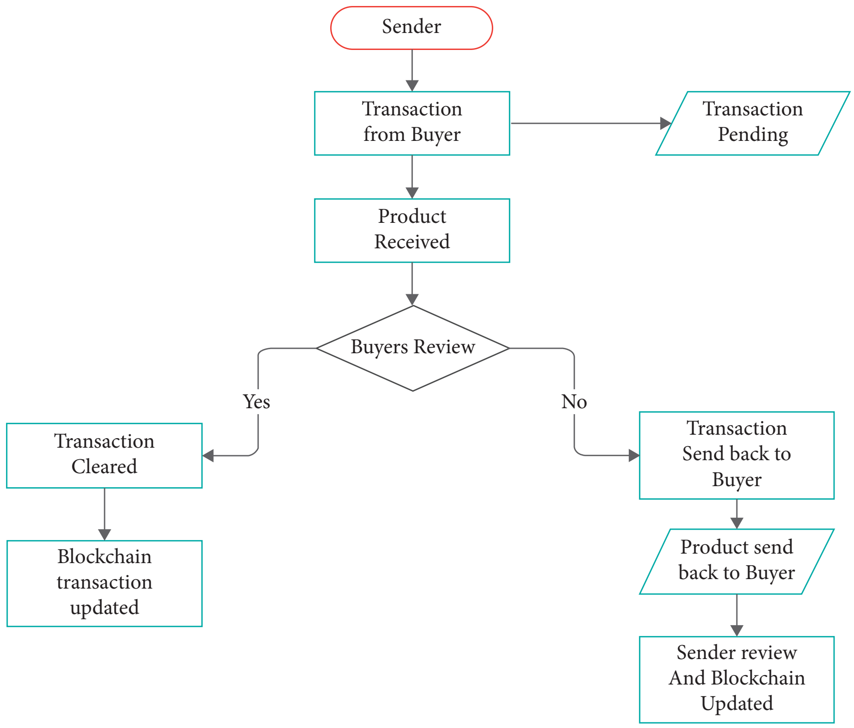

FIGURE 2: The flowchart demonstrating the algorithm used in this SCM.

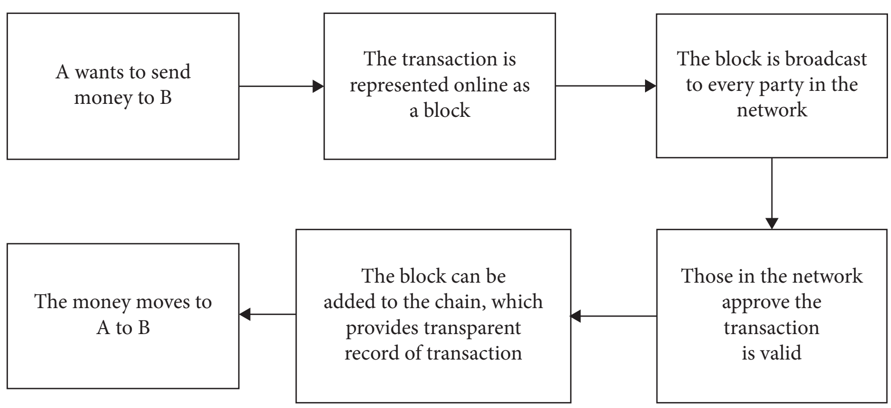

FIGURE 3: Block diagram of the whole system.

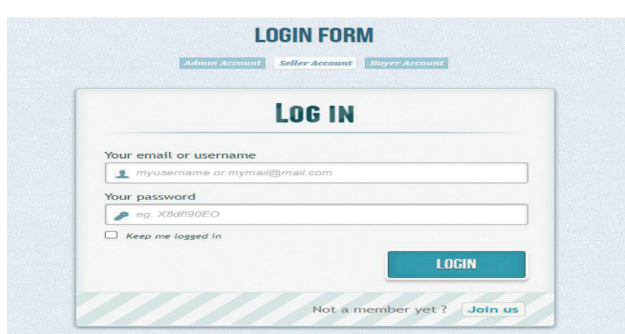

FIGURE 4: Login page for a seller account.

allows you to create three different types of accounts. This page's main features are the admin account, seller account, and buyer account. If the user already has an account, the username and password will be required. However, if someone is creating one for the first time, they will need an e-mail address and a password. Every activity may be controlled and monitored by the admin account. The system requires that the seller and buyer accounts follow the same set of rules. For the development of this website system, it required Javascript, CSS, HTML, and PHP. In Figure 5, the registration page for buyers is shown.

The buyer will fill out the registration form with various pieces of information, like their username, e-mail address, and password. They will also type the password they used to confirm it again. The information will be typed and stored in the local database. Using the administrative control panel, it can be seen.

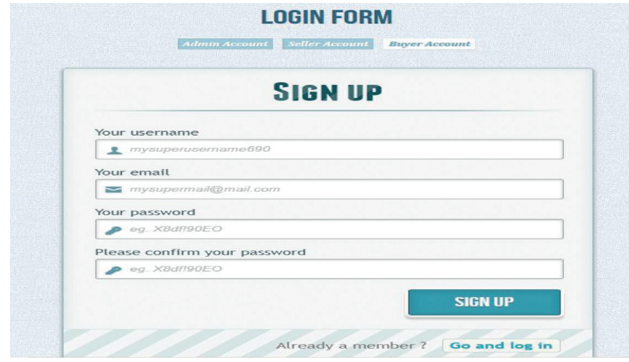

Figure 5: Sign-up page for a buyer account.

2.2. Data Security and Transaction in the Blockchain and Smart Contract. Transactions are not born in the block. When one transaction occurs, the list needs to be empty. Otherwise, it will not get all the separate data. Blocks cannot have the same data in each block. A transaction is put into a block if it is authorized by a majority of the nodes. Each block references the one before it, forming the blockchain. A miner must examine if a transaction is eligible to be processed according to the blockchain history before adding it to their block. The transaction is legitimate and can be included in the block if the sender's wallet balance has sufficient funds according to the current blockchain history. In Figure 6, it is shown that in the traditional system, if we want to buy any big asset, we have to pay for it and, after paying the amount, we get a deed that is the proof of the asset.

If the deed is hacked or manipulated, then the asset owner has no more of their own. It is a volatile way to have ownership, which can be misleading at any time. Someone erases just one line of information, and the asset can lose its license. Client-server networks are used in traditional databases. A user (referred to as a client) may make changes to data that is kept on a central server. The database is still controlled by a specified authority, which verifies a client's credentials before granting access. Because this authority is in charge of database management, the data may be changed or even destroyed if the authority's security is breached. In Figure 7, after using blockchain technology here, we can call it an immutable ledger.

If anyone buys an asset here and keeps all the information in the block, then it is impossible to change the data. Because if any of the data is changed in the block, the whole system gets an alarm as they are all connected with their previous hash number. And it has its own transaction system, which is very secure and trustable. These are the facts that make any traditional ledger an immutable ledger. Public verifiability, provided by integrity and transparency, is a fundamental feature of blockchain technology that differentiates it from conventional database technology.

2.3. Chain and Data Component. This section introduces the basic notion of smart contracts by discussing the nature and types of contracts. From a legal and economic standpoint, we first outline the basic aspects of contracts and their various roles throughout the relationship lifecycle. Then, after examining several ways of defining smart contracts, we offer a broad definition. This part concludes with a critical examination of the role of distributed ledger technology in the idea of smart contracts. In Figure 8, it shows all the functions which have been imported. The date time function is used for each block to have its own timestamp when the block is created and mined. The hashlib function will need to hash the blocks because the hash function will be used here.

Here, using the json function, we will encode the blocks before we hash them. The flask function will be used by the flask library. We will need a flask class because this will use a web application and jsonify, which will take the message and interact with the blockchain with the postman. In the blockchain class, there is a genesis block, a chain function, and a block function that will add a new block and will mine a block. The create_block function will take two arguments: proof and the previous hash number. In Figure 9, proof_of_function has two arguments. One is self, which is for using an instance object that will be created by the class. The other one is previous_proof, for creating a way for miners to solve the problem.

Here, the new_proof value is 1 because after every iteration, it needs to increment by one until it gets the right proof. check_proof will do the checking part to see if it is correct proof or not. The hash_operation contains four leading zeros, which will make mining difficult for the miners, and it is a string of 64 characters. The encode function will encode the string in the right format, which is expected by the sha256 function. In Figure 10, the function of the transaction has been declared. This add_transaction method will conduct the process through the self, sender, and receiver keys of the argument.

This will service the transaction before adding it to the block. This list of data will use the append function to add a new transaction. For every new transaction, it is necessary to add the previous data, which will be done by the previous_blockfunction. Before returning to the previous block function, it will add +1. As a result, the number will automatically rise, the list will grow, and data will be stored.

Figure 6: Traditional ledger with an unwanted security issue.

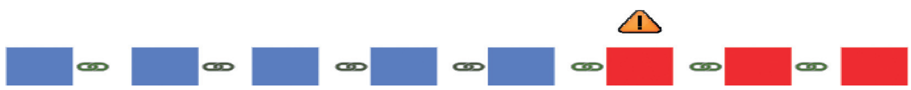

Figure 7: Immutable ledger with high security.

```
import datetime
import hashlib
import json
from flask import Flask, jsonify, request
import requests
from uuid import uuid4
from urllib.parse import urlparse
```

Figure 8: Imported function for the blockchain in spider.

```
def proof_of_work(self,previous_proof):
    new_proof = 1
    check_proof = False
    while check_proof is False:
        hash_operation = hashlib.sha256( str( new_proof**2 - previous_proof**2).encode()).hexdigest()
        if hash_operation[:4] == '0000':
            check_proof = True
        else:
            new_proof += 1
    return new_proof
```

Figure 9: Function for the proof of work in spider.

```
def add_transaction(self, sender,receiver, amount):
    self.transactions.append({'sender': sender,
                              'receiver': receiver,
                              'amount': amount})
    previous_block = self.get_previous_block()
    return previous_block['index'] + 1
```

Figure 10: Function of transaction in spider.

2.4. Transaction Component. After defining the version of solidity, there will be some functions we need to add to connect with my ether wallet and Ganache. We have declared the total amount that people who will mine can use from here. And after that, the coin value of our created coin named "hadcoin." In Figure 11, the transaction method has been initiated. There will be two mining. One is for equity hadcoins and the other is for equity USD, which is for dollars.

Mapping is like a function, but this data will be stored in an array. It is not like a function that takes a variable and returns it. It is more like an array that will have an input variable which will be the investor's address. It will return the equity in hadcoins and the other will be in USD. In solidity, address is a type of work that works as a function. Modifiers can check if the investor can buy or sell any hadcoins or not. In Figure 12, the control panel for the entire system is shown. All of the transactions that have occurred will be added here automatically. It has the ability to monitor and regulate the operations of miners as well as data.

```
contract hadcoin_ico {
    uint public max_hadcoins = 1000000;
    uint public usd_to_hadcoins = 1000;
    uint public total_hadcoins_bought = 0;
    mapping(address => uint) equity_hadcoins;
    mapping(address => uint) equity_usd;
```

Figure 11: Hadcoin creations and adjusting USD in remix.

There will also be information on the buyer and seller, as well as data from Ganache containing transaction details. Details about the buyer's account, the seller's account, and the transaction will be logged here. This section's

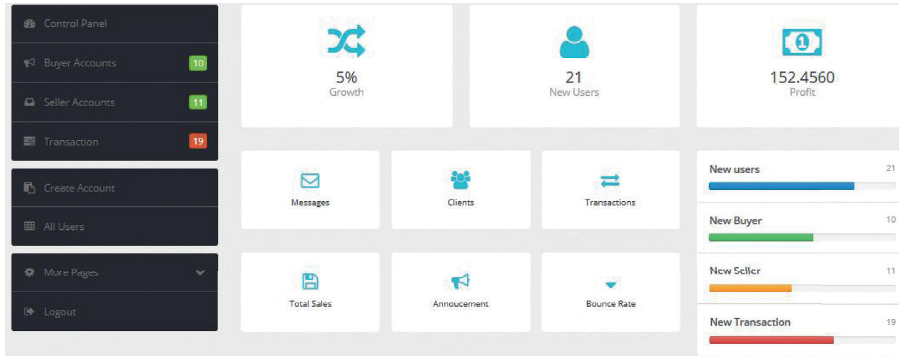

Figure 12: Control panel of the website.

information will be visible to the administrator. Its growth will naturally reflect market conditions. From here, an announcement may be issued. This admin panel will manage all sales, customer information, and bounce rate information. New buyers will be able to see the past information of any previous buyers, making this method extremely trustworthy.

3. Result and Design Analysis

This is the get_chain output. Here, index means the number of the block, as this is the first block, so it has no previous block. Proof indicates the proof of work, which is different for every single block. A Timestamp indicates when the block was created, the exact time, and date with a number. As it is the first block, no transaction happens here. In Figure 13, this is a random block from all the blocks created for mining. Here the index number is different. It has a previous hash which is the hash value of its previous block.

The proof number is different from the first block, which means mining is happening here. The genesis block is the initial block in any blockchain. As this is the first step in the process, it has no prior hash number. It will include evidence of labor, which will be the same for all blocks. Transactions will be placed here using the "hadcoin" coin. As soon as all of the blocks are added to the system, the length will grow and the system will grow too. It will also contain a timestamp, which is a record of the moment when it was first added to the list. In Figure 14, the fourth block is mined. After mining, it will automatically be added here and will show the message text. The difficulty is always set at a certain time interval and then modified every two weeks, such that a block may be constructed at a predetermined time period. As a result, the difficulty of the network sets a predetermined time period between building two blocks, which is roughly 10 minutes (in Bitcoin).

Previous_hash is the hash number of its immediate previous hash and proof is the unique number of each block. The Timestamp function will show the exact time of when it was mined. The most crucial aspect of this system is mining. This mining is done using a fixed algorithm. Many blocks may be mined at once, but only one will get the proper code and be added to the list. This block will get the prize, while the others will not. The procedure, with the exception of mining, will not be particularly genuine. In Figure 15, a block has been mined and this will be added to the main chain. The admin will get to know that with the message "Congratulations, you just mined a block!," this is a confirmation text for miners, and with this, it will ensure mining. The data is then "hashed" by the node, which converts it into a hash value or "hash," which must always include a specific number of zeros. The node determines if a hash satisfies the difficulty requirements. The hash must begin with the appropriate number of zeroes. If the hash satisfies the difficulty requirements, it is disseminated to the rest of the network's miners. The first miner to discover a valid hash converts the block into a new block and is paid for the block reward and fees.

It will display the index number of 4 for this specific block. A message text that confirms whether or not the block has been mined. If mining does not take place, the output will be negative. Every block has a unique number, which for this block is 21391. This system's timestamp shows when it was mined. There is no other way to control this system; it has its own set of rules that it will adhere to throughout the system. In Figure 16, in the transaction section, the amount indicates how many times the sender sends and the sender receives a separate unique number for each transaction. The first miner has a hexadecimal number of sixty-four digits (a "hash") that exceeds or equals the goal hash. It is pretty much a deviation.

This section depicts what the sender and recipient will get once the virtual transaction is completed. The sender and receiver will be reconnected as a result of this procedure, and since they are both unique, they will not be confused by any other customers. For these two clients, both of these figures are produced. Whenever a blockchain transaction flag is raised, there must be a blockchain consensus to update it on the blockchain. Installed on the blockchain network, members nodes in a blockchain consensus protocol agree on a ledger content and cryptographic hate and digital signatures to guarantee the integrity of transactions instead of depending on third parties to broker transactions. These blockchain transactions, if validated, are deemed successful and irrevocable. Transactions depend a lot on hash and hash values. Figure 17 shows that if it is needed to check if the

```
{
    "chain": [
        {
            "index": 1,
            "previous_hash": "0",
            "proof": 1,
            "timestamp": "2021-05-23 03:58:28.604957",
            "transaction": []
        }
    ],
    "length": 1
}
```

Figure 13: Genesis block and details.

```
"index": 4,
"previous_hash": "f972c9ab8ff358c576c2613c567d7035170335f6707d044d16e4c05ed81f4c68",
"proof": 21391,
"timestamp": "2021-05-23 04:03:32.996029",
```

Figure 14: Adding blocks in the list.

```
{
    "index": 4,
    "message": "Congratulations, you just mined a block!",
    "previous_hash": "2a3f053f66fe14ac5feb2b4c6120d9afbd9b8061e710e65c8217d95dbd8e22ef",
    "proof": 21391,
    "timestamp": "2021-05-24 20:48:06.233844"
}
```

Figure 15: After mining text in postman.

```
            "transaction": [
                {
                    "amount": 1,
                    "receiver": "hadcoin5001",
                    "sender": "9f76ed3cb56b4824be8689a91afc2148"
                }
            ]
        }
    ],
```

Figure 16: Transaction occurs in postman.

```
{
    "message": "All good. The blockchain is valid"
}
```

Figure 17: Valid or invalid checking in postman.

blockchain is mining correctly or not, then with the is_valid command, it can be checked. If it stops working, then it will not be valid.

If any sort of unauthentic behavior is detected, the chain will be immediately disrupted. The validation text will not be displayed if this is the case. It will display the phrase “There must be a problem.” As a result, the system’s working process must be halted, and data must be double checked. As previously said, nothing can be altered manually, and each piece of data will have its own unique identification. This is an advantage of the system. Figure 18 is from Ganache after a transaction occurs in a smart contract.

Before the transaction happened, the balance of ethereum was 100 ETH and the TX COUNT was 0. After the transaction occurs, it becomes 99.97 ETH and the TX COUNT becomes 3 because we have mined three times. Here we need to use its private key code, which is just right after the index. In Figure 19, it is shown that all the transaction data will be stored in the transactions section of Ganache.

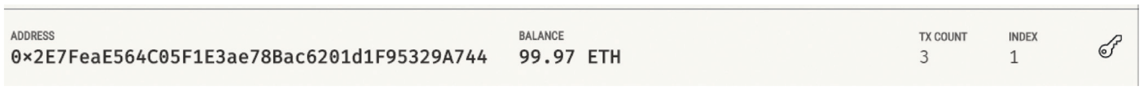

Figure 18: Proof of the transaction data in Ganache.

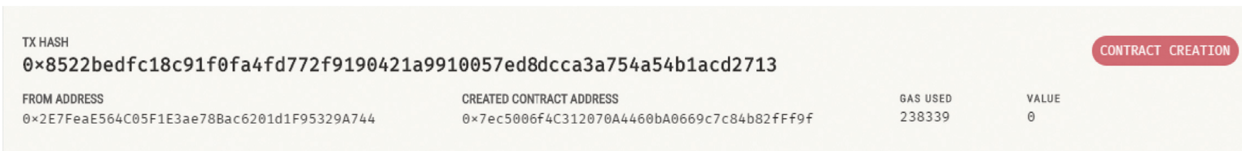

Figure 19: Adding the transaction data in Ganache.

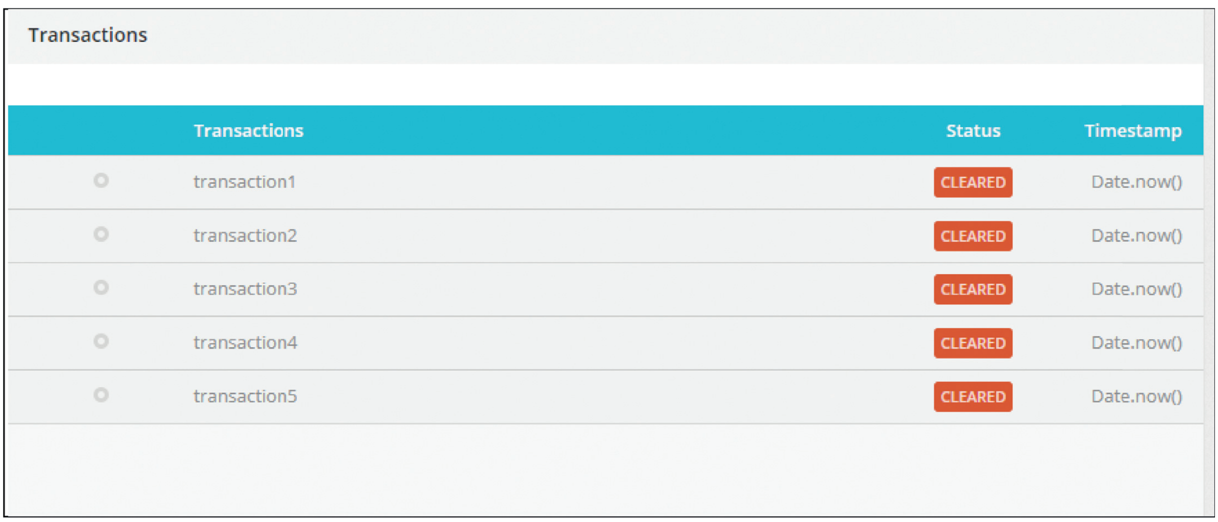

Figure 20: Record of all the transactions.

Table 1: Comparison table between this paper and other papers.

Points of this paper	Points of other papers
(1) Third-party interventions are removed as a result of the deployment of the SCM system described in this article, and strong relationships between peers are formed.	(1) Third-party interventions are frequent in SCM management systems since not every paper proposes their own coin as a currency [4].
(2) The transaction procedure is transparent and highly secure.	(2) The transaction system is broken. Both the vendor and the buyer's trust are affected [5].
(3) This paper contains the strongest immutable ledger technology to prevent cyberattacks, which results in a safe website.	(3) Absence of an immutable ledger on this other paper. If there is any, then it is not secure enough. As a result, the website was hacked [7].
(4) Makes proper use of a smart contract. As a result, the system is more dependable.	(4) There is no proper use of smart contracts. As a result, there's a risk that critical information will be tampered with [11].
(5) This paper's structured SCM is transparent, and refunds are easy to get if a product is defective.	(5) They provide a very difficult refund procedure. Because of this, many unwanted situations are faced by customers [14].

The address of who has made the transaction, how much he has used, and how many times will be stored in this section. The gas used value will be autogenerated by the ganache website from the data of my_wallet account. This is the most secure way to the transaction by using your own coin through ethereum, and the data are also safe and secure. They all have their own distinct worth that cannot be duplicated. The whole system will be separated and secured as a result of this. Hadcoin's approach provides greater security than the conventional method. In Figure 20, it depicts all of the transaction records.

The image is only viewable by accessing the administrator panel. When a transaction between a seller and buyer is successful, the data for the record will be updated in the administration control panel. Additionally, the date and time of the transaction are displayed. Every transaction is recorded here, and the list will become larger as more transactions are made. Only 5 transactions have been made thus far, according to this section. When the status is clear, it indicates that both the buyer and the seller have completed their transaction. The Date now option will provide time information. It contains all of the transaction information.

3.1. Comparison with Other Papers. Table 1 clearly shows the comparison between this paper's materials and the flaws of other papers.

In this article, several very strong security measures have been added, making the system very safe and trustworthy. Other papers, on the other hand, have mostly overlooked these problems, which is why their systems have grown insecure and easy to hack. This paper is up to par since it has an immutable ledger, smart contracts, appropriate transactions, and simple refund and return processes. Every point in previous papers has a flaw. Some of them failed to correctly implement the smart contract, which is the primary cause of the website's failure.

4. Conclusion

The goal of this article is to make supply chain management more intelligent, current, and secure. This framework is immutable and tends to give total transaction transparency. It protects our website from unauthorized access and data manipulation. Furthermore, smart contracts cut the amount of time spent on tedious paperwork. In conventional supply chain management, a lot of documentation is usually necessary. The blockchain keeps the information as proof, making smart contracts immutable. The transaction, immutability, and refundable processes in supply chain management are primarily influenced by this paradigm. This study proposed an end-to-end product supply method. It also allows all customers to return a product if they are unhappy with it and receive a refund for their purchase. Every actor's function and role have been specified. It also means that our framework may be used for a variety of reasons. Smart contracts are also discussed in terms of their structure. The difficulties that individuals experienced with old procedures will be permanently eliminated as a result of the findings of this paper. Among its numerous benefits (the most important of which is the capacity to keep data safe), this research promises to speed up and decrease transaction costs, as well as increase financial inclusion by offering more possibilities for people who do not have easy access to financial services.

This paper is a small-scale and extremely particular piece. However, if there is a large volume of data, the latency may be affected. Blockchain transactions will be extremely beneficial in terms of storage and computational costs. Implementing decentralized databases like BigchainDB and HBasechainDB is another way to boost throughput. Furthermore, in the event of large-scale deployment, tracking devices and more actors can be added to the framework. As the amount of data grows, we may employ off-chain architecture to store the original data, and the proof of existence may be retained on the blockchain itself. This might be a potential future research topic for this investigation.

Data Availability

No data were used to support the findings of this study.

Conflicts of Interest

The authors declare that there are no conflicts of interest regarding the study.

Acknowledgments

The authors are thankful for the support from Taif University Researchers Supporting Project (TURSP-2020/114), Taif University, Taif, Saudi Arabia.

References

[1] C. Prahinski and C. Kocabasoglu, "Empirical research opportunities in reverse supply chains," *Omega*, vol. 34, no. 6, pp. 519–532, 2006.

[2] L. Xiaoming and F. Olorunniwo, "An exploration of reverse logistics practices in three companies," *Supply Chain Management International Journal*, vol. 13, no. 5, pp. 381–386, 2008.

[3] S. Apte and N. Petrovsky, "Will blockchain technology revolutionize excipient supply chain management?" *The Journal of Excipients and Food Chemicals*, vol. 7, no. 3, pp. 76–78, 2016.

[4] S. Alqahtani, X. He, R. Gamble, and M. Papa, "Formal verification of functional requirements for smart contract compositions in supply chain management systems," in *Proceedings of the Hawaii International Conference On System Sciences*, pp. 5278–5287, Maui, USA, January 2020.

[5] O. Alfandi, S. Otoum, and Y. Jaraweh, "Blockchain solution for IoT based critical infrastructures: byzantine fault tolerance," in *Proceedings of the 2020 IEEE Network Operations and Management and Symposium*, pp. 1–4, Budapest, Hungary, April 2020.

[6] D. Magazzeni, P. Mcburney, and W. Nash, "Validation and verification of smart contracts: a research agenda," *Computer*, vol. 50, no. 9, pp. 50–57, 2017.

[7] N. Atzei, M. Bartoletti, and T. Cimoli, "A survey of attacks on ethereum smart contracts (SoK)," *Lecture Notes in Computer Science*, in *Proceedings of the International Conference on Principles of Security and Trust*, pp. 164–186, Thessaloniki, Greece, April 2017.

[8] F. Idelberger, G. Governatori, R. Riveret, and G. Sartor, "Evaluation of logic-based smart contracts for blockchain systems," in *Proceedings of the International Symposium on Rules and Rule Markup Languages for the Semantic Web*, pp. 167–183, New York, USA, June 2016.

[9] L. Luu, D. H. Chu, H. Olickel, P. Saxena, and A. Hobor, "Making smart contracts smarter," in *Proceedings of the ACM SIGSAC Conference On Computer And Communications Security*, pp. 254–269, Vienna, Austria, October 2016.

[10] F. Q. Z. Yao, "BlockChain based supply chain financial risk management research," in *Proceedings of the 2020 International Conference On Mechanical Automation And Computer Engineering (MACE)*, pp. 170–180, Nanchang, China, 2020.

[11] Y. Fu and J. Zhu, "Big production enterprise supply chain endogenous risk management based on blockchain," *IEEE Access*, vol. 7, no. 8626088, pp. 15310–15319, 2019.

[12] S. K. Dwivedi, R. Amin, and S. Vollala, "Blockchain based secured information sharing protocol in supply chain

management system with key distribution mechanism," *Journal of Information Security and Applications*, vol. 54, no. 102554, pp. 1–15, 2020.
[13] E. H. Alfonso-Lizarazo, J. R. Montoya-Torres, and E. G. Franco, "Modeling reverse logistics process in the agro-industrial sector: the case of the palm oil supply chain," *Applied Mathematical Modelling*, vol. 37, no. 23, pp. 9652–9664, 2013.
[14] H. Yuan, H. Qiu, Y. Bi, S.-H. Chang, and A. Lam, "Analysis of coordination mechanism of supply chain management information system from the perspective of block chain," *Information Systems and E-Business Management*, vol. 18, no. 4, pp. 681–703, 2020.
[15] Z. Nehai, P. Piriou, and F. Daumas, "Model-checking of smart contracts," in *Proceedings of the IEEE Smart Data (SmartData)*, pp. 980–987, Halifax, NS, Canada, July 2018.
[16] N. Kshetri, "1 Blockchain's roles in meeting key supply chain management objectives," *International Journal of Information Management*, vol. 39, pp. 80–89, 2018.
[17] S. E. Chang, Y.-C. Chen, and M.-F. Lu, "Supply chain re-engineering using blockchain technology: a case of smart contract based tracking process," *Technological Forecasting and Social Change*, vol. 144, pp. 1–11, 2019.
[18] I. Ahmed and S. Dixit, "Role of technologies in revamping the supply chain management of kirana stores," *Blockchain Applications in IoT Ecosystem*, pp. 275–287, EAI/Springer Innovations in Communication and Computing, Europe, 2021.
[19] R. Kamran, N. Khan, and B. Sundarakani, "Blockchain technology development and implementation for global logistics operations: a reference model perspective," *Journal of Global Operations and Strategic Sourcing*, vol. 14, no. 4, pp. 360–382, 2021.
[20] Z. Liu and P. Guo, "Supply chain decision model based on blockchain: a case study of fresh food E-commerce supply chain performance improvement," *Discrete Dynamics in Nature and Society*, vol. 2021, Article ID 5795547, 14 pages, 2021.
[21] M. Yoo and Y. Won, "A study on the transparent price tracing system in supply chain management based on blockchain," *MDPI AG*, vol. 11, p. 4037, 2018.

Hindawi
Scientific Programming
Volume 2021, Article ID 7953164, 8 pages
https://doi.org/10.1155/2021/7953164

Research Article

Sustainable Development Based on Green GDP Accounting and Cloud Computing: A Case Study of Zhejiang Province

Shanzhong Qi, Zhilei Huang, and Lina Ji

College of Geography and Environment, Shandong Normal University, Jinan 250358, China

Correspondence should be addressed to Shanzhong Qi; shzhqi@sdnu.edu.cn and Zhilei Huang; qshzhsd@163.com

Received 9 August 2021; Accepted 4 September 2021; Published 23 September 2021

Academic Editor: Punit Gupta

Cloud computing is a supercomputing that integrates large-scale and scalable computing, storage, data, applications, and other distributed computing resources for collaborative work in the form of virtualization technology as the basis and the network as the carrier to provide infrastructure, platform, software, and other service's model. Green GDP (GGDP) is an assessment indicator for regional sustainable development. Hence, the evaluation index on GGDP and greening of the national economic accounting system (SNA) are the hotspots of current ecological and economic studies. In the recent years, Zhejiang's economy has achieved rapid development, and there are also problems of high input and high consumption of natural resources, thereby restricting its sustainable development. Based on the statistical data of Zhejiang Province during 2000–2017, the GGDP within the sustainable development context is calculated using the system of integrated environmental and economic accounting (SEEA). The results indicated the following: (1) The GGDP accounted for 79.29%–96.78% of Zhejiang's GDP during the study period, which showed volatility upward trend, resulting from the significant environmental protection and conservation of natural resources in the study area. But economic development was heavily dependent on resources, and the local government still strengthened the work of improving resources and environment. (2) The proportion of secondary industry in Zhejiang Province fluctuated downwards during the period of 2000–2017, and the tertiary industry showed a volatility upward trend, which exceeded the proportion of the secondary industry, indicating that Zhejiang Province is from an industry-led economy to a service-oriented economy change. (3) The GGDP of Zhejiang Province accounted for the highest proportion of GDP in 2008, resulting from the result of a combination of relevant national policies and international competitions.

1. Introduction

Gross domestic product (GDP) is an important index and expounds sustainable development within economic, social, and environmental contexts. In his book *Economics*, Samuelson stated that GDP is one of the greatest inventions of the twentieth century [1], and it is the sum of the values of all services and products which are produced by a country or region in a certain period, and it is a key indicator to evaluate the economic development level for a country or region [2]. For a long time, people have overestimated the positive effect of GDP on promoting economic and social development. Blind pursuit of GDP growth has caused great waste of natural resources and environmental damage. Increasing environmental problems have aroused widespread concern in all countries around the world. In order to achieve sustainable development, governments have actively carried out green GDP (GGDP) accounting projects to compensate for the shortcomings of the original GDP accounting and to reflect more fully and truly the level of national development [3]. GGDP refers to the remaining gross domestic product after deducting the depletion value of ecological resources, such as resource consumption and environmental pollution from traditional GDP [4], which is a compelling method to combine various types of environmental impact with growth within economic context. GGDP can be used to reflect economic growth, to account for the natural resources and environmental conditions, and to allow comparison across countries [5]. GGDP is a compelling approach for combining various types of environmental impact with growth from the economic perspective, and it is an indicator of economic growth with the environmental impacts on that growth factored into the traditional GDP.

Since the 1970s, governments, experts, and scholars have noticed the importance of GGDP and conducted a lot of researches [6]. In 1993, the United Nations Statistical Institute firstly proposed the concept of GGDP in its the System of Integrated Environmental and Economic Accounting (SEEA), which included the integration of resources and environmental costs into the production of the national economy, as the cost of economic production to achieve the adjustment of the original GDP [7]. In addition, the internationally established GGDP accounting system includes the European Statistical Office's European Economic Information Collection System (SERIEE) [8], the Philippine Environmental and Natural Resources Accounting System (ENRAP) [9], and the National Statistical Office of the Netherlands, including the National Accounts Matrix System for Environmental Accounts (NAMEA) [10]. Costanza et al. (1997) measured the service value of the global natural environment for human beings, that is, the ecological service index system (ESI) [11], and Dasily et al. (2000) put forward to evaluate and effectively manage the value of the natural ecosystem, which provides an effective reference for the GGDP accounting [12].

Since the 1990s, Chinese scholars have achieved fruitful results in GGDP theory [13, 14], system construction [15, 16], accounting methods [17–20], and empirical studies [21–23]. Lei (1998) took the lead in designing a resource-economic integration accounting input-output table, taking coal resources as an example to measure China's 1992 GGDP at the national and provincial levels [16]. Shen et al. (2017) used the SEEA system to measure the GGDP of 31 provinces (municipalities and autonomous regions) in China and mainland China from 1997 to 2006 and analysed the spatial pattern according to per capita GGDP and GGDP index [23]. Zhang et al. (2010) used the energy value analysis method to calculate the GGDP of Fujian Province from 2001 to 2006 and used some energy value evaluation indicators to analyze the sustainable development [22]. Lei et al. (2009) calculated the GGDP of Yulin City, Shaanxi Province, by constructing a resource and environmental account index system at the municipal level [21]. Based on the energy value analysis method, Guo et al. (2015) carried out the GGDP accounting of Shangluo city, Shaanxi Province, during the period of 2003–2012 [24]. The GGDP accounting method is mainly divided into two types, namely, direct measurement algorithm and indirect measurement algorithm. The direct measurement algorithm can be calculated by the production method and the expenditure method [19, 20]. The indirect measurement algorithm integrates the resource, environment, and economic factors on the basis of the traditional GDP accounting and obtains the adjustment of the traditional GDP data [25]. It can be found that most accounting studies on the current GGDP are concentrated on the resource-based city level, lacking studies on the GGDP of Zhejiang Province.

Zhejiang Province is a province with the smallest differences within economic development context in China. For example, the GDP per capita in Zhejiang Province is basically above the national level and the per capita disposable income of rural and urban residents for decades is the first among all provinces and cities in China. During the period of 2000–2017, its economy has achieved rapid development, and there are also problems of high input and high consumption of natural resources, thereby restricting Zhejiang's sustainable development. At the same time, the studies are mostly concentrated in a single year from the time scale, or the time span is only 5–10a. Lack of long-term researches may lead to insignificant trends in GGDP. From the perspective of sustainable development, this study aims to introduce a GGDP accounting index system for Zhejiang Province by using the method of SEEA to calculate Zhejiang's GGDP from 2000 to 2017. Further, this study should present a scientific basis for Zhejiang Province to formulate some strategies on its social and economic development and achieve the sustainable development of Zhejiang's resources, environment, economy, and society.

2. Methodology

2.1. Study Area. Zhejiang Province (27°03′~31°11′N and 118°01′~123°25′E) is located in the south wing of the Yangtze River Delta on the southeast coast of China, with an area of 105,500 km^2 and a total population of 49,576,300 (2017). Zhejiang's terrain is stepped from southwest to northeast, with mountains in the southwest, hills in the middle, and alluvial plains in the northeast, and it has a subtropical monsoon climate with four distinct seasons with the annual average temperature of 15–18°C and the annual average rainfall of 980–2000 mm. In the past 18 years, Zhejiang's economy has achieved rapid development, and there are also problems of high input and high consumption of natural resources. In 2017, its GDP achieved 517.768 billion yuan, 8.43 times in 2000, and its average annual GDP growth is 12.1% during 2000–2017. In the same period, the consumption of natural resources increased year by year. In 2000, the total energy consumption of the whole province was 65.6037 million tons of standard coal. In 2017, it reached 210.3001 million tons of standard coal. In the past 18 years, the consumption of energy increased by 3 times, and the average annual growth of energy consumption increased by 7.4%. With the development of industry, the "three wastes" produced by enterprises have a greater negative impact on the environment. In 2017, the industrial exhaust emissions were 3131 billion standard cubic meters, an increase of 4.8 times over 2000, and the industrial solid waste generated 48.28 million tons, an increase of 3.5 times over 2000. If resources and environmental factors are incorporated into the national economic accounting system, traditional GDP will shrink significantly.

2.2. GGDP Accounting Methods. For the accounting of GGDP, the SEEA [26] is commonly used to illustrate the relationship among GDP, environment, and resources; that is, the natural GDP depletion cost and environmental quality degradation cost are subtracted from the gross domestic product, and the resource environment is improved to obtain GGDP as shown

$$\begin{aligned} \text{GGDP} = \text{GDP} - \text{COST}_{\text{Resources}} - \text{COST}_{\text{Environment}} \\ + \text{SAVE}_{\text{Resources–Environment}}, \end{aligned} \quad (1)$$

where $\text{COST}_{\text{Resources}}$ represents the natural resource depletion cost, $\text{COST}_{\text{Environment}}$ represents the environmental quality degradation cost, and $\text{SAVE}_{\text{Resources-Environment}}$ represents the resource environment improvement benefit.

2.3. Indicator Selection of GGDP Accounting. Based on the previous study results, this study combines the main types of natural resource consumption in Zhejiang Province in the past 18 years, classifies the accounts of GGDP accounting into three categories, and selects 10 indicators. The accounting for the depletion of natural resources can be divided into 5 major types of natural resource consumption. The specific indicators are the value of cultivated land depletion, the value of depletion of forest resources, the value of depletion of water resources, the value of energy depletion, and the depletion of mineral resources. The accounting for environmental quality degradation costs is to select various indicators that have a significant impact on the ecological environment of Zhejiang Province, which can be divided into air pollution, water pollution, solid waste pollution, and natural disaster losses. Since the benefits of resource environment improvement are multifaceted and the data are limited, this study only considers the benefits of garden green space, which may have a low impact on the final accounting results.

The evaluation on the depletion value of cultivated land is based on the income multiple method, namely, to calculate the average output value of the first three years of cultivated land and then multiply by the comprehensive maximum multiple of the land compensation fee and resettlement subsidy standard as stipulated in Article 47 of the Land Administration Law, thereby getting the total value of cultivated land, which is divided by the area of cultivated land, and finally get the price of cultivated land per unit area. Finally, by multiplying the obtained cultivated land price per unit area by the cultivated land change area of each year, the value of cultivated land consumption can be obtained [27].

The international common experience method is often used for the value of water resources depletion. The estimation formula is as follows:

$$P_w = \frac{F}{Q}\alpha, \quad (2)$$

where P_w refers to the price of water resources, F refers to the total value created by producers in the water industry (considering the availability of data, F is roughly displaced by the annual GDP increase of Zhejiang Province), Q refers to the total amount of water used each year, and a refers to the consumer's willingness to pay factor. This study does not distinguish between the water industries in the study area and directly estimates the entire area as a whole. According to the formula of the per capita water resources and the empirical method of the willingness coefficient of payment in Zhejiang and other cities from 2000 to 2017, the value is 3% [27].

For the energy depletion value in this study, we use the price of standard coal in 2004, namely, 1,133 yuan/t [28], and then revise through the historical energy price index to obtain the unit energy price in Zhejiang Province over the years from 2000 to 2017.

Exhaust gas, waste water, and solid waste are substances that have a direct negative impact on environment in daily production and life. Considering the availability of data, the objects to be calculated in this study include sulfur dioxide in exhaust gas, smoke dust, industrial wastewater and domestic wastewater in wastewater, industrial solid waste, and domestic waste in solid waste, of which the amount of industrial solid waste is obtained according to the Production Amount-Comprehensive Utilization Amount, and the amount of domestic garbage is obtained according to the Clearance Amount-Harmless Treatment Amount [23]. For the unit treatment cost of various pollutants, the unit cost of sulfur dioxide treatment will be determined according to the 20000 yuan/t formulated by Jiaxing City in the implementation of emissions trading in 2007 [29]. Other governance costs are based on the current year's parameters in the existing study and adjusted according to the historical consumer price index (CPI), so that the average unit cost of smoke dust is 170 yuan/t [30]. When calculating the pollution price, according to the Guidelines for China's Environmental Economic Accounting Technology, the unit treatment cost of industrial wastewater is 4.02 yuan/t, and the unit treatment cost of domestic wastewater is 0.6 yuan/t [31]. The solid waste adopts the national unified standard parameters in 2004; that is, the unit treatment cost of industrial solid waste is 20 yuan/t [32], and the domestic garbage disposal cost is determined to be 110 yuan/t based on the Hangzhou municipal garbage collection and treatment cost report issued by the World Bank in 2002 [29]. Due to the incomplete statistics of pollutants, the results are low. Under the guidance of SEEA, through the above analysis, the accounting method of green GDP in this paper is established (Table 1).

2.4. Data Source. In this study, the data were mainly obtained from the Chinese Statistical Yearbook (National Bureau of Statistics of the People's Republic of China 2001–2018), the *Zhejiang Statistical Yearbook* (Zhejiang Province Bureau of Statistic 2001–2018), the China Land and Resources Statistical Yearbook (Ministry of Land and Resources of the People's Republic of China 2001–2018), and related literature.

A size of 150 mm × 150 mm × 550 mm was used for pore pressure tests. After casting, all the specimens were stored in a standard curing room of concrete with molds for 24 hours; thereafter they were demoded, subjected to water of 20°C, and cured for 28 days. The initial moisture of the specimens was between 4 and 5% by mass.

Table 1: Accounting methods of GGDP.

Account type	Index	Calculation methods
Natural resource depletion cost	Cultivated land depletion value	Cultivated land depletion value = cultivated land consumption × unit price
	Forest resource depletion value	Forest resource depletion value = forest land consumption × unit price
	Water resource depletion value	Water resource depletion value = total water use × unit volume consumers willing to pay the price
	Energy consumption value	Energy consumption value = total energy consumption × unit energy price
	Mineral resource depletion value	Mineral resource depletion value = mineral resource consumption reduction × unit mineral price
Environmental quality degradation cost	Air pollution	SO_2 governance costs = SO_2 emissions × unit SO_2 management fee Smoke dust treatment cost = smoke dust emissions × unit smoke dust treatment costs
	Water pollution	Industrial wastewater treatment cost = industrial wastewater discharge × unit industrial wastewater treatment costs Domestic wastewater treatment cost = domestic wastewater discharge × unit domestic wastewater treatment costs
	Solid waste pollution	Industrial solid waste treatment costs = industrial solid waste × unit solid waste treatment costs Domestic waste treatment cost = amount of domestic garbage × unit management cost
	Natural disaster loss	Direct economic losses caused by natural disasters (geological disasters and forest fires)
Resource and environment improvement benefits	Garden green space benefits	Carbon fixation and oxygen release efficiency = green area × (328.5 × 40.94 × average dollar exchange rate for the year + 12 × 400) [27] Absorbing SO_2 economic benefits = green area × 0.296 × 600 [27] Regulating climate economic benefits = green area × 0.9 × 24 × 189 × 0.7 [33]

3. Results and Discussion

3.1. Analysis of GGDP in Zhejiang Province from 2000 to 2017. According to the GGDP accounting method, relevant data analysis is carried out to obtain the proportion of GGDP and GGDP in GDP of Zhejiang Province from 2000 to 2017 (Table 2). From Table 2, its GDP increased from 614.103 billion yuan in 2000 to 517.768 billion yuan in 2017. The GGDP increased from 5,047.34 billion yuan in 2000 to 481.184 billion yuan in 2017. Moreover, GGDP and GDP maintain a synchronous growth trend (Figure 1), and the proportion of GGDP to GDP generally shows an upward trend, with fluctuations in individual years. The proportion of GGDP to GDP was between 79.29% and 96.78%, with the lowest proportion in 2001, reaching 79.29%; in 2008 the proportion reached the highest, at 96.78%.

From the accounting indicators that constitute GGDP, natural resource depletion costs dominate the GGDP, from 94.214 billion yuan in 2000 to 371.168 billion yuan in 2017. The volatility directly determines the proportion of GGDP to GDP. For example, in 2001, the natural resource depletion cost was 128.344 billion yuan, accounting for the highest value of 18.61% of GDP, making the proportion of GGDP to GDP lower to the lowest point of 79.29%. On the contrary, in 2008, the natural resource consumption reduction cost was reduced linearly to 53.35 billion yuan, accounting for 2.49% of the lowest value in the history, making GGDP account for 96.78% of the highest value of GDP. It dominates the proportion of GGDP to GDP. At the same time, the cost of environmental quality degradation has shown a trend of rising first and then falling, but its proportion of GDP has been declining year by year. It has decreased from 3.00% of GDP in 2000 to 0.21% in 2017, reaching the lowest level in history, indicating research. The environmental quality of the district is improving year by year, and environmental protection work has achieved remarkable results. In addition, although the efficiency of resource and environment improvement has increased year by year, from 3.297 billion yuan in 2000 to 16.619 billion yuan in 2017, its proportion of GDP has increased first and then decreased, indicating that Zhejiang Province should pay attention to resource and environmental improvement to enhance the efficiency of resources and environment. It can be seen that, in 2000–2017, the resource conservation effect of Zhejiang Province was remarkable, and the dependence of economic development on natural resources was gradually weakening, but it is still necessary to further promote the comprehensive utilization of resources.

From the internal analysis of accounting indicators, in the natural resource depletion cost, the energy consumption reduction value accounted for the largest proportion, reaching 62.01–85.83%, which shows that Zhejiang Province has greater dependence on energy during the economic development and should be reduced in the future. The dependence on energy resources is a breakthrough to optimize sustainable development. Among the costs of environmental quality degradation, the cost of SO_2 treatment in air pollution is the main factor. It can be seen that

Table 2: Value of Zhejiang GGDP accounting indicators and the proportion of GDP during 2000–2017.

	Natural resources depletion costs (10^8yuan)	Natural resources depletion costs accounted for % of GDP	Environmental quality degradation cost (10^8yuan)	Environmental quality degradation costs accounted for % of GDP	Resource and environment improvement benefits (10^8yuan)	Resource and environment improvement benefits accounted for % of GDP	GDP (10^8 yuan)	Green GDP (10^8yuan)	Green GDP as a percentage of GDP
2000	942.14	15.34	184.52	3.00	32.97	0.54	6141.03	5047.34	82.19
2001	1283.44	18.61	182.87	2.65	37.80	0.55	6898.30	5469.80	79.29
2002	1189.02	14.86	193.79	2.42	45.22	0.56	8003.70	6666.11	83.29
2003	1400.19	14.43	218.19	2.25	53.51	0.55	9705.02	8140.15	83.88
2004	1576.11	13.53	234.42	2.01	59.92	0.51	11648.70	9898.09	84.97
2005	1601.94	11.94	254.48	1.90	68.66	0.51	13417.70	11629.94	86.68
2006	1992.66	12.68	256.50	1.63	70.53	0.45	15718.47	13539.84	86.14
2007	2193.52	11.70	246.81	1.32	75.06	0.40	18753.73	16388.45	87.39
2008	533.50	2.49	235.18	1.10	77.80	0.36	21462.69	20771.81	96.78
2009	2054.92	8.94	229.16	1.00	78.47	0.34	22998.58	20792.97	90.41
2010	2766.57	9.97	224.97	0.81	83.76	0.30	27747.65	24839.87	89.52
2011	2679.53	8.28	219.44	0.68	107.97	0.33	32363.38	29572.38	91.38
2012	3154.83	9.08	210.16	0.60	120.64	0.35	34739.13	31494.79	90.66
2013	3074.90	8.14	198.78	0.53	125.58	0.33	37756.58	34608.48	91.66
2014	3119.37	7.76	190.06	0.47	127.57	0.32	40173.03	36991.17	92.08
2015	3345.63	7.80	183.39	0.43	134.37	0.31	42886.49	39491.84	92.08
2016	3704.65	7.84	121.54	0.26	158.80	0.34	47251.36	43583.97	92.24
2017	3716.85	7.18	106.76	0.21	166.19	0.32	51768.26	48110.84	92.94

environmental pollution not only increases the cost of pollution control, but also harms human health and ecological environment.

3.2. Industrial Structure Analysis of Zhejiang Province from 2000 to 2017. With the development of social economy of Zhejiang Province, the GDP during 2000–2017 has grown substantially from 614.103 billion yuan in 2000 to 517.768 billion yuan in 2017. In the meantime, the industrial structure has undergone tremendous changes. The GDP of the primary industry (PI), which refers to the department that uses natural forces primarily to produce consumable products or industrial raw materials without further processing, increased from 63.098 billion yuan in 2000 to 193.392 billion yuan in 2017, showing a slow growth phenomenon, but the proportion of the PI in GDP began to decrease from 10.27% in 2000 to that in 2017. The proportion of GDP is only 3.74%, reaching the lowest value of the PI in GDP from 2000 to 2017; the GDP of the secondary industry (SI), which is defined as the mining industry (excluding mining assistance activities), manufacturing (excluding metal products, machinery and equipment repair), electricity, heat, gas and water production and supply, and construction, increased from 327.393 billion yuan in 2000 to 232.328 billion yuan in 2017, showing a slightly faster growth than the PI (Figure 2).

However, the proportion of the SI in GDP has decreased first, then increased, and then decreased year by year. The trend of volatility fell from 53.31% of GDP in 2000 to 51.11% in 2002 and then rose to 54.15% in 2006 and 2007, reaching the highest value of the SI in GDP during the period of 2000–2017, and has since declined. By 2017, the SI will account for 42.95% of GDP, the lowest value of the SI in GDP in the study period; the GDP of tertiary industry (TI) which referred to other industries except the PI and SI, such as wholesale and retail trade, transportation, warehousing, and postal services, increased rapidly from 226.612 billion yuan in 2000 to 2.760226 billion yuan in 2017. With the GDP growth of the TI, it accounts for GDP. Excluding the decline in individual years, the overall growth trend is relatively fast. The proportion of TI in GDP increased from 36.41% in 2000 to 53.32% in 2017. In 2014, the proportion of TI in GDP reached the first time in 15 years. Exceeding the SI's share of GDP, the TI has maintained a leading position in GDP since then. It can be seen that Zhejiang Province vigorously promoted the regulating of industrial structure and the development mode transformation during the period of 2000–2017 and optimized the industrial structure of Zhejiang Province.

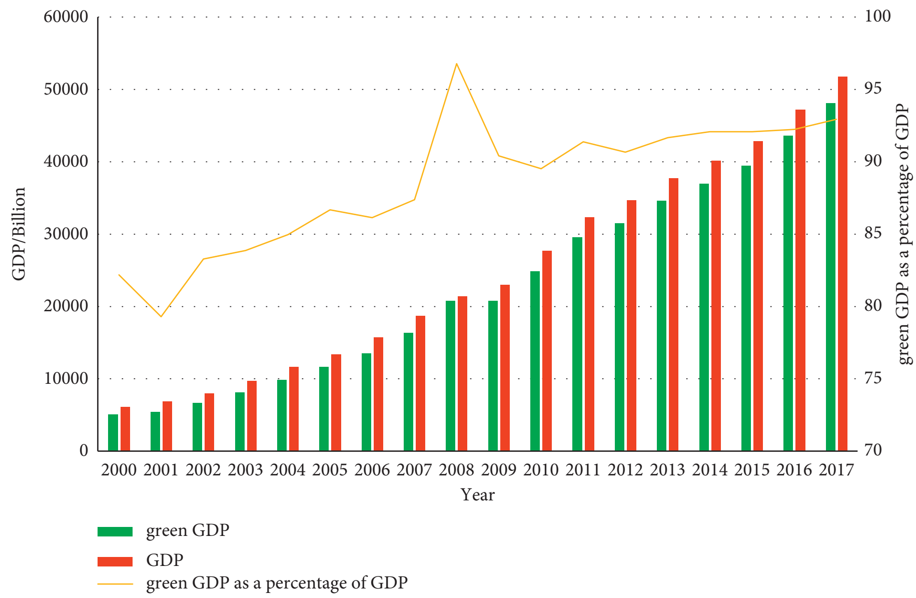

Figure 1: Zhejiang's GGDP, GDP, and GGDP as a share of GDP from 2000 to 2017.

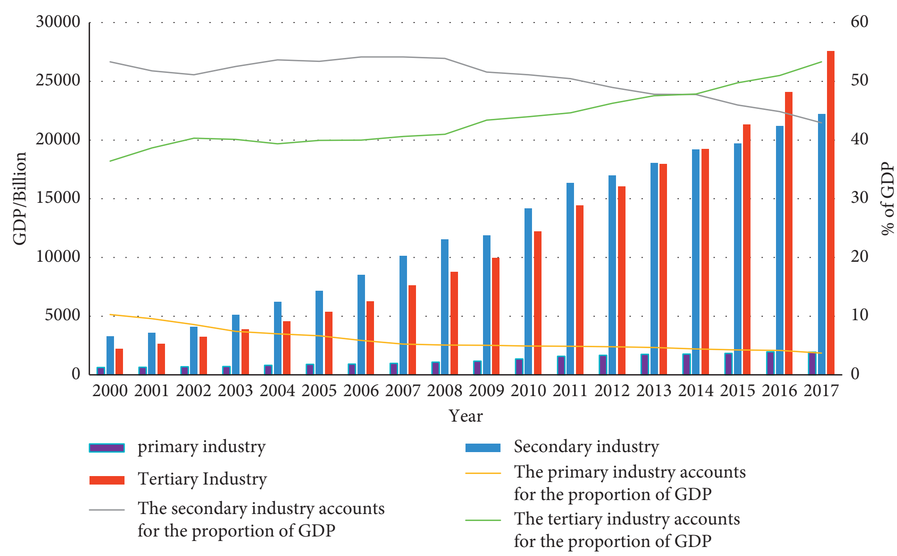

Figure 2: GDP of Zhejiang Province from 2000 to 2017.

4. Conclusions

Based on the data of Zhejiang Province from 2000 to 2017, this study calculates the GGDP in the past 18 years by constructing a GGDP accounting system and draws the following conclusions:

(1) During the period of 2000–2017, the GGDP and GDP of Zhejiang Province maintained a simultaneous growth. The GGDP accounted for 79.29%–96.78% of GDP which showed a volatility upward trend, resulting from the significant environmental protection and conservation of natural resources in the study area.

However, the depletion of natural resources still occupied a dominant position in GGDP. Economic development was particularly dependent on energy resources, and comprehensive utilization of resources had to be strengthened. In a word, the economic development of Zhejiang Province has become less dependent on resources and environment, and the economic development model was gradually optimized.

(2) During the period of 2000–2017, the industrial structure of Zhejiang Province experienced significant changes. The proportion of the PI has been decreasing, and the proportion of the SI fluctuated and declined year by year. The TI showed volatility, surpassing the second after 2014. The proportion of industry and the proportion of the SI and TI were gradually widening, indicating that the economy of Zhejiang Province was transforming from an industry-led economy to a service-oriented economy. This trend was conducive to economic, social, and environmental sustainability development of Zhejiang Province.

(3) In 2008, the GGDP of Zhejiang Province accounted for the highest proportion of GDP during the period of 2000–2017 (Figure 1). The reasons were as follows. First, by analysing the *Zhejiang Statistical Yearbook*, it can be found that the area of cultivated land has increased significantly. It was the main reason. On the other hand, Zhejiang Province promulgated a number of policies on farmland protection around 2008, implemented strict farmland protection systems and land-saving systems, and adopted laws, economics, science, technology, etc. ways to maintain the red line of cultivated land protection and increase the intensity of land construction and land remediation. Second, due to the 2008 Beijing Olympic Games, the country had increased its focus on air quality, increased investment in environmental protection, improved environmental quality, and reduced environmental quality degradation costs. Third, scientific and technological progress had reduced the unit cost of pollutants and reduced the cost of environmental quality degradation. In sum, the result of a combination of relevant national policies and international competitions resulted in that the GGDP of Zhejiang Province accounted for the highest proportion of GDP during the study period.

Data Availability

All data, models, and code generated or used during the study appear in the submitted article.

Conflicts of Interest

The authors declare no conflicts of interest with respect to the research, authorship, and/or publication of this article.

Acknowledgments

This study was supported by the Open Research Fund of State Key Laboratory of Subtropical Silviculture, Zhejiang A&F University (KF201706).

References

[1] Y. P. Li, "Change from development to GDP to green GDP," *Truth Seeking*, vol. 1, pp. 38-39, 2006.

[2] L. X. Wang and Z. Y. Ren, "An elementary discussion and analysis of green GDP calculation methods: a case study of Datong City in Shanxi Province," *Progress in Geography*, vol. 24, no. 2, pp. 100–105, 2005.

[3] M. L. Cao, L. L. Zhang, and H. Zha, "Experience and enlightenment of implementing green GDP accounting at home and abroad," *Environmental Protection*, vol. 4, pp. 63–65, 2014.

[4] Z. L. Zhao, "The new empirical example of local governance guiding by green GDP performance assessment," *Journal of Huazhong University of Science and Technology (Nature Science Edition)*, vol. 6, pp. 6–10, 2017.

[5] B. F. Giannetti, F. Agostinho, C. M. V. B. Almeida, and D. Huisingh, "A review of limitations of GDP and alternative indices to monitor human wellbeing and to manage ecosystem functionality," *Journal of Cleaner Production*, vol. 87, pp. 11–25, 2015.

[6] W. X. Kang, D. Wang, J. L. Zou, Y. P. Hu, and S. S. Cui, "Accounting green GDP in Huaihua based on energy analytic approach," *Acta Ecologica Sinica*, vol. 30, no. 8, pp. 2151–2158, 2010.

[7] H. Jia and X. L. Yu, "The demonetized green GDP accounting system based on the MCDM," *Journal of Arid Land Resources & Environment*, vol. 27, no. 8, pp. 6–13, 2013.

[8] European Commission, *SERIEE European System for the Collection of Economic Information on the Environment 1994 Version*, European Comission, Brussel, 2002.

[9] H. M. Peskin, "Alternative resource and environmental accounting approaches and their contribution to policy," *Ecol. Econ,* vol. 21, pp. 217–229, 1998.

[10] S. J. Keuning and M. D. Han, *Netherlands: What's in a NAMEA? Recent Results*, Springer, Amsterdam, Netherlands, 1998.

[11] R. Costanza, R. d'Arge, R. de Groot et al., "The value of the world's ecosystem services and natural capital," *Nature*, vol. 387, no. 6630, pp. 253–260, 1997.

[12] G. C. Daily, T. Soderqvist, S. Aniya et al., "ECOLOGY: the value of nature and the nature of value," *Science*, vol. 289, no. 5478, pp. 395-396, 2000.

[13] T. Peng and W. L. Wu, "Green GDP accounting: further research and discussion in the context of low-carbon development," *China Popu. Resour. Environ,* vol. 20, no. 12, pp. 81–86, 2010.

[14] H. M. Zhang and C. R. Qiu, "A framework analysis of the green GDP accounting system in China, Financ," *Trade Res*, vol. 3, pp. 37–42, 2004.

[15] N. Lin, "Green GDP accounting system and development of circular economy," *Contemporary Economics*, vol. 11, pp. 53–55, 2006.

[16] M. Lei, "Green GDP accounting," *Journal of Natural Resources*, vol. 13, no. 4, pp. 320–326, 1998.

[17] J. Li, Y. L. Kang, and Y. Lu, "An empirical study of green GDP accounting in Chengdu," *J. Soc. Sci,* vol. 7, pp. 13–16, 2007.

[18] R. X. Xiu, G. Wu, X. A. Zeng, J. G. Sun, and D. Y. Yu, "Research progress of green GDP accounting index," *Chinese J. Ecol,* vol. 26, no. 7, pp. 1107–1113, 2007.
[19] M. G. Chen, "A gross economic indicator under sustainable development: green GDP, China Popu," *Resources and Environment*, vol. 15, no. 1, pp. 1–6, 2005.
[20] Z. Wang, Y. Liu, and Q. B. Zhou, "Research on Shanghai's general growth accounting and green GDP accounting," *Geographical Research*, vol. 25, no. 2, pp. 185–192, 2006.
[21] M. Lei, X. Y. Zhang, and M. M. Cao, "Accounting research of green GDP of resource-dependent cities: a case study of Yulin City in Shaanxi Province," *Journal of Natural Resources*, vol. 24, no. 12, pp. 2046–2055, 2009.
[22] H. Zhang, M. S. Huang, and X. H. Hu, "Green GDP calculation of Fujian province based on energy analysis," *Acta Geographica Sinica*, vol. 65, no. 11, pp. 1421–1428, 2010.
[23] X. Y. Shen, G. H. Wang, and X. J. Huang, "Green GDP accounting and spatio-temporal pattern in China from 1997 to 2013," *Journal of Natural Resources*, vol. 32, no. 10, pp. 1639–1650, 2017.
[24] L. Y. Guo, M. Lei, and X. Q. Liu, "Green GDP accounting research based on emergy analysis method: a case study of Shangluo city in Shaanxi Province," *Journal of Natural Resources*, vol. 30, no. 9, pp. 1523–1533, 2015.
[25] L. Y. Ge, "Green GDP accounting based on sustainable development," *Statistics & Decisions*, vol. 17, pp. 27–29, 2013.
[26] M. Lei, "Trial estimate of 1995' CSEEA and Chinese green GDP," *Syst. Eng. Theor. Pr,* vol. 20, no. 11, pp. 1–9, 2000.
[27] Z. Y. Jin and X. J. Huang, "Accounting of the green GDP in Jiangsu Province based on values of resources and environment," *Areal Res. Dev,* vol. 33, no. 4, pp. 131–135, 2014.
[28] D. Z. Liu, G. E. Zou, and H. Qin, "Empirical study on green GDP accounting in Hebei Province," *J. Hebei GEO Univ,* vol. 29, no. 5, pp. 620–623, 2006.
[29] Y. J. Lou and L. Q. Jin, "An empirical study of green GDP accounting system on Hangzhou," *Reformation Strateg*, vol. 26, no. 10, pp. 122–124, 2010.
[30] X. Z. Xu and S. B. Yan, "Research and application of green GDP accounting in Fujian Province," *J. Anhui Agr. Sci,* vol. 39, no. 19, pp. 11806–11808, 2011.
[31] Y. M. He and S. S. Wu, "Construction of green GDP accounting system based on resource value loss method," *Statistics & Decisions*, vol. 17, pp. 5–10, 2017.
[32] G. L. Guo, *Study ongreen GDP accounting adjusted by environment pollution losses and a case analysis*, Master's thesis, Wuhan University of Technology, Wuhan, China, 2006.
[33] W. J. Zhang, F. Zhang, Z. Yan, and Z. H. Zhang, "Initial Analysis on the ecological service value of the greening land in Lanzhou city," *Pratacultural Science*, vol. 23, no. 11, pp. 98–102, 2006.

Hindawi
Scientific Programming
Volume 2021, Article ID 3713161, 10 pages
https://doi.org/10.1155/2021/3713161

Research Article

Design and Implementation of Multidimensional Interaction in Online English Course under the Assistance of Omnimedia

Ming Cao

School of Humanities and International Education, Xi'an Peihua University, Xi'an, China

Correspondence should be addressed to Ming Cao; caoming@peihua.edu.cn

Received 29 July 2021; Accepted 6 September 2021; Published 18 September 2021

Academic Editor: Dinesh Kumar Saini

The method of multidimensional interaction in online teaching and learning requires teachers to harness the techniques of omnimedia and have an overall course design to achieve similar results as offline learning. Supported by QQ, Lanmo Cloud Class, and WeChat platforms, online English courses implement multidimensional interaction method to enhance language communication. This method compensates for the inefficacy of online teaching and learning which falls short of face-to-face interaction and considers the needs of students. The quasiexperimental study sampled 66 freshmen English major students in an ordinary college via Integrated English Online Course for three months. By using *T*-test of SPSS 26.0, statistics showed that there were significant differences between the experimental class (Number 35) and the control class (Number 31) in students' feedback ($p = 0.044$, < 0.05) and the results of their final examinations ($p = 0.049$, < 0.05). The results indicated that multidimensional interaction in online English course under the assistance of omnimedia appeared effective. It also reflected that both teachers and students should grasp the skills of using new technology and make good use of omnimedia network platform. Teachers need to change traditional teaching concept to student-centered and create effective teaching design while students need to overcome the discomfort and actively engage in online learning to achieve the goals.

1. Introduction

The rapid development of science and technology has provided unlimited possibilities for online teaching and learning. The emergence of new technologies and concepts such as "Internet Plus," "Cloud Computing," and "Big Data," for example, has made online learning more flexible and convenient. New technologies have provided frontline teachers with the resources and opportunities to integrate new technology into English teaching. Liu et al. reported that, in the "Internet Plus" environment supported by Adobe Connect platform, Sino-US cross-culture EFL (English as a foreign language) blended teaching class with real-time technology made a positive impact on the Chinese students' learning behaviours, increased their self-efficacy, and enhanced their understanding of the target culture. At the same time, the unique and rich learning resources and new perspectives they brought into the cyber class benefited students in both countries [1]. "Cloud Computing" is a model of paying by the amount of data using and follows the learning principle of 5A (Anyone, Anytime, Anywhere, Any device, Any form). Yang et al. created a model of smart learning environment based on Cloud Computing. It has been noticed to be of great significance to carry out related research on Cloud Computing and smart learning environment [2]. Although there is less empirical research on the EFL field, some scholars tried to use "Cloud Computing" perspective into college teaching and learning for translation major [3]. In terms of "Big Data," some believe that it is a field that an overlarge and hypercomplex dataset is provided for traditional data system application software to analyze, withdraw, or manage [4]. Others consider that it is so large, fast, or complex that it is difficult or impossible to process using traditional methods [5]. In EFL field, researchers explored many ways of using "Big Data" to design their teaching and learning. It is verified that, by using Google images to be a dataset, students created pictorial annotations for them to remember the target words and integrated them into their prior knowledge [6]. In “Big Data” related English teaching, students’ learning motivation level and learning ability have increased by 16.6% and 14%, respectively [7, 8]. As a result, these physical changes flourish the way of integrating technology into English teaching and learning.

In addition, it has allowed for the change from teacher-centered to student-centered methods, bringing student-centered instruction into practice. Despite the variety of research focused on online teaching and learning in recent years [9, 10], with some spotlight on online interaction strategies [11], there are only a small number of studies on the topic of implementing online teaching with effective interaction. In particular, there has been a lack of attention on the relationship between high quality online teaching at local colleges and the technologies that support the teacher-student interactions. It is reported that teachers’ adaptation is always required to find and solve problems during the teaching practice in an online and offline blended program. Students changed the attitudes gradually under the help of teachers and gain improvement in writing quality [12]. Interaction plays the key role when teachers carry out student-centered instruction. Thus, we need more cases to show how technology integrates into English teaching and learning. Along with the normalization of online or a combination of online-offline teaching and learning, implementing effective Internet-based teaching has become a new challenge for college teachers. This challenge raises some questions: how are we going to draw and maintain students’ attention to make teaching and learning more effective? What do students think of Internet-based learning in central provinces of Chinese mainland? How does online learning impact student results? Interaction strategies have become the key of Internet-based teaching and learning. To achieve student-centered online learning results, we use multidimensional interaction strategies with the assistance of omnimedia in designing the course. New thoughts and ideas may arise during implementation.

1.1. Relevant Concepts

1.1.1. Interaction and Multidimensional Interaction. Interaction is a back and forth activity between subjects and objects. It is a form of communication [13]. Ancient Chinese ideologies include interaction when teaching as a key part of education. For example, during the Warring States Period of ancient China, in Xueji of The Book of Rites, it included “question-answer” and “analysis-explanation” teaching strategies. While teaching, the teacher should not repeat what the book said without first considering what the student knew. Teachers should not give answers until students had no more questions to ask [14]. In 1989, Moore classified interaction and this classification included three types of interaction: student-teacher interaction, student-student interaction, and student-content interaction [15]. Teacher-student interaction is based on the teacher’s hypothesis of how much of the material the students have grasped. Student-student interaction is based on the concept of equality in which students feel free to discuss concepts and what they have understood with their peers when teachers and authority figures are absent. Student-content interaction has been understood to be a unique interaction between students and the content they are learning, including how students understand the learning materials, the concepts from material, and the cognitive structure in students’ minds. This dialogue may also be called “an internal monologue” [15]. Multidimensional interaction stemmed from the context of interaction. Palinscar and Brown put forward the concept of multidimensional interaction in the 1970s last century under the concept of constructivism. They proposed that multidimensional interaction method required teachers to keep the idea of student-centered learning while teaching. Teachers should enable students to shift from passively receiving information to actively and autonomously pursuing information [16]. Evidently, multidimensional interaction method places the emphasis on student-centered learning; by fully understanding the concept of interaction, teachers can utilize multidimensional interaction method to effectively design courses for their students.

Scholars often use online conference, online case analysis, video playback, and virtual activities to achieve multidimensional interaction. They have tried to overcome the limitations of the online learning facilities and optimize online interaction. In addition, they have implemented the multidimensional activities to make student-student, teacher-student, and student-content types of interaction apply in multiangle, multiaspect, and multilevel [17]. Other scholars believe that implementation of multidimensional online teaching or hybrid of online and offline teaching needs teachers to analyze many factors such as students, course contents, students’ learning strategies, and learning environment until we reach the ideal result [10]. If we use different Internet platforms effectively, we may achieve close teacher-student relationship [18]. However, some scholars hold a cautious attitude in how they regard online interaction, as they believe the positive influence for learners is limited to the period of online interaction for the second language vocabulary learning [19]. Consequently, in order to realize online teaching and learning under the assistance of omnimedia and achieve similar results as offline learning, teachers need to not only be familiar with the different online platforms, but also be well-versed about how to design their online course and pay attention to their students’ feedback and feelings. Multidimensional interaction presents an inevitable question to both teachers and students. If we wisely use computer and mobile phones, taking care of those interaction, we will arouse the enthusiasm of students’ motivation, pay attention to learning process, and promote student-centered online teaching and learning.

1.1.2. Omnimedia and English Teaching. There are different explanations to omnimedia. Most of them tend to explain that, by using different media (platform), combining different ways of spreading, and converting or transplanting signals, people have more ways of acquiring information [20]. These ideas assist learners in achieving learning in different places with methods that are less costly and more profitable. The features can be explained using pictures, letters, sounds, light, images, etc., to send messages in certain platforms. Learners may also use computers, mobile phones, tablets, and smart TV sets to receive messages. Hence, everyone can access the learning systems at any time and place by using available terminals to receive the learning content they want and to fully utilize the service [21]. Based on the statistics from the Ministry of Education of People's Republic of China of 2018, China has 2.76 hundred million students in all forms of education at all levels [22]. If we are able to use the omnimedia resources to serve those students, it will provide an opportunity to have a meaningful exploration while combining information technology with education.

Language learning has its own special requirements. The expression of teachers and the practice of students are highly related to interaction. In offline in-person learning, interaction can be all-rounded with the teacher's voice and gestures, including eye contact, facial expression, hand signals, posture, and so forth. These all-rounded expressions with rich emotions are signals to draw students' attention easily. In case that the student is slightly distracted, they may miss the teacher's instruction but still be able to interpret the meaning from the teacher's gestures and expressions. Online learning is a unique situation in which the teachers and students are physically separated making it difficult to fully interact with one another. However, different kinds of Internet platforms provide us another chance to manage this shortcoming. By effectively utilizing pictures, letters, characters, sounds, and images, etc., teachers and students can exchange information attentively and even avoid some other irrelevant distractions to realize a state of highly focused teaching.

1.2. Design. It is not rare to integrate new technology into teaching and learning design in recent years. The common platforms include Facebook, Moodle, Google, Adobe Connect, Tencent, Lanmo Cloud Class, and so forth. The educational potential and advantages have been compared between Facebook and Moodle platforms, Tencent and Lanmo Cloud Class, and others [23, 24]. Currently, many teachers try to use different platforms at the same time to offset the shortage and promote the advantages. To realize multidimensional interaction, English online teaching and learning have mainly relied on QQ, Lanmo Cloud Class, and WeChat platforms. It is called omnimedia as it combines different ways of spreading and converting or transplanting signals. No matter what platform it is, the supporting system such as hardware, software, and Internet also plays an important role. The design can be seen as shown in Figure 1.

1.3. Implementation. QQ platform is one of the application products from Tencent Company. It is user friendly and is also the most frequently used platform. Both teachers and students can use it to perform many tasks such as lecturing, group discussion, and conference, for example. It gives a chance for students to set up their own discussions without instructor interference. Lanmo Cloud Class has many functions such as brainstorming, first-to-answer, light live streaming, messaging, discussion, group discussion, voting, questionnaire, reporting, displaying, debating, and testing. In reality, QQ and Lanmo are synergistically providing support to students. WeChat platform is also from Tencent and is flexible and easy to be handled for teacher-student interaction. It supplements the other two formal platforms as students often communicate with teachers on WeChat platform outside of class.

1.3.1. QQ Platform. QQ platform is the most commonly used platform. It can be used as lecturing, conference, and discussion with multiple interactive functions. It is quite similar to the offline classroom loved by teachers and students. In addition, it contains a mentoring function, which strengthens teacher-student relationship. Students often use this platform to start discussions and complete group assignments. Here are some examples of the QQ platform application (Figure 2).

1.3.2. Lanmo Cloud Class Platform. There are many functions in Lanmo Cloud Class. Teachers use the platform to supplement lectures presented on QQ platform. During the lecture of traditional teaching, teachers often talk by themselves without giving the opportunity to communicate with students. While with student-centered presenting, teachers can cast questions using the Lanmo platform and receive responses immediately. Depending on the content of the lecture, teachers either set up questions for the language learning or explore the supporting information. On the other terminal, students can quickly pick the questions, express their own ideas, and discuss with their peers. When they become familiar with the platform, they will be able to fully take advantage of the available applications. Not only do they learn the technology, but students also develop their thinking, expand their vocabulary, and practice their language skills. Some typical interaction applications are shown as follows:

(1) Brainstorming block: it uses letters, words, and symbols to stimulate interaction. When the teacher posts a question, students can quickly cast their ideas, thoughts, or answers. This mimics offline class in which students present their own ideas to solve the problems and inspire their peers to contribute as well. The brain storming record is shown in Figure 3.

(2) First-to-answer block: it is a good way to draw students' attentions. First, when a question is posted on the screen, students can click the icon to grab the chance to answer. This is called the "raise-your-hand" function. If the question is too difficult, the teacher will give certain clues or delete an option to lower the difficulty. Teachers can also use a specific function to choose one student to answer the question randomly, which is called the "shake-your-phone" function. While using the first function, it is the students who determine the results and in the second available function, it is the teacher who determines the results. Here are screenshots of first-to-answer block (Figure 4)

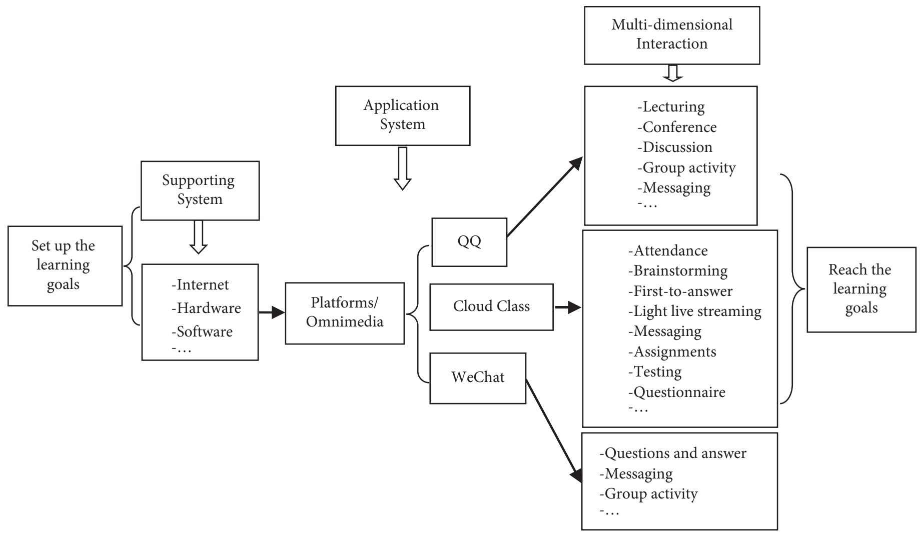

Figure 1: Multidimensional interaction design of online learning.

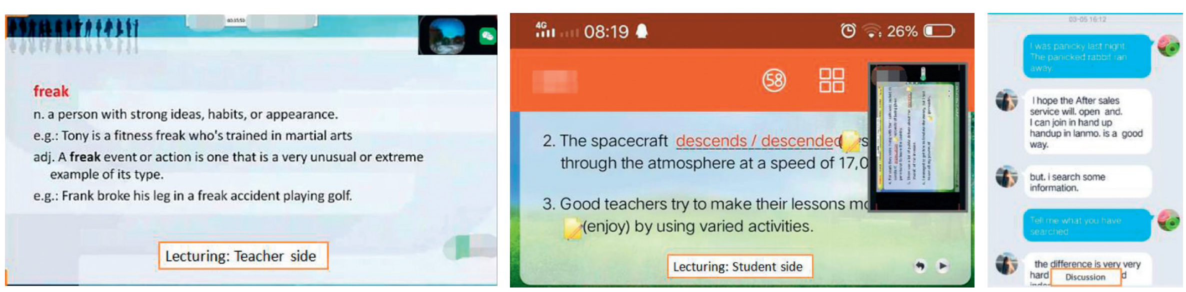

Figure 2: Screenshot of QQ platform interaction.

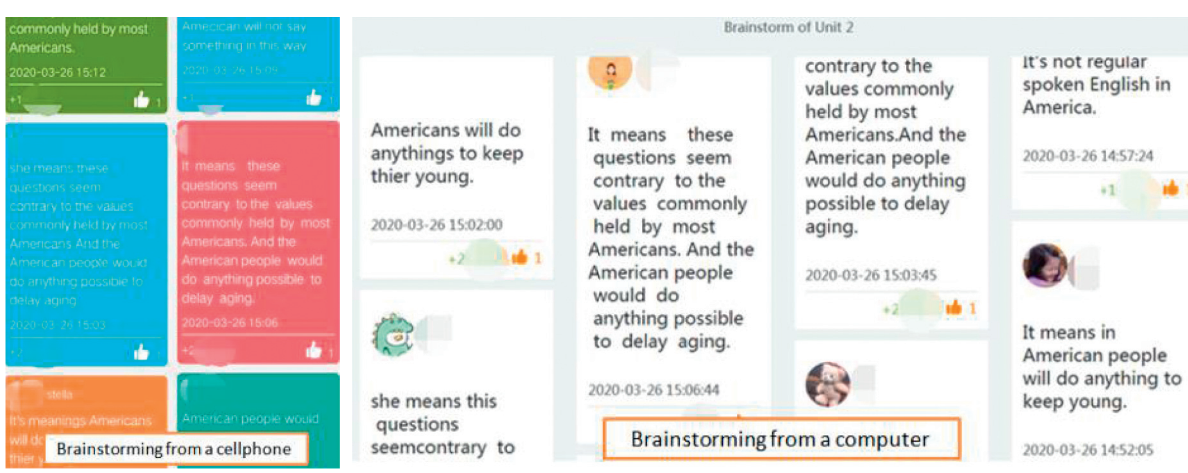

Figure 3: Screenshot of brainstorming on cellphone and computer screen.

(3) Light live streaming block: it, similar to live audio clips, allows teachers to provide short explanations of the course content to students, which lightens their study load and assists their understanding. Teachers are able to explain bit by bit until the students understand. These explanations can take the form of sound message, pictures, or videos. Typed text is seldom used because it is too slow. It can also be used as a discussion forum allowing students to post their ideas in tandem with the explanations. This is a very effective way to involve students in the discussion. Technically, it saves Internet flow of data. Screenshot is as shown in Figure 5.

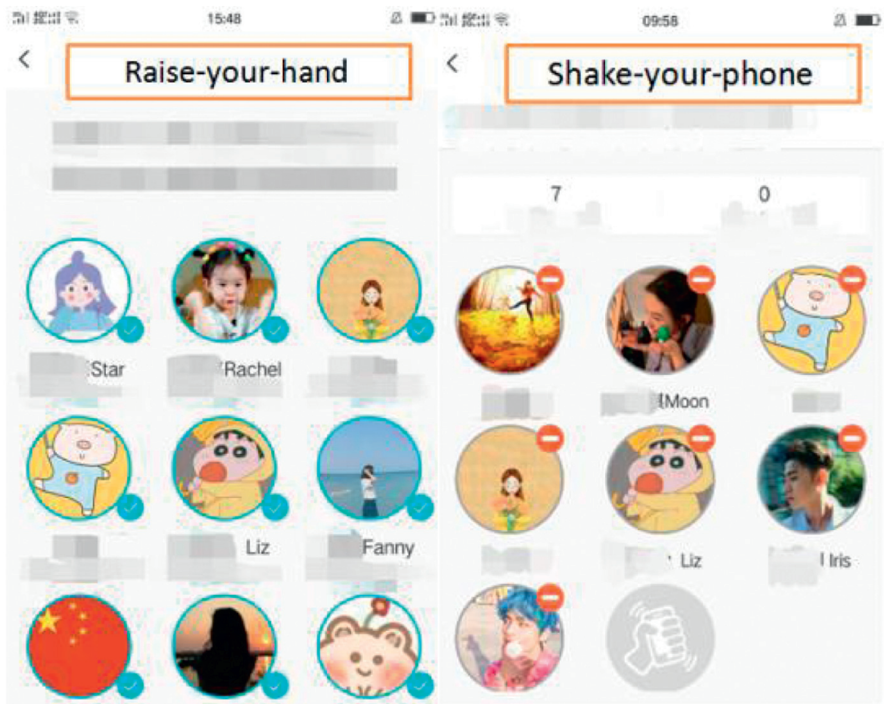

FIGURE 4: Screenshot of "first-to-answer" function.

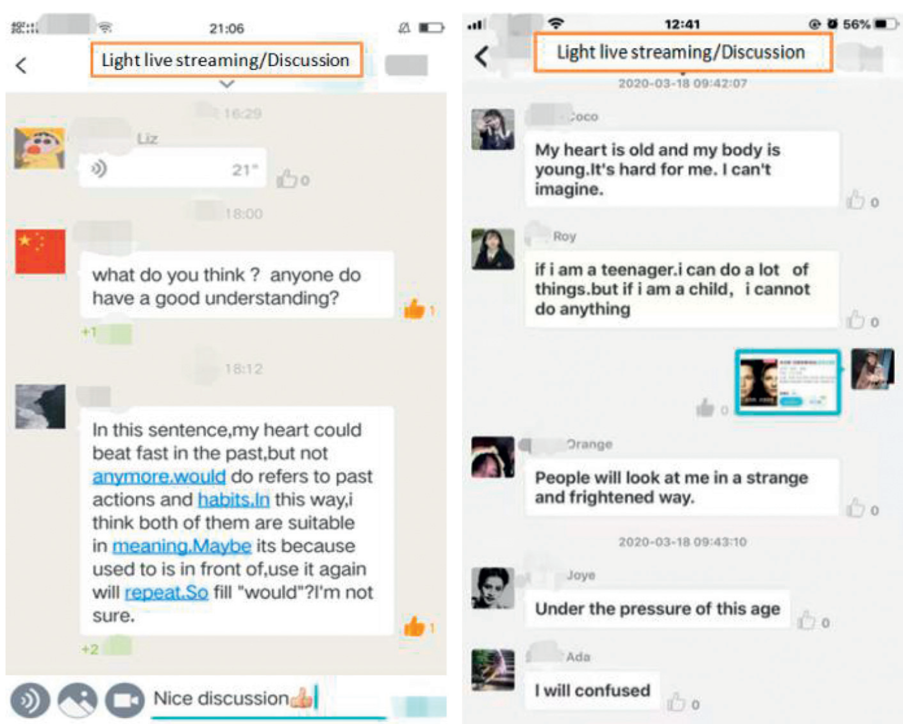

FIGURE 5: Screenshot of light live streaming and discussion.

(4) Messaging block. it is another way to interact and is mainly used outside of class. Teachers can post messages in the online bulletin board and inform or remind students when necessary. Words and text are most frequently used in this form of interaction and the important points can be also highlighted. Here are some examples of messaging block (Figure 6).

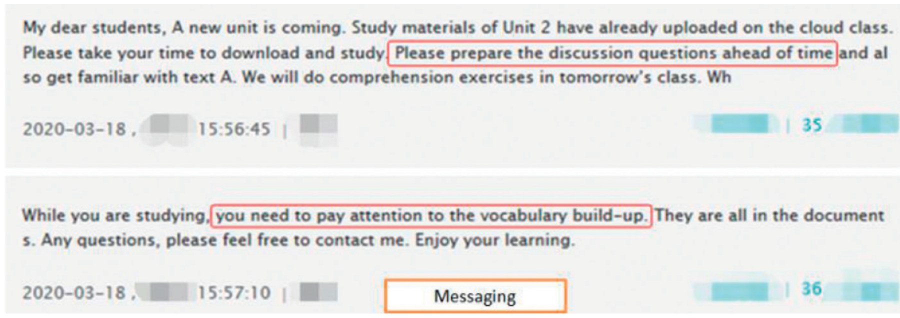

Figure 6: Screenshot of messaging block.

1.3.3. WeChat Platform. WeChat plays an important role as another form of connection between teachers and students outside of class. Not only is it easy to access, but it also allows students to ask questions or leave messages when needed. Moreover, the various lively formats make students and teachers express ideas quickly and effectively. The platform provides letters, characters, words, sound, symbols, audio, and videos and other mixed formats to enhance communication. Here is the WeChat screenshot (Figure 7).

Above are some typical multidimensional interaction examples from QQ, Lanmo Cloud Class, and WeChat platform. There are also other functions that aid interaction. Without any interruptions, words, pictures, sounds, audios, and videos are the main forms of the three-type interactions. It improves participation of teachers and students and embodies the superiority of omnimedia in assistance of online English teaching and learning.

1.4. Quasiexperiment Research. In order to understand and investigate students' feelings and attitudes toward online multidimensional interaction under the assistance of omnimedia, as well as its influence on online English teaching and learning, a self-made questionnaire has been designed. At the same time, we compared the results of students' final examination as a reference point. The questionnaire has been released by one of the most popular online platforms in China, Wen Juan Xing, and the data has been processed by SPSS 26.0.

1.4.1. Investigation of Questionnaire. 66 freshmen English major students have been sampled by random in an ordinary college of a central province in Chinese mainland. These students are English majors taking Integrated English Online Course during research. Multidimensional interaction under the assistance of omnimedia has been applied for experimental group (No. 36) and traditional method under the assistance of single platform for control group (No. 31). The students' score of College Entrance Examination has no significant differences. They were not aware of the experiment. The questionnaire has been designed by Likert classification of five levels with 16 questions in total. The collection rate of the questionnaire for the two groups was 97.22% and 100%, respectively. The 16 questions with responses are shown in Table 1.

The data above have been analyzed by the software of SPSS 26.0. T-test showed that, within the answers "completely agree" and "agree," experimental group (No. 35) has significant differences ($p = 0.44$, < 0.05) compared with the control group (No. 31). It indicated that multidimensional interaction brought different feelings and attitudes toward students' online study. Experimental students showed more acceptable attitudes toward this method. Students who held the neutral attitudes also have significant difference ($p = 0.000$, < 0.001), which means the control group students had more tendency to not care about the interaction or had no sense about interaction in online course. There were no significant differences between two groups in answering "disagree" and "completely disagree." It showed that very few students do not have influences despite the multidimensional interaction mode or traditional mode of online learning (Table 2).

Taking some points as examples, 74.29% experimental group students expressed that there were no big differences but 45.16% expressed that it had differences; 68.57% experimental students believed that, in the online class of multidimensional interaction mode, students can get more chances to open their mouth, whereas only 48.39% control group students feel they had chances to speak out; regarding "shake-your phone" and "raise-your-hand" of interaction, nearly 71.43% experimental group students expressed that they love the portion as they felt like involved in the group, while 54.84% control group had this feeling.

1.4.2. Final Examination Analysis. We used T-test to compare the final examination results between experimental group (No. 35) and control group (No. 31). Statistics showed that the two groups had significant differences ($p = 0.049$, < 0.05) (Tables 3 and 4).

It is clear that the final examination score of experimental group was higher than that of control group and the difference was significant ($p = 0.049$, < 0.05). It indicated that multidimensional interaction had improved students' learning results.

2. Discussion

The above research results show that multidimensional interaction with the assistance of omnimedia has a positive effect on online English learning. In the beginning, students

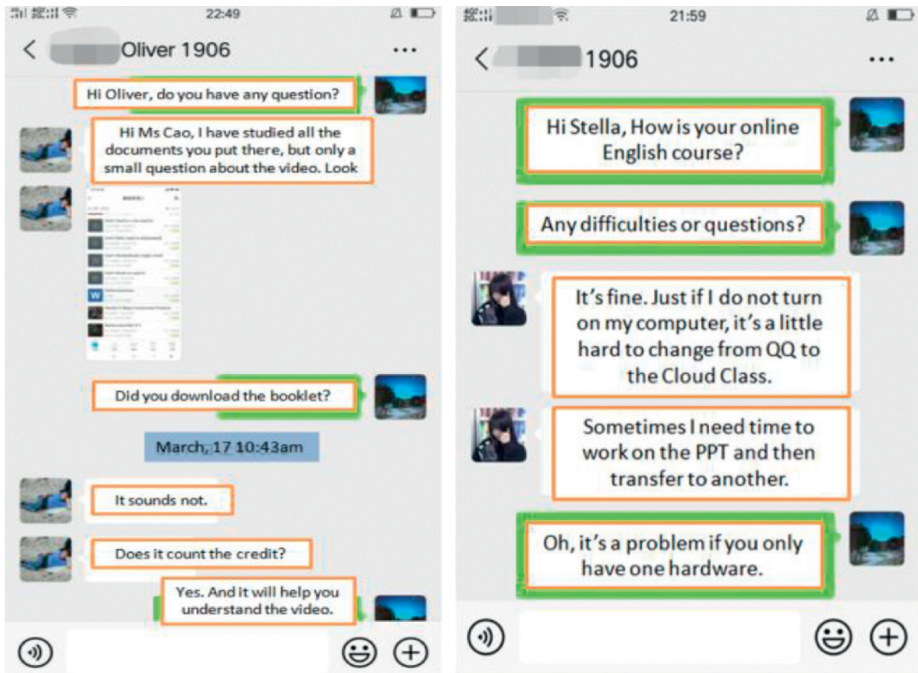

Figure 7: Screenshot of WeChat interaction.

are more concentrated on online English learning as a variety of functions in different platforms have been used. These platforms, which provided words, sounds, pictures, audios, videos, etc., play an important role in drawing students to join various online activities. This increases opportunities for student-teacher and student-student interactions which is comparable to or even exceeded that of offline learning. It also lets the individual students feel they have received more attention. As a result, multidimensional interaction arouses the students' enthusiasm for online learning. It also indicates that most students have a very positive response to the benefits of using online learning with the support of educators [25]. Furthermore, for shy students who tend to be passive, online learning helps them actively answer questions without worrying about other interruptions such as their facial complexion. Overall, shy students tend to speak out in online learning more than offline. The results have coincided with Buelow's et al. research that students just felt that it was a great way for shy students to speak up in online discussion [9]. Besides, online interaction gives students' deep impressions, for many students expose their oral English drawbacks when speaking. They also receive feedback directly from online interaction. When they send messages, they need to review and check the message they have sent, which help them realize their pronunciation drawbacks. Moreover, the final examination results from experimental group and control group have statistically significant differences, meaning that online student engagement has strongly verified the difference of their online learning [11]. For language learning, if students participate in the activities actively, they will have more chances to practice and improve their language competence, whereas those who do not take part in or have limitations to join the multidimensional interactions receive less chances to practice which resulted in lower grades. Although there are significant differences between experimental group and control group in the aspects of questionnaire and final examination, we still need to pay attention to those 30% experimental students who did not feel any superiority of online learning. This could be explained by the students adhering to their own methods to acquire knowledge. Besides, we should not ignore the fact that technology support is also one of the factors affecting students' online learning. As from previous WeChat conversation (Figure 7), students need to transfer from one platform to the other while learning, which is not quite convenient. As teachers, we need to pay more attention to the students' learning needs and learning process. Making good use of online learning superiority, we will improve students' online learning results.

2.1. Reflection. Multidimensional interaction with the assistance of omnimedia reasonably grasps the attention of students in online English teaching and makes the teaching more effective. In classes where multidimensional interaction has been implemented, students rate online learning as more favourable. Multidimensional interaction has a positive effect on the students' study results. Still, we need to pay attention to the following.

From technical aspect, Internet, hardware, and software are the foundation to support the online learning. Easily accessible human-technology interface will yield twice the result with the half effort. Along with technology development, both teachers and students should make good use of omnimedia network platform, especially the commonly used platforms to communicate interactively to improve teaching and learning results.

Table 1: Student survey questions and results (1 = experimental group and 2 = control group).

	Items	Results									
		Completely agree		Agree		Neutral		Disagree		Completely disagree	
		1	2	1	2	1	2	1	2	1	2
1	I was hesitant to speak up in class before, but online class has helped me overcome this fear	8	2	14	8	10	17	3	4	0	0
2	I really enjoy the student-teacher interactions in my English class as my teacher can directly pinpoint my challenges, which helps me remember them	7	5	18	12	9	14	1	0	0	0
3	I am excited during every English class as our teacher gives us many opportunities to participate in discussions	7	4	18	14	9	11	1	2	0	0
4	I think the group activities in the English classes are engaging and there is little difference between online and in-person formats. There is the added benefit of student-teacher evaluation	7	3	19	11	9	14	0	3	0	0
5	I love the debate portion of the English classes as I am supported by my team and I do not feel lonely	5	4	17	10	13	17	0	0	0	0
6	The biggest difference between English classes and other online classes is the additional opportunity to speak up	9	4	15	11	11	15	0	0	0	0
7	I jump at the opportunity to participate in Lanmo activities as they are interesting and vivid	8	6	16	14	11	10	0	1	0	0
8	I have learned more knowledge through online classes that I would not have learned if the class was in-person	5	3	16	9	12	17	2	2	0	0
9	I love the "first-to-answer" portion of the English class as I find it interesting	6	6	15	8	14	16	0	1	0	0
10	I like the value provided through Lanmo's resources and experiences because I would gain experience as long as I downloaded and studied the materials my teacher has uploaded	6	5	19	13	10	11	0	2	0	0
11	I would feel disappointed if I did not get the chance to speak up in my English class	1	1	8	10	21	17	4	3	1	0
12	I felt that my English oral communication skills have improved ever since starting online English classes	3	3	24	16	8	11	0	1	0	0
13	During the online classes only period, I had more time to manage my own study schedule and felt that my improvements are comparable with in-person classes	4	4	16	12	15	14	0	1	0	0
14	I love the brainstorming portion of the Lanmo classes as it allows us to creatively express our opinions	5	5	21	15	9	10	0	1	0	0
15	WeChat has played an important supporting role in online classes as I can directly and conveniently communicate my questions with the teacher privately	7	5	18	14	10	12	0	0	0	0
16	The "shake-your-phone" and "raise-your-hand" methods are also preferable ways to select participants as they resemble a real classroom setting	9	6	16	11	8	14	2	0	0	0

Table 2: *T*-test of experimental group (No. 35) and control group (No. 31).

Items	Groups	Mean	Std. deviation	Sig.
Completely agree and agree	Experimental group	22.94	4.250	0.044*
	Control group	19.75	4.328	
Neutral	Experimental group	11.19	3.331	0.000**
	Control group	15.94	3.473	
Completely disagree and disagree	Experimental group	0.88	1.455	0.331
	Control group	1.88	1.408	

*$p = 0.44$, < 0.05;** $p \leq 0.001$.

Table 3: Data of the final examination.

Groups	Numbers	Mean	Std. deviation	Std. error mean
Experimental	35	67.40	10.094	1.706
Control	31	62.68	8.852	1.590

Table 4: T-test of the final examination (95% confidence interval of the difference).

	t	Sig.	Mean difference	Std. error difference
Equal variances assumed	2.009	0.049*	4.723	2.351
Equal variances not assumed	2.025	0.047	4.723	2.332

*$p = 0.049$, < 0.05.

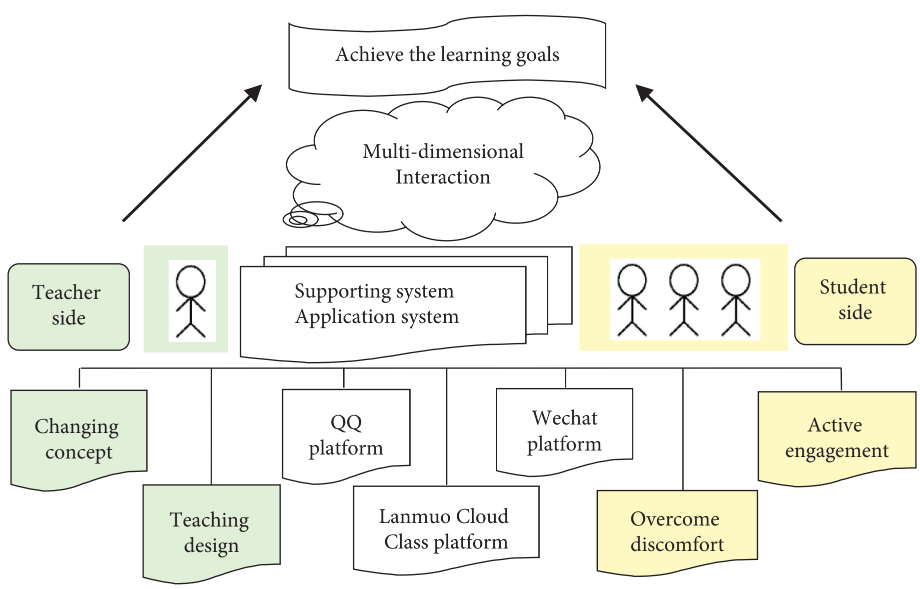

Figure 8: Research results.

From teaching aspect, teachers should diligently create teaching plans to implement online interaction more effectively in order to match the effectiveness of offline teaching. Online teaching should not be regarded as a burden. Teaching with personal bias or strictly adhering to conservative traditional teaching methods is not conducive toward effective online teaching.

For students, overcoming the inner discomfort of online learning and actively participating in the process of interactive learning will bring positive improvements to their online learning experience. Investigation shows that as long as students put enough passion into online learning, actively engage in class activities, and take part in the multidimensional interactions with teachers and classmates, they will realize significant gains from online education (Figure 8).

3. Conclusion

In summary, studying new technologies and conceptions, changing the outdated ideas and habits, and adapting to reformations in technology and education with open minds ultimately facilitate the embodiment of student-oriented teaching process for both students and teachers. This paper explores the teaching modes of online multidimensional interactive English teaching with the assistance of QQ, Lanmo Cloud Class, and WeChat platforms and has shown preliminary results. It helps students to actively engage in online English learning and achieve the satisfactory results. It perhaps opens a window for IT professionals to design more accessible systems for teachers and students and reach the goals of 5A. In the future, additional resources should be dedicated to studying student learning behaviours and processing and accumulating more experience for integrating technology into online-offline hybrid education.

Data Availability

Data sharing is not applicable to this article as no datasets were generated or analyzed during the current study.

Conflicts of Interest

The author declares no potential conflicts of interest with respect to the research, authorship, and/or publication of this article.

Acknowledgments

This study was supported by the Thirteenth Five-Year Plan of Shaanxi Province Education Science Project of 2020 "Study on the English Learning Process of Application-Oriented University Students Based on the Paradigm of PAD," Project no. SGH20Y1475.

References

[1] J. X. Liu, X. X. Wang, and J. Wei, "Effects of blended teaching of English audio-visual & speaking course in the "Internet Plus" environment---Sino-Us cross-culture EFL blended teaching class with real-time technology," *JournalTechnology Enhanced Foreign Language Education*, vol. 6, pp. 105–112+10, 2020.

[2] L. Yang, H. J. Zeng, and B. Y. Gao, "Research on the smart learning environment based on cloud computing," *Journal Modern Educational Technology*, vol. 11, pp. 26–32, 2018.

[3] H. L. Wang, "A probe into the teaching reform of translation major in the era of Cloud Computing," *Journal Theory and Practice of Contemporary Education*, vol. 6, pp. 61-62, 2016.

[4] X. F. Wang and J. B. Gao, "An English-Chinese Artificial Intelligence dictionary," *Shanghai Jiaotong University Press*, vol. 9, p. 18, 2019.

[5] S. A. S. insights, "Big Data Insights. Big Data: What it Is and Why it Matters," 2021SAS Institute Inc., 2021, https://www.sas.com/en_us/insights/big-data/what-is-big-data.html.

[6] D. Zou and H. R. Xie, "Vocabulary learning based on learner-generated pictorial annotations: using Big Data as learning resources," *J Sustainability*, vol. 13, p. 5767, 2021.

[7] L. Xiao, "Motivation of students autonomous learning in English MOOC teaching based on Big Data analysis," *Canadian Journal of Physics: Conference Series*, vol. 1881, no. 2, Article ID 022082, 2021.

[8] Y. Zhang, "Research on College English Online learning platform model based on big data technology," *Canadian Journal of Physics: Conference Series*, vol. 1648, Article ID 042090, 2020.

[9] J. R. Buelow, T. Barry, and L. E. Rich, "Supporting learning engagement with online students," *Journal of Online Learning*, vol. 4, pp. 313–340, 2018.

[10] C. H. Ding, "Research on the multi-dimensional and interactive SPOC blended teaching model," *Journal of Modern Educational Technology*, vol. 7, pp. 102–108, 2017.

[11] S. Mehall, "Purposeful interpersonal interaction in online learning: what is it and how is it measured?" *Journal of Online Learning*, vol. 1, pp. 182–204, 2020.

[12] Y. K. Wang and B. Liu, "A study on the practice of a blended academic English program for postgraduates," *Journal of Foreign Languages and Their Teaching*, vol. 5, pp. 10–19+147, 2019.

[13] Sociology Editorial Board of Encyclopedia of China, *Encyclopedia of China*, Encyclopedia of China Publishing House, Beijing, China, 1991.

[14] B. Z. Wang, Q. J. Guo, and D. H. Liu, *A Brief History of Education in China*, pp. 80-81, Beijing Normal University Publishing Group, Beijing, China, 2008.

[15] G. M. Moore, "Editorial: three types of interaction," *American Journal of Distance Education*, vol. 2, pp. 1–7, 1989.

[16] A. S. Palinscar and A. L. Brown, "Reciprocal teaching of comprehension-fostering and comprehension-monitoring activities," *Journal of Cognition and instruction*, vol. 2, pp. 117–175, 1984.

[17] D. Fu, X. Feng, and Y. Wang, "Application of multi-dimensional interactive online teaching method in the course teaching of "Mechatronics System Design and Practice"," *Journal of Research in Higher Education of Engineering*, vol. 1, pp. 193–196, 2021.

[18] X. Zhou, "The Effect of Multi-dimensional interaction on L2 vocabulary acquisition," *Journal of Modern Foreign Languages*, vol. 5, pp. 647–660, 2018.

[19] X. Y. Bao and Z. L. Liang, "Research on mobile teaching model based on WeChat platform," *Journal of Microcomputer Applications*, vol. 12, pp. 73–77, 2019.

[20] J. Zhou and D. Chen, "The exploration of adults online education models in omnimedia environment," *Journal of Heilongjiang Researches on Higher Education*, vol. 3, pp. 81–84, 2015.

[21] Z. T. Zhu and H. C. Peng, "Omnimedia learning ecology: a practical solution to cope with schooling difficulties during a large-scale epidemic," *Journal of China Educational Technology*, vol. 3, pp. 1–6, 2020.

[22] Ministry of Education of the People's Republic of China, "Statistical Bulletin of the National Education Development in 2018," 2019, https://www.moe.gov.cn/jyb_sjzl/sjzl_fztjgb/201907/t20190724_392041.html.

[23] L. Kazanidis, N. Pellas, P. Fotaris, and A. Tsinakos, "Facebook and Moodle integration into instructional media design courses: a comparative analysis of students' learning experiences using the community of inquiry (CoI) model," *International Journal of Human-Computer Interaction*, vol. 34, no. 10, pp. 932–942, 2018.

[24] H. L. Gao and Y. Y. Qiao, "Online computer course teaching design based on Tencent and Cloud Class platforms," *Journal of Computer Education*, vol. 11, pp. 58–61, 2020.

[25] M. Maskun, T. Rusman, S. Suroto, and F. Rahmawati, Student perceptions of online learning," *International Journal of Multicultural and Multireligious Understanding*, vol. 2, no. 7, pp. 67–73, 2020.

Hindawi
Scientific Programming
Volume 2021, Article ID 7615227, 7 pages
https://doi.org/10.1155/2021/7615227

Research Article

Analysis of the Mental Health of Urban Migrant Children Based on Cloud Computing and Data Mining Algorithm Models

Juan Li

Shandong Management University, School of Arts, Jinan, Shandong 250357, China

Correspondence should be addressed to Juan Li; lijuan_smu@163.com

Received 19 August 2021; Accepted 3 September 2021; Published 16 September 2021

Academic Editor: Punit Gupta

With the rapid development of internet technology, the amount of data generated is also increasing day by day. As a kind of distributed computing, cloud computing has been widely used in the analysis of massive data. With the development of China's economic construction, the integration of urban and rural areas is constantly improving, and the migrant children in the city are also focused on. After moving into the city, migrant children not only face the pressure from the society but also face the pressure from life, which inevitably affects the physical and mental health of urban migrant children. The education of urban migrant children is also a focus that needs attention. How to integrate into the education environment of urbanization and adjust the learning pressure in the process of education is also worthy of our attention. Therefore, this article analyzes the current status of urban migrant children's mental health based on cloud computing and data mining algorithm models. Based on the current research status of urban migrant children and the standards of mental health, this paper conducts a survey of middle and high school students in a certain city through questionnaires, then builds a data mining algorithm model to analyze the survey data, and explores the differences in the grades of students' social identity and the differences in mental health between migrant children and urban children. According to the survey, most of the psychological performances of urban migrant children are very vague. At the same time, there are also some phenomena such as poor adaptability, bad mood, and inferiority complex. During the study period, there are situations such as unwilling to communicate with others, weariness, sensitivity, anxiety, and hostility. The overall incidence of the situation is relatively high in big cities, while the situation of urban children is relatively small.

1. Introduction

Cloud computing is a kind of virtualization technology. In addition to powerful computing power and scalability, it also has the characteristics of high flexibility, high reliability, and on-demand deployment. In recent years, the rapid development of information technology has also promoted the development of cloud computing by leaps and bounds. In scientific research, building algorithm models based on cloud computing can greatly improve research efficiency [1, 2]. In the process of my country's rapid transformation from the traditional economic development model, labor from rural areas has gradually poured into big cities, and most of them are in the family model, bringing young children to the city. According to the data of the sixth national census, in the previous 10 years, the floating population in the city increased greatly, compared with the fifth national census, and there is a very obvious growth trend [3, 4]. Therefore, migrant children have become a huge group in the city [5, 6].

Because there is a big difference between the daily life of modern urban people and that of rural people in China, mobile children, as the second generation of immigrants, passively flow into the city. In daily life, learning, social environment adaptation, and other aspects, mobile children are constantly adjusting their own psychological environment, but in this process, they will experience some confusion, frustration, and loss. Because of the change of the education mode and the influence of bad family environment, it is easy to cause poor communication with peers under the trend of communication and psychological state [7, 8]. In recent years, the mental health problems of migrant children in China's cities have gradually been concerned. Some migrant children are in puberty, which is also out of the rebellious stage. In the face of so many puzzles at this critical moment, whether they can sort out their emotional and psychological problems, bear the pressure brought by the mobile life, and adapt to the environment will have a great impact on the future development and mental health of migrant children. The formation of personality has an important impact [9, 10].

The purpose of this article is to study the mental health of urban migrant children, conduct a questionnaire survey of middle and high school students in a certain city, and then establish a data mining algorithm model in a cloud computing environment, so as to analyze the survey data and differentiate the students from their grades. Look at the changes in the psychological status of urban migrant children [11, 12].

2. Data Mining Algorithm Model Construction Based on Cloud Computing

2.1. Cloud Computing Platform. Cloud computing platforms can be divided into three categories: cloud storage platforms that focus on data storage, cloud computing platforms that focus on data processing, and comprehensive cloud computing platforms that take into account both computing and data storage and processing [13, 14].

As a leading cloud service provider in China, Alibaba Cloud has high stability and practicability and has been widely recognized by users. Compared with international competitors, Alibaba Cloud has a relatively strong price advantage with almost the same computing power [15]. Therefore, this article chooses Alibaba Cloud as the cloud computing platform for research.

2.2. K-Means Clustering Algorithm Model. The number of migrant children in cities is increasing year by year. Due to many reasons such as environmental inadaptability, their mental health problems deserve our attention [16]. Conducting research on urban migrant children to find out the factors that cause their mental health problems can provide parents, teachers, and functional departments with a theoretical basis for solving their psychological problems, so as to better protect this group and enable urban migrant children to grow up healthily [17]. *K*-means algorithm is a classic clustering algorithm for unsupervised learning, which has the advantages of simple thinking, good effect, and easy implementation. It is scientific and practical to analyze the mental health of urban migrant children through the *K*-means algorithm model [18, 19].

(1) Algorithm idea:

Divide n samples into k clusters, and then according to the distance formula or other similarity calculation formulas, the other points in the sample are divided into the nearest cluster; then, calculate the average of all objects in the cluster as the new center point. Iterate repeatedly until the objective function converges.

(2) Algorithm definition:

$$P = \{p_1, p_2 \ldots, p_n\}. \tag{1}$$

$$f(pi, pj) = \sqrt{\left(p_{i1} - p_{j2}\right)^2 + \cdots + \left(p_{in} - p_{jn}\right)^2}. \tag{2}$$

$$\varepsilon_i = \frac{1}{n} \sum_{p \in w_i} p. \tag{3}$$

$$F = \sum_{i=1}^{z} \sum_{p \in w_i} \left|p - n_i\right|^2. \tag{4}$$

(3) Algorithm process:

Selection of the k value:

In the traditional *K*-means algorithm, the number of clusters k is required to be determined in advance, but in practice, it is often difficult to determine the value of k due to the large amount of data and lack of experience. If the value of k is selected too small, it will result in data objects to vary greatly in the same cluster. If the value of k is selected too large, the difference between different clusters will be small. At the same time, improper selection of the k value will also make the final clustering result fall into the local optimum. This paper selects 10 factors that can reflect the mental health of urban migrant children, such as obsessive-compulsive disorder, depression, and anxiety, as a clustered dataset.

Selection of cluster center c:

The steps of selecting cluster centers: first, calculate the maximum value $a1$ and minimum value $b1$ in the sample set, and record where they appear, and then calculate the average rounding to get the cluster center $c1$. Then, remove the maximum value $a1$ and minimum value $b1$, select the approximate maximum value $a2$ and minimum value $b2$ to obtain the cluster center $c2$, and so on; finally, $P = \{c_1 \oplus c_2 \oplus \cdots \oplus c_n\}/n$.

Calculate the distance between the sample and the center: calculate the distance between the sample $P = \{p_1, p_2 \ldots, p_n\}$ and the center c, and divide p_i closest to the center c into the corresponding clusters.

(4) Model establishment:

(a) First, enter the survey data of urban migrant children's mental health problems, check the validity of the data, and normalize the data to ensure the accuracy and reliability of the data. The normalization formula is as follows:

$$H = \frac{Hi - H\min}{H\max - H\min}. \tag{5}$$

(b) Classify the data to ensure that the classified data have strong similarity.
(c) Add the classified 10 groups of data to LSTM for training, and use the powerful time-series feature extraction ability of the LSTM neural network to obtain the feature data of urban migrant children's mental health.
(d) Use the improved K-means algorithm to perform clustering and output the classification results.

Definition 1. Define the dataset that needs to be clustered, as shown in the following formula:

Definition 2. (similarity calculation formula). Here, the Euclidean distance formula is selected as the similarity calculation formula, as shown in the following:

Definition 3. Cluster center point, as shown in the following formula:

Definition 4. Convergence conditions, as shown in the following formula:

3. Survey on the Mental Health of Urban Migrant Children Based on Cloud Computing and Data Mining Algorithms

This article uses a questionnaire survey method to conduct research. The questionnaire survey method mainly refers to a scientific exploratory research method that is generally used to collect information by publishing questions to students in writing. The researcher lists the questions that need to be discussed, fills in the content in the form of face-to-face answers or follow-up interviews, and then collects, sorts out, and comprehensively analyzes the questionnaire to obtain a large amount of data which are closely related to this question and information.

3.1. Research Purpose. It is of great significance to promote the development and improvement of the mental health to urban migrant children. Under the tense pace of life in the city, different children will also face different psychological pressures, which will change children's cognition. How to deal with the possible problems of peer discrimination, inferiority complex, and communication difficulties between families is particularly important. These problems also have a great influence on the formation of children's future personality. From the perspective of social work, it is the most important work to improve the mental health of migrant children.

3.2. Questionnaire Design

3.2.1. Research Object. According to the survey of two schools in a city, this paper randomly selected the reports of two different grades in junior high school and senior high school. According to the reports of these 352 students, the questionnaire is made. After the link was generated, the head teachers shared it with the class group, and the students filled in it anonymously. A total of 330 valid questionnaires were submitted by the two grades; there were 105 questionnaires for migrant children and 95 questionnaires for urban children; there were 65 questionnaires for migrant children in senior one and 64 questionnaires for urban children.

3.2.2. Research Tools

(1) Social identity form:

The social identity of children is investigated by single topic selection. The paper adopts the single question: "you think you are: 1. Rural people. 2. Urban people. 3. Don't know," and through such a questionnaire, we investigate the status of urban migrant children on their own identity.

(2) Self-rating scale of mental health of middle school students in China:

The method used in this scale is five-point scoring, which is divided into 1–5 levels, each of which represents the following: from scratch, occasionally, sometimes, often, and always. It consists of 60 research projects and 10 factors, each of which contains 6 factors. The 10 factors were compulsive symptoms, depression, anxiety, paranoia, interpersonal tension and sensitivity, hostility, learning and stress, psychological disorder, poor adaptability, and out of control. Each factor reflects the following:

① Compulsive symptoms: these symptoms mainly show whether the subjects repeatedly check and count during the homework, always fear that their test results pass, and other unnecessary assumptions and unnecessary forced symptoms
② Depression: depression is mainly the subjects feeling monotonous about life, disappointment, and helplessness to their future and prone to negative emotional experience such as crying and psychological upset
③ Anxiety: anxiety is mainly reflected in the subjects who often show emotional depression and feel very upset, resulting in poor sleep, psychological imbalance, and anger
④ Paranoia: the main problems are feeling that others often say their own bad words behind the back, resulting in unwillingness to communicate with others, feeling that others are wrong in doing anything, others are always targeting themselves because they are foreign people, and they want to bully themselves
⑤ Deal with tension and sensitivity in relationships: the main characteristics reflected by this factor are that the subjects generally think that others do not want to communicate with themselves and despise themselves, and they are always not understood, demanding and blaming others,

believing that others are not friendly to themselves, and are easily hurt by them emotionally

⑥ Hostility: the main feature is that the subjects cannot control their temper, and there is an impulse to smash things, which can easily cause the excitement and quarrel with others

⑦ Study pressure: it shows that the subjects cannot adapt to the change of the learning mode and feel the difficulty of learning, the pressure is great, they are afraid of teachers, the situation of weariness of learning, the dislike of doing homework, and the fear and boredom of the test

⑧ Psychological imbalance: the main performance is that the subjects think that teachers and parents will look at themselves differently, and they will feel that other children are better, often compare themselves with other students, and other problems

⑨ Poor adaptation: the main problems of this factor are that the subjects cannot adapt to school life, teachers' teaching methods, and school environment, contact with more new things, and are unwilling to communicate with people and participate in other extracurricular activities

⑩ Emotional imbalance: the emotional imbalance mainly refers to the subject's emotion which is easy to fluctuate and unstable, which is reflected in the study, which means that the students' attitude towards teachers, classmates, and parents is unstable and changeable

The main evaluation indexes of the mental health self-evaluation scale are as follows: The average score of 10 factors was below 2, indicating that the mental health was very good; the mental health status was mild in 2–2.99; in 3–3.99, it indicates that there are some problems in mental health status; between 4 and 4.99, it indicates that mental health problems are serious and need to be dealt with as soon as possible; if it is 5 points, it means that mental health problems are very serious and should be paid great attention to.

3.2.3. Data Processing. Use SPSS 13.0 for data management and statistical analysis. First, use exploratory analysis to filter the suspicious data so that the complex data can be kept true. Second, analyze the variance of the remaining data, and visually compare the data.

3.2.4. Reliability of the Questionnaire. In order to test the reliability and stability of the questionnaire, firstly, the variance of the questionnaire results was calculated, and then the reliability of the returned questionnaire was tested by the method of "half-half reliability." Using formulas (6)–(8) to calculate the reliability coefficient, the correlation coefficient of the questionnaire is $q = 0.883$. According to the theories and methods of modern scientific research, when the reliability of a test reaches 0.80 or more, it can be regarded as a test with higher reliability. The test results confirm that the questionnaire is reliable.

$$C^2 = \frac{(F - x_1)^2 + (F - x_2)^2 + (F - x_3)^2 + \cdots + (F - x_n)^2}{n}, \tag{6}$$

$$q = 1 - \frac{C^2 (1 - q_1)}{C_n^2}, \tag{7}$$

$$q = \frac{2q_1}{1 + q_1}. \tag{8}$$

4. Research Results and Discussion

4.1. Differences in Social Identity. In order to better understand the real situation of urban migrant children in different grades, this paper analyzes the three levels of social identity of urban migrant children, and the results are shown in Table 1 and Figure 1: there are 65 junior high school students who think they are rural people, accounting for 32.34% of the total number of junior high school students in the survey, 41 junior high school students who think they are urban people, accounting for 20.4% of the total number of junior high school students in the survey, and 95 students with vague identification, accounting for 47.26% of the total number of junior high school students in the survey. There are 24 senior high school students who think they are rural people, accounting for 18.61% of the total number of senior high school students. There are 37 senior high school students who think they are urban people, accounting for 28.38% of the total number of senior high school students. There are 68 senior high school students who have vague identification, accounting for 53.1% of the total number of senior high school students.

It can be seen that the level of social identity of migrant children in different grades is different, as shown in Figure 1. The characteristics are as follows: the migrant children in the first grade of junior high school think that they are rural people more than those in the first grade of senior high school; that is, with the growth of children's age, this concept will decline. The migrant children in grade one are higher than those in grade one in urban identity; that is, with the growth of grade, the identity of urban people is on the rise. In terms of unclear identity, the migrant children in grade one of junior high school think that they are rural people, lower than those in senior high school.

4.2. Differences in Mental Health between Migrant Children and Urban Children. In order to study the difference in mental health between urban children and migrant children, the independent sample t-test method was used to compare the total average mental health scores and ten factors of urban migrant children and urban children. The results in Table 2 indicate the following: Migrant children and urban children have differences in emotional processing and interpersonal relationship processing, migrant children will show sensitivity, anxiety, paranoia, hostility, psychological imbalance, and learning pressure, but there is no significant statistical difference between the

Table 1: Grade differences in social identity.

	Rural identity		City people identity		Not clear	
	Frequency	Percentage	Frequency	Percentage	Frequency	Percentage
First grade	66	33.15	45	22.38	89	44.47
High school	27	20.77	33	25.38	70	53.85

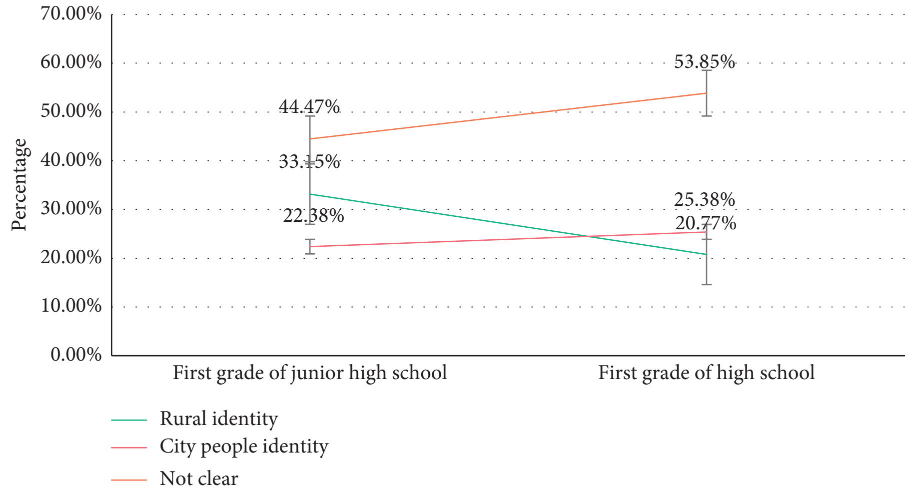

Figure 1: Grade differences in social identity.

total average score. It can be seen from Figure 2 that the total average score of migrant children in maladjustment, emotional imbalance, interpersonal tension and sensitivity, anxiety, paranoia, hostility, psychological imbalance, and learning pressure is higher than that of urban children, which also shows that the mental health of migrant children is lower than that of urban children to a certain extent, and the mental health of urban children is better.

4.3. Analysis of Migrant Children's Mental Health

(1) Lower self-esteem level:

In actual life, migrant children have no way to express their self-esteem clearly, but they will show a sense of loss when their self-esteem is hurt. With the growth of their age, it is possible that those acts of discrimination and hurting their self-esteem will make their body and mind suffer a great deal, leading to the increase of their sense of inferiority and the emergence of psychological problems. Migrant children, because they are still young and immature, tend to imagine themselves as they say, which is easy to confuse their own positioning and has a great impact on the correct self-cognition [20, 21]. To sum up, self-esteem is the basic component of self-cognition to urban migrant children, which reflects a correct positioning and cognition of the individual. Self-esteem refers to the individual itself, which does not include the individual's sensory and evaluation of others, but may be affected by the evaluation from others. Self-esteem is an important form of the development of good mental health. People with strong self-esteem tend to show their own advantages and can naturally accept their own disadvantages. Maintaining high self-esteem is more conducive to the formation of good self-worth, and they can live a positive and enthusiastic life.

(2) Social maladjustment:

Migrant children move from the countryside to the city, especially in the first-tier cities such as Beijing and Shanghai. As the economic level and lifestyle of cities are very different from those of rural areas, differences in living environment will affect migrant children. They will affect them in a subtle way. When migrant children are deeply influenced by the material life of the city, they will imagine a real city person to live like that and learn to accept all this, and their thoughts will become urbanized. Due to the differences in culture, lifestyle, values, and so on, migrant children will need to adapt to these changes through self-regulation when they feel these changes and constantly change their behavior, ideas, and so on, so as to make them better adapt to the rhythm of the city. This process can be defined as the process of adapting to the society. When migrant children perceive the impact of urban culture, they may have a sense of frustration and inferiority, such as being excluded and loneliness rising. Then, they will have psychological discomfort, and their social adaptation will also be biased one after another.

(3) Sensitive discrimination:

From the perspective of the discriminated, discrimination is mainly a phenomenon produced by

Table 2: Differences in mental health between migrant children and urban children.

	Migrant children $M \pm SD$	City children $M \pm SD$	t	p
Maladaptation	1.97 ± 0.63	1.86 ± 0.57	1.932	0.057
Emotional imbalance	2.09 ± 0.66	2.05 ± 0.75	0.568	0.571
Obsessive-compulsive symptoms	2.02 ± 0.58	2.04 ± 0.61	−1.031	0.312
Interpersonal tension and sensitivity	1.91 ± 0.61	1.85 ± 0.63	1.049	0.301
Depression	1.82 ± 0.62	1.83 ± 0.63	−0.198	0.837
Anxiety	1.92 ± 0.76	1.91 ± 0.73	0.382	0.707
Paranoia	1.83 ± 0.65	1.82 ± 0.61	0.601	0.562
Hostility	1.77 ± 0.67	1.76 ± 0.68	0.468	0.641
Psychological imbalance	1.73 ± 0.64	1.69 ± 0.59	0.858	0.387
Study-induced stress	1.91 ± 0.51	2.12 ± 0.82	0.049	0.958

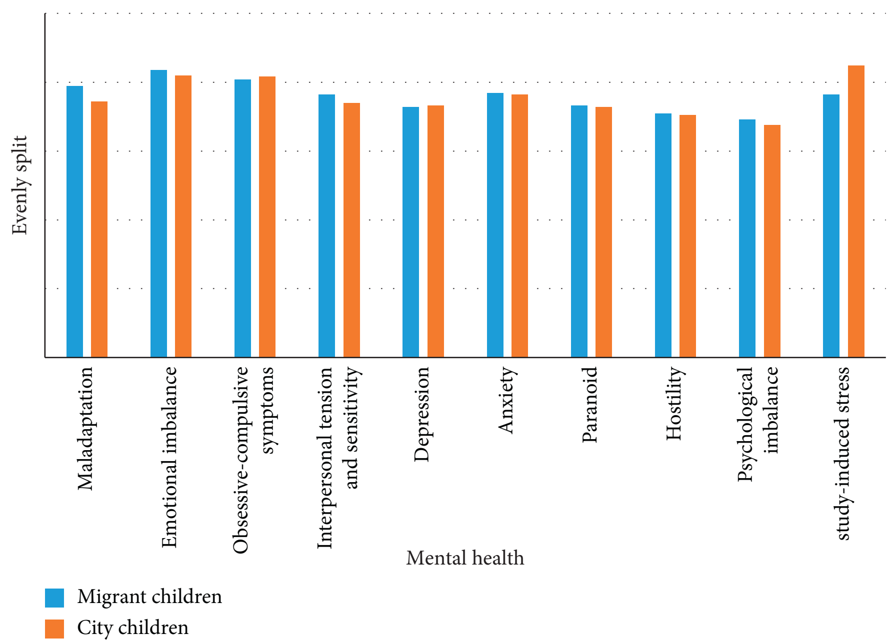

Figure 2: Differences in mental health between migrant children and urban children.

perception. The discriminated can obviously feel the negative impact and the harm brought by discrimination. It is very unfair to treat a person with this perception of discrimination. It is a very unreasonable social system. The manifestation of discrimination may be expressed by actual action, which is very harmful to a person. If urban migrant children encounter discrimination or exclusion, it will cause great harm to them physically and mentally.

5. Conclusions

After the above research, we can draw the following conclusions. From the questionnaire survey, it is found that the problem of unclear social identity of migrant children in this city is universal and ambiguous. There is no significant difference in the ten factors of mental health between urban migrant children and urban children. However, urban migrant children will have sensitivity, anxiety, paranoia, hostility, psychological imbalance, learning pressure, and other problems in adaptability, emotional processing, and interpersonal relationship, and the total average score will be greater than that of urban children, which indicates that the mental health of urban children is better than that of migrant children. We need to help migrant children adapt to the new environment from the heart and accept the new environment, including new culture, new customs, new campus, and new life. Only when they accept the new environment from the heart can they better adapt to the environment and develop better in the city.

Data Availability

Data sharing is not applicable to this article as no datasets were generated or analysed during the current study.

Conflicts of Interest

The author declares that there are no conflicts of interest.

Acknowledgments

This paper is the periodic research results of “Research on the Construction of Relief System for Difficult Children in Shandong Province from the Concept of Multiple Co-governance” (project no. 2020VC12028), a Key Scientific Research Project of Colleges and Universities in Shandong Province in 2020.

References

[1] A. Umer, B. Nazir, and Z. Ahmad, “Adaptive market-oriented combinatorial double auction resource allocation model in cloud computing,” *The Journal of Supercomputing*, vol. 16, no. 1, pp. 1–11, 2021.

[2] G. Baranwal and D. P. Vidyarthi, “A truthful and fair multi-attribute combinatorial reverse auction for resource procurement in cloud computing,” *IEEE Transactions on Services Computing*, vol. 12, no. 6, pp. 851–864, 2019.

[3] L. Ban, S. Guo, R. W. Scherpbier, X. Wang, H. Zhou, and L. J. Tata, “Child feeding and stunting prevalence in left-behind children: a descriptive analysis of data from a central and western Chinese population,” *International Journal of Public Health*, vol. 62, no. 1, pp. 143–151, 2017.

[4] C. Lämmle, O. Wartha, S. Kobel, T. Wirt, A. Kelso, and C. Kutzner, “Intervention effects of the school-based health promotion program “join the healthy boat” on motor abilities of children with migration background,” *Health*, vol. 09, no. 3, pp. 520–533, 2017.

[5] C. W. Pan, B. Shi, H. Zhong, J. Li, and Q. Chen, “The impact of parental rural-to-urban migration on children’s refractive error in rural China: a propensity score matching analysis,” *Ophthalmic Epidemiology*, vol. 27, no. 1, pp. 1–6, 2019.

[6] T. Liu, K. Holmes, and J. Albright, “Urban teachers’ perceptions of inclusion of migrant children in the Chinese educational institution: a comparative study,” *International Journal of Inclusive Education*, vol. 19, no. 9, pp. 1–15, 2016.

[7] J. Fang, “Research on the family language education for migrant children in northwest China: based on the sample of xi’an city,” *Educational Sciences: Theory and Practice*, vol. 18, no. 5, 2018.

[8] K. Antia, J. Boucsein, A. Deckert, P. Dambach, J. Račaitė, and G. Šurkienė, “Effects of international labour migration on the mental health and well-being of left-behind children: a systematic literature review,” *International Journal of Environmental Research and Public Health*, vol. 17, p. 4335, 2020.

[9] A. G. Larsen, “Protection or Participation?: editorial evaluation of two news serials concerning irregular migrant children,” *Journalism Practice*, vol. 11, no. 7, pp. 1–16, 2016.

[10] Q.-F. Dong, D.-K. Chen, and T. Wang, “Urban community structure detection based on the OD of traffic analysis zones,” *Modern Physics Letters B*, vol. 33, no. 13, Article ID 1950164, 2019.

[11] G. Baranwal and D. P. Vidyarthi, “A fair multi-attribute combinatorial double auction model for resource allocation in cloud computing,” *Journal of Systems and Software*, vol. 108, pp. 60–76, 2015.

[12] A. B. Zaslavsky, C. Perera, and D. Georgakopoulos, *Sensing as a Service and Big Data in International Conference on Advances in Cloud Computing*p. 219, ACC-2012, Bangalore, India, 2012.

[13] S. R. Chandra and Y. Wang, “Cloud things construction—the integration of internet of things and cloud computing,” *Future Generation Computer Systems*, vol. 56, no. C, pp. 684–700, 2016.

[14] F. Liang, Y. Quan, A. Wu et al., “Insulin-resistance and depression cohort data mining to identify nutraceutical related DNA methylation biomarker for type 2 diabetes,” *Genes and Diseases*, vol. 8, no. 5, pp. 669–676, 2021.

[15] S. He, D. Luo, and K. Guo, “Analysis of factors affecting the coordinated development of urbanization and the ecological resource environment in southwest China based on data mining,” *Journal of Urban Planning and Development*, vol. 147, no. 3, pp. 71–88, 2021.

[16] Z. Wang, X. Lin, and X. Hou, “Urban adaptation of migrant children and influencing factors-an overview of research in the past 20 Years,” *Journal of Beijing Normal University: Social Science Edition*, vol. 2, pp. 37–46, 2016.

[17] Y. Zhang, A. Du, and Y. Zhou, “The relationship between migrant children’s perception of discrimination and urban adaptation: the multiple mediating effects of social support and identity integration,” *China Special Education*, vol. 8, pp. 55–60, 2017.

[18] T. H. Sardar and A. Anrisa, “An analysis of map reduce efficiency in document clustering using parallel K-means algorithm,” *Future Computing and Informatics Journal*, vol. 3, no. 2, pp. 200–209, 2018.

[19] K. Mostafa, A. Attallab, and T. Hegazy, “Data mining of school inspection reports to identify the assets with top renewal priority,” *Journal of Building Engineering*, vol. 41, no. 3, pp. 99–111, 2021.

[20] G. N. Lima and M. Lombardo, “Urban climatology in Brazil: an analysis based on the methodology of the urban climate system,” *Environment Conservation Journal*, vol. 20, no. 1&2, pp. 1–8, 2019.

[21] J. Gartner, D. B. Larson, and G. D. Allen, “Religious commitment and mental health: a review of the empirical literature,” *Journal of Psychology & Theology*, vol. 19, no. 1, pp. 6–25, 2018.

Hindawi
Scientific Programming
Volume 2021, Article ID 5018917, 8 pages
https://doi.org/10.1155/2021/5018917

Research Article

Model Construction of Enterprise Financial Early Warning Based on Quantum FOA-SVR

Wen-Tsao Pan,[1] Yi Liu,[2] Huan Jiang,[3] Ya-Ting Chen,[3] Ting Liu,[3] Yan Qing,[1] Guo-Hui Huang,[1] and Rong Li[4]

[1]*School of Economics and Management, Hunan University of Science and Engineering, Yongzhou, China*
[2]*School of Management, Guangzhou Huashang College, Guangzhou, China*
[3]*School of Electronics and Information Engineering, Hunan University of Science and Engineering, Yongzhou, China*
[4]*School of Foreign Languages, Hunan University of Science and Engineering, Yongzhou, China*

Correspondence should be addressed to Yi Liu; 619193220@qq.com

Received 2 August 2021; Accepted 30 August 2021; Published 15 September 2021

Academic Editor: Punit Gupta

The sudden outbreak of COVID-19 has a great impact on human life security and global economic development. To deal with the rampant pandemic, many countries have taken strict control measures, including restricting gathering in public places and stopping the production of enterprises; as a result, many enterprises suffered great challenges in survival and development during the pandemic. In order to help enterprises monitor their own financial situation and realize their healthy development under the pandemic, this paper constructs an Enterprise Financial Early Warning Model, in which Quantum Rotation Gate is used to optimize four algorithms, namely, Fruit Fly Optimization Algorithm (QFOA), Bee Colony Optimization Algorithm (QABC), Particle Swarm Optimization (QPSO), and Ant Colony Optimization (QACO). The results show that the ability of the prediction model can be greatly improved by using the Quantum Rotation Gate to optimize these four algorithms.

1. Preface

At present, under the influence of the epidemic, many enterprises have experienced management problems. Therefore, financial early warning has become an important mean for companies to make risk predictions. In order to solve the problem of the lack of effective early warning measures and means for corporate financial risk management, Liu [1] analyzed the basic connotation and causes of marine corporate financial risk and proposed a marine corporate financial risk prevention and control strategy based on the marine economy. Tang [2] put forward some suggestions to better strengthen risk warning based on the forecast of Qingdao marine economy and pointed out that by developing future financial risk assessment models and establishing a sound financial warning mechanism, companies can effectively provide early warning.

Affected by COVID-19, the whole economic market has a tendency to stagnate, and many enterprises face the pressure of tight cash flow, supply chain interruption, and general decline of market supply and demand. Under the background of global economy facing deep recession crisis, the role of financial early warning is particularly important. First, the financial data of 250 enterprises in 2018 and 2019 are collected, and then Quantum Rotation Gate is used to optimize four algorithms, namely, Fruit Fly Optimization Algorithm [3], Bee Colony Optimization Algorithm [4], Particle Swarm Optimization [5], and Ant Colony Optimization [6]. Then, the parameters of SVR neural network are optimized by these optimized algorithms. Afterward, the Financial Early Warning Model is constructed. Finally, the error convergence trend chart and ROC curve of the four models are generated, and the first group of data formed an error narrative statistical table obtained by tests repeated 100 times. The results show that the four algorithms combined with Quantum Rotation Gate can effectively reduce the prediction errors and improve the accuracy and effectiveness of financial early warning.

So far, there are many relevant studies on Quantum Rotation Gate Optimization Swarm Intelligence Algorithm. Mao et al. [7] proposed a hybrid algorithm of Quantum Particle Swarm Optimization and Ant Colony Optimization through the study of glass cutting problem. The research results show that the APSO-ACO algorithm is an effective method to solve glass cutting problems because of its strong optimization ability. Zhao [8] proposed a cloud computing resource scheduling method based on the improved Quantum Particle Swarm Optimization. Through the analysis of its performance through simulation experiments, it is shown that the method can effectively improve the utilization rate of cloud computing resources. Wang [9] proposed an improved multipopulation quantum genetic algorithm and introduced a new Quantum Rotation Gate in the evolution of the algorithm. The research results show that the algorithm has better optimization performance than conventional quantum genetic algorithm and multi-population genetic algorithm. Wu et al. [10] proposed a quantum genetic algorithm to optimize the extreme learning machine. They compared the simulation results of ELM and QGA-ELM on datasets, which showed that QGA-ELM can effectively improve the classification accuracy of ELM networks. Yan and Ye [11] proposed a Hybrid Grasshopper Optimization Algorithm based on quantum computing and carried out simulation experiments, computational complexity analysis, and global convergence proof of the algorithm. The research shows that the Hybrid Grasshopper Optimization Algorithm has stronger global search ability and better convergence accuracy. Guo et al. [12] proposed Quantum Particle Swarm Optimization Based Patch-Graph Sparse Optimization for Large Array. This method is combined with QPSO algorithm. Compared with the traditional Patch-Graph Sparse Optimization, the global search ability is improved and the convergence speed is accelerated. Their simulation results show that the method is effective.

The structure of this paper is as follows: the first section briefly introduces the background and literature review; the second section describes the research methods of this paper; the third section analyzes the verification process and research findings; and the fourth section provides conclusions and suggestions.

2. Research Methods

2.1. Quantum-Optimized Fruit Fly Optimization Algorithm (QFOA). In terms of Quantum Coding Optimization of FOA, the fly position dimension is $3L * 2$, in which 3 represents the three parameters of the SVR model, L represents the number of bits that each parameter needs to be expressed as a binary code, and 2 means two of the quantum gates. The position of Drosophila is the [0,1] range of the zone coordinates.

(1) Fruit fly position initialization: Randomly set a fly position $p0$ within the defined domain, and use a uniform distribution method to randomly generate popsize fruit fly positions.

(2) Move: Find the current optimal fruit fly position "p," and set $p0 = p$.

(3) Release: Take $p0$ as the center and use a uniform distribution method to randomly generate new popsize positions of fruit flies.

(4) Measure the position of the fruit fly code:

In the quantum spin gate, qubits $|0>$ and $|1>$ represent the two base states of tiny particles. According to the principle of superposition, the superposition state of quantum information can be expressed as a linear combination of these two fundamental states; namely, $|\psi \geq a|0\rangle + ß|1\rangle$, where a and $ß$ are complex numbers, representing the probability amplitude of the qubit state, which, respectively, represent the probability that the quantum state $|\psi>$ collapses to the $|0>$ state and $|1>$ state due to measurement and meet the normalization conditions.

In the Quantum Fruit Fly Algorithm, fruit flies use the probability amplitude of qubits for encoding. The encoding scheme is as follows:

$$P_i = \left[\begin{vmatrix} \cos(\theta_{i1}) \\ \sin(\theta_{i1}) \end{vmatrix}\begin{vmatrix} \cos(\theta_{i2}) \\ \sin(\theta_{i2}) \end{vmatrix}\begin{matrix} \Lambda \\ \Lambda \end{matrix}\begin{vmatrix} \cos(\theta_{ik}) \\ \sin(\theta_{ik}) \end{vmatrix}\right], \tag{1}$$
$$\theta_{ij} = 2\pi \times \text{RAND}, \quad i = 1, 2, \ldots n, j = 1, 2, \ldots k.$$

θ is the phase of the qubit, n is the number of fruit flies, k is the number of qubits, which means the dimension of the solution space, and RAND is a random number in the range [0,1]. Each qubit is divided into upper and lower rows, corresponding to the probability amplitudes of the two quantum basic states and satisfying the normalization condition. Therefore, each individual contains two upper and lower cultural coding chains, each of which is a candidate solution to the optimization problem. It can be seen that the Quantum Fruit Fly Algorithm has twice the number of candidate solutions of the Fruit Fly Algorithm when the population size remains unchanged, which increases the diversity of the understanding space and improves the probability of successful optimization.

When measuring the code of fruit flies, the square of each bit of the code is calculated so as to get its binary code.

$$\mathbf{t}_{\text{id}} = \begin{cases} 1, & \text{if } (x_{\text{id}})^2 < \text{RAND}, \\ 0, & \text{if } (x_{\text{id}})^2 \geq \text{RAND}. \end{cases} \tag{2}$$

(5) Convert binary code to decimal decision variable, which means converting the binary code of each decision variable to get the decimal value of the decision variable we need.

(6) Calculate the value of the objective function: Calculate the objective function of the fruit fly position.

(7) Quantum Rotation Gate: The Quantum Rotation Gate is used to change the phase of the qubit to

update the probability range of the qubit, so as to achieve the effect of fruit fly coding mutation. For the operation mode of quantum revolving gate, please refer to [13].

$$\begin{bmatrix} \alpha_i' \\ \beta_i' \end{bmatrix} = \begin{bmatrix} \cos_{\theta i} & -\sin_{\theta i} \\ \sin_{\theta i} & \cos_{\theta i} \end{bmatrix} \begin{bmatrix} \alpha_i \\ \beta_i \end{bmatrix}. \quad (3)$$

2.2. Quantum-Optimized Bee Colony Algorithm (QABC). In terms of Quantum Coding Optimization of Bee Colony Algorithm, the bee position dimension is $3L * 2$, in which 3 represents the three parameters of the SVR model, L represents the number of bits that each parameter needs to be expressed as a binary code, and 2 means two quantum gates. Each dimension range of bee position is the [0,1] range interval of regional coordinates.

(1) Initialization of bee position: Use random initialization of bee position.

(2) Employment stage: A honey bee corresponds to a honey source. The honey bee corresponding to the i^{th} honey source searches for a new nectar source according to the following formula:

$$x_{\text{id}}' = x_{\text{id}}' + \varphi_{\text{id}} \left(x_{\text{id}} - x_{\text{kd}} \right). \quad (4)$$

(3) Selection and wait-and-see phase:

The newly generated possible solutions are

$$x_i' = \{ x_i', x_i', \ldots, x_{i\,D}' \}. \quad (5)$$

The original solutions are $x_i = \{ x_{i1}, x_{i2}, \ldots, x_{i\,D} \}$.

Make comparisons, and use a greedy selection strategy to retain better solutions. Each observation bee selects a nectar source based on probability, and the probability formula is

$$P_i = \frac{\text{fit}_i}{\sum_{j=1}^{SN} \text{fit}_j}. \quad (6)$$

Among them, fit_i is the fitness value of the possible solution X_i. For the selected nectar source, the observation bee searches for new possible solutions according to the above probability formula.

(4) Investigation phase: When all honey bees and observer bees have searched the entire search space, and if the fitness value of a nectar source is not increased within a given step (defined as the control parameter "limit"), then the nectar source is discarded, and the honey bee corresponding to the nectar source becomes a scout bee to search for new possible solutions using the following formula:

$$x_{\text{id}} = x_d^{\min} + r \left(x_d^{\max} - x_d^{\min} \right). \quad (7)$$

(5) Measuring the position of the bee code: In quantum computing, qubits $|0\rangle$ and $|1\rangle$ represent the two basic states of microscopic particles. According to the Principle of Superposition, the superposition state of quantum information can be expressed as the linear combination of two basic states; namely, $|\psi\rangle \ = a\rangle \ \text{e}0\rangle \ +ß\rangle \ e1\rangle$, where a and $ß$ are complex numbers, representing the probability amplitudes of the qubit state, in which the sum, respectively, represents the probability that quantum state $|\psi\rangle$ collapses t $|o0\rangle$ and $|1\rangle$ state due to measurement and satisfies the normalization conditions.

In the Quantum Bee Colony Algorithm, bees use the probability amplitude of qubits for encoding. The encoding scheme is as follows:

$$P_i = \left[\left| \begin{matrix} \cos(\theta_{i1}) \\ \sin(\theta_{i1}) \end{matrix} \right| \left| \begin{matrix} \cos(\theta_{i2}) \\ \sin(\theta_{i2}) \end{matrix} \right| \begin{matrix} \Lambda \\ \Lambda \end{matrix} \left| \begin{matrix} \cos(\theta_{ik}) \\ \sin(\theta_{ik}) \end{matrix} \right| \right],$$
$$\theta_{ij} = 2\pi \times \text{RAND}, \quad i = 1, 2, \ldots n, j = 1, 2, \ldots k. \quad (8)$$

Θ is the phase of the qubit, n is the number of bees, k is the number of qubits, which means the dimension of the solution space, and RAND is the random number in the range of [0,1]. Each qubit is divided into two lines, up line and down line, corresponding to the probability amplitudes of the two quantum fundamental states, and satisfies the normalization condition. Therefore, each individual contains two cultural coding chains, each of which is a candidate solution to the optimization problem. The results show that the number of candidate solutions of Quantum Bee Colony Algorithm is twice as large as that of Swarm Algorithm, which can increase the diversity of solution space and improve the probability of success.

When measuring the code of honey bee, the square of each bit of the code of X_i is calculated.

$$t_{\text{id}} = \begin{cases} 1, & \text{if } (x_{\text{id}})^2 < \text{RAND}, \\ 0, & \text{if } (x_{\text{id}})^2 \geq \text{RAND}, \end{cases} \quad (9)$$

so as to get its binary code.

(6) Binary code conversion to decimal decision variable: Convert the binary code of each decision variable to obtain the decimal value of the decision variable we need.

(7) Quantum Rotation Gate: The Quantum Rotation Gate is used to change the phase of the qubit to update the probability range of the qubit, so as to achieve the effect of bee encoding mutation.

$$\begin{bmatrix} \alpha_i' \\ \beta_i' \end{bmatrix} = \begin{bmatrix} \cos_{\theta i} & -\sin_{\theta i} \\ \sin_{\theta i} & \cos_{\theta i} \end{bmatrix} \begin{bmatrix} \alpha_i \\ \beta_i \end{bmatrix}. \quad (10)$$

2.3. Quantum-Optimized Particle Swarm Optimization (QPSO). The steps of Quantum Coding Optimization of Particle Swarm are as follows:

(1) Set quantum particle algorithm parameters.
(2) Initialize the particle swarm position.
(3) Because the position and velocity of the particle cannot be determined together in quantum space, the wave function *f(x,t)* is used to describe the state of the particle.
(4) Get the probability density function of particles appearing at a certain point in space by solving Schrodinger equation.
(5) The position equation of the particles is obtained by random simulation of Monte Carlo method:

$$x(t) = P \pm \frac{L}{2}\ln\left(\frac{1}{u}\right), \tag{11}$$

where u obeys a uniformly distributed random number on [0,1]; $L(t+1) = 2\beta|\text{mbest}-X(t)|$ is determined. Finally, the evolution equation of the Quantum Particle Algorithm is

$$\begin{aligned} \text{mbest} &= \frac{1}{M}\sum_{i=1}^{M} P_i \\ &= \left(\frac{1}{M}\sum_{i=1}^{M} P_{i1} \cdots \frac{1}{M}\sum_{i=1}^{M} P_{i\,D}\right), \\ P_{\text{id}} &= \phi^* P_{\text{id}} + (1-\phi)^* P_{g\,d}. \end{aligned} \tag{12}$$

2.4. Quantum-Optimized Ant Colony Algorithm (QACO)

(1) Initialize pheromone and heuristic values: Initialize the pheromone intensity of each side and the taboo table of each ant in advance. The pheromone on each edge is initialized to a smaller value *r*0; for each ant, a taboo table is needed to record the nodes that it has passed, and its taboo table is initialized to the node where the ant is located. The length of taboo table is *I*, and the amount of pheromone released by the ants on each side is initialized to 0.
(2) Initialize quantum gate: In quantum computing, qubits |0> and |1> represent the two basic states of microscopic particles. According to the principle of superposition, the superposition state of quantum information can be expressed as a linear combination of these two basic states; namely, $|\psi\rangle = a\rangle\ |0\rangle + ß|1\rangle$, in which a and $ß$ are complex numbers representing the probability amplitude of the qubit state and the sum, respectively, represents the probability that the quantum state $|\psi\rangle$ collapses to $|0\rangle$ and $|1\rangle$ states due to measurement and satisfies the normalization condition. Assign values to a and $ß$ of each qubit $1/\sqrt{2}$ to complete the initialization.
(3) Construct a path: Each ant selects the next node to reach under the constraint of the taboo table according to certain probability rules until a legal path is finally formed. The ant determines the city to be reached next according to a certain probability. The probability is calculated as follows:

$$P_{\text{ij}}(t) = \begin{cases} \dfrac{\left[\tau_{ij}{}^{(t)}\right]^{\alpha}\left[\eta_{ij}\right]^{\beta}\left[\mu_j\right]}{\sum_{k\in\text{allowed}}\left[\tau_{ik}(t)\right]^{\alpha}\left[\eta_{ik}\right]^{\beta}\left[\mu_k\right]} & \text{if } j \in \text{allowed}\, 0, \end{cases} \tag{13}$$

where the pheromone intensity between node i and node j is $[\tau_{ij}(t)]^{\alpha}$, the heuristic value intensity between node i and node j is η_{ij}, and μ_j is the quantum information intensity of node j, which is defined as

$$\mu_j = \frac{1}{\left|\alpha_j\right|^2}, \tag{14}$$

where α_j is the amplitude of the j^{th} quantum gate.

The formula of (1) represents the probability that the ant chooses city *j* from city *i* at time *t*. *a* is the weight of the pheromone in the probability calculation, and the greater its value, the more important the role the pheromone will play in choosing the next city to be visited by the ant. *ß* is the weight of the heuristic factor (usually expressed as the reciprocal of *d* in the TSP problem) in the probability calculation, and the greater its value, the more important the role of the heuristic factor in the process of choosing cities by ants. *allowed* is a collection of cities that are not in the ant taboo list.

The formula of (1) shows that the ants will not choose the cities in the taboo list, so as to ensure the legality of understanding.
(4) Calculate the intensity of quantum information:

$$\mu_j = \frac{1}{\left|\alpha_j\right|^2} \tag{15}$$

where j is the quantum information intensity node and α_j is the amplitude of the j^{th} quantum gate.
(5) Calculate the path length generated by each ant, which is the sum of the length of each side in the path.
(6) Quantum Rotation Gate.
(7) Update pheromone: The pheromone is volatilized from each side, and then the pheromone released by the ants is obtained according to the length of the path produced by each ant. After all ants have completed the pheromone update, record the current shortest path, initialize the taboo table and the pheromone increment value $\triangle T(t,\ t+l)$, and proceed to step 2. Repeat this cycle until the final condition of the Algorithm is satisfied; for example, the solution cannot be further improved or the specified number of cycles is reached.

Table 1: Descriptive statistics of sample data in 2019 and 2018.

				2019					
Var	$X1$	$X2$	$X3$	$X4$	$X5$	$X6$	$X7$	$X8$	$X9$
N	250	250	250	250	250	250	250	250	250
Max	207.50	398.12	96.43	1217.11	3335.51	1126.42	18.49	17.95	3983
Min	−1909.0	−10472	−220.8	−118.87	−17362.4	−473.82	0.03	0.03	4.26
Avg	−36.81	−114.05	31.12	−4.58	−110.23	4.26	2.32	1.87	79.04
Std	422.41	7166.78	7.34	210.31	13580.29	110.99	0.09	0.07	991.44
				2018					
Var	$X1$	$X2$	$X3$	$X4$	$X5$	$X6$	$X7$	$X8$	$X9$
N	250	250	250	250	250	250	250	250	250
Max	169.34	157.28	94.30	876.30	3108.42	1000.28	18.70	17.18	1879.04
Min	−922.79	−890.59	−72.85	−1419.9	−348922.74	−1419.9	0.07	0.04	4.74
Avg	−9.89	−12.84	27.21	−2.62	−2019.64	0.28	2.19	1.81	54.61
Std	90.32	87.30	4.87	141.52	4941745.15	144.56	0.06	0.05	140.41

$$\tau_{ij}(t+1) = \rho\tau_{ij}(t) + \Delta\tau_{ij}(t, t+1), \quad (16)$$

where $\tau_{ij}(t+1)$ represents the pheromone on the edge ij during t iterations. ρ is the pheromone maintenance factor, and $1-\rho$ is the pheromone volatilization factor. $\Delta\tau_{ij}(t, t+1)$ is the sum of the pheromones released by all ants on the edge ij, as in (16).

$$\Delta\tau_{ij}(t, t+1) = \sum_{k=1}^{m} \Delta\tau_{ij}^{k}(t, t+1), \quad (17)$$

where ij belongs to all feasible paths.

Finally, this research uses the same four algorithms, QPSO, QFOA, QABC, and QACO, to optimize the parameter *gamma* and C of the SVR, which greatly improves the predictive ability of the Financial Early Warning Model.

3. Empirical Analysis

3.1. Sample Data and Variables. Considering the demand of sample size, the impact of various factors in 2018 and 2019 on 250 companies in different industries (including 75 crisis companies and 175 normal companies) is studied in this paper. There are nine influencing factors: return on net assets ($X1$), net profit margin ($X2$), gross profit margin ($X3$), shareholder equity growth rate (X4), net profit growth rate ($X5$), net asset growth rate ($X6$), current ratio ($X7$), quick ratio ($X8$), and asset-liability ratio ($X9$). Taking into account the diversity of data, the maximum, minimum, average, and variance of each influencing factor are calculated for the 250 sets of data in 2019 and 2018 in Table 1, so as to compare the differences in financial warning data in the past two years more visually.

3.2. Using Quantum Swarm Intelligence to Optimize SVR Steps. First, in the QFOA optimization of SVR, select the financial early warning data and set the Fruit Fly Optimization Algorithm parameters; then, initialize the position of the fruit fly swarm, taking $p0$ as the center, and the method of uniform distribution is applied, randomly generating new popsize positions of fruit flies. The positions of fruit flies code are measured, and the binary code is converted into a decimal decision variable. Then, the objective function value is calculated, and the qubit phase is changed by Quantum Rotation Gate. Finally, the error is calculated by SVR. In terms of quantum swarm SVR optimization SVR, by employing bees, greedy selection, wait-and-see, reconnaissance, and other stages, the quantum revolving gate is used to change the phase of the qubit and measure the fitness of the swarm. Please refer to relevant literature for details. In the aspect of Quantum Particle Swarm Optimization SVR using SVR, the particle probability density function is obtained by solving the Schrodinger equation, and finally the error is obtained by SVR. Please refer to the relevant literature for details. In the aspect of quantum ant colony using SVR to optimize SVR, each ant constructs a legal path according to a certain probability rule, then calculates the quantum information intensity, calculates the transition probability, and updates the path, that is, calculates the length of the path generated by each ant. Then, use the Quantum Rotating Gate to measure whether the ant colony search is completed. Please refer to the relevant literature for details.

3.3. Result Analysis. According to the convergence trend graph of the four model errors calculated by ESM in Figure 1, QFOA-SVR converges earlier than the other three algorithms, indicating that the algorithm has reached the optimal algorithm. After reaching the optimal algorithm, it can be seen from the trend graph that the QFOA is better than the other three algorithms. The algorithm is more stable, indicating that the QFOA is highly stable. Using Matlab software, the last 50 sets of data in 2018 and 2019 are, respectively, fixed as test data, and the first 200 sets of data are sample; then, repeatedly run QFOA, QABC, and QABC 100 times. After running the four algorithms of QACO and QPSO, count the maximum, minimum, average, variance, and total running time of five indicators of absolute errors, and get the error table that has repeated 100 times, Table 2. It can be seen in the table that the average value of QFOA is smaller than the average of the other three algorithms, indicating that the neural network of QFOA has smaller financial forecast errors than the other three algorithms, and the predicted results are more accurate.

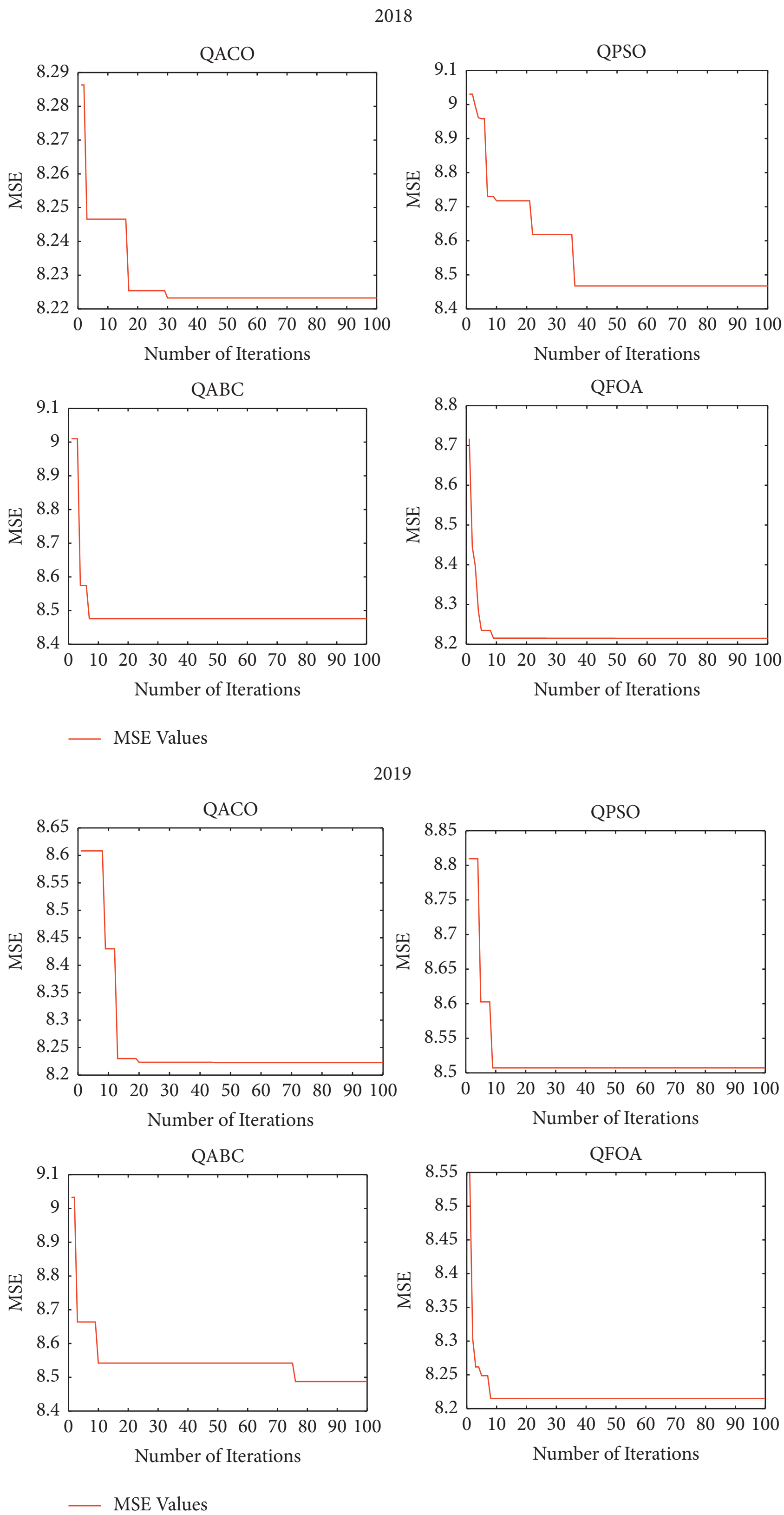

Figure 1: Convergence trend diagram of the four models.

Table 2: Descriptive statistics repeated one hundred times.

	Particular year	Max	Min	Avg	Std	Total time (s)
QABC	2018	1.071907	0.000052	0.273969	0.066597	24.7
	2019	1.054144	0.000044	0.295520	0.062692	23.9
	Particular year	Max	Min	Avg	Std	Total time (s)
QACO	2018	1.065305	0.000037	0.232538	0.058119	21.8
	2019	0.979081	0.000364	0.274045	0.046896	20.7
	Particular year	Max	Min	Avg	Std	Total time (s)
QPSO	2018	1.065305	0.000037	0.229276	0.059667	15.4
	2019	0.866827	0.001849	0.275428	0.045227	13.9
	Particular year	Max	Min	Avg	Std	Total time (s)
QFOA	2018	1.048369	0.001652	0.228247	0.057383	14.9
	2019	0.946589	0.000247	0.274033	0.048588	13.6

Table 3: ROC curve analysis results.

2019	QFOA	QPSO	QACO	QABC	2018	QFOA	QPSO	QACO	QABC
AUC	0.677	0.671	0.623	0.648	AUC	0.701	0.699	0.661	0.664
Gini	0.354	0.342	0.246	0.296	Gini	0.402	0.398	0.322	0.328
Sens	0.43	0.418	0.304	0.43	Sens	0.447	0.461	0.368	0.408
Spec	0.924	0.924	0.942	0.865	Spec	0.954	0.937	0.954	0.92

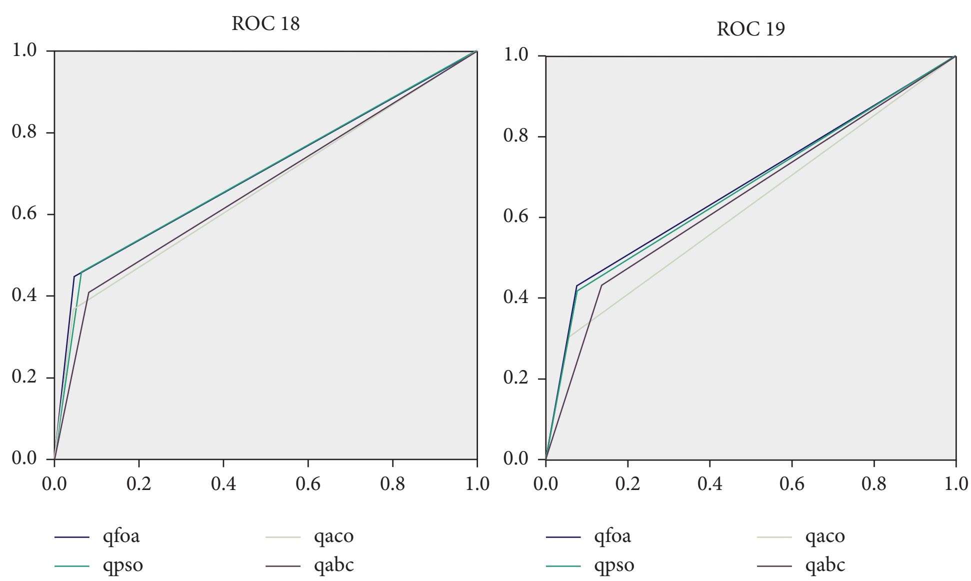

Figure 2: ROC curves of the four models.

It can be seen from Table 3 that the variance of QFOA is smaller than that of the other three algorithms, indicating that the QFOA is the most stable among the four algorithms. In terms of the total time, it can be seen that the QFOA runs for less time compared with the other three algorithms, which indicates that the responsiveness of the Fruit Fly Optimization Algorithm is more sensitive, but the five indicators calculated by the four algorithms are relatively small, and the difference is slight, because we use quantum optimization of four algorithms at the same time; the stability, accuracy, and sensitivity of the optimized algorithm have been greatly improved. The ROC curve and table for 2018 and 2019 are drawn with the SPSS software. Figure 2 is the ROC curve circle, and Table 3 is the ROC table. The ROC table includes clarity, sensitivity, area under the curve, and Gini Coefficient. From the ROC curve and ROC table in 2018, it can be seen that the area, AUC value (0.677), and Gini Coefficient (0.354) of the QFOA are large, indicating that the QFOA is the most accurate of the four algorithms. The sensitivity (0.43) and specificity (0.924) are the highest in QFOA, indicating that the QFOA is more sensitive and responds faster. Moreover, from the ROC curve and ROC table in 2019, the conclusions are the same. Based on the ROC curve of two years, it can be concluded that the QFOA is the one with the most accurate prediction and most sensitive response among the four algorithms.

4. Conclusions and Recommendations

The main contribution of this paper lies in the use of a relatively new Quantum Rotation Gate to optimize algorithms, namely, Fruit Fly Optimization Algorithm, Particle Swarm Optimization, Swarm Optimization Algorithm, and Ant Colony Optimization Algorithm. The results of the study show that the ROC curve is obtained by iterative trend graphs, repeated test data, and ROC curves. In this paper, we find that the Quantum Fruit Fly Optimization Algorithm and the optimized SVR Financial Early Warning Model are superior to the other three algorithms in convergence speed, optimization stability, and financial early warning stability. In addition, it is found that the four models are very close to each other in terms of convergence rate, model stability, and prediction error. Therefore, the Quantum Rotation Gate is superior in the ability to optimize the four algorithms. Therefore, it is suggested that Fruit Fly Optimization Algorithm can be used to optimize SVR to construct Financial Early Warning Model in the future. In this paper, we use Quantum Rotation Gate to optimize the four algorithms, and propose other methods to optimize the four algorithms in the future, such as chaos theory or wavelet theory.

Data Availability

The datasets used and/or analyzed during the current study are available from the corresponding author on reasonable request.

Ethical Approval

Written approval for the publication of this paper was obtained from the Hubei University of Arts and Science and all authors.

Conflicts of Interest

The authors declare no potential conflicts of interest with respect to the research, authorship, and/or publication of this article.

Acknowledgments

This research was funded by the Hunan Philosophy and Social Science Foundation Project no. 20YBA121.

References

[1] X. F. Liu, "Financial risk and financial early warning of marine enterprises based on marine economy," *Journal of Coastal Research*, vol. 112, pp. 177–179, 2020.

[2] Y. Tang, "Financial risk and early warning based on Qingdao marine economic forecast," *Journal of Coastal Research*, vol. 112, pp. 195–198, 2020.

[3] W. T. Pan, "A new fruit fly optimization algorithm: taking the financial distress model as an example," *Knowledge-Based Systems*, vol. 26, pp. 69–74, 2012.

[4] D. Karaboga, *An Idea Based on Honey Bee Swarm for Numerical Optimization*, Technical Report-TR06, Erciyes University, Kayseri, Turkey, 2005.

[5] J. Kennedy and R. Eberhart, "Particle swarm optimization," in *Proceedings of the IEEE International Conference on Neural Networks*, pp. 1942–1948, Perth, Australia, November 1995.

[6] M. Dorigo and T. Stutzle, *Ant Colony Optimization*, MIT Press, Cambridge, MA, USA, 2004.

[7] L. Mao, K. Tong, M. M. Shen, and H. W. Dong, "Research on solving glass cutting problem based on swarm intelligence algorithm," *Computer Engineering*, vol. 15, pp. 171–173, 2010.

[8] L. Zhao, "Cloud computing resource scheduling based on improved quantum particle swarm optimization," *Journal of Nanjing University of Technology*, vol. 2, pp. 223–228, 2016.

[9] H. Wang, "An improved multi population quantum genetic algorithm," *Journal of Zhongkai Agricultural Engineering College*, vol. 4, pp. 40–45, 2017.

[10] Y. R. Wu, H. Wang, and J. H. Li, "Extreme learning machine optimization algorithm for data classification," *Software guide*, vol. 6, pp. 10–13, 2019.

[11] X. Yan and C. M. Ye, "Hybrid grasshopper optimization algorithm for job shop scheduling problem," *Computer engineering and applications*, vol. 6, pp. 257–264, 2019.

[12] Y. X. Guo, Y. Y. Zhang, J. F. Xing, and X. L. Yuan, "Patch-graph sparse optimization for large array based on quantum particle swarm optimization," *Aeronautical Science and technology*, vol. 8, pp. 57–62, 2020.

[13] L. Yu, F. Shi, H. Wang, and F. Hu, *The MATLAB Intelligent Algorithm: 30 Cases Analysis*, Beihang University Press, Beijing, China, 2nd edition, 2015.

Hindawi
Scientific Programming
Volume 2021, Article ID 3022658, 10 pages
https://doi.org/10.1155/2021/3022658

Research Article

Measuring Total Factor Productivity of China Provincial Non-Life Insurance Market: A DEA-Malmquist Index Method

Fangping Yu, Hang Chen, Jiaqi Luo, and Haibo Kuang

Dalian Maritime University, School of Shipping Economics and Management, Dalian 116026, China

Correspondence should be addressed to Jiaqi Luo; lovelyluo@126.com

Received 27 July 2021; Accepted 26 August 2021; Published 15 September 2021

Academic Editor: Punit Gupta

The unbalanced economic development results in the difference in operating efficiency of the non-life insurance industry in China's provinces; based on the DEA-Malmquist index method, this paper investigates the provincial differences, dynamic change characteristics, and causes of non-life insurance productivity in 31 provinces of China from 2004 to 2017. The results show that in the sample period, there are significant differences between provinces and regions in China's non-life insurance efficiency, which generally shows the echelon spatial characteristics of "strong in the west and weak in the east". Technological progress in the western region promotes the rapid growth of total factor productivity, while the low efficiency of technological progress in the eastern region restrains the improvement of total factor productivity. The overall total factor productivity of China's provincial non-life insurance industry is on the rise, mainly due to the improvement of pure technical efficiency and scale efficiency, while technological progress has an inhibiting effect on the contrary. These conclusions are of reference value for relevant stakeholders in China's provincial non-life insurance market to formulate development strategies and business strategies.

1. Introduction

With the rapid development of China's economy, the deepening of financial reform and opening up in recent years has brought substantial changes to the insurance market. The development of the non-life insurance market is particularly rapid. From 2000 to 2019, the non-life insurance premium grows at an annual rate of 206.37%, reaching 287.967 billion US dollars. At present, it is the second-largest non-life insurance market in the world [1]. However, due to China's huge land area, the imbalance of provincial economic development has resulted in differences in the development of the non-life insurance market. According to statistics, the non-life insurance depth (non-life insurance premium/GDP) of China's eastern, central, and western regions in 2019 will be 1.81%, 2.40%, and 1.95%, respectively. Then, is there any obvious regional difference in the efficiency of China's non-life insurance market? At the same time, what are the basic characteristics and dynamic trends? These problems need to be discussed in detail.

The evaluation of insurance market efficiency has always been a hot topic in the academic and industry. Whether it was the efficiency of life insurance, non-life insurance, or the whole insurance market, the vast majority of literature were based on the investigation of insurance companies [2–14];. Only a few researchers took an international perspective to compare the insurance markets of different countries or regions [15–18]. Few studies compared the efficiency of the regional insurance market in a country, especially the non-life insurance market, which was highly related to the development level of the real economy. There were good reasons for this. In addition to the significant imbalance of regional economic development as a prerequisite for the study, it was also very difficult to collect reliable data. Therefore, this paper attempts to use the DEA-Malmquist index method [19–23] to analyze the spatial differentiation characteristics, dynamic trends, and determinants of the efficiency of total factor productivity of non-life insurance market in 31 provinces of China during 2004–2017. It provides important support for China to solve the problem of high-quality and balanced development of the regional non-life insurance market.

This paper has two main contributions to the literature. First, as far as we know, this is the first study focusing on the efficiency of China's provincial non-life insurance market. Therefore, our paper expands the insurance literature of efficiency comparison by comparing the total factor productivity and segmentation efficiency of the developing non-life insurance markets in China. Second, the provincial comparison not only provides the regional distribution characteristics of relative efficiency but also shows the dynamic trend of non-life insurance market efficiency, which increases our understanding of the reasons for the efficiency differences of the provincial non-life insurance market. Evaluating the evolution of provincial-level non-life insurance efficiency in China has important reference significance for relevant stakeholders to formulate development strategies and business strategies.

The remaining part of the paper is organized as follows. In Section 2, the existing relevant studies are summarized. In Section 3, we introduce the principle of measuring the total factor productivity and the DEA-Malmquist index method and describe the selected evaluation index. Section 4 is the result of efficiency analysis and discussion. The conclusion is presented in Section 5.

2. Literature Review

Since the 1990s, the research focus of efficiency evaluation of non-life insurance market has continued till now. Cummins and Weiss [24] analyzed the cost efficiency levels and differences of property-liability insurance companies of different sizes; the results showed that the average efficiency of the large, medium, and small insurance companies were about 90%, 80%, and 88%, respectively, and medium and small insurance companies had more potential to reduce costs. Worthington and Hurley [25] calculated the pure technical efficiency, scale efficiency, allocation efficiency, and cost efficiency of 46 non-life insurance companies in Australia and found that the main cause of inefficiency was allocation inefficiency rather than technical inefficiency. Cummins and Xie [20] investigated the productivity and efficiency effects of mergers and acquisitions in the property-liability insurance industry in the United States. Luhnen [8] made a comprehensive analysis of the efficiency and productivity of the German property-liability insurance industry. It was found that the total factor productivity growth was moderate, the efficiency growth was low, and the market had the potential to improve the technical efficiency by about 20 percentage points and the cost efficiency by about 50 percentage points. Chen et al. [3] discussed whether the efficiency of American property-liability insurance companies has improved before and after the conversion. Sun et al. [26] evaluated the comprehensive technical efficiency, pure technical efficiency, and scale efficiency of 34 Chinese property insurance companies. Cummins and Xie [27] examined the efficiency, productivity, and economies of scale of the property-liability insurance industry in the United States. Yaisawarng et al. [28] examined whether there were economies of scale and technological changes in Thailand's non-life insurance market. Alhassan and Biekpe [19] conducted a comprehensive analysis on the efficiency, productivity, and returns to scale of South Africa's non-life insurance market; the results showed that the inefficiency of non-life insurance companies was about 50%, while about 20% of insurance companies operate at optimal size. Ferro and León [5] evaluated the technical efficiency of non-life insurance companies in Argentina. Venkateswarlu and Rao [23] measured and compared the efficiency change, technology change, and total factor productivity index of Indian public and private non-life insurance companies.

Some scholars have also investigated the different characteristics of the operating efficiency of non-life insurance markets in different countries. For example, Weiss [18] studied the productivity of property-liability insurance companies in the United States, West Germany, Switzerland, France, and Japan during the period 1975–1987. Huang and Eling [16] used the multistage DEA method to analyze the efficiency of non-life insurance companies in BRIC countries. They found that Brazil, Russia, China, and India declined in order and that the environment affected the operating efficiency of non-life insurers in the BRIC countries.

The methods used in the existing insurance efficiency evaluation literature are mainly divided into two categories: one is the parametric method based on stochastic frontier analysis [5, 18, 24, 27], and the other is nonparametric methods based on DEA [8, 16, 25, 26]. Currently, the newly popular DEA-Malmquist index method based on the traditional DEA method is improved [3, 19, 20, 23, 27, 29]. The nonparametric methods can better track the evolution of non-life insurance market efficiency and overcome the prominent problems that the parametric method relies too much on the parametric hypothesis, and the traditional DEA method is not enough to describe the dynamic characteristics.

From the above literature, we can see that although the existing research compares the operating efficiency of the non-life insurance market with the non-life insurance companies in one country or different countries, few studies intend to consider from the perspective of the regional market, especially for the special situation of the large regional difference of non-life insurance.

3. The Measuring Total Factor Productivity of Provincial Non-Life Insurance Market Framework

3.1. The Principle. We investigated the operating efficiency of non-life insurance in China's provinces, mainly based on the following principle. First, an index system of input and output is constructed as a quantitative objective standard for evaluating the operating efficiency of the provincial non-life insurance market. Second, with the help of the DEA-Malmquist index method, the evaluation model of provincial non-life insurance efficiency is constructed. Finally, the data of non-life insurance operations in 31 provinces in

China from 2004 to 2017 were collected for empirical analysis to estimate the total factor productivity and its segmentation efficiency (see Figure 1 for details).

3.2. Input-Output Index. In this paper, the DEA-Malmquist technique is used to measure and analyze the changes and causes of the provincial non-life insurance market efficiency in China. First, the input index and output index should be determined. According to the operating characteristics of China's provincial non-life insurance market, we have determined an evaluation index system, as shown in Table 1. In terms of input index, considering the four basic elements of non-life insurance industry operation, namely "resources, capital, institutions, and manpower", we selected six indexes, including GDP, household consumption level, permanent resident population, total fixed assets of non-life insurance institutions, number of non-life insurance institutions, and non-life insurance practitioners. GDP, household consumption level, and permanent resident population are the input of external resources for the development of the provincial non-life insurance market. The total fixed assets of non-life insurance institutions reflect the investment of capital. The number of non-life insurance institutions refers to the total number of branches in each province, which reflects the density of non-life insurance institutions in the province and reflects the physical input. Non-life insurance practitioners refer to the number of all staff of non-life insurance of province area, including company management personnel, business personnel, and other personnel, reflecting the input of manpower. In terms of output index, we selected three indicators: the premium, insurance indemnity, and underwriting profit. The index of premium reflects the total output capacity of insurance. Insurance indemnity reflects the level of insurance claims. Underwriting profit reflects the benefits of non-life insurance business in the province.

3.3. DEA-Malmquist Index Model. In this paper, the DEA-Malmquist index method [21] is applied to analyze the dynamic changes and causes of operational efficiency in China's provincial non-life insurance market. There are two main reasons to choose the DEA-Malmquist index method. First, it is a nonparametric method, which can avoid the problem that stochastic frontier analysis and other methods rely too much on parameter hypothesis. Second, the overall efficiency can be further subdivided into different seed efficiencies to better understand the dynamic evolution of efficiency and the main reasons.

Since it is difficult to satisfy the constant return to scale in reality, we adopt the BCC-DEA model based on the assumption that the return to scale is variable. The expression is as follows:

$$\begin{cases} \min\left[\theta - \varepsilon\left(\sum_{i=1}^{m} \mathrm{si}^{-} + \sum_{r=1}^{n} \mathrm{sr}^{+}\right)\right], \\ \sum_{j=1}^{m} x_{ij}\lambda_j + si^{-} = \theta x_i k, \\ \sum_{j=1}^{i} y_{rj}\lambda_j - \mathrm{sr}^{+} = y_r k, \\ \sum_{j=1}^{i} \lambda_j = 1, \\ \lambda_j, \mathrm{si}^{-}, \mathrm{sr}^{+} \geq 0, j = 1, 2\ldots, n. \end{cases} \tag{1}$$

The above model measures the efficiency of each DMU from the perspective of input, and the objective function represents the comprehensive efficiency from the perspective of minimizing input, where x_{ij} is the *i-th* input of a decision unit *j*, $x_{ij} \geq 0$, x_i is the *i-th* input, $x_i \geq 0$, y_{rj} is the *r-th* output of a decision unit *j*, $y_{rj} \geq 0$, y_r is the *r-th* output, $y_r \geq 0$, θ is the target programming value, K is the goal of decision-making unit, λ_j is the planning decision variable, ε is non-Archimedean infinitesimal, and si^{-} and sr^{+} are slack variables. If $\theta = 1$, $s^{-} = 0$, and $s^{+} = 0$, then the DEA of the decision-making unit is valid; if $\theta < 1$, DMU is DEA invalid; and if $\theta = 1$ and $s^{-} \neq 0$ or $s^{+} \neq 0$, DMU is weakly efficient.

BCC-DEA model can only compare the efficiency values of different decision-making units in the same period and cannot measure the changes of efficiency values in different periods. For this purpose, we also need to use the Malmquist index [33], whose expression is as follows:

$$\begin{aligned} \mathrm{Tfpch} &= M\left(x^{t+1}, y^{t+1}, x^t, y^t\right) \\ &= \left[\frac{D^t\left(x^{t+1}, y^{t+1}\right)}{D^t\left(x^t, y^t\right)} \times \frac{D^{t+1}\left(x^{t+1}, y^{t+1}\right)}{D^{t+1}\left(x^t, y^t\right)}\right]^{1/2}, \end{aligned} \tag{2}$$

where (x^t, y^t) represents the input and output of the period t, respectively; (x^{t+1}, y^{t+1}) represents the input and output of the period $t+1$, respectively; $D^t(x^t, y^t)$ and $D^t(x^{t+1}, y^{t+1})$, respectively, refer to the distance function of decision unit in t period and $t+1$ period with data in t period as reference set; and $D^{t+1}(x^t, y^t)$ and $D^{t+1}(x^{t+1}, y^{t+1})$, respectively, refer to the distance function of decision units in the t period and $t+1$ period with the data in the $t+1$ period as the reference set. When the Malmquist index of >1 indicates efficiency improvement, the Malmquist index = 1 indicates that the efficiency remains unchanged, and the Malmquist index <1 indicates reduced efficiency.

In this paper, the efficiency of total factor productivity is replaced by Tfpch for short. Tfpch can be further decomposed into the technical efficiency change index (Effch) and technical progress index (Tech) as follows:

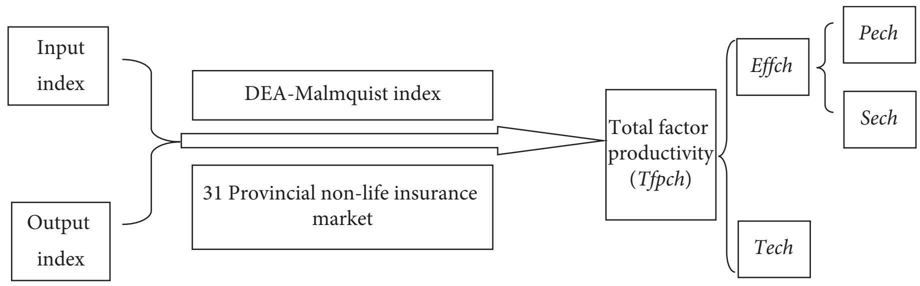

Figure 1: The principle of measuring total factor productivity of China provincial non-life insurance market.

Table 1: Input and output index.

	Detailed indicators	Reference source
Input index	GDP	[16]
	Household consumption level	
	Permanent resident population	
	Total fixed assets of non-life insurance institutions	[10, 16]
	Number of non-life insurance institutions	
	Non-life insurance practitioners	[16, 25]
Output index	The premium	[10, 16, 30]
	Insurance indemnity	[5, 31, 32]
	Underwriting profit	

$$M\left(x^{t+1}, y^{t+1}, x^t, y^t\right) = \frac{D^{t+1}\left(x^{t+1}, y^{t+1}\right)}{D^{t+1}\left(x^t, y^t\right)} \times \left[\frac{D^t\left(x^{t+1}, y^{t+1}\right)}{D^{t+1}\left(x^{t+1}, y^{t+1}\right)} \times \frac{D^t\left(x^t, y^t\right)}{D^{t+1}\left(x^t, y^t\right)}\right]^{1/2}, \tag{3}$$

$$\text{Effch} = \frac{D^{t+1}\left(x^{t+1}, y^{t+1}\right)}{D^{t+1}\left(x^t, y^t\right)}, \tag{4}$$

$$\text{Tech} = \left[\frac{D^t\left(x^{t+1}, y^{t+1}\right)}{D^{t+1}\left(x^{t+1}, y^{t+1}\right)} \times \frac{D^t\left(x^t, y^t\right)}{D^{t+1}\left(x^t, y^t\right)}\right]^{1/2}. \tag{5}$$

In addition, by introducing variable returns into the scale distance function, the technical efficiency change index (Effch) in equation (4) can be subdivided into pure technical efficiency index (Pech) and scale efficiency index (Sech), which can be expressed as follows:

$$\text{Effch} = \frac{D^{t+1}\left(x^{t+1}, y^{t+1}\right)}{D^{t+1}\left(x^t, y^t\right)} = \frac{D_V^{t+1}\left(x^{t+1}, y^{t+1}\right)}{D_V^t\left(x^t, y^t\right)} \frac{D_V^{t+1}\left(x^{t+1}, y^{t+1}\right) D_C^{t+1}\left(x^{t+1}, y^{t+1}\right)}{D_V^{t+1}\left(x^t, y^t\right) D_C^{t+1}\left(x^t, y^t\right)}, \tag{6}$$

where the subscripts V and C refer to variable returns to scale technology and constant return to scale technology, respectively.

$$\begin{aligned} \text{Pech} &= \frac{D_V^{t+1}\left(x^{t+1}, y^{t+1}\right)}{D_V^t\left(x^t, y^t\right)}, \\ \text{Sech} &= \frac{D_V^{t+1}\left(x^{t+1}, y^{t+1}\right) D_C^{t+1}\left(x^{t+1}, y^{t+1}\right)}{D_V^{t+1}\left(x^t, y^t\right) D_C^{t+1}\left(x^t, y^t\right)}. \end{aligned} \tag{7}$$

Therefore, the calculation formula of Tfpch is as follows:

$$\text{Tfpch} = \text{Effch} \times \text{Tech} = \text{Pech} \times \text{Sech} \times \text{Tech}, \tag{8}$$

where Tfpch represents total factor productivity, Effch represents technical efficiency index, Tech represents technological progress index, Sech represents scale efficiency index, and Pech represents pure technical efficiency index. Effch measures whether the input of each factor is wasted. Tech reflects the innovation and improvement of science, technology, and activities in the business operation process to adapt to the future market environment. Sech reflects the influence of scale factors on total factor productivity. Pech is the production efficiency of an enterprise affected by management and technology factors. DEA-Malmquist technology

Table 2: Input and output index basic statistics of 31 provinces during 2004–2017.

	Input index						Output index		
	GDP (100 million yuan)	Household consumption level (yuan per person per year)	Permanent resident population (10 thousand)	Total fixed assets of non-life insurance institutions (10 thousand yuan)	Number of non-life insurance institutions	Non-life insurance practitioners	The premium (10 thousand yuan)	Insurance indemnity (10 thousand yuan)	Underwriting profit (10 thousand yuan)
Minimum	220.34	2,723	276	4,304.74	8	147	14,597	5,351	0.1
Maximum	89,879.23	53,617	11,169	2,987,307	3,263	55,423	11,766,073	5,849,341	1
Mean	15,475.1	12,738.4	4,307.4	427,003.3	933.4	11,714.6	1,553,754.5	821,156.7	0.5
Standard deviation	14,988.9	8,724.8	2,723.6	491,075.3	739.2	10,321.8	1,737,778.4	931,706.8	0.1
Skewness	2.1	1.7	0.6	2.2	0.9	1.7	2.3	2.3	1.2
Kurtosis	5.0	3.9	0.5	6.0	0.2	3.0	6.5	6.0	4.8

can help obtain more dynamic and comprehensive connotation information in the process of evaluating the efficiency of China's provincial non-life insurance market.

4. Experimental Results and Analysis

4.1. Data. In this paper, the efficiency of the non-life insurance industry in 31 provinces of mainland China (excluding Hong Kong, Macao, and Taiwan) during 2004–2017 was studied. The input-output index data used in the evaluation are from the China Insurance Statistical Yearbook and the website of the National Bureau of Statistics of China. Since the input and output indexes in the BCC-DEA model are required to be non-negative, this paper converts the original data of underwriting profit into the data falling within a positive range. It is mainly achieved by the following function [16]:

$$z_{\text{ij}} = 0.1 + 0.9 \times \frac{x_{\text{ij}} - m_j}{M_j - m_j}, \tag{9}$$

where $m_j = \min(x_{\text{ij}}); M_j = \max(x_{\text{ij}}); i = 1, 2, 3..., n; z_{\text{ij}} = [0.1, 1]$.

The basic statistics are shown in Table 2. According to the statistics of minimum, maximum, and mean, there is an obvious gap between the input-output indicators of 31 provinces in China during 2004–2017.

4.2. The Evaluation Outcomes. Figures 2–6 show the basic situation of non-life insurance Tfpch and decomposition efficiency in provinces of China. During the sample period, China's non-life insurance market efficiency showed significant differences among provinces and regions. From the microscopic perspective of specific provinces, the characteristics of non-life insurance efficiency are different. The Tfpch is less than 1 in 15 provinces, including Beijing, Hebei, Shanxi, Inner Mongolia, Liaoning, Shanghai, Jiangsu, Zhejiang, Anhui, Shandong, Guangdong, Chongqing, Sichuan, Ningxia, and Xinjiang. However, Tfpch is greater than 1 in 16 other provinces, which are Tianjin, Jilin, Heilongjiang, Fujian, Jiangxi, Henan, Hubei, Hunan, Guangxi, Hainan, Guizhou, Yunnan, Xizang, Shanxi, Gansu, and Qinghai. In terms of motivation, the 15 provinces with Tfpch of <1 are mainly caused by the low Tech, which indicates that the innovation and improvement of science and technology and activities in the process of enterprise operation have not adapted to the future market environment. In the 16 provinces with Tfpch of >1, it is mainly caused by the improvement of Effch, which indicates that the input of each factor in these provinces has less waste and a high utilization rate. In Tianjin, Heilongjiang, Jiangxi, Henan, Hubei, Hunan, Guangxi, Guizhou, Xizang, Gansu, Qinghai, and other provinces, Effch and Tech play a synergistic role.

From the perspective of geographical space, the efficiency of provincial non-life insurance also presents different characteristics. Tfpch and Tech show the spatial echelon characteristics of "weak in the west and strong in the east". In terms of Effch, Hubei, Shanxi, and other provinces in Central China are relatively high. The Pech shows the spatial echelon characteristic of "strong in the west and weak in the east", and the eastern provinces such as Shandong and Liaoning are relatively high. The Sech is balanced in the whole country, and there is no obvious difference between provinces and regions.

Furthermore, it can be seen from Table 3 that the average non-life insurance Tfpch of eastern, western, and central regions of China is 0.980, 1.027, and 1.013 respectively, and the comprehensive ranking is: western region > central region > eastern region. The non-life insurance total factor productivity in western China grew rapidly, mainly due to technological progress. On the contrary, the low tech inhibits the improvement of Tfpch in the eastern region.

5. Discussion

The dynamic change characteristics of the overall total factor productivity of China's provincial non-life insurance market and its decomposition efficiency are shown in Figure 7. From 2004 to 2017, the average value of the Tfpch was 1.003, showing a general upward trend, but the fluctuation was

Figure 2: Tfpch.

Table 3: Average non-life insurance efficiency of the three regions in China during the sample period.

Area	Tfpch	Tech	Effch	Pech	Sech
Eastern	0.980	0.977	1.004	1.003	1.002
Western	1.027	1.015	1.001	1.001	1.000
Central	1.013	1.007	1.005	1.006	1.004

Note. The provinces in the eastern region include Beijing, Tianjin, Hebei, Liaoning, Shanghai, Jiangsu, Zhejiang, Fujian, Shandong, Guangdong, and Hainan. The provinces in the central region include Shanxi, Jilin, Heilongjiang, Anhui, Jiangxi, Henan, Hubei, and Hunan. The provinces in the western region include Chongqing, Sichuan, Yunnan, Guizhou, Xizang, Ningxia, Xinjiang, Qinghai, Shanxi, Gansu, Guangxi, and Neimenggu.

Figure 3: Tech.

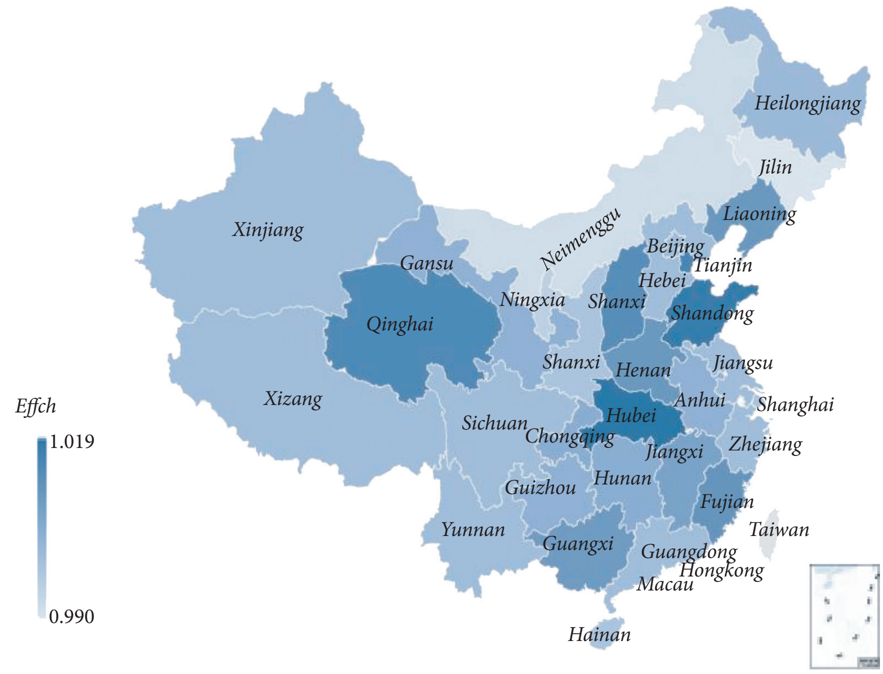

Figure 4: Effch.

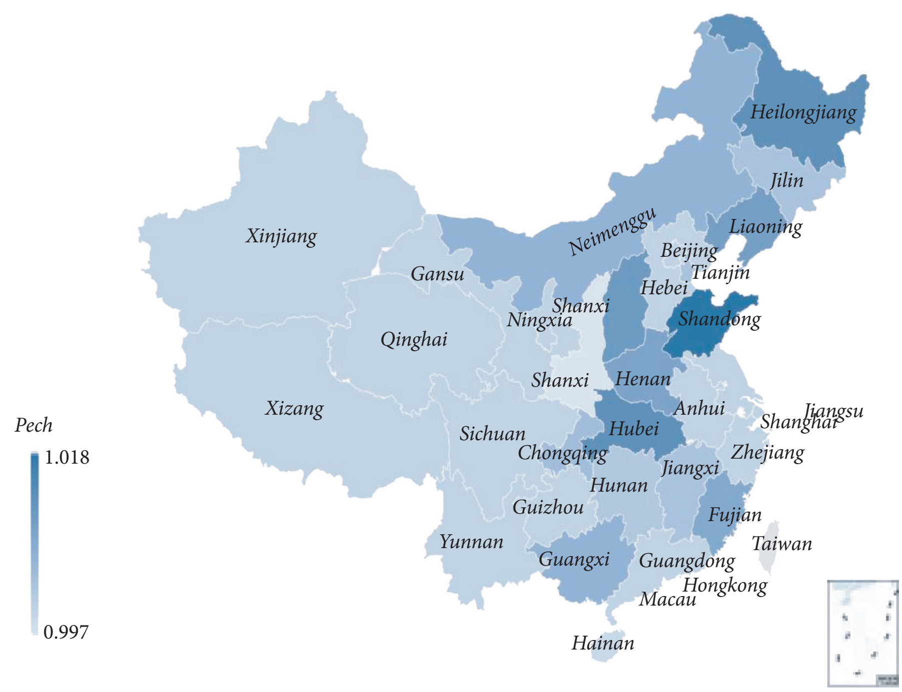

Figure 5: Pech.

large. To be specific, the average annual increase of the Effch was 0.4%, and the average annual decrease of the Tech was 0.1%. Among them, the Sech and Pech increased by 0.1% and 0.3% on average, respectively. This fully shows that the overall management and technical level of the provincial non-life insurance market play a major role in improving the overall efficiency, while the driving effect of technological progress presents a negative effect. In fact, from 2004 to 2017, the development of China's non-life insurance market is mainly driven by costs, manpower, and management and is still in the extensive development stage. It is worth pointing out that during the period of 2013/2014 to 2016/2017, technical efficiency still showed the characteristics of the shock. But the pure technical efficiency index showed a significant upward trend, which promoted the improvement of the overall efficiency.

Figure 6: Sech.

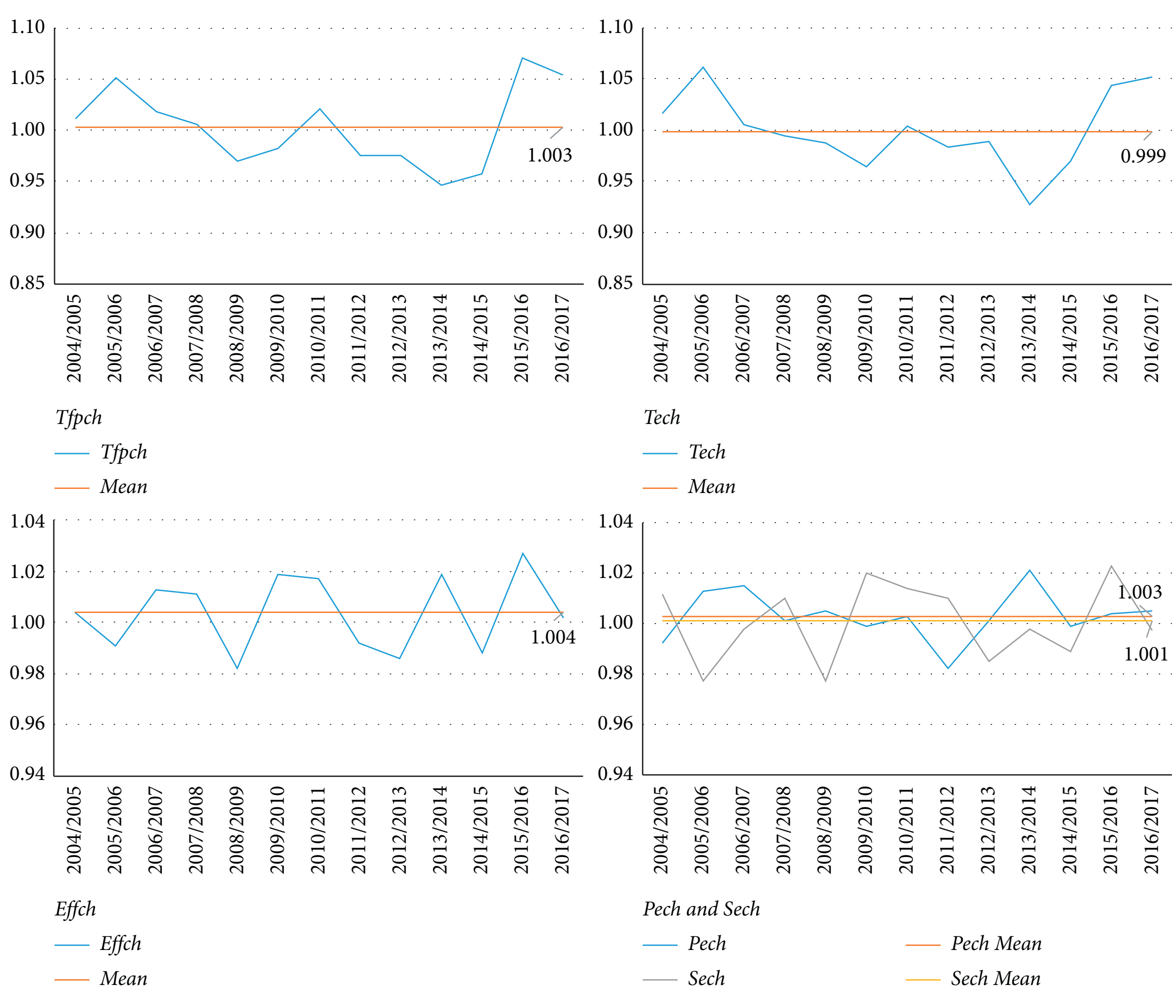

Figure 7: Provincial efficiency during the sample period.

6. Conclusion

Based on the empirical analysis of the differences, evolutionary characteristics, and drivers of non-life insurance market efficiency in 31 provinces of China during 2004–2017, the following conclusions are drawn: (1) from the perspective of provincial efficiency change, total factor productivity of half of the provinces in China has increased. The improvement of total factor productivity in Beijing, Hebei, Shanxi, and other provinces is mainly due to the improvement of technical efficiency index. The improvement of total factor productivity in Neimenggu, Jilin, Hainan, and other provinces is mainly due to the improvement of technological progress. The improvement of total factor productivity in Tianjin, Heilongjiang, Jiangxi, and other provinces is mainly due to the synergistic driving effect of technological efficiency and technological progress. (2) From the perspective of spatial distribution, total factor productivity: western region > central region > eastern region. Total factor productivity in the western region grew rapidly, mainly due to technological progress and improvement of pure technological efficiency. Technological progress in the eastern region shows a downward trend, which indicates that technological progress is the main restriction factor for the improvement of total factor productivity. (3) From the analysis of overall efficiency change, it can be seen that China's non-life insurance total factor productivity is on the rise on the whole, but it is still in an unstable stage. The change of technical efficiency plays a major role in the improvement of total factor productivity, while the driving effect of technological progress is not significant. It reflects that the scale of China's non-life insurance market continues to expand, but the technical level still needs to be improved. There is still much room to improve non-life total factor productivity by improving the technical level. In conclusion, Chinese insurance policymakers and non-life insurance operators should take targeted measures to effectively improve operating efficiency according to the constraints.

Data Availability

Some of the data involved commercial secrets. Therefore, the data in this paper are only used for scientific research and should not be shared.

Additional Points

(i) We investigated originally the provincial differences, dynamic change characteristics, and causes of non-life insurance productivity in 31 provinces of China from 2004 to 2017 using the DEA-Malmquist index method. (ii) The results show that China's non-life insurance efficiency has been on the rise, and there were significant differences between provinces and regions, and the echelon spatial characteristics of "strong in the west and weak in the east".

Conflicts of Interest

The authors declare that they have no conflicts of interest.

Acknowledgments

This research was supported by the National Natural Science Foundation of China (Grant nos. 72072018, 71831002, and 71303026), Changjiang Scholars and Innovation Team Development Plan of the Ministry of Education of China (IRT_17R13), the Fundamental Research Funds for the Central Universities (Grant nos. 3132021256 and 3132021257), and China Postdoctoral Science Foundation (Grant nos. 2019M651101 and 2021T140081).

References

[1] Swiss Re Institute, *World Insurance: Riding Out the 2020 Pandemic Storm*, sigma No 4, 2020.

[2] C. P. Barros, M. Nektarios, and A. Assaf, "Efficiency in the Greek insurance industry," *European Journal of Operational Research*, vol. 205, no. 2, pp. 431–436, 2010.

[3] L.-R. Chen, G. C. Lai, and J. L. Wang, "Conversion and efficiency performance changes: evidence from the U.S. property-liability insurance industry," *The Geneva Risk and Insurance Review*, vol. 36, no. 1, pp. 1–35, 2011.

[4] M. Eling and P. Schaper, "Under pressure: how the business environment affects productivity and efficiency of European life insurance companies," *European Journal of Operational Research*, vol. 258, no. 3, pp. 1082–1094, 2017.

[5] G. Ferro and S. León, "A stochastic Frontier analysis of efficiency in Argentina's non-life insurance market," *The Geneva Papers on Risk and Insurance-Issues and Practice*, vol. 43, no. 1, pp. 158–174, 2018.

[6] H. A. Kader, M. Adams, and P. Hardwick, "The cost efficiency of Takaful insurance companies," *The Geneva Papers on Risk and Insurance-Issues and Practice*, vol. 35, no. 1, pp. 161–181, 2010.

[7] C. Kao and S.-N. Hwang, "Efficiency decomposition in two-stage data envelopment analysis: an application to non-life insurance companies in Taiwan," *European Journal of Operational Research*, vol. 185, no. 1, pp. 418–429, 2008.

[8] M. Luhnen, "Determinants of efficiency and productivity in German property-liability insurance: evidence for 1995-2006," *The Geneva Papers on Risk and Insurance-Issues and Practice*, vol. 34, no. Supplement 3, pp. 483–505, 2009.

[9] M. Nourani, E. S. Devadason, and V. Chandran, "Measuring technical efficiency of insurance companies using dynamic network DEA: an intermediation approach," *Technological and Economic Development of Economy*, vol. 24, no. 5, pp. 1909–1940, 2018.

[10] P. Wanke and C. P. Barros, "Efficiency drivers in Brazilian insurance: a two-stage DEA meta frontier-data mining approach," *Economic Modelling*, vol. 53, no. 2, pp. 8–22, 2016.

[11] S. Anandarao, S. R. S. Durai, and P. Goyari, "Efficiency decomposition in two-stage data envelopment analysis: an application to life insurance companies in India," *Journal of Quantitative Economics*, vol. 17, no. 2, pp. 271–285, 2019.

[12] J. L. Hu and H. E. Yu, "Risk, capital, and operating efficiency: evidence from Taiwan's life insurance market," *Emerging Markets Finance and Trade*, vol. 51, no. Supplement 1, pp. S121–S132, 2015.

[13] Q.-M. Lim, H.-S. Lee, and W.-M. Har, "Efficiency, productivity and competitiveness of the Malaysian insurance sector: an analysis of risk-based capital regulation," *The Geneva Papers on Risk and Insurance-Issues and Practice*, vol. 46, no. 1, pp. 146–172, 2021.

[14] P. A. Purwaningrat, "4. Indonesia," *Intellectual Property and US Relations with Indonesia, Malaysia, Singapore, and Thailand*, vol. 9, no. 3, pp. 27–36, 2018.

[15] M. Eling and M. Luhnen, "Efficiency in the international insurance industry: a cross-country comparison," *Journal of Banking & Finance*, vol. 34, no. 7, pp. 1497–1509, 2010.

[16] W. Huang and M. Eling, "An efficiency comparison of the non-life insurance industry in the BRIC countries," *European Journal of Operational Research*, vol. 226, no. 3, pp. 577–591, 2013.

[17] L. Peng and Z. Lian, "Diversification and efficiency of life insurers in China and India," *The Geneva Papers on Risk and Insurance-Issues and Practice*, 2020.

[18] M. A. Weiss, "Efficiency in the property-liability insurance industry," *Journal of Risk & Insurance*, vol. 58, no. 3, pp. 452–479, 1991.

[19] A. L. Alhassan and N. Biekpe, "Efficiency, productivity and returns to scale economies in the non-life insurance market in South Africa," *The Geneva Papers on Risk and Insurance-Issues and Practice*, vol. 40, no. 3, pp. 493–515, 2015.

[20] J. D. Cummins and X. Xie, "Mergers and acquisitions in the US property-liability insurance industry: productivity and efficiency effects," *Journal of Banking & Finance*, vol. 32, no. 1, pp. 30–55, 2008.

[21] R. Färe, S. Grosskopf, and M. Norris, "Productivity growth, technical progress, and efficiency change in industrialized countries," *The American Economic Review*, vol. 84, no. 5, pp. 1040–1044, 1994.

[22] S. Kaffash, R. Azizi, Y. Huang, and J. Zhu, "A survey of data envelopment analysis applications in the insurance industry 1993-2018," *European Journal of Operational Research*, vol. 284, no. 3, pp. 801–813, 2020.

[23] R. Venkateswarlu and G. Rao, "Productivity analysis of Indian non-life insurance firms using Malmquist total factor productivity index," *International Journal of Operations and Quantitative Management*, vol. 25, no. 2, pp. 91–108, 2019.

[24] J. D. Cummins and M. A. Weiss, "Measuring cost efficiency in the property-liability insurance industry," *Journal of Banking & Finance*, vol. 17, no. 2-3, pp. 463–481, 1993.

[25] A. C. Worthington and E. V. Hurley, "Cost efficiency in Australian general insurers: a non-parametric approach," *The British Accounting Review*, vol. 34, no. 2, pp. 89–108, 2002.

[26] B. Q. Sun, Y. X. Xia, and W. T. Cao, "The efficiency evaluation of property insurance companies based on two-stage correlative DEA models," in *Proceedings of the Management Science and Engineering (ICMSE) 2012 International Conference on*, pp. 699–712, IEEE, Harbin, China, November 2012.

[27] J. D. Cummins and X. Xie, "Efficiency, productivity, and scale economies in the U.S. property-liability insurance industry," *Journal of Productivity Analysis*, vol. 39, no. 2, pp. 141–164, 2013.

[28] S. Yaisawarng, P. Asavadachanukorn, and S. Yaisawarng, "Efficiency and productivity in the Thai non-life insurance industry," *Journal of Productivity Analysis*, vol. 41, no. 2, pp. 291–306, 2014.

[29] N. L. Azad, A. Mozaffari, M. Vajedi, and Y. Masoudi, "Chaos oscillator differential search combined with Pontryagin's minimum principle for simultaneous power management and component sizing of PHEVs," *Optimization and Engineering*, vol. 17, no. 4, pp. 727–760, 2016.

[30] A. Dutta, "Impact of privatization on productivity: a non-parametric analysis of Indian insurance sector," *Global Business Review*, vol. 14, no. 2, pp. 297–314, 2013.

[31] S. L. Hui, F. C. Fan, A. M. Nassir, and A. Nazrul Hisyam, "Does efficiency promote the competitiveness of the insurance industry?" *Journal of Business Economics and Management*, vol. 19, no. 4, pp. 566–591, 2018.

[32] M. Nektarios and C. P. Barros, "A Malmquist index for the Greek insurance industry," *The Geneva Papers on Risk and Insurance - Issues and Practice*, vol. 35, no. 2, pp. 309–324, 2010.

[33] M. J. Farrell, "The measurement of productive efficiency," *Journal of the Royal Statistical Society: Series A*, vol. 120, no. 3, pp. 253–281, 1957.

Hindawi
Scientific Programming
Volume 2021, Article ID 3997648, 13 pages
https://doi.org/10.1155/2021/3997648

Research Article

Adaptive Backstepping Sliding Mode Control for Quadrotor UAV

Sibo Huang,[1] **Jianfeng Huang**,[2] **Zhaoquan Cai**,[3,4] **and Han Cui**[2]

[1]*Network and Information Center, Huizhou University, Huizhou, China*
[2]*School of Electronic Information and Electrical Engineering, Huizhou University, Huizhou, China*
[3]*Shanwei Polytechnic, Shanwei, China*
[4]*School of Computer Science and Engineering, Huizhou University, Huizhou, China*

Correspondence should be addressed to Han Cui; cuihan2010@qq.com

Received 13 August 2021; Accepted 26 August 2021; Published 14 September 2021

Academic Editor: Punit Gupta

Quadrotor UAV has a strong mobility and flexibility in flight and has been widely used in military and civil fields in recent years. An adaptive backstepping sliding mode control (ABSMC) method is proposed to address the trajectory tracking control problem of quadrotor UAV based on actuator fault and external disturbance. In the proposed method, the switching gain of adaptive sliding mode control is constructed in the backstepping design process in order to suppress the chattering effect of sliding mode control effectively by differential iteration. Firstly, the dynamic model of quadrotor UAV with actuator fault and external disturbance is proposed, and then the controllers are designed based on the ABSMC method. Finally, the comparison experiments between sliding mode control (SMC) method and ABSMC method show that the ABSMC method can not only effectively suppress the chattering problem for the SMC method but also perform a perfect control effect.

1. Introduction

In recent years, UAVs have been widely used in military and civilian applications, such as environmental supervision, geological analysis, agricultural operations, search and rescue, and mail delivery [1, 2]. In particular, due to its simple mechanical structure and good maneuverability, the quadrotor UAV can take off vertically, land vertically, hover, or move in a small and disorderly area, which has been developed rapidly [3, 4].

The control problems of a quadrotor UAV are complicated, which contain some parts: its own highly coupled nonlinear problems, unstable and multivariable nature, possibly nonminimum phase, underactuated, existence parameter uncertainties and external disturbances, and the actuator fault [5, 6]. Aiming at the external disturbance encountered during the flight of quadrotor UAV, a double closed-loop active disturbance rejection control scheme was proposed and the extended state observer was used to estimate the external disturbance online and in real time [7]. However, if the observer was used to obtain the external disturbance information in the high-order system, noises can always be introduced. The sliding mode control method [8] was often used to control the nonlinear system with random noise because it was insensitive to noise and did not need to estimate the disturbance online.

And the sliding mode control (SMC) method is widely used in the field of UAV control because it has a strong robustness to disturbance and unmodeled dynamics and good control effect to nonlinear systems [9–12]; however, the setting of its switching gain often causes severe chattering on the control input signal, which often generates a huge burden on the operation of the actuator [13–15]. Usually, setting a small gain can reduce the chattering of the control signal, but it can weaken the robustness of the sliding mode control method under disturbance. Therefore, it is necessary to make the switching gain follow the disturbance or adjust it adaptively according to the corresponding criteria so that it can select the switching gain adaptively under different disturbances. To construct an adaptive switching gain method, the sliding surface was used as a benchmark [16]. The size of the switching gain changes following the change of the sliding surface to ensure that there is an appropriate switching gain corresponding to the tracking error when the tracking error is large or small, which can avoid over adaptation of the gain. In addition, with the help of the neural network model, the switching gain can be considered as a dynamic model approximation value, and the tracking error can be reduced. Neural network was used to estimate unknown dynamics and disturbances [17].

As a kind of controller design method, the backstepping method is widely used because of its brief design process. The designed controller can guarantee the system convergence in finite time, and the convergence time can be proved. Moreover, the combination of the backstepping method and other methods can organically integrate the advantages of the two methods. Accordingly, the backstepping method and sliding mode method were combined to ensure the system convergence [18], where the fuzzy control method combined with the backstepping method was used to control a multi input multi output nonlinear input saturation system [19] so that the controller can make the system converge to the expected value in finite time within a given range. In addition, there are a lot of research studies on controller design [20–25].

Considering that the traditional sliding mode control method is insensitive to the nonlinear problems such as disturbance and failure in the flight of the quadrotor UAV system and the setting of its switching gain can cause huge chattering of input, an adaptive backstepping sliding mode control (ABSMC) method is proposed in this paper, which can estimate the upper bound of the sliding mode switching gain in real time and modify the sliding mode controller in combination with the backstepping method to suppress the chattering of the sliding mode control. The switching gain adaptive method proposed in this paper can update the switching gain adaptively when the upper bound of disturbance is unknown so as to ensure the robustness of sliding mode control as well as the control tracking accuracy. Finally, the effectiveness of the proposed method is verified by comparing the control effect of the ABSMC method with the SMC method.

2. Dynamics Model of Quadrotor UAV

The motion of a quadrotor UAV in space has six degrees of freedom, which are roll, pitch, and yaw around its center of mass and its translational motion in three-dimensional space with two horizontal and one vertical direction. The quadrotor UAV can be regarded as an underactuated rigid body with four inputs. Its thrust is generated by four propellers, which can be controlled by command to keep the UAV in a certain attitude and follow the desired trajectory. Figure 1 shows the structural diagram of the quadrotor UAV.

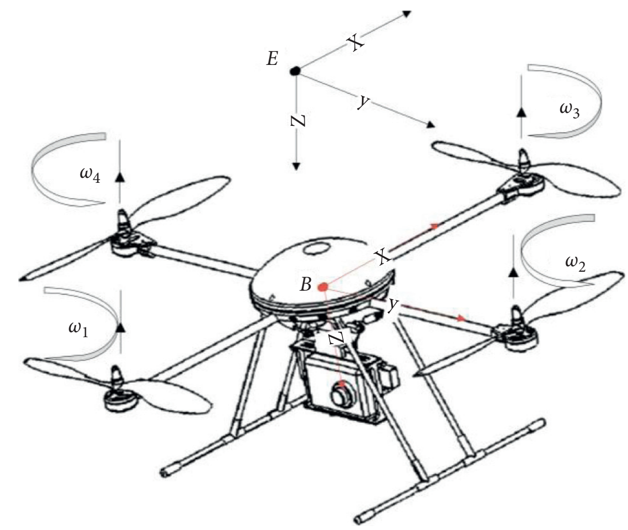

Figure 1: A structure diagram of quadrotor UAV.

According to reference [20, 21], the expression of its dynamic equation is shown in equation (1) based on the actuator fault and external disturbance.

$$\begin{cases} \ddot{x} = \dfrac{1}{m} u_x (U_1 + \varepsilon U_1) + f_1, \\[2ex] \ddot{y} = \dfrac{1}{m} u_y (U_1 + \varepsilon U_1) + f_2, \\[2ex] \ddot{z} = \dfrac{1}{m} (\cos(\phi)\cos(\theta))(U_1 + \varepsilon U_1) - g + f_3, \\[2ex] \ddot{\phi} = \dot{\theta}\dot{\psi}\dfrac{I_y - I_z}{I_x} + \dfrac{J_r}{I_x}\dot{\theta}\omega_r + \dfrac{l}{I_x}(U_2 + \varepsilon U_2) + f_4, \\[2ex] \ddot{\theta} = \dot{\psi}\dot{\phi}\dfrac{I_z - I_x}{I_y} - \dfrac{J_r}{I_y}\dot{\phi}\omega_r + \dfrac{l}{I_y}(U_3 + \varepsilon U_3) + f_5, \\[2ex] \ddot{\psi} = \dot{\phi}\dot{\theta}\dfrac{I_x - I_y}{I_z} + \dfrac{1}{I_z}(U_4 + \varepsilon U_4) + f_6, \end{cases} \tag{1}$$

in which

$$\begin{cases} u_x = \cos(\phi)\sin(\theta)\cos(\psi) + \sin(\phi)\sin(\psi), \\ u_y = \cos(\phi)\sin(\theta)\cos(\psi) - \sin(\phi)\sin(\psi), \\ U_1 = b\left(\omega_1^2 + \omega_2^2 + \omega_3^2 + \omega_4^2\right), \\ U_2 = b\left(\omega_4^2 - \omega_2^2\right), \\ U_3 = b\left(\omega_3^2 - \omega_1^2\right), \\ U_4 = d\left(\omega_2^2 + \omega_4^2 - \omega_1^2 - \omega_3^2\right), \\ \omega_r = \omega_4 + \omega_2 - \omega_1 - \omega_3, \end{cases} \tag{2}$$

where U_1–U_4 are the control input of UAV; εU_1–εU_4 denote the unknown actuator fault; f_1–f_6 are defined as the unknown external interference; I_x, I_y, and I_z present the inertia matrix; b and d are the drag coefficient and lift coefficient, respectively; m is the mass of the quadrotor UAV; g is the gravity acceleration; l represents the length of the quadrotor UAV from the end of each rotor to the center of gravity; J_r is the moment of inertia of the motor rotor; $[\phi, \theta, \psi]$ represent the roll angle, pitch angle, and yaw angle, respectively; $[x, y, z]$ are the position coordinates of the center of mass of the quadrotor UAV relative to the fixed coordinate system; and $\omega_i\,(i = 1, 2, 3, 4)$ are the rotation speed of four propellers of quadrotor UAV.

3. Adaptive Backstepping Sliding Mode Control for Quadrotor UAV

3.1. Control Strategy. The quadrotor UAV is a nonlinear system with strong coupling and is an underactuated system. As an underactuated system, it has only four control inputs, but it has to control six states. The control strategy adopted in this paper is double loop control, and the outer loop is position control, which is composed of altitude and horizontal position. The difference between the real value and the expected value is calculated, and then the altitude and level control of the ABSMC method are used to design control input terms, the desired attitude angle is obtained by inverse solution, and then the inner loop is used for attitude control, which mainly controls the pitch, yaw, and roll motion of UAV. The specific control flow is shown in Figure 2.

3.2. Controller Design. Firstly, the design process of the controller U_1 is given based on the ABSMC method, and then the controllers u_x, u_y, U_2, U_3, and U_4 are obtained based on the same design process.

3.2.1. The Design of the Altitude Controller. Firstly, the controller for quadrotor UAVs' height based on the adaptive backstepping sliding mode method is designed.

In equation (1), the second-order system controlling the height of quadrotor UAV can be equivalent as follows:

$$\ddot{z} = \frac{1}{m}(\cos(\phi)\cos(\theta))U_1 - g + \Delta_z. \tag{3}$$

In equation (3), z represents the height of quadrotor UAV and $\Delta_z = \cos(\phi)\cos(\theta)\varepsilon U_1 + f_3$. Let $z_1 = z$ and $z_2 = \dot{z}$, equation (3) can be rewritten as follows:

$$\begin{cases} \dot{z}_1 = z_2, \\ \dot{z}_2 = \dfrac{1}{m}(\cos(\phi)\cos(\theta))U_1 - g. \end{cases} \tag{4}$$

Firstly, an integral sliding surface is defined as follows:

$$s_{z1} = \int \left(e_z + k_z \dot{e}_z\right). \tag{5}$$

In equation (5), k_z is a positive constant and $e_z = z - z_d$, where z_d is the reference height. The first and second derivatives of equation (5) are defined as follows:

$$\begin{aligned} s_{z2} &= \dot{s}_{z1} \\ &= e_z + k_z \dot{e}_z, \end{aligned} \tag{6}$$

$$\begin{aligned} s_{z3} &= \dot{s}_{z2} \\ &= \dot{e}_z + k_z \ddot{e}_z. \end{aligned} \tag{7}$$

In particular, we use the sliding mode differentiator to obtain the differential value of the state as follows:

$$\begin{cases} \hat{z} = v + k_1 |z - \hat{z}|^{2/3} \operatorname{sign}(z - \hat{z}), \\ \dot{v} = k_2 |z - \hat{z}|^{1/2} \operatorname{sign}(z - \hat{z}), \end{cases} \tag{8}$$

where k_1 and k_2 are normal numbers, and the differentiator can ensure that v converges to $\dot{z}$ in finite time. In the following controller design process, v is used instead of $\dot{z}$ to construct the sliding surface and related error terms.

It can be obtained by combining equations (3), (6), and (7):

$$\begin{cases} \dot{s}_{z1} = s_{z2}, \\ \dot{s}_{z2} = s_{z3}, \\ \dot{s}_{z3} = \dfrac{d}{dt}\left(\dot{e}_z + k_z\left(\dfrac{1}{m}(\cos(\phi)\cos(\theta))U_1 - g + \Delta_z - \ddot{z}_d\right)\right). \end{cases} \tag{9}$$

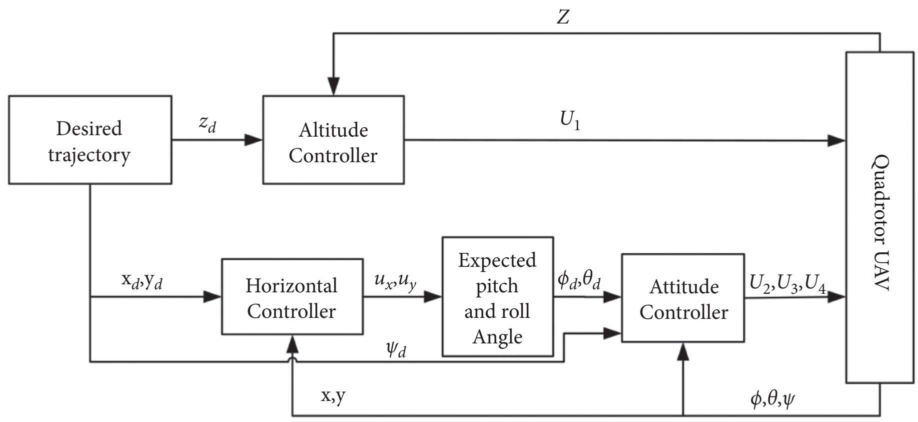

Figure 2: Control flow chart.

Then, according to the backstepping method, combine equations (5)–(7), with following transformation:

$$\sigma_{z1} = s_{z1}, \tag{10}$$

$$\sigma_{z2} = s_{z2} - \alpha_1, \tag{11}$$

$$\sigma_{z3} = s_{z3} - \alpha_2, \tag{12}$$

where α_1 and α_2 are the virtual controllers to be designed.

Combining equation (11) and deriving equation (10), we can get

$$\begin{aligned} \dot{\sigma}_{z1} &= \dot{s}_{z1} \\ &= \sigma_{z2} + \alpha_1. \end{aligned} \tag{13}$$

A Lyapunov function is defined as $V_1 = 1/2\sigma_{z1}^2$. Let the virtual controller $\alpha_1 = -\xi_1\sigma_{z1}$, and we can get the derivative of V_1 as follows:

$$\begin{aligned} \dot{V}_1 &= \sigma_{z1}\left(\sigma_{z2} + \alpha_1\right) \\ &= \sigma_{z1}\sigma_{z2} - \xi_1\sigma_{z1}^2. \end{aligned} \tag{14}$$

In equation (14), ξ_1 is a positive constant. When $\sigma_{z2} = 0$ and $\dot{V}_1 = -\xi_1\sigma_{z1}^2 \leq 0$, σ_{z1} can be asymptotically stable.

Similar to equation (13), by combining equations (11) and (12) with derivation, we can get the following equation:

$$\begin{aligned} \dot{\sigma}_{z2} &= \dot{s}_{z2} - \dot{\alpha}_1 \\ &= \sigma_{z3} + \alpha_2 - \dot{\alpha}_1 \\ &= \sigma_{z3} + \alpha_2 + \xi_1 s_{z2}. \end{aligned} \tag{15}$$

A Lyapunov function is defined as follows:

$$V_2 = V_1 + \frac{1}{2}\sigma_{z2}^2. \tag{16}$$

According to equation (15), the virtual controller α_2 can be defined as the following equation:

$$\alpha_2 = -\xi_2\sigma_{z2} - \sigma_{z1} - \xi_1 s_{z2}. \tag{17}$$

In equation (17), ξ_2 is a positive constant. Combined with equation (17), we can get equation (18) through the differential of equation (16), which is the Lyapunov function V_2 as follows:

$$\begin{aligned} \dot{V}_2 &= \dot{V}_1 + \sigma_{z2}\dot{\sigma}_{z2} \\ &= -\xi_1\sigma_{z1}^2 + \sigma_{z1}\sigma_{z2} + \sigma_{z2}\left(\sigma_{z3} - \xi_2\sigma_{z2} - \sigma_{z1}\right) \\ &= -\xi_1\sigma_{z1}^2 - \xi_2\sigma_{z2}^2 + \sigma_{z2}\sigma_{z3}. \end{aligned} \tag{18}$$

Similar to equation (14), when $\sigma_{z3} = 0$ and $\dot{V}_2 = -\xi_1\sigma_{z1}^2 - \xi_2\sigma_{z2}^2 \leq 0$, σ_{z1} and σ_{z2} can be asymptotically stable.

According to the above derivation, we define a Lyapunov function with the following equation:

$$V_3 = V_2 + \frac{1}{2}\sigma_{z3}^2. \tag{19}$$

Then, combining equations (9) and (19), we obtain the following equation by deriving equation (19):

$$\begin{aligned} \dot{V}_3 &= \dot{V}_2 + \sigma_{z3}\dot{\sigma}_{z3} \\ &= -\xi_1\sigma_{z1}^2 - \xi_2\sigma_{z2}^2 + \sigma_{z2}\sigma_{z3} \\ &\quad + \sigma_{z3}\left(\frac{\mathrm{d}}{\mathrm{d}t}\left(\dot{e}_z + k_z\left(\frac{1}{m}\left(\cos(\phi)\cos(\theta)\right)U_1 - g + \Delta_z - \ddot{z}_d\right)\right) - \dot{\alpha}_2\right). \end{aligned} \tag{20}$$

Thus, the controller U_1 can be designed as follows:

$$U_1 = \frac{m}{k_z\left(\cos(\phi)\cos(\theta)\right)}\left(u_{1n} - u_{1s}\right). \tag{21}$$

In equation (21), u_{1n} and u_{1s} can be given as equations (22) and (23), respectively.

$$u_{1n} = -k_z\left(-g - \ddot{z}\,d\right) - \dot{e}_z + \alpha_2 - \int\left(\xi_3\sigma_{z3} + \sigma_{z2}\right), \tag{22}$$

$$u_{1s} = \int\left(\left(\Lambda_z + \varsigma_z\right)\mathrm{sign}\left(\sigma_{z3}\right)\right). \tag{23}$$

In equations (22) and (23), ξ_3 and ς_z are positive constant and Λ_z is the gain of sliding mode switching. Substituting equation (21) into equation (20) yields the following:

$$\dot{V}_3 = -\xi_1\sigma_{z1}^2 - \xi_2\sigma_{z2}^2 - \xi_3\sigma_{z3}^2 + \sigma_{z3}\frac{\mathrm{d}}{\mathrm{d}t}\left(-u_{1s} + k_z\Delta_z\right)$$
$$\leq -\xi_1\sigma_{z1}^2 - \xi_2\sigma_{z2}^2 - \xi_3\sigma_{z3}^2 - \left(\Lambda_z + \varsigma_z\right)\left|\sigma_{z3}\right| + \Gamma\left|\sigma_{z3}\right|. \quad (24)$$

In particular, it can be seen from equation (24) that if no switching gain is set to counteract the influence of interference, equation (24) needs to be rewritten as follows:

$$\begin{aligned}\dot{V}_3 &\leq -\xi_1\sigma_{z1}^2 - \xi_2\sigma_{z2}^2 - \xi_3\sigma_{z3}^2 + \Gamma\left|\sigma_{z3}\right| \\ &\leq -\xi V_3 + \|\Gamma\|\left|\sigma_{z3}\right|.\end{aligned} \quad (25)$$

In the above equation, $\xi = \min(\xi_1, \xi_2, \xi_3)$; under the influence of interference term $\|\Gamma\|$, V_3 cannot converge to zero but can only converge to the neighbourhood $V_3 \leq \|\Gamma\||\sigma_{z3}|/\xi$. Therefore, by setting the switching gain, i.e., introducing formula (23), the tracking error can be guaranteed to converge to zero.

In equation (24), $\Gamma = k_z(d/dt)\Delta_z$; when $|\Gamma| \leq \Lambda_z$, $\dot{V}_3 \leq -\xi_1\sigma_{z1}^2 - \xi_2\sigma_{z2}^2 - \xi_3\sigma_{z3}^2 \leq -\xi V_3$ is strictly negative, in which $\xi = \min(\xi_1, \xi_2, \xi_3)$. As a result, the proposed control method can ensure that the tracking error converges to zero.

However, uncertain fault or external disturbance Δ_z is usually time-varying in the actual control system, and the upper bound of function Γ cannot be obtained accurately. If the value of switching gain Λ_z is too large, it can counteract the influence of interference Γ and ensure the robustness of the control method, but it will cause chattering to the control input because of the too large switching gain.

If Λ_z in equation (23) is a tiny fixed constant, it cannot well counteract the effect of Δ_z. Thus, we construct an adaptive switching gain function, and then equation (23) can be updated as follows:

$$u_{1s} = \int\left(\left(\widehat{\Lambda}_z + \varsigma_z\right)\mathrm{sign}\left(\sigma_{z3}\right)\right), \quad (26)$$

where $\widehat{\Lambda}_z$ is the adaptive switching gain, and the adaptive law is shown in following equation:

$$\dot{\widehat{\Lambda}}_z = \frac{1}{\delta_z}\left|\sigma_{z3}\right|. \quad (27)$$

In equation (27), δ_z is a positive constant. Let $\widetilde{\Lambda}_z = \widehat{\Lambda}_z - \Lambda_z^*$, where Λ_z^* is the optimal switching gain, and $\Lambda_z^* \geq |\Gamma|$; then, combined with equation (19), we define a Lyapunov function as follows:

$$V_4 = V_3 + \frac{1}{2}\delta_z\widetilde{\Lambda}^2. \quad (28)$$

Then, we can obtain the following equation through deriving equation (28):

$$\dot{V}_4 = \dot{V}_3 + \delta_z\widetilde{\Lambda}\dot{\widetilde{\Lambda}}$$
$$= -\xi_1\sigma_{z1}^2 - \xi_2\sigma_{z2}^2 + \sigma_{z2}\sigma_{z3} + \delta_z\left(\widehat{\Lambda}_z - \Lambda_z^*\right)\dot{\widehat{\Lambda}}_z$$
$$+ \sigma_{z3}\left(\frac{\mathrm{d}}{\mathrm{d}t}\left(\dot{e} + k_z\left(\frac{1}{m}\left(\cos(\phi)\cos(\theta)\right)U_1 - g + \Delta_z - \ddot{z}_d\right)\right) - \dot{\alpha}_2\right). \quad (29)$$

Substituting equations (20) and (21) and equation (26) into equation (29), then equation (29) can be updated as follows:

$$\begin{aligned}\dot{V}_4 &= -\xi_1\sigma_{z1}^2 - \xi_2\sigma_{z2}^2 - \xi_3\sigma_{z3}^2 + \sigma_{z3}\frac{\mathrm{d}}{\mathrm{d}t}\left(u_{1as} + k_z\Delta_z\right) + \delta_z\left(\widehat{\Lambda}_z - \Lambda_z^*\right)\dot{\widehat{\Lambda}}_z \\ &= -\xi_1\sigma_{z1}^2 - \xi_2\sigma_{z2}^2 - \xi_3\sigma_{z3}^2 + \delta_z\left(\widehat{\Lambda}_z - \Lambda_z^*\right)\dot{\widehat{\Lambda}}_z + \sigma_{z3}\left(-\left(\widehat{\Lambda}_z + \varsigma_z\right)\mathrm{sign}\left(\sigma_{z3}\right) + k_z\left(\frac{\mathrm{d}}{\mathrm{d}t}\right)\Delta_z\right) \\ &\leq -\xi_1\sigma_{z1}^2 - \xi_2\sigma_{z2}^2 - \xi_3\sigma_{z3}^2 - \left(\Lambda_z^* + \varsigma_z\right)\left|\sigma_{z3}\right| + \Gamma\left|\sigma_{z3}\right|,\end{aligned} \quad (30)$$

in which $\Lambda_z^* \geq |\Gamma|$, so we have $\dot{V}_4 \leq -\xi_1\sigma_{z1}^2 - \xi_2\sigma_{z2}^2 - \xi_3\sigma_{z3}^2 \leq -\xi V_3$. It can be concluded that $\dot{V}_4 \leq 0$ is strictly negative. Therefore, σ_{z1}, σ_{z2}, and σ_{z3} can converge to zero in limited time eventually, and the system can be asymptotically stable; finally, the UAV can track the expected position accurately.

3.2.2. The Design of Horizontal Plane Motion Controller. The horizontal motion control includes two parts: x-axis and y-axis. The derivation process of horizontal plane motion controller is the same as that of altitude controller; therefore, only the derivation of the x and y direction controller is given here.

The controller in the x direction can be expressed as follows:

$$\begin{cases} u_x = \dfrac{m}{k_x U_1}\left(u_{xn} - u_{xas}\right), \\ u_{xn} = k_x\ddot{x}_d - \dot{e}_x + a_{x2} - \displaystyle\int\left(\xi_3\sigma_{x3} + \sigma_{x2}\right), \\ u_{xas} = \displaystyle\int\left(\left(\widehat{\Lambda}_x + \varsigma_x\right)\mathrm{sign}\left(\sigma_{x3}\right)\right), \\ \dot{\widehat{\Lambda}}_x = \dfrac{1}{\delta_x}\left|\sigma_{x3}\right|. \end{cases} \quad (31)$$

The controller in the y direction can be expressed as follows:

Table 1: Physical parameters of quadrotor UAV.

Parameters	Numerical value	The physical meaning of parameter
m	1.0	The mass of the quadrotor UAV (kg)
g	9.8	Gravity acceleration (m/s^2)
I_y	0.005	The moment of inertias of the Y-axis (kg/m^2)
I_x	0.005	The moment of inertias of the X-axis (kg/m^2)
I_z	0.01	The moment of inertias of the Z-axis (kg/m^2)
l	0.2	The length of the quadrotor UAV from the end of each rotor to the center of gravity (m)
J_r	0.00002	The moment of inertia of the motor rotor (kg/m^2)
b	0.00003	The drag coefficient
d	0.00000006	The lift coefficient

Table 2: Parameters of controller.

The parameters of controllers	Numerical value
$k_i\,(i = x, y, z)$	0.5
$k_j\,(j = \phi, \theta, \psi)$	0.3
$\xi_i\,(i = 1, 2, 3)$	3
$\delta_i\,(i = x, y, z)$	0.5
$\delta_i\,(i = \phi, \theta, \psi)$	5

$$\begin{cases} u_y = \dfrac{m}{k_y U_1}\left(u_{yn} - u_{yas}\right), \\ u_{yn} = k_y \ddot{y}_d - \dot{e}_y + a_{y2} - \displaystyle\int\left(\xi_3 \sigma_{y3} + \sigma_{y2}\right), \\ u_{xas} = \displaystyle\int\left(\left(\widehat{\Lambda}_y + \varsigma_y\right)\mathrm{sign}\left(\sigma_{y3}\right)\right), \\ \dot{\widehat{\Lambda}}_y = \dfrac{1}{\delta_y}\left|\sigma_{y3}\right|, \end{cases} \tag{32}$$

where in equations (31) and (32),

$$\begin{cases} e_x = x - x_d, \quad e_y = y - y_d, \sigma_{x1} = s_{x1}, \sigma_{y1} = s_{y1}, \\ \sigma_{x2} = s_{x2} - \alpha_{x1}, \quad \sigma_{x3} = s_{x3} - \alpha_{x2}, \\ \sigma_{y2} = s_{y2} - \alpha_{y1}, \quad \sigma_{y3} = s_{y3} - \alpha_{y2}, \\ \alpha_{x1} = -\xi_1 \sigma_{x1}, \quad \alpha_{y1} = -\xi_1 \sigma_{y1}, \\ s_{x1} = \displaystyle\int\left(e_x + k_x \dot{e}_x\right), \quad s_{y1} = \displaystyle\int\left(e_y + k_y \dot{e}_y\right), \\ e_x = x - x_d, \quad e_y = y - y_d, \\ s_{x2} = \dot{s}_{x1}, \quad s_{x3} = \ddot{s}_{x1}, s_{y2} = \dot{s}_{y1}, s_{y3} = \ddot{s}_{y1}, \\ k_x, k_y, \delta_x, \delta_y, \varsigma_x, \varsigma_y > 0, \end{cases} \tag{33}$$

where x_d and y_d are the reference values in x direction and y direction, respectively.

3.2.3. The Design of Attitude Controller. Likewise, the design process of attitude controller is the same as that of altitude controller. Therefore, only the derivation of the controllers of attitude ϕ, θ, and ψ is given here.

According to equation (2) and combined with equations (31) and (32), the expected values of pitch angle and roll angle can be obtained as follows:

$$\begin{cases} \phi_d = \arcsin\left(u_x \sin\psi - u_y \cos\psi\right), \\ \theta_d = \arcsin\left(\dfrac{u_x - \sin\phi_d \sin\psi}{\cos\phi_d \cos\psi}\right). \end{cases} \tag{34}$$

The controller of attitude ϕ is as follows:

$$\begin{cases} U_2 = \dfrac{I_x}{k_\phi l}\left(u_{\phi n} - u_{\phi as}\right), \\ u_{\phi n} = -k_\phi\left(\dot{\theta}\dot{\psi}\dfrac{I_y - I_z}{I_x} + \dfrac{J_r}{I_x}\dot{\theta}\omega_r - \ddot{\phi}_d\right) - \dot{e}_\phi + a_{\phi 2} - \displaystyle\int\left(\xi_3\sigma_{\phi 3} + \sigma_{\phi 2}\right), \\ u_{\phi as} = \displaystyle\int\left(\left(\widehat{\Lambda}_\phi + \varsigma_\phi\right)\mathrm{sign}\left(\sigma_{\phi 3}\right)\right), \quad \dot{\widehat{\Lambda}}_\phi = \dfrac{1}{\delta_\phi}\left|\sigma_{\phi 3}\right|. \end{cases} \tag{35}$$

The controller of attitude θ is as follows:

$$\begin{cases} U_3 = \dfrac{I_y}{k_\theta l}\left(u_{\theta n} - u_{\theta as}\right), \\ u_{\theta n} = -k_\theta\left(\dot{\psi}\dot{\phi}\dfrac{I_z - I_x}{I_y} - \dfrac{J_r}{I_y}\dot{\phi}\omega_r - \ddot{\theta}_d\right) \\ -\dot{e}_\theta + a_{\theta 2} - \displaystyle\int\left(\xi_3\sigma_{\theta 3} + \sigma_{\theta 2}\right), \\ u_{\theta as} = \displaystyle\int\left(\left(\widehat{\Lambda}_\theta + \varsigma_\theta\right)\mathrm{sign}\left(\sigma_{\theta 3}\right)\right), \dot{\widehat{\Lambda}}_\theta = \dfrac{1}{\delta_\theta}\left|\sigma_{\theta 3}\right|. \end{cases} \tag{36}$$

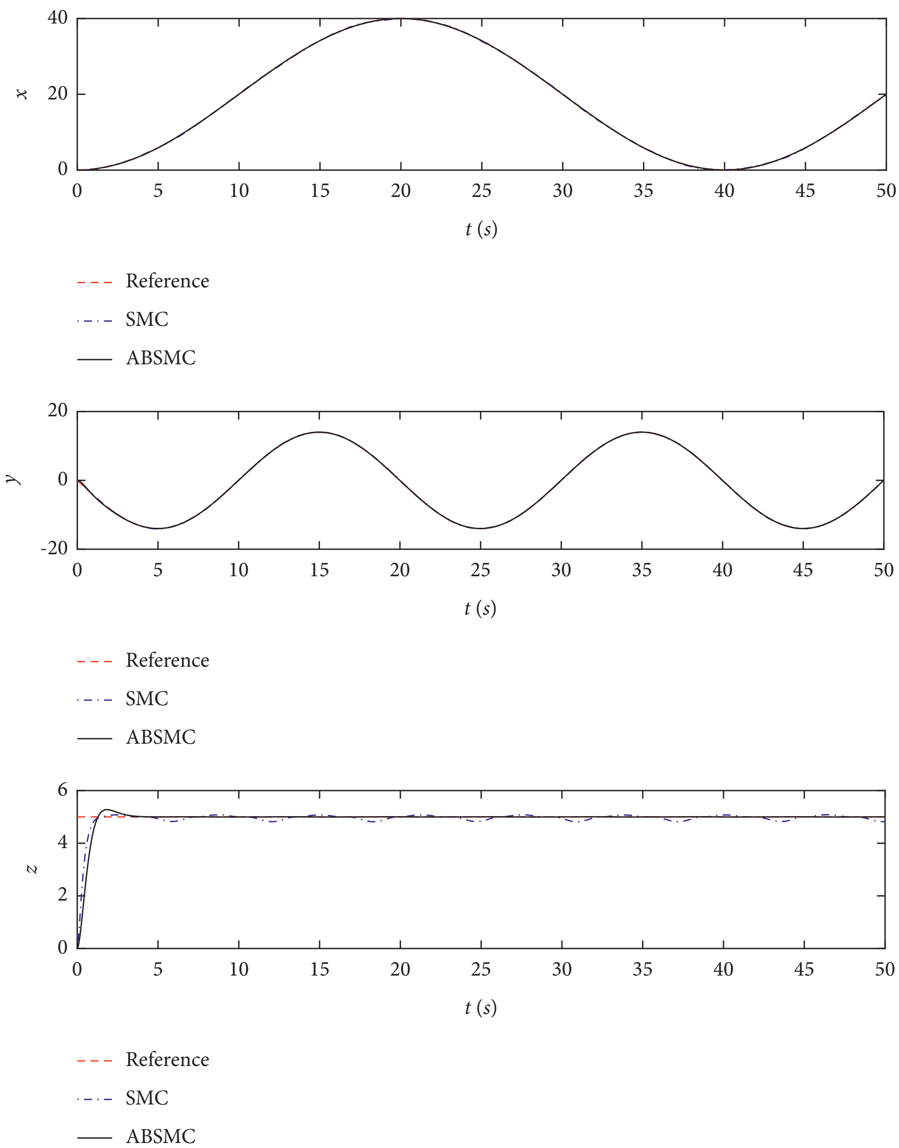

Figure 3: UAV's position tracking.

The controller of attitude ψ is as follows:

$$\begin{cases} U_4 = \dfrac{I_z}{k_\psi l}\left(u_{\psi n} - u_{\psi as}\right), \\ u_{\psi n} = -k_\psi\left(\dot{\phi}\dot{\theta}\dfrac{I_x - I_y}{I_z} - \ddot{\psi}_d\right) - \dot{e}_\psi + a_{\psi 2} - \displaystyle\int\left(\xi_3\sigma_{\psi 3} + \sigma_{\psi 2}\right), \\ u_{\psi as} = \displaystyle\int\left(\left(\widehat{\Lambda}_\psi + \varsigma_\psi\right)\operatorname{sign}\left(\sigma_{\psi 3}\right)\right), \dot{\widehat{\Lambda}}_\psi = \dfrac{1}{\delta_\psi}\left|\sigma_{\psi 3}\right|, \end{cases} \tag{37}$$

where in equations (33) to (35),

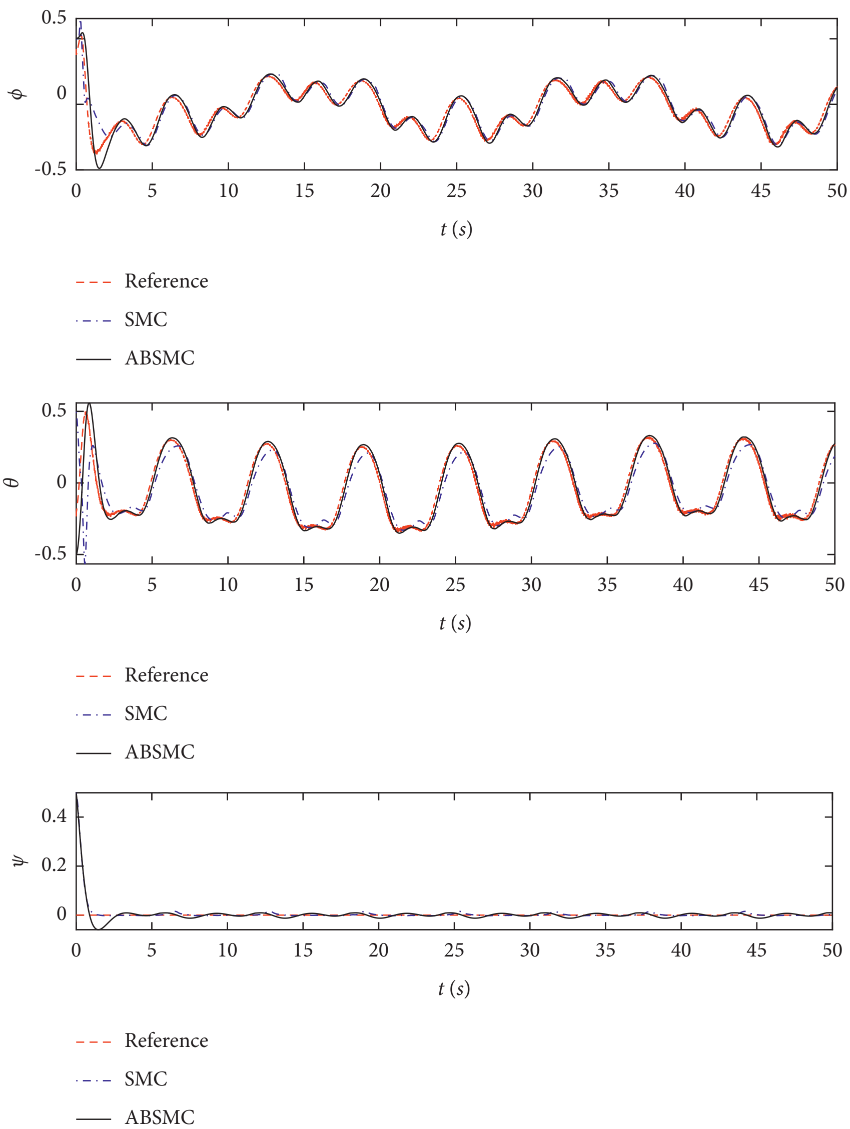

Figure 4: UAV's attitude tracking.

$$\begin{cases} e_\phi = \phi - \phi_d, e_\theta = \theta - \theta_d, & e_\psi = \psi - \psi_d, \\ \sigma_{\phi 1} = s_{\phi 1}, \sigma_{\theta 1} = s_{\theta 1}, & \sigma_{\psi 1} = s_{\psi 1}, \\ \sigma_{\phi 2} = s_{\phi 2} - \alpha_{\phi 1}, & \sigma_{\phi 3} = s_{\phi 3} - \alpha_{\phi 2}, \\ \sigma_{\theta 2} = s_{\theta 2} - \alpha_{\theta 1}, & \sigma_{\theta 3} = s_{\theta 3} - \alpha_{\theta 2}, \\ \sigma_{\psi 2} = s_{\psi 2} - \alpha_{\psi 1}, & \sigma_{\psi 3} = s_{\psi 3} - \alpha_{\psi 2}, \\ \alpha_{\phi 1} = -\xi_1 \sigma_{\phi 1}, \alpha_{\theta 1} = -\xi_1 \sigma_{\theta 1}, & \alpha_{\psi 1} = -\xi_1 \sigma_{\psi 1}, \\ s_{\phi 1} = \int \left(e_\phi + k_\phi \dot{e}_\phi\right), & s_{\theta 1} = \int \left(e_\theta + k_\theta \dot{e}_\theta\right),\ s_{\psi 1} = \int \left(e_\psi + k_\psi \dot{e}_\psi\right), \\ e_\phi = \phi - \phi_d, \quad e_\theta = \theta - \theta_d, & e_\psi = \psi - \psi_d, \\ s_{\phi 2} = \dot{s}_{\phi 1}, & s_{\phi 3} = \ddot{s}_{\phi 1}, s_{\theta 2} = \dot{s}_{\theta 1},\ s_{\theta 3} = \ddot{s}_{\theta 1},\ s_{\psi 2} = \dot{s}_{\psi 1},\ s_{\psi 3} = \ddot{s}_{\psi 1}, \\ k_\phi, k_\theta, k_\psi, \delta_\phi, \delta_\theta, \delta_\psi, \varsigma_\phi, \varsigma_\theta, \varsigma_\psi > 0. \end{cases} \tag{38}$$

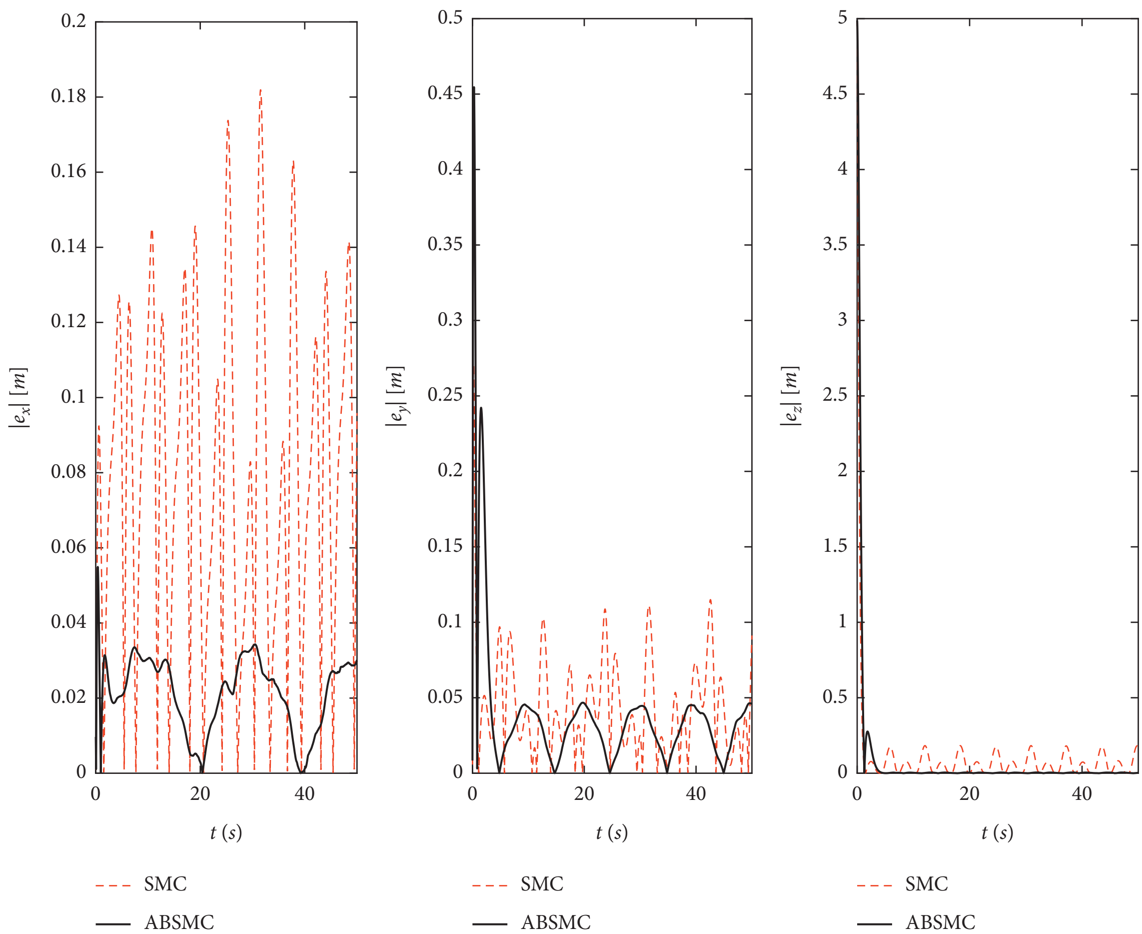

FIGURE 5: The absolute error of UAV's position tracking.

4. Simulation Results

To verify the effectiveness of the proposed ABSMC method, the SMC method and ABSMC method are used to perform trajectory tracking control of quadrotor UAV based on MATLAB 2019b. The expected trajectory of the UAV is set as shown in equation (39). Actuator fault and external disturbance of the aircraft are set as shown in equation (40). The relevant physical parameters of quadrotor UAV are shown in Table 1, and the control parameters are shown in Table 2.

$$\begin{cases} x_d = 20\left(1 - \cos\left(\dfrac{\pi t}{20}\right)\right), \\ y_d = -14 \sin\left(\dfrac{\pi t}{10}\right), \\ z_d = 5, \\ \psi_d = 0, \end{cases} \tag{39}$$

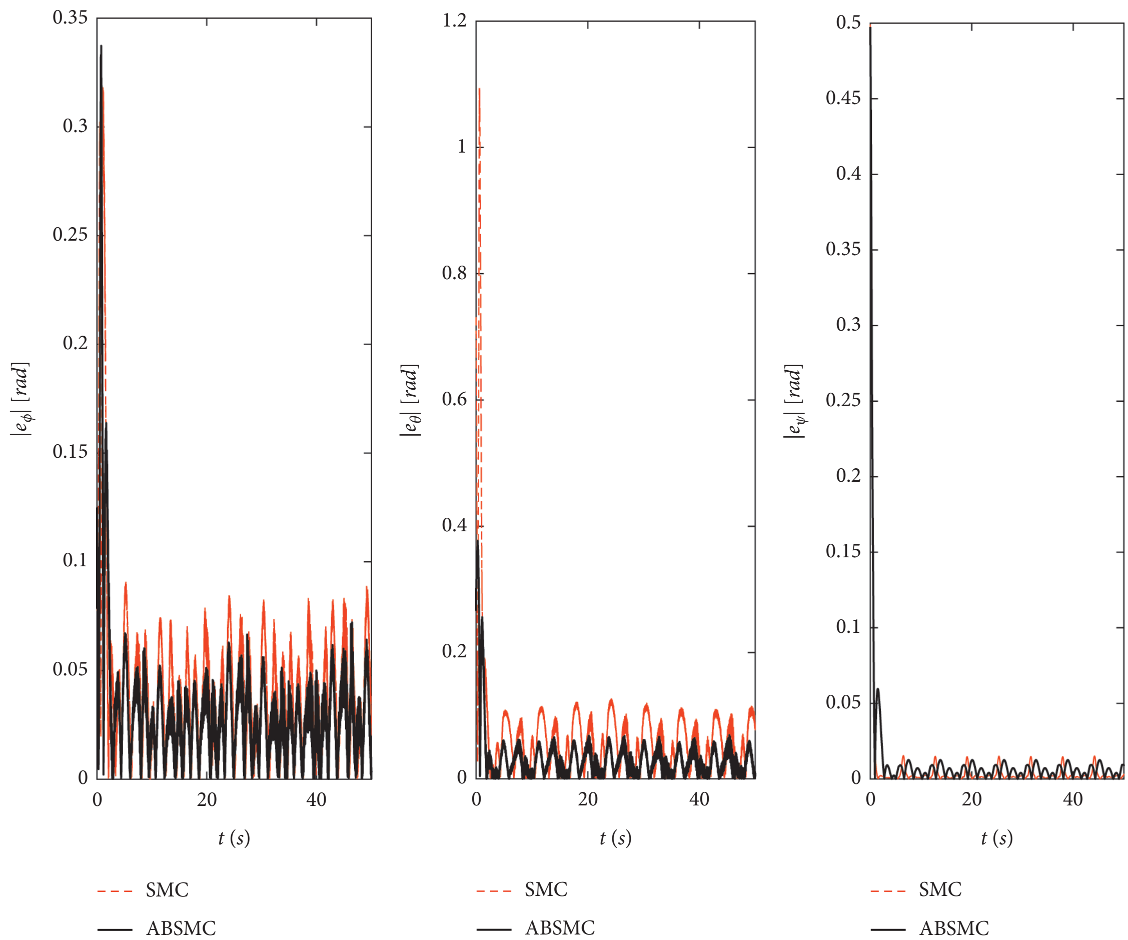

FIGURE 6: The absolute error of UAV's attitude tracking.

$$\begin{cases} \varepsilon U_1 = 0.4\sin(t)U_1, & \varepsilon U_3 = 0.2(\sin(t) + \cos(t))U_3, \\ \varepsilon U_2 = 0.4\cos(t)U_2, & \varepsilon U_4 = 0.2(\sin(t) - \cos(t))U_4, \\ f_1 = -\cos(2t) - 3\cos(t), & f_2 = -\cos(2t) - 3\cos(t), \\ f_3 = -3\cos(t), & f_4 = \cos(2t) + \cos(t), \\ f_5 = -\cos(2t) - 3\cos(t), & f_6 = \cos(2t) + \cos(t). \end{cases} \tag{40}$$

It can be seen that the sliding mode control method has a good control effect in the case of actuator failure and external interference, as shown in Figures 3–6; however, since its switching gain is fixed, it still has disadvantages in the face of interference beyond the upper bound of its gain. At this time, the adaptive backstepping sliding mode control method with adaptive switching gain can adaptively adjust its switching. Compared with the SMC method, it is clear that the ABSMC method significantly suppresses the chattering phenomenon of sliding mode control input after the adaptive switching gain being introduced and the backstepping method being used for correction, as shown in Figures 7 and 8. And the chattering caused by the SMC method is limited in a small range. Therefore, the adaptive backstepping sliding mode control method shows better control performance from the pose tracking effect in Figures 3 to 6.

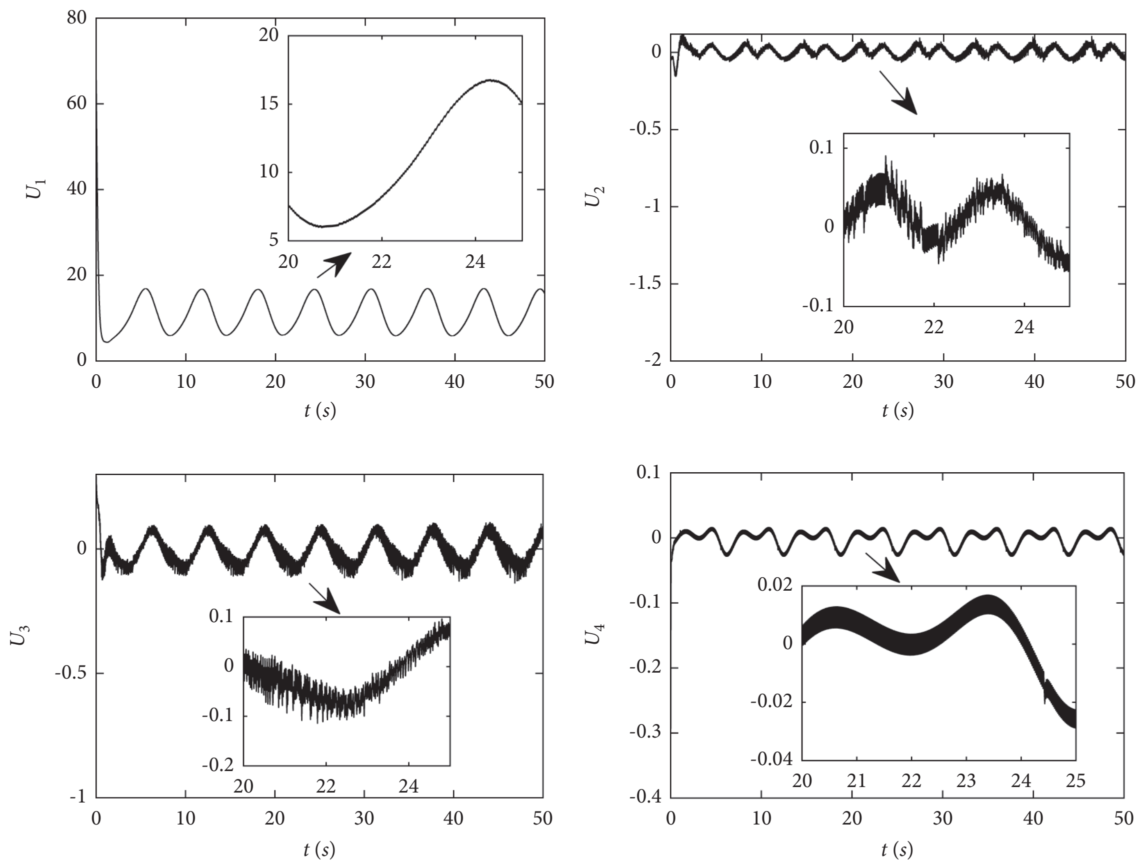

Figure 7: Control input based on the ABSMC method.

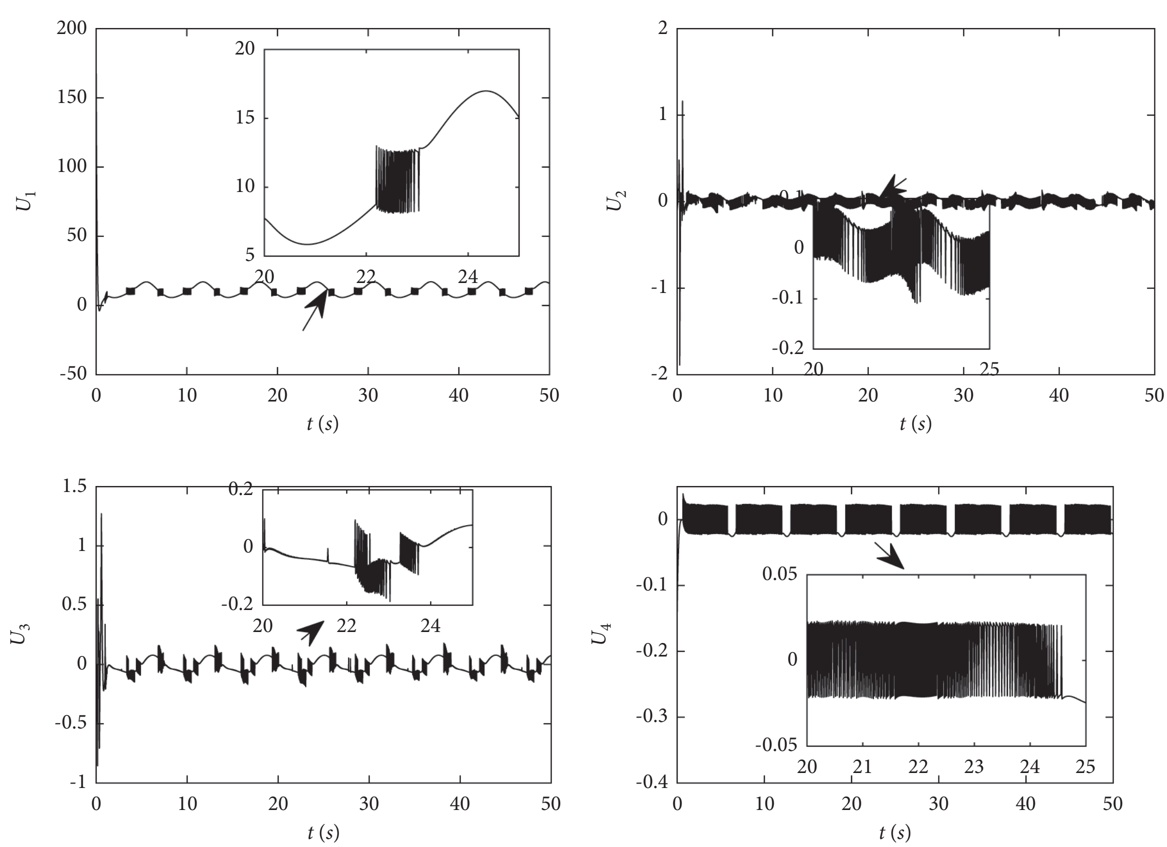

Figure 8: Control input based on the SMC method.

5. Conclusion

Aiming at the trajectory tracking control problem of quadrotor UAV based on actuator fault and external disturbance, the ABSMC method is proposed in this paper by constructing the switching gain of adaptive sliding mode control in the backstepping design process and using differential iteration scheme to suppress the chattering effect of sliding mode control, then the dynamic model of quadrotor UAV is setup, and the control strategy and controllers are designed based on the proposed method. In order to verify the effectiveness of the proposed method, the sliding mode control method and the adaptive stepping sliding mode control method proposed in this paper are used to simulate the actuator fault and external disturbance during the flight of the quadrotor UAV, and the control effect of the two methods is compared. According to the simulation results, it is found that the adaptive backstepping sliding mode control method proposed in this paper not only guarantees the convergence performance of the sliding mode control method but also effectively suppresses the chattering problem caused by the gain of the switching reaching rate. Therefore, the accuracy of trajectory tracking control for quadrotor UAV during external flight disturbances and uncertainties can be improved by the proposed method.

Data Availability

The datasets used and/or analyzed during the current study are available from the corresponding author on reasonable request.

Conflicts of Interest

The authors declare that they have no conflicts of interest.

Acknowledgments

The authors acknowledge the National Natural Science Foundation of China (Grant 61772225), the Major Projects of Guangdong Education Department for Foundation Research and Applied Research (Grants 2017KZDXM081 and 2018KZDXM066), the Featured Innovative Projects of Department of Education of Guangdong Province (Grant 2019KTSCX175), the Key-Area Research and Development Program of Guangdong Province (Grant 2019B010137002), the Guangdong Higher Education Teaching Reform Project (Grant: 2019566) and the Teaching Reform Project of Huizhou University (Grant YYXKC2019003).

References

[1] M. Hassanalian and A. Abdelkefi, “Classifications, applications, and design challenges of drones: a review,” *Progress in Aerospace Sciences*, vol. 91, pp. 99–131, 2017.

[2] G. Macrina, L. Di Puglia Pugliese, F. Guerriero, and G. Laporte, “Drone-aided routing: a literature review,” *Transportation Research Part C: Emerging Technologies*, vol. 120, Article ID 102762, 2020.

[3] H. Mo and G. Farid, “Nonlinear and adaptive intelligent control techniques for quadrotor uav - a survey,” *Asian Journal of Control*, vol. 21, no. 2, pp. 989–1008, 2019.

[4] C. Kanellakis and G. Nikolakopoulos, “Survey on computer vision for UAVs: current developments and trends,” *Journal of Intelligent and Robotic Systems*, vol. 87, no. 1, pp. 141–168, 2017.

[5] S. Mallavalli and A. Fekih, “A fault tolerant tracking control for a quadrotor UAV subject to simultaneous actuator faults and exogenous disturbances,” *International Journal of Control*, vol. 93, no. 3, pp. 655–668, 2020.

[6] Y. Zhong, Y. Zhang, W. Zhang, J. Zuo, and H. Zhan, “Robust actuator fault detection and diagnosis for a quadrotor UAV with external disturbances,” *IEEE Access*, vol. 6, Article ID 48169, 2018.

[7] Y. Zhang, Z. Chen, X. Zhang, Q. Sun, and M. Sun, “A novel control scheme for quadrotor UAV based upon active disturbance rejection control,” *Aerospace Science and Technology*, vol. 79, pp. 601–609, 2018.

[8] B. C. Zheng, X. Yu, and Y. Xue, “Quantized sliding mode control in delta operator framework,” *International Journal of Robust and Nonlinear Control*, vol. 28, no. 2, pp. 519–535, 2018.

[9] S. Modali, S. Ghosh, and S. P.B., “Sliding mode-based guidance for UAV landing on a stationary or moving ground vehicle,” *IFAC-PapersOnLine*, vol. 53, no. 1, pp. 453–458, 2020.

[10] W. Gong, B. Li, Y. Yang, H. Ban, and B. Xiao, “Fixed-time integral-type sliding mode control for the quadrotor UAV attitude stabilization under actuator failures,” *Aerospace Science and Technology*, vol. 95, Article ID 105444, 2019.

[11] X. Wu, B. Xiao, and Y. Qu, “Modeling and sliding mode-based attitude tracking control of a quadrotor UAV with time-varying mass,” *ISA Transactions*, 2019, In press.

[12] E. H. Zheng, J. J. Xiong, and J. L. Luo, “Second order sliding mode control for a quadrotor UAV,” *ISA Transactions*, vol. 53, no. 4, pp. 1350–1356, 2014.

[13] X. Zhang, “Robust integral sliding mode control for uncertain switched systems under arbitrary switching rules,” *Nonlinear Analysis: Hybrid Systems*, vol. 37, Article ID 100900, 2020.

[14] H. Zhao, Y. Niu, and J. Zhao, “Event-triggered sliding mode control of uncertain switched systems under denial-of-service attacks,” *Journal of the Franklin Institute*, vol. 356, no. 18, Article ID 11414, 2019.

[15] X. Zhao, X. Zhang, X. Ye, and Y. Liu, “Sliding mode controller design for supercavitating vehicles,” *Ocean Engineering*, vol. 184, pp. 173–183, 2019.

[16] S. Baek, J. Baek, and S. Han, “An adaptive sliding mode control with effective switching gain tuning near the sliding surface,” *IEEE Access*, vol. 7, Article ID 15563, 2019.

[17] C. Liu, G. Wen, and Z. Zhao, “Neural-network-based sliding-mode control of an uncertain robot using dynamic model approximated switching gain,” *IEEE transactions on cybernetics*, vol. 51, no. 5, 2020.

[18] S. Liu, Y. Liu, and N. Wang, “Nonlinear disturbance observer-based backstepping finite-time sliding mode tracking control of underwater vehicles with system uncertainties and external disturbances,” *Nonlinear Dynamics*, vol. 88, no. 1, pp. 465–476, 2017.

[19] G. Cui, J. Yu, and Q. G. Wang, “Finite-time adaptive fuzzy control for MIMO nonlinear systems with input saturation via improved command-filtered backstepping,” *IEEE Transactions on Systems, Man, and Cybernetics: Systems*, 2020.

[20] J.-J. Xiong and G.-B. Zhang, "Global fast dynamic terminal sliding mode control for a quadrotor UAV," *ISA Transactions*, vol. 66, pp. 233–240, 2017.
[21] Q. Luo, J. Yuan, X. Q. Chen, Q. Zhijian, and T. Jinjun, "Analyzing start-up time headway distribution characteristics at signalized intersections," *Physica A: Statistical Mechanics and its Applications*, vol. 535, no. 1, pp. 1–10, 2019.
[22] M. Labbadi and M. Cherkaoui, "Robust adaptive backstepping fast terminal sliding mode controller for uncertain quadrotor UAV," *Aerospace Science and Technology*, vol. 93, Article ID 105306, 2019.
[23] Q. Luo, J. Yuan, X. Chen, J. Yang, W. Zhang, and J. Zhao, "Research on mixed user equilibrium model based on mobile Internet traffic information service," *IEEE Access*, vol. 7, no. 1, Article ID 164775, 2019.
[24] C. Zhai and W. Wu, "Designing continuous delay feedback control for lattice hydrodynamic model under cyber-attacks and connected vehicle environment," *Communications in Nonlinear Science and Numerical Simulation*, vol. 95, Article ID 105667, 2021.
[25] C. Zhai and W. T. Wu, "Car-following model based delay feedback control method with the gyroidal road," *International Journal of Modern Physics C*, vol. 30, no. 9, Article ID 1950074, 2019.

Hindawi
Scientific Programming
Volume 2021, Article ID 8381550, 7 pages
https://doi.org/10.1155/2021/8381550

Research Article

Malware Detection Using CNN via Word Embedding in Cloud Computing Infrastructure

Rong Wang, Cong Tian, and Lin Yan

School of Computer Science and Technology, Xidian University, Xi'an 710000, China

Correspondence should be addressed to Rong Wang; bilywr@163.com

Received 5 August 2021; Accepted 2 September 2021; Published 13 September 2021

Academic Editor: Punit Gupta

The Internet of Things (IoT), cloud, and fog computing paradigms provide a powerful large-scale computing infrastructure for a variety of data and computation-intensive applications. These cutting-edge computing infrastructures, however, are nevertheless vulnerable to serious security and privacy risks. One of the most important countermeasures against cybersecurity threats is intrusion detection and prevention systems, which monitor devices, networks, and systems for malicious activity and policy violations. The detection and prevention systems range from antivirus software to hierarchical systems that monitor the traffic of whole backbone networks. At the moment, the primary defensive solutions are based on malware feature extraction. Most known feature extraction algorithms use byte N-gram patterns or binary strings to represent log files or other static information. The information taken from program files is expressed using word embedding (GloVe) and a new feature extraction method proposed in this article. As a result, the relevant vector space model (VSM) will incorporate more information about unknown programs. We utilize convolutional neural network (CNN) to analyze the feature maps represented by word embedding and apply Softmax to fit the probability of a malicious program. Eventually, we consider a program to be malicious if the probability is greater than 0.5; otherwise, it is a benign program. Experimental result shows that our approach achieves a level of accuracy higher than 98%.

1. Introduction

Cloud-fog-edge computing, especially cloud computing, is providing a variety of services in many areas throughout the world. The cloud offers a variety of unique security problems, one of which is the detection of malware. Malware is a significant threat to modern computing devices for their illegal purposes, such as unauthorized access, stealing confidential or personal information, implanting ads, and disrupting normal operation. Therefore, some effective approaches and tools for detecting and deactivating malware are required.

A widely used approach for malware detection is behavior-based method, which monitors the behaviors of a program, typically the stream of system calls, to determine whether it is malicious [1, 2]. However, behavior-based malware detection method is inferior in detecting the unseen and continuously modified malware because of its rigid and restrictive nature [3].

In this article, we propose a framework for malware detection that combines behavior-based feature extraction with deep learning. Our work makes the following major contributions:

(1) Unified design of behavior detection and feature extraction: we use a tool Cuckoo Sandbox to collect the behavior information of the program (executable file) when it executed inside a realistic but isolated environment. Then, we construct a map of monitored behavior to a vector space with a method GloVe [4], which trains on a global word-word co-occurrence matrix and produces a word vector space model, to represent each word of the corpus with a real-valued vector.

(2) Representation of the program's behavioral characteristics as a feature map (a matrix consisting of sequential word vectors): this transformation makes behavioral patterns reflected geometrically and

accessible by convolutional neural network, an excellent deep learning algorithm to capture word-level features from the feature maps and further predict the labels of the feature maps, malware or benign.

The rest of this article is organized as follows. Section 2 describes the related work of malware detection. Section 3 studies the problem formulation posed by our approaches. Section 4 introduces the framework of the proposed malware detection model in detail. Section 5 presents the experimental results that are followed by the conclusions in Section 6.

2. Related Work

Malware detection has been a critical challenge in computing since the late 80s, which mainly involves two processes, feature extraction and classification. For feature extraction, many researches focus on using information available in API calls to monitor the behavior of the program that may potentially highlight anomalous and malicious activities.

The work by Alazab et al. [5] studied an automated method of extracting API call features and analysed them to understand their use for malicious purpose. Sundarkumar et al. [6] presented a model, based on the types of API call sequences, using text mining and topic modeling to detect malware. Hachinyan [7] discussed proactive methods based on API call sequences analysis and proposed a method using a multiple sequence alignment to identify malware. Most recently, Pektas, and Acarman [8] presented a runtime behavior-based classification approach for Windows malware, which extracts runtime behaviors for the determination of a malicious sequence of API calls. In this article, we extract API call sequences of program as a baseline to compare with extracting feature from the behavioral information of program in a sandbox environment.

Term Frequency-Inverse Document Frequency (TF-IDF) is a common weighted technique for information retrieval and data mining. Term Frequency (TF) refers to the number of times a given word appears in a document. Jones [9] first puts forward a technical term, later known as Inverse Document Frequency (IDF), which counts the documents containing (or being indexed by) the term in question. TF-IDF has been used for web document clustering and ranking [10], text classification [11], analysis of similarity between important terms in text documents [12], and image retrieval [13]. In this article, we use TF-IDF to extract feature from the corpus of program behavior descriptions as another baseline compared with word embedding and use SVM to classify the numerical characteristics compared with CNN classifying feature maps.

3. Problem Formulation

Several malware detection researches related to Deep Learning have been proved effective, which extract information from log files of program, like API call sequences during execution process, and create a so-called program behavior language model based on this information. But there are two problems:

(1) It is not certain that the resulting textual information from program's log files can describe the nature of programs
(2) The behavior language model established using the GloVe model for API call sequences may lose the syntax information in some dimension

As we all know, the quality of feature extraction has a decisive influence on malware detection. For accuracy and effectiveness, we want more comprehensive, expressive, and available features of programs. On the other hand, byte data in malware can contain multiple types of information, including human-readable text, binary code, images, and even some encrypted content. Therefore, we expect to design a malware detection model that can extract sufficient information from program and be described in a usable format.

4. Methodology

In this section, we propose a new malware detection method with supervised learning. Figure 1 shows an overview of the main steps in our method. This model adopts 5-fold cross validation to process datasets (malware program set and benign program set).

In the training phrase above the dotted line, we first adopt Cuckoo sandbox to extract behavior information of the executable files, such as "Installs itself for autorun at Windows startup," "Installs itself for autorun at Windows startup." Then, we perform a preprocessing to get word sequences, which called Information Unit. We use Glove model to capture the rich semantic and syntactic features of words and vectorize them. The output of GloVe is a dictionary of word embedding for each unique word. After that, we look up in the dictionary to represent every word in the description file as its corresponding vector, thus a feature map of the program is generated. Finally, we obtain a trained CNN by learning from these feature maps.

Below the dotted line, the flowchart describes the detection phrase of our model. More specifically, we first input the executable file from the test set into Cuckoo for analysis to get the Information Unit and then look up in the dictionary of word embedding to get the Information Vector Unit; finally, we use CNN model mentioned above to predict the probability that the executable file is benign or malware. If the probability is higher than 0.5, we consider the program as a benign program, otherwise a malicious program.

4.1. Word Embedding. This stage first utilizes Cuckoo to analyze the executable files that may contain some malicious codes and obtains the program behavior information that described the natural language. Then, the model use GloVe proposed by Jeffrey Pennington to complete the word embedding. Each word w is represented by a 100-dimensional vector v. During this step, we leverage global statistical information by training on the word-word co-occurrence matrix X, where the element X_{ij} presents the number of

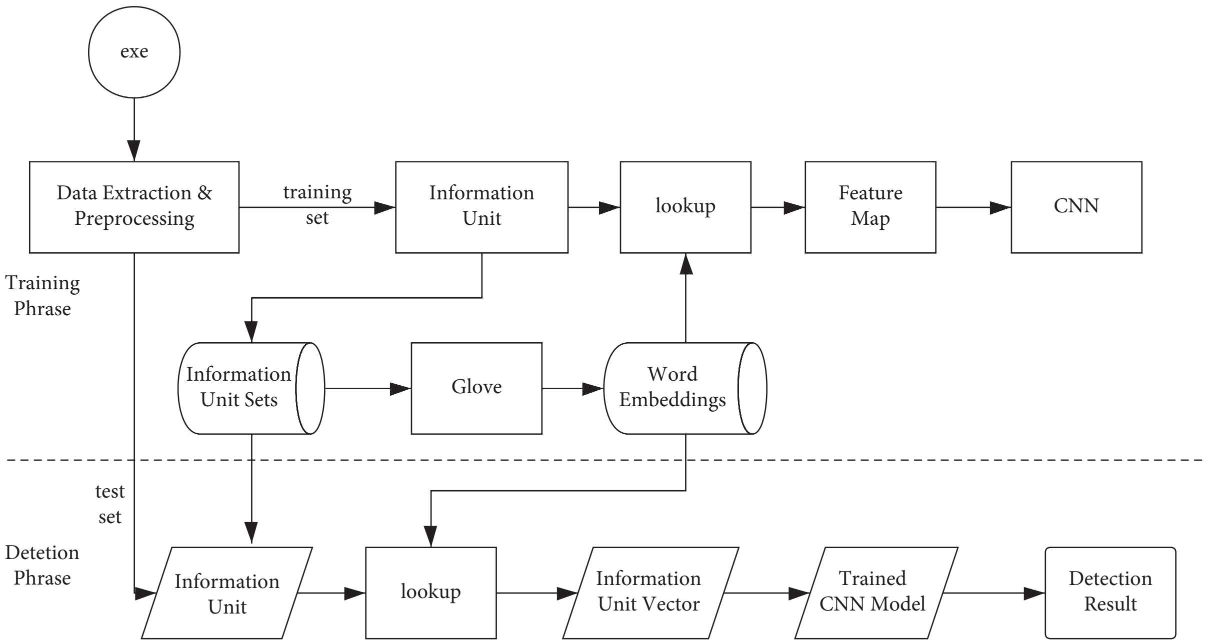

Figure 1: Overview of the main steps.

times that word w_i occurs in the context of word w_i. Let $X_i = \sum_k X_{ik}$ be the number of times that any word appears in the context of word w_i, and

$$P_{i,j} = P\left(w_j \mid w_i\right) = \frac{X_{ij}}{X_i}, \tag{1}$$

be the probability that word w_j appears in the context of word w_i. For three words w_i, w_j, and w_k, the radio P_{ik}/P_{jk} depends on the co-occurrence frequency of words (w_k, w_i) and (w_k, w_j), and the value is contributed to distinguishing relevant words from irrelevant words or discriminate the two relevant words. Let v_i, v_j, and v_k be the word vectors of w_i, w_j, and w_k, since the inherently linear structures of vector space, the radio P_{ik}/P_{jk} can be considered as a function of v_i, v_j, and v_k. Then, the radio P_{ik}/P_{jk} can be measured as follows:

$$F\left(\left(v_i - v_j\right)^T v_k\right) = \frac{X_{ik}}{X_{jk}}. \tag{2}$$

The regression connection function of the model is $P_{ik} = \exp(v_k^T v_i) + a_i + a_k$, where a_i and a_k can be approximated as $\log(X_i)$ and $\log(X_j)$. Then, $v_k^T = \log(P_{ik}) - \log(X_i) - \log(X_k)$ comes naturally. Then, the cost function of Model is $J = \sum_{i,j=1}^{N} f(X_{i,j})(v_i^T v_j + a_i + a_j - \log(X_{i,j}))^2$, where N is the size of the vocabulary (the dimensions of co-occurrence matrix is $N * N$, and v_i, v_j are the vector representations of the words w_i, w_j.

In addition, a weighting function $f(x)$ is needed so that the frequent co-occurrence word pairs will not be overweighted. Various functions can be selected, but we found one work well, which can be parameterized as follows:

$$f(x) = \begin{cases} \left(\dfrac{x}{x^{\max}}\right)^{\alpha}, & \text{if } x < x_{\max}, \\ 1, & \text{otherwise.} \end{cases} \tag{3}$$

Here, $\alpha = 3/4$, and then, the model will perform better to represent the words as vectors containing as many semantic and grammatical information as possible. After getting this word embedding, we can look up in the dictionary to turn word sequences into a two-dimensional feature map, which can also be generated by connecting as:

$$G = v_i \oplus v_j \oplus \cdots \oplus v_k \oplus v_l. \tag{4}$$

The resulting feature map is used as input of CNN.

Figure 2 shows two sample benign feature maps and two sample malware feature maps by their digital gray images. Here, the dimension of a word vector is 100, and different text lengths lead to different image sizes.

4.2. The CNN Architecture. In this work, we treat the feature images as input and perform a convolutional neural network to classify the images. Figure 3 shows the architecture of our CNN used in our model. In general, the basic structure of CNN consists of two layers: feature extraction layer and feature mapping layer. In the feature extraction layer, each neuron's input is connected to the local receptive field of the previous layer, and the local characteristics are extracted. Once the local feature is extracted, the relationship with other characteristics is also determined; In the feature mapping layer, each computing layer of the network consists of multiple feature maps, which can be seen as a plane. The feature mapping structure in our model uses the nonlinear activation function Relu:

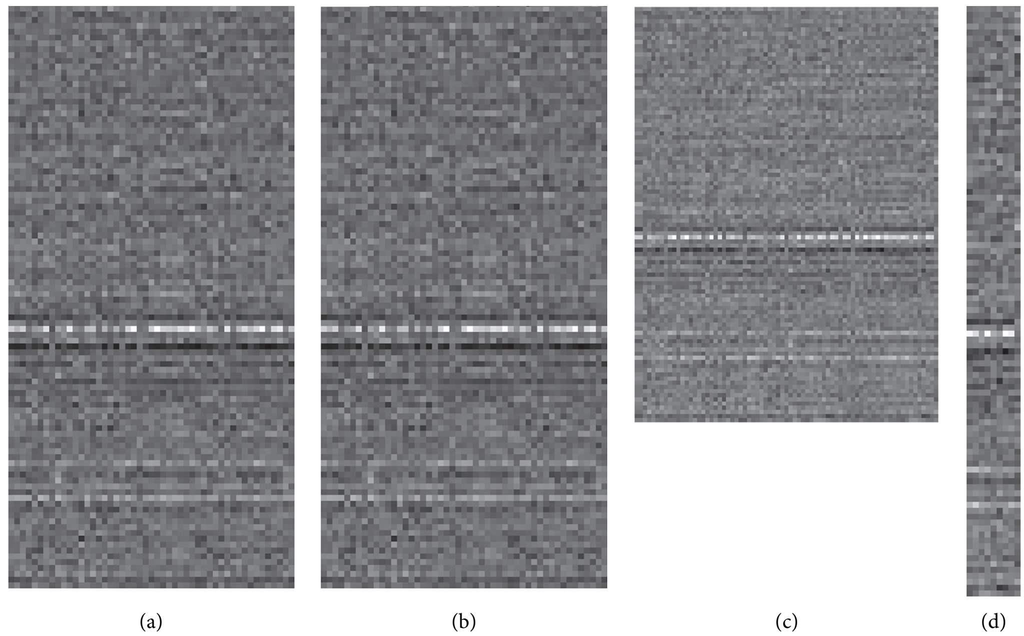

Figure 2: Gray images of two benign feature maps and two malware feature maps.

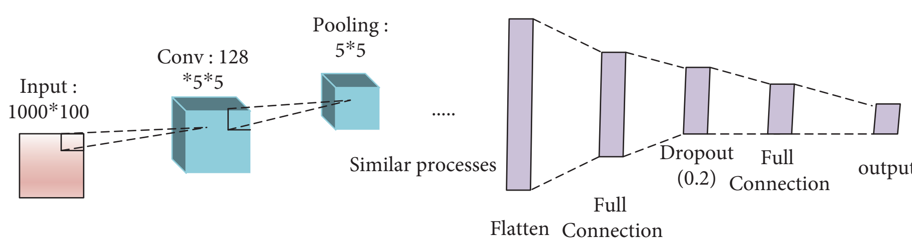

Figure 3: The framework of CNN.

$$f(x) = \max\{0, x\}. \tag{5}$$

4.2.1. Features Extraction. The main task of this stage is to generate a feature map from the complex features within the image. This features extraction stage can be defined as an alternate chain of two different layers (the convolutional layer and the pooling layer).

The convolutional layer applies a series of trainable and learnable K filters (or kernels) to analyze the image. In our CNN, we use the convolutional layer with 128 filters, select the window size of neural network is 5×5, and choose the Relu as the activation function. Each convolution layer in CNN is followed by a calculation layer aimed at the local average and secondary extraction. In the forward calculation, we input a certain size of data (width $w = 1000 *$ height $h = 100$), which dot product with the filter $w \in R^{h\times k}$ (a vector of $h \times k$ dimensions) and add a bias $b \in R^h$.

Then, the pooling layer is designed to compress the data hat produced by the previous convolutional layer and maintain the most relevant features. This layer swipes the filters one by one to form a new output data. More generally, the input is defined by the following parameters: h, w. Here, h represents the height of the volume and w is the width.

When we consider the image processing, for each filter k, the convolutional layer applies a convolution defined as follows:

$$o_{i,j,k} = \sum_{h=0}^{h_k} \sum_{m=0}^{w_k} \left(w_{h,m} \cdot x_{i+h,j+m} \right) + b_k, \tag{6}$$

where the filter k is represented by a $h_k \times w_k$ matrix of weights, b_k is a bias, i and j are the coordinates of the current pixel x in the input volume.

After each convolution layer, we use the pooling method to shrink the parameter space of CNN and filter noises. In this article, we choose the Max-Pooling to obtain the most representative local features. The max-pooling is defined to extract the most critical feature values of the input vectors within a window. So the maximum value of each feature map is obtained as the local optimal feature. After the final flattening, we will get a one-dimensional vector as input for next stage.

4.2.2. Classification. The classification stage receives the input vector from the last layer (convolutional or pooling) of the features extraction stage and then calculates the affinity of the feature map with the classification classes. This stage is structured as a chain of linear layers, which implemented by a Fully Connected Network (FCN). In our model, there are two Fully Connected Networks and one dropout layer to prevent overfitting.

Suppose that the linear layer is composed by J neurons, which are responsible for aggregating the information derived from the previous layer. Then, the output values are expressed as a weighted linear combination of these neurons:

$$o_j = \sum_{i=0}^{I} \left(w_{i,j} \cdot x_i \right) + b_k. \tag{7}$$

Here, $w_{i,j}$ represents the weight, x_i represents the neurons from the previous layer, and b_j represents a bias.

As for the dropout layer, we found that the model works well when the dropout rate was equal to 0.2. The last normalization operator receives the output from the last linear layer and calculates the affinity of the feature image with the classification classes in percentage terms using a SoftMax operator σ: $\sigma_j = e^{x_j} / \sum_{k=1}^{K} e^{x_k}$ for $j = 1, \ldots, K$. Here, x_j means the output of the last linear layer. Then, SoftMax operator enforces the output in range [0, 1]. Thus, this normalized operator output can be seen as the probability of classification.

4.3. Network Training. Convolutional neural network is a supervised learning algorithm. Due to our target of malware detection, the training data should consist of sufficient examples of two classes of application program, malicious program and benign program, so that CNN can learn to capture the relevant features of malware program for further classification more effectively. Fortunately, we have found an efficient method of feature extraction, which collects the global and local statistic information of executable programs. Therefore, the next critical step is to train the vectored data (or feature map) using CNN.

4.4. Dataset and Parameter Settings. In this work, we collected malware samples from some antimalware communities (e.g., Kafan Forum and MalShare) and obtained some benign system programs built in Windows, benign applications from the download site of software (e.g., Greenxf and PConline). Our dataset consists of 1992 programs (executable files), whose size ranges from a few KB to a dozen megabytes. Among them, there are 981 malicious programs, which are considered as negative examples, and 1011 benign programs, which are treated as positive examples. For these programs, we choose 4/5 of dataset as the training set and 1/5 as the testing set, to evaluate the classification results of our model. Batchsize and epoch we choose are 128 and 4, separately. In training process, we use the convolutional layer with 128 filters and the pooling layer alternately before the flatten, after that there are two Full Connection layers and a Dropout behind them for avoiding overfitting and improving the generalization ability of the network.

5. Experiment

We conduct a series of experiments to evaluate the efficiency of our approach. As mentioned before, we extract the textual information by Cuckoo from the program files and describe the behavior of programs in natural language, for example, "Allocatesread-write-execute memory (usually to unpack itself)". It is very critical for us to map the words into the vector space and represents each word with a 100-dimensional vector, which will produce a feature map for each program. Then, we can develop CNN to detect malware with the feature maps obtained before as input. That is the whole process of our model, we will denote it as Method B in the below. In order to compare the efficiency of our model, we design two other groups of experiments: Method A and Method C. Method A also extracts textual information describing the behavior of programs by Cuckoo in natural language but generates the feature vectors by TF-IDF as the input of SVM for malware detection. However, Method C extracts API call sequences of programs and uses GloVe to get the feature map and then uses CNN to detect malware.

5.1. Performance Comparison. As our approach relies on machine learning techniques, we also follow the model evaluation method to assess our experimental results. In this work, our mainly used measurement parameters are Accuracy, Precision, Recall, F1, Kappa, and ROC Curve, for a more comprehensive assessment. For binary classification task, we can divide the sample set into four classes: true positive (TP), false positive (FP), true negative (TN), and false negative (FN), according to the combination of real class and predicted class.

Accuracy is the proportion of the correct sample in the total sample. For a sample set D, the accuracy is defined as accuracy $= \mathrm{TP} + \mathrm{TN}/\mathrm{TP} + \mathrm{FN} + \mathrm{TN} + \mathrm{FP}$. Precision is defined as $P = \mathrm{TP}/\mathrm{TP} + \mathrm{FP}$. Recall is defined as $\mathrm{R} = \mathrm{TP}/\mathrm{TP} + \mathrm{FN}$. Other performance measures take the precision and the recall into account at the same time, such as F1 and kappa. F1 is defined as $F1 = 2 * \text{precision} * \text{recall}/\text{precision} + \text{recall}$.

Kappa is another method of calculating classification accuracy to determine whether the predicted results are consistent with actual results, which is defined as $\kappa = \mathrm{pr}(a) - \mathrm{pr}(e)/1 - \mathrm{pr}(e)$, where the pr(a) is the actual accuracy and pr(e) is the theoretical accuracy.

Receiver operating characteristic (ROC) curve is obtained by selecting the specificity (false-positive rate) and sensitivity (true-positive rate) as the horizontal axis and the vertical axis, respectively. The corresponding area under the receiver operating characteristic (ROC) curve (AUC) is one of the most popular metrics to probabilistically evaluate the performance of classifiers.

5.2. Results. In order to validate our detection method on malwares, we set two baselines for comparison: feature extraction and classification. The experiment performs malware detection task in three different ways on the same dataset, and the results are shown as Table 1. Obviously, the results

Table 1: The TP, TN, FP, precision, recall, accuracy, F1, and kappa of each malware detection method.

Method	TP	TN	FP	Precision	Recall	Accuracy (%)	F1	Kappa
A (CUCKOO + TF-IDF + SVM)	202	186	10	0.953	1	97.5	0.976	0.950
B (CUCKOO + GloVe + CNN)	203	191	4	0.981	1	98.9	0.990	0.980
C (API calls + GloVe + CNN)	193	180	15	0.928	0.951	93.8	0.939	0.87

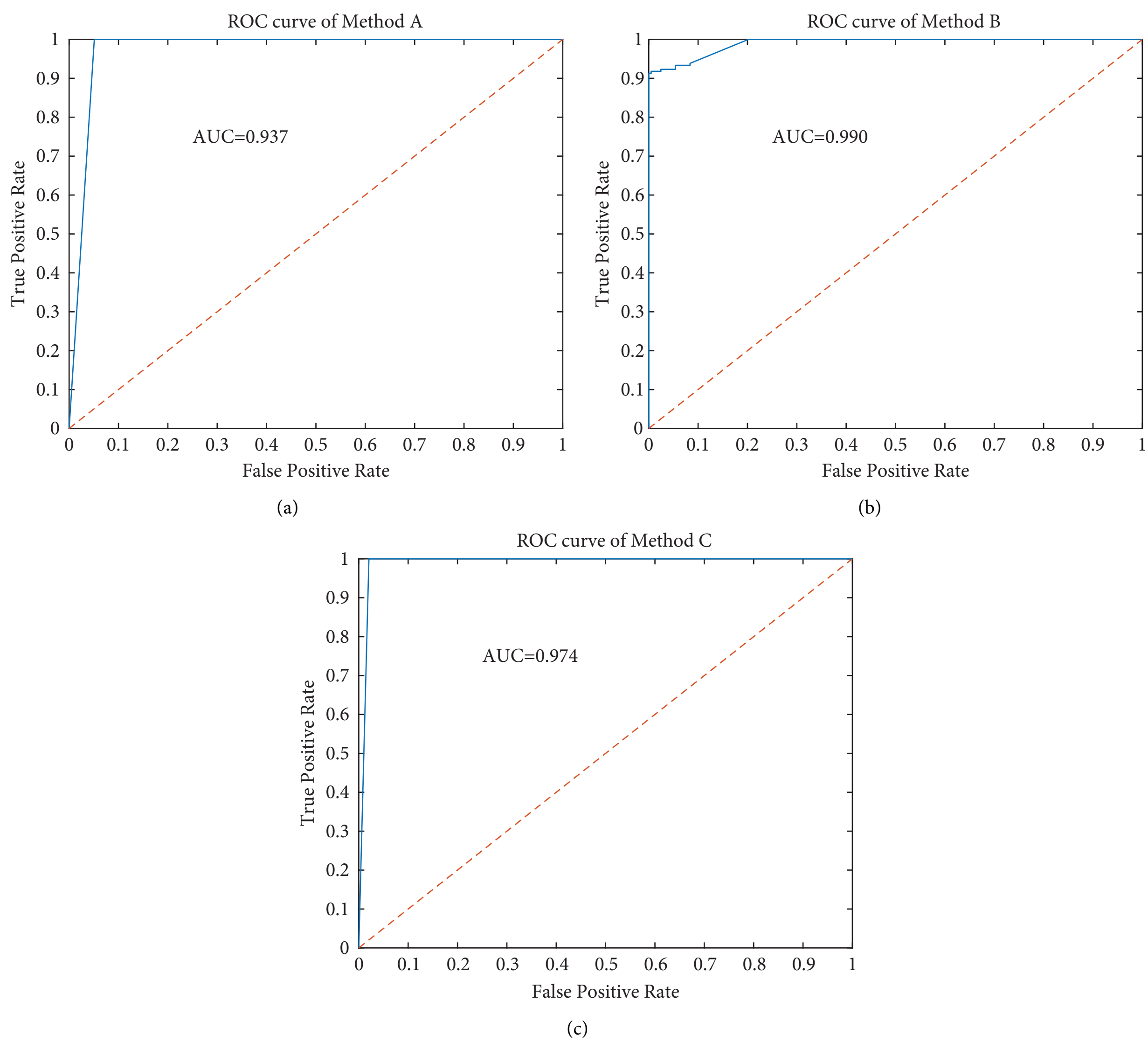

Figure 4: ROC curve of Method A (a), Method B (b), Method C (c).

illustrate that the malware detection method using CNN and Word Embedding outperformed both Method A and Method C in the accuracy, recall, F1, and kappa. Especially, in the aspect of Accuracy, Method A has achieved 98%, which is of great significance in practical for malware detection because the cost of misclassification is very high. As for Recall, the value of Method B is 1, which is equal to Method A . This is the only situation where our model performance is not over other models because its Recall has reached the optimal value 1. In addition, from Figure 4, we can observe that the AUC (area under the ROC curve) of Method B is 0.990, which is superior to 0.974 of Method A and 0.937 of Method B. This means that the model proposed in this article shows better classification ability. Next, we contrast our model with other methods in two stages: the feature extraction stage and the classification stage, respectively.

5.2.1. Feature Extraction with Word Embedding and API Calls Sequence. In the stage of feature extraction, Method C uses Cuckoo to extract the API call sequence of the program as description information for malware detection. Method C divides the API calls sequence information into six categories (socket, memory management, processes, and threads etc.), which simplifies complexity of the feature extraction but also lost some other features. In our model (Method B), Cuckoo takes the natural language description information of program behavior, and GloVe represents the words as vectors remaining the global and local information. On the other hand, the Word Embedding has an inherent advantage in clustering so that the distribution of the similar words roughly similar in vector space. Therefore, it is reasonable that the accuracy of our model is higher than Method C.

5.2.2. Word Vector and TF-IDF. In the stage of classification, Method B and Method A choose different ways to analyze the data obtained previously. Considering that the TF-IDF used in Method A is a type of numerical data, we choose the SVM to complete the classification phase of Method A. Compared with the word embedding in Method A, TF-IDF requires a higher dimension of the space. On the other hand, the word vectors in Method B can express the semantic and grammatical information without removing the stop words because they also contain some grammatical information available for training. Therefore, using the word vectors can extract the features of program behavior more effectively and make the classification more accurate at the same time. The experimental results directly verify that the accuracy of Method B is higher than Method A.

6. Conclusion and Future Work

In this article, we proposed a novel approach for detecting malware using CNN via Word Embedding. Our approach first extracts the natural language description information of program behavior by Cuckoo Sandbox and uses GloVe to map the natural language (word space) into the corresponding vector space, which results in a dictionary of words represented by a real-valued vectors. For each program, the corresponding textual description information extracted by Cuckoo can be represented as a sequence of word vectors, called feature map. The task of malware detection can be equivalent to image classification, and we use the convolution neural network as a classifier to learn the feature maps of programs. In this way, we can make full use of the grammar and sematic information of programs. In the evaluation stage, we created two baselines to compare with our model, one method adopts TF-IDF word representation in the stage of features extraction (Method A) and uses a SVM as classifier in the stage of classification. The other method uses API calls sequences to represent the behavior information of executable program (Method C). The experimental results illustrate that our approach achieves a better performance than others.

Future work should focus on the defensive mechanisms that we identified as potentially helpful to improve our model. Also, the applicability of our detection model to additional domains should be studied. On the other hand, we expect to improve our means of extracting information so that we can generate more valuable features with more expressive ability for the behaviors of executable programs.

Data Availability

The experimental data used to support the findings of this study are available from the corresponding author upon request.

Conflicts of Interest

The authors declare that they have no conflicts of interest.

References

[1] S. Dai, Y. Liu, T. Wang, W. Tao, and Z. Wei, "Behavior-based malware detection on mobile phone," in *Proceedings of the International Conference on Wireless Communications Networking and Mobile Computing*, Niagara Falls, Canada, October 2010.

[2] I. Burguera, U. Zurutuza, and S. T. Nadjm, "Crowdroid:behavior-based malware detection system for android," in *Proceedings of the Acm Workshop on Security and Privacy in Smartphones and Mobile Devices*, Chicago, IL, USA, October 2011.

[3] A. Mujumdar, G. Masiwal, and B. B. Meshram, "Analysis of signature-based and behavior-based anti-malware approaches," *International Journal of Advanced Research in Computer Engineering and Technology*, vol. 2, no. 6, 2013.

[4] J. Pennington, R. Socher, and C. Manning, "Glove: global vectors for word representation," in *Proceedings of the Conference on Empirical Methods in Natural Language Processing*, pp. 1532–1543, Doha, Qatar, October 2014.

[5] M. Alazab, S. Venkataraman, and P. Watters, "Towards understanding malware behaviour by the extraction of api calls," in *Proceedings of the Cybercrime and Trustworthy Computing Workshop*, pp. 52–59, Berlin, Germany, June 2010.

[6] G. G. Sundarkumar, V. Ravi, I. Nwogu, and V. Govindaraju, "Malware detection via api calls, topic models and machine learning," in *Proceedings of the 2015 IEEE International Conference on Automation Science and Engineering (CASE)*, pp. 1212–1217, Gothenburg, Sweden, August 2015.

[7] O. Hachinyan, "Detection of malicious software on based on multiple equations of api-calls sequences," in *Proceedings of the 2017 IEEE Conference of Russian Young Researchers in Electrical and Electronic Engineering (EIConRus)*, pp. 415–418, St. Petersburg and Moscow, Russia, February 2017.

[8] A. Pektas and T. Acarman, "Malware classification based on api calls and behaviour analysis," *IET Information Security*, vol. 12, no. 2, pp. 107–117, 2018.

[9] K. S. Jones, "A statistical interpretation of term specificity and its application in retrieval," *Journal of Documentation*, vol. 60, no. 1, pp. 493–502, 1972.

[10] R. K. Roul, O. R. Devanand, and S. K. Sahay, "Web document clustering and ranking using tf-idf based apriori approach," pp. 34–39, 2014, https://arxiv.org/abs/1406.5617.

[11] K. D. He, Z. T. Zhu, and Y. Cheng, "A research on text classification method based on improved TF-IDF algorithm," *Journal of Guangdong University of Technology*, vol. 33, no. 5, pp. 49–53, 2016.

[12] J. F. Zhang, "Words similarity algorithm based on improved TF-IDF and cosine theorem," *Modern Computer*, pp. 20–23, 2017.

[13] N. Kondylidis, M. Tzelepi, and A. Tefas, "Exploiting Tf-Idf In Deep Convolutional Neural Networks For Content Based Image Retrieval," *Multimedia Tools and Applications*, vol. 77, no. 23, pp. 1–20, 2018.

Hindawi
Scientific Programming
Volume 2021, Article ID 6505253, 16 pages
https://doi.org/10.1155/2021/6505253

Research Article

Adaptive Spiral Flying Sparrow Search Algorithm

Chengtian Ouyang, Yaxian Qiu, and Donglin Zhu

School of Information Engineering, Jiangxi University of Science and Technology, Ganzhou, Jiangxi 341000, China

Correspondence should be addressed to Yaxian Qiu; qiuyaxian@mail.jxust.edu.cn

Received 1 July 2021; Revised 30 July 2021; Accepted 13 August 2021; Published 27 August 2021

Academic Editor: Punit Gupta

The sparrow search algorithm is a new type of swarm intelligence optimization algorithm with better effect, but it still has shortcomings such as easy to fall into local optimality and large randomness. In order to solve these problems, this paper proposes an adaptive spiral flying sparrow search algorithm (ASFSSA), which reduces the probability of getting stuck into local optimum, has stronger optimization ability than other algorithms, and also finds the shortest and more stable path in robot path planning. First, the tent mapping based on random variables is used to initialize the population, which makes the individual position distribution more uniform, enlarges the workspace, and improves the diversity of the population. Then, in the discoverer stage, the adaptive weight strategy is integrated with Levy flight mechanism, and the fusion search method becomes extensive and flexible. Finally, in the follower stage, a variable spiral search strategy is used to make the search scope of the algorithm more detailed and increase the search accuracy. The effectiveness of the improved algorithm ASFSSA is verified by 18 standard test functions. At the same time, ASFSSA is applied to robot path planning. The feasibility and practicability of ASFSSA are verified by comparing the algorithms in the raster map planning routes of two models.

1. Introduction

With the continuous development of scientific research, more and more swarm intelligence optimization algorithms have been proposed. The swarm intelligence optimization algorithm basically abstracts a series of formulas based on the life characteristics or behavior rules of organisms or things and finds high-quality solutions in a certain solution space based on these formulas. Scholars have proposed a series of swarm intelligence optimization algorithms through the behaviors of ant, cat, whale, wolf, and others. Among them, the sparrow search algorithm (SSA) [1], which finds optimal solutions through the sparrow foraging process, is a novel swarm intelligence optimization algorithm proposed by two scholars, Xue and Shen in 2020. This algorithm has fewer population roles and simple principles, and it is easy to understand. Compared with gray wolf optimizer (GWO) [2] and particle swarm optimization (PSO) [3], SSA has higher accuracy, stronger convergence, and better optimization capabilities. Moreover, SSA is now more and more applied in practical engineering. However, SSA also has the common shortcomings of swarm intelligence algorithms, such as easy to get stuck in local and excessive randomness during initialization.

In order to overcome these shortcomings of the swarm intelligence optimization algorithm, scholars have studied the algorithm and successfully applied to practical engineering problems. Lei et al. [4] applied the Levi flight strategy in SSA to avoid local convergence and improve global optimization capabilities. They combine the improved sparrow search algorithm with DV-Hop to enhance the positioning accuracy in WSN. Xin et al. [5] used tent chaotic sequence to initialize the population in turn, and Gaussian mutation operator and tent chaotic disturbance balance the global individual position. A series of strategies increase the population diversity of the algorithm, strengthen the local search ability of the algorithm, and improve the possibility of jumping out of the local area. Tang et al. [6] introduced a cubic mapping strategy to initialize the population, avoiding the decrease of population diversity in the later iterations. The reverse learning strategy and elite particles are added to effectively prevent the algorithm from falling into a local optimum. The sine and cosine optimization algorithm is incorporated into the follower position update to reduce search blind spots and balance algorithm development and search capabilities. Finally, a Gaussian walk strategy is used to help the algorithm leave the stagnant state. The good search ability of the improved algorithm is tested through experiments. Xin et al. [7] also proposed an improved algorithm, adding the flying thoughts in the bird swarm algorithm to the location update of the discoverer and the follower, ensuring global convergence, increasing the diversity of the population, and being able to jump out of the local optimum. In this paper, the improved algorithm is also applied to the multi-threshold image segmentation method, which solves the original low segmentation accuracy and slow segmentation speed. Mao et al. [8] used sin-cosine algorithm, nonlinear dynamic learning factor, and Levy flight strategy to improve the algorithm, speed up the convergence speed, and strengthen the local escape ability. Song et al. [9] proposed to introduce the skew tent map-based chaotic method to initialize the population and strengthen the individual quality of the population. After that, the nonlinear decreasing weight and mutation operator strategies were combined in each stage to dynamically change the search space, increase the diversity of the population, and improve the ability to jump out of the local optimum. Wu and others [10] used tent chaotic mapping, adaptive weight control step size, Cauchy mutation, and Gaussian mutation to improve the original algorithm in turn. Such a series of strategies balance the global search and local search capabilities, enhance the local development capabilities of the algorithm, and improve the search accuracy. Finally, the improved algorithm is applied to the mine intelligent ventilation system, which proves the good optimization effect of the improved algorithm. Zhang and Ding [11] initialized the population by logistic mapping. In the discoverer phase and the early warning phase, adaptive parameters are introduced to expand the search range of the discoverer, dynamically adjust the number of early warning individuals, and better help the sparrow individuals find the best position. The mutation operator strategy is added to the global process to increase the population diversity. The whole improved algorithm enhances the global search capability of SSA. Finally, the improved CSSA is applied to the stochastic configuration network. The results show that CSSA has good performance and improves the regression performance of SCN in solving large-scale data problems. Zhang et al. [12] used the sine cosine strategy to change the way the discoverer updates the location, and improve global and local search capabilities of the algorithm. A labor cooperation structure is added to the discoverer stage and the early warning stage, allowing the discoverer and the early warning individual to share their locations to achieve cooperation, so as to converge to the global optimal solution faster and more stably.

Although these improved strategies can better improve the optimization ability of each algorithm, they do not change the search mechanism of each algorithm itself. And they only improved the search ability of the algorithm in the neighborhood space, and the learning rate was not high, resulting in the algorithm still having drawbacks. This means that when faced with high-dimensional complex problems, these algorithms may also be stuck into the local optimal situation. Therefore, based on the research of many scholars, this paper proposes the adaptive spiral flying sparrow search algorithm (ASFSSA).

In the following paper, Section 2 gives an introduction to the overall work and motivation of the algorithm. Section 3 introduces the sparrow search algorithm. Section 4 illustrates the improvements made by the adaptive spiral flying sparrow search algorithm. Section 5 compares and analyzes the improved algorithm with other intelligent algorithms. In Section 6, the improved algorithm is applied to path planning and compared with the other three algorithms in two different grids. Section 7 summarizes this paper.

2. Related Work and Motivation

In order to improve the search speed and convergence accuracy of individual sparrows and reduce the possibility of falling into the local optimum, adaptive weights and Levy flight strategies are used in the discoverer stage. In order to make the individual sparrow search more detailed and get a better position, a variable spiral search strategy is introduced in the follower stage. The higher the quality of the solution, the better the search ability.

To verify the convergence and optimization ability of the proposed algorithm, six algorithms are used to compare the optimization effects of 18 test functions. As can be seen from the experimental results, the adaptive spiral flying sparrow search algorithm has more significant advantages than other algorithms. Finally, for the purpose of verifying the practicability and performance of the algorithm better, the four algorithms are applied to the path planning of the robot. The results show that the path planning of the adaptive spiral flying sparrow search algorithm is relatively stable and the cost is the least, which reduces the constraints of the immature and randomness in the path planning of the previous algorithms.

3. Sparrow Search Algorithm

The sparrow population is divided into two roles, namely, the discoverer and the follower. They have three behaviors: foraging, following, and reconnaissance. The task of the discoverer is to find food and inform the follower of the location of the food. Therefore, the discoverer needs to search in a large area, and the foraging range of the follower is generally small. This is the formula for updating the position of the discoverer:

$$X_{i,j}^{t+1} = \begin{cases} X_{i,j}^{t} \cdot \exp\left(\dfrac{-t}{\alpha \cdot M}\right), & \text{if } R_2 < \mathrm{ST}, \\ X_{i,j}^{t} + Q \cdot L, & \text{if } R_2 \geq \mathrm{ST}. \end{cases} \tag{1}$$

In formula (1), t and M, respectively, denote the current number of iterations and the maximum number of iterations. $X_{i,j}$ represents the location of the i-th sparrow, and j is the representative dimension. In the above formula, α

and R_2 are both a random number from 0 to 1 (not zero), and R_2 is an important parameter that controls the individual's flight behavior. ST ($\mathrm{ST} \in [0.5,\ 1]$) is a safety threshold and an important parameter to measure whether the location of the discoverer is safe. L is a $1 \times D$ matrix with all elements of 1. If $R_2 < \mathrm{ST}$, it means that the current location is temporarily safe, there are no predators in the surrounding environment, and the discoverer can search for food in a large area. If $R_2 \geq \mathrm{ST}$, it means that the predator's trace is found at the current location, and the discoverer needs to go to other safe areas for foraging activities at this time.

The location update of followers is described as follows:

$$X_{i,j}^{t+1} = \begin{cases} Q \cdot \exp\left(\dfrac{X_{\mathrm{worst}}^{t} - X_{i,j}^{t}}{i^2}\right), & \text{if } i > \dfrac{n}{2}, \\ X_P^{t+1} + \left|X_{i,j}^{t} - X_P^{t+1}\right| \cdot A^{+} \cdot L, & \text{otherwise.} \end{cases} \tag{2}$$

In formula (2), X_P^{t+1} refers to the optimal position occupied by the discoverer in the $t+1$-th iteration so far (the $t+1$-th iteration has not ended) and X_{worst}^{t} represents the worst position occupied by the group in the t-th iteration. A is a $1 \times D$ matrix, and the elements in the matrix are randomly assigned values of 1 or −1, and $A^{+} = A^{T}(AA^{T})^{-1}$. If $i > n/2$, this means that the current follower is at the edge of the entire population and has no food. At this time, the follower needs to go elsewhere for food. Otherwise, the follower will go after the pace of the discoverer for food.

When being aware of the danger, the sparrow population will make antipredatory behavior:

$$X_{i,j}^{t+1} = \begin{cases} X_{\mathrm{best}}^{t} + \beta \cdot \left|X_{i,j}^{t} - X_{\mathrm{best}}^{t}\right|, & \text{if } f_i \neq f_g, \\ X_{i,j}^{t} + K \cdot \left(\dfrac{\left|X_{i,j}^{t} - X_{\mathrm{worst}}^{t}\right|}{(f_i - f_w) + \varepsilon}\right), & \text{if } f_i = f_g. \end{cases} \tag{3}$$

In formula (3), X_{best}^{t} is the global optimal solution obtained in the t-th iteration. In the above formula, β, K, and ε are all parameters in the formula. β is a random number that obeys the standard normal distribution, and it is used to control the step size. K is an arbitrary random number from -1 to 1, it represents the direction in which the individual sparrow moves, and it is also a step control parameter. ε is a relatively small constant, and its function is to prevent the denominator from being zero. f_i represents the fitness value of the i-th individual, and f_g and f_w are the best fitness value and the worst fitness value of the current iteration number, respectively.

If $f_i > f_g$, then this indicates that the individual is at the edge of the population and is easily preyed by natural enemies. If $f_i = f_g$, then this means that the individual is located in the center of the population. At this time, the sparrow needs to be close to other individuals to reduce the probability of being captured.

4. Adaptive Spiral Flying Sparrow Search Algorithm

4.1. Tent Chaotic Mapping Based on Random Variables. Because SSA has the shortcoming of large randomness, it is decided to introduce orderly and uniform tent mapping to improve it. Many scholars have applied tent mapping to solve the optimization problem [13]. However, tent mapping is not very stable. In [7], in order to reduce this influence, tent mapping based on random variables was adopted, which has a good effect. Therefore, in this paper, the tent mapping strategy based on random variables is introduced to improve the initialization of SSA, so that the initialization of the population is more orderly, and the controllability of the algorithm is enhanced. Its specific formula is as follows:

$$z_{i+1} = \begin{cases} 2z_i + \mathrm{rand}(0,1) \times \dfrac{1}{N}, & 0 \leq z \leq \dfrac{1}{2}, \\ 2(1 - z_i) + \mathrm{rand}(0,1) \times \dfrac{1}{N}, & \dfrac{1}{2} \leq z \leq 1. \end{cases} \tag{4}$$

The expression after the Bernoulli transformation is

$$z_{i+1} = (2z_i)\mathrm{mod}1 + \mathrm{rand}(0,1) \times \frac{1}{N}. \tag{5}$$

In formula (5), N is the number of particles in the chaotic sequence.

According to the characteristics of the tent mapping, the sequence flow for generating chaos in the feasible domain is as follows:

(1) Randomly generate the initial value z_0 in (0, 1), and let $i = 1$.

(2) Perform iteration by using that formula (5) to generate a z sequence, and i is increased by 1.

(3) Stop if the number of iterations reaches the maximum, and store the generated z sequence.

4.2. Adaptive Weighting. Weight strategies are common in particle swarm optimization algorithms [14]. Generally, the particle swarm algorithm reduces to some extent the trapping into local optimum by adaptively changing between the set maximum and minimum values. Inspired by this, this paper adds an inertia weight w which varies with the number of iterations in the discoverer stage of sparrow optimization. In the initial stage of the algorithm, it weakens the influence of random initialization and balances the Levy flight mechanism below, so as to enhance the local search and global search of the algorithm.

The discoverer guides other individuals in the population to search for food, so the introduction of adaptive weights improves the quality of individual locations, enabling other individuals to converge faster to optimal locations, and overall accelerates the convergence rate. Based on the characteristics of sparrows, the formula for adaptive weights is as follows:

$$w(t) = 0.2\cos\left(\frac{\pi}{2}\cdot\left(1-\frac{t}{\mathrm{iter}_{\max}}\right)\right). \tag{6}$$

The meaning of formula (6) is that w has the property of nonlinear change between [0, 1]. According to the characteristics of cos function, the weight value is smaller at the beginning of the algorithm, but the optimization speed is faster and the later weight value is larger, but the change speed is slower, so the convergence property of the algorithm is balanced. The improved discoverer location is updated as follows:

$$X_{i,j}^{t+1} = \begin{cases} w(t)\cdot X_{i,j}^{t}\cdot \exp\left(\dfrac{-i}{\alpha\cdot \mathrm{iter}_{\max}}\right), & \text{if } R_2 < \mathrm{ST}, \\ w(t)\cdot X_{i,j}^{t} + Q\cdot L, & \text{if } R_2 \geq \mathrm{ST}. \end{cases} \tag{7}$$

By introducing adaptive weights to dynamically adjust the position changes of sparrows, different guidance modes for the discoverer at different times make the algorithm search flexible. As the number of iterations increases, the individual sparrows converge toward the optimal position, and a larger weight makes the individual move faster, thus increased the convergence speed of the algorithm.

4.3. Levy Flight Mechanism. In SSA, there are few roles in the population, and the same role update position formula is the same, which will result in multiple individuals in the same optimal position. Too high solution repetition rate will reduce the efficiency of the algorithm, which is not conducive to the optimization of the algorithm. The discoverer has a wide search range and globality, and the adaptive weighting strategy is introduced to effectively improve the convergence effect. However, when facing the high-dimensional complex problems, there is still a probability of falling into local optimum. Therefore, the Levy flight strategy is introduced to improve the randomness of the algorithm solution, thereby enriching the diversity of population positions. This can also effectively improve the operating efficiency of the algorithm.

Levy flight obeys the Levy distribution. Principle [15] and the Levy distribution is shown in Figure 1. It uses a random long- and short-distance mechanism to cover a large area. After adding the Levy flight mechanism, the performance of the proposed algorithm can be improved.

The location update format [16] for joining Levy flight strategy is as follows:

$$x_i'(t) = x_i(t) + l \oplus \mathrm{levy}(\lambda). \tag{8}$$

In formula (8), $x_i(t)$ represents the position of the i-th individual in the t-th iteration, $\oplus$ is an arithmetic symbol representing point-to-point multiplication. l denotes a step length control parameter, which is obtained by this formula: $l = 0.01(x_i(t) - x_p)$. levy(λ) is a path that obeys the Levy distribution, which represents the introduced Levy flight strategy and satisfies the following: levy $\sim u = t^{-\lambda}$, $1 < \lambda \leq 3$.

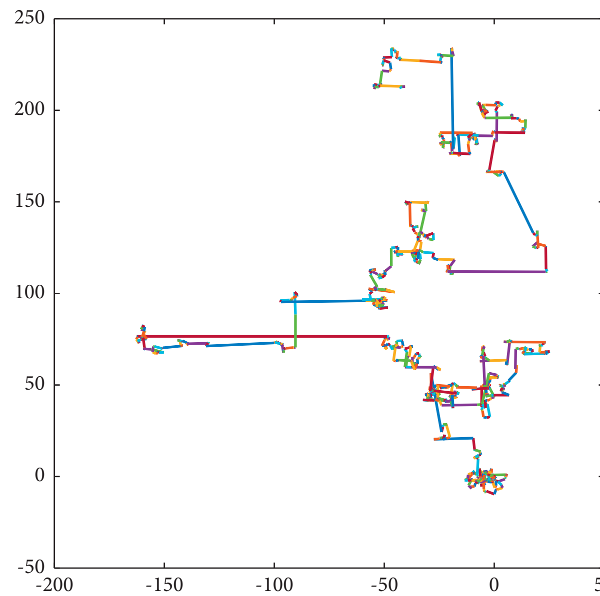

Figure 1: Levy flight diagram.

Because Levy distribution is very complex, Mantegna algorithm is usually used to simulate it [17, 18]. The formula for calculating the step size is as follows:

$$\begin{aligned} s &= \frac{\mu}{|\nu|^{1/\gamma}}, \\ \mu &\sim N\left(0, \sigma_\mu^2\right), \\ \nu &\sim N\left(0, \sigma_\nu^2\right), \\ \sigma_\mu &= \left\{\frac{\Gamma(1+\gamma)\sin(\pi\gamma/2)}{\gamma\cdot\Gamma[(\gamma+1)/2]\cdot 2^{(\gamma+1)/2}}\right\}^{1/\gamma}. \end{aligned} \tag{9}$$

Among them, $\sigma_\nu = 1$, and γ is generally 1.5.

The introduction of the Levy flight strategy makes the sparrows more flexible at this stage and can also lead other individuals to find a better location, free from the constraints of local extremes. Therefore, the combination of Levy flight mechanism and adaptive weights balances the search method, and the quality of each solution obtained is improved to a certain extent, which greatly improves the search ability of the algorithm.

4.4. Variable Spiral Search Strategy. Followers update dynamically with the location of the discoverer, which leads to blindness and singularity in the way they search. Inspired by the rotation operation of the whale algorithm [19, 20], a variable spiral location update strategy is introduced to make follower location updates more flexible, develop a variety of search paths for location updates, and balance the global and local search of the algorithm. The spiral search diagram is shown in Figure 2.

In the follower location update process, the helix parameter z cannot be a fixed shape, which results in monotonous search methods and the possibility of falling into

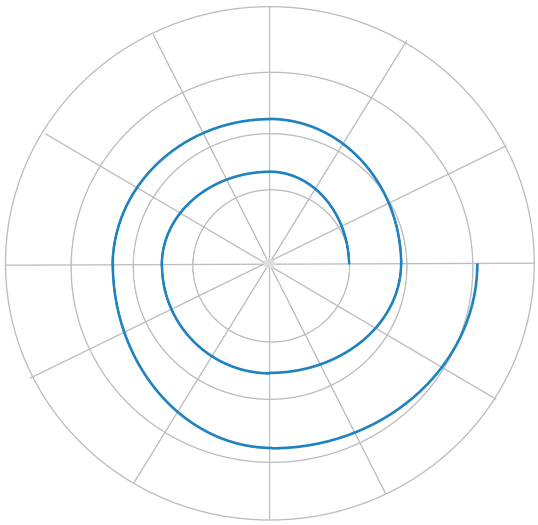

Figure 2: Schematic diagram of spiral search.

local optimum, thus weakens the search ability of the algorithm. The parameter z is designed as an adaptive variable to dynamically adjust the spiral shape of the follower search, which broadens the ability of the follower to explore the unknown region, improves both the search efficiency and the global search performance of the algorithm. The formula for the variable spiral position update strategy is as follows:

$$X_{i,j}^{t+1} = \begin{cases} e^{zl} \cdot \cos(2\pi l) \cdot Q \cdot \exp\left(\dfrac{X_{\text{worst}}^{t} - X_{i,j}^{t}}{i^2}\right), & \text{if } i > \dfrac{n}{2}, \\ X_P^{t+1} + \left|X_{i,j}^{t} - X_P^{t+1}\right| \cdot A^{+} \cdot L \cdot e^{zl} \cdot \cos(2\pi l), & \text{otherwise}, \\ z = e^{k\cdot\cos\left(\pi\cdot\left(1-\left(i/i_{\max}\right)\right)\right)}. \end{cases} \tag{10}$$

The parameter z varies according to the number of iterations and is composed of an exponential function based on e. The size and amplitude of the helix are dynamically adjusted according to the properties of cos function. k is the coefficient of change. According to the optimization characteristics of each function, in order to make the algorithm have a suitable search range, $k = 5$. L is a uniformly distributed random number of $[-1, 1]$. With the range of follower position updating is from large to small, more quality solutions are found in the early stage, and late optimization reduces the increase of idle work, which improves the global optimal search performance of the algorithm. At the same time, according to the spiral characteristics, the optimization accuracy of the algorithm is improved to a certain extent.

4.5. Process for Improving Sparrow Search Algorithm. The sparrow search algorithm has better optimization performance than other algorithms, but it still depends on the initial population so that it is easy to fall into a local optimal state. In order to improve these shortcomings, this paper proposes an adaptive spiral flying sparrow search algorithm. Initially, the population was initialized by tent chaotic mapping based on random variables to provide adequate preparation for the discoverer's optimization. Then, adaptive weights and Levy flight strategies were introduced to make the discoverer's position update method more extensive and flexible, and then a variable spiral was proposed. The strategy makes the follower's search more detailed, avoids premature phenomenon, and speeds up the optimization speed of the algorithm.

The specific implementation steps of ASFSSA are as follows:

Step 1: initialize the sparrow population parameters, for example, the total population pop, the total number of discoverers pNum, the total number of iterations iter, and the solution accuracy ε.

Step 2: use tent mapping to initialize the position of population individuals, and generate pop sparrow individuals.

Step 3: use the correlation function to calculate the fitness value f_i of each population individual, and find the maximum fitness value f_g and the minimum fitness value f_w.

Step 4: sort the population according to the fitness value.

Step 5: select the individuals with the top pNum fitness as the discoverer, and the rest are followers, and use formulas (7) and (8) after adding the strategy to update the position of the discoverer.

Step 6: use formula (10) to update the positions of pop-pNum followers.

Step 7: use formula (3) to update the position of the sparrow that is aware of the danger.

Step 8: after one iteration is completed, recalculate the fitness value f_i of each individual, and update the maximum fitness value f_g, the minimum fitness value f_w, and the corresponding position.

Step 9: judge whether the algorithm has reached the maximum number of iterations or the accuracy of the solution. If it has reached, the optimization result will be output; otherwise, it will return to Step 4.

The specific flowchart is shown in Figure 3.

5. Algorithm Performance Test

To test the optimization capability of the improved algorithm, 18 standard test functions are selected to verify the performance. The test functions are listed in Table 1. The first 10 are unimodal functions, the middle 4 are complex multimodal functions, and the last 4 are fixed-dimension function. In order to increase the experimental convincing, it is necessary to compare the particle swarm algorithm (PSO), gray wolf algorithm (GWO), beetle swarm optimization (BSO), SSA, CSSA, and the proposed algorithm optimization effect. Among them, CSSA is an improved sparrow search algorithm in the literature [5], and BSO [21] is a new

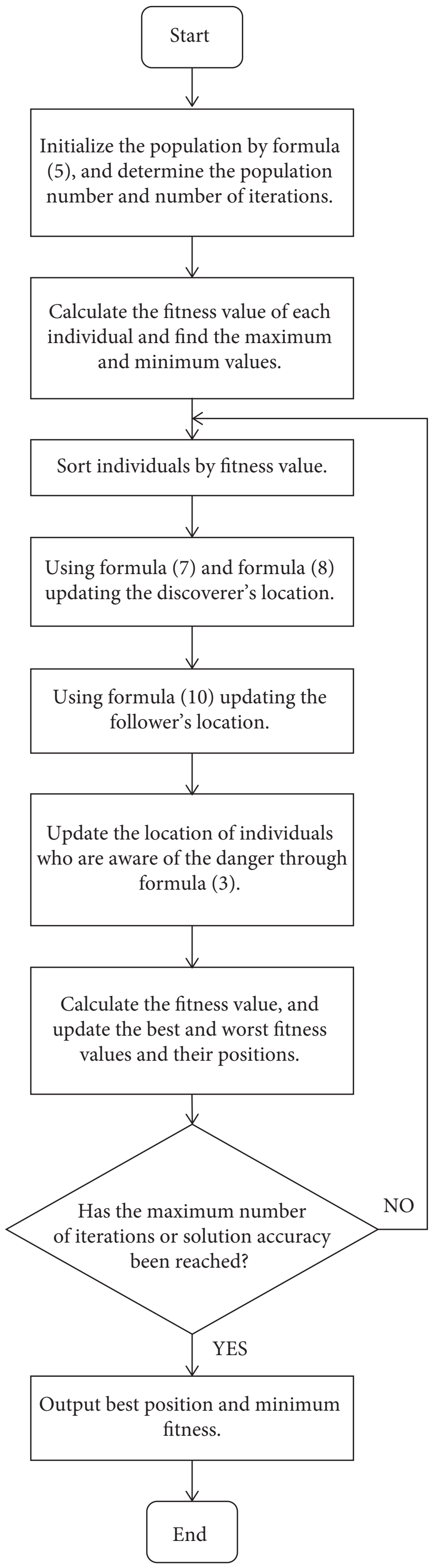

Figure 3: Algorithm flowchart.

algorithm which combines beetle antennae search algorithm (BAS) [22] and PSO, and the research on this algorithm is very popular. The complexity and parameters of all algorithms are shown in Table 2.

The population number of all algorithms is 100; the number of iterations is 200. In PSO, c1 = c2 = 2, $w = 0.728$. The BSO parameter settings are as follows: eta = 0.95, $c = 2$, $k = 0.4$, step0 = 0.9, and step1 = 0.2. The upper and lower limits of all algorithms are given in the test function table. The experimental environment is MATLAB 2018b, the Windows 10 operating system, and the running memory is 8G. In order to enhance the experimental persuasion, exclude the influence of accidental events, and count the minimum (min) value, average (aver) value, and standard (std) deviation of each algorithm, which reflect the optimization ability and stability of each algorithm. The comparison table of optimization effect of each algorithm is shown in Table 3, and the convergence of each algorithm function is shown in Figure 4.

From Table 3, we can see that the ASFSSA has the best performance in function optimization, especially in F_1–F_4, F_7–F_9, F_{16}, and F_{18}, which can find the optimal value each time. The results of CSSA come later, and PSO and GWO are the worst, especially when the boundary is complex. The BSO has good optimization characteristics in the F_{10}, F_{11}, and F_{17} functions, but the effect in other algorithms has great shortcomings, and the effect is the worst. It can be seen that BSO has the limitation of the optimization ability. Among these three functions, the optimization effect of ASFSSA is second only to it. Generally speaking, ASFSSA has a good convergence speed and accuracy on unimodal functions, and it has a strong ability to resist local extremes on multimodal functions. Therefore, the introduction of multiple strategies significantly improves the stability and searching ability of the algorithm.

From Figure 4, we can see that ASFSSA has a significant improvement in convergence speed and accuracy. Especially, the ASFSSA has very fast convergence speed and very high convergence precision in the functions of F_1–F_5, F_7–F_{10}, F_{15}-F_{16} and has obvious ability of resisting local attraction in the functions of F_5, F_{10}, and F_{15}. ASFSSA has good convergence effect in F_6, F_{13}, F_{14}, and F_{17} functions, but there a few differences with other algorithms. BSO has better performance in the three functions of F_{11}-F_{12} and F_{18}, and ASFSSA has the second best performance, but BSO has worse performance in the other functions, and some functions have worse performance than PSO. The convergence effect of other algorithms is insufficient. Thus, it can be seen that the introduction of multistrategy makes the algorithm get rid of the insufficient search mode in the optimization process, open up a more flexible and detailed search, and improve the convergence ability of the algorithm.

5.1. Wilcoxon Rank Sum Test. It is not comprehensive to simply calculate the indexes of the running results of each algorithm. In order to highlight the superiority of the ASFSSA algorithm, it is necessary to carry out the statistical test. In order to reflect the fairness, the Wilcoxon rank sum test [20] is used to verify whether the results of each run of ASFSSA are significantly different from those of other algorithms at the $P = 5\%$ significance level. If $P < 5\%$, it can be considered that there is a significant difference between the two algorithms; if $P > 5\%$, it means that the difference between the two algorithms is not obvious; that is, the

Table 1: Test function table.

Function	Dim (D)	Interval	Min
$F_1(x)=\sum_{i=1}^{n} x_i^2$	30	[−100, 100]	0
$F_2(x)=\sum_{i=1}^{n} \lvert x_i\rvert+\prod_{i=1}^{n} x_i$	30	[−10, 10]	0
$F_3(x)=\sum_{i=1}^{n}(\sum_{j=1}^{n} x_j)^2$	30	[−100, 100]	0
$F_4(x)=\max_i\{\lvert x_i\rvert, 1\le i\le n\}$	30	[−100, 100]	0
$F_5(x)=\sum_{i=1}^{n-1}[100(x_{i+1}-x_i^2)^2+(x_i-1)^2]$	30	[−30, 30]	0
$F_6(x)=\sum_{i=1}^{n}([x_i+0.5])^2$	30	[−100, 100]	0
$F_7=\sum_{i=1}^{d} x_i^2+(\sum_{i=1}^{d} 0.5ix_i)^2+(\sum_{i=1}^{d} 0.5ix_i)^4$	30	[−5, 10]	0
$F_8(x)=\sum_{i=1}^{d/4}[(x_{4i-3}+10x_{4i-2})^2+5(x_{4i-1}-x_{4i})^2+(x_{4i-2}-2x_{4i-1})^4+10(x_{4i-3}-x_{4i})^4]$	30	[−4, 5]	0
$F_9(x)=\sum_{i=1}^{d} \lvert x_i\rvert^{i+1}$	30	[−100, 100]d	0
$F_{10}(x)=\sum_{i=1}^{n} ix_i^4+\text{random}[0,1)$	30	[−1.28, 1.28]	0
$F_{11}(x)=\sum_{i=1}^{n} -x_i\sin(\sqrt{\lvert x_i\rvert})$	30	[−500, 500]	-418.9829n
$F_{12}=418.9829n-\sum_{i=1}^{n} x_i\sin(\sqrt{\lvert x_i\rvert})$	30	[−500, 500]	0
$F_{13}=\sin^2(\pi w_1)+\sum_{i=1}^{d-1}(w_i-1)^2[1+10\sin^2(\pi w_i+1)+(w_d-1)^2][1+\sin^2(2\pi w_d)]$ while $w_i=1+(x_i-1/4)$, $\forall i=1,\ldots,d$	30	[−10, 10]d	0
$F_{14}(x)=\sum_{i=1}^{d-1}((100x_i^2-x_{i+1})^2+(x_i-1)^2)$	30	[−10, 10]d	0
$F_{15}=\sin^2(3\pi x_1)+(x_1-1)^2[1+\sin^2(3\pi x_2)]+(x_2-1)^2[1+\sin^2(2\pi x_2)]$	2	[−10, 10]	0
$F_{16}(x)=2x_1^2-1.05x_1^4+(x_1^6/6)+x_1x_2+x_2^2$	2	[−5, 5]	0
$F_{17}(x)=(1.5-x_1+x_1x_2)^2+(2.25-x_1+x_1x_2^2)^2+(2.625-x_1+x_1x_2^3)^2$	2	[−4.5, 4.5]	0
$F_{18}(x)=(0.002+\sum_{i=1}^{25}1/(i+(x_1-a_{1i})^6+(x_2-a_{2i})^6))^{-1}$, where $a=\begin{pmatrix}-32 & -16 & 0 & 16 & 32 & -32 & \ldots & 0 & 16 & 32\\ -32 & -32 & -32 & -32 & -32 & -16 & \ldots & 32 & 32 & 32\end{pmatrix}$	2	[−65.536.65.536]	0.998

Table 2: The complexity and parameters of each algorithm.

Algorithm	Time complexity	Space complexity	Iteration and population	Parameter setting
ASFSSA	O $(P \times M \times D)$	O $(N \times D)$	Iteration = 200, population = 100	$\varepsilon = 1e-50$
BSO				eta = 0.95, $c = 2$, $k = 0.4$, step0 = 0.9, step1 = 0.2
CSSA				$\varepsilon = 1e-50$
SSA				$\varepsilon = 1e-50$
GWO				—
PSO				c1 = c2 = 2, $w = 0.728$

Table 3: Table of optimization results of each algorithm.

Function	Algorithm	Best	Aver	Std
$F_1(x)$	ASFSSA	0	0	0
	BSO	8.15851	26.3851	14.9876
	CSSA	0	0	0
	SSA	0	$5.192E-251$	0
	GWO	$1.4406E-103$	$1.56961E-97$	$5.36616E-97$
	PSO	$3.8599E-12$	$3.0697E-11$	$2.7076E-11$
$F_2(x)$	ASFSSA	0	0	0
	BSO	0.212219	1.8836	2.13278
	CSSA	0	$3.8973E-160$	$2.1346E-159$
	SSA	0	$2.2022E-144$	$8.4437E-144$
	GWO	$1.6295E-25$	$2.9050E-23$	$4.4358E-23$
	PSO	$8.9056E-08$	$2.5055E-07$	$1.4584E-07$
$F_3(X)$	ASFSSA	0	0	0
	BSO	0.0004945	15.1459	34.9405
	CSSA	0	$4.2858E-192$	0
	SSA	0	$7.7137E-210$	0
	GWO	$2.2250E-04$	0.029431	0.070791
	PSO	22.2592	49.9596	18.1286
$F_4(X)$	ASFSSA	0	0	0
	BSO	0.01503	0.015026	1.40522
	CSSA	0	$4.1077E-141$	$2.2499E-140$
	SSA	$4.0636E-14$	$1.9036E-07$	$2.9266E-07$
	GWO	$2.4178E-06$	$6.4757E-06$	$2.1850E-06$
	PSO	$8.1218E-14$	$6.9044E-13$	$7.0838E-13$
$F_5(X)$	ASFSSA	$2.5510E-09$	$9.6950E-06$	$3.977E-05$
	BSO	553.7041	2543.2161	1657.5282
	CSSA	$1.3357E-08$	$2.6062E-04$	0.0015114
	SSA	$4.7653E-09$	0.00028325	0.00049636
	GWO	45.8565	47.3855	0.89355
	PSO	89.4507	234.8606	104.6002
$F_6(X)$	ASFSSA	$1.2670E-17$	$2.5726E-15$	$4.5874E-15$
	BSO	$1.4135E-19$	$2.7997E-10$	$1.4985E-09$
	CSSA	$1.2204E-17$	$8.1489E-15$	$1.1839E-14$
	SSA	$4.0636E-14$	$1.0936E-07$	$2.9266E-07$
	GWO	$2.4178E-06$	$6.4757E-06$	$2.185E-06$
	PSO	$8.1218E-14$	$6.9044E-13$	$7.0838E-13$
$F_7(X)$	ASFSSA	0	0	0
	BSO	10.9679	76.8897	44.1926
	CSSA	0	$2.6949E-153$	$1.476E-152$
	SSA	0	$6.9176E-139$	$3.7889E-138$
	GWO	$1.1787E-06$	$2.2057E-05$	$2.7228E-05$
	PSO	30.8725	58.7189	18.8337
$F_8(X)$	ASFSSA	0	0	0
	BSO	1.4696	9.2489	5.9505
	CSSA	0	$1.7622E-279$	0
	SSA	0	$2.3385E-270$	0
	GWO	$6.7719E-06$	$5.7427E-05$	$5.9614E-05$
	PSO	0.017546	0.18078	0.14242

Table 3: Continued.

Function	Algorithm	Best	Aver	Std
$F_9(X)$	ASFSSA	0	0	0
	BSO	$7.8221E-46$	$2.0384E-39$	$3.2288E-39$
	CSSA	0	$6.07E-95$	$3.3246E-94$
	SSA	0	$8.7599E-97$	$4.798E-96$
	GWO	0	$9.7069E-251$	0
	PSO	$1.6341E-29$	$6.6714E-24$	$1.2043E-23$
$F_{10}(X)$	ASFSSA	$1.0044E-05$	$9.5155E-05$	$8.3380E-05$
	BSO	0.0038813	0.009674457	0.004701
	CSSA	$9.9226E-06$	0.00026062	0.00016246
	SSA	$5.318E-05$	0.00029582	0.00025735
	GWO	0.00040374	0.0020252	0.89355
	PSO	0.010201	0.030015	0.00096086
$F_{11}(X)$	ASFSSA	−12569.3148	−11107.0762	796.9218
	BSO	−12569.4418	−11820.3055	973.8153
	CSSA	−9859.7543	−8700.9989	615.6127
	SSA	−9374.4498	−8208.1416	501.1037
	GWO	−9055.703	−6452.354	1033.4608
	PSO	−8405.1316	−6176.2342	793.1086
$F_{12}(X)$	ASFSSA	0.490047	1270.9199	964.1809
	BSO	0.03331	848.2818	1061.7445
	CSSA	2529.3974	3661.9962	725.5963
	SSA	3471.670439	4292.617883	529.1990723
	GWO	4866.1835	6134.3633	604.5177
	PSO	5205.7803	7638.9387	1024.9673
$F_{13}(X)$	ASFSSA	$7.2046E-11$	$3.1056E-07$	$6.4439E-07$
	BSO	3.5095	$8.4787E+54$	$3.4748E+55$
	CSSA	$3.6686E-11$	$1.6611E-05$	$6.0978E-05$
	SSA	$1.1633E-09$	$6.0348E-07$	$1.8076E-06$
	GWO	$1.0500E+54$	$1.4300E+57$	$5.7000E+57$
	PSO	$1.5273E+60$	$1.9700E+60$	$2.1400E+59$
$F_{14}(X)$	ASFSSA	0	$4.9628E-05$	$2.5146E-04$
	BSO	$1.3048E-23$	$4.77072E-21$	$6.0171E-21$
	CSSA	$6.2203E-08$	0.0012751	0.0037596
	SSA	$2.9797E-08$	0.00034106	0.00062708
	GWO	$1.0500E+54$	$1.4300E+57$	$5.6800E+57$
	PSO	$2.0728E+87$	$3.3100E+87$	$5.6800E+86$
$F_{15}(X)$	ASFSSA	$1.3498E-31$	$1.3498E-31$	0
	BSO	$1.3498E-31$	$1.3498E-31$	0
	CSSA	$1.4730E-31$	$2.3043E-29$	$3.9261E-29$
	SSA	$1.3498E-31$	$3.9049E-29$	$5.2232E-29$
	GWO	$1.0606E-08$	$8.9305E-07$	$7.8567E-07$
	PSO	$1.30489E-23$	$4.7707E-21$	$6.0171E-21$
$F_{16}(X)$	ASFSSA	0	0	0
	BSO	$1.2475E-42$	$1.8013E-41$	$1.9512E-41$
	CSSA	0	$4.9534E-285$	0
	SSA	0	$3.7547E-237$	0
	GWO	$2.6095E-166$	$2.1062E-131$	$1.0027E-130$
	PSO	$4.0625E-25$	$6.4627E-22$	$1.8985E-21$
$F_{17}(X)$	ASFSSA	$2.9038E-25$	$2.3672E-19$	$7.0572E-19$
	BSO	0	0.2540	0.3592
	CSSA	$4.3789E-21$	$3.2277E-16$	$1.5937E-15$
	SSA	$2.7959E-21$	$1.2661E-16$	$2.7684E-16$
	GWO	$1.2267E-08$	$4.0761E-07$	$4.2024E-07$
	PSO	$1.1013E-22$	$8.1661E-20$	$1.7949E-19$
$F_{18}(X)$	ASFSSA	0.998	0.998	0
	BSO	0.998	1.0311	0.17843
	CSSA	0.998	2.1068	2.9273
	SSA	0.998	2.5594	3.6421
	GWO	0.998	2.8013	2.8092
	PSO	0.998	1.1968	0.3976

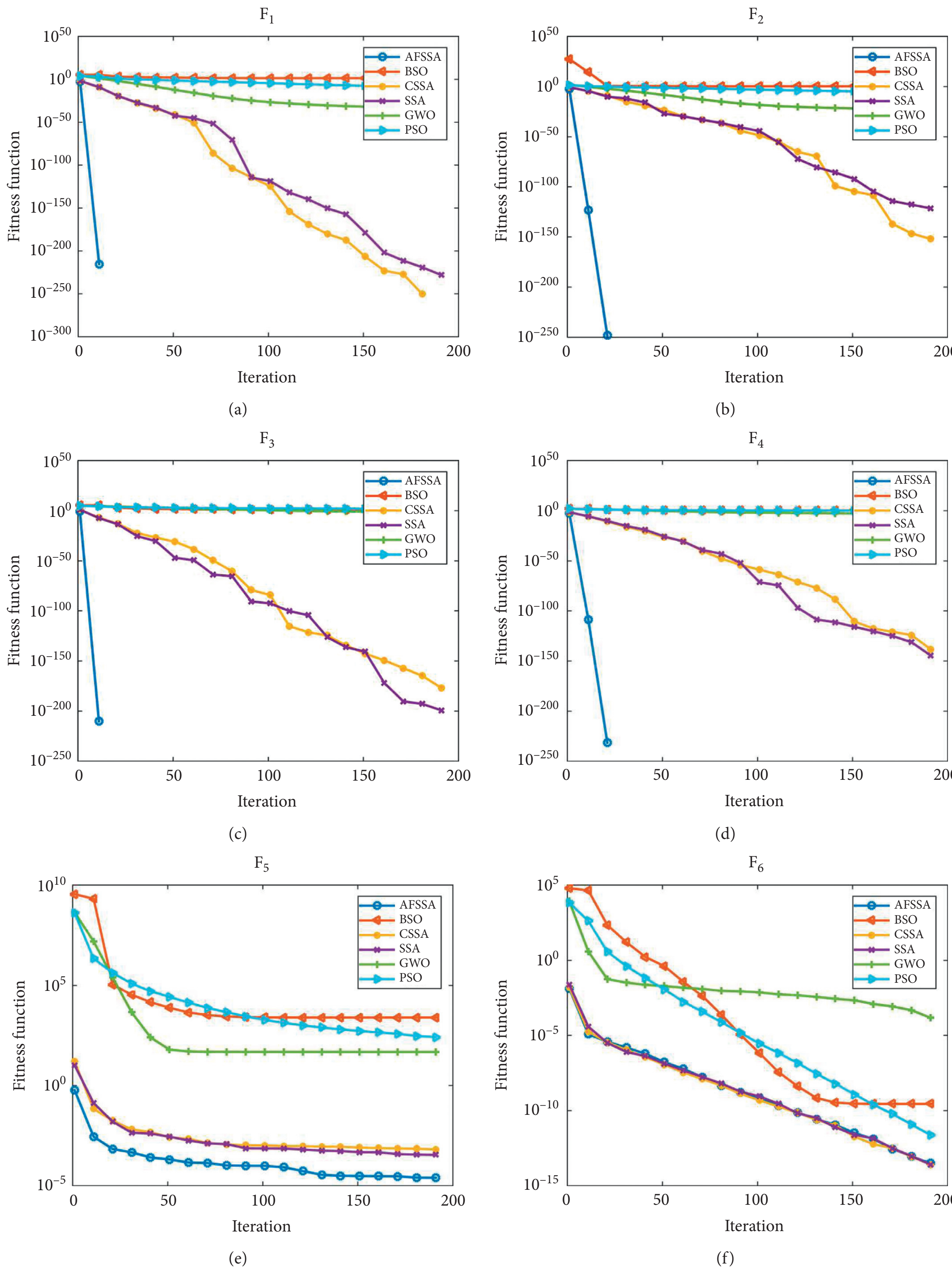

Figure 4: Continued.

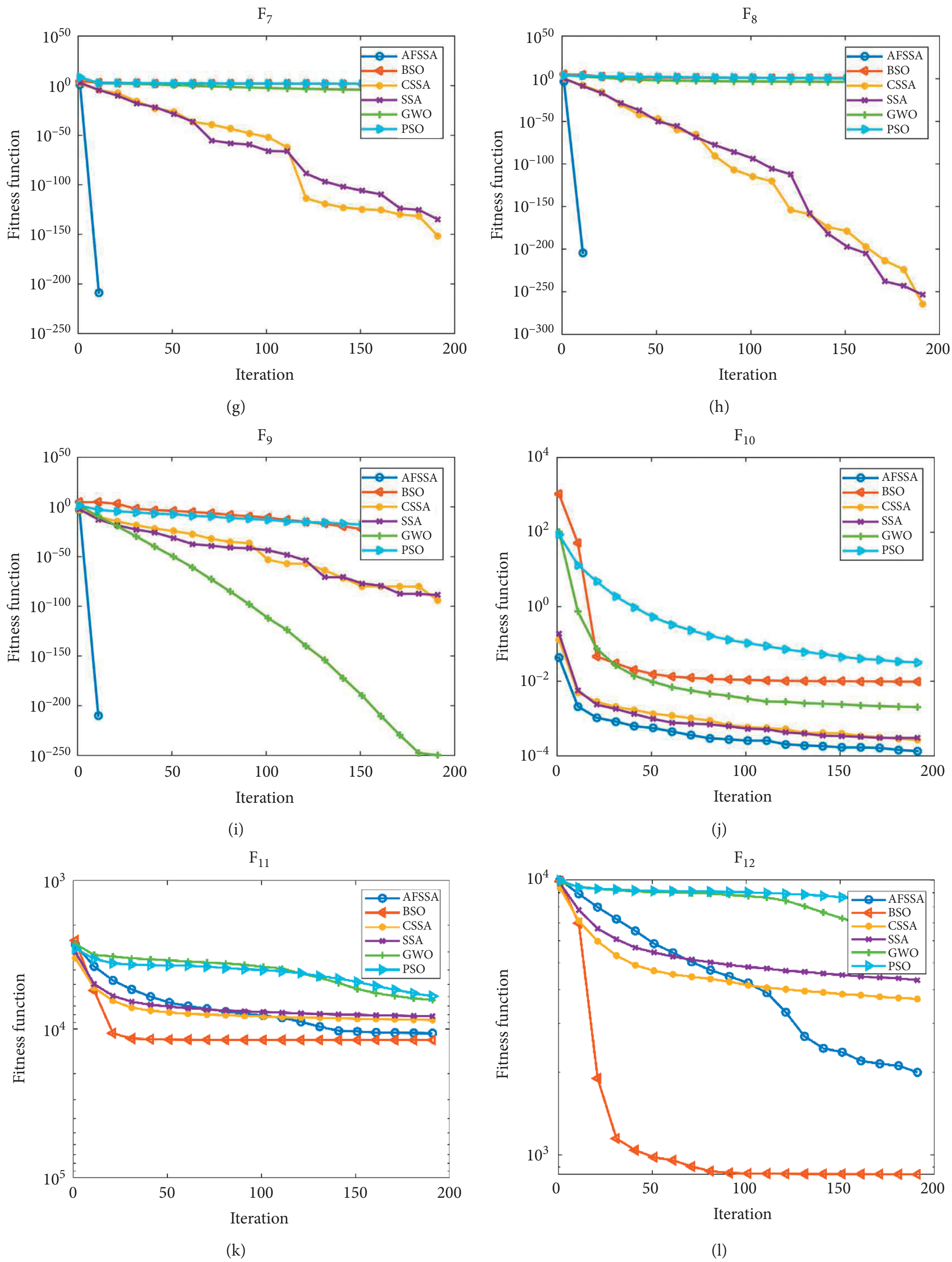

Figure 4: Continued.

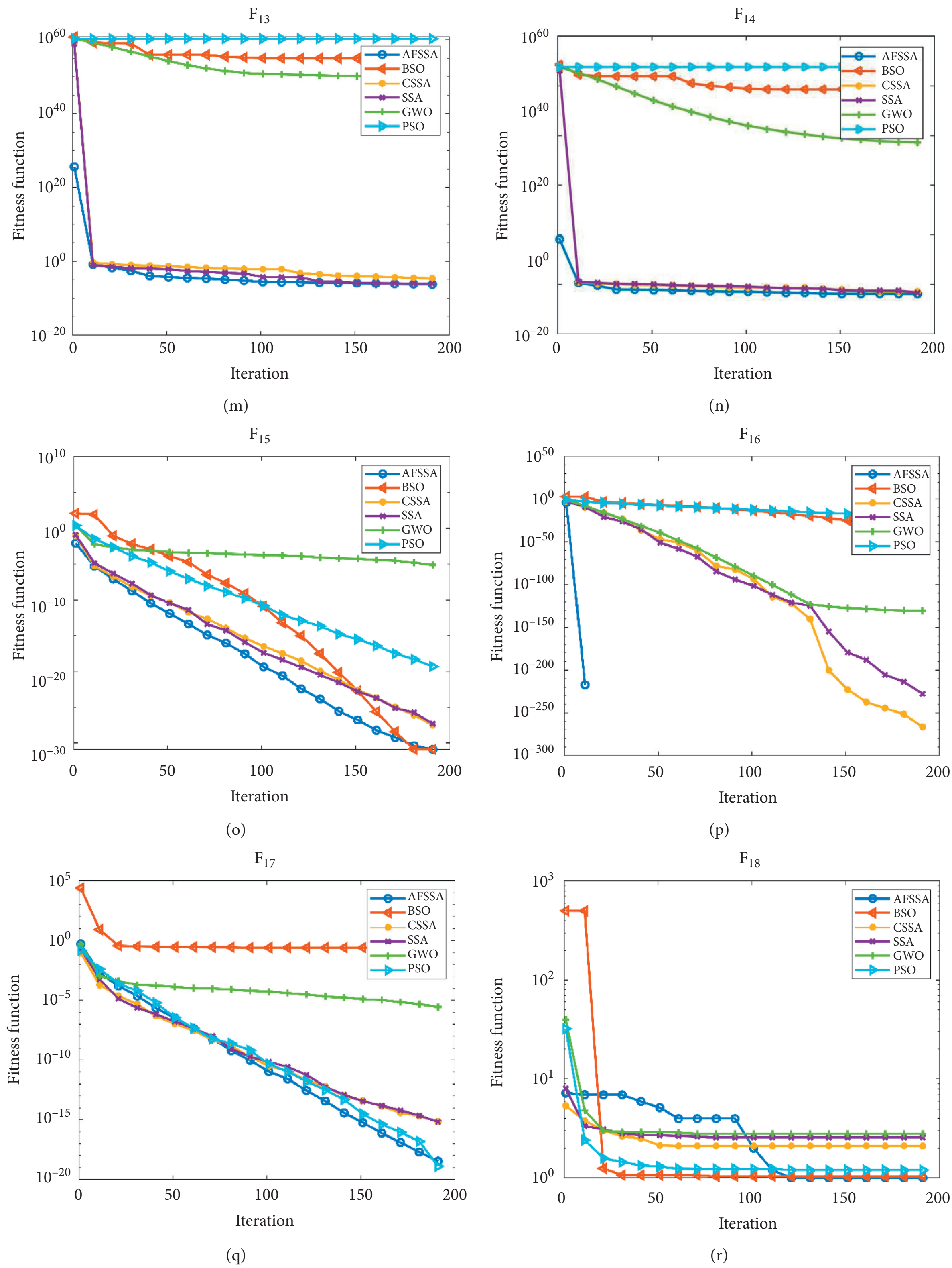

FIGURE 4: Convergence effect diagram of each algorithm. (a) F_1. (b) F_2. (c) F_3. (d) F_4. (e) F_5. (f) F_6. (g) F_7. (h) F_8. (i) F_9. (j) F_{10}. (k) F_{11}. (l) F_{12}. (m) F_{13}. (n) F_{14}. (o) F_{15}. (p) F_{16}. (q) F_{17}. (r) F_{18}.

Table 4: Wilcoxon rank sum test P value.

Function	BSO	CSSA	SSA	PSO	GWO
$F_1(X)$	$1.2118e-12$	N/A	N/A	$1.2118e-12$	$1.2118e-12$
$F_2(X)$	$1.2118e-12$	$8.8658e-07$	$5.3750e-06$	$1.2118e-12$	$1.2118e-12$
$F_3(X)$	$1.2118e-12$	0.0216	N/A	$1.2118e-12$	$1.2118e-12$
$F_4(X)$	$1.2118e-12$	$6.6096e-05$	$6.6096e-05$	$1.2118e-12$	$1.2118e-12$
$F_5(X)$	$3.0199e-11$	0.0184	N/A	$3.0199e-11$	$3.0199e-11$
$F_6(X)$	0.0010	$1.0937e-10$	$1.6132e-10$	$3.0199e-11$	$3.0199e-11$
$F_7(X)$	$1.2118e-12$	0.0056	$1.4552e-04$	$1.2118e-12$	$1.2118e-12$
$F_8(X)$	$1.2118e-12$	0.0419	0.0419	$1.2118e-12$	$1.2118e-12$
$F_9(X)$	$1.2118e-12$	$8.8658e-07$	$3.4526e-07$	$1.2118e-12$	$1.6572e-11$
$F_{10}(X)$	$3.0199e-11$	0.0378	0.0242	$3.0199e-11$	$3.1589e-10$
$F_{11}(X)$	$1.1023e-08$	0.0025	$5.5999e-07$	$4.5043e-11$	$1.2057e-10$
$F_{12}(X)$	$4.8011e-07$	0.0020	$4.5726e-09$	$3.0199e-11$	$3.0199e-11$
$F_{13}(X)$	$3.0199e-11$	N/A	N/A	$3.0199e-11$	$3.0199e-11$
$F_{14}(X)$	$3.0199e-11$	N/A	N/A	$3.0199e-11$	$3.0199e-11$
$F_{15}(X)$	N/A	$1.1970e-12$	$1.6572e-11$	$1.2118e-12$	$1.2118e-12$
$F_{16}(X)$	$1.2118e-12$	N/A	N/A	$1.2118e-12$	$1.2118e-12$
$F_{17}(X)$	N/A	$2.9468e-11$	$2.9468e-11$	$2.9468e-11$	$2.9468e-11$
$F_{18}(X)$	$4.4787e-06$	0.0071	0.0236	0.0200	$1.4930e-11$

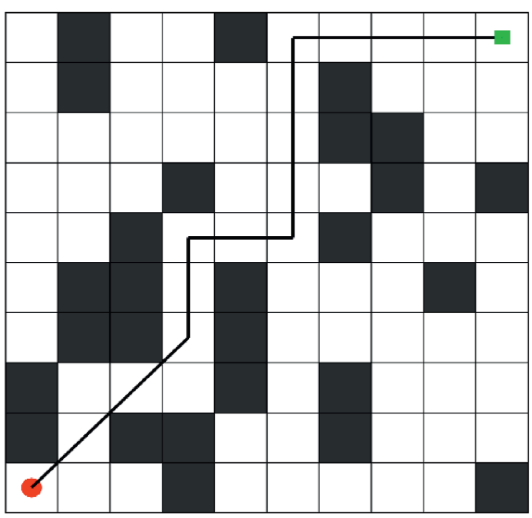

(a)

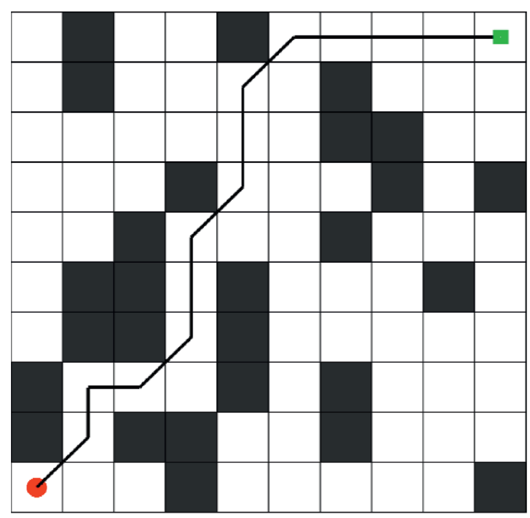

(b)

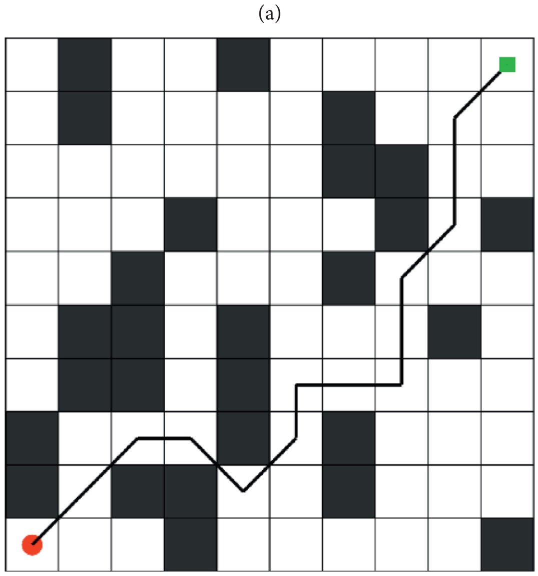

(c)

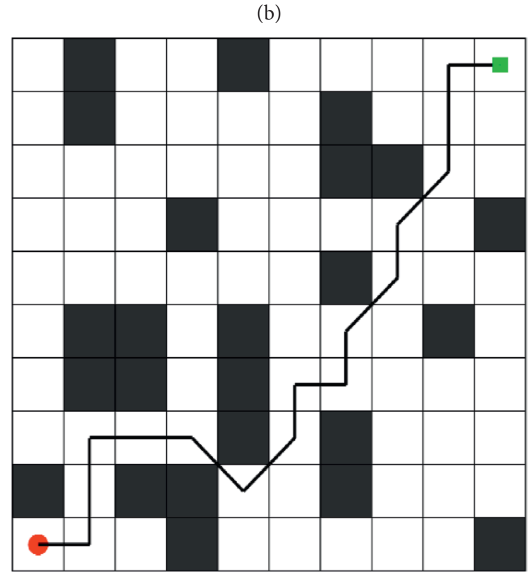

(d)

Figure 5: 10 ∗ 10 shortest path planning diagram. (a) ASFSSA. (b) CSSA. (c) SSA. (d) PSO.

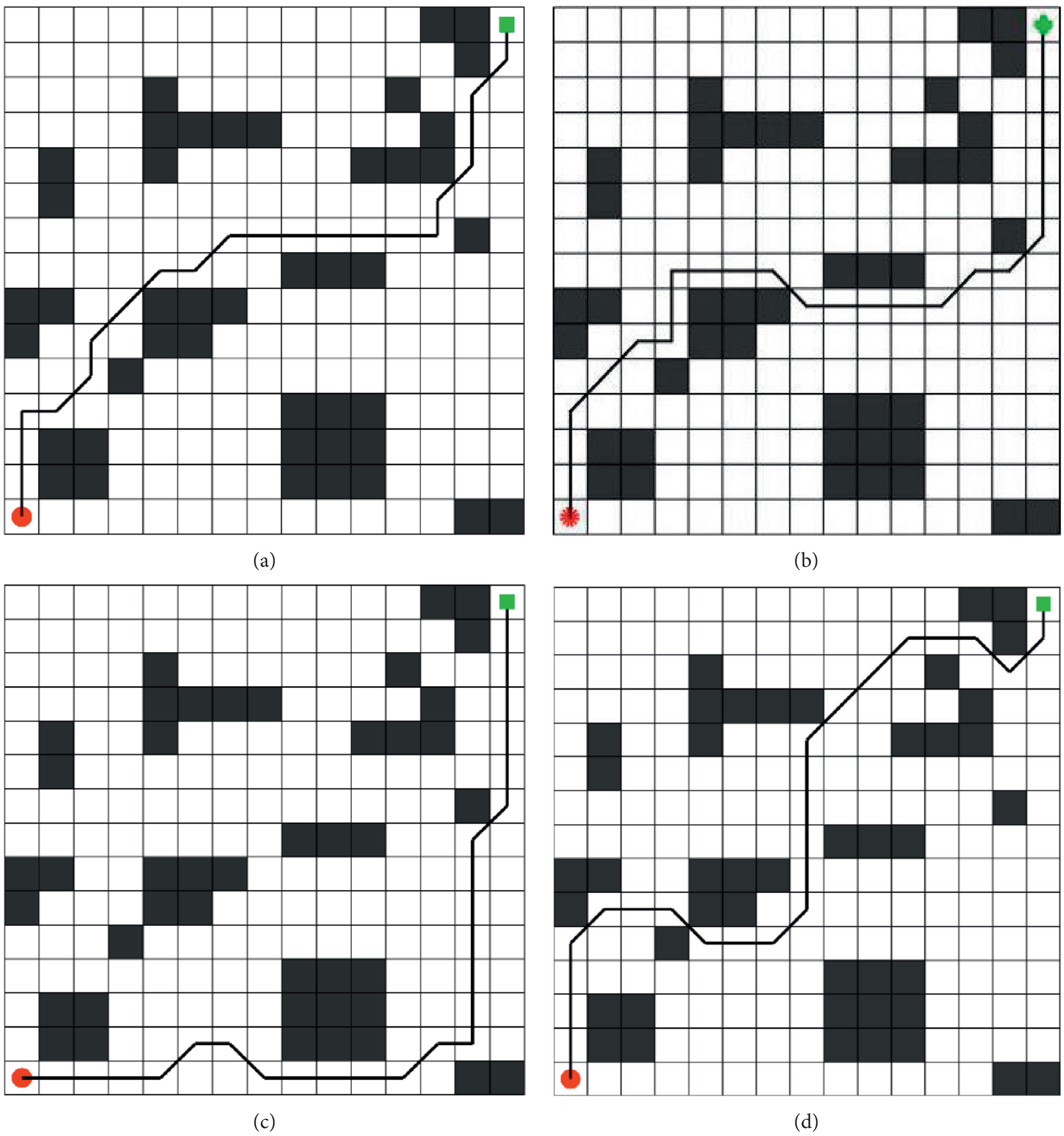

FIGURE 6: 15 ∗ 15 shortest path planning diagram. (a) ASFSSA. (b) CSSA. (c) SSA. (d) PSO.

optimization performance of the two algorithms is equivalent. Table 4 shows the results for ASFSSA and PSO, GWO, BSO, SSA, and CSSA are at a significance level of $P = 5\%$, where N/A indicates that the performance between the two is similar and not comparable.

As can be seen from Table 3, each algorithm is significantly different from the ASFSSA algorithm, with only a few cases of comparable performance. It can be seen that the introduction of multiple strategies improves the disadvantages of the original algorithm and enhances the optimization ability of the algorithm.

6. Robot Path Planning Based on ASFSSA

To verify the feasibility and practicability of the improved algorithm, this paper takes a classic case of robot route planning to explore it. Each individual sparrow is a viable path in routing. Assuming there are N possible paths, dimension D is determined by the number of connections from the starting point to the destination point. Using the raster method to model the environment, the raster method is to use 1 ∗ 1 raster to construct the equivalent working environment, and use the raster value to equivalent the obstacles in the location [23, 24]. This effectively equates the working environment of the robot to a plane, similar to the lattice effect, and then determines the feasible and obstacle zones based on the raster values.

The raster number defines 0 as the feasible domain and 1 as the obstacle zone, so the robot can plan its path on the raster with a value of 0. Dimension D is the number of columns in the raster map and the cost function of the path length of the i-th sparrow individual, as shown in the following equation:

$$f(x_i) = \sum_{j=1}^{D-1} \sqrt{\left(x_{j+1} - x_j\right)^2 + \left(y_{j+1} - y_j\right)^2}. \tag{11}$$

Table 5: Statistics table of optimization route by algorithms.

Map size	Performance index	ASFSSA	CSSA	SSA	PSO
10 ∗ 10	Shortest	12.7279	12.7279	15.5564	15.5564
	Average	13.8593	14.4250	20.6475	21.2132
	Worse	15.5564	20.6475	21.2132	41.0122
20 ∗ 20	Shortest	19.7990	22.6274	22.6274	25.4559
	Average	20.9304	23.7588	24.3244	26.0215
	Worst	22.6274	25.4559	31.1127	31.1127

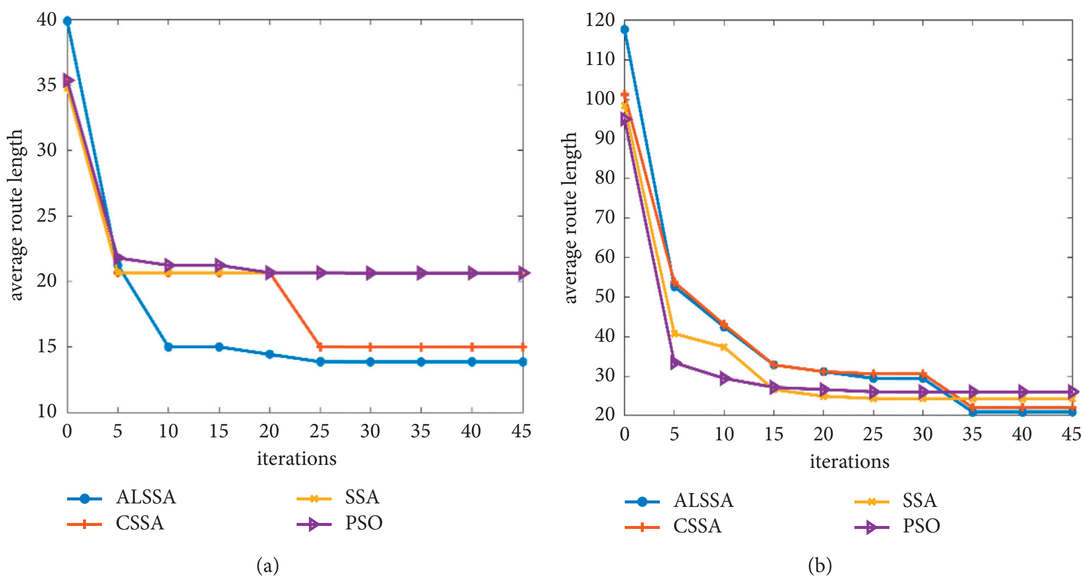

Figure 7: The average route convergence graph of each algorithm. (a) 10 ∗ 10. (b) 15 ∗ 15.

In equation (11), j is the j-th dimension of a sparrow individual.

6.1. Experimental Environment Settings. To better verify the practicability and feasibility of the improved algorithm, the improved algorithm is used to route the raster maps of the two models. Compared with CSSA, SSA, and PSO, the number of population is 20 and the number of iterations is 100. Other environmental parameters are consistent with the above.

6.2. Simulation Results and Analysis. The optimal route of each algorithm in the two model graphs is shown in Figures 5 and 6. In order to eliminate the influence of chance, each algorithm is tested for 10 times, and the shortest, average, and worst route of each algorithm are counted. Three indicators are used to measure the stability and feasibility of each algorithm in this experiment. The optimization statistical table of each algorithm is shown in Table 5, and the average route convergence chart is shown in Figure 7.

As shown in Figures 5 and 6, the ASFSSA route is the simplest and clearest, followed by CSSA, while PSO and SSA are obviously trapped in local optimum. From Table 5, we can see that ASFSSA has the best searching ability and stability in both of raster graphs, and CSSA has better stability. However, from Figure 7, we can see that the convergence of SSA and PSO is insufficient, and the optimization results of SSA and PSO are extremely unstable and poor. Therefore, in the two model diagrams, the introduction of multiple strategies makes the algorithm flexible in the search, greatly improves the search ability of the algorithm, and plans a route with the least cost.

7. Conclusion

The sparrow search algorithm has better performance than other algorithms in optimization, but it is still easy to get stuck in local and rely on population initialization. This paper analyzes these defects and proposes an adaptive spiral flying sparrow search algorithm. Firstly, tent mapping based on random variables is used to initialize the population, which makes the distribution of sparrow individuals uniform and helps the individuals to work better. Secondly, the adaptive weights strategy and Levy flight mechanism are used in the discoverer stage, which makes the discoverer flexible and adaptable in the optimization process and reduces the traditional regular strategy. Finally, the variable spiral search strategy is used in the follower stage, which makes the follower search method more detailed and in-depth, and improves the convergence accuracy of the algorithm. The effectiveness of the improved algorithm is verified by 18 test functions and the comparison of other algorithms. Compared with other algorithms, ASFSSA has significant optimization capabilities. At the same time, the feasibility and practicability of the improved algorithm are verified by the robot path planning study. The path planned by the improved algorithm is clear, and the cost function is the smallest. It can be seen that the introduction of multiple strategies has effectively improved the optimization ability of the basic sparrow search algorithm. However, in some functions, the optimization effect of ASFSSA is second only to the BSO algorithm. In the future research phase, how to improve these optimization effect is the research focus, and it needs to be upgraded to more complex applications.

Data Availability

The data used to support the findings of this study are available from the corresponding author upon request.

Conflicts of Interest

The authors declare that they have no conflicts of interest.

Acknowledgments

This work was financially supported by the Regional Foundation of the National Natural Science Foundation of China (no. 61561024).

References

[1] J. Xue and B. Shen, "A novel swarm intelligence optimization approach: sparrow search algorithm," *Systems Science & Control Engineering*, vol. 8, no. 1, pp. 22–34, 2020.

[2] S. Mirjalili, S. M. Mirjalili, and A. Lewis, "Grey wolf optimizer," *Advances in Engineering Software*, vol. 69, pp. 46–61, 2014.

[3] J. Kennedy and R. C. Eberhart, "A discrete binary version of the particle swarm algorithm," in *Proceedings of the 1997 IEEE International Conference on Systems, Man, and Cybernetics. Computational Cybernetics and Simulation*, vol. 5, IEEE, Orlando, FL, USA, October 1997.

[4] Y. Lei, G. De, and L. Fei, "Improved sparrow search algorithm based DV-hop localization in WSN," in *Proceedings of the 2020 Chinese Automation Congress (CAC)*, Shanghai, China, November 2020.

[5] L. Xin, X. Mu, J. Zhang, and Z. Wang, "Chaotic sparrow search optimization algorithm," *Journal of Beijing University of Aeronautics and Astronautics*, vol. 1–10, 2021.

[6] A. Tang, T. Han, D. Xu et al., "Path planning method of unmanned aerial vehicle based on chaos sparrow search algorithm," *Systems Engineering and Electronics*, vol. 41, no. 7, pp. 2128–2136, 2020, https://kns.cnki.net/kcms/detail/51.1307.TP.20201124.1519.002.html.

[7] L. Xin, X. Mu, and J. Zhang, "Multi-threshold image segmentation based on improved sparrow search algorithm," *Systems Engineering and Electronic Technology*, vol. 43, no. 2, pp. 318–327, 2021.

[8] Q. Mao, Q. Zhang, C. Mao, and J. Bai, "Hybrid sine cosine algorithm and Levy's flying sparrow algorithm," *Journal of Shanxi University (Natural Science Edition)*, pp. 1–6, 2021.

[9] W. Song, S. Liu, X. Wang, and W. Wu, "An improved sparrow search algorithm," in *Proceedings of the 2020 IEEE Intl Conf on Parallel & Distributed Processing with Applications, Big Data & Cloud Computing, Sustainable Computing & Communications, Social Computing & Networking (ISPA/BDCloud/SocialCom/SustainCom)*, England, UK, December 2020.

[10] X. Wu, Z. Han, L. Wei et al., "Intelligent on-demand adjustment algorithm and key technology of mine air flow," *Journal of China University of Mining & Technology*, vol. 50, no. 4, pp. 725–734, 2021.

[11] C. Zhang and S. Ding, "A stochastic configuration network based on chaotic sparrow search algorithm," *Knowledge-Based Systems*, vol. 220, 2021.

[12] J. Zhang, K. Xia, Z. He et al., "Semi-supervised ensemble classifier with improved sparrow search algorithm and its application in pulmonary nodule detection," *Mathematical Problems in Engineering*, vol. 2021, Article ID 6622935, 18 pages, 2021.

[13] Y. Li, M. Han, and Q. Guo, "Modified whale optimization algorithm based on tent chaotic mapping and its application in structural optimization," *KSCE Journal of Civil Engineering*, vol. 24, no. 12, pp. 3703–3713, 2020.

[14] X. Liang, W. Li, Y. Zhang, and M. Zhou, "An adaptive particle swarm optimization method based on clustering," *Soft Computing*, vol. 19, no. 2, pp. 431–448, 2015.

[15] S. N. Chegini, A. Bagheri, and F. Najafi, "PSOSCALF: a new hybrid PSO based on Sine Cosine Algorithm and Levy flight for solving optimization problems," *Applied Soft Computing*, vol. 73, pp. 697–726, 2018.

[16] X. Chen, X. Huang, D. Zhu, and Y. Qiu, "Research on chaotic flying sparrow search algorithm," *Journal of Physics: Conference Series*, vol. 1848, no. 1, Article ID 012044, 2021.

[17] H. Haklı and H. Uğuz, "A novel particle swarm optimization algorithm with Levy flight," *Applied Soft Computing*, vol. 23, pp. 333–345, 2014.

[18] A. A. Heidari and P. Pahlavani, "An efficient modified grey wolf optimizer with Lévy flight for optimization tasks," *Applied Soft Computing*, vol. 60, pp. 115–134, 2017.

[19] S. Mirjalili and A. Lewis, "The whale optimization algorithm," *Advances in Engineering Software*, vol. 95, pp. 51–67, 2016.

[20] X. Tao, W. Guo, Q. Li, C. Ren, and R. Liu, "Multiple scale self-adaptive cooperation mutation strategy-based particle swarm optimization," *Applied Soft Computing*, vol. 89, Article ID 106124, 2020.

[21] T. Wang and L. Yang, "Beetle swarm optimization algorithm: theory and application," 2018, https://arxiv.org/abs/1808.00206.

[22] X. Jiang and S. Li, "BAS: Beetle Antennae Search Algorithm for Optimization Problems," https://arxiv.org/abs/1710.10724.

[23] F. Xu, H. Li, C. M. Pun, and H. Hu, Y. Li, Y. Song, H. Gao, A new global best guided artificial bee colony algorithm with application in robot path planning," *Applied Soft Computing*, vol. 88, Article ID 106037, 2020.

[24] J. Li, "Robot path planning based on improved sparrow algorithm," *Journal of Physics: Conference Series*, vol. 1861, no. 1, Article ID 012017, 2021.

Hindawi
Scientific Programming
Volume 2021, Article ID 1951264, 12 pages
https://doi.org/10.1155/2021/1951264

Research Article

Research on Spatial Pattern Dynamic Evolution Algorithm and Optimization Model Construction and Driving Mechanism of Provincial Tourism Eco-Efficiency in China under the Background of Cloud Computing

Fei Lu,[1] **Wei Qin**,[2] **and Yu-Xuan Wang**[3]

[1]*School of History, Culture and Tourism, Weifang University, Weifang 261061, China*
[2]*School of Innovation and Entrepreneurship, Chongqing University of Posts and Telecommunications, Chongqing 400065, China*
[3]*School of Economics & Management, Beijing Forestry University, Beijing 100083, China*

Correspondence should be addressed to Wei Qin; qinwei@cqupt.edu.cn

Received 19 July 2021; Revised 4 August 2021; Accepted 16 August 2021; Published 26 August 2021

Academic Editor: Punit Gupta

Based on the research of spatial pattern dynamic evolution algorithm and optimization model construction and driving mechanism of provincial tourism eco-efficiency in China under the background of cloud computing, this paper takes 30 provinces in mainland China (excluding Tibet, Hong Kong, Macao, and Taiwan) as the research object and scientifically constructs the measurement index system of tourism eco-efficiency. The Super-SBM-Undesirable model is used to measure the tourism eco-efficiency of each province from 2004 to 2017, and the algorithm and model are optimized. This paper explores the spatial evolution trajectory and path of tourism eco-efficiency by using the barycentric standard deviation ellipse method and constructs a dynamic panel model to identify the factors affecting the evolution trajectory and their driving mechanisms by using the SYS-GMM method. The results show that China's tourism eco-efficiency is at a high level and the eastern region is higher than the central and western regions. From the moving track of the center of gravity, the center of gravity of China's tourism eco-efficiency is located in Henan province, which has experienced a process of moving from southeast to northwest. From the standard deviation ellipse, the spatial distribution direction of China's tourism eco-efficiency presents a "northeast-southwest" pattern, and there is a further strengthening trend of deviation. There is a significant positive correlation between tourism eco-efficiency and tourism industrial structure upgrading, tourism industrial structure rationalization, tourism technology level, and tourism human capital, as well as a significant negative correlation between tourism eco-efficiency and tourism economic development level, environmental regulation intensity, and the degree of opening to the outside world, while the relationship between urbanization and tourism eco-efficiency is relatively vague.

1. Introduction

With the advent of the era of artificial intelligence and cloud computing, the future development of tourism service industry is closely related to artificial intelligence and cloud technology. Since the reform and opening up, the development of China's tourism industry has attracted worldwide attention and created tremendous economic and social value. At the same time, the tourism industry is also suffering from the huge impact of the rapid growth of regional economy. The impact of resource consumption and environmental pollution is prominent, which seriously hinders the transformation of China's tourism industry from high-speed growth to high-quality development stage [1]. During the period of the 13th Five-Year plan, Green Development has become the main theme of China's economic growth. How to seek the balance between tourism economic growth and environmental impact is the current focus of attention [2]. At the Second International Conference on Climate Change and Tourism, the Chinese government called on tourism-related departments in all regions of the world to actively take measures to save energy and reduce emissions. At the same time, the report of the 19th National Congress of the Communist Party of China raised the construction of ecological civilization to an unprecedented level, emphasizing that "the construction of ecological civilization can be considered as a millennium plan related to the sustainable development of the Chinese nation"; therefore, it is necessary to integrate the concept of Green Development into the whole process of tourism economic activities, optimize the structure of tourism industry, change the mode of tourism development, and realize the sustainable improvement of tourism economic growth and tourism environment. Visible, the impact of tourism on the ecological environment has attracted more and more attention. The tourism eco-efficiency is an important judgment index which reflects the two-way effect of the economic value of tourism and environmental impact and can objectively represent how to realize the efficient development of tourism under the background of Green Development, and it provides a new way to measure the level of tourism ecologicalization. Therefore, it is of great theoretical and practical significance to scientifically measure China's provincial tourism eco-efficiency and analyze its spatial pattern dynamic evolution characteristics and driving mechanism for formulating reasonable tourism development policies and promoting the coordinated development of tourism economy and ecological environment.

The idea of eco-efficiency dates back to the 1970s; German scholars Schaltegger and Sturm formally put forward the concept of eco-efficiency in 1990, which is defined as the ratio of economic value added to environmental impact [3]. Subsequently, a number of organizations have developed definitions, analyses, and extensions of eco-efficiency [4, 5], most notably the World Business Council for Sustainable Development (WBCSD), which proposes "creating maximum value with minimal environmental impact." With the development of research on tourism environmental impact, Gössling et al. derived tourism eco-efficiency from the idea of eco-efficiency and defined it as the amount of CO_2 consumed per unit tourism economic value [6]. Since then, tourism eco-efficiency has attracted extensive attention of scholars and has made a wealth of effective research results. From the perspective of the research object, the research object of tourism eco-efficiency is gradually extended from various sectors and different tourism activities to the region, and more and more scholars study the tourism eco-efficiency from the regional perspective [7–9]. From the perspective of measuring methods, the method of measuring tourism eco-efficiency has been extended from single ratio method to DEA and its improved model method, and the methods and models of measuring tourism eco-efficiency have gradually matured and perfected [10]. From the research content, scholars gradually began to pay attention to the time series evolution, spatial pattern, and correlation change of tourism eco-efficiency [11] and, on this basis, use data model to analyze the formation mechanism and influencing factors of spatial-temporal differences of tourism eco-efficiency [12]. Generally speaking, although scholars have carried out in-depth discussion in the field of tourism eco-efficiency, a reference is provided for this paper. However, there are still some problems that need to be further developed: When using DEA and its improved model to measure tourism eco-efficiency, the treatment of undesired output does not conform to the process of tourism economy, and most of the nonexpected output indicators are based on tourism carbon emissions or tourism ecological footprint [13], and some are based on tourism "three wastes" emissions. At the same time, in the empirical analysis of the spatial-temporal evolution of regional tourism eco-efficiency at different scales, the existing literature explored its dynamic characteristics, failed to effectively reflect the spatial evolution characteristics and laws of tourism eco-efficiency, and revealed the influencing factors and mechanism of the evolution process. In view of this, this paper takes China's 30 provinces (excluding Tibet, Hong Kong, Macao, and Taiwan) as the research object and scientifically constructs the index system of tourism eco-efficiency, using Super-SBM-Undesirable model to measure the eco-efficiency of tourism in various provinces from 2004 to 2017, and, on this basis, by means of the method of logarithmic deviation and gravity standard ellipse, to explore the spatial evolution track and path of tourism eco-efficiency, a dynamic panel model is constructed to identify the factors that influence the evolutionary track and its driving mechanism using SYS-GMM.

2. Research Methods

2.1. Models

2.1.1. Super-SBM-Undesirable Model. Common tourism eco-efficiency measurement models are mainly divided into parametric method and nonparametric analysis method. Compared with the parametric method, the nonparametric analysis method does not require a specific function form and residual distribution to explain the deterministic frontier production function. It is easy to apply and has many applications. The nonparametric deterministic frontier production function uses data envelopment analysis (DEA) as the basis. The DEA method is a "data-oriented" analysis method proposed by Charnes in 1978 to measure the relative efficiency of multiple inputs and multiple outputs. Because of the limitation of radial and angle, the traditional DEA model has deviation in efficiency Measure. Tone adds slack variable to the objective function and proposes a nonradial and nonangular SBM model, and the influence of radial and angle selection on efficiency measurement is effectively solved. At the same time, SBM model can also deal with the undesired output according to the production reality. Therefore, Tone extends the SBM model further and proposes an SBM model with undesired outputs [14]. In addition, the traditional DEA model cannot distinguish the differences among multiple DMUs (Decision Making Units) when the efficiency value is 1. In view of this deficiency, Andersen and Petersen put forward the Super Efficiency DEA model which can distinguish the efficient DMUs [15]. The inefficiency of the measure is consistent with the traditional DEA, and the effective value is more than 1, so that the efficient DMUs can be distinguished. SBM model also has problems similar to those of the traditional DEA model. So, Tone extended SBM model, defined it as Super Efficient SBM model, and compared and evaluated DMU which is in the front of production [16]. The model is constructed as follows:

$$\begin{aligned}
\rho^* &= \min \frac{1 + (1/m)\sum_{i=1}^{m} s_i^- / x_{ik}}{1 - (1/(q_1+q_2))\left(\sum_{r=1}^{q_1} s_r^+ / y_{rk} + \sum_{t=1}^{q_2} s_t^{b-} / b_{tk}\right)},\\
\text{s.t.} &\sum_{j=1, j\neq k}^{n} x_{ij}\lambda_j - s_i^- \le x_{ik}, \quad i = 1,2,\ldots,m,\\
&\sum_{j=1, j\neq k}^{n} y_{rj}\lambda_j + s_r^+ \le y_{rk}, \quad r - 1,2,\ldots,q_1,\\
&\sum_{j=1, j\neq k}^{n} b_{tj}\lambda_j - s_t^- \le b_{rk}, \quad k = 1,2,\ldots,q_2,\\
&1 - \frac{1}{q_1+q_2}\left(\sum_{r=1}^{q_1}\frac{s_r^+}{y_{rk}} + \sum_{t=1}^{q_2}\frac{s_t^{b-}}{b_{tk}}\right) > 0, \quad s^- \ge 0, s^+ \ge 0, \lambda \ge 0, j = 1,2,\ldots,n(j \ne k),
\end{aligned} \tag{1}$$

where ρ^* indicates the value of tourism eco-efficiency; λ refers to the Weight Matrix; and s^-, s^+, and s^{b-} represent the slack of input, expected output, and unexpected output, respectively.

2.1.2. Standard Deviation Ellipse. Standard deviational ellipse (SDE) is a spatial pattern statistical method, mainly used to analyze the global characteristics of the spatial distribution of geographic elements. The standard deviation ellipse is a statistical method of spatial pattern, which is mainly used to analyze the global characteristics of spatial distribution of geographical elements [17]. The gravity center, area, standard deviation of x-axis, standard deviation of y-axis, and rotation angle are the basic parameters of this method.

Gravity center is as follows:

$$\begin{aligned}
X &= \frac{\sum_{i=1}^{n} R_i X_i}{\sum_{i=1}^{n} R_i};\\
Y &= \frac{\sum_{i=1}^{n} R_i Y_i}{\sum_{i=1}^{n} R_i}.
\end{aligned} \tag{2}$$

Rotation angle is as follows:

$$\tan\theta = \frac{\left(\sum_{i=1}^{n} R_i^2 X_i^{*2} - \sum_{i=1}^{n} R_i^2 Y_i^{*2}\right) + \sqrt{\left(\sum_{i=1}^{n} R_i^2 X_i^{*2} - \sum_{i=1}^{n} R_i^2 Y_i^{*2}\right)^2 - 4\sum_{i=1}^{n} R_i^2 X_i^{*2} Y_i^{*2}}}{2\sum_{i=1}^{n} R_i^2 X_i^{*2} Y_i^{*2}}. \tag{3}$$

Standard deviation of x-axis is as follows:

$$\sigma_x = \sqrt{\frac{\sum_{i=1}^{n}\left(R_i X_i^* \cos\theta - R_i Y_i^* \sin\theta\right)^2}{\sum_{i=1}^{n} R_i^2}}. \tag{4}$$

Standard deviation of y-axis is as follows:

$$\sigma_y = \sqrt{\frac{\sum_{i=1}^{n}\left(R_i X_i^* \sin\theta - R_i Y_i^* \cos\theta\right)^2}{\sum_{i=1}^{n} R_i^2}}, \tag{5}$$

where (X, Y) is the gravity center of tourism eco-efficiency; (X_i, Y_i) is the geographical center coordinate of province i; R_i is the attribute value of province i; (X_i^*, Y_i^*) is the deviation of (X_i, Y_i) from the ellipse center of province i; (σ_x, σ_y) are the standard deviations of x-axis and y-axis; and the values of the major and minor axes of the ellipse.

2.1.3. Dynamic Panel Metering Model. Panel data has both cross-sectional dimension and time dimension, which can reflect heterogeneous factors (non-time-varying unobservable) and homogeneous factors (time-varying unobservable). Considering the economic inertia, the past economic behavior may have an impact on the current economic behavior. This paper chooses the dynamic panel econometric model. First, it can control the fixed effect; second, it can overcome the omission of variables; and, third, it can overcome the reverse causality problem. The general form of dynamic panel data model is as follows:

$$\mathrm{Ln}Y_{i,t} = \alpha + \beta Y_{i,t-1} + \gamma X_{i,t} + \varepsilon, \quad (6)$$

where $\beta Y_{i,t-1}$ is lag tool variable and γ is the regression coefficient that explains the variable.

2.2. Index System Construction

2.2.1. Index System of Tourism Eco-Efficiency Measurement. Referring to the existing research [18–20] and combining the tourism sustainable development theory and ecosystem theory, this paper constructs the index system of tourism eco-efficiency in China from three aspects of resources, economy, and environment. The input variables include tourism energy consumption, water resource consumption, tourism resource endowment, the number of tourism employees, and tourism capital input. The total tourism consumption and the number of tourism receptions are selected as the expected output, and tourism wastewater, COD, ammonia nitrogen, SO_2, smoke (powder) dust, CO_2 emissions, and the amount of tourism garbage removal were used as undesired outputs. Among them, the tourism capital input is obtained by the method of perpetual inventory and the method of tourism capital stock estimation modified by Wu [21]; tourism resource endowment is determined by Zuo's scenic area weighting method [22]; the consumption of tourism water resources is calculated by using the regional input-output table and "tourism consumption stripping coefficient" [23]; by using the data of domestic and foreign tourists' consumption composition as well as the relevant data of regional input and output, the tourism energy consumption is separated from the specific industry by the "tourism consumption stripping coefficient" [24], and tourism CO_2 emissions are then converted using the IPCC greenhouse gas emission inventory method. It should be noted that the various environmental impact assessments are not homogeneous in the tourism industry, so the entropy method is chosen to integrate the index.

2.2.2. Index of Influencing Factors. Integrating existing research and combining the particularity of tourism and the accessibility of tourism statistics, this paper identifies and analyzes the factors affecting the spatial dynamic evolution of tourism eco-efficiency by seven factors: the level of tourism economic development, the structure of tourism industrial, the technical level of tourism, the intensity of environmental regulation, the human capital of tourism, the degree of opening to the outside world, and urbanization. Specific indicators are shown in Table 1.

2.3. Data Source. All data come from "China Statistical Yearbook" (2005–2018), "China Tourism Statistical Yearbook (Original and Copy)" (2005–2017), "China Tourism Statistical Yearbook 2018," "Tourism Sampling Survey Data" (2006–2018), "China Energy Statistical Yearbook" (2005–2018), "China Population and Employment Statistical Yearbook" (2005–2018), "China Regional Economic Statistics Yearbook" (2005–2018), "China Water Resources Bulletin" (2005–2018)), "China Real Estate Statistical Yearbook" (2005–2018), and the statistical bulletins of national economic and social development of various provinces, statistical bulletins of tourism industry, and statistical bulletins of tourism development from 2004 to 2017. For missing data in some provinces, the average growth rate method is used to fill in.

3. Empirical Study

3.1. Results of Tourism Eco-Efficiency Measurement. Based on the input-output data of tourism eco-efficiency in 30 provinces from 2004 to 2017, using the scale-return constant model of Super-SBM-Undesirable and using MaxDEA Ultra 8.1.2 to measure the tourism eco-efficiency of 30 provinces in the Chinese mainland, the results are shown in Table 2. The MaxDEA Ultra 8.20 software comes from Beijing Revomed Software Co., Ltd.

3.2. Spatial Distribution Characteristics of Tourism Eco-Efficiency. In order to explore the spatial differentiation characteristics of tourism eco-efficiency in different provinces of China, this paper selects four pieces of time-section data of tourism eco-efficiency in 2004, 2009, 2013, and 2017 and uses the software of ArcGIS 10.2 and draws the spatial distribution figure of China's tourism eco-efficiency (as shown in Figure 1). Based on the classification of eco-efficiency and tourism efficiency by Willard and Lu et al. [25] and combining with the research practice, the tourism eco-efficiency can be divided into five grades: high efficiency level (i.e., fully effective) (≥1), near-high efficiency level (0.801–0.999), medium efficiency level (0.601–0.800), near-low efficiency level (0.401–0.600), and low efficiency level (0.101–0.400).

By analyzing the spatial distribution figure of tourism eco-efficiency, it is found that, in 2004, the tourism eco-efficiency of Beijing, Tianjin, Hebei, Shanxi, Shanghai, Jiangsu, Zhejiang, Anhui, Fujian, Jiangxi, Shandong, Henan, Chongqing, Sichuan, Guizhou, Yunnan, and Qinghai is in a completely effective state, accounting for 56.67% of all provinces; it is mainly distributed in the eastern coastal areas and southwest regions, while the rest of the provinces are at a higher level only in Hunan; Xinjiang and Gansu are at a very low level, and China's overall tourism eco-efficiency is at a higher level of efficiency. In 2009, 11 provinces, Tianjin, Hebei, Shanxi, Heilongjiang, Jiangsu, Anhui, Fujian, Shandong, Henan, Chongqing, and Guizhou, achieved full efficiency in terms of tourism eco-efficiency, accounting for 36.67% of all provinces, the high-value areas gradually showed a clear distribution of the eastern coastal areas, and tourism eco-efficiency of China in 2013 was relatively stable compared to that in 2009, and the overall situation did not improve; the tourism eco-efficiency in Liaoning rose from a relatively low level in 2009 to a fully effective level, the medium level in Jiangxi and Shaanxi rose to a fully effective level, and Shanxi, Jiangsu, Anhui, and Henan dropped from a completely effective level to a relatively low level. In 2017, the four provinces of Hebei, Liaoning, Heilongjiang, and Shaanxi showed different degrees of decline in tourism

Table 1: Index system of influencing factors.

Influencing factors	Variable selection	Abbreviations
Level of tourism economic development	Per capita income from tourism	ECON
Structure of tourism industry	Rationalization and optimization of tourism industry structure	SR, SO
Technical level of tourism industry	Energy consumption per unit of tourism income	TECH
Intensity of environmental regulation	Environmental Regulatory Strength Index	GR
Human capital of tourism	Average years of education	HUM
Degree of opening to the outside world	Operating income of foreign-funded star hotels/star hotels	OPEN
Urbanization	Urbanization rate	UR

Table 2: Measurement results of tourism eco-efficiency.

Provinces	Year										
	2004	2006	2008	2010	2011	2012	2013	2014	2015	2016	2017
Beijing	1.098	1.098	0.367	1.002	0.373	0.335	0.410	0.378	0.336	0.338	0.372
Tianjin	1.959	1.299	1.230	1.273	1.454	1.546	1.301	1.323	1.392	1.380	1.254
Hebei	1.019	1.042	1.052	1.117	1.112	1.083	1.019	0.462	0.404	0.422	0.503
Shanxi	1.090	1.076	0.450	0.617	0.435	0.413	0.531	0.574	1.005	1.075	1.168
Neimenggu	0.470	0.527	0.408	0.297	0.266	0.239	0.265	0.286	0.255	0.327	0.345
Liaoning	0.481	0.568	0.476	0.508	0.683	0.559	1.019	1.014	0.541	0.495	0.461
Jilin	0.633	0.493	0.380	0.395	0.394	0.378	0.388	0.402	0.375	0.427	1.016
Heilongjiang	0.678	0.732	0.729	1.122	1.086	1.130	1.132	0.252	0.290	0.272	0.331
Shanghai	1.147	1.174	0.510	1.057	1.003	0.564	1.071	1.044	1.009	1.025	1.035
Jiangsu	1.032	1.138	1.045	0.709	1.046	1.036	0.638	0.581	0.524	1.001	1.006
Zhejiang	1.125	0.689	0.483	0.551	0.482	0.410	0.463	0.455	0.428	0.451	0.486
Anhui	1.249	1.070	1.018	1.085	1.039	1.023	0.679	0.648	0.722	0.652	0.826
Fujian	1.058	1.083	1.794	0.635	0.497	0.396	0.504	0.479	0.444	0.484	0.609
Jiangxi	1.081	1.119	0.479	0.545	0.762	0.726	1.026	0.667	1.021	1.010	1.084
Shandong	1.143	1.207	1.059	1.740	1.724	1.368	1.489	1.377	1.381	1.550	2.283
Henan	1.059	1.230	1.333	1.106	1.073	1.024	1.071	1.084	1.063	1.108	1.119
Hubei	0.616	0.598	0.439	1.019	0.540	0.485	0.629	0.576	0.524	0.558	0.648
Hunan	0.853	0.555	0.501	0.527	0.482	0.454	0.540	0.460	0.484	0.461	0.742
Guangdong	0.537	1.033	0.426	1.003	0.280	0.265	0.459	0.448	0.435	0.340	0.323
Guangxi	0.517	0.508	0.360	0.408	0.439	0.425	0.541	0.484	0.460	0.541	0.653
Hainan	0.399	0.314	0.200	0.063	0.205	0.189	0.177	0.169	0.181	0.285	0.293
Chongqing	1.063	1.024	0.584	1.041	1.109	1.152	1.059	1.113	1.091	1.070	1.117
Sichuan	1.024	1.070	0.485	0.517	0.642	0.453	0.592	0.707	0.519	0.474	0.474
Guizhou	1.028	1.225	1.101	1.002	1.066	1.044	1.064	1.062	1.111	1.169	1.210
Yunnan	1.444	1.040	0.376	0.321	0.306	0.284	0.351	0.366	1.371	0.466	1.023
Shaanxi	0.411	0.717	0.469	0.693	1.056	1.030	1.010	0.755	0.542	0.595	0.770
Gansu	0.360	0.339	0.226	0.288	0.281	0.281	0.294	0.306	0.309	0.332	0.417
Qinghai	1.112	1.018	0.385	0.247	0.235	0.216	0.225	0.205	0.194	0.201	0.201
Ningxia	0.513	0.384	0.290	0.350	0.304	0.329	0.281	0.231	0.193	0.242	0.435
Xinjiang	0.370	0.255	0.153	0.191	0.165	0.157	0.164	0.156	0.145	0.153	1.284
The National	0.886	0.854	0.627	0.714	0.685	0.633	0.680	0.602	0.625	0.630	0.783
Eastern China	1.000	0.968	0.786	0.878	0.805	0.705	0.777	0.703	0.643	0.706	0.784
Central China	0.907	0.859	0.666	0.802	0.726	0.704	0.750	0.583	0.685	0.695	0.867
Western China	0.756	0.737	0.440	0.487	0.534	0.510	0.531	0.516	0.563	0.506	0.721

Note. Not fully listed due to space limitation.

eco-efficiency, while Jiangsu and Yunnan returned to the state of full efficiency, and the overall level of China's tourism eco-efficiency has increased slightly. The regions with higher levels of tourism eco-efficiency are scattered in the three regions, and the differences among the regions are obvious.

3.3. Characteristics of the Spatial Dynamic Pattern of Tourism Eco-Efficiency. After defining the spatial distribution characteristics of China's tourism eco-efficiency, in order to understand the spatial dynamic pattern of China's tourism eco-efficiency, this paper analyzes its spatial pattern evolution by using gravity center and standard deviation ellipse. From the whole distribution of gravity center (as shown in Table 3), the moving path of the of gravity center of tourism eco-efficiency in China experienced the change of "southeast-northeast-north-west-southwest-northwest" during 2004 to 2017. From the three selected characteristic time points of 2004, 2009, 2013, and 2017, the gravity center is in Henan province. In the east-west direction, the tourism eco-efficiency of the western

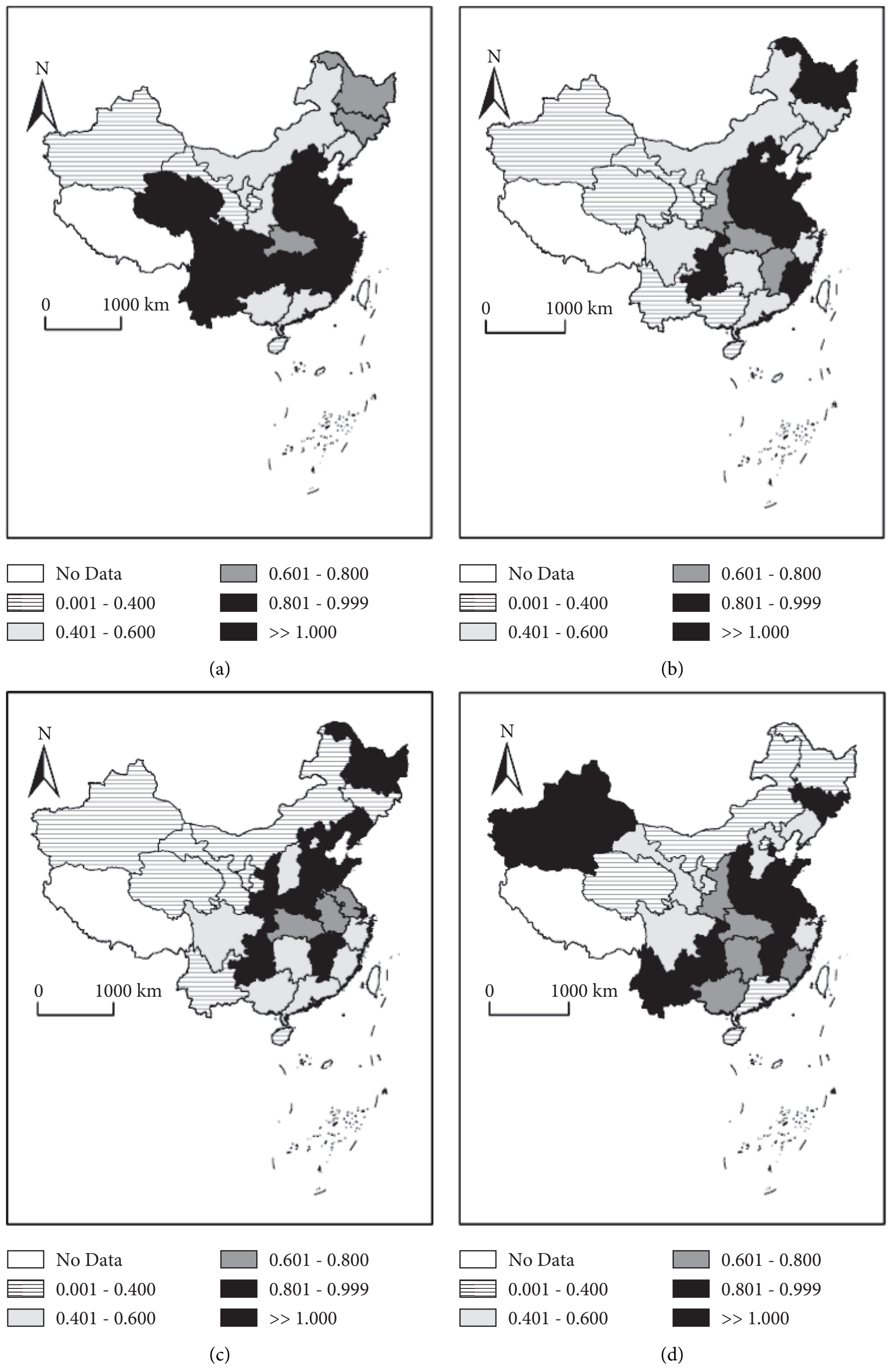

Figure 1: Spatial distribution of tourism eco-efficiency.

provinces is higher than that of other regional provinces. From the perspective of the moving direction of the gravity center, the gravity center of tourism eco-efficiency was near Nanzhao county, Nanyang, Henan province, in 2004. From 2004 to 2009, the gravity center gradually moved to the southeast, with a direction of 54.25° southeast, the gravity center moved from Nanzhao county to Fangcheng county, and the gravity center of tourism eco-efficiency moved to the vicinity of Shangcai county, Zhumadian, with a shift direction of 6.13° southeast in 2009–2013. Thus, the tourism eco-efficiency showed a trend of migration to the southeast from 2004 to 2013, indicating that the tourism eco-efficiency of the provinces in the southeast of China improved greatly during this period, which caused the gravity center to move to the southeast. After 2013, the gravity

Table 3: Direction and distance of the gravity center of tourism eco-efficiency.

Year	Gravity center	Direction	Moving distance (km)	East-west distance (km)	North-south distance (km)	Speed (km/a)	East-west (km/a)	North-south (km/a)
2004	112.76°E, 33.52°N							
2009	112.87°E,33.37°N	Southeast 54.25°	20.54	12.00	16.67	4.11	2.40	8.33
2013	114.15°E,33.23°N	Southeast 6.13°	143.62	142.80	15.34	28.72	35.70	3.84
2017	112.27°E,33.94°N	Northwest 20.54°	222.39	208.26	78.01	55.60	52.07	19.50

center of tourism eco-efficiency began to move to the northwest and moved to Ruyang county of Luoyang, with a direction of 20.54° northwest, which shows that the tourism eco-efficiency of the western region has improved greatly compared with the eastern and central regions during 2013 to 2017. From the perspective of distance and speed of gravity center movement, the distance and speed of gravity center movement of tourism eco-efficiency from 2004 to 2009 are the smallest, which are 20.54 km and 4.11 km/a, respectively. In 2009–2013, the speed of gravity center moving suddenly accelerated, the speed of east-west direction is 35.7 km/a, the speed of north-south direction is 3.84/a, and the speed of gravity center moving eastward is equivalent to the speed of gravity center moving as a whole (28.27 km/a), which indicates that the gravity center of tourism ecological efficiency mainly moves eastward in 2009–2013, and the moving distance is 143.62 km. From 2013 to 2017, the speed and distance of gravity center movement increased again, which were 4.11 km/a and 222.39 km, respectively. This is mainly due to the significant increase of the speed and distance of westward movement in the east-west direction, reaching 52.07 km/a and 208.26 km, respectively. On the whole, the moving speed of the center of gravity of tourism eco-efficiency continues to accelerate.

From the standard deviation ellipse of 4 years (as shown in Figure 2 and Table 4), the range of coverage from 2004 to 2017 is shrinking as a result of expansion. From 2004 to 2013, the standard deviation ellipse scope of tourism eco-efficiency showed a downward trend, and the area decreased from $300.45 \times 10^4\,km^2$ in 2004 to $253.00 \times 10^4\,km^2$ in 2013, reaching the minimum value. Compared with 2004, the space scope continuously reduced, the spatial agglomeration effect of tourism eco-efficiency of provinces in the interior of the standard deviation ellipse increases, but the spatial spillover effect is not obvious. In 2013–2017, the area of standard deviation ellipse increased from $253.00 \times 10^4\,km^2$ in 2013 to $341.83 \times 10^4\,km^2$ in 2017. The area of standard deviation ellipse expanded in all directions, and the overall spatial distribution of tourism eco-efficiency tends to be scattered.

In the spatial direction (as shown in Table 4), the spatial direction of tourism eco-efficiency has two evolutional trends with 2009 as the cut-off point. From 2003 to 2009, the rotation angle θ decreased from 41.39° to 26.83°, indicating that the space direction changed from "northeast-southwest" to "north-south". From 2009 to 2017, the rotation angle θ increased from 26.83° to 72.95°, indicating that the space direction changed from "north-south" to "northeast-southwest." On the whole, the spatial distribution of tourism eco-efficiency in China presents a pattern of "northeast-southwest," and this pattern has a tendency of further strengthening.

3.4. Driving Mechanism Analysis

3.4.1. Panel Data Unit Root and Cointegration Test. The stationary and white noise of variables is the premise of panel data regression estimation; otherwise, it may lead to false regression or spurious regression, and the unit root test must be carried out for variable data. In order to prevent the error caused by the single test method, LLC Test, Breitung Test (for same root), IPS Test, Fisher-ADF Test, and Fisher-PP Test (for different root) are used in this paper. The results are shown in Table 5. LnTE, LnECON, LnSO, LnSR, LnTECH, LnGR, and LnOPEN all reject the null hypothesis of unit root at the 1% level in the 5 test methods, indicating that these 7 variables are all "integrated of order zero," while the sequence of LnHUM and LnUR is stationary after first-order difference, indicating that these two variables are "integrated of order one." All variables are stationary after first-order difference. Therefore, all variables are "integrated of order one."

Variables must be of the same order, so that the panel data can pass the cointegration test. Therefore, the same order is the necessary condition of the panel data cointegration. On the premise of the same-order single integration after difference, it is possible to test whether there is a long-term cointegration relationship between panel data. In order to guarantee the reliability and robustness of cointegration test results, Modified Dickey–Fuller t-test, Dickey–Fuller t-test, Augmented Dickey–Fuller t-test, Unadjusted Modified Dickey–Fuller t-test, and Unadjusted Dickey–Fuller t-test in Kao test are used to test the cointegration of regression equations. It can be seen from Table 6 that all the statistical variables of the equations reject the original assumption that there is no cointegration relationship under the condition of 1%; that is, there is a significant long-term stationary equilibrium relationship between the explanatory variables and the explanatory variables of the equations.

3.4.2. Selection of the Measurement Estimation Method. In terms of model regression for influencing factors, the model identified in this article has lags in the explained variables so as to avoid omitting the dynamics of the model and leading to biased results. At the same time, the explained

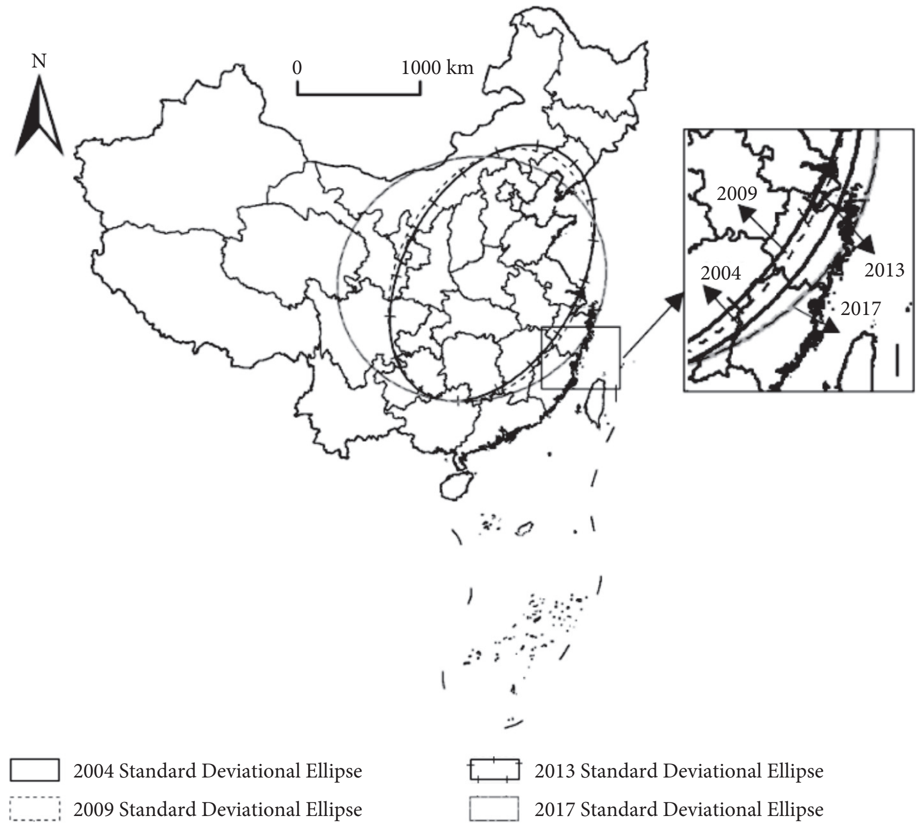

Figure 2: Standard deviation ellipse of tourism eco-efficiency.

Table 4: Standard deviation ellipse parameter of tourism eco-efficiency.

Year	2004	2009	2013	2017
Rotation angle θ (°)	41.39	26.83	29.47	72.95
Standard deviation of x-axis (km)	873.23	752.23	715.06	985.04
Standard deviation of y-axis (km)	1095.25	1085.63	1126.33	1104.67
Area (km^2)	300.45×10^4	256.54×10^4	253.00×10^4	341.83×10^4

Table 5: Unit root test for panel variables.

Variable	LLC Test	IPS Test	Breitung Test	Fisher-ADF Test	Fisher-PP Test
LnTE	-3.260^{***}(0.000)	-2.816^{***}(0.002)	-2.888^{***}(0.001)	180.637^{***} (0.000)	124.832^{***}(0.000)
LnECON	-2.701^{***}(0.003)	2.471^{***}(0.000)	8.990^{***}(0.000)	124.674^{***} (0.000)	117.620^{***}(0.000)
LnSO	-3.983^{***}(0.000)	-0.147^{***}(0.004)	3.191^{***}(0.000)	130.885^{***} (0.000)	53.779^{***}(0.000)
LnSR	-8.066^{***}(0.000)	-3.663^{***}(0.000)	-2.785^{***}(0.002)	217.317^{***} (0.000)	195.529^{***}(0.000)
LnTECH	-5.749^{***}(0.000)	0.237^{*}(0.057)	0.108^{***}(0.000)	161.372^{***} (0.000)	60.725^{***}(0.000)
LnGR	-7.342^{***}(0.000)	-7.856^{***}(0.000)	-10.635^{***}(0.000)	223.499^{***} (0.000)	265.733^{***}(0.000)
D.LnHUM	-8.093^{***}(0.000)	-9.718^{***}(0.000)	-12.054^{***}(0.000)	183.122^{***} (0.000)	474.034^{***}(0.000)
LnOPEN	-22.938^{***}(0.000)	-7.650^{***}(0.000)	-7.586^{***}(0.000)	281.887^{***} (0.000)	263.000^{***}(0.000)
D.LnUR	-2.833^{***}(0.002)	-8.458^{***}(0.000)	-3.199^{***}(0.007)	139.882^{***} (0.000)	478.798^{***}(0.000)

Note. *, **, and ***are significant at the levels of 10%, 5%, and 1%, respectively.

variables and the explanatory variables of the model have a causal relationship with each other, and there are endogenous problems. In dealing with endogenous problems, Manuel Arellano and Stephen Bond believe that the use of ordinary panel regression in the model will lead to deviations in the estimation results, which can be achieved through instrumental variable (IV) and generalized method of moments (GMM) to be eliminated. In the selection of instrumental variables, Anderson and Cheng rely on traditional methods to select instrumental variables that are not related to interference items and then first-order difference, selecting items lagging more than two orders as the instrumental variables of their difference items. Combined with the proposal of dynamic panel theory, differential

Table 6: Panel cointegration test results.

Test method	Value	P value
Modified t	−9.278	0.001
Dickey–Fuller t	−13.71	0.001
Augmented t	−9.392	0.001
Unadjusted Modified t	−17.32	0.001
Unadjusted t	−15.88	0.001

generalized moment estimation (Diff-GMM) and system generalized moment estimation (SYS-GMM) methods have become the mainstream of research. Diff-GMM uses difference to eliminate fixed effects and builds instrumental variables on the basis of difference equations, but the problem of weak instrumental variables cannot be solved. Furthermore, Arellano and Richard proposed the SYS-GMM method, which starts with the information of difference and level equations to select instrumental variables. Compared with other methods, it can better solve the problem of endogeneity, and the model estimation results are also more effective. Based on the above analysis, this paper chooses the SYS-GMM estimation method to estimate the relevant factors of tourism eco-efficiency.

3.4.3. Model Estimates. Considering that SYS-GMM method selects instrumental variables from the information of difference and level equation, it can solve the endogeneity problem better than other methods, and the model estimation results are more effective. Therefore, SYS-GMM method was used for regression analysis in this paper, and the regression results are shown in Table 7. As can be seen from Ward test, the set model is very significant. The Sargan test shows that the setting of the tool variable set is valid.

The regression results of Table 7 show that the tourism economic development level, which is expressed by per capita tourism income, has a negative effect on tourism eco-efficiency, and it is significant at 1% level. The rapid development of tourism economy has not brought about the rational allocation and utilization of resources and energy as well as the scale effect but inhibited the promotion of tourism eco-efficiency. The possible reason is that China's tourism economy is in a transitional stage, and the annual growth rate of tourism income is far higher than the average growth rate of China's GDP in the same period. With the rapid development of the tourism economy, unreasonable low-cost extensive development and operation mode gradually emerged.

The coefficient of tourism industry optimization (SO) passed the test on the level of 5% significance, which shows that the optimization of tourism industry structure has a positive and significant impact on tourism eco-efficiency. In view of the reality of the development of China's tourism industry, in recent years, driven by endogenous technology, the internal and external integration of the tourism industry ("tourism +") and other patterns have achieved a breakthrough in the innovation of tourism products, and its industrial added value has maintained long-term and steady growth; this technology upgrading and value-added growth

Table 7: Regression results of influencing factors.

Independent variable	LnTE
L1.	0.440***(0.000)
LnECON	−0.219***(0.000)
LnSO	0.012**(0.013)
LnSR	0.070**(0.005)
LnTECH	−0.603***(0.000)
Wald test	247.72***(0.000)
Sargan test	0.127
LnGR	−0.057***(0.000)
LnHUM	0.0394***(0.002)
LnOPEN	−0.002***(0.008)
LnUR	−0.150(0.667)
Cons	1.196***(0.000)

Note. *, **, and ***are significant at the levels of 10%, 5%, and 1%, respectively.

is the external performance of the structural adjustment of the tourism industry, which is beneficial to the energy-saving and emission reduction and environmental protection of tourism. The coefficient of tourism industry rationalization (SR) also passed the test at the significant level of 5%, indicating that the rationalization of industrial structure has effectively promoted the eco-efficiency of tourism in China. It can be seen that the flow and reconfiguration of factors of production such as labor and capital among different economic sectors of tourism can effectively utilize all factors and bring about economic growth of tourism, but they do not cause resource depletion and ecological environment deterioration.

The technical level of tourism industry represented by the energy consumption per unit tourism income is a negative indicator. The higher the energy consumption per unit tourism income, the lower the technical level of tourism industry. Its coefficient is obviously negative, which fully shows that enhancing the technical level of tourism is an important way to improve the eco-efficiency of tourism. On the one hand, technological progress can be conducive to the promotion of advanced ecological production and the improvement of energy and resource efficiency of tourism enterprises; on the other hand, technological progress can promote pollution reduction and treatment technologies so as to improve the end of pollution control capacity and further promote the generation of clean energy.

The impact of environmental regulation intensity on tourism eco-efficiency is negative, and it has passed the significance test. The possible reasons for the failure of the government's environmental regulation are as follows: Firstly, the relevant environmental policies and measures formulated by the government have not been effectively implemented, there is a lack of supervision, and it cannot effectively correct the negative externalities of environmental pollution in various sectors related to tourism. Secondly, the cost of effective implementation of environmental regulation is too large and the government intervention is difficult to grasp, which leads to the decrease of the coordination between the economic growth of tourism and the development of ecological environment. Thirdly, due to the traditional development concept, the extensive development mode of China's tourism industry has not changed in essence. Compared with developed countries, the intensity of environmental regulation is still relatively low, and the innovation effect of environmental regulation has not been effectively triggered.

The effect of tourism human capital on tourism eco-efficiency is positive at the significance level of 1%. The main reason is that the education level can, to a certain extent, reflect the social environmental protection consciousness, and environmental protection consciousness enhancement helps consciously perform the obligation of environmental protection; at the same time, tourism practitioners are the higher level of education, and professional skills and technical innovation ability are higher, which is good for energy saving and "three wastes" emissions.

The impact coefficient of the degree of opening to the outside world on tourism eco-efficiency is negative and significant. The amount of foreign investment in tourism reflects the region's ability to attract foreign investment in some aspects, but it is not conducive to improving the regional tourism eco-efficiency. The following are the possible reasons: Firstly, the foreign investment to consider more for tourism is China's rich tourism resources, vast market and its cheap labor supply, foreign investment in the process of actual operation, and the development of tourism resources using a double standard only for the purpose of economic interests of predatory development brought about great pressure to the ecological environment. Secondly, the purpose of China's introduction of foreign capital is to consider the structural and technological effects of foreign investment and the "spillover effect" of management experience and eco-production techniques as well as the "demonstration effect" of high standards of environmental protection brought about in the process of promoting employment and economic development in the region, thus promoting the structural transformation and upgrading of local tourism industry; however, the ecological damage and environmental pollution caused by pollution-intensive foreign capital inflow offset the benefits to some extent. Finally, some local governments relax environmental regulation in order to attract foreign investment in tourism and promote the development of tourism economy at the expense of the environment, thus restraining the promotion of tourism eco-efficiency.

4. Conclusion and Discussion

4.1. Conclusion. In this paper, the Super-SBM-Undesirable model is used to measure the tourism eco-efficiency of 30 provinces in China from 2004 to 2017. On the basis of clarifying the spatial distribution characteristics of tourism eco-efficiency, this paper explores the spatial evolution track and path of tourism eco-efficiency with the help of the the method of gravity center and standard deviation ellipse, constructs a dynamic panel model, and uses SYS-GMM to identify the factors influencing the evolution track and its driving mechanism. The results are as follows: Firstly, during the study period, the overall eco-efficiency of tourism in China is at a high level, and the eastern region is higher than the central and western regions. The provinces with higher tourism eco-efficiency are scattered in three regions, with obvious differences in each region. Secondly, from 2004 to 2017, the gravity center of China's tourism eco-efficiency is distributed in Henan province, and its movement track is "Nanyang (Nanzhao county)-Nanyang (Fangcheng county)-Zhumadian (Shangcai county)-Luoyang (Ruyang county)," the change pattern of the gravity center is first to the southeast and then to the northwest, and the moving speed of the center of gravity is continuously accelerating. Thirdly, from the perspective of the standard deviation ellipse, the overall spatial distribution pattern of China's tourism eco-efficiency tends to disperse, and the rotation angle shows a process of "shrinking a little, increasing a little, then increasing"; the result shows that the spatial distribution of China's tourism eco-efficiency shows a pattern inclined northeast-southwest and has the trend of further strengthening. Fourthly, the optimization of tourism industry structure, the rationalization of tourism industry structure, the technical level of tourism industry, and tourism human capital are positively correlated to tourism eco-efficiency; the development level of tourism economy, the intensity of environmental regulation, and the degree of opening to the outside world are negatively related to tourism eco-efficiency, while the relationship between urbanization and tourism eco-efficiency is ambiguous.

4.2. Policy Implications. In order to promote the sound and coordinated development of China's provincial tourism industry and ecological environment and promote the high-quality development of tourism economy, the following policy recommendations are put forward: First, we should put the protection of tourism ecological environment in a prominent position in combination with the current big data analysis and research and promote the process of nationalization of ecological civilization theory education, as well as change the evaluation index system of tourism development only based on total tourism revenue and tourist receptions. Second, we should combine big data artificial intelligence technology to promote the precise coordination of the allocation of tourism industry elements and comprehensively weigh the impact of tourism economic growth and ecological environment deterioration brought about by the flow of technology, capital, information, labor, and other factors, increase the proportion of green, circular, and low-carbon economy in the tourism industrial structure, and promote the coordinated development of various economic sectors of tourism, as well as comprehensive use of tourism industry planning and policy means to optimize and integrate tourism production factors from the source, while effectively supplying, to avoid duplication of factors, blind investment, and overcapacity. Thirdly, combined with the development of artificial intelligence technology, precise, informationized, and scientific economic policies such as finance and taxation should be adopted to provide support for tourism enterprises adopting advanced ecological technology, accelerate the pace of popularizing pollution control and prevention technology, gradually establish energy statistics and auditing system for tourism industry, and encourage the development of energy-saving and consumption-reducing tourism enterprises. Moreover, we should improve the access standards of foreign investment in tourism industry, change from attracting investment to selecting investment, and select appropriate technologies consistent with the regional tourism economic development environment so as to improve the utilization efficiency of advanced ecological management and technology. Finally, we will make full use of the strictest eco-environmental protection system in the National New-Type Urbanization Plan (2014–2020) and continue to strengthen the construction of tourism eco-environment and improve the efficiency of tourism eco-environment under the mechanism of green, circular, and low-carbon development. The planning of urbanization should consider the present situation of tourism ecological carrying capacity, enhance the support of Environmental Protection Industry, comprehensively study the change characteristics of regional wind direction and the location of tourism service facilities, and rationally plan and arrange the industrial location. Combining the tourism planning with the urbanization ecological planning and on the basis of the tourism planning, setting out a single ecological control index to guide the development and construction of tourism, it also plans energy-saving and emission reduction targets for water-saving rate, rainwater utilization rate, and carbon emission rate of tourism service facilities. The corresponding indicators of tourism ecological response indicators will be brought into the government performance appraisal, improve tourism infrastructure, fully tap the consumption potential of regional tourism market, and vigorously develop green tourism and ecotourism.

4.3. Discussion. Based on the theory of sustainable tourism development and the theory of ecosystem, this paper attempts to construct an index system for the measurement of China's provincial tourism eco-efficiency in order to comprehensively evaluate China's tourism eco-efficiency and to study the dynamic evolution of the spatial pattern of China's tourism eco-efficiency and its driving mechanism by means of artificial intelligence thinking logic, geographical methods, and dynamic panel model. However, there are still some shortcomings to be further explored: on the one hand, the input-output indicators of tourism industry involved in the measurement index system of tourism eco-efficiency are quantifiable indicators. Some social and environmental indicators that are difficult to quantify are not involved, and it is assumed that environmental pollution is homogeneous and stable in all industries. On the other hand, due to the strong correlation of tourism industry, the influencing factors of the spatial dynamic pattern evolution of tourism eco-efficiency are very complex, and it is difficult to fully cover the selection of indicators, and it is impossible to cover all the influencing factors in the regression model. In this sense, the results of empirical analysis in this paper cannot fully explain the actual situation but only have statistical significance in probability. Therefore, in the future, more variables should be included in the theoretical analysis model in the process of factor analysis.

Data Availability

Data sharing is not applicable to this article as no datasets were generated or analyzed during the current study.

Conflicts of Interest

The authors declare no conflicts of interest with respect to the research, authorship, and/or publication of this article.

Acknowledgments

This work was supported by Weifang University Phd Foundation Project (2021SB43).

References

[1] P. Wu and S. Yue, "Research progress on energy demand and carbon dioxide emission of tourism industry," *Tourism Tribune*, vol. 28, no. 7, pp. 64–72, 2013.

[2] Y. Ma and J. Liu, "The core value and promotion strategy of tourism ecological efficiency under the background of green development," *Tourism Tribune*, vol. 31, no. 9, pp. 1–3, 2016.

[3] S. Schaltegger and A. Sturm, "Ökologische rationalität: ansatzpunkte zur ausgestaltung von ökologieorientierten managementinstrumenten," *Unternehmung*, vol. 44, no. 4, pp. 273–290, 1990.

[4] R. Côté, A. Booth, and B. Louis, "Eco-efficiency and SMEs in nova scotia, Canada," *Journal of Cleaner Production*, vol. 14, no. 6, pp. 542–550, 2006.

[5] M. Braungart, W. Mcdonough, and A. Bollinger, "Cradle-to-cradle design: creating healthy emissions – a strategy for eco-effective product and system design," *Journal of Cleaner Production*, vol. 15, no. 13, pp. 1337–1348, 2007.

[6] S. Gössling, P. Peeters, J.-P. Ceron et al., "The eco-efficiency of tourism," *Ecological Economics*, vol. 54, no. 4, pp. 417–434, 2005.

[7] H. S. Peng, J. .H. Zhang, Y. Han, G. R. Tang, and Y. Zhang, "SBM-DEA model and empirical analysis of tourism destination ecological efficiency measurement," *Acta Ecologica Sinica*, vol. 37, no. 2, pp. 628–638, 2017.

[8] W. .K. Lin and B. Lin, "Evaluation of ecological efficiency of regional tourism industry and its spatial difference: a case study of Jiangxi Province," *East China EconomicManagement*, vol. 32, no. 6, pp. 19–25, 2018.

[9] Z. G. Yao, T. Chen, S. .B. Yin, and X. G. Li, "Empirical analysis of regional tourism ecological efficiency: a case study of Hainan Province," *Geographic Science*, vol. 36, no. 3, pp. 417–423, 2016.

[10] P. Sabine, S. Ana, and S. Matthias, "The greenhouse gas intensity of the tourism sector: the case of Switzerland," *Environmental Science & Policy*, vol. 13, no. 2, pp. 131–140, 2010.

[11] H. Cheng, Q. Xu, and M. Y. Zhao, "Research on spatial correlation network structure and its influencing factors of tourism ecological efficiency in China," *Ecological Science*, vol. 39, no. 5, pp. 169–178, 2020.

[12] Z. F. Wang and Q. F. Liu, "Spatiotemporal evolution of tourism eco efficiency in the Yangtze River economic belt and its interaction with tourism economy," *Journal of Natural Resources*, vol. 34, no. 9, pp. 1945–1961, 2019.

[13] M. Lenzen, Y. Y. Sun, F. Faturay et al., "The carbon footprint of global tourism," *Nature Climate Change*, vol. 8, no. 6, pp. 522–544, 2018.

[14] K. Tone, "A slacks-based measure of efficiency in data envelopment analysis," *European Journal of Operational Research*, vol. 130, no. 3, pp. 498–509, 2001.
[15] P. Andersen and N. C. Petersen, "A procedure for ranking efficient units in data envelopment analysis," *Management Science*, vol. 39, no. 10, pp. 1261–1264, 1993.
[16] K. Tone, "A slacks-based measure of super-efficiency in data envelopment analysis," *European Journal of Operational Research*, vol. 143, no. 1, pp. 32–41, 2002.
[17] A. Mamuse, A. Porwal, O. Kreuzer et al., "A new method for spatial centrographic analysis of mineral deposit clusters," *Ore Geology Reviews*, vol. 36, no. 4, pp. 293–305, 2009.
[18] J. P. Cha, "Development efficiency, emission reduction potential and emission reduction path of China's low carbon Tourism," *Tourism Tribune*, vol. 31, no. 9, pp. 101–112, 2016.
[19] J. Liu, L. Huang, L. J. Wu et al., "Study on direct and virtual water consumption of rural tourism in Qingcheng Houshan heritage site," *Tourism Tribune*, vol. 9, pp. 108–116, 2018.
[20] J. Liu and Y. Ma, "Perspective of sustainable tourism development: a review of tourism ecological efficiency," *Tourism Tribune*, vol. 32, no. 9, pp. 47–56, 2017.
[21] Y. M. Wu, "Spatial panel econometric analysis of tourism economic growth and its spillover effect," *Tourism Tribune*, vol. 29, no. 2, pp. 16–24, 2014.
[22] B. Zuo, "Analysis on growth factors and contribution of China's tourism economy," *Business Economy and Management*, vol. 10, pp. 82–90, 2011.
[23] J. F. Li and M. Y. Li, "Calculation of tourism industry and tourism added value," *Tourism Tribune*, vol. 5, pp. 16–19+76, 1999.
[24] J. Liu and Q. Y. Song, "Spatial network structure and formation mechanism of green innovation efficiency of China's tourism industry," *China Population, Resources and Environment*, vol. 28, no. 8, pp. 127–137, 2018.
[25] L. W. Lu, D. Y. Song, and X. F. Li, "Research on green efficiency of urban development in Yangtze River economic belt," *China Population, Resources and Environment*, vol. 26, no. 6, pp. 35–42, 2016.

Hindawi
Scientific Programming
Volume 2021, Article ID 5395988, 9 pages
https://doi.org/10.1155/2021/5395988

Research Article

SWOT Analysis of China's Ceramic Industry and the Use of Computers for Scientific and Technological Innovation Research

Ye Tian[1] **and Xiaobing Hu**[2]

[1]*Graduate School, Jingdezhen Ceramic University, Jingdezhen 333000, Jiangxi, China*
[2]*Fine Art School, Anqing Normal University, Anqing 246001, Anhui, China*

Correspondence should be addressed to Xiaobing Hu; 1976hxb@aqnu.edu.cn

Received 28 July 2021; Accepted 7 August 2021; Published 16 August 2021

Academic Editor: Punit Gupta

Chinese ceramics have a long history and have been deeply recognized by the world after centuries of changes. The current world ceramic industry is diversified. Under this background, there is a huge challenge to the development of Chinese ceramics. The update of materials, the participation of computers in ceramic design, and the demonstration of ingredients all constitute technological factors that cannot be ignored in the development of the ceramic industry. Therefore, this study uses the SWOT analysis method to analyze the development of Chinese ceramics, puts forward its advantages and disadvantages, opportunities, and threats, and under the background of advanced technology, and how to use computer software to demonstrate raw materials and color matching to make Chinese ceramics. The development achieves the goal of self-improvement and then completes the upgrade of its production process and production. Through the research of this study, it is found that the current development of China's ceramic industry should be good at using SWOT analysis, face up to its shortcomings and pressure from other ceramic production areas in the world, give full play to its advantages, maximize strengths and avoid weaknesses, and use technological innovation, combined with technical factors from other disciplines, to promote ceramic industry design and production capabilities and provide a reference for the current ceramic industry development.

1. Introduction

SWOT analysis is also known as situation analysis [1]; it can also be called TOWS analysis or Dawes matrix analysis. In the early 1980s, this method was mainly proposed by a professor of management at the University of San Francisco Weihrich [1]. Each letter in SWOT stands for a certain aspect of the situation. S stands for strengths, W stands for weaknesses, O stands for opportunities, and T stands for threats. S and W belong to internal factors, while O and T belong to external factors. In the context of the rapid development of international ceramics, SWOT has been applied to the development analysis of the ceramic industry in recent years. Some studies focus on the development of regional ceramics [2, 3]. Some research studies use the SWOT analysis method; this study analyzes the Jingdezhen ceramic culture creative industry under the environment of existing market competition advantages, disadvantages, opportunities, and threats of development, and based on this, put forward the Jingdezhen ceramic culture creative industry core competitiveness promotion strategy [4]; in some studies by the SWOT analysis of the ceramic export competitiveness [5], the export of ceramics industry is systematically analyzed. These studies all take SWOT analysis as the research method from different angles to explore the development of the ceramics industry. This study used the SWOT analysis method from a macro perspective to explore China's ceramic industry development in the present situation and the advantages and disadvantages, and in the context of science and technology innovation, analysis using a computer to carry on the technological innovation, show the advantages such as material, color is tie-in, to improve the efficiency of ceramic design and production, and to provide a reference for the ceramic production and design.

2. Advantages and Disadvantages of the Development of Chinese Ceramics

2.1. Advantages. The advantages shown by China's ceramic industry focus on the following aspects:

2.1.1. Has a Long History of Ceramic Culture. Time-honored ceramics belong to the treasure of Chinese civilization. The cultural development of Chinese ceramics has a very long history, extensive and profound. The original celadon had appeared in China over 3,000 years, during the Shang Dynasty (Figure 1). Every different historical stage of ceramics in China shows its completely different artistic style and expression. Chinese ceramic culture has developed into the most core competitive advantage of Chinese ceramics.

Figure 1: Primitive celadon.

2.1.2. Production Is Large Scale and Low Cost. At present, China has become the world's largest ceramic production country, accounting for more than half of the world's total ceramic production output. After a long-term accumulation, China's ceramic industry has formed a very strong scale effect and has great potential to be explored. At the same time, because the labor cost of China's ceramic industry is relatively low, the raw materials are also of high quality and cheap price, and they are very abundant, which has a strong cost advantage; these provide strong raw material support for the development of the ceramic industry.

2.1.3. Domestic Market Has Great Development Potential. The advantage of China's ceramic industry development also lies in a huge domestic market. According to the Seventh National Census Bulletin of 2020 (Number 8) [6], China has a total population of more than 1.4 billion and has a new population of about 20 million per year. In the long run, the investment in real estate development will certainly continue to grow. In recent years, the annual urban real estate development investment is more than 300 billion yuan, the annual completion area of housing has reached 1.5 billion square meters, and the residents' construction decoration cost has reached the annual scale of more than 400 billion yuan. In addition, some big cities in China have also begun to stipulate that the sale of rough houses will not be allowed, so the real estate developers will surely become another very important buyer of construction pottery products. With the rapid improvement of people's living conditions, the need for construction ceramics will certainly remain at a relatively high level. In addition, with the gradual increase of the Chinese government's support for the great development of the west, the marketing of the ceramic market has gradually developed rapidly from the east to the west, the capacity of the domestic ceramic market has undergone qualitative changes, and has gradually developed into one of the most growth potential markets in the domestic building materials industry. In the foreseeable future, in the next 10 years, or even 20 years, the strong domestic market demand will still maintain the rapid and stable development of China's construction pottery industry.

2.2. Disadvantages

2.2.1. Development and Design Lacks Internal Motivation. Compared with the international advanced ceramics, the development and design level of domestic ceramics is far behind. Most ceramic enterprises in China lack the sense of innovation, invest very little investment in design, and have an insufficient investment in research and development. As a result, Chinese ceramic products show three characteristics of homogeneity, trend, and imitation. Ceramic products lack innovation and style; design and color varieties change slow, single style. No matter in the variety, quality, specifications, model, color is very close, and what products are good to sell, used to imitation and cloning, this makes it difficult for ceramic products to occupy not only a strong share in the international market but also cause ceramic products market backlog.

2.2.2. Lack of Standardization of Process and Technology. Foreign ceramic industry in the overall industrial technology, its automation, and intelligence degree is relatively high. It uses more modern processes and technology. Ceramic production generally adopts a professional division of labor, with a standardized, commercialized raw material base, and professional auxiliary material suppliers. Although China's ceramic industry has greatly improved the level of process equipment through the introduction, digestion, and absorption of foreign advanced equipment, most enterprises are still mainly semimechanized equipment. Many ceramic enterprises, especially nonceramic cluster area enterprises, lack standardization and the supply of specialized raw materials and auxiliary materials, resulting in great product quality fluctuations and difficulty in meeting the requirements of the high-grade ceramic production process. In addition, there is also a huge gap in the production of molding and mold materials and machinery and equipment manufacturing industry serving the ceramic industry, which all restrict the improvement of product quality and competitiveness of the industry [7].

2.2.3. The Quality of the Products Is Mixed. Most Chinese enterprises are affected by production, processing, technical personnel, quality control, and other factors. Product quality and grade are low, and the overall quality level is to be improved. The internal quality and appearance quality are still great compared with well-known foreign ceramic brands. In addition, in recent years, due to low industry thresholds that have launched various ceramic lines, market expansion leads to disorderly competition between brands and price reduction, and it is difficult to effectively guarantee the ceramic quality.

2.2.4. Corporate Management Lacks a Strong International Concept. Many domestic ceramic enterprises adopt an extensive management mode, and the international modern enterprises, mainly manifested as lack of advanced management ideas, methods, and means, low strategic decision-making level, weak management foundation, low information technology management level, and lack of management personnel familiar with international trade and market operation rules; operation and management mechanism does not adapt to the requirements of market competition and lack of international marketing experience [8].

3. Opportunities and Threats

3.1. Opportunity

3.1.1. Opportunities Brought about by China's Rapid Economic Development. This opportunity is mainly manifested in the following three aspects. First of all, the development level of urbanization is constantly improving. With the further implementation of the "agriculture, rural areas and farmers" policy, the farmers have also been further improved at the residential level, and the amount of ceramic tile use will be very huge in the future. In the past, in the countryside, in this piece, the amount of ceramic use is very few, mainly because the economy of many places is not too rich; when building a house that stick ceramic tile is very little, after farmers have money, the area that stick ceramic tile will gradually increase.

Second, the urbanization development level of our country is relatively low, with only 36%. A very important measure of the current country is to vigorously promote the process of urbanization development. The acceleration of the urbanization development process will further and quickly improve our infrastructure construction speed, and the improvement of the infrastructure construction speed will usually further drive the rapid development of the real estate industry. This will also further drive the rapid development of the building materials industry because this is synchronous development; therefore, the demand for building materials in this respect will also appear under the role of continuous growth.

Finally, the international market provides a very good opportunity, and the current number of ceramic exports is increasing by more than 50% per year. These factors together create a very good environment for the development of the building materials industry.

3.1.2. Opportunities Brought by WTO Entry. After joining the WTO, the development of Chinese ceramic enterprises mainly from domestic market to international market adjust the industrial structure according to the needs of the international market, participate in the international division of labor and collaboration [9] through external competitive mechanisms and the introduction of advanced technologies, and eliminate backward products and equipment, so as to further realize the sustainability of the ceramic industry development. After joining the WTO, China's ceramic industry can further expand its exports, while driving domestic economic growth, with the transparency of the law and the further realization of the national treatment. The investment environment was further improved, forming a new advantage of attracting foreign investment. Then, it will open a very broad development channel for foreign businessmen to invest in the ceramic industry and realize transnational operation. After joining the WTO, ask for more ceramic companies to operate under internationally recognized business rules, establish a modern enterprise system adapted to the market economy competition, further improve the management system and operation mechanism of enterprises, and vigorously promote the improvement of business efficiency and the rapid improvement of international competitiveness.

3.2. Existing Threats

3.2.1. The Threat of World Ceramic Power and Well-Known Foreign Ceramic Enterprises. Some global ceramic powers have a large number of large-scale well-known enterprises with strong competitiveness. These enterprises all have very strong capital, very perfect management experience and marketing strategies, and are at the high-end level in the global value chain. On the contrary, China's ceramic industry has a low position in the world, is at the low end of the value chain, and is also at a disadvantage in the process of very fierce international market competition in the future. In addition, with the gradual opening of the Chinese market and the further reduction of tariffs, well-known foreign ceramic enterprises have also further seized the domestic ceramic market, thus increasing the impact and threat to the domestic ceramic market.

3.2.2. Antidumping Threat. Antidumping mainly refers to a boycott of the dumping of foreign goods in their domestic markets. Because China's ceramic products have a very strong price competitive advantage, with the rapid development of the current world economy, the export growth is relatively fast and the export market is very concentrated, leading to the intensified conflict between China's export products and importing countries. At the same time, some enterprises lack deep understanding and communication of the international community, and many countries do not understand China's market economy reform and the development process, to China's market economy development situation, leading to some countries for China has very big trade discrimination, "China threat theory" and "nonmarket economy" black hat are very deeply rooted in these countries, so that China's ceramic enterprises were subjected for extensive foreign antidumping investigation. Not only the developed economies but even emerging economies in daily ceramics, especially in BRICS countries and China, are gradually increasing. In recent years, the European Union, the United States, India, Brazil, and other countries have formed an antidumping investigation on China's ceramic industry.

3.2.3. Threats of Technical Trade Barriers. Technical barriers to trade (TBT) mainly refers to the trade barriers formed by some mandatory and nonmandatory technical regulations and standards formulated by a country or regional organization on the grounds of maintaining its basic safety, ensuring the health and safety of humans and animals and plants, protecting the environment, preventing fraud, and ensuring the quality of products. Technical trade barriers are another obstacle to the export of Chinese ceramic products. To protect the interests of their ceramic manufacturers from damage, many countries, with their own technical and economic advantages, prevent China from exporting ceramics to them by formulating a variety of more demanding technical barriers. These technical barriers include standards and technical regulations, technical certification systems, conformity assessment, labeling and packaging, green technology, and e-commerce technology. In the face of technical trade barriers, Chinese ceramic enterprises have exposed incomplete information mastery, immature technical ability, and high copying costs. In the current situation of the ceramic industry, it is very difficult for some Chinese ceramic enterprises to cross these barriers, cause a few obstacles to the export of China's ceramic, and greatly hinder China's ceramics to participate in the international market competition [7].

4. Scientific and Technological Innovation, Optimization, and Upgrading of Contemporary Ceramic Art

4.1. Use of the Polymer to Enhance the Clay Materials

4.1.1. Cured the Clay Material with Cyanoacrylate. The basic operating idea is to dry the prepared clay billet and soak it in the solution of α-acetyl cyanoacrylate. Because the composition of α-cyanoacrylate adhesive is mainly α-ethyl cyanoacrylate, it contains only a small amount of thickener and stabilizer, can play a rapid curing role, can be combined under the catalytic action of trace water in the air, and can quickly cure and bond clay, which can form a very solid cold ceramic.

4.1.2. Cured Clay Materials by the Radiation Method

(1) Idea. After drying the prepared clay billet, it is soaked with a methyl methacrylate monomer solution and then irradiated with a ^{60}Co radiation source, thus forming the polymer effect, forming a polymethyl methacrylate (also known as organic glass), further forming a very solid cold ceramic.

Among them, two radiation methods are involved, namely, radiation crosslinking and radiation polymerization. Radiation crosslinking mainly connects two polymer chains in some way, and the net effect of crosslinking is the increasing molecular weight until the 3D network structure is formed, so once the polymer is aligned, it makes the clay material very difficult to dissolve and melt.

Radiation polymerization mainly uses radiation to stimulate the monomer, causing polymerization. The gas, solid, liquid, and emulsion polymerization of acrylic monomer can be realized by radiation. High polymer materials prepared by the radiation method are usually characterized by high molecular weight and high purity.

(2) Relevant Production Steps. First, use the clay maker type and second, the prepared device type Yin dry, so that it is gradually dehydrated. Again, the dewatered clay billet is put into a methyl methacrylate monomer solution to be fully absorbed. Finally, the clay billet absorbing the methyl methacrylate monomer is irradiated at a ^{60}Co radiation source for the polymerization reaction to occur.

The main advantage of producing cold pottery by the radiation method is that without high temperature, the clay can well preserve the color and texture without burning.

4.2. Computer-Aided Design of Ceramic Color Matching

4.2.1. Methodology. Ceramic glaze patterns need to change at a high temperature of 1000°C or higher, which usually makes it difficult for artists to intuitively design the glaze color of ceramic art. The idea here is mainly based on the glazing code, computer-aided design; the first step should be the direct pattern design in the computer, convert the design pattern to the coded glaze coloring scheme, and finally, the glaze drawing on the ceramic billet. The contents shown in Figures 2 and 3 and Tables 1 and 2 are derived from the introduction of the ceramic products by Ferro [10].

4.2.2. Related Cases

(1) Rob Kessler Ceramic Art Design. Wolfgang Stuppy, a renowned botanist in Keyou District, has made a very careful analysis of the sexual reproductive complexity of plants with the visual artist Rob Kesscler [11]. Rob Kesscler microphotographs of wild pollen in the Royal Wild Botanical Gardens, with many wonderful photographs, striving to reproduce the image of the natural world, plants, and flowers migrated to all aspects of society.

Rob Kessler scanned the wild pollen microphotos into a transparent laser film, before printing the painted paper on screen printing. After drying, the printed pattern coating paper is soaked in water so that the pattern can fall off the paper base and be transferred onto the blank of the product and burned between 750°C and 900°C (Figure 4).

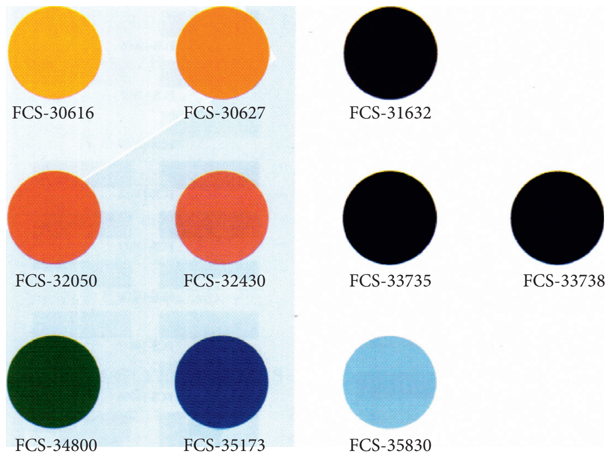

Figure 2: Billet body color chromatography.

In addition to this, digital technology can also bring great convenience and style breakthrough to pattern design.

(2) Blue and White Issued by Adobe Software Design. "Blue and White" (2007 Adobe China Shall We Dance Digital Art Competition Gold Award, created by Fan Yongguang) is a blue and white porcelain plate (Figure 5). The traditional decoration and transparent colorfully show the Chinese blue and white porcelain is very delicate and smooth. On careful observation, the above patterns are arranged by various tool icons commonly used in Adobe software. Thus, the author took great effort and made full use of the time to design and make the porcelain plate.

The overall design of the work is very in line with the relevant requirements of "Chinese wind," in the very representative Chinese blue and white porcelain as its main carrier at the same time can be the Adobe elements that are very perfectly integrated into them, and not only fully embodies the beauty of Chinese traditional culture but also shows the infinite charm brought by the digital tools. This also belongs to the Chinese culture where modern digital art is gradually valued and is very closely combined with Chinese culture into an excellent external form of expression.

(3) Cultural and Creative Products of Local Opera Elements. "Zodiac Huangmei—Zodiac Dog," [12] a glazed cultural and creative porcelain plate (Figure 6), is one of the twelve zodiac Huangmei series; the combination of traditional decoration and animation image fully highlights the vividness of the visual image of the product. The above pattern is designed with Adobe image-making software. The author spent a lot of time creating, examining the local drama culture, refining the visual image with a sense of design, and designing and producing a series of cultural and creative works in the form of the twelfth Chinese zodiac.

The overall design of the work is very in line with the relevant requirements of "Chinese style," and using the very representative Chinese ceramic as the main carrier, the cultural elements of Huangmei Opera are perfectly integrated into it. It not only fully embodies the beauty of Chinese drama culture but also shows the artistic charm brought by digital media tools.

4.3. Mathematical Thinking in Ceramic Art

4.3.1. Mathematical Configurations in Ceramic Art. In the creation of ceramic art, using relevant theories, theorems, laws, logical thinking methods, and techniques, analyze, describe, process, and check the design methods of ceramic design processes and objects. You can use various geometric curves and geometric graphs to divide and combine ellipticals, squares, and triangles by certain rules. It can be combined into various monomers and matching ceramic shapes.

The geometric structure ceramic artworks designed by Mr. Han Meilin show a simple, concise, and lively feature, full of joy. He cut and combined different circles and arcs, producing a very rational and very simple body language, full of philosophical thinking (Figure 7).

Professor Zhang Jingjing's works mainly extend some curves in mathematics into curved surfaces and then integrated the brittle characteristics of ceramics and the soft mathematical curves (Figure 8).

4.3.2. Topological Composition in Ceramic Art. Topology is an independent branch of mathematics formed in the 19th century, studying the nature of geometry based on continuous deformation. In topology, each size and shape can be bent and changed. Because a large number of natural phenomena have typical continuity, many practical things can be transformed into the topology. Explain the collection of space for mastering the different functional relations between spaces. Figure 9 shows the topological ceramic works created by Mr. Bai Ming. He can play the simple elements of nature into the ultimate elegance. His art has vitality and is constructive at the same time. Ceramics has been a transformative sublimation here as said by Bai Ming. Some of his works include creative cracks, folds, and broken lines, from which his thinking about history and the passage of time are seen [13].

5. Optimization and Upgrading of Ceramic Products

For a long time, China's ceramic industry is mainly engaged in low-grade products and is currently in the development stage from quantity growth to quality and efficiency. The focus should be in the future on improving product quality and grade. The improvement of the product grade will lead to a corresponding increase in the sales price, resulting in a profit increase, which will moderately increase the product cost, which also means that the company can use clean and pollution-free fuel to implement technological transformation and equipment upgrading. Purchasing and utilization of energy conservation and environmental protection equipment to improve the level of energy conservation and emission reduction can promote the improvement of product grade and finally realize a virtuous cycle. Improving

Figure 3: Chromatography for glaze material.

Table 1: Biomaterial.

Code	Description	Composition	Maximum temperature (°C)	Residue #400
FCS-30616	Buff	Ti-Sb-Cr	1300	<1
FCS-30627	Buff	Ti-Sb-Cr	1300	<1
FCS-31632	Brown	Fe-Cr-Al-Zn	1300	<1
FCS-32050	Red	Yb-Ca-Cr	1300	<1
FCS-32430	Pink	Mn-Al	1300	<1
FCS-33735	Cobalt-free black	Fe-Cr	1300	<1
FCS-33738	Cobalt black	Fe-Cr-V	1300	<1
FCS-34800	Green	Cr-Al	1300	<1
FCS-35173	Cobalt blue	Co-Al	1300	<1
FCS-35830	Turquoise blue	V-Zr	1300	<1

product quality and grade requires ceramic industry enterprises to actively develop new products and vigorously develop ceramic products with high technical content, good economic efficiency, low resource consumption, and small environmental pollution. During the 13th Five-Year Plan period, China should develop more environmental-conscious sanitary ceramic products, further increase its proportion, research, and development of new products with high technical content and antibacterial, self-cleaning, light storage, conductivity, noise reduction, filtration, health, insulation, and achieve industrialization. We should advocate the reduction of resources, solve the major technical and equipment problems in technology, technology, equipment, specification, and application due to the reduction of thickness, and vigorously promote the thinning process of ceramic bricks. Developing and promoting the application

Table 2: Glazing colors.

Code	Description	Composition	Maximum temperature (°C)	Residue #400
FCS-10401	Yellow	Zr-Pr-Si	1230	<0.4
FCS-11015	Coral	Zr-Fe-Si	1230	<0.4
FCS-11020	Coral	Zr-Fe-Si	1230	<0.4
FCS-11037	Peach	Zr-Fe-Pr-Si	1230	<0.4
FCS-11039	Chocolate brown	Fe-Cr-Zn	1230	<0.4
FCS-11133	Dark brown	Fe-Cr-Ni-Zn	1230	<0.4
FCS-11135	Dark brown	Fe-Cr-Ni-Zn	1230	<0.4
FCS-11500	Golden brown	Fe-Cr-Zn-Al	1230	<0.4
FCS-11508	Dark brown	Fe-Cr-Zn-Al	1230	<0.4
FCS-11510	Brown	Fe-Cr-Al-Zn	1230	<0.4
FCS-11515	Red brown	Fe-Cr-Al-Zn	1230	<0.4
FCS-12012	Maroon	Sn-Cr-Ca-Si	1230	<0.4
FCS-12025	Light maroon	Sn-Cr-Ca-Si	1230	<0.4
FCS-13001	Nickel grey	Co-Ni	1230	<0.4
FCS-13005	Dark grey	Co-Mn	1230	<0.4
FCS-13006	Light grey	Fe-Cr-Mn-Ni	1230	<0.4
FCS-13011	Tin grey	Sn-Sb	1230	<0.4
FCS-13018	Cobalt black	Fe-Cr-Co-Mn	1230	<0.4
FCS-13023	Cobalt-free black	Fe-Cr	1230	<0.4
FCS-14000	Peacock blue	Co-Al-Cr	1230	<0.4
FCS-14027	Peacock green	Cr-Co-Zn	1230	<0.4
FCS-14056	Apple green	Zr-Si-Pr-V	1230	<0.4
FCS-14570	Chrome green	Cr-Al	1230	<0.4
FCS-15063	Blue	Co-Al-Zn	1230	<0.4
FCS-15090	Turquoise	Zr-Si-V	1230	<0.4
FCS-15500	Cobalt blue	Co-Si	1230	<0.4
4FCS-16035	Yellow	S-Se-Zr-Si-Cd	1230	<0.4
FCS-16037	Red	Zr-Cd-Se-Si	1230	<0.4
FCS-16038	Orange	Zr-Cd-Se-Si	1230	<0.4

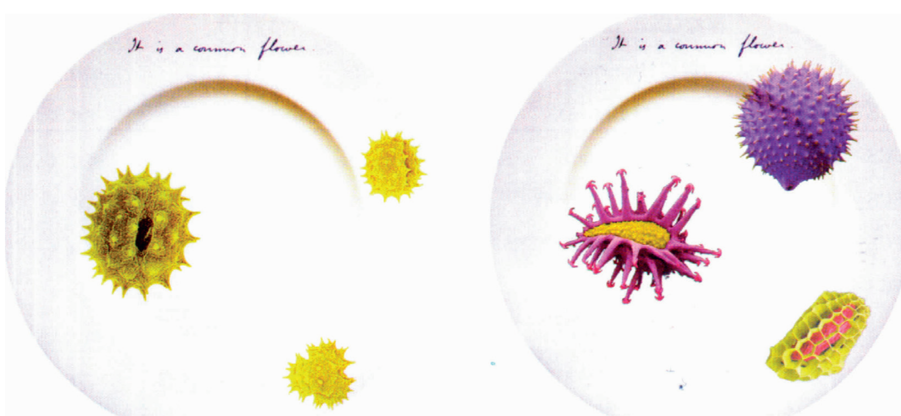

Figure 4: Rob Kessler ceramic art.

of aquatic products and accelerating the lightweight of products, for large and overweight toilets with luxury characteristics and various vertical urinals, should reduce production as much as possible.

The ceramic industry should actively develop and promote new technologies and new equipment for energy conservation and emission reduction. According to the "13th Five-Year Plan" Science and Technology Development Plan of Construction Materials Industry issued by China Federation of Construction Materials Industry [14], during the 13th Five-Year Plan period, key technologies for the development and application of Chinese building sanitary ceramics include supporting technologies for the production and application of thin building tiles (boards), continuous ball grinding process technology, new dry legal powder technology and complete set of equipment technology, energy-efficient multilayer roller dryer, new high-efficient coal gasification (self) purification equipment, ceramic decoration, spray drawing and printing technical equipment, laser printing technology equipment, new automatic ceramic tile selection and packaging technology, powder standardization and functional inkjet inks, production and

Figure 5: “Blue and white” ornamentation designed by computer.

Figure 6: Zodiac dog.

Figure 7: Works “kangaroo” by Mr. Han Meilin.

Figure 8: Spring up.

Figure 9: Taihu Lake Stone.

application of supporting technology for lightweight water-saving and sanitary ceramics, low-pressure rapid drainage forming technology of sanitary ceramics, high-pressure forming technology, intelligent production technology and complete equipment of sanitary ceramics (including robot glaze technology with self-learning function, initialization of the sanitary ceramic model, 3D additive printing technology, sanitary ceramic grouting robot, sanitary ceramic billet robot, sanitary ceramic kiln robot, sanitary ceramic intelligent, and efficient drying system), model development of CNC machining technology, new antibacterial and self-cleaning glaze manufacturing technology, improving the intelligent and healthy use of sanitary ceramics, developing the application of low-grade raw materials and new waste products, accurate automatic ingredient technology of raw material standardization and flexibility, and raw material online monitoring and correction system. Wide-body energy-saving kiln, low temperature burning technology, waste heat utilization technology, robot application technology, automatic storage, and transfer production line, intelligent three-dimensional storage technology, efficient dust removal, desulfurization, defluorine technology and equipment, creative and other building health ceramic product technology, and manufacturing technology, are to develop functional new materials suitable for life decoration (sound insulation, sterilization, and fresh air). Especially in the postepidemic era, we advocate the concept of green ceramic design and production and make more products that are in harmony with human and natural development to benefit the global ecological development.

6. Conclusion

At present, the world porcelain pattern has undergone great changes. Under this background, China, as a traditional porcelain country, has both opportunities and threats, as well as advantages and disadvantages. Only by adhering to scientific and technological innovation as the leading role, promoting industrial optimization and upgrading, and creating green ceramic industry blocks, China's ceramic industry can achieve healthy and proud development. Based on SWOT analysis, this study analyzes the opportunities and disadvantages of China's ceramic industry development, challenges, and opportunities that coexist in the background, analyzes how to use scientific and technological innovation, with the help of interdisciplinary technology, better and stronger development, and hopes to provide theoretical reference for the current ceramic design and production.

Data Availability

The data supporting this study cannot be shared as no datasets were generated or analyzed during the current study.

Conflicts of Interest

The authors declare that they have no conflicts of interest.

Acknowledgments

The authors acknowledge the 2021 University Discipline (Professional) Top Talent Academic Fund Project (gxbjZD2021005).

References

[1] H. Weihrich, *Management: A Global Perspective*, Economic Science Press, Beijing, China, 11th edition, 2005.
[2] H. Yao and Q. Gu, "SWOT analysis of the competitiveness of Dehua ceramics industry and its improvement countermeasures," *Journal of Minnan Normal University (Philosophy and Social Sciences Edition)*, vol. 7, no. 3, pp. 96–101, 2012.
[3] S. Li, "SWOT analysis and countermeasures of Zibo ceramic exports," *Northern Economy*, vol. 7, no. 11, pp. 27-28, 2007.
[4] J. Huang, H. Haiwang, W. Jiang et al., "SWOT analysis and countermeasures of the core competitiveness of Jingdezhen ceramics cultural creative industry," *Science and Technology Information*, vol. 32, no. 6, p. 2, 2012.
[5] H. Zhang, "SWOT analysis of Zibo ceramics export competitiveness," *Ceramics*, vol. 314, no. 4, pp. 17-18, 2013.
[6] T. Tao, "Consumption trends from the seventh census data," *Knowledge-Economy*, vol. 50, no. 6, p. 4, 2021.
[7] G. Li, "Ten gaps alert the Chinese ceramic industry," *Modern Technology Ceramics*, no. 3, pp. 44–46, 2008.
[8] Y. Huang, "Research on the international competitiveness of China ceramic industry," *Economic and Trade Practice*, no. 13, pp. 42-43, 2016.
[9] X. Zhang and X. Zheng, "Research progress in low-temperature ceramic ceramics," *Micro-Nanoelectronic Technology*, vol. 56, no. 10, pp. 32–40, 2019.
[10] W. Stape, R. Keseller, W. Stuppy et al., *The Miracle of the Plant Kingdom: The Mystery of the Fruit*, People's Post & Telecommunications Press, Beijing, China, 2015.
[11] X. Hu and Y. Zhang, "Research on the development and visual image of opera culture creative products," *Journal of Visual Art and Design*, vol. 12, no. 2, pp. 144–156, 2021.
[12] Y. Li and S. Zou, "Strategic choice for improving the international competitiveness of China's ceramic industry after WTO," *University of South China: Social Sciences*, vol. 3, no. 1, pp. 44–49, 2002.
[13] H. Chen, ""The country of—Bai" appeared at Beijing Minsheng modern museum," *Chinese Poamist*, no. 2, pp. 37–40, 2017.
[14] Anonymous, "Construction materials industry 13th five-year plan science and technology development plan," *Commercial Concrete*, no. 7, pp. 23–31, 2016.